

This document was produced
by scanning the original publication.

Ce document est le produit d'une
numérisation par balayage
de la publication originale.

Geological Survey of Canada
Commission géologique du Canada

PAPER 86-1B
ÉTUDE

CURRENT RESEARCH PART B
RECHERCHES EN COURS PARTIE B



(Pages 1-420)

Notice to Librarians and Indexers

The Geological Survey's twice-yearly *Current Research* series contains many reports comparable in scope and subject matter to those appearing in scientific journals and other serials. All contributions to *Current Research* include an abstract and bibliographic citation. It is hoped that these will assist you in cataloguing and indexing these reports and that this will result in a still wider dissemination of the results of the Geological Survey's research activities.

Avis aux bibliothécaires et préparateurs d'index

La série *Recherches en cours* de la Commission géologique paraît deux fois par année; elle contient plusieurs rapports dont la portée et la nature sont comparables à ceux qui paraissent dans les revues scientifiques et autres périodiques. Tous les articles publiés dans les *Recherches en cours* sont accompagnés d'un résumé et d'une bibliographie, ce qui vous permettra, nous l'espérons, de cataloguer et d'indexer ces rapports, d'où une meilleure diffusion des résultats de recherche de la Commission géologique.



GEOLOGICAL SURVEY OF CANADA
PAPER 86-1B

COMMISSION GÉOLOGIQUE DU CANADA
ÉTUDE 86-1B

CURRENT RESEARCH PART B

RECHERCHES EN COURS PARTIE B

Issued in two sections/Publiée en deux volumes:
pages 1-420 and/et pages 421-880

© Minister of Supply and Services Canada 1986

Available in Canada through

authorized bookstore agents and other bookstores

or by mail from

Canadian Government Publishing Centre
Supply and Services Canada
Ottawa, Canada K1A 0S9

and from

Geological Survey of Canada offices:

601 Booth Street
Ottawa, Canada K1A 0E8

3303-33rd Street N.W.,
Calgary, Alberta T2L 2A7

100 West Pender Street
Vancouver, British Columbia V6B 1R8
(mainly B.C. and Yukon)

A deposit copy of this publication is also available
for reference in public libraries across Canada

Cat. No. M44-86/1BE Canada: \$20.00
ISBN 0-660-53302-2 Other countries: \$24.00

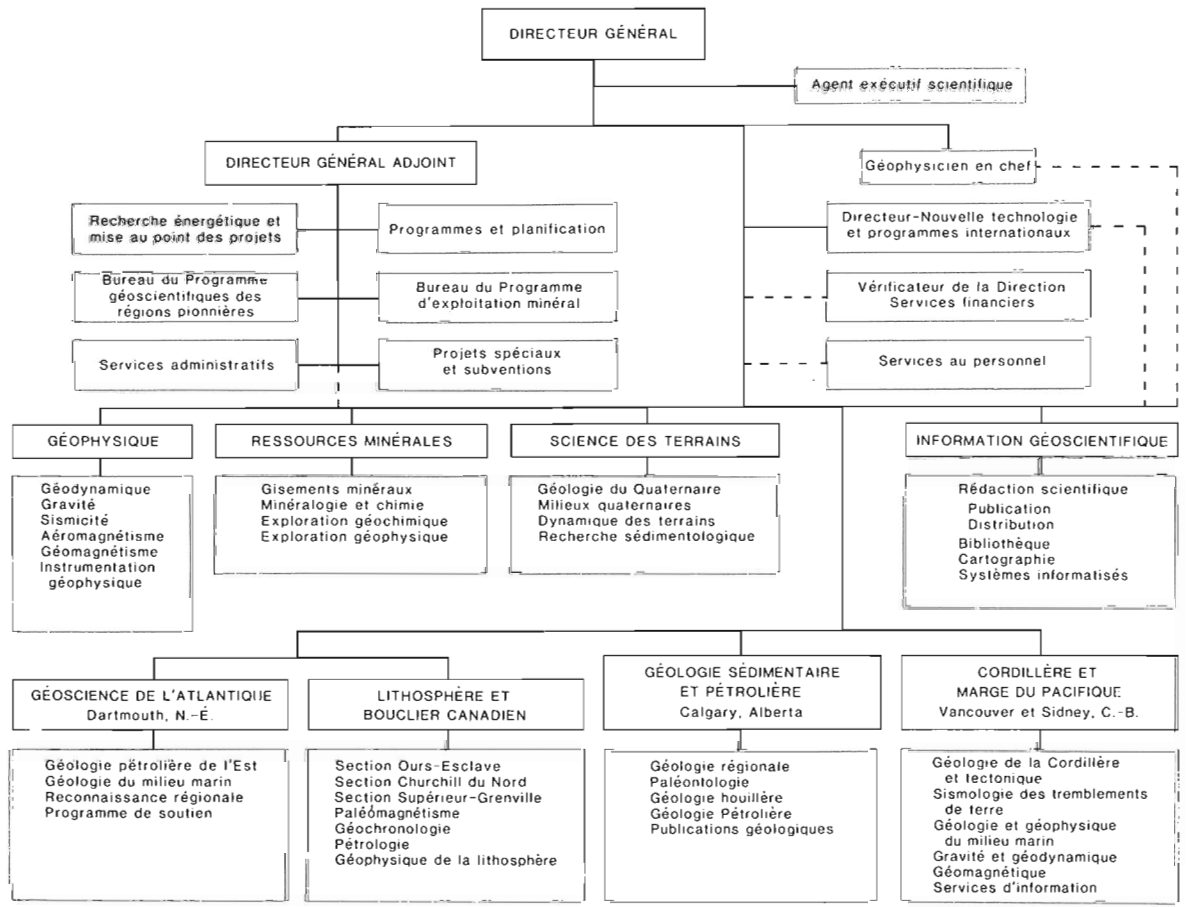
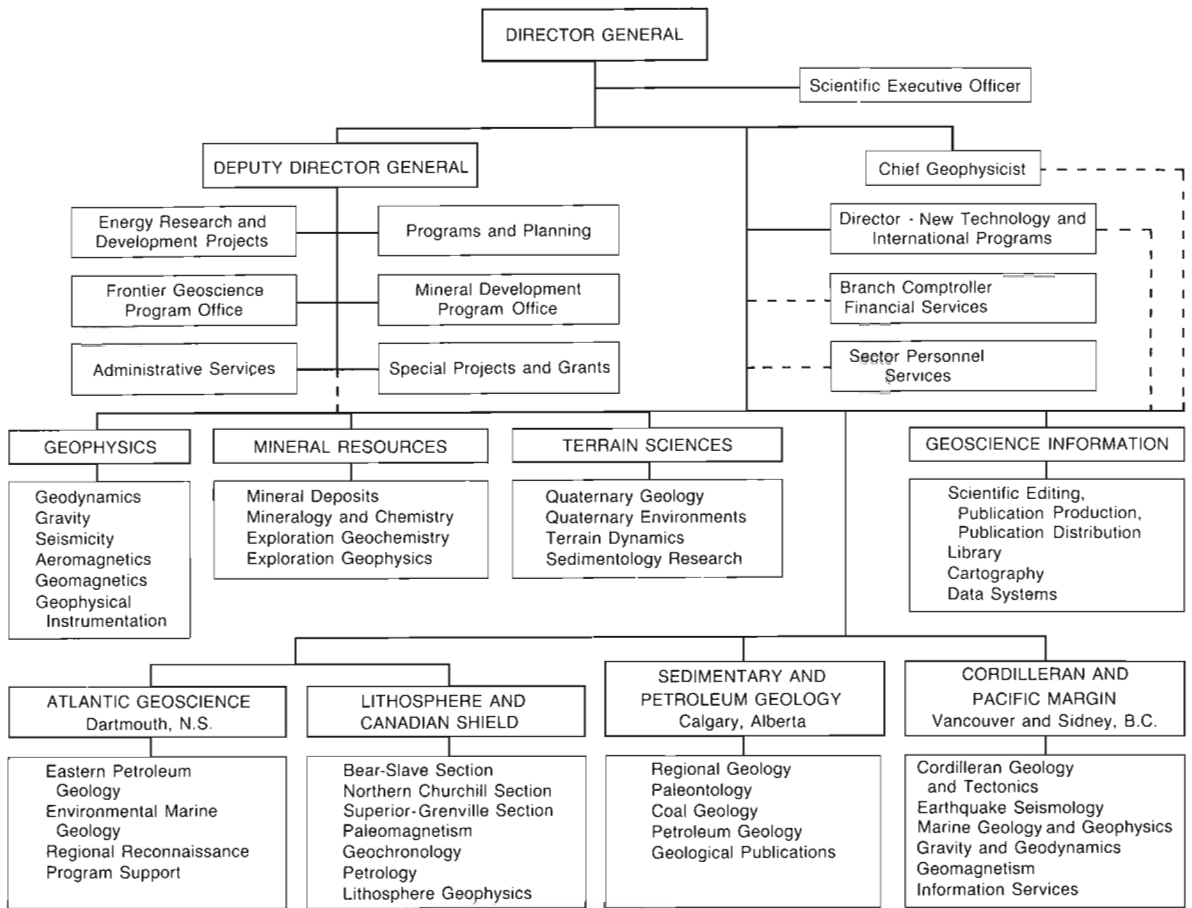
Price subject to change without notice

Sold in sets

Cover

Aerial view eastward from MacMillan Glacier along the north side
of Baird Inlet, Ellesmere Island.

This illustration appears in report 26, p. 241, by W. Blake, Jr.



Separates

A limited number of separates of the papers that appear in this volume are available by direct request to the individual authors. The addresses of the Geological Survey of Canada offices follow:

601 Booth Street,
OTTAWA, Ontario
K1A 0E8

Institute of Sedimentary and Petroleum Geology,
3303-33rd Street N.W.,
CALGARY, Alberta
T2L 2A7

Cordilleran and Pacific Margin Division,
100 West Pender Street,
VANCOUVER, B.C.
V6B 1R8

Atlantic Geoscience Centre,
Bedford Institute of Oceanography,
P.O. Box 1006,
DARTMOUTH, N.S.
B2Y 4A2

When no location accompanies an author's name in the title of a paper, the Ottawa address should be used.

Tirés à part

On peut obtenir un nombre limité de "tirés à part" des articles qui paraissent dans cette publication en s'adressant directement à chaque auteur. Les adresses des différents bureaux de la Commission géologique du Canada sont les suivantes:

601, rue Booth
OTTAWA, Ontario
K1A 0E8

Institut de géologie sédimentaire et pétrolière
3303-33rd, St. N.W.,
CALGARY, Alberta
T2L 2A7

Division de la Cordillère et marge du Pacifique
100 West Pender Street
VANCOUVER, Colombie-Britannique
V6B 1R8

Centre géoscientifique de l'Atlantique
Institut océanographique de Bedford
B.P. 1006
DARTMOUTH, Nouvelle-Ecosse
B2Y 4A2

Lorsque l'adresse de l'auteur ne figure pas sous le titre d'un document, on doit alors utiliser l'adresse d'Ottawa.

SCIENTIFIC AND TECHNICAL REPORTS RAPPORTS SCIENTIFIQUES ET TECHNIQUES

COAL/CHARBON

F. GOODARZI and T. JERZYKIEWICZ: Petrology of a burning bituminous coal seam at Coalspur, Alberta	421
A.R. CAMERON, D.K. NORRIS, and K.C. PRATT: Rank and other compositional data on coals and carbonaceous shale of the Kayak Formation, northern Yukon Territory	665
F. GOODARZI: Comparison of morphology and reflectance of macerals from a tectonically thickened coal seam from Mist Mountain, British Columbia	671

ECONOMIC GEOLOGY/GÉOLOGIE ÉCONOMIQUE

S.M. ROSCOE, S.B. GREEN, and S.S. GANDHI: Uranium, gold and selenide minerals locally concentrated in drift at Twin Lakes near Bathurst Inlet, N.W.T.	47
C. MORETON and P.F. WILLIAMS: Structural and stratigraphic relationships at the B-zone orebody, Heath Steele Mines, Newcastle, New Brunswick	57
K.H. POULSEN, D.E. AMES, S. LAU, and W.C. BRISBIN: Preliminary report on the structural setting of gold in the Rice Lake area, Uchi Subprovince, southeast Manitoba	213
R. MASON, N. MELNIK, C.F. EDMUNDS, D.J. HALL, R. JONES, and B. MOUNTAIN: The McIntyre-Hollinger investigation, Timmins, Ontario: stratigraphy, lithology and structure	567
R. MASON and N. MELNIK: The McIntyre-Hollinger investigation, Timmins, Ontario: a gold dominated porphyry copper system	577
R. DAHL and D.H. WATKINSON: Structural control of podiform chromitite in Bay of Islands ophiolite, the Springer Hill area, Newfoundland	757
Y.T. MAURICE: Distribution and origin of alluvial gold in southwest Gaspésie, Quebec	785

GEOCHEMISTRY/GÉOCHIMIE

D.C. GREGOIRE: Inductively coupled plasma-mass spectrometry at the Geological Survey of Canada	39
M.R. GIBLING, M. ZENTILLI, H. MAHONY, and R.G.L. McCREADY: An isotopic evaluation of sulphur recycling from evaporites to coals in the Carboniferous Sydney Basin, Nova Scotia	73
K. HATTORI and K. HICKS: Preliminary report on the gold mineralization at Bell Creek, Timmins, Ontario	77

J.B. WHALEN: Geochemistry of the mafic and volcanic components of the Topsails igneous suite, western Newfoundland	121
J. DAVID and C. GARIEPY: Geochemistry of the Lower Silurian Pointe aux Trembles and Lac Raymond formations, central Quebec Appalachians: a preliminary report	131
C.J. PARK and G.E.M. HALL: Electrothermal vapourization as a means of sample introduction into an inductively coupled plasma mass spectrometer: a preliminary report of a new analytical technique	767

GEOCHRONOLOGY/GÉOCHRONOLOGIE

J.K. MORTENSEN: U-Pb ages for granitic orthogneiss from western Yukon Territory: Selwyn Gneiss and Fiftymile Batholith revisited	141
C.E. RAVENHURST, P.H. REYNOLDS, and M. ZENTILLI: Strontium isotopic studies of rock and mineral samples in the Shubenacadie Basin, Nova Scotia	547
R.T. BELL and R.I. THORPE: Pb-Pb isochron age of uraniferous phosphorite at the base of the Menihék Formation, Labrador Trough	585
O. VAN BREEMEN and S. HANMER: Zircon morphology and U-Pb geochronology in active shear zones: studies on syntectonic intrusions along the northwest boundary of the Central Metasedimentary Belt, Grenville Province, Ontario	775

GEOPHYSICS/GÉOPHYSIQUES

B.D. LONCAREVIC, M.D. HUGHES, and I. HIMMLER: Evaluation of sea gravimeters: comparison of Bodenseewerk KSS30 and KSS31 systems	85
T.S. HAMILTON and D.C. NOBES: DC resistivity and CSAMT profiles of the southwestern Fraser River delta, British Columbia	741

MARINE GEOSCIENCE/ÉTUDES GEOSCIENTIFIQUES DU MILIEU MARIN

P.U. CLARK and H.W. JOSEPHANS: Late Quaternary land-sea correlations, northern Labrador and Labrador shelf	171
I.S. AL-AASM and B.D. BORNHOLD: Stable isotope studies of planktonic foraminifera <i>Globigerina bulloides</i> from cores in the northeast Pacific Ocean	201
G.B.J. FADER and R.O. MILLER: A reconnaissance study of the surficial and shallow bedrock geology of the southeastern Grand Banks of Newfoundland	591
B. MACLEAN, G.L. WILLIAMS, A. JENNINGS, and C. BLAKENEY: Bedrock and surficial geology of Cumberland Sound, N.W.T.	605
B. MACLEAN, G.L. WILLIAMS, B.V. SANFORD, R.A. KLASSEN, C. BLAKENEY, and A. JENNINGS: A reconnaissance study of the bedrock and surficial geology of Hudson Strait, N.W.T.	617
J.L. LUTERNAUER, J.J. CLAGUE, T.S. HAMILTON, J.A. HUNTER, S.E. PULLAN, and M.C. ROBERTS: Structure and stratigraphy of the southwestern Fraser River delta: a trial shallow seismic profiling and coring survey	707

**MATHEMATICAL AND COMPUTATIONAL GEOLOGY/APPLICATION DES MATHÉMATIQUES ET
DES MÉTHODES MATHÉMATIQUES DE L'ANALYSE À LA GÉOLOGIE**

J.D. HUGHES, D.J. MACNEILL, and P. WATSON: Computerization of coal exploration data for Nova Scotia: a joint Federal-Provincial project	417
J.D. HUGHES and V.P. NEIMANIS: A computer-based system for quantifying surface-mineable coal resources according to environmental characteristics and ownership of the overlying land surface	507

PALEOMAGNETISM/PALÉOMAGNETISME

W.F. FAHRIG: Paleomagnetism of Neohelikian Korok sheets and dykes, and of a possible Mackenzie dyke from southeast of Ungava Bay	65
----------------------------------------------------------------------------------------------------------------------------------------	----

PALEONTOLOGY/PALÉONTOLOGIE

T.E. BOLTON: Early Silurian Bryozoa from the Clemville Formation of the Port Daniel region, Gaspésie Peninsula, Quebec	97
T.E. BOLTON: Chaetitopora (Anthozoa, Tabulata) in the Upper Ordovician rocks of central and eastern Canada	107
J.A. JELETZKY: Pseudoeurypychites : a new polyptychitid ammonite from the Lower Valanginian of the Canadian and Eurasian Arctic	351
M.J. COPELAND: Bullaluta kindlei n. gen., n. sp. (Ostracoda, Archaeocopida) from Zone 5 (Late Cambrian, Cedaria – Crepicephalus) of the Cow Head Group, western Newfoundland	399
W.W. NASSICHUK and C.M. HENDERSON: Lower Permian (Asselian) ammonoids and conodonts from the Belcher Channel Formation, southwestern Ellesmere Island	411
R.A. MCLEAN: The rugose coral Pachyphyllum Edwards and Haime in the Frasnian (Upper Devonian) of Western Canada	443
W.W. NASSICHUK, G.R. DAVIES, and B.L. MAMET: Microcodiaceans in the Viséan Emma Fiord Formation, Devon Island, Arctic Canada	467
A.E.H. PEDDER: Species of the rugose coral genus Minussiella from the Middle Devonian of western and Arctic Canada	471
P. SARTENAER: A new late Eifelian rhynchonellid genus from western North America	489
E.H. DAVIES and T.P. POULTON: Upper Jurassic dinoflagellate cysts from strata of northeastern British Columbia	519

PETROLEUM GEOLOGY/GÉOLOGIE PÉTROLIÈRE

K.G. OSADETZ and L.R. SNOWDON: Speculation on the petroleum source rock potential of portions of the Lodgepole Formation (Mississippian) of southern Saskatchewan	647
-------------------------------------------------------------------------------------------------------------------------------------------------------------------------	-----

QUATERNARY GEOLOGY/GÉOLOGIE DU QUATERNAIRE

Mapping, stratigraphic studies, and sedimentology/Cartographie, études stratigraphiques et sédimentologie

M. RAPPOL: Aspects of ice flow patterns, glacial sediments, and stratigraphy in northwest New Brunswick	223
A. DUK-RODKIN, L.E. JACKSON, JR., and O. RODKIN: A composite profile of the Cordilleran ice sheet during McConnell Glaciation, Glenlyon and Tay River map areas, Yukon Territory	257

**Exploration technology and glacial dispersal studies/Techniques d'exploration
et études de la dispersion glaciaire**

C.A. KASZYCKI and R.N.W. DILABIO: Surficial geology and till geochemistry, Lynn Lake-Leaf Rapids region, Manitoba	245
W.W. SHILTS and S.L. SMITH: Stratigraphic setting of buried gold-bearing sediments, Beauceville area, Quebec	271
M. LAMOTHE: Reconnaissance geochemical sampling of till, south-central Miramichi Zone, New Brunswick	279
M.A. BOUCHARD and C. MARCOTTE: Regional glacial dispersal patterns in Ungava, Nouveau-Québec	295
P.P. DAVID and P. BEDARD: Stratigraphy of the McGerrigle Mountains granite trains of Gaspésie, Quebec	319

**Paleoenvironmental studies and geochronology/Étude des paléoenvironnements
et géochronologie**

C. CAUSSE et C. HILLAIRES-MARCEL: Géochimie des familles U et Th dans la matière organique fossile des dépôts interglaciaires et interstadières de l'est et du nord du Canada: potentiel radiochronologique	11
W. BLAKE, JR.: New AMS radiocarbon age determinations from east-central Ellesmere Island; applications to glacial geology	239
S. LICHTI-FEDEROVICH: Diatom dispersal phenomena: diatoms in precipitation samples from Cape Herschel, east-central Ellesmere Island, Northwest Territories – a quantitative assessment	263
R.J. MOTT, J.V. MATTHEWS, JR., D.R. GRANT, and G.J. BEKE: A late glacial buried organic profile near Brookside, Nova Scotia	289

REGIONAL GEOLOGY/GÉOLOGIE RÉGIONALE

Appalachian region/Région des Appalaches

Y.D. GAGNON et R.A. JAMIESON: Étude de la semelle métamorphique du complexe du Mont Albert, Gaspésie, Québec	1
P. ERDMER: Geology of the Long Range Inlier in Sandy Lake map area, western Newfoundland	19
J.V. OWEN and P. ERDMER: Precambrian and Paleozoic metamorphism in the Long Range Inlier, western Newfoundland	29
J.T. VAN BERKEL, H.P. JOHNSTON, and K.L. CURRIE: A preliminary report on the geology of the southern Long Range, southwestern Newfoundland	157
A.M. O'BEIRNE-RYAN, S.M. BARR, and R.A. JAMIESON: Contrasting petrology and age of two megacrystic granitoid plutons, Cape Breton Island, Nova Scotia	179
A.M. O'BEIRNE-RYAN and R.A. JAMIESON: Geology of the West Branch North River and the Bothan Brook plutons of the south-central Cape Breton Highlands, Nova Scotia	191
H.E. PLINT, K.A. CONNORS, and R.A. JAMIESON: Geology and mineral occurrences of the Jumping Brook Complex, Cheticamp-Pleasant Bay area, Cape Breton Island, Nova Scotia	557

Arctic Islands/Archipel Arctique

A.F. EMBRY: Stratigraphic subdivision of the Blind Fiord and Bjerne formations (Lower Triassic), Sverdrup Basin, Arctic Islands	329
------------------------------------------------------------------------------------------------------------------------------------------	-----

A.F. EMBRY: Stratigraphic subdivision of the Awingak Formation (Upper Jurassic) and revision of the Hiccles Cove Formation (Middle Jurassic), Sverdrup Basin, Arctic Islands	341
B.D. RICKETTS: New formations in the Eureka Sound Group, Canadian Arctic Islands	363
B.D. RICKETTS and D.J. MCINTYRE: The Eureka Sound Group of eastern Axel Heiberg Island: new data on the Eurekan Orogeny	405

Cordilleran region/Région de la Cordillère

J. DIXON: Comments on the stratigraphy, sedimentology and distribution of the Albian Sharp Mountain Formation, northern Yukon	375
D.A. LECKIE and A.E. FOSCOLOS: Paleosols and Late Albian sea level fluctuations: preliminary observations from the northeastern British Columbia foothills	429
J.A. MOTT, J.M. DIXON, and H. HELMSTAEDT: Ordovician stratigraphy and the structural style at the Main Ranges-Front Ranges boundary near Smith Peak, British Columbia	457
T.S.T. HEAH, R.L. ARMSTRONG, and G.J. WOODSWORTH: The Gambier Group in the Sky Pilot area, southwestern Coast Mountains, British Columbia	685
J.H. SEVIGNY and E.D. GHENT: Metamorphism in the northern Adams River area, northeastern Shuswap Complex, Monashee Mountains, British Columbia	693
J.W.H. MONGER: Geology between Harrison Lake and Fraser River, Hope map area, southwestern British Columbia	699
A.J. ARTHUR: Stratigraphy along the west side of Harrison Lake, southwestern British Columbia	715
M.G. MIHALYNUK and E.D. GHENT: Stratigraphy, deformation and low grade metamorphism of the Telkwa Formation near Terrace, British Columbia	721
D.W.A. MCMULLIN and H.J. GREENWOOD: Metamorphic pressures and temperatures in the Barkerville and Cariboo terranes, Quesnel Lake, British Columbia: preliminary results	727
C.A. EVENCHICK: Structural style of the northeast margin of the Bowser Basin, Spatsizi map area, north-central British Columbia	733
J. O'BRIEN: Jurassic stratigraphy of the Methow Trough, southwestern British Columbia	749

Canadian Shield/Bouclier canadien

P.M. CLIFFORD: Petrological and structural evolution of the rocks in the vicinity of Killarney, Ontario: an interim report	147
K.E. ASHTON and K.J. WHEATLEY: Preliminary report on the Kisseynew gneisses in the Kisseynew-Wildnest lakes area, Saskatchewan	305
S.L. JACKSON and T.M. GORDON: Metamorphic studies in the transition zone between the Lynn Lake Greenstone Belt and the Kisseynew gneiss belt, Laurie Lake, Manitoba	539
S.M. ROSCOE and A.R. MILLER: Outliers of porphyritic alkaline volcanic rocks of the Christopher Island Formation at Snowbird Lake, N.W.T.	679
F. FUETEN, P.-Y. F. ROBIN, and M.E. PICKERING: Deformation in the Thompson Belt, central Manitoba: a progress report	797
S. HANMER and J.N. CONNELLY: Mechanical role of the syntectonic Laloche Batholith in the Great Slave Lake Shear Zone, District of Mackenzie, N.W.T.	811

B.A. BARHAM and E. FROESE: Geology of the New Fox alteration zone, Laurie Lake, Manitoba	827
A. DAVIDSON and S.M. GRANT: Reconnaissance geology of western and central Algonquin Park and detailed study of coronitic olivine metagabbro, central Gneiss Belt, Grenville Province of Ontario	837

Interior Plains/Plaines intérieures

I. BANERJEE: Lower Mannville sedimentation in the "Edmonton Channel", central Alberta	383
D.A. LECKIE and R.J. CHEEL: Tidal channel facies of the Virgelle Member (Cretaceous Milk River Formation), southern Alberta	637
T. JERZYKIEWICZ and A.R. SWEET: Caliche and associated impoverished palynological assemblages: an innovative line of paleoclimatic research onto the uppermost Cretaceous and Paleocene of southern Alberta	653

STRATIGRAPHY/STRATIGRAPHIE

H.M. STEELE-PETROVICH: Lithostratigraphy and a summary of the paleoenvironments of the lower Middle Ordovician sedimentary rocks, upper Ottawa Valley, Ontario	493
----------------------------------------------------------------------------------------------------------------------------------------------------------------------------	-----

STRUCTURAL GEOLOGY/GÉOLOGIE STRUCTURALE

A. LEGER and P.F. WILLIAMS: Transcurrent faulting history of southern New Brunswick	111
----------------------------------------------------------------------------------------------	-----

SCIENTIFIC AND TECHNICAL NOTES NOTES SCIENTIFIQUES ET TECHNIQUES

J.V. BARRIE and J.L. LUTERNAUER: Titaniferous placers on the central continental shelf off western Canada	849
S.S. GANDHI: Garnetiferous gneisses and a quartz syenite intrusive sheet at Lynx Lake, Northwest Territories	853
P. MORGAN: Sediment transport study at King Point, Yukon Territory	859
J.Y. VAN BOSSE, I.M. SAMSON, and A.E. WILLIAM-JONES: Illite crystallinity studies around the Roberts metal deposit, Eastern Townships, Quebec	865
M. CLOUTIER et P. CORBEIL: Géologie du Quaternaire de la région du Mont Alexandre, Gaspésie, Quebec	869

CANADA-NEWFOUNDLAND MINERAL DEVELOPMENT AGREEMENT 1984-1989 CANADA-TERRE-NEUVE: ENTENTE D'EXPLOITATION MINÉRALE 1984-1989	875-880
------------------------------------------------------------------------------------------------------------------------------------	---------

AUTHOR INDEX/INDEX DES AUTEURS	420a/883
--------------------------------------	----------

Errata	881
--------------	-----

SCIENTIFIC AND TECHNICAL REPORTS RAPPORTS SCIENTIFIQUES ET TECHNIQUES

- 1 -

Étude de la semelle métamorphique du complexe du Mont Albert, Gaspésie, Québec¹

Y. Denis Gagnon² et Rebecca A. Jamieson²

Division de la lithosphère et du Bouchier canadien

Gagnon, Y.D., et Jamieson, R.A., Étude de la semelle métamorphique du complexe du Mont Albert, Gaspésie, Québec; dans Recherches en cours, Partie B, Commission géologique du Canada, Étude 86-1B, p. 1-10, 1986.

Résumé

La semelle métamorphique du Mont Albert représente une zone de cisaillement à haute température. Se situant structurellement au-dessous de la péridotite, elle possède les principales caractéristiques des « auréoles dynamothermales » associées aux complexes ophiolitiques. Plusieurs coupes géologiques faites dans le secteur nord-est de ce complexe caractérisé par d'intenses déformations, la présence de protolithes, une association structurale avec la péridotite sus-jacente, ainsi que de forts gradients thermiques et barométriques inverses, ont permis de distinguer la superposition, à l'intérieur même de la semelle métamorphique, de quatre terrains distincts composés d'amphibolite et de métasédiments. Les études pétrologiques et structurales semblent indiquer que sa formation aurait débuté en milieu océanique pour se terminer en bordure de la marge continentale et se serait produite de la façon suivante :

- 1) transport et métamorphisme sous la péridotite des roches de plus haut degré; puis
- 2) incorporation successive des roches de degré moins élevé à la semelle métamorphique alors que la péridotite chevauchait des terrains plus riches en sédiments et à température plus basse.

Abstract

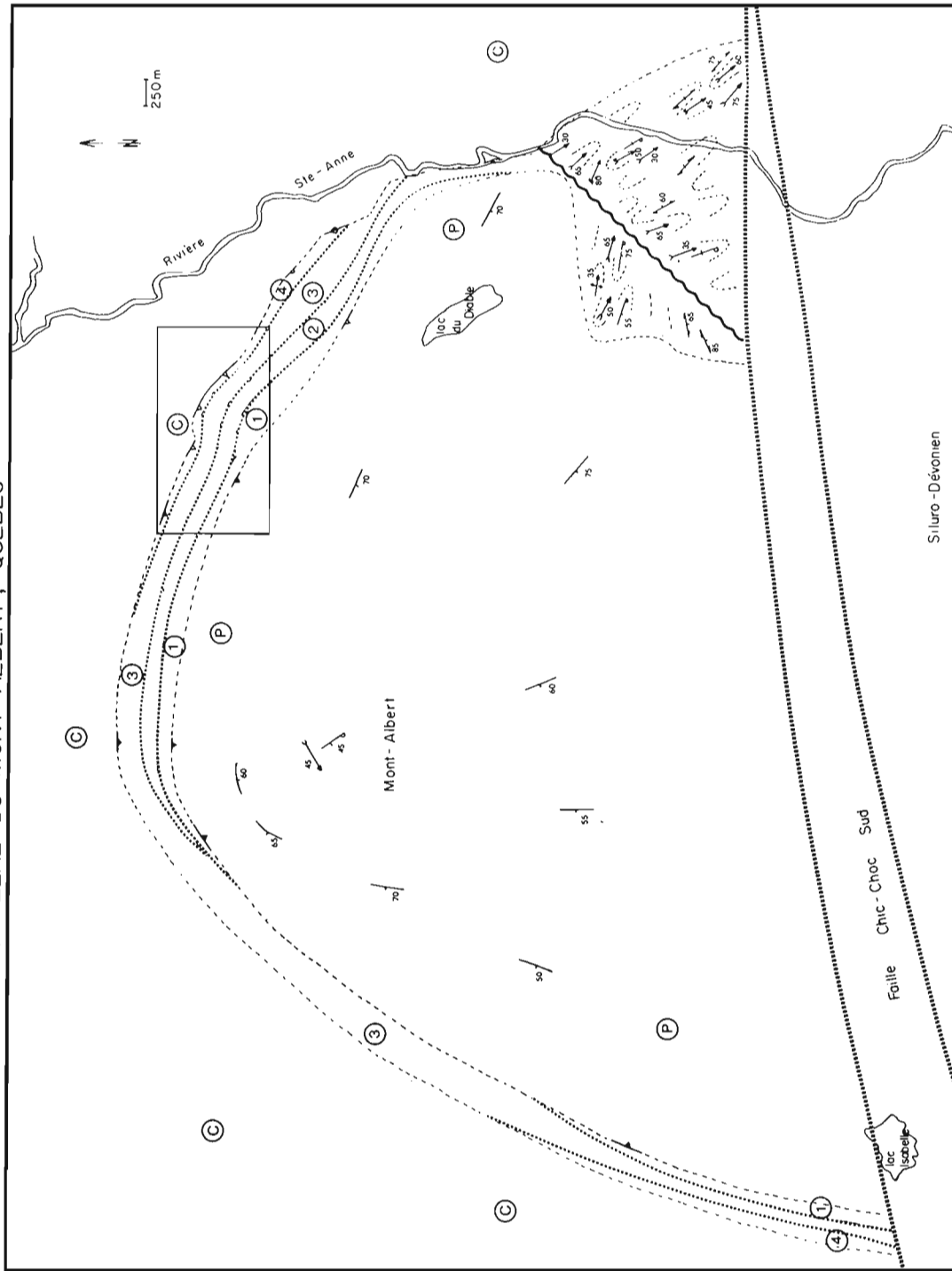
The metamorphic sole of the Mount Albert complex is a high temperature shear zone, structurally underlying the peridotite and showing the main characteristics of dynamothermal aureoles associated with ophiolite complexes. Several geological sections in the northeast part of this complex, characterized by intense deformation, the presence of protoliths, a structural association with the overlying peridotite, as well as high inverted temperature and pressure gradients, have led to the recognition, within the metamorphic body, of four superimposed zones composed of amphibolite and metasediments. Petrographic and structural studies seem to indicate that formation of the metamorphic body began in an oceanic environment and ended along the edge of the continental margin, and involved:

- 1) transportation and metamorphism, under the peridotite, of the highest grade rocks, followed by
- 2) successive incorporation of lower grade rocks into the metamorphic sole while the peridotite overthrust lower-temperature terranes that were richer in sediments.

¹ Contribution au Plan de développement économique Canada/Gaspésie et Bas Saint-Laurent, Volet Mines 1983-1988

² Département de géologie, université Dalhousie, Halifax, Nouvelle-Écosse B3H 3J5

LE COMPLEXE DU MONT ALBERT, QUEBEC



LEGENDE

(P)	Péridotite
(1)	terrain 1
(2)	terrain 2
(3)	terrain 3
(4)	terrain 4
(C)	Groupe des Chic-Choc
— —	contact majeur
- - -	contact entre différents terrains
- - -	métasédiments
↗↘	foliation
↗↘	axe de plis
— —	zone de fracture
↗↘	rubonnement de la péridotite
↗↘	surface axiale des plis

Figure 1.1. Le complexe du Mont Albert, Québec. Légende commune également aux figures 1.2 et 1.3.

Introduction

La péridotite du Mont Albert se situe dans les monts Chic-Choc, en Gaspésie (66°10' longitude O; 48°50' latitude N; SNRC:22B/16). Elle se retrouve à la bordure sud-est du domaine interne des Appalaches québécoises (St-Julien et Hubert, 1975), en Gaspésie, et se présente sous forme d'un klippe semi-circulaire de 5 sur 8 km. Elle se compose essentiellement de bandes métriques d'harzburgite et de dunité partiellement serpentinisées et repose structuralement sur, et est entourée par, une « semelle métamorphique » composée d'amphibolites et de métasédiments. Il s'agit en outre de roches foliées et plissées. Le complexe du Mont Albert, qui inclut la péridotite et la semelle métamorphique sous-jacente, est entouré sur trois côtés par les roches métasédimentaires et métavolcaniques du groupe des Chic-Choc et est bordé au sud par la faille Chic-Choc Sud (fig. 1.1).

Les résultats des travaux sur le terrain exécutés au cours de l'été 1984 viennent appuyer les conclusions de Beaudin (1983) fondées sur des considérations structurales, pétrographiques et régionales, et aux termes desquelles cet auteur suggère que la péridotite du Mont Albert soit une péridotite de type alpin plutôt qu'intrusif (MacGregor, 1962, 1964; MacGregor et Basu, 1976, 1979). Dans le cadre du présent rapport, l'observation détaillée des roches métamorphiques entourant la péridotite semble indiquer que le degré du métamorphisme augmente vers la péridotite depuis le groupe des Chic-Choc, mais qu'il ne s'agit pas d'une progression continue du métamorphisme ainsi que l'ont indiqué MacGregor (1964) et Beaudin (1983). En outre, il a été souligné (Gagnon et Jamieson, 1985) que les roches métamorphiques qui entourent la péridotite du Mont Albert sont structurellement et pétrographiquement très différents des roches du groupe des Chic-Choc et ne peuvent dériver du métamorphisme des roches métavolcaniques et métasédimentaires du groupe des Chic-Choc ainsi que l'ont précédemment suggéré MacGregor (1964) et Beaudin (1983).

À la suite de récents travaux effectués au cours de l'été 1985, il appert que les roches métamorphiques qui entourent la péridotite forment une semelle métamorphique comportant les

principales caractéristiques structurales et pétrographiques des « auréoles dynamothermales » associées aux péridotites alpines (Williams et Smyth, 1973; Coleman et Irwin, 1977; Jamieson, 1980; Spray, 1984). Dans son ensemble, la semelle métamorphique du Mont Albert montre d'intenses déformations associées au métamorphisme, de rapides variations lithologiques, pétrographiques et texturales ainsi qu'une association structurale avec la péridotite sus-jacente. Les résultats obtenus à partir de coupes géologiques faites depuis la péridotite jusque dans le groupe des Chic-Choc ont permis de distinguer la superposition de plusieurs terrains lithologiquement et pétrologiquement distincts.

La discussion qui suit porte sur la description détaillée de ces coupes géologiques faites depuis la partie nord-est de la péridotite du Mont Albert jusque dans le groupe des Chic-Choc. Cette localité a été choisie en raison de la présence d'une couverture végétale très peu développée et de son profil topographique représentatif de la structure interne de la semelle métamorphique. L'analyse de ces coupes géologiques permet de distinguer quatre différents types de terrain à partir de critères pétrographiques, texturaux et structuraux. Aux fins de description, ils porteront les numéros 1, 2, 3, 4, allant du premier (terrain 1) situé en bordure du contact de la péridotite et de la semelle métamorphique au quatrième (terrain 4), à la base de la semelle métamorphique en bordure du groupe des Chic-Choc (fig. 1.2).

Descriptions lithologiques des terrains

Terrain 1

Le terrain 1 borde la péridotite. Il se compose d'hornblendite, d'hornblendite à grenat, d'amphibolite à clinopyroxène et d'amphibolite à clinopyroxène et grenat. Les hornblendites sont composées essentiellement de hornblende en cristaux trapus de 3 à 6 mm que l'on peut appeler des hornblendites à grenat lorsqu'elles contiennent des quantités appréciables de grenat. Des bandes riches en grenat ou en clinopyroxène, ou les deux, se retrouvent dans une foliation donnée par l'orientation planaire des cristaux de hornblende, formant ainsi les

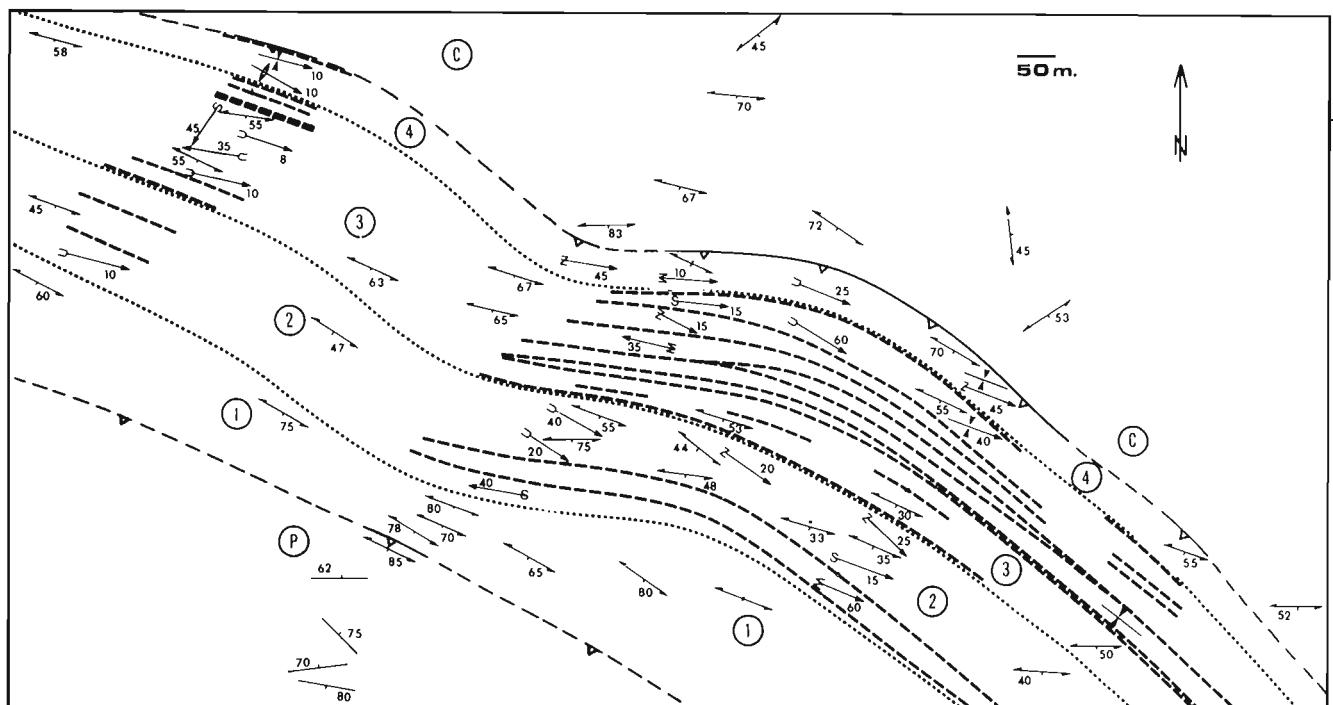


Figure 1.2. La semelle métamorphique du Mont Albert, secteur nord-est. Voir la légende à la figure 1.1

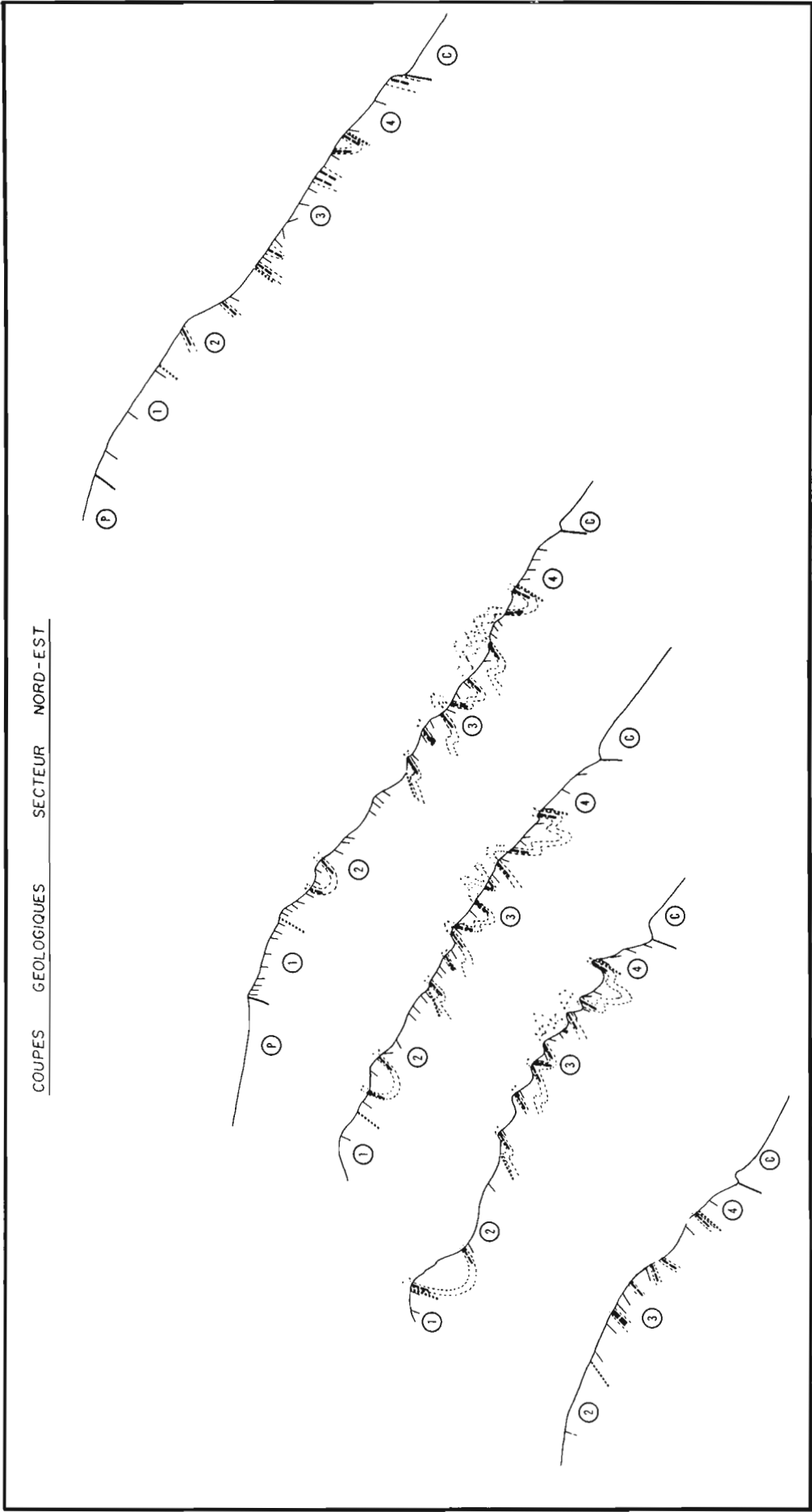


Figure 1.3. Coupes géologiques, secteur nord-est. Voir la légende à la figure 1.1.

amphibolites à clinopyroxène et les amphibolites à clinopyroxène et grenat. Ces dernières, caractérisées par la taille moyenne de leurs grains, présentent des textures granoblastiques où porphyroclastiques. Ces roches contiennent des quantités variables de plagioclase et d'épidote et sont ainsi également caractérisées par un rubanement produit par de très importantes variations compositionnelles et texturales.

Terrain 2

Le terrain 2 se compose de hornblendite, d'amphibolite à clinopyroxène, d'amphibolite à clinopyroxène et épidote, d'amphibolite felsique, d'amphibolite à grenat et de métasédiments. Dans le terrain 2, les amphibolites sont caractérisées par un rubanement compositionnel dû principalement à la présence de bandes riches en épidote ou riches en plagioclase. Le clinopyroxène, la hornblende et le quartz se retrouvent en quantités variables. Des lentilles de hornblendite à grains moyens se manifestent, en moindre quantité, dans les amphibolites. Des bandes riches en épidote et clinopyroxène proviennent du cisaillement et de l'allongement de socles et lentilles à clinopyroxène et plagioclase. À l'échelle de l'échantillon, la formation de l'épidote associée aux bandes à clinopyroxène semble s'être effectuée aux dépens du plagioclase. Dans les amphibolites felsiques, des porphyroclastes de feldspath de l'ordre de un à trois centimètres se retrouvent allongés dans le plan de la foliation principale. Un dyke tardif, composé essentiellement de plagioclase, a été trouvé en un seul endroit du terrain 2; ce dyke à texture pegmatitique recoupe la foliation principale. L'amphibolite à grenat n'est présente que localement, soit en bordure de bandes métasédimentaires. Les métasédiments, présentés en ordre décroissant d'importance, consistent en des gneiss quartzo-feldspathiques à biotite et grenat, des schistes à biotite et muscovite (avec ou sans grenat), des quartzites à grenat, et des gneiss feldspathiques à biotite et muscovite. Chacune de ces roches se retrouve en bandes où lentilles d'épaisseur variable (10 à 30 cm) qui, assemblées, constituent les bandes métasédimentaires mégascopiques représentées sur les coupes géologiques (fig. 1.3). Leurs foliations sont généralement bien développées et concordantes avec la foliation des amphibolites adjacentes.

Sur le terrain, on observe une interdigitation partielle des bandes métasédimentaires et des amphibolites, là où elles sont en contact. Il en résulte localement la production d'une roche « mélangée » contenant à la fois des matériaux métasédimentaires et metabasiques. Cette interdigitation semble la cause de la réapparition du grenat dans les amphibolites en bordure de bandes métasédimentaires (souvent riches en grenat dans le terrain 2).

Terrain 3

Dans le terrain 3, l'amphibolite dominante est de nature felsique (riche en plagioclase et quartz), à grains fins, et à texture généralement protomylonitique. Les feldspaths se retrouvent parfois sous forme de porphyroclastes allongés dans le plan de la foliation. Ils sont d'échelle centimétrique et souvent entourés d'un fin revêtement de hornblende. Il s'agit généralement de quartz intersticiel. Ces amphibolites felsiques se retrouvent avec des quantités variables de bandes d'amphibolite à épidote. Ces dernières sont généralement plus cisillées et à grains plus fins que les amphibolites felsiques. De fines lentilles de hornblendite à grains fins se manifestent entre des bandes d'amphibolite à épidote et d'amphibolite felsique. On peut alors observer une diminution de la quantité de plagioclase du côté de l'amphibolite felsique adjacente.

Les bandes mégascopiques de métasédiments sont composites et ces derniers, d'aspect gneissique ou schisteux, se reconnaissent à leur nature feldspathique ou quartzo-

feldspathique souvent caractérisée par une abondance de muscovite et de biotite. On retrouve également de petites quantités de grenat, de chlorite et d'épidote. Ces bandes font preuve, entre elles, de contacts francs et cisailants. Ces roches se manifestent en bandes de 10 cm à 1 m d'épaisseur. La foliation de ces roches est généralement bien développée, grossière et subconcordante avec la foliation des amphibolites adjacentes.

Comme dans le deuxième terrain, on peut parfois observer une interdigitation partielle des métasédiments et des amphibolites aux endroits de contact. Il en résulte ici une augmentation de la quantité de feldspath dans les amphibolites adjacentes. Une lentille métrique de marbre a été trouvée à un endroit dans une zone légèrement bréchifiée du terrain 3.

Terrain 4

Le terrain 4 se compose essentiellement d'amphibolite avec des quantités variables d'épidote, de plagioclase, de hornblende et de quartz formant un rubanement compositionnel, qui consiste d'amphibolite felsique et d'amphibolite à épidote. Ces bandes d'épaisseur centimétrique, montrent des contacts cisailants et francs. Une granulométrie très fine et une texture mylonitique avec une orientation préférentielle très bien développée caractérisent les roches composantes. Une linéation minérale également bien développée est donnée par l'alignement de fines aiguilles de hornblende dans le plan de la foliation principale. Le quartz, généralement intersticiel, y est abondant.

À l'ouest du Mont Albert, les péridotites du Mont du Sud et du Mont Paul occupent la même position tectonostratigraphique que celle du Mont Albert. Le Mont du Sud possède une semelle métamorphique similaire à celle du Mont Albert. On y retrouve, dans les mêmes positions respectives, un terrain de type 1 et un terrain de type 3 fortement plissés. Ce complexe repose sur les roches du groupe des Chic-Choc. La péridotite du Mont Paul, pour sa part, repose directement sur les roches du groupe des Chic-Choc. Sa mise en place a produit la déformation et le métamorphisme des roches proximales du groupe des Chic-Choc.

Structure

Le rubanement général de la péridotite dessine un pli macroscopique couché avec un axe orienté selon 240-45° et une surface axiale, selon 140-45° (fig. 1.1). Les plus importantes concentrations de chromite se retrouvent dans la charnière de ce pli. En outre, il est important de noter la nature discordante du rubanement dans la péridotite par rapport au contact de la péridotite et de la semelle métamorphique. Toutefois, en bordure du contact avec la semelle métamorphique (à moins de 40 m), la péridotite est mylonitisée et montre une foliation parallèle au contact de la péridotite et de la semelle métamorphique. Les contacts entre, d'une part, la péridotite et la semelle métamorphique et, d'autre part, l'auréole et le groupe des Chic-Choc sont représentés par des failles majeures. Les contacts entre les terrains 1 et 2, 2 et 3, et enfin 3 et 4 correspondent à des variations lithologiques rapides, et cela dans des zones à intensité de cisaillement relativement élevée. Il faut également noter que l'extension latérale de chacun des terrains peut s'avérer variable en raison de la nature composite de la semelle métamorphique. Ces terrains se retrouvent en bandes subparallèles au contact de la péridotite et de la semelle métamorphique dans la partie ouest, nord et nord-est du complexe. Dans la partie sud-est, des mouvements de faille semblent avoir influencé leur répartition.

Dans le terrain 1, un seul épisode de déformation se traduit par le développement de la foliation principale superposée au rubanement. Aucune structure antérieures ou postérieures n'y ont été observées. Le rubanement métamorphique se

distingue par des variations minéralogiques et granulométriques très importantes. L'épaisseur des bandes varie entre 1 et 5 cm. Les contacts entre ces mêmes bandes sont transitionnels ou francs. La foliation principale est dessinée par l'orientation planaire des cristaux tabulaires de hornblende. Le long de contacts entre les bandes de différente composition, l'on peut par endroits observer des lentilles centimétriques de quartz, ainsi que la présence de quelques plis intrafoliaux. Ces derniers sont isoclinaux, aux charnières détachées, et caractérisés par la présence d'agrégats quartzeux centimétriques. De fines veinules millimétriques d'épidote, ou de calcite (plus rare), recourent la foliation de ces roches.

Dans le terrain 2, un premier épisode de déformation est à l'origine du développement de la foliation principale superposée au rubanement métamorphique. Comme dans le cas du terrain 1, l'on peut observer quelques plis intrafoliaux dessinés par des agrégats quartzeux. Toutefois, on peut de plus observer que la foliation principale a été plissée par des plis P2 pincés fortement inclinés vers le sud et le sud-ouest. L'amplitude de ces plis atteint 20 à 40 cm et la foliation principale correspond à la surface axiale. Ces plis P2 s'observent généralement dans des zones ayant subi un cisaillement ductile intense (contacts entre les terrains 2, 3 et 4). La foliation principale des roches du terrain 2 a été reprise par des plis majeurs P3 aux axes orientés selon 90-150° et 20-60°, et aux surfaces axiales subparallèles au contact de la péridotite et de la semelle métamorphique, ce qui explique leur grande dispersion. Leurs surfaces axiales sont généralement deversées vers le nord. L'amplitude de ces plis un peu fermés atteint 50 m et plus. Aucun indice structural n'a été observé qui permettrait de préciser la chronologie relative des deux plissements reprenant la foliation. Toutefois la géométrie des plis P2 semble indiquer que les déformations cisailantes à l'origine de la foliation auraient également été responsables de la formation de ces plis.

Dans le terrain 3, un premier épisode de déformation ductile et cisailante est à l'origine du développement de la foliation principale (superposée au rubanement). Quelques plis P2 reprenant la foliation principale ont été observés en bordure du terrain 4 et dans les zones de contact et d'interdigitation partielle entre les bandes métasédimentaires et les amphibolites. Par endroits, une linéation minérale donnée par l'alignement d'agrégats de hornblende se retrouve dans l'axe de ces plis P2. Dans l'ensemble du terrain 3, la foliation principale a été reprise par les plis majeurs P3. Vers la base du terrain 3, les surfaces axiales de ces plis tendent à se redresser (fig. 1.3). Les axes de ces plis se distinguent souvent par la présence d'un alignement d'agrégats de hornblende.

Dans le terrain 4, le développement de la foliation superposée au rubanement s'est produit lors d'un épisode de déformation cisailante également responsable de la création de textures mylonitiques bien développées ainsi que de la production de plis intrafoliaux de nature isoclinale et centimétrique. La foliation a par la suite été reprise par les plis majeurs P3. Dans le terrain 4, il s'agit de plis pincés aux surfaces axiales relativement redressées. Dans ces roches, la hornblende se retrouve généralement en prismes aciculaires dessinant une bonne linéation minérale dans le plan de la foliation; ces linéations, toujours subparallèles aux axes des plis majeurs P3, semblent indiquer une cristallisation syntectonique associée au plissement P3.

Métamorphisme

À l'intérieur de la semelle métamorphique, le degré du métamorphisme augmente vers la péridotite depuis le groupe des Chic-Choc, mais il ne s'agit pas d'une progression continue. Cette augmentation ne peut résulter d'un métamorphisme progressif des roches du groupe des Chic-Choc.

Les roches du terrain 1 se distinguent par un rubanement textural et compositionnel extrêmement bien développé. Localisées dans la partie supérieure de la semelle métamorphique, elles représentent les roches ayant atteint le degré de métamorphisme le plus élevé et se composent principalement de hornblende, de grenat et de clinopyroxène.

Le grenat est abondant en bordure du contact de la péridotite et de la semelle métamorphique, et disparaît vers la base du terrain 1; il s'agit d'un grenat de couleur rouge foncé, souvent fracturé et aux bordures arrondies. Les grenats analysés ont des compositions variant entre l'almandin (33-55), la spessartine (1,3-4,3), le pyrope (22-27) et la grossulaire (14-33) (fig. 1.4). Il peut contenir des inclusions d'épidote, de hornblende, de plagioclase, de clinopyroxène, de rutile et de minéraux opaques; il arrive que certains grenats présentent un centre bourré d'inclusions et une bordure libre d'inclusions. Le grenat est souvent entouré d'un fin revêtement composé soit de plagioclase et hornblende, ou d'épidote et hornblende. L'épidote et la hornblende dessinent alors parfois des textures symplectiques autour du grenat, indiquant à la fois un métamorphisme rétrogressif et une cristallisation post-tectonique. En outre, cette texture semble indiquer qu'autour des grenats, la hornblende et l'épidote se sont cristallisées simultanément. La hornblende est généralement de forme prismatique allongée (hypidiomorphe), de couleur bleu vert et aux bordures irrégulières. Les cristaux analysés ont des compositions variant entre les hornblendes du type édénitique ou ferro-pargasitique et la pargasite (fig. 1.4). Invariablement orientée dans le plan de foliation des roches et fortement zonée, la hornblende peut contenir des inclusions d'épidote, de plagioclase, de sphène, de zircon ou de minéraux opaques, les inclusions d'épidote étant les plus fréquentes. Le clinopyroxène caractéristique est vert pâle, pouvant se présenter sous forme de porphyroclastes ou d'agrégats formant les bandes d'amphibolite à clinopyroxène. Les clinopyroxènes analysés ont la composition chimique de la salite (fig. 1.4). Ils sont invariablement amphibolitisés, pouvant contenir des inclusions de plagioclase, d'épidote, de sphène, et de minéraux opaques. On peut les retrouver avec une bordure soit d'oxydes, soit de chlorite et épidote, ou soit d'oxydes et chlorite. Des cristaux de clinopyroxène ont été observés en inclusions, également partiellement amphibolitisés, dans des grenats; ce phénomène indique que la cristallisation du clinopyroxène a précédé, ou s'est produite, pendant celle du grenat. Les plagioclases sont généralement séricitisés et parfois entourés d'un revêtement d'épidote. En outre, des traces de scapolite ont été trouvées à proximité du contact avec la péridotite et des traces d'apatite ont été observées dans des hornblendites.

La présence de clinopyroxène, de grenat, et de hornblende formés de façon précoce indique que le faciès des amphiboles et écolites pourrait avoir été atteint lors du premier épisode métamorphique M1 (Trzienski, 1984). Toutefois, l'assemblage caractéristique du faciès des écolites est l'omphacite qu'accompagne un grenat riche en pyrope mais, à partir de l'étude des amphibolites, on a établi que les compositions chimiques de ces deux phases sont très différentes. En outre, à l'échelle du rubanement, on peut observer des variations compositionnelles extrêmes : par exemple, des bandes centimétriques composées essentiellement de clinopyroxène, de hornblende, de hornblende et grenat, de hornblende et plagioclase ou de hornblende et clinopyroxène et grenat, peuvent se retrouver en contact dans un même échantillon. Ces assemblages, ainsi que la chimie des minéraux constituants, sont probablement contrôlés par des variations chimiques importantes. On estime que de telles variations compositionnelles sont dues à un rubanement antérieur qui, par la suite, a été intensifié par des déformations cisailantes et une ségrégation métamorphique.

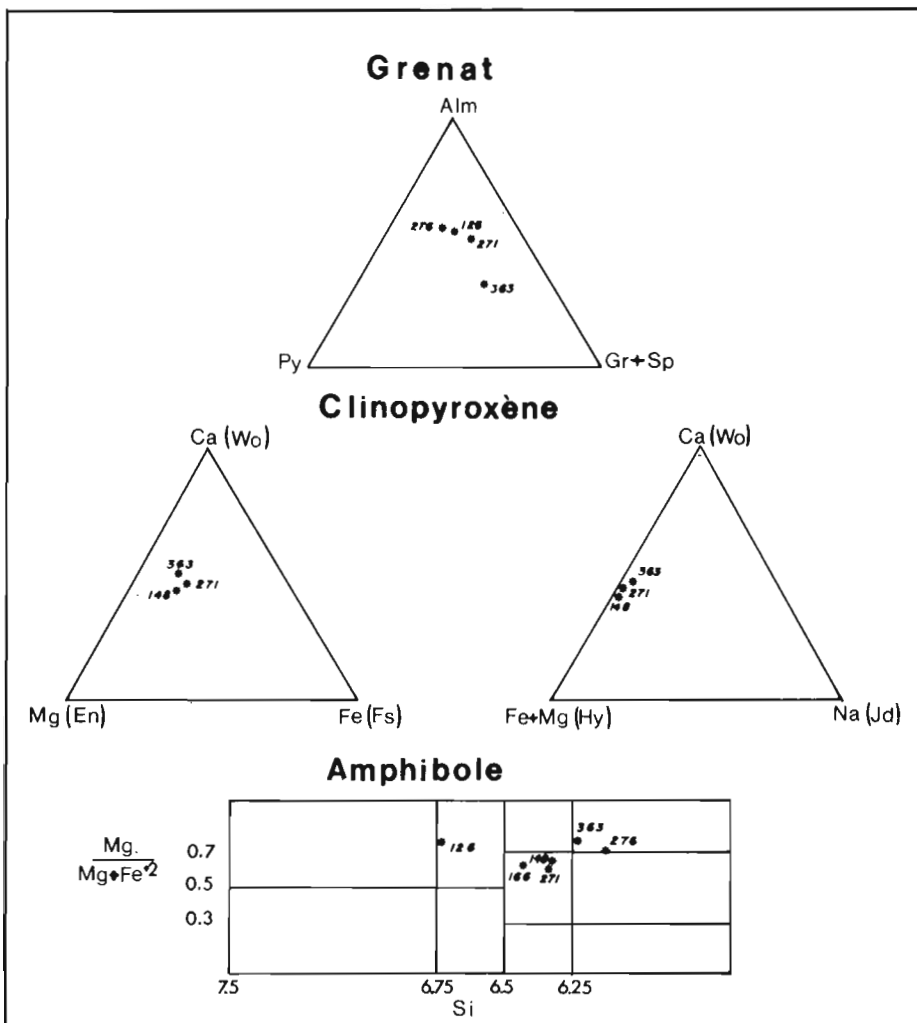


Figure 1.4. Chimie des minéraux

La présence de revêtements de hornblende et épidote autour de grenats et la déstabilisation des clinopyroxènes en hornblende, indiquent un métamorphisme rétrogressif dans les conditions associées au faciès à épidote-amphibolite. Il est intéressant de noter que, plus ces roches sont cisillées dans le plan de la foliation principale, plus les produits de ces réactions rétrogressives sont abondants. Cette observation s'applique aussi aux terrains 2 et 3.

Terrain 2

Les amphibolites du terrain 2 sont caractérisées par un rubanement compositionnel causé par des bandes riches en épidote ou en plagioclase. Toutes deux peuvent contenir des quantités variables de hornblende, de clinopyroxène et de quartz. Dans le terrain 2, la hornblende est généralement hypidiomorphe, bleu-vert, trapue ou allongée, et contient de fréquentes inclusions d'épidote, de quartz, de plagioclase et de minéraux opaques. La hornblende est toujours orientée dans le plan de la foliation des amphibolites. On peut toutefois la retrouver néoformée autour de grains de clinopyroxène. Les clinopyroxènes, pour leur part, se retrouvent sous forme d'aggrégats dans les bandes d'amphibolite à épidote et clinopyroxène ou dans les lentilles à clinopyroxène et plagioclase; généralement déformés, ils présentent des bordures arrondies et sont invariablement amphibolitisés. L'épidote est commune dans ces amphibolites; elle se retrouve sous forme d'aggrégats ou de grains isolés, généralement hypidiomorphes, et se distingue par la présence de nombreuses inclusions concentrées

au centre des grains. Le plagioclase est déformé ou recristallisé, ou les deux, presque toujours séricitisé et remplacé, partiellement ou complètement, par l'épidote. Dans les amphibolites, on retrouve des bandes composées essentiellement d'épidote. Elles peuvent résulter soit du cisaillement et de la rétrogression de concentrations de plagioclase, soit du cisaillement de veines d'épidote. Sur le terrain, on note que les bandes riches en épidote et clinopyroxène proviennent du cisaillement de lentilles de clinopyroxène et plagioclase. Des observations détaillées, ont permis d'établir qu'il s'agit possiblement de clinopyroxènes ignés (résiduels) plutôt que métamorphiques dans certains cas. Ainsi, ces derniers ne pourraient contenir d'informations précises sur les conditions physiques du métamorphisme prograde M1. De plus amples indices texturaux sont nécessaires afin de pouvoir conclure à ce sujet.

Dans la partie supérieure du terrain 2, de fines veinules peu déformées, de composition gabbro-anorthositique (Pl + Cpx + Hb + Sph), recoupent par endroits la foliation principale des amphibolites. Ces veines témoignent de la présence de phénomènes intrusifs synchrones à la déformation et au métamorphisme. Dans les amphibolites, le clinopyroxène est de moins en moins abondant vers la base du terrain 2. En outre, en se dirigeant vers la base du terrain 2, les amphibolites deviennent de plus en plus intensément épidotisées, et cisillées dans le plan de la foliation. En combinant ces observations, il semble que l'effet dynamique du cisaillement a permis une meilleure rééquilibration des assemblages associés au métamorphisme rétrograde et ce, dans les conditions associées au faciès à épidote-amphibolite.

Les principaux éléments constitutifs des roches quartzo-feldspathiques sont le feldspath, le quartz, la muscovite, la biotite, le grenat, l'épidote et la chlorite. Lorsque présent, le grenat contient souvent de nombreuses inclusions bien alignées. La biotite se retrouve en paillettes isolées ou bien elle se forme au détriment de la muscovite ou autour des grenats. Les feldspaths, généralement séricitisés, se manifestent par endroits sous forme de porphyroclastes; ces derniers donnent l'impression d'être de caractère orthogneissique. Les quartzites à grenat, les schistes à biotite et muscovite et la majorité des gneiss quartzo-feldspathiques sont sans aucun doute des roches métasédimentaires. Toutefois, il n'est pas exclu que certains gneiss quartzo-feldspathiques dérivent du cisaillement et du métamorphisme de roches ignées felsiques.

Terrain 3

Ces amphibolites sont rubanées dans le plan de la foliation principale. L'épaisseur des bandes varie entre 1 et 4 cm et l'on peut observer d'importantes variations texturales et granulométriques d'une bande à l'autre. Les contacts entre ces bandes sont francs ou transitionnels (texturaux, minéralogiques et granulométriques). Ainsi que déjà mentionné, les textures granoblastiques et protomylonitiques dominent dans les amphibolites du terrain 3. Ces textures ont été produites par d'intenses déformations cisailantes qui ont effacé les indices permettant de préciser la nature texturale des protolites. Les amphibolites du terrain 3 sont caractérisées par l'assemblage de hornblende, épidote, plagioclase et quartz. La hornblende, minéral dominant généralement de forme prismatique allongée, est fortement zonée et orientée dans le plan de la foliation principale. L'épidote et le plagioclase sont zonés et se manifestent sous forme d'aggrégats de grains arrondis ou entre les cristaux de hornblende. Le quartz est généralement interstitiel mais peut se retrouver par endroits sous forme de fines lentilles dans la foliation principale.

Dans le terrain 3, la distinction entre différents épisodes métamorphiques n'est pas nette. Cela peut dépendre du fait que, même s'il y a eu différents épisodes métamorphiques, ces derniers se sont tous produits à l'intérieur des faciès des amphibolites et à épidote-amphibolite. Toutefois, un métamorphisme rétrograde dans les conditions associées au faciès à épidote-amphibolite, accompagné d'importants cisaillements et du plissement P3, caractérise maintenant ces roches. On peut distinguer que les bandes d'amphibolite les plus intensément cisillées (protomylonitiques) sont celles contenant le plus d'épidote et que cette dernière se forme souvent au détriment des plagioclases adjacents. L'épidotisation des plagioclases semble ainsi avoir été aidée par des déformations cisailantes lors du métamorphisme rétrograde. Le rutile, l'ilménite et le sphène se retrouvent comme minéraux connexes; dans ces roches, le sphène remplace l'ilménite et le rutile.

Terrain 4

On trouve dans le terrain 4, des amphibolites felsiques et des amphibolites à épidote très bien rubanées. L'épaisseur de ces bandes varie entre 2 et 4 cm et les roches présentent des textures de nature mylonitique et protomylonitique. L'épidote, très abondante, se présente sous des formes variables, fortement pléochroïque, zonée et souvent en aggrégats avec le quartz. Le plagioclase est hypidiomorphe ou xénomorphe, et se manifeste généralement sous forme de grains intergranulaires séricitisés. Un seul assemblage de hornblende, épidote, quartz et plagioclase se distingue dans les amphibolites du terrain 4. Cet assemblage résulte d'un métamorphisme dynamique qui s'est opéré dans les conditions associées au faciès à épidote-amphibolite. Cet épisode de métamorphisme a été accompagné d'intenses cisaillements ductiles dans le plan de la foliation principale, ainsi que du plissement majeur P3.

Dans l'ensemble de la semelle métamorphique, l'on trouve de fines veinules tardives d'épidote. Elles suivent et recoupent la foliation principale des roches, phénomène qui semble indiquer que le métamorphisme rétrogressif a touché l'ensemble des roches de la semelle métamorphique.

Géochimie

Les résultats préliminaires indiquent que les hornblendites à grenat, les amphibolites à clinopyroxène, et les amphibolites à clinopyroxène et grenat sont des roches méta-ultrabasiques avec des teneurs en SiO₂ variant entre 41 et 45 %. Les amphibolites à clinopyroxène et grenat ont des teneurs plus faibles en P₂O₅, TiO₂ et Na₂O que les hornblendites à grenat. Les amphibolites felsiques et les amphibolites à épidote, elles, sont des roches metabasiques dont la teneur en SiO₂ varie entre 45 et 51 %. Selon la classification adoptée par Whitehead et Goodfellow (1978), ces roches se situent dans le domaine subalcalin. Les metabasites du groupe des Chic-Choc situés à proximité du complexe du Mont Albert contiennent, pour leur part, entre 46 et 53 % de SiO₂. Dans l'ensemble, les diagrammes de Na₂O, Al₂O₃, MgO, CaO, FeO/(FeO + MgO), P₂O₅ et TiO₂ par rapport à SiO₂, montrent que les amphibolites felsiques et les amphibolites à épidote ont une chimie transitionnelle entre les roches méta-ultramafiques et les metabasites du groupe des Chic-Choc (fig. 1.5). Toutefois, les roches de la semelle métamorphique se distinguent par leur teneur plus faible en SiO₂, TiO₂, Na₂O et P₂O₅, et leur teneur plus élevée en MgO, CaO, Cr(ppm) et Ni(ppm) que les metabasites du groupe des Chic-Choc. Ces derniers sont d'affinité différente, se situant dans le domaine alcalin (Whitehead et Goodfellow, 1978). De plus amples analyses éventuelles pourront possiblement mettre en évidence les variations chimiques entre les différents terrains ainsi que celles à l'intérieur même de chaque terrain.

Sommaire et conclusion

Les analyses géochimiques n'ont relevé aucun indice de métamorphisme. Le métamorphisme, dans son ensemble, peut être considéré comme isochimique. Les protolites du terrain 1 paraissent de composition ultrabasique, riches en FeO (total) et en Ni (ppm) et pauvres en Na₂O et K₂O. Il semble qu'il se soit agi de ferrogabbros rubanés issus de la croûte océanique. Les protolites du terrain 2 paraissent basiques et riches en FeO (total); il s'agit, ici encore, de ferrogabbros de la croûte océanique. Ils étaient possiblement rubanés avant l'épisode de métamorphisme. Toutefois, dans ce terrain, la ségrégation métamorphique accompagnée de déformations cisailantes pourrait expliquer à elle seule les variations compositionnelles du rubanement. Plus d'indices texturaux sont nécessaires afin de conclure à ce sujet. Dans le terrain 2, la présence de métasédiments dans les amphibolites s'explique facilement si l'on considère que leur insertion a eu lieu lors de l'incorporation de ce terrain à la semelle métamorphique en voie d'assemblage. En outre, la présence localisée d'activité magmatique synchrone à la déformation et à un métamorphisme de haute pression peut être reliée au transport du complexe au-dessus d'une zone de subduction. Ce phénomène expliquerait alors l'insertion de lentilles sédimentaires dans les roches gabbroïques de la croûte océanique. Les roches du terrain 3 semblent résulter du métamorphisme et de la déformation d'une intercalation de sédiments et de basaltes subalcalins de composition tholléitique. La présence de grandes quantités de métasédiments quartzo-feldspathiques, de schiste et d'un peu de marbre intercalés dans ces metabasites semble indiquer une provenance à proximité de la marge continentale. Les protolites du terrain 4 paraissent basiques et d'affinité subalcaline. Il peut s'agir de basaltes tholléitiques pauvres en Na₂O et K₂O. Lors de leur incorporation à la base de la semelle métamorphique, ils devaient se trouver dans le milieu de transition entre le domaine océanique

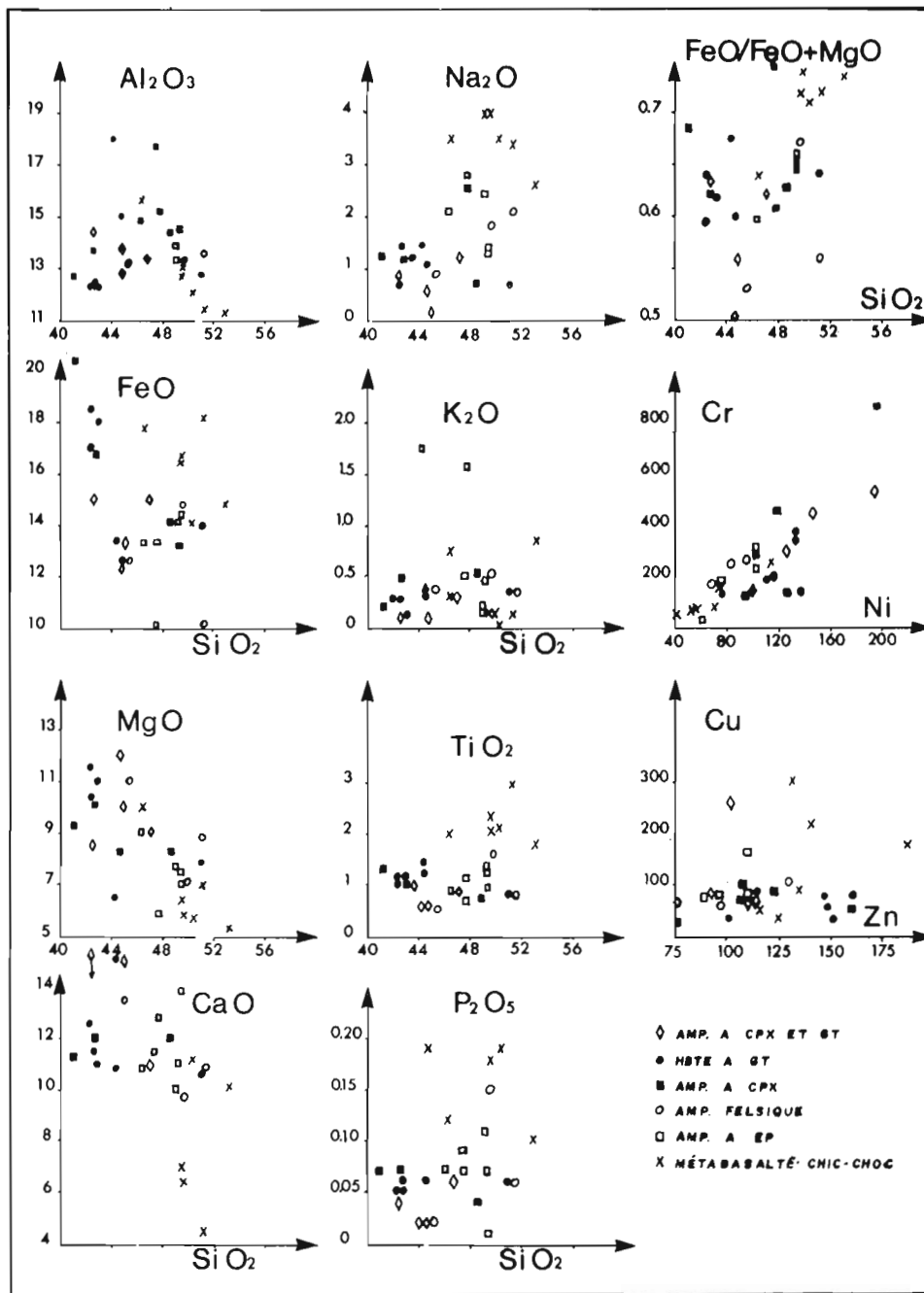


Figure 1.5. Chimie des roches

et la marge continentale, ou sur cette dernière. Cependant, on ignore si ces basaltes se sont épanchés à cet endroit ou s'ils y ont été transportés. Dans ce dernier cas, il n'est pas exclu que la cause en soit le chevauchement du complexe ophiolitique vers la marge continentale.

Bref, les amphibolites des terrains 1 et 2 résultent du métamorphisme de roches intrusives ultrabasiques et basiques de composition ferro-gabbroïque (tabl. 1.1). Les amphibolites des terrains 3 et 4 sont les produits du métamorphisme de roches basaltiques de composition tholléitique. Les topologies des amphibolites des terrains 1, 2, 3 et 4 représentent, respectivement, les faciès à amphibole-éclogite et épidote-amphibolite, amphibolite à degré élevé et épidote-amphibolite, amphibolite et épidote-amphibolite, puis épidote-amphibolite (tabl. 1.1). Les roches de la semelle métamorphique sont structurellement, pétrographiquement et géochimiquement très différentes des roches du groupe des Chic-Choc; elles ne dérivent pas d'un

métamorphisme prograde des roches métavolcaniques et métasédimentaires du groupe des Chic-Choc.

La pétrologie et la structure de la semelle métamorphique du Mont Albert semblent indiquer que les roches de plus haut degré ont été les premières à être transportées et métamorphosées sous la péridotite, puis que les roches de degré moins élevé ont été successivement incorporées à la semelle métamorphique pendant la période de refroidissement de la péridotite qui chevauchait des terrains plus riches en sédiments et à température plus basse. La phase terminale d'incorporation des matériaux est représentée, dans la partie nord-est du complexe, par la présence d'un lambeau d'amphibolite mylonitique, en contact avec les roches du groupe des Chic-Choc. Il semble donc que le processus de formation de la semelle métamorphique a débuté dans le domaine océanique pour se terminer en bordure de la marge continentale. Ces observations, ajoutées aux données géochronologiques de la région, corres-

Tableau 1.1. Lithologie, texture, structure, métamorphisme et chimie des terrains 1, 2, 3 et 4.

	LITHOLOGIES	TEXTURES	STRUCTURE	MÉTAMORPHISME	CHIMIE
①	Hornblendite Gr. Amp. a Cpx. Amp. a Gr. et Cpx.	Porphyroblastique gr. moyens	Une foliation princ. avec plis intra- foliaux	1° Gnt + Cpx + Hbl 2° Hbl + Ep	Ultra-basique
②	Hornblendite Amp. a Cpx et Ep Amp. felsique Amp. a Gr. LOCAL Metasédiments	Protomylonitique gr. moyens et fins	Une foliation princ. P2 - décim. axes \approx Sud-50 P3 - > 30 m. axes \approx // crc. (P) SE ou NO	1° Cpx + Pl local Gr. 2° Hbl + Ep	Ultra-basique et basique
③	Amp. fels Amp. a Ep Hornblendite (LOCAL) Metasédiments	Protomylonitique gr. fins	Une foliation p. P2 + LOCAL li. axes \approx 210°-50° P3 + LOCAL li.	1° Hb + Pl + Ep 2° Hb + Ep + Qtz	Basique, sub-alcaline
④	Amp. a Ep. Amp. fels.	Mylonitique	Une foliation p. P2 LOCAL P3 + bonne li.	1° Hb + Ep + Pl + Qtz	Basique, sub-alcaline

pondent à l'interprétation généralement admise du développement des processus orogéniques des Appalaches du Nord, au cours du Taconique, ainsi que clairement décrits par St-Julien et Hubert (1975). Il s'en dégage que les ophiolites des Appalaches du Nord représentent des sections de la lithosphère proto-Atlantique. Ainsi, l'histoire du complexe du Mont Albert est liée au développement et à la destruction de la marge proto-Atlantique de l'Amérique du Nord.

Remerciements

L'appui et les précieux conseils de M. K.L. Currie ont permis le bon déroulement des travaux sur le terrain ainsi que la rédaction du présent ouvrage. Les commentaires constructifs de MM. T. Feininger, J. Waldron et D.B. Clarke ont été fort appréciés, ainsi que l'aide habile de M. F. Thibert qui a agi à titre d'assistant aux travaux effectués sur le terrain au cours de l'été 1985. En outre, les analyses géochimiques réalisées par M. C. Gariépi de l'Université du Québec à Montréal ont également été grandement appréciées. La Commission géologique du Canada a gracieusement défrayé la totalité des frais reliés aux travaux sur le terrain. Les auteurs remercient, respectivement, le Département de géologie de l'Université Dalhousie pour l'appui financier complémentaire accordé depuis 1984 et le C.N.R.E.S. pour les bourses d'opération accordées depuis 1979.

Bibliographie

- Beaudin, J.
1983: Analyse structurale du groupe des Chic-Choc et de la péridotite alpine du Mont Albert, Gaspésie; thèse de doctorat, université Laval.
- Coleman, R.G and Irwin, W.P. (editors)
1977: North American ophiolites.
- Gagnon, Y.D. and Jamieson, R.A.
1985: Geology of the Mont Albert region, central Gaspé peninsula, Quebec; Geological Survey of Canada, Current research. Paper 85-1A p. 783-787.
- Jamieson, R.A.
1980: The formation of metamorphic aureoles beneath ophiolite suites -Evidences from the St-Antony complex northwestern Newfoundland; *Geology* 8, p. 151-154.
- MacGregor, I.D.
1962: Geology, petrology and geochemistry of the Mont Albert and associated ultramafic bodies of central Gaspé, Quebec; Msc. thesis, Queen's University.
1964: A study of the contact metamorphic aureole surrounding the Mont Albert ultramafic intrusion; Ph.D. thesis, Princeton University.
- MacGregor, I.D. and Basu, A.R.
1976: Geological problems in estimating mantle geothermal gradients; *American Mineralogist*. 61, p. 715-724.
1979: Petrogenesis of the Mont Albert ultramafic massif, Quebec; *Geological Society of America Bulletin*, part 2, vol 90, p. 1529-1627.
- Spray, J.
1984: Possible cause of upper mantle decoupling and ophiolite displacement; *Geological Society London* 13, p. 255-268.
- St-Julien, P. and Hubert, C.
1975: Evolution of the Taconic orogen in Canadian Appalachians; *American Journal of Science*, 275-A, p. 337-362.
- Trzcinski, W.E.
1984: Amphibole Eclogite from Mt. Albert, Gaspé, Quebec, Canada; (Transcription, American Geophysical Union 65, p. 290 (Abstract).
- Whitehead, R.E.S. and Goodfellow, W.D.
1978: Geochemistry of volcanic rocks from Tetagouche group, Bathurst, New Brunswick, Canada; *Reply, Canadian Journal of Earth Sciences* 15 (10) p. 1681.
- Williams, H. and Smyth, R.
1973: Metamorphic aureoles beneath ophiolite suite and alpine peridotites : tectonic implications with West Newfoundland examples; *American Journal of Science* 273, p. 594-621.

Géochimie des familles U et Th dans la matière organique fossile des dépôts interglaciaires et interstadières de l'est et du nord du Canada: potentiel radiochronologique

Convention de recherche EMR 198/04/85

Christiane Causse¹ et Claude Hillaire-Marcel¹
Division de la science des terrains

Causse, C. et Hillaire-Marcel, C., Géochimie des familles U et Th dans la matière organique fossile des dépôts interglaciaires et interstadières de l'est et du nord du Canada: potentiel radiochronologique; dans Recherches en cours, Partie B, Commission géologique du Canada, Étude 86-1B, p. 11-18, 1986.

Résumé

Des travaux récents permettaient de concevoir une application de la méthode Th/U en radiochronologie à la datation de la matière organique de nature fossile. L'analyse d'une cinquantaine d'échantillons de bois provenant d'unités interstadières et interglaciaires de l'est et du nord-ouest du Canada a conduit les auteurs à nuancer cette proposition. Une bonne concordance des données Th/U et ¹⁴C, et une cohérence d'ensemble des résultats n'apparaissent qu'en autant que le sédiment d'où proviennent les échantillons a constitué un milieu géochimiquement clos. Pergélisols et sédiments argileux à faibles gradients hydrauliques semblent constituer a priori les milieux les plus favorables. Cette méthode peut fournir, avec précaution et en particulier en ce qui a trait au dernier cycle glaciaire, des éléments chronostratigraphiques particulièrement précieux en l'absence d'une autre méthode applicable.

Abstract

Recent work in radiochronology has led to the development of a method for dating fossilized organic matter using U-Th. After analyzing about fifty samples of wood from interstadial and interglacial units in eastern and northeastern Canada, the authors were able to qualify this proposed method. Good agreement between U-Th and ¹⁴C data and general consistency of results are possible only when the sediments from which the samples are taken formed a geochemically closed environment. Permafrost and clay-rich sediments with low hydraulic gradients would seem a priori to form the best environments. Used with care, this method can supply chronostratigraphic information that is especially useful, particularly for the most recent glacial cycle, since no other method can be used.

¹ GEOTOP, Université du Québec à Montréal, B.P. 8888, succursale A, Montréal, H3C 3P8 et Laboratoire de Géologie du Quaternaire du CNRS, Marseille-Luminy, 13288, CEDEX 9, France.

Introduction

Les unités interglaciaires et interstadias de l'est et du nord du Canada sont représentées par des dépôts alluviaux, lacustres, palustres (tourbes) ou marins, en général discontinus dans le temps et dans l'espace (Prest, 1970; Fulton, 1984). Les corrélations des unes aux autres s'appuient par conséquent sur leur datation <<absolue>>. Au-delà du Wisconsinien moyen, toutefois, les fossiles organiques qu'ils renferment ne peuvent être datés par le ^{14}C , malgré l'accès aux mesures par spectrométrie de masse (Tendrons, Tandems Van de Graaf, etc.); l'enrichissement isotopique ne permet guère, non plus, d'étendre le domaine chronologique du carbone radioactif, eu égard au poids croissant des contaminations éventuelles.

Parmi les méthodes donnant accès à une chronologie <<absolue>> au-delà des quarante derniers milliers d'années environ, le déséquilibre radioactif Th/U constitue l'une des plus éprouvées (Ivanovich et Harmon, 1982). Cependant, son application à la datation des dépôts continentaux (et même littoraux) n'est pas immédiate. Parfois appliquée avec succès aux carbonates, comme les concrétions karstiques (voir p. ex. Gascoyne et coll., 1978), elle a été envisagée dans quelques rares cas pour établir l'âge de bois ou de tourbes fossiles (Vogel et Kronfeld, 1980).

Vu la rareté des carbonates authigènes dans les dépôts non glaciaires de l'est et du nord du Canada, il était tentant de vérifier le potentiel radiochronologique des bois fossiles, relativement plus abondants. Plusieurs dossiers analytiques ont ainsi pu être établis sur des échantillons provenant de séquences sédimentaires bien étudiées, dans les provinces de l'Atlantique et le golfe du Saint-Laurent (Nouvelle-Écosse, Îles-de-la-Madeleine), et dans le nord-ouest du pays (îles Banks et Victoria, Territoire du Yukon et delta du Mackenzie). Les données géologiques sur la plupart des sites échantillonnés ont par ailleurs été publiées; le présent rapport fait simplement état des données géochimiques complémentaires.

Méthode analytique

Des travaux antérieurs, notamment sur la matière organique de la coupe-type de Grande Pile (Woillard et Mook, 1982), ont démontré que contrairement aux observations de Vogel et Kronfeld (1980), les tourbes constituaient un milieu trop poreux et donc géochimiquement ouvert, impropre à l'utilisation de la méthode Th/U. Des échantillons de bois fossile qui, a priori, pouvaient constituer un milieu plus propice, ont donc été sélectionnés; au total, plus de 50 échantillons ont été analysés. Tous ont subi un traitement identique. La plupart d'entre eux sont des morceaux de troncs ou de grosses branches; seuls quelques échantillons de l'Arctique se présentent sous la forme de minces branchettes.

Après un nettoyage mécanique soigneux, ayant pour objet de débarrasser l'échantillon des sédiments englobants, la partie centrale de chaque morceau de bois a été prélevée de façon à finalement conserver, aux fins d'analyse, une partie aliquote de 20 à 100 g, selon le cas. Placé dans une coupelle de quartz, l'échantillon a été par la suite calciné, sous atmosphère, dans un four porté à 800°C . Les cendres recueillies ont été mises en solution dans de l'acide chlorhydrique (HCl) concentré. La séparation des isotopes de l'uranium et du thorium a été effectuée sur résine échangeuse d'ions, selon la méthode traditionnelle de Goldberg et Koide (1962), après avoir introduit des traceurs dans la solution: en l'occurrence, un mélange connu de ^{232}U (émetteur α), ^{228}Th (émetteur α) et ^{234}Th (émetteur β) destiné à déterminer les rendements chimiques et de comptage des préparations. Le double traçage en thorium permet de contrôler le déséquilibre radioactif éventuel entre

les isotopes 228 et 232 du thorium dans l'échantillon, à la suite, par exemple, de la migration de ^{228}Ra (isotope du radium, intermédiaire entre ^{232}Th et ^{228}Th) dans le fossile. Quoi qu'il en soit, le dépôt d'uranium et celui de thorium s'effectuent sur disques d'acier poli, par électrolyse, assurant ainsi une géométrie parfaite de la couche active, particulièrement importante pour une bonne définition des spectres d'énergie des radioisotopes. Ces derniers sont obtenus dans un ensemble de spectromètres α (EGG-ORTEC) couplés à un analyseur multicanaux (Davidson) et à un microordinateur (IBM-XT), permettant d'obtenir, de stocker et d'analyser directement les spectres d'émission α . Un deuxième calcul du rendement chimique de l'extraction du thorium est assuré par comptage β du ^{234}Th , à l'aide d'un détecteur à barrière de surface.

Dans la plupart des cas, on obtient des rendements chimiques de l'ordre de 60 %, en uranium comme en thorium; au comptage, ceux-ci sont réduits au tiers, environ. Il est à noter que, dans plusieurs cas, la qualité des spectres obtenus à partir des électrodépôts est telle que la résolution théorique des détecteurs est effectivement observée (ici: 25 keV environ).

Les échantillons des provinces de l'Atlantique et du golfe du Saint-Laurent

On trouvera dans de Vernal et Mott (1985) et de Vernal et coll. (sous presse), toutes les informations concernant les sites échantillonnés, notamment sur l'île du Cap-Breton, et dans Grant et coll. (1985), celles relatives aux bois fossiles des Îles-de-la-Madeleine.

Dans la plupart de ces entroits, le point critique concerne la fermeture relative du système géochimique depuis la fossilisation. En effet, contrairement aux milieux plus septentrionaux (voir plus bas), où la persistance quasi continue du pergélisol a permis de limiter la circulation d'eau dans les sédiments et, par suite, la remobilisation des isotopes des familles radioactives de l'uranium et du thorium, les dépôts situés aux anciennes marges est de l'inlandsis ont connu des alternances de périodes de gel (au moment de la glaciation, par exemple), et de dégel. À l'Holocène, en particulier, une percolation importante susceptible d'ouvrir considérablement le système géochimique Th/U, a affecté la plupart des coupes dans les dépôts meubles.

L'ouverture du système géochimique apparaît dans plusieurs paramètres: une dispersion significative des teneurs en uranium, dans des échantillons provenant d'une même unité géologique, en est un indice certain. Un accroissement de la teneur en uranium s'accompagne systématiquement d'une diminution des âges apparents des spécimens (par ex. la localité d'East Bay: unité I; tabl. 2.1). On note, parallèlement, un fort accroissement des proportions de ^{232}Th , par rapport au ^{230}Th , dans ces mêmes échantillons. Celui-ci ne peut migrer, à l'intérieur des morceaux de bois (en compagnie d'ailleurs d'une certaine proportion de ^{230}Th <<initial>>), qu'à la faveur d'une alternance de phases de dessiccation et de réhumidification qui altère le tissu ligneux et permet, par conséquence, l'incorporation des phyllites argileuses porteuses.

En comparant l'ensemble des données, il s'avère irréaliste d'accorder le moindre crédit chronologique aux échantillons renfermant plus de 30 %, environ, de ^{232}Th (par rapport au ^{230}Th). De même, le meilleur indice empirique d'une relative fermeture du système radioactif $^{230}\text{Th}/^{234}\text{U}$ réside dans l'homogénéité des concentrations et des rapports d'activité des isotopes de l'uranium. Tout échantillon présentant des écarts importants, par rapport aux valeurs observées dans l'ensemble de l'unité géologique considérée, devient suspect. De façon pratique, la porosité du sédiment englobant et les gradients hydrauliques sont déterminants: les

Tableau 2.1. East Bay

Numéro échantillon /terrain /Labor.	²³⁸ U (p.p.m.)	²³⁴ U/ ²³⁸ U rap.d'act.	²³² Th (p.p.m.)	²³⁰ Th/ ²³² Th	²³⁴ U/ ²³² Th	²³⁰ Th/ ²³⁴ U	Âge brut	Localité	Identification échant.
MS 84-20B UQT-126	0,011 0,000	1,235 0,043	0,014 0,003	2,078 0,264	2,973 0,363	0,699 0,069	123400 +30000 -23400	East Bay	-
MS 84-20A UQT-175	0,041 0,001	1,221 0,042	0,030 0,004	3,561 0,290	5,031 0,420	0,708 0,032	126400 +15000 -12800	East Bay	-
MS 8236WIC UQT-108	0,109 0,003	1,110 0,035	0,176 0,007	1,314 0,025	2,073 0,078	0,634 0,023	106600 +9600 -8600	East Bay	Pinus strobus
MS 8236WID UQT-179	0,447 0,010	1,190 0,024	0,514 0,029	1,360 0,043	3,132 0,152	0,434 0,020	60800 +5100 -5000	East Bay	Juniperus sp.

Les nombres en caractère gras indiquent la valeur de la déviation normale

Tableau 2.2. Nouvelle-Écosse et golfe du Saint-Laurent

Numéro échantillon /terrain /labor.	²³⁸ U (p.p.m.)	²³⁴ U/ ²³⁸ U rap.d'act.	²³² Th (p.p.m.)	²³⁰ Th/ ²³² Th	²³⁴ U/ ²³² Th	²³⁰ Th/ ²³⁴ U	Âge brut	Localité	Identification échant.
Unité I									
MS 84-20A UQT-175	0,041 0,001	1,221 0,042	0,030 0,004	3,561 0,290	5,031 0,420	0,708 0,032	126400 +15000 -12800	East Bay	-
MS 82-4E UQT-184	0,864 0,027	1,453 0,032	0,579 0,060	3,823 0,098	6,577 0,296	0,581 0,024	89400 +8000 -7100	Le Bassin	Pinus strobus
MS 82-4B UQT-183	0,661 0,015	1,399 0,024	0,405 0,047	4,491 0,116	6,921 0,275	0,649 0,022	106400 +8400 -8000	Le Bassin	Pinus strobus
MS 82-4A UQT-182	0,770 0,021	1,390 0,028	0,624 0,146	3,282 0,140	5,202 0,425	0,631 0,048	101700 +17000 -14200	Le Bassin	Pinus strobus
MS 82-38B UQT-181	1,725 0,019	1,115 0,006	0,862 0,135	4,540 0,096	6,768 0,270	0,671 0,024	117400 +10000 -8800	Green Point	Juniperus sp.
Unité II									
MS 8236W2C UQT-109	0,173 0,005	2,096 0,062	0,104 0,018	6,151 0,176	10,547 0,445	0,583 0,020	86900 +6000 -5700	East Bay	Tsuga canadensis
PL 75-83A UQT-185	0,763 0,016	1,229 0,019	0,130 0,048	12,098 0,625	21,854 1,314	0,554 0,020	84900 +6500 -6100	East Milford	Picea sp.
PL 75-83D UQT-186	0,178 0,005	1,317 0,038	0,100 0,025	3,953 0,180	7,140 0,562	0,554 0,038	84200 +11300 -10100	East Milford	Abies balsamea
Unité III									
MS 84-23W UQT-177	0,234 0,007	1,202 0,029	0,006 0,012	66,907 10,251	151,603 23,760	0,441 0,018	62100 +5000 -4600	East Bay	Picea sp.
MS 8222 BA UQT-178	4,073 0,087	1,539 0,011	0,049 0,399	138,797 24,955	386,178 72,992	0,359 0,022	47000 +4700 -4300	Bay St-Laurt.	Larix laricina

Les nombres en caractère gras indiquent la valeur de la déviation normale

échantillons enveloppés dans une argile saturée dans des endroits caractérisés par des gradients hydrauliques faibles, présentent la plus grande homogénéité et sont donc susceptibles de fournir les meilleurs données radiochronologiques.

En tout état de cause, les âges radiométriques obtenus sur les unités interglaciaires et interstadières de Nouvelle-Écosse et du golfe du Saint-Laurent (tabl. 2.2) doivent être pris à titre indicatif: sur 20 échantillons analysés, neuf ne répondent pas aux critères retenus ci-dessus. Dans l'ensemble, il s'agit de milieux relativement peu favorables à l'application de la méthode. Il reste, cependant, que l'on observe une concordance acceptable des âges calculés pour la plupart des formations considérées; en appui au dossier palynostratigraphique établi par MM. R. Mott et A. de Vernal (voir plus haut), ils permettent d'attribuer raisonnablement chaque unité à un épisode climatostratigraphique reconnu (par ex: unité I = stade isotopique 5e; voir fig. 2.1). Un dernier argument permet d'appuyer ces conclusions. Les couples de valeurs $y = ({}^{230}\text{Th}/{}^{232}\text{Th})$ et $x = ({}^{234}\text{U}/{}^{232}\text{Th})$ de l'ensemble des échantillons de l'unité I, incluant ceux présentant des teneurs élevées en ${}^{232}\text{Th}$, définissent une droite de régression linéaire obéissant à l'équation:

$$y = 0,69 x - 0,28$$

avec un coefficient de corrélation de 0,97. L'ordonnée à l'origine, proche de zéro, semble indiquer qu'une certaine quantité d'uranium a systématiquement été introduite dans les échantillons, probablement après la dernière déglaciation; elle interdit tout calcul de la valeur du rapport initial ${}^{230}\text{Th}/{}^{232}\text{Th}$, correspondant à la composante «détritique» du système radioactif. Cependant, au vu du coefficient de corrélation, il semble que l'on puisse accorder un certain crédit à la pente de la droite de corrélation qui, il ne faut pas oublier, représente le rapport ${}^{230}\text{Th}/{}^{234}\text{U}$ significatif de l'âge des échantillons (voir également Schwarcz et Skoflek, 1982). Dans le cas présent, la pente de 0,69 livre un âge de 120 000 ans environ, compte tenu des rapports ${}^{234}\text{U}/{}^{238}\text{U}$ moyens observés. Cette approche permet d'observer une certaine confirmation de l'âge proposé à partir des rapports isotopiques des échantillons considérés comme les plus fiables.

Les échantillons des îles Banks et Victoria

Dans des milieux où domine le pergélisol, il n'est pas surprenant d'observer des proportions beaucoup plus faibles que précédemment de thorium «détritique» dans les échantillons de bois, comme l'indiquent les rapports ${}^{230}\text{Th}/{}^{232}\text{Th}$ du tableau 2.3. Par ailleurs, les âges calculés, après correction des apports détritiques (sur la base des rapports d'activité d'un échantillon holocène), répondent exactement aux attentes que les études stratigraphiques (Vincent, 1983; Vincent et coll., 1983) laissaient entrevoir. La surprise, dans le cas présent, vient des déterminations d'âges Th/U sur les coquilles de mollusques fossiles des unités marines associées d'origine interglaciaire ou interstadière, ou les deux. En particulier, les faunes attribuées à la mer Big, considérée comme datant du dernier interglaciaire, sinon de la déglaciation qui lui a précédé, montrent une dispersion que n'explique aucune anomalie géochimique. Quoiqu'il soit communément admis que les mollusques s'avèrent des échantillons peu propices aux mesures d'âges radiométriques Th/U (Kaufman et coll., 1971), ce point de vue n'est pas en totalité partagé (voir Hillaire-Marcel et coll., sous presse). Dans le cas présent, les coquilles ont conservé leur nature aragonitique initiale; les proportions de ${}^{232}\text{Th}$ restent faibles; les teneurs en ${}^{18}\text{O}$ et en ${}^{13}\text{C}$ n'indiquent aucune ouverture du système carbonaté; rien, par conséquent, ne permet de mettre en doute la représentativité chronologique des

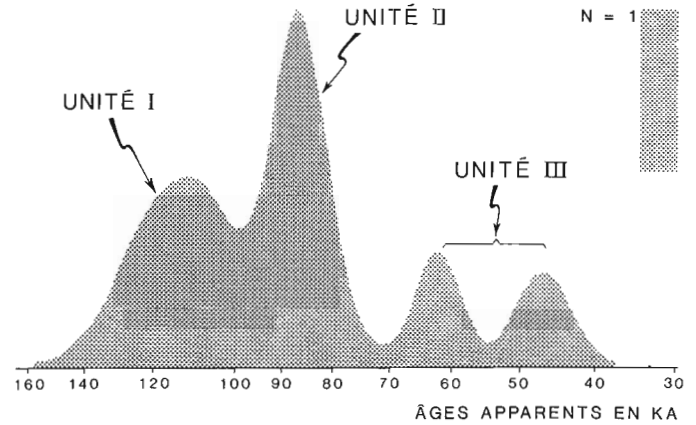


Figure 2.1. Histogramme de fréquence des âges ${}^{230}\text{Th}/{}^{234}\text{U}$ obtenus sur les échantillons de bois des provinces de l'Atlantique. De ce diagramme, sont exclus les échantillons présentant plus de 30 % de ${}^{232}\text{Th}$ (c. ${}^{230}\text{Th}$). L'histogramme est construit en tenant compte de la distribution gaussienne des résultats, entre $\pm 3\sigma$, soit dans un intervalle de confiance de plus de 99 %. On observe un bon regroupement des échantillons, notamment ceux des unités palynostratigraphiques I et II, respectivement autour d'environ 110 000 et de 87 000 ans.

rapports Th/U. Il est difficile de tirer une conclusion en ce qui a trait à la contradiction apparente entre les données géochimiques et celles des études de terrain. Il suffit de rappeler, cependant, que la plupart des échantillons proviennent de dépôts deltaïques attribués à la mer Big sur des bases uniquement morphostratigraphiques; par ailleurs, des indices de remaniement ont été signalés (Vincent, 1983). Le seul échantillon indubitablement prélevé en place a livré un âge de l'ordre de 100 000 ans qui s'accorde relativement bien avec la chronologie attendue. On peut signaler, à ce propos, que des mesures des taux de racémisation des acides aminés, dans les mêmes échantillons attribués à la mer Big, ont livré des résultats aussi «dispersés» que les rapports isotopiques Th/U mentionnés plus haut (Occhietti, comm. per.); ces échantillons pourraient donc refléter une histoire géologique plus complexe qu'il ne paraissait à première vue: y a-t-il eu mélange de populations d'âges différents? ou mise en place de deltas et de dépôts marins au cours d'un épisode relativement long, en relation avec la situation de marge glaciaire de l'île Banks? Des anomalies de ce type ont, par exemple, été observées par Blake (1975) et England (1983) sur les côtes de l'île d'Ellesmere. Finalement, les faunes recueillies dans les autres unités glaciomarines, plus récentes que la mer Big, ne présentent aucune anomalie chronologique particulière, au-delà des corrections mineures dues à la présence d'une faible quantité de thorium «détritique».

Les échantillons du district de Mackenzie

Les données lithostratigraphiques sont ici d'une grande imprécision: niveaux repères très rares, remaniement très fréquent des dépôts à la faveur de conditions thermokarstiques ou bien de mouvements glaciaires, ou les deux; bois fossiles souvent allochtones (J.-S. Vincent, comm. pers.). Les données radiochronologiques Th/U peuvent donc être d'un grand intérêt dans un tel domaine, d'autant plus que l'existence d'un pergélisol leur assure une certaine validité. On comprendra cependant, au vu des discussions précédentes, qu'une approche statistique s'impose.

Tableau 2.3. Ile Banks – Ile Victoria

Numéro échantillon /terrain /labor.	²³⁸ U (p.p.m.)	²³⁴ U/ ²³⁸ U rap.d'act.	²³² Th (p.p.m.)	²³⁰ Th ²³² Th	²³⁴ U/ ²³² Th	²³⁰ Th/ ²³⁴ U	Âge brut	Âge corrigé	Initial	Formation
Mollusques fossiles										
VH 74-042 UQT-141	1,049 0,023	1,265 0,032	0,293 0,025	2,048 0,126	13,726 0,823	0,149 0,007	17500 +1100 -1200	10200*	1,2	mer de Schuyter Point
VH 77-104 UQT-142	0,971 0,022	1,351 0,034	0,506 0,037	2,767 0,081	7,865 0,304	0,352 0,012	46000 +2700 -2300	34300	1,2	mer East Coast
VH 83-011 UQT-143	0,818 0,019	1,408 0,038	0,218 0,058	9,507 0,569	16,033 1,038	0,593 0,021	92400 +7000 -6400	87000	1,2	mer Pré-Amundsen
VH 77-075 UQT-221	2,128 0,031	1,531 0,021	0,127 0,052	13,538 1,023	77,979 6,059	0,174 0,006	20500 +1000 -1000	19300	1,2	mer Big
VH 77 051 UQT-220	1,242 0,034	1,480 0,042	0,108 0,048	16,976 1,270	51,565 4,122	0,329 0,012	42300 +2600 -2400	40600	1,2	mer Big
VH 77-065 UQT-145	0,704 0,018	1,333 0,039	0,160 0,033	6,935 0,381	17,788 1,080	0,390 0,015	52500 +3400 -3400	47400	1,2	mer Big
VH 77-114 UQT-146	0,773 0,020	1,602 0,045	0,306 0,059	5,794 0,266	12,247 0,680	0,473 0,019	66500 +5000 -4600	59300	1,2	mer Big
VH 77-92 UQT-80	0,534 0,012	1,934 0,050	0,169 0,060	12,198 0,952	18,503 1,473	0,659 0,022	104600 +7600 -6800	100400	1,2	mer Big
VH 77-060 UQT-144	0,682 0,013	1,466 0,033	0,151 0,074	13,543 1,128	20,026 1,745	0,676 0,027	113000 +10000 -9400	108700	1,2	mer Big
Bois fossiles										
VH B1032c UQT-116	0,372 0,010	1,248 0,039	0,023 0,006	7,967 0,601	60,758 4,874	0,131 0,005	15200 +1000 -1000	13700	1,2	-
VH 82-125 UQT-230	1,457 0,032	1,344 0,034	0,586 0,099	5,021 0,297	10,139 0,644	0,495 0,019	71800 +5200 -5100	62800	1,2	Interstadiare Wisconsinien
VH 81-066 UQT-117	1,258 0,034	1,268 0,035	0,107 0,074	21,995 1,973	45,381 4,308	0,485 0,020	69900 +6000 -5100	68000	1,2	Cap Collinson
VH 77-132 UQT-118	3,176 0,065	0,824 0,013	0,590 0,212	11,701 0,572	13,456 0,785	0,870 0,032	>200 000	>200 000	1,2	Morgan Bluffs
VH 81-012A UQT-229	1,046 0,026	1,046 0,033	0,640 0,112	5,489 0,295	5,186 0,312	1,058 0,042	>200 000	>200 000	1,2	Morgan Bluffs
Les nombres en caractère gras indiquent la valeur de la déviation normale										
* Âge au carbone radioactif de VH 74-042 : 10 200 ans B.P. (± 170) (CGC-2990)										

Comme dans le cas de l'île Banks, on observe des quantités faibles de ²³²Th (voir tabl. 2.4); à une exception près, le rapport d'activité ²³⁰Th/²³²Th reste supérieur à 6,66. Les trois âges les plus élevés (>150 000 ans environ) correspondent bien aux échantillons appartenant aux sédiments considérés comme les plus anciens d'après les informations stratigraphiques (J.-S. Vincent, comm. pers.). Toutefois, tous les autres échantillons étaient, jusqu'à preuve du contraire, attribués à un épisode associé au stade 5 de la climatostratigraphie isotopique océanique (ibid.). Trois d'entre eux ont livré effectivement des âges Th/U compatibles avec cette interprétation: ils pourraient appartenir à un épisode corrélatif des sous-stades 5c ou 5a, ou les deux. Trois autres, cependant, ont livré des âges apparents moins élevés. Rien n'empêche de croire que ceux-ci ne sont pas représentatifs, dans la mesure où

l'existence d'unités interstadiaries du Wisconsinien moyen n'est pas écartée. Il faut cependant mentionner le fait que l'échantillon le plus <<jeune>> (UQT-233) a fait l'objet d'une mesure d'âge radiométrique ¹⁴C (CGC-4075) contradictoire: >36 000 B.P. Ainsi qu'en fait état plus loin le présent rapport, dans la plupart des autres cas de double contrôle, les deux chronologies sont cohérentes. Dans le cas présent, aucune anomalie géochimique n'est perceptible à partir des seules données analytiques Th/U; il se peut que le milieu englobant l'échantillon n'a pas pu maintenir une fermeture du système géochimique: il serait souhaitable de procéder à un nouvel échantillonnage de la localité en s'efforçant de recueillir des morceaux de bois dans les parties les moins poreuses du milieu. Il se peut, en effet, que certains échantillons, dont ce dernier, aient incorporé secondairement de l'uranium, à la faveur d'une circulation d'eau, telle qu'elle se produirait dans un mollisol.

Les échantillons du Territoire du Yukon

La majorité des échantillons recèle, ici encore, une fraction détritique peu importante (voir tabl. 2.5). Les concentrations en uranium sont très faibles, dans tous les cas inférieures au $\mu\text{g/g}$. Les rapports d'activité $^{234}\text{U}/^{238}\text{U}$ sont très peu différents d'une valeur moyenne proche de 1,4. Deux échantillons ont cependant livré des rapports des isotopes de l'uranium beaucoup plus faibles (UQT-171 et UQT-170). Rien n'empêche de croire, eu égard à la remarquable homogénéité des valeurs observées dans l'ensemble, que ces échantillons ont connu une remobilisation partielle de l'uranium; ce phénomène aurait pour effet de livrer des âges apparents plus élevés que les âges réels. Quoi qu'il en soit, les échantillons de bois paraissent provenir d'unités interglaciaires et interstadias d'âges variés alors que, d'après les données de terrain, on pouvait raisonnablement tous les attribuer au dernier interglaciaire ou à des épisodes non glaciaires antérieurs (J.-S. Vincent, comm. pers.). À défaut d'une conclusion, on peut cependant avancer quelques éléments qui permettent de donner foi, dans une certaine mesure, aux données radiochronologiques Th/U. En effet, un échantillon (UQT-198) donnait un rapport d'activité $^{230}\text{Th}/^{234}\text{U}$ <<anormalement>> bas (0,19) qui, compte tenu de la présence d'une quantité non négligeable de ^{232}Th , donc de thorium d'origine <<détritique>>, pouvait correspondre à celui auquel l'on s'attendrait d'un échantillon d'âge holocène (p. ex. UQT-116, tabl. 3). Sur cette base, une datation par la méthode du ^{14}C a été effectuée: un âge de $8\,250 \pm 80$ B.P. (CGC-4005) est venu confirmer l'interprétation basée sur les seules données Th/U. Par ailleurs, cet âge radiométrique ^{14}C permet de calculer un rapport d'activité $^{230}\text{Th}/^{232}\text{Th}$ initial

(phase <<détritique>>) de l'ordre de 0,4 qui pourrait appartenir à des phyllites argileuses originellement pauvres, ou appauvries par lessivage, en uranium.

Un autre indice d'une stratigraphie complexe, dans ce territoire, peut être donné: une population de mollusques, prélevés en place, par J.-S. Vincent, a fait l'objet de trois analyses indépendantes. La première, d'une partie aliquote de 7 g environ (UQT-110); les deux autres, de parties aliquotes de 30 g environ (UQT-301 et UQT-366). La dispersion relative des résultats (tabl. 2.6) reste acceptable, si l'on tient compte du fait qu'il s'agit de coquilles constituant un milieu géochimiquement ouvert pendant la phase originelle de fossilisation, c'est-à-dire, celle de la fixation de l'uranium. Les deux derniers résultats, obtenus sur des quantités plus grosses de matériel (donc <<homogénéisant>> mieux les mélanges éventuels de populations, quoique ceux-ci soient peu probables, d'après les observations de terrain), ont livré des rapports $^{230}\text{Th}/^{234}\text{U}$ égaux respectivement à $0,30 \pm 0,01$ et $0,33 \pm 0,01$ ($\pm 1\sigma$). Ces rapports donnent au calcul un âge moyen de l'ordre de $40\,000 \pm 3\,000$ ans, si l'on ne tient pas compte de la présence d'une faible part de ^{230}Th non authigène, indiquée par le ^{232}Th . Si l'on suppose un rapport initial $^{230}\text{Th}/^{232}\text{Th}$ égal à 1, l'âge corrigé tomberait aux environs de 30 000 ans; ce dernier est <<minimal>>, puisqu'il correspond au temps de résidence moyen de l'uranium. Si l'on admet que la plus grosse partie de l'uranium est fixée au cours des premiers milliers d'années suivant l'enfouissement des coquilles (voir p. ex. Stearns, 1980), celles-ci, dans le cas présent, dateraient néanmoins du Wisconsinien moyen et se situeraient, hélas, aux limites, sinon au-delà, de la méthode de datation au carbone radioactif.

Tableau 2.4. District de Mackenzie

Numéro échantillon /terrain /labor.	^{238}U (p.p.m.)	$^{234}\text{U}/^{238}\text{U}$ rap.d'act.	^{232}Th (p.p.m.)	$^{230}\text{Th}/^{232}\text{Th}$	$^{234}\text{U}/^{232}\text{Th}$	$^{230}\text{Th}/^{234}\text{U}$	Âge brut
VH 83-212 UQT-233	0,882 0,010	1,043 0,009	0,014 0,017	42,889 4,775	198,633 22,468	0,216 0,007	26400 +1000 -1100
VH 83-183 UQT-231	3,912 0,077	1,214 0,022	0,251 0,172	17,164 1,458	57,396 5,280	0,299 0,013	38200 +2600 -2600
VH 83-220a UQT-235	0,550 0,007	1,064 0,016	0,033 0,023	24,794 2,627	53,139 5,733	0,467 0,014	67800 +3600 -3600
VH 83 171b UQT-232	1,251 0,018	1,092 0,017	0,259 0,073	8,778 0,524	16,009 1,028	0,548 0,019	85100 +6000 -5600
VH 83-169b UQT-201	0,196 0,005	1,190 0,038	0,108 0,016	3,920 0,197	6,526 0,394	0,601 0,027	96600 +10000 -9000
VH 83-190 UQT-207	0,151 0,004	1,114 0,036	0,032 0,011	9,894 1,343	15,765 2,188	0,628 0,027	104800 +10800 -9600
VH 83-217 UQT-234	0,083 0,002	1,342 0,034	0,028 0,008	9,731 0,851	11,877 1,062	0,819 0,028	164400 +18000 -15400
VH 83-188 UQT-205	4,748 0,118	1,075 0,026	0,247 1,014	61,002 7,870	62,632 9,140	0,974 0,070	>200,000
VH 83-149 UQT-200	0,059 0,001	1,241 0,038	0,191 0,009	1,402 0,047	1,152 0,048	1,217 0,048	non calculable
Les nombres en caractère gras indiquent la valeur de la déviation normale							

Tableau 2.5. Territoire du Yukon

Numéro échantillon /terrain /labor.	^{238}U (p.p.m.)	$^{234}\text{U}/^{238}\text{U}$ rap.d'act.	^{232}Th (p.p.m.)	$^{230}\text{Th}/^{232}\text{Th}$	$^{234}\text{U}/^{232}\text{Th}$	$^{230}\text{Th}/^{234}\text{U}$	Âge brut
VH 83-090 UQT-198	0,708 0,017	1,468 0,036	0,965 0,020	0,622 0,018	3,265 0,118	0,191 0,007	22700 +1300 -1300
VH 83-071 UQT-196	0,336 0,009	1,414 0,038	0,137 0,024	5,322 0,257	10,532 0,593	0,505 0,020	73400 +5700 -5300
VH 83-072 UQT-197	0,291 0,008	1,444 0,041	0,213 0,020	2,900 0,122	5,982 0,298	0,485 0,020	69300 +5300 -5100
VH 83-0596 UQT-171	0,198 0,004	0,985 0,029	0,079 0,015	5,113 0,373	7,491 0,569	0,683 0,029	124900 +14800 -12200
VH 83-023 UQT-168	0,200 0,005	1,481 0,046	0,163 0,023	4,867 0,224	5,510 0,292	0,883 0,033	188700 +25000 -20600
VH 83-043 UQT-169	0,044 0,001	1,436 0,036	0,110 0,009	2,291 0,117	1,739 0,092	1,317 0,051	non calculable
VH 83-052 UQT-170	0,154 0,003	1,131 0,026	0,510 0,024	1,221 0,038	1,036 0,046	1,178 0,050	non calculable
VH 83-123 UQT-199	0,483 0,013	1,612 0,045	0,160 0,086	18,621 1,392	14,739 1,178	1,263 0,047	non calculable

Les nombres en caractère gras indiquent la valeur de la déviation normale

Tableau 2.6. Territoire du Yukon : échantillon VH 83-088

N° de l'analyse	^{238}U (p.p.m.)	$^{234}\text{U}/^{238}\text{U}$ (rapports d'activité)	$^{232}\text{Th}/^{230}\text{Th}$	Âge non corrigé (Th initial nul)	Âge corrigé ¹
UQT-110	0,115 ± 0,003	1,45 ± 0,05	0,20 ± 0,02	68,600 ± 5,000	63,800
UQT-301	0,121 ± 0,003	1,46 ± 0,04	0,32 ± 0,02	37,900 ± 2,000	28,000
UQT-366	0,091 ± 0,002	1,45 ± 0,04	0,27 ± 0,01	42,100 ± 3,000	30,600

¹ Selon l'hypothèse: ($^{232}\text{Th}/^{230}\text{Th}$)=1, au temps zéro.
Les nombres en caractère gras indiquent la valeur de la déviation normale

Conclusions

L'échantillon UQT-198, décrit ci-dessus, comme les autres spécimens dont l'âge permettait un contrôle par le ^{14}C (UQT-116, UQT-141, UQT-178), tendrait à convaincre de la validité de l'hypothèse de travail retenue: pour autant que le milieu présente des indices de relative fermeture géochimique, en l'occurrence des circulations d'eau très restreintes, la chronologie Th/U peut constituer un outil radiochronologique applicable aux fossiles ligneux. Toutefois, dans son ensemble, le dossier analytique qui vient d'être examiné ne permet pas de considérer la méthode Th/U comme une panacée. Ainsi que déjà mentionné, en introduction, les tourbes semblaient présenter un milieu très propice à la fixation de l'uranium mais, par suite, peu favorable à la fermeture du système radioactif Th/U; la même restriction s'applique à tout échantillon de bois fossilisé en milieu géochimiquement ouvert. En première approximation, l'échantillonneur, sur le terrain, peut donc être en mesure d'évaluer l'applicabilité de la méthode, selon les conditions de fossilisation et de préservation qu'il peut déduire de ses observations et de sa connaissance du milieu. Il repose sur lui d'échantillonner avec clairvoyance pour que l'analyse ultérieure ait son utilité: entre le morceau de bois enfoui dans le pergélisol, et celui, pourtant d'accès plus aisé, pris dans le mollisol, le choix du premier s'impose. De même, un échantillon prélevé dans une couche de graviers très perméables ne présente aucun intérêt du point de vue radiochronologique. Finalement, dans tous les cas de figure, un échantillon isolé ne pourra donner lieu à une interprétation certaine; la cohérence d'un ensemble de données géochimiques est la meilleure garantie de clôture d'un système radioactif. Il reste que cette méthode peut apporter des éléments chronostratigraphiques, lorsque d'autres font défaut, notamment au-delà des dernières dizaines de milliers d'années couvertes par la méthode de datation au ^{14}C .

Remerciements

Les auteurs remercient les membres de la Commission géologique du Canada qui ont recueilli la plupart des échantillons, et dont les critiques ont aidé à parfaire le manuscrit, soit MM. J.-S. Vincent et R.J. Mott. Ces travaux ont été partiellement financés par la Commission géologique du Canada (convention EMR no. 198), mais essentiellement par le Conseil de la recherche en sciences naturelles et en génie (subvention A-9156).

Bibliographie

- Blake, W., Jr.
1975: Radiocarbon age determinations and post-glacial emergence of Cape Storm, Southern Ellesmere Island, Arctic Canada; *Geografiska Annaler*, series A, v. 57, p. 1-71.
- de Vernal, A. et Mott, R.J.
1985: Palynostratigraphie du Pléistocène supérieur dans la région du lac Bras d'Or, île du Cap-Breton, Nouvelle-Écosse; *Journal canadien des sciences de la Terre*.
- de Vernal, A., Causse, C., Hillaire-Marcel, C., Mott, R.J., and Occhietti, S.
- Palynostratigraphy and Th/U ages of Upper Pleistocene Interglacial and Interstadial deposits on Cape Breton Island, eastern Canada; *Geology*. (in press)
- England, J.
1983: Isostatic adjustments in a full glacial sea; *Canadian Journal of Earth Sciences*, v. 20, p. 895-917.
- Fulton, R.J. (editor)
1984: Quaternary stratigraphy of Canada: a Canadian contribution to IGCP project 24; Geological Survey of Canada, paper 84-10.
- Gascoyne, M., Schwarcz, H.P., and Ford, D.C.
1978: Uranium series dating and stable isotope studies of speleothems: part I Theory and techniques; *British Cave Research Association*, v. 5, p. 91-111.
- Goldberg, E. and Koide, M.
1962: Geochronological studies of deep sea sediments by the Io/Th method; *Geochimica et Cosmochimica Acta*, v. 26, p. 417-449.
- Grant, D.R., Prest, V.K., Dredge, L.A., and Mott, R.J.
1985: Lithostratigraphy and Quaternary history, Magdalen Islands, Quebec; in *abstracts of Geological Association of Canada*, annual meeting, Fredericton, New Brunswick, p. A22.
- Hillaire-Marcel, C., Carro, O., Causse, C., Goy, J.-L., and Zazo, C.
- Th/U dating of *Strombus bubonius* bearing marine terraces in southeastern Spain; *Geology*. (in press).
- Ivanovich, M. and Harmon, R.S.
1982: Uranium series disequilibrium: applications to environmental problems; Clarendon Press, Oxford, 571 p.
- Kaufman, A., Broecker, W.S., Ku, T.L., and Thurber, D.L.
1971: The status of U-series methods of mollusk dating; *Geochimica et Cosmochimica Acta*, v. 35, p. 1155-1183.
- Prest, V.K.
1970: Quaternary Geology of Canada; in *Geology and Economic Minerals of Canada*, Geological Survey of Canada, Economic Geological Report, v. 1, p. 675-764.
- Schwarcz, H.P. and Skoflek, I.
1982: New dates for the Tata, Hungary archaeological site; *Nature*, v. 295, p. 590-591.
- Stearns, C.E.
1980: A Molluscan revival?; in *Actes du Colloque <<Niveaux marins et tectonique quaternaires dans l'aire méditerranéenne>>*, Centre National de la Recherche Scientifique, Paris, p. 15-26.
- Vincent, J.-S.
1983: La géologie du Quaternaire et la géomorphologie de l'île Banks, Arctique canadien; Commission géologique du Canada, Mémoire 405, 118 p.
- Vincent, J.-S., Occhietti, S., Rutter, N., Lortie, G., Guilbault, J.P., and de Boutray, B.
1983: The Late Tertiary-Quaternary stratigraphic record of the Duck Hawk Bluffs, Banks Island, Canadian Arctic Archipelago; *Canadian Journal of Earth Sciences*, v. 20, p. 1694-1712.
- Vogel, J.C. and Kronfeld, J.
1980: A new method for dating peat; *South African Journal of Science*, v. 76, p. 557-558.
- Woillard, G.M. and Mook, W.G.
1982: Carbon-14 dates at Grande Pile: correlation of land and sea chronologies; *Science*, v. 215, p. 159-161.

Geology of the Long Range Inlier in Sandy Lake map area, western Newfoundland¹

DSS Contract 27ST.23233-5-0005

Philippe Erdmer²

Erdmer, P., Geology of the Long Range Inlier in Sandy Lake map area, western Newfoundland; in Current Research, Part B, Geological Survey of Canada, Paper 86-1B, p. 19-27, 1986.

Abstract

The Long Range Inlier, the largest external Precambrian basement massif in the Appalachians, comprises mainly high grade polydeformed quartzofeldspathic gneisses of plutonic origin with wispy remnants of supracrustal rocks. The complex is intruded by granitoid and gabbroic plutons of Middle Proterozoic age, by an Eocambrian mafic dyke swarm, and by a Devonian granite. Greenschist facies retrogression of earlier granulite and amphibolite assemblages occurred in the Late Proterozoic and Early Paleozoic.

Cambro-Ordovician platformal strata deposited on the Precambrian were penetratively deformed in the Middle Paleozoic, but the basement was not. The major structural detachment this implies, westward thrusting of the inlier over the platformal rocks and over Taconic allochthonous rocks, and the fact that fabrics in the Precambrian rocks do not control Appalachian trends, suggest that the Precambrian terrane was involved in thin-skinned Appalachian deformation, and forms a thrust slice rather than a basement massif. Carboniferous redbeds unconformably overlie parts of the inlier and adjacent Silurian and Devonian rocks.

Résumé

La fenêtre Long Range est le plus grand massif externe du socle précambrien des Appalaches, elle se compose principalement de gneiss quartzofeldspathiques plutoniques fortement métamorphisés qui ont subi de multiples déformations. De petites inclusions de roches supracrustales sont parsemées dans ce complexe gneissique. On y trouve des intrusions de plutons granitoïdes et gabbroïques datant du Protérozoïque moyen, ainsi qu'un groupe de filons mafiques de l'Éocambrien et un granite dévonien. La rétro-morphose en faciès de schistes verts d'anciennes associations de granulites et d'amphibolites s'est produite au Protérozoïque supérieur et au Paléozoïque inférieur.

Les couches de roches clastiques et carbonatées cambriennes-ordoviciennes de plate-forme qui se sont déposées sur les roches précambriennes ont été déformées par pénétration au cours du Paléozoïque moyen, ce qui ne fut pas le cas du socle. Cette séparation structurale importante entre le socle et la couverture, le charriage vers l'ouest de la fenêtre sur les roches de la plate-forme et, localement, sur les roches allochtones de la phase taconique et le fait que la structure des roches précambriennes ne commande pas les directions générales appalachiennes laissent supposer que le terrane précambrien a subi une déformation superficielle des Appalaches, il constitue un lambeau de charriage plutôt qu'un massif de socle. Les couches rouges du Carbonifère reposent en discordance sur certaines parties de la fenêtre et des roches siluriennes et dévoniennes adjacentes.

¹ Contribution to Canada-Newfoundland Mineral Development Agreement 1984-1989. Project carried by Geological Survey of Canada, Lithosphere and Canadian Shield Division.

² Department of Geology, University of Alberta, Edmonton, Alberta, T6G 2E3.

Introduction

Extending across most of the width of the Humber Zone, the Long Range Inlier is the largest of the Precambrian external basement massifs of the Appalachian Orogen. It forms a resistant block of high grade crystalline rocks uplifted in the mid-Paleozoic through an unconformably overlying Cambro-Ordovician clastic and carbonate platformal cover. It separates regional structural depressions occupied by major Taconic klippen (e.g. Humber Arm and Hare Bay allochthons), and Silurian, Devonian(?), and Carboniferous rocks.

A systematic investigation of the inlier, until now the largest single unmapped part of the Island of Newfoundland, has been initiated under the Canada-Newfoundland Mineral Development Agreement 1984-1989. Field work in 1985 covered half of the unmapped portion of the inlier (Fig. 3.1), an area of 3000 km² in Sandy Lake map area (NTS 12H). It included an extensive remote portion of Gros Morne National Park being considered for development by park authorities.

Two projects were carried out simultaneously, (1) complete reconnaissance mapping, and (2) detailed mapping of an area of 800 km² in NTS 12H/11 map area where preliminary work showed the widest variety of rock types. The report of reconnaissance mapping is presented here; the results of detailed mapping were described by Owen (1986). This report will be complemented by an open file map at 1:100 000 scale incorporating results of petrography and geochemistry. The isotopic age determinations reported here are results of work in progress.

Previous and related work

A summary of previous geological investigations in various parts of the inlier since Murray and Howley's (1881) first survey is given by Erdmer (1984). Recent and current work in rocks surrounding the inlier has been carried out by Knight (1985), Knight and Boyce (1984), Nyman et al. (1984), Williams (1985), and Williams et al. (1984, 1985). These studies have established in particular that moderate westward transport (a few tens of

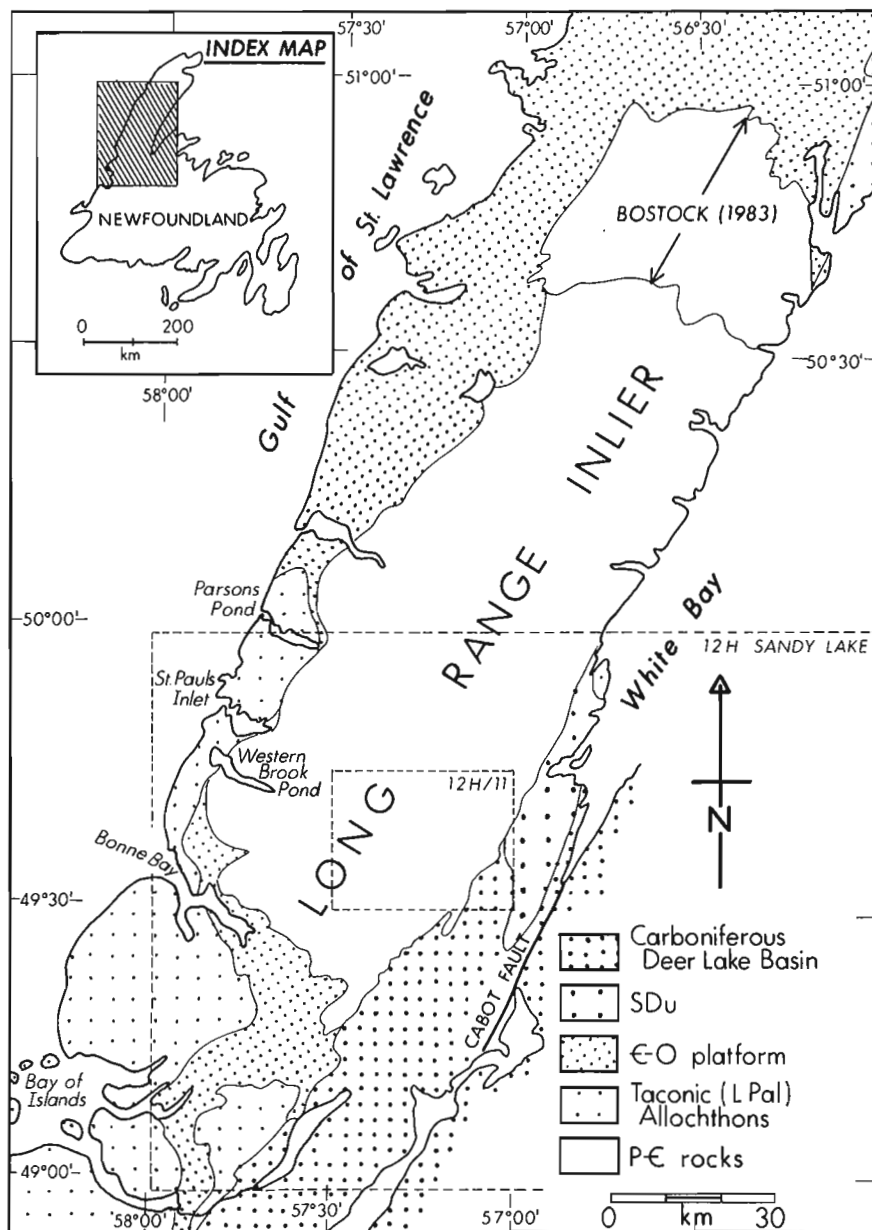


Figure 3.1. Main tectonic divisions of northwestern Newfoundland, and location of NTS 12H and 12H/11 map areas. The extent of mapping by Bostock (1983) is outlined. Abbreviations: PC = Precambrian, C-O = Cambrian and Ordovician, SDu = Silurian and Devonian (?) rocks undifferentiated.

kilometres at the widest part of the structural salient, on the basis of regional truncation of litho-stratigraphic belts) of the Precambrian rocks has occurred over both platformal and allochthonous sedimentary rocks, along brittle thrusts of mid-Paleozoic age.

Hyde (1982; personal communication, 1983) reported the occurrence of metamorphosed and tightly folded Lower Paleozoic platformal strata (now marble, quartzite, and mica schist) at several locations along the southeastern margin of the inlier. These rocks separate the Precambrian crystalline rocks from the unconformably overlying Carboniferous strata of the Deer Lake Basin.

Smyth and Schillereff (1981, 1982) mapped the southeast contact of the inlier with Cambro-Ordovician cover rocks. The unconformable contact with overlying clastic and carbonate rocks is commonly reworked and is mostly a steeply east-dipping fault. Dunford (1984) mapped approximately 25 km² of the terrane underlain by the Devils Room Granite, a late tectonic, massive pluton of Early Devonian age.

General geology

In its structure and internal stratigraphic relations, the southern part of the inlier is broadly comparable to the northern portion described by Bostock (1983), and is characterized by large lithotectonic units (Fig. 3.2). The oldest rocks within the inlier comprise a heterogeneous basement complex of leucocratic to mesocratic polydeformed quartzofeldspathic gneisses. The widespread occurrence of thick lenses of granitoid orthogneiss and the scarcity of clearly supracrustal rocks suggest that the complex is mostly of plutonic origin. As fabrics in the complex are truncated by a suite of granites of Grenvillian age, the minimum structural age of the gneisses is Middle Proterozoic (time scale of Palmer, 1983).

Supracrustal rock types are graphitic and hematitic quartzite, sillimanite schist, diopside marble and calc-silicate, quartz- and muscovite-rich schist, biotite psammite and quartz-rich gneiss. A large number of small basic plutons and dykes that are now variably foliated amphibolite, metagabbro, hypersthene diorite and leucogabbro were intruded into the gneiss throughout the area.

A large intrusive body of olivine gabbro to metagabbro, gabbroic anorthosite and diorite appears to be younger than most of the small basic plutons. It is massive and locally displays primary cumulate layering. Regional metamorphism of granulite grade occurred before or with the emplacement of the basic rocks, and may be related to them. Its products, although commonly retrograded by later events, are preserved in many places.

Several large, distinctive megacrystic or massive granodioritic to granitic plutons postdate the granulite metamorphism, and they record only greenschist overprinting. Quartz diorite and hornblende diorite plutons that cut across the regional foliation may be tectonic contemporaries of the granitic to granodioritic suite. Smaller bodies similar in composition to these plutons occur throughout the area. Basic and metabasic dykes that intrude nearly all the above rocks trend largely northeast, and are correlated with the Long Range swarm described by Bostock (1983). A massive, fresh granite, the Devils Room pluton (Smyth and Schillereff, 1981) of Devonian age, postdates both the high grade metamorphism and the other granitoid plutons.

Retrograde greenschist facies minerals, mainly chlorite, epidote and muscovite, are widespread throughout the terrane, and are inferred to be Proterozoic (Grenvillian) and (or) Paleozoic (Acadian).

Deformation of the basement gneiss has been polyphase, with a northwest-striking fabric predominating. In the western part of the area, this fabric defines large steeply plunging folds (10 to 15 km amplitude) in the uniformly banded or "straightened" gneiss. In the centre and east, superposed deformation, possibly accompanying the basic intrusions, has produced complex interference patterns.

The emplacement of the megacrystic plutons rotated fabrics and rock units into parallelism with the margins of the plutons, which suggests a relatively deep level of intrusion. The plutons are massive in the centre, becoming progressively more foliated outward. Inclusions of host rocks are rare.

The Devils Room granite cuts across all fabrics and contacts at a high angle, suggesting a higher level of intrusion than the megacrystic granites.

Paleozoic deformation is restricted to the fringe zone of the inlier and is not regionally penetrative; it developed most intensely in the small prong at the southern tip of the inlier. Brecciation and recementing, iron staining, pervasive chloritization and quartz veining characterize many brittle shear zones; these truncate the contact with overlying Cambrian rocks at a high angle. The zones are locally diffuse and exhibit a wide range of strains. They are commonly the locus of normal, strike-slip and reverse faults of mid-Paleozoic age, especially along the southwestern margin of the inlier.

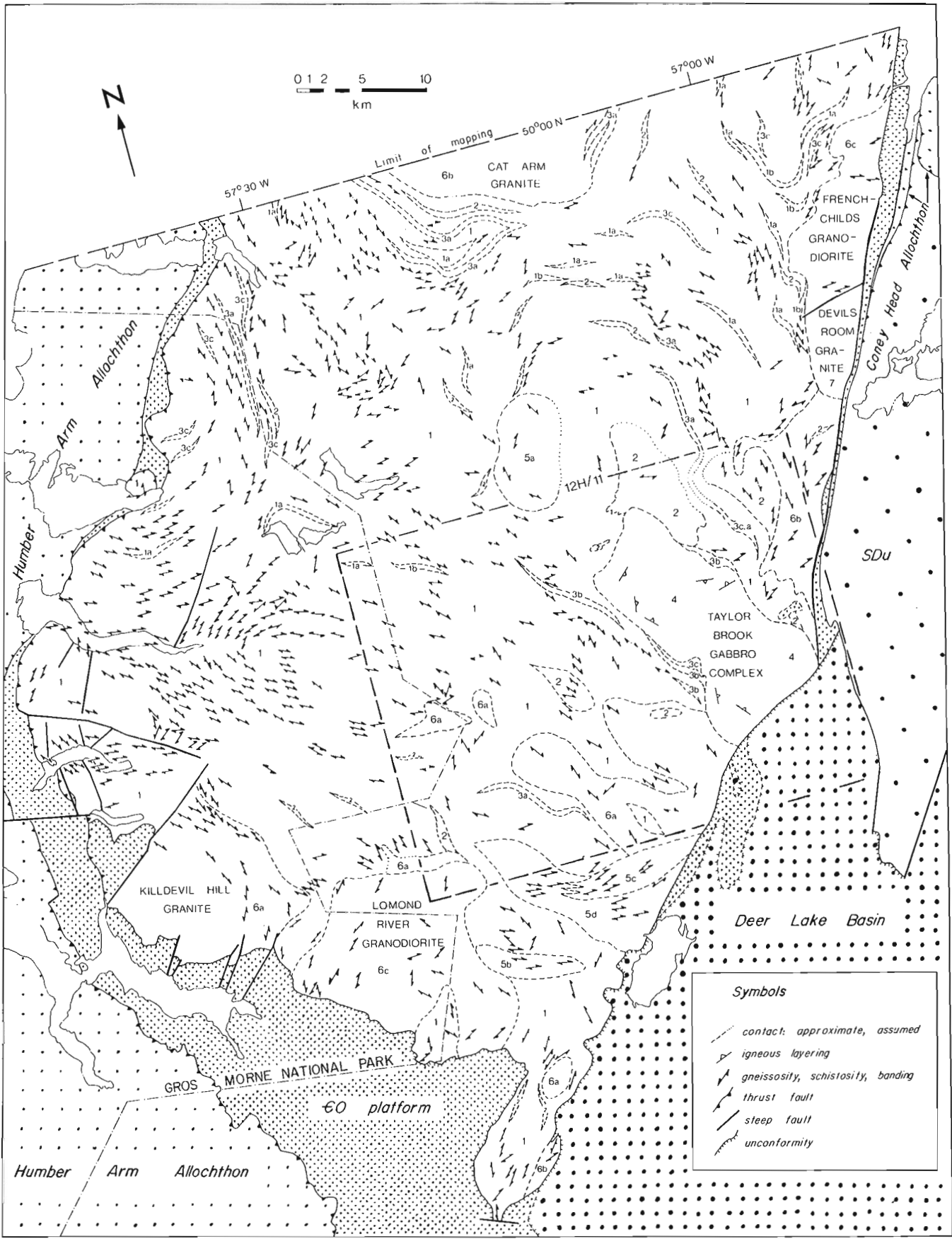
Map units

Metamorphic basement gneiss.

Heterogeneous basement gneiss underlies approximately two-thirds of the terrane. It comprises leucocratic, medium-to coarse-grained, two-pyroxene or hypersthene-biotite (+ chlorite) quartzofeldspathic gneisses of overall granitic to dioritic composition. The rocks are pink to buff to light grey, heterogeneous, commonly nebulitic, and generally well layered in outcrop and approximately equigranular in hand specimen (Fig. 3.3). Hornblende, or epidote, or both, occur together with biotite locally. Migmatite layers of at least two generations (older, folded layers, and undeformed crosscutting ones) are common. In outcrops where migmatitic transposition is not pervasive, areas of homogeneous rock are almost invariably granitoid orthogneiss that grades into the surrounding more complex gneiss. The most homogeneous of these areas (Fig. 3.4) are differentiated in Figure 3.2. The proportion of plutonic protoliths appears high; this is also the case in nearby inliers to the south which are dominantly metaplutonic, such as the Indian Head and Steel Mountain inliers. This contrasts with Bostock's (1983) interpretation of a chiefly metasedimentary origin for the northern part of the inlier. Radiometric U-Pb dating of zircon in two-pyroxene orthogneiss near the head of Western Brook Pond yields an age of approximately 1250 Ma.

Supracrustal layers in individual outcrops include quartz-rich gneiss, pelitic and semipelitic schist, marble and calc-silicate-rock, quartzite, and a wide range of nebulitic or gradational rock types intermediate between these homogeneous end members. The largest of the supracrustal layers are differentiated in Figure 3.2 and are described below.

Amphibolite layers, lenses, and boudins (Fig. 3.5) are common inclusions throughout the gneiss complex and constitute up to 90% of the outcrop locally. As they commonly cut across the foliation in adjacent gneisses (they are only locally conformable), they are interpreted as being largely metabasic dykes intruded at several stages of the gneiss history. Large more equidimensional bodies of amphibolite differentiated on Figure 3.2 are inferred to represent mafic plutons of various ages.



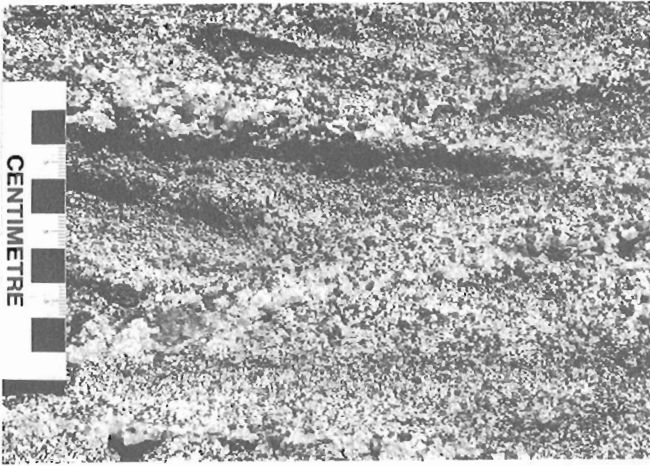


Figure 3.3. Nebulitic appearance of heterogeneous migmatitic gneiss near the centre of the inlier, south of the Cat Arm pluton. This texture characterizes many outcrops in the gneiss complex.

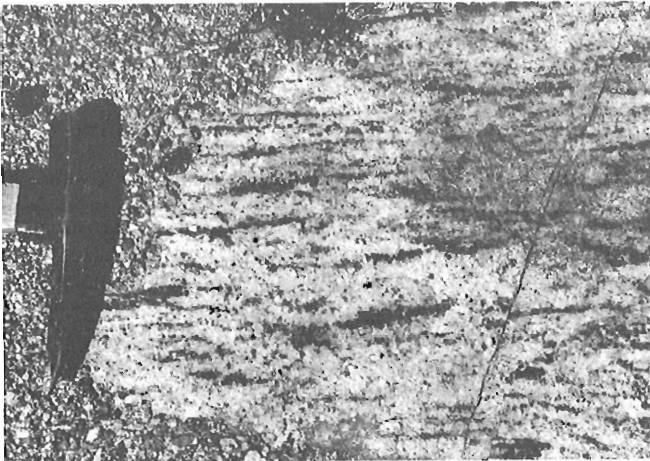


Figure 3.4. Foliated granitic orthogneiss in the gneiss complex.

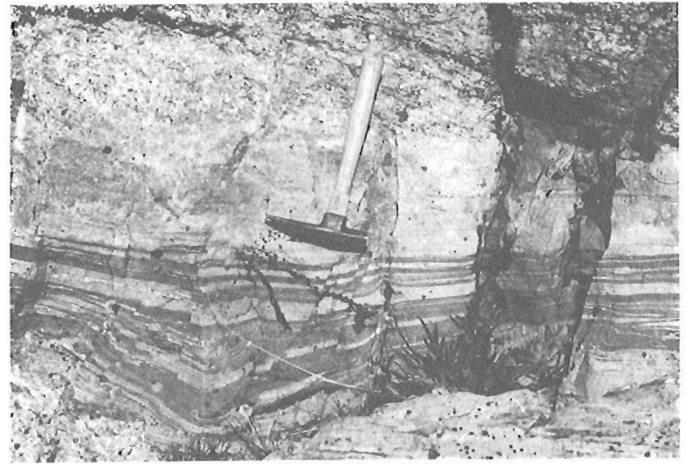


Figure 3.5. Striped amphibolite inclusion in a granodiorite lens in the gneiss complex. The hammer rests on an aplitic phase of the orthogneiss.

Relationships between the protoliths of the gneiss complex have been obscured by deformation so that relative ages are difficult to establish. The oldest components are of Middle to Early Proterozoic age.

Supracrustal rocks forming map-scale bodies

Nearly pure, glassy, white to pale grey, massive to locally well banded quartzites form resistant uniform ridges up to 20 km long near the southern margin of the Cat Arm Granite, south of Parsons Pond, north of the Taylor Brook Gabbro Complex, and northeast of the Lomond River Granodiorite. These quartzite layers are commonly more than 100 m thick; fine, dusty banding and laminations which may be transposed bedding are outlined by graphite and hematite specks. A reddish to light orange or pure white weathering is characteristic. Some of the quartzite layers coincide with distinctive positive anomalies on 1:50 000 scale aeromagnetic maps.

Pelitic and psammitic schist and gneiss occur as rusty weathering commonly recessive biotite-rich layers up to several hundred metres thick, in which sillimanite is locally extremely abundant. An outcrop 25 m across near the margin of the Taylor Brook Gabbro Complex is more than 90% sillimanite, which shows development in at least two separate generations in this section.

Figure 3.2. Geology of the inlier south of 50°00 N. Legend as follows: 1. granitic to tonalitic biotite and (or) hornblende migmatitic gneiss complex, undifferentiated; with abundant amphibolite inclusions; 1a. granitic orthogneiss; 1b. granodioritic orthogneiss; 2. amphibolite, amphibolitic gneiss, foliated metagabbro; 3. supracrustal rocks; 3a. massive to banded glassy quartzite or minor quartz-rich gneiss; 3b. marble and (or) calc-silicate rock; 3c. pelitic or psammitic schist or gneiss; 4. massive to foliated gabbro, olivine gabbro, metagabbro, and anorthositic gabbro; 5. dioritic plutons; 5a. hornblende quartz diorite; 5b. hornblende diorite; 5c. quartz diorite to tonalite; 5d. gneissic phase of 5c; 6. massive to foliated granitoid suite; 6a. biotite granite; 6b. megacrystic granite; 6c. megacrystic granodiorite; 7. massive, fresh granite; SDu, Silurian and Devonian(?) rocks, undifferentiated. C-O, Cambrian and Ordovician. Geology in NB 12H/11 is largely interpreted from Owen (unpublished data, 1985). Geology at periphery of the inlier from Williams (1985), Williams et al. (1984, 1985), Hyde (1982), and Smyth and Schillereff (1981).

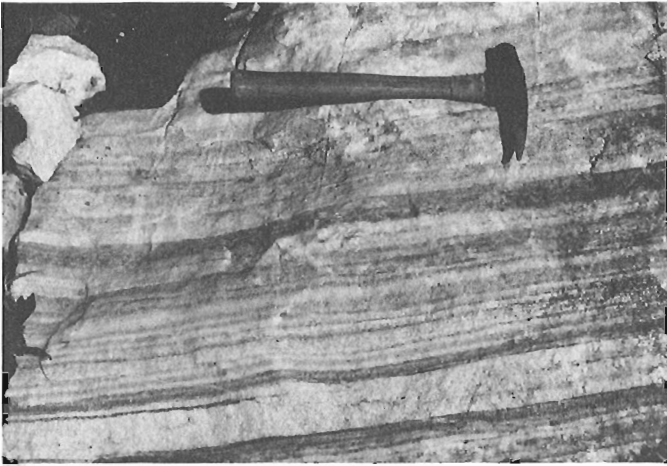


Figure 3.6. Well banded graphitic tremolite and diopside marble along the southern margin of the Taylor Brook Gabbro Complex.

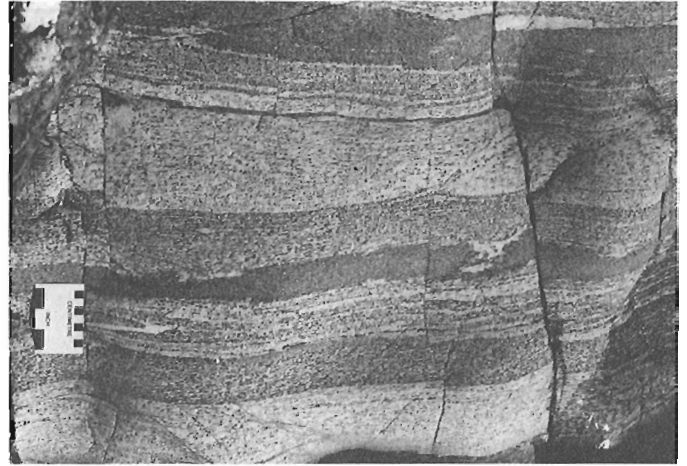


Figure 3.9. Well foliated interlayered quartz diorite and tonalite that grade into a homogeneous gneissic phase near the southern boundary of the inlier.

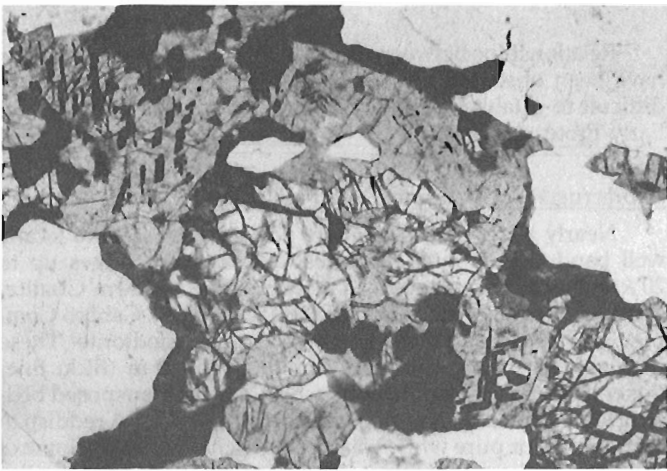


Figure 3.7. Olivine rimmed by orthopyroxene in gabbro of the Taylor Brook Gabbro Complex (high relief grain in centre of field). Photomicrograph under plane light; field of view 2 cm (long dimension).

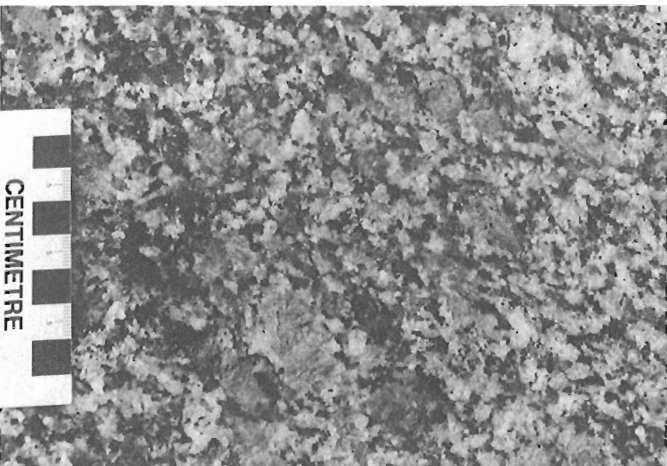


Figure 3.8. Massive to megacrystic biotite granite of the granitoid suite (Cat Arm pluton). This suite is inferred to be tectonically equivalent to late granitoids along the eastern margin of the inlier north of 50°00 N (see Erdmer, 1984).

Characteristically mauve garnet up to 2 cm across is common in the pelitic schist. Psammitic layers that do not contain mesoscopic aluminosilicates grade into the sillimanite layers locally, and occur alone elsewhere. Hybrid, quartz-rich, biotite and/or muscovite-epidote-bearing gneisses and schists are included with the supracrustal rocks in Figure 3.2

Marble (Fig. 3.6) and sandy calc-silicate rocks are exposed along the periphery of the Taylor Brook Gabbro Complex. They form layers up to a few hundred metres thick in which tremolite, diopside and graphite are locally abundant. These rocks are treated in detail in the description of NTS 12H/11 (see Owen, 1986). Scapolite was found in a thin section of a small (5 cm across, 30 cm long) carbonate lens within the gneiss complex on the north shore of Western Brook Pond. Similar wispy, minute metacarbonate nodules were noted in a few other outcrops in the gneiss complex.

Homogeneous plutonic rocks

Zones of orthogneiss occur throughout the complex gneiss in most outcrops; however, their contacts with the gneiss are nebular or gradational and their original relations are unknown. They do not generally form mappable units. The oldest of the large, clearly intrusive bodies in the map area appears to be the large, locally olivine-bearing mafic complex (Fig. 3.7) that straddles the Upper Humber River near the southeast margin of the inlier, named here the Taylor Brook Gabbro Complex. It is described in detail by Owen (1986).

Members of a voluminous suite of megacrystic to equigranular, leucocratic, mostly biotite bearing granites and granodiorites occur along the periphery of the inlier. The largest of these plutons are named here the Cat Arm Granite (Fig. 3.8; pink, megacrystic biotite granite which may be the southern tip of the Lake Michel Pluton of Bostock, 1983; Pringle et al. (1971) obtained an Rb-Sr age of 1130 ± 90 Ma for the Lake Michel Pluton), the French-Childs Granodiorite (pink, mostly megacrystic (K-spar) granodiorite with a characteristically dark chlorite groundmass in its eastern part), the Lomond River Granodiorite (pink, megacrystic biotite granodiorite), and the Kill-devil Hill Granite (buff, equigranular biotite granite). All these plutons have similar ages of crystallization; U-Pb zircon determinations yield an age of 1042^{+22}_{-11} Ma for the suite. Several other bodies of similar composition and comparable size, and many smaller plutons are included in this group. These plutons

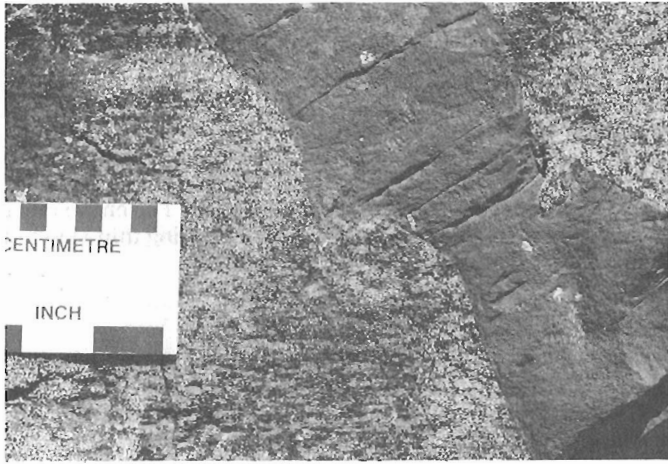


Figure 3.10. *Small mafic dyke correlated with the Long Range swarm, cutting across granitic gneiss. The vertical cooling joints strike east-southeast.*

are characteristically massive and homogeneous in their centre and strongly foliated at their margins, where they contain gneissic inclusions. Contacts with the adjacent gneisses are gradational, and structurally concordant.

A hornblende diorite to monzonite (?) pluton more than 5 km across that is locally garnetiferous occurs northwest of the Taylor Brook Gabbro Complex. A hornblende quartz diorite to tonalite pluton which grades southward into a homogeneous gneiss of similar composition (Fig. 3.9) occurs east of the Lomond River Granodiorite. These plutons appear to be more strongly foliated than those of the megacrystic suite, and their relation to the latter is unknown.

Basic metadykes of dominantly 020-030° strike occur throughout the inlier; the only unit in which they were not observed is the Devils Room Granite. Their width ranges from more than 40 m along the east margin to commonly (but not invariably) less than one metre in the western part of Gros Morne National Park (Fig. 3.10); they appear to decrease in frequency and to be less metamorphosed towards the west. They are correlated with the Long Range swarm of Bostock (1983). A few mafic dykes striking 070° occur in the eastern part of the inlier; these have been noted by other workers (J. Tuach and V. Owen, personal communications, 1985). They may belong to a later, Paleozoic swarm as they are parallel to similar dykes cutting cover rocks along the eastern margin of the inlier near 50°N.

The massive Devils Room Granite (Smyth and Schillereff 1981, 1982; Dunford 1984) cuts across all fabrics in the adjacent gneiss. Few xenoliths occur along its margins. It includes both biotite- and muscovite-bearing phases, and is largely megacrystic. Violet to mauve fluorite occurs along its eastern margin in small veins and cryptocrystalline silica-rich fracture fillings (J. Tuach, personal communication, 1985). The boundary with the French-Childs pluton to the north is a steep lineament, interpreted as a faulted, originally intrusive contact. Radiometric U-Pb determination of zircon ages yield 398 ± 7 Ma.

Fresh, leucocratic, white to buff to pale pink quartz-feldspar porphyry dykes a few metres wide were noted in the eastern part of the terrane 10 km south of the Devils Room pluton, and in several outcrops in 12H/11 map area (V. Owen, personal communication, 1985). These rocks are massive, and form thin flinty shards when broken. They are interpreted to be Paleozoic, and may be related to Silurian volcanism to the east.

Structural geology

The inlier displays structures resulting from several periods of Precambrian and Paleozoic deformation. Deep-seated ductile fabrics characterize most portions of the basement gneiss; these were affected by the intrusion of the mafic and granitoid plutons, which are in turn foliated along their margins together with the gneiss. A major phase of brittle strain coincided with the mid-Paleozoic phase of the uplift of the terrane and subsequent readjustment of its cover.

The penetrative gneissosity, schistosity, and/or migmatitic banding visible in most of the gneissic terrane is commonly folded isoclinally in outcrop; open, irregular folds of migmatitic layers and boudinaged mafic layers are also present. However, large areas of the gneiss complex have regular, "straight" foliation on the scale of the map, as in most of Gros Morne National Park. The broad, large-amplitude folds characterizing these areas clearly predate the emplacement of the granitoid plutons (e.g. Killdevil Hill, Lomond River), because the granulite facies mineralogy in the gneiss defines the fabric, and it is absent in the plutons. A dominant northwest fabric trend characterizes most of the central and eastern part of the inlier. This trend is modified in the vicinity of major plutons into parallelism with their margins for a distance of up to 5 km (e.g. around the French-Childs pluton). This trend is also modified into complex interference patterns where it intersects the large folds exposed in the northern part of Gros Morne National Park.

The prominent quartzite layer exposed south of the Cat Arm Granite forms a refolded isoclinal fold on the scale of the map; the quartzite shows faint graphitic banding parallel to its margins that may be transposed sedimentary layering or a tectonic fabric. This suggests that two (three, if the banding is tectonic) distinct structural events affected most of the basement gneiss, and that the supracrustal rocks were involved in all of them. This is further supported by the local occurrence of at least two fabrics at low angles to each other in outcrops of gneiss. Where migmatization is not extensive, one of the fabrics is invariably seen to cut across or overprint the other(s), and the fabrics appear unrelated.

The fabrics in the gneisses and in the outer portions of the granitoid plutons are parallel, suggesting that at least one deformation event postdates the intrusion of most of the plutons. The age of this deformation is probably Late Grenvillian. It appears to be younger than the emplacement of the granitoid intrusive suite.

The intrusion of the Long Range dykes, which are high-level extensional features, in latest Precambrian time implies that most of the uplift of the inlier had taken place by that time. This is further supported by the occurrence of flood basalts of the Lighthouse Cove Formation, the extrusive equivalents of the Long Range dykes, that rest unconformably on the Precambrian rocks in the northern part of the inlier.

Paleozoic deformation is expressed as moderately to steeply east-dipping thrust faults that place Precambrian rocks above Paleozoic sedimentary strata along the southwestern margin of the inlier, and by steep faults and brittle shear zones that truncate both Precambrian and Paleozoic rocks. Williams et al. (1985) discussed the evidence for overthrusting of the inlier in Gros Morne National Park and concluded that displacement is restricted to a maximum of a few tens of kilometres. The depth of involvement of the basement rocks is unclear; the observation that the Appalachian structural front lies about 15 km offshore near the north end of Gros Morne National Park (P. Gordy, personal communication, 1985) raises the possibility that deeper thrusts underlie the basement and the Paleozoic rocks at the western margin of the inlier. A deep geophysical transect through the structural salient defined by Williams et al. (1985) would help establish relations in this critical area.

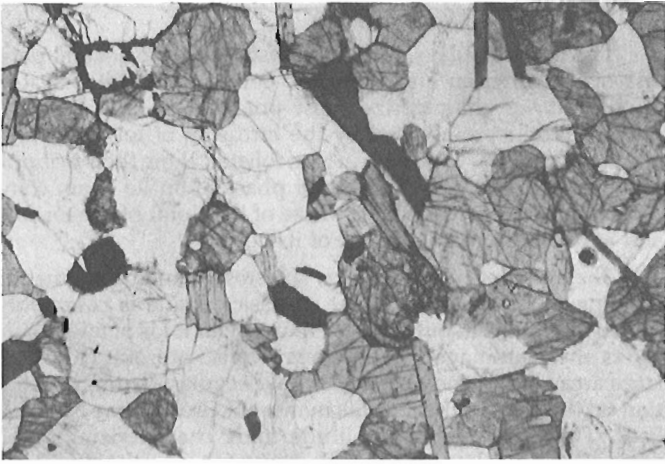


Figure 3.11. Granoblastic texture of fresh two-pyroxene granulite gneiss in the central part of Gros Morne National Park. Photomicrograph under plane light; field of view 1 cm (long dimension).

The steep faults and brittle shear zones postdate the thrusting at least in part, as a portion of the Humber Arm Allochthon shows horizontal separation along a fault that also truncates Precambrian rocks. These faults form two main sets, striking northwest and northeast, that are best developed in Gros Morne National Park. Movement along the faults is generally oblique slip with the major component down dip to the west. These faults are restricted to the zone of maximum overlap of basement onto platformal and allochthonous rocks (the structural salient suggested by Williams et al., 1985). Their map pattern is consistent with brittle fracturing of a thin sheet of competent rock (Precambrian gneiss) above or in a more ductile stack (Lower Paleozoic sedimentary strata) during thin-skinned tectonism. The age of this deformation is constrained between Late Ordovician (thrusting postdates emplacement of the Taconic allochthons) and Early Devonian (intrusion of the Devils Room granite).

Rocks in the vicinity of the steep faults and along the frontal Long Range thrust are commonly reddish, brecciated and re cemented, and they locally contain a dark fine granular cement separating lenses of crushed rock. Strong chloritization of joint faces and the development of chlorite seams along late quartz veins are also characteristic. This deformation is most pervasive in the small 10 km long prong at the southern tip on the inlier.

The steep northeast-trending fault along the east side of the inlier follows the sub-Cambrian unconformity. It cuts either up or down section locally, as evidenced by the preservation of undeformed pockets of basal clastic Cambrian strata in places and the direct juxtaposition of Doucers Marble (Smyth and Schillereff, 1982) against the Precambrian rocks in others. As these structurally higher Paleozoic cover rocks record penetrative deformation that is absent in the basement, a major detachment between cover and Precambrian basement must be situated close to the unconformity. This fault surface is interpreted to predate the Devils Room pluton, i.e. the pluton would have stitched the detachment. However, as the pluton is clearly faulted in the east, regional post-Acadian strike-slip is thought to have reactivated the Lower Paleozoic west-verging detachment. Additional study is required to resolve this question. The detachment is similar to that observed along the southwest margin of the inlier by Nyman et al. (1984), and westerly thrust-

ing of the Lower Paleozoic cover rocks above the Precambrian terrane is suggested by mesoscopic kinematic indicators in at least one place near the Taylor Brook Gabbro Complex (Owen, 1986).

Paleozoic faults cut indiscriminately across Precambrian structural trends, which suggests that the latter had no influence during Appalachian tectonism; this implies tectonic control at deeper levels than those now exposed. The entire inlier appears to have behaved as a discrete slice during thin-skinned Appalachian deformation.

Metamorphism

Granulite and amphibolite facies mineral assemblages are developed in many places. Retrograde greenschist facies metamorphism affected these assemblages heterogeneously; it is strongest in the eastern third of the inlier, where higher grade minerals are commonly completely altered. This retrogression appears to decrease gradually westward.

Hypersthene (Fig. 3.11) is present in most outcrops of the gneiss complex in Gros Morne National Park and occurs sporadically across the terrane, to within 10 km of the eastern margin of the inlier (Owen, 1986). Sillimanite is present in pelitic horizons in several localities. Pervasive migmatization characterizes most outcrops of the gneiss complex. The age of this high grade metamorphism is older than 1042 Ma, as the granitoid plutons cut across foliations defined by the high grade minerals, and are themselves only weakly metamorphosed.

These products of peak metamorphism are commonly replaced by lower grade assemblages in the greenschist and (lower) amphibolite facies: fresh amphibole and biotite are widespread and characterize large areas of the gneiss complex. They are developed in the plutons of the granitoid suite and in the Taylor Brook Gabbro Complex. Epidote, chlorite, and minor actinolite locally replace higher grade minerals in all rock types including the Long Range dykes, with the exception of the Devils Room Granite. The epidote and chlorite are associated locally with rocks that contain at least two separate generations of biotite. Radiometric sphene ages cluster around 400 Ma. It is not clear whether one or two episodes of greenschist facies metamorphism, as suggested by Bostock (1983) in the north, affected the inlier. Structurally continuous Lower Paleozoic rocks surrounding the inlier are metamorphosed to lower greenschist grade along the margin of the inlier, and the Long Range dykes are similarly affected.

This evidence of Lower- to Middle Paleozoic metamorphism suggests that the greenschist metamorphism of the Precambrian rocks is largely of Appalachian origin. However, on the basis of the truncation of chlorite-defined schistosity by the Long Range dykes and of greenschist metamorphism of the Precambrian rocks along the western margin of the terrane, where Paleozoic rocks are barely metamorphosed, at least part of the greenschist metamorphism is Precambrian.

Acknowledgments

Exemplary field assistance was provided by James Unterschultz (University of Alberta). The logistical help of Stuart Cochrane (Newfoundland Department of Mines and Energy) and the use of the A.K. Snelgrove Core Library in Pasadena are acknowledged. Contributions to the geology were made by John Tuach (NDME), Victor French (Labrador Mining and Exploration), Peter Cawood, Richard Hyde, and Harold Williams (Memorial University of Newfoundland). This summary report has benefitted from critical reading by Henry Charlesworth (U of A).

References

- Bostock, H.H.
1983: Precambrian rocks of the Strait of Belle Isle area; *in* Geology of the Strait of Belle Isle, northwestern insular Newfoundland, southern Labrador, and adjacent Quebec; Geological Survey of Canada, Memoir 400, p. 1-73.
- Dunford, W.T.
1984: Geology of the Devils Room Granite; unpublished B.Sc. Honours thesis, Memorial University of Newfoundland, 121 p.
- Erdmer, P.
1984: Summary of fieldwork in the northern Long Range Mountains, western Newfoundland; *in* Current Research, Part A, Geological Survey of Canada, Paper 84-1A, p. 521-530.
- Hyde, R.S.
1982: Geology of the Carboniferous Deer Lake Basin; Newfoundland Department of Mines and Energy, Mineral Development Division, Map 82-7
- Knight, I.
1985: Geological mapping of Cambrian and Ordovician sedimentary rocks of the Bellburns (12I/5 & 6), Portland Creek (12I/4), and Indian Lookout (12I/3) map areas, Great Northern Peninsula, Newfoundland *in* Current Research, ed. K. Brewer, D. Walsh, and R.V. Gibbons, Newfoundland Department of Mines and Energy, Mineral Development Division, Report 85-1, p. 79-88.
- Knight, I. and Boyce, W.D.
1984: Geological mapping of the Port Saunders (12I/11), St. John Island (12I/4), and parts of the Torrent River (12I/10) and Bellburns (12I/6) map sheets, northwestern Newfoundland; *in* Current Research, ed. M.J. Murray, J.G. Whelan, and R.V. Gibbons, Newfoundland Department of Mines and Energy, Mineral Development Division, Report 84-1, p. 114-124.
- Murray, A. and Howley, J.P.
1881: Geological Survey of Newfoundland from 1864 to 1880; Edward Stanford, London, 536 p.
- Nyman, M., Quinn, L., Reusch, D., and Williams, H.
1984: Geology of Lomond map area, Newfoundland; *in* Current Research, Part A, Geological Survey of Canada, Paper 84-1A, p. 157-164.
- Owen, J.V.
1986: Geology of the Silver Mountain area, western Newfoundland; *in* Current Research, Part A, Geological Survey of Canada, Paper 86-1A, p. 515-522.
- Palmer, A.R. (compiler)
1983: The Decade of North American Geology 1983 Geological Time Scale; Geology, v. 11, p. 503-504.
- Pringle, I.R., Miller, J.A., and Warrell, D.M.
1971: Radiometric age determinations from the Long Range Mountains, Newfoundland; Canadian Journal of Earth Sciences, v. 8, p. 1325-1330.
- Smyth, W.R. and Schillereff, H.S. (cont.)
1982: The pre-Carboniferous geology of southwest White Bay; *in* Current Research, ed. C.F. O'Driscoll and R.V. Gibbons, Newfoundland Department of Mines and Energy, Mineral Development Division, Report 82-1, p. 78-98.
1982: The pre-Carboniferous geology of southwest White Bay; *in* Current Research, ed. C.F. O'Driscoll and R.V. Gibbons, Newfoundland Department of Mines and Energy, Mineral Development Division, Report 82-1, p. 78-98.
- Williams, H.
1985: Geology of Gros Morne area, 12H/12 (West Half), western Newfoundland; Geological Survey of Canada, Open File 1134.
- Williams, H., James, N.P., and Stevens, R.K.
1985: Humber Arm Allochthon and nearby groups between Bonne Bay and Portland Creek, western Newfoundland; *in* Current Research, Part A, Geological Survey of Canada, Paper 85-1A, p. 399-406.
- Williams, H., Quinn, L.A., Nyman, M., and Reusch, D.
1984: Geology of Lomond map area, 12H/5, western Newfoundland; Geological Survey of Canada, Open File no. 1012.

Precambrian and Paleozoic metamorphism in the Long Range Inlier, western Newfoundland¹

Project 840024

J. Victor Owen² and Philippe Erdmer³

Owen, J.V. and Erdmer, P., Precambrian and Paleozoic metamorphism in the Long Range Inlier, western Newfoundland; in *Current Research, Part B, Geological Survey of Canada, Paper 86-1B, page 29-38, 1986.*

Abstract

Gneisses in the southern part of the Long Range Inlier record a polymetamorphic history spanning late Precambrian to early Phanerozoic times. They preserve a granulite facies mineralogy which crystallized at ca. $800 \pm 50^\circ\text{C}$ and moderate pressure (≥ 6 kbar). U-Pb (zircon) data indicate an early Grenvillian age (ca. 1250 Ma) for this event. The granulites are retrogressed to amphibolite facies assemblages, particularly where overprinted by a W- to NW-trending schistosity. This schistosity occurs in discordant Grenvillian granites (ca. 1040 Ma) but not in the ca. 605 Ma Long Range mafic dykes or an Acadian granite (ca. 398 Ma). It is attributed to post-plutonic Grenvillian orogenesis. Effects of Phanerozoic orogenesis are recorded by the Long Range dykes. Their polyphase, medium grade metamorphic mineralogy indicates a low pressure event, followed by higher pressure metamorphism. The higher pressure event is attributed to burial by Cambro-Ordovician platformal rocks thrust westward over the inlier during the Taconic Orogeny. A greenschist facies overprint may reflect an early Acadian thermal event accompanied by regional granite plutonism.

Résumé

L'analyse des orthogneiss et des paragneiss affleurant dans la partie méridionale de la fenêtre Long Range dans l'ouest de Terre-Neuve révèle une histoire polymétamorphique s'étendant du Précambrien supérieur jusqu'au Phanérozoïque inférieur. Les gneiss présentent une minéralogie étendue du faciès des granulites et se sont cristallisés à environ $800 \pm 50^\circ\text{C}$ et à une pression modérée (≥ 6 kbar). Une datation U-Pb (zircon) indique que le métamorphisme élevé a eu lieu au début du Grenvillien (il y a environ 1 250 Ma). Les granulites sont rétro-morphosées de façon variable en faciès d'amphibolites, en particulier là où il y a eu superposition d'une schistosité bien formée à orientation ouest-nord-ouest. Cette schistosité s'observe également dans les granites discordants du Grenvillien (env. 1 040 Ma) mais pas dans le groupe de filons mafiques Long Range datant d'environ 605 Ma et dans un granite acadien (env. 398 Ma) contenu dans la fenêtre. Elle est donc attribuable à un épisode post-plutonique ultérieur de l'orogénèse du Grenvillien. Les effets de l'orogénèse phanérozoïque sont enregistrés dans les filons Long Range. La minéralogie des filons indique un métamorphisme moyen polyphasique incluant un stade initial à pression relativement basse suivi d'un métamorphisme à pression plus élevée. Ce métamorphisme à pression plus élevée peut-être attribuable à l'enfouissement de parties de la fenêtre par des roches de plate-forme du Cambrien-Ordovicien charriées vers l'ouest par-dessus la fenêtre au cours de l'orogénèse du Taconique. La superposition du faciès des schistes verts relevée localement dans les filons et leurs roches encaissantes peut-être le résultat d'un événement thermique remontant au début de l'Acadien, accompagné d'un plutonisme granitique régional.

¹ Contribution to Canada-Newfoundland Mineral Development Agreement 1984-1989. Project carried by Geological Survey of Canada, Lithosphere and Canadian Shield Division.

² Department of Mines and Energy, 95 Bonaventure Ave., St. John's, Newfoundland A1C 5T7

³ Department of Geology, University of Alberta, Edmonton, Alberta T6G 2E3

Introduction

Crystalline rocks of the Long Range Inlier form the core of the Great Northern Peninsula of western Newfoundland. They include high grade ortho- and paragneisses, intruded by mafic to felsic plutonic rocks, which together record the effects of both Grenvillian and early Phanerozoic orogenesis.

Approximately half of the Long Range Inlier has been mapped on a reconnaissance scale (Fig. 4.1). The northern portion has been described by Bostock (1983), while the geology of the southern and eastern parts of the inlier was reported by Erdmer (1984, 1986) and Owen (1986). Bostock (1983) described amphibolite facies gneisses, anorthosite, mangerite, and associated rocks from the northern portion of the inlier. He inferred a sedimentary protolith for most of the gneisses, and concluded that the rarity of orthopyroxene in these rocks demonstrated that granulite facies conditions were barely, and only locally, attained. He further noted a spatial relationship between orthopyroxene-bearing gneisses and plutonic rocks of the anorthosite-mangerite suite, and suggested (Bostock, 1983, p. 17) that "regional folding...which accompanied the metamorphic maximum, occurred...perhaps about the same time as the emplacement of the mangerite plutons". This implies that the high grade gneisses in the northern part of the inlier record the thermal imprint of the plutonic rocks. This does not appear to be the case farther south, where orthogneisses are more extensive, in places have migmatitic fabrics clearly cut by plutonic rocks, and contain a granulite facies mineralogy across much of the inlier.

This report summarizes and interprets features of high grade gneisses from the southern part of the Long Range Inlier in light of new U-Pb isotopic dating and analyses of mineral assemblages used to estimate metamorphic P-T conditions. The results provide the first available quantitative constraints for the evolution of this Precambrian massif. A preliminary appraisal of the effects of Paleozoic metamorphism in the area is also presented.

Petrography

The bulk of the gneisses exposed in the southern part of the inlier are quartzofeldspathic rocks interpreted to have plutonic protoliths. Major rock units of the gneiss complex and younger, plutonic rocks of the inlier are listed in Table 4.1. Three categories of felsic orthogneiss have been recognized in this area. Although not distinguished on the generalized geological map (Fig. 4.2), their distribution has previously been depicted in the Silver Mountain area (NTS 12H/11, Fig. 4.1) by Owen (1986). Felsic orthogneiss comprises quartz dioritic, tonalitic, and granitic variants, which show a limited range of modal composition within and between outcrops. Mafic gneisses are grouped as a single unit including amphibolite and dioritic gneiss, which consist of amphibole, plagioclase (andesine in at least one sample), and locally biotite, quartz, clinopyroxene, and/or orthopyroxene.

Felsic orthogneiss consists principally of quartz, oligoclase (An₂₀₋₂₈), and microcline in varying proportions; textural features and the mafic mineralogy are also diagnostic of the three compositional variants. Tonalitic gneiss is characterized by a granoblastic texture and the common occurrence of both clinopyroxene and orthopyroxene; biotite and amphibole may also be present. Granitic gneiss typically is migmatitic, biotite, locally with orthopyroxene ± clinopyroxene, is the principal mafic mineral in this unit. Quartz dioritic gneiss has a distinctive "flecked" texture defined by 5-10 mm ovoid aggregates of amphibole and/or biotite; orthopyroxene was observed in the gneiss at only one locality in the study area. In a few places, bands of garnetiferous granitic gneiss up to about 100 m wide occur in the quartz diorite gneiss.

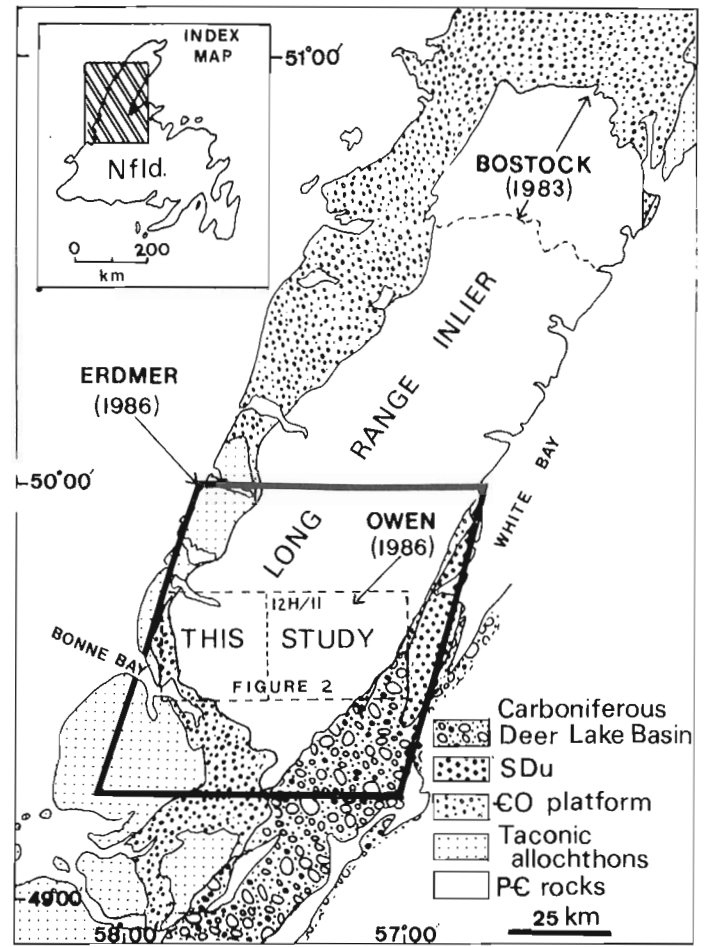


Figure 4.1. Geological setting of the Long Range Inlier, showing the location of the study area and the extent of mapping by Bostock (1983), Erdmer (1986), and Owen (1986). Abbreviations: PE = Precambrian, CO = Cambrian and Ordovician, SDu = Silurian and Devonian(?) rocks.

Table 4.1. Major rock units of the southern Long Range Inlier

PLUTONIC ROCKS	
	Biotite granite-granodiorite
	K feldspar-megacrystic biotite granite
	K feldspar-megacrystic biotite ± hornblende granodiorite-granite
	Biotite + hornblende granodiorite
	Pyroxene + olivine metagabbro, pegmatitic leucogabbro (Taylor Brook Gabbro Complex)
GNEISS COMPLEX	
(1) Paragneiss	Quartzite Pelitic gneiss Marble, calc-silicate rock
(2) Orthogneiss	Amphibolite, dioritic gneiss Granitic (to granodioritic) gneiss Quartz dioritic (to granodioritic) gneiss Tonalitic (to quartz dioritic) gneiss

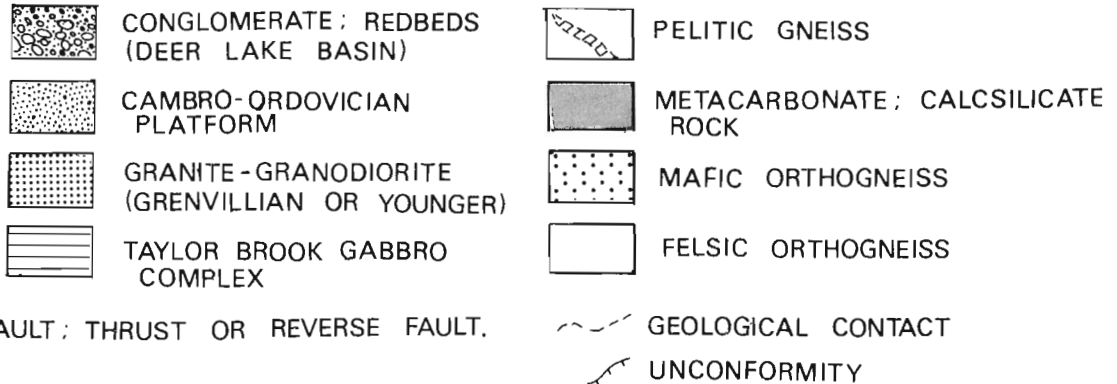
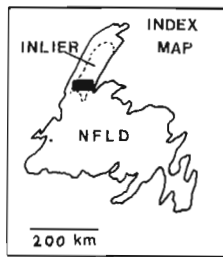
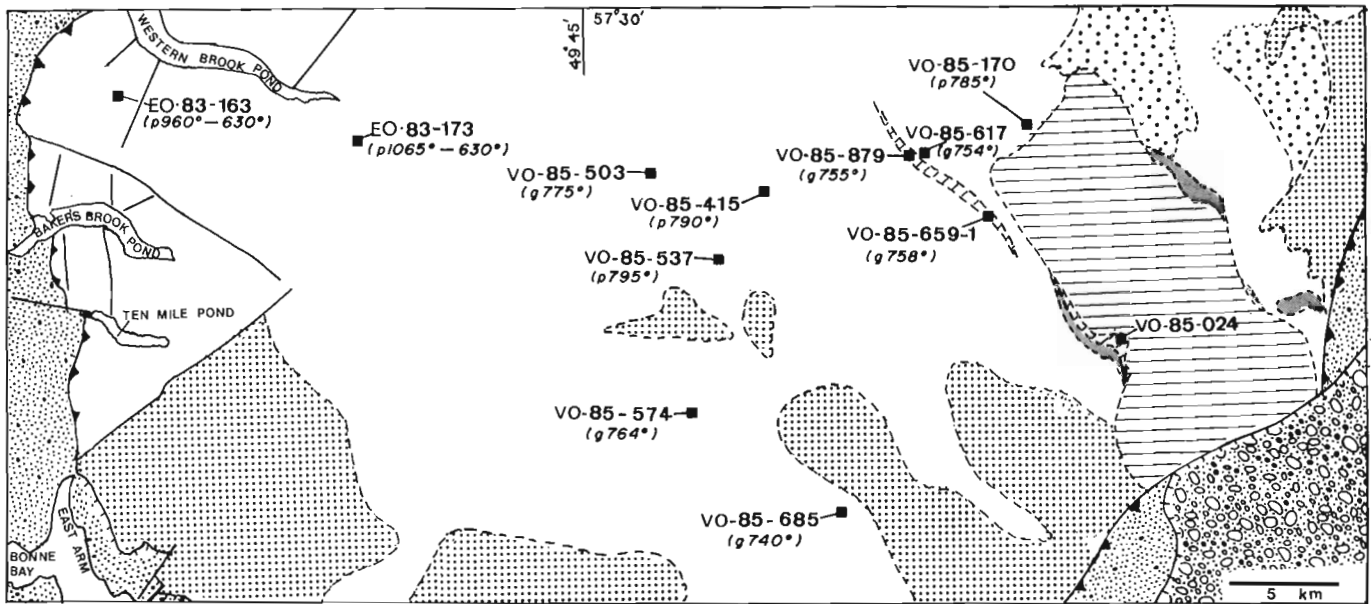


Figure 4.2. Simplified geological and sample location map of the southern Long Range Inlier of the northern Long Range mountains. Numbers in brackets are average peak metamorphic temperatures ($^{\circ}\text{C}$) determined by two-pyroxene geothermometry ("p" prefix; clinopyroxene temperatures; Lindsley's (1983) calibration) and garnet-biotite geothermometry ("g" prefix, Perchuk and Lavrent'eva's (1983) calibration). Pyroxene data for EO83-163, -173 show core and rim temperatures determined for zoned clinopyroxene.

Paragneiss is a minor but distinctive component of the gneiss complex. It includes the derivatives of both clastic and chemical sedimentary rocks. The metaclastic rocks include both quartzose and pelitic strata. Massive, grey or white orthoquartzite (Erdmer, 1986; Owen, 1986) occurs as bands up to 250 m wide in orthogneiss. Although the metaquartzite locally contains narrow pelitic screens, pelitic gneiss more typically occurs as bands up to 0.5 km wide near metacarbonate rocks (e.g. enveloping the Taylor Brook Gabbro Complex, see Erdmer, 1986 and Fig. 4.2). In addition to quartz, plagioclase (An_{33-46}) and biotite, these pelites locally contain variably perthitic microcline, orthopyroxene, cordierite, graphite, garnet and/or sillimanite; in places the latter two minerals are replaced by fine grained hercynite and cordierite.

The metacarbonate rocks form bands up to 0.5 km wide, and consist of grey, buff, or white marble commonly with centimetre- to metre-scale layers of dark grey calc-silicate rock. With one exception, the metacarbonate rocks, although commonly folded, lack a penetrative tectonic fabric. Marble typically consists of carbonate with minor forsterite and/or diopside, whereas calc-silicate rocks contain carbonate, forsterite, diopside, phlogopite, and rare spinel. Forsterite in both rock types is variably serpentinized; the carbonate is magnesian

calcite (1-3% MgO). One sample of tectonized calc-silicate rock from the northeast flank of the Taylor Brook Gabbro Complex consists of wollastonite-rich bands (typically ≤ 1 cm wide), and diopside clinopyroxene (salite) + plagioclase (An_{74}) rich bands (typically ≥ 1 cm wide). The compositional layering in this sample is tightly folded about a steeply northeast-dipping (75°NE) axial planar fabric, which may coincide either with the development of early (F1) isoclinal folds seen elsewhere in the gneiss complex, or with the W- to NW-trending schistosity formed after the emplacement of Grenvillian granitic plutons in the area.

Mineral chemistry

Analyses of mineral assemblages suitable for estimating metamorphic P-T conditions were performed using the JEOL JXA-50A wavelength dispersive electron probe microanalyzer at the Department of Earth Sciences, Memorial University of Newfoundland, using a beam current of 22 nanoamps and an accelerating voltage of 15 kV. Counts were made for 30 seconds or to a maximum of 60,000. Bence-Albee corrections were employed in data reduction. Analyses were performed using calibrations based on natural and synthetic standards, and were checked periodically against two of these (FCPX and ACPX,

Appendix 1). Where possible, the same calibration was utilized in analyzing different unknowns in order to maintain consistency between analyses. The oxidation ratio of iron ($= \text{Fe}^{3+}/(\text{Fe}^{3+} + \text{Fe}^{2+})$) was estimated indirectly by the method of Papike et al. (1974). This method is highly sensitive to variations in SiO_2 , and it is recognized that results obtained using other empirical methods may differ significantly. Pyroxene analyses are presented in Table 4.2; analyses of coexisting garnet and biotite are listed in Table 4.3. Pyroxene analyses were recalculated to 6 oxygens, biotite to 22 oxygens, and garnet to 24 oxygens.

Metamorphic temperatures in the southern part of the inlier were estimated by garnet-biotite and two-pyroxene geothermometry; metamorphic pressures were evaluated both directly, by clinopyroxene-plagioclase-quartz geobarometry, and indirectly, from the mineralogy of pelitic gneiss. Coexisting garnet-biotite was analyzed in four samples of granitic gneiss and two samples of pelitic gneiss, and clino- and orthopyroxene pairs were analyzed in three samples of tonalitic gneiss and two samples of granitic gneiss. The mineralogy of the analyzed samples is listed in Appendix 2.

Estimation of the ferric iron content of biotite by stoichiometric means is hampered by site vacancies. Furthermore, in the present case, utilization of the same calibration in the microprobe analysis of biotite and garnet led to somewhat high (ca. 103%) totals for garnet analyses, despite good stoichiometry (Table 4.3). Resolution of the microprobe is at best $\pm 1.5\text{-}2\%$ (relative). We therefore consider that errors resulting from high oxide totals for the garnet analyses are insignificant, since potential "between-calibration" errors were minimized by retaining the same calibration for analysis of garnet and biotite in these samples.

Garnet occurs as porphyroblasts up to 3 mm in diameter in granitic and pelitic gneiss (Fig. 4.3). Garnet in grey-rose granitic gneiss bands (VO-85-503, -574, -685) enclosed by garnet-free quartz diorite gneiss is a solid solution of almandine (64-74 mol.%) and pyrope (30-38%), with minor grossular (2-4%) and spessartine (1-2%). Garnet in these samples is crisscrossed by thin, phyllosilicate-bearing fractures. Garnet in a sample of green-brown porphyroclastic granitic gneiss (VO-85-617) is relatively rich in almandine (74%) and grossular (14%) and poor in pyrope (10%). Garnet in pelitic gneiss (VO-85-659-1, -879) contains 61-67% almandine, 27-30% pyrope, 3-8% grossular and 1-2% spessartine. Garnets in both granitic and pelitic gneiss show a core-to-rim increase in Fe and Mn with a concomitant decrease in Mg.

Biotite is an essential constituent of both granitic and pelitic gneiss. It occurs principally as subidiomorphic to idiomorphic crystals (Fig. 4.3), although it is also present in the pelites as xenomorphic crystals fringing opaques (ilmenite?), and in places it contains symplectic quartz intergrowths. Only non-symplectic, (sub)idiomorphic biotite was analyzed in this study. All biotites are unzoned with respect to Mg/Fe. Biotite in granitic gneiss is brown to greenish brown, with an Mg number ($= \text{Mg}/(\text{Mg} + \text{Fe})$) of 0.45-0.59, with Ti = 0.29-0.32 per formula unit (p.f.u.), and Alvi (octahedral Al) = 0.39-0.54 p.f.u.; biotite from sample VO-85-617 has a higher Fe/Mg and Ti content, and lower octahedral Al (Table 4.3). Biotite in pelitic gneiss is reddish brown, reflecting a relatively high Ti content (0.51-0.59 p.f.u.); these biotites have an Mg number of about 0.38, with Alvi = 0.33-0.44 p.f.u.

Orthopyroxene occurs as subidiomorphic grains in orthogneiss. The pyroxene-bearing gneisses typically have a granoblastic texture (Fig. 4.4); although they are locally partly replaced by amphibole, for the most part pyroxenes are fresh. The orthopyroxene in these rocks is hypersthene or ferrohypsthene, with an Mg number of 0.60-0.62 in tonalitic

gneiss, and 0.41-0.51 in granitic gneiss. The orthopyroxene is unzoned, even where it is in contact with clinopyroxene, and shows no sign of exsolution.

Clinopyroxene is subordinate to orthopyroxene in orthogneiss. It occurs either as xenomorphic grains attached to larger, better formed orthopyroxene crystals (Fig. 4.4), or as subidiomorphic porphyroblasts. Clinopyroxene in the tonalitic gneiss is typically unzoned with respect to Ca/Fe, although it may show within- and between-grain variations in Al_2O_3 content, and some grains in one sample (VO-85-170) contain minute exsolution lamellae (orthopyroxene?). In contrast, the two samples of pyroxene-bearing granitic gneiss (EO83-163, -173) contain zoned clinopyroxenes showing a marked core to rim increase in Ca/Fe.

Metamorphic P-T conditions

Garnet-biotite geothermometry

Since the composition of biotite is sensitive to the effects of down-temperature re-equilibration, temperatures determined using the garnet-biotite geothermometer should be interpreted

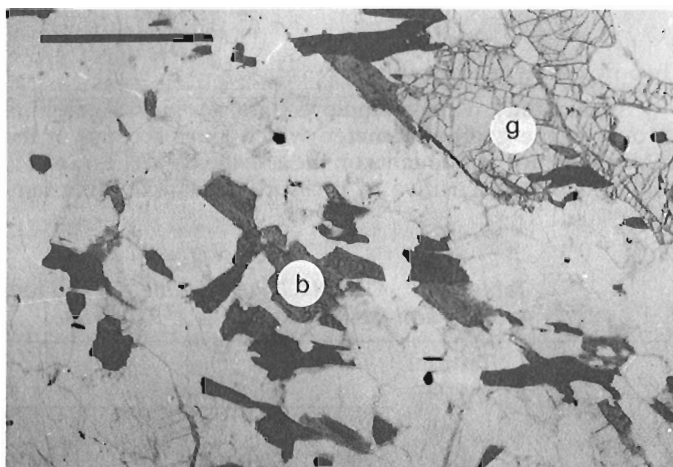


Figure 4.3. Subidiomorphic garnet (g) and biotite (b) from granitic gneiss. Sample VO-85-503; plane polarized light; bar = 1 mm.

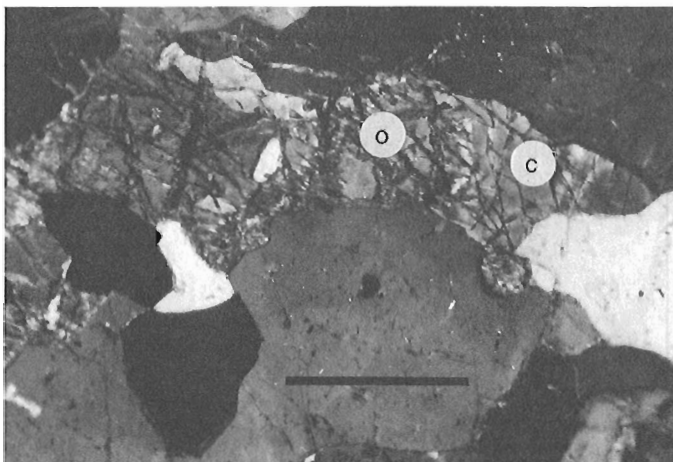


Figure 4.4. Granoblastic texture typical of tonalitic gneiss showing xenomorphic clinopyroxene (c) in contact with a larger orthopyroxene (o) porphyroblast. Sample VO-85-415; crossed nicols; bar = 0.5 mm.

in conjunction with textural features of the analyzed samples. For example, Indares and Martignole (1985a) have shown that rim compositions of touching garnet-biotite pairs yield lower temperature estimates than core compositions of garnet and biotite grains isolated by quartz and feldspar. This also applies to the present samples. We have employed two calibrations of the garnet-biotite geothermometer in this study. Perchuk and Lavrent'eva's (1983) calibration yields temperatures ranging from 735-775°C (mean = 757°C, n = 8) for core compositions of "isolated" garnet and biotite grains (Table 4.2); rim compositions of garnet from the same samples yield temperatures up to 180°C lower (Table 4.4). Somewhat higher temperatures (mean = 841°C, core compositions) were derived using the Indares and Martignole (1985b) calibration, which is based on Ferry and Spear's (1978) experimental expression, but incorporates thermodynamic and empirical correction factors to account for the influence of Ca and Mn in garnet, and Ti and Al⁶⁺ in biotite, respectively, in granulite facies rocks. The results of this calibration are considered to be particularly reliable since Indares and Martignole's empirical evaluation of the extent of the non-ideality of the garnet-biotite exchange reaction is based on the composition of natural assemblages which crystallized at temperatures (ca. 800°C) similar to those independently determined below.

Two-pyroxene geothermometry

In this study, we have employed Lindsley's (1983) graphical two-pyroxene geothermometer, which takes account of the effects of minor components on the activities of Wo, En and Fs, and which is insensitive to pressure at metamorphic tem-

peratures (i.e. <1000°C). We have chosen this method over numerical calibrations, some of which appear to consistently overestimate metamorphic temperatures (e.g. Bohlen and Essene, 1979). Davidson and Lindsley (1985) have recently revised Lindsley's (1983) geothermometer by incorporating the non-convergent, cation site-disorder model of Davidson (1985). Lindsley's (1983) isotherms yield metamorphic temperatures some 25°C lower than the revised method. The most consistent temperature estimates were obtained from pyroxene pairs from tonalitic gneiss, which are generally unzoned except for some grains in sample VO-85-170, which was sampled close to the TBGC (Fig. 4.2). Unzoned clinopyroxenes from tonalitic gneiss straddle Lindsley's (1983) 800°C isotherm on the pyroxene quadrilateral (Fig. 4.5), and are inferred to comprise part of an equilibrium assemblage in these samples. In contrast, clinopyroxene from granitic gneiss shows marked core-to-rim variations in Ca/Fe. Zoning in these clinopyroxenes suggests compositional disequilibrium, and the resultant temperature estimates should be interpreted with caution. Clinopyroxene core and rim compositions from these samples indicate temperatures of approximately 830-1090°C and 580-680°C, respectively. The lower estimate may indicate the temperature at which clinopyroxenes were quenched; however, the significance of the higher temperature estimate is unclear. Orthopyroxenes in all samples yield relatively low temperatures (≤700°C; Fig. 4.5). This is typical of orthopyroxenes from granulites, and, in the present case, may reflect incorrect portrayal of the isotherms for low-Ca pyroxenes, a possibility acknowledged by Lindsley (1983). It should be noted that visual estimation of temperatures by this method (Fig. 4.5, Table 4.2) is probably at best accurate to ± 20-30°C for clinopyroxene compositions, and to ± 30-50°C for orthopyroxenes.

Table 4.4. Compositional parameters and temperature estimates of coexisting garnet and biotite from granitic and pelitic gneiss.

VO-85-	Textural type	Garnet				Biotite				T°C*	
		X Mg	X Fe	X Ca	X Mn	X Mg	X Fe	X Ti	X Al ⁶⁺	A	B
503	1	—	—	—	—	.459	.406	.054	.081	775	926
	3 c*	.303	.638	.038	.021	.532	.349	.053	.066	697	750
574	3 r*	.383	.583	.033	.001	.591	.275	.051	.083	700	718
	1 c	.379	.575	.033	.013	.533	.324	.055	.088	764	872
617	2 r	.047	.793	.134	.026					565	512
	c	.100	.742	.138	.021	.230	.639	.090	.041	745	875
	1 u*	.092	.743	.144	.021	.202	.654	.095	.049	762	911
659-1	1 c	.317	.640	.032	.010	.449	.383	.103	.066	781	810
	1 c	.277	.676	.036	.012	.436	.379	.106	.079	735	700
685	1 r	.268	.697	.023	.012					617	554
	c	.382	.580	.027	.010	.549	.304	.053	.094	740	806
879	1 r	.218	.677	.081	.024	.477	.375	.090	.058	650	622
	c	.300	.610	.075	.014					755	829

Textural types: 1-(sub)idiomorphic biotite isolated from garnet porphyroblast
2-subidiomorphic biotite touching garnet porphyroblast
3-idiomorphic biotite inclusion in garnet porphyroblast
*c = garnet core analysis; *r = garnet rim analysis;
*u = unzoned garnet
*T = temperature determined from (A) Perchuk and Lavrent'eva's (1983) and (B) Indares and Martignole (1985b, "model B") calibration of the garnet-biotite geothermometer adopting a model pressure of 6 kbar.

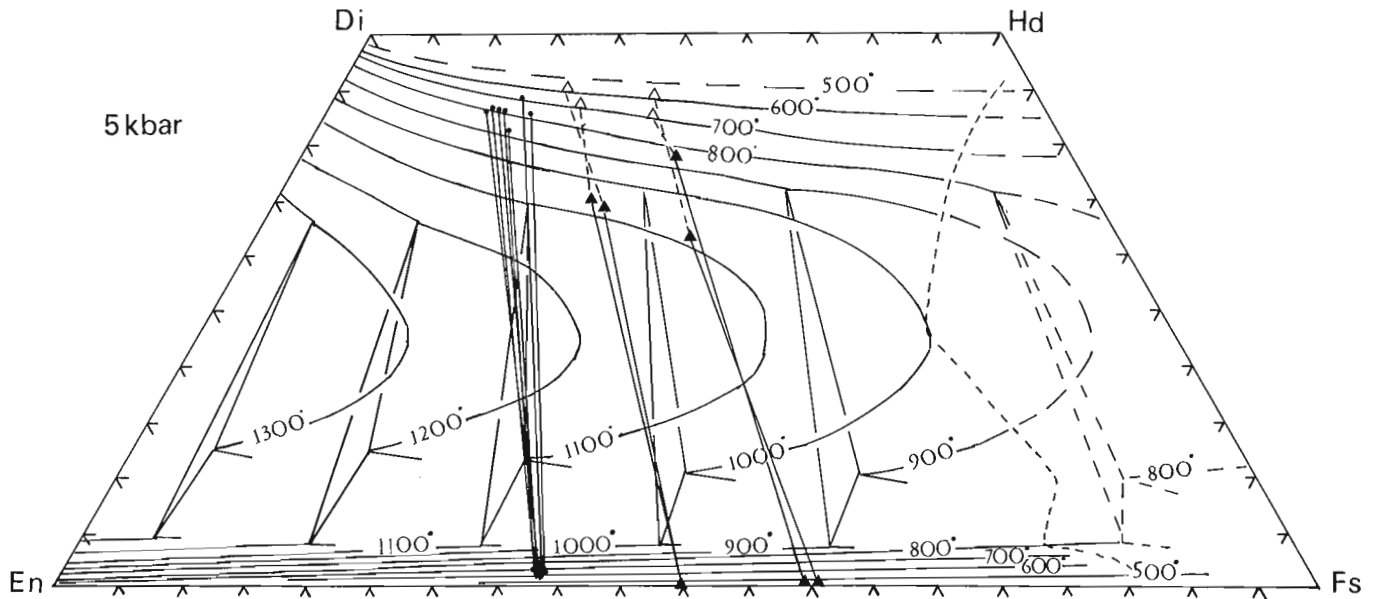


Figure 4.5. End-member compositions of coexisting clinopyroxene and orthopyroxene from tonalitic (dots) and granitic (black triangles-cores, open triangles-rims) gneiss. Isotherms are from Lindsley (1983).

The regional pattern of metamorphic temperatures determined here is depicted in Figure 4.2. The temperature of ca. $800 \pm 50^\circ\text{C}$ determined from garnet-biotite and two-pyroxene-bearing assemblages is consistent with the mineralogy of metacarbonate rocks in the area, specifically the high temperature assemblage forsterite ($\text{Fo} > 90$) + spinel ($> 90\% \text{MgAl}_2\text{O}_4$) (see Schenk, 1984), and coexisting wollastonite, bytownite and diopside (see Boettcher, 1970) present in some samples of calc-silicate rock. However, the metacarbonate rocks (together with some pelitic gneiss) partly envelop the Taylor Brook Gabbro Complex. It is therefore possible that the metacarbonate rocks may in part record thermal effects of the intrusion of the gabbro, and not only regional granulite facies metamorphism.

Metamorphic pressures

Metamorphic pressures associated with the granulite facies event can be indirectly evaluated from the mineralogy of pelitic gneiss, and can be quantified using the clinopyroxene-plagioclase-quartz geobarometer (Ellis, 1980) for tonalitic gneiss.

Sillimanite in the pelitic gneiss suggests moderate metamorphic pressures, but since it does not form an equilibrium assemblage with the garnet in sample VO-85-659-1, the Al_2SiO_5 -garnet-plagioclase-quartz geobarometer is inapplicable. Sillimanite and garnet coexisting on a domainal scale in sample VO-85-659-1 are enclosed and separated from each other by a fine grained mosaic of cordierite (Mg number = 0.70) and hercynite (Mg number = 0.24) (Fig. 4.6). This suggests the reaction:



Harris (1981) described this as a pressure-sensitive reaction with a slightly positive slope in P-T space. The lower pressure assemblage spinel + cordierite develops at $P < 6$ kbar for the temperatures determined above (ca. $800 \pm 50^\circ\text{C}$) assuming $P(\text{H}_2\text{O}) = P(\text{total})$. It should be noted that garnet-biotite temperatures for this sample (Table 4.4) are consistent with those determined for other samples despite textural evidence for retrogression. This is attributed to the fact that only the com-

positions of garnet showing no evidence for partial replacement by spinel and cordierite (e.g. garnets isolated from sillimanite by quartz and feldspar) were used for garnet-biotite thermometry.

It is not possible to determine the P-T trajectory in VO-85-659-1 since reaction [1] may proceed by an isothermal pressure decrease, an isobaric temperature increase, or any number of intermediate paths. The proximity (0.8 km) of the sample to the Taylor Brook Gabbro Complex is noteworthy in this regard, since the formation of spinel and cordierite at the expense of garnet and sillimanite in high grade pelitic gneiss is typical of some medium-pressure thermal aureoles (e.g. Owen, in press). We suggest that reaction [1] was instigated in sample VO-85-659-1 by the thermal imprint of the Taylor Brook Gabbro Complex during uplift of the pelitic gneiss following regional high grade metamorphism in the area.

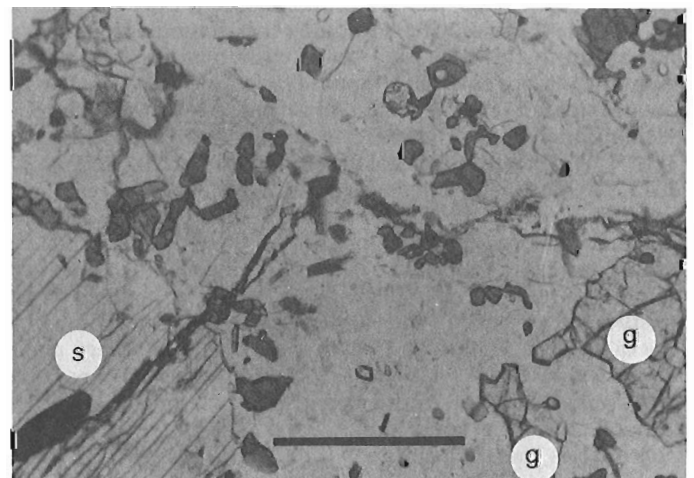


Figure 4.6. Cordierite (pale grey) and hercynite (small, dark grey crystals) enclosing and separating garnet (g) and sillimanite (s) in pelitic gneiss. Sample VO-85-659-1; plane polarized light; bar = 0.5 mm.

Sample VO-85-024 is from the band of pelitic gneiss flanking the southwest margin of the TBGC. In contrast to VO-85-659-1, this sample is impoverished in quartz (<5%), is free of K feldspar, and contains texturally stable porphyroblasts of cordierite, garnet and hypersthene, although the latter two minerals have not been observed in contact in the thin section examined. The garnet, however, is in texturally stable contact with porphyroblasts of cordierite. Bearing in mind the proximity of the TBGC (Fig. 4.2), the occurrence of stable garnet may be attributed to the absence of sillimanite in the sample. Possible thermal effects associated with the emplacement of the TBGC on the mineralogy (and/or mineral compositions) of VO-85-024 are, therefore, uncertain, and it is not presently known whether the cordierite (and/or garnet, hypersthene) porphyroblasts should be attributed to the thermal imprint of the TBGC, or to the earlier, regional, granulite facies event. Coexisting hypersthene–cordierite–garnet–quartz is indicative of pressures of ca. 6-7 kbar over the temperature range determined above (cf. Hensen and Green, 1973; Powers and Bohlen, 1985), although additional thin sections are required to conclusively demonstrate that all four minerals form a stable paragenesis in the sample. Compositional data (presently unavailable) for the stable garnet and cordierite porphyroblasts should further constrain metamorphic P-T conditions. On the basis of the petrography of samples VO-85-024 and VO-85-659-1, we postulate a minimum pressure of ca. 6 kbar for the granulite facies event.

This interpretation is supported by clinopyroxene–plagioclase–quartz geobarometry (Ellis, 1980) utilized in three samples of tonalitic gneiss (Table 4.5). We have calculated pressures assuming a model temperature of 800°C (the approximate mean temperature determined by two-pyroxene and garnet–biotite geothermometry). Pressures of 5.9 and 6.8 kbar were determined for samples VO-85-170 and VO-85-537, respectively, but a higher pressure of 11.0 kbar was determined for the relatively aluminous clinopyroxene (and relatively sodic plagioclase) in VO-85-415. All three samples have a granuloblastic texture, and the clinopyroxenes used in geobarometry are unzoned, consequently the relatively high pressure determined for VO-85-415 is difficult to interpret. We conclude that metamorphic pressures associated with granulite facies metamorphism in the study area were at least 6 kbar.

Timing of metamorphism

Granoblastic, two-pyroxene granitic gneiss from the southern part of the inlier yields a preliminary U-Pb (zircon) age of ca. 1250 Ma (Erdmer, 1986) indicating that granulite facies metamorphism in this area may be an early manifestation of the Grenvillian Orogeny. The granulite facies gneisses were subsequently folded (Owen, 1986) and intruded by granite plutons yielding analytically identical (e.g. within-error) isotopic ages of 1130 ± 90 Ma (Rb-Sr, whole-rock; Pringle et al., 1971), and 1042 ± 22 Ma (U-Pb, zircon; Erdmer, 1986). These Grenvillian granites contain a W- to NW-trending schistosity. Where this schistosity is present in the gneisses (cf. Owen, 1986, Fig. 62.9), granulites are largely retrograded to amphibolite facies assemblages (e.g. hornblende + oligoclase). The regional schistosity is inferred to be a late Grenvillian feature, since it is cut by the ca. 605 Ma (Stukas and Reynolds, 1974) Long Range mafic dyke swarm. However, widespread retrogression of the granulites may in addition record an early Paleozoic event, since the mineralogy of the Long Range dykes is indicative of amphibolite facies metamorphism, with a minor greenschist facies imprint. Several samples of the Long Range dykes contain brown, hornblende amphibole enclosed by green hornblende. The brown amphibole has a markedly higher Ti/Al ratio than the green amphibole, a feature characteristic of amphiboles from low-pressure metamorphic terranes (Hynes, 1982). Both

amphiboles pseudomorph primary igneous (i.e. subophitic) textures in the dykes, but the brown hornblende is absent in highly strained (schistose) mafic dykes and in similarly oriented (N to NE) high strain zones transecting diverse mafic rocks. We infer that the low pressure (brown) amphibole crystallized during a period of partial hydration of the Long Range dykes at relatively shallow crustal levels soon after emplacement. West-directed thrusting (Owen, 1986) of the Cambro-Ordovician Coney Arm Group (Smyth and Schillereff, 1982) over the inlier would permit the subsequent crystallization of the higher pressure, green hornblende in the dykes. The N- to NE-trending schistose fabrics in the Coney Arm Group are defined by greenschist facies mineral assemblages (e.g. chlorite + albite + epidote in mafic schist). Granitoid rocks along the east margin of the inlier contain a similarly oriented, low grade fabric inferred to coincide with the development of the Coney Arm schists. This low grade fabric is cut by an Acadian granite (Devils Room pluton, 398 ± 27 Ma; Erdmer, 1986), and is thus considered to have developed during the Taconic Orogeny; it is probably the youngest widespread structural element in the southern part of the inlier. The greenschist facies imprint in the Long Range dykes, principally recorded by patches of actinolite and chlorite, is not associated with a tectonic fabric; it may have developed during late Taconic uplift, or, perhaps more likely, it may be related to a regional thermal overprint accompanying emplacement of early Acadian granites.

Discussion

Isotopic dating of gneisses and plutonic rocks indicates that the intrusive, structural and metamorphic evolution of the southern part of the Long Range Inlier of western Newfoundland spans early Grenvillian times to Paleozoic times (Acadian Orogeny), a period of at least 850 Ma. The data presently available suggest that effects of the Grenvillian Orogeny in this area are recorded by at least three principal features. The Grenvillian Orogeny began with granulite facies metamorphism at ca. $800 \pm 50^\circ\text{C}$ and moderate pressures (≥ 6 kbar) around 1250 Ma. This was followed by a plutonic episode (ca. 1040-1130 Ma) encompassing the intrusion of large volumes of granite (and possibly mafic rocks e.g. the Taylor Brook Gabbro Complex). Finally, a W- to NW-trending regional schistosity developed in the gneisses and granitic intrusive rocks during a period of amphibolite facies metamorphism prior to the emplacement of the ca. 605 Ma Long Range dykes.

Effects of early Phanerozoic orogenesis are less readily evaluated, but are recorded by the metamorphism of the Long Range dykes and by analogous metamorphic features locally present in their host rocks. A post-Grenvillian structural and metamorphic imprint attributed to the Taconic Orogeny is locally evident, and is recorded by polyphase, pseudomorph replacement of primary igneous minerals, chiefly by amphibole, in the Long Range dykes, and by N- or NE-trending, low

Table 4.5. Compositional parameters and pressure estimates of coexisting clinopyroxene and plagioclase (+ quartz) from tonalitic gneiss.

VO-85-	cpx		plag	Kd*	P (kbar) at 800°C
	Al ⁶⁺	X CaTs	X An		
170	.024	.021	.270	.072	5.9
415	.042	.036	.205	.197	11.0
537	.025	.022	.255	.084	6.8

*Kd = $X_{\text{cpx}} / X_{\text{plag}}$ (Ellis, 1980)
CaTs An

grade fabrics locally present in the gneisses and Grenvillian intrusive rocks near the east margin of the inlier. These fabrics are interpreted to have developed during west-directed thrusting of Cambro-Ordovician platformal rocks over the inlier; structural burial of parts of the inlier is inferred to have instigated partial, pseudomorphic recrystallization of the Long Range dykes under medium-pressure, amphibolite facies conditions. North- to northeast-trending, amphibolite facies high strain zones in the inlier may date this structural burial; however, their kinematic significance is unclear. Owen (1986) reported that a north-trending shear zone in the south-central part of the inlier is associated with small scale (a few metres) dextral offset of the regional, northwest-trending, late Grenvillian(?) fabric. Examination of thin sections of mafic and intermediate rocks transected by this (and other) high strain zone(s) reveals a lower amphibolite facies mineralogy (not greenschist facies as originally reported by Owen, 1986) consistent with the mineralogy of N- to NE-trending mafic dykes (Long Range dykes?) containing a schistose fabric (Owen, unpublished data). The significance of medium grade, high-strain zones with a strike slip component in the interior of the inlier is unclear in the context of a regional, west-directed, low grade thrust régime during the Taconic Orogeny. Evaluation of the age and extent of displacement of the inlier relative to adjacent Cambro-Ordovician rocks awaits further mapping in the central part of the inlier.

Pb-Pb and U-Pb sphene ages of both Grenvillian and Acadian granites in the inlier cluster around 400 Ma, and are similar to a preliminary U-Pb zircon age obtained for the Gull Lake granite farther to the east. The implication is that an early Acadian thermal event accompanied by regional granite intrusion affected large parts of the inlier. Greenschist facies assemblages possibly related to this intrusive event include actinolite and chlorite in the Long Range dykes and pervasive epidotization of their host rocks.

Acknowledgments

We thank Flemming Mengel for use of his programs of the clinopyroxene-plagioclase-quartz geobarometer and the garnet-biotite geothermometer (Indares and Martignole, 1985b, calibration). This report has benefitted from a critical review by Ken Currie.

References

- Boettcher, A.L.
1970: The system $\text{CaO-Al}_2\text{O}_3\text{-SiO}_2\text{-H}_2\text{O}$ at high pressures and high temperatures; *Journal of Petrology*, v. 11, p. 337-379.
- Bohlen, S.R. and Essene, E.J.
1979: A critical evaluation of two-pyroxene thermometry in Adirondack granulites; *Lithos*, v. 12, p. 335-345.
- Bostock, H.H.
1983: Precambrian rocks of the Strait of Belle Isle area; in *Geology of the Strait of Belle Isle, northwestern insular Newfoundland, southern Labrador, and adjacent Quebec*; Geological Survey of Canada, Memoir 400, p. 1-73.
- Cawthorn, R.G. and Collerson, K.D.
1974: The recalculation of pyroxene end-member parameters and the estimation of ferrous and ferric iron content from electron microprobe analyses; *American Mineralogist*, v. 59, p. 1203-1208.
- Davidson, P.M.
1985: Thermodynamic analysis of quadrilateral pyroxenes. Part I. Derivation of the ternary non-convergent site-disorder model; *Contributions to Mineralogy and Petrology*, v. 91, p. 383-389.
- Davidson, P.M. and Lindsley, D.H.
1985: Thermodynamic analysis of quadrilateral pyroxenes. Part II. Model calibrations from experiments and applications to geothermometry; *Contributions to Mineralogy and Petrology*, v. 91, p. 390-404.
- Ellis, D.J.
1980: Osumilite-sapphirine-quartz granulites from Enderby Land, Antarctica: P-T conditions of metamorphism, implications for garnet-cordierite equilibria and the evolution of the deep crust; *Contributions to Mineralogy and Petrology*, v. 74, p. 201-210.
- Erdmer, P.
1984: Summary of field work in the northern Long Range Mountains, western Newfoundland; in *Current Research, Part A*, Geological Survey of Canada, Paper 84-1A, p. 521-530.
1986: Geology of the Long Range Inlier in Sandy Lake map area, western Newfoundland; in *Current Research, Part B*, Geological Survey of Canada, Paper 86-1B, report 3.
- Ferry, J.M. and Spear, F.S.
1978: Experimental calibration of the partitioning of Fe and Mg between biotite and garnet; *Contributions to Mineralogy and Petrology*, v. 66, p. 113-117.
- Harris, N.
1981: The application of spinel-bearing metapelites to P/T determinations: an example from south India; *Contributions to Mineralogy and Petrology*, v. 76, p. 229-233.
- Hensen, B.J. and Green, D.H.
1973: Experimental study of the stability of cordierite and garnet in pelitic compositions at high pressure and temperature. III. Synthesis of experimental data and geologic applications; *Contributions to Mineralogy and Petrology*, v. 38, p. 151-166.
- Hynes, A.
1982: A comparison of amphiboles from medium- and low-pressure metabasites; *Contributions to Mineralogy and Petrology*, v. 81, p. 119-125.
- Indares, A. and Martignole, J.
1985a: Biotite-garnet geothermometry in granulite-facies rocks: evaluation of equilibrium criteria; *Canadian Mineralogist*, v. 23, p. 187-193.
1985b: Biotite-garnet geothermometry in the granulite facies: the influence of Ti and Al in biotite; *American Mineralogist*, v. 70, p. 272-278.
- Lindsley, D.H.
1983: Pyroxene thermometry; *American Mineralogist*, v. 68, p. 477-493.
- Owen, J.V.
1986: Geology of the Silver Mountain area, western Newfoundland; in *Current Research, Part A*, Geological Survey of Canada, Paper 86-1A, p. 515-522.
Géologie de la région du lac Leif, Nouveau Québec; Ministère de l'Énergie et des Ressources (Québec), Rapport Intérimaire (in press).

- Papike, J.J., Cameron, K.L., and Baldwin, K.
1974: Amphiboles and pyroxenes: Characterization of OTHER than quadrilateral components and estimates of ferric iron from microprobe data; Geological Society of America, Abstracts with Programs, v. 6, p. 1053-1054 (abstract).
- Perchuk, L.L. and Lavrent'eva, I.V.
1983: Experimental investigation of exchange equilibria in the system cordierite-garnet-biotite; in Kinetics and Equilibrium in Mineral Reactions, ed. S.K. Saxena; Springer-Verlag, New York, p. 199-239.
- Powers, R.E. and Bohlen, S.R.
1985: The role of synmetamorphic igneous rocks in the metamorphism and partial melting of metasediments, northwest Adirondacks; Contributions to Mineralogy and Petrology, v. 90, p. 401-409.
- Pringle, I.R., Miller, J.A., and Warrell, D.M.
1971: Radiometric age determinations from the Long Range Mountains, Newfoundland; Canadian Journal of Earth Sciences, v. 8, p. 1325-1330.
- Schenk, V.
1984: Petrology of felsic granulites, metapelites, metabasites, and metacarbonates from southern Calabria (Italy): prograde metamorphism, uplift and cooling of a former lower crust; Journal of Petrology, v. 25, p. 255-298.
- Smyth, W.R. and Schillereff, H.S.
1982: The pre-Carboniferous geology of southwest White Bay; in Current Research, Newfoundland Department of Mines and Energy, Mineral Development Division, Report 82-1, p. 78-98.
- Stukas, W.R. and Reynolds, P.H.
1974: $^{40}\text{Ar}/^{39}\text{Ar}$ dating of the Long Range dykes of Newfoundland; Earth and Planetary Science Letters, v. 22, p. 256-266.

Appendix 1

Comparison of published values with microprobe analyses of natural pyroxene standards FCPX and ACPX.

	FCPX			ACPX		
	Publ. Value	Probe Value	s	Publ. Value	Probe Value	s
SiO ₂	49.85	50.79	.55	50.73	50.54	.34
TiO ₂	.83	.80	.02	.74	.84	.03
Al ₂ O ₃	7.86	7.98	.19	7.86	7.96	.33
Cr ₂ O ₃	nd	.04	.02	nd	.16	.02
FeO	6.17	6.08	.15	7.86	6.32	.28
MnO	.14	.11	.03	.13	.12	.05
MgO	15.47	15.84	.32	16.65	16.66	.33
CaO	17.75	16.83	.74	15.82	15.84	.36
Na ₂ O	1.27	1.22	.09	1.27	1.27	.15
n =		22			8	

Appendix 2

Sample mineralogy (listed in approximate decreasing modal abundance)

<u>Tonalitic gneiss</u>	
VO-85-170:	plag(An ₂₇) - qz - opx - hbl - cpx - opq - bi - ap - zirc
VO-85-415:	plag(An ₂₀) - qz - opx - opq - cpx - bi - hbl - ap
VO-85-537:	plag(An ₂₅) - qz - opx - opq - cpx - amph - ap
<u>Granitic gneiss</u>	
EO83-163:	Ksp - qz - plag - cpx - opx - opq - hbl
EO83-173:	Ksp - qz - plag - cpx - opx - bi - hbl - opq
VO-85-503:	Ksp - qz - plag(An ₂₆) - bi - gt - opq - zirc
VO-85-574:	Ksp - plag(An ₂₈) - qz - bi - gt - opq - zirc - sp
VO-85-617:	Ksp - qz - plag(An ₂₅) - gt - bi - opq - zirc - ap
VO-85-685:	Ksp - qz - bi - gt - plag(An ₂₂) - opq - zirc
<u>Pelitic gneiss</u>	
VO-85-024:	Plag(An ₄₆) - opx - cd - gt - bi - qz - opq - ap - sp - zirc
VO-85-659-1:	Ksp - qz - plag(An ₃₃) - gt - bi - sil - sp* - cd* - opq (including graphite) - zirc
VO-85-879:	plag(An ₃₉) - qz - bi - pseudomorph* after opx - Ksp - gt - opq - mu* - zirc
* retrograde phase	

Inductively coupled plasma-mass spectrometry at the Geological Survey of Canada

Project 830041

D. Conrad Grégoire
Mineral Resources Division

Gregoire, D.C., Inductively coupled plasma-mass spectrometry at the Geological Survey of Canada; in Current Research, Part B, Geological Survey of Canada, Paper 86-1B, p. 39-45, 1986.

Abstract

Inductively Coupled Plasma-Mass Spectrometry (ICP-MS) is a new analytical technique capable of determining trace level concentrations of stable isotopes for most elements of the periodic table. Research into fundamental aspects of ICP-MS indicates that the technique is subject to interference effects from concomitant elements, however, these can be compensated for by the proper choice of sample preparation technique. The determination of boron isotope ratios in geological materials is demonstrated. Boron isotope ratios can be determined with a precision of 1%.

Résumé

La spectrométrie de masse par plasma à couplage inductif (ICP-MS) est une nouvelle technique analytique capable de déterminer de faibles concentrations d'isotopes stables de la plupart des éléments du tableau périodique. Les recherches portant sur les aspects fondamentaux de cette technique indiquent qu'il peut y avoir une interférence causée par des éléments concomitants; toutefois, on peut y remédier en utilisant une technique appropriée de préparation des échantillons. La détermination des rapports isotopiques du bore contenu dans les matériaux géologiques est démontrée. Il est possible de déterminer avec une précision de 1 % les rapports isotopiques du bore.

Introduction

The development of an entirely new analytical technique is relatively rare in the field of inorganic analytical chemistry. In the area of trace metal analysis, the development of electrothermal vapourization techniques some twenty years ago was followed by the introduction of plasma emission technology about ten years later. Together these techniques allowed for the sub-ppb determination of most elements of the periodic table. As well, simultaneous multielement determinations could be accomplished during the same measurement period.

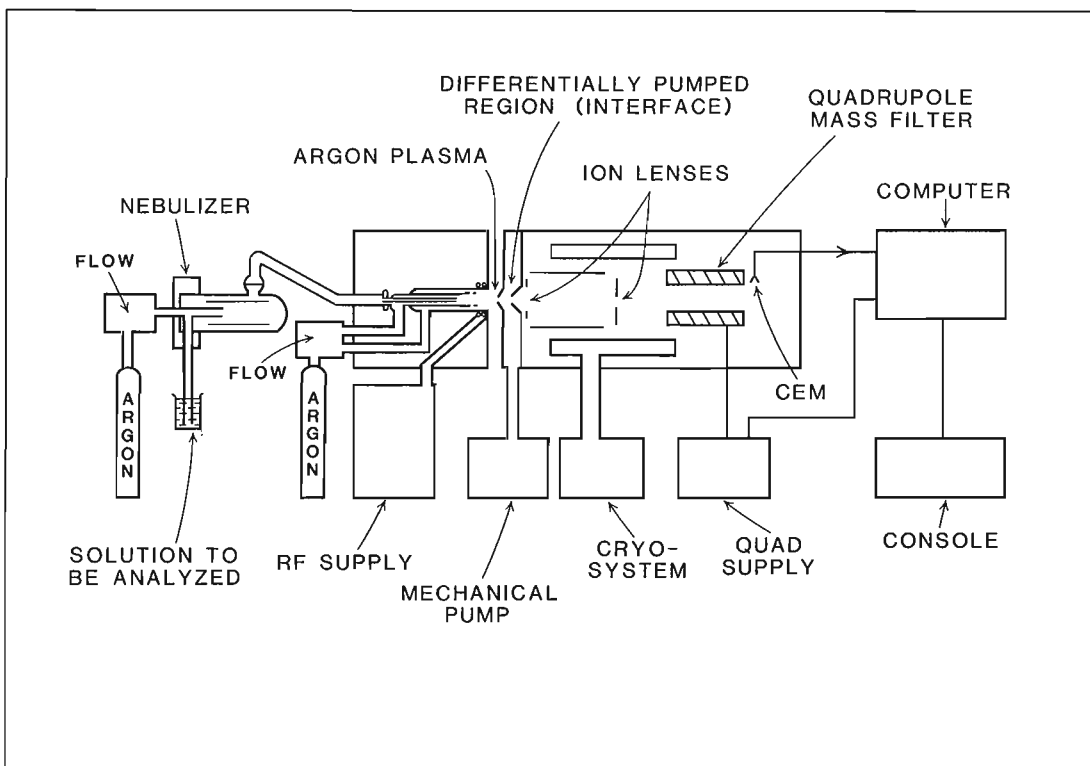
With the delivery of the first commercially available inductively coupled plasma-mass spectrometers in 1984, a new analytical capability was made available. It was now possible to determine the isotopic composition (isotope ratio) of an analyte in a sample solution as well as determine its total concentration.

The instrument comprises a standard inductively coupled plasma torch and a quadrupole mass filter. The novel aspect of this device is the interface which makes it possible to join these two components together. Figure 5.1 is a block diagram of the Sciex Elan ICP-MS instrument. The interface consists of two water-cooled nickel cones each containing a small orifice at the centre. These cones (one placed behind the other) are directed into the plasma (at one atmosphere of pressure) and serve to extract a small amount of ionized gas from the plasma. While passing through the interface, the gases expand adiabatically (to a pressure of 10^{-5} torr) through two successive vacuum chambers and are then introduced into the quadrupole mass filter.

The inherent advantages of each of the two major components of ICP-MS instruments combine to produce a powerful analytical tool. For example, the argon plasma is a good source of ions which is primarily due to its high

temperature (4000-6000°K) and is capable of ionizing all elements whose ionization potential is at or below that of argon (15.8 eV). The argon plasma is a chemically simple flame and thus will not introduce many interfering isobaric species. Samples can be rapidly and conveniently introduced into the plasma as a liquid aerosol, gas or vapourized solid. As well, the quadrupole mass filter is capable of electronically scanning the entire mass spectrum (0 to 300 amu) in seconds, and has a resolving power of better than 0.6 amu. What results from this combination is an instrument capable of 1) performing rapid (one sample every two minutes) mass spectrometry of solutions; 2) analyzing for many elements during the same run; 3) determining stable isotopes (and isotope ratios) at the trace level for most elements of the periodic table (metals and non-metals); 4) taking advantage of the inherent power of isotope dilution analysis; and 5) producing calibration curves whose linear dynamic range spans 4 to 5 orders of magnitude.

Table 5.1 is a comparison of detection limits (3 sigma) for ICP-MS, graphite furnace atomic absorption spectrometry (GFAAS) and inductively coupled plasma emission spectrometry (ICP-ES). Although detection limits for single element solutions seldom reflect the actual detection limits obtainable in sample solutions, these numbers are valuable for comparison purposes. For most elements, detection limits obtainable by ICP-MS are better than or approximately equivalent to those obtainable by GFAAS, and with few exceptions, far superior to those obtainable by ICP-ES. The few elements not determinable by ICP-MS include those originating from atmospheric gases and water (H, O, N, C) and plasma gases (Ar and other rare gases to a lesser extent). Elements whose degree of ionization in the plasma (i.e., ratio of positive ions to neutral atoms produced) is very low (e.g., F, Cl, P and S) are determinable only at concentrations in the ppm range. The ever-present



GSC

Figure 5.1. Block diagram of Sciex Elan Model 250 inductively coupled plasma-mass spectrometer (from operators manual, June, 1985).

large quantity of ^{40}Ar ions severely degrades the detection capability of ICP-MS for ^{39}K and ^{40}Ca (Table 5.1). There are, however, elements for which ICP-MS is very sensitive and which are not easily determined by other spectroscopic techniques. Among these elements are Sn, W, U, Th, Rb, Ta and Cs.

Figure 5.2 is the mass spectrum obtained for several platinum-group metals. The test solution contained 100 ppb of Ru, Rh and Pd. Evident is the extremely high sensitivity of the instrument and the ability of the mass spectrometer to easily resolve adjacent masses. The time required to obtain this scan was less than one minute. Figure 5.3 is the mass spectrum obtained for a solution containing 100 ppb of each of the rare-earth elements. The fourteen rare-earth elements (including La) completely fill the spectrum from mass 139 to mass 176. In spite of the fact that there are many isobaric overlaps, there is a free mass number for each of the rare-earth elements. This means that although one may not always be able to use the most abundant stable isotope for every analyte, it is generally possible to find a

Table 5.1. Comparison of detection limits

Element	Detection Limit/PPB		
	ICP-MS	GFAAS	ICP-ES
Aluminum	0.1	0.01	20
Antimony	0.02	0.2	50
Arsenic	0.4	0.2	50
Barium	0.02	0.04	0.5
Bismuth	0.06	0.1	40
Boron	0.08	20	4
Cadmium	0.07	0.003	4
Calcium	5	0.05	0.1
Chromium	0.02	0.01	5
Cobalt	0.01	0.02	6
Copper	0.03	0.02	3
Gold	0.08	0.1	10
Iron	0.2	0.02	3
Lead	0.02	0.05	40
Lithium	0.06	0.3	5
Magnesium	0.1	0.004	0.3
Manganese	0.04	0.01	1
Mercury	0.08	2	75
Molybdenum	0.08	0.02	5
Nickel	0.03	0.1	10
Niobium	0.02	-	20
Phosphorous	2 PPM	40	25
Platinum	0.08	0.2	30
Potassium	1 PPM	0.02	100
Selenium	1	0.5	50
Silicon	10	0.1	10
Silver	0.04	0.005	5
Sodium	0.06	0.5	30
Sulphur	1 PPM	-	50
Tantalum	0.02	-	20
Tellurium	0.04	0.1	75
Thallium	0.05	0.1	60
Tin	0.03	0.2	30
Titanium	0.06	0.5	2
Tungsten	0.06	-	30
Uranium	0.02	-	50
Vanadium	0.03	0.2	5
Zinc	0.08	0.001	2
Zirconium	0.03	-	4

mass suitable for analysis. Alternatively, it is possible to correct for an isobaric interference by subtracting the contribution to the total signal attributable to the interfering element(s).

The potential impact of ICP-MS on the geosciences is significant. Applications published to date include the determination of lead isotopes in crude oils (Hausler, 1985) and rocks (Brooker and Eagles, 1985; Date and Gray, 1983); the determination of osmium and ruthenium isotopes in geological materials (Russ et al., 1985); and the application of lead isotopes for identifying types of gold and base-metal occurrences (Smith et al., 1984). The quantitative determination of the rare-earth and platinum group metals by ICP-MS has been reported (Doherty et al., 1985) as well as the determination of transition-group metals in natural waters (Taylor and Garbarino, 1985) and rocks and minerals (Lichte and Meier, 1985). ICP-MS has also been applied to the determination of trace elements in coastal seawater reference material (McLaren et al., 1985) following a pre-concentration and separation step.

Current Research

Fundamental Studies

ICP-MS is very new and little is known about those factors which can effect a quantitative analysis. For this reason, it is important to investigate these effects while at the same time develop specific applications. Of particular interest to analysts are non-spectroscopic or so-called matrix interferences. This type of interference is defined as the effect any concomitant element can have (enhancement or suppression) on the ion-sensitivity of a given analyte element. Non-spectroscopic interferences can cause large analytical errors. It is clear from recent experiments (this laboratory) that the degree of severity of any non-spectroscopic interference is dependant on instrumental conditions such as the type of nebulizer used, plasma flow rates, forward plasma power, sample uptake rate and ion lens settings. For example, at a sample uptake rate of two mL per minute, 55% of the scandium signal is lost when a five-fold molar amount of lead is added. At a sample uptake rate of one mL per minute, only 25% of the signal is lost from the same solution.

Not so apparent, however, are the actual causes for these interferences. There are at least two factors which are important in assessing the nature of non-spectroscopic interferences: the relative masses of the interfering and analyte elements and the degree of ionization of these elements in the argon plasma. Figure 5.4 shows the effect of increasing interferent concentration on the normalized ion

Table 5.2. Degree of ionization in argon plasma

Element	Degree of ionization/%
Au	7.9
Ca	99
Cd	35
Fe	74
K	100
Li	99
Mg	85
Na	99
P	3.4
Pt	13
Se	3.7
Si	41
Sr	99

PLATINUM GROUP ELEMENTS

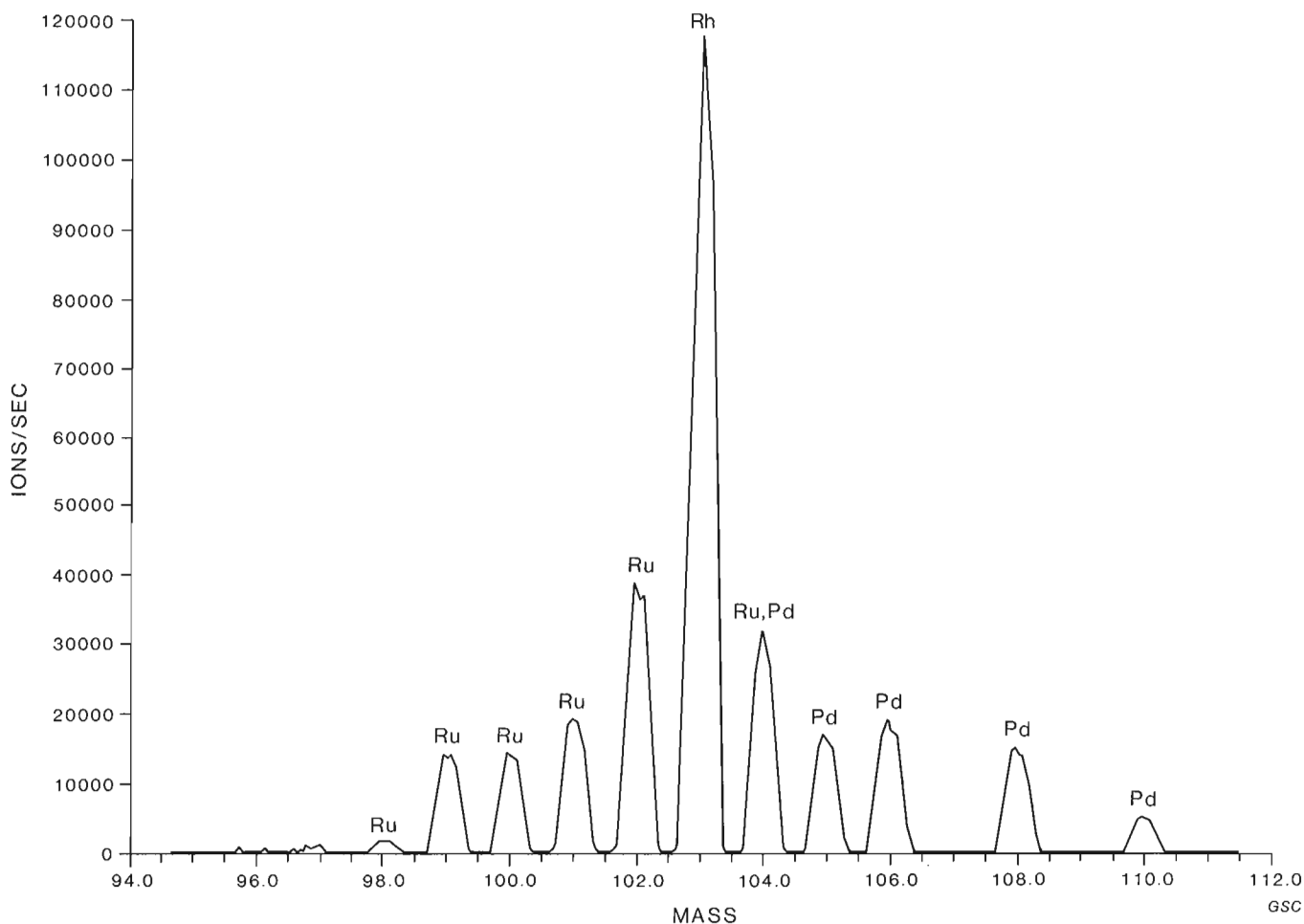


Figure 5.2. Mass spectrum of ruthenium, palladium and rhodium.

signal obtained from a 10 ppm boron solution. A normalized intensity of 1.0 indicates no ion suppression while a normalized intensity of 0 indicates total loss of signal. The serious influence that concomitant elements can have on analyte signal is clearly shown in Figure 5.4. Also included with each interferent curve is the first ionization potential (electron volts) of each of the interfering elements. The loss in boron ion signal shown in Figure 5.4 cannot solely be explained by a shift in the ionization equilibria since this would show a more direct relationship between ion suppression and interferent ionization potential. For example, magnesium and lead have very similar ionization potentials and yet the degree of ion signal suppression is much greater for lead at the same molar concentration.

When comparing the extent of ion signal suppression sustained on ^{11}B by an equimolar amount of interferent, a relationship such as the one shown in Figure 5.5 is obtained. In this figure, the ordinate is given in atomic mass units of interfering element. Table 5.2 lists the approximate degree of ionization expected (in the axial channel of the argon plasma) for each of the elements represented in Figure 5.5

(Boumans, 1966; deGalan et al., 1968). The line in Figure 5.5 is drawn only through those points representing elements whose degree of ionization approaches 100% (Table 5.2). This is done in order to equilibrate any effect due to ionization suppression caused by the interferent elements. Equimolar (relative to boron) quantities of interferent normalizes the number of free electrons which can be produced and thus eliminates ionization suppression as a factor. What remains is a very serious mass effect with the heavier elements causing the greatest ion suppression. All other elements not lying on this line are poorly ionized in the plasma and, despite their atomic masses, do not show the same effect as is observed for the more fully ionized elements. For example, gold has an atomic mass of 197 amu, but suppresses the ^{11}B signal by only about 35%. This is due to the relatively low degree of ionization (7.9%) of gold in the plasma.

We can conclude from these studies that the heavier the interferent and the more ionized it is in the plasma, then the greater will be the change in ion intensity for any given analyte. These observations may be consistent with an ion-repulsion or collisional type of mechanism which is likely the principal cause of these ion suppression effects.

Table 5.3. $^{11}\text{B}/^{10}\text{B}$ isotope ratios for some minerals

	Amberlite XE-243	Std. addn.	Dowex 50W-X8
<u>COLEMANITES</u>			
NMC 17559	4.016 ± .018	4.221 ± .173	4.085 ± .025
NMC 17561	4.055 ± .048	3.926 ± .022	4.056 ± .050
<u>TOURMALINES</u>			
Villeneuve, P.Q.	4.019 ± .043	3.835 ± .063	4.090 ± .050
Ice Claim, Y.T.	4.007 ± .059	4.261 ± .085	4.011 ± .030
New Pascalis Prop., P.Q.		3.848 ± .054	3.959 ± .040
Leduc Mine, P.Q.		4.014 ± .046	4.015 ± .120
Presque Isle Lk., P.Q.		4.039 ± .048	4.004 ± .013
Louvicourt Mine, P.Q.			4.016 ± .092

RARE-EARTH ELEMENTS

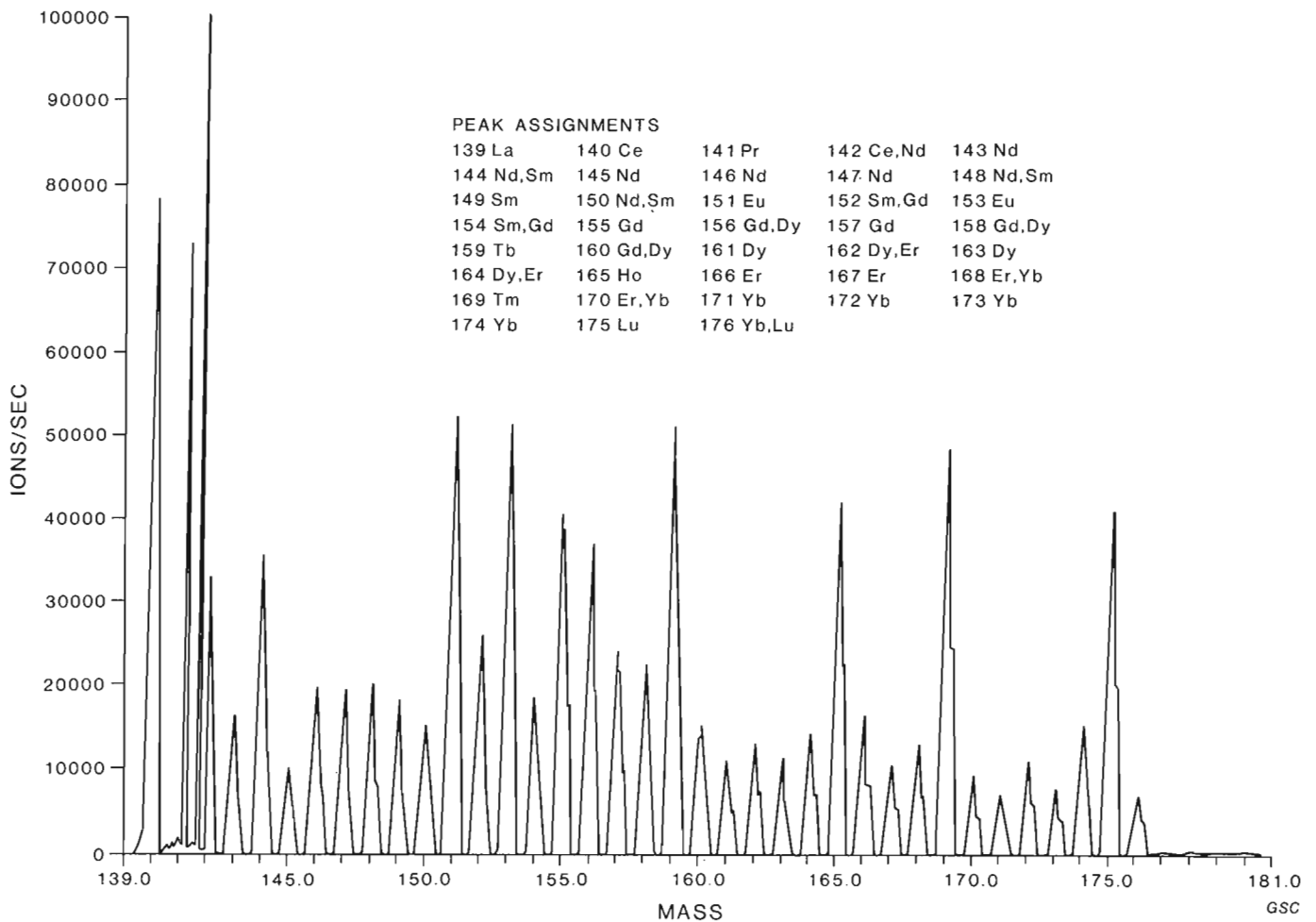


Figure 5.3. Mass spectrum of the rare-earth elements.

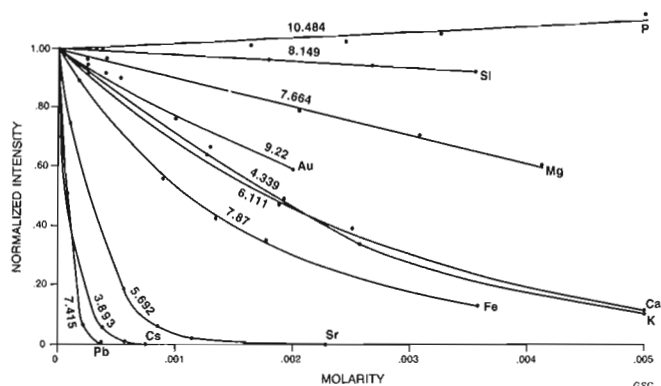


Figure 5.4. Effect of concentration of concomitant elements on the ion sensitivity of ^{11}B .

Determination of Boron Isotope Ratios

The abundance of boron in nature varies greatly and is found associated with many minerals. Boron isotopes are known to fractionate in nature (Shergina and Kaminiskaya, 1963) and therefore it is possible that the study of fractionation patterns may help solve geological problems. Because of analytical problems associated with the determination of boron isotope ratios, very few applications of boron isotope data appear in the literature particularly as applied to exploration geochemistry. For these reasons, research is underway into finding new methods for the determination of boron isotopes in geological materials. The objectives of this work are to accurately determine boron isotope ratios at the trace level (ppm-range) and to do so rapidly in such a way that many samples can be determined per workday.

Initial studies have indicated that the determination of boron isotopes is made difficult by the presence of concomitant elements (Fig. 5.4). In addition to this, it was discovered that concomitant elements also introduced a mass discrimination effect. The effect was greatest (up to 20%) for those elements that caused the greatest change in analyte ion signal. For this reason it became necessary to investigate techniques that either separated boron from the matrix elements or corrected for these effects. Samples used during this phase of study included a series of tourmalines and two colemanites. All samples were brought into solution using a sodium carbonate fusion technique. The procedure comprised fusing 0.2 g of sample (-150 mesh) with 0.5 g of sodium carbonate at a temperature of 850°C for 15 minutes. The resulting melt was dissolved in 10 mL of distilled deionized water.

Sample solutions were then prepared for isotope ratio measurement by three separate techniques. First, boron was separated completely from the matrix by applying an ion-exchange procedure developed by Carlson and Paul (1968). The procedure uses a boron-specific resin (Amberlite XE-243) to remove boron from basic solutions. The resin-bound boron is then converted to the fluoride and eluted with sodium hydroxide which is then passed through a second resin (Dowex 50W-X8) which serves to remove sodium from solution. The eluate contains only boron in solution. This technique not only removes interfering metal ions, but can also be used as a pre-concentration technique for samples low in boron. The second preparation technique used 100 μL of sample solution (dissolved fusion melt) which was diluted to 5 mL with distilled water. One gram of Dowex 50W-X8 was then added and allowed to equilibrate for 8 hours. The resulting solutions were free of matrix elements and could be

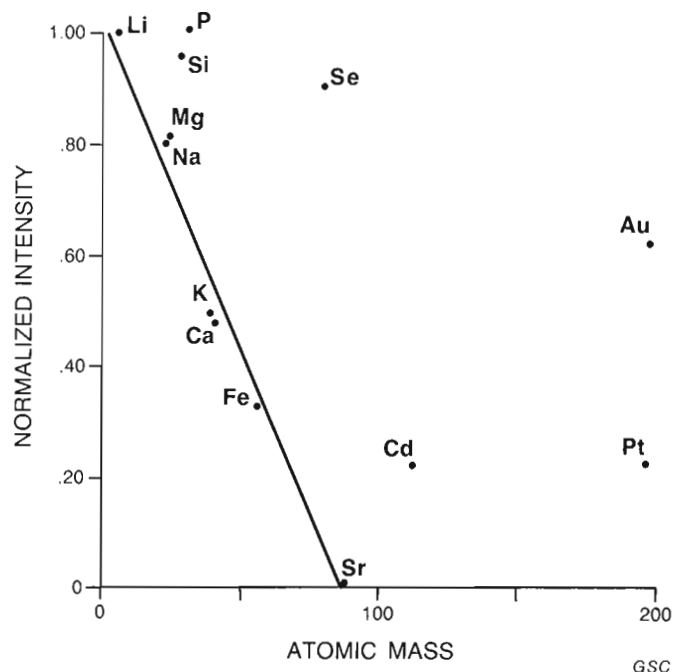


Figure 5.5. Effect of concomitant mass on ion sensitivity of ^{11}B at a 1:1 molar concentration ratio.

nebulized directly into the argon plasma. The third technique applied the method of standard additions in order to compensate for any effects due to concomitant elements. Three separate 100 μL aliquots of sample solution were diluted to 5 mL with distilled water. To two of these, a measured quantity of standard (NBS SRM 951) boron of known isotopic composition was added. The ^{10}B and ^{11}B composition of these solutions were then measured and the isotopic concentration determined by a "double" standard addition calculation.

Table 5.3 summarizes the results obtained using the above sample preparation techniques. In each case, the boron isotope ratio is determined with a precision of approximately 1% (3 replicates). The absolute value of the isotope ratio obtained by each of the three methods was not always consistent for each sample. Values obtained for the isotope ratio using the Amberlite and Dowex resin separation techniques compare well with one another, however, the ratios obtained using the method of standard additions appear to be high for samples NMC 17559 and Ice Claim and low for the Villeneuve tourmaline sample. These results indicate that the method of standard additions cannot be relied upon to compensate for non-spectroscopic matrix effects.

Research is continuing on other sample preparation techniques such as solvent extraction and methyl-ester vapourization of boron as well as extending the determination of boron isotopes to materials containing less than 5 ppm boron.

Electrothermal Vapourization Techniques

Work has been initiated on a new sample introduction technique using a rhenium filament and graphite boat electrothermal vapourization unit. This collaborative project is being carried out by G.E.M. Hall (Head, Geochemical Laboratories) and C.J. Park (visiting fellow), who is continuing his research on the application of electrothermal vapourization (ETV) techniques in ICP-MS.

ETV techniques involve the vapourization of a sample (liquid or solid) by the resistive pulsed-heating of a metal on graphite ribbon. The sample is placed on the ribbon and, once vapourized, is carried into the argon plasma by a stream of argon gas. This technique has already been shown (Park, 1985) to give sub-picogram detection limits in microgram amounts of sample. The technique is initially being applied to the determination of tungsten in geological materials.

Acknowledgments

The author is grateful to E.M. Cameron and I.R. Jonasson for providing the colemanite and tourmaline samples. G.E.M. Hall and E.H.W. Hornbrook are thanked for reviewing the manuscript.

References

- Boumans, P.W.J.M.
1966: Theory of Spectrochemical Excitation; Hilger and Watts Ltd., London, Chapter 7.
- Brooker, E.J. and Eagles, T.E.
1985: The application of plasma-mass spectrometry to analytical chemistry problems of interest to geochemists; Workshop on Applications of Inductively Coupled Plasma-Mass Spectrometry, Toronto, Ontario, Oct. 3-4.
- Carlson, R.M. and Paul, J.L.
1968: Potentiometric determination of boron as tetrafluoride; Analytical Chemistry, v. 40, p. 1292-1295.
- Date, A.R. and Gray, A.L.
1983: Isotope ratio measurements on solution samples using a plasma ion source; International Journal of Mass Spectrometry Ion Physics, v. 48, p. 357-360.
- Doherty, W., Vander Voet, A., and Wong, P.
1985: Application of ICP-MS for the determination of trace elements in geological samples - an overview with examples; Workshop on Applications of Inductively Coupled Plasma-Mass Spectrometry, Toronto, Ontario, Oct. 3-4.
- deGalan, L., Smith, R. and Winefordner, J.D.
1968: The electronic partition functions of atoms and ions between 1500 K and 7000 K; Spectrochimica Acta, v. 23B, p. 521-525.
- Hausler, D.W.
1985: Measurement of trace elements and isotope ratios in petrogeological samples by ICP-MS; Paper no. 238, 27th Rocky Mountain Conference, Denver, Colorado, July 14-18.
- Lichte, F.E. and Meier, A.L.
1985: Optimization of ICP-MS for the analysis of silicate materials; Paper no. 236, 27th Rocky Mountain Conference, Denver, Colorado, July 14-18.
- McLaren, J.W., Mykytiuk, A.P., Willie, S.N., and Berman, S.S.
1985: Determination of trace metals in seawater by inductively coupled plasma mass-spectrometry with pre-concentration on silica immobilized 8-hydroxyquinoline; Analytical Chemistry, v. 57, p. 2907-2911.
- Park, C.J.
1985: Feasibility study of an electrothermal vaporizer/inductively coupled plasma/mass spectrometry system; unpublished Ph.D. Thesis, University of Toronto, 144 p.
- Russ, G.P., Mazan, J.M., and Leich, D.A.
1985: Osmium isotopic ratios for nanogram-sized samples; Paper no. 232, 27th Rocky Mountain Conference, Denver, Colorado, July 14-18.
- Shergina, Yu.P. and Kaminiskaya, A.B.
1963: Isotopic composition of boron in nature; Geochemistry, v. 8, p. 756-763.
- Smith, R.G., Brooker, E.J., Douglas, D.J., Quan, E.S.K., and Rosenblatt, G.
1984: The typing of Au and base-metal occurrences by plasma-mass spectrometry: initial results; Journal of Geochemical Exploration, v. 21, p. 385-393.
- Taylor, H.E. and Garbarino, J.R.
1985: Inductively coupled plasma-mass spectrometry for the quantitative analysis of natural waters; Paper no. 234, 27th Rocky Mountain Conference, Denver, Colorado, July 14-18.

Uranium, gold and selenide minerals locally concentrated in drift at 'Twin Lakes' near Bathurst Inlet, N.W.T.

Projects 770055 and 770024

S.M. Roscoe, S.B. Green, and S.S. Gandhi
Mineral Resources Division

Roscoe, S.M., Green, S.B., and Gandhi, S.S., Uranium, gold and selenide minerals locally concentrated in drift at 'Twin Lakes' near Bathurst Inlet, N.W.T.; in *Current Research, Part B, Geological Survey of Canada, Paper 86-1B*, p. 47-56, 1986.

Abstract

Concentrations of pitchblende, selenide minerals, native gold and carrollite occur in clasts within drift at 'Twin Lakes' in the southern part of the Bathurst Inlet area (66°35.5'N, 108°00'W), N.W.T. These occurrences were discovered by Cominco Limited in 1975. U, Se, Au, Pb, Hg, Bi, Co, Cu and minor amounts of Ni are concentrated in the distinctive mineral suite which resembles assemblages found at Nicholson Mine and in the D uranium orebody at Cluff Lake in Saskatchewan, at Christopher Island in the Baker Lake area, District of Keewatin, and in the Otish Mountain Group in Quebec. Most of the highly radioactive detritus consists of small pebbles or granules of pitchblende and other metallic minerals in some cases attached to quartz or siltstone. Larger mineralized float fragments up to 25 cm long, however, are sparingly present and are composed of clasts of siltstone and quartz in a granular quartzose matrix.

A $^{207}\text{Pb}/^{206}\text{Pb}$ date of 901 Ma on pitchblende represents a minimum age and indicates that it and other intimately associated minerals in the suite were probably deposited in late Helikian time like unconformity-related uranium deposits in Saskatchewan. The mineralized breccia source may be concealed subcrop of fanglomerate of the Helikian Tinney Cove Formation rather than fault breccia or intrusive breccia.

Résumé

Des concentrations de pechblende, de minéraux sélénides, d'or natif et de la carrollite sont présentes dans des fragments rocheux du drift de Twin Lakes dans la partie sud de la région de l'inlet Bathurst (66°35,5'N, 108°00'W), T.N.-O. Ces gisements ont été découverts par la Cominco Ltée en 1975. L'U, Se, Au, Pb, Hg, Bi, Co, Cu et les faibles quantités de Ni se concentrent dans la suite minérale similaire aux associations relevées à la mine Nicholson et dans le gisement d'uranium D au lac Cluff en Saskatchewan, à l'île Christopher dans la région du lac Baker, district de Keewatin et dans le groupe des monts Otish au Québec. La plupart des détritiques à radioactivité élevée sont de petits galets ou granules de pechblende ou d'autres minéraux métalliques qui sont reliés, dans certains cas, à du quartz ou de siltstone. Des fragments minéralisés de grande dimension pouvant atteindre 25 cm, y sont disséminés et se composent de fragments de siltstone et de quartz dans une matrice quartzeuse granulaire.

Une datation au $\text{Pb}^{207}:\text{Pb}^{206}$ d'un pechblende l'évaluant à 901 Ma représente un âge minimal et indique que ce minerai et d'autres minéraux intimement associés dans cette suite ont probablement été déposés à la fin de l'Hélikien comme d'autres gisements d'uranium reliés à des discordances et situés en Saskatchewan. La source de la brèche minéralisée était peut-être un sous-affleurement caché d'un cône alluvial cimenté de la formation hélikienne de Tinney Cove plutôt qu'une brèche de faille ou une brèche intrusive.

Introduction

A rare assemblage of pitchblende, selenide minerals and native gold occurs as rich concentrations in clasts ranging in size from granules to small boulders within thin drift at a locality (66°35.5'N, 108°00'W) in NTS 76J and K, 15 km west of Bathurst Inlet and 30 km south of Bathurst Inlet Lodge at the delta of the Burnside River (Fig. 6.1). These concentrations were discovered in 1975 during a uranium prospecting program by Cominco Limited who staked the JCW claim group to cover the occurrences, and conducted various surveys and exploratory tests in the area between 1976 and 1979. Cominco Limited subsequently allowed the claims to lapse, and in 1984 Glen Warner of Yellowknife staked the GBC group of claims covering the anomalous float occurrences. The occurrences have been described previously in very general terms by Roscoe (1984).

The precise location of the bedrock source of the gold and uranium-bearing detritus may never be discovered, but studies of this detritus may enable us to draw some useful conclusions about the character of the source deposit and of rocks that might be prospected for similar deposits. On initial visits to the locality (Gandhi in 1978, Roscoe in 1979), we tended to seek and collect specimens no more than a few centimetres in size composed largely of pitchblende, other metallic minerals, and native gold. Roscoe revisited the occurrences in 1981 and collected much larger samples of rock clasts containing subordinate concentrations of the unusual mineral assemblage. These have provided better clues to the character of the bedrock source concentrations as well as additional material for mineralogical studies.

Geological setting

The clasts containing pitchblende, gold and selenides have been found in clusters in a drift-covered area between two northerly trending lakes ('Twin Lakes') that are about 1 km long (Fig. 6.2). These clusters, along with areas of anomalous radioactivity and radon concentrations, occur within an area about 600 m by 300 m in extent (Fig. 6.3). Several pits reached fractured bedrock at depths of about 1 metre and several diamond drill holes were drilled by Cominco Limited beneath the area of greatest concentrations of exotic clasts. Bedrock strata, siltstones of the Aphebian Goulburn Group, dip gently east. Beds in outcrops and subcrop near the pits are predominantly grey siltstone and pyritic shale beds, and these are underlain by varicoloured and grey siltstones and thin beds of red granular hematite-jasper iron-formation. The latter beds indicate that the strata are probably correlative with the Mara Formation rather than the upper part of the Burnside River Formation as shown in Figure 6.1 which was based on mapping by Campbell and Cecile (1976b). Their map shows the Mara Formation, which they had earlier considered an upper member of the Burnside River Formation, wedging out 7 km southwest of the locality of interest.

As indicated in Figure 6.1, the Mara Formation overlain successively to the southeast by stromatolitic carbonate of the Quadyuk Formation (unit 8), mudstone rhythmites of the Peacock Hills Formation (unit 9), carbonate of the Kuuvik Formation (unit 10) and arkose and siltstone of the Brown Sound Formation (unit 11). At East Twin Lake and at the east margin of the anomalous drift area, however, the Mara Formation is truncated by the Tub Fault, an important northwesterly-striking branch of the Bathurst Fault, and is in fault contact with the Peacock Hills Formation according to mapping by Campbell and Cecile (1976b). Helikian strata of the Ellice and Tinney Cove formations are preserved in grabens formed by major branches of the Bathurst Fault system 10 to 18 km to the northeast. These formations, respectively sandstone with conglomerate and locally distributed subjacent conglomerate with arkose, were deposited on the eroded and weathered surfaces of the various deformed formations of the Goulburn Group and, south and north of the inlet, on Archean igneous and metamorphic rocks.

LEGEND

(from Roscoe, 1984 after Campbell and Cecile, 1976b)

19 Gabbro sheets/diabase dykes, in part interpreted from aeromagnetics

HELIKIAN

18 ALGAK FORMATION : arkose, siltstone

17 EKALULIA FORMATION : basalt flows

16 KANUYAK FORMATION : dolomite

15 PARRY BAY FORMATION : dolomite, grey shale

14 ELLICE FORMATION : kaolinitic quartzite and conglomerate

13 TINNEY COVE FORMATION : arkose, polymictic conglomerate

APHEBIAN (Goulburn Group)

Intrusive sedimentary breccia

12 AMAGOK FORMATION : arkose, minor conglomerate

11 BROWN SOUND FORMATION : arkose, siltstone, minor basalt flows

OMINGMAKTOOK MEMBER: solution collapse breccia

10 KUUVIK FORMATION : stromatolitic and clastic carbonate

9 PEACOCK HILLS FORMATION : mudstone rhythmites

8 QUADYUK FORMATION : stromatolitic carbonate

7 MARA FORMATION : siltstone, sandstone, hematitic ironstone, pisolitic dolomite

6 BURNSIDE RIVER FORMATION : quartzite, conglomerate; minor siltstone, dolomite

5 WESTERN RIVER FORMATION : quartzite, argillite, siltstone, dolomite

4 Massive to foliated granitic rocks

3 Gneiss, in part derived from 1 and 2

2 Metasedimentary rocks

Metavolcanic rocks

Units 1,3,4,15-18 are not represented in Fig. 1

Geological contact (approximate)

Bedding (inclined, vertical)

Fault (assumed)

PROTEROZOIC

ARCHEAN

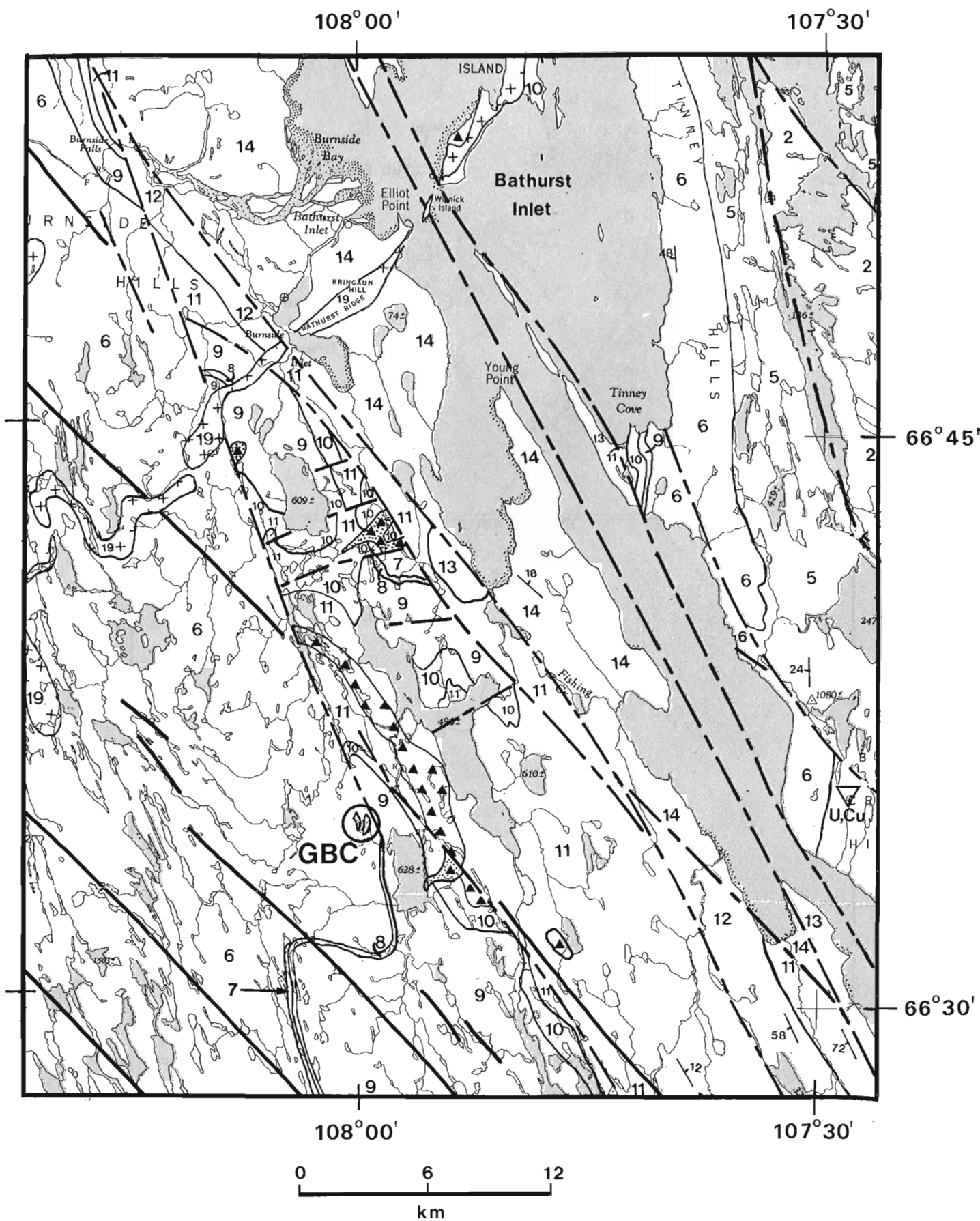


Figure 6.1. Map of the southern portion of Bathurst Inlet showing the location of the GBC claim group (from Roscoe, 1984, after Campbell and Cecile, 1976b).

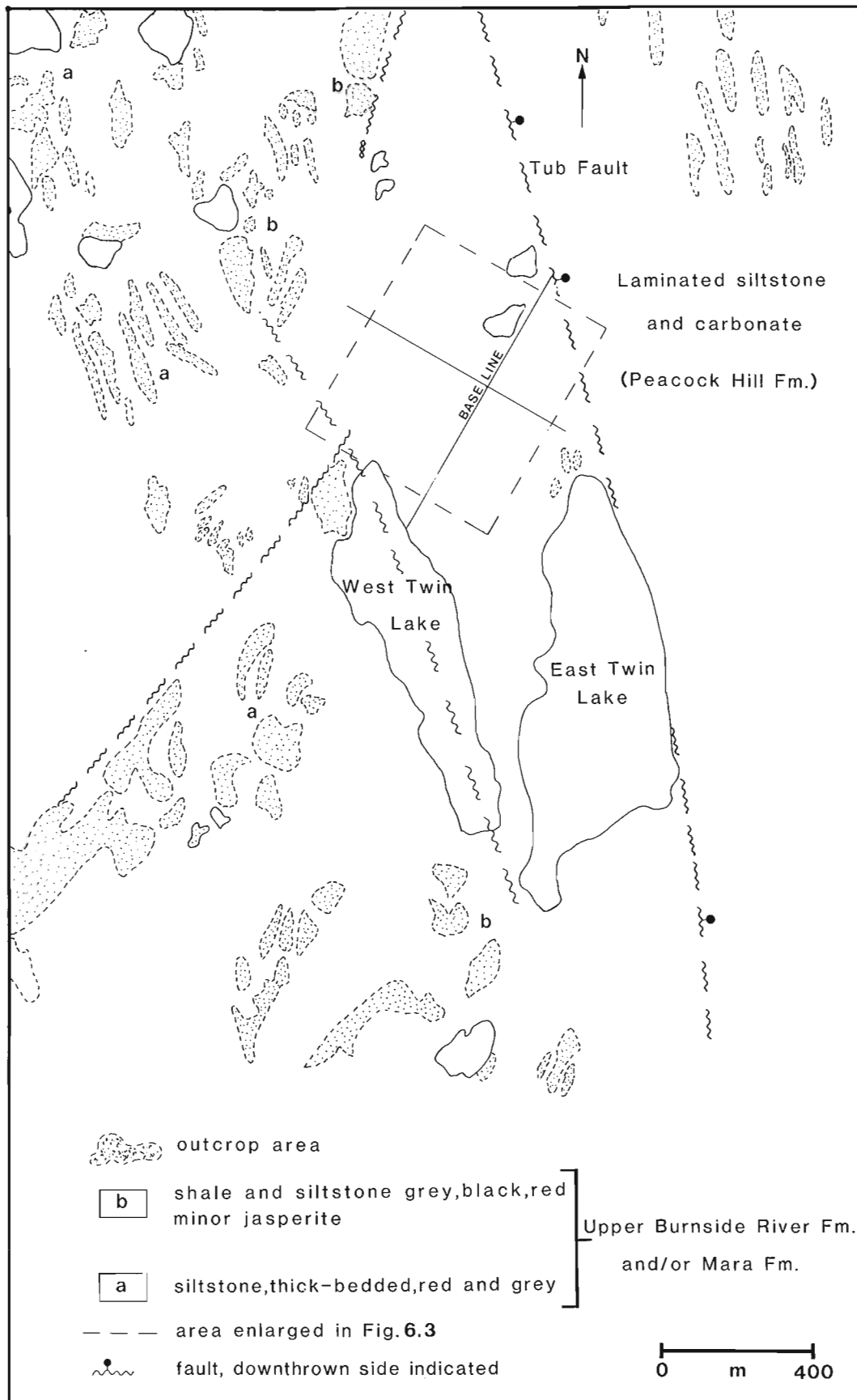


Figure 6.2. Geology map of the 'Twin Lakes' area.

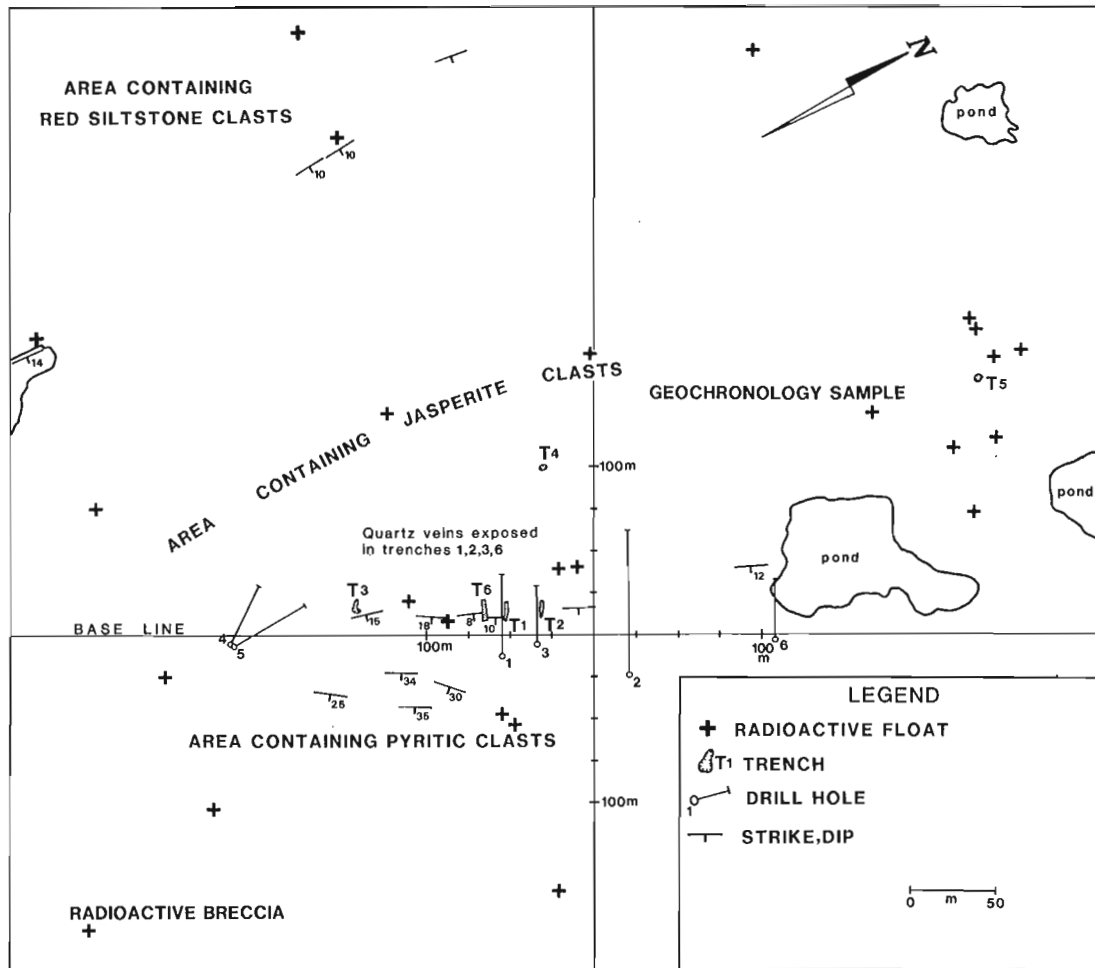


Figure 6.3. Map showing drillholes, trenches, and sample locations on GBC claim group.

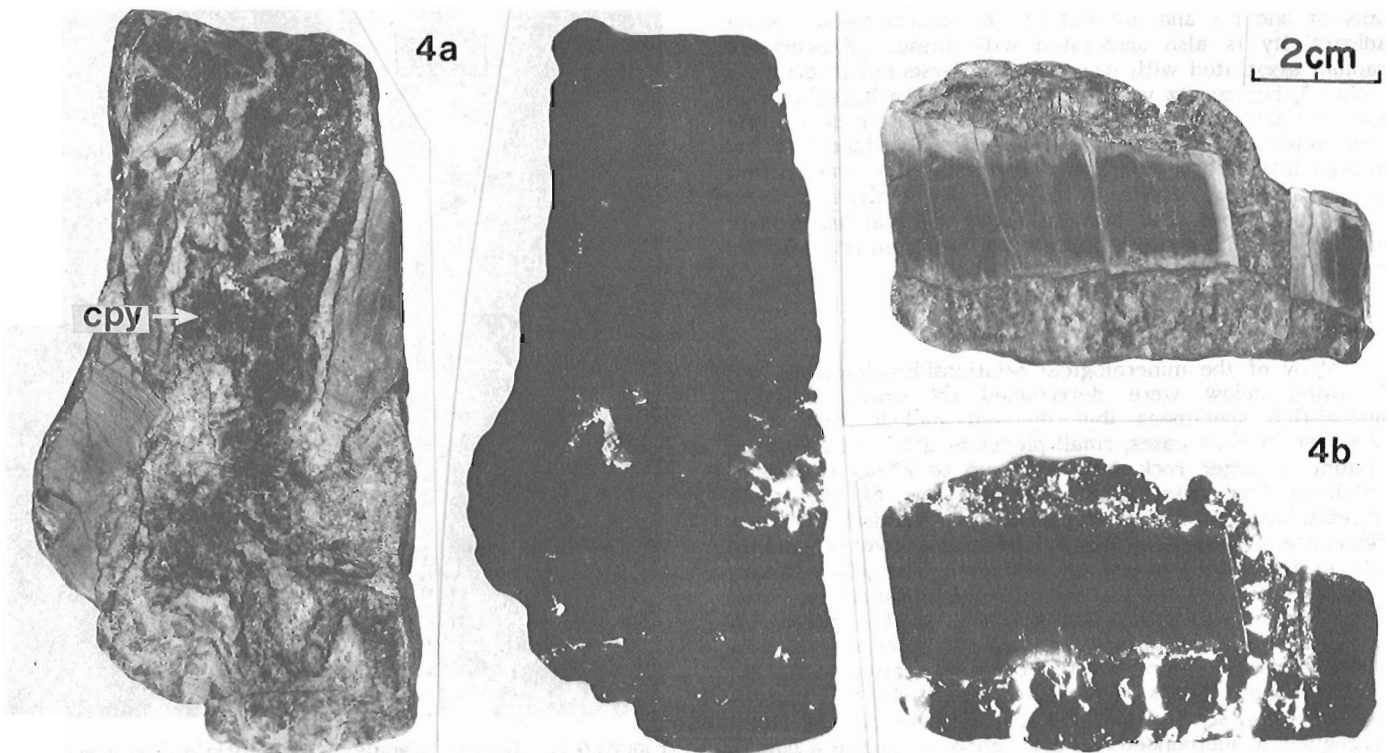


Figure 6.4. Rock fragments composed of clasts of siltstone, vein quartz, quartzite, jasper and chert. Corresponding autoradiographs show location of pitchblende in the samples.

The drift containing the exotic mineral-bearing clasts at 'Twin Lakes' appears to be different from the widespread till which was transported from a direction of about 155°. The former has a relatively intact framework, a hummocky surface, and is rich in pebble-size siltstone clasts. An examination of air photos led W.W. Shilts (personal communication, 1986) to suggest that it may have been transported by a glaciofluvial stream perhaps flowing from a direction around 200° judging from alignments of eskers and scoured areas. There are no distinctive lithologies in sourceward areas and amongst unmineralized clasts in the drift to indicate whether the distance of transport was short or long.

Several uranium concentrations are known in bedrock southeast and east of the 'Twin Lakes' drift occurrence (Roscoe, 1984). These include pitchblende and copper minerals in brecciated, quartz-injected sedimentary rocks of the Western River Formation on the YON claims 24 km to the east, and pitchblende with chalcocite and calcite in veins in arkose and basalt of the Brown Sound Formation on the Pomie claims 63 km to the southwest. Several other radioactive mineral occurrences have been found between 'Twin Lakes' and the Pomie claims, including: uranium-enriched ferruginous arkose beds in the Brown Sound Formation; mineralized fractures in a zone 1.5 km long in dolomite breccia (Omingmaktook Member) in the lower part of the Brown Sound Formation and adjacent to a diabase dyke; and in dolomitic siltstone of the Quadyuk Formation. According to Campbell and Cecile (1976a), mudstones and siltstones of the Mara Formation are everywhere distinctly radioactive. High radioactivities due to pitchblende-bearing clasts in the pit areas made it impossible to determine whether any of the bedrock siltstone, supposed to be Mara Formation, is especially radioactive.

The main pits uncovered a northerly-striking, steeply-dipping quartz vein up to 30 cm thick cutting gently east-dipping siltstone beds. The vein contains pyrite and chalcopyrite and is radioactive at the bedrock surface beneath the uraniumiferous drift. Quartz stringers, dipping gently westward are present in the highly fractured bedrock walls of one pit and are cut by the quartz vein. Some radioactivity is also associated with these. Appreciable uranium associated with quartz was intersected in drillhole number 5, but quartz veins and country rocks intersected in other drillholes were barren or nearly so. The radioactivity found in pits dug into the fractured bedrock surface probably resulted from recent migration of uranium downwards from highly uraniumiferous detritus in the drift. Certainly, there is no reason to suppose that the distinctive mineral assemblage found in the drift could have been derived from immediately subjacent bedrock and quartz veins.

Clasts containing exotic minerals

Many of the mineralogical relationships described and illustrated below were determined on small, metallic mineral-rich specimens that did not include host rocks excepting, in some cases, small pieces of attached quartz or siltstone. Larger rock fragments, up to 25 cm in length, containing less spectacular concentrations of the same minerals, however, can be found locally in the drift (note the occurrence indicated in Fig. 6.3 of radioactive breccia in drift in the southern end of the anomalous area), within dumps at several of the pits – especially pit number 5 – and, in one case, in situ within drift at the edge of pit number 5. These fragments are angular and are composed of clasts of siltstone, coarse vein quartz, pale quartzite, hematitic quartzite and perhaps jasper and brown chert (Fig. 6.4). Laminations in some siltstone clasts are curved. The clasts are angular to subrounded and are tightly packed in a quartz

sandstone matrix. Some clasts were broken and the space between separated parts was filled with sandstone of the matrix. All clasts are fractured to some extent and the fractures are filled by chalcedony.

A variety of massive to laminated, pale to dark greenish grey siltstone clasts are present. Some have red and pale tan alteration rims up to 5 mm thick, reflecting hematization, sericitization and perhaps leaching. Quartz arenite pebbles and quartz granules in the matrix show peculiar multiple overgrowths and hematitic rims on quartz grains (Fig. 6.5). Clasts of coarse grained vein quartz contain pyrite and chalcopyrite and are commonly rimmed by thin films of hematite. Other types of clasts also contain sulphides but in finer grains and lesser abundance. Pitchblende, selenides, and native gold occur in veins and in delicate intergranular networks of veinlets within matrices between clasts and also within clasts.

It is clear that the bedrock source of mineralized clasts in the drift is not a veined zone but a breccia zone or conglomerate unit containing clasts of country rock and quartz veins.

Mineralogy

The following metallic minerals were identified in selected radioactive drift specimens by A.L. Littlejohn, Mineralogical Laboratories, Geological Survey of Canada, and their distribution and relationships studied by S.B. Green: botryoidal pitchblende; sooty pitchblende mixed with limonite and hematite; clausthalite (PbSe); cobaltian clausthalite; tiemannite (HgSe); paraganajuatite ($\text{Bi}_2(\text{Se},\text{S})_3$); carrollite (CuCo_2S_4) with trace amounts of Ni and Se; and native gold.

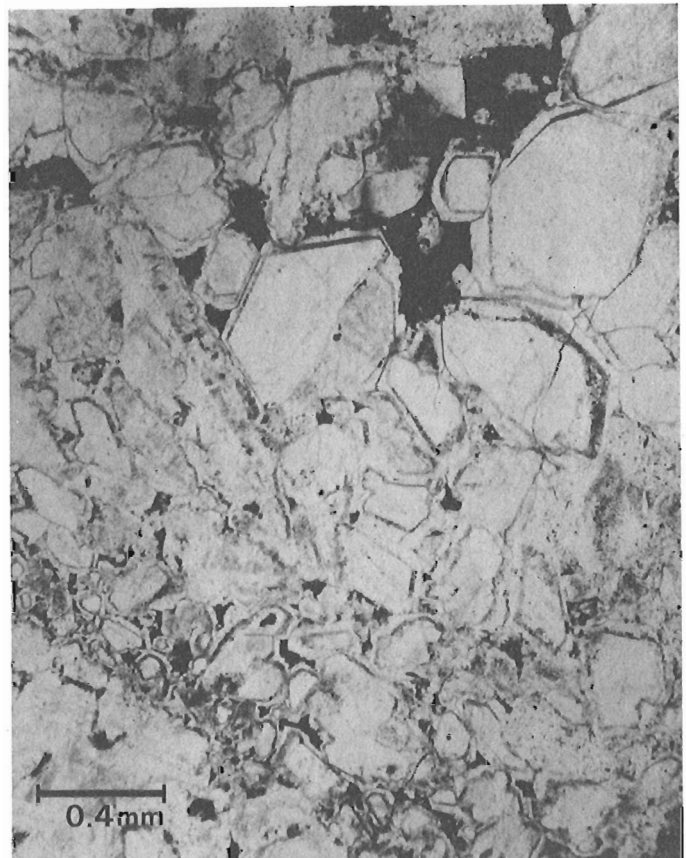


Figure 6.5. Quartz granules with multiple overgrowths and hematitic rims.

Most pitchblende is concentrated in veinlets and small masses in the sandy matrix supporting the siltstone and other clasts (see autoradiographs, Fig. 6.4). It has also been introduced into fractures within siltstone clasts. Colloform pitchblende along with grains of gold were noted within veinlets of paraguanaujatite in one specimen (Fig. 6.6a).

Native gold occurs interstitially within granular quartz matrices, in some cases in association with paraguanaujatite (Fig. 6.6b). It also occurs abundantly in intimate association with clausthalite, carrollite, and pitchblende in distinctive rosette-like clusters (Fig. 6.7a). The rosettes have multiple irregular-shaped gold cores surrounded by cobaltian clausthalite which itself is enclosed by a circular chain of colloform pitchblende grains connected by veinlets of clausthalite, pitchblende and carrollite. A ring of clausthalite forms the outer shell of each rosette. Tiemannite occurs in lieu of gold in some rosettes (Fig. 6.7b). Carrollite is most common within rosettes lacking gold cores.

Chalcopyrite occurs locally as angular grains interstitial to coarse grained, late, open-space filling quartz (Fig. 6.4a).

Pyrite and chalcopyrite were probably present in quartz veins before they were broken up and incorporated in breccia or conglomerate that became the host for the exotic suite of minerals, and that itself was subsequently broken up to form the clasts found in the drift. Hematitic rims on siltstone clasts and some of the oxidation of sulphides to form limonite (Fig. 6.8a, b) were likely products of weathering during the initial erosion of the siltstone and sulphide-bearing quartz veins. Ferric iron concentrations in veinlets, however, are

difficult to date relative to pitchblende-selenide-gold concentrations and it appears likely that some of them, eg. intimate mixtures of limonite, hematite and pitchblende as shown in Figure 6.8c, are coeval with the exotic mineral assemblage.

A close parallel to the 'Twin Lakes' mineral suite has been described from the Consolidated Nicholson Mine on the north shore of Lake Athabaska 3 km east of the former site of the settlement of Goldfields, Saskatchewan. Here, the assemblage colloform pitchblende, native gold, tiemannite, niccolite, pyrite, and chalcopyrite was observed by Robinson (1955) in a vein of carbonate-rich gouge from a surface trench along part of the No. 2 Zone. The 'Twin Lakes' concentrations of U, Se, and Au are also similar to mineralization in the unconformity-related D Zone orebody of Amok Ltd. in sandstone at Cluff Lake, Saskatchewan (Ruhmann, 1985), to veins at Christopher Island in the Baker Lake area of the District of Keewatin (Miller and LeCheminant, 1985), and to concentrations in the Otish Mountain Group in central Quebec (Ruzicka and LeCheminant, 1984).

The suite has distinct geochemical similarities to many sub-Athabaska and other unconformity-related uranium deposits in addition to the Cluff Lake D Zone deposit mentioned above. Its principal chemical difference from most of these deposits is its lack of arsenic and paucity of nickel. This does not necessarily mean that nickel and cobalt arsenides are absent in the mother deposit as these minerals are readily decomposed during weathering.

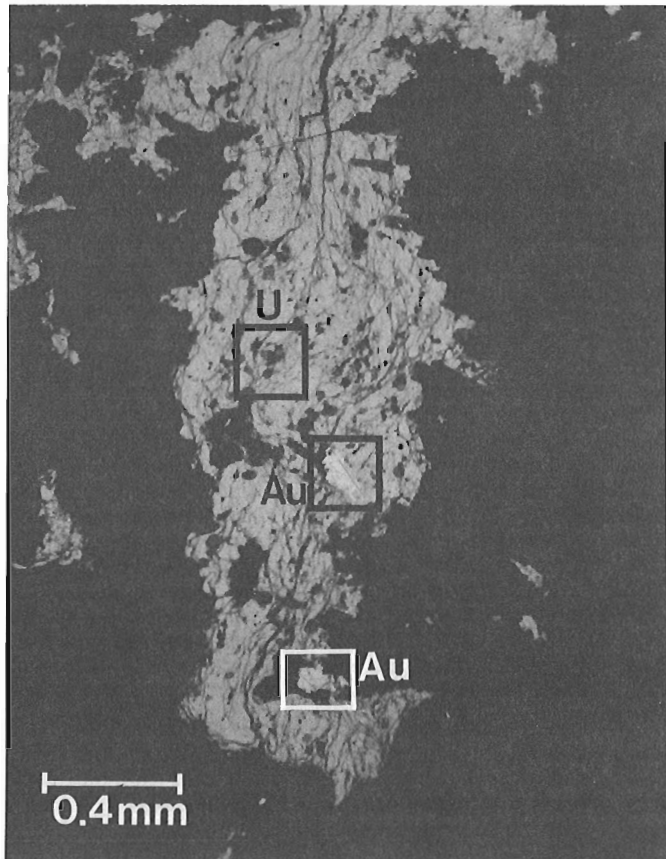


Figure 6.6a. Veinlet of paraguanaujatite with small spheres of colloform pitchblende and grains of gold.

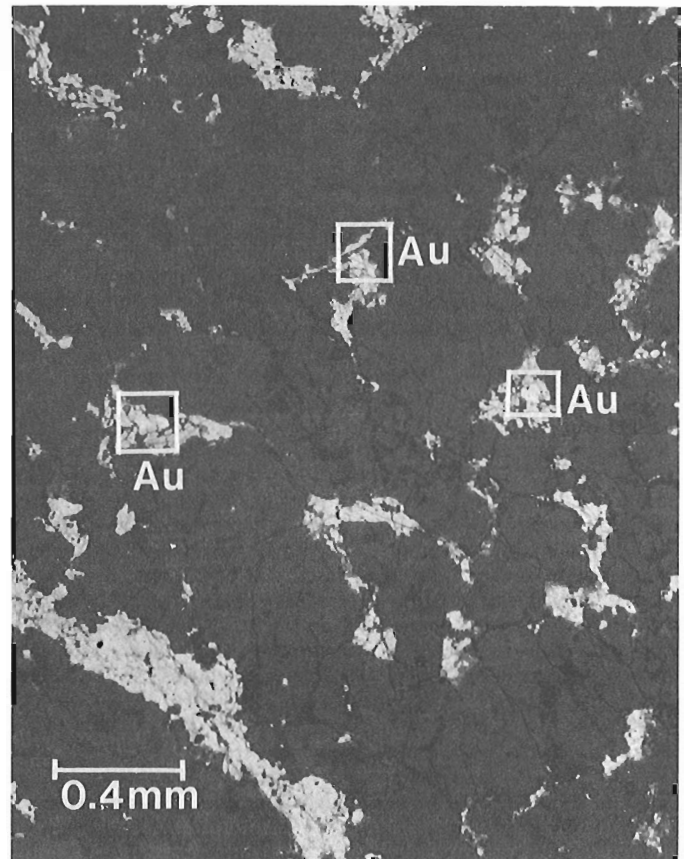


Figure 6.6b. Grains of gold set in paraguanaujatite interstitial to quartz grains.

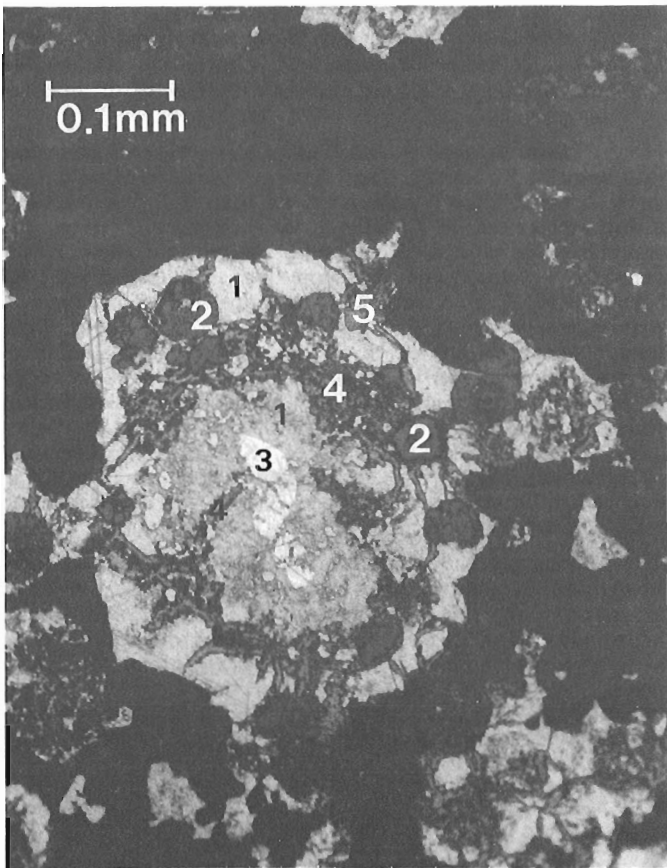


Figure 6.7a. Gold-cored rosette (3) with concentric shells of clausthalite (1), pitchblende (2), and a network of pitchblende connected by veinlets composed of a mixture of clausthalite, pitchblende and carrollite (4). An unidentified selenide mineral (5) also occurs in this rosette.

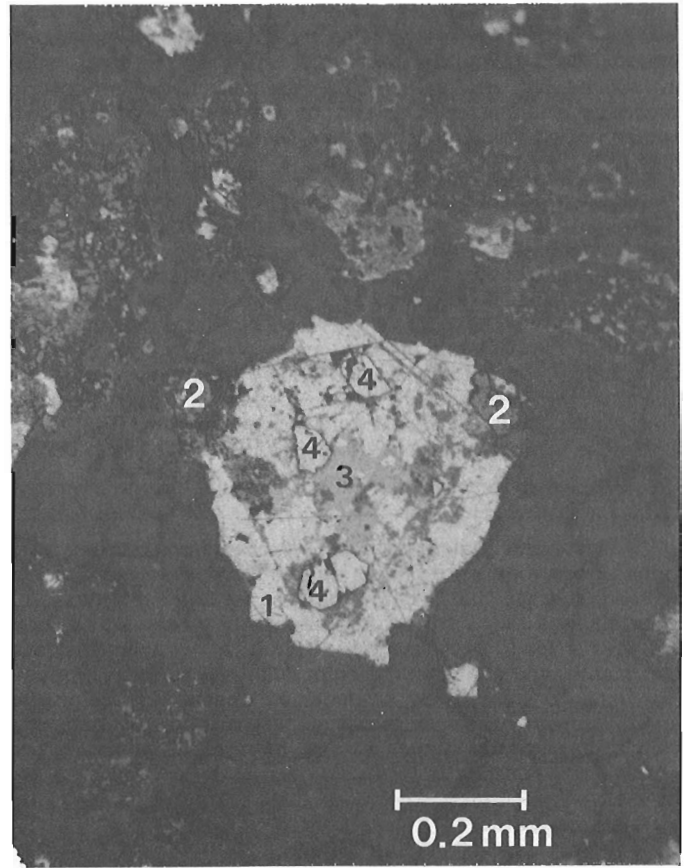


Figure 6.7b. Tiemannite-cored rosette (3) with subhedral crystals of carrollite (4) set in a ring of clausthalite (1) with minor pitchblende (2).

Isotopic dating of pitchblende

Uranium-lead isotopic compositions and dates were determined by Geospec Consultants Limited, Edmonton, on a sample of pitchblende (GFA-78-JCW-2-4) collected at the 'Twin Lakes' site by S.S. Gandhi. Technical data from the analyses are given in Appendix A. Calculated dates are:

$${}^{207}\text{Pb}/{}^{206}\text{Pb} - 901 \text{ Ma}; {}^{207}\text{Pb}/{}^{235}\text{U} - 770 \text{ Ma};$$

$${}^{206}\text{Pb}/{}^{238}\text{U} - 726 \text{ Ma}$$

The discordant dates are considered to reflect lead loss, and the ${}^{207}\text{Pb}/{}^{206}\text{Pb}$ ratio date of 901 Ma is believed to be a minimum date, younger – but perhaps no more than about 200 Ma younger, than the actual time of formation or important modification of the pitchblende-bearing mineral assemblage in the undiscovered deposit that was the source of the mineralized clasts. This places the source deposit in the same general Neohelikian age bracket as sub-Athabaska unconformity deposits in Saskatchewan. For example, massive mineralization in the "zone à boules" in the Cluff Lake D deposit has yielded a ${}^{207}\text{Pb}/{}^{206}\text{Pb}$ date of $1050 \pm 30 \text{ Ma}$ (Gancarz, 1979, as cited by Tona et al., 1985), and pitchblende-selenide mineralization in the same deposit has given a ${}^{206}\text{Pb}/{}^{238}\text{U}$ and a ${}^{207}\text{Pb}/{}^{235}\text{U}$ date of $1150 \pm 25 \text{ Ma}$ (Devilliers and Nordmann, 1974, as cited by Tona et al., 1985).

Discussion

The clasts containing pitchblende, selenide minerals and gold clearly have had a complex history. Their original source was a coarse fragmental rock – a breccia or a conglomerate. The apparently sorted quartz grains forming

the matrix between clasts, the varied character of clasts and the varied alterations of rims of siltstone clasts indicate that this source rock may have been a sedimentary breccia, or a conglomerate, rather than a breccia developed in a fault zone or intruded in some manner like an exotic breccia 5 km southeast of 'Twin Lakes' (Cecile and Campbell, 1977). It is suggested here that the conglomerate was a fanglomerate, correlative with the Tinney Cove Formation, deposited at the base of a scarp formed along a fault zone cutting the eroded surface of Mara Formation siltstones. More tenuous, it may be supposed that quartz veins, locally abundant along the fault, contained pyrite and chalcocopyrite and that their siltstone wall rocks also contained disseminated sulphides. Vein quartz, siltstone and other clasts transported short distances were covered with quartz sand of the Helikian Ellice Formation which also filled interstices between clasts. Silica was introduced as an authigenic cement and also in veins in the consolidated rock. Concentrations of U, Se, Co, Hg, Bi, Cu and minor Ni were formed through reactions involving reduction of introduced fluids and oxidation of sulphides and perhaps carbonaceous material in rock clasts.

The suggestion that the source of the mineralized clasts was a mineral deposit formed in fanglomerate of the Tinney Cove Formation requires an assumption that Helikian rocks once overlay the Mara Formation at 'Twin Lakes' and that a small pocket of these rocks survived in the area at least until the Pleistocene.

The hypothesis outlined above implies that there is a possibility that unconformity-type uranium deposits are present beneath known Helikian rocks preserved in extensive grabens in the Bathurst Inlet area, an idea previously suggested by Roscoe (1984). Exploration for such deposits

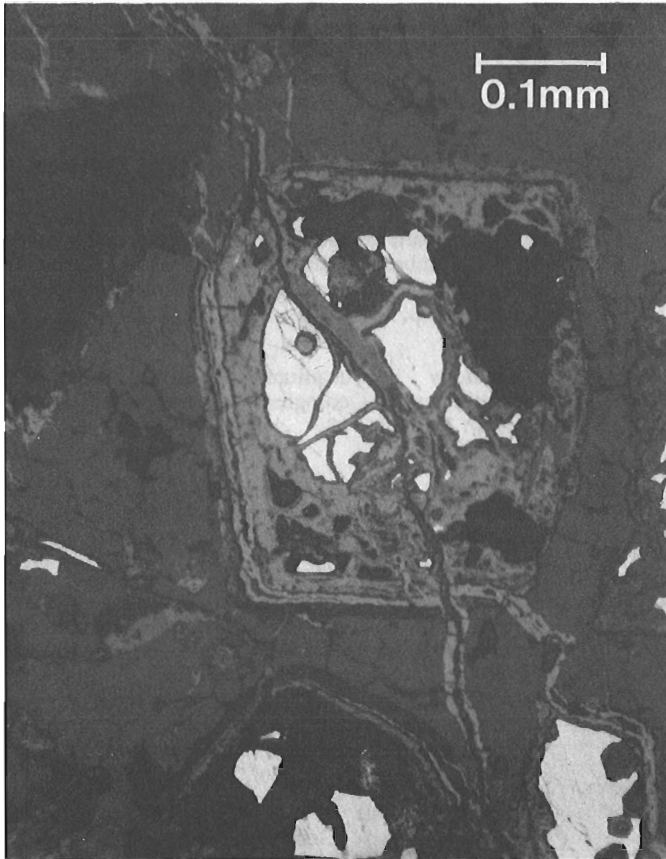


Figure 6.8a. Pyrite crystal oxidized to limonite. Several crystals have been partially to totally replaced by limonite which also forms the small veinlets seen in the photo.

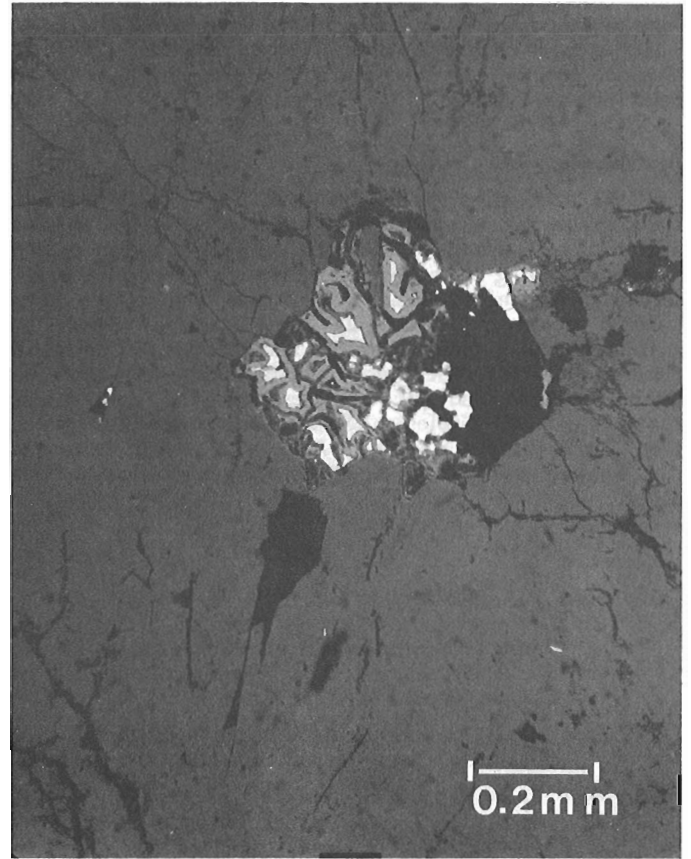


Figure 6.8b. Pyrite and chalcopyrite (shard-like grains in the left centre of the mass being replaced) oxidized and replaced by limonite.

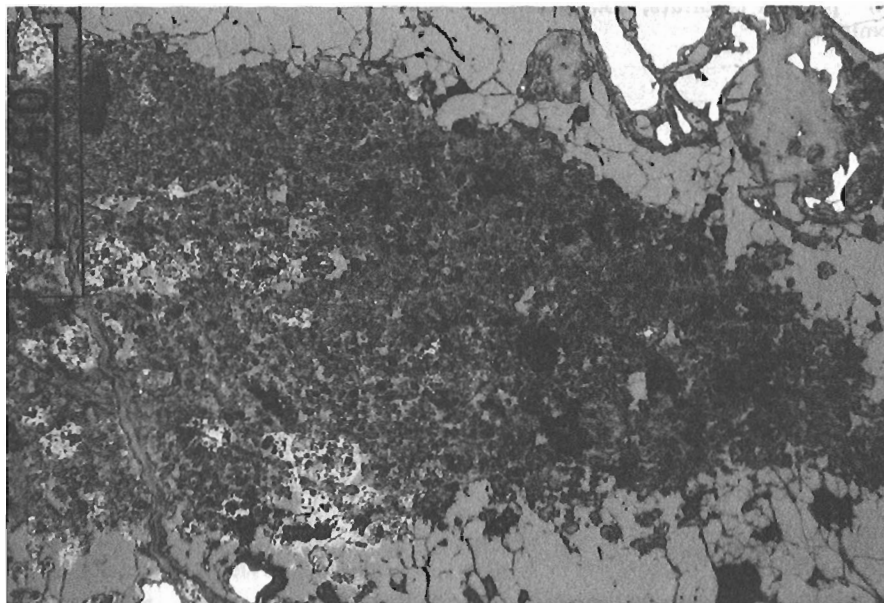


Figure 6.8c. Amorphous pitchblende with limonite and hematite. Rounded sulphide grains are pyrite.

along buried low-angle unconformities between sedimentary rock sequences would be more difficult than in Saskatchewan where steeply-dipping metamorphic rocks beneath sandstone provide geophysical discontinuities that are useful in delimiting exploration drillhole target zones.

Acknowledgments

We thank Glen Warner, owner of the GBC claim group, for permission to publish this report. Paul Wilton and Jim Smith of Cominco Limited provided guidance and hospitality during our early field visits. Bathurst Inlet Lodge served as a comfortable base for a later visit to the 'Twin Lakes' locality. Mineral identifications were by A.L. Littlejohn, Mineralogical Laboratories, Geological Survey of Canada. Geospec Consultants Limited made the pitchblende-lead isotopic analyses reported here under contract with the Geological Survey of Canada. Reviews of the initial manuscript by A.R. Miller, R.T. Bell and D.C. Findlay resulted in significant improvements in this paper.

References

Campbell, F.H.A. and Cecile, M.P.
 1976a: Geology of the Kilohigok Basin, Goulburn Group, Bathurst Inlet, District of Mackenzie; in Report of Activities, Part A, Geological Survey of Canada, Paper 76-1A, p. 369-377.
 1976b: Geology of the Kilohigok Basin; Geological Survey of Canada, Open File 332, 1:500 000 scale map.
 Cecile, M.P. and Campbell, F.H.A.
 1977: Large scale stratiform and intrusive sedimentary breccias of the lower Proterozoic Goulburn Group, Bathurst Inlet, N.W.T.; Canadian Journal of Earth Sciences, v. 14, p. 2364-2387.
 Devilliers, C. et Nordmann, F.
 1974: Datation du minerai uranifère de Cluff (Saskatchewan) – premier résultats; Commissariat a l'Energy Atomique.

Gancarz, A.J.
 1979: Chronology of the Cluff Lake area uranium deposit, Saskatchewan, Canada; International Uranium Symposium on the Pine Creek Geosyncline, N.T., Australia, p. 91-99 (abstract).
 Miller, A.R. and LeCheminant, A.N.
 1985: Geology and uranium metallogeny of Proterozoic supracrustal successions, central District of Keewatin, N.W.T., with comparisons to northern Saskatchewan; in Geology of Uranium Deposits, ed. T.I.I. Sibbald and W. Petruk; Canadian Institute of Mining and Metallurgy, Special Volume 32, p. 167-185.
 Robinson, S.C.
 1955: Mineralogy of uranium deposits, Goldfields, Saskatchewan; Geological Survey of Canada, Bulletin 31, p. 16-18.
 Roscoe, S.M.
 1984: Assessment of mineral resource potential in the Bathurst Inlet Area, NTS 76J,K,N,O including the proposed Bathurst Inlet National Park; Geological Survey of Canada, Open File 788.
 Ruhlmann, F.
 1985: Mineralogy and metallogeny of uraniferous occurrences in the Carswell Structure; in The Carswell Structure Uranium Deposits, Saskatchewan, ed. R. Laine, D. Alonso and M. Svab; Geological Association of Canada, Special Paper 29, p. 106-119.
 Ruzicka, V. and Le Cheminant, G.M.
 1984: Uranium deposit research, 1983; in Current Research, Part A, Geological Survey of Canada, Paper 84-1A, p. 50.
 Tona, F., Alonso, D., and Svab, M.
 1985: Geology and mineralization in the Carswell Structure – a general approach; in The Carswell Structure Uranium Deposits, Saskatchewan, ed. R. Laine, D. Alonso and M. Svab; Geological Association of Canada, Special Paper 29, p. 1-18.
 Wright, R.L.
 1976: JCW Group: Geology, ground track etch and radiometric survey report; Bathurst Inlet area, District of Mackenzie (76J/12, K/9); Cominco Limited; Document N061590 (confidential), Department of Indian and Northern Affairs, Ottawa.

Appendix A

Technical data, isotopic analysis by Geospec Consultants Limited of pitchblende sample GFA-78-JCW-2-4 from Bathurst Inlet area

GFA78-JCW-2-4				MICROMOLES PB FROM 8/6 88/7 (OR 7/6) RATIO			
SAMPLE ATOMIC PERCENT				RATIO			
0.00419	93.26270	6.50040	0.23277	0.24346	0.24402		
PB TRACER ATOMIC FRACTIONS(4,6,7,8)				SAMPLE EX BLANK			
0.0	0.0022	0.0005	0.9973	0.00408	93.26808	6.49922	0.22864
				0.24344	LESS BLANK		
U TRACER(FRAC)235,238		TH TRACER(FRAC)230,232		RADIOGENIC PB (AS ATOMIC FRACTION)			
0.99872	0.00128	0.92040	0.07960	-0.0	0.93202	0.06436	0.00083
SAMPLE (MG.) PB ALIQUOT (MG.)		U-TH ALIQUOT (MG.)		PB207/PB206 PB206/U238 PB207/U235 PB208/TH232			
0.50000E+02	0.3742E+01	0.3742E+01		0.6906E-01	0.1192E+00	0.1135E+01	0.0
PB TRACER WT. U TRACER WT. TH TRACER WT. (MICROGM.)				U CONC TH CONC PB CONC (PPM)			
3.9201	9.5896	0.0		0.1220E+06	0.0	0.1340E+05	
PB BLANK (MICROGM.) AND ITS RATIOS 6/4, ETC.				COMMON PB (MICROGM.) % OF TOTAL CONC. IN PPM.			
0.0040	18.350	15.640	38.220	0.1398E+00	0.28	0.3737E+02	
PB SAMPLE RATIOS (7/6, 8/6, 4/6)				T7/6 M.Y. T6/8 M.Y. T7/5 M.Y. T8/2 M.Y.			
0.0696999	0.0024958	0.0000449		900.7	725.9	770.1	0.0
PB MIXTURE RATIOS (7/6, 8/6) 8/7 (CALC.)							
0.0698822	0.0852703	1.2201996					
U MIXTURE (238/235)		TH MIXTURE (232/230)					
34.8973999		0.0					
COMP. OF COMMON PB(6/4, 7/4, 8/4)							
16.118	15.420	35.805	1500Ma Common Pb				

Structural and stratigraphic relationships at the B-zone orebody, Heath Steele Mines, Newcastle, New Brunswick¹

Contract OST85-00258

Christopher Moreton² and P.F. Williams²

Moreton, C. and Williams, P.F.; Structural and stratigraphic relationships at the B-zone orebody, Heath Steele Mines, Newcastle, New Brunswick; in Current Research, Part B, Geological Survey of Canada, Paper 86-1B, p. 57-64, 1986.

Abstract

The B-zone at Heath Steele Mines is a base metal massive sulphide deposit. Pelitic, semipelitic and psammitic metasedimentary rocks, with minor beds of quartz crystal tuff, are dominant in the footwall, whereas felsic porphyritic rocks are exposed in the hanging wall. A possible alteration zone (acid tuff), concordant with the sulphide deposit, is restricted to the immediate footwall of the orebody. The deposit youngs to the north.

Five fold groups are distinguished on the basis of style and orientation. Relative ages (fold generations) are assigned to the groups using mesoscopic overprinting relationships. Only D₂ structures significantly affect the orebody: earlier structures are inferred so that their effect on the sulphide body is, as yet, indeterminable. The B-zone is inclined to the main transposition foliation (S₂) and is interpreted as being parallel to the F₂ enveloping surface.

Résumé

La zone B de la *Heath Steele Mines* est un gisement de sulfure massif à métal commun. Les roches métasédimentaires pélitiques, semi-pélitiques et psammitiques comprenant de faibles couches de tuf à cristal de quartz, dominent dans le mur, tandis que les roches porphyritiques felsiques affleurent dans le toit. Une zone d'altération possible (tuf acide), concordante avec le gisement de sulfure, se limite au mur du gisement de minerai. Vers le nord, le gisement est d'origine de plus en plus récente.

On distingue cinq groupes de plis en fonction du style et de l'orientation. Les âges relatifs (générations de plis) sont attribués aux groupes en fonction des relations de superposition mésoscopique. Seules les structures D₂ influent de façon marquée sur le gisement: il existe probablement des structures plus anciennes, mais il n'est pas encore possible de déterminer les effets qu'elles ont sur le gisement de sulfur. La zone B est inclinée vers la principale foliation de transposition (S₂) et est interprétée comme étant parallèle à la surface enveloppante F₂.

¹ Contribution to Canada-New Brunswick Mineral Development Agreement 1984-1989. Project carried by Geological Survey of Canada, Lithosphere and Canadian Shield Division.

² Department of Geology, University of New Brunswick, Fredericton, N.B. E3B 5A3

Introduction

Heath Steele Mines is located 60 km northwest of Newcastle, New Brunswick (Fig. 7.1) in the northern part of the Miramichi Zone (Fyffe et al., 1981). Five significant deposits are exposed on the mine property, known as the A-C-D, B and E zones (Fig. 7.2), and all are hosted by the Cambro (?) - Ordovician Tetagouche Group (Skinner, 1974). The latter is a metamorphosed and intensely deformed sequence of volcanic, volcanoclastic and sedimentary rocks of disputed island arc affinity (Helmstaedt, 1971; Davies, 1980).

The B zone has a tabular shape and dips steeply to the north. It has reserves of 24.4 million tonnes grading 4.25% Zn, 1.41% Pb, 1.24% Cu and 68.9 grammes/tonne silver (Davies et al., 1984).

Mine stratigraphy

A workable mine stratigraphy (Fig. 7.3) has been defined by McBride (1976). Except for the acid volcanic rocks, which apparently are in fault contact, the sequence is thought to be continuous and younging to the north. The following is a brief summary of the mesoscopic and microscopic characteristics of the rock types exposed at Heath Steele Mines, based on the work of McBride (1976) and the authors' observations.

Acid volcanic rocks

An absence of quartz phenocrysts and a relative abundance of feldspar phenocrysts (2-3 mm) and felsic lithic clasts (1-2 mm) in a blue-grey, massive siliceous matrix characterizes this rock type. Locally, the matrix displays compositional banding which may be either primary or secondary (metamorphic differentiation).

Footwall crystal tuff

This rock is composed of varying proportions of felsic lithic clasts and quartz and feldspar phenocrysts set in a light to dark grey siliceous matrix. Locally, one or more of these components

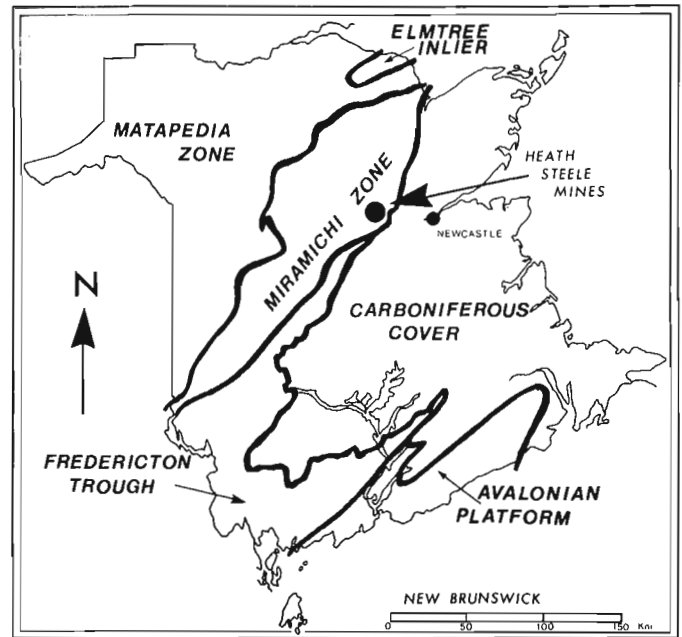


Figure 7.1. Location map for Heath Steele Mines.

is present in sufficient quantities to define a crude bedding. Correlation of these beds, however, is difficult due to rapid facies changes. In the upper parts of the unit finer grained tuffaceous rocks are commonly interbedded with quartz crystal tuff layers. Although albite is present, orthoclase tends to be the dominant phenocryst.

The "Sedimentary" Sequence

According to McBride (1976) three types of clastic "sedimentary" rocks comprise the sequence: mudstone, siltstone

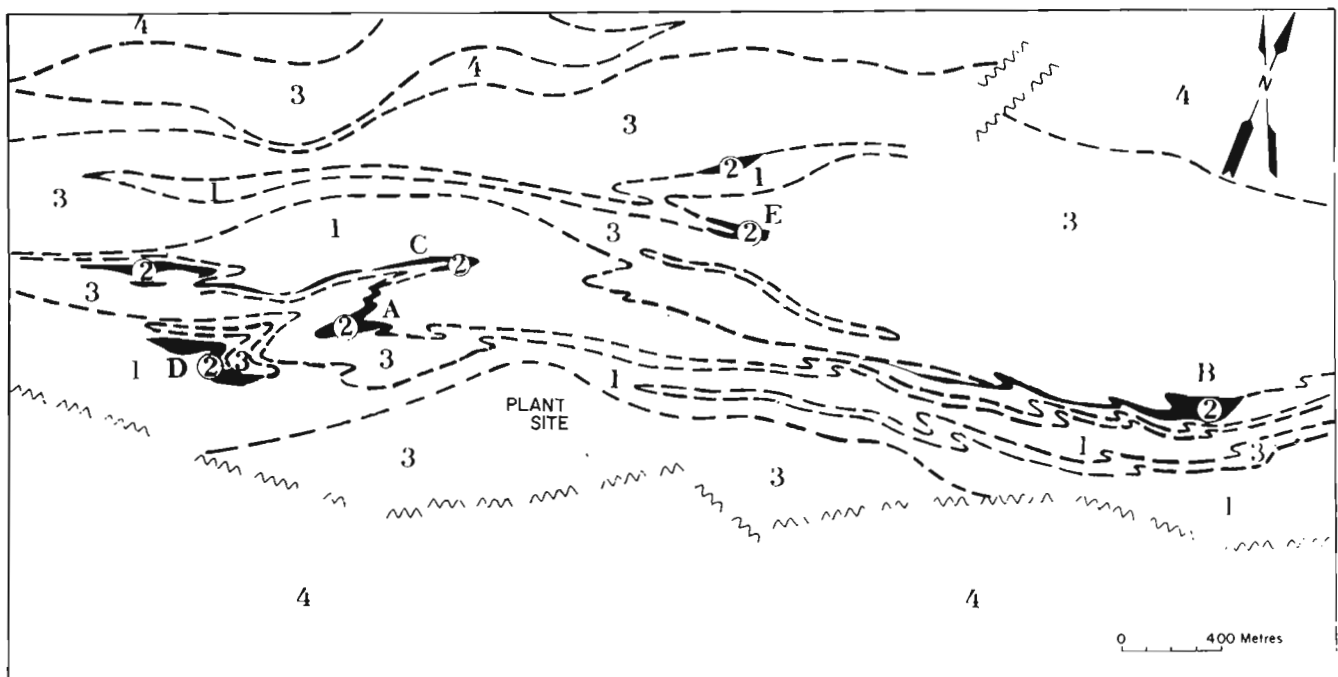


Figure 7.2. Simplified geology map of the mine showing A-C-D, E and B zones. Legend: 1 - metasediments; 2 - massive sulphides; 3 - quartz and quartz-feldspar crystal metatuff; 4 - acid volcanic rocks (from Davies et al., 1984).

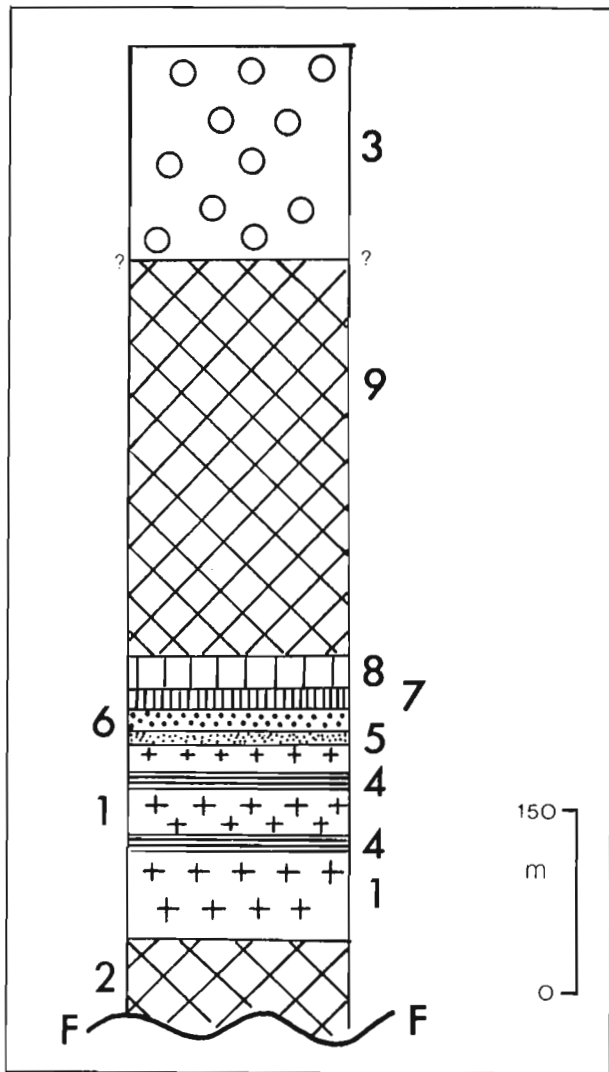


Figure 7.3. Mine stratigraphy (from McBride, 1976).
 Legend: 1 – pelitic metasediments; 2 – footwall quartz-feldspar porphyry; 3 – acid volcanic rocks; 4 – footwall quartz crystal metatuff; 5 – acid tuff; 6 – massive sulphides; 7 – iron-formation; 8 – hanging wall quartz crystal metatuff; 9 – hanging wall quartz-feldspar porphyry; F – fault; (?) – contact not exposed.

and sandstone. Each is defined by the variation in the proportion of phyllosilicate: quartz minerals. Primary sedimentary structures are rare and since these rocks contain greenschist facies mineral assemblages the authors prefer the terms pelite, semi-pelite and psammite respectively, to describe these rock types.

Pelitic rocks. An abundance of phyllosilicate minerals and quartz veins is characteristic. The mine term for these rocks is “chlorite tuff” which is misleading since the chlorite content is <10% and the term tuff carries the genetic connotation of a volcanic origin, something that is not readily substantiated. The colour of the “tuff” is due to microscopically abundant green (PPL) sericite and/or phengite (>40%). The remainder of the minerals in the pelitic rocks are fine-grained quartz ± albite.

Locally, beds of semi-pelite (siltstone) and psammite (sandstone) are present, but they have a limited lateral extent and correlation between exposures is not possible. A general facies change, from pelite in the east to pelite-psammite in the west, has been identified in the footwall of the B-zone.

Psammitic rocks: Relatively coarse grained quartz and a lower content of phyllosilicate minerals are characteristic for this rock type. Massive exposures, with a weak fracture cleavage, are common to the east of the B1 open pit.

Semi-pelite: Mineralogically this rock type is the same as the pelites and psammites, differing only in the proportion of phyllosilicates to quartz.

Acid tuff

This is restricted to the immediate footwall of the B-zone. Apart from disseminated sulphides (principally pyrite) and a light grey-buff weathering it is mineralogically identical to the pelite, i.e. it is a quartz-sericite schist with minor chlorite and carbonate. Opinion is divided as to its origin: a primary facies variation of the ‘normal’ pelite has been suggested (McBride, 1976), as has a secondary alteration product of the pelite (Owsiacki, 1980).

Massive sulphides

Chalcopyrite, sphalerite and galena are the principal sulphide minerals of the B-zone, the latter two being concentrated in the stratigraphic top (north) of the orebody. A mineral banding is generally present in this part of the orebody and may be bedding since, locally, it is deformed by D_2 structures. A gossan, enriched in gold, is variably developed as a capping to the deposit. An economically significant portion of the orebody is a pyrrhotite-chalcopyrite breccia zone (average grade 1-2% Cu) exposed on the southside of the sulphide body (stratigraphic base). Its origin is uncertain and both a primary debris-type flow deposit (Owsiacki and McAllister, 1979) and a tectonic faulting mechanism (McDonald, 1984) have been proposed.

Iron formation

Above the sulphides a discontinuous iron-formation (maximum thickness, 6 m) is found. Three facies are developed at Heath Steele Mines: 1) Oxide facies typified by magnetite; 2) carbonate facies composed predominantly of siderite; and 3) silicate facies where Fe-chlorite is dominant. Banding on a millimetre scale, generally subparallel to the main foliation (S_2), and local lithic clasts have been identified by McBride (1976). The principal minerals of the three facies are fine grained (<0.1 mm) and occur in association with very fine grained quartz (<0.01 mm), which probably is recrystallized chert. Minor minerals present include pyrrhotite, sphalerite, galena and biotite.

Ooids (<1 mm) in the siderite facies of the iron-formation have been identified by McMillan (1969) and McBride (1976). Both interpreted their presence as suggesting a shallow water environment during deposition of the iron-formation.

Quartz crystal tuff

Overlying the iron-formation is a more or less continuous horizon of quartz porphyry. Locally, beds rich in lithic clasts (of pelitic/psammitic composition) occur, suggesting that the porphyry is a tuffaceous unit. At the contact with the iron-formation a chlorite-rich matrix is common, grading northwards into a sericite-dominated matrix. Recrystallized lapilli (?) and orthoclase phenocrysts are minor components in the dominantly siliceous matrix.

Mesoscopic similarities with the footwall quartz crystal tuff are striking and it is only the stratigraphic position of this unit that differentiates the two.

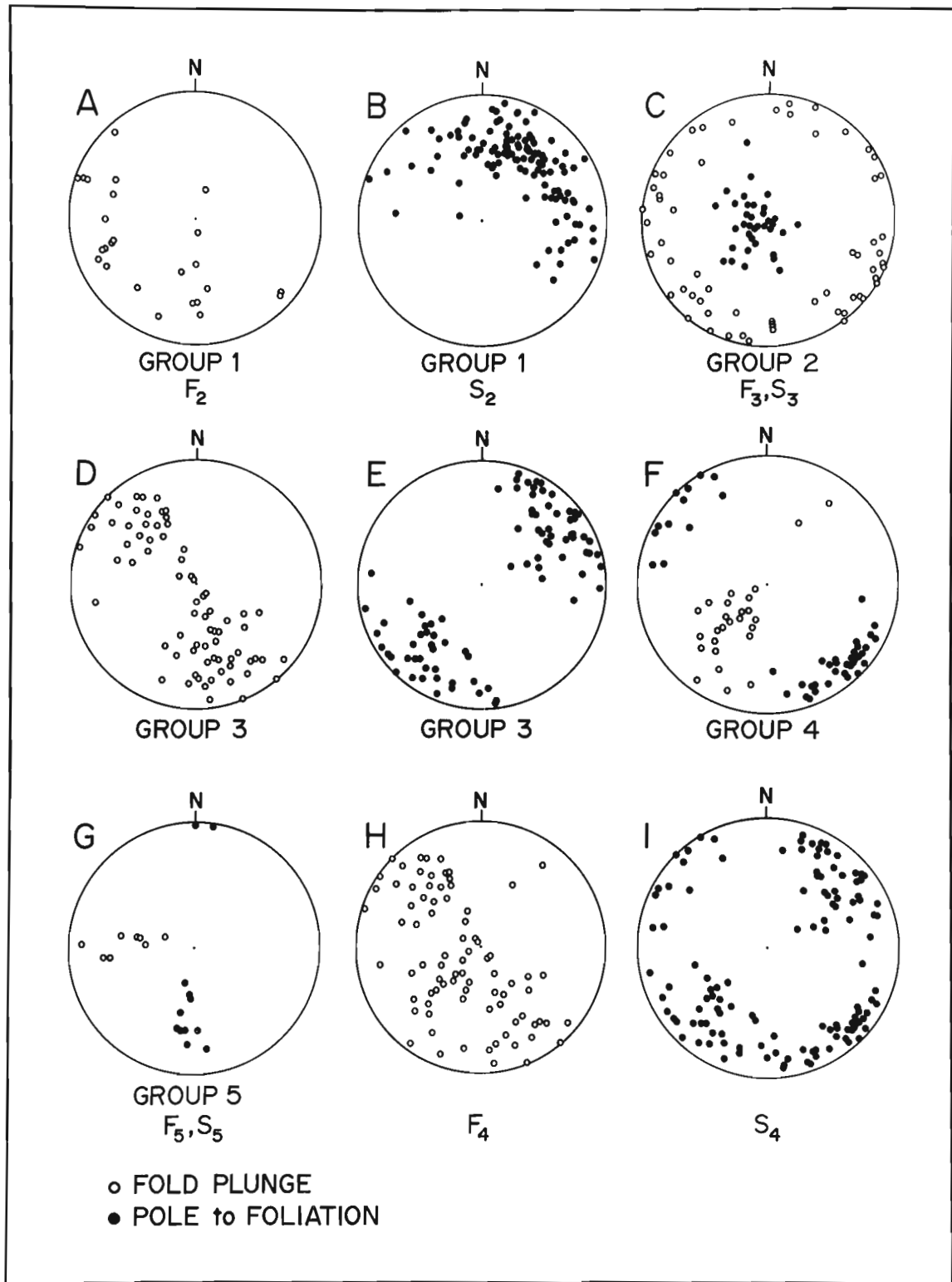


Figure 7.4. Lower hemisphere equal area projections for fold plunges and poles to foliations divided into both style/orientation groups (e.g. Group 1) and fold generations (e.g. F_3). Figures 7.4H and I combine groups 3 and 4.

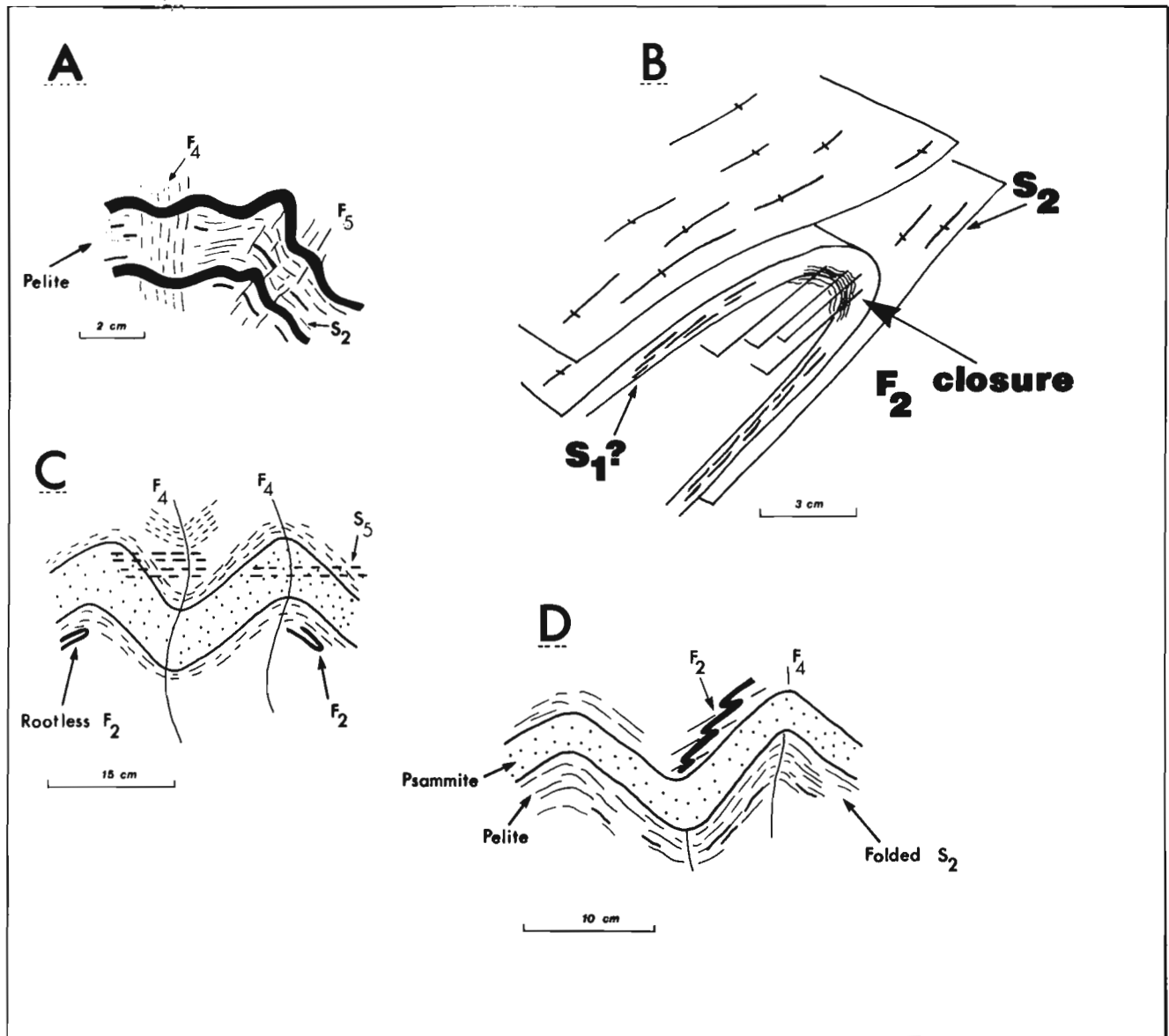


Figure 7.5. Examples of overprinting relationships (at various scales) observed at Heath Steele Mines.

Quartz-feldspar porphyry

A wide outcrop of banded quartz-feldspar porphyry is exposed in the hanging wall of the B-zone. A "clean" appearance is typical, as are pulled-apart feldspar phenocrysts that define a stretching lineation parallel to F_2 fold axes. Banding reflects variations in the phenocryst content, lithic clast content and mineralogical changes in the matrix.

In summary, a mixed sequence of volcanic and sedimentary rocks is exposed at Heath Steele Mines. The favourable horizon for mineralization is the contact of the footwall sedimentary sequence and the hanging wall quartz-feldspar porphyry. Although classified as a base metal volcanogenic massive sulphide deposit (Franklin et al., 1981) it should be noted that there is a significant sediment component to the footwall rocks; "millrock" type lithologies (Sangster, 1972) are not present.

Mesoscopic structural observations

Unequivocal overprinting relationships are not common at Heath Steele Mines. Consequently, the first step in determining

a structural history is the establishment of groups of structures on the basis of style and orientation. Using these criteria five style/orientation groups can be defined (Fig. 7.4).

Group 1

Rootless, intrafolial folds in quartz veins are characteristic although locally group 1 folds are defined by a folded foliation (Fig. 7.5B). In the latter case the axial plane foliation is a crenulation cleavage and this is thought to be the cleavage type for all group 1 folds. Typically, this foliation, known as the main foliation, dips at moderate to steep angles towards the southwest (Fig. 7.4B).

Group 1 fold plunges are variable (Fig. 7.4A) since the majority of the data are from folds in quartz veins. They define a girdle coincident with the main foliation. Since the group 1 folds are isoclinal, any layering present in the rocks is parallel to the axial plane crenulation cleavage, except in fold hinges. The main foliation is therefore a transposition surface (see e.g. Hobbs et al., 1976; Williams, 1983) defined by both the axial plane cleavage and all earlier surfaces rotated into the same orientation.

Group 2

Horizontal folds with flat or gently inclined axial surfaces are distinctive structures at Heath Steele Mines and are labelled as group 2 structures. These folds have an open form (interlimb angle $> 90^\circ$) and an axial plane crenulation cleavage. Group 2 folds form a horizontal girdle (Fig. 7.4C) coincident with the intersection of the axial surface with the various orientation of the group 1 foliation.

Groups 3 and 4

Folds belonging to these groups are considered together because of their similarity in style: they are open, vertical folds with an axial plane crenulation cleavage, locally defined by mica-rich layers. The two groups are differentiated on the basis of orientation: group 3 fold plunges define a NW/SE girdle (Fig. 7.4D) whereas group 4 folds plunge predominantly to the SW (Fig. 7.4F). Axial surfaces of both groups dip steeply and trend NW/SE for group 3 and NE/SW for group 4 (Fig. 7.4E, F).

Group 5

Group 5 folds are rare and have only been documented in exposures adjacent to the B1 open pit. Typically they are open to tight folds of quartz veins, plunging at moderate angles to the west. They have an axial plane crenulation cleavage which is vertical or steeply dipping to the north.

Overprinting relationships

From a limited amount of overprinting observed in surface and underground exposures some constraints can be placed on the relative ages of folds of the five style/orientation groups. The most consistently developed mesoscopic overprinting relationship is that of a foliation cutting an older fold closure (Fig. 7.5); true fold interference patterns are rarely observed.

Group 1 structures are overprinted by folds of all other style/orientation groups implying that the rootless, intrafolial folds and their associated axial planar cleavage, are the oldest folds on the mine property. However, some group 1 folds are seen to fold an earlier foliation, the origin of which could be interpreted as either sedimentary or tectonic. We have no cogent evidence for either origin but interpret the foliation as tectonic on the basis of observations made outside the area described here. Pre-main foliation folds have been recognized in the Brunswick Mines (van Staal and Williams, 1984) and the Sevogle River areas (Irrinki, 1979; Cullen, 1984) and several writers have claimed a pre-main foliation deformation on the grounds of an earlier foliation (Helmstaedt, 1971; McBride, 1976). Thus, we interpret group 1 structures as products of a second generation deformation and name them F_2 and S_2 .

In underground exposures group 2 folds overprint F_2 folds and are themselves overprinted by a group 4 foliation. Thus group 2 is younger than F_2 and older than group 4. No overprinting relationships have been observed for group 3 structures so that we have no basis for ascribing them to a generation. Since they have the same style as group 4 and since, in geometrical terms, groups 3 and 4 form a conjugate pair we tentatively group them together. Group 5 overprints groups 3 and 4 making it the youngest generation. Thus, in summary, we interpret group 2 as third generation (F_3 and S_3), groups 3 and 4 as fourth generation (F_4 and S_4) and group 5 as fifth generation (Fig. 7.4).

Macroscopic structure

The B-zone is basically a north-dipping, tabular body of sulphides that is locally modified by small folds. There are



Figure 7.6. Geological cross-section of the B-zone. Legend same as Figure 7.3 (from Davies et al., 1984).

isoclinal folds that have their axial surfaces oriented parallel to the enveloping surface to the orebody as well as more open folds that have axial surfaces inclined at various angles to the enveloping surface (Fig. 7.6).

Poles to the S_2 transposition define a fully occupied girdle with a maximum indicating a dominant southwesterly dip. The

girdle suggests a southwesterly plunging fold which is approximately parallel to the group 4 (F_4) folds. However, these folds are too open ($>90^\circ$) to account for the girdle. Further possibilities that may explain the S_2 distribution is that the girdle is due either to incomplete transposition of earlier foliations into the S_2 orientation or that it is a result of a combined affect of both fold generations (F_2 and F_4). To distinguish between these possible interpretations it is necessary to establish smaller domains (Turner and Weiss, 1963 p. 94) and to this end more detailed measurement is in progress.

Since we cannot define S_2 domains (i.e. S_2 occupies a girdle rather than a point maximum) the remaining data plots cannot be adequately interpreted. Never-the-less two points can be discussed concerning the S_2 foliation:

1) S_2 dips predominantly to the south (Fig. 7.4B; see also McBride, 1976) and is nowhere parallel to the orebody, which dips north (Fig. 7.6). S_2 is known to be a transposition foliation and where layering can be recognized adjacent to the orebody contact, the two are parallel (McAllister personal communication, 1986). Thus, the orebody must define the regional enveloping surface. The only alternative interpretation is that the orebody is discordant to S_2 . We consider this unlikely in view of the parallelism of the layering and orebody contact.

2) Those folds in the orebody with axial surfaces parallel to the enveloping surface may be overprinted by S_2 but exposure does not allow this interpretation to be confirmed. The point is, their axial planes are inclined to the general S_2 orientation and it is unlikely that they are younger than S_2 in view of their tightness. They may, therefore, be F_1 folds. Another possibility is that they are F_2 folds and where S_2 passes into the incompetent orebody layer it is strongly refracted. Because the orebody is generally inaccessible such a refraction would not be reflected in our observations.

Conclusion

The B-zone at Heath Steele Mines is a north-dipping, tabular body of base metal sulphides. Franklin et al. (1981) classified it as volcanogenic even though the bulk of the footwall rocks are metasediments. Quartz crystal tuffs are interbedded with the metasediments but the majority of volcanic rocks are exposed in the hanging wall (quartz and quartz-feldspar porphyry). Four facies of iron-formation are present: sulphide, silicate, carbonate and oxide. The latter facies is a discontinuous capping to the sulphides exposed in the hanging wall.

A structural history for the B-zone is difficult to define because of a lack of unequivocal overprinting relationships. It is necessary to first define fold groups and then interpret their relative ages through the use of limited overprinting of structures belonging to different groups. Five fold generations are documented using this technique, although the earliest generation structure (F_1) is inferred. In contrast to previous workers we note that the main foliation (S_2) is, in general, inclined to the orebody and interpret the orebody as being parallel to the F_2 enveloping surface.

Acknowledgments

A.L. McAllister criticized the draft manuscript.

References

- Cullen, R.C.
1984: Structural geology of the North Branch Big Seovgle River; Unpubl. B.Sc. thesis, University of New Brunswick, 70 p.
- Davies, J.L.
1980: Geology of the Bathurst-Newcastle area; Geological Association of Canada, Annual Meeting, Halifax, May 1980, Field Trip Guidebook 16, p. 1-16.
- Davies, J.L., Fyffe, L.R. and McAllister, A.L.
1984: Geology and massive sulphides of the Bathurst area, New Brunswick; in Field Trip Guidebook to Stratabound Sulphide Deposits, Bathurst Area, N.B., Canada and West-Central New England, U.S.A., ed. D.F. Sangster; Geological Survey of Canada, Miscellaneous Report 36, p. 16-21.
- Franklin, J.M., Lydon, J.W., and Sangster, D.F.
1981: Volcanic-associated massive sulphide deposits; Economic Geology, 75th Anniversary Volume, p. 485-627.
- Fyffe, L.R., Pajari, G.E. Jr., and Cherry, M.E.
1981: The Acadian plutonic rocks of New Brunswick: Maritime Sediments and Atlantic Geology, v. 17, p. 23-26.
- Helmstaedt, H.
1971: Structural geology of Portage Lake area, Bathurst-Newcastle district, New Brunswick; Geological Survey of Canada, Paper 70-28, 42 p.
- Hobbs, B.E., Means, W.D., and Williams, P.F.
1976: An Outline of Structural Geology; Wiley, New York, 571 p.
- Irrinki, R.R.
1979: Geology of North and South Little Seovgle Rivers, North Branch Little Southwest Miramichi River, McKendrick and Catamaran Lakes. Map areas 0-12, N-13 part of 21-J16; Mineral Resources Branch, Department of Natural Resources, New Brunswick. Map Report 79-1.
- McBride, D.E.
1976: The structure and stratigraphy of the B-zone, Heath Steele Mines, Newcastle, New Brunswick; Unpublished Ph.D. thesis, University of New Brunswick, 227 p.
- McDonald, D.W.A.
1984: Fragmental pyrrhotite ore at Heath Steele Mines, New Brunswick; Unpublished M.Sc. thesis, University of New Brunswick, 177 p.
- McMillan, R.N.
1969: A comparison of geological environments of the base metal sulphide deposits of the B-zone and North Boundary zone at Heath Steele Mines, New Brunswick; Unpublished M.Sc. thesis, University of Western Ontario, 192 p.
- Owsiacki, L.
1980: The geology of the C-zone, Heath Steele Mines, New Brunswick; Unpublished M.Sc. thesis, University of New Brunswick, 226 p.

- Owsiacki, L. and McAllister, A.L.
1979: Fragmental massive sulphides at Heath Steele Mines, New Brunswick; Canadian Institute of Metallurgy and Mining, Bulletin, p. 93-100.
- Sangster, D.F.
1972: Precambrian volcanogenic massive sulphide deposits in Canada: A review; Geological Survey of Canada, Paper 72-22, 44 p.
- Skinner, R.
1974: Geology of the Tetagouche Lakes, Bathurst and Nepisiguit Falls map-areas, New Brunswick; Geological Survey of Canada, Memoir 371, 133 p.
- Turner, F.J. and Weiss, L.E.
1963: Structural Analysis of Metamorphic Tectonites; McGraw-Hill, New York, 545 p.
- van Staal, C.R. and Williams, P.F.
1984: Structure, origin and concentration of the Brunswick No. 12 and No. 6 orebodies; Economic Geology, v. 79, p. 1669-1692.
- Williams, P.F.
1983: Large scale transposition by folding in northern Norway; Geologischt Rundschau, v. 72, p. 589-604.

Paleomagnetism of Neohelikian Korok sheets and dykes, and of a possible Mackenzie dyke from southeast of Ungava Bay

Project 840020

W.F. Fahrig
Lithosphere and Canadian Shield Division

Fahrig, W.F., Paleomagnetism of Neohelikian Korok sheets and dykes, and of a possible Mackenzie dyke from southeast of Ungava Bay; in Current Research, Part B, Geological Survey of Canada, Paper 86-1B, p. 65-71, 1986.

Abstract

Neohelikian Korok sheets and dyke from southeast of Ungava Bay whose ages are between 1350 and 1400 Ma have a paleopole at $133^{\circ}\text{W}, 09^{\circ}\text{S}$. A second dyke also from this area yielded a virtual pole at $166^{\circ}\text{W}, 03^{\circ}\text{N}$ which is close to the poles of the 1220 Ma Mackenzie dykes.

Résumé

Les strates et le dyke Korok du Néohélikien situés au sud-est de la baie Ungava et dont l'âge varie de 1 350 à 1 400 Ma comportent un paléopôle se situant à $133^{\circ}\text{W}, 09^{\circ}\text{S}$. Un deuxième dyke de cette région comporte un pôle virtuel se situant à $166^{\circ}\text{W}, 03^{\circ}\text{N}$, ce qui se rapproche des pôles des dykes du Mackenzie datant de 1 220 Ma.

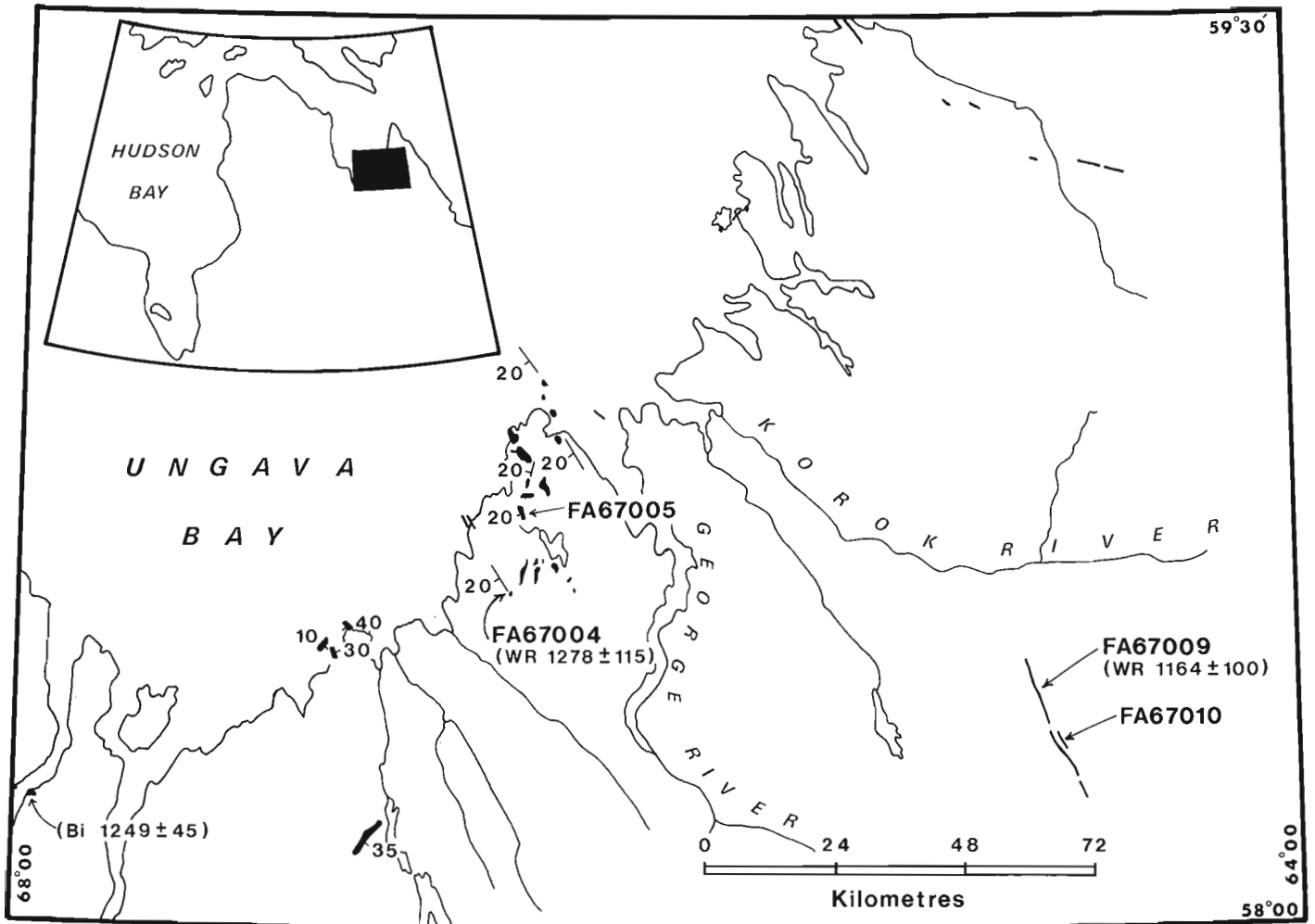


Figure 8.1. Neohelikian sheets (Korok) and dykes (Korok and Mackenzie?) southeast Ungava Bay (Taylor, 1979). Locations sampled for paleomagnetic study and for K-Ar age determinations (WR = whole-rock; Bi = biotite). Thick strike symbols indicate sheets, thinner symbols the strike of a nearby sheet.

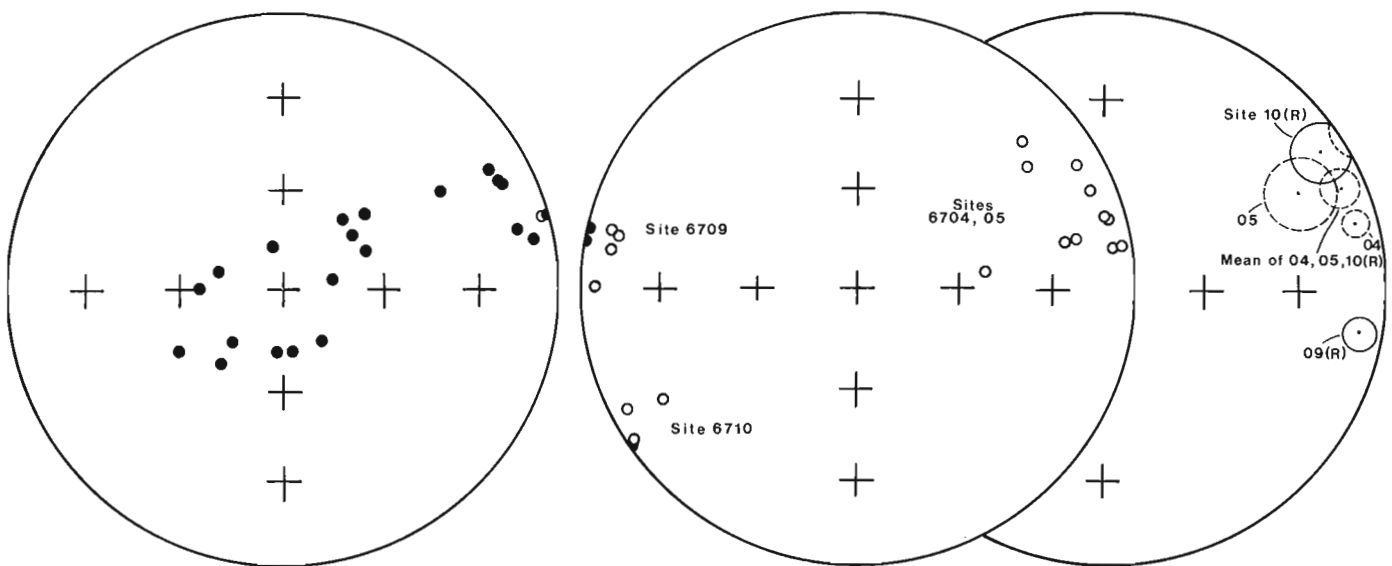


Figure 8.2. Sample directions before (left) and after (centre) AF cleaning. Solid circles down directions, open circles up directions. Site mean directions (right) with circles of confidence (dashed circles, up direction; continuous circles, down direction). Note that sites FA6709 and 10 have been reversed (R) in the right diagram.

Introduction

Although diabase related to the Korok sheets and dykes may have been described previously from elsewhere in the shield, the main body of intrusions was first described by Taylor (1979) under the heading "Neohelikian diabase". As he indicated, the intrusions southeast of Ungava Bay (Fig. 8.1) occur predominantly in the form of gently SSW dipping sheets with, in some localities, the sheets lying in the plane of the host gneisses. Taylor concluded from regional structural consideration that the tilt of the sheets is primary. The sheets range in thickness up to a few tens of metres but in many places are only a few metres thick. Taylor (1979) reported 2-10% olivine in the diabase of these sheets. Three chemical analyses, one of chilled, and two of coarser material from the sheets, and four from dykes, two chilled and two coarse, indicate that the dykes are somewhat more alkalic than are the sheets. The sheets contain about 10% normative olivine whereas the dykes contain almost twice this. Samples from the chilled margins of both dykes contain small amounts of normative nepheline.

The locations from which Neohelikian diabase material was taken for K-Ar age determinations are also indicated on Figure 8.1. Two analyses were reported by Taylor (1979) on chilled material from the edges of the intrusions, and a third on a biotite concentrate. The ages on Figure 8.1 and mentioned below are slightly higher than those quoted by Taylor (1979) because they have been recalculated using the

modern decay constant. One biotite and one chilled whole-rock yielded ages of 1249 ± 45 Ma and 1278 ± 115 Ma respectively, suggesting an age of intrusion between 1350 and 1400 Ma. A third analysis on chilled material from a 25 km long NNW-trending dyke yielded 1164 ± 100 Ma. This age may be significantly different from the two mentioned above, particularly in the light of paleomagnetic results. This would support Taylor's suggestion of two unrelated Neohelikian mafic intrusive events in this part of the Canadian Shield.

Paleomagnetic sampling and laboratory results

Twenty-two samples were drilled from four Neohelikian intrusions (Fig. 8.1) and separately oriented by solar compass. Two specimens were cut from each core and one specimen from each core was AF demagnetized in ten to fifteen steps. At least one specimen from each site was subjected to detailed thermal demagnetization. The remaining specimens were AF demagnetized in five or more steps (Fig. 8.2). Initial intensities ranged from .14 to 1.6 A/m.

Site FA6704. All six samples of this diabase sheet proved to be exceptionally stable in response to both AF and thermal demagnetization (Fig. 8.3). The samples contained only one significant component with a slightly up ENE direction. This is unusual since diabase almost invariably contains a sizable soft component related to the recent earth's field direction.

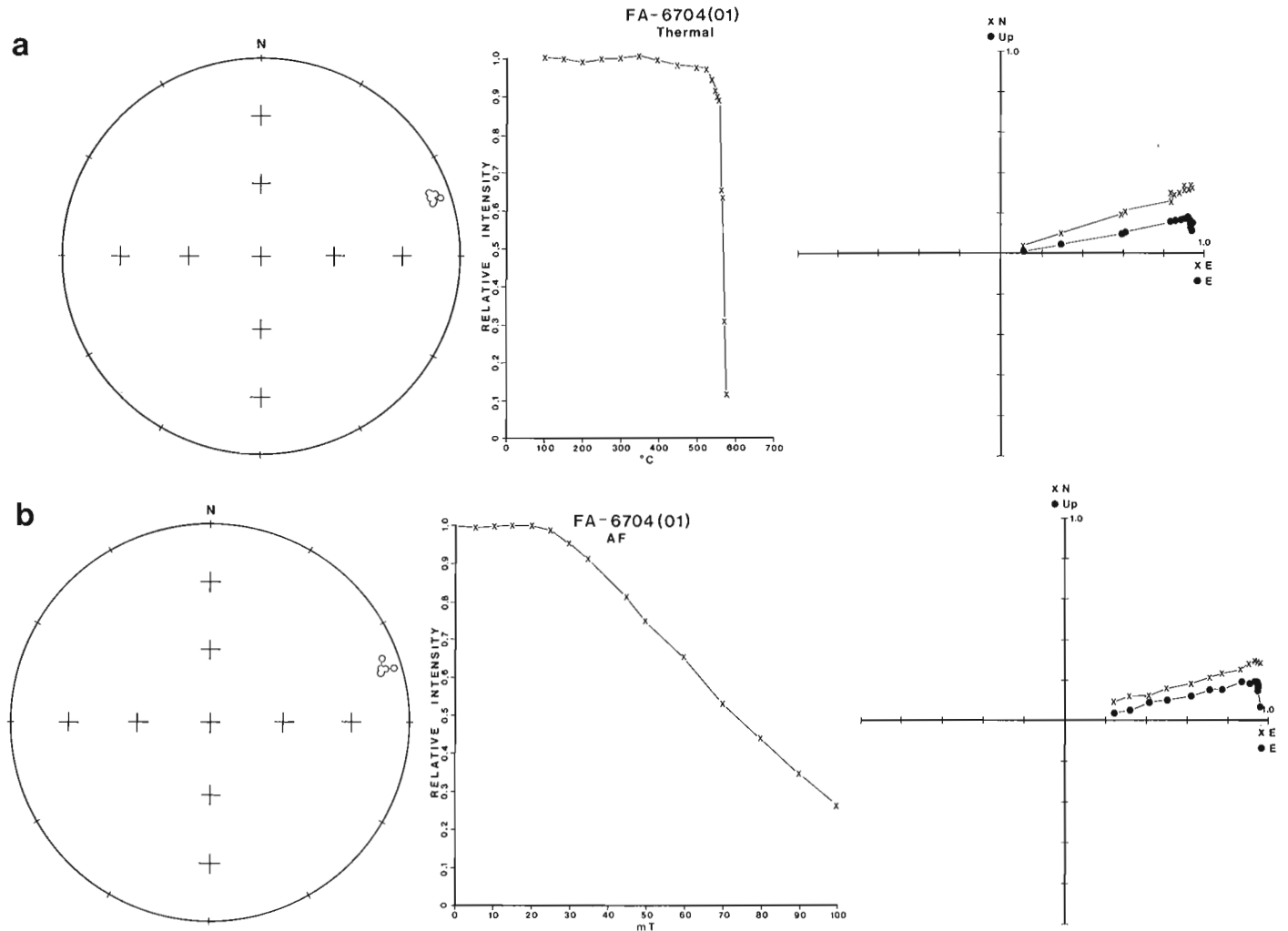


Figure 8.3. Characteristic response of specimens from site FA6704 to thermal (a) and alternating field (b) demagnetization.

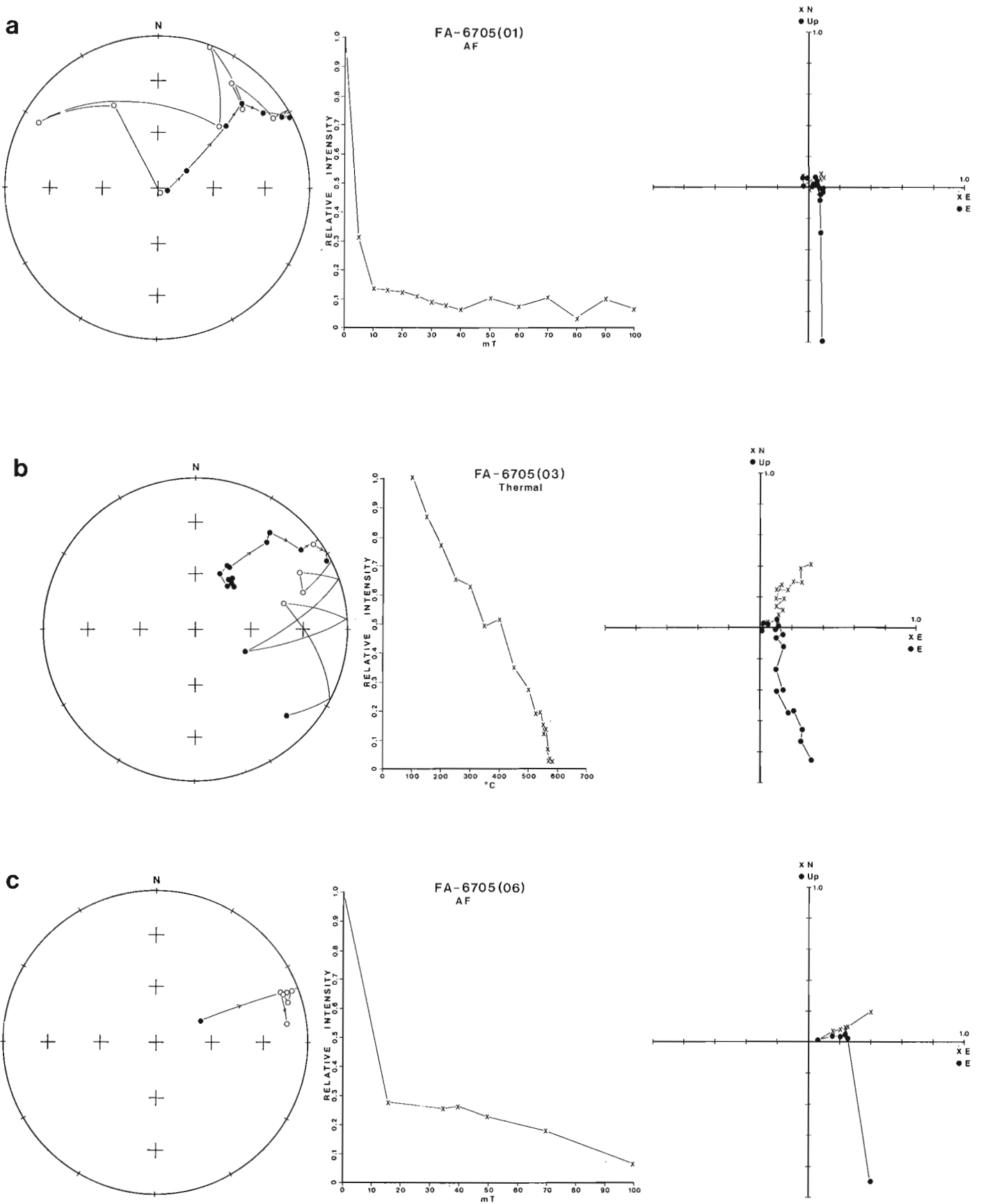


Figure 8.4. Characteristic response of specimens from site FA6705 to alternating field demagnetization to 100 mT (a) and (b) and thermal (c) demagnetization.

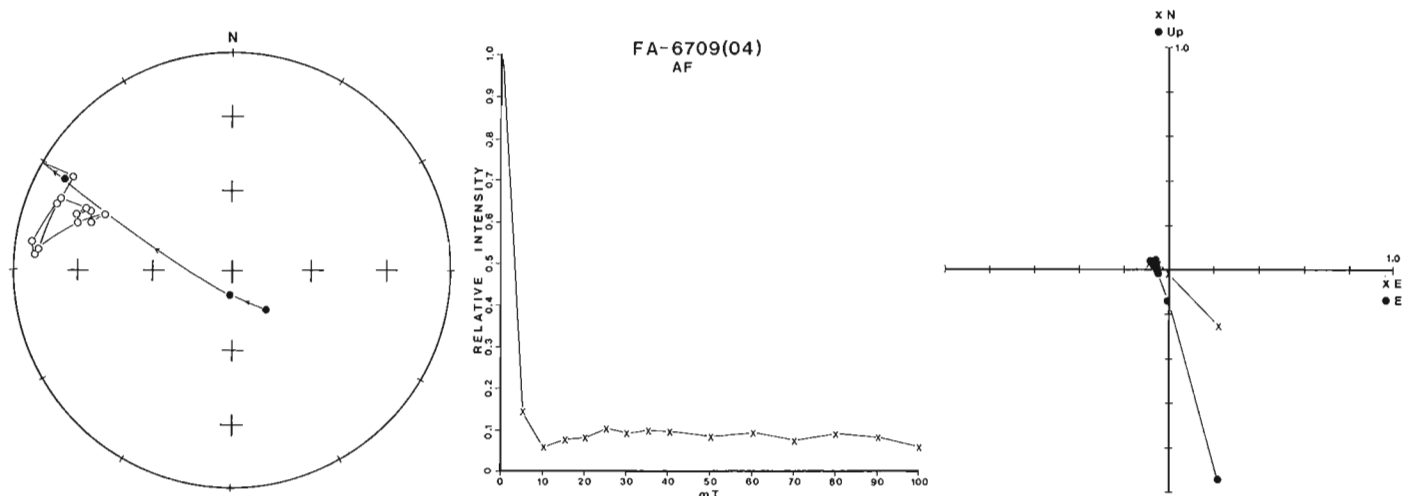


Figure 8.5. Characteristic response of specimens from site FA6709 to alternating field demagnetization.

Table 8.1. Paleomagnetic data for 3 Korok sites and one possible Mackenzie site

Site	N	D	NRM			AF (mT)	D	Cleaned		
			I	K	α_{95}			I	K	α_{95}
KOROK										
FA6704	6	069.0°	08.0°	59	9°	800	074.5°	-07.5°	192	05.0°
FA6705	5*	060.0°	47.5°	12	23°	350-800	063.0°	-21.0°	34	13.0°
FA6710	4	239.0°	66.0°	32	17°	800	237.0°	-08.0°	66	11.5°
Mean direction of 3 sites above (FA6710 reversed) n = 15, D = 066.2°, I = -07.9°, K = 24, α_{95} = 8°										
Mean pole position from mean direction 133.4°W, 08.7°S, dm = 8.0°, dp = 4.0°										
Mean pole position from site poles (FA6710 reversed) n = 3, 132.4°W, 09.7°S, K = 48, α_{95} = 18°										
MACKENZIE										
FA6709	6	168.5°	84.5°	20	15°	800	281.5°	-07.0°	125	06.0°
Virtual pole from site mean direction 166.3°W, 2.8°N, dm = 6.0°, dp = 3.0°										
N = number of cores collected at a site; D = declination; I = inclination K = Fisher's estimate of precision; α_{95} = semi axis of circle of confidence at P = .05; AF = peak alternating field; dm,dp = semi axes of ellipse of confidence at P = 0.05, n = number of sets of data used in calculation of the mean. *The results from one sample of this site were not included because the cleaned direction was more than two standard deviations away from the site mean direction.										

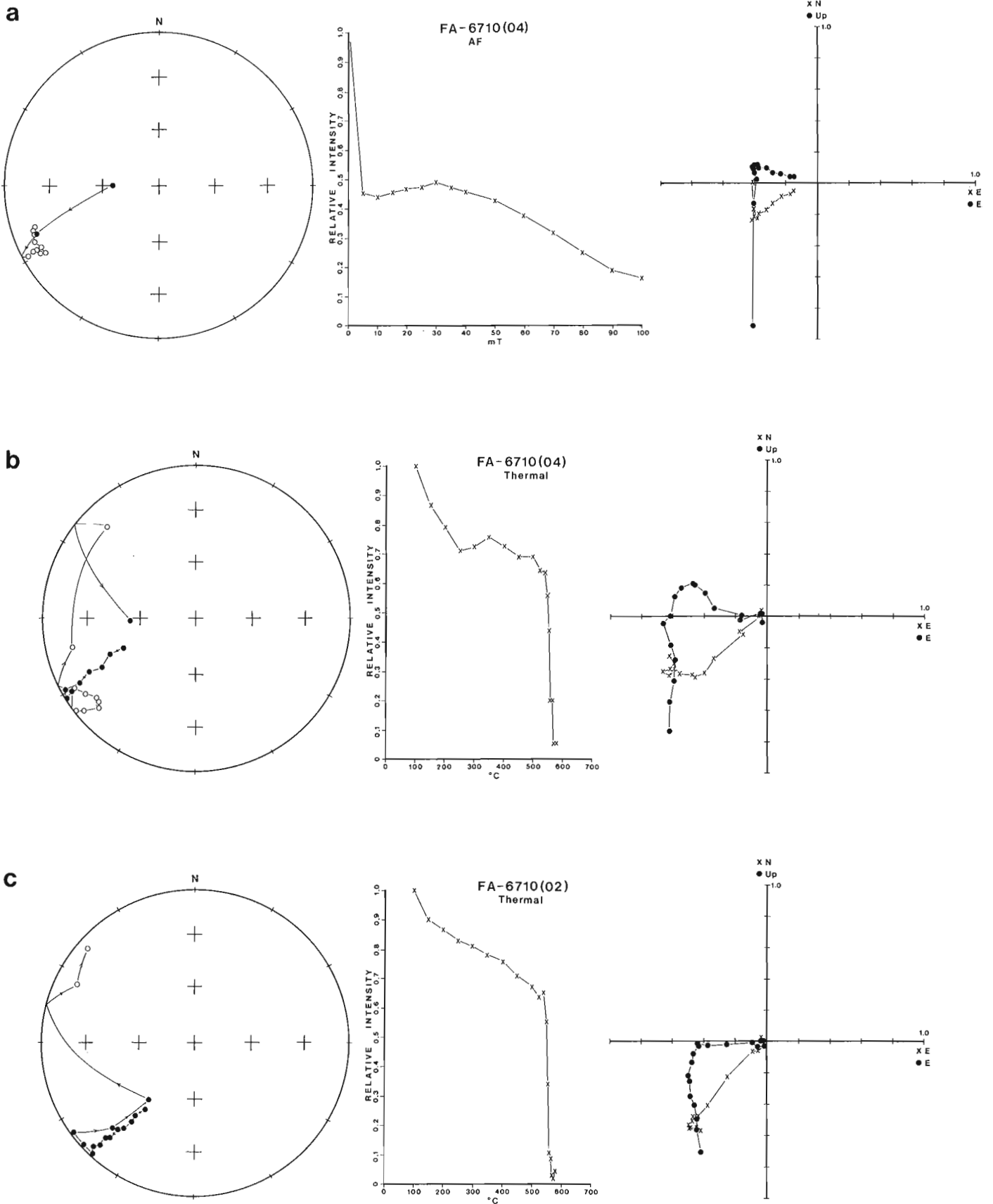


Figure 8.6. Characteristic response of specimens from site FA6710 to alternating field (a) and thermal demagnetization (b) and (c).

Site FA6705. Specimens from this site were far less stably magnetized than those of FA6704 containing both the ENE up component and a significant steeply down component. Results of AF and thermal demagnetization of stably and less stably magnetized specimens are illustrated on Figure 8.4. The high field, high temperature component has a direction similar to that of FA6704.

Site FA6709. Specimens of this dyke site contained a strong steeply down component removed by AF cleaning at 10 mT. AF cleaning to 100 mT revealed only a stable WNW up component (Fig. 8.5).

Site FA6710. The specimens of this dyke site were very stably magnetized, a soft steeply down component being removed by AF cleaning at 5 to 10 mT. The single stable component isolated by AF and thermal demagnetization has a shallow SW up direction (Fig. 8.6).

Interpretation

Paleomagnetic results suggest that two of the sheets sampled, FA6704 and FA6705, and one dyke, FA6710, are the results of a single igneous episode; although FA6710 is reversed relative to the other two sites (Table 8.1). The pole position for these sites at 133.4°W, 09.0°S is close to those of similar age (1350-1400 Ma) from the Canadian Shield (Irving et al., 1972; Berger and York, 1980; and the overprint referred to in the Mistassini dykes of Fahrig et al. (in press) and consistent with the 1350-1400 Ma indicated by K-Ar dating. The paleomagnetic result suggests an age closer to 1400 Ma.

The fourth site, FA6709 from a dyke 25 m thick and 25 km long yielded a virtual pole at 166.3°W, 2.8°N which is close to that for the 1220 Ma Mackenzie igneous rocks (Fahrig and Jones, 1969; Patchett et al., 1978). The chilled whole-rock K-Ar age of 1164 ± 100 Ma is also consistent with a Mackenzie age. This introduces the possibility that Mackenzie dykes extended into this part of the Shield.

References

- Berger, G.W. and York, D.
1980: Reinterpretation of the North American apparent polar wander curve for the interval 800-1500 Ma; Canadian Journal of Earth Sciences, v. 17, p. 1229-1235.
- Fahrig, W.F. and Jones, D.L.
1969: Paleomagnetic evidence for the extent of Mackenzie igneous events; Canadian Journal of Earth Sciences, v. 6, p. 679-688.
- Fahrig, W.F., Christie, K.W., Chown, E.H., Jones, D., and Machado, N.
- The tectonic significance of some basic dyke swarms in the Canadian Superior Province with special reference to the geochemistry and paleomagnetism of the Mistassini swarm, Quebec, Canada; Canadian Journal of Earth Sciences. (in press)
- Irving, E., Park, J.K., and McGlynn, J.C.
1972: Paleomagnetism of the Et-Then Group and Mackenzie diabase in the Great Slave Lake area; Canadian Journal of Earth Sciences, v. 9, p. 744-755.
- Patchett, P.J., Bylund, G. and Upton, B.G.J.
1978: Paleomagnetism and the Grenville Orogeny: new Rb-Sr ages from dolerites in Canada and Greenland; Earth and Planetary Science Letters, v. 40, p. 349-364.
- Taylor, F.C.
1979: Reconnaissance geology of a part of the Precambrian Shield, Quebec, Northern Labrador and Northwest Territories; Geological Survey of Canada Memoir 393, 99 p.

An isotopic evaluation of sulphur recycling from evaporites to coals in the Carboniferous Sydney Basin, Nova Scotia

EMR Research Agreement 233/04/85

Martin R. Gibling¹, Marcos Zentilli¹, Hadi Mahony¹, and
Ronald G.L. McCready²

Gibling, M.R., Zentilli, M., Mahony, H., and McCready, R.G.L., An isotopic evaluation of sulphur recycling from evaporites to coals in the Carboniferous Sydney Basin, Nova Scotia; in *Current Research, Part B, Geological Survey of Canada, Paper 86-1B*, p. 73-76, 1986.

Abstract

The ratios of ^{32}S and ^{34}S were analyzed for pyrite and soluble sulphate extracted from twelve coal samples from the Pennsylvanian Morien Group and for eight gypsum and anhydrite samples from the Mississippian Windsor Group that underlies the Sydney Basin, Nova Scotia. The evaporite samples show a narrow range of $\delta^{34}\text{S}$ values averaging above +15‰, whereas the coal pyrite and soluble sulphate show a wide range of $\delta^{34}\text{S}$ values averaging about +15‰ to -5‰. The results are consistent with the hypothesis that the sulphur in the coals was derived from dissolution of Windsor evaporites, with anaerobic reduction of sulphate to pyrite in the Morien peat swamps, followed by chemical transformation of sulphate to pyrite during burial and coalification.

Résumé

Les rapports de ^{32}S et ^{34}S ont été analysés dans de la pyrite et du sulfate soluble extraits de douze échantillons de charbon provenant du groupe pennsylvanien de Morien et de huit échantillons de gypse et d'anhydrite du groupe mississippien de Windsor sous-jacent au bassin Sydney en Nouvelle-Écosse. Les échantillons d'évaporite révèlent une gamme étroite de valeurs $\delta^{34}\text{S}$ dont la moyenne est d'environ de +15%, tandis que la pyrite de charbon et le sulfate soluble révèlent une large gamme de valeurs $\delta^{34}\text{S}$ dont la moyenne se situe entre +15% et -5%. Les résultats confirment l'hypothèse selon laquelle le soufre contenu dans les charbons provient de la dissolution d'évaporites du groupe de Windsor, le sulfate a été transformé en pyrite par réduction anaérobie dans les tourbières du Morien, et par suite le sulfate a été transformé chimiquement en pyrite au cours de l'enfouissement et de la houillification.

¹ Department of Geology, Dalhousie University, Halifax, Nova Scotia B3H 3J5

² Biotechnology Section, Mineral Sciences Laboratories, CANMET, 555 Booth Street, Ottawa, Ontario K1A 0G1

Introduction

High sulphur contents in coals are normally explained by the proximity of the original peat to marine waters during deposition (Williams and Keith, 1963; Casagrande et al., 1977). The abundant sulphate ions in seawater provide a ready source of sulphur which can be incorporated into the sediment as iron disulphides and as organically-bound sulphur by inorganic and biochemical processes. Sulphur-rich coals normally occur in marginal marine settings, such as back-barrier and coastal swamps, or are intercalated with marine bands formed by periodic flooding of the swamps by the sea (Horne et al., 1978).

The Carboniferous Sydney Basin contains Canada's major economic coal seams, which form part of the Morien Group of Pennsylvanian age (Hacquebard, 1983). The sulphur content of some seams reaches 8% by weight and restricts the commercial utilization of the coal. No marine strata have been discovered in the Morien Group, and the sedimentary evidence indicates deposition on broad alluvial plains with an entirely freshwater biota (Hacquebard and Donaldson, 1969; Rust et al., 1983; Gibling and Rust, 1984). Proximity to a marine source of sulphate cannot be adduced to explain the high levels of sulphur in the coals.

An alternative hypothesis for the sulphur enrichment was outlined by Haites (1951), following earlier work by Bell (1928) and Newman (1935). He suggested that the sulphur was derived from dissolution of evaporites in the Mississippian Windsor Group which underlies the Morien Group. The Morien river could have carried a high dissolved load of sulphate ions, which could have been transported into the peat swamps. The sulphur content in some seams is higher adjacent to fluvial sandstone bodies (Newman, 1935). A similar hypothesis was applied to the Minto coals of New Brunswick by Hacquebard and Barss (1970). The Windsor Group in the region contains thick sulphate-evaporites (Boehner, 1983) and locally forms an erosional surface over which the Morien Group was deposited.

Tests for Windsor evaporites as a sulphur source

Anhydrite and gypsum of the Windsor Group in mainland Nova Scotia have $\delta^{34}\text{S}$ values of about +14‰, reflecting their derivation from Mississippian seawater (Akande and Zentilli, 1984; Thode and Monster, 1965). If no isotopic fractionation occurred during evaporite dissolution, soluble sulphate carried to the Morien swamps should have had a $\delta^{34}\text{S}$ of about +14‰ (McCready and Krouse, 1980). During the decomposition of plant material, an anaerobic environment develops in peat swamps allowing anaerobic reduction of sulphate in groundwaters to H_2S (Casagrande et al., 1977). Numerous studies indicate that the H_2S is enriched in the lighter ^{32}S isotope by 15‰ or more and reacts with indigenous heavy metal ions to produce biogenic metal sulphides (McCready, 1975; Kaplan, 1975). Primary pyrite produced within the swamps should have $\delta^{34}\text{S}$ values of -1‰ or less (Sweeney and Kaplan, 1973; Kemp and Thode, 1968; Goldhaber and Kaplan, 1974).

During burial and the transformation of peat to coal with increasing pressure and temperature, organic sulphur and sulphate esters indigenous to the peat may be reduced chemically to H_2S and subsequently react with metal ions, producing secondary metal sulphides (Casagrande et al., 1977). However, because these are produced chemically at higher temperatures, the isotopic fractionation will be much less than that observed in the biogenic metal sulphides (Sakai, 1968).

Cape Breton coals contain average values of about 4% pyritic sulphur, 1% organic sulphur, and 1% sulphur as inorganic sulphate (McCready, 1983, 1984). If the sulphate is

residual sulphate which has not undergone biological reduction or chemical transformation during coal diagenesis, it should be enriched in the heavier isotope (McCready et al., 1975, 1976; Krouse and McCready, 1979), resulting in $\delta^{34}\text{S}$ values more positive than +14‰. The associated pyrite should have a $\delta^{34}\text{S}$ value of about -1‰, if it has originated by anaerobic decomposition.

The geochemical model outlined above involves several assumptions. Firstly, the model assumes a closed system in which soluble sulphate is partitioned between pyrite, organically-bound sulphur and residual sulphate in solution, all of which are retained within the sediment. Secondly, the model tests the probability that the sulphur isotope values are compatible with derivation from Mississippian sulphates; although there were progressive changes in seawater composition during the Carboniferous, the tests are unlikely to preclude a Pennsylvanian seawater source.

Sampling and analysis

Twelve coal samples were obtained from drillcore, mine workings and outcrop of the Gardiner, Sydney Main, Hub and Point Aconi seams of the Sydney Basin. Two seams were sampled layer by layer through the entire thickness. The pyrite is in the form of small grains and aggregates up to a few tens of microns in diameter, apart from the sample from the Point Aconi seam which was a large (ca. 5 cm) pyritic nodule collected from outcrop. Four gypsum and four anhydrite samples were selected from the Kempt Head 84-1 drillcore in the Sydney Basin, located close to coal sample localities. The evaporite samples were spaced evenly through 318 m of core and are considered to be representative of the evaporites in the upper part of the Windsor Group. Their mineralogical purity was checked by X-ray diffraction analysis.

The coal samples were finely crushed, split, and pyrite was separated from coal dust using the heavy liquid tetrabromoethane. The pyrite was converted to barium sulphate prior to analysis. Soluble sulphate was extracted from an additional subsample and converted to barium sulphate (American Society for Testing and Materials, 1977). The sulphur from the pyrite, soluble sulphate, gypsum and anhydrite was analyzed for sulphur isotopes by C.C. McMullen at McMaster University. Two duplicated pyrite samples showed differences in $\delta^{34}\text{S}$ of 0.3 and 2.1‰, and two duplicated evaporite samples showed differences of 0.1 and 0.3‰.

Results

The evaporite samples showed low variability in $\delta^{34}\text{S}$, ranging from +15.8 to +14.55‰ (Table 9.1). Gypsum and anhydrite showed similar values, and no vertical trends in δ values were observed through the stratigraphic section sampled. The values lie close to those for Windsor evaporites elsewhere in Nova Scotia (Akande and Zentilli, 1984) and to mean values for Mississippian seawater (Thode and Monster, 1965).

The pyrite samples from the coals showed high variability in $\delta^{34}\text{S}$, ranging from +14.65 to -5.0‰ (Table 9.1). Vertical variability within the Gardiner and Sydney Main seems is high and no systematic vertical trends were observed within the seams. The Gardiner seam, stratigraphically lower than the other three seams, shows much lower δ values. The pyrite δ values range from very close to the evaporite values to negative values but none are more positive than the evaporites.

The soluble sulphate samples from the coals showed high variability in $\delta^{34}\text{S}$, ranging from +18.5 to -5.5‰ (Table 9.1), a similar range to the pyrite δ values.

Table 9.1. Sulphur isotope ratios ($\delta^{34}\text{S}$) for Morien Group coals and Windsor Group evaporites, Sydney Basin

Materials	No. of samples	$\delta^{34}\text{S}$
Pyrite from coal		
Point Aconi seam	1	+10.7
Hub seam	1	+14.3
Sydney Main seam	5	+14.65 to +4.0
Gardiner seam	4	+3.8 to -5.0
Soluble sulphate from coal		
Point Aconi seam	1	+10.9
Hub seam	1	+18.5
Sydney Main seam	5	+14.5 to +0.9
Gardiner seam	5	+7.8 to -5.5
Evaporites		
Gypsum	4	+15.8 to +14.5
Anhydrite	4	+15.1 to +14.5

The δ values range from very close to the evaporite values to negative values, with one sample more positive than the evaporites. The soluble sulphate values are generally more positive than those of the associated pyrites in the Gardiner, Hub and Point Aconi Seams, but are generally more negative than the associated pyrites in the Sydney Main seam. The δ values of pyrite and soluble sulphate from the sample differ by up to 6.8‰.

Discussion

The $\delta^{34}\text{S}$ values of pyrite in the Sydney coals are consistent with derivation of the sulphur from a Windsor evaporite source of about +15‰, followed by isotopic fractionation to more negative values during pyrite formation. Following the geochemical model, the Gardiner seam pyrites, two of which show $\delta^{34}\text{S}$ values less than -1‰, formed mainly by anaerobic reduction of the evaporitic sulphate in the Morien swamps. The relatively positive values for the other seams suggest that the pyrite formed in part by chemical reactions involving evaporitic sulphate during burial.

The soluble sulphate values are difficult to interpret. The sulphate is unlikely to be modern groundwater sulphate derived from the dissolution of Windsor evaporites. It could be residual sulphate left over from pyrite precipitation during anaerobic reduction or later chemical transformation; however, only one sample showed a more positive value than the evaporite sulphate, as required by the model. Two possible explanations are suggested:

- The seams were part of an open groundwater system. Pyrite precipitated over a period of time from groundwater derived from evaporite sulphate but of fluctuating δ value. Thus no consistent relationship resulted between the mean values for pyrite and residual soluble sulphate.
- The soluble sulphate is derived from recent oxidation of pyrite, accompanied by migration or mixing of fluids with different δ values.

Conclusions

$\delta^{34}\text{S}$ values of pyrite from high-sulphur Sydney coals are consistent with the hypothesis that the source of sulphur was dissolved sulphate from the underlying Mississippian

Windsor Group (Haites, 1951). A Pennsylvanian seawater source cannot, however, be precluded, although considered improbable on sedimentological grounds. A fuller evaluation of the hypothesis would require isotopic analyses for more coal seams and far more samples vertically and laterally within each seam, as the isotopic variability is great.

Acknowledgments

We thank Peter Hacquebard for discussion, C.C. McMullen and co-workers at MacMaster University for sample analysis, George Caines at the National Research Council, Halifax, for laboratory assistance, and Kevin Gillis of the Nova Scotia Department of Mines and Energy for making samples available. We are grateful for funding through an EMR Research Agreement.

References

- Akande, S.O. and Zentilli, M.
1984: Geologic, fluid inclusion, and stable isotope studies of the Gays River lead-zinc deposit, Nova Scotia, Canada; *Economic Geology*, v. 79, p. 1187-1211.
- American Society of Testing and Materials
1977: Standard test method for forms of sulfur in coal; American Society of Testing and Materials, Paper D2492-77, p. 322-326.
- Bell, W.A.
1928: Discussion of paper by F.W. Gray; *Proceedings, 2nd Empire Mining and Metallurgy Congress*, Montreal, p. 159-165.
- Boehner, R.C.
1983: Loch Lomond basin, Cape Breton Island, Windsor Group project - an update; Nova Scotia Department of Mines and Energy, Report 83-1, p. 97-104.
- Casagrande, D.J., Siefert, K., Berschinski, C., and Sutton, N.
1977: Sulfur in peat-forming systems of the Okefenokee Swamp and Florida Everglades: origins of sulfur in coal; *Geochimica et Cosmochimica Acta*, v. 41, p. 161-167.
- Gibling, M.R. and Rust, B.R.
1984: Channel Margins in a Pennsylvanian braided, fluvial deposit: the Morien Group near Sydney, Nova Scotia, Canada; *Journal of Sedimentary Petrology*, v. 54, p. 773-782.
- Goldhaber, M.B. and Kaplan, I.R.
1974: The sulfur cycle: in *The Sea*, ed. E.D. Goldberg; Wiley Interscience, New York, v. 5, p. 569-655.
- Hacquebard, P.A.
1983: Geological development and economic evaluation of the Sydney coal basin, Nova Scotia; in *Current Research, Part A*; Geological Survey of Canada, Paper 83-1A, p. 71-81.
- Hacquebard, P.A. and Barss, M.S.
1970: Paleogeography and facies aspects of the Minto coal seam, New Brunswick, Canada; 6th Carboniferous Congress, Sheffield, v. 3, p. 861-872.
- Hacquebard, P.A. and Donaldson, J.R.
1969: Carboniferous coal deposition associated with flood-plain and limnic environments in Nova Scotia; *Geological Society of America, Special Paper 114*, p. 143-191.

- Haites, T.B.
1951: Some geological aspects of the Sydney coalfield with reference to their influence on mining operations; Canadian Institute of Mining and Metallurgy, Transactions, v. 54, p. 215-225.
- Horne, J.D., Ferm, J.C., Caruccio, F.T., and Baganz, B.P.
1978: Depositional models in coal exploration and mine planning in Appalachian region; American Association of Petroleum Geologists, Bulletin, v. 62, p. 2379-2411.
- Kaplan, I.R.
1975: Stable isotopes as a guide to biochemical processes; Royal Society of London, Proceedings, Series B., v. 189, p. 183-211.
- Kemp, A.L.W. and Thode, H.G.
1968: The mechanism of the bacterial reduction of sulfate and of sulfite from isotope fractionation studies; Geochimica et Cosmochimica Acta, v. 32, p. 71-91.
- Krouse, H.R. and McCready, R.G.L.
1979: Reductive processes in sulfur cycling; in Biochemical Cycling of Mineral-forming Elements, ed. P.A. Trudinger and D.J. Swaine; Elsevier, Amsterdam.
- McCready, R.G.L.
1975: Sulphur isotope fractionation by *Desulfovibrio* and *Desulfomaculum* species; Geochimica et Cosmochimica Acta, v. 39, p. 1395-1401.
1983: The metabolism of Thiobacilli and their role in environmental sulfur pollution; National Research Council Canada, 22525, Technical Report 44.
1984: Microbiological studies on high sulfur coals; National Research Council Canada, 23601, Technical Report 50.
- McCready, R.G.L. and Krouse, H.R.
1980: Sulfur isotope fractionation by *Desulfovibrio vulgaris* during metabolism of BaSO₄; Geomicrobiology Journal, v. 2, p. 55-62.
- McCready, R.G.L., Laishley, L.J., and Krouse, H.R.
1975: Stable isotope fractionation by *Clostridium pasteurianum*, I. ³⁴S/³²S: inverse isotope effects during SO₄²⁻ and SO₃²⁻ reduction; Canadian Journal of Microbiology, v. 21, p. 235-244.
1976: Biogeochemical implications of inverse sulphur isotope effects during reduction of sulphur compounds by *Clostridium pasteurianum*; Geochimica et Cosmochimica Acta, v. 40, p. 979-981.
- Newman, W.R.
1935: Microscopic features of the Phalen seam, Sydney coalfield, Nova Scotia; Canadian Journal of Research, v. 12, p. 533-553.
- Rust, B.R., Masson G., Dilles, S., and Gibling, M.R.
1983: Sedimentological studies in the Sydney Basin, 1982; Nova Scotia Department of Mines and Energy, Report 83-1, p. 81-95.
- Sakai, H.
1968: Isotopic properties of sulfur compounds in hydrothermal processes; Geochemical Journal (Japan), v. 2, p. 29-49.
- Sweeney, R.E. and Kaplan, I.R.
1973: Pyrite granitoid formation: laboratory synthesis and marine sediments; Economic Geology, v. 68, p. 618-634.
- Thode, H.G. and Monster, J.
1965: Sulphur isotope geochemistry of petroleum, evaporite and ancient seas; American Association of Petroleum Geologists, Memoir 4, p. 367-377.
- Williams, E.G. and Keith, M.L.
1963: Relationship between sulfur in coals and the occurrence of marine roof beds; Economic Geology, v. 58, p. 720-729.

Preliminary report on the gold mineralization at Bell Creek, Timmins, Ontario

EMR Research Agreement 260

K. Hattori^{1,2} and K. Hicks¹
Mineral Resources Division

Hattori, K. and Hicks, K., Preliminary report on the gold mineralization at Bell Creek, Timmins, Ontario; in Current Research, Part B, Geological Survey of Canada, Paper 86-1B, p. 77-83, 1986.

Abstract

Gold mineralization at Bell Creek, Timmins, occurs in east-west striking, finely banded, silica-rich zones hosted by basaltic and ultramafic volcanic rocks. Mineralized zones are mainly composed of carbonates, quartz and albite with lesser amounts of chlorite, muscovite, rutile and pyrrhotite. There are minor amounts of tourmaline, sphalerite, chalcopyrite and pyrite. A prominent foliation parallel to the strike of the ore zone is displayed by the preferred orientation of chlorite, muscovite and rod-shaped aggregates of sulphide minerals. Intense shearing of the ore zones is shown by crushed and milled rutile crystals, which are in some cases incorporated in recrystallized quartz and carbonate grains. Gold is associated mainly with sulphides, which are mostly confined to highly sheared zones. The distribution of the sulphides, lack of pressure shadows around the sulphides, and absence of evidence of strong deformation within the sulphides grains suggest that the metallic mineralization was contemporaneous with the intense deformation.

Résumé

La minéralisation aurifère du ruisseau Bell, à Timmins, se trouve dans des zones finement rubannées riches en silice, orientées d'est en ouest, contenues dans des roches volcaniques basaltiques et ultramafiques. Les zones minéralisées sont principalement composées de carbonate, de quartz et d'albite et en moindres quantités de chlorite, de muscovite, de rutile et de pyrrhotite. Il y a aussi de faibles quantités de tourmaline, de sphalérite, de chalcopryrite et de pyrite. Une foliation saillante parallèle à la zone minéralisée est mise en évidence par l'orientation principale du chlorite, de la muscovite et des agrégats de minéraux de sulfure en forme de baguettes. Un cisaillement intense des zones minéralisées est indiqué par des cristaux de rutile broyés qui sont dans certains cas incorporés dans du quartz et des grains de carbonate recristallisés. L'or est associé principalement aux sulfures qui se trouvent en grande partie dans les zones fortement cisillées. La répartition des sulfures, l'absence d'ombres de pression tectonique autour des sulfures et l'absence de signes d'importante déformation à l'intérieur des grains de sulfure indiquent que la minéralisation métallique est contemporaine de la déformation intense.

¹ Department of Geology, University of Ottawa, Ottawa, Ontario K1N 6N5

² Derry Laboratory, Ottawa - Carleton Centre for Geoscience Studies

Introduction

The Bell Creek gold deposit, with current reserves of 1 102 677 tonnes of 6.65 g/t Au (Northern Miner, April 14, 1986), is located approximately 12 km northeast of Timmins in the southwestern corner of Hoyle Township. Underground mining is expected to start in the summer of 1986. Two producing gold mines, Owl Creek and Hoyle Pond, are also located in Hoyle Township. All three deposits occur on strike and are hosted in basaltic volcanic rocks at or near the contact with carbonaceous shale. The discovery of the Bell Creek deposit in 1981 was made after extensive geochemical analyses of overburden and subsequent geophysical exploration (Middleton et al., 1984). Because the discovery was made recently, there are no publications describing the mineralization. The objective of this project, which commenced in the spring of 1985, is to describe the gold mineralization in the township and to evaluate the role of the carbonaceous shale in its formation. This report describes preliminary results of a petrographic and geochemical study of the North A ore zone at Bell Creek.

Local geology

Due to the scarcity of outcrops, the geology of the township has not been well documented. The first study was carried out by Hurst (1939) in the southern margin of the township. Berry (1941) examined the sparse outcrops in eight townships including Hoyle Township. Their studies are incorporated into the regional map of Timmins-Kirkland Lake (Ontario Division of Mines, 1973).

Although the stratigraphic study by Pyke (1982) does not extend to the township, the volcanic rocks appear to belong to the lower formation of the Tisdale Group. The lower formation consists mainly of ultramafic and basaltic lavas and pyroclastic rocks. Carbonaceous shale trends west-northwest on a regional scale and displays a "Z" shaped fold east of the mineralization (Fig. 10.1). Pillow top determinations in the basalt, now covered by mine buildings, suggest that the steeply-dipping strata young to the south (Fig. 10.2). Farther to the south, on Highway 101, the top of

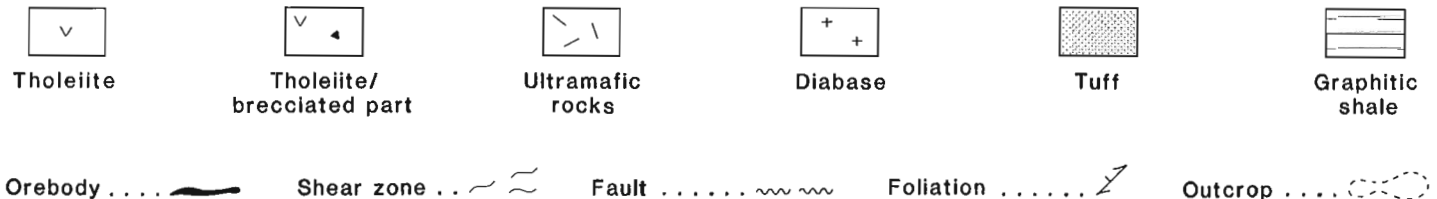
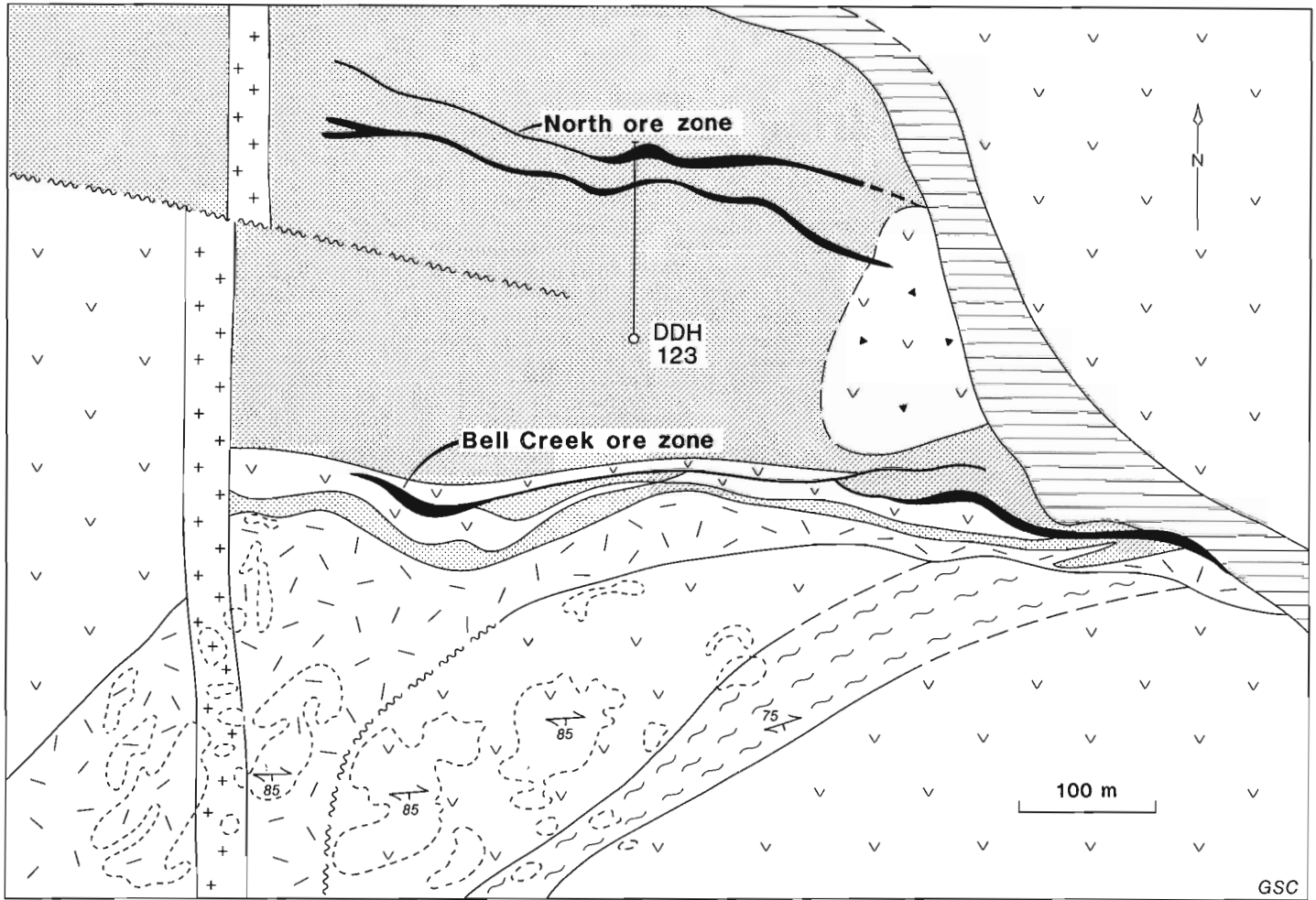


Figure 10.1. Preliminary geological map at Bell Creek. Modified after the preliminary map by Al Philipp of Canamax Resources, 1984.

the volcanic sequence is to the north. This may indicate a fold, supporting the inferred synclinal axis south of the deposit (Ontario Division of Mines, 1973).

Rocks near the mine are commonly highly foliated and several intense shear zones with tectonic fragments were observed in outcrop (Fig. 10.3). The foliation and shear zones strike 80° to 110°, dipping about 85° south, roughly parallel to the regional stratigraphic layering. Other deformation of the volcanic rocks is manifested by a highly brecciated zone near the "Z" fold in the carbonaceous shale (Fig. 10.1). The size of the angular fragments are variable and chlorite outlines breccia fragments. Since the breccia zone is not exposed on surface, its extent is not known.

The area underlain by the ore zones is mostly covered by glacial till and swamp and, as a result, geological information was obtained principally from drill core. Intense alteration and deformation around the ore made exact identification of the protolith impossible.



Figure 10.2. Pillowed basalt showing the top to the south at the main shaft. The exposure is now covered by the mine building.



Figure 10.3. A dextrally-rotated, foliated, tectonic fragment relative to the foliation in the host "leucoxene" basalt, giving a right lateral sense of direction to the shearing. The foliation in the host is east-west. The magnet for scale is six inches.

Lithological units

Basalts

Cation ratios of relatively unaltered basalts indicate that basalts in the area are of tholeiitic affinity. The basalt is characterized by the occurrence of feathery white "leucoxene", which is a composite Ti-Fe-O-OH phase. The basalts in the vicinity of the mine are pervasively altered. They typically comprise chlorite, quartz, actinolite, clinozoisite, "leucoxene", plagioclase, rutile, sphene, carbonates and sulphides. The planar orientation of chlorite defines the foliation in the rocks.

Ultramafic units

Ultramafic rocks occur in the western part of the mine property (Fig. 10.1). They are extensively altered and rarely retain primary textures or minerals. Poorly preserved polysuturing suggests an extrusive origin. Alteration minerals include carbonates, quartz, muscovite, serpentine, rutile and sulphide minerals. Green Cr-rich micas are interpreted to be the alteration product of Cr-bearing minerals in the ultramafic rocks. Thus the lithologies with green mica near the ore zones are mapped as ultramafic flows. Prominent east striking foliation is displayed by the distribution of finely milled rutile grains, and quartz veinlets and preferred orientation of serpentine veinlets in the rocks.

Carbonaceous shale

Black, carbonaceous sedimentary rocks were only observed in core samples. The rocks are fissile, due to the abundant slip planes along the foliation. This fine foliation is caused by the preferred orientation of carbonaceous material, chlorite, lenticular sulphide grains and quartz stringers. Sulphide minerals in the shale include pyrrhotite, chalcopyrite and pyrite.

"Tuffaceous" rocks

This rock type is not exposed at the surface. Finely banded units near the ore zones were all interpreted as "tuffs" and "pyroclastic rocks". To maintain consistency with this mine terminology, the name "tuff" is used here to describe these highly altered and well foliated rock units. The precise identification of the primary rock type was impossible, due to the intense alteration and deformation. The foliation is defined by chlorite, carbonaceous material, muscovite and elongated aggregates of sulphides, pyrrhotite and chalcopyrite. Carbonate and quartz are also abundant. Some of the units contain finely crushed rutile and albite crystals, similar to those in the sheared basalts. Evidence that may support a tuffaceous origin includes the presence of carbonaceous material in some samples. There are, however, other alternatives. The unit could be an interflow sediment or intensely deformed and altered basalt. In the latter case, the carbonaceous material could have been introduced during the intense deformation and hydrothermal alteration as observed near the carbonaceous shale at the Hoyle Pond deposit (Downes et al., 1984) and the Owl Creek deposit (Gagnon, 1986). Underground mapping of the unit may answer some of the questions.

Diabase

All the rocks, including the mineralization, are cut by a north-south striking diabase dyke. The dyke cuts quartz veins and the foliation (Fig. 10.4), demonstrating post-deformation intrusion. The diabase comprises plagioclase (average 20 vol.%), augite (25 vol.%), hypersthene (10 vol.%), chlorite (15 vol.%), sericite (10 vol.%), serpentine (15 vol.%), magnetite (5 vol.%) and pyrite (<1 vol.%). Relict olivine

crystals are pseudomorphed by serpentine. Chlorite occurs as an alteration product of pyroxenes. Sericite replaces plagioclase. The strike, the size and the mineralogy of the dyke are consistent with the dykes belonging to the olivine-bearing variety of the Archean Matachewan Swarm in the Timmins area (Pyke, 1982).

Since the dyke is relatively magnetic, its position is well outlined on the ground magnetic map and it is offset along and near the carbonaceous shale (Middleton et al., 1984). These offsets suggest the carbonaceous shale represented a zone of weakness for subsequent faulting.

Mineralization

Gold mineralization on the property occurs in three main zones, the North zone, the Bell Creek zone (Fig. 10.1) and the Marlhill zone. The Marlhill zone occurs to the north of the carbonaceous shale. Both the Bell Creek and the North zones contain two sub-zones, an upper 'A' horizon and a lower 'B' horizon. Since the mineralization appears to occur roughly concordant to the regional stratigraphy, the ore zones were named "horizons". The ore zones run east-west and are roughly parallel to each other. In addition to these main zones, numerous mineralized lenses, mostly parallel to the foliation, are found nearby. All the ore zones consist mainly of finely banded carbonates, quartz and albite with late coarse veins and veinlets of calcite, quartz and albite. In some cases, late veins crosscut and, in other cases, they parallel the foliation.

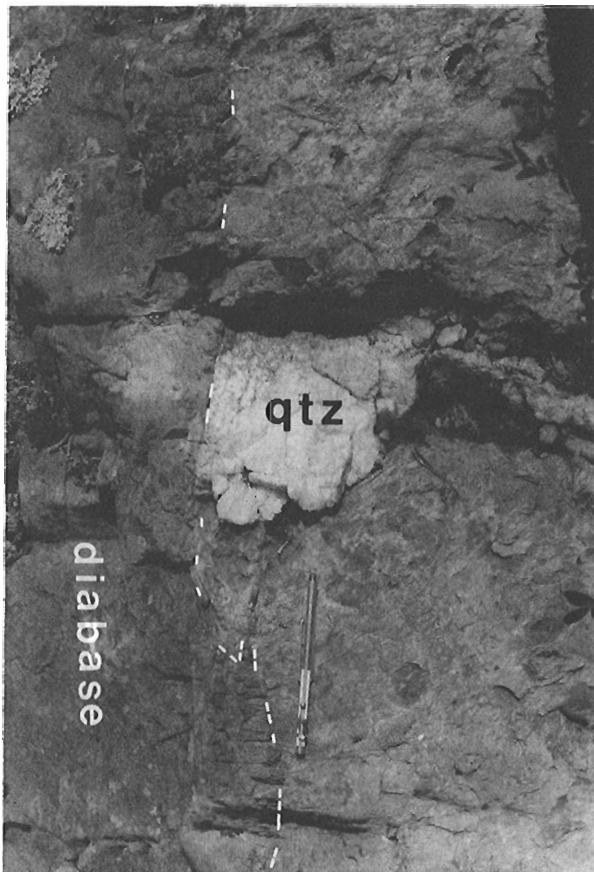


Figure 10.4. Contact between the diabase dyke and highly foliated ultramafic rocks. Note that the diabase dyke cuts a hydrothermal quartz vein and that no foliation exists in the diabase.

The A horizon of the North zone was selected for detailed petrographic study. It strikes is 103° and dips 70° to the south. The ore zone may be either a vein or a completely replaced host rock. The zone is accompanied by a quartz vein about 20 cm wide parallel to the ore zone in the intensely altered and foliated hanging wall. The rocks in the ore zone are classified into three sub-units based on cross-cutting relations, textures, and mineralogy; unit 1, undeformed, coarse grained; unit 2, well-foliated, fine grained; unit 3, coarse grained late veinlets. The fine grained, well-foliated unit contains crushed albite grains and ground carbonates and rutile grains, indicating grain size reduction due to the intense deformation.

Unit 1 occurs as patches in unit 2 and as lenses adjacent to the wall rocks. Some of the coarse unit is cut by unit 2. The absence of grain recrystallization and minor strain deformation is taken as the criterion for identification of this unit 1. It comprises mostly carbonate, quartz, and albite and rutile. The occurrence suggests that the unit 1 may represent the remnant of the vein material prior to intense deformation.

Unit 2 comprises most of the A horizon. This off-white coloured rock has a sedimentary, cherty appearance due to its fine layering with a prominent mineral lineation. Under the microscope, it is characterized by intensely crushed and milled anhedral fine minerals (<0.05 mm) (Fig. 10.5). The mechanical deformation is especially well expressed in rutile, which is ground and broken to fine grains (average 0.02 mm), compared to subhedral prisms averaging 0.2 mm in size in coarse grained parts. Diffused grain boundaries suggest that a certain amount of recrystallization took place. The rock consists of carbonates, quartz, albite, chlorite, muscovite, rutile, pyrrhotite, chalcopryrite, and pyrite. A strong foliation is defined by the orientation of iron-rich chlorite (ferroan clinocllore), muscovite and small rods of sulphide minerals. Each small sulphide rod is an aggregate of anhedral pyrrhotite, chalcopryrite and/or sphalerite and/or pyrite.

Sulphide grains within the small rods have random crystallographic orientation and display only minor internal deformation. Because pyrrhotite is relatively incompetent, ductile flow may be expected in grains under a high strain regime, if pyrrhotite was formed before the deformation. Pyrrhotite associated with more competent grains, such as

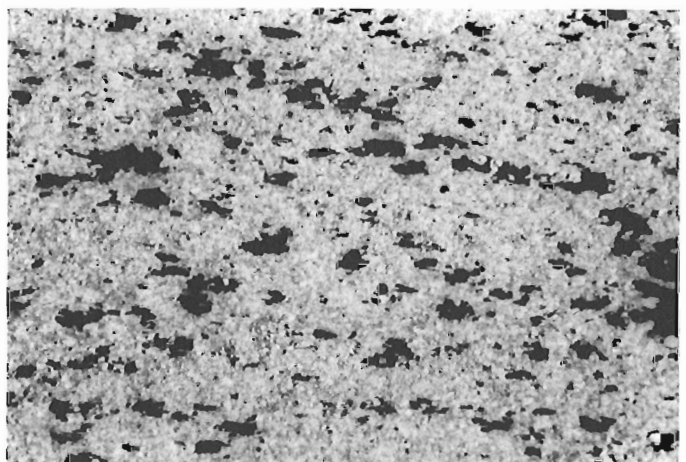


Figure 10.5. Photomicrograph (2 mm across) of the typical unit 2 in the North A ore zone. The foliation is defined by the orientation of chlorite and small lenticular rods of sulphides. Rod-shaped opaque minerals are composed of pyrrhotite, chalcopryrite, and sphalerite with minor pyrite. Matrix is a mixture of fine anhedral grains of ankerite, quartz, albite, rutile and chlorite.

pyrite and sphalerite, does not show any signs of deformation (Fig. 10.6). Combined with the absence of pressure shadows around the small sulphide rods, and a low sulphide content in coarse grained units, the occurrence of sulphides seems to suggest that the introduction of sulphides and their crystallization took place during deformation. Assay data indicate that gold mainly occurs in unit 2. Metallurgical study suggests that gold is associated with pyrrhotite (unpublished report, Canamax Resources). Gold, therefore, seems to have been introduced during the deformation together with sulphide minerals.

Diffused grain boundaries and the occurrence of finely ground rutile enclosed within quartz grains indicate that minor recrystallization proceeded in unit 2. Some parts of the unit display increases in grain size due to the recrystallization process (Fig. 10.7). The mineralogy of the recrystallized part is similar to the fine grained part and the boundary may be gradational (Fig. 10.7). Patches of fine, milled grains were common in the recrystallized part. Quartz and carbonate start to exhibit recrystallization, enclosing dust-like fine mineral inclusions on the former grain boundaries (Fig. 10.8). Well crystallized tourmaline is noted in this part. The foliation in the recrystallized part is not as prominent as in the fine grained part, however, the overgrown minerals in lenticular sulphides exhibit weak orientation parallel to the foliation.

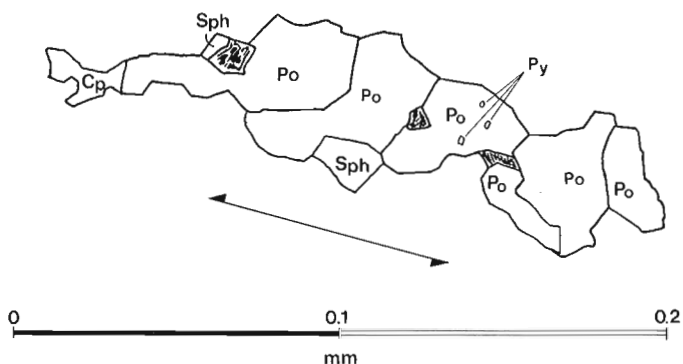


Figure 10.6. Typical occurrence of a small sulphide rod in the unit 2. Random crystallographic orientation of pyrrhotite is well displayed under the reflected light microscope due to the anisotropic optical character. Cp, chalcopyrite; Py, pyrite; Po, pyrrhotite; Sph, sphalerite.

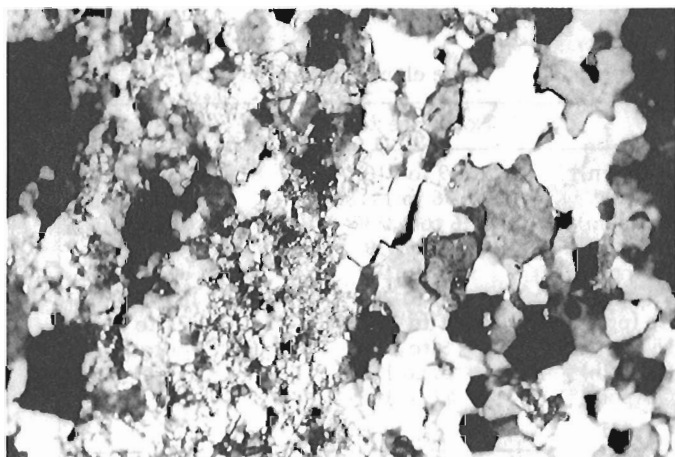


Figure 10.7. Photomicrograph (1.3 mm across) of recrystallized unit in the right and fine grained portion in the left. Note the gradational boundaries.

Late stage veinlets cut all the above units within the North 'A' horizon. Some are monomineralic and some are composed of quartz, calcite and/or albite. Calcite commonly displays pressure twins, indicating the prolonged nature of the deformation (Fig. 10.9). Carbonates in the unit are mostly ankerite and calcite.

Alteration

All the rocks in the mine except diabase are pervasively altered. The alteration mineral assemblage, clinzoisite-actinolite-albite-chlorite-"leucosene"-calcite, may represent the products of the early sub-sea floor alteration or the regional metamorphism of greenschist facies. Primary plagioclase is characteristically replaced by albite in the rocks.

Closer to the ore zones, the amounts of actinolite and clinzoisite decrease and the amounts of carbonates, quartz and sulphides increase. Muscovite, tourmaline and ankerite only appear near the mineralization. The intense deformation and hydrothermal activity related to the Au mineralization appears to have obscured any previous

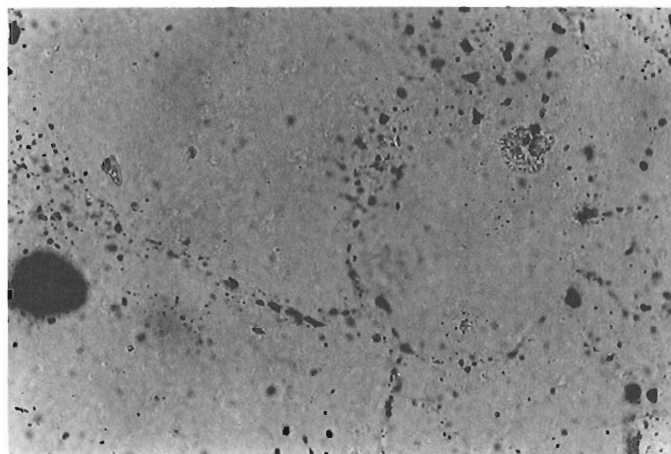


Figure 10.8. Photomicrograph (0.35 mm across) showing recrystallization of quartz. Note fine mineral inclusions inside a single quartz grain.

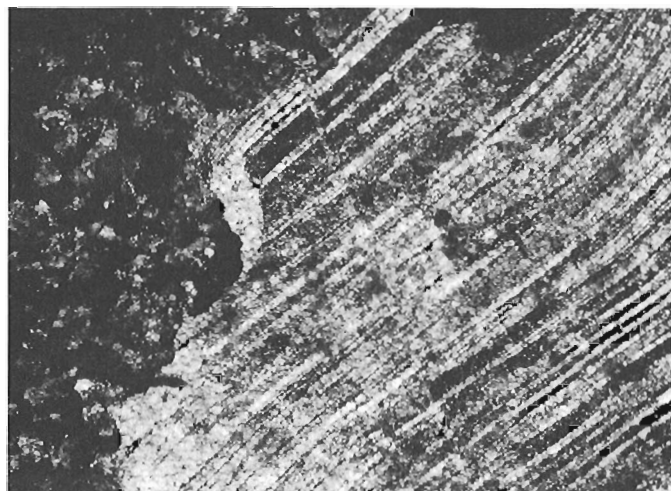


Figure 10.9. Photomicrograph (0.35 mm across) of coarse calcite with pressure twins. The coarse calcite veinlets (unit 3) cut the unit 2, which is seen in the upper right corner.

alterations in the basalts near the ore zones and in ultramafic rocks. Immediate wall rocks are typically composed of ankerite, quartz, albite, muscovite, rutile, quartz, chlorite, pyrite and pyrrhotite. Serpentine may occur in ultramafic rocks. The fact that similar alteration mineral assemblages are found in basalts and in ultramafic units near the mineralization emphasizes the intense nature of the hydrothermal activity related to the Au mineralization.

Geochemistry

Major and trace element contents were determined by an ICP total digestion method using perchloric-nitric-hydrofluoric acids. Samples include fairly unaltered basalts, North A and B ore "horizons", and the wallrocks of the ore zones. The contents of W, As and Sb in the ore zones and the immediate wallrocks were determined by neutron activation analysis. Levels of trace elements are highly variable, but the following general patterns were observed (Fig. 10.10, Table 10.2):

- i) enrichment of As, W, Cu, Zn, Fe, Ni in and near the ore zones, and
- ii) enrichment of Ba, P, K and Na in the wallrocks and ore zones.

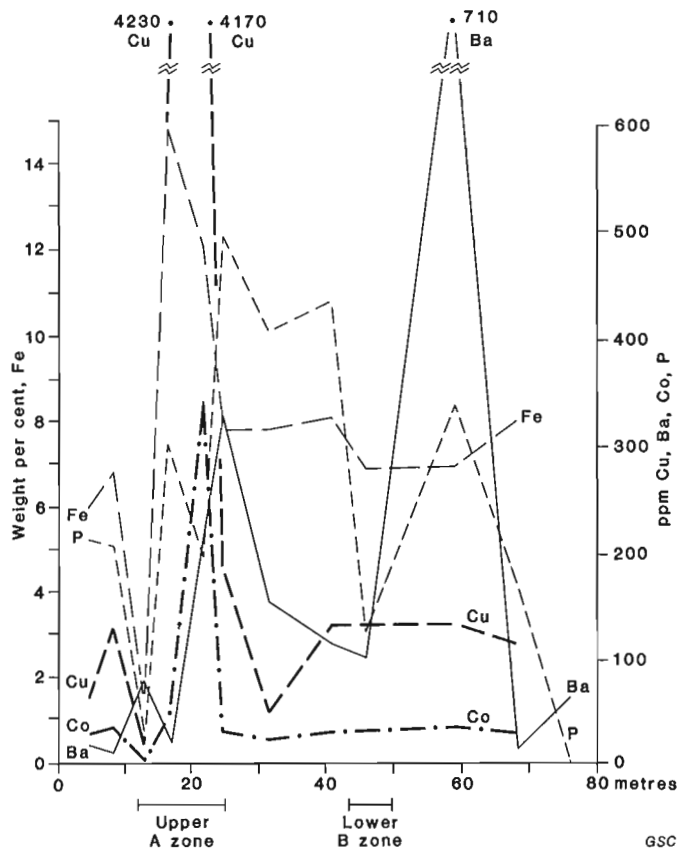


Figure 10.10. Variations of total Fe, K, Na, Ba, P contents in wall rocks and North ore zones. The samples are taken from DDH 123 (see Fig. 10.1) which intersects the ore zones at 75 to 80°. Ore zone samples represent a fine grained unit 2, except for the sample on the boundary between the Upper 'A' zone and the hanging wall rock. The sample is from a late stage coarse quartz vein parallel to the ore zone.

The abundance of Fe, Cu and Zn is apparently due to the introduction of pyrite, chalcopyrite, and sphalerite in the ore zones described. The enrichment of Ni and Co is correlated with the content of Fe, suggesting substitution in pyrrhotite. The occurrence of muscovite in the ore and wallrocks explains the observed enrichment of K and probably Ba, which can replace K in muscovite. P may be present in fine apatite or in muscovite. The variation of Fe, P, Ba, K and Na are plotted with the distance from the ore zones in Figure 10.10.

Discussion

The ore zones were originally interpreted to be of sedimentary origin since they were believed to be exhalative cherty beds hosted in "tuffaceous" units, ultramafic and

Table 10.1. Mineralogy of the North A zone, Bell Creek gold deposit

undeformed coarse grained unit 1	well-foliated fine grained unit 2	late veins unit 3†
quartz (40-60%*)	carbonate** (20-70%)	monomineralic quartz vein
albite (25-40%)	quartz (15-40%)	monomineralic calcite vein
carbonate** (10-20%)	albite (2-30%)	quartz-calcite vein
rutile (1-3%)	chlorite (0-50%)	calcite-quartz vein
	muscovite (1-3%)	quartz-calcite-albite vein
	rutile (1-5%)	
	pyrrhotite (2-7%)	
	chalcopyrite (1-3%)	
	pyrite (0-2%)	
	sphalerite (0-4%)	
	gold	

* volume per cent
 ** mainly ankerite with some calcite
 † some late quartz veins contain visible gold

Table 10.2. Trace element contents

	North ore zones	Wall rocks
Zn (ppm)*	9 to 910	60 to 110
Fe (%)*	0.36 to 14.87	4.56 to 8.53
Cu (ppm)*	6 to 4,230	41 to 410
W (ppm)†	22 to 39	<2 to 13
As (ppm)†	59 to 190	<1 to 480
P (ppm)*	15 to 295	165 to 780
Co (ppm)*	1 to 335	22 to 40
Ni (ppm)*	9 to 163	40 to 100
Ba (ppm)*	20 to 160	<15 to 710
Cr (ppm)*	47 to 100	50 to 110

* ICP analyses
 † neutron activation analyses

basalt flows. Lack of surface exposure in the area makes it difficult to identify the protoliths of the host rocks and the relationship between the ore zones and host rocks. This preliminary study shows the intense and complicated nature of the deformation, hydrothermal activity, and recrystallization of the deformed rocks in the area. At least some of the "tuff" beds seem to be highly deformed basalts. Some "tuff" beds with carbonaceous material may have been true pyroclastic units or possibly an intensely altered and deformed basalt.

The ore zones mostly consist of intensely sheared bands with later coarse hydrothermal veinlets. The preferred orientation of small rods of sulphides, muscovite and chlorite in a mixture of fine grained quartz, carbonates and albite produces the cherty, fine layered appearance. The recrystallization of quartz and carbonate along foliation planes suggest that hydrothermal activity took place during the intense deformation. The abundance of sulphides within the intensely deformed zones, the rod-shaped occurrence of the sulphide aggregates parallel to the foliation, random orientation of sulphides within the small rods and the lack of internal deformation in sulphides all seem to suggest that the introduction of metals took place during deformation.

In Hoyle Township the two gold producers are Hoyle Pond and Owl Creek. These, together with Bell Creek, are located near the contact with a thick carbonaceous shale unit, although the style of the mineralization in the deposits is different. The ore zones at Bell Creek appear to be parallel to the regional stratigraphy. The ore zones at the other two mines are apparently hosted in crosscutting, coarse quartz-carbonate veins. This study indicates that mineralization at Bell Creek is similar to that at Owl Creek (Gagnon, 1986) and Hoyle Pond (Downes et al., 1984) in mineralogy, alteration and styles of deformation in and around the ore. The gold mineralization near the contact with the carbonaceous shale at Owl Creek is interpreted to be due to a large competency difference between carbonaceous shale and basalt under high strain regime (Gagnon, 1986). Brittle basalt near the ductile carbonaceous shale may have provided dilatant zones for gold mineralization. The carbonaceous shale near the mineralization at Bell Creek may have played the same role. The brecciated zone in basalts near the carbonaceous shale and the "Z" shaped highly deformed nature of the carbonaceous shale may support this view.

Detailed underground mapping may determine the nature of the host rock types and the relationships among the ore zones and host rock types. A comparison of the three deposits in Hoyle Township may provide further information on the nature of the mineralization.

Acknowledgments

The authors are grateful to Germain Lauzier and Al Philipp of Canamax Resources Ltd., Timmins, who permitted sampling, provided unpublished maps, drill logs and using their preliminary map in this report. Assistance in the field by Al Philipp is greatly appreciated, who also kindly encouraged the preparation of this report. Critical reading by F. Robert, E.M. Cameron and D.C. Findlay of Mineral Resources Division, GSC, greatly improved the manuscript. The study was funded by EMR Research Agreement 260.

References

- Berry, L.G.
1941: Geology of the Bigwater Lake area; Ontario Department of Mines, Annual Report, 1939, 48-12, 11 p.
- Downes, M.J., Hodges, D.J., and Dewedumen, J.
1984: A free carbon- and carbonate-bearing alteration zone associated with the Hoyle Pond gold occurrence, Ontario Canada; in *Gold '82: The Geology, Geochemistry and Genesis of Gold Deposits*, ed. R.P. Foster, p. 435-448.
- Gagnon, D.
1986: Hydrothermal alteration at Owl Creek gold deposit, Timmins, Ontario; unpublished B.Sc. thesis, University of Ottawa.
- Hurst, M.E.
1939: Porcupine area, District of Cochrane, Ontario; Ontario Department of Mines, Map 47A, scale 1 inch to 2000 feet.
- Middleton, R.S., Durham, R.B., Harron, G.A., and Philipp, A.
1984: Geophysical and geochemical techniques for gold exploration in the Timmins area, Ontario; in *Proceedings of Canadian Institute of Mining and Metallurgy Symposium: Geophysics For Gold*, 12-13 November, 1984, p. 97-132.
- Ontario Division of Mines
1973: Timmins-Kirkland Lake Geological Compilation Series, Cochrane, Sudbury and Timiskaming District, Ontario Division of Mines Map 2205, 1 inch to 4 miles.
- Pyke, D.R.
1982: Geology of the Timmins area, District of Cochrane; Ontario Geological Survey Report 219, 141 p.

Evaluation of sea gravimeters: comparison of Bodenseewerk KSS30 and KSS31 systems

Project 810037

B.D. Loncarevic, M.D. Hughes, and I. Himmler¹
Atlantic Geoscience Centre, Dartmouth

Loncarevic, B.D., Hughes, M.D., and Himmler, I., Evaluation of sea gravimeters: comparison of Bodenseewerk KSS30 and KSS31 systems; in *Current Research, Part B, Geological Survey of Canada, Paper 86-1B*, p. 85-96, 1986.

Abstract

A new KSS31 sea gravimeter system was evaluated during a ten day cruise onboard **CFAV Quest**. The system shows an improvement in performance by a factor of 2 over the older KSS30 system. Standard deviation on 20 track crossovers is 0.298 mGal for KSS31 and 0.535 mGal for KSS30 system.

Résumé

Un nouveau système gravimétrique marin KSS31 a été évalué au cours d'une expédition de dix jours à bord du **CFAV Quest**. Le rendement de ce système a été amélioré d'un coefficient deux par rapport au réseau KSS30 plus ancien. L'écart-type sur 20 points d'intersection est de 0,298 mGal pour le système KSS31 et de 0,535 mGal pour le système KSS30.

¹ Bodenseewerk Geosystem GmbH, Ueberlingen, F.R. Germany

Introduction

The KSS30 sea gravimeter system, manufactured by Bodenseewerk Geosystem GmbH of Meersburg, F.R. Germany, has been in use since 1981. A significant improvement in the system performance was achieved recently by re-designing the gyro-stabilized platform. A 10 day test cruise was organized on board **CFAV Quest** in November 1985 to evaluate the new system and measure the improvements in performance over the old system. The cruise program included a southerly track to a working area in the vicinity of 37°N, 63.5°W (south of the Gulf Stream), five days of acoustic experiments in the working area, a northerly return track and approximately 11 hours of work on the Gravity Test Range, 80 km south of Halifax (Goodacre, 1964). This report deals with the observations on the Gravity Test Range.

Instrumentation

The KSS30 and KSS31 sea gravity systems have identical sensors and similar electronics. The difference between the two systems is in the platform design. The KT30 platform (used in the KSS30 system) is of a cantilevered design and uses a large gyro manufactured by Anschuetz Co. and modified by Bodenseewerk Geosystem GmbH. The gyro is mounted on the platform base and is outside the erection loop. The new platform design (designated KT31) incorporates inner and outer gimbals, symmetrically supported and balanced. The reference gyro, manufactured by SAGEM in France, is smaller than the old Anschuetz gyro. It is mounted on the inner gimbals and so is a part of the erection loop. Because of the symmetrical design and lighter gyro, the off-levelling errors are reduced and the platform response is improved.

The two systems available for comparison used sensors serial number 12 (owned by GSC/AGC) mounted on KT30 platform (KSS30-12 or K12 for short) and serial number 26 (loaned by BSW/G) mounted on KT31 platform (KSS31-26 or K26). The outputs of the two instruments were merged and logged at 10 s intervals on a custom designed system named CIGAL (Macnab et al., 1985). The navigation was provided by the new, improved, version of Bedford Institute of Oceanography integrated navigation system, BIONAV (Wells and Grant, 1981). This system provides the time reference and the 'shot point' control at 10s intervals for recording the readings. In addition to the positions, BIONAV supplied the course and speed information for calculation of the Eotvos correction and for calculation of short term horizontal accelerations affecting the platform erection.

The navigational system utilized Loran-C radio signals in range-range mode (Grant, 1973) with a rubidium vapour oscillator for time reference. The clock was rated by comparison with Transit satellite fixes. The ship's log was not operational so the velocity correction to Transit fixes had to be estimated. The overall positional accuracy of the system is estimated at about 100 m RMS (Grant, 1977).

Adjustment of readings

The gravimeters were mounted side-by-side in close proximity to the ship's roll and pitch axes. There was no need therefore to make any adjustment for the difference in position and it is assumed that the acceleration environment was common to both instruments.

The harbour base station for the cruise was an excentre on Jetty 2A of the Halifax dockyard. The reference gravity value is 980 564.95 mGal at a nominal

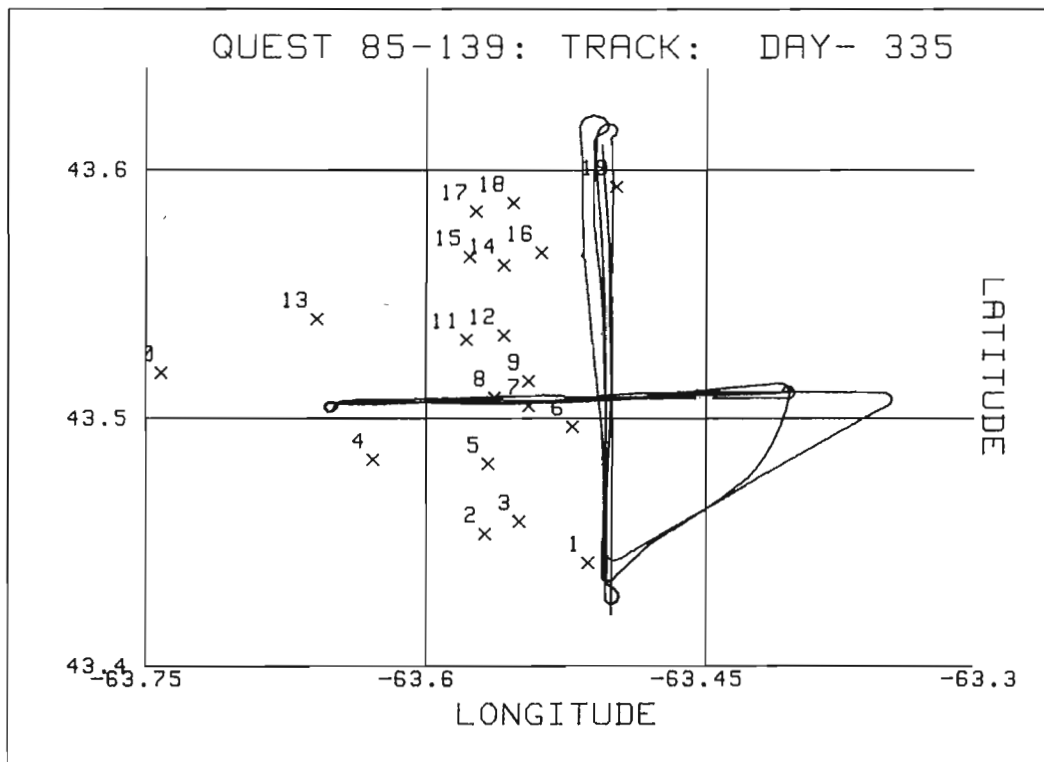


Figure 11.1. The ship's track on the Halifax Gravity Test Range between 00 and 11 hrs GMT on 01 December, 1985. Crosses indicate the location of bottom gravimeter stations given in Table 11.1.

height of 3.2 m above the mean sea level. The height of the gravimeter below this datum was 2.56 m and a correction of -0.79 mGal was applied to correct for this height difference. The reference readings for K12 gravimeter were established before and after the cruise by a simple regression of the gravimeter readings against the tidal height giving values at mean sea level of -228.17 on day 325 at 0300 GMT and -227.48 on day 336 at 1600 GMT. The calculated drift was therefore 0.69 mGal in 11.542 days or 4.8096E-5 mGal/min. The drift correction of this amount was applied to all K12 readings.

There were instrumental difficulties with the installation of the K26 gravimeter and a good base value could not be obtained before the departure. There was also some uncertainty about the calibration factor of K26 which was calibrated only by a tilt method. For these reasons, K26 was calibrated against K12 gravimeter by performing a multiple regression on the difference between K26 and K12 readings against the latitude and time. The long north-south tracks to and from the main working area were particularly suitable for this type of inter calibration.

The multiple regression gave as the mean difference between base readings of the two instruments a value of 251.12 mGal, a calibration constant correction factor of (1-0.009295) and a drift of -8.962E-5 mGal/min (in the opposite direction from the drift of K12).

Observations on the Gravity Test Range

A total of nine, mutually orthogonal lines were run between 00:00 and 10:51 hours GMT on 1 December 1985 (day 335). There were four E-W and five N-S lines. The ship's track on the test range is shown in Figure 11.1.

The lines were run in good weather with wind of less than 15 kts and a slight sea running. The bridge was asked to steam along 63° 30' West for N-S lines and along 43° 30' North for E-W lines but as can be seen from Figure 11.1, there was a set in the northwesterly direction at the eastern end of the E-W lines and at the north end of the N-S lines. The E-W lines were consistently displaced to the north and the N-S lines to the west probably because of the different navigational systems used. Bridge used Loran C in hyperbolic mode without any corrections, while we used Loran C in range-range mode with corrections for overland propagation delays (ASF or additional secondary-phase factor).

The E-W lines covered the same ground while the N-S lines were somewhat dispersed at the north end. All the lines converged on a point near 43°30' N, 63°30' W which was considered the control crossover point.

This particular section of the Gravity Test Range was chosen for the evaluation because the gravity field variations along either line are fairly small (typically less than 2 mGal). This can be seen from Figure 2 in Goodacre (1964). (Note: The gravity values published by Goodacre were based on the old Potsdam system (International Gravity Formula, 1930). To convert to the IGNS 1971 system approximately 16 mGal should be subtracted from Goodacre's values.)

As shown in Figure 11.1, there are a number of bottom gravimeter stations in the vicinity of our tracks. The positional data and gravity values for these stations are given in Table 11.1. The surface gravity values have been corrected as described by Goodacre and the reference system has been changed to IGNS 1971. The range of station values

Table 11.1. Positional data and gravity values for bottom gravimeter stations

EPB. Stn. #	Latitude	Longitude	Depth	Surface gravity
7620	43 26.5N	63 30.8W	171	980 494.57
7643	43 27.2N	63 34.1W	172	980 493.73
7644	43 27.5N	63 33.0W	175	980 492.85
7642	43 28.9N	63 34.0W	171	980 494.30
7624	43 29.0N	63 37.7W	194	980 493.25
15193	43 29.8N	63 31.3W	164	980 493.36
7623	43 30.3N	63 32.7W	172	980 493.17
7641	43 30.5N	63 33.8W	175	980 493.18
7698	43 30.5N	63 33.8W	175	980 493.28
7665	43 30.9N	63 32.7W	178	980 492.05
7604	43 31.1N	63 44.5W	221	980 492.09
7651	43 31.9N	63 34.7W	190	980 492.07
7640	43 32.0N	63 33.5W	177	980 493.28
7605	43 32.4N	63 39.5W	209	980 493.77
7639	43 33.7N	63 33.5W	188	980 492.77
7606	43 33.9N	63 34.6W	195	980 492.25
7666	43 34.0N	63 32.3W	194	980 491.60
7652	43 35.0N	63 34.4W	203	980 491.02
7638	43 35.2N	63 33.2W	198	980 492.98
7697	43 35.2N	63 33.2W	198	980 492.88
7516	43 35.6N	63 29.9W	170	980 495.37
7607	43 35.6N	63 30.0W	167	980 496.29

Note: There are two repeat stations: 7641/7698 and 7638/7697. Only the first of each pair is plotted.

is from 980 491.02 to 980 496.29 mGal. The high values are at the extremes of north-south lines. Disregarding these three stations (EPB station numbers 7620, 7516 and 7607) the mean for the remaining 19 stations is 980 492.84 with all the stations within ± 1.6 mGal of the mean.

The purpose of the Gravity Test Range experiment was: 1) to check the repeatability of readings over the same tracks; 2) to compare readings of the two gravimeters; 3) to check for any dependence of gravity readings on the ship's heading; and 4) to check the crossover accuracy at the central control point.

Repeatability of readings

Repeatability of readings over the same track is shown in Figure 11.2 for north-south and in Figure 11.3 for east-west lines. In both cases, K12 gravimeter produced a much noisier record than the K26 gravimeter. For both instruments, the north-south tracks were noisier than the east-west ones. The envelope of the profiles is about ± 1 mGal for K26 gravimeter except at the north end where track positions diverged. For the K12 gravimeter, the envelope is approximately ± 1.5 mGal for E-W lines and over ± 2 mGal for north-south lines. The N-S lines are particularly disturbed on lines 1N and 2S with three large negative 'bumps' exceeding 5 mGal in amplitude. We suspect that these 'bumps' are a consequence of platform errors caused either by a defective gyro, faulty platform bearings, or both.

K26 profiles agree well with bottom gravimeter stations. Goodacre estimated random errors in gravity values (reduced to the surface) of the order of 1 mGal. It is therefore not possible to use these values to estimate the accuracy of K26 readings but, qualitatively, we conclude that the repeatability is better than 1 mGal, probably between 0.5 and 1.0 mGal. For K12 readings, the repeatability is probably between 1 and 2 mGal except when large 'bumps' are present.

Comparison

Comparison of two gravimeters is illustrated with the plots of the difference K26-K12, shown in Figure 11.4. The mean difference of all the lines (with two exceptions) is close to zero, demonstrating the overall accuracy of each instrument and justifying our choice of the adjustment factors. The 1N and 2S lines showed a systematic level displacement of about +2 mGal (indicating that K12 was lower, probably because of a steady off-leveling error). These two lines were the lines where the biggest 'bumps' occurred. There were no adjustments of the instrumental settings or configuration between the beginning and the end of the test. It is possible that there was some subtle change in the spectrum of ship's accelerations (perhaps due to a shift in wind direction relative to the predominant swell direction or a change in tidal current direction) but these were not perceptible to the watchkeepers.

A detailed comparison of the performance of the two gravimeters is shown in Figure 11.5. The upper plot (Figure 11.5a) shows a 'good' line; the two instruments agree with each other well, within a fraction of a milligal, along the whole length of the profile. The raw gravity is smooth indicating small horizontal accelerations and a smooth progress of the ship through the water without sudden course alterations or speed changes. The two corrected traces (profiles 3 and 4) follow each other and are smooth everywhere except for a small 'bump' just north of 43°32'N. This bump is introduced by the data processing and does not represent gravity change sensed by the instrument since it does not appear on the raw gravity trace. The cause of this

error in Eotvos correction calculation are the spikes in both course and velocity profiles caused by an update within BIONAV processing system.

The lower plot (Fig. 11.5b) is an example of a poor line; the agreement between the two instruments is not very good. There is an overall DC shift of KSS30-12 so that its readings are almost 2 mGal lower. Even more disturbing are the negative 'bumps', the largest of which (just south of 43°32'N) exceeds 5 mGal.

The causes of such significant differences between two lines only six hours apart are difficult to pinpoint but a possible clue may be seen from an examination of the ship's heading i.e. raw gyro-compass readings (Fig. 11.6). Ship's heading and the course calculated by the navigation computer are shown on an expanded scale (and offset by ten degrees for greater legibility).

The upper profile in each plot shows a strong periodic component. The auto pilot is difficult to adjust properly to avoid hunting. In most ships some degree of hunting is unavoidable but its amplitude and frequency differ from ship to ship, from time to time (depending on the adjustments of the feedback loop) and also depends on the sea state etc. The **Quest** has twin rudders and a rather fast response to rudder angle, therefore the autopilot oscillations may be somewhat exaggerated in this case. On line 7 N the hunting had about ± 2 degree amplitude and a period of 1.2 minutes. On line 2 S the amplitude was about 20% greater and the period was about 20% longer. We surmise that this change in hunting characteristics of the autopilot may have been the primary cause of poorer performance on lines 1 N and 2 S.

The mean heading on line 7 N was steady and close to 000°. On line 2 S the heading was changing as the ship struggled to get to the prescribed track. The mean heading started at 353°, changed to 356° at 43°33'N, to 359° just before 43°32'N and finally to 001° at 43°30'N. The change from 356° to 359° was in phase with the autopilot hunting. Although the course change was only three degrees the actual swing of the ship's head was close to ten degrees. This swing would produce a considerable horizontal acceleration which may have been responsible for the bump on the KSS330-12 trace. The new platform and the new gyro obviously can cope with such horizontal accelerations better.

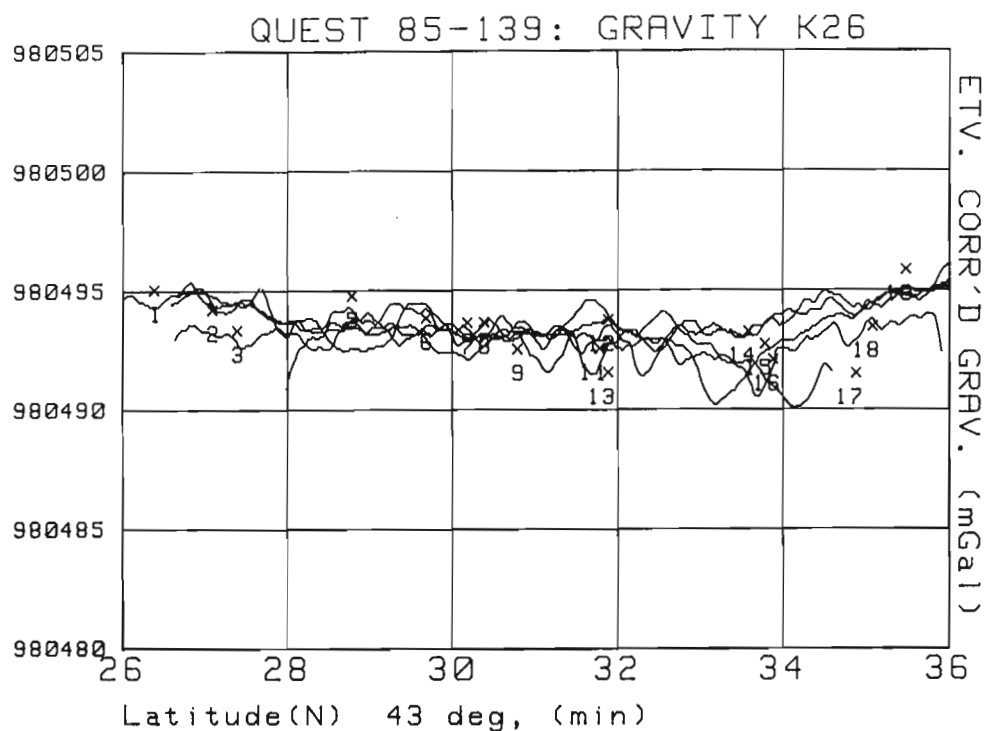
Figure 11.6 also illustrates well the difference between the ship's heading and the course made good. In Figure 11.6a the heading was steady yet the mean true course showed some variation. The most pronounced change is over the northern half of the line where the true course falls off to the west ending up 5 degrees off true north. Since the heading was steady, this falling off would indicate a localized, west flowing, surface current.

On N-S courses, Eotvos effect is dependent primarily on course. As the ship swings to port on a northerly course, the Eotvos effect increases and the raw gravity readings increase as can be seen from Figure 11.5a.

Heading Correction

A heading correction or a permanent platform tilt as a function of ship's heading could be a serious shortcoming in the sea gravimeter performance. Such an effect was suspected following an earlier comparison of a KSS30 and a LaCoste and Romberg SL1 gravimeter (Macnab et al., 1985). It was thought that the heading error may be due to a bug in software since the roll compensation signals in KT30 had opposite sign from those in KT31. Careful search through software code following the cruise failed to detect such a bug.

a. Profiles for gravimeter sensor K26 (K5531 system).



b. Profiles for gravimeter sensor K12 (K5530 system).

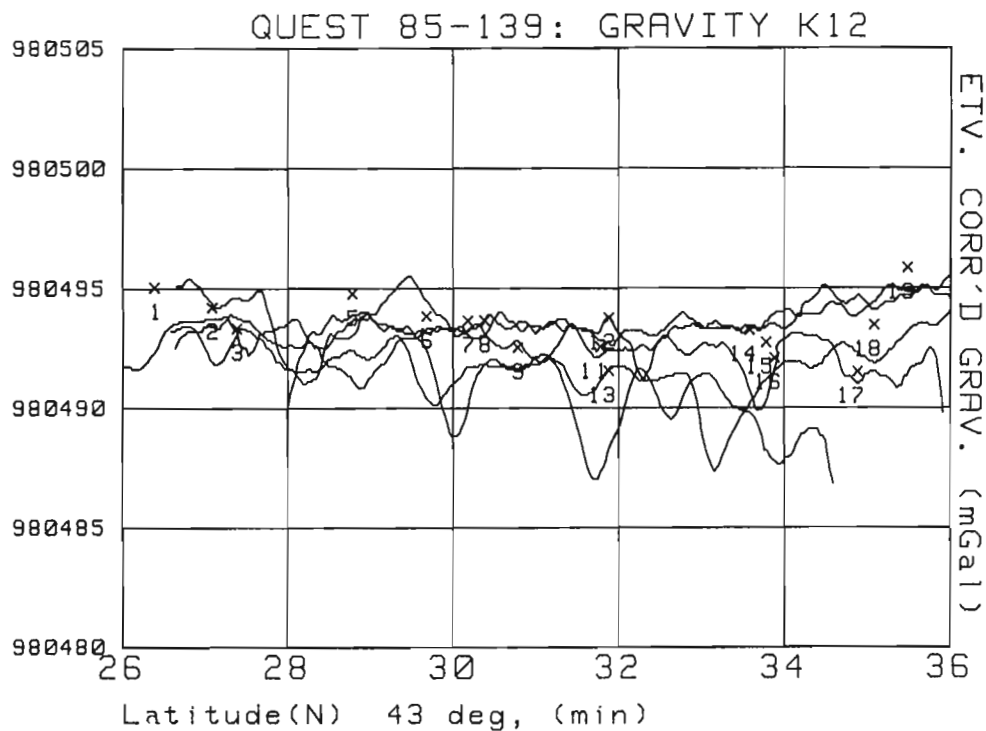
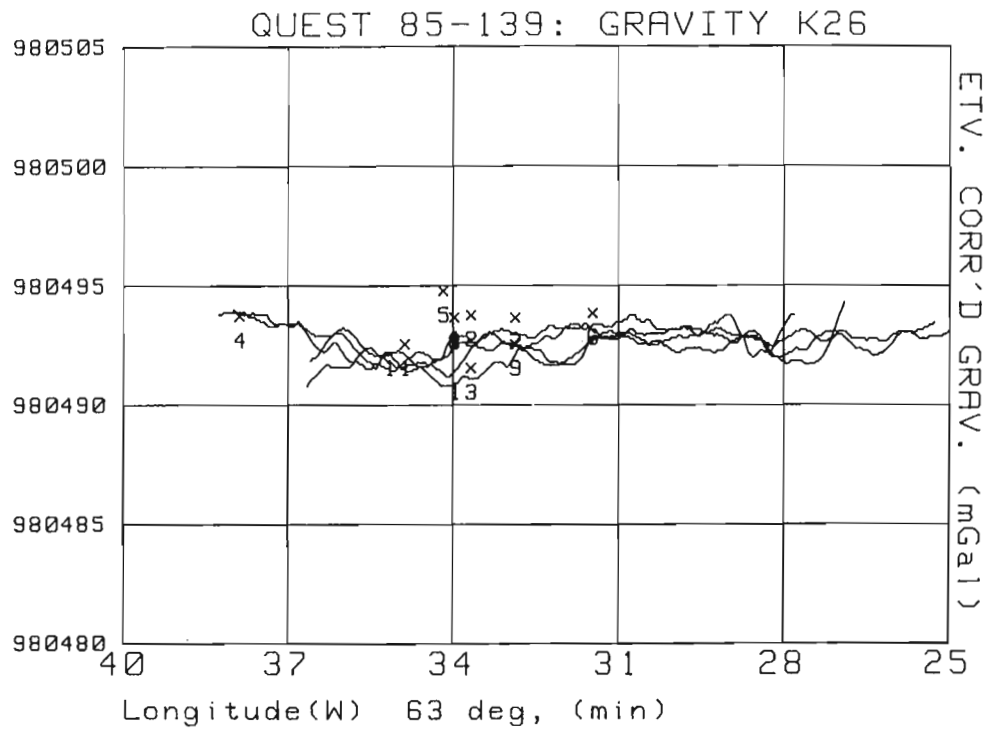


Figure 11.2. Gravity profiles along north-south tracks. Crosses are the surface gravity values at bottom gravimeter stations shown in Figure 11.1.

a. Profiles for gravimeter sensor K26 (KSS31 system).



b. Profiles for gravimeter sensor K12 (KSS30 system).

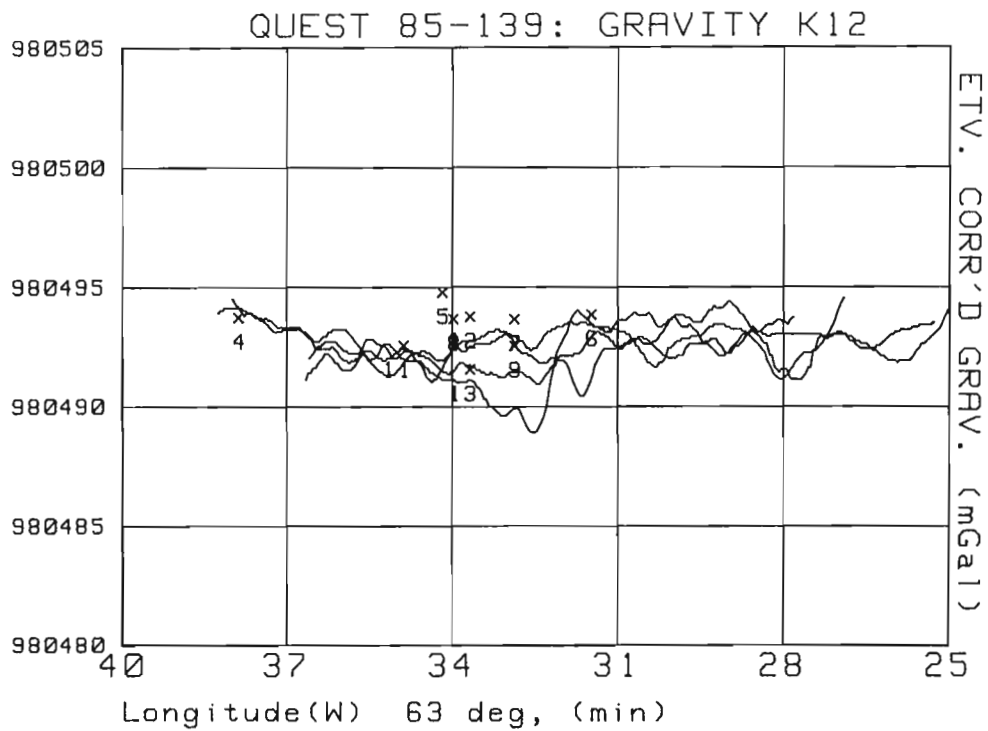


Figure 11.3. Gravity profiles along east-west tracks. Crosses are the surface gravity values at bottom gravimeter stations shown in Figure 11.1.

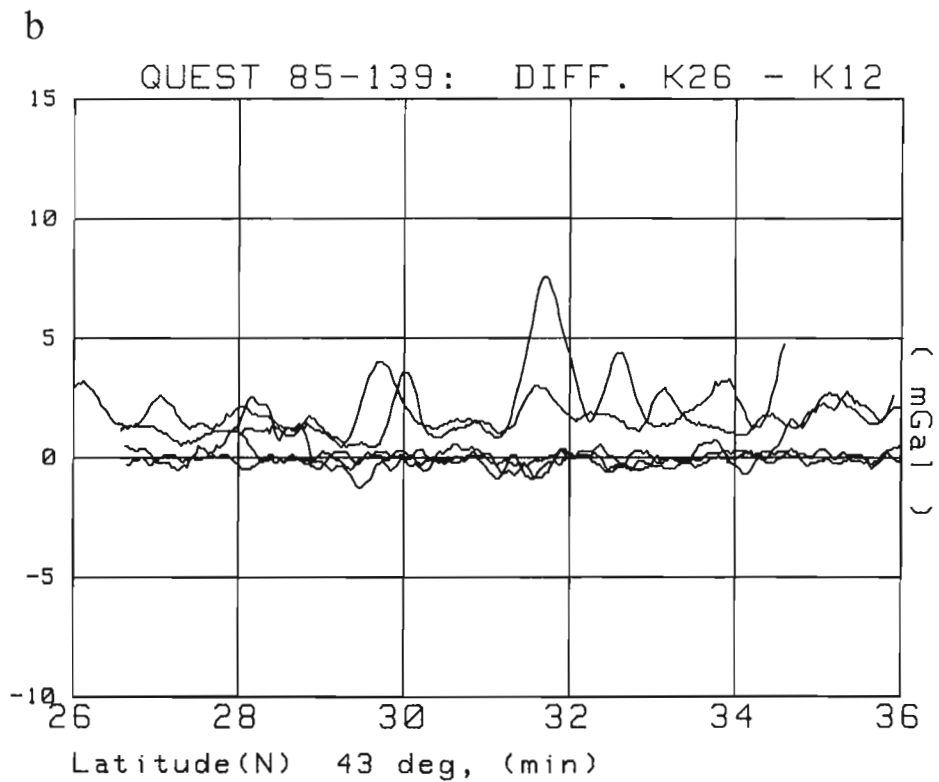
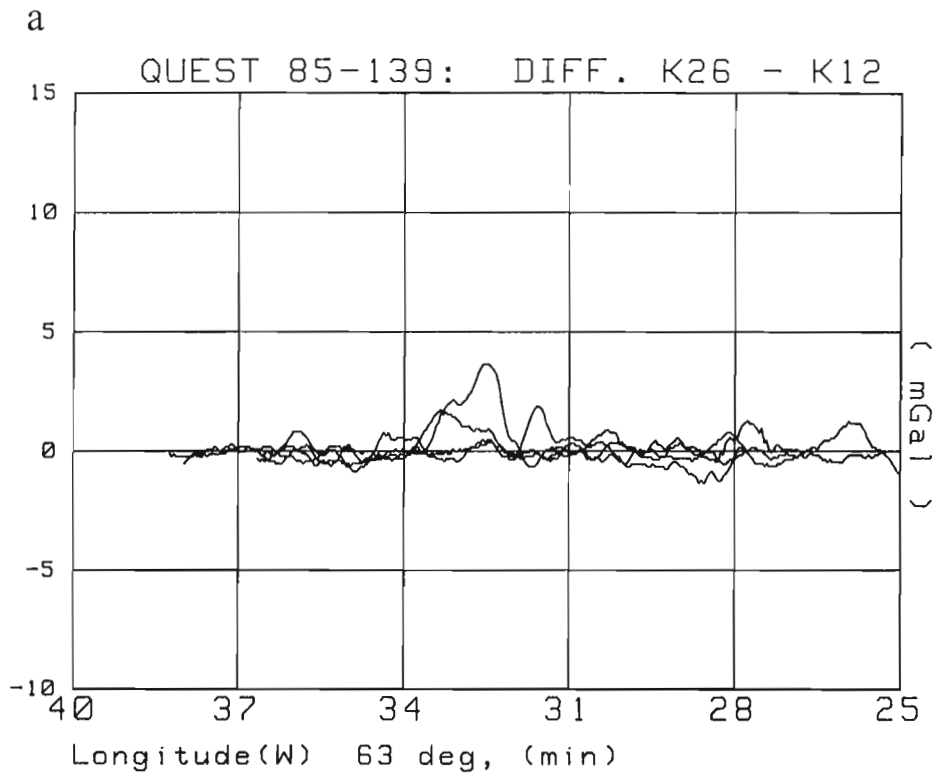


Figure 11.4. The difference between the readings of two gravimeters along
 a. East-west tracks and
 b. North-south tracks. The two displaced profiles in (b) are lines 1N and 2S.

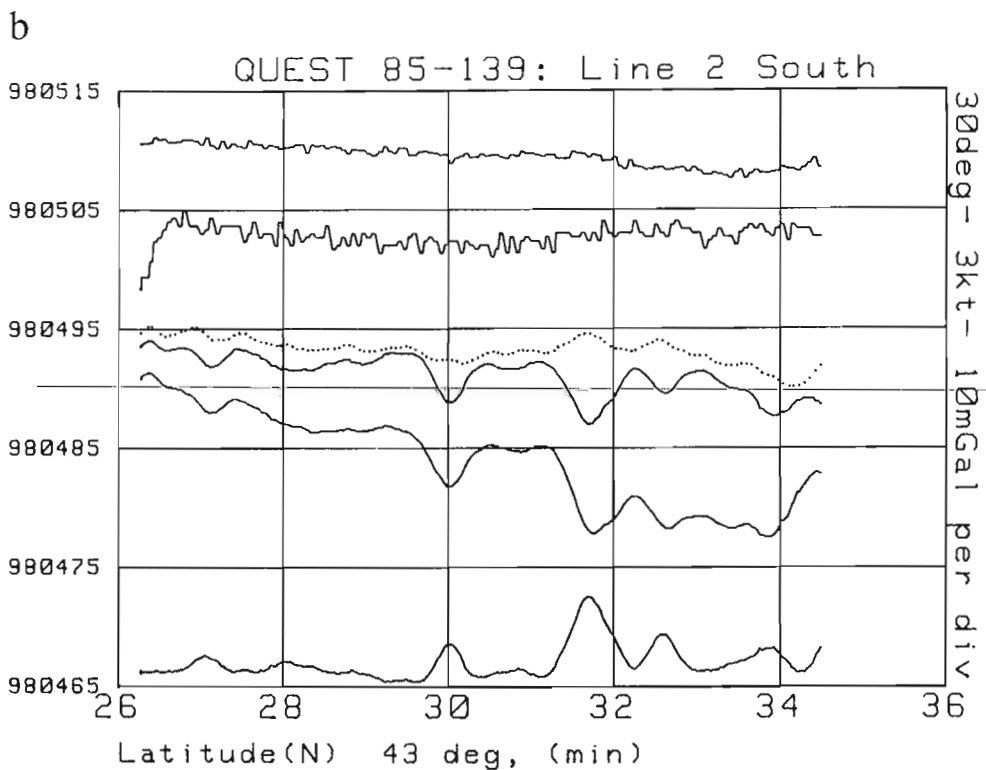
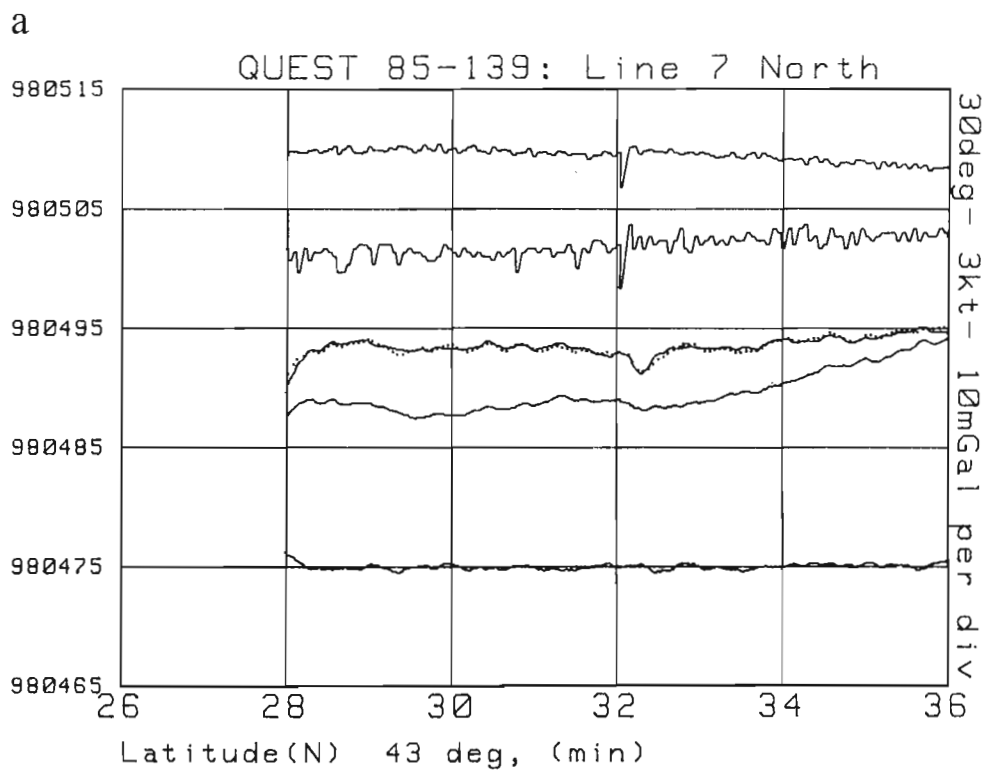


Figure 11.5. Detailed comparison of two gravimeters on a. line 7 North, and b. line 2 South. The six profiles in this figure are from top to bottom: 1, ship's velocity and 2, ship's course from BIONAV; 3, KSS31-26 corrected for Eotvos effect (dashed); 4, KSS30-12 corrected for Eotvos effect; 5, raw gravity for KSS30-12 (this profile is displaced down by 5 mGal so as not to interfere with the two corrected profiles above it); and 6, the difference between corrected readings of K26-K12 (in a. the Y-axis origin is at -10 mGal; in b. the origin is at 0 mGal).

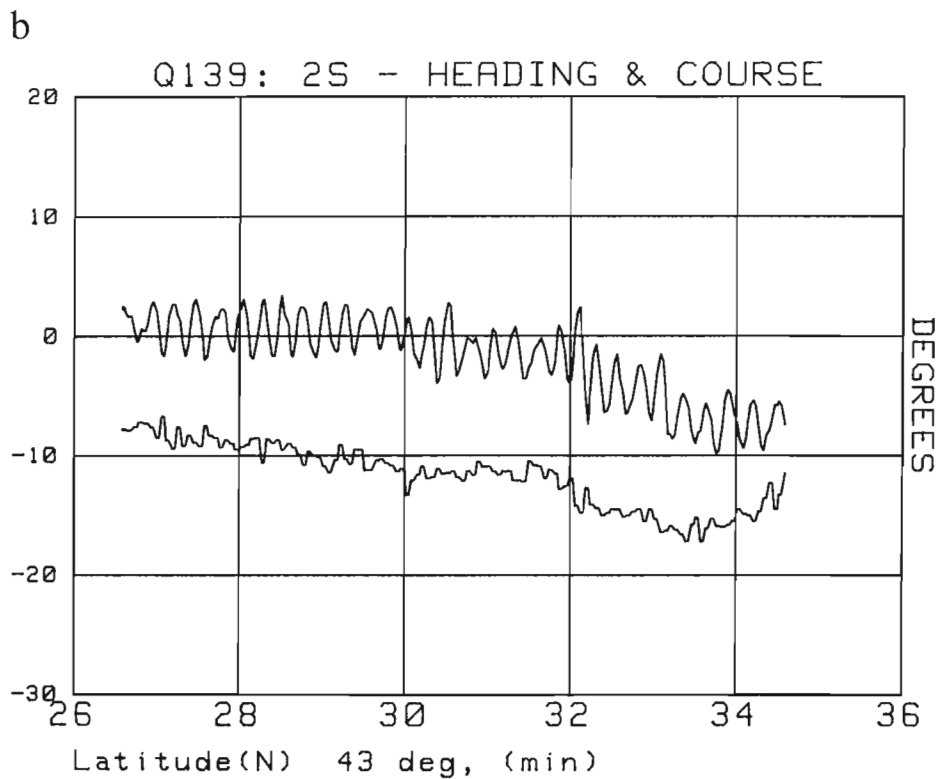
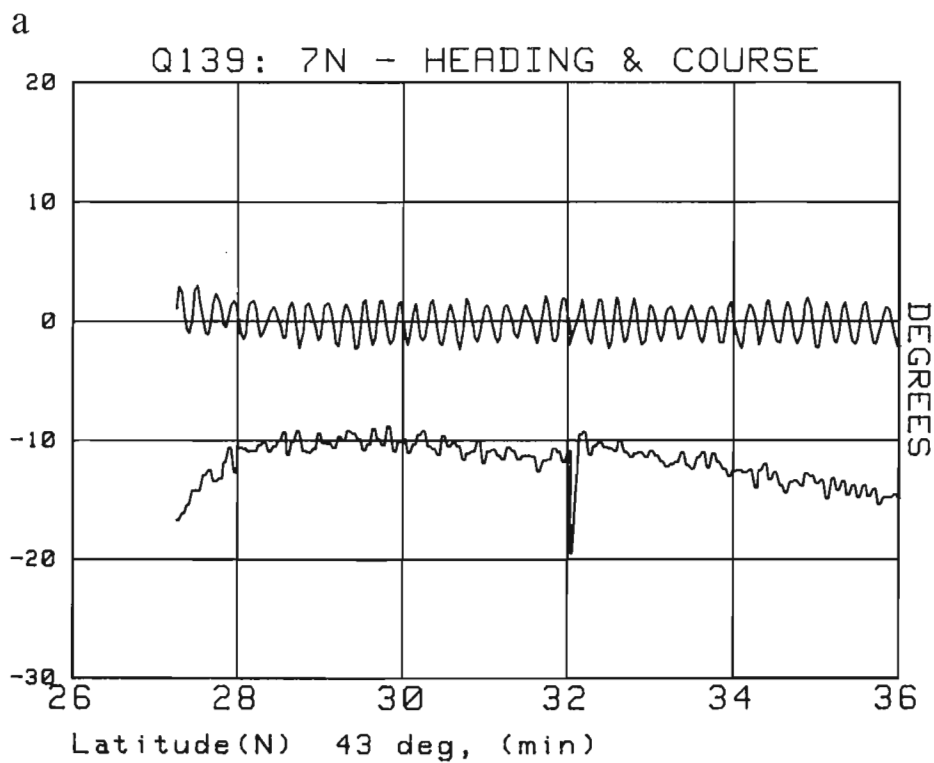


Figure 11.6. Ship's heading (given by the gyro compass) and course (calculated by the BIONAV navigation system). Two profiles are displaced by ten degrees for clarity. Oscillations of the heading are caused by the auto pilot feedback loop. Note lower frequency and higher amplitude of heading oscillations on Line 2S (Fig. 11.6b) compared to Line 7N (Fig. 11.6a).

The tests reported here show no evidence of a heading correction unless both instruments had experienced identical effects. This is unlikely since the two platforms represent radically different designs. The tests do show that KSS30 could be systematically off level (Fig. 11.4b) but this off-leveling is not consistently dependent on heading. It appears that the off-leveling may be a function of the past history, i.e. course, velocity and accelerations experienced some hours earlier may affect later readings. It is difficult to propose a mechanism for this effect, but we note that the ship's speed for the 36 hour period before the arrival at the test range was 13.5 knots and then was dropped to 11.5 knots during the tests. This may have caused a subtle change in the acceleration spectrum, already mentioned.

There is also a possibility of a hidden mechanical fault in the KT30 platform resulting in 'sticky' bearings. The Anschuetz gyro (serial number 109) used on this cruise was suspected of malfunction after the completion of the cruise and has been sent to the manufacturers for the 5000 hour overhaul.

Crossover accuracy

Crossover accuracy was evaluated from 20 crossovers of 4 E-W with 5 N-S lines. The area of crossover points is shown in Figure 11.7. The scale of this plot is greatly enlarged; 0.005 degrees of latitude represents 555 m on the ground. The spread of crossovers is about 600 m in E-W direction and 200 m in N-S direction (indicating a better course keeping in E-W direction).

The results of crossover observations are given in Table 11.2. The values of gravity of both instruments at the time of the closest approach to the intersection are tabulated

together with the differences which indicate the crossover accuracy. Table 11.2 also gives the tidal correction necessary to bring all the crossover values to the mean sea level. These corrections are small but not insignificant. The largest correction of 0.21 mGal for crossover 7/3 reduces the discrepancy from 0.88 mGal to 0.67 mGal for K26 and from 1.68 mGal to 1.47 mGal for K12.

The standard deviation of less than 0.3 mGal for K26 is an excellent result (Table 11.3). With a much larger number of crossovers (say several hundred) it would probably go down and approach that reported by seismic exploration companies. If adequate care is taken, the gravity measurements on a seismic exploration vessel could be more accurate than those on a routine hydrographic survey or on an oceanographic research cruise. The reason for this is that seismic exploration cruises often use dedicated, special purpose, navigational systems (e.g. Argo, Syledis etc.), the vessels steam at a reduced speed of 3 to 5 knots (thus reducing the wave-induced accelerations) and the long seismic cable acts as a sea anchor further steadying the ship's progress through the sea.

Conclusions

From the results reported here, we conclude that shipboard gravity surveys with an expected probable error of less than 1 mGal for a single observation are now within reach using a KSS31 system. To achieve this accuracy, good navigation is essential with a positional accuracy of the order of 50 m and the accuracy of east-west velocity of better than 0.02 knots (0.5 cm/s). In addition, the ship should not be much smaller than the **Quest** (2200 tons displacement). Our tests were carried out in good weather. Unfavourable

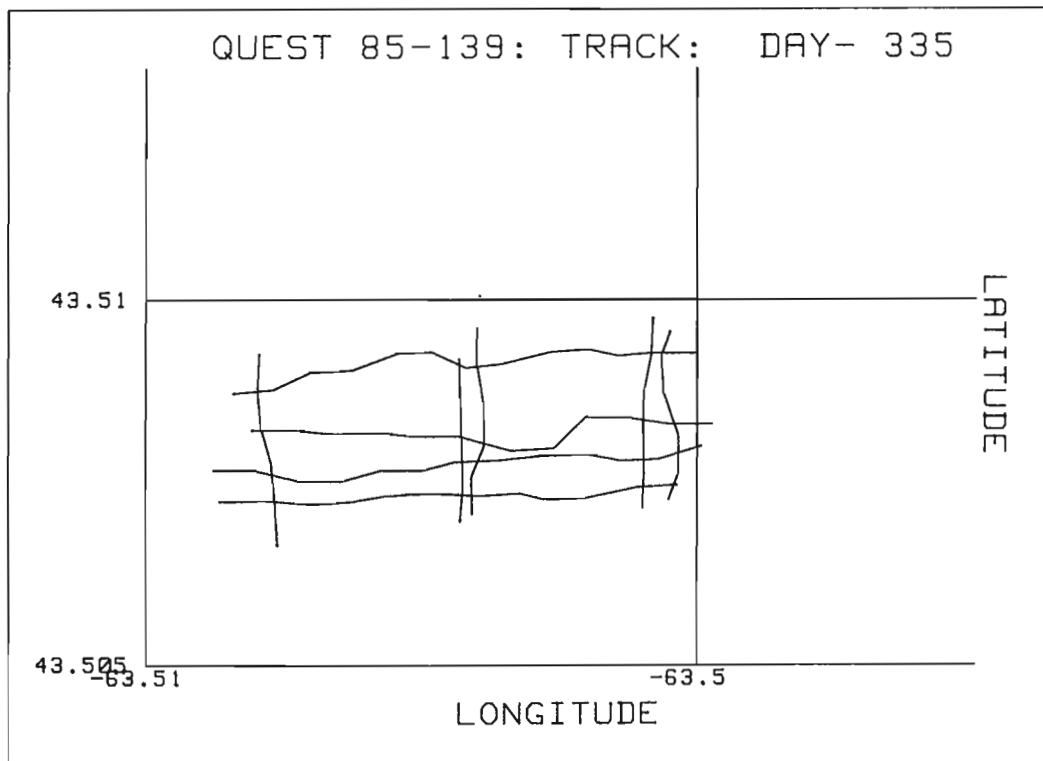


Figure 11.7. Detail of tracks in the vicinity of crossover points. The roughness of the lines is probably due to random noise in navigation rather than jerky motions of the ship through the water. The distance between latitude lines is approximately 555 m and between longitude lines is 806 m.

Table 11.2. The results of crossover observations

Cross over #	Times X1	Times X2	DLat (minutes)	DLon (minutes)	Tidal corr'h	g1	g2	K26 Gravimeter diff.	Tdiff.	g1	g2	K12 Gravimeter diff.	Tdiff.
1/3	00:29:01	3:07:27	0.002	0.008	0.09	3.25	2.80	0.45	0.39	1.73	2.43	0.70	0.60
1/4	00:28:31	4:24:14	0.010	0.002	0.09	3.05	2.26	0.79	0.80	1.73	2.02	0.31	0.28
1/5	00:28:41	5:12:53	0.010	0.010	0.09	3.15	3.16	0.01	0.07	1.73	3.62	1.89	1.81
1/6	00:28:31	6:26:01	0.011	0.022	0.09	3.05	3.17	0.12	0.01	1.73	3.17	1.44	1.31
2/3	01:45:09	3:08:16	0.007	0.008	0.16	3.07	2.61	0.46	0.47	1.93	2.61	0.68	0.67
2/4	01:45:39	4:23:24	0.011	0.015	0.16	2.87	2.66	0.21	0.29	2.03	2.66	0.63	0.55
2/5	01:45:29	5:13:14	0.008	0.004	0.16	2.97	3.16	0.19	0.04	2.03	3.16	1.13	0.99
2/6	01:45:29	6:25:11	0.013	0.007	0.16	2.97	2.98	0.01	0.18	2.03	2.98	0.95	0.75
7/3	08:00:08	3:08:16	0.003	0.011	-0.06	3.49	2.61	0.88	0.67	3.51	1.83	1.68	1.47
7/4	07:59:48	4:23:24	0.015	0.005	-0.06	3.69	2.66	1.03	0.87	3.91	2.32	1.59	1.45
7/5	07:59:38	5:13:43	0.022	0.027	-0.06	3.59	3.16	0.43	0.34	3.71	3.32	0.39	0.32
7/6	07:59:18	6:25:11	0.013	0.017	-0.06	3.79	2.98	0.81	0.79	3.91	2.82	1.09	1.07
8/3	09:17:26	3:09:06	0.001	0.017	-0.05	2.96	2.51	0.45	0.25	2.61	1.83	0.78	0.58
8/4	09:17:56	4:22:34	0.000	0.017	-0.05	3.16	2.56	0.60	0.47	2.91	2.82	0.09	0.04
8/5	09:17:36	5:14:33	0.002	0.010	-0.05	2.96	3.57	0.61	0.67	2.71	3.82	1.11	1.17
8/6	09:17:46	6:24:21	0.006	0.020	-0.05	2.81	2.97	0.16	0.17	2.81	2.62	0.19	0.18
9/3	10:17:24	3:07:27	0.001	0.003	-0.03	3.83	2.80	1.03	0.85	4.01	2.43	1.58	1.30
9/4	10:16:54	4:24:04	0.012	0.008	-0.03	3.23	2.36	0.87	0.76	3.41	2.02	1.39	1.28
9/5	10:17:04	5:13:03	0.009	0.016	-0.03	3.43	3.16	0.27	0.23	3.71	3.62	0.09	0.05
9/6	10:16:54	6:26:01	0.011	0.016	-0.06	3.23	3.17	0.06	0.04	3.41	3.62	0.21	0.20

Note

1. Times of crossovers are given to the nearest ten second logging interval. Considering limitations of navigational accuracy, it is not worth interpolating to the nearest second.
2. Differences of latitude and longitude give an idea of the closeness of approach. The largest distance is on crossovers 7/5. It amounts to 54 m.
3. Tidal correction is given in mGals relative to the mean sea level of 1.300 m.
4. 980 490 mGal should be added to gravimeter readings on crossover points (g1 and g2).

Table 11.3. Summary of results on crossovers

	KSS31-26	KSS30-12
Mean observation at crossover points (N=40)	980 493.05	980 492.81
Mean difference at crossovers (N=20)	0.47	0.90
Standard deviation	0.341	0.574
Mean difference at crossovers after tidal correction (N=20)	0.42	0.80
Standard deviation	0.298	0.535
Mean of bottom stations (N=19)		980 492.84

weather conditions will degrade the accuracy of measurements with a cutoff for useful measurements around 30 to 40 knots wind speed.

The probable error of the KSS30 system is larger than that of the new KSS31 system. It is difficult to estimate the magnitude of the KSS30 probable error because of the suspected malfunction of the gyro but it is most likely between 1 and 1.5 mGal.

Acknowledgments

We are indebted to the Superintendent, Defence Research Establishment Atlantic (DREA) and to Al Bruce, the Chief Scientist for Cruise **Quest** 85-139 for allowing us to participate. Hank Boudreau and Mike McConnell operated BIONAV and assisted with navigation. Everett Coldwell assisted with shipboard data acquisition and post-cruise data reduction. We are grateful to Bodenseewerk Geosystem GmbH for the loan of the KSS31 system used in this project.

References

- Goodacre, A.K.
1964: A shipborne Gravimeter Testing Range near Halifax, Nova Scotia; *Journal of Geophysical Research*, v. 69, p. 1-9.
- Grant, S.T.
1973: Rho-Rho Loran-C combined with satellite navigation for offshore surveys; *International Hydrographic Review*, Monaco, v. 50, p. 35-54.
1977: A user-developed integrated navigation system; *International Congress of Surveyors, Proceedings*, v. 15, Stockholm, p. 99-113.
- Macnab, R.F., Loncarevic, B.D., Cooper, R.V., Girouard, P.R., Hughes, M.D., and Shouzhi, F.
1985: A regional marine multiparameter survey south of Newfoundland; *in* *Current Research, Part B*, Geological Survey of Canada, Paper 85-1B, p. 325-332.
- Wells, D.E. and Grant, S.T.
1981: An adaptable integrated navigation system: BIONAV; *in* *Proceedings of Colloquium III on Petroleum Mapping and Surveys in the 80's*; The Canadian Petroleum Association, Banff, Alberta.

Early Silurian Bryozoa from the Clemville Formation
of the Port Daniel region, Gaspésie Peninsula, Quebec

Project 740084

Thomas E. Bolton
Director General's Office

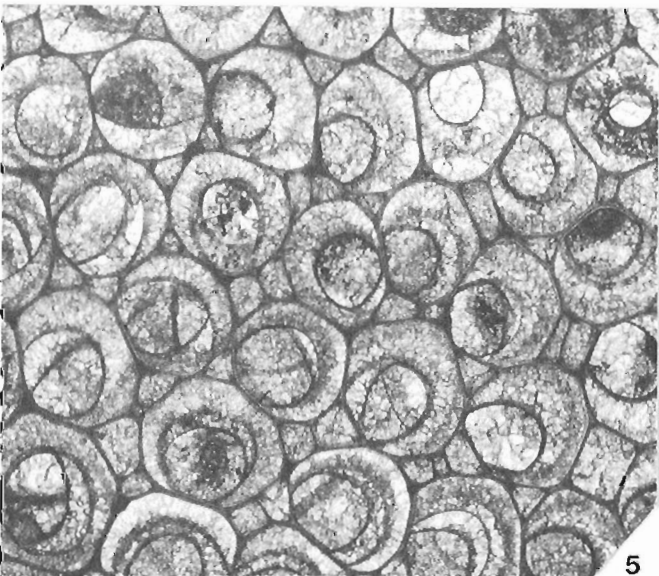
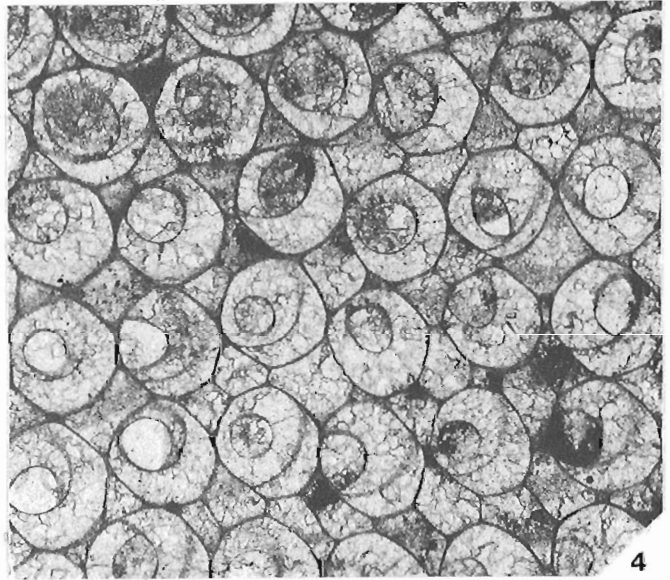
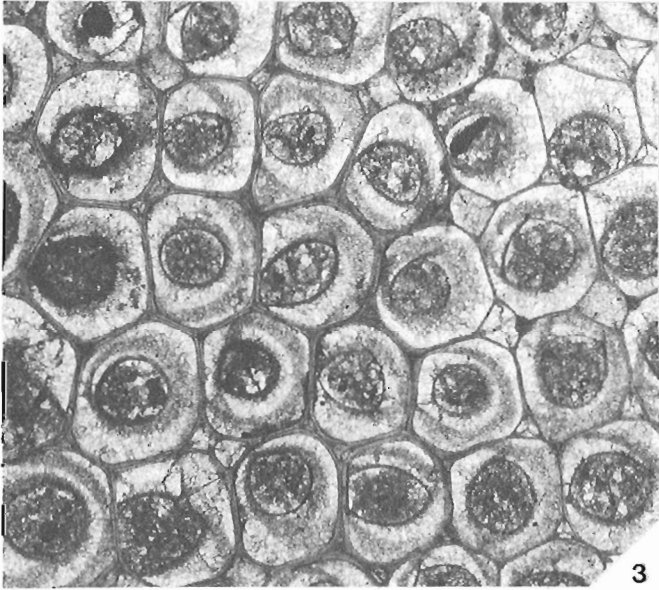
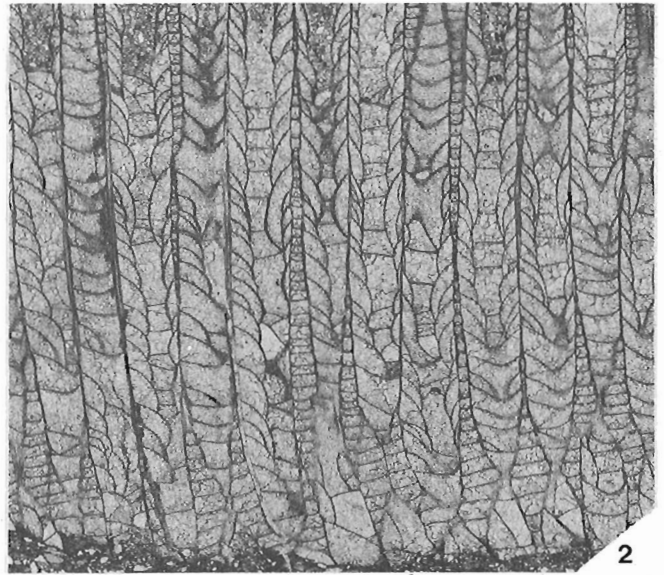
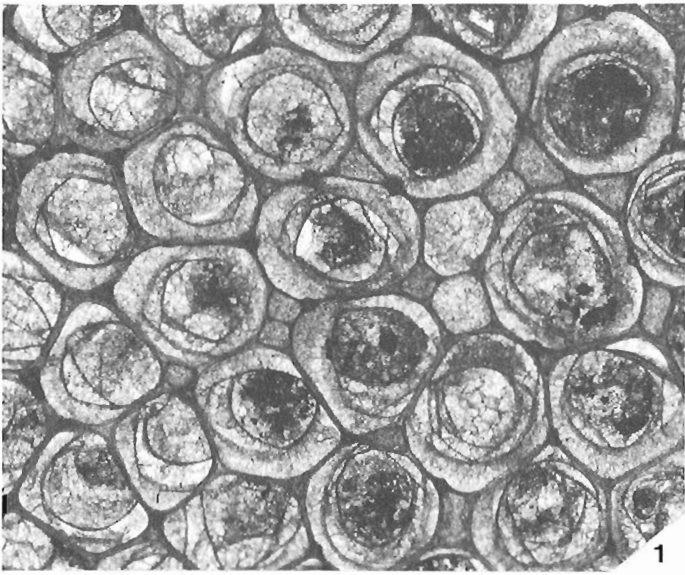
Bolton, T.E., Early Silurian Bryozoa from the Clemville Formation of the Port Daniel region, Gaspésie Peninsula, Quebec; in Current Research, Part B, Geological Survey of Canada, Paper 86-1B, p. 97-106, 1986.

Abstract

A unique bryozoan fauna composed of the common Ordovician genus **Peronopora** in association with **Hallopora magnopora** (Foerste) and **Stictoporella** sp. is described from the Early Silurian pre-Llandoveryan C₁-C₂ beds of the Clemville Formation, Gaspésie Peninsula, Quebec.

Résumé

L'étude décrit des bryozoaires uniques, composés du genre commun **Peronopora** de l'Ordovicien, associés à des **Hallopora magnopora** (Foerste) et **Stictoporella** sp., provenant des couches pré-llandovériennes C₁-C₂ du début du Silurien et faisant partie de la formation de Clemville, en Gaspésie, au Québec.



Introduction

Bryozoa are never abundant in the Silurian rocks of Canada. Their scarcity, plus poor preservation in comparison with Ordovician and Devonian Bryozoa, does not encourage studies of such forms. They have been described from the Middle Silurian (Wenlockian) Rochester Formation of the Niagara Peninsula region, southern Ontario, and neighbouring United States (Bassler, 1906; Bolton, 1966a, Pl. 11), Early Silurian (Alexandrian-Llandoveryan) Manitoulin Formation of the Bruce Peninsula and Manitoulin Island, southern Ontario (Bolton, 1957), Early Silurian (Anticosti-Llandoveryan) of Anticosti Island, Quebec (Bassler in Twenhofel, 1928; Ross, 1960, 1961) and Late Silurian (Ludlovian and Pridolian) of the Canadian Arctic Archipelago (Bolton, 1966b).

Investigations into the Silurian bryozoan faunas of Arctic Canada and Anticosti Island are continuing. These studies, along with the present report detailing a well-preserved association from the Early Silurian (Llandoveryan) Clemville Formation of Gaspésie Peninsula, Quebec, hopefully will enlarge our knowledge sufficiently that establishment of a biostratigraphic framework based on Bryozoa might become feasible.

At least 15 genera have been recognized within the Early Silurian bryozoan fauna of the Manitoulin Formation. *Hallopora*, *Subretopora*, *Helopora*, *Phaenopora*, *Ptilodictya*, *Pachydictya* and *Rhinopora* dominate this assemblage. The earliest Silurian beds of Anticosti Island, Quebec (member 6 of the Ellis Bay Formation and lower beds of the overlying Becscie Formation – Bolton, 1981a) are characterized by *Stictoporella*, *Phaenopora*, *Cyphotrypa*, *Hallopora*, *Helopora*, *Nematopora*, *Ptilodictya* and *Pachydictya*, with cryptostome bryozoans again the most common. Three genera of Bryozoa are described herein from the Clemville Formation, *Peronopora*, *Hallopora*, and *Stictoporella* sp. The Clemville Formation was studied by M.J. Copeland and T.E. Bolton in 1966, 1977 and 1981, and G.S. Nowlan in 1979 and 1981. Thin sections were prepared by G.P. Martin, photography by R.J. Kelly.

Clemville Formation

The Clemville Formation of Bourque and Lachambre (1980, p. 32-35), as exposed along the Little Port Daniel River southwest of the village of Clemville (Bourque, 1981, p. 44, fig. 31), is a heterogeneous 105 m thick sequence of alternating mudstone, thin calcareous sandstone

and siltstone. It is underlain unconformably by the Middle Ordovician Mictaw Group and overlain conformably by the Weir Formation (Nowlan, 1981, p. 268-270).

A Rhuddanian (Llandoveryan A₃-A₄) age *Stricklandia lens typica* brachiopod zone has been delineated in the upper 20 m of the formation (Boucot and Bourque, 1981, p. 317), and Llandoveryan A? – C₂ age *Oulodus? nathani* and *Distomodus kentuckyensis* conodont zones have been described (Nowlan, 1981, p. 270; 1983, p. 102). A few thin coralline beds are present at various levels of the formation. Colonies of the tabulate coral *Paleofavosites* sp. (Bolton, 1981b, Pl. I, Fig. 1-3), *Acidolites clemvillensis* (Parks), *Propora conferta* Milne – Edwards and Haime, *Syringopora* sp. indet. and the rare solitary coral *Streptelasma? sp.* have been identified from 40-41 m below the top of the formation in the type section. A second pocket of *Paleofavosites* sp. was located in beds exposed on the east side of the river, upstream from the type section, south flank of the Clemville anticline, 36.5 to 37.5 m above the base.

The bryozoan beds occur some 3 to 10 m above the base of the formation on the south flank of the Clemville anticline, and to at least 36.8 m above the base on the north flank, some 30 m below the first occurrence of C₁-C₂ conodonts (G.S. Nowlan, personal communication, 1985). All three bryozoan species, *Peronopora juvenis* n. sp. (Pl. 12.1, Fig. 1-6; Pl. 12.3, Fig. 4, 6; Pl. 12.4, Fig. 5), *Hallopora magnopora* (Foerste) (Pl. 12.2, Fig. 1-6; Pl. 12.3, Fig. 1, 2) and *Stictoporella* sp. (Pl. 12.3, Fig. 3-6), occur together 6.7 m to 13.4 m above the base.

Systematic paleontology

Order Trepostomata Ulrich 1882

Family Monticuliporidae Nicholson 1881

Genus *Peronopora* Nicholson 1881, emended Boardman and Utgaard 1966

Type species. *Chaetetes decipiens* Rominger 1866.

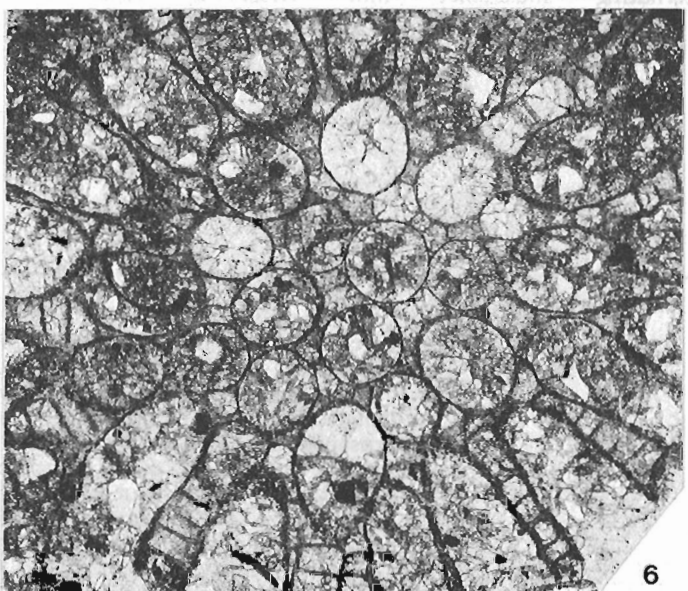
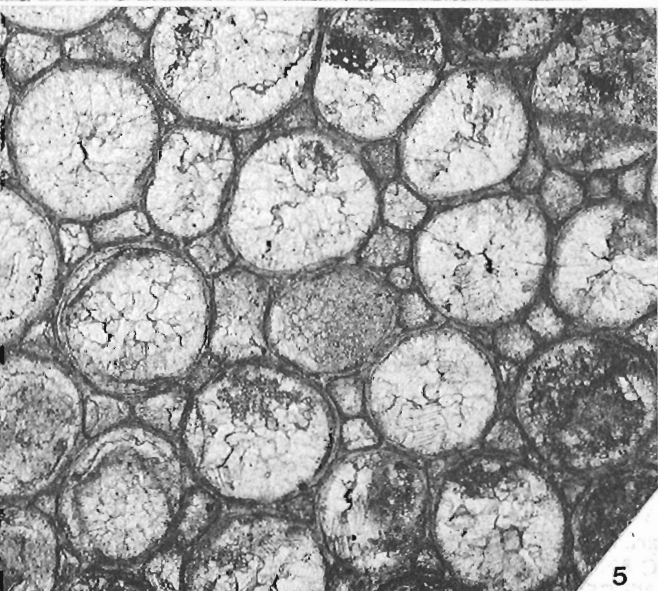
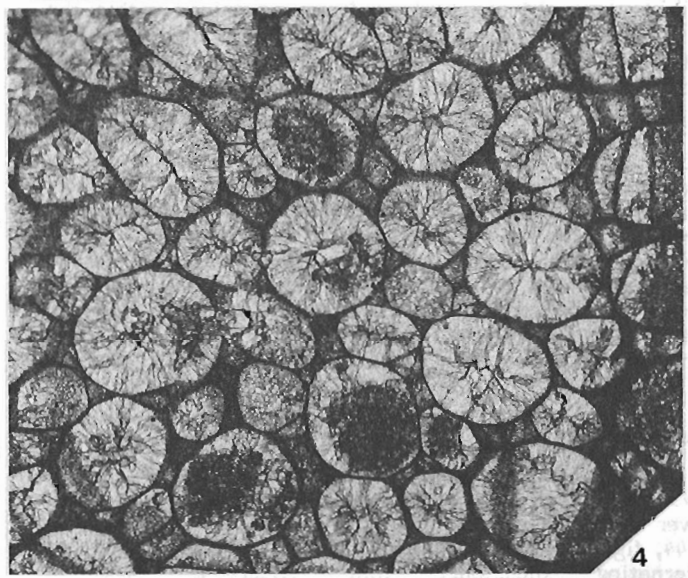
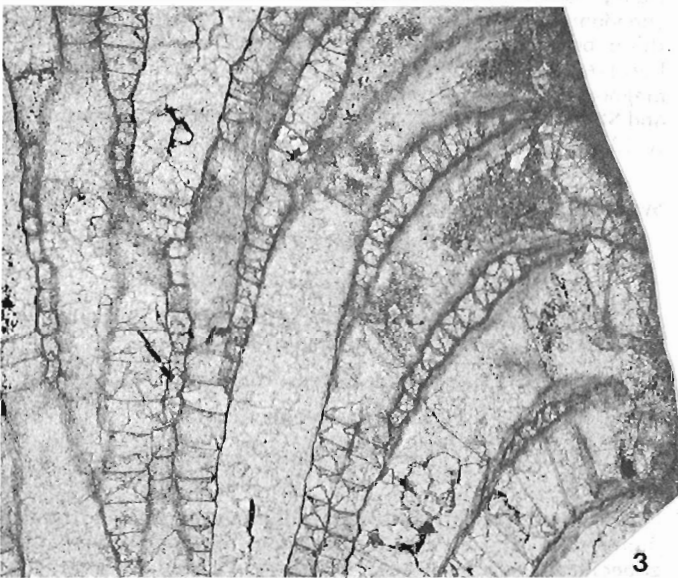
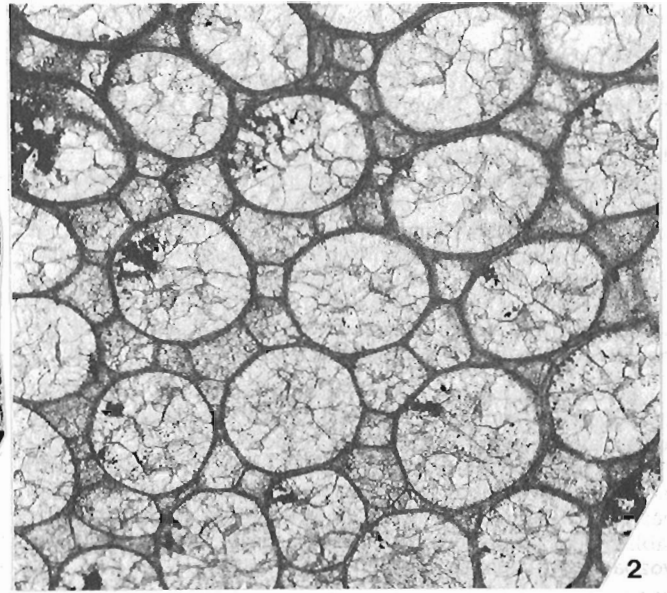
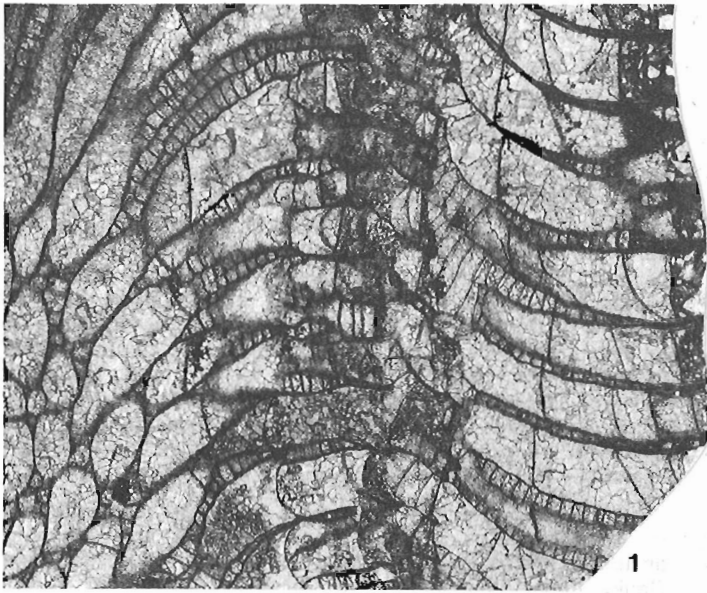
Peronopora juvenis n. sp.

Plate 12.1, figures 1-6; Plate 12.3, figures 4, 6;
Plate 12.4, figure 5

Description. Zoaria non-bifoliate laminar expansion from 1 to 5 mm thick, flat or slightly elevated. In tangential sections, zooecia are subcircular to 5-, 6- or 7-sided, in contact or

PLATE 12.1

- Figures 1-6. *Peronopora juvenis* n. sp. Clemville Formation.
1. Tangential section through maculae showing large mesozooecia and acanthopores in corners and walls, x 40; GSC locality 98406, paratype, GSC 82125.
 - 2, 4. Longitudinal section showing zooecia directly arising from epitheca, abundant *Prasopora*-like cystiphragms lining both walls and resulting central siphuncle-like structure, and long, clear acanthopore tubes or styles, x 20, and tangential section showing thin walls, abundant mesozooecia and rare acanthopore in corner, x 40; GSC locality 98032, paratype, GSC 82133.
 3. Tangential section showing thick integrate walls, rare large acanthopore in corners, x 40; GSC locality 98409, paratype, GSC 82135 (see Pl. 12.4, fig. 5).
 - 5, 6. Tangential and longitudinal sections, x 40; GSC locality 98420, holotype, GSC 82123.



separated at corners by small angular mesozooecia of various sizes (Pl. 12.1, fig. 3, 5), rarely surrounded by larger mesozooecia (Pl. 12.1, fig. 4), walls generally thin; zooecia range from 0.36 to 0.56 mm in diameter, largest in maculae (Pl. 12.1, fig. 1), 5 to 5 1/2 in 2 mm length, 4 to 7 whole zooecia in 1 mm square, 1 to 11 whole mesozooecia in 1 mm square, 4 to 5 on the average; maculae contain 3 to 4 zooecia in 1 mm square with 6 mesozooecia and 3 acanthopores; round acanthopores 0.04 to 0.06 mm in diameter, 0 to 6 in 1 mm square normally, located at corners and rarely in walls, clear centres (Pl. 12.1, fig. 1).

In longitudinal sections, zooecia arise directly from base (Pl. 12.1, fig. 2; Pl. 12.3, fig. 4, 6), rarely recumbent for a very short distance from the epitheca; walls uniformly thin except where thickened by clear straight and hooked acanthopore rods or styles (Pl. 12.1, fig. 2, 6); zooecia with straight diaphragms only, low overlapping cystiphragms along one wall and short straight diaphragms, and overlapping cystiphragms lining both walls with short straight diaphragms restricted to a central tube as in *Prasopora* (see Ross, 1967, p. 406, text-fig. 2A), spacing variable; mesozooecia long, with horizontal diaphragms evenly spaced 11 to 13, rarely 16, in 1 mm length.

Discussion. Boardman and Utgaard (1966) redefined *Peronopora* to include zoaria with and without a median layer (bifoliate and non-bifoliate encrusting). The new species falls within the latter type, with mature specimens similar to the encrusting *Peronopora* sp. illustrated by Boardman and Utgaard (compare their Pl. 136, fig. 4b with Pl. 12.1, fig. 6 herein). They recognized 10 species of *Peronopora*, 3 of which were encrusting forms, whereas Astrova (1978, p. 94) listed 14 species, all from Ordovician rocks.

Within the Ordovician trepostomate bryozoan faunas of Anticosti Island, Quebec, Bassler (in Twenhofel, 1928) established *Prasopora canadensis* n. sp. characteristic of the Richmondian Vaureal Formation and *Aspidopora siluriana* n. sp. restricted to the overlying members 1 and 2 of the Gamachian Ellis Bay Formation. The older species might best be assigned to the genus *Monticulipora* d'Orbigny 1849, whereas the younger species was reassigned to the genus *Peronopora* Nicholson 1881 by Boardman and Utgaard (1966, p. 1097).

Zoaria of *A. siluriana* Bassler (in Twenhofel 1928, p. 149, Pl. 7, fig. 4; Pl. 8, fig. 4, 5) are small laminar expansions 1 to 2.2 mm thick, frequently encrusting brachiopods (Pl. 12.4, fig. 6). In tangential sections (Pl. 12.4, fig. 1, 3), the zooecia are rounded to oval to 5- or 6-sided, normally in contact or separated at the corners by small angular mesozooecia, with an average diameter of 0.28 mm but ranging from 0.2 to 0.36 mm, 6 to 10 in 2 mm length, 10 to 15 whole zooecia in 1 mm square; zooecial walls thin, clear, amalgamate; acanthopores round, 0.02 mm in diameter, located only in corners, arranged in clusters. In longitudinal sections (Pl. 12.4, fig. 2, 4, 6), zooecia are rarely recumbent, walls thin with rare hollow acanthopore rods, with single continuous rows of overlapping large cystiphragms, 4 to 6 in 1 mm length, and straight complete diaphragms both present; mesozooecia long, in single or double rows with abundant evenly spaced thin horizontal diaphragms, 16 to 16 1/2 in 1 mm length.

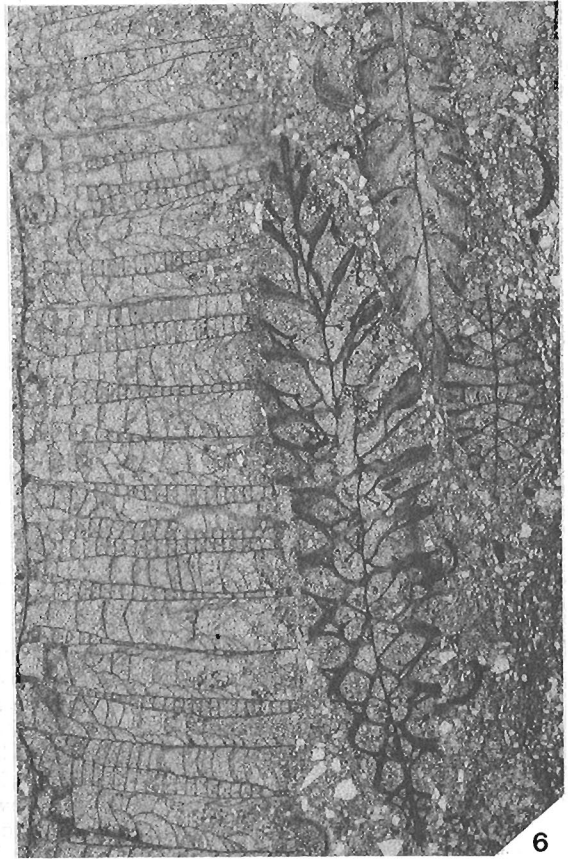
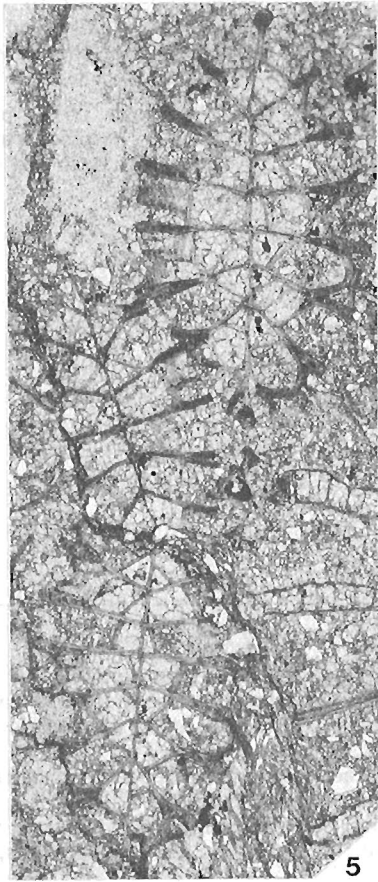
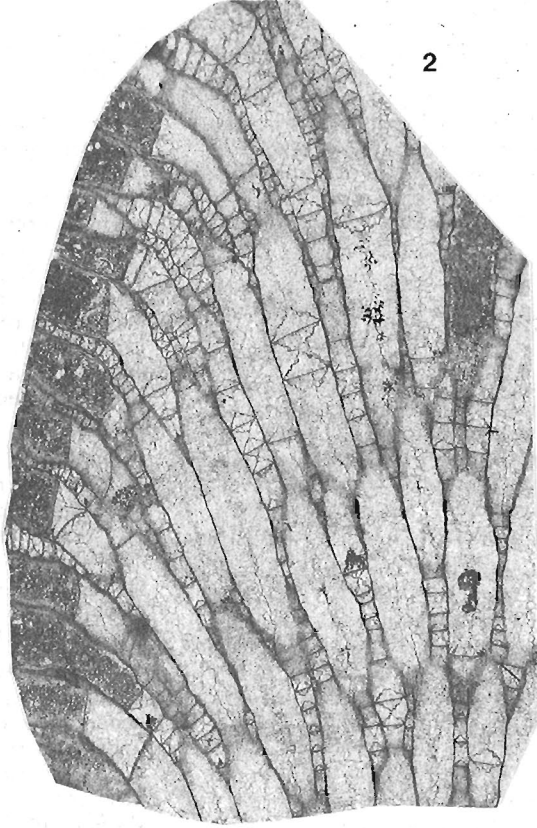
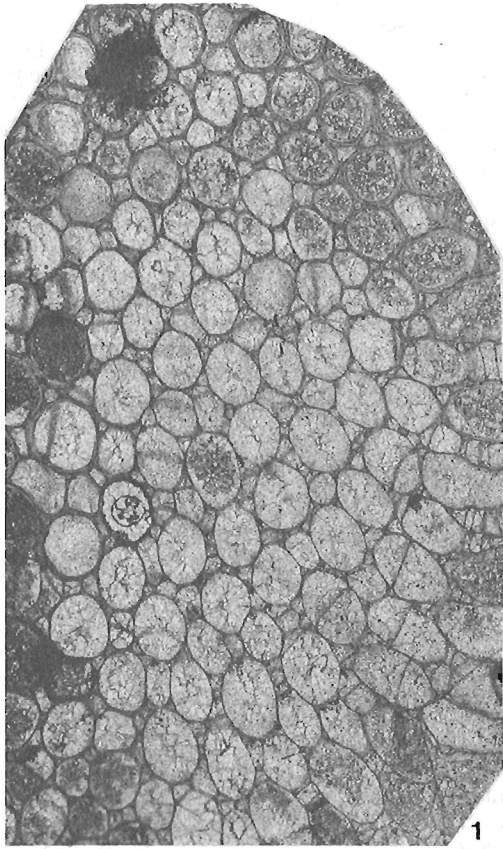
Several of the thinner (1 to 1.5 mm) laminar expansions of *P. juvenis* n. sp. in longitudinal section display single rows of cystiphragms (ie., Pl. 12.3, fig. 6 (right side); Pl. 12.4, fig. 5) and mesozooecial zones up to 0.8 mm wide that closely resemble *P. siluriana* (Pl. 12.4, fig. 6). The presence of double rows of overlapping cystiphragms in thicker sections of *P. juvenis* n. sp. and acanthopores located in both corners and zooecial walls separate the two species.

The development of double rows of these overlapping cystiphragms within the exozone or throughout mature zooecia indicates a close relationship between *Peronopora juvenis* n. sp. and *Prasopora*. Thick colonies of *P. juvenis* n. sp. in particular are similar to the Middle Ordovician *Prasopora simulatrix* Ulrich 1886 (compare, Ross, 1967, Pl. 47, fig. 1 with Pl. 12.1, fig. 2 herein), but in the new species the zooecia are consistently larger (0.36 to 0.56 mm compared to 0.2 to 0.3 mm), the cystiphragms are lower (longer vertically and thus narrower), and the horizontal diaphragms of the mesozooecia are more separated (11 to 13 compared to 9 to 28 in 1 mm length).

Astrova (1978, p. 90) listed 19 species of *Prasopora* (including *Aspidopora* species which she considered synonymous) from the Middle Ordovician, 10 from the Upper

PLATE 12.2

- Figures 1-6. *Hallopora magnopora* (Foerste). Clemville Formation.
- 1, 3. Longitudinal sections showing variation in number of diaphragms in zooecia and long mesozooecia in endozone and exozone, x 20 and x 40; GSC localities 98414 and 98039, hypotypes, GSC 82140, 82139.
 - 2, 5. Tangential sections showing abundant mesozooecia frequently isolating the zooecia, x 40; GSC locality 98414, hypotypes, GSC 82141, 82140.
 - 4, 6. Transverse sections showing oval zooecia and variation in size and number of mesozooecia, x 40; GSC localities 98411 and 98406, hypotypes, GSC 82137, 82136.



Ordovician and 2 from the Silurian. *P. gothlandica* Hennig 1908 from the Lower Ludlovian Hemse Group (Borg, 1965, p. 55) consists of zooecia averaging 0.14 mm in diameter according to Borg (1965, p. 57) or 0.2 to 0.25 mm and 7 to 8 in 2 mm length according to Hennig (1908, p. 28); the characteristic prasopoid cystiphragms are not well developed so that the exact generic assignment of this species is uncertain. *P. parmula* Foerste 1887 from the Brassfield Formation of Ohio has been assigned to *Aspidopora* Ulrich 1882. An additional Silurian form, *P. codonophylloides* Yang and Xia 1976 from Yunnan, China, is characterized by zooecia ranging from 0.22 to 0.27 mm in diameter and 6 to 9 in 2 mm length (Yang and Xia, 1976, p. 49) – this might be a species of *Monticulipora* d'Orbigny 1850 as mesozooecia are rare. Accordingly, the genus *Prasopora* may be restricted to Ordovician rocks.

Types. Holotype, GSC 82123, GSC locality 98420, basal 3 m of the Clemville Formation as exposed in the north flank of the Clemville anticline, east shore Little Port Daniel River just upriver from Mictaw Group exposure; paratypes, GSC 82124-82126, GSC locality 98406, 6.7 mm above base just downriver from Mictaw Group exposure, GSC 82127-82130, GSC locality 98420, GSC 82131, 82132, GSC localities 98411 and 98412, 13.4 m above base, GSC 82133, 82134, GSC locality 98032, 15.5 m above base, and GSC 82135, GSC locality 98409, 36.8 m above base, all upriver from Mictaw Group exposure.

Family Halloporidae Bassler 1911

Genus *Hallopora* Bassler 1911

Types species. *Callopora elegantula* Hall 1852

Hallopora magnopora (Foerste) 1887

Plate 12.2, figures 1-6; Plate 12.3, figures 1, 2

Callopora magnopora Foerste, 1887, p. 173, Pl. 16, fig. 5.

Callopora magnopora Foerste. Bassler, 1906, p. 42, Pl. 15, fig. 1-8; Pl. 26, fig. 3.

Description. Zoaria irregularly ramose. In tangential section, zooecia are oval (Pl. 12.2, fig. 4, 6; Pl. 12.3, fig. 1), to subpolygonal, in contact or separated by angular mesozooecia varying in size and number (Pl. 12.2, fig. 2, 5), 0.32 to 0.48 mm in diameter, rare 0.56 mm in maculae, 2 to 2 1/2 present in 1 mm length, 3 to 5 whole zooecia in 1 mm square, 7 to 8 or rarely 10 whole mesozooecia in 1 mm square; walls thin, thickest in exozone; no spines present as in *H. elegantula* (Hall) as defined by Ross (1969, p. 271) and Corneliussen and Perry (1973, p. 191).

In longitudinal section, zooecia open either obliquely (Pl. 12.3, fig. 2) or directly to surface, flat diaphragms in endozone rare, one or two diaphragms normally in exozone turning upward into walls (Pl. 12.2, fig. 3; Pl. 12.3, fig. 2), and two or three closer, flat to inclined diaphragms near periphery (Pl. 12.2, fig. 1); mesozooecia usually long in exozone, 8 to 14 diaphragms in 1 mm length.

Discussion. Some Clemville specimens differ from *H. magnopora* Foerste as determined by Bassler (1906) in that the mesozooecia can be more abundant in the latter. In occasionally opening obliquely to the surface (Pl. 12.3, fig. 2) the specimens resemble *H. obliquipora* Bolton, 1957 from the Early Silurian Manitoulin Formation of Ontario, but zooecia in that species are slightly smaller (3 in 1 mm length) and mesozooecia are more abundant.

Types. Hypotypes, GSC 82136, GSC locality 98406, GSC 82137, GSC locality 98411, GSC 82138, 82139, GSC locality 98039, 32 mm above base, and GSC 82140, 82141, GSC locality 98414, 36 m above base of the Clemville Formation, all collections upriver from Mictaw Group exposure.

PLATE 12.3

- Figures 1, 3. *Hallopora magnopora* (Foerste). Clemville Formation. Oblique transverse section showing oval zooecia with thin and thick amalgamate walls, rare zooecial diaphragm, and longitudinal section with diaphragms in both endozone and exozone, and long mesozooecia, x 20; GSC locality 98039, hypotype, GSC 82138.
- 3-6. *Stictoporella* sp. Clemville Formation. Longitudinal and oblique longitudinal sections displaying well developed short superior and long inferior hemisepta (fig. 3, 6) or long superior and short inferior hemisepta (fig. 4), and transverse sections with no median tubuli in mesotheca (fig. 5, 6), x 40, x 40, GSC locality 98406 and x 40, x 20, GSC locality 98032, fig. specs., GSC 82143, 82142, 82144, a, b, 82145, a, b (associated with *Peronopora juvenis* n. sp., paratypes, GSC 82124 (fig. 4), 82134 (fig. 6).

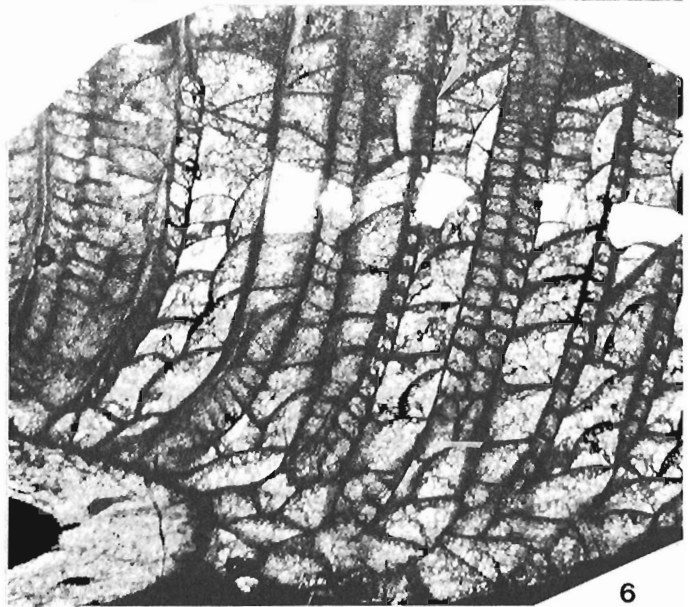
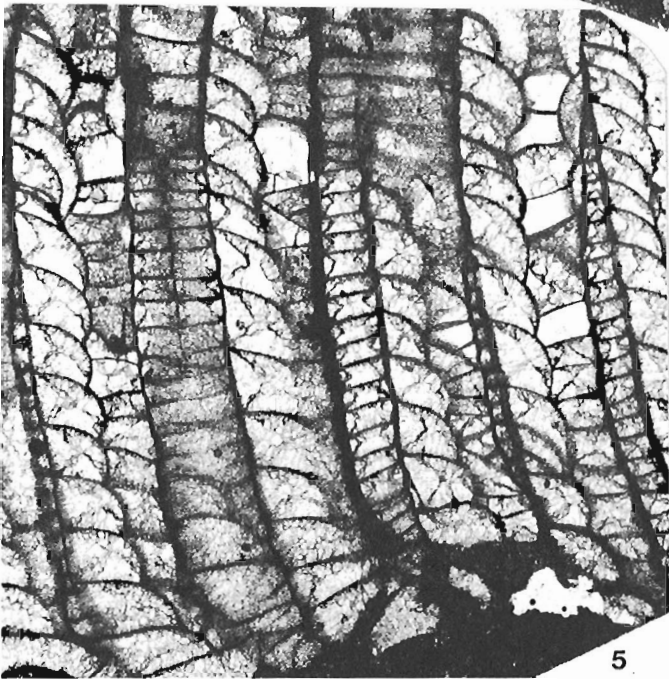
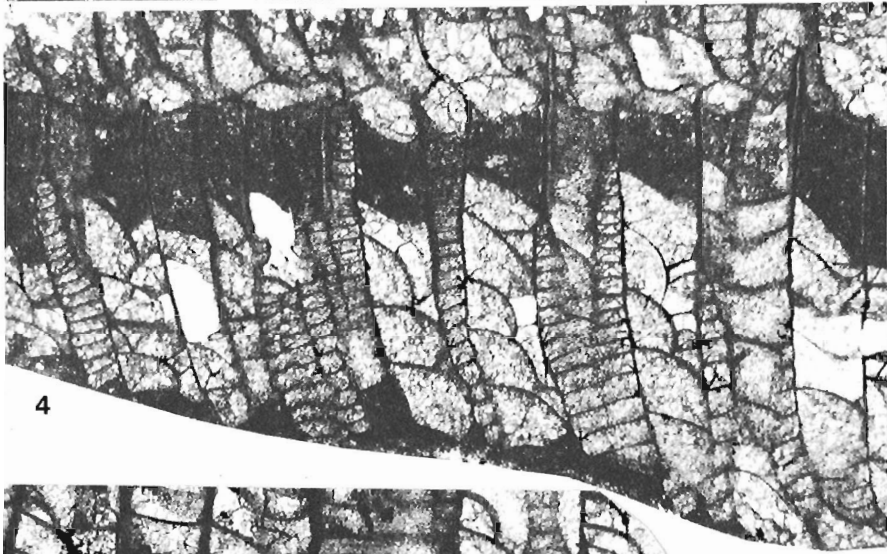
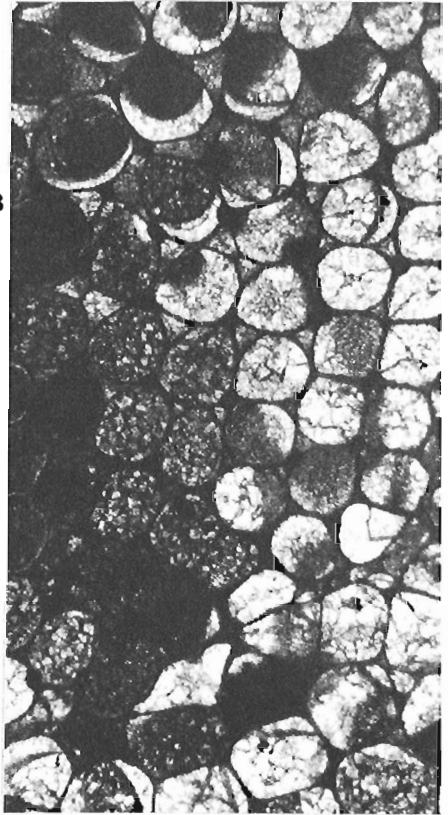
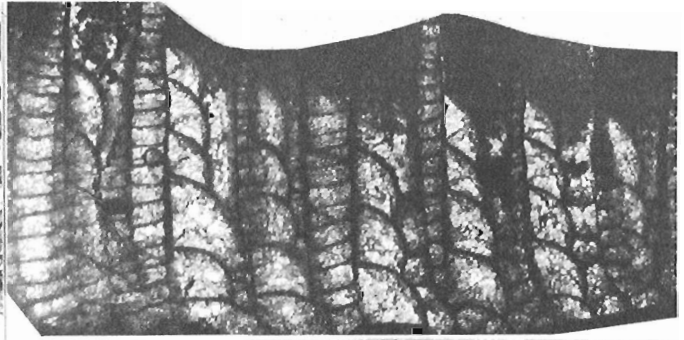
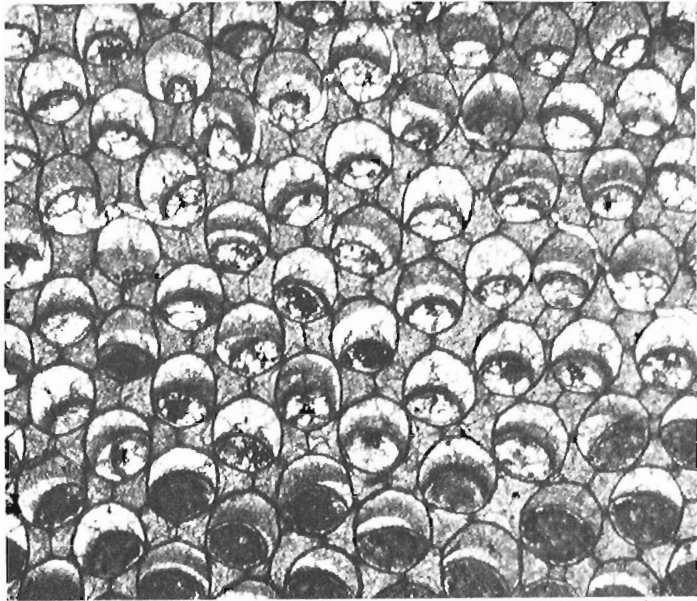


PLATE 12.4

- Figures 1-4, 6. *Peronopora siluriana* (Bassler). Ellis Bay Formation, Upper Ordovician, Anticosti Island, Quebec.
- 1, 2. Oblique tangential and longitudinal sections, x 40; Junction Cliff, holotype, USNM 79499.
 - 3, 4. Longitudinal section showing large cystiphragms, few diaphragms, wide mesozooecia and distally located hollow acanthopore rods, and tangential section showing small and large zooecia and large acanthopores in corners, x 40; GSC locality 62137 (BF 121), La Loutre road 3.8 km south of main highway, hypotype, GSC 82875.
 6. Longitudinal section of encrusting form showing long acanthopore rod and equal development of cystiphragms and diaphragms, x 40; same locality as figure 3, hypotype, GSC 82876.
- Figure 5. *Peronopora juvenis* n. sp. Clemville Formation. Longitudinal section showing zooecia arising directly from epitheca, abundant continuous overlapping cystiphragms as in *P. siluriana* (compare with fig. 6) and rare lining of both zooecial walls, x 40; GSC locality 98409, paratype, GSC 82135 (see Pl. 12.1, fig. 3).

References

- Astrova, G.G.
1978: Evolution, systematics and phylogeny of Bryozoa of the Order Trepostomata; Academy of Sciences USSR, Transactions of the Paleontological Institute, v. 169, 183 p.
- Bassler, R.S.
1906: The bryozoan fauna of the Rochester Shale; U.S. Geological Survey, Bulletin 292, sec. C., Systematic Geology and Paleontology, no. 78, 65 p.
- Boardman, R.S. and Utgaard, J.
1966: A revision of the Ordovician genera *Monticulipora*, *Peronopora*, *Heterotrypa*, and *Dekayia*; Journal of Paleontology, v. 40, no. 5, p. 1082-1108.
- Bolton, T.E.
1957: Silurian stratigraphy and palaeontology of the Niagara Escarpment in Ontario; Geological Survey of Canada, Memoir 289, 141 p.
1966a: Illustrations of Canadian fossils Silurian faunas of Ontario; Geological Survey of Canada, Paper 66-5, 46 p.
1966b: Some late Silurian Bryozoa from the Canadian Arctic Islands; Palaeontology, v. 9, pt. 3, p. 517-522.
1981a: Ordovician and Silurian biostratigraphy, Anticosti Island, Québec; IUGS Subcommittee on Silurian Stratigraphy, Ordovician-Silurian Boundary Working Group. Field Meeting, Anticosti-Gaspé, Québec 1981, Volume II: Stratigraphy and Paleontology, p. 41-59.
1981b: Early Silurian Anthozoa of Chaleurs Group, Port Daniel-Black Cape region, Gaspé Peninsula, Québec; IUGS Subcommittee on Silurian Stratigraphy, Ordovician-Silurian Boundary Working Group. Field Meeting, Anticosti-Gaspé, Québec 1981, Volume II: Stratigraphy and Paleontology, p. 299-314.
- Borg, F.
1965: A comparative and phyletic study on fossil and recent Bryozoa of the suborders Cyclostomata and Trepostomata; Arkiv for Zoolgie, ser. 2, Bd. 17, nr. 1, 191 p.
- Boucot, A.J. and Bourque, P.-A.
1981: Brachiopod biostratigraphy of the Llandoverian rocks of the Gaspé Peninsula; IUGS Subcommittee on Silurian Stratigraphy, Ordovician-Silurian Boundary Working Group. Field Meeting, Anticosti-Gaspé, Québec 1981, Volume II: Stratigraphy and Paleontology, p. 315-321.
- Bourque, P.-A.
1981: Baie des Chaleurs area; IUGS Subcommittee on Silurian Stratigraphy, Ordovician-Silurian Boundary Working Group. Field Meeting, Anticosti-Gaspé, Québec 1981, Volume I: Guidebook, p. 42-56.
- Bourque, P.-A. and Lachambre, G.
1980: Stratigraphie du Silurien et du Devonien basal du sud de la Gaspésie; Ministère de l'Énergie et des Ressources, Québec, Étude Scientifique 30, 123 p.
- Corneliussen, E.F. and Perry, T.G.
1973: *Monotrypa*, *Hallopora*, *Amplexopora* and *Hennigopora* (Ectoprocta) from the Brownsport Formation (Niagaran), western Tennessee; Journal of Paleontology, v. 47, no. 2, p. 151-220.
- Hennig, A.
1908: Gotlands Silur-Bryozoer; Arkiv for Zoologie, Bd. 4, nr. 21, 61 p.
- Nowlan, G.S.
1981: Late Ordovician-Early Silurian conodont biostratigraphy of the Gaspé Peninsula - a preliminary report; IUGS Subcommittee on Silurian Stratigraphy, Ordovician-Silurian Boundary Working Group. Field Meeting, Anticosti-Gaspé, Québec 1981, Volume II: Stratigraphy and Paleontology, p. 257-297.

Nowlan, G.S. (cont.)

1983: Early Silurian conodonts of eastern Canada; *Fossils and Strata*, no. 15, p. 95-110.

Ross, J.P.

1960: Larger cryptostome Bryozoa of the Ordovician and Silurian, Anticosti Island, Canada – Part I; *Journal of Paleontology*, v. 34, no. 6, p. 1057-1076.

1961: Larger cryptostome Bryozoa of the Ordovician and Silurian, Anticosti Island, Canada – Part II; *Journal of Paleontology*, v. 35, no. 2, p. 331-344.

Ross, J.P. (cont.)

1967: Evolution of ectoproct genus *Prasopora* in Trentonian time (Middle Ordovician) in northern and central United States; *Journal of Paleontology*, v. 41, no. 2, p. 403-416.

1969: Champlainian (Ordovician) Ectoprocta (Bryozoan), New York State, Part II; *Journal of Paleontology*, v. 43, no. 2, p. 257-284.

Twenhofel, W.H.

1928: *Geology of Anticosti Island*; Geological Survey of Canada, Memoir 154 (1927), 350 p.

Yang Kingehik and Xia Fengsheng

1976: The Silurian bryozoans from Qujing of Yunnan; *Acta Palaeontologica Sinica*, v. 15, no. 1, p. 41-53.

Chaetipora (Anthozoa, Tabulata) in the
Upper Ordovician rocks of central and eastern Canada

Project 740084

Thomas E. Bolton
Director General's Office

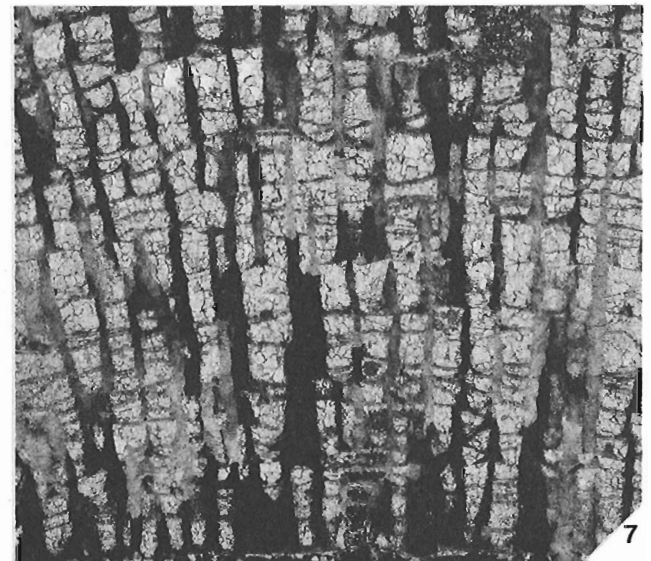
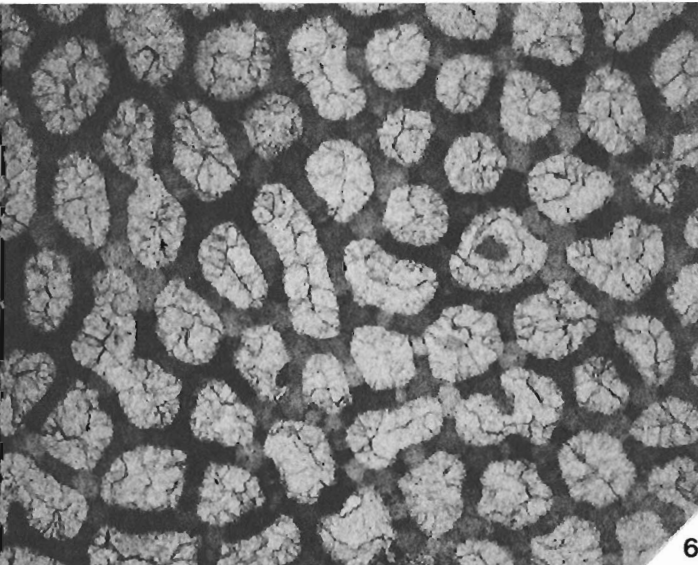
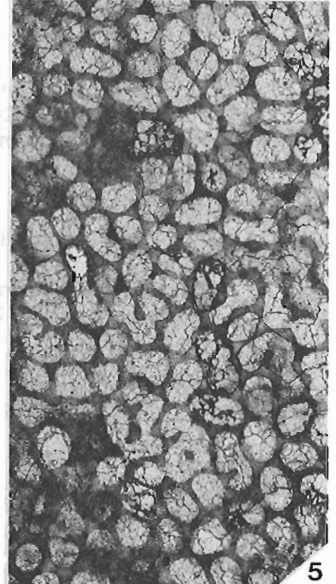
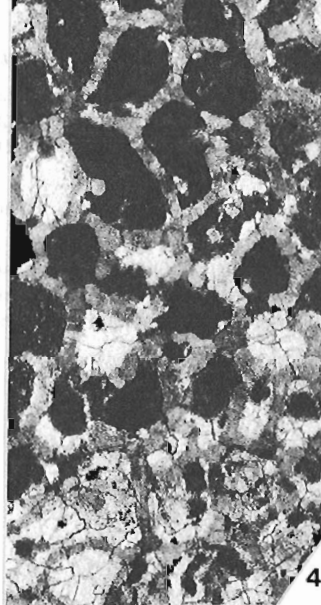
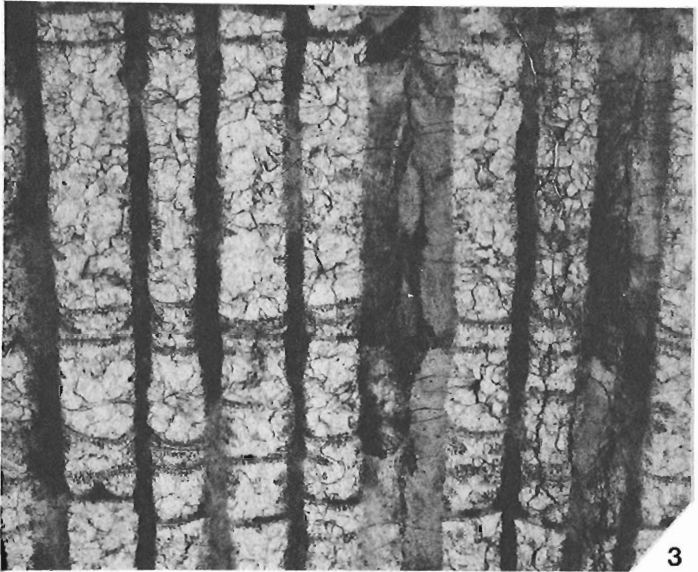
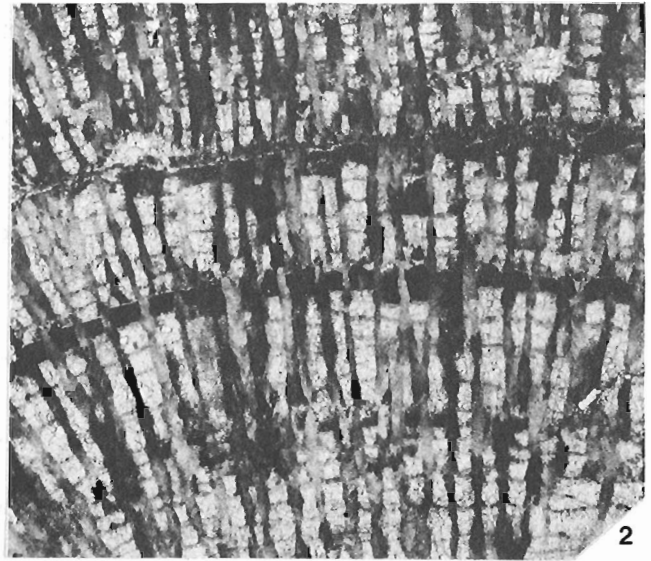
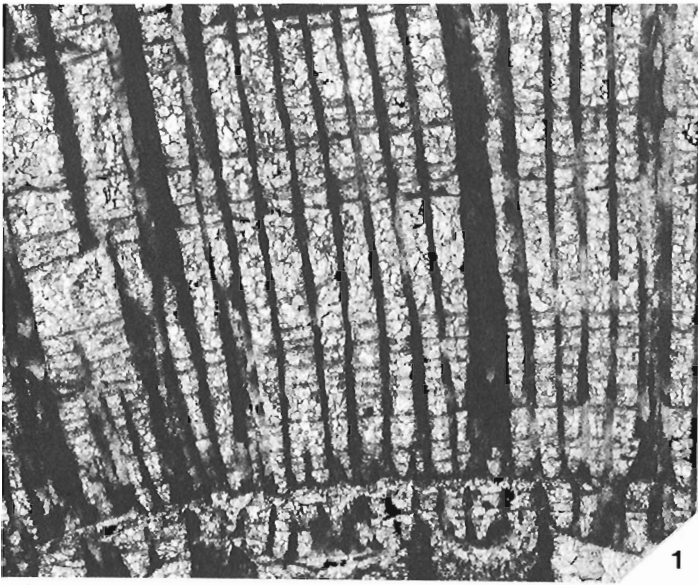
Bolton, T.E., *Chaetipora* (Anthozoa, Tabulata) in the Upper Ordovician rocks of central and eastern Canada; in Current Research, Part B, Geological Survey of Canada, Paper 86-1B, p. 107-110, 1986.

Abstract

Three chaetetid coral specimens from the Late Ordovician (Richmondian-Gamachian) of Anticosti Island, Quebec and northeastern Manitoba are assigned to ***Chaetipora ellesmerensis*** Norford, a species originally described from northern Ellesmere Island, Canadian Arctic.

Résumé

Trois échantillons de coraux chaététides datant de la fin de l'Ordovicien (Richmondien-Gamachien) de l'île d'Anticosti au Québec et du nord-est du Manitoba ont été classés dans l'espèce ***Chaetipora ellesmerensis*** Norford, une espèce décrite à l'origine à partir d'échantillons recueillis dans le nord de l'île Ellesmere, en Arctique canadien.



Introduction

Three chaetetid Ordovician species have been described from widely separated regions of Canada within the Red River-Stony Mountain Solitary Coral Province of Elias (1983, p. 924, text. fig. 1): *Chaetetes perantiquus* Whiteaves, 1897 – Selkirk Member, Red River Formation (late Maysvillian-Richmondian), 'Lower Fort Garry', southern Manitoba; *Chaetetes akpatokensis* Oakley, 1936 – Richmondian, Akpatok Island, District of Franklin; *Chaetetipora ellesmerensis* Norford, 1971 – Richmondian, Daly River, Judge Daly Promontory, northern Ellesmere Island, District of Franklin. Each species was based on a single corallum, and distinguished essentially on the difference in corallite diameter. Flower (1961, p. 17, 61) included *C. akpatokensis* as one of three species within his new coral genus *Trabeculites*. Subsequently, Norford (1971) included all three chaetetid species in the genus *Chaetetipora* Struve, 1898. More recently, specimens of *Chaetetipora* sp. cf. *C. ellesmerensis* Norford, associated with *Paleofavosites* sp. and *Calapoecia* sp., have been reported from the Late Ordovician in the White Mountains of the Fairbanks-Ramparts area, central Alaska (Oliver et al., 1975, p. 24, Pl. 4, fig. 3-6).

The present study records two more occurrences, again from widely separated localities (northern Manitoba and Anticosti Island, Quebec), in both Richmondian (Caution Creek and Vaureal formations) and slightly younger Gamachian (Ellis Bay Formation) strata, containing three colonies best assigned to *C. ellesmerensis* Norford. Hill's (1981, p. F506) assignment of chaetetids to tabulate corals rather than *Sclerospongia* is herein followed. Comments by O.A. Dixon, University of Ottawa, and B.S. Norford, Geological Survey of Canada, were welcomed.

Systematic paleontology

Family Chaetetidae Milne-Edwards and Haime, 1850

Genus *Chaetetipora* Struve, 1898

Type species. *Chaetetipora confluens* Struve, Visean of U.S.S.R.

Chaetetipora ellesmerensis Norford, 1971

Plate 13.1, figures 1-7

Chaetetipora ellesmerensis Norford, 1971, p. 4-5, Pl. 1, fig. 1, 2.

Description. Coralla range from massive, encrusting either a *Sarcinula* (holotype, GSC 25522) or a *Saffordophyllum churchillensis* (Nelson) (GSC 69251) corallum, nodular

PLATE 13.1.

Chaetetipora ellesmerensis Norford, 1971. Fig. 1, 3, 6, longitudinal (x 10, anchored in corallites of *Saffordophyllum churchillensis* Nelson and x 20, showing light and dark walls) and transverse (x 20, showing oval and meandroid corallites and incomplete wall development producing mural pore-like structures) sections, hypotype, GSC 69251; fig. 2, longitudinal section (x 10, showing bifurcating continuous walls), hypotype GSC 69252; fig. 4, transverse section (x 20), holotype, GSC 25522a; fig. 5, 7, transverse (x 10, showing oval and meandroid corallites) and longitudinal (x 10, showing both complete and incomplete walls) sections, hypotype, GSC 69253.

(GSC 69253), or nodose laminar (GSC 69252) in shape. Corallites vary from meandroid to rarely subpolygonal (holotype, Pl. 13.1, fig. 4), to oval (0.32-0.6 mm in diameter), to subpolygonal to submeandroid with openings varying from 0.28 x 0.56 to 0.40 x 0.80 mm in outline (Pl. 13.1, fig. 5, 6). Corallite walls thin clear to thicker trabeculate that in transverse sections display distinct light and dark areas.

In longitudinal sections, the thicker dark walls contain V-shaped to shallow U-shaped coccoserid-type trabeculae fibers, are continuous in encrusting coralla (Pl. 13.1, fig. 1, 3), rarely bifurcating, but more discontinuous in nodular and laminar coralla. Tabulae complete, horizontal to gently convex and upturned into the walls, irregularly spaced; in some coralla zones of closely spaced tabulae occur that form stromatoporoid-like laminae and pillar structures (Pl. 13.1, fig. 2, 7). No tabellae.

Discussion. The new specimens differ from the holotype in displaying fewer meandroid corallites, and the development of more distinct zones of more closely spaced tabulae, particularly in nodular forms; the maximum transverse corallite diameter also is greater by 0.2 mm. The small cerioid to meandroid nature of the corallites favours assignment of these chaetetid forms to *Chaetetipora* rather than the closely similar genus *Chaetetella* Sokolov, 1962; elsewhere both essentially range from Middle Devonian to Carboniferous. In wall structure, *C. ellesmerensis* closely resembles examples of the cerioid coral genus *Trabeculites*. The meandroid nature and consistently small diameter of the corallites serve to separate the genera.

Types. Holotype, GSC 25522. Hypotypes, GSC 69253, lower member, Caution Creek Formation, Churchill River Group, GSC locality 25384 (not 25304 – see Nelson, 1963, Fig. 4), South Knife River, northeastern Manitoba, collector: S.J. Nelson, 1951; GSC 69251, upper member, Vaureal Formation, GSC locality 36276 (BF 92b), Jupiter River road (1964), 76.8 km from Port Menier, 2.4 km south of main highway, collector: T.E. Bolton, 1958; GSC 69252, member 4 bioherm, Ellis Bay Formation, GSC locality 84385 (BF 403 – see Copeland, 1981, Fig. 8), east bank Vaureal River, second bend above main highway bridge, collector: T.E. Bolton, 1981.

References

- Copeland, M.J.
1981: Latest Ordovician and Silurian ostracode faunas from Anticosti Island, Québec; Subcommission on Silurian Stratigraphy, Ordovician-Silurian Boundary Working Group. Field Meeting, Anticosti-Gaspé, Québec 1981, v. II: Stratigraphy and Paleontology, p. 185-195.
- Elias, R.J.
1983: Late Ordovician solitary rugose corals of the Stony Mountain Formation, southern Manitoba, and its equivalents; *Journal of Paleontology*, v. 57, no. 5, p. 924-956.
- Flower, R.H.
1961: Part I Montoya and related colonial corals; New Mexico Institute of Mining and Technology, Memoir 7, p. 1-97.

- Hill, D.
1981: Systematic description: Tabulata; Geological Society of America and University of Kansas, Treatise on Invertebrate Paleontology, Part F Coelenterata, Supplement 1 Rugose and Tabulata, p. F506-F669.
- Nelson, S.J.
1963: Ordovician paleontology of the northern Hudson Bay Lowland; Geological Society of America, Memoir 90, 110 p.
- Norford, B.S.
1971: Upper Ordovician corals Chaetetipora and Sibiriolites from northern Ellesmere Island, District of Franklin; Geological Survey of Canada, Bulletin 197, p. 1-7.
- Oliver, W.A., Jr., Merriam, C.W., and Churkin, M., Jr.
1975: Ordovician, Silurian and Devonian corals of Alaska; U.S. Geological Survey, Professional Paper 823-B, p. 13-44.

Transcurrent faulting history of southern New Brunswick¹

Contract 23233-005-0073

Albert Leger and Paul F. Williams²

Leger, A. and Williams, P.F., Transcurrent faulting history of southern New Brunswick; in Current Research, Part B, Geological Survey of Canada, Paper 86-1B, p. 111-120, 1986.

Abstract

Southern New Brunswick is transversed by two prominent sets of faults; NE-trending and NNW-trending. The NE-trending faults are long, straight and have undergone a long history of movement, both in the ductile and brittle regimes. They are associated with mylonite zones. In the Acadian ductile regime, the movement in the shear zones was dextral transcurrent, now shown by various kinematic indicators. In the Carboniferous, brittle movements on those faults varied from dextral and sinistral transcurrent to high-angle reverse and normal faulting. Thrusting associated with the Variscan Orogeny occurred at high levels on the shore of the Bay of Fundy.

The NNW-trending faults are brittle faults, are not associated with mylonite zones, and show both dextral and sinistral strike-slip movements. Most of these faults are not indicated on the published geological maps but can be recognized on topographic maps and interpreted by association with similarly oriented features mapped as brittle faults throughout the northern Appalachians.

Résumé

Deux grands groupes de failles, l'un orienté nord-est et l'autre nord-nord-ouest, traversent la partie sud du Nouveau-Brunswick. Les failles à orientation nord-est sont longues et droites et ont subi une longue histoire de mouvement ductile et cassant. Ces failles sont associées à des zones de mylonite. Dans le régime ductile acadien, divers indicateurs cinématiques révèlent qu'il y a eu décrochement dextre dans les zones de cisaillement. Au cours du Carbonifère, les mouvements cassants le long des failles ont varié des décrochements dextres et senestres aux failles inverses et normales à angle presque droit. Le charriage associé l'orogénèse du Varisque s'est produit à des niveaux élevés sur le littoral de la baie de Fundy.

Les failles à orientation nord-nord-ouest, de nature cassante, comportaient des décrochements dextres et senestres; elles ne sont pas associées aux zones de mylonite. La plupart de ces failles ne sont pas identifiées sur les cartes géologiques publiées mais peuvent être reconnues sur les cartes topographiques et interprétées par association à d'autres éléments à orientation similaire qui y sont représentés comme des failles cassantes que l'on trouve partout dans le nord des Appalaches.

¹ Contribution to the Canada-New Brunswick Mineral Development Agreement 1984-1989. Project carried by Geological Survey of Canada, Lithosphere and Canadian Shield Division, Project 850023.

² Department of Geology, University of New Brunswick, Fredericton, New Brunswick, E3B 5A3

Introduction

The area studied is situated in southern New Brunswick, and is part of the "Avalon terrane" (Williams, 1979; Williams and Hatcher, 1983). Major NE-trending faults bound the Avalon terrane (Haworth and Lefort, 1979; Hanmer, 1981; Keppie, 1982), but the exact nature of the movements on those faults is unknown. The uncertainty regarding the ages and types of faulting in southern New Brunswick might be due to the inability of most early workers to differentiate between an early ductile period of faulting and a later brittle period.

Most workers in New Brunswick described only the latest movements on the faults (Brown and Helmstaedt, 1970; Garnett and Brown, 1973; Gussow, 1953; Webb, 1963, 1969) which correspond to Carboniferous faulting. Although fault terminology may be confusing (Higgins, 1971; Zeck, 1974; Sibson, 1977; Wise et al., 1984; Mawer, 1985), ductile shear zones and brittle faults produce similar results (i.e. the relative displacement of various rock units) and both should be included in the study of any fault system to understand the extent and complete history of faulting.

This study will demonstrate that faulting in southern New Brunswick has had a long and complicated history, both in the ductile and brittle regimes. These results are consistent with the histories of other parts of the Avalon and Meguma terranes.

Previous work

The New Brunswick faults have received a great deal of attention throughout the years. They have been interpreted in all possible ways, i.e. as: a) high angle reverse and thrust faults, b) normal (and oblique) faults, and c) dextral and sinistral strike-slip faults.

a) High angle reverse and thrust faults. Gussow (1953), in his synthesis of Carboniferous rocks and structure, proposed a series of NE-trending "master" faults (Belleisle, Kennebecasis, Clover-Hill, and Harvey Hopewell faults; Fig. 14.1) that were listric thrust faults with movement in the Carboniferous from the NW towards the SE. His interpretation was based on seismic profiles combined with extensive geological mapping. Other workers have suggested thrusting or high angle reverse movement on one or all of these master faults (Brown and Helmstaedt, 1970; Brown, 1972; Garnett and Brown, 1973; McCutcheon, 1981; Ruitenberg and McCutcheon, 1982) but with a thrusting direction from SE to NW. Thrusting on these NE-trending faults was consistent with a NW – SE maximum principal stress direction determined from fracture analyses performed in both New Brunswick and Nova Scotia (Eisbacher, 1969, 1970; Anderson, 1972; Garnett, 1972). One can argue about the validity of the fracture analyses but an overall NW-SE shortening is a reasonable interpretation in view of fold and fault orientations for at least part of the deformation history.

Thrusting has also been demonstrated on the southern coast of New Brunswick where the faults are shallowly dipping. This thrusting was associated with Variscan deformation (Rast and Grant, 1973a,b; Rast and Currie, 1976; Rast and Dickson, 1982; Currie and Nance, 1983; Rast et al., 1984; Nance, 1982; Nance and Warner, 1986; Plint and Van de Poll, 1984). It occurred at a higher crustal level than the faults discussed above and produced fairly limited displacements (Currie, 1986).

b) Normal (and oblique) faults. Belt (1968), with his rift-valley model for the development of the Carboniferous sedimentary basins, proposed that the major faults in the Maritimes were of the high-angle normal type. He based his interpretation on sedimentological data. Bradley (1982) combined dextral strike-slip and normal movements on the major faults (oblique slip) to explain the formation of the same basins, as pull-apart basins.

c) Dextral and sinistral strike-slip faults. Carboniferous dextral strike-slip movement was first proposed by Webb (1963, 1969). Webb suggested there was as much as 64 km of dextral movement on the Belleisle fault and a total of about 200 km for the New Brunswick fault system as a whole. The distance was determined from the displacement of Carboniferous markers across the faults, and dextral motion was further supported by the orientation of subsidiary folds and faults with respect to the master faults. This latter evidence is only valid if the subsidiary folds and faults can be shown to have formed synchronously with, and in response to, the same deformation as the master faults. Anderson (1972) proposed dextral strike-slip on the Catamaran fault and Ludman (1981) the same movement on the Fredericton fault.

Sinistral motion was first proposed by Wilson (1962) for the Cabot fault, based on the orientation of minor faults in the Notre Dame Bay area of Newfoundland. Further detailed study in the area by one of us (P.F.W.) reveals that the brittle faulting pattern is extremely complex and Wilson's simple model is not substantiated. Wilson's extrapolation of the Cabot fault (*ibid.*) into New Brunswick has also been shown recently (Avalon Workshop at the Atlantic Geoscience Society annual meeting in Amherst, Nova Scotia, January 1986) to be a much more complex issue than he suggested.

Currie (1984) proposed sinistral movement on the Belleisle fault to account for the formation of small north-trending Carboniferous grabens formed by tension along the fault. Currie (1986) further proposed sinistral movement on the Belleisle fault in Precambrian time to account for some north-trending basic dykes in the Seven Mile Lake – Loch Alva area.

A 1500 km sinistral motion on the Fredericton fault was proposed by Kent and Opdyke (1978, 1979, 1980). This proposal was based on paleomagnetic data, and many paleomagneticians agreed with the Kent and Opdyke model and lent supporting data (Morris, 1976; Van der Voo et al., 1979; Van der Voo and Scotese, 1981; Lefort and Van der Voo, 1981). This model was discredited, however, when Roy and Morris (1983) showed that the paleopoles for Upper Devonian and Lower Carboniferous rocks calculated by the previous workers were in fact paleopoles resulting from a Late Carboniferous and Permian (Kiaman) overprint (see also Irving and Strong, 1984; Kent and Opdyke, 1984; Seguin et al., 1985; Seguin and Gahe, 1985). No geological data were ever presented in support of such a magnitude of sinistral movement on the Fredericton fault or any other fault in New Brunswick.

Acadian ductile faulting

Ductile shear zones in southern New Brunswick are characterized by mylonites (Rast and Currie, 1976; Rast and Dickson, 1982; Ruitenberg and McCutcheon, 1982). These are NE-trending and occur only in Precambrian rocks. We propose that these mylonites are of Acadian (Devonian) age, and the evidence is presented and discussed below.

The Pocologan mylonite zone

Introduction. The Pocologan mylonite, a Precambrian basement rock belonging to the Avalon Zone (Williams, 1979) has been described by Rast and Currie (1976), Rast (1979), and Rast and Dickson (1982). They interpreted it as the product of a major transcurrent zone of unknown sense of shear. Rast and Dickson (1982) observed two overprinting cleavages. The first cleavage, trending 060°, was interpreted as Precambrian. The overprinting cleavage, trending 090°, was interpreted as Carboniferous because they observed that it was better developed near the Carboniferous thrust planes. The authors are at variance with the above interpretation and suggest that the two

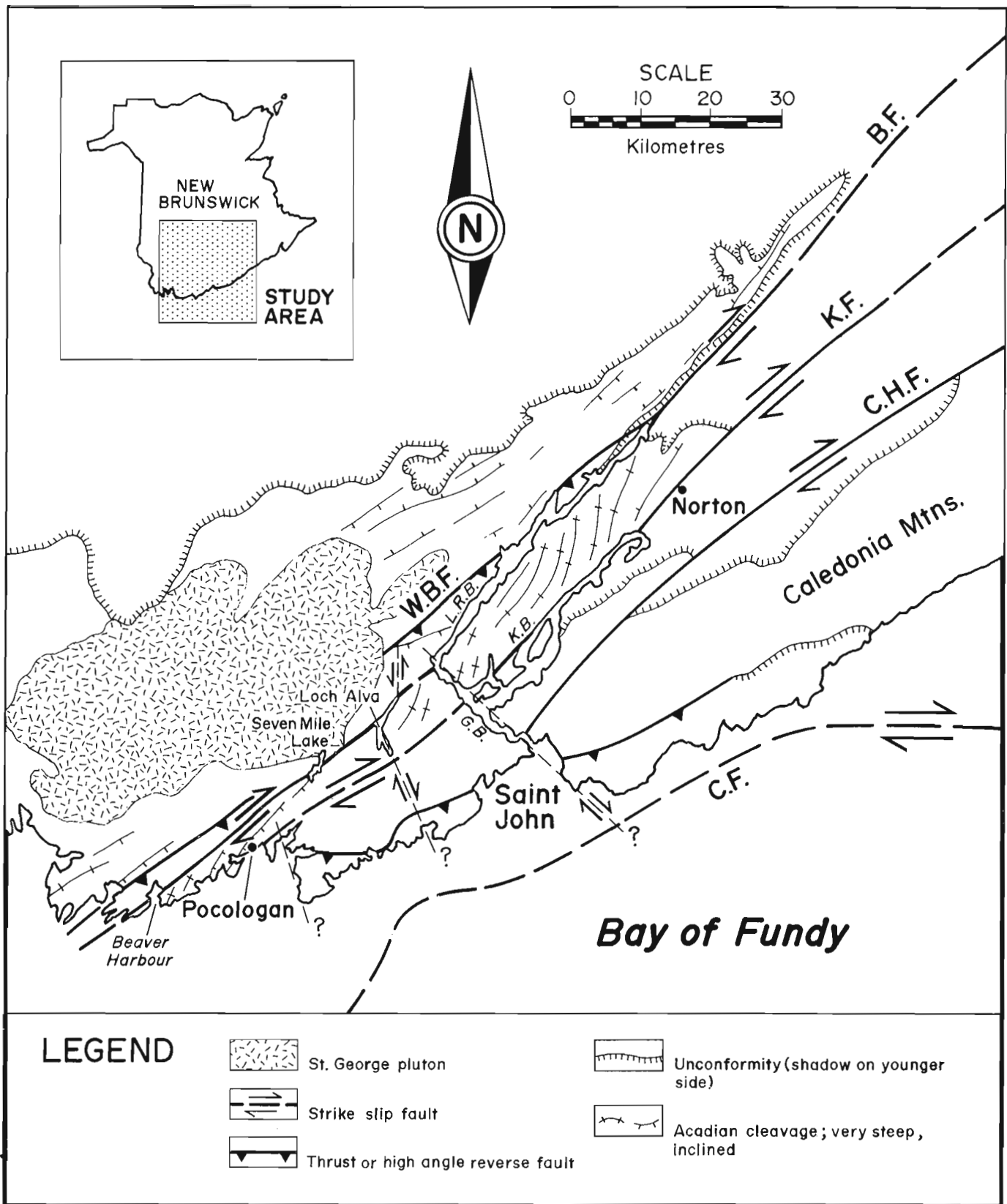


Figure 14.1. Regional geological and structural map of southern New Brunswick after Chandra, 1982, BF – Belleisle fault; KF – Kennebecasis fault; CHF – Clover Hill, (Caledonia fault); CF – Cobequid Fault; KB – Kennebecasis Bay; GB – Grand Bay; LRB – Long Reach.

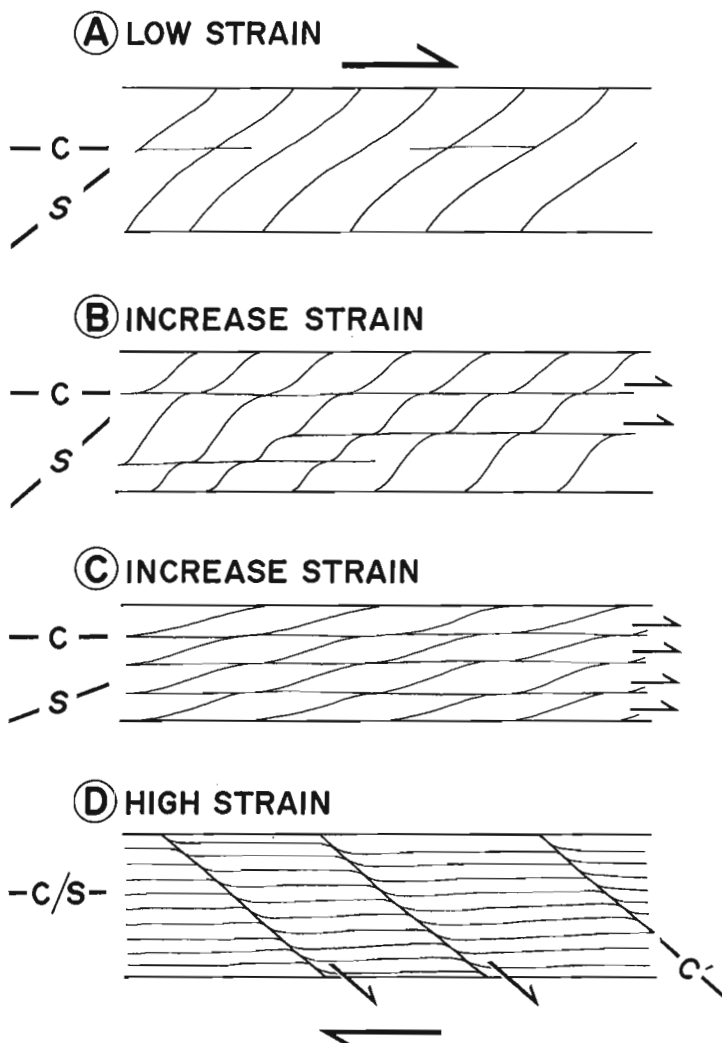


Figure 14.2. Evolution of an idealized shear zone, with development of S, C and C' foliations. Adapted from Simpson, 1984.

cleavages are related to the same period of Acadian deformation.

Field observations. Very well developed by S-C and C-C' structures (Fig. 14.2; Berthe et al., 1979a,b; Simpson, 1984) along with subhorizontal mineral stretching lineations (Fig. 14.3) are observed throughout the Pocologan area, and they indicate a dextral sense of shear.

a) **Petrology.** The protoliths of the Pocologan mylonite are granitoids, volcanics, and acidic and basic intrusions (Rast and Dickson, 1982; Ruitenberg and McCutcheon, 1982; Poole, 1980) and were dated as Late Precambrian by Poole (1980). The metamorphic conditions during the ductile deformation were in the albite-amphibolite facies based on the assemblage quartz – albite – epidote – hornblende in the basic rocks (Miyashiro, 1973). Temperatures of approximately 450°C are also compatible with the observation that quartz crystals were deformed ductilely into ribbons (Vauchez, 1980) while the feldspars were broken (see Tullis, 1983).

b) **Structure.** S-C mylonites (Lister and Snoke, 1984) are found throughout the Pocologan area. In the granitoids, abundant occurrences of very well developed C-C' (or Sm-Ss) mylonites (Fig. 14.4; Platt, 1979; White et al., 1980; Berthe et al., 1979a,b; Platt and Vissers, 1980; Gapais and White, 1982; Weijermars and Rondeel, 1984; Simpson, 1984) clearly demonstrate that the motion was dextral and that the bulk strain was large.

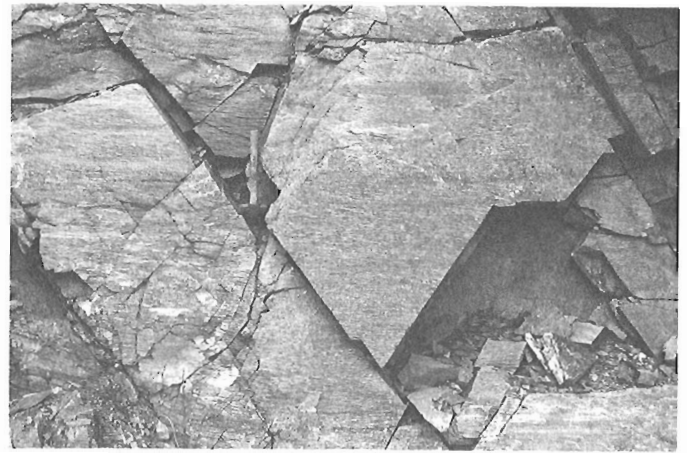


Figure 14.3. Subhorizontal mineral stretching lineation, Pocologan. The outcrop surface is vertical, hammer is 38 cm long.

At Pocologan, the "C" foliation (for "cisaillement", Berthe et al, 1979a) trends 060°, parallel to the regional Acadian cleavage. The "C'" foliation ["shear band" or "extensional crenulation cleavage" (Platt, 1979; White et al., 1980)] trends 090°. This 30° angle between the two cleavages is characteristic of C-C' mylonites (*ibid.*). The "C'" cleavage developed late during the mylonite formation and often appears to overprint the "C" foliation, but is still related to the same deformation event. Also, especially if a compressional motion is associated with the strike-slip (transpression, Harland, 1971), the shear zone may attain higher crustal levels while deforming, causing the second cleavage to show more brittle features than the first (Fig. 14.4d).

Seven Mile Lake

Work in progress in the Seven Mile Lake area (Fig. 14.1) suggests that the ductile deformation was due to a dextral movement on the Belleisle fault. This interpretation is based on large steeply plunging "Z"-folds.

Norton

Exposures along Bloomfield Brook and Bloomfield Creek just west of Norton (Fig. 14.1) show the sharp transition between highly deformed Precambrian Kingston Complex rocks to the north and unmetamorphosed but folded Mississippian sediments of the Albert Formation to the south. The contact, the Kennebecasis fault, does not outcrop but one may approach to within a few metres of it. Field observations did not lead to any conclusion concerning the sense of the ductile movement, but thin section observation reveals asymmetric structures (Fig. 14.5) that indicate dextral sense of shear (Simpson and Schmid, 1983).

Carboniferous brittle faulting

Based on the conclusions stated above, the Acadian ductile deformation must have occurred at depths of approximately 15 km. Uplift due to oblique movement or to transpression gradually brought the rocks to higher crustal levels. In a transpressive shear zone environment such as the Alpine fault of New Zealand, uplift along the fault may attain a rate of 1 mm a year (Sheppard et al., 1975), so rocks deformed at depth in a ductile regime during Acadian times could easily be raised to the surface and subjected to brittle deformation by the Carboniferous. It is this Carboniferous deformation that has received the attention of most previous fault studies.

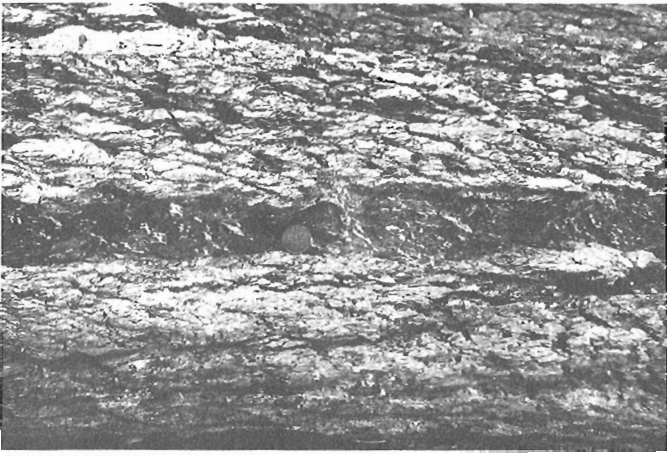


Figure 14.4.a. Well developed C – C' structure, Pocologan. Plan view, penny for scale.

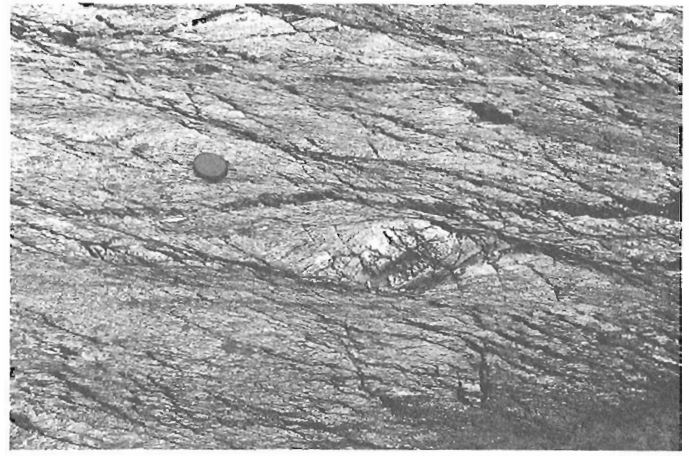


Figure 14.4.b. C – C' structure, Pocologan, showing how the C' foliation overprints the mylonitic C foliation. Plan view, camera lens cap for scale.



Figure 14.4.c. Photomicrograph of section from Pocologan, showing the mylonitic foliation and the shear band foliation. Shear bands are heterogeneously distributed throughout the section. Note shear band through ductile quartz deformed in upper left corner. Crossed polars, scale bar is 1 mm.

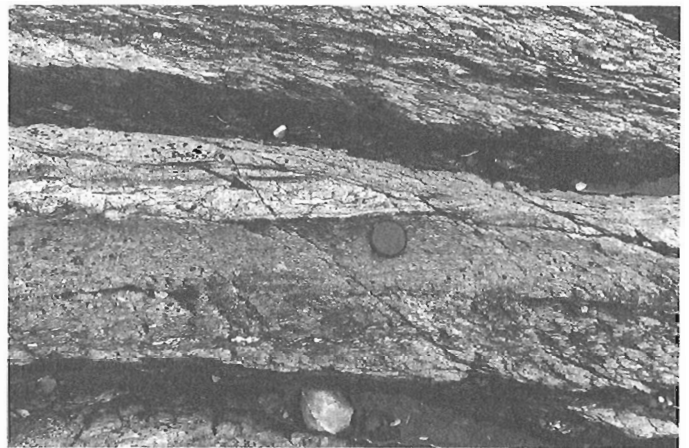


Figure 14.4.d. Well developed shear band overprinting the mylonitic foliation (shown by arrow), Pocologan. Plan view, camera lens cap for scale.

Brittle faulting was extensive in the Carboniferous. Every master fault was reactivated and new faults were initiated. The movement was generally transcurrent and the pattern of faulting is predictably complex with bends in the faults leading to positive and negative flower structures. Thrusting, folding, and basin formation can all be explained in this manner (Aydin and Nur, 1982; Reading, 1980; Mann et al., 1983).

Northeast-trending brittle faults

Belleisle fault. The Belleisle fault was active as a brittle fault in the Carboniferous. At Beaver Harbour, in southwestern New Brunswick, it juxtaposed Precambrian Coldbrook Group and Carboniferous Beaver Harbour Group rocks. The fault there is subvertical and has been interpreted as dip-slip by Helmstaedt (1968).

At Seven Mile Lake, northeast of Beaver Harbour, Carboniferous movement on the Belleisle fault juxtaposed mylonitized Precambrian felsic volcanics and relatively un-

deformed Late Devonian granitoids. Garnett (1972) described a zone of fault gouge associated with the movement and noted that it was at an angle to the mylonitic foliation. He interpreted the fault as reverse, and the movement as minor, because he could follow some lithologies across the fault.

The nature of the brittle Carboniferous movement on the Belleisle fault is difficult to assess. Webb's (1963, 1969) proposal of a 64 km dextral movement was based on the displacement of Carboniferous markers across the fault. Belt (1968) pointed out that across the fault in New Brunswick and in Prince Edward Island, Horton Group sediments (Upper Devonian – Lower Carboniferous) range in thickness from zero on the platform side of the fault to more than 3000 m on the basin side, thus suggesting a large normal component for the Carboniferous movement. Further, the rapid facies change from shale and sandstone on one side to fanglomerates on the other side indicates that movement and sedimentation were synchronous.

A volcanic ash bed at the base of the Hillsborough Member of the Carboniferous Moncton Formation has been interpreted

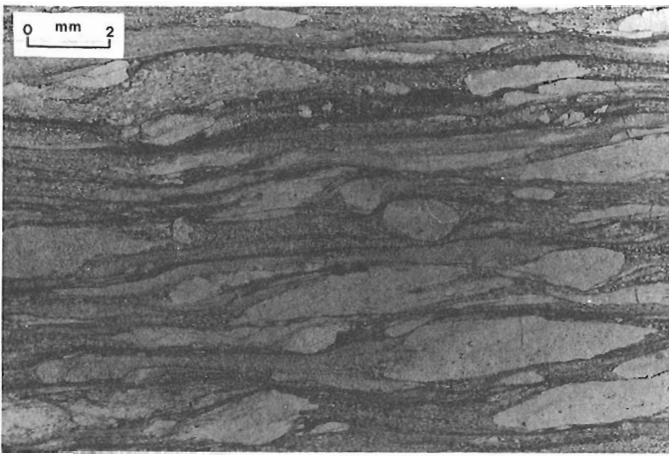


Figure 14.5. Photomicrograph of section from Bloomfield Brook, near Norton. This section is taken from the Precambrian rocks north of the Kennebecasis fault. Asymmetric augens suggest dextral sense of shear. Plane polarized light. Scale bar is 2 mm.

as indicating an extensional regime (Bradley, 1982), which would also suggest a normal component of movement.

Wheaton Brook fault. The Wheaton Brook fault lies just northwest of the Belleisle fault. It was described as a high angle thrust fault by McCutcheon (1981) owing to a revised stratigraphy in the Long Reach area. Currie (1984), however, proposed that the Wheaton Brook fault was a major sinistral strike-slip fault. He objected to NW-directed high angle reverse or thrust movement on the fault because unmetamorphosed Cambrian strata to the southeast of the fault is juxtaposed with hornfelsed Silurian rocks to the northwest.

Kennebecasis fault: In the Kingston Uplift – Indian Mountain area, a late normal faulting event is probable, and the Kingston Uplift is almost certainly a horst-type structure (Greiner, 1962). The extent of the Kennebecasis fault is unknown, as it does not show continuity on the aeromagnetic map and does not outcrop in the Moncton Subbasin.

Slickenside orientations recorded along the Kennebecasis fault are very variable and include horizontal and vertical striae. It would be reasonable to interpret them as a product of transcurrent faulting accompanied by related or later normal faults.

Clover-Hill (Caledonia) fault: The Clover-Hill fault does not outcrop but juxtaposes the Precambrian Caledonia Mountains to the south and the Carboniferous sediments of the Moncton subbasin to the north. Along the trace of the fault, numerous Carboniferous fanglomerates composed of Precambrian boulders indicate a north side down movement. According to Gupta (1974), geophysical evidence indicates a SE dip on the fault and he therefore interpreted it as a reverse fault. Whether or not strike-slip movement was associated with the reverse faulting is unknown.

North-northwest trending brittle faults

The shoreline directions that predominate on the south coast of New Brunswick are NE and NNW. The same directions are prominent inland as lineaments and are reflected in the orientation of lakes and rivers (e.g. stretches of the Saint John River, Grand Bay, Long Reach, Belleisle Bay, Kennebecasis Bay, Loch Alva). We interpret these lineaments as a reflection of the northeast-trending faults discussed above and of another group of faults that trend north-northwest. The latter do not generally

outcrop in the study area. Faults of this approximate orientation are, however, well known to us from Newfoundland and Nova Scotia and are known from the Bathurst area of New Brunswick (A.L. McAllister personal communication, 1986). Ongoing work by one of us (PFW) reveals that these faults in Newfoundland and Nova Scotia have a horizontal separation that is generally sinistral but locally dextral.

One fault belonging to this group has been described from New Brunswick: the Oak Bay fault, interpreted as transcurrent and sinistral (Donohoe, 1978).

Even in areas of good outcrop large faults belonging to this group generally do not outcrop well. Smaller mesoscopic examples can, however, be seen in coastal outcrops and in Nova Scotia and Newfoundland. They are commonly gradational with kinks. This point is demonstrated on a large scale in Nova Scotia where the faults and associated kinks are readily seen on the Aeromagnetic Vertical Gradient Map for Country Harbour (Geological Survey of Canada, 1985). There, as elsewhere, the faults cut all earlier structures.

Discussion

At the southern boundary of the Avalon terrane in the Musquash Harbour area, Currie (1986) explained an en echelon distribution of ductile faults in terms of an overall dextral transcurrent zone within which the movement was accommodated by short faults, where, as one fault dies, an adjacent fault takes up the movement. However, since we know that despite their lack of outcrop, brittle faults are regionally abundant, the en echelon pattern can be explained equally well by late offset by the north-northwesterly striking faults. If the ductile faults were originally all segments of a single zone the late faults would have to have a dextral component whereas most faults of this orientation have a sinistral component. Both senses of movement are known on these faults in the Meguma terrane and in Newfoundland.

At the northern boundary of the Avalon terrane, in the Loch Alva area, the same model may be applied to the Belleisle and Wheaton Brook faults. They appear as en echelon to the left, but could have been the same ductile fault, later displaced by a north-trending sinistral brittle fault. Currie (1986) noted that the Welsford complex (Silurian) was offset sinistral by several hundred metres along a north-trending lineament starting at the northeast end of Loch Alva. Thus, the lineament is known to be the site of sinistral faulting in post-Silurian times.

Movement on northeasterly trending brittle faults remains a problem. Faults of this orientation and relative age (i.e. post ductile faulting) are known in Newfoundland where they have a strong strike slip component. In New Brunswick there is good evidence for vertical components but no cogent evidence that the faults are primarily transcurrent. Suitable markers for indicating horizontal movements on such faults are, however, generally lacking in New Brunswick.

Large transcurrent movement on a planar fault of infinite extent cutting normal crust, will juxtapose rocks of different metamorphic grade, stratigraphic history etc. without any vertical movement taking place, thus giving the illusion of vertical movement. Large transcurrent displacement of real faults, which are neither planar nor infinite in extent, must produce real vertical movements. It is therefore not meaningful to say that a fault is clearly normal or reverse because of evidence of vertical displacement.

Vertical displacements obviously occurred in southern New Brunswick and slickensides indicate that horizontal movement also occurred. Thus, in view of observations outside the area and in view of the compatibility of the vertical movements

with transcurrent faulting, we tentatively interpret the north-east-trending brittle faults as primarily transcurrent structures, with related vertical movements.

Age of faulting

The age of ductile faulting in southern New Brunswick is a controversial issue. One school favours a Precambrian age, the other an Acadian age. The two proposals are discussed in this section.

Precambrian faulting

Precambrian Cadomian deformation has been well documented in the Maritime provinces (Currie et al, 1981; Ruitenberg and McCutcheon, 1982; Keppie, 1982, 1985). The question is whether or not this Precambrian deformation event is related to the deformation associated with the large scale faults described here.

Rast and Currie (1976) contended that the Pocologan mylonite zone was Precambrian based on their observations that no Phanerozoic rocks in the area showed a similar intensity of deformation. If this age is correct, it seems strange that the mylonite zone exactly parallels the regional Acadian trend right across southern New Brunswick and that Devonian, Silurian and Cambrian rocks show similarly oriented foliation, even though they are apparently less strongly deformed.

Rast (1979) and Rast and Dickson (1982) proposed that the Pocologan mylonite zone had been the site of the opening of the Iapetus Ocean in Late Precambrian times. The dyke swarm observed in the Coldbrook Group would have resulted from the extension during the creation of Iapetus. They further observed that the dyke swarm was in part "later than the most intense mylonitization" (Rast and Dickson, 1982, p. 251), thus giving a Precambrian age for the mylonite. They supported the Precambrian age by noting that the dykes were of amphibolite grade, while amphibolites of that type were not found in any of the Phanerozoic rocks of the area.

The authors are at variance with that interpretation. First, in an area of large ductile transcurrent faulting, rocks showing different metamorphic grades can easily be brought into juxtaposition. Second, the metamorphic hornblende and epidote found in the Precambrian basic rocks of the Seven Mile Lake area define the regional Acadian cleavage. We thus suggest that an epidote-amphibolite grade metamorphism accompanied the deformation of the Coldbrook Group. These were subsequently brought to the surface by oblique or transpressional faulting. Thus the amphibolite grade of the Pocologan dykes and sheets are not incompatible with an Acadian metamorphism.

McLeod (1979) suggested that the Coldbrook rocks of Campobello Island had suffered a period of penetrative deformation prior to the deposition of the Silurian Quoddy Formation. He suggested an unconformity between the two terranes, even though the unconformity is never seen in outcrop (McLeod, personal communication, 1985). However, all that he demonstrated was a difference in the development of deformational features, a difference that is readily explained by attributing the deformation to ductile faulting which is normally heterogeneous in its distribution.

The Kingston Complex dyke swarm was used by Currie (1986) as evidence for sinistral faulting on the Belleisle fault in Precambrian time. He observed that a regional sinistral movement parallel to the NE-trending fault would create E-W extension along the north-trending lineament, thus allowing Precambrian dykes to intrude the Kingston Complex. Some problems exist, however, with that model.

First, we do not know the relative positions of the Wheaton Brook and Belleisle faults at the time of formation; they may have been one continuous structure. We do know that their extremities are joined now by a north-trending lineament which, from independent evidence is believed to represent a sinistral fault of Silurian age. If in fact the two faults were originally one, there is no reason for any special extensional area between them. Secondly, if the dykes are old, it is unlikely that their original orientation has been preserved. Thus, we do not consider that a strong case can be made for Precambrian sinistral faulting, on the basis of the dykes, until we have a better knowledge of the history of emplacement and deformation of the dykes.

In summary, the evidence for Precambrian faulting is not convincing. It is based on tenuous interpretations rather than on cogent evidence.

Acadian faulting

Throughout this paper, we have proposed that the mylonitization was Acadian. This is based on the following observations.

a) The mylonitic cleavage at Pocologan, Seven Mile Lake, and Norton parallels the regional Acadian cleavage. This NE-trending cleavage is present in all Paleozoic rocks of southern New Brunswick where penetrative deformation occurs.

b) The strain is similar in Precambrian and Lower Paleozoic rocks of the Beaver Harbour area (Brown, 1972) thus suggesting that the first penetrative deformation in that area was Acadian. Ludman (1981) showed the same relationship for northeastern Maine.

c) Helmstaedt (1968) published a date of 369 ± 21 Ma for actinolite crystals of the Coldbrook dykes in the Beaver Harbour area, and proposed that it represented the age of the first penetrative deformation in the area.

d) The same pattern of ductile and brittle faulting is consistent throughout the Atlantic provinces. In Newfoundland and Nova Scotia, where the outcrop is better than in New Brunswick, the ductile faults cut Paleozoic rocks, including some Devonian plutons and/or their metamorphic aureoles. Further, in Newfoundland, they overprint thrusts and folds of Llandoveryan and younger age (Karlstrom et al., 1982) bracketing the ductile faults as Silurian or younger.

Conclusions

The faulting history of southern New Brunswick is extremely complex and efforts to unravel it have been hindered by the poor exposure. It involves ductile faulting in Paleozoic times (presumably Acadian) on NE-trending faults and younger brittle faulting that was active at least during the Carboniferous. The brittle faults trend NE and NNW and overprint mylonites associated with the earlier faults.

Mylonites in the Pocologan area exhibit very well preserved S-C and C-C' structures which demonstrate that the Acadian ductile faulting there was dextral. Other kinematic indicators indicate the same sense of shear for the Belleisle fault and the Kennebecasis fault.

Brittle transcurrent faults in southern New Brunswick cannot be demonstrated at this time but evidence of such movements in other better exposed parts of the northern Appalachian suggests that the same pattern may have existed in New Brunswick. The vertical movements observed on many of the New Brunswick faults are not incompatible with transcurrent movement, especially in a region of oblique or transpressive faulting.

Acknowledgments

We are grateful to C.G. Elliot and K.L. Currie for discussion and review of the manuscript, to P. Chenard for drafting assistance, and to R. Northrup for word processing.

References

- Anderson, F.D.
1972: The Catamaran fault, north-central New Brunswick; *Canadian Journal of Earth Sciences*, v. 9, p. 1278-1286.
- Arthaud, F. and Matte, P.
1977: Late Paleozoic strike-slip faulting in southern Europe and northern Africa: Result in a right-lateral shear zone between the Appalachians and the Urals; *Geological Society of America, Bulletin*, v. 8, p. 1305-1320.
- Aydin, A. and Nur, A.
1982: Evolution of pull-apart basins and their scale independence; *Tectonics*, v. 1, p. 91-105.
- Belt, E.S.
1968: Post-Acadian rifts and related facies, Eastern Canada; in *Studies of Appalachians, Northern and Maritime*, ed. Zen et al., p. 95-113.
- Berthe, D., Choukroune, P., and Jeguzo, P.
1979a: Orthogneiss, mylonite and non-coaxial deformation of granites: the example of the South Armorican Shear Zone; *Journal of Structural Geology*, v. 1, p. 31-42.
- Berthe, D., Choukroune, P., and Gapsis, D.
1979b: Orientations préférentielles du quartz et orthogneissification progressive en régime cisailant: l'exemple du cisaillement sud-armoricain; *Bulletin de Mineralogie*, v. 102, p. 265-272.
- Bradley, D.C.
1982: Subsidence in late Paleozoic basins in the northern Appalachians; *Tectonics*, v. 1, p. 107-123.
- Brown, R.L.
1972: Appalachian structural style in southern New Brunswick; *Canadian Journal of Earth Sciences*, v. 9, p. 43-53.
- Brown, R.L. and Helstaedt, H.
1970: Deformation history in part of the Lubec Belleisle zone of southern New Brunswick; *Canadian Journal of Earth Sciences*, v. 7, p. 748-767.
- Chandra, J.
1982: Structural map of New Brunswick compiled from geology, gravity and magnetics; New Brunswick Department of Natural Resources, Mineral Resources Branch, Map Plate 82-178.
- Currie, K.L.
1984: A reconsideration of some geological relations near St. John, New Brunswick; in *Current Research, Part A*, Geological Survey of Canada, Paper 84-1A, p. 193-201.
1986: The boundaries of the Avalon tectonostratigraphic zone, Musquash Harbour – Loch Alva region, southern New Brunswick; in *Current Research, Part A*, Geological Survey of Canada, Paper 86-1A, p. 333-341.
- Currie, K.L. and Nance, R.D.
1983: A reconsideration of the Carboniferous rocks of St. John, New Brunswick; in *Current Research, Part A*, Geological Survey of Canada, Paper 83-1A, p. 29-36.
- Currie, K.L., Nance R.D., Pajori, G.E., and Pickerill, R.K.
1981: A reconsideration of the pre-Carboniferous geology of Saint John, New Brunswick; in *Current Research, Part A*, Geological Survey of Canada, Paper 81-1A, p. 23-30.
- Donohoe, H.V., Jr.
1978: Analysis of structures in the St. George area, Charlotte County, New Brunswick; unpublished PhD thesis, U.N.B., Fredericton, N.B.
- Eisbacher, G.H.
1969: Displacement and stress field along part of the Cobequid Fault, Nova Scotia; *Canadian Journal of Earth Sciences*, v. 6, p. 1095-1104.
1970: Deformation mechanics of mylonitic rocks and fractured granites in the Cobequid Mountains, Nova Scotia, Canada; *Geological Society of America, Bulletin*, v. 81, p. 2009-2020.
- Gapsis, D. and White, S.H.
1982: Ductile shear bands in a naturally deformed quartzite; *Textures and Microstructures*, v. 5, p. 1-17.
- Garnett, J.A.
1972: Structural analysis of part of the Lubec-Belleisle Fault Zone, southwestern New Brunswick; unpublished PhD thesis, University of New Brunswick, Fredericton, N.B.
- Garnett, J.A. and Brown, R.L.
1973: Fabric variation in the Lubec-Belleisle Zone of southern New Brunswick; *Canadian Journal of Earth Sciences*, v. 10, p. 1591-1602.
- Geological Survey of Canada.
1985: Aeromagnetic vertical gradient map, County Harbour, Nova Scotia; Geological Survey of Canada, Geophysical Series maps 11F/4 & 11C/13.
- Greiner, H.R.
1962: Facies and sedimentary environments of Albert shale, New Brunswick; *American Association of Petroleum Geologists, Bulletin*, v. 36, p. 219-234.
- Gupta, V.K.
1974: An interpretation of aeromagnetic and gravity data of Caledonian area in southern New Brunswick; unpublished PhD thesis, University of New Brunswick, Fredericton, N.B.
- Gussow, W.C.
1953: Carboniferous stratigraphy and structural geology of New Brunswick; *American Association of Petroleum Geologists, Bulletin*, v. 37, p. 1713-1816.
- Hanmer, S.
1981: Tectonic significance of the northeastern Gander Zone, Newfoundland: an Acadian ductile shear zone; *Canadian Journal of Earth Sciences*, v. 18, p. 120-135.
- Harding, T.P.
1985: Seismic characteristics and identification of negative flower structures, positive flower structures and positive structural inversion; *American Association of Petroleum Geologists, Bulletin*, v. 69, p. 582-600.
- Harland, W.B.
1971: Tectonic transpression in Caledonian Spitsbergen; *Geological Magazine*, v. 108, p. 27-42.
- Helmstaedt, H.
1968: Structural analysis of the Beaver Harbour area, Charlotte County, New Brunswick; unpublished PhD thesis, U.N.B., Fredericton, N.B.

- Haworth, R.T. and Lefort, J.P.
1979: Geophysical evidence for the extent of the Avalon zone in Atlantic Canada; *Canadian Journal of Earth Sciences*, v. 16, p. 552-567.
- Higgins, M.W.
1971: Cataclastic rocks; U.S. Geological Survey, Professional Paper 687, 97 p.
- Irving, E. and Strong, D.F.
1984: Evidence against large-scale Carboniferous strike-slip faulting in the Appalachian-Caledonian orogen; *Nature*, v. 30, p. 762-764.
- Karlstrom, K.E., van de Pluijm, B.A., and Williams, P.F.
1982: Structural interpretation of the eastern Notre Dame Bay area, Newfoundland; regional post-middle Silurian thrusting and asymmetrical folding; *Canadian Journal of Earth Sciences*, v. 20, p. 1757-1758.
- Kent, D.V.
1982: Paleomagnetic evidence for Post-Devonian displacement of the Avalon Platform, Newfoundland; *Journal of Geophysical Research*, v. 87, p. 8709-8716.
- Kent, D.V. and Opdyke, N.D.
1978: Paleomagnetism of the Devonian Catskill red beds: evidence for motion of the coastal New England – Canadian Maritime region relative to cratonic North America; *Journal of Geophysical Research*, v. 83, p. 4441-4450.
1979: The Early Carboniferous paleomagnetic field of North America and its bearing on tectonics of the Northern Appalachians; *Earth and Planetary Sciences Letters*, v. 44, p. 365-372.
1980: Paleomagnetism of Siluro – Devonian rocks from eastern Maine; *Canadian Journal of Earth Sciences*, v. 17, p. 1653-1665.
1984: A revised paleopole for the Mauch Chunk Formation of the Appalachians and its tectonic implications. *EOS Transactions*, v. 65, no. 16, p. 200.
- Keppie, J.D.
1982: The Minas Geofracture; *Geological Association of Canada, Special Paper 24*, p. 263-280.
1985: The Appalachian Collage; in *The Caledonide Orogen, Scandinavia and related areas*, ed. D.G. Geo and B. Sturt; Wiley, N.Y., U.S.A.
- Lefort, J.P. and Van der Voo, R.
1981: A kinematic model for the collision and complete suturing between Gondwanaland and Laurasia in the Carboniferous; *Journal of Geology*, v. 89, p. 537-550.
- Lister, G.S. and Snoke, A.W.
1984: S-C mylonites; *Journal of Structural Geology*, v. 6, p. 617-638.
- Ludman, A.
1981: Significance of transcurrent faulting in Eastern Maine; *American Journal of Science*, v. 281, p. 463-483.
- Mann, P., Hempton, M.R., Bradley, D.C., and Burke, K.
1983: Development of pull-apart basins; *Journal of Geology*, v. 91, p. 529-554.
- Mawer, C.K.
1985: Comment on Wise et al., 1984: "Fault-related rocks; suggestions for terminology"; *Geology*, v. 13, p. 378.
- Miyashiro, A.
1973: *Metamorphism and Metamorphic Belts*; George Allen and Unwin, London, 492 p.
- Morris, W.A.
1976: Transcurrent motion determined paleomagnetically in the northern Appalachians and Caledonides and the Acadian Orogeny; *Canadian Journal of Earth Sciences*, v. 13, p. 1236-1243.
- McCutcheon, S.R.
1981: Revised stratigraphy of the Long Reach area, southern New Brunswick; evidence for major NW – directed Acadian thrusting; *Canadian Journal of Earth Sciences*, v. 18, p. 646-656.
- McLeod, M.J.
1979: The geology of Campobello Island, southwestern New Brunswick; unpublished MSc thesis, University of New Brunswick, Fredericton, N.B.
- Nance, R.D.
1982: Structural reconnaissance of the Green Head Group, St. John, New Brunswick; in *Current Research, Part A, Geological Survey of Canada, Paper 82-1A*, p. 37-43.
- Nance, R.D. and Warner, J.B.
1986: Variscan tectonostratigraphy of the Mispec Group, southern New Brunswick; structural geometry and deformational history; in *Current Research, Part A, Geological Survey of Canada, Paper 86-1A*, p. 351-358.
- Platt, J.P.
1979: Extensional crenulation cleavage; *Journal of Structural Geology*, v. 1, p. 95-96.
- Platt, J.P. and Vissers, R.L.M.
1980: Extensional structures in anisotropic rocks; *Journal of Structural Geology*, v. 2, p. 397-410.
- Plint, A.G. and Van de Poll, H.W.
1984: Structural and sedimentary history of the Quaco Head area, southern New Brunswick; *Canadian Journal of Earth Sciences*, v. 21, p. 753-761.
- Poole, W.H.
1980: Rb-Sr age of some granitic rocks between Ludgate Lake and Negro Harbour, southwestern New Brunswick; in *Current Research, Part C, Geological Survey of Canada, Paper 80-1C*, p. 170-173.
- Rast, N.
1979: Precambrian meta-diabase of southern New Brunswick – the opening of the Iapetus Ocean?; *Tectonophysics*, v. 59, p. 127-137.
- Rast, N. and Currie, K.L.
1976: On the position of the Variscan Front in southern New Brunswick and its relation to Precambrian basement; *Canadian Journal of Earth Sciences*, v. 13, p. 194-196.
- Rast, N. and Dickson, W.L.
1982: The Pocologan mylonite zone; *Geological Association of Canada, Special Paper 24*, p. 249-261.
- Rast, N. and Grant, R.H.
1973a: Transatlantic correlation of the Variscan-Appalachian Orogeny; *American Journal of Science*, v. 273, p. 572-579.
1973b: The Variscan Front in southern New Brunswick; New England Intercollegiate Geological Conference, Annual Meeting, p. 4-11.

- Rast, N., Grant, R.H., Parker, J.S.D., and Teng, H.C.
1984: The Carboniferous succession in southern New Brunswick and its state of deformation; 9ieme Congres International du Carbonifere, v. 3, p. 13-22.
- Reading, H.G.
1980: Characteristics and recognition of strike-slip fault systems. International Association of Sedimentology, Special Publication 4, p. 7-26.
- Roy, J.L. and Morris, W.A.
1983: A review of paleomagnetic results from the Carboniferous of North America; the concept of Carboniferous geomagnetic field horizon markers; Earth and Planetary Science Letters, v. 65, p. 167-181.
- Ruitenbergh, A.A. and McCutcheon, S.R.
1982: Acadian and Hercynian structural evolution of southern New Brunswick; Geological Association of Canada, Special Paper 24, p. 131-148.
- Seguin, M.K. and Gahe, E.
1985: Paleomagnetism of Lower Devonian volcanics and Devonian dykes from north-central New Brunswick, Canada; Physics of the Earth and Planetary Interiors, v. 38, p. 262-276.
- Seguin, M.K., Singh, A., and Fyffe, L.
1985: New paleomagnetic data from Carboniferous volcanics and red beds from central New Brunswick; Geophysics Research Letters, v. 12, p. 81-84.
- Sheppard, D.S., Adams, C.J., and Bird, G.W.
1975: Age of metamorphism and uplift in the Alpine Schist Belt, New Zealand; Geological Society of America, Bulletin, v. 86, p. 1147-1153.
- Sibson, R.H.
1977: Fault rocks and fault mechanisms; Geological Society of London, Journal, v. 133, p. 191-213.
- Simpson, C.
1984: Borrego Springs – Santa Rosa mylonite zone: a late Cretaceous west-directed thrust in southern California; Geology, v. 12, p. 8-11.
- Simpson, C. and Schmid, S.M.
1983: An evaluation of criteria to deduce the sense of movement in sheared rocks; Geological Society of America, Bulletin, v. 94, p. 1281-1288.
- Tullis, J.A.
1983: Deformation of feldspars; in *Feldspar Mineralogy*, ed. P.H. Ribbe, Short Course Notes, Mineralogical Society of America, no. 42, Second Edition, p. 297-323.
- Van der Voo, R., French, A.N., and French, R.B.
1979: The paleomagnetic pole position from the folded upper Devonian Catskill red-beds, and its tectonic implications; Geology, v. 7, p. 345-348.
- Van der Voo, R. and Scotese, C.
1981: Paleomagnetic evidence for a large (2000 km) sinistral offset along the Great Glen Fault during Carboniferous time; Geology, v. 9, p. 583-589.
- Vauchez, A.
1980: Ribbon texture and deformation mechanisms of quartz in a mylonitized granite of great Kabylie (Algeria); Tectonophysics, v. 67, p. 1-12.
- Wardle, R.J.
1978: The stratigraphy and tectonics of the Greenhead Group: its relationship to Hadrynian and Paleozoic rocks, southern New Brunswick; unpublished PhD thesis, University of New Brunswick, Fredericton, N.B.
- Webb, G.W.
1963: Occurrence and exploration significance of strike-slip faults in southern New Brunswick; American Association of Petroleum Geologists, Bulletin, v. 47, p. 1904-1927.
1969: Paleozoic wrench faults in the Canadian Appalachians; American Association of Petroleum Geologists, Memoir 12, p. 754-786.
- Weijermars, R. and Rondeel, H.E.
1984: Shear band foliation as an indicator of sense of shear: field observations in central Spain; Geology, v. 12, p. 603-606.
- White, S.H.
1979: Large strain deformation; report on a tectonic studies group discussion meeting held at Imperial College, London; Journal of Structural Geology, v. 1, p. 333-339.
- White, S.H., Burrows, S.E., Carreras, J., Shaw, N.D., and Humphreys, F.J.
1980: On mylonites in ductile shear zones; Journal of Structural Geology, v. 2, p. 175-187.
- Williams, H.
1979: Appalachian Orogen in Canada; Canadian Journal of Earth Sciences, v. 16, p. 792-807.
- Williams, H. and Hatcher, R.D.
1983: Appalachian suspect terranes; Geological Society of America, Memoir 158, p. 33-53.
- Wilson, J.T.
1962: Cabot fault, an Appalachian equivalent of the San Andreas and Great Glen faults and some implications for continental displacement; Nature, v. 195, p. 135-138.
- Wise, D.U., Dunn, D.E., Engelder, J.T., Geoser, P.A., Hatcher, R.D., Kish, S.A., Odom, A.L., and Schamel, S.
1984: Fault-related rocks; suggestions for terminology; Geology, v. 12, p. 391-394.
- Zeck, H.P.
1974: Cataclastites, hemiclastites, holoclastites, blastoditto, and myloblastites – cataclastic rocks; American Journal of Science, v. 274, p. 1064-1073.

Geochemistry of the mafic and volcanic components of the Topsails igneous suite, western Newfoundland

Project 730044

Joseph B. Whalen
Lithosphere and Canadian Shield Division

Whalen, J.B., Geochemistry of the mafic and volcanic components of the Topsails igneous suite, western Newfoundland; in Current Research, Part B, Geological Survey of Canada, Paper 86-1B, p. 121-130, 1986.

Abstract

The Topsails igneous terrane consists of a complex suite of bimodal volcanic and intrusive rocks which, based on recent U-Pb zircon ages, formed during a brief span in the Early Silurian. The earliest intrusive component, the Rainy Lake complex, may be transitional between subduction-related volcanism and the later, extension-related, within-plate basalts and mafic intrusions of the Topsails suite. The felsic volcanics, which are mainly subalkaline, bear a close chemical resemblance to some intrusive components of the suite, but contrast markedly with the voluminous peralkaline intrusive phases. Fractional crystallization along with magma-mixing may be viable processes to generate the various components of the suite. Comparisons with other Silurian igneous rocks of western Newfoundland should outline large scale igneous suites and provide a better understanding of early Silurian tectonics.

Résumé

Le terrane igné de Topsails se compose d'une suite complexe de roches volcaniques et intrusives bimodales qui, d'après les âges obtenus récemment par datation de l'U-Pb dans les zircons, se seraient formées au cours d'une brève période du Silurien ancien. L'élément intrusif le plus ancien, qui porte le nom de complexe de Rainy Lake, pourrait représenter une transition entre le volcanisme lié à la subduction et la mise en place plus récente, à l'intérieur de la plaque, d'intrusions mafiques et de basaltes de la série de Topsails qui sont liés à des phénomènes d'extension. La chimie des roches volcaniques felsiques, qui sont surtout de nature subalkaline, ressemble étroitement à celle de certains éléments intrusifs de la série, mais font fortement contraste avec les phases intrusives peralkalines volumineuses. La cristallisation fractionnée et le mélange magmatique pourraient avoir donné lieu aux divers éléments de la série. Une comparaison de ces roches et d'autres roches ignées siluriennes dans l'ouest de Terre-Neuve devrait permettre de délimiter les grandes séries ignées et de mieux connaître l'histoire tectonique du Silurien ancien.

Introduction

The Topsails igneous terrane separates the probably allochthonous oceanic volcanic sequences of central Newfoundland from the autochthonous miogeoclinal terrane of western Newfoundland (Fig. 15.1). Though formerly regarded as a Devonian batholith (Poole et al., 1970; Williams, 1978), recent mapping (Whalen and Currie, 1982, 1983a, b) summarized in simplified form in Figure 15.2, showed the Topsails terrane to exhibit a complex sequence of intrusive relations and to be as old as contiguous terranes but of different character. U-Pb zircon and whole rock Rb-Sr geochronological data (Whalen et al., in press b) have established a tightly constrained early Silurian age for the voluminous, bimodal intrusive and volcanic rocks (Topsails igneous suite – map units 6 to 8 in Fig. 15.2) and a middle Ordovician age for the screens and roof pendants of older intrusive rocks. This, along with other recent work on the volcanics (Graves, 1983), and on correlative early Silurian volcanic and intrusive rocks to the north (Coyle et al., 1985, 1986; Coyle and Strong, 1986; Kontak and Strong, 1986; Chandler et al., in press), indicates that the genetic relationship between the various early Silurian igneous rocks in western Newfoundland is of great importance. In this paper, emphasis is put on the volcanic and mafic intrusive rocks and their generic relationship to the felsic plutonic rocks.

General geology

A U-Pb zircon age of 438 ± 8 Ma (Whalen et al., in press b) established the Rainy Lake complex (unit 6, Fig. 15.2) as the oldest component of the Topsails suite. It consists of a distinctive, massive, mildly saussuritized gabbro with clots of pyroxene, biotite and amphibole. Various mesocratic diorites, tonalites and granodiorites cut the gabbro. Most of the intrusive rocks are fine- to medium-grained, have quartz and K-feldspar as minor late interstitial phases and are characterized by light to strong actinolitic amphibole plus chlorite and epidote alteration of mafic silicates. The rocks contain accessory apatite, titanite, zircon and opaque minerals. The Rainy Lake complex intrudes the Glover Formation (unit 4) and is cut by dykes of potassic granite equivalent to unit 8. As the Rainy Lake

complex bears a close lithological resemblance to recent island-arc intrusive complexes (Whalen, 1985), it was previously regarded as a deeper level equivalent of the middle Ordovician Glover Formation (Whalen and Currie, 1983a).

Bimodal volcanics, thought to be equivalent to the Springdale Group volcanics to the north, outcrop in the central and northern parts of the Topsails igneous terrane. The volcanic assemblage has been folded and the fold axes are sinuous and appear to wrap around neighbouring unit 8 plutons by which they are intruded, indicating the volcanics form screens or pendants in the younger granitic intrusions. The Springdale Group correlatives in the Topsails terrane consist of abundant felsic volcanics, lesser basalts and very minor sediments. The main type of felsic volcanic is a brick red to dark brown, flow banded rhyolite which generally contains small (1-3 mm) bipyramidal quartz and euhedral K-feldspar phenocrysts. Rhyolites with spheroidal structures ranging in size from 2-3 mm to 2-3 cm are common. Felsic flows which contain flattened pumice fragments (fiamae) and chaotic flow breccias are thought to represent ignimbrite type deposits. Some of these flows contain evidence of magma mixing: flattened, bleb-like, grey dacitic inclusions occur in a red rhyolitic matrix. The textures suggest the two compositions were liquid at the same time. There are also some minor beige to red, fine grained, laminated, probably water-laid, quartz and feldspar crystal tuffs. The felsic volcanic rocks consist of alkali feldspar and quartz forming finely spheroidal and botryoidal structures; mafic silicates are altered to chlorite plus sericite and opaque minerals and they contain accessory zircon, fluorite and secondary titanite. The rocks are generally intensely fractured, and commonly have chlorite plus carbonate fracture fillings. A sample of flow banded rhyolite yielded a U-Pb zircon age of 429 ± 4 Ma (Whalen et al., in press b), essentially identical to the zircon age of 430 ± 6 Ma obtained by Chandler et al. (in press) from a Springdale Group rhyolite to the north.

Reddened basalt flows with frothy vesicular tops, indicating subaerial extrusion, are present in the lower part of the sequence, which outcrops on the west side of the Topsails terrane. The amygdules are filled with epidote plus chlorite and carbonate and the host basalts are extensively altered. Mafic silicates are replaced by epidote plus chlorite and plagioclase is albitized. Limited areas of volcanics are thought to be slightly stratigraphically younger, due to their less altered and deformed state and their close spatial association with younger subvolcanic intrusions (unit 8e). Fairly flat lying, orange, quartz-K-feldspar porphyritic rhyolite and minor basalt flows occur northwest of Hinds Lake, fringing the north side of an ovoid quartz-K-feldspar intrusion. Peralkaline rhyolite, which is underlain and cut by dykes of quartz-K-feldspar porphyry (unit 8e), cap the summit of Mt. Seemore, just west of Sheffield Lake. This rhyolite, the only studied felsic volcanic in which the mafic mineralogy is well preserved, contains spectacular poikilotic arfvedsonite, aegerine and aenigmatite phenocrysts.

The youngest and most characteristic rocks of the Topsails suite form a rather diverse group of syenites and granites. Based on degree of alteration and intrusive relations, a group of intrusions ranging in composition from gabbro through syenite and granite (unit 8a), appear to be older than the other granitic rocks in unit 8. Within this suite, there are zones and elongate curved screens of agmatite (unit 8b), complex mixtures of diverse mafic fragments in a matrix of variously hybridized granitoid rocks. The hybrid host is itself cut by sinuous, locally boudinaged, mafic dykes and its contacts with other granitic subunits of unit 8 appear to be gradational. Peralkaline, coarse grained, white to red, amphibole granite (unit 8c) with prominent quartz grains and a distinctive interstitial habit to the mafic

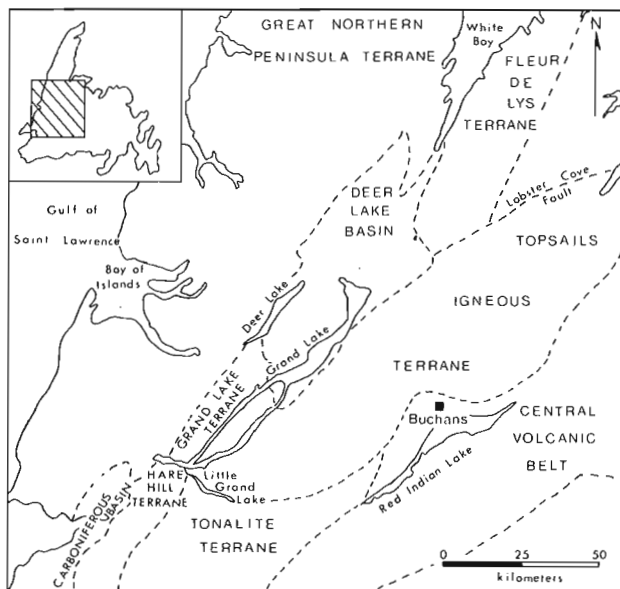


Figure 15.1. Location of the Topsails igneous terrane in relation to other tectonic terranes of western Newfoundland.

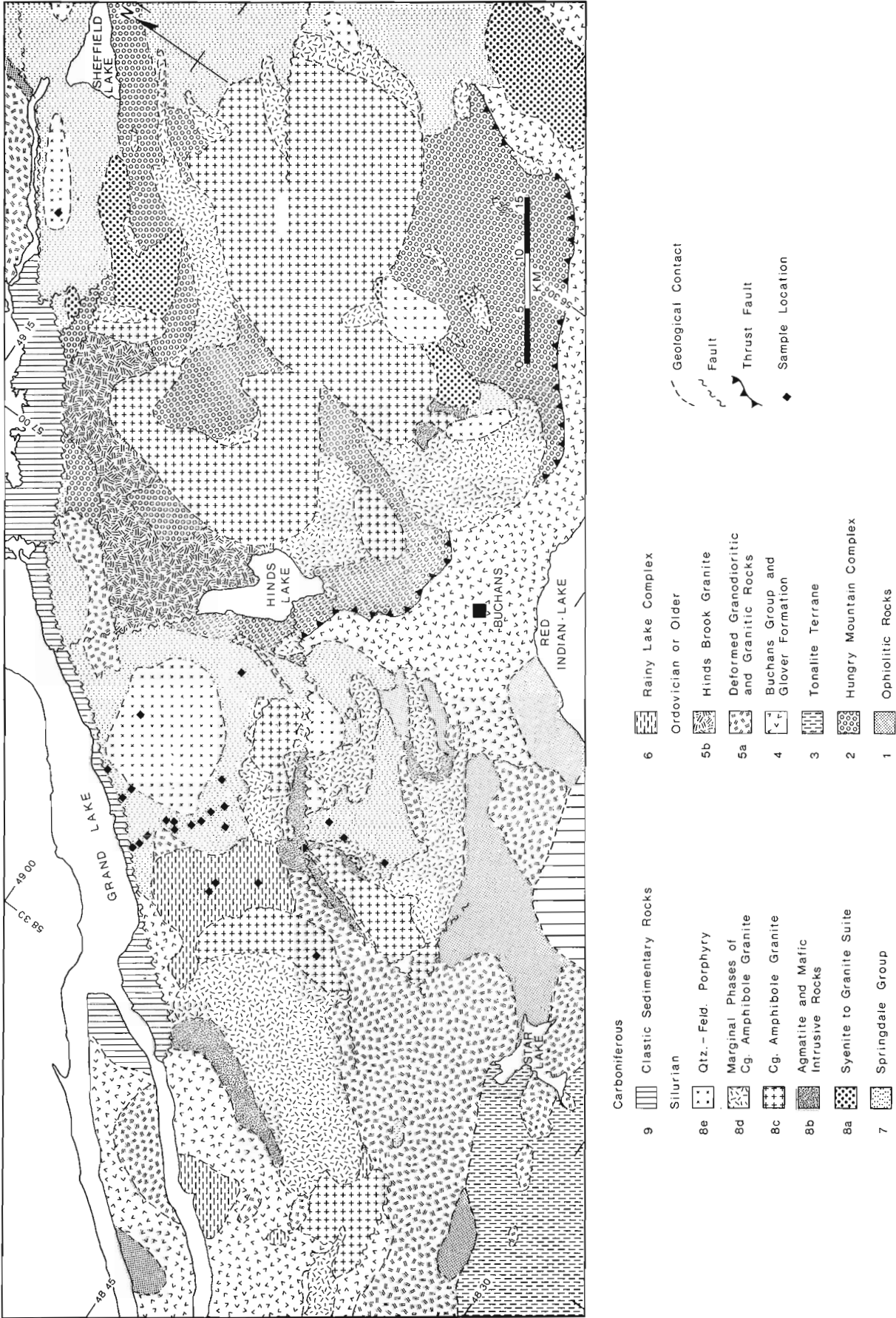


Figure 15.2. Simplified geological map of the Topsails igneous terrane (after Whalen and Currie, 1983b). Locations of samples in Table 15.1 are given.

Table 15.1. Representative Analyses of Topsails Suite Mafic and Volcanic Rocks 1

Unit Sample	6 TB23	6 TB30	6 TB25	7a JG79	7a JG18	7a B1016	7a JG20	7a JG2	7a JG84	7a JG27	7a B1101	7a JG77	7a B1062	7a B1042	7a JG28
SiO ₂	50.55	56.00	66.30	44.05	45.17	45.95	46.33	46.45	47.00	49.05	49.55	51.05	53.55	57.95	63.95
TiO ₂	0.78	0.66	0.68	1.51	1.86	1.89	1.98	2.01	1.37	2.58	2.60	1.68	2.35	1.11	1.42
Al ₂ O ₃	13.75	18.25	15.70	15.65	15.53	15.85	16.77	16.65	15.60	13.50	12.95	14.45	14.00	16.65	12.85
Fe ₂ O ₃	1.94	2.12	1.70	2.70	10.43	10.85	4.27	5.45	2.90	8.85	9.15	1.90	7.45	4.40	5.80
FeO	5.00	3.75	2.20	7.05	0.77	0.75	6.80	6.05	5.80	3.85	3.15	6.35	3.80	2.55	0.70
MnO	0.15	0.09	0.08	0.22	0.23	0.24	0.18	0.21	0.20	0.21	0.21	0.19	0.29	0.18	0.30
MgO	9.87	4.46	1.60	5.39	7.14	7.43	7.80	7.11	6.44	4.08	4.57	3.50	4.55	3.08	2.87
CaO	12.30	8.13	3.60	8.10	6.28	6.08	10.23	8.29	7.20	7.80	6.75	6.85	4.80	4.10	3.07
Na ₂ O	2.35	3.37	4.30	2.05	3.13	3.55	1.53	2.00	1.65	4.15	4.45	1.85	3.35	4.35	3.85
K ₂ O	0.65	1.41	3.15	1.89	1.66	1.75	0.56	1.79	1.60	0.66	0.20	1.92	0.89	2.51	1.74
P ₂ O ₅	0.10	0.21	0.17	0.14	0.22	0.22	0.23	0.32	0.16	0.38	0.43	0.31	0.59	0.25	0.38
S	0.02	0.03	0.01	0.04	0.01	0.01	ND	0.02	0.01	ND	ND	0.03	0.02	ND	0.01
Cl	0.04	0.02	0.06	NA	NA	NA	NA	NA	NA	NA	NA	NA	NA	NA	NA
F	0.02	0.03	0.05	NA	NA	NA	NA	NA	NA	NA	NA	NA	NA	NA	NA
H ₂ O	2.05	1.50	0.80	4.55	3.93	4.00	3.33	3.35	4.85	2.60	3.10	3.90	3.15	1.85	1.95
CO ₂	0.10	0.15	0.10	6.15	2.53	1.85	0.10	0.10	5.50	2.00	3.05	5.05	0.25	0.20	0.80
rest	0.13	0.15	0.18	0.05	0.09	0.08	0.08	0.10	0.06	0.07	0.08	0.07	0.13	0.09	0.18
Total	99.82	100.33	100.68	99.54	98.98	100.50	99.99	99.90	100.34	99.78	100.24	99.10	99.17	99.27	99.87
Trace Elements (ppm)															
Li	16	12	18	NA	NA	NA	NA	NA	NA	NA	NA	NA	NA	NA	NA
Ba	205	300	830	NA	NA	NA	NA	NA	NA	NA	NA	NA	NA	NA	353
Rb	21.5	47.5	84	74	50	54	12.5	84	38.5	9.5	NA	55	19.5	47.5	45.0
Sr	405	565	411	117	511	505	414	498	151	240	263	142	362	388	278
Pb	10	8	17	NA	NA	NA	NA	NA	NA	NA	NA	NA	NA	NA	NA
Th	2.5	5.5	14.5	0.7	0.5	0.4	0.6	1.0	1.6	2.3	2.7	3.4	8.9	4.3	16.2
U	0.5	0.5	2.5	NA	NA	NA	NA	NA	NA	NA	NA	NA	NA	NA	NA
Zr	67	77	202	133	139	145	148	202	213	235	312	276	452	175	651
Nb	3	3	9	4	6	6	5	8	6	10	13	5	13	6	14
Y	12	10	15	31	31	35	29	38	25	33	45	26	48	25	50
Ce	23	30	43	15.8	20.8	20.4	19.7	27.2	26.9	41.0	40.4	44.4	72.7	44.6	80.0
Nd	NA	NA	NA	11.0	16.7	17.2	13.0	17.8	16.2	25.2	27.0	23.7	35.8	22.4	73.0
Sm	NA	NA	NA	3.1	4.2	4.4	3.4	4.5	4.2	5.7	NA	4.9	7.5	4.7	NA
Eu	NA	NA	NA	1.10	1.50	1.40	1.30	1.60	1.20	1.90	2.00	1.70	2.50	1.30	2.70
Tb	NA	NA	NA	0.6	0.7	0.8	0.6	0.8	0.7	1.0	1.0	0.7	1.0	0.7	1.0
Tm	NA	NA	NA	0.4	0.3	0.4	0.4	0.4	0.4	0.4	0.4	0.4	0.4	0.3	0.5
Yb	NA	NA	NA	2.2	2.0	2.0	1.8	2.7	2.4	2.7	2.5	2.2	3.1	2.3	3.1
Hf	NA	NA	NA	2.2	2.5	2.3	2.4	3.2	3.9	4.3	4.5	5.0	6.5	3.6	9.4
Ta	NA	NA	NA	0.1	0.3	0.3	0.3	0.4	NA	0.5	0.5	0.6	1.0	0.3	0.8
Sc	49	22	10	NA	NA	NA	NA	NA	NA	NA	NA	NA	NA	NA	NA
V	182	147	66	NA	NA	NA	NA	NA	NA	NA	NA	NA	NA	NA	NA
Mn	1170	740	565	NA	NA	NA	NA	NA	NA	NA	NA	NA	NA	NA	NA
Ni	142	47	13	NA	NA	NA	NA	NA	NA	NA	NA	NA	NA	NA	NA
Cu	39	4	7	NA	NA	NA	NA	NA	NA	NA	NA	NA	NA	NA	NA
Zn	98	56	61	111	126	35	100	119	115	106	125	85	276	124	228
Ga	14.5	18.0	18.0	NA	NA	NA	NA	NA	NA	NA	NA	NA	NA	NA	NA
(Ce/Y) _n	4.72	7.38	7.05	1.25	1.65	1.43	1.67	1.76	2.65	3.06	2.21	4.20	3.73	4.39	3.94
Ga/Al	1.99	1.86	2.17	NA	NA	NA	NA	NA	NA	NA	NA	NA	NA	NA	NA
A.I.	0.33	0.39	0.67	0.35	0.45	0.49	0.17	0.31	0.29	0.56	0.58	0.35	0.46	0.59	0.64

NA= not analyzed; ND= not detected

1. Analytical techniques: major elements by X.R.F. at the G.S.C. except Na₂O by A.A.S., FeO by titration, volatiles by infra-red, and Cl and F by electrode; REE, Hf and Ta by I.N.A.A. from Graves (1983), Li by A.A.S. and other traces by X.R.F.

minerals appears, to be lithologically and chemically homogeneous over very large areas of the Topsails terrane. It yielded a concordant U-Pb zircon age of 429+/-3 Ma (Whalen et al., in press b). Younger, finer grained marginal phases (unit 8d) are diverse and vary from peralkaline granite to amphibole-poor biotite granite, or even granodiorite and diorite close to agmatite zones. The more mafic compositional variations can be explained by mixing of granitic and basaltic magmas (Whalen and Currie, 1984), which locally has produced spectacular composite dykes. Based on field evidence and chemical data, the mafic magma involved in magma mixing, also forms diabase dykes which cut the coarse grained amphibole granite (unit 8c). Unlike the host rocks, which are fresh, these mafic dykes are altered and, on large outcrop surfaces, have been seen to be broken-up into segments, presumably by movement in a still hot granitic host. The diabases contain ophitic-textured plagioclase, clinopyroxene and opaque minerals. The fact that a high proportion of the mafic minerals are altered to

actinolitic amphibole plus biotite, chlorite and epidote and there is sericitic alteration of plagioclase, suggests a late-stage potassic alteration. High-level intrusive quartz-K-feldspar porphyries form substantial, presumably subvolcanic plutons (unit 8e), which locally exhibit flow banding and may grade to rhyolite with rare interbedded basalt. The porphyries range in composition from alkaline to peralkaline and, based on field relations, are thought to represent a separate intrusive pulse rather than being simply higher level exposures or equivalents of the granites (units 8c and 8d). A sample from the intrusion west of Hinds Lake yielded a U-Pb zircon age of 427+/-3 Ma (Whalen et al., in press b), not significantly younger than the age of the coarse grained amphibole granite. The U-Pb zircon ages indicate a maximum age span of 22 Ma (446 to 424 Ma) and a minimum age span of less than 1 Ma for the Topsails igneous suite (units 6 through 8 in Fig. 15.2) (Whalen et al., in press b).

7h TB42	8b TB135	8b TB29	8b TB33	7c JG82	7c TB102	7c TB14	7c TB13	7c TB97	7c JG83	7c TB56	7c JG7	7c 81096	7d TB2	7e TB45
47.40	43.14	48.65	55.10	74.35	76.85	77.15	77.20	77.35	77.95	78.20	78.90	79.10	72.25	75.40
3.36	4.03	3.27	1.59	0.13	0.12	0.11	0.12	0.11	0.18	0.08	0.12	0.17	0.39	0.19
13.20	14.34	12.75	15.40	12.20	11.75	11.70	12.15	12.05	11.55	11.35	11.05	10.95	13.10	10.65
6.17	5.27	4.35	2.92	1.50	1.36	0.89	0.79	1.18	1.65	0.67	1.40	2.05	1.12	1.99
7.30	10.63	8.75	5.80	0.30	0.55	0.85	0.80	0.55	0.25	0.80	0.20	0.25	1.25	1.60
0.28	0.28	0.34	0.18	0.06	0.02	0.01	0.02	0.06	0.01	0.01	0.02	0.02	0.04	0.06
4.63	6.46	4.69	4.23	0.09	0.03	0.03	0.02	0.16	0.11	0.02	0.01	0.07	0.54	0.06
6.39	9.03	7.45	5.85	1.47	0.41	0.27	0.28	0.34	0.07	0.12	0.06	0.10	0.44	0.19
4.46	2.78	3.77	4.24	3.55	3.67	3.36	3.03	2.58	2.10	2.91	2.40	4.00	3.52	4.40
0.69	1.02	2.21	1.32	4.19	4.36	4.84	5.21	5.55	4.41	5.50	4.98	2.60	5.60	4.62
1.28	0.57	0.24	1.84	ND	0.01	ND	0.01	ND	ND	ND	0.01	ND	0.05	ND
0.02	0.13	0.09	0.16	ND	0.02	0.02	0.02	0.01	ND	0.02	ND	0.02	0.01	0.01
0.02	0.02	0.04	0.02	NA	0.01	0.03	0.01	0.01	NA	0.02	NA	NA	0.02	0.03
0.18	0.06	0.06	0.12	NA	0.03	0.10	0.07	0.08	NA	0.04	NA	NA	0.08	0.08
3.15	2.28	2.20	2.30	0.40	0.30	0.45	0.50	0.55	1.00	0.30	0.40	0.45	0.70	0.40
1.70	0.32	0.15	0.50	1.40	0.30	0.10	0.10	0.25	0.15	0.10	0.05	0.15	0.30	0.05
0.16	0.17	0.17	0.17	0.11	0.10	0.10	0.12	0.11	0.08	0.08	0.08	0.15	0.18	0.27
100.39	100.53	99.18	101.74	99.75	99.89	100.01	100.45	100.94	99.51	100.22	99.68	100.08	99.59	100.00
84	20	16	26	NA	2	4	4	9	NA	3	NA	NA	12	58
310	265	480	455	NA	54	26	30	18	NA	36	62	NA	600	8
12.5	37.0	28.5	71	81	130	152	193	229	161	178	123	83	175	209
164	357	351	269	49	19.0	19.0	17.0	20.0	38.0	11.0	17.5	30.5	63	5.0
8	4	13	12	NA	7	6	24	7	NA	8	NA	NA	10	28
3.0	0.5	3.5	6.5	21.5	22.0	23.0	22.5	22.0	27.8	22.0	17.8	23.3	24.5	33.5
0.5	1.0	0.5	2.0	NA	4.5	10.0	6.0	4.0	NA	4.0	NA	NA	5.5	11.0
392	210	216	337	602	444	406	458	380	NA	274	402	967	462	1660
12	9	9	11	42	30	38	31	36	54	34	30	36	25	61
64	32	53	36	96	71	86	86	79	165	54	NA	116	59	172
75	44	74	72	105.5	123.2	96.7	126.3	133.9	103.3	96.9	51.0	66.3	136	216
NA	NA	NA	NA	51.5	64.8	59.1	75.1	66.0	42.3	51.4	22.8	33.6	NA	NA
NA	NA	NA	NA	NA	14.0	13.6	14.3	19.5	11.1	12.2	NA	NA	NA	NA
NA	NA	NA	NA	0.10	0.40	0.08	0.40	0.06	0.70	0.06	0.04	0.60	NA	NA
NA	NA	NA	NA	2.3	2.0	2.3	2.6	2.4	2.9	1.8	1.5	2.4	NA	NA
NA	NA	NA	NA	1.1	NA	NA	NA	NA	1.5	NA	1.3	1.1	NA	NA
NA	NA	NA	NA	11.3	7.5	8.0	8.1	8.9	14.7	5.8	7.9	13.0	NA	NA
NA	NA	NA	NA	16.4	12.0	11.2	12.2	12.4	23.9	9.4	12.6	19.6	NA	NA
NA	NA	NA	NA	3.1	2.1	2.5	2.2	2.5	3.5	2.2	2.1	2.8	NA	NA
39	30	40	25	NA	ND	ND	ND	ND	NA	ND	NA	NA	4	ND
250	395	186	182	NA	ND	ND	ND	ND	NA	1	NA	NA	17	ND
2010	1770	2170	1380	NA	200	110	165	440	NA	40	NA	NA	345	440
3	61	16	22	NA	ND	ND	ND	ND	NA	ND	NA	NA	ND	ND
12	41	9	16	NA	4	ND	3	ND	NA	3	NA	NA	ND	5
142	129	158	102	44	11	27	36	43	114	18	51	72	220	250
20.5	23.5	20.5	19.0	NA	21.0	21.0	21.5	23.0	NA	18.5	NA	NA	18.5	29.5
2.88	3.38	3.43	4.92	2.70	4.27	2.77	3.61	4.17	1.54	4.41	NA	1.41	5.67	3.09
2.93	3.10	3.04	2.33	NA	3.38	3.39	3.34	3.61	NA	3.08	NA	NA	2.67	5.23
0.61	0.40	0.67	0.55	0.85	0.92	0.92	0.87	0.85	0.71	0.95	0.85	0.86	0.90	1.15
2.	Units:													
6.	Rainy Lake complex													
7a.	lower Springdale Group type basalt													
7b.	upper Springdale Group type basalt													
7c.	Springdale Group type rhyolite													
7d.	quartz-K-feldspar porphyritic rhyolite													
7e.	peralkaline rhyolite													
8b.	diabase dykes													

Geochemistry

Three geologically distinct types or groups of mafic rocks identified in the Topsails terrane and represented in Table 15.1 are, in order of decreasing age:

1. the Rainy Lake complex (unit 6)
2. subaerial basalt flows equivalent to the Springdale Group (unit 7a and b)
3. basaltic rocks associated with acid-mafic magma mixing in units 8b and 8d and diabase dykes cutting the cg. amphibole granite (unit 8c).

Geochemical comparisons will be made between these rocks, and also with the mantle derived (M-type), Uasilau-Yau Yau island arc intrusive suite (Whalen, 1985). The Rainy Lake complex was suggested by Whalen and Currie (1982, 1983a) to be an M-type suite.

Based on the silica contents, the majority of the analyzed mafic samples are clearly basaltic (Table 15.1), though a few samples (81042 and JG28) and components of

the Rainy Lake complex are andesitic to dacitic in composition. This is in keeping with the field observation that the volcanic suite is bimodal and is not thought to reflect a sampling bias. On most chemical plots, there is no clear separation between the various Topsails suite mafic igneous rocks. Alkalis versus silica (Miyashiro, 1978) and TiO₂ versus Zr/P₂O₅ (Floyd and Winchester, 1975) plots (Fig. 15.3a) indicate the subalkaline to alkaline character of the Topsails mafic volcanics and dykes and the less alkaline character of the Rainy Lake complex. Also, the Rainy Lake complex, like the Uasilau-Yau Yau complex, is less enriched in the incompatible trace elements Zr, Nb, Ce and Y than the other basic rocks (Table 15.1). Most chemical discrimination diagrams for basic rocks show a clear separation between the Topsails basic rocks, which plot in the within-plate basalt field, and the Uasilau-Yau Yau suite which plots in the island arc basalt field on the Zr/Y versus Zr diagram of Pearce and Norry (1979) or the ocean floor basalt field on the Ti-Zr-Y triangular diagram of Pearce and Cann (1973). On a MgO-FeO-Al₂O₃ diagram (Pearce et al., 1977) (Fig. 15.3b), mafic components of the Rainy Lake and the Uasilau-Yau Yau

complexes plot together in the orogenic basalt-andesite field, whereas the other Topsails mafic rocks plot in the continental basalt field. REE data for Springdale basalts (Table 15.1, Fig. 15.4a, b) indicate they have slight to moderate chondrite normalized Ce/Yb ratios (1.8 to 6.0). Abundances and slopes of the patterns are very similar to transitional basalts (at the same TiO₂ content) produced in the Gregory Rift, Kenya (Barker et al., 1977) and early rift volcanics in the Camels Hump Group, Vermont (Coish et al., 1985) (Fig. 15.4c).

Various components recognized in the felsic volcanics and represented in Table 15.1 are:

1. a lower sequence with abundant flow banded rhyolite (unit 7c)

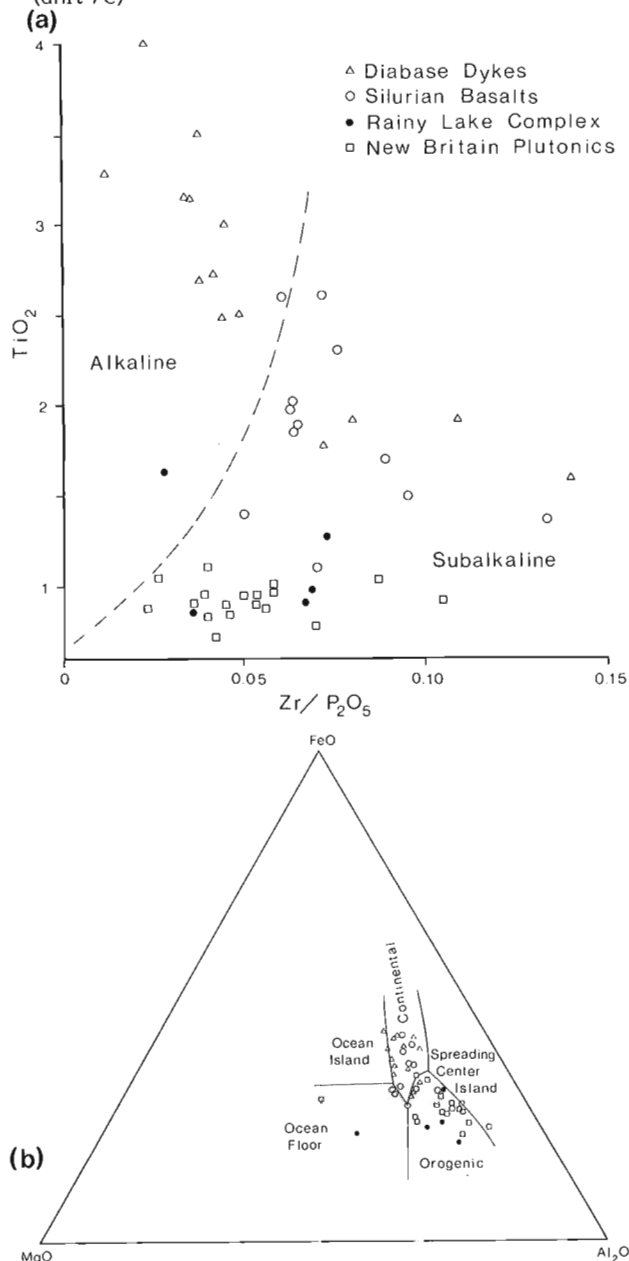


Figure 15.3. Chemical discrimination diagrams for mafic rocks of the Topsails igneous suite and also island arc intrusive rocks of the Uasilau-Yau Yau complex, New Britain (Whalen, 1985): (a) TiO₂-Zr/P₂O₅ plot (after Floyd and Winchester, 1975); (b) FeO-MgO-Al₂O₃ plot (after Pearce et al., 1977).

2. restricted areas of orange quartz-K-feldspar porphyritic rhyolite (unit 7d)
3. a small area of peralkaline rhyolite capping Mt. Seemore (unit 7e).

The last two components, which are closely associated with quartz-K-feldspar porphyry intrusions (unit 8e), may be stratigraphically younger. Chemically (Table 15.1), the quartz-K-feldspar porphyritic rhyolite is less felsic (73 versus 76 to 79 wt.% SiO₂) and has significantly higher TiO₂, FeO*, Ba and (Ce/Y)_n and lower Nb and Ga/Al than the other analyzed rhyolites. In the type Springdale Group to the north, Coyle and Strong (1986) documented the presence of a high-silica and a low-silica group of rhyolites with silica differences which closely approximate those between unit 7e and 7d rhyolites. However, comparison of distinctive trace elements such as Rb, Sr, Nb, Y, Zr and Zn indicates that all the rhyolites from the Topsails suite resemble the high-silica rhyolites. The peralkaline rhyolite, which has been suggested by Coyle et al. (1986) to have obtained its peralkaline character through metasomatism by the subjacent quartz-K-feldspar porphyry intrusion, is also chemically distinct in having high FeO*, Ga/Al, Zr, Nb, REE and Zn.

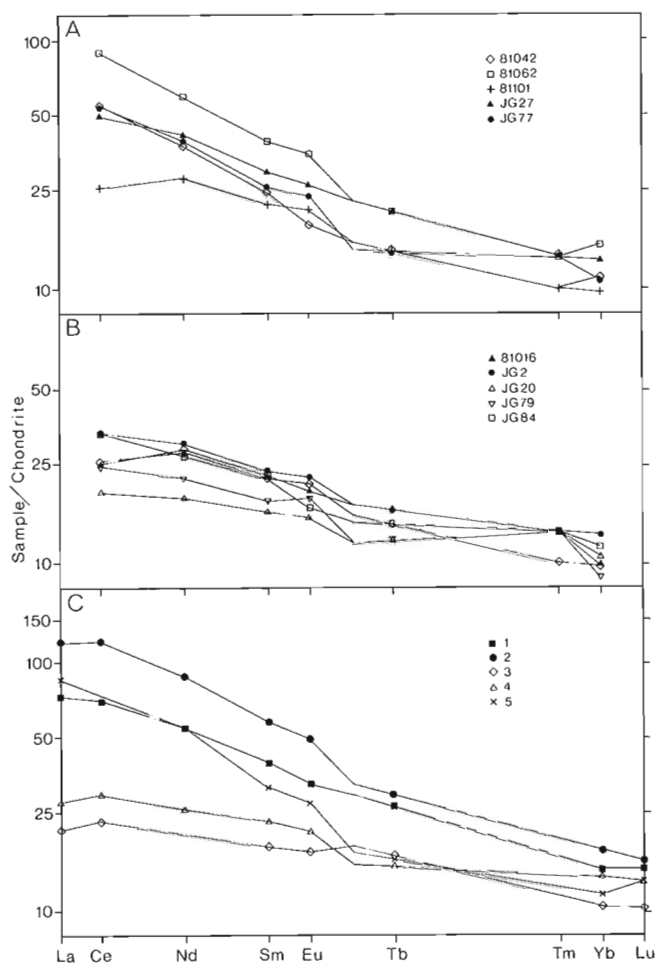


Figure 15.4. Chondrite normalized REE patterns for Topsails suite basalts (A) with (Ce/Yb)_n > 3.0, (B) with (Ce/Yb)_n < 3.0 and (C) various average early rift basalt units of the Camels Hump Group, Vermont (patterns 1 to 4) (Coish et al., 1985) and for average transitional rift basalt of the Gregory Rift, Kenya (pattern 5) (Barker et al., 1977).

Comparison of chemical data from the Topsails felsic plutonic rocks (units 8a, c, d, e) with the felsic volcanic rocks, indicates that many of the rhyolites are more siliceous and have high K_2O/Na_2O values (Fig. 15.5). These features can be attributed to a minor degree of silicification and alteration associated with contact metamorphism. Other than these differences, the felsic volcanic rocks and many of the subalkaline (biotite-amphibole and amphibole-biotite bearing) marginal plutonic phases (unit 8d) bear a very close chemical resemblance. Both are chemically distinct on many chemical plots from the major peralkaline intrusive phases (units 8c and 8e) in having lower TiO_2 , FeO^* , MgO , Sc , Mn and Zr . Ga/Al , an excellent index of the alkaline character of felsic intrusions (Whalen et al., in press a), should be less susceptible to alteration than apatitic index. Figure 15.6A illustrates the lower Ga/Al and Zr values and, thus, less alkaline character of the felsic volcanics, except for the peralkaline Mt. Seemore rhyolite. In contrast, a plot of chondrite normalized Ce/Y versus Ga/Al (Fig. 15.6B) suggests that the felsic volcanics have less fractionated REE patterns than the otherwise chemically similar subalkaline marginal intrusive phases. $(Ce/Y)_n$ values for the rhyolites are similar to those for the peralkaline intrusive phases (units 8c and 8e) and, like these units, $(Ce/Y)_n$ values decrease with increasing alkaline character (higher Ga/Al values). Chondrite normalized REE patterns for the rhyolites (Table 15.1 and Fig. 15.7A, B) are, as indicated by the chondrite normalized Ce/Y data, not strongly fractionated ($Ce/Y = 1.3$ to 4.3) and have very pronounced Eu anomalies ($Eu/Eu^* = 0.012$ to 0.168).

Although complete REE data are not yet available from my samples of Topsails intrusive rocks, some published granite REE data from the northern part of the area (Taylor et al., 1981) are appropriate for comparing the gross features of the felsic intrusive and volcanic rocks of the suite (Fig. 15.7C). Syenites have relatively unfrac­tionated (average $Ce/Yb = 3.6$) chondrite normalized REE patterns

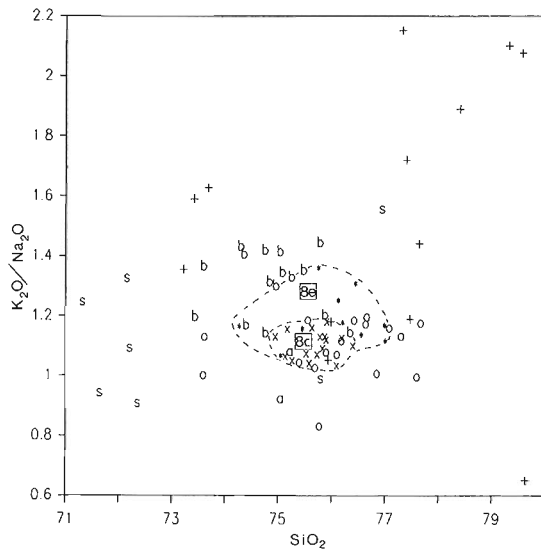


Figure 15.5. SiO_2 versus K_2O/Na_2O plot for felsic rocks of the Topsails igneous suite; fields of various intrusive phases are outlined and labelled with the map unit number, symbols used are:

- (+) Silurian felsic volcanics (units 7c, d and e)
- (s) syenite to granite (unit 8a)
- (b) biotite-amphibole bearing
- (a) amphibole-biotite bearing marginal intrusive phases (unit 8d)
- (o) amphibole-aegirine bearing
- (x) cg. amphibole granite (unit 8c)
- (*) quartz-K-feldspar porphyry (unit 8e)

which lack Eu anomalies. In the order biotite granite, hornblende-biotite granite, peralkaline granite and quartz-feldspar porphyry, there is a decrease in average Eu anomalies (average $Eu/Eu^* = 0.13, 0.34, 0.40$ and 0.42 , respectively) and, though there is an increase in total REE abundance, there is not much change in degree of fractionation of REE patterns (average $Ce/Yb = 4.0, 4.2, 4.8$ and 4.0 , respectively). Within the peralkaline granite the range of chondrite normalized Ce/Yb values (5.1 to 1.8) suggests a trend of decreasing fractionation of REE patterns with increasing alkalinity, as noted in the chondrite normalized Ce/Y data (Fig. 15.6B). Comparison of the REE patterns of the intrusive rocks with that of the felsic volcanics indicates that REE abundances and slopes for the rhyolites and the peralkaline intrusions are essentially identical, except for the extreme Eu anomalies of the rhyolites. The peralkaline rhyolite of Taylor et al. (1981) was collected from the site of sample TB45 in Table 15.1. It has a similar pattern to the other rhyolites but contains a greater abundance of REE.

Discussion

The differences between the Rainy Lake complex and the other early Silurian mafic igneous rocks of the Topsails suite suggests it is transitional between subduction related

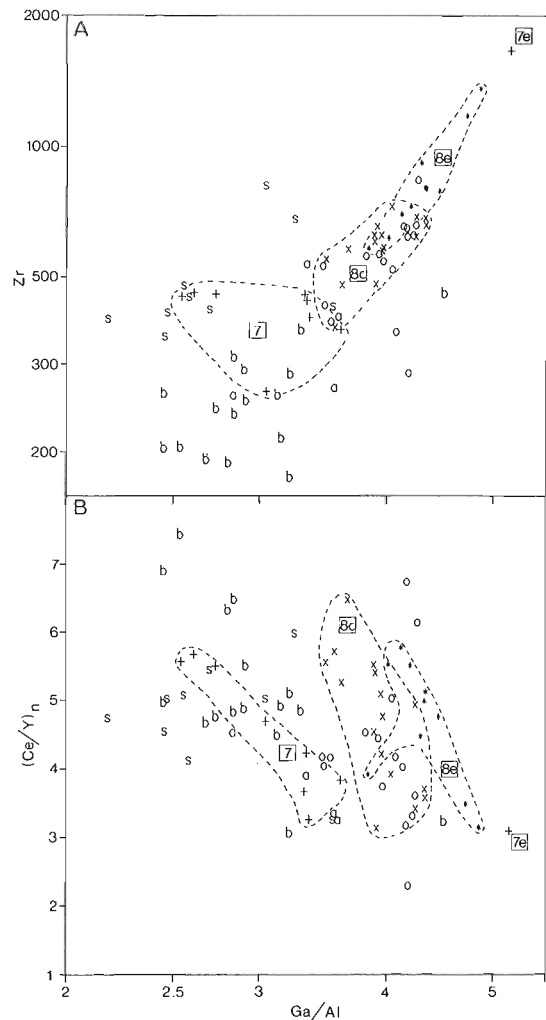


Figure 15.6. Ga/Al versus (A) Zr and (B) $(Ce/Y)_n$ plots for the felsic rocks of Topsails igneous suite; fields and symbols as in Figure 15.5.

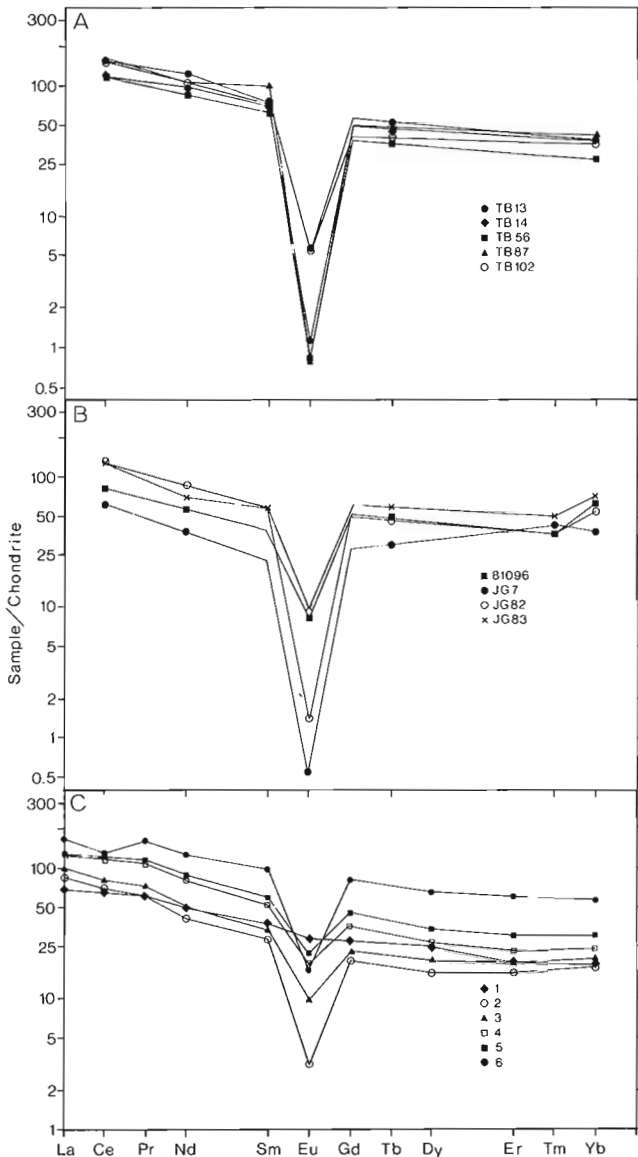


Figure 15.7. Chondrite normalized REE patterns for Topsails suite rhyolites (A) with $(Ce/Yb)_n > 3.0$, (B) with $(Ce/Yb)_n < 3.0$, and (C) for averaged data of Taylor et al. (1981) from northern Topsails terrane.

magmatism and extension related within-plate volcanism. The identical chemical nature of the basalts equivalent to the Springdale Group and the diabase dykes cutting the Topsails granites, granites which intrude these volcanics, suggests there was no change in the composition of mafic magmatism during the main period of Topsails igneous activity. Though the geochemical data do not enable a distinction between a within-plate oceanic or continental setting, the subaerial nature of the volcanics and the vast volumes of felsic versus mafic igneous rocks in the complex clearly indicate a within continental plate tectonic setting. The bimodal character of the volcanic suite in the Topsails igneous terrane is in marked contrast to the calc-alkaline series from basalts to rhyolites documented in the type Springdale Group to the north (Coyle and Strong, 1986). The reason for this difference is unclear, though it may result from a greater amount of mafic-felsic magma mixing, as was described from the Topsails suite by Whalen and Currie (1984).

The close chemical similarities but also differences between the felsic volcanic and plutonic rocks of the Topsails suite may provide information crucial to an understanding of their petrogenesis. It is very notable that the Topsails suite silicic volcanic rocks, and also the type Springdale Group volcanics (Coyle and Strong, 1986), contain a vast predominance (>98%) of non-peralkaline compositions. By contrast, of the plutonic rocks, the major intrusive units (8c, 8e and a large portion of 8d) are alkaline to peralkaline. Arguments have been presented by Taylor et al. (1980, 1981), for the prime importance of fluid metasomatism in the formation of peralkaline rocks, with such features as the upward shift in heavy REE for the peralkaline rocks in Figure 15.7C being attributed to metasomatism. This assertion is far from substantiated; such features may better be explained by more generally accepted igneous processes. Felsic igneous sequences have been the subject of considerable recent controversy regarding the cause of their extreme fractionation in minor and trace elements (Whalen, 1983; Miller and Mittlefehldt, 1984). It has been argued (Hildreth, 1979, 1981) that such trends result from liquid-state fractionation, termed thermogravitational diffusion (TGD), rather than the fairly generally accepted process of crystal-liquid fractionation. Problems with fractional crystallization models for such rocks are, in large part, due to insufficient data on the effects of fractionating REE-rich accessory phases and a lack of appropriate mineral/liquid distribution coefficient data for such rocks (Barker and McBirney (1985) and Wolff and Storey (1984)). Recent sanidine/glass distribution coefficient data for subalkaline to peralkaline silicic rocks (Leeman and Phelps, 1981; Drexler et al., 1983; Nash and Crecraft, 1985) indicate a large variation in values for Sr (3.1 to 28), Ba (3.2 to 24) and Eu (0.16 to 9.06). Drexler et al. (1983) found a negative correlation between apatitic index and Eu distribution coefficient values (sanidine $DEu = 3.04$ and 0.16 for rhyolites with glass apatitic indices = 0.90 and 1.26, respectively). Recent data from accessory mineral phases in felsic rocks such as allanite (Brooks et al., 1981) and monazite (Miller and Mittlefehldt, 1982) have indicated the possible prime role of minute quantities of such phases in drastically altering REE distribution patterns. Experimental work by Watson (1979) on the solubility of Zr in felsic melts has indicated that solubility increases dramatically in melts with an apatitic index greater than 1.0. Thus, trace element behaviour in alkaline to peralkaline silicic melts is complex: differences in melt composition, temperature and volatile content affect melt structure and, as a result, mineral partition coefficient patterns (see Nash and Crecraft, 1985; Barker and McBirney, 1985).

Even though they contain a minor phenocryst content, the Topsails suite rhyolites can be readily argued to closely approximate liquid compositions. The plutonic rocks of the suite, based on petrographic evidence, are melt derived (ie. restite or refractory melt residue free), but may, as has been documented elsewhere (McCarthy and Hasty, 1976; Whalen, 1983, 1985), represent cumulate-melt mixtures. Removal of substantial K-feldspar from a melt with a composition like the subalkaline marginal phases would enrich the heavy REE somewhat more than the light REE and greatly deplete Eu and Ba. In agreement with such a model, the rhyolite and also the quartz-K-feldspar porphyry intrusions (unit 8e), exhibit a trend of decreasing Ba with decreasing $(Ce/Y)_n$ (Fig. 15.8). In contrast, the coarse grained amphibole granite (unit 8c) exhibits the opposite trend and lacks the large Eu anomalies of the rhyolites. These features indicate that the granites may contain a significant volume of K-feldspar cumulates. A careful evaluation of the felsic volcanic and plutonic rock geochemical data and detailed modelling are required to

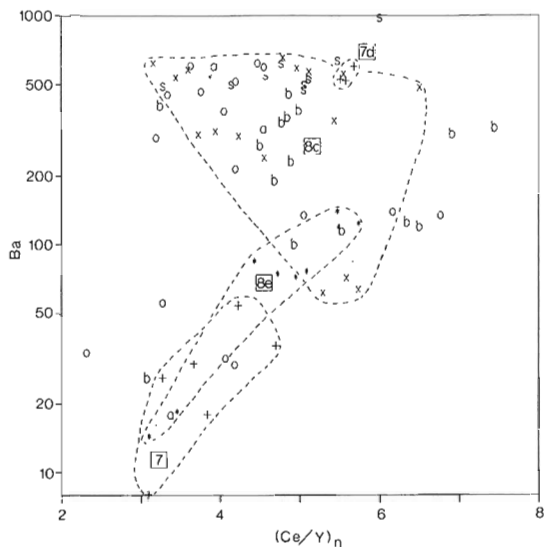


Figure 15.8. $(\text{Ce}/\text{Yb})_n$ versus Ba plot for felsic igneous rocks of Topsails igneous suite; fields and symbols as in Figure 15.5.

quantitatively evaluate a fractional crystallization model for the Topsails suite. However, this process, in combination with magma mixing (Whalen and Currie, 1984), does appear capable of explaining some significant geochemical features of the suite. In addition, comparison of Topsails suite geochemical data with data from other Silurian igneous rocks in Newfoundland (eg. Coyle and Strong, 1986; Kontak and Strong, 1986) may enable large scale suites to be recognized and general conclusions to be reached on the tectonic significance of Silurian magmatism.

Acknowledgments

I thank Jennifer Graves for permission to use unpublished geochemical data and K.L. Currie for helpful discussions and critical reading of the manuscript.

References

- Barker, B.H. and McBirney, A.R.
1985: Liquid fractionation. Part III: Geochemistry of zoned magmas and the compositional effects of liquid fractionation; *Journal of Volcanology and Geothermal Research*, v. 24, p. 55-81.
- Barker, B.H., Gordon, G.G., Leeman, W.P., and Lindstrom, M.H.
1977: Geochemistry and petrogenesis of a basalt-benmoreite-trachyte suite from the southern portion of the Gregory Rift, Kenya; *Contributions to Mineralogy and Petrology*, v. 64, p. 303-332.
- Brooks, C.K., Henderson, P., and Ronsbo, J.G.
1981: Rare-earth partition between allanite and glass in the obsidian of Sandy Braes, Northern Ireland; *Mineralogical Magazine*, v. 44, p. 157-160.
- Chandler, F.W., Sullivan, R.W., and Currie, K.L.
- The age of the Springdale Group, Western Newfoundland and correlative rocks - evidence for a Llandovery overlap assemblage in the Canadian Appalachians; *Transactions of the Royal Society of Edinburgh*. (in press)
- Coish, R.A., Fleming, F.S., Larsen, M., Poyner, R., and Seibert, J.
1985: Early rift history of the proto-Atlantic ocean: geochemical evidence from metavolcanic rocks in Vermont; *American Journal of Science*, v. 285, p. 351-378.
- Coyle, M. and Strong, D.F.
1986: Geology of the southern and northern margins of the Springdale caldera, Newfoundland; in *Current Research, Part A, Geological Survey of Canada, Paper 86-1A*, p. 499-506.
- Coyle, M., Strong, D.F., and Dingwell, D.B.
1986: Geology of the Sheffield Lake group, west-central Newfoundland; in *Current Research, Part A, Geological Survey of Canada, Paper 86-1A*, p. 455-459.
- Coyle, M., Strong, D.F., Gibson, D., and Lambert, E.
1985: Geology of the Springdale Group, central Newfoundland; in *Current Research, Part A, Geological Survey of Canada, Paper 85-1A*, p. 157-163.
- Drexler, J.W., Bornhorst, T.J., and Noble, D.C.
1983: Trace element sanidine/glass distribution coefficients for peralkaline silicic rocks and their implications to peralkaline petrogenesis; *Lithos*, v. 16, p. 265-271.
- Floyd, P.A. and Winchester, J.A.
1975: Magma type and tectonic setting discrimination using immobile elements; *Earth and Planetary Science Letters*, v. 27, p. 211-218.
- Graves, J.C.
1983: A petrographic and geochemical interpretation of a bimodal volcanic suite from the Rainy Lake map area, Newfoundland, in terms of its origin and plate tectonic environment; unpublished B.Sc. thesis, University of Waterloo, 46 p.
- Hildreth, E.W.
1979: The Bishops Tuff: evidence for the origin of zoned magma chambers; in *Ash Flow Tuffs*, ed. C.E. Chapin and W.E. Elston; *Geological Society of America; Special Paper 180*, p. 43-72.
- 1981: Gradients in silicic magma chambers: implications for lithospheric magmatism; *Journal of Geophysical Research*, v. 86, p. 10153-10192.
- Kontak, D.J. and Strong, D.F.
1986: The volcano-plutonic King's Point complex, Newfoundland; in *Current Research, Part A, Geological Survey of Canada, Paper 86-1A*, p. 465-470.
- Leeman, W.P. and Phelps, D.W.
1981: Partitioning of rare earth elements and other trace elements between sanidine and coexisting volcanic glass; *Journal of Geophysical Research*, v. 86, p. 10193-10199.
- McCarthy, T.S. and Hasty, R.A.
1976: Trace element distribution patterns and their relationship to the crystallization of granitic melts; *Geochimica et Cosmochimica Acta*, v. 40, p. 1351-1358.
- Miller, C.R. and Mittlefehldt, D.W.
1982: Light rare earth element depletion in felsic magmas; *Geology*, v. 10, p. 129-133.

- Miller, C.R. and Mittlefehldt, D.W. (cont.)
 1984: Extreme fractionation in felsic magma chambers: a product of liquid-state diffusion or fractional crystallization?; *Earth and Planetary Science Letters*, v. 68, p. 151-158.
- Miyashiro, A.
 1978: Nature of alkalic volcanic rock series; *Contributions to Mineralogy and Petrology*, v. 66, p. 91-104.
- Nash, W.P. and Crecraft, H.R.
 1985: Partition coefficients for trace elements in silicic magmas; *Geochimica et Cosmochimica Acta*, v. 49, p. 2309-2322.
- Pearce, J.A. and Cann, J.R.
 1973: Tectonic setting of basic volcanic rocks determined using trace element analyses; *Earth and Planetary Science Letters*, v. 19, p. 290-300.
- Pearce, J.A. and Norry, M.J.
 1979: Petrogenetic implications of Ti, Zr, Y, and Nb variations in volcanic rocks; *Contributions to Mineralogy and Petrology*, v. 69, p. 33-47.
- Pearce, T.H., Gorman, B.E., and Birkett, T.C.
 1977: The relationship between major element chemistry and tectonic environment of basic and intermediate volcanic rocks; *Earth and Planetary Science Letters*, v. 36, p. 121-132.
- Poole, W.H., Sanford, B.V., Williams, H., and Kelly, D.G.
 1970: Geology of southeastern Canada; in *Geology and Economic Minerals of Canada*, ed. R.J.W. Douglas, Geological Survey of Canada, Economic Geology Report 1, p. 227-304.
- Taylor, R.P., Strong, D.F., and Fryer, B.J.
 1981: Volatile control of contrasting trace element distributions in peralkaline granitic and volcanic rocks; *Contributions to Mineralogy and Petrology*, v. 77, p. 267-271.
- Taylor, R.P., Strong, D.F., and Kean, B.F.
 1980: The Topsails igneous complex: Silurian-Devonian peralkaline magmatism in western Newfoundland; *Canadian Journal of Earth Sciences*, v. 17, p. 425-439.
- Watson, E.B.
 1979: Zircon saturation in felsic liquids: experimental results and applications to trace element geochemistry; *Contributions to Mineralogy and Petrology*, v. 70, p. 407-419.
- Whalen, J.B.
 1983: The Ackley City batholith, southeastern Newfoundland: evidence for crystal versus liquid state fractionation; *Geochimica et Cosmochimica Acta*, v. 47, p. 1443-1457.
 1985: Geochemistry of an island arc plutonic suite: the Uasilau-Yau Yau intrusive complex, New Britain, P.N.G.; *Journal of Petrology*, v. 26, p. 603-632.
- Whalen, J.B. and Currie, K.L.
 1982: Volcanic and plutonic rocks in the Rainy Lake area, Newfoundland; in *Current Research, Part A, Geological Survey of Canada, Paper 82-1A*, p. 17-22.
 1983a: The Topsails igneous terrane of western Newfoundland; in *Current Research, Part A, Geological Survey of Canada, Paper 83-1A*, p. 15-23.
 1983b: The Topsails igneous terrane, western Newfoundland; *Geological Survey of Canada, Open File 923*.
 1984: The Topsails igneous terrane, western Newfoundland: evidence for magma mixing; *Contributions to Mineralogy and Petrology*, v. 87, p. 319-317.
- Whalen, J.B., Currie, K.L., and Chappell, B.W.
 - A-type granites: geochemical characteristics and discrimination; *Contributions to Mineralogy and Petrology*. (in press a)
- Whalen, J.B., Currie, K.L., and van Breemen, O.
 - Episodic Ordovician-Silurian plutonism in the Topsails igneous terrane, western Newfoundland; *The Royal Society of Edinburgh, Transactions*. (in press b)
- Williams, H.
 1978: Tectonic lithofacies map of the Appalachians; *Memorial University of Newfoundland, Map 1*.
- Wolff, J.A. and Storey, M.
 1984: Zoning in highly alkaline magma bodies; *Geological Magazine*, v. 121, p. 563-575.

Geochemistry of the Lower Silurian Pointe aux Trembles and Lac Raymond formations, central Quebec Appalachians: a preliminary report¹

Contract 24ST, 23233-5-0072

Jean David² and Clément Gariépy³

David, J. and Gariépy, C., Geochemistry of the Lower Silurian Pointe aux Trembles and Lac Raymond formations, central Quebec Appalachians: a preliminary report; in Current Research, Part B, Geological Survey of Canada, Paper 86-1B, p. 131-140, 1986.

Abstract

The Pointe aux Trembles Formation consists of conglomeratic and breccia flows, tuffs and rare lavas which accumulated during early Silurian times. It is only moderately altered and the spectrum of compositions observed (53-69 wt% SiO₂) is thought to be primary. The major, trace and REE data unambiguously show that the volcanics are analogous to calc-alkaline series rocks found along modern convergent plate boundaries and imply the existence of an ensialic volcanic arc in the Appalachians, during Llandoveryian times.

The Lac Raymond Formation, the lateral equivalent of the Pointe aux Trembles Formation, comprises mafic sills of unknown age intruded in mudstones, epiclastics and tuffaceous sandstones. The sills are restricted to gabbroic compositions (49-54 wt% SiO₂) but their magmatic affinity remains ambiguous: they could either be equivalent to high-alumina basalts from volcanic arcs or similar to alkaline (?) basalts erupted in Gaspésie during lower Devonian times. Nevertheless, their REE distribution indicates that they are not cogenetic with the Pointe aux Trembles volcanics.

Résumé

La Formation de Pointe aux Trembles qui s'est accumulée au Silurien inférieur, est composée principalement de coulées de brèche, de conglomérats volcaniques, de tufs et de rares épanchements de laves. Le chimisme de ces roches n'a été que légèrement affecté par l'altération et présente des variations de composition (53-69 wt% SiO₂) que l'on considère comme étant primaire. Leurs teneurs en éléments majeurs, en éléments traces et en éléments des Terre-Rares présentent toutes les caractéristiques des séries calco-alkalines que l'on retrouve actuellement à la frontière de plaques convergentes. Les caractéristiques chimiques impliquent aussi l'existence, pendant le Llandoveryien, d'un arc volcanique ensialique dans les Appalaches.

On trouve dans la Formation de Lac Raymond, l'équivalent latéral de la Formation de Pointe aux Trembles, une série de sills mafiques, qui se sont mis en place à l'intérieur de mudstones, d'épiclastites et de grès tufacés et dont l'âge reste incertain. Les sills sont gabbroïques (49-54 wt% SiO₂) et leur affinité magmatique demeure cependant ambiguë. Ils pourraient s'apparenter autant aux basaltes hyper-alumineux associés des arcs volcaniques qu'à des basaltes alcalins (?) semblables à ceux mis en place dans la péninsule gaspésienne pendant le Dévonien inférieur. Leur contenu en éléments des Terre-Rares indiquent toutefois qu'ils ne peuvent pas être cogénétiqes avec les roches volcaniques de la Formation de Pointe aux Trembles.

¹ Contribution to the Canada Economic Development Plan for Gaspé and Lower St. Lawrence, Mineral Program 1983-1988. Project carried by Geological Survey of Canada, Lithosphere and Canadian Shield Division.

² Département de Géologie, Université de Montréal, C.P. 6128, Succ. "A", Montréal, Québec H3C 3J7

³ Département des Sciences de la Terre, Université du Québec à Montréal, C.P. 8888, Succ. "A", Montréal, Québec H3C 3P8

Introduction

Silurian-Devonian assemblages are the most abundant group of rocks exposed in the northeastern Quebec Appalachians. However, the global tectonic evolution of these Siluro-Devonian terranes is still poorly understood. For example, there is a debate as to whether the deformation of these rocks results from large-scale intra-cratonic oblique compression (Arthaud and Matte, 1977; Béland, 1982) or to collision at a plate boundary (Bird and Dewey, 1970; Ruitenberg et al., 1977; Osberg, 1978). One way of contributing to the problem is to establish, through the use of geochemical parameters, the tectonic environment of the volcanic and intrusive series found within these terranes. This method is not new and, in the Appalachians alone, several studies have shown the usefulness of this approach (e.g. Hynes, 1976; Strong, 1977; Pajari et al., 1977; Pintson et al., 1985).

At present, geochemical studies of Siluro-Devonian rocks, from Gaspésie, have mainly focused on the younger magmatic

products i.e. the late Silurian and lower Devonian volcanics of Gaspésie (Laurent and Bélanger, 1984; Bédard, 1985) and the Devonian granitoid intrusives (e.g. Whalen, 1985; Whalen and Gariépy, 1986). Here we report on the geochemistry of early Silurian volcanics from the Pointe aux Trembles Formation and of mafic sills from the Lac Raymond Formation to outline the main geochemical features of both units and discuss simple genetic implications; we defer a more elaborate study of their petrogenesis to a future publication.

Geological outline

The Pointe aux Trembles and Lac Raymond Formations are part of a sedimentary and volcanoclastic pile which stretches for 125 km within the northeastern Quebec Appalachians, close to the boundary with the province of New-Brunswick and the state of Maine (Fig. 16.1). The belt likely extends southwestward, within the state of Maine, where a very similar sequence has been described (Boudette et al., 1976). The stratigraphy of

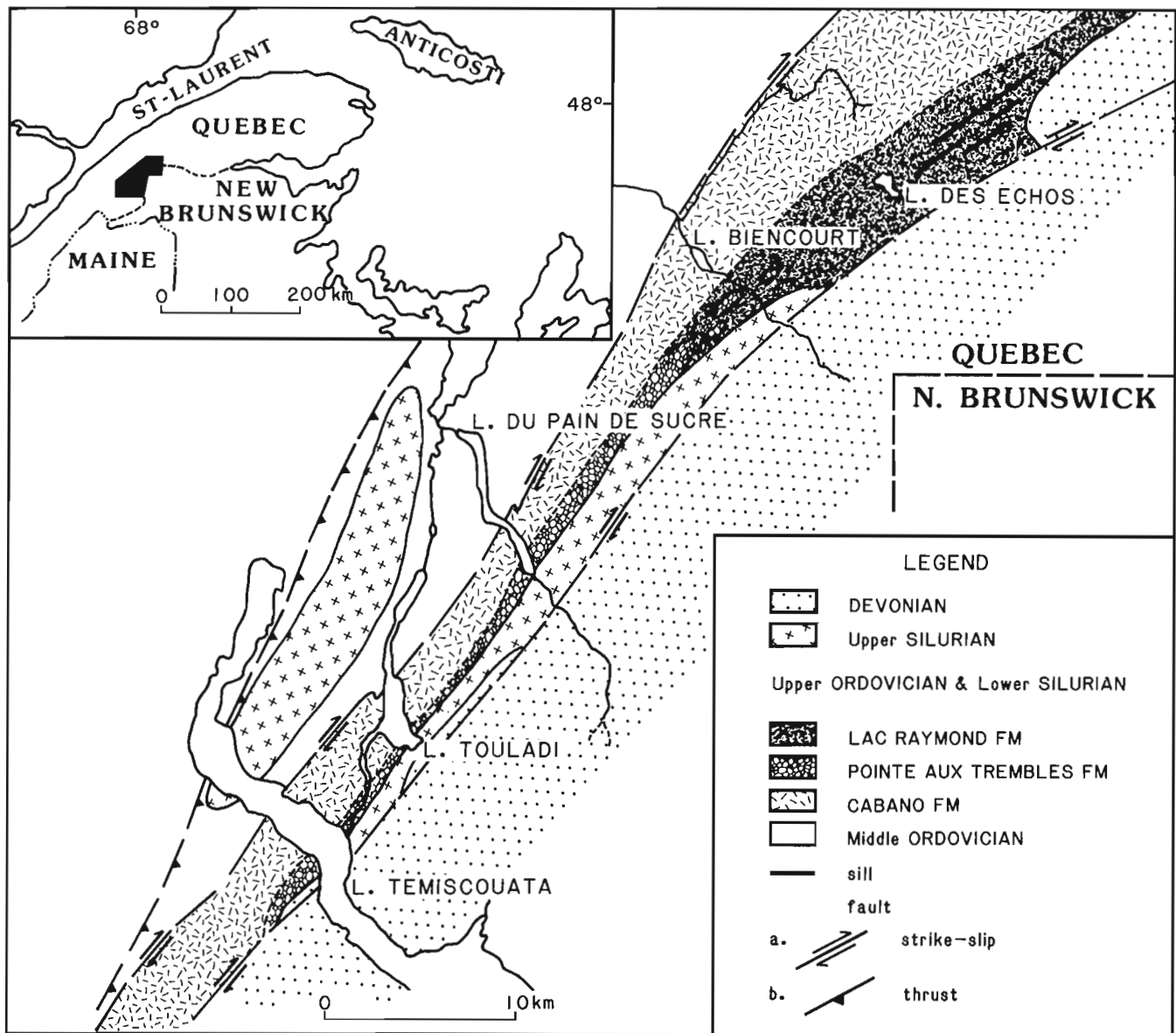


Figure 16.1. Generalized geological map of the area showing the location of the Pointe aux Trembles and Lac Raymond formations (modified from David et al., 1985).

the studied area has been summarized by David et al. (1985) and comprises Upper Ordovician (Caradoc) to Lower Silurian (Llan-doverly) rock units (see legend, Fig. 16.1).

The lowermost unit, Cabano Formation, is a thick pile of coarse- and fine-grained terrigenous sediments. It is conformably overlain by volcanoclastics and volcanics of the Pointe aux Trembles Formation, which have been assigned a Llan-doverly C_{1-5} age (Lespérance and Greiner, 1969). The Lac Raymond Formation is a lateral equivalent of the Pointe aux Trembles Formation (Fig. 16.1) comprising mostly terrigenous sedimentary rocks intruded by mafic sills. Both the Pointe aux Trembles and Lac Raymond formations are unconformably overlain by Upper Silurian limestones.

Lajoie et al. (1968) considered the lowermost Cabano Formation as unconformably overlying Middle Ordovician units which have been deformed during the Taconic Orogeny. Recent fieldwork has, however, brought up evidence that the contact between the Taconic domain and the Upper Ordovician to Lower Silurian (UO-LS) sequence is more likely a fault zone. The UO-LS sequence is located in a sector that Williams and Hatcher (1983) considered as the southwestern limit of the post-Taconic continental margin: accordingly this miogeocline should comprise a continental sedimentary series. The UO-LS sequence, however, shows relatively deep marine facies (David et al., 1985) and the sedimentary and volcanic rocks must have accumulated farther away from the continental margin, in a series of basins that were tectonized during the Acadian Orogeny. This could, in part, explain the lack of similar sequences within the Siluro-Devonian stratigraphy of the north-eastern Quebec Appalachians.

Petrography and sampling

The Pointe aux Trembles and Lac Raymond formations appear to be homoclinal units which barely show any evidence of internal deformation: no cleavage is present within the volcanic rocks and the volcanic fragments present in breccia or conglomeratic flows are not elongated or rotated along the regional schistosity. However, both units have been moderately altered and metamorphosed. The metamorphic grade is sub-greenschist, and prehnite and pumpellyite are frequently found as amygdule fillings and in the matrix of volcanoclastic flows together with quartz and chlorite. Epidote is ubiquitous in the whole sequence and systematically fills the fracture planes. However, when compared to other prehnite-pumpellyite grade rocks (Gélinas et al., 1982; Zen, 1974; Ritcher and Roy, 1976) the alteration is less pervasive: more than 50% of the thin sections examined still contained plagioclase in the range An_{35} to An_{25} instead of the albite-epidote-calcite assemblage characterizing the most altered samples.

Several types of volcanic rocks are present within the Pointe aux Trembles Formation; these were sampled in a proportion that roughly represents their field abundance. Most of the samples were collected along stratigraphic cross-sections which were measured in detail.

The most abundant group of rocks, representing more than 50% of the unit, comprises flow breccias and volcanic conglomerates containing lava and tuff fragments (generally 5 to 50 cm in diameter) of intermediate to felsic composition. The lava fragments generally show trachytic textures and variable grain size (0.1 to 5 mm). Some fragments contain 5 to 20% of amygdules (1 to 5 mm in size) whereas others are completely massive. Their oxidation state varies from west to east becoming less oxidized eastward. In addition, the proportion of highly felsic fragments decreases eastward. The samples collected from the flow breccias are lava fragments covering the range of petrographic types observed in the field. Several lava fragments

were sometimes collected within the same flow horizon in order to evaluate the range of chemical compositions present in a single flow.

The second group of rocks selected for analysis are tuff horizons interstratified with the flow breccias. These tuffs are of two different types. A crystal tuff horizon outcrops close to the top of the Lac Témiscouata type-section (Fig. 16.1). It comprises massive beds, 30 to 50 cm thick, covered by a thin layer of fine ash; this horizon can be followed over a distance of 15 km. The tuff beds are made of broken plagioclase laths, angular fragments of clinopyroxene and rare fragments of basic and intermediate volcanics set in a dust of altered and oxidized glass.

The other tuff horizon analyzed is located close to the base of the section, within the central part of the formation, to the northeast of Lac du Pain de Sucre (Fig. 16.1). It is a vitreous tuff, more than 4 m thick, made of very thin beds showing undulose laminations. A third type of tuffaceous horizon is present in the Pointe aux Trembles Formation which is more widespread than the former two. However, this material was not analyzed as we believe it to be tuffaceous sandstones which did not accumulate through volcanic events.

The third group of samples analyzed are from rare intermediate lava flows which are found in the topmost portion of the formation. Some of these flows formed highly vesicular pillow lavas. The lavas contain plagioclase (30 to 50%) and clinopyroxene (5 to 15%) phenocrysts set in a matrix of plagioclase microlites, oxides and glass.

Finally, a group of gabbro samples was analyzed in order to evaluate if their occurrence within the Lac Raymond Formation, the lateral equivalent of the Pointe aux Trembles Formation, could be genetically linked to the extrusive rocks. These gabbros occur as irregular 20 to 70 m thick sills which extend laterally over a distance of 3 km. The sills are located about 4 km to the northeast of Lac des Echos (Fig. 16.1) and they were intruded in the upper half of the Lac Raymond Formation, in mudstones, epiclastics and tuffaceous sandstones. The sills are massive and show very little textural or grain size variation, except for thin quench zones at their borders. They display 5 to 10 mm long plagioclase phenocrysts set in a fine grained matrix of clinopyroxenes and opaques. No country rock xenolith has been observed within the sills and no dyke has been found within the Lac Raymond Formation or in the underlying units. Although the sills must be younger than the Lac Raymond and Pointe aux Trembles formations, their age remains unknown and they could be significantly younger than the UO-LS sequence. However, these must have been intruded before the UO-LS sequence was juxtaposed on the Taconic domain as the gabbro sills and the volcanics show the same regional metamorphic grade.

Analytical techniques

The samples were reduced into centimetre-sized fragments using a hydraulic piston and only the freshest, vein-free fragments were powdered in a tungsten carbide shatter-box. The geochemical analyses were completed at the Université de Montréal using the following techniques: major element analyses were carried out on glass discs using an automated X-ray fluorescence (XRF) spectrometer; the CO_2 and H_2O^+ contents were measured by gas chromatography using the method outlined by Brooks et al. (1969); trace element analyses were completed by XRF on pressed powder pellets (Schroeder et al., 1980) except for Sc, Cr, Co, Cs, As, Sb, Hf, Ta, Th, U and the rare-earth elements (REE) which were determined by instrumental neutron activation analysis using the SLOWPOKE reactor and the method of Bergerioux et al. (1979).

Table 16.1 Representative chemical analyses from the Pointes aux Trembles and Lac Raymond formations.

#	GABBROS			FRAGMENTS				TUFS		LAVA
	398 G	451 G	184 G	4F4 F	4F24 F	4FA F	4FC F	2TV T	5TL T	1LAV L
SiO ₂	49.35	52.47	54.46	53.65	57.80	61.80	68.28	68.85	60.85	54.77
TiO ₂	2.13	1.58	1.54	1.19	1.23	1.08	0.73	0.61	0.85	1.45
Al ₂ O ₃	16.73	18.49	17.08	18.41	16.87	16.23	13.50	14.55	17.38	19.42
Fe ₂ O ₂	11.71	8.79	9.22	8.61	7.09	6.15	4.66	4.39	5.87	6.98
MnO	0.20	0.10	0.00	0.14	0.07	0.07	0.05	0.06	0.08	0.08
MgO	6.86	4.77	7.01	6.32	3.40	4.69	3.87	2.87	4.04	4.41
CaO	8.24	8.64	6.85	4.27	5.27	3.52	3.36	1.85	2.93	5.38
Na ₂ O	3.72	3.19	3.08	5.24	6.11	4.55	4.60	5.23	5.19	3.96
K ₂ O	0.77	1.55	0.44	1.88	1.81	1.63	0.74	1.50	2.59	3.26
P ₂ O ₅	0.29	0.41	0.31	0.30	0.36	0.26	0.20	0.20	0.21	0.28
H ₂ O ⁺	4.22	2.95	4.19	4.14	2.37	3.52	2.39	1.91	3.67	3.05
CO ₂	0.21	0.08	0.11	0.04	0.08	0.06	0.11	0.06	0.16	0.06
Sc	22.5	23.3	24.0	nd	nd	13.7	12.1	8.7	13.0	20.0
Cr	213	128	178	140	230	81	138	95	121	71
Co	34	30	37	nd	nd	21	23	16	23	30
Ga	19	20	20	29	19	20	14	14	17	22
Rb	21	33	11	60	40	71	33	35	78	68
Sr	656	638	664	703	564	486	504	394	610	761
Y	39	31	32	21	26	21	15	15	17	31
Zr	130	210	254	280	250	262	188	199	231	313
Nb	nd	nd	9	nd	nd	12	8	10	12	11
Hf	4.9	4.8	5.9	nd	nd	6.2	4.3	5.0	5.6	7.6
Ta	0.8	1.1	0.7	nd	nd	0.8	0.8	0.8	0.9	1.0
Th	3.1	3.8	5.0	nd	nd	10.2	7.7	11.6	11.5	11.5
U	0.9	1.0	1.2	nd	nd	2.2	1.7	2.2	2.4	2.6
La	24.7	33.5	34.7	nd	nd	33.5	29.6	30.7	35.9	40.0
Ce	48.4	66.7	73.4	nd	nd	70.9	52.9	53.7	72.7	79.9
Nd	22.7	28.2	29.5	nd	nd	29.6	21.1	21.8	30.8	31.9
Sm	5.46	6.50	6.91	nd	nd	6.33	4.49	4.56	6.65	7.38
Eu	1.44	1.74	1.78	nd	nd	1.46	1.04	1.02	1.50	1.65
Tb	0.74	0.84	1.05	nd	nd	0.75	0.48	0.44	0.58	1.03
Yb	2.53	2.47	2.92	nd	nd	1.55	1.24	1.20	1.33	2.18
Lu	0.36	0.38	0.39	nd	nd	0.24	0.20	0.20	0.21	0.34

– nd: not determined

– major elements are expressed in wt% and normalize to 100% on a volatile-free basis.

– trace elements are expressed in ppm.

Results

Representative rock analyses are listed in Table 16.1 and the data currently available are illustrated in Figures 16.2 to 16.5. In this paper, the data obtained on the gabbro sills are plotted together with the results from the Pointe aux Trembles volcanics; however, and as mentioned above, we do not *a priori* imply that both magma suites are cogenetic.

Major elements

The major element distribution is shown on binary diagrams (Fig. 16.2) using the silica content as a differentiation index (note that the elemental abundances are expressed in molar percentage). The use of other common differentiation indexes, such as the Fe/Mg ratio or the MgO content, would essentially yield similar variation patterns.

When dealing with metamorphosed rocks, one important question is to assess whether part, if not most, of the geochemical variations were caused by interactions with fluid phases. There are several observations which indicate that the composition of the gabbro sills and the volcanics was not pervasively

modified by secondary events. First, in more than half of the rocks examined, the clinopyroxene and plagioclase are primary. Second, the CO₂ content of the samples is systematically low and rarely exceeds 0.2 wt%. Thirdly, the elements which are usually very mobile (such as the alkalis or the alkaline earths) are not correlated with the water content of the samples. However, the rocks show H₂O⁺ contents up to 4.3 wt% and MgO is positively correlated with H₂O whereas both FeO* and SiO₂ are negatively correlated (see Fig. 16.2F). In our opinion, this is only reflecting the higher proportion of mafic minerals (easily transformed into chlorite and epidote) present in the more mafic samples. Nevertheless, this interpretation is not taken for granted and the problem will be evaluated through future geochemical studies.

Altogether, the samples analysed show a wide spectrum of silica contents: the gabbro sills vary from 49 to 54 wt% SiO₂ whereas the volcanics are more evolved, ranging from 53 to 69 wt% SiO₂. The former are thus restricted to basaltic compositions while andesites, dacites and rhyodacites are present within the Pointe aux Trembles Formation with the andesites and dacites being, by far, the most abundant rock types. The salient features of the eruptive series are summarized below:

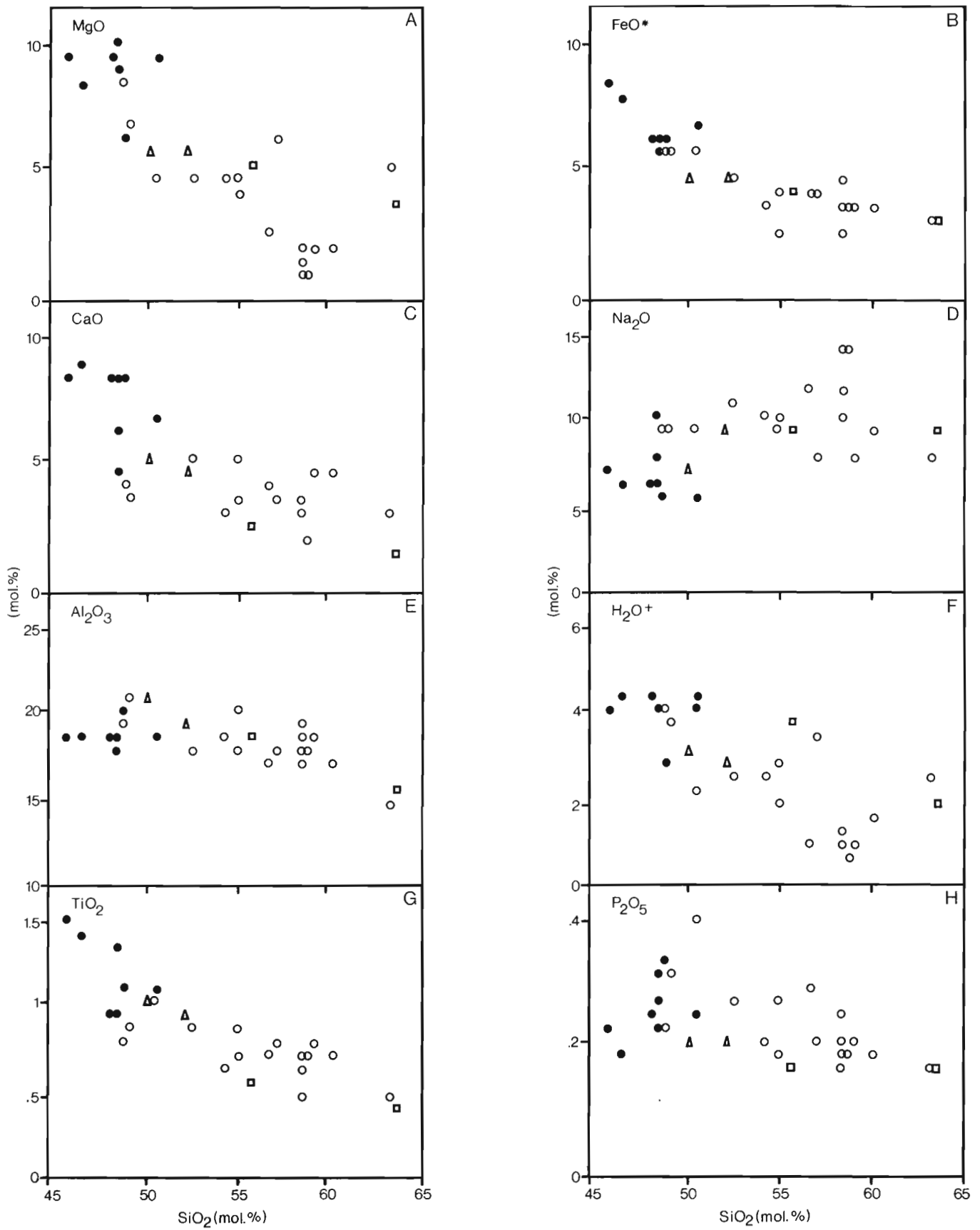


Figure 16.2. Representative variation diagrams of the major elements expressed in molar %, except for H₂O⁺ (wt%). Open circles = fragments from conglomeratic and breccia flows; triangles = lavas; squares = tuffs, filled circles = gabbro sills.

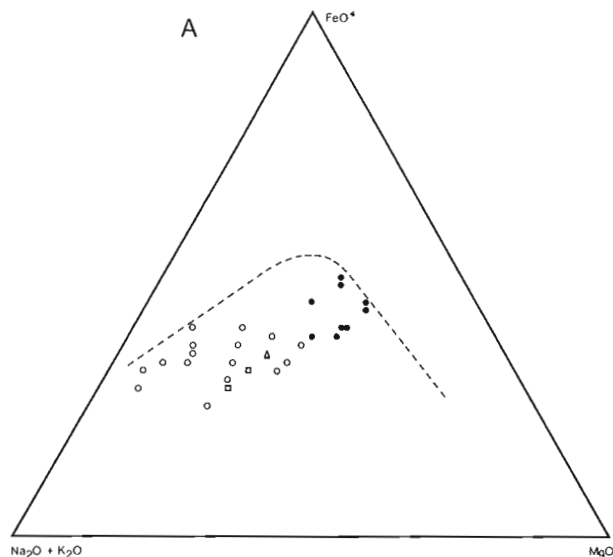
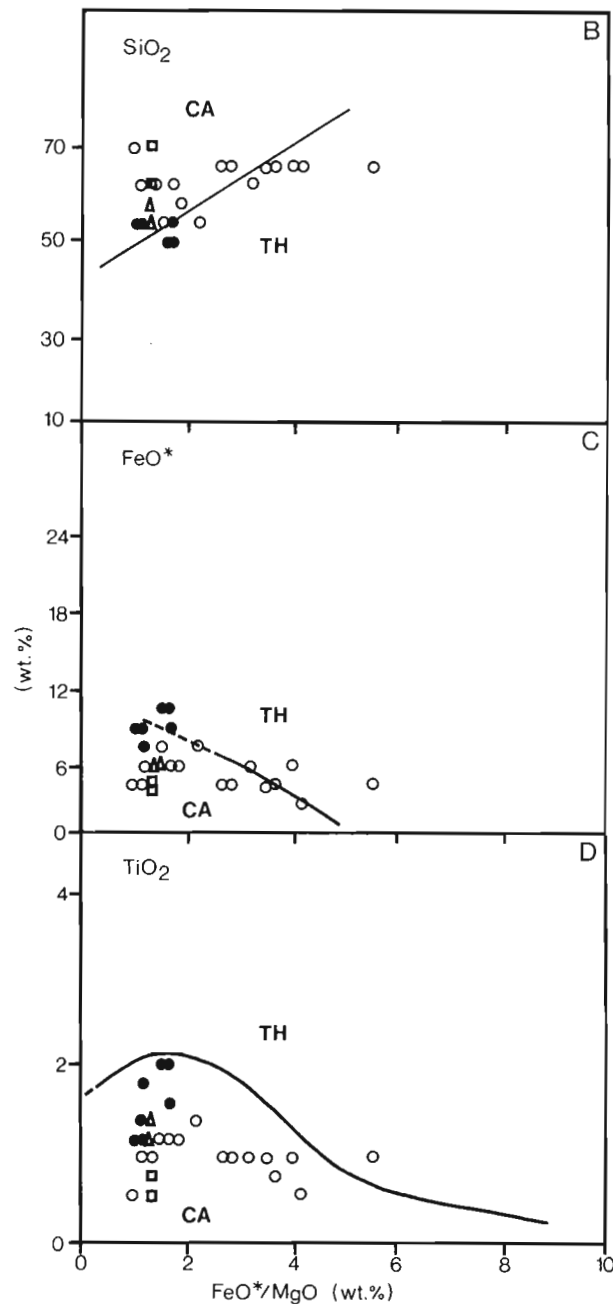


Figure 16.3. Major element discriminant diagrams showing the boundary between calc-alkaline (CA) and tholeiitic (TH) domains. Boundaries are taken A.: from Irvine and Baragar (1971) and B., C. and D.: from Miyashiro (1974). Values are in wt% and symbols as in Figure 16.2.

- 1) The volcanics are silica sursaturated and yield 3 to 20% normative quartz.
- 2) Within a given conglomeratic or breccia flow, the fragments show a variation of their chemical composition that is significantly larger than the analytical precision. However, in a given flow, the range in composition remains relatively narrow and does not spread over the entire range observed in the volcanic pile.
- 3) The major elements show a coherent behaviour with the MgO (7.4 – 0.8 wt%), MnO, FeO* (10.5 – 3.5 wt%), CaO (9.2 – 1.8 wt%), TiO₂ (2.1 – 1.6 wt%) and P₂O₅ (0.4 – 0.2 wt%) contents decreasing with increasing silica saturation level (Fig. 16.2A, B, C, G, H). The tuffs and lavas plot coherently with the fragments, suggesting that they are cogenetic.
- 4) The alumina content is high, ranging mainly from 17 to 19 wt%, and Al₂O₃ defines a negative trend with increasing SiO₂ contents (Fig. 16.2E).
- 5) The alkali content is relatively high, with Na₂O and K₂O ranging from 3 to 8 wt% and 0.7 to 3.3 wt% respectively, but is not apparently correlated with the silica content (Fig. 16.2D).

One of these observations needs to be emphasized, as it is not commonly seen in fractionated series: TiO₂ and P₂O₅ do not behave as incompatible elements indicating either that their abundances are controlled by mineral phases present on the liquidus or by mixing phenomena.

When compared to the eruptive rocks, the gabbro sills exhibit, on most diagrams, very similar geochemical trends (Fig. 16.2). The gabbros, however, are restricted to the silica-poor end of the range and show correspondingly higher MgO (5 – 7.5 wt%), FeO* (7.5 – 10.5 wt%), CaO (4.8 – 9 wt%), TiO₂ (1.3 – 2.1 wt%) and P₂O₅ (0.24 – 0.41 wt%) contents as well as lower Na₂O (3 – 5.8 wt%) and K₂O (< 1.5 wt%) abundances.



On the AFM diagram of Figure 16.3A, the samples show a trend of enrichment in alkali elements, a classical feature of calc-alkaline suites. This is confirmed by diagrams using FeO*/MgO as a differentiation index (Fig. 16.3B-D) where most of the samples plot within the calc-alkaline fields defined by Miyashiro (1974). No iron-enrichment trend is defined. Consequently, the alkali-enrichment trend of Figure 16.3A is most likely a primary feature and not due to pervasive alteration of the samples.

Trace elements

Selected trace elements are plotted against the silica content in Figure 16.4. The gabbros have relatively low Rb, Ba and Sr contents in the range of 10 to 30 ppm, 250 to 600 ppm and 550 to 700 ppm respectively. In comparison, the volcanics yield higher, but still overlapping abundances of Rb (20 to 80 ppm),

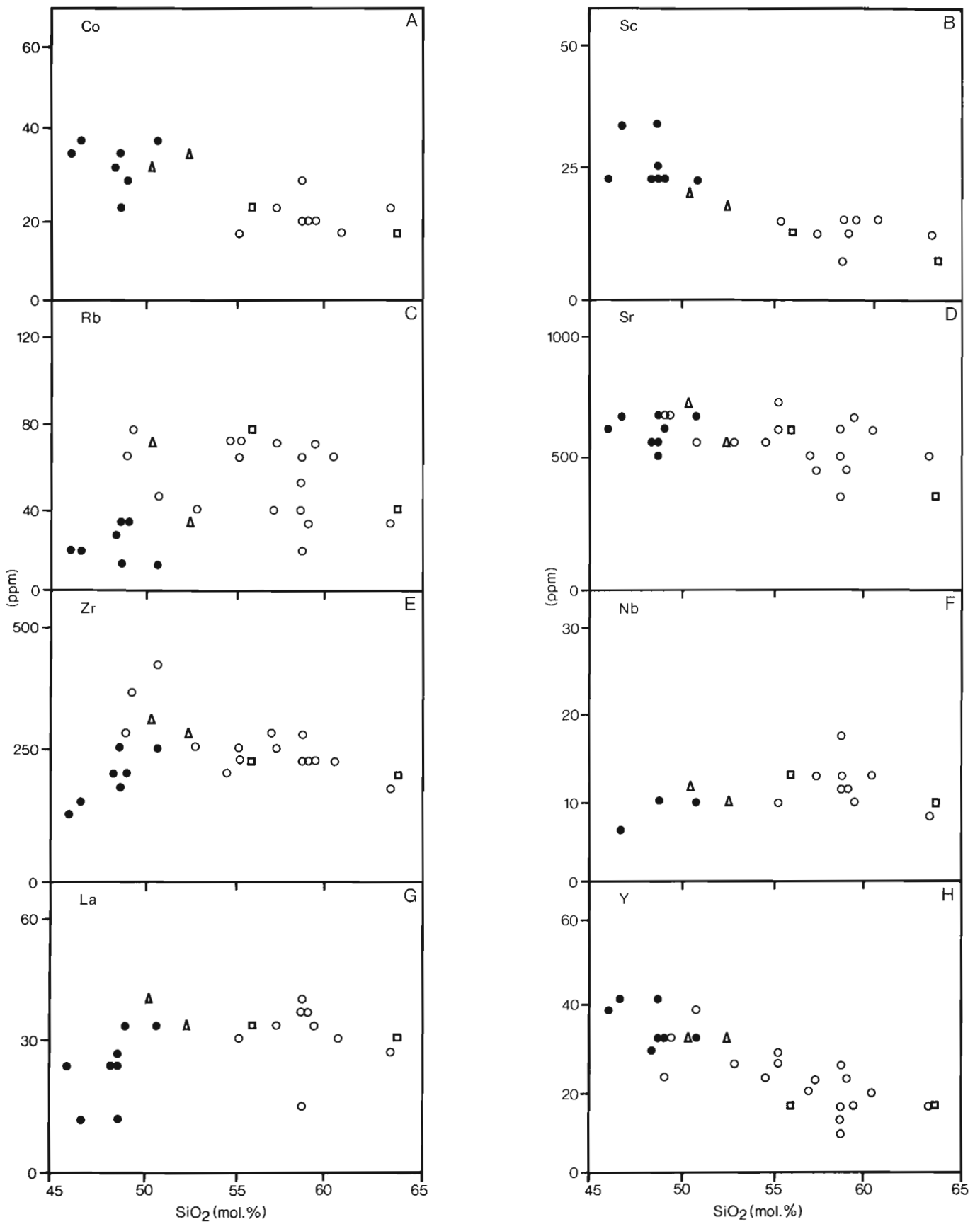


Figure 16.4. Representative trace element abundances (ppm) plotted against the SiO₂ content (mol.%). Symbols as in Figure 16.2.

Ba (130 to 1140 ppm) and Sr (360 to 760 ppm). Amongst these, only Sr displays a negative trend with increasing SiO_2 (Fig. 16.4D) parallelling the calcium behaviour (Fig. 16.2C). The erratic distribution of Rb and Ba is not understood and could be due to alteration and/or more complex processes.

The distribution of Sc and Co, which like Ni and Cr are controlled by mafic mineral phases, is shown in Figure 16.4A and B. The Co content varies from 30 to 40 ppm in the gabbros and from 16 to 35 ppm in the volcanics whilst the Sc abundances range from 22 to 35 and 7 to 20 ppm respectively. Both elements show well defined negative trends with increasing differentiation.

In several cases the so-called incompatible elements do not behave as such in the eruptive rocks. For example, Zr (430 – 190 ppm) and Y (30 – 10 ppm) display negative trends (Fig. 16.4E, H) while Nb and La show flat distributions (Fig. 16.4F, G). The gabbro samples show essentially the same trends except for Zr which does behave as an incompatible element (Fig. 16.4E) in the sills.

Rare-earth elements

Chondrite normalized REE patterns for the various rock types are presented in Figure 16.5. The fragments sampled in the conglomeratic and breccia flows exhibit essentially parallel patterns with La contents in the range of 50 to 110 times chondrite, (La/Yb)_N ratios in the range of 12 to 20 and no important Eu anomaly. On the basis of their REE patterns, the tuff samples are indistinguishable from the fragments (Fig. 16.5A) confirming that they are cogenetic. Similarly, the lavas exhibit REE patterns parallel to the fragments (Fig. 16.5B), but slightly more fractionated and with negative Eu anomalies, suggesting a plagioclase control. In comparison, the gabbro samples (Fig. 16.5C) exhibit slightly lower light REE contents and significantly higher abundances of heavy REE, corresponding to (La/Yb)_N ratios in the range of 6 to 9.

Discussion

Based on the geochemical data presented above some constraints can be placed on the magmatic affinity and the processes involved in the fractionation of the Pointe aux Trembles and Lac Raymond igneous rocks.

The Pointe aux Trembles volcanics exhibit several of the classical features of orogenic andesitic suites (Gill, 1981) associated with convergent plate boundaries. Firstly, they are quartz normative and rich in alumina, and they do not define any iron-enrichment trend (Fig. 16.3). Their low content of transition metals (Ni, Cr, Co and Sc) is also compatible with this interpretation while their alkali abundances (Na, K, Rb, Ba) are comparable to those of high-K andesites: however, we do not know to what extent the alkali content has been modified by secondary processes. Nevertheless, other trace elements, usually considered less mobile, also indicate that the volcanics are similar to high-K calc-alkaline suites. These are the high Sr (>500 ppm) and Th (>5 ppm) contents and the high Th/U (>4), La/Ta (>30) and La/Ca (>3) ratios (see Gill, 1981). Similarly, the REE abundances and the La/Yb ratios are comparable to those of high-K andesitic suites and the decrease of heavy REE and Y contents with silica, although not typical, has been reported from calc-alkaline suites of continental margins (Gill, 1981).

Secondly, there is good evidence that the spectrum of compositions observed in the Pointe aux Trembles volcanics evolved through fractional crystallization:

- 1) Based on outcrop area, the largest proportion of the suite is made of andesitic materials ($\approx 70\%$) and only a small

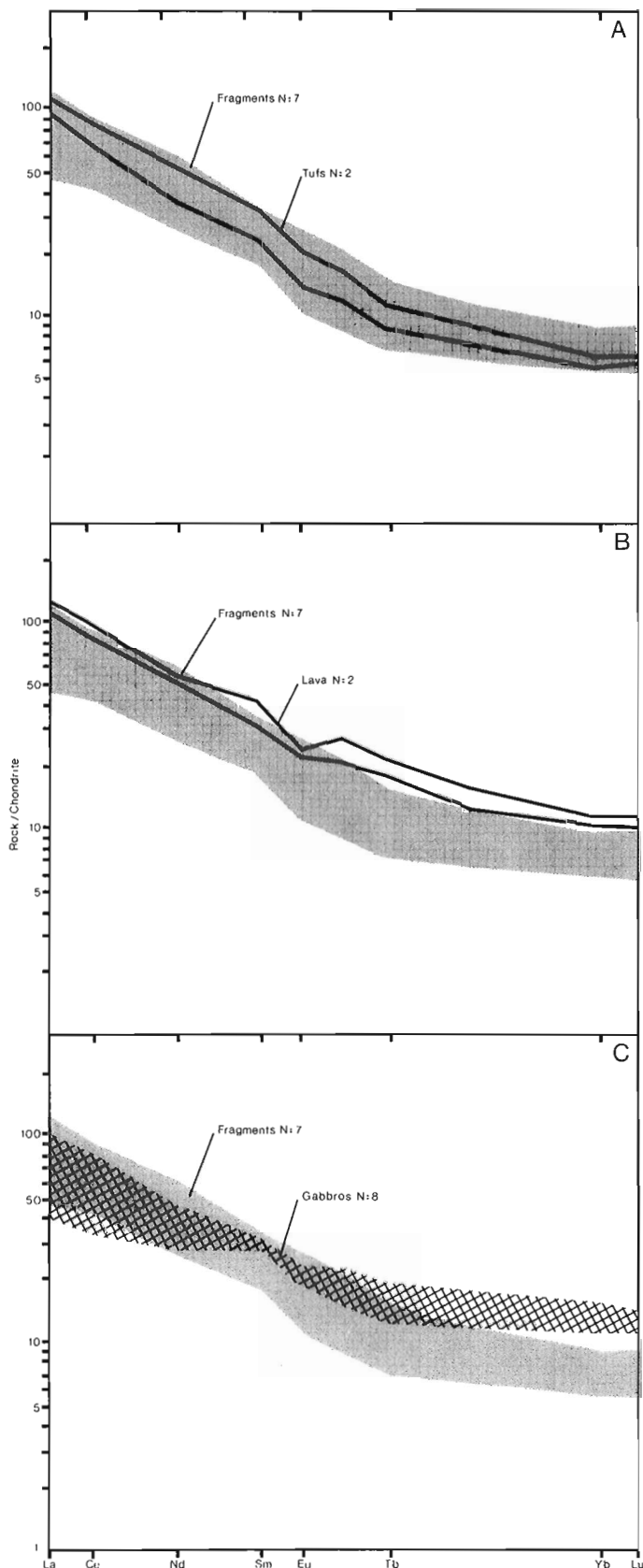


Figure 16.5. Whole-rock REE data normalized to chondritic abundances (Taylor and Gorton, 1977). Shaded field = fragments from conglomeratic and breccia flows (7 analyses), (A) tuff samples; (B) lavas; (C) gabbros (8 analyses).

proportion is dacitic ($\approx 20\%$) or rhyodacitic ($\approx 10\%$); this is close to what would be expected from fractional crystallization of a single parent magma.

- 2) The decrease of MgO, FeO*, CaO, Al₂O₃ and of the transition metals with silica can be explained by removal of clinopyroxene (?), hornblende and plagioclase.
- 3) Removal of magnetite or ilmenite would short-circuit the iron enrichment process and explain the decrease in Ti content with silica. This, however, would not explain the behaviour of an element like Zr which has a high field strength, and does not enter magnetite or ilmenite (Gill, 1981).
- 4) The observation that incompatible elements such as P, Y or Zr, show consistent decreases throughout the suite is taken as evidence for a control by accessory phases such as apatite and titanite (e.g. Exley, 1980; Fourcade and Allègre, 1982).
- 5) Fractionation of hornblende plus plagioclase could explain the absence of important Eu anomalies: hornblende has a lower partition coefficient for Eu than the trivalent REE (Arth and Baker, 1976), and it could compensate the opposite effect caused by plagioclase fractionation.

Alternatively, several of the linear trends illustrated in Figures 16.2 and 16.4 could be explained by mixing between two components. At present, this is considered improbable on the basis of the following observations:

- 1) There is no petrographic evidence, such as corroded or resorbed xenocrysts, for widespread mixing.
- 2) The felsic end member would have to be silica-rich, extremely depleted in compatible elements and in some incompatible trace elements (e.g. Zr, Y and Sr), while curiously undepleted in others (e.g. Nb or La).
- 3) The high viscosity of such magmas would work against efficient mixing.

Nevertheless, this possibility will have to be evaluated when more data are available, especially considering that crustal contamination or assimilation would promote crystal fractionation. The problem of the ultimate origin of the andesitic magmas is beyond the scope of this paper.

The magmatic affinity of the Lac Raymond gabbros is more difficult to ascertain as a large part of the chemical variations observed might result from fractionation during the cooling and crystallization of the sills: see for example the behaviour of Zr with silica (Fig. 16.4E). On one hand, the gabbros exhibit several features characterising calc-alkaline basaltic series.

- 1) They do not show any iron-enrichment trend (Fig. 16.3) and have a high alumina content.
- 2) They have relatively low abundances of the transition metals (Sc and Co).
- 3) On a ternary Ti/100 – Y/3 – Zr diagram (not illustrated) they plot in the calc-alkaline basalt fields as defined by Pearce and Cann (1973).

On the other hand, when compared to high-alumina basalts from the Circum-Pacific region (e.g. Lopez-Escobar et al., 1977), they yield higher TiO₂, P₂O₅, Cr, Sr and heavy REE abundances. Actually, they closely look like early Devonian basalts from Gaspésie which were analyzed by Laurent and Bélanger (1984). These authors equally hesitated to assign this type of composition to either one of a high-alumina or an alkaline series (Laurent and Bélanger, 1984). Future work on the chemistry of the clinopyroxenes might help solving the dilemma. Nevertheless, the gabbros are probably not genetically linked to the Pointe aux Trembles volcanics. This can be shown by comparing the chemical composition of gabbro (sample

number 184) to that of lava (sample 1LAV; Table 16.1). Both samples have a similar bulk composition but exhibit radically different REE patterns: they cannot be linked by fractional crystallization of any phase assemblage and must be derived from different parent magmas.

Conclusion

The Pointe aux Trembles volcanic suite exhibits all the classical features of calc-alkaline series rocks formed at convergent plates boundaries, indicating that subduction was active in the Appalachians during early Silurian times. This may have important implications for reconstructing the tectonic history of the northeastern Quebec Appalachians but should be considered a preliminary interpretation.

Acknowledgments

We are grateful to J.N. Ludden for providing access to his geochemical facilities, to G. Gauthier and R. Lapointe for their technical help, to D. Surprenant for drafting the figures. The first author would like to thank J. Lajoie and P.J. Lespérance for scientific and financial support.

References

- Arth, J.G., and Baker, F.
1976: REE partitioning between hornblende and dacitic liquid and implications for the genesis of trondhjemitic-tonalitic magmas; *Geology*, v. 4, p. 534-536.
- Arthaud, F., and Matte, P.
1977: Late Paleozoic strike-slip faulting in southern Europe and northern Africa: result of a right-lateral shear zone between the Appalachians and the Urals; *Geological Society of America, Bulletin*, v. 88, p. 1305-1320.
- Bédard, J.H.
1985: La pétrogénèse et les mécanismes de différenciation des magmas anorogéniques: Exemples de la Gaspésie, de la Nouvelle-Angleterre et des Collines Montérégiennes; unpublished Ph.D. thesis, Université de Montréal.
- Béland, J.
1982: *Geology of the Quebec Appalachians; in Guide Book to excursion 7B: Paleozoic Continental Margin Sedimentation in the Quebec Appalachians*, ed. R. Hesse, G.V. Middleton, and B.R. Rust; 11th International Congress on Sedimentology, McMaster University, p. 11-23.
- Bergerioux, C., Kennedy, G., and Zikovskiy, L.
1979: Use of the semi-absolute method in neutron activation analysis; *Journal of Radioanalytical Chemistry*, v. 50, p. 229-234.
- Bird, J.M., and Dewey, J.F.
1970: Lithosphere plate-continental margin tectonics and the evolution of the Appalachian Orogen; *Geological Society of America, Bulletin*, v. 81, p. 1031-1060.
- Boudette, E.L., Hatch, N.L., and Harwood, D.S.
1976: Reconnaissance bedrock geology of the Upper St-John and Allagash River Basins, Maine; U.S. Geological Survey, Bulletin 1406.
- Brooks, C., Hart, S.R., Krogh, T.E., and Davis, G.L.
1969: Carbonate contents and ⁸⁷Sr/⁸⁶Sr ratios of calcites from Archean meta-volcanics; *Earth and Planetary Science Letters*, v. 6, p. 35-38.

- David, J., Chabot, N., Marcotte, C., Lajoie, J., and Lespérance, P.J.
1985: Stratigraphy and sedimentology of the Cabano, Pointe aux Trembles, and Lac Raymond formations, Témiscouata and Rimouski counties, Quebec; in *Current Research, Part B, Geological Survey of Canada, Paper 85-1B*, p. 491-497.
- Dupré, B., Chauvel, C., and Arndt, N.T.
1984: Pb and Nd isotopic study of two Archean komatiitic flows from Alexo, Ontario; *Geochimica et Cosmochimica Acta*, v. 48, p. 1965-1972.
- Exley, R.A.
1980: Microprobe studies of REE-rich accessory minerals; implications for Skye granite petrogenesis and REE mobility in hydrothermal systems; *Earth and Planetary Science Letters*, v. 48, p. 97-110.
- Fourcade, S., and Allègre, C.J.
1982: Trace element behavior in granite petrogenesis: a case study. The calc-alkaline plutonic association from the Qerigut complex (Pyrénées, France); *Contributions to Mineralogy and Petrology*, v. 76, p. 177-195.
- Gélinas, L., Mellinger, M., and Trudel, P.
1982: Archean mafic metavolcanics from the Rouyn-Noranda district, Abitibi Greenstone Belt, Quebec. 1. Mobility of the major elements; *Canadian Journal of Earth Sciences*, v. 19, p. 2258-2275.
- Gill, J.B.
1981: *Orogenic Andesites and Plate Tectonics*; Springer Verlag, Berlin, 390 p.
- Hynes, A.
1976: Magmatic affinity of Ordovician volcanic rocks in northern Maine, and their tectonic significance; *American Journal of Science*, v. 276, p. 1208-1224.
- Irvine, T.N., and Baragar, W.R.A.
1971: A guide to the chemical classification of the common volcanic rocks; *Canadian Journal of Earth Sciences*, v. 8, p. 523-548.
- Lajoie, J., Lespérance, P.J., and Béland, J.
1968: Silurian stratigraphy and paleogeography of Matapédia-Témiscouata region, Québec; *American Association of Petroleum Geologist, Bulletin*, v. 52, p. 615-640.
- Laurent, R. and Bélanger, J.
1984: Geochemistry of Silurian-Devonian alkaline basalt suites from the Gaspé Péninsula, Quebec Appalachians; *Maritime Sediments and Atlantic Geology*, v. 20, p. 67-78.
- Lespérance, P.J. and Greiner, H.R.
1969: Région de Squatek-Cabano, Comtés de Rimouski, Rivière-du-Loup et Témiscouata; *Ministère des Richesses Naturelles du Québec, Rapport géologique* 128.
- Lopez-Escobar, L., Frey, F.A., and Vergara, M.
1977: Andesites and high-alumina basalts from the central-south Chile High Andes: geochemical evidence bearing on their petrogenesis; *Contributions to Mineralogy and Petrology*, v. 63, p. 199-228.
- Miyashiro, A.
1974: Volcanic rock series in island arcs and active continental margins; *American Journal of Science*, v. 274, p. 321-355.
- Nisbet, E.G., and Pearce, J.A.
1977: Clinopyroxene composition in mafic lava from different tectonic settings; *Contributions to Mineralogy and Petrology*, v. 63, p. 149-160.
- Osberg, P.H.
1978: Synthesis of the geology of the northeastern Appalachians, U.S.A.; in *Caledonian-Appalachian Orogen of the North Atlantic Region*; Geological Survey of Canada, Paper 78-13, p. 137-147.
- Pajari, G.E., Rast, N., and Stringer, P.
1977: Paleozoic volcanicity along the Bathurst-Dalhousie geotraverse, New Brunswick, and its relation to structure in *Volcanic Regimes in Canada*, ed. W.R.A. Baragar, L.C. Coleman, and J.H. Hall; Geological Association of Canada, Special Publication 16, p. 111-124.
- Pearce, J.A., and Cann, J.R.
1973: Tectonic setting of basic volcanic rocks determined using trace element analyses; *Earth and Planetary Science Letters*, v. 19, p. 290-300.
- Pintson, H., Kumarapeli, P.S., and Morency, M.
1985: Tectonic significance of the Tibbit Hill volcanics: geochemical evidence from Richmond area, Quebec; in *Current Research, Part A, Geological Survey of Canada, Paper 85-1A*, p. 123-130.
- Ritcher, D.A., and Roy, D.C.
1976: Prehnite-pumpellyite facies metamorphism in central Aroostook County, Maine; *Geological Society of America, Memoir* 146, p. 239-261.
- Ruitenbergh, A.A., Fyffe, L.R., and McCutcheon, S.R.
1977: Evolution of pre-Carboniferous tectonostratigraphic zones in the New-Brunswick Appalachians; *Geoscience Canada*, v. 4, p. 171-181.
- Schroeder, B., Thompson, G., Sulanowski, M., and Ludden, J.N.
1980: Analysis of geological materials using an automated X-ray fluorescence system; *X-ray Spectrometry*, v. 9, p. 198-205.
- Strong, D.F.
1977: Volcanic regimes of the Newfoundland Appalachians; in *Volcanic Regimes in Canada*, ed. W.R.A. Baragar, L.C. Coleman, and J.H. Hall; Geological Association of Canada, Special Publication 16, p. 61-90.
- Thirwall, M.F.
1983: Isotope geochemistry and origin of calc-alkaline lavas from a Caledonian continental margin volcanic arc; *Journal of Volcanology and Geothermal Research*, v. 18, p. 589-631.
- Taylor, S.R., and Gorton, M.P.
1977: Geochemical application of spark source mass spectrometry - III element sensitivity, precision, and accuracy; *Geochimica et Cosmochimica Acta*, v. 41, p. 1375-1380.
- Whalen, J.B.
1985: The McGerrigle plutonic complex, Gaspé, Quebec: evidence of magma mixing and hybridization; in *Current Research, Part A, Geological Survey of Canada, Paper 85-1A*, p. 795-800.
- Whalen, J.B., and Gariépy, C.
1986: Petrogenesis of the McGerrigle plutonic complex, Gaspé, Quebec: a preliminary report; in *Current Research, Part A, Geological Survey of Canada, Paper 86-1A*, p. 265-274.
- Williams, H., and Hatcher, R.D.
1983: Appalachian suspect terranes; in *Contributions to the Tectonics and Geophysics of Mountain Chains*, ed. R.D. Hatcher, H. Williams, and I. Zietz; Geological Society of America, *Memoir* 158, p. 33-53.
- Zen, E-an.
1974: Prehnite- and pumpellyite-bearing mineral assemblages, west side of the Appalachian metamorphic belt, Pennsylvania to Newfoundland; *Journal of Petrology*, v. 15, p. 197-242.
- Zindler, A.
1982: Nd and Sr isotopic studies on komatiites and related rocks; in *Komatiites*, ed. N.T. Arndt and E.G. Nisbet, p. 399-420.

U-Pb ages for granitic orthogneiss from western Yukon Territory: Selwyn Gneiss and Fiftymile Batholith revisited

Project 830006

J.K. Mortensen
Lithosphere and Canadian Shield Division

Mortensen, J.K., U-Pb ages for granitic orthogneiss from western Yukon Territory: Selwyn Gneiss and Fiftymile Batholith revisited; *in* Current Research, Part B, Geological Survey of Canada, Paper 86-1B, p. 141-146, 1986.

Abstract

Four new U-Pb zircon analyses from two bodies of granitic orthogneiss from the Yukon-Tanana terrane in western Yukon Territory (Selwyn Gneiss and Fiftymile Batholith) establish crystallization ages for these units of $355.4 \pm 13.7/-6.1$ Ma and $362.4 \pm 10.2/-5.5$ Ma, respectively. These bodies are therefore correlative with the Simpson Range Plutonic Suite in southeastern Yukon Territory in terms of age, lithology, and U-Pb systematics.

Résumé

Quatre nouvelles analyses radiochronologiques ont été effectuées sur des zircons provenant de deux masses d'orthogneiss granitique du terrane Yukon-Tanana, dans l'ouest du Yukon (gneiss de Selwyn et batholite Fiftymile). Cette datation à l'U-Pb révèle que ces unités se sont cristallisées il y a $355,4 \pm 13,7/-6,1$ Ma et $362,4 \pm 10,2/-5,5$ Ma, respectivement. Il est donc possible d'établir une corrélation entre l'âge, la lithologie et la systématique U-Pb de ces roches et de celles de la suite plutonique de Simpson Range dans le sud-est du Yukon.

Introduction

Granitic orthogneiss forms an important component of the Yukon-Tanana terrane in west-central Yukon Territory (Fig. 17.1). Although Mesozoic metamorphic mineral ages are available from several of these orthogneiss bodies, intrusive ages are poorly constrained. Tempelman-Kluit and Wanless (1980) reported U-Pb zircon analyses for two separate gneiss bodies, the Selwyn Gneiss and Fiftymile Batholith (Fig. 17.1). In that study, three zircon fractions were analyzed from each sample, and results suggested a middle or late Paleozoic (probably Permian) age for the Selwyn Gneiss, and an early or middle (probably Devonian) age for the Fiftymile Batholith. All of the analyses were very discordant, however, the calculated concordia intercept ages were somewhat equivocal. Subsequent U-Pb and Rb-Sr dating studies of granitic orthogneiss in the Yukon-Tanana terrane of western Yukon (Mortensen, in press) and southeastern Yukon (Mortensen, 1983, and unpublished data; Mortensen and Jilson, 1985), and in the extension of the terrane into Alaska (Aleinikoff et al., 1981a, b; Dusel-Bacon and Aleinikoff, 1985) have identified two major periods of granitoid intrusion, in Early Permian and in Late Devonian-Early Mississippian time. Better resolution of emplacement ages for the Selwyn Gneiss and Fiftymile Batholith was therefore desirable. To this end, four additional analyses have been carried out on zircon separated from the original concentrates studied by Templeman-Kluit and Wanless (1980). Together with the earlier analyses, the new data provide relatively precise crystallization ages for the two bodies, and permit regional correlations with intrusive events recognized elsewhere in the terrane.

Analytical techniques

Analytical techniques for the original analyses, which were done in 1974, are discussed in Tempelman-Kluit and Wanless (1980). Zircon fractions analyzed were separated from the less magnetic bulk concentrate by sieving, and consisted of at least 95% zircon; further purification by handpicking was not employed. The new analyses reported here are from samples that were carefully handpicked from the least magnetic portion of the original zircon concentrates to isolate the most euhedral, fracture- and inclusion-free grains for analysis. This material was then split into a weakly paramagnetic and a nonmagnetic fraction using a magnetic "pin" as described by Krogh (1982a). Both fractions were abraded to remove surface portions of the grains which are most susceptible to alteration and Pb-loss (Krogh, 1982b). Chemical procedures were modified from Krogh (1973), and concentration data were obtained using a mixed $^{205}\text{Pb}/^{235}\text{U}$ tracer prepared by Krogh and Davis (1975). Isotopic analyses were carried out on a MAT 261 mass spectrometer equipped with a fully adjustable multiple collector and electron multiplier, using data collection procedures outlined by Roddick et al. (in press).

Complete analytical results for both the 1974 analyses and the new analyses are shown in Table 17.1. Analytical results for the 1974 analyses reported by Templeman-Kluit and Wanless (1980) have been recalculated using an initial nonradiogenic Pb composition corresponding to 350 Ma on the Stacey and Kramers (1975) two-stage growth curve, and the U and Th decay constants recommended by Steiger and Jager (1977). Discordia line parameters have been calculated with a modified York II line-fitting model (Parrish and van Breemen, 1985). All errors are reported at the 95% confidence level.

Sample descriptions and analytical results

Selwyn Gneiss

The Selwyn Gneiss is a compositionally homogeneous, variably foliated biotite-hornblende granodiorite, which occurs as a gently dipping sheet about 2 km thick (Templeman-Kluit and Wanless, 1980). Zircons in the analyzed sample are euhedral, stubby (length:width of 2-3), and completely colourless. Most grains analyzed were completely free of inclusions, although a small percentage contained fine, colourless rods and tubes. There was no evidence of xenocrystic cores in any of the grains analyzed.

Five zircon analyses from Selwyn Gneiss are plotted in Figure 17.2. The three original analyses were tightly clustered slightly below concordia at about 275 Ma. The new analyses yield considerably older Pb/U and Pb/Pb ages. A best-fit line through all of the data has a M.S.W.D. of 2.69, and calculated upper and lower concordia intercept ages of 355.4 ± 13.7 – 6.1 Ma and 156.2 ± 88.0 – 93.5 Ma, respectively. The old analyses are 38 to 43% discordant, whereas the new analyses are only 6.5% discordant. This much reduced discordance corresponds to the much lower U-content of the zircon dated in this study (213–238 ppm vs. 724–1155 ppm, Table 17.1). The data array is considered to reflect normal discordance due to post-crystallization Pb-loss, and the upper intercept age of 355.4 Ma (Early Mississippian) is therefore the best estimate for the crystallization of the Selwyn Gneiss.

K-Ar metamorphic ages (recalculated with decay constants recommended by Steiger and Jager, 1977) for biotite from this sample, and for biotite and muscovite from a separate sample of Selwyn Gneiss from about 3 km to the northwest are 167.5 ± 6 Ma, 165.0 ± 6 Ma, and 164.1 ± 6 Ma, respectively (Templeman-Kluit and Wanless, 1975). These ages are close to the calculated lower intercept

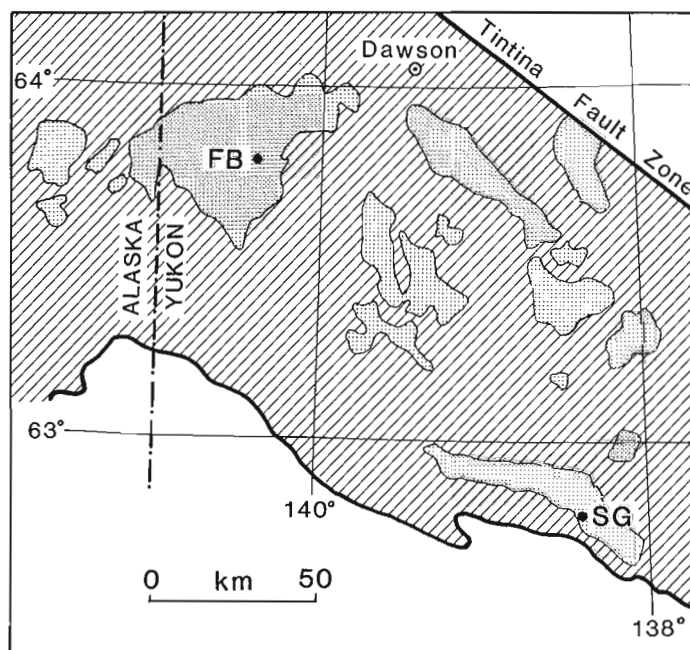


Figure 17.1. Distribution of granitic orthogneiss (dense stipple) in the Yukon-Tanana terrane (hatchure) in western Yukon Territory and eastern Alaska. Sample localities are shown by solid circles; FB = Fiftymile Batholith; SG = Selwyn Gneiss. Modified from Tempelman-Kluit and Wanless (1980), Dusel-Bacon and Aleinikoff (1985), and Mortensen (in press). Terrane boundaries from Monger and Berg (1984).

age for the U-Pb zircon analyses (156.2 Ma); however, because of the very large errors associated with this lower intercept age, the similarity is not necessarily significant.

Fiftymile Batholith

Where sampled, the Fiftymile Batholith is a banded, gneissic, biotite quartz monzonite containing up to 25% by volume of K-feldspar augen. Younger felsic sills are widespread and locally abundant within the unit. Zircons separated for analysis were very pale pink to very pale yellow, euhedral grains with square cross-sections and pyramidal to slightly rounded terminations. Most grains contain abundant thin colourless rods and irregular tubes, but there was no evidence for xenocrystic cores.

The three 1974 zircon analyses (A-C) are plotted in Figure 17.3, along with two new analyses (D-E). The three original analyses, when recalculated, form a linear array that nearly parallels concordia. The two new analyses plot near point C (Fig. 17.3), but considerably closer to concordia. Although together, the five points still define a crudely linear array, the highly precise analyses of fractions D and E, in comparison to the very high blank level, large amount of included nonradiogenic Pb, and consequently low measured $^{206}\text{Pb}/^{204}\text{Pb}$ (202.8) obtained for point C make this point suspect. A best-fit line through the remaining four points yields upper and lower intercept ages of $362.4 \pm 10.2/-5.5$ Ma and $102.2 \pm 79.3/-82.5$ Ma, respectively, with a M.S.W.D. of 0.16. Because of the large errors associated with point C, its inclusion in the regression does not significantly affect the quality of fit (M.S.W.D. = 1.0) or the calculated intercept ages ($362.6 \pm 10.4/-5.6$ Ma and $104.1 \pm 79.1/-82.4$ Ma). Ages and associated errors calculated without this point, however, are considered to be the most reliable. As with the Selwyn Gneiss sample, there is no evidence for an inherited xenocrystic zircon component from either grain appearance or from isotopic systematics, and observed discordance is attributed to simple Pb loss.

Although the K-Ar metamorphic age of 100.0 ± 3.7 Ma (Templeman-Kluit and Wanless, 1975, recalculated to new decay constants) on biotite from the Fiftymile Batholith is very close to the calculated lower intercept age (102.2 Ma), the large errors associated with the lower intercept age indicate that this similarity is not necessarily significant.

Discussion

Field mapping and geochronological studies of granitic orthogneisses in several portions of the Yukon-Tanana terrane in Yukon and Alaska have resulted in the recognition of three distinct intrusive events based on lithology, age, and Sr and U-Pb isotopic systematics. The most widely distributed of these includes large bodies of granitic to quartz monzonitic augen orthogneiss that range in age from about 360 to 340 Ma (Early Mississippian; Mortensen, 1983, in press, unpublished data; Mortensen and Jilson, 1985; Aleinikoff et al., 1981a, b; Dusel-Bacon and Aleinikoff, 1985). These rocks are generally strongly S-type in character, and typically display extremely high Sr initial ratios. Xenocrystic cores are present in most zircon separates, and an inherited Early Proterozoic Pb component is reflected in most U-Pb zircon analyses.

A second plutonic suite, termed the Simpson Allochthonous Assemblage by Templeman-Kluit (1979) and the Simpson Range Plutonic Suite by Mortensen (1983) and Mortensen and Jilson (1985), does not appear to be as widespread as the augen gneiss suite. The plutons consist of hornblende-biotite quartz diorite to quartz monzonite, and yield U-Pb zircon ages of 370 to 350 Ma (Late Devonian to Early Mississippian; Mortensen, 1983; Mortensen and Jilson, 1985). They are typically I-type in character, and Sr initial ratios are generally less than 0.710. No evidence for inherited cores is seen in either the zircon separates themselves, or in the U-Pb isotopic compositions.

Table 17.1. Analytical data, U-Pb analyses of zircon

Sample No.	Characteristics ^C	Wt. (mg)	Pb blank	Concentrations (ppm) ^{**}		Measured $^{206}\text{Pb}/^{204}\text{Pb}$	Isotopic Compositions ^{**}			Isotopic Age $^{207}\text{Pb}/^{206}\text{Pb}$
				U total	Pb [*]		$^{206}\text{Pb}/^{238}\text{U}$	$^{207}\text{Pb}/^{235}\text{U}$	$^{207}\text{Pb}/^{206}\text{Pb}$	
Selwyn Gneiss[#]										
A ^{\$}	-37	5.98	2.03	1154.9	54.82	477.5	0.04422 (2.2)	0.31930 (2.2)	0.052371 (.28)	302.0
B ^{\$}	37-44	4.95	1.65	973.4	43.99	472.7	0.04264 (2.2)	0.31057 (2.2)	0.052829 (.28)	321.5
C ^{\$}	93-149	20.56	3.93	723.9	32.83	3414.2	0.04336 (1.8)	0.31464 (1.8)	0.052625 (.18)	312.8
D [@]	+149; A; <M	0.274	0.084	212.8	12.22	1685.8	0.05451 (0.5)	0.40239 (0.5)	0.053542 (0.1)	351.8
E [@]	+149; A; >M	0.217	0.084	237.6	13.63	1719.0	0.05443 (0.5)	0.40102 (0.5)	0.053433 (0.1)	347.2
Fiftymile Batholith[#]										
A ^{\$}	-37	21.70	3.94	850.1	41.67	495.0	0.04278 (2.2)	0.31242 (2.2)	0.052965 (.28)	327.2
B ^{\$}	37-44	10.03	2.03	868.6	44.95	310.7	0.04498 (2.2)	0.32992 (2.2)	0.053196 (.28)	337.0
C ^{\$}	93-149	12.69	10.48	914.2	55.06	202.8	0.05432 (2.2)	0.40609 (2.2)	0.054242 (.28)	381.0
D [@]	+105; A; <M	0.231	0.084	545.8	34.95	1809.5	0.05424 (0.5)	0.40126 (0.5)	0.053658 (0.1)	356.7
E [@]	+105; A; >M	0.226	0.084	792.0	49.81	2451.3	0.05453 (0.5)	0.40337 (0.5)	0.053650 (0.1)	356.4
Notes:										
‡ All samples are from the least magnetic zircon fraction; A = abraded; <M = monmagnetic with "pin"; >M = magnetic with "pin".										
* Pb* denotes radiogenic Pb (after removal of blank).										
** Corrected for blank Pb. Errors in isotopic compositions (in parentheses) are given in percentage at the 95% confidence level.										
\$ Analyses from Templeman-Kluit and Wanless (1980), recalculated with revised U and Th decay constants and initial nonradiogenic Pb composition.										
@ New analyses, using mixed $^{205}\text{Pb}/^{235}\text{U}$ tracer.										
# Sample localities: Selwyn Gneiss, 62°36'00"N; 137°15'00"W; Fiftymile Batholith, 63°47'30"N; 140°28'00"W.										

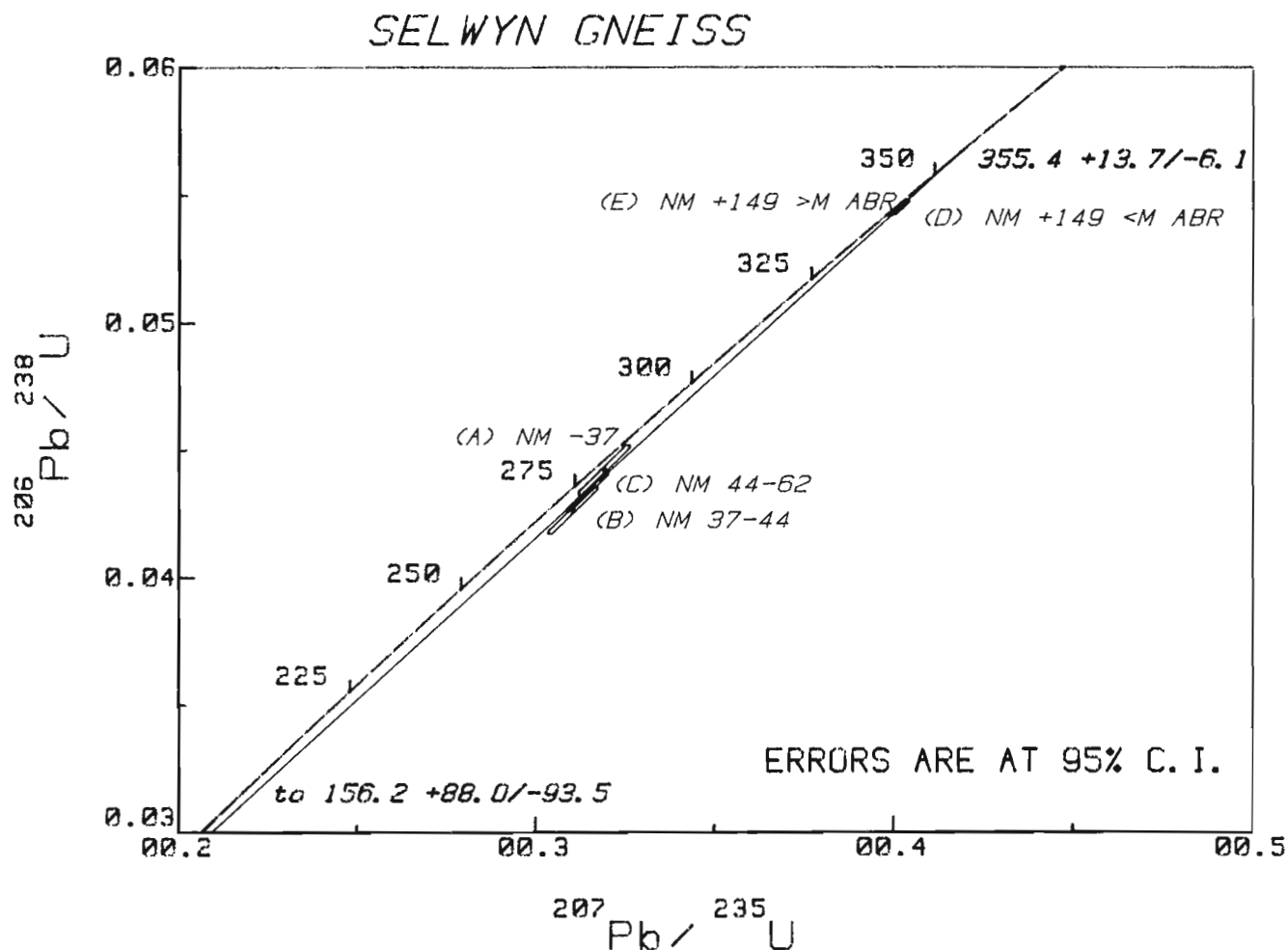


Figure 17.2. U-Pb concordia plot for Selwyn Gneiss zircon analyses. Open symbols represent early analyses recalculated from Tempelman-Kluit and Wanless (1980); solid symbols are new analyses.

A third, somewhat younger intrusive suite has only been recognized in the Klondike District of west-central Yukon (Mortensen, in press). A single body of batholithic dimensions, named the Sulphur Creek Orthogneiss, is present in this area. It is a gneissic biotite quartz monzonite, and has yielded a concordant U-Pb zircon age of 263.8 ± 3.8 Ma (Early Permian), with no evidence for an inherited Pb component (Mortensen, in press).

Although Tempelman-Kluit (1979) and Tempelman-Kluit and Wanless (1980) suggested on lithological grounds that the Selwyn Gneiss was correlative with the Simpson Range Plutonic Suite, their early zircon results appeared to contradict this. The new data reported here confirm that both the Selwyn Gneiss and Fiftymile Batholith are similar in both lithology and age to the Simpson Range Plutonic Suite.

Geochemical and preliminary U-Pb zircon dating results from the westernmost portion of the Fiftymile Batholith in Alaska, and from a separate orthogneiss body that immediately adjoins it to the west, however, led Dusel-Bacon and Aleinikoff (1985) to include the western part of the batholith in the suite of S-type augen orthogneiss. The Fiftymile Batholith may therefore be a composite body of Devon-Mississippian age consisting of elements of both the Simpson Range Plutonic Suite and the augen orthogneiss.

Acknowledgments

I thank W.D. Loveridge and R.R. Parrish for discussion of the dating results, and for critical reviews of an earlier version of the manuscript.

FIFTYMILE BATHOLITH

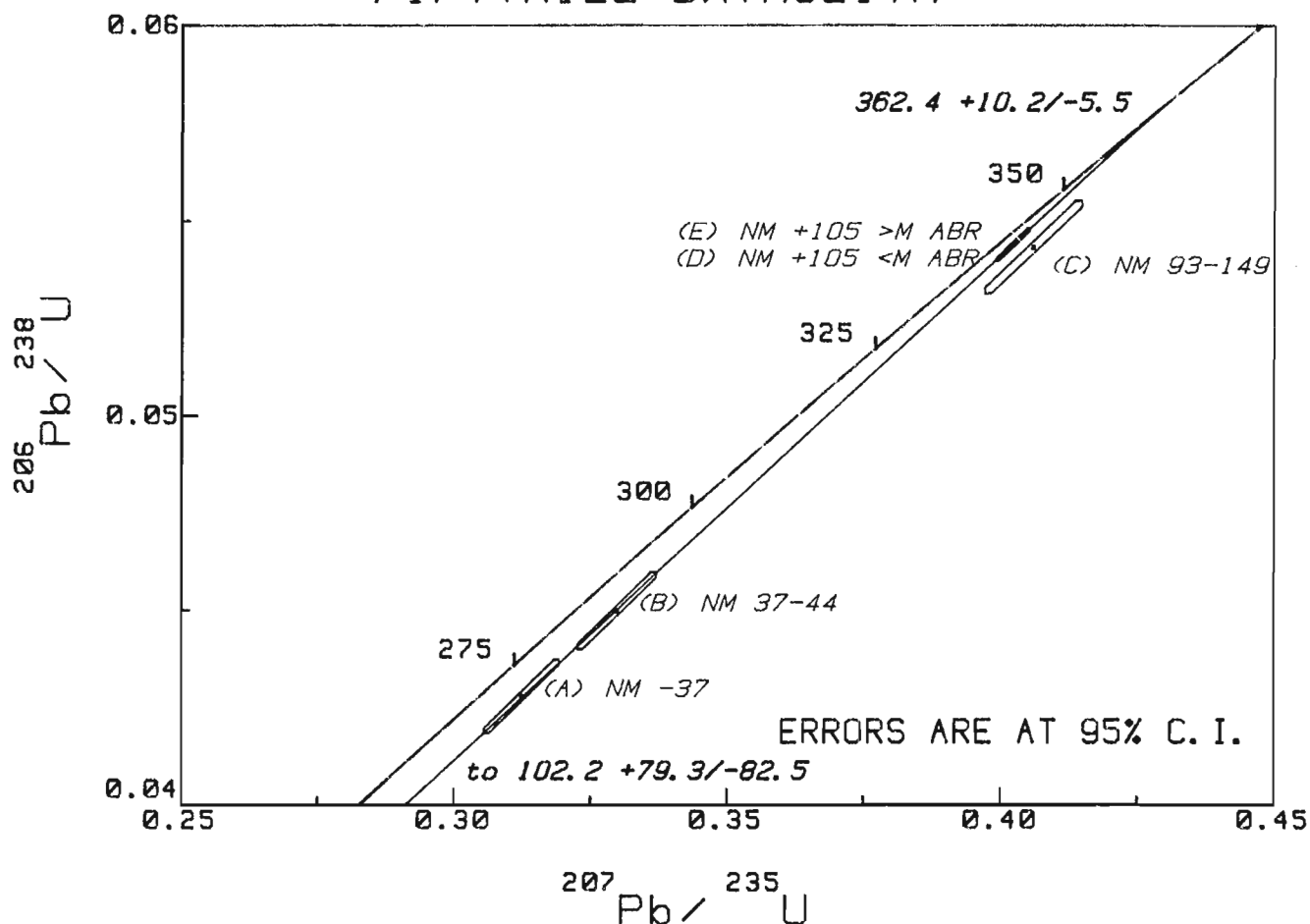


Figure 17.3. U-Pb concordia plot for Fiftymile Batholith zircon analyses. Open symbols represent early analyses recalculated from Templeman-Kluit and Wanless (1980); solid symbols are new analyses.

References

- Aleinikoff, J.N., Dusel-Bacon, C., Foster, H.L., and Futa, L.
1981a: Proterozoic zircon from augen gneiss, Yukon-Tanana Upland, east-central Alaska; *Geology*, v. 9, p. 469-473.
- Aleinikoff, J.N., Dusel-Bacon, C., and Foster, H.L.
1981b: Geochronologic studies in the Yukon-Tanana Upland, east-central Alaska; U.S. Geological Survey Circular 823-B, p. B34-B37.
- Dusel-Bacon, C. and Aleinikoff, J.N.
1985: Petrology and tectonic significance of augen gneiss from a belt of Mississippian granitoids in the Yukon-Tanana terrane, east-central Alaska; *Geological Society of America, Bulletin*, v. 96, p. 411-425.
- Krogh, T.E.
1973: A low contamination method for hydrothermal decomposition of zircon and extraction of U and Pb for isotopic age determinations; *Geochimica et Cosmochimica Acta*, v. 37, p. 485-494.
- Krogh, T.E. (cont.)
1982a: Improved accuracy of U-Pb zircon dating by selection of more concordant fractions using a high gradient magnetic separation technique; *Geochimica et Cosmochimica Acta*, v. 46, p. 1-5.
1982b: Improved accuracy of U-Pb zircon ages by the creation of more concordant systems using an air abrasion technique; *Geochimica et Cosmochimica Acta*, v. 46, p. 6-13.
- Krogh, T.E. and Davis, G.L.
1975: The production and preparation of ^{205}Pb for use as a tracer for isotope dilution analyses; *Carnegie Institution of Washington, Year Book*, v. 74, p. 416-417.
- Monger, J.W.H. and Berg, H.C.
1984: Lithotectonic terrane map of Western Canada and southeastern Alaska; U.S. Geological Survey, Open File 84-0523-B, p. B1-B31.
- Mortensen, J.K.
1983: The age and evolution of the Yukon-Tanana terrane in southeastern Yukon Territory; unpublished Ph.D. dissertation, University of California (Santa Barbara), 155 p.

- Mortensen, J.K. (cont.)
- Geology and U-Pb geochronology of the Klondike District, west-central Yukon Territory; Canadian Journal of Earth Sciences. (in press)
- Mortensen, J.K. and Jilson, G.A.
- 1985: Evolution of the Yukon-Tanana terrane: evidence from southeastern Yukon Territory; Geology, v. 13, p. 806-809.
- Parrish, R. and van Breemen, O.
- 1985: Geochronology of the Baie Verte Peninsula, Newfoundland: implications for the tectonic evolution of the Humber and Dunnage zones of the Appalachian orogen: a discussion; Journal of Geology, v. 93, p. 510-511.
- Roddick, J.C., Loveridge, D.W., and Parrish, R.
- Precise U/Pb dating of sub-milligram quantities of zircon; Terra Cognita. (in press)
- Stacey, J.S. and Kramers, J.D.
- 1975: Approximation of terrestrial lead isotope evolution by a two-stage model; Earth and Planetary Science Letters, v. 26, p. 207-221.
- Steiger, R.H. and Jager, E.
- 1977: Subcommittee on geochronology: convention on the use of decay constants in geo- and cosmochronology; Earth and Planetary Science Letters, v. 36, p. 359-362.
- Tempelman-Kluit, D.J.
- 1979: Transported cataclasite, ophiolite and granodiorite in Yukon: evidence of arc-continent collision; Geological Survey of Canada, Paper 79-14, 27 p.
- Tempelman-Kluit, D.J. and Wanless, R.K.
- 1975: Potassium-argon age determinations of metamorphic and plutonic rocks in the Yukon Crystalline Terrane; Canadian Journal of Earth Sciences, v. 12, p. 1895-1909.
 - 1980: Zircon ages for the Pelly Gneiss and Klotassin granodiorite in western Yukon; Canadian Journal of Earth Sciences, v. 17, p. 297-306.

Petrological and structural evolution of the rocks in the vicinity of Killarney, Ontario: an interim report

EMR Research Agreement 165/04/85

Paul M. Clifford¹
Lithosphere and Canadian Shield Division

Clifford, P.M., Petrological and structural evolution of the rocks in the vicinity of Killarney, Ontario: an interim report; in Current Research, Part B, Geological Survey of Canada, Paper 86-1B, p. 147-155, 1986.

Abstract

Composed of leucogranite, hypabyssal porphyry and a variety of mainly felsic volcanic and pyroclastic rocks, the Killarney Triangle Zone lies at the southwest extremity of the exposed Grenville Front, forming a wedge between folded Huronian strata of the Southern Province and gneissic rocks of the Grenville Province. The granite intruded Huronian rocks and, along with its related volcanic rocks, was deformed before northwest-directed displacement and associated mylonitization that mark the Grenville Front Boundary Zone. The volcanic-plutonic suite may be related to similar middle Proterozoic rocks that underlie much of mid-continental North America.

Résumé

La zone triangulaire Killarney, formée de leucogranite, de porphyre hypabyssal et d'une variété de roches majoritairement volcaniques felsiques et pyroclastiques, se situe à l'extrémité sud-ouest de la partie affleurante du front grenvillien; elle forme un prisme entre les couches plissées huroniennes de la province du Sud et les roches gneissiques grenvilliennes. Le granite, qui injecte les roches huroniennes et où se trouvent aussi des roches apparentées aux volcaniques, a été déformé avant le mouvement en direction nord-ouest et associé à la mylonitisation qui caractérise la zone limite du front grenvillien. La séquence volcano-plutonique est peut-être reliée aux roches semblables du Protérozoïque moyen qui forment l'assise principale du mid-continent nord-américain.

¹ Department of Geology, McMaster University, Hamilton, Ontario L8S 4M1

Introduction

The crudely triangular study area lies around the settlement of Killarney, Ontario, and is here termed the Killarney Triangle Zone (KTZ; Fig. 18.1). It is bounded on the north by Huronian metasediments of the Southern Province, and to southwest and south by Paleozoic cover and the waters of Lake Huron. Mylonites of the Grenville Front Boundary Zone (GFBZ) from the eastern boundary, beyond which lie undoubted Grenville Province gneisses and plutonic igneous rocks, some of which possess only weak or no foliation. The area is traversed by Highway 637 which gives generally good access; numerous lakes ensure well distributed inland exposure for the most part, but there are nonetheless large patches devoid of outcrop. The coast and nearby islands of Lake Huron afford excellent exposures.

The overriding reason for studying the KTZ is to try to fix its proper position in the geological history of this portion of the Precambrian of North America. It is evident, even on the basis of the incomplete mapping reported here, that the KTZ contains some rocks unlike the generality of the Southern and Grenville provinces, as well as the Killarney granite which is usually regarded as one of the several "granites" referred to as Grenville Front granites or, more recently, the Killarney batholith (Frarey, 1985). Rocks of somewhat similar aspects have been reported from Proterozoic terranes in the U.S.A.; they span an age range of 1070-1790 Ma, (van Schmus, 1976) and have been regarded in

part as anorogenic. It is remotely possible that KTZ rocks are part of this assemblage. More immediate goals involve detailed structural and lithological mapping to supplement the available general map (Frarey, 1985), and provision of a useful outline of the nature of the volcanic and plutonic rocks, and of the structural history.

This is a provisional report; mapping in summer 1985 covered perhaps 70% of the area. Further work is required to complete the map, and to refine boundaries and structural relationships now seen as inadequate.

Lithologies

The map (Fig. 18.1) gives a simplified outline of the lithologies of the area. Detail waits on petrography and chemistry, especially for the silicic plutonic rocks.

Huronian metasediments

Along the northern edge of the KTZ, members of the Gordon Lake, Bar River and Lorrain formations have been intruded and thermally metamorphosed by the Killarney granite. The contact relationships are displayed particularly well on the islands northwest of Killarney Village and on the mainland southwest of La Morandière Bay, where granite has wedged along bedding to pry apart and rip off large pieces of quartzite and siltstone.

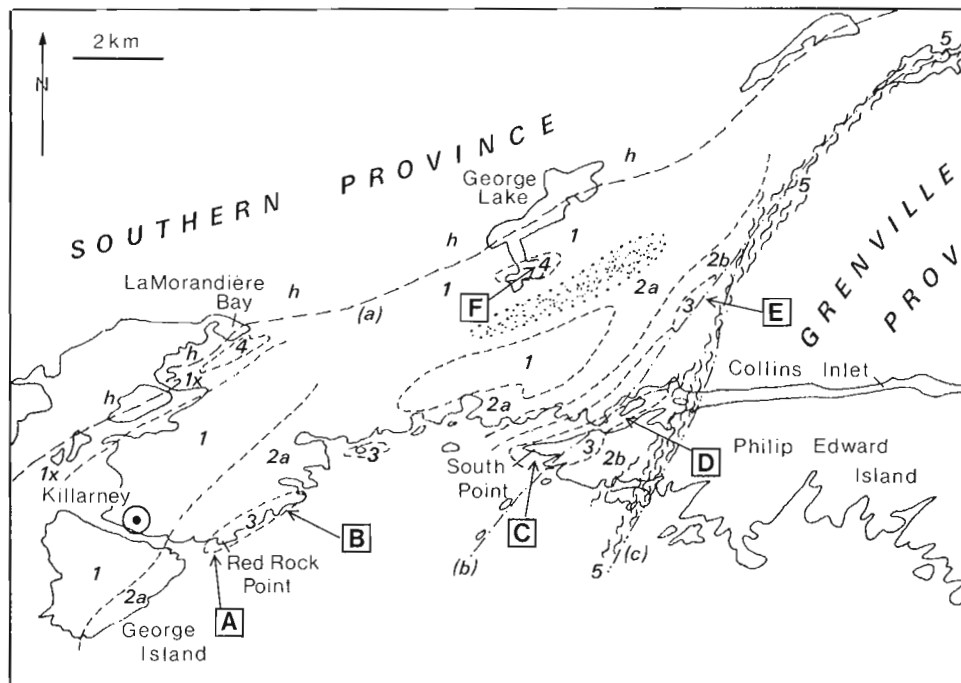


Figure 18.1. Generalized distribution of lithologies in the Killarney Triangle Zone (KTZ). 1 – Silicic plutonic rocks, including Killarney granite; quartz monzonite. 1x – Xenolith-bearing marginal phase. 2a – 'Nail-head' porphyry. 2b – 'Pin-head' porphyry. 3 – Silicic fragmental volcanic and related rocks; includes monomict fragmentals at Red Rock Point, polymict fragmentals at South Point and 4 km to the northeast. 4 – Andesitic volcanic rocks; includes airfall ash and lapilli tuff at George Lake and vesiculated flow rocks at George Lake and La Morandière Bay. 5 – Mylonitic zone. h – Huronian metasediments. Stippled area is covered by glacial deposits. (a) – Boundary of KTZ against Huronian metasediments, intrusive where mapped to date (Frarey, 1985). (b) – Grenville Front Boundary Fault of Card (1978). (c) – Grenville Front Boundary Fault (Davidson, 1984; this project). Letters identify locations mentioned in the text.

Metavolcanics

These rocks (Fig. 18.1) occupy much of the KTZ and probably include high-level, hypabyssal intrusive rocks (as opposed to the coarser grained silicic plutonic rocks described below).

- i) South of LaMorandière Bay, enclosed in Killarney granite, are numerous xenoliths of andesite, one of them upwards of a kilometre long. This is a dark grey-green rock, mottled in outcrop. In large xenoliths, there are signs of flow brecciation, as well as signs of breakage due to incorporation in the granite. Some patches also appear flow-banded or to have a mildly fluidal fabric mottled by feldspar phenocrysts.

A possible andesitic flow rock also outcrops on the shore of George Lake, opposite the western beach of the campsite. This is vesiculated, weathers pale grey, and contains amphibole and plagioclase.

- ii) Over much of the area, the marked (2) on Figure 18.1, there are feldspar-phyric rocks, now with variably developed foliation. These weather in shades of pink, but may be pink to dark grey on a fresh surface. One facies (2a) – a "nail head porphyry" – has feldspars up to 5 mm in diameter scattered through it, but not aligned or clustered. Another facies, 2b, is a "pin-head porphyry" where the feldspar is never more than 2 mm across (Fig. 18.2). Facies 2b lies to the south and east of 2a for the most part; the contact of the



Figure 18.2. "Pin-head" porphyry, without foliation. About 3 km southwest of western tip of Carlyle Lake.

two facies appears to be conformable and no apophyses or xenoliths of one have been seen in the other. A scan of thin sections shows K-feldspar to be strongly twinned, zoned, locally in glomeroporphyritic clusters, and essentially undeformed. Groundmass includes quartz, K-feldspar, a little plagioclase and muscovite as the persistent mineral species. There is a limited preferred orientation of muscovite, and, in some rocks, a tendency to strips of matrix alternating with strips rich in phenocrysts. These rocks are interpreted as porphyritic flows or hypabyssal intrusives of silicic composition. Marsh (1984) suggested that the crystallinity – volume fraction of magma actually crystallized – as the magma approaches the site of emplacement or emission has an upper bound if the magma is to appear as lava: 50% crystallinity is the bound for basalt but lower values apply at higher silica contents. The porphyry has a crystallinity ranging from 15 to 40%, treating the phenocryst population as the crystal population just prior to emplacement, and the matrix crystals as post-emplacement phases. This permits an interpretation of the porphyry as lava; but so far, no outcrop evidence of flow processes have been seen in the porphyry.

- iii) In several patches, assemblages of volcanic clastic rocks, some definitely pyroclastic, are exposed. At Red Rock Point (Fig. 18.1, A) and for 250 m northeast, outcrops reveal (a) pumice-bearing pyroclastic rock possibly ignimbritic; (b) autobrecciated flow with ashy material filling large irregular void spaces; (c) possible thermally cracked and altered flow material; all somewhat intermixed (Fig. 18.3).

Farther northeast (Fig. 18.1, B) a quartz-rich elliptical mass is surrounded to east, south and west by a breccia. The main mass shows possible flow banding; the breccia is totally unorganized. Together these are tentatively interpreted as a rhyodactite dome/flow plus spall-off breccia resting on porphyritic rock.

Between 7 and 10 km east-northeast of Red Rock Point, two more patches of clastic rocks, interpreted as volcanic, outcrop along South Point at the west end of Philip Edward Island (Fig. 18.1, C) and thence east, and on the north side of the channel 2 km east of South Point (Fig. 18.1, D). These patches are flanked by porphyritic rock. Within these outcrops the rocks range from volcanic breccias having



Figure 18.3. Presumed disrupted flow with alteration zones along fractures. Near Red Rock Point.

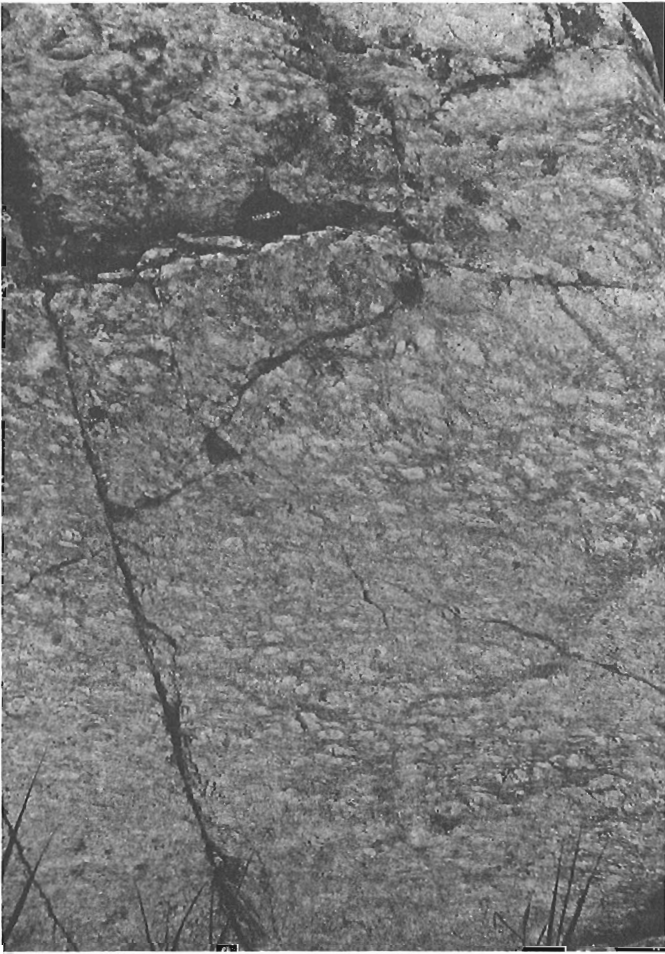


Figure 18.4. Lapilli tuff; clasts not very obviously aligned; moderate percentage of ash matrix. North side of Philip Edward Island, about 1 km east of South Point.

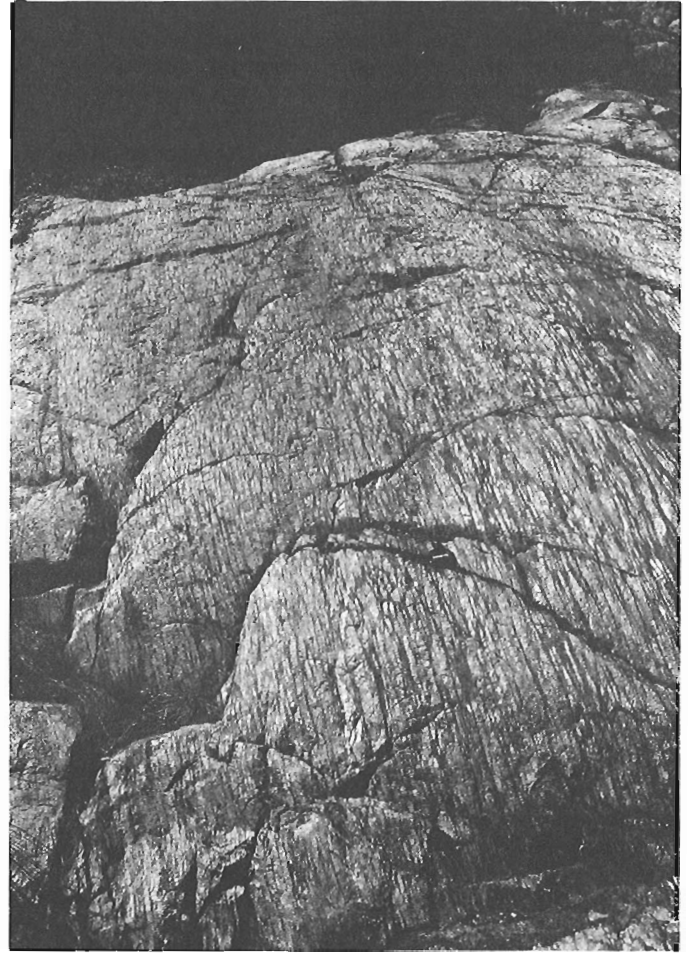


Figure 18.6. Lapilli tuff, severely flattened, with a matrix more basic than clasts. George Lake, west end of south arm.



Figure 18.5. Lapilli tuff; clasts aligned by tectonism. Poorly sorted, high percentage of ash matrix. West end of Philip Edward Island.

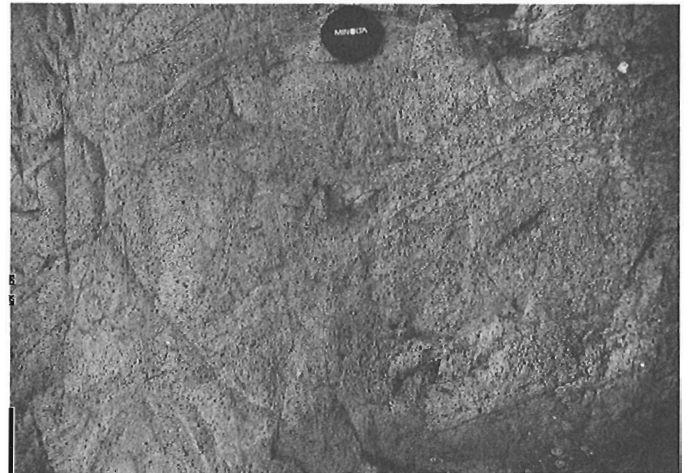


Figure 18.7. Vesiculated and brecciated flow, probably andesite. George Lake, north shore of south arm.

apparently angular silicic clasts, poorly sorted and unaligned in a matrix of similar composition (Fig. 18.4) which forms up to 50% of the outcrop, to discontinuously striped outcrops which are almost certainly much deformed polymict breccias (see below, clast extension lineation). Between these two extremes there occur deformed but recognizable breccias having perhaps 30% ash matrix (Fig. 18.5). All these rocks are lapilli breccias.

There is another patch of possible lapilli breccia, very poorly exposed, some 3 km inland from Collins Inlet at the eastern boundary of the area (Fig. 18.1, E). All clasts are thoroughly extended.



Figure 18.8. Coarse grained, rather poorly sorted unlayered lapilli tuff on left and right (due to ash flow activity?); airfall ashes in centre. George Lake, north shore of south arm.

Finally, at George Lake (Fig. 18.1, F) there occur silicic lapilli breccias in a more basic matrix. All clasts are thoroughly flattened and stretched (Fig. 18.6), locally defining a foliation oblique to primary layering. There is also vesiculated andesite (see above); and some finely layered material against the andesite and also on the eastern side of the southern arm of the lake which is interpreted as probable airfall ash or perhaps a proximal epiclastic unit (Fig. 18.7, 18.8).

These pyroclastic and possible pyroclastic units imply somewhat violent subaerial explosive volcanic activity, with this activity occurring on top of a hypabyssal or flow assemblage. At location B (Fig. 18.1) xenoclasts of ignimbritic fragmental material and of pink porphyritic (?) lava are incorporated in possible flow-banded rhyolites.

Silicic plutonic rocks

Along the western and northern margins of the KTZ and also in its centre there are extensive outcrops of silicic plutonic rocks. So far, boundaries between the two major facies are recognized in only two places: one in the road cut just east of the restaurant outside Killarney, and the other southeast of the restaurant in a small outcrop in the bush.

On the western the northern margin, as mapped to date, is Killarney granite. This is a coarse to very coarse grained rock dominated by K-feldspar with about 20-25% quartz and a little plagioclase. Biotite ranges from near zero to 10%. This confirms Card's (1978) designation of this rock as granite and quartz monzonite.

South and east of the Killarney granite is a medium to coarse grained leucogranite usually lacking dark mica. There is also a pale purple, medium grained quartz monzonite in outcrop along Highway 637, 1-2 km east of George Lake Park entrance. Nothing has been established about its relationship to other units.

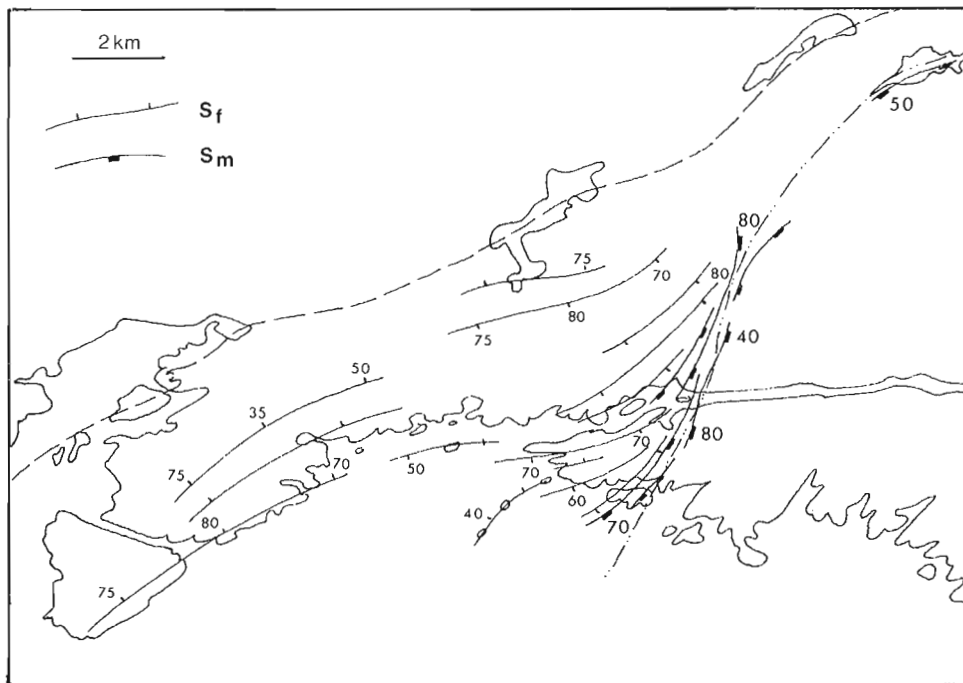


Figure 18.9. Foliation trends in the KTZ. Regional foliation (S_f) is marked mainly by phyllosilicates and includes short-range (?) shears. Mylonitic foliation (S_m) is restricted to the Grenville Front Boundary Fault. Dips shown are local averages.

All of these rocks have either no imposed foliation or an indifferently developed one.

Pegmatites are confined mainly to the eastern part of the area and are commonly modified into the mylonite series. Where not deformed, they are exceedingly coarse grained. They are composed generally of about 60% K-feldspar and 40% quartz, though there is considerable variation and some contain muscovite.

Boundaries range from sharp in areas away from the mylonitic zone, and where the pegmatites cut through the near-isotropic granite and porphyry, to somewhat diffuse in the vicinity, and just to the east, of the mylonite zones. The sharply-bounded pegmatites cut across the planar structural elements which have been developed in granite and porphyry.

Killarney granite obviously intrudes Huronian meta-sediments. It is therefore younger than those metasediments, as it is also probably younger than porphyry which it invades at the southern tip of George Island. Its relationship to other silicic plutonic rocks is currently obscure. One outcrop has been interpreted as having Killarney granite cut the medium grained leucogranite; another suggests the inverse relationship. Finally, xenoclasts of porphyry and pumice-rich fragmentals in rhyodacite suggest that the subaerial volcanics are younger than the porphyries and the ignimbrites.

Structure

With so much initially massive, near-isotropic rock in the KTZ, development of folds has been extremely limited and the generation of mesoscopic fabric elements is areally restricted and quite variable in character.

Foliation, S_f (Fig. 18.9)

In the far west, the Killarney granite and associated coarse grained plutonic rocks lack foliation. Some of the xenoliths are internally layered, but such layering is

clearly primary. Moving generally to the east, there is (a) the appearance of zones of slight distortion of primary fabric: slightly elongate feldspars, short wafers of quartz, local, short-range alignment of phyllosilicates. These zones rarely persist for more than a few metres and dissipate by anastomosis and fingering into undeformed host. Some zones are actually very small shear zones, with local positive dilation marked by quartz precipitation. Such zones appear to be discoidal and always have $X = Y \gg Z$. There follows farther east, (b) definite alignment of aggregates of minerals, and preferred orientation of minerals, especially



Figure 18.10. Mylonitic foliation. Note feldspar "beads" in feldspar-rich layer; also intrafolial-style folds in upper left portion of photo. Island south of Philip Edward Island (GFBZ).

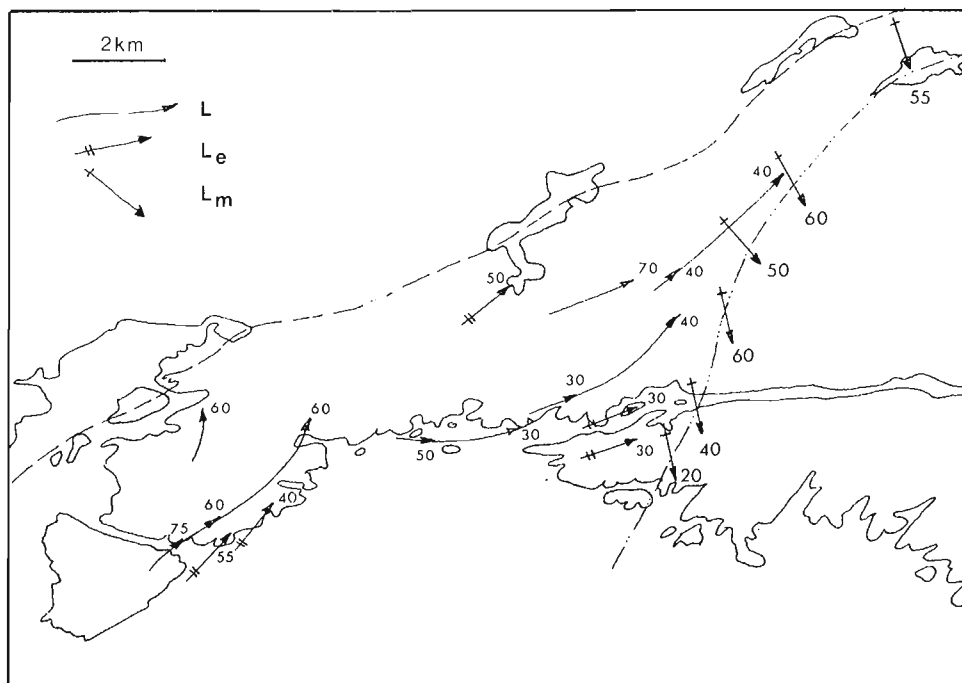


Figure 18.11. Lineation trends in the KTZ. L – regional lineation; L_e – mean long (X) axis of pyroclasts; L_m – ribbon (stretching) lineation in the mylonitic foliation (S_m). Plunges shown are local averages.

phyllosilicates, to yield a faint but persistent planarity. In the same rocks, there may be rounding and/or elongation of feldspars; and quartz is further drawn out. Part at least of this change in character is due to the lithological change from coarse grained silicic plutonics to finer grained, possible hypabyssal or volcanic rocks.

This foliation persists to the eastern boundary of the area, its intensity being somewhat variable. Approaching that boundary, however, it turns from ENE strikes to NNE strikes, towards parallelism with the trend of mylonitic foliation of the GFBZ.

Mylonitic foliation, S_m (Fig. 18.9)

Along the eastern boundary of the KTZ, there occurs a strip about 200 m wide across strike, within which all rocks have been drastically modified into members of the mylonite series. There is no monotonic sense of change of fabric: ultramylonite layers may be sandwiched between layers which are protomylonite, each with a differently developed, through parallel, foliation. This foliation appears as layering down to scales less than 1 mm; each layer may be extremely persistent in mylonite developed from relatively homogeneous parent, or layers may change from pink to white to pink again, as K-feldspar or quartz contributes to the layer. Grain shapes are drastically changed in mylonitic layers, the most obvious examples being a quartz ribbon lineation and rolled feldspars with tails. Grain size is also



Figure 18.12. Isoclinal fold in mylonitic foliation. Note strung out and isolated feldspar. Small Island, 2.5 km southeast of South Point (GFBZ).

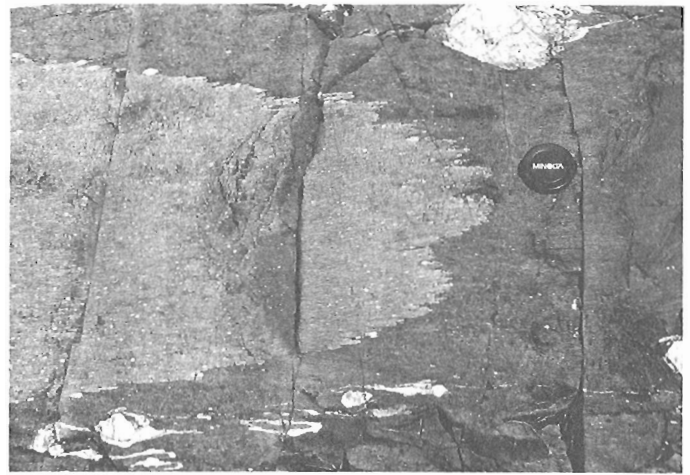


Figure 18.13. Fold in mylonitic foliation, shown by lithological contrast. Axial surface is also the plane of a mylonitic foliation. Island south of Philip Edward Island (GFBZ).



Figure 18.14. Outcrop pattern of pinnate extension fractures on a lineated mylonitic foliation surface. Movement up, from lower left to upper right, of block above this surface.

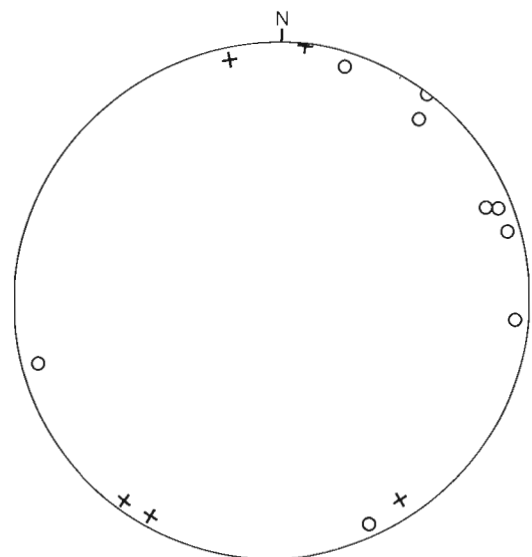


Figure 18.15. Poles to planes of shear zones. Circles are left-handed, crosses are right-handed shears. Implied principal stress directions are: σ_1 -110/00, σ_2 - vertical, σ_3 -020/00, but the scatter of points makes such an implication weak.

drastically changed; much material is barely resolvable under the microscope. In outcrop, the two most spectacular versions are a very fine grained, grey-black, vaguely layered rock with isolated rounded feldspars marginally comminuted (Fig. 18.10) and a pink-and-white striped/layered rock, clearly of pegmatitic parentage. Mylonites are found only at the eastern boundary; they always are in a pegmatite-rich zone.

Flattened clasts

At George Lake, both east and west sides (Fig. 18.6), and also close to Red Rock Point, pyroclasts are obviously distorted into crude triaxial ellipsoids, collectively aligned with their XY planes defining a planarity not visible in the matrix. In both locations, Z is approximately horizontal, NNW-SSE; where noticeably different from Y, X has a low plunge (<20°) ENE-WSW. In both locations, the pyroclastic rocks lie between units of much more homogeneous material, which are undeformed or nearly so.

Clast extension lineation, L_e (Fig. 18.11)

In four of the outcrop patches of pyroclastic material, clasts have been deformed in a very particular way. Seen in YZ section, clasts can appear angular, poorly sorted, and non-aligned. But any section containing X, roughly, shows these clasts to be markedly extended and strongly aligned, such that $X > Y = Z$, with X/Y reaching 10 in one case. The parallelism of X axis is very strong $\cdot L_e$, measured as mean X, is invariably horizontal or subhorizontal. No cleavage occurs in such cases.

Folds, with fold axes, L_f

A very few folds have been defined, all of them small, non-regional. They fall into two groups:

- a. Isoclinal to subisoclinal folds, found mainly on small islands south of Philip Edward Island, close to or in the GFBZ. Folds are developed in mylonitic foliation with rounded feldspars dotted along the limbs (Fig. 18.12). In one of these folds, a mylonitic foliation lies parallel to the axial surface (Fig. 18.13). In all such folds, lineation is highly consistent (see below) in style and orientation.
- b. Somewhat open folds with rounded axial zones, also developed in mylonitized, pegmatite-bearing rocks. Fold axes are of moderate plunge but inconsistent in orientation. The quartz-ribbon lineation of the mylonitic foliation is bent around these folds, to give a quite erratic distribution when plotted on a stereonet. These are post-mylonitization at least locally.

All these folds occur in, and very close to, the GFBZ; no folds have been seen elsewhere.

Mylonite "stretching" lineation, L_m (Fig. 18.11)

In all mylonite outcrops, there is a lineation. Commonly this is a flat ribbon of quartz, perhaps with stretched feldspar accompanying it, but there is also a ribbing on many foliation surfaces not totally of one mineral which is just as conspicuous as the ribbon lineation. In the absence of later folding, this "stretching" lineation is remarkably consistent in orientation.

Kinematic indicators

In the mylonites, rotated feldspars with tails occur in abundance locally. In the same mylonite, pinnate en echelon extension fractures (Fig. 18.14) cut the quartz ribbon lineation. Both imply southeast over northwest thrusting on highly inclined planes. The same inference can be drawn

from the few field occurrences seen of C-S fabric. The angle between C and S planes is always less than 30°, suggesting substantial shear strain. These kinematic indicators occur only in rocks having mylonitic foliation, S_m , and stretching lineation, L_m .

The distribution and generalized orientation of these fabric elements are shown in Figures 18.9 and 18.11.

Fractures and faults

The entire area is cut by joint sets which extend from the KTZ into the Southern Province at least. Most of these are unexceptional, but there is a double fracture set, presumed to be conjugate, which merits comment. Zones of discoloured rocks are actually occupied by sets of en echelon dilatant cracks. Some of these gape up to 0.5 cm; others contain quartz filling. For any given local set, (a) set orientation is very consistent over several zones; (b) set spacing is locally fairly constant; (c) individual cracks in a zone are very consistently spaced, and equally consistently oriented; (d) the angle between an individual fracture and set mean orientation rarely exceeds 20°, and (e) every individual crack is curved at its tips, and shows a slight "twist" of its overall plane moving up the crack. The two sets have a dihedral angle between them ranging from 10 to 40°. Sinistral sets outnumber dextral sets by a factor of 3 at least. These sets are so unlike the generality of fractures here that they may well imply an independent mechanism. Further work is to clarify this possibility.

Orientations of these fracture arrays are quite varied; Figure 18.15 is a stereoplot of poles to fracture zones. There is no systematic distribution of these fractures in terms of their strike direction; they are clearly later than any other structural feature, but do not imply a unique stress field as being responsible for their formation.

Faults are hardly ever seen; but there are a few places where airphotos show conspicuous lineaments, which turn out to have strips and patches of cataclastic breccia in appropriate outcrops. Neither sense nor amount of displacement can be determined. Trends of such faults coincide with one or another of the common regional joint trends, and seem to have no connection with GFBZ.

Comments and conclusions

The abundance of silicic plutonic rocks and of subaerial volcanics of comparable composition clearly sets the KTZ apart from the Southern Province; probably also from the Grenville Province, though there is a chance that such rocks might occur, much deformed and recrystallized beyond recognition, in Grenville assemblages.

It seems clear also that the KTZ can be viewed as a volcanic-plutonic complex (cf. Davidson, 1984). The granites can be seen as solidified sources for the overlying pyroclastic rocks. Distribution of pyroclastic material is patchy; in part, outcrop is probably missing, but in part this reflects an original discontinuous distribution.

Deformation has affected these rocks in several steps. A foliation and lineation has been produced in the porphyries, and, to a lesser extent, in the silicic plutonic rocks. This foliation is variably developed, but generally is more obviously expressed in the eastern portion of the area. Probably at the same time as foliation development, clasts in the pyroclastic rocks were flattened and elongated. There were clearly steep strain gradients between pyroclastic and flow rocks; also variations in the form of the strain ellipsoid, from discoidal ($X = Y > Z$) at George Lake to blade-like at Red Rock Point ($X > Y > Z$), to cigar-shaped ($X \gg Y = Z$) on Philip Edward Island.

Superimposed on this earlier fabric is a mylonitic foliation and lineation along the eastern margin of the KTZ. Mylonite ranges from protomylonite to ultramylonite, with isolated rotated feldspars in an ultra-fine grained matrix as the extreme version. Ribbon lineation is powerfully developed. Nearby there are a few examples of C-S fabric. This fabric, rolled feldspars and pinnate shear fractures in the ribbon lineation all imply a southeast side up-and-over displacement on this mylonitic foliation of GFBZ.

Clearly, substantial shortening of this block is implied by the flattening and extension of clasts; and by the mylonites, which suggest overthrusting from southeast to northwest.

References

Card, K.D.

- 1978: Geology of the Sudbury-Manitoulin area, Districts of Sudbury and Manitoulin; Ontario Geological Survey, Report 166, 238 p.

Davidson, A.

- 1984: The Killarney granite and its relationship to the Grenville Front southwest of Sudbury, Ontario; Geological Association of Canada, Programs with Abstracts, v. 9, p. 56.

Frarey, M.J.

- 1985: Proterozoic geology of the Lake Panache-Collins Inlet Area, Ontario; Geological Survey of Canada, Paper 83-22, 61 p.

Marsh, B.D.

- 1984: On the crystallinity, probability of occurrence, and rheology of lava and magma; Contributions to Mineralogy and Petrology, v. 78, p. 85-98.

van Schmus, W.R.

- 1976: Early and middle Proterozoic history of the Great Lakes area, North America; Phil. Royal Society of London, Transactions, Series A280, p. 605-628.

A preliminary report on the geology of the southern Long Range, southwest Newfoundland¹

Project 850017

**J.T. van Berkel, H.P. Johnston and K.L. Currie
Lithosphere and Canadian Shield Division**

van Berkel, J.T., Johnston, H.P., and Currie, K.L., A preliminary report on the geology of the southern Long Range, southwest Newfoundland; in Current Research, Part B, Geological Survey of Canada, Paper 86-1B, p. 157-170, 1986.

Abstract

The southern Long Range consists of four, fault-bounded segments, namely the Steel Mountain Terrane, dominated by an anorthosite massif; the Central Gneiss Terrane, composed of metasedimentary gneisses intruded by granite and granodiorite and containing thin (3-300 m), elongate (up to 50 km) strips of tectonized ultramafic rocks; the Annieopsquotch Terrane, dominated by gabbro and diabase of ophiolitic affinities and overlain by Silurian redbeds and acid volcanics; the Rocky Ridge Pond Terrane composed of migmatitic metasedimentary rocks invaded by megacrystic biotite granite. On the west rocks of the southern Long Range are unconformably overlain by easterly-derived Carboniferous sedimentary rocks.

In the Steel Mountain and Central Gneiss terranes, mesoscopic fold axes tend to trend north to northwest. Structures in the Rocky Ridge Pond Terrane trend northeast. All terranes are cut by a multitude of faults and high strain zones, both ductile and brittle. Faults coinciding with terrane boundaries are major transcurrent faults. Northeast to southwest trending faults and high-strain zones are post-Lower Ordovician. However, some of the major transcurrent faults like the Long Range Fault may date back as far as the Grenvillian Orogeny (1100 Ma).

Résumé

La région sud du complexe de Long Range est constituée de quatre segments limités par des failles, notamment la région de Steel Mountain dominée par un massif d'anorthosite; la région de Central Gneiss, composée de gneiss métasédimentaires à intrusion de granite et de granodiorite, et contenant de longues bandes (jusqu'à 50 km) minces (3 à 300 m) de roches ultramafiques tectonisées; la région d'Annieopsquotch dominée par du gabbro et de la diabase à affinités ophiolitiques et recouvertes de couches rouges et de roches volcaniques acides du Silurien; la région de Rocky Ridge Pond, composée de roches métasédimentaires migmatitiques envahies de granite à biotite renfermant des macrocristaux. À l'ouest, les roches de la région sud du complexe de Long Range sont recouvertes de façon discordante par des roches sédimentaires du Carbonifère provenant de l'est.

Dans les régions de Steel Mountain et de Central Gneiss, les axes mésoscopiques des plis sont orientés vers le nord et le nord-ouest. Dans la région de Rocky Ridge Pond, les structures sont orientées vers le nord-est. Une multitude de failles et de zones de déformations élevées de roches à la fois malléables et cassantes recourent toutes les régions. Les failles qui coïncident avec les limites de ces régions sont d'importantes failles à déplacement horizontal.

¹ Contribution to the Canada-Newfoundland Mineral Development Agreement 1984-1989. Project carried by Geological Survey of Canada.

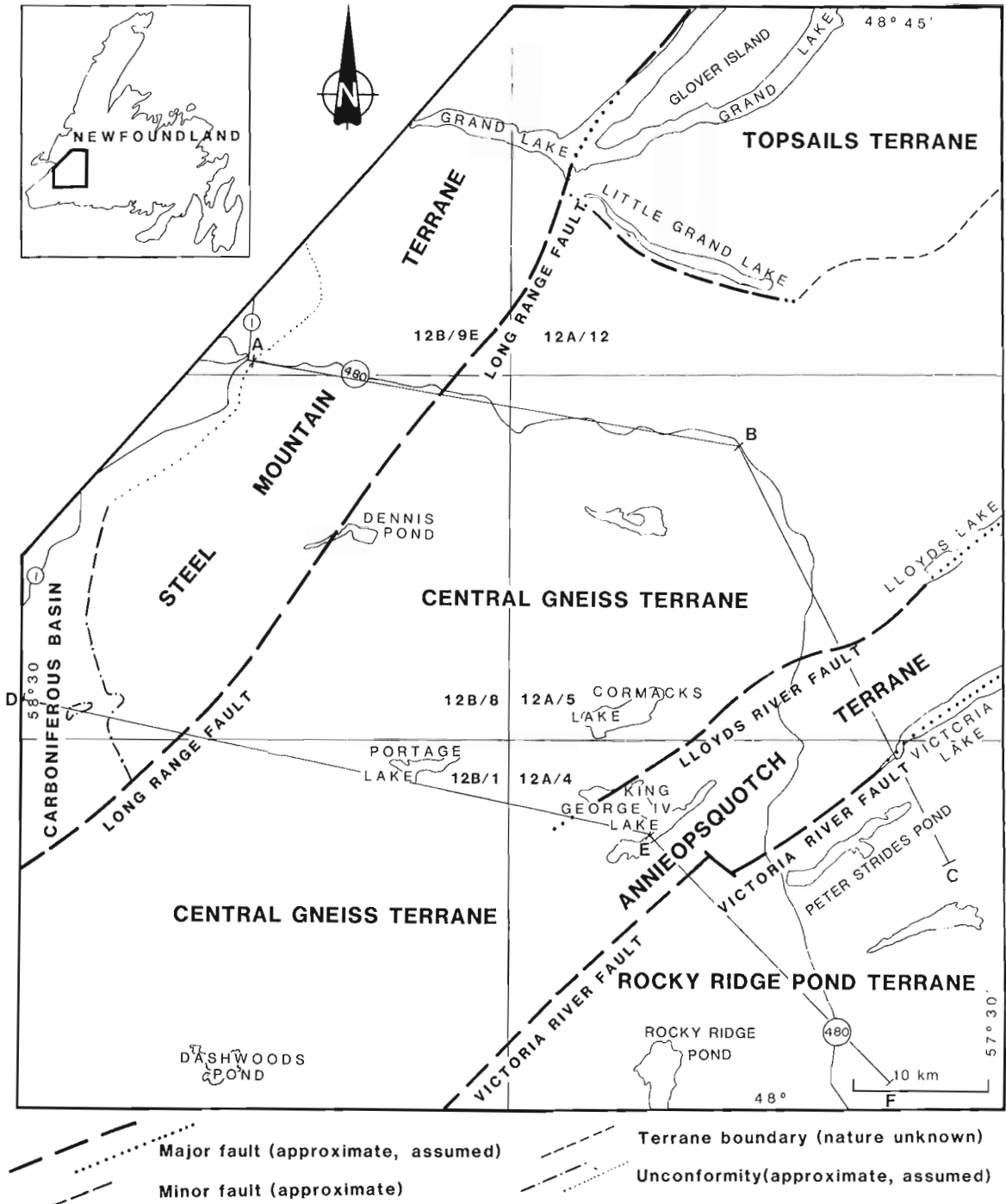


Figure 19.1. Tectonic terranes and major topographic features in the southern Long Range, southwest Newfoundland. Distribution of 1:50 000 map sheets is indicated.

Introduction

The southern Long Range of western Newfoundland forms an elevated, deeply dissected plateau underlain by a variety of plutonic rocks. Due to difficulty of access, geological complexity and the reconnaissance nature of previous geological mapping, the geological history of this region was poorly understood. Williams (1979) showed the boundary between his Humber and Dunnage tectonostratigraphic zones passing through this region. The Humber Zone displays Precambrian Grenville basement and a late Precambrian to early Paleozoic cover sequence, locally veneered by early Paleozoic ophiolitic allochthons derived from the Dunnage Zone. Similar successions have been suggested southeast of the boundary drawn by Williams (1979), for example by Brown (1975, 1977) and by Herd and Dunning (1979). However, Chorlton (1980, 1983) and Wilton (1983) did not see any conclusive evidence for exposure of Grenvillian basement to the southwest of the study area. The region northeast of the southern Long Range (Topsails Terrane; Fig. 19.1) exhibits an assemblage of massive, epizonal igneous rocks separated from surrounding terranes by major tectonic breaks (Whalen and Currie, 1983a,b). The relatively equant shape of the Topsails region suggests that western Newfoundland could be a tessellate assemblage of terranes (e.g. Whalen and Currie, 1984; Keppie, 1986), rather than a few elongate strips as envisaged by Williams (1979). Uncertainties in the geological interpretation of southwestern Newfoundland strongly affect large-scale interpretation of the Appalachian Orogen, since this region is one of the links between the much studied geology of north-central Newfoundland and the rest of the Appalachians.

In order to resolve problems of correlation and structure in this key region, a helicopter-supported operation was launched to map the whole of the southern Long Range (Fig. 19.1) at 1:100 000 scale. During the 1985 field season the Dashwoods Pond (NTS 12B/1) and Main Gut (NTS 12B/8) map sheets were completed, as well as parts of Harrys River (NTS 12B/9E) and Little Grand Lake (NTS 12A/12). Much of this area was previously covered by 1:250 000 reconnaissance maps (Riley, 1957, 1962). In addition, parts of Puddle Pond (NTS 12A/5) and King George IV Lake (NTS 12A/4) were examined in order to integrate the mapping of Herd and Dunning (1979) and Kean (1983) with the present work.

The barren uplands of this region generally exhibit good bedrock exposure, although parts of the Dashwoods Pond sheet are largely drift covered. In the wooded valleys, exposure is poor or non-existent.

General geology

The southern Long Range consists of at least four distinct terranes separated by tectonic breaks. West of the Long Range Fault (Fig. 19.1) in the Steel Mountain Terrane (Humber Zone), anorthosite, tonalite-diorite, norite and hornblende-biotite and psammitic gneiss form a basement of presumed Grenvillian age which is overlain by lower grade pelitic to calcareous schists, probably correlative with the Fleur de Lys Supergroup of late Precambrian to early Paleozoic age (Knapp et al., 1979; Martineau, 1980; Kennedy, 1981; Hibbard, 1983a,b; Williams, 1985). Autochthonous Cambrian and Ordovician carbonate units lie northwest of this terrane (Kennedy, 1981; Williams, 1985). To the west Carboniferous sedimentary rocks unconformably overlie or are in fault contact with the igneous and metamorphic rocks (Knight, 1983).

The Central Gneiss Terrane (Fig. 19.1), between the Long Range Fault and the Lloyds River/Victoria River faults, consists of migmatized psammitic, pelitic and calcareous gneiss intruded by numerous, large plutons of late tectonic granite to granodiorite. The paragneisses, perhaps equivalent to the Fleur

de Lys Supergroup, contain several thin strips of foliated, mostly serpentinized, ultramafic rocks. The northeastern portion of the Central Gneiss Terrane consists mainly of fine grained diabase and medium grained gabbro intruded by minor amounts of granite to diorite. This region may be a separated portion of the Annieopsquotch Terrane.

Between the Lloyds River Fault and the Victoria River Fault the rocks consist mainly of medium grained gabbro and fine grained diabase intruded by minor late tectonic granite to granodiorite (Annieopsquotch Terrane). A large portion of the mafic rocks has been interpreted to be part of an ophiolite fragment (Dunning and Herd, 1980; Dunning, 1981, 1984; Kean, 1983) of Lower Ordovician age (480 Ma; Dunning and Krogh, 1985). These rocks are unconformably overlain by a Silurian sequence of red sandstone and felsic volcanics (Chandler and Dunning, 1983). Along the southeastern side of the Annieopsquotch Terrane, a belt of volcanic rocks and sediments was correlated by Kean (1983) with the Ordovician Victoria Lake Group (Kean, 1977) and Devonian (Emsian; C. McGregor, personal communication, 1981, in Chandler, 1982) Windsor Point Group. This belt pinches out to the southwest, and should perhaps be considered a separate terrane.

Southeast of the Victoria River Fault (Rocky Ridge Pond Terrane) the rocks consist of medium grained granoblastic paragneisses (including volcanics?) intruded by large plutons of late tectonic granites, many of them megacrystic (Kean, 1983). Large-scale compilation maps (Williams, 1978; Hibbard, 1983b) show this region as part of the Central Mobile Belt (Gander and Dunnage Zone) of Newfoundland, but lithologically the rocks at a distance of up to 5 km (in the northeast) or 15 km (in the southwest) from the Victoria River Fault resemble those of the Central Gneiss Terrane. Farther southeast rocks are of typical Dunnage and Gander Zone affinity.

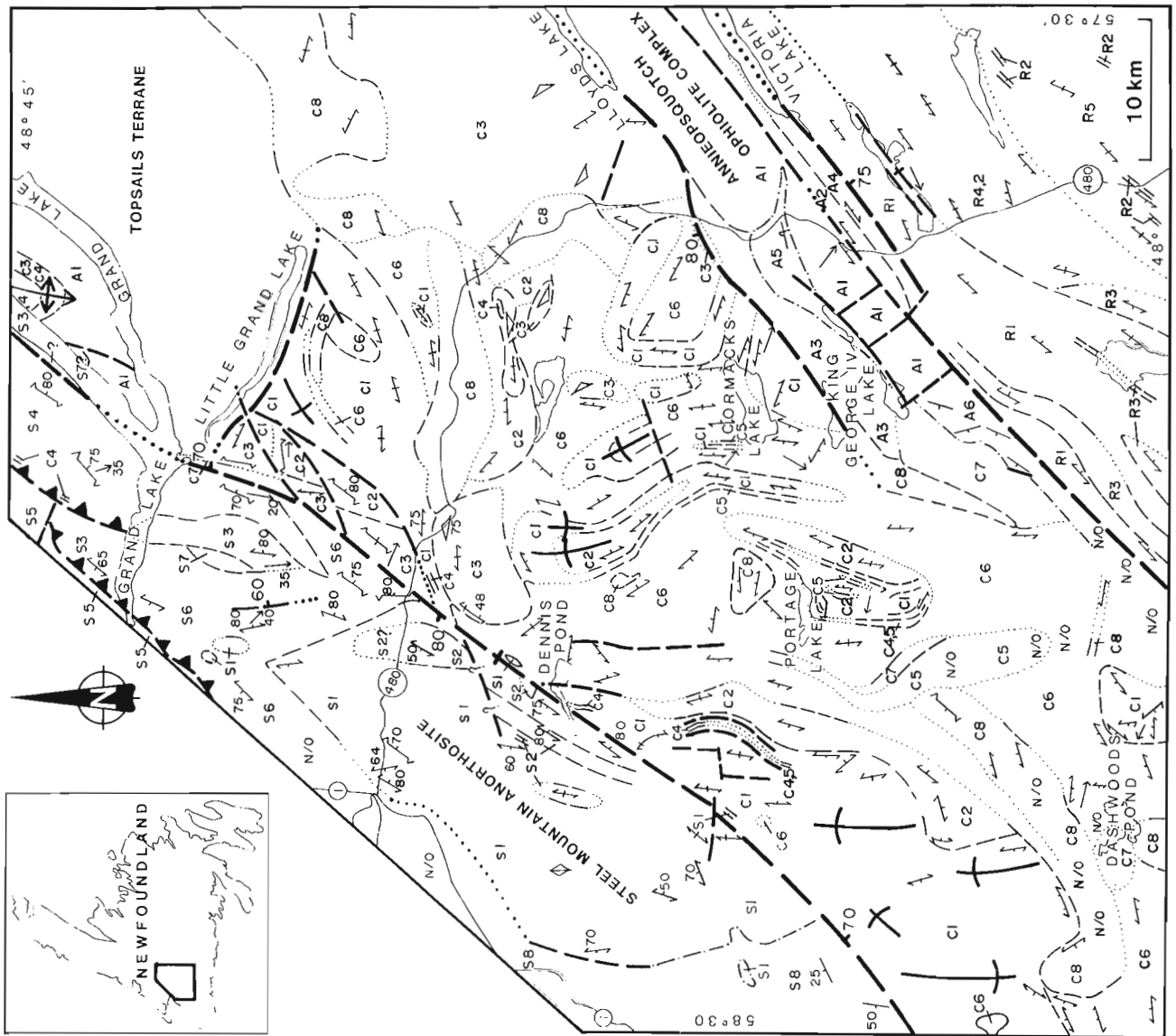
Description of rock units

At present we consider correlation of units between the four terranes defined above to be quite speculative. We therefore describe the lithological units in each terrane separately, and subsequently suggest possible correlations.

Steel Mountain Terrane

The Steel Mountain anorthosite (Fig. 19.2, unit S1) forms a body 40 by 15 km on the west side of the Long Range Fault. Two small, presumably related bodies of anorthosite occur just to the north of the main mass. The Steel Mountain anorthosite consists mainly of a white to mauve, medium grained, polygonal, recrystallized anorthosite with a colour index less than 10. Primary and layered igneous textures are locally preserved. Spectacular anorthositic pegmatites, with pyroxene crystals up to 3 m long, occur west and north of Dennis Pond. Pockets and layers of titaniferous magnetite are often present (Baird, 1943, 1954). Noritic phases are common. Much of the anorthosite is pervasively epidotized. Two sparse swarms of amphibolite dykes, one trending northwest, the other northeast, cut the anorthosite. The Steel Mountain anorthosite is a massif-type anorthosite (Simmons and Hanson, 1978), and resembles the Grenvillian Indian Head anorthosite (Heyl and Ronan, 1954; Colman-Sadd, 1974) located some 15 km to the west.

Along its eastern margin, the Steel Mountain anorthosite contains enclaves up to several kilometres across of tonalite-diorite and norite (unit S2). Although the tonalite-diorite locally displays good foliation, the bulk of these rocks are essentially massive. Contacts between these rocks and the anorthosite are very poorly exposed and unambiguous crosscutting relations were not observed. The tonalite-diorite and norite probably represent facies of the Steel Mountain anorthosite.



- MAJOR FAULT (APPROXIMATE, INCLINED, VERTICAL; ASSUMED)
- MINOR FAULT (APPROXIMATE, INCLINED, VERTICAL; ASSUMED)
- THRUST FAULT (APPROXIMATE)
- STEEPLY-PLUNGING TIGHT TO ISOCLINAL FOLD;
- PLUNGING ANTICLINE
- N/O NO OUTCROP
- BEDDING (INCLINED, OVERTURKED)
- FOLIATION (INCLINED, VERTICAL)
- LINEATION (PLUNGING)
- SHEAR ZONE (INCLINED, VERTICAL)
- IGNEOUS LAYERING (INCLINED, VERTICAL)
- GEOLOGIC BOUNDARY (DEFINED, APPROXIMATE, ASSUMED)
- UNCONFORMITY (APPROXIMATE, ASSUMED)

CARBONIFEROUS	STEEL MOUNTAIN TERRANE	CENTRAL GNEISS TERRANE	ANNIEOPSQUOTCH TERRANE	ROCKY RIDGE POND TERRANE
	S8 Codroy* and Anguille* Groups: conglomerate, sandstone; minor, shale, limestone, dolomite, evaporites			
DEVONIAN			A6 Windsor Point Group*: grey sandstone, grit, mudstone, conglomerate (Emsian Fossils, ± 372 Ma)	R5 megacrystic biotite granite*
SILURIAN	S7 conglomerate		A5 red sandstone, conglomerate, rhyolite*(431 Ma), pyroclastic rocks	
	S6 Leucogranite, peralkaline granite, hybrid granite; minor gneiss(S3) and schist(S4)		A4 Rogerson Lake Conglomerate: conglomerate, sandstone	
ORDOVICIAN	S5 Table Head* and Grand Lake Brook* Groups: limestone, dolomite, marble, shale	C8 mafic dykes C7 diorite-tonalite*; minor granite C6 megacrystic biotite granite C5 leucogranite, granite, granodiorite C4 metagabbro, amphibolite C3 serpentinite, metagabbro C2 gabbro, diabase C1 hbl-biotite granite, granodiorite; migmatite mafic dykes C1 psammitic, pelitic and calcareous gneiss	A3 leucogranite, granite, granodiorite A2 Victoria Lake Group*: felsic to mafic volcanics, sandstone A1 gabbro*, diabase*, basalt; minor ultramafics (480 Ma)	R4 granoblastic quartz-feldspathic gneisses; minor granite; grano- diorite and tonalite R3 biotite granite, leucogranite, R2 Bay du Nord Group*: psammitic, pelitic and quartzitic metasediments; minor calcareous sediments and tuff mafic dykes R1 psammitic and pelitic gneiss
CAMBRIAN				
LATE UPPER PROTEROZOIC	S4 Fleur de Lys*: pelitic and calcareous schist; quartzite			
UPPER PROTEROZOIC	S3 mafic dykes hornblende-biotite gneiss, psammitic gneiss S2 tonalite, diorite, norite S1 anorthosite*			

GEOLOGY BY J.T. VAN BERKEL, H.P. JOHNSTON, K.L. CURRIE, J.C. MARTIN, S. DAWSON AND M.-A.J. PIASECKI, 1985. PARTLY AFTER HERD (1978; 12A/5, 12A/12), HERD AND DUNNING (1979; 12A/5), KNAPP ET AL. (1979; 12B/9E and 12A/12), MARTINEAU (1980; 12B/9E), KENNEDY (1981; 12B/9E and 12A/12), CHANDLER (1982; 12A/4 and 12A/5), KEAN (1983; 12A/4), DUNNING (1984; 12A/4 and 12A/5), WHALEN AND CURRIE (1983a and 1983b; Topsails Terrane) AND WILLIAMS (1985; 12B/9E).

Figure 19.2. Generalized geological map of the southern Long Range, southwest Newfoundland. An asterisk indicates that the age of the unit is reasonably well known. All other age assignments are speculative. Serpentinite and metagabbro (unit C4) could be as old as Cambrian, 20 to 30 Ma older than the dated unit A1. Unit R5 is either Upper Ordovician or Devonian. Some gabbroic rocks of units A1 and C3 may be as young as uppermost Lower Ordovician (Dunning, personal communication, 1985).

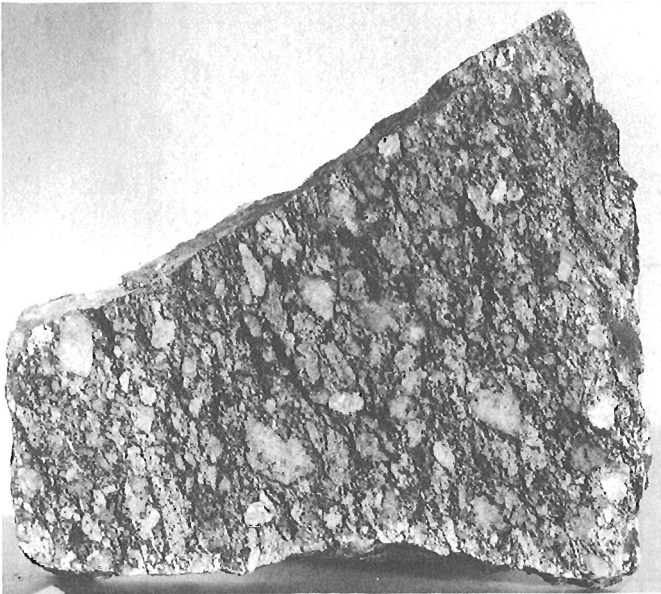


Figure 19.3. Conglomerate of Silurian (?) age or younger (unit S7), south of Grand Lake. Sample is 23 cm long. GSC-204318

Hornblende-biotite gneiss occurs south of Grand Lake (unit S3). These rocks consist of alternating, plagioclase- and hornblende-rich layers, a few millimetres thick, which may show intricate small-scale folding. Numerous layers of psammitic gneiss up to 10 cm thick form 10 to 60% of the outcrop. Biotite locally veneers the amphibole. Migmatitic "sweats" of granite occur as thin seams, or as spectacular ellipsoids up to 30 cm in diameter. No contact between the hornblende-biotite gneiss and the Steel Mountain anorthosite complex has been observed.

Metasedimentary schists of low metamorphic grade (unit S4) occur near the Long Range Fault in the Grand Lake area. Other units in this sequence, described by Martineau (1980) include marble and calcareous pelitic schists. Most outcrops of this sequence are strongly deformed, so that the schists are phyllitic, or show cataclasis. These rocks have been correlated with the late Precambrian-early Cambrian Fleur de Lys Super-group (Knapp et al., 1979; Kennedy, 1981; Hibbard, 1983a,b; Williams, 1985).

The hornblende gneiss and metasedimentary rocks are intruded by granites (unit S6) which may be massive, megacrystic or strongly foliated. Locally, these leucogranites are strongly peralkaline (riebeckite + aegirine +/- aenigmatite) as noted by Whalen and Currie (1984). The most typical feature of the peralkaline rocks is the widespread pseudomorphic replacement of the mafic minerals by ilmenite. Granite types range from one feldspar, peralkaline varieties, through various two feldspar leucogranites, to spectacular hybrid rocks, apparently formed by mixing of acid and basic components. They are correlated with similar Silurian intrusive rocks of the Topsails Terrane (Fig. 19.1; Whalen et al., in press).

Cambrian and/or Ordovician carbonate units of the Grand Lake Brook and Table Head groups (S5) are in thrust contact with the metaplutonic and metasedimentary rocks to the southeast (Kennedy, 1981; Williams, 1985). These carbonate units were not studied by us. A variably deformed, but low grade metamorphosed conglomerate (unit S7; Fig. 19.3) contains cobbles of granites resembling those of unit S6. The occurrence south of Grand Lake is probably surrounded by faults. The con-

glomerate is younger than the Silurian (?) granites (unit S6) and is correlated with Knapp's (1982) Silurian (?) Red Point Formation outcropping along the southwest shore of Glover Island (unit S7; Fig. 19.1, 19.2), 13 km to the northeast. Carboniferous conglomerate and sandstone of the Bay St. George Subbasin, mainly derived from sources southeast of the Long Range Fault (Knight, 1983), unconformably overlie the Steel Mountain anorthosite in the southwestern corner of the map area. West and northwest of the Steel Mountain anorthosite the contact is probably faulted (compare Riley (1962) and Knight (1983) who showed the whole contact as a fault).

Central Gneiss Terrane

The oldest rocks of the Central Gneiss Terrane comprise tightly folded, medium- to high-grade psammitic and calcareous gneisses (Fig. 19.4), with minor pelitic and marble interbeds (unit C1). Boudinaged amphibolitic layers and inclusions are common, and may be composed entirely of mafic minerals. Trains of amphibolite inclusions may be highly deformed and disrupted dykes. In the region south of Dennis Pond, paragneisses are well preserved, but elsewhere the gneisses are highly recrystallized, and commonly exhibit a medium grained granoblastic texture with prominent feldspar porphyroblasts (Fig. 19.5). Stromatic and nebulitic migmatites exhibit ghost stratigraphy suggesting that they are first cycle migmatites.

Psammitic paragneisses in the southeastern half of the Central Gneiss Terrane contain abundant gedrite-pyrite-magnetite instead of the more usual hornblende-biotite-magnetite assemblage. In the area around Cormacks Lake zones richer in pyrite weather out as conspicuous 1-5 m wide rusty zones (Herd and Dunning, 1979). Some quartzo-feldspathic gneisses east of Dashwoods Pond exhibit similar mineralogies (see also Chorlton, 1980, p. 8 for the southern extension of this unit). At present we are uncertain whether these gedrite-bearing gneisses represent a facies of a single paragneiss sequence, or should be considered as a separate unit.

Granitoid rocks (units C2 and C6) comprise the bulk of the Central Gneiss Terrane. In broad terms, the granitoid rocks fall into two categories, namely inclusion-rich foliated hornblende-biotite granite (unit C2), and presumably younger, leucogranite or biotite granite to granodiorite which are massive to weakly foliated (unit C6), or megacrystic (unit C7) with locally preferentially oriented feldspar megacrysts. Presently available information suggests units C6 and C7 are of similar age. Each granite type exhibits a considerable range in composition and structure, and further subdivision of the granite may be possible with additional fieldwork. The hornblende-bearing granite commonly develops adjacent to metasedimentary rocks, exhibits transitions to migmatite, and contains numerous inclusions of the paragneiss. The leucocratic and biotite granites to granodiorites in many cases form discrete, well-bounded plutons which are massive or weakly deformed.

The northeastern part of the Central Gneiss Terrane is underlain by weakly deformed gabbro and diabase (unit C3). Diabase has a subophitic texture and contains more plagioclase than the gabbro. Despite poor outcrop, it can be shown that the mafic rocks form large northeast striking units intruded by sheets and veins of granite to diorite, probably offshoots of units C6 and C8. Coarser grained gabbro (unit C3) forms bodies throughout the Central Gneiss Terrane, and locally exhibits well developed igneous layering (e.g. along the Burgeo Road (Route 480), 6 km east of the Long Range Fault). One gabbro body (16 km north-northeast of Cormacks Lake) contains a 200 m thick serpentinite (unit C4) layer. Zircon dating (Dunning, personal communication, 1985) and a K-Ar hornblende date (455 ± 65 Ma; R.K. Herd, in Stevens et al., 1982, p. 47) of the gabbro body (unit C3) at and south of the Burgeo Road (Route 480),



Figure 19.4. *Tightly to isoclinally folded psammitic and pelitic paragneisses (unit C1). Fold axes plunge steeply, axial planes dip subvertical. Geological hammer for scale. GSC-204311.*

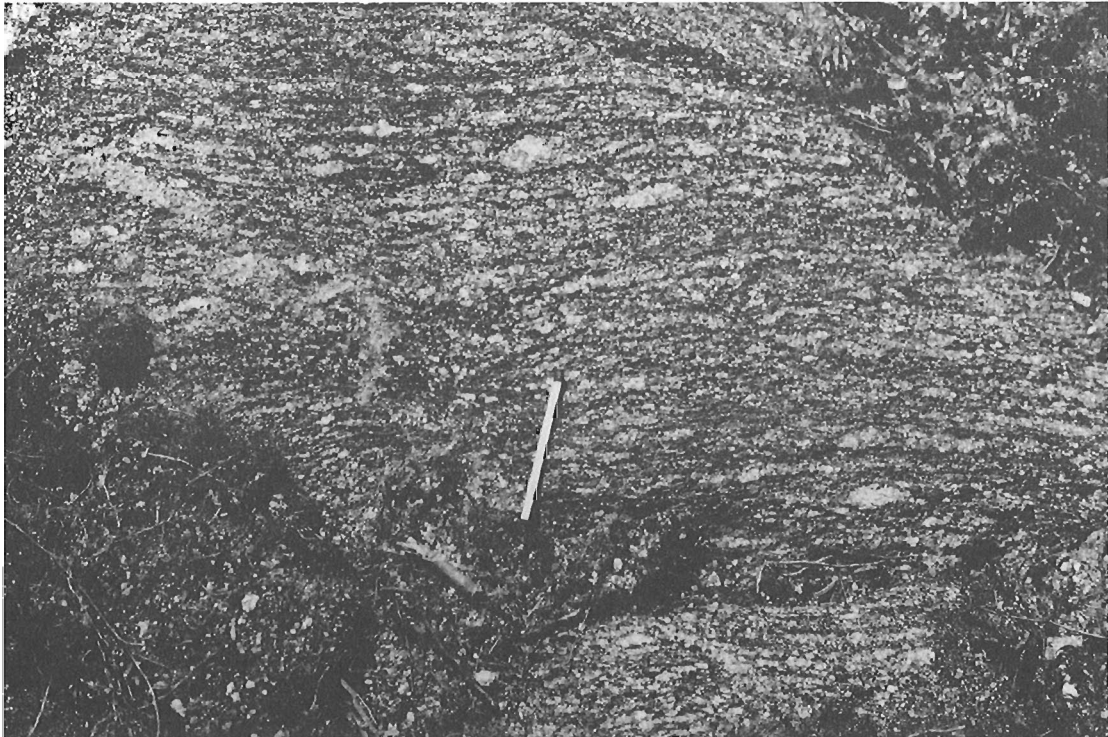


Figure 19.5. *Granoblastic psammitic paragneiss with feldspar porphyroblasts (unit C1). Match for scale. GSC-204311-C.*

5 km southeast of the Long Range Fault (Fig. 19.2), suggest that some of these mafic plutons may have been emplaced in the uppermost Lower Ordovician, although the zircons suggest a complex history.

Small diorite-tonalite plutons (unit C8) occur throughout the Central Gneiss Terrane. East of Dennis Pond, such a pluton clearly truncates a massive granite (unit C6). Diorite-tonalite plutons often contain mafic inclusions, possibly derived from the gabbro-diabase complex (unit C3). Dunning (personal communication, 1985) obtained an uppermost Lower Ordovician

age on zircons from these rocks along the Burgeo Road (Route 480), 7.5 km east of the Long Range Fault. A K-Ar determination on hornblende from a deformed tonalite, also along the Burgeo Road (Route 480) but more to the east, gave a similar age (455 ± 14 Ma; R.K. Herd, *in* Stevens et al., 1982, p. 46).

The most distinctive units of the Central Gneiss Terrane are thin (3-300 m), highly deformed serpentinite layers (unit C4), locally associated with deformed gabbro (units C3 and C5), in the paragneisses (unit C1). Commonly gneisses on opposite sides of such layers appear to be identical. Paragneiss-

Table 19.1: Pd, Pt and Au analyses (in ppb) of serpentized dunite(?), harzburgite and diabase from the Central Gneiss Terrane and the Annieopsquotch Terrane. Samples from ophiolite (?) slivers (SDZ = sheeted dyke zone). Analyses by Bondar-Clegg & Company Ltd., Ottawa. Method fire assay/DC plasma.

Sample number	Element (in ppb)			Location	Rock type	Unit
	Pd	Pt	Au			
5VM210A	< 2	< 15	27	10 km SSW of Dennis Pond	serpentized dunite (?)	C4
5VM210B	< 2	< 15	3	10 km SSW of Dennis Pond	same sample	C4
5VM226	< 2	< 15	< 2	south of Portage Lake	serpentized dunite	C4
5VM226A	< 2	< 15	< 2	south of Portage Lake	same sample	C4
5VM226B	4	< 15	< 2	south of Portage Lake	same sample	C4
5VM229	42	81	< 2	south of Portage Lake	harzburgite	C4
5VM568A	< 2	< 15	13	17 km SSW of Dennis Pond	serpentized dunite (?)	C4
5VM568B	< 2	< 15	6	17 km SSW of Dennis Pond	same sample	C4
5VM594A	< 2	< 15	< 2	18 km NNE of Cormacks Lake	serpentized dunite (?)	C4
5VM594B	8	< 15	< 2	18 km NNE of Cormacks Lake	same sample	C4
5VM608	4	< 15	3	Annieopsquotch Complex	m.gr. diabase in SDZ	A1
5VM610	< 2	< 15	9	Annieopsquotch Complex	very f.gr. diabase in SDZ	A1
5VM611	< 2	< 15	< 2	Annieopsquotch Complex	m.gr. diabase in SDZ	A1
5VM652	< 2	< 15	< 2	10 km NE of Dennis Pond	serpentized dunite (?)	C4
5VM740A	< 2	< 15	< 2	3 km SW of Little Grand Lake	harzburgite	C3
5VM740B	< 2	< 15	4	3 km SW of Little Grand Lake	harzburgite	C3

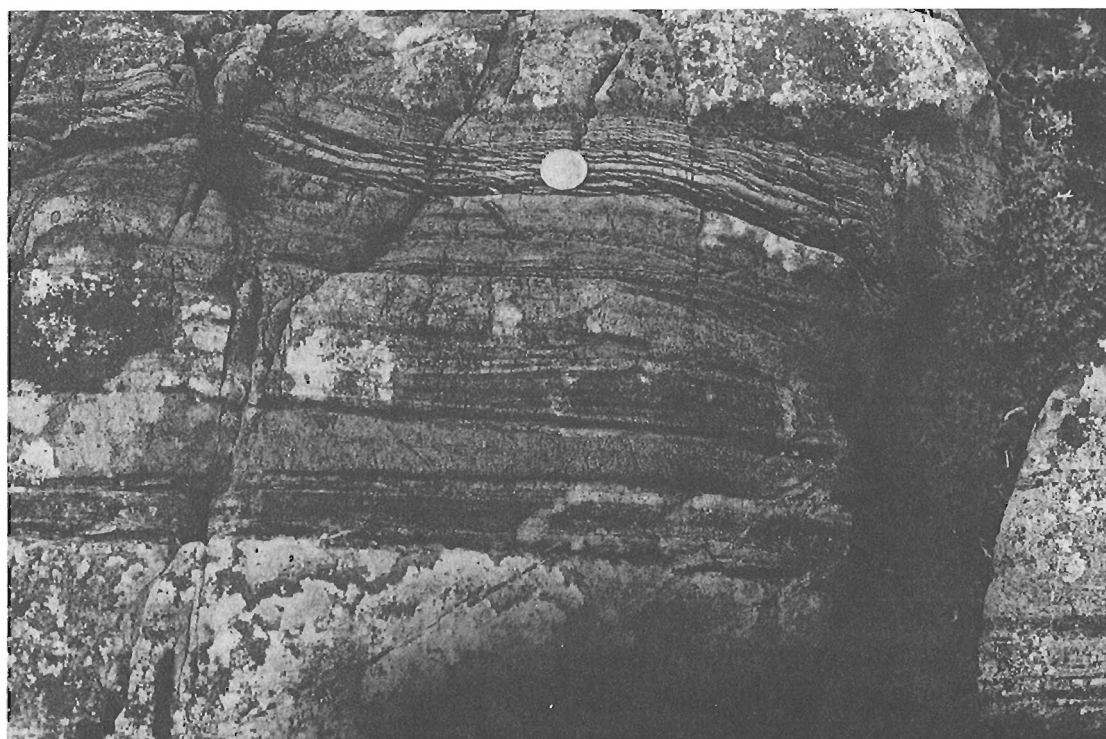


Figure 19.6. Highly deformed serpentinite with isoclinal folds (?), mostly with broken hinges. Dark layers oblique to dominant foliation (around coin) are later asbestos veins. Serpentinite strip (unit C4) 10 km south-southwest of Dennis Pond. GSC-304311-K.

serpentinite contacts are parallel to the foliation in each rock unit. Both units are highly deformed. Internally the mafic-ultramafic layers may be isoclinally folded (Fig. 19.6). Chromite and magnetite may occur as thin seams (Fig. 19.7) or as dispersed euhedral crystals. Veins of talc and asbestos are common. Serpentinite layers in the northwestern part of the terrane are commonly partially chloritized. The serpentinite layer south of Portage Lake exhibits well preserved igneous texture, and displays an east to west transition from serpentinized dunite to harzburgite with minor pyroxenite to gabbro. Veins of serpentinized dunite intrude the harzburgite and pyroxenite. This occurrence appears to be identical to ophiolitic allochthonous material of the Bay of Islands Igneous Complex of western Newfoundland (cf. Smith, 1958). However, it structurally lies next to a north-trending, steeply-dipping zone of pelitic paragneiss and migmatites. Serpentinite lenses or layers hosted by metasedimentary or granitoid rocks appear to be quite common in this part of western Newfoundland. They have been described by Herd (1978) and Herd and Dunning (1979) for the area around the Burgeo Road (Route 480) in the Puddle Pond map sheet (NTS 12A/5) and just to the west (Fig. 19.2), by Kennedy (1981) northwest of Grand Lake (Fig. 19.2) and by Chorlton (1983) and Dunning and Chorlton (1985, Fig. 3) for the Grandys Lake area (southwest of the map area).

Annieopsquotch Terrane

The region between the Lloyds River and Victoria River faults has been studied extensively (Dunning and Herd, 1980; Dunning, 1981, 1984; Chandler, 1982; Kean, 1983), mainly in connection with the Annieopsquotch ophiolite complex. According to Dunning (1981, 1984) and Dunning and Chorlton (1985) the region between King George IV Lake and Victoria Lake comprises a large ophiolite fragment of Lower Ordovician age (480 Ma), invaded by younger uppermost Lower Ordovician mafic igneous rocks to the southwest (Boogie Lake gabbro and related rocks, included in unit A1). We have examined only selected localities in the Annieopsquotch complex (map unit A1). In the sheeted dyke zone southwest of Loon Echo Pond (see Dunning and Herd, 1980, Fig. 35.1) we found about 70% of the outcrops contain a medium grained gabbro or diabase host which appears petrographically identical to the gabbro-diabase of the Central Gneiss Terrane. The dykes trend 160 to 190°.

Dunning (1984) predicted that a basal fault should bound the Annieopsquotch complex to the northwest. We have been unable to find such a basal fault. Two almost completely exposed sections from the high hills down to Lloyds River expose medium grained gabbro cut by fine grained mafic dykes and medium grained granitic veins. This succession closely resembles that northwest of Lloyds River Fault. The Lloyds River Fault itself forms a narrow ductile shear zone dipping 80° to the northwest. The fault affects both the mafic rocks (unit C3) and later granitoid intrusions (unit C6, A3). Southwest of Lloyds Lake, it is flanked on both sides by gabbro with minor granite veining. The Lloyds River Fault could offset the basal fault (Fig. 19.10) or be a ramp of a moderately to gently dipping basal fault.

Sheets and stocks of late tectonic granite to granodiorite and minor tonalite to diorite (unit A3) intrude the mafic rocks. These rocks are unconformably overlain by Silurian redbeds, with associated felsic volcanics (unit A5) which have been dated at 431 ± 5 Ma (Chandler and Dunning, 1983). These rocks are in turn unconformably overlain by grey sandstones (unit A6) from which Devonian (Emsian, about 372 Ma) spores have been recovered (C. McGregor, personal communication 1981, in Chandler, 1982).

Mafic and felsic volcanic rocks with minor clastic sedimentary rocks of the Victoria Lake Group (unit A2), outcrop in a narrow zone southeast of the Annieopsquotch complex (Dun-

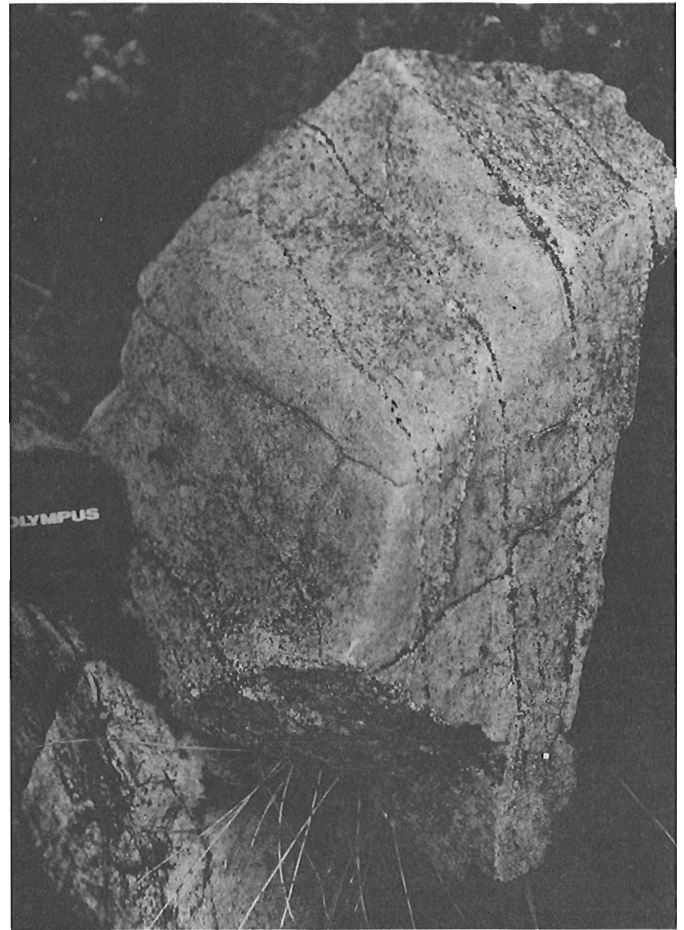


Figure 19.7. Chromite-magnetite layers (black) in serpentinite (unit C4) at Dennis Pond. GSC-204311-D.

ning, 1984; Kean, 1983). This zone pinches out to the southwest. A red, intensely flattened conglomerate (unit A4) of the southeastern margin of the zone has been correlated with the Silurian (?) Rogerson Lake conglomerate to the northeast (Kean, 1983). The whole region is intensely deformed and cut by numerous shear zones.

Rocky Ridge Pond Terrane

Southeast of the Victoria River Fault the dominant rock types are migmatitic psammitic paragneiss and subordinate pelitic schist (unit R1). Discrete plutons of granitoid rocks (enclosed by unit R1) consist of rather leucocratic, medium grained biotite granite (unit R3). Near its contact with the paragneisses, the leucocratic biotite granite tends to be finer grained and contains hornblende. Unit R1 grades to medium grained granoblastic quartzo-feldspathic gneisses (unit R4). The grain size of these gneisses is so coarse (5 mm) that they can easily be confused with felsic intrusive rocks. Granite, granodiorite and tonalite (part of unit R4) dominate this neosome (Kean, 1983) forming 50 to 100 m thick sheets in the paragneisses. The megacrystic biotite granite (unit R5) is probably of Devonian age (B.F. Kean, personal communication, 1986). It contains numerous enclaves of Bay du Nord clastic sediments (unit R2) which were also seen in rocks of unit R4. Both granites and paragneisses contain narrow, late, biotite-rich shear zones. These shear zones parallel the Victoria River Fault.

Deformation and metamorphism

Northwest of the Long Range Fault, medium- to high-grade fabrics (Grenvillian?) occur in the hornblende-biotite gneiss. The Steel Mountain anorthosite does not exhibit a pervasive penetrative foliation, presumably because it behaved as a rigid block during deformation. Later metasediments (unit S4) exhibit low- to medium-grade mineral assemblages. This later metamorphism has altered much of the medium- to high-grade fabrics in the older rocks.

In the Central Gneiss Terrane the oldest rocks, the paragneisses, were tightly to isoclinally folded during regional medium- to high-grade metamorphism. The axial planes of macroscopic and mesoscopic folds are subvertical and strike northwest to northeast, with a predominance of north to northwest strikes (e.g. Herd and Dunning, 1979). Large gabbro-diorite bodies were not affected by this regional deformation and associated medium- to high-grade metamorphism, either because they behaved as rigid blocks (Dunning, 1984), or because they are younger. They only have the later low grade metamorphic fabric. Serpentinized ultramafic-gabbro sheets have also been highly deformed and metamorphosed, but the talc-chlorite-serpentine dominant mineralogy of these bodies demonstrates that they either have undergone extensive retrogression or a second phase of low-grade metamorphism, similar to their host rocks. Late-tectonic granite, granodiorite and tonalite-diorite bodies exhibit only a weakly preferred orientation of mafic minerals and may be completely massive.

Ten kilometres south-southwest of Dennis Pond, two narrow north-trending zones exhibit a high concentration of foliation-parallel quartz veins with quartz plates (cf. Piasecki, 1980), indicating that these zones have undergone high strain. We interpret them to be major shear zones. The western zone separates calcareous gneisses from psammitic gneisses. The eastern zone lies within the calcareous gneisses, but contains a 5-10 m thick, more than 500 m long, highly deformed serpentinite layer. These shear zones predate the emplacement of the late tectonic granitoid rocks as they are intruded by those granitoids.

Regional northeast-striking ductile fault zones of low metamorphic grade overprint all earlier fabrics. The latest fabrics are high level, brittle deformation zones, such as that exposed south of Grand Lake along the Long Range Fault (Fig. 19.2). Megacrystic granite on the east side of the fault exhibits a pervasive cataclastic fabric, and portions of the rock are reduced to mica schist along anastomosing shears (Fig. 19.8). Garnet schist on the west side of the fault is highly crenulated, and contains numerous tension gashes filled with quartz fibres grown perpendicular to the gashes. Along the Burgeo Road (Route 480), just west of the trace of the Long Range Fault, anorthositic rocks exhibit an earlier, medium grade gneissic fabric overprinted by a low grade, laminated, fine grained fabric (Fig. 19.9). Both fabrics trend north-northwest. This indicates a very long and complex history for the Long Range Fault. Many small ductile and ductile/brittle shear zones occur throughout the southern Long Range. They are usually oriented parallel to the major northeast-striking regional faults, but some north- to north-northwest-trending zones were also observed in the Central Gneiss Terrane.

Economic geology

The Steel Mountain anorthosite contains numerous small pockets of titaniferous magnetite. Baird (1943, 1954) described large lenses north of Flat Bay Brook, which contained about 7% TiO_2 . Psammitic paragneisses (unit C1) locally contain accessory amounts of magnetite or pyrite, or both. Gedrite-bearing units may be particularly rich in pyrite, resulting in a distinctive rusty

weathering surface. Gold assays of 12 samples from various localities with "rusty" gneisses show a concentration below detection limit (2 ppb). A concordant magnetite layer 3-20 cm wide and more than 2 m long was observed in quartzitic and pelitic gneiss south of Dennis Pond. One outcrop of layered gabbro (unit C3) on Burgeo Road (Route 480), 7.5 km east of the Long Range Fault, contains layers rich in magnetite.

Serpentinite layers (unit C4) locally contain up to 10% chromite and magnetite in the form of thin seams (Fig. 19.7) or as dispersed euhedral crystals. Au-Pt-Pd analyses (Table 19.1) of various serpentinite layers (unit C4) yield up to 27 ppb Au, below detection limit Pt (15 ppb), and up to 8 ppb Pd. A harzburgite (sample 5VM229) with primary igneous textures which occurs together with the serpentinite (unit C4) south of Portage Lake contains 81 ppb Pt, 42 ppb Pd, but below detection limit Au (2 ppb). Assays of serpentinized dunite from this locality (sample 5VM226) show a concentration below detection limit for Au (2 ppb), Pt (15 ppb) and Pd (2 ppb). A harzburgite (sample 5VM740; part of unit C3) 3 km southwest of Little Grand Lake contains very little Au, Pt and Pd.

Discussion

The mapping completed this year raises a host of questions about the tectonics of southwestern Newfoundland. Williams and St-Julien (1982) considered that a major feature of the Appalachian Orogen, the Baie Verte - Brompton Line, divided autochthonous, continental-based material to the west from oceanic, possibly allochthonous material to the east. They showed the Baie Verte-Brompton Line passing down Grand

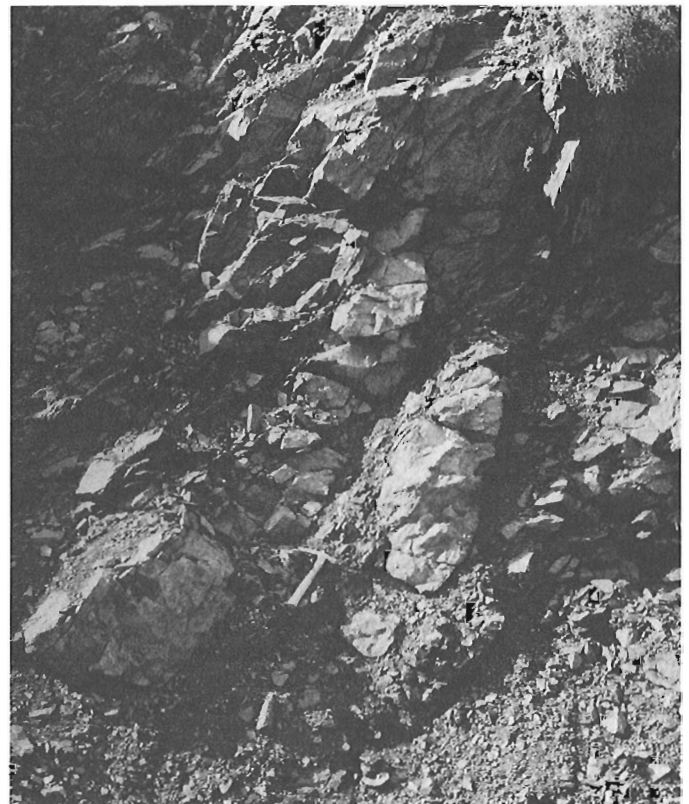


Figure 19.8. Megacrystic granite (unit C7) with large anastomosing shears (e.g. fine grained highly fractured material at geological hammer). Long Range Fault outcrop south of Grand Lake. GSC-204311-E.

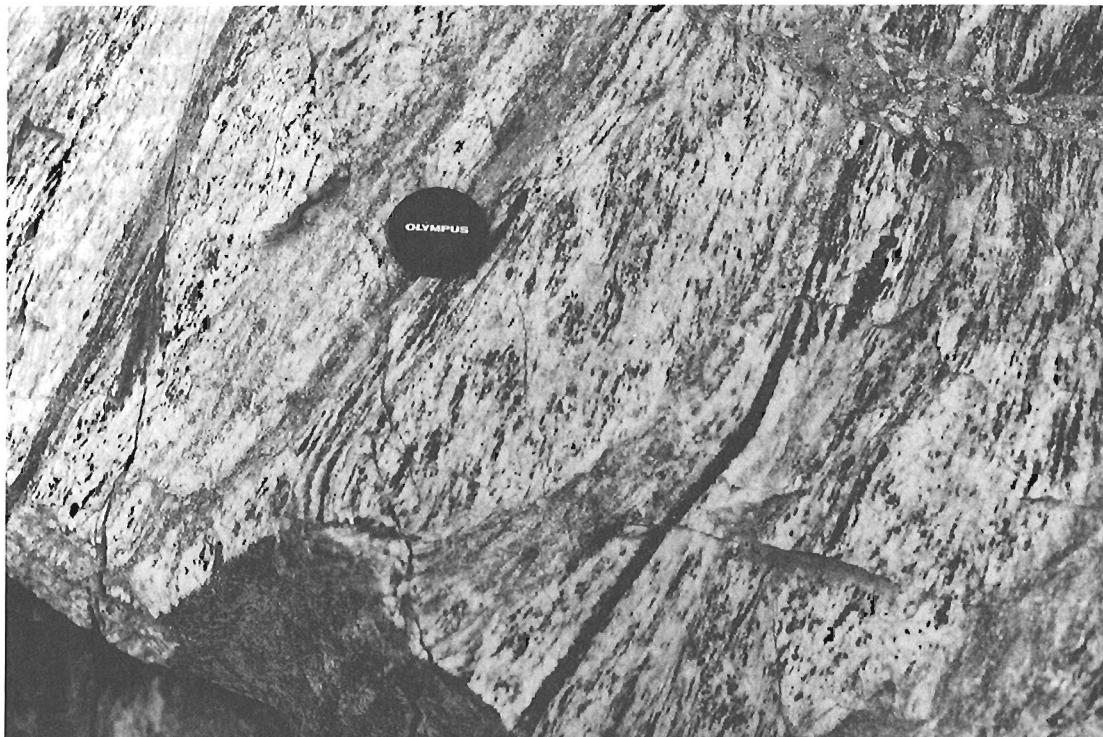


Figure 19.9. Anorthositic gneiss (unit S1) with later fine grained shears (grey; e.g. at lens cap). Outcrop on Burgeo Road (Route 480), just west of the Long Range Fault. GSC-204311-E.

Lake, and then stepping, along Little Grand Lake, to the Lloyds and Victoria River faults. Our mapping of the Central Gneiss Terrane shows it to be dominated by metasediments of shelf affinities (quartz-rich psammitic and calcareous gneisses with minor pelitic and marble interbeds) with potassium feldspar-rich granitic rocks. Except for mafic-ultramafic serpentinitized layers, lithologies correlative to the Central Mobile Belt of Newfoundland appear to be absent. On the other hand, the north-eastern part of the Central Gneiss Terrane contains a gabbro-diabase terrane which we cannot distinguish lithologically from the Annieopsquotch Terrane, except that it contains numerous granite to diorite intrusions (units C6 and C8).

We suggest that in southwest Newfoundland the Baie Verte – Brompton line may not be a narrow zone but a wide zone composed of stacked thrust slices of continental and oceanic/island arc material. We envisage the width of this zone to be at least 50 km and to span the entire Central Gneiss Terrane. Our major argument is the widespread distribution of mafic-ultramafic serpentinitized layers in paragneisses. Such strips and inclusions have been found from the south coast of Newfoundland, northwest of the Cape Ray fault (Chorlton, 1983; Dunning and Chorlton, 1985, Fig. 3), as far as the northwest side of Grand Lake (Kennedy, 1981), spanning the two western terranes described by us. Some occurrences exhibit obvious ophiolitic affinities, e.g. the outcrop south of Portage Lake. We interpret the mafic-ultramafic strips to map the trace of major thrust faults (Fig. 19.10). In the map area they coincide with high strain zones. The Annieopsquotch – King George IV ophiolite sheet dips moderately to steeply to the southeast (Dunning, 1984) and may be floored by a thrust fault (Fig. 19.10). The apparent absence of a basal décollement beneath the Annieopsquotch complex could be attributed to west side down movements along the later, steeply dipping Lloyds River Fault. The basal décollement may surface west of the gabbro-diabase occurrence (unit C3) which is also considered to be part of the Annieopsquotch – King George IV ophiolite sliver. A moderate

to steep southeast dip for this ophiolite sliver along the Burgeo Road (Fig. 19.10) is confirmed by asymmetric peaks in gravity and magnetic profiles (H. Miller, personal communication, 1986).

North- to northwest-trending structures are ubiquitous in the Central Gneiss Terrane. Such structures were first observed around Cormacks Lake by Herd and Dunning (1979) who argued that they were older than the northeast-trending structures. Although the exact timing of deformation and metamorphism remains speculative in the absence of sufficient dating, some clues can be obtained if it is assumed that the entire gabbro-ultramafic suite is of Lower Ordovician age, as suggested by Dunning (1984) and Dunning and Krogh (1985). The metamorphic and structural complexity of the gneisses suggests that several older events are present, which would imply a Precambrian to Cambrian age for the paragneisses. The mafic-ultramafic rocks are cut by granitoid rocks, which must therefore be younger than early Ordovician. The dated Silurian rocks (Chandler and Dunning, 1983) do not contain any hint of younger granitoid plutonism. Hence it seems probable that much of the plutonism in the Central Gneiss Terrane may be middle Ordovician to Silurian (see also Dunning and Chorlton, 1985). Extensive plutonism of this age has been documented in western Newfoundland by Whalen et al. (in press). Except for the megacrystic granite in the Rocky Ridge Pond Terrane, we see no strong evidence for Devonian (Acadian) plutonism or metamorphism in the parts of the southern Long Range examined by us.

An uppermost Lower Ordovician zircon age obtained from a tonalite-diorite (unit C8; Dunning, personal communication, 1985) is compatible with K-Ar mineral ages of similar rocks. This age suggests that there was at least one major event of granitoid plutonism (diorite to granite) around 460-450 Ma, 20 to 30 Ma after the youngest known ophiolites (Dunning and Krogh, 1985).

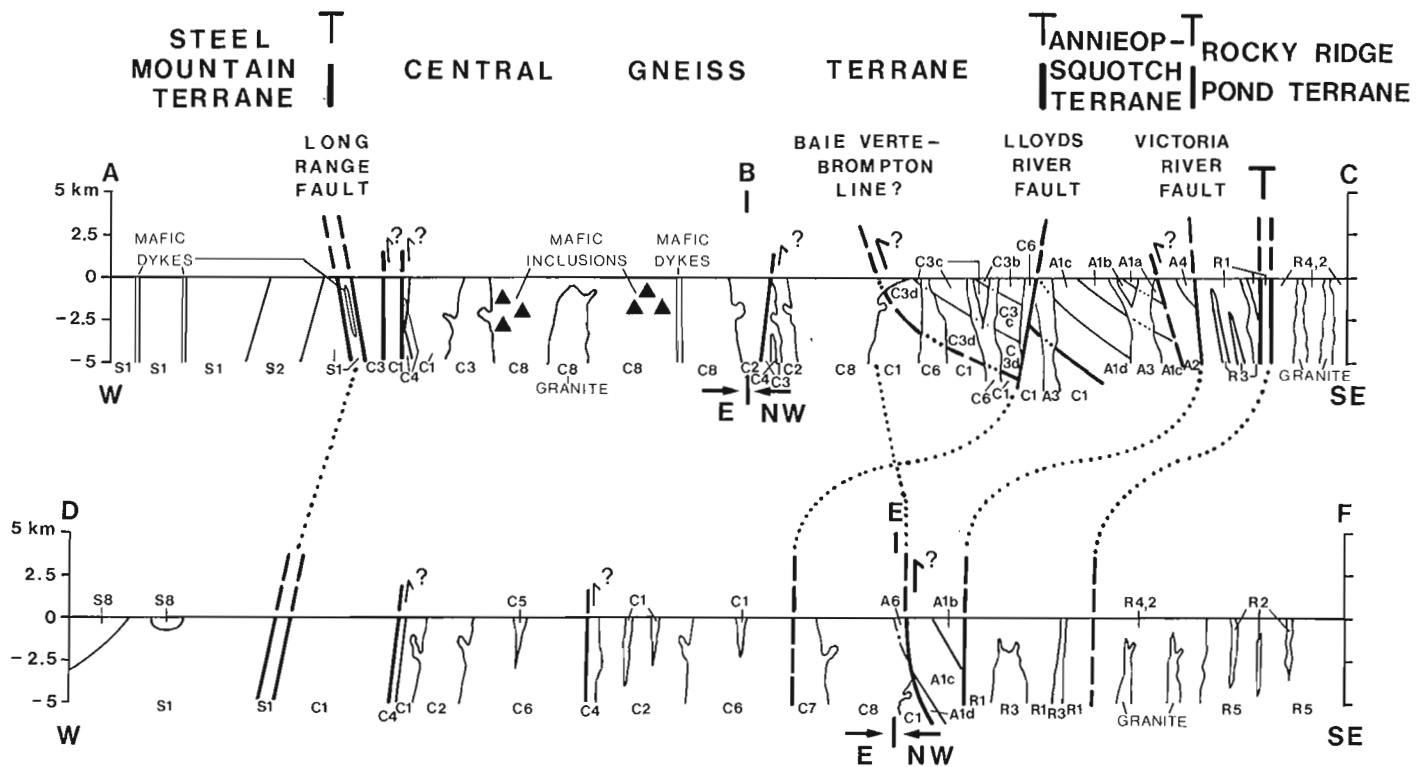


Figure 19.10. Schematic profiles across the map area. For profile lines see Figure 19.1. For symbols see legend of Figure 19.2. High strain zones characterized by the occurrence of serpentine strips are interpreted to be early thrust faults (marked with an arrow). The thrust faults are steepened by continuing deformation or another phase of crustal shortening. Steep to vertical, later faults (marked with a T) may coincide with terrane boundaries. Letters a, b, c and d added to the symbols for the ophiolitic rocks (symbols C3 and A1) refer to: a, pillow lava zone; b, sheeted dyke zone; c, gabbro zone; and d, zone with mainly ultramafic rocks.

Stratigraphic correlation between the various terranes is speculative at this stage of the investigation, particularly in the absence of adequate radiometric age determinations. However a number of possible correlations suggest themselves. These have been synthesized in the legend of Figure 19.2, which we consider a tentative hypothesis to be tested by further mapping. Our correlation implies that the migmatization and formation of granite gneiss is most likely to be late Precambrian to Cambrian, predating emplacement of mafic rocks, which are assumed to be Lower Ordovician. The Long Range, Lloyds River and Victoria River faults, are major northeast-striking transcurrent faults with moderate to large displacement. Because of the large displacement along the Long Range and Victoria River faults, rock types and metamorphic grade changes across these faults.

Gold deposits in Newfoundland tend to be related to ultramafic rocks of ophiolitic affinity (J. Lydon, personal communication, 1986), or to major ductile shear zones, e.g. the Cape Ray Fault in southwest Newfoundland (Wilton, 1985) which coincides with a boundary between two contrasting terranes (Brown, 1975; Chorlton, 1980, 1983). In the map area the ultramafic rocks occur in high strain zones characterized by numerous shear-plane parallel quartz veins and lenses. Shear-plane parallel quartz veins and lenses also occur in the major northeast-striking transcurrent fault zones which separate terranes. Besides 1:50 000 scale regional mapping in NTS 12B/1, 12B/8 and 12B/9E, detailed studies in key areas will be undertaken in the 1986 field season to analyze the relation between high strain zones, ultramafic rocks, quartz veins and gold potential.

Acknowledgments

We are greatly indebted to M.A.J. Piasecki, University of Hull (England) for field mapping assistance and stimulating discussion. We also acknowledge the assistance of Jeff Martin and Steve Dawson. The manuscript was reviewed by S.P. Colman-Sadd, S.J. O'Brien, B.F. Kean, W.L. Dickson, G.R. Dunning, L. Chorlton, R.K. Stevens and J. Lydon. Viking Helicopter of Pasadena supplied and moved the field parties efficiently. We thank the Pasadena Forest Research Station, Environment Canada, for supplying base camp space and logistical help. We thank Kruger Inc., and Abitibi-Price Ltd for permission to use woods roads.

References

- Baird, D.M.
 1943: Titaniferous magnetites in anorthosite, east of St. Georges, Newfoundland; unpublished M.Sc. thesis, University of Rochester, Rochester, New York, U.S.A., 102 p.
 1954: The magnetite and gypsum deposits of the Sheep Brook-Lookout area; Geological Survey of Canada, Bulletin 27, p. 20-41.
- Brown, P.A.
 1975: Basement-cover relations in southwest Newfoundland; unpublished Ph.D. thesis, Memorial University of Newfoundland, St. John's, Newfoundland, 221 p.

- 1977: Geology of the Port aux Basques map area (11O/10), Newfoundland; Newfoundland Department of Mines and Energy, Mineral Development Division, Report 77-2, 11 p.
- Chandler, F.W.
1982: Sedimentology of two middle Paleozoic terrestrial sequences, King George IV Lake area, Newfoundland and some comments on regional paleoclimate; *in* Current Research, Part A, Geological Survey of Canada, Paper 82-1A, p. 213-219.
- Chandler, F.W. and Dunning, G.R.
1983: Fourfold significance of an early Silurian U-Pb zircon age from rhyolite in redbeds, southwest Newfoundland; *in* Current Research, Part B, Geological Survey of Canada, Paper 83-1B, p. 419-421.
- Chorlton, L.
1980: Geology of the La Poile River area (11O/16), Newfoundland; Newfoundland Department of Mines and Energy, Mineral Development Division, Report 80-3, 86 p.
1983: Geology of the Grandys Lake area (11O/15), Newfoundland; Newfoundland Department of Mines and Energy, Mineral Development Division, Report 83-7, Part 1, 116 p.
- Colman-Sadd, S.P.
1974: Iron deposits of the Indian Head Range; *in* Metallogeny and Plate Tectonics. A Guidebook to Newfoundland Mineral Deposits, ed. D.F. Strong; NATO Advanced Studies Institute, p. 150-158.
- Dunning, G.R.
1981: The Annieopsquotch ophiolite complex, southwestern Newfoundland, and its regional relationships; *in* Current Research, Part B, Geological Survey of Canada, Paper 81-1B, p. 11-15.
1984: The geology, geochemistry, geochronology and regional setting of the Annieopsquotch Complex and related rocks of southwest Newfoundland; unpublished Ph.D. thesis, Memorial University of Newfoundland, St. John's, Newfoundland, 403 p.
- Dunning, G.R. and Chorlton, L.B.
1985: The Annieopsquotch ophiolite belt of southwest Newfoundland: Geology and tectonic significance. Geological Society of America, Bulletin, v. 96, p. 1446-1476.
- Dunning, G.R. and Herd, R.K.
1980: The Annieopsquotch ophiolite complex, southwest Newfoundland, and its regional relationships; *in* Current Research, Part A, Geological Survey of Canada, Paper 80-1A, p. 227-234.
- Dunning, G.R. and Krogh, T.E.
1985: Geochronology of ophiolites of the Newfoundland Appalachians; Canadian Journal of Earth Sciences, v. 22, p. 1659-1670.
- Herd, R.K.
1978: Geology of Puddle Pond area, Red Indian Lake map sheet, Newfoundland; *in* Current Research Part A, Geological Survey of Canada, Paper 78-1A, p. 195-197.
- Herd, R.K. and Dunning, G.R.
1979: Geology of Puddle Pond map area, southwestern Newfoundland; *in* Current Research, Part A, Geological Survey of Canada, Paper 79-1A, p. 305-310.
- Heyl, A.V. and Ronan, J.J.
1954: The iron deposits of Indian Head area; *in* Contributions to the Economic Geology of Western Newfoundland, Geological Survey of Canada, Bulletin 27, p. 42-62.
- Hibbard, J.
1983a: Notes on the metamorphic rocks in the Corner Brook area (12A/13) and regional correlation of the Fleur de Lys Belt, western Newfoundland; *in* Current Research, Newfoundland Department of Mines and Energy, Mineral Development Division, Report 83-1, p. 41-50.
- Hibbard, J. (compiler)
1983b: Geology of the Island of Newfoundland; Newfoundland Department of Mines and Energy, Mineral Development Division, Map 83-106.
- Kean, B.F.
1977: Geology of the Victoria Lake map area (12A/6), Newfoundland; Newfoundland Department of Mines and Energy, Mineral Development Division, Report 77-4, 11 p.
1983: Geology of the King George IV Lake map area (12A/4); Newfoundland Department of Mines and Energy, Mineral Development Division, Report 83-4, 67 p.
- Kennedy, D.P.
1981: Geology of the Corner Brook Lake area, western Newfoundland; unpublished M.Sc. thesis, Memorial University of Newfoundland, St. John's, Newfoundland, 370 p.
- Keppie, J.D.
1986: The Appalachian collage. *in* The Caledonide Orogen, Scandinavia and Related Areas ed. D.G. Gee and B. Sturt; John Wiley and Sons Inc., New York.
- Knapp, D.A.
1982: Ophiolite emplacement along the Baie Verte - Brompton Line at Glover Island, western Newfoundland; unpublished Ph.D. Thesis, Memorial University of Newfoundland, St. John's, Newfoundland, 337 p.
- Knapp, D.A., Kennedy, D.P., and Martineau, Y.A.
1979: Stratigraphy, structure and regional correlation of rocks at Grand Lake, western Newfoundland; *in* Current Research, Part A, Geological Survey of Canada, Paper 79-1A, p. 317-325.
- Knight, I.
1983: Geology of the Carboniferous Bay St. George Subbasin, western Newfoundland; Newfoundland Department of Mines and Energy, Mineral Development Division, Memoir 1, 358 p.
- Martineau, Y.A.
1980: The relationships among rock groups between the Grand Lake Thrust and Cabot Fault, western Newfoundland; unpublished M.Sc. thesis, Memorial University of Newfoundland, St. John's, Newfoundland, 150 p.
- Piasecki, M.A.J.
1980: New light on the Moine rocks of the Central Highlands of Scotland. Geological Society of London, Journal, v. 137, p. 41-59.

- Riley, G.C.
 1957: Red Indian Lake (west half), Newfoundland; Geological Survey of Canada, Map 8-1957 (scale 1:250 000 with marginal notes).
 1962: Stephenville map area, Newfoundland; Geological Survey of Canada, Memoir 323, 72 p.
- Simmons, E.C. and Hanson, G.N.
 1978: Geochemistry and origin of massif-type anorthosites; *Contributions to Mineralogy and Petrology*, v. 66, p. 119-135.
- Smith, C.H.
 1958: Bay of Islands Igneous Complex, western Newfoundland; Geological Survey of Canada, Memoir 290, 132 p.
- Stevens, R.D., Delabio, R.N. and Lachance, G.R.
 1982: Age determinations and geological studies. K-Ar isotopic ages, Report 16. Geological Survey of Canada, Paper 82-2, 56 p.
- Whalen, J.B. and Currie, K.L.
 1983a: The Topsails igneous terrane of western Newfoundland; *in* Current Research, Part A, Geological Survey of Canada, Paper 83-1A, p. 15-23.
 1983b: Geology of the Topsails igneous terrane; Geological Survey of Canada, Open File Report 923 (1:100 000 scale map with marginal notes).
 1984: Peralkaline granite near Hare Hill, south of Grand Lake, Newfoundland; *in* Current Research, Part A, Geological Survey of Canada, Paper 84-1A, p. 181-184.
- Whalen, J.B., Currie, K.L. and van Breemen, O.
 – Episodic Ordovician-Silurian plutonism in the Topsails igneous terrane, western Newfoundland. *Canadian Journal of Earth Sciences* (in press).
- Williams, H.
 1978: Tectonic Lithofacies Map of the Appalachian Orogen; Memorial University of Newfoundland, Map No. 1.
 1979: Appalachian Orogen in Canada; *Canadian Journal of Earth Sciences*, v. 16, p. 792-807.
 1985: Geology, Stephenville map area, Newfoundland; Geological Survey of Canada, Map 1579A (scale 1:100 000 with marginal notes).
- Williams, H. and St-Julien, P.
 1982: The Baie Verte – Brompton Line: Early Paleozoic continent-oceanic interface in the Canadian Appalachians; *in* Major Structural Zones and Faults of the Northern Appalachians, ed. P. St-Julien and J. Béland; Geological Association of Canada, Special Paper 24, p. 177-207.
- Wilton, D.H.C.
 1983: The geology and structural history of the Cape Ray Fault Zone in southwestern Newfoundland; *Canadian Journal of Earth Sciences*, v. 20, p. 1119-1133.
 1985: REE and background Au/Ag evidence concerning the origin of hydrothermal fluids in the Cape Ray electrum deposits, southwestern Newfoundland; *Canadian Institute of Mining and Metallurgy, Bulletin*, v. 78, p. 48-59.

Late Quaternary land-sea correlations, northern Labrador and Labrador Shelf

Project 810037

Peter U. Clark¹ and H.W. Josenhans
Atlantic Geoscience Centre, Dartmouth

Clark, P.U. and Josenhans, H.W., Late Quaternary land-sea correlations, northern Labrador and Labrador Shelf; in Current Research, Part B, Geological Survey of Canada, Paper 86-1B, p. 171-178, 1986.

Abstract

Late Quaternary glacial and postglacial units in the Torngat Mountains are correlated with units mapped on the adjacent continental shelf. Correlations are based on acoustic stratigraphic continuity from shelf to fiord bottom sediments, composition, and radiocarbon dating control. We suggest that pre-late Wisconsinan glacial sediments in the Torngat Mountains correlate with (unit 3a) on the shelf. Late Wisconsinan glacial sediments on land south of Ikkudliayuk Fiord correlate with Upper Till (unit 3b) on the shelf, while late Wisconsinan glacial sediments north of Ikkudliayuk Fiord correlate with Hudson Strait Till (unit 3c). Postglacial raised marine deposits on land correlate with glaciomarine sediments (unit 4) on the shelf.

Résumé

Le présent document compare des unités glaciaires et post-glaciaires du Quaternaire récent dans les monts Torngat avec les unités cartographiées de la plate-forme continentale contiguë. Ces comparaisons sont basées sur la continuité stratigraphique acoustique établie à partir de la plate-forme jusqu'aux sédiments du fond du fjord, et sur la composition et le contrôle par datation au carbone radioactif. On suppose que les sédiments glaciaires de toute la période s'échelonnant du pré-Wisconsinien jusqu'à la fin de cette ère dans les monts Torngat peuvent être corrélés avec les sédiments glaciaires de la même période (unité 3a) sur la plate-forme continentale. Les sédiments glaciaires du Wisconsinien supérieur sur les terres au sud du fjord Ikkudliayuk peuvent être mis en corrélation avec le till superficiel (unité 3b) de la plate-forme continentale, alors que les sédiments glaciaires du Wisconsinien supérieur au nord du fjord Ikkudliayuk correspondent au till du détroit d'Hudson (unité 3c). Les dépôts marins soulevés datant de la période post-glaciaire que l'on retrouve sur les terres correspondent aux sédiments glaciomarins (unité 4) de la plate-forme.

¹ Department of Geological Sciences, University of Illinois, Chicago, IL 60680

Introduction

For over 100 years, investigators have debated the extent of the late Wisconsinan Laurentide Ice Sheet in the coastal Torngat Mountains, Labrador (Lieber, 1861; Bell, 1884; Koch, 1891; Daly, 1902; Coleman, 1921; Odell, 1938; Flint, 1943; Tanner, 1944; Ives, 1957, 1958, 1976, 1978; Løken, 1962a; Mayewski et al., 1981; Hughes et al., 1981; Clark, 1984; Prest, 1984). More recently, the debate has included the adjacent continental shelf (Fillon and Harnes, 1982; Josenhans, 1983; Josenhans et al., in press). In this paper, we correlate late Quaternary glacial and post-glacial sediments between the Torngat Mountains and adjacent continental shelf (Fig. 20.1). We propose that glacial deposits in the Torngat Mountains were deposited by eastward-flowing outlet glaciers draining the Laurentide Ice Sheet. These glaciers advanced onto the continental shelf, where they coalesced and deposited regional till sheets. The extent of ice onto the shelf was probably controlled by the net discharge of the outlet glaciers. Ice sheet advance off the coast of the Torngat Mountains onto the shelf during the late Wisconsinan was less extensive than north (Hudson Strait) or south of the Torngat Mountains.

Physiography

The physiography of northern Labrador is dominated by the Torngat Mountains which have relief in excess of 1300 m. They form a highly dissected uplifted plateau, the elevation of which decreases to the west towards Ungava Bay. The location of stream valleys is largely structurally controlled and glaciation has further modified these into typical U-shaped valleys. These U-shaped valleys extend offshore to the eastern edge of the Precambrian basement contact.

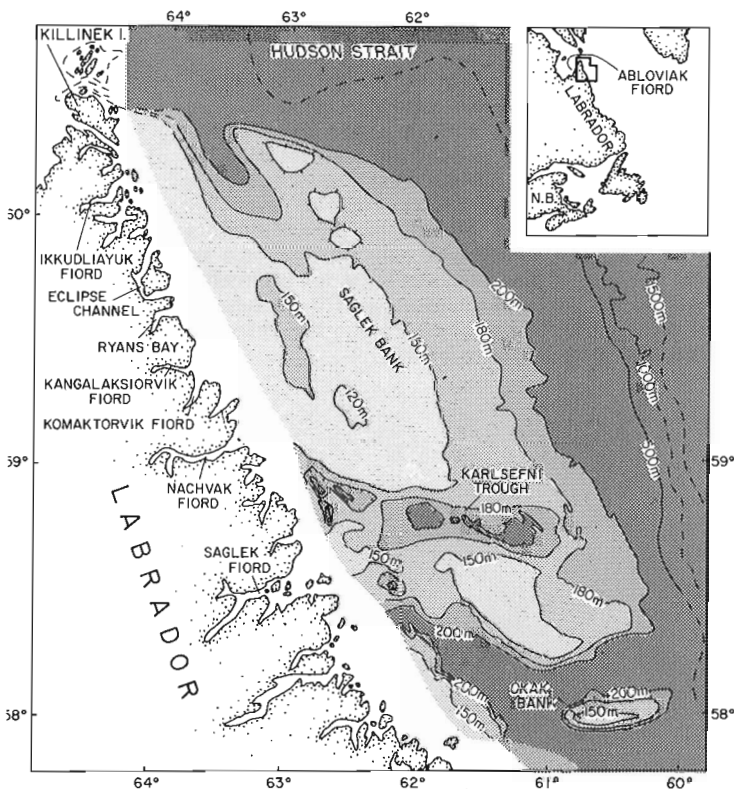


Figure 20.1. Location map, generalized bathymetry, and place names referenced in the text.

Bedrock geology

The bedrock of the Torngat Mountains has been mapped by Taylor (1979), Greene (1970), Wardle (1983), and Ryan et al. (1983). Taylor (1971) identified Precambrian Nain and Churchill structural geological provinces. Archean granites and quartzofeldspathic gneisses, dating to 3.6 Ga (Hurst et al., 1975), underlie most of the Nain Province. Churchill Province rocks are Proterozoic age and include gneisses, quartzites, and marbles (Taylor, 1979). The Ramah Group, which outcrop between Saglek Fiord and Nachvak Fiord, is an Apebian supracrustal sequence comprised of folded siliciclastic, argillaceous, and carbonate rocks, and has been included within the Churchill Province (Morgan, 1975).

The bedrock underlying the Labrador Shelf includes Precambrian crystalline rock forming an inner shelf, adjacent to the mainland, and sedimentary rocks of early Paleozoic to Cretaceous-Tertiary ages forming an outer shelf (Sanford et al., 1979).

Methods

On land, surficial deposits were mapped in the areas of Saglek, Nachvak, Komaktorvik, Kangalaksiorvik, and Ryans Bay fiords (Fig. 20.1) during the 1981, 1982, 1984, and 1985 field seasons. In addition, deposits in interior Labrador-Quebec between Kangalaksiorvik and Ablöviak fiords were mapped during 1982. The remaining area of the Torngat Mountains north to Killinek Island was mapped by air photo interpretation.

Soils developed in glacial deposits were described from hand-dug soil pits on stable sites on moraine crests. Soil description methods and horizon nomenclature follow those of Birkeland (1984). Unweathered glacial deposits were sampled for analysis of matrix (<2 mm) mineralogy and clast (>4 mm) lithology. Till composition north of Eclipse Channel to Killinek Island was reported by Bell (1884) and Løken (1964).

Offshore, the stratigraphic placement and lateral distribution of Quaternary sediments was mapped by a combination of medium (40 cubic inch airgun) and high (Huntec DTS) resolution seismic systems. These acoustic stratigraphic units were sampled where they occur within reach of the piston and grab samplers. The samples were analyzed for sedimentological structure, texture, radiocarbon dates, lithology, foraminifera, and pollen (Josenhans et al., in press).

Late Quaternary sediments

Torngat Mountains

Moraines. Moraines delimiting the extent of late Wisconsinan Laurentide ice draining east through the Torngat Mountains and recessional phases are common throughout the mountains (Fig. 20.2). These moraines are characterized by well-preserved, massive, high-crested morphologies that have undergone little post-depositional modification (Fig. 20.3). The moraine system defining the maximum extent of late Wisconsinan ice includes those moraines defined as Saglek Moraines in the Nachvak and Koroksoak Valley watersheds (Ives, 1976), but not the moraines in the Saglek Fiord area defined as Saglek Moraines by Ives (1976), which are recessional (see below). The Saglek Moraines in the Torngat Mountains were deposited during the maximum extent of late Wisconsinan Laurentide ice.

Glacial sediments deposited during a pre-late Wisconsinan glaciation have low relief moraine ridges which have been substantially modified by cryoturbation and slope processes (Fig. 20.3). These sediments project from beneath and are distal to the younger late Wisconsinan sediments.

Soils. Soils in glacial deposits of the Torngat Mountains show a systematic progression in degree of development with age, and are qualitatively useful for distinguishing deposits of different age. Temporal trends are indicated by development and thickening of the solum and reddening of the B horizon. Differences between soils developed in deposits of different age are consistent throughout the mountains provided that climate, vegetation, parent material, and topography are comparable.

Soils described on late Wisconsinan moraine crests are weakly developed with thin to moderately thick (3-10 cm) A horizons over weakly expressed and thin (< 10 cm) cambic B horizons or directly over Cox horizons. Cambic B horizons are one hue redder than Cox horizons and may have lower values than Cox horizons. Soils described on pre-late Wisconsinan moraine crests are weakly to moderately developed, with thin A horizons overlying cambic B horizons up to 36 cm thick. Cambic B horizons are two hues redder than underlying Cox horizons.

Composition. Late Quaternary glacial sediments in the Torngat Mountains south of Ikkudliayuk Fiord are derived entirely from underlying Precambrian bedrock (metamorphic and igneous rocks of the Churchill and Nain provinces). Detailed pebble and heavy mineral studies of late Wisconsinan glacial sediments along a transect from Abloviak Fiord east to Kangalaksiorvik Fiord showed that maximum distances of transport are 16 km, although most lithologies are derived from within 5 km of their bedrock source (Clark, 1984). Postglacial raised marine sediments south of Ikkudliayuk Fiord commonly contain Paleozoic limestone erratics, whereas glacial drift comprises only local Precambrian bedrock lithologies.

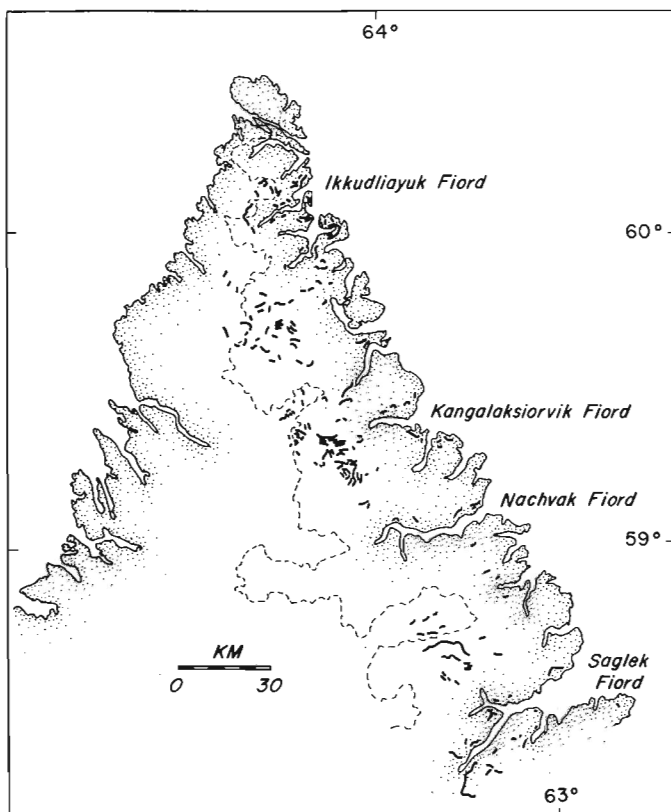


Figure 20.2. Map of late Wisconsinan moraines (heavy solid lines) (include Saglek Moraines and recessional moraines) in the Torngat Mountains.

North of Ikkudliayuk Fiord (60°N), Bell (1884) and Løken (1964) reported abundant sedimentary clasts among glacial till. These were primarily carbonate limestone clasts, but red sandstone lithologies were also observed on Killinek Island (Bell, 1884). Sedimentary carbonate lithologies were probably derived from Paleozoic bedrock flooring Ungava Bay and Hudson Strait (Sanford et al., 1979; MacLean and Williams, 1983). Red sandstone may have been derived from the Labrador Trough or the Dubawnt Group in the District of Keewatin (cf. Shilts, 1980).

Age. A radiocarbon date of $18\,210 \pm 1900$ years BP (GX-6362) (Table 20.1) on varved sediments cored in Square Lake (58°38'N; 63°37'W) (Clark et al., 1986) provides an age for deposition of late Wisconsinan glacial sediments and the Saglek Moraines. Radiocarbon dates on shells of 9110 ± 410 years BP (GX-9293) from outer Kangalaksiorvik Fiord (Clark, 1984) and 9000 ± 200 years BP (L-642) from inner Eclipse Channel (Løken, 1962b) (Table 20.1) provide minimum ages for deglaciation of fiords and deposition of postglacial raised marine sediments.

Saglek Fiord

Moraines bordering the southwestern arm of Saglek Fiord (Ugjuktok Fiord) were mapped as Saglek Moraines by Ives (1976). Field work during 1985 has refined this mapping and demonstrates that these are recessional moraines. Moraines above and distal to the system mapped by Ives (1976) delimit the maximum extent of late Wisconsinan ice in Saglek Fiord (Fig. 20.4). Saglek Moraines mapped by Ives (1976) north of Saglek Fiord in the Nachvak Brook and Koroksoak River watersheds were deposited during the late Wisconsinan maximum and are correlative to the previously unrecognized system shown in Figure 20.4.

Soil profiles were described on moraine crests delimiting the extent of late Wisconsinan ice (Saglek Moraines) and on adjacent, older glacial deposits distal to the moraines (Fig. 20.4). In both examples, a clear weathering break is indicated, thus suggesting an age difference associated with the degree of soil development in glacial sediments.

Ice surface profiles reconstructed from moraines deposited during the late Wisconsinan maximum (Saglek Moraines) and the recessional phase are similar in form (Fig. 20.4). The basal shear stress calculated for these profiles is 0.3-0.4 bar (Clark, listed data).

A radiocarbon date on basal sediments in a core sampled from a lake dammed by a recessional moraine (cf. Ives, 1976, Fig. 5) is $11\,160 \pm 520$ years BP (GX-5522) (Table 20.1) which, although stratigraphically consistent, must be considered as a maximum age because of low organic content of the sample (Short, 1981).

Labrador Shelf

Stratigraphy. Offshore, the glacial-postglacial sedimentary sequence consists of a Lower Till (unit 3a) and an Upper Till (unit 3b) which are overlain by well-stratified glacial marine sediments which are, in turn, overlain by ponded muds in the deep (> 170 m) shelf basins (Josenhans et al., in press). The distribution of the Lower Till is more extensive on the shelf than the Upper Till (Fig. 20.5). The Upper Till is an unsorted, unstratified pebbly-bouldery mud, the coarse fraction of which largely reflects the lithology of the adjacent mainland. The fine fraction is mostly derived from the underlying semiconsolidated bedrock. The till contains no limestone fragments.

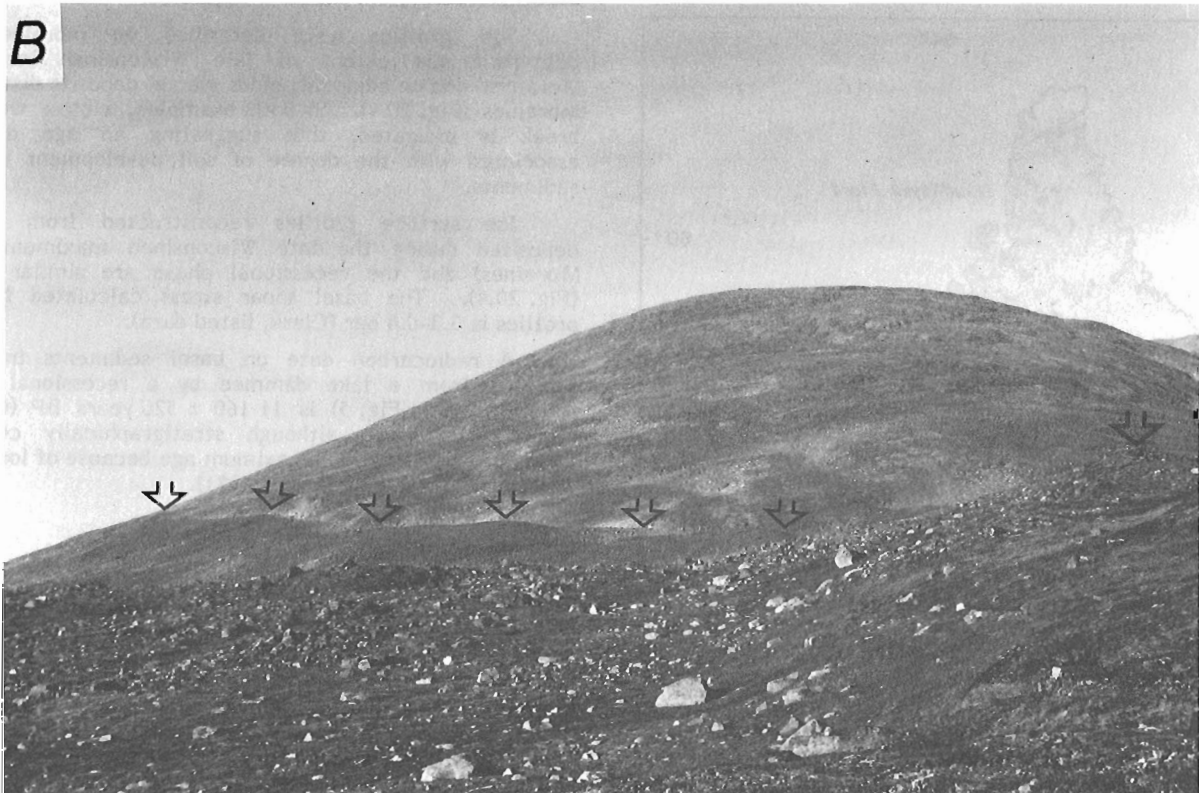
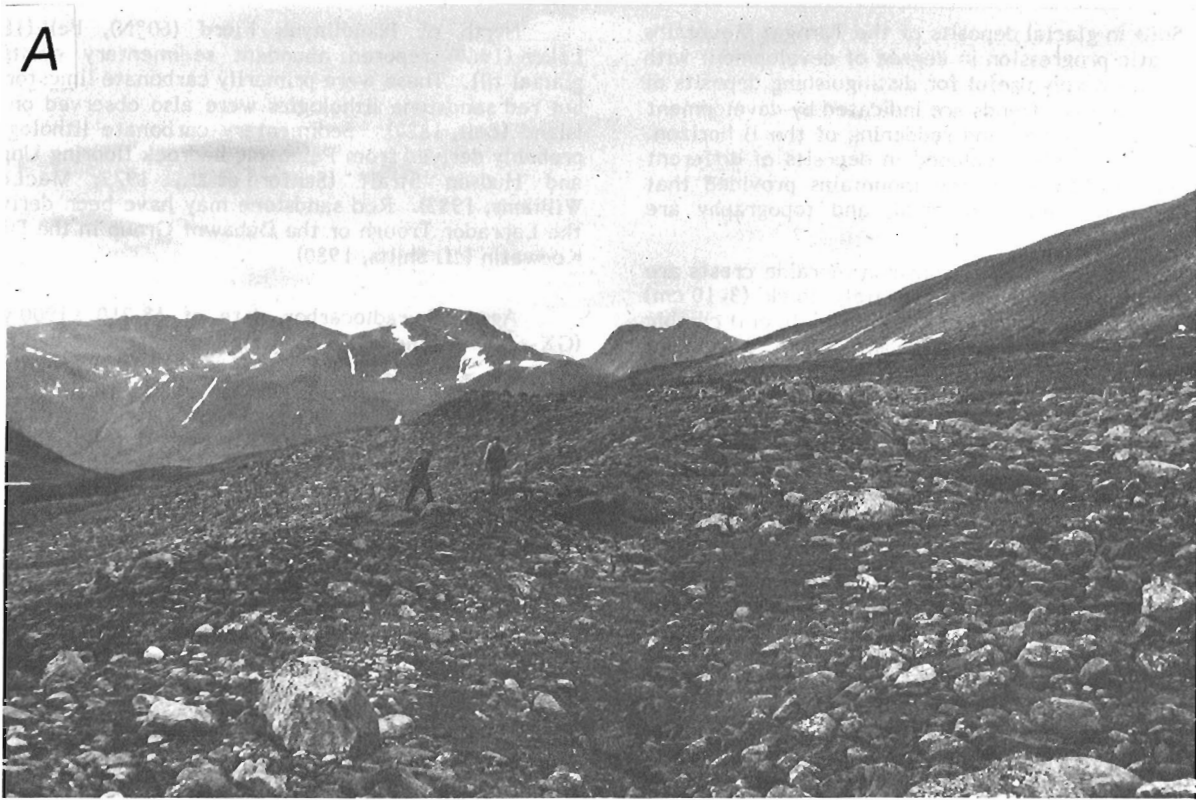


Figure 20.3. (A) Late Wisconsinan left lateral Saglek Moraine on north side of Nachvak Fiord; ice flow toward viewer. Pre-late Wisconsinan glacial sediments mantle hillslope above (distal to) moraine. (B) Late Wisconsinan left lateral Saglek Moraine in Saglek Fiord; ice flow toward viewer. Arrows point to crest of moraine, which runs down hillslope and bends toward viewer. Pre-late Wisconsinan glacial sediments mantle hillslope above (distal to) moraine. Soils from this moraine crest and pre-late Wisconsinan sediments are described in Figure 20.4 on north side of Saglek Fiord.

The glacimarine stratified silt (unit 4, Qeovik Silt) which conformably drapes over the till is a well-stratified muddy sediment with numerous ice-rafted dropstones. In contrast to the underlying tills, this unit is characterized by up to 80% limestone content within the sand fraction.

In the closed depressions (> 170 m) on the outer shelf, the glacimarine silt is overlain by ponded silty muds designated as unit 5a (Makkaq Clay). These muds are poorly stratified and heavily bioturbated. In contrast to the underlying glacimarine silt, unit 5a is almost entirely devoid of limestone.

In Hudson Strait, another younger till (unit 3c; Hudson Strait Till) overlies the Qeovik Silt. This till is confined to the deep portions of Hudson Strait (Fig. 20.5), is rich in limestone content and is interpreted to have been deposited by a late glacial advance that rapidly flowed over unit 4, reworking it into a homogeneous till (Josenhans et al., in press).

Age. Many radiocarbon dates exist from Labrador Shelf sediments, but these show inconsistencies due to incorporation of old carbon and the problem of dating total organic carbon for which the source is unknown. Josenhans et al. (in press) reviewed all available dates (ranging from 9 670 to 31 400 years BP) and concluded that deposition of the Upper Till began at approximately 20 000 years BP. The Qeovik Silt was deposited following ice retreat until ca. 8000 years BP, at which time Makkaq Clay began to be deposited under a current regime and depositional environment which generally exists to the present day. The readvance (surge) of ice from Hudson Strait is interpreted to have occurred just prior to the onset of Makkaq Clay deposition ca. 8000 years BP.

Correlations

Glacial and postglacial units in the Torngat Mountains are correlated with those identified on the adjacent continental shelf by (1) acoustic stratigraphic continuity from fiord basins onto the shelf, (2) similarities in lithologic properties of the units, and (3) ages of the units suggested by radiocarbon dates.

Postglacial raised marine sediments on land are correlated with unit 4 (Qeovik Silt) on the shelf. Both units contain abundant carbonate lithologies. Furthermore, radiocarbon dates are similar, although they suggest deposition of unit 4 began earlier on the shelf ($\pm 15\ 000$ years BP) than on land (± 9000 years BP).

Glacial sediments on land north of Ikkudliayuk Fiord are tentatively correlated with unit 3c (Hudson Strait Till) because: (1) both units contain abundant carbonate lithologies; and (2) the southern limit of carbonate rich till on land (Ikkudliayuk Fiord) and on the shelf can be correlated (Fig. 20.5). However, these glacial sediments on land may also in part be correlated with the older unit 3b (Upper Till).

Late Wisconsinan glacial sediments south of Ikkudliayuk Fiord on land, the limits of which are defined in the mountains by the Saglek Moraines, are correlated with unit 3b (Upper Till) because: (1) both units comprise pebble lithologies derived only from the Labrador continent (although the Upper Till on the shelf also includes matrix lithologies derived from underlying shelf bedrock); and (2) radiocarbon dates, while subject to some error (cf. Fillon et al., 1981), suggest that both units are late Wisconsinan.

Older, pre-late Wisconsinan glacial sediments on land may be correlative to unit 3a (Lower Till) on the shelf, although numerical ages are required to support this hypothesis.

Table 20.1. Radiocarbon dates from Northern Labrador

Laboratory Number ^a	Radiocarbon Date ^b	Source	Material	Comments
L-642	9000 \pm 200	Løken (1962b)	Shell	Collected from glacimarine sediments at head of Eclipse Channel at 29 m a.s.l.
GX-9293	9110 \pm 470	Clark (1984)	Shell	Collected from glacimarine sediments containing carbonate pebbles at Shoal Cove, outer Kangalaksiorvik Fiord at 2 m a.s.l.
GX-5522	11 160 \pm 520	Short (1981)	Total Organic Matter	Basal sandy mud from a 90 cm core taken from lake dammed by recessional moraine (see Fig. 20.4). Low organic content.
GX-6362	18 210 \pm 1900	Short (1981)	Total Organic Matter	Basal silty clay from 97.5 cm core taken from Square Lake dammed by Saglek Moraine. Low organic content (0.105 gm carbon).
^a L-Lamont, GX-Geochron. ^b All radiocarbon dates are reported as received from laboratories. No corrections for shell dates are made based on age of sea water.				

Discussion

Correlations presented here suggest that, during the late Wisconsinan, the Laurentide Ice Sheet drained through major valleys and fiords of the Torngat Mountains as a system of outlet glaciers which deposited the Saglek Moraines along their margins. Large upland areas of the Torngat Mountains remained ice-free. The outlet glaciers advanced onto the continental shelf, spreading out and coalescing as low-sloping thin piedmont glaciers which deposited the Upper Till (unit 3b) (Fig. 20.6). Ice flow on the shelf was also controlled by topography, and the Upper Till is only found at depths greater than 160 m. The lateral continuity of the Upper Till below 160 m suggests that ice must have been grounded, although it was probably close to hydrostatic equilibrium. If the ice had been floating, stratified sediment would have been deposited instead of till.

Laurentide ice draining through the Torngat Mountains as outlet glaciers was probably characterized by high velocities such as found for outlet glaciers draining the Greenland and Antarctica ice sheets (Carbonnell and Bauer, 1968; Bindschadler, 1984; McIntyre, 1985). Ice advanced 30-50 km onto the continental shelf off the coast of the Torngat Mountains (Fig. 20.5, 20.6A), except for east of Saglek Fiord where ice advanced farther onto the shelf through Karsefni Trough (Fig. 20.6B).

North and south of the Torngat Mountains, ice advanced farther onto the shelf than it did east of the mountains (Fig. 20.5) (Josenhans et al., in press). We interpret this as reflecting the influence of the Torngat Mountains on ice sheet flow because: (1) divergence of ice sheet flow around the mountains led to greater discharge onto the shelf north and south of the mountains; and (2) ice flow from Labrador south of the Torngat Mountains onto the shelf was not restricted to a source from several outlet glaciers but was instead characterized by sheet flow. Consequently, ice did not thin as rapidly on the shelf and the grounding line was able to advance deeper and farther onto the shelf.

Late Wisconsinan glacial sediments on land and on the shelf south of Ikkudliayuk Fiord contain only locally derived crystalline and shelf bedrock lithologies, while glacial sediments north of Ikkudliayuk Fiord contain a significant percentage of sedimentary carbonate lithologies which were derived from possible sources of early to middle Paleozoic carbonate bedrock underlying Hudson Strait, Foxe Basin, Ungava Bay, and Hudson Bay. The carbonate rich till (Hudson Strait Till) was deposited by an ice stream flowing through Hudson Strait. Josenhans et al. (in press) argued that deposition of this till continued after deposition of unit 3b.

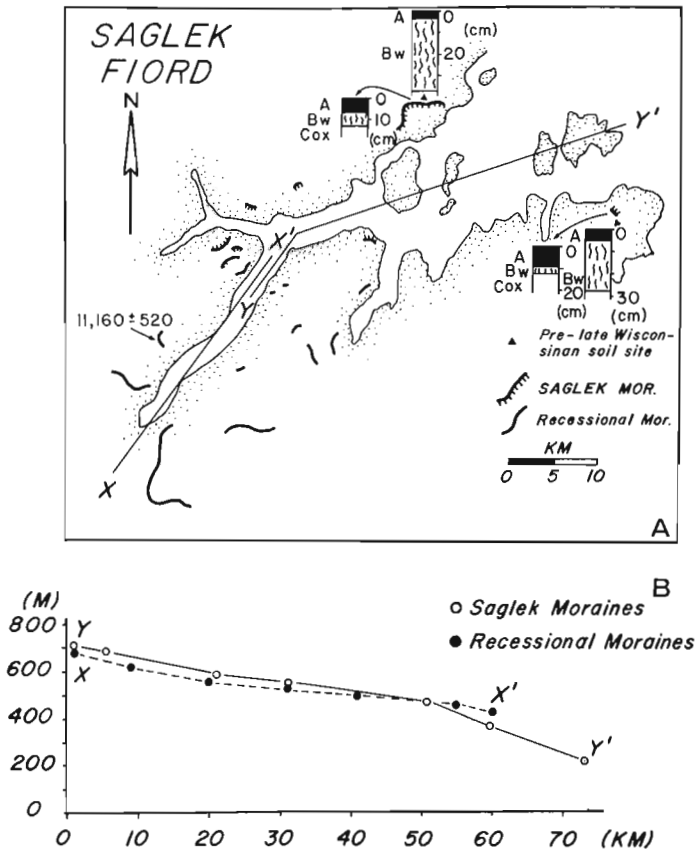


Figure 20.4. (A) Late Wisconsinan moraines (Saglek Moraines and recessional moraines) in Saglek Fiord area. Soil profiles shown were described on crests of Saglek Moraines and on pre-late Wisconsinan sediments distal to Saglek Moraines. **(B)** Profiles X-X and Y-Y are ice surfaces reconstructed from recessional moraines previously mapped as Saglek Moraines by Ives (1976) (X-X) and Saglek Moraines identified in this paper (Y-Y). Note that the two ice surfaces are superimposed, although in fact they are separated in space (Fig. 20.4A).

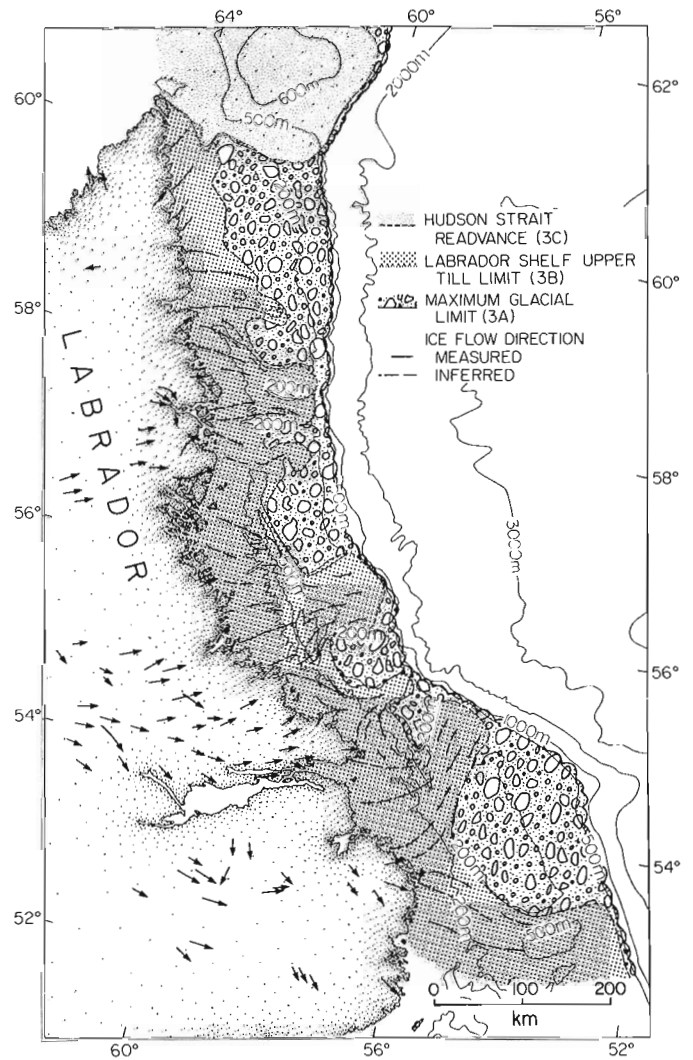


Figure 20.5. Inferred ice flow directions and lateral extent of major Labrador shelf glacial advances.

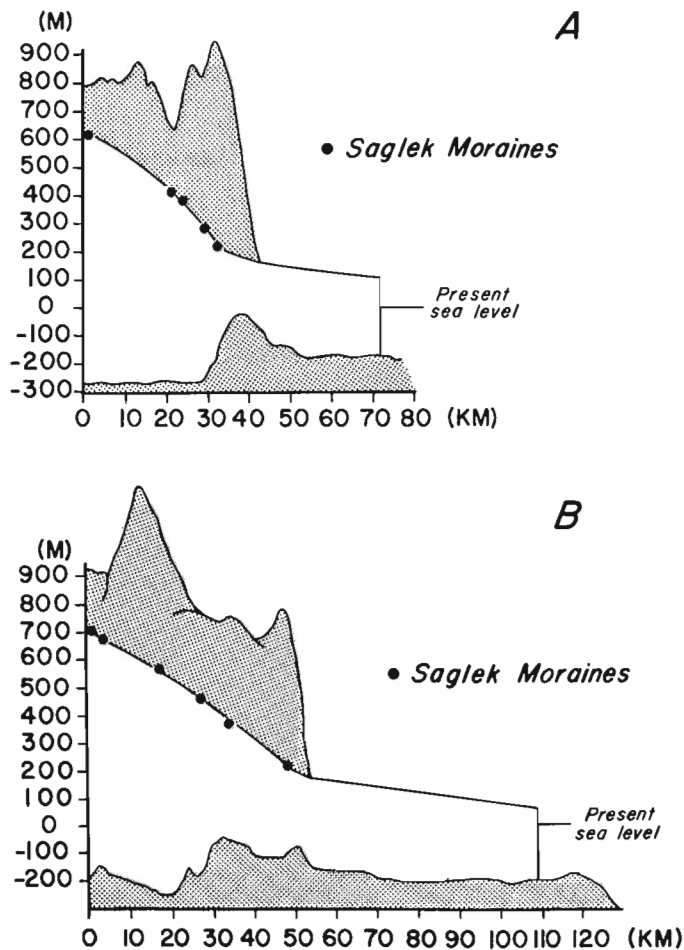


Figure 20.6. Profiles of late Wisconsinan ice surfaces reconstructed from Saglek Moraines in the Torngat Mountains and distribution of unit 3b on shelf. (A) Nachvak Fiord. (B) Saglek Fiord.

This suggests that ice withdrew from the shelf and onto the land south of Ikkudliayuk Fiord while an ice stream remained in Hudson Strait.

The carbonate rich glacial marine stratified sediment (raised marine sediments and unit 4) were deposited after ice had retreated from the continental shelf. Because the underlying tills and bedrock contain no carbonate sediments, the most likely source for the limestone in this unit is Hudson Strait. The timing of Hudson Strait deglaciation is well known based on many radiocarbon dates on shells (Blake, 1966; Clark, 1985; Stravers, 1986), and deglaciation was complete by 8000 years BP. We suggest that the disappearance of a calving ice margin in Hudson Strait resulted in the termination of the carbonate supply to the Labrador shelf. The onset of carbonate-free deposition (Makkaq Clay) at ca. 8000 years BP suggests that the timing of these events agrees well with the Hudson Strait chronology.

Acknowledgments

K. Eckerstrom, V. Hammond, K. Wallace, and J. Fabel provided able field assistance. Discussions with J.T. Andrews, G.H. Miller, J.T. Hollin, and W.D. McCoy have been very helpful. Critical reviews by D.J.W. Piper and J.A. Stravers improved the manuscript. Field work in the

Torngat Mountains was supported by the Arctic Institute of North America, Sigma XI, Geological Society of America, University of Colorado Graduate School, Explorers Club, Geological Survey of Canada, the University of Illinois Research Board, and National Science Foundation Grant EAR-81-21296. Offshore work was supported by the Geological Survey of Canada.

References

- Bell, R.
1884: Observations on geology, mineralogy, zoology, and botany of the Labrador coast, Hudson Strait and Bay; Geological Survey of Canada, Report of Progress, 1882-83-84, Part DD.
- Bindschadler, R.A.
1984: Jakobshavn glacier drainage basin: A balance assessment; *Journal of Geophysical Research*, v. 89, p. 2066-2072.
- Birkeland, P.W.
1984: *Soils and Geomorphology*; Oxford University Press, New York, New York, 372 p.
- Blake, W.
1966: End moraines and deglaciation chronology in northern Canada with special reference to southern Baffin Island; Geological Survey of Canada, Paper 66-26, 32 p.
- Carbannel, M. and Bauer, A.
1968: Exploitation des couvertures photographiques aeriennes repeties du front des glaciers velant dans Diske Bugt en Umanak Fjord, Juin-Juillet, 1964; *Meddelelser Groenland*, no. 173, p. 1078.
- Clark, P.
1984: Glacial geology of the Kangalaksiorvik-Abloviak region, northern Labrador, Canada; unpublished Ph.D. thesis, University of Colorado, Boulder, 248 p.
1985: A note on the glacial geology and postglacial emergence of the Lake Harbour region, Baffin Island, N.W.T.; *Canadian Journal of Earth Sciences*, v. 22, p. 1864-1971.
- Clark, P. Andrews, J.T., Short, S.K., Williams, K., and Melcer, A.
1986: Late-glacial and Holocene paleoenvironmental record from Square Lake, Torngat Mountains, Labrador; *American Quaternary Association, Abstracts with Programs*, v. 9.
- Coleman, A.P.
1921: Northeastern part of Labrador and New Quebec; Geological Survey of Canada Memoir 124, 56 p.
- Daly, R.A.
1902: The geology of the northeast coast of Labrador; *Harvard University Museum of Comparative Zoology Bulletin*, 38, p. 205-270.
- Fillon, R.H. and Harmes, R.A.
1982: Northern Labrador shelf glacial chronology and depositional environments; *Canadian Journal of Earth Sciences*, v. 19, p. 162-192.
- Fillon, R.H., Hardy, I.A., Wagner, F.J.E., Andrews, J.T., and Josenhans, H.W.
1981: Labrador Shelf: Shell and total organic matter C date discrepancies; Geological Survey of Canada, Paper 81-1B, p. 105-111.
- Flint, R.F.
1943: Growth of the North American ice sheet during the Wisconsinan age; *Geological Society of America Bulletin*, v. 54, p. 325-363.

- Greene, B.A.
1970: Geological Map of Labrador; Mineral Development Division, Newfoundland Department of Mines and Energy.
- Hughes, T.J., Denton, G.H., Andersen, B.G., Schilling, D.H., Fastook, J.L., and Lingle, C.S.
1981: The last great ice sheets: A global view; in *The Last Great Ice Sheets*, ed. G.H. Denton, and T.J. Hughes; John Wiley and Sons, New York, p. 275-318.
- Hurst, R.W., Bridgwater, D., and Collerson, K.D.
1975: 3600 m.y. Rb-Sr ages from very early Archean gneisses from Saglek Bay, Labrador; *Earth and Planetary Science Letters*, v. 27, p. 393-403.
- Ives, J.D.
1957: Glaciation of the Torngat Mountains, northern Labrador; *Arctic*, v. 10, p. 66-87.
1958: Glacial geomorphology of the Torngat Mountains, northern Labrador; *Geographical Bulletin*, v. 12, p. 47-75.
1976: The Saglek Moraines of northern Labrador: A commentary; *Arctic and Alpine Research*, v. 8, p. 403-408.
- Josenhans, H.W.
1983: Evidence of Pre-Late Wisconsinan glaciation on Labrador Shelf-Cartwright Saddle region; *Canadian Journal of Earth Sciences*, v. 20, no. 2, p. 225-235.
- Josenhans, H.W., Zevenhuizen, J., and Klassen, R.A.
- The Quaternary geology of the Labrador Shelf; *Canadian Journal of Earth Sciences*, v. 23. (in press)
- Koch, K.R.
1891: History of the supplementary expedition under Dr. K.R. Koch to Labrador; in G. Neumayer, *Die Deutschen Expeditionen und ihre Ergebnisse*, Band I, *Geschichtliches Theil*; Verlag von A. Asher, Berlin, p. 145-188.
- Leiber, O.M.
1861: Sketch showing the geology of the coast of Labrador; United States Coast Survey Report for 1860, Washington, DC.
- Løken, O.H.
1962a: On the vertical extent of glaciation in northeastern Labrador-Ungava; *Canadian Geographer*, v. 6, p. 106-119.
1962b: The late glacial and postglacial emergence and the deglaciation of northernmost Labrador; *Geographical Bulletin*, v. 17, p. 23-56.
1964: A study of the late and postglacial changes of sea level in northernmost Labrador; unpublished report to the Arctic Institute of North America, 80 p.
- MacLean, B. and Williams, G.L.
1983: Geological investigations of Baffin Island shelf in 1982; in *Current Research*, Part B, Geological Survey of Canada, Paper 83-1B, p. 309-315.
- Mayewski, P.A., Denton, G.H., and Hughes, T.J.
1981: Late Wisconsin ice sheets of North America: in *The Last Great Ice Sheets*, ed. G.H. Denton and T.J. Hughes; John Wiley and Sons, New York, New York, p. 67-178.
- McIntyre, N.F.
1985: The dynamics of ice-sheet outlets; *Journal of Glaciology*, v. 31, p. 99-107.
- Morgan, W.C.
1975: Geology of the Precambrian Ramah Group and basement rocks of the Nachvak Fiord-Saglek Fiord area, north Labrador; Geological Survey of Canada, Paper 74-54, 42 p.
- Odell, N.E.
1938: The great ice age: in *Northernmost Labrador mapped from the air*, ed. A. Forbes; American Geographical Society Special Publication no. 22, p. 204-215.
- Prest, V.K.
1984: The late Wisconsinan glacier complex; Geological Survey of Canada, Paper 84-10, p. 21-36.
- Ryan, A.B., Martineau, Y., Bridgwater, D., Schiotte, L., and Lewry, J.
1983: The Archean-Proterozoic boundary in the Saglek Fiord area, Labrador: Report 1; in *Current Research*, Part A, Geological Survey of Canada, Paper 83-1A, p. 297-304.
- Sanford, B.V., Grant, A.C., Wade, J.A., and Barss, M.S.
1979: Geology of eastern Canada and adjacent areas; Geological Survey of Canada, Map 1401A.
- Shilts, W.W.
1980: Flow patterns in the central North American ice sheet; *Nature*, v. 286, p. 213-218.
- Short, S.K.
1981: Radiocarbon Date List I: Labrador and Northern Quebec, Canada; Institute of Arctic and Alpine Research, Occasional Paper No. 36, 33 p.
- Stravers, J.A.
1986: Glacial geology of outer Meta Incognita Peninsula, southern Baffin Island; unpublished Ph.D. Thesis, University of Colorado, Boulder, 232 p.
- Tanner, C.
1944: Outlines of the geography, life, and customs of Newfoundland-Labrador; *Acta Geographica*, v. 8, p. 1-906.
- Taylor, F.C.
1971: A revision of Precambrian structural in provinces in northeastern Quebec and northern Labrador; *Canadian Journal of Earth Sciences*, v. 8, p. 579-584.
1979: Reconnaissance geology of a part of the Precambrian Shield, northeastern Quebec, northern Labrador, and Northwest Territories; Geological Survey of Canada Memoir 393, 99 p.
- Wardle, R.J.
1983: Nain-Churchill Province cross-section, Nachvak Fiord, northern Labrador; Newfoundland Department of Mines and Energy, Mineral Development Division, *Current Research Report 83-1*, p. 68-90.

Contrasting petrology and age of two megacrystic granitoid plutons, Cape Breton Island, Nova Scotia¹

Contract 27ST23233-5-0403

A.M. O'Beirne-Ryan², S.M. Barr³, and R.A. Jamieson²

O'Beirne-Ryan, A.M., Barr, S.M., and Jamieson, R.A., Contrasting petrology and age of two megacrystic granitoid plutons, Cape Breton Island, Nova Scotia; *in* Current Research, Part B, Geological Survey of Canada, Paper 86-1B, p. 179-190, 1986.

Abstract

Although texturally and mineralogically similar, the Cameron Brook and Margaree plutons in the Cape Breton Highlands of Nova Scotia are not similar in age or petrogenesis. Based on Rb-Sr whole-rock isochrons, the Cameron Brook pluton is late Ordovician to early Silurian whereas the Margaree pluton is Devonian-Carboniferous. The Cameron Brook pluton contains plagioclase and less abundant alkali feldspar megacrysts which generally lack rapakivi texture. The Margaree pluton contains predominantly alkali feldspar megacrysts with widespread development of rapakivi texture. Chemical and isotopic characteristics of the two plutons are very different, suggesting different processes were involved in their development. Elevated potassium content and polybaric history during crystallization are thought to be mainly responsible for development of rapakivi texture in the Margaree pluton.

Résumé

Bien que la texture et la minéralogie des plutons de Cameron Brook et de Margaree, dans les hautes-terres du Cap Breton, en Nouvelle-Écosse, soient similaires, l'âge et la pétrogenèse des deux plutons sont différentes. D'après les isochrones Rb-Sr de la roche entière, le pluton de Cameron Brook daterait de l'Ordovicien récent ou du Silurien ancien et le pluton de Margaree, du Dévonien-Carbonifère. Le pluton de Cameron Brook contient du plagioclase et des mégacristaux moins nombreux de feldspath alcalin généralement sans structure rapakivique. Le pluton de Margaree contient surtout des mégacristaux de feldspath alcalin et présente une structure rapakivique répandue. Les caractéristiques chimiques et isotopiques des deux plutons sont très différentes, ce qui porte à croire que des processus distincts ont joué dans leur évolution. La teneur élevée en potasse et l'histoire polybarique qui ont caractérisé la cristallisation auraient été en grande partie responsable de l'évolution de la structure rapakivique dans le pluton de Margaree.

¹ Contribution to the Canada-Nova Scotia Mineral Development Agreement 1984-1989. Project carried by Geological Survey of Canada, Mineral Resources Division, Project 700059.

² Department of Geology, Dalhousie University, Halifax, Nova Scotia B3H 3J5

³ Department of Geology, Acadia University, Wolfville, Nova Scotia BOP 1X0

Introduction

Megacrystic granitoid rocks tend to be grouped together as a distinctive rock type (e.g. Bell et al., 1977; Speer et al., 1979; Strong, 1980) and within a given area, a similar origin and age are commonly inferred. In many cases, however, the similarities may be more apparent than real. This paper discusses two megacrystic granitoid plutons from the north-central Cape Breton Highlands – the Cameron Brook and the Margaree plutons (Barr et al., 1985) – which despite textural and mineralogical similarities, have contrasting petrology, geochemistry, and age.

The Cameron Brook pluton is located in the east-central Highlands, west of Ingonish (Fig. 21.1). It is subcircular with an area of about 25 km². It intruded gneissic, metasedimentary and tonalitic rocks of inferred Late Hadrynian to Ordovician age (Wiebe, 1972; Barr et al., 1985). Wiebe (1972) described the pluton as coarse- to medium-grained granodiorite to adamellite with locally abundant microcline phenocrysts up to 5 cm in length. He suggested that the pluton may have formed approximately contemporaneously with associated metavolcanic units to the west, and inferred an age of about 560 Ma. Samples for the present study were collected mainly from the southern part of the pluton (Fig. 21.1).

The Margaree pluton is located in the west-central Highlands (Fig. 21.1). It is elongate north-south and about 90 km² in area. It intruded varied gneissic rocks of probable Late Hadrynian to Early Palaeozoic age (Barr et al., 1985). The pluton has been previously noted by Currie (1975) and

Jamieson and Craw (1983) who described it as megacrystic hornblende-biotite monzogranite. Jamieson and Craw (1983) reported a preliminary Rb-Sr isochron age of 365±46 Ma. Samples for the present study were collected from the southern half of the pluton (Fig. 21.1).

Textural and mineralogical features

The Cameron Brook pluton consists mainly of coarse grained megacrystic granite, with less abundant medium grained non-megacrystic granodiorite. Aligned biotite grains produce a well defined foliation in the granodiorite and both amphibole and biotite are present (15-20%). The megacrystic granite is weakly foliated, amphibole is absent and the proportion of mafic minerals is slightly less than in the granodiorite (10-15%). Metasedimentary xenoliths are present in both units.

Large subhedral to euhedral grains of plagioclase occur in both units. Both normal and reverse zoning are displayed, and compositions range from An₂₄ to An₈ (Table 21.1). Plagioclase is also present in the groundmass where it is essentially unzoned, with composition about An₂₅ to An₂₃. Potassium feldspar occurs both as large subhedral grains (Or₈₈; Table 21.2) and as interstitial groundmass grains. String perthite is typically present in the large grains, but absent in the groundmass grains. Grid twinning is common in both varieties. Some of the alkali feldspar is replacing plagioclase; however most appears to be primary. Rapakivi texture is rarely developed. Alteration of feldspars throughout the pluton is relatively minor, and is dominated by

Table 21.1. Microprobe analyses* of plagioclase in the Cameron Brook (A-F) and Margaree (G-M) plutons

	A		B		C		D		E		F
	core	rim	core	rim	core	rim	core	rim	core	rim	
SiO ₂	64.56	63.13	62.66	64.51	65.64	65.03	61.30	65.81	64.43	66.26	62.96
Al ₂ O ₃	22.28	22.31	23.70	22.29	20.69	21.89	23.36	21.55	21.58	20.83	23.49
CaO	3.48	2.84	5.04	3.63	1.98	2.60	4.17	2.50	2.83	1.73	4.97
Na ₂ O	10.00	9.75	8.82	9.69	10.48	9.92	8.42	10.64	9.63	10.73	8.85
K ₂ O	0.13	0.41	0.27	0.39	0.17	0.40	0.76	0.13	0.05	0.23	0.17
Total	100.45	98.26	100.49	100.51	98.96	99.84	98.01	100.63	98.52	99.78	100.44
An	16	14	24	17	9	12	21	11	14	8	23
Ab	83	84	75	81	90	86	75	88	86	91	76
Or	1	2	1	2	1	2	4	1	tr	1	1
	G	H		I		J	K	L	M		
		core	rim	core	rim				core	rim	
SiO ₂	62.17	61.93	63.50	60.85	67.53	63.50	63.22	63.99	61.91	64.76	
Al ₂ O ₃	23.60	23.79	21.97	23.27	19.64	22.36	22.25	22.59	24.03	21.68	
CaO	5.14	5.06	3.48	5.04	0.50	3.72	3.63	3.70	5.60	2.85	
Na ₂ O	8.71	8.89	9.71	8.69	11.57	9.45	9.42	9.72	8.33	9.98	
K ₂ O	0.44	0.34	0.38	0.51	0.13	0.26	0.16	0.15	0.56	0.10	
Total	100.06	100.01	99.04	98.36	99.37	99.29	98.68	100.15	100.43	99.37	
An	24	23	16	24	2	18	17	17	26	13	
Ab	74	75	82	73	97	81	82	82	71	86	
Or	2	2	2	3	1	1	1	1	3	1	
Cameron Brook: A-E = megacrysts; F = groundmass.											
Margaree: G = inclusion in K-feldspar megacryst; H, I, M = megacrysts; J, K = synneusitic megacrysts; L = groundmass.											
* Cambridge Instruments Micoscan 5 with Ortec Energy Dispersive Analyser, Dalhousie University.											

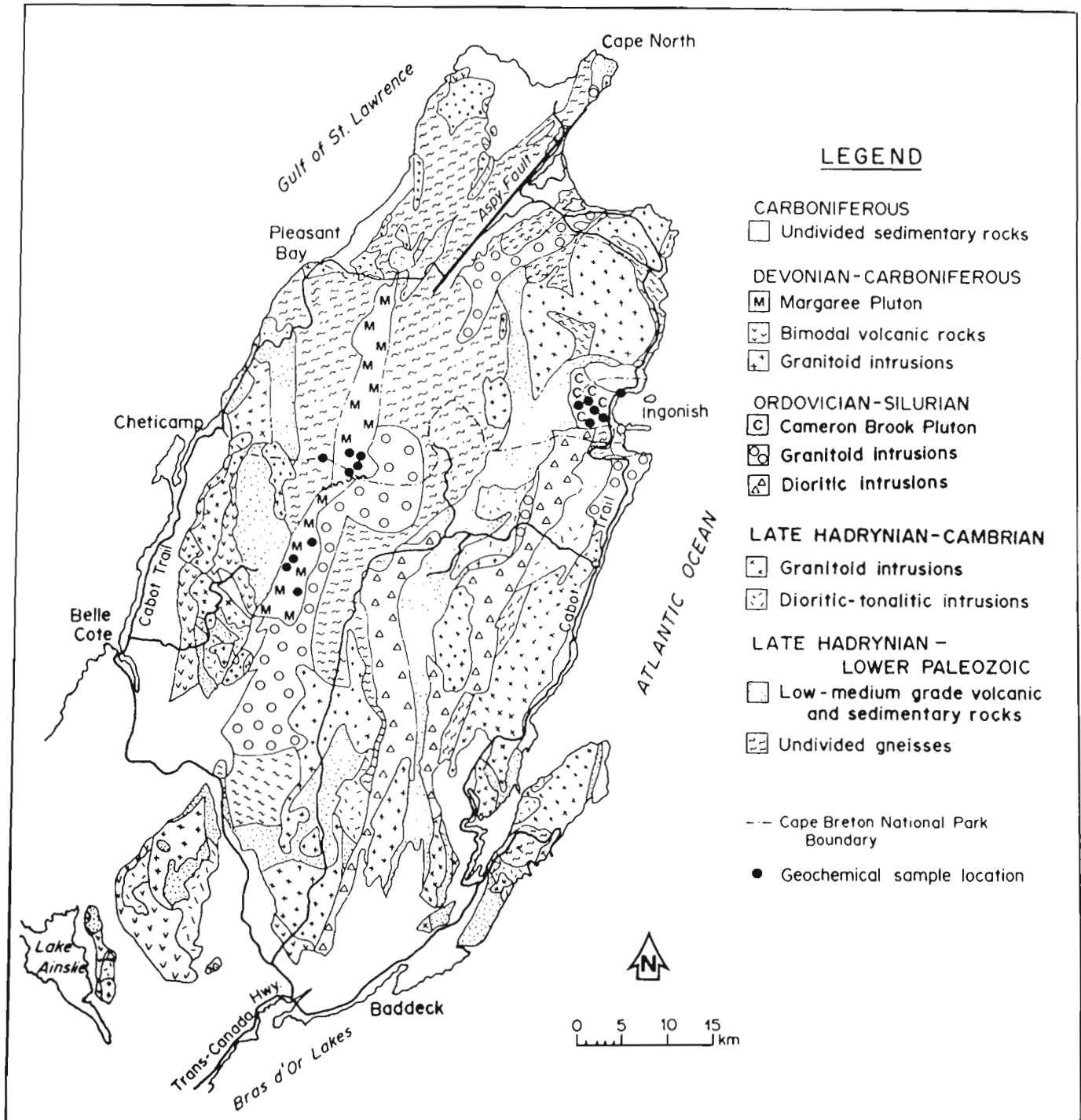


Figure 21.1. Generalized geological map of the Cape Breton Highlands, showing the Cameron Brook and Margaree plutons. (After Barr et al., 1985).

Table 21.2. Microprobe analyses* of K-feldspar from the Cameron Brook and Margaree plutons

	A	B	C	D	E	F	G	H
SiO ₂	64.25	63.93	63.79	63.85	63.55	64.67	64.20	63.93
Al ₂ O ₃	18.48	18.40	17.97	18.02	18.01	18.39	18.08	18.26
CaO	0.08	0.00	0.00	0.00	0.00	0.00	0.00	0.10
Na ₂ O	1.30	2.20	0.69	0.90	0.19	1.09	0.52	0.73
K ₂ O	15.23	13.19	15.93	15.13	16.34	15.13	16.10	15.66
Total	99.34	97.72	98.38	97.90	98.09	99.38	98.90	98.68
An	tr	--	--	--	--	--	--	tr
Ab	12	20	6	8	2	10	5	7
Or	88	80	94	92	98	90	95	93

Cameron Brook: A = megacryst
 Margaree: D, E, F, G, H = megacrysts; B = groundmass; C = inclusion in plagioclase megacryst.
 * Cambridge Instruments Micoscan 5 with Ortec Energy Dispersive Analyser, Dalhousie University.

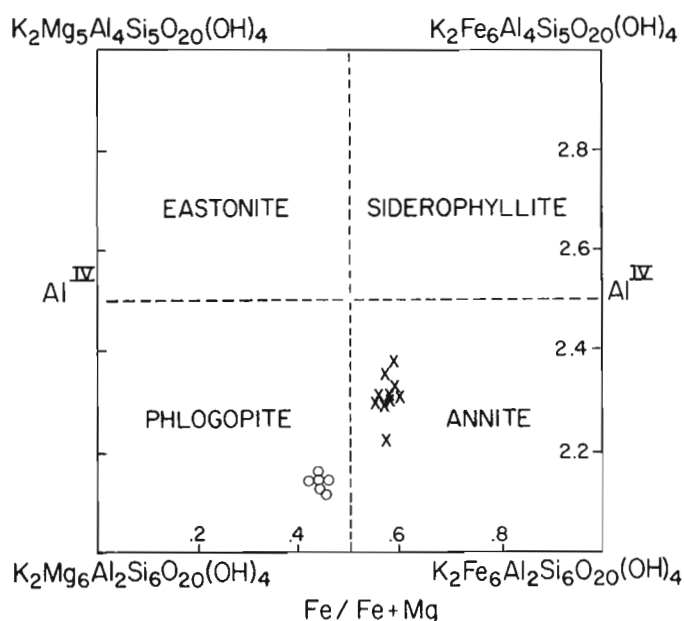


Figure 21.2. Biotite compositions in terms of Al vs. Fe/(Fe+Mg) (biotite quadrilateral); o = Cameron Brook; x = Margaree.

saussuritization and/or sericitization of plagioclase and in some instances, the development of muscovite. Alkali feldspar is typically unaffected. Biotite occurs as large subhedral to euhedral grains, suggesting that it grew early in the crystallization history of the pluton. It is Mg-rich (Table 21.3) and plots in the phlogopite field on the biotite quadrilateral (Fig. 21.2). Amphibole, where present in the granodiorite, is always subordinate to biotite. It is intensely chloritized, and no reliable analyses were obtained. Interstitial anhedral quartz grains show extensive subgrain development, particularly in the more foliated samples. Accessory minerals include abundant apatite, sphene, and opaque oxides. Kinking and undulose extinction in biotites and feldspars, and subgrain development in quartz, indicate post-intrusion deformation of the Cameron Brook pluton.

The Margaree pluton consists mainly of reddish coarse grained megacrystic granite with less abundant medium grained porphyritic granite, and medium grained equigranular granite. Although a sharp contact between megacrystic

granite and equigranular granite was observed in a boulder, relationships appear to be mainly gradational, at least between the porphyritic and megacrystic types, with the porphyritic granite containing smaller and less abundant phenocrysts.

Alkali feldspar, commonly with rapakivi texture, is the dominant feldspar in the Margaree granite, in contrast to the higher proportion of plagioclase in the Cameron Brook pluton. It occurs both as megacrystic grains and in the groundmass. Compositions range from Or₈₀ to Or₉₈ (Table 21.2), with no obvious difference in composition between groundmass and megacrysts. The megacrysts of alkali feldspar are up to 5 cm in length, and are perthitic, with both patch and string perthite developed. Twinning is not common, but where present is mainly simple, with minor grid twinning more commonly developed in the groundmass grains. The megacrysts are typically blocky rather than ovoid, a feature in common with the rapakivi granites of southeastern United States (Speer et al., 1979). Some megacrysts are compound, made up of three or four individual grains, each with plagioclase, or more rarely, quartz mantles, similar to those described by Vormea (1975). Rapakivi texture is common but by no means ubiquitous, and partial mantling is present locally. The mantling plagioclase generally occurs as small individual grains, commonly strongly altered to sericite, and in various orientations relative to the enclosed alkali feldspar.

Less abundant megacrysts of plagioclase occur as large individual zoned grains (An₂₀₋₁₅ core, An₁₆₋₂ rim), and as compound synneusitic grains (An₂₀₋₁₅), (Table 21.1). Rare graphic-like intergrowths with quartz also occur, as observed in the rapakivi granites of the Salmi Massif (Sviridenko, 1968). Biotite is subhedral to anhedral, commonly with ragged boundaries, and occurs both as individual grains and in clusters with amphibole, where it appears to have locally replaced the amphibole. Microprobe analyses indicate that the biotites are Fe-rich (average Fe/Mg = 1.36), and moderately high in TiO₂ (2.1-3.7%) relative to the Cameron Brook pluton (Table 21.3). They plot in the annite field of the biotite quadrilateral (Fig. 21.2), similar to those of the post-tectonic granites of the southeastern United States (Speer et al., 1979). Lack of euhedral grains, the replacement relationship with amphibole, and the overall interstitial nature of the biotite suggest that it grew late in the sequence of crystallization. Amphibole is present in the coarse grained megacrystic unit, except in the south, where the granite is notably more leucocratic. It is

Table 21.3. Microprobe analyses* of biotite from the Cameron Brook and Margaree plutons

	1001-1	1001-2	1009-1	1009-2	1009-3	1009-4	477-1	477-2	477-3	478-1	478-2	478-3	479-1	479-2	479-3	479-4
SiO ₂	38.67	38.99	39.13	38.39	39.16	38.97	36.75	36.86	36.61	35.97	36.47	37.10	37.85	37.71	36.79	37.60
TiO ₂	2.20	2.34	2.32	2.25	2.38	2.25	3.68	2.66	2.86	2.16	2.48	3.11	3.10	3.24	3.67	3.74
Al ₂ O ₃	14.83	13.92	13.95	13.88	14.20	14.14	14.30	14.03	14.20	15.00	13.95	14.04	13.98	13.26	13.31	13.92
FeO	16.48	17.74	18.16	18.22	17.93	17.29	21.76	21.74	22.02	23.06	23.72	23.68	22.76	22.31	22.76	22.76
MnO	0.16	0.22	0.29	0.24	0.16	0.18	0.53	0.59	0.45	0.67	0.59	0.65	0.71	0.62	0.37	0.54
MgO	12.35	12.63	12.80	11.97	12.09	12.44	9.54	10.09	9.23	9.42	9.59	9.05	10.19	9.80	9.46	9.67
K ₂ O	9.27	10.13	10.07	9.71	9.98	10.10	9.25	9.03	9.16	8.01	8.52	9.16	9.66	9.64	9.40	9.60
H ₂ O**	3.96	3.99	4.01	3.93	3.99	3.97	3.90	3.88	3.84	3.84	3.85	3.90	3.98	3.91	3.87	3.96
Total	97.92	99.96	100.73	98.59	99.89	99.34	99.71	99.08	98.37	98.13	99.17	100.69	102.31	100.49	99.63	101.79
IONIC PROPORTIONS																
Si	5.86	5.36	5.84	5.86	5.89	5.88	5.65	5.70	5.71	5.62	5.67	5.69	5.69	5.77	5.70	5.69
Al ^{iv}	2.14	2.14	2.16	2.14	2.12	2.13	2.35	2.30	2.29	2.38	2.33	2.31	2.31	2.23	2.30	2.31
Z site	8.00	8.00	8.00	8.00	8.00	8.00	8.00	8.00	8.00	8.00	8.00	8.00	8.00	8.00	8.00	8.00
Al ^{vi}	0.51	0.32	0.30	0.35	0.39	0.39	0.24	0.25	0.32	0.38	0.23	0.23	0.17	0.17	0.13	0.17
Ti	0.25	0.26	0.26	0.26	0.27	0.26	0.43	0.33	0.34	0.25	0.29	0.36	0.35	0.37	0.43	0.43
Fe	2.09	2.23	2.27	2.33	2.25	2.18	2.80	2.81	2.87	3.01	3.09	3.04	2.86	2.86	2.95	2.88
Mn	0.02	0.03	0.04	0.03	0.02	0.02	0.07	0.08	0.06	0.09	0.08	0.08	0.09	0.08	0.05	0.07
Mg	2.79	2.83	2.85	2.72	2.71	2.80	2.19	2.33	2.15	2.19	2.22	2.07	2.29	2.24	2.18	2.18
Y site	5.66	5.67	5.72	5.69	5.64	5.65	5.73	5.80	5.74	5.92	5.91	5.78	5.76	5.72	5.74	5.73
K	1.79	1.94	1.92	1.89	1.91	1.94	1.81	1.78	1.82	1.60	1.69	1.79	1.85	1.88	1.86	1.85
X site	1.79	1.94	1.92	1.89	1.91	1.94	1.81	1.78	1.82	1.60	1.69	1.79	1.85	1.88	1.86	1.85
H	4.00	4.00	4.00	4.00	4.00	4.00	4.00	4.00	4.00	4.00	4.00	4.00	4.00	4.00	4.00	4.00
O	24.00	24.00	24.00	24.00	24.00	24.00	24.00	24.00	24.00	24.00	24.00	24.00	24.00	24.00	24.00	24.00
PHLOG	56.95	55.62	55.28	53.61	54.36	55.93	43.27	44.60	42.26	41.43	41.28	39.86	43.23	43.62	42.16	42.51
ANN	42.63	43.83	44.01	45.78	45.23	43.61	55.37	53.92	56.57	56.90	57.28	58.52	52.22	54.66	56.91	56.14
Mn	0.42	0.55	0.71	0.61	0.41	0.46	1.37	1.48	1.17	1.67	1.44	1.63	1.55	1.73	0.94	1.35
F/M	0.76	0.80	0.81	0.86	0.84	0.79	1.31	1.24	1.37	1.41	1.42	1.51	1.29	1.31	1.37	1.35
F/FM	0.43	0.44	0.45	0.46	0.46	0.44	0.57	0.55	0.58	0.59	0.59	0.60	0.56	0.57	0.58	0.58

Margaree pluton: 477-1, -2; 478-1, -2, -3; 479-1, -2, -3, -4.

Cameron Brook pluton: 1001-1, -2; 1009-1, -2, -3, -4.

* Cambridge Instruments Microscan 5 with Ortec Energy Dispersive Analyser, Dalhousie University.

** H₂O-calculated based on the stoichiometry of biotite.

Table 21.4. Microprobe analyses* of amphibole from the Margaree pluton

	479-3	479-4	479-5	478-1	478-2
SiO ₂	42.85	43.82	43.73	44.31	40.78
TiO ₂	1.30	1.65	1.51	1.42	0.48
Al ₂ O ₃	8.12	7.69	8.18	7.46	9.81
FeO	21.51	20.47	20.22	19.83	24.03
MnO	0.79	0.97	0.86	0.90	0.91
MgO	8.27	8.96	8.37	9.09	6.20
CaO	10.84	11.02	10.06	10.87	10.99
Na ₂ O	1.73	1.69	2.26	1.86	1.55
K ₂ O	1.00	0.94	0.94	0.93	1.26
Total	96.41	97.21	96.13	96.67	96.01
Si	6.65	6.73	6.78	6.83	6.46
Al ^{iv}	1.35	1.27	1.22	1.17	1.54
Z site	8.00	8.00	8.00	8.00	8.00
Al ^{vi}	0.14	0.13	0.27	0.19	0.29
Ti	0.15	0.19	0.18	0.17	0.06
Fe ^{3+**}	0.37	0.19	0.17	0.08	0.42
Fe ²⁺	2.43	2.44	2.45	2.48	2.76
Mg	1.91	2.05	1.93	2.09	1.47
Y site	5.00	5.00	5.00	5.00	5.00
Mn	0.10	0.13	0.11	0.12	0.12
Ca	1.80	1.81	1.67	1.80	1.87
Na	0.09	0.06	0.22	0.09	0.01
X site	2.00	2.00	2.00	2.00	2.00
Na	0.43	0.44	0.46	0.47	0.46
K	0.20	0.18	0.19	0.18	0.26
A site	0.63	0.62	0.65	0.65	0.72
Total	15.62	15.63	15.65	15.65	15.72

** Calculated after Holland and Richardson (1979).
* Using Cambridge Instruments Microscan 5 with Ortec Energy Dispersive Analyser, Dalhousie University.

absent in the porphyritic variety. Microprobe analyses of several grains are given in Table 21.4. Following the nomenclature proposed by Leake (1978), these are ferroedenitic hornblendes to ferroedenites; their Fe-rich compositions are similar to rapakivi granites elsewhere (Simonen and Vormaa, 1969; VanSchmus et al., 1975). Accessory minerals include apatite, sphene and opaque oxides.

Alteration varies from moderate to intense; many samples display complete chloritization of biotite and amphibole, and extensive sericitization of plagioclase. The alkali feldspar is relatively unaltered. Veinlets of epidote, quartz, and chlorite are common.

Overall, although both the texture and mineralogy are broadly similar in the Margaree and Cameron Brook plutons, the following exceptions are significant: (i) the proportion of plagioclase to potassium feldspar is greater in the Cameron Brook pluton; (ii) rapakivi texture is rare in the Cameron Brook pluton, but widespread in the Margaree pluton; (iii) biotite compositions are more Mg-rich and Ti-poor in the Cameron Brook pluton; (iv) more intense deformation has occurred in the Cameron Brook pluton than in the Margaree pluton, with extensive subgrain development in quartz, and deformed feldspars and biotites; (v) alteration is more intense in the Margaree pluton.

Geochemistry

Despite the presence of two lithologies within the Cameron Brook pluton, the analyzed samples are relatively uniform chemically (Table 21.5). A weak negative correlation with SiO₂ exists for Fe₂O₃t, MgO, CaO, and Al₂O₃ and a positive correlation for TiO₂ and P₂O₅ (Fig. 21.3). K₂O, Na₂O and MnO contents are relatively uniform throughout the suite. Although the granite is represented by the more highly differentiated samples, there is a gradational relationship between the granodiorite and the granite.

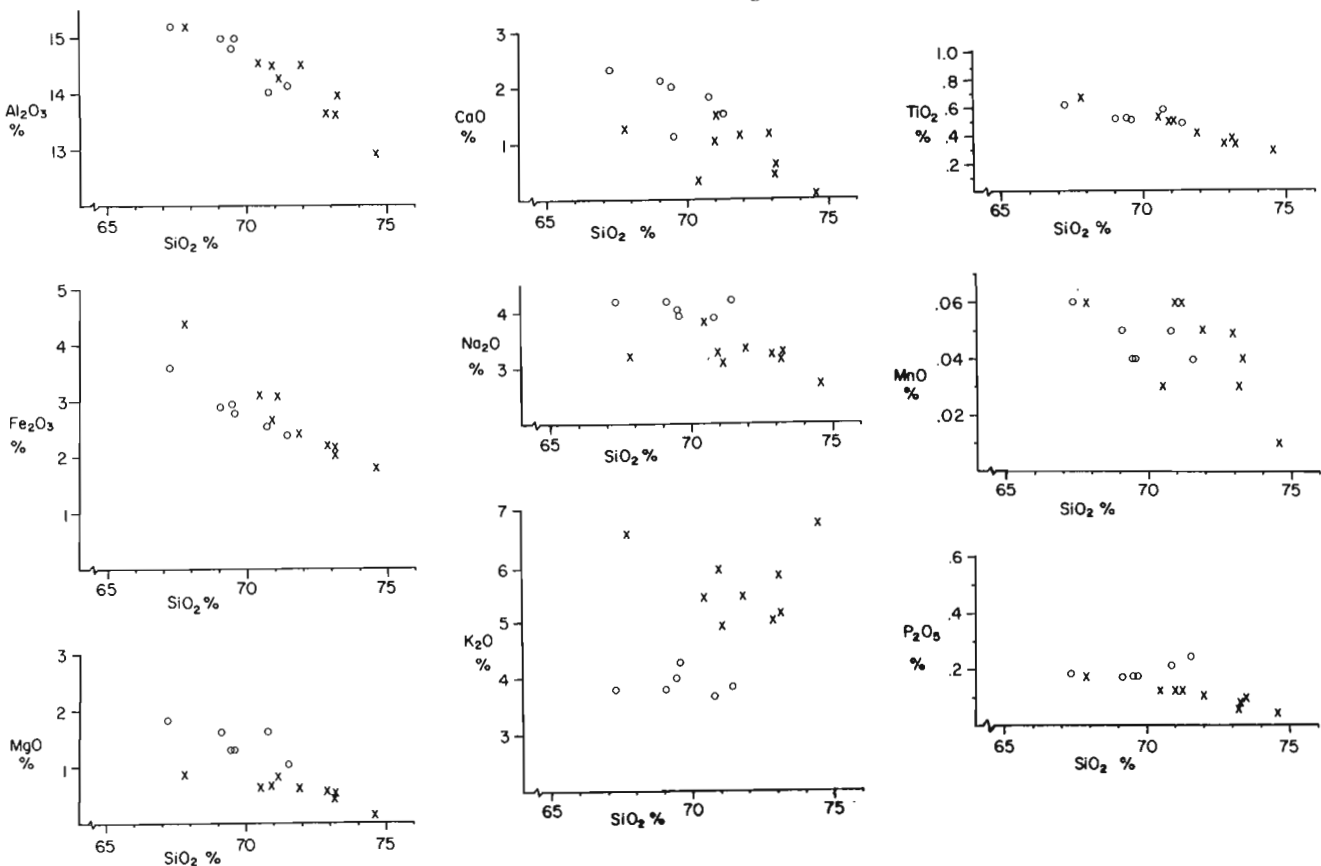


Figure 21.3. Major element geochemistry plotted on SiO₂ variation diagrams. Symbols as in Figure 21.2.

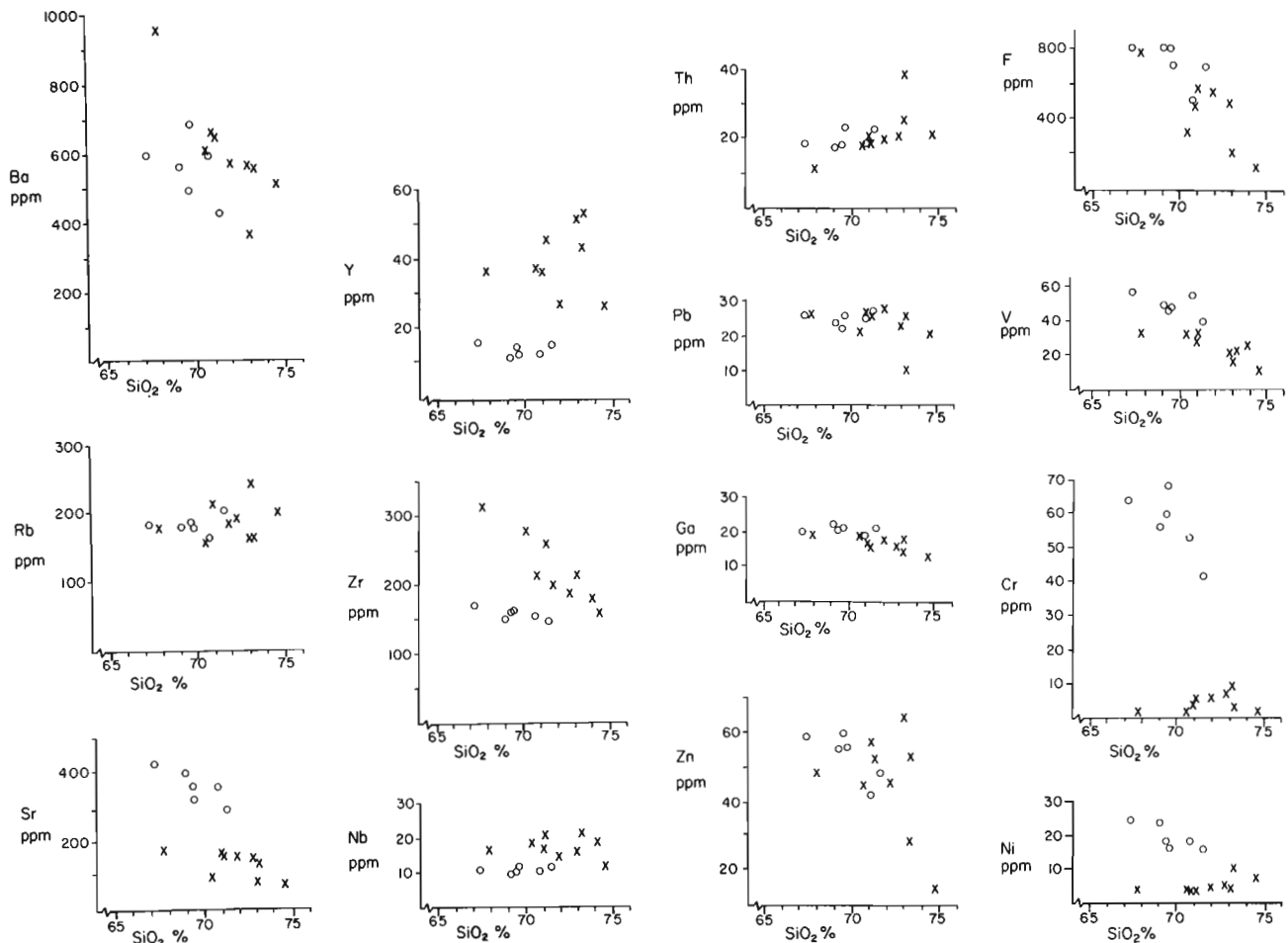


Figure 21.4. Trace element geochemistry plotted on SiO_2 variation diagrams. Symbols as in Figure 21.2.

Trace element data (Fig. 21.4) for the Cameron Brook samples show negative correlation with SiO_2 for Cr, V, Sr, Zn, and F and a poorly defined negative correlation for Ba and Zr. Pb, Th, Nb, Ga, Rb and Y show no correlation.

The Margaree pluton shows a wider geochemical range than the Cameron Brook pluton, but no consistent differences related to textural varieties are apparent. With the exception of Na_2O , which is relatively uniform, and K_2O , which is high and variable, all other oxides show a negative correlation with SiO_2 . With the exception of Ba, Zr and to a lesser extent V, F, Zn, and Th, all of which decrease with increasing SiO_2 , trace element contents appear to be independent of SiO_2 .

High SiO_2 , K_2O and Fe_2O_3 and low CaO are associated with the Margaree pluton, when compared to the Cameron Brook pluton. Sederholm (1925) considered high SiO_2 , K_2O and low MgO, CaO and Al_2O_3 to be characteristic of rapakivi granites in Finland. Emslie (1978), in discussing features of anorogenic granites, and in particular rapakivi granites, noted higher $(\text{Na}_2\text{O} + \text{K}_2\text{O})/\text{CaO}$ and $\text{FeO}^t/(\text{FeO}^t + \text{MgO})$ compared to calc-alkaline granites. $(\text{Na}_2\text{O} + \text{K}_2\text{O})/\text{CaO}$ ratios for the Margaree granite are extremely variable (6-65), although values in general are high relative to the Cameron Brook pluton (3-7). $\text{FeO}^t/(\text{FeO}^t + \text{MgO})$ ranges from 0.78-0.93 for the Margaree pluton, consistently higher than the Cameron Brook pluton (0.60-0.68). An AFM diagram (Fig. 21.5) clearly shows this FeO^t and alkali enrichment in the Margaree granite relative to the Cameron Brook pluton.

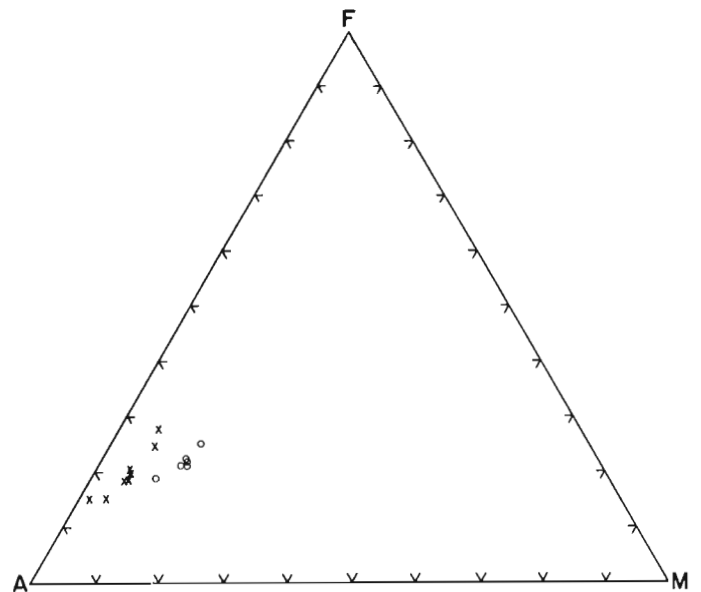


Figure 21.5. Ternary $\text{Na}_2\text{O} + \text{K}_2\text{O} - \text{FeO} - \text{MgO}$ diagram. Symbols as in Figure 21.2.

Table 21.5. Major¹ and trace² element geochemistry and CIPW normative mineralogy of samples from the Cameron Brook (1000, 1001, 1004, 1005, 1008, 1010), and Margaree (338, 340, 474, 476, 477, 478, 478B, 479, 547) plutons

	340	479	477	476	478	547	478B	338	474	1000	1001	1004	1005	1008	1010
SiO ₂	71.89	70.94	71.11	67.82	72.86	73.14	73.21	74.55	70.45	70.8	69.1	67.3	71.5	69.6	69.5
Al ₂ O ₃	14.53	14.47	14.26	15.20	13.65	13.17	13.94	12.88	14.57	14.0	15.0	15.2	14.3	15.0	14.8
Fe ₂ O ₃	1.12	0.98	1.62	1.55	0.97	1.23	1.06	1.54	1.39	1.4	1.9	2.7	1.6	1.0	2.0
FeO	1.14	1.49	1.34	1.99	1.09	0.71	0.98	0.25	1.55	1.1	0.9	0.8	0.7	1.6	0.9
MgO	0.60	0.66	0.79	0.85	0.52	0.40	0.49	0.13	0.62	1.6	1.6	1.8	1.0	1.5	1.5
CaO	1.13	1.00	1.45	1.25	1.16	0.38	1.17	0.11	0.30	1.8	2.1	2.3	1.5	1.1	2.0
Na ₂ O	3.34	3.26	3.10	3.22	3.26	3.17	3.25	2.64	3.81	3.9	4.2	4.2	4.2	3.9	4.0
K ₂ O	5.48	5.95	4.95	6.61	5.05	5.85	5.16	6.76	5.45	3.7	3.8	3.8	3.8	4.3	4.0
TiO ₂	0.05	0.06	0.06	0.06	0.05	0.03	0.04	0.01	0.03	0.05	0.05	0.06	0.04	0.04	0.04
P ₂ O ₅ ^{tot}	0.10	0.12	0.12	0.17	0.09	0.06	0.08	0.04	0.12	0.21	0.17	0.17	0.24	0.17	0.17
H ₂ O	1.06	0.84	0.97	0.96	0.84	0.89	0.83	0.95	1.00	1.0	0.8	0.7	0.7	1.3	0.8
Total	100.82	100.26	100.26	100.34	99.86	99.38	100.52	100.14	99.84	100.12	100.13	99.63	100.04	100.01	100.22
Q	28.21	25.96	30.19	19.79	31.50	31.52	31.42	33.25	26.10	28.53	23.87	21.41	28.68	26.05	25.01
Or	32.49	35.41	29.49	39.34	30.17	35.13	30.59	40.13	32.62	22.08	22.63	22.72	22.63	25.77	23.80
Ab	28.33	27.75	26.42	27.41	27.85	27.23	27.58	22.52	32.61	33.29	35.77	35.92	35.77	33.43	34.04
An	4.96	4.20	6.45	5.12	5.22	1.52	5.30	0.29	0.71	7.62	9.37	10.41	5.91	4.40	8.86
Hy	2.13	2.89	2.41	3.53	2.08	1.01	1.71	0.33	2.42	4.05	4.01	4.53	2.51	5.16	3.76
Mt	1.63	1.43	2.37	2.26	1.42	1.39	1.54	0.03	2.04	2.05	1.60	1.05	1.06	1.47	1.56
Him	0.00	0.00	0.00	0.00	0.00	0.29	0.00	1.53	0.00	0.00	0.81	2.01	0.88	0.00	0.93
Il	0.72	0.94	0.94	1.26	0.61	0.67	0.59	0.54	1.06	1.07	0.98	1.15	0.88	0.96	0.97
Ap	0.23	0.28	0.28	0.40	0.21	0.14	0.19	0.09	0.28	0.49	0.40	0.40	0.56	0.40	0.40
C	1.29	1.14	1.46	0.88	0.93	1.09	1.07	1.12	2.17	0.81	0.57	0.41	1.13	2.36	0.66
Ba	574	661	656	957	565	363	555	514	610	542	571	586	427	681	497
Rb	184	210	186	173	161	242	160	199	155	158	176	179	198	181	185
Sr	151	154	152	172	143	68	127	73	94	347	393	422	285	325	354
Y	28	37	46	37	52	44	55	27	38	13	12	16	16	13	15
Zr	198	213	257	310	187	176	207	156	277	153	149	167	137	166	161
Nb	14	16	20	16	15	18	18	11	18	11	10	11	12	12	11
Th	20	21	19	11	21	39	25	21	18	19	18	19	24	24	19
Pb	28	27	26	26	23	10	26	20	21	26	24	26	26	26	23
Ga	18	17	17	19	16	18	14	13	19	19	22	20	21	21	23
Zn	44	57	51	47	64	27	52	13	44	47	56	58	48	56	60
Ni	5	3	3	4	5	4	10	7	4	18	24	25	15	16	18
V	25	27	32	33	20	17	21	10	32	54	49	56	39	47	46
Cr	6	4	6	2	7	3	9	2	2	53	56	65	42	68	59
F	549	474	574	769	482	206	n.d.	135	314	540	750	790	650	730	700

¹ Cameron Brook: by atomic absorption spectrometry, Dept. of Geol., Acadia University; analyst J. Cabilio.

Margaree: by atomic absorption spectrometry, Dept. of Geol., Dalhousie University; analyst S. Parikh.

² Analyses by XRF at N.S. Regional x-ray fluorescence centre, St. Mary's University, Halifax, except F, by ion-sensitive electrode at Dalhousie University (Margaree) and at CLIM Laboratory, Tech. Univ. of Nova Scotia (Cameron Brook samples).

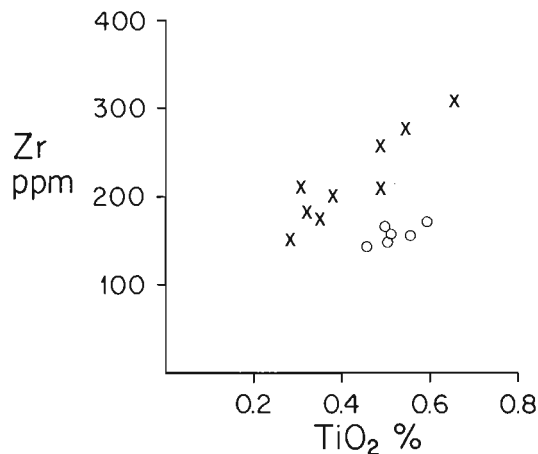


Figure 21.6. Plot of Zr against TiO_2 . Symbols as in Figure 21.2.

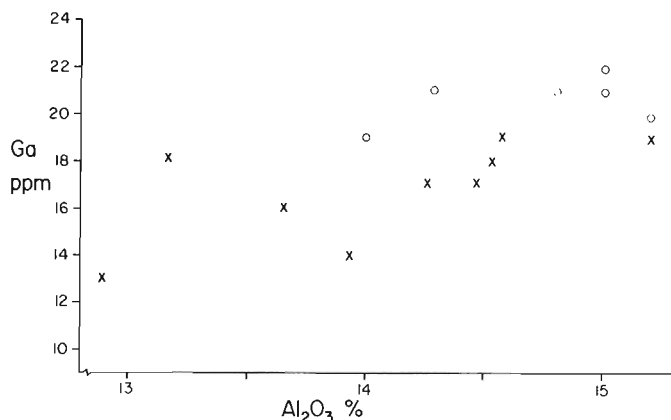


Figure 21.7. Plot of Ga against Al_2O_3 . Symbols as in Figure 21.2.

There is a notable enrichment in Cr, Ni, V and Sr in the Cameron Brook pluton relative to the Margaree pluton, and a corresponding depletion in Y, Zr, and Nb. These differences cannot be accounted for by the higher SiO_2 content in the Margaree pluton. A plot of Zr against TiO_2 (Fig. 21.6) further shows the sharp distinction between the two suites. However, they do show parallel trends, suggesting that both represent differentiation sequences.

Collins et al. (1982) concluded that Zr, Y, Nb, Ga, and Zn are enriched in anorogenic (A-type) granites of Australia. The differences were attributed in part to partial melting of a relatively anhydrous lower crust in which elevated F activity enhances solubilities of Ga and Zr. Elevated concentrations of Zr, Y, and Nb in the Margaree pluton could reflect a similar origin. However, Ga/Al enrichment was not observed (Fig. 21.7) nor do F contents appear to be unusually high (Table 21.5) although Currie (in press) reported fluorite in the northern part of the pluton.

The possible effects of alteration on the geochemistry, particularly in relation to the Margaree granite, cannot be overlooked. The scatter on the SiO_2 variation diagrams is possibly the result of alteration; however, with the exception of K_2O , Na_2O , CaO and MnO, the overall variation is consistent with differentiation-dominated processes. The lack of correlation for K_2O , CaO and to a lesser extent Na_2O and MnO, strongly suggests post-magmatic mobility. On the basis of mineralogical and textural observations, however, the elevated K_2O contents and the depleted CaO

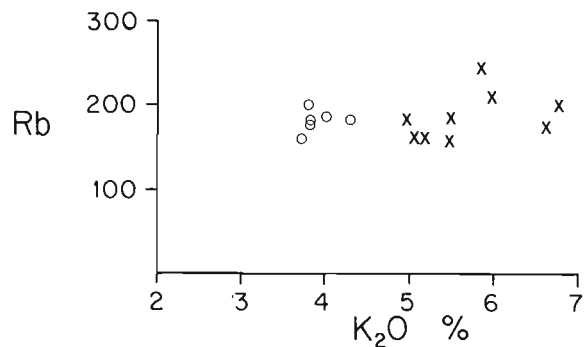


Figure 21.8. Plot of Rb against K_2O . Symbols as in Figure 21.2.

contents are considered to reflect magmatic processes. Thus relative proportions of these oxides, rather than absolute contents, are significant.

Scatter on the variation diagrams for Rb, Sr, Pb, Zn, F and Th can similarly be explained in terms of post-magmatic alteration. It is considered significant that Sr closely mimics CaO distribution. Rb is scattered with respect to K_2O distribution (Fig. 21.8), suggesting some mobilization during alteration.

Given the inherent difficulty of relating granite geochemistry unambiguously to source rocks, the reconnaissance level of mapping of both plutons, the relatively limited number of samples included in this study, and possible alteration effects, it is considered premature to model the geochemistry of either pluton in terms of its source rock, tectonic setting, or crystallization history without further sampling based on more detailed mapping.

Rapakivi texture

The origin and petrogenetic significance of rapakivi texture, that is, the mantling of potassium feldspar by plagioclase, have been the subjects of much controversy as the observed features apparently require a reversal in the normal crystallization sequence of granites (plagioclase followed by alkali feldspar). Rapakivi texture has been variously attributed to selective replacement of early plagioclase by later K-feldspar (eg. Stewart, 1959; Dawes, 1966; Stull, 1979), crystallization of K-rich granitic magmas (Tuttle and Bowen, 1958), and disequilibrium crystallization of granitic magma, combined with pressure-quench effects (Cherry and Trembath, 1978).

The following observations suggest that replacement processes are not responsible for the development of rapakivi texture in the Margaree pluton: (i) plagioclase grains in the mantles of the K-feldspar are typically not in optical continuity, and thus appear to have grown independently of each other; (ii) veinlets of "micrograins" of plagioclase cut the K-feldspar in random orientations, suggesting a late migration of Na-rich as well as K-rich fluids; (iii) plagioclase grains within the megacrysts are commonly in random orientation, unlikely if the K-feldspar represents a replacement phase; (iv) a highly prophyritic dyke, with well developed rapakivi texture, which cuts schists just west of the main pluton, contains alkali feldspar grains which are largely subhedral to euhedral, suggesting early magmatic growth. It thus seems likely that rapakivi texture in the Margaree pluton results from early co-crystallization of K-feldspar and plagioclase. The presence of both K-feldspar and plagioclase megacrysts in some samples (including the dyke) suggests that both feldspars (with quartz) were present early in the crystallization history. Mantled grains are

Table 21.6(a). Rb-Sr isotopic data for the Cameron Brook pluton. Analyses by Geochron Laboratories Division, Krueger Enterprises Inc., Cambridge, Massachusetts.

Sample	Rb*	Sr*	$^{87}\text{Rb}/^{86}\text{Sr}$	$^{87}\text{Sr}/^{86}\text{Sr}^{**}$
1000	165	363	1.316+/-1%	0.71191(13)
1005	203	296	1.976+/-1%	0.71611(06)
1010	196	377	1.499+/-1%	0.71320(08)

* in ppm.
** errors given as 2 sigma in the last digits.

Table 21.6(b). Rb-Sr isotopic data for the Margaree pluton. Analyses at Memorial University using techniques described by Taylor and Fryer (1983). Decay constant for ^{87}Rb is $1.42 \times 10^{-11}/\text{yr}$ (Steiger and Jager, 1977).

Sample	Rb*	Sr*	$^{87}\text{Rb}/^{86}\text{Sr}$	$^{87}\text{Sr}/^{86}\text{Sr}^{**}$
340	184.1	151.7	3.519+/-0.035	0.72393(09)
476	183.7	172.9	3.080+/-0.031	0.72171(05)
477	187.2	154.2	3.519+/-0.035	0.72365(13)
478	160.6	141.0	3.302+/-0.033	0.72283(21)
478B	161.5	131.0	3.562+/-0.036	0.72364(49)
479	201.1	155.4	3.572+/-0.038	0.72532(08)
547	247.4	67.7	10.947+/-0.109	0.75922(07)

* in ppm.
** errors given as 2 sigma in the last digits.

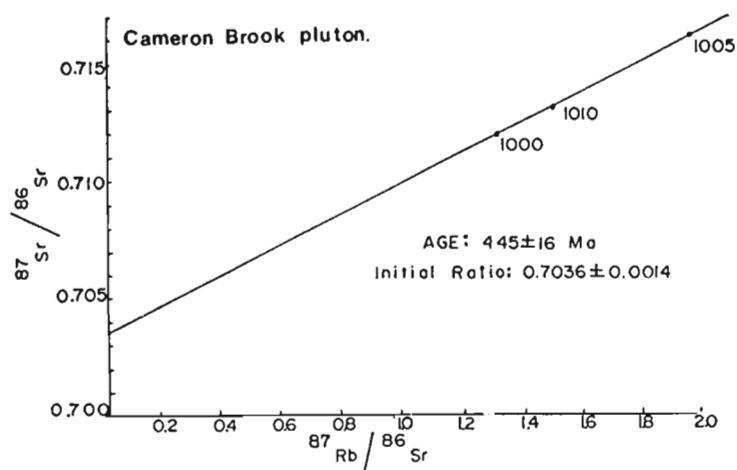


Figure 21.9a. Plot of $^{87}\text{Sr}/^{86}\text{Sr}$ against $^{87}\text{Rb}/^{86}\text{Sr}$ for the Cameron Brook pluton.

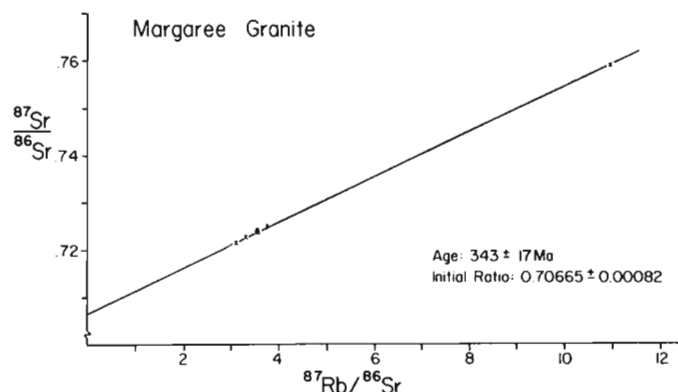


Figure 21.9b. Plot of $^{87}\text{Sr}/^{86}\text{Sr}$ against $^{87}\text{Rb}/^{86}\text{Sr}$ for the Margaree pluton.

significantly more common in the porphyritic varieties of the pluton, suggesting a possible relationship between pressure quenching and the development of rapakivi texture. The K-rich bulk composition of the Margaree pluton may have stabilized K-feldspar at an unusually early stage. This is in contrast to the Cameron Brook pluton, in which rapakivi texture is rare, and the K_2O concentration is lower. In both plutons, the growth of megacrysts is partially attributable to high volatile contents in the melts enhancing diffusion and therefore growth rates of phenocrysts.

Age

A three-point Rb-Sr isochron from the Cameron Brook pluton (Table 21.6, Fig. 21.9a) has yielded a late Ordovician – early Silurian date of 445 ± 16 Ma. Deformation within the Cameron Brook pluton is moderate to strong, and it is possible that there has been some isotopic migration, causing the scatter in the data points. It is unlikely, however, that the data have been completely reset from an original Devonian – Carboniferous date. Similar Ordovician – Silurian ages have been obtained from other granitoids in the area (Cormier, 1972). Thus the age difference between the Cameron Brook pluton and the Margaree pluton (discussed below) is considered significant.

A six-point Rb-Sr whole rock isochron date of 343 ± 17 Ma has been obtained from the southern part of the Margaree pluton (Table 21.5, Fig. 21.9b). This is the youngest date yet obtained on a large pluton in the Highlands, and is very similar to the age of the Fisset Brook Formation and related subvolcanic plutons in the Lake Ainslie area (French and Barr, 1984; Huard and Teng, 1984). This is younger than the Salmon Pool pluton (365 ± 10 , -5 Ma; Jamieson et al., in press) part of which has been reported to cut the Margaree

pluton north of the study area (eg. Currie, in press). A preliminary ^{40}Ar - ^{39}Ar cooling age on biotite from the Margaree pluton has given a significantly older date (ca. 380 Ma) than the Rb-Sr isochron (P.H. Reynolds, personal communication, 1986). This conflict in the date raises the possibility that the Rb-Sr systematics have been disturbed by alteration.

Discussion

The data presented above show that, although the Cameron Brook and Margaree plutons are superficially similar, there are significant differences, particularly in geochemistry and age. These differences must reflect a combination of their source rocks, their crystallization histories, subsequent alteration processes, and the tectonic setting in which the plutons formed. Not all of these possible sources of variation can be evaluated with the present data; however, the following points are considered significant.

In the Cameron Brook pluton plagioclase dominates over K-feldspar, despite the presence of K-feldspar megacrysts, and the rocks are modally granodiorites to granites. The Margaree pluton contains a higher proportion of K-feldspar and the rocks are modally granites. The Cameron Brook pluton contains less K_2O , Y and Zr than the Margaree pluton, and higher MgO, Na_2O , Cr, Ni and Sr. These features suggest that the Cameron Brook pluton is

petrologically less evolved than the Margaree pluton, but the role of crystallization versus melting and source rock factors in creating these differences is not clear. However, the early crystallization of both alkali feldspar and plagioclase in the Margaree pluton suggests this pluton acquired its K-rich characteristics at a relatively early stage. Although both plutons contain normative corundum, the lack of a primary peraluminous mineralogy and the abundance of hornblende and sphene suggest that this feature may result from alteration, and cannot be used to infer the nature of the source material.

The relatively low $^{87}\text{Sr}/^{86}\text{Sr}$ initial ratios for both plutons suggest that neither pluton was derived entirely from a highly radiogenic source rock such as an ancient cratonic basement. The Cameron Brook pluton has a significantly lower $^{87}\text{Sr}/^{86}\text{Sr}$ initial ratio than the Margaree pluton - 0.7036 ± 0.0014 versus 0.7067 ± 0.008 . The different ages of the plutons allow for the possibility of different tectonic environments and different source rocks at the time the plutons formed. However, until a better understanding of the Paleozoic tectonic history of the Cape Breton Highlands is achieved, the characteristics of individual plutons cannot easily be related to tectonic processes.

The development of rapakivi texture in the Margaree pluton and its near absence in the Cameron Brook pluton testifies to the variable mechanisms of formation of megacrystic granites. Growth of Mg-rich biotite early in the crystallization history of the Cameron Brook pluton and the presence of abundant pegmatites (Wiebe, 1972) suggest that the melt was relatively hydrous, which may have encouraged the growth of large crystals. On the other hand, high K-concentrations and a polybaric crystallization history probably influenced the widespread development of rapakivi texture in the Margaree pluton.

Acknowledgments

This study was funded by Research Agreements (51-4-80, 83-4-81, 254-4-82, 205-04-84) and contract 27ST23233-5-0403 from Energy Mines and Resources Canada (to R.A. Jamieson); Operating Grants from the Natural Sciences and Engineering Research Council (to S.M. Barr), and financial support from the Nova Scotia Department of Mines and Energy (to S.M. Barr).

References

- Barr, S.M., Jamieson, R.A., and Raeside, R.P.
1985: Igneous and metamorphic geology of the Cape Breton Highlands: GAC-MAC Field Guide, Excursion 10, 48 p.
- Bell, K., Blenkinsop, J., and Strong, D.F.
1977: The geochronology of some granitic bodies from eastern Newfoundland and its bearing on Appalachian evolution; *Canadian Journal of Earth Sciences*, v. 14, p. 456-476.
- Cherry, M.E. and Trembath, L.T.
1978: The pressure-quench formation of rapakivi texture; *Contributions to Mineralogy and Petrology*, v. 63, p. 1-6.
- Collins, W.J., Beams, S.D., White, A.J.R., and Chappell, B.W.
1982: Nature and origin of A-type granites with particular reference to southeastern Australia; *Contributions to Mineralogy and Petrology*, v. 80, p. 189-200.
- Cormier, R.F.
1972: Radiometric ages of granitic rocks, Cape Breton Island, Nova Scotia; *Canadian Journal of Earth Sciences*, v. 10, p. 1074-1085.
- Currie, K.L.
1975: Studies of granitoid rocks in the Canadian Appalachians; in *Report of Activities, Part A; Geological Survey of Canada, Paper 75-1A*, p. 265-268.
- Relations between metamorphism and magmatism near Cheticamp, Nova Scotia; *Geological Survey of Canada Bulletin*. (in press)
- Dawes, Peter R.
1966: Genesis of rapakivi; *Nature*, v. 209, p. 569-571.
- Emslie, R.F.
1978: Anorthosite massifs, rapakivi granites, and late Proterozoic rifting of North America; *Precambrian Research*, v. 7, p. 61-68.
- French, V.A. and Barr, S.M.
1984: Age and petrology of the Gillanders Mountain intrusive complex, Lake Ainslie area, Cape Breton Island, Nova Scotia; GAC-MAC Program with Abstracts, v. 9, p. 32.
- Holland, T.J.B. and Richardson, S.W.
1979: Amphibole zonation in metabasites as a guide to the evolution of metamorphic conditions; *Contributions to Mineralogy and Petrology*, v. 70, p. 143-148.
- Huard, A.A. and Teng, H.C.
1984: A study of the Fisset Brook Formation at Lake Ainslie, western Cape Breton Island; *Maritime Sediments and Atlantic Geology*, v. 20, p. 86.
- Jamieson, R.A. and Craw, D.
1983: Reconnaissance mapping of the southern Cape Breton Highlands - a preliminary report; in *Current Research, Part A; Geological Survey of Canada, Paper 83-1A*, p. 263-268.
- Jamieson, R.A., van Breemen, O., Sullivan, R.W., and Currie, K.L.
- The age of igneous and metamorphic events in the western Cape Breton Highlands, Nova Scotia; *Canadian Journal of Earth Sciences*. (in press)
- Leake, B.E.
1978: Nomenclature of Amphiboles; *American Mineralogist*, v. 63, p. 1023-1052.
- Sederholm, J.J.
1925: The average composition of the earth's crust in Finland; *Bulletin Commission Geologique, Finland*, No. 70.
- Simonen, A. and Vormaa, A.
1969: Amphibole and biotite from rapakivi; *Bulletin Commission Geologique, Finland*, No. 238, 28 p.
- Speer, J.A., Beck, S.W., and Farrar, S.S.
1979: Field relations and petrology of the post-metamorphic, coarse-grained granitoids and associated rocks of the Appalachian Piedmont; in *The Caledonides of the U.S.A.*, ed. R. Wones; *International Geological Correlation Program, Virginia Polytechnical Institute and State University, Blackburg, Virginia*, v. 27, p. 137-148.
- Steiger, R. and Jager, E.
1977: Subcommission on geochronology: Convention on the use of decay constants in geochronology cosmochronology; *Earth and Planetary Science Letters*, v. 35, p. 359-362.
- Stewart, D.B.
1959: Rapakivi granite from eastern Penobscot Bay, Maine; *20th International Geological Congress, Mexico, Report 9A*, p. 293-320.

- Strong, D.F.
 1980: Granitoid rocks and associated mineral deposits of eastern Canada and western Europe; in *The Continental Crust and its Mineral Deposits*, ed. D.W. Strangway; Geological Association of Canada, Special Paper no. 2, p. 741-770.
- Stull, R.J.
 1979: Mantled feldspars and synneusis; *American Mineralogist*, v. 64, p. 514-518.
- Sviridenko, L.P.
 1968: Petrology of rapakivi granites in the Salmi Massif; *International Geological Review*, v. 10, p. 507-519.
- Taylor, R.P. and Fryer, B.J.
 1983: Strontium isotope geochemistry of the Santa Rita porphyry copper deposit, New Mexico; *Economic Geology*, v. 78, p. 170-174.
- Tuttle, O.F. and Bowen, N.L.
 1958: Origin of granite in the light of experimental studies in the system $\text{NaAlSi}_3\text{O}_8 - \text{KAlSi}_3\text{O}_8 - \text{SiO}_2 - \text{H}_2\text{O}$; *Geological Society of America Memoir*, v. 74, p. 153.
- VanSchmus, W.R., Medaris, L.G., and Banks, P.O.
 1975: Geology and age of the Wolf River Batholith, Wisconsin; *Bulletin of the Geological Society of America*, v. 86, p. 907-914.
- Vorma, A.
 1975: Alkali feldspars of the Wiborg rapakivi massif in southeast Finland; *Bulletin Commission Geologique, Finland*, v. 246, p. 72.
- Wiebe, R.A.
 1972: Igneous and tectonic events in northeastern Cape Breton Island, Nova Scotia; *Canadian Journal of Earth Sciences*, v. 9, p. 1262-1277.

Geology of the West Branch North River and the Bothan Brook plutons of the south-central Cape Breton Highlands, Nova Scotia¹

Contract 27 ST23233-5-0403

A.M. O'Beirne-Ryan² and R.A. Jamieson²

O'Beirne-Ryan, A.M. and Jamieson, R.A., Geology of the West Branch North River and the Bothan Brook plutons of the south-central Cape Breton Highlands, Nova Scotia; in Current Research, Part B, Geological Survey of Canada, Paper 86-1B, p. 191-200, 1986.

Abstract

The West Branch North River and Bothan Brook plutons are an intrusive complex of granodioritic to granitic rocks, in the south-central Cape Breton Highlands. Preliminary mineralogical, geochemical, and isotopic studies suggest that they represent a comagmatic suite of late Devonian age. The Sarach Brook shear zone divides the West Branch North River pluton into an upthrust block of granodiorite in the west, and monzogranite in the east. Alteration, contamination, and deformational features are considered contributors to the observed chemical variability. Hematite-rich breccia zones in the West Branch North River monzogranite, and extreme alteration in the Bothan Brook granite, have been identified and warrant examination for their mineral potential.

Résumé

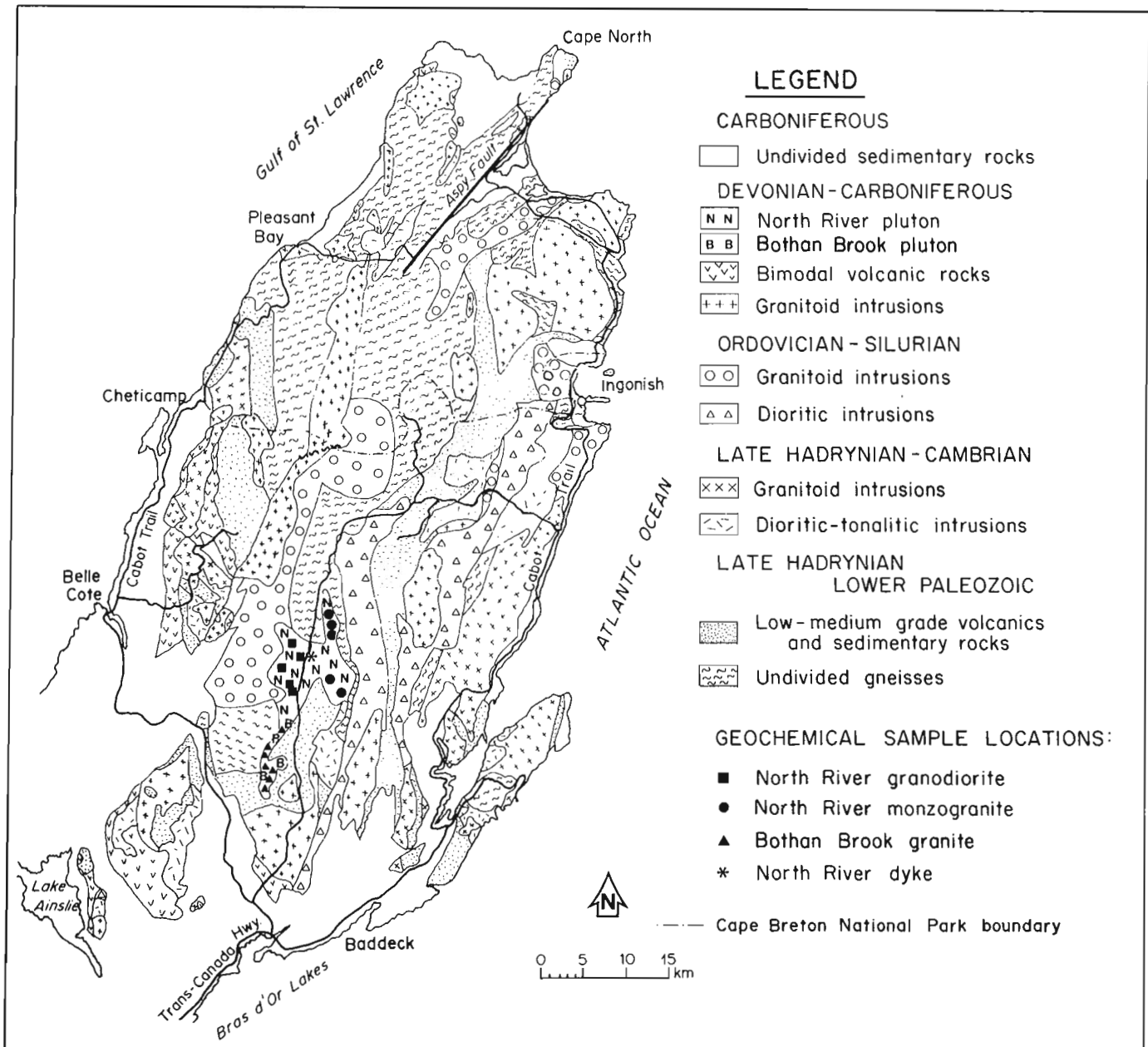
Les plutons de West Branch North River et de Bothan Brook forment un complexe intrusif de roches granodioritiques à granitiques dans la partie centrale du sud des hautes-terres du Cap Breton. L'étude provisoire de la minéralogie, de la géochimie et des isotopes porte à croire que ces plutons représentent une suite comagmatique d'âge tardi-dévonien. La zone de cisaillement de Sarach Brook divise le pluton de West Branch North River en un bloc soulevé de granodiorite à l'ouest et en monzogranite à l'est. L'altération, la contamination et la déformation auraient contribué à la grande variabilité chimique observée. On a examiné des zones de brèches riches en hématite dans le monzogranite de West Branch North River, ainsi que des zones fortement altérées dans le granite de Bothan Brook; ces zones mériteraient d'être étudiées de plus près pour en vérifier les possibilités minérales.

¹ Contribution to the Canada-Nova Scotia Mineral Development Agreement 1984-1989.
Project carried by Geological Survey of Canada, Mineral Resources Division, Project 700059.
² Department of Geology, Dalhousie University, Halifax, Nova Scotia B3H 3J5

Introduction

Diversity in age and composition of the plutonic rocks of the Cape Breton Highlands makes distinctions and comparisons difficult (eg. Barr et al., 1985). Some suites of cogenetic plutons exhibit variations in alteration that mask petrological similarities. On the other hand, some unrelated plutons are very similar. This paper discusses the petrology, geochemistry, and age of the West Branch North River and Bothan Brook plutons of the south-central Cape Breton Highlands (Fig. 22.1) as an example of the first case; a companion paper (O'Beirne-Ryan et al., 1986) discusses an example of the second problem.

The plutons are located in the Middle River area of the south-central Cape Breton Highlands, where they intrude metavolcanic and gneissic rocks of probable Late Proterozoic age (Jamieson and Doucet, 1983). The West Branch North River pluton comprises two distinct phases separated by a shear zone, whereas the Bothan Brook pluton was mapped as a separate unit, whose relation to the West Branch North River pluton was unknown (Jamieson and Doucet, 1983). The present study suggests that the plutons are related, and that the differences noted in the field reflect variable degrees of alteration, deformation and contamination.



- = WBNR granodiorite;
- = WBNR monzogranite;
- ▲ = BB granite.
- * = granitic dyke in WBNR

Figure 22.1. Generalized geological map of the Cape Breton Highlands, showing the West Branch North River and Bothan Brook granites (after Barr et al., 1985).

Table 22.1. Petrography of the West Branch North River (WBNR) and Bothan Brook (BB) plutons

	Plagioclase	Alkali feldspar	Quartz	Biotite	Amphibole	Accessories	Alteration	Textures
Bothan Brook Granite	Subhedral, zoned An ₂₉₋₂₁ . Inclusions of quartz, biotite amphibole and opaques	Anhedral, interstitial, well developed grid-twinning. Or ₈₉₋₉₄ .	Interstitial, deformed, some subgrain development.	Brown, pleochroic subhedral. Inclusions of quartz, apatite, zircon, sphene and opaques. Annite.	Green, pleochroic euhedral-subhedral. Edenitic hornblende.	Zircon, apatite, sphene, opaques, associated with mafic minerals.	Plagioclase: sericitic-mild to strong. Some epidote development. Mafics: chloritization, mild to strong. Alkali feldspar: relatively fresh.	Minor antiperthite. Minor myrmekite. Foliation variably developed.
	35-50%	2-10%	10-20%	10-20%	1-15%	<5%		
North River Monzogranite	Subhedral, zoned An ₁₂₋₂ . Bent twins common.	Perthitic, patchy grid twinning. Anhedral, irregular boundaries, may enclose groundmass. Also interstitial, non-perthitic, well-defined grid twinning. Or ₉₂₋₉₆ .	Anhedral, sutured boundaries, deformed.	Brown, pleochroic subhedral inclusions of accessories.	Absent.	Minor. Rare apatite, sphene, zircon and opaques. Associated mainly with biotite.	Plagioclase: Sericitic-moderate to intense-development of muscovite and epidote. Mafics: 50-90% of biotite chloritized. Alkali feldspar: relatively unaltered. Partial replacement of plagioclase by potassium feldspar.	Megacrystic in part. Minor myrmekite. Replacement textures common.
	30-40%	34-45%	10-25%	<6%		<1%		
North River Granodiorite	Subhedral, zoned An ₁₂₋₁ . May be bent, deformed.	Large, subhedral grains, irregular patchy grid twinning. Perthitic. Or ₈₉₋₉₆ . Interstitial grains microperthitic, grid twinning well developed.	Anhedral, undulatory extinction. Also as "bleb" shaped inclusions in alkali feldspar.	All altered to chlorite, as individual grains and as veinlets.	Absent.	Rare, apatite, secondary sphene zircon, opaques.	Plagioclase: Sericitic-moderate to intense, up to 1% modal muscovite developed. Minor epidote. Mafics: 100% altered to chlorite. Alkali feldspar: relatively unaltered.	Myrmekite development. Breccia veinlets common.
	20-35%	26-40%	30-40%	<4%		<1%		

Field relations

The West Branch North River (WBNR) pluton is a small, composite body, consisting of foliated granodiorite, monzogranite, and associated dykes. It intrudes gneiss and foliated granite in the west, and Late Hadrynian undifferentiated diorite and pelitic schists and gneisses in the east (Fig. 22.1; Barr et al., 1985; Jamieson and Craw, 1983; Jamieson and Doucet, 1983). The Bothan Brook (BB) pluton is a small north-south elongate body, that outcrops due south of the WBNR pluton.

The WBNR granodiorite outcrops in the western portion of the pluton and is associated with hybrid rocks along its western margin. The Sarach Brook shear zone (Jamieson and Doucet, 1983) separates the granodiorite from the monzogranite and bounds the Bothan Brook pluton on the west. Foliation in the granodiorite is more intense near the shear zone. The monzogranite outcrops in the eastern portion of the pluton, and has been observed in intrusive contact with foliated diorite in at least one outcrop along its eastern margin. Contact relations in the BB pluton have not been observed.

Mineralogy

The granodiorite is a medium- to coarse-grained, inhomogeneous, variably foliated, hypidiomorphic inequigranular rock. Mineralogical, textural and alteration features are summarized in Table 22.1. Modal and normative data classify this phase as diorite/granodiorite (Streckeisen, 1976); for consistency with field terminology, this phase is referred to as granodiorite throughout the text. The monzogranite is a medium- to coarse-grained, relatively homogeneous rock, with megacrysts of alkali feldspar locally developed. Mineralogical, textural and alteration features are given in Table 22.1. Both modal and normative data classify this phase as monzogranite.

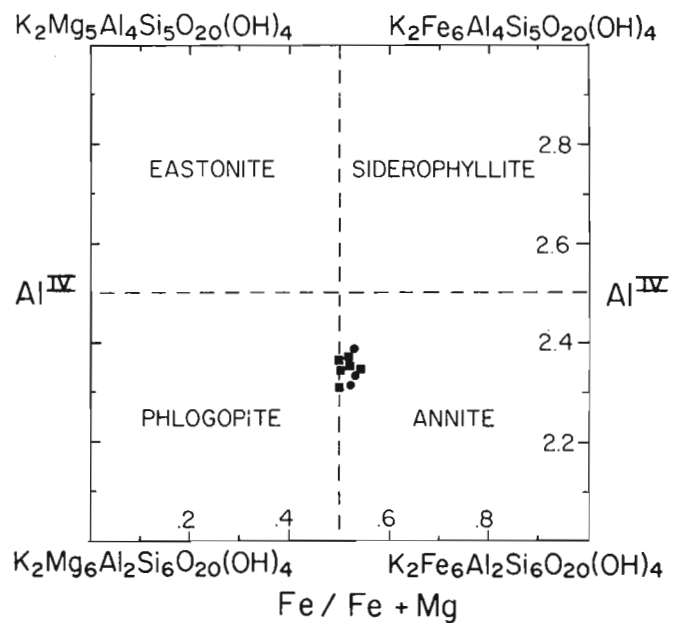


Figure 22.2. Biotite compositions in terms of Al vs Fe/Fe+Mg for the West Branch North River (WBNR) pluton. Symbols as in Figure 22.1.

The Bothan Brook granite is reddish, highly leucocratic, coarse grained, and relatively homogeneous. Petrographic features are summarized in Table 22.1. Alteration within the Bothan Brook pluton is strong throughout. Modal and normative mineralogy indicate that this phase falls in the monzogranite field, however, throughout the text, it is referred to as the Bothan Brook granite.

Feldspars throughout the suite (ie. both the West Branch North River and the Bothan Brook plutons) are all highly sodic (oligoclase-albite) and potassic (Or₈₀ to Or₉₆; Table 22.2). Biotites in the granodiorite and the monzogranite show a restricted compositional range within the annite field (Fig. 22.2), although Mn contents of the monzogranite biotites are notably higher (Table 22.3). Biotites from the Bothan Brook granite have been completely chloritized, hence no comparison of biotite compositions is possible. Amphiboles in the granodiorite are relatively Fe-rich, with a narrow compositional range (Table 22.4),

and similar Fe/(Fe+Mg) to biotite. Amphibole is absent from the WBNR monzogranite and from the BB granite. The mineralogy throughout the suite has been variably modified by alteration, however, it is generally consistent with a cogenetic intermediate to felsic sequence from granodiorite to monzogranite to granite.

Geochemistry

Major and trace element geochemistry and normative mineralogy are listed in Table 22.5. SiO₂ variation diagrams for major and trace element data are plotted in Figures 22.3 and 22.4 respectively.

The bimodal nature of the West Branch North River pluton is clearly defined by the geochemical data (Fig. 22.3, 22.4). There is a gap in SiO₂ contents between 64 and 70% that is reflected by all the other major oxide proportions, with the exception of Na₂O, which remains

Table 22.2. Microprobe analyses* of plagioclase and alkali feldspar from the West Branch North River (WBNR) and Bothan Brook (BB) plutons

	A	B	C	D	E	F	G	H	I	J
SiO ₂	62.77	63.72	63.58	64.51	63.72	64.53	64.60	64.76	64.27	63.98
Al ₂ O ₃	18.18	18.37	18.19	18.49	18.42	18.15	18.27	18.58	18.37	18.12
CaO	0.00	0.00	0.00	0.00	0.00	0.00	0.00	0.00	0.00	0.00
Na ₂ O	0.62	1.26	0.61	0.88	0.50	0.60	0.58	1.26	0.44	0.57
K ₂ O	15.60	14.73	15.70	15.67	16.12	16.10	16.25	15.24	16.28	15.99
Total	97.17	98.08	98.08	99.55	98.78	99.38	99.70	99.84	99.36	98.66
An	-	-	-	-	-	-	-	-	-	-
Ab	6	12	6	8	5	5	5	11	4	5
Or	94	88	94	92	95	95	95	89	96	95

	K		L		M	N		O		P	
	core	rim	core	rim		core	rim	core	rim	core	rim
SiO ₂	61.50	61.94	61.05	61.89	60.71	62.55	62.97	60.83	61.59	61.01	62.55
Al ₂ O ₃	23.83	23.40	23.85	23.53	24.87	23.13	23.19	24.12	23.35	23.80	23.13
CaO	5.28	4.79	5.08	4.74	6.11	4.37	4.64	5.68	4.95	5.48	4.59
Na ₂ O	8.76	9.09	8.76	8.99	8.25	8.62	9.34	8.55	8.73	8.53	9.14
K ₂ O	0.21	0.21	0.16	0.16	0.14	0.24	0.16	0.17	0.12	0.14	0.08
Total	99.58	99.43	98.81	99.31	100.02	98.91	100.30	99.35	98.74	98.96	99.49
An	25	22	24	22	29	22	21	27	24	26	22
Ab	74	77	74	77	70	77	78	72	76	73	78
Or	1	1	1	1	1	1	1	1	1	1	tr

	Q	R		S		T	U	
		core	rim	core	rim		core	rim
SiO ₂	67.46	65.72	67.99	65.44	64.25	67.34	64.59	69.43
Al ₂ O ₃	19.75	19.48	19.28	22.23	21.91	20.02	21.47	19.95
CaO	0.45	0.63	0.25	3.07	2.67	0.83	2.52	0.32
Na ₂ O	11.71	11.21	11.81	10.33	9.95	10.58	9.84	11.81
K ₂ O	0.32	0.22	0.18	0.25	0.09	1.21	0.66	0.21
Total	99.63	97.26	99.45	101.22	98.87	99.98	99.08	101.72
An	2	3	1	14	13	4	12	2
Ab	96	96	98	85	87	89	84	97
Or	2	1	1	1	tr	7	4	1

Microprobe analyses of alkali feldspar (A-J) and plagioclase (K-S) from the WBNR and BB plutons. WBNR granodiorite: A,B,C,K,L,M,N,O,P; WBNR monzogranite: D,E,F,G,Q,R,S; BB granite: H,I,J,T,U.

*Cambridge Instruments Microscan 5 with Ortec Energy Dispersive Analyzer, Dalhousie University.

Table 22.3. Microprobe analyses* of biotites from the West Branch North River (WBNR) granodiorite and monzogranite

	489-1	489-2	489-3	297-1	297-2	297-3	486-1	486-2	486-3
SiO ₂	38.00	37.24	37.44	36.83	37.23	37.37	37.80	38.26	37.60
TiO ₂	1.67	2.86	3.08	2.60	2.75	2.94	3.02	2.83	2.46
Al ₂ O ₃	15.73	15.27	15.72	15.37	15.36	15.89	15.68	15.98	16.06
FeO	20.62	20.06	19.75	20.70	20.33	19.72	20.18	19.99	20.83
MnO	0.14	0.05	0.09	0.09	0.16	0.29	0.56	0.39	0.50
MgO	11.63	10.96	10.92	10.18	10.89	10.67	10.27	10.64	10.57
K ₂ O	9.44	9.41	9.40	9.12	9.14	9.53	9.67	9.77	9.84
H ₂ O**	4.00	3.95	3.98	3.90	3.95	3.98	4.00	4.04	4.01
Total	101.23	99.80	100.38	98.79	99.81	100.39	101.18	101.90	101.87
Ionic proportions									
Si	5.69	5.65	5.64	5.66	5.65	5.63	5.67	5.68	5.62
Al ^{iv}	2.32	2.35	2.37	2.34	2.35	2.37	2.34	2.32	2.38
Z site	8.00	8.00	8.00	8.00	8.00	8.00	8.00	8.00	8.00
Al ^{vi}	0.46	0.38	0.42	0.45	0.40	0.45	0.43	0.48	0.45
Ti	0.19	0.33	0.35	0.30	0.31	0.33	0.34	0.32	0.28
Fe	2.58	2.55	2.49	2.66	2.58	2.48	2.53	2.48	2.63
Mn	0.02	0.01	0.01	0.01	0.02	0.04	0.07	0.05	0.06
Mg	2.59	2.48	2.45	2.33	2.46	2.40	2.29	2.36	2.35
Y site	5.84	5.72	5.72	5.75	5.77	5.70	5.66	5.69	5.77
K	1.80	1.82	1.80	1.80	1.77	1.83	1.85	1.85	1.88
X site	1.80	1.82	1.80	1.80	1.77	1.83	1.85	1.85	1.88
H	4.00	4.00	4.00	4.00	4.00	4.00	4.00	4.00	4.00
O	24.00	24.00	24.00	24.00	24.00	24.00	24.00	24.00	24.00
PHLOG	49.96	49.27	49.52	46.60	48.64	48.72	46.87	48.19	46.89
ANN	49.70	50.60	50.25	53.17	50.95	50.52	51.68	50.80	51.85
Mn	0.34	0.13	0.23	0.23	0.41	0.75	1.45	1.00	1.26
F/M	1.00	1.03	1.02	1.15	1.06	1.05	1.13	1.08	1.13
F/FM	0.50	0.51	0.51	0.53	0.51	0.51	0.53	0.52	0.53
WBNR granodiorite: 489-1, -2, -3; 297-1, -2, -3.									
WBNR monzogranite: 286-1, -2, -3.									
* Cambridge Instruments Microscan 5 with Ortec Energy Dispersive Analyzer, Dalhousie University.									
** H ₂ O – calculated based on the stoichiometry of biotite.									

uniform throughout. A well defined negative correlation with silica exists for TiO₂, MgO and P₂O₅; Al₂O₃, CaO and MnO show a somewhat less uniform decrease with increasing SiO₂ contents. Only K₂O shows a positive correlation. The variability in the proportion of mafic minerals in the granodiorite is reflected in the data point scatter for this phase in general. The somewhat variable CaO contents throughout the suite may be explained by the localized occurrence of microscopic veinlets of epidote. The monzogranite is relatively homogeneous, and shows little systematic variation in geochemistry, with the exception of CaO, Al₂O₃ and K₂O contents, whose variation is consistent with the replacement features observed petrographically.

In the Bothan Brook granite, SiO₂ is uniformly high (72.35–75.76 wt%), with correspondingly low TiO₂, MgO, Fe₂O₃ and P₂O₅ and Al₂O₃, all these oxides decreasing slightly with increasing SiO₂ contents. CaO contents are very low and uniform, and K₂O values are high, but show a broad scatter. Na₂O contents are low relative to the West Branch North River samples. These features reflect the more intense alteration of the Bothan Brook granite. Major element geochemistry of the West Branch North River and the Bothan Brook plutons are therefore compatible with derivation from a single source.

Trace element data are plotted in Figure 22.4, and with the exceptions discussed below, are within the range expected for rocks of these compositions. Ba shows somewhat anomalous behaviour in this suite, and a non-linear trend on the SiO₂ variation diagram (Fig. 22.4). The Ba values of the granodiorite remain uniformly high, and this is followed by a sharp decrease in Ba contents with increasing SiO₂. The overall decrease in Ba throughout the sequence, is similar to that observed for granitic rocks by Lee and Doring (1974). In contrast to the behaviour of Ba, Sr shows a sharp decrease with increasing SiO₂ in the granodiorite, followed by a uniformly lower, though relatively constant (156–318 ppm), set of values for the monzogranite, and a very low, though relatively constant (101–284 ppm) set of values for the Bothan Brook samples. Rb contents increase steadily with increasing SiO₂ in the West Branch North River samples, but are relatively lower and uniform in the Bothan Brook granite. A plot of Rb against K₂O shows the depletion of Rb relative to K₂O in the Bothan Brook samples (Fig. 22.5).

Although the behaviour of these elements can in part be explained by alteration, that is, they are depleted relative to the elements for which they substitute during post-magmatic changes, it is possible that the observed trends are a feature of the magmatic phase, and reflect crystal fractionation.

Plagioclase fractionation will strongly deplete Sr relative to Ba, which does not become "compatible" until K-feldspar begins to crystallize (Cox et al., 1979, p. 337). This can also explain the relatively constant Sr contents, and corresponding decreasing Ba contents in the monzogranite and in the Bothan Brook granite. Rb is concentrated preferentially in biotite, and the virtual absence of this mineral in the Bothan Brook granite may account for the strong depletion of this element in these samples.

Fluorine contents show a negative correlation with SiO₂, similar to trends recorded for several other granitic plutons in Cape Breton (Barr et al., 1982). Alteration can modify F-concentrations (eg. Bailey, 1977; Godfrey, 1962), thus the F-contents may not truly reflect the F-concentrations of the magma. Alternatively, as F tends to be concentrated in minerals such as apatite, biotite, sphene, and to a lesser extent, amphibole (Bailey, 1977), it is possible that the observed distribution simply reflects the higher concentration of these minerals in the granodiorite.

Zr, Y, Zn and Cr decrease overall with increasing SiO₂ contents, although there is considerable scatter, particularly within the granodiorite. It is possible that this scatter is the result of contamination by the host rocks, however, more data are required to evaluate this possibility.

Age

One sharp contact between the WBNR monzogranite and dioritic rocks to the east has been observed in the field, and the pluton does crosscut regional trends in the west. A Rb-Sr isochron date of 399.6 ± 4.6 Ma on samples from the WBNR granodiorite and monzogranite suggests intrusion of the pluton in the early stages of the Acadian orogeny (Table 22.6; Fig. 22.6). Preliminary cooling ⁴⁰Ar/³⁹Ar dates of ca. 380 Ma have been obtained on biotites from these units (P.H. Reynolds, personal communication, 1986). The Bothan Brook pluton is highly altered throughout, thus no samples have been dated. The possible effects of alteration on the isochron from the WBNR pluton are considered in the next section.

Discussion

The geochemical data raise questions as to the relationship among the three units. On the basis of field observations, mineralogy, alteration features, and isotopic studies, we suggest that all three units represent different phases of the same intrusion. This preliminary interpretation is based on limited data, and we recognize that other interpretations are also possible.

The WBNR and BB plutons are quite different in the field in terms of overall appearance, however, a strong case can be made on the basis of geochemistry and mineralogical similarities that the BB granite is a more evolved phase of the WBNR monzogranite. The mineralogy is consistent with this interpretation, considering the extent of alteration, particularly in the BB granite, and the bulk chemical data overlap and fall along essentially the same trend.

The geochemical data from the WBNR pluton exhibit a distinct compositional gap between the granodiorite and the monzogranite (Fig. 22.3, 22.4). In any attempt to determine the significance of this feature, the field relations, isotopic data and mineralogy need to be considered. In the field, the most mafic part of the granodiorite, and the most felsic part of the monzogranite are clearly different in terms of overall appearance. However, locally there are outcrops in which it is difficult to distinguish between them. Thus field observations suggest a gradation between the granodiorite and the monzogranite. Furthermore, the shear zone that separates them has a component of thrusting from north to

Table 22.4. Microprobe analyses* of amphiboles from the granodiorite of the West Branch North River (WBNR) pluton

	489-1	489-2	489-3	297-1	297-2	297-3
SiO ₂	44.78	44.09	44.70	43.79	44.58	44.28
TiO ₂	1.69	1.16	0.98	1.69	1.42	1.64
Al ₂ O ₃	8.89	8.89	8.67	8.99	9.24	8.57
FeO	18.31	18.26	18.44	18.63	18.75	17.85
MnO	0.31	0.19	0.24	0.24	0.22	0.27
MgO	10.61	10.71	10.53	10.19	10.33	10.64
CaO	11.38	11.67	11.47	11.25	11.25	11.35
Na ₂ O	1.77	1.35	1.16	1.62	1.56	1.69
K ₂ O	1.10	0.94	0.97	1.05	1.06	0.91
Total	98.93	97.26	97.16	97.45	98.41	97.20
Ionic proportions						
Si	6.64	6.61	6.70	6.59	6.61	6.66
Al ^{IV}	1.36	1.39	1.30	1.41	1.39	1.34
Z site	8.00	8.00	8.00	8.00	8.00	8.00
Al ^{VI}	0.20	0.18	0.23	0.18	0.23	0.18
Ti	0.19	0.13	0.11	0.19	0.16	0.19
Fe ³⁺ **	0.34	0.57	0.59	0.49	0.56	0.39
Fe ²⁺	1.93	1.72	1.72	1.85	1.77	1.86
Mg	2.35	2.40	2.35	2.29	2.29	2.39
Y site	5.00	5.00	5.00	5.00	5.00	5.00
Mn	0.04	0.02	0.03	0.03	0.03	0.03
Ca	1.81	1.88	1.84	1.81	1.79	1.83
Na	0.15	0.10	0.13	0.16	0.18	0.14
X site	2.00	2.00	2.00	2.00	2.00	2.00
Na	0.36	0.29	0.21	0.31	0.27	0.35
K	0.21	0.18	0.19	0.20	0.20	0.17
A site	0.56	0.47	0.40	0.51	0.47	0.52
Total	15.58	15.47	15.40	15.51	15.48	15.53
* Cambridge Instruments Microscan 5 with Ortec Energy Dispersive Analyzer, Dalhousie University.						
** Calculated after Holland and Richardson (1979).						

south (Jamieson and Doucet, 1983). It is therefore possible that the granodiorite represents a deeper structural level of the pluton, brought up by thrusting. This could also account in part for the foliation observed in the granodiorite. Both the granodiorite and the monzogranite plot on the same Rb-Sr whole rock isochron (Fig. 22.5). When samples from the granodiorite and the monzogranite are plotted separately, the isochron is essentially the same. Although the proportions of mafic to felsic minerals change dramatically between the two, alkali feldspar and biotite compositions are similar in both, and consistent with crystallization from a common parent. As outcrop in the area is poor and sporadic, and detailed mapping was not undertaken, it is possible that the data reflect a selection effect rather than the presence of two completely different intrusions. Alternatively, the presence of hybrid rocks along the eastern margin of the granodiorite, and the variable proportions of mafic minerals within the granodiorite itself, suggest possible contamination of the granodiorite by the host rock.

If the WBNR granodiorite, the WBNR monzogranite, and the BB granite represent different phases of the same intrusion, at least some of the variation may be explained by alteration effects. The BB granite owes its distinctive appearance in part to intense alteration that has reddened the feldspars and completely chloritized the biotite. The intensity of alteration may reflect proximity to the Sarach Brook shear zone, which borders the granite to the west.

Table 22.5. Major¹ and trace element² geochemistry and CIPW normative data from the West Branch North River (WBNR) and Bothan Brook (BB) plutons

	097	297	104	280	489	283	284	483	484	486	488	118	413	425	364	139	326	328
SiO ₂	57.08	54.52	62.27	63.74	62.03	70.43	73.24	71.57	72.62	71.59	73.60	75.29	74.43	72.35	74.71	73.89	75.06	75.76
Al ₂ O ₃	18.07	17.61	17.77	17.11	16.57	15.34	14.53	14.57	14.36	14.43	14.59	13.58	13.22	14.19	13.29	13.32	13.20	13.33
Fe ₂ O ₃	2.04	2.79	1.56	1.55	1.57	0.94	0.76	0.65	1.08	0.88	0.59	0.90	0.80	1.15	0.89	0.65	0.52	0.71
FeO	3.21	4.69	2.31	2.30	3.43	1.32	0.68	1.08	0.94	1.03	0.84	0.66	0.58	1.31	0.23	0.49	0.36	0.25
MgO	3.36	3.48	2.08	1.96	2.68	0.99	0.44	0.59	0.62	0.65	0.34	0.44	0.32	0.54	0.17	0.33	0.17	0.15
CaO	4.99	5.04	3.65	3.30	3.64	1.50	0.39	1.49	1.60	1.56	1.37	0.16	0.19	0.24	0.31	0.32	0.31	0.46
Na ₂ O	4.26	3.85	4.25	4.11	4.00	3.91	4.07	3.91	3.89	3.88	1.67	3.17	3.56	3.51	3.23	3.25	3.16	2.93
K ₂ O	1.93	2.37	2.56	2.84	2.94	4.17	4.83	4.35	3.62	3.72	5.09	5.37	5.32	5.76	5.60	4.97	5.62	5.81
TiO ₂	0.85	1.38	0.84	0.85	0.99	0.55	0.25	0.28	0.35	0.32	0.21	0.34	0.18	0.46	0.16	0.29	0.15	0.16
MnO	0.07	0.09	0.05	0.06	0.03	0.03	0.02	0.03	0.04	0.04	0.02	0.02	0.01	0.03	0.01	0.02	0.01	0.01
P ₂ O ₅	0.41	0.75	0.29	0.26	0.35	0.13	0.05	0.08	0.09	0.09	0.07	0.05	0.03	0.09	0.02	0.03	0.01	0.01
H ₂ O _{tot}	2.49	2.81	2.63	1.79	1.41	1.27	1.05	0.64	1.04	0.96	0.52	0.60	0.37	1.20	0.76	1.01	0.67	0.85
Total	99.46	99.38	100.26	99.87	99.67	100.58	100.31	99.24	100.20	99.15	98.91	100.38	99.01	100.83	99.38	98.57	99.24	100.43
Q	10.03	7.53	17.30	19.32	15.38	27.22	28.24	28.24	32.13	30.95	41.47	35.50	32.93	28.57	34.08	35.72	34.75	35.43
Or	11.77	14.52	15.51	17.12	17.70	24.84	28.78	26.10	21.59	22.41	30.60	31.83	31.90	34.20	33.59	30.13	33.72	34.51
Ab	37.17	33.73	36.83	35.45	34.40	33.31	34.69	33.55	33.19	33.43	14.36	26.88	30.54	29.81	27.71	28.19	27.12	24.89
An	22.76	20.81	16.60	14.95	16.05	6.64	1.62	6.97	7.41	7.28	6.44	0.47	0.76	0.60	1.43	1.43	1.49	2.23
Hy	11.66	13.32	7.00	6.64	10.33	3.28	1.35	2.54	1.93	2.37	1.62	1.00	0.94	2.10	0.43	0.84	0.43	0.38
Mt	3.05	4.19	2.32	2.32	2.32	1.37	1.11	0.96	1.51	1.30	0.87	1.21	1.18	1.67	0.31	0.82	0.76	0.38
Hm	0.00	0.00	0.00	0.00	0.00	0.00	0.00	0.00	0.00	0.00	0.00	0.07	0.07	0.00	0.69	0.10	0.00	0.45
Il	1.66	1.80	1.63	1.65	1.91	1.05	0.48	0.54	0.67	0.62	0.41	0.65	0.35	0.88	0.31	0.56	0.29	0.31
Ap	0.98	1.80	0.69	0.61	0.83	0.30	0.12	0.19	0.21	0.21	0.17	0.12	0.07	0.21	0.05	0.07	0.02	0.02
C	0.91	1.39	2.12	1.93	1.05	1.99	2.03	0.92	1.36	1.42	4.07	2.18	1.35	1.96	1.41	2.13	1.39	1.41
Ba	1216	1336	1236	1174	1245	907	635	684	521	541	627	966	274	645	339	371	226	198
Rb	46	54	70	64	98	136	179	174	159	154	283	125	140	159	131	152	140	139
Sr	1129	1489	868	777	740	318	156	311	298	313	170	284	108	101	159	146	123	121
Y	21	24	17	18	19	10	9	9	11	14	13	11	10	30	14	9	8	8
Zr	255	185	221	238	317	162	100	113	134	138	159	126	113	230	96	105	83	88
Nb	n.d.	15	9	9	12	11	10	10	11	0	12	8	11	13	8	12	8	9
Th	n.d.	0	0	8	8	22	23	24	27	19	54	20	23	15	23	28	27	59
Pb	n.d.	7	14	15	11	20	23	30	26	27	32	17	23	26	22	23	22	26
Ga	n.d.	20	21	20	22	15	17	17	17	19	18	14	15	17	15	17	14	14
Zn	64	91	61	61	89	28	15	35	39	38	39	29	15	43	12	21	22	21
Ni	57	23	22	21	32	12	5	8	3	4	6	2	3	6	0	2	4	3
V	n.d.	184	87	78	104	40	18	25	28	32	15	22	12	26	6	16	4	9
Cr	42	5	49	43	52	24	8	7	9	11	4	8	4	5	6	17	2	4
F	n.d.	1074	731	687	964	419	284	455	417	534	304	183	165	278	164	157	177	119

WBNR granodiorite (097,297,104,280,489), WBNR monzogranite (283,284,483,484,486) and associated dyke (488), and BB granite (118,413,425,364,139,326,328).

¹ Analyses by atomic absorption spectrometry, Dalhousie University; analyst S. Pärkh.

² Analyses by XRF at Nova Scotia Regional X-ray fluorescence centre, St. Mary's University, Halifax, except F by ion-sensitive electrode at Dalhousie University.

Alteration is, however, evident throughout the intrusion in the form of epidote (in veinlets and after plagioclase), sericite (which affects plagioclase more strongly than alkali feldspar), chlorite (after biotite and hornblende) and local development of secondary K-feldspar (after plagioclase and in veinlets). These observations suggest widespread redistribution of K, Na, and Ca and associated Rb and Sr, and possibly account for scatter observed in these and other elements (eg. Al, Ba, Zn, Pb and F) on the SiO₂ variation diagrams (Fig. 22.3, 22.4). The alteration, however,

either occurred shortly after intrusion, or was not sufficiently intense to reset the isochron totally, or to disrupt the geochemical trends severely.

Alteration throughout the area is intensified in proximity to shear zones. These commonly contain quartz-albite pods, suggesting mobilization of Na from the granites where, in general, plagioclase is more severely altered than K-feldspar. Within the monzogranite, subvertical breccia zones up to two metres thick trend about 130°. These are rich in hematite, quartz and monzogranite fragments.

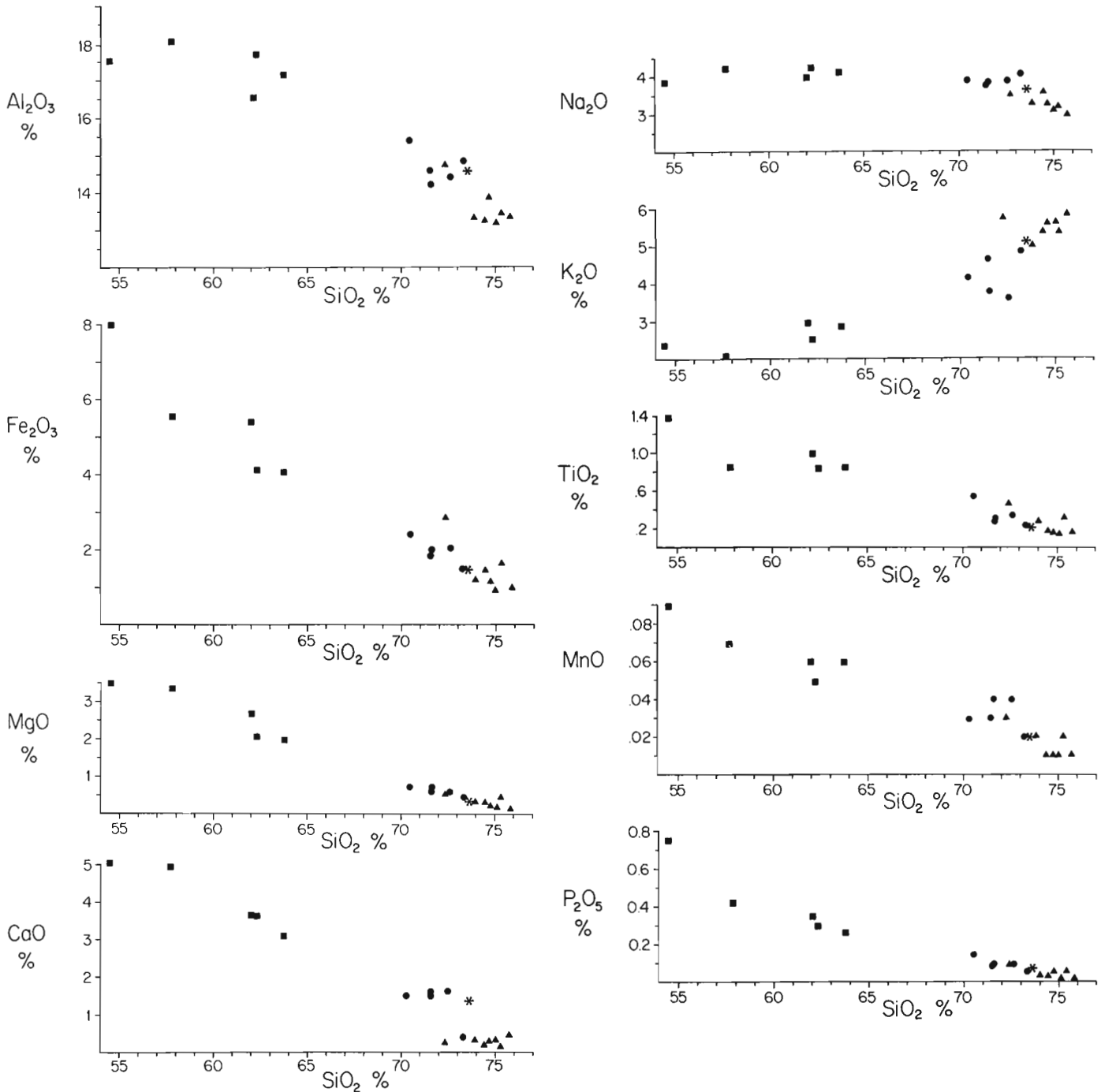


Figure 22.3. Major element geochemistry plotted on SiO₂ variation diagrams. Symbols as in Figure 22.1.

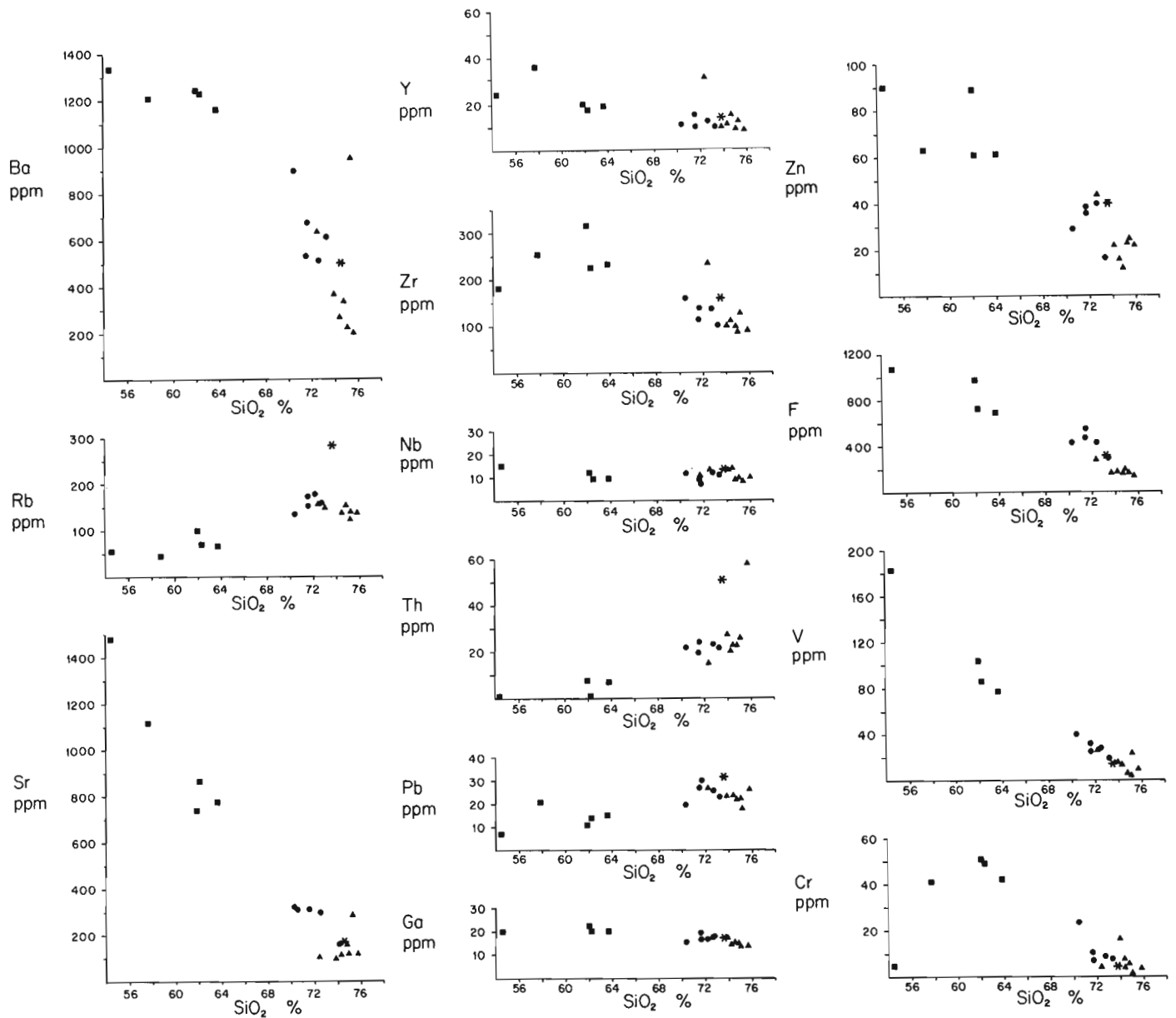


Figure 22.4. Trace element geochemistry plotted on SiO₂ variation diagrams. Symbols as in Figure 22.1.

Table 22.6. Rb/Sr isotope date from the West Branch North River (WBNR) pluton

Sample	Rb	Sr	⁸⁷ Rb/ ⁸⁶ Sr	⁸⁷ Sr/ ⁸⁶ Sr*
097	47.5	1149.7	0.1195±0.0012	0.70453(05)
104	72.2	899.1	0.2325±0.0023	0.70536(05)
280	66.0	807.1	0.2366±0.0024	0.70528(09)
489	94.5	778.1	0.3511±0.0035	0.70581(07)
283	138.1	331.6	1.2058±0.0121	0.71094(05)
284	179.4	157.9	3.2933±0.0329	0.72227(06)
486	154.5	322.8	1.3815±0.0138	0.71181(10)
488	283.5	173.8	4.7336±0.0473	0.73104(06)

WBNR granodiorite = 097, 104, 280, 489; WBNR monzogranite = 283, 284, 286; WBNR dyke = 488.

Analyses at Memorial University using techniques described by Taylor and Fryer (1983). Decay constant for ⁸⁷Rb is 1.42 × 10⁻¹¹/yr (Steiger and Jager, 1977).

Rb and Sr in ppm; *errors given as 2 sigma in the last digits.

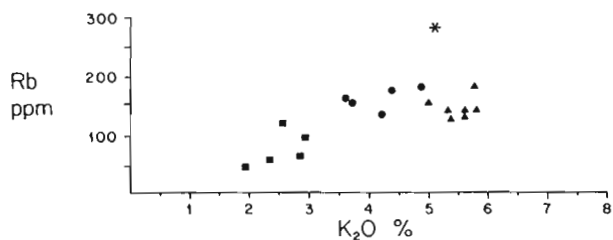


Figure 22.5. Plot of Rb against K₂O for the West Branch North River (WBNR) and the Bothan Brook (BB) plutons. Symbols as in Figure 22.1.

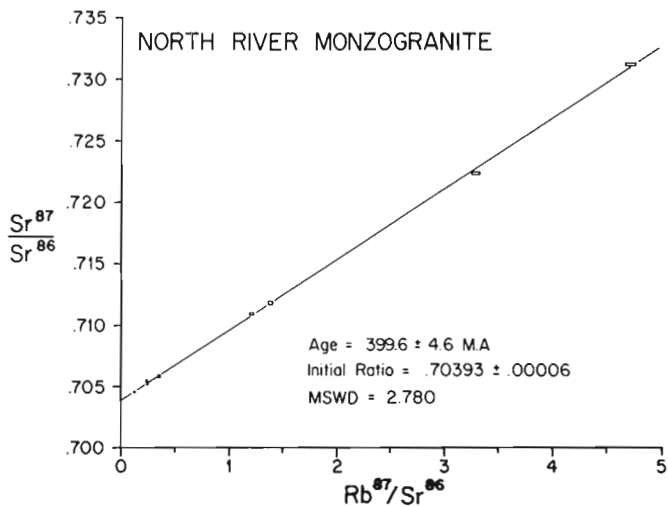


Figure 22.6. Plot of $^{87}\text{Sr}/^{86}\text{Sr}$ against $^{87}\text{Rb}/^{86}\text{Sr}$ for the West Branch North River (WBNR) pluton.

Near the breccia zones, the monzogranite is reddened and has discontinuous pods and veinlets of specular hematite. The complexity of alteration styles and the ubiquitous nature of the alteration suggest that the intrusion, and in particular the breccia zones, may merit examination for their mineral potential.

Acknowledgments

This study was funded by Research Agreements (51-4-80, 83-4-81, 254-4-82, 205-04-84) from Energy Mines and Resources Canada (to R.A. Jamieson) between 1979 and 1985 as well as the current contract 27 ST23233-5-0403. The authors also acknowledge the assistance of the technical and clerical staff of the Department of Geology at Dalhousie University.

References

Bailey, J.C.
1977: Fluorine in granitic rocks and melts: a review; *Chemical Geology*, v. 19, p. 1-42.

Barr, S.M., O'Reilly, G.A., and O'Beirne, A.M.
1982: Geology and geochemistry of selected granitoid plutons of Cape Breton Island; Nova Scotia Department of Mines and Energy, Paper 82-1, 176 p.

Barr, S.M., Jamieson, R.A., and Raeside, R.P.
1985: Igneous and metamorphic geology of the Cape Breton Highlands; Geological Association of Canada - Mineralogical Association of Canada Field Guide, Excursion 10, 48 p.

Cox, K.G., Bell, J.D., and Pankhurst, R.J.
1979: The Interpretation of Igneous Rocks; George Allen and Unwin Publ., 450 p.

Godfrey, J.D.
1962: The deuterium content of hydrous minerals from the east central Sierra Nevada and Yosemite National Park; *Geochimica et Cosmochimica Acta*, v. 26, p. 1215-1245.

Holland, T.J.B. and Richardson, S.W.
1979: Amphibole zonation in metabasites as a guide to the evolution of metamorphic conditions; *Contributions to Mineralogy and Petrology*, v. 70, p. 143-148.

Jamieson, R.A. and Craw, D.
1983: Reconnaissance mapping of the southern Cape Breton Highlands - a preliminary report; in *Current Research, Part A*, Geological Survey of Canada, Paper 83-1A, p. 263-268.

Jamieson, R.A. and Doucet, P.
1983: The Middle River-Crowdis Mountain area, southern Cape Breton Highlands; in *Current Research, Part A*, Geological Survey of Canada, Paper 84-1A, p. 269-275.

Lee, D.E. and Doring, W.P.
1974: Barium in hybrid rocks of the southern Snake Range, Nevada; *USGS Journal of Research*, v. 2, p. 671-673.

O'Beirne-Ryan, A.M., Barr, S.M., and Jamieson, R.A.
1986: Contrasting petrology and age of two megacrystic granitoid plutons, Cape Breton Island, Nova Scotia; in *Current Research, Part B*, Geological Survey of Canada, Paper 86-1B, report 21.

Steiger, R. and Jager, E.
1977: Subcommittee on geochronology: convention on the use of decay constants in geochronology cosmochronology; *Earth and Planetary Science Letters*, v. 36, p. 359-362.

Streckeisen, A.
1976: To each plutonic rock its proper name; *Earth Science Review*, v. 12, p. 1-33.

Taylor, R.P. and Fryer, B.J.
1983: Strontium isotope geochemistry of the Santa Rita porphyry copper deposit, New Mexico; *Economic Geology*, v. 78, p. 170-174.

Stable isotope studies of planktonic foraminifera *Globigerina bulloides* from cores in the northeast Pacific Ocean

Contract 21St.23233-3-1322

Ihsan S. Al-Aasm¹ and Brian D. Bornhold²
Cordilleran and Pacific Margin Division

Al-Aasm, I.S. and Bornhold, B.D., Stable isotope studies of planktonic foraminifera *Globigerina bulloides* from cores in the northeast Pacific Ocean; in *Current Research, Part B, Geological Survey of Canada, Paper 86-1B*, p. 201-212, 1986.

Abstract

Oxygen and carbon isotopes were determined on 161 individual samples of the planktonic foraminifera *G. bulloides*. The samples are from two cores in the northeast Pacific Ocean and cover the Holocene and Pleistocene time span (about 700 000 years). The $\delta^{18}\text{O}$ profiles resemble previously published Pleistocene data and show 18 glacial/interglacial cycles. The magnitude of each glacial/interglacial cycle is about 2‰. *G. bulloides* apparently secreted its test in isotopic disequilibrium with ambient ocean water; this disequilibrium representing combined vital effect and variation in the rate of calcification with increasing depth. The studied species shows also a clear ^{13}C depletion, which may be a consequence of ^{12}C enriched CO_2 (from photosynthesis by symbiotic algae) in ambient waters.

Résumé

On a déterminé les isotopes d'oxygène et de carbone dans 161 échantillons différents du foraminifère planctonique *G. bulloides*. Les échantillons proviennent de deux carottes prélevées dans le nord-est du Pacifique et datent de l'Holocène et du Pléistocène ancien à récent (environ 700 000 ans). Les profils de l'isotope $\delta^{18}\text{O}$ sont similaires aux données déjà publiées sur le Pléistocène et révèlent qu'il y a eu 18 cycles glaciaires/interglaciaires. L'ampleur de chaque cycle glaciaire/interglaciaire est d'environ 2‰. Le test de *G. bulloides* aurait été formé en déséquilibre isotopique par rapport à l'eau ambiante de l'océan; ce déséquilibre représente l'effet vital et la variation de la vitesse de calcification avec l'accroissement de la profondeur. L'espèce examinée est manifestement dépourvue de ^{13}C , ce qui pourrait être le résultat de la présence, dans l'eau ambiante, de CO_2 riche en ^{12}C (produit de la photosynthèse par les algues symbiotiques.)

¹ Derry Laboratory, Department of Geology, University of Ottawa, Ottawa, Ontario K1N 6N5

² Pacific Geoscience Centre, Sidney, B.C. V8L 4B2

Introduction

Starting with the pioneering work of Emiliani (1955, 1966, 1978), planktonic foraminifera have been utilized extensively as a paleo-oceanographic tool for biostratigraphic, ecological, and isotopic stratigraphy (Vincent and Berger, 1981). Emiliani showed that the Quaternary record consists of a series of regular glacial-interglacial fluctuations of saw-tooth pattern. Others (e.g. Shackleton, 1967, 1981; Shackleton and Opdyke, 1973; Hays et al., 1976; Berger, 1979; Broecker, 1981; Duplessy, 1981; Pisias and Moore, 1981) have concentrated on oxygen isotopes not only as a stratigraphic tool but addressed also the problem of ice volume, and the question of climatic oscillations. Such studies, however, were hampered by difficulties arising from several considerations. Firstly, it is not clear whether the $\delta^{18}\text{O}$ and $\delta^{13}\text{C}$ in these foraminifera represent isotopic values in equilibrium with their ambient ocean waters or whether they reflect isotopic disequilibrium as a consequence of interactions between organic and inorganic phases (e.g. foraminifera and other organisms, seawater and atmosphere; Shackleton et al., 1973; Grazzini, 1976; Broecker and Peng, 1982, Chapter 6). Secondly, the magnitude of the "ice volume effect" during glacial-interglacial transitions is not well established and the problem remains unsolved despite 25 years of studies (Hays et al., 1976, Emiliani, 1978; Savin and Yeh, 1981; Shackleton, 1981; Mix and Ruddiman, 1984).

The major goals of the present contribution are the following: (1) elucidation of variations in $\delta^{18}\text{O}$ and $\delta^{13}\text{C}$ in oceanic sediments of the northeast Pacific cores END 77-28 and END 77-29 in terms of their Holocene and Pleistocene evolution, (2) correlation of these variations with paleo-oceanographic records for adjacent oceanic areas, (3) contribution to the understanding of the oceanic carbon cycle from consideration of the established $\delta^{13}\text{C}$ record, and (4) determination whether *Globigerina bulloides* secrete their calcitic tests in isotopic equilibrium with the ambient seawater.

Materials and methods

Two cores from the northeast Pacific Ocean were utilized in this study. These are the core END 77-28 located at $48^{\circ}15.60'\text{N}$, $134^{\circ}30.27'\text{W}$ at a water depth of 3725 m, and END 77-29 located at $48^{\circ}34.24'\text{N}$, $133^{\circ}56.69'\text{W}$ at a water depth of 3695 m (Fig. 23.1).

G. bulloides was separated from the prewashed core subsamples and usually the density was sufficient for isotopic studies, but some intervals were devoid of measurable specimens.

161 samples of *G. bulloides* from both cores and various stratigraphic intervals were selected for oxygen and carbon isotopic analysis. A single sample contains as many as

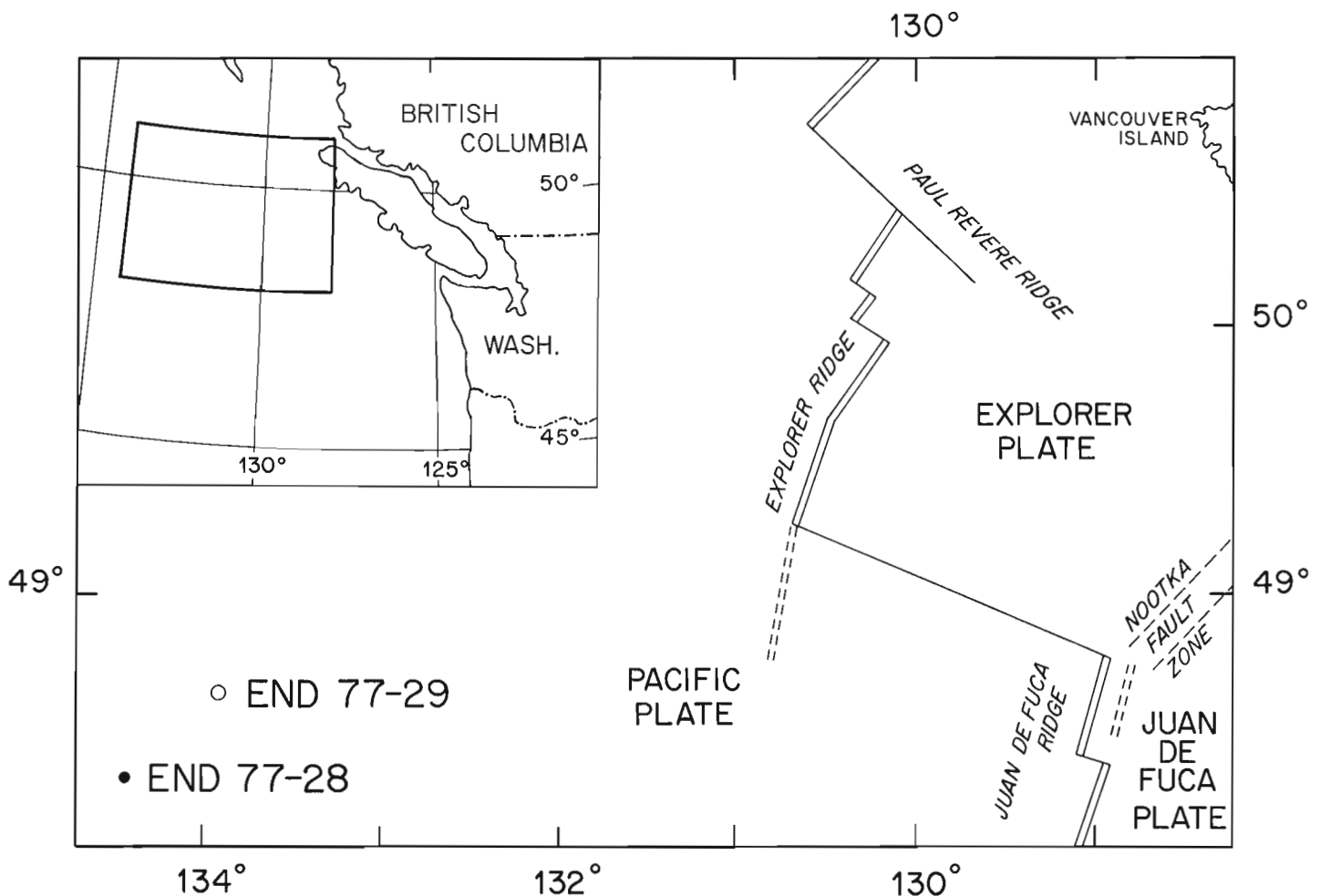


Figure 23.1. Location map of the studied cores.

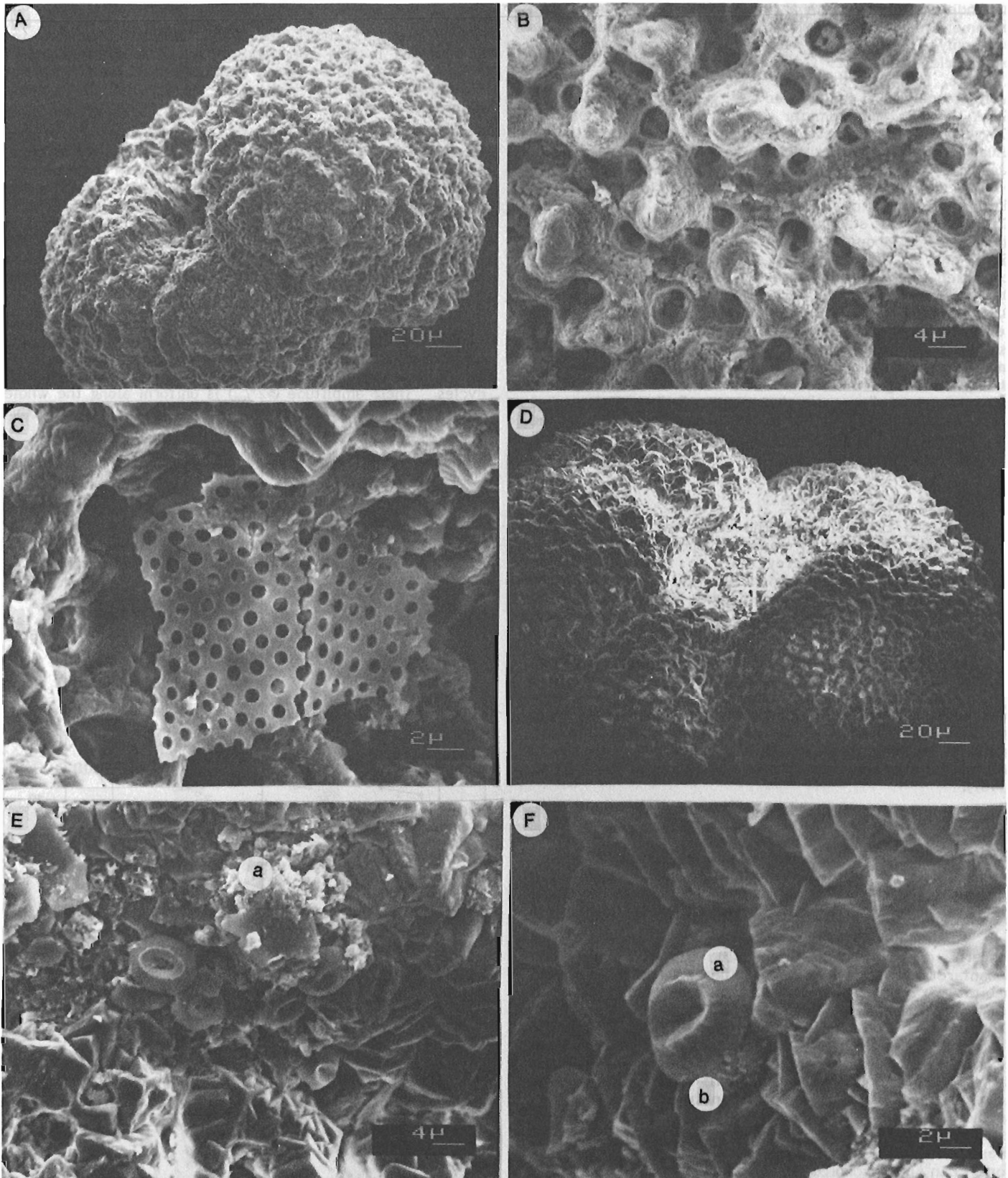


Figure 23.2. (A) SEM micrograph of *G. bulloides* (sample No. 158) showing well preserved texture of the test; (B) closeup of the wall texture showing the pores; (C) radiolarian plate occupying open space in the test; (D) *G. bulloides* (sample No. 570) showing well preserved test; (E) partial dissolution of test wall (a); and (F) coccolith plate (a) and submarine cementation (b).

100 individuals, each with a diameter of about 100-400 μm . In some 40 samples, however, the total number of individuals was only 10-25. Each sample was treated with 100% phosphoric acid at 25°C in a water bath *in vacuo* for 12 hours, following the procedure of McCrea (1950). The isotopic analysis of the evolved CO_2 gas was carried out on a SIRA-12 mass spectrometer at the University of Ottawa. Oxygen and carbon isotopic ratios are expressed in the usual δ notation and given in per mil relative to PDB standard. Calibration was made via the standard carbonate NBS-19 and carbonatite NBS-18. Precision of the data was determined by daily analysis of calcite I (University of Ottawa internal standard equivalent to NBS-18) and by duplication of about 7% of all samples (1 s.d. = 0.11‰ for $\delta^{13}\text{C}$ and 0.13‰ for $\delta^{18}\text{O}$). The average accuracies, as compared to the values given by Coplen et al. (1983), were 0.05‰ for $\delta^{13}\text{C}$ and 0.06‰ for $\delta^{18}\text{O}$ for calcite I and 0.08‰ for $\delta^{13}\text{C}$ and 0.18‰ for $\delta^{18}\text{O}$ for NBS-18. The relatively large standard deviation for foraminiferal samples is believed to be the result of isotopic heterogeneity in the monospecific samples. In addition to isotopic studies, an SEM survey (utilizing NANOLAB 7 SEM) was conducted to detect the presence of diagenetic phenomena. Sedimentation rates were determined by a ^{230}Th method carried out in the Department of Oceanography at the University of British Columbia (Huntley et al., in press).

Lithology of the studied cores

(1) Core END 77-29: The core length is 589.5 cm. Lithologically, the first 70 cm are composed of silty lutite, which is grey to olive grey, soft to firm and rich in foraminifera and diatoms. In the interval from 71-82.5 cm foraminifera are absent. The remainder of the core consists of greyish to brownish grey lutite, with mottled character, and variable concentrations of foraminifera and diatoms.

(2) Core END 77-28: The core length is 238 cm. Lithologically, the first 50 cm are composed of soft mottled, foraminifera-rich, yellowish brown lutite. The sediments become harder below this interval with mottled appearance, and some stratification. They are greyish brown lutites with variable foraminifera content. Further lithological information for these two cores is available in Bornhold et al. (1981).

Results

All isotopic results for *G. bulloides* from northeast Pacific Ocean cores are presented in Appendix 1. Included in this table are calculated shifts from equilibrium $\delta^{18}\text{O}$ and $\delta^{13}\text{C}$ values for assumed summer and winter conditions.

G. bulloides is a spirally coiled spinose species with modern ocean concentrations in the subarctic and subantarctic provinces (Vincent and Berger, 1981). The depth habitat of recent *G. bulloides* is in the upper 100 m of seawater, but they predominate at all depths of 50 to 100 m (Berger, 1969; Durazzi, 1981; Khan and Williams, 1981). The tests of *G. bulloides* are characterized by spinose wall texture (Fig. 23.2). Living specimens have long acicular spines which are represented in fossils as short bases. The test wall is flat with large pores penetrating an unmodified surface (Vincent and Berger, 1981). The original low-Mg calcitic tests are usually mineralogically and texturally well preserved (Fig. 23.2A, D). The pores are usually vacant but some can be occupied by sediments and/or by other micro-organisms, such as diatoms (Fig. 23.2C) and coccolithophorids (Fig. 23.2F). Evidence for partial dissolution of planktonic tests, due to the increasing depth below the carbonate compensation line (CDD), is rare (Fig. 23.2E). Submarine cementation, occluding pores and cavities, has been observed in some specimens (Fig. 23.2B, F).

Core END 77-29

Figure 23.3 shows the $\delta^{18}\text{O}$ and $\delta^{13}\text{C}$ records for *G. bulloides* in this core and includes the percentage of CaCO_3 . It should be noted that carbonate values may not coincide in depth precisely with the samples for isotopic determinations.

Oxygen isotopic values of *G. bulloides* in this core range from +1.30 to 4.73‰ (Appendix 1). The observed isotopic fluctuations (Fig. 23.3) may be correlated with some success with isotopic stages deduced from planktonic and benthic foraminifera from other oceans. These include the composite isotopic record for the Caribbean (Emiliani, 1978) as well as the equatorial Pacific cores V28-238 and V28-239 (Shackleton and Opdyke, 1973, 1976). Using a sedimentation rate of about 0.8-0.9 cm/1000 y, the presently studied core covers a period of about 700 000 years.

Accepting that the sedimentation rate in the core END 77-29 has been slow (about 0.85 cm/1000 year) and uniform throughout glacial and interglacial stages, the $\delta^{18}\text{O}$ record indicates more than 18 successive glacial-interglacial cycles. Their amplitude (>2‰) is uniform along the whole core depth. If interpreted in terms of temperature, this

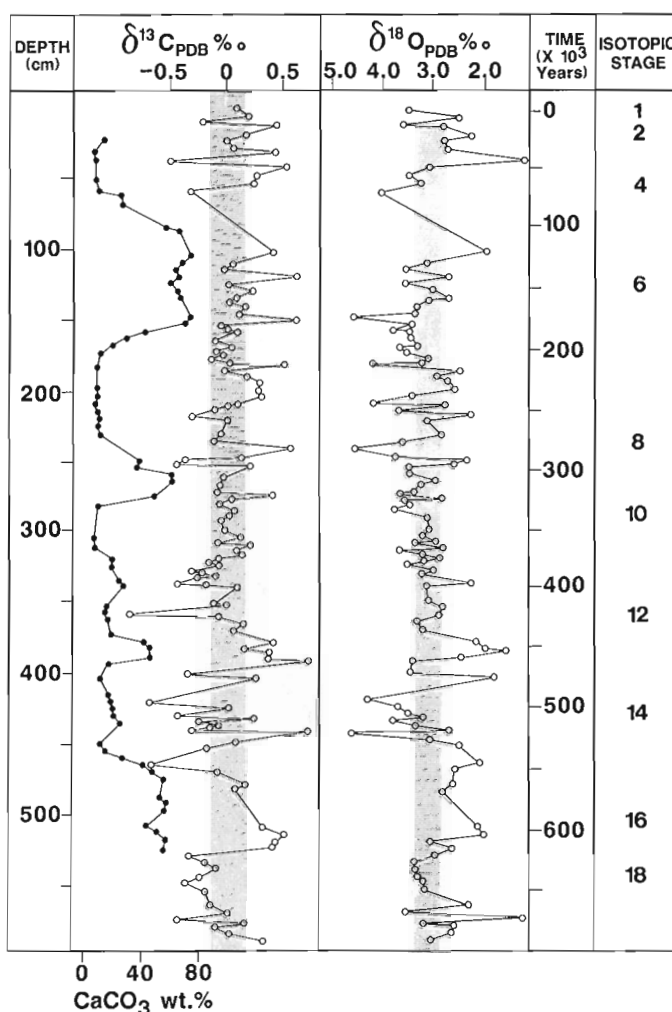


Figure 23.3. $\delta^{18}\text{O}$, $\delta^{13}\text{C}$ (with respect to PDB) in planktonic foraminifera *G. bulloides* and carbonate content (as % CaCO_3) of core END 77-29. Isotopic stages are those estimated by Shackleton and Opdyke (1973) and Emiliani (1978). Time (in thousands of years) is predicted on the assumption that the sedimentation rate was 0.85 cm/1000 years.

would suggest about 8°C difference between glacial and interglacial maxima. This estimate exceeds temperature variations deduced by others for the Pleistocene record, but a proportion of this $\delta^{18}\text{O}$ variance is due to glacial effects. Emiliani (1955, 1966, 1971) advocated that the latter effect accounted for approximately 30% (0.5‰) of the glacial-to-interglacial change in the isotopic composition of shallow tropical seawater, while Dansgaard and Tauber (1969), Savin and Stehli (1974) and Berger and Gardner (1975) advocated about 1‰ change. For bottom waters, Shackleton (1967) argued for about 1.4 to 1.6‰ change in isotopic composition of seawater. The curve, however, is noisier than the Caribbean curves. This is probably due to the slow sedimentation rates which cause blurring of the record due to bioturbation by burrowing organisms (cf. Shackleton, 1977).

The $\delta^{13}\text{C}$ values for all *G. bulloides* samples (Fig. 23.3) show wide variations with depth, but the calculated average is close to 0‰ PDB. The $\delta^{13}\text{C}$ of planktonic foraminifera as well as of other calcareous nannofossils can reflect regional variations in $\delta^{13}\text{C}$ of the total dissolved carbon (TDC) in the oceans (Broecker and Peng, 1982). Shackleton (1977) believed that planktonic foraminifera grown during glacial times have a lower $^{13}\text{C}/^{12}\text{C}$ ratio than do those grown during interglacial times, but this proposition has been disputed by Berger and Killingley (1977). Some of the $\delta^{13}\text{C}$

variations in *G. bulloides* correlate inversely with $\delta^{18}\text{O}$, perhaps as a result of glacial effects. Other parts of the core, however, show opposite relationships (Fig. 23.3). This complexity is a consequence of the fact that $\delta^{13}\text{C}$ variations may be a result of a multitude of parameters, such as changes in TDC, nutrient supply, test growth rates, and metabolic activity (cf. Berger and Killingley, 1977; Erez, 1978; Berger, 1979; Broecker and Peng, 1982).

The CaCO_3 content of this core (Fig. 23.3) suggests 4 maxima and 4 minima, and they appear to correlate partly with the $\delta^{13}\text{C}$ curve. Preceding work on carbonate variations in the Pacific Ocean showed a temporal relation between foraminiferal solution cycles and glacial-interglacial events as determined by isotopic data (Thompson and Saito, 1974). In detail, however, the rate of carbonate solution depends strongly on the location of the sample site relative to the lysocline and to the carbonate compensation depth (Berger, 1970). These effects are difficult to predict and evaluate.

Core END 77-28

This core covers a time span of about 290 000 years, providing the sedimentation rate was about 0.85 cm/1000 year. Appendix 1 and Figure 23.4 show the

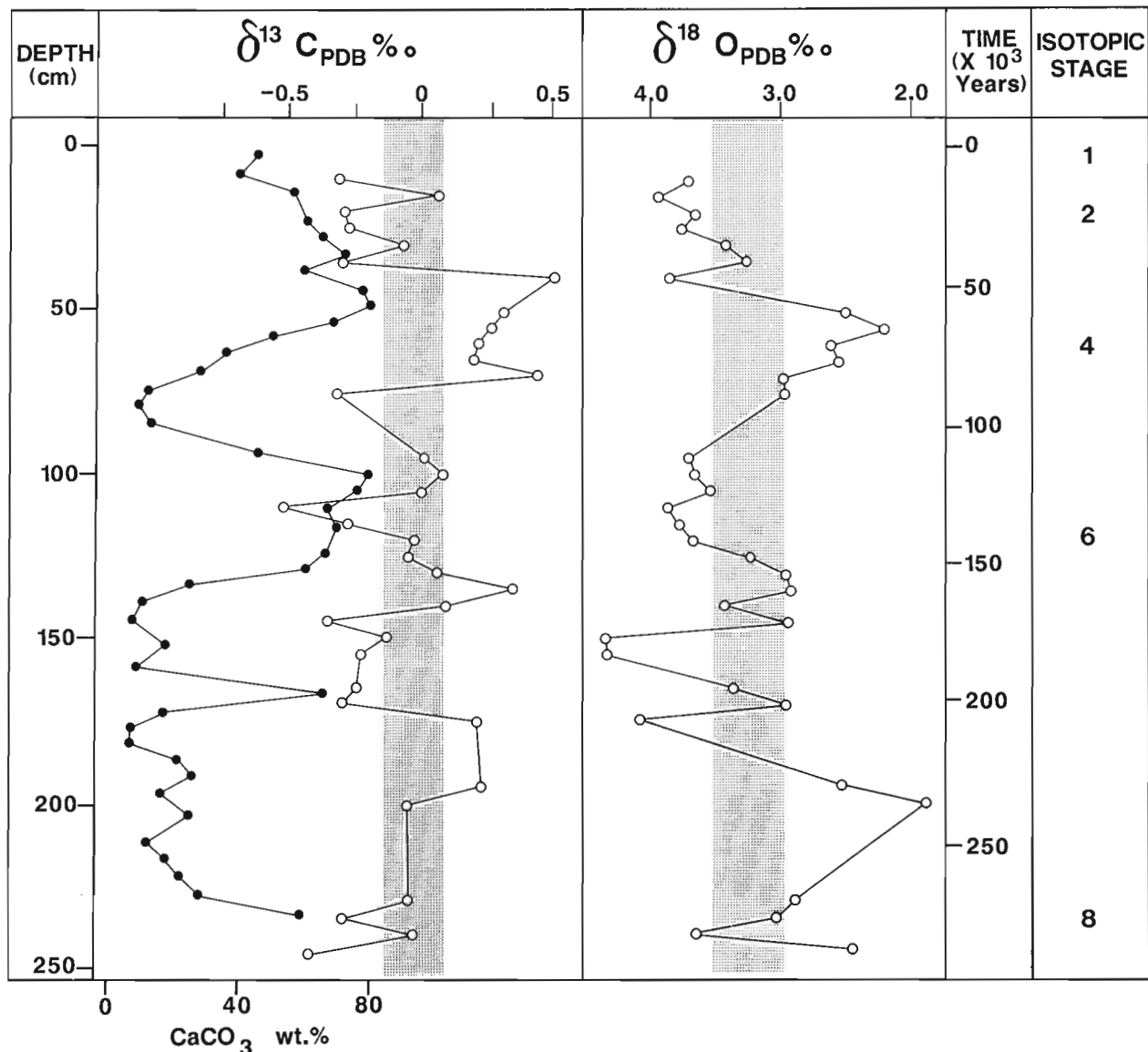


Figure 23.4. Isotopic value and carbonate content of *G. bulloides* of core END 77-28. Time is predicted on the assumption that sedimentation rate was 0.85 cm/1000 years (see text).

stratigraphic variations in isotopic values for *G. bulloides* as well as the associated CaCO_3 contents. The $\delta^{18}\text{O}$ values range from +1.92 to +4.38‰ PDB and the oxygen isotopic record in this core shows 8 glacial-interglacial cycles. These are possibly the cycles 1, 2, 3, 4, 5, 6, 7 and 8. They correlate fairly well with the isotopic stages of Shackleton and Opdyke (1973) and Emiliani (1978). The amplitude of isotopic variations between maxima and minima is about 2‰.

The carbon curve (Fig. 23.4) shows less variation with depth than was the case for the core END 77-29, but the calculated average $\delta^{13}\text{C}$ is again about 0.0‰ PDB. The fluctuations in $\delta^{13}\text{C}$ appear to correlate inversely with $\delta^{18}\text{O}$ and the latter correlate reasonably well with core END 77-29. This agreement suggests comparable paleo-oceanographic conditions. Because of the agreement between carbonate content and $\delta^{18}\text{O}$ (Fig. 23.4), glaciation results in heavy oxygen isotopic composition of the coeval seawater.

Discussion

Oxygen isotopes

The general rules for utilization of oxygen isotope paleothermometry are well established (Urey, 1947; Emiliani, 1955; Shackleton and Opdyke, 1973; Berger, 1979; Savin and Yeh, 1981). For planktonic foraminifera, the

estimated temperature will be a reflection not only of surface water temperatures but also of changes in its isotopic composition due to waxing and waning of ice sheets (Shackleton and Opdyke, 1973; Duplessy, 1981; Zahn et al., 1985). Furthermore, this estimate may also depend on diagenetic alterations of the tests though Imbrie et al. (1973) demonstrated that this factor is negligible for most Pleistocene foraminifera. Overall, planktonic foraminifera are thought to be secreting their CaCO_3 tests at, or close to, isotopic equilibrium with seawater, although some may show small disequilibrium (Shackleton et al., 1973; Grazzini, 1976). It is also generally believed (Hays et al., 1976; Curry and Matthews, 1981; Durazzi, 1981) that *G. bulloides* secretes its test at, or close to, isotopic equilibrium. Thus, the observed $\delta^{18}\text{O}$ variations should reflect a combination of habitat depth (temperature), size variations of the tests, "ice volume effect", and lateral temperature changes. However, Khan and Williams (1981), argued that the so called oxygen depth ranking of the living *G. bulloides* from the northeast Pacific Ocean reflects, in fact, the relative magnitudes of vital effects. The present data are in accord with this proposition.

The ambient oxygen paleotemperature can be calculated as follows (Craig, 1965):

$$T = 16.9 - 4.38(\delta c - \delta w) + 0.13(\delta c - \delta w)^2 \quad (1)$$

where T = is the temperature in celsius degrees; δc = in the oxygen isotopic composition of foraminiferal calcite, and δw = is the oxygen isotopic composition of seawater.

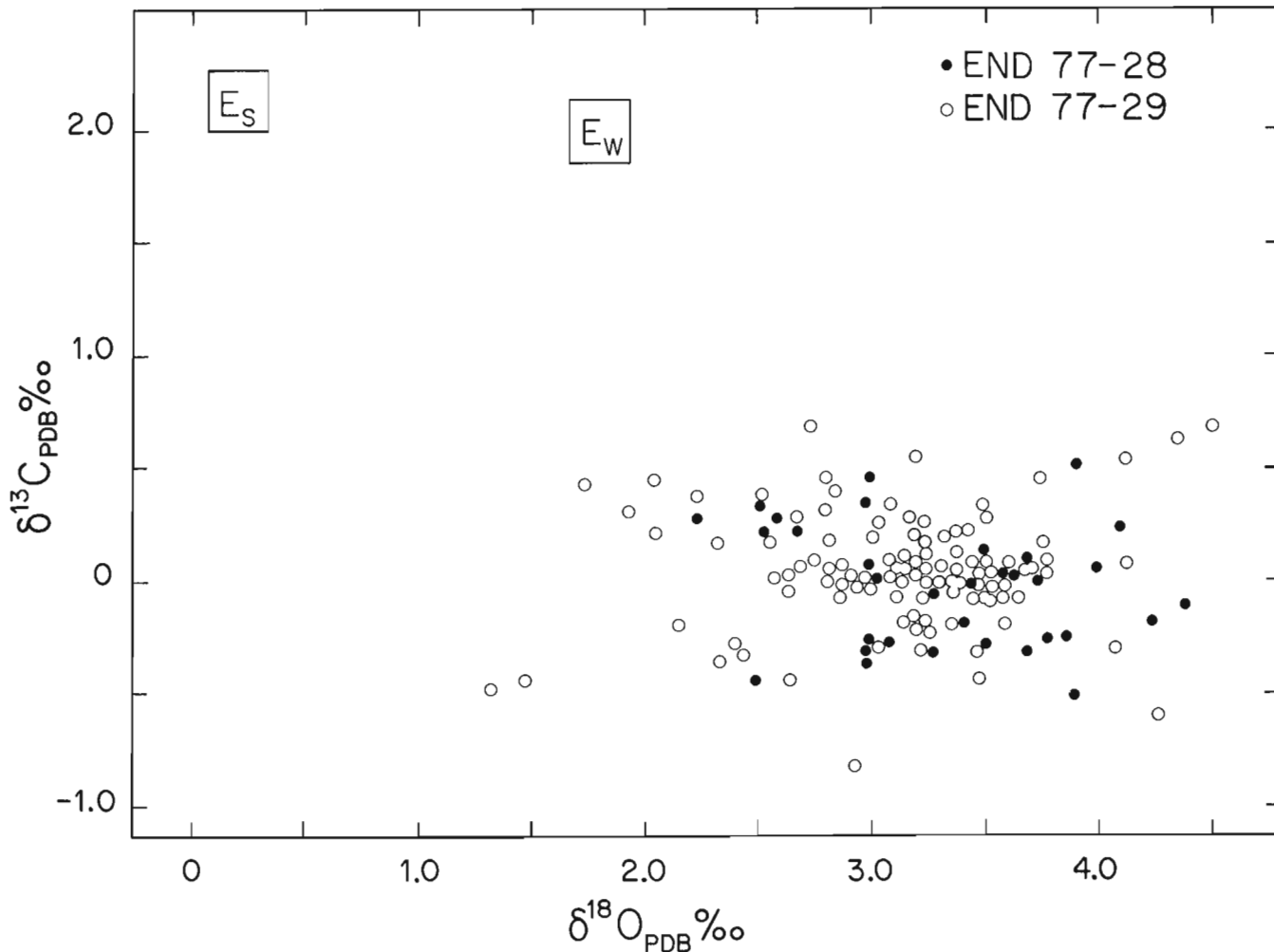


Figure 23.5. $\delta^{13}\text{C}$ vs $\delta^{18}\text{O}$ scatter diagram for all *G. bulloides*. Es and Ew are the estimated values for calcite in equilibrium with seawater for summer and winter, respectively (see text).

Studies of preferable depth habitats for the Holocene *G. bulloides* indicate that the species thrives in the uppermost 100 m, with maximal concentration at 50-75 m depth (Berger, 1969; Durrazzi, 1981; Khan and Williams, 1981). The winter temperature at about 50 m depth at the core localities is approximately 6°C. This estimate is based on the mean January 1978 monthly surface water temperature of 7.5°C (Thomson, 1981) and the vertical temperature gradient taken from the profile for the Ocean station "P" (NE Pacific; Khan and Williams, 1981). The August water temperature at comparable depth is assumed to have been about 12°C. The accepted salinity is 32.45‰ (Thomson, 1981). Utilizing the above temperature and salinity measurements, and $\delta^{18}\text{O}$ of surface water of -1.03‰ PDB-1 (average of 12 subarctic water masses; Khan and Williams, 1981), the $\delta^{18}\text{O}$ in equilibrium calcite should be about 1.73‰ PDB in winter and 0.15‰ PDB in summer. The measured values are much heavier (Fig. 23.5), and the departure is even more striking if one considers that calcification is more effective in summer (see Fig. 23.6). The differences observed between theoretical and measured values range from +1.15 to +4.34‰ in summer and from -0.43 to +2.76‰ in winter (Appendix 1). The most frequent $\Delta^{18}\text{O}$ in summer is +3.25‰, while in the winter it is +2.25‰ (Fig. 23.6). Consequently, all "paleotemperatures" are much less than the present day temperatures reported by Thomson (1981). It may be proposed that the discrepancy is due to the fact that calcification proceeds at some depth below the surface, with calcification rate higher during summer months when the tests are heavier and thus sink into relatively deeper and colder parts of the water column (cf. Vincent and Berger, 1981).

This interpretation, however, is at variance with the observed preferred depth of habitat for *G. bulloides*. If seasonal variations are accepted as a cause of the above oxygen isotope discrepancy, they do not appear to satisfy the observed magnitude of $\delta^{18}\text{O}$ trends. This leaves vital effect as the only viable explanation for the heavy $\delta^{18}\text{O}$ record, although a secondary contribution by some of the above mechanisms is possible.

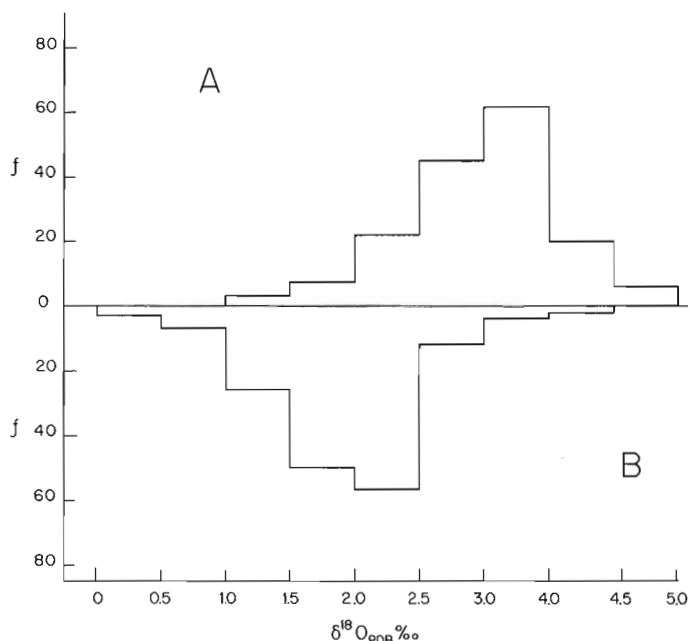


Figure 23.6. Histogram plot of $\Delta\delta^{18}\text{O}$ for predicted summer (A) and winter (B).

To utilize the absolute $\delta^{18}\text{O}$ values of *G. bulloides* for paleoclimatological purposes, a correction of values is essential. Such corrections are, however, unnecessary if only the pattern of variations is considered. Consequently, the primary usefulness of the data is in monitoring the glacial-interglacial intervals.

Carbon isotopes

The variations in $\delta^{13}\text{C}$ of foraminifera may provide information on the source of carbon utilized by organisms during calcification. This, in turn, may reflect nutrient concentrations and hydrographic properties of seawater (Williams et al., 1977). Many planktonic and benthic foraminifera secrete their CaCO_3 tests in isotopic disequilibrium with seawater (Shackleton et al., 1973; Grazzini, 1976; Williams et al., 1977; Erez, 1978; Khan and Williams, 1981; Killingley et al., 1981). In order to ascertain the situation for *G. bulloides*, it is essential to consider hydrographic data. In their absence, it is assumed that: (a) $\delta^{13}\text{C}$ of CO_2 at 50 m depth is 1.7‰ (Kroopnick et al., 1970, 1977); and (b) the fractionation of C isotope follows the relationship of Rubinson and Clayton (1979), with

$$\delta^{13}\text{C}_{\text{calcite}} = \delta^{13}\text{C}_{\text{dissolved bicarbonate}} + 0.9 + 0.035(T - 25^\circ\text{C}) \quad (2)$$

The summer and winter water temperature T in the above equation is as discussed in the section dealing with oxygen isotopes. The utilized temperature-dependent fractionation coefficient of 0.035 is that of Emrich et al. (1970). The $\delta^{13}\text{C}$ of bicarbonate is approximated by that of CO_2 (Kroopnick et al., 1977; Williams et al., 1977; Broecker and Peng, 1982). With such assumptions, the $\delta^{13}\text{C}$ of equilibrium calcite should be +1.93‰ PDB at 6°C and +2.14‰ PDB at 12°C. Again, most tests are considerably lighter in $\delta^{13}\text{C}$ (Fig. 23.5), and the average $\Delta^{13}\text{C}$ foraminifera-equilibrium calcite (Appendix 1) is roughly -2‰ (Fig. 23.7), regardless of whether summer or winter is considered. The lack of seasonal difference in $\delta^{13}\text{C}$ may be a consequence of the fact that isotopic fractionation of carbon is not as strongly temperature dependent as is the oxygen ($\Delta^{13}\text{C}_{\text{HCO}_3^- - \text{CaCO}_3}$ of about 0.035‰ per °C; Emrich et al., 1970).

The departure from equilibrium for $\delta^{13}\text{C}$ in *G. bulloides* could be a consequence of the following factors:

1. the presence of ^{13}C -depleted metabolic CO_2 in the solution from which the calcite was precipitated (cf. Williams et al., 1977; Erez, 1978);
2. the role of photosynthesis of symbiotic algae, which in turn increases the amount of isotopically depleted metabolic CO_2 in the internal CO_2 of *G. bulloides* (cf. Erez, 1978; Khan and Williams, 1981). Symbiotic algae, represented by species from Coccolithophorids (Fig. 23.2E), have been associated with *G. bulloides* utilized in this study; and
3. Kinetic fractionation of carbon isotopes during test growth (cf. Vincent and Berger, 1981). In this latter case, the initial shell nucleation is followed by a slower, near equilibrium, thickening of the test. The small foraminifera would presumably have lighter carbon than the larger massive ones (Grazzini, 1976). Khan and Williams (1981), studying recent *G. bulloides* from the northeast Pacific Ocean, showed that most of their surficial collections contained predominantly small juveniles, whereas those from greater depths contained larger specimens which also had a heavier $\delta^{13}\text{C}$ isotopic composition. These authors attributed the increase in heavy $\delta^{13}\text{C}$ to test size and believed that it reflected a physiological ontogenetic decrease in the intensity of

vital effect during primary calcification and not a change in the depth of their habitat. At present, We are not certain which single or combined factors are involved in this carbon isotopic departure from equilibrium. The observed disequilibrium is, however, more or less uniform throughout the cores.

The relative pattern of fluctuations in $\delta^{13}\text{C}$ of *G. bulloides* downcore may have some bearing on glacial-interglacial episodes. The light peaks may perhaps signify high nutrient supply in surface water during glacial times and thus reflect variations in TDC with time (cf. Berger and Killingley, 1977; Berger, 1979).

Conclusions

Studies of stable isotopic composition of tests of *G. bulloides* from two northeast Pacific cores, and the associated variations in carbonate content, indicate that:

1. The investigated cores cover a time span of 700 000 years, that is the whole Holocene and much of the Pleistocene.
2. The $\delta^{18}\text{O}$ values in cores END 77-29 and END 77-28, indicate 18 and 8 glacial-interglacial cycles, respectively. These cycles coincide more or less with the Pleistocene glacial-interglacial stages recorded elsewhere. The magnitude of each glacial-interglacial cycle is about 2‰.
3. The measured $\delta^{18}\text{O}$ values in both cores are heavier than expected for calcite in equilibrium with seawater. This is believed to be a consequence of varying rates of calcification of foraminiferal tests with depth or of some other vital effects.

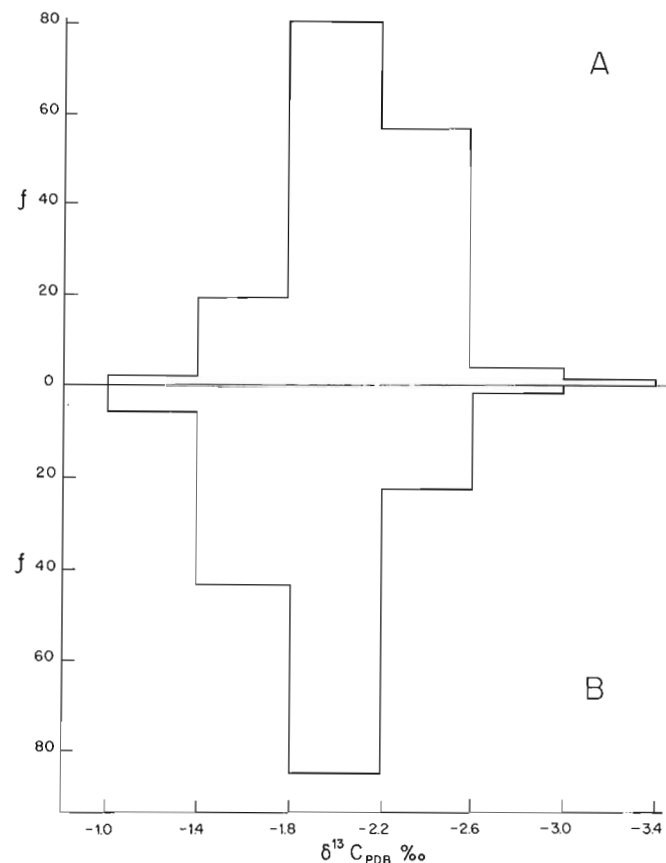


Figure 23.7. Histogram plot of $\Delta\delta^{13}\text{C}$ for predicted summer (A) and winter (B).

4. In contrast to oxygen, the measured $\delta^{13}\text{C}$ values are lighter than expected for calcite in equilibrium with ambient waters. This depletion may be due to the presence of ^{13}C depleted CO_2 in ambient waters, perhaps as a consequence of photosynthesis by symbiotic algae. Alternatively, kinetic fractionation or other factors may be important. The $\delta^{13}\text{C}$ values may reflect total variations in TDC and thus the amount of nutrients in subsurface waters during glacial-interglacial periods.
5. Carbonate content fluctuates downcore and the pattern of these fluctuations correlates positively with $\delta^{13}\text{C}$, and to a lesser extent with $\delta^{18}\text{O}$. The increase in carbonate content at some intervals may signify periods of glaciation.

Acknowledgments

The authors thank J. Veizer for giving the senior author the opportunity to conduct this study and for reading the manuscript; B. Taylor and D. Ryan for technical advice; D. Naldrett for reading the manuscript; the Chemistry Department of the University of Ottawa for the access to the SEM facility; S.E. Calvert and M. Soon of the Department of Oceanography at University of British Columbia for the determination of sedimentation rates using ^{230}Th ; J. Hayes for typing the manuscript, and Alison Steele for drafting. This work has been financially supported by a Post-Doctoral Fellowship from an EMR contract to J. Veizer.

References

Berger, W.H.
 1969: Ecologic patterns of living planktonic foraminifera; Deep-sea Research, v. 16, p. 1-24.
 1970: Biogenous deep-sea sediments: fractionation by deep-sea circulation; Geological Society of America, Bulletin, v. 81, p. 1385-1402.
 1979: Stable isotopes in foraminifera; Society of Economic Paleontologists and Mineralogists, Short Course No. 6, p. 156-198.

Berger, W.H. and Gardner, J.V.
 1975: On the determination of Pleistocene temperatures from planktonic foraminifera; Journal of Foraminifera Research, v. 5, p. 102-113.

Berger, W.H. and Killingley, J.S.
 1977: Glacial holocene transition in deep-sea carbonates: selective dissolution and the stable isotope signal; Science, v. 197, p. 563-566.

Bornhold, B.D., Tiffin, D.L., and Currie, R.G.
 1981: Trace metal geochemistry of sediments, northeast Pacific Ocean; Geological Survey of Canada, Paper 80-25, 21 p.

Broecker, W.S.
 1981: Glacial to interglacial changes in ocean and atmosphere chemistry; in Climatic Variations and Variability Facts and Theories, ed. A. Berger; D. Reidel Publ. Co., p. 109-120.

Broecker, W.S. and Peng, T.H.
 1982: Tracers in the sea; Lamont-Doherty Geological Observatory Publication, Columbia University, Palisades, N.Y., 690 p.

Coplen, T.B., Kendall, C., and Hopple, J.
 1983: Comparison of stable isotope reference samples; Nature, v. 302, p. 236-238.

- Craid, H.
1965: The measurement of oxygen isotope paleotemperatures; in *Stable Isotopes in Oceanographic Studies and Paleotemperatures*, Spoleto, ed. E. Tongiorgi; Consiglio Nazionale delle Ricerche Laboratorio di Geologia Nucleare, Pisa, p. 161-182.
- Curry, W.B. and Matthews, R.K.
1981: Paleo-oceanographic utility of oxygen isotopic measurements on planktonic foraminifera: Indian Ocean core-top evidence; *Palaeogeography, Palaeoclimatology, Palaeoecology*, v. 33, p. 173-191.
- Dansgaard, W. and Tauber, H.
1969: Glacier oxygen-18 content and Pleistocene ocean temperatures; *Science*, v. 166, p. 499-502.
- Duplessy, J. Cl.
1981: Oxygen isotope studies and Quaternary marine climates; in *Climatic Variations and Variability*, ed. A. Berger; D. Reidel Publ. Co., p. 181-192.
- Durazzi, J.T.
1981: Stable-isotope studies of planktonic foraminifera in north Atlantic core tops; *Palaeogeography, Palaeoclimatology, Palaeoecology*, v. 33, p. 157-172.
- Emiliani, C.
1955: Pleistocene temperatures; *Journal of Geology*, v. 63, p. 538-578.
1966: Paleotemperature analyses of Caribbean cores P6304-8 and P6304-9 and a generalized temperature curve for the part 425 000 years; *Journal of Geology*, v. 74, p. 109-126.
1971: The amplitude of Pleistocene climatic cycles at low latitudes and the isotopic composition of glacial ice; in *The Late Cenozoic Glacial Ages*, ed. K.K. Turkajin; Yale University Press, New Haven, p. 183-197.
1978: The cause of the ice age, *Earth and Planetary Science Letters*, v. 37, p. 349-352.
- Emrich, K., Ehhalt, D.H., and Vogel, J.C.
1970: Carbon isotope fractionation during the precipitation of calcium carbonate; *Earth and Planetary Science Letters*, v. 8, p. 363-371.
- Erez, J.
1978: Vital effects on stable-isotope compositions seen in foraminifera and coral skeletons; *Nature*, v. 273, p. 199-202.
- Grazzini, C.V.
1976: Non-equilibrium isotopic compositions of shells of planktonic foraminifera in the Mediterranean Sea; *Paleogeography, Paleoclimatology, Paleoecology*, v. 20, p. 263-276.
- Hays, J.D., Imbrie, J., and Shackleton, W.J.
1976: Variations in the Earth's orbit: pacemaker of the ice ages; *Science*, v. 194, p. 1121-1132.
- Huntley, D.J., Nissen, M., Thomson, J., and Calvert, S.E.
- An improved alphascintillation counting method for determination of Th, U, Ra-226, Th-230 excess and Pa-231 excess in marine sediments; *Canadian Journal of Earth Sciences*. (in press)
- Imbrie, J., Van Donk, J., and Kipp, N.G.
1973: Paleoclimatic investigation of a Late Pleistocene Caribbean Deep-Sea Core: comparison of isotopic and faunal methods; *Quaternary Research*, v. 3, p. 10-38.
- Khan, M.J. and Williams, D.F.
1981: Oxygen and carbon isotopic composition of living planktonic foraminifera from the northeast Pacific Ocean; *Paleogeography, Paleoclimatology, Paleoecology*, v. 33, p. 47-69.
- Killingley, J.S., Johnson, R.F., and Berger, W.H.
1981: Oxygen and carbon isotopes of individual shells of planktonic foraminifera from Ontong-Java Plateau, equatorial Pacific; *Paleogeography, Paleoclimatology, Paleoecology*, v. 33, p. 193-204.
- Kroopnick, P., Deuser, W.G., and Craig, H.
1970: Carbon 13 measurements on dissolved inorganic carbon at the North Pacific (1969) Geosecs station; *Journal of Geophysical Research*, v. 75, p. 7668-7671.
- Kroopnick, P., Margolis, S.V., and Wong, C.
1977: ¹³C variations in marine carbonate sediments as indicators of the CO₂ balance between atmosphere and oceans; in *The Fate of Fossil Fuel CO₂ in the Oceans*, ed. N.R. Anderson and A. Malahopp; Plenum, New York, N.Y., p. 295-321.
- McCrea, J.M.
1950: On the isotopic chemistry of carbonates and a paleotemperature scale; *Journal of Chemical Physics*, v. 18, p. 849-857.
- Mix, A.C. and Ruddiman, W.F.
1984: Oxygen-isotope analyses and Pleistocene ice volume; *Quaternary Research*, v. 21, p. 1-20.
- Pisias, N.G. and Moore Jr., T.C.
1981: The evolution of Pleistocene climate: a time series approach; *Earth and Planetary Science Letters*, v. 52, p. 450-458.
- Rubinson, M. and Clayton, R.N.
1969: Carbon-13 fractionation between aragonite and calcite; *Geochimica et Cosmochimica Acta*, v. 33, p. 997-1002.
- Savin, S.M. and Stehli, F.G.
1974: Interpretation of oxygen isotope paleotemperature measurement effect on the ¹⁸O/¹⁶O ratio of seawater, depth stratification of foraminifera and selective solution; in *Les méthodes Quantitatives d'Études des Variations au Cours du Pléistocène*, Colloques Internationaux du CNRS No. 219, p. 183-191.
- Savin, S.M., Yeh, H.W.
1981: Stable isotopes in ocean sediments; in *The Sea*, v. 7, *The Oceanic Lithosphere*, ed. C. Emiliani; Wiley, Interscience, p. 1521-1554.
- Shackleton, N.
1967: Oxygen isotope analyses and Pleistocene temperature reassessed; *Nature*, v. 215, p. 15-17.
1977: The oxygen isotope stratigraphic record of the Late Pleistocene; *Royal Society of London, Philosophical Transactions, Series B*, v. 280, p. 169-182.
1977: Oxygen isotope stratigraphy of the Middle Pleistocene, in *British Quaternary Studies; recent advances*; ed. F.W. Shotton; Clarendon Press, Oxford, p. 1-16.
1981: Palaeoclimatology before our ice age; in *Climatic Variations and Variability*, ed. A. Berger; D. Reidel, Publ. Co., p. 167-179.

- Shackleton, N.J. and Opdyke, N.D.
 1973: Oxygen isotope and palaeomagnetic stratigraphy of equatorial Pacific core V28-238: oxygen isotope temperatures and ice volumes on a 10^5 year and 10^6 year scale; *Quaternary Research*, v. 3, p. 39-55.
 1976: Oxygen-isotope and paleomagnetic stratigraphy of Pacific Core V28-239 late Pliocene to latest Pleistocene; *Geological Society of America, Memoir*, v. 145, p. 449-464.
- Shackleton, N.J., Wiseman, J.D.H., and Buckley, H.A.
 1973: Non-equilibrium isotopic fractionation between seawater and planktonic foraminiferal tests; *Nature*, v. 242, p. 177-179.
- Thompson, P.R. and Saito, T.
 1974: Pacific Pleistocene sediments: planktonic foraminifera dissolution cycles and geochronology; *Geology*, v. 2, p. 333-335.
- Thomson, R.E.
 1981: *Oceanography of the British Columbia Coast*; British Columbia Department of Fisheries and Oceans, 291 p.
- Urey, H.C.
 1947: The thermodynamic properties of isotopic substances; *Journal of the Chemical Society*, p. 562-581.
- Vincent, E. and Berger, W.H.
 1981: Planktonic foraminifera and their use in paleoceanography; in *The sea*, v. 7, ed. C. Emiliani; John Wiley & Sons, p. 1025-1119.
- Williams, D.F., Sommer II, M.A., and Bender, M.L.
 1977: Carbon isotopic compositions of recent planktonic foraminifera of the Indian Ocean; *Earth and Planetary Science Letters*, v. 36, p. 391-403.
- Zahn, R., Murkussen, B., and Thiede, J.
 1985: Stable isotope data and depositional environments in the Late Quaternary Arctic Ocean; *Nature*, v. 314 p. 433-435.

Appendix 1

Isotopic results for *Globigerina bulloides* with estimated deviation
of $\delta^{13}\text{C}$ and $\delta^{18}\text{O}$ from equilibrium values

Depth (cm)	$\delta^{13}\text{C}$ (‰ PDB)	$\delta^{18}\text{O}$ (‰ PDB)	$\Delta\delta^{13}\text{C}$ (Foram-Equi CaCO_3)		$\Delta\delta^{18}\text{O}$ (foram-Equi CaCO_3)		
			summer value	winter value	summer value	winter value	
END 77-29	0	+0.08	+3.40	-2.06	-1.85	+3.25	+1.67
	6	+0.18	+2.56	-1.96	-1.70	+2.41	+0.83
	11	-0.23	+3.58	-2.37	-2.16	+3.43	+1.85
	12	+0.44	+2.82	-1.70	-1.49	+2.670	+1.09
	19	+0.16	+2.29	-1.98	-1.77	+2.14	+0.56
	23	+0.00	+2.79	-2.14	-1.93	+2.64	+1.06
	27.5	+0.06	+2.65	-2.08	-1.87	+2.50	+0.92
	31	+0.45	+2.77	-1.69	-1.48	+2.62	+1.04
	37	-0.49	+1.30	-2.63	-2.42	+1.15	-0.43
	42	+0.56	+3.17	-1.58	-1.37	+3.02	+1.42
	47	+0.26	+3.47	-1.88	-1.67	+3.32	+1.74
	53	+0.25	+3.23	-1.89	-1.68	+3.08	+1.50
	59	-0.31	+4.02	-2.45	-2.24	+3.87	+2.29
	102	+0.45	+2.05	-1.69	-1.48	+1.90	+0.32
	110.5	+0.07	+3.11	-2.07	-1.86	+2.96	+1.38
	115	+0.00	+3.49	-2.14	-1.93	+3.34	+1.76
	120	+0.67	+2.72	-1.47	-1.26	+2.57	+0.99
	125	+0.02	+3.50	-2.12	-1.91	+3.35	+1.77
	130	+0.25	+3.01	-1.89	-1.68	+2.86	+1.28
	135	+0.10	+2.73	-2.04	-1.83	+2.58	+1.0
	136	+0.04	+3.12	-2.10	-1.89	+2.97	+1.39
	141	+0.19	+3.32	-1.95	-1.74	+3.17	+1.59
	147	+0.12	+3.32	-2.02	-1.81	+3.17	+1.59
	150	+0.69	+4.49	-1.45	-1.24	+4.34	+2.76
	154	-0.04	+3.43	-2.18	-1.97	+3.28	+1.70
	157	+0.03	+3.72	-2.11	-1.90	+3.57	+1.99
	158	+0.10	+3.44	-2.24	-1.83	+3.29	+1.71
	164	-0.09	+3.41	-2.23	-2.02	+3.26	+1.68
	168	+0.05	+3.27	-2.09	-1.88	+3.12	+1.54
	170	+0.06	+3.62	-2.08	-1.87	+3.47	+1.89
	171	-0.08	+3.52	-2.22	-2.01	+3.37	+1.79
	174.5	-0.02	+3.50	-2.16	-1.95	+3.35	+1.77
	177.5	-0.08	+3.07	-2.22	-2.01	+2.92	+1.34
	181	+0.03	+3.22	-2.11	-1.90	+3.07	+1.49
	182	+0.52	+4.11	-1.62	-1.41	+3.96	+2.38
	186	+0.00	+2.57	-2.14	-1.93	+2.42	+0.84
	190.5	+0.19	+2.96	-1.95	-1.74	+2.81	+1.23
	194.5	+0.30	+2.76	-1.84	-1.63	+2.61	+1.03
	200	+0.27	+2.65	-1.87	-1.66	+2.50	+0.92
	205	+0.32	+3.43	-1.82	-1.63	+3.28	+1.70
	210	+0.11	+4.08	-2.03	-1.82	+3.93	+2.35
	211	+0.03	+2.78	-2.11	-1.90	+2.63	+1.05
	214.5	-0.09	+3.66	-2.23	-2.02	+3.51	+1.93
	218.5	-0.28	+2.36	-2.42	-2.21	+2.21	+0.63
	222.5	+0.02	+3.14	-2.12	-1.91	+2.99	+1.41
	232	-0.02	+2.83	-2.16	-1.95	+2.68	+1.10
	237	-0.09	+3.58	-2.23	-2.02	+3.43	+1.85
	242	+0.62	+4.39	-1.52	-1.31	+4.20	+2.66
	248.5	+0.14	+3.70	-2.0	-1.79	+3.55	+1.97
	250	-0.33	+2.42	-2.47	-2.26	+2.27	+0.69
	252.5	-0.42	+2.63	-2.56	-2.35	+2.48	+0.90
	254	+0.23	+3.46	-1.91	-1.700	+3.31	+1.73
	259	-0.01	+3.36	-2.15	-1.94	+3.21	+1.63
	264.5	+0.00	+2.95	-2.14	-1.93	+2.80	+1.22
	266	-0.03	+3.24	-2.17	-1.96	+3.09	+1.510
	272	-0.05	+3.33	-2.19	-1.98	+3.18	+1.60
	274	+0.44	+3.71	-1.70	-1.49	+3.56	+1.98
	276	+0.05	+2.80	-2.09	-1.88	+2.65	+1.07
	280	-0.04	+3.50	-2.18	-1.97	+3.35	+1.77
	280.5	-0.02	+3.38	-2.16	-1.95	+3.33	+1.65
	285	+0.06	+3.72	-2.20	-1.99	+3.57	+1.99
	288	+0.02	+3.14	-2.12	-1.91	+2.99	+1.41
	292	-0.02	+3.11	-2.16	-1.95	+2.96	+1.38
	298	+0.00	+3.09	-2.4	-1.93	+2.94	+1.36
	304	+0.14	+3.20	-2.0	-1.79	+3.05	+1.47
	307	-0.07	+2.97	-2.21	-2.0	+2.82	+1.24
	309	+0.19	+3.34	-1.95	-1.74	+3.19	+1.61
	312	+0.15	+2.80	-1.19	-1.78	+2.65	+1.07
	313.5	+0.08	+3.61	-2.06	-1.85	+2.65	+1.07
	317	+0.14	+3.19	-2.0	-1.79	+3.04	+1.46
	318	-0.07	+2.87	-2.21	-2.0	+2.72	+1.14
	322	-0.16	+3.21	-2.30	-2.09	+3.06	+1.48
	323.5	-0.05	+3.49	-2.19	-1.98	+3.34	+1.76
	327	-0.27	+3.00	-2.41	-2.20	+2.85	+1.27
	328	-0.19	+3.20	-2.33	-2.12	+3.05	+1.50
	331.5	-0.03	+3.25	-2.17	-1.96	+3.10	+1.52
	332	-0.23	+3.23	-2.37	-2.16	+3.08	+1.50
	336.5	-0.39	+2.30	-2.53	-2.32	+2.15	+0.57
	337	-0.19	+3.15	-2.33	-2.12	+3.00	+1.42
	340.5	+0.11	+3.10	-2.03	-1.82	+2.95	+1.37
	351.5	-0.08	+3.20	-2.22	-2.01	+3.05	+1.47

Appendix I (cont.)

Depth (cm)	$\delta^{13}\text{C}$ (‰ PDB)	$\delta^{18}\text{O}$ (‰ PDB)	$\Delta\delta^{13}\text{C}$ (foram-Equi CaCO_3)		$\Delta\delta^{18}\text{O}$ (foram-Equi CaCO_3)	
			summer value	winter value	summer value	winter value
353	+0.02	+2.82	-2.12	-1.91	+2.67	+1.09
356.5	-0.86	+2.83	-3.03	-2.79	+2.66	+1.08
360	-0.05	+2.92	-2.19	-1.98	+2.77	+1.19
365	+0.17	+3.29	-1.97	-1.76	+3.14	+1.56
370	+0.09	+3.19	-2.05	-1.84	+3.04	+1.46
379	+0.39	+2.24	-1.75	-1.54	+2.09	+0.51
383	+0.19	+2.04	-1.95	-1.74	+1.89	+0.31
385	+0.39	+1.71	-1.75	-1.54	+1.56	-0.02
390	+0.38	+2.51	-1.76	-1.55	+2.36	+0.78
392	+0.79	+3.34	-1.35	-1.14	+3.19	+1.61
400.5	-0.35	+3.37	-2.49	-2.28	+3.22	+1.64
404	+0.29	+1.89	-1.85	-1.64	+1.74	+0.16
420.5	-0.64	+4.22	-2.78	-2.57	+4.07	+2.49
425	+0.03	+3.61	-2.11	-1.91	+3.46	+1.88
430	-0.42	+3.47	-2.56	-2.35	+3.32	+1.74
432	+0.26	+3.17	-1.88	-1.67	+3.02	+1.44
434	-0.24	+3.75	-2.38	-2.17	3.60	2.02
437	-0.05	+3.31	-2.19	-1.98	3.16	1.58
438	-0.14	+3.21	-2.28	-2.07	3.06	1.48
441	-0.28	+2.70	-2.42	-2.21	2.55	0.97
442	+0.74	+4.73	-1.40	-1.19	4.58	3.0
447	+0.09	+3.08	-2.05	-1.84	2.93	1.35
454	-0.21	+2.58	-2.35	-2.14	2.43	0.85
465	-0.67	+2.19	-2.81	-2.60	2.14	0.46
470	-0.08	+2.62	-2.22	-2.01	2.47	0.89
480	+0.17	+2.67	-1.97	-1.76	2.52	0.94
486	+0.07	+2.90	-2.07	-1.86	2.75	1.17
510	+0.31	+2.23	-1.83	-1.62	2.08	0.50
515	+0.51	+2.18	-1.63	-1.42	2.03	0.45
520	+0.47	+3.07	-1.67	-1.46	2.92	1.34
525	+0.43	+2.66	-1.71	-1.50	2.51	0.93
530	-0.29	+2.97	-2.43	-2.22	2.82	1.24
535	-0.17	+3.35	-2.31	-2.10	3.20	1.62
540	-0.07	+3.33	-2.21	-2.0	3.18	1.60
545	-0.23	+3.28	-2.37	-2.16	3.13	1.55
547	-0.32	+3.17	-2.46	-2.25	3.02	1.44
550	-0.21	+3.30	-2.35	-2.14	3.15	1.57
555	-0.19	+3.18	-2.33	-2.12	3.03	1.45
565	-0.12	+2.35	-2.26	-2.05	2.20	0.62
570	+0.01	+3.50	-2.13	-1.92	3.35	1.77
575	-0.43	+1.47	-2.57	-2.36	1.32	-0.26
577	+0.18	+3.20	-1.96	-1.75	3.05	1.47
580	-0.06	+2.61	-2.20	-1.99	2.46	0.88
585	+0.03	+2.66	-2.11	-1.90	2.51	0.93
591	+0.31	+3.05	-1.83	-1.62	2.90	1.32
END 77-28						
10	-0.32	+3.68	-2.46	-2.25	3.53	1.95
15	+0.06	+3.93	-2.08	-1.87	3.78	2.20
20	-0.30	+3.46	-2.44	-2.23	3.31	1.73
25	-0.26	+3.75	-2.40	-2.19	3.60	2.02
30	-0.08	+3.40	-2.22	-2.01	3.25	1.67
35	-0.33	+3.25	-2.47	-2.26	3.10	1.52
40	+0.52	+3.85	-1.62	-1.10	3.70	2.12
50	+0.32	+2.49	-1.82	-1.61	2.34	0.76
55	+0.26	+2.21	-1.88	-1.67	2.06	0.48
60	+0.23	+2.60	-1.91	-1.70	2.45	0.87
65	+0.21	+2.53	-1.93	-1.72	2.38	0.80
70	+0.46	+2.98	-1.68	-1.47	2.83	1.25
75	-0.32	+2.95	-2.46	-2.25	2.80	1.22
95	+0.02	+3.68	-2.12	-1.91	3.53	1.95
100	+0.12	+3.65	-2.02	-1.81	3.50	1.92
105	+0.01	+3.57	-2.13	-1.92	3.42	1.84
110	-0.52	+3.83	-2.66	-2.45	3.68	2.10
115	-0.29	+3.77	-2.43	-2.22	3.62	2.04
120	-0.01	+3.63	-2.15	-1.94	3.48	1.90
125	-0.09	+3.23	-2.23	-2.02	3.08	1.50
130	+0.07	+2.97	-2.07	-1.86	2.82	1.24
135	+0.38	+2.91	-1.76	-1.55	2.76	1.18
140	+0.10	+3.47	-2.04	-1.83	3.32	1.74
145	-0.35	+2.96	-2.49	-2.28	2.81	1.23
150	-0.13	+4.38	-2.27	-2.06	4.23	2.65
155	-0.21	+4.19	-2.35	-2.14	4.04	2.46
165	-0.22	+3.36	-2.36	-2.15	3.21	1.63
170	-0.29	+2.96	-2.43	-2.22	2.81	1.23
175	+0.24	+4.09	-1.90	-1.69	3.94	2.36
195	+0.25	+2.54	-1.89	-1.68	2.39	0.81
200	-0.04	+1.92	-2.18	-1.97	1.77	0.19
230	-0.03	+2.93	-2.17	-1.96	2.78	1.20
235	-0.27	+3.03	-2.41	-2.20	2.88	1.30
240	-0.01	+3.68	-2.15	-1.94	3.53	1.95
245	-0.42	+2.47	-2.56	-2.35	2.32	0.74

Preliminary report on the structural setting of gold in the Rice Lake area, Uchi Subprovince, southeastern Manitoba¹

**Contract 102-5-3-5
Project 840018 and 102-5-3-5**

**K.H. Poulsen, D.E. Ames, S. Lau² and W.C. Brisbin²
Mineral Resources Division**

Poulsen, K.H., Ames, D.E., Lau, S., and Brisbin, W.C., Preliminary report on the structural setting of gold in the Rice Lake area, Uchi Subprovince, southeastern Manitoba in Current Research, Part B, Geological Survey of Canada, Paper 86-1B, p. 213-221, 1986.

Abstract

The San Antonio gold deposit comprises a quartz vein network hosted by rocks of basaltic composition. Veins also commonly contain ankerite, albite and pyrite and were formed during regional deformation which resulted in the development and subsequent reorientation of penetrative foliation and lineation. Individual veins occupy shear zones and stockworks which are thought to be coeval. Wallrocks adjacent to veins have been intensely carbonatized, sericitized, albitized and sulphidized.

Résumé

Le gîte d'or de San Antonio consiste en un réseau de filons de quartz dans des roches basaltiques. Les filons contiennent aussi de l'ankérite, de l'albite et de la pyrite, et ont été mis en place pendant une déformation régionale qui a produit une foliation et une linéation pénétratives ainsi que leur déformation subséquente. Les filons individuels se manifestent dans des zones de cisaillement et dans des stockwerks contemporains. Les épontes adjacentes aux filons ont été intensément carbonatisées, séricitisées, albitisées et sulfurées.

¹ Contribution to the Canada-Manitoba Mineral Development Agreement 1984-1989. Project carried by the Geological Survey of Canada, Project 840018.

² Department of Earth Sciences, University of Manitoba, Winnipeg, Manitoba.

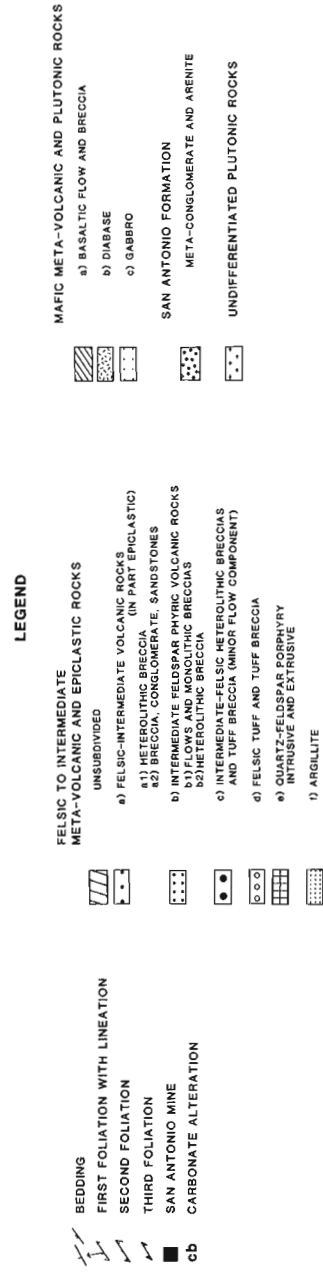
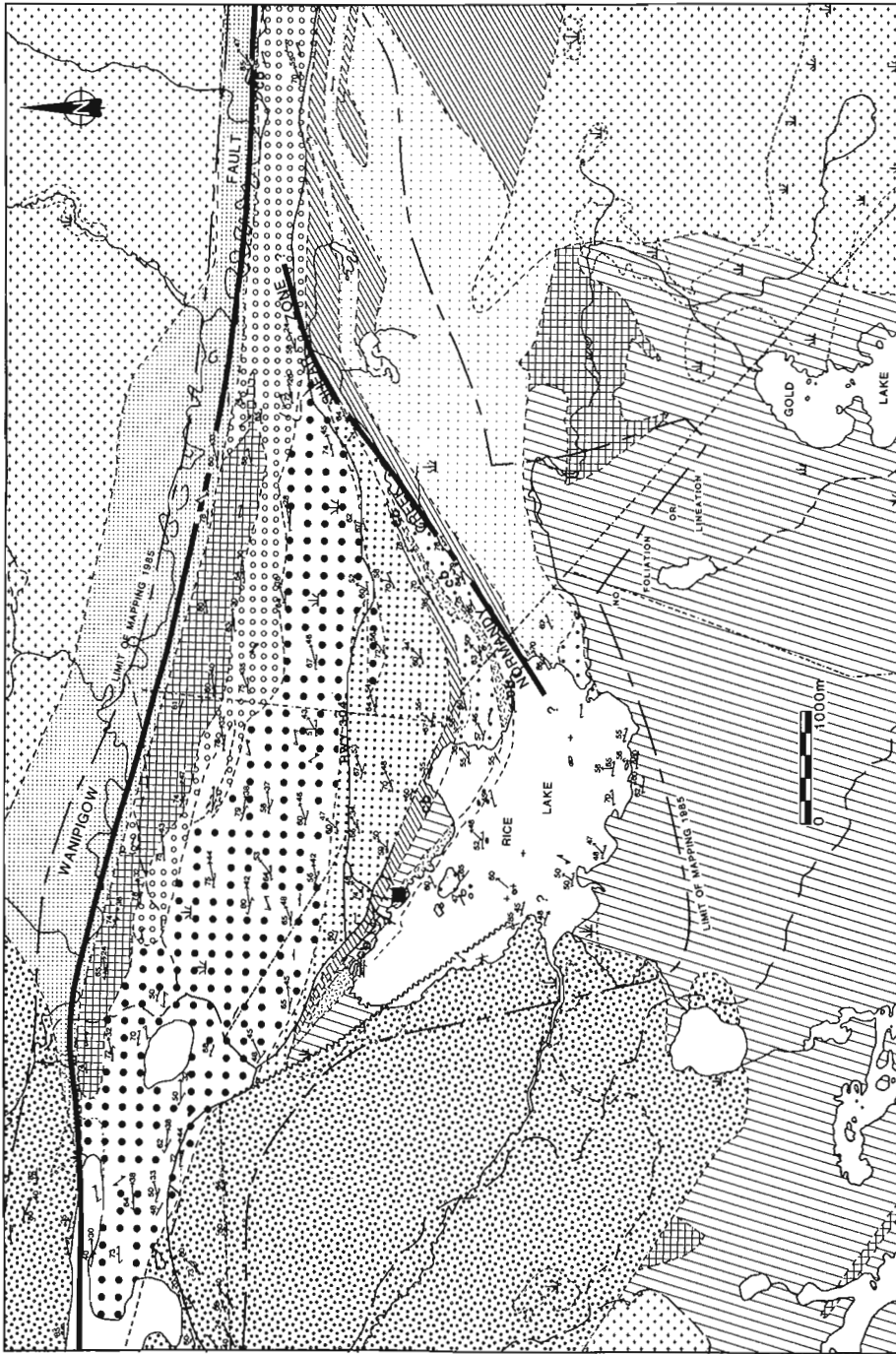


Figure 24.1. Geological map of the Rice Lake area. Complete subdivision of lithological units is only indicated on portions of the map completed in 1985. Other contacts from Stockwell (1938) and Davies (1963).

Introduction

Located within the Rice Lake greenstone belt, the San Antonio mine at Bissett (52 M/4) has been an important past-producer with a yield of 1.36 million ounces of gold (42 300 kg) in the period 1932-1968. Exploration and development have been active at the mine site over the past several years and is continuing at present. This study of structural geology and ore-associated alteration was initiated in the Rice Lake area in 1984 as part of the Canada-Manitoba Mineral Development Agreement. The study involves both regional- and mine-scale examinations of structural, stratigraphic and metamorphic controls on mineralization. D. Ames, A. Galley and H. Poulsen mapped the surface geology in the Rice Lake area in 1985 and underground mapping was undertaken by the authors in 1984 and 1985. This report summarizes our preliminary results with an emphasis on structural geology.

Stratigraphy

The study area (Fig. 24.1) covers a portion of the Archean Rice Lake greenstone belt which has been mapped several times previously at various scales, most notably by Stockwell (1938) and our mapping has not resulted in significant changes in the definition of geological contacts. The area to the south of the Wanipigow Fault was mapped in the greatest detail and is underlain by low grade metamorphic rocks which represent four distinctive lithological associations:

- i) Intermediate volcanic and epiclastic rocks are most abundant in the north-central and southern parts of the area. Rocks of dacitic composition are particularly abundant and occur principally as flows, breccias and volcanic conglomerates.
- ii) Volcanic and intrusive rocks of basaltic composition occur locally around the northern part of Rice Lake and extensively in the east-central part of the map area. These include flows, flow breccias and pillowed flows, as well as metadiabase and metagabbroic rocks. Limited chemical data suggest that these rocks represent a tholeiitic basalt suite.
- iii) Felsic plutonic rocks cut both the intermediate and basaltic supracrustal rocks. A major body of tonalitic composition, the Ross River Pluton, extends into the southeastern portion of the map area and smaller bodies elsewhere may be of equivalent age and/or, as in the case of the elongate body south of the Wanipigow Fault, possibly of synvolcanic origin.
- iv) The San Antonio Formation, composed of crossbedded arenites and minor polymict conglomerates, underlies much of the west-central portion of the map area.

Although mapping of lithological units and establishing structural sequence is straightforward, the interpretation of relationships among units is considerably more problematic. This interpretation is hampered in part by the rarity of unequivocal way-up indicators in the volcanic rocks. The traditional stratigraphic interpretation (Stockwell, 1938) is that the basaltic and intermediate volcanic rocks comprise a northward facing volcanic pile which was intruded by felsic plutons and subsequently unroofed and covered unconformably by sediments of the San Antonio Formation. The present mapping has resulted in no data to the contrary but the recognition of dislocative structures such as the Normandy Creek Shear Zone (see below) within the volcanic rocks makes it unlikely that a simple volcanic succession is preserved.

The large scale structure is dominated by the Wanipigow Fault (McRitchie, 1971) which imparts straight trends in the northern part of the map area and by a prominent "flexure" in

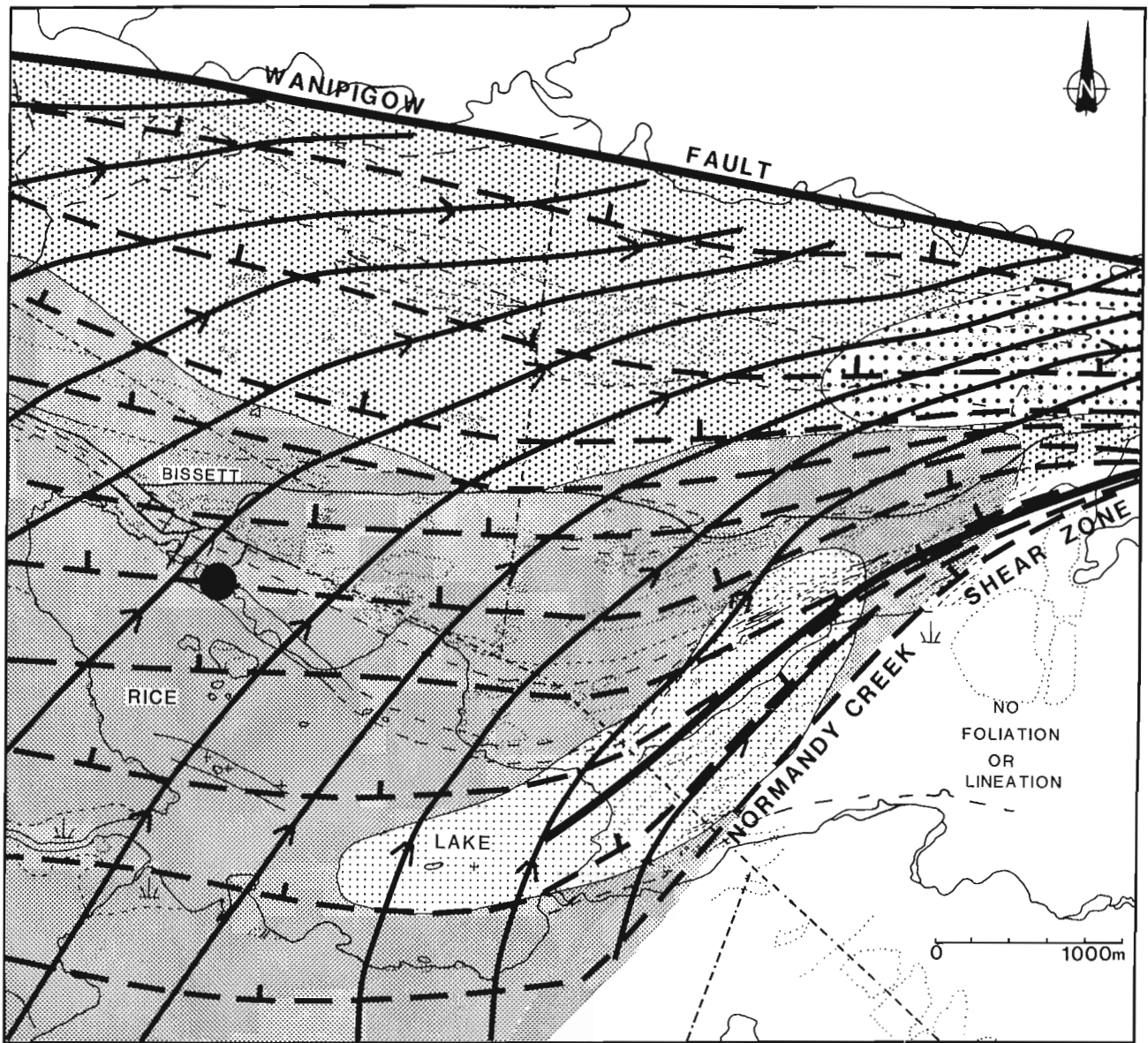
stratigraphic trend centred on Rice Lake. These combine to form a somewhat triangular-shaped domain (Fig. 24.1) which contains the most significant concentrations of gold in the area and has been the focus of most of our studies to date. The southwestern and southeastern edges are inferred to be dislocative on the basis of map relationships. On the southwest side of Rice Lake a back-to-back younging relationship exists between the San Antonio Formation and northeastward-facing volcanic rocks (see Stockwell, 1938, p. 21 for a lucid discussion of the problem). On the southeast side, the evidence for a dislocation along Normandy Creek is much clearer, as lithological units are attenuated and truncated along a zone of intense deformation; this has been identified as the Normandy Creek shear zone (Fig. 24.1). The significance of this structure has not been emphasized previously, although Stockwell (1938) did note a well-developed "schistose structure" in this area.

During the present mapping, mesoscopic structures were documented to supplement the qualitative interpretation given above. Most volcanic, epiclastic and sedimentary rocks in the Rice Lake area contain at least one penetrative foliation and a stretch lineation as well as bedding. Typically, the most widely distributed, best developed and earliest foliation is a continuous to spaced cleavage with a more northerly strike than bedding (i.e. the pole to foliation must be rotated through an acute angle in a clockwise sense to coincide with the pole to bedding). This foliation is well preserved within volcanic clasts and within tuffaceous bedded units. Where elongate clasts are present, their long axes are coincident with the axis of bedding-cleavage intersection. Where three-dimensional exposure is available, as in the mine workings, it is clear that cleavage dips more steeply than bedding. Some rocks contain more than one set of fabric elements: a second foliation, an east-northeast crenulation cleavage was observed near the Wanipigow Fault and a third foliation comprising kink bands and spaced crenulation cleavage, strikes north-northwesterly and occurs locally throughout the area.



Typical attitudes of the various structural elements are shown in Figure 24.1. Figure 24.2 portrays the generalized trajectories of strike of the first foliation and of the trends of lineations within it only for the central part of the map area where sufficient data have been collected to date. Ranges in the value of plunge of the lineations are also shown. The orientations of foliation are largely independent of lithological type and tend to be presently subparallel to the Wanipigow Fault over much of the area; however a major deflection of strike clearly coincides with the inferred position of the Normandy Creek shear zone. Dip of foliation tends to steepen towards both the Normandy Creek and Wanipigow structures. The orientation of lineation is clearly influenced by proximity to the Wanipigow Fault (Fig. 24.2): lineation trends deflect towards parallelism with the fault and magnitudes of plunge decrease as the fault is approached from the south. Steeper lineations, with a larger pitch within foliation, are characteristic of the rocks exposed around Rice Lake proper.

Aside from orientation data, it is clear from our mapping that there are gradients in intensity of foliation and lineation development across the map area. Intense fabric development adjacent to the Normandy Creek shear and Wanipigow Fault contrasts with the virtual absence of fabric southeast of Normandy Creek. Weak to moderate fabrics have been developed in rocks near the town of Bissett.





The patterns of lineation and foliation are consistent with a previous suggestion by McRitchie (1971) that the Wanipigow Fault is a dextral transcurrent structure: the increasing parallelism of strike of foliation and trend of lineation with increasing proximity to the fault, as well as the steepening of foliation and shallowing of lineation, are compatible with their reorientation



LEGEND

-  STRIKE OF FOLIATION
-  TREND OF LINEATION

PLUNGE VALUES OF LINEATION

-  < 30
-  30-45
-  45-60
-  > 60

-  SAN ANTONIO MINE

Figure 24.2. Structural trend map of part of the Rice Lake area. The trajectories show mean strike and trend of first foliation and lineation respectively. Contours show variation in range of values for plunge of the lineations.

by dextral shear if it is assumed that these fabrics predated and were originally oblique to the Wanipigow Fault. Some of the observed crenulation cleavages which superpose earlier fabrics can also be accounted for in this way.

Although transcurrent shear can account for reorientation of earlier foliation and lineation, the observed patterns preclude such shear as an agent responsible for the formation of the fabrics, and an earlier phase of deformation is implied. The Normandy Creek shear seems to be a locus for this earlier deformation and the steep lineation associated with its trace suggests that it may represent a ductile reverse fault with penetrative fabrics developed in its hanging wall to the northwest which is distinct from undeformed footwall rocks to the southeast. We do not have sufficient data at present to speculate on the possible relationship between this earlier deformation and subsequent transcurrent shear.

San Antonio mine

Setting

The San Antonio mine has been developed on a gold-quartz vein deposit within a single lithological unit, which has traditionally been viewed as a sill of metadiabase (Stockwell, 1938) owing to its massive texture and absence of unequivocal volcanic features. Theyer (1983) has suggested that the unit (San Antonio mine unit) comprises mafic flows and tuffs. Unequivocal evidence for either interpretation is presently lacking. The host unit composition is that of tholeiitic basalt, which is distinct from the dacitic rocks on either side. The host unit follows the crescent-shaped outline of the enclosing rocks and the mine is on the west limb of the gentle flexure (Fig. 24.1). For most of its length of nearly 6 km, the unit is only 15 to 90 m thick, but at the mine the thickness is from 120 to 150 m; here the unit strikes N50°-60°W and dips 47°NE (Fig. 24.3). The host unit is cut by an array of northeasterly-striking, steeply-dipping dykes composed primarily of dacitic feldspar porphyry. An envelope of buff-coloured schists with local intense foliation and crenulation surrounds the host unit: this zone of schists is thicker on the footwall side (40 to 140 m) than the hanging wall (1 to 20 m) and has historically been referred to as "footwall sericite schist".

Vein Structure

Two distinctive types of veins form the ore bodies within the host unit (Fig. 24.3). A NE set occupies shear zones which cut across the host unit at a high angle and the second set forms NW stockwork zones which are also discordant to the host, but at a lower angle. Both locally offset feldspar porphyry dykes in the host unit.

The NE veins are also known as shear veins or 16-type in the mine terminology. They occur within restricted tabular zones of foliated host rock and have relatively sharp boundaries (Fig. 24.4a) along which there is commonly some evidence of post-vein displacement. Veins of this set commonly strike N60°E to N75°E and dip 50-60° to the northwest. The shear zones, which contain the veins, are more continuous than the veins themselves and are arranged en echelon with the host unit. The veins pinch and swell within the shear zones and range from a few metres to 150-200 m in length and from a few centimetres to two metres in thickness. The NE veins are composed primarily of quartz, ankerite and albite and commonly are internally zoned away from the vein wall with a quartz-albite-ankerite fringe, an internal contact and a central quartz core with ribbon structures, wall rock fragments and scattered carbonate patches (Fig. 24.5a). Extensional veinlets composed of quartz, carbonate and chlorite commonly cut the main vein fillings at a high angle.

The NW veins are also known as 38-type or "stockworks", each consisting of network of smaller individual veins with different orientations (Fig. 24.4b). The stockwork zones range in strike from N25°-60°W and most dip vertically to steeply NE. They all strike 20-30° more northerly than the host unit and they terminate up and down dip at the hanging wall and footwall contacts. Consequently the long dimensions of these zones plunge gently northwest (Fig. 24.3). The stockworks commonly attain thicknesses of 10 m.

At least three types of extensional veins can occur in a given stockwork. The first is a stacked or "ladder" arrangement of sub-parallel, near-horizontal fractures; the second is a set of sub-vertical fractures of variable strike which link and are coeval with the horizontal ones; the third, later than the other two, comprises vertical fractures which are consistently normal to the strike of the stockwork as a whole. Most stockwork zones contain a central core composed of angular wall rock fragments engulfed in a high percentage (>50%) of vein material. The intensity of fracturing decreases outward from the stockwork core, both along and across strike, so that at the outer margins simple dilation of a reticulate array of fractures is observed. The veins in the stockwork zones have virtually identical compositions to those of the northeasterly-striking set. Individual flat "ladder" veins and some of the vertical veins show an identical arrangement of minerals as well (Fig. 24.5). As with the NE veins, late discordant veinlets contain chlorite as well as quartz and ankerite.

The NE and NW vein sets are auriferous. Additional veins are also locally associated with two other sets of shear zones which are not known to be gold bearing. The first are shear zones of type and strike similar to those hosting the NE veins but which dip to the southeast and offset both NE veins and stockworks. The second set strikes subparallel to the NW veins and dips vertically to steeply southwest. These shear zones offset all other structures in a dextral sense.

The combined distributions of the NE and NW veins define the overall architecture of the San Antonio deposit (Fig. 24.3) which, as a whole, plunges moderately to the northeast. This plunge coincides with the attitude of mesoscopic lineations in volcanic rocks near the mine (Fig. 24.2), suggesting a link between mine scale and regional structures. Furthermore, the NE shear zones within the mine mimic the larger Normandy Creek shear suggesting a temporal relationship between vein formation and the regional deformational history. We at present have insufficient data to permit a unique interpretation of the effects on the deposit of the inferred later transcurrent displacements on the Wanipigow Fault.

Alteration

The wall rocks adjacent to the NE veins are fine grained, schistose and highly altered. They are composed principally of albite, ankerite, sericite, quartz, chlorite, and conspicuous disseminations of pyrite. The wall rocks adjacent to most stockwork zones are structurally massive but contain essentially the same alteration minerals as those adjacent to the NE veins. A distinction is that wallrocks of many of the component veins in a stockwork are visibly "bleached" for a few centimetres from their margins. The bleached rocks are grey compared to the normal dark green host rocks because they lack chlorite and are enriched in albite. The alteration at the vein scale therefore appears to be independent of type (i.e. NE or NW) and involves fixation of carbon dioxide, sulphur and perhaps potassium and sodium as indicated by alteration minerals.

Aside from the observed vein-scale alteration, it is also clear from petrographic, X-ray and chemical analyses of the basaltic mine unit and of adjacent volcanic rocks that CO₂ is also fixed more generally in alteration assemblages at the mine scale.

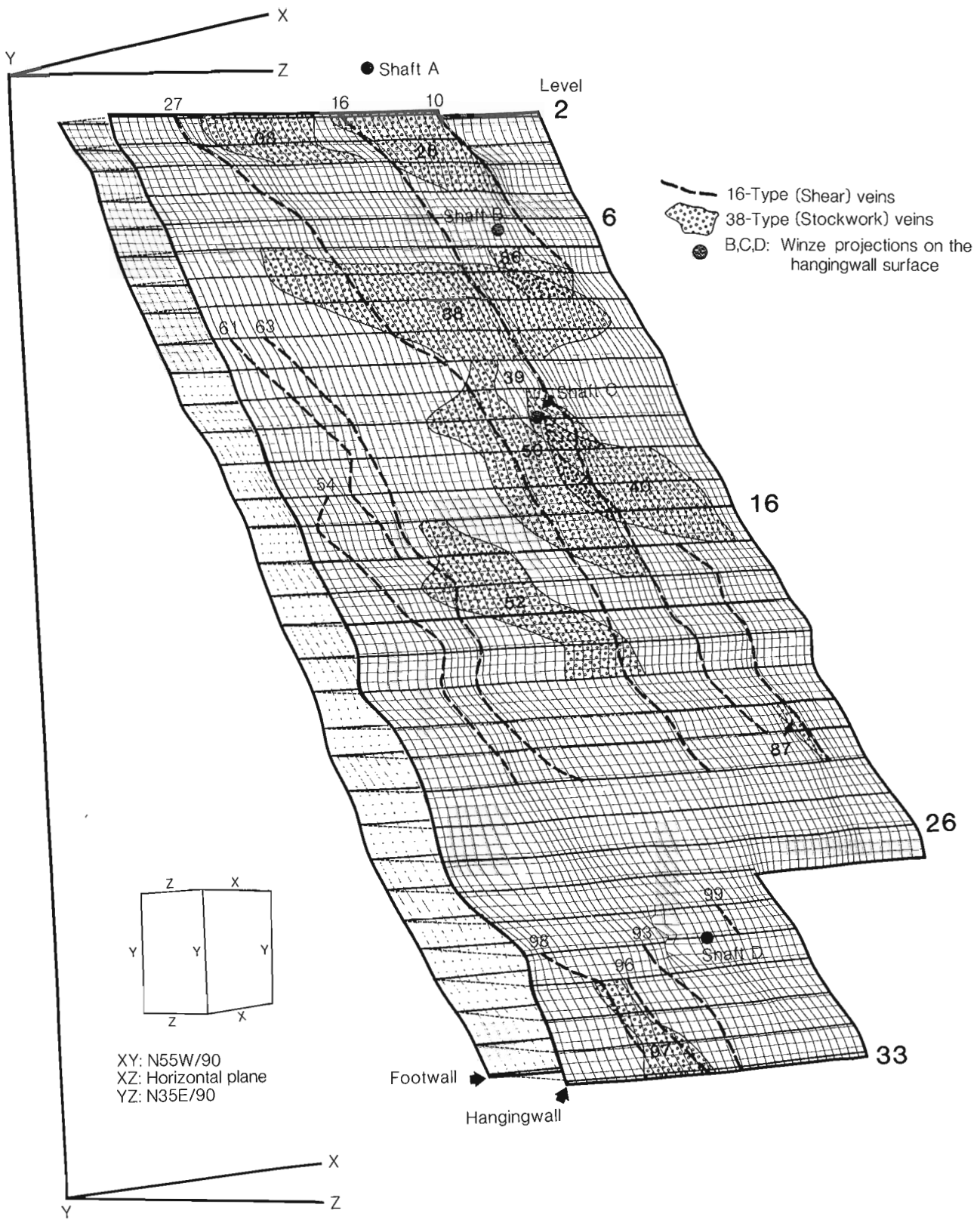


Figure 24.3. Perspective diagram of the mafic host unit to the San Antonio gold deposit. Solid lines show the projection of the NE veins onto the hanging wall surface of the host unit. The NW veins (stockwork zones) lie within the host unit and are also shown projected onto the hanging wall. The diagram shows some distortion of scale: the typical distance between mine levels is 50 m.

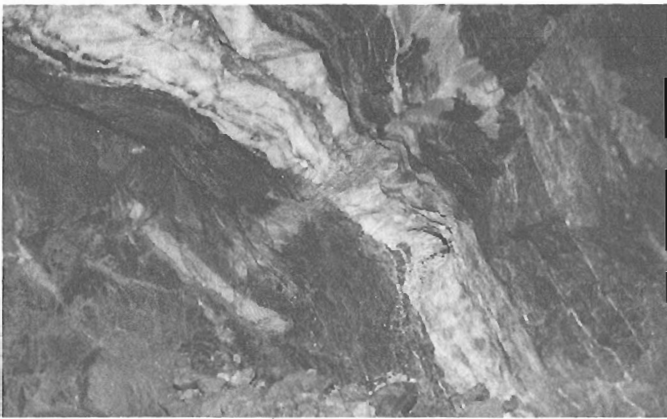


Figure 24.4a. Cross-sectional view of a NE vein, San Antonio Mine. The adjacent wall rock shows the typical zone of schistosity. The vein is cut by a late shear.

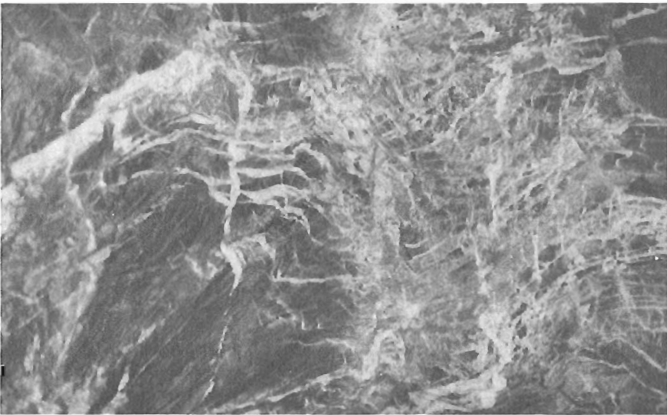
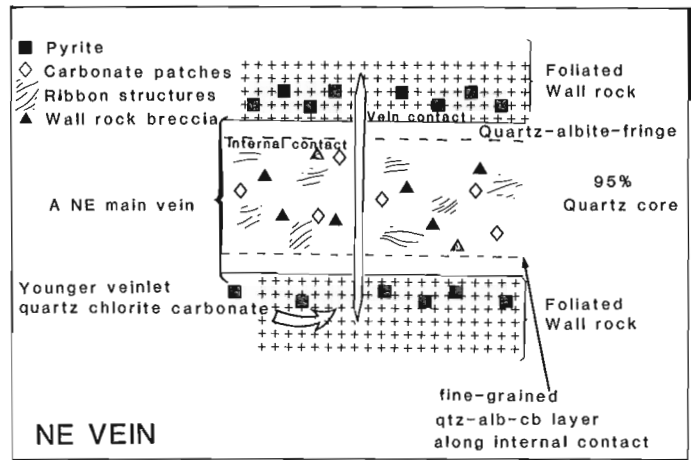
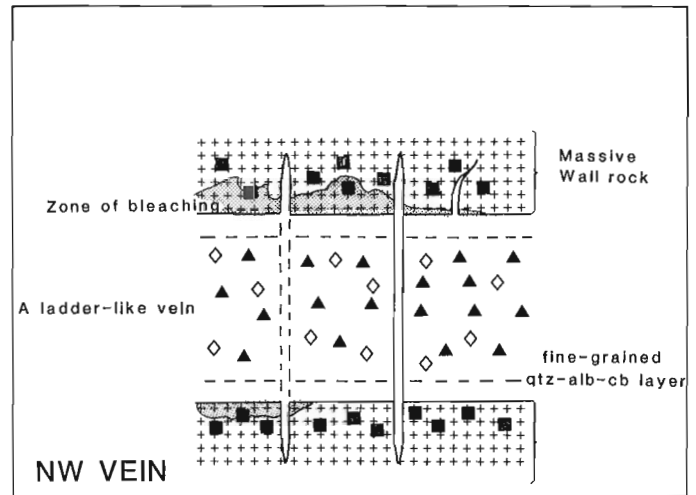


Figure 24.4b. A partially developed central core of a NW vein showing stacks of subhorizontal "ladders" cut by vertical quartz veins together forming the stockwork. The photograph is of a vertical face in the mine parallel to the strike of the vein and therefore is close to a longitudinal view since the vein dips steeply towards the viewer.



(a)



(b)

Figure 24.5. Schematic illustration of the form, composition and alteration for an example of a NE vein (a) and a NW vein "ladder" (b).

Figure 24.6 shows the abundance of calcite and ankerite along a transect from footwall to hanging wall on the 16-level of the mine. Epiclastic rocks well away from the footwall of the host unit are not visibly altered and contain relatively low abundances of calcite and ankerite. Where the transition to "sericite" schist takes place, chlorite is no longer present and the abundance of carbonate minerals increases. It is to be noted that the sericitization does not involve an influx of K_2O , but rather a breakdown of alkali feldspar during carbonatization. Abundant carbonate minerals are developed in the basaltic host rocks of the mine and these are predominantly dolomite/ankerite species (Fig. 24.6). The sericite schists of the hanging wall are similar to those of the footwall and a progressive decrease in carbonate mineral abundance corresponds to increasing distance from the hanging wall contact of the mine unit.

Discussion

From our preliminary appraisal, we conclude that the San Antonio gold deposit comprises a quartz vein system developed during regional deformation. Carbonatization of the basaltic host rock at both the vein- and mine-scale is clearly an important aspect of this deposit. In these respects the deposit is

analogous to others, including the Con mine (Yellowknife), the McIntyre mine (Timmins), and particularly the Mt. Charlotte deposit at Kalgoorlie, Australia (as noted below). The spatial relationship between NE veins and NW stockwork zones, and their similarities in composition, mineral zoning and related alteration strongly suggest that the two are broadly coeval. This is essentially what Stockwell (1938) proposed, but he viewed the structures hosting the auriferous veins as conjugate shears. Our suggestion is that the stockworks are extensional zones which link en echelon shears as shown schematically in Figure 24.7. Such a direct relationship between extensional structures and adjacent shear zones has been clearly demonstrated at other Archean gold deposits, notably the Sigma mine, Quebec (Robert et al., 1983) and Mt. Charlotte, Australia (Finucane, 1965). Further studies are required to test the above structural hypothesis of vein formation, to fully establish the structural history of the map area, and to test the relationships between gold and alteration at the vein, mine, and regional scale.

The data presented above have three implications regarding future exploration in the Rice Lake area. First, considering the analogies drawn above between the San Antonio and other deposits, there may be nothing unique about its host rock that makes it a favourable site for gold. Rather, its tholeiitic basaltic

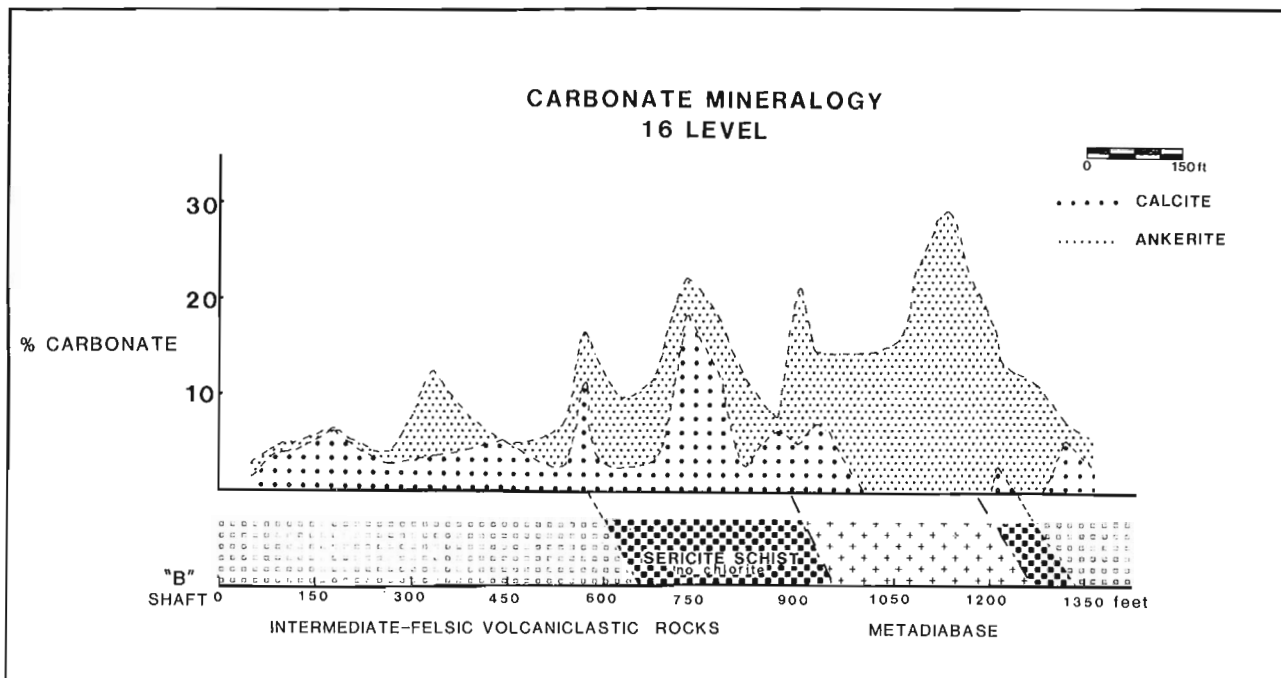


Figure 24.6. Variations in carbonate mineralogy along a profile through the San Antonio mine along crosscuts on the 16-level. The absolute abundances of ankerite and calcite were determined from analysis of total rock CO₂ combined with semiquantitative X-ray diffraction analysis. Note that the total abundance of carbonate minerals is greatest in and adjacent to the mafic host unit and that calcite and chlorite do not coexist in most samples in this zone of CO₂ enrichment.

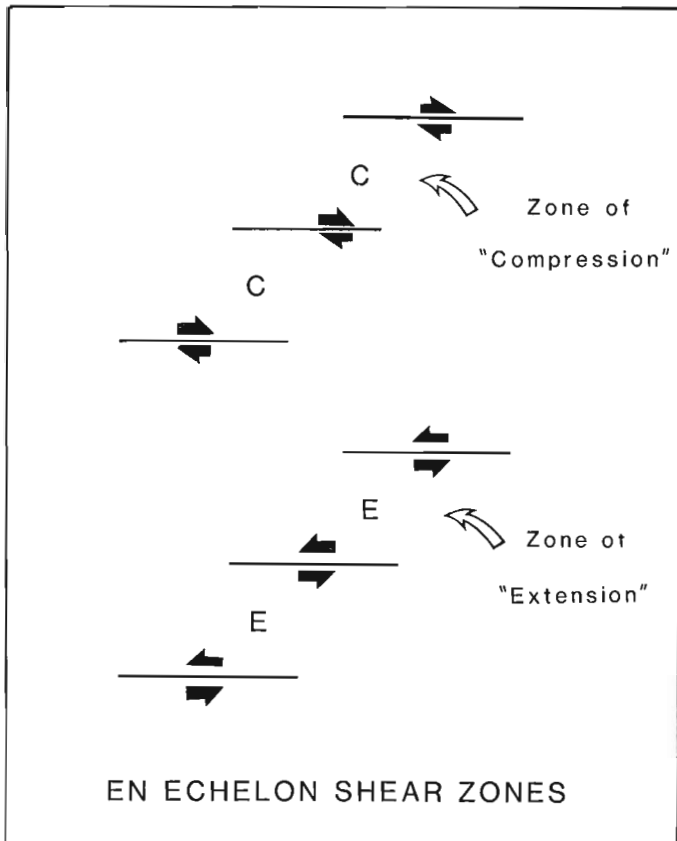


Figure 24.7. Schematic illustrating the well-known principle of extensional (or compressional) zones "linking" en echelon shear zones.

composition seems to be a common attribute for the host rocks of many gold deposits, perhaps because of the availability of iron oxides for reaction with auriferous fluids (Groves et al., 1984). If this is the case, all deformed basaltic rocks in the Rice Lake area could be viewed as potentially favourable targets. Second, it is clear from our preliminary results that significant hydrothermal alteration in the form of carbonatization, sericitization and sulphidation is an important guide to ore. We have observed that such alteration is most common in, though not restricted to, the basaltic rocks. Third, structural studies of the vein systems show the complexity in three-dimensional geometry which can be encountered in exploration. It would be very difficult to infer the correct attitude and spatial relationships of veins from a few intersections in diamond drill core. The particular geometry of veins at the San Antonio mine is likely a function of a "stiff" host unit that has undergone deformation within "softer" volcanic rocks under a local set of deformational constraints. For economic concentrations of gold to have formed elsewhere it is not necessary that the same conditions be reproduced precisely and different structural styles of mineralization might be anticipated (e.g. large single shear zones with no stockworks). Based on the above observations and the results of our mapping, we suggest that deformed, carbonatized mafic rocks near the Normandy Creek shear (and its extension to the northeast) represent favourable targets for future exploration.

Acknowledgments

Our studies have benefitted from the co-operation of industry and provincial government geologists. James Scoates and Patti Tirschmann provided able field assistance. The work by S. Lau and W. Brisbin at the San Antonio mine was performed as part of DSS contract OST-84-00088 to the University of Manitoba. R.I. Thorpe and F. Robert reviewed the manuscripts.

References

- Davies, J.F.
1963: Geology and gold deposits of the Rice Lake-Wanipigow River area, Manitoba; unpublished Ph.D. thesis, University of Toronto, 142 p.
- Finucane, K.J.
1965: Ore distribution and lode structures in the Kalgoolie goldfield; in *Geology of Australian Ore Deposits*, ed. J. McAndrew; Australasian Institute of Mining and Metallurgy, Melbourne, p. 80-86.
- Groves, D.I., Phillips, G.N., Ho, S.E., Henderson, C.A., Clark, M.E., and Waal, G.M.
1984: Controls on distribution of Archean hydrothermal gold deposits in Western Australia; in *Gold '82*, ed. R.P. Foster; Geological Society of Zimbabwe, Sp. Publ. No. 1, p. 689-711.
- McRitchie, W.D.
1971: Geology of the Wallace Lake-Siderock Lake area: a reappraisal; in *Geology and Geophysics of the Rice Lake Region, S.E. Manitoba*, ed. W.D. McRitchie and W. Weber, Manitoba Mines Branch Publication 71-1, p. 107-125.
- Robert, F., Brown, A.C., and Audet, A.J.
1983: Structural control of gold mineralization at the Sigma Mine, Val d'Or, Quebec; *Canadian Institute of Mining & Metallurgy Bulletin*, v. 76, p. 72-80.
- Stockwell, C.H.
1938: Rice Lake-Gold Lake area, southeastern Manitoba; *Geological Survey of Canada, Memoir 210*, 79 p.
- Theyer, P.
1983: Geology of gold environments in the Bisset/Wallace Lake portion of the Rice Lake greenstone belt; in *Manitoba Mineral Resources Division, Report of Field Activities 1983*, p. 101-106.

Aspects of ice flow patterns, glacial sediments, and stratigraphy in northwest New Brunswick¹

Project 690095

**Martin Rappol
Terrain Sciences Division**

Rappol, M., Aspects of ice flow patterns, glacial sediments, and stratigraphy in northwest New Brunswick; in Current Research, Part B, Geological Survey of Canada, Paper 86-1B, p. 223-237, 1986.

Abstract

Records of sedimentation and ice flow patterns in northwest New Brunswick indicate a complex history of glacial cycles, comprising growth and interaction of glaciation centres followed by late glacial events related to relative sea level rise. The stratigraphic record is incomplete, and correlation of tills is hampered by the location of the area in an ice divide zone, the scarcity of useful indicator bedrock lithologies, and the common occurrence of till-like diamictons formed by mass movement processes. Bedrock striations and clast fabric analyses indicate at least three major events, but only two multiple (two) till sections were found.

Résumé

Le registre des taux de sédimentation et des modèles d'écoulement des glaces dans le nord-ouest du Nouveau-Brunswick indiquent des antécédents complexes de cycles glaciaires comprenant la croissance et l'interaction des centres de glaciation, suivis d'événements glaciaires tardifs reliés à une élévation relative du niveau de la mer. Le relevé stratigraphique est incomplet et la comparaison des tills est gênée par l'emplacement de cette région dans une zone de partage des glaces, la pauvreté des indicateurs lithologiques utiles de la roche en place, et la présence fort répandue de diamictons semblables à du till mais formés par des mouvements de masse. Les analyses des stries sur la roche en place et de la structure clastique indiquent au moins trois principaux événements, mais seulement deux sections multiples (2) de till ont été trouvées.

¹ Contribution to the Canada-New Brunswick Mineral Development Agreement 1984-1989. Project carried by Geological Survey of Canada.

Introduction

Since indicators of ice movements in a northern direction in the St. Lawrence Valley area were rediscovered by Lamarche (1971; see Chauvin et al., 1985), many such finds have been reported from the Appalachian regions of southern Quebec (e.g., Lamarche, 1974; Lortie, 1976; Martineau, 1977, 1979; LaSalle et al., 1977; Lebus and David, 1977; Chauvin et al., 1985), northern Maine (Lowell, 1980, 1985), and northwest New Brunswick (Gauthier, 1980; Rampton et al., 1984; Rappol, 1986). These northward ice movements postdate the earlier ice flow directions of Laurentide ice, and are generally assumed to relate to a Late Wisconsinan Appalachian ice divide (Fig. 25.1). Several authors have speculated on the origin of this Appalachian ice divide (e.g., Gadd et al., 1972; Lamarche, 1974; Shilts, 1981; Chauvin et al., 1985), but it seems generally accepted now that the upstream progression of a calving bay in the Saint Lawrence River depression caused separation of ice in the Appalachian region from the main Laurentide Ice Sheet (Chauvin et al., 1985). Rampton et al. (1984), however, depicted an Appalachian ice divide in northwest New Brunswick (their 'North Maine Ice Divide') as a permanent feature of the Late Wisconsinan, while there are also indications that part of Gaspésie peninsula may have experienced only local glacierization during the Late Wisconsinan (Chauvin, 1984).

In northwest New Brunswick and adjacent areas, the geological history predating the northward ice movement is largely unexplored. Older events are poorly preserved in the exposed stratigraphic record, and this poor knowledge has resulted in the development of widely divergent views among researchers on the glacial evolution of the area.

This report summarizes some initial results of current research on glacial sediments in northwest New Brunswick (Fig. 25.1, 25.2), that was undertaken to obtain a more detailed picture of ice flow patterns and glacial stratigraphy. A recent description of physiography and surficial materials, and a summary of previous work in the area is given by Rampton et al. (1984).

Acknowledgments

I am grateful to Christine A. Kaszycki, Michel Lamothe, and William W. Shilts for inspiring discussion and for critical review of the manuscript, and to Jeanette Macey, Louis Michaud, Alain Plouffe, Ineke Prins, and Jillian Sacré for assistance in the field. Till fabric data were processed at the University of Sherbrooke by Luc. St. Pierre.

Chronology Of Ice Flow Directions

Ice flow directions and their relative age were studied primarily through an inventory of glacial striations and clast fabric analysis (Rappol, 1986). A summary of the recorded striations is given in Fig. 25.2. Striated bedrock sites are much more abundant in the northwestern part of the area than in the southeastern part. This is in part an expression of bedrock type, and partially due to a more continuous and thicker cover of unconsolidated sediments in the southeastern part of the area. Moreover, much of the central part of the study area seems similar to zone III of David and Lebus (1985, Fig. 5), in that its surface consists mainly of deeply fractured bedrock with no or a thin cover of loose till.

In the northwestern part of the area, two main directions of ice movement are recorded by glacial striations and related features: an older movement towards east or southeast, and a younger movement towards west or northwest. Along an east-west transect, a gradual change in direction is observed for the youngest ice movement. In northern Maine, latest ice move-

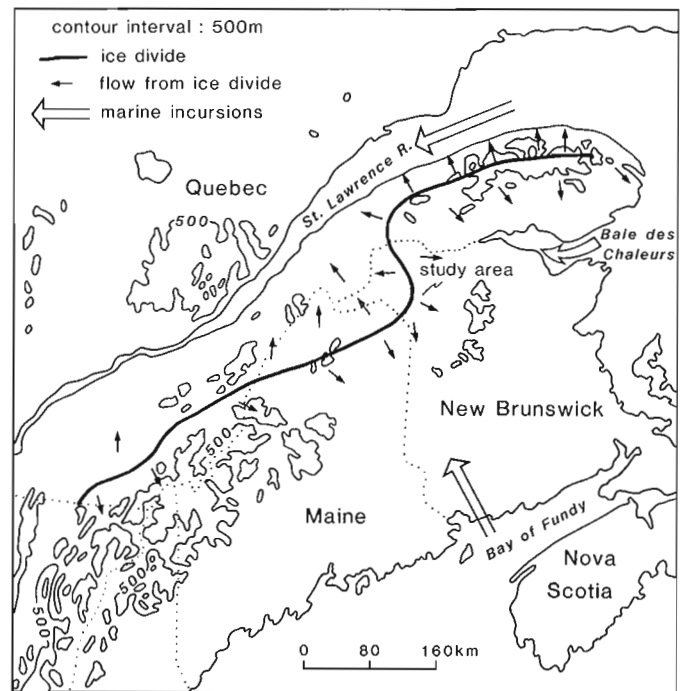


Figure 25.1. Location of the study area, possible position of the Late Wisconsinan Appalachian ice divide, related ice movement directions, and postulated synchronous marine incursions (after various sources).

ment was towards slightly west of north (Kite and Lowell, 1982; Lowell, 1985). It is mainly to the northwest in the northwest panhandle and Edmundston area, and to the west in the area around First Lake. This convergence of ice flow direction, with streaming of ice through the Temiscouata Lake low in the Notre Dame Mountains, may suggest the presence of a northward curve in the course of the Appalachian ice divide, through which it joined the ice divide on Gaspésie Peninsula (Fig. 25.1). Possibly, this configuration developed in response to rising relative sea level accompanied by drawdown in the Chaleur Bay area (Rampton et al., 1984, p. 51).

Northwest flow indicators have been found as far south as 12 km northwest of Grand Falls, where they cross-cut older striations that indicate ice movement towards southwest or south-southwest. This older direction is often encountered in a narrow zone stretching from north of Sisson Branch Reservoir to between Grand Falls and Saint-Léonard (Thibault, 1980, 1985; Rappol, 1986). Southeast of this zone, striations generally indicate ice movement in a southeastern direction. No decisive evidence, however, has been found as to the chronology of the ice movements towards southwest and southeast, respectively.

Elongated clast fabric was determined Fig. 25.3 – 25.5) by measuring orientation and plunge of the a-axis of 25 or 50 elongated clasts. These data were processed by an eigenvalue method (Mark, 1973; Woodcock and Naylor, 1983) and contoured by a method proposed by Starkey (1977), with a counting area of 100/n% of the projection, where n is the sample size. In Figures 25.3, 25.4, and 25.5, the blackened area represents 5 or more clasts per counting area.

Although clast fabric analysis of subglacial till does not provide us with unequivocal evidence of the sense of ice flow direction, in some cases this may be inferred from other features, such as subglacial deformation structures, clast lithology, or striations on and orientation of certain till-embedded boulders (see

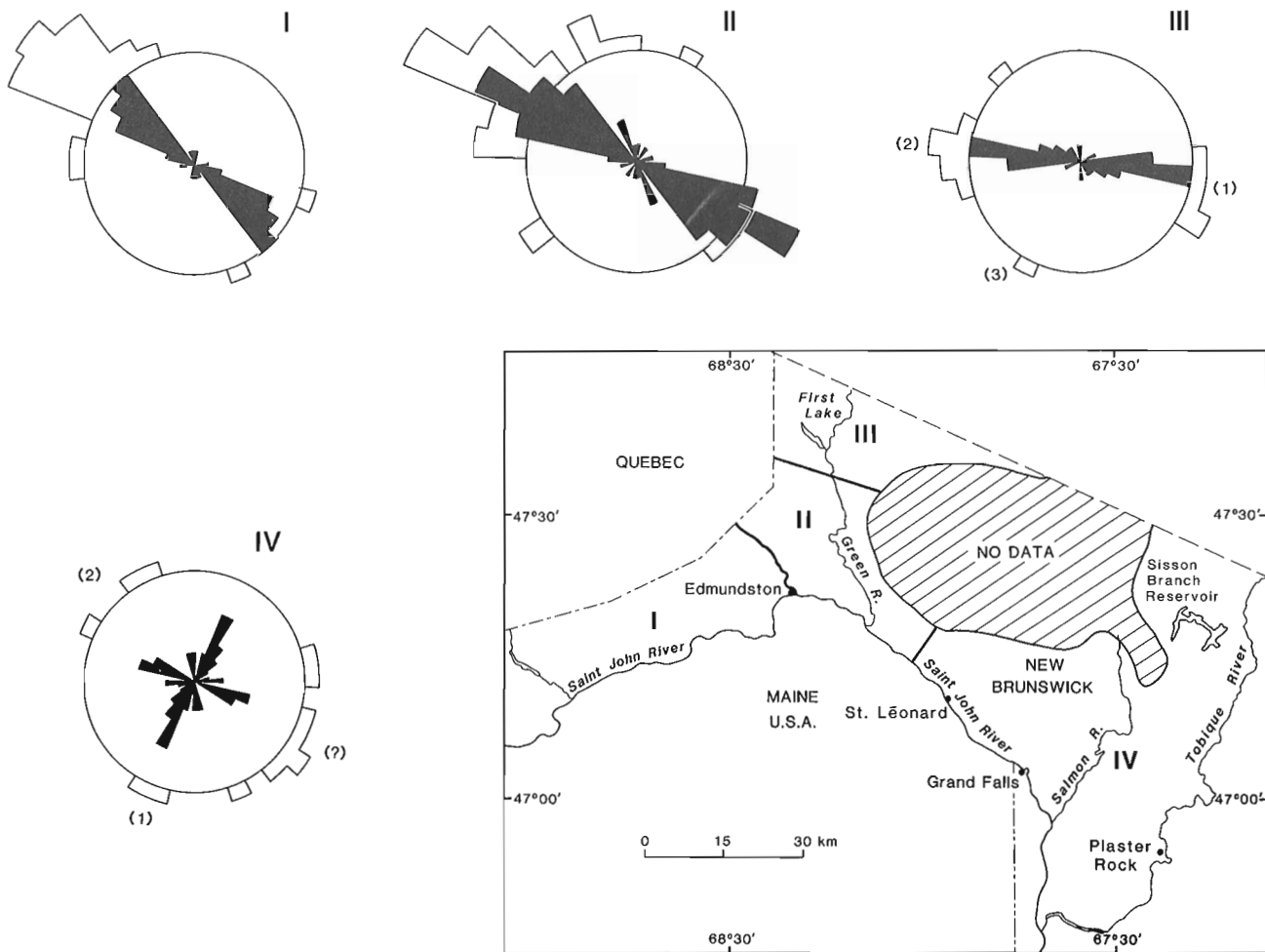


Figure 25.2. Summary of observed bedrock striations for various parts of the study area. Relative age is indicated by numbers; 1 means oldest. Circle represents eight measurements; Striations of known direction are plotted outside the circle. Roman numerals correspond with numbered areas on the map. Data after Thibault (1979, 1980, 1985), Gauthier (1982), and Rappol (1986). Hatched area consists of deeply fractured bedrock, with only a scattered cover of loose till (as zone III of David and Leblais, 1985).

below). Moreover, in some cases and especially in very stony tills, clast imbrication may be so pronounced, that the sense of ice flow direction can be established with a fair level of confidence. For the investigated area, these results are given in Rappol (1986, Fig. 1). In general, trends of elongated clast fabric align with the directions derived from erosional features at nearby sites, but some additional information was gained.

In the northern part of the study area where bedrock striations indicate a latest ice movement towards northwest, elongated-clast fabric measurements in the surface till generally indicate a preferred orientation in the direction northwest-southeast, with, in most cases, a southeastern plunge of the computed principal eigenvector. In places where the lower part as well as the upper part of the till was sampled, this did not give significantly different results (Fig. 25.3). At one site in this area, in the western part of the town of Edmundston, a lower till was observed, separated from the upper till by approximately 6-8 m of sorted sediment. The lower till contains a northeast-southwest oriented clast fabric (Fig. 25.4). This latter direction finds no support in the available striation data from northwest New Brunswick, but an older ice movement in an eastern direction is well known from northern Maine, through striation as well as fabric data (Lowell, 1985; Newman et al., 1985).

At another two till section, along Saint John River, south of Grand Falls (site A in Fig. 10 of Rampton et al., 1984), tills also contain almost perpendicular fabrics (Fig. 25.5). In the upper till, clast orientation suggests ice movement towards south or south-southeast, a direction that was found at several places in Saint John and Salmon River valleys in tills overlying thick gravel deposits. On the plateaus bordering these valleys, the surface till contains a northwest-southeast fabric (Fig. 25.5). The lower till in Saint John Valley shows a fabric with elongated clasts oriented east-west or southwest-northeast (Fig. 25.5). The absence of erratics derived from the Mississippian redbeds of the Plaster Rock area may suggest ice movement in an eastern direction. It is remarkable, however, that in all five samples, the principal eigenvector plunges towards east (Fig. 25.5).

Glacial Deposits

A major concern in present-day glacial stratigraphy and sedimentology is the distinction between till, as a product formed by release of debris directly from the ice, and diamictons formed by resedimentation processes (sediment gravity flow deposits, including flow till, flowed till, etc.). Much work has already been done on the determination of distinguishing

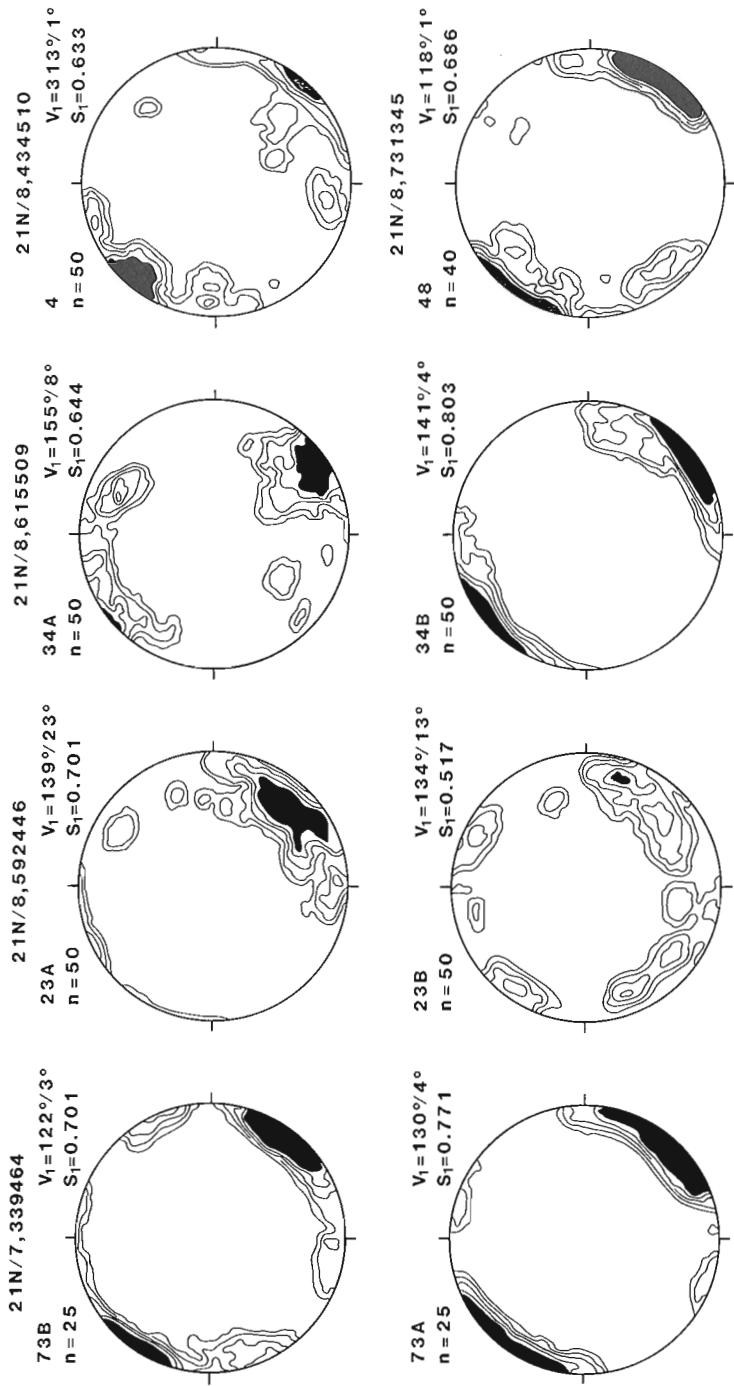


Figure 25.3. (above) Selected clast fabric diagrams from subglacial till in the northern part of the study area. Till was most likely deposited by northwest moving ice from the Appalachian ice divide. V_1 represents trend and plunge of the principal eigenvector, and S_1 the value for the principal normalized eigenvalue as a measure of fabric strength.

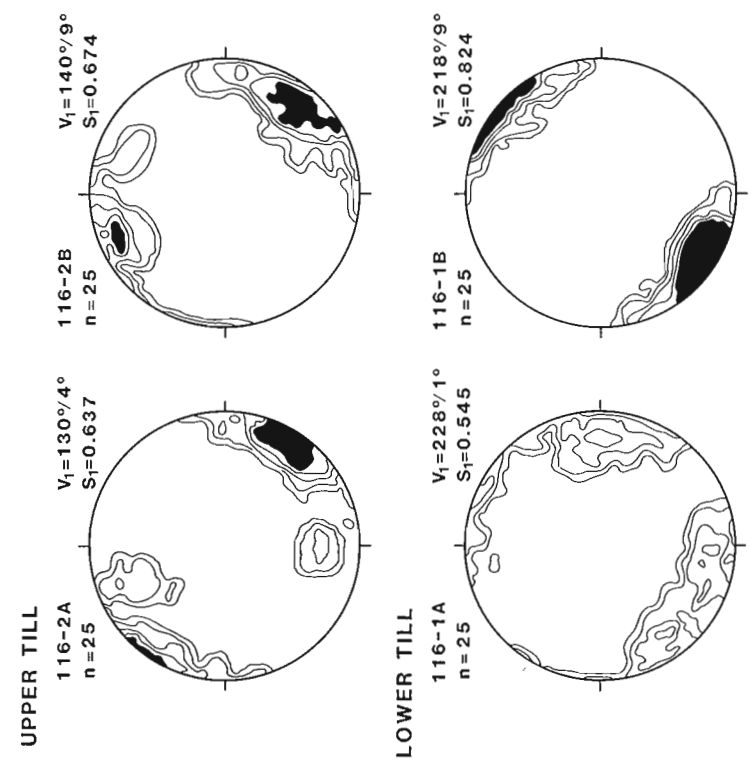


Figure 25.4. (left) Elongated clast fabrics from upper and lower till at Edmondston (21 N/8, 489452). Samples were taken from the middle of the tills, at lateral intervals of about 2 m.

73: 6 m of compact till exposed in a gully at Rang-des-Morneault. 73A: grey till, 4 m below surface; 73B: yellowish brown, oxidized till, 1.5 m below surface

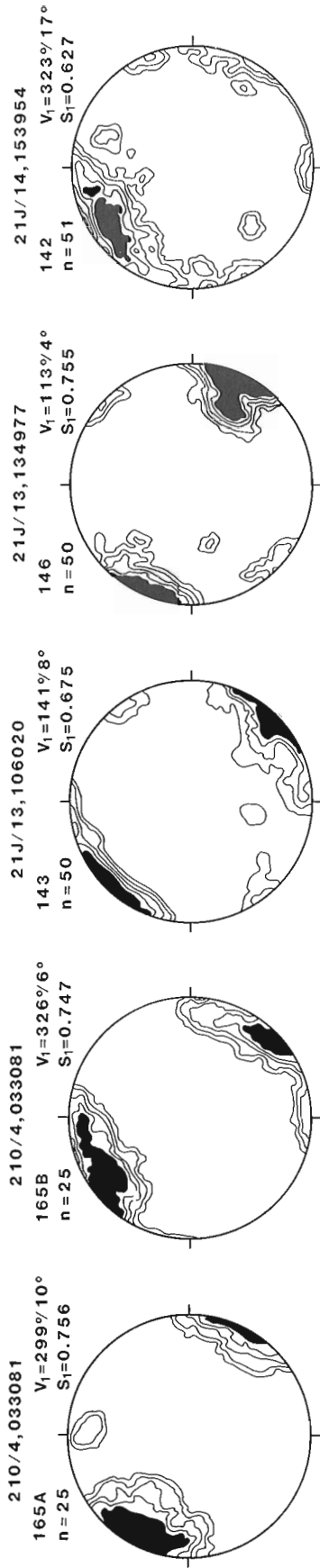
23: 2.5 m of brown, gravelly till overlying sheared sand and gravel deposit near Saint-Basile; 23A: massive, matrix-supported till, 1.5 m below surface; 23B: massive to faintly banded clast-supported base of till, 2.25 m below surface.

34: 4 m of till, overlain by 6 m of gravel and overlying 2-4 m of gravel on deformed lake sediments, Green River valley at mouth of Risseau Thibodeau. 34A: 1 m below top of till (yellowish brown and oxidized); 34B: 0.5 m above base of grey till.

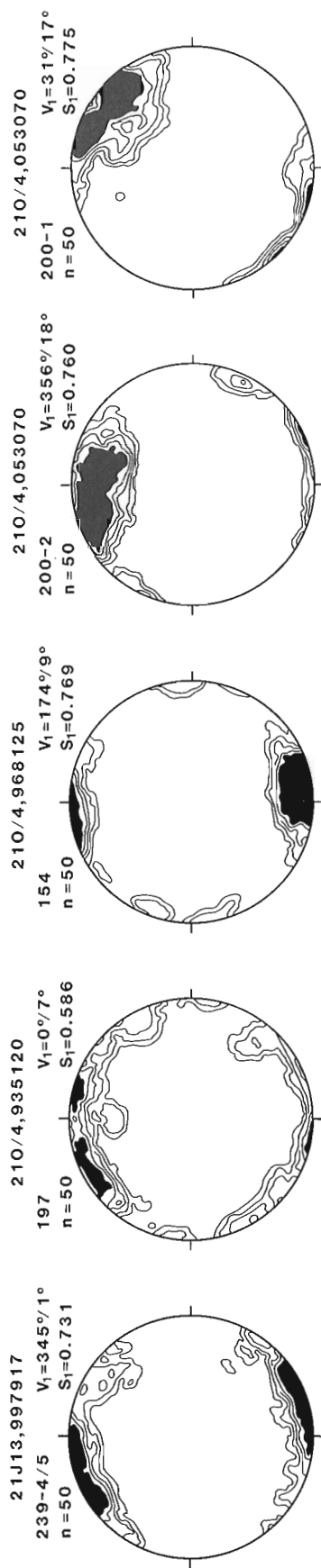
4: 7 m of shear-banded till between gravel deposits; fabric sample at 3 m below top of till.

48: 1 m of local till on weathered bedrock, north of Sainte-Anne-de-Madawaska.

Surface till, plateau east of Saint John River valley



Surface till Saint John, Little and Salmon River valleys



Lower till, Saint John River valley

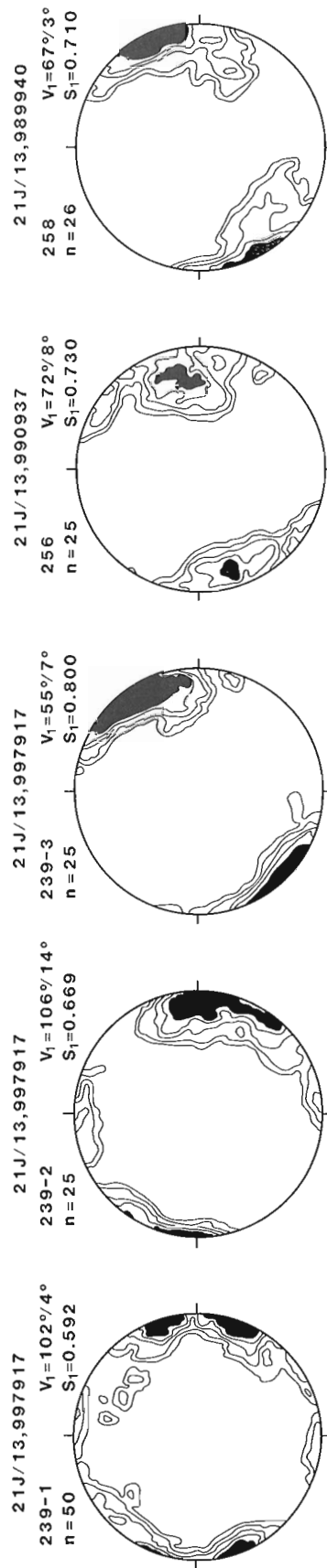


Figure 25.5. Selected clast fabric diagrams from subglacial tills in the southern part of the study area.

properties of these deposits, both in modern and Pleistocene glacial environments (e.g., Boulton, 1971, 1972; Krüger, 1979; Lawson, 1979, 1981; Shilts, 1981; Ehlers, 1982; De Jong and Rappol, 1983; Sharp, 1985; Shaw, 1985), but still, and especially in the case of poor exposure, the distinction between subglacial till and massive stony debris-flow deposits remains problematic. In the following sections some characteristic features of these deposits in New Brunswick will be discussed shortly.

Till

The classical till profile consists of a compact matrix-supported subglacial till overlain by a loose, blocky, and clast-supported ablation till (e.g., Flint, 1971). Although such profiles are common in the Miramichi Highlands, to the east of the study area (Lamothe, this volume), in northwest New Brunswick such profiles are seldom observed in well exposed sections; generally only the subglacial till is present, directly overlain by sorted and stratified glaciofluvial or alluvial gravels.

Deposits interpreted as subglacial till may show one or a number of diagnostic features that distinguish them from similarly textured sediment flow deposits. Firstly, many subglacial tills exhibit a petrographic stratification, ideally with material derived from local rock types most abundant in the lower part of the till, and more far-travelled material increasing upwards (e.g., Rose, 1974; Shilts, 1978; Rappol, 1983). Such an ideal situation may be disturbed, or sometimes even reversed as a result of synsedimentary deformation, but even then, such a petrographic stratification is not normally found in sediment-flow deposits.

This property is well illustrated by the occurrence of brown till on top of red till in the area immediately west of Plaster Rock that is underlain by Mississippian redbeds. Upglacier of this area (towards northwest) till is usually brown (sometimes grey, where unoxidized); upon entering the area underlain by the redbeds from the northwest, a red colouring is immediately observed in the lower part of the till. The boundary between red and brown till is commonly rather diffuse or shows

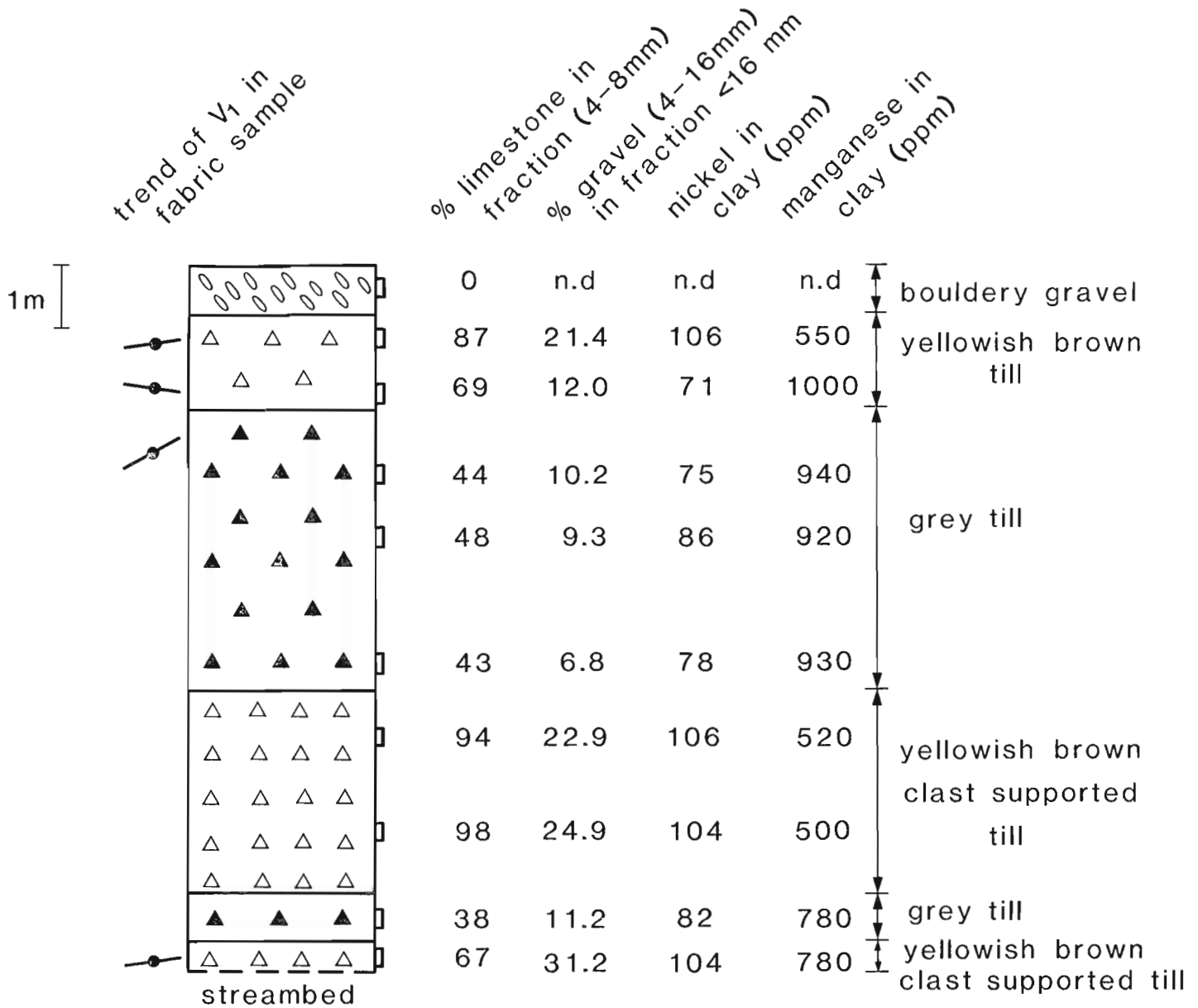


Figure 25.6. Aspects of the compositional variation in a 10 m-thick till section exposed in a gully northwest of Salmonhurst Corner (21 J/13, 037043).

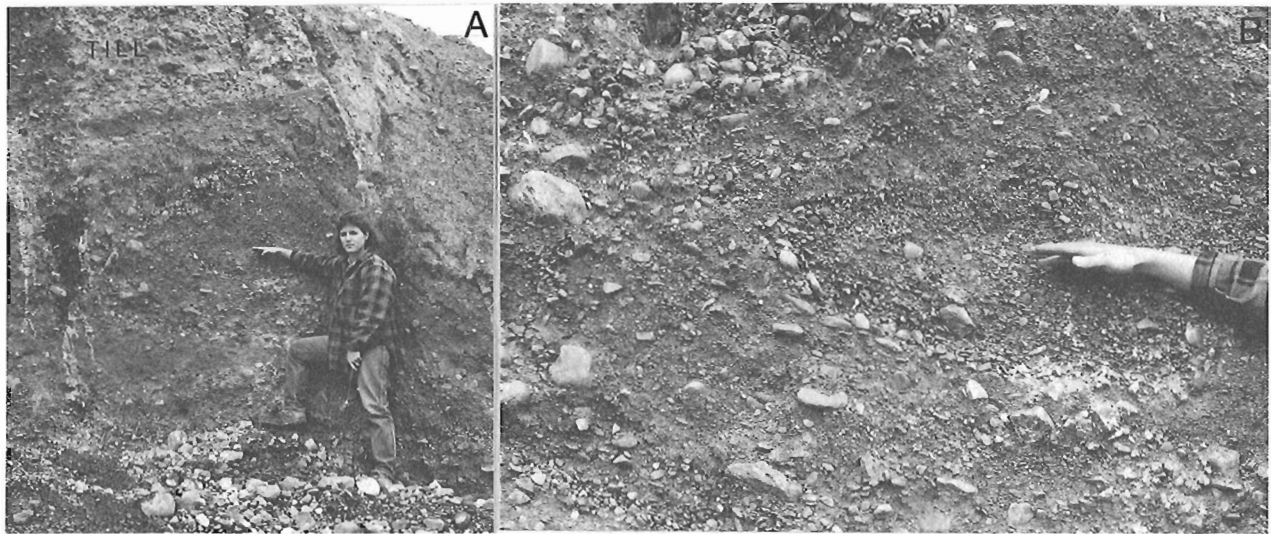


Figure 25.7. A. Deformed subglacial deltaic gravels; gravel pit near north shore of Long Lake, Maine, south of Cleveland (21 N/8). Ice movement was towards the right (southeast). B. Detail of A.

irregularities due to deformation. East of Plaster Rock the entire till is generally red, whereas red colouring extends to more than 15 km eastwards of the area underlain by the redbeds (Gauthier, 1983). Likewise, in the area underlain by limestones and highly calcareous shales, the percentages of these rock types in the gravel fraction of till may vary considerably in vertical profiles (Fig. 25.6). Although in this profile the compositional differences seem to coincide with textural and colour variations, in general grey and (yellowish) brown reflect only the oxidation state of the deposit; it should be stressed that, in the investigated area, till colour cannot be used as a confident stratigraphic tool.

A second characteristic observed in some subglacial tills is the presence of structures that result from deformation styles associated with subglacial shearing. These may be present in the subglacial sediments as well as within the till, and may reflect englacial deformation of debris-rich ice (glaciodynamic structures: Lavrushin, 1971, 1978) or may have been formed subglacially by drag of moving overlying ice (e.g., Boulton, 1976; Rappol, 1983). In combination with till fabric analyses, these structures are important indicators of ice movement direction (e.g., Krüger, 1979; Rappol, 1983; Hicock and Dreimanis, 1985). Subglacial deformation structures are generally well developed where till overlies fine grained sediments, as is the case in most of the north European plain (Lavrushin, 1978; Berthelsen, 1979; Stephan and Ehlers, 1983; Ruszczynska-Szenajch, 1983; Rappol, 1983). In New Brunswick, till is generally observed overlying coarse and porous glaciofluvial gravel that resists deformation; only few examples were observed in the field.

Probably the most common subglacial deformation structure consists of a recumbent fold with slightly up-glacier dipping axial surface. The example shown in Figure 25.7 represents a simple drag structure, in which the lower limb has basically remained in situ. Deformation of the till/subglacial sediment interface may produce up-glacier dipping till wedges, that form the core of tight recumbent folds (Fig. 25.8).

A further distinguishing criterion of subglacial till and sediment flow deposits lies in some characteristics of clast fabric. Elongated clasts in till generally align with the local direction of ice movement, whereas those in sediment flows, if a preferred orientation is present at all, reflect local directions of mass flow that are unrelated to ice movement (e.g., Harrison, 1957;

Boulton, 1971; Lawson, 1979). Moreover, Lawson (1979) found a large difference in fabric strength to exist between subglacial till fabrics and sediment flow fabrics, but in other areas such a sharp distinction may be less clear (e.g., Mills, 1984; Rappol, 1985).

A good indicator for subglacial formation is the presence of a consistent and strong imbrication as present in some stony tills, indicating up-slope transport. This is the case in the lower part of the till section described in Figure 25.6, where ice flow in an eastern direction is indicated.

In the present study, fabric did not play any role in determining sediment genesis, except perhaps in confirming such an interpretation by a parallelism of clast fabric and local striation sites. Compared with samples from two other areas, measured by the same method, the New Brunswick samples occupy an intermediate position in a triangular diagram of the normalized eigenvalues (Fig. 25.9A); this is somewhat better illustrated in Figure 25.9B. In an earlier paper (Rappol, 1985), the data presented by Shaw (1982) were overlooked. He interpreted the till in the Edmonton area as melt-out till, with part of the fabrics

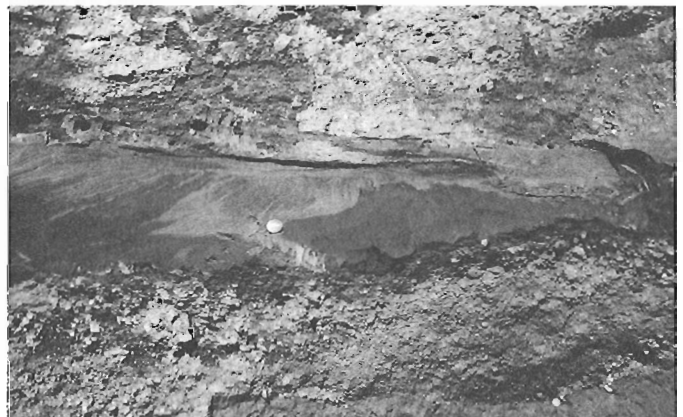


Figure 25.8. Up-glacier dipping till wedge in the core of tight, recumbent fold and deformed subglacial sediments near Saint-Léonard (21 O/4, 822233).

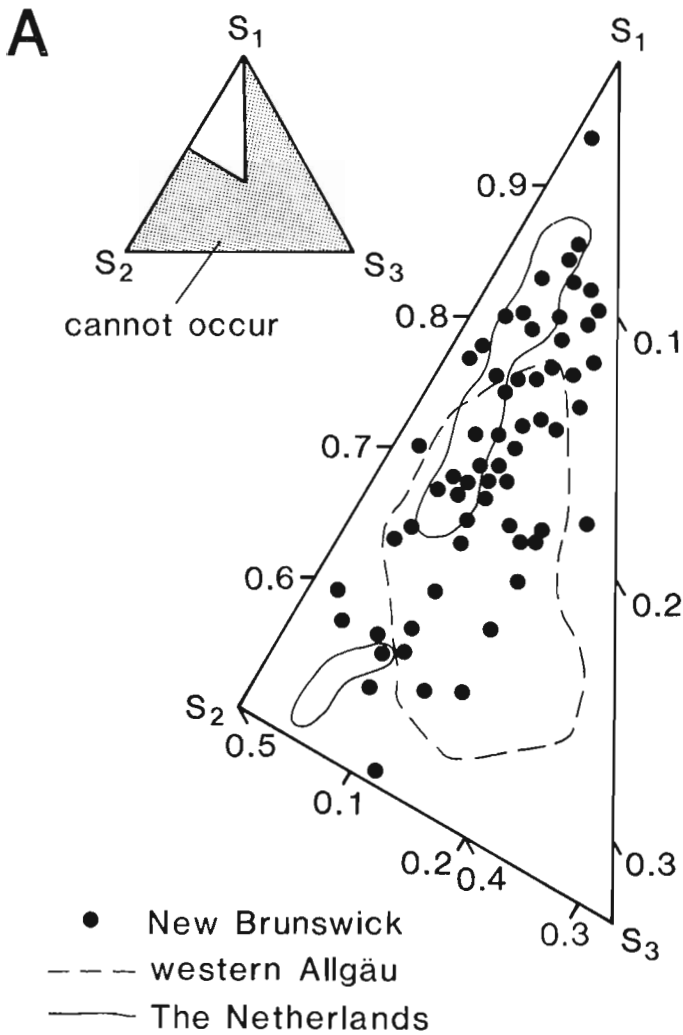


Figure 25.9.

A. Triangular plot of normalized eigenvalues for elongated clast fabrics from New Brunswick, and envelopes for fabric samples from western Allgäu and The Netherlands (from Rappol, 1985).

B. Plot of S_1 and S_3 eigenvalues of clast fabrics in till from different areas, shown as standard deviation around the mean values (see also: Dowdeswell et al., 1985, and data given by Mills, 1984). Fabric data from Lawson (1979) for Matanuska Glacier melt-out till (Mat.), 8 samples; Rappol (1985), Saalian till of The Netherlands (N.L.), 25 samples, and western Allgäu, southern Germany (All.), 37 samples; Mills (1977) for Alpine till (Alp.), 18 samples; Mark (1974), Sumas Till (Sum.), 28 samples; Shaw (1982), till of the Edmonton area (Edm.), 28 samples; and from this report: till in New Brunswick (N.B.), 61 samples.

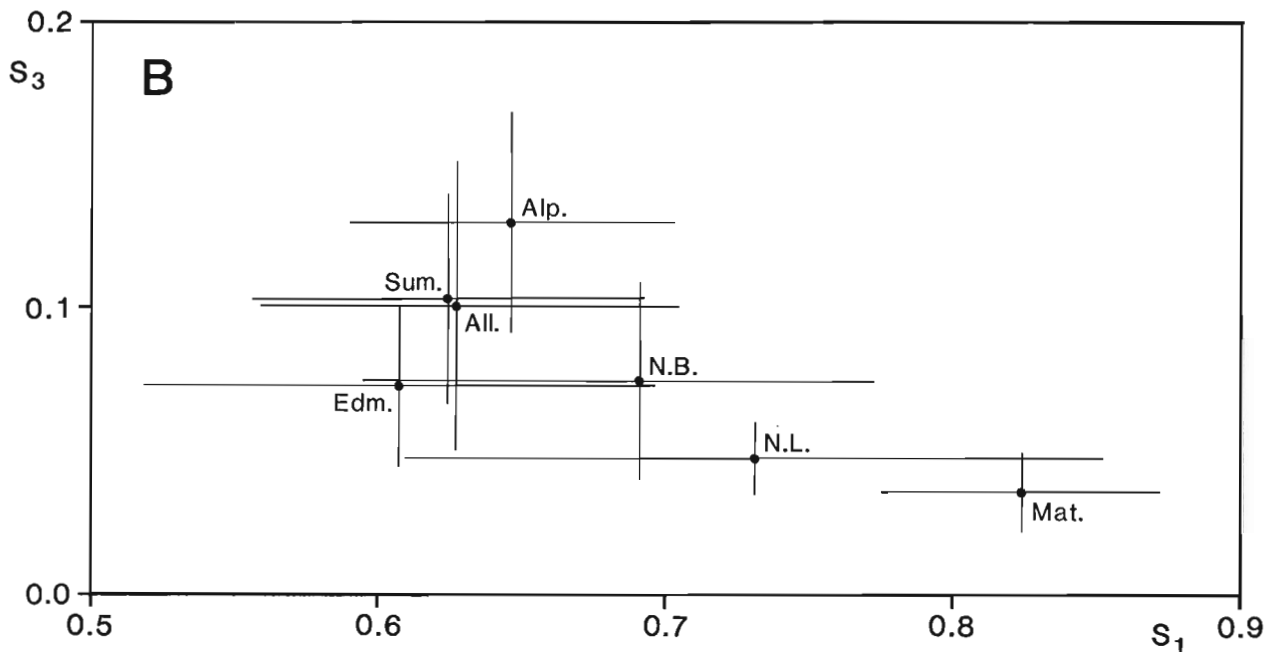




Figure 25.10. Bullet-shaped boulder near base of till overlying glaciofluvial gravels at site 146 (see Fig. 25.5 for till fabric and coordinates). Two sets of striations are present: an older set, parallel to the long-axis of the boulder (180° - 360°) and a younger set (125° - 305°) parallel to the till fabric, with abrasion features indicating ice movement towards the southeast.

suggesting re sedimentation by sediment flow. The range given for the Edmonton samples as given in Figure 25.9B thus represents a mixture of different sediment types, in which the melt-out facies showed the highest fabric strength. Strong fabrics (high S_1 -values) were also measured by Shaw (1979) in melt-out till of the Sveg type in Sweden.

There are several factors that may play a role in the observed variability, although their significance in each case is difficult to assess. These comprise: 1) till texture; during till shear, a higher clast content implies a higher frequency of clast interaction; 2) depositional process, for example, melt-out versus lodgment, including the effect of synsedimentary deformation; and 3) modifications after till formation, e.g. flow or frost action (Derbyshire, 1980; Mills, 1984; Rappol, 1985).

The occurrence of bullet-shaped boulders with stoss-and-lee side forms, and consistent striations parallel to their long axis, is commonly held to be an additional diagnostic criterion for subglacial deposition by lodgment (e.g. Boulton, 1978; Krüger, 1984). Few such boulders were observed in till of the study area, which may be primarily a result of the generally thinly cleaved bedrock of the area, producing mainly flatstones. Moreover, in a few cases, it was observed that bullet-shaped boulders did not obviously align with ice movement. Figure 25.10 shows an example where the boulder was reoriented during some stage of its abrasion and now occupies a position oblique to ice movement as indicated by a younger set of striations and till fabric.

Sediment flow deposits in ice contact sediments

Ice contact sediments deposited during the final deglaciation of the area are characterized by their hummocky topography, and intense faulting or warping of sedimentary layers. They consist of variable amounts of boulders, gravel, sand, and mud, that are commonly interstratified with or overlain by till-like layers (Rampton and Paradis, 1981; Gauthier, 1982).

These till-like layers differ in many aspects from subglacial till, as will be discussed below, and can generally be interpreted as debris flow deposits. Moreover, many sandy gravelly sediments show evidence for emplacement by sediment gravity flow mechanisms, rather than for a strict glaciofluvial origin.

In many cases, ice marginal debris flow deposits are found only at the top of a kame deposit, possibly reflecting their low

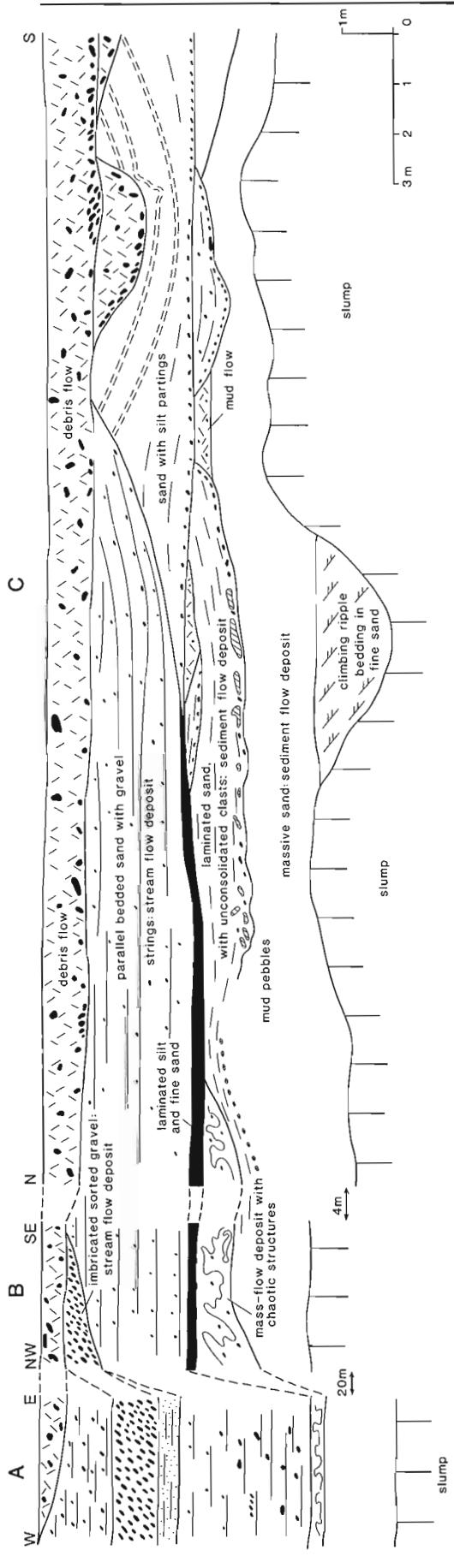


Figure 25.11. Sediments exposed in a gravel pit in the Grande Rivière Valley (21 O/4, 822297). Subaqueous sediment-flow deposits are overlain by glaciofluvial gravelly sand, in turn overlain by subaerial debris-flow deposits.

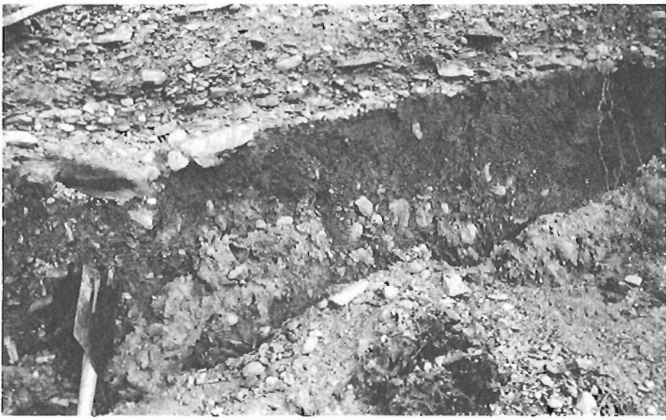


Figure 25.12. Grading in debris flow deposit within ice contact sediments near Comeau Ridge (21 O/4, 996218). The debris flow deposit is overlain by glaciofluvial gravels with an erosive lower bed limit.

preservation potential in the active glaciofluvial environment (Boulton, 1972). Debris flow deposits capping ice contact sediments, commonly contain coarser elements than the underlying sorted sediment, suggesting that they were not formed through simple reworking and colluviation of the sorted sediment, but were probably derived directly from the supraglacial debris.

Stony debris flow deposits may show one or several characteristics that distinguish them from similarly textured subglacial tills. Some debris flow deposits exhibit distinctly gully-shaped lower bed limits (Fig. 25.11), with coarser material commonly concentrated in the gully fill (De Jong and Rappol, 1983). In many debris flow deposits a size grading, vertical as well as lateral, is observable (Fig. 25.12), and a coarse grained traction carpet may be present at the base, showing well developed clast imbrication (Fig. 25.13). The presence of size grading and textural variations between debris flows gives many thick debris flow deposits a stratified appearance and allows the recognition of repetitive debris flow pulses. Also, successive debris flow layers may be separated by a thin layer of diffusely laminated or massive silt, formed at the top of debris flow deposits during water expulsion (Lawson, 1979).

Sediment flow deposits of a sandy gravelly texture were observed in several pits in ice contact kame deposits. These mainly were formed as a result of resedimentation of presorted glaciofluvial or glaciolacustrine deposits, and may have been triggered by the melting of adjacent ice bodies. Figure 25.14 shows an example that probably formed as a result of destabilization of the kame deposit. The massive to faintly banded gravel deposit is underlain by a layer of diffusely laminar sand with dispersed clasts, similar to the shear zone below sandy gravelly mass flow deposits described by Postma et al. (1983).

In the sequence depicted in Figure 25.11, sediment flow deposits constitute the main sediment body of the kame deposit. Several distinct sediment flow facies can be distinguished. Overlying a climbing ripple bed at the bottom of the sequence is a massive sand deposit that is interpreted as a liquefied flow deposit (Lowe, 1976). The only structural feature of this deposit is the presence of many irregular and branching, near vertical channels of a more silty texture (Fig. 25.15) that extend upwards towards the layer of laminated silt and sand, and may represent fluid escape structures. The massive sand layer is overlain by a slightly coarser sand with a laminar structure and a basal conglomerate of unconsolidated mud clasts (Fig. 25.16), that grades laterally in a more chaotically structured

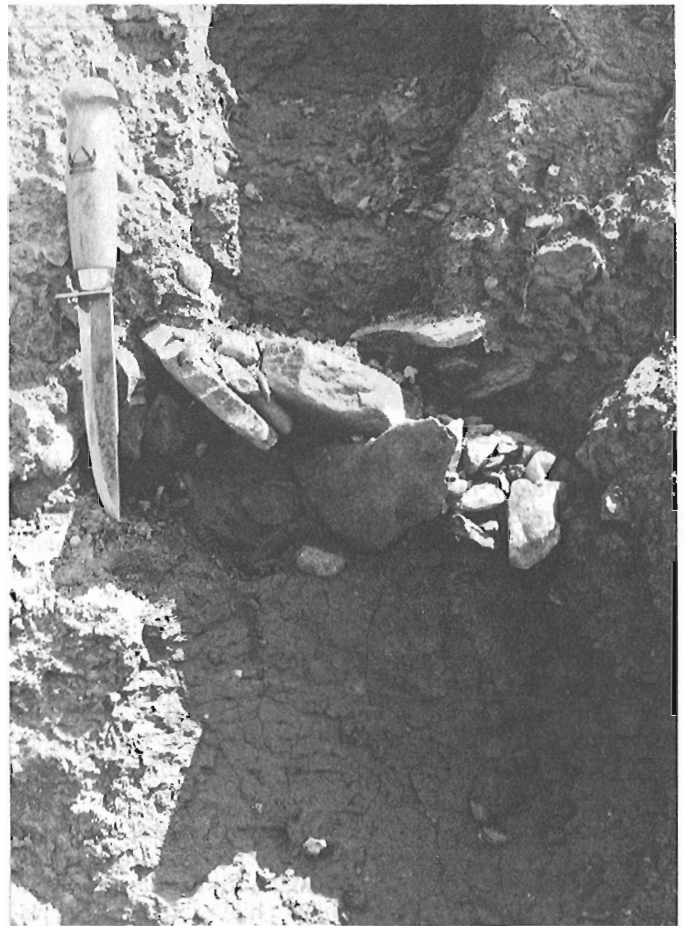


Figure 25.13. Imbricated stone pavement at contact of two debris flow deposits in the debris flow deposit of Figure 25.11.

deposit. The presence of laminated silt and sand, half way up the section, together with the abundant mud clasts in the sediment flow deposits below it, suggests subaqueous deposition of the sediments.

In reconnaissance studies such as this one, it is not possible in most cases to study sediment genesis in much detail at every exposure, and generally one depends on the traditional and rather trivial criteria such as grain size, compaction and overconsolidation, presence or absence of primary pores, thickness and lateral extension of the deposit. Individually, none of these characteristics is of much value in deciphering sediment genesis, but considered in combination and in conjunction with geomorphic and sedimentological setting, reasonably reliable preliminary interpretations can be made.

Stratigraphy

Although Rampton et al. (1984, Fig. 10) indicated at least eight multiple-till sections in the study area, only two sections were found where a significant amount of sorted and stratified deposits separated two tills, that is, in the western part of the town of Edmundston (21 N/8, 489452), and south of Medford in a roadcut on the east bank of Saint John River (21 J/13, 997917; section A in Rampton et al., 1984, Fig. 10).

At Edmundston, the section consists of the following units (from top to bottom):

- i) 0-6 m: alternating gravel and diamict layers (ice-contact gravels and debris-flow deposits)

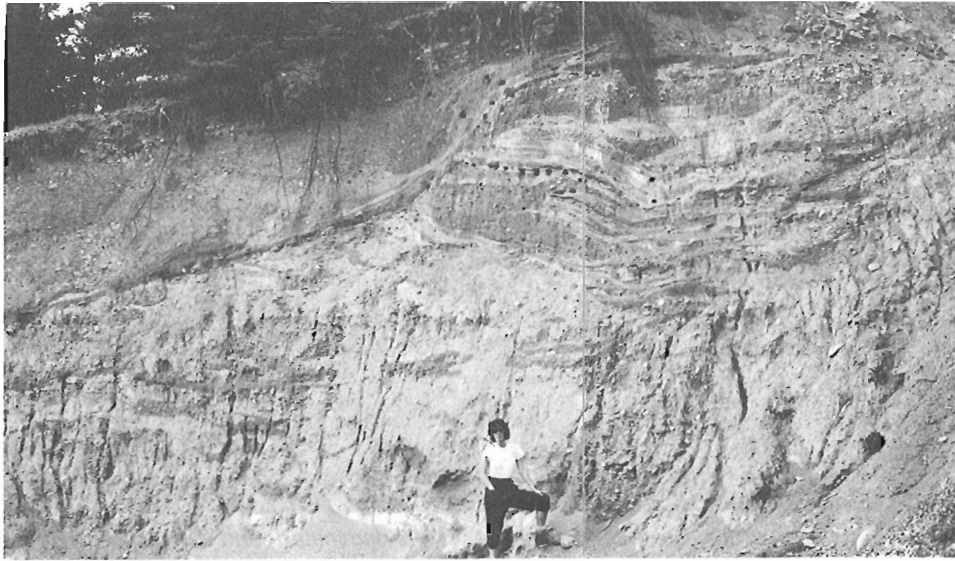


Figure 25.14. Massive clast-supported, gravelly sandy, debris flow deposit underlain by a fine grained shear zone with diffuse banding and dispersed clasts. Exposure in kame deposit near North Tilley (21 J/13, 013883).

- ii) 6-8 m: oxidized, very hard, compact and massive diamicton (upper till)
- iii) 8-10 m: faintly banded sand and silt deposit with a few dispersed clasts (deformation till ?)
- iv) 10-16 m: gravel, sand and silt deposits, commonly deformed bedding, and with a general dip of sedimentary layers towards southeast (ice-contact deposits)
- v) 16-17 m: compact, partly oxidized diamicton, containing deformed sorted layers (lower till)
- 17 m: base of excavation

Figure 25.5 shows that the tills contain a different fabric, suggesting that the sedimentary sequence represents more than a local minor fluctuation of the ice margin.

At the second two-till section, the two tills also have different fabrics (Fig. 25.17). Rampton et al. (1984, p. 15) suggested a possible pre-Wisconsinan age for the lower till, based on a 0.5-1 m-thick oxidized zone at the top of the unit. Oxidation of the upper part of a subsurface till however is common where overlain by porous gravels, as is oxidation of the lower part of till overlying gravels. Also, no sign of weathering in the form of decalcification was observed, as is possibly the case in the upper till (see Fig. 25.17). The decreasing percentage of limestone rock



Figure 25.15.
A. Massive sand deposit overlain by a chaotically structured slump deposit; at the top, horizontally bedded silts and fine sand. (Detail of section B, Figure 25.11).
B. Detail of silty veins in massive sand unit, probably formed by water-escape process.

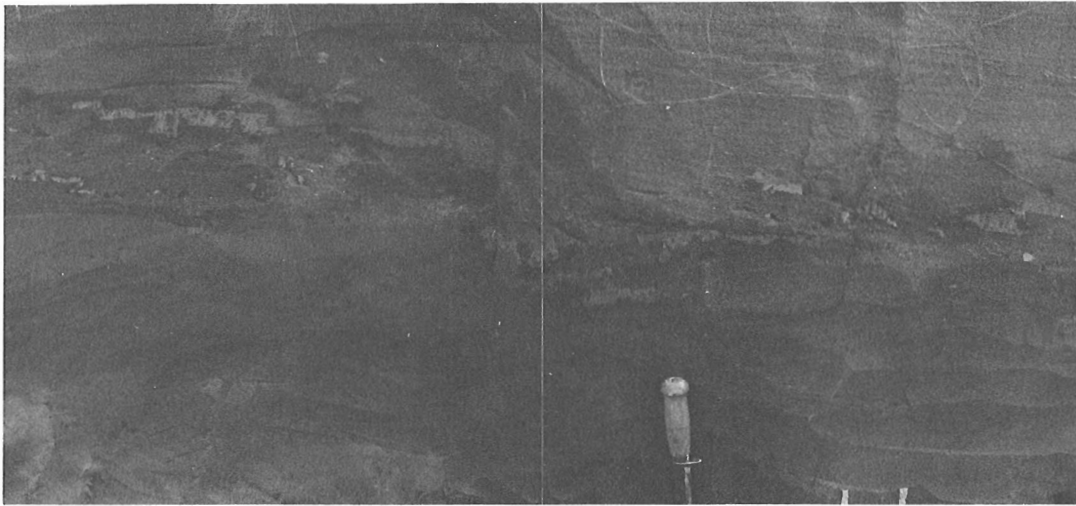


Figure 25.16. Contact of massive sand and base of faintly laminated sand of section C in Figure 25.11, showing the erosive contact and unconsolidated clasts at the base of the upper sediment flow deposit.

fragments towards the top of the upper till could be a primary feature also, when far-travelled noncalcareous material becomes more abundant towards the top of the till.

If the lower tills at these two sites can be correlated, then the intertill gravels suggest a regional deglaciation. If the tills were emplaced by ice moving towards the east or northeast, a correlation with the St. Francis Till of northern Maine (Genes et al., 1981; Newman et al., 1985) seems plausible. In this respect, however, the consistent eastward plunge of the fabrics in the lower till south of Grand Falls remains an unsatisfactory element, which needs future clarification. Ice movement towards the east was inferred from the till depicted in Figure 25.6; this till may be correlative on the basis of fabric trend with the lower till in Saint John Valley.

Of further stratigraphic interest is the sedimentary sequence exposed in the Falls Brook gully (21 0/4, 970113) near Grand Falls. The sediments fill a pre-existing valley, deeply incised in bedrock, and consist of 2-3 m of brown, presumably alluvial gravel, overlying about 5 m of grey till (oxidized and yellowish brown in the upper part), with an apparent north-south fabric, which in turn overlies 20-30 m of mostly gravelly sediments. The subtill gravel consists of two distinct units separated by a thin layer of massive silt.

The lower unit directly overlies limestone and is itself composed throughout its entire thickness almost exclusively of angular limestone clasts (over 90%) that are set in a dense sandy matrix. In the middle of this lower gravel unit, a laminated silt layer (thickness 1-1.5 m) is present, locally overlain by up to 1.5 m of laminated sand (Fig. 25.18). The silt is free of pollen (R.J. Mott, personal communication, 1985) and locally contains dropstones, both suggesting a cold and near-ice environment. The upper subtill gravel consists of well rounded clasts with a mixed petrography and a more open framework, and is probably correlative with similar subtill gravels exposed at many places along Saint John River in the Grand Falls area. The lower subtill gravel is tentatively correlated with Lee's (1962) 'nonglacial' gravel, underlying till and glaciofluvial gravel, recovered from a borehole at Grand Falls (Rappol, 1986). To my knowledge, Lee nowhere indicates the reason for the interpretation of these gravels as being nonglacial, and palynological analyses undertaken to establish this nonglacial origin proved that the gravels are virtually sterile. Unexpectedly, one sample from the overlying glaciofluvial gravel contained a fair amount

of boreal pollen, but these may have been reseeded (R.J. Mott, unpublished GSC Palynological Report 62-32).

In the area of Anfield (21 J/13, 130980) and Blue Bell Lake (21 J/13, 113005), an almost continuous till sheet, about 2 m thick, covers extensive glaciofluvial and deltaic sediments (Thibault, 1980; Rampton et al., 1984). Elevations of the top of the deltaic deposits suggest a lake level around 240 m a.s.l.. This lake must have been blocked by ice in Tobique River valley around Plaster Rock, and in the northwest by an ice lobe in Little Salmon River valley somewhere between New Denmark (21 J/13, 070050) and Blue Bell Lake. Deltaic foresets slope in directions varying between northeast and southeast, and also gravel imbrication in horizontally bedded glaciofluvial gravel indicate streamflow in an eastern direction, and originating from Little Salmon River valley. The deltaic sediments as well as the overlying till contain some granite erratics. Till petrography and fabric indicate ice movement towards southeast.

Subtill sediments were observed at many other places, especially in the Saint John Valley area, but no evidence was found to indicate that these represent anything other than outwash or ice contact deposits associated with an ice advance, with the exception of, perhaps, one section in Green River valley (21 N/8, 615509). Here, a till separates two gravel bodies, and the lower gravel overlies deformed lacustrine sediments. Between the deformed lacustrine silt and overlying gravel deposit, locally a diamict layer is present, consisting primarily of reworked lacustrine deposits with dispersed clasts. Due to poor exposure, it could not be established whether deformations and diamicton were formed as a result of mass movement or as a result of subglacial deformation and till formation.

Discussion

It seems that an explanation of the observed ice flow patterns in different parts of southeast Canada and New England should be sought in an appraisal of the influence and relative importance of the following events: 1) The development of radial outflow from local accumulation centres during the early part of a glacial cycle. More complicated flow patterns would have evolved where such centers merged with each other or, in some areas, with invading Laurentide ice. 2) A readjustment of ice flow pattern, with converging flow towards areas where calving bays induced drawdown of the ice surface, resulting

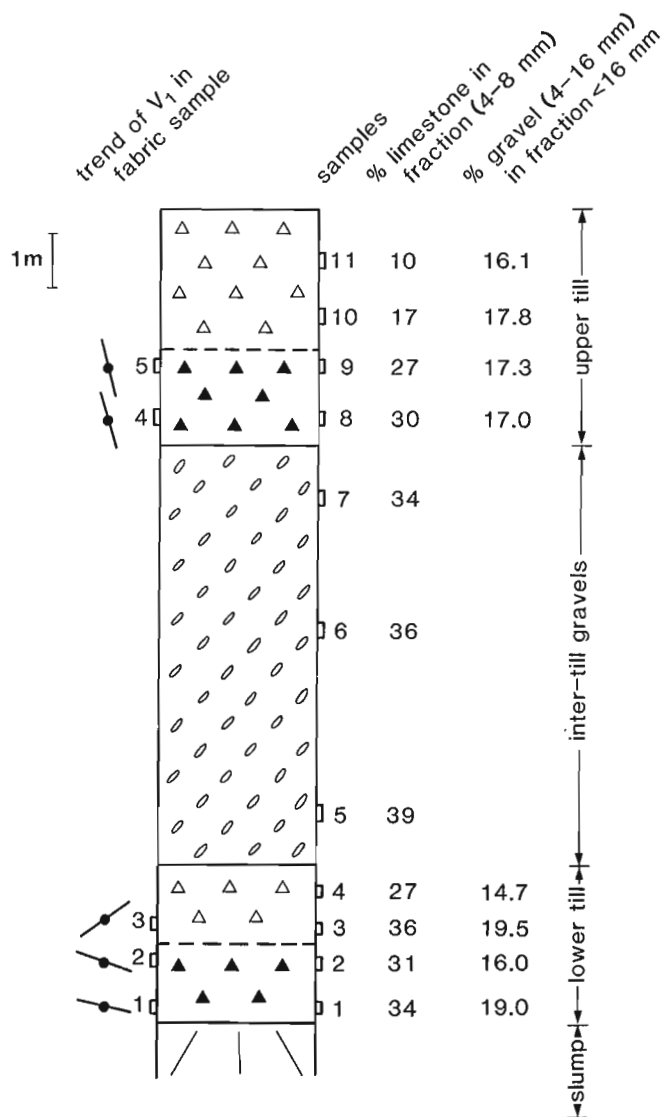


Figure 25.17. Two-till section south of Grand Falls, along Saint John River. Both tills are grey (black triangles) at the base and yellowish brown and oxidized (open triangles) in their upper parts. In the lower till, oxidation is not accompanied by decalcification. Exposures along the opposite river bank show the lower till overlying glaciofluvial gravel on bedrock.

from glacio-isostatic subsidence, and rising marine waters at the end of a glacial cycle.

There are at least two regions where rising marine waters could profoundly influence the ice flow pattern. The first is the St. Lawrence River basin, where the effects of the submergence have now been fairly well documented (see Chauvin et al., 1985, for a review). The occurrence of Laurentide erratics in northwest New Brunswick is well known (e.g., Rampton et al., 1984). At present it is not clear at all during which time of glaciation these have been transported into the area. It is possible that an Appalachian ice divide existed throughout the Late Wisconsinan, and that the marine incursion into St. Lawrence Valley caused the divide to migrate southwards, thereby causing a flow reversal in northwest New Brunswick. In this case, the Laurentide erratics must have been imported during a pre-Late Wisconsinan event.

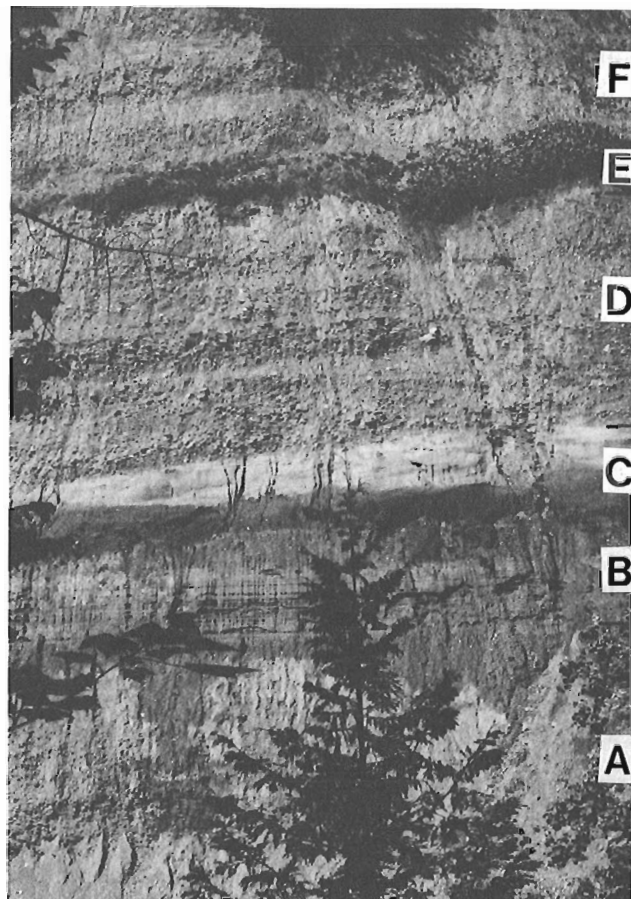


Figure 25.18. View of the lower sub-till gravel deposit (A, D) in the Falls Brook gully, with the laminated silt (B) and overlying sand layer (C). The vegetated horizon (E) is the layer of massive silt separating lower and upper sub-till gravel (F). Laminated silt layer is here about 1.5 m thick.

Alternatively, Laurentide ice may have covered most of the study area during the early Late Wisconsinan and the Appalachian ice divide developed after the marine incursion.

A second area of marine incursion is situated in the Chaleur Bay area (Fig. 25.1); Late Wisconsinan ice flow patterns in response to rising relative sea level in this area was discussed by Rampton et al. (1984) and David and Lebus (1985).

In Saint John Valley and the adjacent Chaleur uplands in the Woodstock area (Rampton et al., 1984) and in coastal Maine (Thompson, 1982) an ice movement to the southeast is followed by one towards the south. Probably the southward ice movement in Saint John and Salmon River valleys of the investigated area, and the southeastward ice movement on the adjacent plateau, are representative of the same chronology. The origin of this change in ice movement direction is not clear yet, but may be a response to drawdown along the Fundy and Maine coast.

For future progress, it is essential to gain a better knowledge of the sedimentology and stratigraphic relations of the deposits predating the surface tills. Planned work involves a detailed sedimentological study of the sub-till sediments in the southern part of the area, and a drilling program in places where preservation of a pre-Late-Wisconsinan sedimentary sequence is expected.

References

- Berthelsen, A.
1979: Recumbent folds and boudinage structures formed by subglacial shear: An example of gravity tectonics; *Geologie en Mijnbouw*, v. 58, p. 253-260.
- Boulton, G.S.
1971: Till genesis and fabric in Svalbard, Spitsbergen; in: *Till, A Symposium*, R.P. Goldthwait (ed.), p. 41-72. Ohio State University Press, Columbus.
1972: Modern arctic glaciers as depositional models for former ice sheets; *Geological Society of London Journal*, v. 128, p. 361-393.
1976: A genetic classification of tills and criteria for distinguishing tills of different origin; *UAM Geografia*, v. 12, p. 65-80.
1978: Boulder shapes and grain size distribution of debris as indicators of transport paths through a glacier and till genesis; *Sedimentology*, v. 25, p. 773-799.
- Chauvin, L.
1984: Géologie du Quaternaire et dispersion glaciaire en Gaspésie: Région de Mont-Louis-Rivière-Madeleine; Ministère de l'énergie et des ressources, ET 83-19, 33 p.
- Chauvin, L., Martineau, G., and Lasalle, P.
1985: Deglaciation of the Lower St. Lawrence region; *Geological Society of America, Special Paper 197*, p. 111-123.
- David, P.P. and Lehuis, J.
1985: Glacial maximum and deglaciation of western Gaspé, Québec, Canada; *Geological Society of America, Special Paper 197*, p. 85-109.
- De Jong, M.G.G. and Rappol, M.
1983: Ice-marginal debris-flow deposits in western Allgäu, southern West Germany; *Boreas*, v. 12, p. 57-70.
- Derbyshire, E.
1980: The relationship between depositional mode and fabric strength in tills: schema and test for two temperate glaciers; *UAM Geografia*, v. 20, p. 41-48.
- Dowdeswell, J.A., Hambrey, M.J., and Ruitang, Wu.
1985: A comparison of clast fabric and shape in Late Precambrian and modern glacial sediments; *Journal of Sedimentary Petrology*, v. 55, p. 691-704.
- Ehlers, J.
1982: Different till types in North Germany and their origin; in: *Tills and Related Deposits*, E. B. Evenson et al. (ed.); Balkema, Rotterdam, p. 61-80.
- Flint, R.J.
1971: *Glacial and Quaternary Geology*; Wiley, New York, 892 p.
- Gadd, N.R., McDonald, B.C., and Shilts, W.W.
1972: Deglaciation of southern Quebec, Canada; *Geological Survey of Canada, Paper 71-47*, 19 p.
- Gauthier, R.C.
1980: Existence of a central New Brunswick ice cap based on evidence of northward moving ice in the Edmundston area, New Brunswick; in: *Current Research, Part A*, Geological Survey of Canada, Paper 80-1A, p. 377-378.
1982: Surficial deposits, northern New Brunswick; *Geological Survey of Canada, Open File 856*.
1983: Surficial materials of northern New Brunswick; *Geological Survey of Canada, Open File 963*.
- Genes, A.N., Newman, W.A., and Brewer, T.B.
1981: Late Wisconsinan glaciation models of northern Maine and adjacent Canada; *Quaternary Research*, v. 16, p. 48-65.
- Harrison, P.W.
1957: A clay-till fabric; its character and origin; *Journal of Geology*, v. 45, p. 275-308.
- Hicock, S.R. and Dreimanis, A.
1985: Glaciotectonic structures as useful ice-movement indicators in glacial deposits: four Canadian case studies; *Canadian Journal of Earth Sciences*, v. 22, p. 339-346.
- Kite, J.S. and Lowell, T.V.
1982: Quaternary geology of the Upper St. John River basin; in: *Guidebook for the 1982 NBQAU Field Trip*, August 18-20, p. 3-16; New Brunswick Quaternary Association.
- Krüger, J.
1979: Structures and textures in till indicating subglacial deposition; *Boreas*, v. 8, p. 323-340.
1984: Clasts with stoss-lee form in lodgement tills: A discussion; *Journal of Glaciology*, v. 30, p. 241-243.
- Lamarche, R.Y.
1971: Northward moving ice in the Thetford Mines area of southern Quebec; *American Journal of Science*, v. 271, p. 383-388.
1974: Southeastward, northward, and westward ice movement in the Asbestos area of southern Québec; *Geological Society of America Bulletin*, v. 85, p. 465-470.
- Lamothe, M.
1986: Reconnaissance geochemical sampling of till, south-central Miramichi Zone, New Brunswick; in: *Current Research, Part B*, Geological Survey of Canada, Paper 86-1B, p.
- LaSalle, P., Martineau, G., and Chauvin, L.
1977: Morainic deposits and glacial striae in Beauce-Notre-Dame-Mountains-Laurentide Park area; *Ministère des richesses naturelles du Québec, DPV-515*, 22 p.
- Lavrushin, Y.A.
1971: Dynamische Fazies und Subfazies der Grundmoräne; *Zeitschrift für Angewandte Geologie*, Bd. 17, p. 337-343.
1978: Texturen, Fazies und stoffliche Zusammensetzung der Grundmoräne; *Schriftenreihe für geologische Wissenschaften*, Berlin, Bd. 9, p. 161-177.
- Lawson, D.E.
1979: Sedimentological analysis of the western terminus region of the Matanuska Glacier, Alaska; *CRREL report 79-9*, 122 p.
1981: Distinguishing characteristics of diamictons at the margin of the Matanuska glacier, *Alaskan Annals of Glaciology*, v. 2, p. 78-84.
- Lehuis, J. et David, P.P.
1977: La stratigraphie et les événements du Quaternaire de la partie occidentale de la Gaspésie, Québec; *Géographie physique et Quaternaire*, vol. 31, p. 275-296.
- Lee, H.A.
1962: Boreholes at Grand Falls, New Brunswick, across a buried channel of ancestral St. John River; *Geological Survey of Canada, Topical Report 59*, 18 p.

- Lortie, G.
1976: Les écoulements glaciaires Wisconsinniens dans les Cantons de l'Est et la Beauce, Québec; Université McGill, Montréal (thèse de MSc.).
- Lowe, D.R.
1976: Subaqueous liquefied and fluidized sediment flows and their deposits; *Sedimentology*, v. 23, p. 285-308.
- Lowell, T.V.
1980: Late Wisconsin ice extent in Maine: evidence from Mount Desert Island and the Saint John River area; University of Maine at Orono (MSc. thesis).
1985: Late Wisconsin ice flow reversal and deglaciation, northwestern Maine; *Geological Society of America, Special Paper 197*, p. 71-83.
- Mark, D.M.
1973: Analysis of axial orientation data, including till fabrics; *Geological Society of America Bulletin*, v. 84, p. 1369-1374.
1974: On the interpretation of till fabrics; *Geology*, v. 2, p. 101-104.
- Martineau, G.
1977: Géologie des dépôts meubles de la région de Kamouraska-Rivière-du-Loupe; Ministère des richesses naturelles du Québec, DPV-545, 17 p.
1979: Géologie des dépôts meubles de la région de Témiscouata; Ministère des richesses naturelles du Québec, DPV-618, 18 p.
- Mills, H.H.
1977: Basal till fabrics of modern alpine glaciers; *Geological Society of America Bulletin*, v. 88, p. 824-828.
1984: Clast orientation in Mount St. Helens debris-flow deposits, North Fork Toutle River, Washington; *Journal of Sedimentary Petrology*, v. 54, p. 626-634.
- Newman, W.A., Genes, A.M., and Brewer, T.
1985: Pleistocene geology of northeastern Maine; *Geological Society of America, Special Paper 197*, p. 59-70.
- Postma, G., Roep, T.B., and Ruegg, G.H.J.
1983: Sandy-gravelly mass-flow deposits in an ice-marginal lake (Saalian, Leuvenumsche Beek Valley, Veluwe, The Netherlands), with emphasis of plug-flow deposits; *Sedimentary Geology*, v. 34, p. 59-82.
- Rampton, V.N., Gauthier, R.C., Thibault, J., and Seaman, A.A.
1984: Quaternary geology of New Brunswick; *Geological Survey of Canada, Memoir 416*, 77 p.
- Rampton, V.N. and Paradis, S.
1981: Quaternary geology of the Woodstock map area (21 J), New Brunswick; New Brunswick Department of Natural Resources, Map Report 81-1, 37 p.
- Rappol, M.
1983: Glacigenic Properties of Till. Studies in glacial sedimentology from the Allgäu Alps and The Netherlands; *Publicaties van het Fysisch-Geografisch en Bodemkundig Laboratorium, Universiteit van Amsterdam*, No. 34, 225 p.
1985: Clast-fabric strength in tills and debris flows compared for different environments; *Geologie en Mijnbouw*, v. 64, p. 327-332.
1986: Ice movements in northwest New Brunswick, Madawaska and Victoria counties; *Friends of the Pleistocene Meeting, Fort Kent, Maine* (in press).
- Rose, J.
1974: Small-scale spatial variability of some sedimentary properties of lodgement till and slumped till; *Geologists' Association of London, Proceedings*, v. 85, p. 223-237.
- Ruszczynska-Szenajch, H.
1983: Lodgement tills and syndepositional glacitectonic processes related to subglacial thermal and hydrologic conditions; *in Tills and Related Deposits*, E.B. Evenson, et al. (ed.); Balkema, Rotterdam, p. 113-124.
- Sharp, M.
1985: Sedimentation and stratigraphy at Eyjabakkajökull – an Icelandic surging glacier; *Quaternary Research*, v. 24, p. 268-284.
- Shaw, J.
1979: Genesis of Sveg tills and Rogen moraines of central Sweden: a model of basal melt out; *Boreas*, v. 8, p. 409-426.
1982: Melt-out till in the Edmonton area, Alberta, Canada; *Canadian Journal of Earth Sciences*, v. 19, p. 1548-1569.
1985: Subglacial and ice-marginal environments; *in Glacial Sedimentary Environments*, G.M. Ashley, J. Shaw, and N.D. Smith (ed.); *Society of Economic Paleontologists and Mineralogists, Short Course 16*, p. 7-84.
- Shilts, W.W.
1978: Detailed sedimentological study of till sheets in a stratigraphic section, Samson River, Quebec; *Geological Survey of Canada, Bulletin 285*, 30 p.
1981: Surficial geology of the Lac Mégantic area, Quebec; *Geological Survey of Canada, Memoir 397*, 102 p.
- Starkey, J.
1977: The contouring of orientation data represented in spherical projection; *Canadian Journal of Earth Sciences*, v. 14, p. 268-277.
- Stephan, H.-J. and Ehlers, J.
1983: North German till types; *in Glacial Deposits in North-West Europe*, J. Ehlers (ed.); Balkema, Rotterdam, p. 239-247.
- Thibault, J.
1979: Granular aggregate resources of the Grandmaison (NTS 21N/9) and the Edmundston (NTS 21N/8) map areas; *New Brunswick Department of Natural Resources, Open File 79-31*, 115 p.
1980: Granular aggregate resources, St. André (210/4), Aroostook (21J/13), New Brunswick; *New Brunswick Department of Natural Resources, Open File 80-6*, 27 p.
1985: Granular aggregate resources and surficial geology of Sisson Branch Reservoir (210/6); *New Brunswick Department of Natural Resources, Open File 85-3*, 46 p.
- Thompson, W.B.
1982: Recession of the late Wisconsin ice sheet in coastal Maine; *in The Wisconsin Glaciation of New England*, G.J. Larson and B.D. Stone (ed.); *Kendall/Hunt Dubugne, Iowa*, p. 211-228.
- Woodcock, N.H. and Naylor, M.A.
1983: Randomness testing in three-dimensional orientation data; *Journal of Structural Geology*, v. 5, p. 539-548.

New AMS radiocarbon age determinations from east-central Ellesmere Island; applications to glacial geology

Projects 570148 and 750063

W. Blake, Jr.
Terrain Sciences Division

Blake, W., Jr., New AMS radiocarbon age determinations from east-central Ellesmere Island: applications to glacial geology; in *Current Research, Part B, Geological Survey of Canada, Paper 86-1B*, p. 239-244, 1986.

Abstract

Radiocarbon dating by means of accelerator mass spectrometry has two great advantages over conventional dating: 1) much smaller samples can be handled and 2) counting time is significantly shorter. Three new age determinations, all on marine mollusc shells of Holocene age from Ellesmere Island, are reported here. In one case the date confirms an earlier AMS result in showing that the front of MacMillan Glacier was well behind its present position 7800 to 7100 radiocarbon years ago. The other two AMS dates reinforce a conventional radiocarbon date and show that the earliest Holocene marine incursion in the Smith Sound-Kane Basin coastal region occurred approximately 9000 radiocarbon years BP.

Résumé

La datation au carbone radioactif par spectrométrie de masse avec accélérateur (SMA) présente deux avantages importants par rapport à la datation classique: 1) manipulation d'échantillons beaucoup moins volumineux et 2) temps de comptage beaucoup plus court. On présente trois nouvelles déterminations d'âge, toutes faites sur des coquilles de mollusques marins de l'Holocène provenant de l'île d'Ellesmere. Dans un de ces cas, la date confirme un résultat précédent obtenu par SMA indiquant que le front du glacier MacMillan était bien loin de sa position actuelle il y a 7800 à 7100 ans. Les deux autres datations établies par SMA appuient une datation radiométrique classique et indiquent que la première incursion marine de l'Holocène dans la région côtière du détroit Smith et du bassin Kane s'est produite il y a environ 9000 ans.

Introduction

A previous report (Blake, 1985) provided three examples to show the usefulness and potential of radiocarbon dating by means of accelerator mass spectrometry (AMS). This note presents additional results from the same area of Ellesmere Island, Arctic Canada.

As emphasized in Blake (1985), the most important advantage of the AMS technique over conventional radiocarbon dating in proportional or scintillation counters is that extremely small samples (milligrams instead of grams) can be utilized, because the method allows direct measurement of the abundance of ^{14}C atoms. A second advantage is that a much shorter counting time is required. Rigorous pretreatment of samples, however, is necessary to remove contaminants, and the various steps in this process, together with the time necessary to load the accelerator (approximately three hours per batch) take far longer than does the actual counting.

Examples of the tiny amounts of materials that can be dated by means of AMS are provided by Oeschger et al. (1985) and Andrée et al. (1986a) – plant macrofossils (mainly *Betula* fruits); Broecker et al. (1985) – foraminifera; Andrews et al. (1985) – marine pelecypods and the organic fraction in marine sediments; Nelson et al. (1986) – blood residues on prehistoric stone tools; and Andrée et al. (1986b) – CO_2 extracted from the air bubbles in polar ice. For a useful general summary the reader is referred to Hedges and Gowlett (1986).

The AMS age determinations reported here were carried out, under contract, by the IsoTrace Laboratory, University of Toronto, where measurements are made on the IsoTrace accelerator mass spectrometer (Litherland, 1984; Kieser et al., 1986; Beukens et al., 1986). The conventional radiocarbon dates from Ellesmere Island were produced in the Radiocarbon Dating Laboratory at the Geological Survey of Canada, where two proportional counters are in operation (Dyck, 1967; Lowdon, 1985).

This report is contribution No. 28 from the Cape Herschel project.

Sample descriptions and results

The first site to be discussed is the one at MacMillan Glacier (site 1, Fig. 26.1) on the north side of Baird Inlet, for which an AMS date was reported earlier (Blake, 1985). The work along this and other glacier margins is part of a continuing program of documenting glacier fluctuations in east-central Ellesmere Island. The collection, at an elevation of approximately 145 m (as determined by repeated measurements with a Wallace and Tiernan surveying altimeter) was made from the surface and side of a small terrace, from a ridge of brown till (7.5YR 5/2) adjacent to the terrace, and from the bed of the stream which flows between the terrace and the lateral moraine along the north edge of MacMillan Glacier (Fig. 26.2).

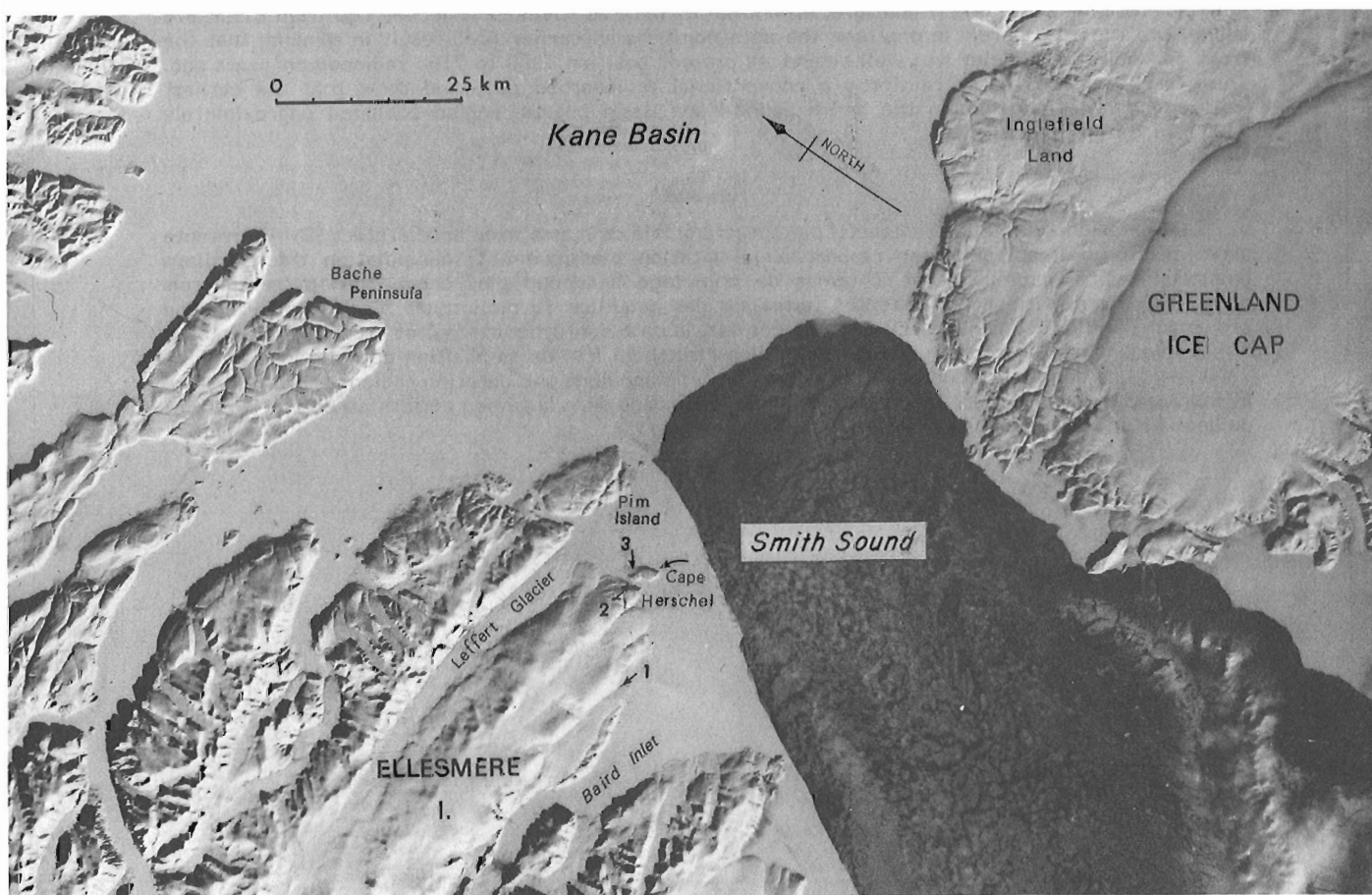


Figure 26.1. LANDSAT image showing Smith Sound and southern Kane Basin. Numerals refer to sites discussed in the text: 1 – MacMillan Glacier; 2 – west side of Cape Herschel; 3 – north side of Cape Herschel. The image shows the development of the 'North Water' on April 4, 1973 (image E-10255-18054, spectral band 7).

Because of the elevation of this sample, slightly above the level believed to represent the limit of Holocene marine submergence, the possibility existed that this sample could be in the 9000 to 9500 year-range. The original age determination, on 105 fragments of *Hiattella arctica*, gave an age of $25\,700 \pm 890$ BP (GSC-3897, Blake, 1985), a result which suggested that the material was partly of Holocene age, partly 'old'.

The newly dated fragment, a partial valve of the pelecypod *Macoma calcarea*, gave an age of 7670 ± 100 BP (TO-244, Table 26.1). This value, corrected to a base of $\delta^{13}\text{C} = 0\text{‰}$, is similar to an earlier result of 7640 ± 60 BP (TO-71), obtained on a single fragment of the barnacle *Balanus balanus* (Table 26.1) from the same collection. It should be noted, however, that at the time the earlier determination was made all IsoTrace dates were being corrected to a base of $\delta^{13}\text{C} = -25\text{‰}$. To make TO-71 comparable with TO-244 and with all GSC age determinations on marine shells, 400 years must be subtracted, giving 7240 ± 60 BP for TO-71 (cf. Mangerud, 1972; Olsson and Osadebe, 1974; Tauber, 1979; Lowdon, 1985).

These two age determinations show, in convincing fashion, that during the interval between approximately 7800 and 7100 radiocarbon years ago, and probably for an even longer period of time, MacMillan Glacier was considerably reduced in size, and the front was several kilometers west of its present position. Until additional dating is carried out, to determine the age of the youngest shells in the deposit, the timing of the readvance which transported the shells is unknown. In this connection it is interesting to note that several age determinations on shells and calcareous algae in a lateral moraine along the south side of Leffert Glacier, a

major outlet glacier 15 km to the north (Fig. 26.1), are in the range of 2280 ± 140 BP (GSC-3515) to 2880 ± 70 BP (GSC-3793; Blake, 1984a, b), so that at that site the readvance has occurred sometime during the last 2000 radiocarbon years. At Leffert Glacier no transported shells as old as those at MacMillan Glacier have been found.

The second site for which comparable age determinations are available is on the west side of the Cape Herschel peninsula (site 2, Fig. 26.1; Fig. 26.3). There, on the deflated surface of a pinkish grey (7.5YR 7/2) silt deposit at an elevation of 11.0 m (determined by levelling instrument), *Macoma calcarea* shells were found to be 8940 ± 100 years old (GSC-2516). This age determination, one of two similar dates in the vicinity (cf. Blake, 1981), is the oldest obtained via conventional counting for marine deposits postdating the last glaciation. Two new AMS determinations on shells from the same site are: 8840 ± 50 BP (TO-225) for *Portlandia arctica* (parts of nine valves) and 9010 ± 150 BP (TO-226) for a single valve of *Macoma calcarea*. These results correspond closely with the earlier GSC determinations, and they show that the earliest Holocene marine incursion in the Smith Sound-Kane Basin coastal region occurred approximately 9000 radiocarbon years BP. The pelecypod-bearing silt is believed to have been deposited in fairly deep water, for *Macoma calcarea* shells collected on the ground surface at 81.5 to 83.5 m at 'Moraine Pond' on the north side of the Cape Herschel peninsula (1.6 km to the east-northeast; site 3, Fig. 26.1) are only 8190 ± 110 years old (GSC-2913; Blake, 1985). The latter shells, themselves reworked, probably relate to the time when a nearby beach deposit, whose surface is at 90.5 m (instrumental levelling), was forming. The pelecypods, however, may have lived when sea



Figure 26.2. Aerial view eastward from MacMillan Glacier along the north side of Baird Inlet, July 9, 1984. The shell collection site for GSC-3897, TO-71, and TO-244 is indicated by the arrow. 201464-0

Table 26-1. Radiocarbon age determinations, east-central Ellesmere Island

Sample elevation m a.s.l.	Dated material ¹	Field sample No.	Laboratory dating No. ²	$\delta^{13}\text{C}$ ‰	Age (Corrected for $\delta^{13}\text{C}$) ^{3,4}	Sample weight (g)	Counter (L)	Pressure (atm)	Counting time (days) ⁵	Comments
145	Hiatella arctica	83-BS-289+ 84-BS-160	GSC-3897	+0.7	25 700 ± 890	6.7	2	2	4	10% HCl leach; mixed with dead gas for counting; aragonitic.
145	Balanus balanus	83-BS-289+ 84-BS-160	TO-71		7 640 ± 60 (7240 ± 60)	268				>20% HCl leach; 64.0 mg after pretreatment; 3 targets counted; calcitic.
145	Macoma calcaria	83-BS-289+ 84-BS-160	TO-244		7 670 ± 100	255				23% HCl leach; 2 targets counted; aragonitic
11	Macoma calcaria	BS-77-163	GSC-2516	-0.1	8 940 ± 100	31.9	2	2	2	20% HCl leach; aragonitic
11	Portlandia arctica	BS-77-163 (B)	TO-225		8 840 ± 50	293				42% HCl leach; 2 targets counted; aragonitic
11	Macoma calcaria	BS-77-163 (A)	TO-226		9 010 ± 150	334				48% HCl leach; 2 targets counted; aragonitic

¹ Marine molluscs and cirripeds identified by W. Blake, Jr.

² Laboratory designations: GSC – Geological Survey of Canada; TO – IsoTrace Laboratory, University of Toronto.

³ All age determinations from the Radiocarbon Dating Laboratory, Geological Survey of Canada, are based on a ^{14}C half-life of 5568 ± 30 years and 0.95 of the activity of the NBS oxalic acid standard. Ages are quoted in conventional radiocarbon years before present (BP) where 'present' is taken to be 1950. All finite age determinations from this laboratory are based on the 2σ criterion; i.e., there is a 95% probability that the correct age in conventional radiocarbon years lies within the stated limits of error. $^{13}\text{C}/^{12}\text{C}$ ratios were determined at the Department of Earth Sciences, University of Waterloo, under the direction of P. Fritz and R.J. Drimmie. Relative to the PDB standard, it is GSC practice to normalize $\delta^{13}\text{C}$ values on terrestrial organic materials and bones of all types to -25.0‰ , whereas marine shells are normalized to 0.0‰ (Lowdon and Blake, 1970).

⁴ At IsoTrace all samples were originally normalized to -25.0‰ , but starting with TO-215, all shell samples are normalized to 0.0‰ . For this reason the age for TO-71 has been 'corrected' to 7240 ± 60 BP. All quoted errors are 68.3% confidence limits. Preparation of the machine-ready sample causes the fractionation of the sample material to vary systematically from the top to the bottom of the target. The computer analysis program uses the $^{13}\text{C}/^{12}\text{C}$ ratio obtained during the measurement, which is the product of this fractionation and the natural fractionation of the sample, to correct the $^{14}\text{C}/^{12}\text{C}$ ratio appropriately. While this procedure yields a highly reliable result for the $^{14}\text{C}/^{12}\text{C}$ ratio, at no time during the measurement is a value of the natural fractionation alone obtained (see IsoTrace Laboratory, 1984 Annual Report, 84-12.31, Chapter II.2, p. 31-64, Radiocarbon Analysis, by R.P. Beukens).

⁵ At IsoTrace each target is given 7 to 8 runs, and each run takes 18 to 22 minutes.



Figure 26.3. View westward at Elison Lake (right foreground) and the head of Herschel Bay (left centre) on the west side of the Cape Herschel peninsula. The open arrow indicates the position of the perched delta whose surface is at 135-140 m a.s.l., the solid arrow indicates the site at 11.0 m where GSC-2516, TO-225, and TO-226 were collected. August 2, 1981. 203107-D

level was even higher relative to the land, although no beaches above 90.5 m have been recognized on the north side of Cape Herschel. One other ^{14}C date, on a fragment of *Clinocardium ciliatum* recovered from sand at 532 cm depth in a core from 'Moraine Pond', resulted in an age of 8510 ± 50 BP (TO-115). As this date is also an early AMS determination from Toronto, correcting it as outlined earlier gives 8110 ± 50 years, a value nearly identical with the age of the shells on the ground surface. Sample TO-115, at 78.0 m elevation, may also relate to the time when the beach at 90.5 m was forming, for *Clinocardium ciliatum* is a species which commonly occurs in a water depth of at least 10 m (Lubinsky, 1980).

Because of these relations between sample age and elevation, it seems likely that when the 9000 year-old pelecypods were living on the south side of the Cape Herschel peninsula, the sea was close to the level of a prominent boulder delta nearby, whose surface is at 135 to 140 m a.s.l. If this assumption is correct, this early Holocene feature is at a higher elevation than the highest ^{14}C dated Holocene marine features to the north of Kane Basin (England, 1983, 1985; Kelly and Bennike, 1985) or to the south of Smith Sound (Blake, 1981), although higher dated features are present on the west side of Ellesmere Island (Hodgson, 1985).

Acknowledgments

Assistance with the collection of the newly dated samples in the field was provided by R.J. Richardson (1977), K.E. Rolko (1983), and K.E. Rolko and C.D. Gault (1984).

E.W. Blake helped as rodman in 1979. Preparation and counting of samples at the GSC was carried out by I.M. Robertson and A. Telka under the supervision of J.A. Lowdon (to October 1981) and R.N. McNeely. I wish to express my appreciation to R.P. Beukens, W.E. Kieser, A.E. Litherland, and their staff at the IsoTrace Laboratory, University of Toronto, for the care with which they have processed samples for the accelerator, and for many useful discussions. Comments which have helped to improve the manuscript have been made by I. Blake, D.A. Hodgson, and J.A. Lowdon.

References

- Andrée, M., Oeschger, H., Siegenthaler, U., Riesen, T., Moell, M., Ammann, B., and Tobolski, K.
1986a: ^{14}C dating of plant macrofossils in lake sediment; *Radiocarbon*, v. 28, p. 411-416.
- Andrée, M., Beer, J., Loetscher, H.P., Moor, E., Oeschger, H., Bonani, G., Hofmann, H.J., Morenzoni, E., Nessi, M., Suter, M., and Wölfli, W.
1986b: Dating polar ice by ^{14}C accelerator mass spectrometry; *Radiocarbon*, v. 28, p. 417-424.
- Andrews, J.T., Jull, A.J.T., Donahue, D.J., Short, S.K., and Osterman, L.E.
1985: Sedimentation rates in Baffin Island fiord cores from comparative radiocarbon dates; *Canadian Journal of Earth Sciences*, v. 22, p. 1827-1834.

- Beukens, R.P., Gurfinkel, D.M., and Lee, H.W.
1986: Progress at the IsoTrace radiocarbon facility; *Radiocarbon*, v. 28, p. 229-236.
- Blake, W., Jr.
1981: Neoglacial fluctuations of glaciers, southeastern Ellesmere Island, Canadian Arctic Archipelago; *Geografiska Annaler*, v. 63A, p. 201-218.
1984a: Post-Hypsithermal advance of Leffert Glacier, Ellesmere Island, Arctic Canada; American Quaternary Association (AMQUA), 8th Biennial Meeting (Boulder, Colorado, 1984), Program and Abstracts, p. 14.
1984b: Geological Survey of Canada radiocarbon date XXIV; Geological Survey of Canada, Paper 84-7, 35 p.
1985: Radiocarbon dating with accelerator mass spectrometry: results from Ellesmere Island, District of Franklin; in *Current Research, Part B, Geological Survey of Canada, Paper 85-1B*, p. 423-429.
- Broecker, W.S., Mix, A.C., Andrée, M., and Oeschger, H.
1985: Radiocarbon measurements on coexisting benthic and planktic foraminifera shells: potential for reconstructing ocean ventilation times over the past 20 000 years; *Nuclear Instruments and Methods in Physics Research*, v. B5, p. 331-339.
- Dyck, W.
1967: The Geological Survey of Canada Radiocarbon Dating Laboratory; Geological Survey of Canada, Paper 66-45, 45 p.
- England, J.
1983: Isostatic adjustments in a full glacial sea; *Canadian Journal of Earth Sciences*, v. 20, p. 895-917.
1985: The late Quaternary history of Hall Land, northwest Greenland; *Canadian Journal of Earth Sciences*, v. 22, p. 1394-1408.
- Hedges, R.E.M. and Gowlett, J.A.J.
1986: Radiocarbon dating by accelerator mass spectrometry; *Scientific American*, v. 254, p. 100-107.
- Hodgson, D.A.
1985: The last glaciation of west-central Ellesmere Island, Arctic Archipelago, Canada; *Canadian Journal of Earth Sciences*, v. 22, p. 347-368.
- Kelly, M. and Bennike, O.
1985: Quaternary geology of parts of central and western North Greenland: a preliminary account; *Rapport Grønlands Geologiske Undersøkelse*, Nr. 126, p. 111-116.
- Kieser, W.E., Beukens, R.P., Kilius, L.R., Lee, H.W., and Litherland, A.E.
1986: IsoTrace radiocarbon analysis – equipment and procedures; *Nuclear Instruments and Methods*, v. B15, p. 718-721.
- Litherland, A.E.
1984: Accelerator mass spectrometry; *Nuclear Instruments and Methods in Physics Research*, v. B5, p. 100-108.
- Lowdon, J.A.
1985: The Geological Survey of Canada radiocarbon dating laboratory; Geological Survey of Canada, Paper 84-24, 19 p.
- Lowdon, J.A. and Blake, W., Jr.
1970: Geological Survey of Canada radiocarbon dates IX; *Radiocarbon*, v. 12, p. 46-86.
- Lubinsky, I.
1980: Marine bivalve molluscs of the Canadian central and eastern Arctic: faunal composition and zoogeography; *Canadian Bulletin of Fisheries and Aquatic Sciences*, Bulletin 207, 111 p.
- Mangerud, J.
1972: Radiocarbon dating of marine shells, including a discussion of apparent age of Recent shells from Norway; *Boreas*, v. 1, p. 143-172.
- Nelson, D.E., Loy, T.H., Vogel, J.S., and Southon, J.R.
1986: Radiocarbon dating blood residues on prehistoric stone tools; *Radiocarbon*, v. 28, p. 170-174.
- Oeschger, H., Andrée, M., Moell, M., Riesen, T., Sigenthaler, U., Ammann, B., Tobolski, K., Bonani, B., Hofmann, H.J., Morenzoni, E., Nessi, M., Suter, M., and Wöflfl, W.
1985: Radiocarbon chronology at Lobsigensee: Comparison of materials and methods; in *Swiss lake and mire environments during the last 15 000 years*, ed. G. Lang; *Dissertationes Botanicae* 87, J. Cramer, Vaduz, p. 135-139.
- Olsson, I.U. and Osadebe, F.A.N.
1974: Carbon isotope variations and fractionation corrections in ^{14}C dating; *Boreas*, v. 3, p. 139-146.
- Tauber, H.
1979: ^{14}C activity of arctic marine mammals; in *Radiocarbon dating*, ed. R. Berger and H.E. Suess (Proceedings of the Ninth International Conference, Los Angeles and La Jolla, California, 1976); University of California Press, Berkeley, Los Angeles, London, p. 447-452.

Surficial geology and till geochemistry, Lynn Lake – Leaf Rapids region, Manitoba¹

Project 780016

C.A. Kaszycki and R.N.W. DiLabio
Terrain Sciences Division

Kaszycki, C.A., and DiLabio, R.N.W., Surficial geology and till geochemistry, Lynn Lake – Leaf Rapids region, Manitoba; in Current Research, Part B, Geological Survey of Canada, Paper 86-1B, p. 245-256, 1986.

Abstract

Morphological evidence, coupled with clast composition and clay mineralogy of tills, suggests that a zone of convergence between Keewatin lobe ice and Hudson lobe ice existed in the Leaf Rapids area. The zone of convergence is marked by a large discontinuous north-south trending esker-like ridge, here defined as the Leaf Rapids interlobate moraine, which marks the maximum western extent of carbonate dispersal in northern Manitoba. The western extent of carbonate erratics in till and dropstones in Lake Aggasiz clay indicates that the confluence between Keewatin and Labradorian ice during deglaciation occurred farther west than previously interpreted.

Reconnaissance till sampling west of the moraine indicates that large areas of metal enrichment in till are related to small scale dispersal from areas of known mineralization and/or from bedrock uniformly enriched in trace metals. A regional As anomaly south of Granville Lake may reflect large scale glacial dispersal (>25 km) from a zone of sulphide mineralization in this area.

Résumé

Des indices morphologiques, conjugués à la composition clastique et la minéralogie de la fraction argileuse des tills semblent indiquer qu'il existait une zone de convergence entre le lobe glaciaire du Keewatin et celui de l'Hudson dans la région de Leaf Rapids. Cette zone de convergence se caractérise par une large crête discontinue à orientation nord-sud; cette dernière, semblable à un esker, est définie dans le présent ouvrage comme étant la moraine interlobaire de Leaf Rapids, qui marque la limite ouest maximale de la dispersion des carbonates dans le nord du Manitoba. La limite ouest des blocs erratiques de carbonate dans le till et de tuf calcaire dans l'argile du lac Aggasiz indiquent qu'au cours de la déglaciation, les glaciers du Keewatin et du Labradorien se sont rencontrés plus à l'ouest qu'on ne l'avait d'abord cru.

L'échantillonnage de reconnaissance du till à l'ouest de la moraine elle-même indique que de vastes zones d'enrichissement métallique dans le till sont liées à une faible dispersion provenant de zones de minéralisation connues ou de la roche en place uniformément enrichie de métaux à l'état de traces, ou les deux. Une anomalie régionale As au sud du lac Granville reflète probablement une dispersion glaciaire d'envergure (plus de 25 km) à partir d'une zone de minéralisation de sulfure dans cette région.

¹ Contribution to the Canada-Manitoba Mineral Development Agreement 1984-1989. Project carried by Geological Survey of Canada.

Introduction

In 1983 a program of systematic till sampling and surficial geological mapping was begun in northwestern Manitoba. The program was undertaken as part of the joint Canada-Manitoba Mineral Development Agreement, to be carried out over a five year period ending in 1989. The primary objective of the sampling is to map variations in chemical and mineralogical components of till which may be related to bedrock mineralization as an aid to mineral exploration in the area. Detailed surficial geological mapping at a scale of 1:125 000 is carried out in conjunction with till sampling in order to develop an understanding of the glacial history of the region as an aid to interpretation of geochemical data. This summary focuses primarily on the surficial geology of the region and secondly, on general aspects of till geochemistry.

Regional setting

The study area is located within the Churchill Structural Province of the Canadian Shield. To date, regional till sampling and surficial mapping have been carried out over four 1:250 000 map areas encompassing the Lynn Lake – Leaf Rapids region (Fig. 27.1). A surficial geology map for Granville Lake (64 C) has been published at a scale of 1:125 000 (Kaszycki et al., 1986), as have till geochemical data for this area (Kaszycki and DiLabio, 1986).

Shield terrane in this region is flanked to the east-northeast and to the south-southwest by Paleozoic carbonate rocks, and to the far west by Mesozoic sedimentary rocks, primarily Cretaceous shales. Throughout the extreme western part of Manitoba, ice flow was from a Keewatin ice centre, at approximately 190-210°. Till in this region is derived predominantly from crystalline shield lithologies. Farther east, ice flow emanated from a more easterly source, with flow directions ranging from 225-260°. Till in this area contains abundant Paleozoic carbonate erratics as well as Proterozoic greywackes of the Omarolluk Formation, which outcrop along the southeastern edge of Hudson Bay, indicating ice flow from a Labradorian ice centre.

During ice retreat, inundation by glacial Lake Agassiz resulted in deposition of calcareous laminated silt and clay throughout a large part of Manitoba. Extensive clay deposition occurred in the central and eastern parts of the basin, as well as along river valleys extending from major inflow channels draining Cretaceous terrane along the western margin of the lake. The composition of Lake Agassiz clay, therefore, reflects provenance related to distal sediment sources along the western edge of the basin, as well as sediment derived from the two ice masses forming the northern and eastern margins of the lake during deglaciation.

Surficial geology

Morphological evidence, coupled with clast composition and clay mineralogy of tills within the region, suggests that a zone of convergence between Keewatin lobe ice and Hudson lobe ice (terminology after Klassen, 1983) existed in the Leaf Rapids area (Fig. 27.2A). The zone of convergent ice flow is marked by a large discontinuous north-south trending ridge composed of ice contact stratified sediment, informally called the *Leaf Rapids interlobate moraine*.

Drift composition and regional ice flow trends

Striae to the east of the moraine record a clockwise rotation of ice flow from approximately 190° (oldest) to approximately 260° (youngest), with prominent directions at 210°, 225°, 240°, and 260° at various locations (Fig. 27.2A). Till in this area contains abundant Paleozoic carbonate erratics from Hudson Bay,

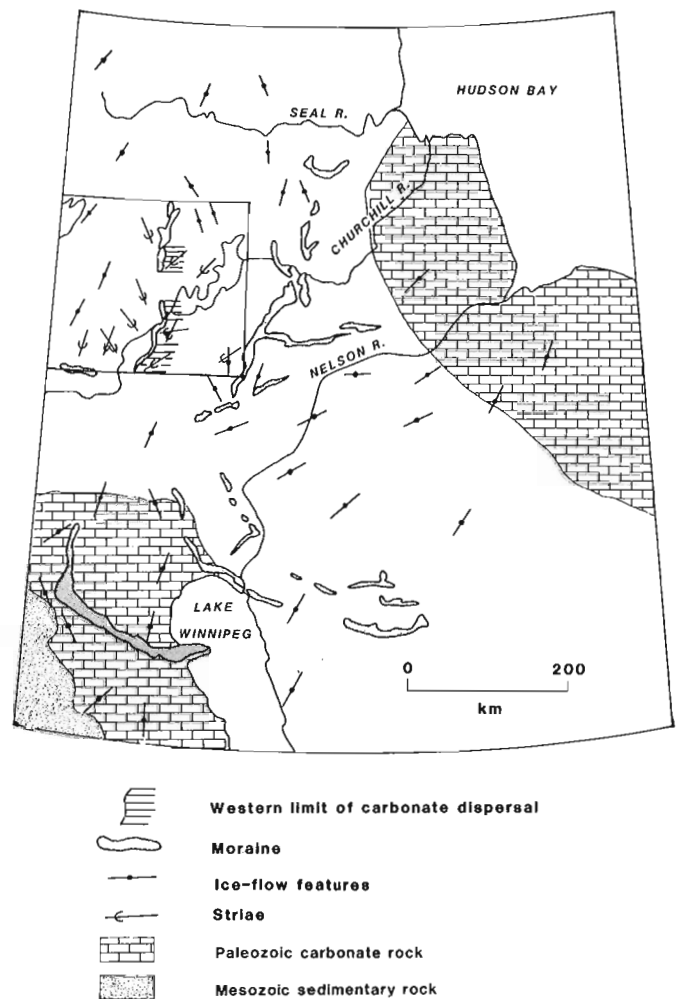


Figure 27.1. Major glacial landforms of northern Manitoba (taken, in part, from Klassen, 1983); Study area is outlined. Striae represent general trends within the region.

as well as Proterozoic greywackes of the Omarolluk Formation which outcrop on the southeastern edge of Hudson Bay, suggesting Labradorian provenance and dominance of Hudson lobe ice at least during the Late Wisconsinan. Till to the west of the moraine contains no carbonate erratics and is dominated by shield lithologies. The earliest ice flow recorded in this area is approximately 190° to 210°, consistent with the oldest ice flow direction mapped to the east. This may suggest that at some time prior to deglaciation Keewatin lobe ice covered the entire region. The youngest striae to the west of the ridge, however, record a late glacial shift of ice flow to the southeast at approximately 165°, producing a late glacial zone of convergent ice flow along the Leaf Rapids interlobate moraine.

Samples of pebbles were collected from till and of dropstones from Lake Agassiz clay along a transect from South Bay to Leaf Rapids and from Leaf Rapids west to Lynn Lake (Fig. 27.3). Sample sites were projected onto an east-west trending profile and per cent carbonate pebbles plotted along the y-axis. The proportion of carbonate pebbles in till east of the moraine varies between 5 and 20%, but trends to zero approximately 8 km east of the interlobate zone. Till on the west side of the moraine contains no carbonate erratics, which is consistent with a Keewatin lobe provenance. The proportion of carbonate pebbles in Lake Agassiz dropstones is erratic but averages

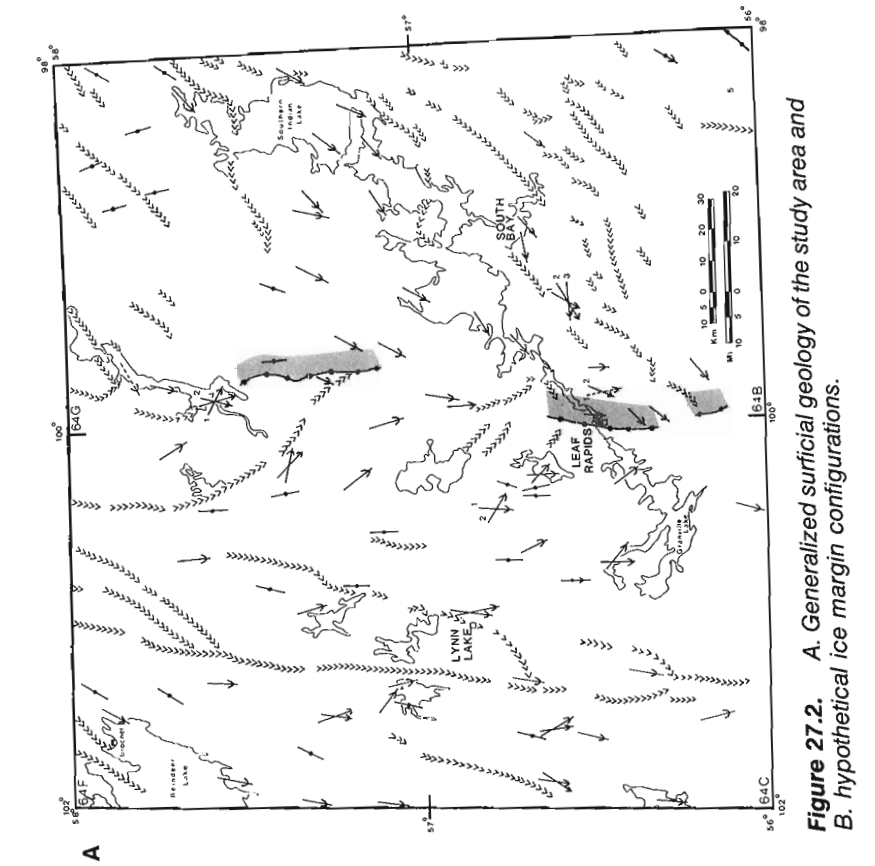
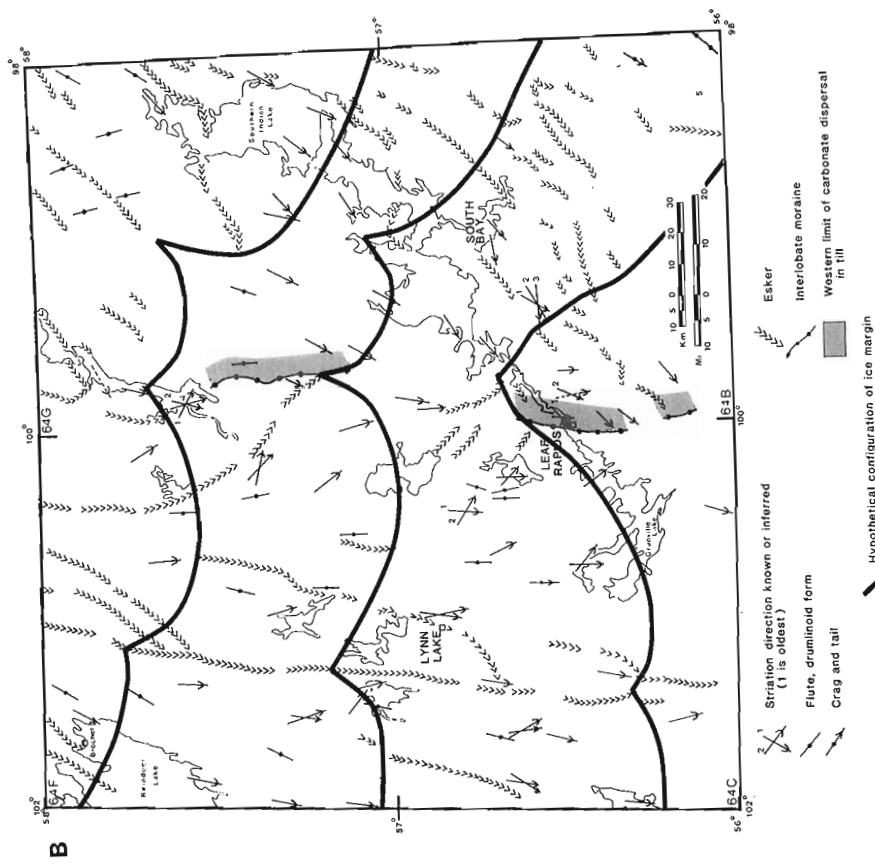


Figure 27.2. A. Generalized surficial geology of the study area and B. hypothetical ice margin configurations.

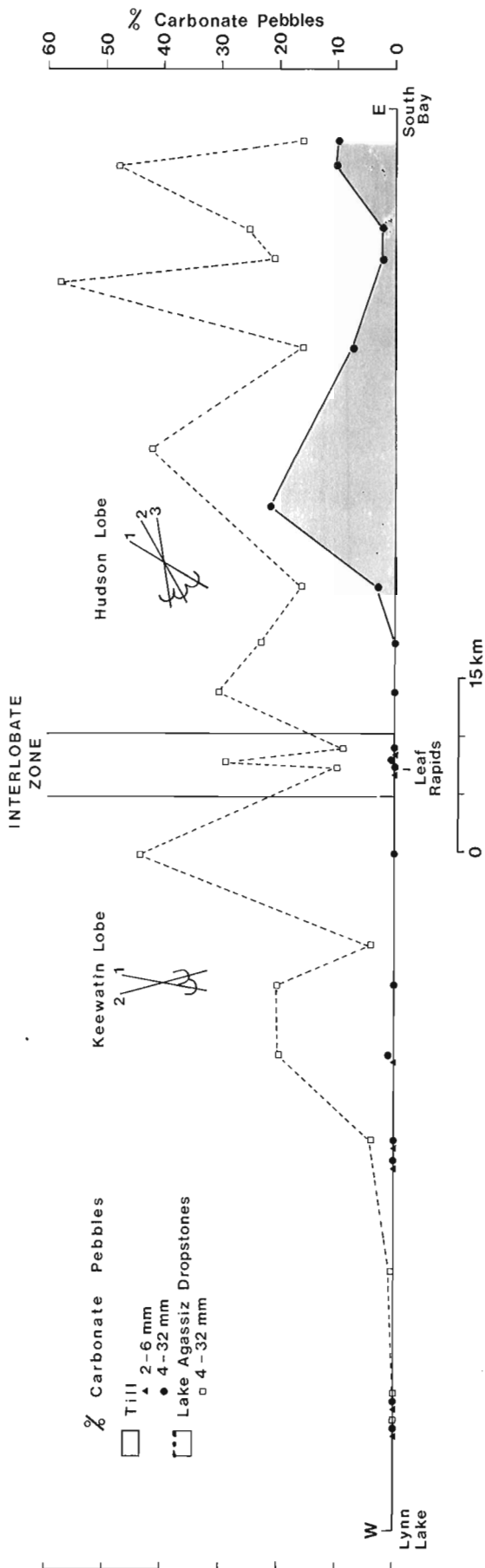


Figure 27.3. Distribution of carbonate pebbles in till and of dropstones in Lake Agassiz clay across the Leaf Rapids interlobate moraine.

approximately 20-30% east of the moraine. Relatively large concentrations persist for approximately 15 km west of the moraine but then steadily decrease to the west, trending to zero approximately 15 km east of Lynn Lake. These relationships indicate that Hudson lobe ice containing carbonate pebbles did not extend westward beyond the Leaf Rapids area and that the margin of this ice lobe bordered the east side of the interlobate moraine during deglaciation and inundation by Lake Agassiz.

Clay mineralogy of tills and Lake Agassiz clay also illustrates the different provenance of all three major sediment types within the region (Hudson lobe till, Keewatin lobe till, and Lake Agassiz clay) (Fig. 27.4). Each sediment type exhibits a distinctive assemblage of clay minerals and, although rigorous testing to enable absolute identification has not been conducted, the general nature of each assemblage is sufficient to characterize each sediment type. Hudson lobe till is characterized by expandable <14 Angstrom clay species, interpreted as vermiculite, illite, minor chlorite, and/or kaolinite, as well as carbonate minerals, and reflects the contribution of sediment from Paleozoic bedrock to the east. Keewatin lobe till exhibits a prominent illite/muscovite peak, chlorite and/or kaolinite, and an absence of carbonate minerals, reflecting Precambrian crystalline source rocks. Lake Agassiz clay, on the other hand, is composed primarily of expandable mixed layer smectite/chlorite, illite, chlorite and/or kaolinite, plus variable amounts of carbonate minerals. The source for smectitic clays is from major inflow channels to the west, draining Cretaceous terrane in Saskatchewan and Alberta. The variable amounts of carbonate and other clay species represent sediment contributed from retreating ice, particularly in the vicinity of moraines and eskers. It appears, however, that most Lake Agassiz clay is derived from extra-basinal sources.

Eskers and kame moraines

Eskers within the study area also exhibit a convergent pattern in the vicinity of the Leaf Rapids interlobate moraine (Fig. 27.2A). To the east of the ridge, eskers exhibit a regional trend to the southwest at approximately 225°. This trend becomes more westerly, approaching 270°, near the terminus of many esker systems, thus paralleling the late glacial shift in ice flow deduced from striation data adjacent to the moraine. West of the moraine, however, eskers exhibit a more complex regional pattern. Major trunk eskers, such as the system immediately west of Lynn Lake (Fig. 27.2A), trend approximately 190-200°. Adjacent to the Leaf Rapids interlobate moraine, however, both major and minor eskers exhibit a pronounced deflection to the southeast and converge on the moraine at approximately 165°, parallel to the youngest striae measured in the area.

Morphology of the moraine is variable, exhibiting a broad, poorly defined crest in some areas and a single sharp crest elsewhere. The internal composition of the Leaf Rapids moraine is characterized, in part, by fining upwards sequences composed of a core of glaciofluvial cobble gravel, which is overlain in turn by crossbedded granular sand, ripple drift cross-laminated fine sand, and capped by laminated silt and clay and/or reworked foreshore beach sand and gravel. The core of glaciofluvial cobble gravel may have been deposited subglacially within conduits or at the ice margin as subglacial meltwater under a large hydrostatic head debouched into Lake Agassiz (Ringrose and Large, 1977). Finer grained sediment was transported away from the ice margin by density underflows, producing a lateral fining sequence down current. Ice margin retreat resulted in successive overlapping sequences characterized by vertical fining upwards trends (Ringrose and Large, 1977). Current indicators within these sequences indicate a southward flow direction although eastward and westward directions have been recorded locally, particularly where minor eskers converge on the moraine (Ringrose and Large, 1977).

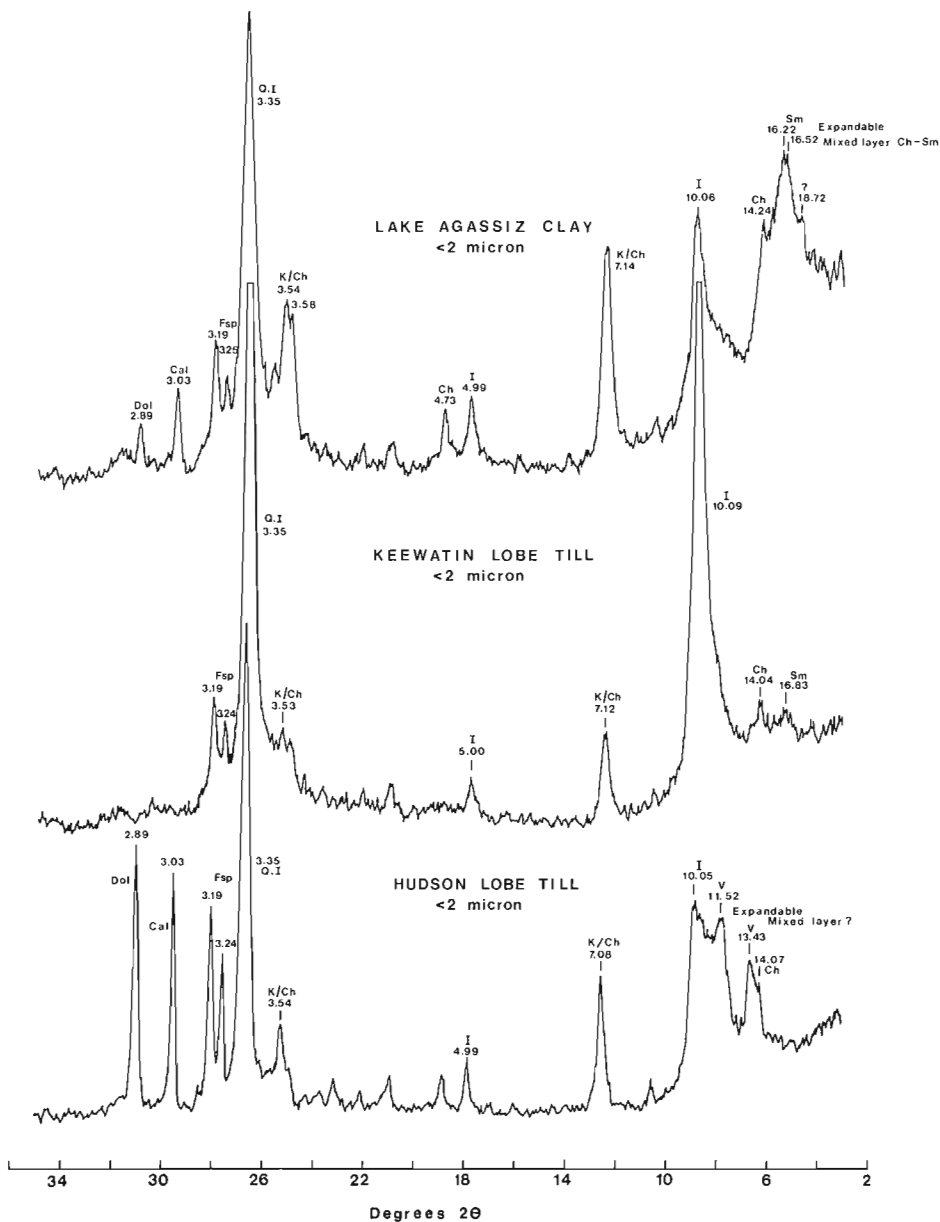


Figure 27.4. Clay mineralogy of tills and Lake Agassiz clay. Clay mineral assemblages in all three sediment types reflect distinctly different source areas.

These relationships suggest convergent ice flow may have been enhanced along the suture between Keewatin and Hudson lobe ice by development of a large re-entrant in the ice front that localized ice marginal sedimentation (Fig. 27.2B). Under these conditions a shift in both ice surface gradient and subglacial hydraulic gradient would have caused meltwater and sediment to be channelled into conduits feeding into the embayment, producing a locus of deposition within this area. Propagation of embayments and feeder conduits in the up-ice direction was generated, most likely, by thermal meltwater erosion and ice recession. Englacial or subglacial conduits and ice surface channels, debouched into glacial Lake Agassiz, producing a long continuous ridge composed of a series of overlapping subaqueous fans (Rust and Romanelli, 1975; Banerjee and McDonald, 1975; Cheel, 1982; Henderson, in press).

Although convergent ice flow was most pronounced at the interlobate position, it also appears to have occurred in the vicinity of large continuous esker systems, as evidenced by the orientation of striae and minor eskers (Fig. 27.2A). Striae in

areas adjacent to trunk eskers occasionally record a deflection of ice flow towards the esker ridge. The orientation of minor eskers parallels this trend, commonly changing direction abruptly to join trunk streams at greater angles than might otherwise be expected. These relationships suggest that laterally restricted zones of convergent ice flow occurred along glacial conduits near the ice margin (Repo, 1954; Shilts, 1984b; Shreve, 1985). Localization of surface and subglacial meltwater along these channels would enhance thermal and fluvial erosion, producing a notch or embayment in the ice front (Fig. 27.2B). Resulting lobation of the ice margin would in turn enhance localized convergent flow and the system would be self-perpetuating. Minor eskers may have formed in short segments near the ice margin (St-Onge, 1984) and, consequently, reflect re-orientation of ice flow and hydraulic gradient within this zone. Trunk eskers deposited under these conditions may be morphologically and sedimentologically indistinct from true interlobate kame moraines, which represent confluence and stagnation between independently active ice masses, and in themselves may be considered a type of interlobate or radial

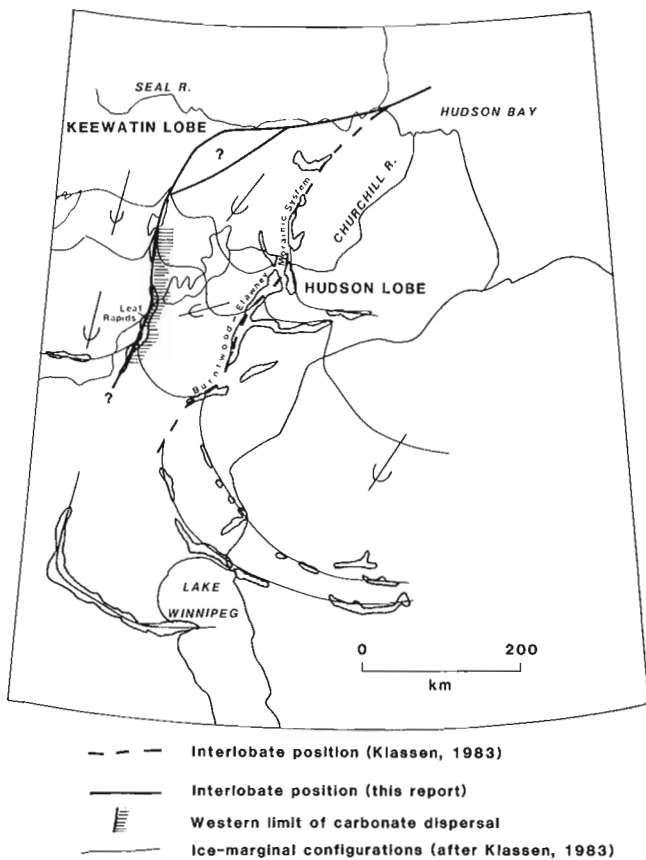


Figure 27.5. Major kame moraines (shaded) in northern Manitoba and hypothetical configurations of the ice margin (after Klassen, 1983).

kame moraine (Dredge, 1983). Overall morphology of the deposit is dependent upon sub-ice topography, the proportion of the sequence deposited within subglacial conduits, and the width of the embayment at the ice margin.

Figure 27.5 illustrates the major kame moraine systems in northern Manitoba (modified from Klassen, 1983). Klassen interpreted the confluence between Labradorean ice (Hudson lobe) and Keewatin ice (Keewatin lobe) during deglaciation to have occurred along a northeast-southwest trending zone represented by a series of linear kame moraines, collectively known as the Burnwood-Etawney morainic system (Elson, 1967). These moraines are thought to have been deposited in Lake Agassiz and represent time-transgressive subaqueous deposition against a retreating ice front (Klassen, 1983). Hypothetical ice margin configurations for northern Manitoba (from Klassen, 1983; Fig. 27.5) indicate that major northeast-southwest trending moraine systems may have developed, in part contemporaneously, along large re-entrants in the ice margin. Development of ice marginal sublobes may have occurred in response to downwasting and thinning of the ice mass during deglaciation (Aario, 1977).

The western extent of carbonate dispersal in till and of Lake Agassiz dropstones, however, indicates that the confluence between Keewatin and Hudson lobe ice during deglaciation occurred farther west, in the Leaf Rapids area. The Burnwood-Etawney morainic system as depicted by Klassen (1983), therefore, may represent a large interlobate or radial kame moraine (Dredge, 1983) developed contemporaneously with the Leaf Rapids interlobate moraine, during degradation of the Hudson ice lobe (Fig. 27.5). Alternatively, the Burnwood-Etawney mor-

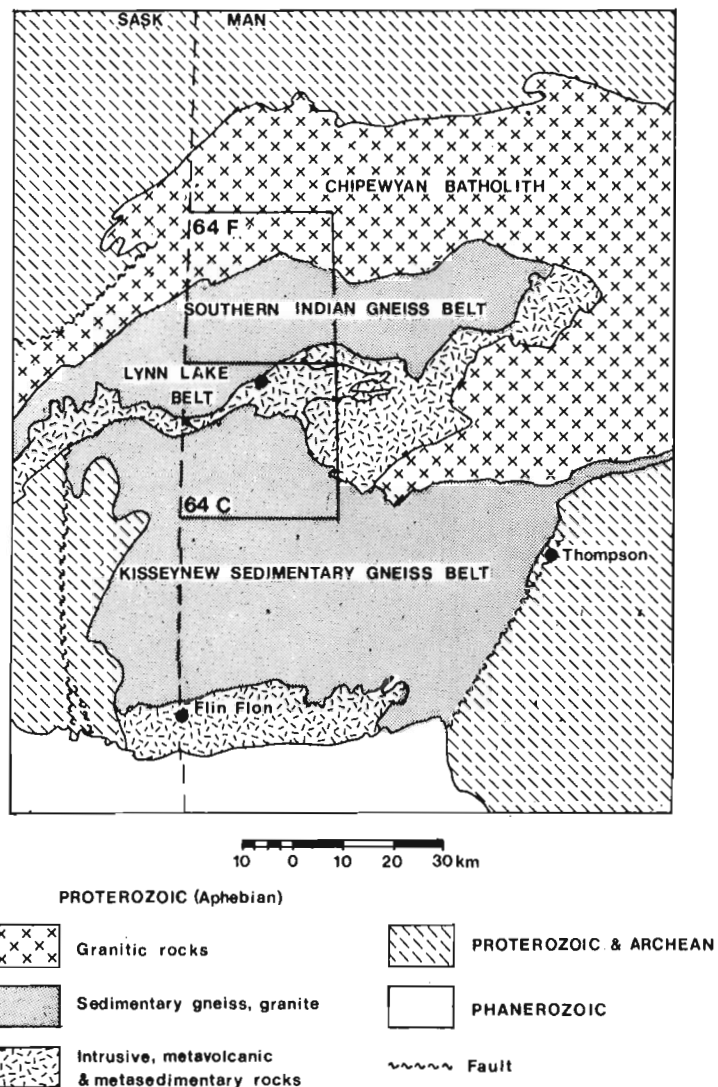


Figure 27.6. Regional lithological and structural setting of the study area (after Gilbert et al., 1980).

ainic system may represent an ice marginal position developed after retreat of Hudson lobe ice from the Leaf Rapids area, and hence may represent a recessional rather than an interlobate moraine (Elson, 1967). Further study of the morphology, composition, internal structure, and paleocurrent indicators of these deposits is required before reliable genetic interpretations can be made.

Glacial dispersal and till geochemistry

The following discussion is based on data from the region west of the Leaf Rapids interlobate moraine and covers map areas 64 C and 64 F. Glacial dispersal and till geochemistry in this area are influenced solely by ice flow from the Keewatin ice centre; the till is derived predominantly from crystalline shield lithologies and is devoid of carbonate erratics. The orientation of flutes and related depositional features has not been significantly influenced by drawdown along the interlobate moraine. To the west of the moraine flutes are oriented approximately parallel to the oldest striae direction, suggesting that large scale dispersal of glacial debris is most likely related to the oldest striae within the region. It is unlikely that late glacial deflection of ice flow towards the moraine significantly altered large scale dispersal patterns.

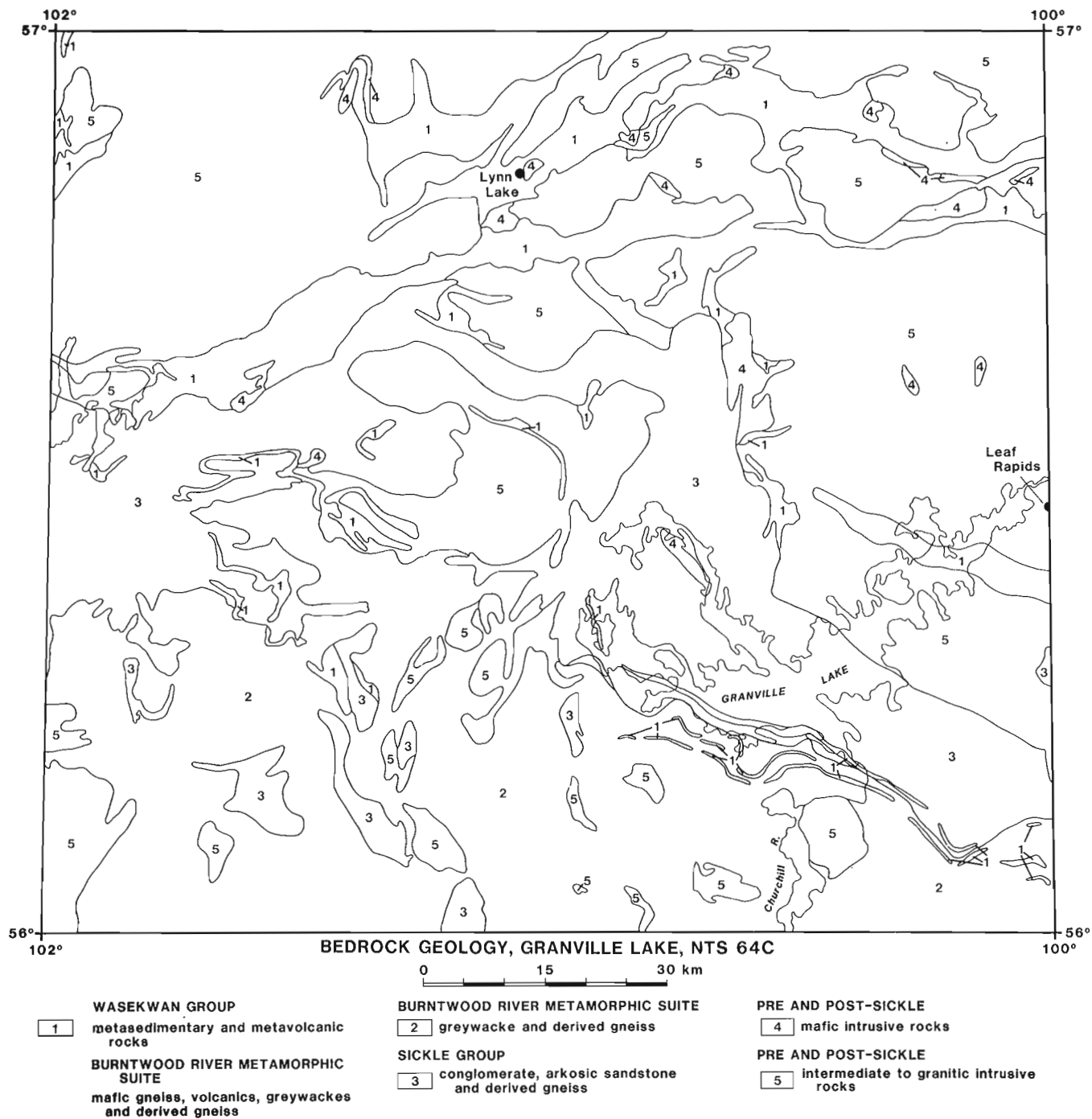


Figure 27.7. Bedrock geology of the Lynn Lake – Granville Lake area (64 C) depicting major lithostratigraphic units (Simplified from Zwanzig, 1980).

Bedrock geology

Bedrock lithologies within this region (64 C and 64 F) comprise metasediments and gneisses of the Kiseynew and Southern Indian gneiss belts, metasediments and metavolcanics of the Lynn Lake Greenstone Belt, and various mafic to felsic intrusive bodies (Fig. 27.6). Most known mineralization is associated with the Lynn Lake Greenstone Belt, located in the southern part of the area (Fig. 27.6). The major lithostratigraphic rock units in this area (Fig. 27.7) are referred to as the Burntwood River Metamorphic Suite (BRMS), composed primarily of meta-greywackes and derived gneisses; the Sickle Group, composed

primarily of meta-arkoses and their derived gneisses; and the Wasekwan Group, composed of metasediments and meta-volcanics of the Lynn Lake Greenstone Belt (Baldwin, 1980).

At several localities, Cu-Zn sulphide and gold mineralization is hosted by Wasekwan Group metasediments and meta-volcanics, and Cu-Ni mineralization is associated with gabbro intrusions within the greenstone belt (Gilbert et al., 1980). Stratiform sulphide mineralization also occurs within the transition zone between rocks of the Sickle Group and BRMS. This includes disseminated and massive iron sulphide, with minor chalcopyrite, arsenopyrite, and sphalerite (Baldwin, 1980).

Procedures

Helicopter-supported sampling was carried out at a density of approximately 2-3 samples per 100 km² (1 sample per 30-50 km²). Care was taken to sample below the postglacial solum, although some samples were collected in profile from unweathered glacial sediment up through modern soil horizons. In nearly all cases, however, samples were collected below surface weathering horizons and represent soil parent material. Where road access was available, more detailed sampling was carried out at approximately 1-2 km intervals. Wherever vertical sections throughout the till were exposed, as in borrow pits, samples were collected in profile to assess in situ variability in till.

In this study, the clay-sized (<2 µm) fraction of all samples was analyzed for trace element composition because: 1) concentrations of trace elements are greater in this fraction than in coarser size fractions due to primary enrichment of metal in the structure of clay-sized minerals (phyllosilicates) (Shilts, 1984a); 2) it provides a more uniform sampling medium than sample subsplits comprising a wider range in grain size (e.g., minus 80 mesh, which commonly contains variable amounts of inert quartz and feldspar); 3) it is known to reflect sulphide mineralization because it will adsorb a representative portion of trace elements released during weathering of labile minerals (Shilts, 1975, 1984a). Clay separated by centrifugation and decantation was analyzed by Bondar-Clegg and Co. Ltd. for Cu, Pb, Zn, Ni, Cr, Mo, Fe, and Mn, using standard atomic absorption techniques after a hot (HNO₃-HCl) leach. Arsenic was analyzed using colorimetric techniques.

Till geochemistry

Trace element concentrations in till reflect, to a first order approximation, variations in regional bedrock lithology. Summary statistics of till geochemical data for each of 64 C and 64 F are presented in Table 27.1. All elements, except Mo and Pb, exhibit markedly larger concentrations in the southern part of the region (64 C). This regional disparity in trace element concentration in till reflects the difference in gross lithology between metasediments and metavolcanics in the Granville Lake - Lynn Lake area (64 C), and metasediments and granitic intrusives to the north (Brochet area, 64 F) (Fig. 27.6). Greater concentrations of Mo and Pb in granitic terrane to the north probably reflect background enrichment of these elements in acid igneous rocks (Boyle, 1968).

Figure 27.8 shows multi-element anomalies mapped for As, Ni, Cr, Cu, and Zn as they represent all known types of mineralization within the region. Anomalous trace element

concentrations were selected as those which exceeded the 90th percentile values. These concentrations were chosen, rather than the 95th percentile values, in order to demonstrate regional trends in element concentrations, as well as locations of truly anomalous samples. The clustering of anomalies in the southern half of the region reflects abundant sulphide mineralization (marked by triangles) associated with metasediments and metavolcanics within this area. Anomalies have been grouped areally as well as by coincident occurrence. For example, a large zone of anomalous As concentration (>11 ppm) occurs along the greenstone belt west of Lynn Lake; some sites also contain anomalous Ni, Zn, and/or Cr. The subzone enclosed by the regional As anomaly represents areas of coincident As, Zn, Ni, and Cr anomalies. Likewise, relatively large regions of anomalous Cr concentration (>100 ppm) occur in the south and southwest parts of 64 C. Subzones enclosed within these regions represent coincident Cr, Ni, and Zn. Although not shown, this area also includes anomalous Mo concentrations (>4 ppm).

In general, anomalous trace-element concentrations in till correspond well with sites of known bedrock mineralization. The highway east of Lynn Lake follows the strike of the greenstone belt in this region, and several samples collected from along the road contain anomalous concentrations for several trace elements, specifically Cu and Zn. These samples were taken a minimum of 300 to 500 m from the road surface to minimize possible contamination by dust from ore trucks. Samples were also collected in vertical profile at 10-20 cm intervals, from the C to the top of the B horizon, at several sites along the highway to assess in situ variability in trace element concentration. No signs of contamination were observed in any of these profiles.

The eastern part of the Lynn Lake Greenstone Belt is strikingly outlined by a zone of anomalous Zn concentration. Subregions of anomalous Cu-Zn and Cr-Ni are located in areas of mafic volcanic and mafic intrusive rocks, respectively. Near the town of Lynn Lake, Cu-Ni and Zn-Ni anomalies reflect several small mafic intrusive bodies.

To the west of Lynn Lake, the greenstone belt is marked by a regional As anomaly which outlines arsenopyrite-bearing metavolcanic rocks trending west-southwest from Lynn Lake. A subzone of anomalous As-Ni-Cr is located near Gemmill Lake, approximately 15 km southwest of Lynn Lake, where a gold prospect is now being investigated (D.A. Baldwin, personal communication, 1985).

A second large As anomaly occurs in the south-southeast part of the area, where a zone of high As concentration (>40 ppm) covers an area of approximately 200 km². At several

Table 27.1. Summary statistics of till geochemical data, 64 C and 64 F.

Element	Minimum		Maximum		Arithmetic mean		Arithmetic S.D.		Geometric mean		90th percentile		95th percentile	
	64C	64F	64C	64F	64C	64F	64C	64F	64C	64F	64C	64F	64C	64C
Cr ppm	20	10	253	127	77.3	44.8	31.3	18.4	72.0	41.2	108	68	123	77
Cu ppm	13	3	292	152	61.6	24.5	40.1	21.1	51.6	19.0	109	50	134	60
Fe %	1.10	.70	9.5	6.8	4.027	3.044	1.355	1.211	3.779	2.813	5.7	4.8	6.1	5.2
Mn ppm	50	46	1467	1080	433.3	314.8	214.7	200.7	381.2	264.5	730	550	805	770
*Mo ppm	1	1	17	37	2.2	2.3	1.5	2.7	1.9	1.8	3	4	4	5
Ni ppm	7	5	446	68	37.2	23.9	27.3	10.1	32.8	21.9	56	36	65	41
*Pb ppm	3	5	57	176	12.1	18.9	4.7	13.0	11.4	16.5	18	24	20	28
Zn ppm	17	11	1350	132	96.9	57.1	79.9	27.9	83.5	50.5	166	104	190	110
As ppm	1	1	110	23	8.1	3.7	12.4	2.1	5.1	3.3	15	6	24	7

* Refers to elements that exhibit larger concentrations in the northern part of the region (64 F).

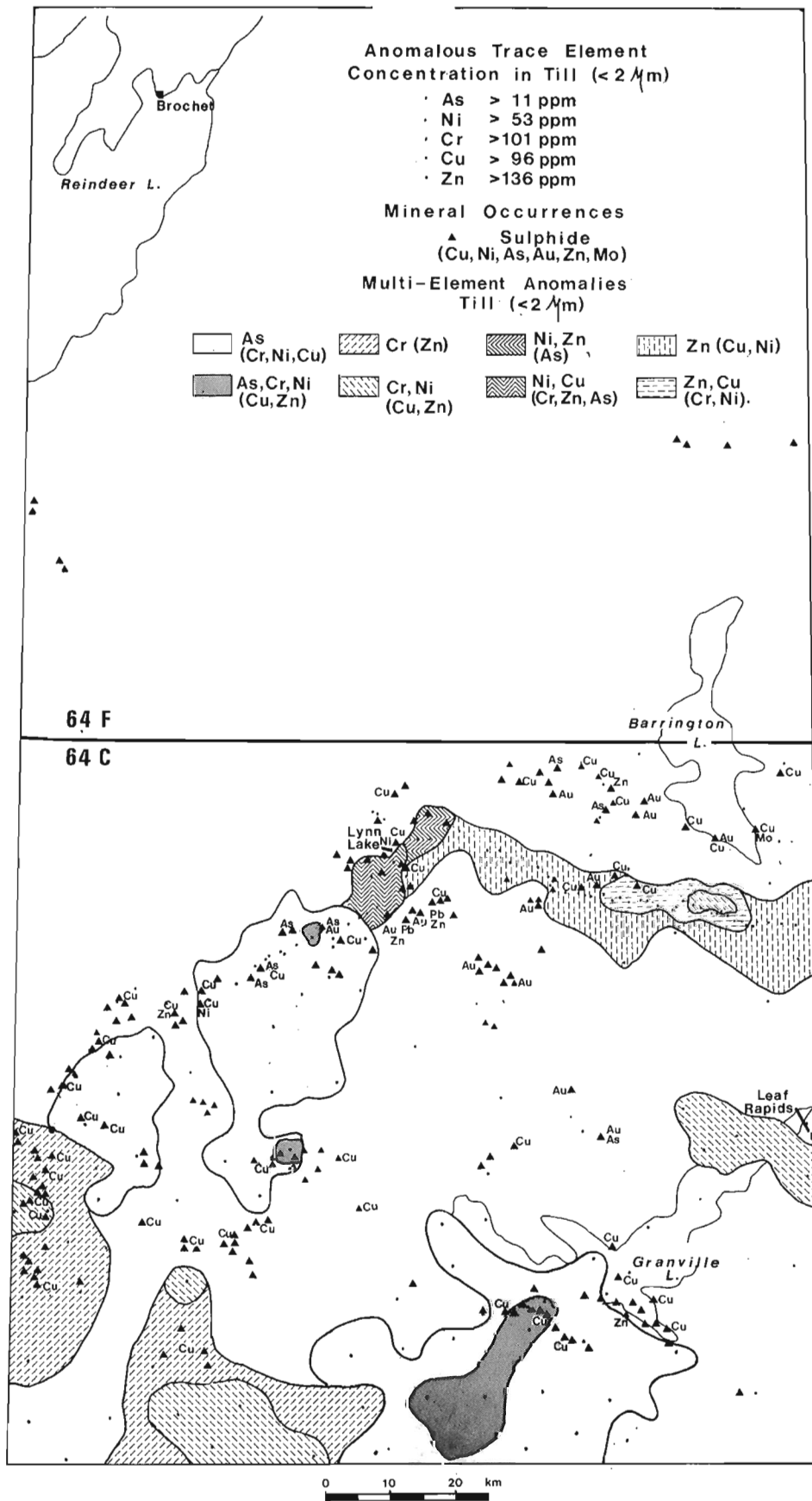


Figure 27.8. Multi-element anomalies in the <2 μm fraction of till. Triangles represent areas of known mineral occurrences (taken from Baldwin, 1980; Gilbert et al., 1980).

sites, Cr, Ni, and Zn anomalies coincide with As and appear to be related to sulphide mineralization in the upper amphibolite units of the BRMS. The highest concentrations of As occur immediately down-ice from a known gold occurrence at Wheatcroft Lake, approximately 5 km southwest of Granville Lake (Barry, 1963).

Two large areas of anomalous Cr concentrations in the west and southwestern part of the region are not as easily interpreted. Both occur near abundant sulphide mineralization, mainly Cu, associated with the BRMS/Sickle Group contact.

Glacial dispersal

Manifestation of geochemically distinctive bedrock components as a dispersal train in till is dependent upon various factors:

- 1) size and topography of both the source and dispersal area;
- 2) erodibility of source rocks;
- 3) rate of dilution by lithologies in the down-ice direction;

- 4) surface weathering; and
- 5) sampling density.

The effects of surface weathering can be controlled by sampling till below the postglacial solum. The remaining factors are a function of bedrock geology and project design. In this study, sampling density is designed to provide reconnaissance level till geochemical data in order to outline regions with potential for further detailed study.

Sulphide mineralization within the region generally occurs as relatively thin stratiform deposits (Baldwin, 1980) with small areas of surface exposure. The size of the source area for glacial erosion and dispersal, therefore, is relatively small. This, coupled with irregular bedrock topography and resistant bedrock lithologies, results in dispersal trains that are relatively short and/or poorly developed. Detailed studies of till geochemistry and glacial dispersal within the Lynn Lake area indicate that down-ice transport of material derived from areas of known sulphide mineralization cannot be traced farther than 1-2 km (E.Nielsen, personal communication, 1986). Based on these

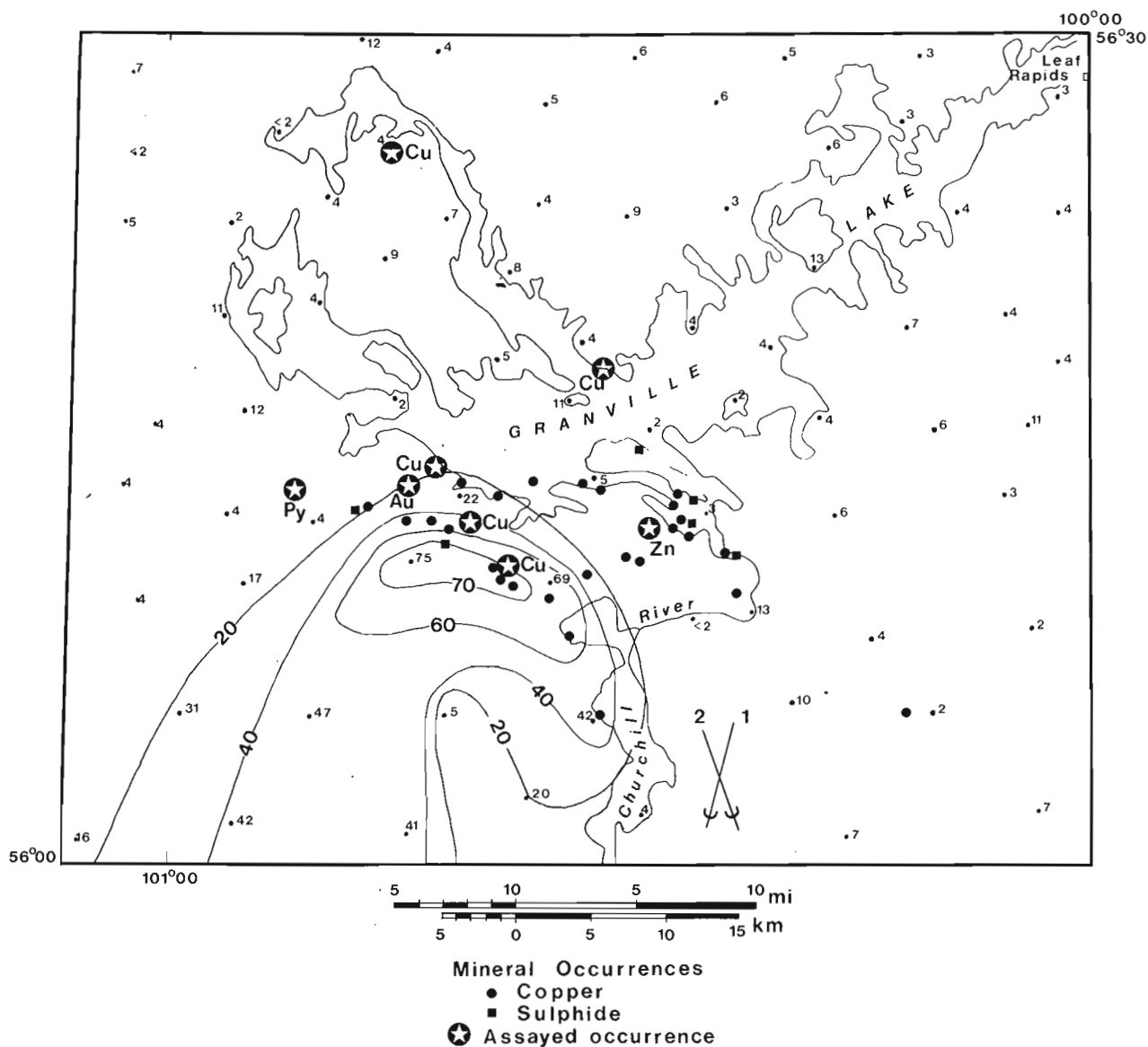


Figure 27.9. Detail of the As anomaly south of Granville Lake and possible dispersal patterns. As values are in ppm; detection limit is 2 ppm. Mineral occurrences from Baldwin (1980).

studies, it is apparent that the sampling density employed in reconnaissance level sampling programs (1 per 30-50 km²) is insufficient to reveal small scale dispersal patterns.

Southward dispersal of trace elements may be marked by a subtle elongation or fingering of concentration contours in that direction. For example, the east-west trending belt of anomalous Zn concentration (90th percentile contour) located east of Lynn Lake (Fig. 27.8) exhibits a slightly lobate southern margin, perhaps reflecting southward dispersal of metals along the greenstone belt. Sample control down-ice of the greenstone belt, however, is not sufficient to document this apparent trend. The large area of anomalous As concentrations west of Lynn Lake trends in a direction compatible with regional ice flow. This pattern, however, likely reflects the occurrence of numerous small outcrops of metavolcanic rocks throughout the area, and therefore represents the cumulative effect of glacial dispersal from a number of small sources (Shilts, 1975).

The regional As anomaly, located south-southwest of Granville Lake may reflect large scale glacial dispersal from a zone of sulphide mineralization along the south shore of Granville Lake. No other sulphide occurrences have been documented south of this belt (Fig. 27.8), although the entire area has been classified as of moderate potential for massive sulphide mineralization (Gale et al., 1980). A contour map of As concentrations in this region is shown in Figure 27.9. The largest concentrations occur immediately down-ice from a known gold occurrence at Wheatcroft Lake. Values decrease systematically to the south-southwest at approximately 190°, and also to the southeast at approximately 165°. These directions parallel both the oldest and youngest ice flow directions mapped in the area. The trend to the southeast, however, parallels a zone of Cu-bearing sulphide mineralization and may not be related to glacial dispersal from a single source. If both trends are related to a single source near Wheatcroft Lake, then dispersal to the southwest appears to have been more prolonged than that to the southeast as concentrations in excess of 40 ppm are maintained up to 25 km down-ice in this direction. Dispersal to the southeast, on the other hand, is limited to approximately 20 km down-ice, at which point As concentrations are reduced to background (<11 ppm). This area is located approximately 20-40 km west of the Leaf Rapids interlobate moraine. These dispersal trends, therefore, are consistent with evidence suggesting a late glacial shift in ice flow towards the southeast, associated with drawdown along the suture between Keewatin and Hudson lobe ice.

At present, sampling density is insufficient to determine whether this areally extensive anomaly was formed solely by glacial dispersal from a single source, or whether it, in part, represents a regional increase in background value associated with scattered sulphide mineralization. In the former case, both the extent of dispersal plus the concentrations of As present within the train would require a comparatively large source area. More detailed sampling within this region is planned in an effort to define patterns of trace metal concentration and to isolate potential source areas of arsenic-bearing mineralization.

Conclusion

The Leaf Rapids interlobate moraine is defined as the large, discontinuous esker-like ridge composed of ice contact stratified sediment that trends north-south through the town of Leaf Rapids. This feature marks the western extent of carbonate-bearing Hudson lobe ice in northern Manitoba. West of the moraine, noncalcareous shield-derived till was deposited by southward flowing Keewatin ice. During deglaciation, ice flow west of the moraine shifted to the southeast producing a zone of convergence with Hudson lobe ice east of the moraine. Klassen (1983) interpreted the confluence between Hudson lobe ice and

Keewatin lobe ice, at the time of deglaciation, to have occurred farther east, at a position marked by the Burntwood-Etawney morainic system. This system, as depicted by Klassen, may represent a large interlobate, or radial kame moraine complex developed contemporaneously with the Leaf Rapids interlobate moraine. Alternatively, it may represent a recessional moraine developed after retreat of Hudson lobe ice from the Leaf Rapids area.

Reconnaissance till sampling within the region indicates that trace element concentrations in till west of the moraine reflect, to a first approximation, variations in regional bedrock lithology. Large areas of metal enrichment in till have been outlined that seem to be related to small scale glacial dispersal from areas of known mineralization and/or from bedrock that is uniformly enriched in trace metals. Because sulphide mineralization within the region occurs as relatively thin stratiform deposits with limited surface exposure, down-ice transport of geochemically distinct bedrock components is limited to a distance of less than 1-2 km. Reconnaissance sampling density of 1 per 30-50 km² is insufficient to reveal these small scale patterns of dispersal. A regional As anomaly south-southwest of Granville Lake, however, may reflect large scale glacial dispersal (<25 km) from a zone of sulphide mineralization along the south shore of Granville Lake. Further study is planned in this area in an effort to isolate potential sources of arsenic-bearing mineralization.

Acknowledgments

The authors would like to thank Erik Nielsen and L.A. Dredge for discussions on related topics. D.J. Ellwood of the Resource Geochemistry and Geophysics Division developed the computer program (APPMAP) used to statistically summarize data and produce computer contour maps, which greatly aided interpretation of analytical results. W.W. Shilts and L.A. Dredge critically reviewed the manuscript.

References

- Aario, R.
1977: Classification and terminology of morainic landforms in Finland; *Boreas*, v. 6, p. 87-100.
- Baldwin, D.A.
1980: Disseminated stratiform base metal mineralization along the contact zone of the Burntwood River Metamorphic Suite and the Sickle Group; Manitoba Department of Energy and Mines, Economic Geology Report ER 79-5, 20 p.
- Banerjee, I. and McDonald, B.C.
1975: Nature of esker sedimentation; in *Glaciofluvial and Glaciolacustrine Sedimentation*, A.V. Jopling and B.C. McDonald (ed.); Society of Economic Paleontologists and Mineralogists, Special Publication No. 23, p. 132-154.
- Barry, G.S.
1963: Geology of the Trophy Lake area (east half) 64 C/2 (east); Manitoba Department of Mines and Natural Resources, Publication 63-3, 47 p.
- Boyle, R.W.
1968: Elemental associations in mineral deposits and indicator elements of interest in geochemical prospecting; Geological Survey of Canada, Paper 68-58, 45 p.
- Cheel, R.J.
1982: The depositional history of an esker near Ottawa, Canada; *Canadian Journal of Earth Sciences*, v. 19, p. 1417-1427.

- Dredge, L.A.
1983: Character and development of northern Lake Agassiz and its relation to Keewatin and Hudsonian ice regimes; in *Glacial Lake Agassiz*, J.T. Teller and Lee Clayton (ed.); Geological Association of Canada, Special Paper No. 26, p. 117-131.
- Elson, J.A.
1967: Geology of glacial Lake Agassiz; in *Life, Land, and Water*, W.J. Mayer-Oakes (ed.); University of Manitoba Press, Winnipeg, p. 34-96.
- Gale, G.H., Baldwin, D.A., and Koo, J.
1980: A geological evaluation of Precambrian massive sulphide deposit potential in Manitoba; Manitoba Department of Energy and Mines, Economic Geology Report ER 79-1, Maps ER 79-1-1 to ER 79-1-23.
- Gilbert, H.P., Syme, E.C., and Zwanzig, H.V.
1980: Geology of the metavolcanic and volcanoclastic metasedimentary rocks in the Lynn Lake area; Manitoba Department of Energy and Mines, Geological Paper GP 80-1, 118 p.
- Henderson, P.J.
Sedimentology of a sublacustrine glaciofluvial deposit on the Frontenac Axis, Ontario; *Canadian Journal of Earth Sciences* (in press)
- Kaszycki, C.A. and DiLabio, R.N.W.
1986: Till geochemistry, Granville Lake (NTS 64 C), Manitoba; Geological Survey of Canada, Open File 1204.
- Kaszycki, C.A., WayNee, V., Neilsen, E., and DiLabio, R.N.W.
1986: Surficial geology, Granville Lake (NTS 64 C), Manitoba; Geological Survey of Canada, Open File 1258, 1:125 000 scale.
- Klassen, R.W.
1983: Lake Agassiz and the late glacial history of northern Manitoba; in *Glacial Lake Agassiz*, J.T. Teller and Lee Clayton (ed.); Geological Association of Canada, Special Paper No. 26, p. 95-115.
- Repo, R.
1954: Om förhållandet mellan rafflor och asar (on the relationship between eskers and striae); *Geologi*, v. 6, No. 5, p. 45.
- Ringrose, S. and Large, P.
1977: Quaternary geology and gravel resources of the Leaf Rapids Local Government District; Department of Mines Resources and Environmental Management, Mineral Resources Division, Geological Report GR 77-2, 93 p.
- Rust, B.R. and Romanelli, R.
1975: Late Quaternary subaqueous deposits near Ottawa, Canada; in *Glaciofluvial and Glaciolacustrine Sedimentation*, A.V. Jopling and B.C. McDonald (ed.); Society of Economic Paleontologists and Mineralogists, Special Publication No. 23, p. 177-192.
- Shilts, W.W.
1975: Principles of geochemical exploration for sulphide deposits using shallow samples of glacial drift; *Canadian Institute of Mining and Metallurgy Bulletin*, v. 68, no. 757, p. 73-80.
1984a: Till geochemistry in Finland and Canada; *Journal of Geochemical Exploration*, v. 21, p. 95-117.
1984b: Esker sedimentation models, Deep Rose Lake map area, District of Keewatin; in *Current Research, Part B*, Geological Survey of Canada, Paper 84-1B, p. 217-222.
- Shreve, R.L.
1985: Esker characteristics in terms of glacier physics, Katahdin esker system, Maine; *Geological Society of America Bulletin*, v. 96, p. 369-646.
- St-Onge, D.A.
1984: Surficial deposits of the Redrock Lake area, District of Mackenzie; in *Current Research, Part A*, Geological Survey of Canada, Paper 84-1A, p. 271-277.
- Zwanzig, H.J.
1980: Geology of the Granville Lake area, NTS 64 C, provisional compilation map; Manitoba Department of Energy and Mines, MRD 1;250 000 scale.

A composite profile of the Cordilleran ice sheet during McConnell Glaciation, Glenlyon and Tay River map areas, Yukon Territory

Project 800001

Alexandra Duk-Rodkin¹, Lionel E. Jackson, Jr., and Oleg Rodkin²
Terrain Sciences Division, Vancouver

Duk-Rodkin, A., Jackson, L.E., Jr., and Rodkin, O., A composite profile of the Cordilleran ice sheet during McConnell Glaciation, Glenlyon and Tay River map areas, Yukon Territory; in *Current Research, Part B, Geological Survey of Canada, Paper 86-1B*, p. 257-262, 1986.

Abstract

During the last (McConnell) glaciation, the Selwyn lobe of the Cordilleran ice sheet covered most of the study area except for isolated nunataks. Well preserved moraine ridges mark the margins of many of these nunataks. A general profile of the Cordilleran ice sheet during McConnell Glaciation was constructed using the inferred McConnell age moraines and ice marginal channels in Glenlyon map area.

Ice streams followed major valleys and the ice surface was elevated on the stoss sides of nunataks presumably due to compressive flow behind these obstructions. An equation for the numerical approximation of a valley glacier-profile profile of the Selwyn lobe.

Résumé

Au cours de la dernière glaciation (McConnell), le lobe Selwyn de l'inlandsis de la Cordillère couvrait la majeure partie de la région à l'étude à l'exception de quelques nunataks isolés. La limite d'un grand nombre de ces nunataks est marquée par des crêtes morainiques bien conservées. Un profil général de l'inlandsis de la Cordillère au cours de la glaciation McConnell a été fait à l'aide des moraines mises en place lors de la glaciation McConnell et des chenaux proglaciaires de la région cartographiée de Glenlyon.

Les langues glaciaires ont suivi les vallées principales et la surface de la glace était surélevée sur les flancs en pente douce des nunataks, probablement en raison de l'écoulement compressif qui se faisait derrière ces obstructions. Une équation utilisée pour trouver l'approximation numérique du profil d'un glacier de vallée constitue la façon la plus précise de reconstituer le profil du lobe Selwyn.

¹ Terrain Sciences Division, Calgary

² Department of Geology, University of Alberta, Edmonton, Alberta T6G 2G7

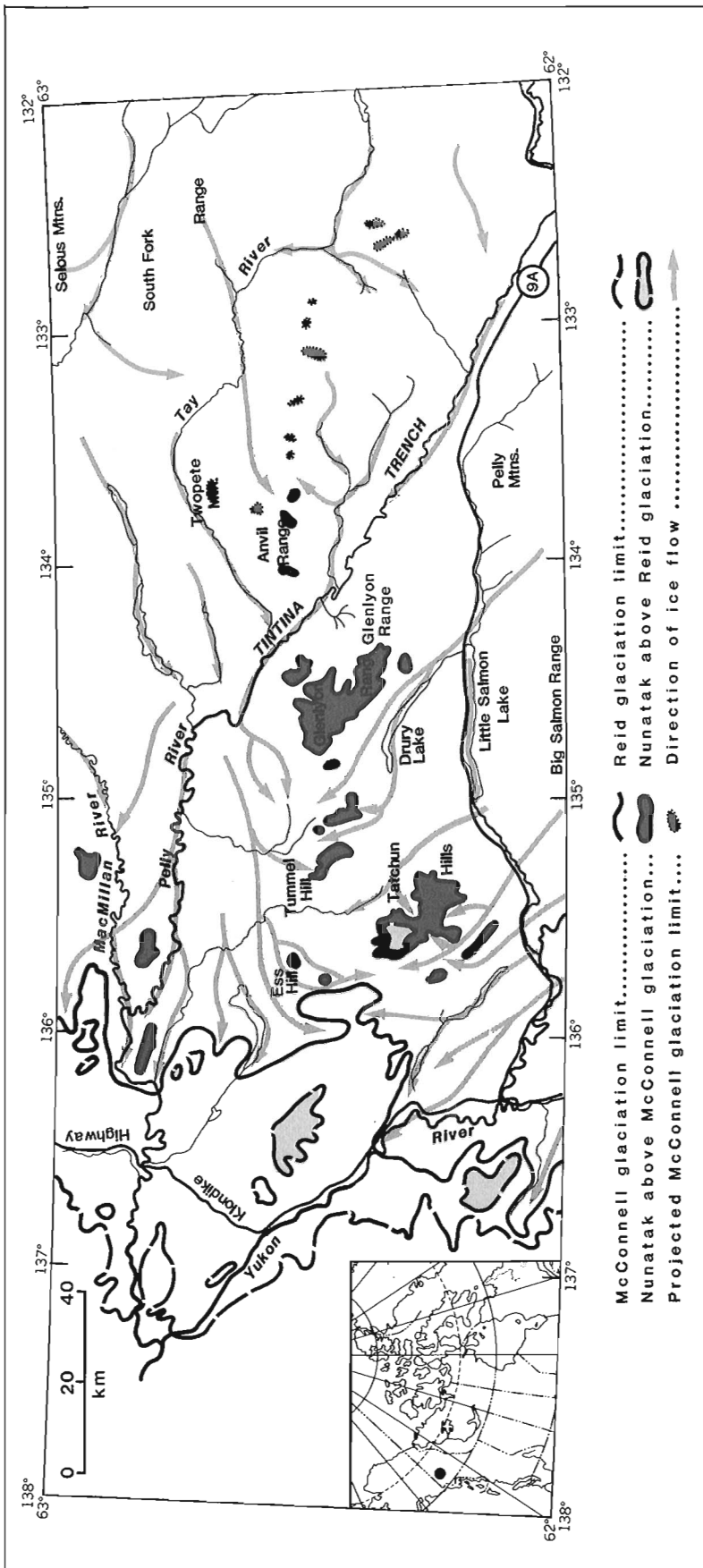


Figure 28.1. Glacial limits and generalized ice flow direction, Carmacks (115 I), Glenlyon (105 L), Tay River (105 K) areas, Yukon Territory.

Introduction

The modes of flow and profiles of the extant ice sheets of the Earth can be determined through direct observation. Similar information for Pleistocene ice sheets can only be inferred from indirect evidence. Profiles can be reconstructed by plotting the upper limits of geomorphic features created at the ice/rock/air interface. Although many profiles have been constructed for valley glaciers, they are relatively rare for ice sheets (Mathews, 1974); unlike valley glaciers, the thicknesses of Pleistocene ice sheets commonly exceeded the relief of the land over which they flowed. In Pelly River basin, topography of the land underlying the Pleistocene ice sheets was close to or locally exceeded ice thickness. Past and present mapping of Quaternary geology in Pelly River basin has generated sufficient data to permit the construction of a composite profile of the Cordilleran ice sheet at its maximum extent during the last glaciation. Such a profile allows the identification of mountain peaks that supported ice caps or otherwise stood above the ice sheet at its maximum thickness but lack definitive geomorphic features. The composite profile also allows comparison and contrast between the modes of flow of extant and Pleistocene ice sheets.

Setting

Carmacks, Glenlyon, and Tay River map areas (115 I, 105 L, and 105 K) include the Glenlyon Range, the MacMillan Plateau sector of Yukon Plateau, and parts of Tintina Trench and Pelly Mountains in the southwest and the Mount Selous Massif, part of Selwyn Mountains, in the northeast (Bostock, 1948; Fig. 28.1). The region is drained by the Pelly and MacMillan river systems. In MacMillan Plateau, the surface is incised by broad anastomosing glaciated valleys, creating high tablelands which are surmounted by small mountain groups.

During the last (McConnell) glaciation of the region, the Selwyn lobe of the Cordilleran ice sheet (Campbell, 1967) covered all the study area except for isolated peaks that stood above the ice sheet as nunataks (Hughes, 1969; Fig. 28.2, 28.3). Glacial deposits here have a freshness characteristic of deposits of McConnell age elsewhere in the territory in contrast to the subdued character of deposits of the penultimate Reid glaciation and of still older Klaza and Nansen glaciations (Bostock, 1966; Hughes et al., 1968).

Drumlinoid till plains are common on the floors of the broad valleys and till extends as a blanket or veneer up valley sides and onto the tableland surfaces. Those valleys that were occupied by glacial lakes during retreat of the ice sheet have glacio-lacustrine silt and clay on their floors.

Glaciofluvial deposits, including outwash plains, eskers, and deltas, are widespread on valley floors and locally small delta complexes are found in association with ice marginal channels that debouched into ponds confined between the ice margin and the mountainside.

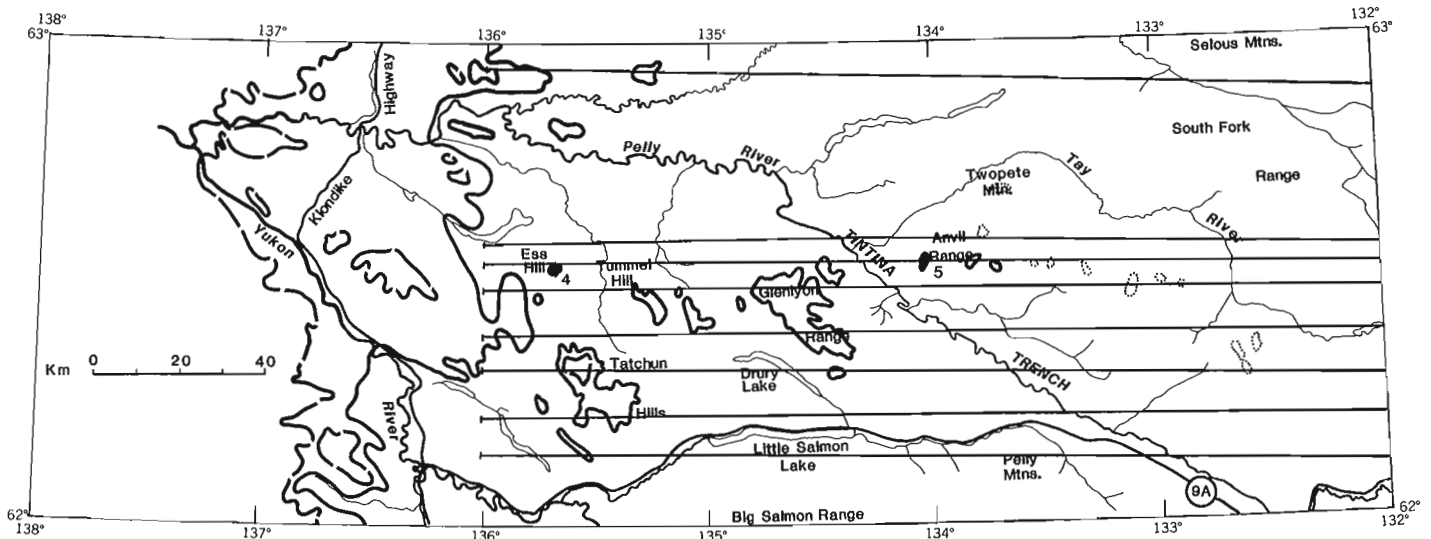


Figure 28.2. Location of topographic profiles and stereopairs.

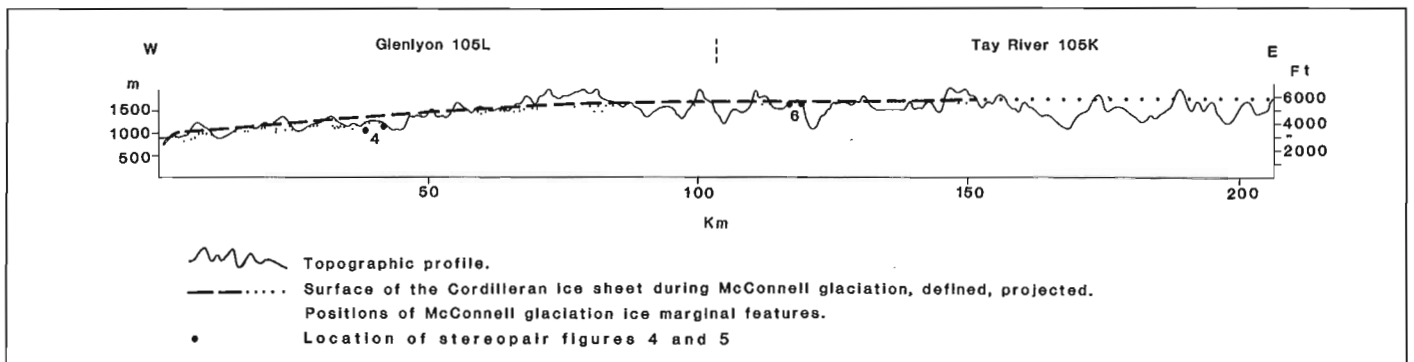


Figure 28.3. Generalized topographic profile oriented east-west, showing the reconstructed upper limit of the McConnell Glaciation.

Regional profile of the Selwyn lobe

The maximum McConnell terminus of the Selwyn lobe is marked by well preserved moraines and sharply incised ice marginal channels in Carmacks and Glenlyon map areas (Bostock, 1966; Campbell, 1967; Hughes et al., 1968); similar features define former nunataks (Fig. 28.4).

In Tay River map area, moraine ridges occur at 1645 m on the south side of Anvil Range and at 1676 m on the north side (Fig. 28.5). The moraines are comparable in degree of preservation to moraines of McConnell age elsewhere in central Yukon and are judged to mark the upper limit of the Cordilleran ice sheet during McConnell Glaciation, when the summits of Anvil Range stood as nunataks above the ice sheet. The Selwyn lobe moved generally westward; the surface of the ice sheet, as reconstructed from moraines and ice marginal channels that mark the upper limit, rises eastwards (Fig. 28.2, 28.3). The moraines in Anvil Range are higher than moraines assigned to McConnell Glaciation at localities farther west, hence their elevations are compatible with the inferred age. To test this compatibility more rigorously, moraines and ice marginal channels in Glenlyon map area, previously identified by Campbell (1967), were replotted on maps at 1:50 000 scale and elevations were determined from topographic maps (contour interval 100 feet). The elevations, together with those of moraines in Tay River map area, were plotted on a composite east-west profile. A generalized profile of the former ice sheet

(Fig. 28.2, 28.3) was drawn over a distance of 114 km from the ice front through the elevations of the locally highest ice marginal features. This reconstructed upper limit indicates the maximum level of McConnell Glaciation but does not reflect the maximum levels of older glaciations. The generalized ice surface profile has an average slope of $0^{\circ}30'$ over the outermost 50 km, $0^{\circ}19'$ over the next 52.5 km, and $0^{\circ}03'$ farther east. Slopes in the profile have not been corrected for isostatic rebound.

A check on the accuracy of this profile was made by extrapolating the ice profile defined by ice marginal features in Glenlyon map area to analogous features in Tay River map area (Fig. 28.3). Moraines in Anvil Range lie close to the extrapolated profile of the ice sheet at the McConnell maximum, supporting the accuracy of the profile and the assignment of a McConnell age to these moraines.

The reconstructed ice profile intersects other ice marginal features on the flanks of upland summits in Tay River map area. They include small ice marginal channels, minor breaks in slope, and abrupt changes in the morphology of upland summit areas. These features apparently mark the upper limit of McConnell ice or lie close to it. Well developed moraines and ice marginal channels, however, are lacking around these other nunataks. Hughes (in press) noted a comparable lack of well defined ice marginal features on former nunataks in Aishihik map area, to the south. He suggested that this was because the ice surface around the

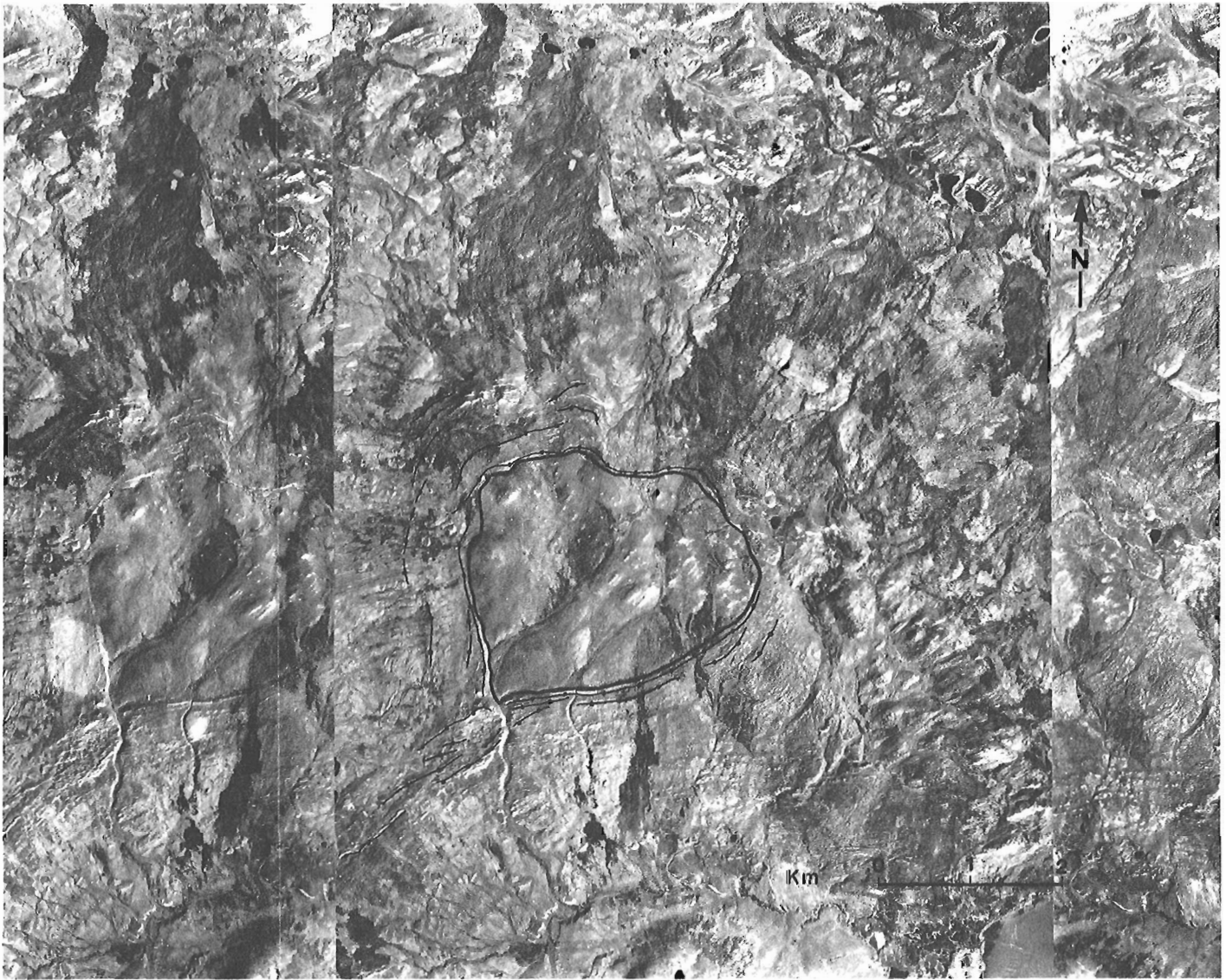


Figure 28.4. Moraine showing the upper limit of McConnell Glaciation on a nunatak (Ess Hill), Glenlyon map area.

nunataks was above the equilibrium level during the climax of glaciation. Because of limited ablation, morainic material and meltwater were insufficient for development of well defined moraines and ice marginal channels.

The data shown in Figure 28.3 have a vertical scatter, particularly near the terminus of the ice sheet. The scatter corresponds to distortion in the distribution of the data points caused by the manner of plotting, in which points within a north-south belt, 100 km wide, were projected onto a single east-west plane. Within that belt, the flow of the ice sheet was controlled strongly by topography: ice flowed along major valleys, bifurcated around nunatak areas, and then rejoined and finally divided into a digitate terminal zone. Within the belt, the flow direction varied as much as 50° from the generalized westward flow (Campbell, 1967). In short, the data points represent several anastomosing flows with variable ice gradients rather than a simple uniform sheet.

Flow characteristics around nunataks

A notable feature of these moraines around nunataks is the common large differences in their elevations measured in the direction of overall flow. Differences of 30 m in the

level of the ice sheet occurred on opposite sides of former nunataks in the Anvil Range whereas there is a difference of 122 m between moraines at the northeast side of the hill and those on the southwest side at Ess Hill (Campbell, 1967; Fig. 28.4). Only approximately 40 to 60% of the ice elevation difference across Ess Hill can be attributed to ice sheet convexity; in the Anvil Range, the figure is probably about 7% (Fig. 28.5). The balance of elevation difference is likely attributable to compressive flow on the stoss side of the nunatak and perhaps extensive flow on its lee side. Observation and mathematical modelling of ice sheet flow over low relief roughness elements (Budd, 1970, 1971) have shown that under the right conditions, small bedrock protuberances (i.e., relative to ice sheet thickness) can cause changes in the surface slope of the overlying ice sheet even to the point of local upslope flow in the direction of general ice flow. The effects of nunatak-scale roughness elements on the flow of ice sheets analogous to the Selwyn lobe are absent from the literature. On the basis of the reconstructed profile of Selwyn ice, significant deviations from laminar flow seem likely.

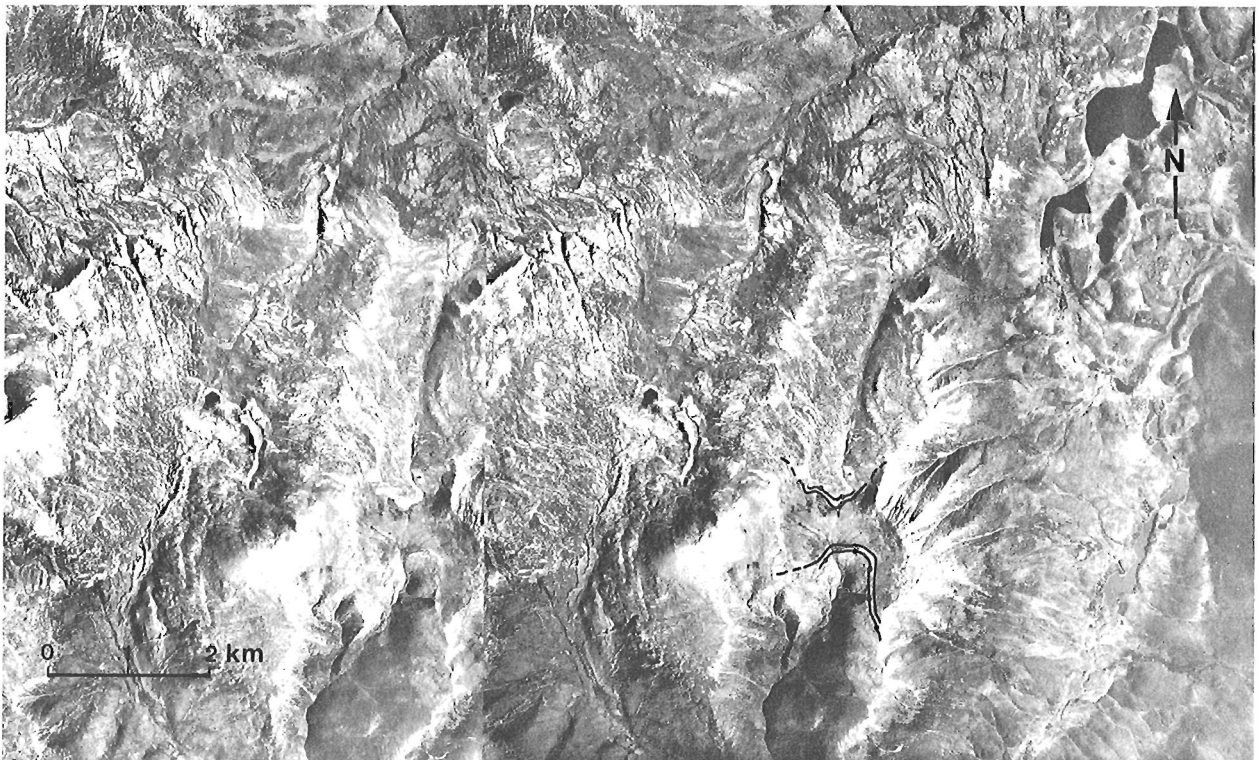


Figure 28.5. Moraine ridges marking the upper limit of the McConnell Glaciation ice in Anvil Range, Tay River map area.

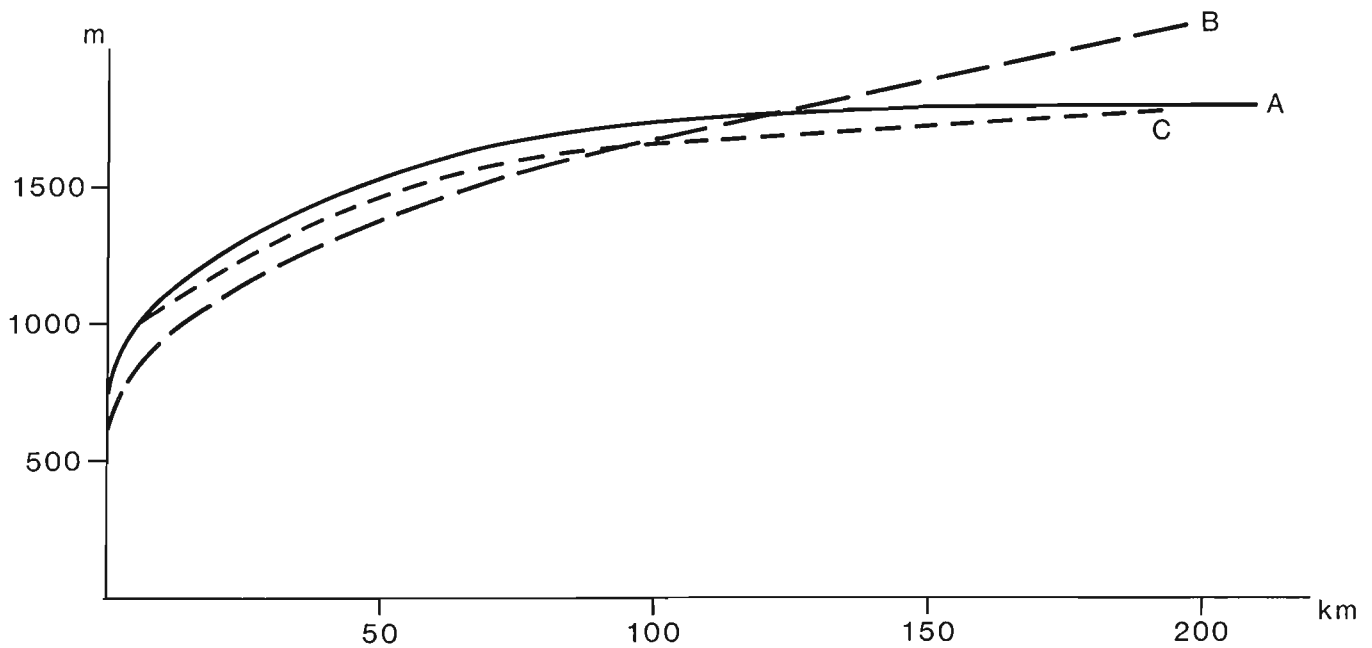


Figure 28.6. Ice surface profiles: (A) Direct evidence as in Figure 28.3, (B) Theoretical curve (parabola), (C) Theoretical curve according to Shilling Hollin (1981).

Numerical reconstruction of the Selwyn lobe and its implications for ice sheet flow

Methods of calculating glacier and ice cap profiles were developed by Orowan (1949); Nye (1952a, b, c, 1959); Robin (1958); and Vialov (1958). These approaches have successfully approximated the profiles of the Greenland and Antarctic ice sheets as parabolas, ellipses, and ellipsoids. All of these figures proved to be inappropriate for the Selwyn lobe.

The Selwyn lobe was much flatter over most of expanse than would be characteristic of a parabola or ellipse. The best approximation was the curvilinear profile generated by the integrated equation of Shilling and Hollin, 1981 after Nye, 1952b, c) for approximating the flow of a valley glacier:

$$h_{i+1} = h_i + \frac{\tau_{av} \Delta x}{\rho g t_i}$$

where: t = ice thickness (m)
 h = ice surface elevation (m)
 r = bedrock elevation (m)
 τ_{av} = average shear stress ($0.8 \times 10^5 \text{ N/m}^2$)
 ρ = ice density (920 kg/m^3)
 g = gravitational acceleration (9.8 m/s^2)
 f = shape factor (0.5)
 h_j and h_{j+1} = ice surface elevations for each Δx step of calculations (m).

A comparison of the profile generated by this equation, the equation for a parabola, and the reconstructed profile appear in Figure 28.6.

Shear stress (τ) is an average because, in valley glacier flow and in the high relief terrain traversed by the Selwyn lobe, shear stress occurs not only along the sole of the glacier, but along valley walls as well; a value of $0.8 \times 10^5 \text{ N/m}^2$ was assumed. The shape factor (f) of Nye (1965) can be calculated from valley geometries obtained from topographic maps using the equation:

$$\frac{A}{P} = ft$$

where:

A = valley cross-sectional area
 P = valley perimeter
 t = ice thickness

A value of $f = 0.5$ was calculated, which is in the 1 to 0.4 range of Weertman (1971); it matches values in Mathews (1967) and is close to the 0.8 value obtained by Denton and Hughes (1981).

The close approximation of a profile assuming valley glacier flow conditions to that reconstructed for the Selwyn lobe using real data suggests its mode of flow was not like the Antarctic, Greenland, and probably the Laurentide ice sheets. The effects of underlying topography on flow were significant. Flow was concentrated as ice streams in major valleys while compressive flow elevated the ice surface behind intervening uplands as indicated by oriented features and moraines.

References

- Bostock, H.S.
 1948: Physiography of the Canadian Cordillera with special reference to the area north of the fifty-fifth parallel; Geological Survey of Canada, Memoir 247, 106 p.
 1966: Notes on glaciation in central Yukon Territory; Geological Survey of Canada, Paper 65-36.
- Budd, W.F.
 1970: Ice flow over bedrock perturbations; Journal of Glaciology, v. 9, p. 29-48.
 1971: Stress variations with ice flow over undulations; Journal of Glaciology, v. 10, p. 177-196.
- Campbell, R.B.
 1967: Reconnaissance geology of Glenlyon map-area, Yukon Territory; Geological Survey of Canada, Memoir 352, 92 p.
- Denton, G.H. and Hughes, T.J. (editors)
 1981: The Last Great Ice Sheets; Wiley Interscience, New York, 484 p.
- Hughes, O.L.
 1969: Distribution of open-system pingos in central Yukon with respect to glacial limits; Geological Survey of Canada, Paper 69-34, 8 p.
 - Surficial geology and geomorphology of Aishihik Lake map area, Yukon Territory; Geological Survey of Canada, Paper. (in press)
- Hughes, O.L., Campbell, R.B., Muller, J.E., and Wheeler, J.O.
 1968: Glacial flow patterns, Yukon Territory south of 65° North Latitude; Geological Survey of Canada, Paper 68-34, 9 p.
- Mathews, W.H.
 1967: Profiles of late Pleistocene glaciers in New Zealand; New Zealand Journal of Geology and Geophysics, v. 10, p. 147-163.
 1974: Surface profiles of the Laurentide ice sheet in its marginal areas; Journal of Glaciology, v. 13, p. 37-43.
- Nye, J.F.
 1952a: A method of calculating the thickness of ice sheets; Nature, v. 169, p. 529.
 1952b: The mechanics of glacier flow; Journal of Glaciology, v. 2, p. 82-93.
 1952c: A comparison between the theoretical and the measured long profile of the Unteraar Glacier; Journal of Glaciology, v. 2, p. 103-107.
 1959: The motion of ice sheets and glaciers; Journal of Glaciology, v. 2, p. 493-507.
 1965: The flow of a glacier in a channel of rectangular, elliptic or parabolic cross section; Journal of Glaciology, v. 5, p. 661-690.
- Orowan, E.
 1949: Report in Joint meeting of the British Glaciological Society, the British Rheologists Club and the Institute for Metals; Journal of Glaciology, v. 1, p. 231-240.
- Robin, G. de Q.
 1958: Glaciology III: Seismic shooting and related observations (Norwegian-British-Swedish Antarctic expedition 1949-1952): scientific results 5; Norsk Polarinstitt, Oslo.
- Shilling, D.H. and Hollin, J.T.
 1981: Numerical reconstructions of valley glaciers and small ice caps; in The Last Great Ice sheets, ed. G.H. Denton and T.J. Hughes; Wiley Interscience, New York, p. 207-220.
- Vialov, S.S.
 1958: Regularities of glacial Shields, movement and plastic flow; International Association of Scientific Hydrology, Publication 47, p. 266.
- Weertman, J.
 1971: Shear stress at the base of a rigidly rotating cirque glacier; Journal of Glaciology, v. 10, p. 31-37.

Diatom dispersal phenomena: diatoms in precipitation samples
from Cape Herschel, east-central Ellesmere Island,
Northwest Territories – a quantitative assessment

Project 720078

Sigrid Lichti-Federovich
Terrain Sciences Division

Lichti-Federovich, S., Diatom dispersal phenomena: diatoms in precipitation samples from Cape Herschel, east-central Ellesmere Island, Northwest Territories – a quantitative assessment; in Current Research, Part B, Geological Survey of Canada, Paper 86-1B, p. 263-269, 1986.

Abstract

The quantitative assessment of the diatom content of freshly fallen snow, collected in two successive years, affirms the effectiveness of atmospheric transport as the main dispersal agent of these micro-algae. Mean numbers of unfragmented diatoms range from 27 to 23 300/100 mL of snow meltwater, with drifting snow yielding the highest concentration.

Résumé

L'évaluation quantitative de la concentration de diatomées dans la neige nouvellement tombée, prélevée au cours de deux années successives, confirme l'hypothèse selon laquelle le transport atmosphérique constitue le principal agent de dispersion de ces algues microscopiques. Les nombres moyens de diatomées non fragmentées varient de 27 à 23 300/100 mL d'eau de fonte des neiges, la neige soufflée donnant la concentration la plus élevée.

Introduction

The report is the third in a series presenting results from an ongoing investigation into diatom dispersal phenomena. This study continues to explore the significance of aerial transport of diatoms in an attempt to confirm previous findings (Lichti-Federovich, 1985) which characterize wind (anemochorous) transport as the chief dissemination mechanism of these micro-algae. The preceding investigation of diatoms in precipitation focused on meltwater samples of rime frost gathered from radio tower support cables at the Cape Herschel base station, east-central Ellesmere Island (Fig. 29.1) and from boulders on the nearby plateau. Here, diatoms found in melted snow samples collected at ground level at the Cape Herschel Base are described.

While the microbial content of bacteria, moulds, yeasts, and fungi in hail, rain, and snow has been repeatedly investigated, microbiological investigations of precipitation samples with regard to diatoms are exceedingly scarce. The only reported occurrences of diatoms in such samples are:

1) Pouchet (1860), on examining the upper layer of freshly fallen snow (volume unknown) from a courtyard in Rouen, France discovered three *Naviculae* and three *Bacillaires*; 2) one diatom, *Navicula minuscula*, was recovered from 200 cm³ of rain water collected on the laboratory roof of the Botanical Institute of the State University at Leiden, Netherlands (Overeem, 1937); and 3) Lichti-Federovich (1985) noted numerous marine and freshwater diatoms in rime frost samples collected from bedrock and radio tower support cables at Cape Herschel, Ellesmere Island.

This report is Contribution No. 27 from the Cape Herschel Project.

Material and methods

The precipitation samples were collected by W. Blake, Jr. in two successive years in the vicinity of the Cape Herschel Base camp (Fig. 29.2). The snow accumulated in a stainless steel pan lined with aluminum foil (Fig. 29.3). The collection pans were flushed with distilled water between

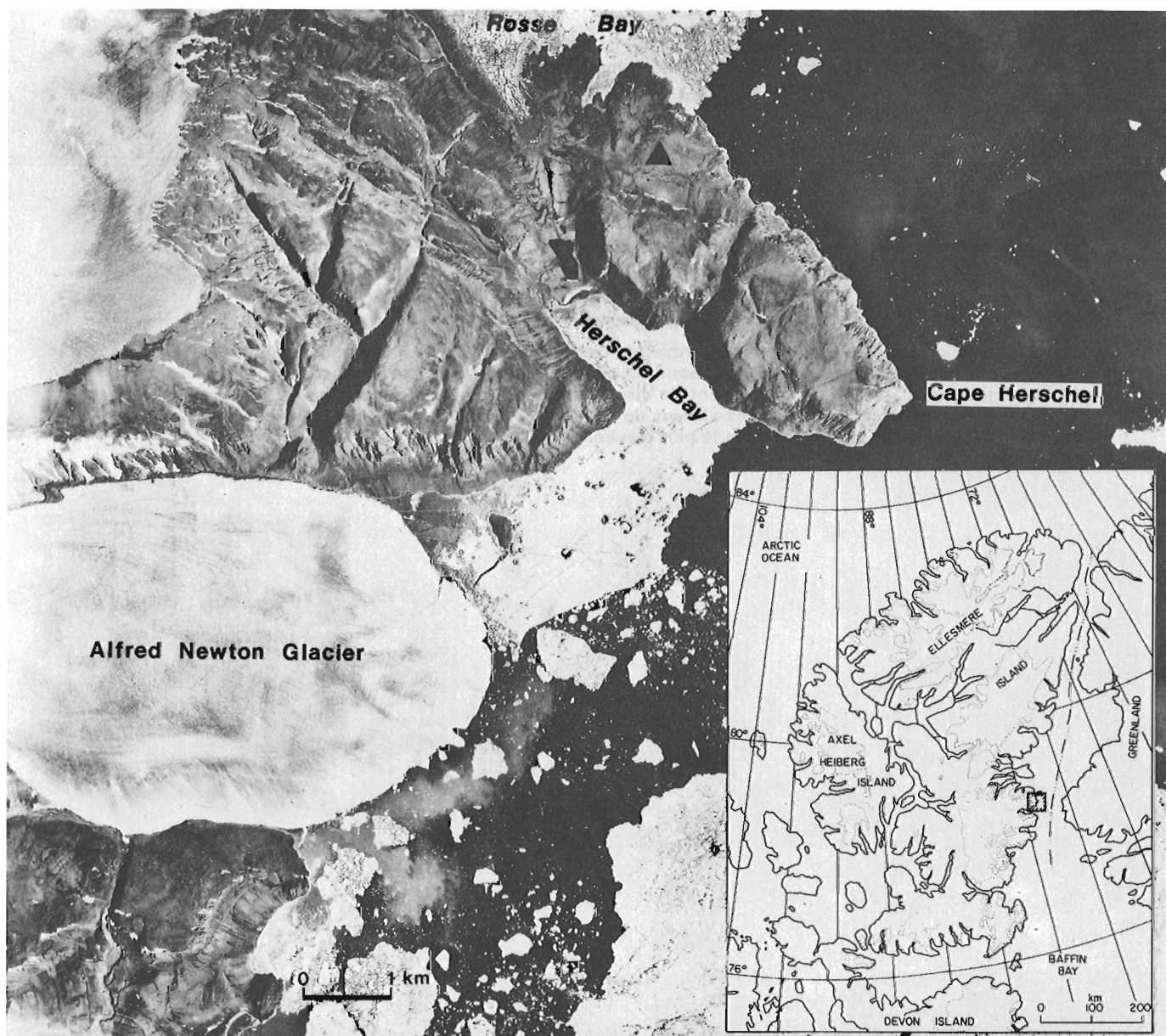


Figure 29.1. Aerial view of Cape Herschel, Ellesmere Island; solid triangle shows the location of Cape Herschel Base.



Figure 29.2. View northwest at collecting pans (arrow) and Cape Herschel Base, May 24, 1984. (Photo courtesy of W. Blake, Jr., 1984).

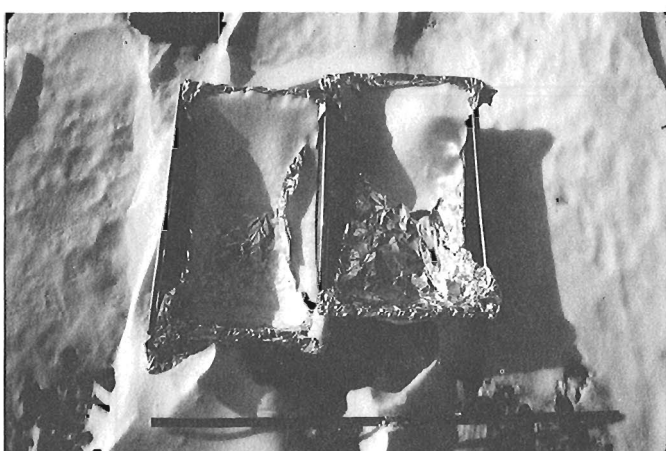


Figure 29.3. Detail of drifted snow (Precipitation sample #1-1984) accumulated on 23/5/1984 in stainless steel pans lined with aluminum foil. (Photo courtesy of W. Blake, Jr., 1984).

each sample collection and lined anew. Water derived from the partially melted snow was transferred to clean plastic bottles and stored in the dark at or near outdoor temperatures. Sample description and attendant meteorological conditions are presented in Table 29.1.

Quantitative analysis is based on at least two 10 mL aliquots of well mixed, unprocessed meltwater from each snow collection, filtered through a 25 mm, 0.8 μm nuclepore filter, thoroughly dried and mounted in Hyrax. Numerical counts were done with a x40 objective using a Leitz Ortholux. Frequency data were derived from the mean number of diatoms adjusted to a 100 mL volume measure.

Meltwater samples intended for scanning electron (SE) micrography were treated as follows: 1) addition of 25% cold HCl with subsequent heating and boiling for 10 minutes; 2) upon cooling, addition of distilled water; after standing overnight, filtration and the addition of 30% cold H_2O_2 with subsequent heating and boiling for 15 minutes; upon cooling, filtration and repeated washings with distilled water using a 3.0 μm filter for the final filtration. SE micrographs were

taken with a Cambridge Instruments Stereoscan 180 at 20 kv. Some floristic elements are illustrated in Plates 29.1 and 29.2.

Results

The numerical counts in Table 29.2 represent the first meaningful absolute abundance determination of diatoms recovered from precipitation samples. The only other significant quantitative analyses of airborne diatoms are the air filtration studies reported by Spitz and Schneider (1964) and by Spitz et al. (1965).

As regards the diatom frequency determinations of the meltwater samples from the Canadian Arctic, certain limitations need be considered. Some diatoms may have been lost during filtration and mounting procedures; therefore, the abundances may be underestimated. Conversely, some ambiguity on a quantification level is introduced by the possible "contamination" through drift dispersal, i.e. the influx of diatoms due to secondary deposition. Although the latter may have had some bearing upon the diatom content of all samples, as snow collection took place at ground level, this phenomenon predominantly affects the sample of drifted snow (Table 29.1). Thirdly, some measure of quantitative inexactitude is based on the incidence of fragmentation. Fragmentation of diatoms may be caused by wind abrasion during aerial transport; it may have occurred during sample storage or preparation, for example as a result of repeated freezing and thawing of sample material or as a consequence of agitation during sample mixing; or the incidence of broken diatoms may simply be a result of the uptake and transport of diatom fragments.

Despite these limitations, the common occurrence of diatoms in these snow samples (Table 29.2) demonstrates the importance of atmospheric transport as a dispersal agent as does the abundant diatom content of rime frost samples (Lichti-Federovich, 1985). Also, there is a striking variation between samples in the number of diatoms, ranging from a mean of 27 whole frustules (#2-1984) to a near 1000-fold increase in concentration (#1-1984). The floristic elements in these meltwater samples also differ, a selection of which is illustrated in Plates 29.1 and 29.2.

Significant numerical variance in the distribution of aerial diatoms is also demonstrated in the series of air filtration studies by Spitz et al. (1965). For example, atmospheric samplings at three different stations, selected from their series, with approximately the same air intake (30.0 m^3/h) and the same time exposure (at differing dates but within one week and a 12 hour exposition time in each case) yielded the following numbers of diatoms: Essen – 142 diatoms, Stuttgart – 38 diatoms, Berlin Tempelhof (Flughafen) – 388 diatoms. Similarly, a previous study conducted by Spitz and Schneider (1964) in Berlin, at a two-month interval with the same total air intake of 1500 m^3 within a 72 hour exposure time resulted in the recovery of 662 diatoms for the time period of April 22 to 24, 1961 and of 1567 diatoms from June 22 to 24, 1961.

These quantitative inconsistencies are caused by widely fluctuating variables such as: the actual number of airborne diatoms in the atmosphere, time of year, locality, and meteorological conditions. With particular reference to the diatom content of the meltwater samples in the present study, the following factors merit special consideration. As mentioned previously, the exceedingly high concentration of diatoms in the sample of drifted snow, undoubtedly originated from proximal terrestrial and aero-aquatic sources in the form of melting residue or windblown detrital matter and either were incorporated directly into the accumulating snow by dry deposition or were picked up as contamination by

Table 29.1. Characterization of precipitation samples from the Cape Herschel base, Ellesmere Island (78°37.0'N, 74°41.4'W; elevation 63 m)

Field/Lab Numbers	Sample material	Volume of meltwater (mL)	Temperature (°C)	Wind direction + date & time of observation	Wind speed (m/s)	Other meteorological data	Date/Time of collection
<i>1984 Precipitation samples</i>							
#1-1984 DT-85-3	drifted snow	190	max. - 7.7 min. - 11.6	SW 23/5 0700	3.6	Visibility 15 km; fog over channel to E and N	23/5/1984 (2400 h)
			max. - 6.5 min. - 7.0	SW 23/5 1900	10.8	Visibility 50+ km; fog over channel to E; blowing snow along ground most of day	
			max. - 5.9 min. - 11.2	- 24/5 0700	no wind	Visibility 50+ km; fog over channel to E	
#2-1984 DT-85-1	newly fallen snow	100	max. - 6.1 min. - 9.6	NNW 24/5 1900	1.5	Visibility 15 km; fog over channels to N and E; wind direction and speed variable; trace of snow	24/5/1984 (2100 h)
			max. - 6.4 min. - 9.8	NE 25/5 0700	0.5	Visibility 0.5 to 1 km in snow; precipitation 30 mm in last 12 h	
<i>1985 Precipitation samples</i>							
#1-1985 DT-85-4	newly fallen snow	285	max. + 0.2 min. - 3.0	SW 22/5 0700	7.2	Visibility 15 km; fog over channel to E; snow (1.8 mm)	22/5/1985 (1800 h)
			max. + 1.3 min. - 3.7	NNW 22/5 1900	1.0	Visibility 0.2 km in fog	
			max. + 1.6 min. - 1.9	N 24/5 1900	5.1	Visibility 50 km	
#2-1985	newly fallen snow	170	max. + 0.6 min. - 1.5	SE 25/5 0700	1.5	Visibility 1.5 km in fog and snow; trace of precipitation	25/5/1985 (0715 h)

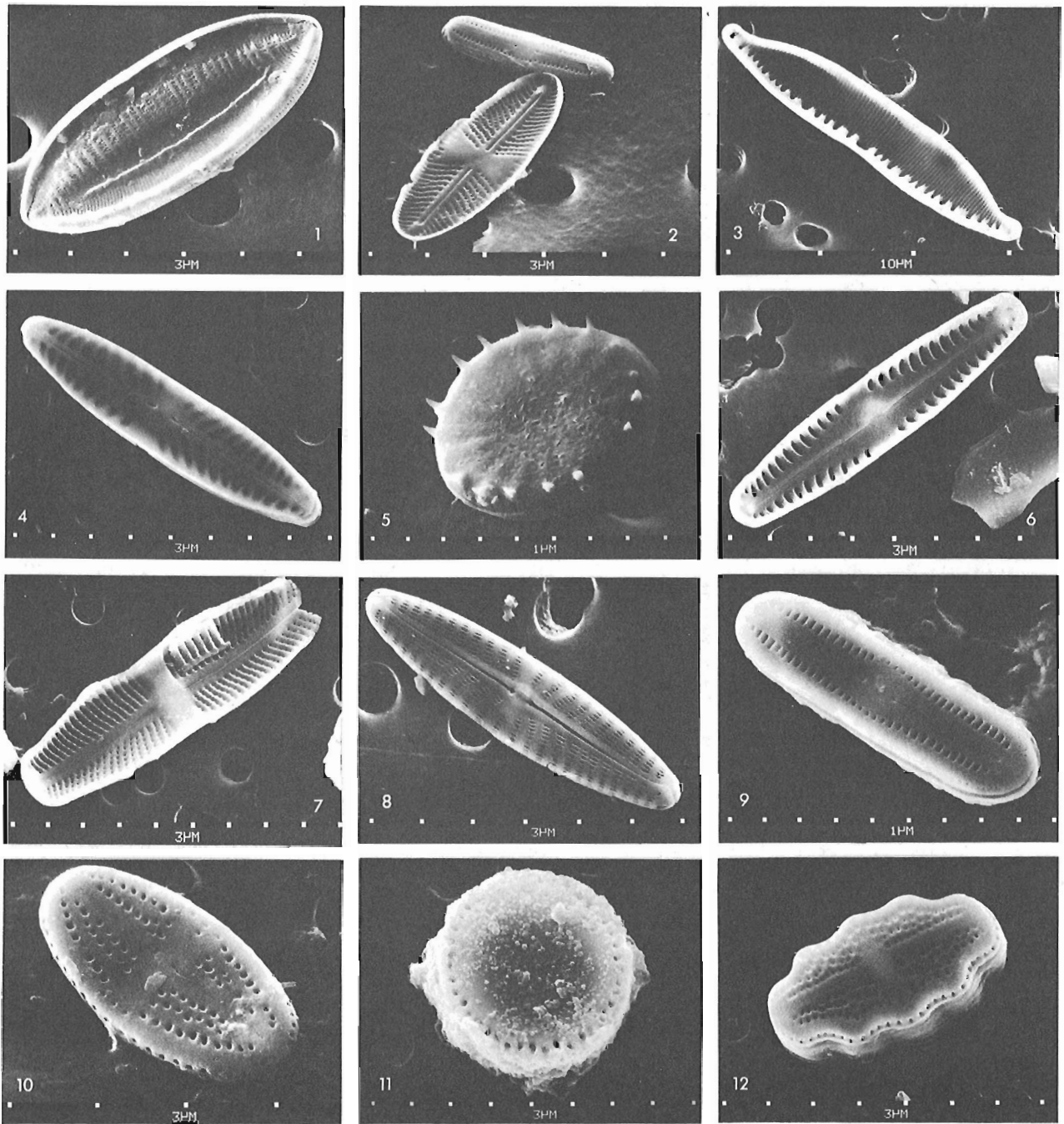


PLATE 29.1

Freshwater diatoms from precipitation samples

- fig. 1. *Nitzschia debilis* (Arn.) Grun. (internal view).
 fig. 2. Two freshwater diatoms (internal and external views).
 fig. 3. *Hantzschia amphioxys* (Ehr.) Grun. (internal view).
 fig. 4. *Pinnularia* sp. (external view).
 fig. 5. *Stephanodiscus* sp. (external view).
 fig. 6. *Pinnularia microstauron* (Ehr.) Cleve (internal view).
 fig. 7. *Achnanthes coarctata* (Bréb.) Grun. (internal view).
 fig. 8. *Navicula cincta* Kuetz. var. *heufleri* (Grun.) V.H. (external view).
 fig. 9. *Navicula contenta* Grun. fo. *parallela* Pet. (external view).
 fig. 10. *Navicula mutica* Kuetz. (external view).
 fig. 11. *Melosira* sp. (external view).
 fig. 12. *Navicula nivalis* Ehr. (external view).

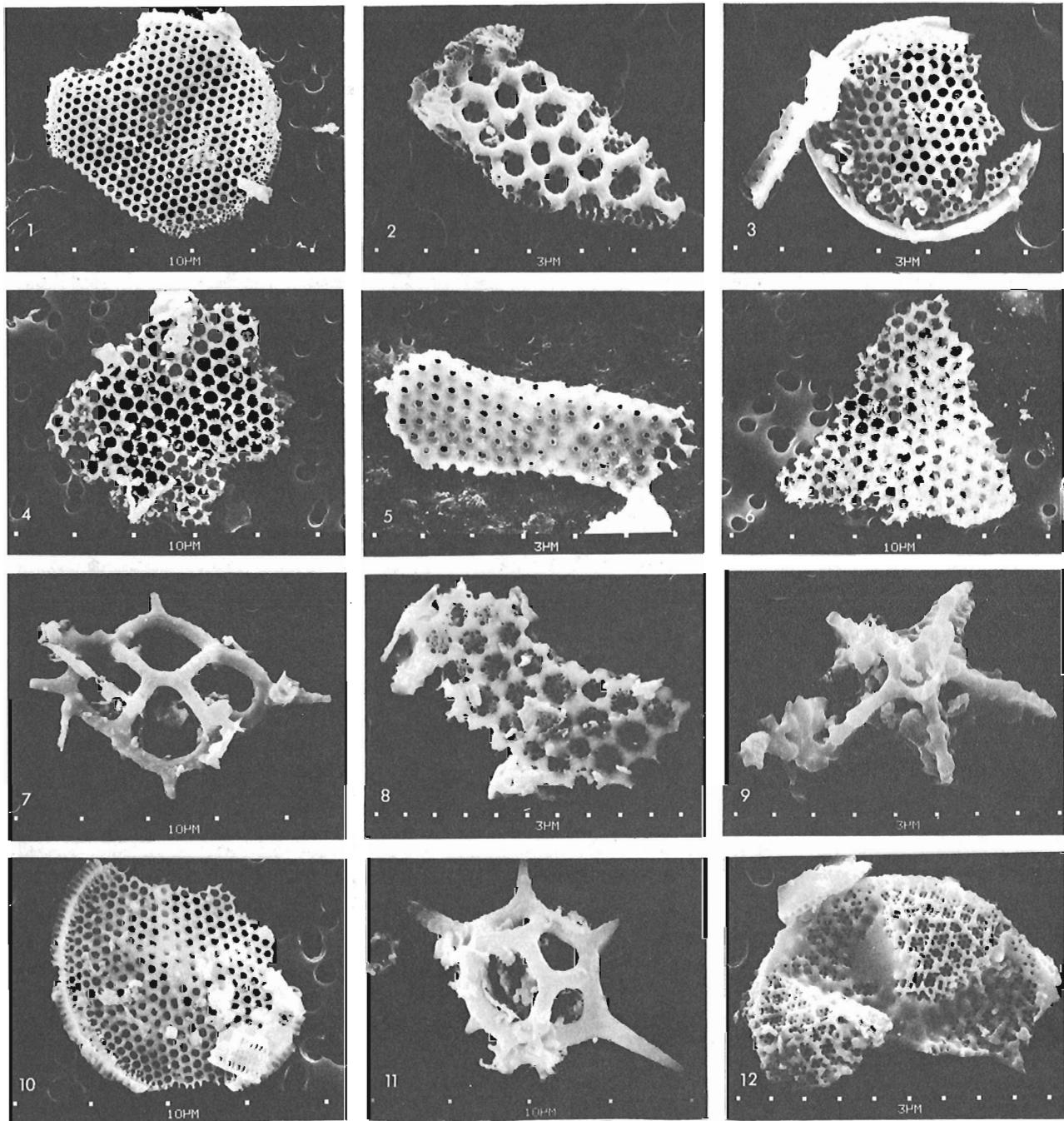


PLATE 29.2

Marine diatoms, diatom fragments, and silicoflagellates from precipitation samples.

fig. 1, 3. *Thalassiosira* spp. (external views).

fig. 2, 4, 5,

6, 8. Various centric fragments.

fig. 7. *Dictyocha fibula* Ehr. (oblique view).

fig. 9. *Discoaster* (?) (external view).

fig. 10. *Thalassiosira* sp. (internal view).

fig. 11. *Distephanus speculum* (Ehr.) Haeck. (oblique view).

fig. 12. *Actinoptychus undulatus* (Bail.) Ralfs (external view).

Table 29.2. Abundance of diatoms in precipitation samples from Cape Herschel, Ellesmere Island

Field/Lab numbers	Sample material	No. of diatoms /100 mL	No. of diatom fragments/100 mL	No. of diatom units/100 mL
<i>1984 Precipitation samples</i>				
#1-1984 DT-85-3	drifting snow	23 230	5 780	29 010
#2-1984 DT-85-1	newly fallen snow	27	10	37
<i>1985 Precipitation samples</i>				
#1-1985 DT-85-4	newly fallen snow	96	150	246
#2-1985 DT-85-5	newly fallen snow	303	336	693

blowing snow drifting along the ground surface. Furthermore, since it is well established that most of the organic and inorganic particles are removed from the atmosphere by precipitation "scour", duration and intensity of precipitation are of paramount importance as are the duration and time of collection. For example, differences in snow accumulation time, other parameters being equal (such as intensity of precipitation), would introduce a dilution factor affecting the sample with the longest collection time because the highest numbers of aerial diatoms are removed at the beginning, and significantly lower numbers or none at all are removed towards the end of a precipitation washout.

As regards the meltwater samples under investigation, the number of diatoms per volume does not accurately reflect the diatom load of the atmosphere. Nor can quantification be utilized on a comparative assessment basis, as the total volume for any sample, even if it were to contain the washout of all available diatoms, introduces a dilution/concentration factor based on duration and intensity of snowfall.

Because of the interplay of these variables, some of which are beyond human control or manipulation, extrapolation of influx rates on a comparative basis, at present, is unjustified. Yet despite the quantitative differences caused by meteorological and other factors, the mechanism itself of anemochorous (wind) dispersal of diatoms is neither rendered ineffective, nor is its impact diminished.

Concluding remarks

The data from this investigation confirm previous findings based on the diatom content of rime frost samples. They conclusively demonstrate the presence of micro-algae, in meaningful numbers, in freshly fallen snow, thus adding to the growing evidence of the effectiveness of aerial transport as a dispersal agent of diatoms.

It is hoped that in a future investigation the viability of airborne diatoms will be studied, in order to ascertain their tolerance towards various adverse conditions during aerial transport. Demonstration of such viability would undoubtedly

establish atmospheric diatom dispersal as a concept which not only explains the cosmopolitan distribution of most diatoms, but also accounts for the continuous recolonization of suitable habitats.

Acknowledgments

I extend my appreciation and gratitude to W. Blake, Jr. for collecting the sample material, for providing photographs, and for recording pertinent meteorological data.

References

- Lichti-Federovich, S.
1985: Diatom dispersal phenomena: diatoms in rime frost samples from Cape Herschel, Central Ellesmere Island, Northwest Territories; in *Current Research, Part B, Geological Survey of Canada, Paper 85-1B*, p. 391-399.
- Overeem, M.A. van
1937: On green organisms occurring in the lower troposphere; *Recueil des travaux Botaniques Neerlandais*, v. 34, p. 388-442.
- Pouchet, M.F.
1860: *Micrographie Atmosphérique. Corps organisés recueillis dans l'air par la neige; Compte rendu des séances de l'académie des sciences, Paris*, v. 50, p. 532-534.
- Spitz, W.U. and Schneider, V.
1964: The significance of diatoms in the diagnosis of death by drowning; *Journal of Forensic Sciences*, v. 9, p. 11-13.
- Spitz, W.U., Schmidt, H., and Fett, W.
1965: Untersuchungen von Luftfiltrationsstreifen aus verschiedenen Gebieten der Bundesrepublik auf ihren Diatomeengehalt. Ein Beitrag zum Beweiswert von Diatomeen für die Diagnose des Ertrinkungstodes; *Deutsche Zeitschrift der gerichtlichen Medizin*, v. 56, p. 116-124.

Stratigraphic setting of buried gold-bearing sediments, Beauceville area, Quebec¹

Project 690095

W.W. Shilts and S.L. Smith
Terrain Sciences Division

Shilts, W.W. and Smith, S.L., Stratigraphic setting of buried gold-bearing sediments, Beauceville area, Quebec; in Current Research, Part B, Geological Survey of Canada, Paper 86-1B, p. 271-278, 1986.

Abstract

Correlation of till sheets at two major, naturally exposed sections along Plantes River and in two boreholes drilled into the buried valley of Gilbert River is made on the basis of relative stratigraphic position, nickel concentrations in the clay size fraction, and the presence of ultramafic pebbles.

At Gilbert River, the uncharacteristic brown colour of the unoxidized tills, probably reflects glacial reworking of the highly weathered, gold-bearing material, thought to be the remnant of a preglacial colluvium, at the bottom of the boreholes. The rarity of occurrence of preglacial sediments and coincidence of preservation of the buried gold placer-bearing strata suggest that the possibility of a second coincidence, such as a local bedrock source for the gold, seems unlikely.

Résumé

La corrélation des couches de till dans deux importantes sections, exposées de façon naturelle, le long de la rivière des Plantes et dans deux trous de sonde forés dans la vallée enfouie de la rivière Gilbert, est faite en fonction de la position stratigraphique relative, des concentrations de nickel dans la fraction argileuse et de la présence de galets ultramafiques.

À la rivière Gilbert, la couleur brune non caractéristique des tills non oxydés reflète probablement le remodelage par les glaces de matériau aurifère très altéré gisant au fond des trous de sonde; il s'agit, croit-on, de restes de colluvions préglaciaires. La rareté de ce phénomène et la coïncidence de la conservation de strates enfouies de matériaux alluvionnaires de nature aurifère semblent indiquer que la possibilité d'une seconde coïncidence, comme un gisement d'or local dans la roche en place, s'avère peu probable.

¹ Contribution to Federal Asbestos Initiatives, Geoscience Research Program 1984-1987. Project carried by Geological Survey of Canada.

Introduction

Detailed descriptions of boreholes continuously cored through unconsolidated deposits to bedrock in 1984-85, as well as natural and man-made sections, were made to improve stratigraphic and sedimentological models of the Tertiary and Quaternary deposits of the Chaudière Valley region (Shilts and Smith, 1986). In order to reconcile modern stratigraphy with that of the buried gold-bearing strata east of Beauceville, two naturally exposed sections along Plantes River, located approximately 10 km northeast of Beauceville (Fig. 30.1), are correlated with two boreholes from Gilbert River. It is expected that the correlation of Gilbert River stratigraphy will aid the interpretation of the genesis of the gold, and subsequently, the methodology of gold exploration in a region long known for its buried and modern placer deposits.

In general, the glacial stratigraphy of Chaudière Valley has been compiled by many workers (Gadd, 1964, 1965, 1971; McDonald, 1967; McDonald and Shilts, 1971; Gadd et al., 1972; LaSalle et al., 1976, 1979; Shilts, 1978, 1981; LaSalle, 1980; Shilts and Smith, 1986) and the major glacial events have been accepted (LaSalle, 1984), but the gold-bearing sediments of Gilbert Valley (Boyle, 1979) have not been previously placed in proper stratigraphic context.

Glacial stratigraphy

Tills deposited by successive glaciers flowing from the northwest (Johnville), northeast (Chaudière), and northwest (Lennoxville) have been identified throughout Chaudière Valley. At present these tills are all thought to be of Wisconsin age.

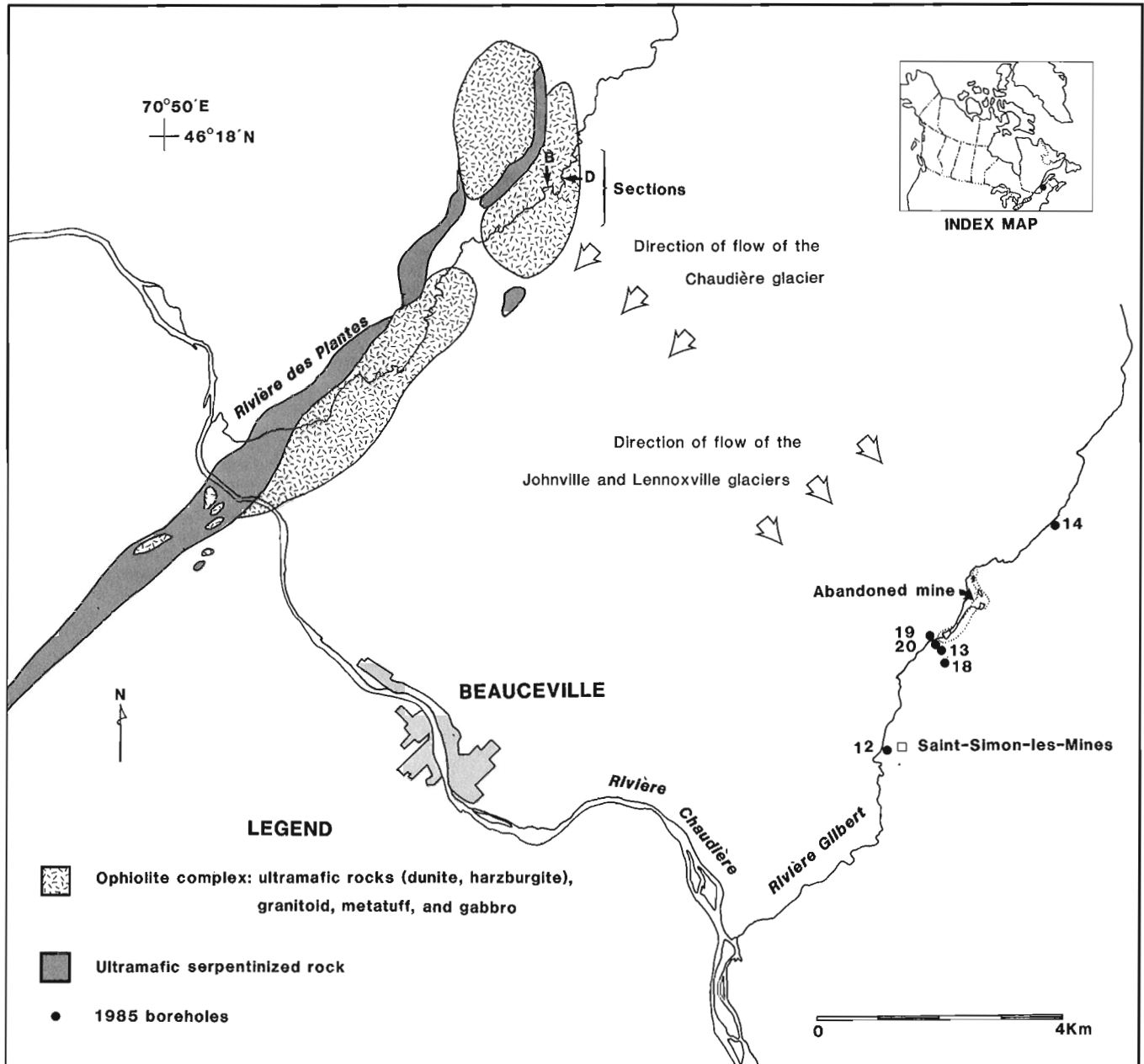


Figure 30.1. Location map showing position of Plantes River sections and Gilbert River boreholes in relation to ultramafic bedrock.

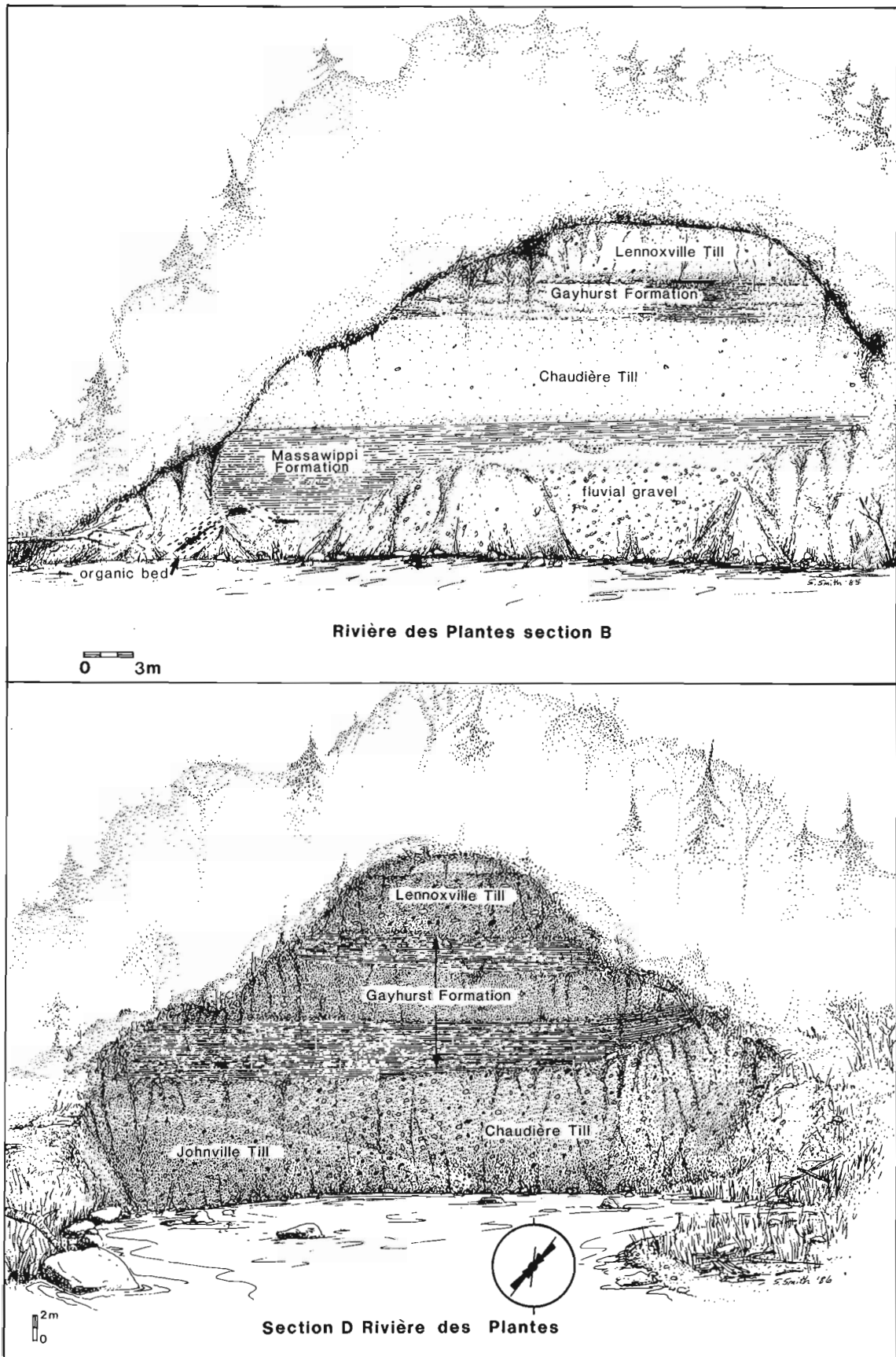


Figure 30.2. Illustrations of Plantes River sections B and D.

Lennoxville Till, representing the most recent glaciation, comprises the surface unit of most of the Chaudière Valley area and is commonly weathered to depths of 2 to 4 m. The oldest till (Johnville Till) also is commonly oxidized at its surface where it is exposed in sections in this region, but Chaudière Till has never been observed to be oxidized in sections or boreholes. All unweathered tills in Chaudière Valley contain abundant pyrite derived from pyritiferous slates and sandstones. Because of their high sulphide content, the tills are susceptible to rapid weathering, rendering them brown or tan. Where this process has occurred, associated sulphides and other labile minerals are destroyed making near-surface geochemical surveys of heavy minerals difficult to interpret. A till containing unoxidized pyrite is considered to be unweathered and is usually grey to olive grey.

A thick sequence of laminated glaciolacustrine silt and clay with deltaic, debris flow and subaqueous fan deposits of the Gayhurst Formation commonly separates the Lennoxville and Chaudière till sheets. The sequence of stratified sediments was deposited in a proglacial lake dammed by a glacier that stood south of St. Lawrence River against the Appalachian Highlands. Up to 75 m of laminated silt and clay deposited in this body of water was encountered in some boreholes of upper Chaudière Valley.

Whenever glaciers stood north of the St. Lawrence, allowing free northward drainage, fluvial sands, gravels, and floodplain deposits were formed. Sediments separating the Chaudière and Johnville tills comprise the Massawippi Formation and consist of fluvial gravels and sands, in some places overlain by laminated silty clay. The laminated sediments are typically mauve and may exhibit primary deformation due to overriding ice.

Pre-Johnville sediments are rare, comprising oxidized fluvial gravel and laminated silt where observed on Grande Coulée River (McDonald and Shilts, 1971).

Plantes River

Most of the major Pleistocene stratigraphic units known from the Appalachians are exposed in two sections 100 m apart along Plantes River (Fig. 30.2). The sections (B, D of Fig. 30.1) are located southeast of ultramafic outcrops that strike northeastward along the north side of Plantes River. Distinctive clasts and minerals eroded from the ultramafic outcrops have been incorporated into tills and associated waterlain sediments by glaciers that flowed from the Canadian Shield, southward or southeastward across the Appalachians. Sediments deposited by glaciers flowing from Appalachian dispersal centres located east or northeast of Plantes and Gilbert valleys contain little ultramafic debris. Sediments predating glaciation and formed by mass wasting and fluvial processes which modified and redistributed material formed by in situ weathering, likewise should not contain ultramafic components outside the drainage basin in which the ultramafic rocks outcrop.

At section D (Fig. 30.2), a compact, stony, grey lower till (Johnville Till) is oxidized to brown or tan at its surface. The hard lower till has a significant concentration of cobble-sized ultramafic clasts, consisting mostly of well rounded serpentized peridotites. Its fabric has not been measured here, but it must have been deposited by ice flowing from northwest in order to bring clasts from the ultramafic outcrops that lie less than 500 m northwest of the section. The lower till is overlain with sharp contact (Fig. 30.3) by a greyish mauve till (Chaudière Till) with fabric striking about northeast-southwest, roughly parallel to the strike of the adjacent ultramafic outcrops. The grey-mauve till is similar in colour and fabric to the lowermost till (Chaudière Till) at section B (Fig. 30.2) that lies on fluvial and lacustrine

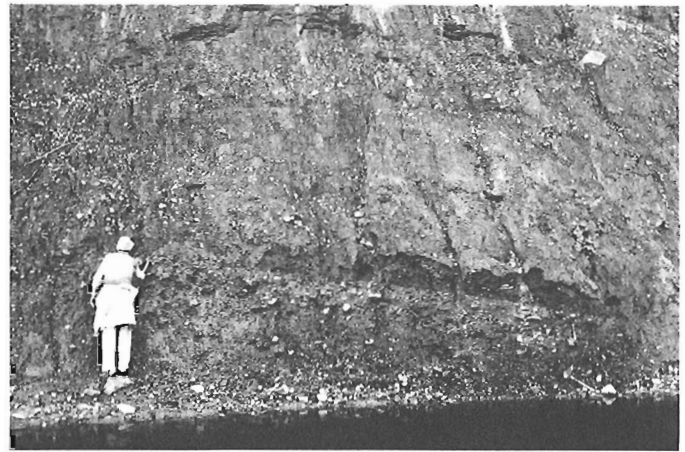


Figure 30.3. Contact of lower (Johnville) till overlain by Chaudière Till, section D, Plantes River.

sediments (Massawippi Formation) and, although not yet studied thoroughly, appears to contain few ultramafic erratics. The apparent lack of ultramafic debris indicates that there has been no reworking of debris from the lower till.

Interlaminated mauve clay and grey silt in 1 cm or thinner couplets underlie the mauve-grey till at section B. The mauve clay laminae presumably account for the slightly mauve hue of the overlying grey-mauve till. The laminated sediments are in turn underlain by a highly Fe-oxide-stained channel gravel flanked by sand (Massawippi Formation). The shape of the channel and texture of its sediments suggest a depositional environment not unlike the fluvial environment of the present site. Organic debris found within and below the base of the laminated sequence (Massawippi Formation) has yet to be satisfactorily dated, apparently being contaminated with modern plant debris where exposed.

In sections B and D, the grey-mauve, ultramafic-poor till (Chaudière Till) is overlain by grey, laminated silty clay (Gayhurst Formation) which is interbedded with compact, grey, matrix-supported, stony diamictos thought to be till and/or subaqueous mudflow deposits, the latter having slumped from a glacier front. The complex interbedding of the stratified unit is seen in both sections but has not yet been studied sufficiently to infer in detail the sedimentological circumstances of deposition. Lennoxville Till at the top of both sections is grey and contains ultramafic clasts.

Because the ultramafic lithologies impart a distinctive geochemistry to the glacial sediments derived from them, the geochemical characteristics of the tills at Plantes River are distinctive and useful as a stratigraphic tool. Nickel, in particular, is strongly enriched in till with ultramafic provenance. The three tills (assuming that the uppermost diamict is Lennoxville Till) exposed at section D have geochemical signatures that are diagnostic of the ice flow direction of their depositing glaciers. The nickel concentrations of the clay (<2 μ m) fraction of till on either side of the contact between the Johnville and Chaudière tills are 1248 ppm and 109 ppm, respectively. The uppermost till contains over 200 ppm nickel in its clay fraction. Similar contrasts could be drawn from chromium and cobalt, which also have a unique provenance in the ultramafic belt.

The geochemistry, fabric, clast lithology, and general sedimentological associations of the sections at Plantes River are easily correlated with the classic three-till stratigraphy of the southeastern Appalachians (McDonald and Shilts, 1971; Shilts, 1981). They probably represent the most complete stratigraphy

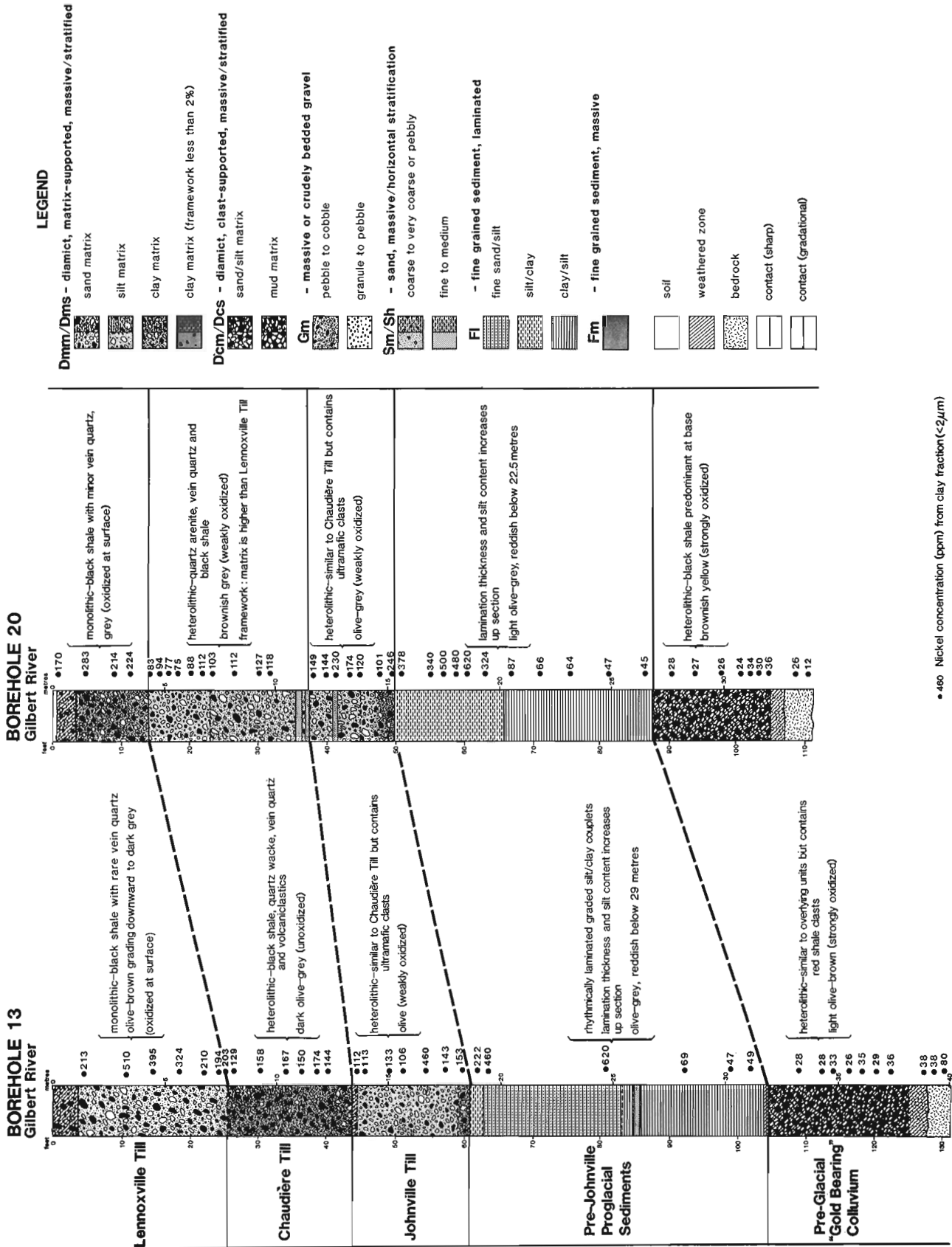


Figure 30.4. Detailed logs of Rivière Gilbert boreholes 13 and 20.

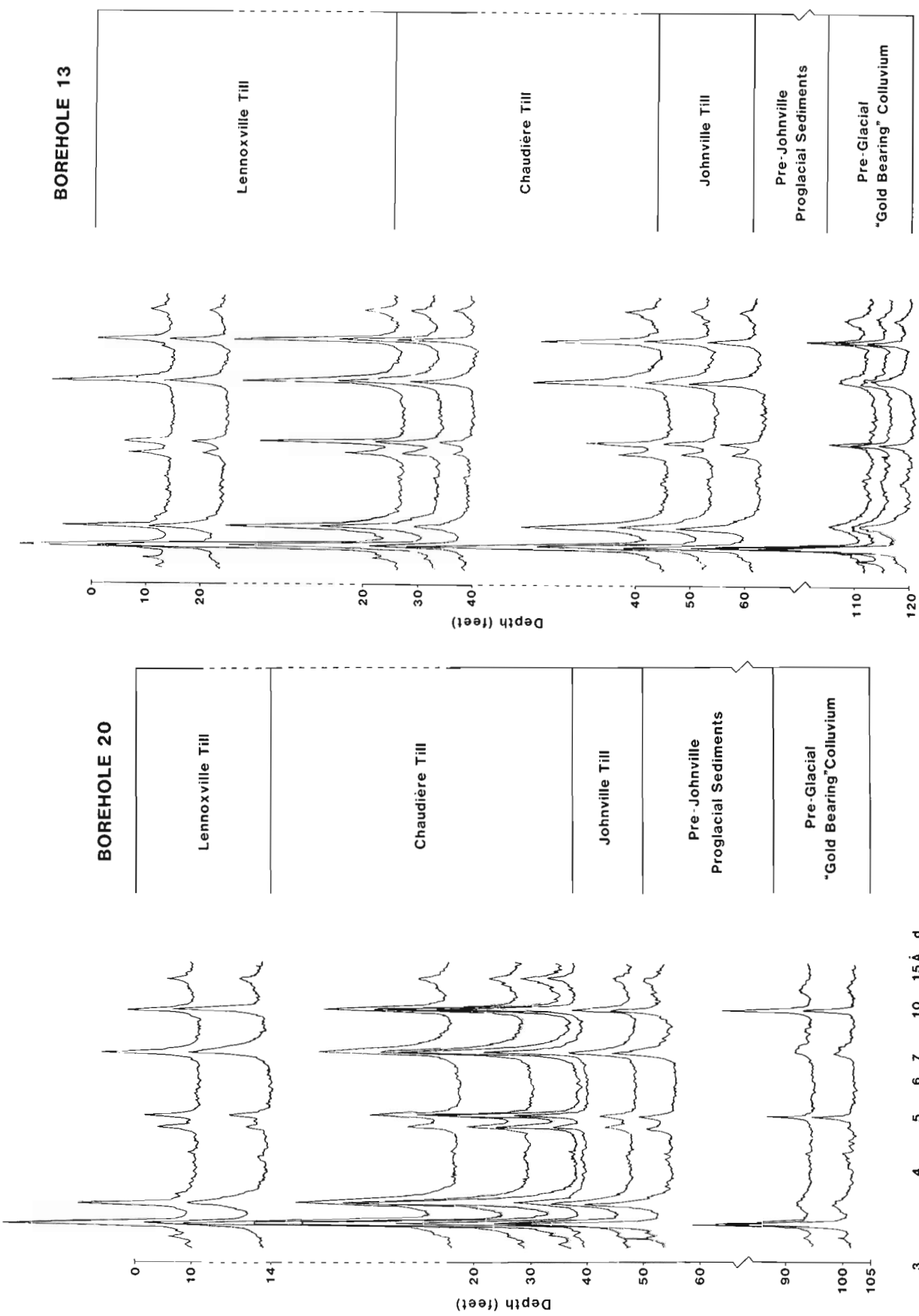


Figure 30.5. X-ray stratigraphy (Ni-filtered, $\text{CuK}\alpha$) of Gilbert River boreholes 13 and 20. Peaks at 14.2, 7.1, 4.7, 3.5 Å are interpreted as chlorite or degraded chlorite/mixed layer; 10.0, 5.0, 3.3 Å peaks are illite or similar mineral; 7.1 and 3.5 Å may include kaolinite, but this is considered unlikely in light of previous studies (Shilts, 1981); diffractograms of untreated samples were at ambient room temperature and humidity.

at any site yet discovered in the region. Section D, in particular, seems to expose almost the entire known Appalachian stratigraphy in one section, lacking only the fluvial beds of the Massawippi Formation to be complete. Massawippi fluvial beds are exposed in their proper stratigraphic position within 100 m of the section, however, and the oxidized upper surface of the lowermost till (Johnville) is almost certainly confirmation that its deposition was followed by a period of subaerial exposure. Conditions favourable for subsurface oxidation by groundwater, a process that easily can be confused with the results of subaerial weathering, are not present at this section.

Gilbert River

A series of boreholes were drilled across Gilbert Valley, just downstream from where a major gold-mining operation was carried out by dredging in the 1950s. The boreholes intersected a stratigraphic sequence that is similar to that described for Plantes River, but with some notable exceptions.

The surface till, exposed along the modern channel of Gilbert River adjacent to the dredge tailings, is compact and grey except near its surface where it is oxidized to a tan colour to a depth of about 2 m. It has strong northwest fabric and serpen-tinized peridotite erratics are readily apparent at its outcrop. There is little doubt that it was deposited by southeastward-flowing ice of the Lennoxville glacier.

The uppermost unit in nearby boreholes 13 and 20 (Fig. 30.4) is similar to the Lennoxville Till. However, this grey till, oxidized to tan at the surface, grades downwards into a sequence of brown tills with minor, interbedded laminated silt-clay and sandy waterlaid units. From the geochemistry, the brown till sequence can be split into nickel-rich and nickel-poor units (Fig. 30.4), permitting at least a tenuous correlation with the alternating nickel-rich (Johnville and Lennoxville) and nickel-poor (Chaudière) tills of Plantes River. On this basis, we have recognized what appears to be the established three-till, Johnville/Chaudière/ Lennoxville glacial sediment sequence. The almost complete lack of waterlain sediments is reminiscent of section D on Plantes River. Without clearly identifiable water-lain marker beds of the Gayhurst and Massawippi formations, and with no opportunity to spot the buried Johnville weathering zone because of the uniform brown or tan colour of all but the uppermost till, it is only on the basis of the geochemical characteristics associated with glacial erosion of the ultramafic complex that we were able to effect any stratigraphic interpretation.

Unlike the Plantes River sections, the Gilbert River till sequence rests on a basal unit of fine grained sand and laminated silt-clay. The silty clays of this sequence are strikingly grey compared to the overlying (Johnville?) till but are similarly enriched in nickel. This suggests that they were deposited in a proglacial lake by meltwater or density currents issuing from a southeast-flowing glacier carrying debris eroded from the ultramafic outcrops 10 km to the northwest along Plantes River.

At the base of boreholes 13 and 20, above highly weathered slate bedrock, 5 m or more of a yellow-brown, clast-supported diamict were cored. This is apparently the richest gold-bearing unit in the overburden and was the target of the numerous shafts sunk in this valley over the past century. It is not presently clear whether the dredge actually tapped the lowermost unit or the higher brown tills which superficially resemble it. No erratics were found in this lowermost unit and a preliminary assessment of its clay mineralogy (Fig. 30.5) indicates that it contains a well crystallized 10Å mica (illite?) and a highly degraded chlorite with possible mixed layer minerals. The clast-supported diamict is impoverished in nickel, containing consistently 26-36 ppm Ni in its clay fraction in both boreholes, the

lowest concentration yet noted in any from among thousands of samples analyzed from the region.

Based on preliminary geochemical and mineralogical examination of the Gilbert River boreholes, we feel that the lower diamict is probably pre-Quaternary in age, representing a pocket of weathered debris that was not completely stripped for some reason, probably topographic, by subsequent glaciations. We found little clear evidence of the fluvial gravel containing placer gold that is usually cited as the exploration target. We suspect that the diamict is a colluvial deposit made especially thick in the paleovalley bottom by contributions from mass wasting of adjacent slopes. It is possible that somewhere in the paleovalley there is a true fluvial gravel with significant gold concentrations, and that the boreholes simply failed to intersect it. Several grains of gold were recovered from the lower diamict as well as the overlying brown tills by Overburden Drilling Management, who processed several large samples.

The brown colour of the overlying tills is thought to result from glacial erosion and reworking of the colluvial deposit which was undoubtedly more extensive in the valley than it is now. If an unusually high amount of gold was concentrated in the colluvium or in associated fluvial sediments, there is probably an anomalous amount in the tills reworked from it, accounting for the high gold concentrations reported from the modern river channel which is cut mainly through the Lennoxville and Chaudière tills. Lennoxville Till was deposited after the colluvial source had been stripped by earlier glaciers or covered by their deposits. Thus, it is grey like most Appalachian tills, bearing, as in the case of Chaudière Till at Plantes River, section D, little reworked material from the underlying strata.

Conclusions

The excellent stratigraphic sections at Plantes River, located less than 10 km from the gold-bearing beds of Gilbert River, expose and confirm the established Appalachian Quaternary stratigraphy and provide a model and numerous petrological criteria with which to compare the sediments recovered from boreholes drilled through the gold-bearing strata in 1985. The same Pleistocene stratigraphic sequence is recognized from boreholes in Gilbert Valley.

Gilbert Valley is the only place known to the authors where preglacial brown colluvium is preserved and is overlain by brown tills, glacially reworked from it, suggesting that this type of gold-bearing sediment is rarely preserved in southeastern Quebec. Even if the colluvium did not outcrop, it could be expected that brown till derived from the colluvium would have been seen or encountered in the hundreds of natural sections and boreholes examined over the years by numerous geologists. Certainly this study shows that it is important to recognize the origin of brown coloration in glacial or other unconsolidated sediments of this region, particularly if the preglacial colluvium is found to have been enriched in gold.

Finally, special conditions that protected the gold-bearing colluvium from glacial erosion in Gilbert Valley are rare in this region, and the occurrence of buried gold placers so rare, that their association in this valley can be considered coincidental. The possibility of a second coincidence, that there happens to be a local bedrock source for the gold, seems unlikely. There is always the chance, however, that some characteristic imposed on the colluvium by a hypothetical mineralized source in the bedrock along ancestral Gilbert River caused the material to resist glacial erosion (cementation?), thus being responsible both for the gold enrichment and for preservation of the deposit. The fact that the colluvium was stripped from areas elsewhere in the valley and incorporated into the till would argue against such a hypothesis.

Acknowledgments

The authors express their thanks to R.N. Delabio for the X-ray diffractograms of samples from boreholes 13 and 20, and to R. Rainbird for his detailed logs and drafted figures for the Gilbert River boreholes. Both the Plantes River section study and the drilling in Gilbert River valley were discussed and carried out in close cooperation with Coniagas mining company through their consultant, Dr. Jacques Locat. Midwest Drilling carried out the stratigraphic drilling under a subcontract to our principal contractor, Roche Ltée. of Quebec City. All geochemical analyses were carried out by Chimitec Ltée. of Quebec City and gold analyses by Overburden Drilling Management of Nepean, Ontario. Thanks go to R.A. Klassen for critically reviewing this manuscript.

References

- Boyle, R.W.
1979: The geochemistry of gold and its deposits; Geological Survey of Canada, Bulletin 280, 585 p.
- Gadd, N.R.
1964: Surficial geology, Beauceville map-area; Geological Survey of Canada, Paper 64-12.
1965: Surficial geology, Chaudière River valley; in Report of Activities, Geological Survey of Canada, Paper 65-1, p. 115-117.
1971: Pleistocene geology of the central St. Lawrence Lowland (with selected passages from an unpublished manuscript "The St. Lawrence Lowland", by J.W. Goldthwait); Geological Survey of Canada, Memoir 359.
- Gadd, N.R., McDonald, B.C., and Shilts, W.W.
1972: Deglaciation of southern Quebec; Geological Survey of Canada, Paper 71-47, 19 p.
- LaSalle, P.
1980: L'or dans les sédiments meubles: Formation des placers, extraction et occurrences dans le sud-est du Québec; Ministère de l'énergie et des ressources du Québec, DPV-745, 26 p.
- 1984: Quaternary stratigraphy of Quebec: A review; in Quaternary Stratigraphy of Canada – A Canadian Contribution to IGCP Project 24, R.J. Fulton (ed.); Geological Survey of Canada, Paper 84-10, p. 155-171.
- LaSalle, P., Martineau, G., and Chauvin, L.
1976: Géologie des sédiments meubles d'une partie de la Beauce et du Bas Saint-Laurent, Québec; Ministère des richesses naturelles, DPV-438, 13 p.
1979: Lits de bryophytes du Wisconsin Moyen, Vallée-Jonction, Québec; Journal canadien des sciences de la terre, Vol. 16, p. 593-598.
- McDonald, B.C.
1967: Pleistocene events and chronology in the Appalachian region of south-eastern Quebec, Canada; Department of Geology, Yale University, 161 p. (Ph.D. thesis).
- McDonald, B.C. and Shilts, W.W.
1971: Quaternary stratigraphy and events in south-eastern Quebec; Geological Society of America Bulletin, v. 82, p. 683-698.
- Shilts, W.W.
1978: Detailed sedimentological study of till sheets in a stratigraphic section, Samson River, Quebec; Geological Survey of Canada, Bulletin 285, 30 p.
1981: Surficial geology of the Lac Mégantic area, Québec; Geological Survey of Canada, Memoir 397, 102 p.
- Shilts, W.W. and Smith, S.L.
1986: Stratigraphy of placer gold deposits; overburden drilling in Chaudière Valley, Quebec; in Current Research, Part A, Geological Survey of Canada, Paper 86-1A, p. 703-712.

Reconnaissance geochemical sampling of till, south-central Miramichi Zone, New Brunswick¹

Project 690095

**M. Lamothe
Terrain Sciences Division**

Lamothe, M., Reconnaissance geochemical sampling of till, south-central Miramichi Zone, New Brunswick; in Current Research, Part B, Geological Survey of Canada, Paper 86-1B, p. 279-287, 1986.

Abstract

Results of the first stage of reconnaissance sampling of till overlying rocks of the mineralized Miramichi Zone in the Woodstock map area are presented. This area is characterized by (1) Sn-W-Mo mineralization associated with extensive granitic intrusion in Devonian to Early Carboniferous time and (2) minor occurrences of sulphides partly associated with the Tetagouche Group. The clay fraction (<2 μ m) of 198 samples of till was analyzed for 16 elements. Geochemical response in till down-ice from known mineralized sources shows definite anomalous patterns. This suggests that a series of similar but isolated anomalies, such as Little Southwest Miramichi River (Cu, Zn, Mo, As), Burtt's Corner (As, Zn), and Bamford Brook Fault (As) areas, may be parts of dispersal trains extending from presently unknown mineralization.

Résumé

Ce rapport présente les résultats préliminaires d'un programme d'échantillonnage de reconnaissance des tills recouvrant les roches de la zone minéralisée de Miramichi, dans la région de Woodstock. La région est caractérisée par 1) une minéralisation de type Sn-W-Mo associée à de larges intrusions granitiques datant du Dévonien au Carbonifère inférieur et 2) quelques manifestations de sulfures en partie associés au groupe de Tétagouche. La fraction argileuse (<2 μ m) de 198 échantillons de till a été analysée pour 16 éléments. La réponse géochimique dans des tills localisés en aval de l'écoulement glaciaire à partir de zones minéralisées démontre l'existence de configurations anormales. Ce phénomène semble indiquer qu'une série d'anomalies isolées comme celles près de la Petite rivière Miramichi Sud-Ouest (Cu, Zn, Mo, As), Burtt's Corner (As, Zn) et l'anomalie d'arsenic avoisinant la faille de Bamford Brook peuvent faire partie de traînées de dispersion développées à partir de zones minéralisées non identifiées à ce jour.

¹ Contribution to Canada-New Brunswick Mineral Development Agreement 1984-1989. Project carried out by Geological Survey of Canada.

Introduction

Prospecting in areas of glaciated terrain has become a major concern in mineral exploration during the last two decades with the drastic reduction of new discoveries of the so-called "easy-to-find" ores. Modern drift exploration techniques have been developed particularly in Finland (Kauranne, 1975; Wennervirta, 1968) and are now being applied to other countries such as Canada (Shilts, 1984).

As part of the Canada-New Brunswick Mineral Development Agreement, the Geological Survey of Canada has initiated a geochemical study of the glacial sediments overlying the mineralized Miramichi Zone in New Brunswick. This preliminary report presents the results of the first stage of a reconnaissance survey conducted over the south-central part of the zone. The area over which tills were sampled is located in the Woodstock map area (Fig. 31.1). The study area is drained by two major rivers, the Saint-John and the Miramichi. Local relief exceeds 400 m; the highest elevations (500 m a.s.l.) are found in the northern part of the map area.

Bedrock geology and mineral occurrences

The pre-Carboniferous rocks of New Brunswick are divided into five tectonostratigraphic zones bounded by major fault systems (Ruitenberg et al., 1977; Fig. 31.1). The Miramichi Zone is a belt mainly composed of Cambrian and Ordovician sedimentary and volcanic rocks (Tetagouche Group), poly-deformed and slightly metamorphosed during the Taconic Orogeny. They were later intruded by large bodies of Devonian to Lower Carboniferous granites during the subsequent Acadian and Hercynian orogenies. These granites underlie a significant part of the map area. The core of the zone, though, is composed of paragneiss, amphibolites, and schists that may be as old as late Precambrian (Fyffe, 1985). Patterns of mineralization in the Miramichi Zone reflect the two major geological events recorded in the area.

The Tetagouche Group hosts the well known stratabound sulphide deposits that have been extensively mined in the Bathurst area to the north. In the Woodstock map area, one such stratiform deposit is worthy of mention, that is, the Sisson

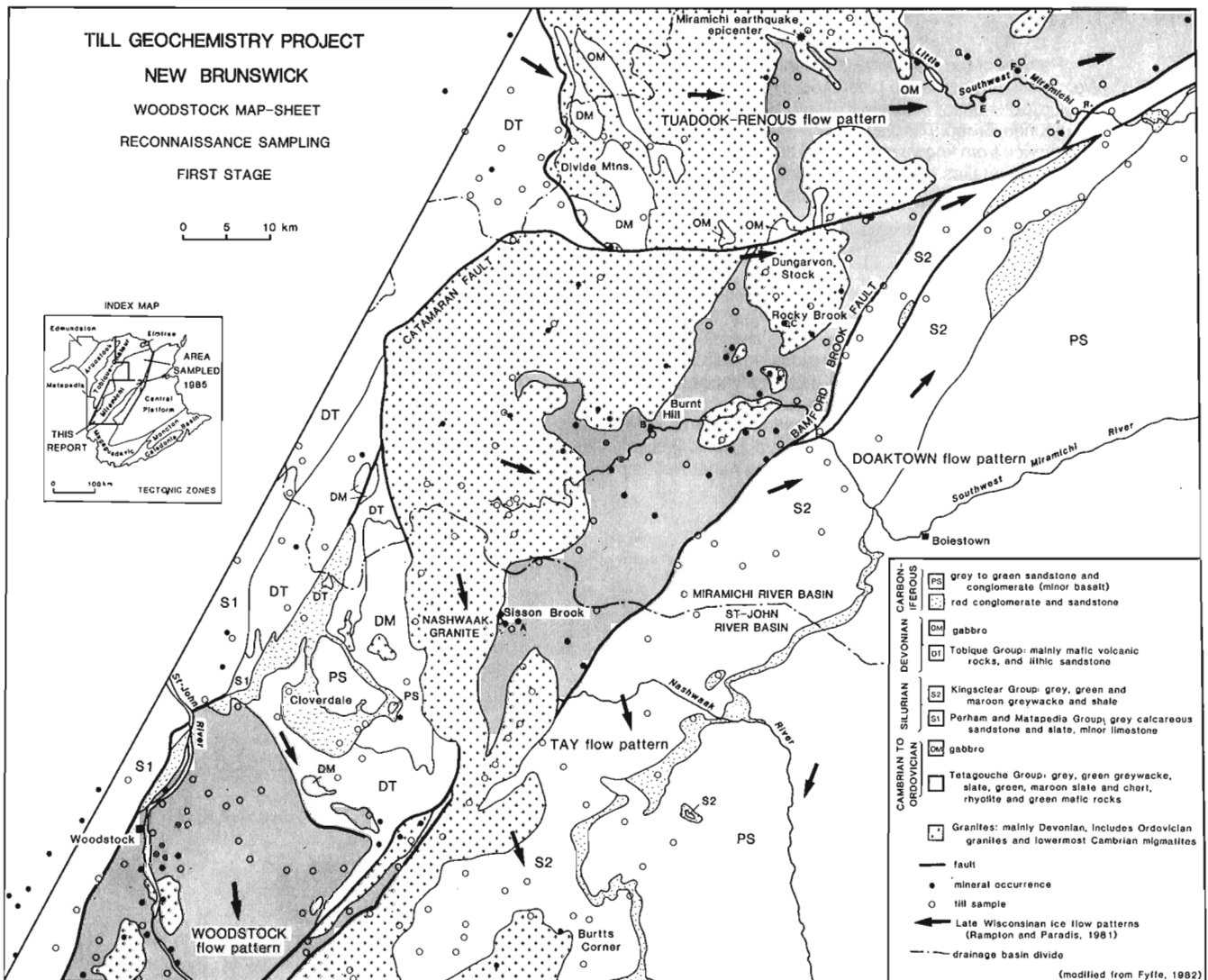


Figure 31.1. Location map and simplified geology map (from Fyffe, 1982) of the study area showing mineral occurrences and till sampling sites. Areas of mineral occurrences discussed in text: A. Sisson Brook East; B. Burnt Hill; C. Rocky Brook; D. Sisson Brook West; E. Little Southwest Miramichi River; F. Shore Camp Brook; G. Guagus Stream.

Brook East deposit (A of Fig. 31.1) which hosts Zn, Ag, Pb, Sb, and Cu. Elsewhere, most mineral occurrences are greisen and related endogranitic veins and disseminations, in general associated with the emplacement of the granite bodies (Ruitenberg and Fyffe, 1985). Tin, tungsten, and molybdenum are the major metals occurring in these deposits with locally important F, Be, Cu, Pb, and Zn. The Burnt Hill deposit (B of Fig. 31.1) is a wolframite-molybdenite-cassiterite-bearing greisen vein swarm that outcrops at the southern edge of the Burnt Hill granite; it was mined until 1956 (Poole, 1963). The Rocky Brook deposit (C of Fig. 31.1), associated with the Dungarvon stock, hosts mainly cassiterite with minor fluorite and beryl. The Sisson Brook deposit (D of Fig. 31.1) occurs in the aureole of the Nashwaak granite. Here, in addition to wolframite and molybdenite, scheelite and metallic sulphides are abundant. The two last deposits have been claimed and surveyed by Kidd Creek Mines Ltd. (Snow and Coker, in press). Numerous vein-type and porphyry-copper showings are documented in the map area (Fig. 31.1) and include Fe, Mn, Cu, Pb, Zn, W, Sn, F, Ag, and Au occurrences. The reader is referred to Fyffe (1982) for the specific nature and location of these occurrences.

Rocks of the Miramichi Zone are bound by deformed Silurian to Devonian sediments and volcanics of the Aroostook and Tobique tectonostratigraphic zones to the northwest and by Silurian greywacke and slates of the Magaguadavic Zone, to the southeast. Minor mineral occurrences have been described in the former. Barren Carboniferous rocks overlie the entire southeastern part of the study area and form two nearly circular outliers in the west, one of which is found in the Cloverdale area. The rocks are gently dipping, nondeformed sandstone, shale, and conglomerate which are mostly green and grey; however, the lower part of the sequence is composed of redbeds.

Aspects of glacial geology

The Quaternary geology of the Woodstock map area has been described by Rampton and Paradis (1981). The area has been glaciated during the last part of the Late Wisconsinan glaciation, and deglaciation was completed by 12.5 ka. Ice flow

patterns based on the youngest generation of striae (Rampton and Paradis, 1981) are shown in Figure 31.1. The divergence one can observe between the Tay and the Doaktown flow patterns is believed to have controlled the last depositional event and could have been caused by the obstruction of the Gaspereau ice centre which was located over the New Brunswick Lowland (Rampton et al., 1984). A study of pebble composition in till is in progress to relate the depositional sequence to the erosional indicators, but geochemical dispersal seems to confirm the trends already suggested by those authors (see below). It is not known if the ice that was flowing over the highlands of the Miramichi Zone during the last glaciation was of Laurentide origin. A major Appalachian ice centre which was present in latest Wisconsinan time over northern Maine and northwestern New Brunswick (Rampton et al., 1984) controlled till deposition in Saint-John River valley (Lowell, 1985; Rappol, this volume). Laurentide erratics are present, however, in the valley down to its confluence with Tobique River. One such cobble, collected in the Grand Falls area, 100 km north of Woodstock, has been dated at ca. 1100 Ma (K-Ar; GSC 80-3100; V.K. Prest, personal communication, 1986). When these rocks were initially transported into the area remains unknown. Moreover, the occurrence of similar appearing paragneiss in the central part of the Miramichi Zone dramatically limits the type of evidence required for any demonstration of a former presence of Laurentide ice in the area.

Over the Miramichi Highlands, till is generally thin (<1.5 m) and displays the classical lodgment-ablation till couple. In most till exposures, the lower part of the till is dense, sandy, and grey. It is yellowish brown where oxidized. The upper part is commonly loose, more stony, and yellowish brown to yellow.

A belt of thick till defines a major NNE-SSW belt that is geomorphologically expressed as hummocky, ribbed, and rolling moraine (Rampton and Paradis, 1981). According to them, this zone represents an ice marginal position of the Millville-Dungarvon phase during deglaciation of the area. The morainic belt, however, is developed preferentially over the granite bodies, some part of which are intensively weathered (Léveillé,

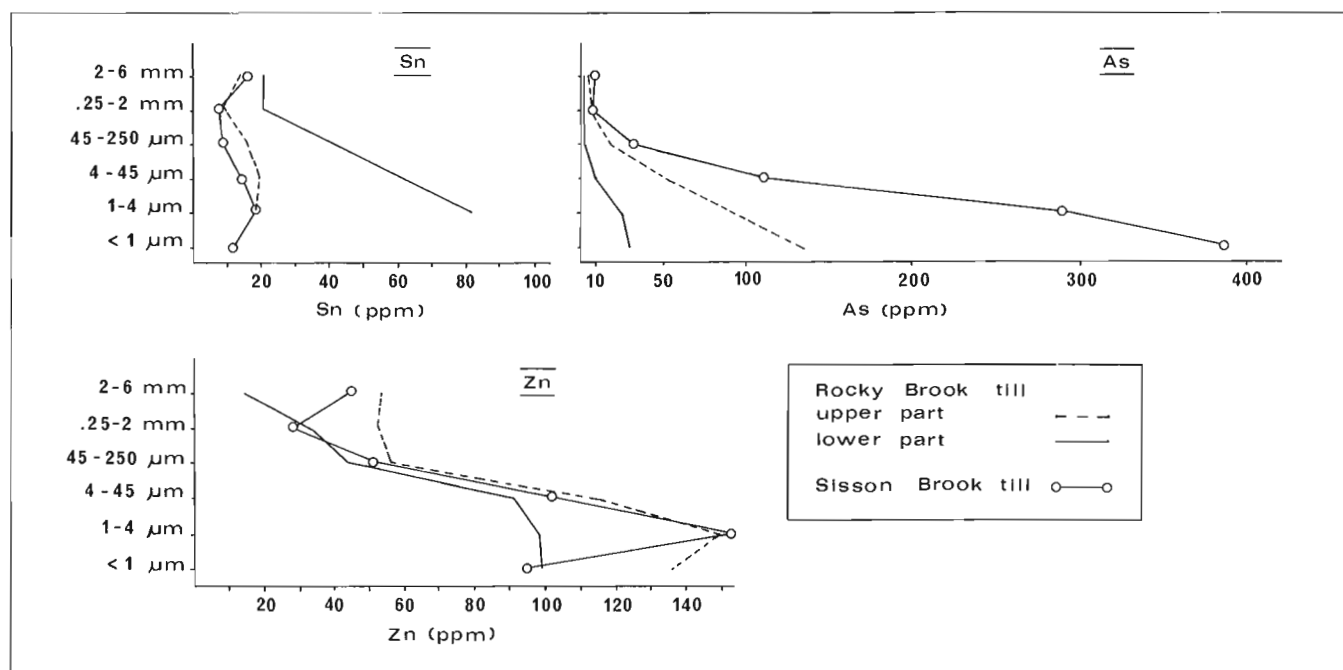


Figure 31.2. Abundance of Zn, Sn, and As in different grain size fractions in till.

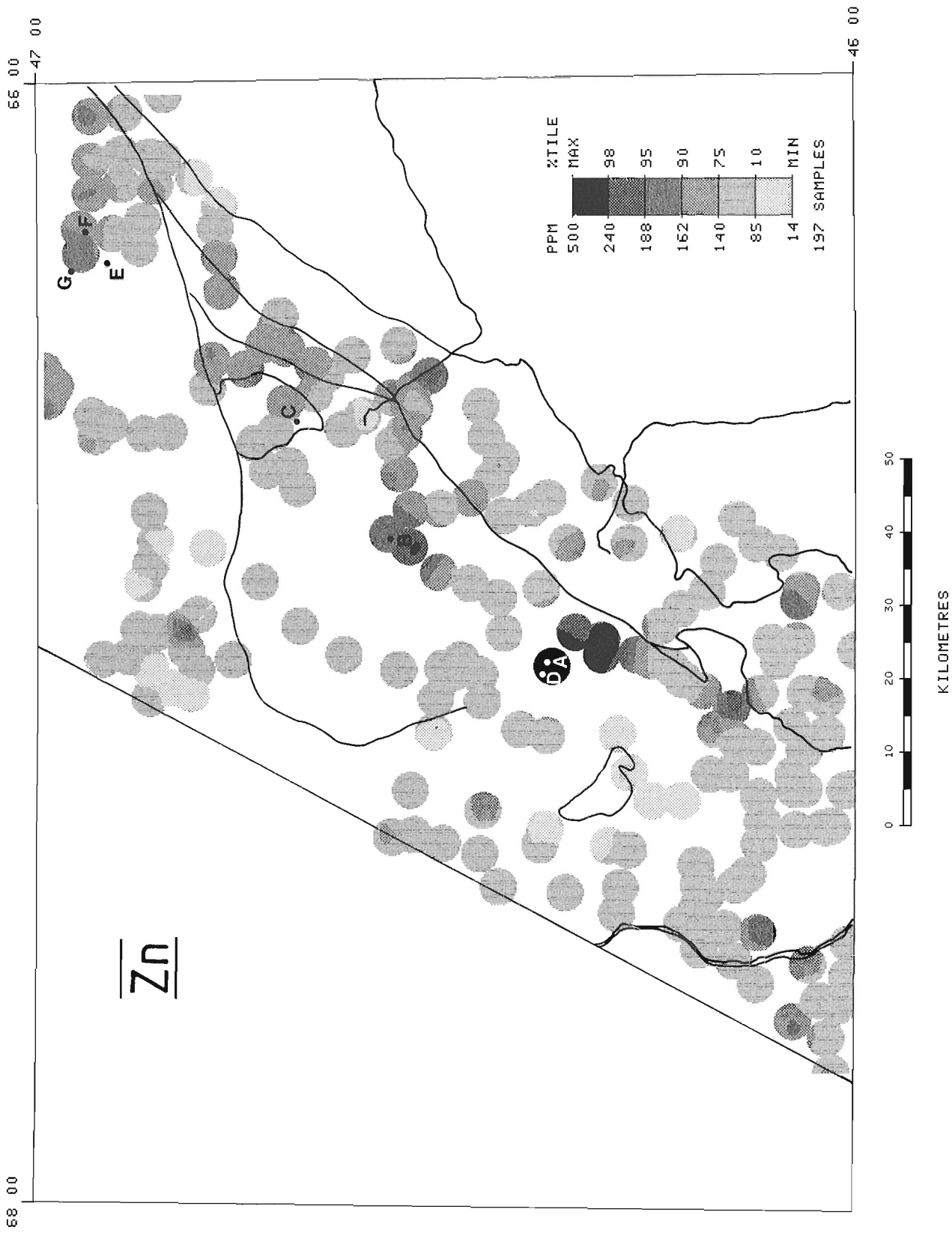


Figure 31.3. Zinc abundance in clay sized fraction of till, south-central Miramichi Zone. A few geological features are shown (cf. Fig. 31.1).

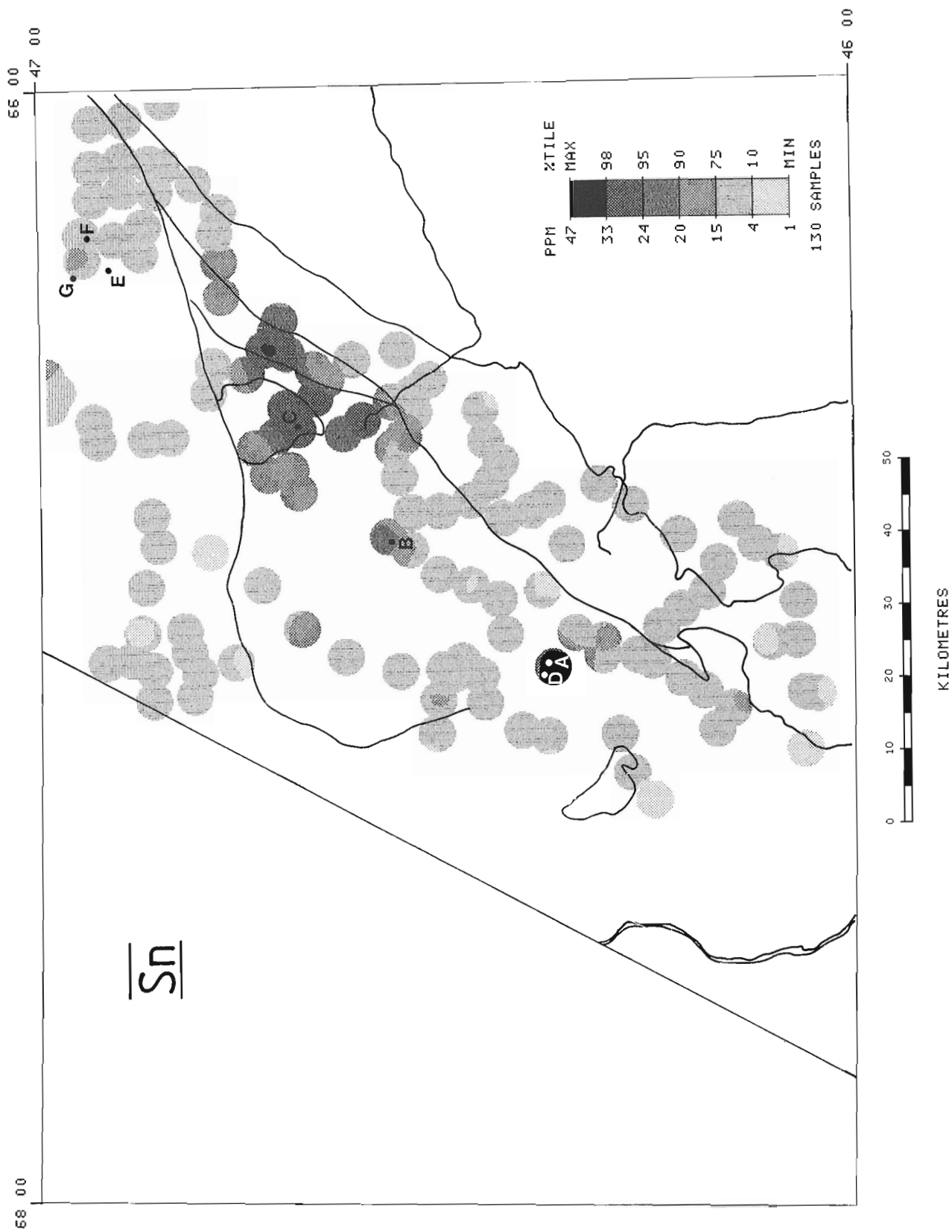


Figure 31.4. Tin abundance in clay sized fraction of till, south-central Miramichi Zone. A few geological features are shown (cf. Fig. 31.1).

1977). A high density of rock debris at the base of the ice could have resulted in ice flow deceleration and extensive subglacial till deposition. The bedrock control on the course of this morainic belt and the paleogeographic implications are discussed elsewhere (Lamothe, 1985).

Reconnaissance till sampling program

During the summer of 1985, samples of till were collected along road exposures at every 5 to 8 km where possible. Some trenches were also visited and sampled in the Rocky Brook and Sisson Brook area, on properties of Kidd Creek Mines Ltd, and in the area of the Miramichi Earthquake Epicenter. Because of lack of time and difficult access, some areas have a low sample density. Some of the data collected by Kettles and Wyatt (1985; 60 samples) were used in the geochemical compilation. The resulting density is one sample per 45 km². Care was taken to sample the tills in the C horizon; most were slightly oxidized. The tills were analyzed for Cr, Mn, Fe, Co, Ni, Cu, Zn, Mo, Ag, Cd, Pb, W, As, U, Sn, and F. Geochemical procedures have been described by Kettles and Wyatt (1985); in addition to these procedures, W was determined by colorimetry and Sn by XRF. Data processing and storage have been described by Burns (1985). Data were contoured for the 10th, 75th, 90th, 95th, and 98th percentiles. Powderized aliquots of 47 samples of clasts in till samples collected in the Dungarvon area (Plouffe, 1986) and selective grain size fractions of three till samples were also analyzed after total leach.

Results and discussion

Statistical data and percentile contours have been processed for each element; however, only the Cu-Pb-Zn and Sn-W-Mo assemblages and the As data will be discussed below. In this report, due to the scale of the geochemical survey, the 90th percentile will be considered as "anomalous".

Metal partitioning in till

Traditionally, geochemical studies in New Brunswick have been concentrated mainly on the heavy mineral fraction of stream sediments (Austria, 1976; Bamwoya, 1978; Poole and Lachance, 1979) or various grain size fractions of soils (Govett, 1973). Research in the geochemistry of tills has demonstrated the enrichment of most metals in the fine fraction of tills (Shilts, 1975, 1984; Nikkarinen et al., 1984). This partitioning is thought to be particularly strong for anomalous samples. W.W. Shilts (GSC) collected three samples from the two Kidd Creek properties and analyzed them after grain size fractionation and total leach; the results shown in Figure 31.2 confirm such partitioning for the metals investigated. Among other elements, Cu, Pb, Zn, As, Sn, W, and Mo are found to be concentrated in the fine fraction of the till. The clay sized fraction of the two Rocky Brook till samples are dominated by chlorite (kaolinite?) and illite with minor mixed layer and/or expandible phyllosilicates. Preglacial weathering may have enhanced the metallic anomalies but since the bedrock is indeed mineralized at this site, some preliminary processes must be responsible for the observed enrichment in the fines. Fine grained metallic dissemination in the vicinity of the ore could be one process. This is particularly true for the till overlying the Sisson Brook deposit from which highly anomalous values are measured. Whatever the nature of the process, the consequence of this partitioning is that the analysis of a bulk till sample may in part depend on the clay content of the sample (Shilts, 1975, 1984). The clay fraction (<2 μ m) of the till samples was therefore analyzed systematically in this reconnaissance program.

Cu-Pb-Zn assemblage

These three elements show similar patterns of distribution. Zinc data are shown in Figure 31.3. Individual data cannot be discussed in this paper but, some general comments can be made.

In spite of limited data, the general background values do not seem to be dependent on rock types, except for the samples located over the Carboniferous redbeds. Those samples have lower metal concentrations, a fact which might reflect the influence of an oxidizing environment at the time of sedimentation.

A series of samples located southeast from the Sisson Brook area, although not closely spaced, suggest the presence of a diffuse dispersal pattern. Anomalous zinc values can actually be traced for at least 5 km from the postulated source, assuming absence of any other zinc source along the glacier path.

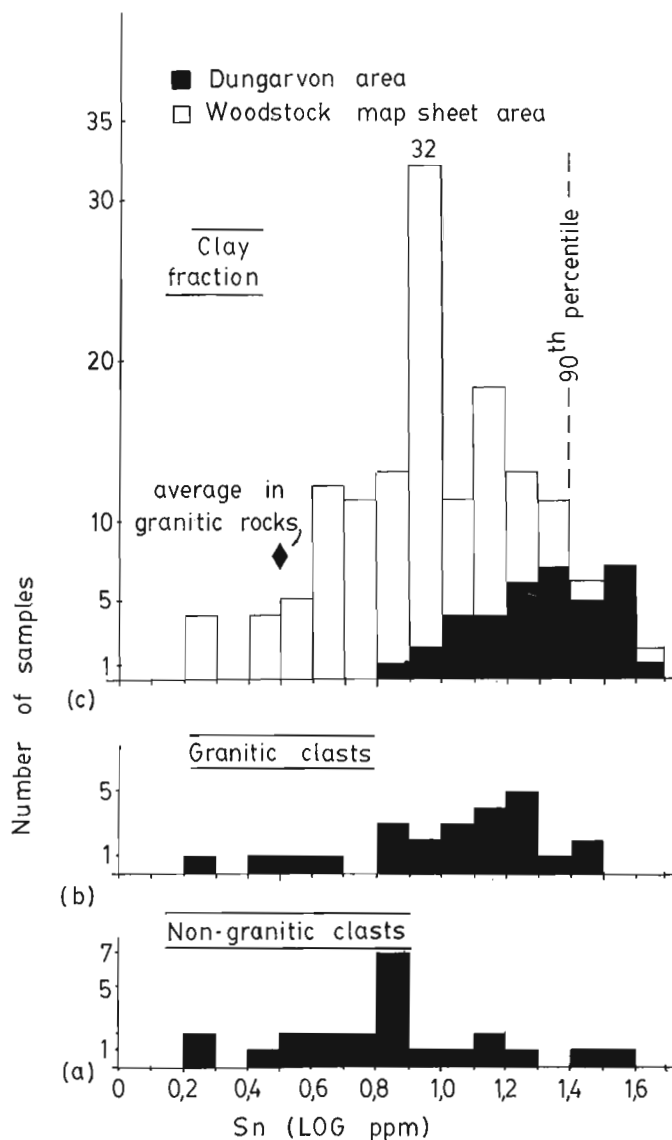


Figure 31.5. Frequency distribution for tin in (a) nongranitic clasts, (b) granitic clasts, and (c) clay sized fraction of till, Dungarvon area.

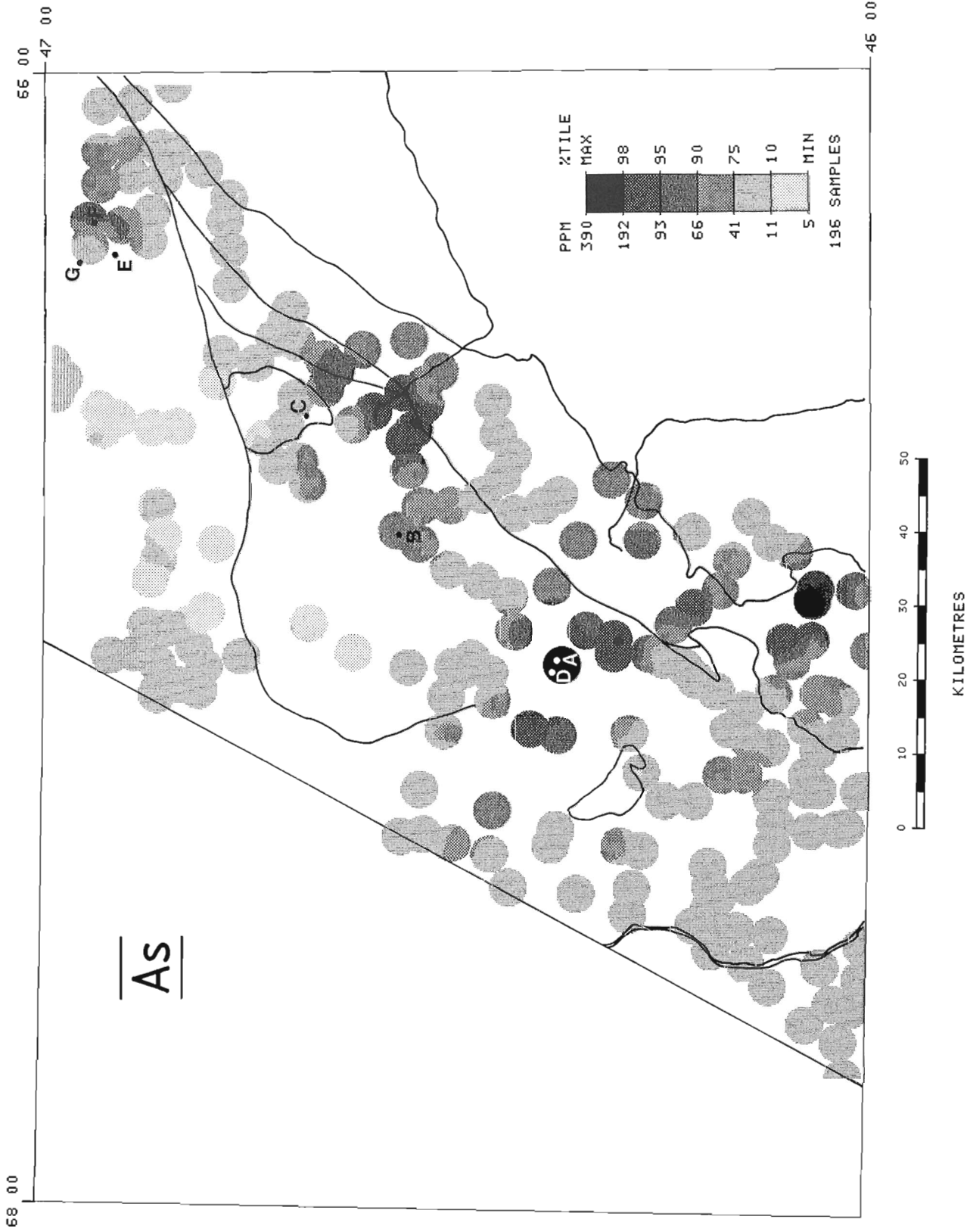


Figure 31.6. Arsenic abundance in clay sized fraction of till, south-central Miramichi Zone. A few geological features are shown (cf. Fig. 31.1).

The northeastern sector (Little Southwest Miramichi) is anomalous with respect to the three metals, especially Cu and Pb. Small scale showings have been documented in the general area surrounding these anomalies (for example, Little Southwest Miramichi (E), Cu, Au; Shore Camp Brook (F), Pb).

Some other anomalous values could belong to unknown dispersal trains or could be false anomalies since, to the knowledge of the author, they do not seem to be related to any nearby mineral occurrence; such is the case in the Burtts Corner area.

Sn-W-Mo assemblage

The contoured data for the "granophile" elements show similar patterns. Tin data are shown in Figure 31.4. (Samples collected by Kettles and Wyatt (1985) were not analyzed for Sn and W).

Overall, the contrast between the 98:95:90th percentile is rather low; this may be due to low crustal abundance. Even with such "poor" contrast, however, the clay geochemistry reflects the mineralization. In Figure 31.5, the histograms of the log normal Sn values obtained from the clay fraction of all the samples analyzed are compared to the Sn values measured for the granitic and nongranitic clasts separated from the tills collected in the Dungarvon area and in the Rocky Brook trenches. These histograms demonstrate that (1) the Dungarvon clay data are grouped in the upper tail of the regional Sn distribution and (2) the Sn values for the clasts are all much higher than the average 3 ppm in granitic rocks (Taylor, 1964) which means that the area is anomalous with respect to Sn and that mineralization is reflected in the nongranitic clasts as well (here the Tetagouche lithologies). This is the result of the common occurrence of granophile mineralization along the edges of the granitic bodies. It should be noted that the contrast between the geochemical data in the clasts is so high that, probably, litho-geochemistry may not have been efficient in detecting the source rock.

Like the metallic sulphides, the Sn-W-Mo assemblage is anomalous southeast of Sisson Brook (D). Weaker anomalous patterns originate from the two other well documented deposits in the Burnt Hill (B) and Dungarvon (C) area. Indeed, a definite anomalous belt extends northeastward from the Rocky Brook (C) tin mineralized zone. This "dispersal" is most probably of glacial origin because it is parallel to the Renous ice flow pattern.

Isolated anomalies occur and could be related to unknown sources. The two sectors already identified as potential sites for sulphides, the Little Southwest Miramichi and Burtts Corner area can also be considered as granophile targets.

As data

Because of renewed interest in gold exploration in New Brunswick (Ruitenberget al., 1985), special attention should be given to one of its pathfinders – arsenic. The contoured data for this element are shown in Figure 31.6. Apart from the till from Sisson Brook, which is anomalous for almost every element analyzed, many other zones are found to be anomalous with respect to As.

The Little Southwest Miramichi River area shows As anomalies which could be related to known gold occurrences such as the Guagus (G) showing.

The Burtts Corner anomaly cannot be linked to any documented occurrence of arsenopyrite or gold based on the geology of the area.

The As anomaly which can be followed along the Bamford Brook Fault could be related to numerous small occurrences of arsenopyrite associated to the Burnt Hill intrusive event (Poole, 1963). These occurrences have been mapped in an up-glacier

direction, west-southwest of the anomaly. The trend of the anomaly, however, is at an angle to both the Doaktown and Renous ice flow patterns.

These two last anomalies in till partly overlie the rocks of the Maguagadavic zone, in which occurs the Lake George Tungsten-Antimony-Gold deposit (Ruitenberget and Fyffe, 1985), located south of the study area.

Conclusions and recommendations for future work

Govett (1973) suggested that glaciation has played a minor role in New Brunswick in the geochemical dispersal of economic elements compared to other surficial physico-chemical factors such as drainage and soil processes. In the south-central Miramichi Zone, however, good geochemical response is found in the clay fraction of the tills. Discrete geochemical anomalies trends originate from known mineralized bedrock source and appear to be displaced for some kilometres in the direction of the last ice flow.

Typical assemblages of metallic sulphides and granophile elements remain relatively coherent in the glacial sediments. This reflects clastic dispersal of the bedrock without influence of major secondary processes, at least at a reconnaissance scale. This is demonstrated, for example, by the association of sulphide to granophile minerals along the Sisson Brook anomaly and the relative depletion of these sulphides in the Burnt Hill and Rocky Brook area, in the bedrock as well as in the tills: "The Sisson Brook Deposit, in the contact aureole of the Devonian Nashwaak Granite, differs from the Burnt Hill Deposit in that scheelite and metallic sulphides are relatively more abundant and the deposit is generally fine-grained." (Ruitenberget and Fyffe, 1985, p. 209).

Future work in 1986 will focus on the following: (1) completion of the reconnaissance coverage; (2) detailed modelling of geochemical, mineralogical, and lithological dispersal trains in areas of major mineral occurrences; attention will be paid to possible hydromorphic and soil-forming processes in oxidized tills; and (3) follow-up sampling in new target areas such as the Little Southwest Miramichi River, Burtts Corner, and Bamford Brook Fault areas.

Acknowledgments

The author wishes to thank W.W. Shilts and M. Rappol for critically reading this report. W.W. Shilts provided the initial input in this project. Thanks are extended to W.W. Gardiner of Kidd Creek Mines Ltd. for permitting access to trenches, M. Rappol for sharing ideas on the glacial geology of New Brunswick, and I.M. Kettles and P.H. Wyatt for the use of their data. N. Blais, J. Macey, L. Michaud, A. Plouffe, and J. Sacré provided field assistance.

References

- Austria, V.
1976: Stream and spring sediment geochemistry map, Napadogan West (21 J/7W); New Brunswick Department of Natural Resources, MP 76-76, 7 maps.
- Bamwoya, J.J.
1978: Exploration geochemistry in the Burnt Hill area, New Brunswick: Distribution of elements in bedrock and in heavy and light fractions of stream sediments; University of New Brunswick, Saint John, 377 p. (PhD thesis).
- Burns, R.K.
1985: Data storage and processing in Terrain Sciences Division; in Current Research, Part B, Geological Survey of Canada, Paper 85-1B, p. 475- 478.

- Fyffe, L.R.
1982: Geology, Woodstock; New Brunswick Department of Natural Resources, Map NR-4.
1985: Amphibolites of the Miramichi Highlands; in New Brunswick Report of Activities, Project Résumés, Abbott A.S. (ed.) p. 26-28 (abstract).
- Govett, G.J.S.
1973: Geochemical exploration studies in glaciated terrain, New Brunswick, Canada; in *Prospecting in Areas of Glacial Terrain*, Institute of Mining and Metallurgy, London, p. 11-24.
- Kauranne, L.K.
1975: Regional geochemical mapping in Finland; in *Prospecting in Areas of Glaciated Terrain*; Institute of Mining and Metallurgy, London, p. 128-137.
- Kettles, I.M. and Wyatt, P.H.
1985: Applications of till geochemistry in southwestern New Brunswick: Acid rain sensitivity and mineral exploration; in *Current Research, Part B*, Geological Survey of Canada, Paper 85-1B, p. 413-422.
- Lamothe, M.
1985: Sédimentologie glaciaire et paléogéographie quaternaire, partie centrale du Nouveau-Brunswick; ACFAS, 54^e Congrès annuel, Montréal (résumé).
- Léveillé, J.
1977: Inventory of weathered granite deposits of New Brunswick; New Brunswick Department of Natural Resources, Open File 77-12, 38 p.
- Lowell, T.V.
1985: Late Wisconsin ice-flow reversal and deglaciation, northwestern Maine; in *Late Pleistocene History of Northeastern New England and Adjacent Quebec*, H.W. Borns, H.W., P. LaSalle, and W.B. Thompson (ed.); Geological Society of America, Special Paper 197, p. 71-83.
- Nikkarinen, M., Kallio, E., Lestinen, P., and Äyräs, M.
1984: Mode of occurrence of copper and zinc in till over three mineralized areas in Finland; *Journal of Geochemical Exploration*, v. 21, p. 239-247.
- Plouffe, A.
1986: Till clay geochemistry and lithology in the vicinity of a tin-bearing granite, south-central New Brunswick; University of Ottawa, Ottawa (BSc thesis).
- Poole, W.H.
1963: Geology, Hayesville, New Brunswick, Geological Survey of Canada, Map 6-1963.
- Poole, W.H. and Lachance, G.R.
1979: Placer pan concentrates, Hayesville and Napadogan map areas (21 J/10, 7), New Brunswick; Geological Survey of Canada, Open File 617, 15 p.
- Rampton, V.N., Gauthier, R.C., Thibault, J., and Seaman, A.A.
1984: Quaternary geology of New Brunswick; Geological Survey of Canada, Memoir 416, 77 p.
- Rampton, V.N. and Paradis, S.
1981: Quaternary geology of Woodstock map area (21 J), New Brunswick; New Brunswick Department of Natural Resources, Map Report 81-1, 37 p.
- Rappol, M.
1986: Aspects of ice flow patterns, glacial sediments, and stratigraphy in northwest New Brunswick; in *Current Research, Part B*, Geological Survey of Canada, Paper 86-1B, p.
- Ruitenbergh, A.A., Fyffe, L.R., McCutcheon, S.R., St-Peter, C.T., Irrinki, R.R., and Venugopal, D.V.
1977: Evolution of pre-Carboniferous tectonostratigraphic zones in the New Brunswick Appalachians; *Geoscience Canada*, v. 4, p. 171-181.
- Ruitenbergh, A.A. and Fyffe, L.R.
1985: Characteristics and tectonic setting of granitoid related deposits in New Brunswick; in *Granite-related mineral deposits*, Taylor, R.P. and Strong, D.F. (ed.), Canadian Institute of Mining and Metallurgy, Geology Division, p. 205-210.
- Ruitenbergh, A.A., McCutcheon, S.R., and Davies, J.L.
1985: Gold environments in New Brunswick; GAC-MAC meeting, Fredericton, Program with Abstracts, p. A-53.
- Shilts, W.W.
1975: Principles of geochemical exploration for sulphide deposits using shallow samples of glacial drift; *Canadian Institute of Mining and Metallurgy, Bulletin* 68, p. 73-80.
1984: Till geochemistry in Finland and Canada; *Journal of Geochemical Exploration*, v. 21, p. 95-117.
- Snow, R.J., and Coker, W.B.
Overburden geochemistry related to the W-Cu-Mo mineralisation at Sisson Brook, New Brunswick, Canada: An example of short and long distance glacial dispersal; *Journal of Geochemical Exploration*, in press.
- Taylor, S.R.
1964: Abundance of chemical elements in the continental crust: A new table; *Geochimica et Cosmochimica Acta*, v. 28, p. 1273-1285.
- Wennervirta, H.
1968: Application of geochemical methods to regional prospecting in Finland; Geological Survey of Finland, *Bulletin* 234, 92 p.

A late glacial buried organic profile near Brookside, Nova Scotia

Projects 690064, 730027, 700056

R.J. Mott, J.V. Matthews, Jr., D.R. Grant, and G.J. Beke¹
Terrain Sciences Division

Mott, R.J., Matthews, J.V. Jr., Grant, D.R., and Beke, G.J., A late-glacial buried organic profile near Brookside, Nova Scotia; in Current Research, Part B, Geological Survey of Canada, Paper 86-1B, p. 289-294, 1986.

Abstract

Organic seams in sand and silt buried by a diamicton date between 11 100 and 11 700 BP. Pollen and plant and animal macrofossils indicate deposition in a shallow pond or marsh environment. Shrub tundra early in the sequence was invaded by spruce trees in a successional response to climate that was similar to that occurring near the present northern tree line. Cessation of organic deposition and burial by mineral sediments suggests deterioration of the climate about 11 000 years ago as seen in numerous other sites throughout Atlantic Canada.

Résumé

Des veines organiques trouvées dans le sable et le limon, enfouies dans un diamicton remontent à environ 11 100 et 11 700 BP. Le pollen et les macrofossiles de plantes et d'animaux indiquent un dépôt dans un milieu constitué d'un étang ou d'un marais peu profond. La toundra broussailleuse qui se trouvait à cet endroit au début de cette période a été envahie par des épinettes à la suite de réactions successives au climat semblables à celles qui se produisent actuellement près de la limite forestière septentrionale. La cessation des dépôts organiques et l'ensevelissement par les sédiments minéraux indiquent la détérioration du climat il y a environ 11 000 ans, comme on peut le voir dans de nombreux autres sites partout dans la région canadienne de l'Atlantique.

¹ Agriculture Canada Research Station, Lethbridge, Alberta T1J 4B1

Introduction

During soil erosion studies in the Brookside area of Nova Scotia by G.J. Beke, an excavation exposed thin organic layers in sandy sediments below a diamicton on which the modern soil profile was developed. A radiocarbon date of $11\,100 \pm 100$ BP (GSC-2930) on one of the richer organic horizons indicated that the site was similar in age to several other buried organic sites found throughout Nova Scotia (Mott, 1985; unpublished report by Mott et al., entitled "A late-glacial climatic oscillation in Atlantic Canada - An Allerød/younger Dryas equivalent"). The obvious value of this occurrence as a record of an important change in postglacial ecological regimes and associated climate prompted further studies of the palynology, chronology, and stratigraphy.

Location and setting

The site is located north of Highway 104 about 1 km east of the junction with Brookside Road northeast of Truro, Nova Scotia ($45^{\circ}24.09'N$, $63^{\circ}14.35'W$) (Fig. 32.1). Excavations were made in a small incipient gully on a south-facing slope at an elevation of 53 m. At present the 9% slope is pasture vegetated with grasses and forbs, but the local indigenous forest is spruce and fir. The area has been strongly disturbed by clearing and cultivation over the last 200 years. Softwood stands of balsam fir (*Abies balsamea*), red spruce (*Picea rubens*), and black spruce (*P. mariana*) remain on noncultivable land such as in gullies and on steeper slopes and uplands. The area falls within the Central Lowlands Section of the Acadian Forest Region (Rowe, 1972) where spruce (white (*Picea glauca*), red and black), balsam fir, eastern hemlock (*Tsuga canadensis*), and white pine (*Pinus strobus*) are intermixed with birch (*Betula papyrifera*), red maple (*Acer rubrum*), sugar maple (*A. saccharum*), yellow birch (*Betula alleghaniensis*), and beech (*Fagus grandifolia*).

Stratigraphy and radiocarbon dates

The 15 m-wide excavation showed approximately 100 cm of reddish sandy silt with some pebbles, overlying 80 cm of mottled, red, silty, sandy loam. Below, 75 cm of silty and sandy sediments containing seams of black organic material rests on red-brown micaceous sands and silts and a basal reddish sandy till typical of the area (Fig. 32.2).

Plant remains (including sedge achenes, moss stems, and spruce needles) washed from the organic horizon at 190-196 cm gave a ^{14}C date of $11\,100 \pm 100$ BP (GSC-2930). Bulk organic matter from the organic horizon at 242-250 cm depth yielded an age of $11\,700 \pm 110$ BP (GSC-3849).

Results

Pollen

Four organic horizons within the silty and sandy unit (Fig. 32.2) were processed for pollen using a modified Erdtman method involving treatment with KOH, HF, HCl, HNO₃, and acetolysis followed by mounting in silicon oil for counting. Results are shown in Table 32.1. Cyperaceae (sedge) dominates all four samples. *Picea* (spruce) is equally abundant in each of the lower three samples but increases significantly in the upper sample. The reverse trend is seen for *Pinus banksiana/resinosa* type (jack pine/red pine type) pollen. *Betula* (birch) has low values at the base, increases slightly, and then declines again. Other trees are represented by only a few grains.

Salix (willow) is the only significant shrub taxon present with relatively abundant representation in the lower three samples. Gramineae (grass), likewise, is more abundant in the lower layers. Other herbaceous taxa are represented by low values except for *Galium* (bedstraw) which is plentiful in the upper horizon.

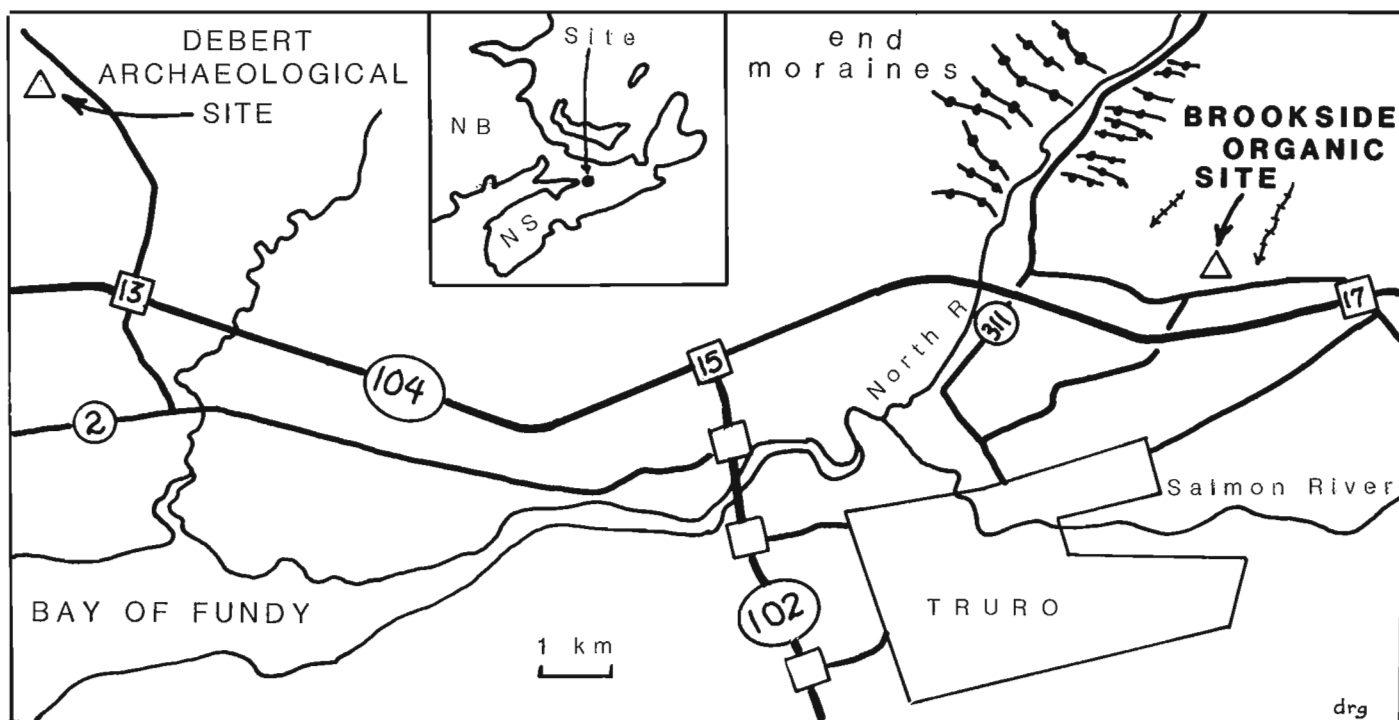


Figure 32.1. Location of Brookside buried organic site in relation to major highways, and to Debert paleo-Indian encampment.

Lycopodium (club-moss) species and Polypodiaceae, *Botrychium*, and *Osmunda* (ferns) spores are generally poorly represented; Polypodiaceae, however, is more pronounced in the lower samples. Other than Cyperaceae, aquatic and bog indicators are scarce with low values for *Sphagnum* (moss) and *Potamogeton* (pondweed) at the base and less abundant higher in the sequence.

Macrofossils

Macrofossils of plants and various animals were isolated from a small sample (approximately 1 L) of the organics at the 190–196 cm level. After soaking in water for several days, the sediments were washed through a number 80 Tyler sieve (0.180 mm opening) and the fossils picked from the residue remaining on the sieve.

The >0.180 mm residue consists predominantly of whole or partly degraded stem fragments, most of which are probably from sedges and, to a lesser extent, bryophytes. Identified plant and animal macrofossils are listed in Table 32.2. *Carex* achenes (some with the enclosing perigynium) dominate the plant macrofossil assemblage. Needles of spruce are also abundant. In addition, spruce needles and seed wing fragments are present. Seeds of a grass, *Rubus idaeus* type (raspberry), *Potentilla palustris* (cinquefoil), and Compositae plus a birch bract are represented.

The animal macrofossil assemblage is dominated by heads, pronota, and elytra of beetles (Coleoptera) and earthworm cocoons. Taxa recovered are listed in Table 32.2. Also present are oribatid mites, a mandible of a dragonfly, and miscellaneous fragments of flies (Diptera), wasps (Hymenoptera), and caddisflies (Trichoptera).

The abundance of earthworm cocoons in the sample is unusual. One of the authors (JVM) has studied many fossil assemblages representing similar biotopes from sites across northern North America but has never encountered the number of earthworm cocoons seen in this sample. Schwert (1979) has reported the presence of several earthworm cocoons from a 10 000 year-old level at the Gage Street site in Kitchener, Ontario. The fossils in the Brookside sample are similar to the Gage Street specimens but probably do not refer to the same species (*Dendrodrilus rubidus*).

Discussion

The radiocarbon dates indicate that deposition of sandy sediment including discrete organic horizons occurred over several centuries between approximately 11 700 and 11 100 BP. The abundant sedge pollen and stems, small numbers of *Sphagnum* spores, and minor pondweed pollen along with sedge achenes and *Potentilla palustris* seeds suggest deposition in a shallow pond, wet sedge meadow, or marsh environment. Several beetle taxa (marked with an "*" in Table 32.2) commonly occur together in and around sedge marsh areas of the type indicated by the plant macrofossils. The basin was presumably a small depression on the undulating till surface. The intercalation of discrete organic layers within a body of mineral sediment shows that a period characterized by influx of detritus, perhaps by slope wash, was periodically interrupted by intervals of stable slopes when organic matter accumulated.

The early pollen spectra, dating from 11 700 BP, indicate that the surrounding landscape supported a vegetation cover mainly comprising willow and grass. Shrub birch may have been present. Spruce trees were probably not present locally and, despite relatively high *Pinus* percentages, pine trees were not present. Various herbs occupied open areas of a shrub tundra-like environment. Gradually birch, probably shrub birch, became more abundant along with willow. Spruce may have been present nearby on suitable sites. The landscape, however, was probably still tundra-like. By 11 100 BP spruce trees had invaded the area, occurring near enough to the site to contribute needles and seeds to the sediments. Even so, spruce probably did not form a continuous cover but grew as scattered groves, with birch and willow, and grasses and herbs in open areas. To some degree, the insect assemblage supports this conclusion, for it conspicuously lacks fossils of bark beetles, normally typical of assemblages that represent closed or nearly continuous forest.

The sequence of changes portrayed by the pollen probably represents local succession rather than ongoing climatic change. This sequence is the expected vegetational response to a climate that had warmed to a level comparable to that prevailing at or near the northern treeline. Several of the Coleoptera taxa support this conclusion.

For example, none of the species of the northern staphylinid beetle genus *Eucnecosum* occur as far south as Nova Scotia (or Newfoundland) today (Campbell, 1984). According to Campbell (1983), the staphylinid *Olophrum rotundicolle*, one of the dominant elements of the assemblage, occurs in northern boreal and tundra habitats from Alaska to Newfoundland and farther south, mostly at higher elevations or in cold bogs (Fig. 32.3A). It does not live in the Truro area today but has been collected to the north on

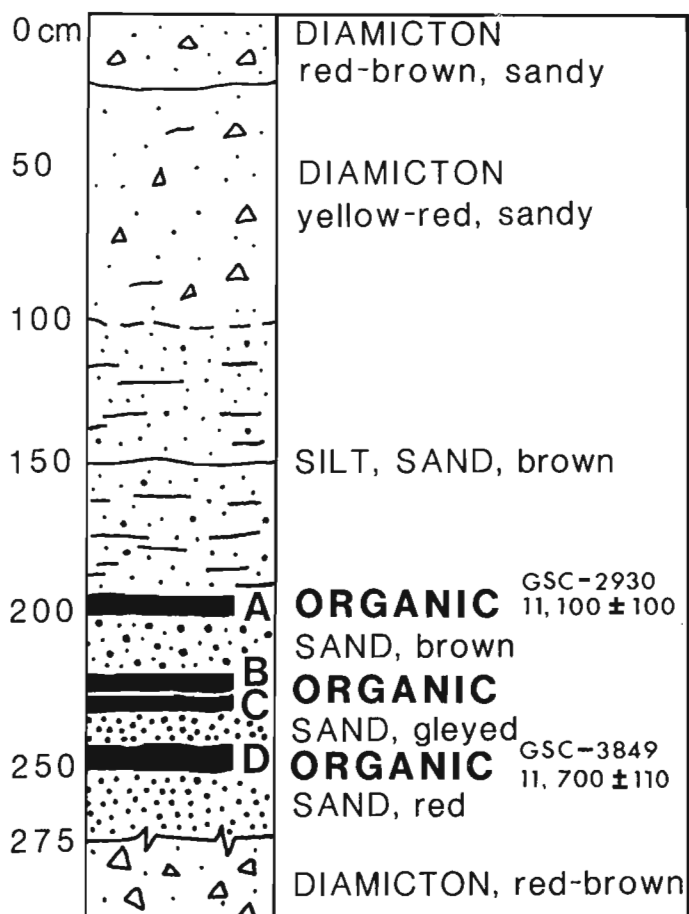


Figure 32.2. Lithological log, showing organic seams interbedded in sand, buried by stony diamicton (depths below ground surface): A-D. Pollen (Table 32.1), A. Macrofossils (Table 32.2).

Table 32.1. Pollen assemblages of the buried organic beds in the Brookside section

Pollen source	Pollen (%)*			
	A (190-196 cm)	B (216-222 cm)	C (222-230 cm)	D (242-250 cm)
Arboreal pollen				
<i>Picea</i>	52.6	20.2	18.8	16.2
<i>Pinus strobus</i>				0.4
<i>P. banksiana/resinosa</i>	3.5	23.6	19.5	12.6
<i>Larix laricina</i>			0.7	
<i>Betula</i>	11.9	15.3	14.2	4.7
<i>Populus</i>	0.3	0.4		
<i>Quercus</i>	1.3	0.8	1.0	2.5
<i>Carya</i>		0.4	0.3	
<i>Fraxinus nigra</i>	0.6	0.4		
<i>Carpinus/Ostrya</i>	0.3			
<i>Alnus</i>		0.4	0.7	0.7
<i>Salix</i>	1.9	11.6	8.9	20.6
<i>Shepherdia canadensis</i>				0.4
<i>Myrica</i>	1.9			0.7
Non-arboreal pollen				
Ericaceae	0.6			
Gramineae	10.6	10.7	23.1	26.4
Tubuliflorae	1.9	0.4	1.3	1.9
Ambrosieae	0.3	0.4	0.7	
<i>Artemisia</i>	0.3	1.7	0.3	1.4
Chenopodiaceae		0.4		
Rosaceae	1.0		2.6	0.4
Caryophyllaceae	0.3	0.8		
<i>Galium</i>	7.7	0.8	0.3	
Spores				
<i>Lycopodium annotinum</i>		2.1	1.3	0.4
<i>L. complanatum</i> type		1.2		
<i>L. clavatum</i>			0.7	
<i>L. selago</i>			0.3	
<i>Selaginella selaginoides</i>		0.4	0.7	
<i>Equisetum</i>	0.3			
Pteridophyta	0.3			0.4
Polypodiaceae	1.6	4.1	3.0	5.8
<i>Botrychium</i>				1.8
<i>Osmunda</i>				0.4
Unidentified	0.3	3.7	1.7	2.5
Aquatics				
Cyperaceae	268.1	160.3	75.2	173.3
<i>Sphagnum</i>	0.6	2.5	3.0	3.2
<i>Potamogeton</i>		0.4	0.7	0.4

* Percentages based on total pollen plus spores, excluding aquatics.

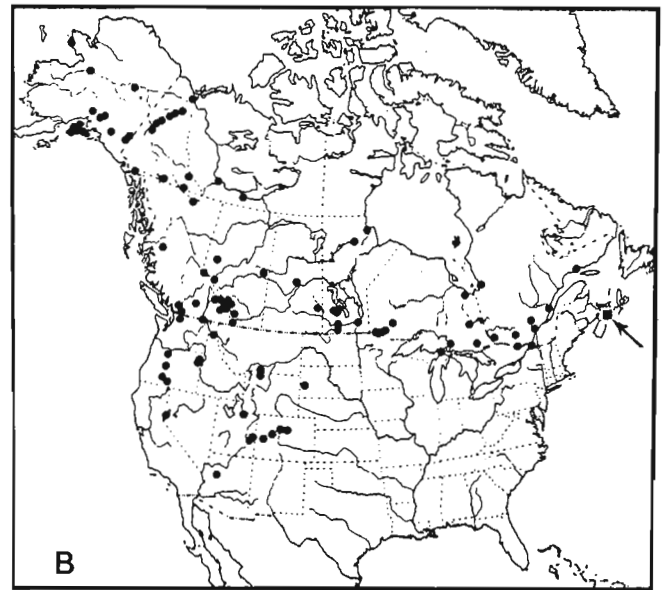
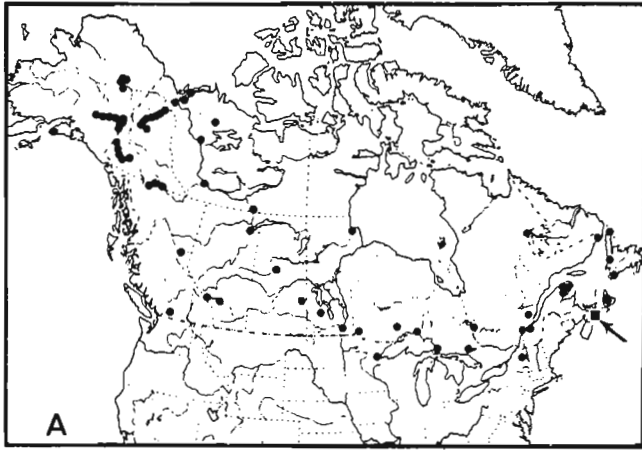


Figure 32.3. North American distribution (closed circles) of A: *Olophrum rotundicolle* (Sahlb.) and B: *Olophrum consimile* Gyll. with respect to the Brookside site (square symbol and arrow) (modified from Campbell, 1983).

Table 32.2. Plant and animal macrofossils from the 190-196 cm level of the Brookside section

PLANTS		ANIMALS (cont.)	
Bryophytes	+	Dytiscidae	
Pinaceae		* <i>Agabus</i> sp.	?(pr, el)
<i>Picea</i> sp.	++nd, sd	* <i>Hydroporus</i> sp.	+ab
Gramineae		Hydrophilidae	
genus?	+sd	* <i>Hydrobius</i> sp.	?el (ff)
Cyperaceae		Hydraenidae	
<i>Carex aquatilis</i> Wahlenb.	++sd	* <i>Ochthebius</i> sp.	+el
<i>Carex diandra</i> type	+sd	Staphylinidae	
<i>Carex rostrata</i> type	+sd	<i>Eucnecosum</i> sp.	?pr
<i>Carex</i> spp.	+sd	* <i>Olophrum rotundicolle</i> (Sahlb.)	++pr, hd, el
Betulaceae		* <i>Olophrum consimile</i> Gyll.	+pr
<i>Betula</i> sp.	+br	* <i>Stenus</i> spp.	+hd, pr, ff
Rosaceae		* <i>Lathrobium</i> sp.	cf (el)
<i>Rubus idaeus</i> type	+sd	Aleocharinae	+pr
<i>Potentilla palustris</i> L.	+sd	* <i>Gymnusa</i> sp.	+el, hd
Compositae		Ptiliidae	
genus?	+sd	* <i>Acrotrichis</i> sp.	+el
		Helodidae	
		* <i>Cyphon</i> sp.	+pr
		Byrrhidae	
		<i>Cytilus alternatus</i> (Say)	+el (ff)
		Chrysomelidae	
		* <i>Donacia</i> sp.	++el, pr, ff
		* <i>Plateumaris</i> sp.	+el
		Curculionidae	
		<i>Phytobius</i> sp.	?el (ff)
		TRICHOPTERA..."caddisflies"	
		Family-genus?	+lv (ff)
		DIPTERA..."flies"	
		Family?	+pp (ff)
		HYMENOPTERA..."wasps and ants"	
		Ichneumonoidea	?hd
		Formicidae	+md
		ARACHNIDA	
		Acari	
		Oribatei..."oribatid mites"	+

Abbreviations: + = taxon present; ++ = taxon abundant; ? = taxon not well enough preserved for positive identification; "cf" indicates adequate preservation but uncertain identity.

Plants: sd = "seed" (achene, fruit, samara, etc.); nd = needle (conifer); br = bractlet.

Insects: * = beetles typical of wet sedge meadows; pr = pronotum; el = elytron; hd = head; md = mandible; pp = puparia; lv = larval; cc = cocoon; ab = abdominal fragments; ff = fragments.

Cape Breton Island (J.M. Campbell, personal communication, 1986). *Olophrum consimile*, represented in this sample by a single pronotum, has a similar distribution (Fig. 32.3B), though it does extend farther south at higher elevations. Together the fossils of these beetle species (especially those of *Olophrum*) suggest that the climate at Brookside was somewhat colder 11 100 years ago than at present. Like the pollen evidence, they suggest a climate more like that of present day Newfoundland, central and northern Quebec, or southern Labrador.

Organic accumulation ceased shortly after 11 100 BP. First, sheets of silt and sand buried the organic sand layers. Ultimately the organic sequence was covered by a thick layer of diamicton. The inferred cause of the destabilized slopes and increased solifluction and slope wash was extensive depletion, if not wholesale loss of the vegetation cover. An abrupt shift to a cooler and possibly wetter climate is implied. A similar and contemporaneous sequence of events is seen at numerous other sites throughout Nova Scotia and New Brunswick, suggesting that a pronounced climatic deterioration interrupted the general deglacial warming over a large area of Atlantic Canada (Mott, 1985; unpublished data).

Finally, this site bears on the late-glacial and archaeological history of the area. It lies just beyond a series of moraines (Fig. 32.1) left by an ice cap over northern Nova Scotia. Perhaps the remnant glacier readvanced during the cooling interval; otherwise the moraines are much older. A few kilometres to the west at Debert, a large hunting encampment of the Maritime archaic culture, which depended on woodland caribou, has been dated to $10\ 903 \pm 48$ BP (the mean age of 13 hearth charcoal samples) (Stuckenrath, 1966). It was probably abandoned because of a shifted migration route, in all likelihood due to the abrupt cooling.

References

- Campbell, J.M.
1983: A revision of the North American Omaliinae (Coleoptera: Staphylinidae), the genus *Olophrum* Erichson; *The Canadian Entomologist*, v. 115, p. 577-622.
1984: A revision of the North American Omaliinae (Coleoptera: Staphylinidae). The genus *Arpedium* Erichson and *Eucnecosum* Reitter; *The Canadian Entomologist*, v. 116, p. 487-527.
- Mott, R.J.
1985: Late-glacial climatic change in the Maritime Provinces; in *Climatic change in Canada 5: Critical Periods in the Quaternary Climatic History of Northern North America*, ed. C.R. Harington; *Syllogeus*, no. 55, p. 281-300.
- Rowe, J.S.
1972: *Forest Regions of Canada*; Department of the Environment, Canadian Forestry Service, Publication Number 1300, 172 p.
- Schwert, D.P.
1979: Description and significance of a fossil earthworm (Oligochaeta: Lumbricidae) cocoon from post-glacial sediments in southern Ontario; *Canadian Journal of Zoology*, v. 57, p. 1402-1405.
- Stuckenrath, R.J.
1966: The Debert archaeological project, Nova Scotia: radiocarbon dating; *Quaternaria*, v. 8, p. 75-80.

Regional glacial dispersal patterns in Ungava, Nouveau-Québec

Project 850051, DSS Contract 245T. 23233-5-009

M.A. Bouchard¹ and C. Marcotte¹
Terrain Sciences Division

Bouchard, M.A. and Marcotte, C., Regional glacial dispersal patterns in Ungava, Nouveau-Québec; in Current Research, Part B, Geological Survey of Canada, Paper 86-1B, p. 295-304, 1986.

Abstract

Thin-section analysis of the coarse grained fraction of over 200 samples of glacial sediments and a systematic study of other glacial flow indicators from aerial photographs and from field survey, allow the following conclusions: (1) Ungava Peninsula was not affected by glacial ice originating from sources to the west, such as Keewatin or Hudson Bay, to the east such as Ungava Bay, or to the north such as Baffin Island or Foxe Basin. (2) Various parts of Ungava at different times were under the influence of three different outflow centres, named here the Ungava, the Payne, and the Caniapiscou centres. (3) The most important flow system for the dispersal of Proterozoic and Archean rocks was that of the Payne centre. (4) Glacial transport distance was at least 6-10 km and 10-15 km, respectively 80 km west and 80 km east of the Payne centre. (5) A dispersal fan of pyroxene-rich granite in till extends at least 70 km northeastward – a distance of 150-200 km east of the Payne centre.

Résumé

L'analyse des lames minces de la fraction grossière de plus de 200 échantillons de sédiments glaciaires et l'étude systématique d'autres indicateurs de la direction d'écoulement glaciaire sur le terrain et à partir de photographies aériennes donnent lieu aux conclusions suivantes: (1) la péninsule d'Ungava n'a pas été touchée par les glaciers venus de l'ouest, par exemple, la glace de Keewatin ou celle de la baie d'Hudson, ni par les glaciers venus de l'est, par exemple, la glace de la baie d'Ungava ou vers le nord, l'île Baffin ou le bassin Foxe; (2) à différents moments, diverses parties de l'Ungava ont été touchées par trois centres d'écoulement distincts, le centre d'Ungava, le centre de Payne et le centre de Caniapiscou; (3) le centre d'écoulement de Payne a contribué le plus à la dispersion des roches protérozoïques et archéennes; (4) la distance de transport glaciaire a été d'au moins 6 à 10 km et 10 à 15 km respectivement à 80 km à l'ouest et à l'est du centre de Payne; (5) un cône de dispersion de granite riche en pyroxène se prolonge vers le nord-est sur au moins 70 km, à une distance de 150 à 200 km à l'est du centre de Payne.

¹ Département de géologie, Université de Montréal, C.P. 6128, Succ. A, Montréal, Québec H3C 3J7

Introduction

Although the ice flow patterns and the large scale glacial geological features of Ungava are relatively well known (see Prest et al., 1968; Lauriol, 1982, Delisle et al., 1984; Gray and Lauriol, 1985; Wilson et al., 1986), little data regarding the glacial dispersal of rocks and minerals had been previously gathered within this region and little attention had been paid to the overall pattern of overlapping flow events.

This report is based on the results of the analysis of the composition of the coarse grained fraction of 284 samples of glacial sediments from Ungava, between latitudes 58° and 61° N (Fig. 33.1); on the examination and measurement of ice flow features visible on aerial photographs from 650 selected locations within the region; and on the measurement in the field of all the various ice flow indicators on outcrops when observed at the sampling sites (Fig. 33.2).

This preliminary report describes the main features of the glacial dispersal patterns, in order to support and assist mineral exploration in this area. In fact, this project was run concurrently with a reconnaissance sampling operation led by Monopros Ltd., Toronto.

Methods

Wherever available, till was the sampled material; fluvio-glacial gravels and sands alternatively were collected. A standard volume of 1 kg of sediment was taken at depths of 10 to 75 cm; surface till samples were taken from mudboils.

Sample preparation and treatment in the field involved drying, water content determination, splitting into various grain size fractions, and subsampling and embedding of granules into small resin cakes. Grain size splitting allowed the measurement of the weight proportion of clasts (larger than 4 mm diameter), granules (larger than 2 mm), sands (2 mm to 63µm), and silt and clay (smaller than 63µm diameter). The resin mounts consisted of approximately 5 g of the granule fraction in 20 mL of fast hardening resin. Thin sections were later prepared from the resin mounts; on average, 75 to 90 granules are available for identification on each thin section.

The composition of the sediment was determined from the examination of thin sections for 209 samples and from the examination of the granule fraction under binocular microscope for the remaining 75 samples. Abundances of a

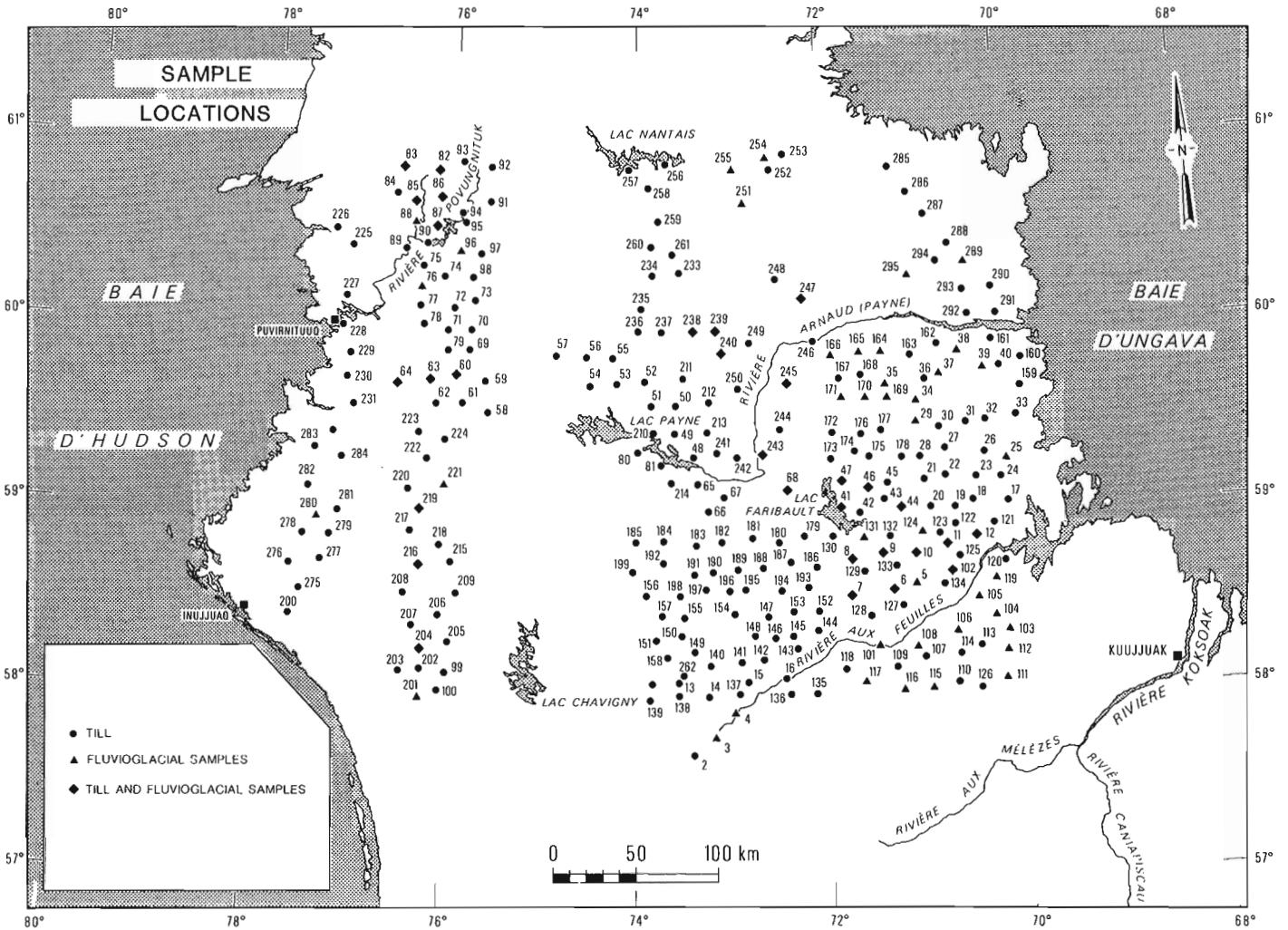


Figure 33.1. Location map showing sampling sites in the study area.

given rock type in a given sample are expressed as a per cent. For those values derived from thin sections, abundance refers to the number of grains of a given type relative to the total number of grains, whereas for those values derived from the binocular study, abundance refers to weight per cent. The sand fraction is presently being examined for its heavy minerals; the silt-clay fraction is being analyzed for its carbonate content (CaCO₃ equivalent) and for its multi-element geochemical make-up. These results are not available and are not discussed here.

In the southeast part of the region the systematic sampling was at an average density of one sample per 225 km². Elsewhere, the sampling strategically covered the area along corridors trending at right angles to the known or presumed glacial flow direction, or extending parallel to and along major geological boundaries.

Glacial ice flow direction

The major first-order ice flow features in Ungava, those visible from satellite imagery or from small scale aerial photographs, all combine to show a conspicuous pattern of outward radiating glacial flow from a central, north-south zone within the Peninsula, which is a segment of a larger feature referred to as the New Québec (Labrador) Ice Divide. The particular segment which appears to have acted as the persistent central area of flow within this region is here

referred to as the Payne outflow centre (Fig. 33.3). Located about halfway between Ungava and Hudson bays, the Payne centre provides an axis of bilateral symmetry with regard to other aspects of the geology and glacial geomorphology, such as the types of morainic terrains and the thickness and continuity of the drift cover on the Peninsula (Fig. 33.4, 33.5). The reader is referred to Lauriol (1982) for further reading on the glacial geomorphology of the area.

No unequivocal evidence in the form of erosional ice flow features has been found that Ungava was under the influence of glacial flow originating from external centres, such as from District of Keewatin or Hudson Bay in the west, or Ungava Bay in the east, or from Baffin Island or Foxe Basin in the north. One of the objectives of this study is to examine whether or not, in spite of the lack of erosional features, there is evidence, in terms of dispersal of foreign erratics, that ice flowed from such external sources.

Some evidence exists, however, that parts of the study area were under the influence of other glacial outflow centres on Ungava, namely in the north and in the southeast. In the north part of the area, scattered observations suggest a southward component of dispersal of the Proterozoic rocks over the Archean subcrop, followed by northward flow from the Payne centre. For example, at the Nouveau Québec Crater, both Currie (1962) and Delisle et al. (1984) recognized the presence of Proterozoic erratics derived from

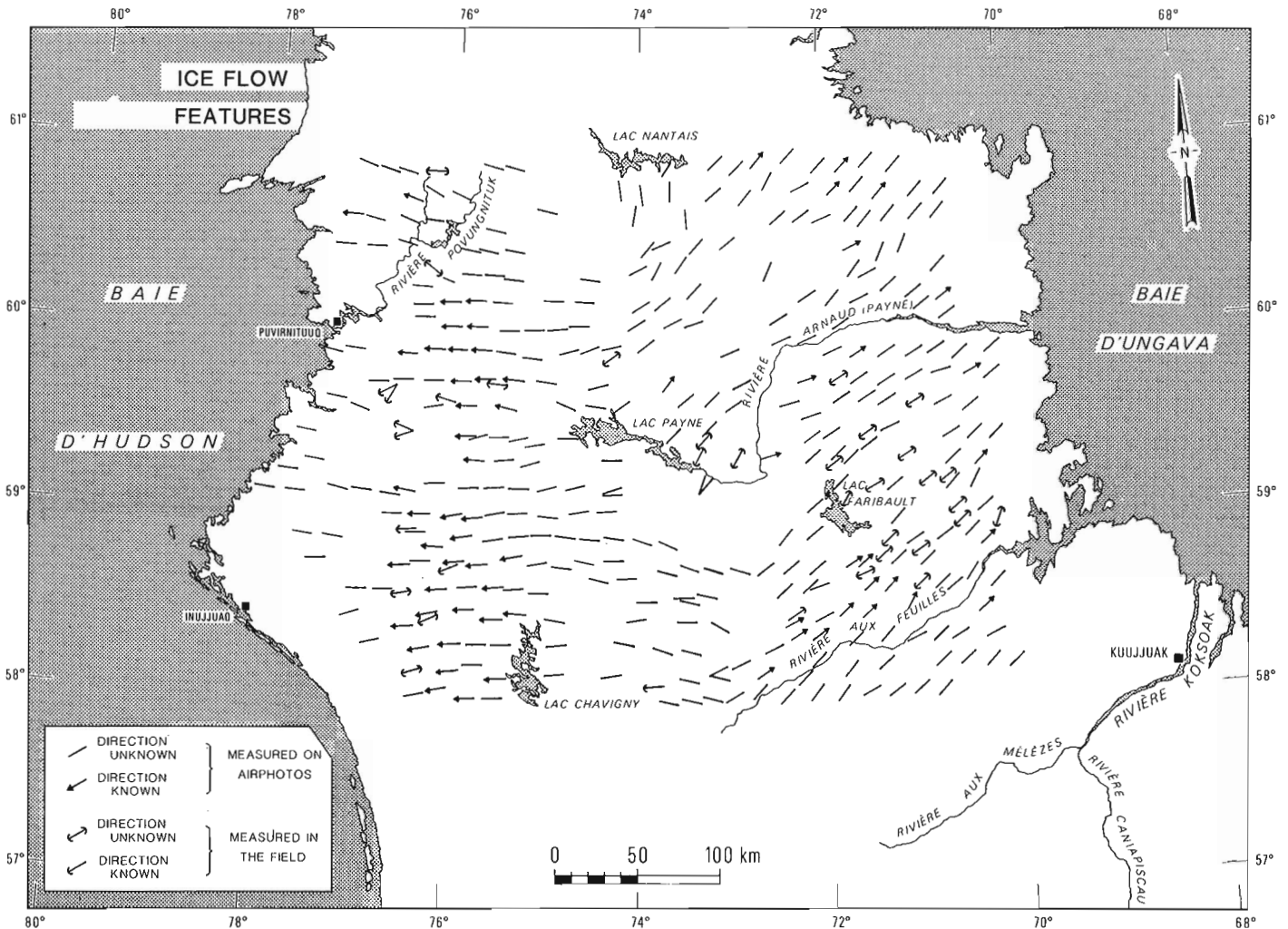


Figure 33.2. Glacial ice flow directions, Ungava Peninsula.

the north, while all other ice flow indicators suggest that the subsequent flow was northeastward, originating from the Payne centre. Similarly, in an area due south of Lac Chukotat, west of Lac Nantais, Proterozoic erratics from the Cape Smith Belt occur south of their source area (Fig. 33.6; J. Moorhead, personal communication, 1985), within a region where most of the flow features indicate a northwestward flow from the Payne centre. These observations indicate that the northern part of Ungava Peninsula was under the influence of an independent ice flow centre located north of the region some time prior to the invasion ice from the Payne centre. The name *Ungava* centre is suggested here for that northern centre which, it is further suggested, was located in the uplands northeast of Povungnituk River (Fig. 33.3), possibly extending east-west along the structural and topographic trend of the Cape Smith Belt. North of this location, all directional ice flow indicators, including the dispersal of the characteristic Proterozoic rocks of the Cape Smith Belt (Fig. 33.6), show a northward component of flow (Delisle et al., 1984; Wilson et al., 1986).

In the southeast, critical information is from Kuujjuak, southeast of the study area, and from the vicinity of Lac Faribault. North of the village of Kuujjuak, on a series of glaciated outcrops, well defined striae and crag-and-tail features show a succession of two glacial events. The first originated from an area west of Kuujjuak, presumably the

Payne centre; it was followed by a more prominent (or better preserved striae) ice flow originating from south of the site (see also Gangloff et al., 1976). Furthermore, south and southeast of Kuujjuak, as everywhere south of Ungava Bay, the influence of a northward ice flow is dominant in the glacial landscape and there is at least one documented report of a dispersal train, tens of kilometres in length, extending northward from a well defined Labrador Trough source (Drummond, 1965). These observations suggest that in the Kuujjuak area, ice flowing from the Payne centre was followed by ice flowing from another segment of the New Québec Ice Divide; the centre must have been in the vicinity of Lac Delorme, (Hughes, 1964; Richard et al., 1982) in the headwater region of the Caniapiscou River, hence the name *Caniapiscou* centre suggested here. The boundary of the Caniapiscou ice domain that overlapped the Payne ice domain is not known (domain is here defined as a region within which all the various ice flow features can be combined into a coherent pattern related to a known or a presumed flow centre). It must have extended at least as far north as Lac Faribault (Fig. 33.3), as shown there by cross-cutting striations and small-scale crag and tail features reported by Monopros Ltd. personnel. Finally, Lauriol (1982) reported multiple striae directions from Lac Bérard and Lac Jourdan, located in the unmapped area of Figure 33.2, between Feuilles and Mèlèzes rivers.

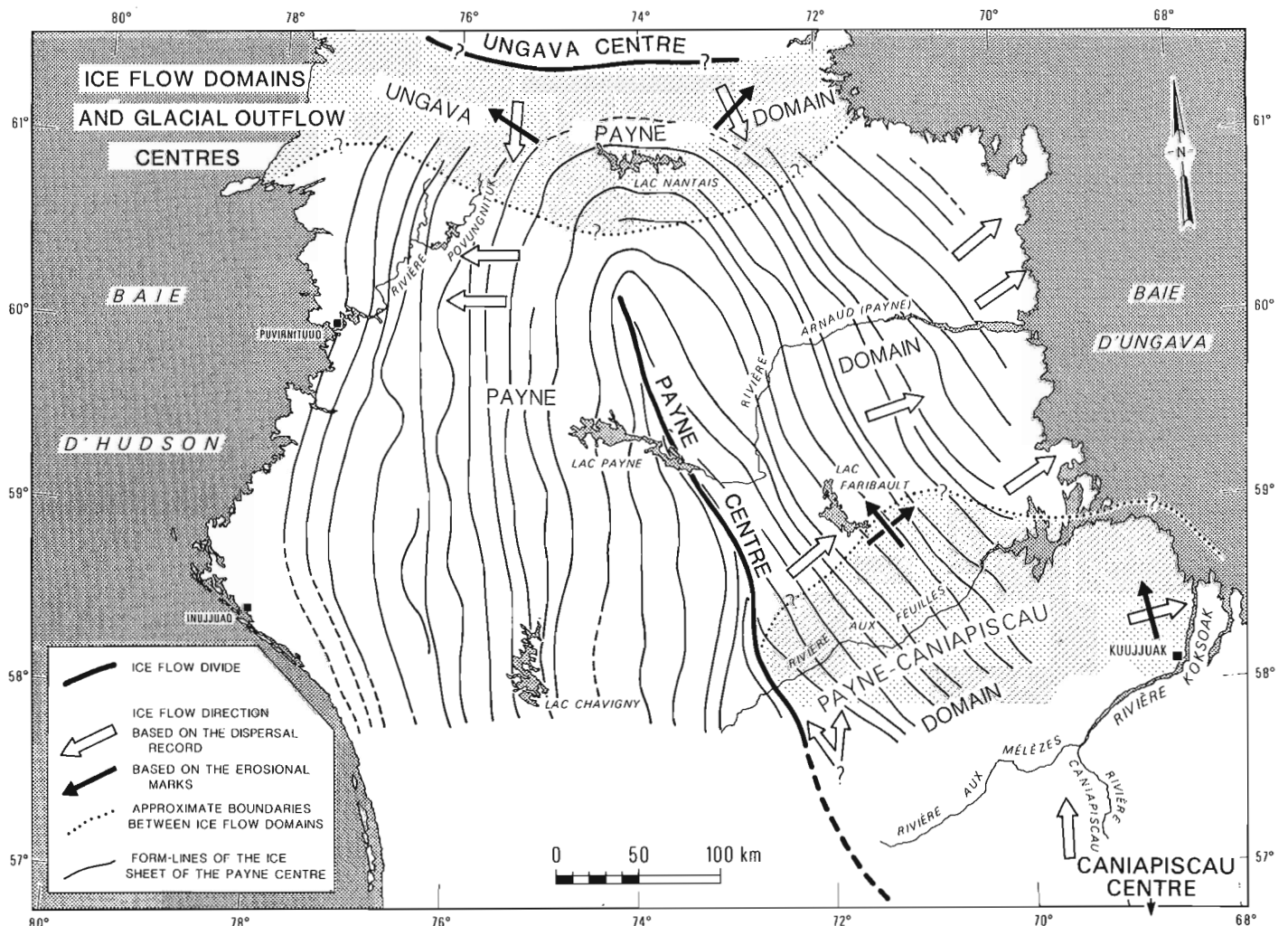


Figure 33.3. Glacial outflow centres and ice flow domains in Ungava. Contour lines are schematic form-lines illustrating the geometry of a glacier complex associated with the Payne centre.

In summary, available information on ice flow directions, as well as from a scanty dispersal record, suggests that three outflow centres influenced the area under study, creating two wide areas of overlapping glacial flow systems. All boundaries of overlapping flow domains are undetermined. The following sections examine the relative influence and magnitude of glacial transport within the various flow domains, especially in areas of flow overlap.

The dispersal of Proterozoic rocks

A simplified bedrock geology map of the part of Ungava under study is shown in Figure 33.5; most of the area is underlain by Archean rocks with little lithological contrast. It is bounded on three sides by belts of distinctive rocks of Aphebian (Proterozoic) age, namely the Belcher Belt to the west, the Cape Smith Belt to the north, and the Labrador Trough to the east (Fig. 33.6). The slightly metamorphosed sedimentary and volcanic rocks derived from these Proterozoic belts are easily identified in thin sections and their tracing poses no methodological difficulties.

Based on the regional distribution pattern of the Proterozoic rock fragments, (Fig. 33.6), it is concluded that there is no evidence of dispersal of rocks from the Belcher

Belt eastward onto the Archean subcrop. Scattered sedimentary rock fragments in surface samples below marine limit on the Hudson Bay seaboard were likely ice-rafted.

No rock fragments derived from the Cape Smith Belt were found by the authors within that part of Ungava covered by the present survey (Fig. 33.1). It is suggested, therefore, that the southward limit of extent of ice flowing from the Ungava centre must lie north of the northern limit of the present survey (Fig. 33.3). Admittedly, however, there is a lack of samples in the northern zone and further discussion of the above matter must await additional sampling. Rock fragments derived from the Labrador Trough were dispersed and transported eastward within the Payne flow domain. The compositional contrast in the till on either side of the western boundary of the Labrador Trough is striking. The abundance of local distinct rock types in the till increases rapidly east of the boundary and peaks at over 50% within 20 km along the Payne flow direction. The relative influence of Payne and Caniapiscau ice on the dispersal pattern is not known. It appears that the well defined dispersal pattern of the Payne flow domain was not modified or altered in any significant way north of Feuilles River by a later flow from the Caniapiscau centre.

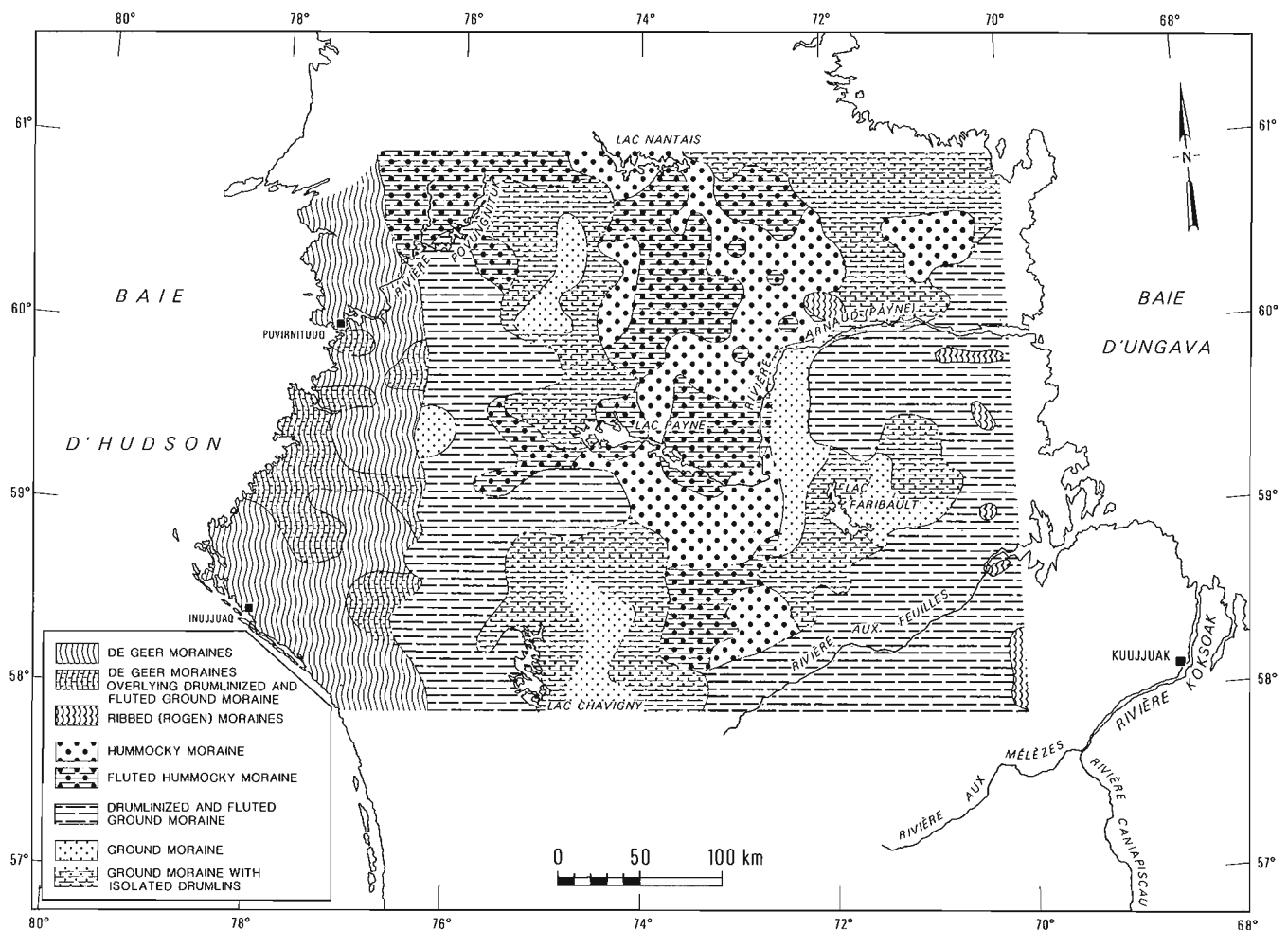
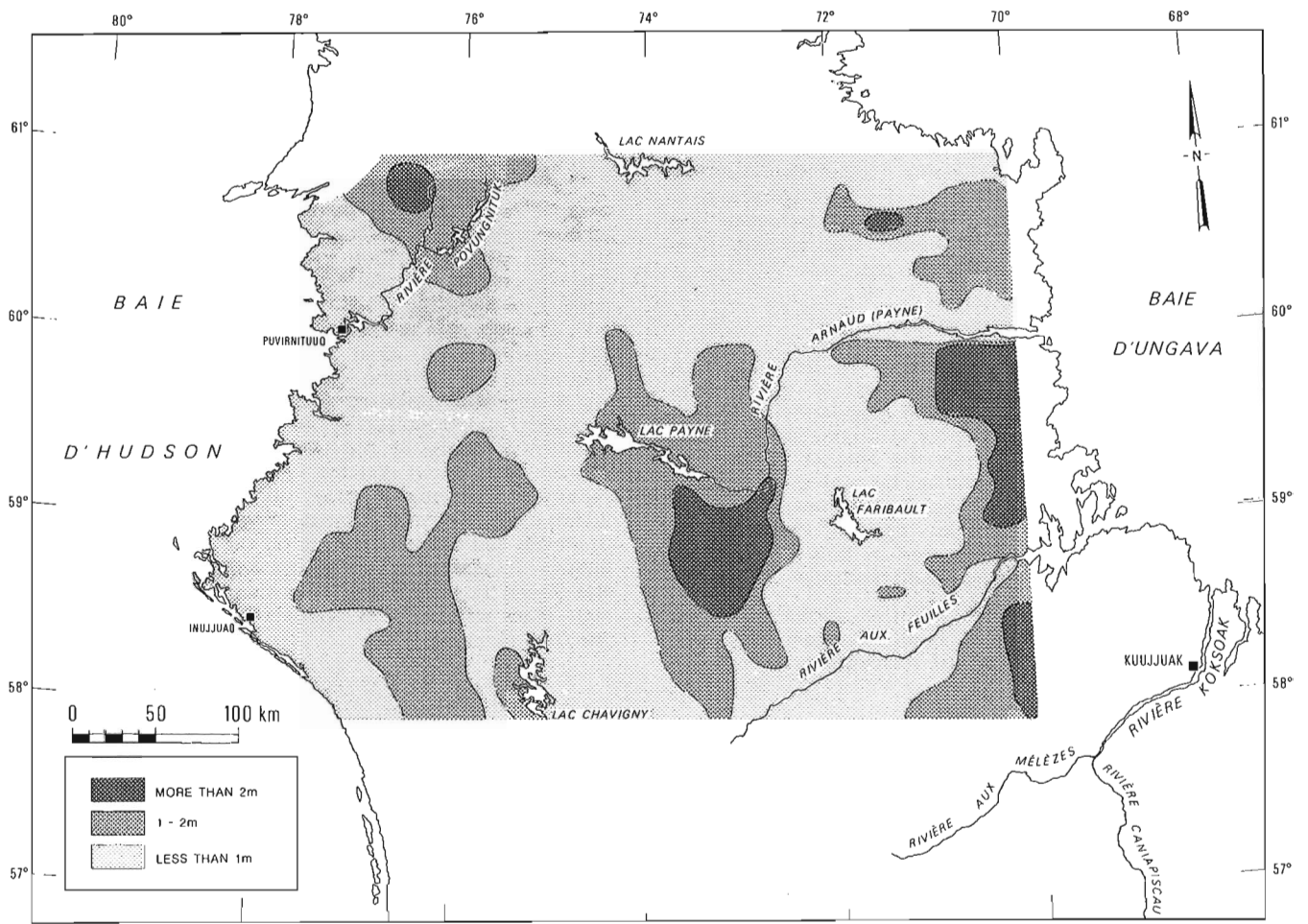
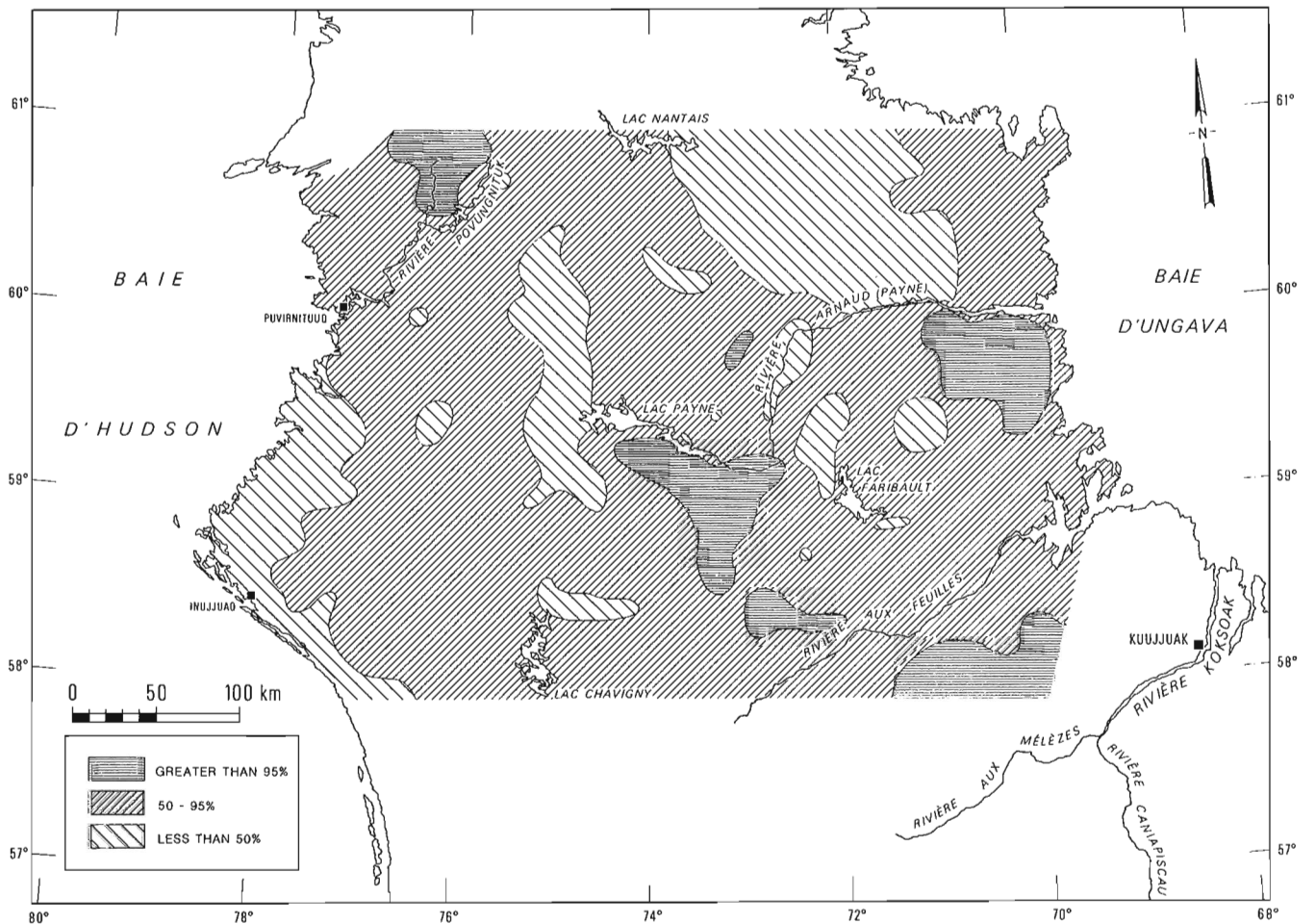


Figure 33.4. Glacial geology compiled from aerial photographs and field survey
A. Types of morainic terrains



33.4B. Estimated thickness of the glacial drift



33.4C. Continuity of the glacial drift cover

In summary, the regional distribution of the rock fragments derived from the peripheral Proterozoic bedrock sources confirm that no evidence exists that Ungava was under the influence of glacial flow originating from external centres, from the west, east, or north. This conclusion is now based on the close examination of nearly 400 samples of glacial sediments scattered throughout Ungava from data in this study and from Wilson et al. (1986). The most influential and consequential glacial flow system for the dispersal of the Proterozoic rocks was that of the Payne flow domain. Glacial transport was at least 20 km, at a distance of some 200 km east of the Payne centre.

The dispersal of Archean rocks

Within the Archean terrain, the study of the regional dispersal pattern is complicated by the low contrast of the bedrock sources or their wide or scattered distribution. Of the seven simplified Archean rock map-units (Fig. 33.5), four make up approximately 95% of the Archean subcrop (Table 33.1), each being bedrock sources of hundreds of square kilometres in extent; these are felsic gneisses, mafic gneisses, granites, and pyroxene-rich granites. The three other map units represent more distinctive lithologies – gabbros; ultramafics; and metasedimentary and metavolcanic rocks which are referred to as "greenstones". They make up approximately 5% of the Archean terrain, each forming

bedrock sources of limited extent; however, unlike the "greenstones" of the Cape Smith belt, they have widely scattered occurrences. Consequently, although the ultramafics and gabbros may be convenient and useful bedrock sources for local dispersal studies, they have very limited use for the present regional study.

In thin sections, eleven different types of grains were recognized (Table 33.1) in addition to the distinct Proterozoic rock fragments already discussed. The abundance of each of the 11 grain types in the various till samples was mapped and contoured. Only two types of grain were found to have either an obvious or a clearly significant relationship to a given bedrock source, allowing a relatively straightforward interpretation of the glacial dispersal patterns in the area: 1) "greenstone" rock fragments, obviously derived from the belts of Archean metasedimentary and metavolcanic rocks and 2) pyroxene-rich polyminerals grains which are most probably derived from the pyroxene-rich granites. For example, Table 33.1 shows that out of 100 samples of till overlying pyroxene-rich granites, 85 samples contained pyroxene-rich polyminerals grains, whereas only 49 and 36 samples contain such grains over mafic and felsic gneiss, respectively. It is concluded therefore, that the occurrence of a pyroxene-rich grain in a till has 85% chance to be derived from the nearest pyroxene-rich granitic bedrock source. Stated differently, the areal distribution of the abundance of the pyroxene-rich grains in Ungava till is

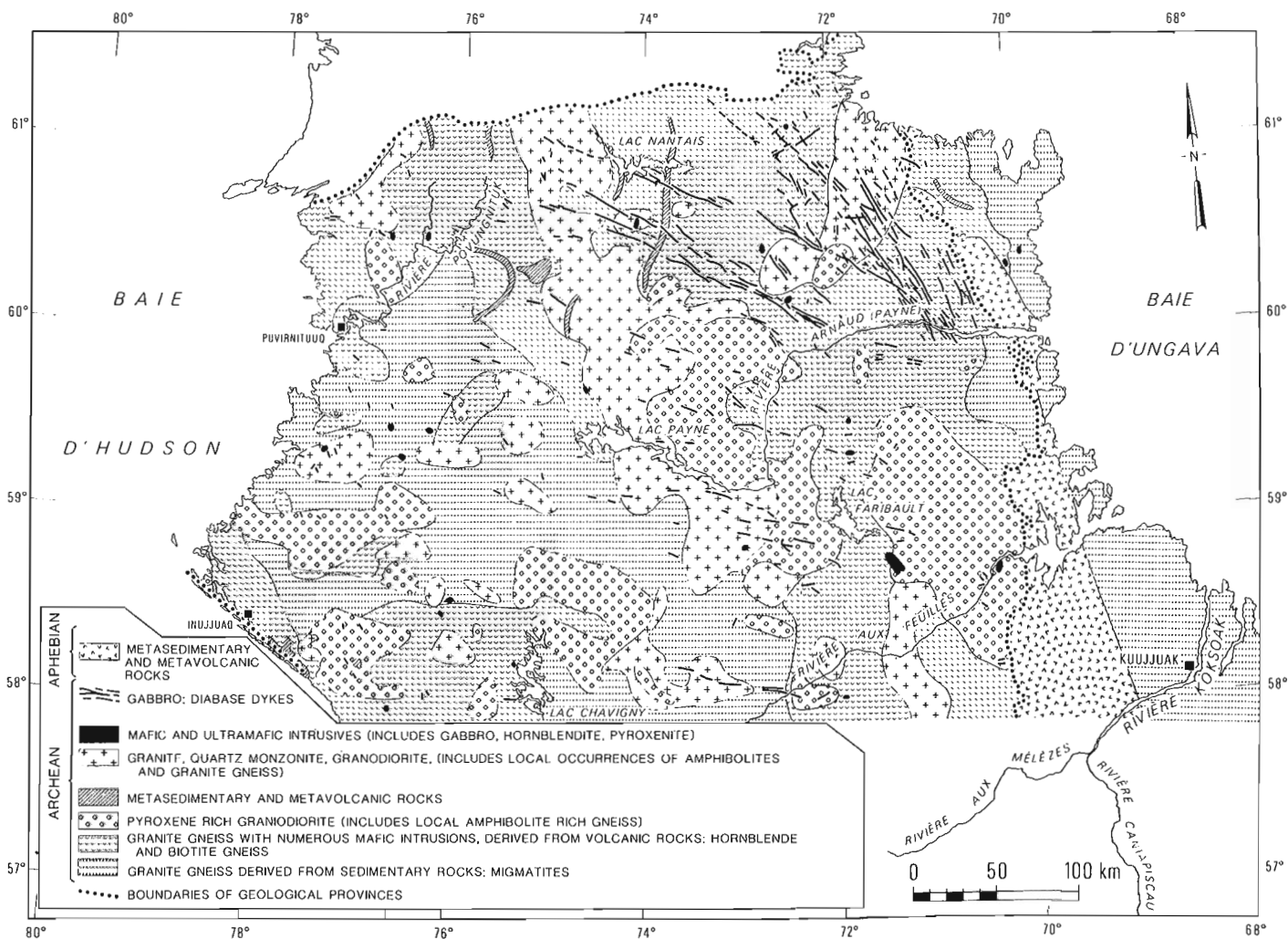


Figure 33.5. Simplified bedrock geology of Ungava Peninsula (modified from Taylor, 1982; Stevenson, 1968; MERQ, 1982).

Table 33.1. Mean abundance and frequency of occurrence of granule types over the Archean map units (cf. Fig. 33.5). Only the widespread map units (95% of the area) are considered.

GRANULE LITHOLOGY												
	Background types						Possible Tracer type					
	Mean Abundance (%) in the Coarse-grained fraction of till over a given map unit						Frequency of occurrence (%) in till over a given map unit					
	1	2	3	4	5	Total	6	7	8	9	10	11
Other granitics	43	39	5	3	3	93	68	56	48	40	4	8
Pyroxene granite	46	40	4	3	4	97	85	57	42	20	5	20
Mafic granite gneiss	47	35	4	3	3	92	49	76	38	24	16	20
Felsic granite gneiss	40	39	7	4	2	93	36	76	39	45	6	21

1 - Quartz + K-Feldspar + (Biotite or hornblende)	6 - Pyroxene granite
2 - Quartz + feldspar	7 - Hornblende/biotite/quartz
3 - Quartz	8 - Amphibole + quartz
4 - K-Feldspar	9 - quartz + plagioclase
5 - Plagioclase	10 - Ultramafic
	11 - "Greenstones"

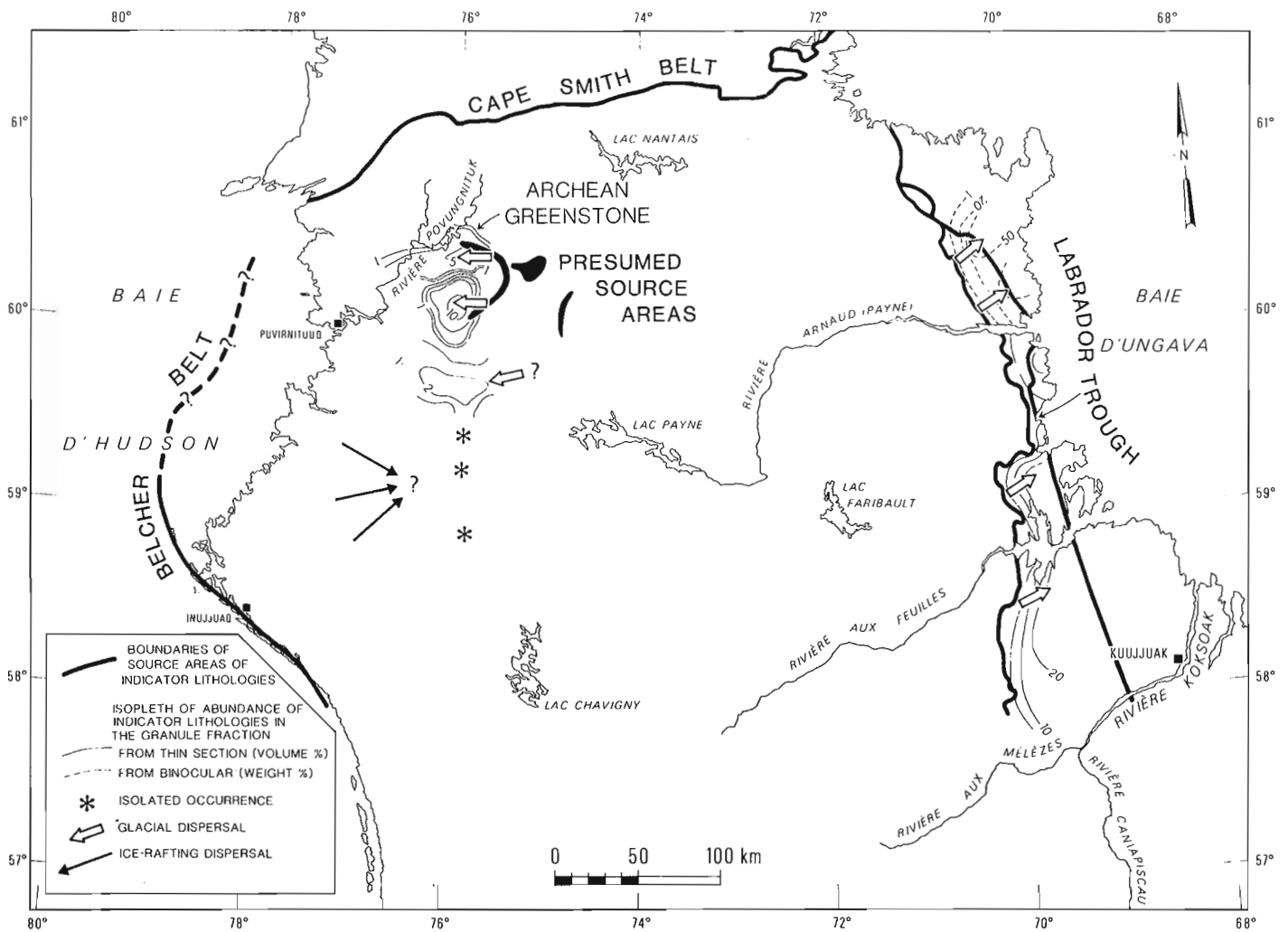


Figure 33.6. Dispersal of Proterozoic rock fragments.

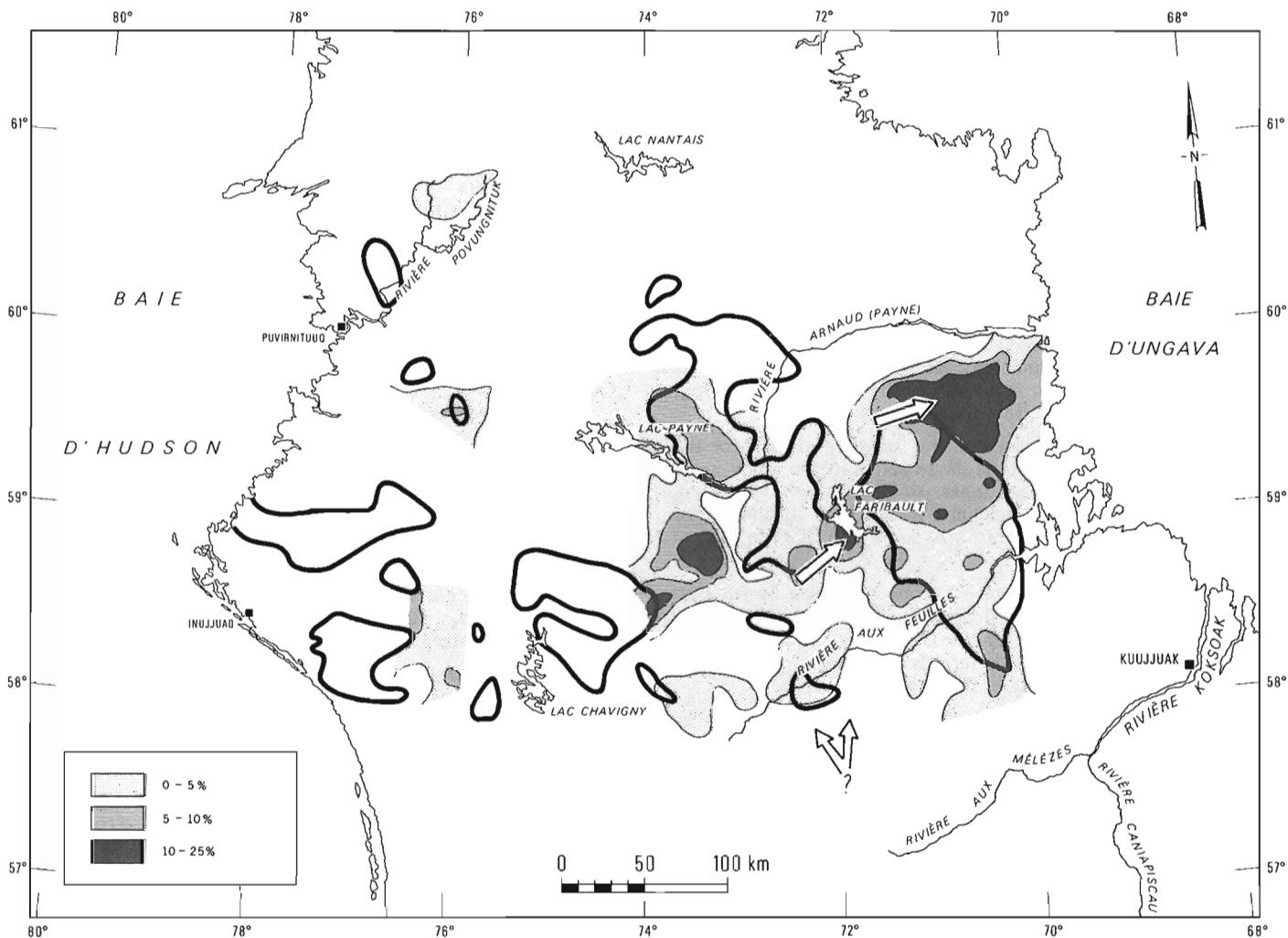


Figure 33.7. Dispersal of Archean rock fragments.

interpreted as a dispersal pattern from the various subcrop areas of the pyroxene-rich granites with approximately 85% confidence.

Distinct greenstone fragments are found in the till, west of a "greenstone" belt, located in the northwest part of the region (Fig. 33.6), with peak abundance (over 10%) occurring some 6-10 km down-ice from the bedrock source. The dispersal pattern obviously belongs to the Payne flow domain and suggests a minimum glacial transport distance of 6-10 km some 80 km west of the Payne centre. A second area of abundant "greenstone" fragments (over 2%) in till occurs south of this location with no known, or mapped, sources to the east. In the vicinity of Lac Nantais, greenstone fragments are high in till directly overlying segments of a north-south trending greenstone belt (not shown on Figure 33.6).

The regional pattern of the abundance of the pyroxene-rich grains is shown in Figure 33.7. East of the Payne centre, pyroxene-rich grains in the till form a dispersal fan extending northeastward from a wide pyroxene-rich bedrock source area between Arnaud R. to the north and Feuilles River to the south. The fan extends for a distance of at least 70 km, into the Labrador Trough region.

Immediately northeast of Lac Faribault, the abundance of the pyroxene-rich grains in the till increases rapidly to 10%, about 10-15 km northeastward from the western boundary of the underlying bedrock source. The dispersal

patterns obviously are related to the Payne ice flow and suggest a minimum glacial transport distance ranging from 10 to 70 km, respectively, some 80 km to some 150-200 km east of the Payne centre.

South of Feuilles River the pattern is less evident. Nevertheless there appears to be some northward component of flow indicated by the extent of pyroxene-rich till 3-5 km northward from a likely bedrock source.

A small zone in which the till contains in excess of 20% of pyroxene-rich grains occurs southwest of Lac Payne, west of the presumed location of the Payne outflow centre (Fig. 33.3). There are possible bedrock sources at about equal distance, both east and west of this zone. There is a notable lack of such rock fragments in the till just east of this location, however, suggesting that the more likely source of the fragments is to the west. This would indicate that at some earlier time the ice divide was located some 60 km west of its presumed final location as shown in Figure 33.3. An alternative explanation might also be the presence of unmapped pyroxene-rich rock units underlying the pyroxene-rich till, which at that particular location forms a thick, continuous cover (Fig. 33.4B, C).

In summary, the regional distribution of Archean tracer lithologies suggests a dispersal pattern predominantly related to the Payne flow domain with limited evidence that some influence of the Caniapiscau centre was felt south of Feuilles River. Glacial transport was at least 6-10 km and 10-15 km,

some 80 km west and east of the Payne centre. Some 150–200 km east of the divide, a dispersal fan at least 70 km long exists.

Summary

Based on presently available evidence, various parts of Ungava Peninsula at different times were under the influence of three different glacial outflow centres, namely, from north to south, the Ungava centre, the Payne centre, and finally the Caniapiscou centre (Fig. 33.3); each centre is related to an ice flow domain of the same name.

Based on the close examination of almost 400 samples of glacial sediments collected throughout Ungava, no evidence exists that Ungava was under the influence of glacial flow from external sources from the west such as Keewatin or Hudson Bay, from the east such as Ungava Bay, or from the north such as Baffin Island or Foxe Basin.

The Payne flow system was the most significant for the dispersal of Proterozoic and Archean rocks in the study area. Glacial transport was at least 6–10 km and 10–15 km, respectively, some 80 km west and 80 km east of the Payne centre; it may have reached 70 km, some 150–200 km east of the divide.

No rock fragments derived from the Cape Smith Belt were found within that part of Ungava covered by the present survey. The southern limit of the Ungava Payne flow domain is however considered still largely undetermined as the sampling was of low density in this part of the region.

The influence of the Caniapiscou flow centre may be recorded by the dispersal data as for north as Rivière aux Feuilles, and perhaps, based on erosional features, up to Lac Faribault.

Implications for the glacial history of Ungava

A speculative reconstruction of the glacier complex to which might have been related the Payne centre is shown in Figure 33.3. The contours were drawn at right angles to all the various large scale and smaller scale glacial flow indicators (Fig. 33.2); spacing of the contours is immaterial. If it is assumed that all the various ice flow indicators are contemporaneous, the contour lines would be form-lines of a large glacier at a given time. Form-lines imitate the glacier surface contour lines, drawn at uneven and unspecified vertical interval. Alternatively, if the flow features are diachronous, the contour lines would indicate the persistence of a given overall geometry of a large glacier complex through time. It can be seen that, notwithstanding the assumptions involved in the reconstruction, the latter provides an astonishingly simple glacier geometry to which is amenable practically all the flow features within Ungava. On the west side, widely divergent striae directions within short distances (Fig. 33.2) suggest small-scale lobations of the ice margin, most likely during the retreat phase, all through the zone that was later inundated by the Tyrrell Sea.

The Ungava centre, appears to have acted independently from the two other centres farther south which are different segments of the larger New Québec Ice Divide. Its influence in Ungava south of 61°N is poorly known as the southern boundary of the Ungava-Payne flow domain could not be determined by the present survey. Whether the Ungava centre remained a separate centre throughout the last glacial phase, or whether it was engulfed by a larger ice mass from the south during the maximum phase of the last glaciation is not known, as the northern boundary of the Payne flow domain is not determined. In the southeast part of the area, along the major ice divide, the Caniapiscou centre outlived the Payne centre, indicating that ice disappeared first from west of Ungava Bay, remaining later in residual centres south of the Bay.

Acknowledgments

The authors wish to express their gratitude to Guy Fortin and Alain Blanchette for their enthusiastic assistance in the field. Jean Veillette suggested that this study be done and deserves all the credit for its eventual usefulness; he read and commented on the final manuscript. Personnel of Monopros Ltd. Toronto were collaborative and made this experience most pleasant. Mrs. Francine Le Gresley word processed the original manuscript. Institut de recherche en exploration minérale – Mineral Exploration Research Institute (IREM-MERI) administered the funds provided for the project and Mrs. Valérie Virard is especially thanked for her efficiency.

References

- Currie, K.L.
1962: The geology of the New Quebec crater; Canadian Journal of Earth Sciences, v. 2, p. 141–160.
- Delisle, C.E., Bouchard, M.A., et André, P.
1984: Les précipitations acides et leurs effets, au nord du 55° parallèle au Québec; Rapport Préliminaire à la Fondation Canadienne Donner, 134 p.
- Drummond, R.N.
1965: The glacial geomorphology of the Cambrian Lake area, Labrador-Ungava; McGill University, Montréal (Ph.D. thesis).
- Gangloff, P., Gray, J.T., et Hillaire-Marcel, C.
1976: Reconnaissance géomorphologique sur la côte ouest de la baie d'Ungava; Revue de Géographie de Montréal, vol. xxx, p. 339–348.
- Gray, J.T. and Lauriol, B.
1985: Dynamics of the Late Wisconsin Ice Sheet in the Ungava Peninsula interpreted from geomorphological evidence; Arctic and Alpine Research, v. 17, p. 289–310.
- Hughes, O.L.
1964: Surficial geology Nichicun-Kaniapiscou map-area, Quebec; Geological Survey of Canada, Bulletin 106, 20 p.
- Lauriol, B.
1982: Géomorphologie Quaternaire du sud de l'Ungava; collection Paléo-Québec, Numéro 15, 173 p.
- Ministère Energie et Ressources du Québec (MERQ)
1982: Carte des gîtes minéraux-Baie d'Hudson; DPV-926.
- Prest, V.K., Grant, D.R., and Rampton, V.N.
1968: Glacial Map of Canada; Geological Survey of Canada, Map 1253A.
- Richard, P.J.H., Larouche, A., et Bouchard, M.A.
1982: Age de la déglaciation finale et histoire post-glaciaire de la végétation dans la partie centrale du Nouveau-Québec; Géographie Physique et Quaternaire, v. 36, p. 63–90.
- Stevenson, M.
1968: A geological reconnaissance of the Leaf River map-area, New-Québec and Northwest Territories; Geological Survey of Canada, Memoir 356, 112 p.
- Taylor, F.C.
1982: Reconnaissance geology of a part of the Canadian Shield, Northern Québec and Northwest Territories; Geological Survey of Canada, Memoir 399, 32 p.
- Wilson, H., Bouchard, M.A., and Delisle, C.E.
1986: Acid neutralizing capacity of glacial sediments of western Ungava, Québec; Water Science and Technology, v. 18, p. 69–85.

Preliminary report on the Kisseynew gneisses in the Kisseynew-Wildnest lakes area, Saskatchewan¹

Contract 14SQ.23233-5-0079

K.E. Ashton² and K.J. Wheatley³

Ashton, K.E. and Wheatley, K.J., Preliminary report on the Kisseynew gneisses in the Kisseynew-Wildnest lakes area, Saskatchewan; in *Current Research, Part B, Geological Survey of Canada, Paper 86-1B*, p. 305-317, 1986.

Abstract

The Kisseynew gneisses immediately north of the Flin Flon volcanic belt, northwest of Flin Flon, Manitoba, consist of a heterogeneous sequence of medium grade, metamorphosed volcanic and sedimentary rocks. They are divided into the Nokomis Group of volcanic and volcanoclastic rocks and greywackes, and the Sherridon Group of predominantly arkosic, volcanic and volcanoclastic rocks. A discontinuous polymictic conglomerate marks the contact between the two groups and apparently indicates at least a locally unconformable relationship. The gneisses have been intruded by several phases of pre- to syn-tectonic granitoid rocks.

Middle amphibolite facies metamorphism has affected all supracrustal rocks and rare kyanite-garnet-biotite assemblages suggest that metamorphic pressures in the area were, at least locally, in excess of 4.8 kb.

Two early phases of folding have been recognized as mesoscopic, tight to isoclinal folds, which may have been recumbent prior to subsequent deformation. Two later phases are more open and upright, and have deformed the pre-existing, gently dipping surfaces into a complicated and irregular outcrop pattern.

Résumé

Les gneiss de Kisseynew, situés immédiatement au nord de la zone volcanique de Flin Flon, au nord-ouest de Flin Flon (Manitoba), constituent une séquence hétérogène de roches sédimentaires et volcaniques métamorphisées, à teneur moyenne. Ils se répartissent entre le groupe de Nokomis, composé de grauwackes, de roches volcaniques et volcanoclastiques, et le groupe de Sherridon, constitué principalement de roches arkosiques, volcaniques et volcanoclastiques. Un conglomérat polygénique discontinu fait le lien entre les deux groupes et laisse supposer une discordance, tout au moins par endroits. Les gneiss ont été pénétrés à plusieurs reprises par des roches granitoïdes variant d'antétectoniques à syntectoniques.

Une phase de métamorphisme caractérisée par un faciès moyen d'amphibolites a altéré toutes les roches supracrustales et de rares associations de disthène-grenat-biotite, et permet de supposer que les pressions métamorphiques ont été supérieures à 4,8 kb dans certains endroits de la région.

Deux premières phases de plissement ont produit des plis mésoscopiques, variant de plis fermés à des plis isoclinaux, qui ont pu passer à des plis couchés avant d'être déformés. En effet, ultérieurement, deux phases de plissement ont créé des plis plus ouverts et plus droits et transformé les surfaces à faible pendage qui existaient déjà en un affleurement à structure complexe et irrégulière.

¹ Contribution to the Canada-Saskatchewan Mineral Development Agreement 1984-1989. Project carried by Geological Survey of Canada, Lithosphere and Canadian Shield Division, Project 850010.

² 1-88 Quebec Street, Kingston, Ontario K7K 1T9.

³ P.O. Box 546, Niagara-on-the-Lake, Ontario L0S 1J0.

Introduction

A four-year project to study the southern flank of the Kiseynew gneisses in Saskatchewan was initiated in 1985. Recent stratigraphic and structural interpretations in Manitoba (Bailes, 1980a,b; Zwanzig, 1984), and renewed economic interest, have created the need for a compilation of previous geological work on the Kiseynew gneisses of Saskatchewan. By supplementing previous work with new field observations, it is hoped that a stratigraphic correlation can be made with the Kiseynew gneisses in Manitoba. In practice, this involves attempting to determine lithological precursors and, if possible, the stratigraphy and geological history of the gneisses.

Fieldwork was begun in an area centred about 30 km northwest of Flin Flon, Manitoba (Fig. 34.1) and includes parts of four 1:50 000 scale map areas (63K/13, 63L/16, 63M/1 and 63N/4). Most of the fieldwork during summer 1985 was on the shores of large lakes, although some traversing was carried out between the lakes to provide continuity.

The regional geology is summarized in Figure 34.1, which is based on a previous compilation by Bailes (1971), with modifications resulting from more recent mapping (Tuckwell, 1979; McRitchie, 1980, 1985; Froese and Gall, 1981; Froese and Goetz, 1981; James, 1983; Zwanzig, 1983, 1984; Froese, 1984, 1985; Schledewitz, 1985). The geology of the western part of the map is based on previous mapping in Saskatchewan (Byers and Dahlstrom, 1954; Cheesman, 1956; Pyke, 1961; Byers et al., 1965; Macdonald, 1975, 1981) and on preliminary results of this study.

The Flin Flon volcanic belt has been divided into the Amisk Group, consisting of predominantly mafic volcanic rocks with minor associated felsic volcanic and volcanoclastic rocks, and the unconformably overlying Missi Group of polymictic conglomerates and clastic quartzofeldspathic sedimentary rocks (Bruce, 1918; Wright, 1933).

The Kiseynew gneiss terrane has been divided into the quartzofeldspathic Sherridon Group (Bateman and Harrison, 1946; Robertson, 1953) and the Nokomis Group of micaceous gneisses (Robertson, 1953). Migmatites and granitoid orthogneisses originally assigned to the Nokomis Group (Robertson, 1953) have been put into a separate unit by Zwanzig (1983) due to their largely igneous derivation.

The relationship between the Flin Flon volcanic belt and the Kiseynew gneisses has been the subject of much debate. The gneisses were originally thought to occur stratigraphically between the Amisk and Missi groups (Bruce, 1918; Wright, 1931), but were later interpreted as their metamorphic equivalents in the Annabel and Kiseynew Lake areas (Wright and Stockwell, 1935; Bateman and Harrison, 1945; Byers and Dahlstrom, 1954). The two belts have also been considered as distinct terranes in fault contact (Harrison, 1951a,b; Kalliokoski, 1952, 1953), but Robertson (1951) found that the local faults recognized along the boundary zone were not part of a major, continuous, structural feature. In fact, Bailes (1980a,b) has recently demonstrated that the Nokomis Group metasedimentary rocks in the File Lake area of Manitoba are the higher grade metamorphic equivalents of Amisk Group epiclastic rocks. The Sherridon Group has subsequently been interpreted as correlative with the Missi Group in the Kiseynew Lake area (Zwanzig, 1984), as was first suggested by Bateman and Harrison (1946). In Saskatchewan, the Kiseynew terrane has been divided largely on the basis of metamorphic mineralogy and, to a lesser extent, on composition (Byers and Dahlstrom, 1954; Cheesman, 1956; Pyke, 1961; Byers et al., 1965; Macdonald, 1975, 1981). A large component of this study is, therefore, directed towards attempting to apply the Nokomis-Sherridon Group stratigraphy to the Kiseynew gneisses in Saskatchewan.

General geology

The preliminary results of geological mapping in the Weetago Bay-Wildnest Lake area are presented in Figure 34.2. The locations of the Tyrrell Lake and Walker Lake granodiorites have been partly taken from a previous map (Byers and Dahlstrom, 1954) to illustrate the regional structure, but the remainder of the geology is based on new fieldwork.

The classification of the Kiseynew gneisses used is generally consistent with that determined by Zwanzig (1983) in the eastern Kiseynew Lake area, but has been modified to accommodate new evidence. It is based on a two-fold division consisting of the Nokomis Group, which is subdivided into metamorphosed volcanic and volcanoclastic rocks and greywackes, and the Sherridon Group, which is predominantly arkosic rocks with lesser amounts of polymictic conglomerates, greywackes, calcareous arkoses, feldspathic quartzites and volcanic and volcanoclastic rocks.

Several terms used by various workers to designate the precursors of some Kiseynew gneisses have been adopted here to aid in the correlative nature of this work, but it is necessary to define them in the present context. Robertson (1953) first pointed out the compositional similarity between the Nokomis graphitic garnet-biotite-quartz-plagioclase gneisses and "greywackes". This term is still in common use in the area (Zwanzig, 1983) and, in this study, refers to clastic sedimentary rocks in which the constituent ferromagnesian minerals amount to 15-40% of the rock. Zwanzig has also used the term "arkose" to describe quartzofeldspathic gneisses of the Sherridon Group. In this study, arkose is used for quartzofeldspathic rocks with less than 15% ferromagnesian minerals. Neither term is intended to carry any genetic connotation other than that of a clastic sedimentary origin. The term "volcanoclastic rock" is used to designate any clastic rock derived from a volcanic source, and includes both pyroclastic and epiclastic varieties.

Nokomis Group

The Nokomis Group consists mainly of graphitic garnet-biotite-quartz-plagioclase gneisses, interpreted as metagreywackes, and a spatially associated, heterogeneous suite of hornblende-bearing gneisses, which are thought to be metamorphosed volcanic and volcanoclastic rocks.

Mafic to intermediate volcanic and volcanoclastic rocks and subvolcanic equivalents

The Nokomis volcanic and volcanoclastic rocks include a variety of compositions but consist mainly of intermediate to mafic, layered gneisses with minor amounts of more felsic, well-layered rocks. No primary textures or structures were recognized.

The intermediate to mafic rocks are generally grey to dark green, fine- to medium-grained and well layered on a scale of millimetres to centimetres. Most are garnet-hornblende-quartz-plagioclase and garnet-biotite-quartz-plagioclase gneisses but clinopyroxene, cummingtonite and carbonate are also important constituents. Other common accessories include apatite, sphene, zircon and opaques. Typical outcrops contain 5-10% medium grained, hornblende-bearing leucosome and 5-10% concordant to discordant, white to pink biotite-quartz-feldspar \pm hornblende \pm garnet pegmatites.

Minor felsic gneisses are interlayered with the more mafic rocks throughout the region but are particularly abundant in the area of northwestern Wildnest Lake, where they are commonly

associated with calc-silicate rocks and cummingtonite-bearing gneisses. Most are garnet-hornblende-biotite-microcline-quartz-plagioclase gneisses, but varieties containing clinopyroxene and carbonate are not uncommon. The locally associated calc-silicate rocks are made up of various proportions of garnet, clinopyroxene, hornblende, biotite, carbonate, scapolite, quartz, microcline and plagioclase, and may be interlayered with the felsic gneisses or occur as large pods in the hinge zones of early folds. The layered, felsic to mafic volcanic and volcanoclastic rocks are commonly interlayered with, or gradational into, Nokomis graphitic greywackes.

A suite of homogeneous, intermediate garnet-hornblende-biotite-quartz-plagioclase rocks occurs on the western sides of Cotteral and Little Mari lakes (Fig. 34.3). They are grey to green on weathered surfaces and show evidence of strong recrystallization. Typical samples contain 2-10% fine grained, red, glassy, equally distributed garnet, 15-35% hornblende and biotite, 15-25% quartz and 35-50% plagioclase. Mafic schlieren occur in these rocks at one locality, and a white, medium grained, hornblende-bearing leucosome constitutes about 5% of most outcrops. They are tentatively interpreted as metamorphosed, subvolcanic tonalites and/or dacites.

Thin units of homogeneous, more mafic, garnet- and hornblende-rich rocks are also widespread but are not common in the area. Most are dark green to black with an average grain size of about 1 mm, and are locally interlayered with fine grained biotite-quartz-feldspar gneisses. They are interpreted as the metamorphosed equivalents of intermediate to mafic volcanic rocks.

This large, heterogeneous suite of mainly hornblende-bearing rocks is thought to represent a variety of precursors, but most, if not all, have likely been derived from volcanic and volcanoclastic rocks. The more calcareous and cummingtonite-bearing compositions in the northwestern Wildnest Lake area may result from the hydrothermal alteration of a volcanic terrane prior to metamorphism rather than the presence of marine carbonates.

Greywackes

The Nokomis greywackes are distinctive due to their relatively consistent composition, texture and mineralogy. They weather grey to rusty and range from homogeneous over several metres to well layered on a scale of centimetres. Most are graphitic garnet-biotite-quartz-plagioclase gneisses, but sillimanite, kyanite, white mica, hornblende and cummingtonite are all locally important constituents. Typical samples contain a total of 20-40% biotite and pink, euhedral, garnet porphyroblasts, and up to several per cent graphite. Hornblende most commonly occurs as coarse porphyroblasts at contacts with other hornblende-bearing rocks and probably marks a transitional composition.

The greywackes are commonly intercalated with, and gradational into, Nokomis volcanic and volcanoclastic rocks. Several Sherridon Group lithologies are also found in contact with the Nokomis greywackes.

The composition and texture of the greywackes is consistent with a clastic sedimentary origin, likely as feldspathic and/or lithic wackes.

Sherridon Group

The Sherridon Group was originally restricted to the sequence of rocks hosting the Cu-Zn mineralization at Sherridon, Manitoba (Bateman and Harrison, 1946), but was later extended to include the majority of supracrustal rocks, and in particular

the quartzofeldspathic gneisses (Robertson, 1953), thought to stratigraphically overlie the Nokomis Group (Zwanzig, 1983). Arkosic gneisses make up most of the Sherridon Group in the area mapped, but polymictic conglomerates, greywackes, feldspathic quartzites and volcanic and volcanoclastic rocks are locally important constituents.

The stratigraphy of the Sherridon Group is poorly understood. A sketch map of the area between Cotteral and Mari lakes illustrates some of the complexities (Fig. 34.3). The stratigraphic order outlined in the accompanying legend is based on field relationships but is tentative. Perhaps the most complicated portion of the Sherridon stratigraphy is the base where facies changes appear to account for a variety of lithologies including polymictic conglomerate (Fig. 34.4), greywacke, calcareous arkose, arkose and volcanic and volcanoclastic rocks. Although the conglomerate is thought to mark a hiatus between the deposition of the two groups, it is not yet clear whether a significant unconformity exists along the entire length of the Nokomis-Sherridon boundary.

Polymictic conglomerate

The polymictic conglomerate occurs at, or within a few metres of, the base of the Sherridon Group, but is discontinuous and cannot be traced for more than a few kilometres along strike. It is strongly foliated and/or lineated and can easily be mistaken for a well-layered gneiss where a down-plunge orientation cannot be observed (Fig. 34.4, 34.5, 34.6). It attains a maximum apparent thickness of 500 m in the hinge zone of the Mari Lake synform (Fig. 34.2), but contains a significant amount of intercalated calcareous greywacke and has been thickened by early folding.

The clasts consist mainly of hornblende-bearing rocks including abundant intermediate hornblende-quartz-plagioclase±garnet gneisses, minor garnet-quartz-feldspar±hornblende quartzofeldspathic gneisses, amphibolites and garnet amphibolites. Many of these lithologies are similar to those of the Nokomis volcanic and volcanoclastic rocks although no Nokomis greywacke clasts were recognized. Granitoid rocks make up 10-20% of the clasts. Most are fine- to medium-grained and contain feldspar phenocrysts, but rare clasts of medium- and coarse-grained, equigranular, granitoid rocks and vein quartz are also present. Original clast size is difficult to determine due to subsequent deformation, but ranges up to at least cobble size.

The conglomerate matrix is not easily distinguished from the clasts but appears to be of greywacke or calcareous greywacke composition and contains abundant garnet, biotite and/or hornblende. Clast-free, matrix-like material is commonly interlayered with the conglomerate and appears to be a lateral equivalent of restricted occurrence.

The polymictic conglomerates are generally found in direct contact with Nokomis greywackes, but are locally separated from them by Sherridon arkoses at the Cotteral Lake occurrence. They are therefore thought to have been deposited at or near the base of the Sherridon Group as a result of erosion of the pre-existing Amisk-Nokomis terrane.

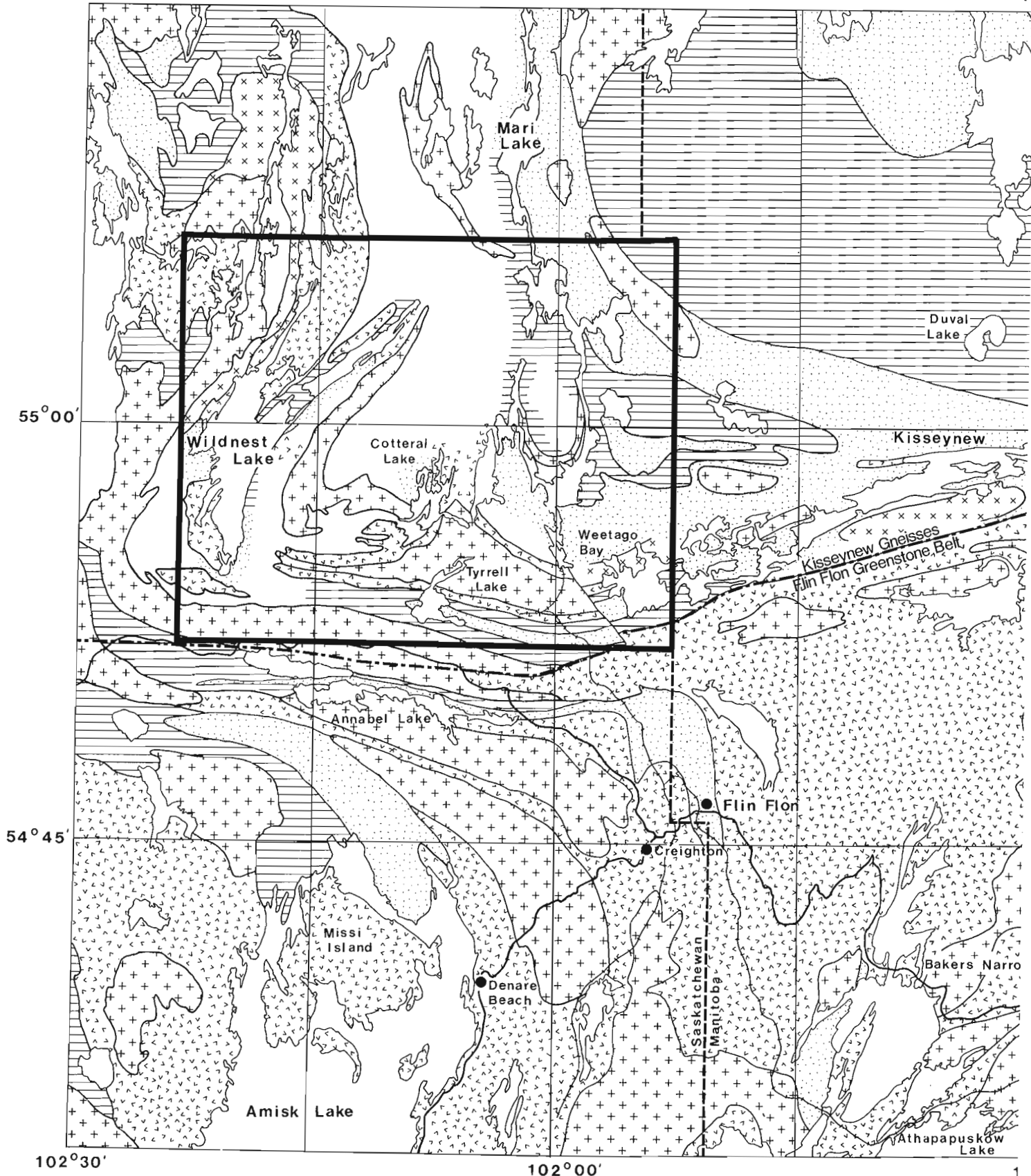
Arkose, calcareous arkose, feldspathic quartzite and greywacke

Sherridon arkoses are common and widespread throughout the area. Most are layered on a scale of centimetres to metres and consist of fine- to medium-grained, white to grey, garnet-biotite-quartz-plagioclase gneisses. Primary textures and structures are generally lacking but deformed crossbedding (Fig. 34.7) was recognized on the southwestern shore of

102°30'

102°00'

10



55°00'

54°45'

102°30'

102°00'

1

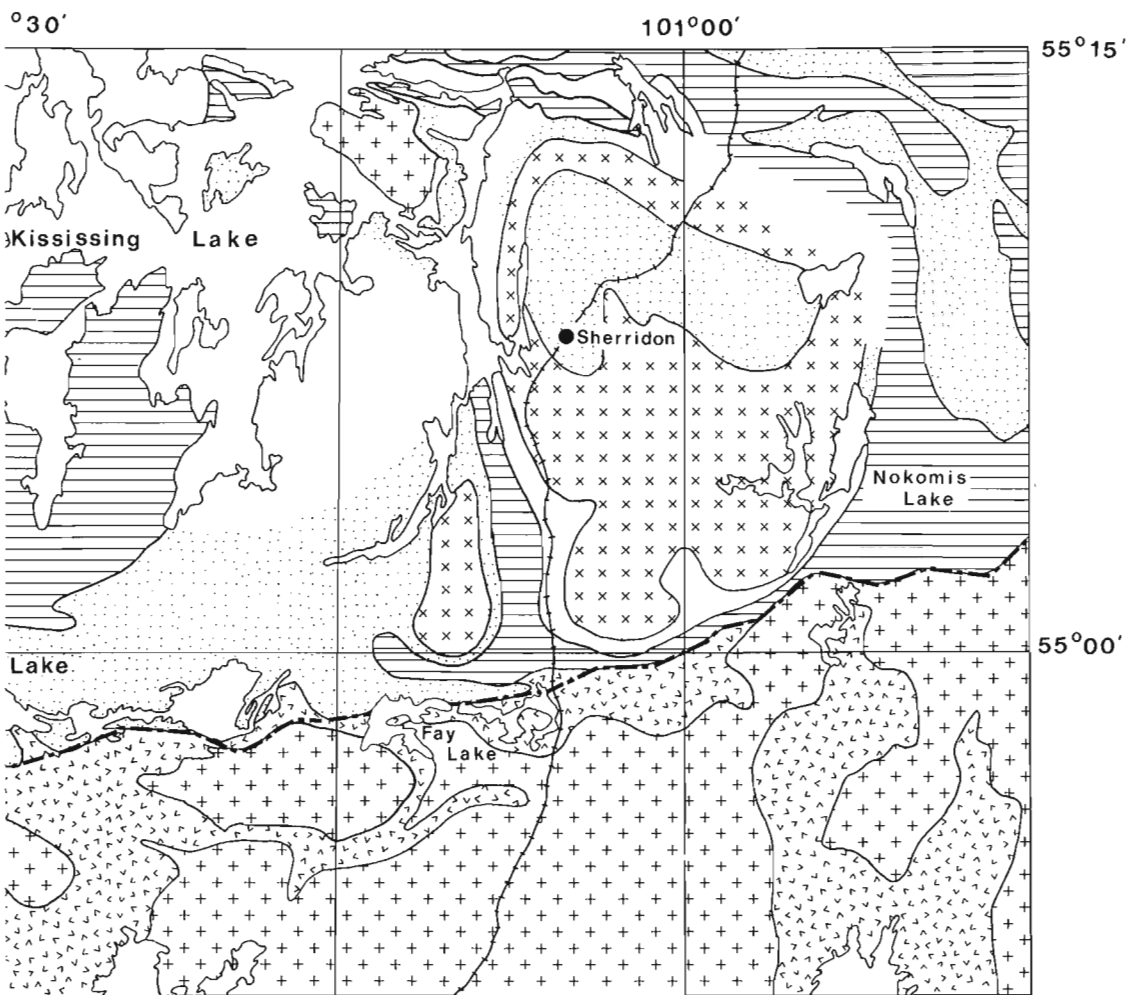
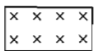


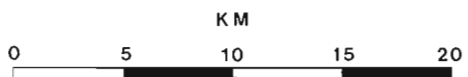


Figure 34.1. Compilation map of the regional geology in the Flin Flon area. See text for sources. Box outlines area of Figure 34.2.

LEGEND

-  Granitoid intrusive rocks
-  Granitoid and migmatitic gneisses
-  Undifferentiated Kisseynew gneisses
-  Missi Group, Sherridon Group
-  Amisk and Nokomis sedimentary rocks
-  Amisk and Nokomis volcanic rocks



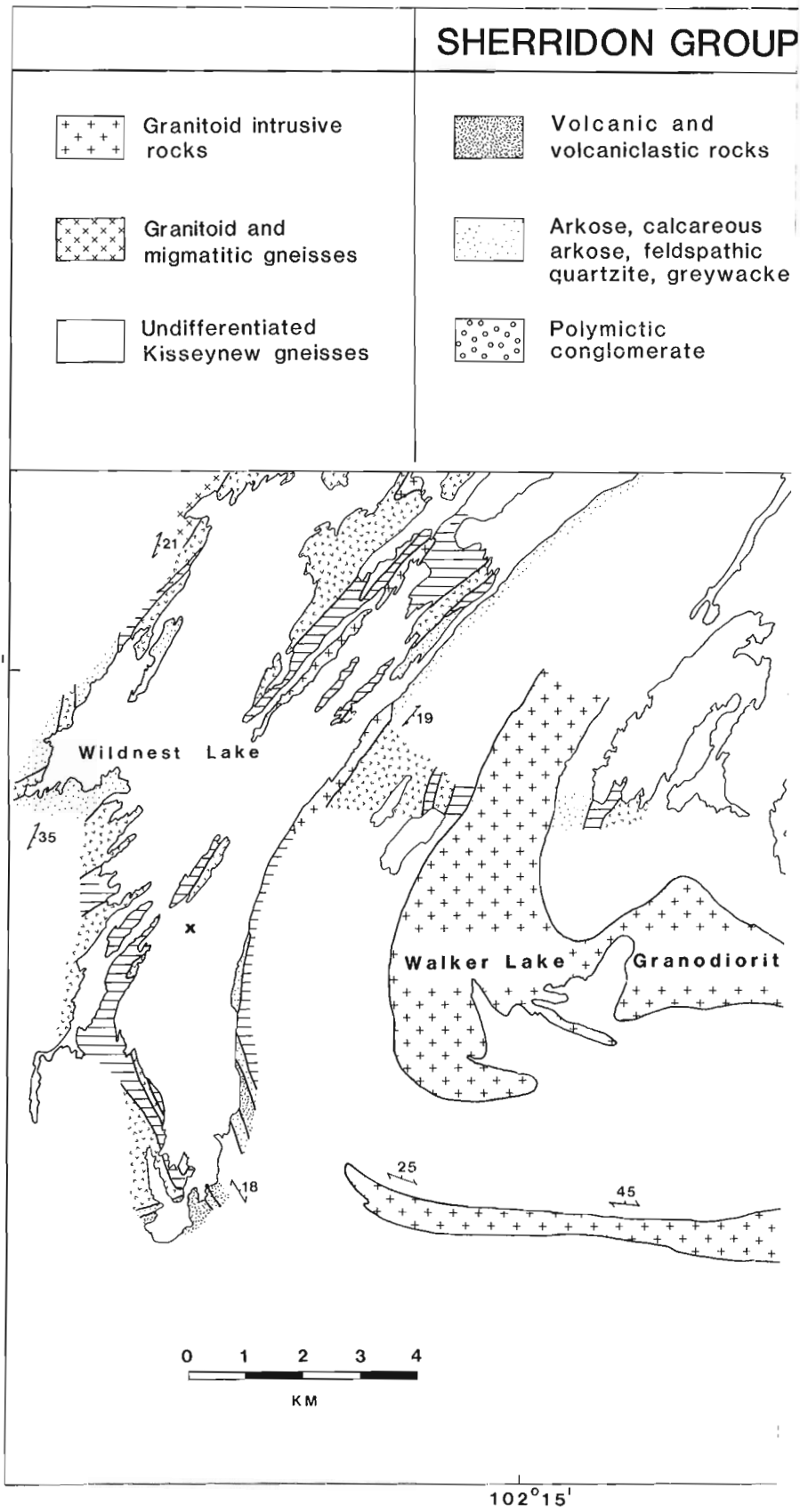




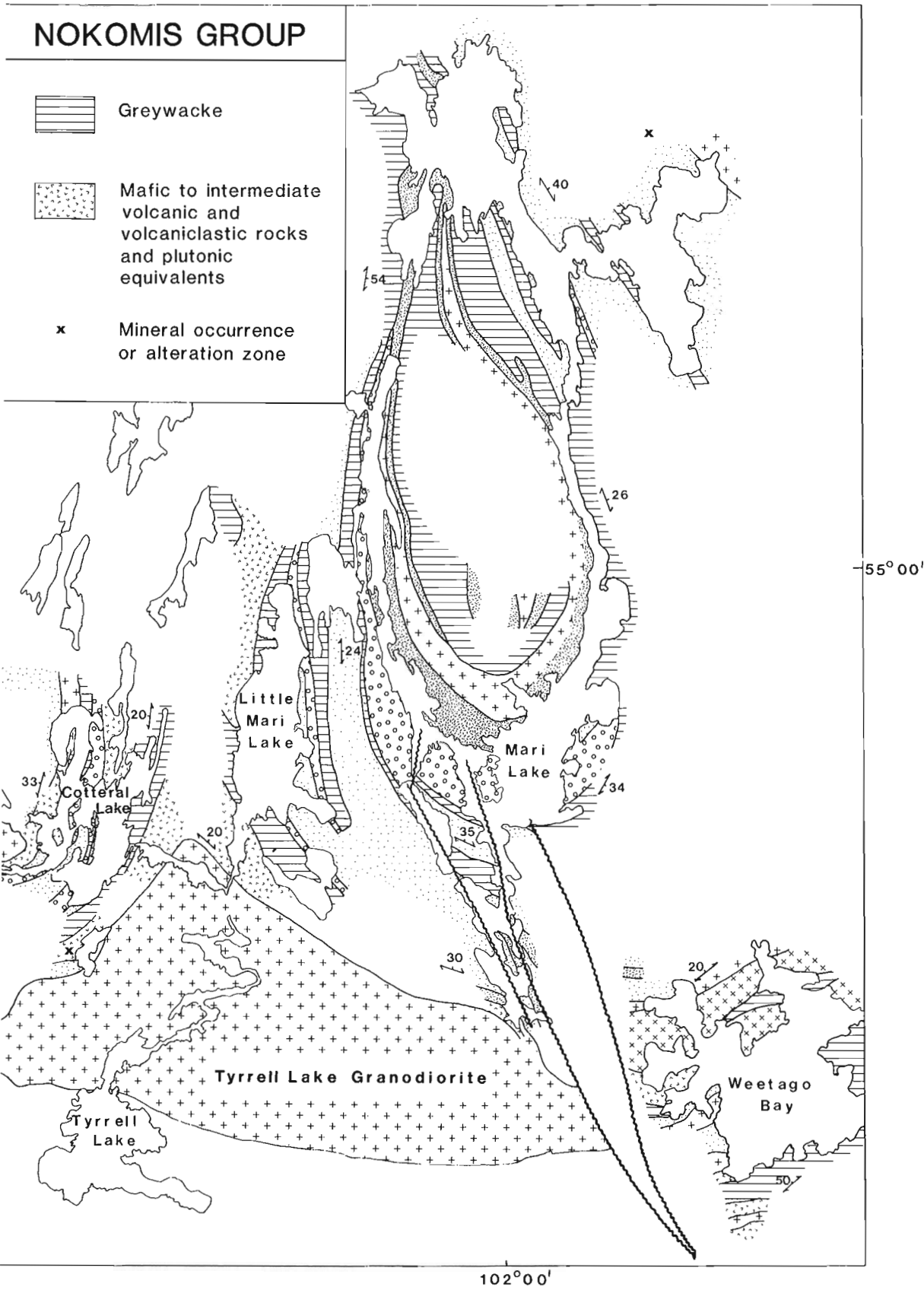
Figure 34.2. Preliminary map of the general geology of the Weetago Bay (Kisseynew Lake) – Wildnest Lake area. The stratigraphy has been simplified for this map and the stratigraphic order is tentative.

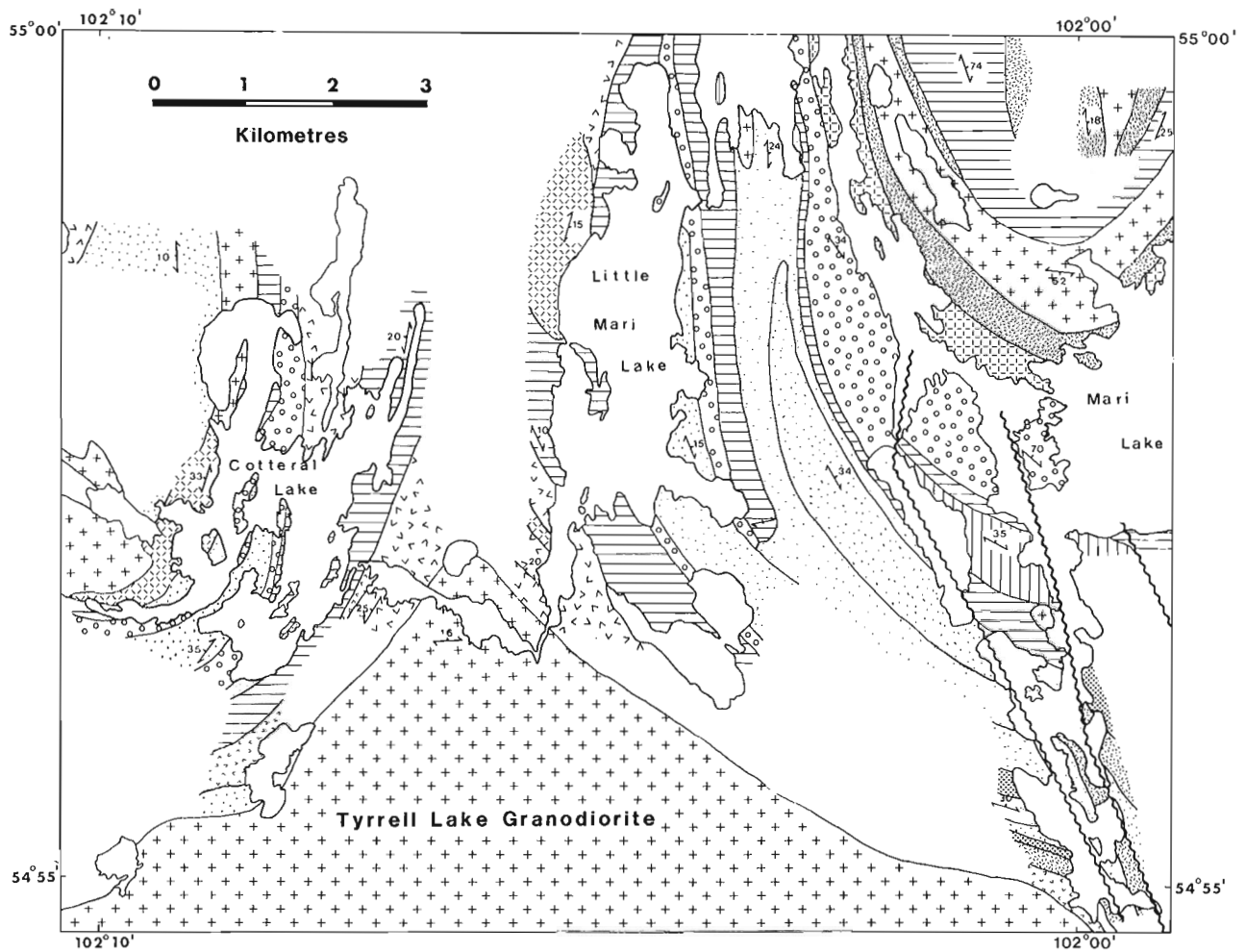
NOKOMIS GROUP

 Greywacke








 Mafic to intermediate volcanic and volcaniclastic rocks and plutonic equivalents

x Mineral occurrence or alteration zone





LEGEND

-  Granitoid intrusive rocks
-  Undifferentiated Kisseynew Group
- SHERRIDON GROUP**
-  Feldspathic quartzite
-  Mafic intermediate volcanic and volcanoclastic rocks
-  Felsic volcanoclastic(?) rocks
-  Arkose
-  Calcareous arkose
-  Greywacke
-  Polymictic conglomerate

NOKOMIS GROUP


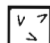


-  Greywacke
-  Layered felsic to mafic volcanoclastic rocks, minor calc-silicate rocks
-  Intermediate volcanic and/or plutonic rocks
-  Mafic volcanic and plutonic rocks

Figure 34.3. Simplified sketch map of the geology in the Mari Lake - Cotteral Lake area. The stratigraphic order is tentative.

Cotteral Lake. Typical samples contain a total of less than 15% biotite and coarse, anhedral, red garnet poikiloblasts in a quartzofeldspathic matrix. The calcareous, hornblende-bearing variety forms a discrete, mappable unit between Little Mari and Mari lakes, where its structural position between Nokomis greywacke and hornblende-free Sherridon arkoses suggests that it locally forms the base of the Sherridon Group. Elsewhere,

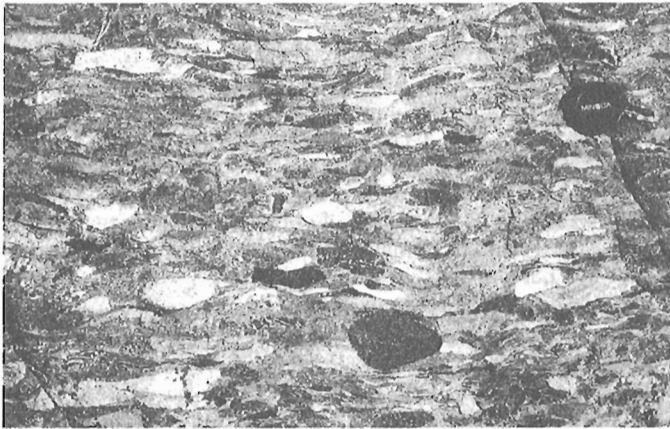


Figure 34.4. Down-plunge view of Sherridon polymictic conglomerate, southern Mari Lake.



Figure 34.5. Sherridon polymictic conglomerate viewed oblique to regional lineation, western Cotteral Lake.

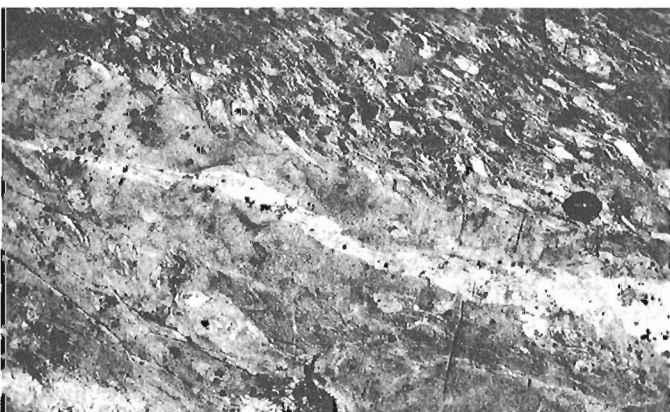


Figure 34.6. Rare example of preserved bedding at contact between Sherridon polymictic conglomerate and arkose, southern Mari Lake. Note the strong, oblique, regional foliation in the polymictic conglomerate.

the hornblende-bearing arkoses occur as thin layers and boudins within the arkoses. Aluminous arkoses generally contain white mica and/or coarse sillimanite faserkiesel. Magnetite and tourmaline are also common accessory phases within the arkoses.

Feldspathic quartzites form discrete units in the Weetago Bay and Wildnest Lake areas and occur elsewhere as centimetre-scale layers within the arkoses. They are typically white, fine- to medium-grained and contain 60-70% quartz, 15-25% plagioclase, and minor amounts of white mica, biotite, garnet, kyanite and sillimanite.

The arkoses and feldspathic quartzites are interpreted as the metamorphosed equivalents of feldspathic, quartz and/or lithic arenites.

A unit of weakly layered to homogeneous biotite-quartz-feldspar greywackes in the southern (Fig. 34.3) and west-central Mari Lake areas is not easily assigned to either the Nokomis or Sherridon Group. Typical samples are white to grey, fine- to medium-grained and contain 10-20% biotite and hornblende, and up to 3% magnetite, in a quartzofeldspathic matrix. The high magnetite content and arkosic composition have led to their tentative assignment to the Sherridon Group, but their structural position within Nokomis greywackes may indicate that they are part of that sequence.

Volcanic and volcanoclastic rocks

Three types of predominantly intermediate to mafic hornblende-rich gneisses have been tentatively interpreted as Sherridon volcanic and volcanoclastic rocks. Due to the presence of rocks of this composition in the Nokomis Group, however, it is particularly difficult to classify specific occurrences. In the Weetago Bay and Wildnest Lake areas, intermediate to mafic garnet-hornblende-quartz-plagioclase gneisses occur between Sherridon arkoses and feldspathic quartzites, and are therefore interpreted as part of the Sherridon Group. They are well layered on a scale of millimetres to centimetres and are only a few metres to tens of metres thick. Typical samples weather dark green and contain 0-8% garnet, 0-7% clinopyroxene, 30-50% hornblende, 0-2% biotite, 10-25% quartz and 30-40% plagioclase. They are interpreted as mainly volcanoclastic rocks but may also contain minor volcanic flows.

In the southern Wildnest Lake area (Fig. 34.2), another compositionally similar suite of intermediate to mafic garnet-hornblende-biotite-quartz-feldspar rocks was recognized. Although the contacts of the unit are not exposed, Sherridon

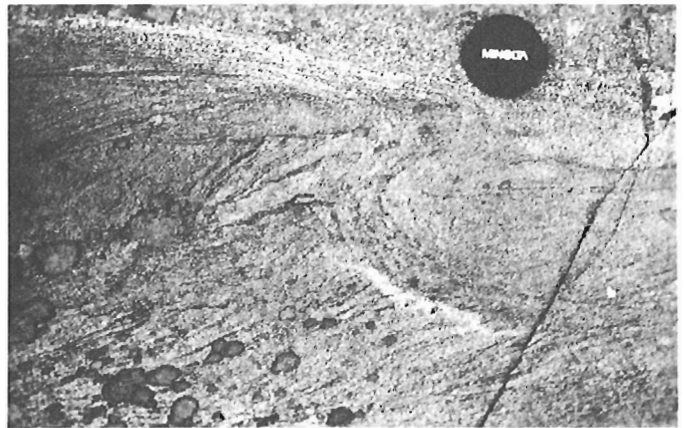


Figure 34.7. Relict crossbedding(?) in folded Sherridon arkose, central Cotteral Lake.

arkoses and feldspathic quartzites occur in the area and may be interlayered. These rocks differ from the mafic gneisses described above in their more homogeneous nature and by containing coarse garnet and/or hornblende poikiloblasts up to 3 cm. They are interpreted as intermediate to mafic volcanic rocks.

A much more heterogeneous suite of hornblende-bearing gneisses occurs in the hinge zone of the Mari Lake synform. They are flanked by granodiorite and Nokomis greywacke to the north and Sherridon polymictic conglomerate to the south. The northernmost unit is a thin, relatively homogeneous garnet-hornblende-quartz-plagioclase rock of intermediate to mafic composition. It grades southward into well layered, intermediate to mafic, garnet-hornblende-biotite-quartz-plagioclase \pm clinopyroxene gneisses, which become progressively more felsic, culminating in heterogeneous, well layered garnet-biotite-quartz-plagioclase \pm hornblende \pm magnetite gneisses along the shore of Mari Lake. The suite is thought to represent a gradation from intermediate to mafic volcanic rocks in the north to felsic volcanoclastic rocks in the south, although there is no evidence to indicate the younging direction of the sequence. The unique structural position of these rocks with respect to the Sherridon stratigraphic succession and their dissimilarity to the well documented Sherridon volcanic and volcanoclastic rocks described above, may lead to their reclassification as Nokomis Group rocks at a future date. A suite of rocks exhibiting a similar compositional variation and structural setting in the eastern Kisseynew Lake area, was assigned to the upper Sherridon Group by Zwanzig (1983).

In the northern Mari Lake area, a suite of mafic dykes intrudes the Sherridon arkoses. Most are now concordant, but rare apophyses, which cut across layering but are overprinted by the regional foliation, indicate a pre-tectonic, intrusive origin. Most are less than a few metres thick and consist of homogeneous, foliated, fine- to medium-grained hornblende-plagioclase \pm garnet rocks. They are interpreted as a set of diabase dykes and small gabbros which may be coeval with the Sherridon volcanic and volcanoclastic rocks in the Weetago Bay and Wildnest Lake areas.

Granitoid and migmatitic gneisses

In the northern Weetago Bay area, fine- to medium-grained gneissic granodiorites, hornblende-biotite-quartz-feldspar \pm garnet \pm clinopyroxene \pm magnetite migmatitic gneisses, diorites and gabbros are interlayered with Nokomis greywackes and volcanoclastic rocks. Centimetre- to metre-scale layering in the gneisses is well defined to nebulitic, where it grades into migmatites and gneissic granodiorites.

The pink, grey or rusty weathering, biotite-rich gneisses typically contain about 5-10% biotite, 25% quartz, 50% plagioclase, 10% microcline and minor amounts of zircon and apatite. Garnet, white mica, hornblende and magnetite are also important constituents in some outcrops.

The hornblende-rich gneisses are generally black and white and contain 10-25% hornblende and biotite, 20-30% quartz, 40-60% plagioclase and 2-5% microcline. Accessory minerals include zircon, apatite, sphene and opaques, and garnet and clinopyroxene were noted in a few outcrops. The hornblende-rich gneisses locally grade into small bodies of metamorphosed, foliated to massive, black and white, fine- to coarse-grained diorite and gabbro containing up to 60% hornblende and 5% garnet.

All of the granitoid and migmatitic gneisses contain schlieren of mafic hornblende gneisses and amphibolites and most also include about 10% leucosome, the composition of which varies with the composition of the associated

melanosome. Most of this leucosome is white, medium- to coarse-grained, biotite-quartz-feldspar material containing up to 5% biotite and locally significant amounts of hornblende, garnet and/or magnetite. Typical outcrops of the migmatitic gneisses also contain granodiorite sills, quartz veins and 10-30% pink biotite-white mica-quartz-feldspar pegmatites.

The granitoid and migmatitic gneisses are thought to be the high grade equivalents of Nokomis and Sherridon Group rocks which have been heavily injected with granodiorite and pegmatite.

Granitoid intrusive rocks

Three types of pre- to syn-tectonic, granitoid intrusive rocks have thus far been distinguished in the Weetago Bay-Wildnest Lake area. They include a suite of tonalites which occur as small plutons within the Nokomis and Sherridon Group rocks, two large hornblende granodiorite plutons named the Tyrrell Lake and Walker Lake Granodiorites by Macdonald (1981), and two smaller granodiorites in the Weetago Bay and Mari Lake areas (Fig. 34.2).

The small tonalite plutons occur along the southern side of Weetago Bay, in the eastern and central Mari Lake areas and along the eastern side of Wildnest Lake. They are typically homogeneous and well foliated, and may be white, grey or pink. Most are medium grained and contain 10-40% hornblende and biotite, with patchy occurrences of coarse garnet porphyroblasts probably resulting from the assimilation of supracrustal material. Schlieren and inclusions of mafic, hornblende-rich material and biotite-quartz-feldspar gneiss are common, and many outcrops contain minor, irregular, coarse grained, hornblende-bearing segregations. Dykes of aplite and fine grained diorite are intrusive into the tonalites in the Weetago Bay area, and pink, pegmatite dykes are a common feature throughout the tonalites.

Little has thus far been seen of the two large hornblende granodiorite plutons. The Tyrrell Lake Granodiorite has only been observed at its northern limit where it is homogeneous, coarse grained and weathers pink to white. Typical samples contain about 5-10% biotite, 1-10% hornblende, 0-5% garnet, 25% quartz, 55% plagioclase and 10% microcline, with minor zircon, apatite, sphene and opaques. The border zone contains rare xenoliths of garnet-hornblende gneiss and arkosic rocks. Pink, hornblende-bearing swaths and pink, crosscutting pegmatite dykes are characteristic of most outcrops.

The Walker Lake Granodiorite is somewhat more mafic, containing 15-30% hornblende and biotite, although this difference may be a function of the small portion of each pluton thus far observed. Typical samples are homogeneous, well foliated, medium grained and white to grey.

The granodiorite bodies in the Weetago Bay and Mari Lake areas are typically medium grained but show evidence of having been recrystallized, with originally coarse feldspar grains deformed into pink, pancake-shaped aggregates of 1-1.5 mm grains. Outcrops may be near homogeneous to well foliated and/or lineated, but most exhibit some nebulitic layering defined by changes in grain size and mineral compositions. Typical samples are white, pink or grey and contain 3-10% biotite. Magnetite, hornblende and garnet are minor components at Mari Lake, probably due to contamination from supracrustal material. Many outcrops contain layers, inclusions and/or schlieren of mafic hornblende-plagioclase rocks and quartzofeldspathic material, and at Weetago Bay, the granodiorites appear to grade into Sherridon arkosic gneisses. Pink pegmatite dykes intrude the granodiorites at both localities.

South of Weetago Bay, a suite of porphyritic tonalites intrude Amisk-Nokomis volcanoclastic rocks and greywackes at the boundary between the Flin Flon volcanic belt and the Kisseynew gneisses. They are white weathering, homogeneous, and fine grained with about 10% white to pink feldspar and 5% hornblende and biotite phenocrysts. A sample studied petrographically contains 6% hornblende, 6% biotite, 5% microcline, 20% quartz, 60% plagioclase, and minor zircon, apatite and opaques. The porphyritic tonalites are intruded by 10% pink, white mica-bearing pegmatite dykes.

Massive, pink and white, granitic pegmatite dykes are common throughout the area. Typical samples contain trace-5% biotite, 0-5% white mica, 20-30% quartz and about 75% feldspar. Tourmaline is a common accessory in some outcrops. A patchy, yellow staining in pegmatite dykes from the Weetago Bay area is similar to that observed farther east in the Kisseynew Lake area where it was shown to be uranophane alteration (McRitchie, 1985).

Structure

The Kisseynew gneisses have been affected by at least four phases of folding which have obliterated virtually all primary igneous and sedimentary features. The earliest recognized structure is a mesoscopic, tight, recumbent fold. It was recognized in the central Mari Lake area and folds a layered Nokomis greywacke so that the strong regional foliation is axial planar to the observed layering (Fig. 34.8).

More common are tight to isoclinal, locally recumbent folds which deform the regional foliation and commonly display shearing along the limbs (Fig. 34.9). They are found in all of the supracrustal rocks as well as the migmatitic gneisses. A strong, regional lineation, best recognized as a stretching lineation in the polymictic conglomerate, was probably developed during this second phase of folding, but could be older and only modified by the second and later phases. The apparent synclines defined by the Sherridon polymictic conglomerate in the Cotteral and Little Mari lakes areas, and by the calcareous arkose between Little Mari and Mari lakes, are tentatively interpreted as belonging to one of these early phases (Fig. 34.3).

At least two phases of more open, near-upright folds post-date the early, tight to isoclinal folding. The gently north-plunging antiform between Cotteral and Little Mari lakes (Fig. 34.2) is an example of one of these later folds. It appears to re-fold the earlier, isoclinal structures defined by the polymictic conglomerate in the Cotteral and Mari lakes areas, and may be part of an extensive set of gently to moderately northeast-plunging folds recognized north (Cheesman, 1956) and northwest (Pyke, 1961) of Wildnest Lake.

The Wormworth Lake synform, outlined by the Walker Lake Granodiorite in the Cotteral Lake-Wildnest Lake area, is a large, open structure resulting from the interference of the synformal analogue to the north-plunging Cotteral Lake antiform and an open, upright, northeast-plunging fold, which is probably part of a set which includes the east-trending Schott Lake antiform north of Wildnest Lake (Cheesman, 1956; Pyke, 1961). The large, open flexure of Amisk strata between Annabel and Amisk lakes in the Flin Flon volcanic belt (Fig. 34.1) is also thought to be related to this later set of northeast-plunging folds. From the mapping of Pyke (1961), it appears that the northeast-plunging set of folds postdates and re-folds the north-plunging set.

The large, irregular, dome-like structure in the Mari Lake area (Fig. 34.2) is also the result of interference of at least two phases of folding. The north-trending part of the structure is near isoclinal and is overturned to the west. Most of the layering

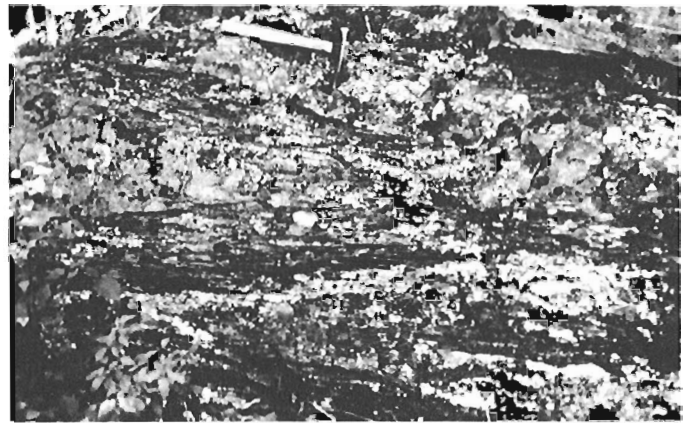


Figure 34.8. Early recumbent fold in bedded Nokomis greywackes, central Mari Lake. Well developed axial planar foliation is parallel to the main regional foliation.

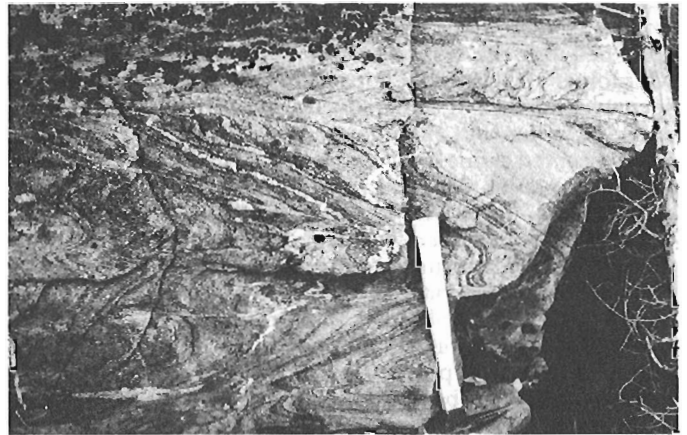


Figure 34.9. Recumbent folds deforming gneissic layering in Sherridon arkoses, southwestern Cotteral Lake. Note the sheared fold limbs.

in the southern hinge zone dips moderately to steeply northward, defining an east-northeast-plunging synform, although dip reversals due to earlier isoclinal folding are common. Since the main regional lineation is folded around the southern hinge zone of the dome, the structure is thought to postdate the two early phases of tight to isoclinal folding, but its isoclinal, overturned nature may indicate deformation related to yet another phase which predates both the north- and northeast-plunging sets of later, open folds.

Few faults have been recognized in the area. Shearing along the limbs of early isoclinal folds has been observed at outcrop scale and may indicate larger-scale, low-angle faulting. Contacts between Sherridon arkoses and Nokomis volcanoclastic rocks along the northeastern side and at the southern end of Wildnest Lake, and between Sherridon polymictic conglomerates and Nokomis greywackes on the eastern side of Little Mari Lake, are strongly sheared and may be examples of such layer-parallel faulting.

Late, north-striking, apparent left-lateral brittle faults (Byers et al., 1965) in the Weetago Bay-Mari Lake area (Fig. 34.2) and northeast-striking faults (Pyke, 1961) in the northwestern Wildnest Lake area are marked by minor brecciation and fractures filled by chlorite and epidote.

Metamorphism

The absence of staurolite in the metagreywackes and of significant anatexis in rocks of granitic composition is consistent with middle amphibolite facies metamorphic conditions (upper medium grade of Winkler, 1979), although the nature of the granitoid and migmatitic gneisses implies slightly higher temperatures in the Weetago Bay area. There is no obvious difference in metamorphic grade between the Nokomis and Sherridon groups, and only a weak metamorphic gradient, marked by a coarsening in average grain size to the north and west, was recognized. Although sillimanite, microcline, white mica and quartz coexist on the scale of a thin section in some Sherridon arkoses, the sillimanite is not in contact with the microcline and does not appear to have grown due to the breakdown of muscovite in the presence of quartz.

The discovery of kyanite in Nokomis greywackes from the Mari Lake area and in Sherridon arkoses from western and northeastern Wildnest Lake was unexpected. Kyanite has been reported from metamorphosed alteration zones near Snow Lake in the Flin Flon volcanic belt (Froese and Moore, 1980) and from late, discordant quartz-feldspar veins in the transition zone between the volcanic belt and the Kisseynew gneisses (Gordon et al., 1985), but apparently not from within the Kisseynew gneisses. It generally occurs as rare, microscopic, anhedral grains, but euhedral porphyroblasts up to 1 cm long were observed at one locality on eastern Mari Lake. Sillimanite and kyanite occur together in some samples, but they are not in contact and appear to result from different reactions. Due to the rare presence and generally anhedral nature of the kyanite, it is thought to have been unstable relative to sillimanite at the peak metamorphic conditions. The presence of euhedral garnet and biotite in the kyanite-bearing samples, however, implies that the assemblage kyanite-garnet-biotite was stable at one time during the metamorphic history of these rocks, which is particularly significant because it implies metamorphic pressures in excess of 4.8 kb (Carmichael, 1978). The appearance of sillimanite rather than kyanite in the File Lake and Snow Lake areas, however, led Bailes and McRitchie (1978) to infer 3.5-5 kb metamorphic pressures for the transition zone between the volcanic belt and gneissic terrane. It is therefore possible that rocks now exposed along the southern flank of the Kisseynew gneisses are indicative of a wide range of metamorphic pressures and crustal depths, and may indicate that tectonic thickening was involved in the development of the steep metamorphic temperature gradient across the Flin Flon volcanic belt - Kisseynew gneiss terrane boundary.

Economic geology

Zones of metamorphosed, hydrothermally altered rocks were observed south of Cotteral Lake and on an island in southern Wildnest Lake (Fig 34.2). Both are characterized by garnet-anthophyllite-cummingtonite assemblages although cordierite was not recognized. The Vass Lake showing, located about 1 km south of Cotteral Lake, has undergone extensive exploration and at one time contained sphalerite, chalcopyrite, pyrite and pyrrhotite (Byers and Dahlstrom, 1954; Beck, 1959). No sphalerite was observed during a cursory look at the occurrence, but samples collected from the alteration zone contain Cu and Fe sulphides, garnet, anthophyllite, spinel and staurolite. The southern Wildnest Lake occurrence is not marked on earlier geological maps and has yet to be thoroughly examined.

The Dolly gold showing (Beck, 1959; Coombe, 1984; Parslow and Gaskarth, 1985), north of the eastern bay on central Mari Lake (Fig. 34.2) has not yet been mapped during this study, but minor chalcopyrite and pyrite were found in a rusty zone within Sherridon arkoses to the southeast, along the shore of the bay.

Acknowledgments

E. Froese, Geological Survey of Canada, J.G. Pearson, Creighton Resident Geologist for the Saskatchewan Geological Survey, D.P. Price, Hudson Bay Exploration and Development Company, and E.C. Syme, Manitoba Mineral Resources Division, all took time to show one of us (KEA) various localities of interest in the Flin Flon area. We also participated in an enlightening field trip to the Kisseynew gneisses in Manitoba led by H.V. Zwanzig, Manitoba Mineral Resources Division. G.R. Parslow, University of Regina, and W.J. Gaskarth, University of Aston, allowed us to accompany them on a tour of mafic rocks in the Mari-Melgurd-Wildnest Lakes area, during which time we also benefitted from discussions with J.G. Pearson and R. Macdonald, Assistant Director of the Saskatchewan Geological Survey. One of us (KEA) also examined a metamorphosed alteration zone in the Kisseynew gneisses northwest of Flin Flon, courtesy of B. Davis, Greenstone Resources.

E. Froese provided encouragement and advice during a mid-summer visit, and A.D. Leclair, Queen's University, supplied assistance and helpful insights into the structure and metamorphism of the area during September.

E. Froese critically reviewed an early draft of this report.

References

- Bailes, A.H.
1971: Preliminary compilation of the geology of the Snow Lake - Flin Flon - Sherridon area; Manitoba Mines Branch, Geological Paper 1/71.
1980a: Geology of the File Lake area; Manitoba Mineral Resources Division, Geological Report 78-1.
1980b: Origin of Early Proterozoic volcaniclastic turbidites, south margin of the Kisseynew sedimentary gneiss belt, File Lake, Manitoba; Precambrian Research, v. 12, p. 197-225.
- Bailes, A.H. and McRitchie, W.D.
1978: The transition from low to high grade metamorphism in the Kisseynew sedimentary gneiss belt, Manitoba; in *Metamorphism in the Canadian Shield*, ed. J.A. Fraser and W.W. Heywood; Geological Survey of Canada, Paper 78-10, p. 155-178.
- Bateman, J.D. and Harrison, J.M.
1945: Mikanagan Lake, Manitoba; Geological Survey of Canada, Map 832A with descriptive notes.
1946: Sherridon, Manitoba; Geological Survey of Canada, Map 862A with descriptive notes.
- Beck, L.S.
1959: Mineral occurrences in the Precambrian of northern Saskatchewan (excluding radioactive minerals); Saskatchewan Department of Mineral Resources, Report 36.
- Bruce, E.L.
1918: Amisk-Athapapuskow Lake district; Geological Survey of Canada, Memoir 105.
- Byers, A.R. and Dahlstrom, C.D.A.
1954: Geology and mineral deposits of the Amisk-Wildnest Lakes area, Saskatchewan; Saskatchewan Department of Mineral Resources, Report 14.
- Byers, A.R., Kirkland, S.J.T., and Pearson, W.J.
1965: Geology and mineral deposits of the Flin Flon area, Saskatchewan; Saskatchewan Department of Mineral Resources, Report 62.

- Carmichael, D.M.
1978: Metamorphic bathozones and bathograds: a measure of the depth of post-metamorphic uplift and erosion on the regional scale; *American Journal of Science*, v. 278, p. 769-797.
- Cheesman, R.L.
1956: The geology of the Mari Lake area, Saskatchewan; Saskatchewan Department of Mineral Resources, Report 23.
- Coombe, W.
1984: Gold in Saskatchewan; Saskatchewan Geological Survey, Open File Report 84-1, 134 p.
- Froese, E.
1984: Geology of the Weldon Bay-Fay Lake area, Manitoba; in *Current Research, Part B*, Geological Survey of Canada, Paper 84-1B, p. 355-358.
1985: Anthophyllite-bearing rocks in the Flin Flon-Sheridon area, Manitoba; in *Current Research, Part B*, Geological Survey of Canada, Paper 85-1B, p. 541-544.
- Froese, E. and Gall, Q.
1981: Geology of the eastern vicinity of Kisseynew Lake, Manitoba; in *Current Research, Part A*, Geological Survey of Canada, Paper 81-1A, p. 311-313.
- Froese, E. and Goetz, P.A.
1981: Geology of the Sherridon Group in the vicinity of Sherridon, Manitoba; Geological Survey of Canada, Paper 80-21.
- Froese, E. and Moore, J.M.
1980: Metamorphism in the Snow Lake area, Manitoba; Geological Survey of Canada, Paper 78-27.
- Gordon, T.M., Jackson, S.L., and Zaleski, E.
1985: Metamorphic processes in the Kisseynew meta-sedimentary gneiss belt, Manitoba; in *Current Research, Part A*, Geological Survey of Canada, Paper 85-1A, p. 511-516.
- Harrison, J.M.
1951a: Possible major structural control of ore deposits, Flin Flon-Snow Lake mineral belt, Manitoba; *Canadian Mining and Metallurgy Institute, Transactions*, v. 54, p. 4-8.
1951b: Precambrian correlation and nomenclature, and problems of the Kisseynew gneisses in Manitoba; Geological Survey of Canada, Bulletin 20.
- James, D.T.
1983: Origin and metamorphism of the Kisseynew gneisses, Kisseynew Lake-Cacholotte Lake area, Manitoba; unpublished M.Sc. thesis, Carleton University, Ottawa.
- Kalliokoski, J.
1952: Weldon Bay map-area, Manitoba; Geological Survey of Canada, Memoir 270.
1953: Interpretations of the structural geology of the Sherridon-Flin Flon region, Manitoba; Geological Survey of Canada, Bulletin 25.
- Macdonald, R.
1975: Compilation geology, Pelican Narrows (63M) and Amisk Lake (63L) areas, Saskatchewan; Saskatchewan Geological Survey, Summary of Investigations 1975, p. 44-47.
- 1981: Compilation and bedrock geology: Pelican Narrows and Amisk Lake areas (NTS 63M, 63L and part 63N and 63K); Saskatchewan Geological Survey, Summary of Investigations 1981, p. 16-23.
- McRitchie, W.D.
1980: Cacholotte Lake (parts of 63K/13,14 and 63N/3,4); Manitoba Mineral Resources Division, Report of Field Activities 1980, p. 65-69.
1985: Kisseynew Project: Geological reconnaissance of Kisseynew Lake West (63K/13 NW); Manitoba Mineral Resources Division, Report of Field Activities 1985, p. 57-63.
- Parslow, G.R. and Gaskarth, W.J.
1985: Kisseynew metallotect geochemical study; Saskatchewan Geological Survey, Summary of Investigations 1985, p. 50-58.
- Pyke, M.W.
1961: The geology of the Attiti Lake area (west half), Saskatchewan; Saskatchewan Department of Mineral Resources, Report 54.
- Robertson, D.S.
1951: The Kisseynew Lineament, northern Manitoba; *The Precambrian*, v. 24, p. 8-11, 13, 23.
1953: Batty Lake map-area, Manitoba; Geological Survey of Canada, Memoir 271.
- Schledewitz, D.C.P.
1985: Kisseynew Project: Kississing Lake, Big Island-Yakushavich Island region; Manitoba Mineral Resources Division, Report of Field Activities 1985, p. 54-56.
- Tuckwell, K.
1979: Stratigraphy and mineral deposits of the Sherridon area; Manitoba Mineral Resources Division, Report of Field Activities 1979, p. 42-45.
- Winkler, H.G.F.
1979: *Petrogenesis of Metamorphic Rocks* (5th edition); Springer-Verlag New York Inc.
- Wright, J.F.
1931: Geology and mineral deposits of a part of northwest Manitoba; Geological Survey of Canada, Summary Report 1930, Part C, p. 1-124.
1933: Amisk Lake, Saskatchewan; Geological Survey of Canada, Summary Report 1932, Part C, p. 73-110.
- Wright J.F. and Stockwell, C.H.
1935: Amisk Lake, Saskatchewan; Geological Survey of Canada, Map 314A with descriptive notes.
- Zwanzig, H.V.
1983: Kisseynew Project: Lobstick Narrows (parts of 63K/13,14 and 63N/3,4); Manitoba Mineral Resources Division, Report of Field Activities 1983, p. 15-22.
1984: Kisseynew Project: Lobstick Narrows-Cleunion Lake, Puffy Lake and Nokomis Lake areas; Manitoba Mineral Resource Division, Report of Field Activities 1984, p. 38-45.

Stratigraphy of the McGerrigle Mountains granite trains of Gaspésie¹

Contract 24ST. 23233-5-0122

Peter P. David² and Pierre Bédard²

David, P.P. and Bédard, P., Stratigraphy of the McGerrigle Mountains granite trains of Gaspésie; in *Current Research, Part B, Geological Survey of Canada, Paper 86-1B*, p. 319-328, 1986.

Abstract

Glacial erratics from the McGerrigle Mountains granite pluton are found over plateau areas across central Gaspésie. They form two well defined linear trains, oriented 160° and 55°, and occur in lesser concentration in areas to the north, west, and southwest of the mountains. Excavations in the southeastern train near the vicinity of the mountains revealed a sequence of preglacial and glacial sediments over the bedrock. The bedrock is solid; fractured, with or without glacial matrix filling the fissures; or weathered to saprolite. Locally, preglacial colluvium overlies the bedrock. Glacial sediments include deformation till, basal till, basal melt-out till, ablation till, train deposit, supraglacial avalanche deposit, and glaciofluvial deposits. Talus and colluvium constitute the postglacial deposits. Sediments of two distinct glaciations have been recognized. A model is proposed to explain the formation of the various glacial lithofacies.

Résumé

Des blocs erratiques d'origine glaciaire se manifestent sur les plateaux du centre de la Gaspésie sous forme de deux traînées de granite provenant du pluton des monts McGerrigle et orientées selon une direction de 160° et 55°, ainsi que sous forme d'une dispersion diffuse et locale des côtés nord, ouest et sud-ouest des monts. Des coupes dans la traînée à orientation sud-est située à proximité des monts, montrent une séquence de dépôts d'origine glaciaire et antérieure à la glaciation reposant sur la roche en place. Cette dernière est soit massive, soit fracturée et, dans ce cas, une matrice d'origine glaciaire peut remplir, par endroits, les fissures, tandis qu'ailleurs, la roche s'est altérée en saprolite. À quelques endroits, la roche en place est recouverte par un colluvion préglaciaire. On compte parmi les divers genres de dépôts glaciaires du till de déformation, du till de fond, du till de fusion, du till d'ablation, des dépôts de traînées, un dépôt d'avalanche supraglaciaire et, finalement, des dépôts fluvioglaciaires. Les dépôts postglaciaires se composent de talus d'éboulis et de colluvions. Des sédiments de deux glaciations distinctes ont été reconnus. On propose un modèle pour expliquer la formation des divers lithofaciès glaciaires.

¹ Contribution to the Canada Economic Development Plan for Gaspé and Lower St. Lawrence, Mineral Program 1983-1988. Project carried by Geological Survey of Canada, Terrain Sciences Division, Project 840035.

² Département de géologie, Université de Montréal, Montréal, Québec H3C 3J7

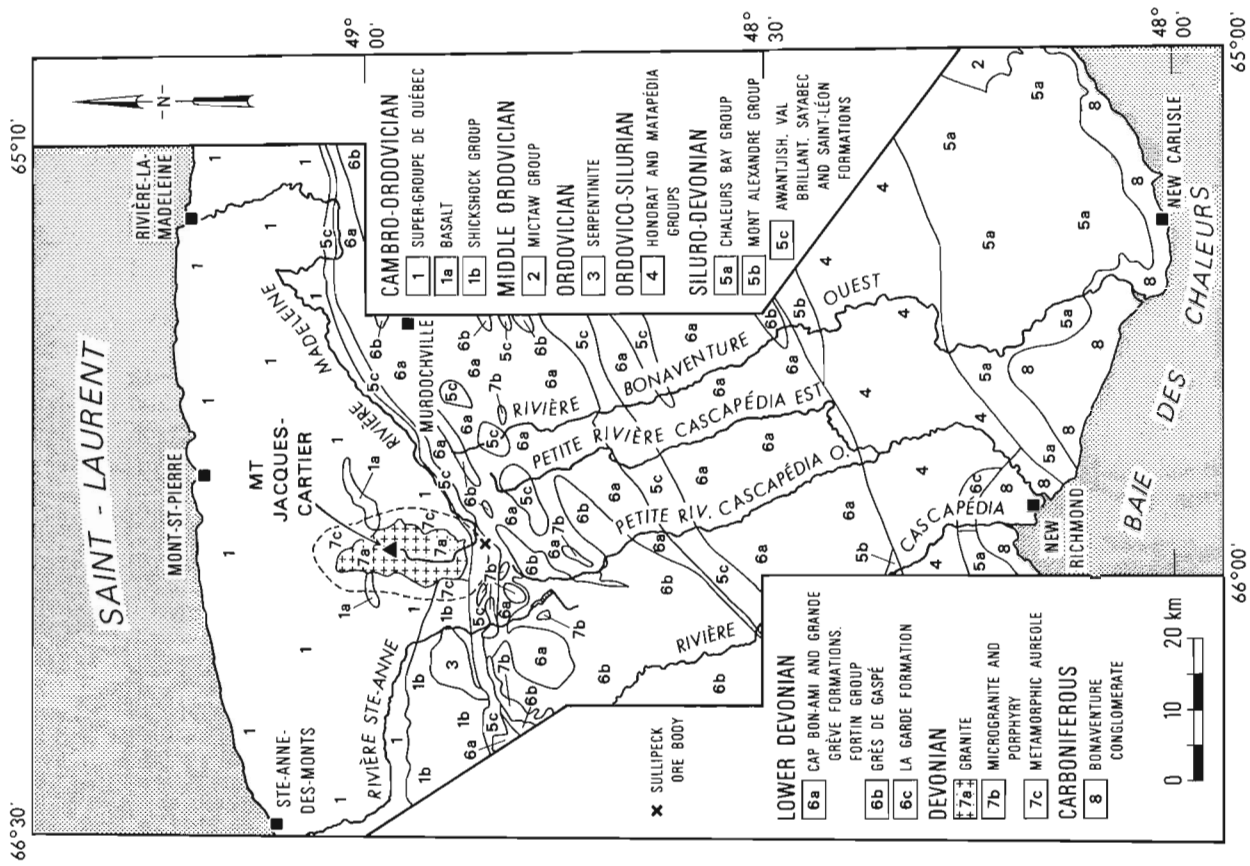


Figure 35.2. Bedrock geology of the study area; the McGerrigle Mountains are shown by units 7a and 7c (geology adapted from McGerrigle and Skidmore, 1967).

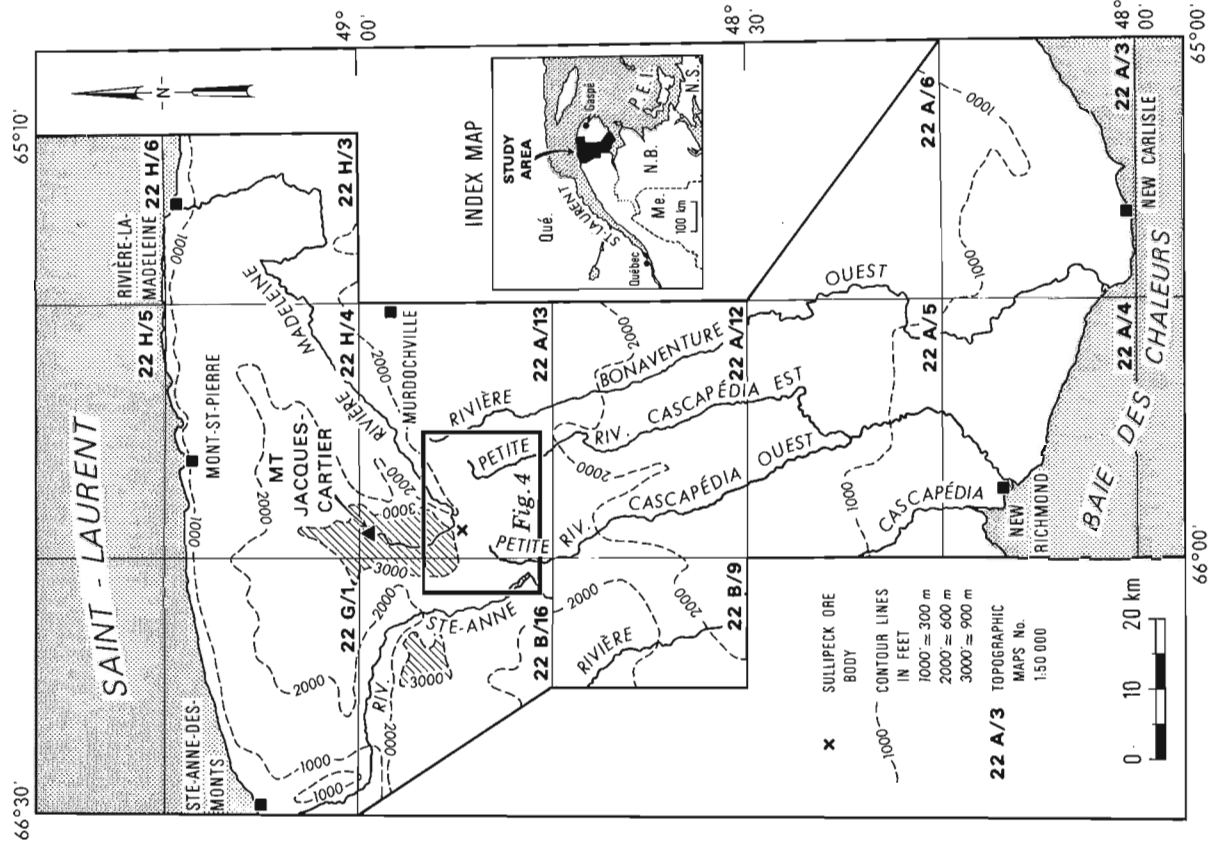


Figure 35.1. Location of study area. Contours approximately delimit the extent of plateau surfaces; hachured areas show land over 3000 feet (the larger area includes the McGerrigle Mountains).

Introduction

This report presents the results of stratigraphic studies conducted in north-central Gaspésie during the summer of 1985 in the proximal part of the southeasterly oriented McGerrigle Mountains granite train. A number of glacial and nonglacial sedimentary units have been identified from excavations along three transects across the train. These units have been correlated with one another and their origin explained. The most important discoveries made are the recognition of a till predating till of the last glaciation, a supraglacial avalanche deposit, as well as the recognition of various glacial sedimentary facies that show the stages of evolution of glacial debris in transport.

Purpose and aim of study

A study of trace element distribution in the fluvial sediments of Gaspésie (Choinière, 1982) has shown that variations in the concentration of the trace elements are related to lithological changes in the underlying bedrock. Even so, Chauvin (1984) observed north of Murdochville (Fig. 35.1) a remarkable correspondence between certain high concentration values of Cu, apparently unrelated to the underlying bedrock, and the local northeasterly ice flow direction. A subsequent detailed study of several of the geochemical maps of Gaspésie by David et al. (1984) has shown that certain linear distribution patterns seem to coincide with the various local glacial flow directions that had been independently identified through mapping of the Quaternary deposits. Since trace element geochemistry forms the basis of mineral exploration in Gaspésie, it has become necessary to identify the nature and amount of glacial contribution to the present trace element distribution through a detailed stratigraphic and geochemical study of a known and geologically well defined extensive glacial deposit. Most suitable for this study are the two granite trains of the McGerrigle Mountains with their associated deposits (Chauvin and David, in press).

Location of the study area

The study area forms a north-south corridor across Gaspésie Peninsula between the St. Lawrence Estuary in the north and Baie des Chaleurs in the south. It is approximately 140 km long, from 40 to 80 km wide, and covers five complete 1:50 000 map areas and parts of six others (Fig. 35.1). Although this region includes the two granite trains with the adjacent areas of low block concentration, it excludes some areas of rare granite block occurrences.

Bedrock geology

Surface lithological contacts and the principal structural elements of the bedrock trend more or less parallel with the elongation of the peninsula and, consequently, the transversely oriented study area includes most of the lithological and structural elements of Gaspésie (Fig. 35.2). For this report, only the granite pluton and its metamorphic aureole forming the McGerrigle Mountains, and the local lithologies immediately south of them, are of particular interest. The metamorphic aureole consists of hornfels, skarn, and metavolcanic rocks. The local lithologies comprise sandstone, limestone, and shale which, in places, are traversed by numerous dykes of porphyric rocks. The Sullipeck ore body occurs at the contact of the aureole and the local rocks.

Physiography

Variations in the topography of the region played an important role in the development and extent of local ice caps and glaciers and in the degree of erosion of the glacial subsurface. In general (Hétu and Gray, 1985), the central portion of Gaspésie is characterized by a high plateau in the north rising above 600 m (2000 foot contour in Fig. 35.1), above which the McGerrigle Mountains highland area projects to over 900 m (3000 foot contour). Southward, across the peninsula, the land surface gradually lowers to a distance about 20 km north of Baie des Chaleurs where it abruptly drops along a south-facing escarpment to the level of a lowland that leads to Baie des Chaleurs.

Glacial geology

David et al. (1984) have summarized five principal ice flow directions which are, from the oldest to the youngest: (1) mostly radial outflow from the high mountains, (2) easterly from the west end of the peninsula, (3) southeasterly across the whole region, (4) east-northeasterly, and (5) northerly in the north.

Various glacial and nonglacial materials occur at the surface over much of the study area (Chauvin, 1984; LaSalle, 1984). In addition, Chauvin and David (in press) observed in geological exploration pits additional sedimentary units overlying and including weathered bedrock. Glacial sediments are more abundant in the north but are locally present in the south as well (LaSalle and David, 1984). Across much of the region, however, they are difficult to identify in the field without excavating because of the rocky nature of the surficial rubble. Bedrock rubble or colluvium is the most common surficial material.

Methods

Field methods

A hydraulic retro-excavator (back-hoe) was used to excavate 72 pits, along three transects across the primary train (Fig. 35.3). The pits range from about 1 to more than 5 m in depth, most of them reaching into the upper few decimetres of the bedrock. At certain locations, the base of the glacial deposits was not reached owing to either their great thickness or their strongly blocky nature. In addition, some 23 of the already existing geological exploration pits were cleared of slump debris and studied. Of the newly excavated pits, 7 were too shallow for sampling and were only described, and only 1 pit was neither described nor sampled because it was judged to be unsafe.

Samples were collected for geochemical, clay and heavy mineral, grain-size, and pebble lithological analyses. Samples for geochemical analysis were taken from the matrix of a deposit using plastic utensils and gloves to avoid contamination. All samples were stored in tightly closed plastic bags in the field to preserve their original moisture content. Every unit was sampled for geochemical analysis, and thick units were sampled at several levels.

Laboratory methods

A total of 241 geochemical samples were prepared in the Quaternary Laboratory of the Université de Montréal, following the method of sample preparation used by the Sedimentology Laboratories of Terrain Sciences Division. These samples are presently being analyzed. Grain sizes analysis using a combined hydrometer-sieve technique has been done on a number of samples and will be statistically treated for the purpose of characterizing the various glacial and nonglacial sediments. Clay and heavy mineral analysis have not yet been performed on the few samples collected for this purpose.

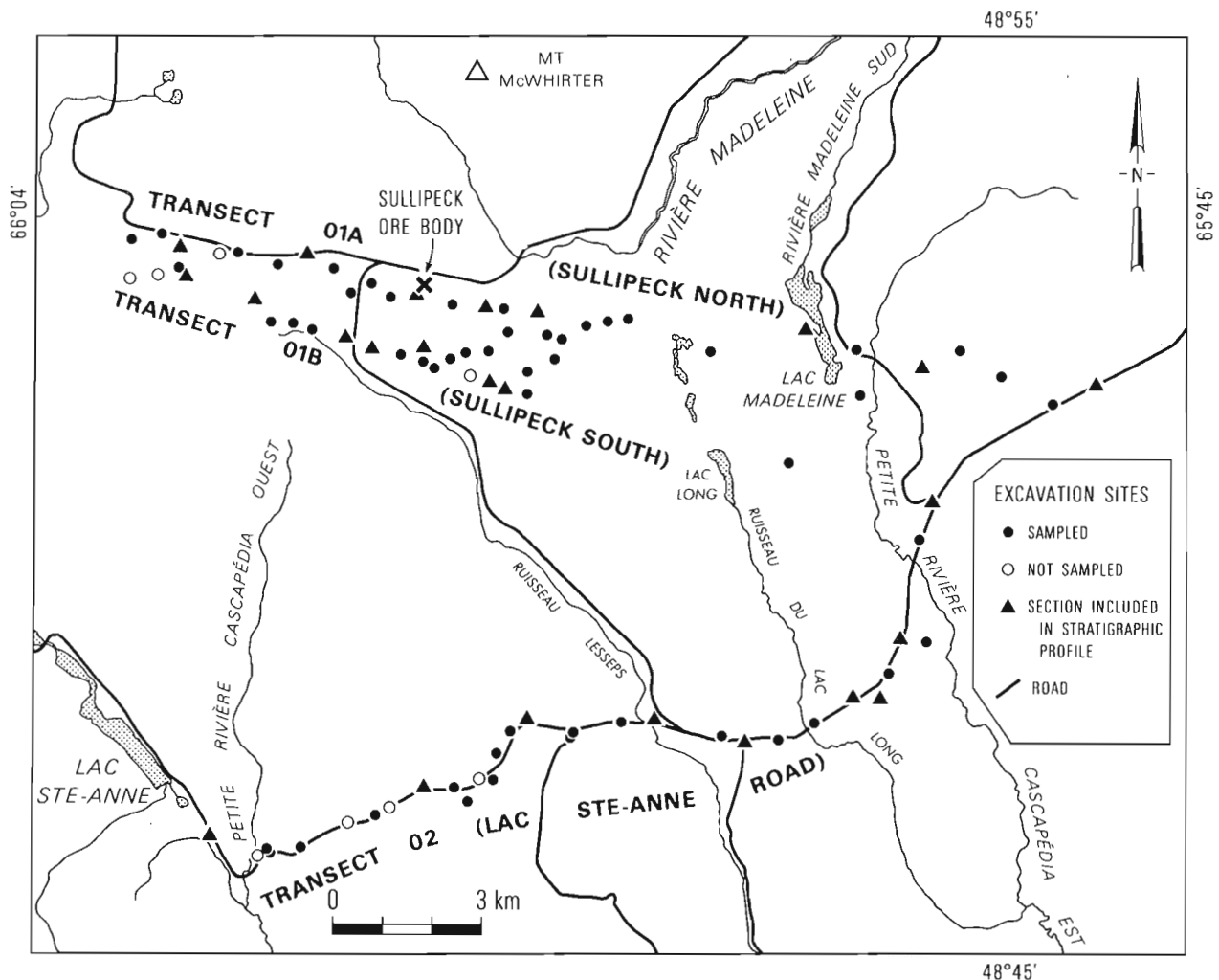


Figure 35.3. Location of excavation sites along three transects across the granite train.

Character and origin of the trains

Description

Blocks of granite derived from the McGerrigle Mountains pluton have been found over plateau areas in all directions around the mountains. They occur (1) in two well defined linear trains, (2) as a blanket of lower concentration of erratics, (3) and as a region of sparse occurrence (Fig. 35.4). The two trains are located to the southeast and northeast of the source area, the blanket lies in a general northerly direction, and the area of sparse occurrence is to the west and southwest. The region of granite block occurrences was mapped by three different surveys which left three small areas on the west side of the mountains unmapped.

The more important one of the two linear trains is oriented southeastward at about 160° and extends from the McGerrigle Mountains to Baie des Chaleurs. It is about 110 km long, 20 km wide in the northern half and more than 50 km wide near Baie des Chaleurs. The other train is oriented northeastward at about 55° to 60° and extends from the mountains to the St. Lawrence estuary near Rivière-la-Madeleine. It is only 40 km long and about 22 km wide.

Origin

The present pattern of dispersal of granite blocks in Gaspésie is the combined result of at least three consecutive glacial phases (Chauvin et al., 1984; David and Lebluis, 1985). The earliest phase of granite dispersal probably occurred during an early, local ice cap-mountain glaciation event when blocks of granite were radially dispersed from the mountains. Because of the paucity of granite blocks in the west, it is presumed that no further transport of granite blocks occurred to the west at any other time. This early phase of glaciation was followed immediately by the southeastward transport of granite blocks by an ice sheet flowing southeastward to beyond the southern limit of the peninsula (LaSalle et al., 1985). This regional ice flow, on the one hand, formed the southeasterly oriented trans-Gaspésian train and, on the other hand, it also redistributed southeastwards the earlier westward-transported blocks giving rise to the sparse granite block occurrences to the west. During the next glacial event that followed the breakup of the ice sheet along the St. Lawrence estuary-gulf system, ice flow changed from southeasterly to northeasterly, and the granite blocks which had already been entrained in the ice, were rerouted northeastward forming the second train. A later northward shift in ice flow formed the blanket of low concentration in the north.

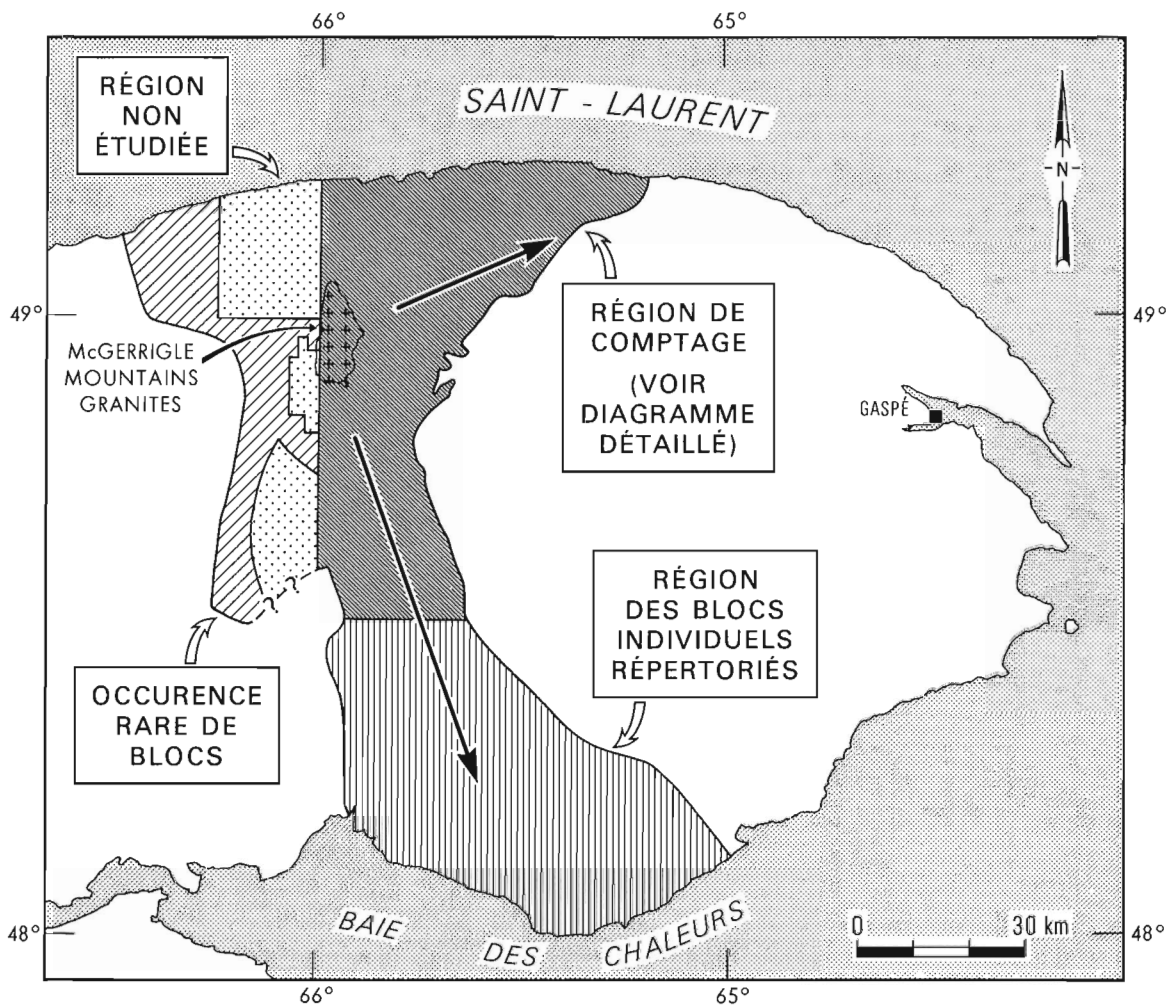


Figure 35.4. Dispersal of granite blocks from the McGerrigle Mountains, showing the granite trains and adjacent areas of low granite erratic concentration.

Chauvin et al. (1984) suggested and later Chauvin and David (in press) have demonstrated that in certain parts of the region, local topography controlled the glacial acquisition of debris for long distance transport. They have shown that those lithologies that formed positive relief and projected well above the general level of the surrounding ground surface were eroded the most and transported the farthest, indicating lesser basal activity in the glacier over low-lying areas, and more rigorous flow at higher levels.

Sub-train stratigraphy

Sedimentary facies and their origin

Excluding the unaltered bedrock, 12 distinct sedimentary units have been identified in the various excavation pits (Table 35.1). Their regional distribution along the three transects is shown through selected sections in Figure 35.5. While at most sites a sequence of only 4 or 5 units can be observed, locally there are as many as seven. These have been identified and characterized by a series of sedimentary and structural parameters (Table 35.1) and by their relative stratigraphic positions (Table 35.2).

The bedrock exposed at the base of most pits varies from place to solid fractured, or fracture-filled with injected glacial matrix.

Saprolite, still showing the original structure of the rock (Fig. 35.6) and containing altered core-stones, is found at a number of locations.

The various till facies have been distinguished from one another on the basis of their degree of maturity reflected in their sedimentary and structural attributes, the relative proportion of clast and matrix fractions, and their relative stratigraphic position (Fig. 35.7). Deformation till is the transitional sediment between fractured bedrock, with glacial matrix injected into the fissures, and basal till. Although matrix-filled fractures in the bedrock are not necessarily glacial in origin, deformation till exists when the rock fragments are displaced in the direction of glacial flow inferred from other sources, and the resulting sediment has an appreciable quantity of fines. The sediment is referred to as basal till of local origin when much of its clast fraction has slightly rounded edges, has a principally clast-supported disposition, and incorporates a small proportion of distal lithologies. A basal till of distal origin has a larger proportion of matrix, becoming principally matrix-supported, has some subrounded clasts, and a larger proportion of distal lithologies. The processes of glacial deformation and reworking forming these deposits also affected the saprolites. At one site, a red and yellow saprolite is overlain by a till of the same lithological composition without any erratics; the clasts in that till consisted of well rounded "fragments" of either one of the prominently coloured units and were emplaced in a homogeneously

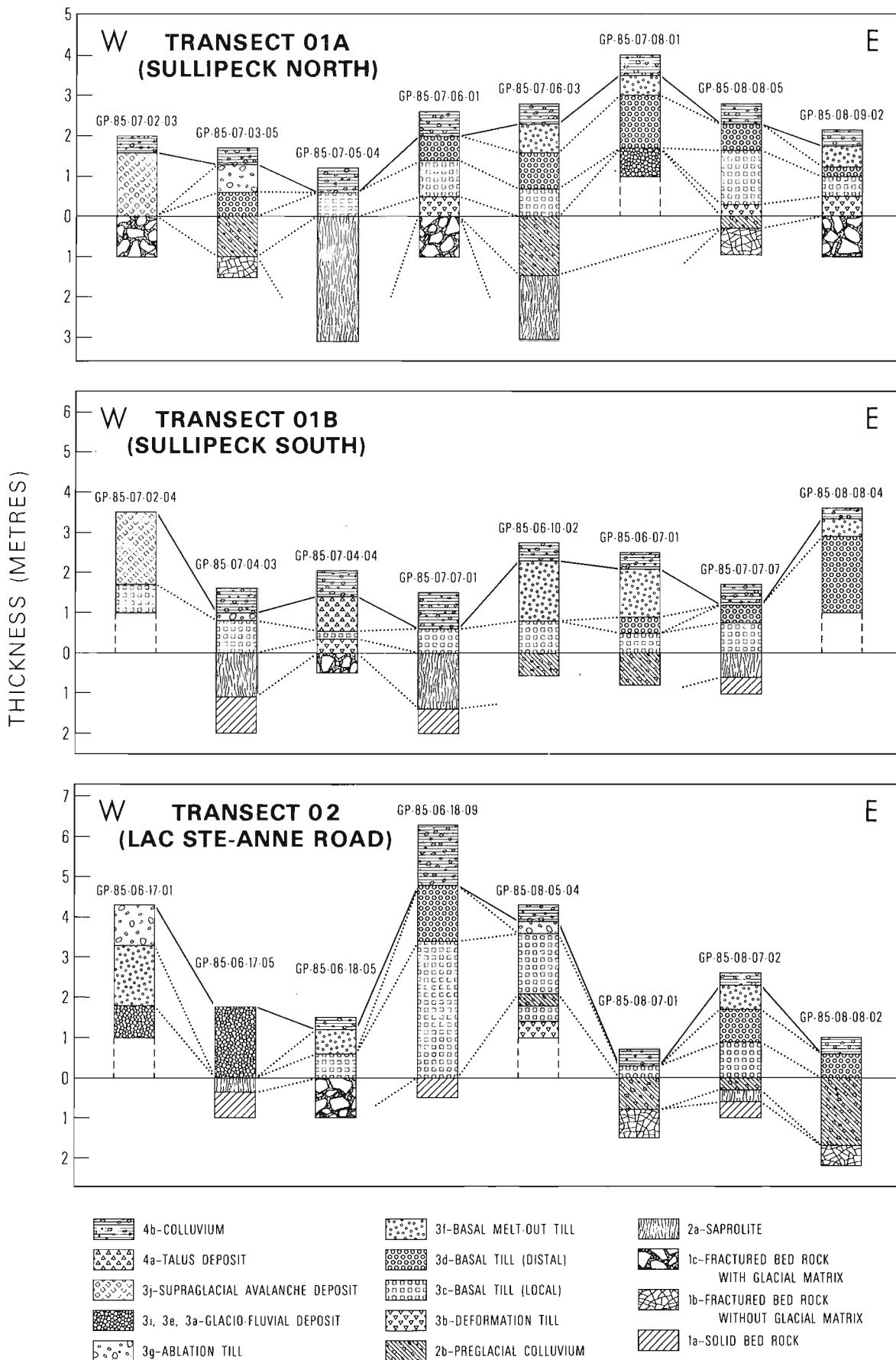


Figure 35.5. Stratigraphic profiles showing the correlation of sedimentary units along the three transects.

Table 35.1. Sedimentary and structural attributes of the various sedimentary units

Description of sediments											
Interpretation	Thickness (m)	Sediment type	Compactness	Clast					Matrix		
				roundness	diam. (m)	disposition	lithology	other	composition	structure	other
colluvium	0.2-1.5	diamict	v L, L	SAN, SRO ANG	<0.3	MS, CS	PL	preferred orientation	silty sand, sand	granular	homogenous
talus deposit	<1.0	blocks	L	ANG	<0.5	CS	ML	rare ALL	sand, silt		little abundant sand layers
glaciofluvial deposit	<2.0	gravel and sand	L	SRO, RON	<0.4	CS	PL	ALL	sand, silty sand		little abundant
supraglacial avalanche deposit	<1.6	blocks	L, C	ANG, SAN	<0.5	CS	almost ML	ALL	sand	—	little abundant
train deposit	—	blocks	—	RON, SRO	<6	at surface	ML	ALL	—	—	—
ablation till	0.2-1.0	diamict	L	SRO, SAN, RON	<0.5	CS, MS	PL	ALL layers	sand, silty sand	little fissile	sand and granule
basal melt-out till	0.2-1.5	diamict	C, L	SRO, SAN	<0.4	MS	PL	preferred orientation	sand, silty sand	fissility 5-10 mm	granule lenses
basal till (distal)	0.2->2.0	diamict	C, v C	SAN, SRO	<0.4	MS	PL	striated, almost AUT	silty sand, clayey silt	fissility 1-5 mm	compact
basal till (local)	0.2-3.5	diamict	C, v C	ANG, SRO	<2	MS, CS	almost ML	striated, AUT blocks	silty sand, clayey silt	fissility 1-5 mm	compact
deformation till	0.3-0.5	diamict	C, v C	almost ANG	—	CS	ML	fractured AUT blocks	silty sand, clayey silt	weak fissility	compact
colluvium (preglacial)	0.2-1.5	diamict	L, C	ANG	<0.3	CS	almost ML	preferred orientation	sand, silt	bedded	
saprolite	0.2->3.2	sand, clay	Va	—	—	—	ML	core-stones	sand, clay	stratified	

L: loose ANG: angular CS: clast supported ML: monolithologic
 C: compact SAN: subangular MS: matrix supported PL: polyolithologic
 v: very RON: rounded ALL: allochtone
 L-C: variable SRO: subrounded AUT: autochtone

Table 35.2. Stratigraphic sequence within the study area

Stratigraphic Sequence			
No.	Sediment	Interpretation	Age
4 b	polyolithologic diamict	colluvium	POST-GLACIAL
4 a	blocks, monolithologic	talus deposit	
3 j	blocks, monolithologic	supraglacial avalanche deposit	GLACIAL
3 i	gravel and sand	glaciofluvial deposit	
3 h	blocks, monolithologic	train deposit	
3 g	diamict, polyolithologic	ablation till	
3 f	diamict, polyolithologic	basal melt-out till	
3 e	gravel and sand	glaciofluvial deposit	
3 d	diamict, polyolithologic	basal till (distal)	
3 c	diamict, monolithologic	basal till (local)	
3 b	diamict, monolithologic	deformation till	
3 a	gravel and sand	glaciofluvial deposit	
2 b	diamict, monolithologic	colluvium	PRE-GLACIAL
2 a	sand, clay	saprolite	
1 c	fractured bedrock with glacial matrix		
1 b	fractured bedrock without glacial matrix	bedrock	
1 a	solid bedrock		



Figure 35.6. Section GP-85-07-04-03, showing colluvium over glaciofluvial gravel over local basal till, overlying saprolite. Inclination of the bedrock strata towards the left is still visible.



Figure 35.7. Section GP-85-07-17-01, showing basal melt-out till over distal basal till, overlying fractured bedrock with glacial matrix filling the fissures.

coloured clayey matrix. Even though matrix-supported, this till was interpreted as a basal till of local origin because of its lithological composition. It was matrix-supported only because of the softness of the easily eroded material.

Even though only some of these till facies occur together at any one site, going from one location to another, one can observe the results of the glacial erosional and comminution processes that must have acted at and near the base of the glacier. The local, patchy preservation of thick saprolites suggests that, within the study area, the base of the glacier was mostly inactive and locally may have been frozen to its base. The reduced activity led to the preservation of the several till facies that represent the different phases of basal erosion, entrainment, and comminution processes.

Basal melt-out till is strongly fissile, has a sandy matrix and almost invariably contains well rounded granite clasts and some of local lithologies. Locally, it has layers of sand and shows a colour banding. In places, it is underlain by glaciofluvial gravels. It is suggested, that the debris which formed the melt-out till was transported in an englacial position just above the basal load and, while incorporating parts of that load, it still remained distinct as an englacial unit. Ablation till is rare in the study pits but occurs at the surface within the study area. Its surficial equivalent, the train deposits are, however, omnipresent. They have been omitted from the sections shown in Figure 35.5. Figure 35.8 shows, in a schematic form, a model for the formation of the above glacial lithofacies.

A supraglacial avalanche deposit has been observed at the west end of the two Sullipeck transects. It consists mostly of angular clast-sized particles of one erratic rock types with rare, subrounded particles of another erratic rock type. The deposit occurs on the south side of a gently sloping small hill that is

separated from the source area to the north by a large low. The supraglacial origin for the deposit is based on its geographical location and on its lithological attributes.

Postglacial colluvium is omnipresent and its thickness varies only slightly from site to site. Its preglacial equivalent is distinguished from it by its relative position and greater compactness.

Glaciofluvial deposits occur in relatively great thickness at the base of two excavations, both located in major valleys, and as thin beds elsewhere, separating the various till facies. They are composed generally of well rounded particles and are poly-lithologic in nature.

Stratigraphic disposition

Preglacial materials include the various forms of the bedrock, its altered equivalent, saprolites, and overlying colluvium. All three units are fairly common to widespread in the study area.

A basal till predating till of the last glaciation is found at one location along the Lac Sainte-Anne road transect (Figure 35.5). The till is overlain by colluvium which is overlain by sediments of the last glaciation. The pre-last till glacial unit seems to show evidence of weathering, though it has not been fully investigated yet.

At the west end of the same transect, and in the eastern half of the Sullipeck North transect, highly inclined stratified glaciofluvial deposits occur. Because they show no evidence of weathering, they are interpreted as having originated from the early phase of ice cap-mountain glaciation and may, in fact, delimit the extent of that glacial expansion.

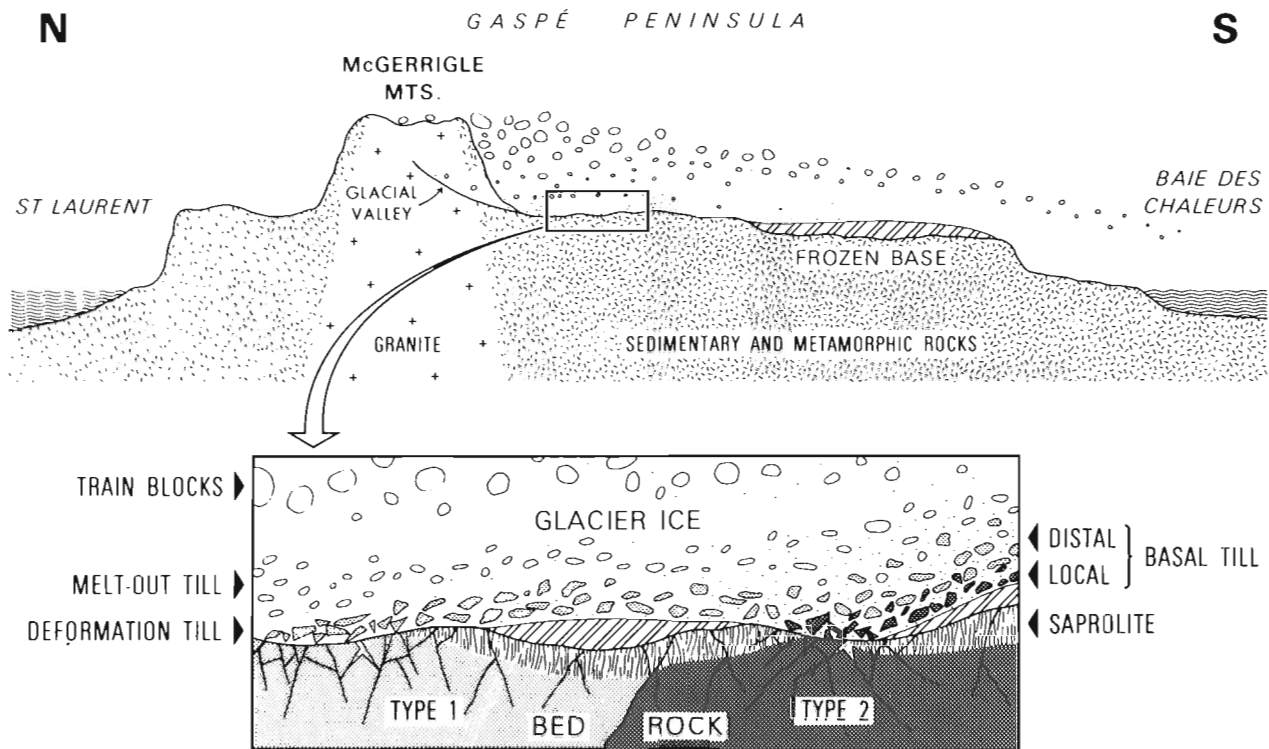


Figure 35.8. Schematic representation of the processes involved in the formation of the glacial lithofacies of the area.

Conclusions

A number of preglacial, glacial, and postglacial stratigraphic units have been identified from excavations made across the southeasterly oriented McGerrigle Mountains granite train in central Gaspésie. The various units differ from one another in their sedimentary, compositional, and stratigraphic attributes. It is believed that these differences will be reflected in the distribution patterns of the ten trace elements for which these units are being analyzed and that they will help determine the role of glacial ice in trace element dispersal in the stream sediments in Gaspésie.

Future field work in the region includes further excavations along the rest of the principal train and along two transects across the secondary train to the northeast.

Acknowledgments

The funds for the project are managed by Institut de recherche en exploration minérale/Mineral Exploration Research Institute (IREM/MERI). The illustrations were drawn by Michel Demidoff of Université de Montréal. The manuscript has been read by J.J. Veillette.

References

- Chauvin, L.
1984: Géologie du Quaternaire et dispersion glaciaire en Gaspésie (région de Mont-Louis-Rivière Madeleine) Ministère de l'Énergie et des Ressources, Québec, ET-83-19, 33 p.
- Chauvin, L. et David, P.P.
— Dispersion glaciaire d'erratiques en Gaspésie centrale et ses applications; Ministère de l'Énergie et des Ressources, Québec, Rapport final. (sous presse)
- Chauvin, L., David, P.P., and LaSalle, P.
1984: Debris production and glacial transport in the Gaspé peninsula, Québec; Geological Society of America, Abstracts with Programs, v. 16, p. 8.
- Choinière, J.
1982: Trace element geochemistry in stream sediments in relation to the bedrock in the Gaspé area, Québec; in *Prospecting in glaciated terrain*, P.H. Davenport (ed.); Canadian Institute of Mining and Metallurgy, p. 105-131.
- David, P.P. and Lebus, J.
1985: The last glacial maximum and deglaciation of the western half of Gaspé Peninsula and adjacent areas, Québec, Canada; Geological Society of America, Special Paper 197, p. 85-109.
- David, P.P., Chauvin, L., Choinière, J., and LaSalle, P.
1984: Ice flow directions and trace element concentration patterns in stream sediments in Gaspé, Québec; Geological Association of Canada, Programs with Abstracts, v. 9, p. 56.
- Héту, B. and Gray, J.
1985: Le modelé glaciaire du centre de la Gaspésie septentrionale, Québec; *Géographie physique et Quaternaire*, vol. 39, p. 47-66.
- LaSalle, P.
1984: Géologie des sédiments meubles de la région de New Richmond - New Carlisle; Ministère de l'Énergie et des Ressources, Québec, DP-83-29.
- LaSalle, P. and David, P.P.
1984: Glacial erosion and transport in southern Gaspé, Québec; Geological Association of Canada, Program with Abstracts, v. 9, p. 82.

LaSalle, P., David, P.P., and Chauvin, L.

1985: Ice limits during the last glacial maximum in Gaspésie, Québec, Canada; Geological Society of America, Abstracts with Programs, v. 17, p. 30.

McGerrigle, H.W. and Skidmore, W.B.

1967: Geological map of Gaspé Peninsula, Québec; Department of Natural Resources, Geological Exploration Service, Map 1642.

Stratigraphic subdivision of the Blind Fiord and Bjerne formations (Lower Triassic), Sverdrup Basin, Arctic Islands

Project 750083

Ashton F. Embry
Institute of Sedimentary and Petroleum Geology, Calgary

Embry, A.F., Stratigraphic subdivision of the Blind Fiord and Bjerne formations (Lower Triassic), Sverdrup Basin, Arctic Islands; in Current Research, Part B, Geological Survey of Canada, Paper 86-1B, p. 329-340, 1986.

Abstract

The Blind Fiord Formation is a Lower Triassic shale/siltstone unit that occurs within the Sverdrup Basin. The formation is divisible into three members, formally named in ascending order: Confederation Point, Smith Creek, and Svartfjeld. Each member consists predominantly of shale in its lower portion and siltstone in its upper portion.

The Bjerne Formation is a sandstone-dominant unit that occurs on the basin margins, and is stratigraphically equivalent to the Blind Fiord Formation. Along the eastern and southeastern basin margins two shale/siltstone units occur within the formation, allowing five members to be recognized. The sandstone-dominant members are formally named in ascending order: Cape Butler, Pell Point and Cape O'Brien. The intervening shale/siltstone members are correlated with the Smith Creek and Svartfjeld members.

The stratigraphic nomenclature reflects the occurrence of three major transgressive-regressive cycles in the Lower Triassic of Sverdrup Basin.

Résumé

La formation de Blind Fiord est une unité de schiste argileux et aleurolite du Trias inférieur qui se trouve dans le bassin de Sverdrup. La formation se divise en trois membres qui portent les noms officiels suivants, donnés en ordre ascendant: Confederation Point, Smith Creek et Svartfjeld. La partie inférieure de chaque membre se compose surtout de schiste argileux et la partie supérieure, d'aleurolite.

La formation de Bjerne, composée surtout de grès, se trouve en bordure du bassin; elle est l'équivalent stratigraphique de la formation de Blind Fiord. La formation comprend deux unités de schiste argileux et aleurolite le long des marges est et sud-est du bassin, ce qui permet d'identifier cinq membres. Les noms officiels des membres, composés surtout de grès, sont donnés en ordre ascendant: Cape Butler, Pell Point et Cape O'Brien. Les membres intercalaires de schiste argileux et aleurolite sont mis en corrélation avec les membres de Smith Creek et de Svartfjeld.

La nomenclature stratigraphique traduit la présence de trois grands cycles de transgression-régression dans le Trias inférieur du bassin de Sverdrup.

Introduction

Lower Triassic strata are widespread in the Sverdrup Basin (Fig. 36.1) and are assigned to either the Bjerne or Blind Fiord formations (Tozer, 1961, 1963a, b). The Bjerne Formation consists predominantly of fine to medium grained sandstone and occurs along the southern and eastern margins of the basin, both in outcrop and the subsurface. The Blind Fiord Formation consists mainly of shale and siltstone with lesser amounts of very fine grained sandstone. The formation forms the basal portion of the Triassic succession on the basin margins where it underlies the Bjerne Formation and thickens basinward to comprise the entire Lower Triassic succession over much of the basin (Fig. 36.1). Outcrops of the formation are common on northern and western Axel Heiberg Island, and it occurs in the subsurface over the central and western Sverdrup Basin. Numerous surface and subsurface sections of these formations have been examined and form the basis for this paper (Fig. 36.1).

Outcrop studies of the Blind Fiord Formation on northern Ellesmere and Axel Heiberg islands have revealed that in those areas, the formation can be divided into three members. Each member, which is usually hundreds of metres thick, consists of a lower, shale-dominant portion and an upper, siltstone-dominant portion. These members are formally defined herein.

Subsurface and outcrop studies of the Bjerne Formation have led to the recognition of five, distinctive, lithologic units within the formation; three sandstone units and two

shale/siltstone units. The sandstone units are formally defined as members herein and the intervening shale units are assigned member names that are defined for the Blind Fiord Formation.

Previous work

Tozer (1963a) defined the Blind Fiord Formation on the basis of fieldwork done during Operation Franklin in 1955. He established a type section north of Blind Fiord on south-western Ellesmere Island. At this locality, the formation is about 1100 m thick and consists of green-grey shale, siltstone and very fine grained sandstone. During Operation Franklin, the formation was also examined by Souther (1963) at Buchanan Lake on east-central Axel Heiberg Island and McMillan (1963) on northwestern Axel Heiberg. Subsequent studies by R. Thorsteinsson and E.T. Tozer on Ellesmere and Axel Heiberg islands in the late fifties and early sixties established the presence of the formation on the northern portions of those islands (Tozer, 1963c). At all localities, the Blind Fiord Formation consists of interbedded shale and siltstone with minor, very fine grained sandstone. It overlies Permian strata and is overlain by black, phosphatic shale of the Murray Harbour Formation (Blaa Mountain Group). Paleontological studies of the Blind Fiord Formation (Tozer, 1961, 1963a, b, 1967) indicate that the entire Lower Triassic is represented in the formation, and Tozer (1965a, 1967) used the ammonite zonation established in the formation to erect four new stages for the Early Triassic.

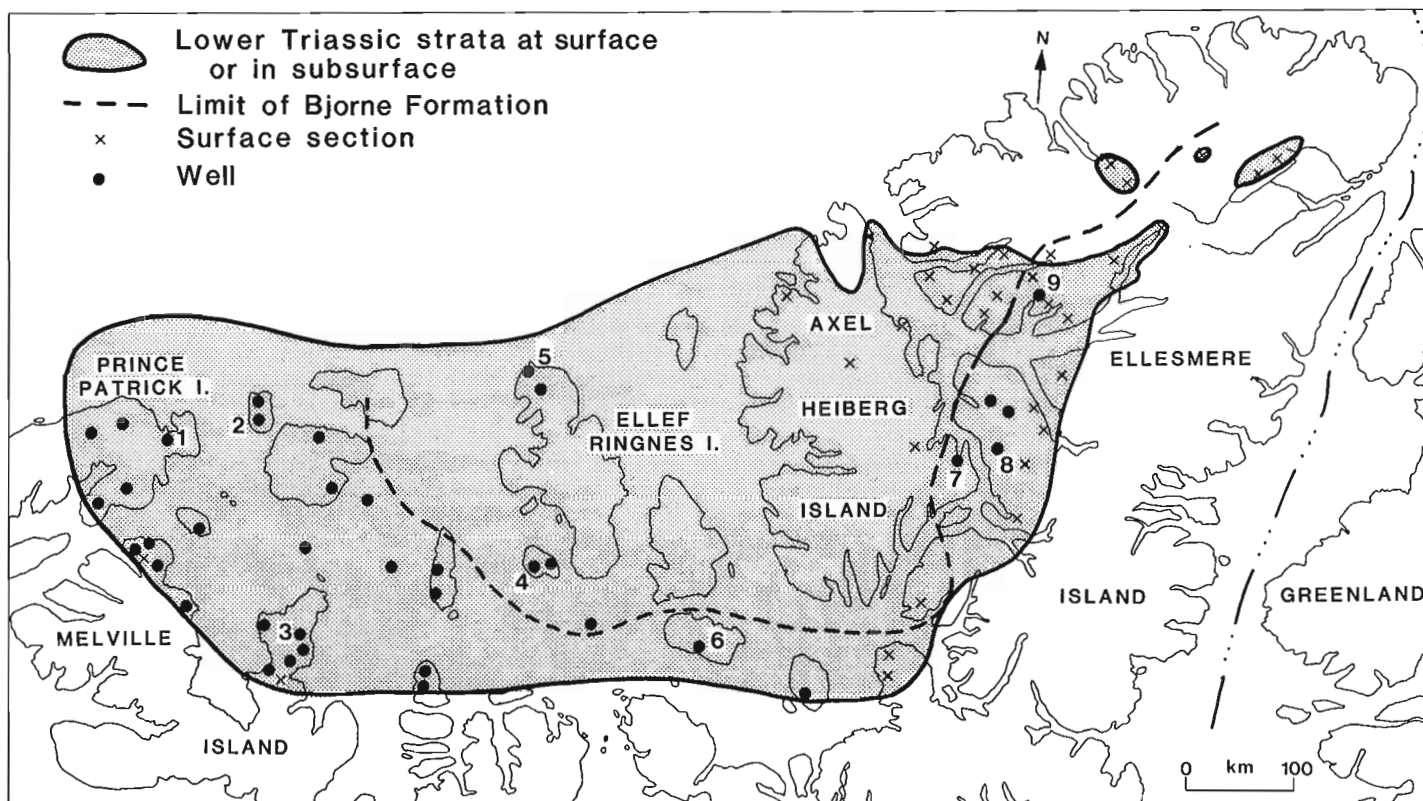


Figure 36.1. Distribution of Lower Triassic strata and control points. Key to wells listed in Appendix:

- | | |
|---------------------|---------------------|
| 1. Satellite F-68 | 6. Cornwall O-30 |
| 2. Brock C-50 | 7. Depot Point L-24 |
| 3. Drake Point D-68 | 8. Fosheim N-27 |
| 4. Sutherland O-23 | 9. Neil O-15 |
| 5. Isachsen J-37 | |

Moore (1981) briefly described the Blind Fiord Formation at three localities on northern Ellesmere Island and noted that sandstone content increased toward the east.

The only published subsurface description of the Blind Fiord Formation is by Balkwill and Roy (1977) of a partial section drilled in the King Christian N-06 well on King Christian Island.

None of the above authors attempted to stratigraphically subdivide the Blind Fiord Formation. However, Tozer (1963c) noted that black shale is a component of the upper part of the Blind Fiord Formation at Smith Creek on northwestern Ellesmere Island. At other localities Tozer (1963c, 1965a) assigned black shales stratigraphically equivalent to those at Smith Creek to the overlying Blaa Mountain Formation. In this paper, these shales are placed in the Blind Fiord Formation.

Tozer (1963b) also defined the Bjerne Formation from studies completed during Operation Franklin. He established a type section on Bjerne Peninsula, southwestern Ellesmere Island, where the formation is 500 m thick and consists mainly of fine to medium grained sandstone. Tozer also examined the Bjerne Formation at Trold Fiord (Tozer, 1963d) and Cameron Island (Tozer, 1963e) during Operation Franklin. Subsequent fieldwork by Tozer and Thorsteinsson established the presence of the formation on Table Island (Tozer, 1961), central and northern Ellesmere Island (Tozer, 1963c) and northern Melville Island (Tozer and Thorsteinsson, 1964). A detailed study of the Bjerne Formation on Melville Island was completed by Trettin and Hills (1966) as a result of the interest in the tar sands that occur in the formation in that area.

Nassichuk and Christie (1968) described the formation in the Tanquary Fiord area of northern Ellesmere Island. Roy (1972) briefly summarizes his studies of the Bjerne Formation on southern and central Ellesmere Island. Roy's field notes also contain much valuable data on the Bjerne and Blind Fiord formations on Ellesmere Island. These data have been incorporated into this study.

Subsurface occurrences of the Bjerne Formation in the Skybattelle Bay C-15 well on Loughed Island have been briefly described by Balkwill et al. (1982), and, in the western Sverdrup by Henao-Londono (1977).

Present work

Tozer (1970) summarized the Lower Triassic stratigraphy of the Sverdrup Basin and demonstrated that the sand-rich Bjerne Formation of the southern and eastern basin margins passes basinward into the argillaceous Blind Fiord Formation. My studies have confirmed this, and it has been found that a thin unit of Blind Fiord Formation occurs at the base of the Lower Triassic succession on the basin margins.

Numerous stratigraphic sections have been measured through the Blind Fiord Formation on northern Ellesmere Island and Axel Heiberg Island (Fig. 36.1). Three members are recognizable in the formation. Each member consists of shale in the lower portion with siltstone dominant in the upper portion (Fig. 36.2, 36.3). These three members are formalized in this paper and are named, in ascending order: Confederation Point, Smith Creek, and Svartfjeld members of the Blind Fiord Formation.

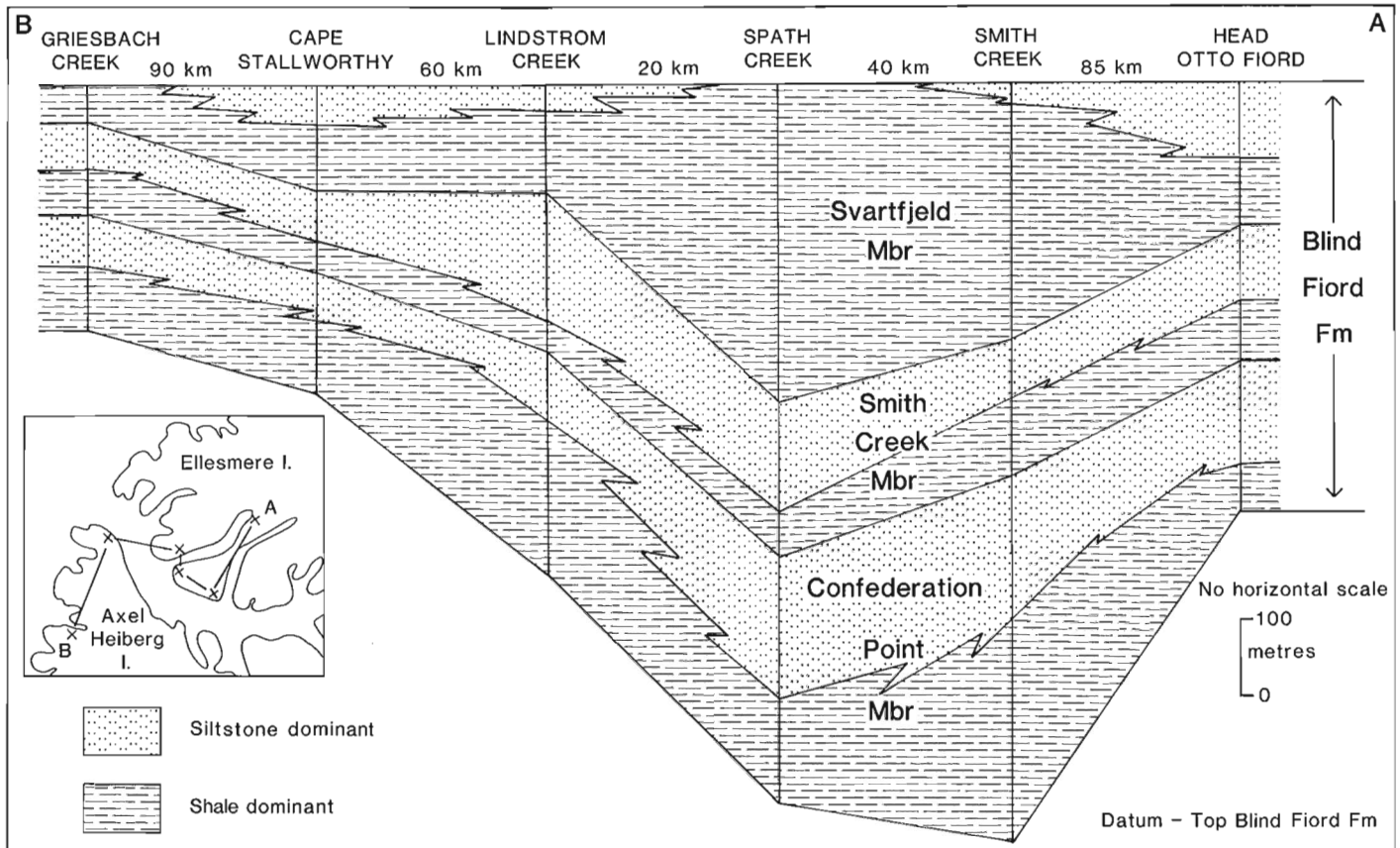


Figure 36.2. Stratigraphic cross-section, Blind Fiord Formation, northeastern Sverdrup Basin.



Figure 36.3. Blind Fiord Formation at head of Otto Fiord, northern Ellesmere Island.

1. Confederation Point Member
2. Smith Creek Member
3. Svartfjeld Member
4. Murray Harbour Formation

On the basin margins, the thin unit of Blind Fiord Formation at the base of the Lower Triassic succession is assigned to the Confederation Point Member and it is overlain by the Bjerne Formation. In many surface and sub-surface sections of the Bjerne Formation, two shale/siltstone units occur within the formation, allowing it to be divided into five subdivisions (Fig. 36.4, 36.5). The three sandstone-dominant units are formally recognized herein as members of the Bjerne Formation and are named, in ascending order: Cape Butler, Pell Point and Cape O'Brien. The intervening shale units, which represent tongues of the Blind Fiord Formation, are assigned member names defined for the Blind Fiord Formation: Smith Creek and Svartfjeld (Fig. 36.6). However, it is important to note that in this case the Smith Creek and Svartfjeld members are part of the Bjerne Formation.

The tops for the new members from selected wells in the Sverdrup Basin are listed in the Appendix. Well cuttings taken at three metre intervals from the type sections of the new members of the Bjerne Formation can be examined at the Institute of Sedimentary and Petroleum Geology, Calgary, Alberta.

Confederation Point Member, Blind Fiord Formation

Definition

The Confederation Point Member consists of medium to dark grey, silty shale with interbeds of argillaceous siltstone that become more common upward. The type section is in an unnamed creek 2 km north of Smith Creek on Svartfjeld Peninsula, northwestern Ellesmere Island (80°37'30"N; 87°39'W) (Fig. 36.7). The member is named for Confederation Point, which is 4 km to the southeast of the type section.

Boundaries

The Confederation Point Member abruptly overlies various Permian strata, including glauconitic sandstone of the Trold Fiord Formation, bioclastic limestone of the Degerbols Formation and argillaceous chert of the Van Hauen Formation. The soft grey shale of the Confederation Point contrasts sharply with the Permian rock types and the contact is placed at the base of the first unit of soft, medium to dark grey shale. The contact is unconformable on the basin margins and becomes conformable within the basin. In the basin, the Confederation Point Member is conformably overlain by the Smith Creek Member of the Blind Fiord Formation, and the contact is placed at the top of the highest siltstone unit above which soft shale is the predominant rock type. On the basin margins the member is conformably overlain by the Bjerne Formation (usually Cape Butler Member) and the contact is placed at the base of the first sandstone above which sandstone is predominant.

Lithology

At the type section, the lower 300 m consists of medium grey, silty shale with thin, widely spaced siltstone interbeds. In the upper 175 m of the member, siltstone units, which are parallel laminated to burrowed and up to 50 m thick, occur interbedded with the grey shale. This description applies to the member over the northern Ellesmere-Axel Heiberg area; interbeds of very fine grained sandstone increase to the southeast.

Thickness and distribution

The Confederation Point Member occurs on northern Ellesmere and Axel Heiberg islands, where it is up to 525 m thick. The member comprises the entire Blind Fiord Formation on the eastern and southern basin margins, where it underlies the Bjerne Formation. Thicknesses in these areas are usually less than 100 m. The member has also been tentatively recognized in wells in the western Sverdrup Basin.

Age

The Confederation Point Member is dated as Griesbachian and Dienerian on the basis of ammonites collected from the member on northern Ellesmere and Axel Heiberg islands (Tozer, 1965a). On the basin margins, the member is probably only Griesbachian.

Environment of deposition

The argillaceous lithologies, marine fauna, and sedimentary structures all suggest an outer shelf to marine slope environment of deposition for the member.

Smith Creek Member, Blind Fiord Formation

Definition

The Smith Creek Member consists of medium to dark grey silty shale with argillaceous siltstone interbeds common in the upper portion. The type section is at the head of an unnamed stream 2 km north of Smith Creek on northwestern Ellesmere Island and is 180 m thick (Fig. 36.7). The name is taken from the nearby Smith Creek.

Boundaries

Within the basin, the Smith Creek Member conformably overlies the Confederation Point Member as previously described. On the basin margins, it conformably overlies the Cape Butler Member of the Bjerne Formation, and the contact is placed at the base of the lowest shale/siltstone unit above which shale and siltstone are predominant.

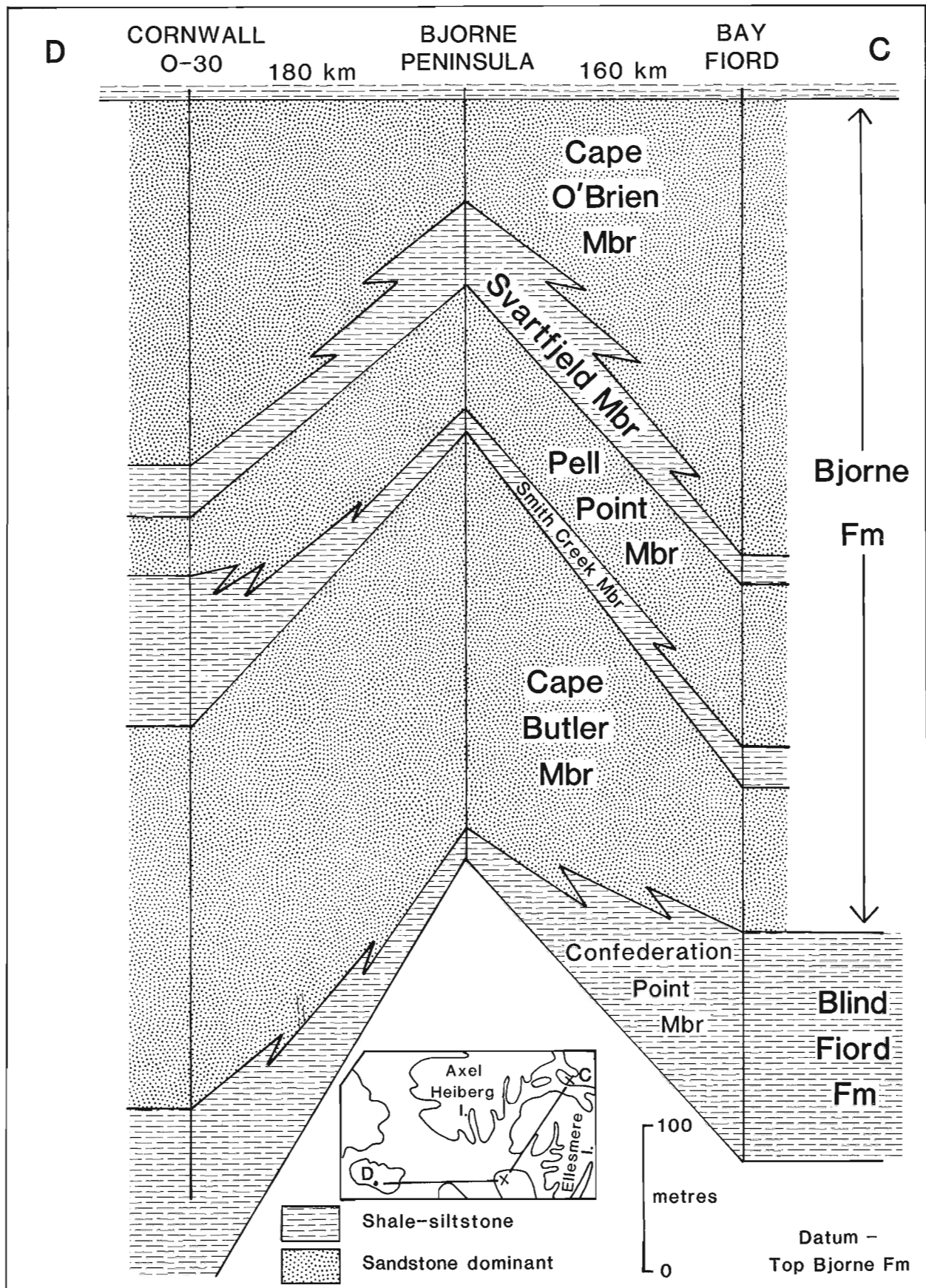


Figure 36.4. Stratigraphic cross-section, Bjorne Formation, southeastern Sverdrup Basin.

The Smith Creek Member in the basin is overlain by the Svartfjeld Member. The contact is placed at the top of the highest siltstone unit above which shale is predominant. Marginward, it is overlain by the Pell Point Member of the Bjerne Formation and the contact is placed at the top of the highest shale/siltstone unit above which sandstone is the predominant lithology.

Lithology

At the type section, the lower 85 m consists of medium to dark grey shale with a few resistant, parallel laminated siltstone units in the upper portion. A distinctive, grey,



Figure 36.5. Portion of Bjerne Formation at the Canyon Fiord locality with shale and siltstone of the Smith Creek Member overlying sandstone of the Cape Butler Member and underlying sandstone of the Pell Point Member.

bioclastic limestone unit 0.5 m thick with a rich ammonite fauna caps the lower portion of the member. The upper 95 m consists of dark grey shale with medium grey siltstone units increasing in thickness and frequency upwards. In other sections, siltstone is more common and usually dominates the upper one half to two thirds of the member. Interbeds of very fine grained sandstone also occur in these sections. Sedimentary structures in the coarser rock types include parallel lamination, ripple crosslamination and a variety of trace fossils.

Thickness and distribution

The Smith Creek Member is recognized in the outcrop of Blind Fiord Formation on northern Axel Heiberg and Ellesmere islands, where it is up to 320 m thick. The member also occurs along the eastern and southeastern basin margins. It has been tentatively recognized in wells in the western Sverdrup.

Age

Ammonites collected on Ellesmere and Axel Heiberg islands indicate a latest Dienerian to Smithian age for the member (Tozer, 1965a).

Environment of deposition

An outer shelf to marine slope environment of deposition is suggested by the argillaceous lithologies and marine fauna.

Svartfjeld Member, Blind Fiord Formation

Definition

The Svartfjeld Member consists of medium grey to black shale with interbeds of siltstone in the upper portion of the member. The type section is on Smith Creek in north-western Ellesmere Island (80°38'N; 87°37'W) where the

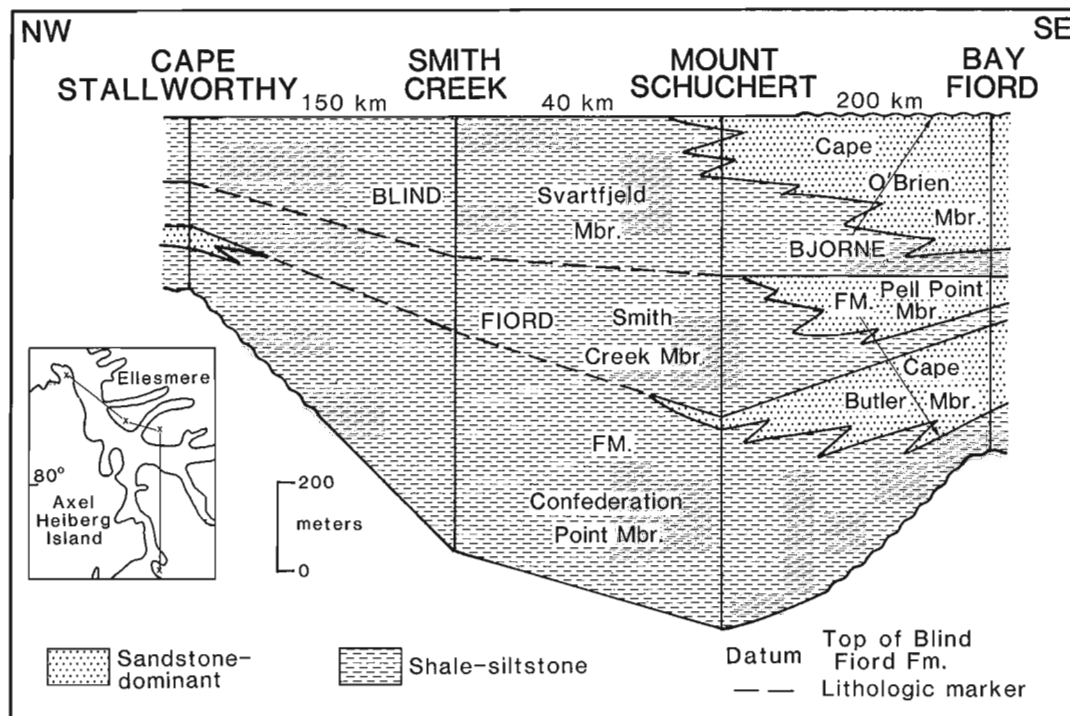


Figure 36.6. Stratigraphic cross-section of Lower Triassic strata, northeastern Sverdrup Basin. Note that Smith Creek and Svartfjeld are members of the Blind Fiord Formation in the north and become members of the Bjerne Formation to the south.

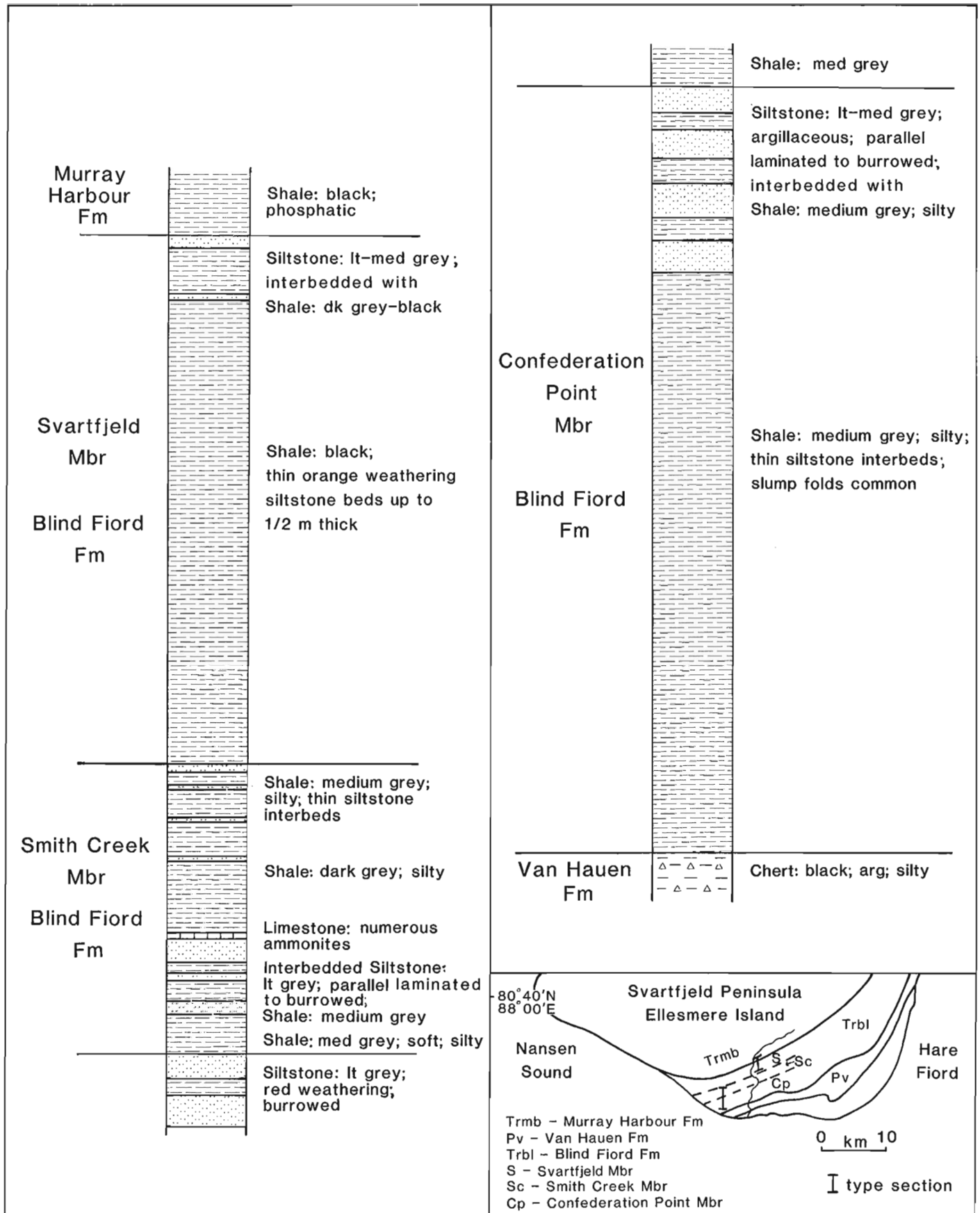


Figure 36.7. Stratigraphic section for the type sections of the Confederation Point, Smith Creek and Svartfjeld members of the Blind Fiord Formation. Accompanying map shows the locations of the type sections.

member is 327 m thick (Fig. 36.7). The member is named after Svartfjeld Peninsula, on which the type section is located.

Boundaries

Within the basin, the member conformably overlies the Smith Creek Member as has been previously described and is conformably overlain by the Murray Harbour Formation of the Blaa Mountain Group (Embry, 1984). The upper contact is placed at the top of the uppermost siltstone unit, which is abruptly overlain by black, calcareous shale with numerous phosphatic concretions.

On the basin margins, the Svartfjeld Member conformably overlies the Pell Point Member of the Bjerne Formation and the contact is placed at the top of the highest sandstone unit above which shale and siltstone are predominant. The upper contact of the Svartfjeld Member is with the Cape O'Brien Member of the Bjerne Formation and is placed at the top of the highest shale/siltstone unit above which sandstone is the main rock type.

Lithology

At the type section, which lies near the axis of the Sverdrup Basin, most of the member consists of black, silty shale with thin, orange weathering beds of calcareous siltstone. The siltstone beds are usually 20 cm thick, massive, and occur about every 10 m. In the uppermost portion of the formation, the siltstone units become thicker and more common. Toward the margins of the basin the shale becomes lighter in colour – mainly medium to dark grey – and siltstone content increases, especially in the upper half of the member. Interbeds of very fine grained sandstone also begin to appear within the upper portion of the member in marginal sections. Sedimentary structures within the siltstone and sandstone units are mainly parallel lamination and ripple crosslamination.

Thickness and distribution

The member is recognized mainly in the eastern and southeastern portions of the Sverdrup Basin and has also been identified in wells in the western portion of the basin. It ranges from a few metres thick in marginal sections to up to 400 m thick within the basin.

Age

Ammonites and pelecypods collected from the member on northern Ellesmere and Axel Heiberg islands indicate that it ranges in age from latest Smithian to Spathian (Tozer, 1965a; unpublished paleontological reports).

Environment of deposition

The argillaceous lithologies and the marine fauna suggest an outer shelf to slope environment of deposition. The presence of black shales within the basinal sections indicate that the bottom waters were oxygen deficient in this area.

Cape Butler Member, Bjerne Formation

Definition

The Cape Butler Member consists predominantly of fine to medium grained sandstone with interbeds of red, green or grey shale and siltstone. The type section is in the Mobil

Cornwall O-30 well (77°29'47"N, 94°38'58"W; spudded June 5, 1979; abandoned October 14, 1979; T.D. 3584 m; K.B. 29.8 m) between 1203 m and 1430 m, and is 227 m thick (Fig. 36.8). The name is taken from Cape Butler on Cornwall Island, which is 28 km from the type well.

Boundaries

The member conformably overlies the Confederation Point Member of the Blind Fiord Formation as previously described and is overlain by the Smith Creek Member. This contact is placed at the top of the highest sandstone above which shale and siltstone become predominant (Fig. 36.8).

Lithology

At the type section, the member consists mainly of fine to medium grained sandstone in units up to 20 m thick. Interbeds of red, green or grey, silty shale and siltstone usually 2 m or less in thickness occur throughout the member. Coarsening-upward cycles occur in lowermost portion of the member and fining-upward cycles are common throughout the remainder of the member. In outcrops on the basin margin, the predominant sedimentary structures are trough and planar crossbeds up to 1 m thick. Ripple crosslamination, horizontal bedding and mudcracks also occur. Mud chip conglomerates are present at the base and within sandstone units. In more basinward sections of the member, burrows are common in association with horizontal bedding and ripple crosslamination.

Thickness and distribution

The member occurs along the southern and eastern basin margins except in the Melville Island area where the Bjerne Formation is undivided. It ranges in thickness from a few metres near its shale-out edge to a maximum of 375 m on Fosheim Peninsula, Ellesmere Island.

Age

The member is dated as Griesbachian to Dienerian on the basis of the established ages of underlying and overlying shale/siltstone units.

Environment of deposition

The lithologies, cycles, and sedimentary structures indicate a spectrum of depositional environments from braided stream to shallow marine shelf. Fluvial strata dominate on the basin margin and are gradually replaced by shoreline to shallow marine strata basinward.

Pell Point Member, Bjerne Formation

Definition

The Pell Point Member consists mainly of fine to medium grained sandstone with interbeds of grey, green and red shale and siltstone. The type section of the formation is in the Mobil Cornwall O-30 well between 1077 m and 1117 m and is 40 m thick (Fig. 36.8). The name is taken from Pell Point on southern Cornwall Island.

Boundaries

The Pell Point Member conformably overlies the Smith Creek Member and is conformably overlain by the Svartfjeld Member as has been previously described.

Lithology

At the type section, the lower 22 m consists of interbedded, very fine to fine grained sandstone, siltstone and shale with individual units usually less than 2 m thick. In outcrop similar lithological associations occur and the sandstone units are sharp-based and have horizontal bedding, ripple crosslamination and burrows. Shale and siltstone units are mainly grey and green with occasional red intervals, and exhibit parallel lamination and bioturbation. The upper 18 m of the type section consist mainly of fine to medium grained

sandstone with only thin siltstone interbeds. Outcrops of similar lithology are dominated by trough crossbedding and horizontal bedding with burrows associated with thin argillaceous beds.

Thickness and distribution

The Pell Point Member occurs along the southern and eastern basin margins except in the Melville Island area. It is thickest near the edge of the basin and the maximum

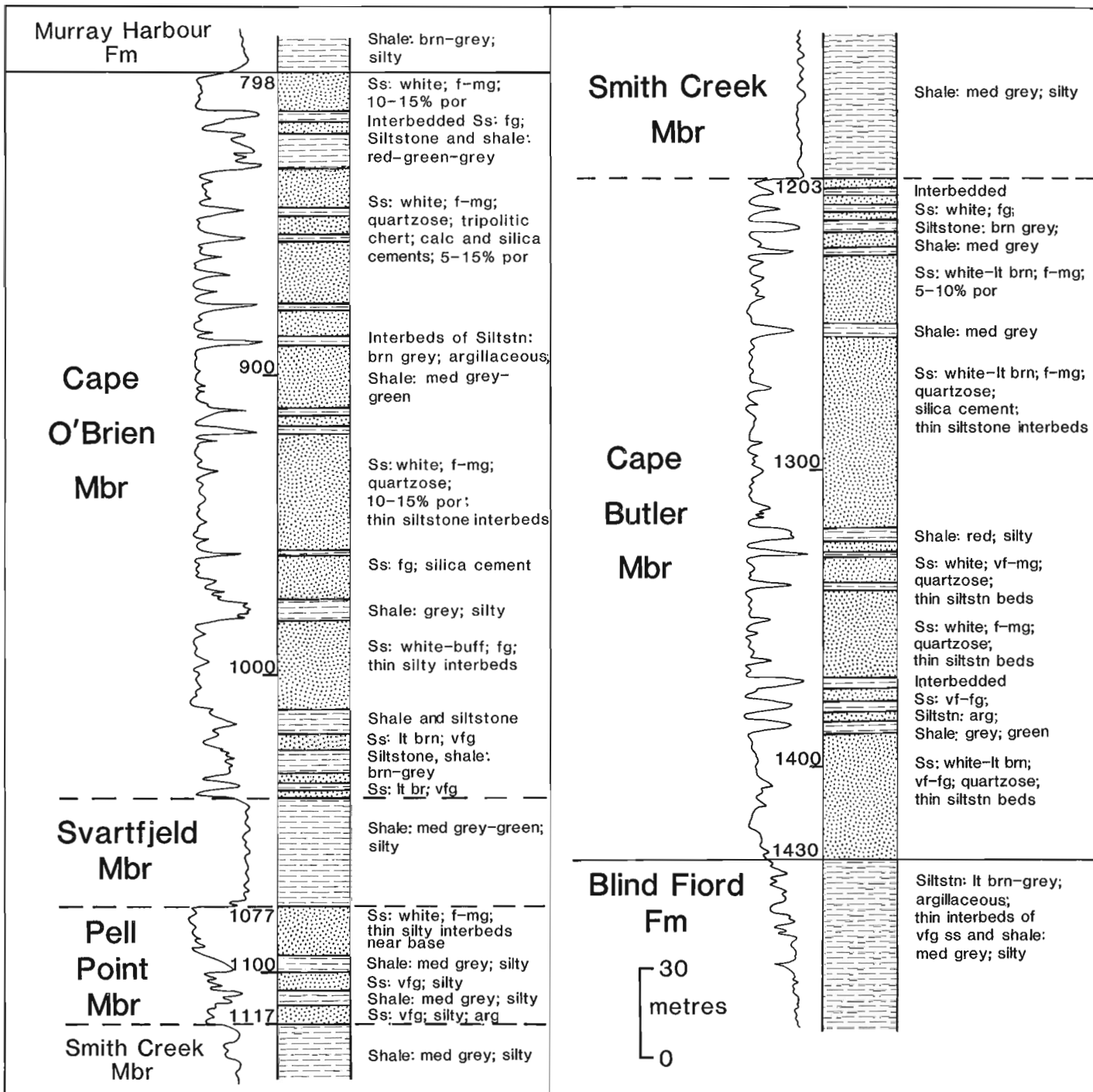


Figure 36.8. Lithology (from samples) and gamma ray curve for type sections of Cape Butler, Pell Point and Cape O'Brien members of the Bjerne Formation; Cornwall O-30 well.

recorded thickness is 555 m (Fosheim Peninsula). The member thins basinward due to facies change to shale and siltstone of the Smith Creek Member (Fig. 36.6) and eventually disappears.

Age

The Pell Point Member is dated as Smithian on the basis of the established ages of the enclosing shale units.

Environment of deposition

The portion of the member that consists of finely interbedded sandstone, siltstone and shale is of shallow shelf origin. The portion dominated by crossbedded sandstone is of shoreface to coastal plain origin, and in some areas includes thick braided stream deposits.

Cape O'Brien Member, Bjorne Formation

Definition

The Cape O'Brien Member consists mainly of fine to medium grained sandstone with thin interbeds of grey, green and red shale and siltstone. The type section is the Mobil Cornwall O-30 well between 798 m and 1042 m, and is 244 m thick. The name is taken from Cape O'Brien on southwest Cornwall Island.

Boundaries

The member conformably overlies the Svartfjeld Member as previously described and is overlain by the Murray Harbour Formation. This contact varies from conformable to unconformable and is placed either at an obvious unconformity or at the top of the highest sandstone above which shale and siltstone predominate.

Lithology

At the type section, the member consists mainly of fine to medium grained sandstone units up to 25 m thick. Coarsening-upward units are most common in the lower portion of the unit, and fining-upward cycles are present in the upper portion. Shale/siltstone units are usually less than 3 m thick and occur throughout the member. Colours range from grey through red and green. In outcrop, the thick sandstone units are dominated by trough crossbedding and horizontal bedding, with scour surfaces and mud chip conglomerates also common. Ripple crosslamination, horizontal bedding and burrows occur in the lower part of the member in basin margin sections and throughout it near its shale-out edge.

Thickness and distribution

The Cape O'Brien Member occurs along the extent of the Bjorne Formation except in the Melville Island area, where the Bjorne Formation is undivided. It is thickest (500 m) in the Fosheim Peninsula area. It thins basinward due to facies change to shale and siltstone (Svartfjeld Member) and eventually shales out.

Age

The member is dated as Spathian (possibly as old as Smithian) on the basis of its equivalence with the well dated Svartfjeld Member.

Environment of deposition

Interbedded sandstone, siltstone and shale arranged in coarsening-upward cycles and containing burrowed horizons are mainly of shallow shelf to strandline origin. The cross-bedded sandstones, which are associated with red shale and siltstone, scour surfaces and fining-upward cycles, and which lack trace fossils are interpreted to be of fluvial origin.

References

- Balkwill, H.R. and Roy, K.J.
1977: Geology, King Christian Island, District of Franklin; Geological Survey of Canada, Memoir 386.
- Balkwill, H.R., Hopkins, W.S. Jr., and Wall, J.H.
1982: Geology, Lougheed Island, District of Franklin; Geological Survey of Canada, Memoir 388.
- Henao-Londono, D.
1977: Correlation of producing formations in Sverdrup Basin; Bulletin of Canadian Petroleum Geology, v. 25, p. 969-980.
- McMillan, N.J.
1963: Lightfoot River to Wading River; in Geology of the north-central part of the Arctic Archipelago, Northwest Territories (Operation Franklin), ed. Y.O. Fortier; Geological Survey of Canada, Memoir 320, p. 501-512.
- Moore, P.R.
1981: Mesozoic stratigraphy in the Blue Mountains and Krieger Mountains, Northern Ellesmere Island, Arctic Canada: a preliminary account; in Current Research, Part A, Geological Survey of Canada, Paper 81-1A, p. 95-101.
- Nassichuk, W.W. and Christie, R.L.
1969: Upper Paleozoic and Mesozoic stratigraphy in the Yelverton Pass region, Ellesmere Island, District of Franklin; Geological Survey of Canada, Paper 68-31.
- Roy, K.J.
1972: Bjorne Formation (Lower Triassic), western Ellesmere Island; in Report of Activities, Geological Survey of Canada, Paper 72-1A, p. 224-226.
- Souther, J.G.
1963: Geological transverse across Axel Heiberg Island from Buchanan Lake to Strand Fiord; in Geology of the north-central part of the Arctic Archipelago, Northwest Territories (Operation Franklin), ed. Y.O. Fortier; Geological Survey of Canada, Memoir 320, p. 426-448.
- Tozer, E.T.
1961: Triassic stratigraphy and faunas, Queen Elizabeth Island, Arctic Archipelago; Geological Survey of Canada, Memoir 316.
- 1963a: Blind Fiord; in Geology of the north central part of the Arctic Archipelago, Northwest Territories (Operation Franklin); Geological Survey of Canada, Memoir 320, p. 380-385.
- 1963b: Northwestern Bjorne Peninsula; in Geology of the north central part of the Arctic Archipelago, Northwest Territories (Operation Franklin); Geological Survey of Canada, Memoir 320, p. 363-370.

Tozer, E.T. (cont.)

- 1963c: Mesozoic and Tertiary stratigraphy, western Ellesmere Island and Axel Heiberg Island, District of Franklin; Geological Survey of Canada, Paper 63-30.
- 1963d: Troid Fiord; *in* Geology of the north central part of the Arctic Archipelago, Northwest Territories (Operation Franklin); Geological Survey of Canada, Memoir 320, p. 370-379.
- 1963e: Northwestern Cameron Island; *in* Geology of the north central part of the Arctic Archipelago, Northwest Territories (Operation Franklin); Geological Survey of Canada, Memoir 320, p. 639-644.
- 1965a: Lower Triassic stages and ammonoid zones of Arctic Canada; Geological Survey of Canada, Paper 65-12.

Tozer, E.T. (cont.)

- 1965b: Latest Lower Triassic ammonoids from Ellesmere Island and northeastern British Columbia; Geological Survey of Canada, Bulletin 123.
- 1967: A standard for Triassic time; Geological Survey of Canada, Bulletin 156.
- 1970: Geology of the Arctic Archipelago, Mesozoic; *in* Geology and Economic Minerals of Canada, ed. R.W. Douglas; Geological Survey of Canada, Economic Geology Report 1, p. 574-583.
- Tozer, E.T. and Thorsteinsson, R.
1964: Western Queen Elizabeth Islands, Arctic Archipelago; Geological Survey of Canada, Memoir 332.
- Trettin, H.P. and Hills, L.V.
1966: Lower Triassic tar sands of northwestern Melville Island, Arctic Archipelago; Geological Survey of Canada, Paper 66-34.

APPENDIX

Stratigraphic tops from selected wells, Blind Fiord and Bjerne formations. Location of wells shown in Figure 36.1.

<u>BP Satellite F-68</u>			<u>Horn River Depot Point L-24</u>		
Bjerne Formation			Bjerne Formation	329 m	(1080 ft)
Cape O'Brien Member	1165 m	(3822 ft)	Blind Fiord Formation	621 m	(2039 ft)
Svartfjeld Member	1189 m	(3900 ft)	Thrust fault ?	822 m	(2696 ft)
Pell Point Member	1302 m	(4272 ft)	Bjerne Formation	822 m	(2696 ft)
Smith Creek Member	1418 m	(4651 ft)	Blind Fiord Formation	864 m	(2835 ft)
Cape Butler Member	1506 m	(4941 ft)	Thrust fault	1507 m	(4945 ft)
Blind Fiord Formation			Bjerne Formation	1507 m	(4945 ft)
Confederation Point Member	1854 m	(6082 ft)	Blind Fiord Formation	1740 m	(5710 ft)
Trold Fiord Formation	1860 m	(6101 ft)	Thrust fault	1971 m	(6468 ft)
			Bjerne Formation	1971 m	(6468 ft)
			Blind Fiord Formation	2100 m	(6889 ft)
			Van Hauen Formation	3608 m	(11837 ft)
<u>Panarctic Drake Point L-67</u>			<u>Panarctic Fosheim N-27</u>		
Bjerne Formation	1561 m	(5123 ft)	Bjerne Formation		
Blind Fiord Formation			Cape O'Brien Member	688 m	(2257 ft)
Confederation Point Member	2874 m	(9428 ft)	Svartfjeld Member	1230 m	(4037 ft)
Van Hauen Formation	3134 m	(10282 ft)	Pell Point Member	1244 m	(4082 ft)
			Smith Creek Member	1835 m	(6021 ft)
			Cape Butler Member	1997 m	(6551 ft)
			Thrust fault	2132 m	(6995 ft)
			Pell Point Member	2132 m	(6995 ft)
			Smith Creek Member	2419 m	(7936 ft)
			Cape Butler Member	2568 m	(8425 ft)
			Blind Fiord Formation		
			Confederation Point Member	3002 m	(9850 ft)
			Van Hauen Formation	3608 m	(11837 ft)
<u>Panarctic Brock C-50</u>			<u>Gulf Neil O-15</u>		
Bjerne Formation			Bjerne Formation		
Cape O'Brien Member	446 m	(1463 ft)	Cape O'Brien Member	1098 m	(3601 ft)
Blind Fiord Formation			Svartfjeld Member	1202 m	(3945 ft)
Svartfjeld Member	494 m	(1620 ft)	Pell Point Member	1255 m	(4117 ft)
Smith Creek Member	795 m	(2608 ft)	Smith Creek Member	1490 m	(4887 ft)
Confederation Point Member	1062 m	(3485 ft)	Cape Butler Member	1508 m	(4946 ft)
Degerbols Formation	1658 m	(5438 ft)	Blind Fiord Formation		
			Confederation Point Member	1579 m	(5180 ft)
			Thrust fault	1964 m	(6442 ft)
			Bjerne Formation		
			Cape Butler Member	1964 m	(6442 ft)
			Blind Fiord Formation		
			Confederation Point Member	1990 m	(6530 ft)
			Trold Fiord Formation	2353 m	(7720 ft)
<u>Dome Sutherland O-23</u>					
Blind Fiord Formation					
Svartfjeld Member	1917 m	(6290 ft)			
Smith Creek Member	2831 m	(9287 ft)			
Confederation Point Member ?					
<u>Panarctic Isachsen J-37</u>					
Blind Fiord Formation					
Svartfjeld Member	1477 m	(4846 ft)			
Smith Creek Member	1796 m	(5891 ft)			
Confederation Point Member	1984 m	(6510 ft)			
Degerbols Formation	2530 m	(8301 ft)			
<u>Mobil Cornwall O-30</u>					
Bjerne Formation					
Cape O'Brien Member	798 m	(2618 ft)			
Svartfjeld Member	1042 m	(3419 ft)			
Pell Point Member	1077 m	(3534 ft)			
Smith Creek Member	1177 m	(3862 ft)			
Cape Butler Member	1203 m	(3947 ft)			
Blind Fiord Formation					
Confederation Point Member	1430 m	(4692 ft)			
Van Hauen Formation	1638 m	(5374 ft)			

Stratigraphic subdivision of the Awingak Formation (Upper Jurassic) and revision of the Hiccles Cove Formation (Middle Jurassic), Sverdrup Basin, Arctic Islands

Project 750083

Ashton F. Embry
Institute of Sedimentary and Petroleum Geology, Calgary

Embry, A.F., Stratigraphic subdivision of the Awingak Formation (Upper Jurassic) and revision of the Hiccles Cove Formation (Middle Jurassic), Sverdrup Basin, Arctic Islands; in Current Research, Part B, Geological Survey of Canada, Paper 86-1B, p. 341-349, 1986.

Abstract

The Awingak Formation is a sandstone-dominant unit of Oxfordian to Tithonian (Late Jurassic) age and it occurs in the eastern and southeastern portion of the Sverdrup Basin. Throughout most of its extent, three members can be recognized within the formation: a lower sandstone, a medial shale/siltstone, and an upper sandstone. These three members are given formal status and are named, in ascending order: Cape Lockwood, Hot Weather and Slidre members.

Correlation of the three members of the Awingak Formation and the underlying Ringnes Formation with sections on western Melville Island and Prince Patrick Island, has revealed that strata previously assigned to the upper portion of the Hiccles Cove Formation are stratigraphically equivalent to the Ringnes Formation and the Cape Lockwood Member of the Awingak Formation. In order to achieve a consistent stratigraphic nomenclature for the Middle-Upper Jurassic succession of the Sverdrup Basin, the upper boundary of the Hiccles Cove Formation is redefined to exclude strata equivalent to the Ringnes and Awingak formations from the Hiccles Cove.

Résumé

La formation d'Awingak, qui se trouve dans les parties est et sud-est du bassin de Sverdrup, est une unité composée surtout de grès d'âge oxfordien à tithonien (Jurassique supérieur). Trois membres sont identifiés sur presque toute l'étendue de la formation: un grès inférieur, un schiste argileux et aleurolite médian et un grès supérieur. Ces trois membres officiels portent les noms suivants, donnés en ordre ascendant: Cape Lockwood, Hot Weather et Slidre.

La mise en corrélation des trois membres de la formation d'Awingak et de la formation sous-jacente de Ringnes avec des colonnes stratigraphiques dans la partie ouest de l'île Melville et dans l'île Prince-Patrick montre que les strates auparavant attribuées à la partie supérieure de la formation de Hiccles Cove sont l'équivalent stratigraphique de la formation de Ringnes et du membre de Cape Lockwood de la formation d'Awingak. Afin d'établir une nomenclature stratigraphique homogène pour la succession du Jurassique moyen à supérieur du bassin de Sverdrup, la limite supérieure de la formation de Hiccles Cove a été redéfinie de façon à exclure de cette formation les couches équivalant aux formations de Ringnes et d'Awingak.

Introduction

The Awingak Formation, defined by Souther (1963), is an Upper Jurassic sandstone-dominant unit that occurs between two shale/siltstone units, the Ringnes Formation below and the Deer Bay Formation above. The type section of the Awingak Formation is southwest of Buchanan Lake in the eastern Sverdrup Basin, and the formation has been traced along the eastern and southern portions of the basin (Fig. 37.1). To the northwest, the Awingak Formation disappears due to facies change, and stratigraphic equivalents occur within the shale/siltstone-dominant Mackenzie King Formation (Embry, 1985).

Numerous surface and subsurface sections of the Awingak Formation are available along its extent (Fig. 37.1). Regional studies have revealed that a shale/siltstone unit within the formation can be correlated through many of the sections, allowing a three-fold stratigraphic subdivision of the formation: a lower sandstone, a medial shale/siltstone, and an upper sandstone. These units are given formal member status in this paper.

Another consequence of the regional correlations of the Awingak Formation is that the delineation of the Hiccles Cove Formation, a sandstone unit occurring between the McConnell Island Formation below and Ringnes Formation above (both shale/siltstone units), has to be revised. It has been found that strata assigned to the upper portion of the Hiccles Cove Formation in the western Melville-Prince Patrick Island area (Embry, 1984) correlate with the Ringnes Formation and lower member of the Awingak Formation. Overlying argillaceous strata previously thought to be the Ringnes Formation (Embry, 1984) actually correlate with the medial shale/siltstone member of the Awingak Formation. Thus only the lower portion of the Hiccles Cove Formation as defined previously in these areas coincides with the original intent of the formation: a regional sandstone unit between

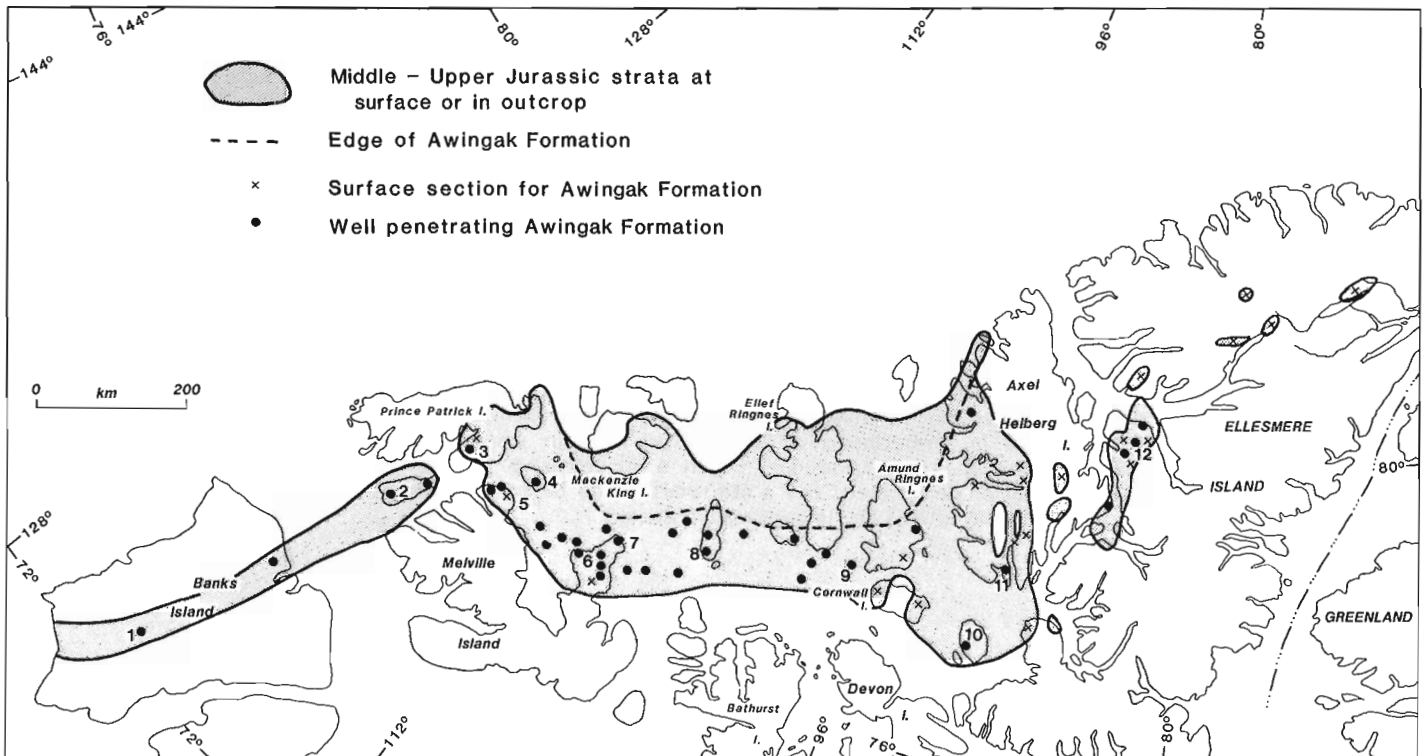
the argillaceous McConnell Island and Ringnes formations. To avoid unnecessary stratigraphic overlap, the Hiccles Cove Formation is redefined in this paper.

Previous work

Souther (1963) defined the Awingak Formation from studies made during Operation Franklin in 1955, when he made a geological traverse across central Axel Heiberg Island. At the type section on east-central Axel Heiberg, Souther recognized four sandstone units separated from each other by shale/siltstone units in the 300 m thick section. Fossils collected below, within, and above the formation established it as Upper Jurassic in age (mainly Oxfordian-Kimmeridgian). Souther (1963) also recognized the Awingak Formation on western Axel Heiberg Island and he commented that the shale content was less in that area. During Operation Franklin, the Awingak Formation was also briefly described – western Axel Heiberg Island by Tozer (1963a) and Cornwall Island by Greiner (1963).

Subsequent studies of the Mesozoic succession of Ellesmere and Axel Heiberg islands by Tozer (1963b) led to the recognition of the Awingak Formation over large areas of these islands. Moore (1981) briefly described two sections of the Awingak Formation measured on northern Ellesmere Island. In the south-central Sverdrup Basin, the Awingak Formation on Cornwall and southern Amund Ringnes islands has been described by Balkwill (1983). In these areas he recognized four mappable sandstone units within the Awingak Formation and demonstrated that they all changed facies to shale and siltstone on central Amund Ringnes Island.

The Awingak Formation was not recognized farther west in the Melville-Prince Patrick Island area by Tozer and Thorsteinsson (1964). Equivalent strata were interpreted to occur within the uppermost portion of a sandstone-dominant,



- | | | |
|----------------------|-----------------------|-------------------------|
| 1. Orksut I-44 | 5. Depot Island C-44 | 9. Linckens Island P-46 |
| 2. Pedder Point D-49 | 6. Hecla J-60 | 10. Graham C-52 |
| 3. Jameson Bay C-31 | 7. North Sabine H-49 | 11. Sherwood P-37 |
| 4. Emerald K-33 | 8. Skybattle Bay C-15 | 12. Romulus C-42 |

Figure 37.1. Distribution of Awingak Formation and control points. Key to numbered wells listed in the Appendix.

Lower-Upper Jurassic unit named the Wilkie Point Formation. Overlying shale and sandstone of mainly Volgian age were placed in the Mould Bay Formation.

Embry (1984) revised the Lower-Upper Jurassic stratigraphy of the Melville-Prince Patrick area. He correlated the shale unit at the base of the Mould Bay Formation with the Ringnes Formation and assigned the overlying sandstone, which composes most of the Mould Bay, to the Awingak Formation. Embry (1984) also raised the Wilkie Point to group status and the uppermost sandstone unit was named the Hiccles Cove Formation. It consists of a lower, sideritic, fossiliferous sandstone and an upper, white, carbonaceous sandstone that is devoid of fossils. The two units are separated by a thin, argillaceous siltstone unit. The lower sideritic sandstone was well dated, using ammonites, as Callovian, but the upper white sandstone did not yield any diagnostic fossils. It was interpreted to be Callovian to Early Oxfordian on the basis of its stratigraphic position.

Subsurface descriptions of the Awingak Formation include Balkwill et al.'s (1982) of the Skybattle Bay C-15 well on Loughed Island and Balkwill's (1983) of the Linckens Island P-46 well northwest of Cornwall Island. Henao-Londono (1977) and Crane (1977) have briefly commented on the reservoir properties of the formation.

Present work

Regional correlation of the subsurface and surface sections of the Awingak Formation have led to the recognition of a three-fold subdivision of the formation along most of its extent (Fig. 37.2). A lower sandstone, a medial shale/siltstone, and an upper sandstone are recognized and are given formal member status herein. They are named, in ascending order, the Cape Lockwood, Hot Weather, and Slidre members of the Awingak Formation. The type sections of all three members are in the Panarctic Romulus C-42 well on Fosheim Peninsula, west-central Ellesmere Island (Fig. 37.1) at 79°51'05"N and 84°22'44"W. The well was spudded on January 28, 1972 and was abandoned on July 25, 1972 at a total depth of 4554 m. The elevation of the K.B. was 160 m. Chip samples taken at three metre intervals from the type sections are available for study at the Institute of Sedimentary and Petroleum Geology, Calgary, Alberta.

In many areas of the basin, the Cape Lockwood Member extends farther basinward than the Slidre Member (Fig. 37.3). Thus in more basinward sections, the Cape Lockwood Member represents the entire Awingak Formation and equivalents of the Hot Weather and Slidre members occur in the lower portion of the Deer Bay Formation (Fig. 37.3).

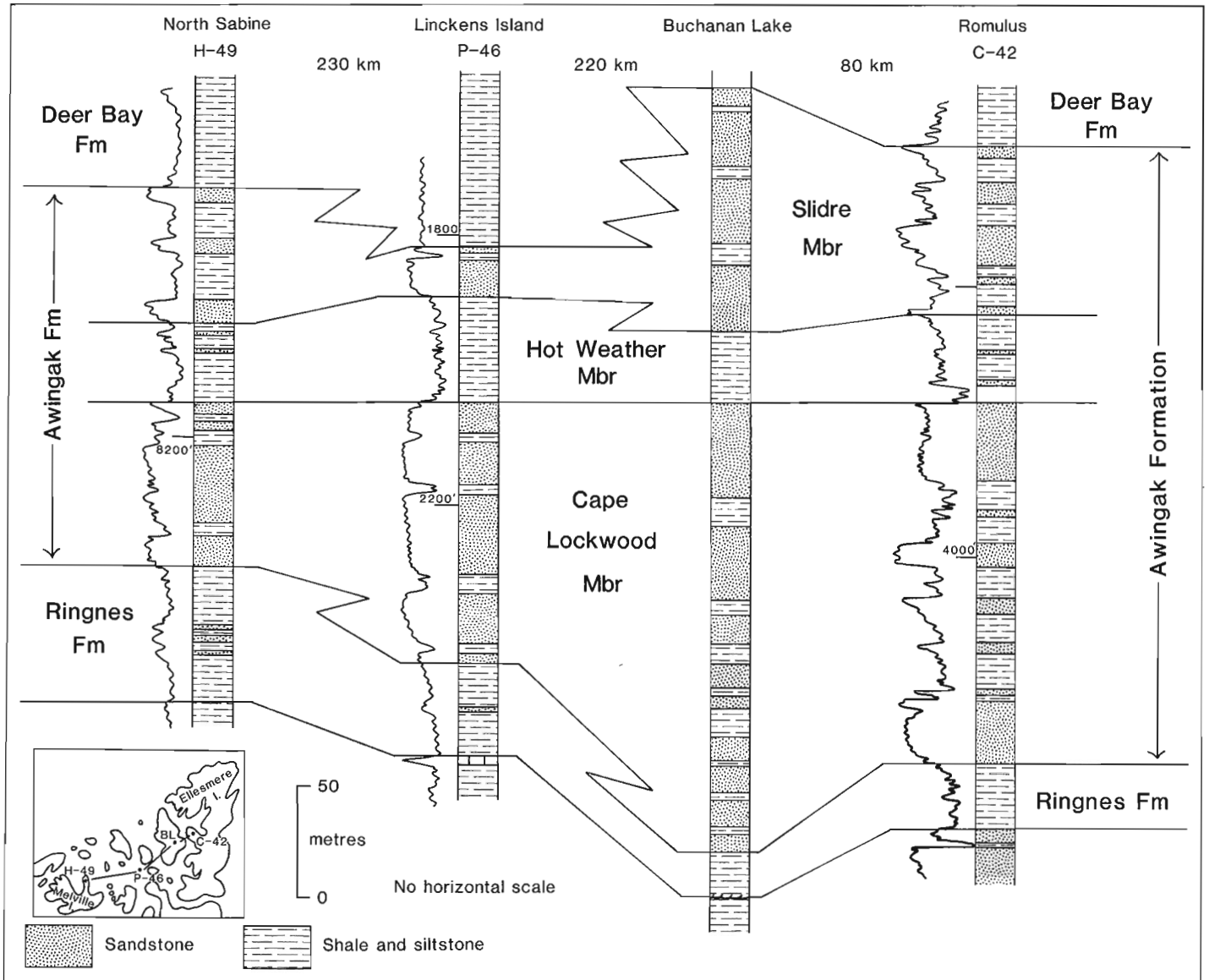


Figure 37.2. Stratigraphic cross-section, Awingak Formation, parallel to basin margin. Gamma ray logs displayed beside rock types.

Correlation of the three members of the Awingak Formation and the underlying Ringnes Formation with western Melville Island and Prince Patrick Island has revealed that the correlation proposed by Embry (1984) for this area is incorrect. Embry (1984) correlated the shale unit overlying the Hiccles Cove Formation with the Ringnes Formation, but recent data indicate this interpretation is wrong. Upper Jurassic pelecypods have been collected from the white sandstone unit of the Hiccles Cove Formation on western Melville Island (Poulton, pers. comm., 1986) and seismic interpretation indicates the equivalence of the top of the white sandstone unit on western Melville with the top of the Cape Lockwood Member of the Awingak Formation on Lougheed Island (Densmore, personal communication, 1986). Also, ammonites and pelecypods collected from the shale overlying the white sandstone are the same as those collected from the Hot Weather Member on Axel Heiberg Island. Taking all these new data into consideration, the white

sandstone unit, which forms the uppermost portion of the Hiccles Cove Formation, is correlated with the Cape Lockwood Member of the Awingak Formation. The underlying argillaceous siltstone unit is correlated with the Ringnes Formation. The shale overlying the white sandstone unit, which was formerly thought to be Ringnes Formation, is now correlated with the Hot Weather Member (or lower Deer Bay Formation where the Slidre Member is absent) (Fig. 37.4, 37.5).

In order to achieve a consistent stratigraphic nomenclature for the Middle-Upper Jurassic succession of the Sverdrup Basin, the Hiccles Cove Formation is herein redefined to include only the lower sideritic sandstone unit. The overlying siltstone unit and white sandstone unit are excluded from the Hiccles Cove Formation and assigned to the Ringnes and Awingak formations. Revised well tops that stem from these changes are included in the Appendix.

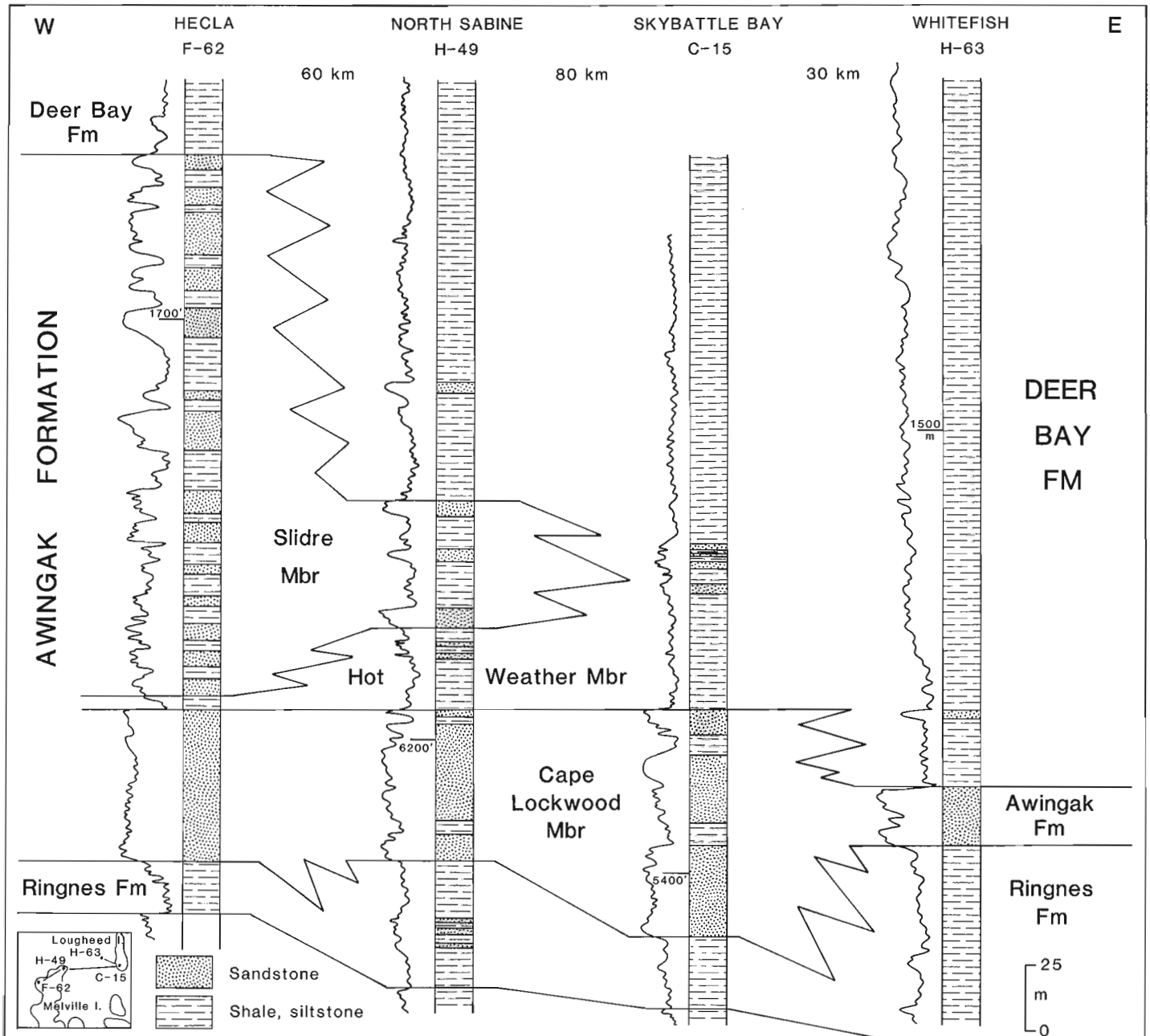


Figure 37.3. Stratigraphic cross-section, Awingak Formation, western Sverdrup Basin. Gamma ray logs displayed beside rock types.

Cape Lockwood Member, Awingak Formation

Definition

The Cape Lockwood Member consists of interbedded very fine to medium grained sandstone, siltstone and shale; sandstone is the dominant rock type. The type section is in

TOZER AND THORSTEINSSON 1964		EMBRY 1984	EMBRY THIS PAPER	
MOULD BAY FM.	UPPER SHALE	DEER BAY FM.	AWINGAK FM.	DEER BAY FM.
	MIDDLE SANDSTONE	AWINGAK FM.		SLIDRE MBR.
	LOWER SHALE	RINGNES FM.		HOT WEATHER MBR. CAPE LOCKWOOD MBR.
WILKIE POINT FM.	UPPER MEMBER	HICCLETS COVE FM.	RINGNES FM.	
	LOWER MEMBER		HICCLETS COVE FM.	
		McCONNELL ISLAND FM.	McCONNELL ISLAND FM.	

Figure 37.4. Past and present nomenclature of Middle-Upper Jurassic stratigraphy, Prince Patrick-Melville Island.

the Romulus C-42 well between 1149 m (3770 ft) and 1311 m (4302 ft) and is 163 m thick. The name is taken from Cape Lockwood, which is on the north coast of Fosheim Peninsula.

Synonyms

1. Lower three sandstone and two shale units of type Awingak Formation (Souther, 1963).
2. Upper member, Wilkie Point Formation, Melville and Prince Patrick islands (Tozer and Thorsteinsson, 1964).
3. Lower two map units of Awingak Formation, Cornwall and southern Amund Ringnes islands (Balkwill, 1983).
4. Upper portion, Hiccles Cove Formation, Melville and Prince Patrick islands (Embry, 1984).
5. Hiccles Cove Formation, Orksut I-44 well, Banks Island (Embry, 1985).

Boundaries

The Cape Lockwood Member conformably overlies the Ringnes Formation. The contact is placed at the base of the lowest sandstone unit above which sandstone becomes the predominant rock type. The member is overlain by the Hot Weather Member of the Awingak Formation or Deer Bay Formation and the contact is placed at the top of the highest sandstone above which shale and siltstone become predominant. In most areas, this contact is conformable, but on Prince Patrick Island the contact becomes unconformable southward and the Hot Weather Member oversteps the Cape Lockwood Member.

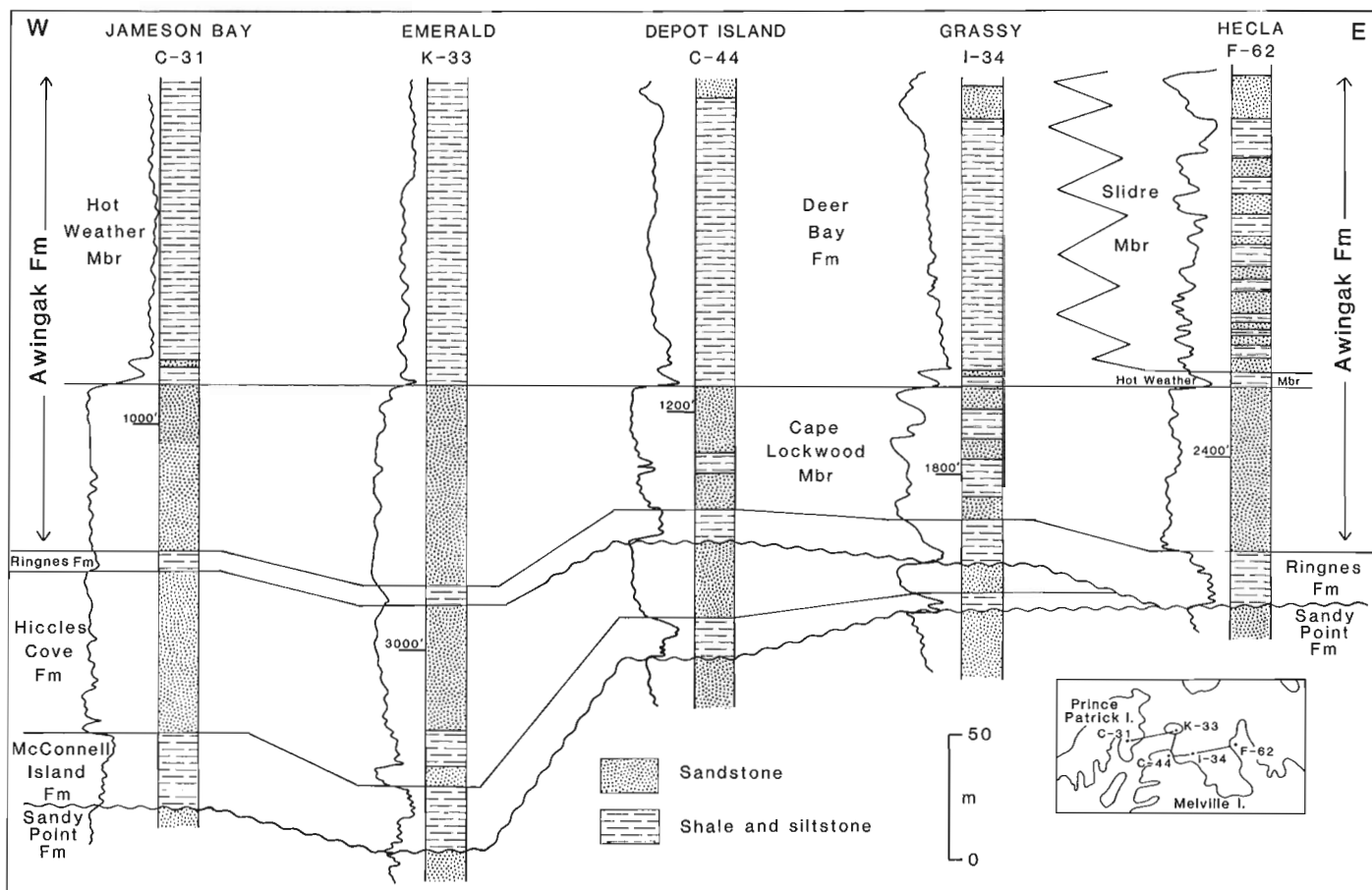


Figure 37.5. Stratigraphic cross-section, Middle-Upper Jurassic strata, Prince Patrick-Melville Island. Gamma ray logs displayed beside rock types. Compare with Figure 33.2 of Embry (1984).

Lithology

In the type section, the member consists of interbedded dark grey shale, siltstone and very fine to medium grained sandstone. The rock types are arranged in coarsening-upward cycles up to 60 m thick (Fig. 37.6). The strata are variably carbonaceous. In outcrops, bioturbation dominates the shale, siltstone and lower portion of the sandstone units. The upper portions of the sandstones commonly are horizontally bedded or massive, with crossbedding occurring infrequently. In the Melville Island-Prince Patrick Island area, the Cape Lockwood Member consists almost entirely of white, fine to medium grained, carbonaceous sandstone with a few thin coal seams near the top.

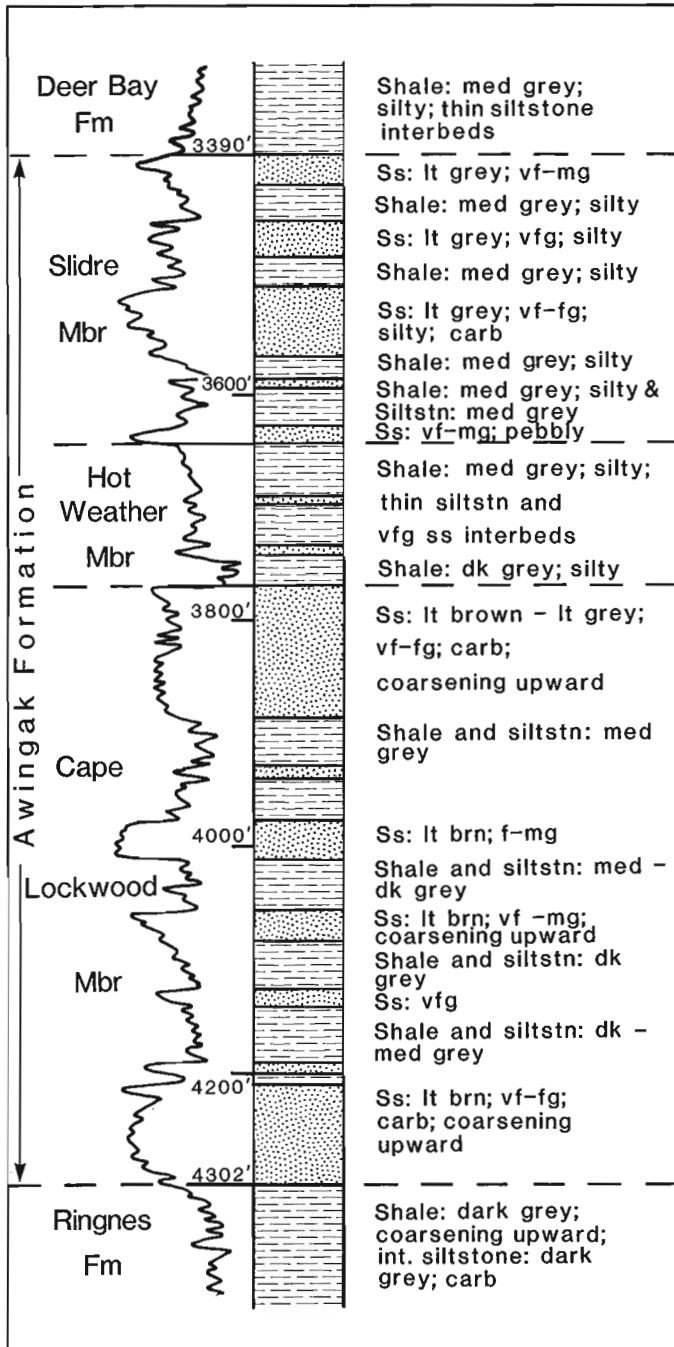


Figure 37.6. Lithology (from samples) and gamma ray curve for type sections of the Cape Lockwood, Hot Weather and Slidre members of the Awingak Formation; Romulus C-42 well.

Thickness and distribution

The Cape Lockwood Member is recognized along the extent of the Awingak Formation except on the southeastern basin margin, where the Awingak Formation is undivided. The maximum recorded thickness is 300 m. The member thins basinward and eventually disappears due to facies change to shale and siltstone.

Age

The member is dated as Oxfordian on the basis of the occurrence of early Oxfordian ammonites in the underlying Ringnes Formation and early Kimmeridgian ammonites and pelecypods in the overlying Hot Weather Member. Early to late Oxfordian dinoflagellates occur within the member (unpublished paleontological reports).

Environment of deposition

The lithology, sedimentary structures and fauna of the coarsening-upward cycles are typical of prograding outer shelf to shallow shelf deposits. In the western Sverdrup, where massive sandstone and coal are present, shallow shelf, strandline and lagoonal environments are represented in the member.

Hot Weather Member, Awingak Formation

Definition

The Hot Weather Member consists of medium to dark grey shale and siltstone with minor very fine grained sandstone. The type section is in the Romulus C-42 well between 1111 m (3644 ft) and 1149 m (3770 ft) and is 38 m thick (Fig. 37.6). The name is taken from Hot Weather Creek on Fosheim Peninsula.

Synonyms

1. Upper shale member, type Awingak Formation (Souther, 1963).
2. Lower shale unit, Mould Bay Formation, Prince Patrick and Melville islands (Tozer and Thorsteinsson, 1964).
3. Ringnes Formation, Prince Patrick Island (Embry, 1984).

Boundaries

The Hot Weather Member overlies the Cape Lockwood Member as previously described and is conformably overlain by the Slidre Member of the Awingak Formation. This upper contact is placed at the top of the uppermost shale/siltstone unit above which sandstone becomes the predominant rock type.

Lithology

At the type section, the basal 7 m consist of dark grey shale, and the overlying 31 m consist of interbedded siltstone and silty shale with minor, very fine grained sandstone. Basinward, dark grey to black shale becomes the main rock type. In some areas, dolomitic concretions up to 4 m across occur within the member.

Thickness and distribution

The Hot Weather Member occurs throughout most of the Awingak Formation's extent. It is absent due to facies change to sandstone in the southeast. It is also not recognized when the overlying Slidre Member is absent, and equivalents occur in the Deer Bay Formation. Its maximum recorded thickness is 210 m.

Age

Ammonite and pelecypod evidence from the member indicates for it a Kimmeridgian age (Souther, 1963; unpublished paleontological reports).

Environment of deposition

The argillaceous lithologies and open marine fauna indicate an offshore marine shelf environment of deposition for the member.

Slidre Member, Awingak Formation

Definition

The Slidre Member consists of interbedded very fine to medium grained sandstone, siltstone and shale. The type section is in the Romulus C-42 well between 1033 m (3390 ft) and 1111 m (3644 ft) and is 77 m thick (Fig. 37.6). The name is taken from Slidre Fiord on west-central Fosheim Peninsula.

Synonyms

1. Uppermost sandstone member, type Awingak Formation (Souther, 1963).
2. Middle sandstone member, Mould Bay Formation, Prince Patrick Island (Tozer and Thorsteinsson, 1964).
3. Upper two Awingak Formation map units, Cornwall and southern Amund Ringnes islands (Balkwill, 1983).
4. Awingak Formation, Prince Patrick Island (Embry, 1984).

Boundaries

The Slidre Member conformably overlies the Hot Weather Member as previously described and is conformably overlain by the Deer Bay Formation. This contact is placed at the top of the uppermost sandstone unit above which shale and siltstone become the predominant rock types.

Lithology

At the type section, the member consists of interbedded grey shale, siltstone and very fine to medium grained sandstone arranged in coarsening-upward cycles up to 30 m thick. Bioturbation is the predominant sedimentary structure and ripple crosslamination and horizontal bedding occasionally occur in the uppermost portions of sandstone units. On Cornwall Island, fining-upward cycles with thin coal seams occur in the upper portion of the member (Balkwill, 1983). In the western Sverdrup the sandstones commonly contain thin pebble layers in basin margin sections.

Thickness and distribution

The Slidre Member occurs along the southern and eastern margins of the Sverdrup Basin. It is not recognized in the southeast (e.g. Graham Island area) where the Awingak Formation is not subdivided. It is also absent on northwestern Melville, and stratigraphic equivalents occur in the Deer Bay Formation. The maximum recorded thickness of the member is 270 m.

Age

The member is interpreted to be mainly Tithonian (Volgian) in age on the basis of pelecypods found within it (Tozer, 1963b; Tozer and Thorsteinsson, 1964; Balkwill, 1983). In basin margin sections, the age of the member may extend down into the late Kimmeridgian and upward into the Berriasian.

Environment of deposition

The rock types, sedimentary structures and fauna of the coarsening-upward cycles are typical of prograding inner to outer marine shelf deposits. The interval with fining-upward cycles and thin coal beds on Cornwall Island represents lower delta plain deposits (Balkwill, 1983).

Hiccles Cove Formation (redefined)

Definition

The Hiccles Cove Formation consists mainly of very fine to fine grained sandstone which is often sideritic and glauconitic. The type section is in the Elf Jameson Bay C-31 well (76°40'12"N, 116°43'45"W; spudded March 11, 1971; abandoned May 18, 1971; T.D. 2539 m; K.B. 63 m) between 369 m (1210 ft) and 442 m (1451 ft) and is 73 m thick (Fig. 37.7). The name is taken from Hiccles Cove on the eastern side of Intrepid Inlet, Prince Patrick Island.

Synonyms

1. Units 5 to 7, Wilkie Point Formation, Intrepid Inlet section, Prince Patrick Island (Tozer and Thorsteinsson, 1964).
2. Jaeger Formation, northern Ellef Ringnes Island (Stott, 1969).
3. Medial sandstone unit, Upper Savik, Cornwall Island (Balkwill, 1983).
4. Lower portion, Hiccles Cove Formation, Prince Patrick and western Melville Island (Embry, 1984).

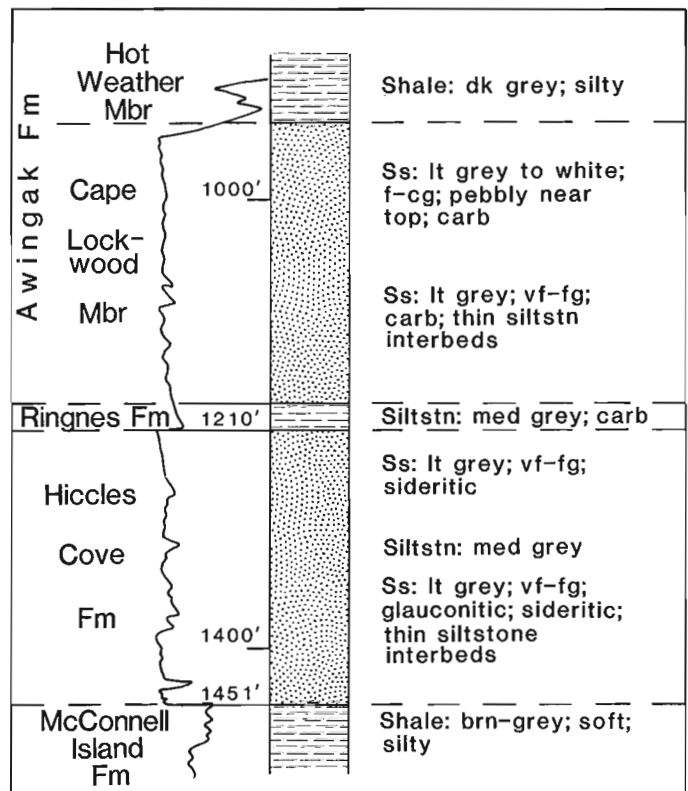


Figure 37.7. Lithology (from samples) and gamma ray curve for the revised type section of the Hiccles Cove Formation; Jameson Bay C-31 well.

Boundaries

The Hiccles Cove Formation conformably overlies the McConnell Island Formation. The contact is placed at the base of the lowest sandstone unit above which sandstone is dominant. The formation is overlain by the Ringnes Formation, and the contact varies from conformable to unconformable. The contact is placed at the top of the highest sandstone unit above which shale and siltstone are predominant.

Lithology

In the type section, the formation consists of interbedded, very fine to fine grained sandstone arranged in coarsening-upward cycles. Beds of ironstone are common and glauconite is a common accessory mineral. Farther basinward, shale and siltstone occur within the formation at the base of the cycles. Burrows, ripple crosslamination and horizontal bedding are the predominant sedimentary structures.

Thickness and distribution

The Hiccles Cove Formation occurs along the basin margins and is up to 70 m thick. Basinward, the formation changes facies to shale and siltstone of the McConnell Island Formation. On the basin edges it is truncated by the Ringnes Formation.

Age

The formation is dated as Callovian on the basis of ammonites collected on Prince Patrick and Ellef Ringnes islands (Tozer and Thorsteinsson, 1964; Stott, 1969).

Environment of deposition

The arenaceous lithologies, sedimentary structures and fauna indicate an inner to mid-shelf environment of deposition for the formation.

References

- Balkwill, H.R.
1983: Geology of Amund Ringnes, Cornwall and Haig Thomas islands, District of Franklin; Geological Survey of Canada, Memoir 390.
- Balkwill, H.R., Hopkins, W.S. Jr., and Wall, J.H.
1982: Geology, Loughheed Island, District of Franklin; Geological Survey of Canada, Memoir 388.
- Crain, E.R.
1977: Log interpretation in the high Arctic; in Transactions of the CWLS Sixth Formation Evaluation Symposium; Canadian Well Logging Society, Calgary, Alberta, p. S1-S32.
- Embry, A.F.
1984: The Wilkie Point Group (Lower-Upper Jurassic), Sverdrup Basin, Arctic Island; in Current Research, Part B, Geological Survey of Canada, Paper 84-1B, p. 299-308.
1985: New stratigraphic units, Middle Jurassic to lowermost Cretaceous succession, Arctic Islands; in Current Research, Part B, Geological Survey of Canada, Paper 85-1B, p. 269-276.
- Greiner, H.R.
1963: Jaeger River, eastern Cornwall Island; in Geology of the north-central part of the Arctic Archipelago, Northwest Territories (Operation Franklin), ed. Y.O. Fortier et al.; Geological Survey of Canada, Memoir 320, p. 533-537.
- Henao-Londono, D.
1977: Correlation of producing formations in Sverdrup Basin; Bulletin of Canadian Petroleum Geology, v. 25, p. 969-980.
- Moore, P.R.
1981: Mesozoic stratigraphy in the Blue Mountains and Krieger Mountains, a preliminary account; in Current Research, Part A, Geological Survey of Canada, Paper 81-1A, p. 95-101.
- Souther, J.G.
1963: Geological transverse across Axel Heiberg Island from Buchanan Lake to Strand Fiord; in Geology of the north-central part of the Arctic Archipelago, Northwest Territories (Operation Franklin), ed. Y.O. Fortier et al.; Geological Survey of Canada, Memoir 320, p. 426-448.
- Stott, D.F.
1969: Ellef Ringnes Island, Canadian Arctic Archipelago; Geological Survey of Canada, Paper 68-16.
- Tozer, E.T.
1963a: South side of Strand Fiord; in Geology of the north-central part of the Arctic Archipelago, Northwest Territories (Operation Franklin), ed. Y.O. Fortier et al.; Geological Survey of Canada, Memoir 320, p. 448-456.
1963b: Mesozoic and Tertiary stratigraphy, western Ellesmere Island and Axel Heiberg Island, District of Franklin; Geological Survey of Canada, Paper 63-30.
- Tozer, E.T. and Thorsteinsson, R.
1964: Western Queen Elizabeth Islands, Arctic Archipelago; Geological Survey of Canada, Memoir 332.

APPENDIX

Selected well tops, Awingak, Ringnes and Hiccles Cove formations, Sverdrup Basin. Location of wells shown on Figure 37.1.

<u>Deminex Orksut I-44</u>			<u>Panarctic North Sabine H-49</u>		
Deer Bay Formation	1457 m	(4781 ft)	Awingak Formation		
Awingak Formation			Slidre Member	2385 m	(7825 ft)
Cape Lockwood Member	1813 m	(5948 ft)	Hot Weather Member	2444 m	(8020 ft)
Cape de Bray Formation (Devonian)	1828 m	(5998 ft)	Cape Lockwood Member	2483 m	(8147 ft)
<u>Panarctic Pedder Point D-49</u>			Ringnes Formation	2557 m	(8390 ft)
Awingak Formation			McConnell Island Formation	2618 m	(8590 ft)
Slidre Member	1085 m	(3560 ft)	<u>Sun Skybattle Bay C-15</u>		
Hot Weather Member	1441 m	(4728 ft)	Awingak Formation		
Cape Lockwood Member	1610 m	(5282 ft)	Cape Lockwood Member	1568 m	(5145 ft)
Ringnes Formation	1710 m	(5610 ft)	Ringnes Formation	1674 m	(5491 ft)
Hiccles Cove Formation	1714 m	(5622 ft)	McConnell Island Formation	1711 m	(5612 ft)
Weatherall Formation (Devonian)	1725 m	(5658 ft)	<u>Sun Linckens Island P-46</u>		
<u>Elf Jameson Bay C-31</u>			Awingak Formation		
Awingak Formation			Slidre Member	554 m	(1818 ft)
Slidre Member		spud	Hot Weather Member	576 m	(1890 ft)
Hot Weather Member	76 m	(250 ft)	Cape Lockwood Member	628 m	(2060 ft)
Cape Lockwood Member	287 m	(942 ft)	Ringnes Formation	732 m	(2400 ft)
Ringnes Formation	359 m	(1178 ft)	McConnell Island Formation	814 m	(2670 ft)
Hiccles Cove Formation	369 m	(1210 ft)	<u>BP Graham C-52</u>		
McConnell Island Formation	442 m	(1451 ft)	Awingak Formation (undivided)	978 m	(3210 ft)
<u>BP Emerald K-33</u>			Ringnes Formation	1272 m	(4174 ft)
Deer Bay Formation	447 m	(1466 ft)	Hiccles Cove Formation	1279 m	(4196 ft)
Awingak Formation			McConnell Island Formation	1318 m	(4325 ft)
Cape Lockwood Member	798 m	(2618 ft)	Jameson Bay Formation	1329 m	(4360 ft)
Ringnes Formation	883 m	(2898 ft)	<u>Imperial Sherwood P-37</u>		
Hiccles Cove Formation	896 m	(2940 ft)	Awingak Formation		
McConnell Island Formation	975 m	(3200 ft)	Cape Lockwood Member		spud
<u>Panarctic Depot Island C-44</u>			Ringnes Formation	269 m	(882 ft)
Awingak Formation			McConnell Island Formation	305 m	(1000 ft)
Cape Lockwood Member	354 m	(1160 ft)	Sandy Point Formation	363 m	(1192 ft)
Ringnes Formation	408 m	(1340 ft)	<u>Panarctic Romulus C-42</u>		
Hiccles Cove Formation	422 m	(1384 ft)	Awingak Formation		
McConnell Island Formation	457 m	(1500 ft)	Slidre Member	1034 m	(3390 ft)
<u>Panarctic Hecla F-62</u>			Hot Weather Member	1111 m	(3644 ft)
Awingak Formation			Cape Lockwood Member	1149 m	(3770 ft)
Slidre Member	440 m	(1444 ft)	Ringnes Formation	1311 m	(4302 ft)
Hot Weather Member	695 m	(2280 ft)	Sandy Point Formation	1350 m	(4428 ft)
Cape Lockwood Member	701 m	(2301 ft)			
Ringnes Formation	771 m	(2528 ft)			
Sandy Point Formation	797 m	(2615 ft)			

Pseudoeuryptychites: a new polyptychitinid ammonite
from the Lower Valanginian of the Canadian and Eurasian Arctic

Project 850026

J.A. Jeletzky¹
Institute of Sedimentary and Petroleum Geology, Ottawa

Jeletzky, J.A., **Pseudoeuryptychites**: a new polyptychitinid ammonite from the Lower Valanginian of the Canadian and Eurasian Arctic; in Current Research, Part B, Geological Survey of Canada, Paper 86-1B, p. 351-361, 1986.

Abstract

A new subgenus **Pseudoeuryptychites** is erected for the **Cadoceras**-like representatives of the early Valanginian genus **Siberyptychites** Kemper and Jeletzky 1977. **Pseudoeuryptychites** is a high Boreal homoeomorph of the European genus **Euryptychites** Pavlow 1914.

Résumé

Un nouveau sous-genre, **Pseudoeuryptychites**, est proposé pour les représentants du type **Cadoceras** du genre **Siberyptychites** Kemper et Jeletzky 1977 du Valanginien inférieur. **Pseudoeuryptychites** est un homéomorphe de l'Extrême nord du genre européen **Euryptychites** Pavlow 1914.

¹ 741 Melfa Crescent, Ottawa, Ontario K2C 0P4

Introduction and acknowledgments

The subgenus *Siberiptychites* Kemper and Jeletzky was published under joint authorship in the stratigraphic paper by Kemper (1977, p. 3) for North Siberian and Arctic Canadian polyptychitids belonging to the species group of *Polyptychites stubendorffi* (Schmidt, 1872). This subgenus was originally "characterized by the combined presence of frequent constrictions and the third auxiliary lobe in the external suture line." *Polyptychites stubendorffi* was designated as the type species of *Siberiptychites*. However, it was recognized that the subgenus includes *Cadoceras*-like forms resembling *Euryptychites* Pavlow 1914 but possessing features diagnostic of *S. stubendorffi*.

Siberiptychites was treated as a full genus by Klimova (1981, p. 74, 80) who also discovered its additional morphological distinctions from *Polyptychites* s.s. This example is followed here, particularly because of Klimova's (1978) previous discovery of the genus *Bodylevskites* in the oldest Valanginian of Northern Siberia. This genus is interpreted here as the immediate ancestor of the predominantly younger *Siberiptychites* ex gr. *stubendorffi*, confirming Kemper and Jeletzky's (in Kemper, 1977) conclusion that *Siberiptychites*, including its *Cadoceras*-like representatives, is only indirectly related to *Polyptychites* s.s. *Siberiptychites* appears, instead, to form an independent high Boreal polyptychitid lineage that (Kemper, 1977, p. 3): "apparently evolved in the same direction as the *Temnoptychites-Thorsteinssonoceras* lineage of Craspeditidae (Jeletzky and Kemper, in prep.) (see Jeletzky, 1979) which also terminated with broad *Cadoceras*-like forms."

The writer's study of *Cadoceras*-like *Siberiptychites* forms revealed that they are a well defined evolutionary offshoot of its main lineage (i.e. *Siberiptychites* ex gr. *stubendorffi*). Furthermore, all of the North Siberian and European Arctic *Cadoceras*-like polyptychitids assigned to the European genus *Euryptychites* by Pavlow (1914, p. 36-38, Pl. XI, figs. 1-3) and subsequent Russian workers (e.g. Voronets, 1962, p. 78-82, Pl. XXXIX, fig. 2; Pl. XL, fig. 2a, b; Pl. XLIX, fig. 1a, b; Pl. XLII, fig. 1; Pl. L, fig. 2; Pl. XLVIII, fig. 1; Pl. LI, fig. 1a, b; Pl. LII, fig. 1; Figures 29-31; Bodylevsky, 1968, p. 313; Pl. 72, fig. 1a, b and Yershova, 1980, Pl. IV, fig. 2) were found to belong to this offshoot. Therefore, in this paper, a new subgenus *Pseudoeuryptychites* is erected for them, and their biochronology and geographical distribution is also described.

Dr. Edwin Kemper (Bundesanstalt fuer Bodenforschung und Rohstoffe, Hannover, Federal German Republic), collected all of the Canadian *Pseudoeuryptychites* material described in this paper, provided the writer with valuable stratigraphic information about it, and made available important comparative material of the polyptychitids from northwest Germany. Dr. Kemper has also contributed to the development of ideas presented in this paper in the course of the preparation of a joint monograph on European and high Boreal Polyptychitinae (Jeletzky and Kemper, in prep.). Ms. J. White prepared the photographs of *Pseudoeuryptychites* reproduced in this paper.

The type specimens are stored at Geological Survey of Canada headquarters in Ottawa.

Systematic descriptions

Genus *Siberiptychites* Kemper and Jeletzky 1977

Subgenus *Pseudoeuryptychites* Jeletzky new subgenus

Type species. *Euryptychites pavlovi* Voronets 1962.

Derivation of name. Intended to stress the superficial morphological similarity of the subgenus to the homoeomorph *Euryptychites* Pavlow 1914.

Diagnosis. Subgenus of *Siberiptychites* characterized by an *Euryptychites*-like shape and proportions of all growth stages with the shell diameter exceeding 40 to 45 mm. The adult external suture line¹ differs in the positioning of all three auxiliary lobes on the umbilical wall. All of these auxiliaries are relatively much larger, more slender and more deeply and complexly denticulated than their counterparts in *Siberiptychites* s.s. and true *Euryptychites*. The subgenus differs from the true *Euryptychites* and all other *Euryptychites*-like European polyptychitids in the same way as *Siberiptychites* s.s. does.

Type area. Central part of Northern Siberia (Anabar-Khatanga basin).

Stratigraphy and age. Lower Valanginian. Regional *Temnoptychites syzranicus* and *Polyptychites michalskii* zones, with probable exception of the lower part of *Temnoptychites syzranicus* Zone (Klimova, 1981, p. 74; Gol'bert et al., 1981, p. 56, 57, Tables 3, 4). See in the descriptions of *Siberiptychites (Pseudoeuryptychites) pavlovi* and *S. (P.)* n. sp. indet. A for further details.

Geographical range. Northern Siberia, Arctic Canada (Sverdrup Basin), and Spitsbergen. Probably present elsewhere in high Boreal basins of the European Arctic also.

Discussion. The purely homoeomorphic nature of the morphological similarity of *Euryptychites* s.s. (as defined by its type species *E. latissimus* (Neumayr and Uhlig, 1881)) with the North Siberian cadicone polyptychitids assigned to that genus by Pavlow (1914, p. 36) and other Russian workers, is revealed first of all by an entirely different ontogenetic development of their sculpture and whorl shape. As indicated below in the description of *Siberiptychites (Pseudoeuryptychites) pavlovi* – the type species of *Pseudoeuryptychites* – this ontogeny is similar to that of *Siberiptychites* s.s. recently described by Klimova (1981, p. 74, 80) using the example of *S. (S.) stubendorffi*. Furthermore, all these cadicones possess numerous *Siberiptychites* s.s. – like constrictions completely absent in true *Euryptychites*. The adult external sutures of these two taxa also differ markedly. Unlike the sutures of *S. (P.) pavlovi* and other *Pseudoeuryptychites* species, those of *E. latissimus* (Neumayr and Uhlig 1881, p. 158, Pl. XXVIII, fig. 1b; this paper, Fig. 38.1) and other *Euryptychites* species have, as a rule, only two auxiliary lobes. These auxiliaries are relatively smaller and simpler structures separated from each other and from the second lateral lobe by relatively wider saddles. Most *Euryptychites* sutures also differ in the stubby, downward-tapering appearance of their lobes.

The resemblance of *Pseudoeuryptychites* to the late early to earliest late Valanginian Central European *Polyptychites* ex gr. *orbitatus-praelatus* is also a matter of homoeomorphy only. These European forms do exhibit a similarly late development of the *Euryptychites*-like shape and proportions of the whorl. However, they always lack the constrictions that are so characteristic of *Pseudoeuryptychites*. Furthermore, *Polyptychites* ex gr. *orbitatus-praelatus* are characterized by a different bundling habit of intermediate whorls, dominated by polyptychoid to tridichotomous bundles (e.g. Koenen, 1902, Pl. III, figs. 1, 3; Pl. LV, fig. 1). The equivalent whorls of all *Pseudoeuryptychites* forms exhibit instead either a trivirgatatipartitious (see Kemper, 1978, p. 188-190, Fig. 1)

¹ Polyptychitid external sutures are considered to be adult when they acquire the maximum number of auxiliary lobes and the arrangement of all their major elements that do not change substantially to the oral end of the adult phragmocone.

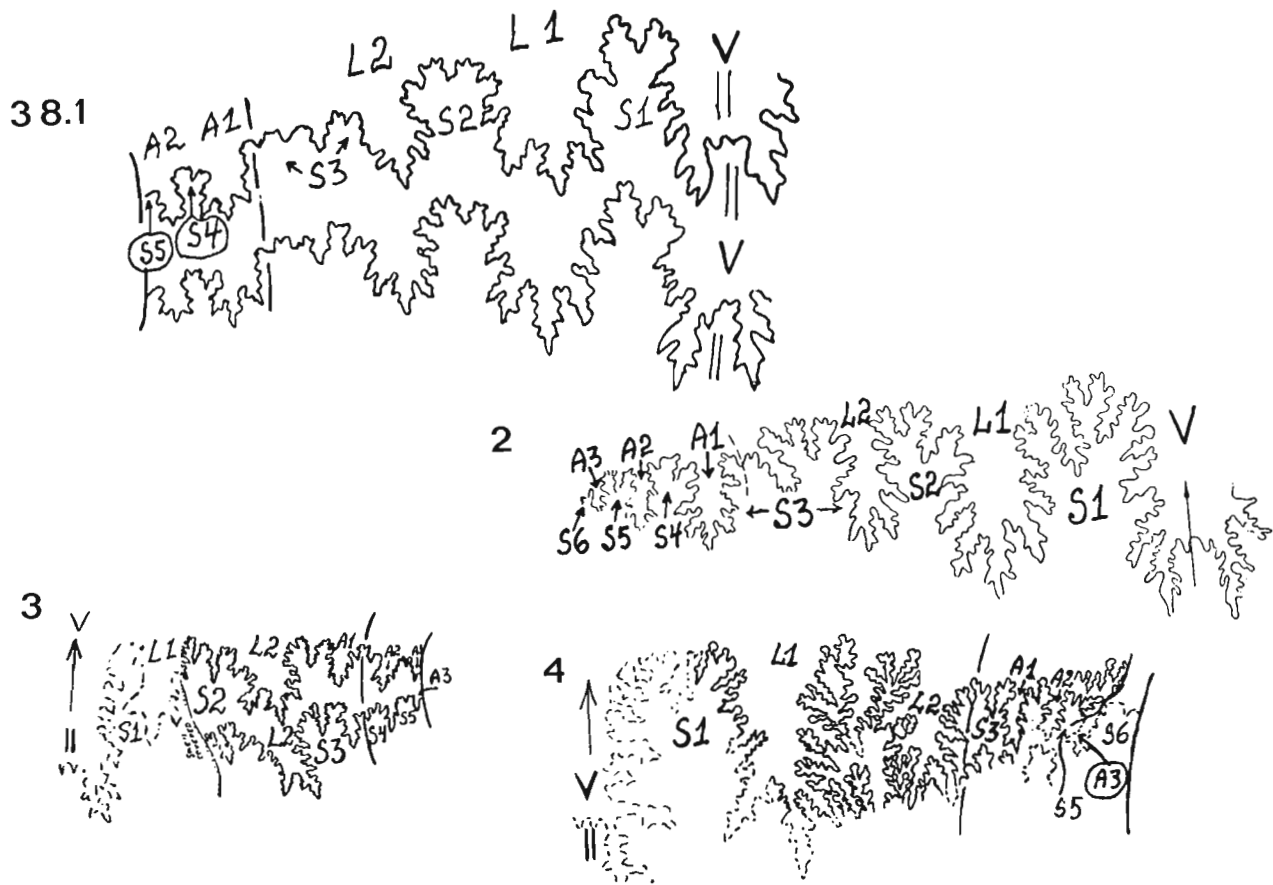


Figure 38.1. *Euryptychites latissimus* (Neumayr and Uhlig 1881). *Polyptychites*-beds, lower Valanginian. Northwest Germany, Buekeburg-Jetenburg. BGR Collection, Hannover kv 396. Early adult external suture line at the whorl diameter of about 23 mm; x2.

Figure 38.2. *Siberiptychites* (*Pseudoeuryptychites*) *pavlovi* (Voronets 1962). Reproduction of the adult external suture of the lectotype originally published by Voronets (1962, p. 79, Fig. 29); x2.

Figure 38.3. *Siberiptychites* (*Pseudoeuryptychites*) n. sp. indet. A. Late juvenile external suture line lacking the ventral and first lateral lobe at the whorl diameter of about 15 mm. Specimen GSC 79414 (otherwise unfigured). The same locality, bed and age as for the specimen GSC 77119 reproduced in Pl. 38.1, fig. 2A-C); x4 (approx.).

Figure 38.4. *Siberiptychites* (*Pseudoeuryptychites*) n. sp. indet. A. Terminal adult external suture lines lacking the ventral lobe and the bulk of the third auxiliary lobe. Estimated whorl diameter of about 50 mm. Specimen GSC 79413 (otherwise unfigured). The same locality, bed and age as for the specimen GSC 77119 reproduced in Pl. 38.1, fig. 2A-C); x1.

The so called "Russian system" of designation of external lobes and saddles is used (see Jeletzky, 1965, p. 2 for further details). V - ventral lobe; L₁ - first lateral lobe; L₂ - second lateral lobe; A₁ - first auxiliary lobe; A₂ - second auxiliary lobe; A₃ - third auxiliary lobe. Lateral saddles are designated S₁ to S₆ inclusive beginning at the venter. No symbol is used for the ventral saddle. Umbilical shoulder marked by dashed line. Umbilical seam marked by solid line. Mid-venter is marked by a double line and an arrow, the head of which points oralward.

or a predominantly quadripartitious bundling habit, which is similar to that of the equivalent and younger whorls of *Siberiptychites* s.s. Finally, all better known representatives of *Pseudoeuryptychites* (e.g. *S. (P.) pavlovi* and *S. (P.) splendens*; see Pavlow, 1914, Pl. XI, fig. 3; Voronets, 1962, Pl. XLII, fig. 1; Bodylevsky, 1968, Pl. 72, fig. 1) exhibit the characteristic *Siberiptychites* s.s. - like sequence of various whorl shapes and sculptural stages that are not present in *Polyptychites* ex. gr. *orbitatus-praelatus*. This sequence of whorl shapes and sculptural stages was recently described by Klimova (1981, p. 74, 80) using *S. (S.) stubendorffi* as an example.

The adult external suture line of *Polyptychites* ex gr. *orbitatus-praelatus* may have either two or three auxiliary lobes (e.g. Koenen, 1902, Pl. III, figs. 1, 4, 8; Pl. IV, figs. 1, 2, 3, 5, 8; Pl. LV, figs. 1, 2). The variant with three auxiliaries resembles closely the adult suture of *Pseudoeuryptychites* (Fig. 38.2, 38.4), except in the positioning of the auxiliaries and the ontogenetic-phylogenetic development. The adult, seven-lobed external suture of *Polyptychites* ex gr. *orbitatus-praelatus* develops out of the six-lobed late juvenile suture via the addition of the third auxiliary at the umbilical seam and the concurrent displacement of the first auxiliary onto the adumbilicalmost part of the flank. Furthermore, the

seven-lobed suture of this species group can be traced back phylogenetically to the adult external suture of ancestral *Polyptychites* ex gr. *pavlovi* that always possesses only two auxiliary lobes. The external suture of *Pseudoeuptychites*, in contrast, has three auxiliary lobes in the earliest growth stages known (Fig. 38.3 and in the description of *S. (P.)* n. sp. indet. A). This late juvenile suture has only two auxiliaries on the umbilical wall and is *Siberiptychites* (*Siberiptychites*)-like in this respect. The adult *Pseudoeuptychites* suture develops out of this juvenile suture via the adumbilical displacement of the first auxiliary onto the outermost part of the umbilical wall (Fig. 38.3, 38.4). Furthermore, the adult *Pseudoeuptychites* suture can be traced phylogenetically first, into the much less denticulated adult external suture of *S. (S.) middendorffi* var. *incrassata* (Pavlow, 1914, Pl. VI, fig. 2c; Jeletzky, 1965, Fig. 1f), and then into that of *S. (S.) stubendorffi* (Pavlow, 1914, Pl. VI, fig. 1c; Klimova, 1981, Fig. 3b), both of which also have three auxiliary lobes. However, only two auxiliaries of these sutures are situated on the umbilical wall. The inferred palaeogenetic evolutionary development of the *Siberiptychites* external suture features a gradual displacement of the first auxiliary lobe onto the outer part of the umbilical wall and a concurrent crowding of all three auxiliaries there combined with a gradual increase in the complexity of the adult suture. This ontogenetic and phylogenetic development is quite unlike the above discussed, well documented, ontophylogenetic development of the external suture of *Polyptychites* ex gr. *orbitatus-praelatus*.

Pseudoeuptychites differs from *Siberiptychites* s.s. first of all in the entirely *Euryptychites*-like shape, and in the proportions of all its advanced to adult whorls, beginning with the shell diameter of 40 to 45 mm. The development of an acute umbilical shoulder (Pavlow, 1914, Pl. XI, figs. 1, 2a-c, 3; Voronets, 1962, Pl. XLII, fig. 1; Pl. XLVII, fig. 1; Pl. LI, fig. 1a, b; Pl. L, fig. 2; Pl. LI, fig. 1a, b; Pl. LII, fig. 1; this paper Pl. 38.1, fig. 1B, 2B) is particularly diagnostic. It is this feature that permits the exclusion of the otherwise similar, adult shells of the ancestral *S. (S.) middendorffi* from *Pseudoeuptychites*. The adult external suture line of *Pseudoeuptychites* differs from that of *Siberiptychites* s.s. in the positioning of all three auxiliary lobes on the umbilical wall combined with a much greater complexity of all its elements. However, the adult external suture of *S. (S.) middendorffi* has a transitional character.

Siberiptychites (*Siberiptychites*) and *Siberiptychites* (*Pseudoeuptychites*) both exhibit frequent constrictions throughout their ontogeny. Furthermore, they exhibit an apparently entirely similar ontogenetic sequence of sculptural growth stages (see in the description of *S. (S.) pavlovi* below). These two subgenera coexist in the same high Boreal basins in approximately contemporary lower Valanginian beds without any intergradation, except near the base of their time ranges (i.e. via *S. (S.) middendorffi*). This indicates that they are independent lineages arising out of the same rootstock (i.e. the earliest known forms of *S. (S.)* ex gr. *stubendorffi*). The morphologically transitional *S. (S.) middendorffi* (Pavlow, 1914, p. 32, 33; Pl. VI, fig. 2; Pl. VII, fig. 1), that is difficult to assign subgenerically, appears to be a connecting link between *S. (S.) stubendorffi* and typical representatives of *Pseudoeuptychites*. The recorded detailed stratigraphic relationships of these forms (see in the specific descriptions below) support this conclusion. *Pseudoeuptychites* appears to be a shortlived offshoot of the main *Siberiptychites* (*Siberiptychites*) stem that died out without issue. Therefore, it is assigned a subgeneric rank only.

***Siberiptychites* (*Pseudoeuptychites*) *pavlovi* (Voronets 1962)**

Figure 38.2

- 1914 *Euryptychites gravesiformis* Pavlow, p. 37, Pl. XI, figs. 2, 3.
 1962 *Euryptychites pavlovi* Voronets, p. 78, 79, Pl. XXXIX, fig. 2; Pl. XL, fig. 2; Pl. XLIX, fig. 1; Figure 29.
 1980 *Euryptychites* aff. *pavlovi* Yershova, 1980, Pl. IV, fig. 2.

Type specimen. Voronets (1962) did not designate the holotype of her new species from four specimens available to her. The only figured specimen, No. 29a, reproduced in Pl. XXXIX, fig. 2 (where it is erroneously designated No. 25a); Pl. XL, fig. 2; Pl. XLIX, fig. 1 and Text-fig. 29 is formally designated by the writer as the lectotype of *Siberiptychites* (*Pseudoeuptychites*) *pavlovi* (Voronets 1962).

Nomenclatorial status of *S. (P.) pavlovi*. "*Euryptychites*" *pavlovi* does not become a homonym of *Polyptychites pavlovi* Koenen 1902 (Pl. I, figs. 1-3) proposed for one of the cotypes of *Olcostephanus keyserlingi* of Neumayr and Uhlig (1881-82, Pl. XXVII, fig. 2, 2a), as it was originally assigned to a different genus. Furthermore, the spelling of the two names is different.

Material. No Canadian polyptychitids definitely assignable to *S. (P.) pavlovi* (Voronets) are known to the writer. However, this species is redescribed here as it is the best known representative and the type species of the subgenus *Pseudoeuptychites* novum.

Description. The following original description of *Siberiptychites* (*Pseudoeuptychites*) *pavlovi* is provided by Voronets (1962, p. 78, 79; writer's translation from Russian): "Whorls are involute, low and thick; the thickness is almost two times greater than the height. Their greatest thickness occurs on the umbilical shoulder. The lateral side is very short and rapidly merges into the wide and flattened siphonal side. The umbilicus is moderately wide, deep and funnel-like shaped. The umbilical shoulder is rounded-acute. The umbilical wall of the inner whorl is covered by primary ribs that begin at the umbilical seam. On its outer whorls these ribs begin in the middle of the umbilical wall. The ribs are fine at first but they become higher as they approach the umbilical shoulder and form the obliquely forward inclined nodes on the latter. There are 16 of these nodes per a complete whorl. The node splits into two secondaries. The anterior secondary is almost of the same size as the node, strongly inclined forward and represents, so to say, the continuation of the node. The posterior secondary is less prominent than the node, splits off the lower part of the latter, and is directed almost radially. An intercalated secondary that adjoins the node may sometimes occur between these two secondaries. These ribs subdivide, in turn, into two branches each. The resulting tertiary ribs are fine and sharp. The distance between them is wider than the thickness of the ribs. There are 8 primary ribs per half whorl; the siphonal side exhibits 44 ribs. The secondary ribs become smooth in the proximity of the nodes as one approaches the living chamber. The distances between the ribs on the siphonal side increase in that direction and then the ribs disappear completely on the living chamber. There are four constrictions on the whorl of which one is very deep and wide. Only a part of the living chamber is preserved.

"The suture line (Fig. 29) is strongly denticulated. The line joining the tops of saddles is oriented almost radially with only its auxiliary saddles being lowered (i.e. descendant; writer's remark). The siphonal lobe is longer than the first lateral one. However, the first lateral lobe is twice as long and wide as the second lateral lobe. The outer (i.e. S₁ of Fig. 38.2; writer's remark) and the second lateral (i.e. S₃ of Fig. 38.2) saddles are very wide. The width of the first lateral (i.e. S₂ of Fig. 38.2) is one-third that of the other two saddles. The second lateral saddle is subdivided into two unequal parts by a long auxiliary lobe.

"Dimensions (in mm)

Shell diameter	74 (100)
Height of whorl	30 (40)
Thickness of whorl	58 (78)
Diameter of the umbilicus	32 (29)"

This description appears to deal only with the lectotype of the species (selected herein) reproduced in Pl. XXXIX, fig. 2; Pl. XL, fig. 2 and Pl. XLIX, fig. 1, but not with the other three unfigured specimens. Therefore, the range of variability of individual morphological features within the type lot remains unknown. This description is also incomplete in other ways.

First, it does not discuss the ontogenetic changes of shape and proportions of the whorl, which were previously described and clearly illustrated by Pavlow (1914, p. 37, Pl. XI, fig. 2c). According to him, the adult, *Euryptychites*-like habitus of *S. (P.) pavlovi*, with its uniformly and very low-arched cross-section of the ventral region, the angular umbilical shoulder, and approximately straight umbilical wall, first appears at a shell diameter of 40 to 45 mm. The preceding two whorls have an entirely different, rounded-rectangular to rounded-trapezoidal, only slightly wider than high cross-section with rounded but clearly defined ventral and umbilical shoulders. This cross-section matches closely, and evidently corresponds to, the *Polyptychites rectangulatus*-like growth stage of *Siberiptychites* recently described by Klimova (1981, p. 77, Fig. 2-5) using the example of *S. (S.) stubendorffi*. The next younger whorl cross-section, which is about 5.5 mm wide and only about 3 mm thick, is again *Euryptychites*-like in its proportions as well as in the uniformly- and low-arched shape. This cross-section is similar and evidently corresponds to the first *Euryptychites*-like growth stage of *Siberiptychites* (Klimova, 1981, p. 77, Fig. 2/1-3).

Second, the description of sculpture is incorrect and omits its ontogenetic development. As visible in Voronets' (1962, Pl. XXXIX, fig. 2) photograph, the earliest exposed intermediate whorl with a terminal shell diameter of about 70 mm, is not ornamented by bidichotomous rib bundles alone. Instead, it exhibits an irregular alternation of regularly bidichotomous, subbidichotomous, quadrivirgati-partitious and quadrifasciculate bundles. The apparently exclusively bidichotomous ornament appears to be restricted to the adapical third of the next older whorl, with a shell diameter of about 76 mm (Voronets, 1962, Pl. XL, fig. 2a). The exact character of bundling is obscured on the oral two thirds of that whorl because of an obliteration of the lower parts of secondary ribs. These parts of ribs become distinct again on the adapical third of the next and last preserved whorl of the lectotype (Voronets, 1962, Pl. XLIX, fig. 1a) with a shell diameter of about 90 mm. However, this oralmost phase of clearly defined ornament is again dominated not by bidichotomous bundles but by true polyptychous bundles, consisting of one trifurcate and one bifurcate branch. On the whole, this ornament is entirely similar and corresponds to the sculptural stage of regularized rib bundles of *Siberiptychites* s.s. recently described by

Klimova (1981, p. 78, Pl. XI, fig. 4, 4a, 6) using *S. (S.) stubendorffi* as an example. The secondary and tertiary ribs are completely detached from the umbilical bullae on the adoral two thirds of the last preserved whorl of the lectotype (Voronets, 1962, Pl. XLIX, fig. 1a, b), which represents the early part of a presumably intermediate (because of the spacing of oralmost sutures; see below) living chamber. Furthermore, the ribs are irregularly spaced and unequally prominent there, in contrast to their regular spacing and equal strength in earlier growth stages. This terminal disorganization of the ornament is similar and corresponds to the terminal phase of the stage of regularized rib bundles in *Siberiptychites* s.s. that was described and illustrated, but not formally segregated, by Klimova (1981, p. 78, Pl. IX, fig. 6). The recurrence of this sculptural stage in *S. (P.) pavlovi* suggests that its earlier, unexposed whorls bear sculpture similar to that of earliest sculptural stages of *Siberiptychites* s.s.

The inner (second penultimate?) whorl of the specimen of *S. (P.) pavlovi* figured by Pavlow (1914, Pl. XI, fig. 2a, b) only differs from its lectotype in an appreciably earlier disorganization of the ornament. Its rib bundles become indistinct at an estimated shell diameter of 50 mm simultaneously with the emergence of the *Euryptychites*-like shape and proportions of the whorl. This earlier, apparently infraspecific, disorganization of the ornament is then followed by its marked but irregular weakening on the living chamber of this specimen (Pavlow, 1914, p. 37, Pl. XI, fig. 2c). The living chamber of *S. (P.) pavlovi* is also characterized by a marked lengthening of umbilical bullae that may become spike-like (Pavlow, 1914, p. 37, Pl. XI, fig. 3).

Finally, this description omits the most diagnostic features of the adult external suture line of *S. (P.) pavlovi*, which are clearly visible in Pavlow's (1914, Pl. XI, fig. 2d) and Voronets' (1962, Fig. 29) drawings. This suture, reproduced in Figure 38.2 of this report, is *Siberiptychites*-like in the presence of three, well developed auxiliary lobes. However, they are relatively larger, more strongly denticulated, and more crowded in comparison with their equivalents. Furthermore, they are all positioned on the umbilical wall. The intervening fourth and fifth lateral saddles are correspondingly narrowed. The extremely wide and rather complexly denticulated third lateral saddle spans the umbilical shoulder and much of the inner (or adumbilicalmost) part of the flank instead of being situated entirely on the umbilical shoulder. It contrasts with the much more narrow second and first lateral saddles, of which the second is the more narrow. The lateral lobes and the first and second lateral saddles are deeply and complexly denticulated. The sutures are well separated on the part of the whorl that provided the published external suture of the lectotype (Voronets, 1962, Pl. XLIX, fig. 1). Therefore, this suture is an early adult one and is followed by an intermediate living chamber.

The external suture line of *S. (P.) pavlovi* figured by Pavlow (1914, Pl. XI, fig. 2, b, d) only differs from that of the lectotype infraspecifically in its generally more slender and more finely and deeply denticulated ventral, first and second lateral, and first auxiliary lobes. The third auxiliary lobe appears to be concealed. There is just enough room for it in the narrow, presumably shell-covered space that separates the second auxiliary lobe from the marked position of the umbilical seam. This suture is also an early adult one as its whorl has a diameter of about 68 mm and is the inner whorl of a much larger specimen that includes the adult living chamber (Pavlow, 1914, Pl. XI, fig. 2c).

Affinities and differences. According to Voronets (1962, p. 81), *S. (P.) pavlovi* differs from her *S. (P.) pateraeiformis* in the greater height of its whorls and their greater thickness.

Furthermore, the sculpture of *S. (P.) pateraeformis* consists mostly of fasciculate and quasifasciculate rib bundles, and its second lateral lobe is differently shaped. Finally, the umbilicus of *S. (P.) pateraeformis* measures 32 to 36 per cent versus 29 per cent in *S. (P.) pavlovi*. The taxonomic value of differences in the bundling habit and the shape of the second lateral lobe is uncertain. These features are variable in *S. (P.) pavlovi* and their range of variation in *S. (P.) pateraeformis* is unknown. However, the rest of the morphological distinctions appear to be valid and sufficient for a full specific differentiation of these two forms. Furthermore, the two also differ in some other important features not noted specifically by Voronets (1962). As already pointed out, the supplementary (this new term covers all ribs, such as secondary, tertiary and intercalated, other than the primary ribs) ribs of *S. (P.) pavlovi* are regularly and closely spaced and equally strong on the intermediate whorls but become variably strong, irregularly distributed and variably oriented on the two to three terminal whorls of its adult shell. In contrast, the supplementary ribs of *S. (P.) pateraeformis* maintain their regular spacing and equal strength to the end of its phragmocone and on the preserved part of its presumably intermediate living chamber (Voronets, 1962, Pl. LII, fig. 2). Furthermore, these ribs maintain the same character until the oral end of the still larger but fully septate Canadian representative of *S. (P.) pateraeformis* (see below). Finally, the supplementary ribs of the lectotype of *S. (P.) pateraeformis* become (abruptly?) considerably more sparse and widely spaced on the living chamber as compared with the phragmocone (compare Voronets, 1962, Pl. LI, fig. 1a, b with Pl. LII, fig. 1).

S. (P.) pavlovi differs from *Siberiptychites (Pseudoeryptychites) splendens* Bодylevsky (1968, p. 313, Pl. 72, fig. 1), which is conspecific with *Siberiptychites (Pseudoeryptychites) sp. nov. indet.* of Voronets (1962, p. 80, 81, Pl. XLII, fig. 1; Pl. L, fig. 2; Fig. 30), in its possession of a considerably smaller number of bullae per whorl (16 versus 20) and a later appearance of an angular umbilical shoulder. Furthermore, its bundling habit is dominated by well defined trifurcate and quadrifurcate bundles at similar whorl diameters. Finally, this *S. (P.) splendens* differs in the persistence of regularly and evenly spaced *S. (P.) pateraeformis*-like supplementary ribbing onto its presumably adult penultimate whorl at least (Voronets, 1962, Pl. L, fig. 2).

Distinctions of *S. (P.) pavlovi* from the Canadian *Siberiptychites (Pseudoeryptychites) n. sp. indet. A* are discussed in the description of the latter.

Stratigraphy and age. In northern Siberia, *S. (P.) pavlovi* was recorded only from its type-locality 29a and 29a.5 at the northeastern end of Paks Peninsula, Lena-Anabar region of North Siberia (Voronets, 1962, p. 18, 79) and from an unspecified locality on Anabar River (Pavlov, 1914, p. 37). At its type-locality, this species was found in the topmost bed of an approximately 50 m thick unit of dark grey shale with thin interbeds and concretions of very hard, grey, argillaceous limestone. The underlying beds of that unit have yielded *S. (P.) pateraeformis*. The rich and allegedly uniform ammonite fauna of this unit was assigned by Voronets (1962, p. 18) to the "Polyptychites Zone of the middle Valanginian." Subsequent, more detailed zonations of this interval of the Paks Peninsula profile (e.g. Bassov et al., 1970; Bassov et al. in Saks et al., 1972, p. 42; Zakharov et al., 1974, p. 124-126; Gol'bert et al., 1981, p. 56-59) assign this unit to some part of the regional upper lower Valanginian *Polyptychites michalskii* Zone (earlier *Polyptychites stubendorffi* Zone). However, it is difficult to determine the position of the *S. (P.) pavlovi*-bearing bed of this unit within the *Polyptychites michalskii* Zone. For some unexplained reason, all above mentioned

workers neither cite any of the "*Euryptychites*" (i.e. *Pseudoeryptychites*) species described by Voronets (loc. cit.) nor offer a correlation of the individual fossiliferous lower Valanginian beds and units (their "pachki") distinguished by them with those recognized previously by Voronets (1962, p. 18). However, the citation of "*Euryptychites*" *gravesiformis* (identification of N.I. Shulgina), from unit XVIII of Zakharov et al. (1974, p. 125) suggests its being

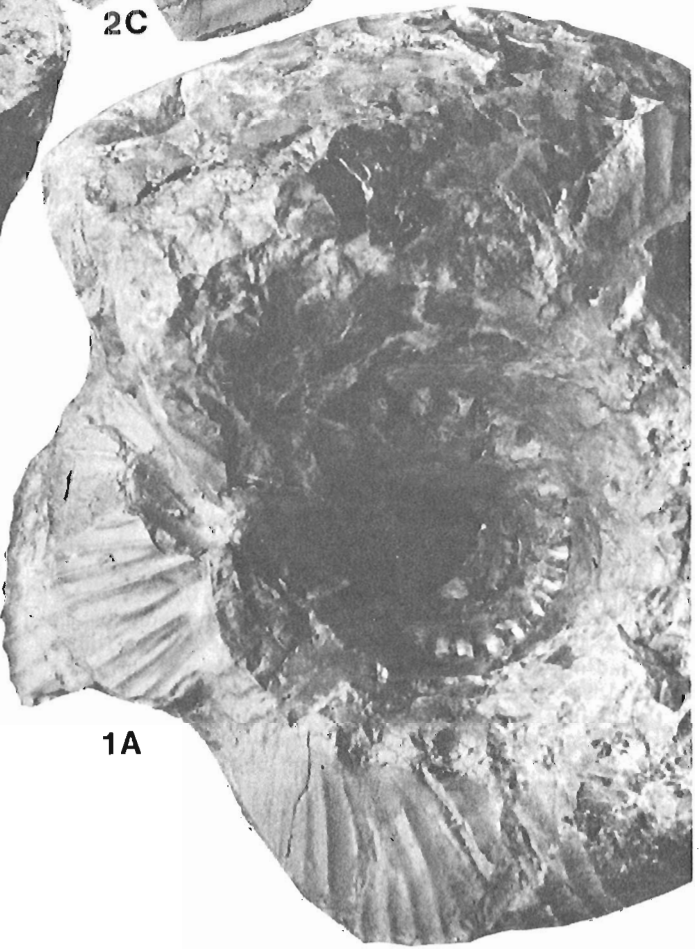
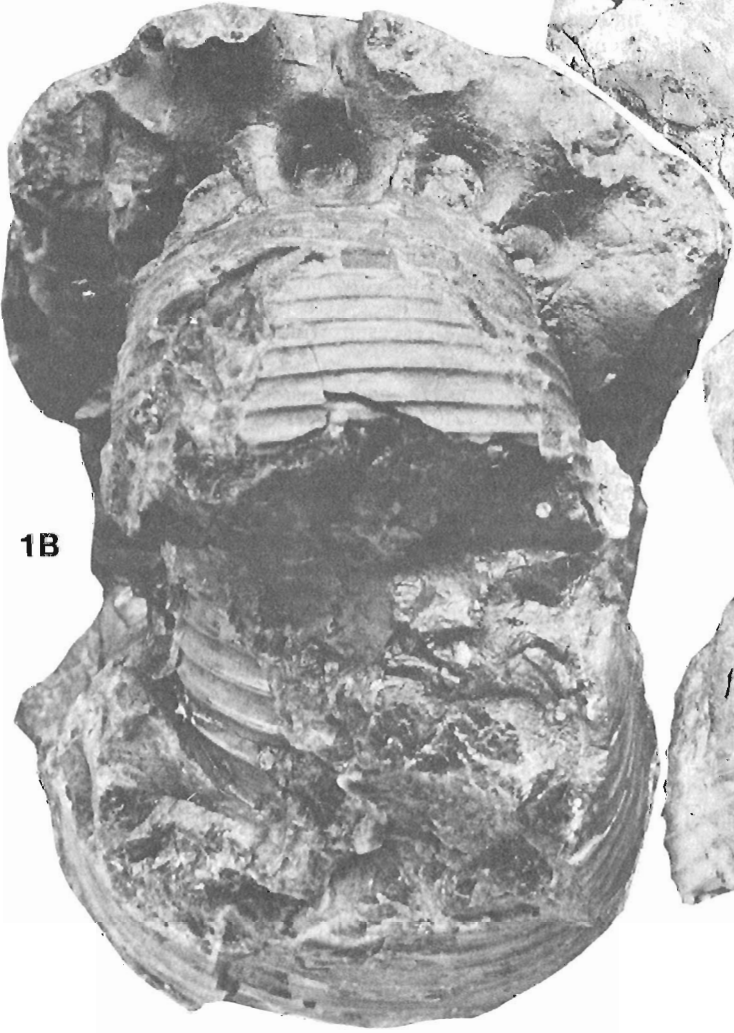
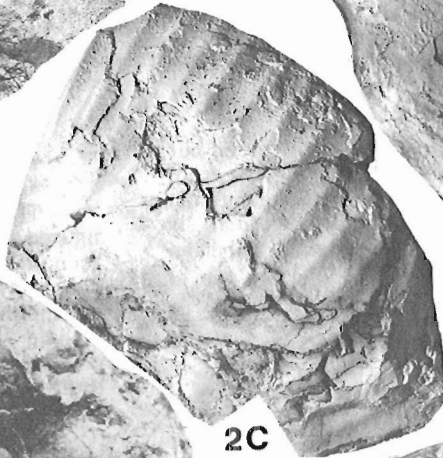
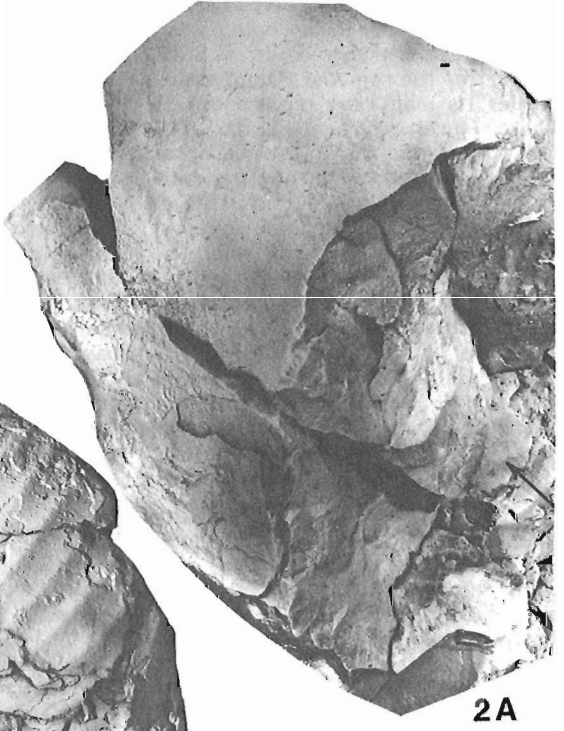
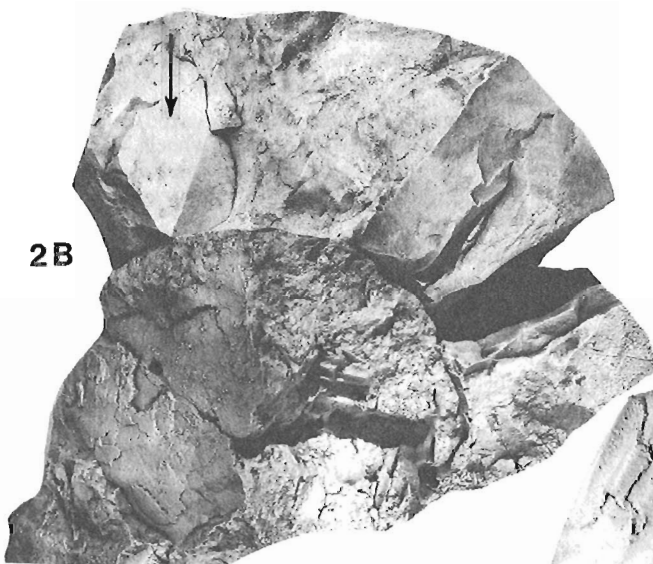
PLATE 38.1

Figure 1A, B. *Siberiptychites (Pseudoeryptychites) pateraeformis* (Voronets 1962).

GSC 77107, GSC loc. 91309. Upper Deer Bay Formation, Section Ke 74/11 (Kemper, 1977, p. 3, Fig. 3), concretionary bed-15 situated between 200 and 225 m stratigraphically below the assigned base of Isachsen Formation; uppermost part of *Siberiptychites*-beds, middle part of lower Valanginian. North Amund Ringnes Island, N.W.T.; Lat. 78°38'26"N.; Long. 94°54'W. Strongly deformed, large but entirely septate representative, xl. 1A. Lateral view; 1B. Terminal cross-section and ventral view of the early part of last preserved (adult penultimate?) whorl. Note the straight umbilical wall and angular umbilical shoulder on the right side of the cross-section that are diagnostic of the subgenus *Pseudoeryptychites novum*.

Figure 2A-C. *Siberiptychites (Pseudoeryptychites) n. sp. indet. A*.

GSC 77119, GSC loc. 93754 (=91308). Upper Deer Bay Formation, Section Ke 76/11 (Kemper, 1977, p. 3, Fig. 3), bed-14 situated about 225 m stratigraphically below the assigned base of Isachsen Formation and about 24 m stratigraphically above the bed-16 that has yielded the youngest representatives of *S. (S.) stubendorffi*; uppermost part of *Siberiptychites*-beds, middle part of lower Valanginian. North Amund Ringnes Island, N.W.T.; Lat. 78°38'26"N.; Long. 97°54'W. 2A. Ventral view of a fragment of apparently smooth, adult living chamber. An obliquely oriented segment of sharp and bullate (two bullae only) umbilical shoulder is visible on the lower left. This umbilical shoulder is also visible on the lower right side of 2B. A small segment of evenly and coarsely ribbed adult penultimate whorl, that is shown in 2C, is visible on the lower right (marked by arrow); 2B. Cross-sections of fragments of the adult ultimate (living chamber) and penultimate whorls shown in 2A and C. Their almost undeformed umbilical walls preserved on the right side are characteristically straight and separated from the evenly arched ventral region (i.e. venter and flank combined) by angular umbilical shoulders. The position of the mid-venter of ultimate whorl is marked by black arrow at the upper left. The left flank and umbilical wall of the penultimate whorl are caved-in, and those of the ultimate whorl are broken off; 2C. Oblique lateral view of the fragment of adult penultimate whorl shown in 2A and B. All figures xl.



correlative, in part at least, with the *S. (P.) pavlovi*-bearing bed of Voronets' (loc. cit.) unit. The Russian workers interpret *Euryptychites gravesiformis* by its North Siberian specimens that are, in my opinion, synonymous with *S. (P.) pavlovi* (see its synonymy). If so, *S. (P.) pavlovi* occurs in the basal part of the regional *Polyptychites michalskii* Zone that underlies its main part represented by the units XIX-XX of Zakharov et al. (1974, p. 125). This basal part of the *Polyptychites michalskii* Zone is apparently correlative with the *Thorsteinssonoceras ellesmerense*-bearing beds of the Deer Bay Formation (Jeletzky, 1979, p. 56-58, Fig. 8) and so is inferred to be older than any part of its next younger *Siberiptychites*-bearing beds where *S. (S.) stubendorffi* and *S. (S.) middendorffi* co-exist and *Pseudoeuryptychites* is unknown. This correlation is consistent with the presence of "*Polyptychites ramulicosta*" (a *Siberiptychites* s.s.?) and "*P. sp. (ex gr. stubendorffi)*" in the basal part of the overlying units XIX-XX of Zakharov et al. (1974, p. 124-125). The overlying, *Pseudoeuryptychites*-bearing beds 15 and 14 (Kemper, 1977, p. 3, Fig. 3) of the Deer Bay Formation are younger yet (see in the description of stratigraphy and age of *S. (P.) pateraeformis* for further details).

The early whorl of *S. (P.) pavlovi* listed and figured but not described by Yershova (1980, p. 70, Pl. IV, fig. 2) from Spitsbergen is assigned to the upper lower Valanginian regional zone of *Polyptychites ramulicosta*, which is approximately equivalent to the regional Siberian *Polyptychites michalskii* Zone.

**Siberiptychites (Pseudoeuryptychites)
pateraeformis (Voronets 1962)**

Plate 38.1, figure 1A, 1B

?1914 *Euryptychites globulosus* Pavlow, p. 38, Pl. IX, fig. 1.
1962 *Euryptychites pateraeformis* Voronets, p. 81, 82, Pl. XLVIII, fig. 1; Pl. LI, fig. 1a, b; Pl. LII, fig. 1, Text-fig. 31.

Type specimen. No type specimen of *Euryptychites pateraeformis* was selected by Voronets (1962) who named this *Siberiptychites (Pseudoeuryptychites)* species. Therefore, the writer selects the specimen No. 29a.8 reproduced in Voronets (1962) Pl. XLVIII, fig. 1; Pl. LI, fig. 1a, b and Pl. LII, fig. 1 as its lectotype.

Material. Six North Siberian specimens, including the lectotype, used by Voronets (1962, p. 81). One large, fully septate, considerably deformed Canadian specimen GSC 77107 from GSC loc. 91309.

Description. The original description of *P. (S.) pateraeformis* provided by Voronets (1962, p. 81) is as follows (writer's translation from Russian): "Whorls involute, low and wide. Width of the outer whorl is almost two times greater than its height. The width of inner whorls is only 1.4 times greater than their height. The greatest width of the whorls occurs at the level of the umbilical shoulder. The surface of the flanks is short and merges immediately into the wide and flattened siphonal side. The umbilicus is wide and deep with a high, abruptly delimited rim (i.e. umbilical shoulder; translator's remark). It is covered by ribs, which bend forward when they cross the shoulder and form forward bent bullae at that level. On the outer whorl, the ribs begin in the middle of the umbilical wall. There are 8 bullae on the inner half of the whorl and there are 15 of them on the whole of the outer whorl. Three fine and high secondary ribs branch off each bulla. The median rib is the continuation of the bulla. The anterior rib separates from its flank and bends forward while

the posterior rib splits off the bulla at the umbilical shoulder and is directed radially. Higher up the ribs bifurcate again at the midflank. Intercalated ribs occur locally. All ribs cross the venter on an almost straight course. There are 51 secondaries per one half whorl. The living chamber occupies almost the whole whorl.

"The bullae become more elevated on the living chamber in comparison with the early whorls. However, the secondary ribs become gradually weakened as they approach the mouth border. There are three constrictions per whorl, one of them near the mouth.

"The suture line (Fig. 31) is characterized by a broad, downward widening second lateral lobe and a wide second lateral saddle (i.e. S_3 of this paper) which is situated at the umbilical shoulder.

"Dimensions (in mm)

Shell diameter	125(100)	80(100)
Height of whorl	44(37)	32(40)
Thickness (i.e. width) of whorl	84(68)	46(57)
Width of umbilicus	45(36)	26(32)"

The description apparently pertains exclusively to the figured lectotype of *P. (S.) pateraeformis* and takes no account of the remaining five specimens available to Voronets (1962, p. 81). This description also suffers from the incomplete preservation of the lectotype that does not include the adult ultimate whorl, may lack the adult penultimate whorl as well, and does not exhibit early intermediate and juvenile whorls. Furthermore, the lectotype does not exhibit a complete external suture line.

In spite of these defects, the presence of three constrictions per whorl of the lectotype, in combination with the *Euryptychites*-like morphology of the two exposed intermediate whorls attests that "*Euryptychites*" *pateraeformis* is a representative of the *Pseudoeuryptychites* subgenus novum.

The incomplete and considerably deformed Canadian specimen GSC 77107 (Pl. 38.1, fig. 1) closely resembles the lectotype of *P. (S.) pateraeformis* in most of the diagnostic features available. The whorl shape and proportions of its only accessible, last preserved whorl are similar to those of the last preserved, appreciably smaller whorl of the lectotype (estimated ratio height/width about 0.50 and the roughly estimated width of the deformed umbilicus between 30 and 35 per cent). There are about 16 small, pronouncedly forward-bent bullae on this fully septate whorl. Wherever the lower flank is preserved (Pl. 38.1, fig. 1A), these bullae split into three fine and sharp secondary ribs that are similar to those of *P. (S.) pateraeformis* in every respect. The intercalated ribs are either rare or absent. Though the supplementary ribs on the venter of this whorl cannot be counted exactly, they are estimated to number between 70 and 80, which compares closely with their number on the last preserved whorl (but not the earlier whorls) of the lectotype (compare Voronets, 1962, Pl. LII, fig. 1). These supplementaries also have about the same degree of thickness, sharpness and elevation and are spaced about as widely as those of the last whorl of the lectotype.

The Canadian specimen GSC 77107 appears to differ from the lectotype of *P. (S.) pateraeformis* in:

1. Its considerably larger dimensions, the terminal shell diameter being in the order of 135 to 140 mm. The Canadian specimen is septate to the end, strongly suggesting that the living chamber of the lectotype is an intermediate rather than adult living chamber.

2. An apparent absence of the abrupt replacement of the very closely spaced ribbing habit of the penultimate whorl of the lectotype (see Voronets, 1962, Pl. LI, fig. 1a, b) by a much more sparse ribbing habit on its last preserved whorl (see Voronets, 1962, Pl. LII, fig. 1). However, a broken off part of the terminal quarter-whorl on the unfigured flank of our specimen exhibits a considerably more dense ribbing of the oralmost preserved part of the preceding whorl. It is inferred therefrom that the ribbing habit of the earlier inaccessible part of that whorl is similar to that of the comparably large penultimate whorl of the lectotype.

Because of the far reaching morphological similarity of the specimen GSC 77107 to the lectotype of *S. (P.) pateraeformis*, and the apparently infraspecific nature of their discernible morphological differences, the former is assigned unreservedly to this North Siberian species.

Affinities and differences. The distinctions of *P. (S.) pateraeformis* from *S. (P.) pavlovi* and the Canadian *S. (P.)* n. sp. indet. A are discussed in the descriptions of these species.

From *Siberiptychites (Pseudoeryptychites) splendens* Bodylevsky (1968, p. 309, Pl. 72, fig. 1 = *Siberiptychites (Pseudoeryptychites)* sp. nov. indet. of Voronets (1962, p. 80, 81, Pl. XLII, fig. 1; Pl. L, fig. 2; Fig. 30) *S. (P.) pateraeformis* differs in a considerably lesser number of umbilical bullae per whorl (15 versus 20) and in the prevalence of well formed trifurcate rub bundles. The material of this *Siberiptychites (Pseudoeryptychites) splendens* is scarce, fragmentary and represented mostly by considerably larger, more advanced (including the early part of ?adult living chamber) whorls than the holotype of *S. (P.) pateraeformis*. Furthermore, its Canadian specimen GSC 77107, which is larger than the lectotype of *S. (P.) pateraeformis*, appears to be morphologically transitional to the Canadian *Siberiptychites (Pseudoeryptychites)* n. sp. indet. A. Therefore, the taxonomic significance of above distinctions cannot be evaluated definitively. The two forms are treated tentatively as specifically distinct but may yet prove to be but extreme morphological variants of the same variable species.

Stratigraphy and age. In Northern Siberia *S. (P.) pateraeformis* is recorded from the Lena-Anabar region only. There it occurs in the Valanginian section exposed on the northeastern end of Paks Peninsula (Voronets, 1962, p. 18, 81), at an unspecified locality in the fourth ridge of Prontshistchev Range (Voronets, 1962, p. 18), and at an unspecified locality on Anabar River (Pavlow, 1914, p. 38, Pl. XI, fig. 1). The *S. (P.) pateraeformis*-bearing beds can be dated and correlated only at its Paks Peninsula locality, where our species occurs in the same unit as, but stratigraphically slightly below, the *S. (P.) pavlovi*-bearing bed (see in the description of its stratigraphy and age for further details). The bed containing *S. (P.) pavlovi* appears to represent the basal part of the regional *Polyptychites michalskii* Zone and to correspond to the *Thorsteinssonoceras ellesmerense* beds of the Deer Bay Formation. Therefore, the next older, *S. (P.) pateraeformis*-bearing beds of the Paks Peninsula section are probably correlative with the upper part (i.e. the *Temnoptychites syzranicus* Subzone) of the next older, regional *Temnoptychites syzranicus* Zone. So interpreted, they would correspond to part or all of the units XVI-XVII of Zakharov et al. (1974, p. 124). If so, these *S. (P.) pateraeformis*-bearing Siberian beds are correlative with part of (?all of) the *Temnoptychites kemperi*-bearing beds of the Deer Bay Formation (see Jeletzky, 1979, p. 56-58, Fig. 8).

The Canadian specimen GSC 77107 of *S. (P.) pateraeformis* was found in bed 15 of the Section 3 (Kemper, 1977, p. 3, Fig. 3), which is correlative with the lower, but not the basal, part of *Polyptychites michalskii* Zone (Jeletzky, 1979, p. 56-58, Fig. 8). Furthermore, *Siberiptychites (Pseudoeryptychites)* n. sp. indet. A was found in the younger bed 14 of that section. These Canadian records appear to be contemporary with the record of "*Euryptychites*" sp. (most likely referable to *Pseudoeryptychites*) in the topmost bed of units XIX-XX of the Saks Peninsula section (Zakharov et al., 1974, p. 126). Therefore, *S. (P.) pateraeformis* appears to be a long-ranging species that existed through part or all of the *Temnoptychites syzranicus* Subzone and through the lower part at least of the overlying *Polyptychites michalskii* Zone. In the Sverdrup Basin, *S. (P.) pateraeformis* has so far been found only in beds that appear to be correlative with the topmost part (i.e. the lower, but not the lowermost part of the *Polyptychites michalskii* Zone) of its time range. Because of a similarly restricted Canadian time range of *Siberiptychites (Siberiptychites) stubendorffi* (Jeletzky, 1979, p. 56-58, Fig. 8), this discrepancy is explained by a strongly delayed eastward migration of *S. (P.) pateraeformis* out of its evolutionary center in the Lena-Anabar Basin of Northern Siberia.

Siberiptychites (Pseudoeryptychites) n. sp. indet. A.

Pl. 38.1, fig. 2A-C; Figures 38.3, 38.4

Material. Four larger and several small, partly deformed to completely squashed fragments from GSC loc. 93754 (=91308). All of them were obviously collected from the float.

Description. Only three subgenerically identifiable larger fragments are discussed below. Though conceivably belonging to more than one specimen, they are sufficiently similar morphologically to be conspecific and are so treated here. Other fragments are only tentatively assigned to our form.

The early whorls less than 40 mm high are too strongly deformed to infer their original shape and proportions. The earliest almost undeformed cross-section of the unfigured example GSC 79414 is about 40 mm high and 45 to 50 mm wide. The shape and proportions of this presumably third penultimate whorl are similar to those of comparably large whorls of *Polyptychites keyserlingi* (compare Jeletzky, 1973, Pl. 3, fig. 2b) and the intermediate variant of *Siberiptychites (Siberiptychites) stubendorffi* (compare Pavlow, 1914, Pl. V, fig. 5b). The next older, apparently second penultimate whorl, that comprises the oralmost part of this fragment, has an *Euryptychites*-like shape and proportions. The same is true of the preserved fragments of the adult penultimate and adult ultimate whorls of the specimens GSC 77119 (Pl. 38.1, fig. 2A-C) and GSC 79113 (unfigured). The complete cross-sections of these terminal whorls must have been considerably wider than high (height/width ratio in order of 0.60-0.65). The entire ventral region must have been evenly and low arched, with the flanks inseparable from the venter proper. The preserved umbilical shoulder is pronouncedly angular. The approximately straight umbilical wall is high and forms an approximately right angle with the adjacent part of the flanks. The umbilicus must have been moderately involute, deep and funnel-like. The fragments of the adult living chamber apparently represent a shell diameter of 130 to 140 mm.

The earliest visible sculpture on the fourth penultimate whorl of the unfigured specimen GSC 79414 (at a whorl diameter of about 15 mm) consists of closely spaced, fine, nonbullate primary ribs that are slightly inclined forward.

They begin on the umbilical shoulder and appear to bifurcate at or near the medial part of the flank. Upper parts of these secondaries are not visible. This sculpture appears to represent the initial, simple dichotomous sculptural phase of the stage of regularized rib bundles characteristic of the genus *Siberiptychites*. The ventral surface of the *Polyptychites*-like second penultimate whorl of this specimen is ornamented by regularly and rather closely spaced (their interspaces are about 2 times wider than the ribs themselves) supplementary ribs that cross the venter with slight forward bends. Neither the bundling habit nor the primaries of this growth stage are exposed.

The ventral region of the adult penultimate whorls of the specimens GSC 77119 (Pl. 38.1, fig. 2C) and GSC 79413 (unfigured) are ornamented by fairly sharp and prominent, moderately heavy but rather sparse (the interspaces being 2 1/2 to 3 times wider than the ribs) supplementary ribs, which are considerably coarser than those of the preceding whorl. They cross the venter with slight forward bend. Neither the bundling habit nor the primaries of this growth stage are visible.

The fragmentary oralmost whorls of the specimens GSC 77119 (Pl. 38.1, fig. 2A, B) and GSC 79413 (unfigured) represent, respectively, the middle part and the very beginning (with a couple of terminal suture lines; see below) of the adult living chamber. They both lack any ornament, except for large but low and round-topped bullae spanning the umbilical shoulder and petering out closely above and below it. The interspaces are about 2 1/2 times wider than the bullae. The surface of the specimen GSC 77119 is, for the most part, appreciably to considerably abraded but that of the specimen GSC 79413 is fairly well preserved.

An early external suture line is visible on the fourth penultimate whorl of the specimen GSC 79414 at an approximate whorl diameter of 15 mm. This suture lacks the ventral and the first lateral lobes (Fig. 38.3). Though this suture already includes all three auxiliary lobes typical of the genus *Siberiptychites*, it is *Siberiptychites* s.s. (i.e. *S. (P.) stubendorffi*)-like rather than *Pseudoeryptychites*-like. The *S. (S.) stubendorffi*-like features include fairly simple to very simple and shallow (especially in the third auxiliary) denticulation of all exposed elements, the positioning of the first auxiliary lobe on the flank, the relatively greater width of the fourth lateral saddle (instead of the third characteristic of *Pseudoeryptychites*), and the relatively small size of all three auxiliary lobes. The suture is, therefore, a late juvenile one. The two terminal external sutures exposed on the specimen GSC 79413 (Fig. 38.4) are, in contrast, entirely *Pseudoeryptychites*-like. Only the first and second lateral lobes of the best preserved last suture are situated on the ventral region. They are separated from the first auxiliary lobe, that is situated entirely on the outermost part of the umbilical wall, by a uniquely wide third lateral saddle, that is at least 2 1/2 times wider than the fourth saddle. The narrow fourth lateral saddle separates this auxiliary lobe from the only partially preserved second auxiliary that occupies the inner part of the outer half of the umbilical wall. Only the fifth lateral saddle and the small adjacent segment of the third auxiliary lobe are preserved, but there is little doubt of the original presence of that auxiliary within the ample expanse of the remaining, deeply eroded, inner half of the umbilical wall. All visible lobes and saddles are similar to those of *S. (P.) pavlovi* (Fig. 38.2) in their shapes and proportions but are more closely spaced (especially the lateral lobes) and considerably more complexly denticulated. This suture either touches, or overlaps with, the second last suture wherever the latter is visible (Fig. 38.4). This indicates the adult nature of this fragment of the living chamber.

Affinities and differences. ***Siberiptychites (Pseudoeryptychites)*** n. sp. indet. A differs from *S. (P.) pateraeformis* in the considerably higher cross-section of its adult ultimate and penultimate whorls. These whorls are also more highly arched, and approximately equally thick throughout (compare Pl. 38.1, fig. 1B with Pl. 38.1, fig. 2B). Furthermore, the adult living chamber of our form is smooth, except for the umbilical nodes, while that of *S. (P.) pateraeformis* bears irregularly spaced and unequally thick, coarse ribs in addition to differently shaped umbilical nodes. Finally, the coarse, prominent and widely spaced supplementary ribs of the adult penultimate and second penultimate whorls of *S. (P.)* n. sp. indet. A contrast less with the fine and closely spaced supplementaries of its earlier whorls than do the equivalent supplementaries of *S. (P.) pateraeformis*.

Unlike the vanishing ribbing habit of *Siberiptychites (Pseudoeryptychites)* n. sp. indet. A, the previously regular ribbing habit of *S. (P.) pavlovi* becomes strongly disorganized on its adult penultimate and second penultimate whorls and this irregular rib pattern persists onto its adult living chamber. Furthermore, *S. (P.) pavlovi* develops closely but irregularly spaced, unequally sized and partly spinose umbilical nodes on the adult living chamber. Finally, the *Euryptychites*-like advanced whorls of *S. (P.) pavlovi*, including the adult living chamber, are relatively much lower, wider and thinner than those of *Siberiptychites (Pseudoeryptychites)* n. sp. indet. A.

Siberiptychites (Pseudoeryptychites) n. sp. indet. A resembles *S. (P.) splendens* Bodylevsky (= *S. (P.)* sp. nov. indet. of Voronets, 1962, Pl. XLII, fig. 1, Pl. L, fig. 2) in the smoothness of its adult living chamber (except for the umbilical nodes) and in the subequal thickness of its cross-section throughout the whorl's width. However, its living chamber is about 1 1/2 times thicker than that of *S. (P.) splendens*. Furthermore, the ventral parts of supplementary ribs of its adult penultimate whorl (Pl. 38.1, fig. 2C) are distinctly coarser, more elevated and more widely spaced than those on the adult penultimate whorl of *S. (P.) splendens* (Voronets, 1962, Pl. L, fig. 2; Bodylevsky, 1968, Pl. 72, fig. 1a, b).

Because of its morphological distinctions from all other formally and informally named representatives of *Pseudoeryptychites*, our form is probably a new species. However, it is described in open nomenclature because of the poor and fragmentary preservation of all its presently known examples.

Stratigraphy and age. All known examples of *Siberiptychites (Pseudoeryptychites)* n. sp. indet. A have been collected at GSC loc. 93754 (=91308) in bed 14 of the section of the upper Deer Bay Formation measured by E. Kemper (1977, p. 3, Fig. 3) on North Amund Ringnes Island. These youngest known Canadian representatives of the subgenus *Pseudoeryptychites* are associated with *Siberiptychites (Siberiptychites)* n. sp. aff. *stubendorffi*. The stratigraphy and age of this bed was already discussed in the description of *S. (P.) pavlovi* and *S. (P.) pateraeformis*.

References

- Bassov, V.A., Zakharov, V.A., Ivanova, E.F., Saks, V.N., Shulgina, N.I., and Yudovnii, E.G.
1970: A zonal subdivision of Upper Jurassic and Lower Cretaceous deposits on the Urduk-Khaya Peninsula; Nauchno-Issledovatel'skii Institut Geologii Arktiki Ministerstva Geologii SSSR, Uchenye Zapiski, Paleontologiya i Biostratigrafiya, no. 29, Leningrad, p. 14-31, 4 Text-figs (in Russian).

- Bodylevsky, V.I.
1968: New Early Cretaceous ammonites of Northern Siberia; In the book: *Novye vidy drevnikh rastenii i zhivotnykh SSSR, Vsesoyuznii Nauchno-Issledovatel'skii Geologicheskii Institut Ministerstva Geologii SSSR*, no. II, pt. 1, p. 308-311, Pls. 71-72 (in Russian).
- Gol'bert, A.V., Bulynnikova, S.P., Grigorieva, K.N., Deviatov, V.A., Zakharov, V.A., Kazakov, A.M., Klimova, I.G., Reshetnikova, M.A., Sanin, V.Ya., and Turbina, A.S.
1981: A standard section of the Neocomian of the northern part of Siberian Platform. Vol. I; Ministerstvo Geologii SSSR, Sibirskii Nauchno-Issledovatel'skii Institut Geologii, Geofiziki i Mineral'nogo Syr'ya, Novosibirsk, 98 pages, 1 Text-fig., 14 Tables (in Russian).
- Jeletzky, J.A.
1965: *Thorsteinssonoceras*: a new craspeditid ammonite from the Valanginian of Ellesmere Island, Arctic Archipelago; Geological Survey of Canada, Bulletin 120, 16 pages, 6 Pls., 1 Text-fig.
1973: Biochronology of the marine boreal latest Jurassic, Berriasian and Valanginian in Canada; The Boreal Lower Cretaceous (a collection of papers), Geological Journal, Special Issue no. 5, p. 41-80, 7 Pls., 3 Text-figs.
1979: Eurasian craspeditid genera *Temnoptychites* and *Tollia* in the lower Valanginian of Sverdrup Basin, District of Franklin: With comments on taxonomy and nomenclature of Craspeditidae; Geological Survey of Canada, Bulletin 299, 89 pages, 14 Pls., 8 Text-figs.
- Kemper, E.
1977: Biostratigraphy of the Valanginian in Sverdrup Basin, District of Franklin; Geological Survey of Canada, Paper 76-32, 6 pages, 3 Text-figs.
1978: Einige neue und stratigraphisch bedeutsame Arten der Ammoniten-Gattung *Dichotomites* des NW-deutschen Ober-Valangin; *Geologisches Jahrbuch*, Ser. A, Bd. 45, Hannover, p. 183-253, 16 Pls., 18 Text-figs.
- Klimova, I.G.
1978: A new ammonite genus from the lower Valanginian of northern part of Central Siberia; *Akademiya Nauk SSSR, Sibirskoye Otdelenie, Geologiya i Geofizika*, no. 12, p. 50-61, 2 Pls., 6 Text-figs. (Russian with English abstract).
1981: Morphogenesis of the Early Cretaceous ammonite *Siberiptychites stubendorffi* (Schmidt); *Akademiya Nauk SSSR, Sibirskoye Otdeleniye, Sbornik Nauchnykh Trudov Sibirskogo Nauchno-Issledovatel'skogo Instituta Geologii, Geofiziki i Mineral'nogo Syr'ya* no. 287: Stratigrafiya i Paleontologiya Sibiri, p. 74-81, Pl. IX, 3 Text-figs., 1 Table (in Russian).
- Koenen, A. von
1902: Die Ammonitiden des Norddeutschen Neocom; *Abhandlungen der Koeniglich Preussischen Landesanstalt und Bergakademie, Neue Folge*, Heft 24, p. 1-451, and an Atlas with 55 Plates.
- Neumayr, M. and Uhlig, V.
1881: Ueber Ammonitiden aus den Hilsbildungen Nordwestdeutschlands; *Palaeontographica*, Kassel, Bd. 27, p. 129-203, Pls. 15-57.
- Pavlov, A.P.
1914: Jurassic and Lower Cretaceous Cephalopoda of Northern Siberia; *Zapiski Imperatorskoi Akademii Nauk, Fisiko-Matematicheskoye Otdelenie*, t. XXI (4), 68 pages, 18 Pls., St. Petersburg (in Russian).
- Saks, V.N., Shulgina, N.I., Bassov, V.A., Burdykina, M.D., Gol'bert, A.V., Dagis, A.S., Zakharov, V.A., Ivanova, E.F., Klimova, I.G., Messezhnikov, M.S., Nal'niaeva, T.I., Pokhiolainen, V.P., Romanova, E.Ye., Ronkina, Z.Z., Sazonova, I.G., Trushkova, L.Ya, and Yudovnii, E.G.
1972: Jurassic-Cretaceous Boundary and the Berriasian stage in Boreal Realm; "Nauka" - Press, Sibirskoye Otdeleniye, Novosibirsk, 371 pages, 46 Pls., 21 Text-figs. 28 Tables (in Russian) (also available in English translation by the Israel Program for Scientific Translation, Jerusalem, 1975, from the U.S. Department of Commerce).
- Voronets, N.S.
1962: The stratigraphy and cephalopod molluscs of the Jurassic and Lower Cretaceous deposits of the Lena-Anabar area; *Nauchno-Issledovatel'skii Institut Geologii Arktiki Ministerstva Geologii i Okhrany Nedr SSSR, Trudy*, t. 110, Gosgeoltekhizdat, Moskva, 237 pages, 61 Pls., 32 Text-figs., 1 corr. table (in Russian).
- Yershova, E.S.
1980: Some early Valanginian ammonites from Spitsbergen Island; *Nauchno-Issledovatel'skii Institut Geologii Arktiki Ministerstva Geologii SSSR, Sbornik Nauchnykh Trudov: Geologiya Osadochnogo Chekhla Arkhipelaga Svalbard, Leningrad*, p. 70-80, 8 Pls. (in Russian).
- Zakharov, V.A., Sanin, V.J., Spiro, N.S., Shulgina, N.I., and Yudovnii, E.G.
1974: Zonal subdivision as well as the lithological-geochemical and paleoecological characters of Lower Cretaceous deposits of the northern part of Pacha Peninsula, Anabar Bay (northern part of Central Siberia); *Akademiya Nauk SSSR, Sibirskoye Otdeleniye, Institut Geologii i Geofiziki, Trudy*, no. 136: Biostratigrafiya boreal'nogo mesozoya, "Nauka" - Press, Sibirskoye Otdelenie, Novosibirsk, p. 121-133, 5 Text-figs. (in Russian).

New formations in the Eureka Sound Group, Canadian Arctic Islands

Project 850043

B.D. Ricketts
Institute of Sedimentary and Petroleum Geology, Calgary

Ricketts, B.D., New formations in the Eureka Sound Group, Canadian Arctic Islands; in Current Research, Part B, Geological Survey of Canada, Paper 86-1B, p. 363-374, 1986.

Abstract

The Eureka Sound Group, in eastern Arctic Islands, is divided into four new, lithologically distinct formations of regional extent. The oldest is the Expedition Formation of middle or late Campanian to early Paleocene age, consisting predominantly of sandstone and minor shale, that originated as wave dominated delta, barrier island and estuarine deposits; a major shale unit, the Strand Bay Formation of early to middle Paleocene age, that represents basin-wide marine transgression (early Paleocene), followed by regressive prodelta and shelf deposits; the Iceberg Bay Formation of middle or late Paleocene to middle Eocene age, consisting of fluvial sandstone and coal (mostly delta plain); and the stratigraphically highest unit, the Buchanan Lake Formation of middle Eocene age, possibly extending into the late Eocene, that consists of syntectonic conglomerate shed from adjacent thrust sheets, and signifying a major phase of the Eureka Orogeny. Correlations are made with Eureka Sound strata on Bylot Island, Amund Ringnes Island, Loughheed Island, Banks Island and at Lake Hazen.

Résumé

Le groupe d'Eureka Sound dans la partie est des îles de l'Arctique est divisé en quatre nouvelles formations lithologiquement distinctes d'étendue régionale. La formation d'Expédition, la plus ancienne, date du Campanien moyen ou supérieur au Paléocène inférieur; elle se compose surtout de grès avec de petites quantités de schiste argileux qui, à l'origine, étaient des dépôts d'estuaire, de crête d'avant-plage et de delta, dominés par l'action des vagues. Une importante unité de schiste argileux, la formation de Strand Bay, du Paléocène inférieur à moyen, représente une transgression marine survenue dans l'ensemble de bassin (Paléocène inférieur), suivie par des dépôts de plate-forme et de prodelta en régression; la formation d'Iceberg Bay, du Paléocène moyen ou supérieur à l'Éocène moyen, se compose de grès et de charbon fluviatiles accumulés en grande partie sur une plaine deltaïque. L'unité stratigraphiquement la plus élevée, la formation de Buchanan Lake de l'Éocène moyen et peut-être même de l'Éocène supérieur, se compose d'un conglomérat syntectonique issu de nappes de charriage contiguës et représentant une importante phase de l'orogénèse d'Eureka. Une corrélation a été établie avec les strates d'Eureka Sound dans l'île Bylot, l'île Amund Ringnes, l'île Loughheed et le lac Hazen et l'île Banks.

Introduction

The Late Cretaceous and Early Tertiary Eureka Sound Formation underlies large tracts of the Arctic Archipelago, especially in the eastern Arctic (Fig. 39.1). Although local map units have been defined in some areas, the succession as a whole has not been subjected to detailed regional mapping. The present investigation, begun in 1983, was undertaken to re-evaluate current concepts in Late Cretaceous and Tertiary basin evolution in the Arctic, to determine more precisely the timing of Eureka orogenesis, and to provide more detailed information on coal resources in the Canadian Arctic. Complete mapping of the Eureka Sound Group, on a scale of 1:50 000, is at present underway (Ricketts, 1984, 1985). Mapping of the Eureka Sound succession on Axel Heiberg and Ellesmere islands has resulted in the identification of four basic lithostratigraphic units of regional extent, and these are formally introduced herein.

Previous terminology

The name Eureka Sound 'group' was first used by Troelsen (1950) for the predominantly nonmarine, coal-bearing, Cenozoic strata underlying Fosheim Peninsula (Table 39.1). Eureka Sound strata were originally interpreted as postdating the last period of orogeny (Troelsen, 1950, 1952) but later were discovered by Thorsteinsson and Tozer (1957) to have been included in the deformation. Following the more extensive investigations of Operation Franklin, Tozer (1963) redefined the unit as a formation, to comply with the current North American stratigraphic practice, and suggested that strata exposed on Fosheim Peninsula were 'typical' of the formation. However, a type section was inadvertently erected by Souther (1963) at Strand Fiord on western Axel Heiberg Island (see discussion by Balkwill, 1983, p. 45), and this designation has continued in the literature.

As a result of preliminary mapping in the Bay Fiord and Strathcona Fiord area of Ellesmere Island, West et al. (1981) identified four informal members within the Eureka Sound Formation. Map unit boundaries established in the same area during the present investigation (Ricketts, 1985, GSC Open File 1182), coincide only approximately with those established by West et al. (1981) and therefore the latter designations are not used here. Miall (1984) has indicated that the Eureka Sound Formation should be raised to group status. Because of considerable lithofacies variations, Miall (1984) considers it unlikely that any unit can be mapped regionally, and suggests that the lithostratigraphic framework should be based on (genetic) depositional systems. As an alternative approach, I intend to introduce a simple nomenclatural scheme based on the general lithological homogeneity of rock units and their mappability.

Rationale

A thick sequence of shale (up to 287 m) has been identified and mapped in the Strand Fiord area, and subsequently found as a distinct mappable unit in the areas surrounding Strathcona and Bay fiords, Vesle Fiord, Canon Fiord and northward along Fosheim Peninsula. At Strand Fiord, the age of the shale sequence is Early to Middle Paleocene (Ricketts, in press) and this age is also confirmed in the other areas (McIntyre, personal communication, 1985). Thus, the shale unit is a particularly useful stratigraphic marker throughout the area. Wherever the shale unit occurs, it is underlain and overlain by thick sequences consisting predominantly of sandstone. The Eureka Sound succession can be divided into four formations based primarily on shale, sandstone or conglomerate content. Although sedimentary facies may vary within any one formation, this feature in itself does not invalidate the scheme, but provides the basis for further subdivision into members. Each formation is also

mappable at a scale of 1:250 000 (Fig. 39.2, 39.3). Corresponding stratigraphic sections are shown schematically in Figure 39.4 (Strand Fiord area), and in Figure 39.5, central Ellesmere Island (Fosheim Peninsula and Strathcona Fiord). Following Miall (1984), the Eureka Sound is now referred to as a group.

Lithostratigraphy

Expedition Formation

Definition. The Expedition Formation is the lowest stratigraphic unit of the Eureka Sound Group, and consists predominantly of quartz-rich sandstone, with subordinate shale and coal. The Expedition Formation is overlain by shale of the Strand Bay Formation. Thickness varies from 500 m at Strand Fiord, to a maximum of 836 m at Canon Fiord; other measured sections are at Strathcona Fiord (502 m+), and at the north end of Fosheim Anticline (632 m). The formation is named after Expedition Fiord on western Axel Heiberg Island.

The type section is located on the east side of Kanguk River, 2.5 km due north of Strand Fiord, latitude 79°16'N; longitude 90°35'W (Fig. 39.2). This lies above the type section of the Kanguk Formation.

Synonyms. The Expedition Formation includes Member I and the lower part of Member II of West et al. (1981).

Contacts. Where the Expedition Formation is conformable with the Kanguk Formation, the contact is flat; where it is in contact with Lower Paleozoic bedrock, basal strata of the Expedition Formation overlie an erosional relief of up to 50 m, with profound unconformity.

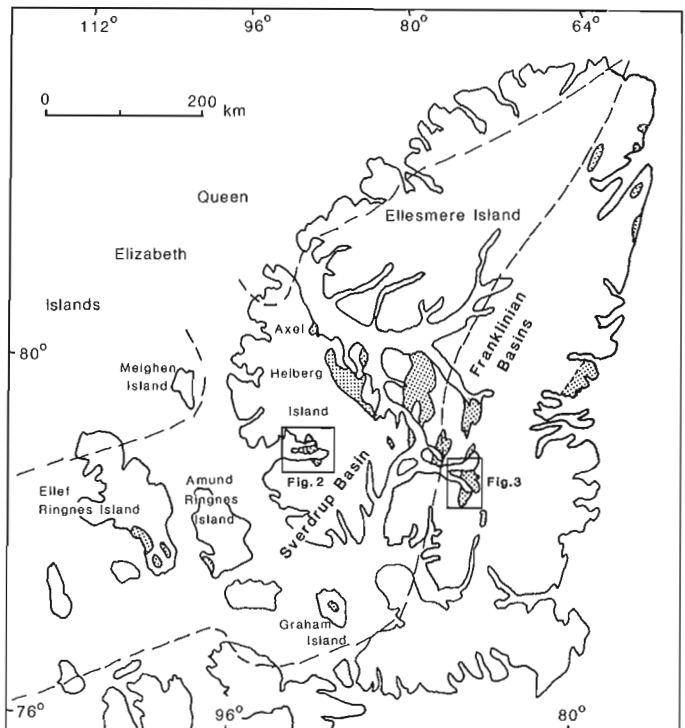


Figure 39.1. A map of the eastern Arctic Islands, showing general distribution of Upper Cretaceous and Tertiary strata (stipple), with respect to Sverdrup Basin and Franklinian bedrock. The insets show the locations of more detailed lithostratigraphic maps in the Strand Fiord and Strathcona Fiord areas.

Table 39.1. Eureka Sound Group nomenclature Axel Heiberg Island and central Ellesmere Island

			Troelsen, 1950	Tozer, 1963	West et al, 1975	This Study	
TERTIARY	EOCENE	U	Eureka Sound Group	Eureka Sound Formation		Buchanan Lake Formation	
		M					
		L					
	PALEOCENE	U	(undivided)	(undivided)	Eureka Sound Fm	member IV	Iceberg Bay Formation
		L				member III	
					member II	Strand Bay Fm	
					member I	Expedition Formation	
CRETACEOUS	MAASTRICHTIAN		Mesozoic	Kanguk Formation	Kanguk Formation	Kanguk Formation	
	CAMPANIAN	U					
		M					

It has been found necessary to modify the definition of the Kanguk Formation – Eureka Sound Group contact, as indicated in the ensuing discussion. In most places the contact is gradational, and Tozer (1963) placed the boundary beneath the first major sandstone bed. However, the thickness of this bed was left undefined, and in fact is quite variable; at many localities the first major sandstone actually forms part of a coarsening- and thickening-upward sequence that is tens of metres thick. An additional problem is encountered at the type section (Fig. 39.6), where the upper part of the Kanguk Formation contains several tens of metres of sandstone and thin interbedded shale, overlain by a 30 m thick unit of shale containing *Inoceramus lundbreckensis* (Jeletzky, personal communication, 1984). Souther (1963) and Tozer (1963) placed the top of the Kanguk Formation immediately above this shale, which would mean that the Kanguk contains a sandstone facies that is identical to sandstone units found elsewhere in the Eureka Sound Group; logically, the sandstone could be included in the Eureka Sound Group. During the present mapping program, a useful criterion for determining the contact was found to be the stratigraphic level above which the sandstone/shale ratio approximates 2:3. At this level the outcrop is much more resistant to weathering and the contact may be mapped clearly.

In most places, contact with the overlying Strand Bay Formation is abrupt. Sandstone at the top of the Expedition Formation is succeeded by thick, blocky weathering shale. Stratigraphic relationships across this contact vary from conformable to unconformable.

Lithology. The proportion of major lithotypes varies considerably across the Eureka Sound Basin. In the area around Strand Fiord, sandstone and shale units are arranged into coarsening- and thickening-upward cycles that rarely are

capped by thin coal seams. Coarsening- and thickening-upward cycles also occur in the lower half of the formation from Strathcona Fiord and north along Fosheim Peninsula. The lowest of these cycles includes the 'basal' white sandstone that is so prominent in the west-central Ellesmere Island area, particularly where the formation overlies Paleozoic bedrock. Coal seams that cap the cycles here are better developed than at Strand Fiord; the number and thickness of seams increase northward toward Hot Weather Creek, thickness ranging from a few centimetres to more than a metre.

Along western Ellesmere Island, the Expedition Formation is easily recognized by two principal criteria: a basal white sandstone unit, and a distinctive, striped weathering pattern in strata above the white sandstone bed, which reflects the thin, regular alternation of sandstone, shale and coal beds. In the upper part of the formation, these rock types are arranged in thin, fining-upward sequences.

Age. The base of the Expedition Formation appears to be diachronous; at Strand Fiord it ranges from middle Campanian to Maastrichtian. Palynological evidence has led to the identification of a disconformity at the top of the Expedition Formation at Strand Fiord (D.J. McIntyre, personal communication, 1984). This disconformity is considered to be a result of nondeposition and possibly local erosion. At the northwest end of Fosheim Peninsula, the Expedition Formation is probably middle Campanian to Early Paleocene. Where the formation directly overlies Paleozoic bedrock, as in the Strathcona – Canon Fiord area, it is Early Paleocene in age (e.g. Canon Fiord). A disconformity like that recognized at Strand Fiord has not been identified at the top of the Expedition Formation in the Fosheim Peninsula – Strathcona Fiord area. However, this does not preclude the possibility of a hiatus, especially if its duration were too short to be resolved by palynological studies.

Interpretation. A variety of facies are represented. At Strand Fiord, the Expedition Formation originated as a series of wave dominated deltas (Ricketts, in press), whereas between Strathcona and Canon fiords, barrier island and estuarine conditions prevailed. Basal strata near Hot Weather Creek and Fosheim anticline also represent barrier island deposition, although upper strata here probably accumulated on delta plains.

Strand Bay Formation

Definition. This unit is easily recognized in most areas as a thick sequence of dark grey shale. Tabular bedded sandstones are minor, composing less than 10 per cent at Strand, Strathcona and Vesle fiords. However, the sandstone component increases north and west along Fosheim Peninsula, and at the north end of Fosheim anticline, sandstone locally

composes up to 60 per cent of the formation; thin coal seams also are present. Maximum thicknesses occur at Strand Fiord and Canon Fiord (287 and 276 m, respectively), and at other localities values range from 122 to 196 m. The Strand Bay Formation is conformably overlain by the Iceberg Bay Formation.

The type section is located on a ridge along the north shore of Strand Fiord, 15.5 km due west of the mouth of Kanguk River and 3 km due east of Twin Diapirs, at latitude 79°14'N and longitude 91°27'W (Fig. 39.2, 39.7). The formation is named after Strand Bay, which marks the entrance to Strand and Expedition fiords on west Axel Heiberg Island.

Synonyms. The Strand Bay Formation includes approximately the upper 200 m of Member II at south Strathcona Fiord, recorded by West et al. (1981).

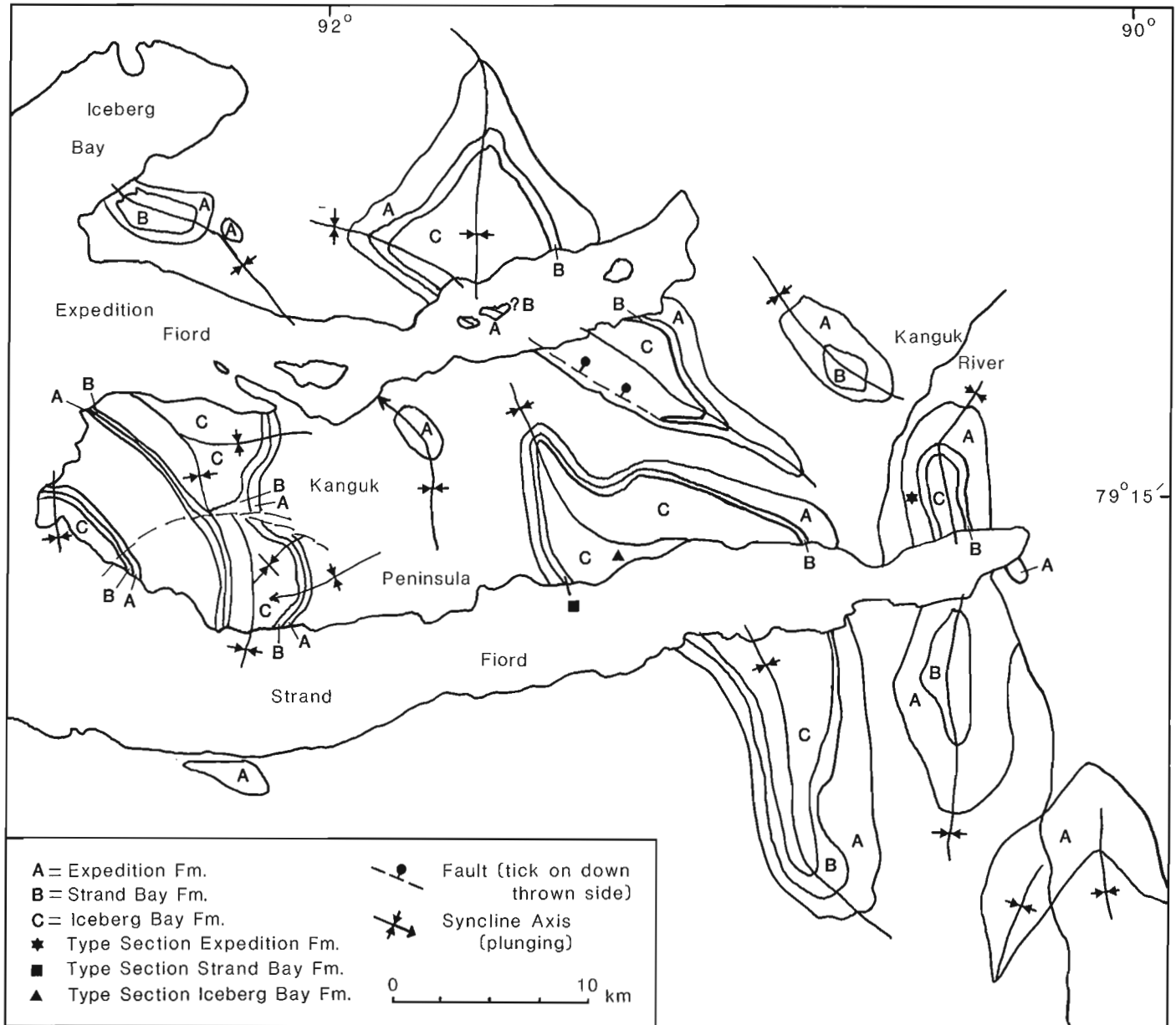


Figure 39.2. Lithostratigraphic map of the Eureka Sound Group at Strand Fiord. The map is summarized from Open File 1147. Formations are designated by letters. Type sections for the Expedition, Strand Bay and Iceberg Bay formations also are located. The map area is shown in Figure 39.1.

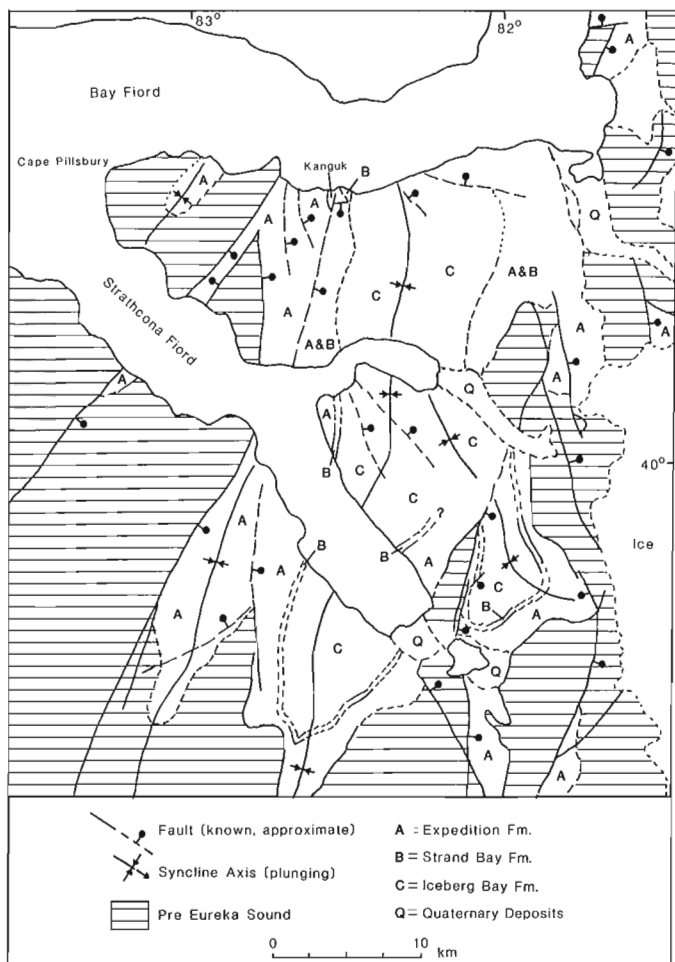


Figure 39.3. Lithostratigraphic map of the Eureka Sound Group in the Strathcona Fiord area. Data has been summarized from Open File 1182. All formations are indicated by letters. The map area is located in Figure 39.1.

Contacts. Contact with the underlying Expedition Formation is described in the preceding section. Contact with sandstone of the superjacent Iceberg Bay Formation generally is conformable and gradational over a few metres of interbedded shale and sandstone. Even in areas of poor exposure, shale of the Strand Bay Formation can be traced as a recessive interval bounded by formations of resistant sandstone.

Lithology. The shale weathers to a grey or blue-grey colour and has a blocky fracture. Resistant sandstone beds that have tabular geometries and cumulative thicknesses of 25 to 30 m occur in the lower third of the formation at Strand Fiord. In comparison, sandstone units exposed at Canon Fiord and elsewhere along Fosheim Peninsula form distinct coarsening- and thickening-upward cycles, that locally are capped by thin coal seams. The proportion of sandstone also increases northward along this trend although shale remains the dominant rock type. Hummocky crossbedding occurs in several cycles at Canon Fiord. Tidal bedding is common in the lower parts of these cycles on Fosheim Peninsula. These features indicate overall eastward- and northward-shoaling trends in the Strand Bay Formation.

Age. Palynological analysis by D.J. McIntyre (personal communication, 1984) indicates an Early to Middle Paleocene age for the Strand Bay Formation. The Paleocene age is generally confirmed by a sparse assemblage of arenaceous foraminifera (J.H. Wall, personal communication, 1985).

Interpretation. Because of its regional extent and abrupt appearance in the stratigraphic succession of the eastern Arctic Islands, the base of the Strand Bay Formation is considered to represent an Early Paleocene marine transgression. Transgression was followed by a depositional phase, and the bulk of the shales and minor sandstone represent prodelta and shelf deposits of the subsequent regression. Continued progradation gave rise to the overlying sandstones of the Iceberg Bay Formation.

Iceberg Bay Formation

Definition. In many areas of the eastern Arctic, the Iceberg Bay Formation is the highest stratigraphic unit preserved. It is characterized by three principal lithotypes: a unit of noncalcareous or slightly calcareous sandstone and shale; a calcareous, flaggy, white siltstone and sandstone unit; and a unit containing sandstone and thick coal seams (Ricketts, 1984, 1985). All units can be mapped separately and, in a future publication, will be designated as members.

The preserved thickness of the Iceberg Bay Formation at its type section at Strand Fiord is 1950 m, with additional thick sections located at Mokka Fiord (1500 m recorded by Bustin, 1977), 1240 m at Strathcona and Bay fiords, 600 m preserved at Canon Fiord, and possibly as much as 2000 m near Hot Weather Creek. In most cases, the top of the formation in these areas is eroded and thickness values are a minimum.

The only continuous and well exposed section through the entire formation is the type section (Fig. 39.8), which is located on the north shore of Strand Fiord, immediately above the type section of the Strand Bay Formation. The base of the section is located at latitude 79°14'N and longitude 91°27'W; the top of the section is latitude 79°14.5'N and longitude 91°15'W, 11 km due west of the mouth of Kanguk River. The formation is named after Iceberg Bay, situated north of Expedition Fiord on west Axel Heiberg Island.

Synonyms

The Iceberg Bay Formation is equivalent to both members III and IV recorded at Strathcona Fiord by West et al. (1981).

Contacts

Where basal strata of the Iceberg Bay Formation include thick brown sandstone (as at Strand Fiord), or calcareous, flaggy siltstone and sandstone (as at Canon Fiord and Strathcona Fiord), the contact with the underlying Strand Bay Shale is easily mapped. The contact is gradational over a few metres, in which the proportion of coarse grained rock types interbedded with shale increases.

Contact with the overlying Buchanan Lake Formation is abrupt and disconformable, although locally it may be conformable, as noted at Lake Hazen by Miall (1979a). At the head of Mokka Fiord, in the footwall of Stolz Thrust and 8 km due south of Mokka Fiord Diapir, the contact is defined by the abrupt transition from pale brown weathering, quartz-rich sandstones interbedded with coal seams, to dark brown, lithic sandstones and diabase-pebble conglomerates.

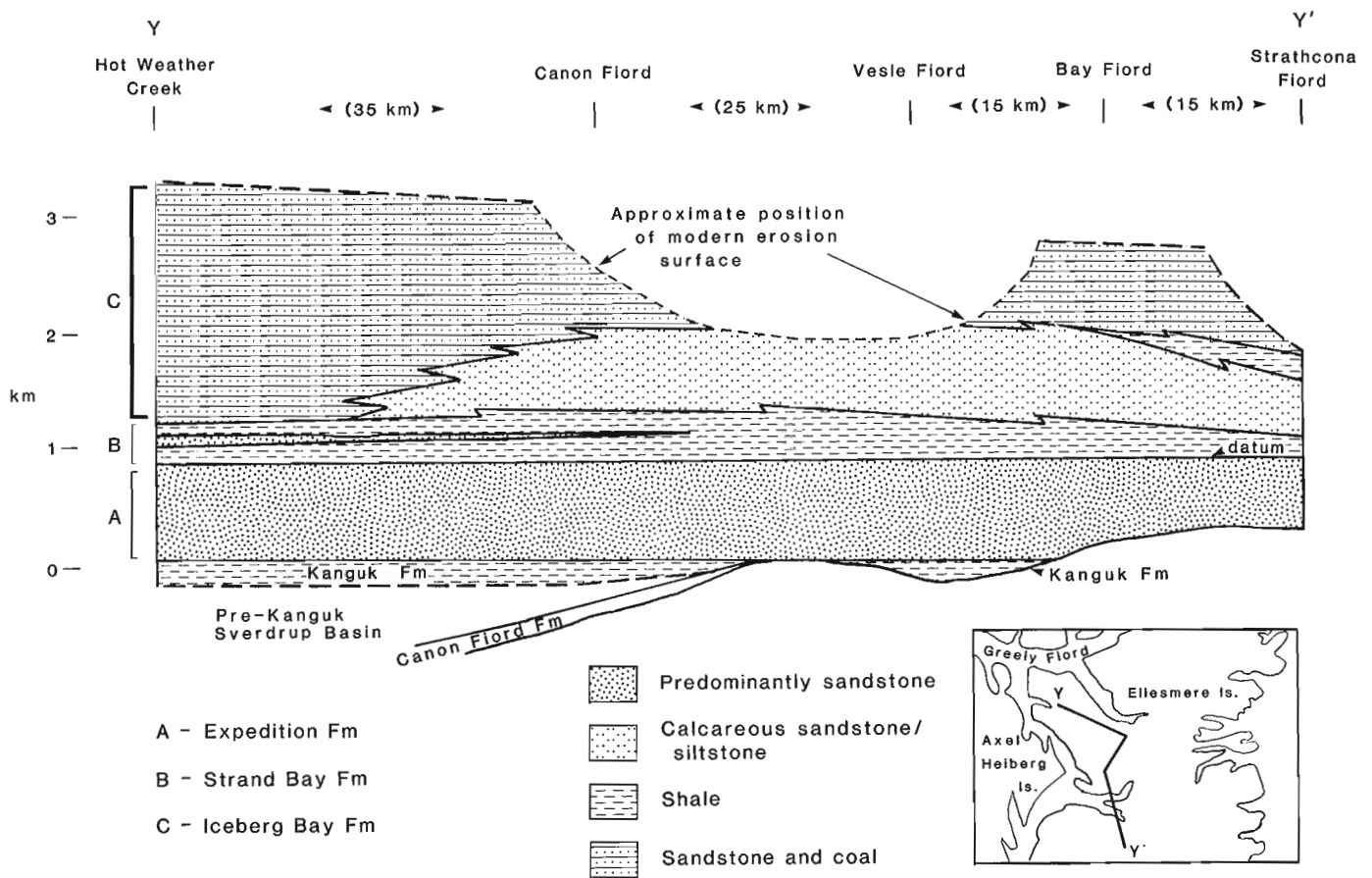


Figure 39.5. A stratigraphic cross-section of the Eureka Sound Group, from Strathcona Fiord to northern Fosheim Peninsula (see map inset). The datum is placed at the base of the Strand Bay Formation. Formations are designated by letters. Stratigraphic thickness is approximate. Note that the Iceberg Bay Formation has been subdivided into three distinct lithological units that in future may be defined as members.

coal-bearing sequence at Strand Fiord (map unit 5, Ricketts, 1984, 1985). Toward the northwest along Fosheim Peninsula, the lower, calcareous rock types are replaced laterally by the coal-bearing sequence, and at Hot Weather Creek the formation consists almost entirely of fining-upward sandstone-coal cycles (Fig. 39.5).

Age. The age of the Iceberg Bay Formation, based primarily on palynomorphs (D.J. McIntyre, personal communication, 1985) ranges from Middle or Late Paleocene to Middle Eocene. Additional evidence is provided by Paleocene calcareous foraminifera (J.H. Wall, personal communication, 1985), found for the first time in the Eureka Sound Group at Strathcona Fiord, and also a diverse assemblage of vertebrate fossils found in Eocene coal-bearing rocks near the top of the formation, south of Bay Fiord (West et al., 1977).

Interpretation. The Middle Paleocene to Middle Eocene regressive phase of deposition at Strand Fiord gave rise to deltaic deposits that reflect a greater fluvial influence than the wave dominated deltas that deposited the Expedition Formation. However, the eastern side of the Eureka Sound Basin (west-central Ellesmere Island) also contain barrier island, lagoon and shelf deposits, in addition to more local prodelta shale. Coal-bearing strata at the top of formation are also of delta plain origin and appear to have extended across the entire basin by Early Eocene time; laterally equivalent delta front facies are probably preserved in the subsurface offshore and beneath Meighen Island (north and west of Axel Heiberg Island).

Buchanan Lake Formation

Definition. Besides being the highest stratigraphic unit in the Eureka Sound Group, the Buchanan Lake Formation is critical because it formed in response to a major period of faulting and folding during the Eureka Orogeny. At Mokka Fiord, interbedded quartz arenite and coal seams belonging to the Iceberg Bay Formation are abruptly overlain by diabase conglomerates, lithic arenites, and minor amounts of siltstone and shale. Thick units of conglomerate with a variety of clast compositions are now known from several localities on Axel Heiberg and Ellesmere islands, and herein are named the Buchanan Lake Formation. Because stratigraphic and structural relationships are reasonably well exposed in the strata along the south shore of Mokka Fiord (Fig. 39.9), the area is designated as the type locality (lat. 79°32'N, long. 87°34'W). At the type locality, the formation occurs in the immediate footwall of the Stolz Thrust and hence the 370 m of section is a minimum value. Similar thicknesses are recorded at Geodetic Hills (possibly up to 1000 m, Bustin, 1982; this study) and Otto Fiord (about 300 m). A thick conglomerate unit (300 m) occurring in the Franklin Pierce Bay area of eastern Ellesmere Island is tentatively placed in the Buchanan Lake Formation. The formation is named after Buchanan Lake, which drains into Mokka Fiord (eastern Axel Heiberg Island).

Synonyms. Conglomerate and sandstone exposed at Geodetic Hills were formerly included in the Beaufort Formation by Bustin (1982), but now are reclassified as

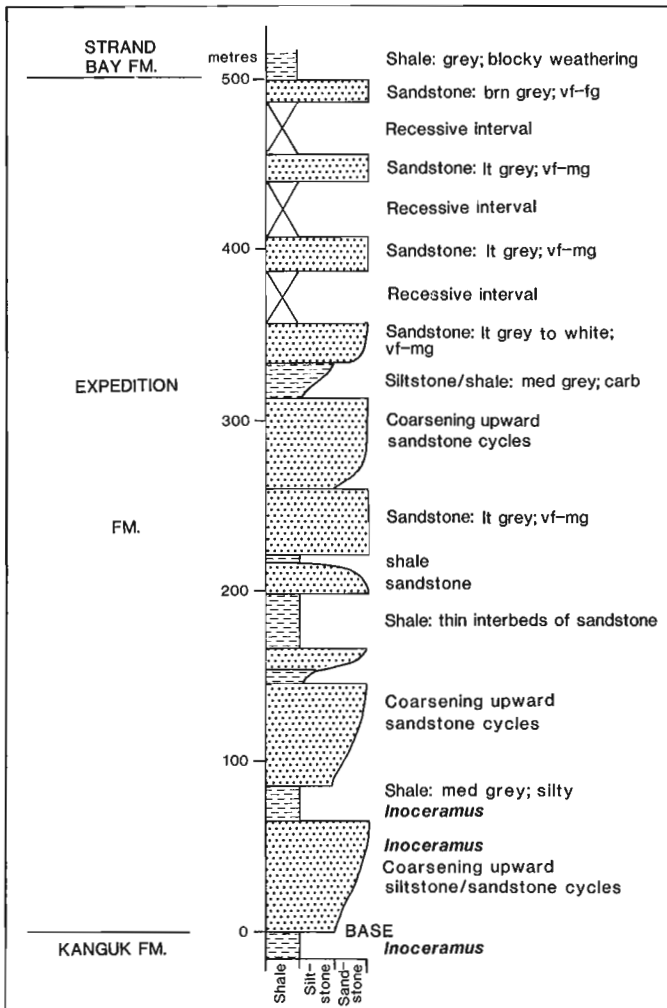


Figure 39.6. A schematic representation of the Expedition Formation type section, east of Kanguk River (lat. 79°16'N; long. 90°35'W). Detailed description of this section is given in Ricketts (in press).

Buchanan Lake Formation (Ricketts and McIntyre, 1986). Conglomerates at the Boulder Hills locality near Lake Hazen (conglomerate member of Miall, 1979a) are also assigned to the Buchanan Lake Formation.

Contacts. As previously noted, the basal contact at Mokka Fiord is disconformable. At other localities along eastern Axel Heiberg Island there is a slight discordance with underlying Mesozoic bedrock (for example 5-8° in exposures due west of Stang Bay). Conglomerates at Boulder Hills, are seemingly in conformable and gradational contact with underlying sandstones and interbedded coal seams that are included in the Iceberg Bay Formation. The basal contact at Franklin Pierce Bay (east coast of Ellesmere Island) appears to be disconformable; conglomerate composed of highly indurated sandstone and limestone clasts overlies Early Paleozoic, Franklinian strata of similar composition. The upper contact of the Buchanan Lake Formation is faulted, and conglomerates lie in the footwalls of major thrusts, such as the Stolz, Parrish Glacier and Lake Hazen thrusts.

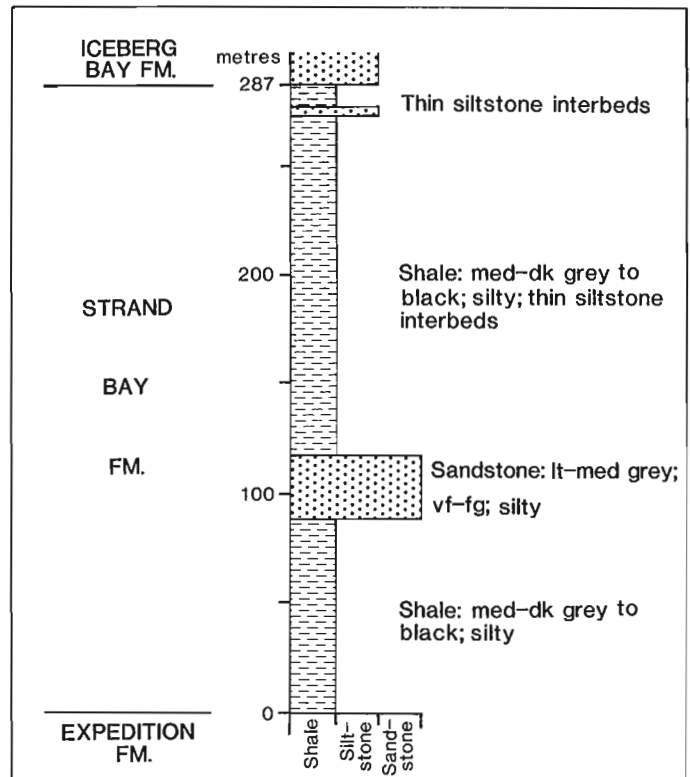


Figure 39.7. A schematic representation of the Strand Bay Formation type section, north shore of Strand Fiord (lat. 79°14'N; long. 91°27'W). Detailed description of this section is given in Ricketts (in press).

Lithology. Internal organization and sedimentary facies in the Buchanan Lake Formation conglomerates are similar from one area of exposure to another, despite considerable differences in clasts composition; crossbedding and channel structures abound. Exposures along eastern Axel Heiberg contain a variety of bedding types, with massive cliff-forming conglomerate in the lower part of the formation, and interbedded conglomerate, sandstone, grey mudstone, and lignitic coal higher in the succession. Pebble composition here and at the type section is predominantly diabasic, with minor amounts of sandstone. Clasts at Franklin Pierce Bay consist predominantly of carbonate and highly indurated sandstone derived from Lower Paleozoic rocks in the hanging wall of the Parrish Glacier Thrust. At Otto Fiord, diabase pebble conglomerate occurs at the base of the sequence, whereas siliceous limestone clasts predominate at stratigraphically higher levels, a compositional change that may reflect an inverse stratigraphic derivation; namely, diabase eroded from sills intruding the Triassic Blaa Mountain Group, and siliceous limestone from the Upper Paleozoic Nansen Formation

Age. Lignite seams and mudstone at Geodetic Hills contain a rich, well preserved flora. The assemblages indicate a Middle Eocene age. A more detailed description of the flora is given in Ricketts and McIntyre (1986).

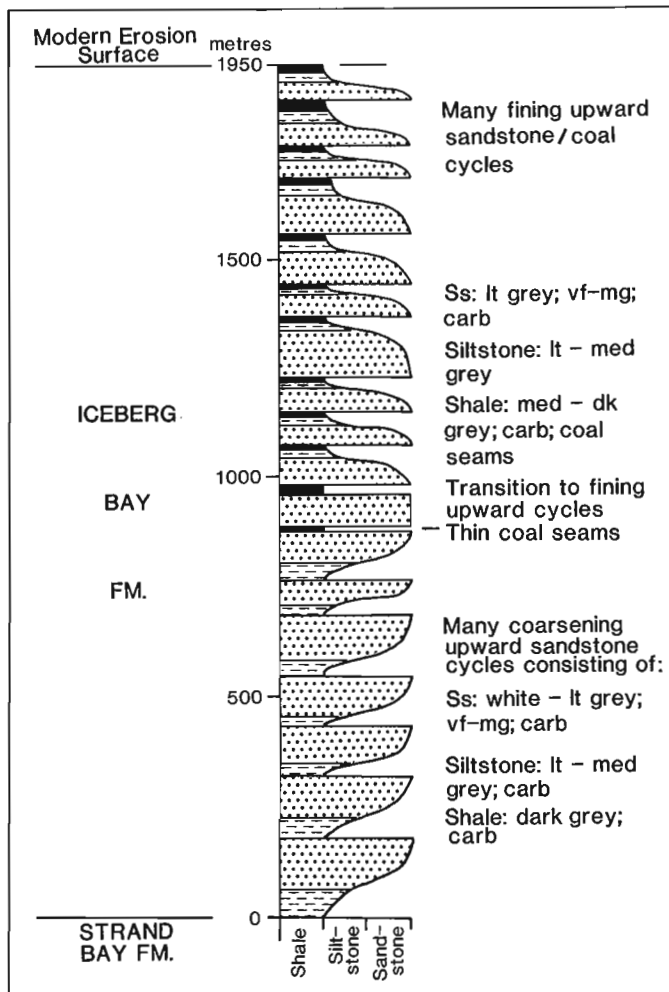


Figure 39.8. A schematic representation of the Iceberg Bay Formation type section, north shore of Strand Fiord (lat. 79°14'N; long. 91°27'W). Detailed description of this section is given in Ricketts (in press).

Interpretation

The conglomerate and sandstone that compose the bulk of the Buchanan Lake Formation were deposited by fluvial processes, commonly braided rivers, and locally, by debris flows. The clastic debris of the alluvial fans and braidplains was derived from adjacent thrust sheets of Mesozoic and Paleozoic bedrock. The Buchanan Lake Formation is syntectonic and represents a major phase of Eureka tectonism.

Use of the Eureka Sound Group nomenclature in other areas of the Arctic Archipelago

The terminology proposed here can be applied to a number of other areas in the Arctic that contain Eureka Sound Group strata (summarized in Table 39.2). Thick bedded conglomerate at Lake Hazen and Judge Daly Peninsula (Miall, 1979a, 1982) display lithological, stratigraphic and structural relationships that are similar to those in the Buchanan Lake Formation. Underlying sandstone, shale and coal, up to 450 m thick and mostly of fluvial origin, can logically be included in the Iceberg Bay Formation.

Changes to the Kanguk-Eureka Sound contact at Bylot Island are suggested. The upper 'sandstone member' of the Kanguk Formation (Miall et al., 1980) correlates with the Expedition Formation, basal Eureka Sound Group; contact relationships with the Kanguk Formation and lithological criteria are similar to those at the type section of the Expedition Formation at Strand Fiord. The 'lower mudstone member' of Miall et al. (1980), which is almost 500 m thick on southwestern Bylot Island, is correlated with the Strand Bay Formation. An abrupt and disconformable basal contact, an upper contact that is gradational with the overlying sandstone, and a general Paleocene age, all are similar features to those of the Strand Bay Formation at its type section. The disconformity at the base of the mudstone member may correlate with a similar hiatus at Strand Fiord. The remainder of the Eureka Sound strata, which consists mainly of sandstone, is assigned to the Iceberg Bay Formation.

On Amund Ringnes and Cornwall islands, approximately 300 m of sandstone and shale, in gradational and conformable contact with the Kanguk Formation and apparently of Late Cretaceous age (Balkwill, 1983), are included in the Expedition formation. A major unconformity between much younger 'unnamed' brown sandstone (possibly Late Paleocene-Eocene) and Triassic and Lower Cretaceous bedrock (Balkwill, 1983), may also correspond to the disconformity discovered at Strand Fiord. These younger sandstones are tentatively included in the Iceberg Bay Formation. The Strand Bay Formation has not been recognized on Amund Ringnes Island.

About 60 m of sandstone, probably of Maastrichtian age (Balkwill et al., 1982), that disconformably overlie Kanguk shale on south-central Loughheed Island, also are correlated with the Expedition Formation.

On Banks Island, Miall (1979b) divided the Campanian to Eocene succession into the Kanguk Formation, with a shale member and an upper sandstone member, and the Eureka Sound Formation, with a shale member and an overlying cyclic member. The lithotypes and ages of these units indicate that the upper sandstone member of the Kanguk Formation can be assigned to the Expedition Formation, the shale member of the Eureka Sound Formation to the Strand Bay Formation, and the overlying cyclic member to the Iceberg Bay Formation.

Acknowledgments

Special thanks are due to A.F. Embry (ISPG), for introducing me to the problem of Eureka Sound basin analysis and for many useful discussions. Also, I gratefully acknowledge the efforts of D.J. McIntyre (ISPG) for palynological determinations, J.H. Wall (ISPG) for microfossil determinations, and R. Thorsteinsson (ISPG) for valuable discussion. Over the last three years of this project, capable assistance in the field has been given by Dave Allen, Michael Slawinski, and Bill Halliday. Most of this paper was written while visiting the Geology Department of Auckland University. Use of facilities in the department is gratefully acknowledged.

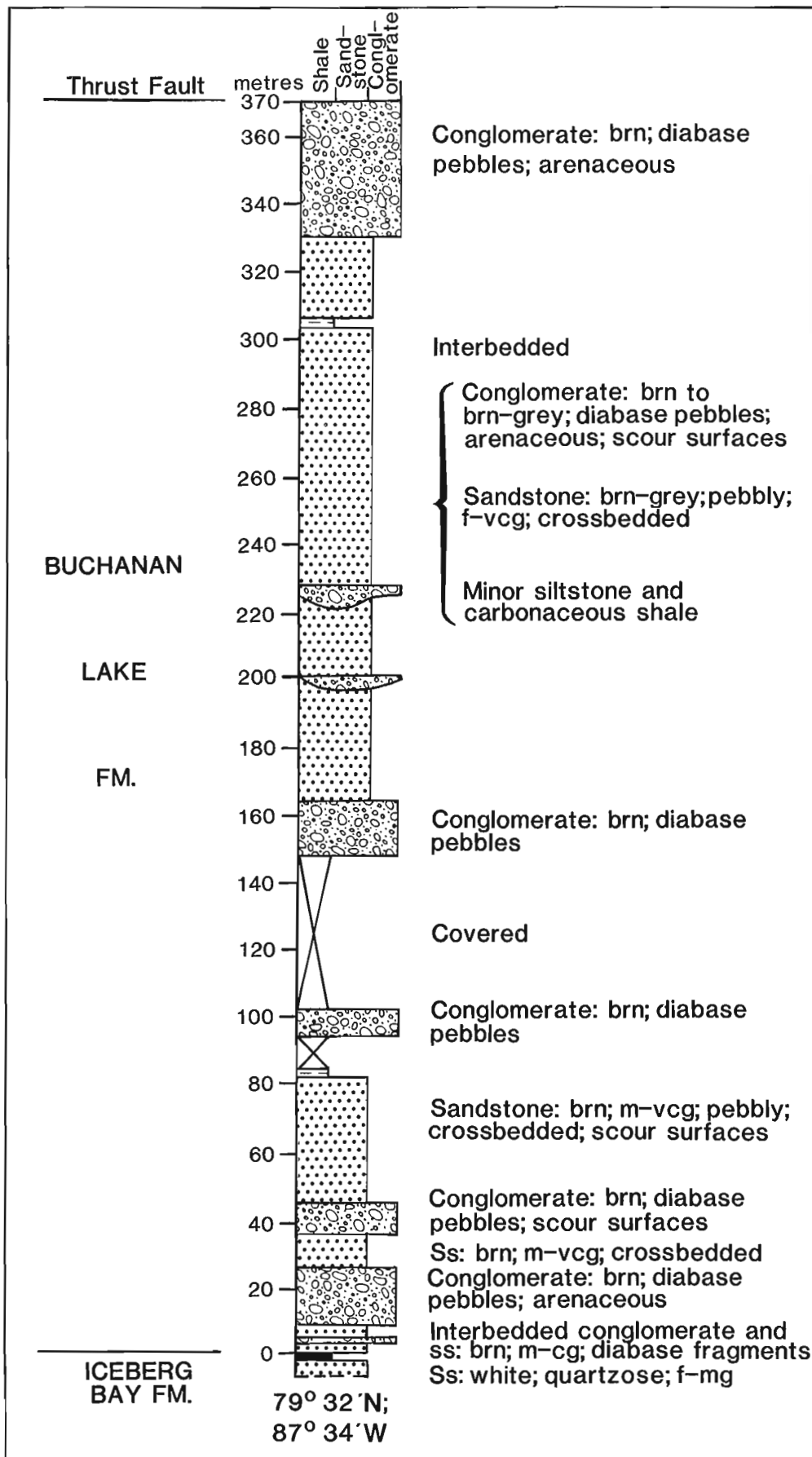


Figure 39.9. Buchanan Lake Formation type section, at the head of Mokka Fiord (lat. 79°32'N; long. 87°34'W).

Table 39.2. Lithostratigraphic correlation of Eureka Sound Group, Arctic Islands

		This Report	LAKE HAZEN Miall, 1979a	BYLOT IS. Miall et al, 1980	AMUND RINGNES IS. Balkwill, 1983	LOUGHEED IS. Balkwill et al, 1982	BANKS IS. Miall, 1979b
EOCENE	U	?					
	M	Buchanan Lake Fm	conglomerate member				
	L	Iceberg Bay Fm	sandstone- mudstone member	Te 4 Te 3	unnamed sandstone Tpe		cyclic member Te 2
PALEOCENE	U						
	M						
	L	Strand Bay Fm		Te 2 lower mudstone member Te 1		?	shale member Te 1
MAASTRICHTIAN		Expedition Fm		sandstone member	?	Eureka Sound Fm sandstone	upper sand mbr Kanguk Fm
				Kanguk Fm Kk 2	Eureka Sound Fm Te		shale member Kanguk Fm
UPPER CAMPANIAN							
MIDDLE CAMPANIAN		Kanguk Fm		Kanguk Fm Kk 1	?	Kanguk Fm	
		Pre- Kanguk					

References

- Balkwill, H.R.
1983: Geology of Amund Ringnes, Cornwall, and Haig Thomas islands, District of Franklin; Geological Survey of Canada, Memoir 390.
- Balkwill, H.R., Hopkins, W.S., and Wall, J.H.
1982: Geology of the Lougheed island and nearby small islands, District of Franklin (parts of 69C, 79D); Geological Survey of Canada, Memoir 395.
- Bustin, R.M.
1977: The Eureka Sound and Beaufort formations, Axel Heiberg and west-central Ellesmere islands, District of Franklin; M.Sc. thesis, University of Calgary, Alberta, 208 p.
1982: Beaufort Formation, eastern Axel Heiberg Island, Canadian Arctic Archipelago; Bulletin of Canadian Petroleum Geology, v. 30, p. 140-149.
- Miall, A.D.
1979a: Tertiary fluvial sediments in the Lake Hazen intermontane basin, Ellesmere Island, Arctic Canada; Geological Survey of Canada, Paper 79-9.
1979b: Mesozoic and Tertiary Geology of Banks Island, Arctic Canada; Geological Survey of Canada, Memoir 387.
1982: Tertiary sedimentation and tectonics in the Judge Daly Basin, northeast Ellesmere Island, Arctic Canada; Geological Survey of Canada, Paper 80-30.
1984: Sedimentation and tectonics of a diffuse plate boundary: The Canadian Arctic Islands from 80 Ma B.P. to the present; Tectonophysics, v. 107, p. 261-277.

- Miall, A.D., Balkwill, H.R., and Hopkins, W.S. Jr.
 1980: Cretaceous and Tertiary sediments of Eclipse Trough, Bylot Island area, Arctic Canada, and their regional setting; Geological Survey of Canada, Paper 79-23.
- Ricketts, B.D.
 1984: Geological Survey of Canada, Open File Map 1147.
 1985: Geological Survey of Canada, Open File Map 1182.
 Delta evolution in the Eureka Sound Group, western Axel Heiberg Island: The transition from wave-dominated deltas; Geological Survey of Canada, Bulletin. (in press)
- Ricketts, B.D. and McIntyre, D.J.
 1986: The Eureka Sound Group of eastern Axel Heiberg Island; new data on the Eureka Orogeny; in Current Research, Part B, Geological Survey of Canada, Paper 86-1B, Report 43.
- Souther, J.G.
 1963: Geological traverse across Axel Heiberg from Buchanan Lake to Strand Fiord; in Geology of the north-central part of the Arctic Archipelago, Northwest Territories (Operation Franklin), ed. Y.O. Fortier et al.; Geological Survey of Canada, Memoir 320, p. 426-448.
- Thorsteinsson, R. and Tozer, E.T.
 1957: Geological investigations in Ellesmere and Axel Heiberg islands, 1956; Arctic, v. 10, p. 2-31.
- Tozer, E.T.
 1963: Mesozoic and Tertiary stratigraphy; in Geology of the north-central part of the Arctic Archipelago, Northwest Territories (Operation Franklin), ed. Y.O. Fortier; Geological Survey of Canada, Memoir 320, p. 74-95.
- Troelsen, J.
 1950: Contributions to the geology of northwest Greenland, Ellesmere Island and Axel Heiberg Island; Meddeleiser om Grønland, v. 149, no. 7.
 1952: Geological investigations in Ellesmere Island; Arctic, v. 5, p. 199-210.
- West, R.M., Dawson, M.R., Hickey, L.J., and Miall, A.D.
 1981: Upper Cretaceous and Paleogene sedimentary rocks, eastern Canadian Arctic and related North Atlantic areas; in Geology of the North Atlantic borderlands, ed. J.W. Kerr and A.J. Ferguson; Canadian Society of Petroleum Geologists, Memoir 7, p. 279-298.
- West, R.M., Dawson, M.R., and Hutchison, J.H.
 1977: Fossils from the Paleogene Eureka Sound Formation, Northwest Territories, Canada: occurrence, climate and paleogeographic implications; in Paleontology and Plate Tectonics, ed. R.M. West; Milwaukee Public Museum, Special Papers in Biology and Geology, no. 2.

Comments on the stratigraphy, sedimentology and distribution of the Albian Sharp Mountain Formation, northern Yukon

Project 850037

J. Dixon
Institute of Sedimentary and Petroleum Geology, Calgary

Dixon, J., Comments on the stratigraphy, sedimentology and distribution of the Albian Sharp Mountain Formation, northern Yukon; in Current Research, Part B, Paper 86-1B, p. 375-381, 1986.

Abstract

The early Albian Sharp Mountain Formation of the Keele Range, northern Yukon, was originally described as a shallow water, marine to alluvial deposit. New outcrop trends are identified and four facies assemblages described: conglomerate, conglomerate-sandstone, sandstone and shale. The sedimentological attributes of these facies favour an origin as sediment gravity flow deposits in basinal areas. Deposits of similar origin in the Blow Trough to the north and the Kandik Basin to the southwest indicate that, during the early Albian, basinal conditions extended throughout much of northern Yukon.

Résumé

La formation de Sharp Mountain de l'Albien inférieur, trouvée dans le chañon Keele, dans le nord du Yukon, a été considérée à l'origine comme étant un dépôt marin ou alluvial accumulé en eau peu profonde. La présente étude identifie de nouvelles orientations d'affleurements et décrit quatre nouveaux assemblages de faciès: un conglomérat, un conglomérat-grès, un grès et un schiste argileux. Les caractéristiques sédimentologiques de ces faciès semblent indiquer que les sédiments se sont accumulés à la suite de coulées par gravité dans un bassin. La présence de dépôts d'origine similaire dans la dépression Blow au nord et dans le bassin Kandik au sud-ouest montre qu'au cours de l'Albien inférieur, des conditions sédimentologiques de bassin régnaient sur une grande partie du nord du Yukon.

Introduction

The early Albian Sharp Mountain Formation was formally described and defined by Jeletzky (1975), and in his publication he concluded that the Sharp Mountain contains strata of alluvial to shallow water marine origin and that these strata formed the western shoreline facies of an early Albian flysch trough.

The objectives of this brief report are to re-evaluate the stratigraphy and sedimentology of the Sharp Mountain Formation and to report on newly identified outcrops. The data for this presentation were collected during the summer of 1985.

Type section

The seven intervals and supplementary section described by Jeletzky (1975, Fig. 2) at Sharp Mountain, in the Keele Range of northern Yukon (Locality 1, figs. 40.1, 40.2) were re-examined and observations made on bedding attitude and thickness, lithology and sedimentary structures. Fossils were looked for but only a few, poorly preserved moulds of bivalves were located in the equivalent of Jeletzky's unit 1.

Jeletzky (1975) identified his unit 1 as an Upper Jurassic sandstone, which can be correlated with the Porcupine River Formation. Unit 2 was a covered interval, and units 3 to 7 were identified as Sharp Mountain Formation. Two units were identified in his supplementary section – a lower conglomerate and an upper sandstone – both of which were placed in the Sharp Mountain Formation. The supplementary section is located to the north of his main section, and he believed there was an anticlinal axis separating the two sections.

In situ material is very scarce in the first four units and in Unit 6; most of the rock is frost-heaved felsenmeer. In units 5 and 7 of Jeletzky, in situ material is more abundant. Faulting, such as that cited by Jeletzky (1975, units 4 and 5), could not be decisively proven; in fact the impression is of a continuous, if poorly exposed, succession dipping to the south. Also, the supplementary section of Jeletzky (1975, p. 241) appears to dip to the south, not to the north as stated by Jeletzky. The upper contact of the Sharp Mountain Formation appears to be a stratigraphic contact with map unit Kwr (Fig. 40.2), not a fault as mapped (Norris, 1981a). The inference from these observations is that there is a continuum of strata at the Sharp Mountain section, from the apparently faulted contact with Paleozoic carbonates in the north, to map unit Kwr on the dip slope of Sharp Mountain in the south. In light of these observations, it is believed that the conglomerate adjacent to the Paleozoic carbonate (unit 1 of Jeletzky's supplementary section) is a Paleozoic unit; the sandstones of unit 2 in Jeletzky's supplementary section are considered to be part of the Upper Jurassic Porcupine River Formation. For the remainder of the section the stratigraphy is considered to be the same as described by Jeletzky (1975).

Distribution

Jeletzky (1975) only identified the Sharp Mountain Formation at its type section and the immediately adjacent area. Norris (1981a) mapped the Sharp Mountain's occurrence on the north and south side of the Porcupine River, near its junction with Driftwood River (localities 2 and 3, Fig. 40.1), and in a narrow outcrop belt extending southwest from Sharp Mountain. During the 1985 fieldwork, it was noted that much of the strata mapped as unit KRR (Rat River Formation) southwest of Sharp Mountain (Norris, 1981a,b) in the Keele Range and northernmost Nahoni Range were actually Sharp Mountain Formation. Most of the examined locations of Norris' Rat River Formation (Fig. 40.1) contained chert-pebble conglomerates, a facies that is unique to the Sharp

Mountain Formation in the Cretaceous succession of the Keele Range and northernmost Nahoni Range. One location (Locality 4, Fig. 40.1) contained an atypical lithotype. It is located west of Heart Mountain, on a low-relief, north-south ridge, and contains an isolated exposure of mudstone near the ridge crest. The age and correlation of the mudstone remain unresolved. Sandstones at localities 5, 6 and 7 (Fig. 40.1), although mapped as KRR (Norris, 1981b), appear to be in structural and stratigraphic continuity with adjacent map unit KWC. Although not all KRR outcrop belts southwest of Sharp Mountain were examined, a sufficient number were visited to suggest that most of the KRR units are Sharp Mountain strata, or its equivalent. At Locality 8 (Fig. 40.1) Albian foraminifera (Institute of Sedimentary and Petroleum Geology internal paleontological report no. 3-DHM-1985) were recovered from a shale unit within a sandstone-conglomerate unit mapped as KRR (Norris, 1981b), lending further support to the correlation of much of map unit KRR with Sharp Mountain Formation.

Between Johnson Creek and Porcupine River, unit KRR was mapped overlying Porcupine River strata (Norris, 1981a, c; localities 9 to 12 of Fig. 40.1). However, Upper Jurassic fossils from Locality 9 (Geological Survey of Canada internal paleontology report no. Km-13-1985-JAJ) and the mappable continuity of the same unit through localities 10 and 11 indicate that map unit KRR is part of the Porcupine River Formation.

Strata at Locality 12 were also mapped as KRR, but in light of the other revisions it seems that these strata are part of some other unit, possibly the Porcupine River Formation. Strata identified as Sharp Mountain Formation in the vicinity of Locality 13 (Fig. 40.1; Norris, 1985a) also are of questionable correlation. They consist of chert-pebble conglomerates very similar in appearance to those of the Sharp Mountain Formation, but the local structural and stratigraphic situation indicates that they are more likely to be equivalent to map unit CKK, the Carboniferous Kekiktuk Formation (Norris, 1981a). The mapped Sharp Mountain Formation in the vicinity of Locality 13 needs to be investigated further to obtain more conclusive answers.

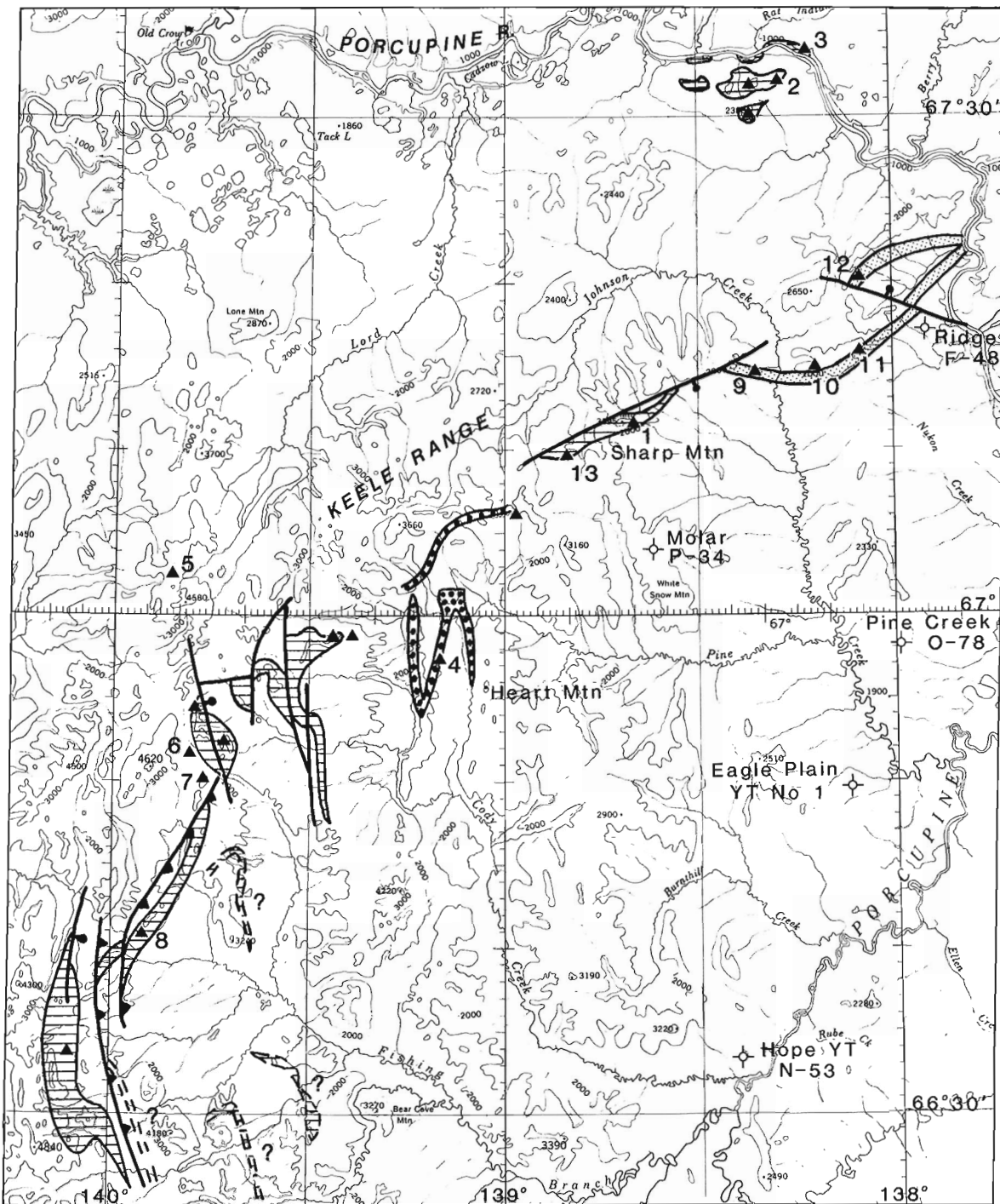
Fifteen kilometres south-southeast of Sharp Mountain, at the north end of White Snow Mountain, is the Socony Mobil Western Minerals Molar YT P-34 well (Fig. 40.1), which penetrated Albian strata between log depths 847.3-2328.8 m. An early to middle Albian age is indicated by the contained microfossils (Chamney, in Norford et al., 1971). Cuttings samples and eight cores of Albian strata indicate that conglomerate and sandstone of the Sharp Mountain Formation are absent in this well. The succession is dominated by mudstone, interlaminated and interbedded with siltstone and very fine grained sandstone. A similar lithological succession is encountered in the basal part of the Albian section in the Hope YT N-53, Pine Creek YT O-78, Eagle Plain YT No. 1, and Ridge YT F-48 wells (Fig. 40.1).

Facies

Four lithofacies can be identified in the Sharp Mountain Formation and equivalent strata: conglomerate, conglomerate-sandstone, sandstone, and shale.

Conglomerate facies

The conglomerate facies contains beds of granulestone to small-pebble conglomerate. Clasts up to 17 cm in long diameter were noted but the majority are less than 2 cm. The clasts are well rounded and generally well sorted. The well sorted character probably accounts for the lack of size grading and the difficulty of distinguishing individual beds. Most of the conglomerates are clast-supported, with a matrix



LEGEND

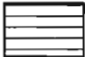





- | | | | |
|-------------------------------------------------------------------------------------|--------------------------------------------------------------------------------|-------------------------------------------------------------------------------------|---------------------------------------------|
|  | Sharp Mtn Fm |  | Examined localities - numbers cited in text |
|  | Newly identified Porcupine River Fm - originally mapped as Rat River Fm(KRR) |  | Normal fault |
|  | Mapped as Sharp Mtn or Rat River formations but stratigraphy remains uncertain |  | Thrust fault |

Figure 40.1. Distribution of Sharp Mountain Formation and localities cited in text.

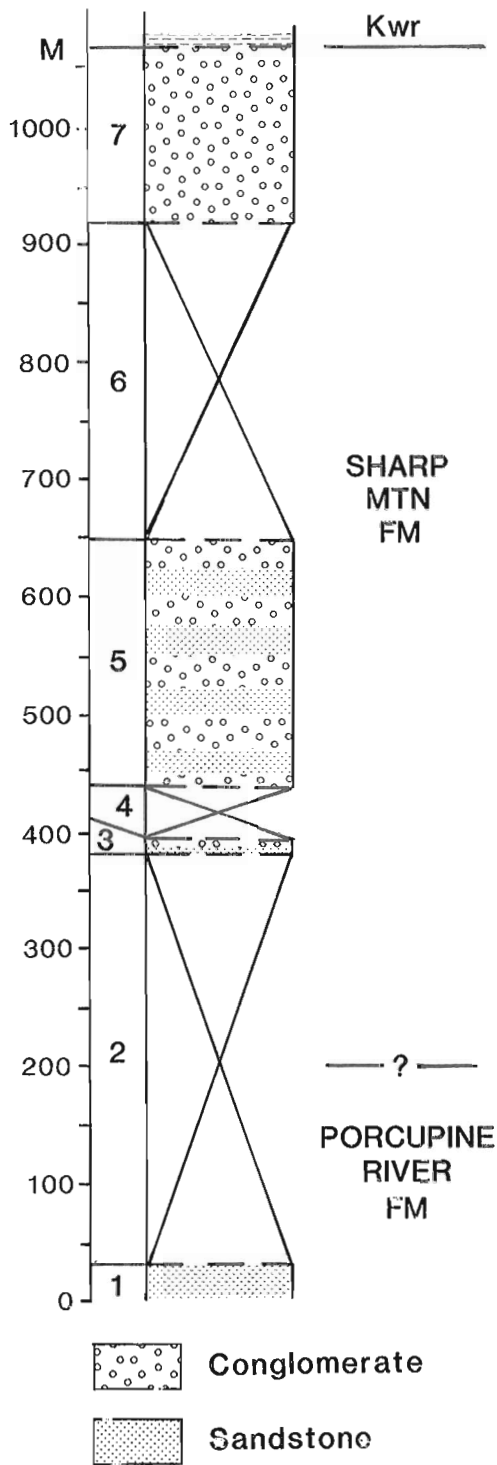


Figure 40.2. Lithological succession in the type section, Sharp Mountain Formation. Numbers refer to Jeletzky's (1975) units. Kwr: unnamed Albian shale succession.

of fine sand to granules. Only a few examples of mud-supported conglomerates were noted. Clasts are mostly black and grey chert, with subordinate numbers of sandstone clasts.

Most of the conglomerates occur in massive-appearing units, where bedding is not always easily seen. However, a few examples of clast-size variation, and the presence of parting planes parallel to regional dip, indicate that individual beds are in the order of 5 to 50 cm thick, although most beds are less than 20 cm thick. Few sedimentary structures were observed; where present they were either crude, subhorizontal bedding or low-angle crossbedding (Fig. 40.3). Where individual beds are discernible, contacts are invariably erosional.

Conglomerate-sandstone facies

Rocks of the conglomerate-sandstone facies are present principally on an isolated hill on the south side of the Porcupine River (Locality 2, Fig. 40.1). Only a few minor occurrences of this facies were noted at other locales. The facies consists of beds up to 30 cm thick in which conglomerate grades up into sandstone. Conglomerate forms 60 to 80 per cent of the bed thickness. Where stacked beds of this facies occur, the basal contacts are erosional. The conglomerate component is very similar in composition and texture to those of the conglomerate facies.

The sandstone component is generally fine to coarse grained, with scattered granules and small pebbles common in many beds. The transition from conglomerate to sandstone is generally abrupt, usually occurring over an interval less than 3 cm thick. Sedimentary structures consist of parallel to subparallel lamination, very low-angle crosslamination and current-ripple lamination.

At its principal place of occurrence, the conglomerate-sandstone facies appears to be transitional between sandstones below and conglomerates above.

Sandstone facies

The sandstone facies consists of fine to coarse grained strata, although the majority are fine to medium grained. Quartz and chert are the principal components, and most beds are extremely well cemented with silica. Many beds contain granules and small pebbles of chert and sandstone, most commonly as a basal layer, one to several pebbles in thickness, but also present as scattered clasts throughout the sandstone. A few examples of disc-shaped mudstone intraclasts were noted. Few sedimentary structures were seen, but when present consisted of fine, parallel laminae. Other sedimentary structures included load casts, flute marks, grooves and bounce marks. Horizontal burrows are commonly associated with the sole marks. In many of the sandstone intervals, bioturbated beds of argillaceous, very fine grained sandstone are not uncommon. Plant impressions were noted at a number of locations, but contrary to Jeletzky's observations (1975, p. 239) no coal or coal-like material was seen in the type section or any other section. Bed thicknesses were difficult to determine in many places due to a lack of in situ material, but when discerned, most beds were in the order of 5 to 15 cm thick.

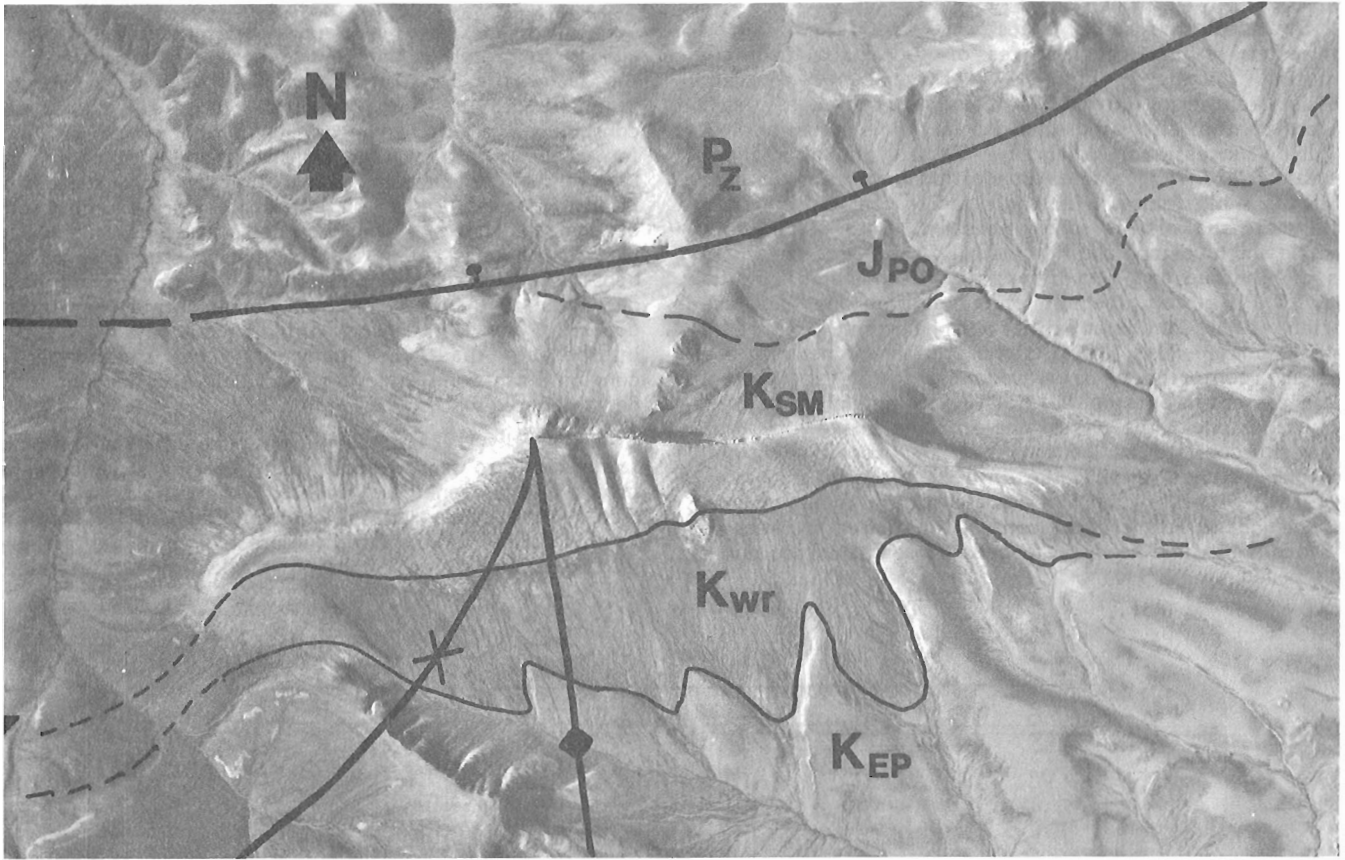


Figure 40.3. Aerial photograph of Sharp Mountain and environs and interpreted geology (National Air Photo Library number A14451-60). Pz - Paleozoic; Jpo - Porcupine River Formation; Ksm - Sharp Mountain Formation; Kwr - Albian shale; Kep - Eagle Plain Formation.

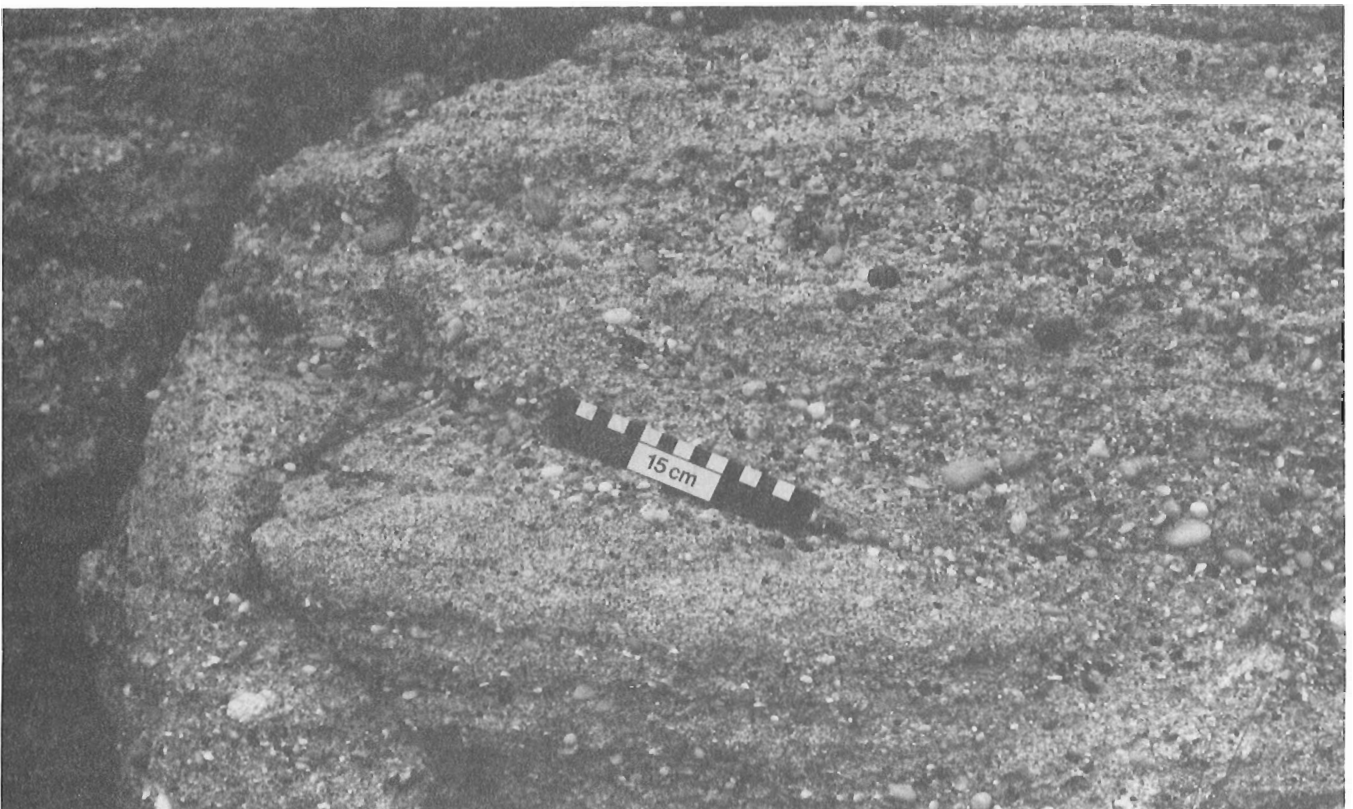


Figure 40.4. Crossbedding in the conglomerate facies, Sharp Mountain Formation; Locality 3 (Fig. 40.1).

Shale facies

Strata of the shale facies were found only in the southwestern outcrop occurrences of the Sharp Mountain Formation (Locality 8, Fig. 40.1). Even in the covered, recessive weathering intervals of the type section, the frost polygons contain only sandstone debris. If the basal part of the Albian succession in Molar YT P-34 is equivalent to Sharp Mountain strata, it represents an additional example of strata within the shale facies. The shale facies consists of black, fissile shale and silty to sandy mudstone. Interbedded with the shale and mudstone are thin (usually less than 2 cm thick) beds of siltstone and very fine grained sandstone. In the Molar YT P-34 well, the siltstone and sandstone beds are invariably finely laminated, either with horizontal or current-ripple laminae. Also, the siltstone and sandstone beds are commonly contorted or show sediment loading structures. Locally present in outcrop, but not very common, are beds of pebbly mudstone. The one example of the latter rock type seen in situ consisted of 1.5 m of matrix-supported chert and sandstone pebbles grading up into silty/sandy mudstone. Other beds of pebbly mudstone are assumed to be present where abundant pebbles were seen on weathered surfaces of the shale facies and no discrete beds of conglomerate could be discerned.

Sedimentology

The presence of sole marks and graded beds, the thin bedded character of the sandstones and conglomerates, and the lack of cross-stratification, all suggest an origin as sediment gravity flow deposits. There is no apparent consistent, vertical arrangement of the facies within the formation. To the south, southwest and east of the type area, the Shale facies becomes quite prominent, suggesting a lateral change to a more distal position from the main source of coarse clastics. The presence of fossils, burrows and bioturbated beds attests to the marine character of many beds. The lack of argillaceous material, and the thin bedded character of the sandstone and conglomerate beds indicate deposition by low density turbidity currents. A lack of interbedded shale in many of the sandstone- and conglomerate-dominant intervals would also account for the dearth of sole marks.

Jeletzky (1975) cited the presence of a shallow-marine fauna; coaly to carbonaceous, plant-bearing sandstones; coal layers; and flattened clay-balls (i.e. intraclasts) as evidence of a shallow-marine depositional environment for his unit 3. For his units 5 to 7 he cited the presence of a well preserved marine fauna, large-scale ripple marks, and the absence of

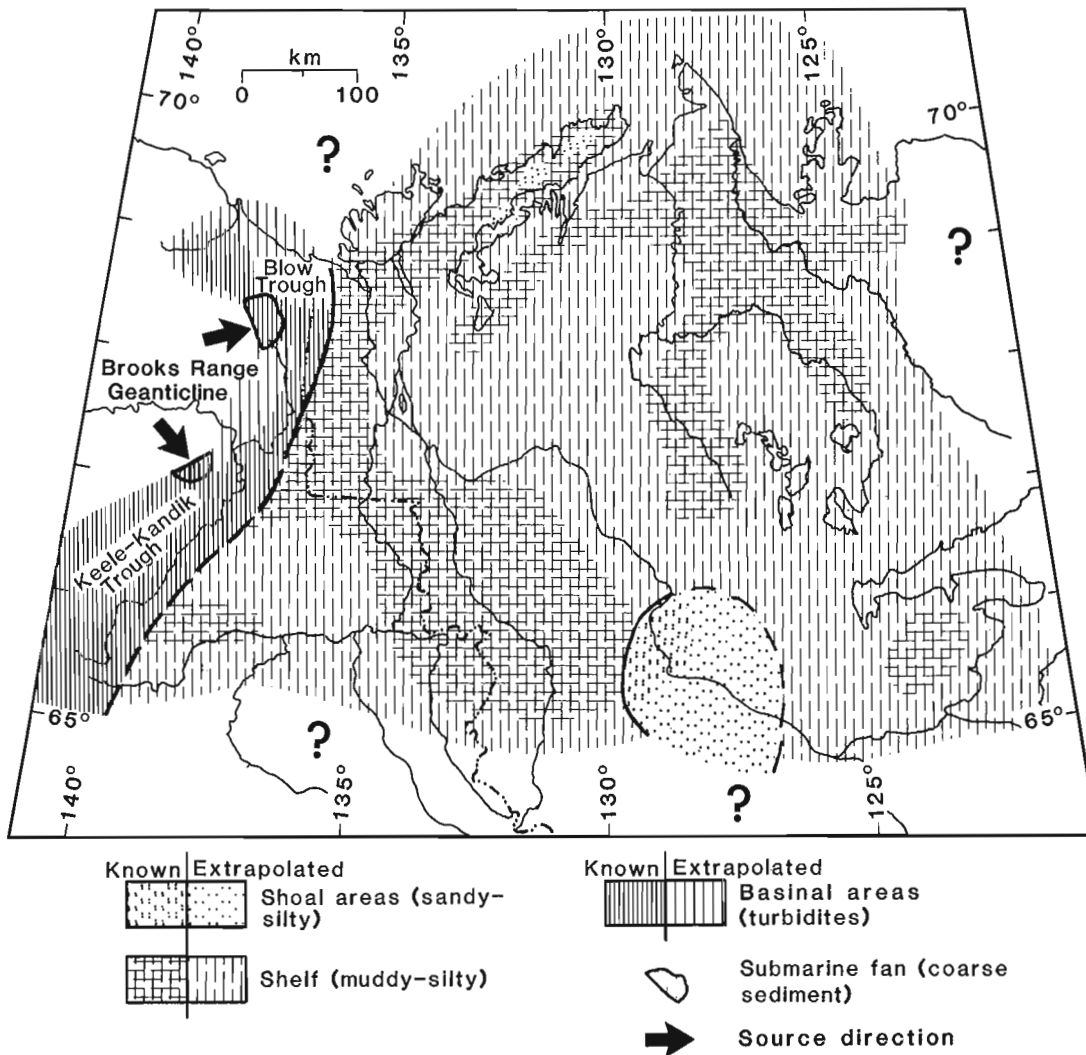


Figure 40.5. Paleogeographic reconstruction for the early Albian (from Dixon, 1986).

features typical of resedimented deposits as evidence of a shallow-marine depositional environment. With the exception of coal beds, none of the features cited by Jeletzky are unique to any specific depositional environment. No coal or coal-like material was ever noted in the type section and other sections of the Sharp Mountain Formation during the 1985 fieldwork. Jeletzky's (1975) suggestion that alluvial deposits are present in the uppermost beds of the formation was a supposition with no supportive evidence.

The Sharp Mountain strata have many similarities to the Albian conglomerates of the Blow Trough (Young, 1972, 1973a, b). In the Blow Trough, the conglomerates also consist of massive-appearing units, and contain well rounded and well sorted pebbles of chert and sandstone. The conglomerates are mostly clast-supported and bedding is difficult to distinguish. Associated with the conglomerates, either overlying them or as lateral equivalents, are interbedded sandstone and mudstone in which Bouma-type sequences of sedimentary structures are present. The sediment gravity flow origin for the Blow Trough beds is generally accepted.

Paleogeographic Implications

The sediment gravity flow origin for Sharp Mountain strata indicates that basinal conditions extended from the Blow Trough into the Keele-Kandik Trough during the early Albian. Although previous authors have implied such a reconstruction (Young et al., 1976, Fig. 11; Young and Robertson, 1984, Fig. 2) there has been no documentation to indicate that Sharp Mountain strata were deposited within the trough as sediment gravity flow deposits. This basinal area was located between the Brooks Range Geanticline to the northwest and west, and broad shelf seas of the craton to the east and south (Fig. 40.5). Like the age-equivalent Albian conglomerates of the Blow Trough, the Sharp Mountain clastics were derived from the uplifted terrain of the Brooks Range Geanticline. The coarse clastic facies of the Sharp Mountain Formation have a limited areal distribution; they shale-out and thin rapidly southward and eastward from the type area. Westward from the type area, the coarser facies become less dominant, and shale is a prominent component of the succession. These trends lend further support to the postulated northerly and northwesterly source for the clastic material.

Acknowledgments

I would like to thank my 1985 field assistant, Lorraine Velcic. I also thank Jacques Cing-Mars of the Archeological Survey of Canada and the Polar Continental Shelf Project for providing logistical support. Accommodation and storage facilities in Inuvik, Northwest Territories, were kindly provided by the Scientific Resource Centre. Comments and criticism by A.P. Hamblin and A.E. Embry greatly improved the manuscript. K. McInnis' help with the drafting is gratefully acknowledged.

References

- Dixon, J.
1986: Cretaceous to Pleistocene stratigraphy and paleogeography, northern Yukon and northwestern District of Mackenzie; *Bulletin of Canadian Petroleum Geology*, v. 34.
- Jeletzky, J.A.
1975: Sharp Mountain Formation (new): A shoreline facies of the Upper Aptian-Lower Albian flysch division, eastern Keele Range, Yukon Territory (NTS-117-0); Geological Survey of Canada, Paper 75-1B, p. 237-244.
- Norford, B.S., Barss, M.S., Brideaux, W.W., Chamney, T.P., Fritz, W.H., Hopkins, W.S., Jr., Jeletzky, J.A., Pedder, A.E.H., and Uyeno, T.T.
1971: Biostratigraphic determinations of fossils from the subsurface of the Yukon Territory and the District of Mackenzie; Geological Survey of Canada, Paper 71-15, 25 p.
- Norris, D.K.
1981a: Geology: Old Crow, Yukon Territory; Geological Survey of Canada, Map 1518A.
1981b: Geology: Porcupine River, Yukon Territory; Geological Survey of Canada, Map 1522A.
1981c: Geology: Bell River, Yukon - Northwest Territories; Geological Survey of Canada, Map 1519A.
- Young, F.G.
1972: Cretaceous stratigraphy between Babbage and Blow rivers Yukon Territory; in *Report of Activities, Part A*, Geological Survey of Canada, Paper 72-1A, p. 229-235.
1973a: Mesozoic epicontinental, flyschoid and molassoid depositional phases of Yukon's north slope; in *Canadian Arctic Geology*, J.D. Aitken and D.J. Glass (eds.); Geological Association of Canada - Canadian Society of Petroleum Geologists, p. 181-201.
1973b: Jurassic and Cretaceous stratigraphy between Babbage and Blow rivers, Yukon Territory; in *Report of Activities, Part A*, Geological Survey of Canada, Paper 73-1A, p. 277-281.
- Young, F.G., Myhr, D.W., and Yorath, C.J.
1976: Geology of the Beaufort-Mackenzie Basin; Geological Survey of Canada, Paper 76-11, 65 p.
- Young, F.G. and Robertson, B.T.
1984: The Rapid Creek Formation: An Albian flysch-related phosphatic iron formation in northern Yukon Territory; in *The Mesozoic of Middle North America*, D.F. Stott and D.J. Glass (eds.); Canadian Society of Petroleum Geologists, Memoir 9, p. 361-372.

Lower Mannville sedimentation in the "Edmonton Channel", central Alberta

Project 820033

I. Banerjee
Institute of Sedimentary and Petroleum Geology, Calgary

Banerjee, I., Lower Mannville sedimentation in the "Edmonton Channel", central Alberta; *in* Current Research, Part B, Geological Survey of Canada, Paper 86-1B, p. 383-397, 1986.

Abstract

The Edmonton Channel of central Alberta has previously been defined as a 300 km-long, northwest-trending paleovalley incised on the surface of a sub-Cretaceous unconformity, and later drowned by an advancing sea. This paper presents a detailed stratigraphic study of the area around the channel.

The lowest stratigraphic unit in the channel, the Ellerslie Formation, has three facies: a lithologically diverse basal transgressive unit, a thick crossbedded sandstone (delta-front), and a bioturbated mudstone (shallow marine and bay). The sedimentary rocks of the Ostracode Zone, which blankets the top of the channel above the Ellerslie Formation, comprise a dark micritic limestone (restricted marine facies), a bioturbated mudstone (lower shoreface facies) and a low-angle-crossbedded, bioturbated sandstone (storm facies).

The study reveals that a drowned river valley is an inappropriate model for the Edmonton Channel, which is an extremely shallow and wide depression (width/depth ratio ~1000) filled with shallow marine and deltaic sediments. A narrow, semi-enclosed, open ocean embayment filled with tidal deltas is proposed as an alternative model.

Résumé

Le chenal d'Edmonton, dans la partie centrale de l'Alberta, a déjà été décrit comme étant une paléovallée de 300 km de long, à orientation nord-ouest, creusée à la surface d'une discordance sub-crétaïque puis inondée par l'avancée de la mer. Ce rapport présente une étude stratigraphique détaillée de la région aux alentours du chenal.

Le membre d'Ellerslie soit l'unité stratigraphique occupant la position la plus basse dans le chenal, comporte trois faciès: une unité transgressive basale à lithologie variée, un grès épais à stratification oblique (front du delta) et une pélite bioturbée (mer peu profonde et baie). Les sédiments de la zone à ostracodes qui recouvre le sommet du chenal au-dessus du membre d'Ellerslie se composent d'un grès micritique foncé (milieu marin restreint), d'une pélite bioturbée (avant-plage inférieure) et d'un grès bioturbé, caractérisé par une stratification oblique à angle faible.

La présente étude révèle que le modèle d'une vallée fluviale submergée ne s'applique pas au chenal d'Edmonton, qui est une dépression large et très peu profonde (rapport largeur/profondeur d'environ 1000), remplie de sédiments de delta et de mer peu profonde. L'auteur croit que ce chenal représente plutôt une baie étroite semi-encaissée, parsemée de deltas de marée, qui donnait sur la haute mer.

Introduction

The Lower Cretaceous Mannville Group (Fig. 41.1), covers most of Alberta in the form of a westward thickening wedge, 100 to 600 m thick (Porter et al., 1982). It is believed to overlie a highly dissected erosional surface with a well developed paleodrainage pattern (Beltz, 1953; Bokman, 1963; Martin, 1966; Martin and Jamin, 1963; Sonneveld and Murray, 1982). Most conspicuous among the paleovalleys is the Edmonton Channel, described and named by Williams (1963). It has been traced for approximately 300 km in Central Alberta, where it trends roughly north-northwest (Fig. 41.2).

Williams believed that in most of the channel, fluvial sediments (Ellerslie Formation) have been preserved, and the channel fill grades upward into the marine sedimentary rocks (Clearwater-Ostracode Zone).

The basis of Williams' reconstruction of the Edmonton Channel is an isopach map of Lower Cretaceous strata, which includes the stratigraphic interval from the post-Mississippian unconformity to the base of the Fish Scale Zone. This interval includes the entire Mannville Group and lower part of the Colorado Group. Williams believed that the isopach pattern reflected the true paleotopography and that the Early Cretaceous paleodrainage system consisted of southward consequent and northwestward subsequent streams. Glaister (1959) and Rudkin (1964) also constructed isopach maps of both the Upper and the Lower Mannville sediments but did not recognize the Edmonton Channel.

Much subsurface data has accumulated since Williams' (1963) work, enabling McLean (1982) to make a special study of the Edmonton Channel. In McLean's interpretation, the direction of flow in the channel was southerly and southwesterly, into the Spirit River Channel, which flowed north-northwest. McLean agreed with Williams' view that the Edmonton Channel later became an arm of the Clearwater Sea.

Ranger (1983) presented computer-generated isopach maps of the Mannville Group, as well as the Lower Mannville (McMurray Formation), from approximately 100 000 wells in Alberta and Saskatchewan. He reconstructed the entire paleodrainage pattern on the basis of these maps, and the Edmonton Channel is recognizable on the basis of a linear isopach "thick" even on the isopach map of the entire Mannville Group (Fig. 41.2).

The present study area was chosen to look at the effect of paleotopography on Mannville stratigraphy and to interpret the nature of the paleogeographic feature, the Edmonton Channel. Maps and cross-sections based on well data, and detailed sedimentological descriptions of cores are presented to illustrate the pattern of sedimentation in the Edmonton Channel. The database used in this study includes: 397 well records (Fig. 41.3) from the Canstrat data files, for the subsurface maps; 107 Canstrat "lithologs" and 150 geophysical logs, used for the cross-sections; and the details of 51 cores, for the facies analysis. This study has revealed that the Edmonton Channel is an extremely shallow and wide paleotopographic depression that probably had some structural control. It is filled with shallow marine and deltaic sediments. The term "channel", therefore, is an inappropriate description of this feature.

Description of the channel

The basic data presented by Williams in support of his concept of the Edmonton Channel were incorporated in his isopach map of Lower Cretaceous strata (Williams, 1963; Fig. 2). The 1100 ft (335 m) contour on this map defines the main channel as well as the tributaries. More recent isopach maps of the Mannville Group and the Lower Mannville

subgroup have been compiled by Ranger (1983), and two similar isopach maps have been prepared from the database used in this study. Compilation of the "axes" of the isopach "thicks" from all sources enables a mean axis for the Edmonton Channel to be defined. This has been used to locate the channel in Figures 41.4 to 41.7.

Studying the structure contour map of the sub-Cretaceous unconformity surface is another way of delineating the Edmonton Channel. In two separate studies, a depression defining the channel was found to persist after all known regional structural effects were removed by statistical filtering (Robinson et al., 1969; Ranger, 1983). Robinson and co-workers found orthogonal undulations with a relief of 60 to 150 m and oriented northeast and northwest, to be a common feature on this surface. They concluded that at least part of this relief reflects the topography. They recognized a structural depression below the Edmonton Channel and suggested that it is underlain by a left-lateral wrench fault with a minimum displacement of 16 km.

Another map of this surface, prepared by Ranger (1983), represents fifth-order residuals, presumably with most structural effects eliminated. The Edmonton Channel, plotted on this map, (Fig. 41.4a) occupies a northwest-trending depression with a maximum relief of 120 m. Although its present form – a closed depression – must record a post-Mannville structure, this depression has

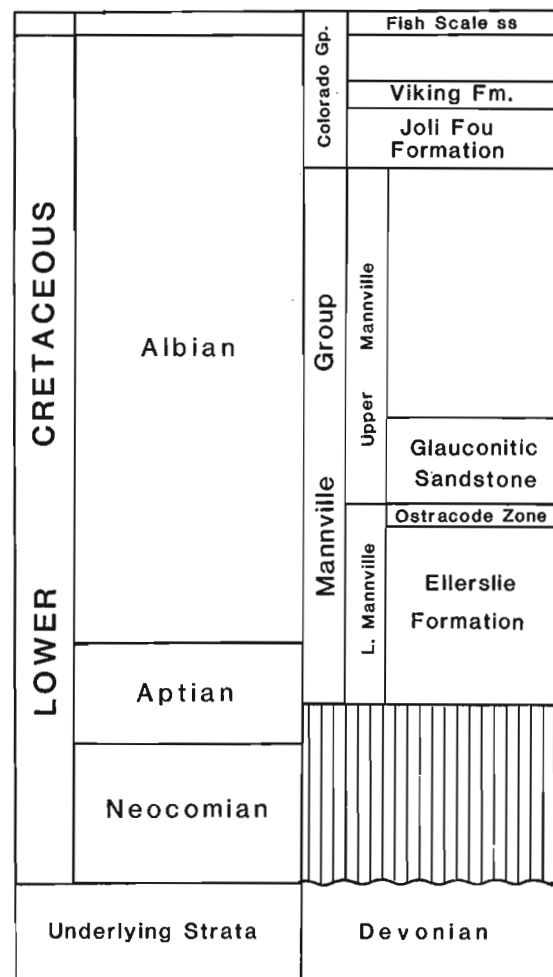


Figure 41.1. Lower Cretaceous stratigraphy of central Alberta (modified after Glaister, 1959).

been assumed to reflect paleotopography, and a cross-section along line AA' reveals its shape (Fig. 41.4b). This can be compared to the stratigraphic cross-section along the parallel line BB' (Fig. 41.4c). Both cross-sections reveal that the Edmonton Channel is an extremely shallow and wide depression. The channel would not be revealed by a true scale representation of its morphology, because of its width/depth ratio of 1000. The representation with a ten times vertical exaggeration shown in Figure 41.4d, gives an approximate visual impression of the depression.

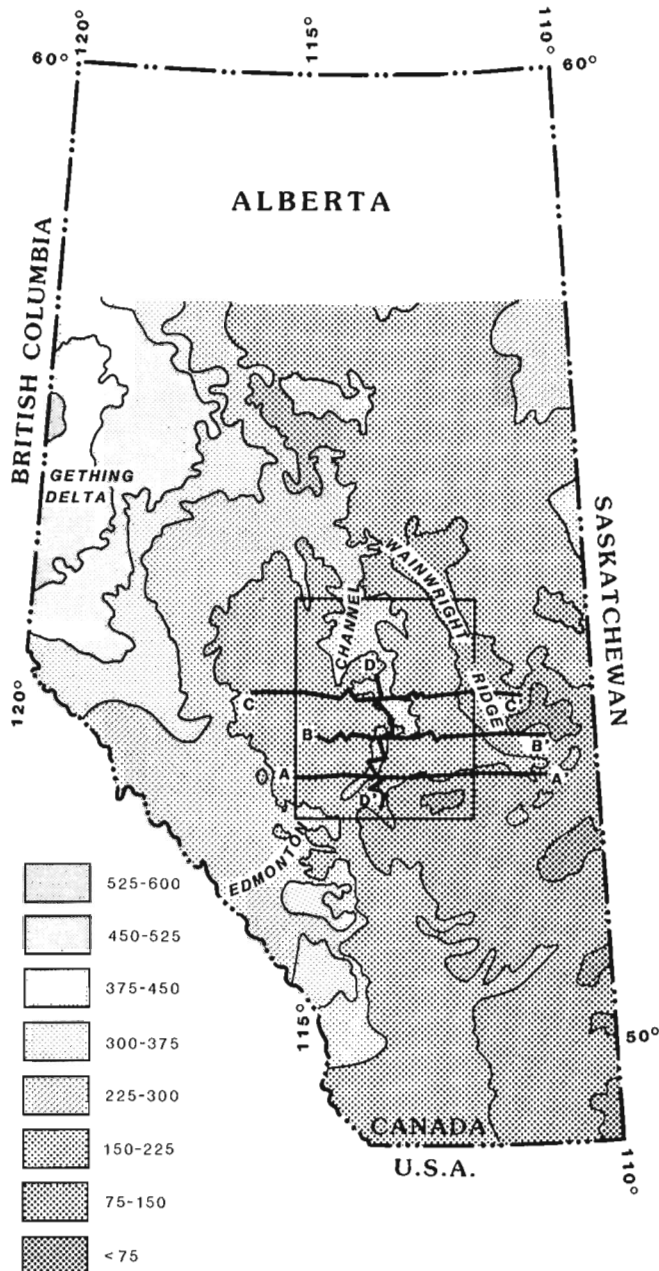


Figure 41.2. The Edmonton Channel (enclosed by the 225-300 m contour) as shown in the regional isopach map of the Mannville Group (modified after Ranger, 1983). The area studied is shown by the rectangle, and the lines AA', BB', CC', DD' are the locations of the cross-sections in Figures 41.8 to 41.11. All isopach contour measurements are in metres.

Lithology of the channel fill

Broad spatial relations

Two isopach maps, and one net sandstone map of the Lower and Upper Mannville subgroups show that:

1. The quasi-linear north-south pattern of total thickness and net sandstone thickness in the channel, as seen in the Lower Mannville (Figs. 41.5, 41.6), is replaced by a more irregular pattern in the Upper Mannville in which a northeasterly trend is detectable (Fig. 41.7). This possibly reflects a change from shore-normal (NW) to shore-parallel (NE) trends of thick sandstone. The shore-parallel Hoadley barrier bar complex of the Glauconitic Sandstone (Chiang, 1985) occurs in this area.
2. Patterns shown in the isopach and net sandstone maps of the Lower Mannville are disjointed and lobate, not strictly linear.
3. The maximum relief of the paleovalley was approximately 140 m (maximum thickness of the Lower Mannville strata), uncorrected for compaction.

Broad relationships in the vertical sequence

The Mannville stratigraphy of the in-channel and off-channel areas has been studied using six cross-sections (of which only four will be illustrated here) prepared from 107 Canstrat lithology logs supplemented by approximately 150 geophysical logs. Lithotypes were generalized to simplify the relationships and the top of the Mannville (the base of the Joli Fou Shale) was taken as the datum in all cross-sections. One longitudinal cross-section (across Ranges 23 and 24W4 extending from Tp. 51 to Tp. 35) and three transverse cross-sections (across Tps. 49, 44 and 39) of the channel were constructed. Note that in these sections, the thicker sandstone bodies shown may contain thinner shale partings, which have been eliminated (i.e. what appears as a single homogeneous sandstone may, in fact, be a composite one), and secondly, thinner beds such as coal and limestone are exaggerated.

A tripartite stratigraphy is illustrated by all four cross-sections (Figs. 41.8-41.11):

1. A thicker sandstone/shale sequence with lenses of conglomerate and at least one thin, continuous limestone unit at the base: Ellerslie Formation.
2. A bioturbated, black mudstone and thin, micritic limestone/coquina sequence in the middle: Ostracode Zone.
3. A shale/coal/sandstone sequence: Upper Mannville.

The following observations have been made:

1. The Ostracode Zone is approximately parallel to the datum and blankets the top of the channel fill, in one instance abutting against the Wainwright Ridge, as illustrated in Figure 41.10. The undulations in this layer, seen in Figures 41.9 and 41.11, are caused by either differential compaction or differential subsidence. The topographic lows seem to have been completely filled in Lower Mannville time. The Upper Mannville sedimentation was little affected by the underlying channel, as shown by the minimal change in its thickness or facies across the area.
2. The longitudinal section along the channel suggests the presence of a series of thick, lenticular and shingled sandstone bodies occurring near the top of the Ellerslie Formation (Fig. 41.11), locally underlain by a thin limestone bed.

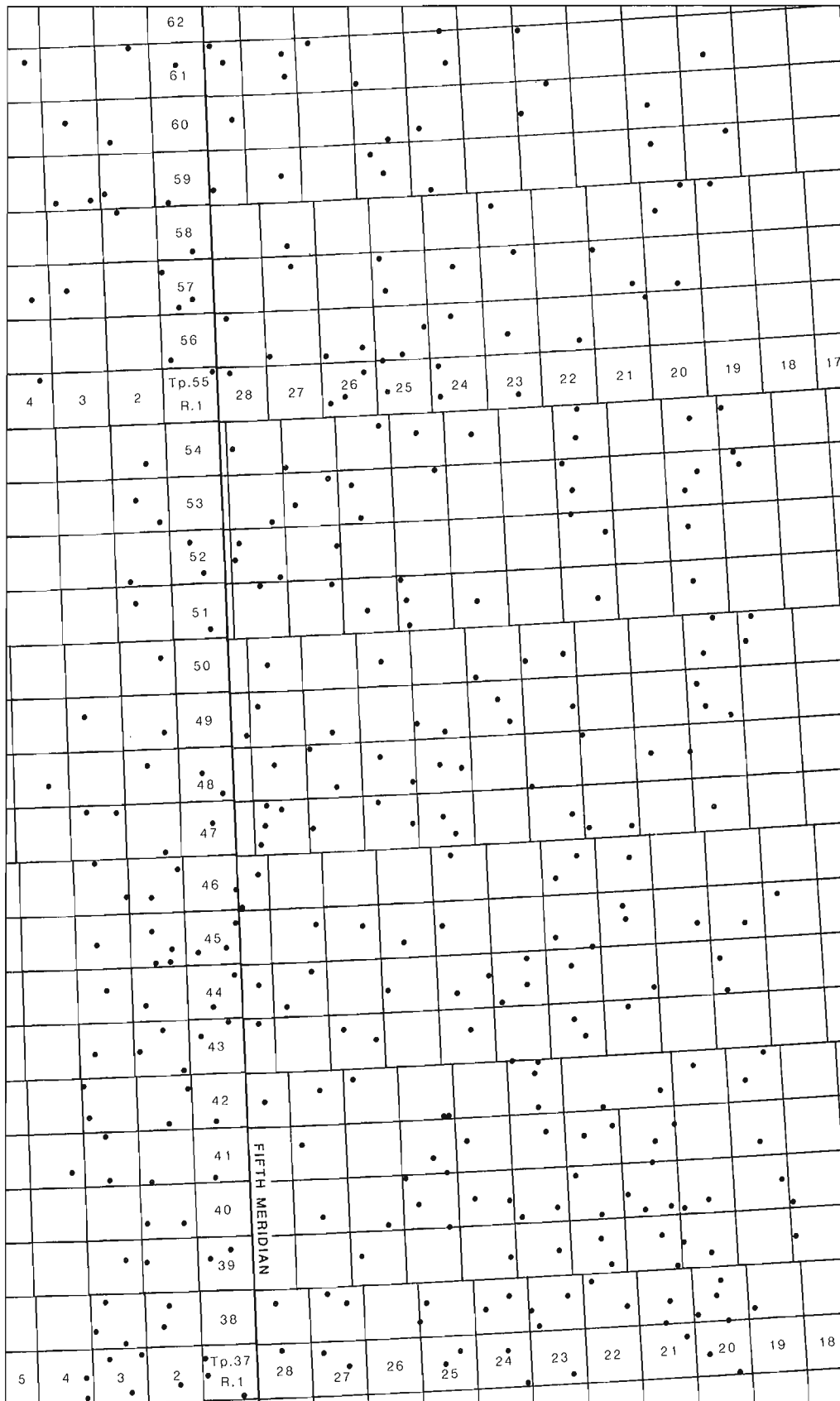


Figure 41.3. Well control for the subsurface maps (Figs. 41.5-41.7).

Facies analysis of the channel sediments

A sedimentological description resulting from the examination of 51 cores of the channel sediments is presented in this section, together with paleoenvironmental interpretations.

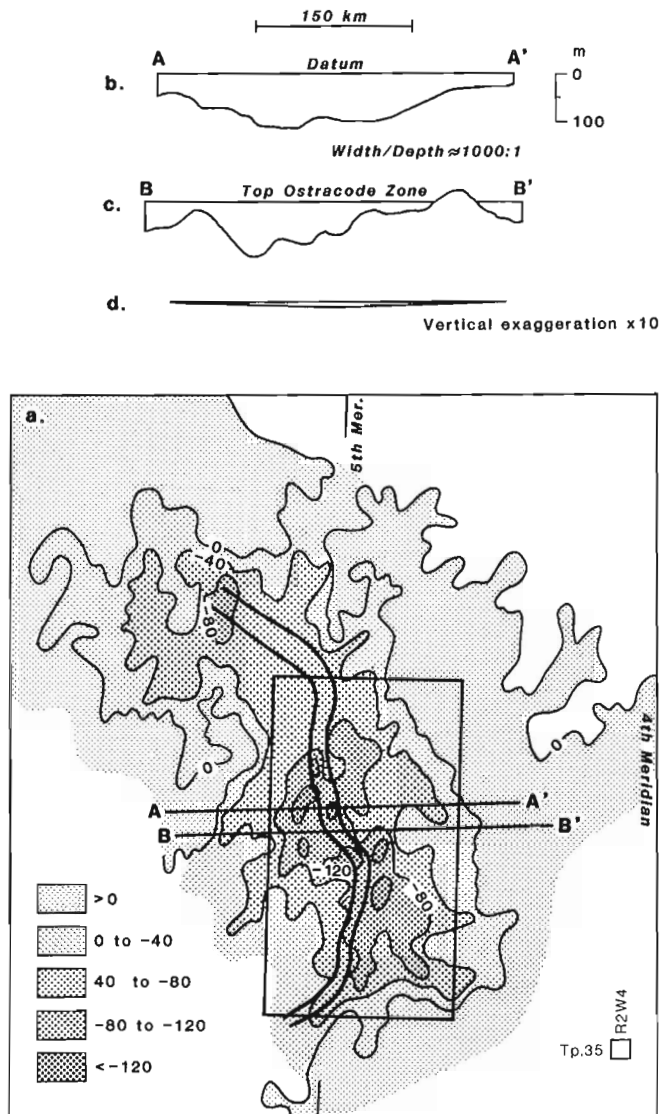


Figure 41.4.

- Structure contour map of the Pre-Cretaceous unconformity surface based on fifth order residuals after removal of structure (modified after Ranger, 1983). Contour interval 20 m. Thick lines outline the Edmonton Channel. The study area is shown by the rectangle.
- Cross-section along line AA' in Fig. 41.4a, showing configuration of the Pre-Cretaceous surface below the Edmonton Channel.
- Stratigraphic cross-section of the Lower Mannville subgroup along line CC' (cross-section in Fig. 41.10).
- Cross-section to show width/depth ratio of the Edmonton Channel derived from Fig. 41.4b and 41.4c with vertical exaggeration of 10.

Ellerslie Formation

This unit comprises thick sandstones, bioturbated sandstone/shale alternations, black shales, shell layers, thin limestones, and sideritic bands. Its stratigraphy is shown in Figure 41.11. The Ellerslie consists of the following units: (i) a basal transgressive sheet unit, (ii) thick lenticular sandstone, enclosed by, (iii) interbedded thin sandstone and shale. These units represent the three basic facies of a coarsening-upward sequence, the typical log signature of which has been recognized in many wells and is illustrated in Figure 41.13.

Basal transgressive facies. Four wells include cored intervals of the basal unit and the top of the Wabamun (Devonian) Formation. They reveal the deposition of different kinds of sediments on the unconformity surface.

The first example is a chert breccia (called the "Deville Member" and, more recently, the Deville Formation) overlying the unconformity surface close to the west flank of the Wainwright Ridge (10-12-35-22-W4; 4900-4953 ft, 1494-1510 m). Angular clasts of white chert are embedded in a medium grained, pyritic sandstone. Contorted and disrupted laminae suggest that the sandstone is strongly bioturbated. It is underlain by a very thin (20 cm) greenish shale and overlain by a sequence of interbedded, bioturbated sandstone and shale. A mixture of weathering residue from the limestone surface and marine mud is the possible basis of this facies. In addition, contortions in the overlying shale and sandstone and brecciation in the limestone probably indicate some slumping.

In the second example (5-5-44-23W4; 4877-4924 ft, 1486-1500 m), an 18 cm thick, coarse to medium grained, moderately sorted sandstone with black, carbonaceous laminae overlies the unconformity surface. It is followed by an interbedded sequence of medium grained sandstone and bioturbated mudstone. In the third example (3-22-46-23W4; 4485-4501 ft, 1367-1372 m), a bioturbated shale/sandstone sequence overlies the unconformity. In the fourth example (6-20-51-23W4; 1250-1268 m, 4101-4160 ft), a 3.5 m thick sequence of black shale directly overlies the Devonian limestone surface. It contains lenses of coal and marlstone and nodules of pyrite. The upper part of the shale displays liquefaction structures. The sandstone overlying the shale is very fine grained, flaser-bedded and apparently bioturbated.

Thick-crossbedded sandstone facies. These thick lenticular sandstones, illustrated in Figure 41.11 are an important part of the Ellerslie lithology and are economically important as reservoir rocks. They exhibit a typical coarsening-upward log signature. The sandstone is overlain and underlain by the bioturbated mudstone facies. The sedimentological characteristics of this facies are illustrated by the core log of a key well in which the entire sandstone has been cored (Fig. 41.13). The sandstone is fairly homogenous from top to bottom (Fig. 41.14a-g). It is a grey, 'salt and pepper', fine grained, well sorted and poorly cemented rock. The top of the sandstone is ripple-laminated and the base has high-angle, tabular crossbeds. The rest of the sandstone exhibits different structures at random: high-angle tabular crossbeds, low-angle crossbeds, parallel beds, and rare trace fossils, mostly *Skolithos*. Bioturbated mudstone partings occur at several levels.

In many cores, a typical structure is a low-angle bedding plane lined with black organic layers that have a crenulated appearance (Fig. 41.14g). These crenulations are probably due to bioturbation. Encased within bioturbated mudstone, and itself containing evidence of bioturbation, the sandstone shows a definite marine influence. The most likely origin of this sandstone will be

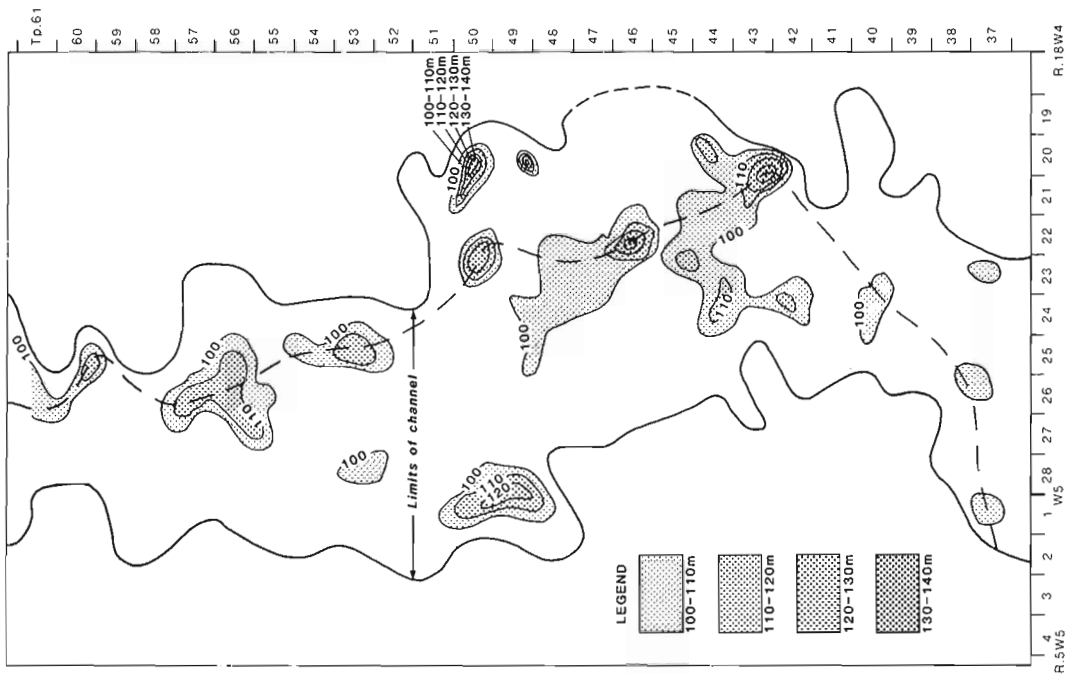


Figure 4.1.5. Isopach map of the Lower Mannville subgroup. Only contours above 100 m are shown. Contour interval is 10 m here and in Figures 4.1.6 and 4.1.7. Limit of the Edmonton Channel is arbitrarily taken at the 60 m contour and a mean axis has been determined from several databases (see text).

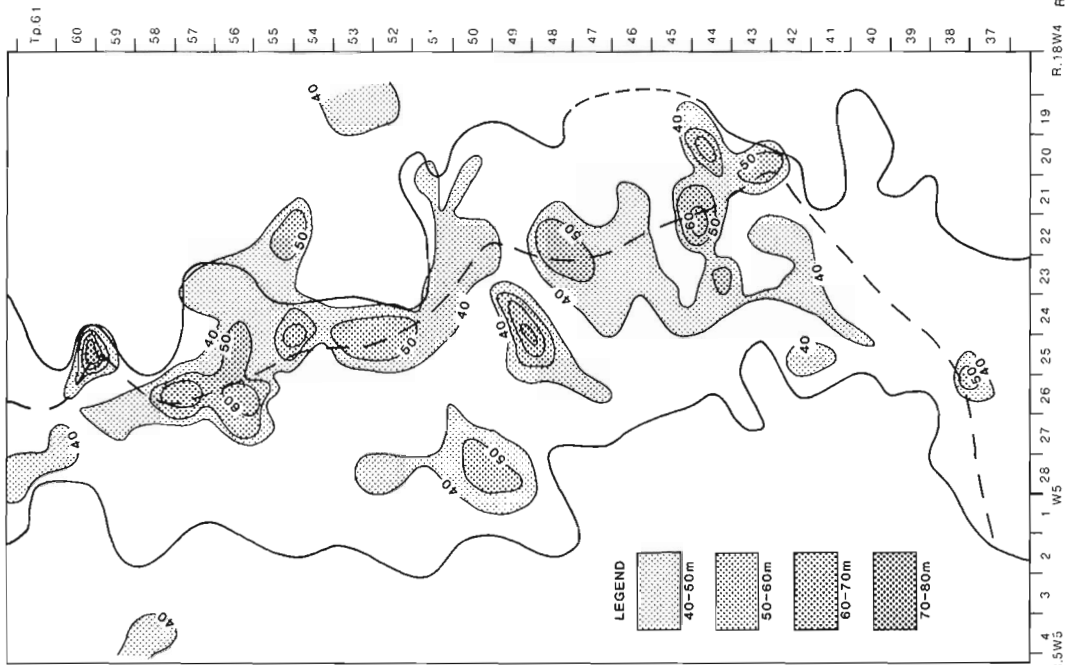


Figure 4.1.6. Lower Mannville net sand. Only net sand thicker than 40 m is shown. Thicker sand areas show irregular patterns with an apparent north-south trend. The dashed line indicates the channel axis. Limits of the channel are shown by the outer lines.

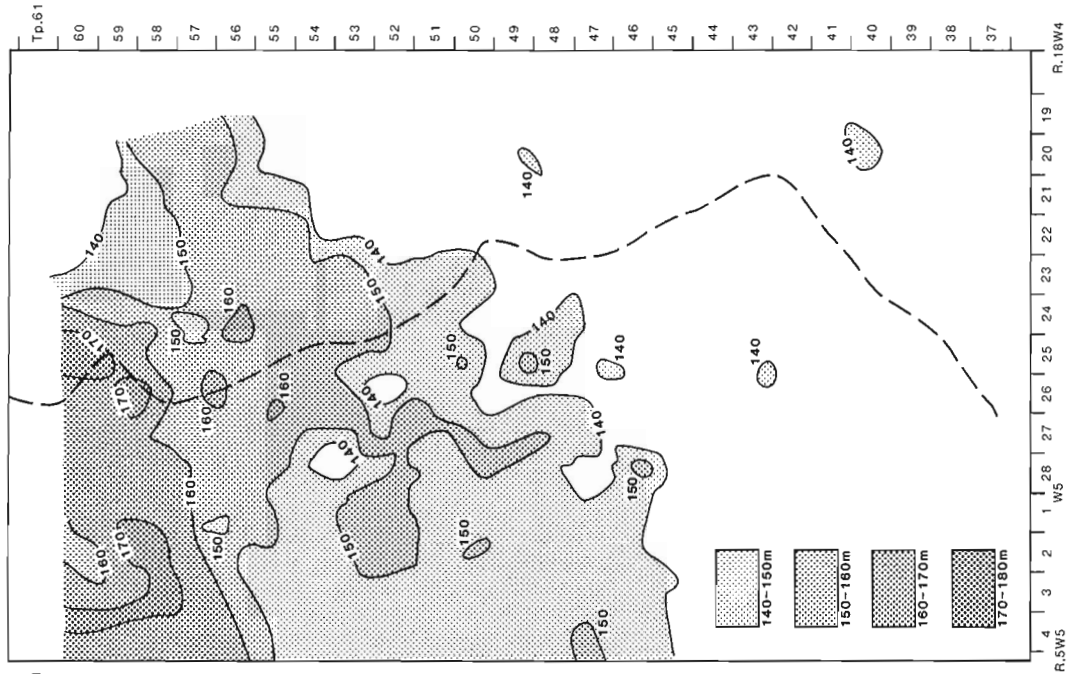


Figure 4.1.7. Isopach map of the Upper Mannville subgroup. Dashed line indicates the channel axis. Linear pattern of the Lower Mannville is replaced by a broad, irregular pattern with a rough NE trend and an increase in thickness to the NW.

discussed later. As the general setting suggests a deltaic origin, the term "delta-front sand" has been used in the environmental interpretation.

Bioturbated mudstone facies. This facies alternates with the thick-crossbedded sandstone facies. Dominantly composed of bioturbated dark mudstone, it also contains thin, fine grained, rippled and bioturbated sandstone, shell debris

and limestone. It shows a serrated log signature caused by the stacking of 2-3 m thick, "coarsening-upward" units. Basic sedimentary units are 10-15 cm thick, sharp-based, very fine grained sandstone or siltstone alternating with black mudstone, both of which are bioturbated (Fig. 41.15). Rarely, there occurs a lone bed of crossbedded, very fine grained sandstone (3-22-46-23W4; 4403-4413 ft, 1342-1345 m). Liquefaction structures with highly contorted laminae are also common. **Asterosoma(?)**, **Chondrites**,

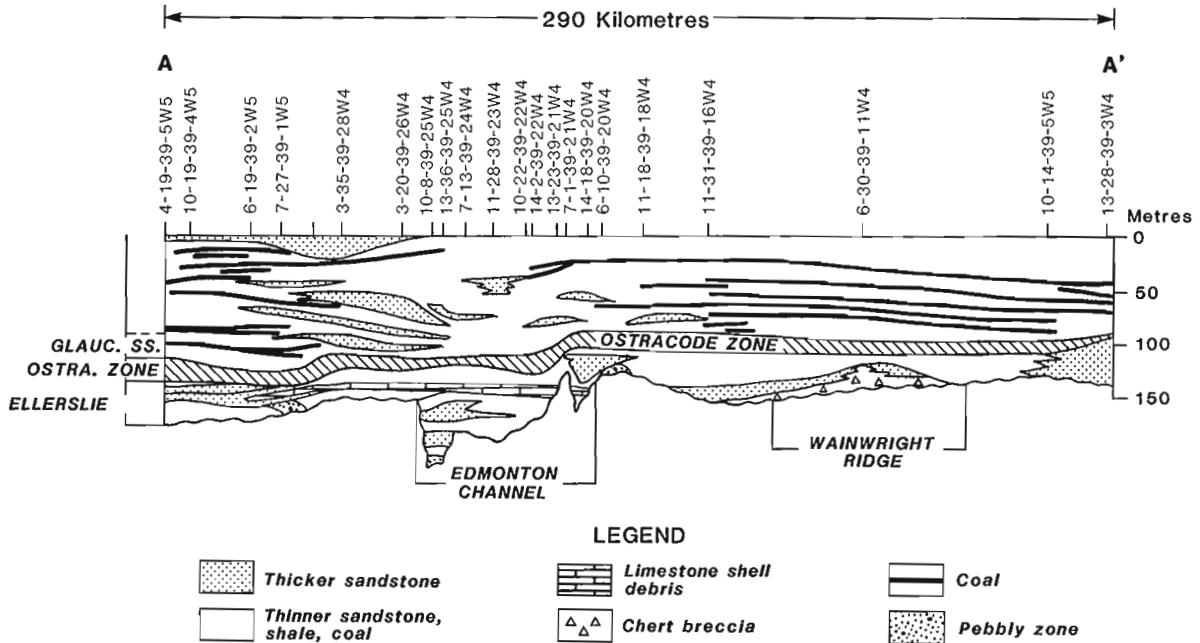


Figure 41.8. Stratigraphic cross-section along Tp. 39 (line AA' in Fig. 41.2) across the southern end of the Edmonton Channel. Note coarse gravelly sand at bottom and chert breccia on the flank of the Wainwright Ridge. The Ostracode Zone is continuous, flat, and blankets the channel topography. The undulations in this layer are controlled both by the bottom topography and compaction. The Upper Mannville shows constant thickness, and continuous coal seams.

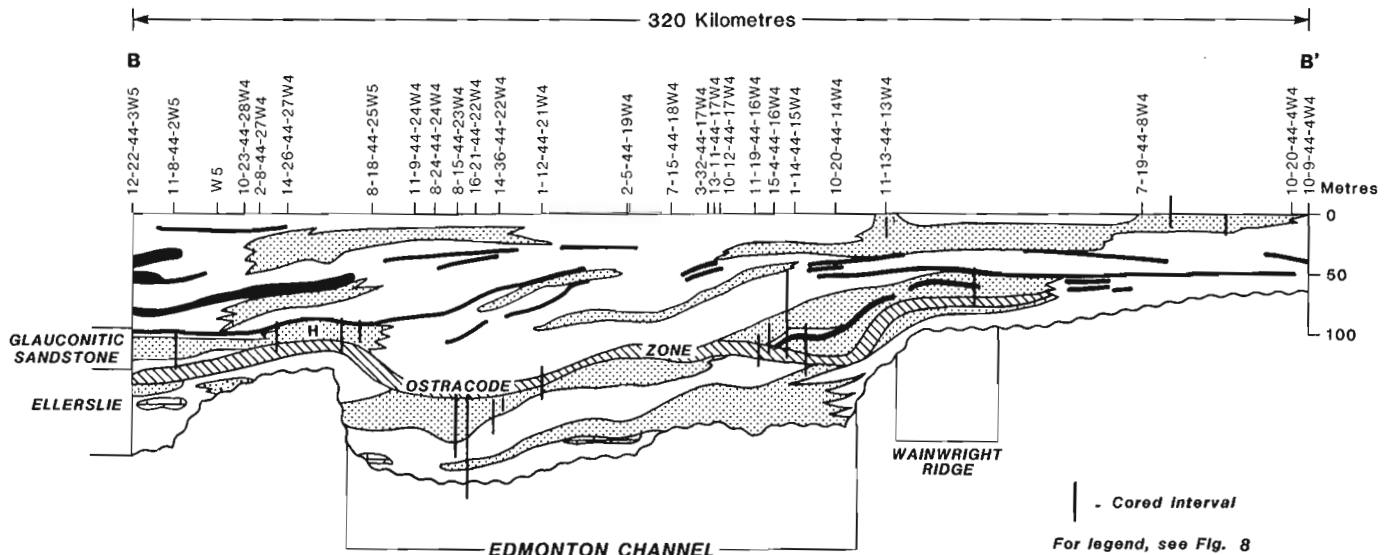


Figure 41.9. Cross-section across the Edmonton Channel along Tp. 44 (line BB' in Fig. 41.2). Note the greater width of the channel and the compactional downward bend of the Ostracode Zone. H, location of Hoadley barrier bar in the Glauc. Sandstone (Chiang, 1985).

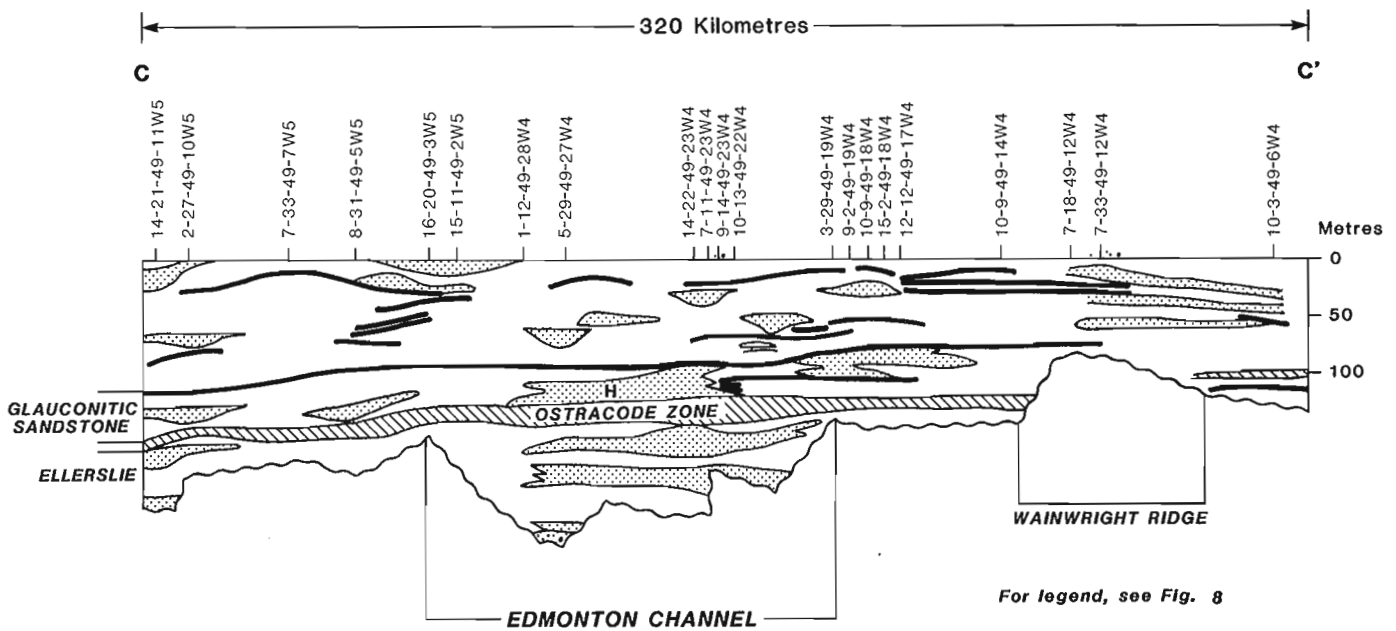


Figure 41.10. Cross-section of the Edmonton Channel along Tp. 49 (line CC' in Fig. 41.2). Note the flat configuration of the Ostracode Zone, covering the channel-fill and abutting against the Wainwright ridge.

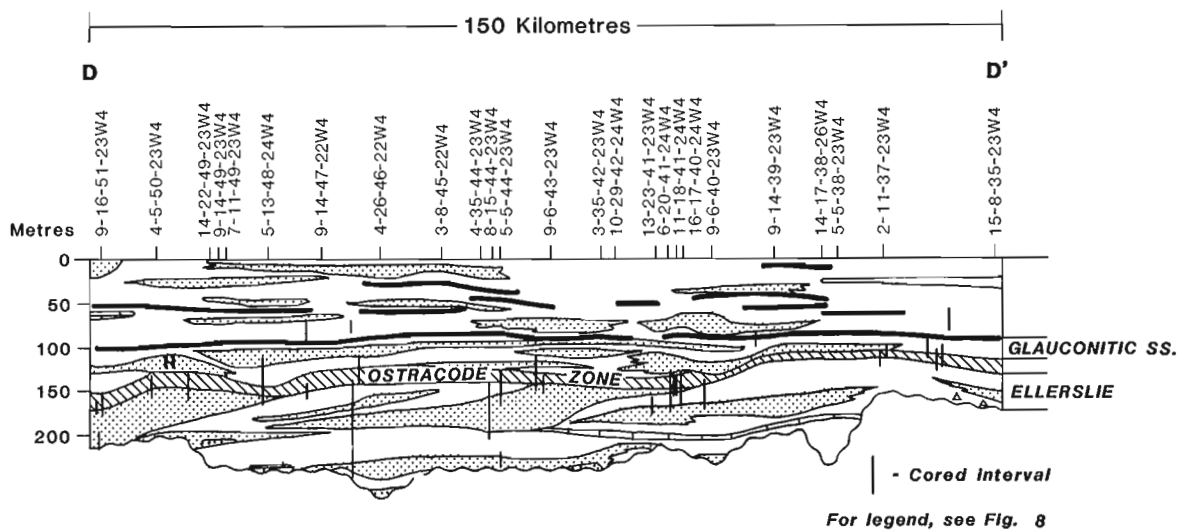


Figure 41.11. Longitudinal section along the Edmonton Channel (line DD' in Fig. 41.2) between Rge. 22 and 24W4 extending from Tp. 35 to 51. The Ostracode Zone is continuous along the channel, capping the sedimentary fill. The undulations seen in the layer follow the bottom topography and are probably caused by differential compaction. Note the lower limestone layer within the channel. Between the two limestone layers are thick, shingled sand bodies. Gravelly coarse sand occupies the deepest part of the channel. H, Hoadley barrier.

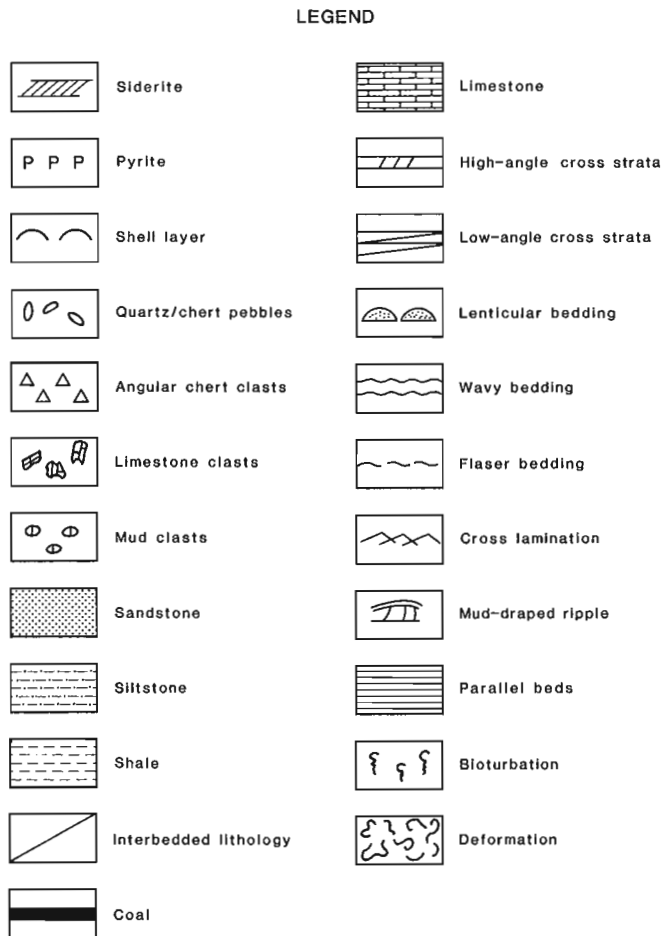


Figure 41.12. Legend for figures 41.13 and 41.16.

Planolites, Skolithos and Teichichnus are the common trace fossils. Two species of dinoflagellates have been found in these sediments at one well near the top of the Ellerslie (8-12-44-21W4; 4228 ft, 1289 m; GSC loc. C-108308).

In deltaic sequences, prodelta or shallow marine sediments underlie thick mouth bar sands, and interdistributary bay sediments overlie them. However, it is sometimes difficult to distinguish them. In the Ellerslie Formation, the bioturbated mudstones overlying and underlying the sandstones are indistinguishable. They are identical both in the way they were deposited and in their trace fossil assemblages (Fig. 41.15), which indicates a **Cruziana** ichnofacies extending from bays and lagoons to open shelves (Pemberton and Frey, 1983). To conclude, this facies has a dominantly shallow marine aspect, but may also, in some places, represent a thin veneer of bay sediments overlying the thick, crossbedded deltaic sandstone bodies.

Ostracode Zone

Hunt (1950) defined the Ostracode Zone in the area as a "calcareous fossiliferous black, brackish water shale approximately 45 feet thick". In this study, limits of the Ostracode Zone are taken at the first and last occurrence of limestone or marlstone beds in this shaly zone.

For recognition of facies within the Ostracode Zone, log signatures are not useful because thin, argillaceous, impure limestones vary widely in their log expressions.

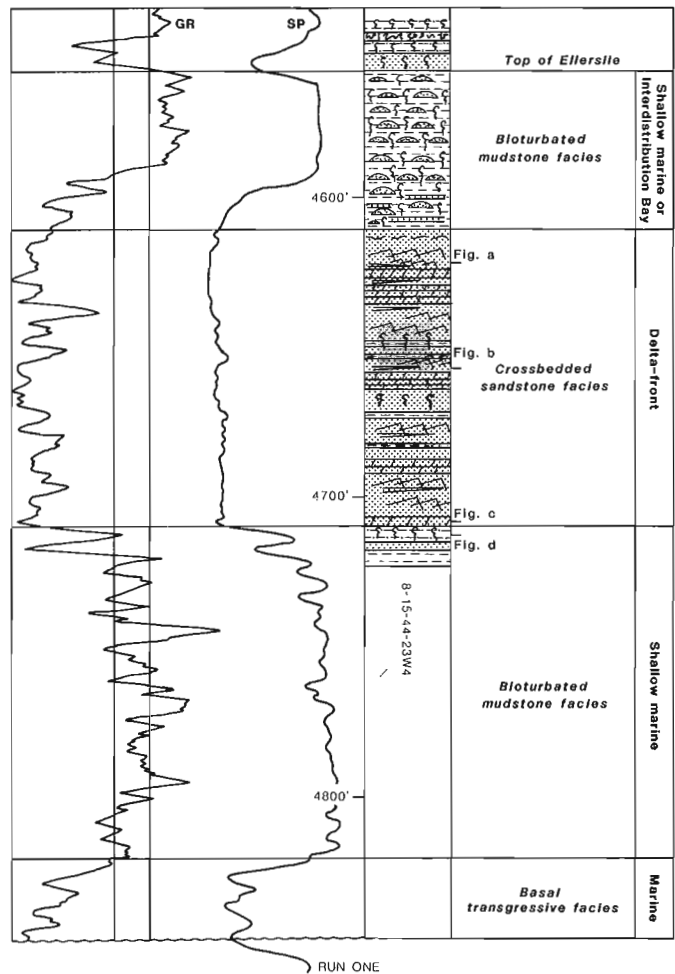


Figure 41.13. Gamma ray and SP logs and lithological succession in the core of the well at 8-15-44-23W4. This well shows typical log signature for all three facies of the Ellerslie, and the core penetrates through a thick interval (40 m) of the facies sequence. a, b, c, and d, locations of cores, photographs of which are shown in Figure 41.14. For legend see Figure 41.12.

A stratigraphic cross-section based on 33 available cores has been constructed to illustrate the facies relationships (Fig. 41.16). There is an onlapping relationship between the beds of the Ostracode Zone and the Lower Mannville sandstone of the Ellerslie Formation.

The topmost thin (0.5 - 1 m) limestone of the Ostracode Zone can be traced continuously within the area and its top has been interpreted as a hiatal surface (Banerjee, 1984). These surfaces, defined by Frazier (1974), record periods of no, or extremely slow, sedimentation during a marine transgression, when the centre of fluvial input shifts far landward. Lack of clastic input and long contact of the water column with the sediment interface leads to precipitation of carbonates (Galloway and Hobday, 1983). Within the Ostracode Zone, which records an extensive marine transgression in Alberta and British Columbia (Finger, 1983; Jackson, 1985; Smith et al., 1985), this recognizable hiatal surface marks the peak of the transgression.

The Ostracode Zone displays three facies:

1. Limestone facies
2. Bioturbated, dark mudstone facies.
3. Bioturbated, very fine grained sandstone facies (minor).

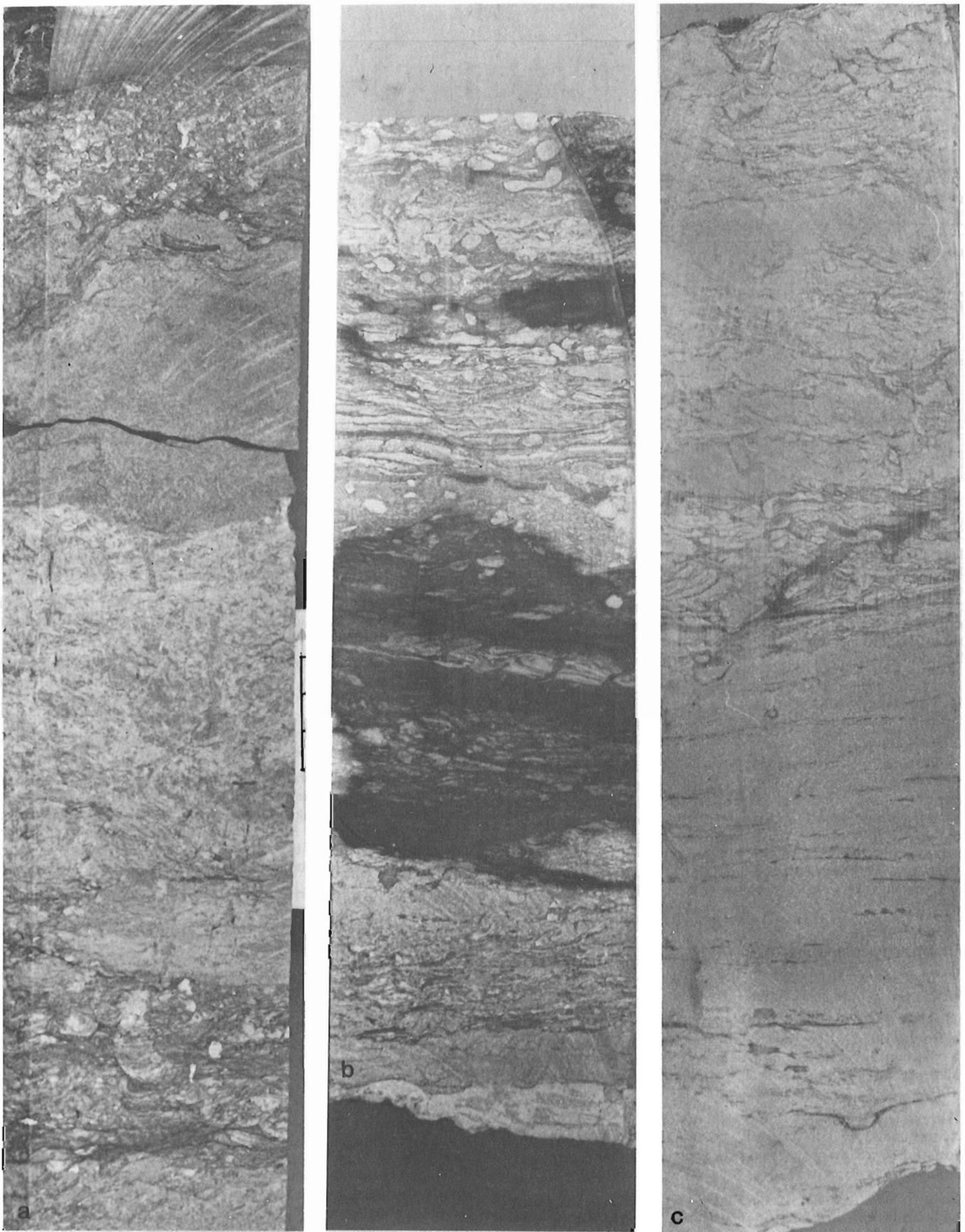
Limestone. This facies can be further subdivided into three subfacies. The first is a micritic, pyritic, partially recrystallized limestone, with varying amounts of shell debris (Fig. 41.17b) and rip-up clasts of laminated lime-mud. It may

be laminated, bioturbated or structureless, and occurs in beds 20-50 cm thick. The second type comprises 2-3 cm thick, graded beds of comminuted shell debris occurring within black shale. Ostracode, pelecypod and gastropod shells account for most of the debris. (Fig. 41.17d). The third subfacies is a limestone breccia, found in the southern end of the channel (Fig. 41.17a). In this rock, angular clasts of micritic limestone that have a maximum length of 8 cm, are set in a matrix of quartz sand and clay, cemented by carbonate. This indicates a very shallow water origin.



- a. Wave ripple laminae with mud drapes (bottom) indicating waning storm or slackening tidal currents.
- b. Low-angle cross-strata showing alternate fine/coarse laminae and crenulated (bioturbation?) mud drapes.
- c. High-angle tabular cross-strata in medium to coarse grained sand.
- d. Bottom of the sequence with bioturbated mudstone and black shale.
- e. (Top) Sandstone with ripple laminae and bioturbated and contorted mudstone. (Bottom) Sandstone with very thin mud laminae with bioturbation. (10-31-49-23W4; 4136 ft, 1260 m).
- f. Mud laminae in fine grained sandstone. (14-36-44-22W4; 4250 ft, 1295 m).
- g. Mud lined low-angle bedding in bioturbated very fine grained sandstone. Subvertical burrow (*Skolithos*). (14-36-44-22W4; 4255 ft, 1297 m). Scale in cm.

Figure 41.14. Photographs of cores of the thick- crossbedded sandstone facies in the Ellerslie Formation. Locations of a, b, c, and d are shown in Figure 41.13.



- a. Bioturbated very fine grained sandstone/mudstone interbeds. Subvertical burrows (*Skolithos*). Large burrow near the bottom is *Teichichnus*. 5142 ft (1567 m).
- b. Same lithology as in a. Trace fossils: *Asterosoma*(?) *Chondrites*, *Planolites* and *Teichichnus*. 5171 ft (1576 m).
- c. Bioturbated and parallel laminated, very fine grained sandstone. Conical burrow at the top is *Conichnus* and those with circular cross-sections in the middle are *Paleophycus*. 5181 ft (1579 m). Scale in cm.

Figure 41.15. Photographs of cores of the bioturbated mudstone facies. All photographs are from the well at 6-26-41-24W4.

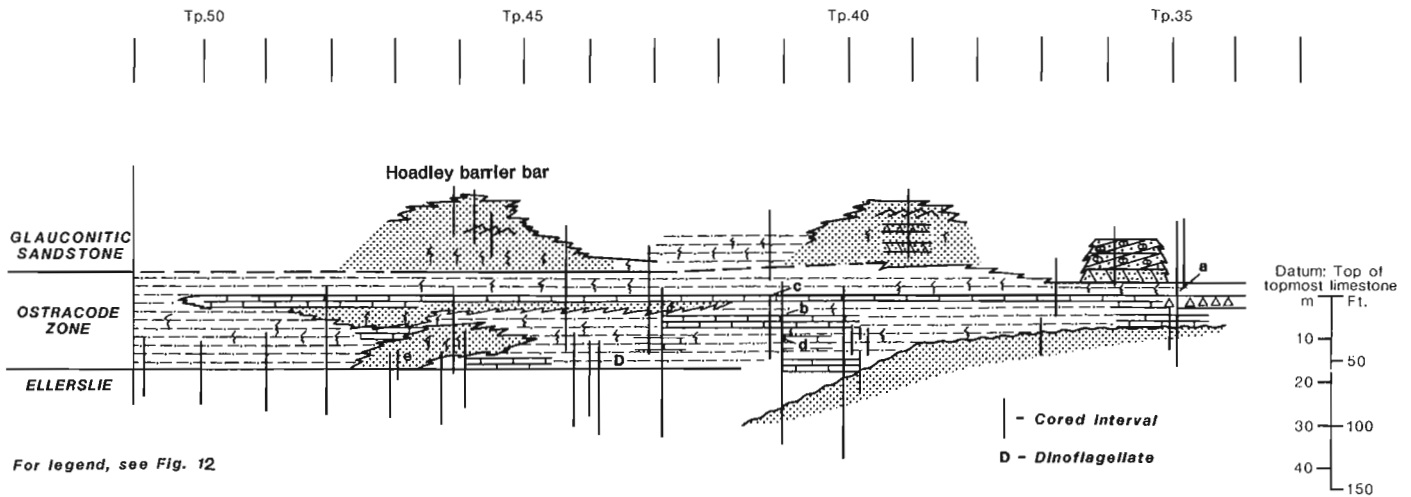


Figure 41.16. Stratigraphic cross-section of the Ostracode Zone based on core data. Core locations shown. Datum is the top of the topmost limestone bed. Note the onlapping relationship of the limestones. a, b, c, d, and e - locations of cores, photographs of which are shown in Figure 41.17.

Bioturbated mudstone. Most of the Ostracode Zone consists of a dark grey or black mudstone, showing lenticular bedding, contorted laminae, and intense bioturbation (Fig. 41.17c). It contains abundant interbeds of bioturbated, very fine grained sandstone. Common trace fossils are: **Chondrites**, **Paleophycus**, **Planolites**, and **Teichichnus**. Slow shallow marine sedimentation with a low input of clastic is indicated.

In one sample from this facies (5-6-41-6W; 2469.8 and 2465.0 m; GSC loc. C-108306), five species of dinoflagellates have been identified (see Fig. 41.16).

Bioturbated sandstone. In this sandstone, beds of hummocky(?) cross-stratified, clean sandstone, 5-10 cm thick, with sharp, in places loaded, bases and normally graded clay-rich tops, typically alternate with intensely bioturbated mudstone (Fig. 41.17e). The whole scenario resembles the episodic sedimentation in the hummocky cross-strata model of Dott and Bourgeois, (1982), but on a smaller scale. The facies in all probability represents shallow shelf storm sedimentation below fairweather wave base.

Summary and conclusions

Significant features of the paleotopographic feature known as the Edmonton Channel are summarized below:

1. Due to their considerable vertical exaggeration, cross-sections illustrating this paleotopographic depression give a distorted picture. In reality, the depression is very shallow and wide, with a width/depth ratio exceeding 1000.
2. Although very shallow, the depression has probably been accentuated by differential subsidence because it was located in a slowly subsiding tectonic zone (Jackson, 1985; Fig. 9a).
3. Isopach and net sandstone maps of the Lower Mannville sediments infilling this depression do not show a well defined linear pattern, but a series of disjointed lobes (Figs. 41.5, 41.6).

4. Cores recovered from drilling through the floor of the depression reveal sediments with a marine aspect (bioturbated mudstone and associated thin sandstone).
5. The longitudinal section along the channel shows a series of thick, shingled sandstones encased in bioturbated mudstones (Fig. 41.11).
6. Cores of these sandstones (Fig. 41.13) show that they are not fluvial. They contain "coarsening-upward" sequences, which grade from intensely bioturbated mudstones at the base to clean, crossbedded sandstones with burrows at the top. Limestone, shell debris and rare dinoflagellates also occur in these infilling sediments.

Both the morphology of the topographic depression and the marginal marine nature of the infilling sediments, as discussed above, suggest an embayment-fill model for the Edmonton Channel. Based on a study of Holocene sediments in southeastern Australia, Roy et al. (1980) proposed three primary types of embayment-fill:

1. Open ocean embayment
2. Barrier estuary
3. Drowned river valley.

Sediments infilling these embayments differ in their basic stratigraphy (Fig. 41.18). At first sight, the Edmonton Channel seems to fit the "drowned river valley" model. But the stratigraphy does not fit that of the model. No fluvial sediments on the valley floor of the Edmonton Channel were observed in the cores examined (see point 4, above).

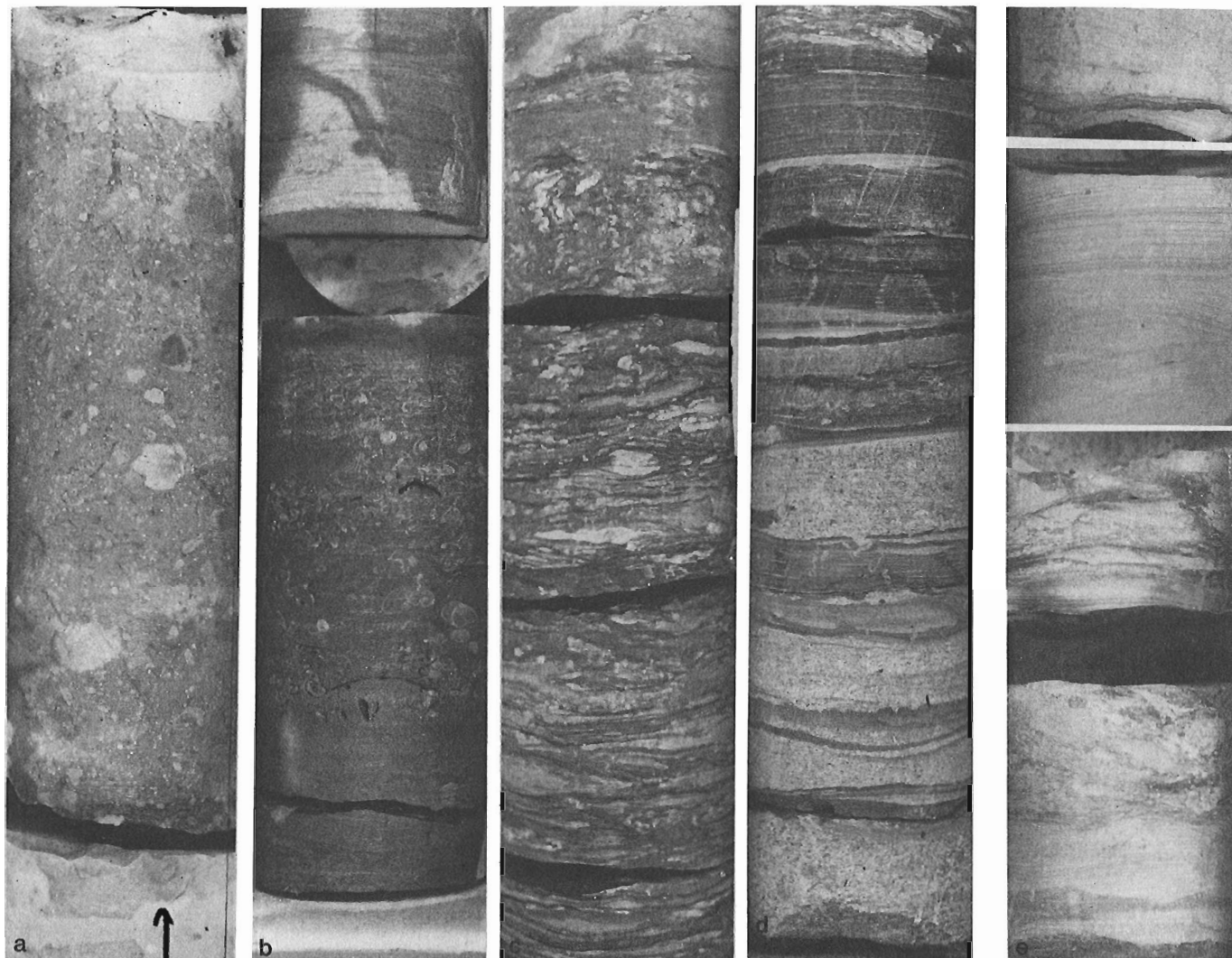
Although Hunt (1950) thought that the lower part of the Ellerslie Formation in the White Mud area was nonmarine, his designation of the facies as a "fluvial-lagoonal-littoral type" suggests that a marginal marine interpretation is also possible. Thick estuarine mud, as shown in the "barrier-estuary" and the "drowned river valley" models, is absent from the Edmonton Channel. The thick sandstone bodies do not have beach or dune structures or other evidence of a barrier origin. A semienclosed, open ocean embayment model, therefore seems to be the best choice. Sands of tidal

deltas were the major infilling sediments during a period of transgression. A complex history of migration and infilling of a V-shaped embayment was responsible for the complex stratigraphy of the Edmonton Channel.

Acknowledgments

An earlier version of the paper was critically read by A.F. Embry and A.P. Hamblin and the present version by D.A. Leckie, all of whom offered many useful suggestions.

D.J. McIntyre identified the dinoflagellates. K.N. Nairn produced the computer-generated subsurface maps with great care. W.B. Sharman patiently processed hundreds of core photographs. The author is greatly indebted to M.J. Ranger of Gulf Canada Ltd. who very kindly allowed the author to use copies of his unpublished isopach and structure contour maps.



- a. Limestone breccia. The lower, light coloured layer is the micrite limestone, possibly the parent rock of the clasts (10-12-35-22W4; 4898 ft, 1493 m).
- b. Shells of ostracodes, pelecypods and gastropods in a dark lime mudstone. (11-5-41-23W4; 4816 ft, 1468 m).
- c. Contorted and bioturbated mudstone (11-8-41-24W4; 5053 ft, 1540 m).
- d. Graded shell debris layers. Note the syneresis cracks and loading at the base of the layers (11-5-41-23W4; 4828 ft, 1471 m).
- e. Bioturbated sandstone shows storm layers. Small-scale hummocky cross-strata in very fine grained sandstone separated by bioturbated mudstone (11-36-47-24W4; 4420 ft, 1347 m). Width of cores 10 cm.

Figure 41.17. Core photographs of different facies of the Ostracode Zone. Location of photographs are shown in Figure 41.16.

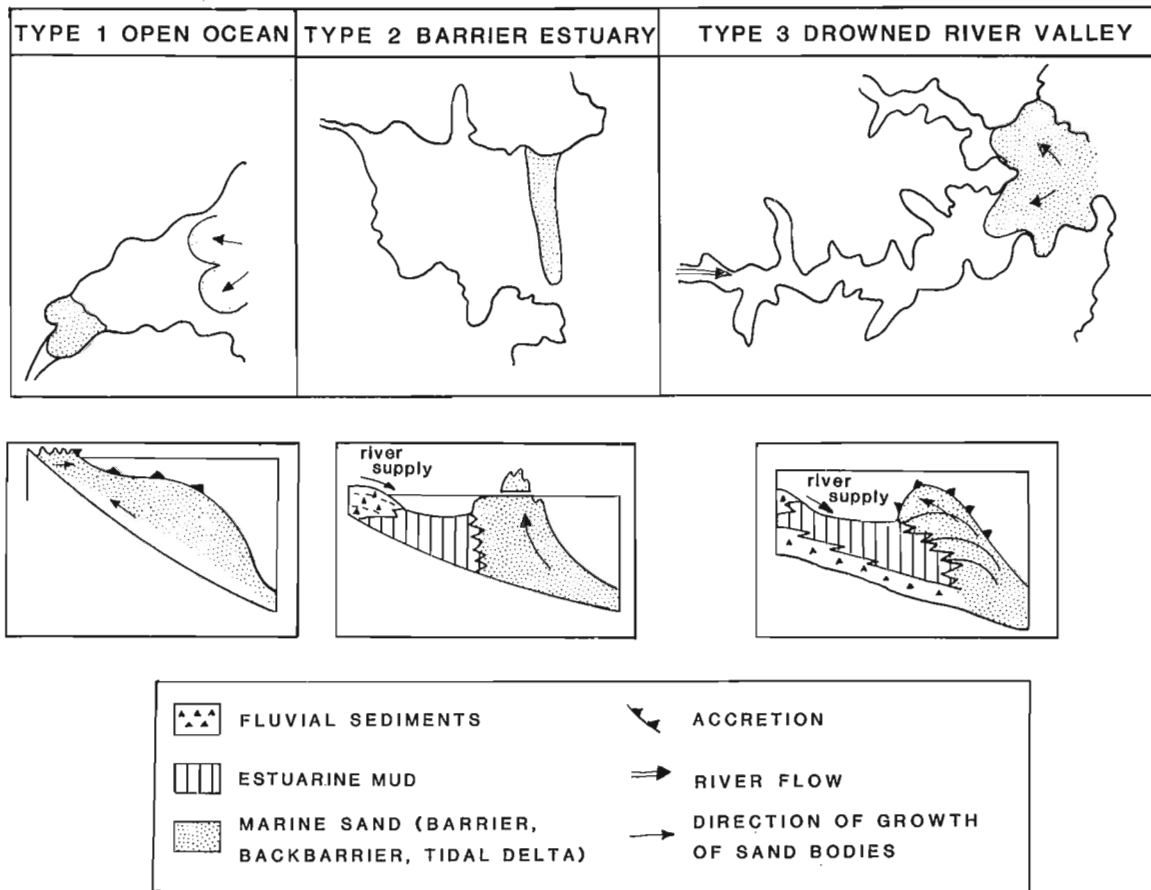


Figure 41.18. Three types of embayment-fill model (Modified from Roy, Thom, and Wright, 1980).

References

Banerjee, I.
 1984: Depositional episode during Mannville sedimentation in southern Alberta; northwest Montana and adjacent Canada, field guidebook and volume of abstracts; Montana Geological Society, 1984, Field Conference and Symposium, Kalispell, p. 8.

Beltz, E.W.
 1953: Topography and geology of eastern Alberta and western Saskatchewan during Early Cretaceous time; Alberta Society of Petroleum Geologists, News Bulletin, v. 1, nos. 1-4, p. 1-3.

Bokman, J.
 1963: Post-Mississippian unconformity in western Canada basin; in *Backbone of the Americas*, ed. O.E. Childs and B.N. Beebe; American Association of Petroleum Geologists, Memoir 2, p. 252-263.

Chiang, K.K.
 1985: The Giant Hoadley Gas Field, south-central Alberta; in *Elmworth-case study of a Deep Basin Gas Field*, ed. J.A. Masters; American Association of Petroleum Geologists, Memoir 38, p. 297-313.

Dott, R.H. (Jr.) and Bourgeois, J.
 1982: Hummocky stratification: significance of its variable bedding sequence; *American Association of Petroleum Geologists Bulletin*, v. 66, p. 138-157.

Finger, K.L.
 1983: Observations on the Lower Cretaceous Ostracode Zone of Alberta; *Bulletin of the Canadian Society of Petroleum Geology*, v. 31, p. 326-337.

Frazier, D.E.
 1974: Depositional episodes: their relationship to the Quaternary stratigraphic framework in the northwestern portion of the Gulf Basin; *Bureau of Economic Geology, University of Texas, Austin, Geological Circular* 71-1.

Galloway, W.E. and Hobday, D.K.
 1983: *Terrigenous Clastic Depositional Systems*; Springer-Verlag, New York, 423 p.

Glaister, R.P.
 1959: Lower Cretaceous of southern Alberta and adjoining areas; *American Association of Petroleum Geologists Bulletin*, v. 43, p. 590-640.

Hunt, C.W.
 1950: Preliminary report on Whitemud oil field, Alberta, Canada; *American Association of Petroleum Geologists, Bulletin*, v. 34, p. 1795-1801.

- Jackson, P.C.
1985: Paleogeography of the Lower Cretaceous Mannville Group of Western Canada; in Elmworth-case study of a Deep Basin gas field, ed. J.A. Masters; American Association of Petroleum Geologists, Memoir 38, p. 49-77.
- Martin, R.
1966: Paleogeomorphology and its application to exploration for oil and gas (with examples from western Canada); American Association of Petroleum Geologists, Bulletin, v. 50, p. 2277-2311.
- Martin, R. and Jamin, F.G.S.
1963: Paleogeomorphology of the buried Devonian landscape in northeastern Alberta; in K.A. Clarke volume, a collection of papers on Athabasca oil sands. Research Council of Alberta, Information Series, v. 45, p. 31-42.
- McLean, J.R.
1982: Early Cretaceous Edmonton Channel in Alberta; in Book of Abstracts; American Association of Petroleum Geologists, Annual Convention, Calgary, 1982, p. 86.
- Pemberton, S.G. and Frey, R.W.
1983: Biogenic structures in Upper Cretaceous outcrops and cores; in The Mesozoic of Middle North America, Field Trip Guidebook no. 8, 161 p.
- Porter, J.W., Price, R.A., and McCrossan, R.G.
1982: The western Canada Sedimentary Basin; Royal Society of London, Philosophical Transactions, v. A305, p. 169-192.
- Ranger, M.
1983: The paleotopography of the Pre-Cretaceous erosional surface in the western Canada Basin; in The Mesozoic of Middle North America, Program and Abstracts, Calgary, Alberta, p. 118.
- Robinson, J.E., Charlesworth, H.A.K., and Ellis, M.J.
1969: Structural analysis using spatial filtering in interior plains of south-central Alberta; American Association of Petroleum Geologists Bulletin, v. 53, p. 2341-2367.
- Roy, P.S., Thom, B.G., and Wright, L.D.
1980: Holocene sequences on an embayed high energy coast: an evolutionary model; Sedimentary Geology, v. 26, p. 1-19.
- Rudkin, R.A.
1964: Lower Cretaceous; in Geological history of Western Canada, ed. R.G. McCrossan and R.P. Glaister; Alberta Society of Petroleum Geologists, Calgary, p. 156-168.
- Smith, D.G., Zorn C.E., and Sneider, R.M.
1985: The paleogeography of the Lower Cretaceous of western Alberta and northeastern British Columbia; in and adjacent to the Deep Basin of the Elmorth area; in Elmworth-case study of a Deep Basin Gas Field, ed. J.A. Masters; Association of Petroleum Geologists, Memoir 38, p. 79-114.
- Sonneveld, E.M. and Murray, J.W.
1982: Influence of the Pre-Cretaceous unconformity on deposition of Lower Mannville clastic sequence, Drumheller, Alberta; in Book of Abstracts; American Association of Petroleum Geologists, Annual Convention, Calgary, 1982, p. 115.
- Williams, G.D.
1963: The Mannville Group (Lower Cretaceous) of central Alberta; Bulletin of Canadian Petroleum Geology, v. 11, p. 350-368.

Bullaluta kindlei n. gen., n. sp. (Ostracoda, Archaeocopida)
from Zone 5 (Late Cambrian, *Cedaria* – *Crepicephalus*)
of the Cow Head Group, western Newfoundland

Project 720072

M.J. Copeland
Institute of Sedimentary and Petroleum Geology, Ottawa

Copeland, M.J., *Bullaluta kindlei* n. gen., n. sp. (Ostracoda, Archaeocopida) from Zone 5 (Late Cambrian, *Cedaria* - *Crepicephalus*) of the Cow Head Group, western Newfoundland; in *Current Research, Part B, Geological Survey of Canada, Paper 86-1B*, p. 399-403, 1986.

Abstract

The ostracode Order Archaeocopida has long been considered ancestral to the Order Leperditicopida because of their general morphological similarities. The presence of the archaeocope *Bullaluta* n. gen. in Upper Cambrian rocks of western Newfoundland strengthens this concept.

Résumé

L'ordre Archaeocopida d'ostracodes a depuis longtemps été considéré comme l'ancêtre de l'ordre Leperditicopida, étant donné leurs similarités morphologiques générales. La présence de l'archaeocope *Bullaluta* n. gen., dans les roches du Cambrien supérieur de l'ouest de Terre-Neuve vient appuyer cette hypothèse.

Introduction

The Cecil H. Kindle collection of Cambro-Ordovician fossils from western Newfoundland consists predominantly of trilobites, but other arthropods are present. This important collection, purchased with the assistance of a grant under the Cultural Property Export and Import Act, is housed in Ottawa, at the Geological Survey of Canada, and is currently being examined by several paleontologists. While studying some of the Cambrian trilobites, Dr. R. Ludvigsen, University of Toronto, discovered the three non-trilobite arthropod specimens reported here and referred them to me for examination. They are morphologically important because biostratigraphically they may represent a stage of ostracode development that includes both archaeocopid and leperditicopid characteristics.

Systematic position

Much has been written about the Cambrian ostracode-like forms that have been referred to variously as Ostracoda, Phyllopoda, Conchostraca, etc. These, and several other uni- or bivalved orders of Crustacea were included in the Order Bradorina erected by Raymond (1935). He proposed this order of the Subclass Archaeostraca, believing it to be ancestral to the Ostracoda, and placed the Ostracoda in a separate subclass. Sylvester-Bradley (1961) erected the Order Archaeocopida of the Class Ostracoda Latreille, 1804 arguing that the morphology of these forms suggested their relationship to the Leperditicopida, and that one genus, *Cambria* Netskaya and Ivanova, might be related to the Beyrichiacea. It is still not certain whether the Leperditicopida should be contained within the Class Ostracoda and little has been forthcoming about the possible ancestry of the Palaeocopida. The ostracode affinity of the Archaeocopida and/or Leperditicopida has been generally accepted (Müller, 1981; Ulrich and Bassler, 1931; Öpik, 1961, 1963; Copeland, 1976; Berdan, 1984, etc.) and it is expected that these orders will be retained within the Class Ostracoda in a future revision of the Treatise.

As stated, the Archaeocopida are generally of Cambrian age but species of one genus, *Ludvigsenites* Copeland, 1974, have been recovered from Middle Ordovician and Middle Silurian (Copeland, 1978) strata of the Northwest Territories of Canada. If this genus represents a true archaeocopid (and at present there is no reason to think otherwise) and if a branch of the Archaeocopida gave rise to the Leperditicopida sometime in the Late Cambrian, it may

be that true archaeocopid ostracodes could have become adapted to a continental slope and/or deeper water habitat about that time, whereas the leperditicopes occupied the shallow to inter-tidal habitats ascribed to them by Berdan (1969, 1984), Copeland (1976) and others. To speculate further, could a branch of the Archaeocopida have given rise to the Myodocopina at about the same time? So little is known of deep water faunas of this age that we may only theorize.

The three specimens discussed here appear to be transitional between representatives of the archaeocopid family Beyrichonidae and the leperditicopid family Isochilinidae, particularly if the genus *Eremos* Moberg and Segerberg, 1906 (represented by *E. bryograptorum* Moberg and Segerberg, 1906) of the Beyrichonidae is compared with the isochilinid genus *Kenodontoichilina* Berdan, 1984 (as represented by its most conservative species *K. nelsoni* (Bassler), 1932 = *Ivia nelsoni* (Bassler) of Schallreuter, 1984). Species of these genera have a broad, complete marginal brim and a distinct, large eye tubercle or adductor node elevated on the valve surface as a boss (bulla).

It was thought that the purported difference in chemical composition and structure of the valves of Archaeocopida (uniform phosphato-chitinous) and Leperditicopida (calcareous; inner dark layer and outer prismatic layer) might serve as criteria on which to base differentiation between specimens of these two orders. Accordingly, the shell of one of the Late Cambrian specimens of *Bullaluta* n. gen (holotype, GSC 80998) and that of a Middle Ordovician leperditiid specimen (*Eoleperditia* sp., unfigured specimen, GSC 80995) from Long Point, western Newfoundland, were analyzed using an electron probe. Both specimens proved to have shells with very high calcium carbonate peaks to the exclusion of other peaks; no evidence of phosphate or a "shadow" that could be interpreted as an organic background was observed on either specimen. Apart from the fact that the Cambrian specimen was obtained from an allochthonous boulder in the Cow Head Group and the Ordovician specimen from bedded strata of the Long Point Group, no difference in the diagenetic history is apparent. Because the shell of the Cambrian specimen is so thin it cannot be ascertained if the Cow Head specimens have uniform or laminated wall structure.

In consultation with Dr. J.M. Berdan (USGS) several characteristics of the three Cambrian specimens were compared with their closest counterparts in the Archaeocopida and Leperditicopida:

	Cow Head specimens	Archaeocopida Beyrichonidae in general	Leperditicopida Isochilinidae in general
Free margin outline	triangular-ovate	triangular-ovate	ovate
Greatest width	posterior	posterior	median
Brim	uniform width	marginal ridge	narrowing ventrally
Shell thickness	thin	thin	thick
Shell texture	randomly pustulose	smooth to wrinkled	usually smooth
Boss	anterodorsal	nodes, ridges	near midvalve
Eye tubercle	none	anterodorsal	distinct
Stop pit(s)	none	none	present/absent
Sulcation	none	usually present	usually present

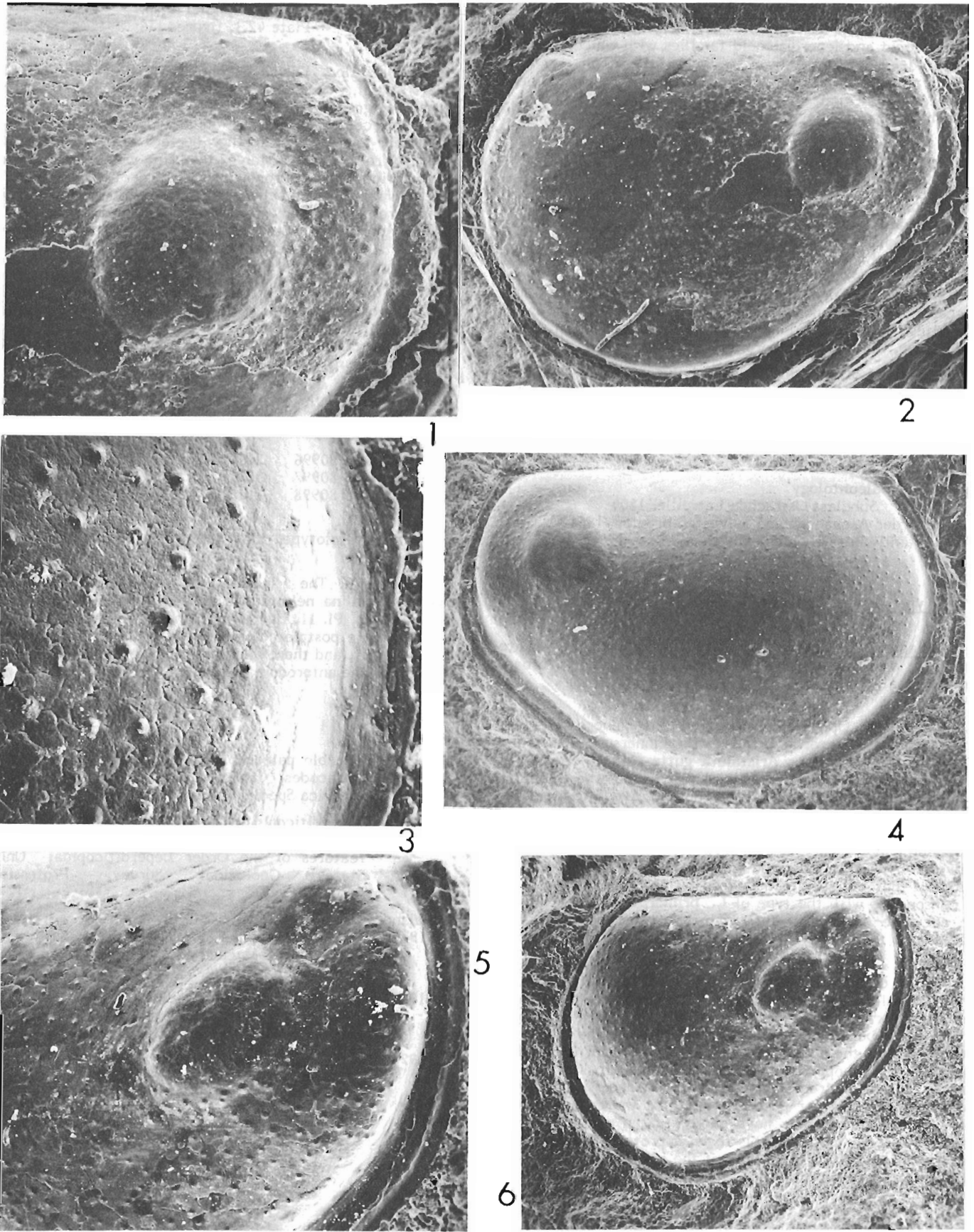


PLATE 42.1

Figures 1-6. **Bullaluta kindlei** n. sp.

- 1, 2. Right valve; x 100 and x 50, paratype, GSC 80996.
 3, 4. Left valve; x 270 and x 45, holotype, GSC 80998.
 5, 6. Right valve; x 80 and x 40, paratype, GSC 80997.

From the above it would appear that significant differences exist between the Cow Head specimens and each of the archaeocopid and leperditicopid families with which they are compared. In general, however, the greater similarity (and the stratigraphic position) of the Cow Head specimens indicates their inclusion in the Order Archaeocopida, and possibly the Family Beyrichonidae.

Stratigraphic position of the specimens

The three specimens were obtained from an allochthonous boulder (no. 28) occurring in *Cedaria* - *Crepicephalus* Zone 5 conglomerate, outcropping along the northeast shore of Cow Head Peninsula, west coast of Newfoundland at an approximate latitude of 49° 55' 30" N, longitude 57° 48' W. The exact position of the boulder (no. 28) within Zone 5 is unknown. Occurring with the archaeocopid specimens in boulder 28 are the following trilobites (identifications by Drs. R. Ludvigsen and S. Westrop, University of Toronto):

"Boulder 28 contains *Deiracephalus* cf. *aster* (Walcott) and *Cedaria* sp. It belongs to our *Deiracephalus* - *Meteoraspis* Fauna (late Marjuman) and to Kindle's (1981) Zone 5." (Written communication, March 10, 1986). A map and photograph of the general area are found in Kindle (1982).

Systematic paleontology

Subclass Ostracoda Latreille, 1804

Order Archaeocopida Sylvester-Bradley, 1961

Family Beyrichonidae Ulrich and Bassler, 1931

Genus *Bullaluta* n. gen.

Type species. *Bullaluta kindlei* n.sp.

Diagnosis. Archaeocopid ostracodes of triangular-ovate outline, with complete marginal brim and broad, anterodorsal, ovate node.

Remarks. Öpik (1961) erected the genera *Svealuta* (type species *Leperditia primordialis* Linnarson, 1863) and *Aristaluta* (type species *Aristaluta gutta* Öpik). Species of both genera have some superficial resemblance to *Bullaluta kindlei* n. sp. However, Öpik's diagnosis of *Svealuta* indicates that its type species bears a dorsal border and two anterodorsal nodes, and those of *Aristaluta* bear two pairs of sulci and a posterodorsal gap between the brims of the two valves. As Öpik indicated in his plate description, it is doubtful that the specimen figured by him (Pl. 24, fig. 1a-e) is conspecific with the type of *L. primordialis* Linnarson, so an accurate definition of *Svealuta* remains unknown until Linnarson's type material is redescribed or topotypic material is found.

It is difficult to assess the role of the large, ovate, anterodorsal node either as an eye tubercle or the position of muscle attachment. It is not possible that both functions would have been combined. If the node is the place of attachment of the adductor it is somewhat too far forward to give sufficient support to the hinge to keep the posterior part of the carapace from being forcibly opened. Of course, because of the greater posterior width of the carapace, the body of the animal may have been situated posteriorly and the furcal rami (assuming this to be a proto ostracode) may have been exsert. The flatness of the posterior valve brims, however, does not support this speculation.

Bullaluta kindlei n. sp.

Plate 42.1, figures 1-6

Description. Valves triangular-ovate in outline; hinge long, straight; cardinal angles abrupt, more than 90°. Postplete; greatest height in posterior half. Free margin with wide, continuous brim of equal width throughout, with a slight near-marginal thickening. Surface of domicilium rising abruptly from proximal side of the brim; greatest valve width in posterior third. Pronounced circular to ovate node in anterodorsal third of valve; surface of node regular except for several very shallow furrows on its posterior side giving that margin of the node a slightly fluted appearance. Margin of node slightly depressed on valve surface. Surface of domicilium with discrete pustules.

No ocular tubercle, although one specimen (Pl. 42.1, fig. 5) appears to have a shallow, rounded, sulcus-like groove extending from the anterodorsal margin of the node toward the anterior cardinal margin. This is not present on the other two specimens.

Measurements of figured specimens (in mm):

	L	H	
Paratype, GSC 80996	1.8	1.4	a partial carapace
Paratype, GSC 80997	1.7	1.1	a right valve
Holotype, GSC 80998	2.0	1.4	a left valve

Types. Holotype, GSC 80998, paratypes, GSC 80996, 80997.

Remarks. The species is somewhat similar to *Kenodontochilina nelsoni* (Ulrich and Bassler) as figured by Berdan (1984, Pl. 11, fig. 12) in being randomly pustulose, but is much more postplete in outline, the shell of the valve is much thinner, and there is no indication of an ocular tubercle anterior of the anterodorsal node.

References

- Berdan, J.M.
 1969: Possible paleoecologic significance of leperditiid ostracodes, (abstract); Geological Society of America Special Paper 121, p. 337.
 1984: Leperditicopid ostracodes from Ordovician rocks of Kentucky and nearby states and characteristic features of the Order Leperditicopida; United States Geological Survey, Professional Paper 1066-J.
 Copeland, M.J.
 1974: Middle Ordovician Ostracoda from southwestern District of Mackenzie; Geological Survey of Canada, Bulletin 244.
 1976: Leperditicopid ostracodes as biostratigraphic indices; in Current Research, Part B, Geological Survey of Canada, Paper 76-1B, p. 83-88.
 1978: Some Wenlockian (Silurian) Ostracoda from southwestern District of Mackenzie; in Current Research, Part B, Geological Survey of Canada, Paper 78-1B, p. 65-71.

- Kindle, C.H.
 1981: Cambrian faunas in the limestone conglomerates of western Newfoundland; in Short papers for the Second International Symposium on the Cambrian System, United States Department of the Interior, Geological Survey, Open File Report 81-743, p. 106-110.
 1982: The C.H. Kindle collection: Middle Cambrian to Lower Ordovician trilobites from the Cow Head Group, Western Newfoundland; in Current Research, Part C, Geological Survey of Canada, Paper 82-1C, p. 1-17.
- Müller, K.
 1981: Arthropods with phosphatized soft parts from the Upper Cambrian "Orsten" of Sweden; in Short papers for the Second International Symposium on the Cambrian System, United States Department of the Interior, Geological Survey, Open File Report 81-743, no. 44, p. 147-151.
- Öpik, A.A.
 1961: The geology and palaeontology of the headwaters of the Burke River, Queensland; Commonwealth of Australia, Department of National Development, Bulletin No. 53.
- Öpik, A.A. (cont.)
 1963: Early Upper Cambrian fossils from Queensland; Commonwealth of Australia, Department of National Development, Bulletin No. 64.
- Raymond, P.E.
 1935: **Leancoilia** and other Mid-Cambrian Arthropoda; Harvard University, Museum of Comparative Zoology, Bulletin, v. 76, no. 6, p. 205-230.
- Schallreuter, R.
 1984: Neufunde der gehörnten Leperditiocopen-Gattung **Kiaeria** (Ostracoda) in silurischen Geschieben Westfalens sowie ihre systematische und phylogenetische Stellung; Palaontologische Zeitschrift, v. 58, nos. 1/2, p. 131-142.
- Sylvester-Bradley, P.C.
 1961: Archaeocopida; in Treatise on Invertebrate Paleontology, Part Q, Arthropoda 3, Geological Society of America and University of Kansas Press, p. Q100-Q105.
- Ulrich, E.O. and Bassler, R.S.
 1931: Cambrian bivalved Crustacea of the Order Conchostraca; Proceedings of the United States National Museum, v. 78, no. 4, p. 1-130.

The Eureka Sound Group of eastern Axel Heiberg Island: new data on the Eureka Orogeny

Projects 850043 and 820035

B.D. Ricketts and D.J. McIntyre
Institute of Sedimentary and Petroleum Geology, Calgary

Ricketts, B.D. and McIntyre, D.J., The Eureka Sound Group of eastern Axel Heiberg Island: new data on the Eureka Orogeny; in *Current Research, Part B, Geological Survey of Canada, Paper 86-1B*, p. 405-410, 1986.

Abstract

The stratigraphy of Tertiary conglomerate, sandstone, mudstone and lignite beds, which outcrop over a wide area of eastern Axel Heiberg Island, is reassessed. The deposits are considered to be synorogenic on the basis of structure (overthrust by older Sverdrup Basin units in the Stolz Thrust zone), lithology and palynology. The deposits are correlated with thick synorogenic conglomerates at Mokka Fiord, and are included in the Buchanan Lake Formation of the Eureka Sound Group. The timing of synorogenic sedimentation can now be interpreted as Middle Eocene, on the basis of well preserved palynofloras. The deposits accumulated in the Axel Heiberg foredeep, which was one of a series of orogenic foredeeps that developed along eastern Axel Heiberg Island and eastern Ellesmere Island.

Résumé

L'étude présente une réévaluation de la stratigraphie des couches tertiaires de conglomérat, de grès, de pélite et de lignite qui affleurent sur une grande région de l'est de l'île Axel Heiberg. La lithologie, la palynologie et la structure des dépôts, qui ont été chevauchés par les unités plus anciennes du bassin de Sverdrup dans la zone de charriage de Stolz, indiquent qu'ils seraient de nature synorogénique. Les dépôts ont été mis en corrélation avec d'épaisses couches de conglomérats synorogéniques au fjord Mokka, et font partie de la formation de Buchanan Lake du groupe d'Eureka Sound. Les palynoflores bien conservées indiquent que la sédimentation synorogénique aurait eu lieu durant l'Éocène moyen. Les dépôts se sont accumulés dans l'avant-fosse Axel Heiberg, qui faisait partie d'une série d'avant-fosses orogéniques formées le long de la partie est de l'île Axel Heiberg et de la partie est de l'île Ellesmere.

Introduction

Tertiary strata, distributed along eastern Axel Heiberg Island from Whitsunday Bay in the south, to Stang Bay (Fig. 43.1), provide information that is critical to an understanding of depositional and tectonic relationships during the latest stages of Sverdrup Basin evolution. In particular, thick sequences of conglomerate and sandstone from areas such as Mokka Fiord and Whitsunday Bay diapir, where coarse diabasic debris was shed off east-directed thrust blocks, have long been recognized as synorogenic (Tozer, 1960). An extensive swath of conglomerate and sandstone also underlies a broad alluvial plain between Mokka Fiord and Stang Bay, and east of Geodetic Hills, that originally was mapped as Eureka Sound Formation by Thorsteinsson and Tozer (Thorsteinsson, 1971). Exposures due east of Geodetic Hills and northwest of Stang Bay were later mapped as latest Tertiary, Beaufort Formation by Balkwill and Bustin (1975) and Bustin (1982).

During 1985, several aspects of the stratigraphy, structure and palynology of the deposits on eastern Axel Heiberg Island were re-examined. Our results indicate that all of the deposits belong to the Eureka Sound Group (Buchanan Lake Formation; see Ricketts, 1986, this volume, for definition of new formations) and previous assignment of the strata to the Beaufort Formation is likely in error. Furthermore, our data show that these deposits can now be dated as Middle Eocene, thus placing much more severe constraints on the timing of Eureka deformation.

Distinguishing features of the Beaufort Formation

The name Beaufort Formation was formally introduced by Tozer (1956) for sand and gravel deposits exposed on Prince Patrick Island, and has since been extended to similar deposits at other localities in the western Arctic and islands of the Arctic Coastal Plain: for example, Meighen Island (Thorsteinsson, 1961), Banks Island (Thorsteinsson and Tozer, 1962), and Melville Island (Tozer, 1970). Beaufort strata overlie Eureka Sound Group and older Mesozoic units of Sverdrup Basin unconformably. Typically, the Beaufort Formation consists of unconsolidated sands and gravels that commonly contain uncompressed, unaltered wood. Well preserved cones of pine and spruce (*Picea banksii* Hills and Ogilvie), and the fossil walnut *Juglans eocinera* Hills, Klován and Sweet, have also been found on Banks Island (Hills and Ogilvie, 1970; Hills et al., 1974).

Strata exposed in the area of Geodetic Hills and Stang Bay, and included in the Beaufort Formation by Bustin (1982), also contain spruce cones that, despite some morphological differences, have been equated, along with the examples from Banks Island, with *Picea banksii* (Hills and Bustin, 1976). However, apart from this apparent similarity in cone type, there are few other similarities between the typical Beaufort of western Arctic, and that designated as Beaufort on Axel Heiberg Island. In the sections that follow, the important differences in lithology and structure are discussed.

Lithological criteria

Recent investigations indicate that the conglomerate, sandstone and coal deposits exposed in ridges and stream-cuts due east of Geodetic Hills, are identical to deposits that cover the entire area mapped as Eureka Sound Group, both north of Stang Bay, and on the broad alluvial plain north of Mokka Fiord. Representative stratigraphic sections from these localities are illustrated in Figure 43.2. Furthermore, the lithotypes are also remarkably similar to those of conglomerates exposed in the footwall of the Stolz Thrust zone at both Mokka Fiord and Whitsunday Bay diapirs. The last two examples are here considered to be some of the youngest deposits in the Eureka Sound Group; they are synorogenic, formed from coarse diabase debris shed from uplifted and thrust faulted Triassic rock farther west, and are themselves overthrust within the Stolz Thrust zone (Tozer, 1963; Balkwill, 1978; Bustin, 1982).

The sequence east of Geodetic Hills has been described by Bustin (1982). Very thick conglomerates, possibly greater than 1000 m thick, occur in a graben between Geodetic Hills and Stolz Thrust; the strata of the sequence dip to the west at 30 to 35°. The degree of induration is reflected in the high ridges and steep, stream-cut bluffs that are incised into the conglomerates. Conglomerate frameworks are clast supported, with cobbles and boulders (mostly diabase) moderately to well rounded. Similar fabrics are observed in thick grey diabase conglomerate at Mokka Fiord.

As indicated in Figure 43.2, most of the sequence along eastern Axel Heiberg Island is made up of conglomerate units, several metres thick, that are interbedded with units of lithic arenite and a few thin lignite seams; fining-upward sequences are common. Trough, planar and ripple cross-bedding abound, along with frequent indications of channeling. As Bustin (1982) has reported, the transition from the more massive, thick conglomerate facies, to the interbedded conglomerate-sandstone facies, is not exposed at Geodetic Hills because of faulting. However, this transition was observed in vertical sections in the area of Mokka Fiord.

A third lithofacies, that Bustin (1982) referred to as the sandstone-mudstone-siltstone facies, occurs in the Geodetic Hills area. The principal exposure of this facies is on a prominent ridge approximately 25 km northeast of Geodetic Hills, and contains thinly interbedded grey mudstone and fine grained sandstone, with numerous lignite seams. These seams contain abundant cones and leaf fossils of *Metasequoia*, and subordinate numbers of spruce cones and broad leaf angiosperms. Rather than being laterally equivalent to the conglomerate-sandstone facies, as suggested by Bustin, the coal-bearing strata, in fact, occur stratigraphically above them.

Comparison of the eastern Axel Heiberg deposits with typical Beaufort strata in the western Arctic Archipelago illustrates some important differences:

1. Some of the conglomerates and sandstones are weakly consolidated; however, the majority, including the thick conglomerates at Geodetic Hills and several calcite cemented units at Stang Bay, show degrees of lithification that are considerably greater than "typical" Beaufort. The degree of lithification is similar to that of some of the sandstones in other areas of Eureka Sound Group exposure, particularly in the uppermost sandstone units of the Iceberg Bay Formation on Fosheim Peninsula.

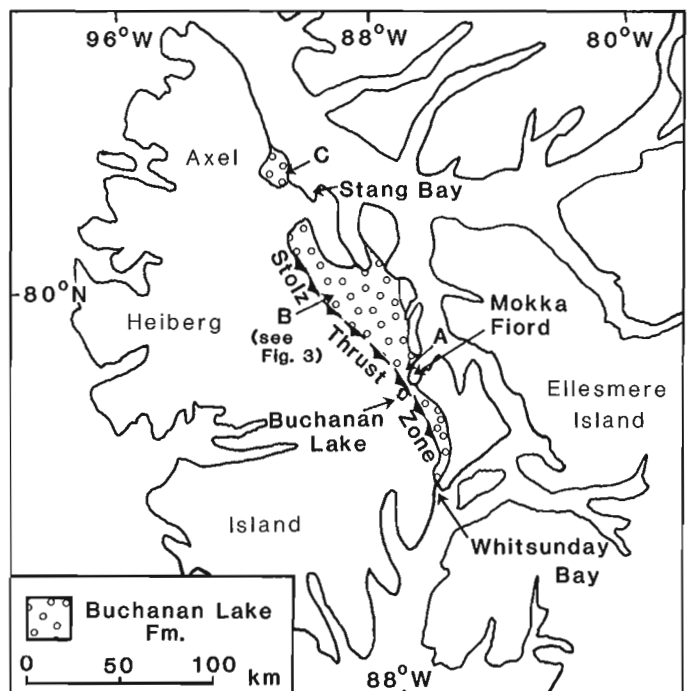


Figure 43.1. Map showing the general location of conglomerate-bearing strata on Axel Heiberg Island, and the stratigraphic sections A, B and C in Figure 43.2.

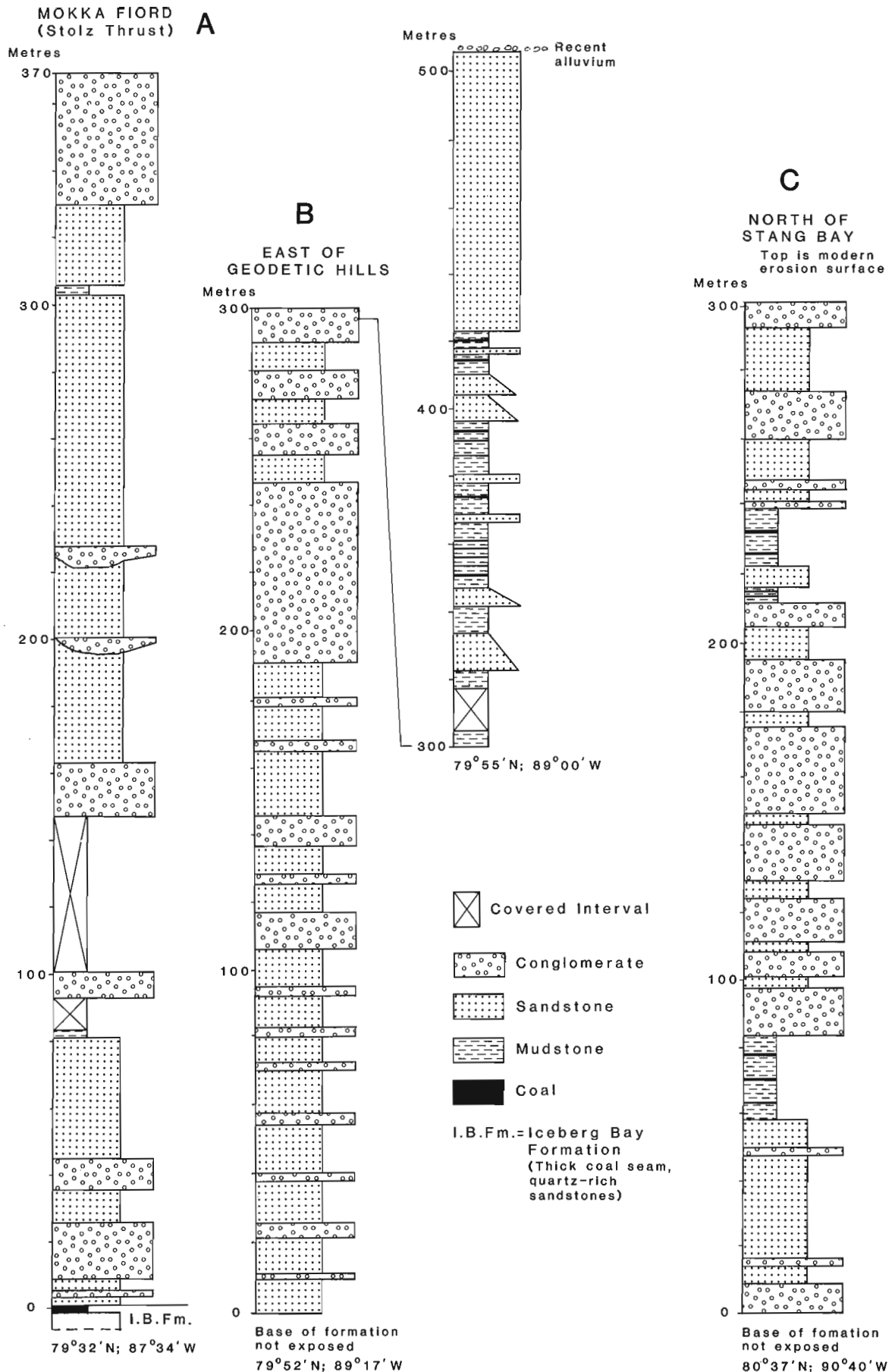


Figure 43.2. Three generalized stratigraphic sections of the Tertiary conglomerate-bearing sequence at Mokka Fiord (A), Geodetic Hills area (B), and north of Stang Bay (C). Note that section (B) is composite.

2. Wood, associated with the lignite beds, commonly is highly compressed (up to 10/1). Much of this wood is altered to low grade lignite, although there is some relatively unaltered wood similar to that present in the Beaufort Formation. This wood can be compared with wood altered to low grade lignite, which occurs in the weakly lithified sandstones at the top of the Eureka Sound Group at Hot Weather Creek. Some beds, especially channel-fill sandstones and conglomerates, contain large wood fragments that are completely mineralized, and are remarkably similar to mineralized wood in the Eureka Sound Group (especially the Iceberg Bay Formation). It is in these beds that the best preserved spruce cones are found.

Structural criteria

Structural and stratigraphic relationships are complex in the area of Geodetic Hills and in the hanging wall of Stolz Thrust (Fig. 43.3). On the original 1:250,000 scale map (Strand Fiord map sheet of Thorsteinsson, 1971), the northern end of Stolz Thrust was depicted as a splay of three normal faults, and the extension of the thrust trace was a fault with an opposite sense of displacement (downthrown to the west). A more logical extension of the thrust would be the eastern-most fault of the splay (downthrown to the east). During the present investigation, an overthrust relationship was observed here, with Triassic strata (Blaa Mountain Group and Heiberg Formation) occurring over the Tertiary conglomerate and sandstone (Fig. 43.3). The thrust plane dips to the west at about 30°. Thus a relationship can reasonably be inferred between the thrusting and deposition of the diabase-rich conglomerates that were derived by erosion of the sills and dykes that abound in the Triassic strata.

The small graben situated east of Geodetic Hills and in the hanging wall of Stolz Thrust (Fig. 43.3), is structurally complex. Here, thick conglomerate overlies, in succession, white sandstone and dark grey shale of the Isachsen and Christopher formations. This implies that differential movement and erosion of older Sverdrup Basin strata took place prior to conglomerate deposition and, therefore, also preceded the main phase of faulting on Stolz Thrust.

Differential movement within the conglomerate-sandstone sequence outboard (east) of Stolz Thrust is also indicated, where thick conglomerate beds exposed near the snout of a large glacier (Fig. 43.3), occur at a topographically lower level than equivalent strata on the adjacent ridge; either there is a substantial east-northeast striking fault, or a broad, open fold within the Tertiary sequence. Large-scale faulting or folding, which resulted in rotation of strata to dips exceeding 40°, also occurs in the area north of Stang Bay.

Palynology

Samples for palynological study were collected from intervals of suitable lithology from each of the stratigraphic sections (Fig. 43.2). The characteristics of the pollen assemblages are summarized in this section; details of the assemblages will be presented in a later publication.

In general, the samples examined contain rich, diverse and well preserved pollen assemblages that are similar to the Middle Eocene microfloras found in the highest stratigraphic levels of sections at Strand Fiord (Axel Heiberg Island) and Strathcona Fiord (Ellesmere Island); viz. the Iceberg Bay Formation.

In the section east of Geodetic Hills, the eight samples from lignite seams and grey mudstone beds, found in the upper 200 m of the Buchanan Lake Formation, yielded rich pollen floras. Common constituents of the assemblages include pollen of *Picea* (occasionally abundant), *Pinus*, *Tsuga*

(rare to common), Taxodiaceae (including *Sequoiapollenites*), *Alnus* and *Betula* (both usually abundant), *Carya* and *Tilia* (both often abundant), *Juglans* (common near top of section), Ericaceae, *Liliacidites*, *Ulmus* and *Quercus*. Other pollen that may be present includes *Nyssapollenites*, *Engelhardtia*, ?*Fagus* and *Tricolporopollenites kruschii* (of Rouse, 1977). Abundant *Metasequoia* cones and leaves and some *Picea* cones occur in some intervals of this section. Reworked palynomorphs (Cretaceous pollen and dinoflagellates, Late Paleozoic spores) are rare in the Geodetic Hills section and are readily distinguished from autochthonous forms.

The Geodetic Hills pollen assemblages are similar to those recorded from Middle and Late Eocene by Rouse (1977) and differ significantly from Oligocene assemblages documented by Peil (1971), Rouse (1977) and Ioannides and McIntyre (1980). *Carya viridifluminipites* (Wodehouse) Wilson and Webster and *C. veripites* Wilson and Webster (both often abundant in Geodetic Hills samples) are common in both the Eocene and Oligocene of the Arctic, whereas *Tilia vespicipites* Wodehouse, usually common in Geodetic Hills samples, and *T. crassipites* Wodehouse were not recorded from the Oligocene in the Arctic by Rouse (1977) although they occur in Oligocene strata in other parts of Canada. Hills et al. (1974) noted, however, the presence of *Tilia* in the Beaufort Formation from northwestern Banks Island. Other pollen types present, which are common in both Eocene and Oligocene strata, include *Tsuga*, *Juglans* and ?*Fagus*. Rouse (1977) recorded *Fagus* no earlier than Late Eocene and *Juglans* from Lower-Middle Eocene. *Tsuga* and *Juglans* were recorded from Lower or Middle Eocene by Ioannides and McIntyre (1980). Pollen of *Engelhardtia* type (*Momipites coryloides* Form A of Rouse, 1977) is common in a

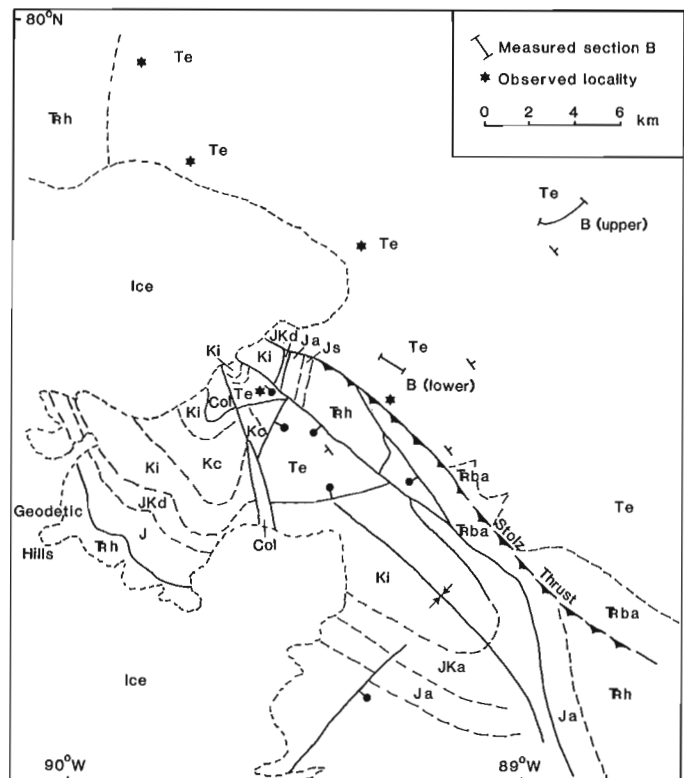


Figure 43.3. Reinterpreted structural relationships along the Stolz Thrust, east of Geodetic Hills (modified from Thorsteinsson, 1971, and Bustin, 1982). Te = Buchanan Lake Fm.; Kc = Christopher Fm.; Ki = Isachsen Fm.; JKd = Deer Bay Fm.; Ja = Awingak Fm.; Js = Savik Fm.; TRh = Heiberg Group; TRba = Blaa Mountain Group; Col = Diapirs. Extensional faults have downthrown block indicated; Stolz Thrust has teeth on upthrust block.

few samples. This type differs from Paleocene forms of *Momipites* and is apparently restricted to the Eocene and possibly Oligocene of northern Canada. *Tricolporopollenites kruschii* was recorded from the Lower-Middle Eocene by Rouse (1977). Species characteristic of the Oligocene (Piel, 1971; Rouse, 1977; Ioannides and McIntyre, 1980) were not seen in the Geodetic Hills samples. However, the Lower-Middle Eocene *Lonicera*-type of Rouse (1977) occurs rarely and the onagraceous pollen recorded by Ioannides and McIntyre (1980), from Paleocene to Middle Eocene strata of the Caribou Hills section of the Mackenzie Delta area, is common in some samples. The presence of *Pistillipollenites mcgregorii* Rouse, not known from rocks younger than Middle Eocene, provides further important evidence for an Eocene age. The palynological evidence, therefore, indicates that the Geodetic Hills samples examined are most likely of Middle Eocene age. There is no evidence that the uppermost part of the section is as young as Late Eocene. Palynological assemblages from the Beaufort Formation of Miocene-Pliocene age were discussed briefly by Craig and Fyles (1960) and Hills et al. (1974). The Beaufort assemblages, however, are apparently less varied than Eureka Sound assemblages and lack the distinctive Eocene pollen forms recorded in the Geodetic Hills material.

In the section north of Stang Bay, lignite seams and mudstone beds compose the upper components of fining-upward sequences of conglomerate and sandstone. The pollen assemblages here are similar to those from Geodetic Hills but are of slightly lower diversity. Reworked Cretaceous palynomorphs are rare in the Stang Bay section. The presence of pollen of *Tsuga*, *Juglans*, *Tilia vesicipites* and *T. crassipites* together suggests a Middle Eocene age. Onagraceous pollen and *Saxonipollis*, both recorded up to Middle Eocene by Ioannides and McIntyre (1980) provide further evidence for Middle Eocene age.

Sections at Mokka Fiord contain lignite only as discontinuous stringers; mudstones occur locally but comprise only a very small proportion of the succession. Pollen assemblages are similar to those from Geodetic Hills but generally contain fewer specimens, although *Carya viridifluminipites*, *Alnus* and Taxodiaceae may be abundant. Reworked Cretaceous spores, pollen and dinoflagellates are abundant in some of the samples. Paleozoic spores may also be present and samples near the top of the section contain some Paleocene pollen, including *Caryapollentis wodehousei* Nichols and Ott, which is also considered to be reworked. The presence of *Tilia vesicipites* (sometimes abundant), *Tricolporopollenites kruschii*, *Pistillipollenites mcgregorii* and *Juglans* indicates that the Mokka Fiord deposits are also of Middle Eocene age.

Conclusions

Important differences in lithology, structure and palynology exist between the Tertiary conglomerate deposits of eastern Axel Heiberg Island, and the Beaufort Formation of the western Arctic. In particular, overthrust relationships observed at Geodetic Hills indicate that the episode of syntectonic sedimentation was the same as that inferred for the Mokka Fiord and Whitsunday Bay areas. All of the criteria presented here demonstrate that the Tertiary strata of eastern Axel Heiberg Island should be equated with syntectonic units of the Eureka Sound Group (Fig. 43.4), representing deposition during the Eureka Orogeny. Therefore, conglomerate-bearing strata at Geodetic Hills, Stang Bay and other areas of eastern Axel Heiberg Island belong to the Buchanan Lake Formation, and correlate with similar synorogenic units at Lake Hazen, Franklin Pierce Bay and Judge Daly Peninsula.

In previous investigations, the age of Eureka deformation has been bracketed between Middle Eocene (the date of the youngest typical Eureka Sound Group), and Early Miocene (an age based primarily on the oldest Beaufort Formation that unconformably overlies Eureka Sound rocks). The lignite seams on eastern Axel Heiberg that are part of the syntectonic deposits contain well preserved pollen floras

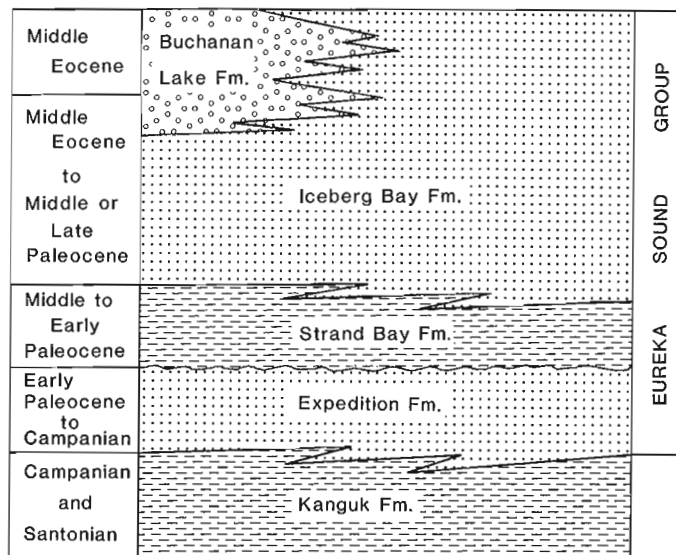


Figure 43.4. Formations of the Eureka Sound Group (see Ricketts, 1986 for details).

that suggest an age range restricted to Middle Eocene. This indicates that thrusting and folding was well underway by the end of the Eocene, but does not preclude the possibility that deformation continued into the Oligocene.

Indications of a much younger (Miocene) age for the conglomerate-bearing sequence on Axel Heiberg Island (Balkwill and Bustin, 1975; Hills and Bustin, 1976) were based primarily on the presence of cones identified as *Picea banksii*. The genus *Picea*, however, occurs throughout the Tertiary, but cones are rarely found in the older strata (compared to Beaufort strata). In comparing the Axel Heiberg spruce cones with *P. banksii* from Beaufort deposits

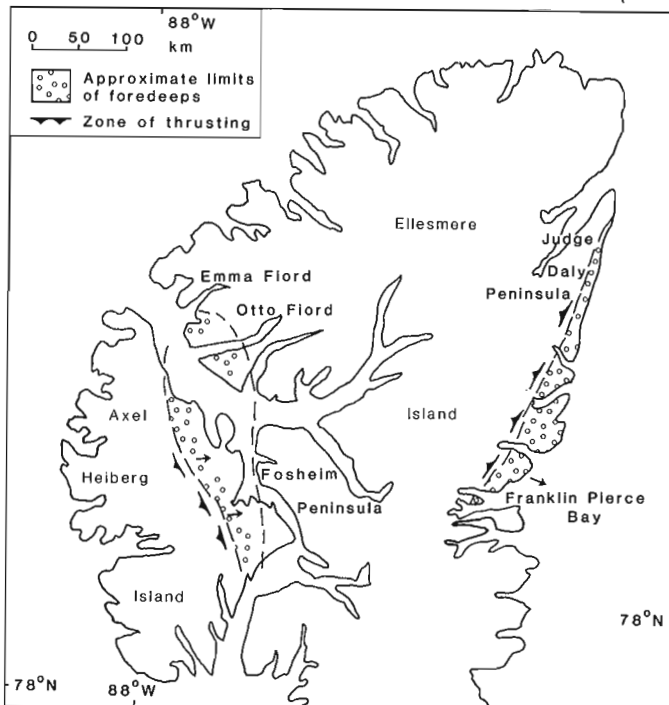


Figure 43.5. The location of orogenic foredeeps on Axel Heiberg and Ellesmere islands, shown schematically. The western limit of the Axel Heiberg foredeep is approximated by the Stolz Thrust zone. The eastern limits are unknown, but can reasonably be inferred to have been no farther east than Fosheim Peninsula, on the basis of lateral facies changes in the conglomerates, and the stratigraphic level of Eureka Sound Group strata exposed on north Fosheim. Thick conglomerates at Otto Fiord and Emma Fiord may represent the northern limits of the Axel Heiberg foredeep.

on Banks Island, Hills and Bustin (1976) noted considerably greater morphological diversity in the Axel Heiberg examples, and attributed these differences to environmental stress; differences in age were discounted. In view of our results, the validity of using this spruce flora in biostratigraphic determinations needs to be reassessed. Either *P. banksii* occurs in deposits that are older than Beaufort Formation, or the cones on Axel Heiberg Island are not comparable to *P. banksii*, but to a different *Picea* species. Bustin (1982) also used microfloral results to support the Miocene/(?Pliocene Beaufort Formation interpretation but did not provide details of the assemblages. Re-examination of these samples shows that the assemblages are also Eocene and do not suggest a younger age.

Implications for tectonic history

Reworked Lower and Upper Cretaceous, older Mesozoic, and Paleozoic palynomorphs are relatively common in the conglomerate deposits at Mokka Fiord. Notably, some reworked Paleocene pollen was also found in a few samples. Sediment transport directions, inferred from crossbed measurements (Bustin, 1982; this study) indicate that the bulk of the syntectonic sequence on eastern Axel Heiberg Island was derived from a terrane farther west. The source rocks apparently ranged in age from Devonian to Paleocene, and therefore would have included reworked Eureka Sound Group strata from central and/or western Axel Heiberg; the younger Sverdrup Basin strata were subsequently stripped from the central Princess Margaret Range.

The coarse grained deposits on eastern Axel Heiberg Island (viz. Buchanan Lake Formation), represent alluvial fan and braidplain sedimentation, where debris was shed east and southeast from uplifted and thrust faulted Mesozoic (and possibly older) strata. Thus, the sedimentary basin can be considered as an orogenic foredeep and is informally referred to here as the Axel Heiberg foredeep. The broadly east-dipping paleoslope also represents a complete reversal of the basin configuration that prevailed during much of the earlier Eureka Sound Group sedimentation in the western Ellesmere Island region. The Axel Heiberg foredeep extended from somewhere north of Stang Bay, almost to the southern end of Axel Heiberg Island (Fig. 43.5).

Correlative conglomerate-bearing strata on eastern Ellesmere Island (Franklin Pierce Bay to Judge Daly Peninsula) also represent sedimentation in an east-southeast dipping foredeep, which developed outboard of the Parrish Glacier Thrust and associated faults, during the Eureka Orogeny (Fig. 43.5).

Eureka Sound Group sedimentation in the Axel Heiberg foredeep may have ended by Middle Eocene time. A main phase of faulting and folding, which represents the Eureka Orogeny, was well underway by the end of the Eocene.

The previous designation of the Axel Heiberg conglomerates, as Beaufort Formation of Miocene or younger age, implied an episode of considerable post-orogenic faulting and folding (or rotation of fault blocks). Much of this faulting can now be attributed to the Eureka Orogeny. However, this does not preclude the possibility of younger extensional faulting. It appears now that deposits correlative with the Beaufort Formation are restricted or possibly absent in the eastern Arctic (onshore).

References

Balkwill, H.R.

1978: Evolution of Sverdrup Basin, Arctic Canada; American Association of Petroleum Geologists, Bulletin, v. 62, p. 1014-1028.

Balkwill, H.R. and Bustin, R.M.

1975: Stratigraphic and structural studies, central Ellesmere Island and eastern Axel Heiberg Island, District of Franklin; in Current Research, Part A, Geological Survey of Canada, Paper 75-1A, p. 513-517.

Bustin, R.M.

1982: Beaufort Formation, eastern Axel Heiberg Island, Canadian Arctic Archipelago; Bulletin of Canadian Petroleum Geology, v. 30, p. 140-149.

Craig, B.G. and Fyles, J.G.

1960: Pleistocene geology of Arctic Canada; Geological Survey of Canada, Paper 60-10.

Hills, L.V. and Bustin, R.M.

1976: *Picea banksii* Hills and Ogilvie from Axel Heiberg Island, District of Franklin; in Current Research, Part B, Geological Survey of Canada, Paper 76-1B, p. 61-63.

Hills, L.V. and Ogilvie, R.T.

1970: *Picea banksii* n. sp., Beaufort Formation (Tertiary), Banks Island, Arctic Canada; Canadian Journal of Botany, v. 48, p. 457-464.

Hills, L.V., Klovan, J.E., and Sweet, A.R.

1974: *Juglans eocinerea* n. sp., Beaufort Formation, southwestern Banks Island, Arctic Canada; Canadian Journal of Botany, v. 52, p. 65-90.

Ioannides, N.S. and McIntyre, D.J.

1980: A preliminary palynological study of the Caribou Hills outcrop section along the Mackenzie River, District of Mackenzie; in Current Research, Part A, Geological Survey of Canada, Paper 80-1A, p. 197-208.

Piel, K.M.

1971: Palynology of Oligocene sediments from central British Columbia; Canadian Journal of Botany, v. 49, p. 1885-1920.

Ricketts, B.D.

1986: New formations in the Eureka Sound Group; in Current Research, Part B, Geological Survey of Canada, Paper 86-1B.

Rouse, G.

1977: Paleogene palynomorph ranges in western and northern Canada; in Contributions of Stratigraphic Palynology, volume 1, Cenozoic Palynology; American Association of Stratigraphic Palynologists, Contribution Series No. 5A, p. 48-65.

Thorsteinsson, R.

1971: Geology, Strand Fiord, District of Franklin; Geological Survey of Canada, Map 1301A.

1961: History and geology of Meighen Island; Geological Survey of Canada, Bulletin 75.

Thorsteinsson, R. and Tozer, E.T.

1962: Banks, Victoria and Stefansson Islands, Arctic Archipelago; Geological Survey of Canada, Memoir 330.

Tozer, E.T.

1956: Geological reconnaissance Prince Patrick, Eglinton and western Melville Islands, Arctic Archipelago, Northwest Territories; Geological Survey of Canada, Paper 55-5.

1960: Summary account of Mesozoic and Tertiary stratigraphy, Canadian Arctic Archipelago; Geological Survey of Canada, Paper 60-5.

1963: Mesozoic and Tertiary stratigraphy, western Ellesmere Island and Axel Heiberg Island, District of Franklin; Geological Survey of Canada, Paper 63-30.

1970: Mesozoic and Cenozoic; in Geology and Economic Minerals of Canada, ed. R.J.W. Douglas; Geological Survey of Canada, Economic Geology Report no. 1, p. 574-589.

Lower Permian (Asselian) ammonoids and conodonts from the Belcher Channel Formation, southwestern Ellesmere Island

Project 680064

W.W. Nassichuk and C.M. Henderson¹
Institute of Sedimentary and Petroleum Geology, Calgary

Nassichuk, W.W. and Henderson, C.M., Lower Permian (Asselian) ammonoids and conodonts from the Belcher Channel Formation, southwestern Ellesmere Island; in *Current Research, Part B*, Geological Survey of Canada, Paper 86-1B, p. 411-416, 1986.

Abstract

A diverse fauna of Lower Permian ammonoids, including representatives of **Neopronorites**, **Daixites**, **Boesites**, **Agathiceras**, **Glaphyrites**, and **Emilites** is associated with representatives of the conodont **Streptognathodus** and the fusulinids **Pseudofusulina** and **Pseudofusulinella** in the lower part of the Belcher Channel Formation at Blind Fiord, southwestern Ellesmere Island. Ammonoids, conodonts and fusulinaceans all indicate an earliest Permian (Asselian) age.

Résumé

Une faune diverse d'ammonoïdés du Permien inférieur, y compris des représentants de **Neopronorites**, **Daixites**, **Boesites**, **Agathiceras**, **Glaphyrites** et **Emilites**, est associée à des représentants du conodonte **Streptognathodus** et des fusulinidés **Pseudofusulina** et **Pseudofusulinella** dans la partie inférieure de la formation de Belcher Channel, à Blind Fiord, dans la partie sud-ouest de l'île Ellesmere. Les ammonoïdés, les conodontes et les fusulinidés datent tous du Permien le plus ancien (Assélien).

¹ Department of Geology, University of Calgary, Calgary, Alberta T2N 1N4

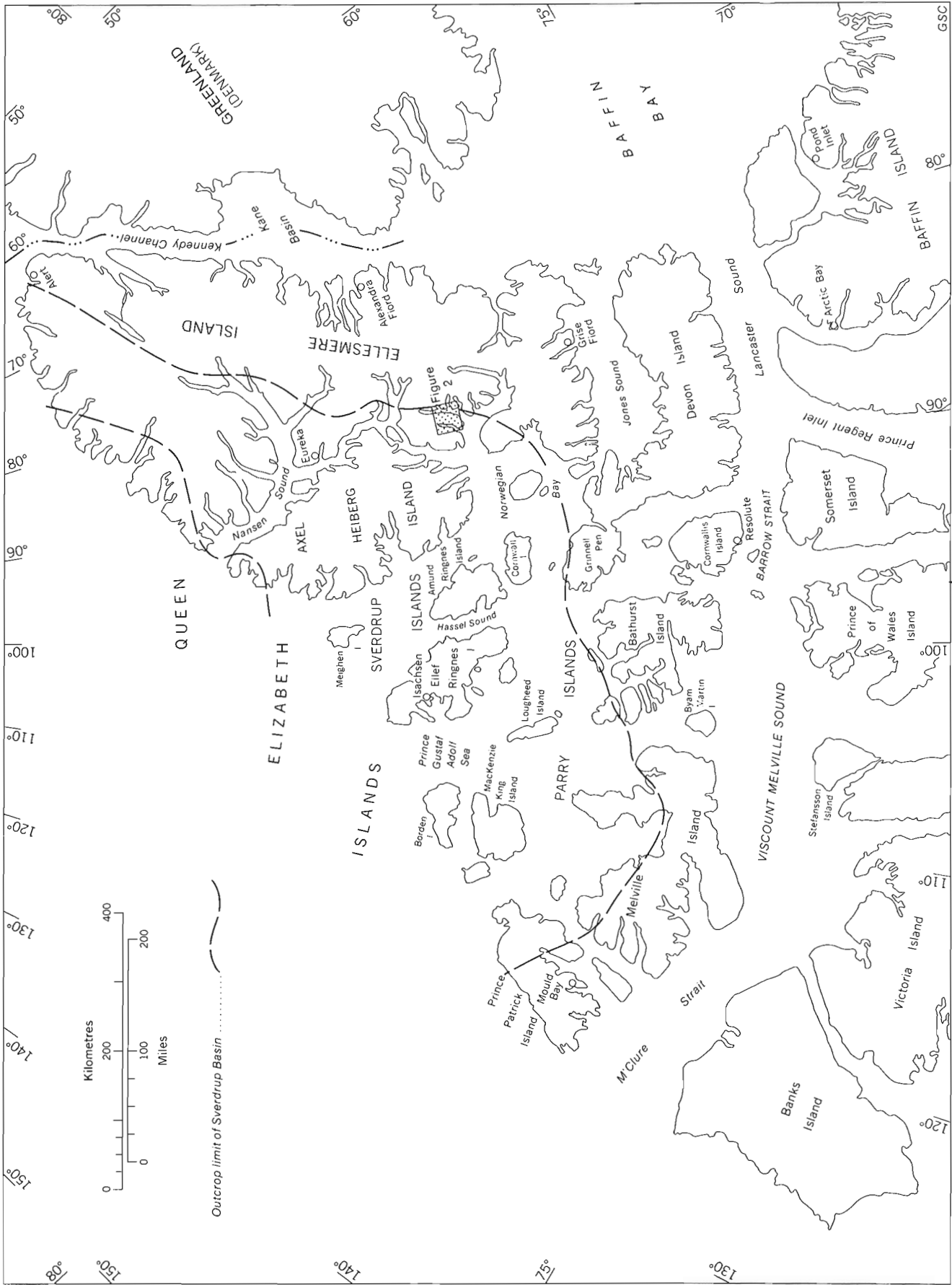


Figure 44.1. Index map of the Canadian Arctic Archipelago showing outcrop limits for the Sverdrup Basin and an inset of the study area at Blind Fiord, Ellesmere Island.

Introduction

Lower Permian ammonoids are widely distributed in the Sverdrup Basin and have been recorded from five formations representing nearshore, deltaic to deeper water basinal deposition from the lowermost Permian (Asselian) to uppermost Early Permian (Roadian). They have been described from Asselian limestone in the Hare Fiord Formation on Ellesmere Island (Nassichuk and Spinosa, 1972), from Artinskian strata in the Sabine Bay and Hare Fiord formations on Melville Island and Ellesmere Island (Nassichuk, Furnish and Glenister, 1966; Nassichuk, 1970), and also from an unnamed formation in southwestern Ellesmere Island that was earlier thought to belong to the Assistance Formation (Nassichuk, 1975). Roadian species are known from the Assistance and van Hauen formations on Melville, Devon and Ellesmere islands (Nassichuk, 1970, 1975).

The first ammonoid fauna ever recovered from the Lower Permian (Asselian-Artinskian) Belcher Channel Formation in the Sverdrup Basin is of Asselian age and contains elements remarkably similar to those described by Nassichuk and Spinosa (1972) from the lower part of the Hare Fiord Formation on northern Ellesmere Island. The ammonoids were discovered in a thin (10 cm) bed of micritic limestone 235 m above the base of the Belcher Channel Section exposed on the west side of Blind Fiord (Fig. 44.1, 44.2). Included in the ammonoid fauna are small and mainly

fragmentary representatives of *Neopronorites* Ruzhencev, *Daixites* Ruzhencev, *Boesites* Miller and Furnish, *Agathiceras* Gemmellaro, *Glaphyrites* Ruzhencev and *Emilites* Ruzhencev.

Stratigraphy

The Belcher Channel Formation is well developed between Blind Fiord and Troid Fiord in southwestern Ellesmere Island (Fig. 44.2) where it attains a thickness of nearly 1000 m. It is composed mainly of argillaceous and bioclastic limestone and is contained within the Marginal Clastic and Carbonate Belt of Thorsteinsson (1974). Between Blind Fiord and Troid Fiord, the Belcher Channel Formation overlies reddish weathering sandstone and sandy limestone of the Moscovian-Asselian Canyon Fiord Formation. It is alternately overlain by black shale of the lower van Hauen Formation or by greenish weathering, argillaceous limestone of an unnamed formation that grades laterally into the lower van Hauen Formation (Fig. 44.3; Nassichuk, 1975; Nassichuk and Wilde, 1977; Beauchamp, personal communication, 1985).

The Belcher Channel Formation is at least 806 m thick in the ammonoid-bearing section on the west side of Blind Fiord (Fig. 44.3) and a detailed description was provided by Nassichuk and Wilde (1977). The base of the formation is obscured and relationships with underlying strata are unknown.

In this section, the Belcher Channel consists of a succession of cyclical carbonates; individual 'cycles' indicate shoaling upward and include wavy bedded, argillaceous

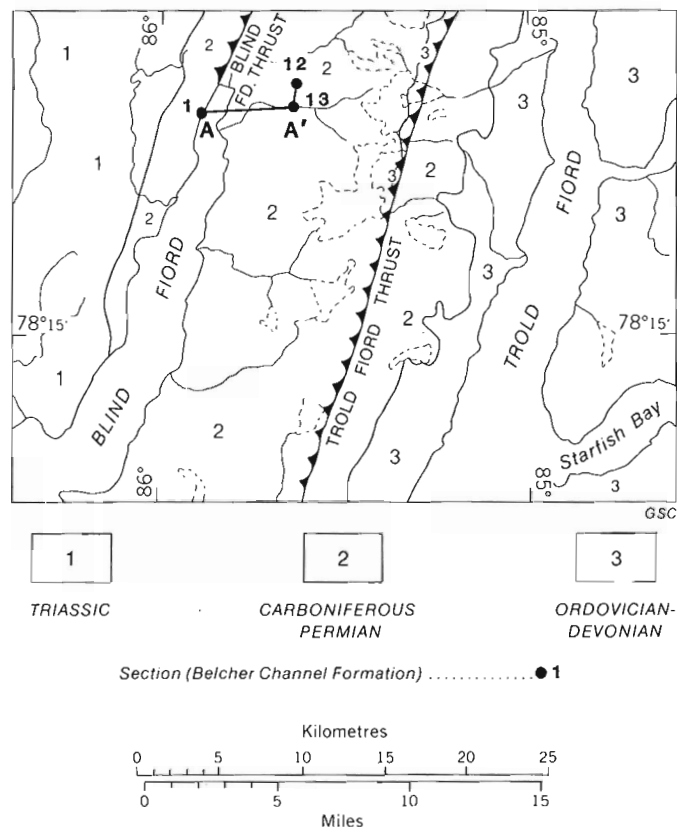


Figure 44.2. Generalized geological map of the area shown in the inset in Figure 44.1, displaying the distribution of Paleozoic and Mesozoic rocks in the Blind Fiord area, the locations of Section 1, from which fusulinaceans, ammonoids and conodonts were recovered from the Belcher Channel Formation, and sections 12 and 13. Carboniferous to Triassic strata are in the Sverdrup Basin and Ordovician to Devonian strata are in the Franklinian Geosyncline.

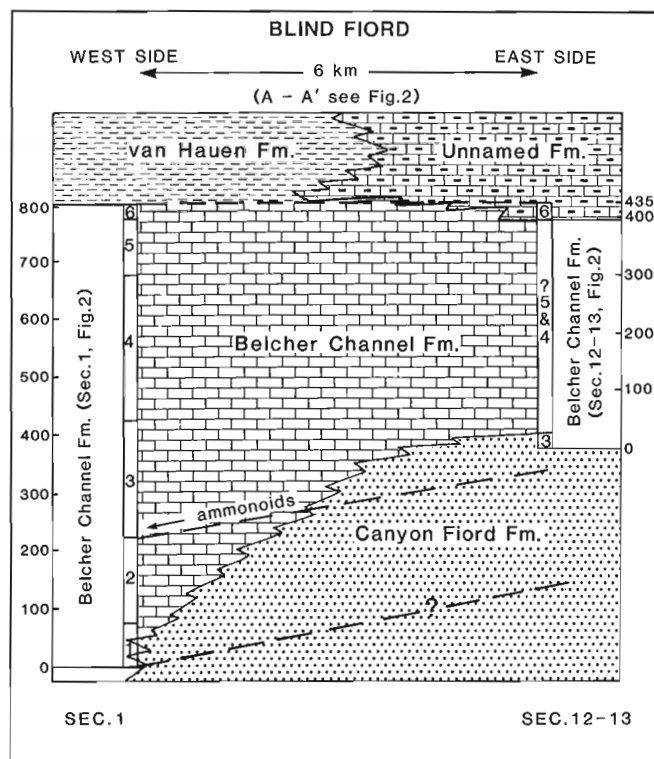


Figure 44.3. Schematic diagram of Lower Permian facies relationships across Blind Fiord. Conodont zones 1 to 3 are of Asselian age (Fig. 44.4) and zones 4 to 6 are of Sakmarian age (zone 6 may include lowest Artinskian strata). The geographic distance between sections on the west side and the east side of Blind Fiord is 6 km, but palinspastic reconstruction reveals that distance between them was probably considerably larger, possibly up to 25 km.

limestone, skeletal wackestone, and grainstone. Moreover, the formation is relatively sandy in its lower part where numerous recessive shaly beds occur. Its upper part, however, is characterized by a succession of thick, resistant carbonate mounds of Sakmarian age that contain the enigmatic organism *Palaeoaplysina* (Davies and Nassichuk, 1973).

Biostratigraphy

General remarks

Nassichuk and Wilde (1977) provided a brief outline of the status of the Carboniferous-Permian boundary in the Soviet Union and indicated that the position of the boundary has been controversial for more than 30 years. In the General Soviet Scale the boundary has been placed for many years between the uppermost Carboniferous (Gzhelian) *Daixina sokensis* Zone and the lowermost Permian (Asselian) *Schwagerina vulgaris*-*Schwagerina fusiformis* Zone. Some Soviet scientists insist, however, that the boundary should be placed at the top of the "*Schwagerina* beds"; that is, at the top of the Asselian, and others think that it should be placed at the base of the *Pseudofusulina uralica* Zone, which is within the Asselian Stage.

Ruzhencev (1950) recognized important distinctions between ammonoid faunas that he considered to be uppermost Carboniferous (Orenburgian), near Orenbourg in the southern Urals, and ammonoids that occur elsewhere in the Urals in apparently younger, Asselian strata. Stratigraphic relationships between Orenburgian and Asselian strata in the Urals remain obscure, but geological mapping in recent years has led some stratigraphers to conclude that differences between the two successions might reflect a change of facies; the upper part of the Orenburgian might be synchronous with the lower Asselian (Pnev, personal communication, 1975).

Recently, a new zone, the *Daixina bosbytauensis*-*Daixina robusta* Zone, was identified between the *Daixina sokensis* (Gzhelian) and *Schwagerina vulgaris*-*Schwagerina fusiformis* (Asselian) zones in the Darvaz region of central Asia and in the Urals (Kotlyar and Leven, personal communication, 1985). The zone contains ammonoids from the *Shumardites*-*Vidrioceras* "genozone" in the upper part of Ruzhencev's (1950) Orenburgian Stage. In addition to the fusulinaceans, after which the zone was named, it includes the first occurrences of *Occidentoschwagerina*, *Rugosochusenella paragregaria*, *Pseudofusulina kljasmica*, *Pseudofusulina modesta*, *Pseudofusulina pseudokrotowi*, *Pseudofusulina anderssoni*, *Pseudofusulina pseudoanderssoni* and *Daixina vozgalensis*.

As a result of decisions taken at a Plenary Session of the ISC Commission on the Carboniferous and Permian systems in the U.S.S.R. in 1984, the Carboniferous-Permian boundary is now placed at the base of the "new" zone in the General Soviet Scale. According to the Soviet scale, the upper part of the Orenburgian is contained within the Asselian Stage. The controversy over the boundary has not diminished, however, and many Permian specialists in the Soviet Union continue to support the traditional view that the boundary should be retained at the top of the "new" zone; that is, at the base of the *Schwagerina vulgaris*-*Schwagerina fusiformis* Zone.

Faunas in the Belcher Channel Formation at Blind Fiord

Nassichuk and Wilde (1977) indicated that fusulinaceans occurring from 135 m to 375 m above the base of the Belcher Channel Formation at Section 1 (Fig. 44.2) on the west side

of Blind Fiord are included in the Asselian assemblage zone of *Pseudofusulina plana* Skinner and Wilde. In addition to *P. plana*, the following are also contained in the zone: *Pseudofusulinella praeantiqua* Nassichuk and Wilde, *Pseudofusulinella tempelensis* Ross, *Pseudofusulinella biconica* Skinner and Wilde and *Pseudofusulina grinnelli* (Thorsteinsson). *Pseudofusulinella grinnelli* is particularly common near the base of the type section of the Belcher Channel Formation on Grinnell Peninsula, Devon Island (Harker and Thorsteinsson, 1960). Ross (in Nassichuk and Davies, 1975) assigned an Asselian age to several other species in the lower part of the type section, including *Eoparafusulina* sp., *Schwagerina* sp., *Pseudofusulina* sp., and *Pseudofusulinella* sp.

Several ammonoids recovered from 235 m above the lowest exposures of the Belcher Channel Formation at Section 1 (Fig. 44.2), including species of *Agathiceras*, *Neopronorites* and *Boesites*, are widely distributed from Upper Carboniferous (Moscovian) through much of the Lower Permian, and indeed, representatives of one of them (*Agathiceras*) extend into the Upper Permian. With the possible exception of the strata on Ellesmere Island, *Emilites* is unknown from strata either older or younger than Orenburgian; Movshovich et al. (1979) concluded that the Orenburgian occurrences in the Urals are in fact in their lower Asselian zone 3. Elsewhere, *Emilites* is known only from Texas, where *E. incertus* (Böse), from Virgillian (= Orenburgian) strata in the Gaptank Formation bears a very close resemblance to the Ellesmere Island species (W.M. Furnish, personal communication, 1986). *Glaphyrites* is common throughout the Upper Carboniferous, but is not known from strata younger than lowest Permian (Asselian). Similarly, *Daixites*, which previously was unknown outside the Ural Mountains, is confined to the interval between the uppermost Carboniferous (Orenburgian) to the lowest Sakmarian.

Accordingly, the ammonoid fauna does not provide a clear distinction between uppermost Carboniferous (Orenburgian) and lowermost Permian (Asselian) but, as discussed earlier, the General Soviet Scale includes the uppermost Orenburgian in the Asselian Stage. Nevertheless, the ammonoids from the Belcher Channel Formation appear to compare more favourably with upper "Orenburgian" and lower to middle Asselian species in the Urals than with upper Asselian species.

Whereas ammonoids and fusulinaceans have been studied for decades in the type area for the Permian in the Ural Mountains, conodont studies were initiated only recently. Already it has been demonstrated that conodonts will become as important in Permian biostratigraphy as they are in the rest of the Paleozoic and, indeed, in the Triassic. Movshovich et al. (1979) have identified three distinct conodont zones for the Asselian ("*Schwagerina* beds") in the Urals (see their zones 3, 4, 5 in our Figure 44.4). In ascending order, their zones are:

- 3) *Streptognathodus* (their *Gnathodus*) *simplex* - *S. elongatus* Zone
- 4) *Streptognathodus elongatus* - *S. wabaunsensis* Zone
- 5) *Streptognathodus barskovi* Zone.

It is difficult to compare lower and middle Asselian conodont faunas of Ellesmere Island with those in the Soviet Union because faunas in the former region are dominated by species of *Adetognathus* and in the latter by species of *Streptognathodus* (Fig. 44.4). Species of *Adetognathus* are generally considered to be long ranging, but one of us (CMH) has recognized several species in the lower (Asselian) part of the Belcher Channel Formation at Section 1 (Fig. 44.2). As taxonomic research on these species is at a preliminary stage, specific identifications cannot be presented in this

URAL MOUNTAINS, U.S.S.R. after Movshovich et al., 1979			BLIND FIORD (Sec.1 of Fig.2) S.W. ELLESMERE ISLAND, CANADIAN ARCTIC ARCHIPELAGO			
SYSTEM	STAGE	CONODONT ZONES	CONODONT ZONES this paper	LITHOLOGY and measurements (m)	FUSULINID ZONES after Nassichuk and Wilde, 1977	
PERMIAN	SAKMARIAN					
	ASSELIAN	5 <i>Streptognathodus barskovi</i>	3 <i>Streptognathodus elongatus</i> - <i>S. barskovi</i>	430 * 230*	435 375 135	<i>Schwagerina whartoni</i> <i>Pseudofusulina plana</i>
		4 <i>S. elongatus</i> - <i>S. wabaunsensis</i>	2 <i>Adetognathus</i> spp. - <i>Idiogonathodus</i> sp.			<i>Pseudofusulinella thompsoni</i>
		3 <i>S. simplex</i> - <i>S. elongatus</i>	1 <i>Adetognathus</i> spp.		80 18	<i>Pseudofusulinella usvae</i> (group)
CARB.	GZHELIAN					

Figure 44.4. Asselian conodont zones in the Ural Mountains and at Blind Fiord. Lithology column reflects thickness of individual cycles. (* = first appearance of *Streptognathodus barskovi*; ** = position of ammonoid locality).

summary report. As a result, the lower two assemblages indicated on the range chart (Fig. 44.4) are simply designated *Adetognathus* spp. The third conodont assemblage at Section 1 is dominated by *Streptognathodus* species that provide a direct comparison with faunas in the Urals. The ammonoids recorded from locality I occur at about the same level as the first appearance of *Streptognathodus elongatus*, whereas *S. barskovi* first appears 22 m above the ammonoid locality. *Streptognathodus barskovi* is restricted to the upper Asselian (zone 5 of Movshovich et al., 1979) in the Ural Mountain sequences. At Section 1, our boundary between zones 2 and 3, which is based on the appearance of *Streptognathodus* spp., can thus be correlated with the upper part of the *S. elongatus* - *S. wabaunsensis* Zone (middle Asselian) of Movshovich et al. (1979).

References

- Davies, G.R. and Nassichuk, W.W.
1973: The hydrozoan *Palaeoaplysina* from the upper Paleozoic of Ellesmere Island, Arctic Canada; *Journal of Paleontology*, v. 47, p. 251-265.
- Harker, P. and Thorsteinsson, R.
1960: Permian rocks and faunas of Grinnell Peninsula, Arctic Archipelago; Geological Survey of Canada, Memoir 309.
- Movshovich, E.V., Kozur, H., Pavlov, A.M., Pnev, V.N., Polozova, A.N., Chuvashov, B.I., and Bogoslovskaya, M.F.
1979: Conodont assemblages of the Lower Permian in the sub-Ural region and problems of correlation of Lower Permian deposits; in *Conodonts of the Urals and their stratigraphic significance*, Symposium, Sverdlovsk, 1979, Academy of Science, Ural Scientific Centre, p. 94-125.
- Nassichuk, W.W.
1970: Permian ammonoids from Devon and Melville Islands, Canadian Arctic Archipelago; *Journal of Paleontology*, v. 44, no. 1, p. 77-97, Pls. 19-22.
1975: The stratigraphic significance of Permian ammonoids on Ellesmere Island; in *Current Research, Part B*, Geological Survey of Canada, Paper 75-1B, p. 277-283.
- Nassichuk, W.W. and Davies, G.R.
1975: The Permian Belcher Channel Formation at Grinnell Peninsula, Devon Island; in *Current Research, Part C*, Geological Survey of Canada, Paper 75-1C, p. 267-277.
- Nassichuk, W.W., Furnish, W.M., and Glenister, Brian F.
1966: The Permian ammonoids of Arctic Canada; Geological Survey of Canada, Bulletin 131.

Nassichuk, W.W. and Spinosa, C.

1972: Early Permian (Asselian) ammonoids from the Hare Fiord Formation, northern Ellesmere Island; *Journal of Paleontology*, v. 46, p. 536-544, Pl. 1.

Nassichuk, W.W. and Wilde, G.L.

1977: Permian fusulinaceans and stratigraphy at Blind Fiord, southwestern Ellesmere Island; *Geological Survey of Canada, Bulletin 268*, 59 p.

Ruzhencev, V.E

1950: Upper Carboniferous ammonites of the Urals; *Academy of Sciences, U.S.S.R., Paleontology Institute, Trudy*, v. 29, p. 1-223, Pls. 1-15.

Thorsteinsson, R.

1974: Carboniferous and Permian stratigraphy of Axel Heiberg Island and western Ellesmere Island, Canadian Arctic Archipelago; *Geological Survey of Canada, Bulletin 224*, 115 p.

Computerization of coal exploration data for Nova Scotia: a joint Federal-Provincial project

Project 810014

J.D.Hughes, D.J.MacNeil¹ and P.Watson²
Institute of Sedimentary and Petroleum Geology, Calgary

Hughes, J.D., MacNeil, D.J., and Watson, P., Computerization of coal exploration data for Nova Scotia: a joint Federal-Provincial project; *in* Current Research, Part B, Geological Survey of Canada, Paper 86-1B, p. 417-420, 1986.

Abstract

The construction of computer files of coal exploration data for Nova Scotia's coalfields is underway through a co-operative Federal/Provincial project. Procedures and computer programs developed by the Geological Survey of Canada for its National Coal Inventory are used for data compilation, interpretation and storage. Products of this work in the short term will be the availability of consistently defined exploration data in a flexible information management system. In the longer term, deposit models suitable for geological, economic and environmental assessment will be developed by applying established methodologies to the analysis of these data. This will give planners in industry and government a flexible, high-resolution planning tool providing the capability for rapid identification of the location and quantity of coal resources that meet any combination of geological, quality, economic or environmental criteria.

Résumé

L'établissement de fichiers informatisées sur l'exploration des houillères en Nouvelle-Écosse se poursuit dans le cadre d'un projet fédéral-provincial. Les méthodes et les programmes machine mis au point par la Commission géologique du Canada pour l'Inventaire national du charbon sont utilisés pour la compilation, l'interprétation et la mise en mémoire des données. À court terme, ce projet assurera la disponibilité de données d'exploration bien définies qui seront présentées dans un système de gestion de l'information souple. À plus long terme, l'analyse des données au moyen de méthodes établies permettra d'élaborer des modèles de gisements susceptibles de servir aux évaluations géologiques, économiques et environnementales. Ce projet fournira aux planificateurs de l'industrie et du gouvernement un outil de planification souple et détaillé qui rendra possible l'identification rapide de l'emplacement et de la quantité des réserves houillères et qui pourra satisfaire à toutes les combinaisons de critères géologiques, qualitatifs, économiques ou environnementaux.

¹ Nova Scotia Department of Mines and Energy, P.O. Box 147, Sydney Mines, Nova Scotia B1V 1Y3

² c/o Nova Scotia Department of Mines and Energy, 1690 Hollis St., Halifax, Nova Scotia B3J 2T3

Introduction

Coal exploration and exploitation have been conducted in Nova Scotia's coalfields for more than two centuries. A large volume of information on the distribution and characteristics of coals in these deposits has accumulated over this period, comprising outcrop and core descriptions, mine plans, analytical data and, more recently, geophysical logs of boreholes. A cooperative project, under the Canada-Nova Scotia Mineral Development Agreement, was initiated in February, 1985, between the Nova Scotia Department of Mines and Energy and the Geological Survey of Canada, to compile this information in a consistently defined, computer-processable format. Once in this format, the information can be manipulated by computer to develop a comprehensive understanding of the geological, resource and economic characteristics of these coal deposits.

This report is intended to provide a brief description of the project in terms of available data, interpretation techniques, data organization and longer term potential in the development of a comprehensive coal resource management tool.

Available Data

A recent overview of coal in Nova Scotia (Calder, 1985) provides background information on the location and geology of Nova Scotia's coalfields. Mining has been carried out in many of these coalfields over long periods, ranging in scale from very small underground and surface operations, to the large under-sea mines operated by the Cape Breton Development Corporation in the Sydney coalfield. Exploration data gathered within the coalfields vary widely in type and quality; the older data is generally somewhat less reliable than more recently collected information. These data comprise surface information obtained from outcrop descriptions and geological maps, subsurface information gathered from boreholes and mines, and other information including coal analyses, topographic maps, seafloor maps and geological reports.

Table 45.1 summarizes the type and amount of coal exploration data available for Nova Scotia. With the exception of the Sydney coalfield, most of the hardcopy data is stored in files of the Nova Scotia Department of Mines and Energy in Halifax. Arrangements have been made with the Cape Breton Development Corporation in Sydney to obtain copies of their data, some of which dates back more than one hundred years, in order to complete hardcopy files for the Sydney coalfield.

Data interpretation and storage

Exploration data are being gathered, interpreted and entered into the computer using methods and computer programs developed by the Geological Survey of Canada for its National Coal Inventory. This process involves the interpretation of geophysical logs and rationalization of other forms of data using a consistent set of procedures, data entry and verification, followed by geological analysis and data manipulation to develop grid models suitable for resource assessment (Irvine 1981; Hughes, 1984; Hughes and Neimanis, 1986). These steps are outlined in Figure 45.1.

At present, this project is directed only toward compiling and verifying data in a computer-processable format. Further processing of the data will be undertaken either using G.S.C. computer facilities in Calgary or yet-to-be-acquired facilities of N.S.D.M.E. in Halifax. Data compilation and verification are being conducted by a two-person team in Halifax, consisting of a geologist and a technician, who utilize database programs on the G.S.C. computer in Calgary via an onsite terminal and Datapac.

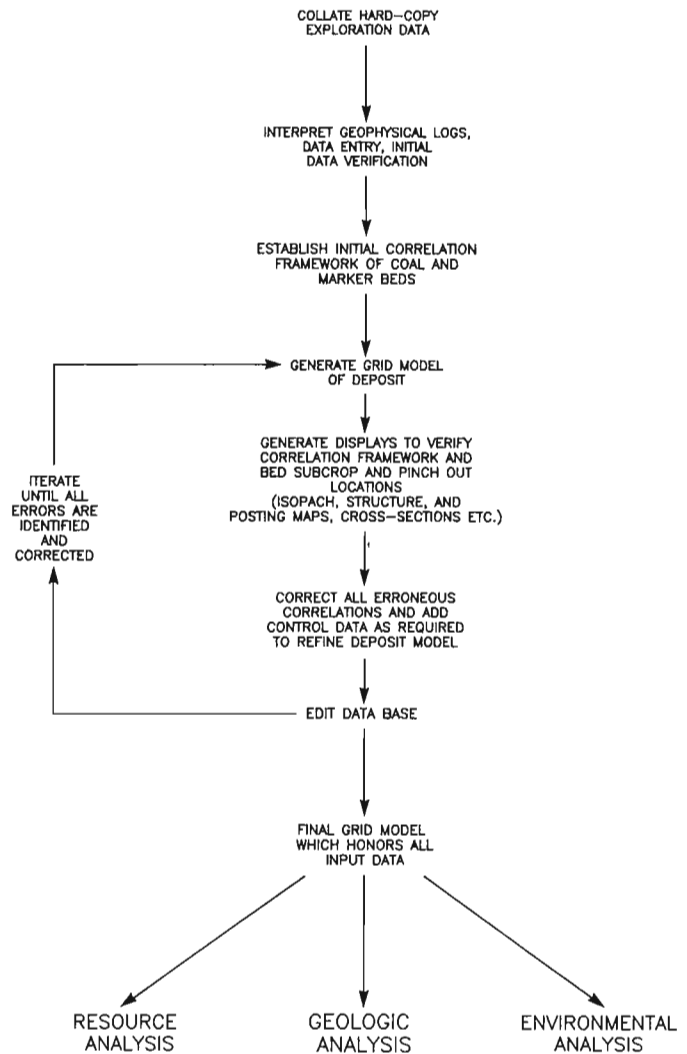


Figure 45.1. Sequence of processes undertaken to develop, from hard-copy exploration data, a computer model of a coal deposit suitable for resource, geological and environmental assessment.

Of utmost importance in the interpretation process is the consistency with which parameters such as coal thickness and lithotypes are determined. In the case of data of a descriptive nature, such as drillers' logs or core descriptions, the data compilers can do little more than transcribe the information using a standardized set of descriptors. If geophysical logs are available, they are interpreted using a standard set of procedures to maximize consistency, and then incorporated with other available data to complete the interpretation for the hole. The interpretation techniques used for geophysical logs have been discussed by Hughes (1984).

Data are stored in a hierarchical database on G.S.C.'s HP3000 computer in Calgary. The structure and contents of the database are illustrated in Figure 45.2. Data entry, modification and retrieval functions available for this database allow efficient input and editing of information. To detect errors, entries are checked against a data dictionary or numeric range on input. Graphic strip logs and listings of the data are also generated for each location and compared with the original information for

Table 45.1. Summary of exploration data available for Nova Scotia coalfields

Coalfield	Borehole data ¹				Outcrops ¹	Analyzed samples	Mines	
	Type 1 ²		Type 2 ³					
Sydney	(495)	40,865	(248)	20,624	(100)	3,000	18,927	yes
St. Rose	(8)	1,000	(11)	2,300	(0)	0	20	yes
Pictou	(198)	25,830	(124)	27,525	(50)	1,500	600	yes
Springhill	(168)	15,534	(133)	16,672	(25)	750	1,000	yes
Joggins	(50)	8,100	(14)	2,091	(25)	750	200	yes
Debert	(11)	3,060	(7)	1,254	(20)	600	50	yes
Others	(20)	4,000	(30)	6,000	(30)	900	100	yes
Totals	(950)	98,389	(567)	76,466	(250)	7,500	20,897	

¹ number of holes or outcrops in brackets, aggregate length in metres

² boreholes with driller's or geologist's description only

³ boreholes with a suite of geophysical logs

EXPLORATION DATA BASE

IDENTIFICATION DATA SET

ID NAME
 ID TYPE - HOLE, TRENCH, ADIT, OUTCROP
 LOCATION - UTM, LATITUDE-LONGITUDE,
 NTS, LEGAL DESCRIPTION
 ELEVATION
 LOCATION AND ELEVATION UNCERTAINTY
 INCLINATION
 AZIMUTH
 TOTAL, LOGGED, FLUID DEPTHS
 DATE DRILLED
 GEOLOGIST
 DRILLER
 DRILLING COMPANY
 LOGGING COMPANY
 DRILLER'S LOG - PRESENCE/ABSENCE
 GEOPHYSICAL LOGS - PRESENCE/ABSENCE
 SOURCE OF DATA
 LOG INTERPRETER
 DATE INTERPRETED
 LAST EDIT DATE

ANALYTICAL DATA SET

ID NAME
 COAL ZONE
 COAL ZONE MODIFIER
 TOP DEPTH
 BOTTOM DEPTH
 THICKNESS
 THICKNESS OF INCLUDED PARTINGS
 SAMPLE METHOD
 PER CENT RECOVERY
 LABORATORY
 SPECIFIC GRAVITY
 RANK - ASTM AND VITRINITE REFLECTANCE
 PROXIMATE ANALYSIS
 CALORIFIC VALUE
 ULTIMATE ANALYSIS
 ASH ANALYSIS
 ASH FUSION ANALYSIS
 TRACE ELEMENT ANALYSIS
 HARDNESS

STRUCTURE DATA SET

STRUCTURE NAME
 STRUCTURE TYPE - LINEAR OR PLANAR
 ORIENTATION - DIP/DIP DIRECTION
 X-Y-Z LOCATION OF TOP AND BOTTOM
 CORRELATION IF APPLICABLE

LITHOLOGY DATA SET

ID NAME
 LITHOLOGY TYPE
 LITHOLOGY MODIFIER
 PRIMARY AND SECONDARY SEDIMENTARY STRUCTURES
 FORMATION
 ZONE CORRELATION
 ZONE MODIFIER CORRELATION
 X-Y-Z LOCATION OF UNIT TOP AND BOTTOM
 THICKNESS
 EXPANDED SCALE GEOPHYSICAL LOGS?
 AVAILABILITY OF SAMPLE
 COLOR

Figure 45.2. Schematic diagram illustrating the structure and contents of the database used to store exploration data for the project.

verification. Retrievals of data can be made on an ad hoc basis using a comprehensive query language, or through a variety of programs linked to the database.

Other information required to develop coal deposit models in near-surface or undersea areas includes topographic and seafloor maps. These maps are being digitized, gridded and converted to a common co-ordinate base for incorporation with gridded exploration data in deposit models.

Objectives and current status

The objectives of this project are several. In the short term, the objective is to collate, interpret and verify all available coal exploration data in Nova Scotia. This will provide industry and government workers in these coalfields with consistently-defined exploration data in a flexible information management system. In the longer term, this information will be used to construct deposit models such as those developed by G.S.C. for coalfields in Western Canada (eg. Hughes, 1984; Hughes and Neimanis, 1986), which can be used to determine the geological, economic, quality and environmental characteristics of a deposit. These deposit models allow the rapid determination of the location and quantity of coal resources meeting any combination of quality, economic, environmental or geological criteria, and can be quickly updated as new information becomes available.

All borehole data and some of the analytical data for the Sydney and St. Rose coalfields were completed in the first year of the project. The remaining analytical data for the Sydney coalfield and all data from the Cumberland coal basin and the Debert coalfield will be completed in 1986-1987. The Pictou and other smaller coalfields will be completed in 1987-1988. The initial application of the data toward expediting the work of the coal industry will occur in mid-1986, when the Sydney database and associated programs are implemented on the Cape Breton Development Corporation's computer in Sydney.

Conclusion

This co-operative project is contributing to a larger effort by the Geological Survey of Canada to compile available exploration data for coal deposits across Canada, and construct consistently defined deposit models suitable for geological, resource and environmental assessment. The rationale behind this National Coal Inventory, beyond providing workers with consistently defined exploration information within the limits of confidentiality of the data, is to provide planners in industry and government with a flexible, high-resolution resource management tool. This tool will allow planners to rapidly determine the location and quantity of coal resources meeting any combination of geological, economic, quality or environmental criteria.

References

- Calder, J.H.
1985: Coal in Nova Scotia; Nova Scotia Department of Mines and Energy, Halifax, Nova Scotia, 79 p.
- Hughes, J.D.
1984: Geology and depositional setting of the Late Cretaceous, upper Bearpaw and lower Horseshoe Canyon formations in the Dodds-Round Hill coalfield of central Alberta – a computer-based study of closely-spaced exploration data; Geological Survey of Canada, Bulletin 361, 81 p.
- Hughes, J.D. and Neimanis, V.P.
1986: A computer-based system for quantifying surface-mineable coal resources by environmental and ownership characteristics of the overlying land surface; *in* Current Research, Part B, Geological Survey of Canada, Paper 86-1B.
- Irvine, J.A.
1981: Canadian coal resource terminology and evaluation methodology; Geological Society of America, Bulletin, Part 1, v. 92, p. 529-537.

Author Index/Index des auteurs

	Page		Page
Al-Aasm, I.S.	201	Hall, D.J.	567
Ames, D.E.	213	Hall, G.E.M.	767
Armstrong, R.L.	685	Hamilton, T.S.	707, 741
Arthur, A.J.	715	Hanmer, S.	775, 811
Ashton, K.E.	305	Hattori, K.	77
Banerjee, I.	383	Heah, T.S.T.	685
Barham, B.A.	827	Helmstaedt, H.	457
Barr, S.M.	179	Henderson, C.M.	411
Barrie, J.V.	849	Hicks, K.	77
Bédard, P.	319	Hillaire-Marcel, C.	11
Beke, G.J.	289	Himmeler, I.	85
Bell, R.T.	585	Hughes, J.D.	507
Blake, W., Jr.	239	Hughes, M.D.	85, 417
Blakeney, C.	605, 617	Hunter, J.A.	707
Bolton, T.E.	97, 107	Jackson, L.E., Jr.	257
Bornhold, B.D.	201	Jackson, S.L.	539
Bouchard, M.A.	295	Jamieson, R.A.	1, 179, 191, 557
Brisbin, W.C.	213	Jeletzky, J.A.	351
Cameron, A.R.	665	Jennings, A.	605, 617
Causse, C.	11	Jerzykiewicz, T.	421, 653
Cheel, R.J.	637	Johnston, H.P.	157
Clague, J.J.	707	Jones, R.	567
Clark, P.U.	171	Josenhans, H.W.	171
Clifford, P.M.	147	Kaszycki, C.A.	245
Cloutier, M.	869	Klassen, R.A.	617
Connelly, J.N.	811	Lamothe, M.	279
Connors, K.A.	557	Lau, S.	213
Copeland, M.J.	399	Leckie, D.A.	429, 637
Corbeil, P.	869	Leger, A.	111
Currie, K.L.	157	Lichti-Federovich, S.	263
Dahl, R.	757	Loncarevic, B.D.	85
David, J.	131	Luternauer, J.L.	707, 849
David, P.P.	319	MacLean, B.	605, 617
Davidson, A.	837	MacNeill, D.J.	417
Davies, E.H.	519	Mahony, H.	73
Davies, G.R.	467	Mamet, B.L.	467
DiLabio, R.N.W.	245	Marcotte, C.	295
Dixon, J.	375	Mason, R.	567, 577
Dixon, J.M.	457	Matthews, J.V., Jr.	289
Duk-Rodkin, A.	257	Maurice, Y.T.	785
Edmunds, C.F.	567	McCready, R.G.L.	73
Embry, A.F.	329, 341	McIntyre, D.J.	405
Erdmer, P.	19, 29	McLean, R.A.	443
Evenchick, C.A.	733	McMullin, D.W.A.	727
Fader, G.B.J.	591	Melnik, N.	567, 577
Fahrig, W.F.	65	Mihalynuk, M.G.	721
Foscolos, A.E.	429	Miller, A.R.	679
Froese, E.	827	Miller, R.O.	591
Fueten, F.	797	Monger, J.W.H.	699
Gagnon, Y.D.	1	Moreton, C.	57
Gandhi, S.S.	47, 853	Morgan, P.	859
Gariepy, C.	131	Mortensen, J.K.	141
Ghent, E.D.	693, 721	Mott, J.A.	457
Gibling, M.R.	73	Mott, R.J.	289
Goodarzi, F.	421, 671	Mountain, B.	567
Gordon, T.M.	539	Nassichuk, W.W.	411, 467
Grant, D.R.	289	Neimanis, V.P.	507
Grant, S.M.	837	Nobes, D.C.	741
Green, S.B.	47	Norris, D.K.	665
Greenwood, H.J.	727		
Gregoire, D.C.	39		

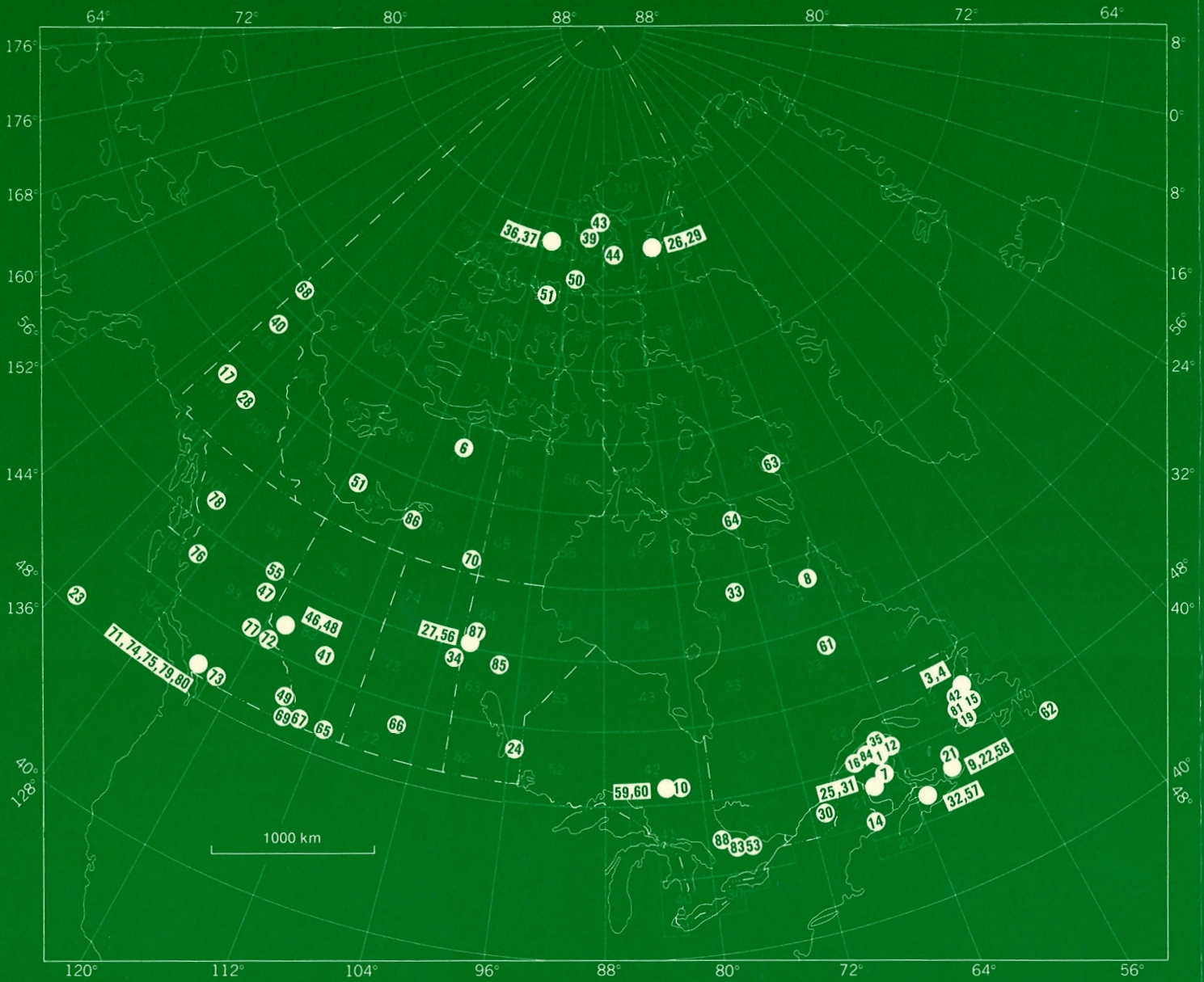
	Page		Page
O'Beirne-Ryan, A.M.	179, 191	Sevigny, J.H.	693
O'Brien, J.	749	Shilts, W.W.	271
Osadetz, K.G.	647	Smith, S.L.	271
Owen, J.V.	29	Snowdon, L.R.	647
		Steele-Petrovich, H.M.	493
Park, C.J.	767	Sweet, A.R.	653
Pedder, A.E.H.	471		
Pickering, M.E.	797	Thorpe, R.I.	585
Plint, H.E.	557		
Poulsen, K.H.	213	van Berkel, J.T.	157
Poulton, T.P.	519	van Bosse, J.Y.	865
Pratt, K.C.	665	van Breemen, O.	775
Pullan, S.E.	707		
		Watkinson, D.H.	757
Rappol, M.	223	Watson, P.	417
Ravenhurst, C.E.	547	Whalen, J.B.	121
Reynolds, P.H.	547	Wheatley, K.J.	305
Ricketts, B.D.	363, 405	William-Jones, A.E.	865
Roberts, M.C.	707	Williams, G.L.	605, 617
Robin, P.-Y.F.	797	Williams, P.F.	57, 111
Rodkin, O.	257	Woodsworth, G.J.	685
Roscoe, S.M.	47, 679		
		Zentilli, M.	73, 547
Samson, I.M.	865		
Sanford, B.V.	617		
Sartenaer, P.	489		

NOTE TO CONTRIBUTORS

Submissions to the *Discussion* section of *Current Research* are welcome from both the staff of the Geological Survey and from the public. Discussions are limited to 6 double-spaced typewritten pages (about 1500 words) and are subject to review by the Chief Scientific Editor. Discussions are restricted to the scientific content of Geological Survey reports. General discussions concerning branch or government policy will not be accepted. Illustrations will be accepted only if, in the opinion of the editor, they are considered essential. In any case no redrafting will be undertaken and reproducible copy must accompany the original submissions. Discussion is limited to recent reports (not more than 2 years old) and may be in either English or French. Every effort is made to include both *Discussion* and *Reply* in the same issue. *Current Research* is published in January and July. Submissions should be sent to the Chief Scientific Editor, Geological Survey of Canada, 601 Booth Street, Ottawa, Canada, K1A 0E8.

AVIS AUX AUTEURS D'ARTICLES

Nous encourageons tant le personnel de la Commission géologique que le grand public à nous faire parvenir des articles destinés à la section *discussion* de la publication *Recherches en cours*. Le texte doit comprendre au plus six pages dactylographiées à double interligne (environ 1500 mots), texte qui peut faire l'objet d'un réexamen par le rédacteur en chef scientifique. Les discussions doivent se limiter au contenu scientifique des rapports de la Commission géologique. Les discussions générales sur la Direction ou les politiques gouvernementales ne seront pas acceptées. Les illustrations ne seront acceptées que dans la mesure où, selon l'opinion du rédacteur, elles seront considérées comme essentielles. Aucune retouche ne sera faite aux textes et dans tous les cas, une copie qui puisse être reproduite doit accompagner les textes originaux. Les discussions en français ou en anglais doivent se limiter aux rapports récents (au plus de 2 ans). On s'efforcera de faire coïncider les articles destinés aux rubriques *discussions* et *reponses* dans le même numéro. La publication *Recherches en cours* paraît en janvier et en juillet. Les articles doivent être renvoyés au rédacteur en chef scientifique: Commission géologique du Canada, 601, rue Booth, Ottawa, Canada, K1A 0E8.



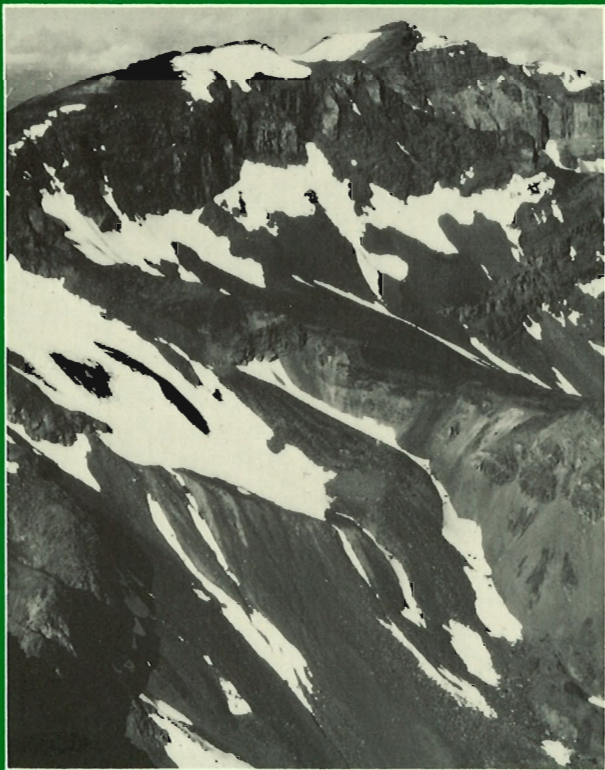
Energy, Mines and
Resources Canada

Énergie, Mines et
Ressources Canada

Geological Survey of Canada
Commission géologique du Canada

PAPER 86-1B
ÉTUDE

CURRENT RESEARCH PART B RECHERCHES EN COURS PARTIE B



(Pages 421-880)

Notice to Librarians and Indexers

The Geological Survey's twice-yearly *Current Research* series contains many reports comparable in scope and subject matter to those appearing in scientific journals and other serials. All contributions to *Current Research* include an abstract and bibliographic citation. It is hoped that these will assist you in cataloguing and indexing these reports and that this will result in a still wider dissemination of the results of the Geological Survey's research activities.

Avis aux bibliothécaires et préparateurs d'index

La série *Recherches en cours* de la Commission géologique paraît deux fois par année; elle contient plusieurs rapports dont la portée et la nature sont comparables à ceux qui paraissent dans les revues scientifiques et autres périodiques. Tous les articles publiés dans les *Recherches en cours* sont accompagnés d'un résumé et d'une bibliographie, ce qui vous permettra, nous l'espérons, de cataloguer et d'indexer ces rapports, d'où une meilleure diffusion des résultats de recherche de la Commission géologique.



GEOLOGICAL SURVEY OF CANADA
PAPER 86-1B

COMMISSION GÉOLOGIQUE DU CANADA
ÉTUDE 86-1B

CURRENT RESEARCH PART B

RECHERCHES EN COURS PARTIE B

Issued in two sections/Publiée en deux volumes:
pages 1-420 and/et pages 421-880

1986

© Minister of Supply and Services Canada 1986

Available in Canada through

authorized bookstore agents and other bookstores

or by mail from

Canadian Government Publishing Centre
Supply and Services Canada
Ottawa, Canada K1A 0S9

and from

Geological Survey of Canada offices:

601 Booth Street
Ottawa, Canada K1A 0E8

3303-33rd Street N.W.,
Calgary, Alberta T2L 2A7

100 West Pender Street
Vancouver, British Columbia V6B 1R8
(mainly B.C. and Yukon)

A deposit copy of this publication is also available
for reference in public libraries across Canada

Cat. No. M44-86/1BE Canada: \$20.00
ISBN 0-660-53302-2 Other countries: \$24.00

Price subject to change without notice

Sold in sets

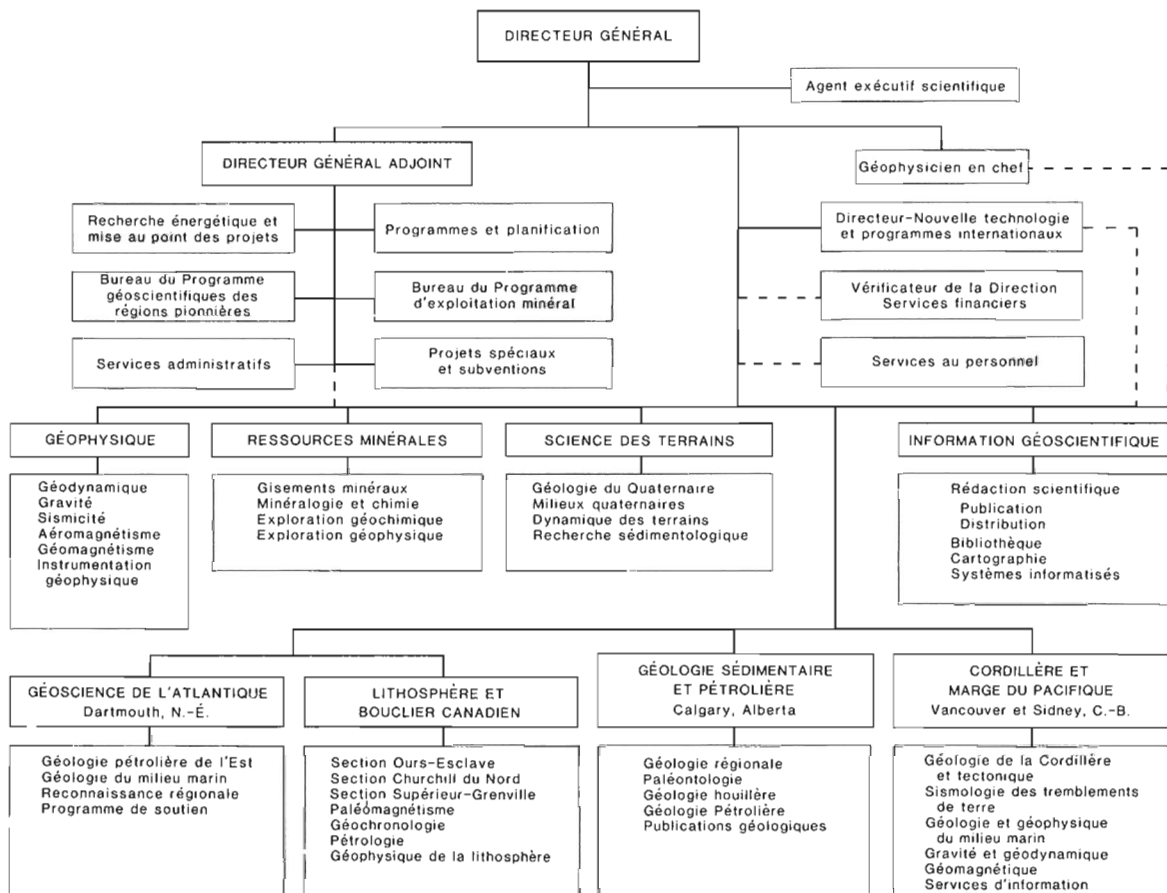
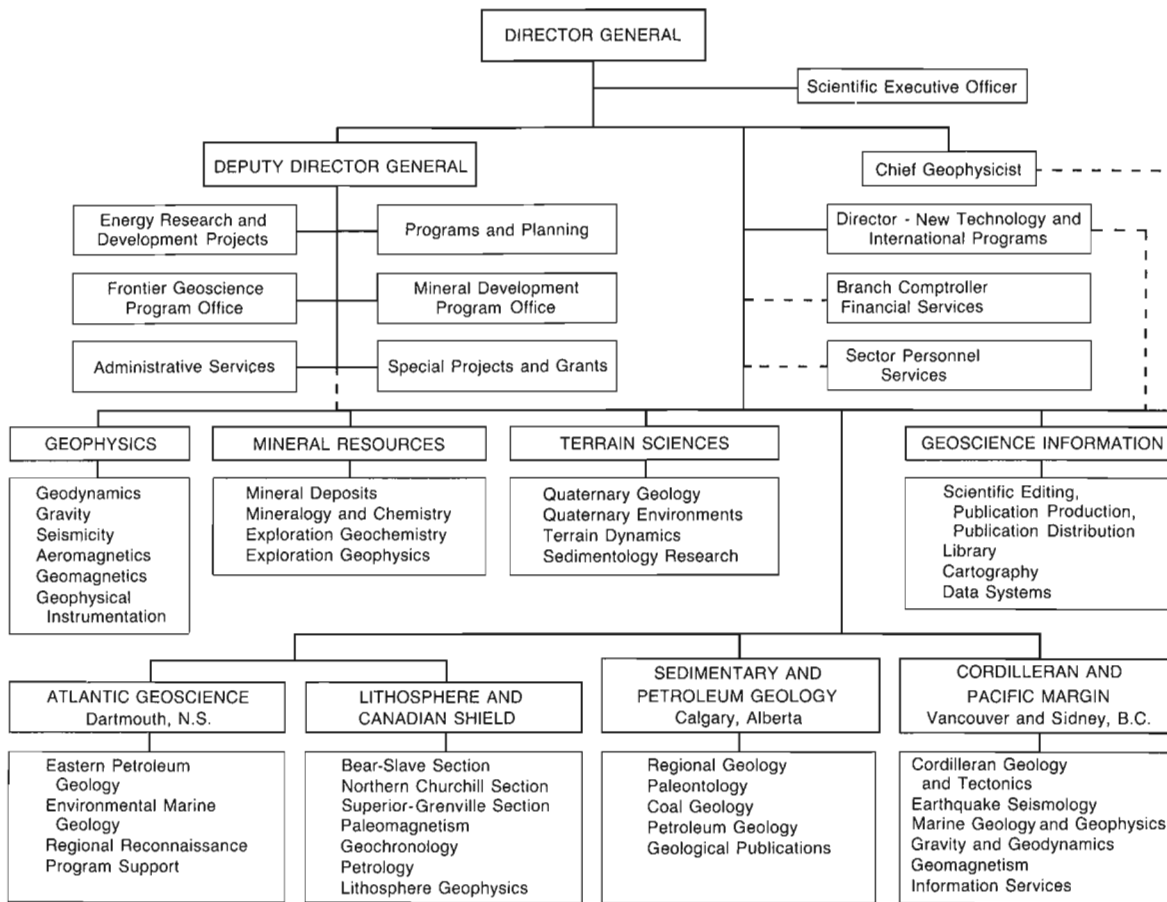
Cover

Left

View west across the Nation Anticline, showing the layering and structural style of the Cold Fish volcanics, Spatsizi map area, north-central British Columbia. See report 78, p. 733-739, by C.A. Evenchick for details.

Right

Sea Data 635-12 directional wave and current meter, in tripod. See note by P. Morgan (p. 859-863) for details.



Separates

A limited number of separates of the papers that appear in this volume are available by direct request to the individual authors. The addresses of the Geological Survey of Canada offices follow:

601 Booth Street,
OTTAWA, Ontario
K1A 0E8

Institute of Sedimentary and Petroleum Geology,
3303-33rd Street N.W.,
CALGARY, Alberta
T2L 2A7

Cordilleran and Pacific Margin Division,
100 West Pender Street,
VANCOUVER, B.C.
V6B 1R8

Atlantic Geoscience Centre,
Bedford Institute of Oceanography,
P.O. Box 1006,
DARTMOUTH, N.S.
B2Y 4A2

When no location accompanies an author's name in the title of a paper, the Ottawa address should be used.

Tirés à part

On peut obtenir un nombre limité de "tirés à part" des articles qui paraissent dans cette publication en s'adressant directement à chaque auteur. Les adresses des différents bureaux de la Commission géologique du Canada sont les suivantes:

601, rue Booth
OTTAWA, Ontario
K1A 0E8

Institut de géologie sédimentaire et pétrolière
3303-33rd, St. N.W.,
CALGARY, Alberta
T2L 2A7

Division de la Cordillère et marge du Pacifique
100 West Pender Street
VANCOUVER, Colombie-Britannique
V6B 1R8

Centre géoscientifique de l'Atlantique
Institut océanographique de Bedford
B.P. 1006
DARTMOUTH, Nouvelle-Ecosse
B2Y 4A2

Lorsque l'adresse de l'auteur ne figure pas sous le titre d'un document, on doit alors utiliser l'adresse d'Ottawa.

SCIENTIFIC AND TECHNICAL REPORTS RAPPORTS SCIENTIFIQUES ET TECHNIQUES

COAL/CHARBON

F. GOODARZI and T. JERZYKIEWICZ: Petrology of a burning bituminous coal seam at Coalspur, Alberta	421
A.R. CAMERON, D.K. NORRIS, and K.C. PRATT: Rank and other compositional data on coals and carbonaceous shale of the Kayak Formation, northern Yukon Territory	665
F. GOODARZI: Comparison of morphology and reflectance of macerals from a tectonically thickened coal seam from Mist Mountain, British Columbia	671

ECONOMIC GEOLOGY/GÉOLOGIE ÉCONOMIQUE

S.M. ROSCOE, S.B. GREEN, and S.S. GANDHI: Uranium, gold and selenide minerals locally concentrated in drift at Twin Lakes near Bathurst Inlet, N.W.T.	47
C. MORETON and P.F. WILLIAMS: Structural and stratigraphic relationships at the B-zone orebody, Heath Steele Mines, Newcastle, New Brunswick	57
K.H. POULSEN, D.E. AMES, S. LAU, and W.C. BRISBIN: Preliminary report on the structural setting of gold in the Rice Lake area, Uchi Subprovince, southeast Manitoba	213
R. MASON, N. MELNIK, C.F. EDMUNDS, D.J. HALL, R. JONES, and B. MOUNTAIN: The McIntyre-Hollinger investigation, Timmins, Ontario: stratigraphy, lithology and structure	567
R. MASON and N. MELNIK: The McIntyre-Hollinger investigation, Timmins, Ontario: a gold dominated porphyry copper system	577
R. DAHL and D.H. WATKINSON: Structural control of podiform chromitite in Bay of Islands ophiolite, the Springer Hill area, Newfoundland	757
Y.T. MAURICE: Distribution and origin of alluvial gold in southwest Gaspésie, Quebec	785

GEOCHEMISTRY/GÉOCHIMIE

D.C. GREGOIRE: Inductively coupled plasma-mass spectrometry at the Geological Survey of Canada	39
M.R. GIBLING, M. ZENTILLI, H. MAHONY, and R.G.L. McCREADY: An isotopic evaluation of sulphur recycling from evaporites to coals in the Carboniferous Sydney Basin, Nova Scotia	73
K. HATTORI and K. HICKS: Preliminary report on the gold mineralization at Bell Creek, Timmins, Ontario	77

J.B. WHALEN: Geochemistry of the mafic and volcanic components of the Topsails igneous suite, western Newfoundland	121
J. DAVID and C. GARIEPY: Geochemistry of the Lower Silurian Pointe aux Trembles and Lac Raymond formations, central Quebec Appalachians: a preliminary report	131
C.J. PARK and G.E.M. HALL: Electrothermal vapourization as a means of sample introduction into an inductively coupled plasma mass spectrometer: a preliminary report of a new analytical technique	767

GEOCHRONOLOGY/GÉOCHRONOLOGIE

J.K. MORTENSEN: U-Pb ages for granitic orthogneiss from western Yukon Territory: Selwyn Gneiss and Fiftymile Batholith revisited	141
C.E. RAVENHURST, P.H. REYNOLDS, and M. ZENTILLI: Strontium isotopic studies of rock and mineral samples in the Shubenacadie Basin, Nova Scotia	547
R.T. BELL and R.I. THORPE: Pb-Pb isochron age of uraniferous phosphorite at the base of the Menihok Formation, Labrador Trough	585
O. VAN BREEMEN and S. HANMER: Zircon morphology and U-Pb geochronology in active shear zones: studies on syntectonic intrusions along the northwest boundary of the Central Metasedimentary Belt, Grenville Province, Ontario	775

GEOPHYSICS/GÉOPHYSIQUES

B.D. LONCAREVIC, M.D. HUGHES, and I. HIMMLER: Evaluation of sea gravimeters: comparison of Bodenseewerk KSS30 and KSS31 systems	85
T.S. HAMILTON and D.C. NOBES: DC resistivity and CSAMT profiles of the southwestern Fraser River delta, British Columbia	741

MARINE GEOSCIENCE/ÉTUDES GEOSCIENTIFIQUES DU MILIEU MARIN

P.U. CLARK and H.W. JOSEPH: Late Quaternary land-sea correlations, northern Labrador and Labrador shelf	171
I.S. AL-AASM and B.D. BORNHOLD: Stable isotope studies of planktonic foraminifera <i>Globigerina bulloides</i> from cores in the northeast Pacific Ocean	201
G.B.J. FADER and R.O. MILLER: A reconnaissance study of the surficial and shallow bedrock geology of the southeastern Grand Banks of Newfoundland	591
B. MACLEAN, G.L. WILLIAMS, A. JENNINGS, and C. BLAKENEY: Bedrock and surficial geology of Cumberland Sound, N.W.T.	605
B. MACLEAN, G.L. WILLIAMS, B.V. SANFORD, R.A. KLASSEN, C. BLAKENEY, and A. JENNINGS: A reconnaissance study of the bedrock and surficial geology of Hudson Strait, N.W.T.	617
J.L. LUTERNAUER, J.J. CLAGUE, T.S. HAMILTON, J.A. HUNTER, S.E. PULLAN, and M.C. ROBERTS: Structure and stratigraphy of the southwestern Fraser River delta: a trial shallow seismic profiling and coring survey	707

MATHEMATICAL AND COMPUTATIONAL GEOLOGY/APPLICATION DES MATHÉMATIQUES ET
DES MÉTHODES MATHÉMATIQUES DE L'ANALYSE À LA GÉOLOGIE

J.D. HUGHES, D.J. MACNEILL, and P. WATSON: Computerization of coal exploration data for Nova Scotia: a joint Federal-Provincial project	417
J.D. HUGHES and V.P. NEIMANIS: A computer-based system for quantifying surface-mineable coal resources according to environmental characteristics and ownership of the overlying land surface	507

PALEOMAGNETISM/PALÉOMAGNETISME

W.F. FAHRIG: Paleomagnetism of Neohelikian Korok sheets and dykes, and of a possible Mackenzie dyke from southeast of Ungava Bay	65
----------------------------------------------------------------------------------------------------------------------------------------	----

PALEONTOLOGY/PALÉONTOLOGIE

T.E. BOLTON: Early Silurian Bryozoa from the Clemville Formation of the Port Daniel region, Gaspésie Peninsula, Quebec	97
T.E. BOLTON: <i>Chaetitopora</i> (Anthozoa, Tabulata) in the Upper Ordovician rocks of central and eastern Canada	107
J.A. JELETZKY: <i>Pseudoeurptychites</i> : a new polyptychitid ammonite from the Lower Valanginian of the Canadian and Eurasian Arctic	351
M.J. COPELAND: <i>Bullaluta kindlei</i> n. gen., n. sp. (Ostracoda, Archaeocopida) from Zone 5 (Late Cambrian, <i>Cedaria</i> – <i>Crepicephalus</i>) of the Cow Head Group, western Newfoundland	399
W.W. NASSICHUK and C.M. HENDERSON: Lower Permian (Asselian) ammonoids and conodonts from the Belcher Channel Formation, southwestern Ellesmere Island	411
R.A. MCLEAN: The rugose coral <i>Pachyphyllum</i> Edwards and Haime in the Frasnian (Upper Devonian) of Western Canada	443
W.W. NASSICHUK, G.R. DAVIES, and B.L. MAMET: Microcodiaceans in the Viséan Emma Fiord Formation, Devon Island, Arctic Canada	467
A.E.H. PEDDER: Species of the rugose coral genus <i>Minussiella</i> from the Middle Devonian of western and Arctic Canada	471
P. SARTENAER: A new late Eifelian rhynchonellid genus from western North America	489
E.H. DAVIES and T.P. POULTON: Upper Jurassic dinoflagellate cysts from strata of northeastern British Columbia	519

PETROLEUM GEOLOGY/GÉOLOGIE PÉTROLIÈRE

K.G. OSADETZ and L.R. SNOWDON: Speculation on the petroleum source rock potential of portions of the Lodgepole Formation (Mississippian) of southern Saskatchewan	647
-------------------------------------------------------------------------------------------------------------------------------------------------------------------------	-----

QUATERNARY GEOLOGY/GÉOLOGIE DU QUATERNAIRE

Mapping, stratigraphic studies, and sedimentology/Cartographie, études stratigraphiques et sédimentologie

M. RAPPOL: Aspects of ice flow patterns, glacial sediments, and stratigraphy in northwest New Brunswick	223
A. DUK-RODKIN, L.E. JACKSON, JR., and O. RODKIN: A composite profile of the Cordilleran ice sheet during McConnell Glaciation, Glenlyon and Tay River map areas, Yukon Territory	257

Exploration technology and glacial dispersal studies/Techniques d'exploration et études de la dispersion glaciaire

C.A. KASZYCKI and R.N.W. DILABIO: Surficial geology and till geochemistry, Lynn Lake-Leaf Rapids region, Manitoba	245
W.W. SHILTS and S.L. SMITH: Stratigraphic setting of buried gold-bearing sediments, Beauceville area, Quebec	271
M. LAMOTHE: Reconnaissance geochemical sampling of till, south-central Miramichi Zone, New Brunswick	279
M.A. BOUCHARD and C. MARCOTTE: Regional glacial dispersal patterns in Ungava, Nouveau-Québec	295
P.P. DAVID and P. BEDARD: Stratigraphy of the McGerrigle Mountains granite trains of Gaspésie, Quebec	319

Paleoenvironmental studies and geochronology/Étude des paléoenvironnements et géochronologie

C. CAUSSE et C. HILLAIRE-MARCEL: Géochimie des familles U et Th dans la matière organique fossile des dépôts interglaciaires et interstadias de l'est et du nord du Canada: potentiel radiochronologique	11
W. BLAKE, JR.: New AMS radiocarbon age determinations from east-central Ellesmere Island; applications to glacial geology	239
S. LICHTI-FEDEROVICH: Diatom dispersal phenomena: diatoms in precipitation samples from Cape Herschel, east-central Ellesmere Island, Northwest Territories – a quantitative assessment	263
R.J. MOTT, J.V. MATTHEWS, JR., D.R. GRANT, and G.J. BEKE: A late glacial buried organic profile near Brookside, Nova Scotia	289

REGIONAL GEOLOGY/GÉOLOGIE RÉGIONALE

Appalachian region/Région des Appalaches

Y.D. GAGNON et R.A. JAMIESON: Étude de la semelle métamorphique du complexe du Mont Albert, Gaspésie, Québec	1
P. ERDMER: Geology of the Long Range Inlier in Sandy Lake map area, western Newfoundland	19
J.V. OWEN and P. ERDMER: Precambrian and Paleozoic metamorphism in the Long Range Inlier, western Newfoundland	29
J.T. VAN BERKEL, H.P. JOHNSTON, and K.L. CURRIE: A preliminary report on the geology of the southern Long Range, southwestern Newfoundland	157
A.M. O'BEIRNE-RYAN, S.M. BARR, and R.A. JAMIESON: Contrasting petrology and age of two megacrystic granitoid plutons, Cape Breton Island, Nova Scotia	179
A.M. O'BEIRNE-RYAN and R.A. JAMIESON: Geology of the West Branch North River and the Bothan Brook plutons of the south-central Cape Breton Highlands, Nova Scotia	191
H.E. PLINT, K.A. CONNORS, and R.A. JAMIESON: Geology and mineral occurrences of the Jumping Brook Complex, Cheticamp-Pleasant Bay area, Cape Breton Island, Nova Scotia	557

Arctic Islands/Archipel Arctique

A.F. EMBRY: Stratigraphic subdivision of the Blind Fiord and Bjerne formations (Lower Triassic), Sverdrup Basin, Arctic Islands	329
---------------------------------------------------------------------------------------------------------------------------------------	-----

A.F. EMBRY: Stratigraphic subdivision of the Awingak Formation (Upper Jurassic) and revision of the Hiccles Cove Formation (Middle Jurassic), Sverdrup Basin, Arctic Islands	341
B.D. RICKETTS: New formations in the Eureka Sound Group, Canadian Arctic Islands	363
B.D. RICKETTS and D.J. MCINTYRE: The Eureka Sound Group of eastern Axel Heiberg Island: new data on the Eurekan Orogeny	405
Cordilleran region/Région de la Cordillère	
J. DIXON: Comments on the stratigraphy, sedimentology and distribution of the Albian Sharp Mountain Formation, northern Yukon	375
D.A. LECKIE and A.E. FOSCOLOS: Paleosols and Late Albian sea level fluctuations: preliminary observations from the northeastern British Columbia foothills	429
J.A. MOTT, J.M. DIXON, and H. HELMSTAEDT: Ordovician stratigraphy and the structural style at the Main Ranges-Front Ranges boundary near Smith Peak, British Columbia	457
T.S.T. HEAH, R.L. ARMSTRONG, and G.J. WOODSWORTH: The Gambier Group in the Sky Pilot area, southwestern Coast Mountains, British Columbia	685
J.H. SEVIGNY and E.D. GHENT: Metamorphism in the northern Adams River area, northeastern Shuswap Complex, Monashee Mountains, British Columbia	693
J.W.H. MONGER: Geology between Harrison Lake and Fraser River, Hope map area, southwestern British Columbia	699
A.J. ARTHUR: Stratigraphy along the west side of Harrison Lake, southwestern British Columbia	715
M.G. MIHALYNUK and E.D. GHENT: Stratigraphy, deformation and low grade metamorphism of the Telkwa Formation near Terrace, British Columbia	721
D.W.A. MCMULLIN and H.J. GREENWOOD: Metamorphic pressures and temperatures in the Barkerville and Cariboo terranes, Quesnel Lake, British Columbia: preliminary results	727
C.A. EVENCHICK: Structural style of the northeast margin of the Bowser Basin, Spatsizi map area, north-central British Columbia	733
J. O'BRIEN: Jurassic stratigraphy of the Methow Trough, southwestern British Columbia	749
Canadian Shield/Bouclier canadien	
P.M. CLIFFORD: Petrological and structural evolution of the rocks in the vicinity of Killarney, Ontario: an interim report	147
K.E. ASHTON and K.J. WHEATLEY: Preliminary report on the Kisseynew gneisses in the Kisseynew-Wildnest lakes area, Saskatchewan	305
S.L. JACKSON and T.M. GORDON: Metamorphic studies in the transition zone between the Lynn Lake Greenstone Belt and the Kisseynew gneiss belt, Laurie Lake, Manitoba	539
S.M. ROSCOE and A.R. MILLER: Outliers of porphyritic alkaline volcanic rocks of the Christopher Island Formation at Snowbird Lake, N.W.T.	679
F. FUETEN, P.-Y. F. ROBIN, and M.E. PICKERING: Deformation in the Thompson Belt, central Manitoba: a progress report	797
S. HANMER and J.N. CONNELLY: Mechanical role of the syntectonic Laloche Batholith in the Great Slave Lake Shear Zone, District of Mackenzie, N.W.T.	811

B.A. BARHAM and E. FROESE: Geology of the New Fox alteration zone, Laurie Lake, Manitoba	827
A. DAVIDSON and S.M. GRANT: Reconnaissance geology of western and central Algonquin Park and detailed study of coronitic olivine metagabbro, central Gneiss Belt, Grenville Province of Ontario	837

Interior Plains/Plaines intérieures

I. BANERJEE: Lower Mannville sedimentation in the "Edmonton Channel", central Alberta	383
D.A. LECKIE and R.J. CHEEL: Tidal channel facies of the Virgelle Member (Cretaceous Milk River Formation), southern Alberta	637
T. JERZYKIEWICZ and A.R. SWEET: Caliche and associated impoverished palynological assemblages: an innovative line of paleoclimatic research onto the uppermost Cretaceous and Paleocene of southern Alberta	653

STRATIGRAPHY/STRATIGRAPHIE

H.M. STEELE-PETROVICH: Lithostratigraphy and a summary of the paleoenvironments of the lower Middle Ordovician sedimentary rocks, upper Ottawa Valley, Ontario	493
----------------------------------------------------------------------------------------------------------------------------------------------------------------------------	-----

STRUCTURAL GEOLOGY/GÉOLOGIE STRUCTURALE

A. LEGER and P.F. WILLIAMS: Transcurrent faulting history of southern New Brunswick	111
----------------------------------------------------------------------------------------------	-----

SCIENTIFIC AND TECHNICAL NOTES NOTES SCIENTIFIQUES ET TECHNIQUES

J.V. BARRIE and J.L. LUTERNAUER: Titaniferous placers on the central continental shelf off western Canada	849
S.S. GANDHI: Garnetiferous gneisses and a quartz syenite intrusive sheet at Lynx Lake, Northwest Territories	853
P. MORGAN: Sediment transport study at King Point, Yukon Territory	859
J.Y. VAN BOSSE, I.M. SAMSON, and A.E. WILLIAM-JONES: Illite crystallinity studies around the Roberts metal deposit, Eastern Townships, Quebec	865
M. CLOUTIER et P. CORBEIL: Géologie du Quaternaire de la région du Mont Alexandre, Gaspésie, Quebec	869

CANADA-NEWFOUNDLAND MINERAL DEVELOPMENT AGREEMENT 1984-1989	875-880
CANADA-TERRE-NEUVE: ENTENTE D'EXPLOITATION MINÉRALE 1984-1989	

AUTHOR INDEX/INDEX DES AUTEURS	420a/883
--------------------------------------	----------

Errata	881
--------------	-----

Petrology of a burning bituminous coal seam at Coalspur, Alberta

Projects 780006 and 810039

F. Goodarzi and T. Jerzykiewicz
Institute of Sedimentary and Petroleum Geology, Calgary

Goodarzi, F. and Jerzykiewicz, T., Petrology of a burning bituminous coal seam at Coalspur, Alberta; in Current Research, Part B, Geological Survey of Canada, Paper 86-1B, p. 421-427, 1986.

Abstract

Samples from a burning bituminous coal seam (%Roil = 0.70) at Coalspur, Alberta, Canada were studied using reflected light microscopy. The burning of coal has taken place in limited areas of the seam that had access to air. Two zones, namely, oxidation-combustion, and distillation, were detected in the coal seam.

Near the surface, the oxidation zone contains chars showing cracks and oxidation rims. The combusted chars in the deeper part of the oxidation zone have a carbonized matrix, and the rims are combusted.

The distillation zone covers most of the coal seam. The chars in this zone have not developed oxidation rims. Distilled chars are mostly in the precarbonization stage, except for chars immediately below the combustion zone, or near the base of the coal seam. Precarbonized chars have developed devolatilization vacuoles and contraction cracks. These chars contain pyrolytic carbon in some horizons. The distilled chars were formed due to heat generated by combustion of coal at the top of the coal seam and also due to transfer of heat from an underlying burning seam through an intercalated, clastic layer.

Résumé

Des échantillons d'un filon de charbon bitumineux en combustion (% de réflectance dans l'huile = 0,70) à Coalspur, en Alberta, ont été examinés à l'aide d'un microscope à lumière réfléchie. La combustion du charbon a lieu dans certaines zones restreintes du filon qui sont exposées à l'air. Deux zones, l'une d'oxydation et de combustion et l'autre de distillation, ont été décelées dans le filon.

Près de la surface, la zone d'oxydation contient des résidus carbonés parsemés de fissures et d'auréoles d'oxydation. Les résidus carbonés dans la partie plus profonde de la zone d'oxydation ont une matrice carbonisée et des auréoles calcinées.

La zone de distillation couvre la plus grande partie du filon houiller. Les résidus carbonés qu'elle contient sont dépourvus d'auréoles d'oxydation. La plus grande partie des résidus carbonés distillés en sont à l'étape de la précarbonisation, sauf les résidus situés immédiatement sous la zone de combustion ou près de la base du filon houiller. Les résidus précarbonisés contiennent des vacuoles laissées par le dégagement des matières volatiles et des fentes de contraction. Dans certains horizons, ces résidus contiennent du carbone pyrolytique. Les résidus distillés ont été formés par la chaleur provenant de la combustion du charbon au sommet du filon et par le transfert, au travers d'une couche clastique intercalaire, de la chaleur dégagée par un filon sous-jacent en combustion.

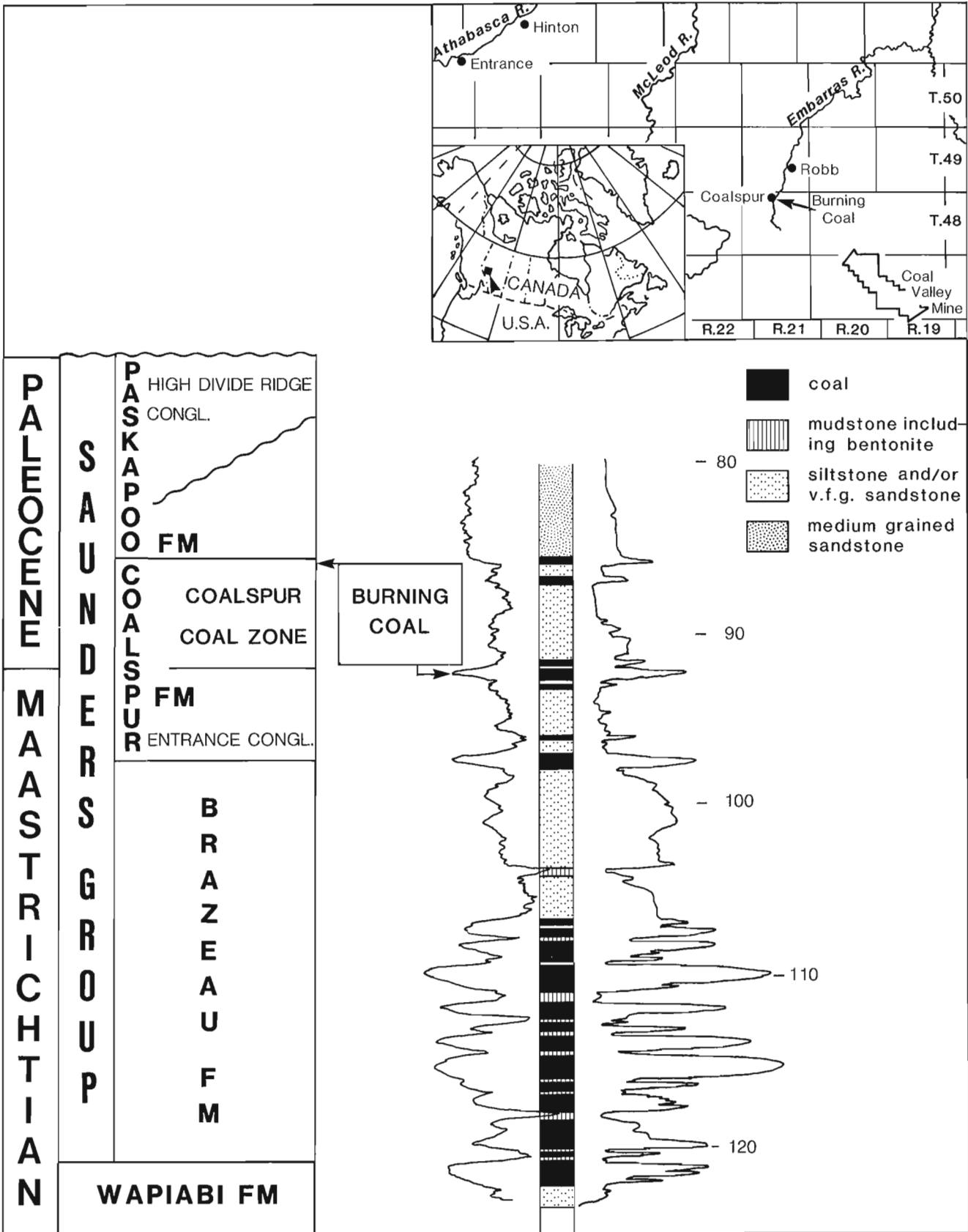


Figure 46.1. Location and geological setting of "burning coal".

Introduction

Natural burning of coal may start as a result of lightning or bush or forest fires (Pearson and Creaney, 1980; Bustin and Matthews, 1982). Pearson and Creaney (1980) have stated that the formation of meta-anthracite with a reflectance of 5.0 per cent at the Fording Coal property, British Columbia, was due to lightning strikes, which started the burning and transformation of a weathered, low volatile coal seam. Bustin and Matthews (1982) have reported that the ignition of a high volatile bituminous (%Roil = 0.96) coal seam in the Lower Cretaceous Mist Mountain Formation, British Columbia, was due to a forest fire. This coal seam was about 6 m thick and its upper 2 to 3 m were completely consumed by fire. The remaining 3 to 4 m were transformed into coke or remained unaltered.

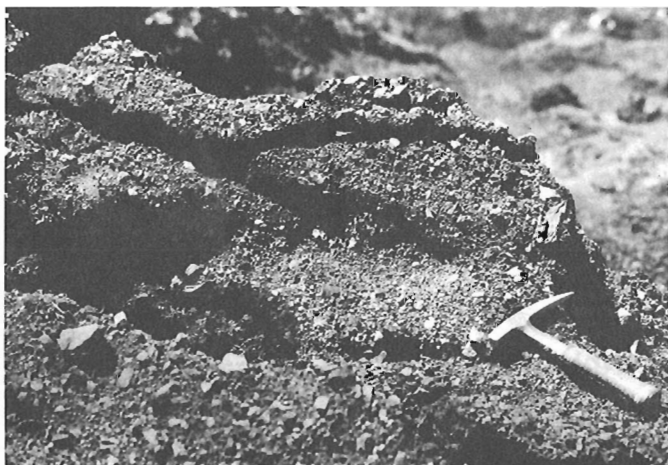


Figure 46.2. Cracks formed on the top and side of the burning coal.

The present work is part of a systematic study of burning coal seams and coal dumps in Western Canada. In this instance, the petrology of a burning bituminous coal seam of Cretaceous age in Coalspur, Alberta (Fig. 46.1) is examined. This and other coal seams have been burning since 1922 (Fryer, 1981). There is no evidence as to how the burning was started.

Geological setting of the "burning coal"

The samples of "burning coal" were collected from the roadcut section of the uppermost part of the Coalspur coal zone at Coalspur (Fig. 46.1). The middle part of the section is occupied by a smoldering and burning coal zone comprising rather thin coal beds interfingering with mudstone, siltstone and very fine grained sandstone intrabeds above the Val d'Or coal seam (Fig. 46.1).



Figure 46.4. Sulphur crystals (S) on the surface fragments near the cracks (C).



Figure 46.3. Emission of volatile matter from burning coal.

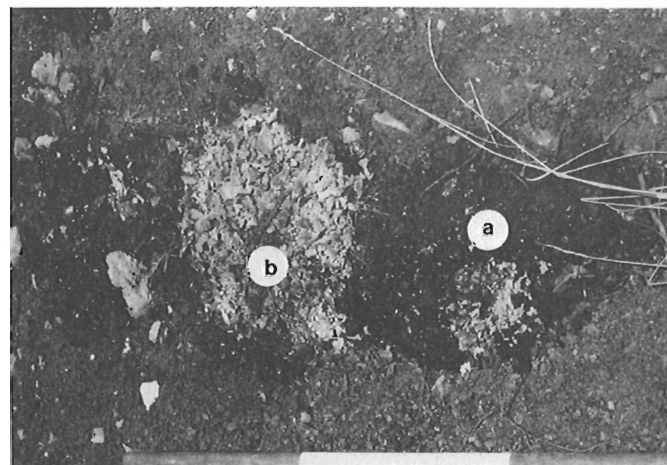


Figure 46.5. Conversion of coal to ash from oxidation zone; (a) from oxidized coal, and (b) from combusted coal. Note the extent of ashing from combusted coal, and also the angular shape of individual particles.

The Coalspur coal zone, which is the upper part of the Coalspur Formation (Fig. 46.1), is considered to be the major Lower Paleocene coal-bearing interval in the Alberta Foothills. It contains several mineable coals seams. Some of them are being exploited in the Coal Valley Mine (Fig. 46.1). The Val d'Or seam is the thickest (over 10 m) and laterally the most continuous. The Coalspur coal zone has been described as originating in an alluvial floodplain environment of deposition (Jerzykiewicz and McLean, 1980).

The roadcut section in Coalspur is the reference section for the uppermost part of the Coalspur Formation and the lowermost Paskapoo Formation in the central Alberta foothills (Jerzykiewicz, 1985).

Experimental procedure

Sample collection

Channel samples of the fresh, oxidized and distilled coal were collected in 5 cm increments after excavation of a trench across the burning zone. The hot, burning residues were cooled in water immediately after sampling to prevent further oxidation and combustion. All samples were stored in water while awaiting further examination. The samples were dried and crushed to pass <20 mesh (>850 nm). Polished samples were prepared following the method of Mackowsky (1982).

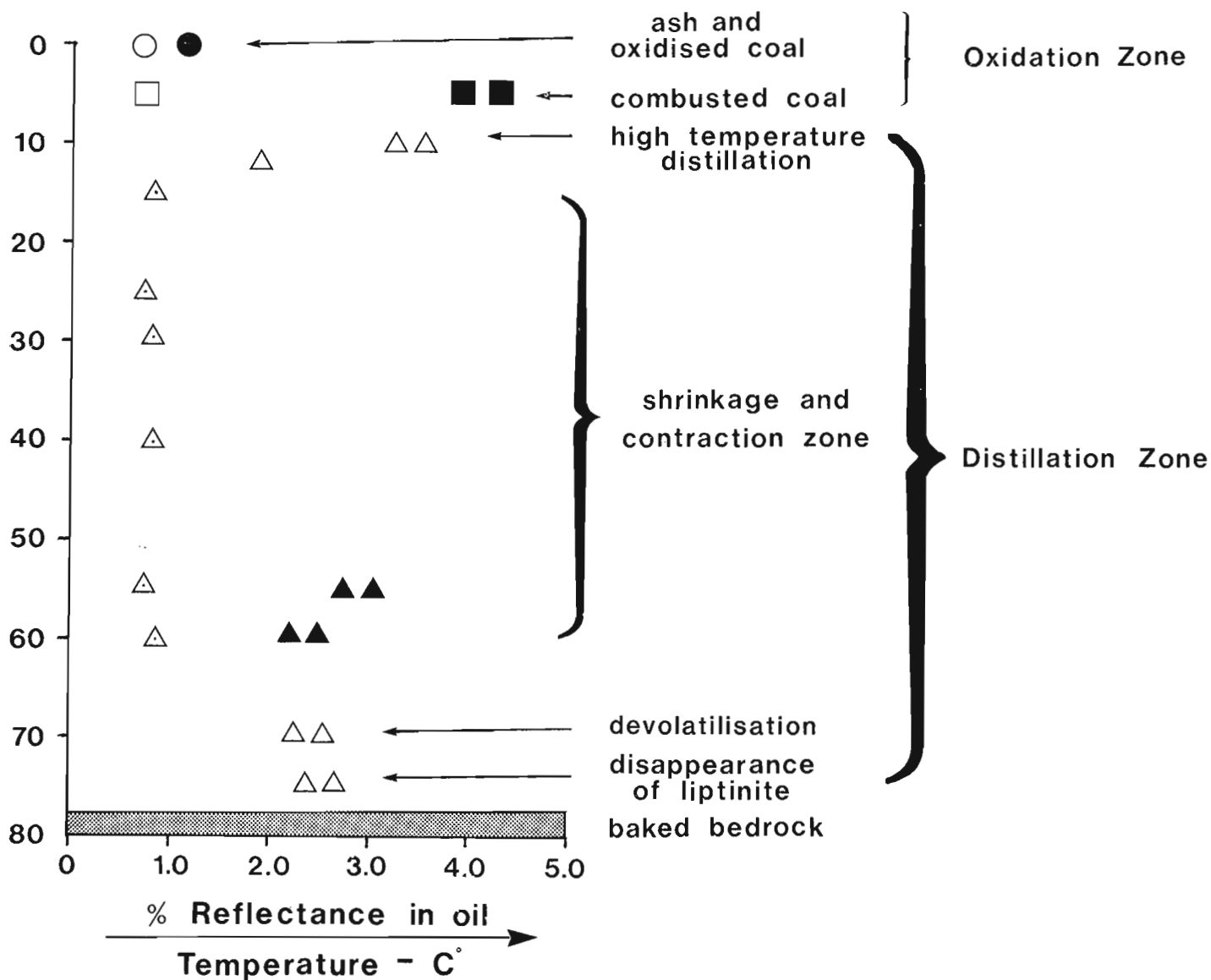


Figure 46.6. Reflectance (maximum and minimum) profile of different zones of burning coal seam. (a) Oxidized coal, centre of particle (○), oxidation rim (●); (b) combusted coal in centre of particle (■), in combustion front (□). Distillation (carbonization) zone: (d) pre-carbonized (△), (c) and (e) carbonized (△), pyrolytic carbon (▲).

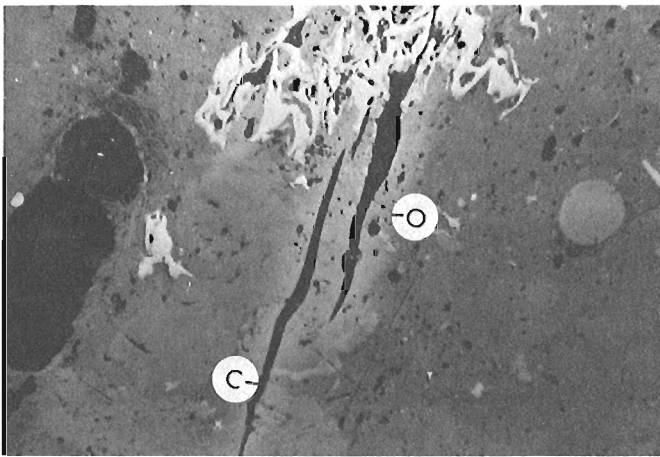


Figure 46.7. Char in oxidation zone showing oxidation rim (O) in the vicinity of cracks (C).

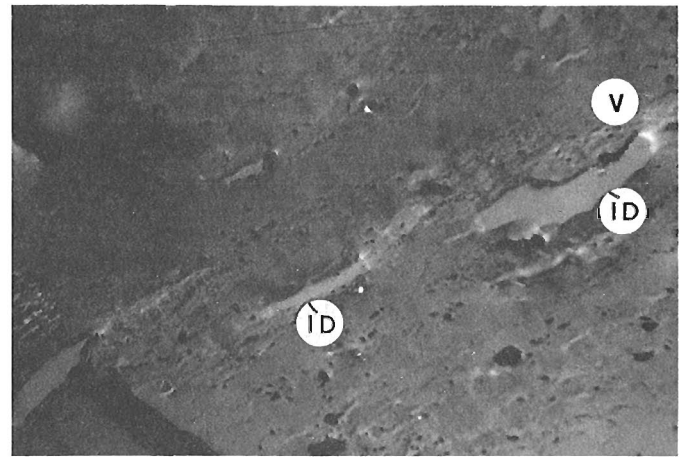


Figure 46.10. Semi-coke in distillation zone showing "anthracitic" morphology. Note vesiculation and also strain anisotropy in the boundaries of inertodetrinite (ID) and vitrinite (V).

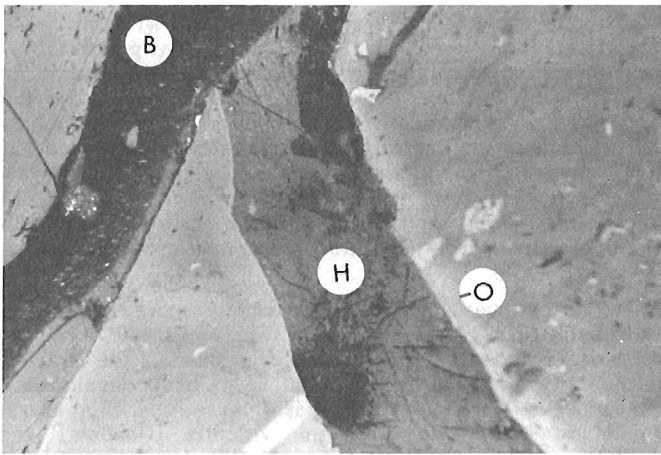


Figure 46.8. Fracture-filling hydrocarbon (H) in cracks; oxidation rim (O); bonding material (B) of grain mount.

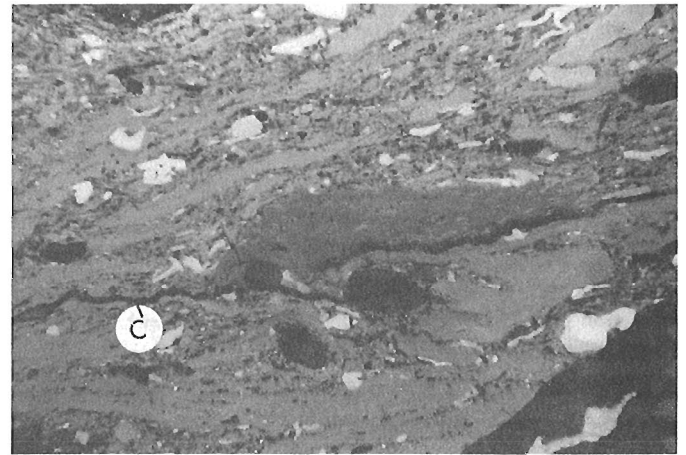


Figure 46.11. Semi-coke in pre-carbonization subzone. Clarite in pre-carbonization zone showing cracks (C); no evidence of oxidation rim is present.

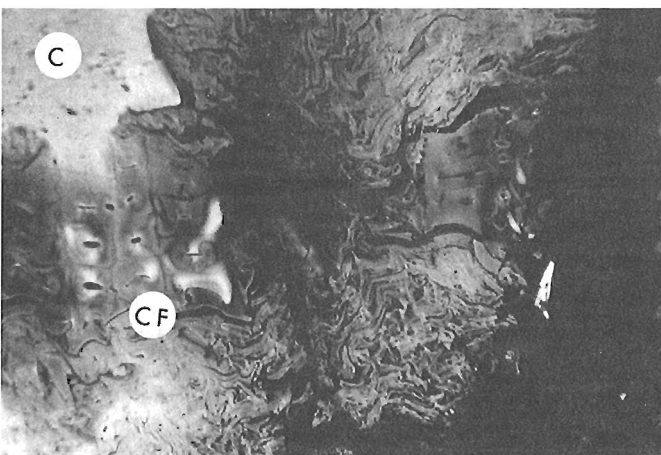


Figure 46.9. Combusted coal showing apparently structureless carbonized matrix (C), combustion front (CF); combusted collinite showing its original cellular morphology.

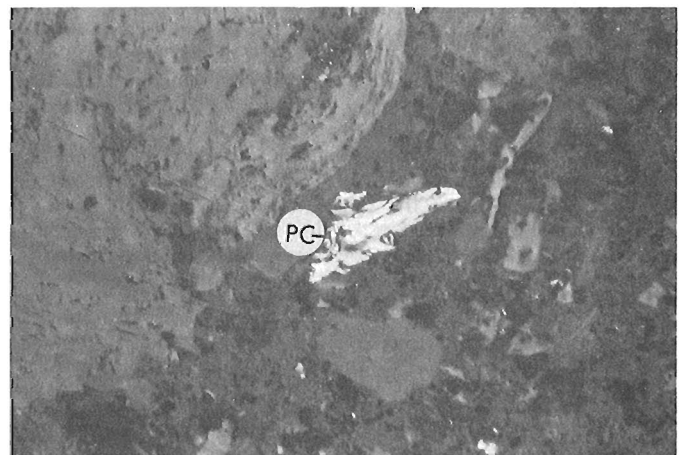


Figure 46.12. Pyrolytic carbon (PC) showing anisotropy in isotropic collinite matrix. Crossed polars.

Microscopy

All samples were examined using a Zeiss MPM II reflected light microscope, fitted with white (halogen) and fluorescent light (HBO) sources, and connected to a Zonax microcomputer and plotter.

Results and discussion

The burning coal at Coalspur may be distinguished from the rest of the coal zone by the emission of water vapour and volatile matter. The area surrounding the burning seam is warm and devoid of surface vegetation. Volatile matter is emitted through cracks (figs. 46.2, 46.3). Surface fragments close to cracks and also the cracks themselves are lined with yellow needles of crystalline sulphur (Fig. 46.4) and coal tar. Samples taken from cracks contain 48 per cent sulphur. Burgundy-coloured ash and red sinters are also found in this area due to total consumption of other coal seams. The burning coal seams are covered by a burgundy coloured ash. It was thought that this ash is the residue of coal that has been completely consumed. To test this idea, samples of hot chars (char in this study refers to oxidized or combusted residues of coals) from different parts of the burning seam were left on the surface overnight. The residues from the combusted zone were converted into ash. The rate of conversion of coal to ash was dependent on the original temperatures of the residue. This rate was greater the higher the temperature (Fig. 46.5).

The burning coal seam can be divided into two zones based on morphology and reflectance of the residues (Fig. 46.6).

Oxidation-combustion Zone

Oxidized Coal

This subzone consists of the uppermost part of the burning coal seam. Chars from this zone show oxidation rims and cracks. The reflectance of the oxidation rims is higher than that of the main body of the char (Fig. 46.7). The oxidation cracks in the upper part of this zone are commonly filled with low reflecting (%Roil = 0.25 to 0.75), homogeneous, soft, fluorescing to nonfluorescing hydrocarbons (Fig. 46.8). Elemental sulphur lines the vent and coats loose surface fragments close to the vent (Fig. 46.4).

Combusted Coal

This subzone represents the hottest part of the burning coal seam. The oxidation reaction in this part is exothermic due to the reaction: $C+O_2 - CO_2$ (King, 1967). Chars immediately below the oxidized coal showed a similar morphology to that of combusted coal (Fig. 46.9) described by Alpern and Chauvin (1958). The combustion front has lower reflectance than the matrix of char (Fig. 46.9), in agreement with results of Alpern and Chauvin (1958). The matrix of char is carbonized and has higher reflectance (Fig. 46.9). The matrix of char away from the combustion front is homogeneous, whereas the char in the combustion front has similar morphology to that of inertinite. Combustion has etched the vitrinite char in the combustion front revealing its original telinitic morphology (Fig. 46.9).

Distillation (Carbonization) Zone

This zone encompasses most of the burning coal seam, and the following two subzones were recognized. The carbonization subzone occurs at both the top and base

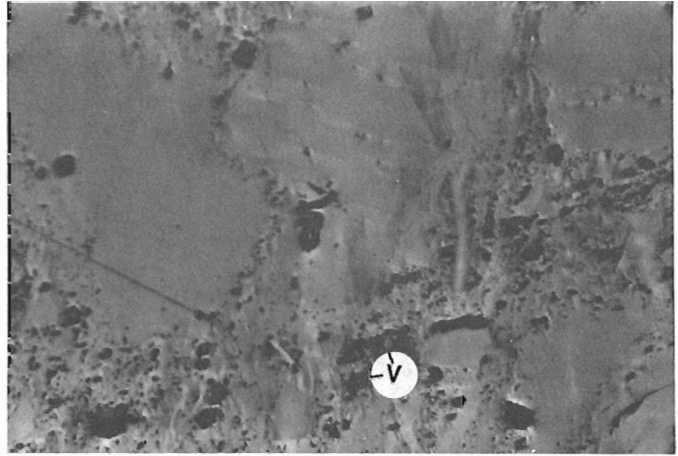


Figure 46.13. Carbonized residue in carbonization subzone showing devolatilization vacuoles (V). This residue has a reflectance of 2.6%, whereas fresh coal has a reflectance of 0.7%.

of the zone. In the upper part of this subzone, the coals below the combusted chars are carbonized and are anisotropic, showing high reflectance (Fig. 46.10a, b). The carbonization of these coals was due to the heat generated by the combustion of coal. The pre-carbonization subzone, in the middle of the zone, consists of residues found under the carbonized coals that, on first inspection, have morphology and reflectance similar to that of unaltered coal and do not show any sign of oxidation or combustion (Fig. 46.11). However, they contain devolatilization vacuoles, contraction cracks (Fig. 46.11), and also pyrolytic carbon (Fig. 46.12). Some of the pyrolytic carbon may be pre-combustion (Goodarzi, 1985).

The residues become progressively more carbonized toward the floor of the coal seam (Fig. 46.13) and form the lower occurrence of the carbonization subzone. The residues in the bottom 25 cm of the coal seam have developed a homogeneous morphology and basic anisotropy (Fig. 46.13) similar to carbonized low rank vitrinite (Goodarzi and Murchison, 1978). The cause of distillation (carbonization) of coal near the floor of the seam was the heat transmitted by the bedrock (baked mudrock), due to combustion of a seam underlying the seam under study and separated from it by a mudrock layer that has become baked. This process is similar to the progressive carbonization of coal in a coke oven, where the coal near the coke oven wall becomes carbonized first and then the carbonization front moves toward the centre of the oven.

Present results could be useful in other studies of combustion in coal seams. Further detailed study of burning coal seams is necessary to determine the morphology of chars from the burning bituminous coal seams and coal dumps, as well as the variation of the reflectance within the burning coals.

Conclusions

1. Combustion of coal in a burning coal seam is limited to the area of the seam in direct contact with air.
2. The coal becomes oxidized initially and then combusted.
3. The coal beneath the combustion subzone in a burning coal seam may become carbonized or remain almost unchanged depending on its proximity to the heat source.

References

- Alpern, B. and Chauvin, R.
1958: Application des méthodes de la microscopie par réflexion à l'étude de la combustion des boulets; *Revue Industrie Minérale*, Paris, p. 210-218.
- Bustin, R.M. and Matthews, W.H.
1982: In situ gasification of coal, a natural example: history petrology and mechanics of combustion; *Canadian Journal of Earth Sciences*, v. 19, no. 3, p. 514-523.
- Fryer, H.
1981: Ghost towns of Alberta; Stage Coach Publishing Co., Langley, British Columbia, Canada, p. 149.
- Goodarzi, F.
1985: Pyrolytic carbon in Canadian coals; *Fuel*, v. 64, p. 1672-1676.
- Goodarzi, F. and Murchison, D.G.
1978: Petrography and anisotropy of carbonized preoxidized coals; *Fuel*, v. 55, p. 141-147.
- Jerzykiewicz, T.
1985: Stratigraphy of the Saunders group in central Alberta Foothills – a progress report; in *Current Research, Part B*, Geological Survey of Canada, Paper 85-1B, p. 247-258.
- Jerzykiewicz, T. and McLean, J.R.
1980: Lithostratigraphical and sedimentological framework of coal-bearing upper Cretaceous and lower Tertiary strata, Coal Valley area, central Alberta Foothills; Geological Survey of Canada, Paper 79-12, 47 p.
- King, J.D.
1967: Fuel – solid, liquid and gaseous; Edward Arnold Ltd., London, England.
- Mackowsky, M.Th.
1982: Methods and tools of examination; in *Stach's Textbook of Coal Petrology*, ed. E. Stach, M.Th. Mackowsky, M. Teichmuller, G.H. Taylor, D. Chandra and R. Teichmuller; Gebruder Borntraeger, Berlin, p. 295.
- Pearson, D.E. and Creaney, S.
1980: Spontaneous carbonization of oxidized high volatile coal by a lightning strike; *Canadian Journal of Earth Sciences*, v. 17, no. 1, p. 36-42.

Paleosols and Late Albian sea level fluctuations: preliminary observations from the northeastern British Columbia foothills

Project 860011

D.A. Leckie and A.E. Foscolos
Institute of Sedimentary and Petroleum Geology, Calgary

Leckie, D.A. and Foscolos, A.E., Paleosols and Late Albian sea level fluctuations: preliminary observations from the northeastern British Columbia foothills; in Current Research, Part B, Geological Survey of Canada, Paper 86-1B, p. 429-441, 1986.

Abstract

Fifteen closely spaced paleosols occur in the Boulder Creek Formation (late Albian) in the foothills of northeastern British Columbia. The paleosols are well developed and 0.7 to 4 m thick. The paleosols are characterized by their grey colour, pedogenic slickensides, vertical roots, preserved peds, absence of sedimentary structures and presence of spherulitic siderite. The paleosols formed during a period when one or more depositional hiatuses or unconformities occurred as a result of either eustatic sea level fluctuations or local tectonic events. The paleosols may be the terrestrial record of these hiatuses/unconformities, when base level changed with accompanying incision and decreasing rates of sedimentation. A scarcity of calcium carbonate indicates a humid to subhumid climate. The water table was high for part of the year but there is also evidence of periodic drying and oxidation of organic debris. Cumulatively, the paleosols appear to represent a very long period of time in which deposition was slow and there was very little erosion.

Résumé

Dans la formation de Boulder Creek (Albien récent), dans les avants-monts du nord-est de la Colombie-Britannique il y a quinze paléosols très rapprochés les uns des autres. Les paléosols sont bien évolués et leur épaisseur varie de 0,7 à 4 m. Ils se caractérisent par leur couleur grise, par la présence de miroirs de faille pédogéniques, de racines verticales et d'agrégats conservés, par l'absence de structures sédimentaires et par la présence de sidérites sphérulitiques. Les paléosols se sont accumulés au cours d'une période caractérisée par la formation d'au moins une lacune ou discordance sédimentaire liée à des fluctuations eustatiques du niveau de la mer ou à des événements tectoniques locaux. Ces paléosols pourraient être la trace sur terre de ces lacunes/discordances, lorsque le niveau de base a changé avec l'incision et la réduction des taux de sédimentation. La rareté du carbonate de calcium indique que le climat était humide ou subhumide. La nappe phréatique était élevée pendant une partie de l'année, mais il y aurait également eu assèchement périodique et oxydation des débris organiques. Dans l'ensemble, les paléosols représenteraient une très longue période marquée par une sédimentation lente et un très faible degré d'érosion.

Introduction

The presence of paleosols in the Cretaceous Western Canada sedimentary basin has not yet been documented, but there is an abundance of nonmarine sediments where fossil soil horizons should be preserved. The purpose of this paper is to document well developed paleosols from the Lower Cretaceous Boulder Creek Formation in the northeastern British Columbia foothills (Fig. 47.1, 47.2). By pointing out and describing macroscopic characteristics of these paleosols it is hoped that other fossil soils in other intervals will also be recognized. These paleosols formed during a period when one or more depositional hiatuses or unconformities occurred (Koke and Stelck, 1984, 1985; Stott, 1982; Caldwell et al., 1978). The hiatuses have been attributed to both tectonic and eustatic causes. The paleosols may be the terrestrial record of these hiatuses/unconformities, when base level changed with accompanying incisement and decreasing rates of sedimentation.

Paleosols are buried soils of the geologic past (Ruhe, 1956). The controlling mechanisms responsible for development of modern soils are: climate, organisms, relief, parent material and time (Jenny, 1941). It is possible to infer how these controls operated in the past by detailed studies of fossil soils, especially on the bases of the geochemistry and mineralogy of the deposits. Macroscopic, geochemical and micromorphological criteria have been used in this study to establish that well developed paleosols are present within the Boulder Creek Formation. In this preliminary report, the results of the macroscopic analyses are presented: geochemical and micro-morphological studies are continuing.

The interval containing the paleosols described here is from a suite of four, closely spaced diamond drill cores (6.75 cm in diameter) that penetrate the whole of the Lower Cretaceous of northeastern British Columbia (Fig. 47.1). Some 15 paleosols, ranging in thickness from 0.7 to 4 m, have been recognized in the Boulder Creek Formation over a

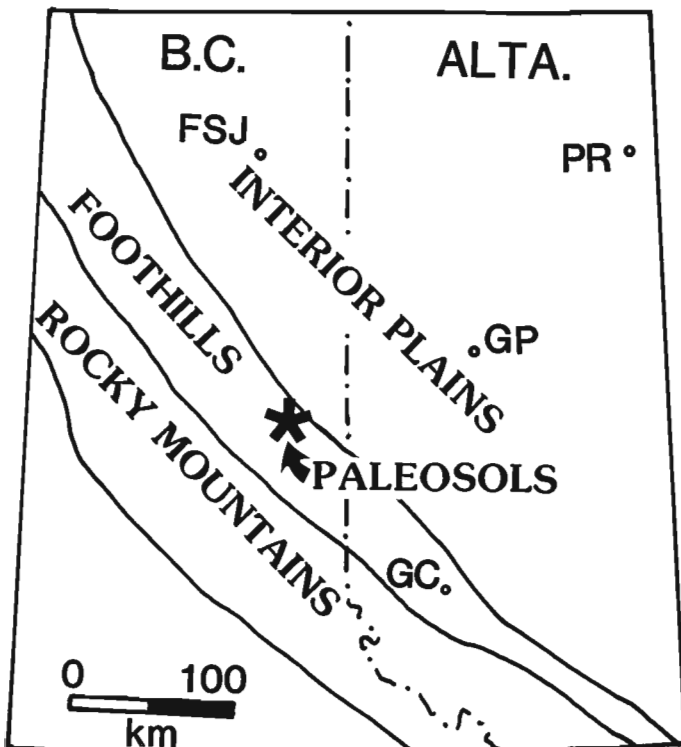


Figure 47.1. Location of the core containing the Boulder Creek paleosols. FSJ - Fort St. John, PR - Peace River, GP - Grand Prairie and GC - Grande Cache.

90 m interval. Five paleosol horizons were studied in detail (numbered 1 to 5 in Fig. 47.4) and two were sampled for geochemical analyses. Measured sections of Profiles 1 and 5 are shown in Figure 47.4, and detailed descriptions are in the Appendix. An example of one of the paleosols is shown in Figure 47.5. All described colours are based on comparison with a Munsell (1954) colour chart. The Boulder Creek paleosols described herein are not unique to this core but occur over a wide areal extent throughout the formation (D.W. Gibson, personal communication, 1986).

Regional Geology

The Hulcross and Boulder Creek formations are interpreted as a fourth order transgressive-regressive cycle of a more extensive third order clastic wedge (Leckie, 1986b). The Boulder Creek Formation in this area consists of 23 m of marine shoreface to foreshore sandstone and conglomerate overlain by 112 m of nonmarine, alluvial plain sandstone, siltstone and shale (Fig. 47.3). A 70 cm thick, high volatile A bituminous coal (W. Kalkreuth, personal communication, 1986) sits directly on the shoreline deposits. Lenticular conglomerate occurs at various stratigraphic positions throughout the alluvial plain deposits (Stott, 1962). The paleosols discussed here occur in the top 90 m of the formation. The underlying Hulcross Formation consists of 87 m of finely interbedded sandstone, siltstone and shale deposited in a shallow shelf setting. The Boulder Creek Formation is overlain by the Shaftsbury Formation, an approximately 300 m thick unit of marine shale (Stott, 1968). Ammonite and foraminiferal zonation schemes date the Boulder Creek sediments as Middle to Late Albian (Jeletzky, 1980; J.H. Wall, personal communication, 1986).

The precise nature and timing of depositional hiatuses or unconformities during the Middle to Late Albian has not yet been resolved (Fig. 47.2). Stott (1982) indicated that a major unconformity occurs from the middle Albian through to the top of the Cenomanian throughout the Alberta Foothills. It was during this time period that the Hulcross and Boulder Creek formations were deposited in northeastern British Columbia. Wickenden (1951) and Koke and Stelck (1984, 1985) indicated a major hiatus between the Paddy and Cadotte members of the Peace River Formation, which are lateral equivalents of the Boulder Creek Formation (Stott, 1982).

Description

There are several macroscopic features that can be used to establish that well developed paleosols are present within the Boulder Creek Formation.

Colour

The initially most notable aspect of these paleosols is their light grey colour in comparison with the parent material. The paleosols are light grey (5Y 7/1) to grey (5Y 6/1) and when wet, have a "waxy" appearance. If the paleosol colour is representative of the original soil colour, then grey and grey-green colours are probably indicative of soils that were originally poorly drained and poorly aerated. Mottling, which is evident in some of the paleosols, may also be the result of impeded drainage. The light colouration may also be caused by leaching of humus and argilluviation (Retallack, 1976).

Roots

In situ vertical roots are one of the most diagnostic characteristics of fossil soils younger than Silurian (Retallack, 1983). The Boulder Creek paleosols are

	FOOTHILLS, PEACE RIVER, B.C (STOTT,1982)	PEACE RIVER PLAINS (STOTT,1982)	PEACE RIVER PLAINS (KOKE AND STELCK,1985)	CENTRAL ALBERTA (KOKE AND STELCK,1985)
CEN	FISH SCALE ZONE			
UPPER ALBIAN	HASLER FM.	SHAFTSBURY FM.		COLORADO SHALES
		PADDY SS.		VIKING FM.
		PADDY MBR. CADOTTE MBR.		JOLI FOU FM.
MIDDLE ALBIAN	BOULDER CREEK FM.	PEACE RIVER FM.	HARMON MBR.	BASAL SS.
	HULCROSS FM.		HARMON SHALE	
LOWER ALBIAN	GATES FM.	SPIRIT RIVER FM.		MANNVILLE FM.
	MOOSEBAR FM.	SPIRIT RIVER FM.		

Figure 47.2. Stratigraphic nomenclature. The paleosols are from the upper part of the Boulder Creek Formation, which, in the subsurface is equivalent to the Paddy Member.

extensively penetrated by in situ vertical roots preserved as carbonaceous films and clay traces 1 to 5 mm in width and centimetres to decimetres long (Fig. 47.6). Fine root traces 1 to 2 mm wide are most common and occur dominantly in the top several decimetres. Several root traces taper and branch downward. Many of the root traces, especially larger ones, are not preserved as carbonaceous films, but are filled with clay. The clay filled root casts suggest oxidation of the original carbonaceous material and infilling of the root casts by clay illuviation.

Vegetation and leaf litter

Fossils of plant remains occur in the Boulder Creek Formation as carbonaceous impressions of leaves and stems and as comminuted carbonaceous debris. Leaf and stem impressions of unidentified gymnosperms do not occur within the paleosols but are common in shale and siltstone directly overlying the fossil soils. Angiosperms have been reported in the Boulder Creek Formation from nearby Belcourt Ridge (Mellon et al., 1963). In some instances, this carbonaceous debris may be representative of the surface A horizon, which was enriched in organic matter. Normally in paleosols, this horizon has been oxidized and cannot be recognized.

The black shales at the top of, or directly overlying, individual profiles have total organic carbon contents, as determined by RockEval pyrolysis, of 1.46 to 2.04 per cent (e.g., at the 0 to 50 cm level in Profile 1, Fig. 47.3). Shale and sandstone within individual profiles have less than 0.1 per cent total organic carbon (e.g., below 50 cm level in Profile 1, Fig. 47.4).

Burrows

Recognizable burrows are uncommon, but some horizontal and subhorizontal burrows occur near the top of some soils. The burrows are round to elliptical and are 5 to 8 mm in diameter.

Peds and slickensides

Peds are naturally occurring aggregates of soil material separated from adjacent peds by cutans or natural voids (Brewer, 1960). Compaction usually destroys most of the original soil peds. In the Boulder Creek Formation, preserved peds are not abundant but, where present, are outlined by pedogenic slickensided clay skins (cutans) (Fig. 47.7) and cracks. Due to compaction none of the original soil voids

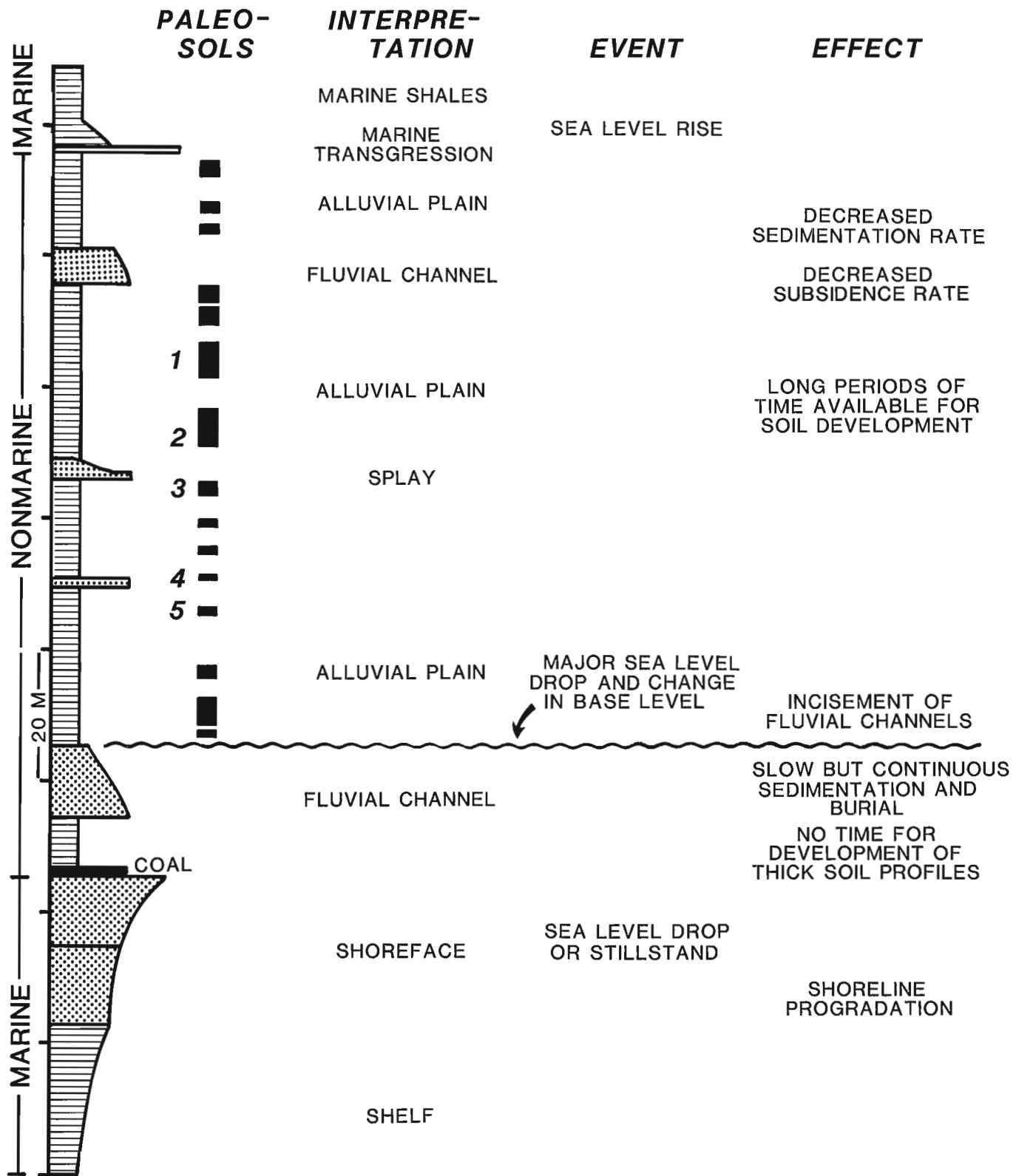


Figure 47.3. Measured section and interpretation of Boulder Creek Formation in diamond drill core MD 80-08. Paleosols are indicated.

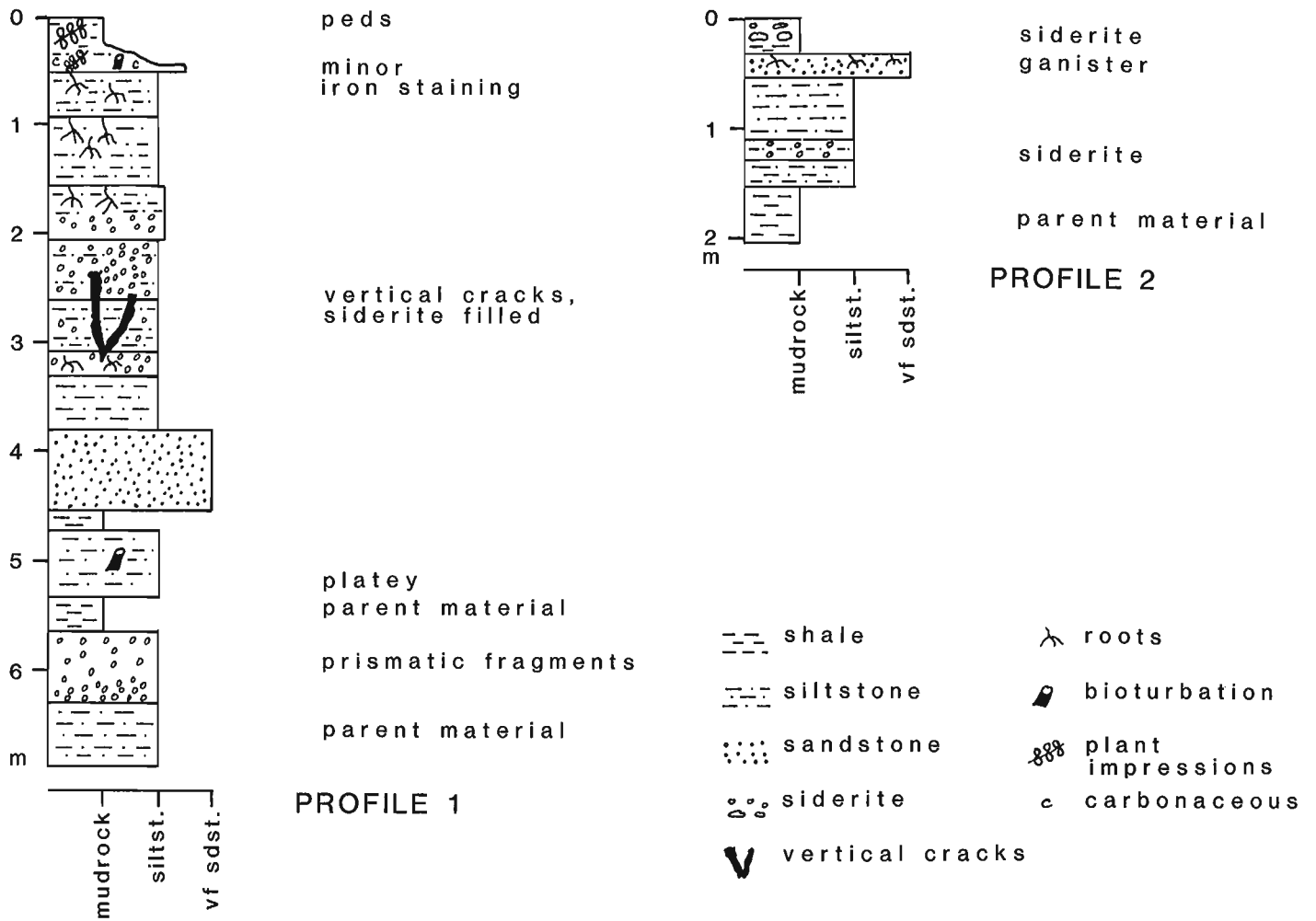


Figure 47.4. Vertical sections of paleosol Profiles 1 and 5. For location of profiles in the Boulder Creek Formation see Figure 47.3.



Figure 47.5. Soil Profile 4 in Borehole MD 80-08. Light coloured sandstone ("G") is a ganister overlain by carbonaceous shale. Below the ganister there is a gradual downward decrease in the extent of alteration of the original parent material until, at some point, original sedimentary structures ("S") are present. Top of the core is to the upper left; bottom is to the lower right.

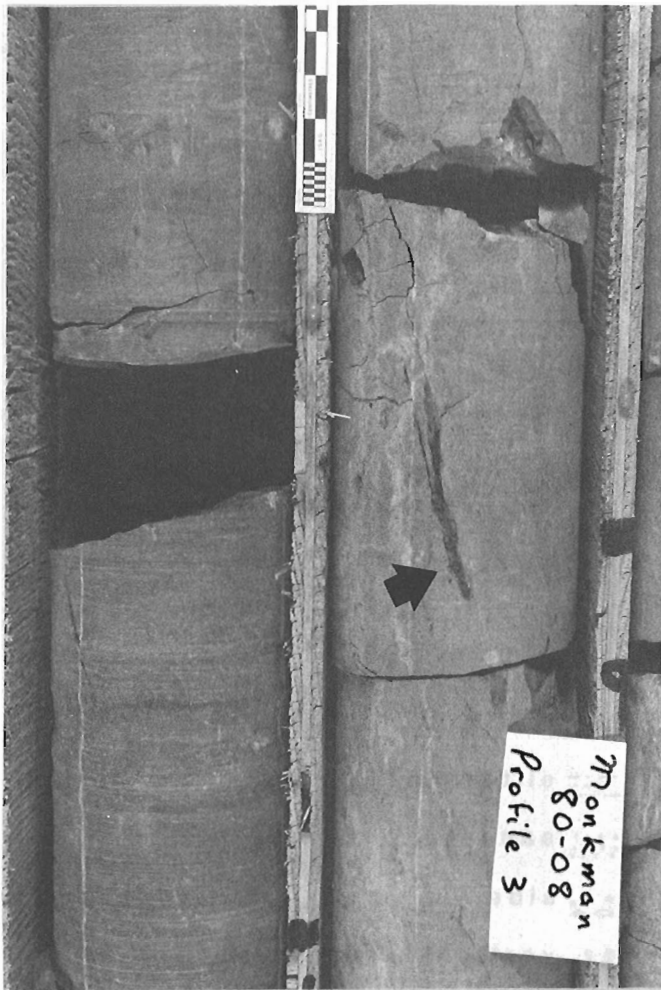


Figure 47.6. In situ vertical root trace in Profile 3.

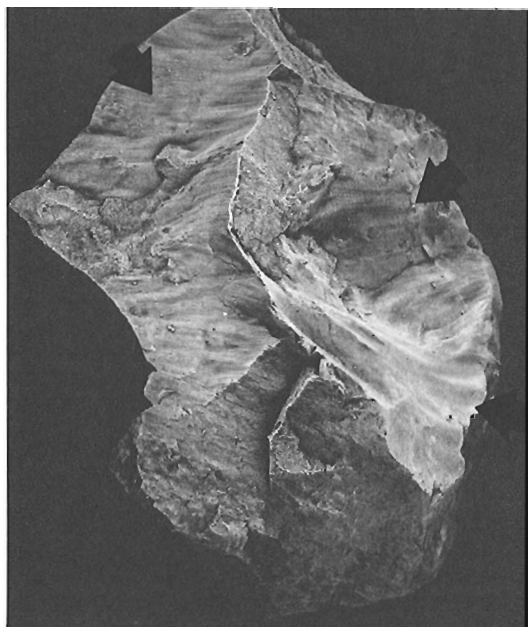


Figure 47.7. Randomly oriented slickensides on clay skins of soil ped.

are preserved. The peds are irregularly shaped, angular to subangular, blocky and prismatic and are 0.5 to 2.0 cm in size. The slickensides are polished and finely grooved surfaces with a waxy lustre occurring as randomly arranged planes. Slickensided surfaces are oriented obliquely to one another and may occur on all sides of the peds. The slickensides are not tectonic in origin but are pedogenic and probably formed as the result of gravitational compaction.

The paleosol intervals throughout the core tend to be broken up into blocky, platy or irregular fragments to a greater degree than the non-soil portions of the core. This breakage may have occurred along pre-existing zones of weakness that were the boundaries of the original peds.

Absence of sedimentary structures

Primary sedimentary structures are absent in the well developed paleosols. Within the profiles there is a gradual downward decrease in the extent of alteration of the original parent material until, at some point, original sedimentary structures are present ("S" in Fig. 47.5). The most common sedimentary structures in the relatively unaltered material are parallel lamination and ripple crosslamination. Destruction of the original sedimentary structures resulted from bioturbation by roots and animals and other soil forming processes.

Ganisters

A ganister is quartzose sandstone composed of subangular grains, 0.15-0.5 mm in diameter, with amorphous silica cement (Williamson, 1967). Ganisters occur in two of the soil profiles (Fig. 47.3, Profiles 4 and 5; Fig. 47.5). The Boulder Creek ganisters are very resilient, light grey in colour (5Y 7/1), are 25 to 30 cm thick, and are made up of very fine grained and silt-sized quartz material. The upper contact is sharp and may be overlain by black, carbonaceous shale with carbonaceous plant imprints. There is a gradational lower contact to finer grained argillaceous sediment. There is no carbonate in the ganisters but 1 to 2 mm siderite grains are concentrated in an underlying horizon of the same profile. The ganisters are underlain by grey (5Y 5/1), massive siltstone that contains horizons of 1 to 2 mm siderite spherules.

The light colour and quartzose nature of the ganisters are the result of leaching and argilluviation (Retallack, 1976). The ganister would have originally been an A₂ or eluvial horizon (Retallack, 1976). The grey, massive siltstone would have been the B horizon, and the siderite, if syndimentary, formed in a water saturated zone of the soil (Retallack, 1976). The lack of carbonate in the ganister suggests an acid to neutral pH (Baas Becking et al., 1960; Krumbein and Garrells, 1952). Retallack (1976) observed that paleosols such as ganisters, which originally had a dry upper portion resting on wetter lower sediments (as indicated by increased clay content, siderite and organic matter), would have had a steep Eh gradient.

Cracking

One well developed paleosol contains vertical cracks infilled with red (2.5 YR 5/6) siderite grains (Fig. 47.8). The cracks are greater than 15 cm in length, up to 13 mm wide, extend across the width of the core and taper downward. Sediment surrounding the cracks is massive.

These cracks are interpreted as shrinkage cracks, formed during soil development. They may indicate intermittent drying of the soil profile. The siderite within the cracks may be the result of a high water table at other times.



Figure 47.8. Siderite filled crack in soil Profile 1. The crack is vertical and tapers downward.

Siderite

Siderite occurs as concretionary nodules and spherulites (sphaerosiderite) in the grey (2.5Y 4/0), massive mudrocks. The presence of siderite was confirmed by X-ray diffraction. The nodules are up to 10 cm in diameter and occur at various levels within the profiles. The spherulites are 1 to 2 mm in diameter and occur in discrete horizons or as the fill within vertical cracks (see above). In thin section, the siderite occurs as isolated spherules or closely packed aggregates. Individual spherules have a radial crystal fabric and accompanying radial extinction patterns. The spherulites form a cristic plasmic soil fabric similar to that described by Brewer (1964).

Synsedimentary siderite nodules and spherulites indicate frequent wet periods with a relatively high water table characteristic of gleyed flood plain horizons. Spherulitic siderite has been reported from seatearths and underclays beneath British coal measures (Tucker, 1981) where iron was derived by eluviation from higher in the soil profile.

Mineralogy and mechanical analysis

Channel samples were collected over 20 cm intervals for Profiles 1 and 5 and subjected to mechanical and mineralogical analyses. Results are presented in Tables 47.1 and 47.2.

Table 47.1 indicates that two and probably three paleosols may exist in Profile 1, making this paleosol profile a cumulosol. One paleosol occurs in samples 1-1 to 1-13, the second from samples 1-15 to 1-27, and the third from 1-29 to 1-31 (Table 47.1). Distinct features amongst the profiles are as follows. From 1-1 to 1-13 the quartz concentration is high, whereas that of illite and mixed layer clays is low (Table 47.1). Siderite is present in the bottom layers; kaolinite concentrations and the <2 μ fraction are relatively constant. From 1-15 to 1-27, the concentration of quartz decreases but the amount of illite and mixed layer clays increases with respect to the overlying material. Siderite becomes scarce, while kaolinite concentration and the <2 μ

Table 47.1. Soil mineralogy, mechanical analysis, pH and organic carbon in paleosol 1

Sample Number	Soil mineralogy							Mechanical analysis				
	Quartz	Feldspar	Illite	Kaolinite	Chlorite	Mixed layer	Siderite	% Sand	% Silt	% Clay	pH 1:5	% Organic C
1-1	65		14	6	2	13		32.55	7.30	60.15	8.08	1.46
1-3	68		14	5		13		35.92	17.58	46.50	7.89	0.10
1-5	87		3	4		5	1	45.70	11.65	42.65	7.63	0.01
1-7	79		5	4		6	6	42.13	14.42	43.45	7.80	0.00
1-9	77		7	5		6	5	34.81	13.74	51.45	7.88	0.00
1-11	76		6	6		7	5	28.25	28.20	49.55	8.07	0.00
1-13	62	trace	10	5		8	15	29.67	23.28	47.05	8.16	0.00
1-15	59		16	5		12	8	25.99	26.91	47.10	8.01	0.05
1-17	57		21	6		16		37.10	15.80	47.10	8.35	0.01
1-19	59		22	6	trace	13		23.20	30.80	46.00	8.32	0.00
1-21	61	trace	15	5	trace	9	10	13.70	38.85	47.45	8.66	0.03
1-23	65	trace	17	5	trace	13		23.29	28.51	48.20	8.41	0.02
1-25	73	trace	12	4		11		23.21	29.89	46.90	8.50	0.01
1-27	68	trace	15	6	trace	11		15.18	27.02	47.40	8.47	0.03
1-29	60	trace	22	5	trace	9	4	36.34	41.06	22.60	8.41	0.07
1-31	69	2	15	6	1	7		25.00	56.60	18.40	8.45	0.03

Table 47.2. Soil mineralogy, mechanical analysis, pH and organic carbon in Profile 5

Sample Number	Soil Mineralogy									Mechanical Analysis				
	Quartz	Feldspar	Illite	Kaolinite	Chlorite	Mixed layers	Calcite	Dolomite	Siderite	% Sand	% Silt	% Clay	pH 1:5	% Organic C
5-1	55		20	7	1	7	3	4	3	27.48	50.17	22.35	8.45	2.04
5-2	60		17	7	1	14				46.54	34.96	18.50	8.64	1.16
5-4	89		trace	6	trace	trace			5	28.96	51.19	19.85	8.07	0.02
5-5	76		4	8	trace	8			4	29.61	53.79	16.60	8.27	0.07
5-6	69		12	8		9			2	19.91	61.49	18.60	8.25	0.02
5-7	60		17	6		13			3	30.53	47.22	22.25	8.54	0.00
5-8	71	1	13	7	trace	8				30.60	54.45	14.95	8.39	0.09
5-9	56		23	5	trace	14			2	25.84	54.21	19.95	8.60	0.05
5-10	55		23	6	trace	16				38.34	41.71	19.95	8.52	0.08

fractions are constant. In this material however, the percent silt increases but the percent sand decreases (Table 47.1). Finally, in samples 1-29 and 1-31, the percent silt increases while the percent of <2 μ fraction decreases substantially with respect to the overlying material.

Samples from Profile 5 resemble the 1-29 and 1-31 samples of Profile 1 in that silt concentration is high with respect to percent clay and percent sand. Siderite is ubiquitous in all samples, whereas calcite and dolomite are present in the uppermost samples.

The pH in all profiles is neutral to slightly alkaline as a result of the presence of carbonate minerals and the saturation of the exchange sites with mono- and divalent cations. The total organic carbon (determined by RockEval pyrolysis) and therefore the organic matter in both profiles, follows the trend of being relatively abundant at the top of the profile and decreasing in abundance downward.

Major and trace element analysis

Major and trace element analyses were carried out by X-ray fluorescence following Trail and Lachance (1965). The results are presented in Tables 47.3 and 47.4.

The results from Profile 1 (Table 47.3) reflect the mineralogical composition. As illite increases K₂O increases. As quartz increases so does SiO₂ while Al₂O₃ decreases. As siderite increases or is present in the sample, Fe₂O₃ increases. Trace element analysis does not show any trends except for Zn. As illite concentrations increase, the amount of Zn also increases.

The results from Profile 5 (Table 47.4) follow the same trend as in Profile 1, that is, the elemental composition is a function of the mineral composition. For example, in sample 5-1 where calcite, dolomite and siderite are present, calcium, magnesium and iron are present in high concentration. In Profile 5, manganese is quite abundant, moreso than the manganese concentration in Profile 1, especially in the upper horizons. The reason for this relative abundance is not understood. There may be a correlation with the presence of siderite, where manganese isomorphically substitutes for iron in the carbonates.

Interpretation

Parent material

The original parent material consists dominantly of floodplain alluvium with siltstone and mudrock making up 77 per cent of the nonmarine portion of the Boulder Creek Formation. Sediments were deposited in meandering rivers,

crevasse splays and lakes. The Boulder Creek deposits contain metamorphic, clastic and sedimentary rock fragments as well as volcanic detritus (Stott, 1968). Whole rock analyses of the parent material in Profiles 1 and 5 (Fig. 47.4; Table 47.5) show that the dominant mineral components are quartz and feldspar (or rutile), and illite, kaolinite and chlorite are the dominant clays.

Climate

Within these paleosols there is an absence of calcium carbonate in the form of caliche, calcrete or even calcareous horizons which, if present, would indicate an arid to semi-arid soil environment. There are rare occurrences of calcite-filled tectonic slickensides associated with fault movement in the Foothills. If indurated carbonates had formed they would have persisted to the present day even under changed environmental conditions and through burial diagenesis (Yaalon, 1971). The absence of calcite/caliche and presence of siderite indicate a wet, sub-humid climate with a high water table. The lack of carbonaceous material but abundance of roots may indicate periodic drying and oxidation of organic debris. The clay-illuviated root channels and sideritic layers indicate that some of the paleosols were wet for most of the year.

Topography

Some of the paleosols appear to have been wet for long periods of time as is evident from their apparent gleyed nature. The wetness does not necessarily imply high rainfall; it could be a function of topography. Wetness would result on a plain with low relief and broad divides where horizontal and downward drainage were very poor. The shale and siltstone would have been relatively impermeable so that drainage was further hindered. The preservation of numerous preserved paleosols indicates that very little erosion took place, which also would have been a consequence of low relief.

Time

Several characteristics of these soil profiles indicate that long periods of time were involved in their formation. These characteristics include: profiles up to 4 m thick; an absence of any relict sedimentary structures throughout the profiles; well differentiated paleosol horizons; and, local occurrences of well developed peds (Retallack, 1976). The ganisters were probably podsols, which can form in a few hundred years but may take up to several thousand years

Table 47.3. Major and trace element analysis in soil Profile 1

Major elements in per cent												
Sample Number	SiO ₂	Al ₂ O ₃	Fe ₂ O ₃	TiO ₂	CaO	MgO	K ₂ O	Na ₂ O	P ₂ O ₅	TGA/Lot*		
1-1	62.99	19.59	3.26	0.81	0.25	1.68	3.10	0.14	0.10	7.90		
1-3	70.78	18.24	1.89	0.91	0.14	1.11	2.68	0.11	0.04	3.90		
1-5	80.11	11.24	1.63	0.88	0.13	0.64	1.17	0.04	0.03	4.00		
1-7	77.15	11.78	2.98	0.74	0.24	0.67	1.36	0.06	0.02	4.85		
1-9	73.73	13.95	3.09	0.75	0.25	0.73	1.67	0.06	0.03	5.60		
1-11	70.82	12.95	5.87	0.65	0.38	0.84	2.00	0.10	0.05	6.20		
1-13	67.44	15.94	4.53	0.83	0.35	1.01	3.03	0.13	0.07	6.50		
1-15	67.71	18.12	2.59	0.81	0.21	1.18	3.37	0.12	0.17	5.50		
1-17	68.68	17.21	3.05	0.81	0.15	1.33	3.39	0.09	0.10	5.00		
1-19	70.63	11.78	6.90	0.82	0.48	1.08	2.36	0.06	0.10	5.80		
1-21	72.66	14.72	2.69	0.81	0.26	1.24	3.03	0.11	0.10	4.20		
1-23	74.01	14.73	1.82	0.84	0.14	1.08	2.63	0.08	0.05	4.45		
1-25	73.16	14.99	2.20	0.79	0.15	1.17	2.89	0.08	0.05	4.55		
1-27	72.52	14.64	3.15	0.79	0.20	1.28	2.76	0.08	0.07	4.35		
1-29	67.92	15.47	4.89	0.77	0.34	1.53	3.13	0.08	0.11	5.55		
1-31	74.61	13.26	2.92	0.72	0.27	1.27	2.60	0.10	0.13	3.95		

Trace elements in p.p.m.												
Sample Number	Pb	Zn	Cu	Ni	Mn	Cr	Zr	Y	Sr	Rb	Ba	
1-1	26	199	42	40	38	91	119	21	160	155	1689	
1-3	19	104	28	25	18	84	181	17	113	132	1698	
1-5	7	64	19	17	39	58	195	10	78	49	847	
1-7	10	69	14	17	127	65	203	14	89	67	1000	
1-9	9	58	11	22	82	65	178	13	90	80	1106	
1-11	31	118	13	20	235	65	135	12	90	98	1192	
1-13	4	133	16	16	205	107	136	17	121	147	1639	
1-15	42	455	24	37	30	72	140	44	255	153	1818	
1-17	15	190	15	43	57	71	129	46	175	149	1744	
1-19	15	218	23	29	454	70	209	21	108	110	1540	
1-21	14	97	9	21	61	54	153	20	121	110	1146	
1-23	18	104	13	25	24	57	147	19	114	130	1367	
1-25	14	86	13	22	25	62	156	19	113	124	1413	
1-27	21	231	29	39	91	92	185	26	119	127	1477	
1-29	16	159	23	32	261	73	140	19	114	142	1601	
1-31	19	214	20	27	87	68	180	18	107	120	1297	

*Thermal gravimetric analysis/loss of ignition

Table 47.4. Major and trace element analysis in soil Profile 5

Major elements in per cent												
Sample Number	SiO ₂	Al ₂ O ₃	Fe ₂ O ₃	TiO ₂	CaO	MgO	K ₂ O	Na ₂ O	P ₂ O ₅	TGA/Lot*		
5-1	59.34	14.19	5.28	0.71	6.51	2.96	2.75	0.13	0.34	7.60		
5-2	62.20	19.16	5.06	0.87	0.30	1.82	3.15	0.21	0.14	6.90		
5-4	76.00	12.37	3.38	0.81	0.17	0.55	0.83	0.28	0.03	5.35		
5-5	73.06	14.63	3.12	0.71	0.16	0.66	1.44	0.13	0.03	5.80		
5-6	71.53	15.85	2.50	0.81	0.13	0.87	2.49	0.15	0.04	5.30		
5-7	66.96	18.38	3.05	0.81	0.15	1.14	3.13	0.31	0.07	5.80		
5-8	77.33	12.52	2.22	0.66	0.09	0.82	2.30	0.10	0.06	3.75		
5-9	69.16	16.56	3.37	0.86	0.14	0.16	3.32	0.16	0.07	5.00		
5-10	66.54	18.45	3.10	0.83	0.10	1.46	3.65	0.28	0.07	5.35		

Trace elements in p.p.m.												
Sample Number	Pb	Zn	Cu	Ni	Mn	Cr	Zr	Y	Sr	Rb	Ba	
5-1	36	214	32	89	597	73	151	23	174	130	1393	
5-2	23	203	28	39	264	89	161	23	156	168	1843	
5-4	4	59	10	17	820	65	185	8	67	36	884	
5-5	12	41	11	20	885	69	163	10	69	61	1087	
5-6	7	46	6	31	978	75	165	14	78	96	1320	
5-7	19	56	23	29	234	89	126	19	147	147	1619	
5-8	17	114	17	20	33	72	228	16	124	102	1252	
5-9	13	96	34	25	66	74	139	21	121	145	1573	
5-10	25	118	22	57	34	85	141	31	161	190	1908	

*Thermal gravimetric analysis/loss of ignition

Table 47.5. Mineralogic composition of parent material underlying Profiles 1 and 5

	Mineral		Per cent	
	Profile 1	Profile 5	Profile 1	Profile 5
Quartz	69.24	55.41		
Illite	15.18	23.13		
Mixed layer clays	7.0	15.0		
Kaolinite	5.94	5.9		
Feldspar or rutile	1.51	-		
Chlorite	1.13	0.57		

(Buol et al., 1980). Cumulatively, the superposed paleosols represent a very long period of time during which deposition was slow and there was very little erosion.

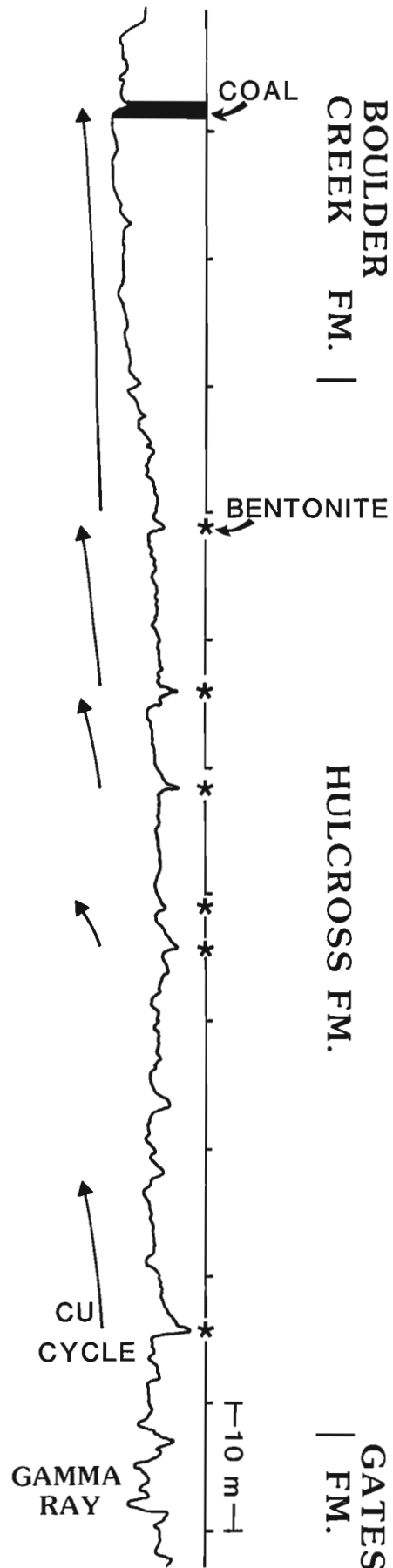
Some of the thick paleosols are probably not a single, well developed soil but are cumulative profiles, where soil formation and sediment influxes occurred concurrently (Nikiforoff, 1949). Cumulative profiles are common on river floodplains.

Regional controls on paleosol development

The conditions under which the Lower Cretaceous coals formed differ from those that formed the paleosols. In explaining the abundant, thick paleosols it is necessary to account for the lack of coals in the Boulder Creek Formation. Cretaceous nonmarine sediments in the underlying Gates Formation, Gething Formation and Minnes Group contain numerous, thick coal seams, but well developed, superposed paleosols are uncommon, although isolated paleosols do occur. The development of peat requires slow, continuous subsidence so that the groundwater table rise coincides with the rising peat surface and there is protection from marine and flood waters and clastic sediment influx (Stach et al., 1975). Organic material will be oxidized if the water table drops or fluctuates. Coal does not form when subsidence slows and the organic material rots or already existing peat is eroded. During deposition of the upper Boulder Creek, the water table, although high enough to form the gleysols, apparently was not high enough for the development of peat, or tended to fluctuate, causing the organic material to oxidize and the paleosols to crack.

In order to evaluate some of the possible controls on soil development (i.e., decreased or interrupted sediment supply, lower water table etc.), it is necessary to evaluate some of the stratigraphic relationships of correlative horizons. The Boulder Creek paleosols formed at a time when a major unconformity was developing throughout the Western interior basin (Fig. 47.2) and, as such, the paleosols are diastems. Although the existence of this unconformity is well accepted, the precise nature of its timing and origin is still controversial.

The cause of the unconformity can be attributed to one of three mechanisms or some combination of them: Late Albian tectonic activity in the rising Cordillera to the west; eustatic sea level fluctuations; and epeirogenic movement associated with the Peace River Arch. The Viking Formation of central Alberta may be correlated with the Paddy Sandstone (sic Koke and Stelck, 1985) and is thus slightly younger or similar in age to the Boulder Creek (Fig. 47.2). Bentonites in the Viking Formation were probably derived from volcanic activity associated with the Crownsnest Volcanics in southwestern Alberta during a period of extensive and frequent volcanism associated with the



Columbian orogen (Amajor, 1985). Further support of Late Albian tectonic activity can be found by examination of Figure 47.9. The Hulcross Formation, which underlies the Boulder Creek Formation, contains six bentonites. Several of the bentonites bracket upward-coarsening cycles or herald their commencement (Fig. 47.6). Thus there appears to be a relationship between the generation of the bentonites and minor progradational sequences which may best be explained as tectonic. The abundance of conglomerate in channel and shoreface deposits (Stott, 1962) may also indicate Late Albian tectonic activity farther to the west. It appears therefore that the Boulder Creek Formation was deposited during a time of intensive volcanic and tectonic activity which caused fluctuations in local relative sea level.

A strong argument can also be made for eustatic sea level fluctuations in the late Albian at about the time of deposition of Boulder Creek sediments. The case for late Albian eustatic sea level change has been strongly made (Kauffman, 1977, 1984; Weimer, 1983; Caldwell, 1984; and Leckie, 1986a) and will not be repeated here. This sea level fluctuation occurred approximately 97 Ma (Weimer, 1983).

The Peace River Arch is a major epeirogenic feature that was subsiding during Albian time and affected sedimentation patterns of the Boulder Creek Formation (Stott, 1968). Regional sedimentation patterns of the Boulder Creek Formation were controlled by the trend of the Peace River Arch (Stott, 1968), however, it is not likely that the major depositional hiatus above or within the Boulder Creek was affected by the Arch.

It appears that eustatic sea level fluctuations played a role, as did tectonic activity in the rising Cordillera to the west, which would have affected sedimentation in the basin. The hiatus illustrated in Figure 47.2 is probably the result of a base level drop, but at this time it is not possible to say whether the cause was a eustatic or tectonic event. The sea level fall would have caused incisement of fluvial channels and reduced rates of sedimentation on the alluvial plain. The formation of several, well developed, superposed paleosols required long periods of time with slow deposition rates and little erosion. The nonmarine expression of this regional sea level drop may be the superposed Boulder Creek paleosols.

CONCLUSIONS

Fifteen well developed paleosols occur in a 90 m interval of the Boulder Creek Formation. Macroscopic criteria used to identify the paleosols are listed in Table 47.6. These criteria can also be applied to the recognition of paleosols in other stratigraphic intervals. On a reconnaissance basis, similar paleosols have so far been observed in the Cardium Formation of northern Alberta, and the Gething and Nikanassin formations of northeastern British Columbia.

In contrast to nonmarine intervals of the underlying Nikanassin, Gething, Gates and lower Boulder Creek formations, where coal is present, the development of numerous well developed, superposed paleosols and the development of coal in the upper Boulder Creek Formation seem to be mutually exclusive. The paleosols appear to have formed in a humid to sub-humid climate with a periodically

Table 47.6. Macroscopic characteristics of Boulder Creek paleosols

- | |
|-------------------------------------------------------------------------------------------------------------------------------------------------|
| i. Slickensides that are not tectonic but indicative of soil formation |
| ii. Preserved blocky, columnar or platy peds |
| iii. In situ vertical roots |
| iv. Waxy, light grey (5Y 7/1) to grey (5Y 6/1) colour |
| v. No sedimentary structures in well developed portion of profile; structures do gradually appear downward in minimally altered parent material |
| vi. Spherulitic siderite |
| vii. Shrinkage cracks filled with siderite |
| viii. Ganisters |

high water table. The paucity of carbonaceous material but abundance of roots suggests periodic drying and oxidation of organic material. The numerous, closely-spaced paleosols suggest that rate of sediment supply was low, probably as a result of base level lowering, and that very little erosion took place as a consequence of low relief. The thickness and number of paleosols indicate a long period of time for their formation, which can be related to a major late Albian unconformity/hiatus that has been documented elsewhere in the Western Canada sedimentary basin. The unconformity is probably the result of regional sea level fall during the Late Albian caused by tectonic or eustatic mechanisms.

Although it is premature to discuss the types of soils that developed and hence to infer the paleoclimatic conditions based on geochemical analysis, it seems that from the limited data available to date, the soils were of the intrazonal group. Topography and especially water table were the main soil forming factors in controlling soil genesis. Ongoing data analyses on the cation exchange capacity, exchangeable cations, and X-ray analysis of the clay fraction may reinforce or modify these conclusions.

Acknowledgments

Earlier versions of this paper were read by D.W. Gibson, R.W. Macqueen, R.J. Cheel and O.L. Hughes. Geochemical analyses were carried out by A. Heinrich and J. Wong.

References

- Amajor, L.E.
1985: Biotite grain size distribution and source area of the Lower Cretaceous Viking bentonites, Alberta, Canada; *Bulletin of Canadian Petroleum Geology*, v. 33, p. 471-478.
- Baas Becking, L.G.M., Kaplan, I.R., and Moore, D.
1960: Limits of the natural environment in terms of pH and oxidation-reduction potentials; *Journal of Geology*, v. 68, p. 243-284.
- Buol, S.W., Hole, F.D., and McCracken, R.J.
1980: *Soil Genesis and Classification*; Iowa State University Press, Ames, 404 p.
- Brewer, R.
1960: Cutans: their definition, recognition, and classification; *Journal of Soil Science*, v. 11, p. 280-292.

Figure 47.9. Gamma ray trace of Hulcross and Boulder Creek formations in diamond drill hole Monkman 81-2. Gamma ray tool measures natural radioactivity of the sediment. Bentonites are highly radioactive and have a high deflection to the right. The bentonites appear to herald the beginning or end of upward coarsening cycles. Occurrences of bentonites were confirmed by core examination.

- Brewer, R. (cont.)
1964: Fabric and mineral analysis of soils; John Wiley and Sons, New York.
- Caldwell, W.G.E.
1984: Early Cretaceous transgressions and regressions in the southern interior plains; in *The Mesozoic of Middle North America*, ed. D.F. Stott and D.J. Glass; Canadian Society of Petroleum Geologists, Memoir 9, p. 173-204.
- Caldwell, W.G.E., North, B.R., Stelck, C.R., and Wall, J.H.
1978: A foraminiferal zonal scheme for the Cretaceous system in the interior plains of Canada; in *Western and Arctic Canadian Biostratigraphy*, ed. C.R. Stelck and B.D.E. Chatterton; Geological Association of Canada, Special Paper 18, p. 497-575.
- Jeletzky, J.A.
1980: New or formerly poorly known, biochronologically and paleobiogeographically important gastropod and ammonitid (Ammonitida) taxa from middle Albian rocks of mid-western and Arctic Canada; Geological Survey of Canada, Paper 79-22, 63 p.
- Jenny, H.
1941: *Factors of Soil Formation*; McGraw-Hill, New York, 281 p.
- Kauffman, E.G.
1977: Geological and biological overview: Western Interior Cretaceous basin; *Mountain Geologist*, v. 14, p. 75-99.
1984: Paleobiogeography and evolutionary response dynamics in the Cretaceous Western Interior Seaway of North America; in *Jurassic-Cretaceous Biochronology and Paleogeography of North America*, ed. G.E.G. Westermann; Geological Association of Canada, Special Paper 27, p. 273-306.
- Koke, K.R. and Stelck, C.R.
1984: Foraminifera of the Stelckiceras Zone, basal Hasler Formation (Albian), northeastern British Columbia; in *The Mesozoic of Middle North America*, ed. D.F. Stott and D.J. Glass; Canadian Society of Petroleum Geologists, Memoir 9, p. 271-280.
1985: Foraminifera of a Joli Fou shale equivalent in the Lower Cretaceous (Albian) Hasler Formation, northeastern British Columbia; *Canadian Journal of Earth Sciences*, v. 22, p. 299-313.
- Krumbein, W.C. and Garrels, R.M.
1952: Origin and classification of chemical sediments in terms of pH and oxidation-reduction potential; *Journal of Geology*, v. 60, p. 1-33.
- Leckie, D.A.
1986a: Tidally influenced, transgressive shelf sediments in the Viking Formation, Caroline, Alberta; *Bulletin of Canadian Petroleum Geology*, v. 34, p. 111-125.
1986b: Rates, controls and sandbody geometries of transgressive-regressive cycles: Cretaceous Moosebar-Gates formations, British Columbia; *American Association of Petroleum Geologists, Bulletin*, v. 70, p. 516-535.
- Mellon, G.B., Wall, J.H., and Stelck, C.R.
1963: Lower Cretaceous section, Mount Belcourt, northeastern British Columbia; *Bulletin of Canadian Petroleum Geology*, v. 11, p. 64-22.
- Munsell Colour Company
1954: *Munsell soil colour charts*; Baltimore.
- Nikiforoff, C.C.
1949: Weathering and soil evolution; *Soil Science*, v. 67, p. 219-223.
- Retallack, G.J.
1976: Triassic paleosols in the upper Narrabeen Group of New South Wales. Part I: features of the paleosols; *Journal of the Geological Society of Australia*, v. 23, p. 383-399.
1983: Late Eocene and Oligocene paleosols from Badlands National Park, South Dakota; *Geological Society of America, Special Paper 193*, 82 p.
- Ruhe, R.V.
1956: Geomorphic surfaces and the nature of soils; *Soil Science*, v. 82, p. 441-455.
- Stach, E., Taylor, G.H., Mackowsky, M., Chandra, D., Teichmüller, M., and Teichmüller, R.
1975: *Stachs textbook of coal petrology*; Berlin, Gebrüder Borntraeger, 428 p.
- Stott, D.F.
1962: Stratigraphy of the Lower Cretaceous Fort St. John Group, Gething and Cadomin formations, Foothills of northern Alberta and British Columbia; *Geological Survey of Canada, Paper 62-39*, 48 p.
1968: Lower Cretaceous Bullhead and Fort St. John groups, between Smokey and Peace rivers, Rocky Mountain Foothills, Alberta and British Columbia; *Geological Survey of Canada, Bulletin 152*, 279 p.
1982: Lower Cretaceous Fort St. John Group and Upper Cretaceous Dunvegan Formation of the Foothills and Plains of Alberta, British Columbia, District of Mackenzie and Yukon Territory; *Geological Survey of Canada, Bulletin 328*, 124 p.
- Traill, R.J. and Lachance, G.
1965: A new approach to X-ray spectrochemical analysis; *Geological Survey of Canada, Paper 64-57*.
- Tucker, M.E.
1981: *Sedimentary petrology: an introduction*; Blackwell Scientific Publications, Oxford, 252 p.
- Weimer, R.J.
1983: Relation of unconformities, tectonics, and sea level changes, Cretaceous of the Denver Basin and adjacent area; in *Mesozoic Paleogeography of the west-central United States*, ed. M.W. Reynolds and E.D. Dolly; Rocky Mountain Paleogeography Symposium 2. Rocky Mountain Section, Society of Economic Paleontologists and Mineralogists, Denver, Colorado, p. 359-376.
- Wickenden, R.T.D.
1951: Some Lower Cretaceous sections on Peace River below the mouth of the Smokey River, Alberta; *Geological Survey of Canada, Paper 51-16*, 47 p.
- Williamson, I.A.
1967: *Coal Mining Geology*; Oxford University Press, Oxford.
- Yaalon, D.H.
1971: Soil-forming processes in time and space; in *Palaopedology: Origin, Nature and Dating of Paleosols*; Jerusalem, I.S.S.S. and Israel Universities Press, Jerusalem, 350 p.

APPENDIX

Paleosol Profile 1 (see Figure 47.3)

0 - 33 cm	- shale: very dark grey (2.5YR 3/0); gymnosperm vegetation, pinnately compound, fern-like leaf imprints; clay skin surfaces on peds; carbonaceous plant imprints; noncalcareous	4.55 - 4.72 m	- silty shale: dark grey (2.5Y 5.0); gradational upper and lower contact; rubbly 0.5-1.5 cm pieces
33 - 40 cm	- siltstone: gradational upper and lower contacts; clear, smooth contacts; dark grey (2.5Y 4/0); carbonaceous; rooted; slightly mottled; colour contrast is faint with sharp boundaries; horizontal oblate burrows, 11 mm; homogenous, poorly sorted; massive	4.72 - 5.33 m	- siltstone: dark grey (10YR 4/1); 6 cm wide, diagonal, burrow(?) at top
40 - 47 cm	- sandstone: light grey (7.5YR 7/0) fine grained; vertical roots 1-2 mm wide, 4 cm long; minor ironstaining; noncalcareous; lower contact abrupt, smooth	5.33 - 5.69 m	- shale: dark grey (2.5YR 4/1); abrupt contacts, platy, part of original parent material
47.0 - 92 cm	- siltstone: dark grey (7.5YR 4/0) at top; grey (5Y 5/1) at base; rooted, 1-3 mm in size; massive; faint mottling; root casts are not carbonaceous but are defined by slightly darker clay; lower boundary abrupt, smooth	5.69 - 6.32 m	- siltstone: dark grey (2.5Y 4/0); prismatic fragments; 1-2 mm sideritic blebs that become more frequent downward; gradual lower contact; this is a new soil horizon
92 cm - 1.57 m	- grey siltstone (5YR 5/5): rooted, 2-3 mm in size; massive; very slightly sandy	6.32 - 6.85 m	- siltstone: massive; parent material
1.57 - 2.02 m	- sandy siltstone: olive grey (5Y 5/2); massive with some peds (angular blocky) and clay skins; carbonaceous roots; mm sized sideritic blebs ≈ 5%.		
2.02 - 2.62 m	- siltstone: noncalcareous; irregularly shaped sideritic blebs mm to 1 cm in size; grey (5Y 5/1) at top - greenish tinge down low, olive (5Y 5/3); dominantly siderite blebs 1-2 mm size; siderite appears concentrated in vertical cracks		
2.62 - 3.09 m	- siltstone: grey (5Y 5/2); vertical cracks filled with sideritic pellets; cracks are >1.5 cm in size, downward tapering, up to 13 mm wide, cut across the core; scattered siderite grains throughout the interval; gradual upper and lower contact; structure is massive		
3.09 - 3.29 m	- siltstone: grey (5Y 5/1) mottled to red (2.5YR 5/6) 30-40% sideritic grains; abrupt lower contact; slightly carbonaceous; massive; siderite occurs as concentrations of 1-2 mm blebs 6 cm thick; 2 mm size roots		
3.29 - 3.81 m	- siltstone: dark grey (5Y 4/1); rubbly, 0.5-1 cm pieces		
3.81 - 4.55 m	- sandstone: grey (5Y 4/1) mottled red (2.5 YR 5/6); argillaceous, massive; upper 15 cm is mottled red due to sideritic blebs 1-2 mm in size; gets greyer downward, with no siderite		

Paleosol Profile 5 (see Figure 47.3)

0 - 10 cm	- shale: dark grey (2.5YR 4/0); sideritic; irregularly shaped red (2.5YR 3/4) sideritic concretions; abrupt upper and lower contacts
10 - 21 cm	- siderite: red (2.5YR 4/0); shaly; abrupt contacts
21 - 32 cm	- shale: dark grey (2.5Y 4/0); carbonaceous; horizontal plant imprints; irregular lower contact, abrupt
32 - 56 cm	- very fine grained sandstone: top 8 cm is grey (5Y 5/1) mottled dark grey (2.5Y 4/0); carbonaceous, massive; looks leached; in situ vertical roots; calcite-filled fractures
56 - 96 cm	- siltstone: dark grey (2.5Y 4/0); abrupt contact; carbonaceous
96 cm - 1.11 m	- siltstone: dark grey (2.5Y 4/0); abrupt contact; massive; mottled with black pellets to 1.5 cm
1.11 - 1.18 m	- grey (2.5Y 4/0) mottled red (2.5Y 3/4) with siderite (<50% siderite), as blebs 0.1 cm to 1.5 cm in size
1.18 - 1.27 m	- siltstone: mottled black and red (2.5Y 3/4); red is siderite (≈10-20%); black is siltstone (5Y 2.5/1) (≈30%)
1.27 - 1.51 m	- siltstone: grey (5Y 4/1); massive
1.51 - 2.06 m	- shale: grey (5Y 4/1); parent material.



The rugose coral *Pachyphyllum* Edwards and Haime in the Frasnian (Upper Devonian) of Western Canada

Project 680093

R.A. McLean¹
Institute of Sedimentary and Petroleum Geology, Calgary

McLean, R.A., The rugose coral *Pachyphyllum* Edwards and Haime in the Frasnian (Upper Devonian) of western Canada; in *Current Research, Part B*, Geological Survey of Canada, Paper 86-1B, p. 443-455, 1986.

Abstract

The genus *Pachyphyllum* is restricted to massive, horseshoe dissepiment-bearing phillipsastreids with the growth morphology of the type species, *P. bouchardi* Edwards and Haime, 1850. Under this interpretation, the genus occurs rarely in Frasnian strata of North America and Western Europe. The new species *P. miniaceum*, *P. anfractum*, and *P. mirusense* are described from Western Canada, while *P. calostrotum* (Crickmay, 1962) is revised, and a form comparable to the Iowa species *P. crassicostratum* Webster, 1889 is discussed.

Résumé

Le genre *Pachyphyllum* désigne uniquement des phillipsastréides à dissépiments en fer à cheval caractérisés par la morphologie de croissance de l'espèce type, *P. bouchardi* Edwards et Haime, 1850. D'après cette interprétation, le genre n'est retrouvé que rarement dans les couches frasniennes de l'Amérique du Nord et de l'Europe de l'Ouest. L'étude présente une description de *P. miniaceum*, *P. anfractum* et *P. mirusense*, de nouvelles espèces de l'Ouest du Canada, une révision de *P. calostrotum* (Crickmay, 1962) et une discussion d'une forme comparable à *P. crassicostratum* Webster, 1889, une espèce trouvée en Iowa.

¹ Amoco Canada Petroleum Company Ltd., 444 - 7th Avenue S.W., Calgary, Alberta T2P 0Y2

Introduction

The genus *Pachyphyllum*, under the restricted interpretation proposed herein, is extremely rare in Frasnian strata worldwide. The recent discovery in Western Canada of a number of forms referable to the genus has prompted the present contribution, which represents the first record of the genus in this country. The localities from which the material was obtained are shown in figures 48.1 to 48.4. Documentation of the other massive phillipsastreids in Western Canada, a large and varied fauna, will be the subject of a forthcoming publication.

Acknowledgments

I am grateful to J.E. Sorauf, State University of New York at Binghamton, for comments on the Iowa representatives of *Pachyphyllum*, and for providing photographs of thin sections of their type material. P.R. Hoover, Paleontological Research Institution, Ithaca, New York, kindly loaned the type material of *Macgeea calostrota* Crickmay and gave permission for the preparation of new thin sections from it.

Some of the material described in this paper was collected by A.S. Hedinger, R.H. Workum and T.E. Nitychoruk. F. Grillo assisted with thin section preparation. Figures 48.1 to 48.5 were drafted by D.C. Decocq, and photography was by R.K. Strom.

The writer publishes with permission of Amoco Canada Petroleum Company Ltd.

Stratigraphy

The stratigraphy and faunas associated with the species described in this paper have been discussed by McLean and Pedder (1984, p. 8-13) and McLean and Pedder (in press). A generalized correlation chart of the stratigraphic sequences is given in Figure 48.5.

The only Frasnian rugose coral species based on subsurface material from Western Canada is *Macgeea calostrota* Crickmay, 1962. Revision of this species, and its assignment to *Pachyphyllum*, necessitates some comments on the age of its type horizon, the Cooking Lake Formation of eastern Alberta. Because correlation of subsurface and outcrop Frasnian sections in Alberta is not yet clear in many cases, a subsurface column has been omitted from Figure 48.5. However, on the basis of brachiopod studies, a generalized correlation of the Cooking Lake Formation with part of the upper Cairn Formation and its equivalents of the Alberta Rocky Mountains can be supported (McLaren, 1962, Fig. 1). Hence, an early Frasnian age may be assigned to the type horizon of *P. calostrota*.

Systematic paleontology

Specimens bearing numbers with the prefix GSC are registered in the type collections of the Geological Survey of Canada, Ottawa. The specimen with the prefix PRI is in the collections of the Paleontological Research Institution, Ithaca, New York.

Family PHILLIPSASTREIDAE Roemer, 1883
Genus *Pachyphyllum* Edwards and Haime, 1850

Pachyphyllum Edwards and Haime, 1850, p. lxxviii.

Type species. *Pachyphyllum bouchardi* Edwards and Haime, 1850, p. lxxviii; 1851, p. 397, Pl. 7, figs. 7, 7a, 7b. Frasnian, Ferques, Boulonnais area, France.

Diagnosis. Massive, phillipsastroid coral genus with thamnasterioid to aphroid coralla, comprising relatively few, large corallites. Distally, corallites show a strong tendency

to be well raised above the main surface of the corallum. Horseshoe dissepiments are well developed adjacent to the tabularium.

Discussion. The generic subdivision of the massive, horseshoe dissepiment-bearing phillipsastroid corals has had an extremely varied history, which was reviewed in detail by Scrutton (1968), and others. Many workers have considered that *Pachyphyllum* should be regarded as a junior subjective synonym of *Phillipsastrea* d'Orbigny, 1849, but Sorauf (1978) produced some compelling reasons for separating the two genera. On the basis of Scrutton's (1968) revision of the type species, *Phillipsastrea hennahi* (Lonsdale, 1840), Sorauf considered that the two genera could be distinguished primarily by *Pachyphyllum* having a more uniform collar of horseshoe dissepiments, pronounced stereome coating of the dissepiments, and a greater tendency to develop an aphroid growth form, larger tabularia and coarser trabeculae. I agree in general with this point of view, but study of the large and diverse fauna of massive, horseshoe dissepiment-bearing phillipsastreids in Western Canada indicates that further subdivision of this group is feasible.

The type species of *Pachyphyllum*, *P. bouchardi* Edwards and Haime, 1850, has a distinctive growth form characterized by a small number of large corallites projecting well above the surface of the main, massive part of the corallum (Edwards and Haime, 1851, Pl. 7, figs. 7, 7a). A similar growth form is shown by *P. crassicostatum* Webster, 1889, as illustrated by Fenton and Fenton (1924, Pl. 8, fig. 1; Pl. 9, figs. 1-5). Such a distinctive growth form, characterized by relatively small coralla with few, very large corallites, is also developed in several Western Canadian species. I consider that this growth form is taxonomically significant, and thus restrict *Pachyphyllum* to only those species that have the general features attributed to the genus by Sorauf, but that, in addition, have the corallum form of *P. bouchardi*, the type species. A similar characterization of *Pachyphyllum* was given by Birenheide (1978, p. 115-116), although he considered *P. bouchardi* to be the only representative of the genus. This interpretation necessitates a separate generic name for the large number of species that have the internal morphology of *Pachyphyllum*, but have the

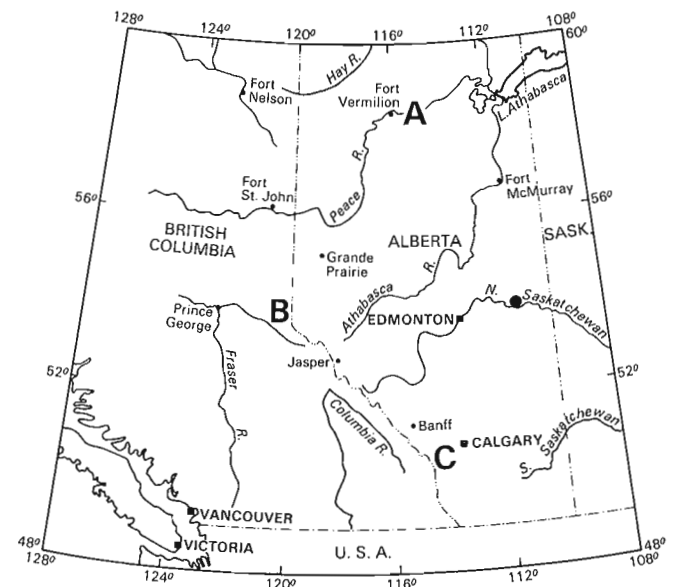


Figure 48.1. Index map of part of Western Canada, showing location of small scale locality maps, figures 48.2-48.4. Black dot indicates location of Imperial Fribourg 12-33-55-9W4 well.

more typical, massive, phillipsastroid growth form, with numerous small corallites. Two of the syntypes of *Medusaephyllum ibergense* Roemer, 1855, type species of *Medusaephyllum* Roemer, were discovered recently by A.E.H. Pedder in the collections of the Institut für Geologie und Paläontologie, Technische Universität Clausthal-Zellerfeld, West Germany. Preparation of new thin sections of these corals, and a planned publication by Pedder, will provide a firm basis for the characterization of this species and genus. The interpretation of the species by Frech (1885, p. 66-67, Pl. 6, figs. 1a, 1b) and Birenheide (1978, p. 117-118), in particular, is substantiated by the type material, and *Medusaephyllum* is the appropriate generic name for species with the internal morphology of *Pachyphyllum*, but lacking the *bouchardi* growth form. I reserve *Phillipsastrea* for those massive phillipsastreids with numerous small corallites that consistently have only intermittently developed horseshoe dissepiments, commonly lack stereome coating of these dissepiments, and have rather weakly developed rhipidacanthine trabeculae.

The species composition of *Pachyphyllum* is as follows:

P. bouchardi Edwards and Haime, 1850. Type species. Ferques Limestone, Boulonnais area, northern France. The holotype of this species was stated to be in the collections of the Museum of Natural History, Paris, by Lang and Smith (1935, p. 554). However, Semenoff-Tian-Chansky in Semenoff-Tian-Chansky et al. (1962, p. 303) was unable to locate this specimen and its whereabouts are still unknown (Hill, 1981, p. F281). A thin section of a topotype was illustrated by Semenoff-Tian-Chansky (in Semenoff-Tian-Chansky et al., 1962, Pl. 9, figs. 1, 2); this topotype is a suitable potential neotype. It is obviously an extremely rare species, as it was not included in comprehensive faunal lists

from the type area provided by Rohart (in Brice et al., 1977, p. 144-145). According to Brice et al. (1979, p. 320), the type horizon corresponds to the Upper *asymmetricus* conodont zone, and is thus of Early Frasnian age.

P. crassicostratum Webster, 1889. Revised by Fenton and Fenton (1924) and Sorauf (1978). Owen Member, Lime Creek Formation, Iowa. Late Frasnian.

P. crassicostratum var. *nanum* Fenton and Fenton, 1924. Cerro Gordo Member, Lime Creek Formation, Iowa. Late Frasnian.

P. calostrotratum (Crickmay, 1962). Cooking Lake Formation, subsurface eastern Alberta. Early Frasnian.

P. miniaceum sp. nov. Mikkwa Formation, northern Alberta. Early Frasnian.

P. anfractum sp. nov. Peechee Member, Southesk Formation, southern Alberta. Middle Frasnian.

P. mirusense sp. nov. Ronde Member equivalent, Southesk Formation, eastern British Columbia. Late Frasnian.

Pachyphyllum calostrotratum (Crickmay, 1962)

Figures 48.6-48.13

Macgeea calostrota Crickmay, 1962, p. 3, Pl. 4, figs. 10-14.

Material. Holotype PRI 27075, Cooking Lake Formation, at 2520-2536 feet (768-773 m) in Imperial Fribourg well, Lsd. 12, Sec. 33, Twp. 55, Rge. 9W 4th Mer., Alberta (see Figure 48.1). A re-examination of the cored interval of this well revealed several further specimens of *P. calostrotratum*;

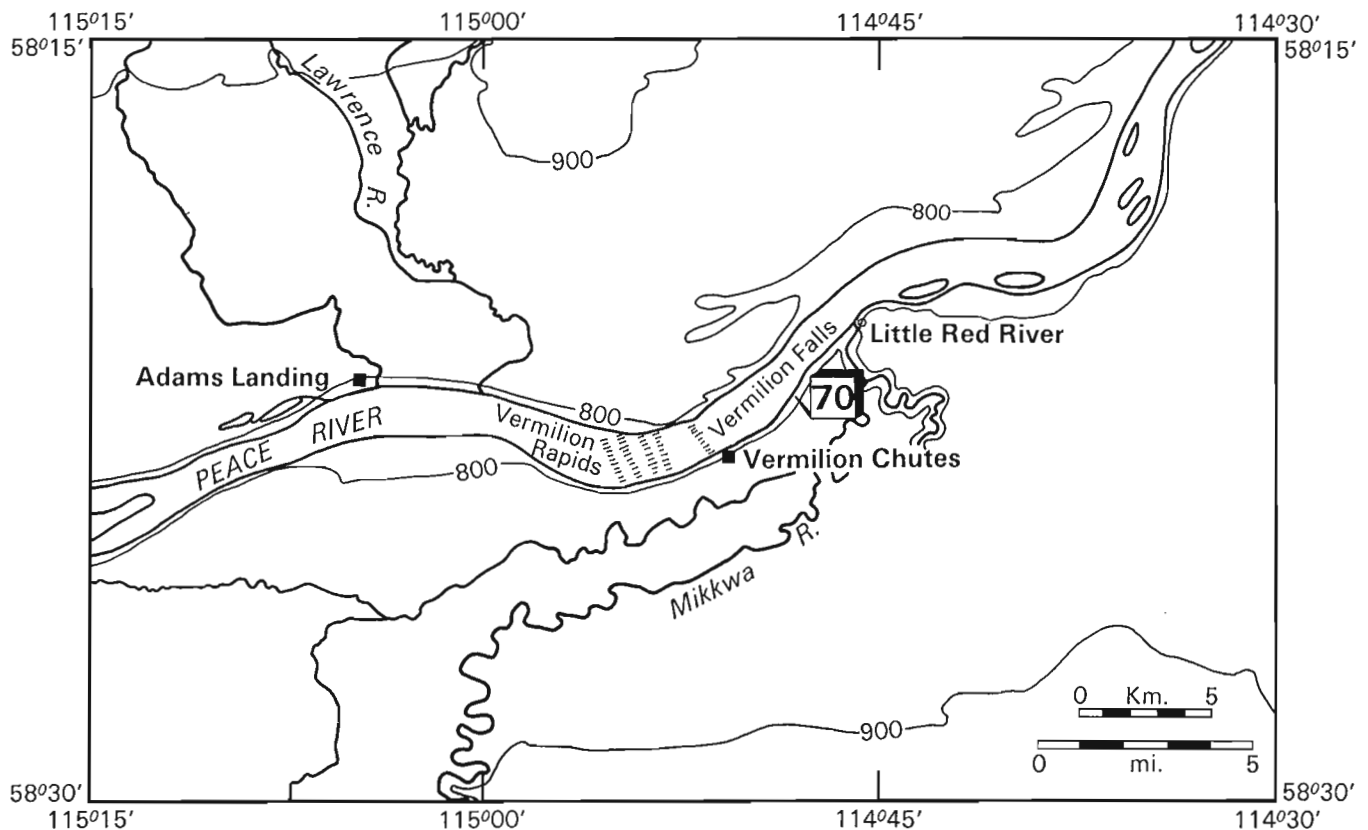


Figure 48.2. Locality map, Vermilion Falls area, northern Alberta (Area A, Fig. 48.1).

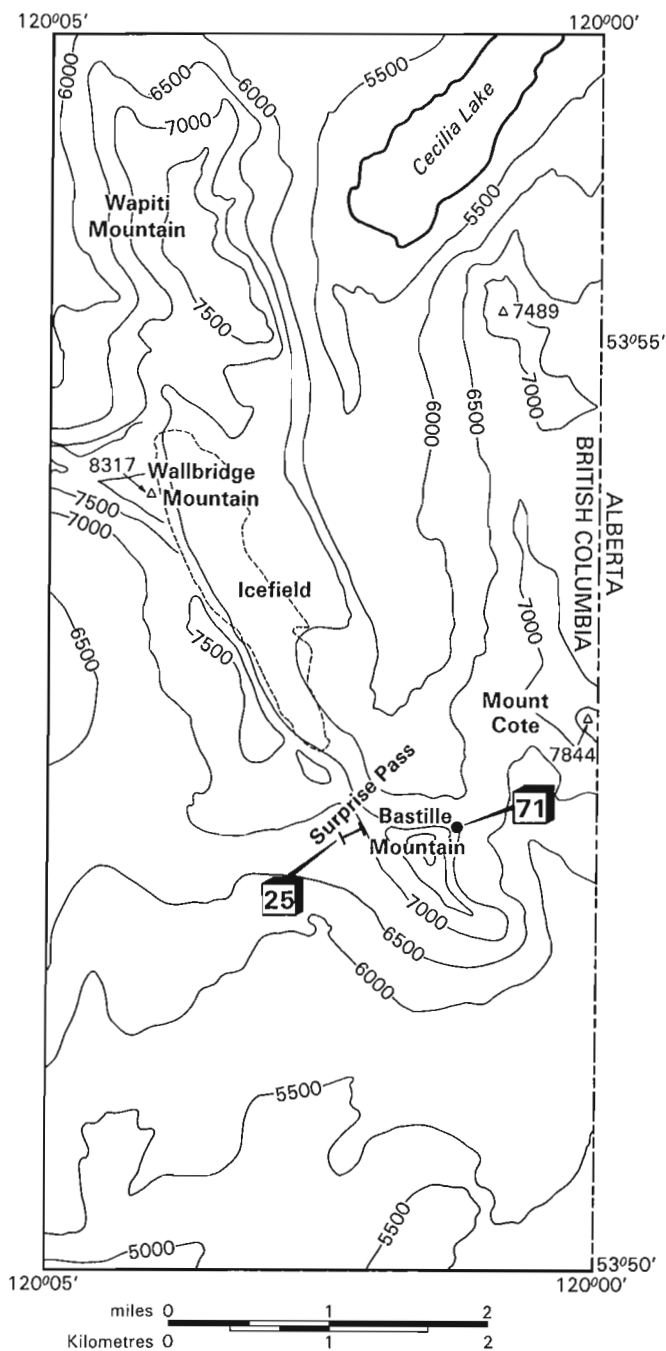


Figure 48.3. Locality map, Bastille Mountain area, eastern British Columbia (Area B, Fig. 48.1).

these are catalogued as GSC 76488 (2520.3 ft; 768.2 m), GSC 76489 (2520.4 ft; 768.2 m), and GSC 76490 (2521.0 ft; 768.4 m). As these specimens are from within the cited stratigraphic range of the holotype, they are regarded as topotypes.

Diagnosis. Corallum is aphyroid to thamnasterioid in early growth stages, with individual corallites extending above main part of corallum in later ontogeny. Ephebic corallite diameter ranges from 11.0 to 13.0 mm, diameter of tabularium ranges from 6.5 to 8.5 mm, and number of major septa varies from 21 to 27. Trabeculae are coarse, commonly obscuring development of small horseshoe dissepiments.

Description. Coralla available for study are all small and generally fragmented. It is apparent, however, that most coralla are massive and aphyroid to thamnasterioid in early growth stages, with a strong tendency for tall, individual corallites to extend above the distal surface of the massive part of the corallum in later ontogeny. Such ephebic corallites reach a diameter of 11.0 to 13.0 mm. Major septa range in number from 21 to 27 in mature corallites and are composed of particularly coarse rhipidacanth. In the vicinity of the collar of horseshoe dissepiments, septa are typically highly dilated, and, with associated stereome, are often in lateral contact. Adaxially, major septa become rapidly thinner in the tabularium, extending to, or almost to, the corallite axis, and become variably twisted. Minor septa extend 0.3 to 0.5 of length of major septa. Horseshoe dissepiments form a regular collar, are generally small, and often are obscured by coarse septal trabeculae. Outer dissepiments are typically large, elongate, and coated by stereome in early growth stages. In later ontogeny, where corallites project above massive portion of corallum, outer dissepiments may be absent. Tabularia range in diameter from 6.5 to 8.5 mm in mature parts of the corallum. Large, elongate tabellae, sloping down toward the corallite axis, occur locally at the outer margin of the tabularium. The remainder of the tabularium comprises a flat, weakly arched, or moderately concave series of widely spaced, complete and incomplete tabulae.

Remarks. The repository and catalogue number of the holotype of *P. calostrotum* were not recorded by Crickmay (1962), when he proposed the species. However, it is now known to be in the collections of the Paleontological Research Institution, Ithaca, New York, where it is registered under the number 27075. Newly prepared thin sections of the holotype are illustrated herein (figs. 48.6, 48.7).

Pachyphyllum calostrotum generally has smaller corallites than other Western Canadian species of *Pachyphyllum*, and is further distinguished from them all by its consistently strongly dilated septa that often obscure the horseshoe dissepiments. *Pachyphyllum crassicosatum* Webster has some small corallites, within the range of those of *P. calostrotum* (Sorauf, 1978, Textfig. 4), but is generally large, and has more septa. In addition, septal dilation in *P. crassicosatum* is not as consistently strong as in *P. calostrotum*.

Pachyphyllum miniaceum sp. nov.

Figures 48.14-48.27

Derivation of name. Latin, *miniaceus* = vermilion, a reference to Vermilion Falls, in the vicinity of the type locality.

Material. Holotype GSC 76491, Mikkwa Formation, Peace River, Vermilion Falls area, Alberta; locality 70 (Amoco loc. 14013) of locality register and Figure 48.2. Paratypes GSC 76492-76495, same horizon and locality.

Diagnosis. Corallum is generally thamnasterioid, more rarely aphyroid, through most of its ontogeny, with mature calices projecting to varying degrees above massive portion of corallum. Ephebic corallite diameter reaches 16.0 mm, tabularium diameter ranges from 8.0 to 13.5 mm, and as many as 33 major septa are present. Septal dilation is weak to moderate, and horseshoe dissepiments are large and well developed.

Description. Available coralla are highly variable in size, and some (e.g. GSC 76493, 76494) are clearly juvenile. Mature coralla reach a diameter of approximately 7 cm and height of

about 4 cm. Corallum is predominantly massive, thamasterioid, or more rarely aphroid. In late ontogeny, individual corallites project above the massive corallum surface for up to 1.5 cm, although generally this is not as pronounced. Corallite diameter is highly variable, increasing rapidly during ontogeny. It reaches 15.0 to 16.0 mm in largest specimens, and corallites are commonly elliptical in calical view. Calices are deep, generally with a low calical boss. There are 29 to 33 major septa in mature corallites, extending to, or slightly withdrawn from, the corallite axis. Near the axis, some major septa are slightly contorted. Minor septa are short, barely projecting adaxially beyond the collar of horseshoe dissepiments. Septa are weakly to moderately dilated in the dissepimentarium, tapering gradually toward the corallite axis, and have a characteristic ragged appearance in transverse section, reflecting coarse rhipidacanthine trabeculae. Stereome commonly coats dissepiments adjacent to the tabularium. Horseshoe dissepiments are well developed, large, locally coated with stereome, and only rarely obscured by septal trabeculae. Outer dissepiments are characteristically small, globose to weakly elongate, and in layers sloping steeply downward from adjacent tabularia. Tabularia range in diameter from 8.0 to 13.5 mm in mature corallites. Tabulae are incomplete and in moderately arched, variably spaced series. In the calical region, where corallites project above the surface of the main, massive part of the corallum, numerous small tabellae may occur in steeply dipping layers between the collar of horseshoe dissepiments and normal tabulae.

Remarks. *Pachyphyllum miniaceum* is the only Western Canadian species of *Pachyphyllum* to be found sufficiently weathered out from the enclosing rock matrix to allow adequate characterization of its external morphology. Consequently, as growth form is an essential diagnostic character of the genus, this species is illustrated in external view (figs. 48.14-48.19).

Although the internal morphology of the type species, *P. bouchardi*, is inadequately known, as discussed above, it appears to have the closest resemblance to *P. miniaceum*. On the basis of Semenoff-Tian-Chansky's (1962) revision, *P. bouchardi* is distinguished by having longer trabeculae, weaker stereome development, generally fewer septa at a greater corallite diameter, and more flattened tabulae. In addition, the original material of Edwards and Haime (1851, Pl. 7, fig. 7) suggests that the corallum of *P. bouchardi* is more erect than that of *P. miniaceum*.

Pachyphyllum calostrotum (Crickmay, 1962) differs from *P. miniaceum* in having smaller corallites and stronger septal dilation.

***Pachyphyllum anfractum* sp. nov.**

Figures 48.28-48.31

Derivation of name. Latin, *anfractus* = winding, referring to the highly convoluted septa of this species.

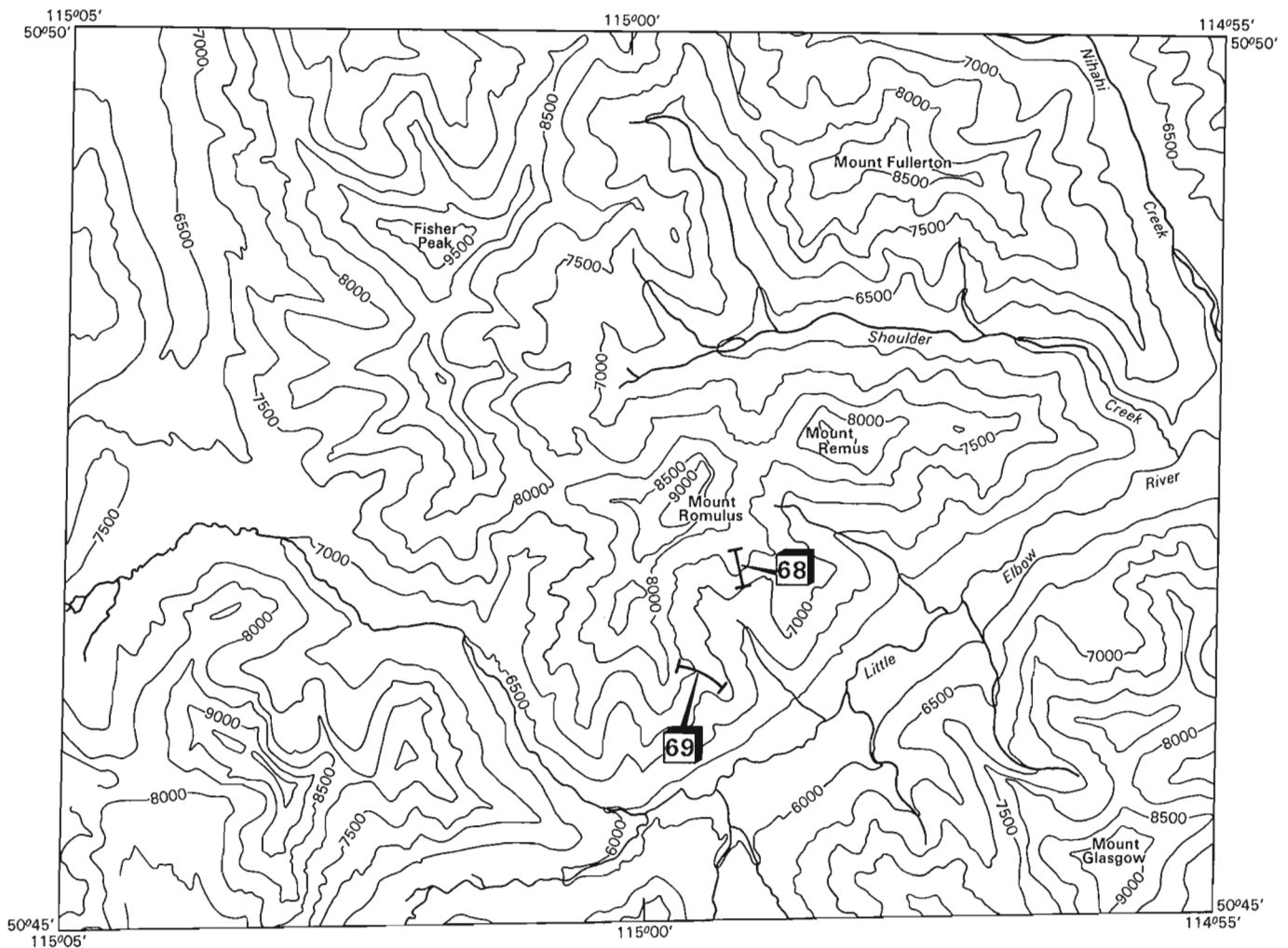


Figure 48.4. Locality map, Mount Romulus area, southern Alberta (Area C, Fig. 48.1).

Material. Holotype GSC 76496, Peechee Member, Southesk Formation, 1.75 km south of Mt. Romulus, Alberta; locality 69 (Amoco loc. 11518) of locality register and Figure 48.4. Paratype GSC 76497, same horizon, Mt. Romulus, Alberta; locality 68 (Amoco loc. 11517) of locality register and Figure 48.4.

Diagnosis. Corallum is loosely thamnasterioid, with individual corallites projecting above massive corallum in late ontogeny. Ephebic corallite diameter ranges up to 17.0 mm, with tabularium diameter of 8.0 to 10.0 mm. There are 24 to 26 major septa in mature corallites; they are characteristically long, thin and highly contorted in the tabularium. Horseshoe dissepiments are very small.

Description. As only two fragmentary coralla of this species are available for study, its full growth habit is not completely known. It is apparent from the holotype, the larger, more mature specimen, that the corallum is loosely thamnasterioid in early ontogeny, with individual corallites projecting well above the massive part of the corallum in late ontogeny, as is typical of *Pachyphyllum*. Corallites reach a diameter of at least 17.0 mm. There are 24 to 26 major septa in ephebic corallites and they generally extend to the corallite axis. They are only weakly dilated in the region of the collar of horseshoe dissepiments in the ephebic stage, but an immature corallite of the paratype (Fig. 48.31) exhibits moderate septal dilation in that area. In the tabularium, major septa are typically very thin and highly contorted, especially in the ephebic stage. Minor septa barely extend into the tabularium. Rhipidacanthine trabeculae are well developed, and are generally fine, reflecting the slender nature of the septa. They occasionally obscure the horseshoe dissepiments, and stereome is not strongly developed. Horseshoe dissepiments form a regular collar and are very small. They are most clearly apparent in the better preserved paratype (Fig. 48.31). Outer dissepiments are very variable in size and shape and form layers sloping steeply downward from the collar of the horseshoe dissepiments. The tabularium ranges in diameter from 8.0 to 10.0 mm in mature corallites, and comprises a weakly arched series of incomplete, well spaced tabulae, with a few peripheral tabellae.

Remarks. Although most species of *Pachyphyllum* show some twisting of septa in the tabularium, it is never as pronounced as in *P. anfractum*. The combination of very slender, highly contorted major septa and small horseshoe dissepiments clearly separates this species from all other known representatives of the genus.

Pachyphyllum sp. cf. *P. crassicostratum* Webster, 1889

Figures 48.32, 48.33

cf. 1889 *Pachyphyllum crassicostratum* Webster, p. 623.

cf. 1924 *Pachyphyllum crassicostratum* Webster; Fenton and Fenton, p. 51, Pl. 8, fig. 1; Pl. 9, figs. 1-5.

cf. 1978 *Pachyphyllum crassicostratum* Webster; Sorauf, p. 827, Pl. 4, figs. 2-5.

Material. GSC 76498, undifferentiated lower Southesk Formation, or lower Ronde Member equivalent of upper Southesk Formation, Bastille Mountain, British Columbia; locality 71 (Amoco loc. 11515) of locality register and Figure 48.3.

Diagnosis. Corallum is predominantly aphroid. Tabularia up to 13.0 mm in diameter; as many as 37 major septa. Major septa are variably withdrawn from corallite axis and moderately dilated at margin of dissepimentarium. Horseshoe dissepiments are generally small and regularly developed. Outer dissepiments are also mostly small.

Description. The only specimen available for study is largely aphroid, especially in mature parts of the corallum. There are as many as 37 major septa in the largest corallite of the specimen, with moderate dilation in the vicinity of the collar of horseshoe dissepiments. They become very slender in the tabularium, extending up to about 0.8 of the tabularium radius. Where dilated, septa show a typical ragged appearance, reflecting constituent rhipidacanthine trabeculae. Minor septa are slightly less dilated than major septa and barely extend into the tabularium. Horseshoe dissepiments are generally small, commonly coated in stereome, and form a regular collar. Outer dissepiments are mainly small, especially adjacent to the horseshoe dissepiments. Tabularia up to 13.0 mm in diameter. Very small tabellae may be present at the margins of the tabularium, but it is normally composed of a weakly arched series of incomplete, closely spaced tabulae.

Remarks. The type material of *P. crassicostratum* Webster, 1889, from the Owen Member of the Lime Creek Formation, Iowa, has not been illustrated in this section. Photographs of thin sections of syntypes of this species, catalogued under the numbers 78628 and 78628A at the U.S. Museum of Natural History, Washington, were kindly provided by J.E. Sorauf. They show apparently thamnasterioid coralla, moderate to strong septal dilation, large, well developed horseshoe dissepiments, and major septa extending almost to the corallite axis. Material from New York State, referred to this species by Sorauf (1978), is closer to the Canadian material, having predominantly aphroid coralla and considerable withdrawal of the major septa from the corallite axis (Sorauf, 1978, Pl. 4, figs. 2, 3). The Canadian specimen can certainly be accommodated in the expanded morphological scope of *P. crassicostratum* proposed by Sorauf, except for having wider tabularia and more septa. According to Sorauf (1978, Textfig. 4), tabularia of this species have a

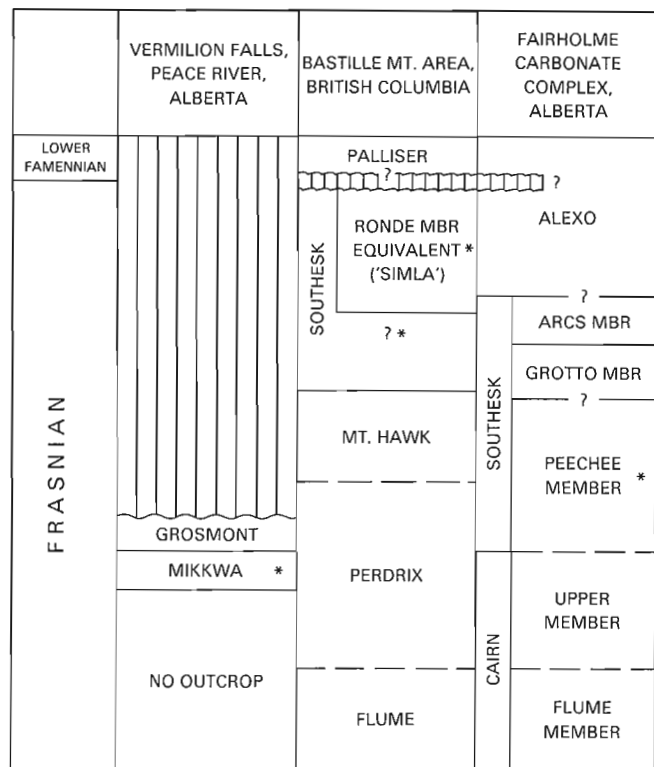


Figure 48.5. Stratigraphic terminology and general correlations. Asterisks indicate horizons bearing corals described in this paper.

diameter of up to about 9 mm, and have as many as 32 major septa. However, Fenton and Fenton (1924, p. 51) indicated that some corallites of the Iowa material reached 22 mm in diameter. Hence, tabularia of the size of the Canadian specimen (13 mm) are quite possible. Pending a more detailed revision of the Iowa fauna, and as only one Canadian specimen is available for study, it is thought to be appropriate at this stage to assign it to *P. crassicostatum* only tentatively.

Fenton and Fenton (1924) erected a new variety of *P. crassicostatum*, *P. crassicostatum* var. *nanum*, from the Cerro Gordo Member of the Lime Creek Formation of Iowa. Despite extensive further collecting, it is known only by the holotype (J.E. Sorauf, pers. comm., 1986). However, on the basis of Fenton and Fenton's illustration (1924, Pl. 9, fig. 6)

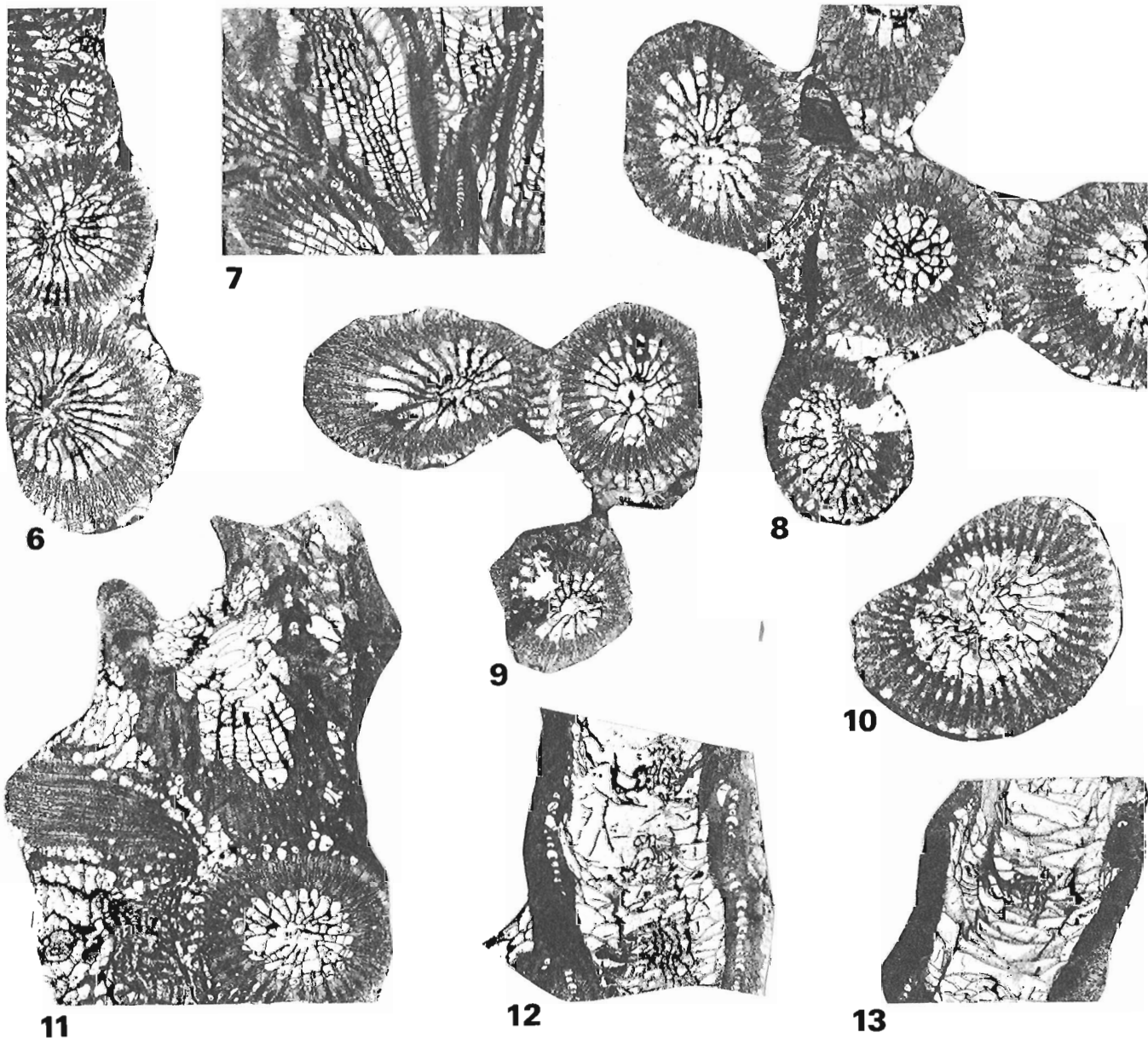
and photographs of thin sections kindly provided by Sorauf, it is a typical representative of *Pachyphyllum*. It differs from *P. crassicostatum* in having smaller corallites and fewer septa.

Pachyphyllum mirusense sp. nov.

Figures 48.34-48.37

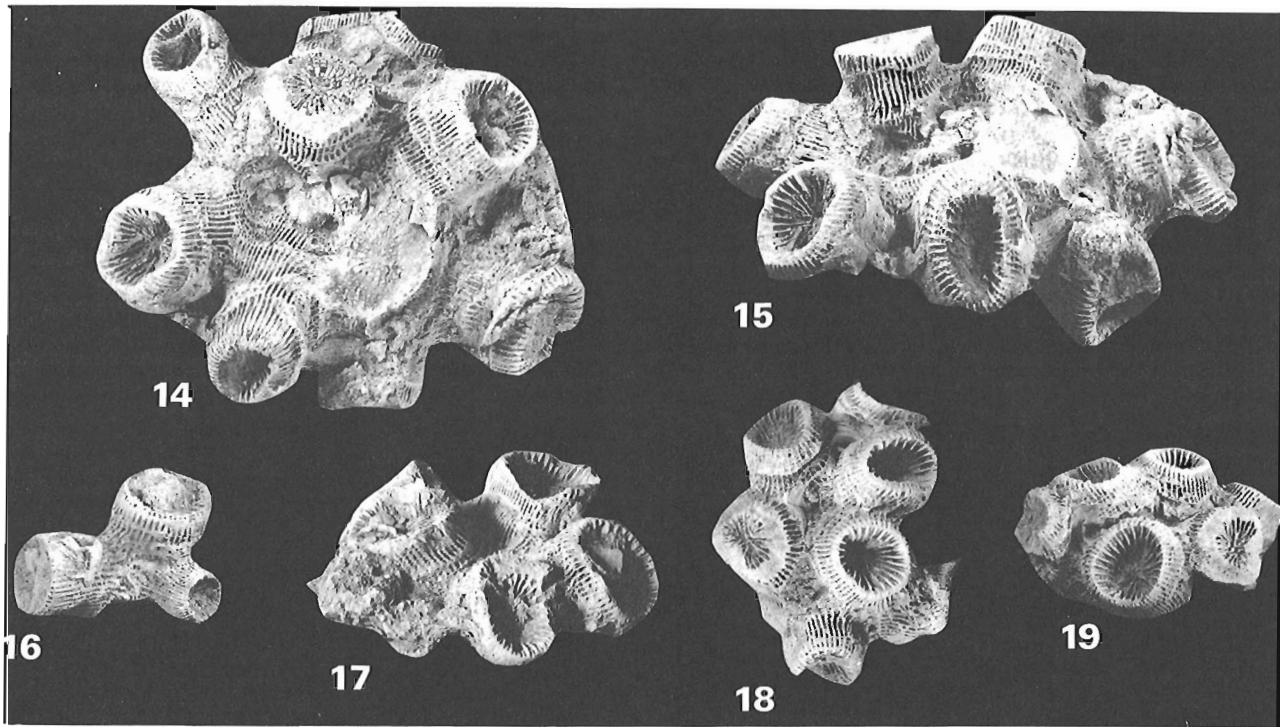
Derivation of name. Latin, *mirus* = surprising, after Surprise Pass, British Columbia, the type locality.

Material. Holotype GSC 76499, Ronde Member equivalent, Southesk Formation, Surprise Pass, British Columbia; locality 25 (Amoco loc. 11513) of locality register and Figure 48.3. Paratype GSC 76500, same horizon and location.



Figures 48.6-48.13. *Pachyphyllum calostrosum* (Crickmay), x3.

- 48.6, 48.7. PRI 27075, holotype, transverse and longitudinal sections.
- 48.8. GSC 76490, topotype, transverse section.
- 48.9. GSC 76488, topotype, transverse section.
- 48.10-48.13. GSC 76489, topotype, transverse, oblique and two longitudinal sections.



Figures 48.14-48.19. *Pachyphyllum miniaceum* sp. nov., x1.

- 48.14, 48.15. GSC 76491, holotype, transverse and lateral views before sectioning.
 48.16. GSC 76494, paratype, lateral view of immature specimen before sectioning.
 48.17. GSC 76492, paratype, lateral view before sectioning.
 48.18, 48.19. GSC 76493, paratype, transverse and lateral views of immature specimen.

Diagnosis. Growth form is dominantly thamnasterioid, mature corallites not extending far above massive part of corallum. Tabularium diameter up to 13.0 mm; 33 to 34 major septa in mature corallites. Major septa are weakly dilated and strongly withdrawn from corallite axis; minor septa are intermittently developed. Horseshoe dissepiments are very variable in size and form an irregular, unevenly developed collar.

Description. Corallum is mainly thamnasterioid, with pronounced, raised calical rims, but apparently without the development of extended individual mature corallites. Calices are deep, as shown in the immature paratype (Fig. 48.37). Septa are typically very slender, showing only weak dilation near the dissepimentarium/tabularium boundary. There are 33 to 34 major septa in the mature holotype; they extend adaxially for only approximately 0.5 of the tabularium radius. Minor septa barely extend into the tabularium and are commonly interrupted by dissepiments. Horseshoe dissepiments are highly variable in size and form an irregular collar. Some of these dissepiments show a tendency to become "unrolled" at their outer margins. Outer dissepiments are abundant and also extremely variable in size and shape. Stereome coating of dissepiments is weak or absent. Tabularia reach 13.0 mm in diameter and comprise a flat to weakly arched series of well spaced, complete and incomplete tabulae.

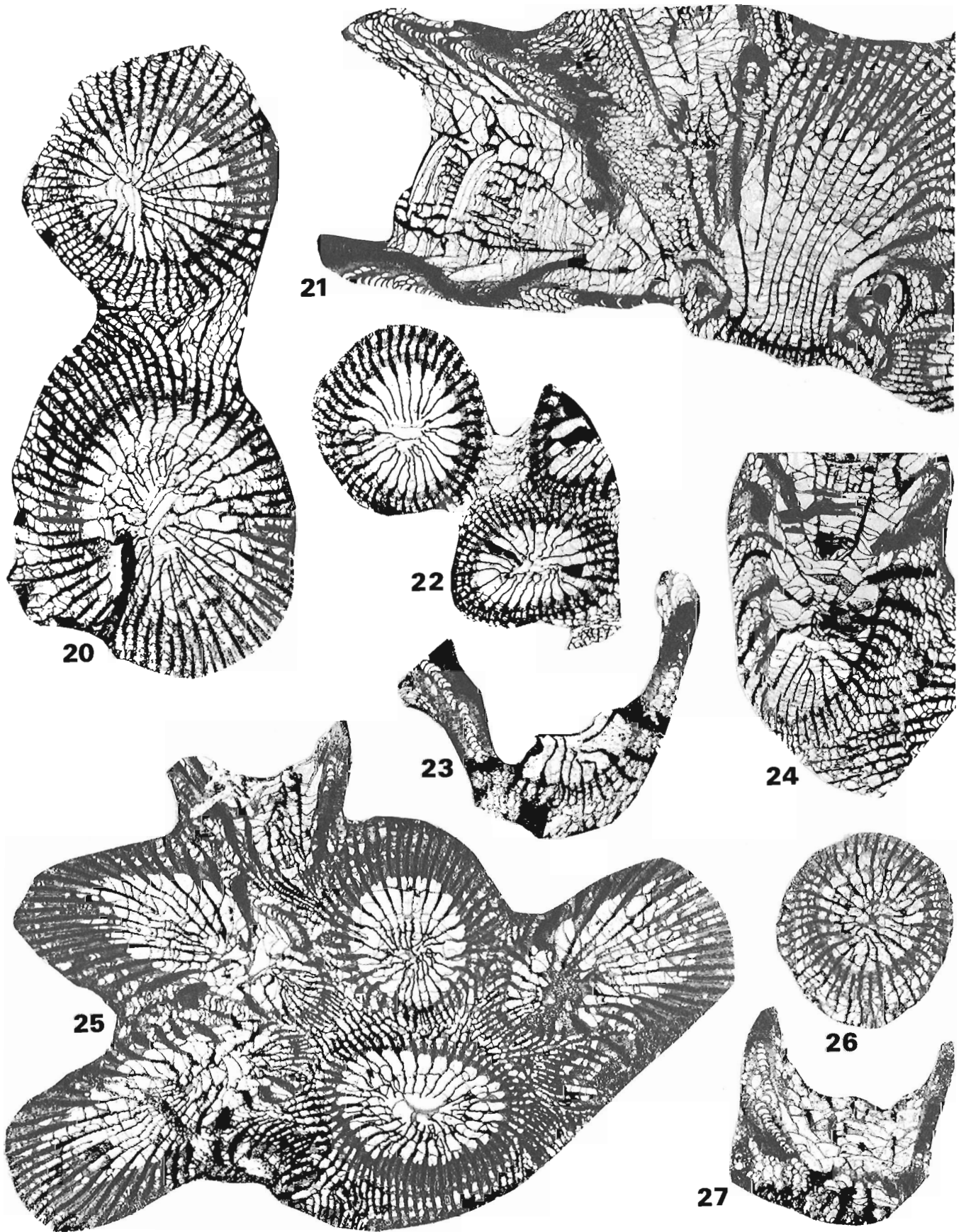
Remarks. The short major septa, weak minor septa, and irregularly developed horseshoe dissepiments distinguish *P. mirusense* from most other known representatives of the genus. The longitudinal section of *P. bouchardi* illustrated by Semenoff-Tian-Chansky et al. (1962, Pl. 9, fig. 2), although poorly preserved, suggests rather unevenly developed

horseshoe dissepiments and similar tabulae to those of *P. mirusense*. However, although the length of the major septa in mature corallites of *P. bouchardi* is not clear, *P. bouchardi* may be clearly distinguished from *P. mirusense* by having more dilated septa, of which there are considerably less at a comparable tabularium diameter.

Locality register

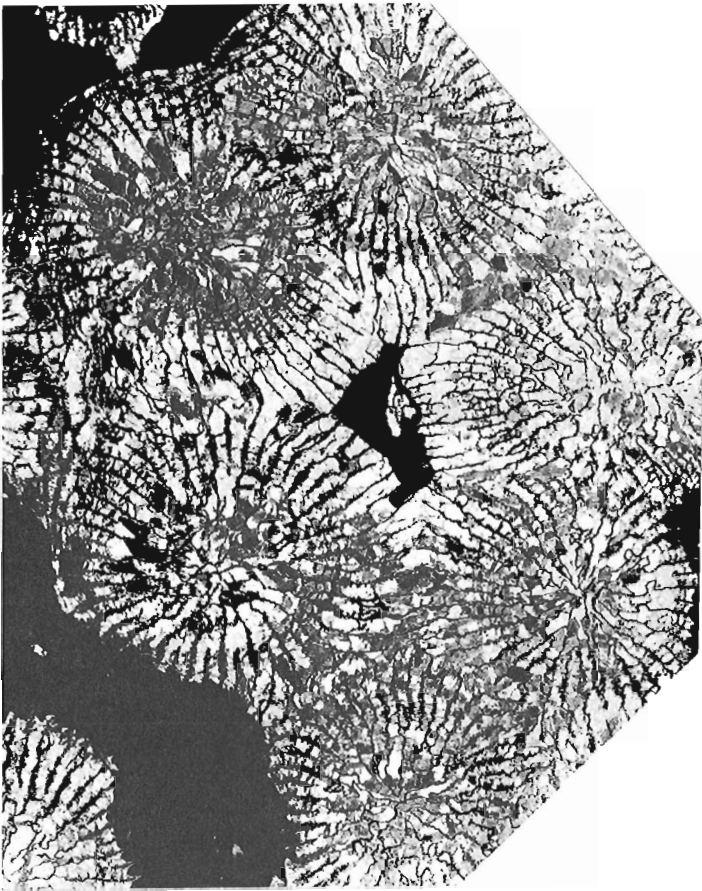
In a series of publications, the writer, partly in conjunction with A.E.H. Pedder, is currently describing the Frasnian rugose coral fauna of Western Canada. To make cross-referencing easier, each coral-bearing locality is assigned a unique number, and that number is used for the locality in each publication. Locality numbers are listed below in numerical order. They can be found on the locality maps, figures 48.2 to 48.4.

25. Amoco loc. 11513, Ronde Member equivalent, Southesk Formation, 70 m below top. South side of Surprise Pass, between Wallbridge and Bastille mountains, British Columbia. 53°52'22"N, 120°02'15"W. Collected by A.S. Hedinger, 1981.
68. Amoco loc. 11517, Peechee Member, Southesk Formation, 14.0 m above base, 14.9 m below top. Southeast flank of Mt. Romulus, Alberta. 50°47'10"N, 114°59'21"W. Collected by R.H. Workum, 1980.
69. Amoco loc. 11518, Peechee Member, Southesk Formation. Approximately 1.75 km south of summit of Mt. Romulus, Alberta. 50°46'37"N, 114°59'47"W. Collected by T.E. Nitychoruk, 1980.
70. Amoco loc. 14013, Mikkwa Formation. Right bank of the Peace River, approximately 4 km downstream from Vermilion Falls, Alberta. 58°22'58"N, 114°48'35"W. Collected by R.A. McLean, 1985.

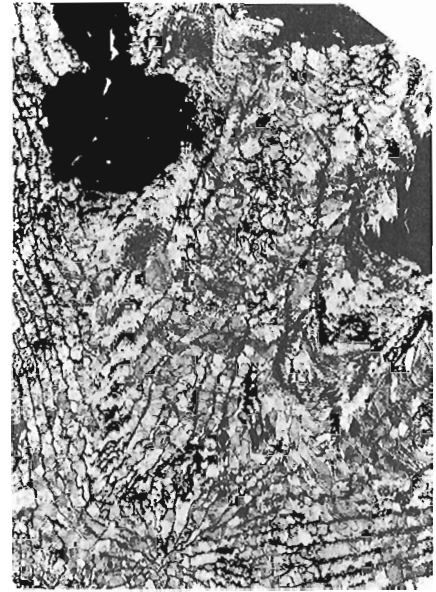


Figures 48.20-48.27. *Pachyphyllum miniaceum* sp. nov., $\times 3$.

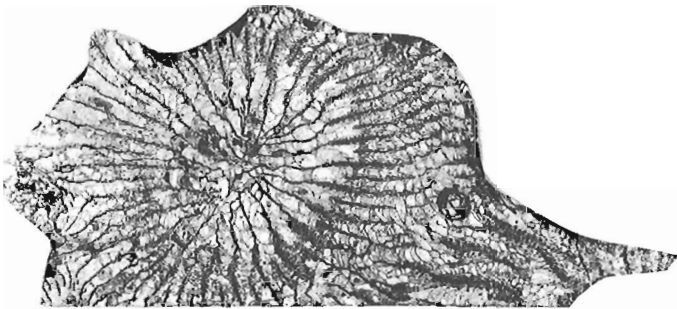
- 48.20, 48.21, 48.24. GSC 76491, holotype, transverse and two longitudinal sections.
 48.22, 48.23. GSC 76495, paratype, transverse and longitudinal sections.
 48.25. GSC 76492, paratype, oblique section.
 48.26, 48.27. GSC 76494, paratype, transverse and longitudinal sections.



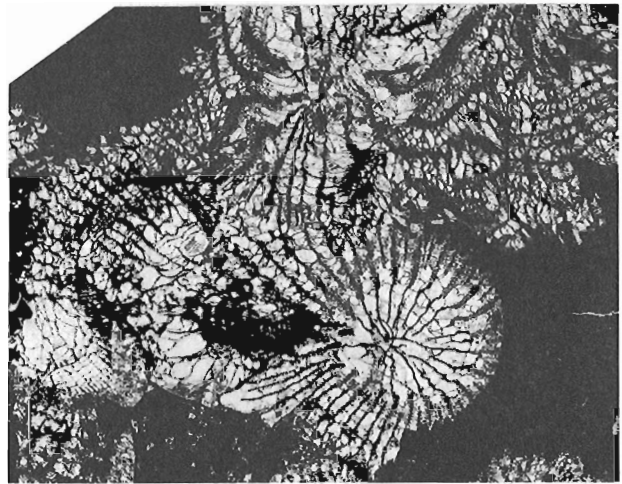
28



29



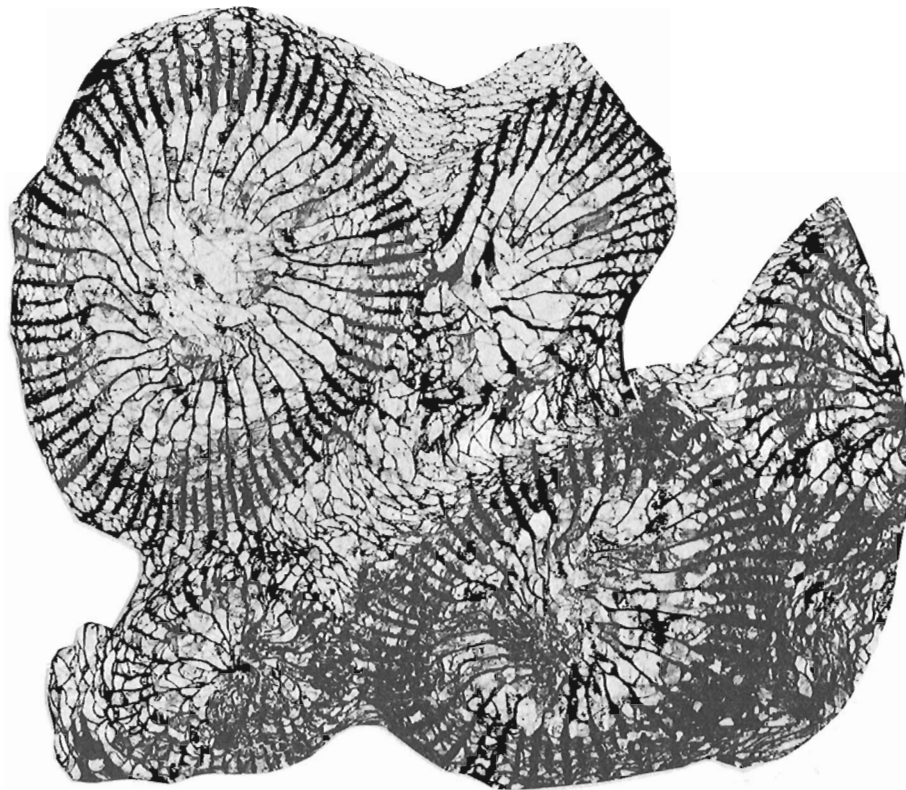
30



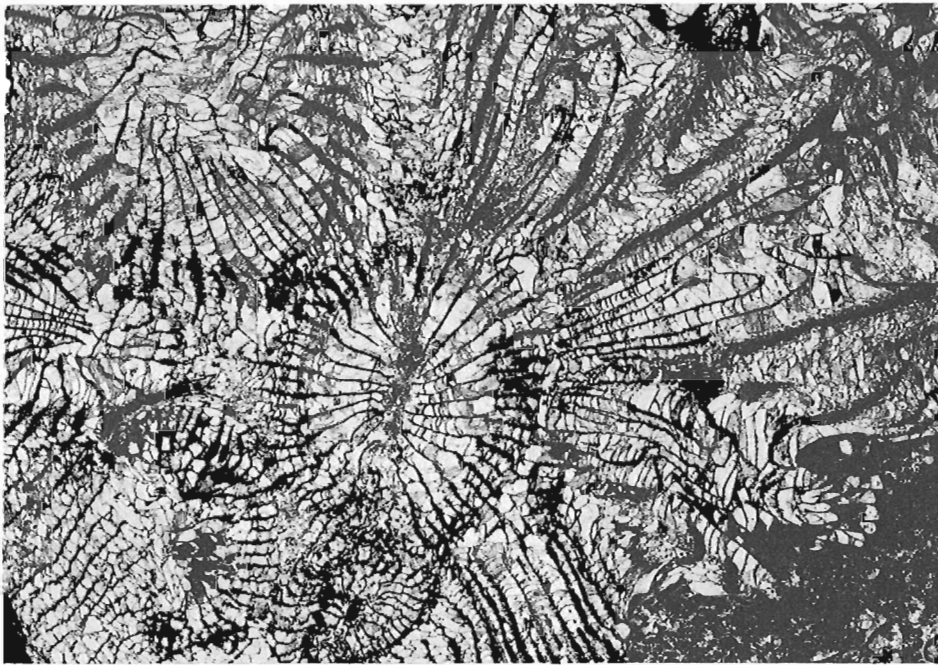
31

Figures 48.28-48.31. *Pachyphyllum anfractum* sp. nov., x3.

48.28, 48.29. GSC 76496, holotype, transverse and oblique sections.
48.30, 48.31. GSC 76497, paratype, transverse and oblique sections.

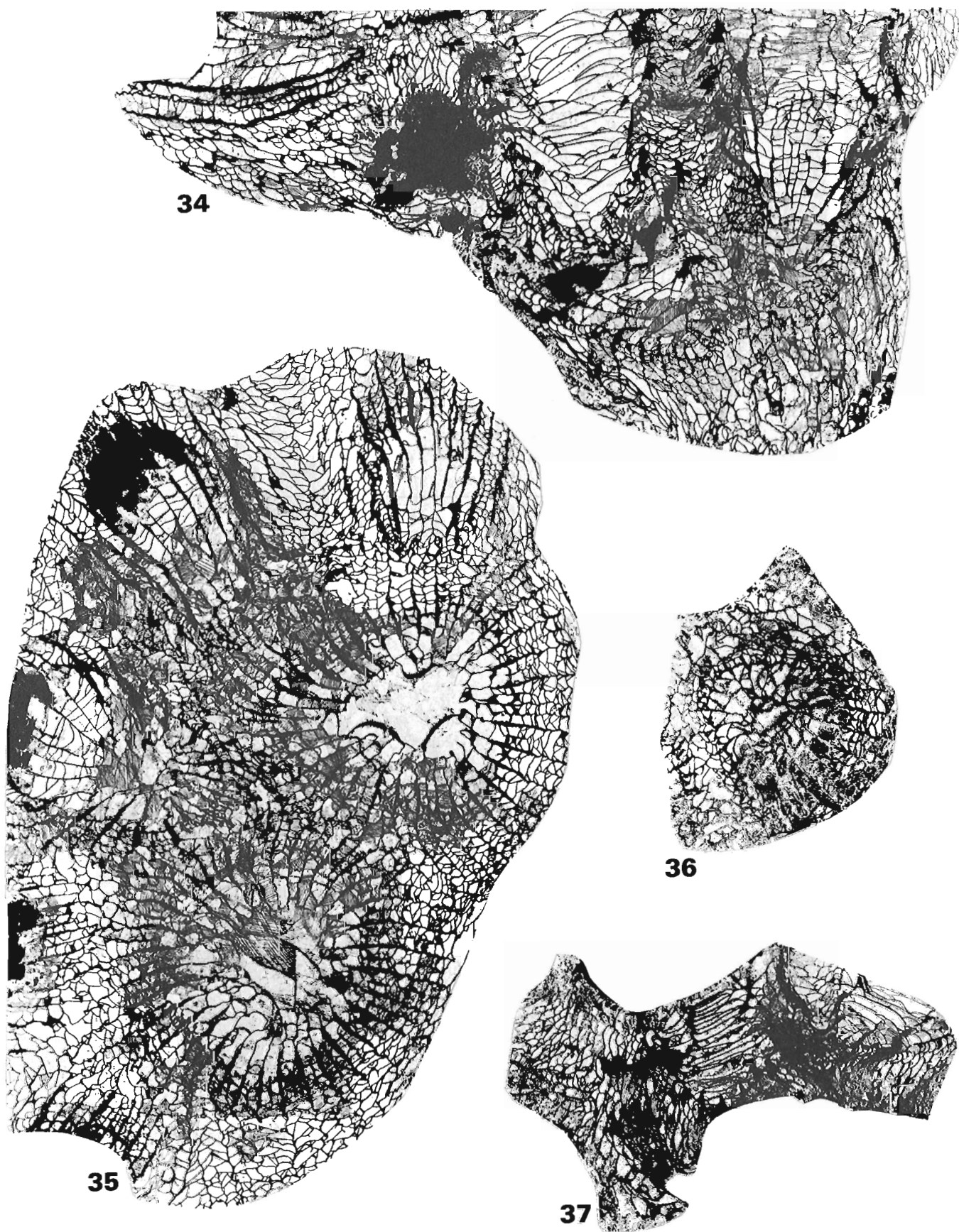


32



33

Figures 48.32-48.33. *Pachyphyllum* sp. cf. *P. crassicostatum* Webster, x3. GSC 76498, transverse and oblique sections.



Figures 48.34-48.37. *Pachyphyllum mirusense* sp. nov., x3.

48.34, 48.35. GSC 76499, holotype, longitudinal and transverse sections.

48.36, 48.37. GSC 76500, paratype, transverse and longitudinal sections of immature specimen.

71. Amoco loc. 11515, scree collection from undifferentiated lower Southesk Formation or lower Ronde Member equivalent of upper Southesk Formation. Eastern flank of Bastille Mountain, British Columbia. 53°52'22"N, 120°00'56"W. Collected by A.S. Hedinger, 1981.

References

- Birenheide, R.
1978: Rugose Korallen des Devon. Leitfossilien Nr. 2; Gebrüder Borntraeger, Berlin, Stuttgart, vi p. + 265 p.
- Brice, D., Bigey, F., Mistiaen, B., Poncet, J., and Rohart, J.-C.
1977: Les organismes constructeurs (Algues, Stromatopores, Rugueux, Tabulés, Bryozoaires) dans le Dévonien de Ferques (Boulonnais, France). Associations – Répartition stratigraphique; Bureau de Recherches Géologiques et Minières, Mémoires, no. 89, p. 136-151.
- Brice, D., Colbeaux, J.P., Mistiaen, B., and Rohart, J.-C.
1979: Les Formations dévoniennes de Ferques (Bas-Boulonnais, France); La Société Géologique du Nord, Annales, t. 98, p. 307-323.
- Crickmay, C.H.
1962: New Devonian fossils from western Canada; published by the author, Calgary, 16 p.
- Edwards, H.M. and Haime, J.
1850: A monograph of the British fossil corals; Part 1, Introduction and corals from the Tertiary and Cretaceous formations; The Palaeontographical Society, London, p. i-lxxxv + p. 1-71.
1851: Monographie des polypiers fossiles des terrains paléozoïques. Muséum d'Histoire Naturelle, Paris, Archives, t. 5, v p. + 502 p.
- Fenton, C.L. and Fenton, M.A.
1924: The stratigraphy and fauna of the Hackberry Stage of the Upper Devonian; Museum of Geology of the University of Michigan, Contributions, v. 1, xi p. + 260 p.
- Frech, F.
1885: Die Korallenfauna des Oberdevons in Deutschland; Deutsche geologische Gesellschaft, Zeitschrift, Bd. 37, p. 21-130.
- Hill, D.
1981: Treatise on invertebrate paleontology; Part F, Coelenterata, Supplement 1, Rugosa and Tabulata, C. Teichert (ed.); The Geological Society of America and University of Kansas Press, Boulder and Lawrence, v. 1, p. i-xl + p. 1-378, v. 2, p. i, ii + p. 379-762.
- Lang, W.D. and Smith, S.
1935: *Cyathophyllum caespitosum* Goldfuss, and other Devonian corals considered in a revision of that species; Geological Society of London, Quarterly Journal, v. 91, p. 538-590.
- McLaren, D.J.
1962: Middle and early upper Devonian rhynchonelloid brachiopods from western Canada; Geological Survey of Canada, Bulletin 86, 122 p.
- McLean, R.A. and Pedder, A.E.H.
1984: Frasnian rugose corals of western Canada. Part 1: Chonophyllidae and Kyphophyllidae; Palaeontographica, Abteilung A, Bd. 184, p. 1-38.
– Frasnian rugose corals of western Canada. Part 2: The genus *Smithiphyllum*; Palaeontographica, Abteilung A. (in press)
- Scrutton, C.T.
1968: Colonial Phillipsastraecidae from the Devonian of south-east Devon, England; The British Museum (Natural History), Bulletin, v. 15, p. 181-281.
- Semenoff-Tian-Chansky, P., Lafuste, J., and Durand Delga, M.
1962: Madréporaires du Dévonien du Chénoua (Algérie); La Société Géologique de France, Bulletin, 7e Série, t. 3, p. 290-319.
- Sorauf, J.E.
1978: Upper Devonian *Pachyphyllum* (rugose coral) from New York State; Journal of Paleontology, v. 52, p. 818-829.
- Webster, C.L.
1889: Contributions to the knowledge of the genus *Pachyphyllum*; The American Naturalist, v. 23, p. 621-625.

Ordovician stratigraphy and the structural style at the Main Ranges-Front Ranges boundary near Smith Peak, British Columbia

Project 850048

J.A. Mott,¹ J.M. Dixon¹, and H. Helmstaedt¹
Institute of Sedimentary and Petroleum Geology, Calgary

Mott, J.A., Dixon, J.M., and Helmstaedt, H., Ordovician stratigraphy and the structural style at the Main Ranges-Front Ranges boundary near Smith Peak, British Columbia; in Current Research, Part B, Geological Survey of Canada, Paper 86-1B, p. 457-465, 1986.

Abstract

The McKay Group, measured to be at least 2100 m thick, is divided into four, broad, lithological units. The Middle Ordovician Skoki and Glenogle formations are found to interfinger; the transitional Outram Formation is not present. The Glenogle Formation coarsens upward from siltstone to sandstone. Eastward, two unconformities, one beneath a Basal Devonian unit, and one beneath the Upper Ordovician Beaverfoot Formation, cut sharply into the stratigraphic sequence and lie in the upper McKay Group. The unconformity beneath the Beaverfoot indicates that a structural basin existed in the central Main Ranges prior to Upper Ordovician sedimentation.

The northern extension of the Gypsum Fault, truncated by later-occurring normal faults, is found to lie west of the Bull River valley. The fault cuts up structurally but down stratigraphically in an overturned panel, indicating structural overturning prior to thrust detachment.

Résumé

Le groupe de McKay, dont l'épaisseur est d'au moins 2 100 m, se divise en quatre grandes unités lithologiques. Les formations de l'Ordovicien moyen de Skoki et de Glenogle sont interdigitées; la formation transitionnelle d'Outram est absente. La formation de Glenogle devient plus grossière vers le haut, passant de siltstone à un grès. Vers l'est, deux discordances, l'une sous une unité dévonienne basale et l'autre sous la formation de Beaverfoot de l'Ordovicien supérieur, tranchent brusquement la séquence stratigraphique et se trouvent dans la partie supérieure du groupe de McKay. La présence d'une discordance sous la formation de Beaverfoot indique qu'il y avait un bassin structural dans la partie centrale du chaînon Main avant la sédimentation de l'Ordovicien supérieur.

La prolongation vers le nord de la faille de Gypsum, coupée par des failles normales plus récentes, se trouve à l'ouest de la vallée de la rivière Bull. La faille est dirigée de façon structurale vers le haut mais de façon stratigraphique vers le bas dans une nappe déversée, ce qui indique qu'un renversement structural a précédé le décollement.

¹ Department of Geology, Queen's University, Kingston, Ontario

Introduction

Three months of geological mapping at a scale of 1:25 000 was undertaken as part of a Ph.D. study at Queen's University in cooperation with M. McMechan of the Geological Survey of Canada. The study area lies at the headwaters of the East White and Bull rivers in the south-eastern corner of the Kananaskis Lakes West-Half map area (NTS 82J/W1/2). The area comprises the eastern boundary of the Main Ranges subprovince of North and Henderson (1954) from latitude 50°04'N to 50°14'N (see Figure 49.1). The Kananaskis Lakes West-Half area was mapped at a reconnaissance scale of one inch to two miles (1:126 720) by G.B. Leech (Leech, 1979) in the early 1960's. The only more recent published work on the region concerns several zinc showings in and on the east side of the Bull River valley immediately southeast of the study area (Gibson, 1979). The area continues to be potentially economically interesting to several petroleum companies. The principal author has benefited from access to private field notes and maps compiled in the early 1960's and made available by Shell Canada Resources, Limited.

Leech (1979; pers. comm., 1985) noted facies changes in Middle and Upper Ordovician formations along the eastern margin of the study area. Leech (1979) shows that the fold-dominated strata underwent an eastward tightening and overturning to the Main Ranges-Front Ranges boundary at this latitude. The rocks of the study area would be expected to represent the hanging wall of the northern extension of the Gypsum Fault mapped in the northern Fernie map area (Benvenuto and Price, 1979), and originally postulated by Leech (1962). Leech (1964) noted that the McKay Group was unusually thick in the study area and Raasch and Bruce (1966) noted that lithological divisions in the McKay Group were evident there, but neither of these observations has ever been documented in a publication.

Stratigraphy

Stratigraphic units in the study area range essentially from the Upper Cambrian and Lower Ordovician McKay Group, through the sub-Devonian unconformity, to a few rare occurrences of Devonian strata. The base of the McKay Group is not visible. A simplified, composite stratigraphic section is illustrated in Figure 49.2 and shows typical unit thicknesses. Figure 49.3 illustrates some of the lateral variation visible at the top of the stratigraphic column. Of the numerous fossil collections made, the majority have been dated by B.S. Norford of the Geological Survey of Canada.

The McKay Group

Leech (1958) noted that the McKay Group in the Fernie map area, south of the present study area, consists of a lower, shale-rich, and an upper, limestone-rich division. The part of the McKay Group observed in the present study area probably constitutes much of the upper division.

Raasch and Bruce (1966) noted six physical subdivisions in the McKay Group at the western boundary of the study area. These divisions are visible as thick, alternating resistant and recessive intervals. Stratigraphic sections provided by Shell Canada Resources Limited and original work (Fig. 49.2) indicate an extremely gradational nature to all McKay Group lithological changes (commonly occurring over 100 m or more of section). It was not clear from the sections provided by Shell to what extent differences in lithology and gross weathering characteristics permit the division of the McKay Group. Resistant intervals of the McKay Group are locally recessive with no evident corresponding lithological change. Two unit contacts described in this study correlate approximately to subdivision contacts made by Shell.

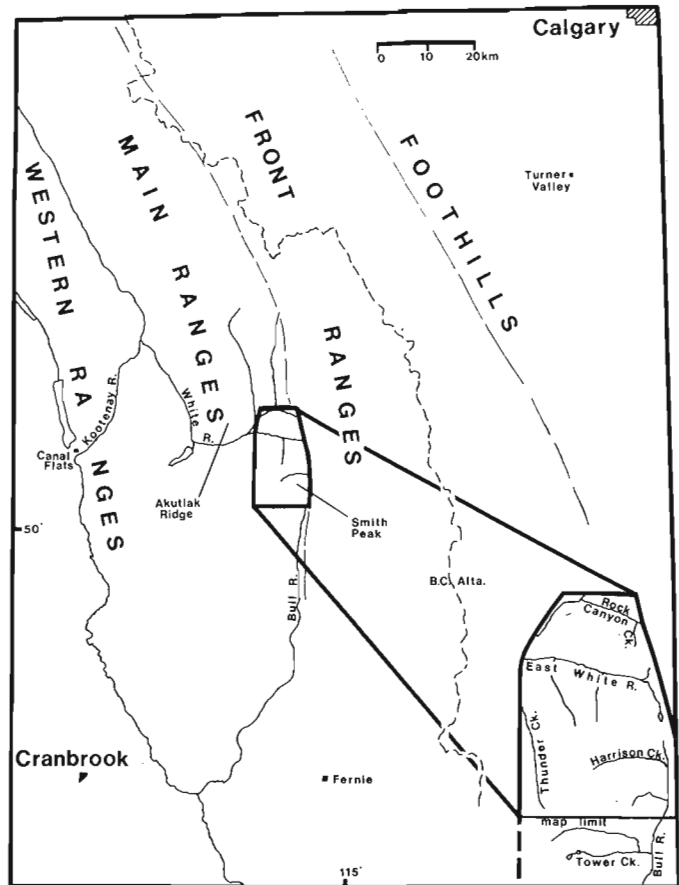


Figure 49.1. Location map illustrating some regional geography and the structural subprovinces of the Rocky Mountains. Rivers and creeks referred to in the text as in, or at the boundaries of, the study area are illustrated in more detail in the bottom right hand corner.

Leech (1979) illustrated (but did not describe) the McKay divided into at least three map units in the western part of the Smith Peak area, but Leech (pers. comm., 1985) has since found the McKay Group divisible into at least seven stratigraphic units. A correlation of this study's McKay units with those of Leech has not yet been made.

The McKay Group is most easily divisible into four broad units, termed from bottom to top: A, B, C, and D, although further subdivisions are possible (Fig. 49.2). Because the base of the McKay is not seen, it should be noted that Unit A, the lowest unit observed, may not be the lowest McKay unit in existence. Each of the units B, C and D is shaly and recessive at the base and becomes more resistant as the proportion of carbonate to shale gradually increases upward. Ignoring some differences in the lithology of the upper portion of each unit and the gradational contacts, repeated sequences of sedimentation, represented by different units, may be visualized. Unit D has been subdivided into lower, shaly D1 and upper carbonate-rich D2 subunits (Fig. 49.5) in an attempt to better illustrate structure. This subdivision will be described later.

Unit A is a commonly calcareous, greyish green phyllite. Most primary textures are obliterated by a strong cleavage, but locally, fine laminae – some seemingly graded – and cobble-sized, turquoise-coloured limestone nodules are present. The nodular limestone fabric appears to be related to the solution cleavage. Up to five per cent of

Unit A consists of isolated 0.2 to 1 m thick beds of skeletal packstone and grainstone (crinoid and brachiopod debris) and, rarely, intraclastic lime rudstone and floatstone with skeletal debris matrices. A thin, resistant interval, consisting of 50 per cent thin bedded, laminated dolostone with the green phyllite, is visible at four isolated localities but has not been measured. This interval is mapped together with Unit A. The overall appearance of Unit A bears a strong resemblance to the Putty Shale Member of the Survey Peak Formation of Aitken and Norford (1967).

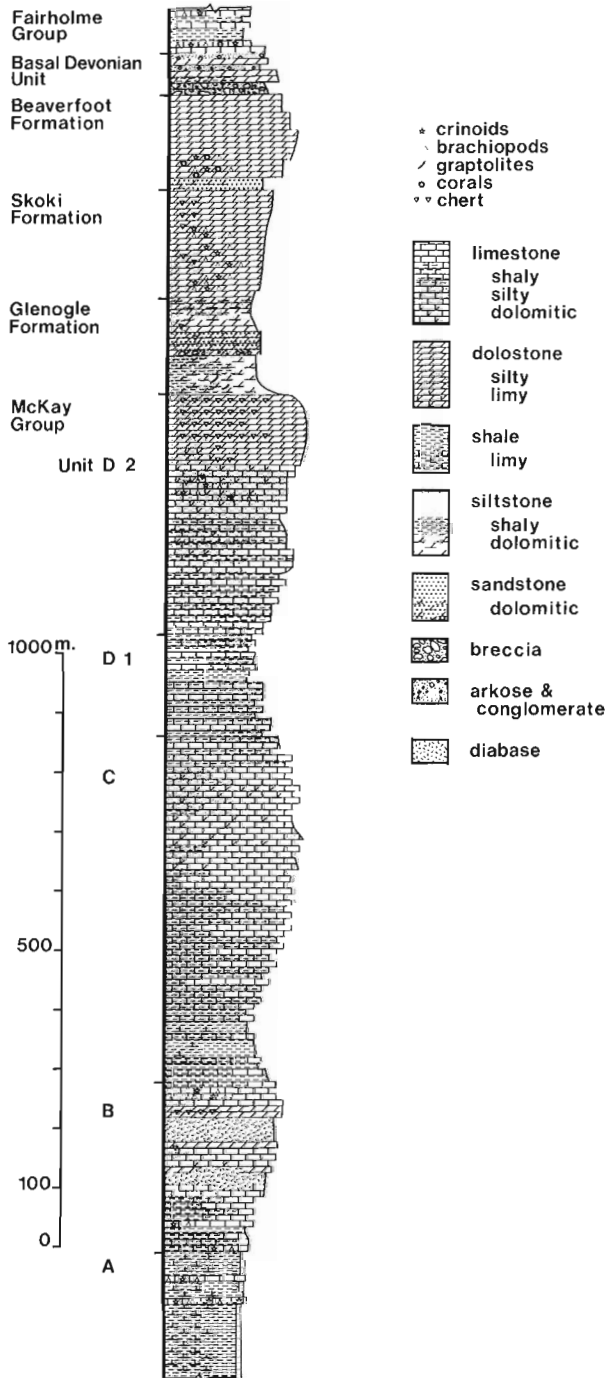


Figure 49.2. Generalized, composite stratigraphic section of all measured map units and formations.

The lower portion of Unit B consists primarily of highly cleaved, light grey, limy shale and very shaly limestone. The contact with Unit A is gradational. The lime content increases upward until the section consists of 50 to 80 per cent microcrystalline limestone; packstone and grainstone is more rare and the rock more resistant. Intervals of very thin bedded, nodular, microcrystalline limestone with 50 per cent light grey to pale orange-brown shale and limy shale matrices are present. The nodular fabric is principally due to a strong solution cleavage, as in Unit A. Silt content of the limestone appears to increase upward. At the top of the unit, limestone beds show up to 60 per cent thick, wavy, cherty dolomite laminae and, more rarely, fine, irregular chert nodules. At a few locations, thin, medium to coarse grained, calcareous sandstone beds are present. Unit B contains thick diabasic sills surrounded by beds of massive dolostone and dolomitic limestone. The proximity of the dolomite to the sills suggests that some dolomitization may have been caused by the intrusives.

The contact between units B and C occurs over as little as 30 m and is the most abrupt of all McKay unit contacts. Resistant, silty limestones of Unit B grade upward into the lower part of Unit C, which consists of whitish grey to light grey shale, limy shale and local phyllite with 10 to 30 per cent thin, isolated, microcrystalline limestone interbeds. Farther upward, limestone content increases until more resistant, 0.5 to 3 m thick, well bedded, medium to dark blue-grey, microcrystalline limestone beds, typical of the upper part of Unit C, are dominant. Cleaved, shaly limestone interbeds persist, creating a pattern of alternating strongly cleaved and uncleaved beds. Limestone with up to 40 per cent partial dolomitization can be observed in some beds. The dolomite is irregularly distributed parallel to bedding and cleavage planes.

Unit D of the McKay Group changes upward from shale to limestone to dolostone. As stated, the shaly portion (D1) of Unit D has been distinguished in order to illustrate the structure of the study area (Fig. 49.5) but, because it grades into the limestones of Sub-unit D2, its map contacts are approximate. The limestone of Subunit D2 and the D1 shale are distinguished on the basis of end-member lithologies. The limestone is similar, and often identical, to the upper portion of Unit C, except that it is typically more silty. The D2 shale also has resistant, microcrystalline limestone and shaly limestone interbeds but is distinguished, often with difficulty, by the presence of very recessive limy shale and shale, typically white to whitish grey in colour.

The dolostone at the top of Unit D and Subunit D2 is a distinct lithological marker. It has not been mapped separately from the limestone of D2 because it varies substantially in thickness at the expense of the limestone. The predominantly microcrystalline dolostone¹ is light grey to pale orange-brown in colour, thick bedded, and weathers massive and resistant. The dolostone contains variable proportions of two distinctive features: up to 30 per cent coarse, irregular to wavy, dark brown, resistant, silty-dolomite laminae, or up to 90 per cent coarse, white to bluish white chert lenses and cobble-sized, irregularly shaped nodules. Generally, chert content increases upward to a maximum at the McKay-Glenogle contact.

The measured thickness of the McKay above Unit A is in excess of 1400 m. In the core of the first overturned anticline east of the western boundary of the map area (Thunder Creek), the base of Unit A was not observed. This indicates that at least an additional 700 m of section is present beneath Unit B. The cumulative thickness of the McKay Group is thus at least 2100 m. Just west of the study area, in the Thunder Creek Anticline, the McKay Group has been measured to be at least 3000 m thick (Leech, 1964).

¹ A rigid classification of observed dolomitic rocks (Todd, 1966) is here avoided until more detailed petrographic studies are complete. The classification of Dunham (1962) modified by the word dolomite, in this text, indicates 100% dolomitization of the rock.

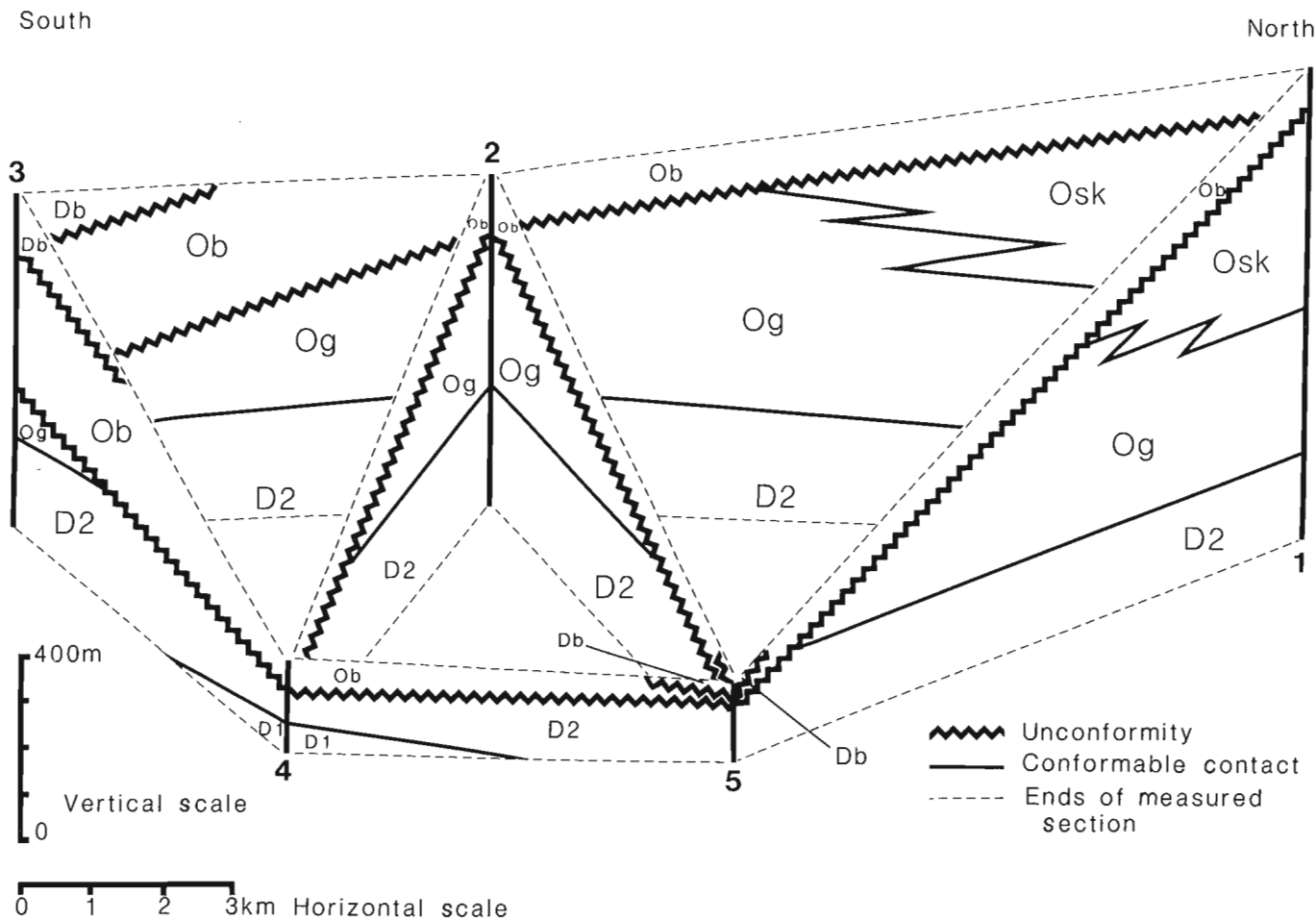


Figure 49.3. Schematic fence diagram of observed stratigraphic changes viewed from the east. Symbols: Db - Basal Devonian; Ob - Beaverfoot; Osk - Skoki; Og - Glenogle; D1, D2 - McKay Group Unit D subunits. Section locations: 1. Rock Canyon Creek; 2. north side of Harrison Creek; 3. south edge of map area; 4. southeast corner of map area; 5. north side of Harrison Creek structurally below Section 2. Note that section locations have been altered relative to each other for clarity, and bear no precise relationship to the horizontal scale.

The Glenogle Formation

The Glenogle Formation is characterized by two rock types. The lower part of the formation is typified by fissile and very recessive, interlaminated, black, slaty siltstone and orange silty dolostone. Locally, the black colour grades abruptly to deep red and, more rarely, green. Fossils are rare, but a graptolite and part of a trilobite in these lower strata (GSC loc. C-108000, B.S. Norford) indicate an Arenig age (Early Ordovician) typical for the base of the Glenogle (B.S. Norford, pers. comm.). The lower contact with the McKay was observed to be conformable at numerous localities, and in the south end of the study area, there are small lenses of fissile red slate and siltstone in the uppermost tens of metres of McKay strata.

Thin, medium to coarse grained, quartz sandstone interbeds increase in concentration upward in the black siltstone. The lithology of the upper portion of the Glenogle is typified by chert-rich, fine to coarse grained quartzites, commonly with carbonate cements. The quartzites are thin bedded or platy and show a variety of primary sedimentary features including crossbedding, flute casts, and some

graded bedding. Lateral variation in cement composition imparts a cherty, often coarse, lensoid character to many beds. The Glenogle Formation is distinctive, but portions of its upper half bear a striking similarity to many of the more chert-rich sections at the top of Unit D in the McKay Group.

Leach (1979) mapped what is here termed Glenogle Formation as the Glenogle and Tipperary formations, undivided. Presumably, the upper portion of the herein-described Glenogle Formation was considered the Tipperary Quartzite. Work presently being done by B.S. Norford above Akutlak Creek, west of the study area, reveals five Glenogle members, of which the lower two fit the descriptions of the lower and upper portions of the Glenogle Formation outlined here (B.S. Norford, pers. comm., 1985). Rocks of the Tipperary Quartzite, as described at their type section (Norford, 1969), are not present in the study area.

One complete section of Glenogle was measured to be 160 m thick, but eastward the formation thins, and is absent altogether between the Beaverfoot Formation and McKay Group (Fig. 49.3).

The Skoki Formation

At the north end of the map area, in the vicinity of Rock Canyon Creek, very silty dolomite overlies Glenogle siltstone and quartzite. Brachiopods collected by B.S. Norford during a field visit with the principal author (GSC loc. C-82891, B.S. Norford) indicate a Whiterockian (early Middle Ordovician) age. The facies closely resembles the Skoki Formation of Mount Wilson (Norford, 1969). The Skoki observed in the study area is primarily a light grey to pale orange-brown, massive weathering, thin bedded dolostone. Many beds are so silty that they border on being dolomitic siltstones. The lower part of the formation may consist of up to 60 per cent thick, wavy, resistant, dark brown, silty-dolomite laminae, resembling parts of the top of Unit D of the McKay Group. The middle of the Skoki Formation comprises thinly interbedded skeletal dolomite mudstone and dolomite grainstone (crinoid, brachiopod and trilobite debris) with lesser peloidal dolomite packstone and dolomite grainstone. The upper portion of the Skoki is a light grey dolomite mudstone with up to five per cent irregularly shaped, dark brown chert nodules. Although a thin interval of dolomite breccia and coarse sand is present near the Glenogle-Skoki contact (Fig. 49.2), the boundary between the two formations appears to be conformable. Interbeds of the lower Skoki-type lithology begin in the Glenogle sands and increase in proportion upsection.

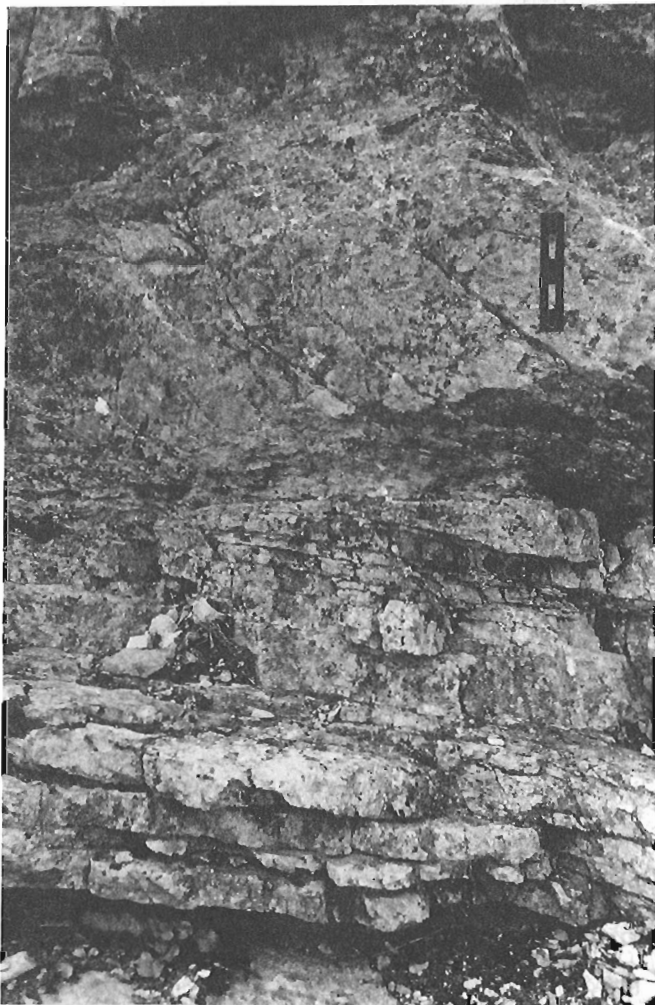


Figure 49.4. Beaverfoot Formation unconformably overlying the McKay Group. Note the angular truncation of McKay Group strata. The scale bar measures 0.5 m.

Studies farther to the north (Norford, 1969) indicate that the Outram Formation (Aitken and Norford, 1967) displays a lithology that is transitional between those of the Skoki and Glenogle formations. No facies attributable to the Outram Formation is observed in the present study area. The sedimentological significance of this absence is presently uncertain.

The Beaverfoot Formation

The Beaverfoot Formation consists of light grey to (rarer) pale orange-brown, thick bedded, massive-weathering dolostone. The lower 100 m typically contain five per cent coarse skeletal debris, principally intact specimens or large fragments of solitary and colonial corals with lesser crinoid and brachiopod debris. The corals are nearly always present and make the Beaverfoot Formation a very distinctive marker unit. The base is characterized by a dark reddish brown, coarse grained dolomitic sandstone that varies from centimetres to metres in thickness. A coarse-pebble conglomerate with rounded dolomite and chert clasts is present locally; its thickness can exceed 10 m. Intraclastic dolomite rudstone, floatstone and wackestone are present in the upper tens of metres of the Beaverfoot Formation.

The base of the Beaverfoot Formation is characterized by a significant unconformity (Fig. 49.4). On the eastern side of Smith Peak, south of Harrison Creek, the Glenogle Formation is visibly truncated beneath the Beaverfoot Formation. Examination of the McKay-Beaverfoot contact shows it to be disconformable, with a minimum of 2 m of local relief. This disconformity was postulated by Leech (1958). The Glenogle Formation is some 800 m thick west of the study area at Akutlak Creek (Norford, pers. comm., 1985). Although the McKay and Glenogle interfinger and their contact may be diachronous (Norford, 1969), the base of the Glenogle at Akutlak Creek and in the study area contain identical fossils (compare GSC locs. C-107997 and C-108000, *protobifidus* zone, B.S. Norford). A significant portion of the Glenogle Formation may have been removed prior to deposition of the Beaverfoot Formation.

In the southeastern corner of the study area, the Beaverfoot Formation overlies the McKay Group with an angular unconformity (Fig. 49.4). The combined dolomite and limestone of Subunit D2 of the McKay Group, ordinarily 500 to 600 m thick, is no more than 100 m thick beneath the Beaverfoot. Eastward, the unconformity cuts down into the McKay Group and is marked by a 2 m thick, dark brown, dolomitic sandstone with rare coral debris. The unconformity is visibly deformed around a small fold.

The presence of a sub-Beaverfoot angular unconformity in the Western Ranges and across the Rocky Mountain Trench has been postulated (Norford, 1981, Fig. 4), because westerly sections show progressively older strata immediately beneath the unconformity. The presence of the unconformity, truncating progressively older strata eastward in the Main Ranges, combined with Norford's (1981) proposal, indicate that a structural basin formed in the central Main Ranges before Beaverfoot deposition. The loss of the Glenogle Formation beneath the unconformity indicates basin development started during or after Glenogle deposition.

In the northernmost portion of the study area, a thin sandstone unit, measured to be a maximum of 18 m thick, is present beneath the Beaverfoot Formation. The unit is composed of coarse conglomerate, dolomitic sandstone, dolomite breccia, and fine to medium grained, crossbedded orthoquartzite. The unit has an abrupt contact with the underlying Skoki Formation but grades into the dolomitic sandstone at the base of the Beaverfoot Formation. This unit was previously mapped as the Mount Wilson Formation (Leech, 1979), but it is regarded as a basal Beaverfoot sand

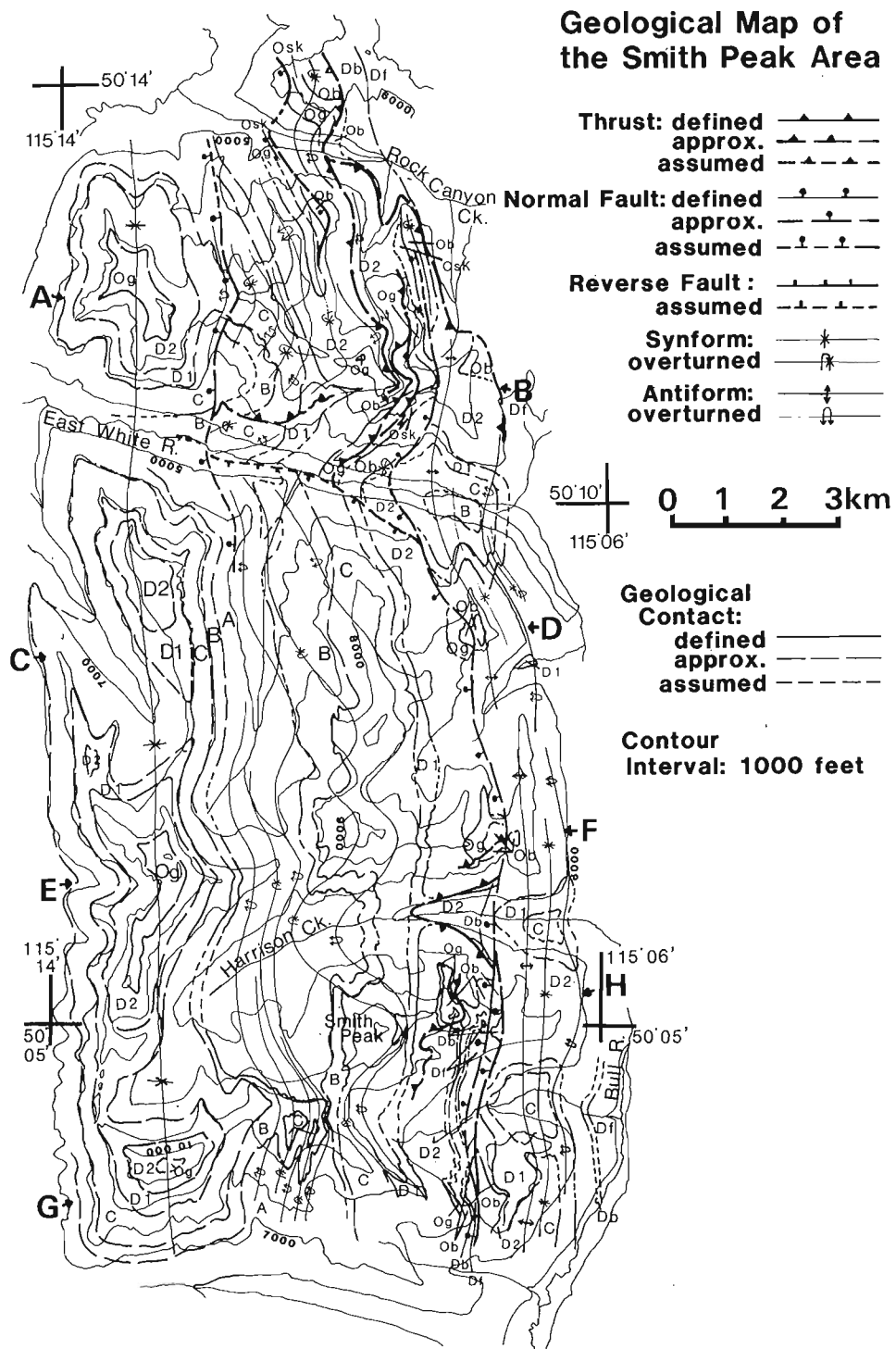


Figure 49.5. Boldface letters indicate the locations of structural sections presented in Figure 49.6. Map unit symbols: A, B, C, D1 and D2 represent the McKay Group, with A stratigraphically the lowest and D2 the highest; Og - Glenogle; Osk - Skoki; Ob - Beaverfoot; Db - Basal Devonian; and Df - Fairholme. Note that the thicknesses of a number of thin map units have been exaggerated for presentation.

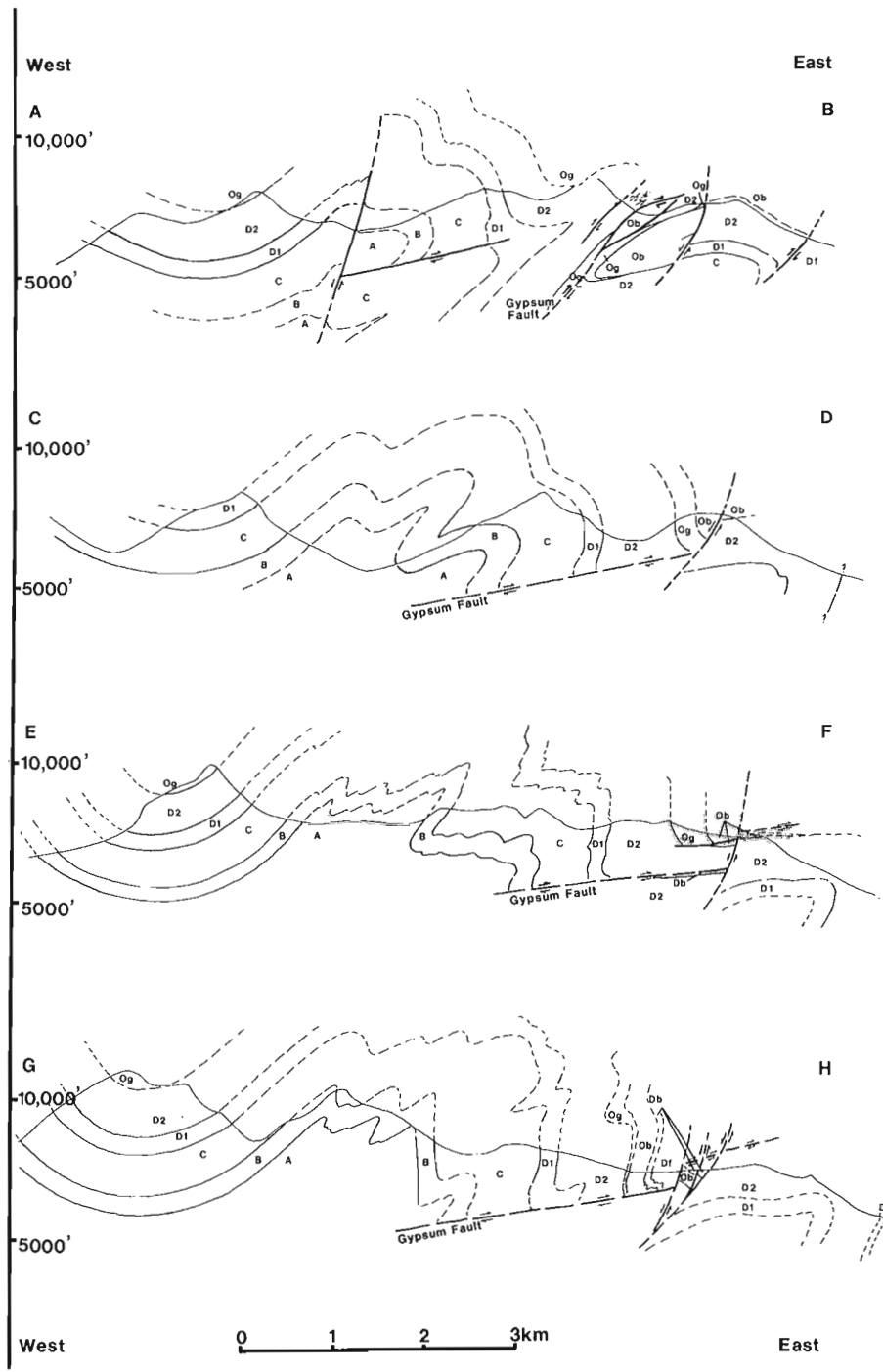


Figure 49.6. Unbalanced structural sections. Letters at the top of each section reveal its location in Figure 49.5. The directional sequence of the sections from top to bottom is north to south. Symbols: A, B, C, D1 and D2 are McKay Group units with A stratigraphically the lowest and D2 the highest; Og - Glenogle; Ob - Beaverfoot; Df - Basal Devonian; Df - Fairholme.

for several reasons: 1. Ketner (1968) argued that the source area for Ordovician quartzites must have been the Peace River Arch. If this interpretation is correct, it is difficult to envision how a presumably proximal conglomerate facies was deposited south of the clean orthoquartzites of the Mount Wilson Formation type section at Mount Wilson (Norford, 1969). 2. Even though many Mount Wilson-Beaverfoot contacts appear conformable, erosion surfaces are sometimes present, and a separate rock type – the Whisky Trail Member of the Beaverfoot – is known to occasionally occur. These features suggest that the Mount Wilson and Beaverfoot formations represent separate depositional events in the Ordovician and that a gradational contact between the two is unlikely. 3. Conglomerate and sandstone are known to occur along the base of the Beaverfoot Formation south of the study area (Leech, 1958).

Devonian strata

Strata lying above the Beaverfoot Formation in the study area fit the descriptions of the Basal Devonian and Fairholme Group map units of Leech (1979). Basal Devonian rocks consist primarily of finely laminated, pale orange-brown dolostone with interbedded white orthoquartzite, deep red, brown and some green arkose, arkosic sandstone, and arkosic conglomerate. Pebble-sized granite and, possibly, metamorphic lithoclasts are observed. Cobble-sized, fine grained, diabase clasts are also present. Some thin, green and grey shale interbeds are present toward the base of the Basal Devonian unit, together with coarse limestone and dolomite breccia. Finely laminated white gypsum was observed in the northernmost part of the study area. The thickness of the Basal Devonian unit appears to be quite variable.

The Basal Devonian unit may directly overlie the McKay Group in the Harrison Creek valley. On the north side of the valley, an apparently conformable contact of Beaverfoot and McKay is observed. The basal dolomitic sand of the Beaverfoot is present, but the formation is only a metre thick beneath the sub-Devonian unconformity and Basal Devonian unit. It is thus possible that the Basal Devonian unit may be present directly over the McKay Group farther to the east in the study area. Immediately south of the study area, at latitude 50°00'N, Leech (1979) mapped an occurrence of Basal Devonian on McKay Group sediments. The contact between the McKay Group and Basal Devonian unit on the south side of Harrison Creek is not exposed and a very thin interval of Beaverfoot Formation could be present. The scales in figures 49.5 and 49.6 do not allow this metre-thick occurrence of Beaverfoot Formation in the Harrison Creek valley to be distinguished.

The Fairholme Group consists of commonly bituminous black shale, black lime mudstone and skeletal wackestone. Skeletal grains include abraded and intact brachiopods, and crinoid, gastropod and stromatoporoid debris.

Structure

Figures 49.5 and 49.6 illustrate the structure of the strata in the study area. The East White River marks a change from a north-south structural strike in the south to a northwest-southeast strike in the north. The central and eastern parts of the study area are characterized by overturned strata, thus the standard stratigraphic age relationships defining thrust and normal faults become complex. Each mapped fault was individually studied in terms of the need for balancing its hanging wall and footwall cutoffs in order to estimate its sense of displacement.

Leech (1979) mapped what must be a steeply dipping thrust fault bringing the McKay Group over Fairholme Group strata in the Bull River valley. Strata in the vicinity of this

thrust fault in the southern part of the study area are overturned and dip steeply westward. Gibson (1979) mapped the southern extension of this fault as a steeply dipping normal fault; this better explains the overturned age relationships across the steeply dipping fault plane. Structure and age relationships at the northeast edge of the study area require McKay to be thrust over Fairholme. However, extension of this northeastern thrust far south of the East White River requires: 1. the dip of the fault to change rapidly from a shallow value to near vertical within the mountains north of the East White River, and 2. the strike of the near vertical fault to change markedly at least twice at the southward bend in the East White River. The possibility of a thin Basal Devonian unit unconformably above the McKay Group weakens stratigraphic arguments for a thrust in the Bull River valley in the southern part of the area. Given the structural difficulties arising from a postulate of a southern extension of the fault, the north-eastermost thrust fault probably loses displacement into an overturned anticline on the west face of the Bull River valley. If a fault is present in the Bull River valley in the southern part of the study area, it probably has a normal sense of displacement.

Approximately 4 km west of the Bull River, a significant thrust fault underlying most of the study area is visible in the Harrison Creek and East White River valleys. This fault is presumably the northern extension of the Gypsum fault and is herein so named. The thrust is clearly delineated by the distinctive Basal Devonian unit in the Harrison Creek valley. Despite good exposure on the northeast side of the Harrison Creek valley, no Basal Devonian outcrop talus or any other structural evidence was found to indicate that the thrust fault extends in a planar fashion to the Bull River valley. West-side-down normal faults are clearly visible on the ridges south of Harrison Creek and are interpreted as cutting the Gypsum Thrust (figs. 49.5 and 49.6). An alternate hypothesis, that the thrust fault is folded, requires that the fault cut downsection in an initially upright panel of McKay Group sediments.

North of the East White River, the Gypsum Thrust dips much more steeply and its surface trace lies west of the normal fault that cuts it farther south (figs. 49.5 and 49.6, Section A-B). A "blind", relatively shallow-dipping thrust west of the Gypsum Thrust is interpreted as a minor contraction structure resulting from tight folding. A tear fault, with significant reverse displacement, is inferred to exist in the valley of the East White River to explain a change in the level of stratigraphy exposed across the valley (Fig. 49.5). Stratigraphy on the north side of the East White River can be traced to the valley bottom. East of the normal fault that cuts the southern portion of the Gypsum Thrust, stratigraphic contacts do not appear to be offset across the East White River. The tear fault is believed to lie only in the hanging wall of the Gypsum Thrust, and may be related to the change in fault geometry across the East White River. While the tear fault is speculative, precedent exists for such structural style in the Kananaskis area (Leech, 1959, 1979).

On the north side of the East White River (Fig. 49.5) the Gypsum Thrust appears to have its displacement transferred to a fault plane immediately to the west. The transfer zone is little more than 100 m wide across strike and is well exposed on the ridgetops. Because the transfer zone is so narrow, the new fault plane extending north may, for our purposes, also be considered as an extension of the Gypsum Thrust.

On the north side of the Harrison Creek, in the hanging wall of the Gypsum Thrust, evidence exists for pre-Beaverfoot displacement on a fault. The fault plane is nearly horizontal and presently shows thrust-fault age relationships. It is suggested that the fault, probably with a normal sense of

displacement, was initiated before Beaverfoot deposition, in part causing the angularity of the sub-Beaverfoot unconformity, and was then reactivated after Beaverfoot deposition, during the latest compressional event. If no pre-Beaverfoot displacement is postulated, then palinspastic restoration of the fault requires that 160 m of Glenogle sandstone and siltstone change facies abruptly into upper McKay dolostone, interfingering over a narrow, vertical zone no more than 150 m wide. Proof of pre-Beaverfoot motion awaits dating of the McKay strata immediately beneath the Beaverfoot Formation.

There is a change in structural style eastward across the study area (figs. 49.5 and 49.6). The syncline on the west edge of the map area is an upright structure, as are folds west of the study area (Leech, 1979). From west to east across the study area, folds are progressively overturned to the east. Folds also are progressively disharmonic eastward across the area, and, on a large scale, many are similar in form.

On the north side of the East White River, the Gypsum Thrust cuts downsection through both its hanging wall and footwall. The thrust fault cuts up structurally but downsection in the overturned hanging wall through the Glenogle and uppermost dolostone of McKay Unit D into limestone of McKay Unit D. Although the structure is complicated by a horse of Beaverfoot Formation, this relationship requires the stratigraphic sequence to be overturned, presumably by fold development, prior to the formation of the fault detachment.

Acknowledgments

The authors would like to thank M.E. McMechan and B.S. Norford of the Geological Survey of Canada for their assistance and advice; C.J. Bruce, F. Frey and P. Fermor (who suggested the project) of Shell Canada Resources Limited for making available unpublished field notes and maps; G.B. Leech for consultation; and S. Peters for excellent assistance in the field.

References

- Aitken, J.D. and Norford, B.S.
1967: Lower Ordovician Survey Peak and Outram formations, southern Rocky Mountains; *Bulletin of Canadian Petroleum Geology*, v. 15, p. 150-207.
- Benvenuto, G.L. and Price, R.A.
1979: Structural evolution of the Hosmer thrust sheet, southeastern British Columbia; *Bulletin of Canadian Petroleum Geology*, v. 27, p. 360-394.
- Dunham, R.J.
1962: Classification of carbonate rocks according to depositional texture, in *Classification of Carbonate Rocks*, W.E. Ham (ed.); American Association of Petroleum Geologists, Memoir 1, p. 108-121.
- Gibson, G.
1979: Geology of the Munroe-Alpine-Boivin carbonate-hosted zinc occurrences, Rocky Mountain Front Ranges, southeastern British Columbia; British Columbia Ministry of Energy, Mines and Petroleum Resources, Preliminary Map no. 46.

- Ketner, K.B.
1968: Origin of Ordovician quartzite in the Cordilleran miogeosyncline; United States Geological Survey, Professional Paper 600-B, p. B169-177.
- Leech, G.B.
1958: Fernie map-area, West-half, British Columbia; Geological Survey of Canada, Paper 58-10.
1959: Canal Flats, British Columbia; Geological Survey of Canada, Map 24-1958.
1962: Structure of the Bull River Valley near latitude 49°30'N; *Journal of the Alberta Society of Petroleum Geologists*, v. 10, p. 396-407.
1964: Kananaskis, West-half (82J W1/2) map area; Geological Survey of Canada, Paper 64-1, p. 30.
1979: Kananaskis Lakes map area; Geological Survey of Canada, Open File no. 634.
- Norford, B.S.
1969: Ordovician and Silurian stratigraphy of the southern Rocky Mountains; Geological Survey of Canada, Bulletin 176.
1981: Devonian stratigraphy at the margins of the Rocky Trench, Columbia River, southeastern British Columbia; *Bulletin of Canadian Petroleum Geology*, v. 29, p. 540-560.
- North, F.K. and Henderson, G.G.L.
1954: Summary of the geology of the southern Rocky Mountains of Canada; in *Guidebook of the 4th Annual Field Conference*; Alberta Society of Petroleum Geologists, p. 15-100.
- Raasch, G.O. and Bruce, C.J.
1966: Notes on Late Cambrian and Early Ordovician biostratigraphy of southeast British Columbia (abstract); *Bulletin of Canadian Petroleum Geologists*, v. 14, p. 600.
- Todd, T.W.
1966: Petrogenetic classification of carbonate rocks; *Journal of Sedimentary Petrology*, v. 36, p. 317-340.

APPENDIX 49.1

GSC loc.	Location and stratigraphic information
C-82891	50°13'45"N, 115°10'30"W. Ridge north of Rock Canyon Creek; Skoki Formation; from a 30 cm bed about 20 m up in the Skoki.
C-107997	50°11'45"N, 115°21'15"W. Akutlak Creek Ridge Section (north-central eastern spur); Glenogle Formation; 14.0-14.1 m above base of section.
C-108000	50°06'45"N, 115°08'30"W. Ridge Crest Section, north of "Harrison Creek" (Bull River) British Columbia; Glenogle Formation; from a 15 cm bed about 30 m above base.

Microcodiaceans in the Viséan Emma Fiord Formation, Devon Island, Arctic Canada

Project 680046

W.W. Nassichuk, G.R. Davies¹, and B.L. Mamet²
Institute of Sedimentary and Petroleum Geology, Calgary

Nassichuk, W.W., Davies, G.R., and Mamet, B.L., Microcodiaceans in the Viséan Emma Fiord Formation, Devon Island, Arctic Canada; in Current Research, Part B, Geological Survey of Canada, Paper 86-1B, p. 467-470, 1986.

Abstract

The Lower Carboniferous (Viséan) Emma Fiord Formation on Grinnell Peninsula of Devon Island contains an abundance of the enigmatic algae **Microcodium** and **Palaeomicrocodium** in sediments of lacustrine origin. The microcodiaceans are associated with a variety of megaplants, ostracodes, serpulid worms, and phosphatic bone fragments. In other reported occurrences, **Palaeomicrocodium** has been found in rocks of shallow marine origin ranging in age from Devonian to Permian. The Emma Fiord discovery confirms that **Palaeomicrocodium** also occurs in nonmarine settings.

Résumé

La formation d'Emma Fiord du Carbonifère inférieur (Viséen), trouvée dans la presqu'île Grinnell, dans l'île Devon, contient de très nombreux fossiles d'algues énigmatiques **Microcodium** et **Palaeomicrocodium** dans des sédiments d'origine lacustre. Les microcodiacéens sont associés à une gamme de plantes macroscopiques, d'ostracodes, de serpules et de fragments osseux phosphatiques. **Palaeomicrocodium** aurait également été trouvé dans des roches dévoniennes à permienne accumulées dans une mer peu profonde. La découverte d'Emma Fiord confirme la présence de **Palaeomicrocodium** dans des milieux non marins.

¹ AGAT Technologies Inc., 3650 - 21 Street N.E., Calgary, Alberta T2E 6V6

² University of Montreal, Department of Geology, Montreal, Quebec H3C 3A7

Introduction

The enigmatic microcodiacean alga *Palaeomicrocodium* Mamet and Roux, 1983, which ranges in age from Devonian to Permian, is common in the Lower Carboniferous (Viséan) Emma Fiord Formation on Grinnell Peninsula of Devon Island in the Canadian Archipelago. It is associated with a close relative, *Microcodium* Glück, 1912, which usually occurs in younger Carboniferous and Permian strata in the Arctic Islands, but which occurs elsewhere in the world in strata as young as Tertiary. Until recently, most authors considered microcodiaceans to be restricted to the Cenozoic, to be associated with a lacustrine environment, and to be indicative of a pedogenic origin. Earlier records of occurrences of microcodiaceans in the Paleozoic were interpreted to be the result of *per descensum* contamination (references in Klappa, 1978; Smith, 1979). However, Maslov (1956), Mamet and Roux (1982, 1983) and Mamet and Pr at (1985) demonstrated that the microcodiaceans thrived in the Devonian, the Carboniferous and the Permian. All cited Paleozoic occurrences of *Palaeomicrocodium* and *Microcodium* are thought to reflect shallow marine deposition. The presence of *Palaeomicrocodium* and *Microcodium* (Fig. 50.2) at several levels in the Emma Fiord Formation on Grinnell Peninsula is the first well documented evidence that representatives of the Microcodiaceae may also have thrived in lacustrine environments during the Paleozoic.

Another enigmatic alga, *Girvanella* Nicholson and Etheridge, 1878, is commonly associated with *Palaeomicrocodium* in the Emma Fiord Formation. *Girvanella* has been documented mostly from shallow marine sediments (Mamet and Roux, 1975), but since it is most probably a cyanophyte, its occurrence is not unexpected in the mainly lacustrine (seasonably fresh to slightly saline) environment that characterized deposition of the Emma Fiord Formation.

Geological setting

The Emma Fiord Formation is the oldest sedimentary rock unit in the Sverdrup Basin, a pericratonic depression that contains more than 15 km of strata ranging in age from Carboniferous to Tertiary. The Emma Fiord Formation is composed of up to 135 m of recessive weathering, black, carbonaceous and calcareous shale with interbeds of crossbedded, fining-upward, granular textured, sandy, oncolitic limestone, chert-pebble conglomeratic limestone, and oolitic grainstone. Minor components include thin beds of grey limestone that contain a variety of plant remains, serpulid worm tubes, ostracodes, and phosphatic bone fragments. Two of us (GRD, WWN) are preparing a more comprehensive manuscript on the Emma Fiord that will include detailed descriptions of facies, biota, depositional setting, thermal maturation, and tectono-climatic implications.

Near the headwaters of Lyall River on Grinnell Peninsula, where the authors measured the stratigraphic sections identified in Figure 50.1, the Emma Fiord Formation is confined to three synclinal depressions that were formed on Devonian and older rocks of the Franklinian Geosyncline. The Emma Fiord rocks are separated from Silurian limestone of the Cape Storm Formation by a prominent unconformity (Kerr, 1976), and are in turn overlain by syntectonic redbed conglomerate of the Upper Carboniferous Canyon Fiord Formation. Deposition of the Emma Fiord predated the onset of the major phases of faulting, rifting and erosion that marked the formation of the Sverdrup Basin during early Late Carboniferous (Namurian) time.

Depositional environment

The Emma Fiord rocks on Grinnell Peninsula are interpreted to be of lacustrine origin for the following reasons:

1. They lack any evidence of marine fossils.
2. They contain an abundance of terrestrial plant detritus, coal, spores, and pollen.
3. They contain abundant tufa-like carbonate clasts and cements analogous to lacustrine tufa in the Quaternary lakes of western and southwestern United States and elsewhere.
4. Ooid grainstone comparable to the ooid grainstone of Great Salt Lake and other ephemeral Quaternary lake systems are present.

Emma Fiord biota

Emma Fiord shales and carbonate rocks from Grinnell Peninsula contain a variety of megaplants, palynomorphs, algae or algal-like clasts, calcareous serpulid worm tubes, small, thin-shelled pelecypods, abundant ostracodes, fish scales and phosphatic bone fragments from small vertebrates. H. Pfefferkorn (personal communication, 1975) examined megaplants from grey limestone in the Emma Fiord on Grinnell Peninsula and reported the following: *Stigmaria ficoides* (in situ), *Lepidostrobophyllum* sp., *Lepidophylloides* sp., "*Lepidodendropsis*" sp.?, *Lepidodendron* sp., cf. *Cardiopteridium* sp., and lycopod twigs. Pfefferkorn (personal communication, 1975) concluded that the limestone is "definitely indicative of fresh water lacustrine conditions" and that the flora, reminiscent of Lower Carboniferous flora in Spitzbergen, is of "Tournaisian to early Vis an age".

As indicated by McGregor and Barsz (in Kerr, 1976), palynomorphs indicate a Vis an age. The flora is currently being studied by Utting (personal communication, 1986) who suggested that it has a number of features in common with the *Aurita* assemblage described from Spitzbergen by Playford (1962, 1963). Moreover, Utting (ibid.) is of the opinion that palynomorphs in the Emma Fiord Formation at Grinnell Peninsula are similar to, but not identical with, those from the type section at Kleybolte Peninsula, northern Ellesmere Island, and similar to those described from the Emma Fiord Formation on northern Axel Heiberg Island by Playford and Barsz (1963).

Palaeomicrocodium, *Microcodium* and *Girvanella* are common in almost all of the grey limestone that we interpret to be lacustrine in the Emma Fiord Formation. *Palaeomicrocodium* does not perforate as strongly as *Microcodium*, but the presence of many corroded *Girvanella* lumps and pellets in the Emma Fiord samples may indicate corrosion by microcodiaceans.

Several samples contain *Girvanella staminea* Garwood, 1931 and *Girvanella wetheredii* Chapman, 1908. Other specimens identified by one of us (BLM) are probably *Tharama*? sp., and "*Batinevia*" Korde; the latter may in fact be *Girvanella* in original growth position.

Palaeomicrocodium and *Microcodium* have a similar ecological range, from very shallow marine carbonate environments, to supratidal mangrove swamps, and, as demonstrated by the Emma Fiord samples, probably to freshwater and saline lacustrine settings.

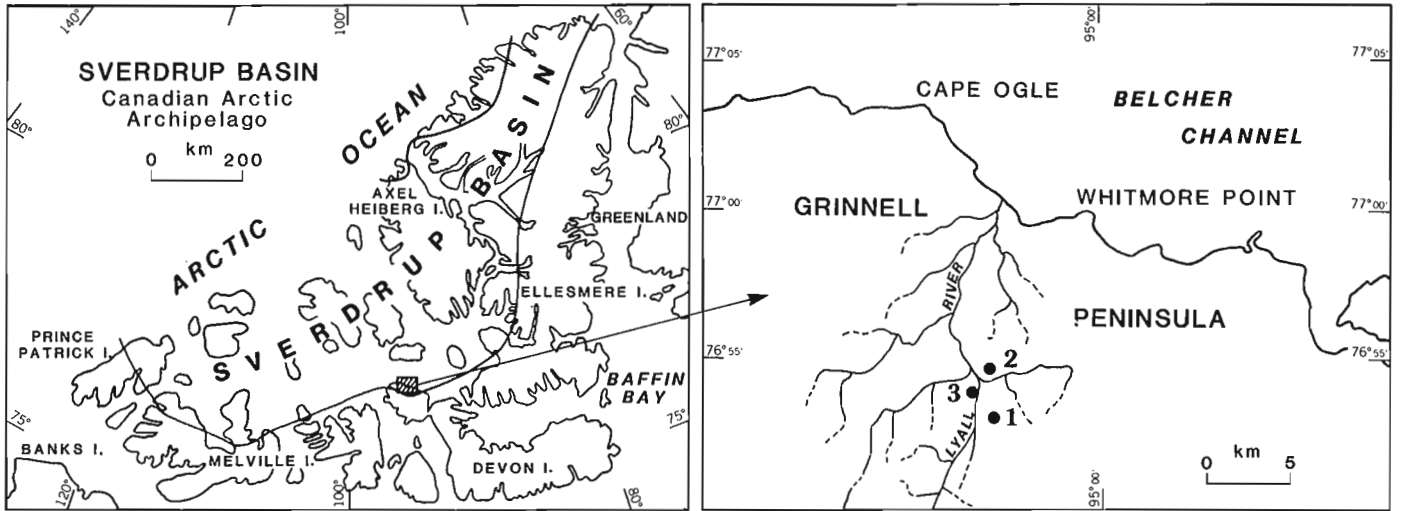


Figure 50.1. Locality map of the Canadian Arctic Archipelago, with detail of northern Grinnell Peninsula on Devon Island showing location of three sections of the Emma Fiord Formation that have yielded microcodiacean algae.

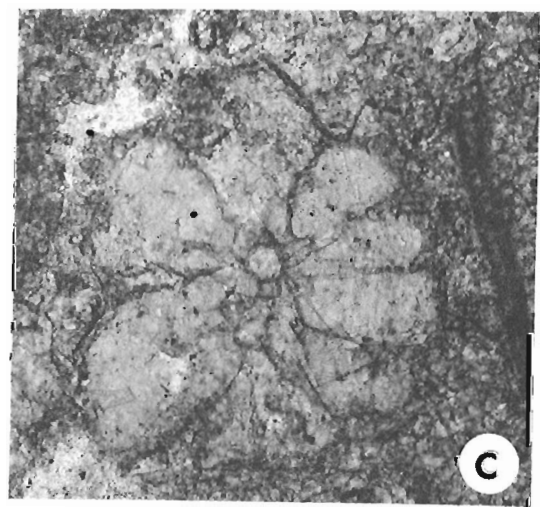
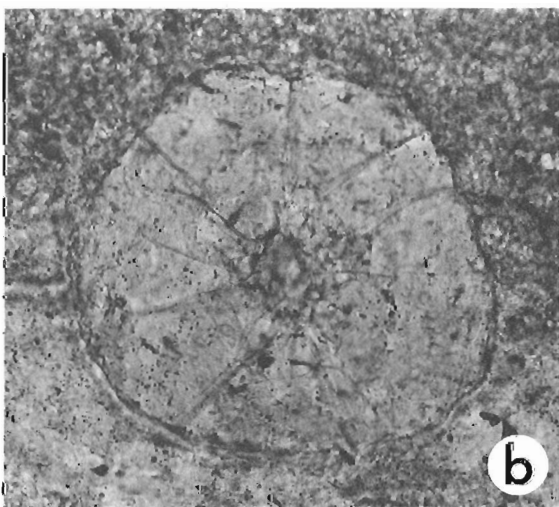
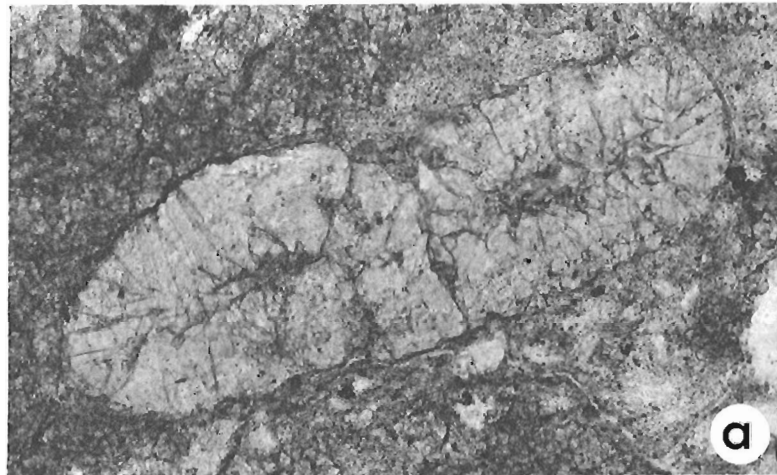


Figure 50.2. Microcodium sp. (a) longitudinal section, GSC 76525; (b) axial section, GSC 76526; (c) axial section, GSC 76527; all x200. Note the radiating crystalline structure with a central cavity, and curved crystal faces. GSC loc. C-32923; 6.5 m above base of Emma Fiord Formation of Section 2 (Fig. 50.1), 76°54'30"N, 95°15'W. Illustrated specimens are stored in the type collection of the Geological Survey of Canada, in Ottawa.

Conclusions

The discovery of **Microcodium** and **Palaeomicrocodium** in Viséan rocks interpreted to be of lacustrine origin expands the range of environments for **Palaeomicrocodium**, and documents the occurrence of **Microcodium** in the Early Carboniferous. It also expands the overall geographic and temporal distribution of the microcodiacean algae.

References

Kerr, J.Wm.

- 1976: Geology of outstanding Arctic aerial photographs-3; in Margin of Sverdrup Basin, Lyaill River, Devon Island; Bulletin of Canadian Petroleum Geology, v. 24, no. 2, p. 139-153.

Klappa, C.F.

- 1978: Biolithogenesis of **Microcodium**: elucidation; Sedimentology, v. 25, p. 489-522.

Mamet, B. and Pr eat, A.

- 1985: Sur la pr esence de **Palaeomicrocodium** (Algue) dans le Giv etien inf erieur de la Belgique; G ebios, v. 18, no. 3, p. 380-392.

Mamet, B. and Roux, A.

- 1975: Algues d evoniennes et carbonif eres de la T ethys occidentale, Troisi eme partie; Revue de Micropal eontologie, v. 19, no. 4, p. 215-266.

Mamet, B. and Roux, A. (cont.)

- 1982: Sur la pr esence de **Microcodium** (Algue? Incertae sedis) dans le Pal eozo ique sup erieur de l'Arctique Canadien; Canadian Journal of Earth Sciences, v. 19, no. 2, p. 357-363.

- 1983: Algues d evono-carbonif eres de l'Australie; Revue de Micropal eontologie, v. 26, no. 2, p. 63-131.

Maslov, V.P.

- 1956: Fossil calcareous algae of the U.S.S.R. (in Russian, translated); Akademiya Nauk SSSR, Trudy Instituta Geologicheskikh, v. 160, 301 p.

Playford, G.

- 1962: Lower Carboniferous microfloras of Spitsbergen Part I, Palaeontology, v. 5, pt. 3, p. 550-618.

- 1963: Lower Carboniferous microfloras of Spitsbergen Part II; Palaeontology, v. 5, pt. 4, p. 619-678.

Playford, G. and Barss, M.S.

- 1963: Upper Mississippian microflora from Axel Heiberg Island, District of Franklin; Geological Survey of Canada, Paper 62-36, 5 p.

Smith, J.

- 1979: **Microcodium**, its earliest occurrence and other considerations; Revue de Micropal eontologie, v. 22, no. 1, p. 44-50.

Species of the rugose coral genus *Minussiella* from the Middle Devonian of western and Arctic Canada

Project 680093

A.E.H. Pedder
Institute of Sedimentary and Petroleum Geology, Calgary

Pedder, A.E.H., Species of the rugose coral genus **Minussiella** from the Middle Devonian of western and Arctic Canada; in Current Research, Part B, Geological Survey of Canada, Paper 86-1B, p. 471-488, 1986.

Abstract

The genus **Minussiella** Bul'vanker, 1952, which was previously recognized only in the Middle Devonian of southern Siberia and western Mongolia, is shown to include four Canadian species. **Minussiella bathurstensis** sp. nov. and **M. goodbodyi** sp. nov. are described from an Eifelian (**costatus** Zone) carbonate on Bathurst Island, Canadian Arctic Archipelago. **Minussiella cornus** (McLaren) and **M. conjuncta** sp. nov. are described from the Givetian (probably Middle **varcus** Zone) organic reef facies of the type Horn Plateau Reef in southwestern District of Mackenzie.

Résumé

Le genre **Minussiella** Bul'vanker, 1952, qui auparavant avait été identifié uniquement dans les roches du Dévonien moyen dans le sud de la Sibérie et dans l'ouest de la Mongolie, comprend quatre espèces canadiennes. **Minussiella bathurstensis** sp. nov. et **M. goodbodyi** sp. nov. qui sont décrites dans cette étude proviennent d'une roche carbonatée eifélienne (zone à **costatus**) dans l'île Bathurst, de l'archipel Arctique canadien. **Minussiella cornus** (McLaren) et **M. conjuncta** sp. nov. proviennent d'un faciès de récif organique givetien (probablement le milieu de la zone à **varcus**) du récif type du plateau de Horn dans le sud-ouest du district de Mackenzie.

Introduction

The genus *Minussiella* was established in 1952 in a work that for many years was overlooked by workers outside the Soviet Union. It was not mentioned in the first edition of the coelenterate part of the *Treatise on Invertebrate Paleontology* (Hill, 1956), nor was it considered by the present writer (Pedder, 1965) when the closely related genus *Chalcidophyllum* was proposed. Records suggest that *Minussiella* is characteristic of several Middle Devonian faunas of southwestern Siberia and Mongolia. The purpose of the present paper is to demonstrate that *Minussiella* is also in the Givetian Horn Plateau fauna of Western Canada, and in an Eifelian carbonate, referred to the Blue Fiord Formation by earlier workers, on Bathurst Island. Three of the Canadian species are new; one of them, named *Minussiella bathurstensis*, is likely to become an important Eifelian index fossil for the Canadian Arctic Archipelago.

Acknowledgments

Q.H. Goodbody, recently of the University of Alberta, Edmonton, has allowed the author free access to large arctic coral collections made by him over several seasons. It is a pleasure to acknowledge this co-operation, especially as one of the species named in this work is known only from his collections. B. Jones, also of the University of Alberta, and T.T. Uyeno, of the Geological Survey of Canada, kindly provided previously unpublished identifications and age determinations of brachiopods and conodonts associated with the corals described in this paper.

Biostratigraphy of the Horn Plateau Formation

The physical stratigraphy of the type Horn Plateau Reef has been outlined by Fuller and Pollock (1972) and Vopni and Lerbekmo (1972). The organic reef facies around the northeastern margin of the exposed reef yields a unique and biostratigraphically enigmatic megafauna. For a Western Canadian Devonian reef facies, this fauna is unusually rich in rugose corals and brachiopods, and correspondingly impoverished in stromatoporoids and tabulate corals.

Most of the commonly occurring corals have been made known by McLaren (in McLaren and Norris, 1964). Species named *Atelophyllum nebracis* and *Grypophyllum cornus* by McLaren are among the more prominent forms. Since the time of McLaren's work, colonial species of *Atelophyllum*, such as *A. nebracis*, have been removed to the genus *Scissoplasma* by Spasskiy and Kravtsov (in Spasskiy et al., 1975, p. 171). The Horn Plateau coral fauna is now further revised by the removal of *Grypophyllum cornus*, which was originally known only from a single specimen, to the genus *Minussiella*. In addition to these, and the new species named *Minussiella conjuncta*, the organic reef facies of the type Horn Plateau Reef includes corals named or identified by McLaren as *Lekanophyllum* sp. cf. *L. punctatum* Wedekind, *Sinospongophyllum* sp. cf. *S. planotabulatum* Yoh, *Neostriphophyllum craigi* McLaren, *Australophyllum* (?) sp. cf. *A. (?) thomasae* (Hill and Jones), *Stringophyllum* (*Sociophyllum*) *redactum* McLaren and *Cyathophyllum* (*Peripaedium*) *gretneri* McLaren. All of these corals are currently under revision by the present author.

Several of the brachiopods described by Norris (in McLaren and Norris, 1964) from the "upper thick-bedded unit" of the Horn Plateau Formation are from the organic reef facies. *Desatrypa nasuta* (Norris), which has been discussed by Copper (1979, p. 313, Text-fig. 6), is the commonest; others are *Schizophoria fascicostella* Norris, *Pentamerella sclavus* Norris, *Longispina whittakeri* Norris, *Spinatrypa hornensis* Norris, *Desatrypa* (?) *hearni* Norris and *Cranaena* (?) *cryptonelloides* Norris.

The age of the exposed organic reef facies of the type Horn Plateau Reef is not easily assessed. Corals suggest that it is intermediate between the ages of the Hume and Ramparts formations, which is to say that it is probably equivalent to some part of the Givetian *ensensis* to Middle *varcus* Zone time span. Conodonts indicate that it is not older than Middle *varcus* Zone, because it overlies the Teilzone of *Polygnathus linguiformis linguiformis* zeta morphotype (identified as *P. linguiformis mucronatus* in Fuller and Pollock, 1972, p. 150), in the lower subsurface part of the reef. Together, these data point to a Middle *varcus* Zone age.

Biostratigraphy of the Eifelian carbonates of northern Bathurst Island

Following the pioneer work of McLaren (in Fortier et al., 1963, p. 606-615), the Middle Devonian carbonates of north-central Bathurst Island have been referred to the Blue Fiord Formation by many workers (Ormiston, 1967; McGregor and Uyeno, 1972; Kerr, 1974; Brice, 1982). However, it is now known that these carbonates are younger than the Emsian type Blue Fiord Formation on Ellesmere Island, and cannot be traced into it by way of Grinnell Peninsula on northwestern Devon Island. In the absence of a suitable name, and in the knowledge of their Eifelian age, these carbonates are referred to here, informally, as Eifelian carbonates. In the Stuart River region of north-central Bathurst Island, they decrease in thickness from 234 m at Twilight Creek, to 183 m at Cut Through

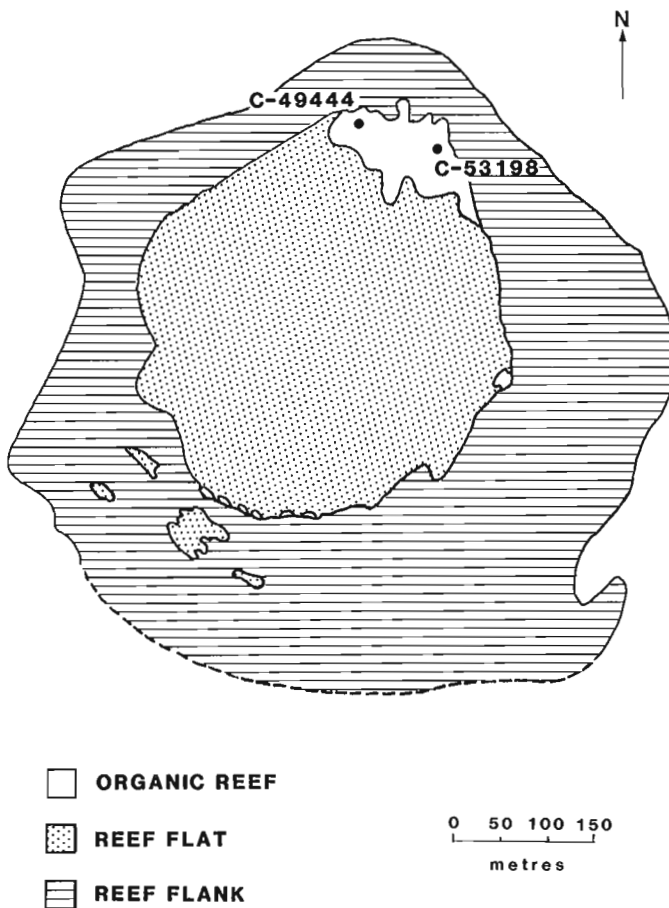


Figure 51.1. Plan of macrofacies on the present surface of the Horn Plateau Reef (after Vopni and Lerbekmo, 1972, Fig. 6). *Minussiella conjuncta* sp. nov. and *M. cornus* (McLaren) occur at both GSC loc. C-49444 and C-53198.

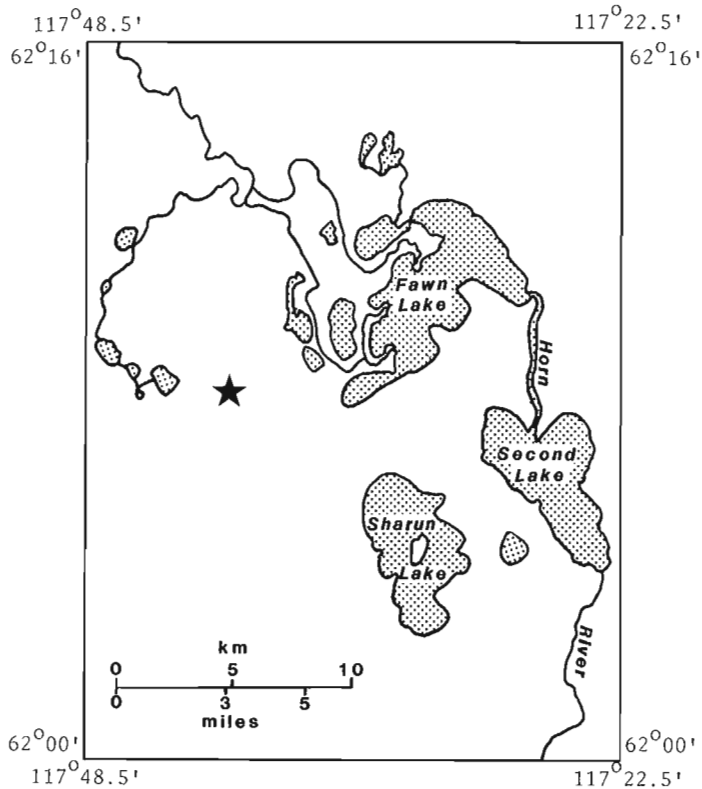


Figure 51.2. Map of the Fawn Lake area, southwestern District of Mackenzie, with the location of the Horn Plateau Reef shown as a star.

Creek (Fig. 51.3, locality 1), 28 m on the north side of Half Moon Bay (Q.H. Goodbody measurement; Fig. 51.3, locality 2), and 14 m on the south side of Half Moon Bay (Kerr, 1974, Fig. 8). Eifelian carbonates do not occur as a mappable unit south of South Dundee Bight, but may be represented by about 4 m of impure limestone at the base of the Bird Formation in a section at latitude 75°52'N and longitude 99°50'W (Johnson and Perry, 1976, p. 616).

Species of *Minussiella* described in this paper from Bathurst Island come from four localities shown in Figure 51.3. The *M. bathurstensis* occurrence on Cut Through Creek (GSC loc. 26536) is not dated by associated fossils, but is believed to be at about the same horizon as *Dechenella (D.) franklini* Ormiston and *Astycoryphe cimelia* Ormiston described by Ormiston in 1967 (p. 92, 118). The horizon is also similar to that of specimens of *Cupularostrum* (?) *pentagonale* Brice, *Quadrithyris* sp. cf. *Q. vijajica* Khodalevitch and *Emanuella bisinuata* Brice from GSC localities 26539, 26540 (Brice, 1982, p. 14). Brice has already pointed to the similarity between the "Blue Fiord" brachiopod fauna in the vicinity of Cut Through Creek and the Eifelian brachiopods described by Johnson and Perry (1976). The principal horizon of Johnson and Perry's fauna (579 m level) has yielded *Polygnathus linguiformis linguiformis* Hinde and *P. linguiformis parawebbi* Chatterton, identified by G. Klapper (Johnson and Perry, 1976, p. 618), and apparently overlies, by a stratigraphic thickness of about 16 m, occurrences of *Icriodus norfordi* Chatterton and *I. orri* Klapper and Barrick, identified by T.T. Uyeno from the same section (GSC loc. C-136351).

University of Alberta (UA) locality PCC 92169, which is the stratigraphically higher of two occurrences of *Minussiella bathurstensis* near Half Moon Bay, is dated as Eifelian *costatus* Zone by its accompanying fauna, listed in the

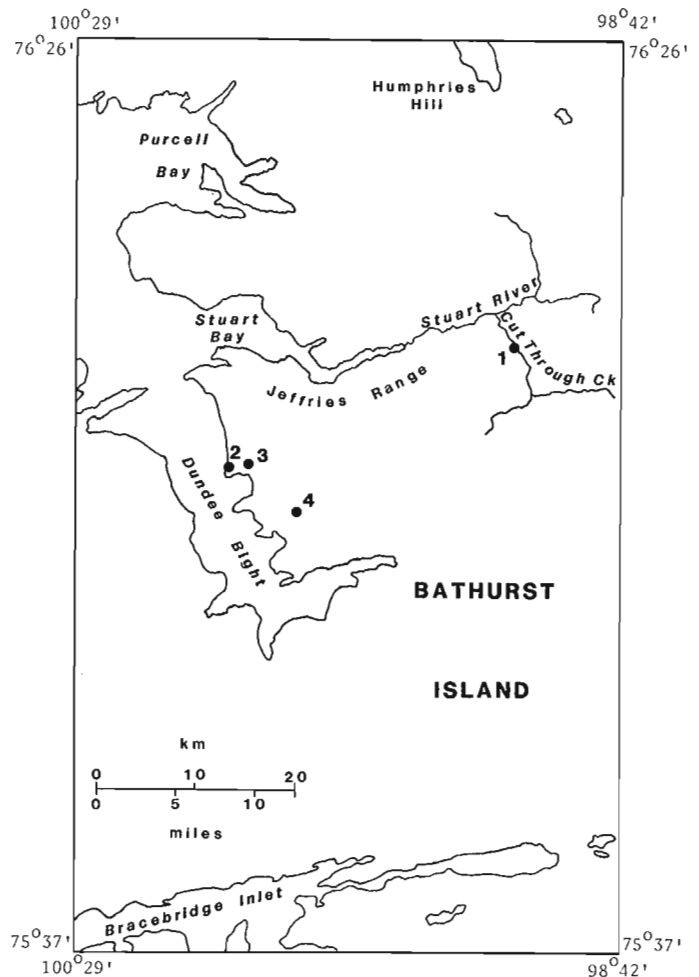


Figure 51.3. Map of part of Bathurst Island showing *Minussiella*-bearing localities. 1, GSC loc. 26536, southern limb of Stuart Bay Anticline. 2, 3 UA loc. PCC 92164 and 92169, respectively, northern limb of Moon Bay Anticline. 4, UA loc. PCC 92160. *Minussiella bathurstensis* sp. nov. occurs at localities 1, 2 and 3, whereas *M. goodbodyi* sp. nov. is known only from locality 4.

locality register. The other occurrence of *M. bathurstensis* in the Half Moon Bay area (UA loc. PCC 92164) is not precisely dated and may equate with the Eifelian part of the *patulus* Zone. In Figure 51.3, these localities are numbered 3 and 2.

The fourth *Minussiella*-bearing locality on Bathurst Island is UA locality PCC 92160. It is the type locality of *M. goodbodyi* and is shown as locality 4 on Figure 51.3. The associated fauna can be dated only as Eifelian, but since the occurrence is at the top of the Eifelian carbonate, and since a *costatus* Zone fauna has been obtained from 9 m below the top of the same carbonate unit near Half Moon Bay (UA locality PCC 92169; locality 2 in Fig. 51.3), *M. goodbodyi* is assumed to be of *costatus* Zone age also.

Systematic paleontology

It is assumed that readers have access to Hill (1981). Original references to genera and their type species discussed in the remarks on *Minussiella* are not repeated, if they are available in Hill (1981).

In addition to the standard abbreviations used in GSC works, The University of Alberta, Edmonton, and the Paleontological Collections Catalogue of the same university are abbreviated UA and PCC.

Remarks. The genus *Minussiella* was originally assigned to the Spongophyllidae because of the presence of presepiments and consequent disruption of the septa in the type species. Soviet authors have generally followed this classification (Ivanovskiy, 1958, p. 343; Spasskiy, 1960, p. 129, 130, 1977, p. 36, 39; Ivaniya, 1965, p. 139, 167; Ulitina, 1980, p. 38, 40). However, many finely septate genera, from different families, develop similar presepiments and disrupted septa, and *Minussiella* may be better placed in the Disphyllidae (Soshkina and Dobrolyubova, 1962, p. 334; Ivanovskiy, 1976, p. 110; Hill, 1981, p. 264, 269) or the Cyathophyllidae (Birenheide, 1978, p. 71, 94). In this work, it is tentatively placed in the Columnariidae, which, in the author's present opinion (Pedder, 1983, p. 228-230), is a senior synonym of the Disphyllidae.

Genus *Minussiella* Bul'vanker

Minussiella Bul'vanker in Rzhonsnitskaya et al., 1952, p. 134.
Pseudocampophyllum Ivanovskiy, 1958, p. 343-344.

Type species of *Minussiella*. *M. beliakovi* Bul'vanker, in Rzhonsnitskaya et al., 1952, p. 135-136, Pl. 7, figs. 2a-3b. Tashtyp Suite, Eifelian; Mount Kulagay (holotype) and Perevozinskaya Village in the region of Mount Kulagay, Minusinsk Basin, southern central Siberia, U.S.S.R. The trivial name is also spelled *beljakovi* in the original description. Bul'vanker spelled it *beliakovi* in 1955 (p. 35, 74) and *beljakovi* in 1958 (p. 160). Here, it is assumed to have been stabilized as *beliakovi* by Bul'vanker's 1955 usage.

Type species of *Pseudocampophyllum*. *P. enisseicum* Ivanovskiy, 1958, p. 344-346, Text-fig. 2, Pl. 1, figs. 1-4. Beyskoe Suite, Givetian; Chaizy-Kozy near Kapchala village, west of Abakan (holotype), and Enisei River, north of Abakan, southern Minusinsk Basin, southern central Siberia, U.S.S.R.

Additional species. *Minussiella kulagaiensis* Bul'vanker, in Rzhonsnitskaya et al., 1952, p. 135-136, Pl. 7, figs. 1a, b. Tashtyp Suite, Eifelian; Mount Kulagay, Minusinsk Basin, southern central Siberia, U.S.S.R.

M. asiatica Bul'vanker in Rzhonsnitskaya et al., 1952, p. 136, Pl. 7, figs. 5a, b. Tashtyp Suite, Eifelian; Mount Kurbezek, Minusinsk Basin, southern central Siberia, U.S.S.R.

M. beiensis Bul'vanker, 1955, p. 35, Pl. 14, figs. 1a-v. Beyskoe Suite, Givetian; region of Ubrus, Minusinsk Basin, southern central Siberia, U.S.S.R.

M. sociabilis Bul'vanker, 1958, p. 160-161, Pl. 69, figs. 1a, b; Pl. 70, fig. 1. Safonovo Beds, Givetian; 1.5 km north of Artsht railway crossing (holotype) and other localities in the Kuznetsk Basin, southern central Siberia, U.S.S.R.

Rejected species. *Minussiella solida* Bul'vanker, 1965, p. 57, Pl. 20, figs. 1a-v. "Eifelian Stage" (probably Emsian); Bisernyi Stream, Omulevsk Mountains, Soviet Far East. Spasskiy and Kravtsov (in Besprozvannykh et al., 1975, p. 56) refer this coral to *Hexagonaria*, but it is probably a species of *Spongonaria* or, since it lacks septal laths, *Leurelasma* Yu and Cai (1983, p. 31, 32, 69, 70).

M. crassiseptata Cherepnina, in Udodov, 1967, p. 143. Eifelian; Uymen Synclorium, Altay Mountains, southwestern Siberia, U.S.S.R. This is apparently a nomen nudum.

Diagnosis. Corallum solitary, fasciculate or subcerioid. Corallites subcylindrical to ceratoid. Corallite wall very thin, with fine septal furrows and much broader, almost flat, interseptal ridges. Septa radially arranged in two orders, typically attenuate, locally discontinuous, especially the minor septa, which are commonly much reduced. Septa variably withdrawn from the axis. Majority of septal bases embedded in the corallite wall. Dissepiments and presepiments form a moderately wide dissepimentarium. Dissepimental surfaces inwardly sloping. Tabulae variable, locally not well differentiated from dissepiments. Tabularial surfaces flat or distinctly sagging.

Remarks. Ulitina (1980, 1982), who believed, probably correctly, that *Minussiella asiatica* and *M. kulagaiensis* are synonymous with *M. beliakovi*, has demonstrated two types of gemmation in colonies of *M. beliakovi* from Mongolia. In early stages of colony development, offsets rapidly grow into mature daughter corallites, whereas in later stages of the colony, offsets usually either fail to develop beyond the initial stage, or lengthen without ever becoming mature.

Comparisons. The more strongly carinate examples of *Minussiella* bear some resemblance to both *Cyathophyllum dianthus* Goldfuss, the type species of *Cyathophyllum* Goldfuss, 1826, and *Spinophyllum spongiosum* (Schlüter), the type species of *Spinophyllum* Wedekind, 1922. Although *Cyathophyllum dianthus* has been revised by Birenheide (1963, p. 376-381, Pl. 46, figs. 1-3; Pl. 50, figs. 19-21; Pl. 51, figs. 22-24), no photographic illustrations of its interior are available. Based on Haller's (1936, Pl. 36, figs. 2a-c; Pl. 37, figs. 1a-3b; Pl. 38, figs. 1a-2b) and Wrzolek's (1982, Pl. 4, figs. 2a-c) photographs of other species admitted to *Cyathophyllum* by Birenheide, *Cyathophyllum* is distinguished from *Minussiella* primarily by having septa that are more carinate and strongly retiform toward the periphery. *Spinophyllum spongiosum* (Schlüter) was never illustrated by Schlüter. Specimens illustrated by Birenheide (1978, Pl. 12, figs. 1a, b) and Hill (1981, Fig. 172, 3a, b) have numerous yardarm carinae, not found in species of *Minussiella*. Chinese corals attributed to *Spinophyllum* by Birenheide and Liao (1985, Pl. 2, figs. 8a-9e, Pl. 3, figs. 10a-c) have fusiform septa, small dissepiments and slightly everted dissepimentaria, none of which is typical of *Minussiella*.

Genera erected after 1952, that resemble *Minussiella*, are *Pseudocampophyllum* Ivanovskiy, 1958, *Mansuyphyllum* Fontaine, 1961, and *Chalcidophyllum* Pedder, 1965.

Ivanovskiy's illustrations of *Pseudocampophyllum enisseicum*, especially the two not reproduced by Hill in 1981 (Ivanovskiy, 1958, Pl. 1, figs. 1, 4), strongly suggest that *P. enisseicum* is conspecific with *Minussiella beiensis*. Both are from the Beyskoe Suite of the Minusinsk Basin, and both have few presepiments, strongly crenulate septa, with a tendency for the adaxial ends of the minor septa to abut the major septa. These minor and inconsistent deviations from the typical morphology of *Minussiella* are probably not sufficient to retain *Pseudocampophyllum* as a separate genus.

Mansuyphyllum Fontaine, 1961, is not an easy genus to diagnose, because of uncertainty regarding the septal structure of *M. annamiticum*, the type species from Viêt-Nam. Interpretations of Fontaine (1966, p. 58-61) and Pedder (in Pedder and Goodbody, 1983, p. 344) are essentially identical, but may be too broad in that they admit to the genus forms with distinctly fusiform septa. Judging from Fontaine's (1961, Pl. 17, figs. 1a-2) figures of *M. annamiticum*, the species is certainly congeneric with a

Givetian coral from the Urals, figured by Soshkina (1941, Fig. 22) as *Ceratinella soeticum*. However, the name *Ceratinella*, which was introduced by Soshkina (1941, p. 36) in an informal manner for corals resembling *Schlueteria*, but differing from it by earlier loss of septal dilation during ontogeny, is unavailable in this context, due to prior use for a living spider (Emerton, 1882, p. 32). Tentatively, *Mansuyphyllum* is differentiated from *Minussiella* by having coarse trabeculae, variably fusiform and, on the whole, more carinate septa that are not disrupted by presepiments.

Chalcidophyllum Pedder, 1965, has been discussed subsequently by the author twice (Pedder et al., 1970, p. 237; Pedder, 1971, p. 378). It is probably a solitary genus, characterized by an invariable continuity between the septal bases and invaginations of the wall at the septal furrows (Pedder, 1965, Pl. 34, figs. 1, 2). The same phenomenon occurs locally in Canadian specimens of *Minussiella* and there is little doubt of the close relationship between the genera. Unlike *Minussiella*, *Chalcidophyllum* is known with certainty only from the Lower Devonian of eastern Australia.

Distribution. Eifelian of the Minusinsk Basin (Rzhonsnitskaya et al., 1952, p. 134-136; Ivaniya, 1965, p. 167-170), Altay Mountains (Spasskiy, 1960, p. 131; Udodov, 1967, p. 142), Mongolian Altay (Spasskiy, 1960, p. 131), western Mongolia (Ulitina, 1980, p. 40-43) and Bathurst Island (this paper). Givetian of the Minusinsk Basin (Bul'vanker, 1955, p. 92), Kuznetsk Basin (Bul'vanker, 1958, p. 160-161) and Western Canada (this paper).

A late Emsian coral from the Obisatit Beds of Uzbekistan, identified by Erina (1978, p. 19, Pl. 41, figs. 8a, b) as *Minussiella* sp., is not identifiable on the basis of the published figures.

Minussiella cornus (McLaren)
Figures 51.4-51.24

?*Disphyllum salicis* McLaren, in McLaren and Norris, 1964, p. 9-10, Pl. 3, figs. 1a-2b.
Grypophyllum cornus McLaren, in McLaren and Norris, 1964, p. 10-11, Pl. 3, figs. 3a-c.

Material. Holotype, GSC 16482. Holotype and paratype of *Disphyllum salicis*, GSC 16469, 16470. These three specimens are from the type Horn Plateau Reef, but their exact stratigraphic and geographic occurrences were not recorded.

Additional material prepared for this work consists of seven specimens from GSC loc. C-53198, registered GSC 76501-76507, and one specimen from GSC loc. C-49444, registered GSC 76508.

Diagnosis. Solitary to weakly fasciculate species of *Minussiella*. Corallites subcylindrical to ceratoid with diameters of 22 to 40 mm at maturity. Septa thin, typically smooth, locally crenulate, and numbering from 30 x 2 to 37 x 2 in mature corallites. Rare, extremely short, third-order septa may be present. Adult dissepimentaria comprise 6 to 10 rows of globose and elongate dissepiments and presepiments.

Description. The only known occurrence of this species is in a high energy organic reef facies. Corallites are subcylindrical to ceratoid. Many were abraded before burial; most, as now collected, are solitary, but some, such as GSC 76502, illustrated in figures 51.7 to 51.9, form loose aggregations assumed to belong to the same colony. Some of

these corallites are mature, with mean diameters varying from 22 to 40 mm; others are not only immature, but also seem to be nonmaturing. Figure 51.7 illustrates one of these. The corallite wall is very thin, 0.09 to 0.12 mm thick, except during periods of rejuvenation when it thickened to as much as 0.5 mm. The exterior surface of the corallite wall bears fine growth rings, narrow and shallow septal furrows and much broader, essentially flat, interseptal ridges. Judging from longitudinal thin sections, the sides of the calice would have been conical and its base would generally have been flat or concave.

Although no fossula is evident, the arrangement of septa is commonly not quite radial, due to suppression of one or more major septa. In addition to the 30 x 2 to 37 x 2 septa present in mature corallites, rare traces of third order septa are visible in some corallites. Immature corallites have about 20 x 2 septa at 6.0 mm diameter, 27 x 2 at 11.0 mm diameter and 29 x 2 at 20.0 mm diameter. Some major, and many of the minor septa are interrupted by presepiments. Septa are very thin, typically only 0.03 to 0.1 mm thick over most of their length. They tend to thicken slightly at the periphery of the corallite and inner margin of the tabularium. During rejuvenescence they may thicken in places to as much as 0.5 mm. Septal bases are generally embedded in the wall, but in rare cases may be continuous with invaginations of the wall. Zigzag carinae may be developed during rejuvenescences, otherwise the septa are smooth, although they may be strongly crenulate. Abaxial withdrawal of the major septa is variable. Trabeculae are either absent or exceedingly fine.

In adult stages, the dissepimentarium usually comprises 6 to 10 rows of globose to elongate dissepiments and some presepiments. Immature corallites rarely have more than three rows of dissepiments. Tabulae and marginal tabellae vary considerably, but usually form depressed tabularial surfaces. Spacing is such that normally 9 to 18 tabulae are counted over a vertical distance of 10 mm.

Remarks. The narrow corallites, which either do not mature, or mature very slowly, the thin wall, thin disrupted septa and sagging tabularium of this species are all consistent with an assignment to *Minussiella*, as the genus is now known through the work of Ulitina (1980, 1982). *Grypophyllum*, which has been discussed by Birenheide (1972, p. 407-422) and Jia (1984, p. 28-29), has a typical ptenophyllid tabularium with incomplete and very closely spaced tabulae that are quite distinct from the innermost dissepiments.

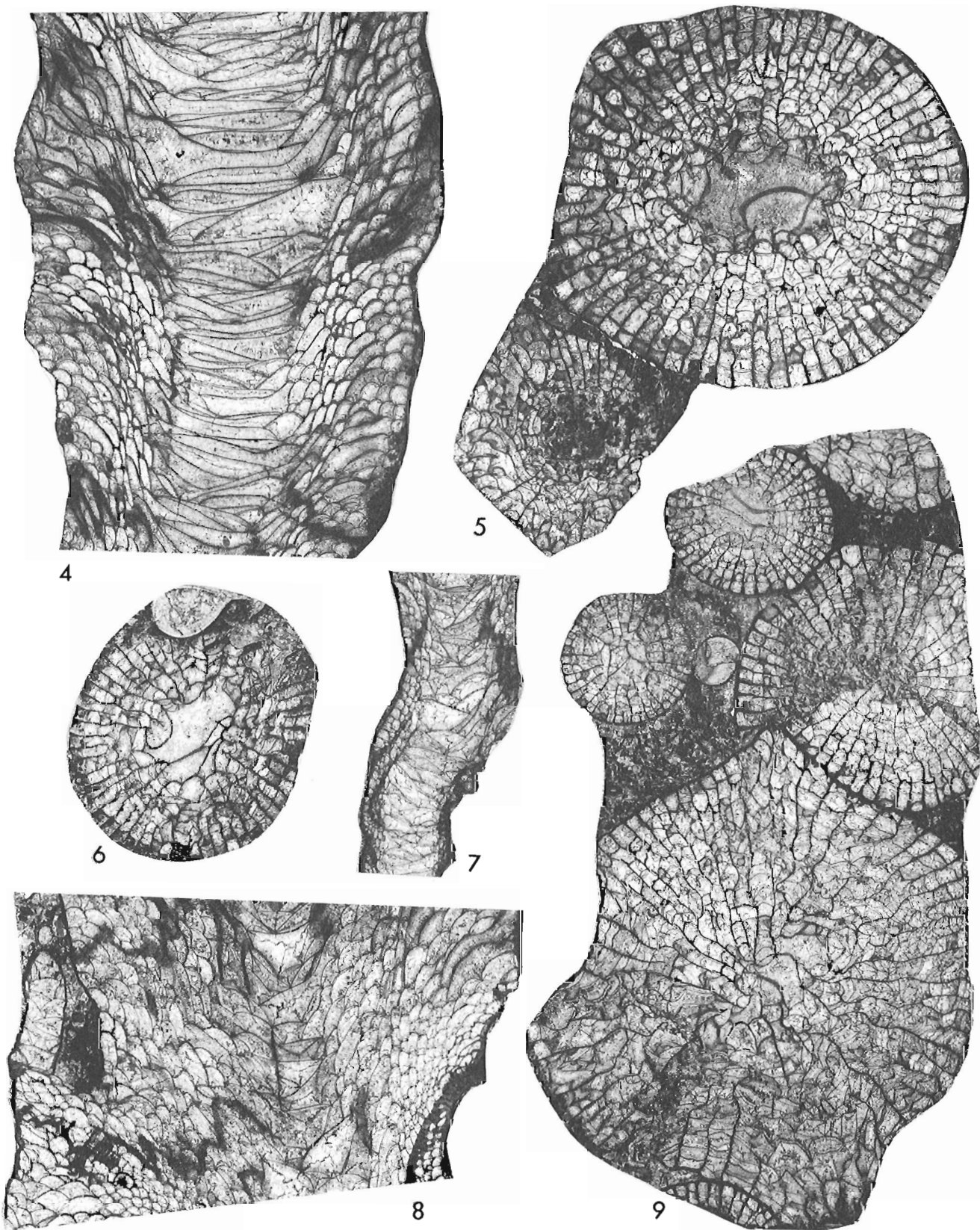
It seems probable that *Disphyllum salicis* is based on two immature corallites of *Minussiella cornus*.

McLaren stated that the trivial name *cornus* is the Latin word *cornu*, a horn. Here, *cornus* is regarded as a noun – either the common form in the genitive case, or the accessory form (Lewis and Short, 1966, p. 471) in the nominative case – and not a corruption of the adjective *corneus*.

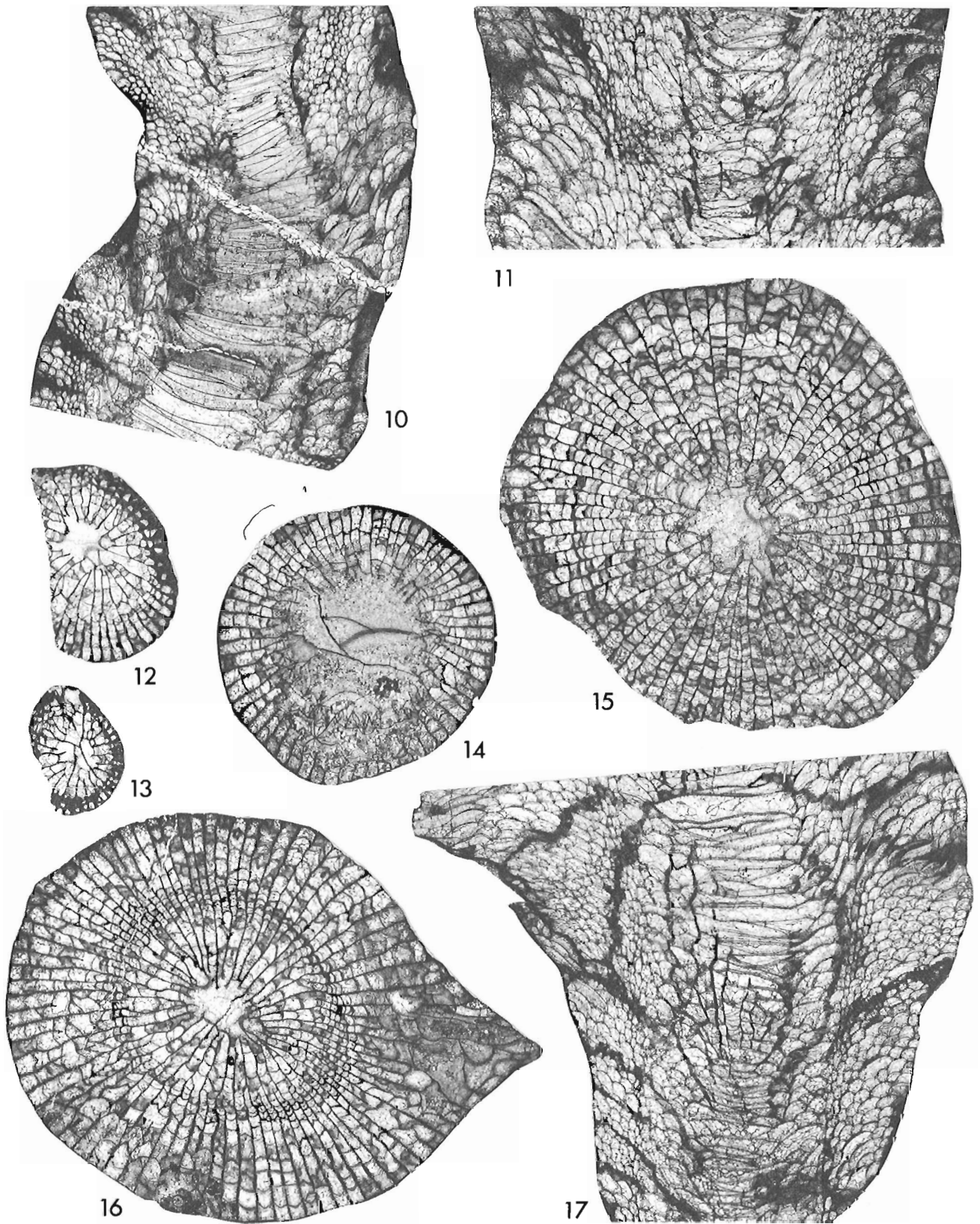
Minussiella conjuncta sp. nov.
Figures 51.25-51.31

Material. Holotype, GSC 76509, and two paratypes, GSC 76510, 76511, from GSC loc. C-49444. One paratype, GSC 76512, from GSC loc. C-53198.

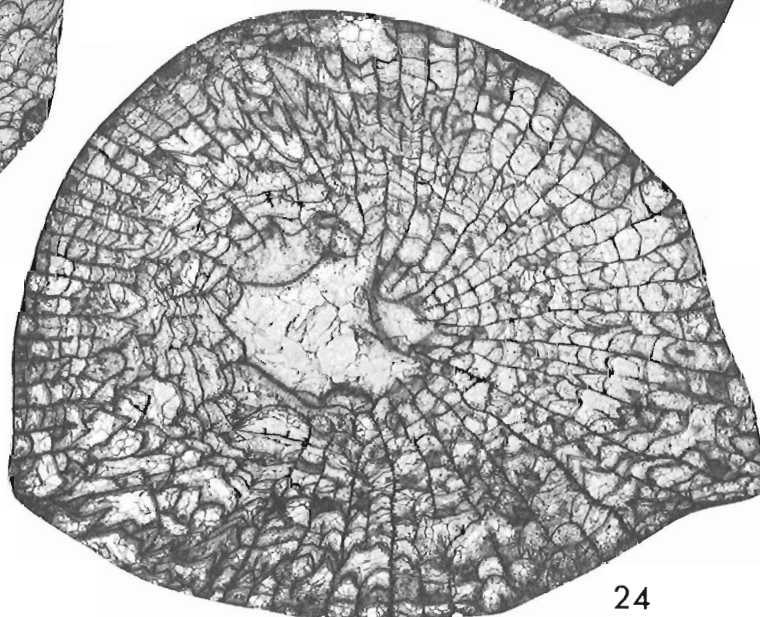
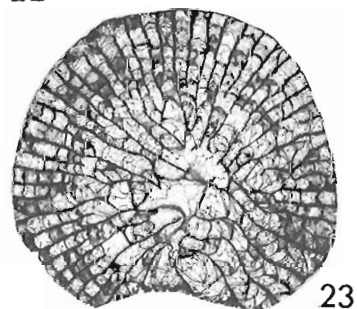
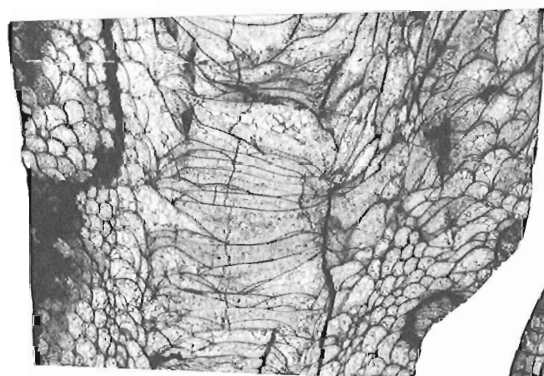
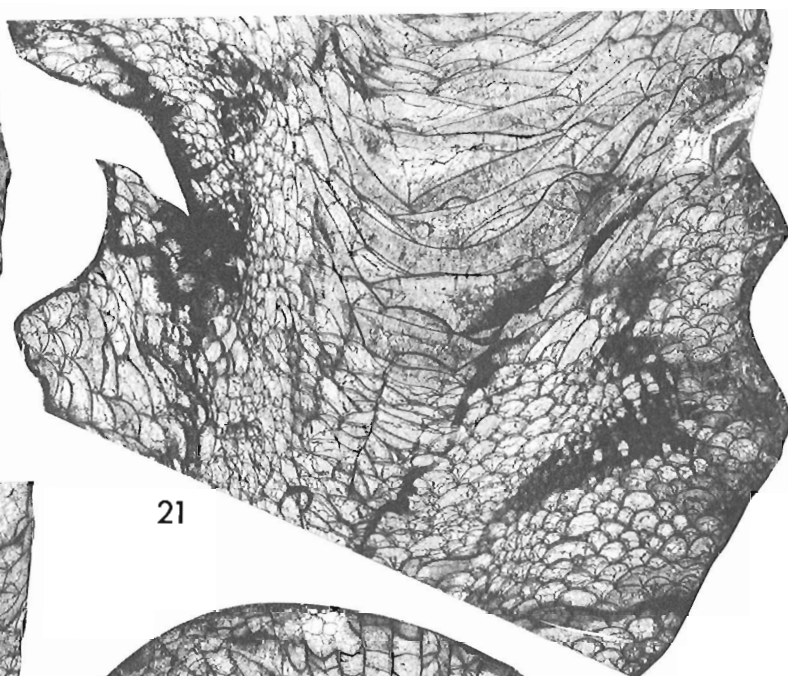
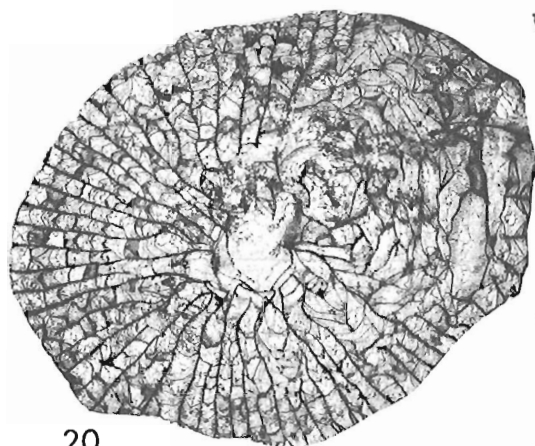
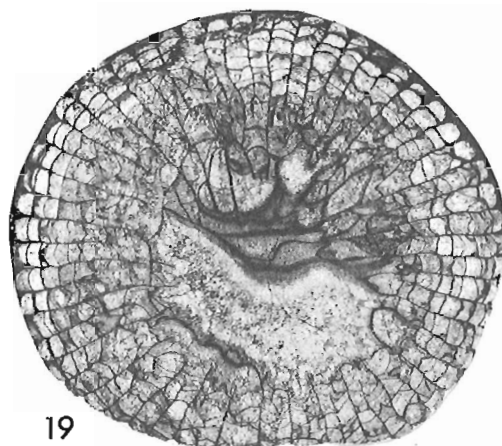
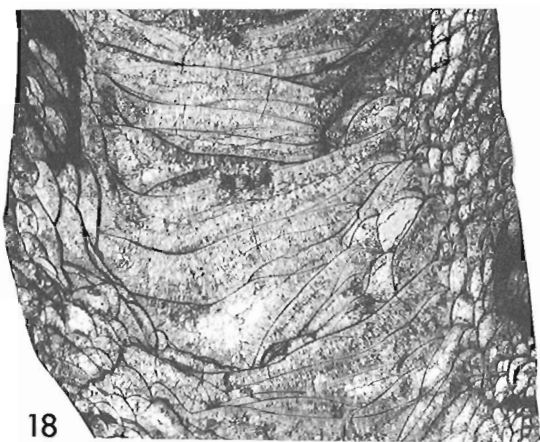
Diagnosis. Subcerioid to cerioid, but not prismatic, species of *Minussiella*. Mature corallites, with mean diameters of 17 to 25 mm, have 23 to 27 major, and typically slightly fewer minor, septa. Septa smooth, very attenuate, and commonly



Figures 51.4-51.9. *Minussiella cornus* (McLaren), longitudinal and transverse thin sections, x3. All from GSC loc. C-53198. 51.4-51.6. GSC 76501. 51.7-51.9. GSC 76502.



Figures 51.10-51.17. *Minussiella cornus* (McLaren), longitudinal and transverse thin sections, x3. All from GSC loc. C-53198. 51.10, 51.12-51.14. GSC 76503. 51.11, 51.15. GSC 76504. 51.16, 51.17. GSC 76505.



Figures 51.18-51.24. *Minussiella cornus* (McLaren), longitudinal and transverse thin sections, x3. 51.18, 51.19. GSC 76508, GSC loc. C-49444. 51.20, 51.22, 51.23. GSC 76506, GSC loc. C-53198. 51.21, 51.24. GSC 76507, GSC loc. C-53198.

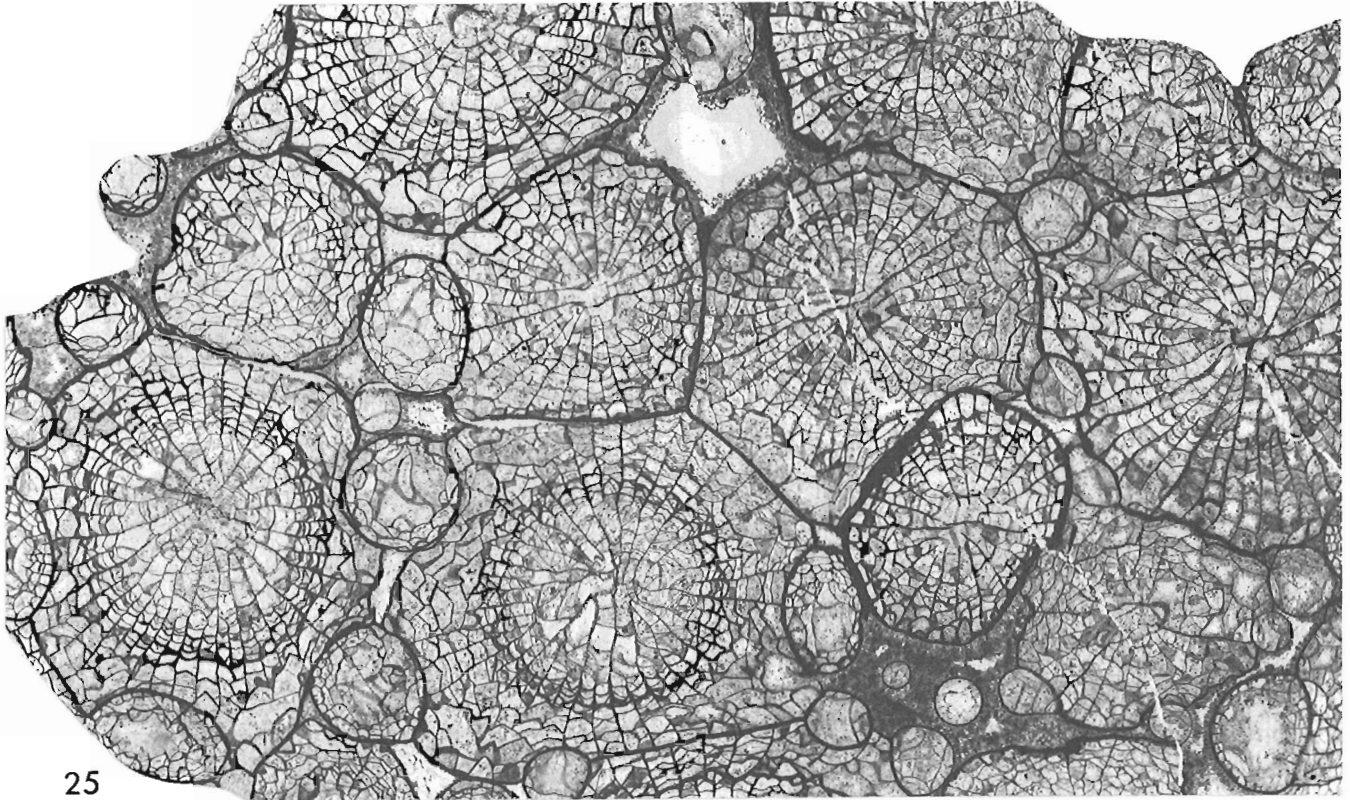


Figure 51.25. *Minussiella conjuncta* sp. nov., GSC 76509, holotype, transverse section, x3, from GSC loc. C-49444.

discontinuous toward the periphery of the corallite. Adult dissepimentaria have 6 to 9 rows of elongate dissepiments and presepiments.

Description. The four type colonies are incomplete and their shape unknown. Two, including the holotype, are subcerioid; the others are cerioid, but not prismatic, since they include many immature rounded corallites. Early mode of corallum increase has not been observed. In distal regions of the colony, offsets are produced marginarily, one or more at a time. Some of these offsets remain stunted without septa; others develop normal septa, but increase very little in diameter, if at all, over several centimetres of vertical growth, and it is doubtful if any ever become full-sized mature corallites. Mean diameters of adult corallites are 17 or 18 mm in the holotype, and 22 to 25 mm in the paratypes. The width of the corallite wall in free corallites, or half the width of intercorallite walls constructed by two adjacent corallites, is only 0.07 to 0.15 mm. Calices are shallow, with sloping sides and generally flat, or depressed bases.

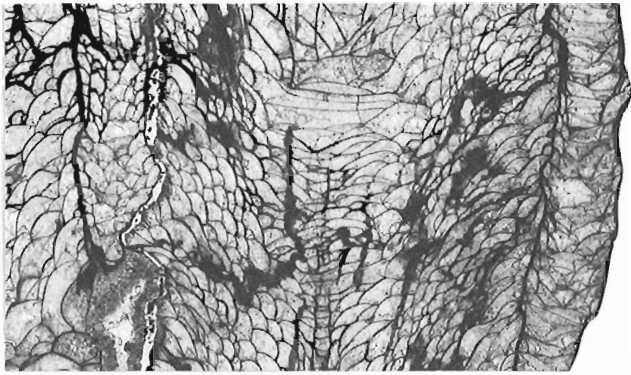
Septal arrangement is essentially radial, although the lengths of septa within a corallite are commonly unequal, with some major septa extending adaxially beyond the axis. Variable reduction of the septa, including total suppression of some minor septa, makes it difficult to summarize septal counts. In mature corallites, with mean diameters of 17 to 25 mm, there are 23 to 27 major septa; in smaller immature corallites, with mean diameters of 8 to 16 mm, the number of major septa is 18 to 22. The septa are generally smooth, extremely attenuate and much disrupted by presepiments in the peripheral region of large corallites.

In adult stages, the dissepimentarium usually comprises 6 to 9 rows of predominantly elongate dissepiments and presepiments. Immature corallites normally lack, or have only one or two rows of dissepiments. The variable tabulae are not consistently distinguishable from marginal tabellae, and the marginal tabellae may not be perceptibly different from the innermost dissepiments or presepiments. Tabularial surfaces range from more or less flat to distinctly depressed. Spacing of the tabulae varies from about 11 to 25 for each centimetre of vertical growth.

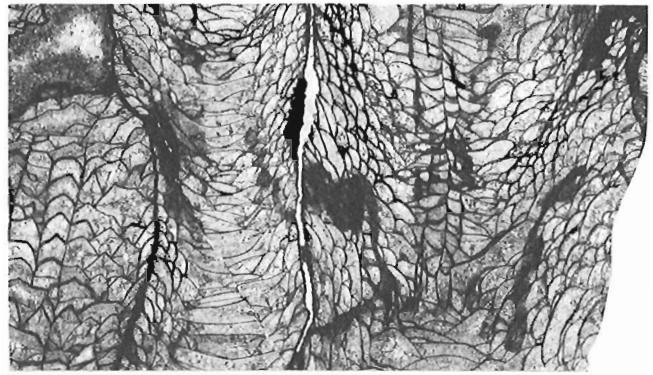
Remarks. The manner of corallum increase in *Minussiella conjuncta* and specimens of *M. beliakovi* studied by Ulitina (1980, 1982) from western Mongolia appear identical, although the intense early gemmation of the Mongolian species cannot be confirmed in the available material of *M. conjuncta*. The overall corallite morphology of the two species is also similar. *Minussiella beliakovi* is distinguished from the new species by the smaller average size of its corallites (diameters rarely more than 20 mm), narrower dissepimentaria (2 to 6 rows of dissepiments and presepiments), fewer disruptions in the septa and its generally fasciculate, rather than subcerioid to cerioid growth form.

Minussiella conjuncta is distinguished from *M. cornus* by its subcerioid to cerioid growth form, smaller corallites and fewer septa (corallites of 22 to 40 mm diameter have 30 x 2 to 37 x 2 septa in *M. cornus*) and more peripheral presepiments.

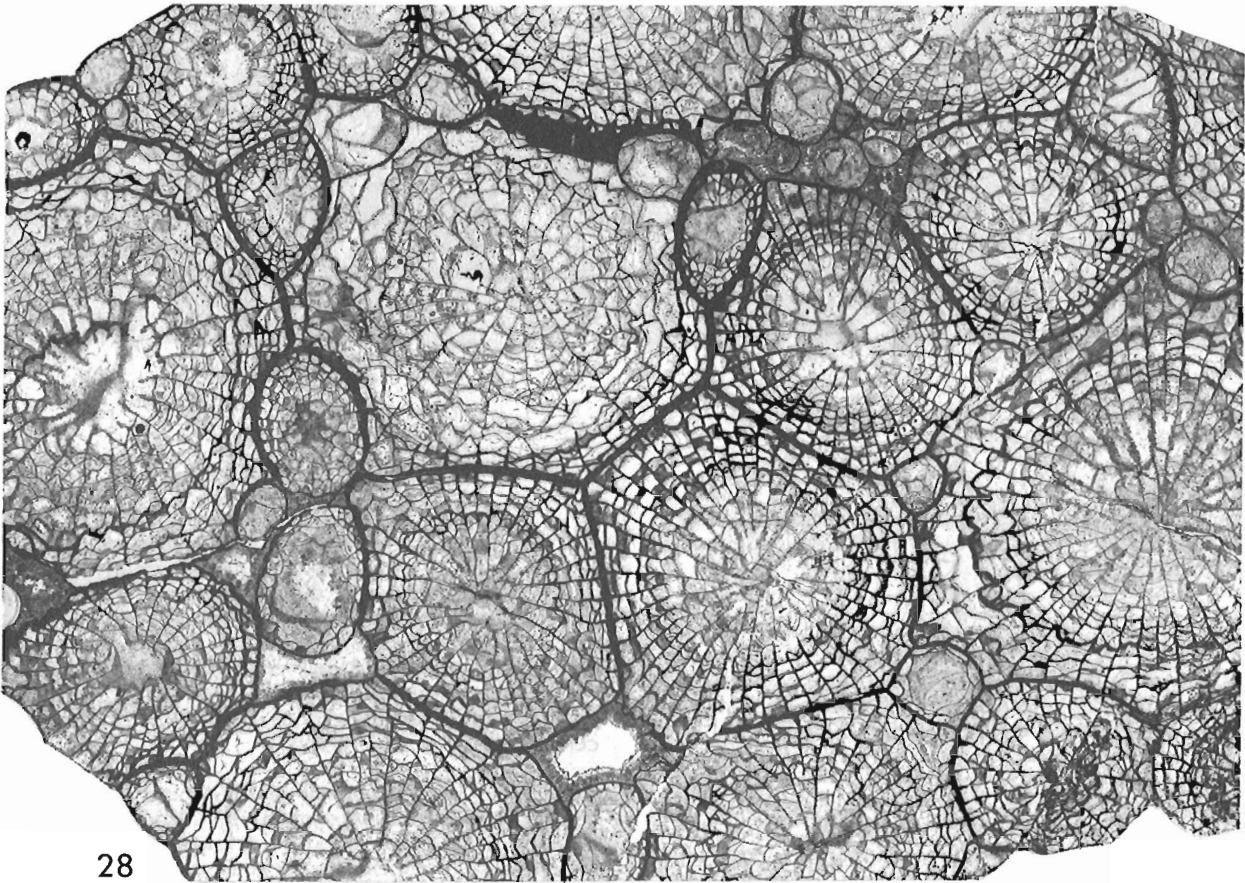
Derivation of name. The trivial name *conjunctus* is the Latin adjective meaning joined together, and is chosen as a reminder of the growth form of the species.



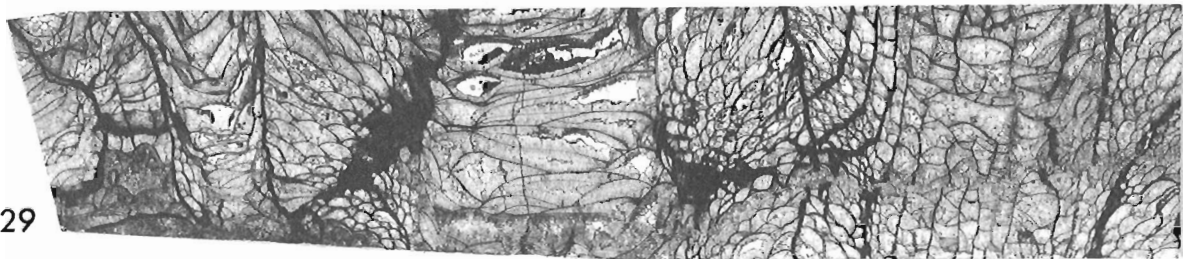
26



27

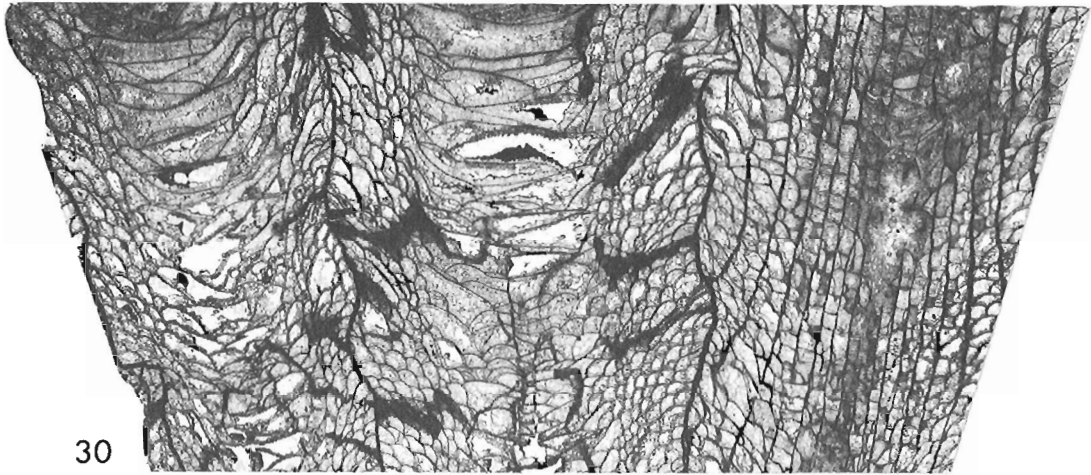


28

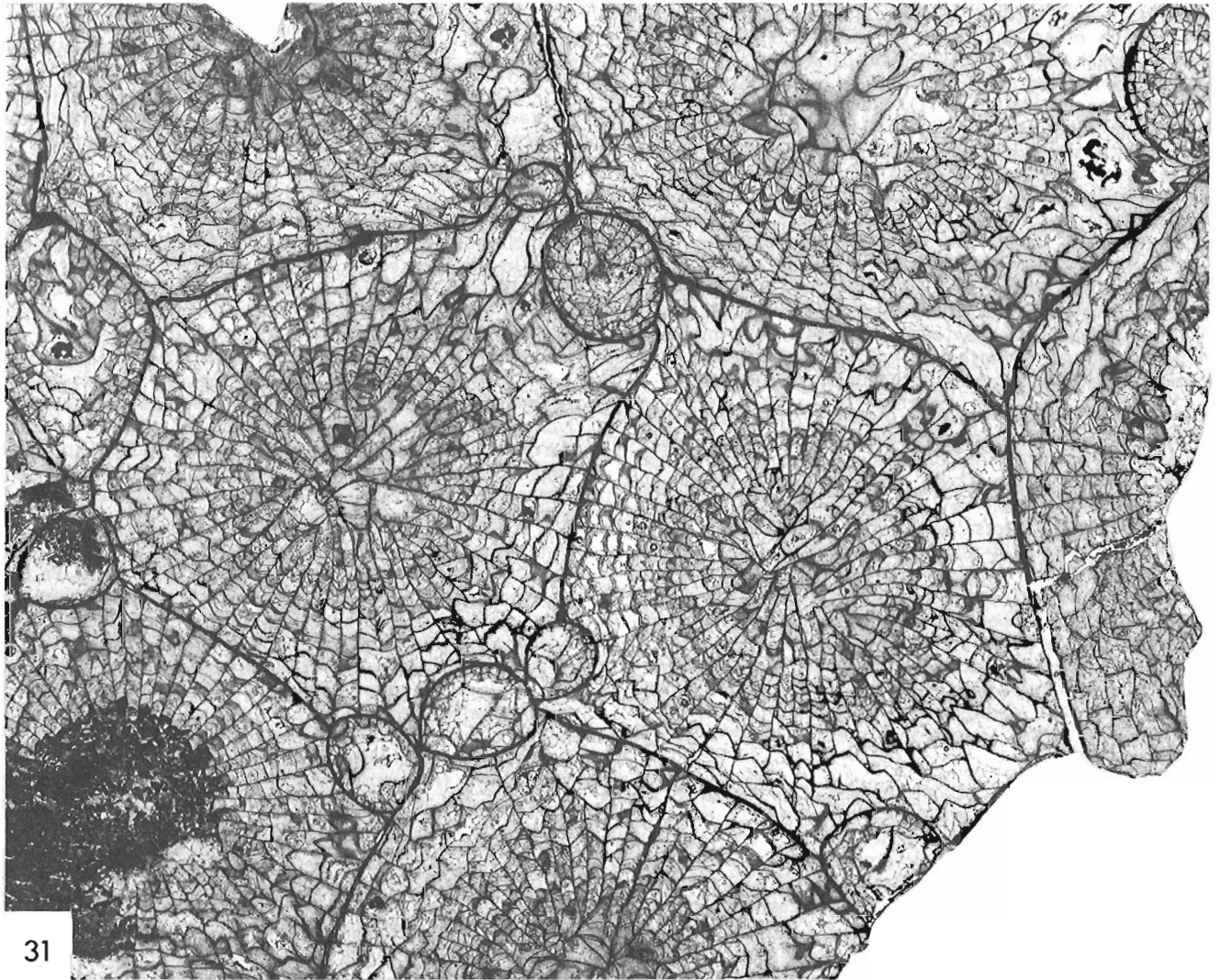


29

Figures 51.26-51.29. *Minussiella conjuncta* sp. nov., longitudinal and transverse thin sections, x3. All from GSC loc. C-49444. 51.26-51.28. GSC 76509, holotype. 51.29. GSC 76510, paratype.



30



31

Figures 51.30, 51.31. *Minussiella conjuncta* sp. nov., GSC 76510, paratype, longitudinal and transverse thin sections, $\times 3$, GSC loc. C-49444.

Minussiella bathurstensis sp. nov.
Figures 51.32-51.51

leptoinophyllid, McLaren, in Fortier et al., 1963, p. 612.

Material. Holotype, UA 7739, and four paratypes, UA 7740-7743, from UA loc. PCC 92169. One paratype, UA 7744, from UA loc. PCC 92164. One paratype, GSC 76513, from GSC loc. 26536.

Diagnosis. Fasciculate species of *Minussiella*. Mature corallites have mean diameters of 16.5 to 21.0 mm, 24 x 2 to 32 x 2 septa, and 6 to 10 rows of dissepiments. Septa are smooth, thin and only rarely disrupted by presepiments.

Description. Field photographs, provided by Q.H. Goodbody, of large - about 1 m in diameter - clumps of more than 100 radiating corallites of this species, indicate a fasciculate growth form. As received by the author, the material from the type locality comprised separate, subcylindrical corallites with maximum mean diameters of 16.5 to 21.0 mm and a maximum length of 115 mm. Non-parricidal gemmation leading to a full-sized daughter corallite was evident in only one of these specimens (UA 7741). However, stunted offsets, such as those illustrated in Figure 51.51, were present on several corallites. Radiciform processes, attaching to the substrate, were developed prior to rejuvenescence in some cases. The corallite wall is only 0.1 to 0.2 mm thick, except for rare situations, probably associated with rejuvenation or gemmation, where it thickens to as much as 0.4 mm. The exterior of the corallite wall bears fine growth rings, narrow and shallow septal furrows and much broader, flat, to gently convex, interseptal ridges. The calice, which is only about 5 to 8 mm deep, consists of a narrow, intermittently developed calicular platform, walls that increase in inclination toward the axis, and a flat or depressed base.

Septa are radially arranged in two orders. Immature corallites of 5 to 16 mm diameter have 20 x 2 to 25 x 2 septa, whereas mature corallites of more than 16 mm mean diameter have 24 x 2 to 32 x 2 septa. Septa are variably withdrawn from the axis and, on the whole, very little disrupted by presepiments, especially those of the major order, which are normally complete. Although they may be crenulate locally, the septa are smooth and only 0.02 to 0.03 mm thick over most of their length. Toward their bases, which are invariably embedded in the corallite wall, the septa expand to a thickness of 0.15 to 0.4 mm. Other limited dilations of the septa appear to be associated with budding or large-scale rejuvenescences. Fine, upwardly and inwardly directed lineations, visible in longitudinal thin sections through a septal plane, appear to represent extremely fine trabeculae.

Immature corallites with diameters in the order of 7 mm have 2 to 4 rows of predominantly globose dissepiments. Mature corallites generally have 6 to 10 rows of elongate as well as globose dissepiments, and a few presepiments. Tabulae and marginal tabellae are variable, and form flat to depressed tabularial surfaces. Spacing of the tabulae ranges from about 18 to 26 for each cm of vertical growth.

Remarks. Corallites of *Minussiella beliakovi* resemble those of *M. bathurstensis* in size and number of septa. *Minussiella bathurstensis* differs from *M. beliakovi* in being loosely fasciculate, by having fewer disruptions in the septa and more numerous dissepiments (dissepiments normally confined to only 2 to 6 rows in *M. beliakovi*).

Minussiella sociabilis is also similar in size to *M. bathurstensis*. The new species is distinguished from *M. sociabilis* by its loosely fasciculate growth form and by its more complete (minor septa, in particular, are considerably reduced in *M. sociabilis*) but less numerous septa (36x2 to 46x2 septa in *M. sociabilis*).

The identification of the paratype, registered GSC 76513, as "a leptoinophyllid" (Fortier et al., 1963, p. 612) was made before Birenheide's (1961, p. 117-123) revision of the type species of *Leptoinophyllum* was available.

Derivation of name. The trivial name *bathurstensis* is coined from Bathurst Island and the suffix *-ensis*.

Minussiella goodbodyi sp. nov.
Figures 51.52-51.63

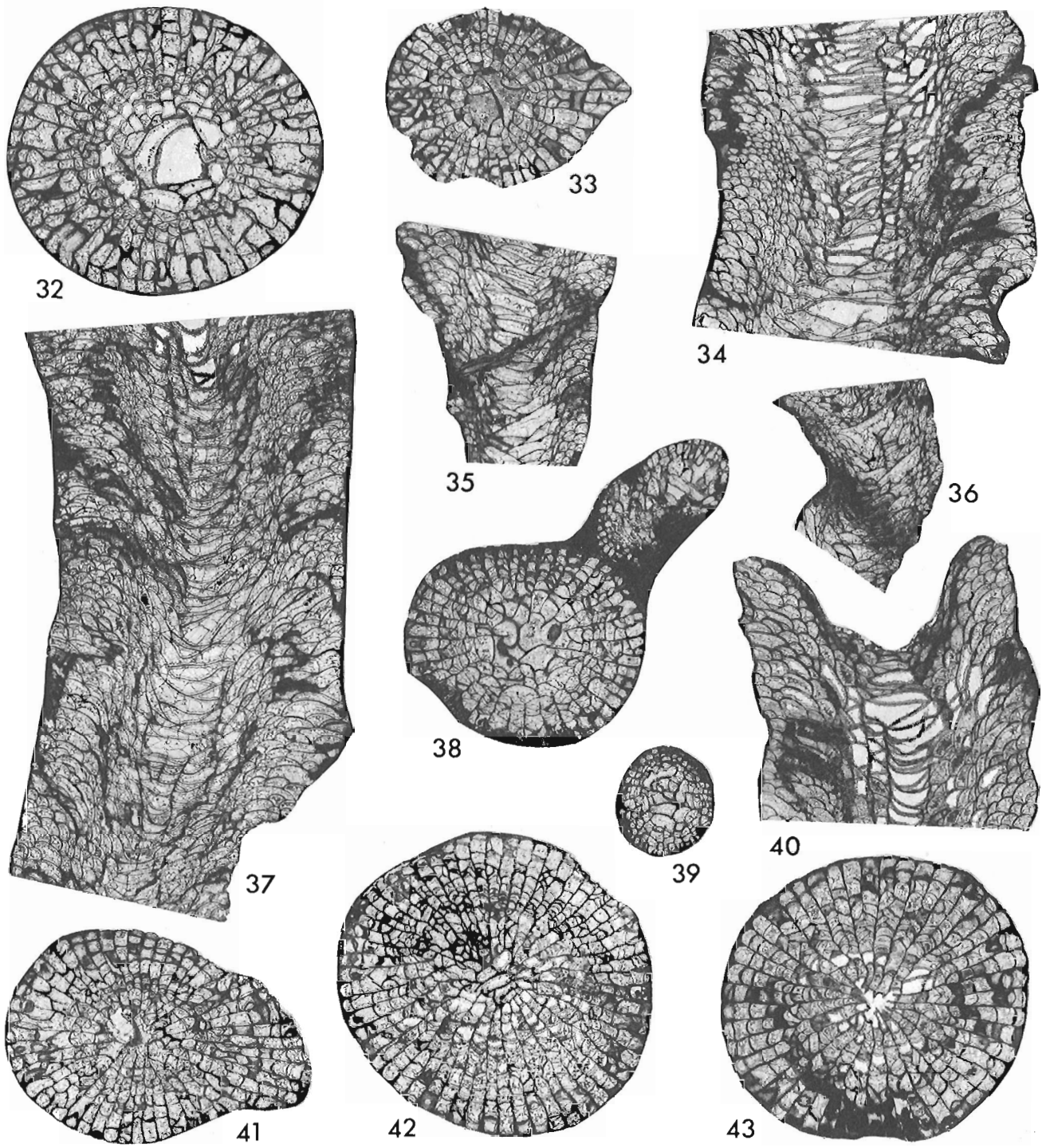
Material. Holotype, UA 7745, and four paratypes, UA 7746-7749, from UA loc. PCC 92160.

Diagnosis. Loosely fasciculate species of *Minussiella*. Mature corallites have mean diameters of 11.0 to 19.0 mm, 22 x 2 to 29 x 2 septa, and 6 to 13 rows of dissepiments. Septa commonly bear zigzag carinae and also are commonly thickened in the inner dissepimentarium. They are rarely disrupted by presepiments.

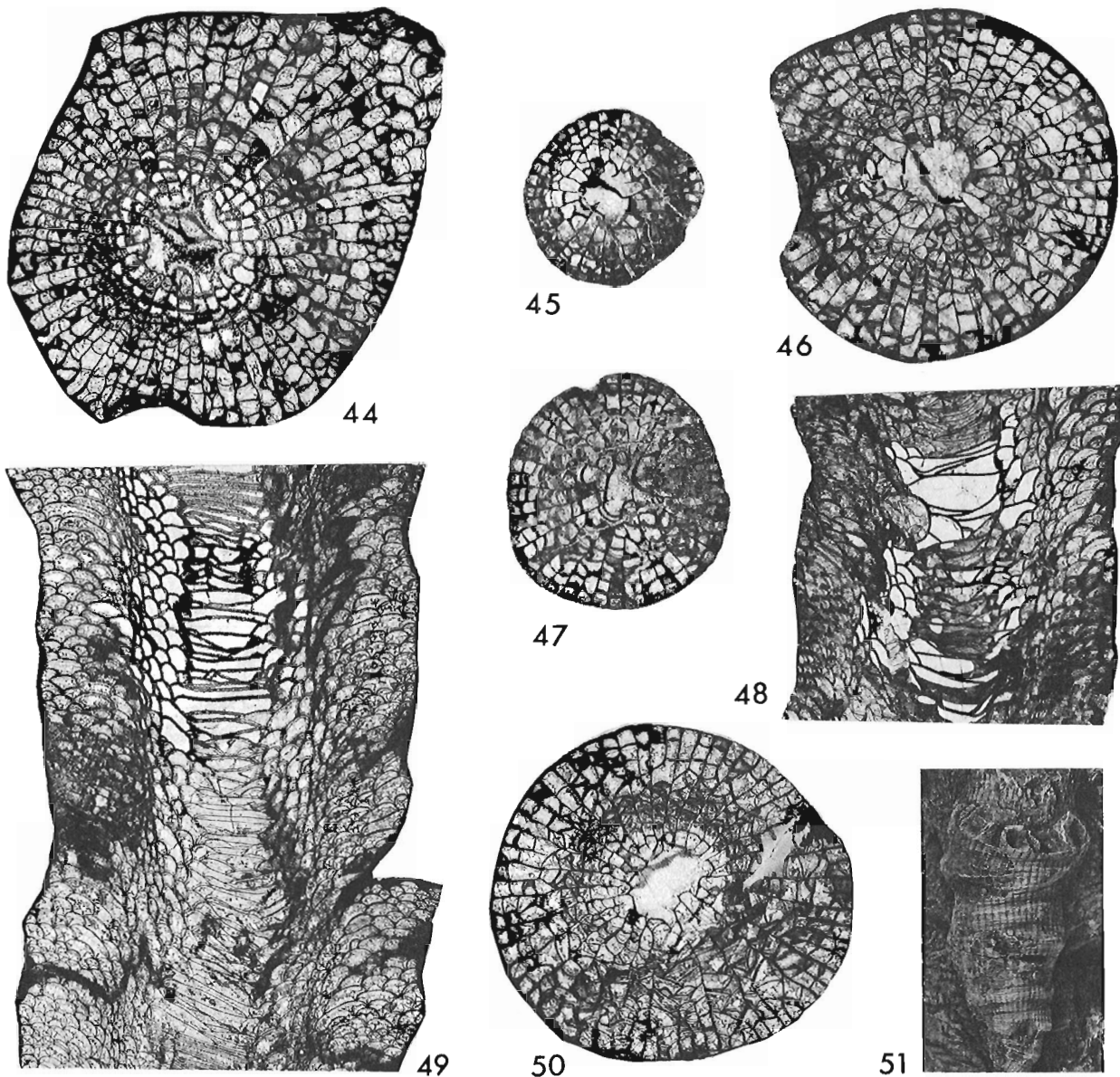
Description. The corallum is presumed to be loosely fasciculate, although the non-parricidally produced offsets, seen in the type series, are all stunted. Adult corallites are subcylindrical with maximum mean diameters ranging from 11.0 to 19.0 mm, and a maximum observed length of 80 mm. The corallite wall is 0.08 to 0.5 mm thick and on the outside bears fine septal furrows and much broader, flat to gently convex interseptal ridges. Below some levels of rejuvenescence, the corallite wall develops short, non-tubular radiciform processes. Calices are 5 to 10 mm deep. A narrow calicular platform is present locally in expanded regions of the corallite. Elsewhere, the calicular wall is inwardly sloping, with the slope increasing adaxially. Bases of the calices are flat to concave.

The septa, of which there are 22 x 2 to 29 x 2 in mature corallites with mean diameters of 13 to 19 mm, are radially arranged and are commonly moderately to strongly carinate. The carinae are zigzag, and, like the septa, vary in coarseness. In places, the septa are only 0.03 mm thick, but in the inner dissepimentarium they are commonly dilated to a thickness of 0.3 mm. They are also dilated at their bases, where their thickness may be as much as 0.55 mm. The majority of septal bases are embedded in the corallite wall, but a few are confluent with it. The septa are variably withdrawn from the axis. Gaps due to disruption by presepiments are rare. Trabeculae are monacanthate and commonly coarse, some having a diameter of 0.3 mm. Near the periphery, many of the trabeculae are vertical; toward the axis they flatten, and are usually directed inward, at 30° to 45° to the horizontal, in the inner dissepimentarium.

In adult corallites, there are normally about 6 to 13 rows of predominantly globose to moderately elongate dissepiments, and a few presepiments. The variable and locally indistinguishable tabulae and marginal tabellae form flat, or more typically depressed, tabularial surfaces. Spacing of the tabulae ranges from about 15 to 34 for each centimetre of vertical growth.



Figures 51.32-51.43. *Minussiella bathurstensis* sp. nov., transverse and longitudinal thin sections, x3. All from UA loc. PCC 92169. 51.32, 51.37, 51.41. UA 7739, holotype. 51.33, 51.35. UA 7740, paratype. 51.34, 51.36, 51.38, 51.39, 51.42. UA 7741, paratype. 51.40, 51.43. UA 7742, paratype.



Figures 51.44-51.51. *Minussiella bathurstensis* sp. nov. 51.44, 51.49, 51.50. UA 7774, paratype, transverse and longitudinal thin sections, x3, UA loc. PCC 92164. 51.45-51.48. GSC 76513, paratype, transverse and longitudinal thin sections, x3, GSC loc. 26536. 51.51. UA 7743, paratype, exterior, x1, UA loc. PCC 92169.

Remarks. The taxonomic problem presented by the corals assigned to this new species is that, while they are clearly closely related to *Minussiella bathurstensis*, they are distinguished principally by strong carination of their septa; this is seen in no other species currently assigned to the genus.

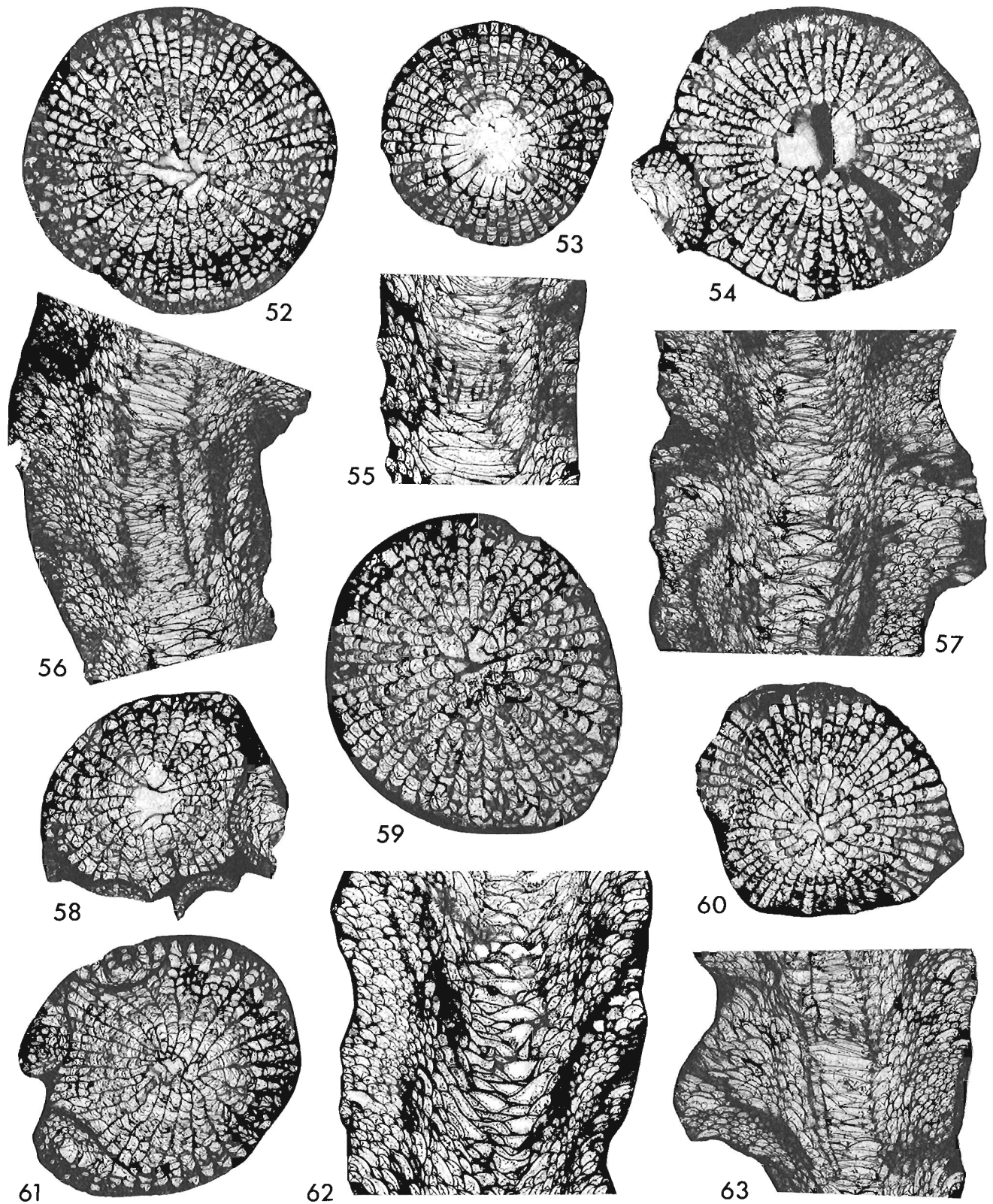
Derivation of name. The trivial name is a patronym for Q.H. Goodbody who collected the type series.

Locality register

GSC locality 26536. Upper beds of a 183 m thick Eifelian carbonate unit. (McLaren in Fortier et al., 1963, columnar section no. 82, sheet 11). Cut Through Creek, southern limb of Stuart Bay Anticline, Bathurst Island;

approximately 76°09.3'N latitude, 99°00'W longitude. Collected by D.J. McLaren, 1955. Fauna includes *Minussiella bathurstensis* Pedder.

GSC locality C-49444. Horn Plateau Formation, organic reef macrofacies (Vopni and Lerbekmo, 1972, p. 506-510), probably Middle varcus Zone, Givetian. Northern end of the surface outcrop of the Horn Plateau Reef, 4.4 km west of the southwestern tip of Fawn Lake, southwestern District of Mackenzie; 62°08'N latitude, 117°41.5'W longitude. Collected by A.E.H. Pedder, 1977. Fauna includes *Scissoplasma nebracis* (McLaren), *Sinospongophyllum* sp. cf. *S. planotabulatum* sensu McLaren, "*Neostriogophyllum craigi*" McLaren, *Psydracophyllum* sp. nov. (= *Australophyllum* ? sp. cf. *A. ? thomasmiae* sensu McLaren), *Sociophyllum redactum* McLaren, *Minussiella conjuncta* Pedder, *M. cornus* (McLaren), *Desatrypa nasuta* (Norris) and *Cranaena(?) cryptonelloides* Norris.



Figures 51.52-51.63. *Minussiella goodbodyi* sp. nov., transverse and longitudinal thin sections, x3.
 All from UA loc. PCC 92160. 51.52, 51.56. UA 7745, holotype. 51.53, 51.55. UA 7746, paratype.
 51.54, 51.57, 51.60. UA 7747, paratype. 51.58, 51.61, 51.63. UA 7748, paratype. 51.59,
 51.62. UA 7749, paratype.

GSC locality C-53198. Horn Plateau Formation, organic reef macrofacies (Vopni and Lerbekmo, 1972, p. 506-510), probably Middle varcus Zone, Givetian. Northeastern margin of the surface outcrop of the Horn Plateau Reef, 4.4 km west of the southwestern tip of Fawn Lake, southwestern District of Mackenzie; 62°08'N latitude, 117°41.5'W longitude. Collected by A.E.H. Pedder, 1977. Fauna includes the forms listed above as occurring at GSC Locality C-49444, as well as *Ozarkodina brevis* (Bischoff and Ziegler), *Polygnathus linguiformis linguiformis* Hinde morphotype indet. and *P. sp. undet.* Another GSC conodont sample from the same outcrop (GSC loc. C-28091) has yielded *Polygnathus linguiformis linguiformis epsilon* morphotype.

UA locality PCC 92160. Eifelian carbonate, isolated sample from top of unit, *costatus* Zone. 5 km southeast of Half Moon Bay, Bathurst Island; 75°53.5'N latitude, 99°47'W longitude. Collected by Q.H. Goodbody, 1980. *Favosites sp.*, *Lythophyllum sp.*, *Digonophyllum sp.*, *Lekanophyllum sp.*, *Minussiella goodbodyi* Pedder, *Schizophoria sulcata* Johnson and Perry, *Spinulicosta sp.*, *Anatrypa (Variatrypa) sp. cf. A. arctica* (Warren), *Warrenella sp.*, *Icriodus sp.*, *Polygnathus sp. cf. P. linguiformis* Hinde and *P. sp.*

UA locality PCC 92164. Eifelian carbonate, 3.2 m above base, 24.8 m below top, and 102.2 m above base of section, *patulus* to *costatus* Zone. Northern side of Half Moon Bay, Dundee Bight, Bathurst Island; 76°03'N latitude, 100°04'W longitude. Collected by Q.H. Goodbody, 1980. *Digonophyllum sp.*, *Lekanophyllum sp.*, *Minussiella bathurstensis* Pedder, *Spinulicosta sp.*, *Ivdelinia grinnellensis* Brice ?, *Anatrypa (Variatrypa) sp. cf. A. arctica* (Warren), *Protathyris ? sp.* and *Nucleospira sp.*

UA locality PCC 92169. Eifelian carbonate, approximately 19 m above base, 9 m below top, *costatus* Zone. Northern side of Half Moon Bay, Dundee Bight, Bathurst Island; 76°03'N latitude, 100°02'W longitude. Collected by Q.H. Goodbody, 1980. *Zonophyllum sp.*, *Lekanophyllum sp.*, *Chostophyllum sp.*, *Minussiella bathurstensis* Pedder, *Schizophoria sulcata* Johnson and Perry, *Spinulicosta sp.*, *Ivdelinia grinnellensis* Brice ?, *Anatrypa (Variatrypa) sp. cf. A. arctica* (Warren), *Warrenella sp.*, *Icriodus norfordi* Chatterton, *Polygnathus costatus costatus* Klapper and *P. sp. cf. P. costatus* Klapper.

References

- Besprozvannykh, N.I., Dubatolov, V.N., Kravtsov, A.G., Latypov, Yu. Ya., and Spasskiy, N.Ya.
1975: Devonskie rugozy Taymyro-Kolym'skoy provintsii; Akademiya Nauk SSSR, Sibirskoe Otdelenie, Institut Geologii i Geofiziki, Trudy, vypusk 228, 172 p.
- Birenheide, R.
1961: Die Acanthophyllum-Arten (Rugosa) aus dem Richtschnitt Schönecken-Dingdorf und aus anderen Vorkommen in der Eifel; Senckenbergiana lethaea, Band 42, p. 77-146.
1963: Cyathophyllum- und Dohmophyllum-Arten (Rugosa) aus dem Mitteldevon der Eifel; Senckenbergiana lethaea, Band 44, p. 363-458.
1972: Ptenophyllidae (Rugosa) aus dem W-deutschen Mitteldevon; Senckenbergiana lethaea, Band 53, p. 405-437.
1978: Leitfossilien. No. 2. Rugose Korallen des Devon; Gebrüder Borntraeger Berlin, Stuttgart. vi p.+ 265 p.
- Birenheide, R. and Liao Wei-hua
1985: Rugose Korallen aus dem Givetium von Dushan, Provinz Guizhou, S-China. 3: Einzelkorallen und einige Koloniebildner; Senckenbergiana lethaea, Band 66, p. 217-267.
- Brice, D.
1982: Brachiopodes du Dévonien inférieur et moyen des formations de Blue Fiord et Bird Fiord des îles arctiques canadiennes; Geological Survey of Canada, Bulletin 326, 175 p. and folder.
- Bul'vankov, E.Z.
1955: Podklass Rugosa. Rugozy; in Polevoy atlas fauny i flory devonskikh otlozheniy Minusinskoy kotloviny, M.A. Rzhonsnitskaya and V.S. Meleshchenko (eds.); Vsesoyuznyy Nauchno-issledovatel'skiy Geologicheskii Institut (VSEGEI), Moskva, 140 p.
1958: Devonskie chetyrekhluchevye korally okrani Kuznetskogo basseyna; Vsesoyuznyy Nauchno-issledovatel'skiy Geologicheskii Institut (VSEGEI), Leningrad, text 212 p. and atlas.
1965: Pervye dannye o devonskikh rugozakh Severo-Vostoka SSSR; in Rugozy paleozoya SSSR, B.S. Sokolov and A.B. Ivanovskiy (eds.); Trudy I Vsesoyuznogo simpoziuma po izucheniyu iskopaemykh korallov SSSR, vypusk 3, p. 54-58.
- Copper, P.
1979: Devonian atrypoids from western and northern Canada; in Western and Arctic Canadian biostratigraphy, C.R. Stelck and B.D.E. Chatterton (eds.); Geological Association of Canada, Special Paper 18, p. 289-331 (imprint 1978).
- Emerton, J.H.
1882: New England spiders of the family Therididae; The Connecticut Academy of Arts and Sciences, Transactions, v. 6, p. 1-86.
- Erina, M.V.
1978: Rugosa; in Atlas paleontologicheskikh tablits. Prilozhenie k Putevoditel'yu ekskursiy, B.S. Sokolov and V.G. Garkovets (eds.); Polevaya sessiya Mezhdunarodnoy podkomissii po stratigrafii devona. Samarkand, SSSR 1978, Tashkent, p. 15-20.
- Fontaine, H.
1961: Les Madréporaires paléozoïques du Viêt-Nam, du Laos et du Cambodge; Archives Géologiques du Viêt-Nam, no. 5, 276 p. and atlas.
1966: Quelques Madréporaires dévoniens du Musée du Service Géologique de Saïgon (collections du Yunnan); Archives Géologiques du Viêt-Nam, no. 9, p. 51-95.
- Fortier, Y.O., Blackadar, R.G., Glenister, B.F., Greiner, H.R., McLaren, D.J., McMillan, N.J., Norris, A.W., Roots, E.F., Souther, J.G., Thorsteinsson, R., and Tozer, E.T.
1963: Geology of the north-central part of the Arctic Archipelago, Northwest Territories (Operation Franklin); Geological Survey of Canada, Memoir 320, 671 p. and accompanying box of maps, table, columnar sections and figures.
- Fuller, J.G.C.M. and Pollock, C.A.
1972: Early exposure of Middle Devonian reefs, southern Northwest Territories, Canada; International Geological Congress, 24th session, Montreal, section 6, p. 144-155.

- Haller, W.
1936: Einige biostratigraphische Untersuchungen in der Rohrer Mulde unter besonderer Berücksichtigung der Keriophyllen; Preussische geologische Landesanstalt zu Berlin, Jahrbuch für das Jahr 1935, Band 56, Heft 1, p. 590-632.
- Hill, D.
1956: Rugosa; in Treatise on invertebrate paleontology. Part F. Coelenterata, R.C. Moore (ed.); Geological Society of America and University of Kansas Press, Lawrence, p. 233-324.
1981: Treatise on invertebrate paleontology. Part F. Coelenterata. Supplement 1. Rugosa and Tabulata, C. Teichert (ed.); Geological Society of America and University of Kansas Press, Boulder and Lawrence, xl+762 p. (2v.).
- Ivaniya, V.A.
1965: Devonskie korally Rugosa Sayano-Altayskoy gornoy oblasti; Izdatel'stvo Tomskogo Universiteta, Tomsk, 398 p.
- Ivanovskiy, A.B.
1958: O Pseudocampophyllum - novom rode korallu Rugosa iz beyskoy svity Yuzhno-Minusinskoy vpadiny; Vsesoyuznyi Neftyanoy Nauchno-issledovatel'skiy Geologorazvedochniy Institut (VNIGRI), Trudy, vypusk 124, p. 341-346.
1976: Ukazatel' rodov rugoz; Akademiya Nauk SSSR, Sibirskoe Otdelenie, Institut Geologii i Geofiziki, Trudy, vypusk 217, 256 p.
- Jia Hui-zhen
1984: Evolutionary sequence in Grypophyllidae with description of two new genera; Acta Geologica Sinica, v. 58, p. 27-34 (Chinese with English abstract).
- Johnson, J.G. and Perry, D.G.
1976: Middle Devonian brachiopods from the Bird Fiord Formation of Bathurst Island, Arctic Canada; Canadian Journal of Earth Sciences, v. 13, p. 615-635.
- Kerr, J.W.
1974: Geology of Bathurst Island Group and Byam Martin Island, Arctic Canada (Operation Bathurst Island); Geological Survey of Canada, Memoir 378, 152 p.
- Lewis, C.T. and Short, C.
1966: A Latin dictionary founded on Andrew's edition of Freund's Latin dictionary; Clarendon Press, Oxford, 2019 p.
- McGregor, D.C. and Uyeno, T.T.
1972: Devonian spores and conodonts of Melville and Bathurst Islands, District of Franklin; Geological Survey of Canada, Paper 71-13, 37 p.
- McLaren, D.J. and Norris, A.W.
1964: Fauna of the Devonian Horn Plateau Formation, District of Mackenzie; Geological Survey of Canada, Bulletin 114, 74 p.
- Ormiston, A.R.
1967: Lower and Middle Devonian trilobites of the Canadian Arctic Islands; Geological Survey of Canada, Bulletin 153, 148 p.
- Pedder, A.E.H.
1965: A revision of the Australian Devonian corals previously referred to Mictophyllum; The Royal Society of Victoria, Proceedings, v. 78, p. 201-220.
- Pedder, A.E.H. (cont.)
1971: Lower Devonian corals and bryozoa from the Lick Hole Formation of New South Wales; Palaeontology, v. 14, p. 371-386.
1983: New Dalejan (Early Devonian) rugose corals from the Blue Fiord Formation of southwestern Ellesmere Island, Northwest Territories; Geological Survey of Canada, Paper 83-1B, p. 223-236.
- Pedder, A.E.H. and Goodbody, Q.H.
1983: New Devonian rugose corals of probable late Dalejan age from the Bird Fiord Formation of southwestern Ellesmere Island, Northwest Territories; Geological Survey of Canada, Paper 83-1B, p. 335-352.
- Pedder, A.E.H., Jackson, J.H. and Philip, G.M.
1970: Lower Devonian biostratigraphy in the Wee Jasper region of New South Wales; Journal of Paleontology, v. 44, p. 206-251.
- Rzhonsnitskaya, M.A., Meleshchenko, V.S., Belyakov, N.A., Dubatolov, V.N., Bul'vank, E.Z., Nalivkin, B.V., Balashev, Z.G., and Maksimova, Z.A.
1952: Materialy k izucheniyu fauny Tashtypskoy svity Minusinskoy kotloviny; Paleontologiya i stratigrafiya, sbornik statey, Vsesoyuznyy Nauchno-issledovatel'skiy Geologicheskii Institut (VSEGEI), Trudy, p. 120-189.
- Soshkina, E.D.
1941: Sistematika srednedevonskikh Rugosa Urala; Akademiya Nauk SSSR, Paleontologicheskii Institut, Trudy, tom 10, vypusk 4, 54 p.
- Soshkina, E.D. and Dobrolyubova, T.A.
1962: Otryad Evenkiellida Soshkina, ord. nov.; in Osnovy paleologii, tom 2. Gubki, arkheotsiaty, kishchnopolostnye, chervi, B.S. Sokolov (ed.); Izdatel'stvo Akademii Nauk SSSR, Moskva, p. 333-339.
- Spasskiy, N. Ya.
1960: Devonskie chetyrekhluchevye korally Yuzhnogo Altaya i prilgayushchikh territoriy; Gornyy Institut Leningradskogo ordenov Lenina i Trudovogo Krasnogo Znameni, Zapiski, tom 37, vypusk 2, p. 108-131.
1977: Devonskie rugozy SSSR (sistematika, stratigraficheskoe i geograficheskoe znachenie); Izdatel'stvo Leningradskogo Universiteta, Leningrad, 344 p.
- Spasskiy, N. Ya., Kravtsov, A.G., and Tsyganko, V.S.
1975: Kolonial'nye tsistimorfy; in Drevnie Cnidaria, Tom 1, B.S. Sokolov (ed); Akademiya Nauk SSSR, Sibirskoe Otdelenie, Institut Geologii i Geofiziki, Trudy, vypusk 201, p. 170-172 (imprint 1974).
- Udodov, V.P.
1967: K voprosu ob eyfel'skikh otlozheniyakh Uymenskogo Sinklinoriya; in Nekotorye voprosy geologii zapadnoy Sibiri, V.A. Khakhlov (ed.); Tomskiy ordena trudovogo krasnogo znameni Gosudarstvennyy Univeristet imeni V.V. Kyubysheva, Uchenye Zapiski, no. 63, p. 141-147.
- Ulitina, L. M.
1980: Nekotorye zakonomernosti kolonial'nogo razvitiya rugoz; Paleontologicheskii Zhurnal, 1980, no. 2, p. 32-43.
1982: Astogeny in some colonial Rugosa; Acta Palaeontologica Polonica, v. 27, p. 137-146.

Vopni, L. K. and Lerbekmo, J.F.

1972: The Horn Plateau Formation: a Middle Devonian coral reef, Northwest Territories, Canada; Bulletin of Canadian Petroleum Geology, v. 20, p. 498-548.

Wrzolek, T.

1982: Rugose coral *Cyathophyllum diffusum* sp. n. from the Frasnian deposits of the Holy Cross Mts.; Acta Geologica Polonica, v. 31, p. 169-175 (imprint 1981).

Yu Chang-min and Cai Zheng-quan

1983: Early Middle Devonian rugose corals from the Lure Formation of Diebu in Gansu Province; Institute of Geology, Geological Bureau of Gansu Province, Bulletin, v. 1, p. 1-78 (Chinese with English Summary).

A new late Eifelian rhynchonellid genus from western North America

Project 700034

Paul Sartenaer¹
Institute of Sedimentary and Petroleum Geology, Calgary

Sartenaer, P., A new late Eifelian rhynchonellid genus from western North America; in Current Research, Part B, Geological Survey of Canada, Paper 86-1B, p. 489-491, 1986.

Abstract

A new genus **Properotundirostrum**, with type species **P. miriam** (Johnson, 1971), is described from the late Eifelian of central Nevada. It will be compared with the genus **Leiorhynchus** Hall, 1860, which will be re-examined in a forthcoming paper, by A.W. Norris, T.T. Uyeno and P. Sartenaer, on the brachiopods and conodonts of the middle Givetian Bituminous limestone member of the Pine Point Formation, on the south side of the Great Slave Lake, District of Mackenzie.

Résumé

Un nouveau genre **Properotundirostrum**, avec **P. miriam** (Johnson, 1971) comme espèce-type, est décrit dans la partie supérieure de l'Eifélien du Nevada central. Il sera comparé au genre **Leiorhynchus** Hall, 1860, qui fera l'objet d'un nouvel examen dans un travail rédigé par M.M. A.W. Norris, T.T. Uyeno et P. Sartenaer; cette publication, à paraître sous peu, est consacrée aux brachiopodes et aux conodontes du membre calcaire bitumineux (Givétien moyen) de la formation de Pine Point sur la rive sud du Grand lac des Esclaves dans le District du Mackenzie.

¹ Royal Institute of Natural Sciences of Belgium, Brussels

Systematic paleontology

Properotundirostrum n. gen.

Derivatio nominis. **Prope** (Latin, adverb) = about; **rotundus, a, um** (Latin) = circular; **rostrum, i** (Latin, neuter) = beak. The name alludes to the subcircular contour of the shell as seen in ventral and dorsal views.

Type species. ***Leiorhynchus miriam*** Johnson, 1971. The species is illustrated in the original publication by numerous photographs, some of which show the internal characters. All specimens are silicified. No attempt is made to discuss the distinction between ***L. miriam miriam*** Johnson, 1971 and ***L. miriam alpha*** Johnson, 1971.

Description. Small to medium sized. Subcircular to subpentagonal in ventral and dorsal views, generally subelliptical in frontal view. Uniplicate. Inequivalve, the thickness of the pedicle valve varying from 25 to 43 per cent of the thickness of the shell. Cardinal line is short and undulating. Posterolateral margins concave near the commissure. Commissure sharp and undulated by the costae. Commissures are located high as seen in lateral profile.

Contour of pedicle valve is low, semi-elliptical in longitudinal and transverse median sections; the semi-ellipse is barely depressed by the sulcus in transverse median sections. The convexity of the valve is thus relatively uniform, although flanks slope more steeply toward the posterolateral commissures. Sulcus is only clearly differentiated from the flanks anteriorly, beginning imperceptibly at a variable but relatively long distance from the beak (35-45 per cent of the length of the shell or 28-43 per cent of the unrolled length of the valve). Sulcus is shallow (one to three times the height of the low costae where it passes to the tongue); bottom of sulcus is generally convex, sometimes flat; width of sulcus at point of origin varies from 30 to 45 per cent of its greatest width (54-70 per cent of the width of the shell) at the junction of the frontal and lateral commissures; thus, it widens gradually. Tongue trapezoidal, moderately high with sharp borders, standing out clearly. Beak wide, thick-set, erect, with a small subcircular foramen. Ventral interarea short, low and ill-defined, but on each side of the beak there is a high, crescent-shaped area separated from the rest of the valve by distinct ridges; these beak ridges fade out laterally.

Brachial valve moderately to strongly convex, sometimes rotund, never grossly inflated, with umbonal region tangential to a vertical plane, only exceptionally extending beyond the pedicle beak. Fold is low, clearly differentiated from the flanks only in its median and anterior parts, begins more or less imperceptibly at a variable distance from the beak. Top of the fold is flat to slightly convex.

Highest part of pedicle valve is located approximately where the sulcus starts or slightly posterior to it. Greatest thickness of brachial valve is located at a point between 35 and 66 per cent of the length of the shell posterior to the frontal commissure; from this point the valve curves gently toward this commissure, and thus, the highest part of the tongue is never the highest part of the shell, but is situated at a point between 12 and 30 per cent of the thickness of the shell below its top. Although width is the largest dimension, width and length have very close values. Maximum width of shell occurs at a point between 52 and 62 per cent of the length of the shell anterior to the ventral beak. Apical angle varies from 100° to 115° (most values are between 105° and 110°).

Umbonal regions smooth. Costae are rounded, regular and low. Median costae are generally simple (rarely a division can be observed), starting at a variable and relatively great distance from the beaks. Width of median costae at the front usually vary between 1.5 and 2.5 mm. Lateral costae simple. Internal lateral costa may start around mid-length; other lateral costae decrease rapidly in length, the most lateral one(s) is (are) often evident only as mere undulation(s) of the commissure. Number of costae few: three to four on the fold, two to three in the sulcus, and up to six on the flanks. No parietal costae. No radial costellae.

Shell is generally thin with occasional secondary thickening of the internal structures. Dental plates are thin, concave anteriorly, very short, strongly convergent, delimiting wide umbonal cavities. Teeth are small, short and stout. Pedicle muscle field is very faintly impressed and flabellate and extends to about mid-length. Hinge plate is thin, short and divided. Septum is thin, short and supports a relatively deep and wide septalium. Dental sockets are narrow. Muscle field of brachial valve is vaguely delimited and extends to about mid-length; the adductor scars form a narrow, spindle-shaped impression.

Diagnostic characters. Small to medium sized. Subcircular to subpentagonal. Shallow sulcus and low fold beginning at a variable distance from the beaks. Moderately high, trapezoidal and clearly conspicuous tongue. Short, low and ill-defined ventral interarea. High crescent-shaped area on each side of the beak, bordered by ridges fading out laterally. Highest part of the tongue is never the highest part of the shell. Width and length similar. Apical angle wide. Few long, rounded and regular costae starting some distance from the beaks. Median costae rarely divided. Lateral costae simple. Thin, very short and strongly convergent dental plates. Wide ventral umbonal cavities. Divided hinge plate. Thin and short septum. Relatively deep and wide septalium.

Comparisons. Some of the features that ***Properotundirostrum*** n. gen. has in common with ***Leiorhynchus*** Hall, 1860 to which the type species was originally attributed, are: size, sharp commissure; shallow sulcus, wide at front; tongue never recurved posteriorly; top of tongue corresponding to the most anterior part of the shell at the frontal margin; low fold; the greatest thickness of brachial valve located posterior to the frontal commissure; the similar number of median costae; the short dental plates; and the well developed umbonal cavities. However, the genus ***Leiorhynchus*** is easily distinguishable by its inflated and globulose aspect; the dorsal umbonal region commonly extending a little more posteriorly than the ventral; the higher tongue, the sulcus and fold starting farther away from the beaks; the high brachial valve; the still lower costae; the frequent divisions of the median costae; the lateral costae not always clearly present; the presence of a crural trough and not of a septalium; and the septum thickened lens-like posteriorly.

McLaren (1962, p. 12, p. 91) suggested that ***Leiorhynchus*** sp. a, cited and figured by Merriam (1940, Table 6, p. 56, Pl. 8, figs. 18, 19), could be ***L. awokanak*** McLaren, 1962 ("probably a small variant of ***L. awokanak***"). Johnson (1971, p. 315, 316) assigned this form, from the "upper part of ***Martinia kirki*** Zone" in the Lone Mountain section in central Nevada, to ***L. miriam***, and pointed out some differences between ***L. awokanak*** and ***L. miriam***, the type species of the middle Givetian genus ***Stenoglossariorhynchus*** Sartenaer, 1970, and ***Properotundirostrum*** n. gen., respectively. These two genera have some similar external features. They both are uniplicate, inequivalve, depressed and thick-set, and they

both have a sharp commissure, weakly developed sulcus and fold starting at a great distance from the beaks, a shallow and narrow sulcus, a low and narrow fold, and median costae starting at a variable but great distance from the beaks. But *Properotundirostrum* n. gen. differs in its internal structures, notably its septalium, as well as in various external characters: a smaller size; a transversely subcircular to subpentagonal contour in ventral and dorsal views; an always clearly undulated frontal commissure; a higher tongue; an erect beak; the presence of clearly defined ventral beak ridges; costae fewer in number and always clearly discernible; rare divisions of median costae; lateral costae not restricted to the margins of the flanks, and a smaller apical angle.

Species attributed to the genus. At present only the type species is attributed to the new genus.

Stratigraphic position and geographic distribution. When Johnson (1971, p. 301, 304-306, 315-317; Pl. 40, figs. 16-30; Pl. 43, figs. 1-26; Tables 1, 2) introduced *Leiorhynchus miriam* from the central Nevada sequence, he distinguished a lower and an upper brachiopod fauna in Merriam's (1940) *Martinia kirki* Zone (= *Warrenella kirki* Zone). He assigned an early Givetian age to this zone although Poole et al. (1967, Fig. 2a, p. 882; Fig. 2b, p. 884; Fig. 2c, p. 886) considered it as equivalent to the upper part of the Eifelian. Johnson (1971, p. 303, 304, 316, 317, 324) recognized *Leiorhynchus miriam alpha* in the upper brachiopod fauna at one locality (loc. FF-24 = UCR loc. 4554 = USNM loc. 17213, between 1530 and 1535 ft (466 and 468 m) above the top of the the Nevada Group) at Lone Mountain; this is the locality where Merriam (1940, Table 6, p. 56, Pl. 8, figs. 18, 19) had found *L. sp. a*, which was later placed in synonymy with *L. miriam*. Johnson (1971, p. 317) also mentioned two specimens from the Woodpecker Limestone in the Sulphur Spring Range, which are "very similar to *L. miriam alpha* but also similar to *L. nevadensis*", occurring "with *L. castanea*". The *L. castanea* Zone was considered by this author at that time as of middle Givetian age. *L. miriam miriam* was reported by Johnson (1971, p. 303-305, 316, 324, Table 1) from the lower brachiopod fauna at two localities in the Lone Mountain area (EF-24 = UCR loc. 4519, and FF-23 = UCR loc. 4553 = USNM loc. 17212, respectively, between 1302 and 1307 ft (397 and 398 m), and between 1330 and 1360 ft (405 and 415 m) above the top of the Nevada Group); and from one locality in the southern Roberts Mountains area (loc. W-28-59 = USNM loc. 10807 present in the Denay Limestone, from which all the figured specimens were derived). Johnson (1971, p. 306, 316, Table 2) also named *L. cf. L. miriam miriam*, a form from the Eifelian *Leptathyris circula* Zone, which he (Johnson, 1966, p. 155, 166, 167, Pl. 24, figs. 8-23) had identified earlier as *L. sp.* from localities in the northern Roberts Mountains and northern Simpson Park Range.

Johnson (in Johnson and Oliver, 1977, Table, p. 1463; Johnson, 1977a, fig. 2, p. 8; and 1977b, p. 24, Table 4, p. 26; in Johnson and Sandberg, 1977, Fig. 2, p. 124-125) introduced faunal Interval 17 as corresponding to the *Warrenella kirki* Zone and revised the early Givetian age to late Couvian ("perhaps all of Interval 17 is in the range of the *kockelianus* Zone"), the upper limit of the Couvian being placed in the middle of Interval 18.

After revision of various intervals, the *W. kirki* Zone was further restricted by Johnson, Klapper and Trojan (1980, p. 79, Fig. 3, p. 80, 81, Fig. 5, p. 84, 85, Table 2, p. 91) to the

upper half of Interval 17, i.e. in the middle part of the *Tortodus kockelianus* Zone; the upper limit of the Eifelian being placed in the middle of Interval 19, i.e., in the middle of the *Polygnathus xylus ensensis* Zone. The distinction of a lower and an upper brachiopod fauna in the *Warrenella kirki* Zone was also abandoned: "Present knowledge does not sustain zonal significance of the two faunas of the *kirki* Zone' together, or either fauna alone".

In short, the genus *Properotundirostrum* is present with certainty in the lower part of the upper Eifelian, or, more precisely, in the middle part of the *Tortodus kockelianus* Zone.

References

- Johnson, J.G.
 1966: Middle Devonian brachiopods from the Roberts Mountains, central Nevada; *Palaeontology*, v. 9, pt. 1, p. 152-181.
 1971: Lower Givetian brachiopods from central Nevada; *Journal of Paleontology*, v. 45, no. 2, p. 301-326.
 1977a: Status of Devonian studies in western and Arctic North America; in *Western North America: Devonian*, ed. M.A. Murphy, W.B.N. Berry, and C.A. Sandberg; University of California, Riverside Campus Museum Contribution 4, p. 1-15.
 1977b: Lower and Middle Devonian faunal intervals in central Nevada based on brachiopods; in *Western North America: Devonian*, ed. M.A. Murphy, W.B.N. Berry, and C.A. Sandberg; University of California, Riverside Campus Museum Contribution 4, p. 16-32.
- Johnson, J.G., Klapper, G., and Trojan, W.R.
 1980: Brachiopod and conodont successions in the Devonian of the northern Antelope Range, central Nevada; *Geologica et Palaeontologica*, v. 14, p. 77-115.
- Johnson, J.G. and Oliver, W.A., Jr.
 1977: Silurian and Devonian coral zones in the Great Basin, Nevada and California; *Geological Society of America, Bulletin*, v. 88, p. 1462-1468.
- Johnson, J.G. and Sandberg, C.A.
 1977: Lower and Middle Devonian continental-shelf rocks of the western United States; in *Western North America: Devonian*, ed. M.A. Murphy, W.B.N. Berry, and C.A. Sandberg; University of California, Riverside Campus Museum Contribution 4, p. 121-143.
- McLaren, D.J.
 1962: Middle and early Upper Devonian rhynchonelloid brachiopods from western Canada; *Geological Survey of Canada, Bulletin* 86.
- Merriam, C.W.
 1940: Devonian stratigraphy and paleontology of the Roberts Mountains region, Nevada; *Geological Society of America, Special Paper* no. 25.
- Poole, F.G., Baars, D.L., Drewes, H., Hayes, P.T., Ketner, K.B., McKee, E.D., Teichert, C., and Williams, J.S.
 1967: Devonian of the southwestern United States; in *International Symposium on the Devonian System*, Calgary, 1967, v. 1, ed. D.H. Oswald; *Alberta Society of Petroleum Geologists*, p. 879-912.

Lithostratigraphy and a summary of the paleoenvironments of the lower Middle Ordovician sedimentary rocks, upper Ottawa Valley, Ontario

Project 05B80-00166

H. Miriam Steele-Petrovich¹
Institute of Sedimentary and Petroleum Geology, Calgary

Steele-Petrovich, H.M., Lithostratigraphy and a summary of the paleoenvironments of the lower Middle Ordovician sedimentary rocks, upper Ottawa Valley, Ontario; in *Current Research, Part B, Geological Survey of Canada, Paper 86-1B*, p. 493-506, 1986.

Abstract

In the upper Ottawa Valley the Middle Ordovician carbonate and terrigenous rocks traditionally assigned to the Pamela, Lowville, Chaumont and Rockland formations, comprise the following ten lithofacies, recorded here in descending order stratigraphically.

10. Bioturbated bioclastic oncolitic wackestone. 9. Coarse grained bioclastic intraclastic packstone. 8. Lime siltstone. 7. Shaly lime mudstone to shaly intraclastic packstone. 6. Sublithographic mudstone. 5. Ooidal peloidal limestone. 4. Skeletal packstone. 3. Lime mudstone to fossiliferous wackestone. 2. Algal/dolomitic carbonate. 1. Terrigenous lithofacies.

These rocks are best subdivided into the following six lithostratigraphic units, which do not correspond completely to the traditional formations: A (lithofacies 1), B (lithofacies 2), C (lithofacies 3, 4, 5), D (lithofacies 6, 7), E (lithofacies 8, 9), and F (lithofacies 10).

The carbonate rocks of this study were deposited on a relatively-shallow lime-mud bank and in its quiet inner lagoon within a tropical transgressive sea; the terrigenous rocks were deposited on intertidal flats.

Résumé

Les roches carbonatées de l'Ordovicien moyen provenant de la partie supérieure de la vallée de l'Outaouais et traditionnellement attribuées aux formations de Pamélie, de Lowville, de Chaumont et de Rockland comprennent dix lithofaciés. Il serait préférable de condenser ces roches en six unités lithostratigraphiques qui pourraient être soit des formations, soit des membres: A (lithofaciés 1), B (lithofaciés 2), C (lithofaciés 3, 4, 5), D (lithofaciés 6, 7), E (lithofaciés 8, 9) et F (lithofaciés 10).

Ces unités lithostratigraphiques (A-F) ne correspondent pas aux formations traditionnelles, mais l'auteur recommande de conserver temporairement la nomenclature traditionnelle utilisée dans la région en attendant que toutes les roches de Black River et de Trenton de la vallée soient réévaluées.

Les roches carbonatées examinées se sont accumulées sur un banc relativement peu profond de boue calcaire et dans une lagune intérieure calme au sein d'une mer tropicale transgressive; les roches terrigènes se sont accumulées sur un vey, probablement avant la formation du banc carbonaté et de sa lagune.

¹ 1463 Valley Road, Bartlesville, Oklahoma, 74003, U.S.A.

Introduction

The Middle Ordovician sediments studied occur between Ottawa and Pembroke in the upper part of the Ottawa Valley (Fig. 53.1). The stratigraphic sequence that is considered here includes the units that have been traditionally called the Pamela, Lowville, Chaumont (or Leray) formations of the Black River Group and the Rockland Formation of the Trenton Group.

The reference section chosen is the only relatively complete stratigraphic section in the upper part of the Ottawa Valley, and is located at Braeside (Fig. 53.1). Different rock units were determined and measured, characteristics and relative stratigraphic positions were recorded, at least one lithological sample was collected from each rock unit, and as many of the contained fossils as possible were identified and collected. Each measured unit was distinguished by macroscopic features such as colour, texture, weathering pattern, physical and biogenic structures, size and composition of constituent particles, faunal composition, and lateral facies changes; a vertical change in any of these features signified a separate unit.

About 50 less-complete sections at other localities (Fig. 53.1) were studied in a similar way. The following terminology was used in the field:

Bed - delineated by bedding planes; with no limiting thickness (Reineck and Singh, 1975, p. 82)

Laminae - layers composing a bed (Reineck and Singh, 1975, p. 83)

Massive bedding - beds generally thicker than 50 cm (term of splitting property of rock)

Very thick bed - bed thicker than 50 cm (thickness term)

(I have followed McKee and Weir here (see Pettijohn, 1957, p. 159) and kept splitting property of the rock and bed thickness separate).

Grain size of terrigenous rocks - Wentworth Scale (see Pettijohn, 1957, p. 19)

Grain size of carbonates

very coarse grained - particles generally larger than 1 cm

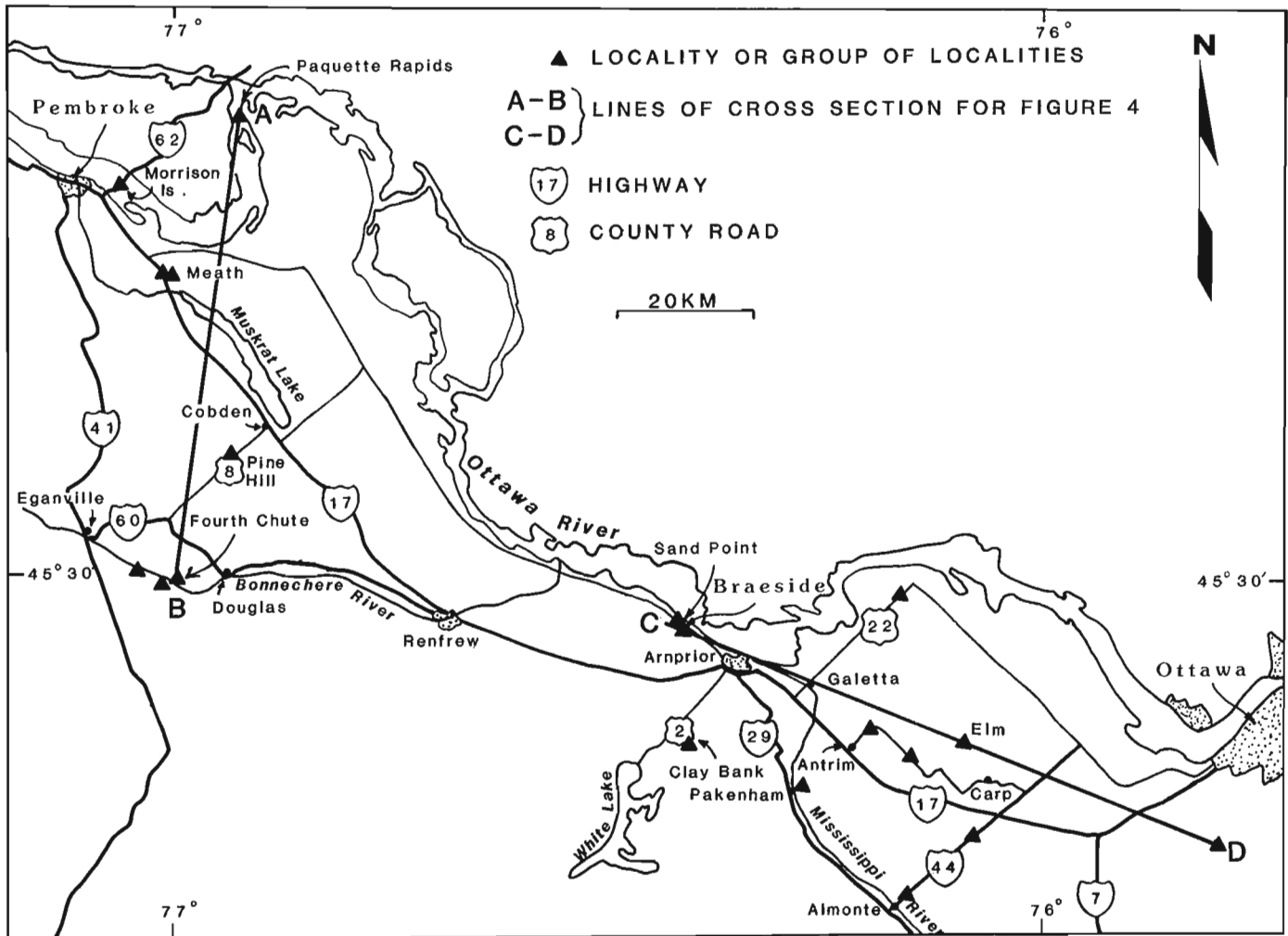


Figure 53.1. Locality map - upper Ottawa Valley.

coarse grained - particles identifiable to naked eye and generally smaller than 1 cm

medium grained - individual particles visible to naked eye but not identifiable

fine grained - individual grains visible with hand lens (10x) but not identifiable

very fine grained - individual grains not visible with hand lens

Stratigraphy

Lithofacies and their spatial relationships

The reference section at Braeside is a composite of 23 separate outcrops, occurring over a horizontal distance of 4 km, on the side of a hill 85 m high (Fig. 53.2). Elevations at the different localities were determined using a level and stadia rod. An almost-complete composite section composed of ten different lithofacies was pieced together (Fig. 53.3). The characteristics of the ten lithofacies, numbered in ascending order stratigraphically, are summarized in Table 53.1.

The field localities of this study are isolated outliers on the Precambrian Shield that are, in general, relatively widely separated along two traverses (AB and CD of Fig. 53.1). Composite stratigraphic sections as projected onto AB and CD are plotted in Figures 53.4A and 53.4B.

Lithostratigraphic subdivisions

Individual lithofacies can rarely be correlated from one locality to another, as interbedding is common between certain lithofacies, and some horizontal intergrading also occurs (Table 53.2). However, groups of interbedded lithofacies form fairly well delineated entities that can be correlated. On the basis of these lithological groups, the Ordovician of the upper Ottawa Valley can be divided into 6 lithostratigraphic units, A-F, defined on the basis of their dominant lithofacies (Table 53.3); these units would have formation (or possibly member) status. When considered in detail, the distribution of lithofacies within the different lithostratigraphic units is not as precise as shown in Table 53.3, as some interbedding occurs across the lithostratigraphic boundaries (Fig. 53.4, Table 53.4). Because of this interbedding, a lithostratigraphic unit cannot necessarily be correctly determined in the field if only a thin stratigraphic interval is present; however, a stratigraphic section one to two metres thick should be adequate in most cases for determining the stratigraphic horizon.

In Figure 53.4, the top of the interbedded group of lithofacies 3, 4 and 5 was arbitrarily chosen as the base line or datum; most of those measured sections that do not include the datum are tied into the correlation along a secondary datum between groups of lithofacies 8 and 9, and 9 and 10; the few remaining sections are fitted into Figure 53.4 where they are best suited lithologically.

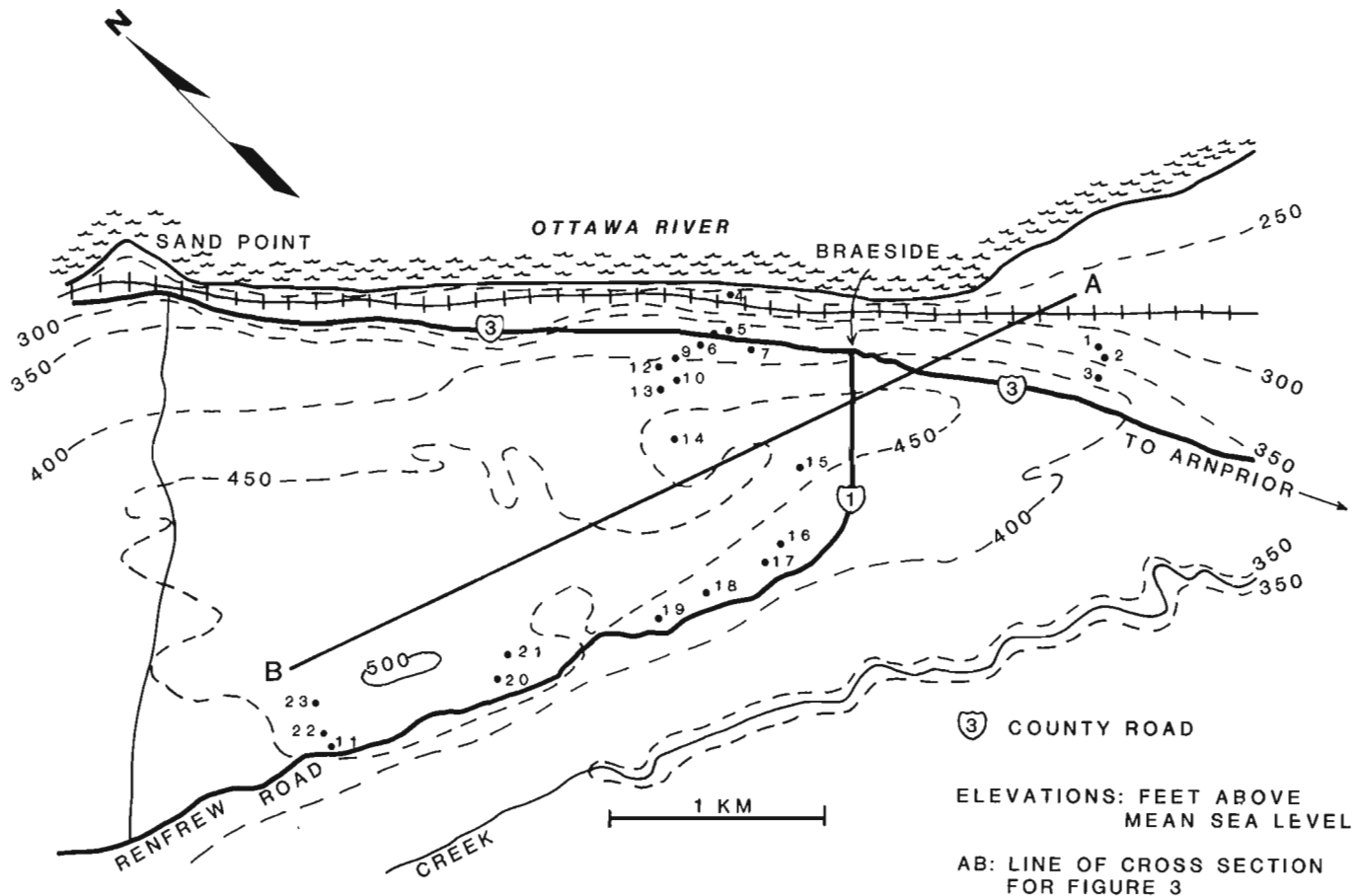


Figure 53.2. Topographic map showing localities of sections making up composite reference section Braeside, Ontario.

Table 53.1. Summary of characteristics of lithofacies as determined in the field

Lithofacies	Composition and texture	Colour	Physical structures	Biological structures	Fossils
1a	<u>Coarse grained quartz arenite</u> Sand grains well sorted, well rounded	White to slightly greenish	Beds few mm to 1 m thick, un laminated, horizontally laminated, or crossbedded; reactivation surfaces rare; upper and lower boundaries sharp	-	-
1b	<u>Very fine grained quartz arenite/siltstone</u> Small quantities of disseminated clay minerals throughout	Very light pink and green	Beds usually 0.5-5 cm thick, un laminated, horizontally laminated, or crossbedded; small-scale ripples common; upper and lower boundaries sharp	-	-
1c	<u>Very fine grained quartz arenite/siltstone and shale</u> Arenite/siltstone as in Lithofacies 1b	Shale red or green, rarely black	Commonly occurs as wavy, flaser, lenticular bedding; cross-laminated sandstone rare; mudcracks common	Horizontal burrows present, diameter 1-3 mm; no vertical burrows; large areas with no burrows	-
1d	<u>Silty shale and shaly siltstone</u> Crumbly when weathered; patches of sand-size quartz grains throughout	Dark green, rusty on weathered surfaces	Beds usually 2-5 cm thick; local patches of lenticular and flaser bedding; mudcracks rare	Abundant horizontal and oblique burrows throughout, diameter 2-3 mm; vertical burrows rare	Lingulids locally abundant
2a	<u>Algal limestone and dolomite</u>				
i	Very fine grained, very homogeneous limestone with conchoidal fracture; dolomite rare	Medium grey, weathers darker grey to light brown	Beds up to 40 cm thick; flat or undulating algal laminae common; mudcracks present, not common	-	Ostracods
ii	Coarsely crystalline; abundant intraclasts and fossil fragments	Dark brown-grey, weathers brown	Beds 1-5 cm thick, weather into chunks locally; sharp boundaries	-	Abundant ostracods
2b	<u>Limestone/dolomite and dolomite</u> Fine to medium grained; commonly crystalline; commonly with sugary appearance	Sooty blue-grey to yellow-green; weathers buff	Beds up to 25 cm thick; mudcracks present locally	Poorly defined horizontal burrows uncommon; vertical burrows rare	Ostracods locally abundant; few molluscs locally common
3	<u>Lime mudstone to fossiliferous wackestone</u> Scattered fossil fragments rare to common in very fine grained lime-mud matrix; inclusions of red and green rounded terrigenous mudstone clasts (approx. 5 cm across) rare to common; fossils and fossil fragments locally replaced by spar; small local patches of fossil debris throughout but not common	Very light to very dark grey; weathers dark grey	Beds 5-15 cm thick; mudcracks rare, ripple marks rare	Bioturbation absent to common	Rare to abundant; diversity low; some in living position

Table 53.1 (cont.)

Lithofacies	Composition and texture	Colour	Physical structures	Biological structures	Fossils
4	<u>Skeletal packstone</u> Coarse grained bioclastic limestone of broken, densely-packed shell fragments in very fine grained limestone matrix; fossils typically replaced by calcite spar; large clasts and thin interbeds of red and green terrigenous mudstone; weathers rubbly	Unweathered matrix medium grey; weathers tan to reddish brown	Bedding poorly defined; beds less than 8 cm thick	-	Disarticulated bivalve shells present
5	<u>Ooidal peloidal limestone</u> Medium to coarse grained, containing scattered to densely packed ooids and peloids; matrix usually fine grained lime mud, rarely spar	brown-grey; weathers buff to grey with rare reddish patches	Beds approx. 2 cm thick to very thick; beds flat lying, cross-laminae very rare; ripples rare	-	Absent to locally abundant; diversity low
6	<u>Sublithographic mudstone</u> Very homogeneous, hard, dense ultra fine grained limestone; breaks with conchoidal fracture	Very light grey, commonly with reddish hue; weathers almost white	Beds commonly very thick; bedding planes smooth, irregularly bumpy, and/or irregularly cracked	Commonly unburrowed; rarely highly burrowed horizontally and vertically so weathers into irregular nodules	Tetradium rare to locally abundant
7	<u>Shaly lime mudstone to shaly fossiliferous wackestone</u> Fossiliferous, shaly limestone with very fine grained matrix; shale content varies	Brown-grey to blue-grey; weathers buff to yellow, rarely bluish	Bedding varies from very thick to flaky, depending on clay content	Horizontal trails of various sizes common on shaly bedding planes	Rare to abundant and very diverse
8	<u>Lime siltstone</u> Fine grained limestone; somewhat scaly on broken surface; ultra-thin, black, platy, organic material common on bedding planes; chert nodules common locally; incipient concretions rare	Brown-grey, weathers grey	Beds 2-15 cm thick; flat laminae common, crosslaminae rare; bedding planes flat or irregularly bumpy, rarely shaly; ripple marks rare; associated hardgrounds and concretions	Burrows absent or vertical and horizontal burrows in range of densities locally; burrows weather into pits on vertical and horizontal surfaces; large, horizontal trails on shaly bedding planes; associated stromatoporoid biostrome, and elongated mounds and depressions	Typically absent except abundant on some shaly bedding planes; low diversity
9	<u>Coarse grained bioclastic intraclastic packstone</u> Coarse to very coarse grained limestone of densely packed, large fossil fragments and to lesser extent, of intraclasts of Lithofacies 8 in finer grained matrix; chert rare; strong petroleum odour from some samples	Usually brown-grey, commonly with reddish hue; weathers light grey to buff	Beds 2-5 cm thick; lower contact generally sharp; upper contact sharp or gradational; dissolution horizons common; crossbeds and cross-laminae common; ripple marks rare.	Associated coral/stromatoporoid/bryozoan biostrome	Common; diversity relatively low
10	<u>Bioturbated bioclastic oncolitic wackestone</u> Matrix fine grained to very fine grained; fossil fragments common; oncolites and rhodolites common to locally abundant, rarely absent	Brown-grey; weathers light grey to buff; may be overgrown by dark grey to black or reddish lichen	Bedding massive; incipient bedding planes occur on weathered faces	Typically bioturbated; well defined vertical and horizontal burrows common	Rare to locally abundant and diverse

Raymond (1912, 1913, 1914) originally subdivided the Black River rocks of the Ottawa region, and applied to them the established formation names for somewhat similar rocks of the same age from New York State (i.e. Pamela, Lowville, Leray formations). Raymond also subdivided the Trenton Group in the Ottawa Valley, but as there were no established formation names for Trenton rocks in New York State, he named several of these higher units, including the Rockland Formation, after sections near Ottawa. Raymond's stratigraphic terms (Table 53.5) are still the most widely used in the Ottawa Valley, although "Chaumont" is substituted commonly for "Leray".

A great deal of confusion exists in the stratigraphic nomenclature of the Ottawa Valley. The Pamela, Lowville, Leray (Chaumont) and Rockland formations were all originally poorly defined and poorly delimited there, permitting a number of interpretations. This original lack of rigour has led to considerable variation in published descriptions of the formations (compare Raymond, 1912; Wilson, 1932, 1936; Kay, 1942; Barnes, 1967), and at times to considerable disagreement (e.g. Barnes, 1968; Kay, 1968; Sinclair, 1968). It has also resulted in the introduction of stratigraphic classifications that have not been widely accepted in the Ottawa Valley (Liberty, 1967; Kay, 1972), using terms that were originally defined for central and southwestern Ontario (e.g. Kay, 1937; Okulitch, 1939; Liberty, 1955, 1969). Although the Pamela, Lowville, Leray (Chaumont) and Rockland formations of the Ottawa Valley were originally defined on the basis of lithology (Raymond, 1912; Wilson, 1932, 1936; Barnes, 1967), their common treatment as biostratigraphic terms (Wilson, 1946; common local use) has increased the level of disagreement and confusion. Kay's (1960) change of the original formation names to the status of stage is also confusing (Fisher, 1962; Barnes, 1968; Walker, 1973), as is Wilson's (1946) suggestion that the Black River and Trenton be turned into time terms. The fact that "Rockland" is preoccupied by an Ordovician limestone in Maine (Fisher, 1962) is potentially difficult; however, as the name is well established in the Ottawa Valley, it need not necessarily be changed there, particularly if its use in Maine is neither well known nor common (North American Commission on Stratigraphic Nomenclature 1983, Article 7c).

The lack of a well defined stratigraphy in the Ottawa Valley makes placing of some of the ten lithofacies noted in this study into the Pamela, Lowville, Chaumont and

Rockland formations (as they are traditionally recognized in the Valley) exceedingly difficult. Specific problems encountered are:

1. Published descriptions of the formations typically note only the dominant rock characteristics (e.g. Raymond, 1912; Wilson, 1932, 1936; Kay, 1942).
2. A number of distinct lithofacies recognized in this study had not been recognized previously.
3. Formation boundaries commonly have not been defined.
4. The formations have been described previously in very general terms (e.g. Raymond, 1912; Wilson, 1932, 1936; Kay, 1942) or according to Twenhofel's terminology (Barnes, 1967). In contrast, lithological descriptions in this study are more detailed, and are based on Dunham's (1962) classification, which attaches considerably greater environmental significance to the lithotypes. As well, a single lithofacies of this study commonly fits previous descriptions of more than one formation.

Assignment of the present lithofacies to the traditionally acknowledged formations has had to be in part according to stratigraphic positions of these lithofacies with respect to formation boundaries as generally accepted in the field by previous workers. Using such criteria, the ten lithofacies of this study would be placed into the lithostratigraphic nomenclature of the Ottawa Valley as shown in Tables 53.3 and 53.6.

In discussing the appropriateness of using for the study area the traditional formation names (Pamela, Lowville, Chaumont and Rockland; tables 53.3, 53.6) one must consider whether the lithofacies, as recognized in this study, naturally fit into the traditionally accepted stratigraphical subdivisions; and, whether the rock types and lithological boundaries as recognized in the type areas are similar to those in this study.

Tables 53.3, 53.4 and 53.6 show that the lithostratigraphic subdivision suggested in this study does not correspond completely to the traditionally accepted lithostratigraphy. The main differences are in the groupings associated with lithofacies 6 (sublithographic mudstone) and 7 (shaly lime mudstone to shaly fossiliferous wackestone). Lithofacies 6 is traditionally assigned to the Lowville Formation and lithofacies 7 to the Chaumont Formation. However, in the study area, lithofacies 6 and 7 are considerably more intimately associated with each other than with other traditional Lowville or Chaumont rocks; thus, on the basis of this study, lithofacies 6 and 7 should be considered a separate formation (Tables 53.3, 53.6; Fig. 53.4). Also, in the study area, there are greater differences between lithofacies 1 (terrigenous rocks) and 2 (algal/dolomitic carbonates), both traditionally assigned to the Pamela Formation, than between the lithofacies of other accepted formations. Therefore, on the basis of this study, lithofacies 1 and 2 should be placed in different formations (Tables 53.3, 53.6; Fig. 53.4).

A comparison of the Black River lithofacies from the type area in New York State (Walker, 1973) with lithofacies 1 to 9 of the present study, (Table 53.1) shows that there are certain similarities between the Pamela and Lowville formations and, as originally noted by Kay (1937, 1939), great differences between the Chaumont formations of the two regions. Also, the rocks that have been assigned to the Rockland Formation in the present study area west of Ottawa appear to differ lithologically from those in the type area of the Rockland Formation, east of Ottawa (Barnes, 1967; personal observations).

Legend for Figure 53.3

Lithofacies (number and name)

- | | |
|----|-------------------------------------------------------|
| 10 | Bioturbated bioclastic oncolitic wackestone |
| 9 | Coarse grained bioclastic intraclastic packstone |
| 8 | Lime siltstone |
| 7 | Shaly lime mudstone to shaly fossiliferous wackestone |
| 6 | Sublithographic mudstone |
| 5 | Ooidal peloidal limestone |
| 4 | Skeletal packstone |
| 3 | Lime mudstone to fossiliferous wackestone |
| 2 | Algal/dolomitic carbonate |
| 1 | Terrigenous lithofacies |

(see Table 53.1 for summary of macroscopic characteristics of 10 lithofacies).

Figure 53.4. Distributions of the ten lithofacies in measured sections.

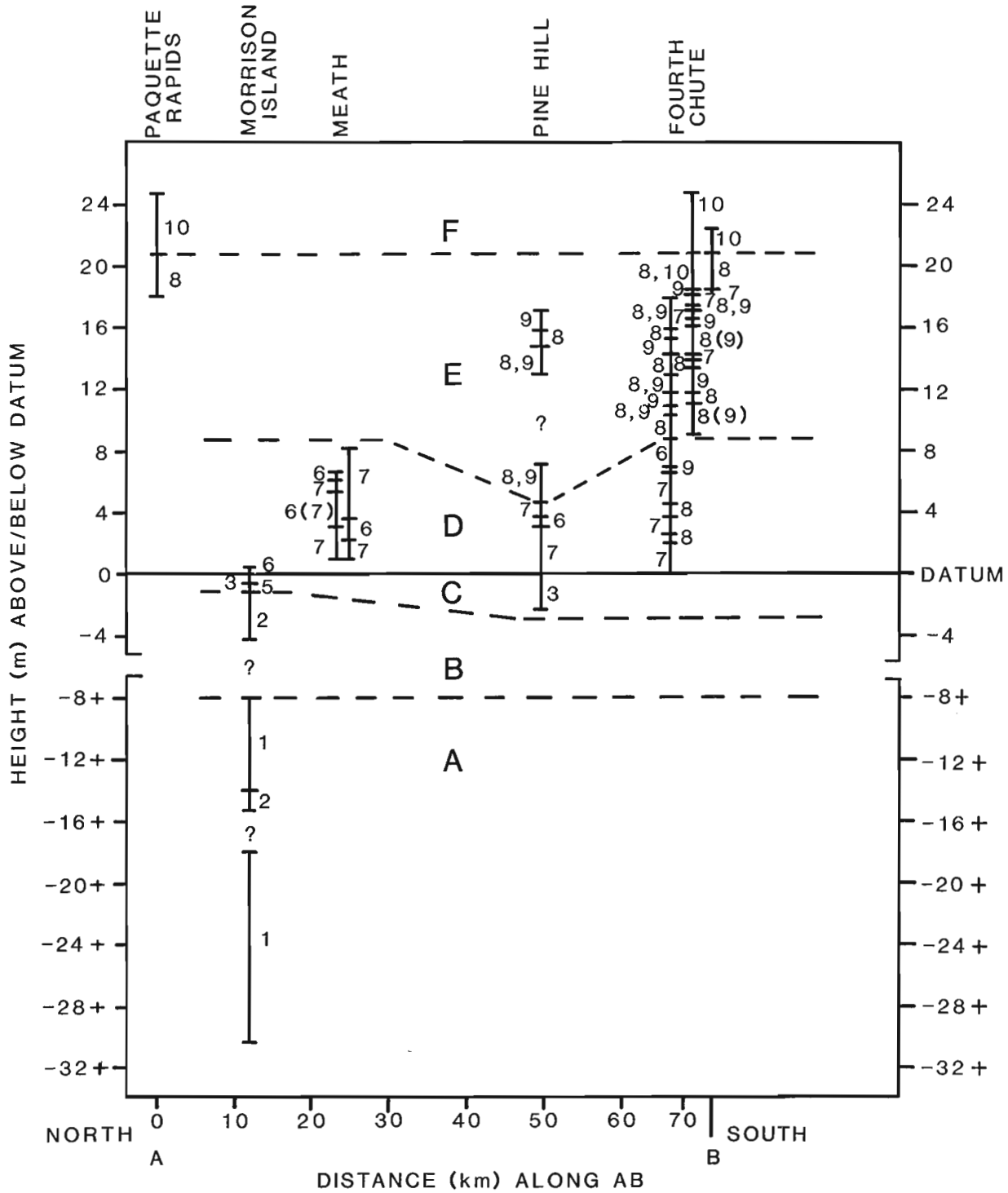


Figure 53.4A. Measured sections, western part of study area.

Legend for Figure 53.4

Lithofacies (number and name)	2	Algal/dolomitic carbonate
10	1	Terrigenous lithofacies
9	8,9	Interbedded lithofacies 8 and 9
8	8 (9)	Major component lithofacies 8, minor component 9
7	?	Covered interval of unknown thickness
6	A-F	Proposed lithostratigraphic subdivisions
5	AB, CD	Traverses shown in Figure 53.1
4		
3		
		(see Table 53.1 for summary of macroscopic characteristics of the ten lithofacies).

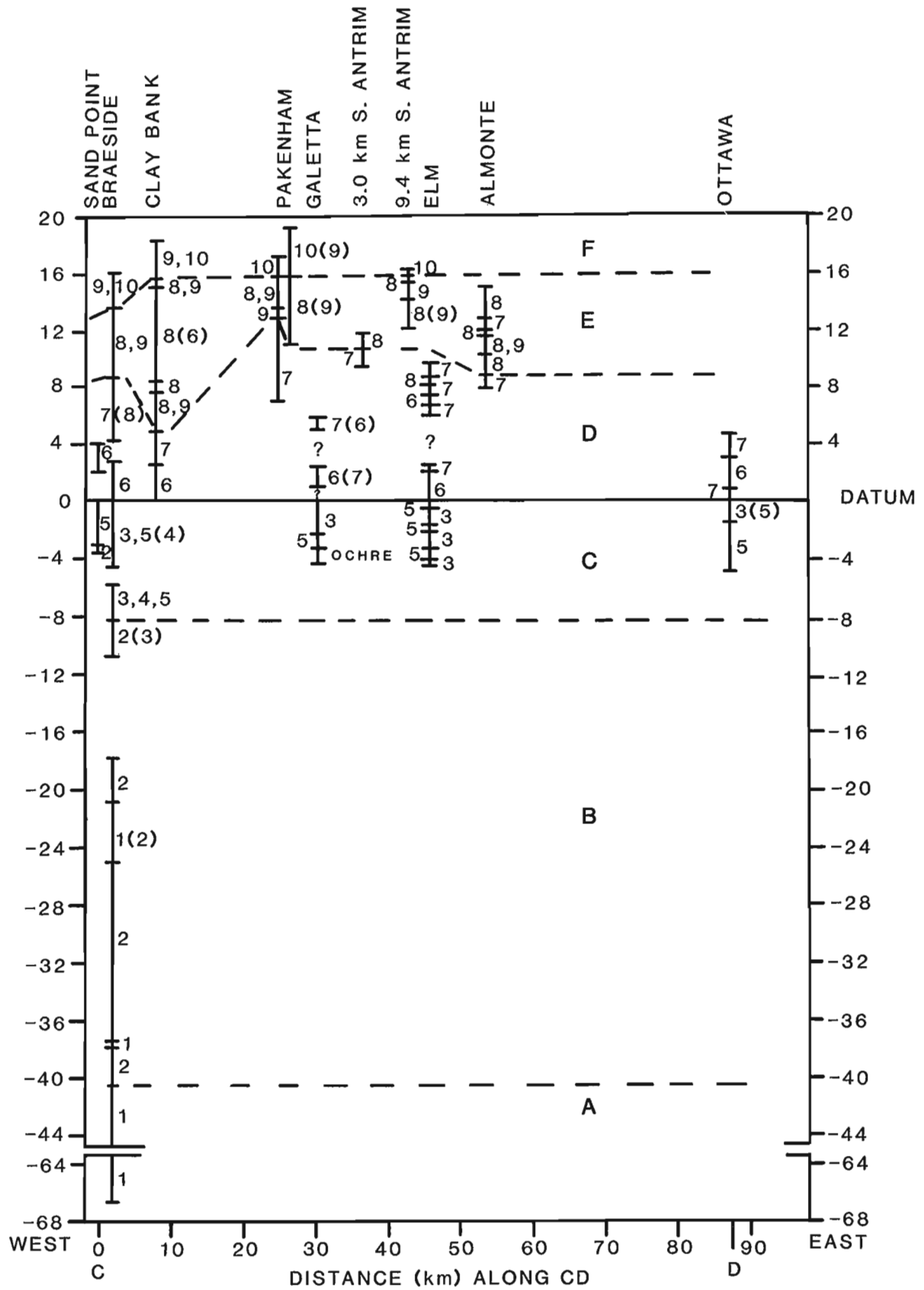


Figure 53.4B. Measured sections, eastern part of study area.

Table 53.2. Interbedding and horizontal intergrading characteristics of the different lithofacies

Lithofacies	Interbedding and intergrading characteristics
2	rarely interbedded with Lithofacies 1 rarely interbedded with Lithofacies 3, 4, 5
3, 4, 5	commonly interbedded on all scales; 3 and 4 generally dominate lower stratigraphically and 5 higher stratigraphically 3 very rarely interbedded with Lithofacies 2
6, 7	6 rarely interbedded with Lithofacies 3, 4, 5 at some localities 6 precedes 7 with little or no interbedding; at other localities 6 and 7 are interbedded to greater extent, with 6 dominating stratigraphically lower and 7 stratigraphically higher thin units of 6 interbedded rarely with Lithofacies 8 and 9 thin units of 7 interbedded very rarely with Lithofacies 8 and 9 rare units with lithological characteristics of both 6 and 7
8, 9	interbedded on all scales 8 rarely interbedded with Lithofacies 6 and 7 8 rarely interbedded with Lithofacies 10 9 usually laterally persistent for tens to hundreds of metres but may grade laterally into or end abruptly against 8
9, 10	interbedding not uncommon, particularly in lower stratigraphic part of 10

The extent of these differences in lithofacies and lithological boundaries between the study area and type localities suggests that the formation names that have been traditionally used in the western part of the Ottawa Valley are inappropriate there. Although there are similarities between the Pamela and Lowville formations of the two areas, these can reflect comparable environments of deposition close to shore in different epeiric seas of similar age.

I can find no evidence in the western part of the Ottawa Valley for a major change in lithology at the Black River/Trenton boundary, and therefore no support for the use of these terms in the study area. In fact, the corresponding Chaumont/Rockland boundary, as determined by Kay (1942) at different outcrops, is commonly very poorly delineated, and at some localities appears to have been arbitrarily chosen. Also, as Wilson (1921, 1937, 1946) noted, there is no evidence in the study area of a hiatus between the Black River and Trenton rocks.

The present study has not been extensive enough stratigraphically to determine the appropriateness of the "Ottawa Limestone", although from my general knowledge of the rocks of the Ottawa Valley it appears to be a useful term in that it identifies a group of sedimentary rocks that are usually thought of as a unit and that may have been deposited in a single sequence. As lithological differences are slight within the Black River and Trenton rocks, further study may indicate that they should be lumped together into the Ottawa Formation as proposed by Wilson (1946); smaller units would then have member status. If the Ottawa Limestone were assigned to group status, its subdivisions would be formations.

Although the new evidence shows that there is a better lithostratigraphic subdivision for the study area than that which is traditionally used, I suggest that the traditional

Table 53.3. Comparison of traditional and proposed lithostratigraphic subdivisions

Traditional formations	Dominant Lithofacies	Proposed lithostratigraphic units	Measured thicknesses
Rockland	10	F	2+ to 4+ m
Chaumont	9	E	3 to 12 m
	8		
	7	D	5 to 9 m
Lowville	6	C	2 to 8 m
	5		
	4		
Pamela	3	B	7+ to 32 m
	2		
lower	1	A	21+ to 27+ m

Table 53.4. Proposed lithostratigraphic subdivision showing both dominant lithofacies and minor interbedded components

Proposed formation/member	Lithofacies
F	10, some 9,
E	most of 8, most of 9, rare 6, rare 7, rare 10
D	most of 6, most of 7, rare 8
C	most of 3, 4, 5, rare 6
B	2, rare 1, rare 3
A	1, rare 2

nomenclature be retained for the present time. This study, dealing only with part of the Black River/Trenton rocks in a corner of the Ottawa Valley, is too restricted both geographically and stratigraphically to attempt a regional stratigraphic revision. A formal revision of the stratigraphy should not be attempted until the Black River and Trenton rocks in the eastern part of the Ottawa Valley also have been restudied. Until that time, the addition of new formation names would probably be largely ignored and would only further clutter the literature (cf. Table 53.5).

It would not be surprising to find that the lithostratigraphy of the western part of the Ottawa Valley is unique, considering the apparent lithological differences between the rocks in the study area and those that occur east of Ottawa; uniqueness would be consistent with the proposed environmental model (see Steele-Petrovich, 1984). If the lithostratigraphy proves to be unique, the proposed lithostratigraphic units (A to F) should then be formally defined and named with respect to the western part of the Ottawa Valley. If a future regional study of stratigraphy shows that the lithostratigraphy of these rocks is the same throughout the Ottawa Valley, the units should be defined and named with respect to the whole region.

If the traditionally accepted lithostratigraphic nomenclature is to be retained for the present time in the upper Ottawa Valley, not only should the traditional formations be characterized in terms of the lithofacies of this study (Tables 53.3, 53.6), but their generally accepted boundaries should be discussed with respect to the field evidence (see below). In order to express doubt about the equivalence of these formations with those of their type localities one might qualify these as Pamela (Upper Ottawa), Lowville (Upper Ottawa), Chaumont (Upper Ottawa), Rockland (Upper Ottawa). Although lithofacies 6 and 7 are intimately associated, they can be retained (albeit not very neatly) in separate formations, for in spite of interbedding, lithofacies 6 is generally found stratigraphically lower than lithofacies 7 (Fig. 53.4). The Ottawa Limestone should have Supergroup status for now in accordance with the Stratigraphic Code (rather than Megagroup as proposed by Swann and Willman, 1961), with Black River and Trenton groups (Table 53.5).

Lower Pamela/upper Pamela boundary. Although the Terrigenous lithofacies (lithofacies 1) of this study more closely fits Kay's (1942) description of the Chazy than Wilson's (1932) description of the lower part of the Pamela Formation, there is no question that these terrigenous sediments are part of the Black River sequence. They form the lowest rocks of the reference section and toward its top are interbedded with the algal/dolomitic lithofacies (lithofacies 2) with no sign of a break in deposition (Fig. 53.4A, B). Raymond (1912) placed the boundary between the lower and upper Pamela at the base of a coarse sandstone unit, but as Wilson (1932) noted, shifting sands close to shore result in beds that usually cannot be traced any distance. In the Braeside and Morrison Island sections (Fig. 53.4A, B), which are the only exposures of the lower part of the sequence in the study area, a relatively well defined boundary between lower and upper Pamela can be placed at the base of the carbonates.

Pamela/Lowville boundary. Placing the Pamela/Lowville boundary at the base of the first bed of sublithographic limestone (lithofacies 6) with a birdseye¹ effect, as suggested by Wilson (1932), is inappropriate in the upper part of the Ottawa Valley, as the birdseye structure is frequently not well developed there, and where present, it occurs stratigraphically above much of lithofacies 3, 4, 5 and 6; which are normally included in the Lowville Formation. With respect to most of the rocks studied here, the bottom of the Lowville is best placed at the base of whichever appears first of lithofacies 3, 4, 5 and 6; this is a rather sharp boundary in the reference section, coinciding with the top of the dolomite facies (lithofacies 2). Where a gradational boundary occurs in other sections (apparently rarely), the boundary can be put at the horizon where lithofacies 3, 4, 5 or 6 begin to dominate.

Lowville/Chaumont boundary. Barnes' (1967) Lowville/Chaumont boundary at the top of a 3 to 5 foot (1-1.5 m) sublithographic unit containing dense *Tetradium cellulatum* does not appear to be practicable for the upper Ottawa Valley. My experience is that although sublithographic limestone commonly immediately underlies Chaumont lithofacies, this is not necessarily the case (compare Table 53.6 and Fig. 53.4), nor is this sublithographic unit necessarily thick or replete with *Tetradium cellulatum*; in fact, it may be highly burrowed and easily broken into nodules, and relatively unfossiliferous. Since sublithographic beds occur sporadically throughout most of the stratigraphic column of this study, it is advisable to place the top of the Lowville at the base of the first significant occurrence of the shaly lime mudstone to shaly fossiliferous wackestone (lithofacies 7), or base of the lime siltstone (lithofacies 8) which usually succeeds lithofacies 7 but, occasionally, appears first.

Chaumont/Rockland boundary. Kay (1942) and Barnes (1967) put the boundary between the Chaumont and Rockland at the same horizon, where, according to Barnes, there is a change in both lithology and crossbedding; these changes could not be discerned during the present fieldwork.

¹ The term "birdseye" was used extensively by palaeontologists during the 19th and part of the 20th centuries to describe vertical, spar-filled tubes of *Phytopsis*, and probably of *Tetradium*, that occur in the Birdseye Limestone (now Lowville Formation) of eastern North America (Raymond, 1931; Wilson, 1936; Wilmarth, 1938, p. 192). Use of the term for primarily horizontal desiccation features came considerably later (Shinn, 1968) and has been widely accepted by carbonate sedimentologists. The two uses can lead to confusion when dealing with the Lowville Formation. Shinn (1983b) now favours the term "fenestrae" over "birdseye" for desiccation features.

Table 53.5. History of rock stratigraphic classification of the Ottawa Valley

Raymond 1912	Raymond 1914 Wilson 1936	Kay 1942	Wilson 1946	Cooper 1956	Swann & Willman 1961	Liberty 1967a	Barnes 1967	Kay 1972	This study
Trenton Fm.	Trenton Group Rockland Fm.	Trenton Group Rockland Fm.	Trenton Subepoch Rockland Member	Wilderness Stage	Ottawa Limestone Megagroup Simcoe Group	Bobcaygeon Fm.	Trenton Group Rockland Fm.	Napance Fm. Selby Fm.	Trenton Group Rockland (Upper Ottawa) Fm.
Black River Fm.	Black River Group Leray Fm.	Black River Group Chaumont Fm.	Black River Subepoch Leray Member	Wilderness Stage	Ottawa Limestone Megagroup Simcoe Group	Gull River Fm.	Black River Group Chaumont Fm.	Water town Fm.	Black River Group Chaumont (Upper Ottawa) Fm.
Lowville Fm.	Black River Group Lowville Fm.	Black River Group Lowville Fm.	Black River Subepoch Lowville Member	Wilderness Stage	Ottawa Limestone Megagroup Simcoe Group	Gull River Fm.	Black River Group Lowville Fm.	Gull River Fm.	Black River Group Lowville (Upper Ottawa) Fm.
Pamelia Fm.	Black River Group Pamelia Fm.	Black River Group Pamelia Fm.	Black River Subepoch Pamelia Member	Wilderness Stage	Ottawa Limestone Megagroup Simcoe Group	Gull River Fm.	Black River Group Pamelia Fm.	Gull River Fm.	Black River Group Pamelia (Upper Ottawa) Fm.
Chazy Fm.	Chazy Series Rockcliffe Fm.	Chazy Series Rockcliffe Fm.	Chazy Subepoch St. Martin Fm. Rockcliffe Fm.	Wilderness Stage	Ottawa Limestone Megagroup Simcoe Group	Gull River Fm.	Black River Group Pamelia Fm.	Gull River Fm.	Black River Group Pamelia (Upper Ottawa) Fm.
Beekmantown Fm.	Canadian Series Beekmantown dolomite	Canadian Series Beekmantown dolomite	Beekmantown Subepoch Oxford Fm. March Fm.	Wilderness Stage	Ottawa Limestone Megagroup Simcoe Group	Gull River Fm.	Black River Group Pamelia Fm.	Gull River Fm.	Black River Group Pamelia (Upper Ottawa) Fm.

Table 53.6. Stratigraphic positions of lithofacies with respect to traditionally accepted nomenclature, showing both dominant lithofacies and minor interbedded components

Traditional formations	Lithofacies
Rockland	10, some 9
Chaumont	most of 7, 8, most of 9, some 6, rare 10
Lowville	most of 3, 4, 5, most of 6, some 7
Upper Pamelia	2, rare 1, rare 3
Lower Pamelia	1, rare 2

Table 53.7. Lithofacies and corresponding environments of deposition

Lithofacies	Depositional environments
	BANK
10	Lime-mud bank
9	Spillover deposits on lee side of bank
	OUTER LAGOON
9	Lagoonal spillover or storm deposits
8	Sheltered zone in lee of bank
	INNER LAGOON
7	Mud bottom
6	Subtidal algal ooze or mat
	LOW INTERTIDAL AND SHALLOW SUBTIDAL REGION
5	Zone of wave impingement
4	Near-shore storm deposits
3	Quiet pools and shallow, level bottom
	INTERTIDAL FLATS
2a, 2b	Carbonate intertidal mud flats
2ai	Protected mud flats or intertidal pools
2aii	Channel deposits
1a - 1d	Clastic intertidal mud flats
1c, 1d	Mixed flats
1a, 1b	Sand flats

However, a slight difference in bedding, although not usually well demarcated, was detected. The bedding character changed from thinner and well-defined to more massive and poorly-defined, apparently coinciding with the beginning of intensive burrowing. The Coarse grained bioclastic intraclastic packstone (lithofacies 9) crosses the Chaumont – Rockland boundary of Kay (1942) and Barnes (1967) and within several feet becomes interbedded and possibly interfingering horizontally with, and appears to finally be succeeded by, the Bioturbated bioclastic oncolitic wackestone (lithofacies 10). In this case, the most natural boundary seems to me to occur at the base of lithofacies 10. Where lithofacies 8 (lime siltstone) and 10 are interbedded, which occurs rarely, the boundary appears to be best placed at the top of the last appearance of lithofacies 8.

It would be useful to redefine at this time two informal units in accordance with recommendations of the Code of Stratigraphic Nomenclature: the Braeside beds and Paquette Rapids beds (see Sinclair in Steele and Sinclair, 1971). The Braeside beds, named for Braeside, Ontario, occur within the Shaly lime mudstone to Shaly fossiliferous wackestone (lithofacies 7) and are distinguished by an abundant and diverse fauna dominated by the molluscs *Cyrtodonta grattanensis*, *Vanuxemia inconstans*, *Lophospira milleri*, and the brachiopods *Doleroides germanus*, *Pionodema cooperi*, *Hallina canadensis* (Steele and Sinclair, 1971). The Paquette Rapids beds, named for Paquette Rapids near Pembroke, occur in the coarse grained bioclastic intraclastic packstone (lithofacies 9) and the bioturbated bioclastic oncolitic wackestone (lithofacies 10). The Paquette Rapids beds are also distinguished by an abundant and diverse fauna, in this case dominated by stromatoporoids, the colonial tabulate coral *Foerstephyllum halli*, the gastropods *Maclurites logani* and several species of *Lophospira*, the brachiopods *Dalmanella paquettensis* and *Hesperorthis tricenaria*, and the codiacean alga *Receptaculites* (Sinclair, in Steele and Sinclair, 1971).

Environmental reconstruction

Each of the ten lithofacies recognized in this study was deposited in a different environment under different physical conditions (Table 53.7). Carbonate deposition here is interpreted as having taken place on a relatively shallow lime-mud bank and in its quiet, inner lagoon at the edge of a tropical, transgressive, epeiric sea; the terrigenous rocks were deposited on intertidal flats, probably before formation of the carbonate bank.

The lime-mud bank was a highly burrowed, biostromal structure that supported a diverse and locally abundant fauna; it lacked a rigid framework even though reef-forming fauna and flora occurred throughout. Blue-green algae were probably the major binding and stabilizing agents. The deepest and quietest part of the lagoon, immediately behind the bank, was normally stagnant near the bottom, and floored by a laminated lime siltstone that was commonly barren; concretions, semihardgrounds and fields of mounds of biotically-trapped sediment occurred but were rare. Intermittent storms tore up the lime siltstone and redeposited it with coarser grained, storm-transported material that had been carried over the bank and into the lagoon. The inner, subtidal part of the lagoon, just below normal wave base, was fully oxygenated and floored in part by a relatively firm carbonate mud that supported an abundant and diverse fauna, and in part by a soft, algal ooze that appears to have inhibited most forms of life. Ooids formed in the wave impingement zone. Shallow, quiet pools occurred in the low intertidal/shallow subtidal region; storm deposits were dumped there rarely. The intertidal lime-mud flats were covered with algal mats, dotted with tidal pools, and dissected by meandering, relatively sluggish tidal channels. The whole setting was exceptionally quiet, and the

sediments throughout were dominated by lime mud. (See Steele-Petrovich, 1984, for detailed discussions of environments).

Acknowledgments

This paper was taken from a part of my Ph.D. dissertation at Yale University. For critically reading the arguments of this paper in the dissertation, I thank D.C. Rhoads, D.E. Schindel, K.M. Waage, K.R. Walker, and particularly R.G.C. Bathurst, C.T. Feazel, R.K. Park, and R. Petrovich. I thank R. Petrovich for helpful comments on the present paper; T.E. Bolton and particularly M.J. Copeland for help at various times; T.E. Bolton and G.S. Nowlan for visiting some of the outcrops and sharing ideas with me; D. Jarvis and F.S. Steele for assistance in the field; and Susan King for superb drafting.

I gratefully acknowledge the following field support for this work: Geological Society of America, Grants 1267-69, 1394-70; Sigma Xi Grants-in-Aid-of-Research, 1969, 1971; Geological Survey of Canada, summer field support 1969 (Graduate Assistant) and 1980 (contract No. OSB80-00166).

References

- Barnes, C.R.
1967: Stratigraphy and sedimentary environments of some Wilderness (Ordovician) limestones, Ottawa Valley, Ontario; Canadian Journal of Earth Sciences, v. 4, p. 209-244.
1968: Reply: stratigraphy and sedimentary environments of some Wilderness (Ordovician) limestones, Ottawa Valley, Ontario, by C.R. Barnes; Canadian Journal of Earth Sciences, v. 5, p. 169-172.
- Dunham, R.J.
1962: Classification of carbonate rocks according to depositional texture; in Classification of Carbonate Rocks, ed. W.E. Ham; American Association of Petroleum Geologists, Memoir 1, p. 108-121.
- Fisher, D.W.
1962: Correlation of the Ordovician rocks in New York State; New York State Museum and Science Service, Geological Survey, Map and Chart Series 3.
- Kay, G.M.
1937: Stratigraphy of the Trenton Group; Geological Society of America, Bulletin 48, p. 233-302.
1939: Ordovician System in Ontario; in Geologie der Erde. Geology of North America, Vol. I, ed. R. Ruedemann and R. Balk; Borntraeger, Berlin, p. 589-593.
1942: Ottawa-Bonnechere Graben and Lake Ontario Homocline; Geological Society of America, Bulletin 53, p. 585-646.
1960: Classification of the Ordovician System in North America; Proceedings of the 21st International Geological Congress, Copenhagen, pt. 7, p. 28-33.
1968: Discussion: stratigraphy and sedimentary environments of some Wilderness (Ordovician) limestones, Ottawa Valley, Ontario, by C.R. Barnes; Canadian Journal of Earth Sciences, v. 5, p. 166-168.
1972: Unpublished Field Guide for Geology 9293x Carbonate Trip – Fall 1972.

- Liberty, B.A.
 1955: Stratigraphic studies of the Ordovician System in central Ontario; Proceedings of the Geological Association of Canada, v. 7, p. 139-147.
 1967: Ordovician stratigraphy of southern Ontario: The Ottawa Valley problem; Abstracts of the Geological Association of Canada and Mining Association of Canada, International Meeting, p. 49-50.
 1969: Paleozoic geology of the Lake Simcoe area, Ontario; Geological Survey of Canada, Memoir 355, 201 p.
- North American Commission on Stratigraphic Nomenclature
 1983: North American Stratigraphic Codes; American Association of Petroleum Geologists, Bulletin 67, p. 841-875.
- Okulitch, V.J.
 1939: The Ordovician Section at Coboconk, Ontario; Transactions of the Royal Canadian Institute, v. 21, p. 319-339.
- Pettijohn, F.J.
 1957: Sedimentary Rocks; second edition; Harper and Brothers, New York, 718 p.
- Raymond, P.E.
 1912: Field Work, Ottawa Valley; Geological Survey of Canada, Summary Report for 1911; p. 351-357.
 1913: Ordovician of Montreal and Ottawa; International Geological Congress Guidebook, 13th Session, No. 3, p. 137-162.
 1914: The Trenton Group in Ontario and Quebec; Geological Survey of Canada, Summary Report for 1912, p. 342-350.
 1931: On the Nature of *Phytopsis tubulosum* Hall; Bulletin of the Museum of Comparative Zoology, Geological Series, v. 55, p. 194-198.
- Reineck, H.-E. and Singh, I.B.
 1975: Depositional Sedimentary Environments with Reference to Terrigenous Clastics; Springer-Verlag, New York, 439 p.
- Shinn, E.A.
 1968: Practical significance of birdseye structures in carbonate rocks; Journal of Sedimentary Petrology, v. 38, p. 215-223.
 1983b: Birdseyes, fenestrae, shrinkage pores, and loferites: a re-evaluation; Journal of Sedimentary Petrology, v. 53, p. 619-628.
- Sinclair, G.W.
 1968: Comment on discussion and reply: Stratigraphy and sedimentary environments of some Wilderness (Ordovician) limestones, Ottawa Valley, Ontario, by C.R. Barnes; Canadian Journal of Earth Sciences, v. 5, p. 172-173.
- Steele-Petrovich, H.M.
 1984: Stratigraphy and paleoenvironments of Middle Ordovician carbonate rocks, Ottawa Valley, Canada; Ph.D. Dissertation, Yale University, New Haven, Connecticut, 477 p.
- Steele, H.M. and Sinclair, G.W.
 1971: A Middle Ordovician fauna from Braeside, Ottawa Valley, Ontario; Geological Survey of Canada, Bulletin 211, 97 p.
- Swann D.H. and Willman, H.B.
 1961: Megagroups in Illinois; American Association of Petroleum Geologists, Bulletin 45, p. 471-483.
- Walker, K.R.
 1973: Stratigraphy and environmental sedimentology of Middle Ordovician Black River Group in the type area - New York State; New York State Museum of Science Service, Bulletin 419, 43 p.
- Wilmarth, M.G.
 1938: Lexicon of geologic names of the United States; United States Department of the Interior, Geological Survey Bulletin 896.
- Wilson, A.E.
 1921: The range of certain Lower Ordovician faunas of the Ottawa Valley with descriptions of some new species; Canada Department of Mines, Bulletin 33, p. 19-57.
 1932: Notes on the Pamelia Member of the Black River Formation of the Ottawa Valley; American Journal of Science, Series V, v. 23, p. 135-146.
 1936: A synopsis of the Ordovician of Ontario and western Quebec and the related succession in New York; Geological Survey of Canada, Memoir 202, p. 1-20.
 1937: Erosional intervals indicated by contacts in the vicinity of Ottawa, Ontario; Transactions of the Royal Society of Canada, Section IV, v. 31, p. 45-60.
 1946: Geology of the Ottawa - St. Lawrence lowland, Ontario and Quebec; Geological Survey of Canada, Memoir 241, 65 p.

A computer-based system for quantifying surface-mineable coal resources according to environmental characteristics and ownership of the overlying land surface

Project 810014

J.D. Hughes and V.P. Neimanis¹
Institute of Sedimentary and Petroleum Geology, Calgary

Hughes, J.D. and Neimanis, V.P., A computer-based system for quantifying surface-mineable resources according to environmental characteristics and ownership of the overlying land surface; in Current Research, Part B, Geological Survey of Canada, Paper 96-1B, p. 507-518, 1986.

Abstract

A computer-based capability has been developed to assess surface-mineable coal resources in relation to the suitability of the overlying land for alternative uses, and in relation to surface ownership. Coal resource quantities categorized by land use and ownership criteria can be derived for entire coal deposits, or for any area within a deposit to a minimum size of one hectare. This capability was developed by combining the capabilities of two pre-existing information systems, Environment Canada's Canada Land Data System, and the Geological Survey of Canada's National Coal Inventory. The combined systems provide policy-makers and planners with a powerful and flexible tool to examine Canada's coal resources in the light of competing land uses, and should in future allow optimal development of these resources. This tool is available to private industry and other government agencies within the limits of the confidentiality of data in the system.

Studies have been completed or are underway for several coalfields in Alberta and Saskatchewan, and will eventually be extended to coal deposits across Canada.

Résumé

Un système informatisé a été mis au point en vue d'évaluer les ressources houillères exploitables en surface par rapport à d'autres utilisations possibles des terres sus-jacentes et à la propriété de la surface. Il est possible de dériver les quantités de ressources houillères en fonction de l'utilisation des terres et des critères de propriété pour l'ensemble des gisements houillers ou pour toute région à l'intérieur d'un gisement dont les dimensions sont supérieures à un hectare. Cette capacité a été mise au point en combinant les capacités de deux systèmes d'information existants, le Système de données sur les terres du Canada d'Environnement Canada et l'Inventaire national du charbon de la Commission géologique du Canada. Ces deux systèmes pris ensemble fourniront aux technocrates et aux planificateurs un outil puissant et souple qui permettra d'examiner les ressources houillères du Canada par rapport à d'autres utilisations des terres et de les mettre en valeur le plus efficacement possible. Cet outil sera mis à la disposition de l'industrie privée et d'autres organismes gouvernementaux sous réserve des limites ayant trait à l'aspect confidentiel des données.

L'étude de plusieurs bassins houillers en Alberta et en Saskatchewan a été terminée ou se poursuit présentement; éventuellement, tous les gisements houillers au Canada seront examinés.

¹ Federal Land Services Division, Land Use Policy and Research Branch, Lands Directorate, Environment Canada, Place Vincent Massey, 351 St. Joseph Blvd., Hull, Quebec K1A 0E7

Introduction

Quantification of surface-mineable coal resources according to quality and economic parameters provides only part of the information required to make decisions on the best development options for these resources. Often of equal importance to knowledge that a mineable deposit exists, is knowledge about the suitability of the land for other uses, and the current disposition of the land in terms of present use and ownership.

This report outlines the capabilities of a computer-based system that allows the consideration of land use characteristics and ownership data in the assessment of development options for surface-mineable coal resources. The system was developed through a co-operative project between the Lands Directorate of Environment Canada (EC), the Coal Division of the Mineral Policy Sector of Energy, Mines and Resources Canada (EMR), and the Geological Survey of Canada (GSC). This project, which was initiated in October, 1982, incorporates digitized environmental and ownership data gathered by EC, with digital coal deposit models developed by GSC from primary exploration data.

The rationale behind the development of this system, and the collection by the participating agencies of the data on which it is based, is to provide a high-resolution planning capability for decision-makers in industry and government to optimize the utilization of Canada's coal and land resources.

Acknowledgments

A. Darragh, of the Coal Division of the Mineral Policy Sector of EMR, provided the impetus for initiating this project, arranged for funding through the Coal Division and provided support throughout. N. Chartrand, of Environment Canada, developed a computer program for grid conversion of the land capability data. K. Nairn, of the Geological Survey of Canada, provided assistance in the development of software to integrate the land capability data with coal deposit information.

Data organization and type

Two information storage and management systems, EC's Canada Land Data System (CLDS) (Crain and Macdonald, 1983; Griffith, 1980) and GSC's National Coal Inventory (Irvine, 1981), form the basis of this project. The type and organization of data in each system is outlined below.

Canada Land Data System

Information contained in CLDS includes land capability assessments for agriculture, forestry, recreation, wildlife-ungulates and wildlife-waterfowl, as well as assessments of historic land use and shoreline location, which were collected under the Canada Land Inventory (CLI). Each capability type is subdivided into seven ordinal classes, with classes 1, 2 and 3 being the highest capability land for each assessment. Data are collected by digitizing the boundaries of classes and subclasses for each assessment from 1:50 000 base maps, and are stored as polygonal outlines grouped by NTS mapsheet in the computer, where they can be manipulated to answer specific land use questions. Additional information collected as a result of this project includes the boundaries of surface-mineable coal areas provided by GSC, and coal land ownership data provided by the respective provincial governments.

The coverages now available in CLDS are shown in Figure 54.1. A description of each coverage is as follows (Lands Directorate, 1978):

1. Soil capability for agriculture: homogeneous land units are mapped according to their general suitability for the production of common field crops, taking into account the effects of climatic and soil limitations in a system of mechanized farming.
2. Land capability for forestry: land units are mapped according to their potential capability for growing commercial timber from indigenous tree species maturing as full-stock stands and assuming good management.
3. Land capability for outdoor recreation: land is classified according to the quantity of outdoor recreation that may be sustained per unit area per year under "perfect" market conditions.
4. Land capability for wildlife-ungulates: the environmental factors that control the numbers of ungulates produced and supported on a unit of land.
5. Land capability for wildlife-waterfowl: denotes the ability of the land or water to support the existence and reproduction of waterfowl.
6. Historic land use: indicates land use/land cover in 1968 according to a fourteen category classification.
7. Shoreline location: denotes the position of land/water boundaries based on National Topographic Series (NTS) maps.
8. Coal tenure: the land is classified according to the tenure owner (freehold, crown, or a specific company), the tenure type (coal application/permit or coal lease) and a special designation to indicate if land is within an area withdrawn from disposition, an area approved for mining, or an excluded area such as a townsite or a park.
9. Surface-mineable coal: denotes the boundaries of areas underlain by surface-mineable coal as determined by GSC.

GSC's National Coal Inventory

Information within GSC's National Coal Inventory includes primary exploration data from boreholes, outcrops, adits and mines, and processed data resulting from comprehensive geological analyses of the primary information. Processed data include geographically referenced variables defining the geometry, thickness, depth, and quality of coal seams, the geometry and distribution of

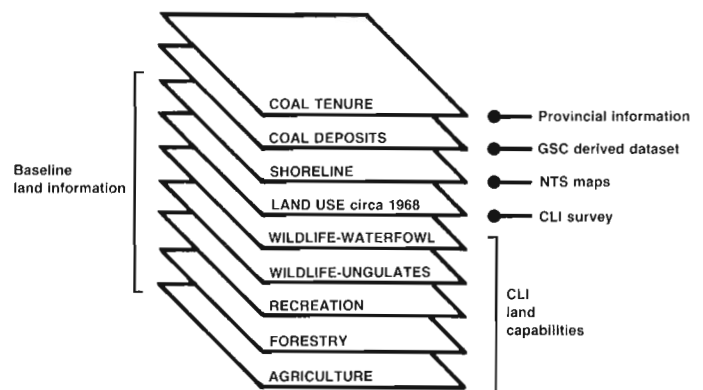


Figure 54.1. Coverages of information available in CLDS (see text).

Figure 54.2

Map showing areas underlain by surface-mineable coal in the Ardley coalfield, plotted by CLDS.

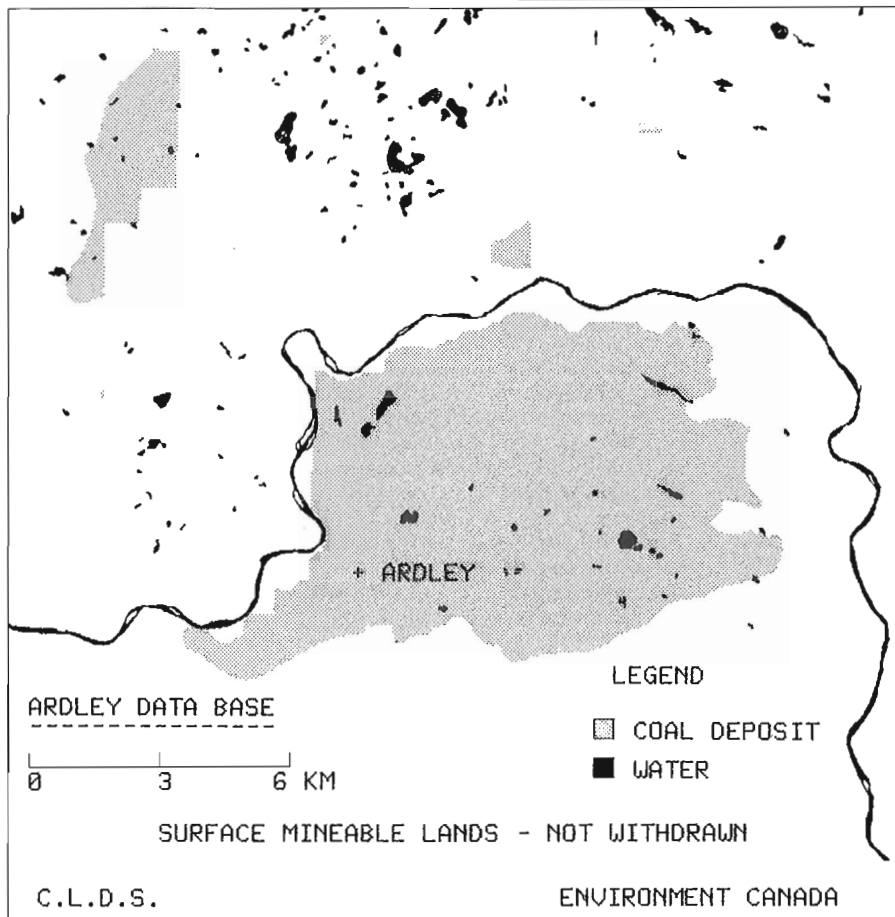
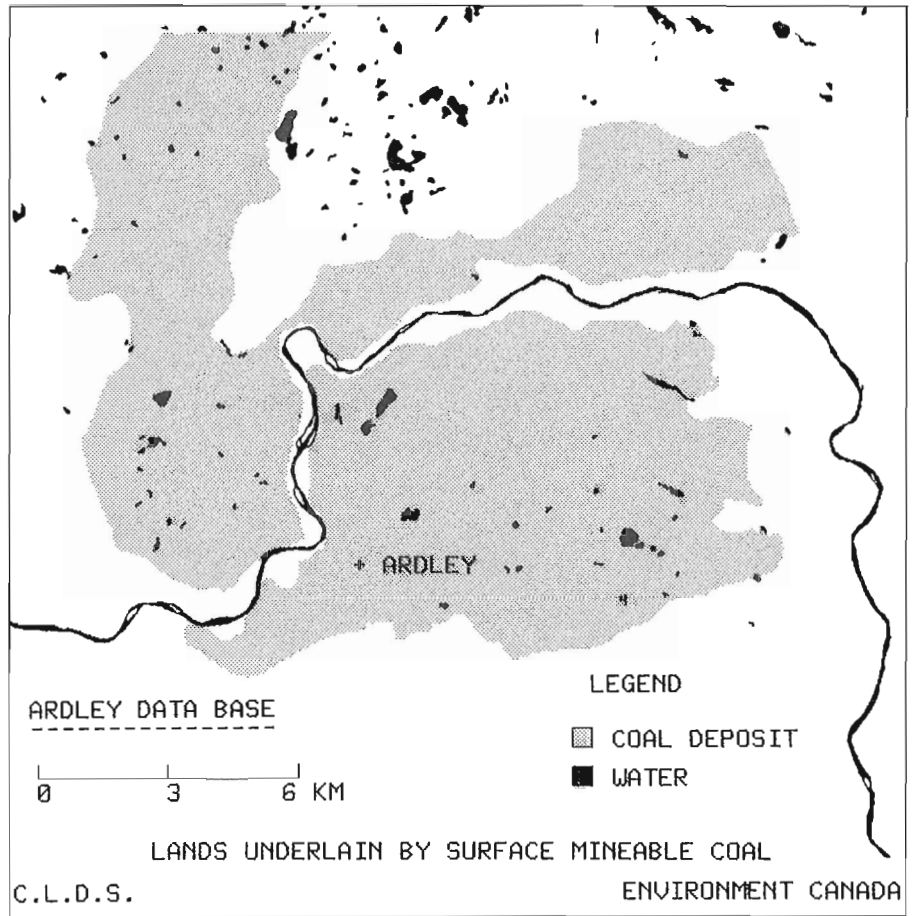


Figure 54.3

Map showing location of surface-mineable coal areas that are not withdrawn from disposition in the Ardley coalfield, plotted by CLDS.

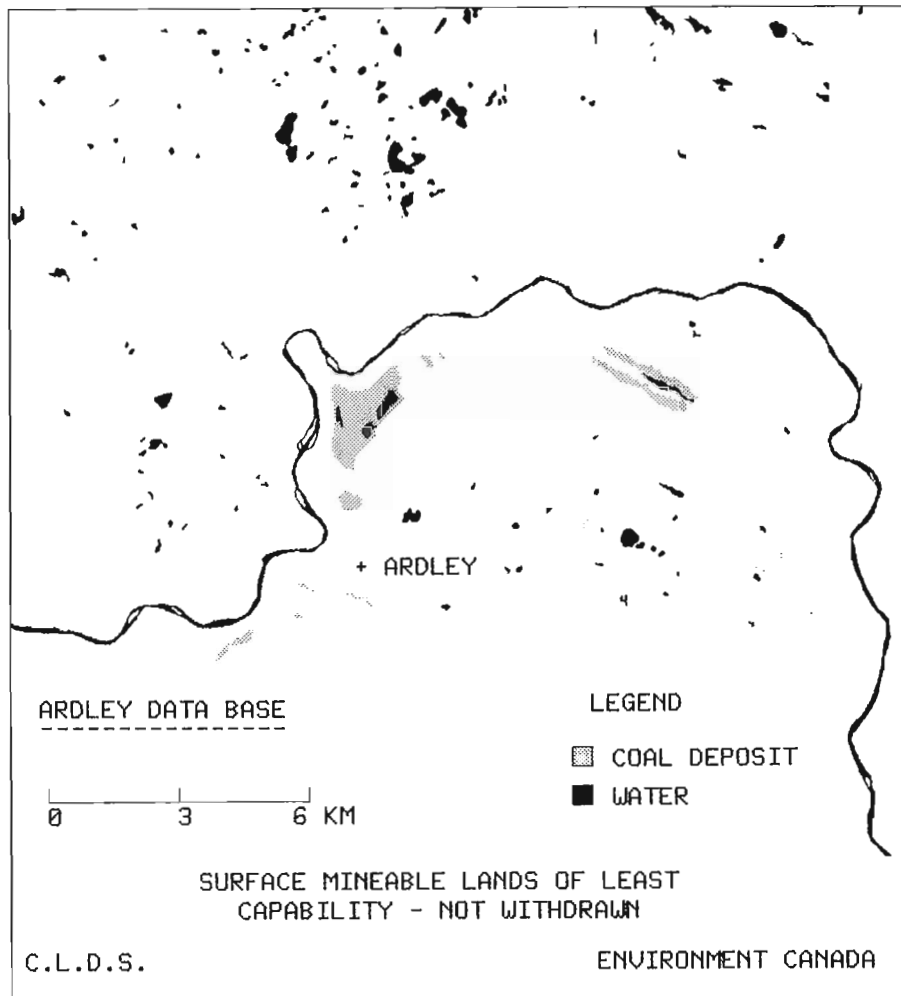


Figure 54.4. Map showing surface-mineable lands of least capability that are not withdrawn from disposition in the Ardley coalfield, plotted by CLDS.

interseam rock units and other geological features, as well as parameters of economic importance such as stripping ratios. The processed data may be interrogated in order to answer highly specific questions as to the development potential of the resource.

A fundamental difference exists in the representation of data in each system. All processed variables in GSC's system are referenced to the nodes of a regular orthogonal grid, with a cell size related to the spacing of primary data. In most deposits with surface-mineable coal, grid nodes are spaced at 100 m intervals so that each cell covers a one hectare area. This allows resource parameters and development potential to be determined for areas within a deposit as small as one hectare.

Information in CLDS, on the other hand, is stored as polygonal outlines of classes and subclasses for each coverage. As only the boundaries of a surface-mineable coal area are represented in the system, land use observations can be related only to the total resource volume, and not to resource volumes underlying smaller areas within its boundaries. This represents a limitation in that the boundaries of surface-mineable areas are established using criteria reflecting current mining technology and economic

conditions, and are therefore subject to change with advances in mining technology and changes in economic relationships affecting coal.

Initially, GSC provided Environment Canada only with the outlines of surface-mineable resource areas defined using current resource criteria. It was recognized, however, that considerably more flexibility could be achieved if CLDS data could be determined at the nodes of the reference grid used by GSC. In 1984, Environment Canada added the capability to their system of representing coverage data as a grid, and provided gridded data on tape to GSC for entry into the National Coal Inventory. This greatly enhanced the flexibility and scope of the questions that could be asked of the combined systems, effectively allowing GSC to subdivide its resource data by CLDS coverages for areas as small as one hectare within a deposit.

Data analysis capabilities

Both CLDS and the National Coal Inventory have considerable capabilities to manipulate data to answer highly specific queries. The following section provides a brief overview of some of these capabilities.

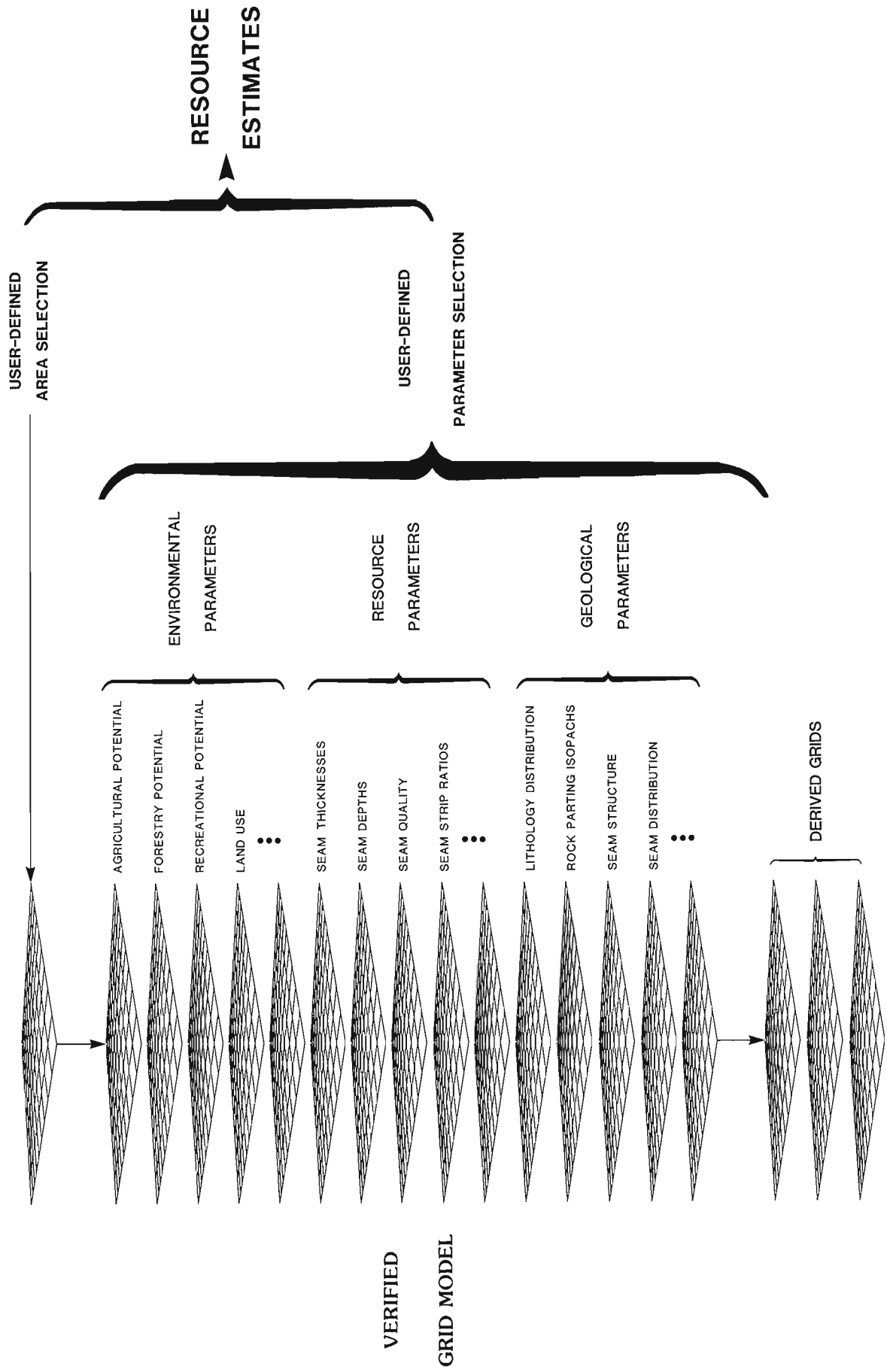


Figure 54.5. Schematic diagram illustrating the representation and type of data in GSC's National Coal Inventory, and its application for the production of resource assessments.

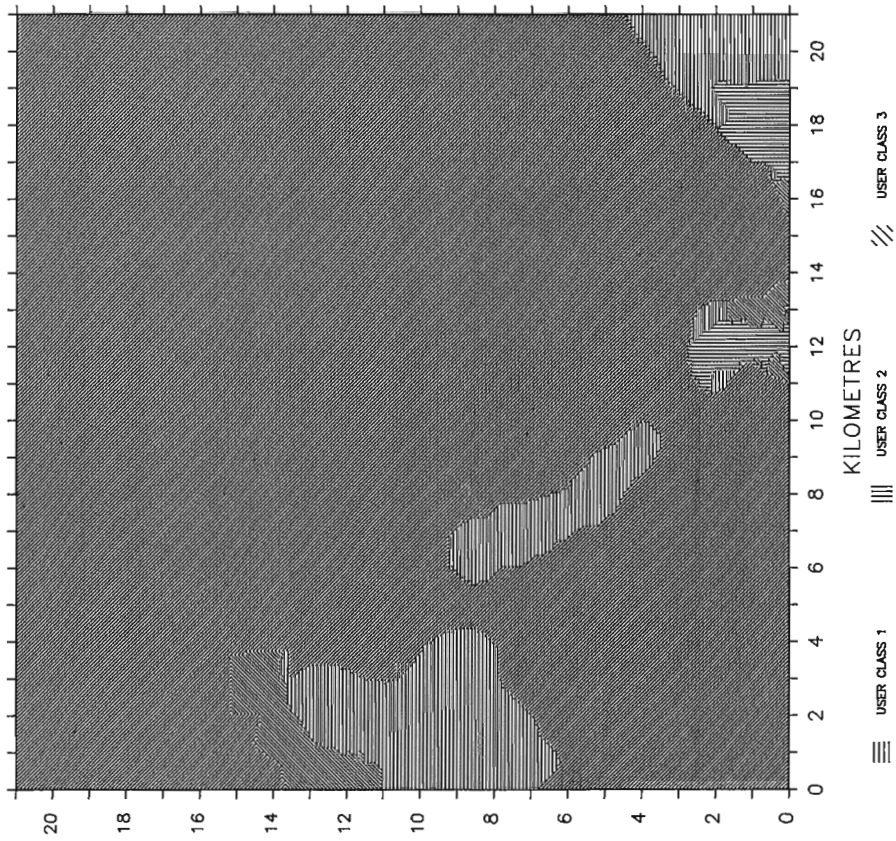


Figure 54.6. Map of Shaunavon coalfield showing distribution of land capability categories resulting from an Environment Canada study. Plotted using gridded data by GSC.

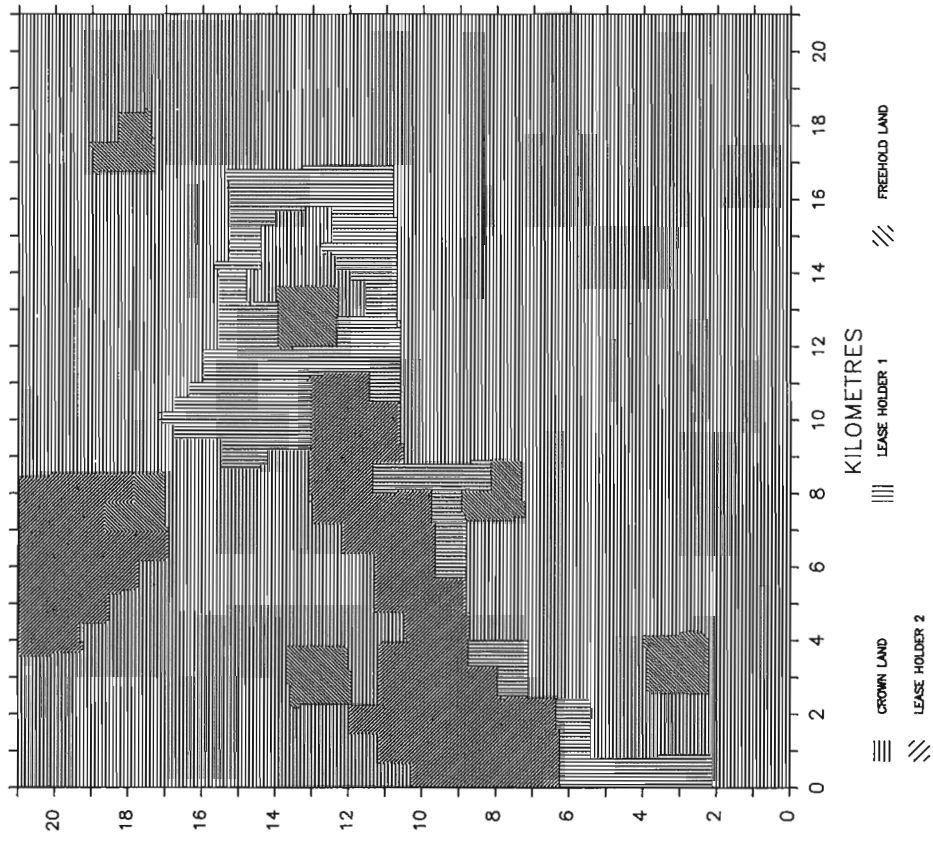


Figure 54.7. Map showing distribution of coal tenure in the Shaunavon coalfield. Plotted using gridded data by GSC.

Interactive capabilities within CLDS allow the investigation and testing of a wide variety of land development scenarios. Statistical and mapped retrievals of any portion of one or of a combination of the coverages shown in Figure 54.1 can be made. For example, records of the lands of least capability underlain by surface-mineable coal can readily be derived. Beyond focusing on land quality, any particular lease holding can also be investigated in terms of the other coverages.

An example of the application of these capabilities to the Ardley Coalfield of central Alberta is given below:

1. Figure 54.2 shows the location of the two areas in the coalfield underlain by surface-mineable coal. They comprise a total of 37 173.4 hectares.
2. Figure 54.3 shows the result of intersecting the surface-mineable areas with the coal tenure classification and selecting only those areas not withdrawn from disposition (according to 1984 Alberta provincial data). It indicates that only 7701 hectares of surface-mineable area are not

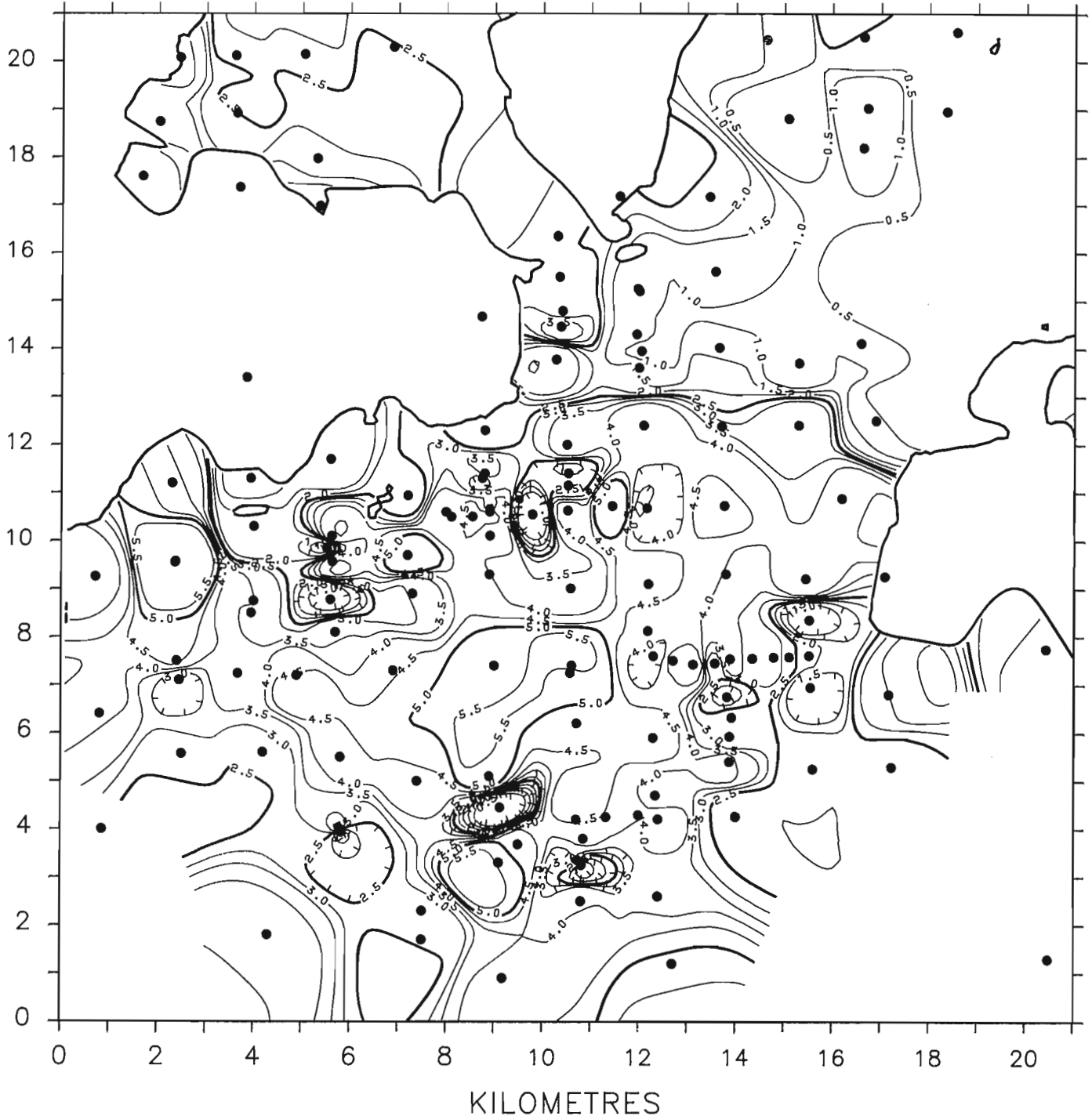


Figure 54.8. Contour map showing the thickness of coal in the Ferris coal zone of the Shaunavon coalfield (in metres) and the location of exploration boreholes (dots). Heavy line indicates location of coal zone subcrop.

already withdrawn from disposition. Within this area, 58% of the coal tenure is freehold, 0.1% Crown, 20% is held by Ardley Coal Ltd., 15% by Fording Coal Ltd., 7% by Luscar Ltd., and the remainder is distributed amongst four other companies.

3. One possible land development scenario tested on this data set was to determine the land areas with least capability in the surface-mineable area not withdrawn from disposition. Least capability was defined to include

class 4, 5, 6 and 7 agricultural lands, class 2 ungulate lands, and class 4, 5, and 6 waterfowl capability lands. This yielded a total of 314 hectares scattered amongst two major and several minor polygons, as illustrated in Figure 54.4.

4. The analysis of the Ardley Coalfield revealed a land area possible for surface-mining of 14 273 hectares. The application of land capability and land tenure criteria, as

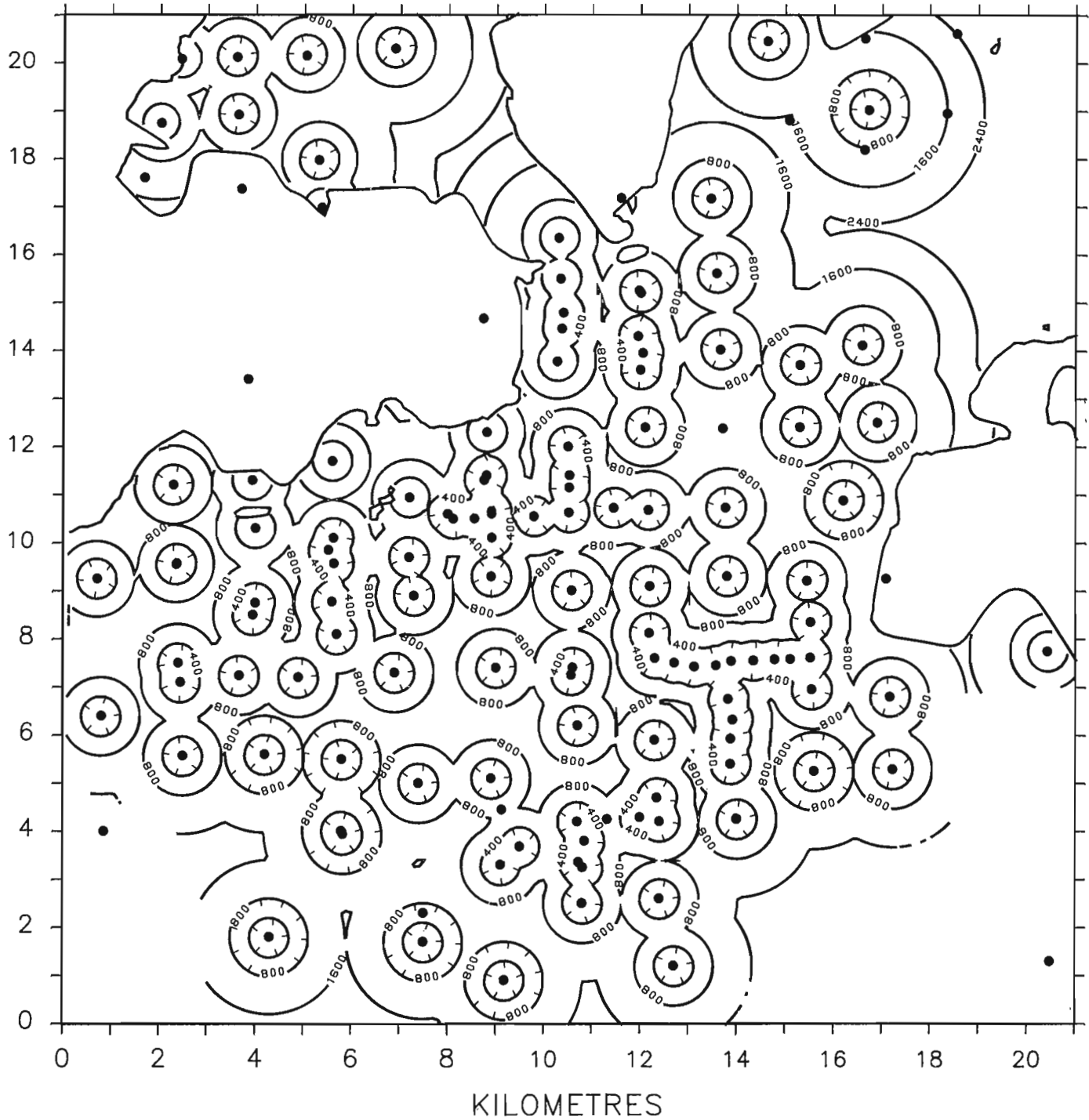


Figure 54.9. Contour map showing the distance from subsurface control points of the Ferris coal zone in the Shaunavon coalfield (in metres) and the location of exploration boreholes (dots). This parameter is used to subdivide coal resource quantities into measured, indicated and inferred categories.

outlined in point 2 (above), significantly influences the surface-mining development options available for this deposit.

GSC's National Coal Inventory

Geological modelling and resource assessment software available within GSC's National Coal Inventory allow the interactive analysis of coal deposits and the estimation of resource quantities categorized by any one or a combination

of economic, geological or land capability attributes, as illustrated in Figure 54.5 (Irvine, 1981; Hughes, 1984). As all attributes are referenced to the nodes of a grid, as previously discussed, resource assessments can be made for areas as small as one grid cell (typically one hectare) within a deposit.

Through this project, Environment Canada has made CLDS data available to GSC in a gridded format, which allows optimal integration with information in GSC's system. GSC has developed software to interactively analyse the land

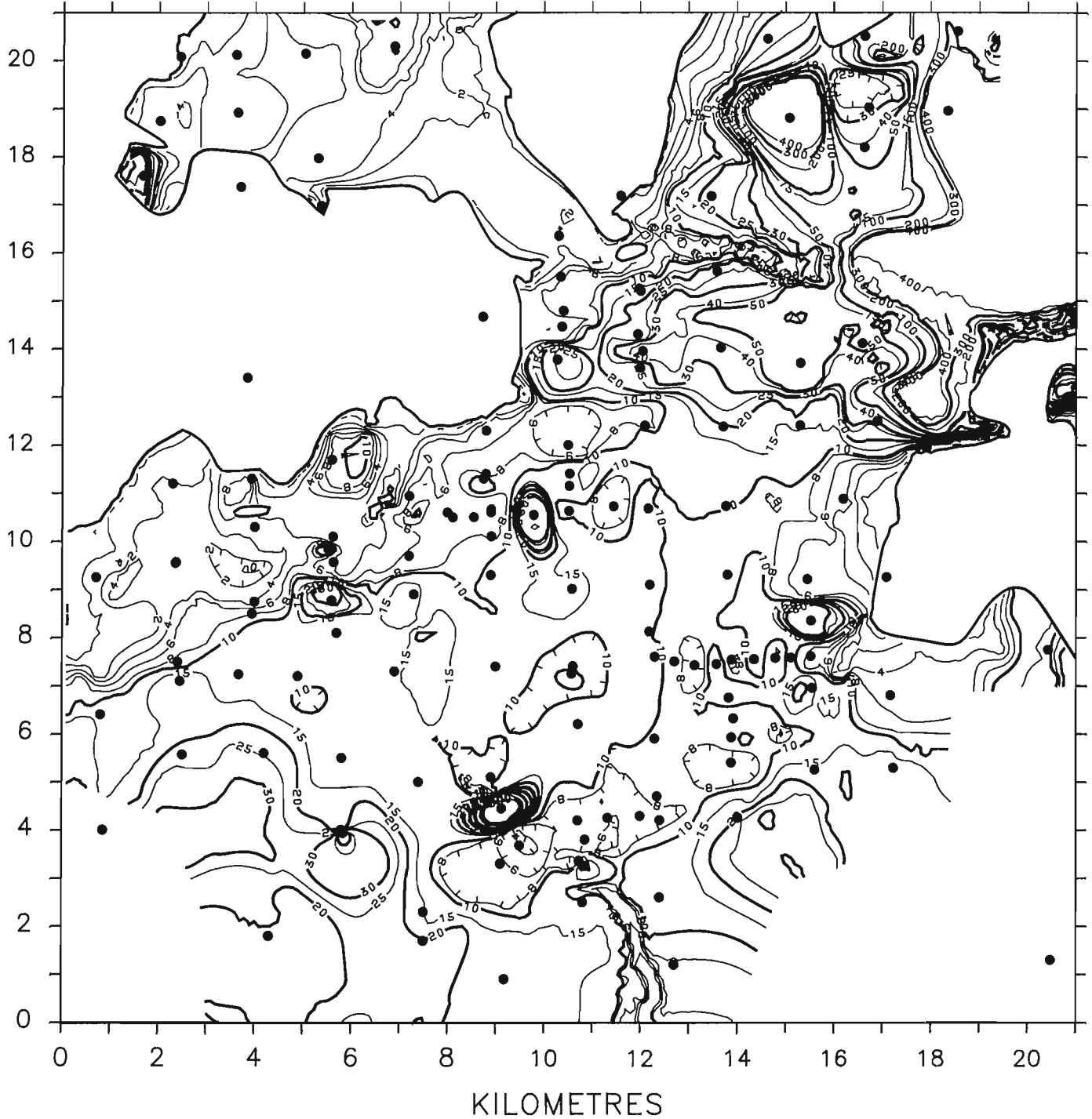
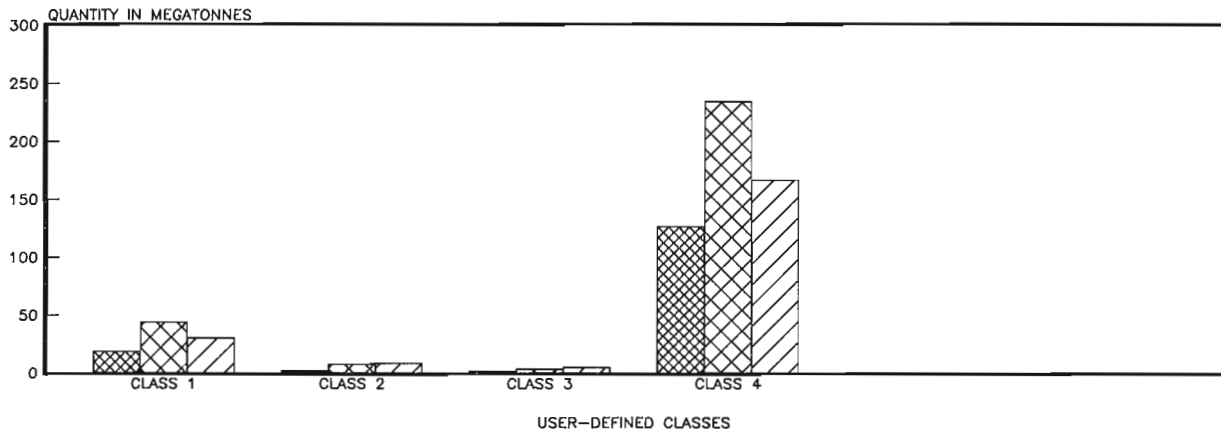


Figure 54.10. Contour map showing the stripping ratio on the Ferris coal zone in the Shaunavon coalfield and the location of exploration boreholes (dots). Stripping ratio is defined as the number of cubic metres of overburden that must be removed in order to recover one tonne of coal.

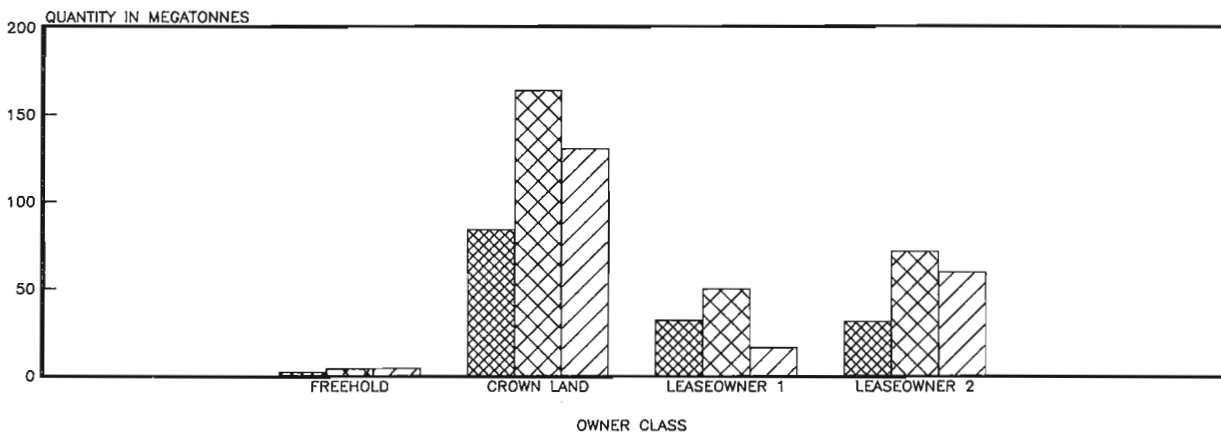
FERRIS COAL RESOURCES BY USER-DEFINED CLASSES

RESOURCES OF IMMEDIATE INTEREST



FERRIS COAL RESOURCES BY OWNERSHIP CLASS

RESOURCES OF IMMEDIATE INTEREST



FERRIS RESOURCES OVERLAIN BY CROWN LAND

RESOURCES IN SEAMS GREATER THAN 1 M THICK

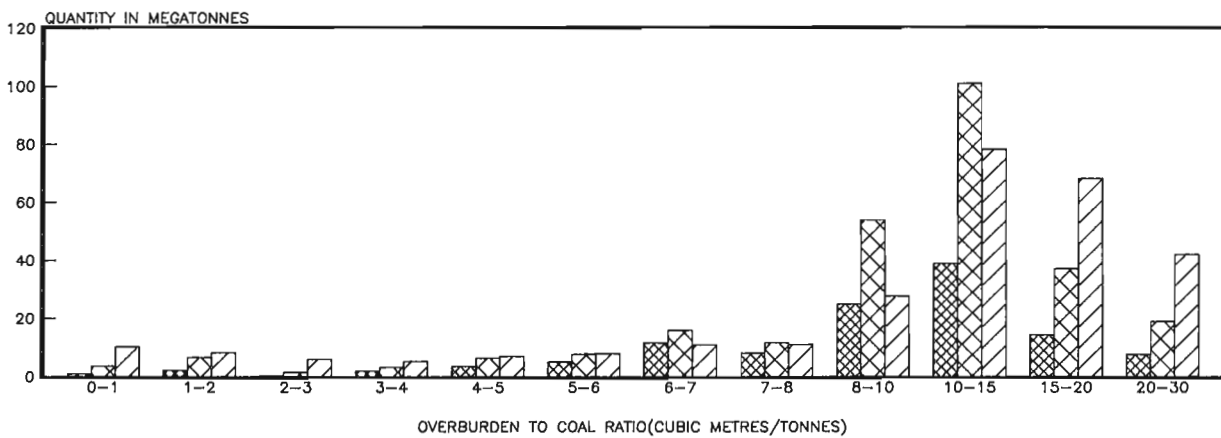
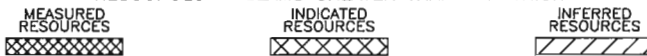
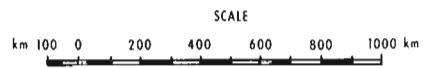
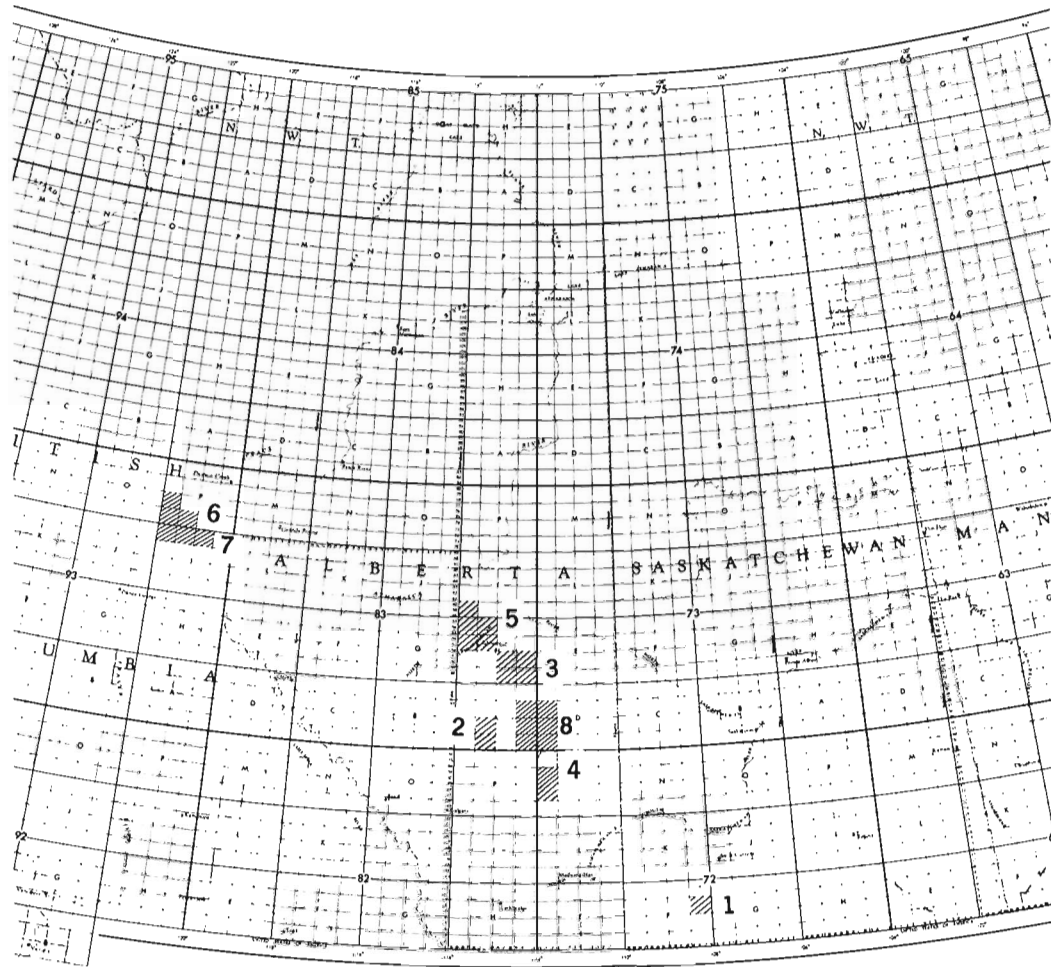


Figure 54.11. Coal resource quantities subdivided by land capability and land tenure categories (see text), for the Ferris zone in the Shaunavon coalfield. In Figure 54.11a (upper), resources are subdivided according to their capability to support alternative activities. In Figure 54.11b (centre), resources are subdivided according to surface coal tenure. In figure 54.11c (lower), resources underlying crown land are subdivided by stripping ratio.

DATA BASE DEVELOPMENT



- | | |
|--------------------------------------------------------------------------------------------------------------------------------------------------------------------------|-----------------------------------------------------------------------------------------------------------------------------------------------------------------------------------------------------------------|
| <p>1-Shaunavon (72F/9)
 2-Ardley (83A/3/6)
 3-Dodds-Round Hill (83H/1/2/7/8)
 4-Sheerness (72M/5&12)</p> | <p>5-Morinville-Legal (83H/11-14 & 83I/4)
 6-Sukunka (93P3W/4/5)
 7-Quintette (93I 13-15, 93P3/4)
 8-Paintearth (83A 1/8/9 & 73D4/5/12)</p> |
|--------------------------------------------------------------------------------------------------------------------------------------------------------------------------|-----------------------------------------------------------------------------------------------------------------------------------------------------------------------------------------------------------------|

Figure 54.12. Map showing location of completed and current study areas.

use data in a manner similar to that available within CLDS, so that Environment Canada's land use analyses, such as the one outlined above for the Ardley coalfield, can be applied to the gridded data provided to GSC.

The following examples from the Shaunavon coalfield of southwestern Saskatchewan illustrate the application of these assessment capabilities and the land use data to resource information within the National Coal Inventory:

1. Figure 54.6 illustrates the distribution, based on gridded data, of land capability classes defined by an Environment Canada study similar to that outlined above for the Ardley coalfield. Class 4 lands are those least suitable for coal extraction activities whereas class 1 lands are those that are most suitable.
2. Figure 54.7 illustrates the coal tenure distribution for the area, again using gridded data provided by the Saskatchewan Department of Mines.
3. Figures 54.8, 54.9 and 54.10 illustrate the distribution of several important resource parameters for the Ferris coal zone, which is the most significant seam in this area. The variation in seam thickness within the area underlain by coal is shown in Figure 54.8, the distance of each part of the coalfield from the nearest subsurface control point is shown in Figure 54.9, and the variation in stripping ratio is shown in Figure 54.10.
4. Coal resource quantity estimates for the Ferris coal zone subdivided by some of the CLDS coverages are given in Figure 54.11. These resources are also subdivided by depth from surface (into immediate interest and future interest categories – only immediate interest resources are shown in Figure 54.11), and by distance from nearest control point (into measured, indicated and inferred categories).
 - In Figure 54.11a, resource quantities are subdivided into land use categories defined by the Environment Canada study. It can be seen that the majority of the resources underlie the least suitable land for coal extraction.
 - In Figure 54.11b, resource quantities are subdivided according to the ownership of the overlying land. As can be seen, the majority of the coal resources in the area are not currently held by private lease holders.
 - In Figure 54.11c, resource quantities underlying crown land are investigated in more detail by further subdividing them by stripping ratio. It can be seen that the majority of these resources are beneath relatively large amounts of overburden, and are therefore uneconomical to mine in the current economic climate. This is the probable reason that these resources have not yet been leased.

Current status

This project is proceeding at a rate governed by GSC's completion of geological studies of coal deposits. Since the initiation of the project, land use studies have been completed on the Shaunavon coalfield of southwestern

Saskatchewan, and on the Ardley and Dodds-Round Hill coalfields of Alberta. Studies are underway on the Sheerness and Morinville-Legal coalfields and will be complete in mid-1986. Studies will commence on the Paintearth coalfield of Alberta and on the Sukunka and Quintette coalfields of northeastern British Columbia in 1986-1987. The locations of these study areas are illustrated in Figure 54.12.

Conclusion

This co-operative project has resulted in a low-cost capability to examine surface-mineable coal resources in the light of land use and ownership constraints. Coal resource volumes meeting highly specific environmental, ownership, quality and geological criteria can be rapidly determined for any studied area, and located with a resolution of one hectare. Coverage could eventually be extended to all coal deposits in Canada, as geological studies are completed by GSC. In addition to meeting EMR's resource planning needs, the availability of this highly flexible tool will enable planners in industry and government to optimize the utilization of Canada's coal and land resources.

References

- Crain, I.K. and MacDonald, C.L.
1983: From land inventory to land management: the evolution of an operational geographic information system; Proceedings of Sixth International Symposium on Automated Cartography, Ottawa, v. 1, p. 41-50.
- Griffith, C.
1980: Geographic information systems and environmental impact assessment; Environmental Management, v. 4, no. 1, p. 21-25.
- Government of Alberta
1984: Coal Licence maps, Department of Energy and Natural Resources, Edmonton.
- Hughes, J.D.
1984: Geology and depositional setting of the Late Cretaceous, upper Bearpaw and lower Horseshoe Canyon formations in the Dodds-Round Hill coalfield of central Alberta – a computer-based study of closely-spaced exploration data; Geological Survey of Canada, Bulletin 361, 81 p.
- Irvine, J.A.
1981: Canadian coal resource terminology and evaluation methodology; Geological Society of America, Bulletin, Part 1, v. 92, p. 529-537.
- Lands Directorate
1978: The Canada Land Inventory objectives, scope and organization; Report 1, Ottawa, Lands Directorate, Environment Canada, 61 p.

Upper Jurassic dinoflagellate cysts from strata of northeastern British Columbia

Project 760042

E.H. Davies¹ and T.P. Poulton
Institute of Sedimentary and Petroleum Geology, Calgary

Davies, E.H. and Poulton, T.P., Upper Jurassic dinoflagellate cysts from strata of northeastern British Columbia; in *Current Research, Part B, Geological Survey of Canada, Paper 86-1B*, p. 519-537, 1986.

Abstract

Dinoflagellate cyst assemblages from the Fernie Formation in northeastern British Columbia indicate an Oxfordian to Tithonian age, rather than a Middle Jurassic age as previously thought. An assemblage from the basal part of the Monteith Formation indicates a late Tithonian age.

The Upper Jurassic sequence lies just above the Lower Jurassic 'Nordegg' Member documenting the presence of a major regional unconformity. This hiatus, supported by both microfossil and macrofossil evidence, suggests that Middle Jurassic strata are absent throughout northeastern British Columbia.

Résumé

Des assemblages de kystes de dinoflagellés provenant de la formation de Fernie dans le nord-est de la Colombie-Britannique datent de l'Oxfordien ou du Tithonien plutôt que du Jurassique moyen. Un assemblage trouvé dans la partie basale de la formation de Monteith daterait du Tithonien récent.

La séquence du Jurassique supérieur repose sur la formation de Nordegg du Jurassique inférieur, ce qui indique la présence d'une importante discordance régionale. L'existence de cette lacune, soutenue par la présence de microfossiles et de macrofossiles, porte à croire que le Jurassique moyen n'est pas représenté dans l'ensemble du nord-est de la Colombie-Britannique.

¹ Bujak Davies Group, 1-2835-19 Street N.E., Calgary, Alberta T2E 7A2

Introduction

Geological setting

The material described in this report comes from Upper Jurassic beds of the Fernie Formation and the basal part of the Monteith Formation in northeastern British Columbia (Stott, 1967; Fig. 55.1).

The Fernie Formation is a dominantly argillaceous epicratonic formation of the Western Canadian miogeocline and platform, outcropping from northeastern British Columbia to southwestern Alberta and southeastern British Columbia (Poulton, 1984). Lower and Middle Jurassic parts of the Fernie contain minor sandstone and carbonate derived mainly from the craton that was exposed east of the trough.

In contrast, upper parts of the Fernie Formation, which are of Late Jurassic age, mainly comprise a coarsening-upward succession that filled the narrow foredeep, i.e. the early stages of the Alberta or Rocky Mountain Trough (Fig. 55.2), adjacent to the first major uplifts of the Columbian Orogen. With a few exceptions, most of these Upper Jurassic rocks are assumed to have been derived from the orogen to the west, and a westward transition to conglomeratic facies is documented in both northeastern and southeastern British Columbia (McMechan and Stott, in Poulton, 1984; Gibson, 1985).

The Monteith Formation (Table 55.1) is one of several of the uppermost Jurassic and lower Cretaceous sandstone formations along the trough, and has components derived from both the east and west (Poulton, 1984; Stott, 1984).

Initial subsidence of the foredeep in the Late Jurassic appears to have been preceded by a period of uplift and erosion along the length of the trough, perhaps the result of a pre-orogenic 'welt' passing eastward across the craton. This is indicated by a regional unconformity below the Oxfordian Green beds of the Fernie Formation, or below the 'upper Fernie shales' where the Green beds are absent. The Green beds themselves are a series of berthierine-rich, condensed, fossiliferous sandstone units, which are interpreted as the basal transgressive facies, deposited as the seas advanced over the unconformable surface and the trough began to subside (Poulton, 1984).

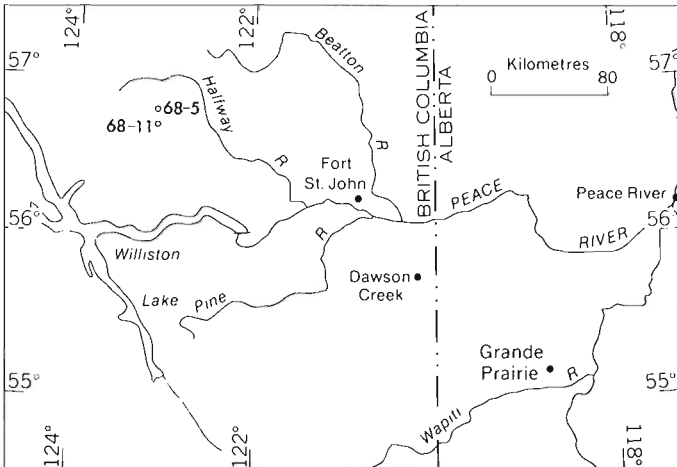


Figure 55.1. Index map, northeastern British Columbia.

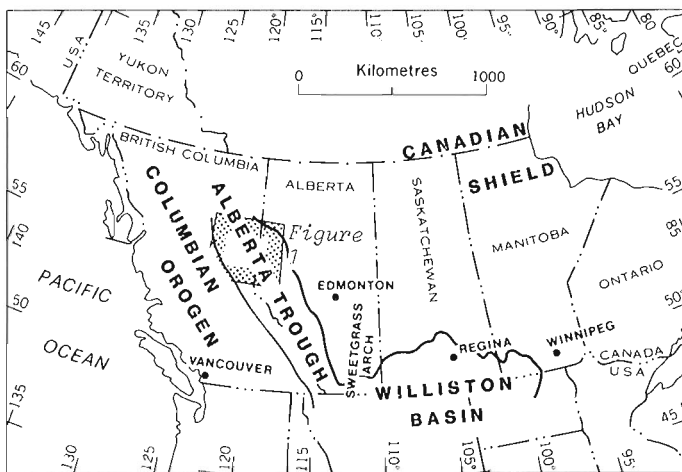


Figure 55.2. Paleogeographic-tectonic framework of Western Canada in latest Jurassic time.

Table 55.1. Table of formations

	NW Alberta -NE B.C.	SW Alberta- SE B.C.	
VOLGIAN	Monteith	Nikanassin	Mist Mtn
	Upper Fernie Shale		Morrissey
KIMMERIDGIAN		Passage beds	Kootenay
		Upper Fernie Shale	
OXFORDIAN		Green beds	
CALLOVIAN			
BATHONIAN		Grey beds	
		Highwood	
BAJOCIAN		Rock Creek	
AALENIAN		Paper shale	
TOARCIAN		Poker Chip Shale	
PLIENSBAKIAN		Red Deer	
SINEMURIAN		Nordegg	
HETTANGIAN			
	Brown beds		

Evidence from the microfossil study of Brooke and Braun (1981) in northeastern British Columbia indicates that, along the strike of the trough, there was significant variation in the amount of sub-Upper Jurassic rocks preserved below the unconformity, and in the nature of the source terranes of the Upper Jurassic sediments. Whereas a considerable thickness of Middle Jurassic rocks characterized the Fernie Formation from the Jasper area south to the U.S. border, none appear to be present north of about 54°N latitude. The northernmost Middle Jurassic fossils that can be confirmed are those listed from the Kvass Creek area by Irish (1954). Additionally, those Upper Jurassic sediments that are derived from an easterly source are thin and localized in the south, whereas those in the northern areas of the prairie provinces appear to be thicker and more extensive (Poulton, 1984). These include the eastern facies of the Monteith Formation (Stott, 1984), and an undated glauconitic sandstone unit in the Peace River Plains area formerly assigned to the Middle Jurassic Rock Creek Member of the Fernie Formation by Lackie (1958). However, the high glauconitic content of this unit is considered to be more characteristic of Upper Jurassic rocks (Poulton, 1984).

The interpretation that a major hiatus involving most of the Middle Jurassic occurs in northeastern British Columbia (Brooke and Braun, 1981) came as a surprise to stratigraphers working in that area. Previous studies of microfauna (Chamney, in Stott, 1967) had indicated the presence of a thick sequence of Bajocian to Callovian shales in the section measured by D.F. Stott. The conclusions of Brooke and Braun (1981) were based on a reinterpretation of the foraminifer and ostracode faunas, which they suggested indicated that Callovian to Oxfordian, or possibly Kimmeridgian, beds rested directly or nearly directly on Lower Jurassic beds. Subsequent palynological and macrofossil studies have supported their interpretation.

The principal additional support for the existence of the hiatus comes from the dinoflagellate studies described in this report. Additional evidence for a major regional unconformity below the Upper Jurassic beds is derived from two sources. In 1983, D.F. Stott collected the Late Oxfordian-Early Kimmeridgian bivalve *Buchia concentrica* (Sowerby) and a poorly preserved ammonite, which may belong to the genus *Amoeboceras* of the same age range, from a section only a few metres stratigraphically above the Lower Jurassic 'Nordegg' Member. This left little, if any, room for Middle Jurassic beds. The section occurs along a tributary of Trench Creek (53°57'N, 119°48'W) in the Mount Robson area. Furthermore, a search of the literature and the fossil collections of the Geological Survey of Canada failed to produce any record of diagnostic Middle Jurassic fossils in the Fernie Formation of British Columbia or Alberta north of about 54° latitude. Similarly, no rock types have been described that would indicate unequivocally a lithological correlation with Middle Jurassic beds farther south. The palynomorphs from one sample collected immediately below those described in this report, and immediately above the Nordegg Member may still be Middle Jurassic, although they cannot be dated conclusively.

The geographic position of the pre-Late Jurassic uplift documented in this report permits speculation regarding its possibly being a short-lived Jurassic rejuvenation of the Early Paleozoic Peace River Arch, and a reversal of the Late Devonian to earliest Jurassic Peace River Embayment. The earliest Jurassic (Hettangian) beds at Williston Lake (Tozer, 1982) are a unique occurrence in the eastern Cordillera, and their preservation, together with the thick Triassic section present in the area, suggest a youngest date for the temporal extent of the embayment. In contrast to these tectonic characteristics, which are restricted to the northeastern British Columbia region, the Upper Jurassic

succession described by Stott (1967) and documented in this report appears to be a basin-fill sequence like that all along the foredeep in the eastern Cordillera.

Previous palynological studies

There are few comprehensive palynological reports on the Jurassic of the Canadian Western Interior. The most significant work so far is by Pocock, who described and illustrated Jurassic terrestrial spores and pollen (Pocock, 1970), and marine dinoflagellates and acritarchs (Pocock, 1972). An informal palynological zonation was proposed (Pocock, 1972) in which seven dinoflagellate assemblage zones (and subzones) were recognized: two for the Early Jurassic, three for the Middle Jurassic and two for the Late Jurassic. The zonation was based on material collected from Manitoba to British Columbia, and from southern Alberta to northern Yukon as well as from scattered locations in the Queen Elizabeth Islands. This work demonstrated a potential for regional correlation using palynology.

Other palynological studies have dealt with local assemblages or species described from short stratigraphic intervals. Reports of Late Jurassic palynomorphs from central, southwestern and northwestern British Columbia and Alberta have been published by Rouse (1959), Gussow (1960), Ziegler and Pocock (1960), Pocock (1961a, b, 1962a, b, 1964, 1970, 1972, and 1980).

Published palynological reports from other areas of western Canada are both geographically and stratigraphically diverse. In northern Yukon and adjacent Northwest Territories, terrestrial and marine palynomorphs, ranging from Sinemurian to Oxfordian in age, have been recorded by Audretsch (in Poulton et al., 1982). Pocock (1970, 1972) recorded Middle to Late Jurassic palynological assemblages from widespread localities. Oxfordian, or possibly Kimmeridgian to Tithonian, assemblages were reported by Pocock (1967, 1976). The most detailed work on the Late Jurassic was published in a series of papers by Brideaux and his colleagues (Brideaux, 1976, 1977; Brideaux and Myhr, 1976; and Brideaux and Fisher, 1976). The spores from the Jurassic-Cretaceous boundary beds from the Aklavik Range have been described by Fensome (in press).

Within the Williston Basin, Jurassic palynological assemblages have been described by Pocock and Jansonius (1961), Pocock (1970, 1972), and Pocock and Sarjeant (1972).

Materials and methods

Forty-two samples from a section in northeastern British Columbia (Table 55.2) were analyzed for dinoflagellate cysts. The section is located at Christina Falls (56°40'N; 123°04'W) and was measured and described by D.F. Stott as section SI68-11; GSC localities C-71959 to C-72007 (Stott, 1968). Stott collected samples from the Fernie Formation and basal part of the Monteith Formation and they were analyzed for microfauna by Brooke and Braun (1981). The microfauna were dated as Callovian(?) to Early Cretaceous. The oldest sample studied in this report occurs about 30 m above what was called the Lower Jurassic Nordegg Member by Stott (1968). It is possible that a thin Middle Jurassic sequence may be represented by the unsampled shale unit above the Nordegg Member. This, however, appears unlikely in view of the regional macrofossil evidence.

Of the 42 samples processed from this section, 40 produced recoverable residues. In general the assemblages contain abundant palynomorphs, which are predominantly

terrestrial miospores. Numerous species of dinoflagellate cysts are present, ranging from 0 to 10, with an average of 5, species per sample.

Based on dinoflagellates, the palynological assemblages can be grouped into five intervals, which may prove to have correlative significance. Four of the intervals, from the upper parts of the Fernie Formation, are late Oxfordian or early Kimmeridgian to late Tithonian in age. The highest interval, which comprises the uppermost parts of the Fernie Formation and the basal parts of the Monteith Formation, is late Tithonian. The Monteith Formation, from which no microfaunas were recovered, was designated Early Cretaceous by Brooke and Braun (1981). The dinoflagellate cyst assemblages can be correlated with the assemblages in the Mackenzie Delta area described by Brideaux and Fisher (1976) and those from the Sverdrup Basin described by Brideaux and Fisher (1976) and Davies (1983).

In addition, ten samples were processed from another section at Cypress Creek (measured by D.F. Stott as section SI-68-5; GSC localities C-71949 to C-71958; 56°48'N; 123°05'W), of which eight produced recoverable residues. The assemblages are generally dominated by terrestrial miospores with only rare specimens of the dinoflagellates *Escharisphaeridia rudis* Davies and *Meiourgonyaulax* sp.

Dinoflagellate cyst assemblages

The assemblages are described from bottom to top and divided into intervals (A-E) according to age. The stratigraphic levels of samples are approximate and are measured from the top of the Fernie Formation.

A. Late Oxfordian - early Kimmeridgian assemblages

Seven samples (SI-68-209 to 216) from between 130 and 115 m below the top of the Fernie Formation were analyzed. *Cribroperidinium ehrenbergii* (Gitmez) Stover and Evitt, *Paragonyaulacysta capillosa* (Brideaux and Fisher) Stover and Evitt and *Escharisphaeridia rudis* are common in most samples within the interval. The lowest sample is only tentatively included in this interval because of the poor recovery of fossil material and the absence of diagnostic fossils. The second lowest sample (SI-68-210) is marked by the lowest occurrence of *Occucysta* sp. A, *Gonyaulacysta dualis* (Brideaux and Fisher) Stover and Evitt, *P. capillosa* and *Glomodinium tripartitum* (Johnson and Hills) Davies.

Tubotuberella eisenackii (Deflandre) Stover and Evitt occurs in the middle of the interval along with the lowest occurrences of *Sentusidinium filiatum* Davies, *Paragonyaulacysta borealis* (Brideaux and Fisher) Stover and Evitt, *Cribroperidinium granuligerum* (Klement) Stover and Evitt and *Apteodinium nuciforme* (Deflandre) Stover and Evitt.

Near the top of the interval (SI-68-214), the lowest occurrence of *Hystrichogonyaulax cladophora* (Deflandre) Stover and Evitt is present along with *Cantulodinium speciosum*. The uppermost sample (SI-68-216) contains the lowest occurrence of *Cribroperidinium globatum* (Gitmez and Sarjeant) Helenes.

The age of this interval is questionably Callovian to Oxfordian, according to Brooke and Braun (1981). They (*loc. cit.*, p. 38) also inferred "an even later age", stating "Kimmeridgian to Portlandian must be considered for the microfauna of the Peace River region". By comparing these dinoflagellate assemblages with the assemblages from the Mackenzie Delta area, an age of late Oxfordian to early Kimmeridgian (Poulton et al., 1982; Brideaux and Fisher, 1976; and Brideaux, 1977) is assignable. Equivalent to

this zone would be the range of *Gonyaulacysta* sp. cf. *G. cladophora* (Brideaux and Fisher, 1976; and Brideaux, 1977) and the upper parts of Opper zone H and Opper zone I from the Sverdrup Basin (Davies, 1983).

B. (?) Mid-Kimmeridgian assemblages

Four samples (SI-68-217 to 219) were analyzed from the interval between 103 and 112 m below the top of the Fernie Formation. The lowest sample (SI-68-217) is marked by common occurrences of *Cribroperidinium perforatum*, *Acanthaulax aceras* Gitmez and Sarjeant and *Ellipsoidictyum reticulatum* (Valensi) Lentin and Williams. *Scriniodinium crystallinum* (Deflandre) Klement is common in the upper parts of this interval. The age has been determined as mid-Kimmeridgian.

C. Late Kimmeridgian assemblages

Eight samples (SI-68-220 to 227) were analyzed from the interval between 100 and 255 ft (30 and 78 m) below the top of the Fernie Formation. An abundance of *Cribroperidinium* sp. A and the presence of *Oligosphaeridium* sp. A characterize this interval. The lowest sample is marked by the first appearance of *Tubotuberella egemenii* (Gitmez) Stover and Evitt and *Cribroperidinium jubaris* (Davies) Lentin and Williams, and by the common presence of *Endoscrinium galeritum* (Deflandre) Vozzhennikova. *Tectatodinium laminatum* Davies is characteristic of the lower parts of the interval, while several other species, such as *Horologinella spinosigibberosa* Brideaux and Fisher, and *Cribroperidinium* (alias *Gonyaulacysta*) sp. F of Gitmez and Sarjeant (1972), first occur in the middle of the interval. *Paragonyaulacysta* sp. cf. *P. borealis* occurs in sample SI-68-225. This species was described recently by Albert et al. (in press) from the Oxfordian to Kimmeridgian of Alaska.

The upper parts of this interval are marked by *Pareodinia prolongata* Sarjeant, *Sentusidinium baculatum* (Dodekova) Stover and Evitt, *Prolixosphaeridium spissum* (McIntyre and Brideaux) Lentin and Williams and *Rhynchodiniopsis hyalodermopsis* (Cookson and Eisenack) Sarjeant, and a peak in abundance of *Sirmiodinium grossii* Warren.

A late Kimmeridgian age is assigned to this interval. This would be equivalent to the range of *Oligosphaeridium asterigerum* sensu Brideaux, 1977 from the Mackenzie Delta area and approximately equivalent to Opper zone J from the Sverdrup Basin.

D. Late Kimmeridgian to late Tithonian assemblages

Eleven samples (SI-68-228 to 238) were analyzed from the interval between 43 and 88 m below the top of the Fernie Formation. This interval is marked by the presence of both *Cribroperidinium* sp. A and *Paragonyaulacysta capillosa*. The lower part is characterized by the presence of *Prolixosphaeridium spissum*, *Rhynchodiniopsis hyalodermopsis* and *Subtilisphaera paeminosa* (Drugg) Bujak and Davies, as well as the highest occurrence of *Apteodinium nuciforme* and the lowest occurrence of *Occucysta monoheuriskos* Gitmez. In the middle of the interval, *Rigaudella aemula* occurs and *Cribroperidinium perforatum*, *Cribroperidinium granuligerum*, *Dichatogonyaulax schizoblata* (Norris) Sarjeant, *Oligosphaeridium* sp. A and *Subtilisphaera paeminosa* (Drugg) Bujak and Davies appear for the last time. The upper parts of this interval are marked by the last occurrences of several taxa, including *Atopodinium prostaticum* Drugg, *Cribroperidinium* sp. A, *Paragonyaulacysta borealis* and *P. capillosa*, along with the occurrence of *Ctenidodinium panneum* (Norris) Lentin and Williams.

The assemblages present within this interval are comparable to assemblages found within the range of *Lanterna saturnalis* Brideaux and Fisher from the lower parts of the *Buchia piochii* Zone in the Mackenzie Delta and those of Opper zones J and K of the Sverdrup Basin (late Kimmeridgian-Tithonian-?Berriasian). The age, therefore, is considered to be late Kimmeridgian to late Tithonian.

E. Late Tithonian assemblages

Eleven samples (SI-68-239 to 249) were analyzed from the interval between 14 and 40 m below the top of the Fernie Formation. The presence of the thin-walled cavate pareodinioid cyst *Netrelytron parum* Sarjeant is characteristic of assemblages in this interval. At the foot of the interval, *Apteodinium bucculiatum*, *Tubotubella egemenii*, and *Sentusidinium filiatum* are present. *Cribroperidinium jubaris* and *Sirmiodinium grossi* do not occur above the middle parts of this interval, and *Cometodinium* sp. A of Habib (1972) is present.

The upper parts are characterized by the presence of *Veryhachium* sp. A, *Canningia ringnesiorum* Manum and Cookson and *Tetranguladinium* sp. A, as well as *Cribroperidinium granuligerum*, the highest occurrence of which is in this part of the interval. The age of this interval is late Tithonian. It is equivalent to the uppermost parts of Opper zone K and the lower parts of Opper zone L from the Sverdrup Basin.

The highest sample (SI-68-250) collected from the Monteith Formation 18 m above its base is also assigned to this zone. Although it is dominated by terrestrial miospores, the dinoflagellate cysts *Lanterna sportula* Dodekova and *Netrelytron parum* are present, indicating most probably a late Tithonian age. The former species may range higher into the Berriasian. However, it is generally abundant in the Tithonian (Portlandian) of the Jeanne d'Arc Basin, northeastern Grand Banks (Bujak and Williams, 1977; Davies, unpublished data). This sample was assigned a Lower Cretaceous age by Brooke and Braun (1981) but they did not give supporting fossil evidence. The basal 60 m or so of the Monteith Formation has yielded bivalves that have been assigned to the *Buchia fischeriana* zone, of Late Jurassic (Volgian) age (Jeletzky, unpublished data).

Descriptions of informal taxa

Cribroperidinium sp. A. Plate 55.5, figure 7

Description: An oblate species of *Cribroperidinium* with a smooth to granulate ornament. Growth marks are suppressed, but occasionally evident by the alignment of granules. The adcingular flanges are slightly more developed than other sutural crests. The cyst is generally rounded except at the apex where there is a distinctive apical horn (14 μm long), sharply terminating with a short solid antennule (5 μm long). Width, 88 μm ; length, 82 μm ; one measured specimen.

Remarks. This species may be conspecific with *Gonyaulacysta* sp. C of Gitmez and Sarjeant (1972).

Nannoceratopsis? sp. A Plate 55.3, figures 4, 7

Description. A species questionably assigned to the genus *Nannoceratopsis* with long apical (17 μm) and antapical (39-51 μm) horns, which are constricted at their bases.

The cyst wall is covered by a coarse, imperfect reticulate pattern, except over the horns where the surface is smooth. Width, 40 μm ; length, 122 μm ; one measured specimen.

Remarks. This species has affinities to *Nannoceratopsis pellucida* Deflandre. The large epicyst and the difference in ornamentation between the antapical horns and the body of the cysts indicates, however, that a new genus is most probably required.

Occisucysta sp. A. Plate 55.5, figures 2, 8

Description. A species of *Occisucysta* with a coarsely granulate ornament. The archeopyle is 2P. The apical horn is short and round giving the epicyst a conical shape. The hypocyst is also conical but with a more rounded antapex. The plate sutures are low and obscured by the granulation. Both apical and lateral compressions are common. Width, 80 μm ; length, 104 μm ; one measured specimen.

Oligosphaeridium sp. A (Plate 55.2, figures 1, 4)

Description. A species of *Oligosphaeridium* in which the processes (18-30 μm) are two thirds the diameter of the cyst body. The processes are complete distally, hollow and often perforated and strongly buccinate. Short, rudimentary cingular processes are rarely present. Body diameter, 43 to 53 μm ; three measured specimens.

Remarks. This species is similar to *Oligosphaeridium pulcherrimum* sensu Gitmez (1970) from the Kimmeridgian of Great Britain.

Tetranguladinium? sp. A Plate 55.3, figure 9

Description. A species with affinities to *Tetranguladinium* with strong cavations well developed in each corner of the rhomboidal cyst. These cavations protrude as rectilinear pairs (29-34 μm). Striations are also present along the corner projections. A cingulum, sulcus or archeopyle is not evident. Width, 42 μm ; length, 121 μm ; one measured specimen.

Veryhachium sp. A Plate 55.4, figure 9

Description. A large species of *Veryhachium* with a long slender process at each corner of the cyst. The processes terminate in a solid spine for approximately one third of the length. Process length, 20 μm ; body diameter, 40 μm ; one measured specimen.

Acknowledgments

The two sections were measured, described and sampled in 1968 by D.F. Stott. Gratitude is extended to D.F. Stott and D.J. McIntyre for their constructive criticism of this manuscript. The samples were processed by the palynological laboratories of the Eastern Petroleum Geology Section, GSC Dartmouth, Nova Scotia.

References

- Albert, N.R., Evitt, W.R. and Stein, J.A.
- **Lacrymodinium** gen. nov., a Gonyaulacoid dinoflagellate with intercalary archeopyle, from the Jurassic and Early Cretaceous of California and Alaska; *Micropaleontology*. (in press)
- Brideaux, W.W.
1975: Status of Mesozoic and Tertiary dinoflagellate studies in the Canadian Arctic; *American Association of Stratigraphic Palynologists, Contributions Series no. 4*, p. 15-28.
1976: Taxonomic notes and illustrations of selected dinoflagellates from the Gulf Mobil Parsons N-10 well; in *Report of Activities, Part B, Geological Survey of Canada, Paper 76-1B*, p. 251-257.
1977: Taxonomy of Upper Jurassic-Lower Cretaceous microplankton from the Richardson Mountains, District of Mackenzie, Canada; *Geological Survey of Canada, Bulletin 281*.
- Brideaux, W.W. and Fisher, M.J.
1976: Upper Jurassic-Lower Cretaceous dinoflagellate assemblages from Arctic Canada; *Geological Survey of Canada, Bulletin 259*.
- Brideaux, W.W. and Myhr, D.W.
1976: Lithostratigraphy and dinoflagellate cyst succession in the Gulf Mobil Parsons N-10 well, District of Mackenzie; in *Report of Activities, Part B, Geological Survey of Canada, Paper 76-1B*, p. 235-249.
- Brooke, M.M. and Braun, W.K.
1981: Jurassic microfossils and biostratigraphy of northeastern British Columbia and adjacent Alberta; *Geological Survey of Canada, Bulletin 183*.
- Bujak, J.P. and Williams, G.L.
1977: Jurassic palynostratigraphy of offshore eastern Canada; in *Stratigraphic Micropaleontology of Atlantic Basin and Border Lands*, F.M. Swain (ed.); Elsevier Scientific Publications, p. 321-339.
- Davies, E.H.
1983: The dinoflagellate Opper-zonation of the Jurassic-Lower Cretaceous sequence in the Sverdup Basin, Arctic Canada; *Geological Survey of Canada, Bulletin 359*.
- Fensome, R.A.
- Taxonomy of schizaeacean spores from the Aklavik Range, northern Richardson Mountains, Northwest Territories; *Palaeontographica Canadiana*. (in press)
- Gibson, D.W.
1985: Stratigraphy, sedimentology and depositional environments of the coal-bearing Jurassic-Cretaceous Kootenay Group of Alberta and British Columbia; *Geological Survey of Canada, Bulletin 357*.
- Gitmez, G.U.
1970: Dinoflagellate cysts and acritarchs from the basal Kimmeridgian (Upper Jurassic) of England, Scotland and France; *Bulletin of the British Museum (Natural History) Geology*, v. 18, p. 231-331.
- Gitmez, G.U. and Sarjeant, W.A.S.
1972: Dinoflagellate cysts and acritarchs from the Kimmeridgian (Upper Jurassic) of England, Scotland, and France; *Bulletin of the British Museum (Natural History) Geology*, v. 21, p. 171-257.
- Gussow, W.C.
1960: Jurassic-Cretaceous boundary in western Canada and late Jurassic age of the Kootenay; *Transactions of the Royal Society of Canada*, v. LIV, Series III, p. 45-64.
- Habib, D.
1972: Dinoflagellate stratigraphy, Leg 11, Deep Sea Drilling Project; in *Initial Reports of the Deep Sea Drilling Project 11*, C.D. Hollister and J.E. Ewing et al. (eds.), p. 367-425.
- Irish, E.J.W.
1954: Kvass Flats, Alberta; *Geological Survey of Canada, Paper 54-02*.
- Lackie, J.H.
1958: Subsurface Jurassic of the Peace River area; in *Jurassic and Carboniferous of western Canada*, A.J. Goodman (ed.); *American Association of Petroleum Geologists, John Andrew Allan Memorial Volume*, p. 85-97.
- Pocock, S.A.J.
1961a: Microspores of the genus **Murospora** Somers from Mesozoic strata of western Canada and Australia; *Journal of Paleontology*, v. 35, p. 1231-1234.
1961b: The microspore genus **Cingulatisporites** Thomson 1953; *Journal of Paleontology*, v. 35, p. 1234-1236.
1962a: Microflora analysis and age determination of strata at the Jurassic-Cretaceous boundary in the western Canada plains; *Palaeontographica, Abteilung B, Band 111*, p. 1-95.
1962b: Comparison of Canadian and European Jurassic-Cretaceous boundaries by means of microfossils; *Oil in Canada, February 8, 1962*, p. 36-40.
1964: Palynology of the Kootenay Formation at its type section; *Bulletin of Canadian Petroleum Geology*, v. 12, Special Guide Book Issue - Flathead Valley, p. 500-511.
1967: The Jurassic-Cretaceous boundary in northern Canada; *Review of Paleobotany and Palynology*, v. 5, p. 124-136.
1970: Palynology of the Jurassic sediments of western Canada; Part 1, terrestrial species; *Palaeontographica, Abteilung B, Band 130*, p. 12-72, 73-136.
1972: Palynology of the Jurassic sediments of western Canada; Part 2, Marine species; *Palaeontographica, Abteilung B, Band 137*, p. 85-153, Pl. 22-29.
1976: A preliminary dinoflagellate zonation of the uppermost Jurassic and lower part of the Cretaceous, Canadian Arctic, and possible correlation in the western Canada Basin; *Geoscience and Man*, v. XV, p. 101-111.
1980: Palynology at the Jurassic-Cretaceous boundary in North America; *Palynology Congress, Lucknow (1976-77)*, v. 2, p. 377-385.
- Pocock, S.A.J. and Jansonius, J.
1961: The pollen genus **Classopollis** Pflug, 1953; *Micropaleontology*, v. 7, p. 439-449.
- Pocock, S.A.J. and Sarjeant, W.A.S.
1972: The Partitomorphae, a new subgroup of acritarchs from the Triassic and Jurassic of Canada and Greenland; *Bulletin of the Geological Society of Denmark*, v. 21, p. 346-357.

- Poulton, T.P.
 1984: Jurassic of the Canadian Western Interior, from 49°N Latitude to Beaufort Sea; in *The Mesozoic of Middle North America*, D.F. Stott and D. Glass (eds.); Canadian Society of Petroleum Geologists, Memoir 9, p. 15-41.
- Poulton, T.P., Leskiw, K. and Audretsch, A.P.
 1982: Stratigraphy and microfossils of the Jurassic Bug Creek Group of northern Richardson Mountains, northern Yukon and adjacent Northwest Territories; Geological Survey of Canada, Bulletin 325.
- Rouse, G.E.
 1959: Plant microfossils from Kootenay Coal Measures strata of British Columbia; *Micropaleontology*, v. 5, p. 303-324.
- Stott, D.F.
 1967: Fernie and Minnes strata north of Peace River, Foothills of northeastern British Columbia; Geological Survey of Canada, Paper 67-17, Part A.
 1968: Fernie and Minnes strata north of Peace River, Foothills of northeastern British Columbia; Geological Survey of Canada, Paper 67-19, Part B.
- Stott, D.F. (cont.)
 1984: Cretaceous sequences of the foothills of the Canadian Rocky Mountains; in *The Mesozoic of Middle North America*, D.F. Stott and D.J. Glass (eds.); Canadian Society of Petroleum Geologists, Memoir 9, p. 85-108.
- Tozer, E.T.
 1982: Late Triassic (Upper Norian) and earliest Jurassic (Hettangian) rocks and ammonoid faunas, Halfway River and Pine Pass map-areas, British Columbia; Geological Survey of Canada, Paper 82-1A, p. 385-391.
- Williams, G.L. and Bujak, J.P.
 1980: Palynological stratigraphy of Deep Sea Drilling Project Site 416; Atlantic Geoscience Centre, Bedford Institute of Oceanography, Dartmouth, Nova Scotia, Canada.
- Ziegler, W.H. and Pocock, S.A.J.
 1960: The Minnes Formation; Edmonton Geological Society, 2nd Annual Field Conference, Guidebook, p. 43-71.

Plate descriptions

The name of the species is followed by the field sample number, the GSC locality number, the England Finder coordinates, with the lower right corner of the slide as the fixed reference, and the GSC type specimen number. All specimens were photographed under phase contrast (unless otherwise stated) and reproduced at x750 magnification; a 20 μm bar is present in figure 1 of each plate.

PLATE 55.1

- | | | |
|---------|-------|----------------------------------------------------------------------------------------------------------------------------------------------------------------------------|
| figure | 1. | Paragonyaulacysta borealis , SI-68-237, GSC loc. C-71987, V40/0, GSC 76271. |
| figures | 2, 3. | Paragonyaulacysta sp. cf. P. borealis , with a short apical horn, SI-68-224, GSC loc. C-71974, T47/1, GSC 76272. Figure 3 is with bright field illumination. |
| figures | 4-8. | Netrelytron sp. A. |
| | 4. | SI-68-240, GSC loc. C-71990, 038/2, GSC 76276. |
| | 5. | SI-68-240, GSC loc. C-71990, P51/3, GSC 76277. |
| | 6. | SI-68-240, GSC loc. C-71990, L43/4, GSC 76280. |
| | 7. | SI-68-240, GSC loc. C-71990, J36/3, GSC 76275. |
| | 8. | SI-68-250, GSC loc. C-72000, U41/3, GSC 76287. |
| figure | 9. | Subtilisphaera paeminosa , SI-68-229, GSC loc. C-71979, N42/3, GSC 76291. |

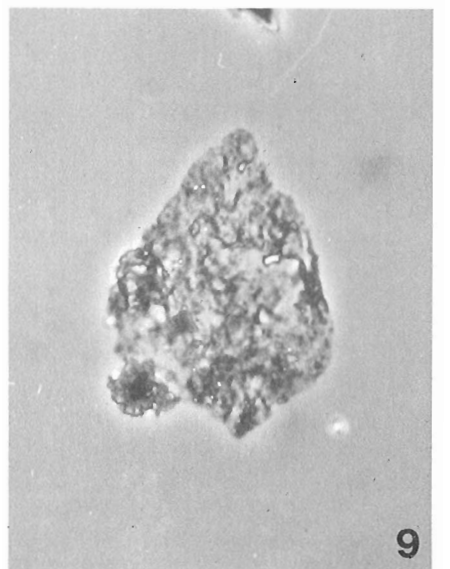
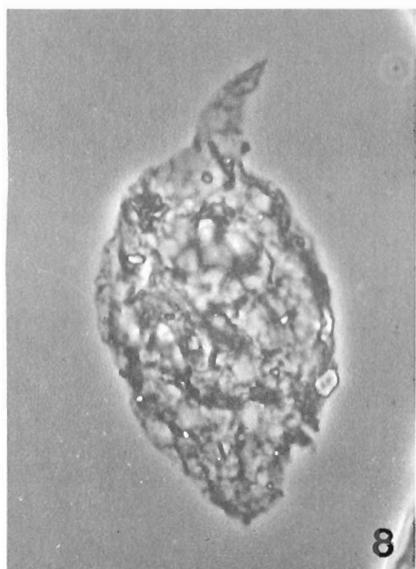
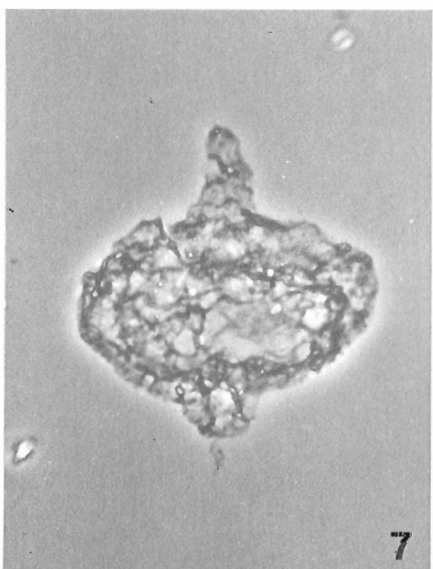
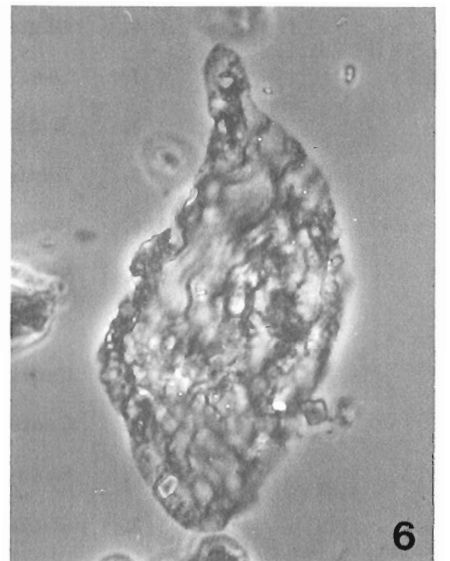
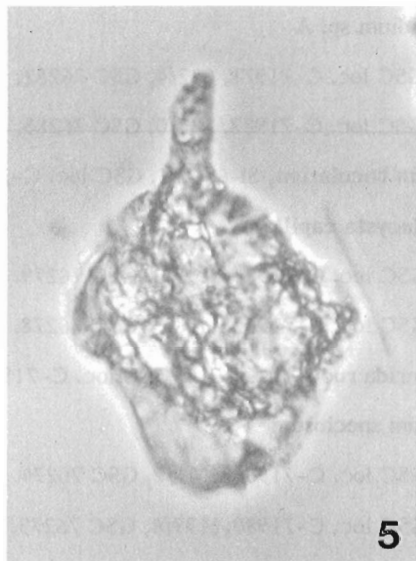
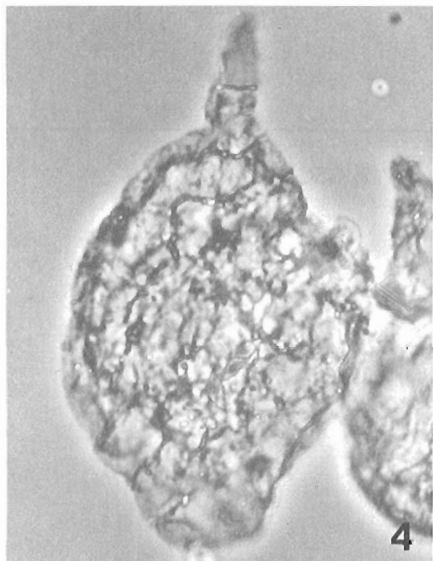
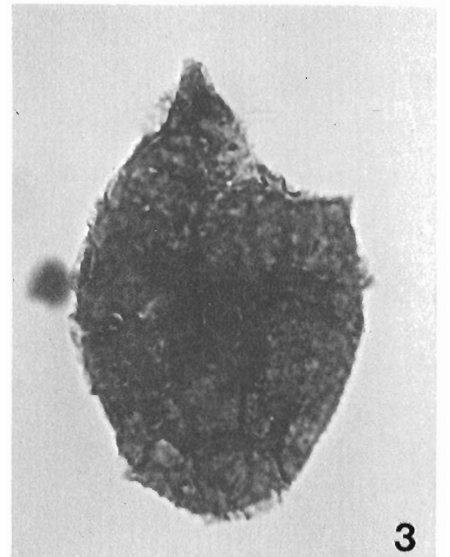
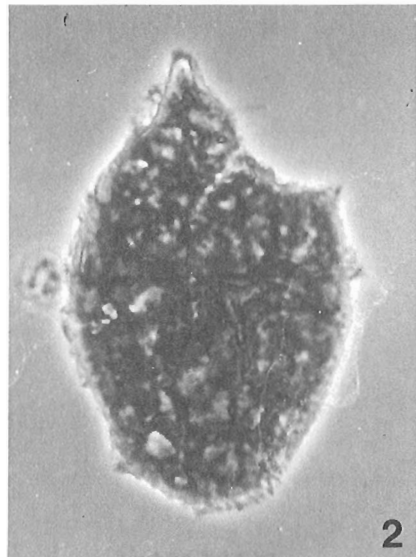
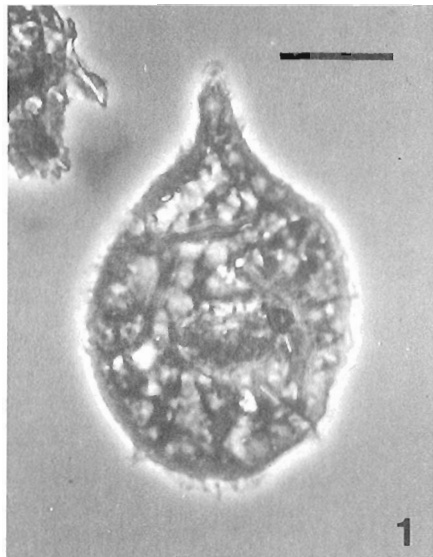


PLATE 55.2

- figures 1, 4. **Oligosphaeridium** sp. A
1. SI-68-221, GSC loc. C-71971, 042/4, GSC 76282.
4. SI-68-232, GSC loc. C-71982, S32/0, GSC 76283.
- figure 2. **Sentusidinium baculatum**, SI-68-226, GSC loc. C-71976, P37/2, GSC 76293.
- figures 3, 6. **Paragonyaulacysta capillosa**
3. SI-68-234, GSC loc. C-71984, C35/2, GSC 76279.
6. SI-68-217, GSC loc. C-71967, H38/3, GSC 76278.
- figure 5. **Escharisphaerida rudis**, SI-68-210, GSC loc. C-71960, M 43/0, GSC 76281.
- figures 7, 8. **Cantulodinium speciosum**
7. SI-68-214, GSC loc. C-71964, K41/2, GSC 76274.
8. SI-68-230, GSC loc. C-71980, M 39/4, GSC 76273.
- figure 9. **Sentusidinium filiatum**, SI-68-236, GSC loc. C-71986, K36/3, GSC 76528.

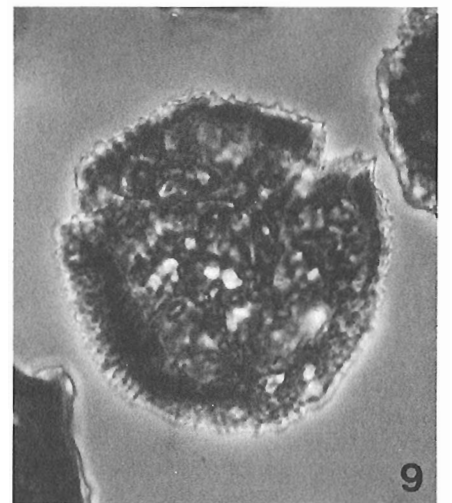
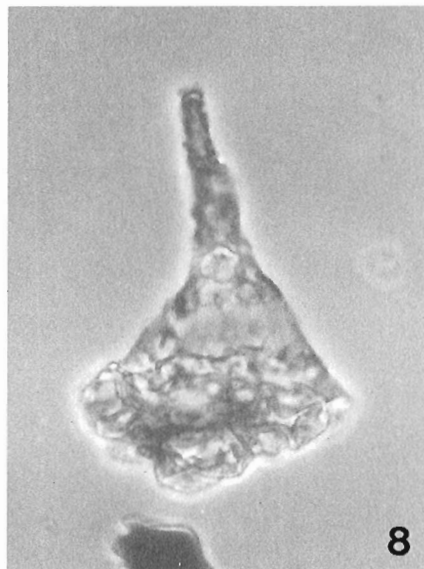
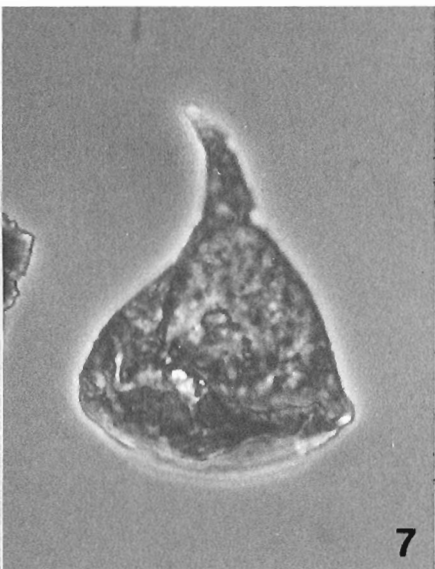
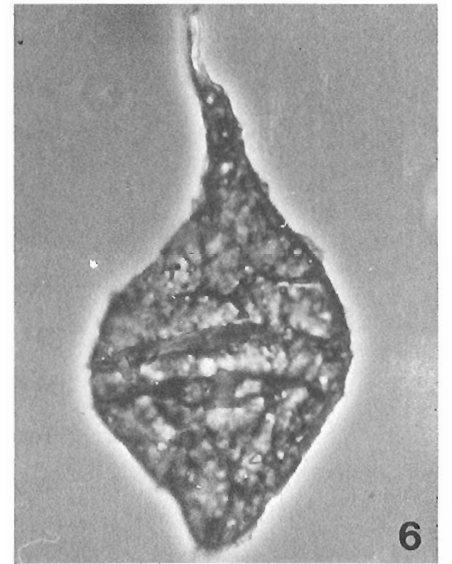
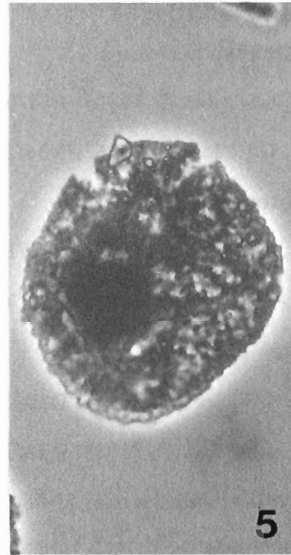
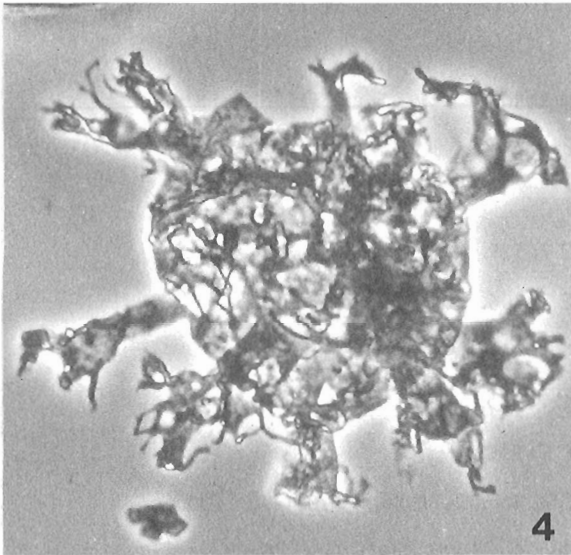
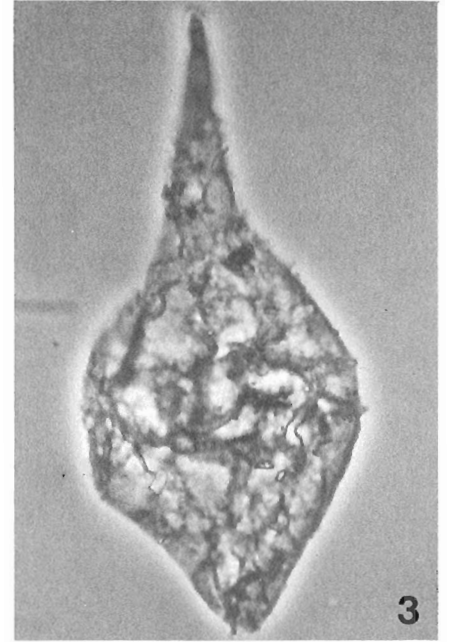
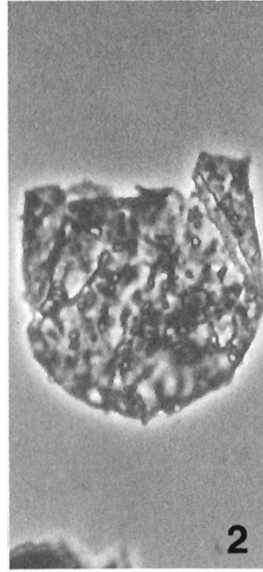
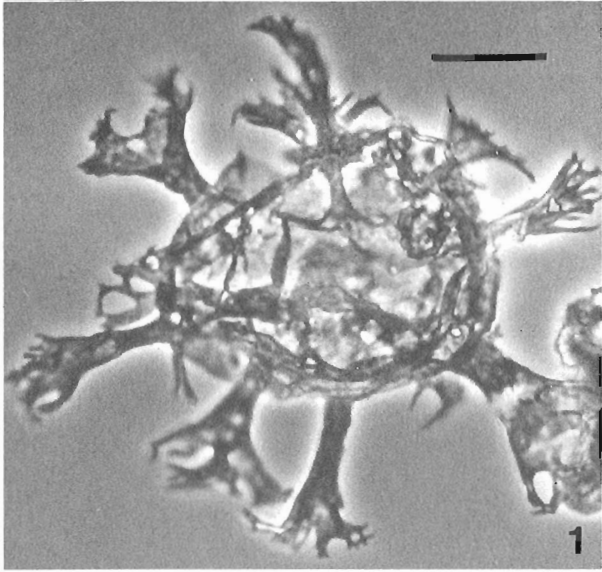


PLATE 55.3

- figure 1. **Gonyaulacysta dualis**, SI-68-225, GSC loc. C-71975, V52/2, GSC 76304.
- figures 2, 3. **Cribroperidinium perforans**
2. SI-68-217, GSC loc. C-71967, P44/0, GSC 76300.
3. SI-68-217, GSC loc. C-71967, N36/2, GSC 76301.
- figures 4, 7. **Nannoceratopsis?** sp. A
4. SI-68-237, GSC loc. C-71987, T46/1, GSC 76529.
7. SI-68-210, GSC loc. C-71960, E28/4, GSC 76306.
- figures 5, 6. **Atopodinium prostatum**
5. SI-68-222, GSC loc. C-71972, D30/0, GSC 76285.
6. SI-68-238, GSC loc. C-71988, Q33/3, GSC 76530.
- figure 8. **Tubotuberella rhombiformis**, SI-68-236, GSC loc. C-71986, S39/0, GSC 76305.
- figure 9. **Tetranguladinium** sp. A, SI-68-249, GSC loc. C-71999, J34/1, GSC 76303.

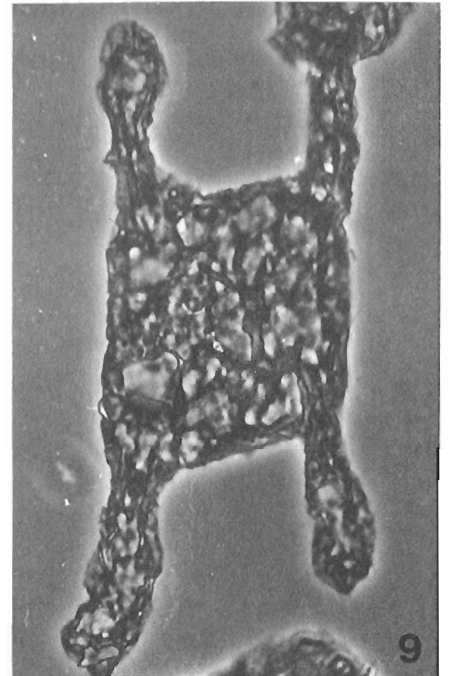
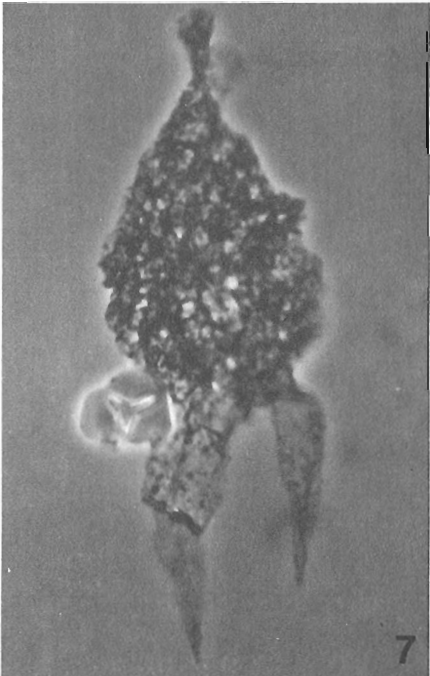
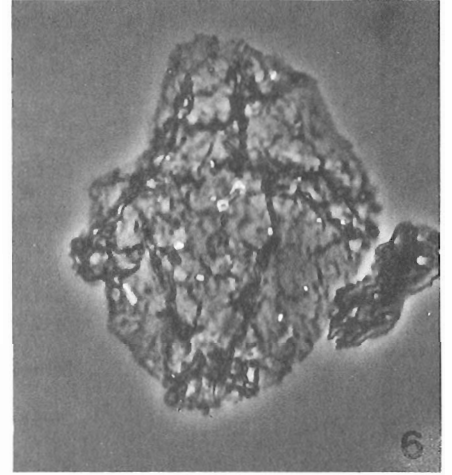
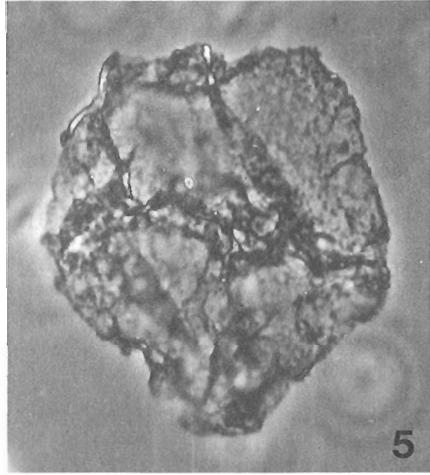
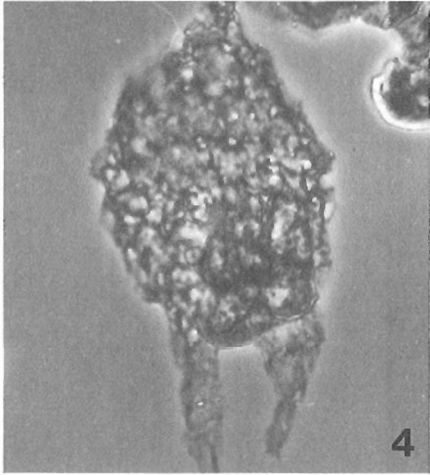
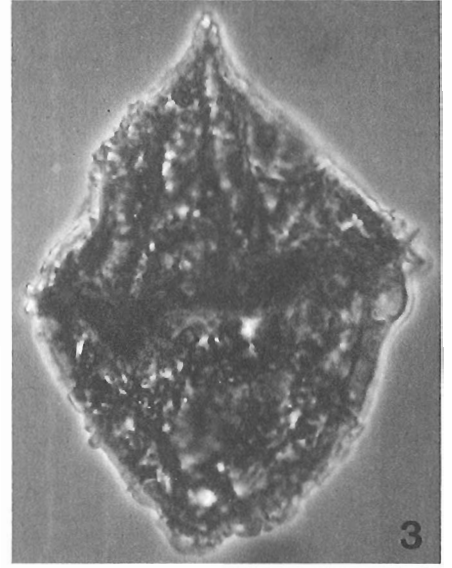
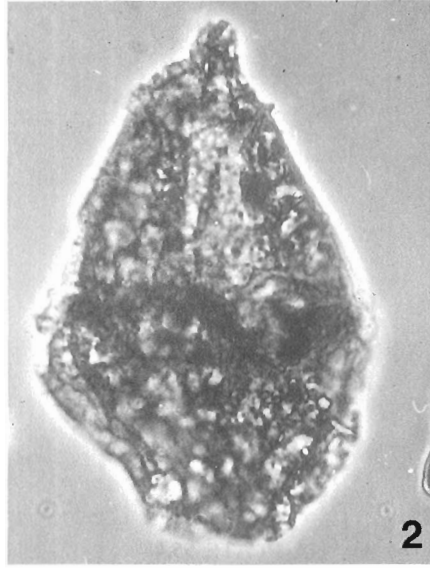
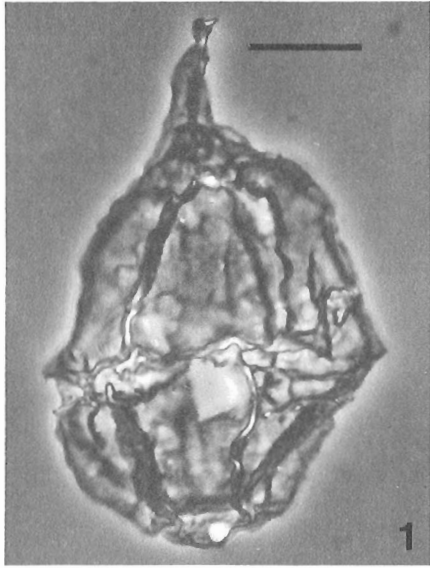


PLATE 55.4

- figures 1, 4. **Cribopteridinium jubaris**
1. SI-68-228, GSC loc. C-71978, T35/4, GSC 76290.
4. SI-68-243, GSC loc. C-71993, W33/3, GSC 76289.
- figures 2, 5, 8. **Occisucysta monoheuriskos**
2. SI-68-231, GSC loc. C-71981, N38/1, GSC 76531.
5. SI-68-231, GSC loc. C-71981, F37/0, GSC 76292.
8. SI-68-230, GSC loc. C-71980, G33/3, GSC 76532.
- figures 3, 6. **Scriniodinium crystallinum**
3. SI-68-219, GSC loc. C-71969, U45/2, GSC 76295.
6. SI-68-220, GSC loc. C-71970, S32/1, GSC 76296.
- figure 7. **Acanthaulax aceras**, SI-68-217, GSC loc. 71967, W34/1, GSC 76533.
- figure 9. **Veryhachium** sp. A., SI-68-246, GSC loc. C-71996, P40/1, GSC 76288.

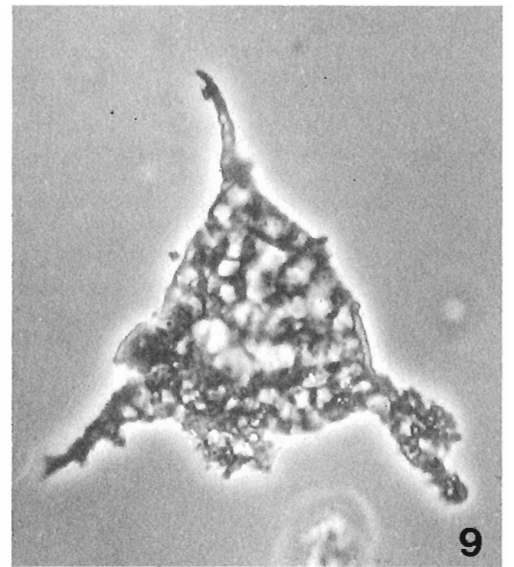
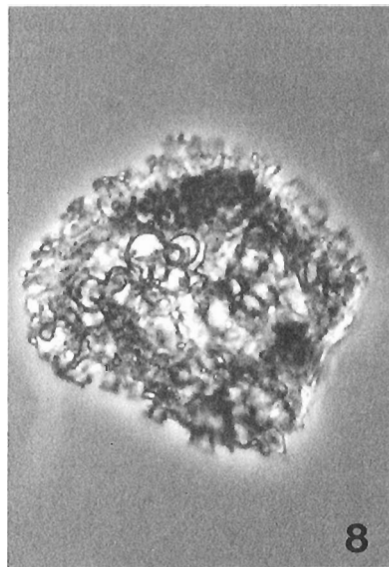
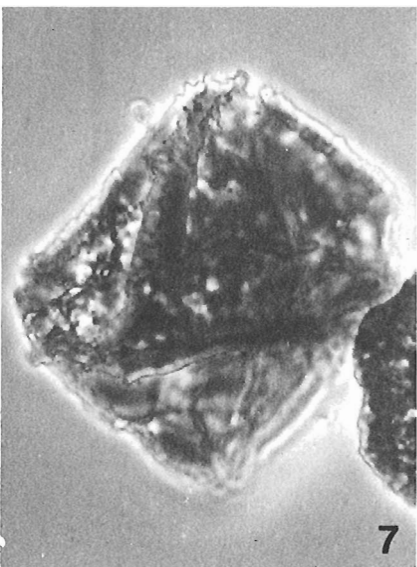
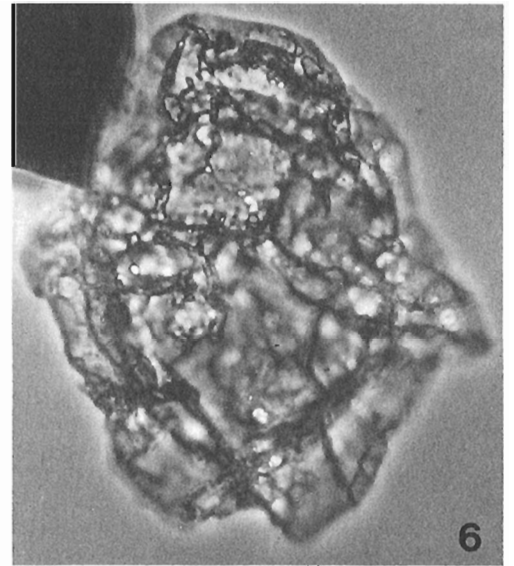
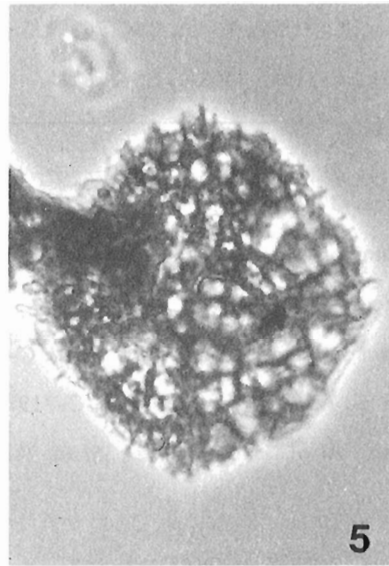
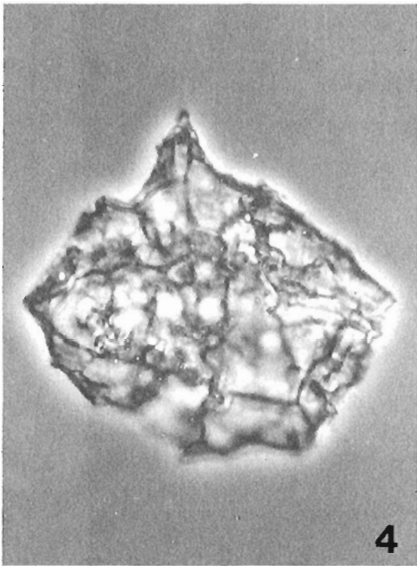
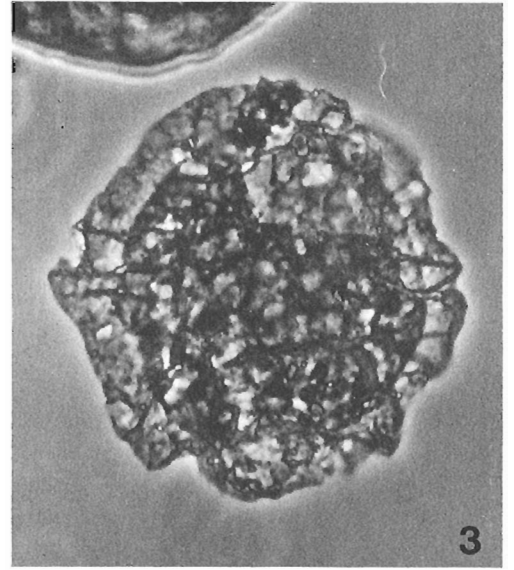
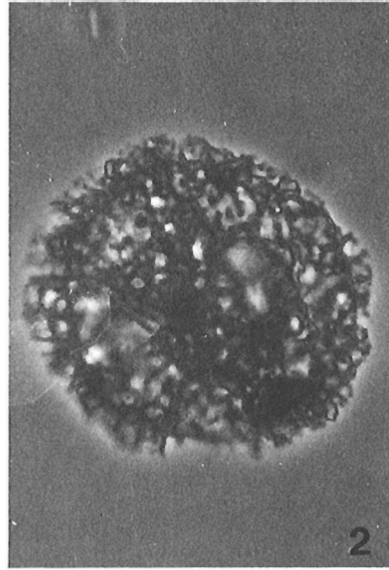
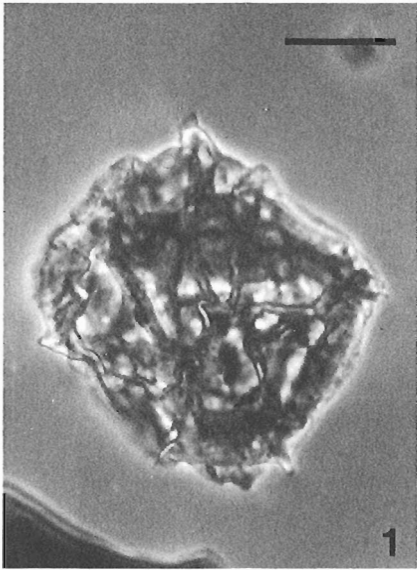
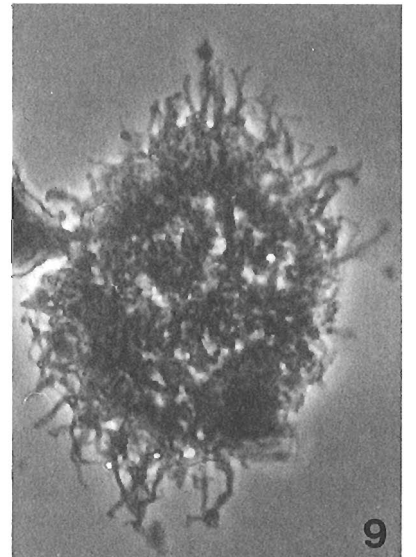
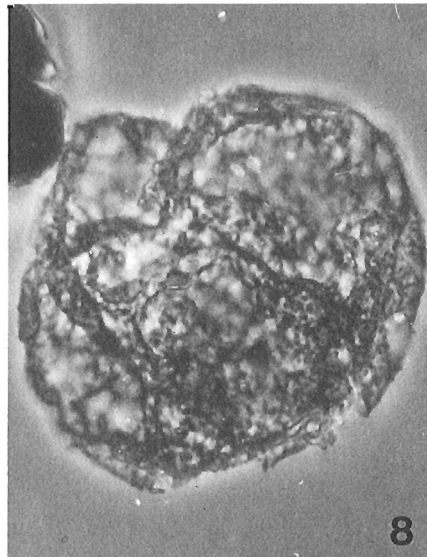
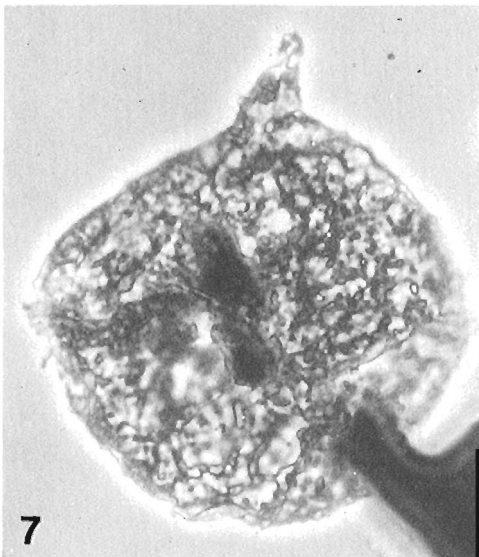
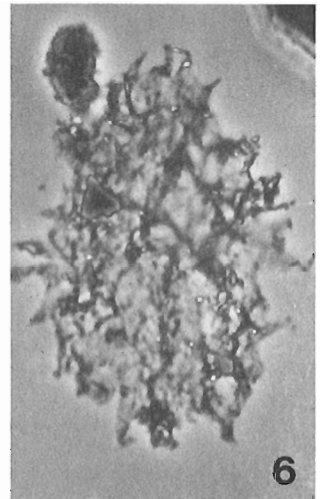
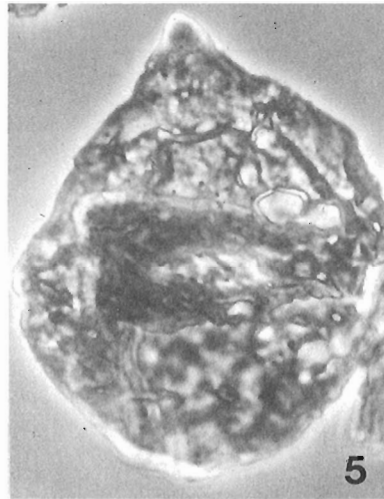
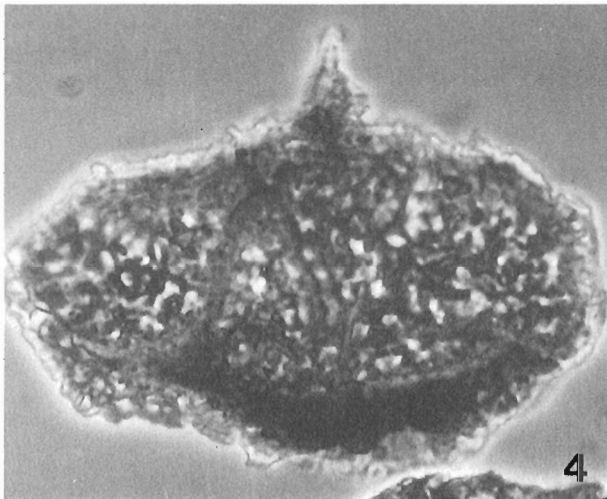
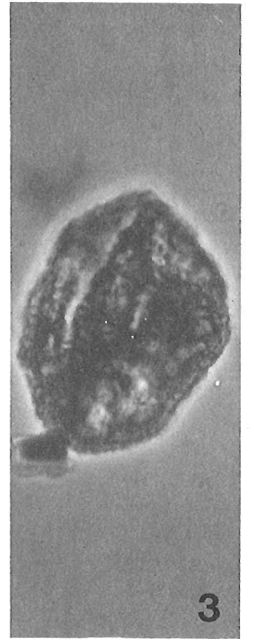
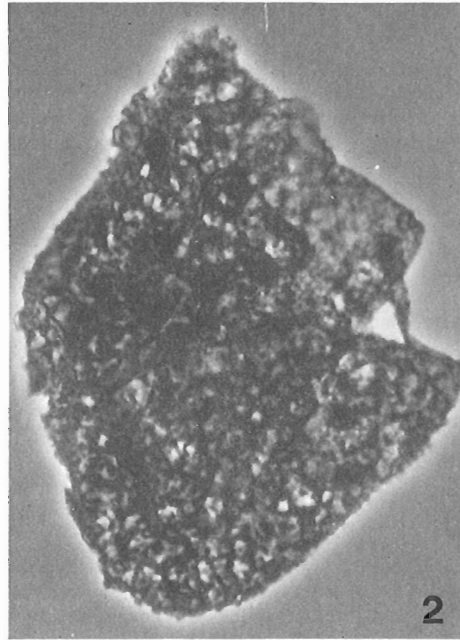
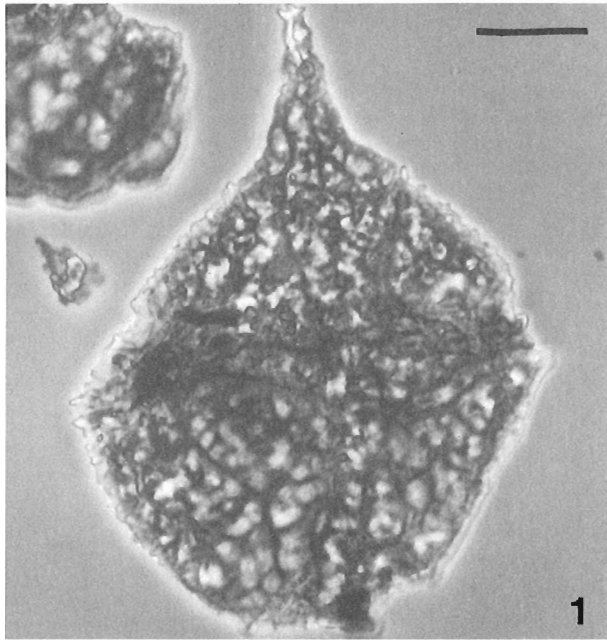


PLATE 55.5

- figures 1, 4. **Cribroperidinium** (alias **Gonyaulacysta**) sp. F of Gitmez and Sarjeant (1972).
1. SI-68-222, GSC loc. C-71972, T35/1, GSC 76299.
4. SI-68-231, GSC loc. C-71981, Q48/1, GSC 76534.
- figures 2, 8. **Occisucysta** sp. A
2. SI-68-210, GSC loc. C-71962, V30/0, GSC 76297.
8. SI-68-212, GSC loc. C-71960, W37/1, GSC 76298.
- figure 3. **Tectatodinium laminatum**, SI-68-221, GSC loc. C-71971, O43/3, GSC 76284.
- figure 5. **Apteodinium bucculiatum**, SI-68-223, GSC loc. C-71973, C50/2, GSC 76294.
- figure 6. **Prolixosphaeridium spissum**, SI-68-228, GSC loc. C-71978, R35/4, GSC 76286.
- figure 7. **Cribroperidinium** sp. A, SI-68-224, GSC loc. C-71974, T43/1, GSC 76302.
- figure 9. **Cometodinium** sp. A of Habib (1972), SI-68-242, GSC loc. C-71992, K41/1, GSC 76535.



Metamorphic studies in the transition zone between the
Lynn Lake Greenstone Belt and the Kisseynew Gneiss Belt,
Laurie Lake, Manitoba¹

Project 850025

S.L. Jackson and T.M. Gordon
Lithosphere and Canadian Shield Division

Jackson, S.L. and Gordon, T.M., Metamorphic studies in the transition zone between the Lynn Lake Greenstone Belt and the Kisseynew Gneiss Belt, Laurie Lake, Manitoba; in Current Research, Part B, Geological Survey of Canada, Paper 86-1B, page 539-546, 1986.

Abstract

The Laurie Lake region in Manitoba lies at the transition zone between the Lynn Lake Greenstone Belt and the Kisseynew Gneiss Belt. Pressure-temperature estimates within the region range from 4.5 kb and 650°C to 5.5 kb and 750°C. Migmatite development in aluminous metasedimentary rocks of the Wasekwan Group/Burntwood River Metamorphic Suite is progressive from unmigmatized rocks in the northeast to extensively migmatized rocks in the southwest. Sickle Group/Sickle Metamorphic Suite rocks contain assemblages appropriate for constraining a sillimanite-K feldspar isograd.

Résumé

La région du lac Laurie au Manitoba, se trouve dans une zone de transition entre la zone de roches vertes de Lynn Lake et la zone de gneiss de Kisseynew. Les estimations de la pression et de la température dans cette région varient de 4,5 kb et 650°C à 5,5 kb et 750°C. Un développement de migmatite dans des roches métasédimentaires alumineuses du groupe de Wasekwan et de la suite métamorphique de Burntwood River se migmatise progressivement du nord-est vers le sud-ouest. Les roches du groupe de Sickle et de la suite métamorphique Sickle contiennent des assemblages appropriés pour l'établissement d'une courbe isograde sillimanite-feldspath potassique.

¹ Contribution to the Canada-Manitoba Mineral Development Agreement 1984-1989. Project carried by Geological Survey of Canada.

Introduction

Metamorphosed supracrustal rocks of the Lynn Lake Greenstone Belt in the Churchill Structural Province of Manitoba are Aphebian in age (Clark, 1980; Baldwin et al., 1985). These rocks belong to two main groups. The older Wasekwan Group contains mainly metavolcanic rocks and mafic to aluminous metasedimentary rocks. Quartzofeldspathic metasedimentary rocks of the Sickle Group lie unconformably on the Wasekwan Group (Milligan, 1960; McRitchie, 1974; Gilbert et al., 1980).

The Kisseynew Gneiss Belt, south of the greenstone belt, includes two suites of high grade metasedimentary rocks, the Burntwood River Metamorphic Suite and the Sickle Metamorphic Suite (Gilbert et al., 1980), which are believed to be correlative with the Wasekwan Group and the Sickle Group respectively.

The Laurie Lake region (Fig. 56.1) lies at the transition zone between the greenstone belt and the Gneiss Belt. Within the region, volcanic and sedimentary rocks of the Wasekwan Group may be traced southwestwards into the Kisseynew Gneiss Belt (Zwanzig, 1976). Elsewhere, quartzofeldspathic rocks of the Sickle Group separate the two belts. This makes the Laurie Lake region well suited for studies of the relationship between the two belts.

The transition zone exhibits lithologic changes (Zwanzig, 1976), structural complications, and increasing metamorphic grade from northeast to southwest. The present investigation is concerned with the metamorphism and structure of this transition zone. Metamorphic studies conducted during the past year focussed on: 1) microprobe analyses of garnet, biotite, and plagioclase to estimate the physical conditions of metamorphism; 2) field documentation of migmatite development in aluminous metasedimentary rocks of the Wasekwan Group/Burntwood River Metamorphic Suite; and 3) collection of mineral assemblage data from the Sickle Group/Sickle Metamorphic Suite to constrain a sillimanite-K feldspar isograd.

In this report, symbols for minerals and components (Table 56.1) are from Kretz (1983). Migmatite nomenclature follows that of Johannes (1983). Evaluation of precision errors in chemical analyses, atomic ratios, mole fractions, and distribution coefficients follow procedures outlined by Kretz (1985).

Microprobe analyses and P-T estimates

Ten element (Si, Al, Fe, Mg, Mn, Ca, Ti, Cr, Na, and K) chemical analyses of garnet, plagioclase, and biotite co-existing with quartz and sillimanite were obtained from three samples (Fig. 56.2) using an energy dispersive system on the Queen's University ARL-SEMQ electron microprobe. Operating conditions were 15 kV accelerating voltage, 120 second count times, and beam widths of 2, 10 and 15 μm for garnet, plagioclase, and biotite respectively. Spectra collected from these minerals were compared to spectra collected from garnet, biotite, and glass (NBS 4709 K-412) standards, and corrections were made using the Bence-Albee method.

The three samples (one from below the sillimanite-Kfeldspar isograd and two from above) were chosen for both their distribution over the map area and lack of alteration. Within each sample, analyses were obtained from two to three different domains separated from each other by 10 mm. Within each domain the minerals chosen for analysis were separated from one another by several mineral grains. Rim analyses of minerals are from locations where the adjacent mineral was quartz. Garnets were analyzed one to four times at several locations from core to rim. Plagioclase cores and rims were each analyzed three times; those of biotite were analyzed twice.

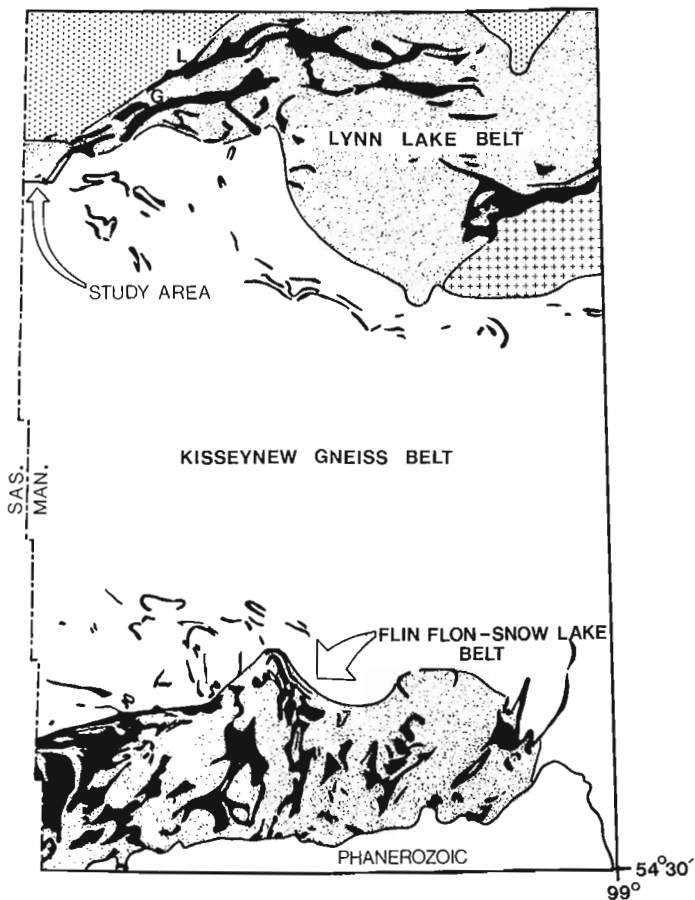


Figure 56.1. Location of Laurie Lake region (study area) and major lithostructural domains in northern Manitoba. Solid black regions represent amphibolite. Stipples and crosses represent granitic intrusive rocks.

Table 56.1. Mineral and component symbols

MINERALS		COMPONENTS	
		an	anorthite
And	andalusite		
Ap	apatite		
Bt	biotite		
Gr	graphite		
Grt	garnet	grs	grossular
Ilm	ilmenite		
Kfs	K feldspar		
Ky	Kyanit		
Mag	magnetite		
Ms	muscovite		
Pl	plagioclase		
Qtz	quartz		
Sil	sillimanite		
Tur	tourmaline		

Analyzed biotites and plagioclases do not exhibit any compositional zoning at the 0.95 confidence level of precision. Hence, both rim and core compositions were averaged.

Garnets display compositional zoning in the outer 10 to 30 per cent of their radii. Except for MnO in one garnet, the variation in concentration of all oxides is less than one weight

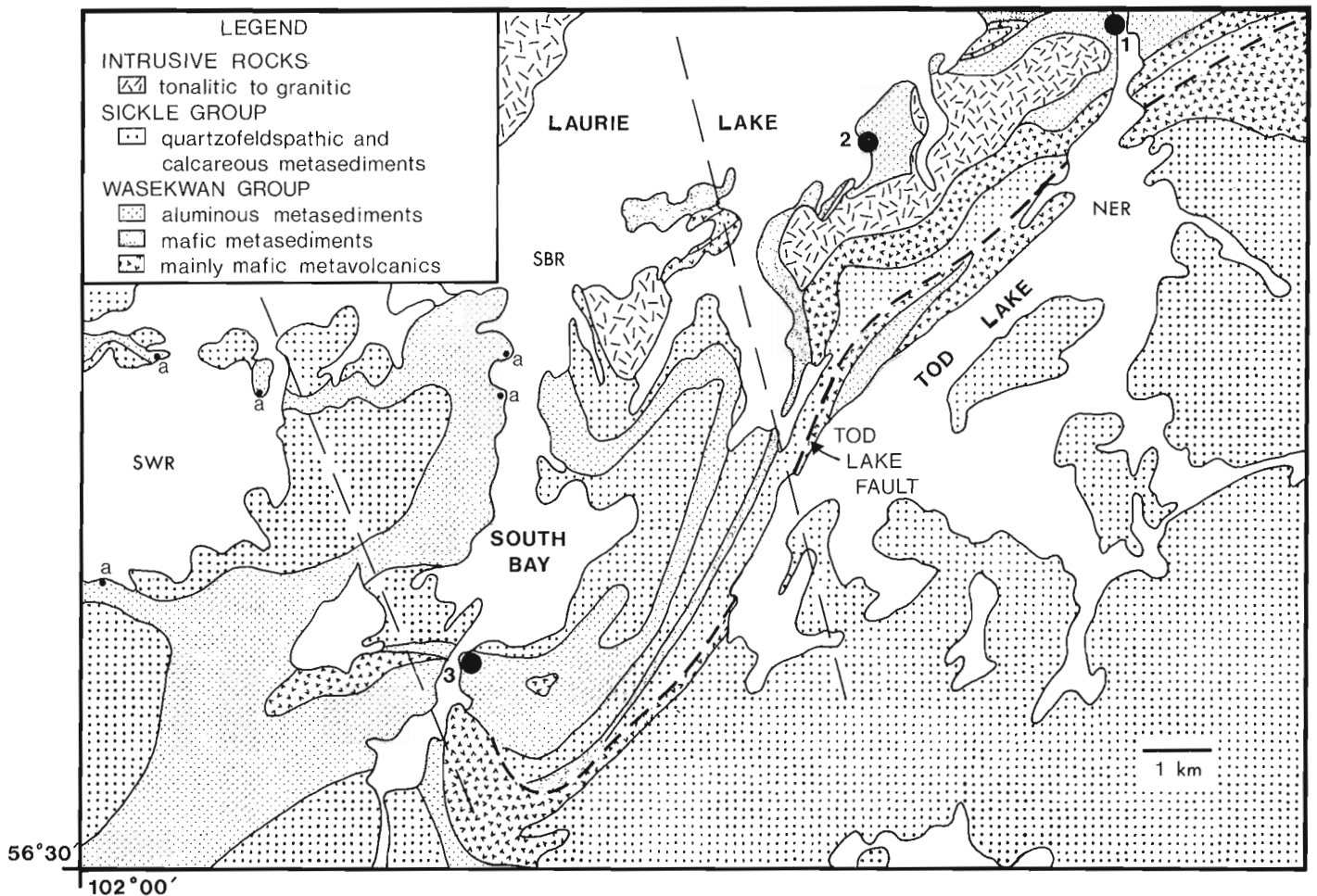


Figure 56.2. Geology of Laurie Lake region. Distribution of lithologies modified after Zwanzig (1980). Dashed NNW trending lines divide map into northeast (NER), South Bay (SBR), and southwest (SWR) regions referred to in text. Numbers 1, 2 and 3 indicate locations of samples used for P-T estimates. "a" indicates locations of retrograde andalusite in leucosomes of migmatites.

per cent. FeO and CaO exhibit flat composition profiles whereas MgO (and thus atomic Mg/Fe ratio) decreases and MnO increases. MnO displays the most pronounced zoning. An example of one garnet profile is shown in Figure 56.3.

Grant and Weiblen (1971) and Tracy et al. (1976) studied garnets with zoning characteristics similar to those in this study. They attributed the zonation patterns to retrograde reaction since most prograde continuous reactions in pelitic rocks result in increasing the Mg/Fe ratio and decreasing the concentration of Mn from core to rim. This interpretation is adopted in this study.

In calculation of P-T estimates, two assumptions were made concerning mineral compositions. First it was assumed that garnets were compositionally homogeneous at peak metamorphic conditions and that the observed zoning resulted from retrograde reaction. Secondly, because the garnet rims are volumetrically insignificant in comparison to the volume of matrix biotite, it was assumed that the compositional adjustment of biotite during retrogression was negligible (Tracy et al., 1976). Therefore interior garnet, average biotite, and average plagioclase compositions were used in the calculations.

Mg/Fe ratios of garnet and biotite (Table 56.2) used in the geothermometer of Ferry and Spear (1978) are combined with X_{Grt}^{Gr} and X_{An}^{Pl} values used in the geobarometer of Ghent (1976) as modified by Ghent et al (1979) to yield unique P-T estimates

for each domain in each sample. Accounting for precision errors in mineral analyses results in an estimate of a range of P and T for each domain (Fig. 56.4). The confidence level chosen for calculation of precision errors is 0.95. Accuracy and errors in the calibration of the geothermometer and geobarometer have not been considered. To obtain the most probable P-T estimate for each sample the distribution coefficients (calculated from Mg/Fe ratios and mole fractions in Table 56.2) from each domain in a sample were averaged. This procedure greatly reduced the estimated fields of pressure and temperature (Fig. 56.4, 56.5). The results agree with the increase in metamorphic grade from northeast to southwest (Jackson and Gordon, 1985; Milligan, 1960; Zwanzig, 1976); however, the temperature estimate for sample 3 appears to be high (~750°C) since no orthopyroxene is present in mafic rocks (as would be expected if the rocks attained the estimated temperature).

Migmatites in the Wasekwon Group/Burntwood River Metamorphic Suite

Migmatized and nonmigmatized aluminous metasedimentary rocks of the Wasekwon Group/Burntwood River Metamorphic Suite generally contain the same mineral assemblage: Grt + Bt + Sil + Pl + Qtz + Gr + Tur +/- Ap, Ilm, and Ms (retrograde). Exceptions to this include: the presence of relict staurolite in the northeast region, retrograde andalusite in

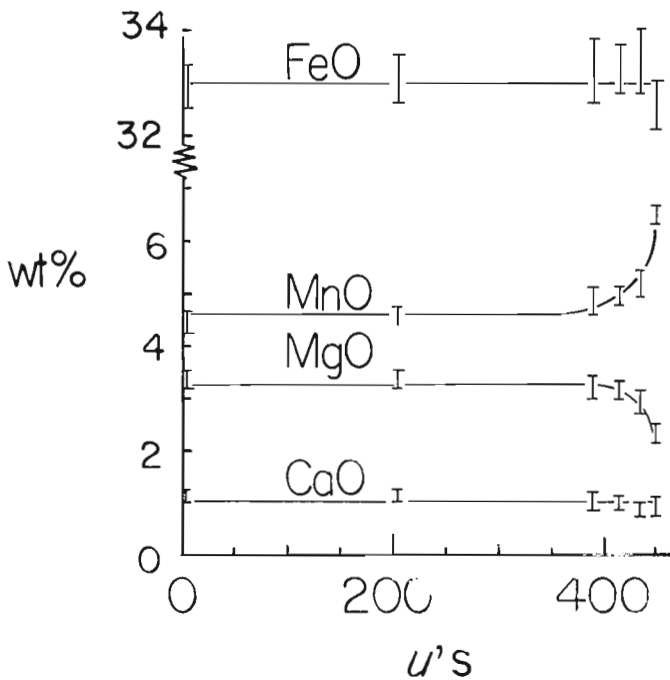


Figure 56.3. Chemical zonation profile of a garnet from sample 1. Note increase in MnO at the rim. Error bars calculated at 0.95 confidence level.

leucosomes of the southwest region and the western portion of the South Bay region, and cordierite as an additional phase in the southwest region. Petrographic work and staining of several specimens did not confirm the presence of K feldspar in cordierite-bearing rocks previously reported by Jackson and Gordon (1985).

The progression from unmigmatized to extensively migmatized rocks is documented by an increase in the variety of leucosome present, an increase in the percentage of leucosome present, an increase in grain size of mesosomes, and an increasingly aluminous nature of melanosomes.

The northeast, South Bay, and southwest regions in Figure 56.2 contain 4, 6, and 7 major types of leucosome, respectively. The four leucosome types present in the northeast region (also present in the other regions) are: quartz veins, quartz veins with plagioclase-rich rims, discordant pegmatites (Jack-

son and Gordon, 1985), concordant pegmatites (op. cit.). In the South Bay region two additional types of leucosomes exist: coarse to very coarse grained quartz-plagioclase veins (Fig. 56.6), and individual or clusters of several plagioclase porphyroblasts (Fig. 56.7). In the southwest region a seventh type of leucosome, an equigranular coarse grained tonalite, is present.

Leucosome material increases in abundance from less than 5% to greater than 40% from the northeast to southwest regions. The increase in degree of migmatization is due mainly to an increase in the abundance of the quartz-plagioclase veins and also to an increase in the individual and clusters of plagioclase porphyroblasts. The other leucosome types, with the possible exception of the coarse grained equigranular tonalite, are only locally significant. The equigranular tonalite variety may increase in abundance to the southwest of the map area.

The quartz-plagioclase veins, individual and clusters of several plagioclase porphyroblasts, and the coarse grained equigranular tonalite commonly display well developed biotite rich melanosomes. These melanosomes become more aluminous from northeast to southwest as indicated by an increase in the amount of sillimanite and garnet present.

The quartz-plagioclase leucosomes are the dominant type of leucosome and their abundance reflects the degree of migmatization. The leucosomes are coarse grained with euhedral to subhedral plagioclase ranging from 0.5 mm to 4 cm (most of the adjacent mesosome plagioclase is less than 1 to 2 mm). The plagioclase grains commonly are fractured and turbid. In addition to the minerals present in adjacent mesosomes, the leucosomes may contain retrograde muscovite and andalusite, tourmaline porphyroblasts, and concentrations of graphite. Fold and boudinage structures are common features of these leucosomes.

Hydrothermal processes and partial melting are considered to be the two major mechanisms by which migmatites may develop in regional metamorphic belts (Yardley, 1978). It is not yet clear which mechanism or combination of mechanisms resulted in the formation of migmatites in the aluminous metasedimentary rocks of the Wasekwan Group/Burntwood River Metamorphic Suite. Nevertheless, the above observations indicate that the migmatite-forming process(es) had the following attributes: boron and CO₂ were involved (tourmaline and graphite), no phase was eliminated, and plagioclase and quartz became extremely coarse grained and formed segregations. Subsequently, post migmatization strain and retrogression has affected to varying degrees the morphologies and compositions of the various parts of the migmatite.

Table 56.2. Atomic Mg/Fe ratios in garnet and biotite and X_{grs}^{Grt} and X_{an}^{Pl} values.

Sample	Domain	Mg/Fe Grt	Mg/Fe Bt	X _{grs} ^{Grt}	X _{an} ^{Pl}
1	1	.190 ± .009	.836 ± .059	.030 ± .0021	.224 ± .009
	2	.194 ± .009	.849 ± .022	.031 ± .0021	.207 ± .012
	3	.181 ± .009	.831 ± .026	.033 ± .0021	.248 ± .006
2	1	.224 ± .007	.917 ± .025	.033 ± .0017	.230 ± .007
	2	.233 ± .007	.909 ± .087	.027 ± .0017	.262 ± .007
	3	.240 ± .007	.950 ± .100	.034 ± .0017	.271 ± .006
3	1	.221 ± .009	.830 ± .050	.026 ± .0021	.249 ± .005
	2	.241 ± .009	.855 ± .057	.034 ± .0021	.250 ± .006

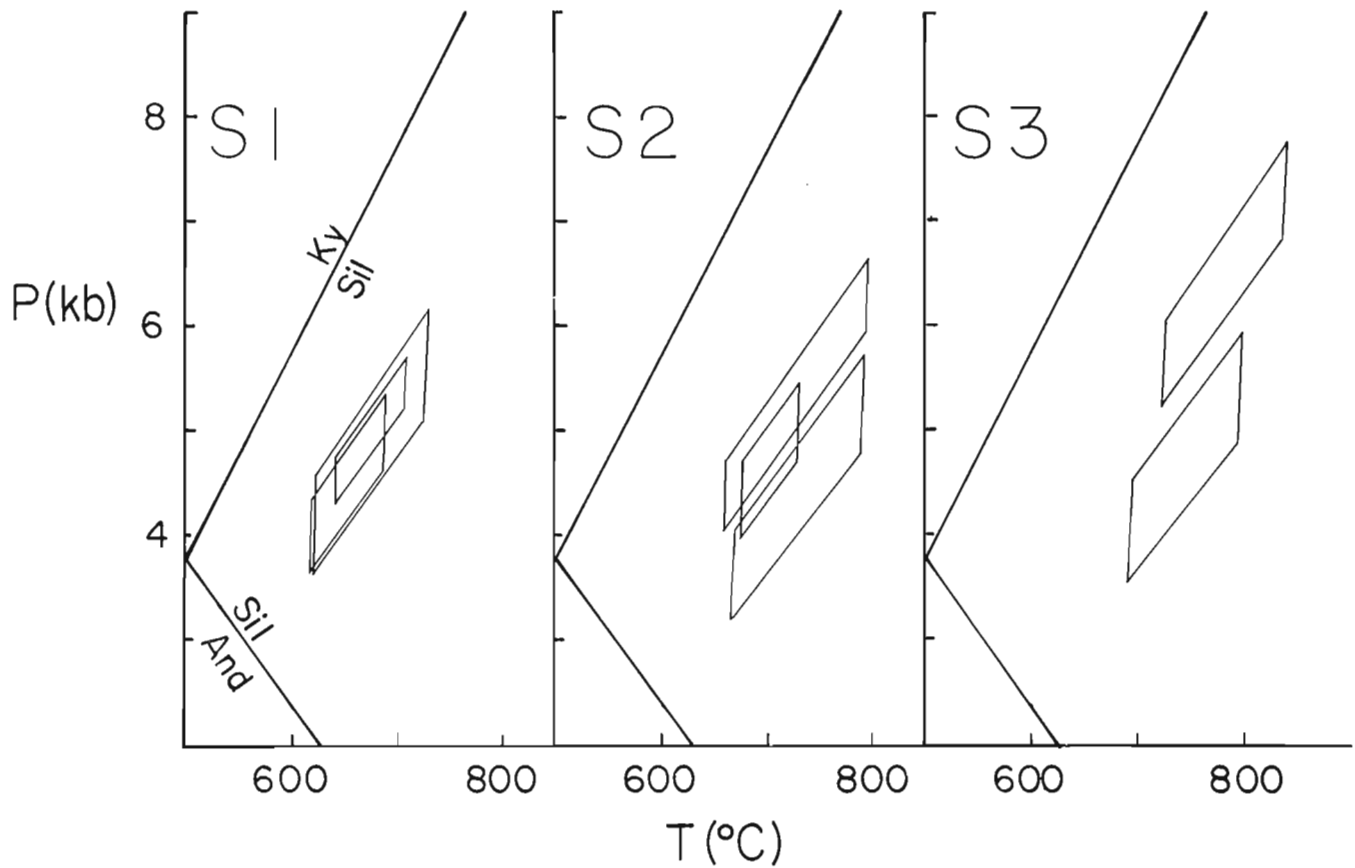


Figure 56.4. *P-T estimates for each domain from three garnet-biotite-sillimanite bearing rocks. See Figure 56.2 for locations. Quadrilaterals represent estimates calculated at the 0.95 confidence level. Ky, And, and Sil stability fields taken from Holdaway (1971).*

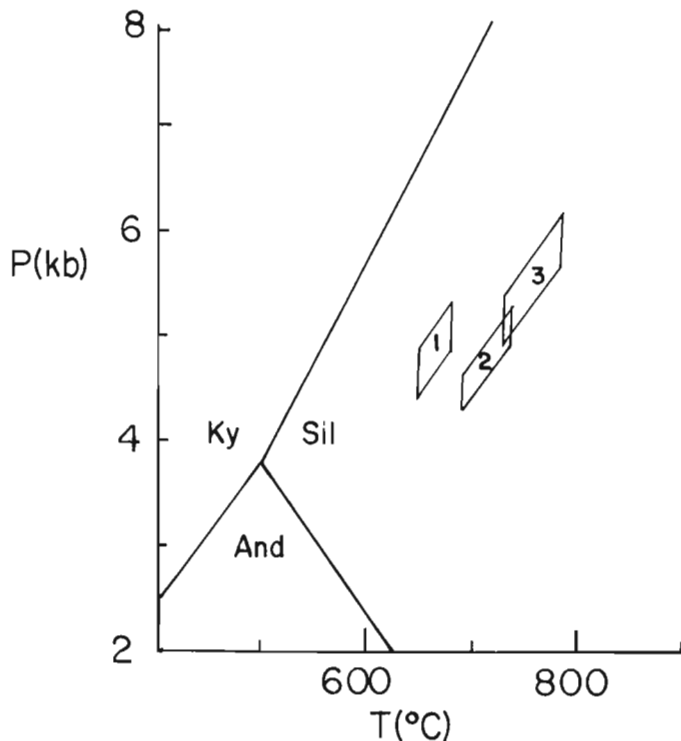


Figure 56.5. *P-T estimates for each sample when the domain values (from Fig. 56.4) are averaged and precision errors treated according to Kretz (1983). Estimates calculated at the 0.95 confidence level. Ky, And, and Sil stability fields taken from Holdaway (1971).*

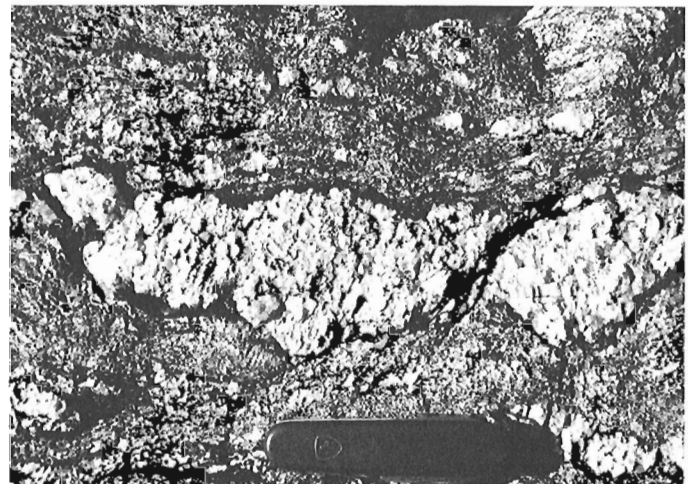


Figure 56.6. *Coarse grained quartz plagioclase vein from South Bay region (Fig. 56.2). Note the well developed biotite melanosome.*

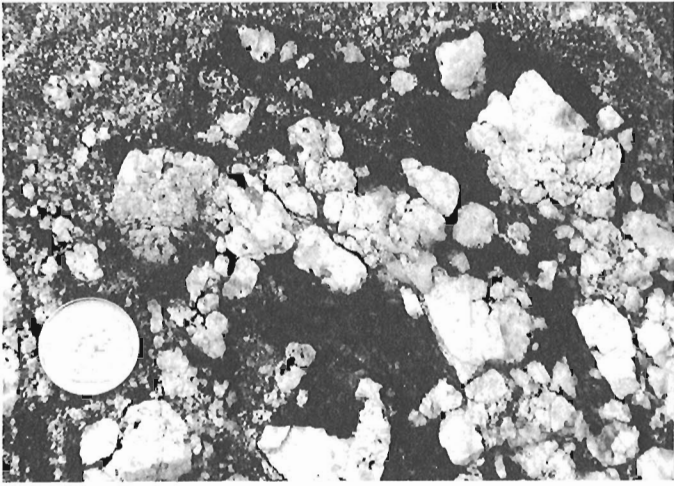


Figure 56.7. Clusters of coarse grained plagioclase porphyroblasts in biotite rich matrix from South Bay Region (Fig. 56.2). Twenty-five cent piece for scale.

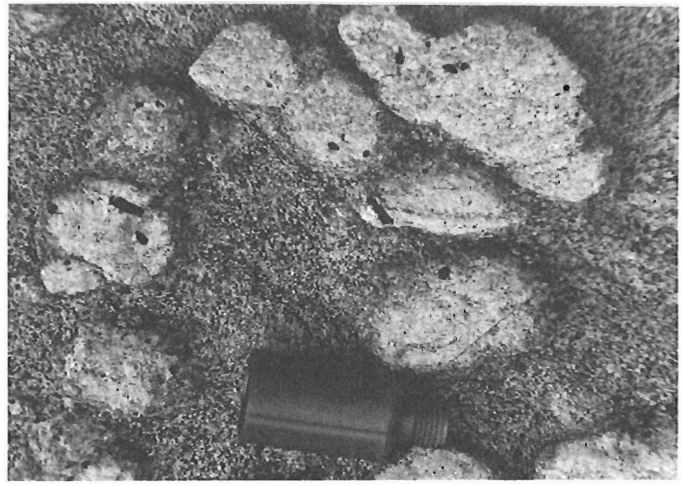


Figure 56.9. Quartz-sillimanite nodule in quartzofeldspathic rocks of the Sickie Group. Note that the tourmaline porphyroblasts are concentrated within these segregations.

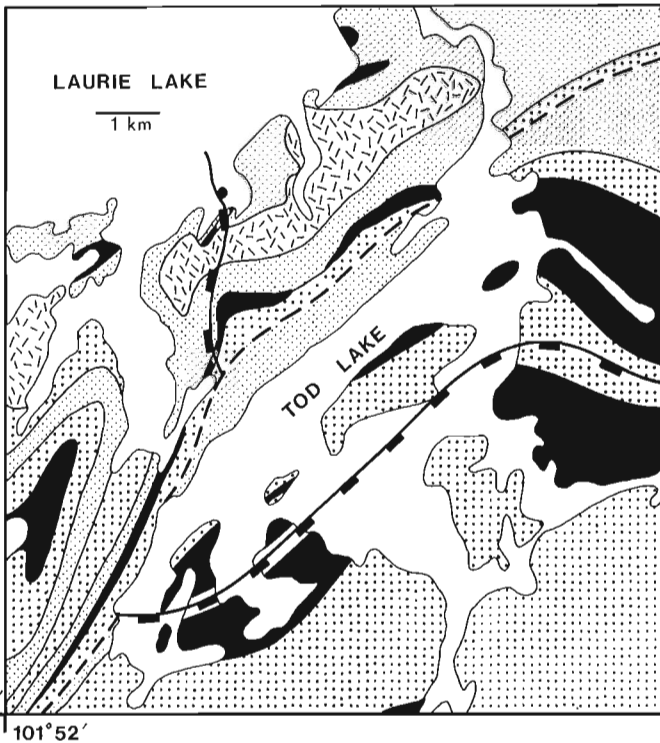


Figure 56.8. The sillimanite-K feldspar isograd in the Laurie Lake region (rectangles on high grade side). Solid black regions represent quartzofeldspathic rocks of the Sickie Group of appropriate composition to constrain the isograd. Heavy stippling represents Sickie Group metasediments. Light stippling represents the Wasekwan Group. Dashed symbols represent intrusive rocks. Heavy dashed line represents the Tod Lake Fault.

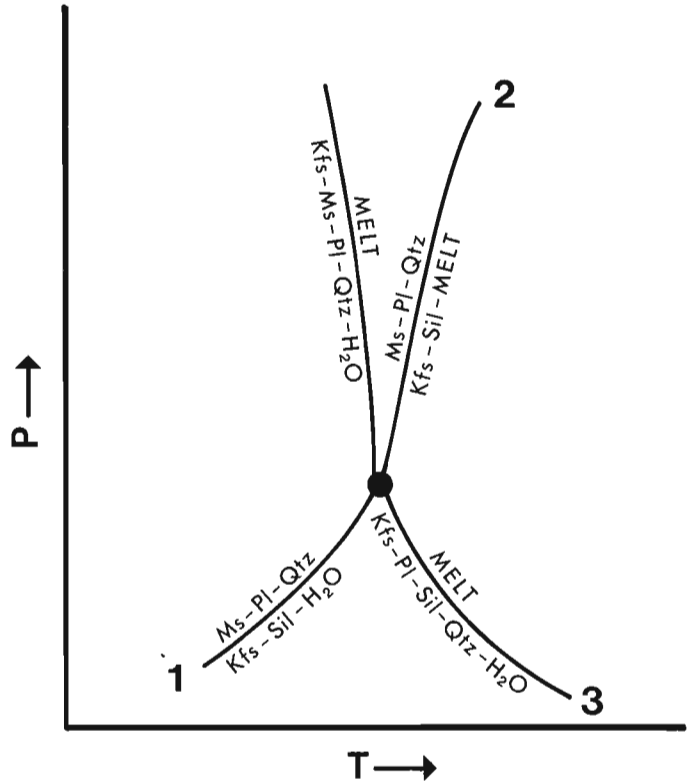


Figure 56.10. Schematic P-T diagram illustrating phase relations in the model KNASH system. Numbered curves correspond to numbered reactions in text.

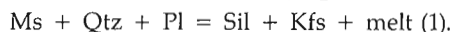
Sillimanite-Kfeldspar isograd in the Sickle Group/Sickle Metamorphic Suite

Quartzofeldspathic rocks of the Sickle Group near Tod Lake and eastern Laurie Lake contain mineral assemblages appropriate for constraining an isograd based on the first appearance of sillimanite (and/or retrograded quartz-feldspar-sillimanite knots now consisting mostly of muscovite). From the configuration of the isograd it is inferred that 3.5 km of post-metamorphic right-lateral strike-separation occurred along the Tod Lake Fault (Fig. 56.8).

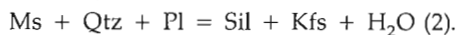
On the low grade side of the isograd rocks contain $Pl + Kfs + Qtz + Ms + Bt + Mag + / - Tur$. On the high grade side of the isograd sillimanite is present in addition to these phases. The higher grade assemblage is easily recognized in the field by the appearance of sillimanite and quartz in ovoid knots approximately 1 to 2 cm in diameter (Fig. 56.9). Muscovite is present but decreases in abundance with increasing distance above the isograd for several kilometres. Based on these observations it is clear that, although this isograd marks the first appearance of sillimanite in the Sickle Group/Sickle Metamorphic Suite, it corresponds to what is commonly referred to as the "second sillimanite isograd" or sillimanite-K feldspar isograd in metapelites.

Some small granitic veins (5 mm to several centimetres in width, totalling less than 1% of the total outcrop) and discordant tourmaline-bearing pegmatites are present below and above the isograd. The veins do not increase in abundance immediately above the isograd; however, a kilometre or more above the isograd granitic veins are abundant. It is not yet known if the granitic veins below the isograd represent the products of a melt phase present during peak metamorphic conditions.

If the granitic material on the low-grade side of the isograd represents a melt phase that was present during peak metamorphic conditions, then the isogradic reaction in the model system $K_2O-Na_2O-Al_2O_3-SiO_2-H_2O$ (KNASH) would be:

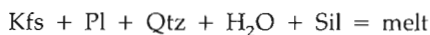


If this material does not represent a quenched melt phase then the isogradic reaction would be:



Reaction (1) would occur under P-T conditions where a melt is stable whereas reaction (2) would occur under conditions where a melt is not stable (Fig. 56.10) either due to a lower P or lower activity of water.

Since there is no notable increase in the amount of granitic material present immediately above the isograd, reaction (2) is tentatively adopted as the K feldspar-sillimanite producing reaction. To be consistent with this hypothesis, the increase in the amount of granitic material a kilometre or more above the isograd would be due to the model KNASH reaction:



Reactions (1) and (2) would be univariant in the model system KNASH. Muscovite coexisting with K feldspar and sillimanite several kilometres upgrade of the isograd indicates that the actual reaction was not univariant. A model system involving additional phases and components should provide a more accurate approximate to the rocks. Mineral compositions are being determined so as to provide constraints on the reactions that produce sillimanite, K feldspar, and melt.

Summary and conclusions

- 1) P-T estimates range from approximately 4.5 kb and 650°C to 5.5 kb and 750°C from the northeast to southwest regions.
- 2) Migmatite development in the Wasekwan Group/Burntwood River Metamorphic Suite is progressive. This sup-

ports correlation of the aluminous sedimentary rocks between the greenstone belt and the gneiss belt (eg. Milligan, 1960; McRitchie, 1974; Zwanzig, 1976).

- 3) An isograd based on the first appearance of sillimanite has been mapped. The reaction that produced sillimanite and K feldspar may have occurred in the absence of a melt phase. If this is true, and if the pressure estimates are valid, then the P-T intersection of the muscovite breakdown reaction and the granite minimum-melt reaction must have occurred at pressures above 5 kb. Kerrick (1972) has shown that this situation may arise if X_{H_2O} is less than 0.8.

Acknowledgments

D.M. Carmichael (thesis supervisor), and E. Froese are thanked for both discussions and comments made during a visit to the study area and for comments which improved this report. P. Roeder and D. Kempson are thanked for their guidance in the use of the electron microprobe. H.V. Zwanzig and D.A. Baldwin (Manitoba Mineral Resources Division) are once again thanked for discussions related to the geology of the field area.

References

- Baldwin, D.A., Syme, E.C., Zwanzig, H.V., Gordon, T.M., Hunt, P.A., and Stevens, R.D.
1985: U/Pb zircon ages from the Lynn Lake and Rusty Lake metavolcanic belts, Manitoba: Two ages of Proterozoic magmatism (Abstract); Geological Association of Canada, Annual Meeting, Program with Abstracts.
- Clark, G.
1980: Rubidium-Strontium geochronology in the Lynn Lake Greenstone Belt, Northwestern Manitoba; Manitoba Mineral Resources Division, Geological Paper GP8D-2.
- Ferry, J.M. and Spear, F.S.
1978: Experimental calibration of the partitioning of Fe and Mg between biotite and garnet; Contributions to Mineralogy and Petrology, v. 66, p. 113-117.
- Ghent, E.D.
1976: Plagioclase-garnet- Al_2SiO_5 -quartz: a potential geobarometer-geothermometer; American Mineralogist, v. 61, p. 710-714.
- Ghent, E.D., Robbins, D.R., and Stout, M.Z.
1979: Geothermometry, geobarometry and fluid compositions of metamorphosed calc-silicates and pelites, Mica Creek, British Columbia; American Mineralogist, v. 64, p. 874-885.
- Gilbert, H.P., Syme, E.C., and Zwanzig, H.V.
1980: Geology of the metavolcanic and volcanoclastic metasedimentary rocks in the Lynn Lake area; Manitoba Mineral Resources Division, Geological Paper GP 80-1, 118 p.
- Grant, J.A. and Weiblen, P.W.
1971: Retrograde zoning in garnet near the second sillimanite isograd; American Journal of Science, v. 270, p. 281-296.
- Holdaway, M.J.
1971: Stability of andalusite and the aluminum silicate phase diagram; American Journal of Science, v. 271, p. 97-131.
- Jackson, S.L. and Gordon, T.M.
1985: Metamorphism and structure of the Laurie Lake region, Manitoba; in Current Research, Part A, Geological Survey of Canada, Paper 85-1A, p. 753-759.

- Johannes, W.
 1983: On the origin of layered migmatites; *in* *Migmatites, Melting and Metamorphism*, ed. M.P. Atherton and C.D. Gribble, p. 225-248.
- Kerrick, D.M.
 1972: Experimental determination of the muscovite + quartz stability with $P_{H_2O} < P_{total}$; *American Journal of Science*, v. 272, p. 946-958.
- Kretz, R.
 1983: Symbols for rock-forming minerals; *American Mineralogist*, v. 68, p. 277-279.
 1985: Calculation and illustration of uncertainty in geochemical analyses; *Journal of Geological Education*, v. 33, p. 40-44.
- Milligan, G.C.
 1960: Geology of the Lynn Lake District; Manitoba Mines Branch Publication 57-1.
- McRitchie, W.D.
 1974: The Sickle-Wasekwan debate: a review; Manitoba Mines Branch Geological Paper 1/74.
- Tracy, R.S., Robinson, P., and Thompson, A.B.
 1976: Garnet composition and zoning in the determination of temperature and pressure of metamorphism, central Massachusetts; *American Mineralogist*, v. 61, p. 762-775.
- Yardley, B.W.D.
 1978: Genesis of the Skagit Gneiss migmatites, Washington, and the distinction between possible mechanisms of migmatization; *Bulletin of the Geological Society of America*, v. 89, p. 941-951.
- Zwanzig, H.V.
 1976: Laurie Lake area (Fox Lake project); *in* *Report of Field Activities, 1976*, Manitoba Mineral Resources Division, p. 26-32.
- Zwanzig, H.V., Thomas, M.W., and Keay, J.P.
 1980: Laurie Lake; Manitoba Mineral Resources Division, Map GP 80-1-3.

Strontium isotopic studies of rock and mineral samples in the Shubenacadie Basin, Nova Scotia¹

Contract OST85-00052

C. E. Ravenhurst², P.H. Reynolds², and M. Zentilli²

Ravenhurst, C.E., Reynolds, P.H., and Zentilli, M., Strontium isotopic studies of rock and mineral samples in the Shubenacadie Basin, Nova Scotia; in Current Research, Part B, Geological Survey of Canada, Paper 86-1B, p. 547-555, 1986.

Abstract

Mineral deposits and occurrences of lead, zinc, and/or barite that exist at the margin of the Carboniferous Shubenacadie basin of Nova Scotia, occur near the disconformity between the older Horton Group continental clastic rocks and the overlying Windsor Group marine carbonates. Strontium isotopic analyses of calcite and barite indicate that there is a genetic link between these mineral occurrences. The ore-stage minerals of the larger and/or higher grade deposits such as the Gays River Pb-Zn deposit, have a relatively high $^{87}\text{Sr}/^{86}\text{Sr}$ ratio ($= 0.712$), suggesting a massive influx of a mineralizing fluid considerably different from Carboniferous marine water as recorded in the host carbonates ($^{87}\text{Sr}/^{86}\text{Sr} = 0.708$). Thus, strontium isotopic data have potential applications in prospect evaluation within this basin.

No unique source for the calcium or barium component of the mineralizing fluids can be ascertained.

Résumé

Les gisements de minéraux et les venues de plomb, de zinc et de barite qui existent à la limite du bassin Shubenacadie datant du Carbonifère au Nouveau-Brunswick se trouvent près de la discordance stratigraphique entre les roches clastiques continentales de l'ancien groupe de Horton et les carbonates marins du groupe de Windsor qui les recouvrent. Des analyses isotopiques au strontium de la calcite et de la baryte indiquent qu'il y a un lien génétique entre ces venues minérales. Les minéraux considérés comme minerai constituant les gisements plus importants ou plus riches comme le gisement de Pb-Zn de la rivière Gays ont un rapport relativement élevé $^{87}\text{Sr}/^{86}\text{Sr}$ ($= 0,712$), indiquant un influx massif de fluides minéralisés très différents de l'eau de mer du Carbonifère comme l'indiquent les carbonates d'hôtes ($^{87}\text{Sr}/^{86}\text{Sr} = 0,708$). Les données isotopiques (strontium) peuvent donc être appliquées pour ce genre d'évaluation à l'intérieur de ce bassin.

On ne peut affirmer qu'il existe une source unique de calcium ou de baryum dans les fluides de minéralisation.

¹ Contribution to the Canada-Nova Scotia Mineral Development Agreement 1984-1989. Project carried by Geological Survey of Canada, Mineral Resources Division, Project 700059.

² Department of Geology, Dalhousie University, Halifax, Nova Scotia B3H 3J5.

Introduction

The Shubenacadie Basin of Nova Scotia is a small (65 × 16 km) Carboniferous basin in the southeastern portion of the Minas sub-basin, which is part of the evaporite/carbonate platform of the main Fundy/Magdalen Basin (Fig. 57.1). The Shubenacadie Basin contains a stratified sequence of sedimentary rocks with an estimated maximum thickness of 2000 m (Boehner, 1981). The basal Tournaisian Horton Group clastic rocks lie unconformably on metamorphic basement rocks of the Cambro-Ordovician Meguma Group and are in turn overlain (disconformably in most places) by carbonate, evaporite and clastic rocks of the Windsor and Canso groups (Fig. 57.2). Picou Group rocks unconformably overlie the Canso rocks. Windsor Group rocks unconformably overlap the Meguma Group along the southeastern margin of Shubenacadie Basin and in Musquodoboit Basin (Giles and Boehner, 1979). Pb-Zn-Ba concentrations are found in Windsor Group carbonate (e.g. Gays

River Pb-Zn deposit), within a short distance of the Horton/Windsor contact (e.g. Smithfield Pb deposit), and in the upper Horton Group clastic rocks (e.g. Brookfield Ba deposit).

Genetic hypotheses for the Carboniferous "carbonate-hosted" Pb-Zn-Ba deposits in Nova Scotia include: (1) sabkha-type deposition (MacLeod, 1975); (2) formation from late diagenetic mineralizing fluids laterally secreted from the adjacent sedimentary basins (Lydon, 1978); and (3) deposition from fluids from a "deep source" (Krebs and Macqueen, 1984). The sabkha model has been ruled out by fluid inclusion temperatures (>200°C) measured in sphalerite by Akande (1982; Akande and Zentilli, 1984), at the Gays River deposit. Isotopic information on the components of the mineralization places constraints on the other genetic hypotheses.

Strontium isotopes are useful for tracing the calcium and barium component of minerals such as calcite, barite and

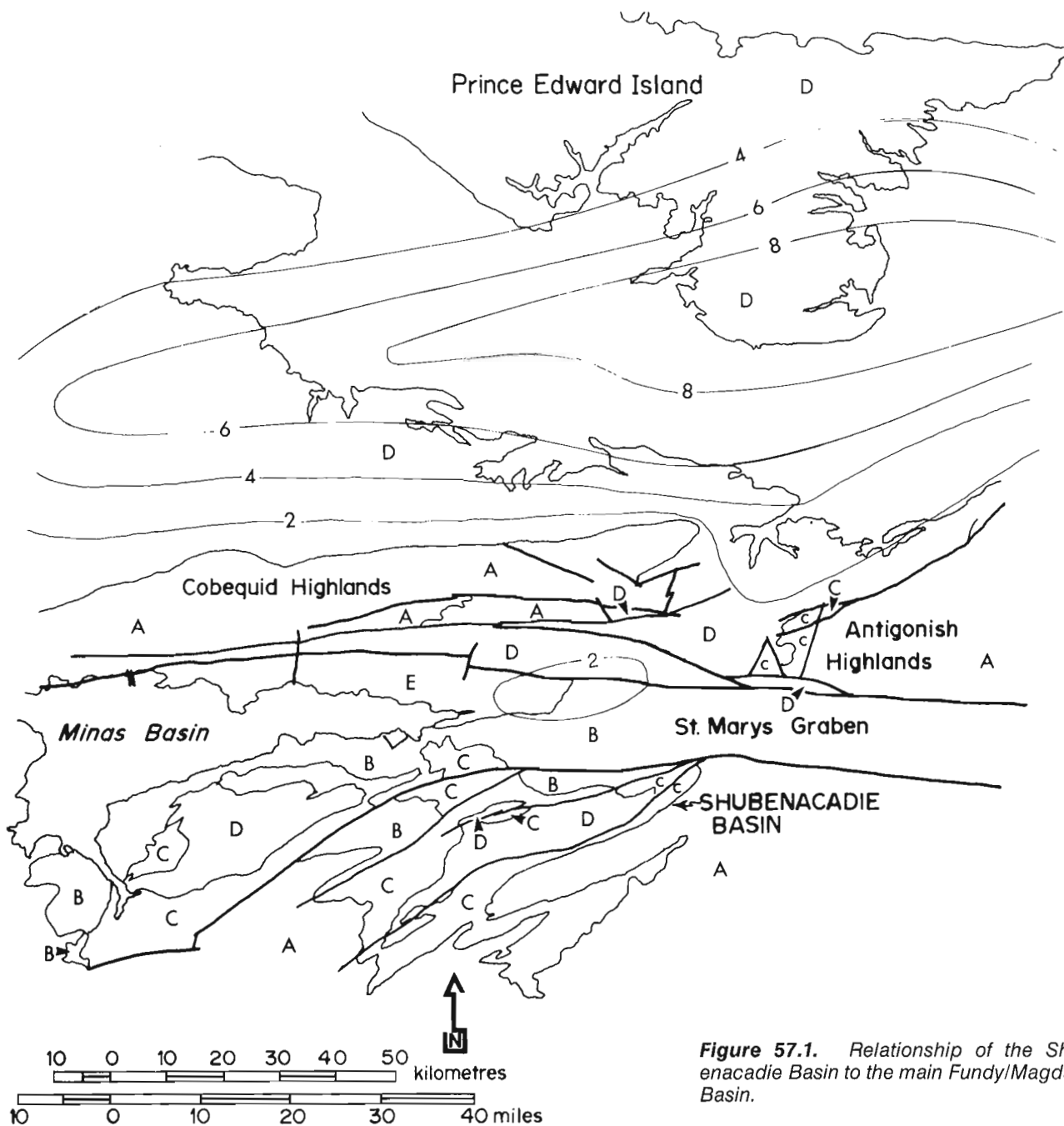


Figure 57.1. Relationship of the Shubenacadie Basin to the main Fundy/Magdalen Basin.

fluorite. Because these minerals usually contain negligible quantities of rubidium, their strontium isotope ratios are a measure of the isotopic composition of the strontium in the mineralizing fluids. The strontium isotope ratios in gangue minerals from Mississippi Valley-type (MVT) deposits indicate that where mineralization is sparse, the minerals precipitated from fluids that were in local isotopic equilibrium with the host carbonates. Conversely, in districts with major deposits, the ratios are anomalous and increase as mineralization progresses. In these districts, the process appears to be that of mixing of fluids containing strontium derived from the silicate minerals in the sedimentary succession, with locally derived strontium-bearing fluids (Kessen et al., 1981). Thus, within a given basin, prospects in which calcite, barite or fluorite have relatively high $^{87}\text{Sr}/^{86}\text{Sr}$ ratios may represent good exploration targets.

Rubidium-strontium information is available on some of the possible source rocks which may have equilibrated with the mineralizing fluids. Clarke and Halliday (1980) reported that in the South Mountain batholith, granodiorite (371.8 ± 2.2 Ma) had an initial ratio ($^{87}\text{Sr}/^{86}\text{Sr}$) of 0.7076 – 0.7090; adamellite (364.3 ± 1.3 Ma), with a ratio ($^{87}\text{Sr}/^{86}\text{Sr}$) of 0.70942; and porphyry (361.2 ± 1.4 Ma) with a ratio ($^{87}\text{Sr}/^{86}\text{Sr}$) of 0.71021. A suite of Meguma country rock samples had $^{87}\text{Sr}/^{86}\text{Sr} = 0.7113 - 0.7177$ at the time of intrusion of the batholith. Work on the Meguma Group black slates (Lambert et al., 1984), indicates a possible age of 490 ± 10 Ma with an initial ratio of 0.7130. Preliminary data on turbidites give an initial ratio ($^{87}\text{Sr}/^{86}\text{Sr}$) of 0.711. No data exist for the Horton Group clastic rocks which may have undergone equilibration of strontium (at least in glauconite or 2M-illite) either during burial, a low temperature regional metamor-

phism, or during a fluid flow event (e.g. Clauer, 1982; Stein and Kish, 1985).

The purpose of this study is to determine: 1) if a genetic link exists between the different deposits around the margin of the Shubenacadie basin; 2) if the mineralizing fluids may have derived at least their calcium and barium components from Horton Group clastic rocks, ascertaining the age of homogenization of strontium in the rocks, and thus the age of a possible hydrothermal event would be an added bonus; and 3) if strontium isotopic analyses of ore-stage minerals is a useful exploration tool.

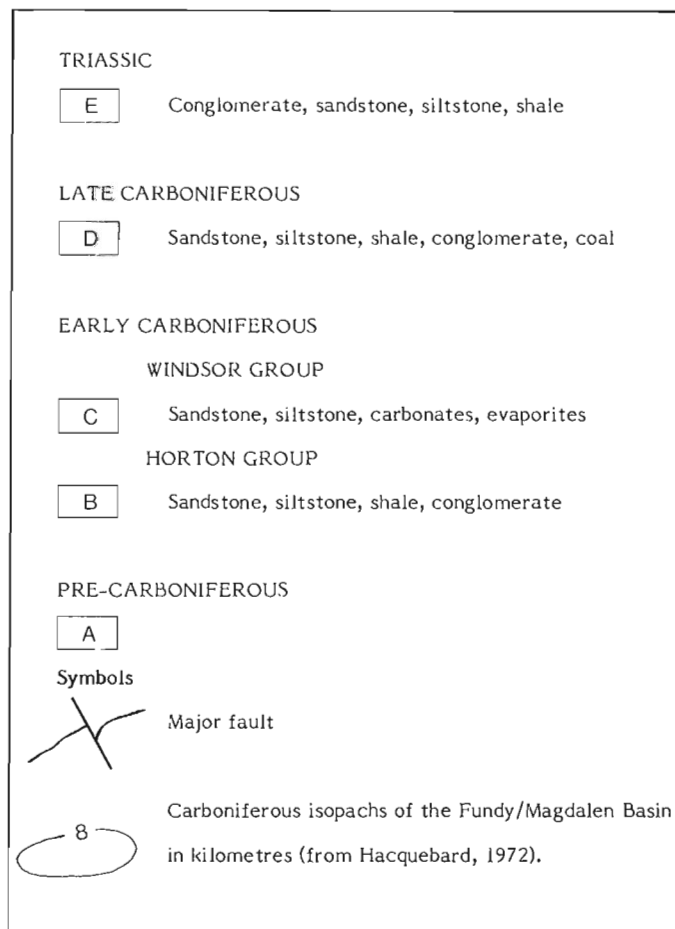
Description of sample localities

Samples of barite, calcite and host rock carbonate were selected from a number of mineral deposits around the margin of the Shubenacadie Basin (Fig. 57.3). The Gays River Pb-Zn deposit contains about 12 million tons of 7% combined lead and zinc hosted in a dolomitized carbonate bank of Gays River Formation (Akande and Zentilli, 1984). The Southvale Ba occurrence is a small layer of fine grained to cryptocrystalline barite showing replacement characteristics, and underlain by the basal dolomitic limestone of the Windsor Group (Felderhof, 1978). The lead at Pembroke occurs as galena in calcite veins and with vug-filling calcite, in a limestone of the Windsor Group (Ponsford, 1983). The Smithfield Pb-Zn-Cu-Ba occurrence contains 500 000 tons of 6% combined lead and zinc and occurs in a brecciated basal Windsor limestone, disconformably overlying highly pyritized Horton clastic rocks (Felderhof, 1978; Walker, 1978). Barite mineralization at the Middle Stewiacke occurrence is structurally controlled and is hosted in massive limestone and limestone breccia of the upper Windsor Group, where it is in fault contact with Horton clastic rocks. The Brookfield Ba deposit contains at least 62 000 tons of 50% barite and is a replacement and vein deposit hosted entirely in Horton clastic rocks. The barite at Hilden occurs as a vein in basal limestone and limestone breccia of the Windsor Group. The barite at Lake Fletcher occurs as a vein in Meguma slates (Felderhof, 1978). Only clean, unweathered samples were used. Sample selection was based on position in the paragenetic sequence, location in the deposit, and colour (Table 57.1).

Sample preparation

Samples of 2 to 4 kg of grey Horton sandstone were selected at regular stratigraphic intervals at site 1A (Fig. 57.3). As much of the weathered material as physically possible was removed from the outcrop before sampling. The site is remote from any large mineral occurrences and was sampled from a large cliff section directly stratigraphically below the Horton-Windsor contact. The area is structurally complex with steeply dipping (75°NE) Windsor strata occurring just north of the sample site, but flat-lying overturned strata at the sample site itself.

A careful sample preparation procedure was followed. The calcite and host carbonate samples were broken up with a percussion mortar and sieved in plastic sieves to obtain the +20 to -40 mesh (841 – 355 μ) fraction. This fraction was hand-picked to give approximately 2 grams of very clean sample. The samples were then washed repeatedly with super-clean ethyl alcohol in a sonic bath. The dry samples were crushed using an agate mortar and pestle. Relatively strontium-rich barite samples were prepared in a similar manner, but in a separate location to avoid contamination. One portion of calcite sample RSB-32 (32a) was prepared in the same laboratory as the barite samples and another portion (32b) in the separate location. A comparison of the two results gives a good indication of the cleanliness of the preparation system. Sieves were cleaned with compressed air and super-clean ethyl alcohol between



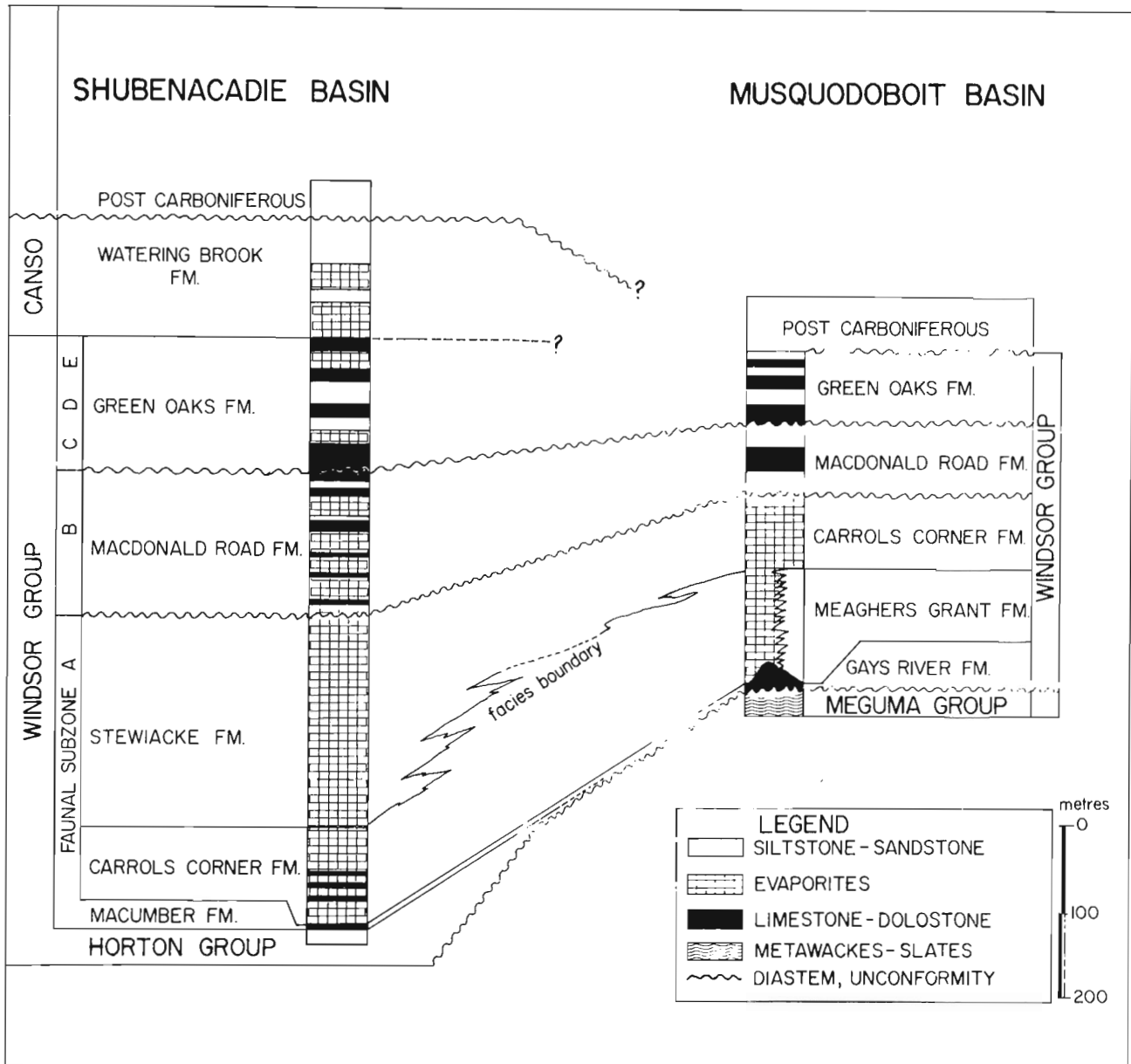


Figure 57.2. Stratigraphy of the Mississippian Windsor Group in the Shubenacadie and Musquodoboit Basins (simplified from Giles and Bohner, 1979).

samples and the mortar and pestle were cleaned with quartz between samples.

Sample preparation procedure for clays was modified from Halliday (1978). The samples were crushed to -18 mesh (<1 mm) and dry sieved in a sieve shaker for 20 minutes. About 100 to 600 grams of the -230 mesh (<63 μ) fraction of each sample was stirred into 1 or 2 L of distilled water in beakers. After 48 hours the water was siphoned off and samples let dry until sticky/wet. Then using weighing paper (which adhered to the surface), about 1 mm of the clays was "skimmed" off the top. Semi-oriented smears of the samples were run on the X-ray diffractometer for a qualitative determination of the relative amount of illite in each. At this point, about half of the original samples were rejected. The remaining illite-rich samples are tabulated in Table 57.2. All samples contained some quartz and albite in addition to illite, muscovite and chlorite. No detailed mineralogical study has been completed.

Analytical methods

All the isotopic analyses were carried out at the Department of Geology, Carleton University, Ottawa, on a Finnigan-MAT 261 multi-collector mass spectrometer. The estimated precision in the $^{87}\text{Sr}/^{86}\text{Sr}$ analysis is ± 0.00003 (2 standard deviations). The measured $^{87}\text{Sr}/^{86}\text{Sr}$ ratios for the Eimer and Amend Standard and NBS 987 were 0.70802 ± 0.00002 and 0.71023 ± 0.00003 , respectively. All analyses were normalized to $^{88}\text{Sr}/^{86}\text{Sr} = 8.37521$.

The carbonate samples were first dissolved in 3N HCl and strontium was then isolated by conventional cation exchange techniques. Barite was first fused with LiBO_2 in a graphite crucible, then dissolved in dilute HCl. The clay samples were dissolved in hydrofluoric and perchloric acids. Rubidium and strontium concentrations in clays were determined by X-ray fluorescence techniques (to a precision of about $\pm 0.5\%$).

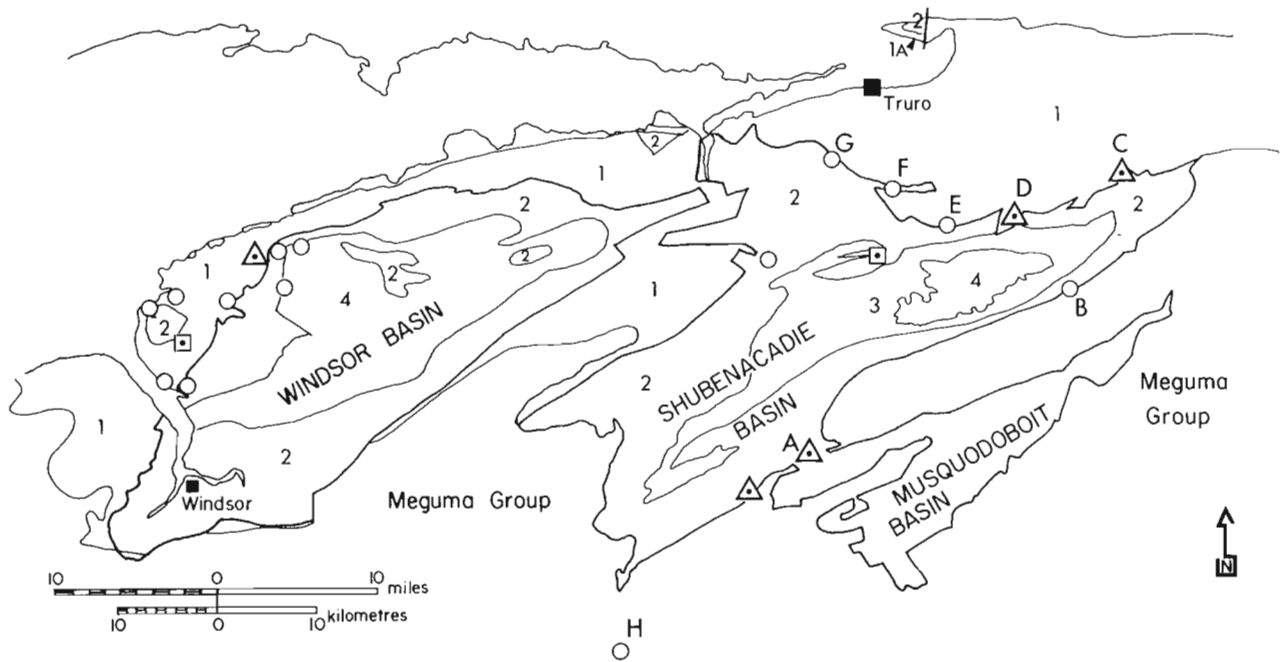


Figure 57.3. Carboniferous basins and associated mineral occurrences of the Minas sub-basin, central Nova Scotia (after Felderhof, 1978). A = Gays River, B = Southvale, C = Pembroke, D = Smithfields, E = Middle Stewiacke, F = Brookfield, G = Hilden, H = Lake Fletcher.

UPPER CARBONIFEROUS	
PICTOU GROUP	
4	Sandstone, siltstone, shale, coal
CANSO GROUP	
3	Sandstone, siltstone, shale
LOWER CARBONIFEROUS	
WINDSOR GROUP	
2	Sandstone, siltstone, carbonates, evaporites
HORTON GROUP	
1	Sandstone, siltstone shale, conglomerate, dolostone, coal
Symbols	
△	Carbonate-hosted Pb-Zn occurrence
○	Barite occurrence
□	Fluorite occurrence

Results

Analytical results are tabulated in Tables 57.1 and 57.2 and plotted in Figures 57.4 and 57.5. The paths with arrows in Figure 4 indicate the change in strontium ratios along the paragenetic sequence of the mineralization event at each mineral occurrence.

Data in Figure 57.4 show that the strontium ratio of host rock carbonate is almost identical to that of Mississippian seawater. Calcite in the Gays River and Pembroke deposits, and the barite at Brookfield all have strontium isotope ratios substantially higher than that of the carbonate host rock. This result is similar to that found by Kessen et al. (1981) in the major Mississippi Valley districts. Post-ore calcite at Gays River contains lower strontium ratios. Strontium ratios in barite at Southvale, Smithfield, Middle Stewiacke and Hilden are intermediate between the host rock and highly anomalous values. The highest strontium ratios were found in barite within Meguma Group slates at Lake Fletcher.

Clay samples separated from Horton rocks (Table 57.2) all contained illite, but some had substantial amounts of muscovite and chlorite. The samples covered approximately 10 m (stratigraphically) of the Horton section. Five of the six samples define an isochron (i.e. the points fit a single line within the estimated uncertainty: MSWD = 1.0) (Fig. 57.5). The indicated age is 300 ± 6 Ma with an initial ratio of 0.7096 ± 0.0002 (2σ errors quoted). Sample RSB-101, which has the highest Rb/Sr ratio, does not plot on the isochron. The reason for this is not known.

Discussion

The 300 ± 6 Ma isochron age may be the time at which the strontium contained in the clay fraction of the rocks was

Table 57.1. Sample descriptions and strontium isotope ratios

Map	Location	Sample number	Composition	Description	⁸⁷ Sr/ ⁸⁶ Sr
A	Gays River	AGR-137	Pre-ore dolomite	Recrystallized micrite host rock	0.70825
	Gays River	AGR-139	Pre-ore	Recrystallized micrite host rock	0.70847
	Gays River	SPA-105-1	Ore-stage calcite	Vein calcite intergrown with sphalerite	0.71200
	Gays River	AGR-119-2	Post-ore calcite	Vug-filling calcite overgrowths on galena	0.7083
	Gays River	AGR-201-2	Post-ore calcite	Vug-filling calcite in fracture-related cavity	0.71050
	Gays River	NE-105-1	Post-ore calcite	Scalenohedral calcite in vugs	0.70868
	Gays River	AGR-131	Post-ore calcite	Recrystallized secondary limestone (dedolomite)	0.70890
	Gays River	AGR-133a	Post-ore calcite	Recrystallized limestone breccia	0.70895
	B	Southvale	RSB-47	Barite	White barite in basal Windsor carbonate
C	Pembroke	FHd	Pre-ore dolomite	Skeletal grainstone host rock	0.70851
	Pembroke	P13-VN	Mineralized calcite	Vein calcite with galena	0.71193
	Pembroke	RSB-46	Mineralized calcite	Vein calcite with galena	0.70837
	Pembroke	P9-VN	Unmineral. calcite	Vein calcite	0.70833
D	Smithfield	RSB-31	Pre-ore calcite	Carbonaceous limestone host rock	0.70775
	Smithfield	RSB-34b	Pre-ore calcite	Limestone host from quarry 800 m. west	0.70816
	Smithfield	RSB-27	Barite	Pink crystalline barite	0.70978
	Smithfield	RSB-28a	Barite	Reddish crystalline barite	0.70875
	Smithfield	RSB-28b	Barite	White crystalline barite	0.70990
	Smithfield	RSB-29a	Barite	White crystalline barite	0.71002
	Smithfield	RSB-32	Post-ore calcite	Vein calcite a) prep with barites b) prep with calcites	0.70867 0.70864
E	Middle Stewiacke	RSB-51	Pre-ore calcite	Limestone host rock	0.70812
	Middle Stewiacke	RSB-49	Barite	Red vein barite	0.70958
	Middle Stewiacke	RSB-50	Barite	Pink to white vein barite	0.70977
	Middle Stewiacke	RSB-54	Barite	Vein barite which cuts calcite veins	0.70912
	Brookfield	RSB-40	Pre-ore calcite	Porous crystalline Windsor limestone	0.70808
F	Brookfield	RSB-35	Barite	Pink massive barite from quarry centre	0.71175
	Brookfield	RSB-36	Barite	Red massive barite from quarry centre	0.71171
	Brookfield	RSB-37	Barite	Pink massive barite from SW quarry wall	0.71145
	Brookfield	RSB-38	Barite	White massive barite from SW quarry wall	0.71144
	Brookfield	RSB-39	Barite	Pink massive barite from quarry centre	0.71127
	G	Hilden	RSB-67	Barite	Pink vein barite
Hilden		RSB-68	Barite	Pink massive barite assoc with siderite	0.70904
H	Lake Fletcher	RSB-62	Barite	White vein barite in Meguma slate	0.71230
	Lake Fletcher	RSB-63	Barite	White vein barite in Meguma slate	0.71228

Table 57.2. Horton Group (Tournaisian) sandstone samples selected for Rb/Sr and $^{87}\text{Sr}/^{86}\text{Sr}$ analyses.

Map Location	Sample number	Description	Composition analysed	$^{87}\text{Rb}/^{86}\text{Sr}$ ($\pm 1.5\%$)	$^{87}\text{Sr}/^{86}\text{Sr}$ ($\pm 0.004\%$)
1A Upper Brookside	RSB-98	Unweathered upper Horton sandstone with hematite	chlorite muscovite illite	1.05	0.71407
	RSB-101	Horton sandstone 1.5 m "below" Windsor. Weathered outcrop	muscovite illite chlorite	8.13 (omitted from isochron)	0.74636
	RSB-102	Horton sandstone 3.0 m "below" Windsor. Weathered outcrop	illite muscovite chlorite	failed	failed
	RSB-103	Horton sandstone 4.5 m "below" Windsor. Unweathered	illite muscovite chlorite	5.89	0.73506
	RSB-104	Horton sandstone 6.0 m "below" Windsor. Some weathering	muscovite illite chlorite	4.93	0.73048
	RSB-105	Horton sandstone 8.0 m "below" Windsor. Some weathering	illite muscovite chlorite	6.21	0.73631
	RSB-106	Horton sandstone 10 m "below" Windsor. Some weathering	illite muscovite chlorite	3.19	0.72293

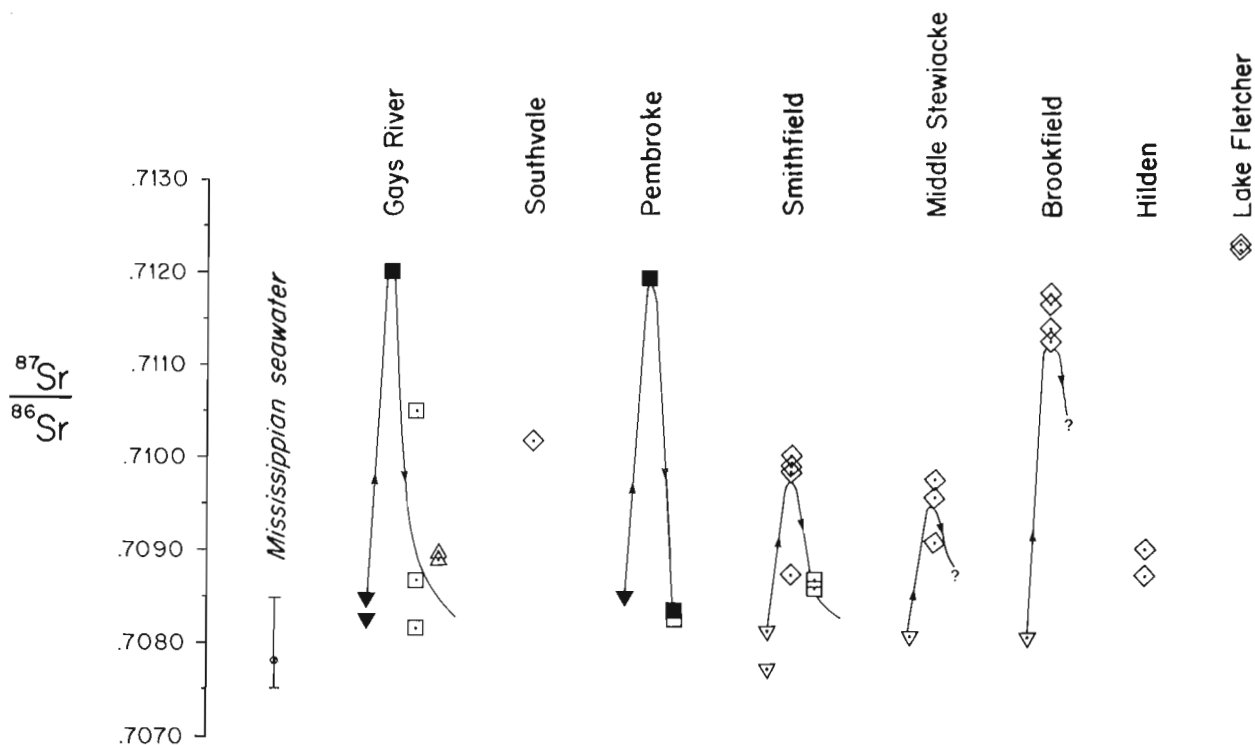


Figure 57.4. Strontium isotopic compositions of barite, calcite and host rock carbonate from mineral occurrences around the Shubenacadie Basin. ∇ = host limestone (Visean); \blacktriangledown = host dolomite (Visean); \blacksquare = mineralized vein or vug-filling calcite; \diamond = barite; \square = postore and/or unmineralized calcite; \triangle = postore dedolomitized limestone. Analytical errors fall within the symbols. Average Mississippiian seawater and range of analyses from Burke et al. (1982). Lines with arrows show probable paragenetic sequence at each deposit.

homogenized at a scale of tens of metres. This would have been possible only in the presence of a common permeating fluid in hydraulic continuity. The fluids may have entered the basement rocks along fractures as well as moving through the Horton clastic rocks. The $^{87}\text{Sr}/^{86}\text{Sr}$ ratios (at 300 Ma) for the Meguma Group metasediments (0.7124–0.7244) and the granodiorites (0.7104–0.7127) (calculated from data in Lambert et al., 1984, and Clarke and Halliday, 1980) indicate that either could have been a source for the strontium in calcite and barite with high strontium ratios present at some of the deposits. The Horton Group clastic rocks at site 1A could not have been the sole source or conduit for the Gays River, Pembroke and Brookfield occurrences, but, the initial strontium ratio existing at site 1A at 300 Ma is in the range of strontium ratios measured at some of the other deposits. The Horton Group is very heterogeneous, however, and other parts of the Horton strata may have homogenized at a higher initial ratio.

The barite vein in Meguma slates at Lake Fletcher could not have been formed from the South Mountain granites ($t = 374$ to 360 Ma) because the strontium available would have had an isotopic ratio that was too low. However, it may have been formed at that time by barium- and strontium-rich fluids originating within the Meguma Group. This type of deposit could then have been the source for the later Carboniferous mineralization. It may also have formed at this later time; the range of strontium ratios available in the Meguma metasedimentary rocks is too large to rule out either possibility.

Conclusions

No genetic link appears to exist between the mineral occurrences around the Shubenacadie basin. High strontium ratios are associated with larger and/or higher grade deposits, that probably had a massive influx of mineralizing fluids. Smaller, lower grade deposits have strontium ratios that are probably a mixture of high fluid ratios and low host rock ratios.

No single source for the calcium and barium components of the mineralizing fluids can be determined. The Horton clastic rocks at site 1A north of Truro could not have been a major source or conduit for the fluids. But, the Rb-Sr isotopic data do indicate an anomalous temperature or fluid-flow event, sufficient to locally homogenize strontium isotopes, in the Horton at about 300 Ma, during the Hercynian Maritime disturbance (Poole, 1967). This is the first good age determination of an event which affected Horton clastic rocks in the Pennsylvanian and which may be related to the mineralization in the Shubenacadie Basin.

The exploration significance of this study is two-fold: 1) We now have an age for an event, in the Horton clastic rocks, which may have acted as a conduit for mineralizing fluids (though not at site 1A); and 2) the size and/or grade of a deposit in the Minas sub-basin is reflected by the $^{87}\text{Sr}/^{86}\text{Sr}$ ratio of the ore-stage calcite and barite in the deposit.

Acknowledgments

We are indebted by J. Blenkinsop of Carleton University for the high quality strontium isotope analyses. The work of Akande (1982) and Ponsford (1983) contributed samples to this study. The financial contributions to this research through operating grant A-9036 to M.Z. from the Natural Sciences and Engineering Research Council (NSERC) of Canada, and Graduate Scholarships to C.R. from NSERC and Petro-Canada Ltd. are gratefully acknowledged.

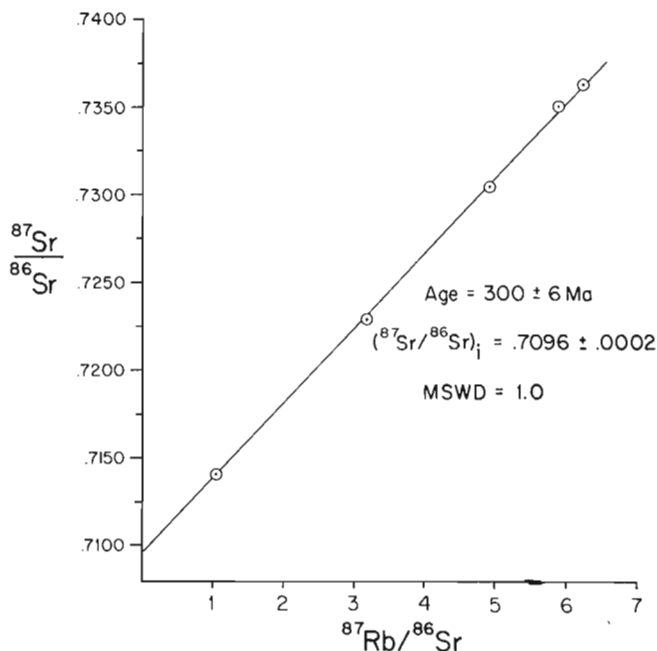


Figure 57.5. Isochron formed from Rb/Sr and $^{87}\text{Sr}/^{86}\text{Sr}$ analyses of five of the clay samples separated from Horton sandstone.

References

- Akande, S.O.
1982: Genesis of the lead and zinc mineralizations at Gays River, Nova Scotia, Canada: a geologic, fluid inclusion and stable isotopic study; unpublished Ph.D. thesis, Dalhousie University, Halifax, Nova Scotia, 349 p.
- Akande, S.O. and Zentilli, M.
1984: Geologic, fluid inclusion, and stable isotope studies of the Gays River lead-zinc deposit, Nova Scotia, Canada; *Economic Geology*, v. 79, p. 1187-1211.
- Boehner, R.C.
1981: Stratigraphy and depositional history of marine evaporites in the lower Carboniferous Windsor Group, Shubenacadie and Musquodoboit structural basins, Nova Scotia, Canada; Nova Scotia Department of Mines and Energy, Open File Report 468, 28 p.
- Burke, W.H., Denison, R.E., Heatherington, E.A., Koepick, R.B., Nelson, H.F. and Otto, J.B.
1982: Variation of seawater $^{87}\text{Sr}/^{86}\text{Sr}$ throughout Phanerozoic time; *Geology*, v. 10, p. 516-519.
- Clarke, D.B. and Halliday, A.N.
1980: Strontium isotope geology of the South Mountain batholith, Nova Scotia; *Geochimica et Cosmochimica Acta*, v. 44, p. 1045-1058.
- Clauer, N.
1982: The rubidium-strontium method applied to sediments—certitudes and uncertainties; in *Numerical Dating in Stratigraphy*, ed. G.S. Odin; Wiley, p. 245-276.

- Felderhof, G.W.
1978: Barite, celestite and fluorite in Nova Scotia; Nova Scotia Department of Mines and Energy, Bulletin 4, 463 p.
- Giles, P.S. and Boehner, R.C.
1979: Windsor Group stratigraphy in the Shubenacadie and Musquodoboit basins, central Nova Scotia; Nova Scotia Department of Mines and Energy, Open File Report 410.
- Hacquebard, P.A.
1972: The Carboniferous of eastern Canada; *Compte Rendu 7e, International Congress of Carboniferous Stratigraphy and Geology*, p. 69-90.
- Halliday, A.N.
1978: $^{40}\text{Ar}/^{39}\text{Ar}$ stepheating studies of clay concentrates from Irish orebodies; *Geochimica et Cosmochimica Acta*, v. 42, p. 1851-1858.
- Kessen, K.M., Woodruff, M.S., and Grant, N.K.
1981: Gangue mineral $^{87}\text{Sr}/^{86}\text{Sr}$ ratios and the origin of Mississippi Valley-type mineralization; *Economic Geology*, v. 76, p. 913-920.
- Krebs, W. and Macqueen, R.
1984: Sequence of diagenetic and mineralization events, Pine Point lead-zinc property, Northwest Territories, Canada; *Bulletin of Canadian Petroleum Geology*, v. 32, p. 434-464.
- Lambert, R.St.J., Chamberlain, V.E., and Muecke, G.K.
1984: Rubidium-strontium age and geochemistry of the Halifax Formation, Meguma Group, Nova Scotia; *Geological Association of Canada, Program with Abstracts*, v. 9, p. 81.
- Lydon, J.W.
1978: Observations on some lead-zinc deposits of Nova Scotia; in *Current Research, Part A, Geological Survey of Canada Paper 78-1A*, p. 293-298.
- MacLeod, J.
1975: Diagenesis and sulfide mineralization at Gays River, Nova Scotia; unpublished B.Sc. thesis, Dalhousie University, Halifax, Nova Scotia, 132 p.
- Ponsford, M.A.
1983: Geologic, fluid inclusion and stable isotope study of a carbonate-hosted lead deposit at Pembroke (Glenberrie), Colchester county, Nova Scotia; unpublished B.Sc. thesis, Dalhousie University, Halifax, Nova Scotia.
- Poole, W.H.
1967: Tectonic evolution of Appalachian region of Canada *Geological Association of Canada, Special Paper 4*, p. 9-51.
- Stein, H.J. and Kish, S.A.
1985: The timing of ore formation in southwest Missouri-rubidium-strontium glauconite dating at the Magmont Mine, Viburnum Trend; *Economic Geology*, v. 80, p. 739-753.
- Walker, S.D.
1978: Geological and mineralogical studies at the Smithfield lead-zinc prospect, Colchester County, Nova Scotia; Unpublished B.Sc. thesis, Dalhousie University, 93 p.

Geology and mineral occurrences of the Jumping Brook Complex, Cheticamp – Pleasant Bay area, Cape Breton Island, Nova Scotia

Contract 27 ST23233-5-0403¹

H.E. Plint², K.A. Connors², and R.A. Jamieson²

Plint, H.E., Connors, K.A., and Jamieson, R.A., Geology and mineral occurrences of the Jumping Brook Complex, Cheticamp – Pleasant Bay area, Cape Breton Island, Nova Scotia; in *Current Research, Part B, Geological Survey of Canada, Paper 86-1B*, p. 557-566, 1986.

Abstract

The Jumping Brook Complex is part of a belt of metamorphosed volcanic and sedimentary rocks which hosts small polymetallic sulphide deposits in northwestern Cape Breton Island. Detailed geological mapping (1:10 000) of the Jumping Brook Complex in the Cheticamp-Pleasant Bay area has been conducted in order to 1) document the structure, stratigraphy and metamorphism of the complex and its geological relationships to higher grade rocks to the east (Pleasant Bay Gneiss Complex), 2) determine the relative and absolute ages of the complexes, and 3) determine sulphide-host rock relations of three known deposits in the southern part of the map area. Bedding transposition and ambiguous younging indicators preclude determination of a depositional stratigraphy in the Jumping Brook Complex. Mafic pillow lavas have been documented in the southern part of the map area. A progressive, east to west, metamorphic increase from chlorite to staurolite-kyanite grade in the Jumping Brook Complex continues into the Pleasant Bay Gneiss Complex. All three sulphide occurrences are hosted by the metavolcanic rocks of the Jumping Brook Complex and two of the deposits are hosted by felsic tuffs. Sulphide-host rock textures indicate that mineralization pre-dates metamorphism and deformation, and is probably syngenetic. Locally, however, mineralization has been remobilized by shearing.

Résumé

¹ Contribution to the Canada-Nova Scotia Mineral Development Agreement 1984-1989. Project carried by Geological Survey of Canada, Mineral Resources Division, Project 700059.

² Department of Geology, Dalhousie University, Halifax, Nova Scotia, B3H 3J5

Introduction

Rocks of the Cape Breton Highlands (Fig. 58.1) host numerous, small, polymetallic Cu, Zn, Au, Ag (Pb, Fe) deposits (eg. Milligan, 1970; Chatterjee, 1980; Ponsford and Lyttle, 1984). Many of these deposits are associated with a discontinuous belt of low- to medium-grade metavolcanic and metasedimentary rocks informally referred to as the western Highlands volcanic-sedimentary complex (Barr et al., 1985). Although exploration and very limited mining have been conducted in different parts of the belt (eg. Gold Brook, Sarach Brook, Faribault Brook areas, Milligan, 1970; McNabb et al., 1976; Covey, 1978, 1979; Chatterjee, 1980; Doucet, 1983) it is unknown whether the deposits are mainly syngenetic or epigenetic, what role shearing has played in their present configuration, or to what extent the deposits differ from each other. The problem is complicated by the lack of a detailed geological understanding of the volcanic and sedimentary host rocks. This paper discusses the geology of the Jumping Brook — Faribault Brook area, where several small sulphide deposits occur, in an attempt to clarify the depositional, structural, and metamorphic history and their bearing on the formation of the mineral deposits.

Previous work

Currie (1975, 1982, in press) included the low grade metavolcanic and metasedimentary rocks of the Cape Breton Highlands north and east of Cheticamp in the Jumping Brook Complex, which he interpreted to be Silurian and separated from high grade gneissic rocks to the east (Pleasant Bay Gneiss Complex; Currie, 1975) by an unconformity. Craw (1984), in a detailed study of the Cheticamp River area, recognized low, medium, and high grade metamorphic belts which he interpreted as representing different structural levels of the same volcanic-sedimentary sequence. Conrod (1984) studied the transition from low to high grade metamorphic rocks exposed along Jumping Brook, but did not find conclusive evidence of either an unconformity or a continuous metamorphic transition. A late Proterozoic age for the volcanic rocks was suggested by Jamieson and Craw (1983) as the nonfoliated Cambrian Cheticamp pluton intrudes similar rocks on its eastern border (Barr et al., in press).

Covey (1978) described the geology and mineral deposits of the Faribault Brook area based on drill core and outcrop investigations. He noted the importance of quartz-sericite schist as the host rock for many sulphide-rich zones. Chatterjee (1980) gave a detailed description of the sulphide mineralogy and preferred a hydrothermal replacement origin for the deposits on the basis of geochemistry. The syngenetic versus epigenetic origin of the deposits is therefore still open to question, particularly in terms of their association with previously unrecognized felsic volcanic rocks (Connors, 1986).

Present work

Mapping was carried out during the summer of 1985 at a 1:10 000 scale with the following objectives.

- a. To document the stratigraphy, structure, and metamorphism of the volcanic and sedimentary rocks of the Jumping Brook Complex.
- b. To find evidence bearing on the relative and absolute ages of the low grade volcanic and sedimentary rocks and the high grade metamorphic rocks to the east.
- c. To document the relationship of the sulphides to their host rocks as a guide to the origin of the deposits.

Stratified rocks

Late Proterozoic (?)

Pleasant Bay Gneiss Complex. The Pleasant Bay Gneiss Complex (Currie, 1975, 1982) forms a north-south belt which extends from approximately 8 km south of the Cheticamp River northwards to the Pleasant Bay area where it is in sheared contact with the Cape North tectonic zone (S.M. Barr, personal communication, 1986). It is bounded to the west by the Jumping Brook Complex and intruded in the east by a Devonian megacrystic granite (Margaree Pluton, see O'Beirne-Ryan et al., 1986).

The dominant lithological units of the complex are: (1) biotite schist and paragneiss; (2) felsic muscovite-garnet orthogneiss; (3) amphibolite, and (4) granodioritic megacrystic gneiss. Contacts between these units are generally concordant and the rocks are well foliated. The degree of deformation in the complex precludes the recognition of primary stratigraphy but relative ages of some units are determinable.

The biotite schists and paragneisses (including pegmatite and amphibolite discussed below) comprise approximately 70% of the complex. This unit is composed primarily of fine- to medium-grained, grey, pelitic to semipelitic metasedimentary rocks. Pelitic lithologies are most common in exposures along Fishing Cove River and Benjies Lake Brook (Fig. 58.1).

Gneissic layering is due to variation in the relative proportion of biotite to quartz and feldspars, but is emphasized over most of the complex by the intrusion of sills of biotite granodiorite, fine grained mafic rocks (now metamorphosed to biotite-hornblende schists and amphibolites), medium grained granitoids, undeformed to strongly sheared muscovite-granite pegmatites, and veins of quartz \pm feldspar. Pegmatites and amphibolites also commonly truncate the layering. A sedimentary protolith for this unit is suggested by its aluminous composition and by pelitic to semipelitic layering.

Felsic muscovite-garnet orthogneiss, locally interlayered with unit 1, is exposed along the South Branch of Fishing Cove River (Fig. 58.1). It is a minor component in the complex and elongate feldspar and quartz porphyroclasts define the foliation.

Granodioritic, megacrystic gneiss, locally garnet- or magnetite-bearing, makes up about 30% of the complex. It varies from a K-feldspar megacrystic gneiss (up to approximately 30% megacrysts) to a coarse grained, foliated gneiss with rare megacrysts, and is intruded by biotite granodiorite and granite pegmatite dykes and sills.

Grande Anse biotite schists. Fine- to medium-grained, calcareous, biotite schists, amphibolites, and rare marble outcrop along the northwestern tributaries of the Grande Anse River. Locally, the schists contain small rounded feldspar porphyroclasts. Pinch and swell quartz-feldspar-muscovite veins trend parallel to the schistosity, and where abundant, give the rock a migmatitic appearance. These schists are interpreted to have sedimentary protoliths but their geological affinities are unknown, due to poor exposure, and they are grouped with the high grade gneisses (Pleasant Bay gneiss) in Figure 58.1.

Jumping Brook Complex

The Jumping Brook Complex trends north-south between Jumping Brook and the Cheticamp River (Currie, 1982; in press; Fig. 58.1). It is faulted and sheared against the Cheticamp pluton and intruded by the Devonian Salmon Pool pluton in the south (Jamieson and Craw, 1983; Craw, 1984; Barr et al., in press; Jamieson et al., in press). In the north and east it is bounded by the Pleasant Bay Gneiss Complex; the nature of the northern

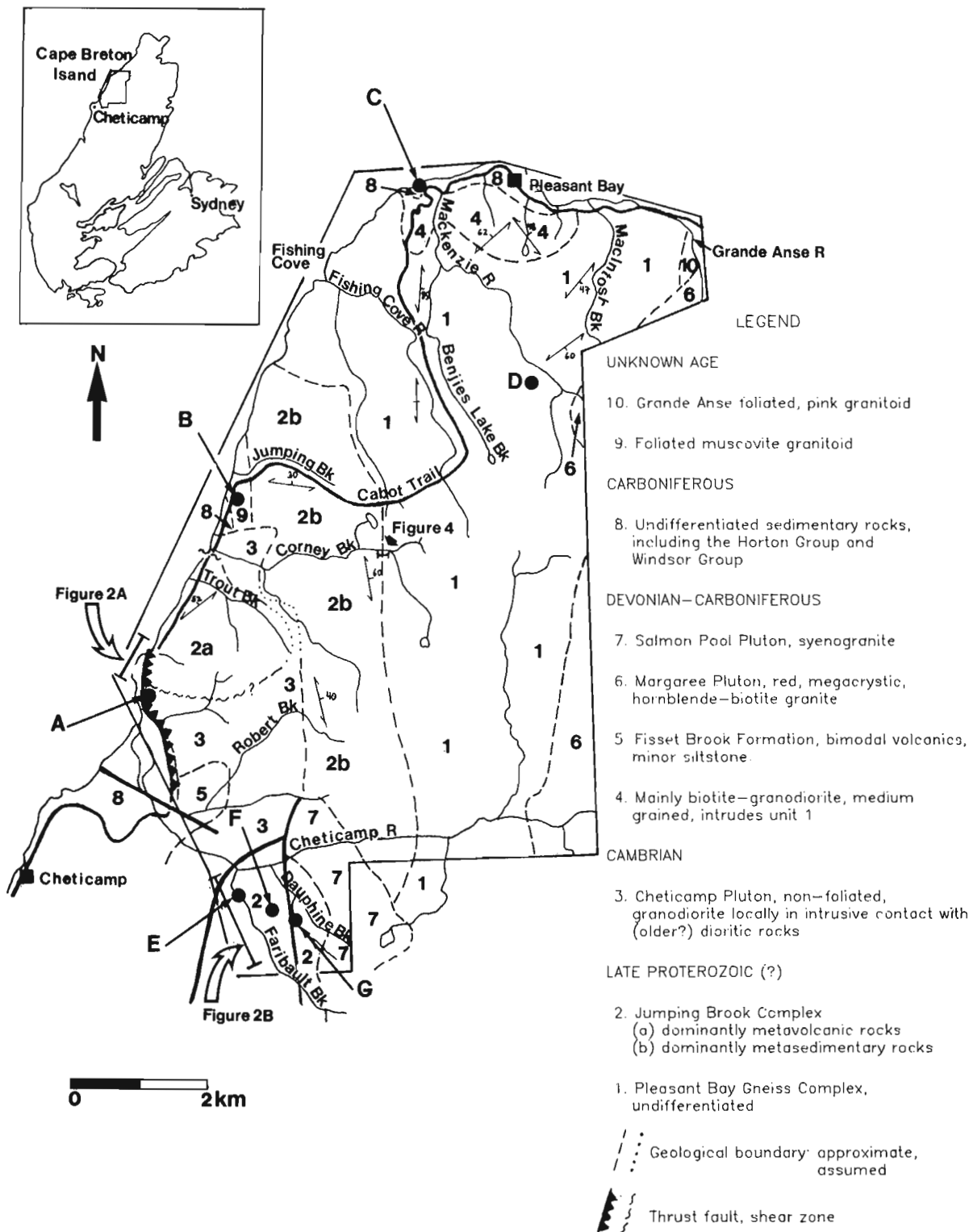
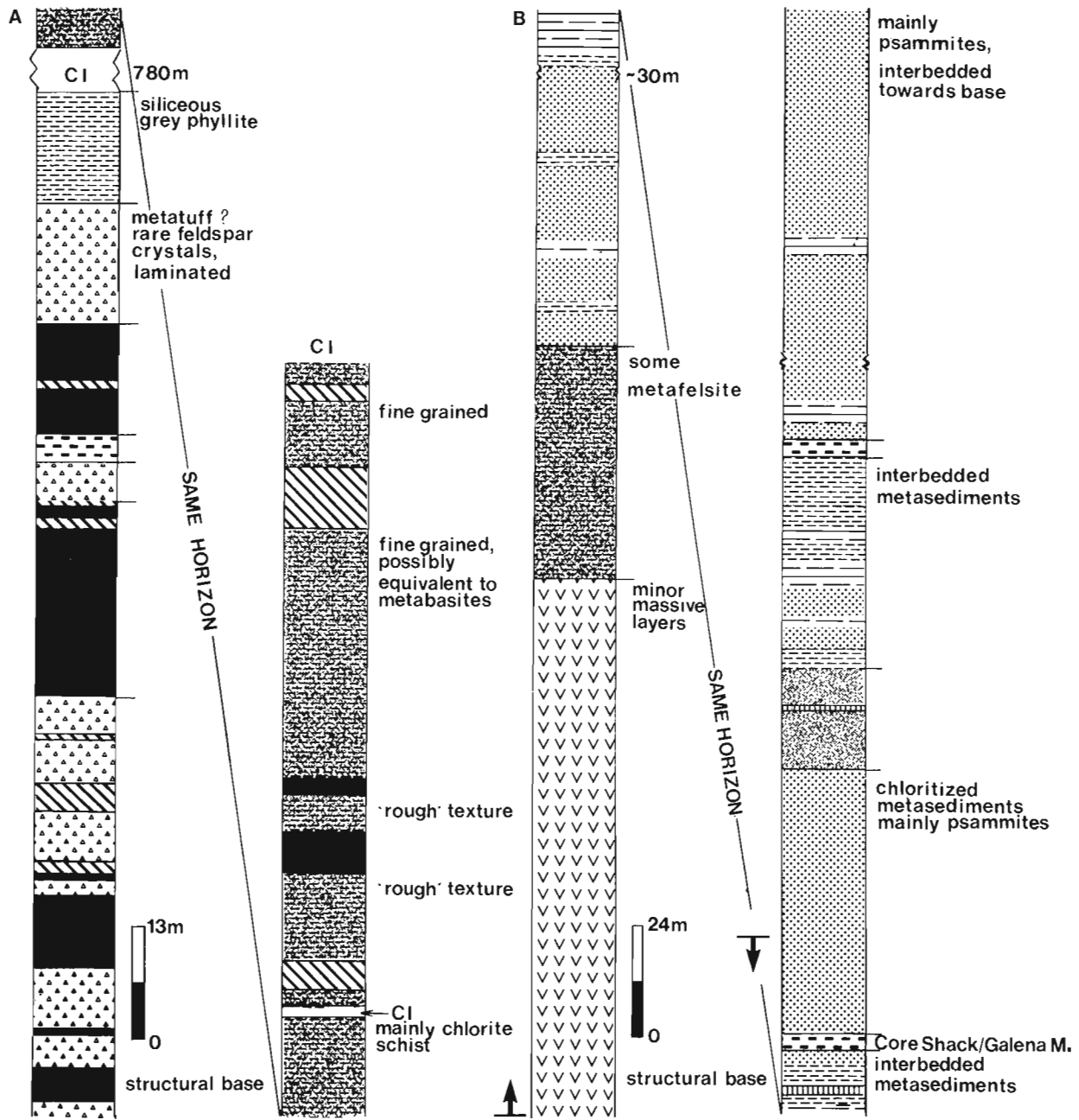


Figure 58.1. General geology of the area, modified on basis of 1985 field work, after compilations by Jamieson and Craw (1983), Barr et al. (1985) and Currie (in press). Inset gives regional location of study area. Heavy lines denote faults (after Jamieson and Craw, 1983). Regional structural trends are shown. Locations of lithological sections in Figure 58.2 and 58.4 are indicated. Mineral occurrences are: A = K10-06 (after Ponsford and Lytle, 1984), B = K10-11, C = K15-03, E = "Galena Mine", F = "Core Shack" and G = "Silver Cliff" as referred to in the text. Cabot Trail is omitted for clarity in the vicinity of thrust fault.



LEGEND

psammite	meta-tuff	chlorite sch.	pillowed mafic	quartz-sericite schist	mineralized zone
semi-pelite	metabasite	chlorite alteration	meta-volc.		
pelite	metafelsite				

Figure 58.2. Lithological sections through the western Highlands metavolcanic-metasedimentary complex. Note difference in scales between (A) and (B).

(A) Section as exposed along the Cabot Trail. CI = covered interval and is not to scale. Thicknesses of units are visual estimates. All data from this study.

(B) Section through the Faribault Brook area, modified after Covey (1978) with surface exposure mapped in this study. Arrow denotes part of section based primarily on findings in this study. Interbedded metasedimentary units are schematic.

boundary is not clear but in the east the transition may be gradational (see below). Carboniferous sedimentary rocks of the Horton Group are faulted against the Jumping Brook Complex in the west.

The main lithologies (Fig. 58.2) include mafic metavolcanic rocks with relict pillow structures, felsic to intermediate phyllites and schists, and pelitic, semipelitic and psammitic phyllites and schists which structurally overlie the mafic metavolcanics and are locally interlayered with the felsic to intermediate rocks. Younging indicators (apparent graded and crossbedding) yield conflicting data and are commonly poorly preserved. The degree to which the present distribution of rock types reflects depositional versus tectonic processes is not clear, but all the rocks are strongly deformed.

Metamorphosed mafic volcanic rocks dominate in the Fairbault Brook – Dauphinee Brook area south of the Cheticamp River and probably continue northwards as metabasite layers within felsic to intermediate phyllites and schists (hereafter referred to collectively as schists), although an extrusive origin is not proven in this area. Deformed pillow lavas, in the Fairbault Brook – Dauphinee Brook area are recognized by ellipsoidal pillows, lava tubes and rare, radial fractures. The metabasites are massive, fine grained, dark green rocks whose contacts are sharp and concordant with the surrounding schists.

Felsic to intermediate schists occur throughout the metavolcanic rocks and dominate the metavolcanic units north of the Cheticamp River. The intermediate schists are fine grained, chloritic and commonly exhibit centimetre-scale compositional layering. The felsic schists consist of (1) a very fine grained, commonly fissile, pink to green, banded schist (metafelsite in Fig. 58.2) and (2) a medium grained, buff, quartz-sericite schist, commonly containing abundant quartz porphyroclasts, which is host to sulphides (see below). All these rocks, with the local exception of the chlorite schists, contain plagioclase porphyroclasts in which relict primary twinning and euhedral outlines are locally preserved and quartz porphyroclasts which exhibit rare prismatic terminations. These features suggest close affinities to similar rocks at Money Point (Macdonald and Smith, 1980) and Sarach Brook (Jamieson and Doucet, 1983) where a volcanic origin has been clearly established. The quartz-sericite schists, therefore, are interpreted to be metamorphosed silicic tuffs. The banding and general paucity of porphyroclasts in the banded schists suggests they are meta-ophiolites but a tuffaceous origin cannot be precluded. Where porphyroclasts are abundant, the chloritic schists are interpreted to be metatuffs (Fig. 58.2) but where porphyroclasts are rare or absent, a protolith is indeterminate.

The metasedimentary schists (Fig. 58.3, 58.4) are subdivided on the basis of lithology and metamorphic grade from west to east (structurally up section), into (1) a low grade package of interbedded pelitic, semipelitic and psammitic phyllites, (2) a medium grade pelitic schist-dominated package and (3) a medium to high grade semipelitic schist-dominated package and (4) a high grade porphyroblastic pelitic schist and interbedded semipelitic schist. The contact between units 1 and 2 is obscured by the Cheticamp Pluton, between units 2 and 3 it is gradational and between units 3 and 4 it is not exposed but assumed concordant as foliations are consistent from one unit to the other.

The low grade pelitic, semipelitic and psammitic phyllites are interpreted to be metamorphosed equivalents of shales, siltstones and arkoses. The pelitic phyllites are mainly composed of fine grained quartz, muscovite, feldspar, chlorite, and idioblastic garnet and chloritoid. The semipelitic phyllites are distinguished from the pelitic phyllites by a greater percentage of quartz and the presence of small (1-3 mm) quartz porphyroclasts. Abundant blue quartz porphyroclasts characterize

the psammitic phyllites for which a poorly sorted protolith is suggested by local feldspar porphyroclasts and local gradations into quartz-feldspar metaconglomerate.

The medium grade pelitic schists are similar in composition to the low grade pelitic phyllites but are distinguished by the development of biotite porphyroblasts, hornblende porphyroblasts in associated mafic rocks (see below), and a slight increase in grain size. Minor, concordant, metre-scale zones of semipelitic schist outcrop in the pelitic schists. The medium to high grade semipelitic schists are fine- to medium-grained rocks composed of quartz, plagioclase, and muscovite in varying proportions and porphyroblastic garnet and biotite. Centimetre-scale compositional layering is common throughout the metasedimentary rocks. Minor, concordant metre-scale zones of grey quartzites, foliated metagabbros (presumed to be sills), fine grained amphibolites and siliceous, muscovite schists outcrop within units 2 and 3 and one metre-scale zone of marble is exposed within unit 3.

The semipelitic schists are succeeded eastwards by an interlayered sequence of quartz-feldspar-mica-garnet semipelitic schists and well foliated, highly aluminous, staurolite-garnet-mica-kyanite schists. Reconnaissance mapping to the south has revealed similar lithologies in the Robert Brook area (Fig. 58.1), suggesting its regional extent is greater than indicated by McLaren (1955).

Devonian-Carboniferous

Stratified rocks of this age include the Fisset Brook Formation and Horton Group and Windsor Group sedimentary rocks. These lithologies have been studied by other workers (eg. Currie, 1975; Jamieson and Craw, 1983; Blanchard et al., 1984) and were not investigated in this study.

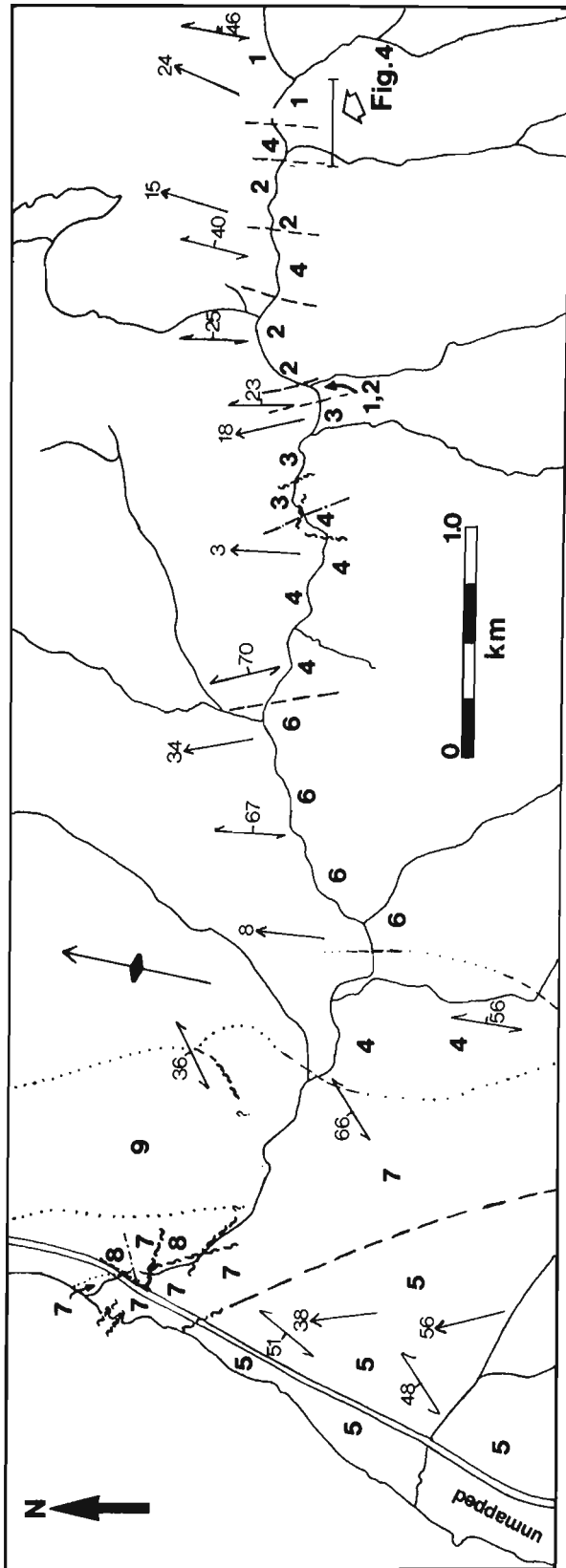
Intrusive rocks

Proterozoic (?)

Foliated Muscovite Granitoid. In the vicinity of Jumping Brook, foliated muscovite granitoid cuts semipelitic schists of the Jumping Brook Complex (Conrod, 1984). A sheared contact between the Cheticamp Pluton and the granitoid was observed on the south side of French Mountain near the mouth of Corney Brook but otherwise contact relations are unknown. Foliation in the pink, medium grained granitoid is defined by muscovite and quartz. The age of this pluton is unknown, but its foliation suggests that it is older than the Cheticamp Pluton and therefore probably Proterozoic.

Dioritic Rocks. Foliated to undeformed diorite is common near the Cheticamp Pluton (cf. Barr et al., 1985). Contacts between the Cheticamp Pluton and diorite are visible in Corney Brook and nearby coastal sections but it is unclear which unit is later. Foliated diorite is exposed along George Brook and within metasedimentary rocks along Corney Brook. Contact relations are not exposed but pervasive foliation in the diorite is parallel to that in the surrounding lithologies suggesting that the sedimentary rocks and diorite have shared at least one period of deformation. Locally the foliated diorites grade into or crosscut amphibolites; the latter also occur interlayered with or discordant to the medium and high grade schists exposed in Corney Brook.

Medium- to fine-grained biotite (\pm hornblende) schists and amphibolites are exposed within the medium grade pelitic package along Corney Brook (Fig. 58.3). On the basis of composition and fabric, these rocks may be foliated diorites but rare feldspar and quartz porphyroclasts and the local abundance of biotite in the schists allow the possibility of extrusive or volcanoclastic protoliths.



LEGEND

UNKNOWN AGE

9. Foliated muscovite granitoid

CARBONIFEROUS

8. Horton Group, undivided clastic sedimentary rocks

CAMBRIAN

7. Cheticamp Pluton

LATE PROTEROZOIC (?)

6. Dioritic rocks, undeformed to foliated; amphibolites, biotite +/- hornblende schists

JUMPING BROOK COMPLEX

5. Low grade interbedded pelitic, semipelitic, and psammitic schists (undivided)

4. Medium grade pelitic package (see text)

3. Medium to high grade semipelitic package (see text)

2. Staurolite-garnet-mica-(kyanite) schists and interlayered semipelitic schists

PLEASANT BAY GNEISS COMPLEX

1. Biotite schists and minor amphibolite, granite pegmatite and two-mica granite

↗₃₀ Main foliation

↗₃₀ Mineral lineation and crenulation fold axes

--- Geological boundary: defined, gradational, approximate, assumed

~ Fault or shear

↖ Late macroscopic antiformal fold axis

Figure 58.3. Detailed map of the metasedimentary lithologies of the Jumping Brook Complex exposed along Corney Brook. Rock units are described in text.

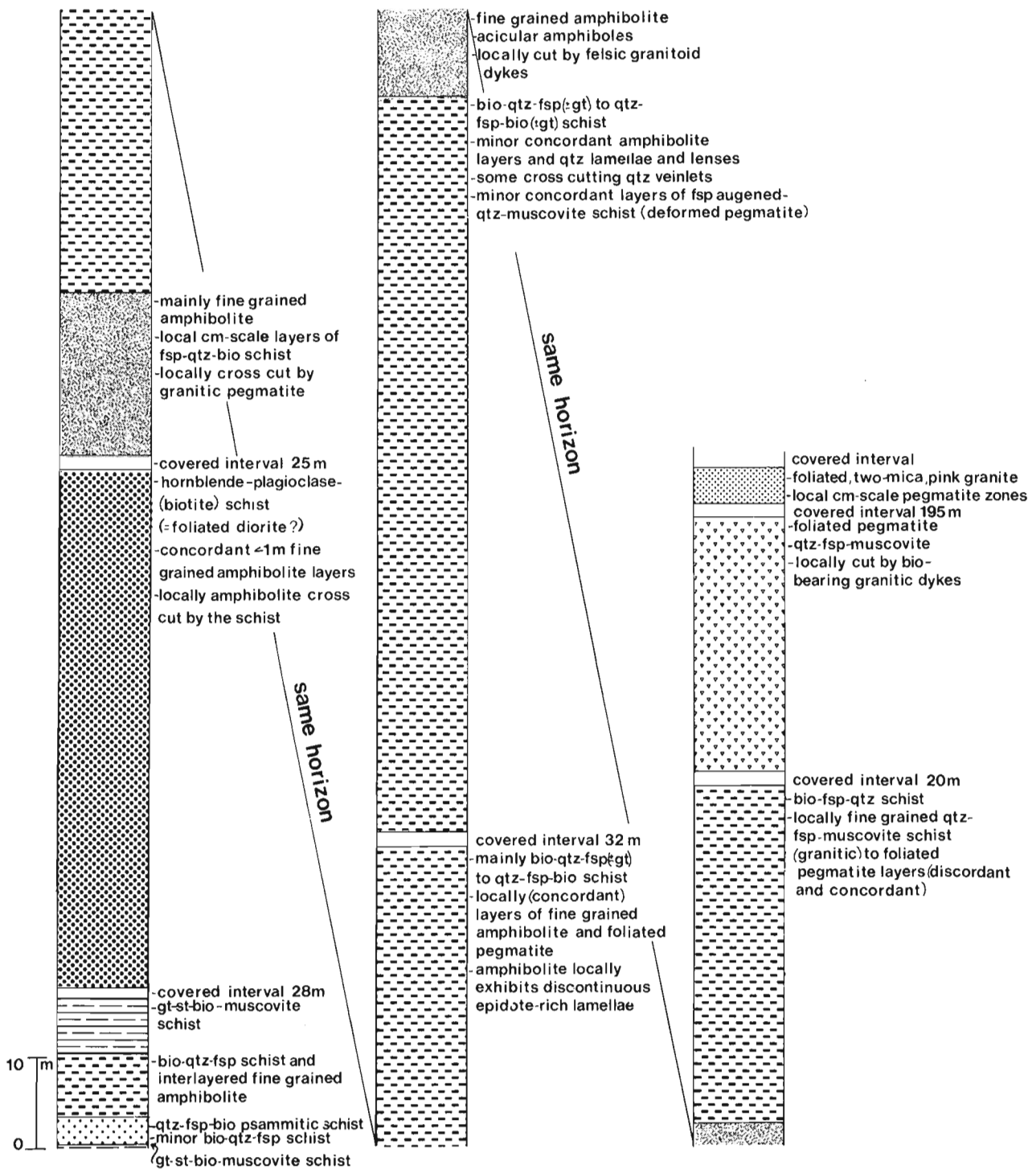


Figure 58.4. Lithological section through transition zone between the Jumping Brook and Pleasant Bay Gneiss complexes as exposed along Corney Brook. Note that the covered intervals are not to scale. Thicknesses of units are visual estimates.

The age of the diorites, amphibolites and biotite/hornblende schists in the Cheticamp area is unknown but as they are commonly strongly deformed, they are shown as Precambrian in Figure 58.3.

Cambrian

Cheticamp Pluton. The Cheticamp Pluton outcrops in a narrow belt along the western margin of the Cape Breton High-

lands from Corney Brook to the Northeast Margaree River (Currie, 1975, 1982, in press; Jamieson and Crow, 1983; Barr et al., 1985, in press). Barr et al. (1985) reported that the pluton intrudes the Pleasant Bay Gneiss Complex. In the map area, its contacts with the Jumping Brook Complex are faulted or sheared. Cataclastic deformation in the pluton results from thrust faulting which has brought the pluton westward over the Fisset Brook Formation in the southern part of the study area (Currie, 1975, 1982; Barr et al., 1985). Along the coast near

Corney Brook, and in exposures in the mouth of Corney Brook, numerous small scale faults and several northwest-trending ductile shears, interpreted to be related to this faulting, occur within the pluton.

The age of the Cheticamp Pluton has been determined by Rb-Sr geochronology to be 530 ± 44 Ma (Cormier, 1972, as revised by Keppie and Smith, 1978). A similar U-Pb age has been obtained from zircons (Jamieson et al., in press) and confirmed by further Rb-Sr work (Barr et al., in press).

Devonian-Carboniferous

Biotite Granodiorite. The Pleasant Bay Gneiss Complex is intruded by sills and dykes of a massive, locally foliated, equigranular biotite (muscovite) granodiorite which locally contains enclaves of the megacrystic gneiss. Pegmatites and fine grained, granitic and dioritic dykes intrude the granodiorite. An age of 398 Ma (Rb-Sr whole-rock) obtained for the granodiorite (Fairbairn et al., 1960) and crosscutting relationships imply that the granodiorite is probably Devonian.

Margaree and Salmon Pool plutons. These plutons were not investigated in detail and their extent as shown in Figure 58.1 is based on previous compilations (eg. Currie, 1982, in press; Craw, 1984; Jamieson and Craw, 1983). Both the Salmon Pool (U-Pb) and Margaree (Rb-Sr) plutons are dated as Late Devonian to Carboniferous and they intrude the Jumping Brook and Pleasant Bay gneiss complexes respectively (Jamieson et al., in press; O'Beirne-Ryan et al., 1986).

Unknown age

Grande Anse granitoid. Along the northern part of the Grande Anse River, south of the Cabot Trail, a fine- to medium-grained, pink feldspar-quartz-(biotite) granitoid is exposed. Foliation is variably developed and locally minor shear zones trend parallel to the pervasive foliation. A pre-Devonian age is suggested by the presence of a foliation in an area where the Devonian Margaree Pluton is unfoliated.

Structure

No pre-metamorphic structures are observed in the Pleasant Bay Gneiss Complex. An early foliation (S_{g1}) is locally preserved in rootless, isoclinal folds, to which the pervasive foliation (S_{g2}), is axial planar. Whether S_{g2} development correlates with D_1 in the Jumping Brook Complex (see below) is unknown. It is unclear if the pervasive foliation (S_{g2}) is of the same generation throughout the complex, but S_{g2} orientations define an apparent, macroscopic, close, NNE-trending, anti-form.

Pervasive foliation (S_{j1}) in the Jumping Brook Complex is commonly parallel or nearly parallel to bedding (S_0). Mesoscopic and microscopic, rootless, isoclinal folds in S_0 , transposed along S_{j1} , small scale, recumbent isoclinal folds to which S_{j1} is axial planar and local bedding-foliation intersection angles of 30 to 45° support Craw's (1984) interpretation that S_{j1} is axial planar to recumbent, macroscopic, isoclinal folds (D_1). Ductile, foliation-parallel shears in the Faribault Brook area are probably related to this folding. The Jumping Brook Complex has been refolded into a moderately north-plunging, close, macroscopic, NNE-trending antiform (D_2). Fine crenulations (S_{j2}), mineral lineations (defined mainly by biotite) and some small scale upright fold axes trend parallel to the macroscopic fold axis and are interpreted to result from the same deformation event (D_2). Extensional fractures are commonly developed perpendicular to the fine crenulations and locally form a well developed cleavage (S_{j3}).

Extensive kinking, some low amplitude, large wavelength crenulations, and faulting along the coast within the Jumping Brook Complex define late stage deformation (D_4). Minor late stage faults and shears also occur locally within the Pleasant Bay Gneiss Complex and associated granitoids.

Metamorphism

Metamorphic grade in the study area varies from greenschist to upper amphibolite facies (eg. Currie, 1975, 1982; Craw, 1984; Conrad, 1984). A progressive increase in metamorphic grade is observed from west to east within the Jumping Brook Complex through chlorite, biotite, garnet and staurolite-kyanite grade. Evidence is found for only one episode of prograde metamorphism. Porphyroblasts almost always overgrow the pervasive foliation (S_{j1}) indicating that the thermal maximum postdates D_1 (cf. Currie, 1982, in press; Craw, 1984; Conrad, 1984; Connors, 1986). In addition, garnet overprints the fine crenulations (D_2) in the low grade metasedimentary rocks, and apparently retrograde chlorite porphyroblasts overprint S_{j1} in the medium to high grade schists. Currie (1982, in press) also reported chloritoid, cordierite and andalusite in the medium and high grade schists. These are not confirmed by this work although chloritoid is abundant in the low grade pelitic phyllites.

Garnet and hornblende are developed in the biotite schists, paragneisses and amphibolites of the Pleasant Bay Gneiss Complex and are syntectonic with respect to S_{g2} . Post-tectonic (relative to S_{g2}) kyanite is common in the aluminous zones within the semipelitic schists and paragneisses and is variably retrograded, ranging from fresh to almost entirely pseudomorphed by muscovite.

The maximum metamorphic grade in the Jumping Brook Complex (staurolite-kyanite zone) is similar to the metamorphic grade in the adjacent gneisses; no evidence is found for a structural or metamorphic break.

Mineral deposits

The most important sulphide deposits of the area occur within metavolcanic rocks of the Jumping Brook Complex. In the course of this study, three deposits in the Faribault Brook area were examined in detail (Galena Mine, Silver Cliff, and Core Shack; Connors, 1986) and several minor showings were confirmed (K10-06, K15-21; Ponsford and Lyttle, 1984).

Faribault Brook Area. The Galena Mine deposit contains galena, sphalerite, and arsenopyrite, with minor chalcopyrite and pyrrhotite, concentrated near the top of a 3-4 m thick quartz-sericite schist layer within a zone of interlayered pelitic, semipelitic, and psammitic schists. Chatterjee (1980) reported rare stibnite and bismuthinite from the deposit. The sulphides occur in lenses but overall the deposit appears stratiform. Hand samples and thin sections reveal folding and shearing in the sulphide-rich zones, which therefore must pre-date the main deformation in the area (D_1). Similarly, pre- D_1 , pyrite occurs in quartz-sericite schist north of the Cheticamp River.

At the Core Shack showing, the sulphides are concentrated in layers within a 5-6 m thick quartz-sericite schist which is truncated by a late fault. Arsenopyrite is the dominant sulphide with sphalerite, galena, and pyrite visible in hand specimen; in addition, pyrrhotite, argentite and chalcopyrite were reported by Chatterjee (1980). In hand sample and thin section, deformation of the sulphides is evident, indicating a pre-tectonic origin.

The Silver Cliff deposit is now covered by debris, but Chatterjee (1980) described a 2-8 m mineralized zone with sulphides present in concordant to discordant folded lenses. The host

rock is a chlorite schist, probably of volcanic origin, with the sulphides closely associated with a massive quartz-carbonate unit. The main minerals are sphalerite, arsenopyrite, galena, pyrite, chalcopyrite and pyrrhotite; tetrahedrite, argentite, bismuthinite, and lollingite were also reported by Chatterjee (1980). The arsenopyrite is recrystallized and commonly intergrown with chalcopyrite and sphalerite.

The association of the sulphides with the quartz-sericite schist unit, identified in this study as a metamorphosed felsic tuff, is considered significant. The Silver Cliff deposit is not associated with the silicic rocks but does occur in a chlorite schist of probable volcanic origin. Simple lithological association, therefore, suggests a connection between the volcanic rocks and the sulphides which is consistent with a syngenetic origin.

Detailed petrographic investigations of the sulphides and their host rocks (Connors, 1986) showed clearly that in most cases mineralization pre-dated deformation and metamorphism. Disseminated sulphides have been strongly deformed in the plane of the foliation in some samples. In other samples, garnet has nucleated on, and overgrown, previously deformed sulphide stringers; the pattern of deformation in one sample suggests that the host rock was a volcanic breccia. These observations are also consistent with formation of the sulphide deposits during or shortly after volcanism.

In some areas, however, mobilization of the sulphides in later shear zones has occurred: this may also explain some of the features of the Silver Cliff deposit. These shear zones are particularly common in the pillowed sequence, where coarse grained arsenopyrite is replaced by sphalerite and chalcopyrite. Late stage mobilization of the sulphides in shear zones has been noted in other parts of the western Highlands volcanic-sedimentary complex (eg. Doucet, 1983). This masks the primary features of the deposits and probably accounts for the previous lack of agreement on their origin.

Minor occurrences. Disseminated sulphides, including galena, arsenopyrite and sphalerite with less abundant chalcopyrite, pyrrhotite and pyrite, are common accessory phases (combined totals up to 10%) of some psammitic and semipelitic layers within the metasediments. In these rocks, the sulphides clearly pre-date the deformation. This study has not determined any systematic distribution of these layers. In the meta-volcanic exposures north of the Cheticamp River, rare sphalerite occurs in the chlorite schists in carbonate lenses parallel to the foliation and disseminated pyrite blebs and stringers along the foliation are common within the metabasites and intermediate schists. Sulphides are only rarely associated with the pillow lavas, except in late shear zones as discussed above, but accessory arsenopyrite, sphalerite, pyrite, and galena are intergrown with amphibole and ilmenite in some diorites along Faribault Brook.

Showing K10-06 consists of chalcopyrite-carbonate veins along the margin of the mafic dyke which intrudes the Cheticamp Pluton; showing K15-21 consists of a minor amount of arsenopyrite and pyrite in a fault zone in unit 1 of the Pleasant Bay Gneiss Complex. Showing K10-11 (Ponsford and Lyttle, 1984) was not investigated but is reportedly hosted in the Horton Group rocks and therefore not related to those in the Faribault Brook area. Showing K15-03, apparently hosted in the foliated muscovite granitoid, was not confirmed.

Discussion

No stratigraphic sequence can be defined in the Jumping Brook Complex as bedding is transposed along S_{11} and top indicators give conflicting results. However, mafic pillow lavas

(previously unrecognized) and felsic tuffs (quartz-sericite schist) have been documented in the Faribault Brook area in this study. Our observations strongly suggest that the Jumping Brook Complex was originally a mafic to felsic volcanic complex gradational into poorly sorted sedimentary and volcanoclastic rocks. Chemistry of the mafic pillow lavas suggests an island arc origin (Connors, 1986).

Our structural data support the interpretation (Currie, 1975, 1982; Craw, 1984) of early, now recumbent, macroscopic, isoclinal folding of bedding (S_0) and subsequent refolding into a close, north-plunging, nearly upright, NNE-trending antiform.

The region between the complexes is marked by north-south, nearly vertical foliation suggesting some form of tectonized contact exists. No evidence is found for an unconformity or faulted contact between the complexes but the transition (as indicated by Currie, in press) along Corney Brook is obscured by foliated diorites. Foliations are conformable and a metamorphic progression is observed from the Jumping Brook Complex to the Pleasant Bay Gneiss Complex suggesting a continuous transition between the complexes. Other workers have proposed a continuous sequence for the Jumping Brook Complex and Pleasant Bay Gneiss Complex (Craw, 1984) and correlated rocks (Macdonald and Smith, 1980; Doucet, 1983).

The depositional age of the Jumping Brook Complex is not apparent from field relations. The complex is, however, strongly foliated and therefore probably pre-dates the intrusion of the nonfoliated Cambrian Cheticamp pluton.

Sulphide-host rock textural relations strongly suggest that most of the sulphides are syngenetic with respect to felsic volcanism. Sulphides have been affected by deformation and metamorphism and locally remobilized by later shearing. Thus, an understanding of the pre-metamorphic distribution of sulphides and their host rocks and the effects of deformation and metamorphism are important in assessing the economic potential of these deposits.

Acknowledgments

This project has been funded by GSC Contract No. 27ST23233-5-0403 to RAJ. KC was supported in part by this grant and by an NSERC Undergraduate Summer Research Award. HP was supported in part by a Killam Memorial Scholarship from Dalhousie University and an NSERC Postgraduate Scholarship. The co-operation of the Cape Breton Highlands National Park staff in providing access to private roads and allowing sample collection within the park boundaries is greatly appreciated. We have benefited from discussions with R.P. Raeside, S.M. Barr, M. Zentilli, A.M. O'Beirne-Ryan, A. Sangster and others.

References

- Barr, S.M., Jamieson, R.A., and Raeside, R.P. 1985: Igneous and metamorphic geology of the Cape Breton Highlands; GAC/MAC 1985 Excursion 10 Guidebook, 48 p.
- Barr, S.M., Macdonald, A.S., and Blenkinsop, J. The Cheticamp pluton, an early Cambrian peraluminous granitoid intrusion in the western Cape Breton Highlands, Nova Scotia; Canadian Journal of Earth Sciences (in press).
- Blanchard, M.C., Jamieson, R.A., and Moore, E.B. 1984: Late Devonian-Early Carboniferous volcanism in western Cape Breton Island, Nova Scotia; Canadian Journal of Earth Sciences, v. 21, p. 762-774.

- Chatterjee, A.K.
1980: Mineralization and associated wall rock alteration in the George River Group, Cape Breton Island, Nova Scotia; unpublished Ph.D. thesis, Dalhousie University, 197 p.
- Connors, K.A.
1986: Relationships between sulphide minerals, metamorphism, and deformation in the Faribault Brook area of the Cape Breton Highlands, Nova Scotia; unpublished B.Sc. thesis, Dalhousie University, 105 p.
- Conrod, D.M.
1984: The relationship between low and high grade metamorphic rocks in the French Mountain area, Cape Breton Highlands, Nova Scotia; unpublished B.Sc. thesis, Dalhousie University, 214 p.
- Cormier, R.F.
1972: Radiometric ages of granitic rocks, Cape Breton Island, Nova Scotia; Canadian Journal of Earth Sciences, v. 9, p. 1074-1085.
- Covey, G.
1978: Nova Scotia Department of Mines and Energy Assessment File 11K/10B, 7-J-09(48).
1979: Nova Scotia Department of Mines and Energy Assessment File 11K/10B, 7-J-09(49).
- Craw, D.
1984: Tectonic stacking of metamorphic zones in the Cheticamp River area, Cape Breton Highlands, Nova Scotia; Canadian Journal of Earth Sciences, v. 21, p. 1229-1244.
- Currie, K.L.
1975: Studies of granitoid rocks in the Canadian Appalachians; in Report of Activities, Part A, Geological Survey of Canada Paper 75-1A, p. 265-270.
1982: Paleozoic supracrustal rocks near Cheticamp, Nova Scotia; Maritime Sediments and Atlantic Geology, v. 18, p. 94-103.
– Relations between metamorphism and magmatism near Cheticamp, Cape Breton Island, Nova Scotia; Geological Survey of Canada, Paper 85-23 (in press).
- Doucet, P.
1983: The petrology and geochemistry of the Middle River area, Cape Breton Island, Nova Scotia; unpublished M.Sc. thesis, Dalhousie University, 339 p.
- Fairbairn, H.W., Hurley, P.M., Pinson, W.H., and Cormier, R.F.
1960: Age of the granitic rocks of Nova Scotia; Geological Society of America, Bulletin, v. 71, p. 399-414.
- Jamieson, R.A. and Craw, D.
1983: Reconnaissance mapping of the southern Cape Breton Highlands — a preliminary report; in Current Research, Part A, Geological Survey of Canada, Paper 83-1A, p. 263-268.
- Jamieson, R.A. and Doucet, P.
1983: The Middle River-Crowdis Mountain area, southern Cape Breton Highlands; in Current Research, Part A, Geological Survey of Canada, Paper 83-1A, p. 269-275.
- Jamieson, R.A., van Breemen, O., Sullivan, R.W., and Currie, K.L.
The age of igneous and metamorphic events in the western Cape Breton Highlands, Nova Scotia; Canadian Journal of Earth Sciences (in press).
- Keppie, J.D. and Smith, P.K.
1978: Compilation of isotopic age data of Nova Scotia; Nova Scotia Department of Mines, Report 78-4.
- Macdonald, A.S. and Smith, P.K.
1980: Geology of Cape North area, Northern Cape Breton Island, Nova Scotia; Nova Scotia Department of Mines and Energy, Paper 80-1, 60 p.
- McLaren, A.S.
1955: Cheticamp River, Inverness and Victoria Counties, Cape Breton Island, Nova Scotia; Geological Survey of Canada, Preliminary Map 55-36.
- McNabb, B.E., Fowler, J.H., and Covert, T.G.N.
1976: Geology, geochemistry, and mineral occurrences of the Northeast Margaree River drainage basin in parts of Inverness and Victoria Counties, Cape Breton, Nova Scotia; Nova Scotia Department of Mines and Energy, Paper 76-4, 30 p.
- Milligan, G.C.
1970: Geology of the George River Series, Cape Breton; Nova Scotia Department of Mines, Memoir Z, 111 p.
- O'Beirne-Ryan, A.M., Barr, S.M., and Jamieson, R.A.
1986: Contrasting petrology and age of two megacrystic granitoid plutons, Cape Breton Island, Nova Scotia; in Current Research, Part B, Geological Survey of Canada, Paper 86-1B, report 21.
- Ponsford, M. and Lyttle, N.A.
1984: Metallic mineral occurrences map and data compilation, Eastern Nova Scotia; Nova Scotia Department of Mines and Energy, Open File Report 600.

The McIntyre-Hollinger investigation, Timmins, Ontario: stratigraphy, lithology and structure

Project 850052

R. Mason¹, N. Melnik¹, C.F. Edmunds¹, D.J. Hall¹, R. Jones¹, and B. Mountain¹
Mineral Resources Division

Mason, R., Melnik, N., Edmunds, C.F., Hall, D.J., Jones, R., and Mountain, B., The McIntyre-Hollinger investigation, Timmins, Ontario: stratigraphy, lithology and structure; in *Current Research, Part B*, Geological Survey of Canada, Paper 86-1B, p. 567-575, 1986.

Abstract

The McIntyre-Hollinger gold complex is enclosed by a sequence of Archean volcanic rocks, the Tisdale Group, which surround a felsic porphyry intrusion (the Pearl Lake porphyry), and is folded into a periclinal structure – the Central Tisdale anticline. The volcanic rocks consist of iron and magnesium tholeiitic flows, flow breccias and interflow sedimentary units. The flows may be massive or pillowed, and the pillowed flows may be variolitic or amygdaloidal and four major volcanic formations have been established in and around the Central Tisdale anticline.

The Pearl Lake porphyry contains xenoliths of volcanic rocks and transgresses the stratigraphy. Marginal heterolithic intrusion breccias occur at its contacts with the volcanic rocks, but its intrusive nature is partly obscured elsewhere by intense hydrothermal alteration and shear deformation. The shear deformation has resulted in the development of cleavage, linear fabrics, shear zones and faults related to the Hollinger Fault system. It has modified the original shapes of the porphyry and the Central Tisdale anticline through flattening in the plane of the cleavage and extension parallel to the linear fabric.

Résumé

Le complexe aurifère McIntyre-Hollinger est enfermé dans une séquence de roches volcaniques de l'Archéen, le groupe de Tisdale, qui entoure une intrusion de porphyre felsique (le porphyre de Pearl Lake), et il est plissé dans une structure périclinale, l'anticlinal Central Tisdale. Les roches volcaniques sont composées de coulées tholéitiques de fer et de magnésium, de brèches de coulées de laves et d'unités sédimentaires intercalées. Ces coulées peuvent être massives ou en coussins et celles en coussins peuvent être variolitiques ou amygdalaires; de plus, quatre importantes formations volcaniques ont été identifiées dans cet anticlinal de Central Tisdale et autour de ce dernier.

Le porphyre de Pearl Lake contient des zéolithes de roches volcaniques et ne respecte pas la stratigraphie. Il y a des brèches d'intrusion hétérolithique marginale à ses points de contact avec les roches volcaniques, mais sa nature intrusive est en partie cachée par une altération hydrothermique intense et de la déformation du cisaillement. Cette déformation tectonique a entraîné le développement de zones de cisaillement, de clivages et de structures linéaires apparentés au système de la faille Hollinger. Elle a modifié la forme originale du porphyre et de l'anticlinal Central Tisdale par un aplanissement dans le plan de clivage et une extension parallèle à la structure linéaire.

¹ Department of Geology, Queen's University, Kingston, Ontario K7L 3N6

Introduction

A systematic geological appraisal of copper and gold mineralization at the McIntyre and Hollinger mines was initiated in June 1984. This paper, together with its companion Mason and Melnik (1986) record a summary of findings to date. All available information in mine records and publications have been utilized, together with investigations of available underground workings and the surface outcrops over the two properties. The McIntyre mine was investigated during summer 1984: No. 6 shaft allowed access to the mine workings on the western part of the property from 1000 level to 1875 level, and No. 11 shaft provided access to the central and eastern parts of the property from 1000 level to 3875 level. Below 3875 level, No. 12 shaft served the mine to 6825 level, but it was not in regular use and is being closed down. Traverses were completed on 4175 level. The upper parts of the mine from surface to 900 level are closed and inaccessible. In addition to the McIntyre investigations, a limited amount of work was carried out underground at the Hollinger mine.

During summer 1985 a detailed surface map was made of the outcrops on McIntyre and Hollinger properties and a compilation of geological information from mine records is being made. A major petrographic study of the Pearl Lake porphyry, its hydrothermal alteration and associated copper and gold mineralization is also being undertaken by N. Melnik.

Outline of geology

The Timmins gold camp, situated within the city limits of Timmins in northern Ontario, forms part of a volcanic complex in the western part of the Archean Abitibi greenstone belt.

The McIntyre mine is part of a larger mineralized complex which includes the Hollinger mine and associated properties to the west and the Coniaurum mine to the east (Fig. 59.1). The Pearl Lake porphyry, on the southern limb of the Central Tisdale anticline forms the core of the complex. It intrudes a sequence of volcanic flows, breccias and thin interflow sedimentary units of the Tisdale Group (Fig. 59.1). Most of the important gold mineralization occurs in veins within the Central Formation of the Tisdale Group in which volcanic breccias dominate a sequence of magnesian and iron tholeiitic basalt flows.

Figure 59.2 summarizes the geological history at McIntyre and the Timmins gold camp in general, up to the time of the Matachewan-type diabase dyke intrusions. The geology of the Timmins area has been documented by Burrows (1925), Ferguson (1968) and Pyke (1982).

Tisdale volcanism was followed by a period of structural disturbance which resulted in folding and faulting followed by uplift and erosion prior to the deposition of the Timiskaming sedimentary sequence with angular unconformity on the tilted Tisdale rocks. These events were followed by the intrusion of felsic porphyries, the largest

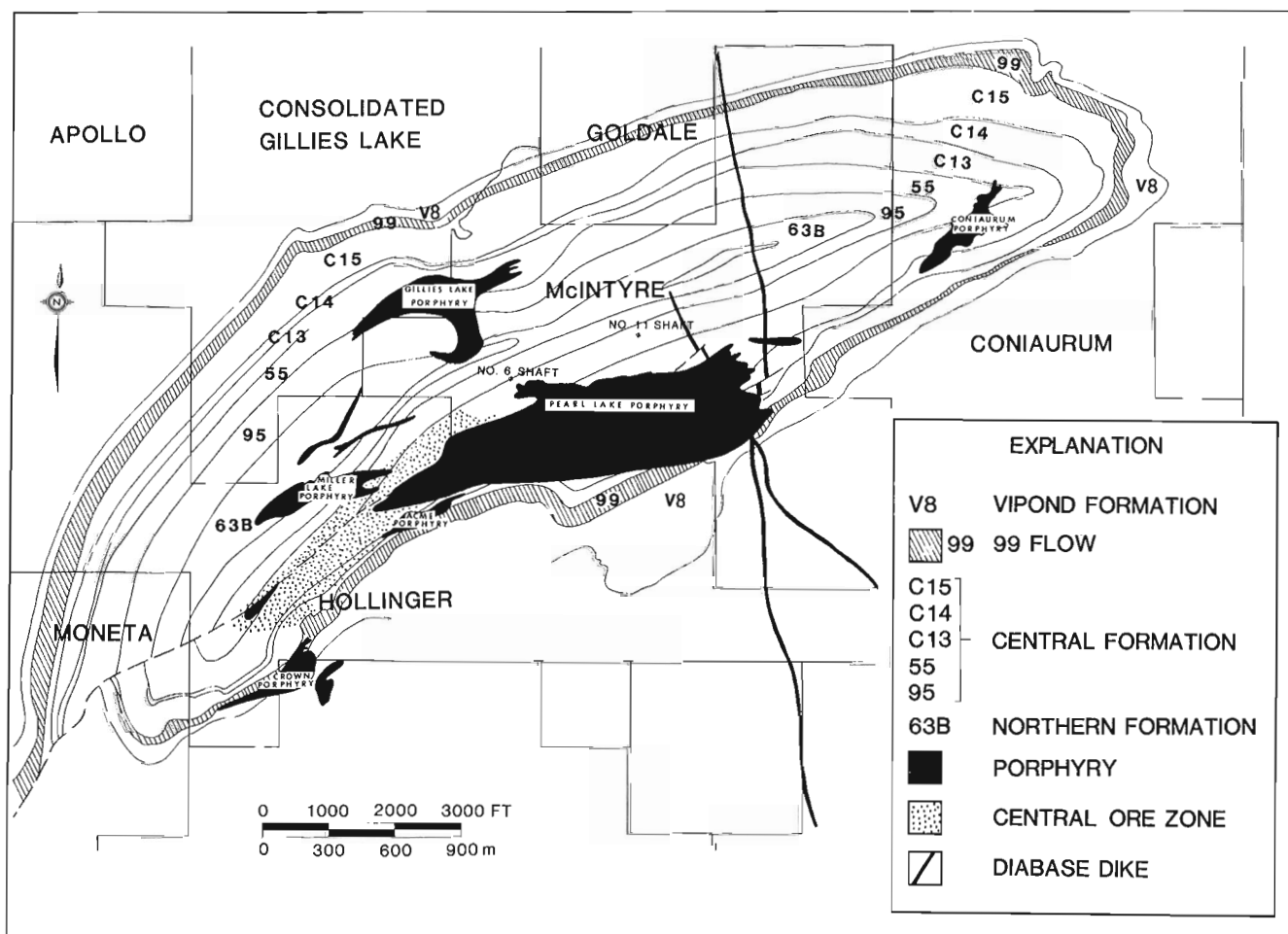


Figure 59.1. Geological map of the Central Tisdale anticline, Timmins.

SEQUENCE OF EVENTS AT MCINTYRE

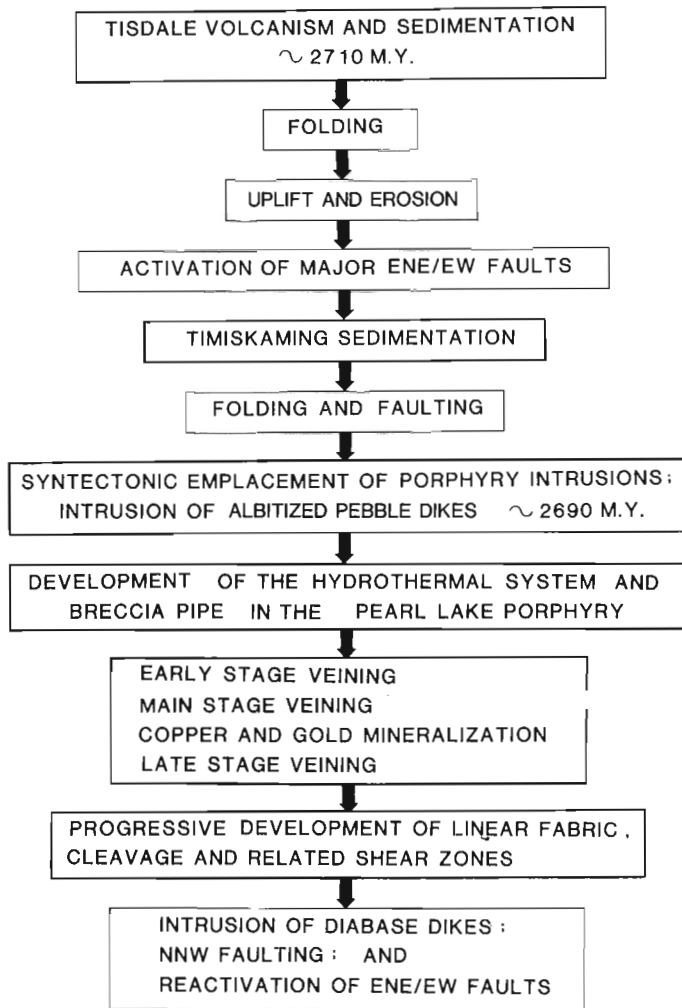


Figure 59.2. Sequence of events at McIntyre mine, Timmins.

of which, at surface, is the Pearl Lake porphyry, and the emplacement of heterolithic breccia dykes, pipes and albitite dykes. A breccia pipe was formed in the Pearl Lake porphyry, with early hydrothermal alteration dominated by albitization and sericitization followed by carbonate alteration and mineralizing events which generated the copper-molybdenum-gold stockwork associated with the breccia pipe, and auriferous quartz veins close to the contacts of the porphyry and within the enclosing volcanic sequence. The mineralizing events were followed by regional deformation which modified the geometry of the entire complex and resulted in the development of a pervasive cleavage and linear fabric and the development of shear zones and faults.

The later part of the geological record is represented by a series of major NNW-trending diabase dykes, thought to be Proterozoic (Matachewan-type) and these dykes are themselves disrupted by late reactivation of ENE-trending faults.

Stratigraphy and lithology

Historical approach

The stratigraphy at McIntyre (Robinson, 1923; Hurst, 1936; Langford, 1941; Furse, 1948) was originally established by careful mapping of the tops and bottoms of

individual flow and interflow were sedimentary units. Lithological and structural differences was noted; massive flows were distinguished from pillowed and brecciated flows; amygdaloidal pillowed flows were distinguished from variolitic pillowed flows, and the continuity of certain units was established. Brecciated flows at the base of the Central Formation (the "McIntyre Series" of Hurst, 1936 and Langford, 1941) provided good marker units to the north of the Pearl Lake porphyry.

Following a major re-appraisal of the geology and the potential for further ore at McIntyre, Griffis (1962 and, in Ferguson, 1968) reported on the convenience of adopting the use of the terms "uniform lava" and "structured lava" as a means of distinguishing massive flow units from those flows which exhibited pillows, flow textures and other primary structures. Instead of the emphasis on flow contacts and related features as a means of establishing volcanic stratigraphy, major compilations at 1:100 scale were prepared at that time, using only "uniform" versus "structured" as the principal means of correlation.

Unfortunately, as the earlier geologists had discovered, massive units grade into structured units along strike and vice versa, so that correlation of massive or structured units from underground exposures and borehole information is generally inaccurate and misleading. The geological interpretation at McIntyre therefore changed from a simple south-facing sequence of volcanic units disrupted by the Pearl Lake porphyry intrusion (1923-1954) to a complexly folded and abnormally thickened volcanic sequence, and Ferguson's (1968) compilation of mine plans reflects this.

The present study

Figure 59.3 illustrates the stratigraphy and lithologies at McIntyre. It is based on all previous work summarized by Griffis (1960), and modified in the light of the present investigation.

Northern Formation. As its name implies, the Northern Formation occurs to the north of the mine workings at McIntyre and Hollinger, where it forms the core of the Central Tisdale anticline as defined by our underground investigations and recent surface mapping (Fig. 59.1). Jones (1948) recorded reversals of younging directions to the north of the Hollinger boundary, on the Gillies Lake Property, where he observed duplication of the basal stratigraphy (95/55 flow units) of the Central Formation.

The Northern Formation outcrops extensively on the McIntyre and Hollinger properties (Timmins golf course area), and consists of pillowed amygdaloidal basalts (magnesian tholeiites) and massive, uniform basalts (iron and magnesian tholeiites) with related flow top breccias, pillow breccias and polysutured (polygonite) flows. At Hollinger the core of the Central Tisdale anticline consists of generally thick but discontinuous units of iron tholeiite interlayered with amygdaloidal pillow lavas (N51-N59 flows recognized by Graton, in Ferguson, 1968). At McIntyre (Fig. 59.3) these units were named 51A and 51B respectively). Above the lower part of the Northern Formation, the N63 flow units have been traced on Moneta, Hollinger and McIntyre, and they comprise a lower massive iron tholeiite overlain by a pillowed amygdaloidal basalt, itself overlain by a prominent and persistent interflow sedimentary unit which marks the boundary with the Central Formation. This interflow horizon is important because of the well developed veins and orebodies associated with it at McIntyre (5, 3 and 25 veins), Hollinger (91 vein) and the Moneta vein system.

Central Formation. The Central Formation encloses all the major gold orebodies at McIntyre (Fig. 59.3). In both mines the Central Formation is characterized by a

STRATIGRAPHY OF THE TISDALE ANTICLINE

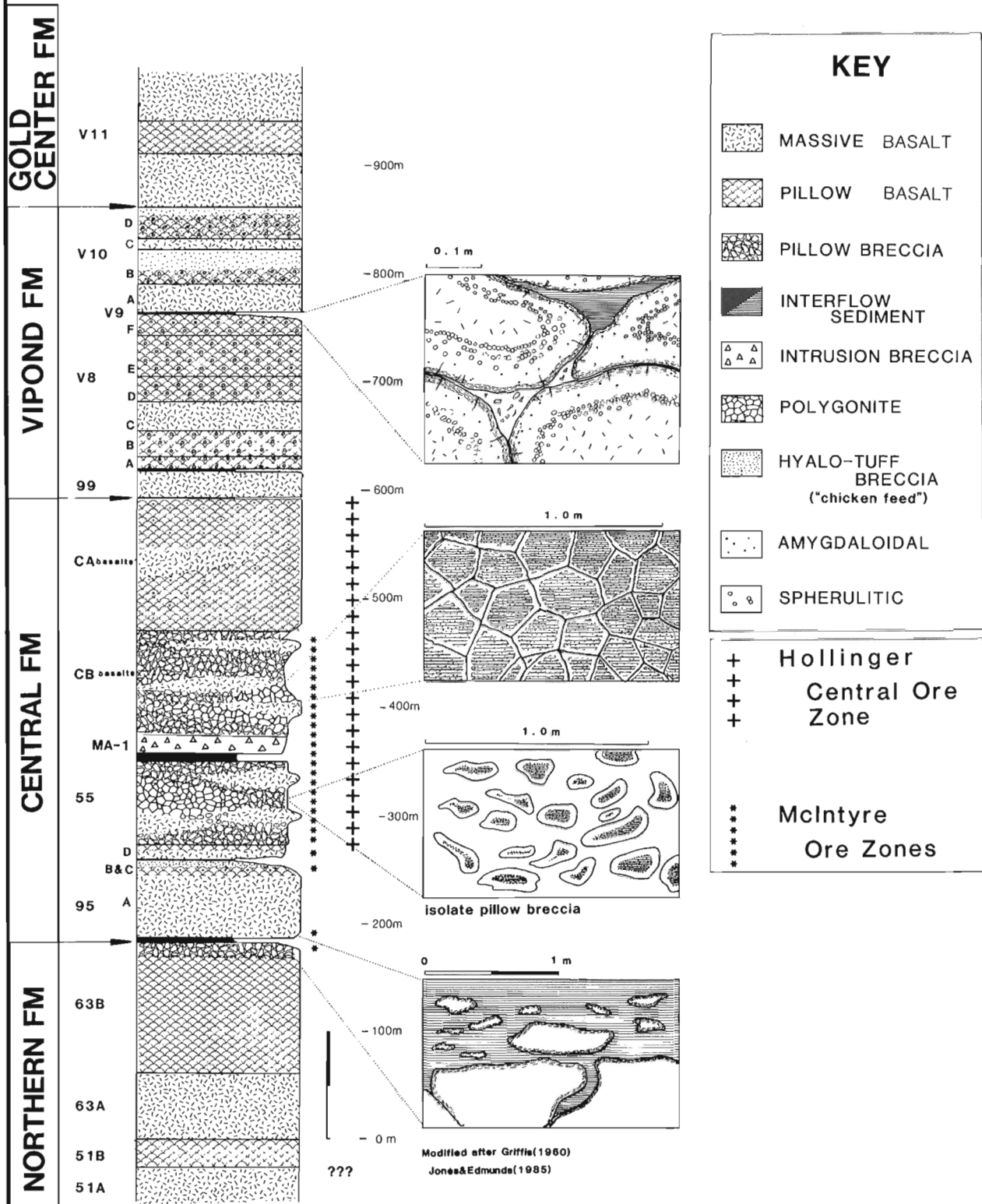


Figure 59.3. Stratigraphy and lithology of the Central Tisdale anticline.

heterogeneous sequence of magnesian tholeiite flows, pillow breccias, hyaloclastite breccias, polygonite units, pillowed flows which may or may not be amygdaloidal, and discontinuous units of leucoxene-bearing massive iron tholeiite. The upper part of the Central Formation consists of several alternating amygdaloidal pillowed basalt and massive basaltic units. The best exposed sections of the Central Formation occur in several crosscuts in the No. 6 shaft area on McIntyre.

The "95 flow" forms the base of the Central Formation and varies in thickness from 95 to 135 m at McIntyre up to 160 m at Moneta. Griffis (1960) recognized four subdivisions of the 95 flow and assigned the letters A-D to these subdivisions (from the base to the top). 95A is a thick (75-100 m) and consistent unit of massive and uniform, dark green, chloritic, leucoxene-bearing iron tholeiite which may have locally developed pillowed zones in its basal section. This unit grades upwards into 95B which consists of a discontinuous unit (0-20 m) of amygdaloidal pillow basalt and pillow breccia. The pillows tend to be small (20-30 cm) and often display dark grey to black carbonaceous pillow selvages. Varioles and brecciated varioles are locally developed.

The 95C unit is a conspicuous and consistent stratigraphic marker at McIntyre, Hollinger and Moneta, and shows both gradational and sharp contacts with the 95B unit. It consists of brecciated variolitic and amygdaloidal basaltic material in which broken, angular and poorly sorted porcellaneous clasts are set in a fine grained chloritic and carbonaceous matrix, with a typical "chicken-feed" hyaloclastite texture. Isolated pillow fragments and pillows occur as clasts surrounded by the hyaloclastite matrix. The thickness of the 95C unit varies from 0-20 m and it is overlain by a thin (0-2 m), discontinuous carbonaceous sedimentary horizon. The 95C breccia and its associated carbonaceous sedimentary horizon is host to 7 vein at McIntyre.

The 95D unit consists of a 2-3 m thick unit of small diameter amygdaloidal pillow lava (maximum dimension of pillows 20-30 cm).

The "55 flow" overlies the 95 flow (Fig. 59.3) and has been traced from Moneta through Hollinger and across McIntyre with a consistent thickness of about 90 m. Facies variations within the 55 flow are characteristic. Thus discontinuous units of leucoxene-bearing, massive iron tholeiite are separated by polysutured magnesian tholeiites (polygonite units) and related amygdaloidal pillowed basalts with pillow breccias and isolated pillow breccias. In some sections the massive iron tholeiites predominate but in others they are subordinate to the polygonite flows and pillow breccias. The isolated pillow breccias display a conspicuous and characteristic alteration pattern with a thin, dark chloritic rind enclosing a bleached margin around irregular lava fragments and globules ("doughnut" structure; Fig. 59.3). The top of the 55 flow is commonly marked by a breccia zone with local development of hyaloclastite material, and this is succeeded by a carbonaceous interflow sedimentary unit which is usually about a metre thick but which may vary from 0-10 m in thickness.

In the No. 6 shaft area on McIntyre and on Hollinger, the 55 flow is commonly separated from the upper part of the Central Formation by a heterolithic breccia unit (MA 1, Fig. 1.3) which maintains its stratigraphic position until it merges with the heterolithic intrusion breccia fringing the northwestern margins of the Pearl Lake porphyry. Thus, although it is usually included as part of the stratigraphic sequence and has previously been described as "agglomerate" and "breccia", the MA 1 unit is clearly related to the heterolithic intrusion breccias associated with the Pearl Lake porphyry, and to similar breccias associated with the

Northern porphyry, the Miller Lake and Millerton porphyries at Hollinger, and the Coniaurum porphyry. The MA 1 unit varies from 0-60 m in thickness. The heterolithic breccia consists of a variety of irregularly shaped and sized volcanic lithologies (lava and breccia fragments), fragments of interflow sedimentary material and porphyry fragments, all set in a highly altered, fine grained matrix which may be chloritic and/or carbonaceous in part.

A thick but locally developed sequence of magnesian tholeiitic pillow breccias, isolated pillow breccias ("doughnut" structure) and polygonite structured flows, overlies the 55 flow around the southern, western and eastern margins of the Pearl Lake porphyry where it is host to the 10 and 22 vein complexes. We have named this sequence "CB" breccia" (Fig. 59.3), and it appears to be thicker and better developed at McIntyre (maximum 300 m), and it thins out westwards onto Hollinger where it becomes sheared together with the 55 flow in the main ore zone, and lenses out eastwards towards Coniaurum. This dominantly brecciated sequence is interrupted by discontinuous units of leucoxene-bearing massive iron tholeiite, and it is very similar to the breccia-dominated sections of the 55 flow. Only Furse (1954), of the previous workers at McIntyre, recognized this as a separate sequence.

In the 10 vein area south of No. 6 shaft a thin carbonaceous interflow sedimentary unit separates the "CB" sequence from the overlying amygdaloidal pillow lavas and massive flows at the top of the Central Formation. These "CA lavas" (Fig. 59.3) form a 100-150 m thick sequence between the CB breccia sequence and the "99 flow" at the base of the overlying Vipond Formation. The convention of correlating and numbering flows (C11-C16), according to whether they were pillowed (C11, C13 and C15) or massive (C12, C14 and C16), had its most serious repercussions in this section of the stratigraphy (see above), and led to the misinterpretation of both stratigraphy and structure at McIntyre, and to an exaggerated estimate of thickness for the Central Formation as a whole (Griffis, 1960, and stratigraphic sections in Ferguson, 1968). The amygdaloidal pillow lavas and interlayered massive flow units form a distinctive stratigraphic sequence below the "99 flow", which can be traced around the southern edges of the Pearl Lake porphyry and around the Central Tisdale anticline (Fig. 59.1).

Vipond formation. At McIntyre a fairly complete section of the Vipond Formation (Fig. 59.3) occurs to the south of the Pearl Lake porphyry where it is well exposed in the 1250 level crosscut (Fig. 59.4). The basal 99 flow is a massive leucoxene-bearing iron tholeiite unit bounded by thin interflow sedimentary units which are in part graphitic. Overlying the 99 flow is a sequence of variolitic pillowed iron tholeiite flow units (V8, A, B, D, E, F, Griffis, 1960).

Griffis (1960) subdivided the V10 lava sequence into four units: A at the base and C being massive, leucoxene-bearing iron tholeiites, and B and D being prominent variolitic pillowed units with large pillows and characterized by brecciated varioles and hyaloclastite breccia material in the interstices of the pillows. The V10B and D units were used by Furse (1954) as marker horizons for the Timmins camp as a whole. The V8E unit is characterized by large mattress-type pillows with wide rims, and the V8F unit at the top has hyaloclastite breccia material in the interstices of variolitic pillows and is overlain by a thin carbonaceous interflow sedimentary unit, which in turn is followed by the V10 lava sequence.

Above the V10, Griffis (1960) recorded massive lava units (V11) which were intersected in drill cores and were assigned to the Gold Centre Formation which outcrops to the south of the Pearl Lake porphyry.

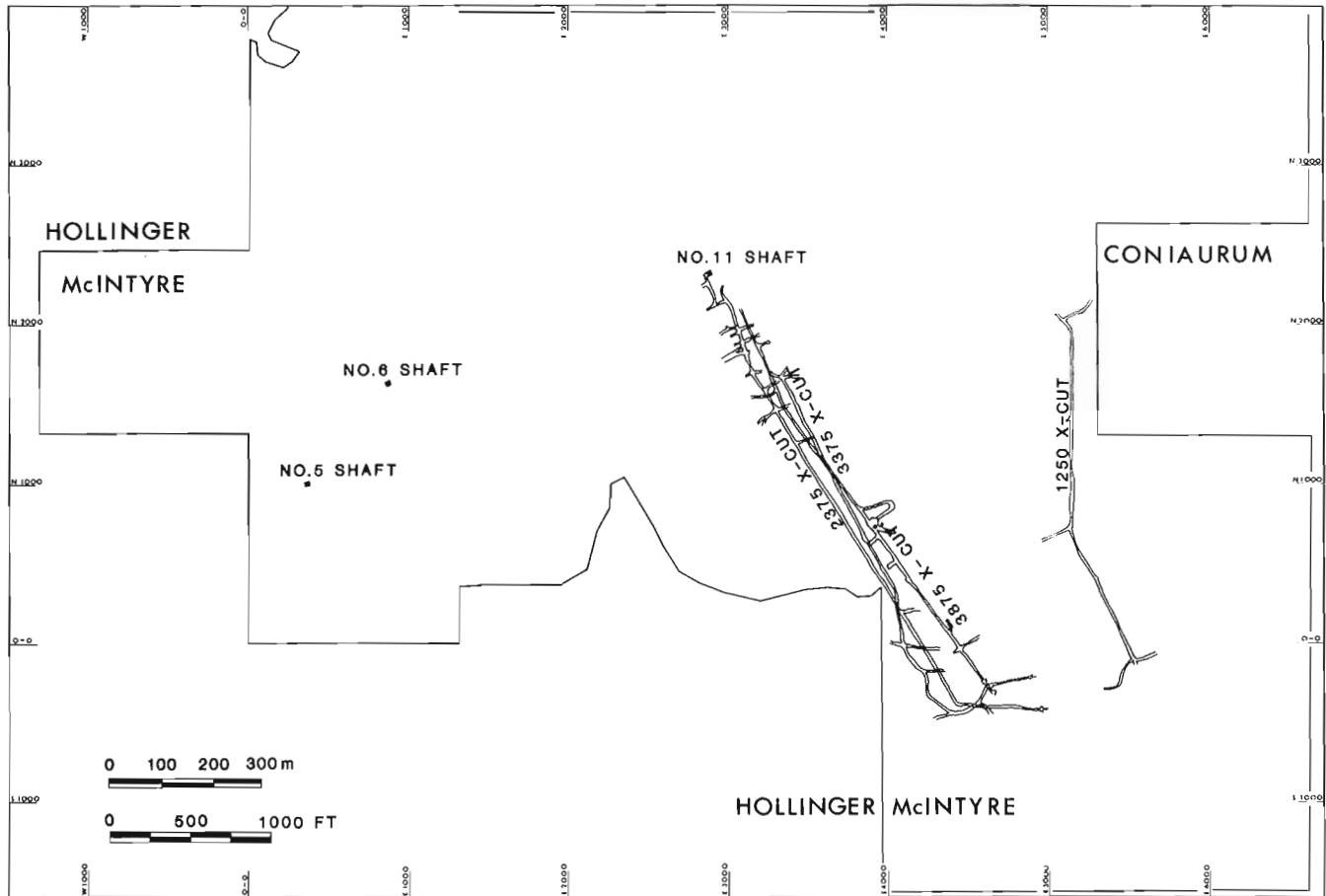


Figure 59.4. Location map showing shafts and crosscuts at McIntyre mine.

Pearl Lake porphyry and related intrusions

Two district types of quartz-feldspar porphyry are present: one is pervasively altered, selectively mineralized and sheared, whereas the other is less altered and less deformed. The first type includes the Pearl Lake, Millerton, Acme and Coniaurum porphyry intrusions (Fig. 59.1) and the second type includes the subsurface Northern Porphyry on McIntyre and the Crown Porphyry on Hollinger. The porphyries are accompanied by marginal heterolithic breccias which may form dyke-like apophyses extending into the country rocks, usually parallel or sub-parallel to stratigraphy but occasionally being strongly discordant and obviously intrusive. Post-porphyry, but pre-mineralization albitite dykes (albitized "pebble-dykes") represent the latest phase of felsic intrusive activity in the area.

The Pearl Lake porphyry intruded the brecciated flows of the Central Formation within the Central Tisdale anticline and appears to have been emplaced within the volcanic sequence prior to being flattened and stretched by a major regional deformation. Thus its original configuration and relationships to the surrounding volcanic sequence have been strongly modified and much of the past debate as to the nature and origin of the Pearl Lake porphyry has stemmed from lack of understanding of this modification.

The Pearl Lake porphyry is elliptical in plan, with an average long axis, striking ENE, of about 1500 m, and an average width of about 500 m. The porphyry tapers and interfingers with the volcanic sequence along strike, but has subconcordant and strongly sheared north and south margins.

The observed relationships and plan shape of the porphyry strongly suggest translation along shear zones and shortening of the original strike length. The plan shape, dimensions and style of the porphyry are maintained to at least 1500 m below surface. The position of the porphyry shifts eastwards with depth since the body plunges about 50° to the east on a bearing of approximately 075°.

Volcanic stratigraphy is disrupted by the porphyry and although the northern and southern contacts appear to be concordant or subconcordant on any one level, the porphyry contacts transgress the stratigraphy markedly between surface and 4175 level (Fig. 59.5, 59.6). Since exposures of the porphyry contacts in the mine tend to be related to development of mineralized areas adjacent to the porphyry contacts, these contacts are commonly hydrothermally altered and sheared. The distinctions between porphyry and strongly bleached, silicified and sericitized volcanic rocks become blurred, and careful inspection to determine the presence or absence of relict volcanic textures and structures is essential.

Numerous xenoliths of a variety of volcanic country rocks and interflow sedimentary material occur within the main body of the porphyry, providing further evidence of the intrusive nature of the porphyry. Where the porphyry has intruded interflow sedimentary units it tends to be strongly sheared and contains large amounts of carbonaceous material. In extreme cases the porphyry develops into a dark grey graphitic quartz-sericite schist, with evidence of translation of slivers of porphyry along interflow sedimentary units, and the development of so-called "graphitic faults".

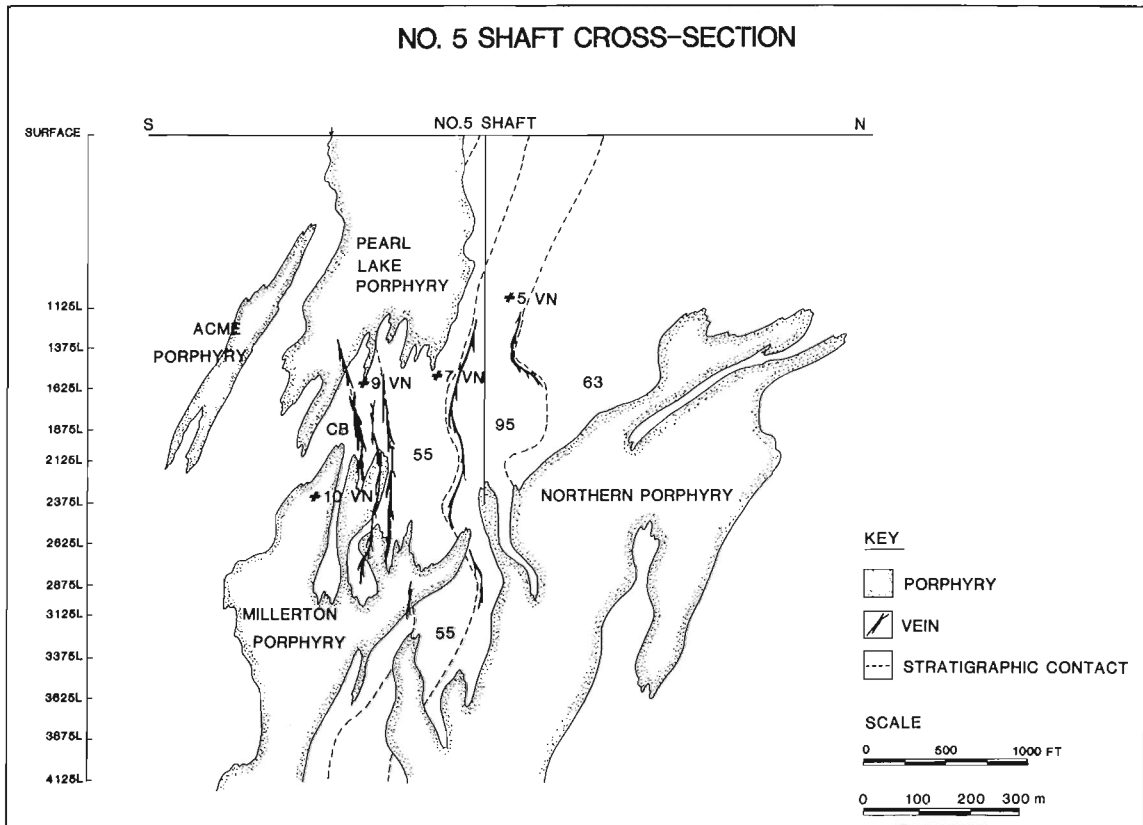


Figure 59.5. Generalized cross-section through No. 5 shaft at McIntyre mine.

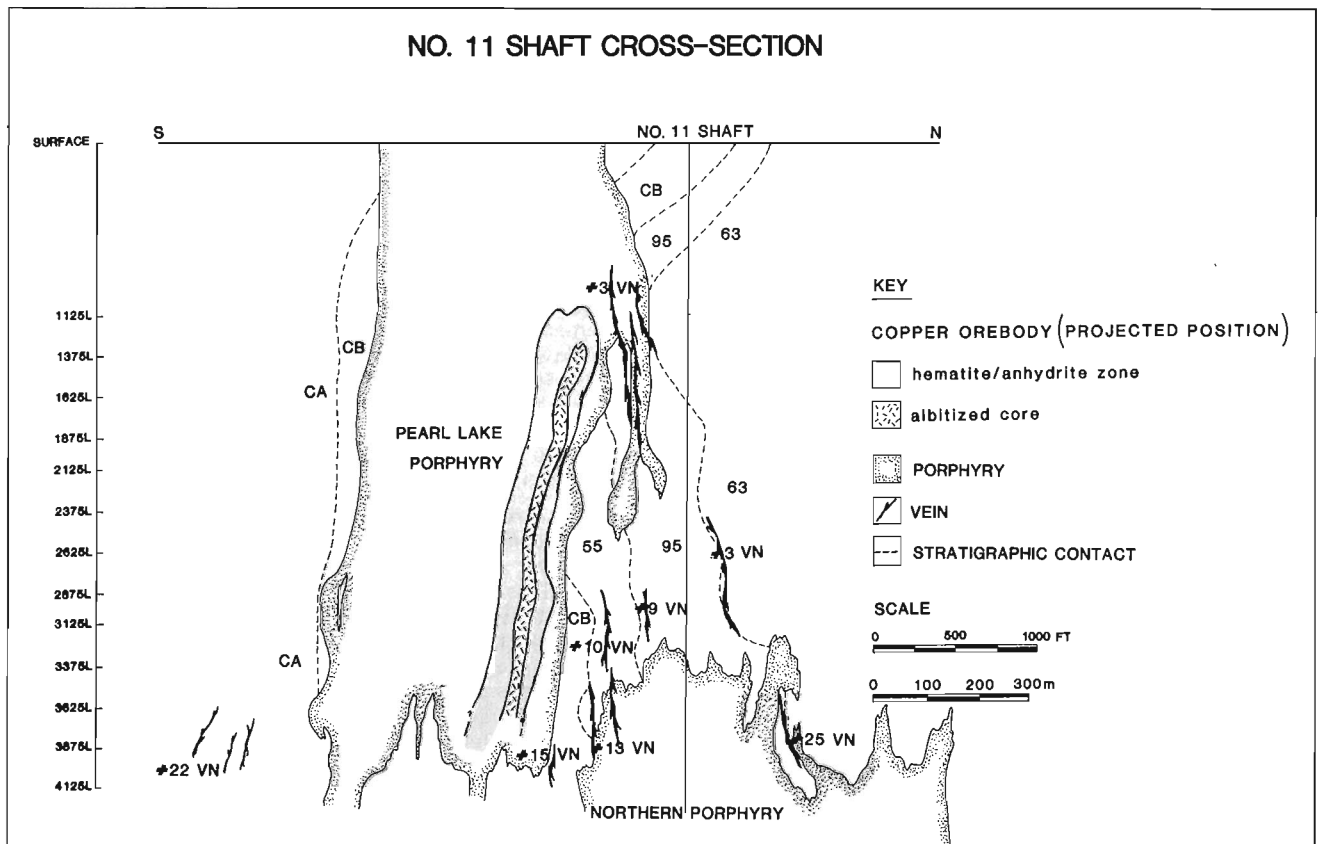


Figure 59.6. Generalized cross-section through No. 11 shaft at McIntyre mine.

Evans (1944) described the occurrence of carbon as inclusions in feldspars and as coatings on sericite in carbonaceous quartz-sericite schist from the Pearl Lake porphyry. In the area to the southwest and south of No. 6 shaft the porphyry is fringed by heterolithic breccias. Similar breccias have been mapped on Hollinger and these are closely associated with the Acme and Miller Lake porphyries.

The Pearl Lake porphyry is generally strongly altered and sheared, and could be described as a carbonated pyritic-quartz-albite-sericite schist with a quartz-albite-sericite-ankerite groundmass and a linear fabric defined by curvilinear sericitic foliae. Prominent albite tablets and rounded quartz grains are partly enveloped by the sericitic foliae. The quartz grains show various degrees of deformation from unstrained to severely strained and broken and the albite tablets usually display evidence of rotation. Alteration associated with a deformed, pipe-like zone of copper mineralization in the Pearl Lake porphyry southeast of No. 11 shaft, is described separately by Mason and Melnik (1986).

Albite dykes cut the Pearl Lake porphyry, and intrude the surrounding volcanic rocks on McIntyre and Hollinger. They are in turn cut by mineralized veins and both are deformed by the cleavage and linear fabric. Langford (1941) described the dykes as having "a matrix of sodic plagioclase, interstitial quartz and a little biotite altering the chlorite, with inclusions of granitoid holocrystalline rock fragments made up chiefly of sodic plagioclase, microperthite, some microcline and subordinate quartz. These inclusions commonly have the size and shape of goose eggs, hence the rock is locally named "goose egg dyke". Some inclusions, however, as large as 10 by 60 cm, and 45 by 75 cm have been found.

The dykes appear to be albitized pebble dykes, of a type commonly associated with copper porphyry systems in the United States and elsewhere, and they seem to be closely related to the initiation of the hydrothermal system and the mineralization at McIntyre and Hollinger.

Structure

Following the deposition of the Tisdale volcanic sequence there was a period of uplift and erosion, which resulted in the Porcupine sedimentary sequence being deposited on an erosion surface across tilted volcanic rocks of the Tisdale Group (Burrows, 1925). No pre-Porcupine Group folds have been positively identified but there is no doubt that the volcanic sequence was tilted (and thus probably folded) and it was eroded prior to deposition of the sedimentary sequence. Hodgson (1983) has suggested that the tilting resulted from listric normal faults which may also have controlled deposition of the sedimentary sequence and provided loci for the subsequent porphyry intrusions. The Central Tisdale anticline and related folds in the Timmins area were, however, developed prior to intrusion of the porphyries.

Figure 59.2 illustrates the sequence of structural events at McIntyre and in the Timmins area. It is based on a synthesis of all previous work and the present investigation.

There is no evidence of stratigraphic duplication due to folding in the area of the McIntyre mine workings to the north and south of the Pearl Lake porphyry and there is a continuous steeply dipping (70-85°) south-facing sequence through the Tisdale Group along the eastern boundary in the upper levels of the mine. This has recently been confirmed by detailed mapping of surface outcrops at McIntyre and Hollinger. Post-mineralization deformation has modified the geometry of all pre-existing rock formations, structures and

mineralization in the area. A pervasive E- to ENE-trending cleavage and associated linear fabric (plunging about 50° eastwards) characterizes the whole area. Local zones of high strain are represented by shear zones which are best developed in the mineralized areas.

ENE-trending shear zones envelope the Pearl Lake porphyry and die out eastwards and downwards in the McIntyre mine, and coalesce westwards and upwards into the central ore zone on Hollinger where they form a single zone over 300 m in width close to surface. Here they split again into discrete shear zones which generally die out westwards with the exception of strong shear zones associated with the Hollinger fault. The Hollinger fault system strikes ENE and dips between 60 and 70° SSE, and shows evidence of repeated brittle and ductile deformation, all of which postdates the gold-quartz mineralization in the shear zones, and in general the mineralized veins are disrupted by faulting.

Subsidiary shear zones envelope some of the gold veins and parts of the copper orebody at McIntyre, but some of the major veins exhibit only minor shearing of the wallrocks, and some of the shear zones contain no veins. Wherever shearing is observed close to mineralization, the shear fabric is superimposed on wallrock alteration. Thus although the mineralization must have originally been emplaced in open spaces related to brittle fractures, in many cases subsequent ductile deformation has obscured the original relationship. This might lead the casual observer to assume a closer relationship between the mineralization and the shear zones than is actually the case.

A study to determine the finite strain of varioles from the V10B spherulitic pillow lava was made on oriented samples collected from the 1250 W crosscut in the southeastern corner of the McIntyre mine property. The varioles consist of felsic material enclosed by mafic pillow lava material, and since the varioles would have been more brittle than the enclosing mafic material, strain determinations on the varioles represent minimum estimates.

In downplunge cross-sections the varioles appear to be relatively undeformed and are typically rounded to subrounded (slightly flattened and ovoid). In the plane of maximum extension the varioles are extremely prolate with relatively smooth curvilinear margins and ragged ends. In this plane the varioles display intense internal cracking, development of cymoid structures and transposition along small anastomosing shear planes which result in the ragged appearance of the tips of the varioles with slivers of felsic material protruding into the country rock. This configuration is remarkably similar to that of the Pearl Lake porphyry and its relationship to the enclosing volcanic rocks at a larger scale. Where tongues and slivers of the porphyry project into the volcanic sequence at the western and eastern ends of the Pearl Lake intrusion, they are bounded by faults or shear zones and are themselves strongly schistose, suggesting transposition related to shearing.

The results of the study showed that the varioles were elongated more than three times and shortened to less than half their original diameter, based on the reasonable assumptions that they were originally spherical and that deformation occurred under constant volume conditions. If the downplunge plan projection dimensions of the Pearl Lake porphyry are considered, it is apparent that the ratio of long to short axes is similar to the average ratio for the spherules, suggesting that the Pearl Lake intrusion may also have been roughly circular in plan shape prior to deformation. On an even larger scale, the same could be said for the Central Tisdale anticline itself which has also been modified by the deformation.

Acknowledgments

The project is sponsored by the Mineral Resources Division of the Geological Survey of Canada, through DSS contracts OST84-00077 and OST85-00077, and by Pamour Porcupine Mines Ltd. at Timmins.

References

Burrows, A.G.

1925: The Porcupine gold area; Ontario Department of Mines, Annual Report, v. 33, pt. 2, 1924, 112 p.

Evans, J.E.L.

1944: Porphyry of the Porcupine district, Ontario; Geological Society of America, Bulletin, v. 55, p. 1115-1142.

Ferguson, S.A.

1968: Geology and ore deposits of Tisdale Township, District of Cochrane; Ontario Department of Mines, Geology Report 58, 177 p.

Furse, G.D.

1948: McIntyre Mine; in Structural Geology of Canadian Ore Deposits, v. 1; Canadian Institute of Mining and Metallurgy, p. 482-496.

1954: Geology of the Pearl Lake section of the Porcupine gold area; Canadian Institute of Mining and Metallurgy, Bulletin, v. 47, p. 197-201.

Griffis, A.T.

1960: Stratigraphy at McIntyre; unpublished report, McIntyre Mine.

1962: A geological study of the McIntyre Mine; Canadian Institute of Mining and Metallurgy, Bulletin, v. 55, no. 598, p. 76-83.

Hodgson, C.S.

1983: The structure and geological development of the Porcupine Camp – a re-evaluation. p. 211-225 in The Geology of Gold in Ontario, ed. A.C. Colvine; Ontario Geological Survey, Miscellaneous Paper 110, 278 p.

Hurst, M.E.

1936: Recent studies in Porcupine area; Canadian Institute of Mining and Metallurgy, Transactions, v. 39, p. 448-458.

Jones, W.A.

1948: Hollinger Mine; in Structural Geology of Canadian Ore Deposits, v. 1; Canadian Institute of Mining and Metallurgy, p. 464-481.

Langford, G.B.

1941: Geology of the McIntyre mine; American Institute of Mining and Metallurgy, Engineering Transactions, v. 144, p. 151-169.

Mason, R. and Melnik, N.

1986: The McIntyre-Hollinger investigation, Timmins, Ontario: a gold dominated porphyry copper system; in Current Research, Part B, Geological Survey of Canada, Paper 86-1B, report 60.

Pyke, D.R.

1982: Geology of the Timmins area, District of Cochrane; Ontario Geological Survey, Report 219, 141 p.

Robinson, H.S.

1923: Geology of the Pearl Lake area, Porcupine District, Ontario; Economic Geology, v. 18, p. 753-771.

The McIntyre-Hollinger investigation, Timmins, Ontario: a gold dominated porphyry copper system

Project 850052

R. Mason¹ and N. Melnik¹
Mineral Resources Division

Mason, R. and Melnik, N., The McIntyre-Hollinger investigation, Timmins, Ontario: a gold dominated porphyry copper system; in *Current Research, Part B, Geological Survey of Canada, Paper 86-1B*, p. 577-583, 1986.

Abstract

The McIntyre-Hollinger complex is interpreted as a gold dominated, subvolcanic porphyry system, in which the original configuration of the system and its orebodies has been modified by subsequent deformation.

Stockwork copper-molybdenum-gold-pyrite mineralization occurs in a breccia pipe within the Pearl Lake porphyry intrusion at the McIntyre mine. The breccia pipe was the focus of intense albitization and hydraulic fracturing. An albitite core is surrounded by a zone of hematite-anhydrite alteration which grades out into an extensive pyritic halo. A zone of auriferous quartz-ankerite-albite veins occurs around the periphery of the pyritic halo, culminating in the central ore zone at Hollinger. Gold bearing veins are localized in preferred stratigraphic sites which have been loci of brittle failure, vein emplacement and subsequent complex shear deformation. Mineralized veins are characterized by sericitic alteration and pyritization of wall rocks.

Post-mineralization brittle and ductile shear deformation resulted in the formation of a pervasive cleavage and linear fabric, and the Hollinger fault system. The hydrothermal alteration and veining associated with the complex appear to have promoted deformation by weakening the country rocks and enhancing ductility contrasts.

Résumé

Le complexe McIntyre-Hollinger est décrit comme étant un système de porphyre subvolcanique contenant principalement de l'or et dans lequel la configuration originale et ses masses minéralisées ont été modifiées par une déformation ultérieure.

Un stockwerk de minéralisation de cuivre, de molybdène, d'or et de pyrite est présent dans la brèche d'une cheminée volcanique à l'intérieur de l'intrusion de porphyre de Pearle Lake, à la mine McIntyre. Cette cheminée bréchique a été l'objet d'une albitisation et d'un fractionnement hydraulique intenses. Un noyau d'albitite est entouré d'une zone d'altération hématite-anhydrite qui arrive à la surface en formant une grande auréole pyritique. Une zone de veines aurifères de quartz, d'ankérite et d'albite entoure l'auréole pyritique et se termine dans la zone minéralisée centrale de Hollinger. Des filons aurifères se trouvent dans des sites stratigraphiques de choix dans lesquels il y a eu des cas de ruptures de roche, d'emplacement de la veine et d'une déformation subséquente d'un cisaillement complexe. Les veines minéralisées sont caractérisées par une altération séricitique et une pyritisation des roches de la paroi.

Une déformation de cisaillement cassante et ductile de post-minéralisation a entraîné la formation d'un clivage envahissant et d'une structure linéaire, ainsi que du système de failles Hollinger. L'altération hydrothermique et le veinage associés à ce complexe semblent avoir favorisé la déformation en affaiblissant la roche encaissante et en renforçant les contrastes de plasticité.

¹ Department of Geology, Queen's University, Kingston, Ontario K7L 3N6

Introduction

The McIntyre mine contained low grade, stockwork-type copper-gold orebodies which were exploited from 1963 to 1982, in addition to the vein-type gold orebodies which have been exploited from 1912 to the present day.

The gold veins extended westwards from McIntyre onto the Hollinger property and eastwards onto the Coniaurum property. In total the complex has produced about 35 million ounces of gold, 7 million ounces of silver and 100 000 tons of copper, of which McIntyre produced one third of the precious metals and all of the copper. Hollinger produced most of the rest, with Coniaurum contributing just over 1 million ounces of gold.

To date, the copper mineralization has tended to be regarded as separate and unrelated to the gold mineralization, but the present study has shown that the two are intimately related. Several convergent lines of evidence support the suggestion by Kirkham and Thorpe (1973) that the mineralization represents a gold dominated porphyry copper system with related peripheral precious metal veins. At the outset it should be emphasized that both the copper and gold mineralization post-date the intrusion of the Pearl Lake porphyry and related albitite dykes, and they pre-date the regional shear deformation with its related cleavage and linear fabric development. Thus timing of the mineralizing events in relation to porphyry intrusion and hydrothermal alteration and subsequent deformation in the complex imposes limitations on genetic hypotheses.

Evidence for post-porphyry timing of mineralization includes the selective superposition of the copper stockwork mineralization and its related hydrothermal alteration on the Pearl Lake porphyry, and by the presence of gold-quartz veins which occur within the porphyry and also cut across the contacts between the porphyry and the surrounding volcanic rocks. The common association of these auriferous quartz-ankerite albite veins emplaced within albitite dykes, demonstrates that the mineralized veins post-date the emplacement of the albitite dykes. This is especially clear at McIntyre in the No. 11 shaft area immediately north of the Pearl Lake porphyry between 2000 level and 3500 level and in the 22 vein complex south of the Pearl Lake porphyry (12 shaft), and in the central ore zone at Hollinger.

Evidence for pre-deformation emplacement of the mineralization includes 1) the intense deformation of the copper stockwork mineralization, with lined streaks of chalcopyrite in the stockwork and remobilized hackly aggregates of chalcopyrite in boudinaged and folded quartz veins within the copper orebodies; 2) the lenticular elongate geometry of the individual copper orebodies and their plunge parallel to the linear fabric; 3) boudinaged and folded auriferous quartz veins with sheared sericitized margins observed in all productive stopes, and 4) the orientation of orebodies (in the copper zone) and payshoots (in the auriferous veins) parallel to the linear fabric. All the mineralized veins and stockworks are deformed to a greater or lesser degree. The less deformed appearance of some of the flat veins in the complex is explained by their initial orientation in planes parallel to the maximum compressive stress, and their preservation in low strain zones.

The copper system is mainly contained within a flattened and stretched, ellipsoidal, pipe-like zone of albitization, with associated brecciation and intense hydrothermal alteration in the Pearl Lake porphyry. The gold-quartz veins occur in lithostructural sites within the volcanic rocks along the northern and southern margin of the porphyry and generally within 200 m of the porphyry contact. The copper orebodies were mined between 1125 level and 4175 level and copper mineralization has been found in drilled extensions down to 4625 level, and upwards to 600 level.

Most of the copper ore was produced from the interval between 1500 level and 3250 level. The top of the system probably outcrops under Pearl Lake, and the base of the copper mineralization appears to occur about 5075 level in the downplunge extensions on the Coniaurum (Westfield Minerals) property. These limits also define nearly all of the productive gold veins with the exception of the lower (and less significant) parts of 22 vein complex (see later) which have been mined down to 6825 level. Most of the gold produced from McIntyre has been won from veins mined between 1000 level and 4625 level and by far the bulk of this was produced from the interval between 1000 level and 3000 level (Fig. 60.1).

The development of the regional cleavage, linear fabric and major shear zones must be taken into consideration in any discussion of the limits of productive mineralization. The estimates of prolate strain (Mason et al., 1986) would suggest that the original, pre-deformation vertical interval for optimum development of most of the productive mineralization was about 300 m.

Copper mineralization

The copper mineralization consists of a pyrite-chalcopyrite-bornite-tennantite stockwork containing less important but significant molybdenite and gold. From information available and our own observations, molybdenite occurs as smears on slip surfaces and in veinlets within the copper orebodies and appears to increase in abundance in the lower sections of the copper zone (below 3000 level). The zone plunges eastwards from a position south of No. 11 shaft close to surface, to a position across the McIntyre boundary on Coniaurum below 3875 level (Fig. 60.2). It extends about 300 m along an east-west strike and is about 100 m wide. These dimensions are proportionately remarkably similar to those of the Pearl Lake porphyry.

The orebodies are shaped like flattened cigars, being elliptical in plan and elongate with greatest continuity downplunge. They occur in a series of an echelon pods

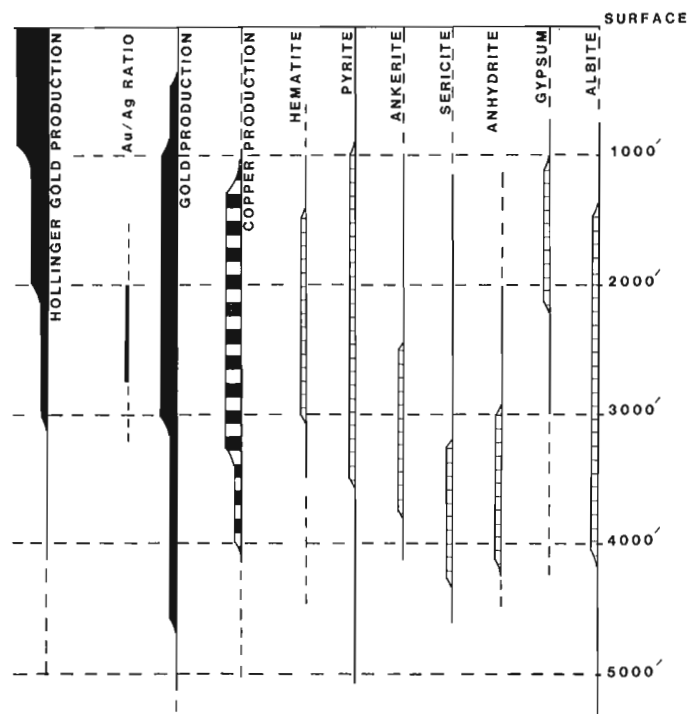


Figure 60.1. Vertical distribution of gold, copper and alteration related to copper zone at McIntyre mine.

within, but discordant to, a flattened annular zone of fracturing and alteration around and within the albitite pipe (Mercereau, 1985). The orebodies were defined using a 0.65% copper cut off grade, and about 10 million tons have been produced or were in reserve at a grade of about 0.8% cu and 0.025 oz Au as of 1982. Most of the intensely fractured and altered zone mentioned above, together with other zones in the Pearl Lake porphyry, would average better than 0.1% Cu. At least two boreholes have been drilled across the width of the Pearl Lake porphyry and systematically assayed for copper along the entire length of core recovered. These holes contained copper mineralization throughout, varying from a low of 300 ppm to over 2% copper in ore grade intersections, suggesting that the Pearl Lake porphyry contains a much bigger sub-economic copper system than the mine production indicates.

Apart from the brief but perceptive description by Kirkham and Thorpe (1973), Davies and Luhta (1978) have published the only description of the copper orebody at McIntyre. They were the first to recognize the hydrothermal alteration and its relationship to the copper mineralization. These authors recognized an early phase of hydrothermal alteration with an albitite core zone surrounded by a zone of hematite-anhydrite alteration, and showed that sulphide veins were emplaced after the early hydrothermal alteration. They interpreted the Pearl Lake porphyry as a metasomatic replacement of felsic volcanics, with the copper mineralization interpreted to be post-tectonic.

Karvinen, (1981) has interpreted the entire complex as a volcanic centre with partly remobilized exhalative gold mineralization associated with carbonate units. The Pearl Lake porphyry, however, is clearly an intrusive subvolcanic body and both the copper and gold mineralization are associated with hydrothermal alteration which postdate the intrusion. The present configuration of both is a result of the deformation which resulted in the superimposition of a cleavage and linear fabric on both the mineralization and its enclosing host rocks.

The present study has confirmed the major alteration patterns outlined by Davies and Luhta (1978) but with some additions and modifications. First, the Pearl Lake porphyry is thoroughly affected to a greater or lesser extent by pervasive hydrothermal alteration and shearing. This in itself separates the intrusion from most of the other porphyries in the district, which are well preserved and do not show the same degree of alteration or shearing (e.g. the Northern Porphyry). Three other small porphyry intrusions in the complex have characteristics similar to the Pearl Lake porphyry; the Acme and Millerton porphyries on Hollinger, and the Coniaurum porphyry. In fact at depth (downplunge) the Acme and Millerton porphyries merge with the Pearl Lake porphyry.

Second, the alteration is dominated by carbonatization (ankerite), and sericitization, as well as albitization, the latter becoming intense in the centre of the copper zone.

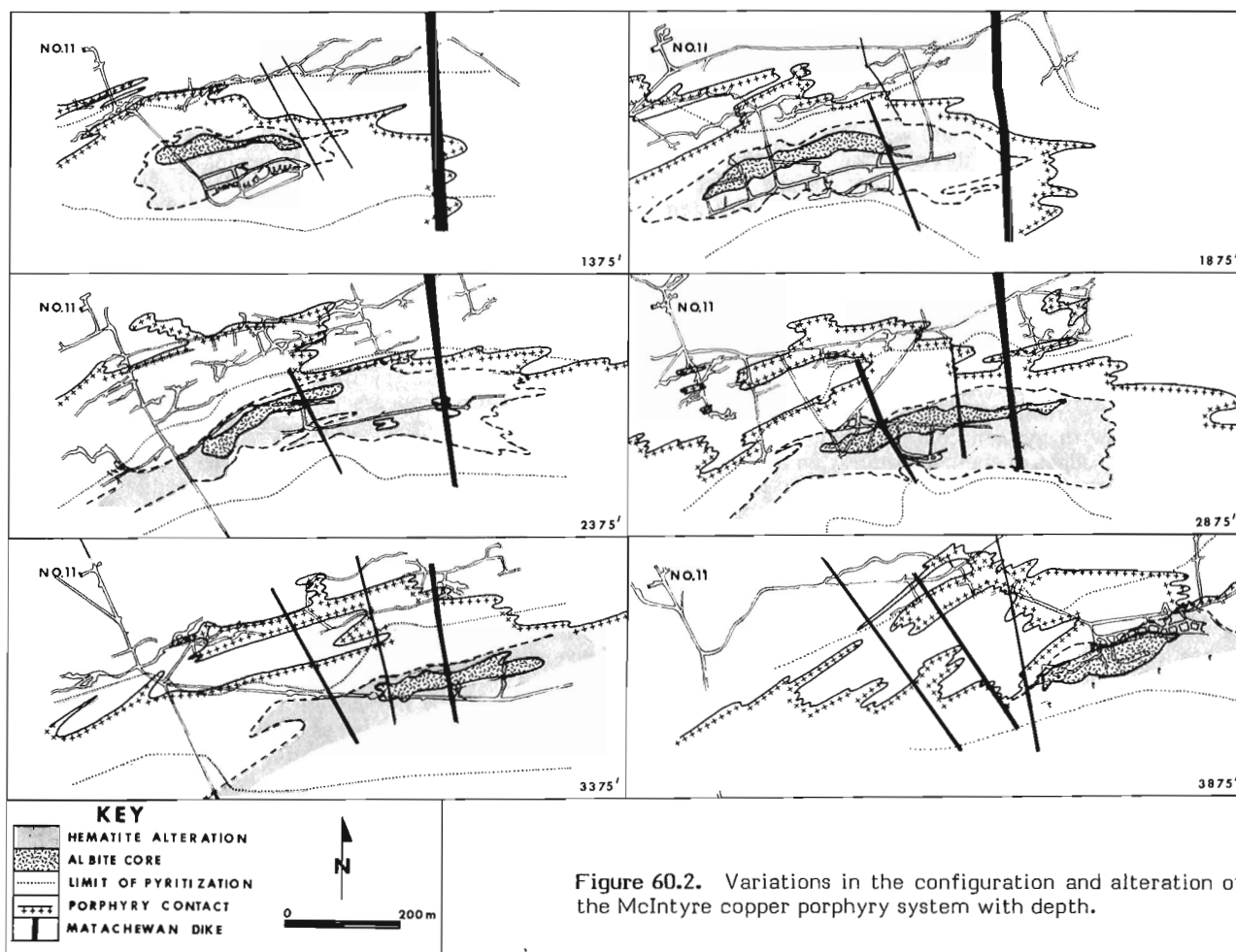


Figure 60.2. Variations in the configuration and alteration of the McIntyre copper porphyry system with depth.

The intensely albitized inner core is creamy-grey and generally more massive than the surrounding highly fractured outer zone which is characterized by pink-buff-orange and red alteration caused by the development of hematite and anhydrite (Fig. 60.2). The internal boundary between the grey inner zone and the red outer zone is generally sharp except at the top of the system (above 1500 level) and towards the base of the system below 3625 level. The outer limit of red alteration is not well defined and typically consists of a transition zone of more patchy, localized hematization which merges outward into pyritic quartz-albite-sericite schists. The fracture-controlled hematite-anhydrite alteration which characterizes the outer core zone is pervasive between 1375 level and 3875 level, with most intense and widespread alteration of this type between 1875 level and 2875 level.

Sulphides were introduced after the formation of the main core alteration, and sulphide veinlets in the hematite-anhydrite zone commonly show bleaching along their margins as a result of reduction of the iron oxides. The copper sulphides were deposited in the stockwork together with swarms of quartz-albite-ankerite-chalcopyrite veins which developed in the central core. The wallrocks of these veins are characterized by well developed buff/khaki-green sericite. Individual veins contain gold, and some contain tourmaline and minor scheelite; thus these veins are identical in all respects, other than being hosted by porphyry, to the gold veins peripheral to the porphyry.

A pyritic halo is developed around the central alteration core of the copper zone and pyritization is widespread and intense around the northern and eastern margins of this zone between 1500 level and 3000 level. Here pyrite and quartz-pyrite veins occur in addition to pyritic stockwork mineralization. As observed by Davies and Luhta (1978), the area immediately north of the copper zone tends to be locally silicified as well as being heavily pyritized. In addition, parts of this area are consistently rich in ankerite, especially along and adjacent to the northern contact of the Pearl Lake porphyry. The ankerite enrichment is especially prominent below 2375 level.

In the copper zone granoblastic anhydrite is dominant in veinlets within the central alteration core, and increases in both quartz-albite-ankerite and sulphide veins with depth. Gypsum (the low temperature sulphate) is the predominant vein sulphate above 1875 level, with relatively rare anhydrite outside the central alteration core. Below 1875 level anhydrite (the high temperature sulphate) becomes the dominant sulphate with gypsum confined to narrow veinlets and stringers at the edges of the main alteration zone. There is a noticeable increase in vein anhydrite below 3375 level. Calcite is common in late stage veins throughout the Pearl Lake porphyry and adjacent volcanic rocks. It occurs as replacements and segregations in selected zones within and peripheral to the mineralized areas which are themselves characterized by development of ankerite, especially to the north of the ankerite enrichment and to the east of the copper zone and the porphyry contacts. The zonation of carbonates with calcite peripheral to ankerite, was first recognized by Graton and McKinstry (1932) and Keyes (1940), and has been confirmed by Whitehead et al. (1980), Smith et al. (1984), and Smith and Kesler (1985).

Gold mineralization

The gold mineralization occurs in quartz veins and pyritized wall rocks in structural sites which have developed in specific stratigraphic locations such as interflow contacts (with or without interflow sedimentary beds), volcanic breccia zones, and along the north and south contact zone of the Pearl Lake porphyry. Although there is a general tendency for veins to be subconcordant to particular

stratigraphic sites, and the major productive veins characteristically follow such sites along strike and down dip, there is obvious local discordance of veins and vein complexes where structural sites do not maintain particular stratigraphic positions.

The mineralized veins nearly always contain ankerite and commonly contain albite, and wall rocks are sericitized, pyritized and commonly sheared. The development of hydrothermal sericite, ankerite and pyrite appears to be almost a prerequisite for gold mineralization, although given every possible favourable circumstance, there is still no guarantee of economic concentrations of gold in a particular vein, a factor which has traditionally added interest and frustration to the evaluation and development of most vein-type gold deposits. Tourmaline and pyrrhotite occur in 22 vein complex, and pyrrhotite is typically developed in preference to pyrite in the No. 12 shaft sections of 22 vein complex (below 3875 level). Tourmaline is otherwise a minor vein constituent at McIntyre, whereas it is important in the Hollinger veins. Chalcopyrite is reported from McIntyre as a common, but subordinate sulphide in many of the gold veins, and sphalerite is locally important (3 vein was noted for occurrences of sphalerite). Scheelite occurrences were common in the 22 vein complex and in the veins at the western end of the Pearl Lake porphyry, but no significant concentrations have been reported from McIntyre, such as those developed on Hollinger (Allen and Folinsbee, 1944).

More than one generation of pyrite and several generations of quartz are commonly developed in the veins, and evidence for deformation and repeated crack and seal textures in the quartz are typical, although much of this could be interpreted as a post-mineralization feature related to deformation. Early pyrites tend to be strongly deformed and two separate sets of pyritic veins can be identified both in the copper and gold zones. These veins are superposed on early syndepositional pyrites associated with interflow sedimentary units and on disseminated pyrite in the Pearl Lake porphyry associated with stockwork fracture development. Graton and McKinstry (1932), Hurst (1935) and Keyes (1940), recognized three dominant phases of quartz deposition. Fracturing of early smoky quartz and development of ankerite was associated with gold mineralization, whereas a second phase of white quartz, and a third phase of clear glassy quartz were interpreted as post-gold mineralization. Much of the gold, however, occurs associated with pyrite in altered wallrocks and this mineralization appears to pre-date the free-gold associated with late stage cracks in the quartz veins.

The gold orebodies at McIntyre include a wide variety of vein types which are specific to their own individual habitats, and are enclosed by a variety of wallrocks of differing composition. The veins with best strike and down-dip plunge continuity are those situated along or closely related to major contacts, especially those along interflow sedimentary units (such as 3, 5 and 25 veins, all along the contact between the Northern, and Central Formation), 7 and 9 vein associated with the 95C "chickenfeed" hyaloclastite breccia unit, and 10 vein associated with the Central breccias and disrupted by the eastern extension of the Hollinger fault zone at the western edges of the Pearl Lake porphyry. It is noteworthy that the pyritization and sericitization associated with the wallrocks of 7, 9 and 10 veins are more widespread and intense, and there is much more shearing adjacent to the veins than in the case for 3, 5 and 25 veins. This appears to be a reflection of the nature of the wallrocks, and proximity to the source of the mineralizing fluids. Thus there is intense pyritic replacement of interfragmental material in the volcanic breccias (7, 9 and 10 veins) closer to the Pearl Lake porphyry, as opposed to localized alteration of more massive wallrocks (3, 5 and 25 veins) farther from the porphyry.

The 10 and 22 vein complexes, which lie on the south side of the Pearl Lake porphyry, are situated in the pillow breccias and related rocks in the lower part of the Central Formation, and are characterized by strong and extensive pyritic replacement of matrix material in the breccias for considerable distances from the veins, as well as by correspondingly larger sericitized zones associated with the veins. Thus intensity of alteration is more a function of wall rock reactivity, permeability and porosity than of anything else within the gold zone. Both 10 and 22 vein complexes extend for over 5000 m down plunge adjacent to the Pearl Lake porphyry, and both are characterized by an echelon clusters of veins and vein swarms enveloped and interspersed with sericitized, pyritized and selectively sheared volcanic breccias.

A linear zone of gold-bearing quartz veins has been mined between the copper zone and the northern contact of the Pearl Lake porphyry between 1125 level and 2375 level. This is an easterly extension of 10 vein complex which is situated at the western end of the Pearl Lake porphyry. Another gold vein was mined between 600 level and 800 level on the south side of the copper zone in the Pearl Lake porphyry.

The 3750 and 3875 crosscuts from No. 11 shaft south across the Pearl Lake porphyry expose the highly altered, pyritic crest of the 22 vein complex, recognized as such prior to development of the productive part of the complex by the geological staff at McIntyre in 1932 (Annual report of McIntyre Mines for 1932). Silicification, sericitization and pyritization continue and weaken upwards to the 2375 cross cut, south of No. 11 shaft along the southern fringes of the porphyry, although the productive top of the 22 vein complex at McIntyre lies at 3500 level, close to the Hollinger boundary. There is evidence from compilations of the gold orebodies at Hollinger and McIntyre to suggest that 10 vein and 22 vein complexes are down plunge extensions from Hollinger, and the abnormal development (for McIntyre) of tourmaline in 22 vein complex would also support this suggestion.

The northern contact zone of the Pearl Lake porphyry is strongly altered and sheared, and can be traced as a shear zone along an ENE strike onto Coniaurum. The zone weakens, along strike towards Coniaurum, and down dip following the 55 flow - CB breccia stratigraphic units. It hosts a series of narrow, en echelon quartz-ankerite veins of the 12, 13, 14, 15 and 18 vein series which are themselves well mineralized but which form lower grade orebodies because of the narrow vein widths and increased dilution from barren wallrocks.

The veins at McIntyre range from single quartz veins of widths from a few centimetres to 50 m, through complex vein swarms and an echelon arrays to pyritic replacement zones with irregular quartz stringers and lenses. The veins are typically irregular and, as exposed in productive stopes, include several generations of quartz and are boudinaged and folded. The wallrocks adjacent to the veins are usually bleached and characterized by sericitic alteration, pyritization and shearing.

Productive vein systems tend to merge into zones of silica enrichment of the country rocks with barren quartz-calcite veining at their lateral and vertical extremities (Van Weichen, personal communication, 1984). These silicified zones frequently impart a layering in the volcanic host rocks which may in part resemble banded chert, and although disseminated pyrite is common, gold is either weakly developed or absent. The transition from a typical quartz vein system to a silicified fringe zone can occur in the space of a few metres.

Longitudinal sections of the veins at McIntyre reveal a tendency for the development of a plunge to the east in sympathy with the linear fabric throughout the area. Robinson (1923) showed a "graphitic zone" in 5 vein plunging to the east, and the western edge of the vein has the same attitude. The 25 vein has a similar overall plunge to the east and sections of all the other veins display the same feature. Further work on gold distribution is needed to determine if there is any systematic development of, and attitude to, higher grade ore shoots within the veins such as reported from Hollinger (Graton and McKinstry, 1932). This is probable, since vein systems were deformed when the linear fabric formed in the area.

Discussion

Gold distribution at McIntyre follows a well defined pattern, with about 90% of all gold produced situated between 1000 level and 4625 level and the majority of that being produced from between 1000 level and 3125 level (Fig. 60.1). In a study of gold/silver ratios at McIntyre, Pearson (1947) showed that there was a pronounced peak in the fineness of gold between 2000 level and 3000 level with silver levels increasing above and below. The gold associated with the copper zone has an average gold-silver ratio of 1:6.5 as opposed to the average ratio for the peripheral gold orebodies of 4.5:1. Taking the major development of the copper orebodies into consideration, the optimum conditions for copper concentration developed in the zone between 1500 level and 3000 level.

Thus, if the copper and gold systems are integrated, there is a central copper-rich zone with subordinate gold and molybdenum and a low gold to silver ratio. This grades outwards into increasingly high grade gold veins, with a high gold to silver ratio and with the 5-3-25 vein system being the richest and most productive, but lying farther away from the copper system than other veins. Smith (1948) suggested a marked thermal zonation around the centre of the Pearl Lake porphyry from work based on decrepitation studies of pyrites at McIntyre. He showed a high temperature (570°C) core grading outwards to lower temperature zones (420°C) associated with the peripheral vein systems (5-3-25 vein system), and suggested that there must be some link between a hydrothermal system centred on the Pearl Lake porphyry and the gold veins around it. The copper zone and the other evidence to support this suggestion lay undiscovered at that time.

Optimum depositional and concentrating factors were developed within the same vertical interval for both copper and gold mineralization, irrespective of wallrock type or composition, strongly suggesting that temperature and pressure were the most sensitive and critical variables involved in the formation of the various orebodies, within the physical limitations of structural site preparation and creation of access for mineralizing fluids. Productive veins occur in Fe and Mg tholeiite flows and breccias, interflow sedimentary units (both graphitic and non-graphitic), in the porphyry and within albitite dykes, so that is difficult to ascribe significance to any particular wall rock in terms of ore deposition.

At Hollinger (Jones, in Ferguson, 1968) most of the gold production from the central ore zone which is situated in the same stratigraphic zone (63 flow up to the Central Subgroup breccias) as the major productive veins on McIntyre. The central ore zone represents the culmination "up plunge" of the McIntyre vein systems and, as would be expected, the significant vertical interval for gold production extends from surface down to about 2000 level. Furthermore the uniquely massive concentration of auriferous quartz veins and

associated alteration at Hollinger suggests that the central ore zone represents the apical portion of a very large hydrothermal system. Graton and McKinstry (1932) and Jones (1948) drew attention to the pitch of ore shoots within the Hollinger veins which follows the regional plunge of the linear fabric, but the bases of individual orebodies on Hollinger and McIntyre appear to coincide with a plane dipping at about 30° east. This led Graton and McKinstry (1932) to suggest that this plane probably represented an original basal surface of deposition to the hydrothermal system as a whole.

It is suggested that the McIntyre-Hollinger copper-gold mineralization is part of a porphyry-type system, probably of island-arc type, dominated by albitization, sericitization and carbonatization, and with strongly developed peripheral gold veins. The mineralization developed in structural sites which were probably opened as a result of porphyry intrusion and related hydrothermal activity, with extensive development of hydraulic fracturing and most intense copper mineralization around a pipe-like albitite core zone in the Pearl Lake porphyry. The intrusion of the Pearl Lake porphyry, the initiation of the hydrothermal system, and emplacement of the mineralization were probably interrelated, and appear to have occurred within a relatively short time.

The porphyry system and its associated gold veins were strongly deformed with dominant prolate strains, and this resulted in spectacular but predictable adjustments to original geometries and the present elongate shape of the system. The deformation of the copper stockwork at McIntyre has undoubtedly condensed the mineralized zone into a more compact entity, and as the grade in mineralized stockworks depends to a large extent on fracture density in the stockwork, shortening of the stockwork as a result of deformation would have much the same effect as increasing the fracture density, with concentration of ore into high grade shoots aligned with the stretch lineation. The practical implications of this type of deformation are fairly obvious, but there are also implications in the easily mistaken interpretation of this type of deformed mineralization as stratabound or even stratiform.

On a regional scale it would be instructive to determine to what extent the structural style of the Hollinger-McIntyre complex is typical of gold-bearing environments. Many major gold deposits seem to be intimately associated with localized complex deformation zones, with perhaps the closest comparisons to the Hollinger-McIntyre complex being the Campbell-Dickenson complex at Red Lake and the Kerr Addison mine at Virginiatown.

The association of hydrothermal gold systems, felsic intrusions, and major structural discontinuities, all of which postdate regional folding in Archean granite greenstone terranes, has been noted by geologists since the beginnings of gold mining in Archean gold camps throughout the world. It is only recently, however, that there has been a realization that the association is accompanied by widespread shear deformation and regional cleavage which overprint earlier regional folding. This major association marks the climax of late Archean crustal evolution between 2.6 and 2.7 Ga, and appears to represent one of the most significant event in terms of generating most of the world's significant economic concentrations of gold (Mason, 1985).

The major structural discontinuities such as the Destor-Porcupine, Cadillac and Kirkland Lake "breaks" appear to mark boundaries between crustal blocks or strike-slip fault zones within them. The association of felsic intrusions, hydrothermal systems, gold deposits and shear deformation with these discontinuities, is seen as part of the response to amalgamation of such crustal blocks into the first large plates of continental lithosphere during the late Archean.

Acknowledgments

This project was initiated from a Queen's University Advisory Research Committee Award, and partly supported by NSERC operating grant number AO620, both of which are gratefully acknowledged.

Particular acknowledgment is made to Warren Holmes, General Manager of Pamour Porcupine Mines, whose support and encouragement has been much appreciated. Pamour Porcupine Mines provided accommodation and office facilities during the period spent at Timmins. Bill Longworth, Tony Van Weichen, and Hugh Lockwood gave logistic and technical support throughout the project. Karl Hauser and Henry Dougherty were especially helpful in expediting our underground work at McIntyre, and Bill Fink assisted with arrangements for mapping on Hollinger. Phil Walford was responsible for encouraging the project from its conception, and his early support was invaluable.

The foundations of the project are the mine records at McIntyre and Hollinger, built up by numerous geologists over a period of some seventy years. Their work is respectfully acknowledged and is cited where appropriate.

The active encouragement and support of D.C. Findlay, J.M. Franklin and K.H. Poulsen of the Mineral Resources Division of the Geological Survey of Canada is gratefully acknowledged.

References

- Allen, C.C. and Folinsbee, R.R.
1944: Scheelite veins related to porphyry intrusives, Hollinger Mine; *Economic Geology*, v. 39, p. 340-348.
- Davies, J.F. and Luhta, L.E.
1978: An Archean "porphyry-type" disseminated copper deposit, Timmins, Ontario; *Economic Geology*, v. 73, p. 383-396.
- Ferguson, S.A.
1968: Geology and ore deposits of Tisdale Township, District of Cochrane; Ontario Department of Mines, Geological Report 58, p. 57-158 (and maps).
- Graton, L.C. and McKinstry, H.E.
1932: Geology of the Hollinger Mine; unpublished report on Hollinger Mine.
- Hurst, M.C.
1935: Vein formation at Porcupine, Ontario; *Economic Geology*, v. 30, p. 103-127.
- Jones, W.A.
1948: Hollinger Mine; in *Structural Geology of Canadian Ore Deposits*, v. 1; Canadian Institute of Mining and Metallurgy, p. 464-481.
- Karvinen, W.O.
1981: Geology and evolution of gold deposits, Timmins area, Ontario; in *Genesis of Archean Volcanic Hosted Gold Deposits*, ed. E.G. Pye and R.G. Roberts; Ontario Geology Survey, Miscellaneous Paper 97, p. 29-46.
- Keyes, M.R.
1940: Paragenesis in the Hollinger veins; *Economic Geology*, v. 35, p. 611-628.
- Kirkham, R.V. and Thorpe, R.I.
1973: Studies of gold-copper deposits suggests red metal may be used as a guide to gold; *Northern Miner*, November 1973, p. 55.

- Mason, R.
1985: Tectonic setting of late Archean gold deposits; in Abstracts with Program, 6th International Conference on Basement Tectonics, Santa Fe, New Mexico.
- Mason, R., Melnik, N. Edmonds, C.F., Hall, D.J., Jones, R., and Mountain, B.
1986: The McIntyre-Hollinger investigation, Timmins, Ontario: Stratigraphy, lithology and structure; in Current Research, Part B, Geological Survey of Canada, Paper 86-1B, Report 59.
- Mercereau, B.G.
1985: The evaluation of the Copper Orebody of the Pamour Porcupine Mine using the Climax ore zoning method; unpublished B.Sc. thesis, Queen's University, Kingston, 31 p.
- Pearson, H.A.
1947: Report on the variation of the Au-Ag ratio at McIntyre Porcupine Mines Ltd.; unpublished report, McIntyre Mines Ltd.
- Robinson, H.S.
1923: Geology of the Pearl Lake area, Porcupine District, Ontario; Economic Geology, v. 18, p. 753-771.
- Smith, F.G.
1948: The ore deposition temperature and pressure at the McIntyre Mine, Ontario; Economic Geology, v. 43, p. 627-637.
- Smith, T.J., Cloke, P.L. and Kesler, S.E.
1984: Geochemistry of fluid inclusions from the McIntyre-Hollinger gold deposit, Timmins, Ontario, Canada; Economic Geology, v. 79, p. 1265-1285.
- Smith, T.J. and Kesler, S.E.
1985: Relation of fluid inclusion geochemistry to wallrock alteration and lithogeochemical zonation at the Hollinger-McIntyre gold deposit, Timmins, Ontario, Canada; Canadian Institute of Mining and Metallurgy, Bulletin, v. 78, no. 876, p. 35-46.
- Whitehead, R.E.S., Davies, J.F., and Cameron, R.A.
1980: Carbonate and alkali alteration patterns in the Timmins gold mining area; Grant 30, in Geoscience Research Grant Program; Summary of Research, 1979-1980, ed. E.G. Pye; Ontario Geology Survey, Miscellaneous Paper 93, p. 244-256.

Pb-Pb isochron age of uraniferous phosphorite at the base of the Menihek Formation, Labrador Trough

Projects 750069 and 780032

R.T. Bell and R.I. Thorpe
Mineral Resources Division

Bell, R.T. and Thorpe, R.I., Pb-Pb isochron age of uraniferous phosphorite at the base of the Menihek Formation, Labrador Trough; *in* Current Research, Part B, Geological Survey of Canada, Paper 86-1B, p. 585-589, 1986.

Abstract

Basal units of the Menihek Formation are dated as about 1704 Ma by preliminary lead isotope studies on uraniferous phosphatic sediments. This date may reflect the onset of the main orogeny which terminated the last cycle of sedimentation in the Labrador Trough.

Résumé

Les unités basales de la formation Menihek datent d'environ 1704 Ma selon des études préliminaires faites avec l'isotope Pb sur des sédiments phosphatiques uranifères. Cette date correspond probablement au commencement de la principale orogénèse qui a terminé le dernier cycle de sédimentation dans la fosse du Labrador.

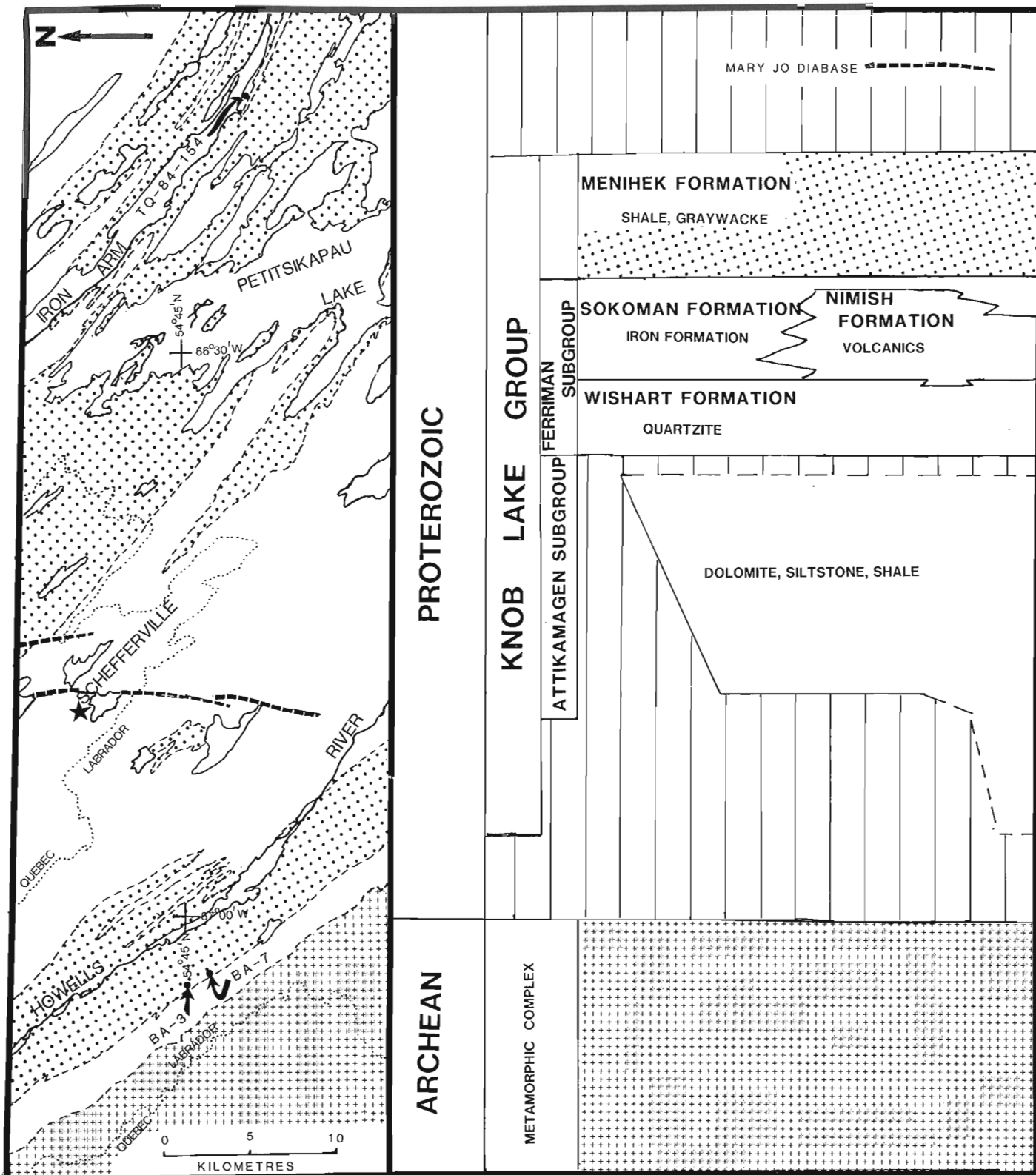


Figure 61.1. Location of specimens, and main areas of Menihek Formation near Schefferville, Quebec (after Wardle, 1982) with summary of stratigraphic units and main lithologies.

Introduction

Uraniferous phosphatic rocks in a black clastic sequence near the base of the Menihék Formation in the Labrador Trough, Québec, were described by Bell and Ruzicka (1985). They lie within 10 m above the top of the Sokoman Formation (iron-rich beds) and are best developed in the basal 2 m of the Menihék. The lead isotope compositions of some specimens from these radioactive phosphatic beds were determined in an attempt to date the uranium mineralization and the host sedimentary sequence.

For this preliminary report the following points are important:

1. Phosphorites in cherty black shales fix uranium during sedimentation and early diagenesis, and considering the relative impermeability of these rocks in comparison with phosphorites in carbonates, arenites and at unconformities, we believe the Pb-U system can stay effectively closed after early diagenesis until disturbed by high grade metamorphism.
2. Records of Precambrian phosphorites are relatively rare compared with Phanerozoic ones. Recent discoveries, however, suggest that Precambrian phosphorites are not so scarce as has been generally believed.
3. The first lead isotope studies of phosphatic sediments were by Soviet scientists (Golubchina, 1962; Tugarinov et al., 1963). In view of the success of these studies it is surprising that so few Pb-Pb and U-Pb isotope studies have been done. A more recent study in Finland (Vaasjoki et al., 1980) of uranium phosphatic rocks adjacent to iron-formation (analogous to this study except the Finnish rocks have been metamorphosed) prompted us to make a preliminary investigation of the Menihék phosphorites.

We propose to discuss at greater length in a succeeding paper, some of the more general aspects of phosphorites, and of Precambrian phosphorites in particular, and to review the isotope dating of these rocks.

Description of the Menihék-hosted phosphorite

The general character of phosphatic material at the base of the Menihék Formation (Fig. 61.1) has been described by Bell and Ruzicka (1985). The phosphatic layers and angular fragments of phosphorites are in turbidite beds that are enclosed and overlain by black, carbonaceous, siliceous and pyritic mudstones, and very fine grained sandstones. The turbidite beds are underlain by lean carbonate iron-formation of the Sokoman Formation. The basal 2 to 4 m of the Menihék sequence contains graded turbidites with angular clasts of cherty and carbonaceous pelite, fine grained sandstone and rarely of pelletal and carbonate iron-formation. The clasts are commonly less than 2 cm in diameter and rarely greater than 5 cm. Larger clasts (in drill core up to 20 cm apparent diameter) of banded black siltstone-mudstone that have been deformed and show diffuse boundaries with the matrix, are encountered locally.

The angular clasts are interpreted to be from Sokoman-Menihék transitional beds. These were lithified very early. The angularity testifies to rapid processes of erosion and redeposition. The less siliceous and sandy clasts are more rounded. The large deformed non-cherty clasts and the matrix are interpreted to have been carried by turbidity currents from up-slope sites of semiconsolidated lower Menihék sediments. The deformation in the larger clasts is interpreted to be related to the processes of removal and resedimentation.

The conglomeratic layers fine upwards and are overlain by laminated siltstone and mudstone over the first 4 m of section. Conglomeratic layers are uncommon in the next 6 m. At more than 10 m from its base, the Menihék is a monotonous sequence of 0.1 to 1 cm layered, black organic-rich shale, siltstone and very fine sandstone characterized by finely disseminated grains (5 μ m size) and clots (100 μ m) of pyrite. Thin (0.5 cm) layers of cherty mudstone or chert also are present. The total interval examined in drill core is the basal 50 m of the Menihék Formation.

Specimens were collected from two drill holes near Howells River (BA-7 at 54°44'N, 67°03'W and BA-3 at 54°45'N, 67°03'W) and from an outcrop near Iron Arm (TQ-84-154 at 54°43'N, 66°16'W) (Fig. 61.1). The specimens selected represented the most radioactive sections and thus were judged sufficiently enriched in uranium to warrant lead isotope analyses. The characteristics of representative specimens are illustrated by figures in the report by Bell and Ruzicka (1985). The specimens from outcrop at Iron Arm are from the crest of an anticline and appear to have been brecciated, perhaps in response to folding.

Methods of analysis

Lead isotope analyses of six uranium phosphatic specimens were supplied by Geospec Consultants Ltd., Edmonton, in 1985 under contract to the Geological Survey of Canada. The methods of analysis have been reported by Thorpe et al. (1984). The analytical uncertainties (at 2σ) of the lead isotope ratios, as determined by numerous analyses on the NBS 981 standard lead, are reported to be 0.042%, 0.052%, 0.058% and 0.014% for the ratios $^{206}\text{Pb}/^{204}\text{Pb}$, $^{207}\text{Pb}/^{204}\text{Pb}$, $^{208}\text{Pb}/^{204}\text{Pb}$ and $^{207}\text{Pb}/^{206}\text{Pb}$, respectively.

Table 61.1. Lead isotope analyses by Geospec Consultants Ltd. for uranium phosphate specimens from the Menihék Formation, Labrador Trough

No.	Field specimen no.	$^{206}\text{Pb}/^{204}\text{Pb}$	$^{207}\text{Pb}/^{204}\text{Pb}$	$^{208}\text{Pb}/^{204}\text{Pb}$
1	BA 3A	25.522	16.459	38.586
2	BA 7E	92.902	23.637	36.552
3	BA 7C	89.509	22.962	36.465
4	BA 7G	106.32	24.705	36.772
5	TQ 84-154 (dark)	283.61	43.132	36.412
6	TQ 84-154 (light)	334.34	48.605	36.511

Results and interpretation

The lead isotope analyses are listed in Table 61.1. Four of the six analyses are collinear within analytical uncertainties (Fig. 61.2) and at least squares regression of these data, taking account of correlated errors (York, 1969), yields a calculated slope (Pb-Pb isochron) age of 1704 ± 7 Ma. Since the $^{208}\text{Pb}/^{204}\text{Pb}$ ratios are comparable for 5 of the 6 specimens, a comparable plot can be prepared using ^{208}Pb , rather than ^{204}Pb , as the reference isotope. The same specimens are essentially collinear in this plot (Fig. 61.3) and the indicated age is approximately 1709 Ma, in accord with the previous result. The analyses for specimens 1 and 2 (Table 61.1) lie very slightly off of the 4-point line. Slight postdepositional disturbance of the U-Pb systems could account for this pattern.

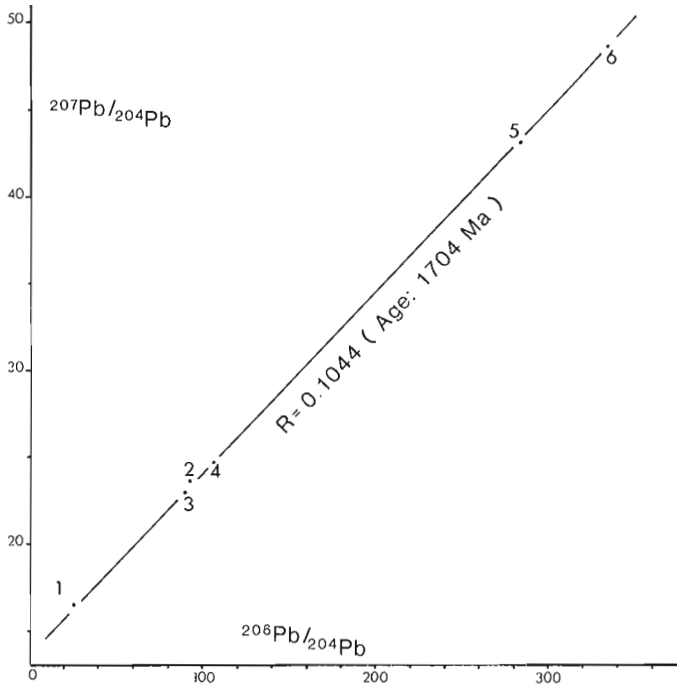


Figure 61.2. Standard Pb-Pb isochron (^{204}Pb reference) for uraniferous phosphorite, Menihek Formation.

This lead isotope date for phosphorite in the basal Menihek Formation reflects, in our opinion, a pencontemporaneous date for the onset of Menihek deposition. In that the Menihek is interpreted as flysch and is followed by molasse sediments (Dimroth et al., 1970; Dimroth, 1978; Wardle and Bailey, 1981), the date (1704 ± 7 Ma) could reflect the onset of the main orogeny affecting the Labrador Trough and which terminated the last cycle of Trough sedimentation.

Discussion

Fryer (1972) reported the results of a Rb-Sr geochronology study of sedimentary rocks, including banded iron-formations, from the Labrador Trough and from the Lake Mistassini area, Quebec. For the Menihek Formation he reported an age of 1816 ± 74 Ma (with the presently accepted ^{87}Rb decay constant of $1.42 \times 10^{-11} \text{a}^{-1}$; Steiger and Jager, 1977) and an initial $^{87}\text{Sr}/^{86}\text{Sr}$ ratio of 0.7033 ± 0.0085 . This is not in good agreement with the Pb-Pb isochron age reported here for uraniferous phosphorite at the base of the Menihek Formation. However, a replot of Fryer's data (Fig. 61.4) indicates that 4 of his 7 analyses are in accord, as shown by the line in Figure 61.4, with an age of about 1713 Ma. If this interpretation is correct, the scatter of his remaining 3 points would have to be attributed to a relatively broad scatter in initial isotope ratios and/or postdepositional disturbance of the Rb-Sr system. Fryer's analyses for dolomites from the Belcher Basin, Mistassini Basin and Knob Lake area do indicate that these rocks had a wide range in initial strontium isotope ratios.

Two other dates (Clark, 1984; Dressler, 1975) give us more concern. Clark (1984) presented a U/Pb date of 2142 Ma for zircons in rhyolite in a unit mapped as Mistamisk Formation in the north-central Trough. The Mistamisk Formation is correlated either with the Menihek Formation or the pre-Ferriman Bacchus Formation. Considering the

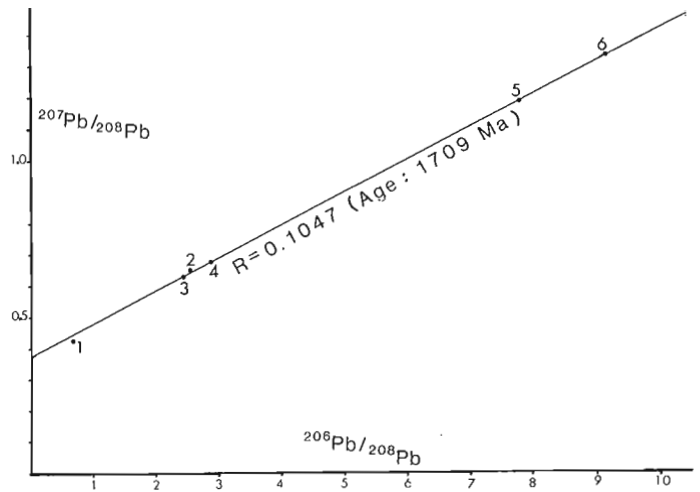


Figure 61.3. Pb-Pb isochron (^{208}Pb reference) for uraniferous phosphorite, Menihek Formation.

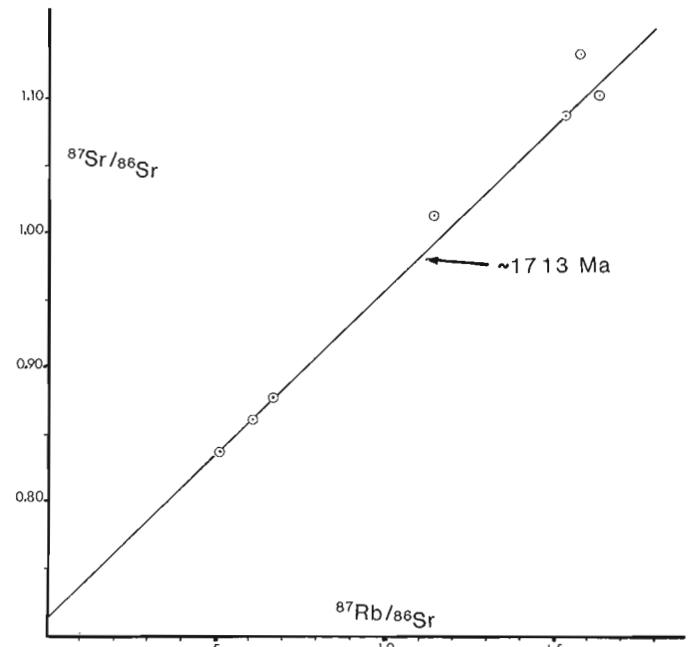


Figure 61.4. Rb-Sr isochron plot for Menihek shale based on data from Fryer (1972). The line plotted represents an age of about 1713 ± 74 Ma ($\lambda^{87}\text{Rb} = 1.42$ for 4 analyses selected from the 7 by Fryer). The two points lying above the line cannot define an isochron in combination with the lowermost 3 points, because the required initial $^{87}\text{Sr}/^{86}\text{Sr}$ value is unreasonably low.

tenuous nature of the correlation with Menihek (Dimroth, 1978) we prefer the pre-Ferriman correlation. If our date of 1704 Ma for early Menihek sedimentation is valid then a fairly substantial temporal difference exists between basal Menihek and pre-Ferriman rocks.

We are more concerned about our date when compared with a whole-rock K-Ar date of 1875 ± 53 Ma on lamprophyres which are clearly documented to cut Sokoman and older rocks but to be older than Menihek Formation in the north-central Trough (Dressler, 1975). If our date on basal Menihek and interpretation that it is approximately

synsedimentary is valid, it implies a break of more than 100 Ma between (late?) Sokoman sedimentation and the commencement of Menihék sedimentation on a regional scale. The alternative is that most, if not all, uranium was introduced later and selectively absorbed by the phosphorites. The autoradiographs of the drillcore samples, (see Fig. 19.1, Bell and Ruzicka, 1985) indicate that distribution of uranium is related to bedding lamination and selected resedimented phosphate clasts, which we consider implies synsedimentary and early diagenetic emplacement. In view of the good linearity of the analyses, resetting of the U-Pb systems during a subsequent metamorphic or other event would require essentially complete removal of the accumulated radiogenic lead component. Thus resetting is not the favoured interpretation.

Summary and conclusions

The lead isotope analyses for the phosphatic sedimentary rocks of the Menihék Formation yield an isochron age of 1704 ± 7 Ma. This date is tentatively considered to represent the time of accumulation of the uraniumiferous phosphate during sedimentation of a character that signals the onset of the orogeny that subsequently terminated the last cycle of sedimentation within the Labrador Trough.

Comparison with other dates suggests there may be a 400 Ma interval between pre-Ferriman rocks and those of the Menihék, and a break in the order of 100 Ma between the Ferriman and Menihék. Without doubt further stratigraphic work is in order throughout the Trough.

We recognize that the validity of interpreting an age as young as 1704 Ma as the true age of the basal Menihék Formation will be questioned despite the foregoing arguments. In order to better evaluate the results of Pb-Pb and U-Pb isotope studies of phosphorites we recommend comparative studies at localities where the ages are better constrained. At the same time more dating of igneous and metamorphic events within the Trough is needed to throw light on this situation. With regard to the Menihék Formation, more material should be obtained from the localities for which data are reported here, as well as from additional sites and further Pb-Pb and U-Pb studies should be pursued.

Acknowledgments

Geospec Consultants Ltd. supplied the lead isotope analyses under contract to the Geological Survey of Canada. A.T. Avison of Norcen Energy Resources Ltd. allowed sampling during the 1984 field season. We gratefully acknowledge constructive discussions with A.T. Avison, G.A. Gross, T. Birkett, and S.M. Roscoe but take responsibility for the conclusions.

References

- Bell, R.T. and Ruzicka, V.
1985: Uranium in the Circum-Ungava Belt, northern Quebec and Labrador: new information from the central Labrador Trough; in *Current Research, Part A*, Geological Survey of Canada, Paper 85-1A, p. 145-149.
- Clark, T.
1984: Géologie de la région du lac Cambrien, Territoire du Nouveau-Québec; Ministère de l'Énergie et des Ressources, Direction de la recherche géologique, ET 82-02, 71 p.
- Dimroth, E.
1978: Région de la fosse du Labrador entre les latitudes $54^{\circ}30'$ et $56^{\circ}30'$; Ministère des Richesses Naturelles du Québec, Rapport géologique 193, 396 pp.
- Dimroth, E., Baragar, W.R.A., Bergeron, R., and Jackson, G.D.
1970: The filling of the Circum-Ungava geosyncline; in *Symposium on Basins and Geosynclines of the Canadian Shield*, ed. A.J. Baer; Geological Survey of Canada, Paper 70-40, p. 45-142.
- Dressler, B.
1975: Lamprophyres of the north-central Labrador Trough, Quebec, Canada; *Neues Jahrbuch für Mineralogie, Mon. Heft 6*, p. 268-280.
- Fryer, B.J.
1972: Age determinations in the Circum-Ungava geosyncline and the evolution of Precambrian banded iron-formations; *Canadian Journal of Earth Sciences*, v. 9, no. 6, p. 652-663.
- Golubchina, M.N.
1962: Determination of the absolute age of phosphorite by the lead-isotopic method; *Infrom. Sb., Vsesoyuznyy Nauchno-Issledovatel'skiy Geologicheskiiy Institut*, no. 54, p. 27-29.
- Steiger, R.H. and Jäger, E.
1977: Subcommittee on geochronology: conventions on the use of decay constants in geo- and cosmochronology; *Earth and Planetary Science Letters*, 36, p. 359-362.
- Thorpe, R.I., Guha, J., Franklin, J.M., and Loveridge, W.D.
1984: Use of the Superior Province lead isotope framework in interpreting mineralization stages in the Chibougamau District; in *Chibougamau - and Mineralization*, ed. J. Guha and E.H. Chown; Canadian Institute of Mining and Metallurgy, Special Volume 34, p. 496-516.
- Tugarinov, A.I., Zykov, S.I., and Bibikova, E.V.
1963: Determination of the age of sedimentary rocks by the lead-uranium method; *Geochemistry*, No. 3, p. 284-300.
- Vaasjoki, M., Aikas, O., and Rehtijarvi, P.
1980: The age of mid-Proterozoic phosphatic metasediments in Finland as indicated by radiometric U-Pb dates; *Lithos*, v. 13, no. 3, p. 257-262.
- Wardle, R.J.
1982: Geology of the south-central Labrador Trough; Mineral Development Division, Department of Mines and Energy, Government of Newfoundland and Labrador, Maps 82-5, 82-6 and legend.
- Wardle, R.J. and Bailey, D.G.
1981: Early Proterozoic sequences in Labrador, in *Proterozoic Basins of Canada*, ed. F.H.A. Campbell; Geological Survey of Canada, Paper 81-10 supplement, p. 331-359.
- York, D.
1969: Least squares fitting of a straight line with correlated errors; *Earth and Planetary Science Letters*, v. 5, p. 320-324.

A reconnaissance study of the surficial and shallow bedrock geology of the southeastern Grand Banks of Newfoundland

Project 730072

Gordon B.J. Fader and Robert O. Miller
Atlantic Geoscience Centre, Dartmouth

Fader, G.B.J. and Miller, R.O., A reconnaissance study of the surficial and shallow bedrock geology of the southeastern Grand Banks of Newfoundland; in *Current Research, Part B*, Geological Survey of Canada, Paper 86-1B, p. 591-604, 1986.

Abstract

Tertiary bedrock occurs at a shallow depth of from 0 to 15 m below the seabed. Fluvial and glacial bedrock channels are largely confined to the eastern edge of the Grand Banks. A 30 m-thick deposit of till and glaciomarine sediment occurs in a 30 km wide zone along the southwestern edge of the Grand Banks. These glacial sediments, together with rounded boulders and gravel on the southern area of Grand Bank, suggest that glaciers extended across the entire area possibly during Wisconsinan glaciation.

The surface of the southeastern Grand Banks is dominated by large sand ridge bedforms, up to 4 km in wavelength. Erosion of the sand ridges is suggested by zones of straight-crested, wave-generated ripples developed within 1 to 2 m large depressions on the surfaces of the sand ridges.

Five surficial geological formations are proposed for the Grand Banks of Newfoundland: Grand Banks Drift, Downing Silt, Adolphus Sand, Grand Banks Sand and Gravel, and Placentia Clay.

Résumé

L'assise rocheuse tertiaire se trouve à une faible profondeur, de 0 à 15 m, sous le fond marin. Les chenaux fluviaux et glaciaires de la roche en place sont principalement limités au bord oriental des Grands Bancs. Un dépôt de moraine glaciaire et de sédiments glacio-marins d'une épaisseur de 30 m se trouve le long de la bordure sud-ouest des Grands Bancs dans une zone de 30 km de large. La présence de ces sédiments glaciaires ainsi qu'une multitude de gros blocs et de graviers arrondis dans la partie méridionale du Grand Banc indiquent que les glaciers couvraient toute la superficie de cette région, possiblement au cours de la glaciation du Wisconsin.

La surface de la partie sud-est des Grands Bancs est dominée par d'importants reliefs de crêtes sableuses de 4 km de long. L'érosion des crêtes sableuses est suggérée par la présence de zones d'ondulations aux arêtes rectilignes produites par les vagues produites dans des dépressions de 1 à 2 m de large à la surface des crêtes de sable.

Cinq formations géologiques superficielles sont donc proposées pour les Grands Bancs de Terre-Neuve: matériaux détritiques des Grands Bancs, silt Downing, sable Adolphus, sable et graviers des Grands Bancs et argile Placentia.

Introduction

Previous studies of the surficial geology of the Grand Banks of Newfoundland by the Atlantic Geoscience Centre concentrated on Quaternary geology of the Hibernia hydrocarbon discovery areas of northeast Grand Bank (Fader and King, 1981; and Fader et al., 1986), and on the near surface bedrock geology of a Paleozoic sedimentary basin on the inner shelf of the Grand Banks (King et al., in press).

This paper presents the preliminary results of a three-week regional cruise (Hudson 85-005) and a two-week cruise (Pandora 85-057) using the submersible *Pisces IV*, during which lithologic and stratigraphic information on surficial and near surface bedrock geology of the southeastern Grand Banks was collected (Fig. 62.1). The data set completes a regional geological-geophysical survey of the southeastern Grand Bank region at a reconnaissance level and leaves only the Whale Bank/Green Bank area to be systematically studied for mapping purposes. Significant new interpretations are presented on glacial limits, sea level history, Tertiary stratigraphy, bedform and iceberg furrow distributions and characteristics.

Objectives

The objectives of the regional cruise (Hudson 85-005) were: (1) to collect surficial and bedrock data to determine the area's geological history, (2) to determine the extent of the last (Wisconsinan) and earlier glaciations across the Grand Banks of Newfoundland, and the sediments deposited by the glaciers, (3) to study the morphology, distribution and characteristics of bedforms at the seabed (sand ridges, waves, ribbons, ripples), (4) to determine late Quaternary changes in relative sea level, (5) to quantitatively map reflectively of seabed sediments and associated parameters, (6) to study the regional distribution of relict and modern iceberg furrows and their relationship to seabed materials, (7) to understand and describe the Holocene transgression history of the Grand Banks (subaerial channelling, terraces, unconformities, overconsolidated and dessicated sediments), and (8) to assess the mineralogy of the coarse sediment and the non-fuel aggregate potential of the area.

The objectives of the *Pisces IV* submersible program were to ground truth the interpretation of the geophysical data collected on the Hudson 85-005 cruise. Specific dive targets were: (1) "Superfarrow", a 200 m-wide, 12.5 m-deep, large iceberg furrow in glacial till sediments of Avalon Channel; (2) shell beds - circular to linear acoustic sonar anomalies interpreted as shellfish communities on the Southeast Shoal area; (3) sand ridges, 3 km-wavelength, 15 m-high bodies of sand overlying lag gravels on southern Grand Bank; and (4) iceberg pits and furrows, in the Hibernia area of northern Grand Bank. Because of bad weather conditions, submersible dives were completed only on the superfarrow and sand ridge dive sites but high quality sidescan sonograms were collected to further define the distribution and detailed character of the iceberg pits and shell bed areas.

The Hudson 85-005 cruise also undertook testing of a new underwater drill developed by Nordco Ltd. for sampling unconsolidated sediments and subsurface bedrock.

Methods

An integrated geophysical-geological approach was used in the collection of the data. For seismic reflection information, a 40 in³ airgun and Hunttec deep-towed high resolution system (DTS) were deployed. The DTS was equipped with an Acoustic Reflectivity Unit (ARU) that produced on-line acoustic reflectivity values to provide

lithologic information on seabed materials (Parrott et al., 1980). Bathymetric data were collected with EDO Western and Kelvin Hughes echo sounder systems. A 70 kHz sidescan sonar developed by the Bedford Institute of Oceanography, and a Klein, 100 kHz sidescan sonar system provided sonograms of the seafloor. Navigation control was provided by integrated Loran C and satellite systems.

For sampling the seabed, small Van Veen grabs and a large 1 m³ system, designed by the Institute of Continental Shelf Research, Norway, were used. Piston cores were collected with a Benthos split piston system. For underwater bottom photographs a UMEL camera system was operated. Samples of benthic shellfish were collected with an epibenthic sled.

Bedrock geology

Over most of the study area the bedrock occurs less than 10 m below the seabed and is commonly exposed, especially in the troughs of some of the larger bedforms and at the shelf edge near canyons. In these areas it is generally covered by thin gravel-boulder lag deposits. This is similar to the geological setting of northeastern Grand Bank in the Hibernia region (Fader and King, 1981).

The age of the pre-Quaternary bedrock (Fig. 62.2) for the southeastern Grand Banks is interpreted to be Tertiary on the basis of well control and seismostratigraphic correlation from the Hibernia area. However, in the Tail of the Bank area sample control does not exist and it is possible that the sequence includes Pleistocene rocks. The thin surficial cover over most of Grand Bank provides easy access to the bedrock for obtaining ground truth.

The Tertiary rocks appear as continuous coherent reflections dipping seaward 1-2° on the high resolution seismic reflection profiles (Fig. 62.3). Wedge shaped bodies of prograded sediment are widespread, occurring between major parallel reflections and may represent shelf edge outbuilding during Tertiary times of lowered sea level. A major unconformity of regional extent is developed across the region, and is generally flat with little relief. In areas of

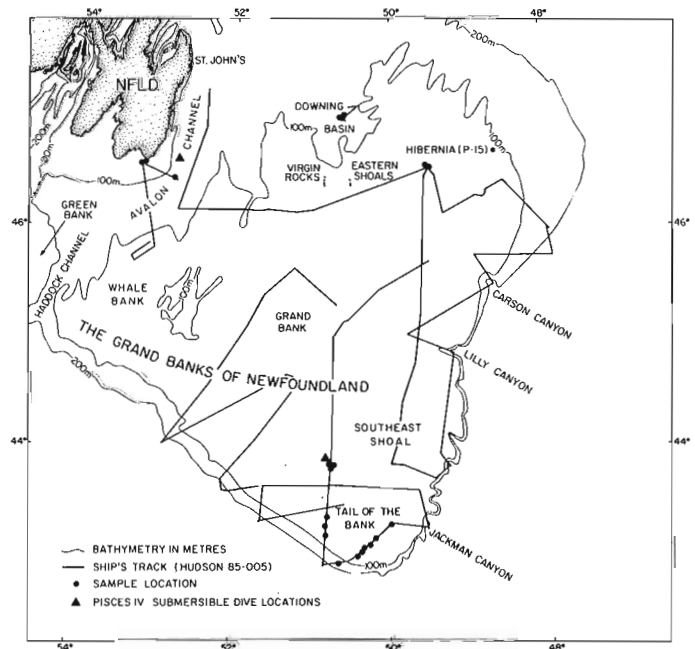


Figure 62.1. Index for the eastern Grand Banks of Newfoundland showing the ship's tracks for Hudson cruise 85-005 and the submersible dive locations of *Pisces IV*.

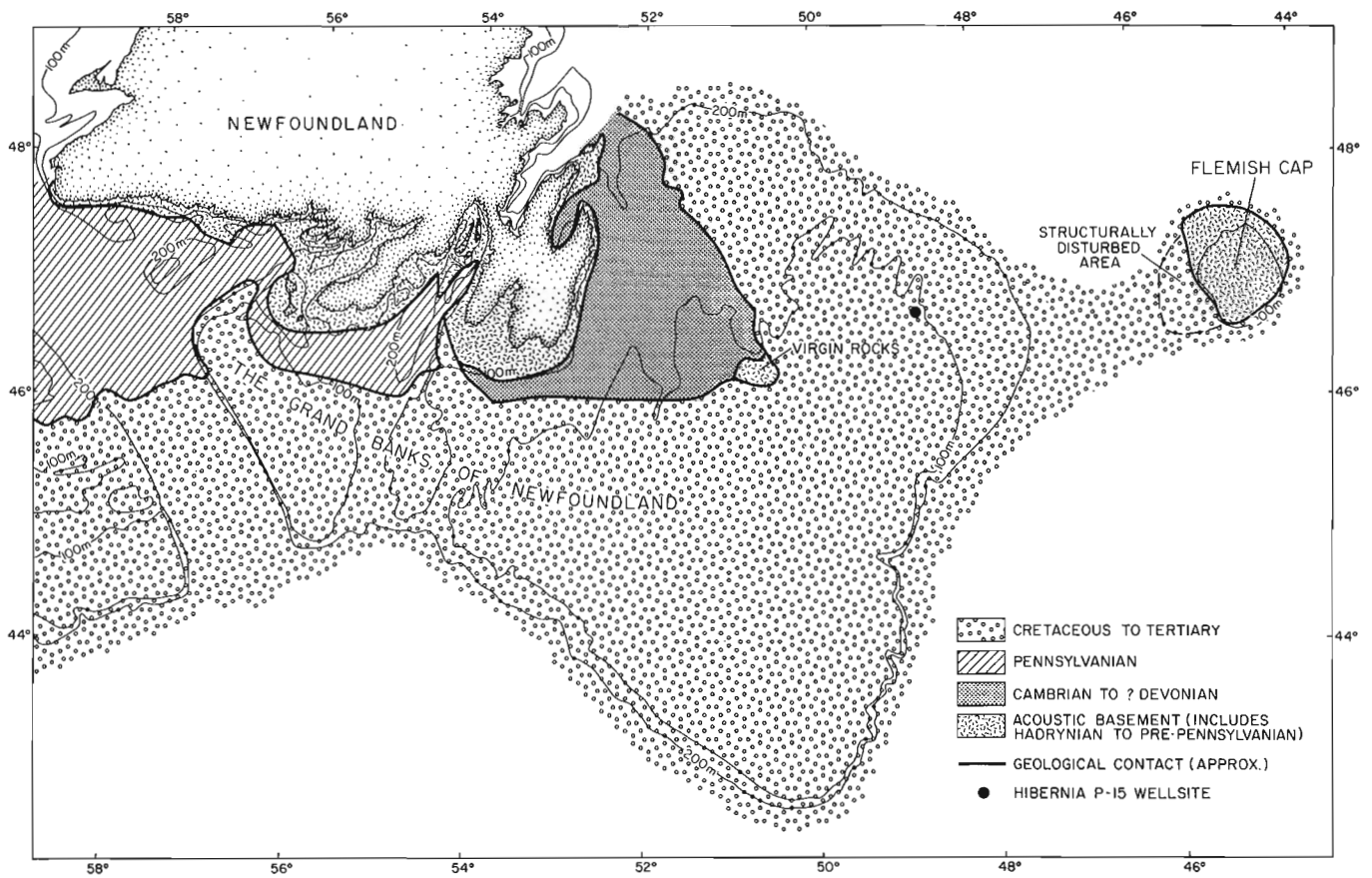


Figure 62.2. Regional bedrock geology of the Grand Banks of Newfoundland interpreted on the basis of seismic reflection profiles and samples collected with the Bedford Institute electric rock core drill and exploration drilling (King et al., in press; King et al., 1985; Fader et al., 1982).

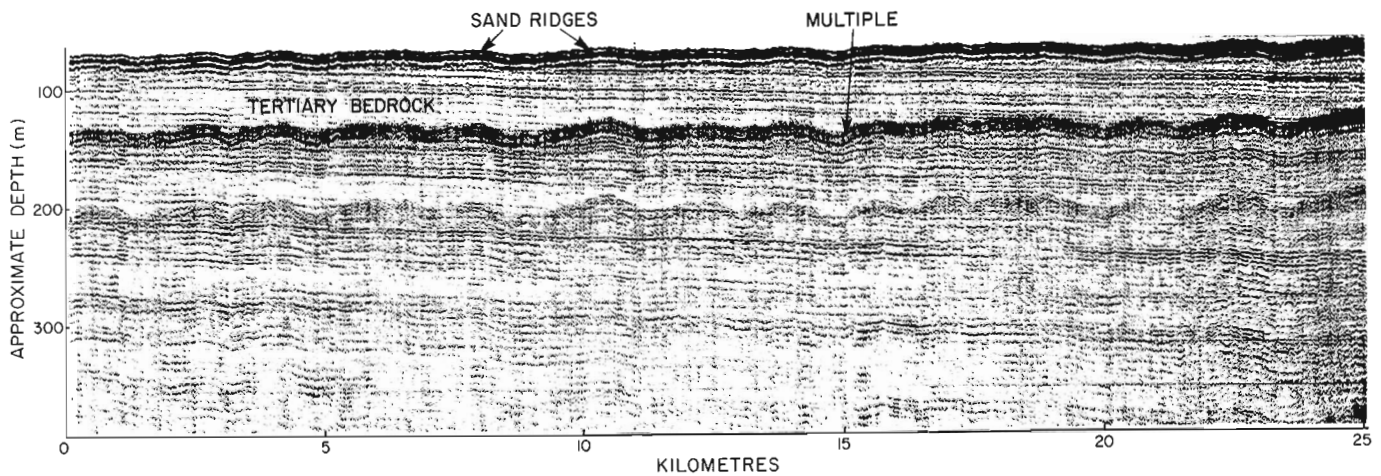


Figure 62.3. Airgun seismic reflection profile from the south-central area of Grand Bank showing a typical sequence of Tertiary shallow dipping reflections to the south. The reflections terminate in the seafloor bubble pulse of the profile and indicate that the overlying surficial sediment is less than 10 m thick. Note the absence of channeling within the Tertiary sequence. The undulations at the seabed are sand ridges.

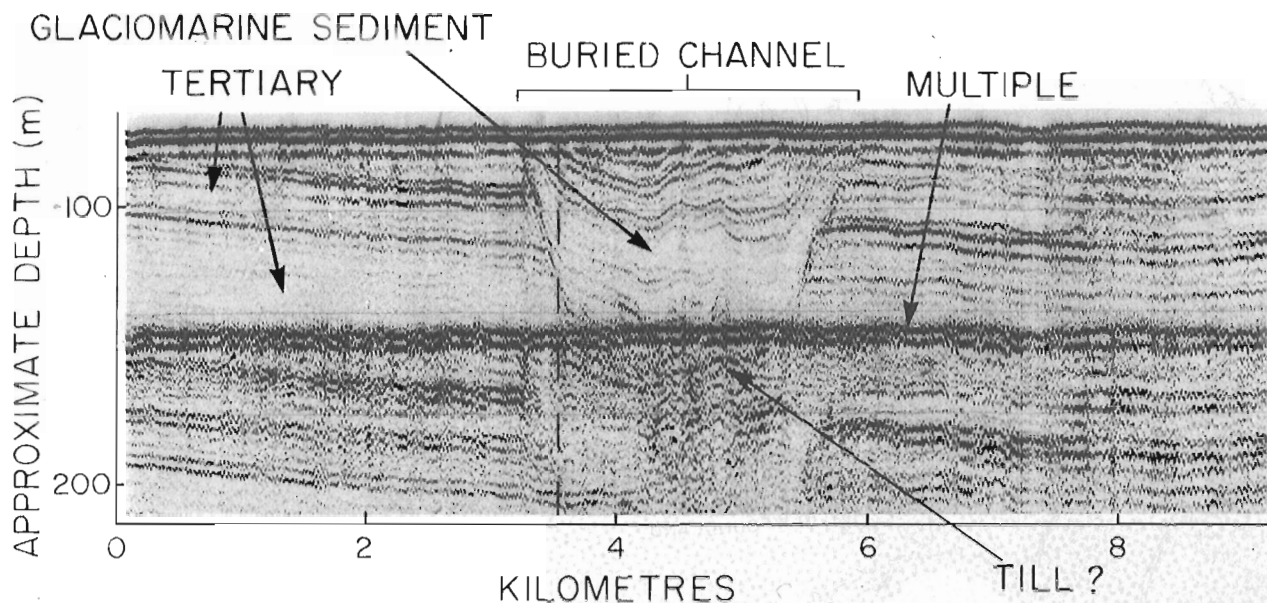


Figure 62.4. Airgun seismic reflection profile from the northern area of Grand Bank showing an isolated buried bedrock channel. The conformable nature, seabed unconformity and continuous-coherent character of infilling sediments suggest that they are glaciomarine sediments overlying possible till. The channel is cut into Tertiary rock.

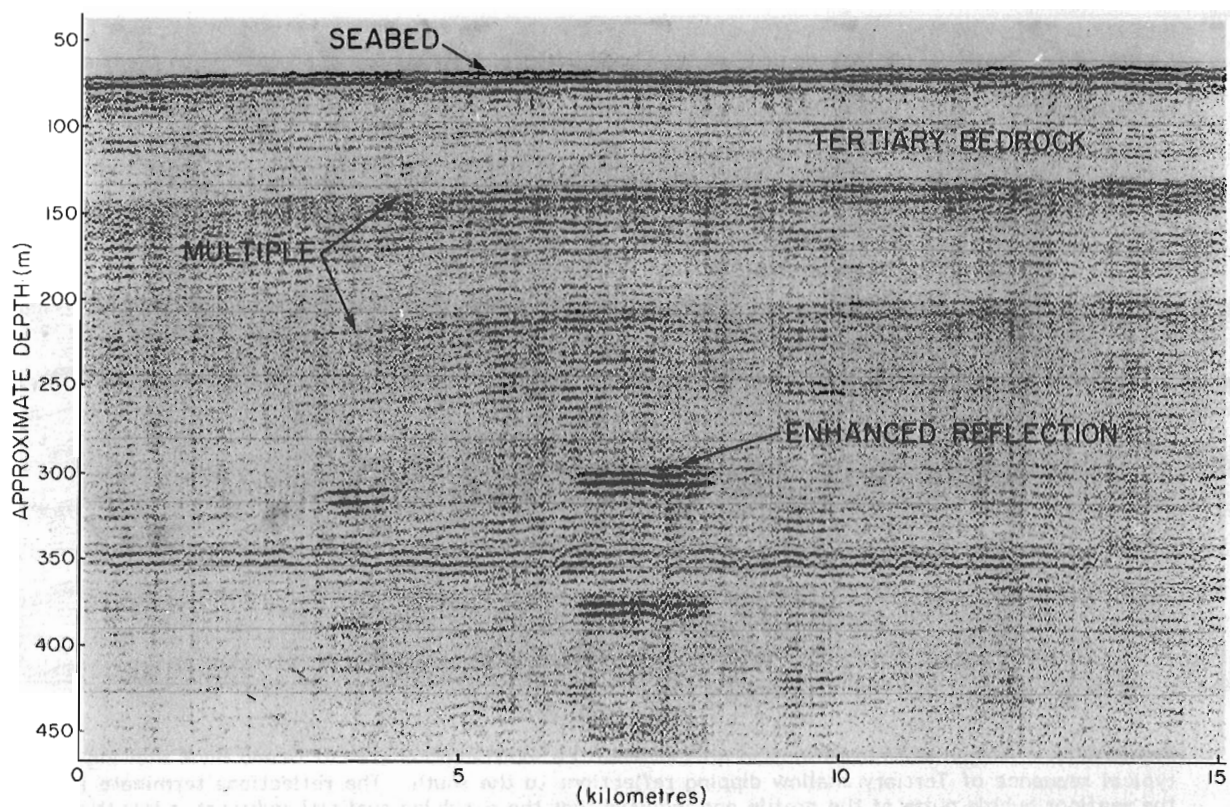


Figure 62.5. Airgun seismic reflection profile from the Tail of the Bank showing the occurrence of an acoustic anomaly of high intensity (bright spot) interpreted as shallow gas within Tertiary rocks.

central Grand Bank, reflections dip in a northward direction contrary to the regional seaward dip and may represent periods during the Tertiary when large areas of the southern Grand Banks were subaerially exposed and prograded northward.

Channelling is generally absent from most areas of Grand Bank, however, along the eastern flank of the bank, many deep, incised channels, up to 300 m in depth occur. They probably connect with the major shelf edge canyons (Fig. 62.1) which cut the eastern edge of Grand Bank. In addition, a few isolated channels (Fig. 62.4) near the Hibernia area of northeast Grand Bank extend to a depth of 60 m. Many of the channels are interpreted to be infilled with glaciomarine sediments as evidenced by the conformable structure of the continuous coherent reflections on the seismic reflection profiles. These glaciomarine sections occur beneath thin sand and gravel deposits and have not been sampled.

Numerous acoustic anomalies of high intensity (bright spots), interpreted as shallow gas, occur within the Tertiary succession in the Tail of the Bank area (Fig. 62.5). They range in depth from 300-500 m below the seabed and represent a possible hazard to hydrocarbon exploration.

Surficial geology

Formations

As a result of interpretation of the regional data base collected on this cruise and other previous investigations, as well as the need for a common stratigraphic framework, we hereby propose a surficial nomenclature for the Grand Banks of Newfoundland. Table 62.1 is a correlation diagram of the surficial formations with those of the adjacent Scotian Shelf (King, 1970) to the west and the Labrador Shelf (Josenhans, in press) to the north.

The Grand Banks Drift is a formation of glacial till which conformably overlies the bedrock surface and was deposited directly beneath grounded ice. It is confined to the deeper basins, channels, and the saddles between offshore banks. Overlying and interbedded with the till is the Downing Silt, a glaciomarine sediment. It is named after the type section found in Downing Basin. The Adolphus Sand is a sublittoral deposit of sand and muddy sand which occurs in the peripheral areas of the banks and in the adjacent saddles. It is named after the first discovery well of liquid hydrocarbons in the Hibernia area of northern Grand Bank. The Grand Banks Sand and Gravel Formation is a basal transgressive deposit which occurs on the bank surfaces in water depths shallower than 100 m. A wide variety of bedforms are developed across the Grand Banks Sand and Gravel. The Placentia Clay, named after the type section in Placentia Bay, is a late Pleistocene-Holocene clay deposited

in the basinal areas of the shelf. The sediment was derived by winnowing during transgression of the tills and glacial sediments on the bank areas in late Pleistocene-Holocene time. In contrast to the LaHave Clay of the Scotian Shelf, the Placentia Clay has a significant coarse ice-rafted component.

Surficial sediment thickness

The surficial sediment on the Grand Banks of Newfoundland varies to over 300 m in thickness. In water depths less than 100 m the average thickness of sand ridges on the bank tops is approximately 5 m, with the thickest sand ridges ranging to 15 m. The few buried channels near the Hibernia area extend to 60 m in depth while those on the eastern edge of Grand Bank are over 300 m in depth. A unique sediment section extending from the Tail of the Bank area, west to Whale Bank, is a continuous seaward thickening wedge up to 30 m thick, of glacial sediments overlain by muddy sand (Fig. 62.6).

Tertiary outcrop, lag gravels and boulders

Tertiary bedrock occasionally outcrops at the seabed in the western part of the study area. The outcropping beds appear as irregular, linear features of high reflectivity with thin patches of sand scattered across their surface. The strike of the outcropping beds on the sonograms conforms to the regional structure of the Tertiary strata as interpreted from the seismic reflection data.

Beneath the sand ridges and occurring over large areas of the seabed, is a lag gravel deposit which overlies the regional unconformity developed on Tertiary bedrock. The lag gravel outcrops between sand ridges and this helps to define their outline on sidescan sonograms (Fig. 62.9). Sidescan sonar data and submersible observations have been used to estimate the number of boulders larger than 0.5 m (the resolution of the system) distributed across the seabed of the southeastern Grand Banks. Figure 62.12 shows that the boulders are widespread and occur in densities of up to 1400/km². From submersible observations it is evident that there are at least as many boulders in the substrate which slightly protrude from the seabed which would not show on sidescan sonar. On central Grand Bank the frequent high sand ridges have masked the boulders; on the Tail of the Bank the mud deposit has buried the boulders, accounting for their absence in these areas. The rocks are subrounded in shape.

The lithology of the boulders is difficult to determine from submersibles because of the density of organic growth on their surfaces. Large volume samples, however, indicate a predominance of lithologies that show affinities to rocks exposed on the Avalon Peninsula and in the adjacent offshore area. The distribution of these boulders and their lithology and shape have a direct bearing on an understanding of the extent of glaciations across the Grand Banks.

Bedforms

Perhaps the most conspicuous geological aspect of the surficial geology of the study area of southern Grand Bank is the complex distribution of bedforms and their textural and morphological variability. The largest of the bedforms, which also covers the largest area of the seabed, are sand ridges. These features range in thickness to 15 m, with wavelengths up to 4 km (Fig. 62.7). They appear as isolated features on lag gravel, in fields with individual bedforms maintaining separation, and as overlapping features where it is difficult to separate one bedform from another. The upper surfaces of most sand ridges are incised by 1-3 m depressions of wave-formed ripples (Fig. 62.7) which have a wavelength of 1-3 m and heights of 0.5-1 m. The incised zones of ripples

Table 62.1. Correlation of surficial formations with the Scotian Shelf and Labrador Shelf

Scotian Shelf (after King, 1970)	Grand Banks of Newfoundland	Labrador Shelf (after Josenhans, in press)
LaHave Clay	Placentia Clay	Makkaq Clay
Sable Island Sand & Gravel	Grand Banks Sand & Gravel	--
Sambro Sand	Adolphus Sand	Sioraq Sand
Emerald Silt	Downing Silt	Qeovik Silt
Scotian Shelf Drift	Grand Banks Drift	Labrador Shelf Drift

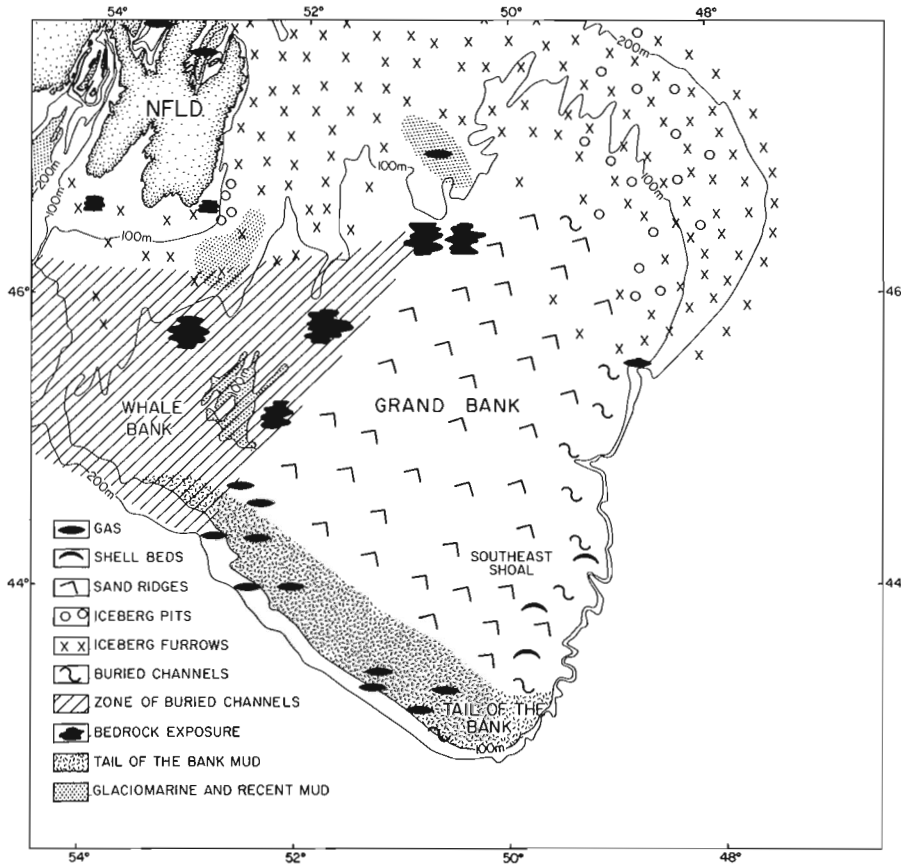


Figure 62.6

Regional distribution of significant geological characteristics for the southeastern Grand Banks of Newfoundland.

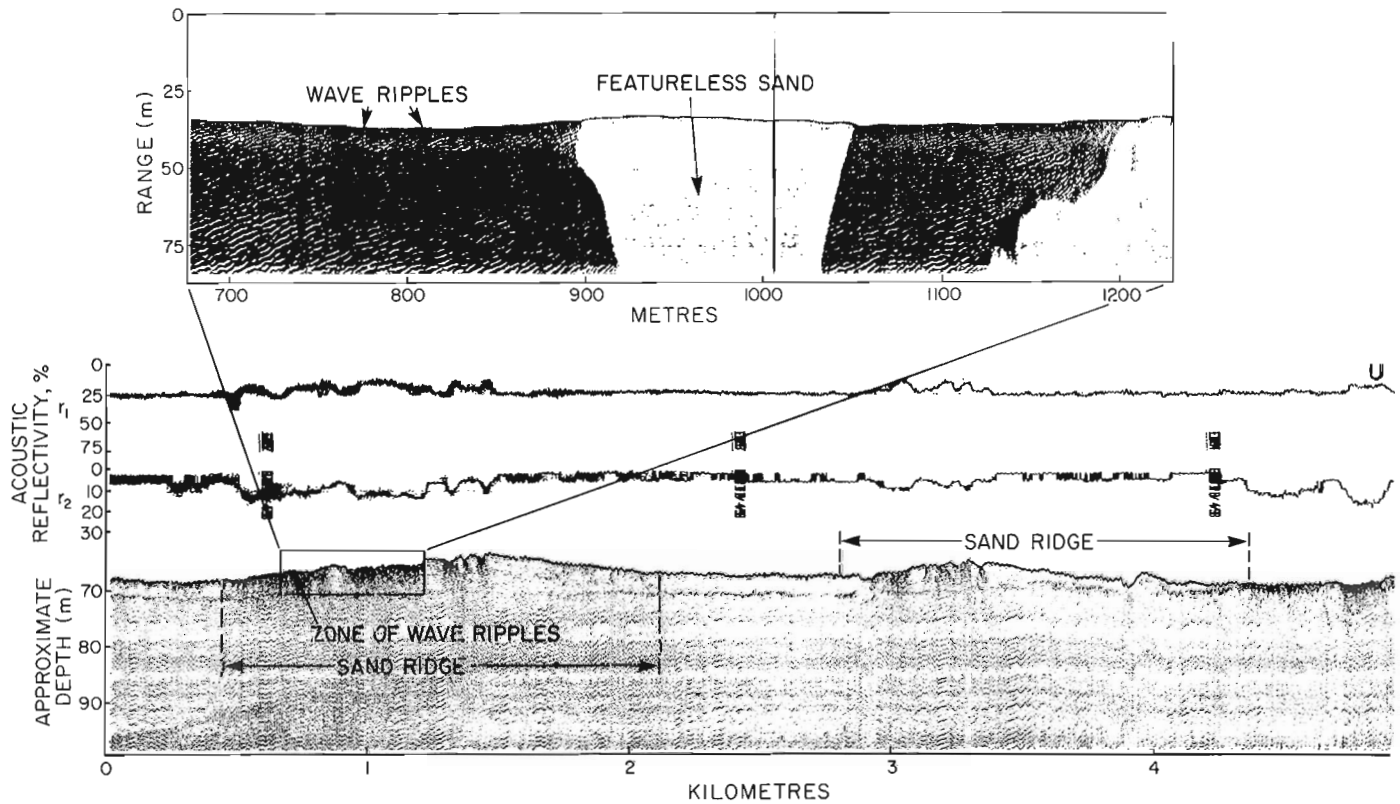


Figure 62.7. Huntec DTS profile and 100 kHz sidescan sonogram across an area of sand ridges on Grand Bank. Note the incised wave-formed rippled seabed on the upper surface of the sand ridges. These rippled areas consist of coarse sand and gravel with broken shell debris in the troughs of the ripples. Sand ridges occur across the seabed of southern Grand Bank.



Figure 62.8

Submersible bottom photograph across the wave-formed rippled area shown on the sonogram in Figure 62.7. Note the preferential deposition of gravel-sized sediment in the troughs of the bedforms.

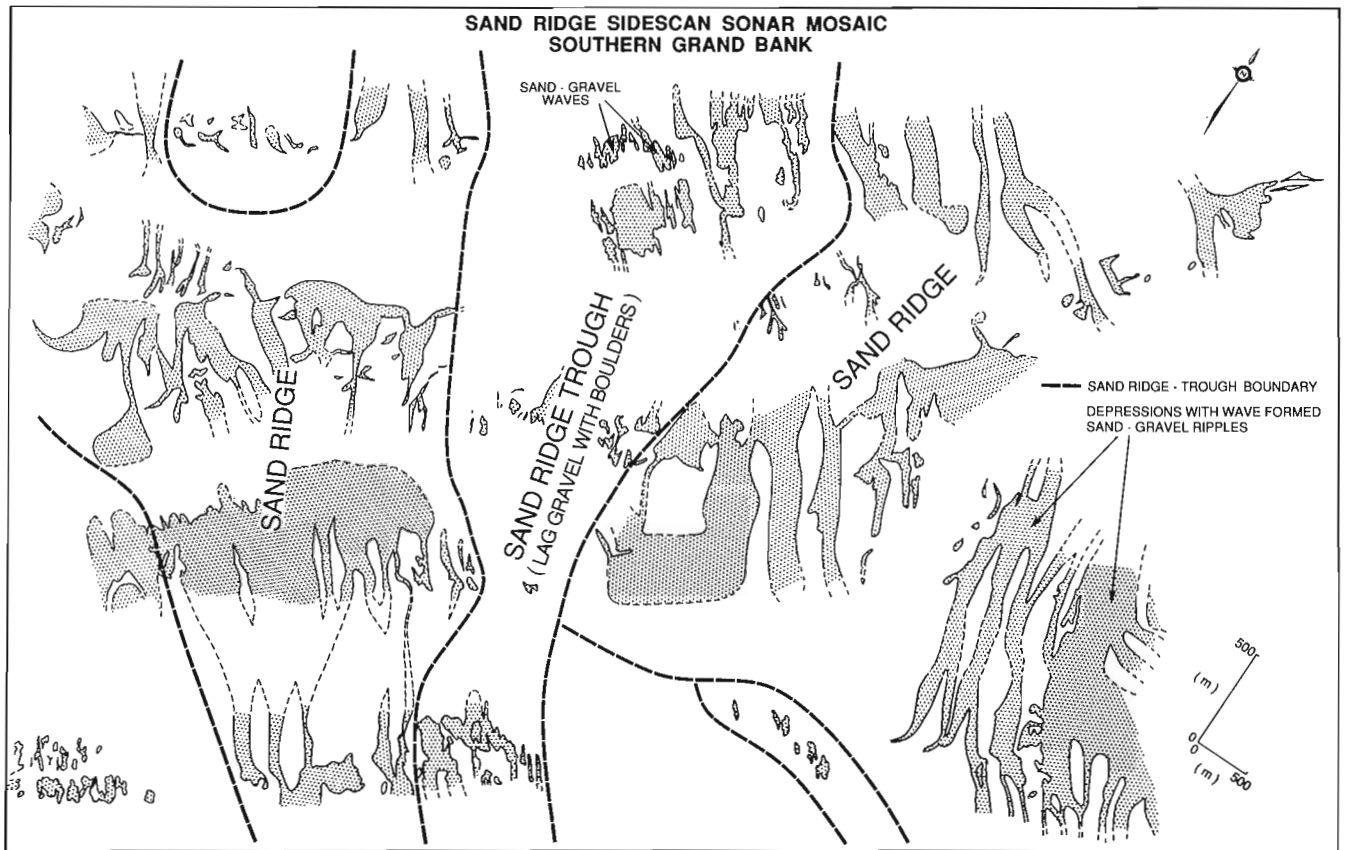


Figure 62.9. Sidescan sonar mosaic of an area of the southern Grand Bank sand ridge field investigated with the *Pisces IV* submersible. The orientation of the sand ridges could not be determined from the mosaic because of their large size, wavelengths up to 4 km. Note the sinuous pattern on the upper sand ridge surfaces of incised wave-formed rippled areas, and the boulder strewn gravel lag areas between ridges.

appear as curvilinear features of extreme complexity and range in width from a few metres to over 1 km. The wave-formed ripples within the depressions generally tend to be straight crested but bifurcate occasionally. Similar, channel-like depressions containing large sand ripples have been reported in water depths up to 65 m along the continental shelf off California (Cacchione et al., 1984). They interpreted the channel-like depressions to form under storm-generated bottom currents associated with coastal downwelling and the large straight-crested ripples to form by large-amplitude, long-period surface waves generated by winter storms. Samples and submersible observations of the wave-formed ripples indicate that they are composed of both gravel and sand-sized material. The coarser sediment, including shell debris, is often preferentially accumulated in the troughs of the wave-formed ripples (Fig. 62.8). These incised zones (Fader and King, 1981) based on acoustic reflectivity measurements and limited sample control, together with low resolution sidescan sonograms, were previously interpreted as "shell beds". We now know this to be incorrect and that indeed the depressions are zones of wave-formed ripples. As to the origin, an interplay of currents and wave base is presently suspected to be responsible for their formation. The incised ripple fields may be similar to subaerial sand dune blowouts which are of common occurrence on land and may indicate a gradual degradation of the sand ridges with time.

Over most of the eastern survey area, the wave-formed ripples consist of a unidirectional pattern suggesting one storm or current event for their origin and the freshness of the sharp crests of the waves indicates recent formation. Toward the western part of the study area, two and in some cases three patterns can be seen superimposed.

Because of the large size of the sand ridges, their coalesced nature and the narrow swath width of the sidescan sonar systems, it is difficult to map the orientation of the sand ridge field. In addition the sand ridges must be isolated over lag gravels to define their edges. Figure 62.9 is an attempt to construct a sidescan sonar mosaic of the sand ridge field investigated with the *Pisces IV* submersible in the Tail of the Bank area.

Other bedforms such as linguoid ripples, sand waves, sand ribbons and two- and three-dimensional megaripples (Amos and King, 1984) are widespread across the area. Near the mouths of the many canyons which incise the shelf edge, fields of three-dimensional megaripples are found. They may form in response to increased currents as a result of the canyon topography.

South of the Hibernia area on northern Grand Bank, a unique pattern of W-shaped bedforms occur on gravel. They are defined on the sidescan sonograms by sand overlying gravel and may be isolated (Fig. 62.10) or connected (Fig. 62.11). They point southwest parallel to the Labrador current. On the higher resolution sidescan sonograms gravel waves occur within the W-shaped bedforms.

Shell beds

Isolated, circular to linear depressions of high acoustic reflectivity, occur on the Southeast Shoal area of Grand Bank (Fig. 62.6). They occur as isolated features, in small groups, in large groups, or as continuous or discontinuous linear patches (beaded) (Fig. 62.14). Epibenthic sled tows show that the features are composed of shells. Unfortunately, submersible observations were prevented by bad weather. The linear distributions, in some areas, may be controlled by low relief megaripples of sand which are in active transport across the seabed.

Iceberg related features

Iceberg furrows are rare on southern Grand Bank. This is in direct contrast to the Hibernia region (d'Apollonia and Lewis, 1981) where many occur at the seafloor and in the deeper Avalon Channel area (Fig. 62.15) where the seabed is entirely covered with furrows. The few that occur on southern Grand Bank are not clearly defined and are degraded. Figure 62.16 shows a large furrow at 46°34.22'N latitude and 52°48.0'W longitude with internal ribs normal to the iceberg furrow track. The internal ridges are interpreted to be formed by the rocking of a tabular iceberg and subsequent sediment molding, as it moved across the seabed.

During the submersible cruise, dives were planned at the Hibernia area over features termed iceberg pits (Fader and King, 1981; Fader et al., 1986; Barrie et al., 1986). Bad weather again precluded dives on the features, however, high quality sidescan images show the details of these features (Fig. 62.17). No pits were found in the southern study area. Interpretation of the lack of iceberg furrows in the southern area must be tempered by the fact that the large fields of sand ridges on the seabed may be mobile enough to obliterate evidence of iceberg furrows. However, the areas of exposed bedrock and gravel lag are free of iceberg furrows.

Extent of glaciation across the Grand Banks of Newfoundland

Earlier studies have postulated that glacier ice did not extend across the Grand Banks (Grant and King, 1984). King and Fader (1985) found evidence in Downing Basin and Whale Basin on the north central and southwestern Grand Banks, and Fader et al. (1982) on St. Pierre Bank and Placentia Bay to support an interpretation that Wisconsinan ice advanced at least to these areas. The problem of ice advance is complicated by the late Pleistocene-Holocene transgression of the Grand Banks which effectively eroded previously deposited evidence for glaciation (ie. glaciomarine sediments and tills).

The occurrence of a wide distribution of gravel including boulders distributed across the area, and the dominance of Avalonian lithologies within the gravel assemblage suggests a glacial rather than iceberg origin. The rounded shape of the boulders is due to the passage through a high energy beach zone of the transgressing sea, hence, glacial deposition before transgression. Seismic reflection profiles of the Tail of the Bank mud deposit show acoustic signatures similar to well-sampled sections of glaciomarine sediments and till from other areas of the bank (King and Fader, 1985) and suggest that ice extended across the Tail of the Bank area and deposited till and glaciomarine sediments beneath a floating ice shelf. Buried channels south of Hibernia and along the eastern flank of Grand Bank, are up to 300 m in depth and are infilled with sediments that have acoustic characteristics similar to sampled glaciomarine sections in Placentia Bay and Downing Basin. The absence of iceberg furrows across the southern Grand Banks and the absence of iceberg rafted boulders in the Tail of the Bank mud deposit supports a glacial origin for the coarse debris. Icerafted coarse sediments would tend to be regionally distributed. These characteristics of the southeastern Grand Banks support the interpretation that glacier ice did extend across the entire Grand Banks of Newfoundland and that this ice was probably of Wisconsinan age.

Sea level history

The depth of a late Pleistocene-Holocene low sea level stand is critical to the distribution of the surficial formations on the southeast Canadian continental shelf. For the

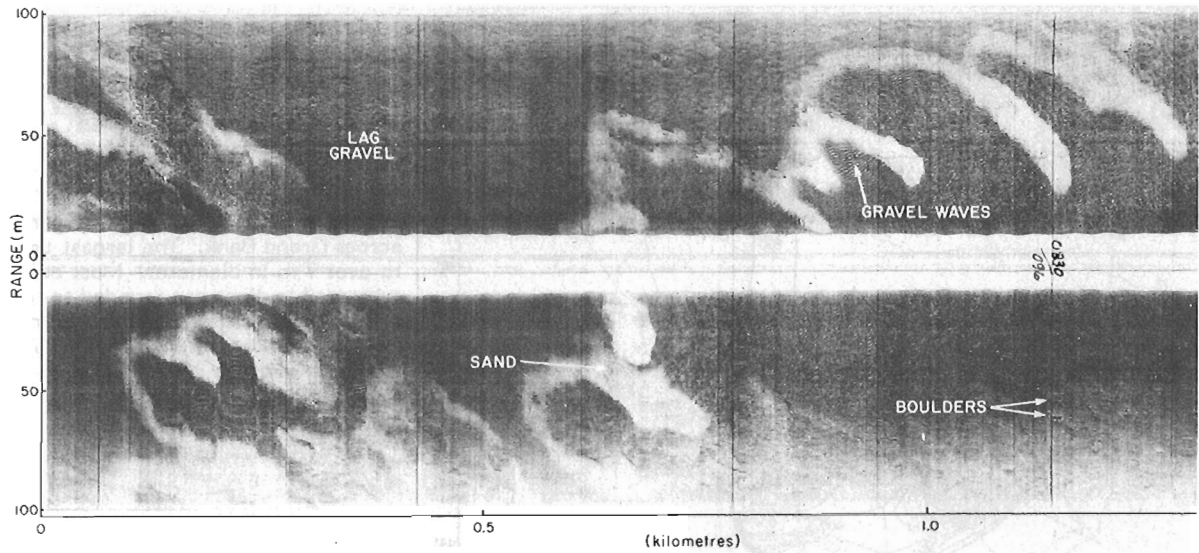


Figure 62.10. A Klein 100 kHz sidescan sonogram collected south of the Hibernia area of northern Grand Bank, showing bedforms termed "W" developed over a gravel surface. The "W" shaped features are defined by low reflectivity sand with gravel waves developed in the central areas of the "W"-shaped structures. They can occur isolated or connected together to form long chains (Fig. 62.11).

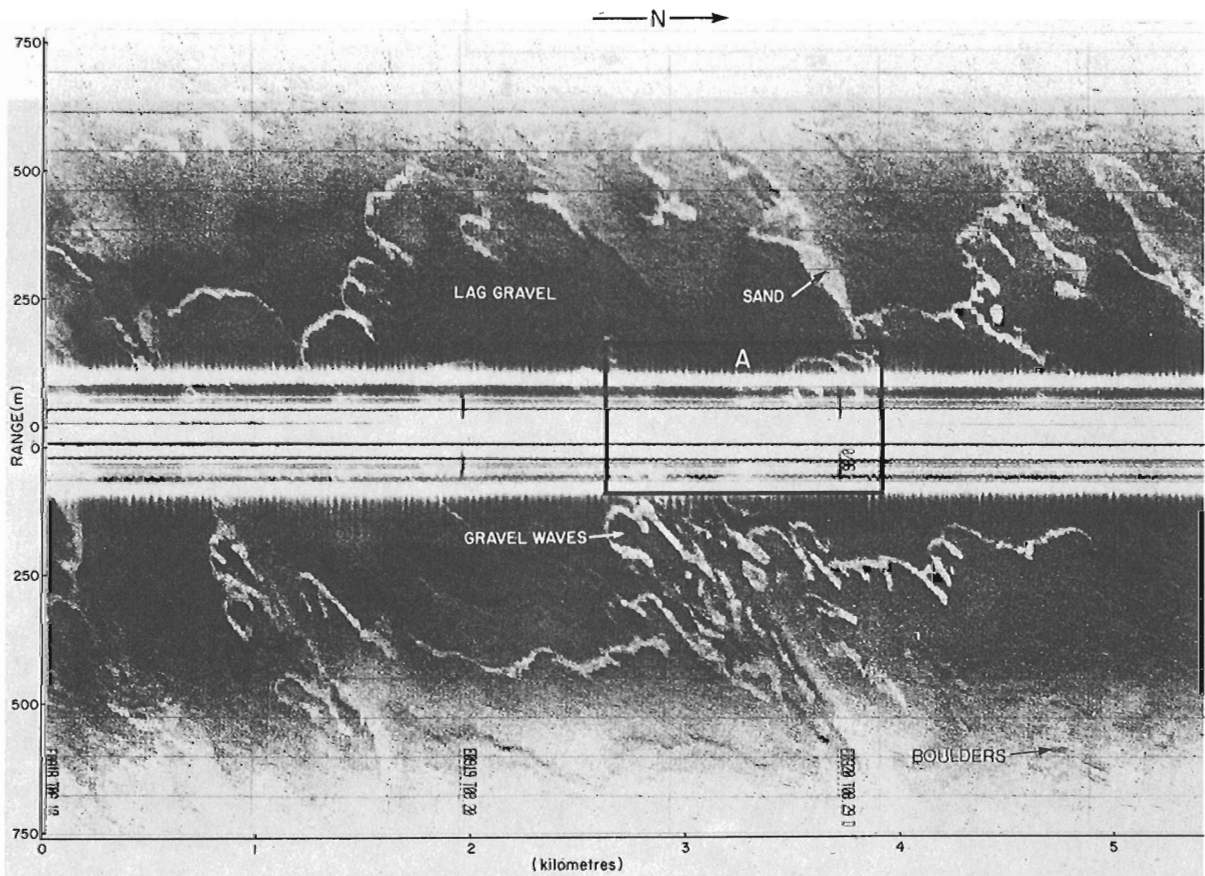


Figure 62.11. A 70 kHz sidescan sonogram of the area in Figure 62.10 showing the regional distribution of "W" shaped bedforms and surficial sediments in an area south of Hibernia, northern Grand Bank. The individual gravel waves seen in Figure 62.10 are not resolved on this sonogram.

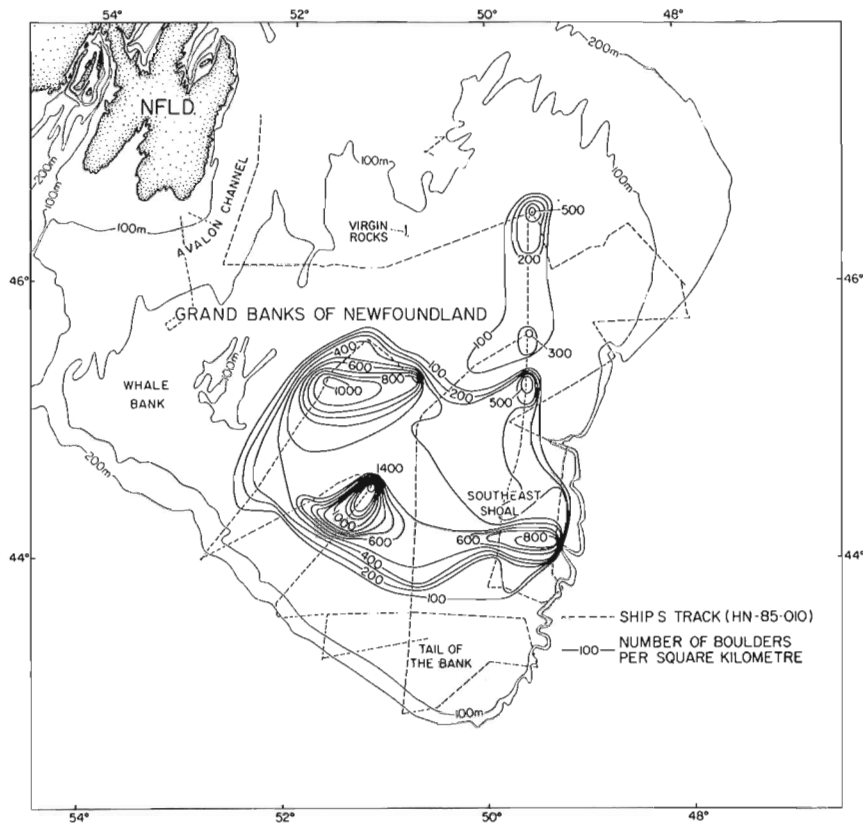


Figure 62.12

Distribution of boulders larger than 0.5 m across Grand Bank. The largest boulders range to over 7 m in diameter. Most observed on the submersible dives are rounded to subrounded in shape. This large population is interpreted to have been deposited largely by advancing glaciers across the Grand Banks of Newfoundland and not from ice rafting by icebergs.

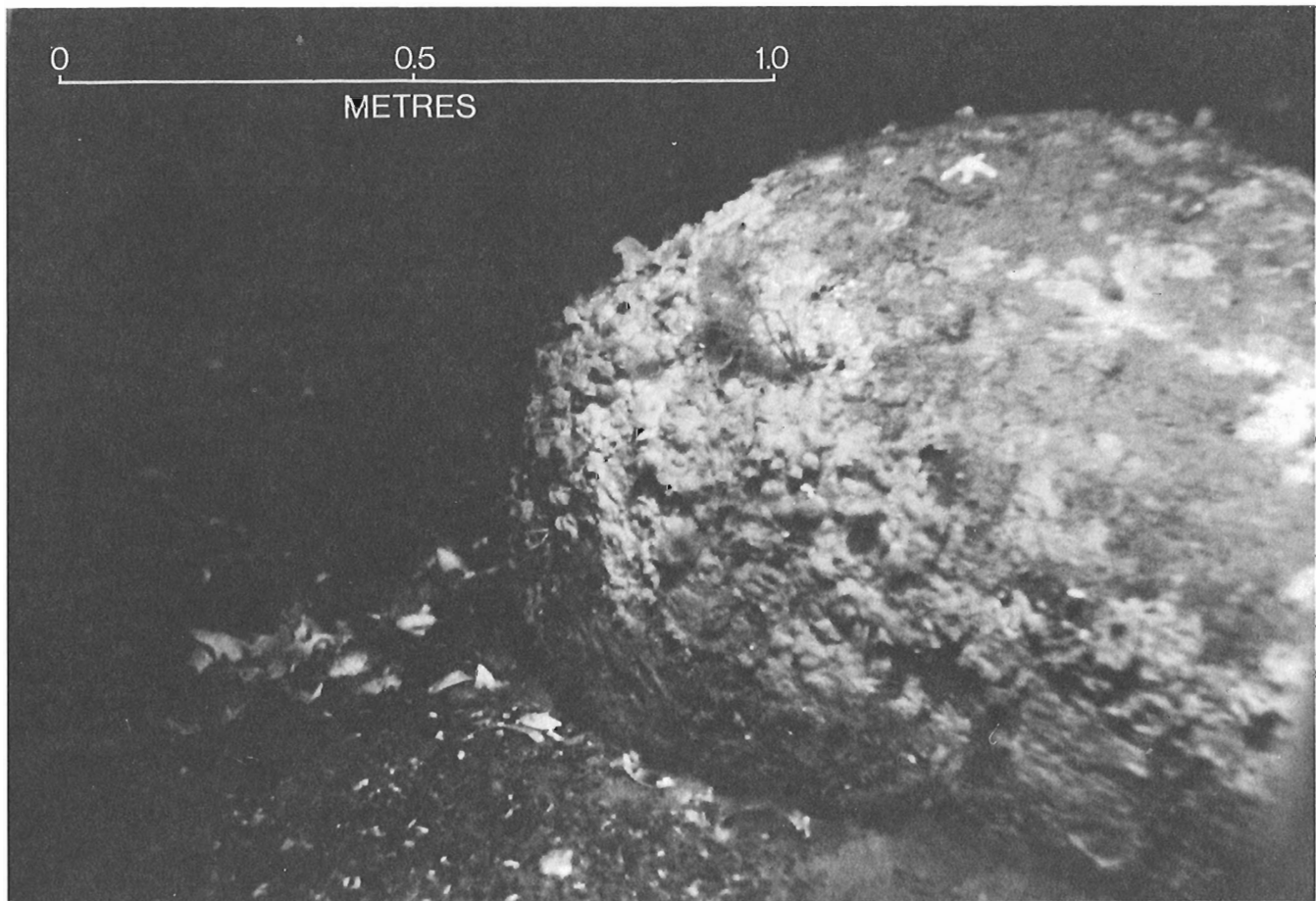


Figure 62.13. Bottom photograph of a large rounded boulder at the seabed, collected from the Pisces IV submersible in the southern area of Grand Bank. The lithology of the boulder population is difficult to determine because of the large amount of biogenic growth covering their surfaces.

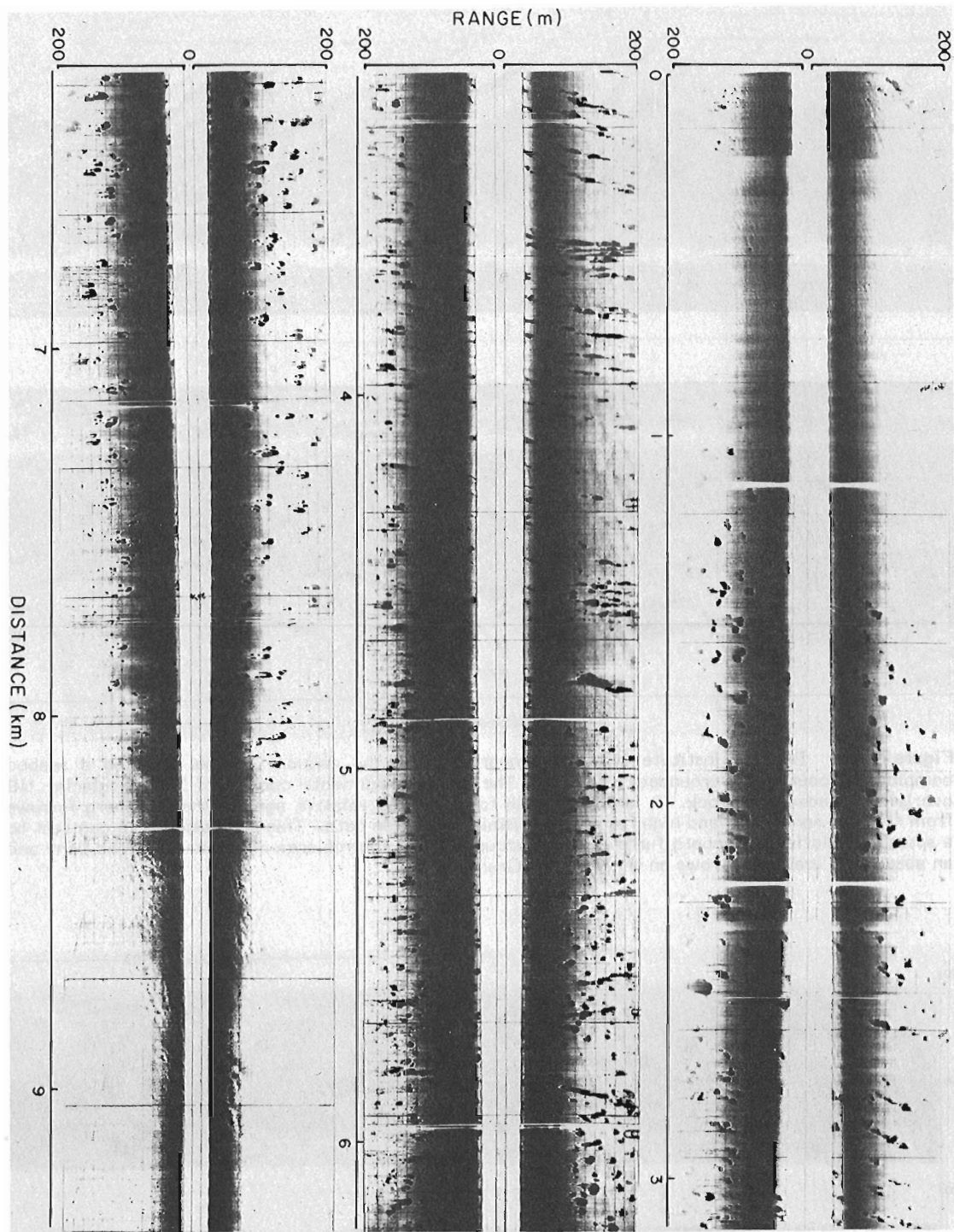


Figure 62.14. Sidescan sonogram (100 kHz Klein) across an area of "shell beds" from the Southeast Shoal area of Grand Bank. Note the wide variety in shapes and patterns of the patches (represented by dark areas of high acoustic reflectivity). The seafloor consists of sand-sized sediment.

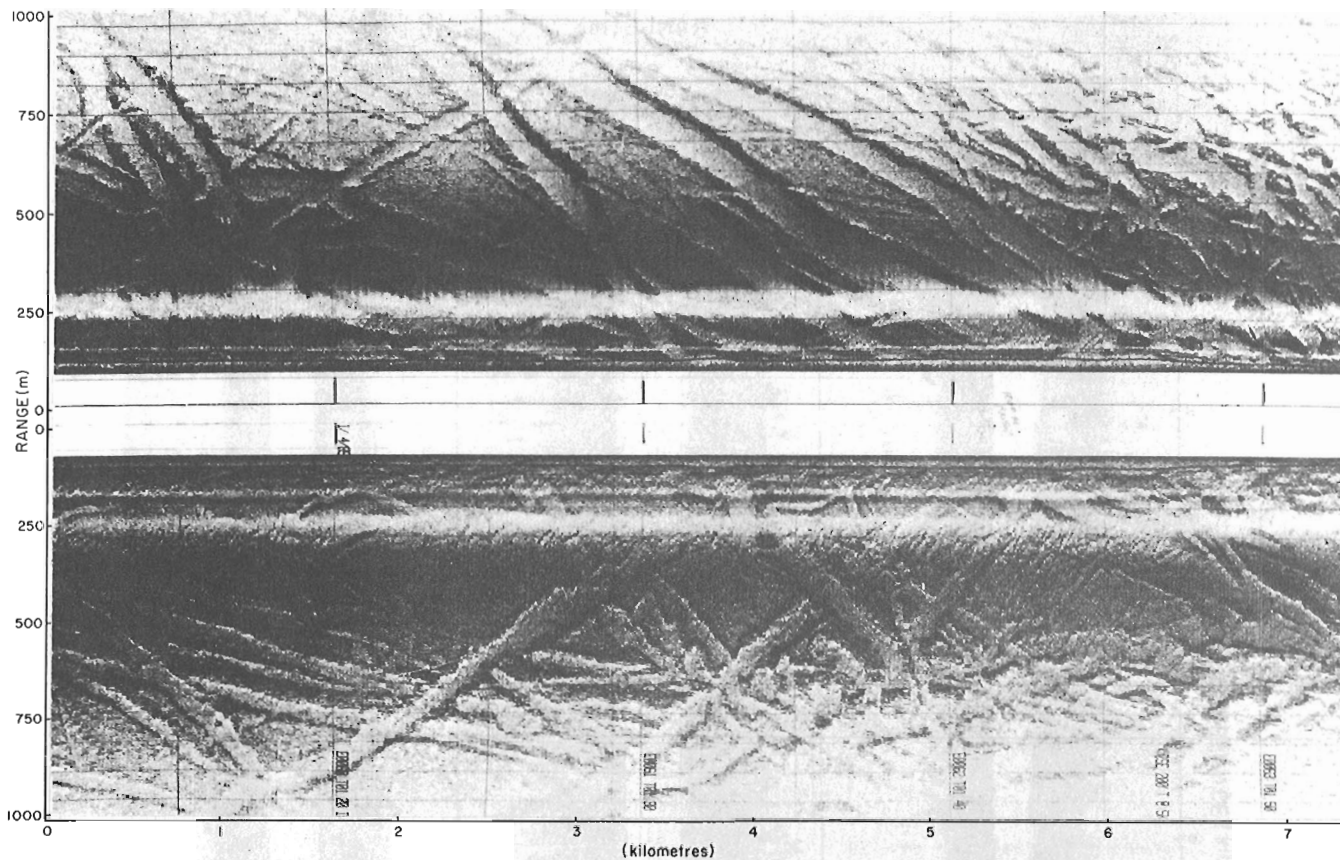


Figure 62.15. Bedford Institute (70 kHz) sonogram from the Avalon Channel showing a seabed completely scoured by grounded icebergs. The seabed sediments consist of 3 m of glacial till overlying Paleozoic bedrock. It is not possible to determine relative ages of these iceberg furrows from study of sonograms and high resolution seismic reflection data. This population is in contrast to a sparse population of iceberg furrows which occurs in the Hibernia area of northeast Grand Bank and an absence of iceberg furrows on the southern Grand Banks.

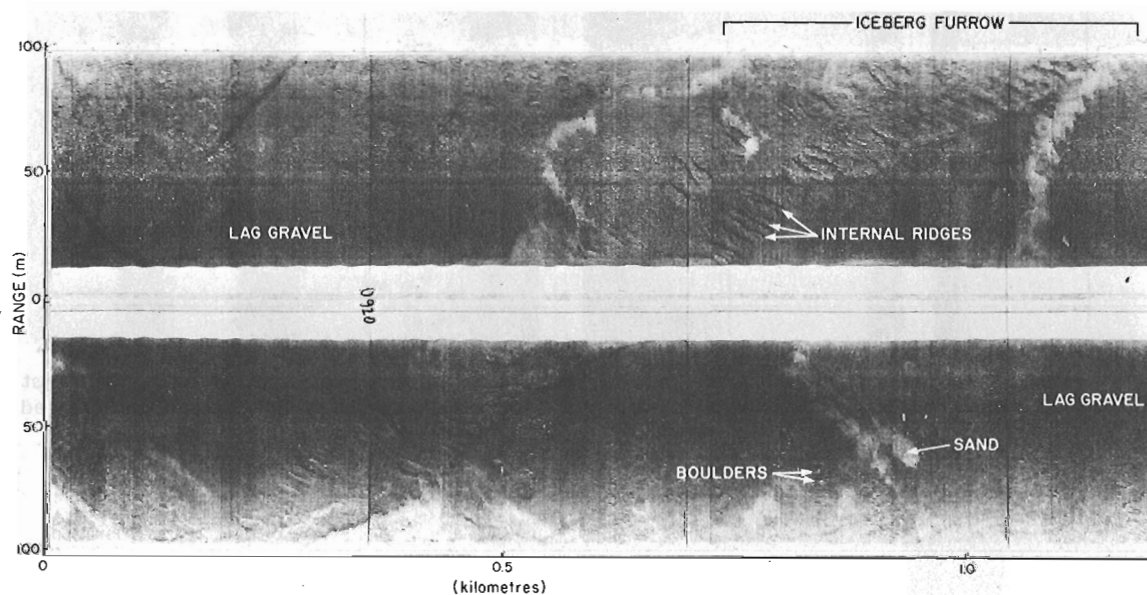


Figure 62.16. A 100 kHz Klein sidescan sonogram from northern Grand Bank showing a large iceberg furrow developed on Grand Banks Sand and Gravel. The internal ribs or ridges in the furrow, which resemble tractor tread imprints, are interpreted to be formed by the rocking motion of a grounded tabular iceberg and sediment molding.

adjacent Scotian Shelf this depth has been determined to occur at a present depth of 110-120 m (King and Fader, 1985). Above this depth previously deposited glacial sediments were eroded during the marine transgression and the basal transgressive sand and gravel formation was developed. As a result of late glacial rebound local variation in the depth of the low sea level stand occurs at the approaches to the Bay of Fundy (Fader et al., 1977) and in the offshore along the south coast of Newfoundland (Fader et al., 1982).

In the Hibernia area of Grand Bank, the depth of the low sea level stand occurred at approximately 100 m (Fader et al., 1986). It is difficult to define precisely the minimum sea level position because of the low gradients of the shelf in this area. In the Avalon Channel area and western Placentia Bay we interpret the low sea level stand at 90 m (Fader et al., 1982). This differential warping may result from the presence of late glacial ice on the adjacent land areas which delayed the rebound of the nearshore zone.

The Tail of the Bank mud deposit (Fig. 62.6) is a regionally continuous glaciomarine section of 30 m thickness, which occurs in water depths as shallow as 55 m along the entire southwestern edge of Grand Bank. If a post-glacial low stand of sea level occurred below the depth of occurrence of this section, it would be expected that it would largely be eroded in the subsequent transgressing sea, as is the case along the flanks of most of the bank areas of the Scotian Shelf (King and Fader, 1985). Its preservation in water depths as shallow as 55 m suggests that the sediments were not transgressed, and that the low sea level stand in this area is less. In order to account for the shallow distribution of these glacial sediments and the small amount of relative sea level lowering, we propose a large late glacial ice dome located on the southern Grand Banks area, as a mechanism for delaying isostatic rebound of the Tail of the Bank region. Cores through the glacial section collected on the Hudson 85-005 cruise will be analyzed to substantiate this hypothesis.

Acknowledgments

We thank the Captain, officers and crew of *CSS Hudson, M.V. Pandora II*, Chief Pilot Frank Chambers and pilots of the *Pisces IV* submersible, and the Atlantic Geoscience Centre Program Support technicians for their assistance and co-operation during field studies. The interpretation and compilation of the boulder distribution was undertaken by Heather Joyce. We also wish to thank C.L. Amos for helpful discussions on bedforms and classification. The submersible cruise was enhanced by the assistance and observations of P. Hale, COGLA and T. Lambert, Atlantic Oceanographic Laboratory. The manuscript was reviewed by D.J.W. Piper and G. Vilks.

References

Amos, C.L. and King, E.L.
1984: Bedforms of the Canadian eastern seaboard: a comparison with global occurrences; *Marine Geology*, v. 57, p. 167-208.

Barrie, J.V., Collins, W.T., Clarke, J.I., Lewis, C.F.M., and Parrott, D.R.
1986: Submersible observations and origin of an iceberg pit on the Grand Banks of Newfoundland; in *Current Research, Part A, Geological Survey of Canada, Paper 86-1A*, p. 251-258.

Cacchione, D.A., Drake, D.E., Grant, W.D., and Tate, G.B.
1984: Rippled scour depressions on the inner continental shelf off Central California; *Journal of Sedimentary Petrology*, v. 54, no. 4, p. 1280-1291.

d'Apollonia, S.J. and Lewis, C.F.M.
1981: Iceberg scour data maps for the Grand Banks of Newfoundland between 46°N and 48°N; *Geological Survey of Canada, Open File 819*, 13 p.

Fader, G.B.J. and King, L.H.
1981: A reconnaissance study of the surficial geology of the Grand Banks of Newfoundland; in *Current Research, Part A, Geological Survey of Canada, Paper 81-1A*, p. 45-56.

Fader, G.B.J., King, L.H., and Josenhans, H.J.
1982: Surficial geology of the Laurentian Channel and Western Grand Banks of Newfoundland; *Geological Survey of Canada, Paper 81-22*.

Fader, G.B.J., King, L.H., and MacLean, B.
1977: Surficial geology of the Eastern Gulf of Maine and Bay of Fundy; *Geological Survey of Canada, Paper 76-17*, 23 p.

Fader, G.B.J., Lewis, C.F.M., Barrie, J.V., Parrott, D.R., Collins, W., Miller, R.O., and d'Apollonia, S.
1986: Quaternary Geology of the Hibernia area of northeast Grand Bank; *Geological Survey of Canada, Open File 1222*.

Grant, D.R. and King, L.H.
1984: A stratigraphic framework for the Quaternary history of the Atlantic Provinces; in *Quaternary Stratigraphy of Canada - A Canadian Contribution to IGCP Project 24*, ed. R.J. Fulton; *Geological Survey of Canada, Paper 84-10*, p. 173-191.

Josenhans, H.J.
- Quaternary formations of the Labrador Shelf; *Lexicon of Canadian Stratigraphy, Volume 6, Atlantic Canada*, ed. G.L. Williams and J.A. Watt; *Canadian Society of Petroleum Geologists, Special Edition*. (in press)

King, L.H.
1970: Surficial geology of the Halifax-Sable Island map area; *Marine Sciences Branch, Paper 1*, Department of Energy, Mines and Resources, Ottawa, Ontario.

King, L.H. and Fader, G.B.J.
1985: Wisconsinan glaciation of the continental shelf, southeast Atlantic Canada; *Geological Survey of Canada, Open File 1126*.

King, L.H., Fader, G.B.J., Jenkins, W.A.M., and King, E.L.
- Occurrence and regional geological setting of Paleozoic rocks on the Grand Banks of Newfoundland; *Canadian Journal of Earth Sciences*. (in press)

King, L.H., Fader, G.B., Poole, W.H., and Wanless, R.K.
1985: Geological setting and age of the Flemish Cap Granodiorite, east of the Grand Banks of Newfoundland; *Canadian Journal of Earth Sciences*, v. 22, no. 9, p. 1286-1292.

Parrott, D.R., Dodds, D.J., King, L.H., and Simpkin, P.G.
1980: Measurement and evaluation of the acoustic reflectivity of the seafloor; *Canadian Journal of Earth Sciences*, v. 17, no. 6, p. 722-737.

Bedrock and surficial geology of Cumberland Sound, N.W.T.

Project 760015

B. MacLean, G.L. Williams, A. Jennings¹, and C. Blakeney
Atlantic Geoscience Centre, Dartmouth

MacLean, B., Williams, G.L., Jennings, A., and Blakeney, C., Bedrock and surficial geology of Cumberland Sound, N.W.T.; in Current Research, Part B, Geological Survey of Canada, Paper 86-1B, p. 605-615, 1986.

Abstract

The southwestern half and inner parts of Cumberland Sound are underlain by Precambrian rocks whereas the outer part is underlain by Ordovician carbonates which extend northwestward for 70 km. Cretaceous (Barremian-Cenomanian) semi-consolidated mudstones and siltstones underlie the northeastern half of Cumberland Sound. Palynomorph assemblages indicate deposition of the Cretaceous strata occurred in a nonmarine to marginal marine environment.

Cumberland Sound is a graben that appears to have been active subsequent to Barremian-Cenomanian time and possibly earlier.

The main accumulation of surficial sediments is in the outer half of the northeastern side of the sound. The sequence, 25-50 m thick, includes both unstratified and stratified sediments. Surficial sediments in southwestern and inner parts of the sound form a thin (<1-2 m) discontinuous cover over rough Precambrian rocks and comprise lag gravels and sands.

Résumé

La moitié sud-ouest et des parties intérieures du détroit de Cumberland sont formées de roches précambriennes, alors que la partie extérieure repose sur des carbonates de l'ordovicien qui s'étendent vers le nord-ouest sur une distance de 70 km. Des mudstone et des siltstone semi-consolidés du Crétacé (Barrémien-Cénomaniens) se trouvent sous la moitié nord-est du détroit. Des assemblages palynomorphes indiquent que le dépôt des strates du Crétacé s'est fait dans un milieu variant de continental à marin marginal.

La détroit de Cumberland est un fossé qui semble avoir été actif après le Barrémien-Cénomaniens et peut-être même avant.

La principale accumulation de sédiments superficiels se trouve dans la moitié extérieure, du côté nord-est du détroit. La séquence qui, à cet endroit, a une épaisseur de 25 à 50 m comprend des sédiments à la fois non stratifiés et stratifiés. Les sédiments superficiels des parties sud-ouest et intérieure du détroit forment une couverture discontinue (inférieure à 1 à 2 m) qui couvrent des roches rugueuses du Précambrien et comprend des résidus de déflexion graveleux et sableux.

¹ Institute of Arctic and Alpine Research, University of Colorado, Boulder, Colorado

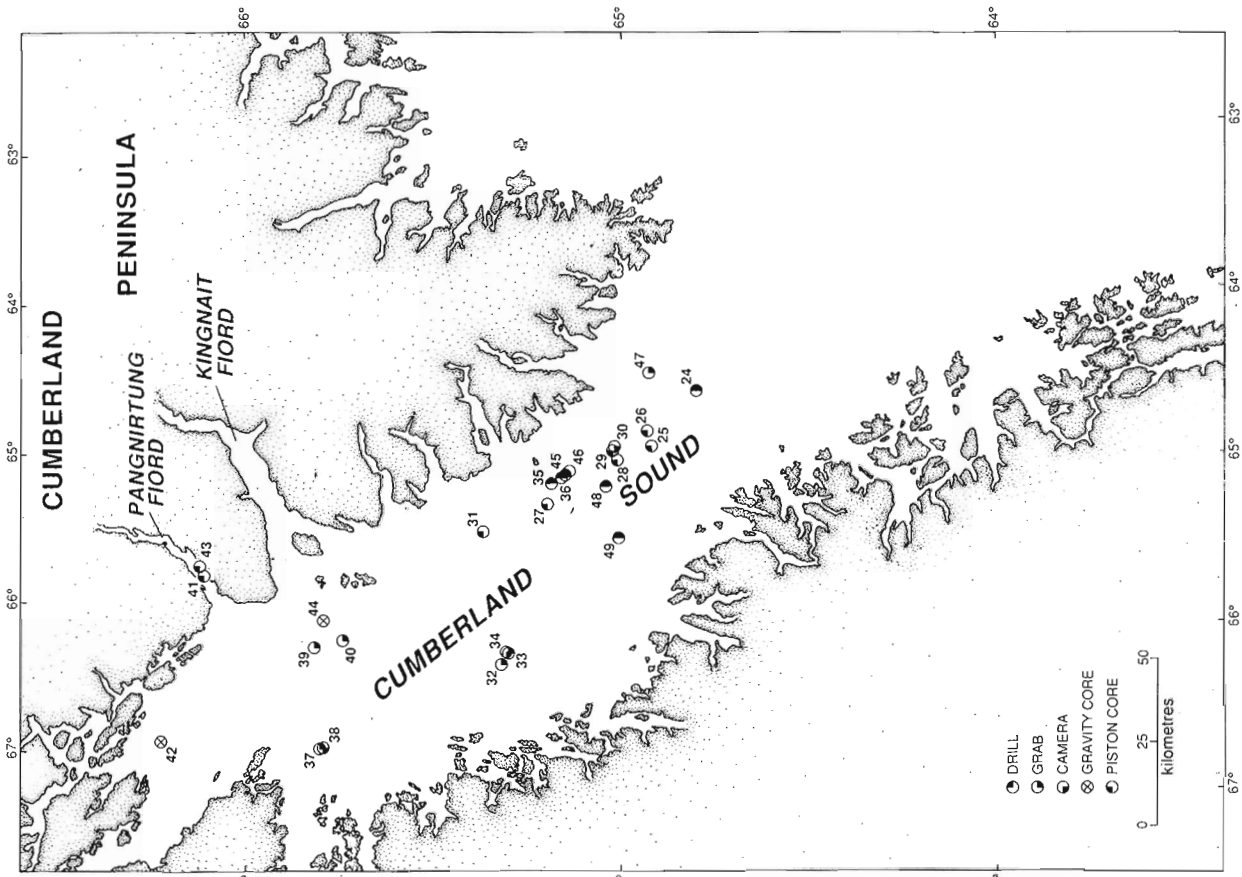


Figure 63.2. Sample station locations.

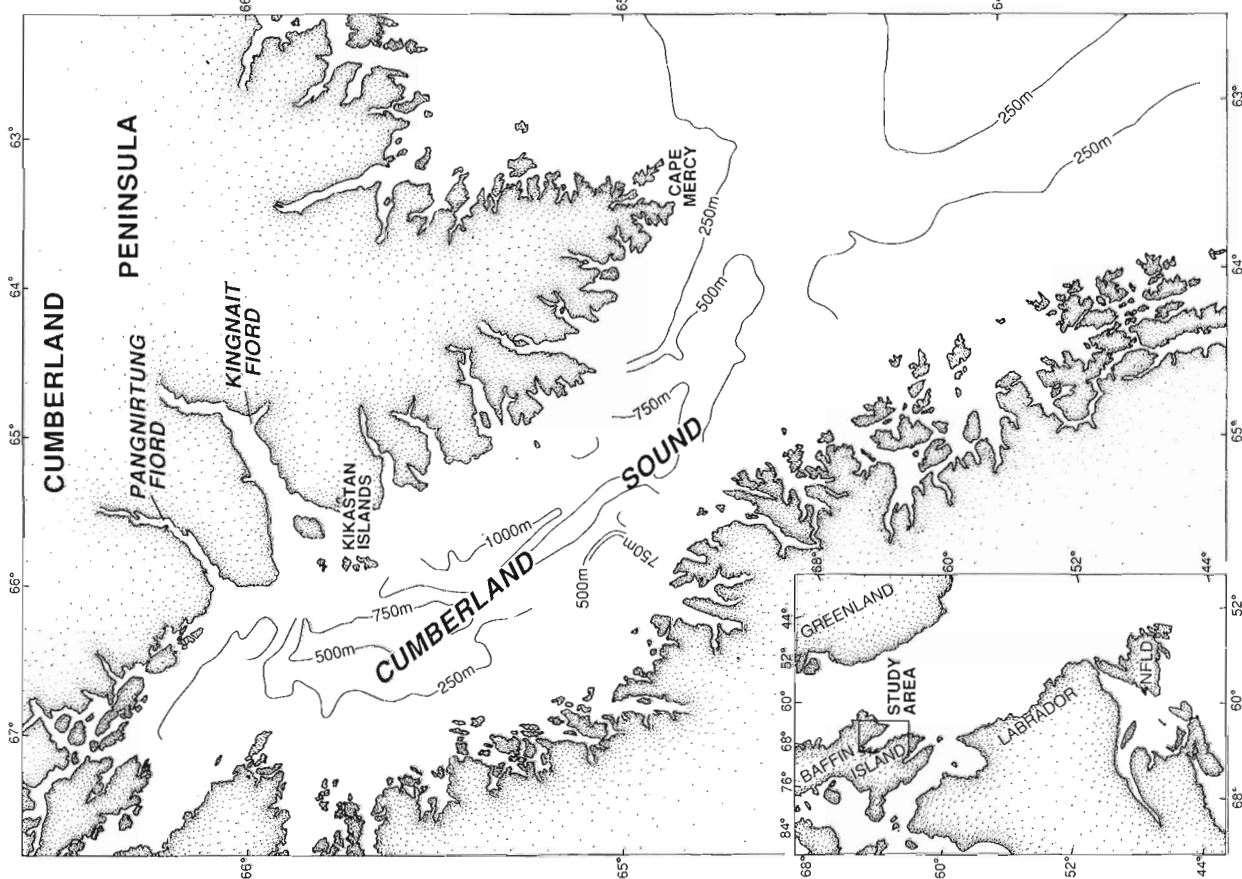


Figure 63.1. Generalized bathymetry in Cumberland Sound.

Introduction

The Cumberland Sound phase of CSS Hudson cruise 85-027 was carried out from 2 to 10 October 1985. The major objectives were to delineate the areal extent of the bedrock and surficial units and to obtain lithostratigraphic, biostratigraphic, and physical property data.

Cumberland Sound forms a major embayment, 280 km long by 70 km wide, in southeastern Baffin Island (Fig. 63.1). It is bounded by the Precambrian rocks of Cumberland

Peninsula to the north and Hall Peninsula to the south. The onshore topography ranges up to 1830 m with the highest elevation being on Cumberland Peninsula, which supports the Penny Ice Cap, several smaller ice caps, and numerous cirque and valley glaciers. The coast of Cumberland Sound is cut by deep fiords particularly along the southwest shore of Cumberland Peninsula. The largest of these fiords, Kingnait and Panqnirtung, are 83 km and 33 km long, respectively. There are numerous small islands and emergent rocks along the inner southwest margin and at the head of the sound (Canadian Hydrographic Chart 7051).

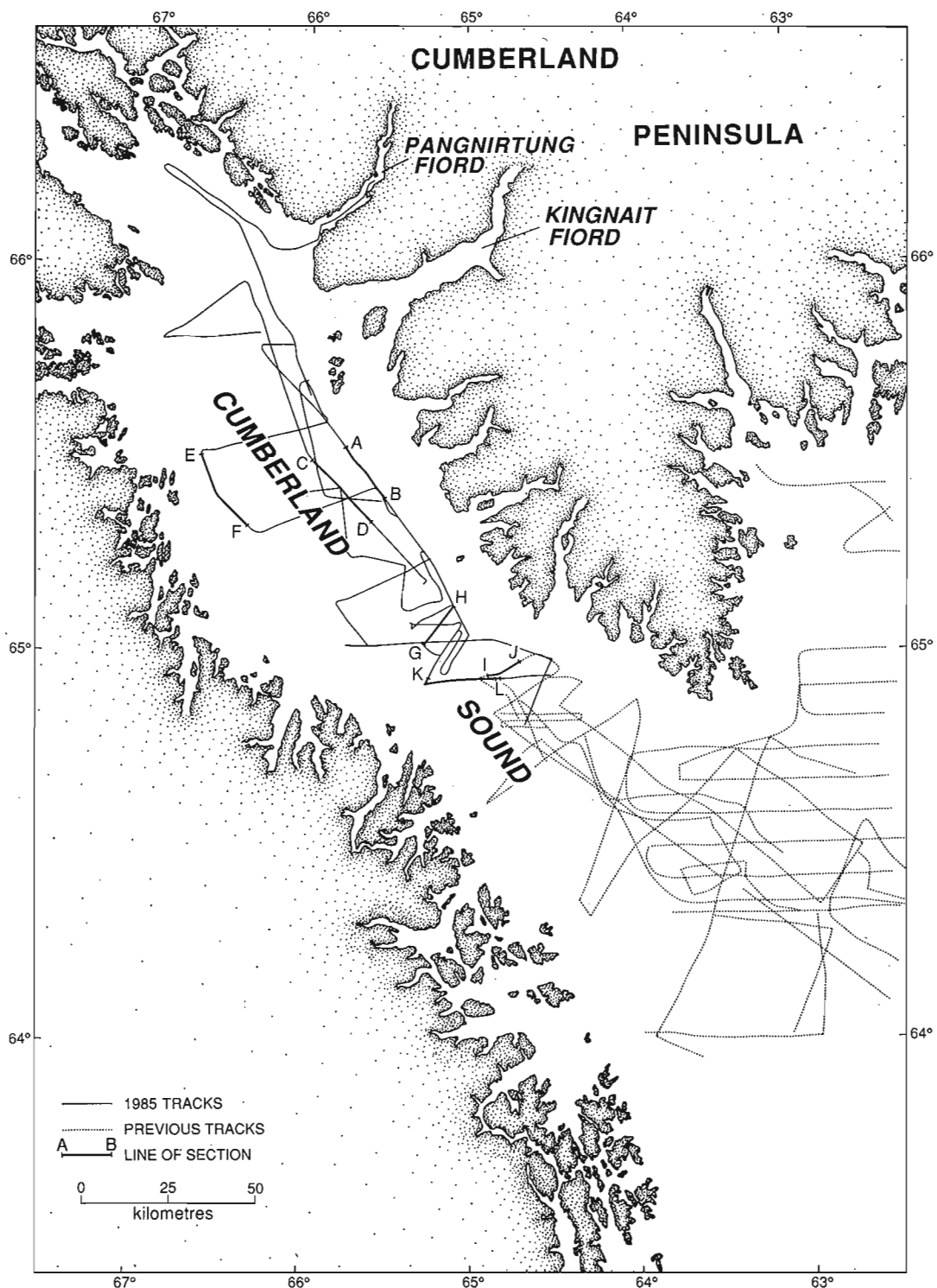


Figure 63.3. Survey tracks, cruise 85-027 and previous. Locations of profile sections are indicated.

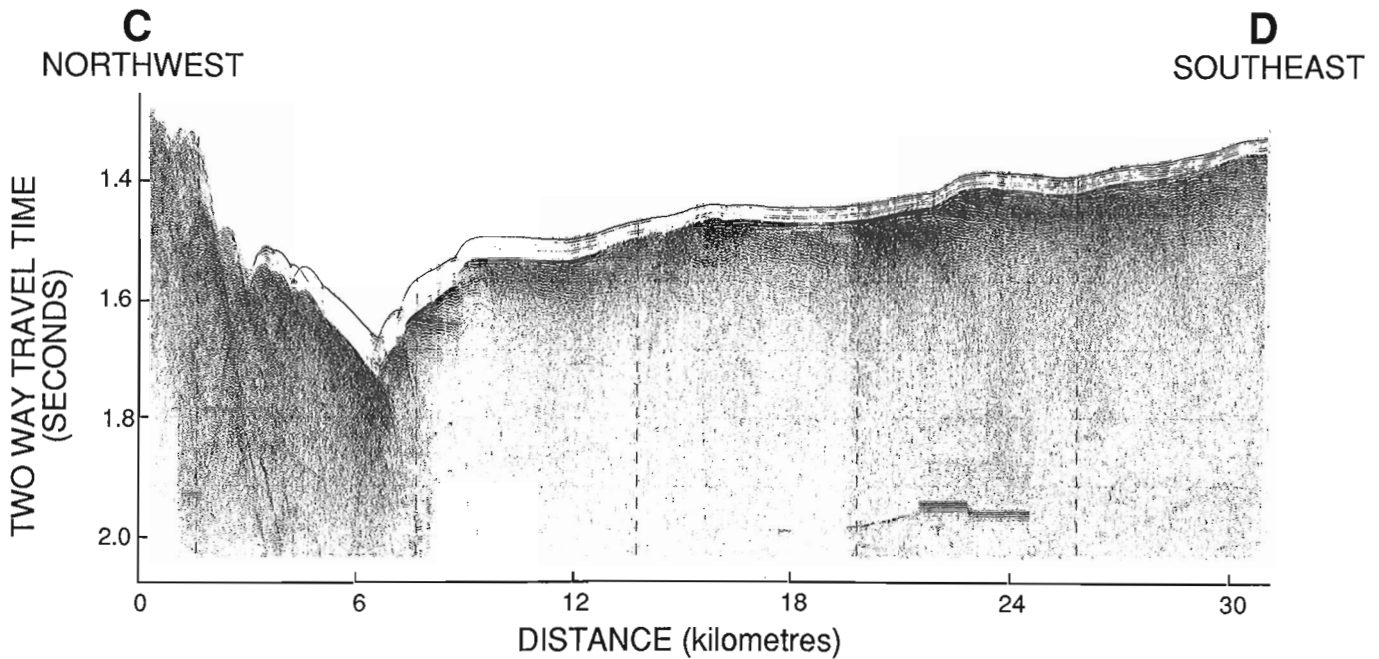


Figure 63.4. Section C-D: Seismic reflection profile illustrating gently dipping Cretaceous strata in probable fault contact with Precambrian rocks. A relict erosional "marginal channel" is developed at the contact. Up to 30 m of mainly stratified surficial sediments mantle the bedrock (see Fig. 63.3 for section location).

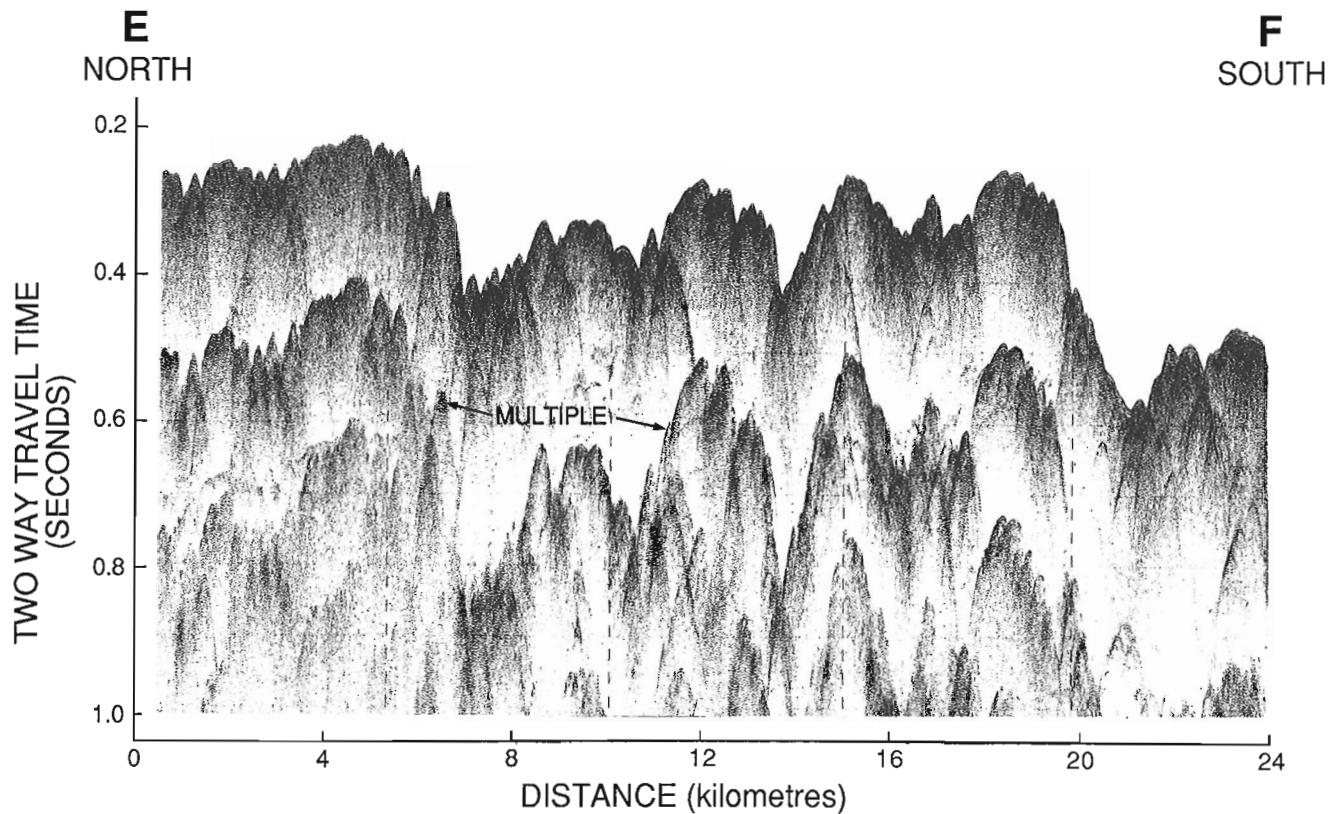


Figure 63.5. Section E-F: Seismic reflection profile across Precambrian rocks on the southwest side of Cumberland Sound; this illustrates the irregular topography associated with occurrences of these rocks and the absence of significant overburden (see Fig. 63.3 for section location).

Survey methods

The on board program included the collection of geophysical data and bedrock and sediment samples (Fig. 63.2, 63.3). Geophysical data were obtained using a single channel seismic reflection system (655 cm³ compressed air source), Hunttec high resolution deep tow seismic system, Bedford Institute of Oceanography sidescan, and Varian magnetometer. Bedrock cores in Cumberland Sound were obtained by means of the Bedford Institute of Oceanography rock core drill which can penetrate up to 9 m into the seafloor. Acoustic information was obtained using: a Nova Scotia Research Foundation 6 m hydrophone; a SE 30 m hydrophone; and Hunttec fitted with an internal hydrophone and a towed streamer. These systems provided good delineation of the near surface bedrock and overlying sediments. Such data were also the basis for locating drill sites. Surficial sediments were sampled principally by Benthos piston corer with 1360 kg head and by IKU clam shell sampler. UMEL cameras were used for seabottom topography at selected stations.

Navigational positioning was by the Bedford Institute navigational system BIONAV – which integrated data from rho-rho Loran C, Satellite Navigation, and log and gyro, and by radar.

Previous studies

Onshore

Precambrian metamorphic rocks form the onshore bedrock surrounding Cumberland Sound. The composition and distribution of these rocks have been reported by Riley (1960), Blackadar (1967), and Jackson and Taylor (1972).

Dyke et al. (1982) mapped the surficial materials of Cumberland Peninsula. The deposits include: till, felsenmere, raised marine deposits (mainly deltaic), lacustrine sediments, alluvium, and colluvium.

The land areas surrounding Cumberland Sound appear to have been glaciated at various times during the Quaternary: by the Laurentide ice sheet flowing eastward from Foxe Basin; by an expanded Penny Ice Cap; by local fiord and valley glaciers emanating from cirques (Dyke, 1977; Dyke et al., 1982); and possibly by local ice caps on Hall Peninsula (Miller, 1985b).

The late Foxe glacial maximum is marked by the Ranger Moraine which lies at the head of Cumberland Sound (Dyke, 1977; Miller, 1985b). It correlates with the Frobisher Bay Moraine of Hall Peninsula (Blake, 1966; Miller, 1985b).

Offshore

Aeromagnetometer surveys have shown that Cumberland Sound is a graben containing in excess of 8 km of sediments (Hood and Bower, 1975). Grant (1975), from seismic reflection and magnetometer data in the outer part of the sound, postulated the presence of Paleozoic-Mesozoic sedimentary rocks. MacLean and Williams (1983) on the basis of core material and seismic reflection data concluded that the stratigraphic section included

rocks of Aptian-Cenomanian age. MacLean et al. (1982) outlined the occurrence of Lower Cretaceous and lower Tertiary strata on the shelf seaward of Cumberland Sound.

Bathymetry

The general trend of bathymetric features is approximately parallel to the axis of Cumberland Sound (Fig. 63.1). Water depths are greatest in the northeastern half where they exceed 1100 m. The seafloor in that area is fairly smooth and consists of sedimentary rocks and unconsolidated sediments (Fig. 63.4). This contrasts with the highly irregular seafloor morphology in the southwestern and inner parts of the sound which are underlain by Precambrian metamorphic rocks (Fig. 63.5). The bathymetry is generally uncharted in a 15 km wide zone adjacent to the coast, thus the shoreward limit of deep water along the northeast side of the sound has been established only in a few localities which lie in the outer part. There the transition from deep to shallower depths is abrupt and spatial relationships suggest that a similar condition probably prevails along most of the northeast side of the sound. Though bathymetry on the southwest side of the sound is highly irregular, shallowing appears to be more gradual.

The lack of bathymetric data in the zone adjacent to the coast constrained the geological survey, particularly the definition of bedrock and surficial sediment boundaries and structural relationships on the northeast side.

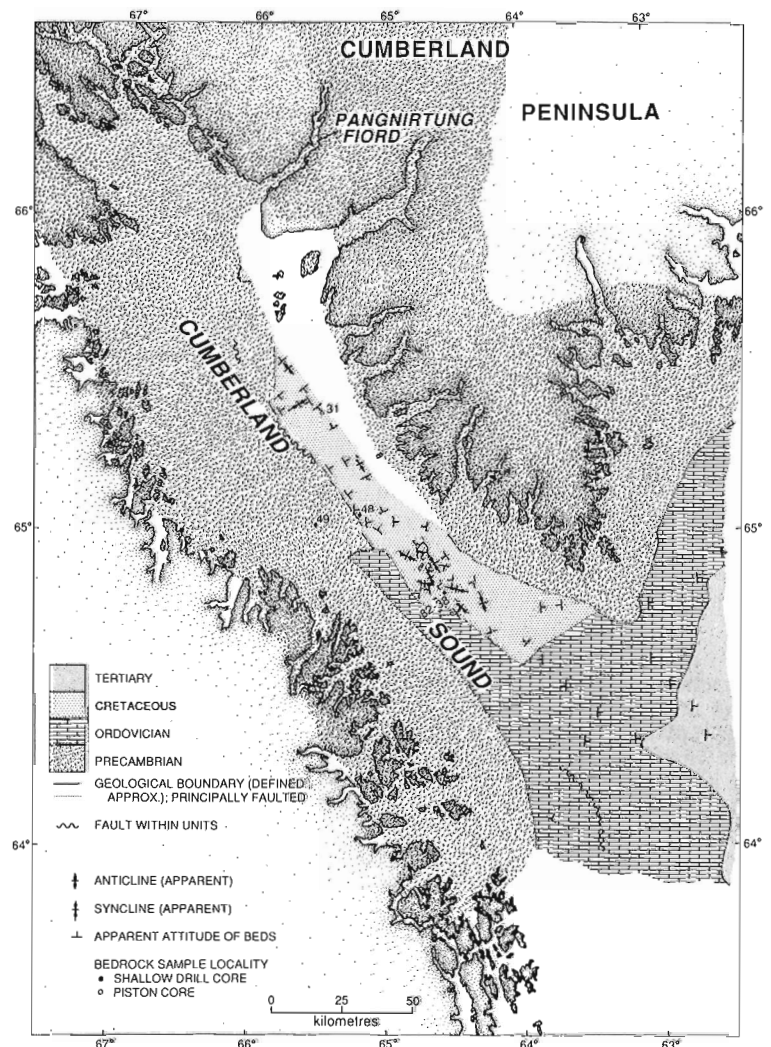


Figure 63.6

Bedrock geology of Cumberland Sound.

Bedrock geology

Precambrian metamorphic and granitic rocks that surround Cumberland Sound and form most of eastern Baffin Island (Riley, 1960; Blackadar, 1967; Jackson and Taylor, 1972) make up the bedrock beneath the southwestern half and inner part of the sound (Fig. 63.6). Seabed morphology across these areas is highly irregular (Fig. 63.5), a characteristic typical of Precambrian rocks on the inner part of the Baffin Island shelf. Where sampled at station 49 (Fig. 63.2, 63.6, Table 63.1), these rocks consisted of hornblende-pyroxene gneiss. Usually the Precambrian rocks in Cumberland Sound are either covered by less than 1-2 m of surficial sediments or are bare.

Sedimentary rocks interpreted to be Ordovician carbonates on the basis of their seismic character form the bedrock at the mouth of the sound. They extend northwestward in a 10-15 km wide band for 70 km along the southwest part of Cumberland Sound. They are in apparent fault contact with adjacent rocks (Fig. 63.7). Ordovician rocks underlie much of the southeast Baffin shelf between Cumberland Sound and Frobisher Bay and have been sampled at five localities (MacLean et al., 1977; MacLean and Falconer, 1979). These rocks are interpreted to extend northward along the shelf to the vicinity of Cape Dyer and possibly farther (Grant, 1975; MacLean et al., 1982).

Cretaceous (Barremian-Cenomanian) sedimentary rocks underlie the northeastern half of the sound. The age assignment is based mainly on spores and sparse dinoflagellates in samples from three localities (Fig. 63.2). The shallow drill core sample from station 48 (Fig. 63.6, 63.8, Table 63.1) consists of semi-consolidated mudstone and contains Barremian-Aptian palynomorphs. Lithologically it is similar to Aptian-Cenomanian sediments obtained 40 km to the southeast in core 82-034-38 (MacLean and Williams, 1983). Further confirmation of an early Cretaceous age was obtained at station 31 (Fig. 63.6, Table 63.1) where a benthos piston core cutter recovered black friable siltstone and mudstone. Palynomorphs in this core indicate that it is similar in age to the strata sampled at station 48, and suggest that these strata are terrestrial to marginal marine in origin. Throughout the area these rocks display a consistent acoustic signature, with penetration being substantially greater than that associated with the Paleozoic rocks.

The stratigraphic and structural characteristics of the Cretaceous rocks are illustrated in Figures 63.4, 63.7-63.9. The strata have been folded and faulted and extensively bevelled by erosion. In places (e.g. Fig. 63.4) a relict marginal channel exists at the contact between Precambrian and Cretaceous rocks. Boundary relations as seen on the seismic profiles suggest that these rocks are in fault contact. Low relief of Precambrian rocks adjacent to the contact (Fig. 63.4) suggests that they too have been faulted.

The Precambrian-Cretaceous contact on the northeast side of Cumberland Sound has not been established, as it lies in uncharted waters. In the outer part of the sound, where some soundings are available, the contact is coincidental with an abrupt transition from deep to shallow water. The narrow zone in which the transition must occur (both geologically and bathymetrically) along most of the northeast side of the sound suggests that the change is equally abrupt. This contact is interpreted to be a fault scarp.

Cumberland Sound thus appears to be a graben that has been active subsequent to Barremian-Cenomanian time. The presence of Ordovician rocks in Cumberland Sound suggests that pre-Barremian structural displacement may also have occurred. The post-Cenomanian faulting in the sound appears to be consistent with the time of rifting proposed in seafloor spreading models for northern Labrador Sea - Davis Strait - Baffin Bay (McMillan, 1973; Srivastava et al., 1981).

Table 63.1. Listing of samples from Cumberland Sound.

STATION NUMBER	SAMPLE TYPE	JULIAN DAY/TIME	LATITUDE	LONGITUDE	DEPTH (MTRS)	GEOGRAPHIC LOCATION	NOTES
24	DRILL	2751952	64 49.23N	64 37.03W	750	CUMBERLAND SOUND	BIO DRILL. NO SAMPLE.
24-G	GRAB/DRL	2751952	64 49.23N	64 37.03W	750	CUMBERLAND SOUND	GRAB SAMPLE TAKEN FROM THE LEG OF THE DRILL.
25	CORE	2752349	64 56.43N	64 57.78W	823	CUMBERLAND SOUND	PISTON CORE. LENGTH: 630 CM.
26	CORE	2760104	64 57.16N	64 52.19W	816	CUMBERLAND SOUND	PISTON CORE. LENGTH: 860 CM.
27	CORE	2761557	65 13.44N	65 21.22W	896	CUMBERLAND SOUND	PISTON CORE. LENGTH: 1150 CM.
28	CORE	2761744	65 01.88N	65 03.36W	850	CUMBERLAND SOUND	PISTON CORE. LENGTH: 1020 CM.
29	CORE	2761908	65 02.57N	64 59.51W	814	CUMBERLAND SOUND	PISTON CORE. LENGTH: 1140 CM.
30	CAMERA	2762015	65 02.35N	64 58.66W	823	CUMBERLAND SOUND	UMEL UNDERWATER CAMERA.
31	CORE	2772028	65 26.46N	65 30.82W	896	CUMBERLAND SOUND	PISTON CORE. LENGTH: 800 CM.
32	GRAB	2772305	65 19.98N	66 22.29W	350	CUMBERLAND SOUND	IKU GRAB.
33	GRAB	2780008	65 19.22N	66 17.13W	95	CUMBERLAND SOUND	IKU GRAB.
34	CAMERA	2780026	65 19.39N	66 16.81W	66	CUMBERLAND SOUND	UMEL UNDERWATER CAMERA.
35	DRILL	2781457	65 12.37N	65 12.06W	823	CUMBERLAND SOUND	BIO DRILL. NO SAMPLE.
35-G	GRAB/DRL	2781457	65 12.37N	65 12.06W	823	CUMBERLAND SOUND	GRAB SAMPLE TAKEN FROM THE LEG OF THE DRILL.
36	DRILL	2781908	65 10.32N	65 08.93W	845	CUMBERLAND SOUND	BIO DRILL. NO SAMPLE.
36-G	GRAB/DRL	2781908	65 10.32N	65 08.93W	845	CUMBERLAND SOUND	GRAB SAMPLE TAKEN FROM THE LEG OF THE DRILL.
37	GRAB	2791431	65 48.94N	66 56.01W	147	CUMBERLAND SOUND	IKU GRAB.
38	CAMERA	2791510	65 48.30N	66 55.67W		CUMBERLAND SOUND	UMEL UNDERWATER CAMERA.
39	GRAB	2791742	65 50.21N	66 16.21W	760	CUMBERLAND SOUND	IKU GRAB.
40	GRAB	2791903	65 45.57N	66 13.30W	680	CUMBERLAND SOUND	IKU GRAB.
41	CORE	2801453	66 08.31N	65 48.55W	165	PANGNIRTUNG FIORD	PISTON CORE. LENGTH: 930 CM.
42	CORE	2800829	66 14.36N	66 54.77W	310	CUMBERLAND SOUND	GRAVITY CORE. LENGTH: 151 CM.
43	CORE	2801649	66 08.28N	65 48.40W	165	PANGNIRTUNG FIORD	PISTON CORE. LENGTH: 600 CM.
44	CORE	2810422	65 48.75N	66 05.92W	1024	CUMBERLAND SOUND	GRAVITY CORE. LENGTH: 158 CM.
45	DRILL	2811446	65 10.79N	65 09.92W	845	CUMBERLAND SOUND	BIO DRILL. LENGTH: 24 CM. OF GNEISS.
45-G	GRAB/DRL	2811446	65 10.79N	65 09.92W	845	CUMBERLAND SOUND	GRAB SAMPLE TAKEN FROM THE LEG OF THE DRILL.
46	CORE	2812113	65 10.82N	65 09.93W	845	CUMBERLAND SOUND	PISTON CORE. LENGTH: 492 CM.
47	GRAB	2812341	64 56.82N	64 30.23W	475	CUMBERLAND SOUND	IKU GRAB.
48	DRILL	2831213	65 03.73N	65 12.98W	890	CUMBERLAND SOUND	BIO DRILL. LENGTH: 9 CM. MUDSTONE/SILTSTONE.
48-G	GRAB/DRL	2831213	65 03.73N	65 12.98W	890	CUMBERLAND SOUND	GRAB SAMPLE TAKEN FROM THE LEG OF THE DRILL.
49	DRILL	2831547	65 01.78N	65 32.98W	220	CUMBERLAND SOUND	BIO DRILL. LENGTH: 37 CM. OF GNEISS.
49-G	GRAB/DRL	2831547	65 01.78N	65 32.98W	220	CUMBERLAND SOUND	GRAB SAMPLE TAKEN FROM THE LEG OF THE DRILL.

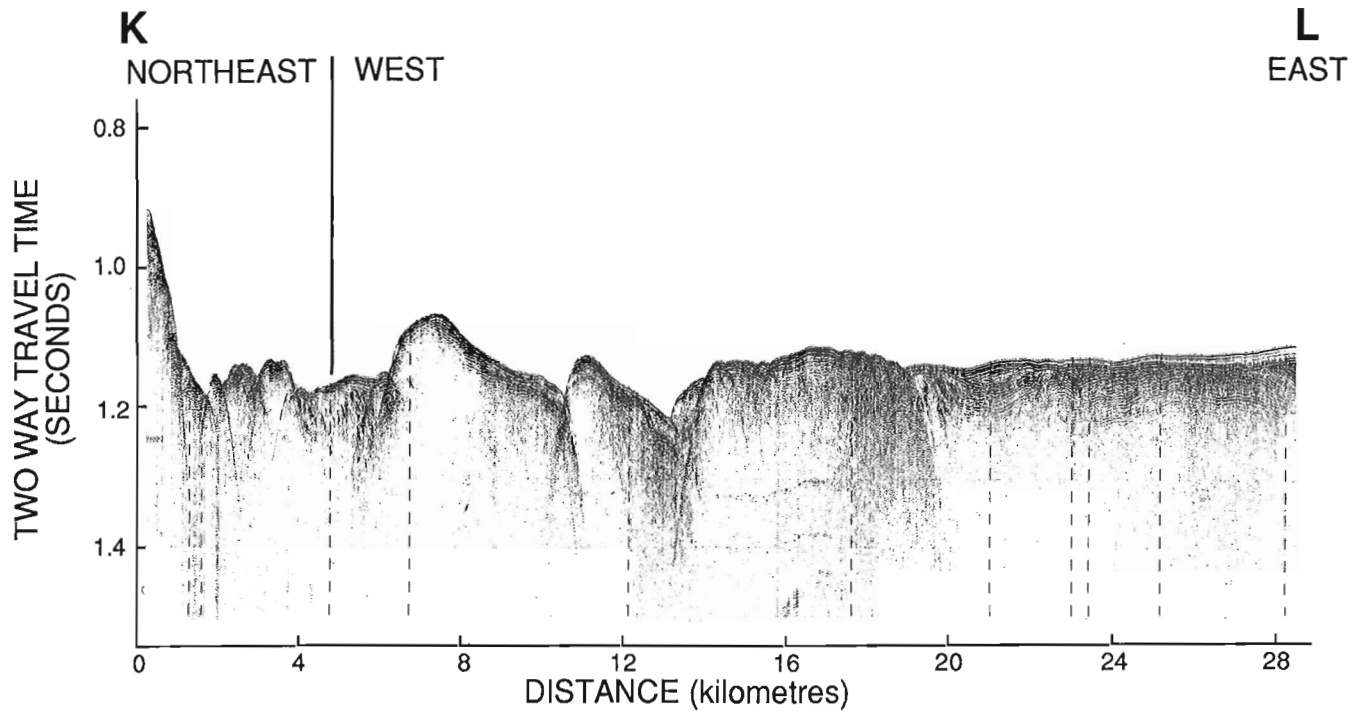


Figure 63.7. Section K-L: Seismic reflection profile west to east illustrating inferred Lower Paleozoic rocks in apparent fault contact with Precambrian and Cretaceous rocks, 4 km and 20 km respectively, along the section (see Fig. 63.3 for section location).

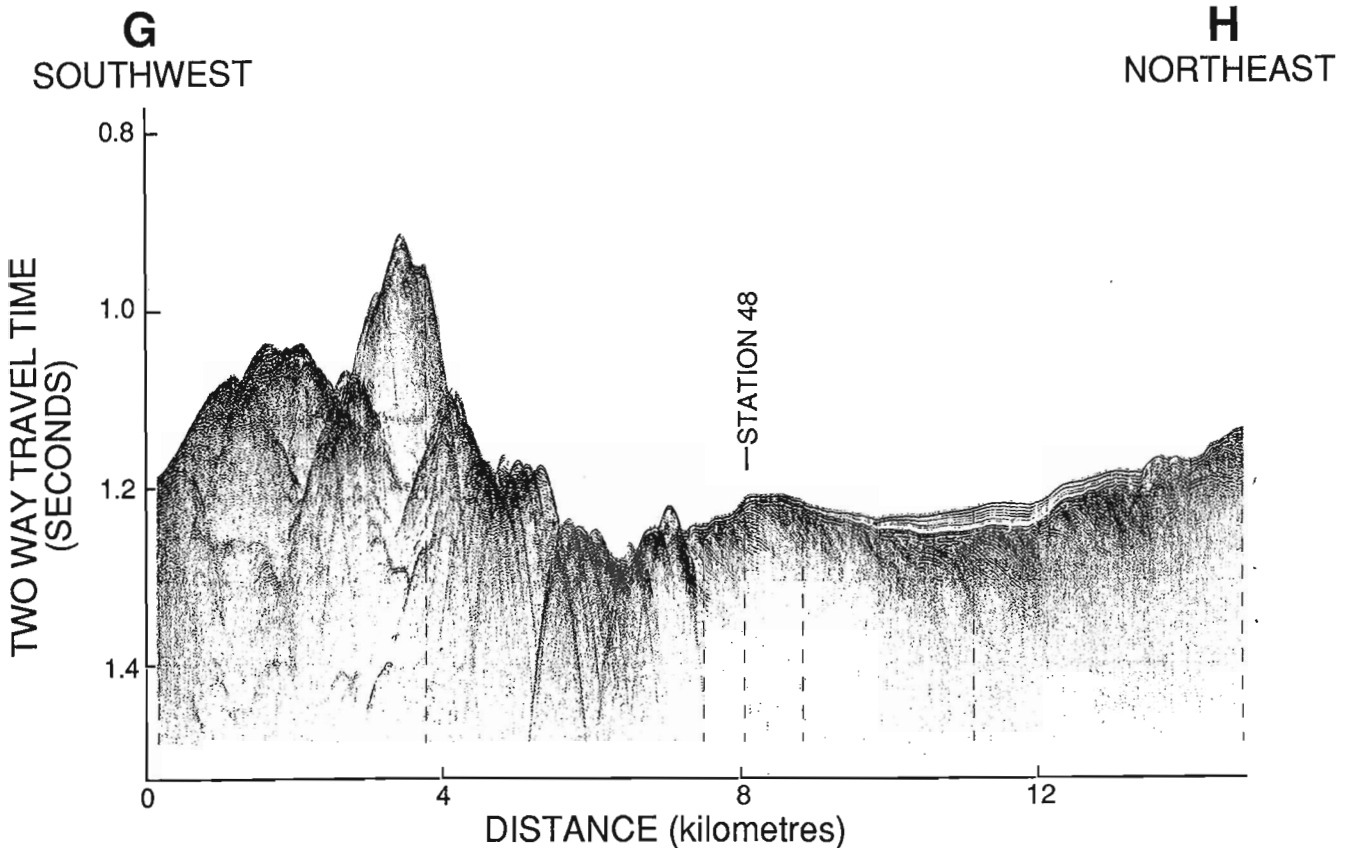


Figure 63.8. Section G-H: Seismic reflection profile illustrating: easterly dipping Cretaceous strata at bedrock sample locality, Station 48; the contact with Precambrian rocks at approximately 7 km; and the distribution of surficial sediments (see Fig. 63.3 for section location).

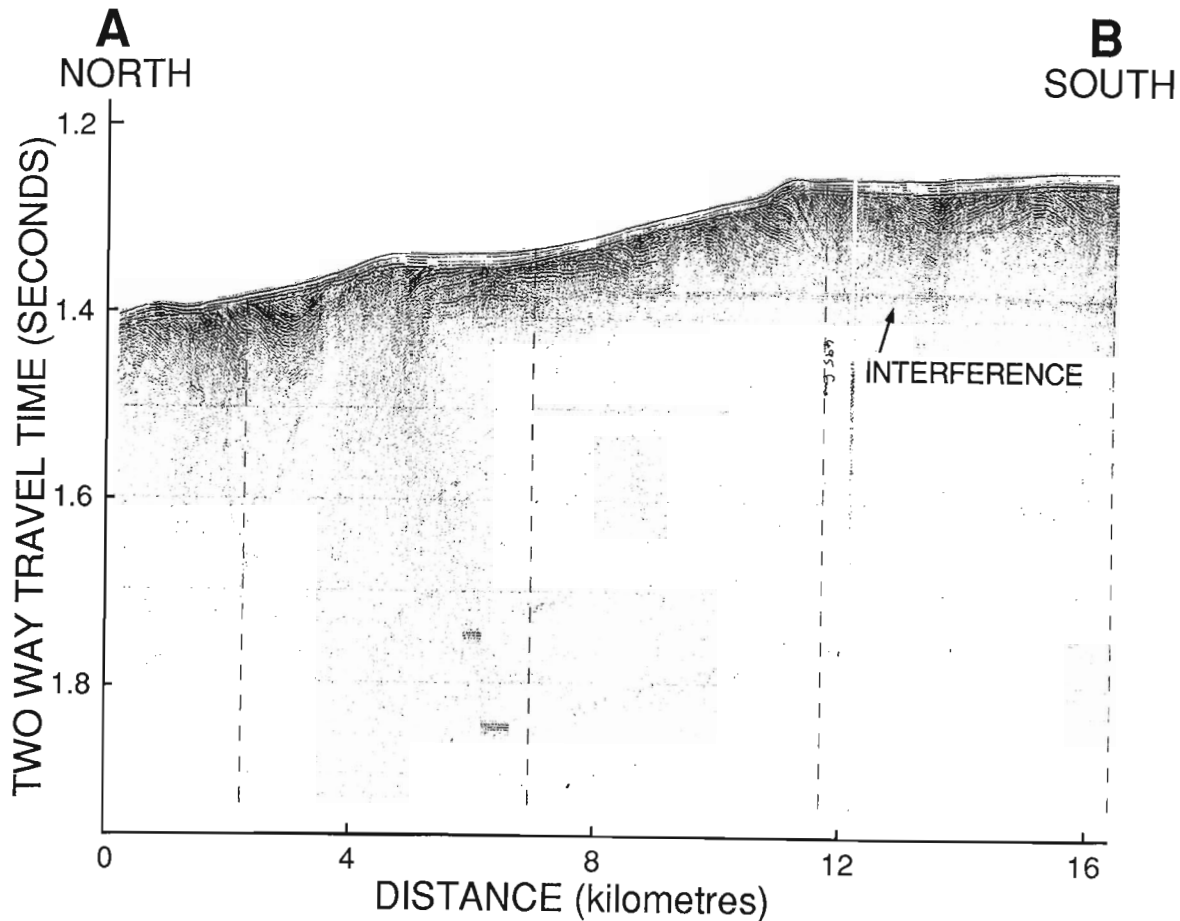


Figure 63.9. Section A-B: Seismic reflection profile northwest to southeast showing folding and possible faulting within Cretaceous rocks along the east side of Cumberland Sound, and erosional beveling of the strata (see Fig. 63.3 for section location).

The sedimentary rocks on the continental shelf east of Cumberland Sound have been extensively bevelled by erosion subsequent to the early Eocene (MacLean et al., 1982). Similar beveling of the Cretaceous beds in Cumberland Sound may relate to this event. Glacial erosion also presumably affected the seabed. To date no indication of Tertiary strata has been seen in Cumberland Sound; it appears either they were not deposited or they subsequently have been removed.

Surficial sediments

The main accumulation of unconsolidated sediments in Cumberland Sound occurs in the deeper northeast half (Fig. 63.4, 63.7, 63.8, 63.10). In the inner part of this area the unconsolidated sediments are generally underlain by Cretaceous strata. The surficial sediments are up to 30 m thick in this area and are up to 50 m thick in the outer part of the sound. Five units are recognized from acoustic profiles. The basal unit is unstratified and is interpreted as a till. It occurs in marginal areas and locally fills bedrock depressions and forms constructional features (Fig. 63.11). A second, acoustically stratified unit composed of black, very pebbly, sandy mud locally overlies the till and bedrock. These sediments are overlain by a basin wide unit that is poorly to well stratified and moderately transparent on seismic profiles. It may be a correlative of the Davis Strait Silt mapped on the southeast Baffin shelf (Praeg et al., 1986). Core data suggest that this unit includes unbioturbated black

and grey laminated mud with some sand beds overlain by bioturbated mud, sandy mud, and pebbles. The youngest unit in the basin sequence appears as a laminated basin fill sediment on high resolution seismic profiles. The unit is a correlative of the post-glacial marine Tiniktartuq Silt and Clay which occurs in the outer part of Cumberland Sound and on the Baffin shelf (Praeg et al., 1986) (Fig. 63.11). It consists of olive grey and sandy mud with indistinct banding.

Isolated patches of soft Quaternary sediments also are present: off Kingnait Fiord, 14 km northwest of the main body of sediments, locally in a small area at the head of the sound, and at another locality toward the southwest side (Fig. 63.10).

In the southwest and inner parts of Cumberland Sound surficial sediments mainly form a thin (<1-2 m) discontinuous cover over rough Precambrian bedrock (Fig. 63.5, 63.10). The seafloor sediments are mainly lag gravels and sands presumably formed by current modification of the underlying sediments. These commonly consist of mud, sand and gravel mixtures that appear to include till. Acoustic profiles show thicker, localized accumulations in some valley bottoms.

Cores of the surficial sediments were obtained at 10 localities and IKU grab samples at 6 others (Fig. 63.2, Table 63.1). Analyses of these samples should yield information on sediment textures, depositional environments, paleoceanographic and paleoclimatic conditions, geochronology, geotechnical, and related parameters.

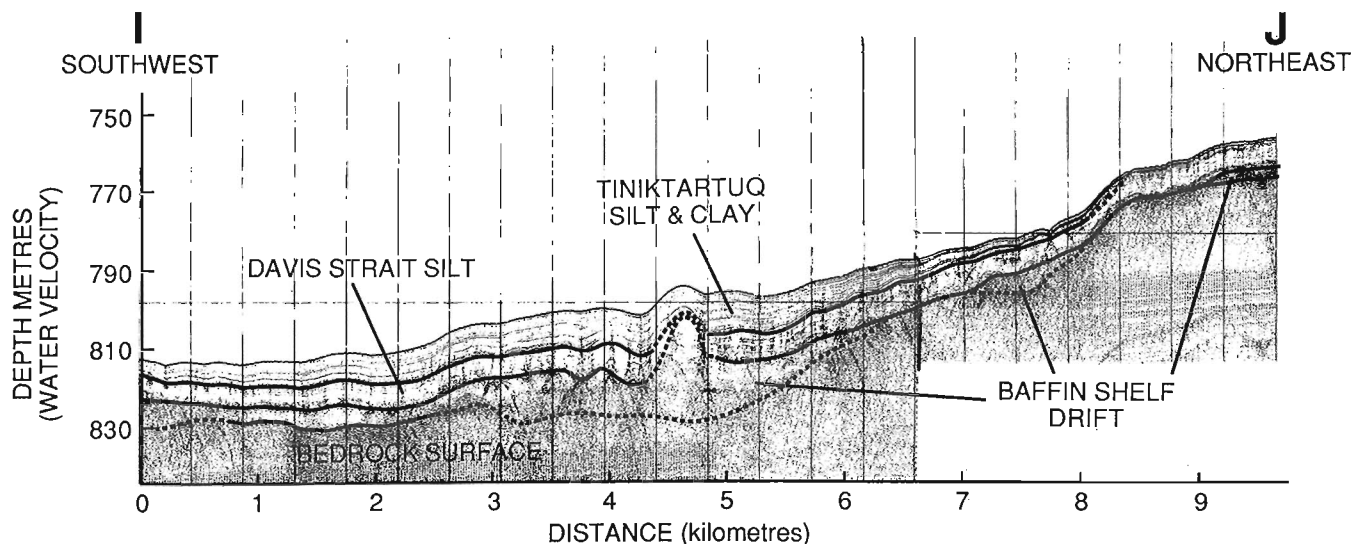


Figure 63.11. Section I-J: Huntex high resolution seismic reflection profile west to east in outer Cumberland Sound from Praeg et al. (1986); this illustrates glacial till of Baffin Shelf Drift which is overlain by Davis Strait Silt stratified glacial marine sediments and basin fill muds of the Tiniiktartuq Silt and Clay (see Fig. 63.3 for section location).

Acknowledgments

We sincerely thank Captain F.W. Mauger, officers, crew and scientific staff aboard **CSS Hudson** for their excellent co-operation and dedicated efforts in carrying out the program. Special thanks also are due P. Ryall and C. Walls, Dalhousie University and J. Coombes, NORDCO Ltd. for support of the drill core sampling, and S. Lau, University of Manitoba for geotechnical measurements. We are also grateful to our colleague A.C. Grant for helpful discussion and thank both he and J.A. Stravers for review of this manuscript.

References

- Andrews, J.T. and Miller, G.H.
1984: Quaternary glacial and nonglacial correlations for the Eastern Canadian Arctic; in *Quaternary Stratigraphy of Canada - A Canadian Contribution to IGCP Project 24*, ed. R.J. Fulton; Geological Survey of Canada, Paper 84-10, p. 101-115.
- Blackadar, R.G.
1967: Geological Reconnaissance, southern Baffin Island, District of Franklin; Geological Survey of Canada, Paper 66-47, 32 p.
- Blake, W., Jr.
1966: End moraines and deglacial chronology in northern Canada with special reference to southern Baffin Island; Geological Survey of Canada, Paper 66-26, 31 p.
- Dyke, A.S.
1977: Quaternary geomorphology, glacial chronology, and climatic and sea level history of southwestern Cumberland Peninsula, Baffin Island, N.W.T.; Ph.D. thesis, University of Colorado, Boulder, Colorado, 207 p.
- Dyke, A.S., Andrews, J.T., and Miller, G.H.
1982: Quaternary geology of Cumberland Peninsula, Baffin Island, District of Franklin; Geological Survey of Canada, Memoir 403, 32 p.
- Grant, A.C.
1975: Geophysical results from the continental margin off southern Baffin Island; in *Canada's continental margins and offshore petroleum exploration*, ed. C.J. Yorath, E.R. Parker, and D.J. Glass; Canadian Society of Petroleum Geologists, Memoir 4, p. 411-431.
- Hood, P. and Bower, M.
1975: Aeromagnetic reconnaissance of Davis Strait and adjacent areas; in *Canada's continental margins and offshore petroleum exploration*, ed. C.J. Yorath, E.R. Parker, and D.J. Glass; Canadian Society of Petroleum Geologists, Memoir 4, p. 433-451.
- Jackson, G.D. and Taylor, F.C.
1972: Correlation of major Aphebian rock units in the northeastern Canadian Shield; *Canadian Journal of Earth Sciences*, v. 9, p. 1650-1669.
- Locke, W.W. III
1980: Quaternary geology of the Cape Dyer area, southern Baffin Island, Canada; Ph.D. thesis, University of Colorado, Boulder, Colorado, 305 p.
- MacLean, B.
1986: Cruise report - CSS Hudson cruise 85-027; Bedford Institute of Oceanography, unpublished report.
- MacLean, B., Jansa, L.F., Falconer, R.K.H., and Srivastava, S.P.
1977: Ordovician strata on the southeastern Baffin Island shelf revealed by shallow drilling; *Canadian Journal of Earth Sciences*, v. 14, p. 1925-1939.
- MacLean, B. and Falconer, R.K.H.
1979: Geological/geophysical studies in Baffin Bay and Scott Inlet-Buchan Gulf and Cape Dyer-Cumberland Sound areas of the Baffin Island shelf; in *Current Research, Part B*, Geological Survey of Canada, Paper 79-1B, p. 231-244.
- MacLean, B., Srivastava, S.P., and Haworth, R.T.
1982: Bedrock structures off Cumberland Sound, Baffin Island shelf; core samples and geophysical data; in *Arctic Geology and Geophysics*, ed. A.F. Embry and H.R. Balkwill; Canadian Society of Petroleum Geologists, Memoir 8, p. 279-295.

- MacLean, B. and Williams, G.L.
 1983: Geological investigations of Baffin Island shelf in 1982; *in* Current Research, Part B, Geological Survey of Canada, Paper 83-1B, p. 309-315.
- McMillan, N.J.
 1973: Shelves of Labrador Sea and Baffin Bay, Canada; *in* The Future Petroleum Provinces of Canada, ed. R.G. McCrosson; Canadian Society of Petroleum Geologists, Memoir 1, p. 473-517.
- Miller, G.H.
 1980: Late Foxe glaciation of southern Baffin Island, N.W.T., Canada; Geological Society of America Bulletin, v. 91, p. 399-405.
 1985a: Aminostratigraphy of Baffin Island Shell-bearing deposits; *in* Quaternary environments eastern Canadian Arctic, Baffin Bay and western Greenland, ed. J.T. Andrews; George Allen and Unwin, London, p. 394-427.
 1985b: Moraines and proglacial lake shorelines, Hall Peninsula, Baffin Island; *in* Quaternary environments eastern Canadian Arctic, Baffin Bay and western Greenland, ed. J.T. Andrews; George Allen and Unwin, London, p. 546-559.
- Praeg, D.B., MacLean, B., Hardy, I., and Mudie, P.
 1986: Quaternary geology of the southeast Baffin Island continental shelf, N.W.T.; Geological Survey of Canada, Paper 85-14, 38 p.
- Riley, G.S.
 1960: Petrology of the gneisses of Cumberland Sound, Baffin Island, N.W.T.; Geological Survey of Canada, Bulletin 61, 68 p.
- Osterman, L.E., Miller, G.H., and Stravers, J.A.
 1984: Late and mid-Foxe glaciation of southern Baffin Island; *in* Quaternary environments, eastern Canadian Arctic, Baffin Bay, and west Greenland, ed. J.T. Andrews; George Allen and Unwin Ltd., London, p. 520-545.
- Srivastava, S.P., Falconer, R.K.H., and MacLean, B.
 1981: Labrador Sea, Davis Strait, Baffin Bay: geology and geophysics – a review; *in* Geology of the Atlantic borderlands and basins, ed. J.W. Kerr and A.J. Fergusson; Canadian Society of Petroleum Geologists, Memoir 7, p. 333-398.

A reconnaissance study of the bedrock and surficial geology of Hudson Strait, N.W.T.

Project 760015

B. MacLean, G.L. Williams, B.V. Sanford¹, R.A. Klassen²,
C. Blakeney, and A. Jennings³
Atlantic Geoscience Centre, Dartmouth

MacLean, B., Williams, G.L., Sanford, B.V., Klassen, R.A., Blakeney, C. and Jennings, A., A reconnaissance study of the bedrock and surficial geology of Hudson Strait, N.W.T.; in *Current Research, Part B, Geological Survey of Canada, Paper 86-1B*, p. 617-635, 1986.

Abstract

The preservation of Paleozoic and possibly younger strata beneath the strait is controlled by half grabens at the eastern and western ends, and in the central part by a regional synclinal structure.

Preliminary lithologic correlations of Paleozoic strata in Hudson Strait were made with rocks exposed on Southampton, Coats, and Mansel islands in northern Hudson Bay and in the Premium Homestead Akpatok L-26 well in Ungava Bay. These correlations and regional stratigraphic relationships recorded on seismic profiles suggest that carbonate rocks of Ordovician age underlie most of the western part of the strait, but occur together with Silurian and possibly younger rocks in the eastern part. The seismic data also suggest that 2000 m or more of strata may be present in the area.

Surficial sediments include glacial till and stratified sediments. Greatest accumulations, 95 m and 130 m, are in the eastern and western basins, respectively. Moraines have been observed on both north and south sides and in the western part of the strait. In places they include more than one till.

Résumé

La préservation des couches du Paléozoïque et de strates probablement plus jeunes sous le détroit est confirmée par la présence de sémi-fossés aux extrémités est et ouest, et dans la partie centrale par une structure synclinale régionale.

Les corrélations lithologiques préliminaires des strates du Paléozoïque dans le détroit d'Hudson ont été effectuées à l'aide de roches exposées sur les îles Southampton, Coats et Mansel dans la partie septentrionale de la baie d'Hudson et dans le puits Premium Homestead Akpatok L-26 dans la baie d'Ungava. Ces corrélations et les rapports stratigraphiques régionaux enregistrés sur des profils sismiques indiquent que des roches carbonatées de l'Ordovicien se trouvent sous la majeure partie de la région occidentale du détroit, mais qu'elles sont mêlées à des roches du Silurien et d'autres roches probablement plus jeunes dans la partie orientale. Les données sismiques indiquent également que cette strate a probablement une épaisseur de 2000 m ou plus à cet endroit.

Les sédiments superficiels comprennent du till et des sédiments stratifiés. Les plus grandes accumulations, 95 m et 130 m, se trouvent respectivement dans les bassins est et ouest. Des moraines ont été observées du côté nord et du côté sud et dans la partie occidentale du détroit. À certains endroits, elles comprennent plus d'un type de till.

¹ Lithosphere and Canadian Shield Division, Ottawa

² Terrain Sciences Division, Ottawa

³ Institute of Arctic and Alpine Research, University of Colorado, Boulder, Colorado

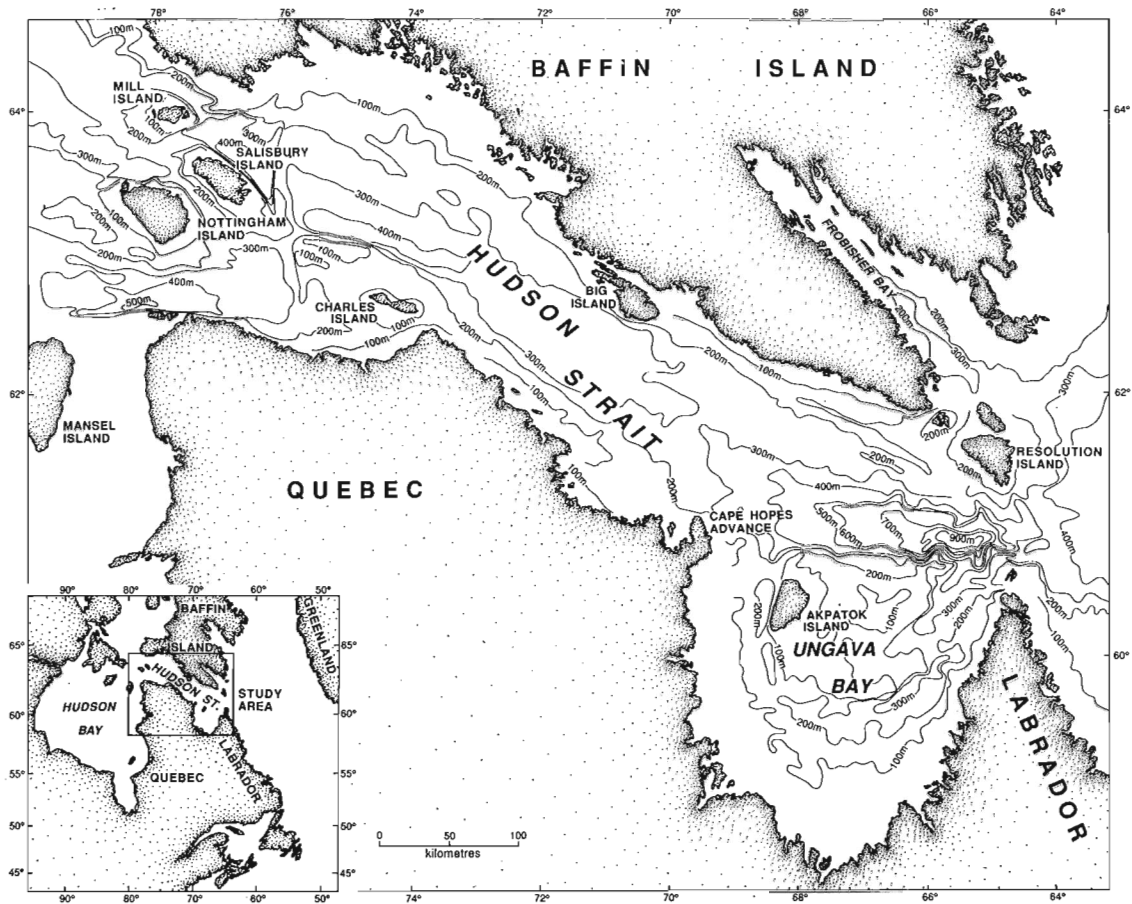


Figure 64.1

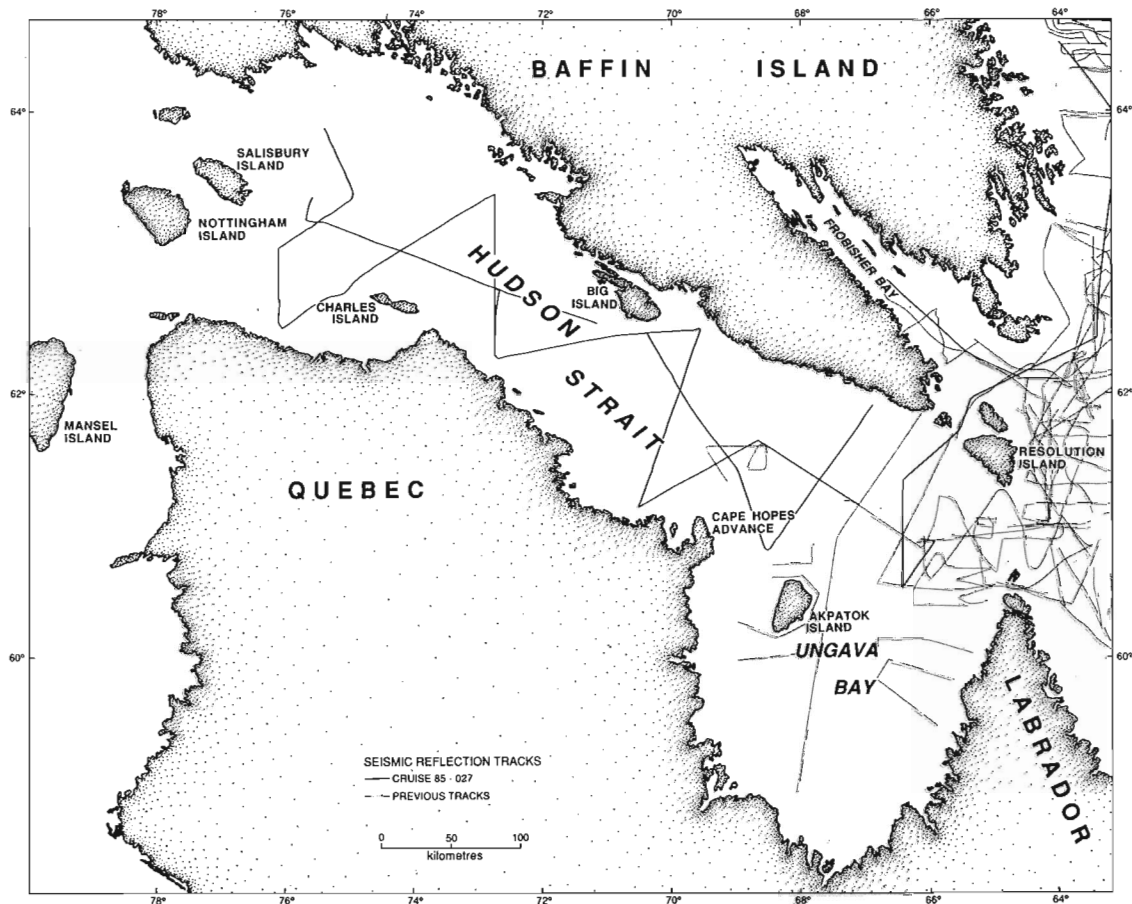


Figure 64.2

Introduction

A reconnaissance survey of the bedrock and surficial geology of Hudson Strait was carried out from **CSS Hudson** from 11 to 24 October 1985, during cruise 85-027.

Objectives of the studies were to delineate the regional distribution of the main bedrock and surficial geological units and to obtain lithostratigraphic, biostratigraphic and physical property data to provide information on their composition, age, depositional history and other properties.

Hudson Strait separates Baffin Island from Labrador and northern Quebec and connects Hudson Bay and Foxe Basin with the Labrador Sea (Fig. 64.1). It is 800 km long and ranges in width from 90 km to 340 km across Ungava Bay. Nottingham, Salisbury, and Mill islands constrict the strait at its western end.

Generalized bathymetry is shown in Fig. 64.1. Water depths in excess of 200 m are continuous along the strait from the continental shelf at its eastern end to the west side

of Foxe Basin, with branches into Ungava Bay and northern Hudson Bay (Canadian Hydrographic Service, charts 5.04, 5450). Greatest depths, in excess of 900 m, occur in an elongate depression in the eastern end of the strait north of Ungava Bay. This is separated from the Labrador Sea by a narrow sill with a depth of about 400 m. A depression in the western part of the strait contains water depths in excess of 400 m. It commences east of Nottingham Island and extends eastward parallel to the axis of the strait for 130 km. Major fault scarps control the bathymetry along the south side of both of these depressions. Water depths increase progressively southward into these half graben basins. In contrast, the bathymetric profile of the central part of the strait is broadly u-shaped. On a smaller scale, bedrock cuestas or small fault ridges, morainal or other surficial sediment deposits, and small channels locally influence the bathymetry (e.g. Fig. 64.8, 64.9, 64.11).

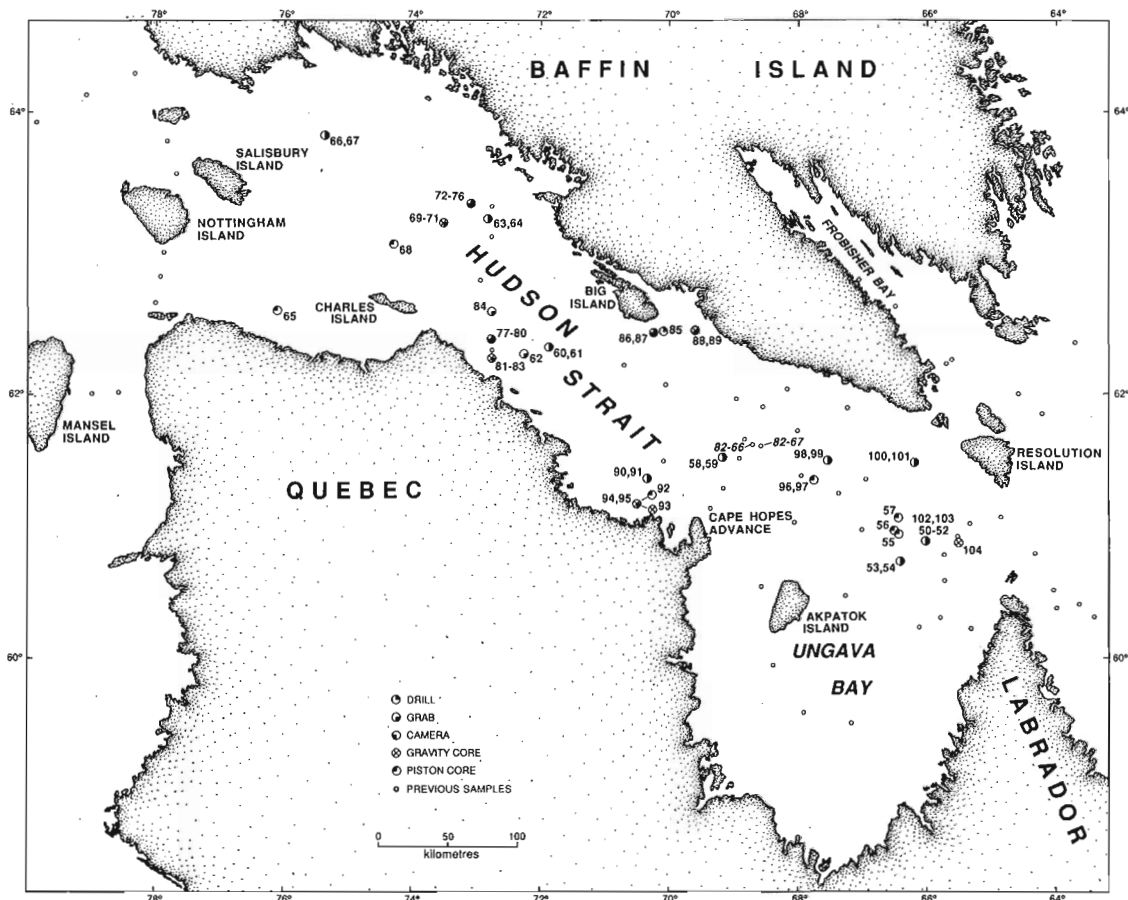


Figure 64.3

Figure 64.1. (opposite) Generalized bathymetry of Hudson Strait.

Figure 64.2. (opposite) Tracks along which single channel seismic reflection data have been acquired. Huntec high resolution seismic data were also acquired along all 1985 tracks. See Grant and Manchester (1970), Grant (1975) and MacLean and Williams (1983) for previous track information in Hudson Strait and Ungava Bay.

Figure 64.3. Sample stations from cruise 85-027 and other cruises, mainly cruises 82-027 and 82-034.

Methods

The survey included the collection of both geophysical data and samples of bedrock and Quaternary sediments (Fig. 64.2, 64.3). Geophysical data were obtained with a single channel seismic reflection system using a 655 cm³ compressed air source and Nova Scotia Research Foundation and Seismic Engineering hydrophones, a Huntec high resolution seismic system fitted with a towed streamer as well as internal hydrophone, a Varian magnetometer, and a Bedford Institute of Oceanography sidescan sonar.

Bedrock samples were collected at 12 sites (Fig. 64.4). They were obtained with the Bedford Institute of Oceanography underwater electric drill with up to 9 m seafloor penetration capability, which has been used extensively on the Baffin Island shelf and elsewhere, and a newly developed NORDCO drill. The NORDCO unit consists

of a 6 m auger through which a diamond drill can be extended 6 m farther. This unit proved very effective in augering through overburden down to the bedrock surface, and thus disposing of gravel fragments that commonly jam in the diamond drill barrel. Some problems, however, were encountered with core retention.

Surficial sediment samples were obtained principally with a Benthos piston corer and large IKU clamshell sampler, but gravity and Lehigh corers also were used, and some grab samples were obtained from the drill legs. Photographs of the seabed were obtained at selected stations with UMEL underwater cameras.

Navigational positioning was by means of BIONAV, the Bedford Institute integrated navigation system which utilizes rho-rho Loran C, Satellite navigation, log and gyro, and by radar.

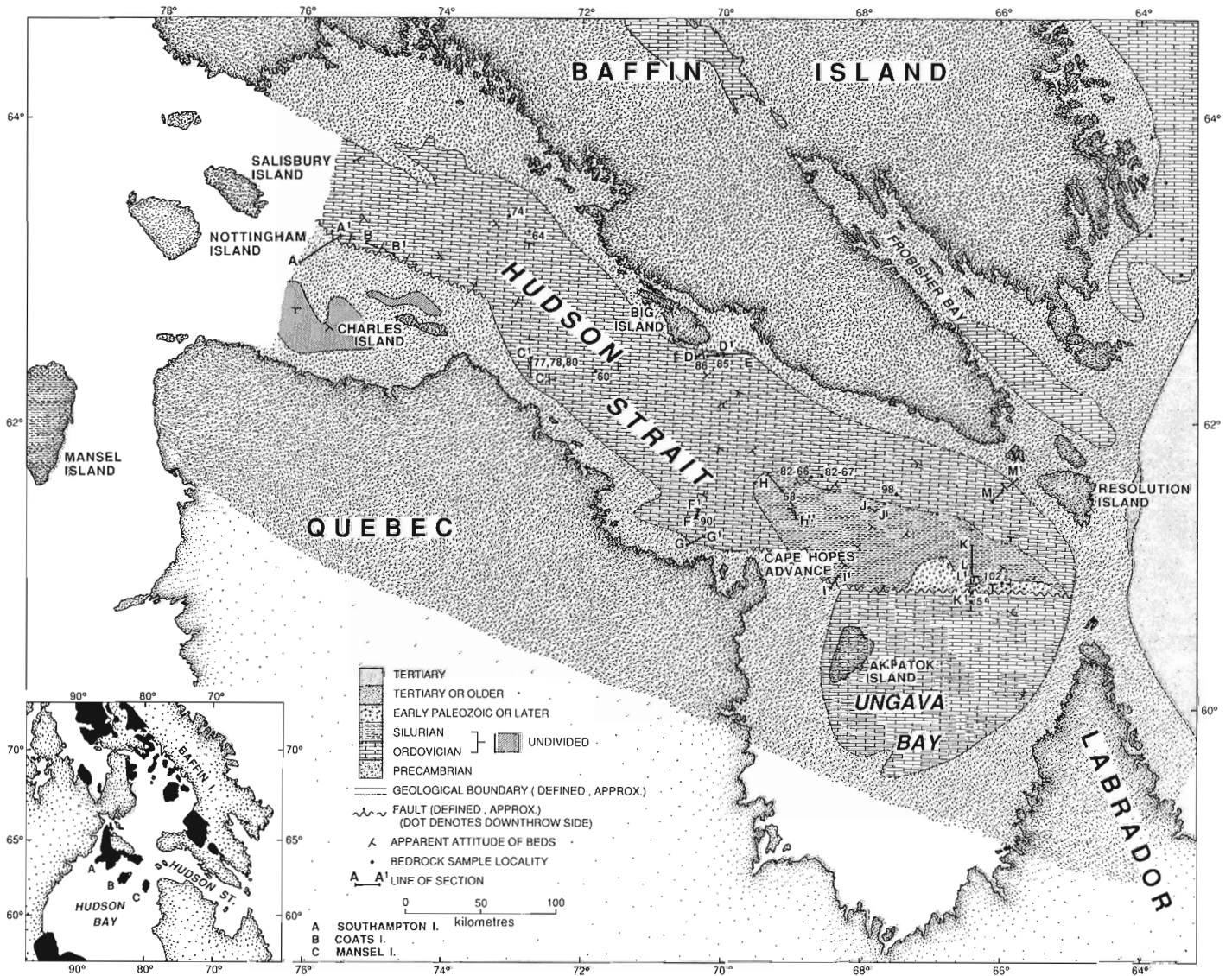


Figure 64.4. Geological map showing tentative units represented. Age assignments are on the basis of preliminary lithologic correlations with rocks on Southampton, Coats and Manse islands, in the Akpatok well, and seismic relationships. Ungava Bay geology is after Grant and Manchester (1970), Grant (1975) and Sanford et al. (1979). Black areas on the inset map show the distribution of Ordovician and Silurian rocks in the region.

Previous studies

The most pertinent previous onshore investigations relative to bedrock geology are: Sanford in Heywood and Sanford (1976) on the Paleozoic rocks of Southampton, Coats and Mansel islands in northern Hudson Bay; Workum et al. (1976) on stratigraphy from the Premium Homestead Akpatok L-26 well on Akpatok Island in Ungava Bay; Blackadar (1966) – geology of southern Baffin Island; and Taylor (1979 and 1982) – geology of parts of northern Quebec and Ungava. The Quaternary geology of southern Baffin Island has been studied by Blake (1966), Stravers (1986), Stravers and Miller (1984), Miller (1982), and Clark (1985), of northern Quebec and Labrador by Løken (1978), Gray and Lauriol (1985), and Gray et al. (1985). Previous offshore studies included: seismic reflection, magnetometer and dredge sampling investigations of Ungava Bay and eastern Hudson Strait by Grant and Manchester (1970), Grant (1975); synthesis of existing offshore, onshore, and well data by Sanford (1974), and Sanford et al. (1979) to postulate the distribution of Paleozoic rocks in the strait; investigations of surficial sediments at the eastern end of the strait through profiling and sampling by Fillon et al. (1981), Fillon and Harnes (1982); seismic reflection surveys and bedrock sampling in eastern Hudson Strait by MacLean and Williams (1983); collection of sediment samples as part of chemical, physical and biological oceanographic investigations of Hudson Strait by Jones and Drinkwater (1982), and studies of tidal currents by Drinkwater (1983).

For a broader overview of the bedrock and surficial geological data and problems in the region the reader is referred to Andrews et al. (1983), Shilts (1980, 1984), Osterman et al. (1985), Praeg et al. (1986), MacLean (1985), Bolton et al. (1977), and Trettin (1975).

Bedrock geology

A preliminary interpretation of the bedrock geology of Hudson Strait, presented in Figure 64.4, is based on: tentative lithologic correlations of samples recovered from 12 offshore localities (Table 64.1) with strata mapped on Southampton, Coats and Mansel islands in northern Hudson Bay (Heywood and Sanford, 1976), and in the Premium Homestead Akpatok L-26 well on Akpatok Island (Workum et al., 1976); and stratigraphic relations and acoustic characteristics of bedrock units from seismic reflection profiles. The resultant division of units in general agrees quite well with the onshore and well data both lithologically and in approximate formation thickness. Paleontological data, however, is as yet unavailable from the offshore samples so the proposed age of the strata should be considered tentative. The correlations suggest that the strait is underlain mainly by carbonate rocks of Ordovician and Silurian age. Younger strata may also occur adjacent to the fault scarp in the eastern part of the strait (Fig. 64.5, Section K-K¹, 24-34 km along the profile).

Interpretations of data from the Premium Homestead Akpatok L-26 well on Akpatok Island (Workum et al., 1976) and seismic reflection data (Grant and Manchester, 1970) indicate that Ungava Bay is floored mainly by carbonate rocks of the Ordovician Bad Cache Rapids Group. The core samples recovered from station 85-027-54 are lithologically consistent with this. The lower 264 m (70-334 m below sea level) in the well contains poorly consolidated shale, sandstone and carbonate rocks which may outcrop around the periphery of the carbonate platform in Ungava Bay. Precambrian rocks were encountered at a depth of 335 m below sea level.

The eastern part of the strait north of Ungava Bay and the western part north of Charles Island are half graben features in which strata have been down faulted against older rocks to the south (Fig. 64.5, 64.6).

The contact between Precambrian metamorphic rocks that make up the adjacent landmass on both sides of the strait and the Lower Paleozoic rocks under the strait occurs close to the present shoreline in many areas. Precambrian rocks, however, are present locally in the western part of the strait north and west of Charles Island.

Lower Paleozoic (Ordovician) strata onlap Precambrian rocks on the north side of the strait where they commonly form cuesta ridges (Fig. 64.7). However, faulting may be associated with ridges near Big Island (Fig. 64.8).

From Big Island westward the strait is underlain by rocks that appear mainly to be equivalents of the Ordovician Bad Cache Rapids and Churchill River groups, and Red Head Rapids Formation, as well as older Ordovician beds described by Heywood and Sanford (1976) and Workum et al. (1976). Silurian strata possibly occur locally southwest of Charles Island (undivided in Fig. 64.4). The possibility of post-Ordovician beds in the western graben north of Charles Island cannot be ruled out.

The stratigraphy in the eastern part of the strait is more complex. Here a sequence of younger strata that thickens southward (Fig. 64.9) forms a stratigraphic section some 725 m in thickness (using an assumed velocity of 4 km/s). These beds overlie strata that closely resemble Red Head Rapids Formation where sampled at station 82-67 (MacLean and Williams, 1983) and Churchill River-Bad Cache Rapids groups at e.g. stations 85, 86, 90, 82-66. A sample of reddish brown calcareous sandstone was recovered from the younger unit at Station 58. This is tentatively correlated with the Silurian Kenogami River Formation. If this correlation is correct, the section here presumably also includes equivalents of the earlier Silurian Severn River, Ekwan River and Attawapiskat formations. The change in acoustic character (greater penetration and more closely spaced reflectors) of these beds relative to the Ordovician strata which they onlap presumably reflects the less massive nature of some of these beds: for example thin bedded limestones of the Severn River and parts of the Ekwan River formations. Small, irregular, somewhat dome-shaped features interrupt the seismic reflectors in part of the sea floor in the eastern depression. These features may represent reefal developments in possible Attawapiskat and Ekwan River formations, this being a common characteristic of these units on Southampton, Coats and Mansel islands (Heywood and Sanford, 1976).

Strata identified in Figure 64.4 as "Early Paleozoic or Later" occur mainly in an elongated ridge on the floor of the eastern depression adjacent to the fault scarp north of Ungava Bay (e.g. Fig. 64.5, 24-34 km along the section). These rocks have been down dropped relative to the adjacent seafloor to the north as well as to the south (Fig. 64.5). They attain thicknesses of 850 or 1130 m respectively, if velocity corrections to 3 km/s or 4 km/s are applied. The beds were penetrated to a depth of 4.5 m at station 102 by the NORDCO drill, but only a 2 cm core of brown fairly friable sandstone was recovered. Grant (1975) previously obtained a dredge sample of possible Silurian age from this area. The exact stratigraphic and structural position of these beds relative to the Ordovician and Silurian strata to the north and west has not yet been determined due to discontinuities in the reflectors. The general relationships inferred from the seismic reflection profiles and the apparently softer more

Table 64.1. Listing of sample locations, Hudson Strait

STATION NUMBER	SAMPLE TYPE	JULIAN DAY/TIME	LATITUDE	LONGITUDE	DEPTH (NTRS)	GEOGRAPHIC LOCATION	NOTES
50	DRILL	2851306	60 52.98N	66 00.47W	815	HUDSON STRAIT	BID DRILL. NO SAMPLE. MALFUNCTIONED.
50-G	GRAB/DRL	2851306	60 52.98N	66 00.47W	815	HUDSON STRAIT	GRAB SAMPLE TAKEN FROM THE LEG OF THE DRILL.
51	GRAB	2851350	60 52.95N	65 59.73W	795	HUDSON STRAIT	LARGE VAN VEEN GRAB.
52	DRILL	2851430	60 53.05N	65 58.55W	840	HUDSON STRAIT	BID DRILL. NO SAMPLE.
53	GRAB	2851714	60 44.71N	66 25.69W	345	HUDSON STRAIT	LARGE VAN VEEN GRAB.
54	DRILL	2851804	60 44.89N	66 25.30W	355	HUDSON STRAIT	BID DRILL. LENGTH: 50 CM LIMESTONE/21 CM. PEBBLE.
54-G	GRAB/DRL	2851804	60 44.89N	66 25.30W	355	HUDSON STRAIT	GRAB SAMPLE TAKEN FROM THE LEG OF THE DRILL.
55	CORE	2852034	60 56.72N	66 25.84W	805	HUDSON STRAIT	PISTON CORE. LENGTH: 1062 CM.
56	CORE	2852200	60 58.11N	66 29.73W	777	HUDSON STRAIT	PISTON CORE. LENGTH: 1181 CM.
57	CORE	2852325	61 04.26N	66 25.60W	790	HUDSON STRAIT	PISTON CORE. LENGTH: 1190 CM.
58	DRILL	2861730	61 31.89N	69 08.21W	346	HUDSON STRAIT	NORDCO DRILL. 16 CM. OF REDDISH/BROWN LIMESTONE.
58-G	GRAB/DRL	2861730	61 31.89N	69 08.21W	346	HUDSON STRAIT	GRAB SAMPLE TAKEN FROM THE LEG OF THE DRILL.
59	GRAB	2862349	61 31.86N	69 09.45W	355	HUDSON STRAIT	VAN VEEN GRAB.
60	DRILL	2881725	62 20.46N	71 50.30W	357	HUDSON STRAIT	NORDCO DRILL. LENGTH: 5 CM.
60-G	GRAB/DRL	2881725	62 20.46N	71 50.30W	357	HUDSON STRAIT	GRAB SAMPLE TAKEN FROM THE LEG OF THE DRILL.
61	GRAB	2881938	62 20.22N	71 49.40W	357	HUDSON STRAIT	IKU GRAB. 2ND ATTEMPT.
62	GRAB	2882110	62 17.89N	72 14.18W	320	HUDSON STRAIT	IKU GRAB.
63	GRAB	2891631	63 15.08N	72 46.61W	212	HUDSON STRAIT	IKU GRAB.

Table 64.1. (cont.)

STATION NUMBER	SAMPLE TYPE	JULIAN DAY/TIME	LATITUDE	LONGITUDE	DEPTH (MTRS)	GEOGRAPHIC LOCATION	NOTES
64	DRILL	2891855	63 15.19N	72 47.17W	209	HUDSON STRAIT	NORDCO DRILL. LENGTH: 8 CM. OF LIMESTONE.
64-G	GRAB/DRL	2891855	63 15.19N	72 47.17W	209	HUDSON STRAIT	GRAB SAMPLE TAKEN FROM THE LEG OF THE DRILL.
65	CORE	2902111	62 35.92N	76 07.02W	333	HUDSON STRAIT	PISTON CORE. LENGTH: 300 CM.
66	DRILL	2911837	63 49.77N	75 21.86W	230	HUDSON STRAIT	NORDCO DRILL. NO SAMPLE.
66-G	GRAB/DRL	2911837	63 49.77N	75 21.86W	230	HUDSON STRAIT	GRAB SAMPLE TAKEN FROM THE LEG OF THE DRILL.
67	GRAB	2912048	63 49.90N	75 22.23W	228	HUDSON STRAIT	IKU GRAB.
68	CORE	2921124	63 04.50N	74 18.55W	435	HUDSON STRAIT	PISTON CORE. LENGTH: 1060 CM.
69	CORE	2921343	63 14.00N	73 31.47W	305	HUDSON STRAIT	LEHEIGH CORE. NO SAMPLE.
70	GRAB	2921402	63 13.91N	73 31.29W	305	HUDSON STRAIT	IKU GRAB.
71	CORE	2921431	63 13.92N	73 31.33W	310	HUDSON STRAIT	LEHEIGH CORE. LENGTH: 34 CM.
72	DRILL	2921717	63 21.78N	73 03.97W	230	HUDSON STRAIT	BIO DRILL. NO SAMPLE.
73	CAMERA	2921802	63 21.84N	73 04.67W	232	HUDSON STRAIT	UMEL UNDERWATER CAMERA.
74	DRILL	2922011	63 21.76N	73 04.20W	225	HUDSON STRAIT	BIO DRILL. LENGTH: 10 CM
74-G	GRAB/DRL	2922011	63 21.76N	73 04.20W	225	HUDSON STRAIT	GRAB SAMPLE TAKEN FROM THE LEG OF THE DRILL.
75	DRILL	2922129	63 20.22N	73 04.22W	233	HUDSON STRAIT	BIO DRILL. NO SAMPLE.
75-G	GRAB/DRL	2922129	63 20.22N	73 04.22W	233	HUDSON STRAIT	GRAB SAMPLE TAKEN FROM THE LEG OF THE DRILL.
76	GRAB	2922223	63 20.81N	73 04.63W	230	HUDSON STRAIT	IKU GRAB.
77	DRILL	2930920	62 23.09N	72 44.94W	210	HUDSON STRAIT	BIO DRILL. LENGTH 48 CM.

Table 64.1. (cont.)

STATION NUMBER	SAMPLE TYPE	JULIAN DAY/TIME	LATITUDE	LONGITUDE	DEPTH (MTRS)	GEOGRAPHIC LOCATION	NOTES
77-G	GRAB/DRL	2930920	62 23.09N	72 44.94W	210	HUDSON STRAIT	GRAB SAMPLE TAKEN FROM THE LEG OF THE DRILL.
78	DRILL	2931220	62 23.09N	72 44.94W	210	HUDSON STRAIT	BID DRILL. LENGTH: 35 CM.
78-G	GRAB/DRL	2931220	62 23.09N	72 44.94W	210	HUDSON STRAIT	GRAB SAMPLE TAKEN FROM THE LEG OF THE DRILL.
79	CAMERA	2931543	62 23.28N	72 45.61W	214	HUDSON STRAIT	UMEL UNDERWATER CAMERA.
80	DRILL	2931853	62 23.45N	72 45.77W	216	HUDSON STRAIT	NORDCO DRILL. LENGTH: 61 CM.
80-G	GRAB/DRL	2931853	62 23.45N	72 45.77W	216	HUDSON STRAIT	GRAB SAMPLE TAKEN FROM THE LEG OF THE DRILL.
81	CORE	2932120	62 15.03N	72 45.42W	151	HUDSON STRAIT	LEHEIGH CORE. NO SAMPLE.
82	GRAB	2932132	62 15.15N	72 44.98W	155	HUDSON STRAIT	IKU GRAB.
83	GRAB	2932201	62 14.95N	72 45.45W	155	HUDSON STRAIT	IKU GRAB.
84	GRAB	2940030	62 34.94N	72 45.43W	340	HUDSON STRAIT	IKU GRAB.
85	DRILL	2941518	62 27.02N	70 05.04W	210	HUDSON STRAIT	BID DRILL. LENGTH: 45 CM
86	DRILL	2941713	62 26.69N	70 13.76W	250	HUDSON STRAIT	NORDCO DRILL. LENGTH: 45 CM.
86-G	GRAB/DRL	2971713	62 26.69N	70 13.76W	250	HUDSON STRAIT	GRAB SAMPLE TAKEN FROM THE LEG OF THE DRILL.
87	CAMERA	2941826	62 26.71N	70 13.59W	250	HUDSON STRAIT	UMEL UNDERWATER CAMERA.
88	CORE	2942037	62 26.85N	69 35.45W	143	HUDSON STRAIT	LEHEIGH CORE. EMPTY ON BOTH ATTEMPTS.
89	GRAB	2942049	62 26.90N	69 35.28W	143	HUDSON STRAIT	IKU GRAB.
90	DRILL	2951352	61 21.73N	70 21.27W	165	HUDSON STRAIT	NORDCO DRILL. LENGTH: 64 CM.
91	GRAB	2951544	61 21.84N	70 20.53W	164	HUDSON STRAIT	IKU GRAB.

Table 64.1. (cont.)

STATION NUMBER	SAMPLE TYPE	JULIAN DAY/TIME	LATITUDE	LONGITUDE	DEPTH (MTRS)	GEOGRAPHIC LOCATION	NOTES
92	CORE	2951747	61 12.50N	70 26.99W	171	HUDSON STRAIT	PISTON CORE. LENGTH: 249 CM. BENT CORE BARREL.
93	CORE	2951839	61 09.48N	70 29.98W	171	HUDSON STRAIT	LEHEIGH CORE. LENGTH: 100 CM.
94	CORE	2951854	61 09.27N	70 29.49W	171	HUDSON STRAIT	LEHEIGH CORE. LENGTH: 94 CM.
95	GRAB	2951928	61 10.09N	70 26.34W	143	HUDSON STRAIT	IKU GRAB.
96	CORE	2961629	61 20.72N	67 44.70W	392	HUDSON STRAIT	PISTON CORE. LENGTH: 717 CM. NO TRIGGER CORE.
97	CORE	2961735	61 20.69N	67 44.43W	392	HUDSON STRAIT	PISTON CORE. LENGTH: 162 CM. NO TRIGGER CORE.
98	DRILL	2962104	61 29.87N	67 30.84W	290	HUDSON STRAIT	NORDCO DRILL. 21 CM. ARGILLACEOUS LIMESTONE.
99	GRAB	2962317	61 29.92N	67 31.21W	285	HUDSON STRAIT	VAN VEEN GRAB.
100	DRILL	2971151	61 28.93N	66 08.72W	203	HUDSON STRAIT	NORDCO DRILL. NO SAMPLE.
101	GRAB	2971329	61 28.99N	66 08.95W	205	HUDSON STRAIT	VAN VEEN GRAB.
102	DRILL	2971857	60 53.14N	65 59.91W	798	HUDSON STRAIT	NORDCO DRILL. LENGTH: 2 CM. OF BROWN SANDSTONE.
103	GRAB	2972156	60 52.76N	65 01.77W	775	HUDSON STRAIT	VAN VEEN GRAB.
104	CORE	2980000	60 52.86N	65 29.52W	950	HUDSON STRAIT	LEHEIGH CORE. NO SAMPLE.

acoustically penetratable character of the strata (Fig. 64.5, 24-34 km), as previously noted by Grant and Manchester (1970), suggest that this section may contain the youngest beds in the strait, but whether they are in part equivalents of the adjacent Ordovician and Silurian rocks, or closely related to them stratigraphically, or significantly younger is not known.

Structural relationships

Calculations along profiles southward from Baffin Island into the eastern depression indicate that the Ordovician-Silurian sections attains a thickness of at least

800 to 930 m when corrected to 3 km/s and 4 km/s velocities, respectively¹. Inclusion of the beds of the "Early paleozoic and Later" unit (Fig. 64.4) increases the probable minimum thickness to between 1650 and 2060 m. This is in agreement with Grant and Manchester's (1970) estimate of 2000 m depth to basement. They suggested a displacement of 600 m (water velocity) at the fault. The 85-027 cruise data suggest this may be as much 900 m or more after allowing for velocity corrections.

Thickness calculations for Ordovician and Silurian strata along a seismic profile from near Big Island in the north southeastward to the intersection with basement rocks 50 km east of Cape Hopes Advance (Fig. 64.9, section H-H¹)

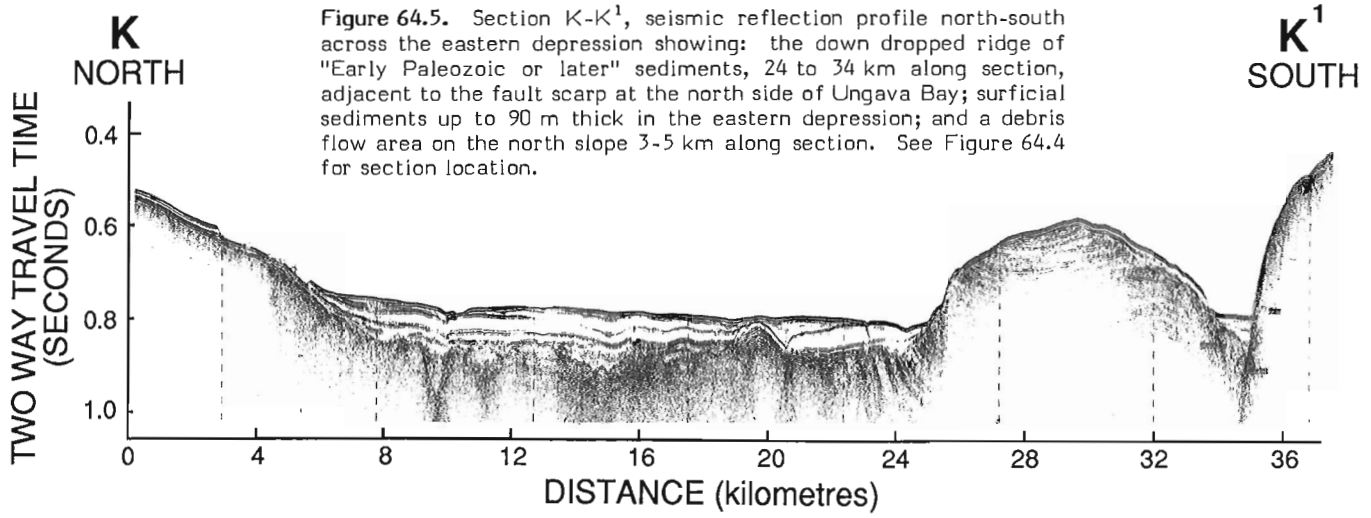


Figure 64.5. Section K-K¹, seismic reflection profile north-south across the eastern depression showing: the down dropped ridge of "Early Paleozoic or later" sediments, 24 to 34 km along section, adjacent to the fault scarp at the north side of Ungava Bay; surficial sediments up to 90 m thick in the eastern depression; and a debris flow area on the north slope 3-5 km along section. See Figure 64.4 for section location.

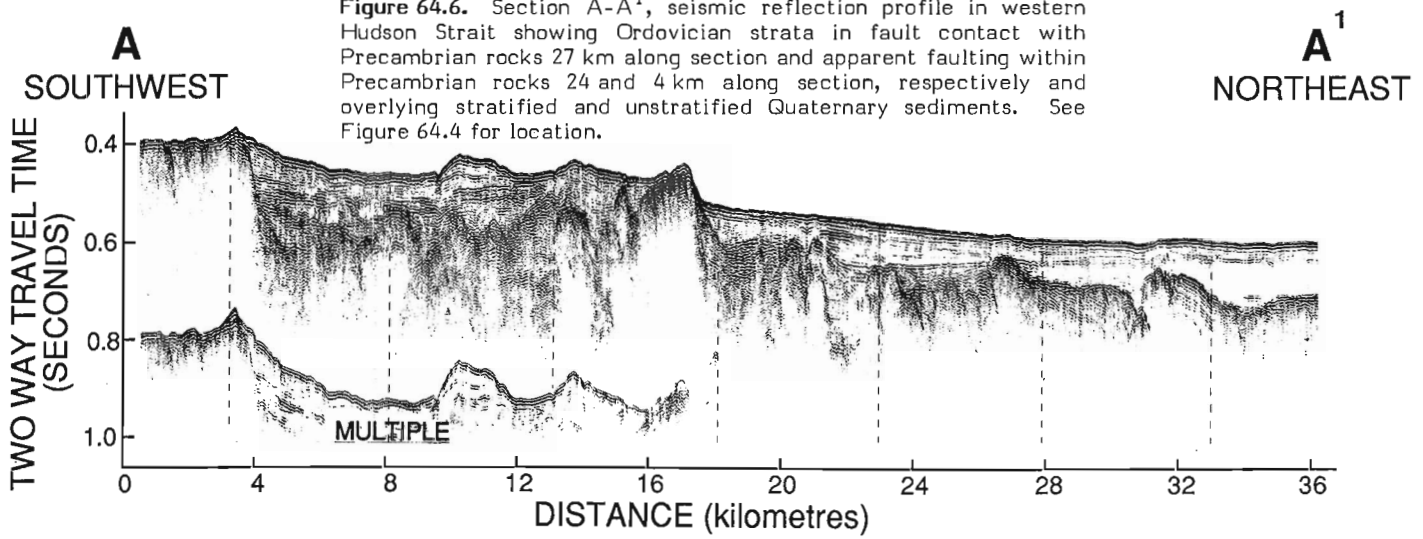


Figure 64.6. Section A-A¹, seismic reflection profile in western Hudson Strait showing Ordovician strata in fault contact with Precambrian rocks 27 km along section and apparent faulting within Precambrian rocks 24 and 4 km along section, respectively and overlying stratified and unstratified Quaternary sediments. See Figure 64.4 for location.

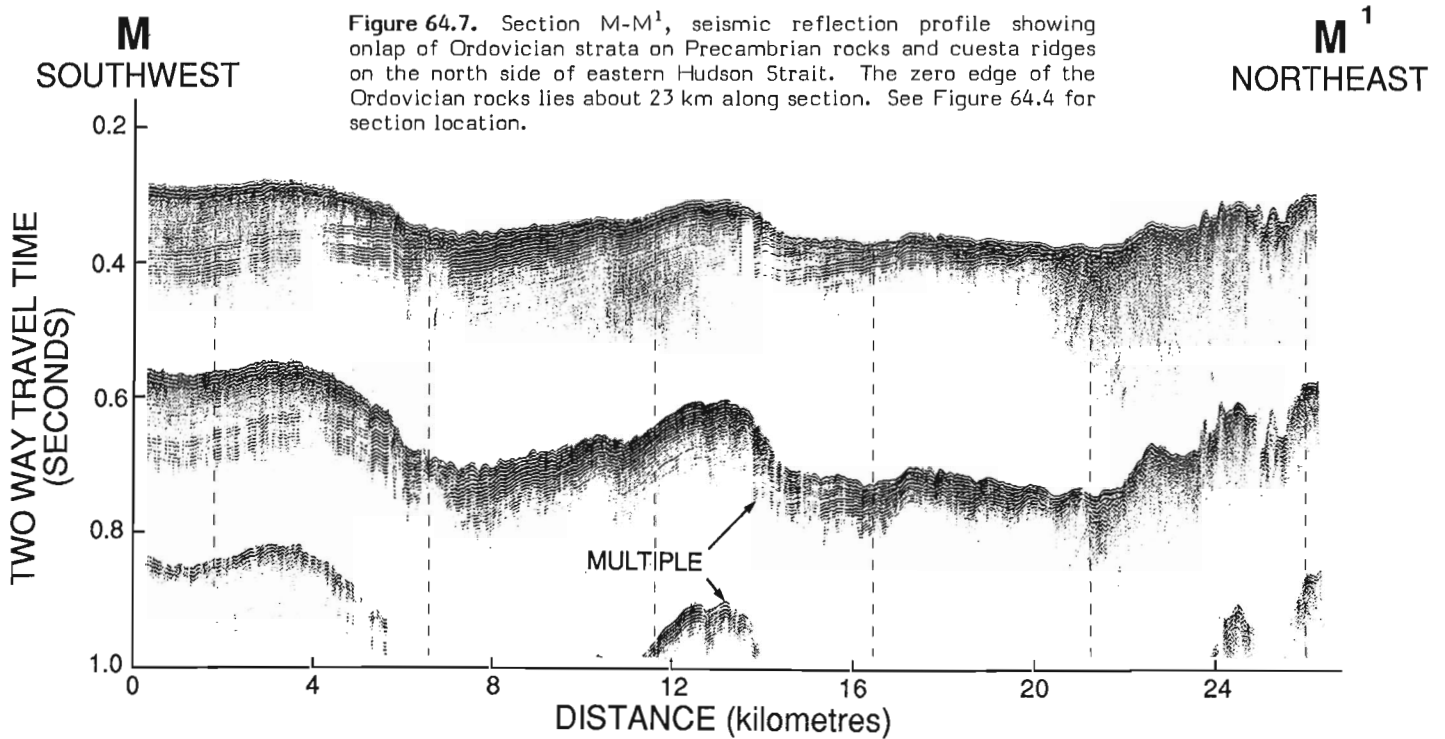


Figure 64.7. Section M-M¹, seismic reflection profile showing onlap of Ordovician strata on Precambrian rocks and cuesta ridges on the north side of eastern Hudson Strait. The zero edge of the Ordovician rocks lies about 23 km along section. See Figure 64.4 for section location.

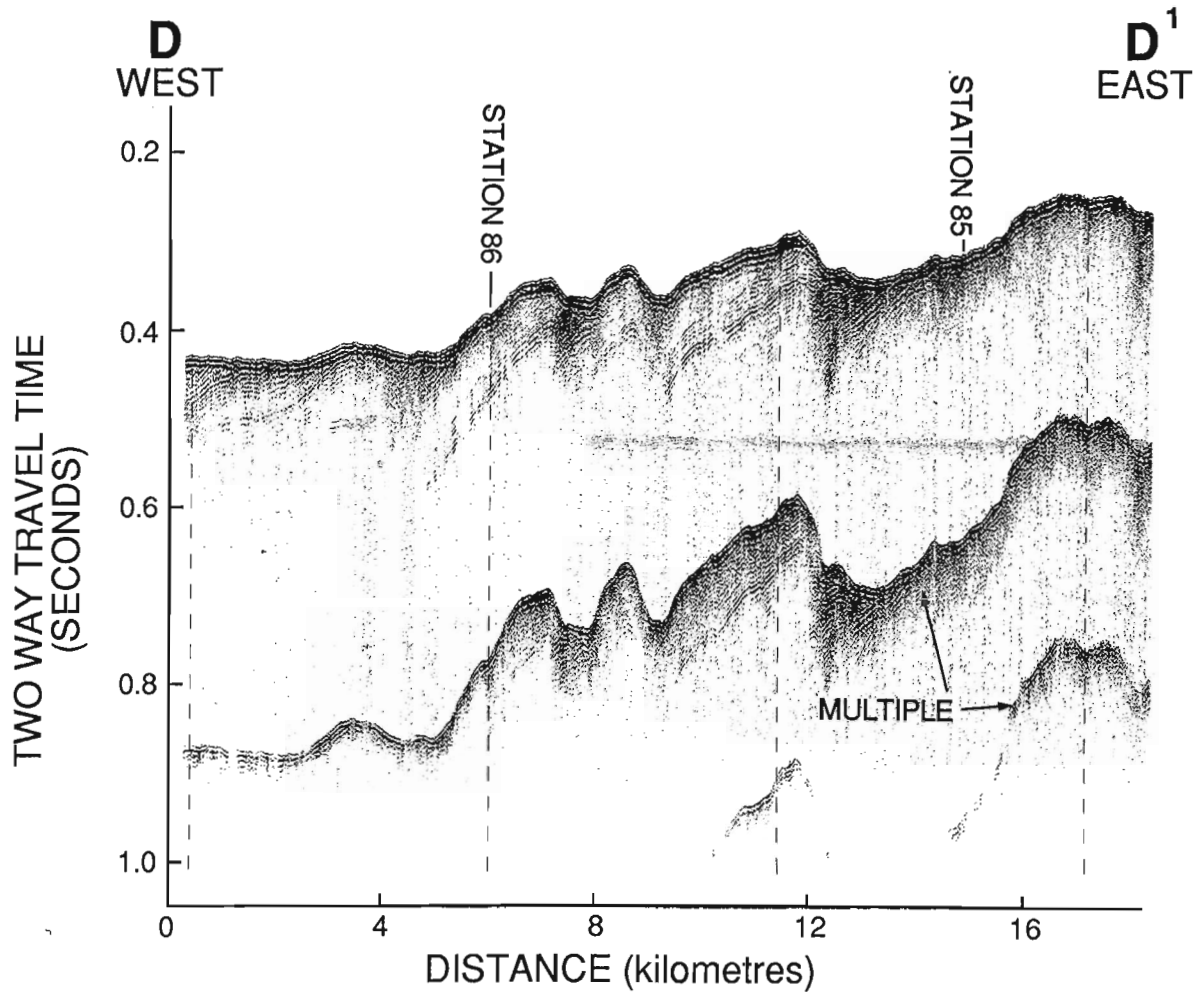


Figure 64.8. Section D-D¹, seismic reflection profile illustrating cuesta-like but possibly fault controlled ridges in Ordovician rocks near Big Island on the north side of the strait. Locations of samples stations 85 and 86 are indicated. See Figure 64.4 for section location.

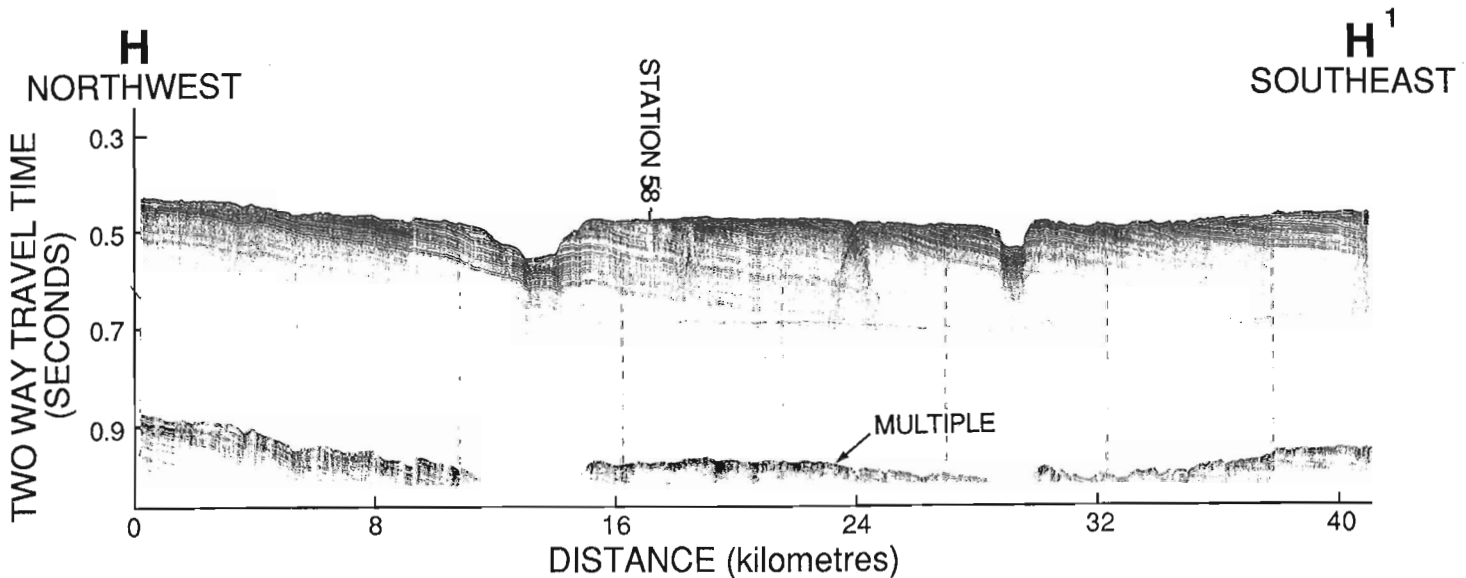


Figure 64.9. Section H-H¹, seismic reflection profile illustrating the southerly thickening succession of "Silurian" strata in eastern Hudson strait. These beds have been extensively bevelled by erosion. Two former erosional channels cut the strata. See Figure 64.4 for location.

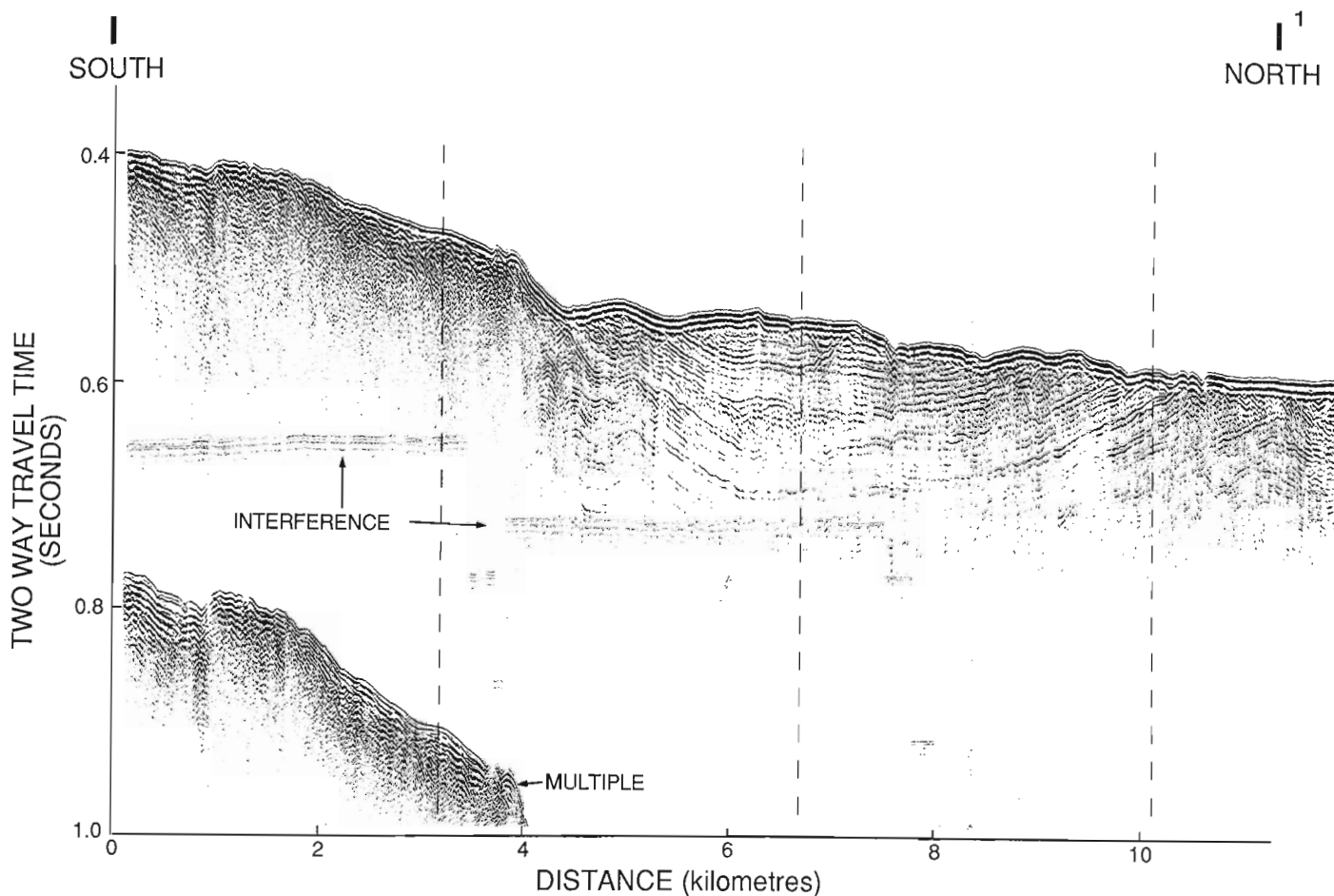


Figure 64.10. Section I-I¹, seismic reflection profile showing "Silurian strata" in fault contact with Precambrian rocks on the south side of the strait 65 km east of Cape Hopes Advance. Calculations of the strata thickness suggest that some 875-1170 m of vertical movement has occurred at the fault. See Figure 64.4 for location.

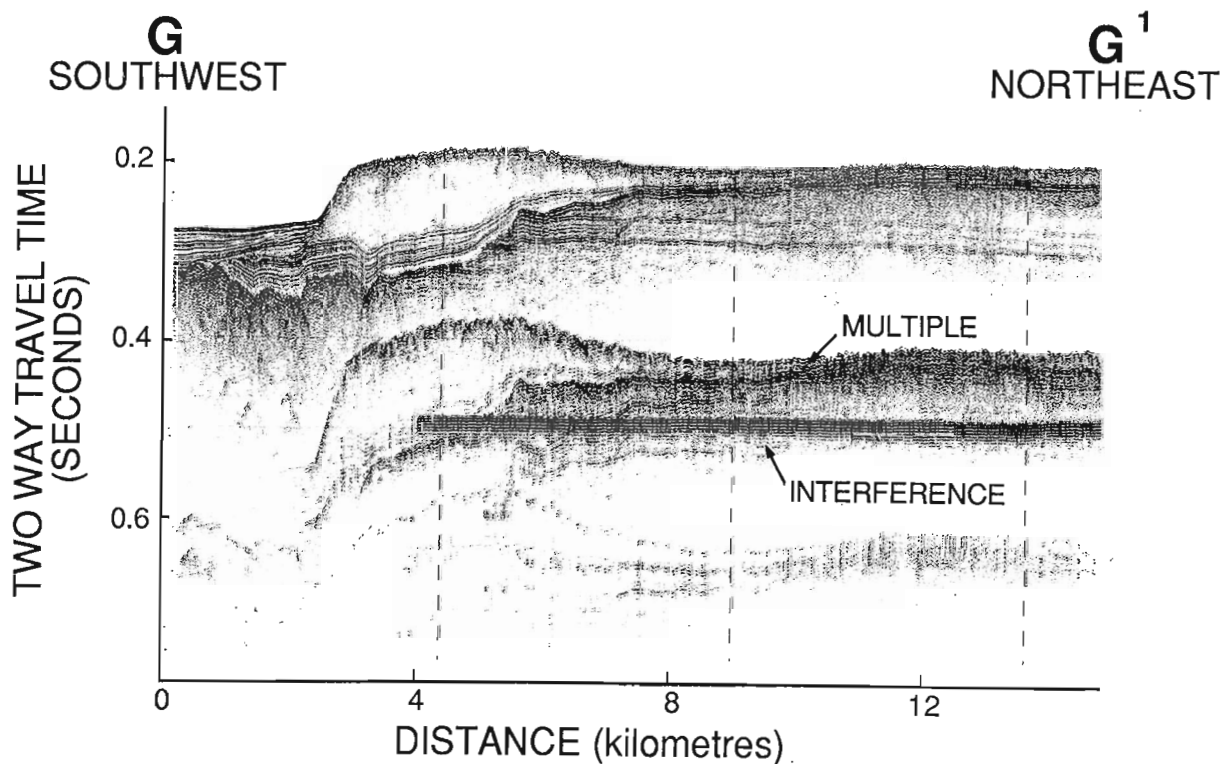


Figure 64.11. Section G-G¹, seismic reflection profile showing a moraine up to 70 m thick lying on earlier stratified sediments of presumed Quaternary age, which unconformably overlie truncated Ordovician strata and Precambrian rocks on the south side of the strait 52 km west of Cape Hopes Advance. Shoreward of the moraine the underlying Quaternary sediments are unconformably overlain by a younger sequence of stratified sediments. See Figure 64.4 for location.

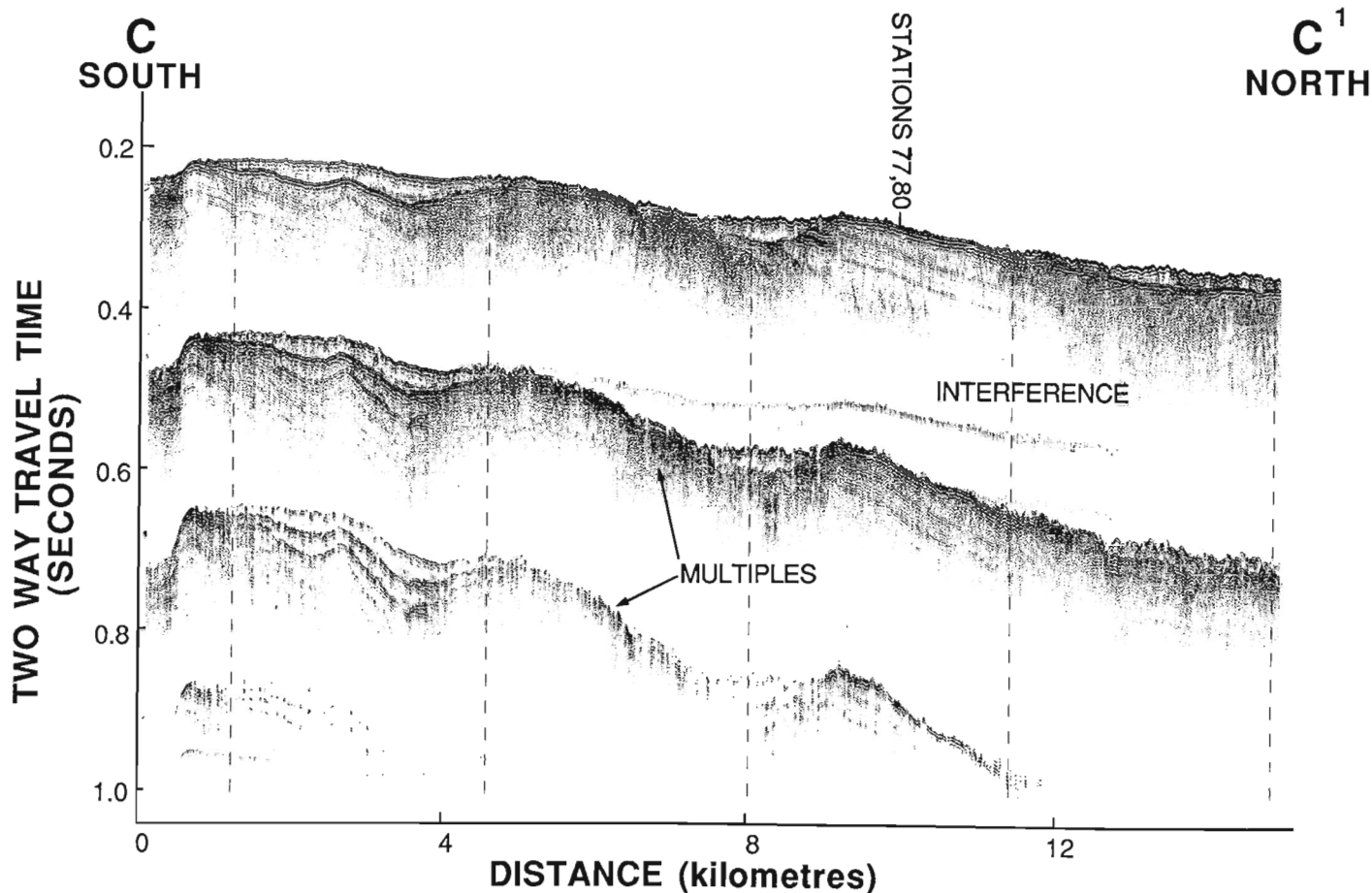


Figure 64.12. Section C-C¹, seismic reflection profile showing cuesta ridges in northward dipping Ordovician strata on the south side of the strait. Glacial drift up to 30 m thick fills the depressions on the bedrock surface. See Figure 64.4 for location.

indicate the section at the south side of the strait in this area is 875 to 1170 m thick assuming velocities of 3 km/s and 4 km/s respectively¹. The strata here are in fault contact with the Precambrian rocks (Fig. 64.10) and displacement is in the order of 875 to 1170 m on the basis of the measurements and velocities indicated above¹. This is in good agreement with the calculated displacement farther east indicated above.

Where intersected 52 km west of Cape Hopes Advance the structure there has become more synclinal in character. Ordovician rocks at the contact with the Precambrian have been truncated by erosion (Fig. 64.11). If there has been faulting at this contact it is not evident that the displacement is as large as that farther east. Some structural adjustment, however, occurs at a fold flecture 61 km to the northeast. About 175 km to the west, (Fig. 64.12), a cuesta development in Ordovician rocks on the south side of the strait is covered by Quaternary sediments and is not unlike cuestas along the north side of the strait.

Structural disturbance recorded by the Paleozoic strata in Hudson Strait thus appears to be most intense along the fault north of Ungava Bay.

Surficial sediments

Information on unconsolidated surficial sediments was obtained with high resolution and single channel seismic reflection systems along tracks indicated in Figure 64.2 and

from eight piston cores, eighteen grab samples, and three camera stations during cruise 85-027 (Table 64.1). Locations of these and previous sample stations are indicated in Figure 64.3. Bulk samples were also obtained from surficial sediments adhering to the legs of the drill at several stations.

Hudson Strait is an important area in terms of the Quaternary history of the region. It has been regarded as a major dispersal route for glacial ice from one or more inland ice centres. Evidence on eastern Meta Incognita Peninsula (southeastern Baffin Island between Frobisher Bay and Hudson Strait) indicative of northeastward movement of ice has been interpreted to indicate impingement of Hudson Strait ice (Blake, 1966; Stravers, 1986) and also inundation by ice flowing out of Ungava Bay and across Hudson Strait from a dispersal centre on Labrador or Ungava (e.g. Miller, 1982; Andrews and Miller, 1983).

The presence of till in the seafloor of Hudson Strait, moraines, and multiple tills on the shelf at its eastern entrance testify that glacial ice has occupied Hudson Strait. Analyses of the samples obtained during cruise 85-027, except for a preliminary assessment of coarse fraction (gravel size) lithologies, are as yet incomplete and textural, paleontological and geochronological data which are important to delineating the history of late Quaternary events in the strait are not yet available. However, data from the acoustic profiles do permit a preliminary outline of surficial sediment thickness and to some extent their general makeup.

¹ Determinations on samples from the Ordovician unit indicate velocities in the order of 5-6 km/s (P. Ryall and C. Walls, personal communication, 1986). Probable section thicknesses thus are 100-200 m greater than indicated.

Surficial sediments are generally thin (5-10 m) throughout most of the strait and preferentially thicken in the deep basins (Fig. 64.13). They often completely infill minor bedrock depressions thus smoothing the seafloor morphology of Hudson Strait. Greatest accumulations are found in the eastern and western basins where sediments reach 90 m and 130 m in thickness, respectively (e.g. Fig. 64.5, 64.15). In Ungava Bay the most significant accumulations (up to 70 m) also occur within basins (Grant and Manchester, 1970).

The seismic records indicate that the surficial sediments in Hudson Strait consist of four or more unstratified and stratified units, although the complete sequence is not everywhere present. The stratigraphy is complex in some areas, for example in the thick sedimentary sequence of the eastern basin (Fig. 64.5, 64.14) and in some morainal occurrences (Fig. 64.11).

The lowermost of the surficial units recognized generally is acoustically unstratified and massive, and is interpreted as till (Fig. 64.15). The contact with overlying sediments is well defined and locally the unit thickens to

form mounds or ridges interpreted as moraines (Fig. 64.16). Surface and subsurface deposits of till appear to be widespread in the floor of Hudson Strait.

The till unit is overlain in the basins by an acoustically massive unit that is nearly transparent on the Hunttec records and appears to lack internal reflectors (Fig. 64.14). The upper contact of this unit commonly is well defined but sometimes is irregular and poorly defined. The origin of this unit has not been established. Acoustically similar units occur in the sediment sequences of Lake Melville (G. Vilks, personal communication, 1985), in Scott Trough on the northeastern Baffin Island shelf, and in the fiords of Baffin Island (Gilbert, 1982). Hunttec data indicate that acoustically similar material occurs on the north side of the eastern depression in Hudson Strait where sediments from a debris flow have come to rest adjacent to the bottom of the slope (flow area and sediment accumulation are illustrated in Fig. 64.5, 3-9 km along the profile). The subbottom unit in Hudson Strait thus may represent debris flow sediments. Alternately, a lightly compacted, relatively fine grained till containing few coarse clasts would probably have similar

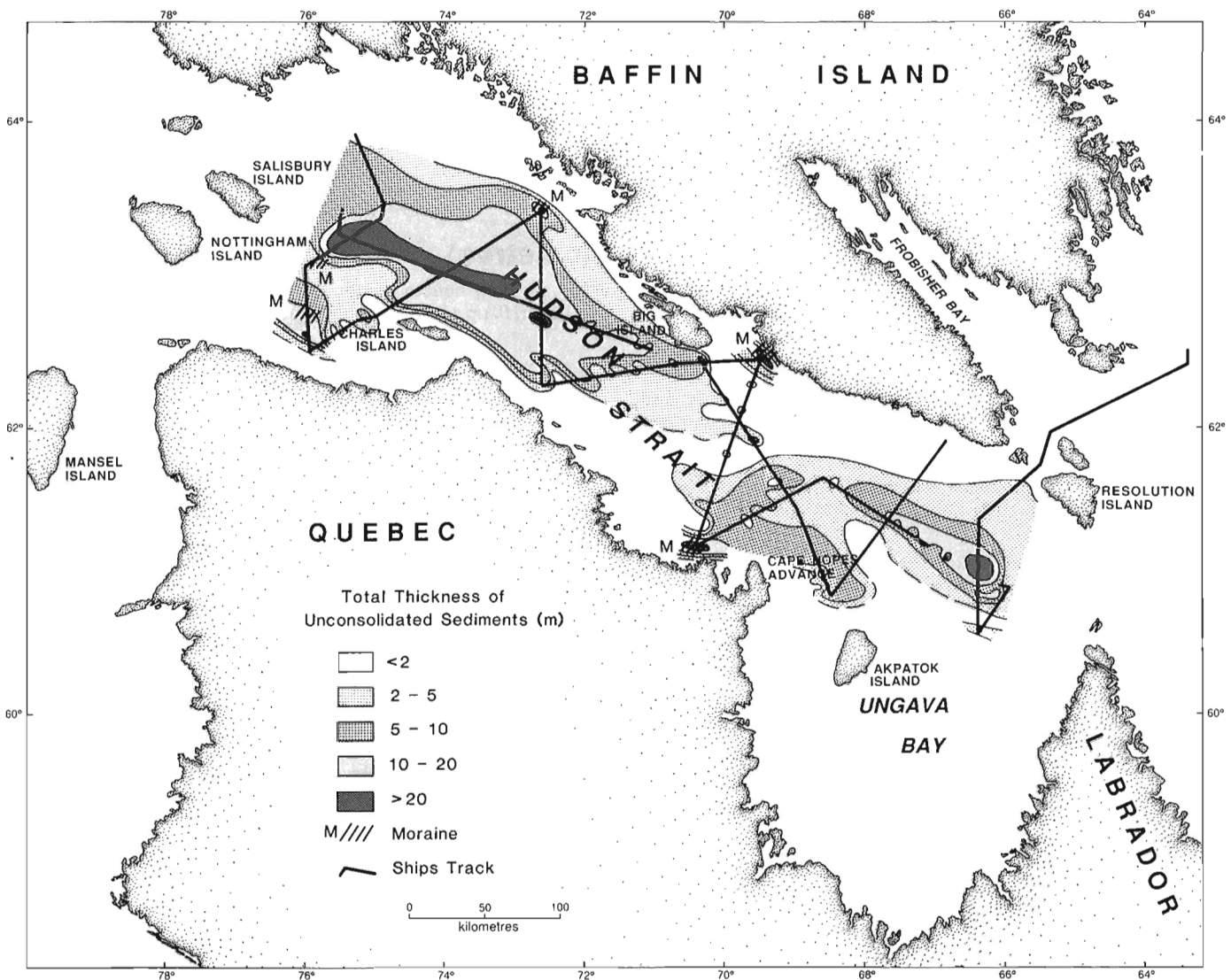


Figure 64.13. Isopach map of Quaternary sediments in Hudson Strait. The interpretation refers only to areas investigated in Hudson Strait in 1985.

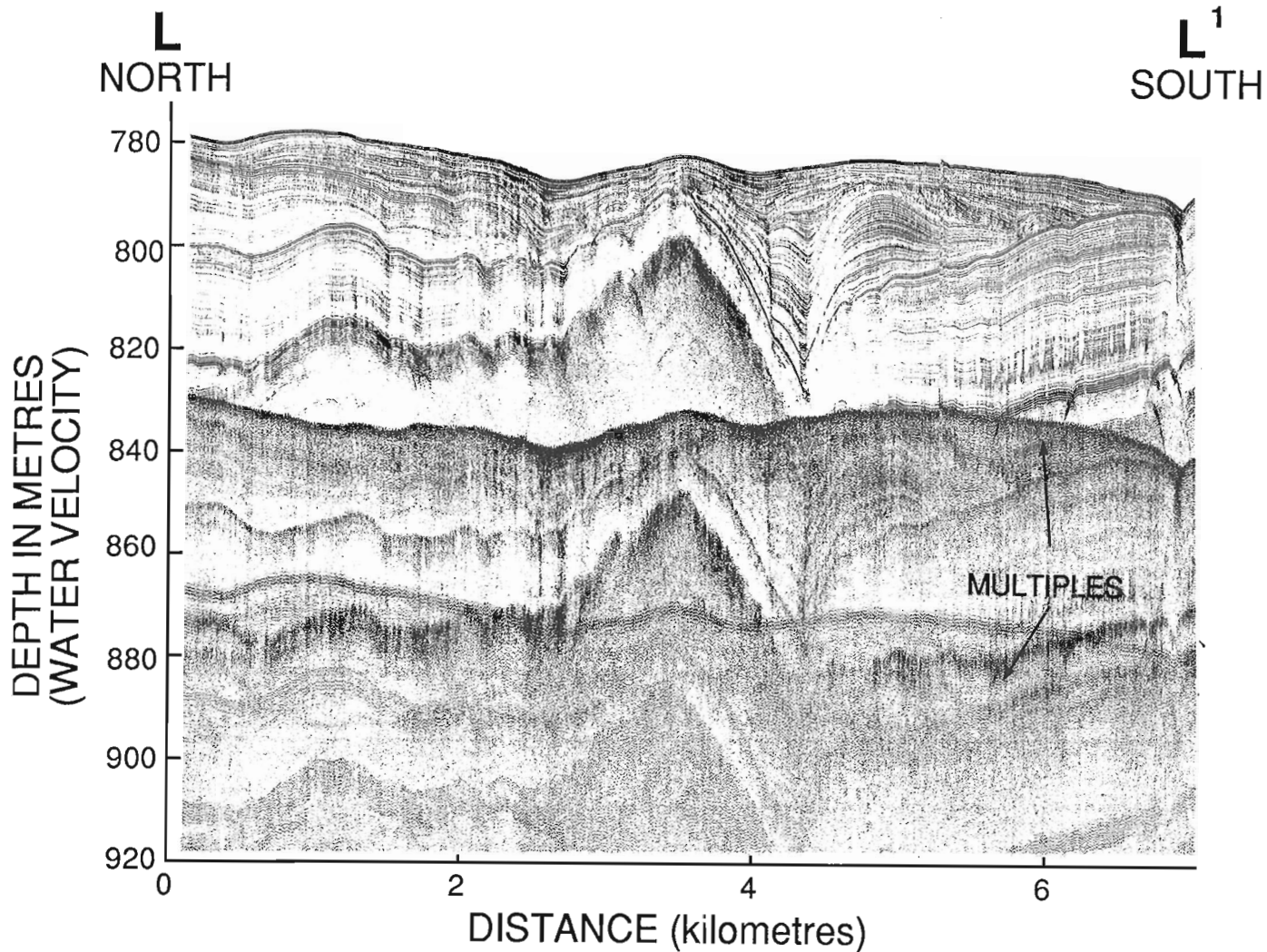


Figure 64.14. Section L-L¹, Huntex high resolution seismic reflection profile illustrating the complex pattern of sediment deposition in the eastern depression. This figure provides greater detail of the area between 16 and 24 km in section K-K¹ (Fig. 64.5).

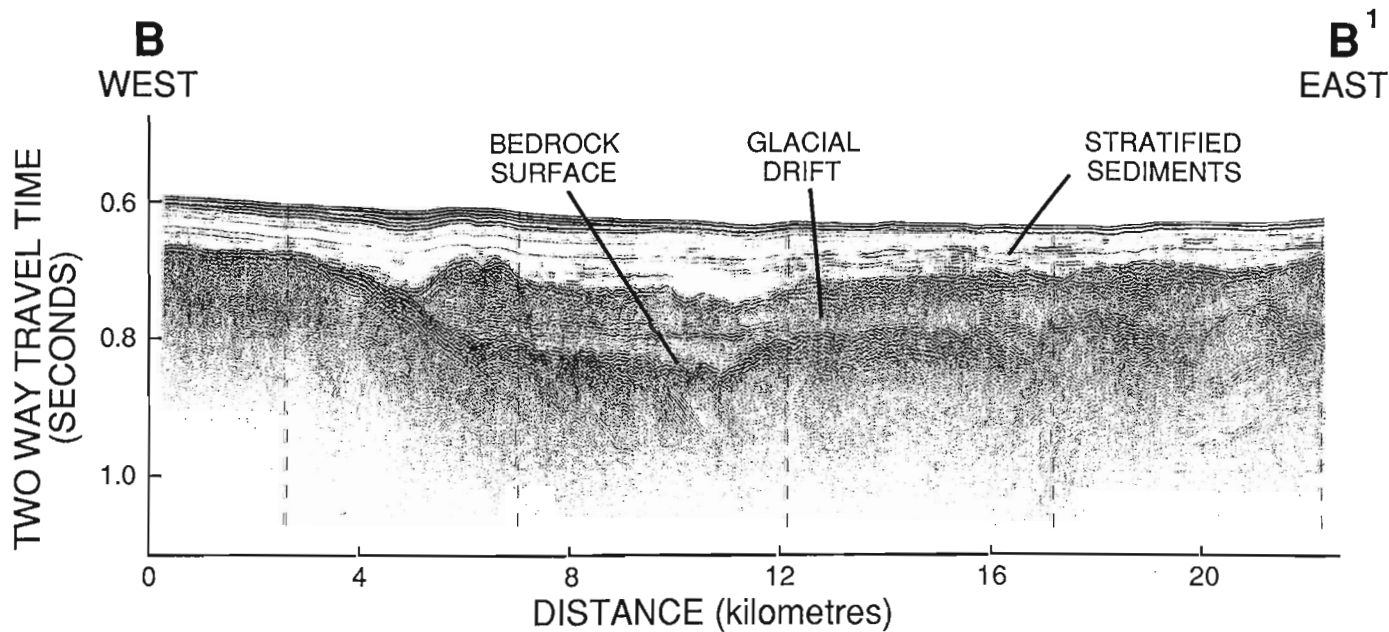


Figure 64.15. Section B-B¹, seismic reflection profile illustrating sediments in the western depression consisting of two or more tills up to 70 m thickness overlain by stratified sediments of about equal thickness. See Figure 64.4 for location.

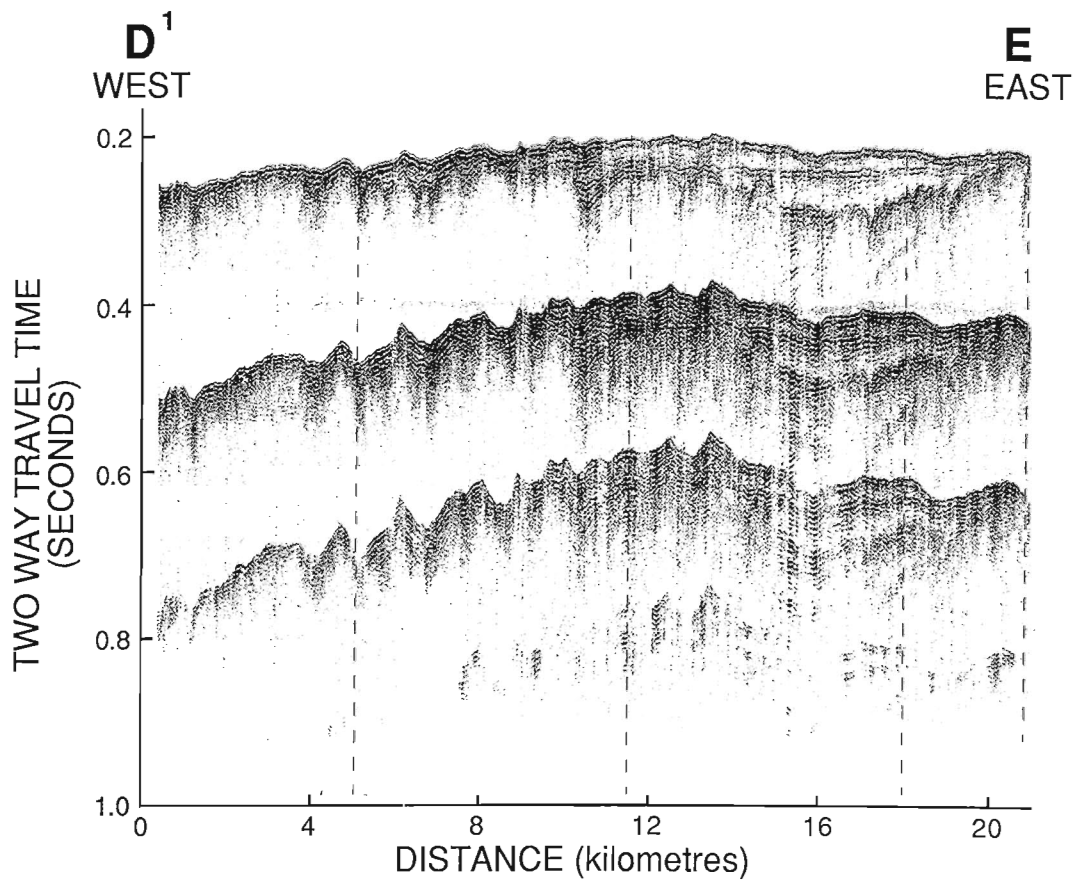


Figure 64.16. Section D¹-E, seismic reflection profile showing multiple till deposits forming moraines near Big Island on the north side of the strait. See Figure 64.4 for location.

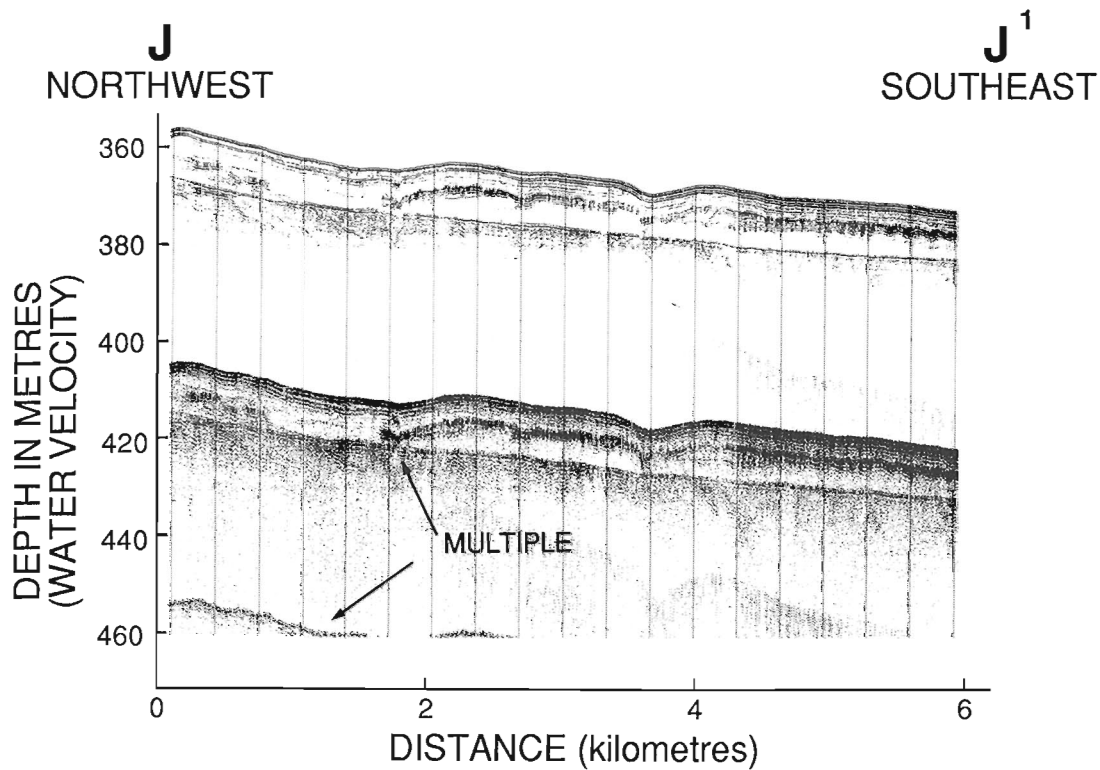


Figure 64.17. Section J-J¹, Huntec high resolution seismic profile illustrating glacial till up to 5 m thick lying on a smooth gently sloping erosional surface on "Silurian" rocks in eastern Hudson Strait. The till is overlain by 1-2 m of a stratified basal diamicton and 5-6 m of softer stratified sediments. See Figure 64.4 for location.

acoustic characteristics. Gilbert (1985) suggested the Baffin fiord unit may consist of fine sediments deposited in quiescent conditions when the glaciers that were the major source of sediment supply had retreated.

The massive units in many areas are overlain by stratified sediments (Fig. 64.15, 64.17) that consist of mud, sandy mud, and some pebbles. The acoustic data indicate that two or more acoustic units often are represented in these sediments. The lower part of the section commonly is characterized by well-defined, evenly spaced acoustic reflectors that are generally conformable with the surface of the underlying sediments.

The uppermost part of the section is well to poorly stratified on acoustic profiles, and the reflecting layers generally are not as well defined as in the underlying sediments. The boundary between these units in some areas is unconformable. In the eastern basin the stratified sediments can be divided into at least three units on the basis of their unconformable relations (Fig. 64.14), but they do not differ significantly from one another in acoustic character. Cores previously collected from sediments in the eastern basin 52 km east of where seismic profiles and cores were obtained in 1985 yielded dates of 8730 and 9100 years BP on shells from core depths 102-110 and 200-300 cm (Fillon et al., 1981; Fillon and Harmes, 1982) and 22 900 BP (Beta No. 8899) on total organic matter from a core depth of 540-550 cm. Extrapolation of these data to acoustic units basin wide is not yet possible because of the complex stratigraphy.

Most of the grab samples collected during cruise 85-027 appear to represent sediments deposited in glacial or glacio-marine environments; post-glacial sedimentation appears to be minimal and represented by relatively thin accumulations

that are mainly restricted to basal areas. The samples indicate that a gravel lag or partially modified sediments apparently resulting from winnowing by seabottom currents are prevalent in many areas except in the deeper parts of the strait where finer sediments and presumably quieter current conditions prevail.

Preliminary studies of pebble lithologies in grab samples indicate there are up to three times as many sedimentary as crystalline rock fragments. The sedimentary rock debris is typically carbonate, carbonate cemented sandstone and mudstone, and is commonly fossiliferous. Possible sources of this material include Paleozoic successions in Foxe Basin, Hudson Bay and the floor of Hudson Strait and Ungava Bay. Red clastic sandstones represent less than 1%, although they are a widespread component. The crystalline rock debris is typically grey gneiss and granitic rock characteristic of northern Quebec and southern Baffin Island. Indicator rocks, which are rocks having more clearly defined bedrock source areas, include iron-formation from the circum-Ungava fold belt, and volcanic rocks from the fold belt in northern Quebec. Volcanic rocks, although uncommon, are scattered throughout the strait. Iron-formation, including oolitic jasper and hematite and magnetite fragments, appears restricted to the eastern reaches of the strait (approximately east of the longitude of Akpatok Island). The pebble fraction of grab samples from the moraine 52 km west of Cape Hopes Advance is predominantly (80%) of crystalline lithology in contrast with sediments elsewhere in the strait that typically are composed of 50% or more of sedimentary rock. The crystalline composition of the rocks of the moraine suggests a northern Quebec origin for the ice that deposited this moraine, although the data are not considered conclusive.

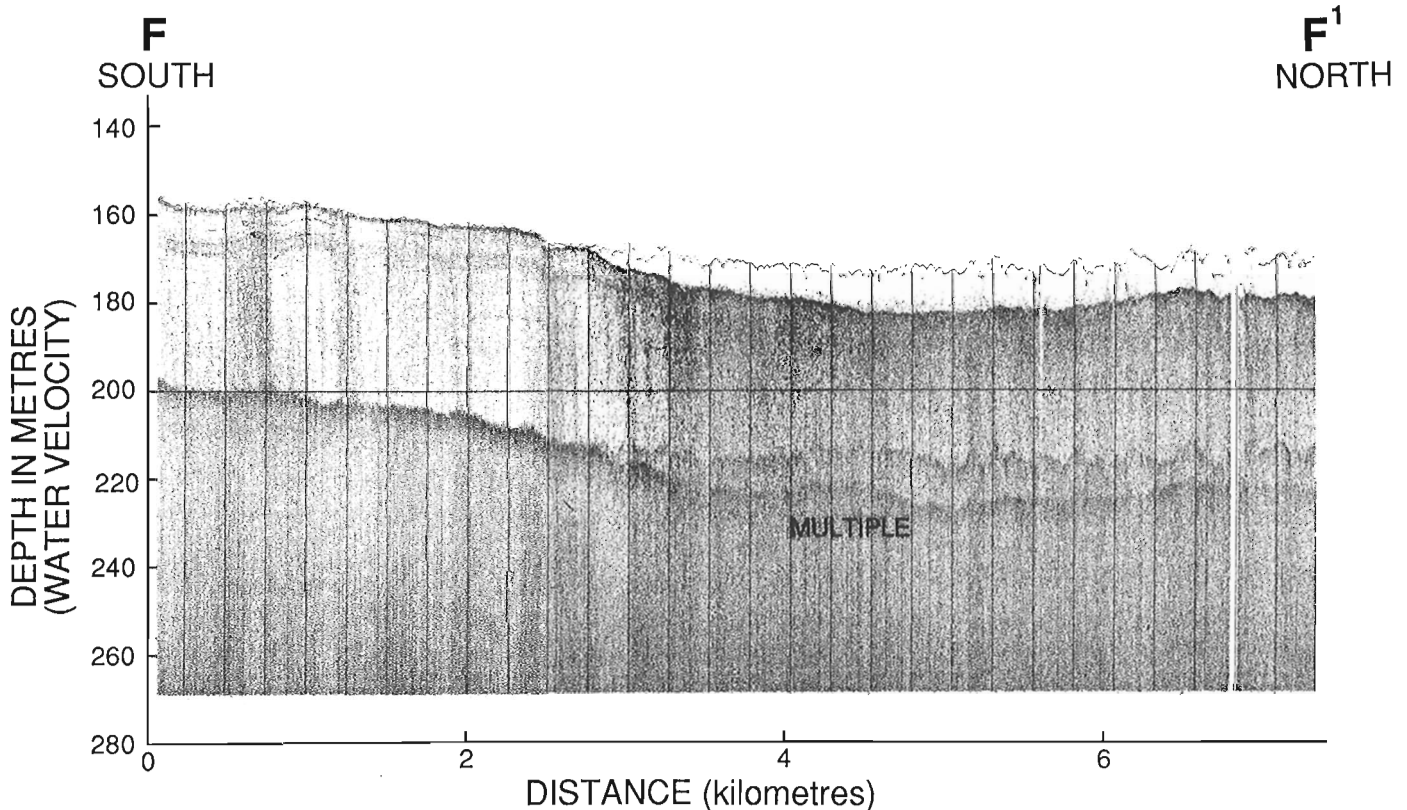


Figure 64.18. Section F-F¹, Hunttec high resolution seismic profile illustrating intensely ice scoured, unstratified, acoustically transparent till or other ice modified sediment exposed at the seafloor in 160 m of water. The surficial sediments range from 0 to 12 m in thickness. See Figure 64.4 for location.

Morainal accumulations of glacial sediments have been observed at several localities. Fifty-two km west of Cape Hopes Advance a moraine overlies stratified sediments of presumed Quaternary age at the bedrock contact between Paleozoic strata and Precambrian crystalline rocks (Fig. 64.11). Southwest of the moraine, toward the coast of northern Quebec, stratified sediments underlying the moraine are unconformably overlain by a younger sequence of stratified sediments. Multiple tills occur in a moraine near Big Island on the north side of the strait (Fig. 64.16), and in the western part of the strait, southeast of Nottingham Island two stratigraphically superimposed moraines of contrasting acoustic character are present. The older of these is significantly more acoustically opaque and massive than the succeeding one.

At present the extent of the moraines along the coasts, and their origins are not known. Those observed all lie west of Ungava Bay and thus may be related either to ice flowing into the strait from adjacent land areas, or to ice flowing generally eastward along the strait.

Post depositional modification of the surficial sediments through scouring by grounded icebergs is evident in Hudson Strait down to depths of 350-365 m below sea level (e.g. Fig. 64.18). Scours reach to 5 m in depth and, from limited sidescan sonar records, generally trend along the east-west axis of the strait. As indicated previously, modification of sediments has also occurred through winnowing by seabottom currents and locally through slumping or debris flows.

Acknowledgments

The authors are grateful to Captain F.W. Maugher, officers, crew and scientific staff aboard **CSS Hudson** for their co-operation and assistance in carrying out these studies; to J. Coombs, B. Henderson, A. Fagan, D. Milan, NORDCO Ltd., and C. Walls, Dalhousie University, and W. MacKinnon, AGC for dedicated support of the drill core sampling; to G. Standen, Hunttec (70) Ltd., and S. Lau, University of Manitoba, for operation of the Hunttec high resolution system, and geotechnical measurements, respectively, to H. Weile for photographic services at sea and in the lab; and to all the Atlantic Geoscience Centre staff who participated in the cruise for their fine support and co-operation. Sincere thanks are also extended to A.C. Grant and H.W. Josenhans for very helpful discussion and for review of the manuscript.

References

- Andrews, J.T. and Miller, G.H.
1983: Grant EAR-79-26061: Quaternary history of the Northeast sector of the Laurentide ice sheet and the mid-Wisconsin sea level problem; Institute of Arctic and Alpine Research, University of Colorado, Final report to the National Science Foundation, 43 p.
- Andrews, J.T., Shilts, W.W., and Miller, G.H.
1983: Multiple deglaciations of the Hudson Bay Lowlands, Canada, since deposition of the Missinaibi (last interglacial?) formation; *Quaternary Research*, v. 19, p. 18-37.
- Blackadar, R.G.
1966: Geological reconnaissance, southern Baffin Island, District of Franklin; Geological Survey of Canada, Paper 66-24, 32 p.
- Blake, W., Jr.
1966: End moraines and deglaciation chronology in northern Canada with special reference to southern Baffin Island; Geological Survey of Canada, Paper 66-26, 32 p.
- Bolton, T.E., Sanford, B.V., Copeland, M.J., Barnes, C.R., and Rigby, J.K.
1977: Geology of Ordovician rocks, Melville Peninsula and region, southeastern District of Franklin; Geological Survey of Canada, Bulletin, 269, 134 p.
- Clark, P.
1985: A note on the glacial geology and post glacial emergence of the Lake Harbour region, Baffin Island, N.W.T.; *Canadian Journal of Earth Sciences*, 22, p. 1864-1871.
- Drinkwater, K.F.
1983: Moored current meter data from Hudson Strait, 1982; Canadian Data Report, Fisheries and Aquatic Sciences, No. 381, 46 p.
- Fillon, R.H. and Harmes, R.A.
1982: Northern Labrador Shelf glacial chronology and depositional environments; *Canadian Journal of Earth Sciences*, 19, p. 162-192.
- Fillon, R.H., Hardy, I.A., Wagner, F.J.E., Andrews, J.T., and Josenhans, H.W.
1981: Labrador Shelf: shell and total organic matter - C¹⁴ discrepancies; In *Current Research, Part B*, Geological Survey of Canada, Paper 81-1B, p. 105-111.
- Gilbert, R.
1982: The Broughton Trough of eastern Baffin Island. *Canadian Journal of Earth Sciences*, v. 19, p. 1599-1607.
- Grant, A.C.
1975: Geophysical results from the continental margins off southern Baffin Island; in *Canada's continental margins and offshore petroleum exploration ed.*; C.J. Yorath, E.R. Parker and D.J. Glass; *Canadian Society of Petroleum Geologists, Memoir 4*, p. 411-431.
- Grant, A.C. and Manchester, K.S.
1970: Geophysical investigations in the Ungava Bay - Hudson Strait region of northern Canada; *Canadian Journal of Earth Sciences*, v. 7, p. 1062-1076.
- Gray, J. and Lauriol, B.
1985: Dynamics of the Late Wisconsin ice sheet in the Ungava Peninsula interpreted from geomorphological evidence; *Arctic and Alpine Research*, v. 17, p. 289-310.
- Gray, J., Lauriol, B., and Ricard, J.
1985: Glacio-marine outwash deltas, early ice retreat and stable ice fronts in the northeastern coastal region of Ungava; 14th Arctic Workshop, Bedford Institute of Oceanography, Dartmouth, N.S., Nov. 6-8, 1985, Program and Abstracts, p. 15-153.
- Heywood, W.W. and Sanford, B.V.
1976: Geology of Southampton, Coats, and Mansel Islands, District of Keewatin, Northwest Territories; Geological Survey of Canada, Memoir 382, 35 p.

- Jones, E.P. and Drinkwater, K.
1982: Report of cruise 82-027, CSS Hudson, August 12 to September 8, 1982, Bedford Institute of Oceanography, unpublished report.
- Løken, O.H.
1978: Postglacial tilting of Akpatok Island, Northwest Territories; *Canadian Journal of Earth Sciences*, 15, p. 1547-1553.
- MacLean, B.
1985: Geology of the Baffin Island Shelf; in *Quaternary Environments: eastern Canadian Arctic, Baffin Bay, and western Greenland*, ed. J.T. Andrews; George Allen and Unwin, London, p. 154-177.
- MacLean, B. and Williams, G.L.
1983: Geologist investigations of Baffin Island Shelf in 1982; in *Current Research, Part B*, Geological Survey of Canada, Paper 83-1B, p. 309-315.
- Miller, G.H.
1982: Glaciation of southeastern Meta Incognita Peninsula, Baffin Island: evidence for a Labradorian ice-dispersal centre; in *11th Annual Arctic Workshop, Institute of Arctic and Alpine Research, Boulder, Colorado, March 1982, Program and Abstracts*, p. 65-67.
- Osterman, L.E., Miller, G.H., and Stravers, J.A.
1985: Late and mid-Foxe glaciation of southern Baffin Island; in *Quaternary Environments: eastern Canadian Arctic, Baffin Bay and West Greenland*, ed. J.T. Andrews; George Allen and Unwin, London, p. 530-545.
- Praeg, D.B., MacLean, B., Hardy, I.A., and Mudie, P.J.
1986: Quaternary geology of the southeast Baffin Island continental shelf; Geological Survey of Canada, Paper 85-14, 38 p.
- Sanford, B.V.
1974: Paleozoic geology of the Hudson Strait region; in *Report of Activities, Part B*, Geological Survey of Canada, Paper 74-1B, p. 144-146.
- Sanford, B.V., Grant, A.C., Wade, J.A., and Barss, M.S.
1979: Geology of Eastern Canada and adjacent areas; Geological Survey of Canada, Map 1401A, scale 1:2 000 000.
- Shilts, W.W.
1980: Flow patterns in the central North American ice sheet; *Nature*, v. 286, p. 213-218.
1984: Quaternary events – Hudson Bay Lowland and southern District of Keewatin; Geological Survey of Canada, Paper 84-10, p. 117-126.
- Stravers, J.A.
1986: Glacial geology of outer Meta Incognita Peninsula, southern Baffin Island, Arctic Canada; unpublished Ph.D. Thesis, University of Colorado, Boulder, Colorado, 311 p.
- Stravers, J.A. and Miller, G.H.
1984: Provenance studies and Foxe/Wisconsin age glacial reconstruction of the Meta Incognita Peninsula, southern Baffin Island; 5th Congress AQQUA, Abstracts, p. 51.
- Taylor, F.C.
1979: Reconnaissance geology of a part of the Precambrian Shield, northeastern Quebec, northern Labrador and Northwest Territories; Geological Survey of Canada, Memoir 393, 99 p.
1982: Reconnaissance geology of a part of the Canadian Shield, northern Quebec and Northwest Territories; Geological Survey of Canada, Memoir 399, 32 p.
- Trettin, H.P.
1975: Investigations of Lower Paleozoic geology, Foxe Basin, Northeastern Melville Peninsula and parts of northwestern and central Baffin Island; Geological Survey of Canada, Bulletin 251, 175 p.
- Workum, R.H., Bolton, T.E., and Barnes, C.R.
1976: Ordovician geology of Akpatok Island, Ungava Bay, District of Franklin; *Canadian Journal of Earth Sciences*, v. 13, p. 157-178.

Tidal channel facies of the Virgelle Member (Cretaceous Milk River Formation), southern Alberta

Project 860011

D.A. Leckie and R.J. Cheel¹
Institute of Sedimentary and Petroleum Geology, Calgary

D.A. Leckie, and Cheel R.J., Tidal channel facies of the Virgelle Member (Cretaceous Milk River Formation), southern Alberta; in *Current Research, Part B, Geological Survey of Canada, Paper 86-1B*, p. 637-645, 1986.

Abstract

Sandstones of the Virgelle Member (Cretaceous Milk River Formation) are well exposed in three dimensions in hoodoos along the Milk River valley in southern Alberta. The exposure allows detailed analysis of ebb- and flood-tidal channel facies. The basal Virgelle Member comprises a lower shoreface facies characterized by amalgamated, hummocky cross-stratified sandstone passing upward into horizontally laminated and swaley cross-stratified sandstone. The lower shoreface facies is overlain by cross-stratified sandstones interpreted as deposits of tidal channels and associated facies that are locally ebb or flood dominated. Evidence of tidal activity includes: superposed bipolar, planar tabular cross-strata; reversing paleocurrent directions along strike; reactivation surfaces; mud-layer couplets; and tidal bundles. The ebb-dominated facies is characterized by northward dipping, planar tabular cross-strata sets, with up to 3 m relief, bounded by lateral accretion surfaces. The flood-dominated facies is characterized by planar tabular cross-stratification with shale rip-up clasts. Southward dipping cross-strata predominate.

Résumé

Des grès du membre de Virgelle (formation de Milk River datant du Crétacé) sont bien exposés dans des cheminées de fée de trois dimensions le long de la vallée de la rivière Milk, dans le sud de l'Alberta. Cette exposition permet une analyse détaillée des faciès des chenaux d'étiage et de crue. Le membre de Virgelle basal comprend un faciès de la zone infratidale inférieure caractérisé par du grès amalgamé à des stratifications entrecroisées à creux et à bosses, passant vers le haut à une couche horizontale de grès laminé à stratifications entrecroisées. Le faciès de la zone infratidale inférieure est recouvert par des grès à stratification entrecroisée interprétés comme étant des dépôts de chenaux et de deltas de marée dominés par endroit par les étiages ou les crues. Les signes d'activité de marée comprennent: des strates entrecroisées planes, bipolaires; des paléocourants inversés en direction du sillon; des surfaces de réactivation; des couches de boue couplées et des amoncellements produits par la marée. Le faciès dominé par la marée est caractérisé par des ensembles de strates entrecroisées planes en pente douce vers le nord d'un relief atteignant 3 m, bordés par des surfaces d'accrétion latérale. Le faciès dominé par la crue est caractérisé par une stratification entrecroisée plane accompagnée de fragments de schistes argileux fragmentés. La stratification entrecroisée inclinée vers le sud prédomine.

¹ Department of Geology, Brandon University, Brandon, Manitoba R7A 6A9

Introduction

Evidence for tidal influence on sedimentation in the Cretaceous epeiric seaway of Western Canada has been inconclusive and based on sparse observations of tide-formed structures (R. Rahmani, pers. comm., 1986; Leckie and Walker, 1982; Leckie, 1985; Leckie, 1986; Chiang, 1984; McCrory and Walker, 1986). Shaw (1964) categorically stated that significant tides would not develop in shallow epeiric seas. Slater (1985) argued that, based on numeric modelling of the Western Interior Seaway, the maximum tidal range that could develop was 0.86 m, with maximum current velocities of 10 cm/s. Conversely, Klein and Ryer (1978) used sedimentological evidence to argue that epeiric seas were characterized and dominated by tides. Pannella and MacClintock (1968) and Berry and Barker (1975) suggested that the presence of daily growth rings indicated that Upper Cretaceous bivalves of the seaway were affected by tidal rhythms.

Outcrops of the Virgelle Member (Cretaceous Milk River Formation; Fig. 65.1) at Writing on Stone Provincial Park in southern Alberta (Fig. 65.2) has provided a unique opportunity to describe abundant evidence of deposition in a tidally-influenced shoreline setting. This paper presents preliminary documentation of the sedimentology and lateral variability of both ebb- and flood-dominated portions of a tidal channel, which are exposed in three dimensions in hoodoos along a section of the incised Milk River valley.

Geological setting

The Milk River Formation (Santonian-Campanian) is exposed in outcrop along the Milk River in southern Alberta, where the strata dip gently to the northeast on the eastern flank of the Sweetgrass Arch (Fig. 65.2). The three members of the Milk River Formation (Meijer Drees and Myhr, 1981; Fig. 65.1, 65.3) include: the lowermost, Telegraph Creek Member (marine shelf sandstone and shale), the middle, Virgelle Member (shoreface sandstone with tidal channel deposits), and the uppermost, Dead Horse Coulee Member (nonmarine sandstone and shale). The Milk River Formation comprises a coarsening-upward sequence to the top of the Virgelle Member where it is locally capped by coals and floodplain sediments of the Deadhorse Coulee Member (Fig. 65.3). Figure 65.3 shows the stratigraphic context of the tidal channel facies as it occurs in the nearby subsurface. Overall, the Milk River sequence preserves sediments deposited in a progradational shelf to terrestrial setting.

Meijer Drees and Myhr (1981) interpreted the Milk River Formation as a west-northwest trending shoreline with beach-barrier facies that prograded in a northerly direction. The Virgelle Member thins northeastward (Slipper and Hunter, 1931) and is laterally replaced by the thinly interbedded marine sandstone and shale of the Alderson Member (Meijer Drees and Myhr, 1981; McCrory and Walker (1986) interpreted the Virgelle Member as being deposited on a wave and tidally influenced, progradational shoreline. In this paper, we build on the earlier work of Meijer Drees and Myhr (1981) and McCrory and Walker (1986) and deal specifically with the effects of ebb- and flood-variability evident within the tidal channel. The source area of the Virgelle sediments is to the southwest, with K-feldspar and clear quartz derived from the Elkhorn volcanics of Wyoming and Montana (L. Rosenthal, pers. comm., 1985).

Facies of the Virgelle sandstone

For the purposes of description and interpretation, the Virgelle Member is subdivided into two major facies: lower shoreface facies and tidal channel facies. The latter varies

along strike due to local dominance of either ebb- or flood-tidal sediment transport along the paleoshoreline. In the following descriptions, we begin at the base of the progradational sequence and describe deposits that occupied increasingly landward positions in the overall depositional system.

Lower shoreface facies

The lowest sediments exposed are 2 m of interbedded shale and hummocky, cross-stratified, very fine grained sandstone. These are overlain by approximately 20 m of very fine to fine grained sandstone exhibiting amalgamated, hummocky cross-stratification and horizontal lamination, passing upward into fine grained sandstone with swaley cross-stratification and horizontal lamination. There is minimal bioturbation, with *Ophiomorpha* sp. the only burrows recognized. These sediments were deposited below fair weather wave base on the lower shoreface of a wave-dominated coastline. McCrory and Walker (1986) provide a detailed description and interpretation of this facies.

Tidal channel facies

The upper 8 to 9 m of the Virgelle Member consist predominantly of fine to medium grained, planar-tabular cross-stratified sandstone (Fig. 65.4a), erosionally overlying the lower shoreface deposits. This sandstone displays abundant evidence of tidal currents during deposition, including: superposed, bipolar, planar-tabular crossbeds (Fig. 65.4b); reactivation surfaces (Fig. 65.4b); mud-layer couplets (Fig. 65.4c) and tidal bundles (Fig. 65.4c; Boersma, 1969; Visser, 1980); and reversing paleocurrents along strike (Fig. 65.5). This facies occurs as distinctly ebb-dominated

PERIOD / STAGE		SOUTHEASTERN ALBERTA (MEIJER DREES AND MYHR, 1981)	
UPPER CRETACEOUS	CAMPANIAN	BEARPAW FM	
		JUDITH RIVER FM	
		PAKOWKI FM	LEA PARK FM
	SANTONIAN	MILK RIVER FM	ALDERSON MBR
		DEAD-HORSE COULEE VIRGELLE TELE-GRAPH CREEK	
	COLORADO GP	LLOYD-MINSTER FM	

Figure 65.1. Stratigraphic nomenclature.

(Sec. 1) or flood-dominated deposits (Sec. 2) as shown in Figure 65.5. In this figure the paleocurrents from each section are contrasted with the orientation of the paleoshoreline (landward to the south). The tidal deposits are also sufficiently different, sedimentologically, to warrant their subdivision into ebb- and flood-dominated facies described below.

Ebb-dominated channel facies. Figure 65.6 illustrates the sequence preserved in an ebb-dominated portion of a tidal channel (Sec. 1, Fig. 65.2). A legend is shown in Figure 65.7. The lower part of the sequence is dominated by sets of planar tabular cross-strata (up to 0.3 m thick) bounded by surfaces dipping at 10 to 20 degrees in a direction perpendicular to the dip of the cross-strata (Fig. 65.6), and becoming flatter down-dip. The total change in relief along the bounding surfaces is up to 3 m. The planar tabular cross-strata decrease in scale upward along the bounding surfaces (Fig. 65.8) and dip in a northward (seaward) direction (Fig. 65.6). The bounding surfaces dip variably along strike in either an easterly or westerly direction (parallel to the coastline), although at Section 1 they dip consistently to the east. One set of bounding surfaces was traced laterally along strike for 39 m.

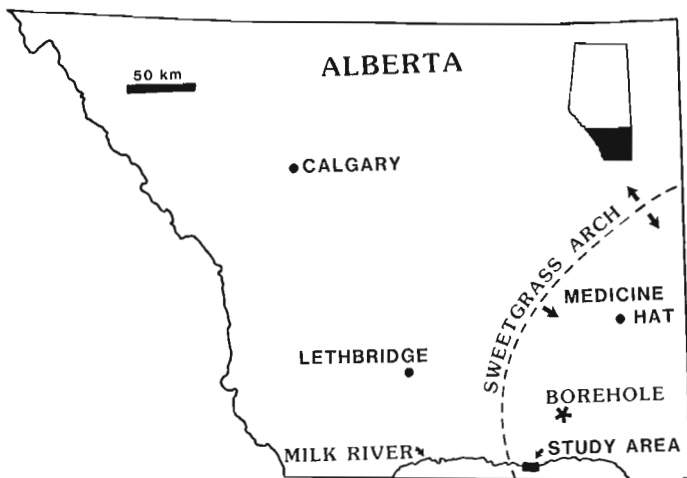
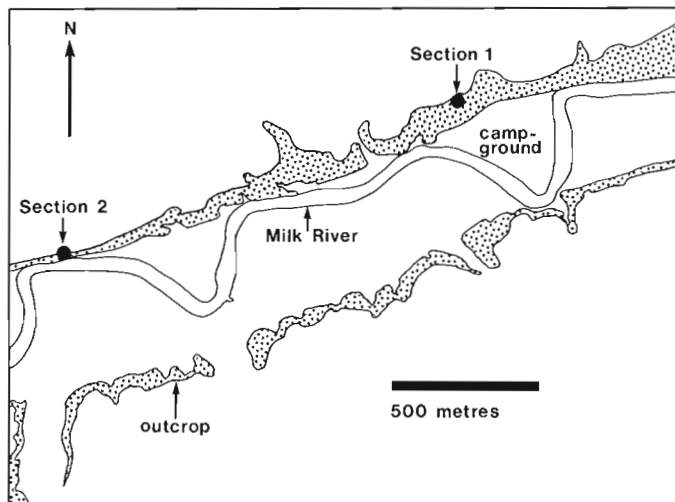


Figure 65.2. Location map: a) detail of the study area with Sections 1 and 2 shown in Figures 65.6 and 65.9, respectively; b) location of the study area at Writing on Stone Provincial Park in southern Alberta. Borehole refers to location of gas well shown in Figure 65.3.

The bounding surfaces are interpreted as the result of lateral accretion of the channel margin due to longshore drift (McCrory and Walker, 1986). An example of lateral accretion surfaces from another hoodoo is shown in Figure 65.8. Planar tabular cross-strata (Fig. 65.8b) formed by migration of sand waves within the channel, in response to ebb-tidal currents (to the north, Fig. 65.6b). The channels were probably also sites of flood-tidal currents, but these would have been considerably weaker than the ebb currents; thus flood-oriented crossbedding (southwards) is not preserved.

Lateral accretion surfaces are absent above approximately 2 m in Section 1 (Fig. 65.6) where fine grained sandstone displays trough cross-strata sets that thin upward from 0.5 m to 0.2 m (Fig. 65.6a). A 0.6 metre thick wedge of current ripple crosslaminated, fine grained sandstone, containing abundant, comminuted, carbonaceous debris,

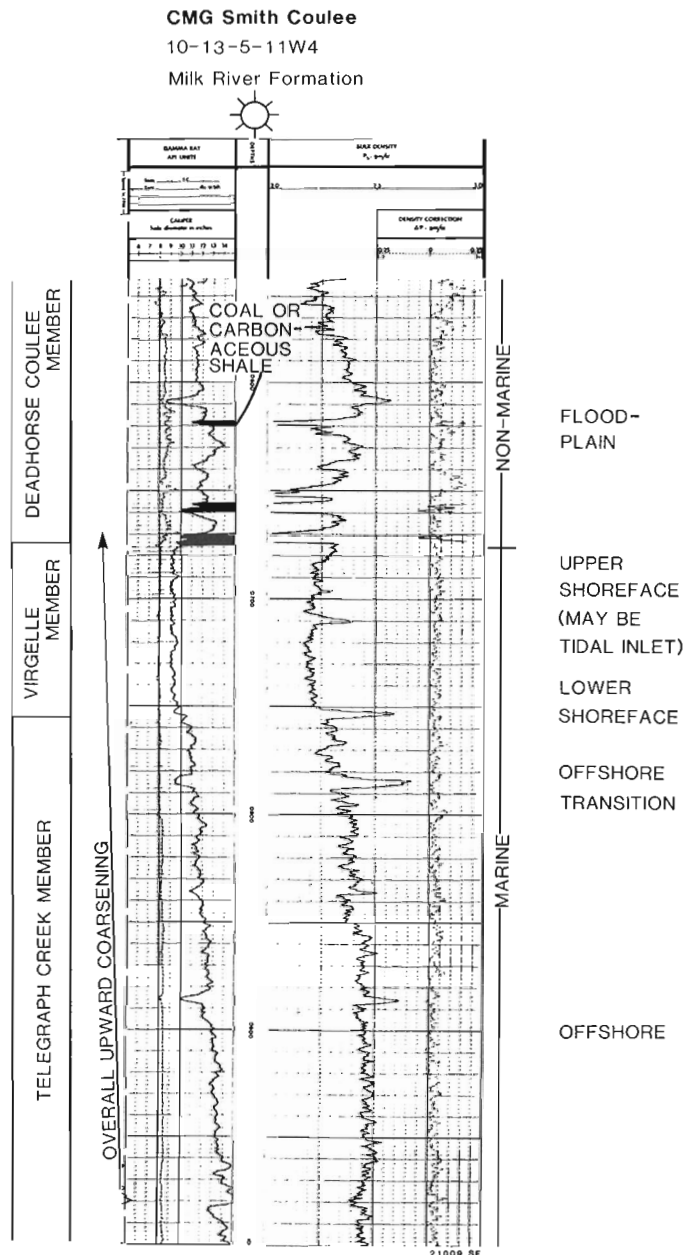


Figure 65.3. Gamma ray-density log of the Milk River Formation from gas well near Writing on Stone Provincial Park (see Fig. 65.2 for location of well). Interpretations are based on the motifs of the log patterns; application of stratigraphy is based on Meijer Drees and Myhr (1981).

occurs within the trough cross-stratified unit (Fig. 65.6a). Paleocurrents of the trough cross-strata were in a seaward direction (Fig. 65.6b). Above the trough cross-stratified sandstone is one planar tabular set overlain by a bed of current ripple crosslaminated, fine grained sandstone. Changes in structures reflect variation in flow strength through the ebb portion of the channel. The uppermost unit comprises shale with an interbed of ebb-oriented, current ripple crosslaminated, fine grained sandstone. These were deposited under relatively quieter conditions, possibly on a tidal flat or in a lagoon that was drained by the channel. Similarly, a wave ripple crosslaminated, fine grained sandstone at the top of Section 1 was deposited in a setting that was largely protected from strong tidal currents. Evidence of subaerial exposure of these "quiet-water" deposits is notably lacking. All were probably deposited under subtidal conditions.

The units above 2 m in Section 1 do not exhibit evidence of lateral accretion because they were deposited sufficiently landward to be unaffected by the longshore drift

that caused the lateral migration at the seaward edge of the channel. It might be argued that the accretion surfaces were formed by the lateral migration of a fluvial channel (as in meandering rivers or a distributary). However, if this were the case, overlying strata should show similar features. Furthermore, the predominance of planar tabular cross-stratification at the base of the channel is not typical of meandering rivers (Allen, 1970).

Flood-dominated channel facies. The flood-dominated channel facies is exposed at Section 2 and is characterized by evidence of paleocurrents flowing predominantly to the south (toward the paleoshoreline, Fig. 65.5). An example of the flood-tidal sequence is illustrated in Figure 65.9 (Sec. 2, Fig. 65.2), based on exposure along several adjacent hoodoos. The lowermost unit shown in each column in Figure 65.9 is the swaley cross-stratified lower shoreface, the top of which is exposed only at the eastern end of Section 2 (Fig. 65.9, col. 1 at 0.7 m), where it is erosively overlain by a medium grained sandstone of the channel facies, with abundant

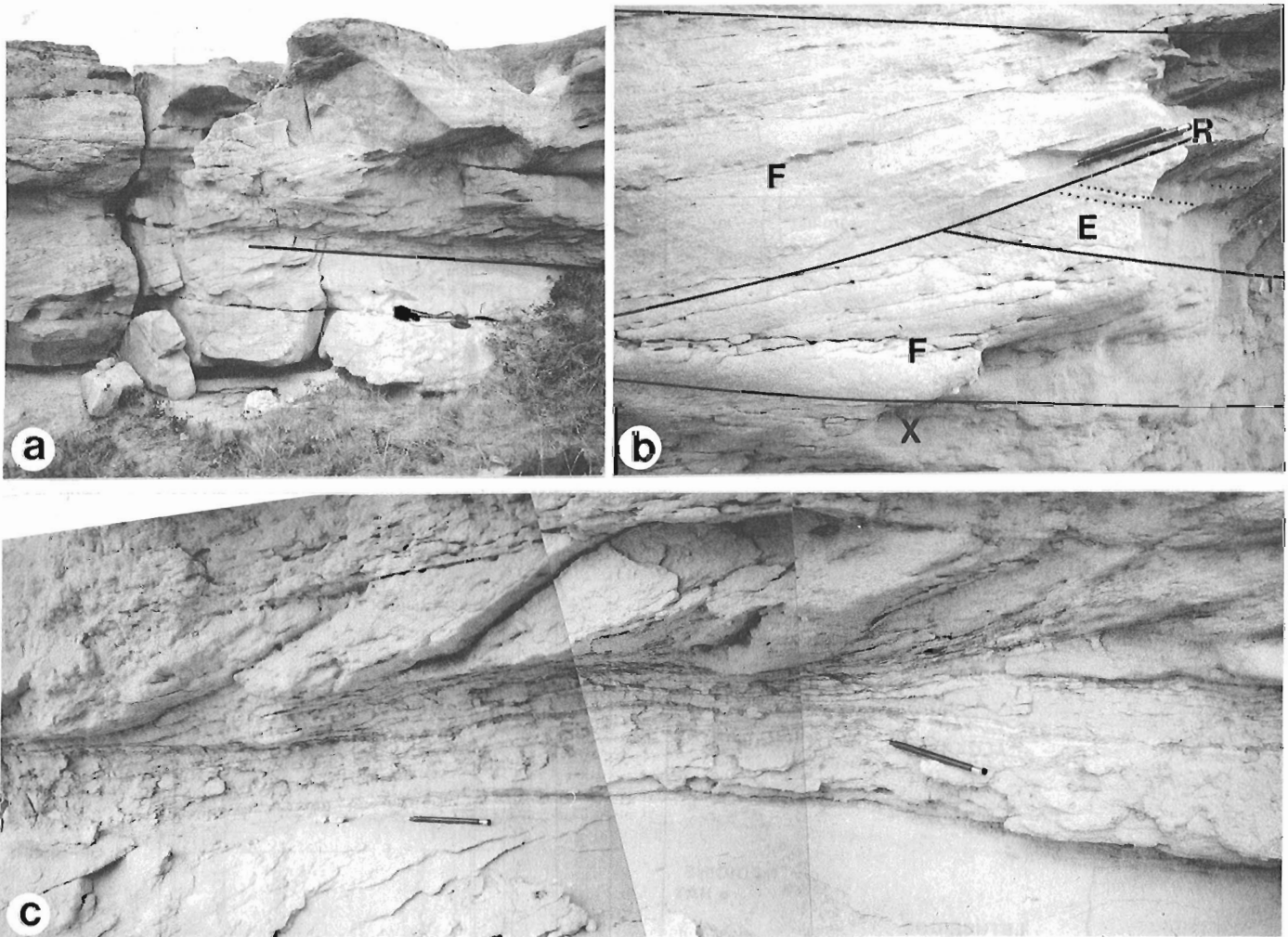


Figure 65.4. a) Flood-oriented planar tabular cross-strata sets climbing up a very gentle northward (seaward) dipping surface (solid line), interpreted as flood ramp. Flood direction is to the left. Camera for scale. b) Two flood-oriented planar tabular cross-strata sets (F) separated by a wedge of ebb-oriented planar tabular cross-strata (E). Lowermost unit is current ripple cross-stratified (x) sandstone. A reactivation surface (R) separates the flood-oriented sets. The flood-oriented sets have dips oriented N146°, 16°W and N151°, 18°W. The ebb-oriented set has dips of N172°, 10°E. These sets can be traced along strike to make sure they are not trough cross-stratified. Small pockmarks in sandstone are molds of weathered-out shale clasts. Pencil for scale. c) Tidal bundles and mud-layer couplets on flood-oriented planar tabular cross-strata. Lower portions of foreset strata are separated by mud drapes.

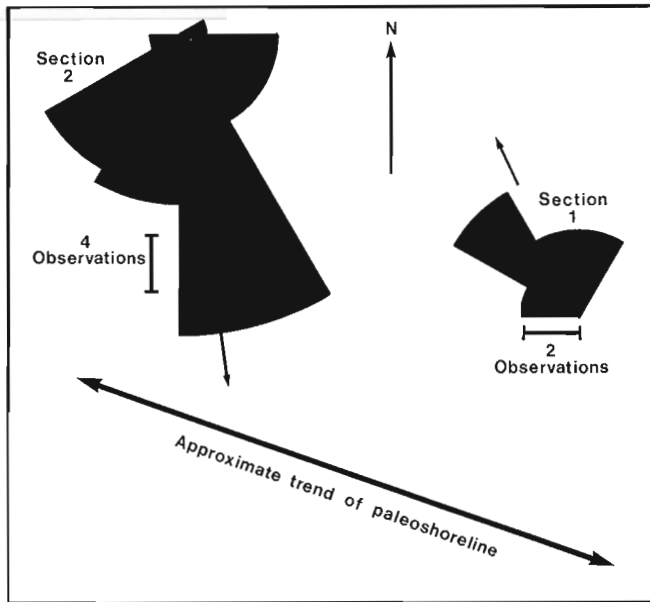


Figure 65.5. Summary of paleocurrent data from each of the two sections. These data indicate that Section 1 is ebb-dominated whereas Section 2 is flood dominated. Locations of the sections are shown in Figure 65.2. Trend of the shoreline is from Rice (1980) and Meijer Drees and Myhr (1981).

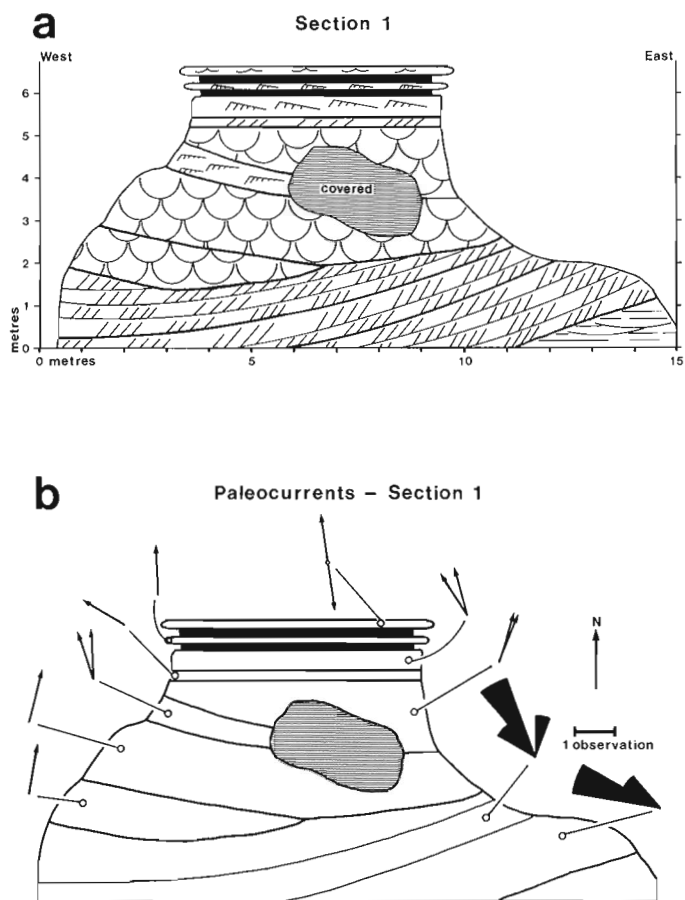


Figure 65.6. Ebb-dominated portion of tidal channel at Section 1. a) Sedimentary structures; b) Paleocurrents from different parts of the section. Location shown in Figure 65.2. For legend see Figure 65.7.

carbonaceous debris and shale rip-up clasts up to 18 cm in size. Lateral accretion surfaces are notably absent in the flood-dominated deposits, probably because flood-tidal currents do not result in significant deposition on the seaward side of the channel where longshore currents are active.

The flood facies is dominated by planar tabular, cross-stratified, fine grained sandstone, with set thicknesses ranging from 0.1 m to approximately 1 m (Fig. 65.4a), formed by sandwave migration in response to flood currents. The extreme domination by flood-tidal currents is evident from the consistent southward component of the dip direction of planar foresets (Fig. 65.5, Sec. 2). One exception occurs at approximately 5.8 m up column IV, Section 2 (Fig. 65.9), where a small planar tabular set with northward-dipping foresets lies between planar tabular sets with southward-dipping foresets (Fig. 65.4b), forming herringbone cross-stratification. In this case, ebb-tidal currents were locally strong enough to erode the lee side of a flood-oriented sandwave and construct a sandwave that migrated in the ebb direction, forming the northward-dipping foresets.

Another ebb-current feature is a reactivation surface between southward-dipping planar tabular sets, at 5.5 m up column IV, Section 2 (Fig. 65.9). This structure formed when the ebb current was sufficiently strong to erode the front of a flood-oriented sandwave, and perhaps sufficient to construct an ebb-oriented bedform, but any stratification formed by ebb migration was destroyed by the subsequent flood currents.

A third feature of the planar tabular sets that reflects the tidal influence are tidal bundles, which consist of sandstone foresets bounded above and below by subparallel layers of shale that thicken down the foresets (Fig. 65.4c). Bundles developed in sub-tidal environments, where slack water mud draped foresets that formed in response to the dominant tidal current. These are similar to tidal bundles described by Visser (1980) but lack erosional surfaces cutting foresets in response to a subordinate flow (which would be an ebb flow in the case described here). Allen (1984) suggested that this particular type of tidal bundle forms where there is a strong asymmetry in the tidal flow, with no significant sediment transport by the subordinate current. This interpretation is supported by only rare preservation of ebb-oriented structures at Section 2. A horizontal bed of interlaminated sandstone and shale, approximately 6 cm thick, composes the bottomsets of one planar tabular set (Fig. 65.4c; Fig. 9, col. I at 3.1 m). The shale layers are

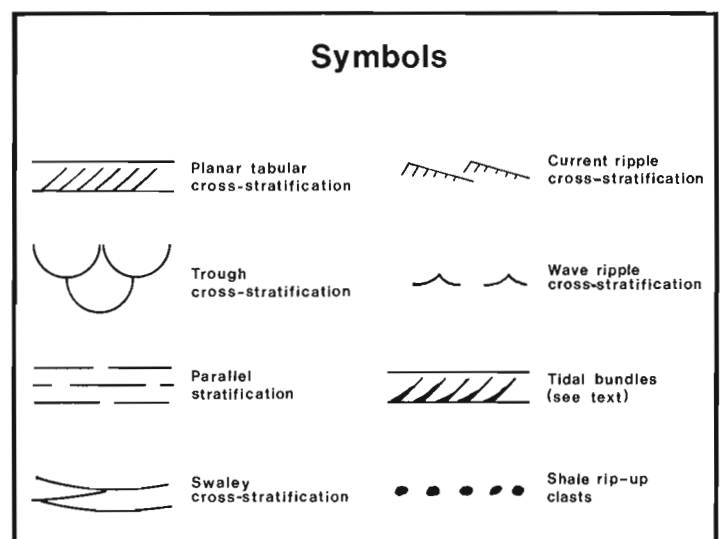


Figure 65.7. Legend for Figures 65.6 and 65.9.

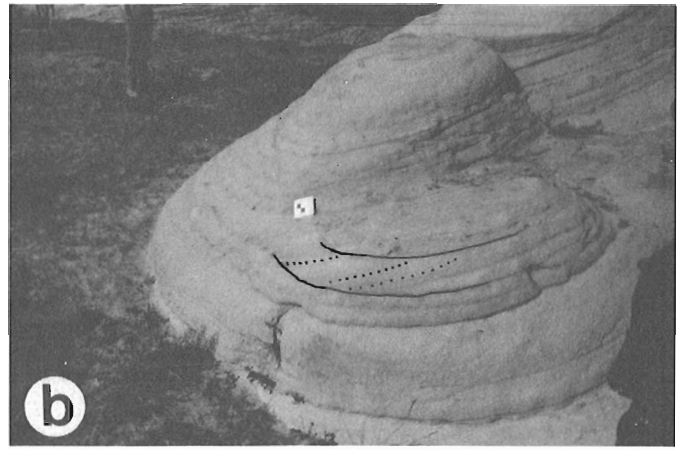
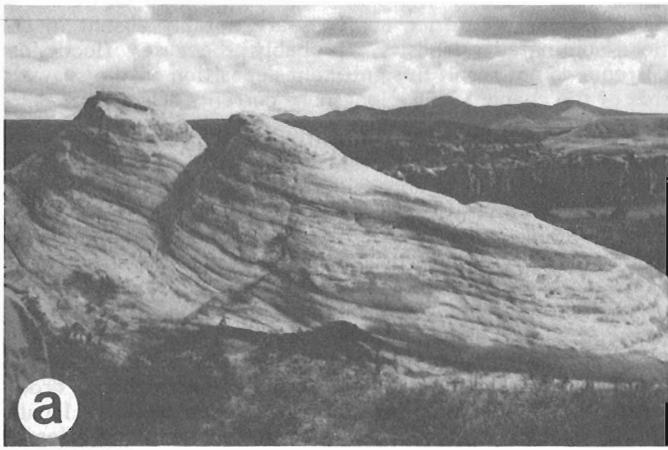


Figure 65.8. a) Westerly dipping lateral accretion surfaces; b) Bedding within the lateral accretion surfaces displays ebb-oriented, planar tabular cross-stratification.

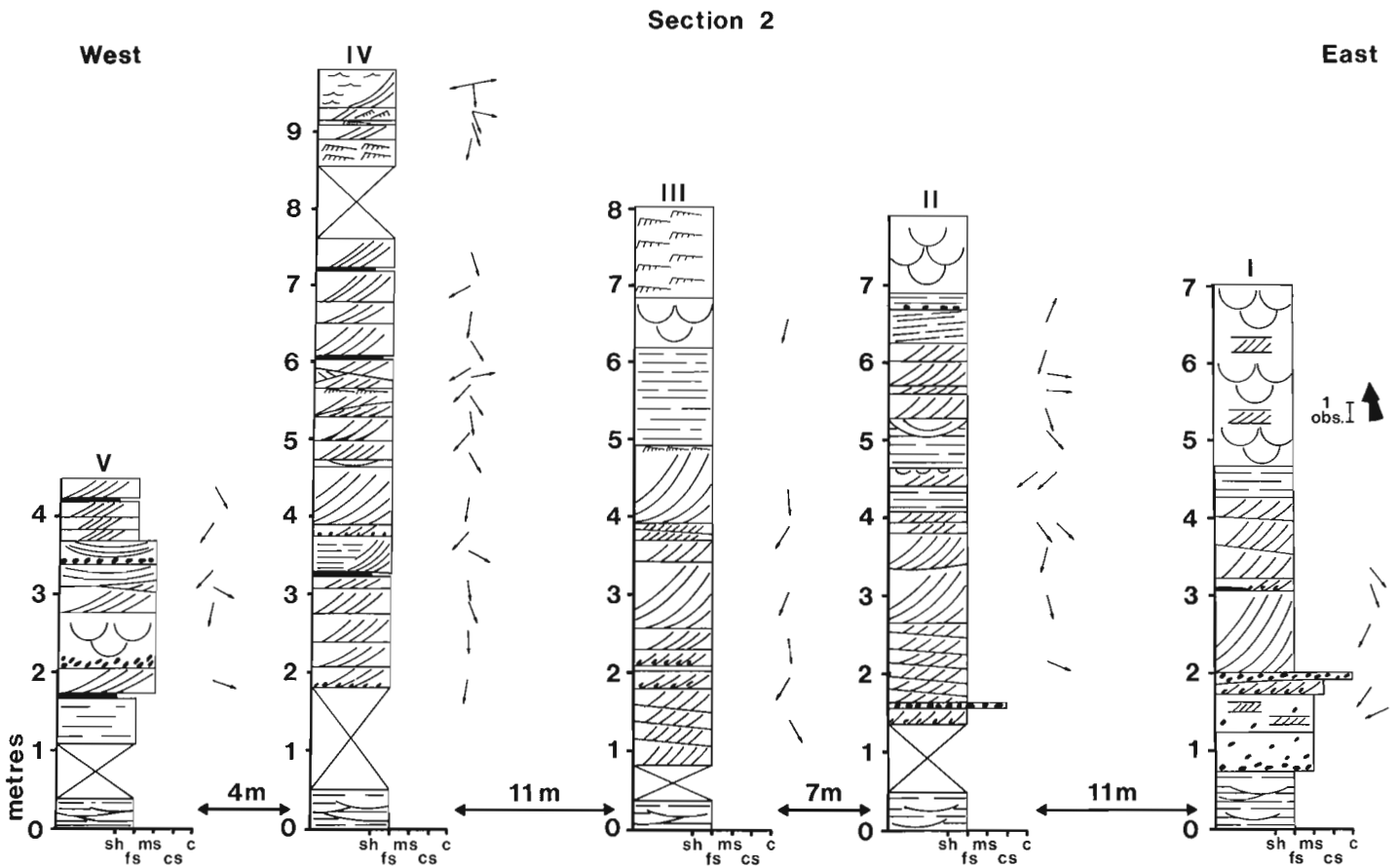


Figure 65.9. Flood-dominated portion of tidal channel at Section 2, consisting of five individual sections (I to IV) illustrating the sequence of structures at this location (Fig. 65.2). Arrows indicate current direction. Grain size is shown on the lower horizontal scales: sh = shale, fs = fine sand, ms = medium sand, cs = coarse sand, and c = conglomerate. For legend see Figure 65.7.

thicker (up to 1 cm) than the sandstone layers (a few millimetres), which appear to be structureless. This interlaminated shale and sandstone bed is interpreted as sets of "mud couplets" (Visser, 1980) and is thought to reflect alternating slack water deposition (mud) and current deposition (sand) in the lee of the advancing sandwave that produced the planar tabular cross-stratification. Shale rip-up clasts occur in many of the planar tabular sets, along the base of foresets in the lower part of the channel facies. There are also several beds in the lower part of the sequence that are predominantly composed of shale rip-up clasts. Thin shale beds (generally less than 5 cm thick) are preserved intact largely in the two western sections (IV and V, Fig. 65.9). These shale beds are probably ebb and flood, slack water deposits laid down in areas protected from significant sand transport, or more extensively during neap tide when the currents were least competent. Regardless, similar mud deposits probably provided the source of mud that was reworked into the shale rip-up clasts preserved in this facies.

Sets of large scale, flood-oriented, trough cross-stratification, in fine grained sandstone, occur near the top of the flood tidal sequence (Fig. 65.10). This form of cross-stratification develops with the migration of large, sinuous bedforms (megaripples) under more energetic flows than the straight-crested sandwaves, which form planar tabular cross-stratification. In the progradational setting in which the Virgelle Member was deposited, the trough cross-stratified sandstone occupied a more landward position than the lower sandstone, which displays planar tabular sets. The specific setting of deposition may have been in relatively deep, narrow flood channels that developed around sand bars in the channel. Flow through these channels would be faster than in the broad, seaward channels in which the sandwaves formed, and thus capable of forming the sinuous megaripples. The bed of low-angle, northward (seaward) dipping, parallel stratified, fine grained sandstone at 6.5 m, column II, Section 2 (Fig. 65.9) may reflect such a bar, or the flood ramp of a flood-tidal delta, where deposition was under upper plane bed conditions, forming laminae parallel to the seaward-sloping surface of the bar. Trough sets occurring lower in the sequence (e.g. Fig. 65.9, col. V at 2.5 m) probably formed in the deepest part of the main channel when tidal currents were especially fast (e.g. spring tide).

Horizontally laminated, fine grained sandstone occurs in the upper portion of the sequence, which preserves relatively shallow water portions of the prograding channel and shoreline. This sandstone was deposited under upper

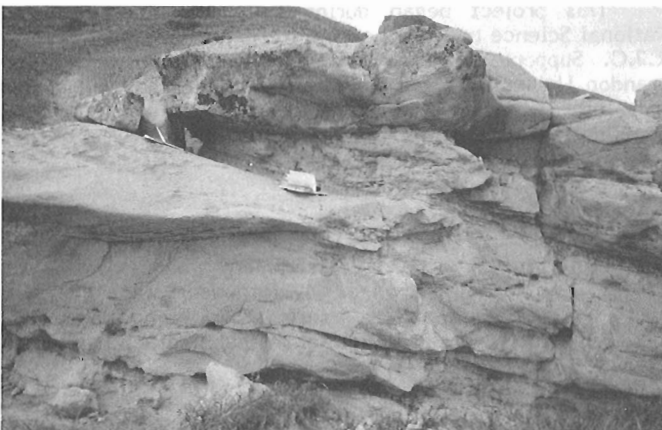


Figure 65.10. Flood-oriented, trough cross-stratified sandstone with interformational shale clasts from immediately west of flood ramp, planar tabular sandstone shown in Figure 65.4a. These cross-strata were deposited in the tidal channel.

plane bed conditions. Rare, vertical escape burrows have been observed in identical horizontally laminated sandstones along strike from Section 2, documenting the response of organisms to rapid deposition. Current ripple crosslamination in fine grained sandstone near the top of the sequence reflects relatively shallow-water deposition under lower flow strengths than the horizontally laminated deposits. Wave ripple crosslamination illustrated at the top of column IV, Section 2 (Fig. 65.9), formed in response to relatively shallow water, wind-generated waves in areas adjacent to the landward side of the tidal channel. Rare root casts are preserved in this uppermost sandstone, penetrating downward and originating from the overlying recessive Deadhorse Coulee Member, which is not well exposed.

Discussion

Our results show a complexity of tidal facies rarely shown in other outcrop studies. Most studies of barrier channels concentrate on the channel and place little significance on preservation of tidal delta facies (Kumar and Sanders, 1974; Reinson, 1979; Carter, 1978). The sequence of flood-oriented structures in Section 2 (Fig. 65.9) was

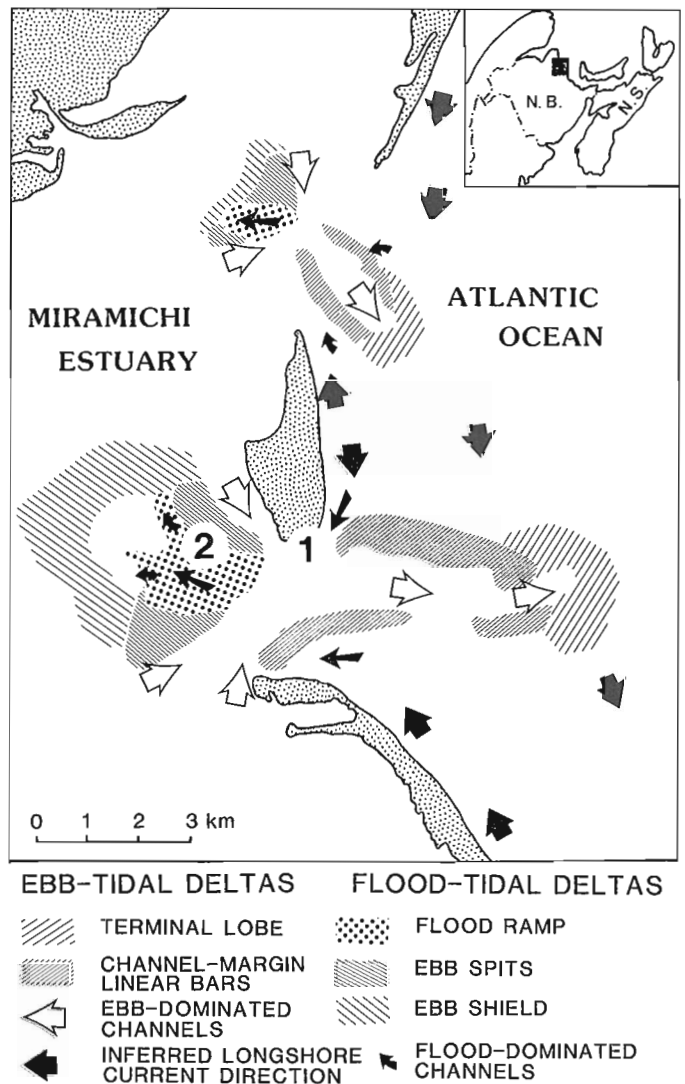


Figure 65.11. Barrier islands and inlets of the Miramichi estuary (modified from Reinson, 1977). The numbers "1" and "2" refer to positions of Sections 1 and 2 (Fig. 65.6, 65.9) on a hypothetical "fossilized" Miramichi estuary.

deposited as part of a flood-tidal delta complex and bears little resemblance to the hypothetical sequences proposed by Hayes (1976) and Hubbard and Barwis (1976). Many of these studies on modern tidal inlets comment on the migration of the inlet over time. The Milk River example is one of the first documented examples of this lateral migration preserved in the ancient record (McCrorry and Walker, 1986).

The tidal deltas and channels of the Miramichi estuary in New Brunswick (Reinson, 1977a, b) are a suitable modern analogue for the deposits of the Virgelle Member (Fig. 11). The locations of sections 1 and 2 (Fig. 65.6, 65.9), as they would occur on a hypothetical, fossilized Miramichi estuary, appear in Figure 65.11. The lateral accretion surfaces are interpreted as belonging to the lower portion of the main ebb-channel, which was dominated by ebb-tidal currents. One variation from the Miramichi analogue occurs in the Virgelle sandstone, where the ebb current was directly beside the outer margins of the tidal channel. On the Miramichi estuary (Reinson, 1977a, b) and estuaries of the Carolina coast (Hubbard and Barwis, 1976) the flood currents typically flow adjacent to the channel margins. The bidirectionality that occurs in the lateral accretion surfaces along the strike of the outcrop can be explained by the Miramichi analogue (Fig. 65.11) where reversals of longshore drift occur due to differences in the directions of wave approach (Reinson, 1976).

We agree with McCrorry and Walker (1986) that the paleoshoreline was storm and tidally influenced. The abundance of hummocky and swaley cross-stratification in the nonchannel intervals of the shoreface indicate a strong wave influence. We see very little evidence to indicate a well developed ebb-tidal delta system. The lateral accretion surfaces and ebb-directed planar tabular and trough cross-stratified sands were deposited within the channel close to the shoreline. The abundance of lateral accretion surfaces indicates well developed longshore drift patterns. Wave dominated inlets generally have only a small ebb-tidal delta that is close to the shore and a large, complex flood-tidal delta complex (Hubbard, 1977). Swash bars and swash platforms are poorly developed (Hubbard, 1977). Our observations indicate that Section 2 belongs to a large, flood-tidal delta complex that developed in the upper Virgelle Member.

Table 65.1. Comparison of ebb- and flood-dominated portions of the tidal channel

Ebb-dominated	Flood-dominated
No lag of shale clasts	More commonly a lag of shale rip-up clasts at base of deposit
Lateral accretion surfaces dipping variably along strike of paleo-shoreline	Abundant shale rip-up clasts on lower foresets and toesets
Offshore dipping (northward) cross-strata	Onshore-dipping cross-strata
Decreasing set thickness upward	Very gentle, seaward-dipping surface covered with onshore-dipping, planar tabular cross-strata (flood ramp)
In general, fewer shale rip-up clasts than in the flood-dominated facies	
In general, trough cross-stratification is more common	

Although there was a strong ebb-tidal influence within the channel, there is little evidence for a large, well developed ebb-tidal delta. If the channels were just tide dominated, with little wave influence, the flood-tidal delta complex would not have developed (Hubbard, 1977).

At this time it is difficult to assign a definite tidal range. However, we tentatively assign a mesotidal range (2-4 m) to the tidal amplitude. The grounds for this are that modern microtidal (<2 m) barrier islands and estuaries are characterized by abundant washover fans, small flood-tidal deltas, numerous spits and aligned beaches (Hayes, 1975). Modern mesotidal barrier islands are dominated by tidal deltas and channels (Hayes, 1975; Kumar and Saunders, 1970). The upper part of the Virgelle Member that we have examined to date is dominated by tidal delta and channel facies and, as such, a mesotidal assignment may be appropriate. Assuming a 10 per cent reduction in thickness resulting from compaction (Ingles and Grant, 1975), the tidal channels were in the order of 7 to 9 m deep.

Conclusions

Hoodoos in the Virgelle Member at Writing on Stone Provincial Park in southeastern Alberta provide an opportunity to study the ebb- and flood-dominated portions of a tidal channel and their geometric relationships. Evidence of tidal activity includes: superposed bipolar tabular cross-strata, reversing paleocurrent directions along strike, reactivation surfaces, mud-layer couplets, and tidal bundles. A summary of criteria for differentiating ebb and flood portions of the channel is presented in Table 65.1. The ebb-dominated facies is characterized by seaward-dipping, planar tabular cross-strata sets, with up to 3 m of relief, bounded by lateral accretion surfaces. The lateral accretion surfaces dip at angles of 10 to 15 degrees and form sets which dip variably, along strike, to the east and west (alongshore). The cross-strata sets between surfaces decrease in thickness upward. The flood-dominated facies, interpreted as a flood-tidal delta complex, is characterized by planar tabular cross-stratification (set thicknesses of 0.2 to 1.0 m) with common shale rip-up clasts on lower foresets and toesets. Landward-dipping cross-strata predominate. In one case, planar tabular sets climb up a low-angle (4°), seaward-dipping surface, interpreted as a flood ramp, located on the landward side of the channel. The tidal channel was probably wave dominated with a small ebb-tidal delta, but a large flood-tidal delta complex. The tidal range was probably mesotidal.

Acknowledgments

This project began during fieldwork financed by a National Science and Engineering Research Council Grant to R.J.C. Support for later fieldwork was provided by the Brandon University Research Grants Committee and is also gratefully acknowledged. The comments of Jim Dixon, Tom Jerzykiewicz, and Erik Johannessen improved an earlier version.

References

- Allen, J.R.L.
 1970: Studies in fluvial sedimentation: a comparison of fining upward cyclothems, with special reference to coarse-member composition and interpretation; *Journal of Sedimentary Petrology*, v. 40, p. 298-323.
 1984: Sedimentary structures, their character and physical basis; *Developments in Sedimentology*, v. 30, Elsevier, New York, 663 p.
 Berry, W.B.N. and Barker, R.M.
 1975: Growth increments in fossil and modern bivalves; in *Growth Rhythms and the History of the Earth's Rotation*, ed. G.D. Rosenberg and S.K. Runcord; London, Wiley, p. 9-25.

- Boersma, J.R.
1969: Internal structures of some tidal megaripples on a shoal in the Westerschelde estuary, the Netherlands; *Geologie en Mijnbouw*, v. 48, p. 409-414.
- Carter, C.H.
1978: A regressive barrier and barrier-protected deposit: depositional environment and depositional setting of the Late Tertiary Cohansey Sand; *Journal of Sedimentary Petrology*, v. 48, p. 933-950.
- Chiang, K.K.
1984: The giant Hoadley gas field, south-central Alberta; in *Elmworth – case study of a deep basin gas field*, ed. J.A. Masters; American Association of Petroleum Geologists, Memoir 38, p. 297-315.
- Hayes, M.O.
1975: Morphology of sand accumulation in estuaries; in *Proceedings of the Second International Estuarine Research Conference*, ed. L.E. Cronin; Academic Press, New York, p. 3-22.
1976: Transitional-coastal environments; in *Terrigenous clastic depositional environments*, ed. M.O. Hayes and T.W. Kana; American Association of Petroleum Geologists Field Course, University of South Carolina, Technical Report no. 11-CRD, p. I32-II11.
- Hubbard, D.K.
1977: Variations in tidal inlet processes and morphology in the Georgia embayment; University of South Carolina, Technical Report no. 14-CRD, 79 p.
- Hubbard, D.K. and Barwis, J.H.
1976: Discussion of tidal inlet sand deposits: examples from the South Carolina coast, ed. M.O. Hayes and T.W. Kana; American Association of Petroleum Geologists Field Course, University of South Carolina, Technical Report no. 11-CRD, III28-III42.
- Ingles, O.H. and Grant, K.
1975: The effect of compaction on various properties of coarse-grained sediments; in *Compaction of coarse-grained sediments*, ed. G.V. Chilingarian and K.H. Wolf; Elsevier, New York, p. 293-348.
- Klein, G. de V and Ryer, T.A.
1978: Tidal circulation patterns in Precambrian, Paleozoic and Cretaceous epeiric and mioclinal shelf seas; *Geological Society of America, Bulletin*, v. 89, p. 1050-1058.
- Kumar, N. and Sanders, J.E.
1974: Inlet sequence: a vertical succession of sedimentary structures and textures created by the lateral migration of tidal inlets; *Sedimentology*, v. 21, p. 491-532.
- Leckie, D.A.
1985: The Lower Cretaceous Notikewin Member (Fort St. John Group), northeastern British Columbia: a progradational barrier island system; *Bulletin of Canadian Petroleum Geology*, v. 33, p. 39-51.
1986: Tidally-influenced, transgressive shelf sediments in the Viking Formation, Caroline, Alberta; *Bulletin of Canadian Petroleum Geology*, v. 34.
- Leckie, D.A. and Walker, R.G.
1982: Storm and tidal dominated shorelines in Cretaceous Moosebar-Gates interval: outcrop equivalents of Deep Basin gas trap in Western Canada; *American Association of Petroleum Geologists, Bulletin*, v. 66, p. 138-157.
- McCrary, V.L.C. and Walker, R.G.
1986: A storm and tidally-influenced prograding shoreline – Upper Cretaceous Milk River Formation of southern Alberta, Canada; *Sedimentology*, v. 33.
- Meijer Drees, N.C. and Myhr, D.W.
1981: The Upper Cretaceous Milk River and Lea Park formations in southeastern Alberta; *Bulletin of Canadian Petroleum Geology*, v. 29, p. 42-72.
- Pannella, G. and MacClintock, C.
1968: Paleontological evidence of variations in length of synodic month since Late Cambrian; *Science*, v. 162, p. 792-796.
- Reinson, G.E.
1976: Channel and shoal morphology in the entrance to the Miramichi estuary, New Brunswick; in *Report of Activities, Part C*, Geological Survey of Canada, Paper 76-1C, p. 33-45.
1977a: Tidal-current control of submarine morphology at the mouth of Miramichi estuary, New Brunswick; *Canadian Journal of Earth Sciences*, v. 14, p. 2524-2532.
1977b: Examination of bedforms in shallow water using side-scan sonar, Miramichi Estuary, New Brunswick; in *Report of Activities, Part B*, Geological Survey of Canada, Paper 77-1B, p. 99-105.
1979: Barrier island systems; in *Facies Models*, ed. R.G. Walker; Geoscience Canada, Reprint Series 1, p. 57-74.
- Rice, D.D.
1980: Coastal and deltaic sedimentation of Upper Cretaceous Eagle Sandstone: relation to shallow gas accumulation, north-central Montana; *American Association of Petroleum Geologists, Bulletin*, v. 64, p. 316-338.
- Shaw, A.B.
1964: *Time in stratigraphy*; New York, McGraw-Hill Book Co., 365 p.
- Slater, R.D.
1985: A numerical model of tides in the Cretaceous seaway of North America; *Journal of Geology*, v. 93, p. 333-345.
- Slipper, S.E. and Hunter, H.M.
1931: Stratigraphy of Foremost, Pakowki and Milk River formations of southern plains of Alberta; *American Association of Petroleum Geologists, Bulletin*, v. 15, p. 1181-1196.
- Visser, M.J.
1980: Neap-spring cycles reflected in Holocene subtidal large-scale bedform deposits: a preliminary note; *Geology*, v. 8, p. 543-546.

Speculation on the petroleum source rock potential of portions of the Lodgepole Formation (Mississippian) of southern Saskatchewan

Project 780003

K.G. Osadetz and L.R. Snowdon
Institute of Sedimentary and Petroleum Geology, Calgary

Osadetz, K.G. and Snowdon, L.R., Speculation on the petroleum source rock potential of portions of the Lodgepole Formation (Mississippian) of southern Saskatchewan; in Current Research, Part B, Geological Survey of Canada, Paper 86-1B, p. 647-651, 1986.

Abstract

Significant oil resources occur in Mississippian rocks of southeastern Saskatchewan. The source of these oils is commonly inferred to be the Bakken Formation (Devonian-Mississippian). The overlying Lodgepole Formation (Mississippian) has been previously attributed no source potential. Significant potential petroleum source rocks do occur in a mappable shale in the lower part of the Lodgepole Formation. Their significance as an effective petroleum source rock remains to be determined.

Résumé

Les roches du Mississippien du sud-est de la Saskatchewan renferment d'importantes ressources pétrolières. La source de ces gisements est généralement considérée comme étant la formation de Bakken (Dévonien-Mississippien). On a déjà estimé que la formation de Lodgepole (Mississippien) qui la recouvre ne présentait aucune possibilité comme source d'hydrocarbures. Une zone de schistes argileux cartographiée dans la partie inférieure de la formation de Lodgepole contient des roches qui sont probablement une source importante de pétrole. Il reste à établir l'importance de cette source.

Introduction

In excess of 250 million cubic metres of recoverable oil is entrapped at or near the subcrop of Mississippian rocks in southwestern Manitoba and southeastern Saskatchewan (Lee et al., 1985). It is commonly believed that thin yet rich potential petroleum source rocks of the Bakken Formation (Devonian-Mississippian) were the source of these oils (Price et al., 1984). This report identifies significant potential petroleum source rocks in the Mississippian Lodgepole Formation that may have been contributing sources to the oil pools of southeastern Saskatchewan.

Samples of potential petroleum source rocks in the Lodgepole Formation, examined to date, are marginally mature. Possibly these potential source rocks are mature either in regions of higher heat flow or where they have been more deeply buried. The latter possibility appears to be restricted to American portions of the Williston Basin.

Method of study

The RockEval pyrolysis technique allows the evaluation of potential petroleum source rocks: it indicates shows of oil or gas, the oil and gas generation potential, the thermal maturity, and an inferred organic matter type (Tissot and Welte, 1978, p. 443-447). The RockEval pyrolysis-organic carbon analysis gives five parameters: S1, S2, S3, TOC and Tmax. The S1 parameter is a measure of the free or adsorbed hydrocarbons that are volatilized at moderate temperatures during the pyrolysis experiment. The S2 parameter is the quantity of hydrocarbons and hydrocarbon-like compounds that are liberated from the kerogen in the rock sample during the pyrolysis experiment. The S3 parameter is a measure of the CO₂ generated from the kerogen. All of these parameters are measured in milligrams of product per gram of rock sample (equivalent to kilograms of product per tonne of sample). The Total Organic Carbon analysis, TOC, is measured in weight per cent. Tmax is the temperature corresponding to the maximum hydrocarbon generation (S2 peak) during the pyrolysis experiment.

The source rock potential of a rock sample is determined by the amount of Total Organic Carbon as a function of lithology, and the S2 parameter value (Table 66.1). Thermal maturity is determined by both the Tmax and Hydrogen Index-Oxygen Index parameters (Macauley et al., 1985, p. 5). The petroleum potential of the sample, S1 + S2, can be employed to rank the generative potential of different source rocks.

Potential petroleum source rocks in the Lodgepole Formation

Good to excellent potential petroleum source rocks are present in both the Bakken Formation and Madison Group in southern Saskatchewan (Osadetz and Snowdon, 1986).

Table 66.1. Criteria for rating potential source rocks

TOTAL ORGANIC CARBON (TOC) VALUE (WEIGHT PER CENT)		
% TOC IN SHALES	SOURCE RATING	% TOC IN CARBONATES
0.00 - 0.50	Poor	0.00 - 0.12
0.50 - 1.00	Fair	0.12 - 0.25
1.00 - 2.00	Good	0.25 - 0.50
2.00 - 4.00	Very good	0.50 - 1.00
4.00 and greater	Excellent	1.00 and greater
S2 VALUE (mg HYDROCARBON / gm OF ROCK)		
S2 VALUE	SOURCE RATING	
Less than 2.00	Poor	
2.00 - 5.00	Fair	
Greater than 5.00	Good	

KGO-86 gsc

This paper identifies potential petroleum source rock intervals in the Lodgepole Formation in the Imperial Garville well (8-23-3-24W2). Some indication of source rock potential in the lower portion of the Lodgepole Formation was recognized in the Norcanols Parry No.1 well (16-8-9-21W2; Osadetz and Snowdon, 1986). Shales correlative with the potential source interval identified in the Garville well are present in the Broadview Crown well (8-36-16-6W2) but they give no indication of petroleum source rock potential. Two wells west of the third meridian, Shell Amerada Crown S-A (5-31-2-11W3) and Imperial Tidewater Climax No.1 (6-10-3-18W3) contain no potential source rock interval in the Lodgepole Formation. Presumably they lie west of the depositional limit of potential petroleum source rocks. The result of the anhydrous pyrolysis experiments for samples from the Bakken Formation and Madison Group for the Garville well is listed in Table 66.2.

In the Garville well, good to excellent potential petroleum sources are present in samples of the middle sandstone and lower shale members of the Bakken Formation. The upper shale member of the formation was not examined. Several potential petroleum source rock intervals are present in the Madison Group. Potential sources are extensively developed in the Lodgepole Formation and sporadically developed in the Mission Canyon Formation. There are three potential source rock intervals in the Lodgepole Formation. Except for sporadic source rocks in basal portions of the formation, the first potential source rocks occur in shales and argillaceous carbonates in the interval from 6350 to 6500 ft (1936-1981 m) in the well (Fig. 66.1). This interval is characterized by an increase in the abundance of Total Organic Carbon upward through the section to a maximum of 5.26 per cent at the top of the interval. S1 yields reach 1.00 mg hydrocarbon per gram of rock (mg HC/gm) and S2 yields exceed 30.00 mg HC/gm. Hydrogen Index values exceed 350 in argillaceous carbonates and the potential source is considered to be dominated by Type II, marine, organic matter. Tmax is 430°C, on average. Tmax and Productivity Index values, not commonly exceeding 10 per cent, suggest that, in the Garville well, the interval is marginally mature.

The second and third potential source rock intervals are developed in the intervals 6240 to 6280 ft (1902-1914 m), and 6020 to 6120 ft (1835-1865 m), respectively. The latter interval does not represent a continuous source interval; potential sources are developed discretely and sporadically. The source potential of individual samples from these intervals is commonly good (Table 66.2), although TOC values rarely exceed 2.50 per cent and S1 yields are very poor (less than 0.25 mg HC/gm).

Correlation and distribution of potential sources

The lowermost potential source interval (6350-6500 ft, 1936-1981 m) in the Garville well is a regionally persistent lithological unit, recognizable as far east as Imperial Halkett 15-7-3-8W2 (6100-6240 ft, 1859-1902 m). To the north, the unit is recognized in both the Norcanols Parry No.1 well, where it has limited good source rock potential (5605-5710 ft, 1708-1740 m; Osadetz and Snowdon, 1986) and in the Tidewater Broadview Crown No.8-36 well (8-36-16-6W2; 2926-2939 ft, 892-896 m), where it has no source rock potential. To the west, the section becomes condensed and this interval converges with underlying beds to become the basal beds of the formation. No source rock potential is recognizable in the two wells that have been examined in the area west of the third meridian, Shell Amerada Crown S-A and Imperial Tidewater Climax No.1.

The second potential source interval (6240-6280 ft, 1902-1914 m) occurs at a stratigraphic position equivalent to the top of the Lodgepole Formation as inferred from

Table 66.2. RockEval pyrolysis results (0.5% TOC cutoff)

Imperial Garville 8-23-3-24W2 K.B. 2524 feet (769.3 m)										
DEPTH in feet	(m)	TOC	PI	S1+S2	TMAX	S1	S2	S3	HI	OI
Charles Formation (5323 ft, 1623 m)										
5380	(1640)	1.00	0.7	1.84	436	.12	1.72	.72	172	72
Mission Canyon Formation (5423 ft, 1653 m)										
5480	(1670)	1.10	.06	1.78	430	.10	1.68	.48	152	43
5500	(1676)	1.99	.02	4.57	435	.11	4.46	.89	224	44
5580	(1701)	1.00	.16	3.16	436	.52	2.64	1.10	264	109
5640	(1719)	.74	.10	1.18	431	.12	1.06	.78	143	105
Lodgepole Formation (5677 ft, 1730 m)										
5680	(1731)	.92	.05	1.91	439	.10	1.81	.62	196	67
5720	(1744)	1.44	.05	3.27	430	.16	3.11	1.04	215	72
5740	(1750)	.75	.04	1.34	440	.05	1.29	.37	172	49
5760	(1756)	1.31	.07	2.81	432	.21	2.60	.77	198	58
5780	(1762)	1.66	.03	3.72	422	.12	3.60	1.18	216	71
5860	(1786)	.86	.04	1.22	436	.05	1.17	.51	136	59
5920	(1804)	1.09	.04	1.36	434	.05	1.31	.31	120	28
5940	(1811)	.81	.04	1.82	438	.08	1.74	.42	214	51
5960	(1817)	.50	.04	.90	435	.04	.86	.20	172	40
5980	(1823)	.78	.02	2.30	433	.05	2.25	.27	288	34
6000	(1829)	1.01	.03	2.00	434	.07	1.93	.61	191	60
6020	(1835)	1.00	.04	2.51	442	.09	2.42	.63	242	63
6060	(1847)	1.33	.03	4.87	430	.13	4.74	.77	356	57
6100	(1859)	1.14	.05	2.48	433	.12	2.36	1.08	207	94
6120	(1865)	2.65	.02	9.69	424	.23	9.46	1.72	356	64
6160	(1878)	.91	.06	1.78	434	.10	1.68	.68	184	74
6180	(1884)	.62	.05	1.26	433	.06	1.20	.42	193	67
6200	(1890)	.74	.05	1.84	432	.10	1.74	1.38	235	186
6220	(1896)	.55	.05	2.04	432	.10	1.94	.48	352	87
6240	(1902)	1.28	.05	2.65	429	.12	2.53	.84	197	65
6260	(1908)	.60	.10	3.10	433	.30	2.80	.96	466	160
6280	(1914)	.90	.08	3.34	431	.28	3.06	1.08	340	120
6320	(1899)	.52	.05	1.68	433	.09	1.59	.63	305	121
Unnamed argillaceous carbonate (6350 ft, 1936 m)										
6350	(1935)	5.26	.03	29.51	430	.84	28.67	2.54	545	48
6353	(1936)	3.00	.06	17.54	448	1.00	16.54	.57	551	19
6356	(1937)	4.97	.03	32.93	430	1.00	31.93	2.10	642	42
6360	(1938)	.64	.06	2.47	429	.14	2.33	1.55	364	242
6380	(1945)	.65	.06	2.36	431	.14	2.22	.40	341	61
6400	(1951)	.94	.10	4.04	429	.39	3.65	1.07	388	113
Unnamed clay shale (6410 ft, 1954 m)										
6420	(1957)	1.79	.12	3.34	430	.38	2.86	1.63	159	91
6440	(1963)	2.90	.11	4.37	432	.48	3.89	2.48	134	85
6460	(1969)	1.15	.18	1.52	432	.28	1.24	1.14	107	99
6480	(1975)	3.44	.10	5.13	427	.53	4.60	2.70	133	78
Unnamed carbonate (6487 ft, 1977 m)										
6500	(1981)	1.44	.04	5.78	425	.22	5.56	1.27	386	88
6600	(2012)	1.23	.20	2.60	432	.53	2.07	.90	168	73
6660	(2030)	1.62	.15	8.70	427	1.30	7.40	2.03	456	125
Bakken Formation, upper shale member (6670 ft, 2033 m)										
Bakken Formation, middle sandstone member (6676 ft, 2035 m)										
6700	(2042)	1.13	.23	3.22	430	.74	2.48	1.82	219	161
6720	(2048)	1.69	.23	4.27	431	1.00	3.27	1.95	193	115
Bakken Formation, lower shale member (6723 ft, 2049 m)										
6740	(2054)	14.15	.13	64.44	420	8.65	55.79	4.70	394	33
6740	(2054)	14.37	.13	67.71	419	9.10	58.61	5.18	407	36
Torquay Formation (6748 ft, 2057 m)										

IMPERIAL GARVILLE

(8-23-3-24W2)

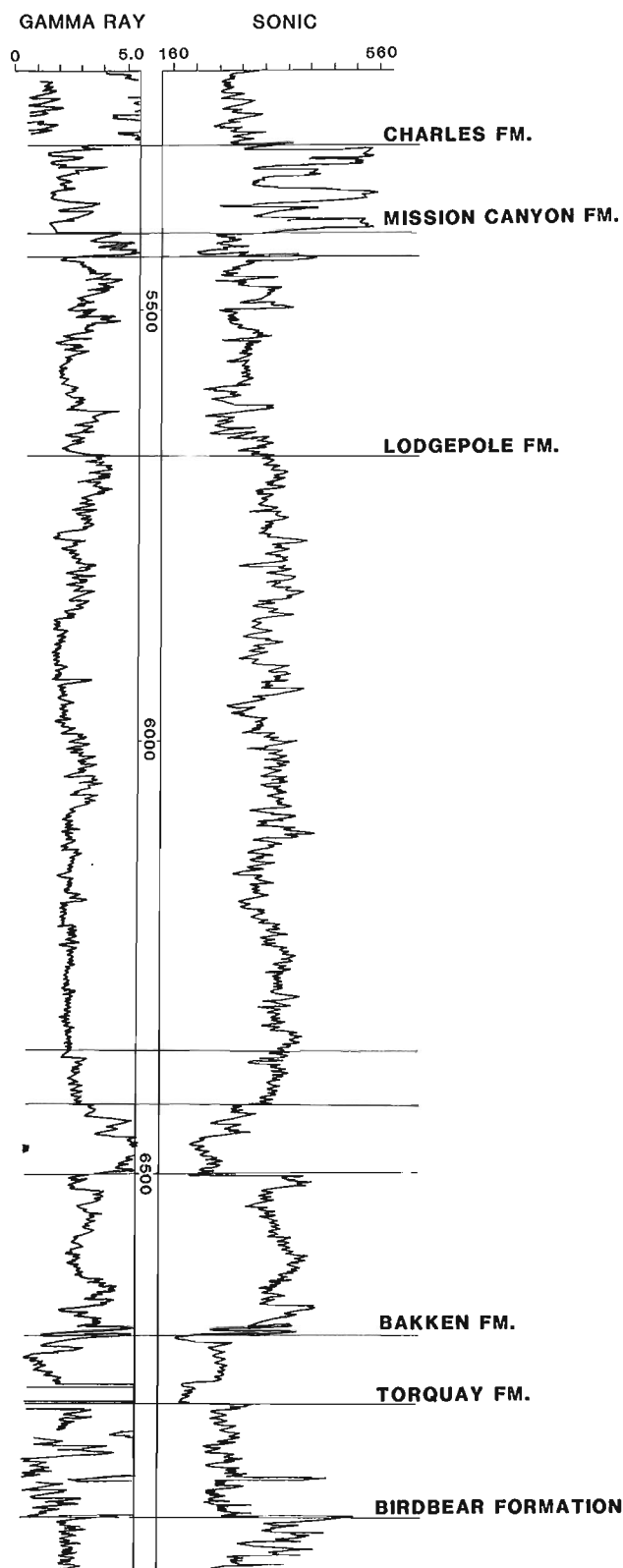


Figure 66.1. Gamma ray and sonic logs of the Lodgepole, Bakken and over- and underlying formations from the Imperial Garville (8-23-3-24W2) well.

MacDonald's maps (MacDonald, 1956). The third potential source interval (6020-6120 ft, 1835-1865 m) in the Garville well occurs in beds of argillaceous wackestones to bioclastic grainstones. These beds are correlative with argillaceous beds underlying the endothyrid foraminiferal grainstone beds recognized by MacDonald at the base of the Mission Canyon Formation (as picked in this study) in the nearby Buffalo Gap No. 1 well (MacDonald, 1953, p. 121; 1956). Significant potential petroleum source rocks have not been identified in other wells, in strata correlative to either the second (6240-6280 ft, 1902-1914 m) or third (6020-6120 ft, 1835-1865 m) intervals of potential petroleum sources identified in the Garville well. Only the lower interval (6350-6500 ft, 1936-1981 m) is considered a significant potential petroleum source rock.

Discussion

Recently, considerable attention has been focused on the petroleum source rock potential for the Fammenian and Tournaisian shales of the Bakken Formation and laterally equivalent strata (Dembicki and Pirkle, 1985; Leenheer, 1984; Price et al., 1984; Webster, 1984; Schmoker and Hester, 1983). The present authors agree that this formation should be assigned a high source rock potential (Table 66.2; Osadetz and Snowdon, 1986). Extensive investigation of the Bakken Formation as a unit containing potential petroleum source rocks has been strongly influenced by the correlation of oils in Mississippian reservoirs to solvent extracts from the Bakken Formation (Williams, 1974). Dow (1974) suggested that, "All other formations between the Devonian Prairie salt and the Charles salt contain insufficient organic matter to generate the amount of Type II oil discovered in the basin." This view has prevailed, as indicated by the recent review of petroleum source rocks in the greater Rocky Mountain region (Meissner et al., 1984).

Data obtained from this study indicate that extensive, correlative shale and argillaceous carbonate intervals in the lower portion of the Lodgepole Formation have significant petroleum source rock potential. Further work is required to document the significance of this potential.

Acknowledgments

Well cuttings for this study were donated by Suncor Inc. of Calgary. This project was formulated under the guidance of the O.E.R.D. 6.1.1 Government-Industry review committee, and the authors are grateful for their commitment to the guidance of this project.

References

- Dembicki, H., Jr. and Pirkle, R.L.
1985: Regional source rock mapping using a source potential rating index; American Association of Petroleum Geologists, Bulletin, v. 69, no. 4, p. 567-581.
- Dow, W.G.
1974: Application of oil-correlation and source-rock data to exploration in Williston Basin; American Association of Petroleum Geologists, Bulletin, v. 58, no. 7, p. 1253-1262.
- Lee, P.J., Podruski, J.A., Barclay, J.E., Osadetz, K.G., Hamblin, A.P., Taylor, G.C., and Procter, R.M.
1985: Conventional oil resources of western Canada (light and medium gravity); Geological Survey of Canada, unpublished manuscript prepared by the Petroleum Resource Appraisal Secretariat, Institute of Sedimentary and Petroleum Geology, Calgary, 33 p.

- Leenheer, M.J.
1984: Mississippian Bakken and equivalent formations as source rocks in the Western Canadian Basin; *Organic Geochemistry*, v. 6, p. 521-532.
- Macauley, G., Snowdon, L.R., and Ball, F.D.
1985: Geochemistry and geological factors governing exploitation of selected Canadian oil shale deposits; Geological Survey of Canada, Paper 85-13, p. 65.
- MacDonald, G.H.
1956: Subsurface stratigraphy of the Mississippian rocks of Saskatchewan; Geological Survey of Canada, Memoir 282, 46 p.
1953: The Mississippian of Saskatchewan; University of Toronto, unpublished Ph.D. thesis, Toronto, 193 p.
- Meissner, F.F., Woodward, J., and Clayton, J.L.
1984: Stratigraphic relationships and distribution of source rocks in the greater Rocky Mountain region; in *Hydrocarbon source rocks of the greater Rocky Mountain region*, ed. J. Woodward, F.F. Meissner, and J.L. Clayton; Rocky Mountain Association of Geologists, Denver, p. 1-34.
- Osadetz, K.G. and Snowdon, L.R.
1986: Petroleum source rock reconnaissance of southern Saskatchewan; in *Current Research, Part A*, Geological Survey of Canada, Paper 86-1A, p. 609-617.
- Price, L.C., Ging, T., Daws, T., Love, A., Pawlewicz, M., and Anders, D.
1984: Organic metamorphism in the Mississippian-Devonian Bakken shale, North Dakota portion of the Williston Basin; in *Hydrocarbon source rocks of the greater Rocky Mountain region*, ed. J. Woodward, F.F. Meissner, and J.L. Clayton; Rocky Mountain Association of Geologists, Denver, p. 83-134.
- Tissot, B.P. and Welte, D.H.
1978: *Petroleum Formation and Occurrence*; Springer-Verlag, Berlin, p. 538.
- Schmoker, J.W. and Hester, T.C.
1983: Organic carbon in the Bakken Formation, United States portion of Williston Basin; *American Association of Petroleum Geologists, Bulletin*, v. 67, no. 12, p. 2165-2174.
- Webster, R.L.
1984: Petroleum source rocks and stratigraphy of the Bakken Formation in North Dakota; in *Hydrocarbon source rocks of the greater Rocky Mountain region*, ed. J. Woodward, F.F. Meissner, and J.L. Clayton; Rocky Mountain Association of Geologists, Denver, p. 57-81.
- Williams, J.A.
1974: Characterization of oil types in Williston Basin; *American Association of Petroleum Geologists, Bulletin*, v. 58, no. 7, p. 1243-1252.

Caliche and associated impoverished palynological assemblages:
an innovative line of paleoclimatic research onto
the uppermost Cretaceous and Paleocene of southern Alberta

Projects 810039 and 710091

T. Jerzykiewicz and A.R. Sweet
Institute of Sedimentary and Petroleum Geology, Calgary

Jerzykiewicz, T. and Sweet, A.R., Caliche and associated impoverished palynological assemblages: an innovative line of paleoclimatic research into the uppermost Cretaceous and Paleocene of southern Alberta; *in* Current Research, Part B, Geological Survey of Canada, Paper 86-1B, p. 653-663, 1986.

Abstract

Glaeular paleosol and pedogenic limestone in the Willow Creek Formation should be recognized as important features in paleoclimatic interpretations. A semiarid floodplain environment of the Willow Creek Formation in the southern Foothills can be contrasted with the poorly drained, swampy floodplain (Coalspur coal zone) of the central Foothills. Such an interpretation for the Willow Creek Formation, based on sedimentology, is supported palynologically by the exceptionally high number of low-yield samples, the low diversity of the Late Maastrichtian assemblages and the occurrence of **Classopollis**. The abundance of **Concentricystes** in many samples, which are otherwise nearly barren of palynomorphs, suggests a well drained soil as its ecological niche.

The correlation and paleoenvironmental comparison between the Willow Creek Formation and the Coalspur coal zone is now possible by the recognition of the Cretaceous-Tertiary boundary within the Willow Creek Formation. An age range of Early to Middle Paleocene is suggested for the Porcupine Hills Formation.

Résumé

Il faudrait reconnaître, dans la formation de Willow Creek, l'importance du paléosol caractérisé par la présence de glèbes et du calcaire pédogénique, dans les interprétations paléoclimatiques. Le milieu de plaines d'inondation semi-arides de la formation de Willow Creek, dans la partie sud des Foothills, contraste avec la plaine d'inondation marécageuse et mal drainée (zone houillère de Coalspur) de la partie centrale des Foothills. Cette interprétation de la formation de Willow Creek, basée sur la sédimentologie, est appuyée palynologiquement par le nombre exceptionnellement élevé d'échantillons à faible rendement, la faible diversité des assemblages du Maastrichtien récent et la présence de **Classopollis**. L'abondance de **Concentricystes** dans bien des échantillons, qui sont ordinairement presque exempts de palynomorphes, semble indiquer qu'un sol bien drainé a servi de niche écologique.

La corrélation et la comparaison paléo-environnementale entre la formation de Willow Creek et la zone houillère de Coalspur est maintenant rendue possible par la reconnaissance de la limite du Crétacé et du Tertiaire à l'intérieur de la formation de Willow Creek. Quant à la formation de Porcupine Hills, on suggère un éventail d'âges allant du Paléocène inférieur à moyen.

Introduction

Caliche (syn.: calcrete, cornstone or kankar) is a general term used to define low-magnesium calcite deposits, occurring in states ranging from chalky to well cemented and highly indurated, formed within a soil in or on pre-existing sediments, soil or rocks in semiarid environments (Bretz and Horberg, 1949; Esteban and Klappa, 1983; Goudie, 1983). A great variety of morphological types of caliche have been described from both ancient and modern continental deposits (Gile, 1961, 1970; Brewer and Sleeman, 1964; Gile and Hawley, 1966; Blokhuis et al., 1969; Reeves, 1970, 1976; Strakhov, 1970; Singh and Singh, 1972; Steel, 1973; Esteban and Klappa, 1983; Goudie, 1983). Concretions and nodules as well as crusts and hardpan are the most common types of caliche.

Such features were recorded in the Willow Creek Formation of southern Alberta over one hundred years ago by Dawson (1884, p. 67): "In some clayey layers, peculiar whitish-weathering, irregularly reniform, and generally small sized concretions abound". Williams and Dyer (1930, p. 59) noticed that "Many of the clay beds are characterized by white weathering, small, irregular-shaped nodules of calcite." Bell (1949, p. 11) gave the first interpretation of these features stating: "These concretions, it may be added, consist of lime carbonate, and are similar to cornstone or kankur" (kankar).

Although the occurrence of the limestone concretions was often cited in descriptions of the Willow Creek Formation (Douglas, 1950; Tozer, 1953, 1956), no attempt was made to use them as an indication of paleoclimate. The purpose of this paper is to draw attention to the paleoclimatic research based on the knowledge of the spatial distribution of caliche-bearing versus coal-bearing deposits and associated palynological assemblages in the uppermost Cretaceous and Paleocene in Alberta.

Acknowledgments

The introduction to the general stratigraphy of the study area by L.V. Hills during a field trip in spring, 1985, is acknowledged.

D.W. Gibson, G.G. Smith and J.H. Wall are thanked for their helpful criticisms, which led to improvements in the manuscript. B. Davies and R.M. Kalgutkar are recognized for their skilful preparation of the palynological samples.

Results

Stratigraphic setting of the caliche-bearing deposits

Observations of the caliche features in the Willow Creek and Porcupine Hills formations were made at the well known sections along Crowsnest, Oldman, and Castle rivers near Cowley (Fig. 67.1) and from cores located about 6 km northeast of Pincher Creek (Fig. 67.1, locality 9; Fig. 67.2, sections 9, 9a, 9b).

The stratigraphic nomenclature of Douglas (1950) and Tozer (1956) is applied to the study area. This study has allowed us to place the Cretaceous-Tertiary boundary within the Willow Creek Formation precisely, to differentiate the Willow Creek and Porcupine Hills formations palynologically, and to assign a minimum age of Middle Paleocene to the top, noneroded part of the Porcupine Hills Formation (Figs. 67.1, 67.2).

The lower part of the Willow Creek Formation is of Late Maastrichtian age, based on its relative stratigraphic position and the presence of dinosaur bones (Tozer, 1952, 1953, 1956; Abler, 1984). Additionally, the presence of

Azolla barbata Snead 1969 (Fig. 67.2, fig. 15, section 5, samples C-137585 and C-137587), known only from the Late Maastrichtian (Snead, 1969; Sweet, 1972, 1978), including records from the Willow Creek Formation (Snead, 1969), supports this age. Single specimens of *Cranwellia rumseyensis* Srivastava 1966, and possibly *Aquilapollenites conatus* Norton 1965 (Fig. 67.2, fig. 11, 12, respectively) were seen in sample C-137587. As these species or allied species range into the Campanian, a reworked origin cannot be excluded. Of the Upper Maastrichtian samples counted, in which *Concentricystes* is absent or only an accessory species, angiosperm pollen dominates in two (Fig. 67.2, section 4, C-132746 and C-132750) and is subdominant in one (Fig. 67.2, section 5, C-137587); a dominance of angiosperm pollen is characteristic of the Late Maastrichtian (Jerzykiewicz and Sweet, in press; Sweet and Hills, 1984).

The Cretaceous-Tertiary boundary occurs near the top of member D (Fig. 67.2, section 5, between samples C-137587 and C-137588). Recovery from sample C-137587, from a 0.3 m thick, greenish grey mudstone, is relatively poor. In addition to *Azolla barbata*, and the single specimens of *Cranwellia* and *Aquilapollenites* mentioned above, this sample contains a relatively high percentage of angiosperm pollen (23%) and a miospore assemblage dominated by *Cyathidites* (22%, compared with *Laevigatosporites* at 20%) giving it an overall Late Maastrichtian character. In sample C-137588, from a 3 cm thick, dark grey mudstone overlying the greenish mudstone, the percentage of angiosperm pollen is low (6%) and the miospore assemblage is dominated by *Laevigatosporites* (28.9%, compared with *Cyathidites* at 6.8%). In the next higher sample, C-137589, from a 2 cm thick coaly shale, the relative abundances remain the same but *Azolla schopfii* Dijkstra 1961, the range of which starts immediately above the Cretaceous-Tertiary boundary (Snead, 1969; Sweet, 1972, 1978; Sweet and Hills, 1984), is also present. A shift to a low relative abundance of angiosperm pollen, and from a dominance of *Cyathidites* to a dominance of *Laevigatosporites*, within the miospore assemblage are characteristics of the floral changes that occur across the Cretaceous-Tertiary boundary in Alberta (Jerzykiewicz and Sweet, in press; Sweet and Hills, 1984).

Relatively diverse assemblages occur in the uppermost part of member D (Fig. 67.2, top part of section 5) and member E (lower part of section 9a, samples C-131402 at 62.5, 90.6, and 111.5 m) of the Willow Creek Formation. An Early Paleocene age for these intervals is confirmed by the presence of *Brevicolporites colpella* Anderson 1960, *Kurtzipites trispissatus* Anderson 1960, and *Paraalnipollenites alterniporus* (Simpson) Srivastava 1975 (Fig. 67.2, figs. 8, 7 and 9, respectively) in combination with *Momipites waltmanensis* Nichols and Ott 1978, *M. wyomingensis* Nichols and Ott 1978 (Fig. 67.2, figs. 6 and 5, respectively). Associated taxa include *Alnus trina* Stanley 1965, *Ericaceoipollenites rallus* Stanley 1965, *Pandaniidites typicus* (Norton) Sweet 1986, *Retitricolpites crassus* Samoilovich 1965, *Syncolporites minimus* Leffingwell 1971 and *Ulmoideipites krempii* Anderson 1960. The coal-bearing members of the Scollard and Coalspur formations (Snead, 1969; Sweet and Hills, 1984; Jerzykiewicz and Sweet, in press) contain a similar suite of angiosperm pollen. This observation, in combination with the respective positions of the Cretaceous-Tertiary boundary, indicates a correlation between the coal-bearing members of the Scollard and Coalspur formations and the upper part of members D and E of the Willow Creek Formation. These stratigraphic intervals correspond to zone P1 and the initiation of zone P2 of Nichols and Ott (1978).

The occurrence of *Momipites waltmanensis* in the upper part of section 9b (Fig. 67.2, C-131401 at 35.4, 38.1, and 58.8 m) and the absence of species typical of the Early Paleocene, suggest an age at least as young as the P2 Zone of Nichols and Ott (1978) for the presumed basal beds of the Porcupine Hills Formation. By implication, this suggests that the basal beds of the Porcupine Hills Formation correlate with those of the Paskapoo Formation, although the evidence for this is based more on what is absent rather than on what is present.

Grey mudstones (Fig. 67.2, section 10; samples C-119747 and C-119748) from a location north of the main area of research yielded a well diversified assemblage.

The presence of *Aquilapollenites spinulosus* Funkhouser 1961, *Momipites ventifluminis* Nichols and Ott 1978, *Tilia danei* Anderson 1960, and *Momipites anellus* Nichols and Ott 1978 (Fig. 67.2, fig. 1-4, respectively) indicates a correlation between the uppermost part of the Porcupine Hills Formation and the Middle Paleocene, Zone P3 of Nichols and Ott (1978). In common with the Early Paleocene is the presence of *Alnus trina*, *Momipites waltmanensis*, *M. wyomingensis*, *Pandaniidites typicus*, *Syncolporites minimus* and *Ulmoideipites krempii*. This total assemblage is similar to that from a roadside outcrop of the Paskapoo Formation near Big Hill Springs west of Calgary (Wall and Sweet, 1982) and is comparable to that of "zone" C (Snead, 1969) from the

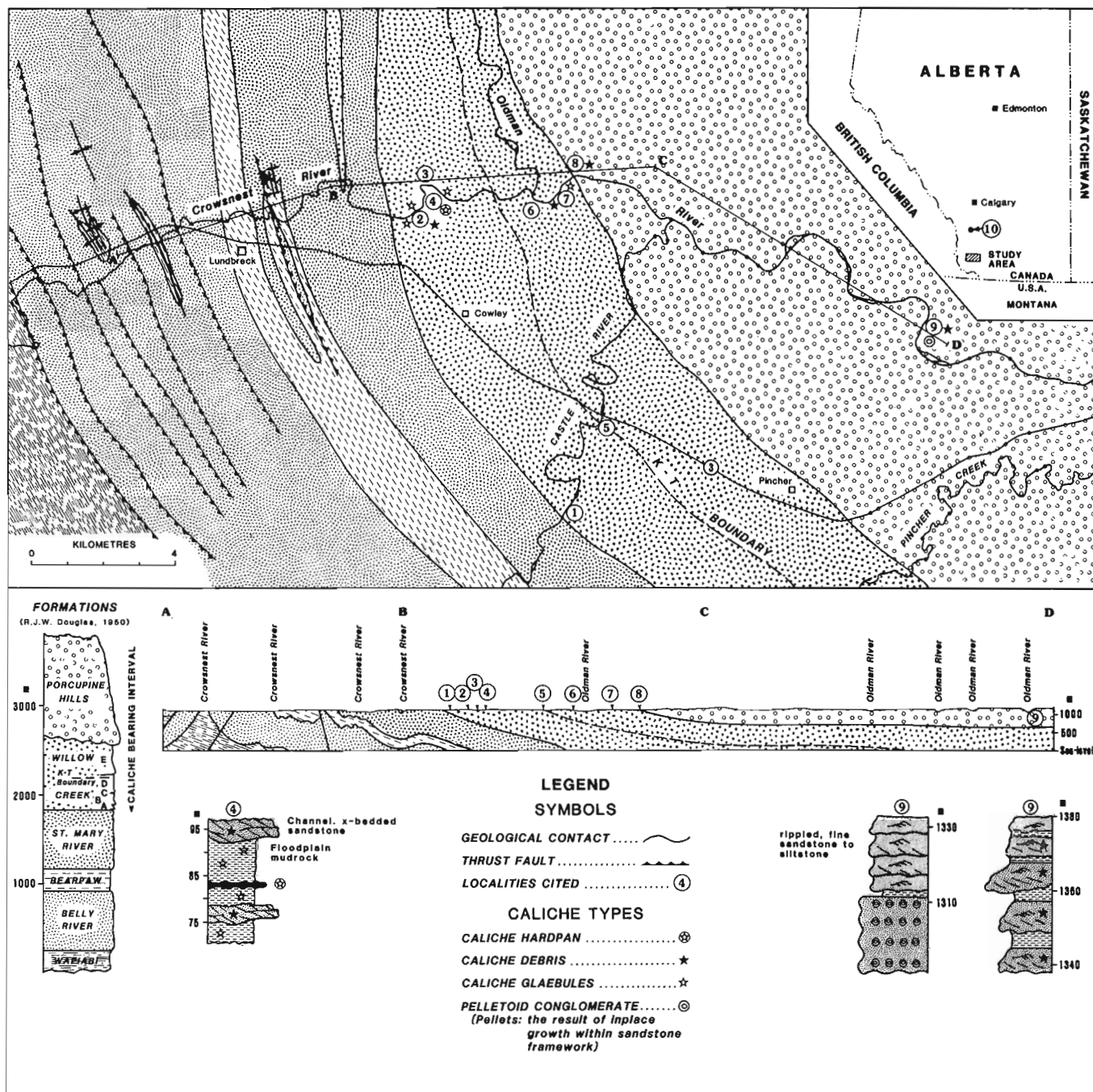
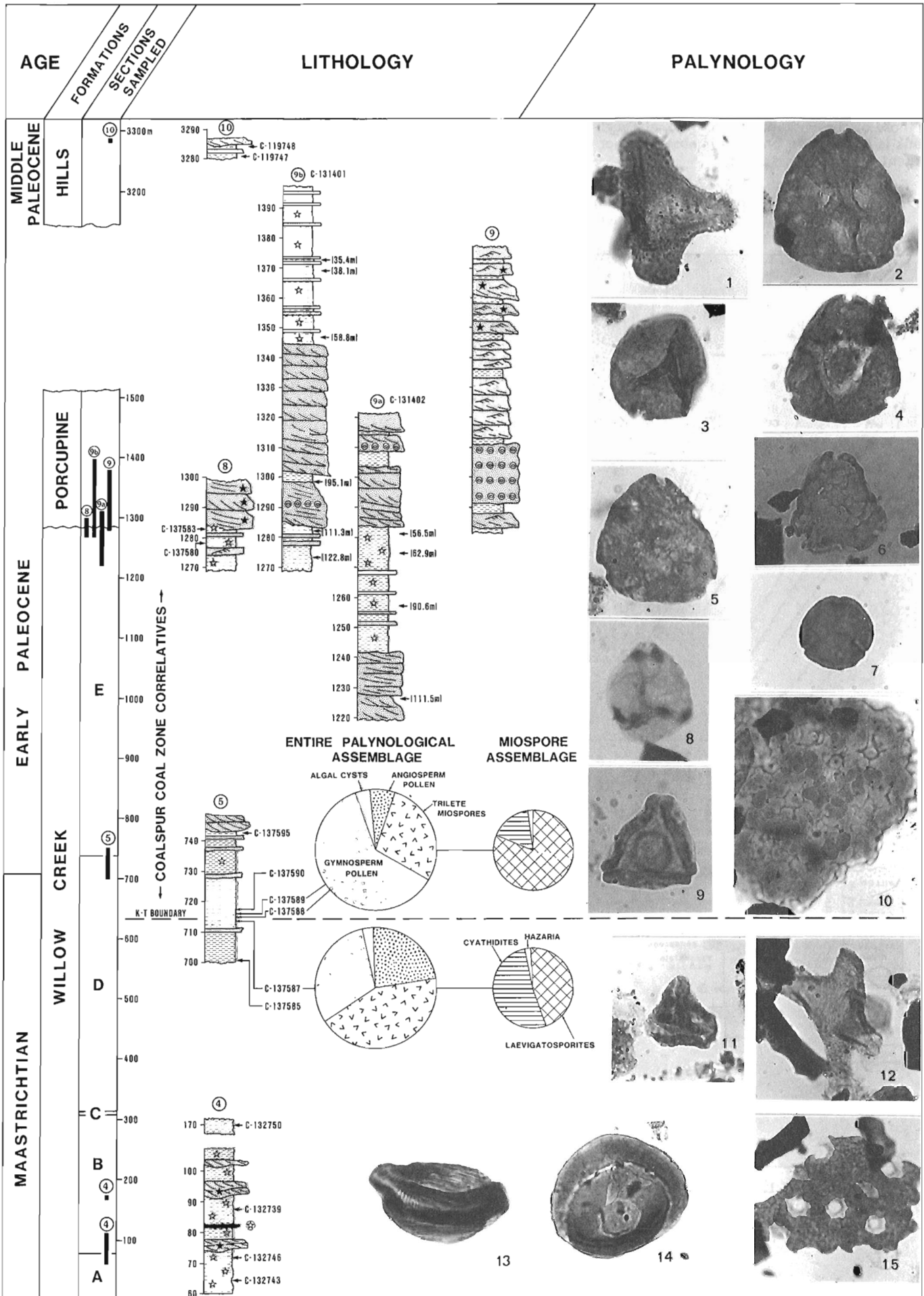


Figure 67.1. Caliche in the Willow Creek and Porcupine Hills formations of southern Alberta. (Geology modified after Hage, 1945).



Paskapoo Formation. These observations contradict Carrigy's (1971) conclusion that the Porcupine Hills Formation postdates the Paskapoo.

Caliche in the Willow Creek and Porcupine Hills formations

The following caliche types occur in the Willow Creek and/or Porcupine Hills formations: 1. glaeboles; 2. hardpan; 3. pelletoid conglomerate; and 4. caliche debris (Pl. 67.1). The first three types are due to alteration and replacement of the original host sediment in situ and the fourth type is a product of redeposition of one of the first three.

Caliche glaeboles¹ are common throughout the Crowsnest, Oldman and Castle rivers sections of the Willow Creek Formation (Fig. 67.1). They occur as a rule within the recessive mudrock intervals of the sections (Fig. 67.1, 67.2; Pl. 67.1, fig. 1). The glaeboles are easy to identify in outcrop because of their characteristic shape, surface texture, difference in colour from the surrounding mudrock, and greater resistance (Pl. 67.1, fig. 7). For this reason, many outcrops of the Willow Creek Formation are strewn with loose caliche glaeboles.

Pebble-sized glaeboles (nodules and septaria) seem to be the most common, but their size ranges from sand sized to

several centimetres in diameter. The most common are glaeboles that internally reveal patches of irregularly shaped cryptocrystalline micrite (Pl. 67.1, fig. 5) and cracks infilled with sparry cement (Pl. 67.1, fig. 6). X-ray emission energy spectra show the main mineral constituent of both micrite and sparry cement to be low-magnesium calcite.

Large glaeboles are usually composed of several smaller pedological features and may be referred to as the "compound types" of Brewer and Sleeman (1964). In some cases, the glaeboles tend to coalesce along horizontal surfaces, forming hardpan, which occurs as resistant layers of limestone in the mudstone intervals of the Willow Creek Formation. The thickest hardpan observed in member B of the formation is up to 0.5 m thick and can be traced over a distance of two hundred metres at locality 4 north of Cowley (Fig. 67.1, 67.2; Pl. 67.1, fig. 1).

Coalescent glaeboles are visible on the lower, bulbous surface of the hardpan (Pl. 67.1, fig. 2) as well as in any section through it. The internal structure, composed of coalescent glaeboles built up with microcrystalline calcite, as well as channels and cracks infilled with sparry calcite (Pl. 67.1, figs. 3, 3a), is diagnostic of a caliche facies (Esteban and Klappa, 1983).

Figure 67.2. Stratigraphic framework and palynology of the caliche-bearing sections. Locality for section 4, Lsd. 13, Sec. 28, Twp. 1, Rge. 1, W5 Mer.; section 5, Lsd. 4, 5, Sec. 12, Twp. 7, Rge. 1, W5 Mer.; section 8, Lsd. 10, Sec. 35, Twp. 7, Rge. 1, W5 Mer.; section 9, Sec. 17, Twp. 7, Rge. 30, W4 Mer.; and section 10, Sec. 9, Twp. 15, Rge. 1, W5 Mer.

Pie diagrams (inset) illustrate the shift in dominance within the flora midway through section 5. This provides part of the evidence for the placement of the Cretaceous-Tertiary boundary.

Micrographs are of biostratigraphically and paleoenvironmentally significant species. All figures x800, unless otherwise specified. In descriptions of figures, the GSC locality number is followed by the slide number, stage co-ordinates, and the GSC type number.

figures 1-4. Species restricted to the middle Paleocene.

1. *Aquilapollenites spinulosus* Funkhouser 1961; GSC loc. C-119747; P2664-1b, 40.3 x 112.4; GSC 76131.
2. *Momipites ventifluminis* Nichols and Ott 1978; GSC loc. C-119747; P2664-1a, 19.2 x 122.7; GSC 76132.
3. *Tilia danei* Anderson 1960; GSC loc. C-119747; P2664-1a, 27.8 x 119.4; GSC 76133.
4. *Momipites anellus* Nichols and Ott 1978; GSC loc. C-119747; P2664-1b, 41.3 x 112.2; GSC 76134.

figures 5, 6, 10. Species from throughout the Paleocene.

5. *M. wyomingensis* Nichols and Ott 1978; GSC loc. C-119747; P2664-1b, 28.8 x 119.6; GSC 76135.
6. *Momipites waltmanensis* Nichols and Ott 1978; GSC loc. C-131401, 58.8 m; P2795-13c, 26.7 x 118.4; GSC 76136.
10. *Azolla schopfii* Dijkstra 1961; GSC loc. C-137589; P2814-5a, 25.5 x 114.0; GSC 76140; x400.

figures 7-9. Species restricted to the Early Paleocene.

7. *Kurtzipites trispissatus* Anderson 1960; GSC loc. C-137590; P2814-6c, 12.3 x 120.7; GSC 76137.
8. *Brevicolporites colpella* Anderson 1960; GSC loc. C-131402/90.6 m; P2796-14a, 22.4 x 114.0; GSC 76138.
9. *Paraalnipollenites alterniporus* (Simpson) Srivastava 1975; GSC loc. C-131401/122.8 m; P2795-21c, 18.3 x 118.4; GSC 76139.

figures 11, 12, 15. Species restricted to the Late Maastrichtian.

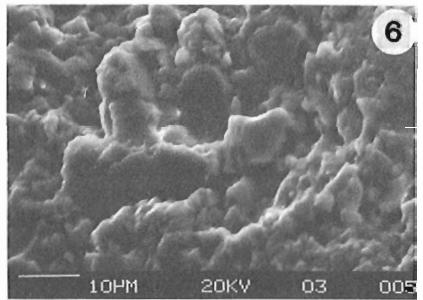
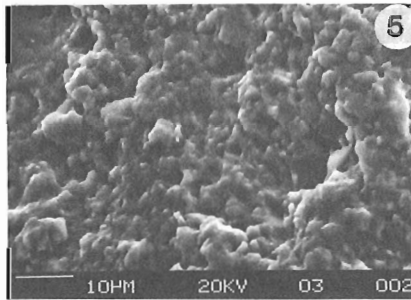
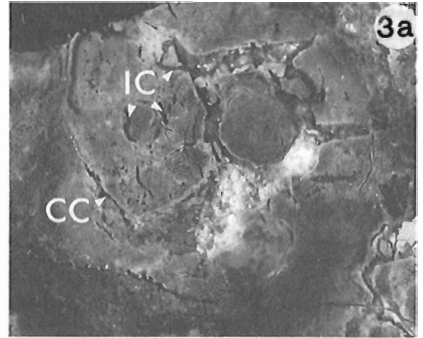
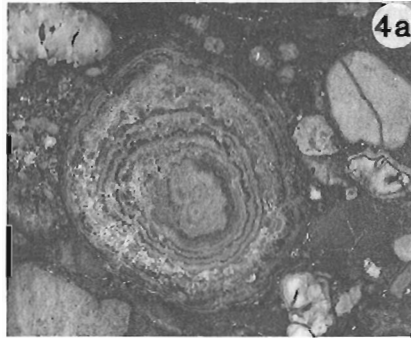
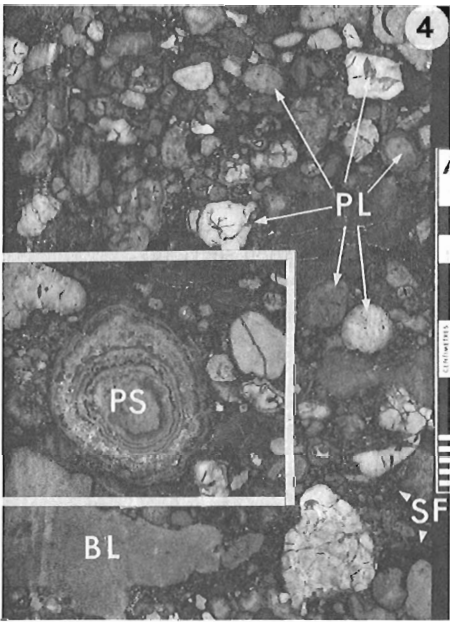
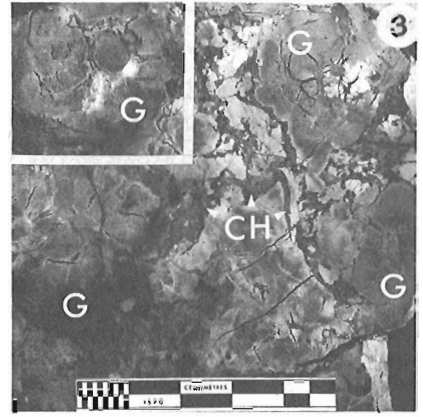
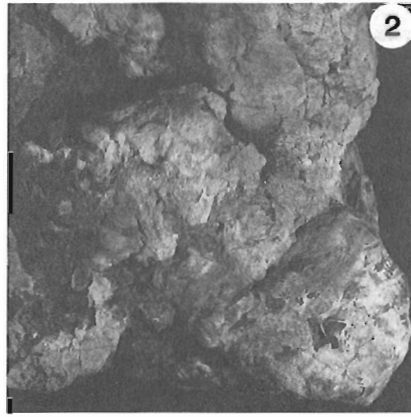
11. *Cranwellia rumseyensis* Srivastava 1966; GSC loc. C-137587; P2814-3a, 18.2 x 124.0; GSC 76141.
12. *Aquilapollenites conatus* Norton 1965; GSC loc. C-137587; P2814-3b, 32.4 x 114.3; GSC 76142.
15. *Azolla barbata* Snead 1969; GSC loc. C-137585; P2814-1a, 21.2 x 121.0; GSC 76143; x400.

figures 13, 14. Species with probable paleoenvironmental significance.

13. *Concentricystes* sp.; GSC loc. C-132743; P2679-0Aa, 19.8 x 123.2; GSC 76144.
14. *Classopollis* sp.; GSC loc. C-132736; P2812-4b, 33.2 x 116.3; GSC 76145.

¹ "Glaebules" is a general term for a broad group of three-dimensional pedological features embedded in the matrix of soil material (Brewer and Sleeman, 1964). They include "nodules" (internally structureless), "concretions" (concentric), "septaria" (with a distinctive, superimposed pattern of cracks) as well as "pedoles", "glaebular haloes" and "papules", which reveal a more compound internal fabric (Pettijohn, 1949; Brewer and Sleeman, 1964).

PLATE 67.1



Pellets, ooids and pisolites¹ consisting of micritic calcite occur occasionally in the sandstone layers of the Porcupine Hills Formation. They may be dispersed throughout the sandy matrix or may form a conglomerate comprising closely packed pellets, ooids and pisolites (Pl. 67.1, fig. 4, 4a). This pelletoid conglomerate occurs in the basal part of the Porcupine Hills Formation (Figs. 67.1, 67.2; sections 9, 9a, 9b)

All constituents of the conglomerate that are larger than the sand fraction are of authigenic origin and consist principally of micritic calcite with some admixtures of iron oxide pigments, which produce the yellow to brown hues of most of the pellets. Some of them, however, are dark grey to black and are of particular interest. They might be compared with black "caliche-algal micrite", which forms a caliche crust near hypersaline lakes (Ward et al., 1970).

Further investigation is needed in order to identify the nature of the black pigmentation of these pellets before any firm paleoclimatic conclusion is drawn (see Discussion of the results in this paper).

Debris consisting of subangular limestone fragments derived from caliche, as well as almost intact redeposited glaeboles, are common in some channel lag deposits of the Willow Creek and Porcupine Hills formations. The caliche clasts are easily distinguished from the extraformational pebbles, which consist of clasts of quartz, quartzite and chert.

Associated palynological assemblages

As in Snead's (1969) study, recovery from samples of the Willow Creek Formation was found to be generally low. Of the 90 samples processed from the Willow Creek and Porcupine Hills formations, mostly grey and dark grey mudstones, 24 samples were effectively barren of indigenous palynomorphs and only 14 samples yielded assemblages that were sufficiently rich to be counted. The recovery of indigenous palynomorphs was sparse in the remaining 52 samples.

In addition to the erratic recovery, the diversity of palynomorphs in the lower, Maastrichtian part of the Willow Creek Formation is very low. The three samples with abundant angiosperm pollen contained few species; the pollen assemblage was dominated by *Ulmoideipites tricostatus* and/or *U. hebridicus* (C-132746 and C-132750), or simple tricolpate pollen (C-137587). In contrast, in the upper, Early Paleocene portion of the Willow Creek Formation (uppermost beds of member D and member E), assemblages recovered from three samples (C-137590 and C-131402 from 90.6 and 111.5 m) are as diverse as those usually recovered from the upper, coal-bearing member of the Coalspur Formation (Jerzykiewicz and Sweet, in press) and Scollard Formation (Snead, 1969; Sweet, unpublished data) of Early Paleocene age. Similarly, the total diversity of the assemblages from the Porcupine Hills Formation appears similar to that recorded for the Paskapoo Formation (Snead, 1969; Jerzykiewicz and Sweet, in press).

Another aspect of the Late Maastrichtian and Paleocene assemblages of southern Alberta with possible paleoenvironmental significance (see Discussion of results) is the occurrence of *Classopollis* and *Concentricystes*. *Classopollis* sp. (Fig. 67.2, fig. 14) occurs in several samples, in which there is no evidence of its having been reworked. This species makes up about 6 per cent of the assemblage in sample C-137587 from just below the Cretaceous-Tertiary boundary, 3 per cent in sample C-137583 and 1 per cent in sample C-137580 (the last two are near the top of the Willow Creek Formation), in addition to its being present in several other samples. Another unique character of many of the assemblages is the conspicuous presence of excellently preserved specimens of *Concentricystes* (Fig. 67.2, fig. 13). *Concentricystes* is commonly the dominant, if not the only, species in samples that do not have enough specimens to establish a relative abundance. This estimated dominance of *Concentricystes* is confirmed by the relative abundances obtained from samples C-132739 (near the base of the Willow Creek Formation), and C-131402 (from 56.5 m, near the top of the Willow Creek Formation), in which *Concentricystes* makes up 60 per cent and 57 per cent of the assemblages, respectively. Accompanying *Concentricystes* in several samples are relatively common fungal spores and hyphae.

PLATE 67.1

Examples of caliche features in the Willow Creek and Porcupine Hills formations

- figure 1 Resistant hardpan layer (indicated by arrow) in mudstone interval of the Willow Creek Formation. Locality 4.
- figure 2 Coalesced caliche glaeboles revealed on the lower, bulbous surface of the hardpan. The sample was taken from the horizon visible in figure 1.
- figure 3 Internal structure of the same sample sectioned parallel to the sole of the hardpan. Note the coalesced glaeboles built up with microcrystalline calcite (G), and the channels and cracks infilled with sparry calcite cement (CH). The frame indicates the outline of figure 3a.
- figure 3a Close-up view showing details of caliche glaeboles affected by circumgranular (CC) and intergranular (IC) cracks.
- figure 4 Pelletoid conglomerate. Porcupine Hills Formation. Locality 9. All pellets resulted from in place growth within a sandstone framework. Note the pattern of recemented cracks and rims around and within some pellets. PL, limestone pellet; BL, black limestone pellet; PS, pisolite, SF, sandstone framework. The frame indicates the outline of figure 4a.
- figure 4a Close-up view showing details of the pisolite and adjacent pellets within the sandstone framework.
- figures 5, 6 Scanning electron micrographs of caliche glaebole sections. Figure 5 shows microcrystalline calcite from the body of the glaebole. Figure 6 shows sparry calcite cement infilling the channels and cracks. Note partially dissolved calcite crystals.
- figure 7 Caliche glaeboles from the Willow Creek Formation. Locality 4.

¹ The terminology by Hay and Wiggins (1980) has been adopted here: **pellet** refers to a spherical or oval particle of authigenic origin lacking a nucleus; **oid** refers to a spherical or oval particle less than 2 mm in diameter comprising a nucleus enclosed by one or more laminae. The majority of ooid coatings are concentrically banded; **pisolites** are structurally similar to ooids, but greater than 2 mm in diameter.

Discussion of the results

A major environmental difference must have existed between the central and southern Alberta Foothills in Late Maastrichtian and Early Paleocene time, because the stratigraphic correlative of the coal-bearing deposits (Coalspur coal zone) in the southern Foothills is the barren Willow Creek Formation (Fig. 67.2). The lack of coal in the southern Foothills is the most dramatic, but not the only, facies difference between the two areas. The common occurrence of caliche throughout the Willow Creek Formation, the presence of redbeds in its lower part, and the impoverished palynological assemblages, seem to be of prime importance for the reconstruction of its depositional environment.

Although caliche is known to occur in many parts of the world, including polar regions, significant calcium carbonate accumulations of this type are characteristic of the soil in warm, semiarid regions (Reeves, 1976; Esteban and Klappa, 1983; Goudie, 1983). The amount and frequency of precipitation seem to be the most important controlling factors. If precipitation is excessive, leaching of the soil is complete and no calcium carbonate will accumulate. If rainfall is not sufficient, the degree of leaching is inadequate to mobilize calcium carbonate, and only minor accumulations of calcite occur in the soil. The most favourable conditions for caliche formation exist in the regions where annual rainfall is between 400 and 600 mm (Goudie, 1983). Essential for caliche formation also appears to be the sporadic distribution of rainfall, i.e. alternation of periods of rainfall and long-lasting droughts (Woolnough, 1930). It also has been proven that the depth of the caliche zone in the soil profile depends on the amount of annual rainfall (Jenny and Leonard, 1939). With increased annual rainfall, the zone of caliche formation moves to a greater depth and finally will disappear when the annual precipitation (in temperate regions) exceeds 1000 mm (Blatt et al., 1980).

From the common and well developed caliche in the overbank deposits of the Willow Creek Formation, we can visualize the depositional environment as a semiarid floodplain. The overbank mudstone with scattered glaebules should be interpreted in terms of glaebular soil (Bernard and Le Blanc, 1965; Blokhuis et al., 1969; Singh and Singh, 1972), which represents stages I and II of caliche development (Gile et al., 1966). The hardpan can be described in terms of the pedogenic limestone (Gile, 1961, 1970; Gile and Hawley, 1966; Reeves, 1970), representing stages III and IV in the morphogenic scheme of caliche development (Gile et al., 1966).

The position of the caliche in the overbank deposits of the Willow Creek Formation is very similar to that described in the Old Red Sandstone (Allen, 1974; Leeder, 1975; 1976). The overall sedimentological character (the fining-upward cycles) and the distribution of redbeds within the Old Red Sandstone and the Willow Creek Formation also show some similarities. Redbeds in the Willow Creek Formation occur within the fine members of the fining-upward cycles while the coarse, channel member is, as a rule, drab. Such contrasting colours between the coarse and fine members in the Old Red Sandstone have been explained by Friend (1966) as follows: in the floodplain environment, abundant iron hydroxides were deposited with the clay-rich suspended load. Because of periodic drying, and lowering of the water table, oxidizing conditions prevailed and iron hydroxides eventually altered into haematite. In the channel environment, however, the sediment remained mostly below the water table after deposition. In areas where substantial organic matter was present, bacterial consumption of oxygen created a reducing environment in which ferric hydroxides were unstable and were removed in solution, and the channel sediments ultimately became drab. This explanation can be applied to the floodplain environment of the

Willow Creek Formation. Presumably the groundwater table was low during dry periods, causing oxidizing conditions and the evaporation of vadose water. This led to the upward capillary movement of soil water and the precipitation of calcium carbonate. Even during rainy seasons, the groundwater table was low enough to prevent formation of extensive peat swamps, which were well developed in the Willow Creek Formation correlatives of the central Alberta Foothills (Coalspur coal zone). The plant matter accumulations that are present in rare, organic-rich, dark mudstone of the Willow Creek Formation might have been deposited on the floodplain in local and ephemeral lakes.

Somewhat puzzling is the occurrence of black limestone pellets in the basal part of the Porcupine Hills Formation. The black colour of similar limestone has been attributed to the preservation of finely disseminated organic matter of algal origin, and possibly to the presence of iron sulphide (Ward et al., 1970). These authors suggested that layers of fragmented, dark-coloured limestone may indicate subaerial exposure adjacent to hypersaline water. The depositional setting of the Porcupine Hills Formation, far from a marine shoreline, seems to preclude any consideration of a marine influence in the formation of the black limestone pellets. Further research is needed in order to explain their association with the caliche deposits in the study area.

The semiarid depositional environment of the lower part of the Willow Creek Formation is reflected in the impoverished palynological assemblage. The Upper Maastrichtian and Lower Paleocene strata of central Alberta are usually very productive in terms of yield per unit volume of sample, with the Upper Maastrichtian high in terms of floral diversity (Snead, 1969; Srivastava, 1970; Sweet, 1978; Jerzykiewicz and Sweet, in press; and unpublished data). An inference of an environment of deposition not generally amenable to plant growth is compatible with the observed overall low productivity of Late Maastrichtian and Early Paleocene samples from southwestern Alberta.

The assemblages from the Upper Maastrichtian of southwestern Alberta have only a few, probably wind-distributed, angiosperm pollen species. This contrasts sharply with the abundant, relatively large and exotic angiosperm pollen species that together form a significant portion of Late Maastrichtian assemblages from the central Alberta Foothills (Jerzykiewicz and Sweet, in press). Whereas in central Alberta the Early Paleocene was the time of lowest diversity, samples from member E, or the upper (Lower Paleocene) part of the Willow Creek Formation in southwestern Alberta contain the greatest diversity of angiosperm pollen. This reversal in the usual trend toward decreased diversity going from the Late Maastrichtian to Early Paleocene can adequately be explained by differences in local environmental conditions overriding regional trends in diversity.

The lower (Maastrichtian) part of the Willow Creek Formation contains the highest proportion of red, maroon and green beds, and the largest and most abundant calcrete glaebules. In member E (the upper part of the Willow Creek Formation), red and green beds occur infrequently, and although there are zones bearing calcrete glaebules, these are less frequent and the glaebules are generally smaller and less common. Additionally, restricted organic-rich horizons occur. Presumably these changes from older to younger strata represent an amelioration of the climate, allowing for the coexistence of a greater diversity of plants. Hence, in its correspondence with the observed lithological changes, the upward increase in diversity of the angiosperms supports our contention that in southwestern Alberta a biologically stressed environment existed during the Late Maastrichtian and that this environment improved in the Early Paleocene.

The paleoenvironmental significance of **Classopollis** and **Concentricystes** (Fig. 67.2, fig. 13, 14, respectively) is somewhat more ambiguous. A relatively wide range of habitats has been ascribed to **Classopollis**-bearing plants (Srivastava, 1976; Vakhrameev, 1981; Alvin, 1982). It seems likely that during the Late Cretaceous their ecological niche was xerophytic, becoming slightly more humid toward the end of the Cretaceous (Pons et al., 1980). Vakhrameev (1981) makes a direct correlation between the occurrence of a high relative abundance of **Classopollis** and either a warm arid, or a warm semiarid climate during the Jurassic, suggesting a greater adaptability within this group for drier habitats than expressed either by other gymnosperms or ferns. With the advent of the angiosperms as a dominant group in the Late Cretaceous, warm, arid or semiarid habitats may have provided the final refugiums for the **Classopollis**-bearing plants.

Concentricystes and allied, if not synonymous, genera occurring in relatively low abundance have been documented worldwide (e.g., Shugayevskaya, 1969; Hekel, 1972; Christopher, 1976; and Kedves, 1977). Greater abundances have been recorded from coal and coal-bearing strata (Thiergart and Frantz, 1962; Norris, 1965; Shugayevskaya, 1969), in clastics associated with indicators of a humid climate (Rossignol, 1962), as well as from clastics with some associated semiarid characteristics (Hekel, 1972; Christopher, 1976). From the above discussion it is apparent that the characteristics of the ecological niches preferred by the organism producing **Concentricystes** are far from being established. The occurrences identified in this study are compatible with its being derived from a soil fungus inhabiting well drained soils.

Concluding remarks

Palynology has been used to amplify two separate aspects of this study. It has contributed not only to the paleoenvironmental interpretation, but has also refined the correlation between Upper Maastrichtian and Lower Paleocene formations in different parts of the Foothills Belt. Our ability to define the Cretaceous-Tertiary boundary in both the central and southern Foothills has established an exact correlation between a horizon within the top of member D of the Willow Creek Formation and the bases of the Nevis and Mynheer coal zones within the Scollard and Coalspur formations, respectively. The Porcupine Hills Formation is concluded to be coeval with the lower part of the Paskapoo Formation.

As a result of the data presented herein, it is obvious that the previous paleogeographic picture of the Cretaceous-Tertiary boundary interval in Alberta requires some modification. A new component, the semiarid floodplain, should be added to the spectrum of depositional environments occurring within a vast alluvial plain extending eastward from the flanks of the rising Rocky Mountains. Such a modification opens a new line of paleoclimatic and paleoecological research in the area, with implications for the distribution of coal along the Alberta Foothills, the composition of the flora in the interval spanning the Cretaceous-Tertiary boundary, and the ecological niches available to the dinosaurs in the Late Maastrichtian.

Russell (1977, p.110) portrays the general paleo-environmental setting of the Late Maastrichtian **Triceratops** fauna as being a moist floodplain crossed by large, sediment-laden, meandering rivers. He visualized the floodplains as being covered by a canopied wetland forest. However, Russell, citing the presence of apparently abundant protoceratopsids and ankylosaurs, astutely observed that the present central Alberta region bordered another major environment. We have now provided evidence for this other environment.

References

- Abler, W.L.
1984: A three-dimensional map of a paleontological quarry; *Contributions to Geology*, University of Wyoming, v. 23, p. 9-14.
- Allen, J.R.L.
1974: Sedimentology of the Old Red Sandstone (Siluro-Devonian) in the Cleve Hills Area, Shropshire, England; *Sedimentary Geology*, v. 12, p. 73-167.
- Alvin, K.L.
1982: Cheirolepidiaceae: Biology, structure and paleoecology; *Review of Palaeobotany and Palynology*, v. 37, p. 71-98.
- Bell, W.A.
1949: Uppermost Cretaceous and Paleocene floras of western Alberta; *Geological Survey of Canada, Bulletin* 13, 231 p.
- Bernard, H.A. and Le Blanc, R.J.
1965: Résumé of Quaternary geology of the Northwestern Gulf of Mexico; in *The Quaternary of the United States*, ed. H.E. Wright and D.G. Frey; Princeton University Press, Princeton, New Jersey, p. 137-185.
- Blatt, H., Middleton, G., and Murray, R.
1980: Origin of sedimentary rocks; Prentice-Hall, Inc., 782 p.
- Blokhuis, W.A., Pape, T., and Slager, S.
1969: Morphology and distribution of pedogenic carbonate in some vertisols of the Sudan; *Geoderma*, v. 2, p. 173-200.
- Bretz, J.H. and Horberg, L.
1949: Caliche in southwestern New Mexico; *Journal of Geology*, v. 57, p. 491-511.
- Brewer, R. and Sleeman, J.R.
1964: Glaebules: their definition, classification and interpretation; *Journal of Soil Science*, v. 15, p. 66-78.
- Carrigy, M.A.
1971: Lithostratigraphy of the uppermost Cretaceous (Lance) and Paleocene strata of the Alberta Plains; *Research Council of Alberta, Bulletin* 27, 161 p.
- Christopher, R.A.
1976: Morphology and taxonomic status of **Pseudoschizaea** Thiergart and Frantz ex R. Potonie emend.; *Micropaleontology*, v. 22, p. 143-150.
- Dawson, G.M.
1884: Report on the region in the vicinity of Bow and Belly Rivers, North West Territory; *Geological Survey of Canada, Report of Progress* 1882-83, pt. C.
- Douglas, R.J.W.
1950: Callum Creek, Langford Creek, and Gap map-areas, Alberta; *Geological Survey of Canada, Memoir* 255, 124 p.
- Esteban, M. and Klappa, C.F.
1983: Subaerial exposure environment; in *Carbonate Depositional Environments*, ed. P.A. Scholle, D.G. Bebout, and C.H. Moore; American Association of Petroleum Geologists, *Memoir* 33, p. 1-54.

- Friend, P.F.
1966: Clay fractions and colours of some Devonian red beds in the Catskill Mountains, U.S.A.; Geological Society of London, Quarterly Journal, v. 122, p. 273-292.
- Gile, L.H.
1961: A classification of Ca horizons in soils of a desert region, Dona Ana County, New Mexico; Soil Science Society of America, Proceedings, v. 25, p. 52-61.
1970: Soils of the Rio Grande Valley border in southern New Mexico; Soil Science Society of America, Proceedings, v. 34, p. 465-472.
- Gile, L.H. and Hawley, J.W.
1966: Periodic sedimentation and soil formation on an alluvial-fan piedmont in southern New Mexico; Soil Science Society of America, Proceedings, v. 30, p. 261-268.
- Gile, L.H., Peterson, F.F., and Grossman, R.B.
1966: Morphological and genetic sequences of carbonate accumulation in desert soils; Soil Science, v. 101, p. 347-360.
- Goudie, A.S.
1983: Calcrete; in Chemical sediments and geomorphology: precipitates and residues in the near-surface environment, ed. A.S. Goudie and K. Pye; Academic Press, p. 93-131.
- Hage, C.O.
1945: Cowley; Geological Survey of Canada, Map 816A.
- Hay, R.L. and Wiggins, B.
1980: Pellets, ooids, sepiolite and silica in three calcretes of the southwestern United States; Sedimentology, v. 27, p. 559-576.
- Hekel, H.
1972: Pollen and spore assemblages from Queensland Tertiary sediments; Geological Survey of Queensland, Publication no. 355, 31 p.
- Jenny, H. and Leonard, C.D.
1939: Functionable relationships between soil properties and rainfall; Soil Science, v. 38, p. 363-381.
- Jerzykiewicz, T. and Sweet, A.R.
- The Cretaceous-Tertiary boundary in the central Alberta Foothills: stratigraphy; Canadian Journal of Earth Sciences. (in press)
- Kedves, M.
1977: Scanning electron-microscopic investigations on the pollen grains of the Operculati Venk. et Gocz. 1664; Acta Biologica Szeged, v. 22, p. 29-36.
- Leeder, M.R.
1975: Pedogenic carbonates and flood sediment accretion rates: a quantitative model for alluvial arid-zone lithofacies; Geological Magazine, v. 112, p. 257-270.
1976: Palaeogeographic significance of pedogenic carbonates in the topmost upper Old Red Sandstone of the Scottish border basin; Geological Journal, v. 11, p. 21-28.
- Nichols, D.J. and Ott, H.L.
1978: Biostratigraphy and evolution of the *Momipites-Caryapollenites* lineage in the Early Tertiary in the Wind River Basin, Wyoming; Palynology, v. 2, p. 93-112.
- Norris, G.
1965: Triassic and Jurassic miospores and acritarchs from the Beacon and Ferrar Groups, Victoria Land, Antarctica; New Zealand Journal of Geology and Geophysics, v. 8, p. 236-277.
- Pettijohn, F.J.
1949: Sedimentary rocks; Harper and Brothers, New York, 1st edition, 526 p.
- Pons, D., Lauerjat, J., and Broutin, J.
1980: Paléoclimatologie comparée de deux gisements du Crétacé supérieur d'Europe occidentale; Société Géologique de France, Mémoires, Paris, no. 139, p. 151-158.
- Reeves, C.C. Jr.
1970: Origin, classification and geologic history of caliche on the south-eastern High Plains, Texas and eastern New Mexico; Journal of Geology, v. 78, p. 352-362.
1976: Caliche: origin, classification, morphology and uses; Lubbock, Texas, Estacado Books, 233 p.
- Rosignol, M.
1962: Analyse pollinique de sédiments marins Quaternaires en Israël II. - Sédiments Pléistocènes; Pollen et Spores, v. 4, p. 121-148.
- Russell, D.A.
1977: A Vanished World. The dinosaurs of western Canada; National Museum of Canada, Natural History Series, no. 4, 142 p.
- Shugayevskaya, O.V.
1969: Lower Cretaceous *Chomotriletes* miospores from the Suyfun depression; Paleontological Journal, v. 2, p. 270-272.
- Singh, L. and Singh, S.
1972: Chemical and morphological composition of Kankar nodules in soils of the Vindhyan region of Mirzapur, India; Geoderma, v. 7, p. 269-276.
- Snead, R.G.
1969: Microfloral diagnosis of the Cretaceous-Tertiary boundary, central Alberta; Research Council of Alberta, Bulletin 25, 148 p.
- Srivastava, S.K.
1970: Pollen biostratigraphy and paleoecology of the Edmonton Formation (Maestrichtian), Alberta, Canada; v. 7, p. 221-276.
1976: The fossil genus *Classopollis*; Lethaia, v. 9, p. 437-457.
- Steel, R.J.
1973: Cornstone (fossil caliche) - Its origin, stratigraphic, and sedimentological importance in the New Red sandstone, western Scotland; Journal of Geology, v. 82, p. 351-359.
- Strakhov, N.H.
1970: Principles of lithogenesis, vol. 3; Plenum Publishing Company, New York, 577 p.
- Sweet, A.R.
1972: The taxonomy, evolution and stratigraphic value of *Azolla* and *Azolopsis* in the Upper Cretaceous and Lower Tertiary boundary, central Alberta; Ph. D. thesis; University of Calgary, Calgary, Alberta, 403 p.
1978: Palynology of the Ravenscrag and Frenchman formations; in Coal Resources of Southern Saskatchewan: A model for evaluation methodology; Geological Survey of Canada, Economic Geology Report 30, p. 29-38.

- Sweet, A.R. and Hills, L.V.
 1984: A palynological and sedimentological analysis of the Cretaceous-Tertiary boundary, Red Deer River Valley, Alberta, Canada (Abstract); Sixth International Palynological Conference, Calgary 1984, p. 160.
- Thiergart, F. and Frantz, U.
 1962: Some spores and pollen grains from a Tertiary brown coal deposit in Kashmir; *Palaeobotanist*, v. 10, p. 84-86.
- Tozer, E.T.
 1952: The St. Mary River - Willow Creek contact on Oldman River, Alberta; Geological Survey of Canada, Paper 52-3, 9 p.
 1953: The Cretaceous-Tertiary transition in southwestern Alberta; Third Annual Field Conference and Symposium, Alberta Society of Petroleum Geologists, Calgary, p. 23-31.
 1956: Uppermost Cretaceous and Paleocene non-marine molluscan faunas of western Alberta; Geological Survey of Canada, Memoir 280, 125 p.
- Vakhrameev, V.A.
 1981: Pollen *Classopollis*: indicator of Jurassic and Cretaceous climates; *The Palaeobotanist*, v. 28-29, p. 301-307.
- Wall, J.H. and Sweet, A.R.
 1982: Upper Cretaceous-Paleocene stratigraphy, micro-paleontology and palynology of the Bow Valley area, Alberta; 1982 Alberta Association of Petroleum Geologists-Canadian Society of Petroleum Geologists Field Trip 10; Canadian Society of Petroleum Geologists, Calgary, 47 p.
- Ward, W.C., Folk, R.L., and Wilson, J.L.
 1970: Blackening of eolianite and caliche adjacent to saline lakes, Isla Mujeres, Quintana Roo, Mexico; *Journal of Sedimentary Petrology*, v. 40, p. 548-555.
- Williams, M.Y. and Dyer, W.S.
 1930: Geology of southern Alberta and southwestern Saskatchewan; Geological Survey of Canada, Memoir 163, 160 p.
- Woolnough, W.G.
 1930: The influence of climate and topography in the formation and distribution of products of weathering; *Geological Magazine*, v. 67, p. 123-132.

Rank and other compositional data on coals and carbonaceous shale of the Kayak Formation, northern Yukon Territory

Project 850044

A.R. Cameron, D.K. Norris, and K.C. Pratt
Institute of Sedimentary and Petroleum Geology, Calgary

Cameron, A.R., Norris, D.K., and Pratt, K.C., Rank and other compositional data on coals and carbonaceous shales of the Kayak Formation, northern Yukon Territory; in Current Research, Part B, Geological Survey of Canada, Paper 86-1B, p. 665-670, 1986.

Abstract

The Mississippian Kayak Formation was examined and sampled systematically at five locations in northern Yukon Territory in order to assess the number, thickness, rank, petrographic characteristics, ash and sulphur content of exposed seams in relation to their tectonic setting in the Cordilleran orogenic system.

All of the seams examined are anthracites, suggesting thermal upgrading through a combination of deep burial and differential exposure to higher temperatures from igneous intrusions. All have a relatively high content of inertinite. One of the seams, with a measured thickness of about 5.5 m, has an ash content of under 7 per cent and an average sulphur content of about 0.5 per cent, and thus is a prospective source of good quality thermal coal. The high rank of the Kayak coals, however, suggests that the Mississippian and older rocks are not good oil prospects, although some parts of the Yukon Coastal Plain may be within the gas window.

Résumé

La formation de Kayak d'âge mississipien a été étudiée et échantillonnée de façon systématique à cinq endroits dans le nord du Territoire du Yukon afin d'évaluer le nombre, l'épaisseur, le rang, les caractéristiques pétrographiques, la teneur en cendres et en soufre des couches exposées par rapport à leur cadre tectonique dans le système orogénique de la Cordillère.

Toutes les couches étudiées sont des anthracites, phénomène qui semble indiquer un accroissement thermique vers le haut à la suite d'un enfouissement profond et d'une exposition différentielle à des températures élevées provenant d'intrusions ignées. Les couches ont toutes une teneur relativement élevée en inertinite. Une de ces couches, d'une épaisseur mesurée d'environ 5,5 m, a une teneur en cendres inférieure à 7 % et une teneur moyenne en soufre d'environ 0,5 %, ce qui en fait une source éventuelle de charbon thermique de bonne qualité. Le rang des charbons de Kayak semble cependant indiquer que les roches datant du Mississipien et plus anciennes présentent peu de chances de renfermer du pétrole, bien que certaines parties de la plaine côtière du Yukon fassent partie de la zone gazière.

Introduction

Coal seams and carbonaceous shales of the Mississippian Kayak Formation were sampled at five locations in northern Yukon Territory during the field season of 1985 (Fig. 68.1, Table 68.1). The general geographic position of these sites is as follows: Station 1 southeast of Barn Mountains; Station 2 near the headwaters of the Spring River; and Stations 3, 4 and 5 in the British Mountains near Malcolm River. Of these locations, the most important in terms of economic interest is Station 1, where a seam of anthracite 5.53 m thick was discovered and sampled in detail. The seam is exposed in a shallow gully on the divide between the headwaters of the Blow River and Johnson Creek (Fig. 68.2). At Stations 2 and 4, the black beds sampled proved to be weathered shales relatively lean in carbonaceous matter. At Station 3, float coal from an unlocated seam was sampled. A seam of high ash coal, at least 0.3 m thick, was sampled at Station 5, and coal from a second seam of undetermined thickness and stratigraphic position also was collected there. Rank evaluation by reflectance measurement was carried out on a number of these samples along with maceral, ash and sulphur determinations. Some were also submitted for palynological analysis.

Geological setting

The coal-bearing, Lower Carboniferous Kayak Formation in northern Yukon occurs in association with three structural highs in the Cordilleran orogenic system. These are, from east to west, Hoidahl Dome, Barn Uplift and Romanzof Uplift (Norris and Yorath, 1981). The structural depressions surrounding them on the mainland are filled primarily with Jurassic and younger Mesozoic and Tertiary clastics. Offshore, on the northeast flank of Romanzof Uplift, these clastics thicken to constitute the bulk of the post-Precambrian stratigraphic succession on the continental shelf of southern Beaufort Sea.

The Hadrynian(?) Neruokpuk Formation and unnamed graptolitic clastics coeval with the Road River Formation, exposed in these structural highs, were acutely deformed in the Ellesmerian Orogeny. They host granite plutons of Early Silurian age (430 Ma), including Mt. Fitton and Mt. Sedgwick stocks. The host rocks are overlain with angular unconformity by the Mississippian Kekiktuk and Kayak formations and, in turn, by a thick succession of Upper Paleozoic and younger rocks (Norris, 1981a, 1981b). The Kekiktuk and Kayak are widely exposed around the periphery of the uplifts and, in the case of Romanzof Uplift, on the top as well.

Relative to the Neruokpuk and Road River equivalents, the coal-bearing Kayak is only mildly deformed. It dips gently southward off the flank of Hoidahl Dome (Station 1). At the headwaters of Spring River (Station 2) it dips about 30° northeast in the footwall of a major, high-angle reverse fault. It is flat-lying to gently folded on the crest of Romanzof Uplift (Stations 3, 4 and 5). The region underwent epeirogenic uplift in the mid-Triassic and Early Jurassic and block faulting in the mid-Cretaceous. It was the Late Cretaceous and early Tertiary Laramide Orogeny, however, that folded and reverse-faulted the Kayak as we see it today.

Palynological analysis of the suite of samples collected for the present study indicates a Viséan age for sample 855 NC at Station 3 and a possible late Tournaisian(?) / early Viséan(?) age for the clastics immediately over the coal at Station 1 (J. Utting, pers. comm., 1986).

Sampling and experimental methodology

Samples from the beds under investigation were collected in the field as channels, and the thicker beds, like those at Station 1, were divided into subchannels. Specific details of the field sampling are as follows:

- Station 1: A single coal seam 5.53 m thick; sampled mainly in 0.5 m increments (see Table 68.2 for thickness of individual increments) from bottom to top. Samples labelled with field numbers HD-1 through HD-14. HD-1 and HD-14 represent clastic material in the floor and roof, respectively. Samples identified as series GSC loc. C-099883.
- Station 2: Two black shale beds sampled from outcrop on ridge top. Lower one represented by samples series GSC loc. C-099884, with individual field-numbered samples and thicknesses as follows: 922 NC (1A), 30 cm; 922 NC (1B), 24 cm; 922 NC (1C), 32 cm; 922 NC (1D), 50 cm; bed sampled in ascending order; bottom and top not seen. Some 10 m above the lower bed, a second black shale occurs, which was sampled in the following order: sandstone under shale, 922 NC (2A); 35 cm black shale, 922 NC (2B); overlying coaly siltstone, 922 NC (2C). This second set of samples is identified as GSC loc. C-099885.
- Station 3: GSC loc. C-099890. A single sample of coaly fragments and clastics collected from a shallow depression on hillside. Field number 855 NC. No coal found in place.
- Station 4: Two samples series representing two black shales were collected at this site. Lower series (GSC loc. C-099886), with following individual samples identified by field number arranged in ascending order: 1526 NC (A), brown mudstone; 1526 NC (B), 4 cm rusty brown sandstone; 1526 NC (C), 7 cm black shale; 1526 NC (D), 21 cm black shale; 1526 NC (E), 49 cm black shale; 1526 NC (F), deeply weathered grey shale. A second shale bed 10 m higher was sampled as follows: underlying sandstone, 1526 NC (G); black shale, 1526 NC (H). Samples from the second bed assigned series number GSC loc. C-099887.

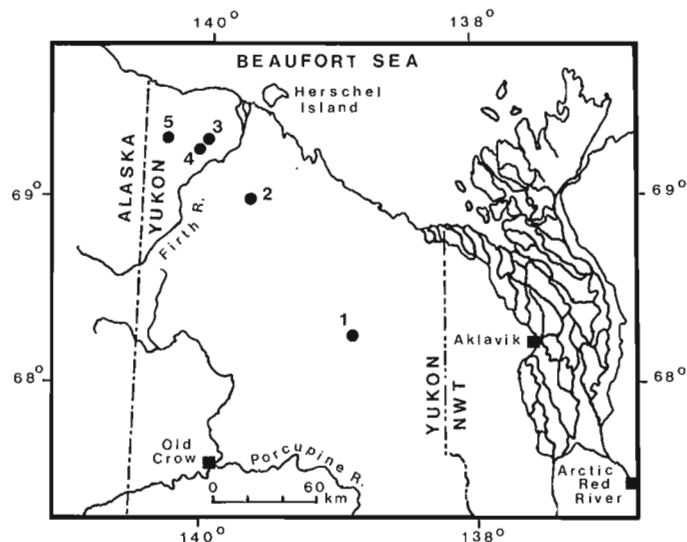


Figure 68.1. Location map for sampling stations in Kayak Formation, northern Yukon Territory (see Table 68.1).

Station 5: Four samples were collected at this site. A black shale and coal bed 17 m above top of Kekiktuk Formation was sampled in the following ascending order: grey shale, 873 NC (A); 70 cm black shale, 873 NC (B); 30 cm coal, 873 NC (C); top of coal not found. A fourth sample of float material from a stratigraphically higher seam was collected at this site and identified as GSC loc. C-099889 (field number 873 NC (D)).

In the laboratory, the samples were stage crushed and riffled to provide representative splits of minus 20 mesh (<850 nm) size. Splits of a selected number of samples were moulded into grain mounts with epoxy resin and polished for

microscopic examination in accordance with ASTM procedures (ASTM, 1979). Splits of a selected number of samples were further ground to minus 100 mesh (<149 nm) for ash and sulphur analyses. Ash content was determined at 1000°C in a muffle furnace and sulphur at 2600°C in a Leco analyser. Petrographic analyses consisted of measurement of both maximum and minimum reflectance on vitrinite A (50 points per sample) and maceral determinations by point count (500 points per sample). A Leitz Orthoplan microscope equipped with MPV II photometric accessories was used for the petrographic examinations. All samples were tested for radioactivity with a Geiger counter. None showed readings above background.

Table 68.1. Locality data for Kayak Formation sampling stations (see Fig. 68.1)

Station	Map area	NTS	Longitude	Latitude	C-number sample series	Field number
1	Blow River	117A	137°52'	68°17'	C-099883	1529 NC
2	Herschel Is.	117D	139°22'	69°01.5'	C-099884 C-099885	992 NC
3	Demarcation Point	117C	140°04'	69°20'	C-099890	855 NC
4	Demarcation Point	117C	140°14'	69°17.5'	C-099886 C-099887	1526 NC
5	Demarcation Point	117C	140°42'	69°19'	C-099888 C-099889	873 NC

Table 68.2. Chemical data for Kayak Formation samples

Sample series	Subsample number	Thickness (metres)	% Moisture (as rec'd)	% Ash (dry)	% Sulphur (dry)
C-099883	HD-13	0.33	1.31	12.31	0.51
	HD-12	0.50	1.12	7.42	0.46
	HD-11	0.50	1.09	2.89	0.53
	HD-10	0.50	1.24	2.86	0.54
	HD-9	0.50	1.17	3.30	0.56
	HD-8	0.50	1.15	3.56	0.52
	HD-7	0.50	1.01	4.88	0.50
	HD-6 ¹	0.14	0.51	64.76	0.19
	HD-5	0.70	0.90	7.18	0.47
	HD-4	0.50	0.94	4.65	0.47
	HD-3	0.50	1.19	4.20	0.51
	HD-2	0.50	0.94	23.34	0.41
Average			1.13	6.81	0.50
C-099888	873 NC (C)	0.30	0.94	41.44	0.26
C-099889	873 NC (D) ²	float	1.39	13.78	0.41
¹ Data not included in calculating average values for seam.					
² The seam from which this coal originated was not located but is stratigraphically higher than sample 873 NC (C).					



Figure 68.2. Outcrop of 5 m thick coal seam at Station 1. GSC photo no. 2421-190.

Results

Chemical analyses

Results from the chemical analyses are given in Table 68.2. Although most of the samples were submitted for determination of ash content, only those that could be classified as coal are listed. As mentioned earlier, some of the black beds sampled were impoverished in carbonaceous matter, with ash contents of 90 per cent or more.

The most impressive suite of samples with respect to ash and sulphur content are those from the single seam collected at Station 1. One parting, 14 cm thick (sample HD-6) occurs in the seam and has a high ash content. The samples immediately adjacent to floor and roof (samples HD-2 and HD-13, respectively) also show a relatively high ash content. The remainder of the seam is

remarkably clean, with a calculated average ash content of 6.8 per cent, including samples HD-2 and HD-13. Sulphur content is also low, with a seam average of 0.50 per cent, and the distribution is very uniform from roof to floor. Much of this sulphur must be in organic form; no pyrite was seen during the microscopic examination. The lateral extent of this seam is unknown; the exposure described in this report was the only one discovered.

The samples from Station 5 are also low in sulphur but one of them, 873 NC (C), contains 41.4 per cent ash. Sample 873 NC (D), the second sample from this station, has a moderately low ash yield of 13.8 per cent.

Maceral composition

The maceral data shown in Table 68.3 are mainly derived from the series of samples from Station 1, the exceptions being the two coals from Station 5. Because these are high rank coals, macerals of the liptinite group could not be determined, so that maceral distribution data are limited to the other two main groups, namely vitrinite and inertinite.

Maceral distribution for the HD set of samples (Station 1) shows a moderately high content of inertinite. Values among individual increments range from 30 per cent in HD-11 to 50 per cent in HD-10. Average vitrinite content for the whole seam, excluding increment HD-6, is 61 per cent, with a corresponding inertinite content of 39 per cent on the mineral-matter free basis.

Inertinite is fairly abundant in all increments, especially the macerals macrinite, inertodetrinite and semifusinite. The common occurrence of inertodetrinite suggests an energy level in the peat swamp that was conducive to the reworking and attrition of materials such as pyrofusinite, which would have been formed during the accumulation of the peat. The overall relatively high content of inertinite further suggests that the water cover in the swamp must have been relatively low, and uniformly so

Table 68.3. Maceral composition (MMF) of Kayak coals; data in volume per cent

Sample	Vitrinite A	Vitrinite B	Total Vitrinite	Semi-fusinite	Fusinite	Macrinite	Intertodetrinite	Micrinite	Sclerotinite	Total Inertinite
HD-13	22.0	38.0	60.0	13.2	3.0	11.4	10.6	1.4	0.4	40.0
HD-12	12.4	56.4	68.8	6.1	1.2	10.4	9.8	3.7	0.0	31.2
HD-11	25.4	45.2	70.6	7.4	0.8	12.4	6.2	2.6	0.0	29.4
HD-10	13.6	36.4	50.0	7.6	0.8	21.4	15.6	4.6	0.0	50.0
HD-9	16.0	39.8	55.8	8.2	1.2	23.4	9.4	1.8	0.2	44.2
HD-8	10.5	43.4	53.9	11.5	0.0	23.3	9.4	1.5	0.4	46.1
HD-7	11.2	43.8	55.0	10.0	0.4	18.9	12.5	3.0	0.2	45.0
HD-6	NOT ANALYZED									
HD-5	18.0	51.9	69.9	6.6	1.2	12.1	6.8	3.4	0.0	30.1
HD-4	10.7	41.2	51.9	9.5	0.6	17.9	13.3	6.2	0.6	48.1
HD-3	26.2	39.1	65.3	8.7	1.8	12.5	8.3	2.8	0.6	34.7
HD-2	23.4	41.2	64.6	12.4	4.4	9.4	8.2	1.0	0.0	35.4
Ave.	17.0	43.6	60.6	8.9	1.9	15.7	9.8	2.9	0.2	39.4
873 NC (C)	9.5	52.2	61.7	10.0	0.0	11.4	14.9	2.0	0.0	38.3
873 NC (D)	9.9	47.8	57.7	17.8	0.4	13.4	8.3	2.4	0.0	42.3

Table 68.4. Reflectance data on coals and carbonaceous shales of Kayak Formation

Sample series	Sample number	Romax	Standard deviation	Romin	Standard deviation	N	Bireflectance Romax-Romin	Station
C-099883	HD-13	2.99	0.07	2.39	0.18	50	0.60	1
	HD-12	3.01	0.09	2.51	0.21	50	0.50	
	HD-11	2.95	0.07	2.36	0.19	50	0.59	
	HD-10	2.95	0.10	2.45	0.20	50	0.50	
	HD-9	2.86	0.08	2.29	0.17	50	0.57	
	HD-8	3.00	0.08	2.45	0.26	50	0.55	
	HD-7	2.99	0.07	2.43	0.26	50	0.56	
	HD-5	2.99	0.10	2.42	0.26	50	0.57	
	HD-4	2.94	0.08	2.43	0.23	50	0.51	
	HD-3	2.93	0.08	2.38	0.24	50	0.55	
	HD-2	2.88	0.10	2.21	0.22	50	0.67	
	Ave. HD	2.95		2.39			0.56	
C-099885	922 NC (2B)	2.72	0.18	2.03	0.14	9	0.69	
C-099884	922 NC (1D)	2.77	0.34	2.12	0.41	11	0.65	2
	922 NC (1C)	2.99	0.23	2.30	0.20	10	0.69	
	922 NC (1B)	3.03	0.19	2.43	0.18	10	0.60	
	922 NC (1A)	2.33	0.20	1.65	0.17	10	0.68	
C-099890	855 NC	3.55	0.13	2.69	0.29	23	0.86	3
C-099886	1526 NC (D)	3.78	0.15	2.85	0.44	14	0.93	4
	1526 NC (C)	3.62	0.38	2.97	0.40	10	0.65	
C-099889	873 NC (D)	4.03	0.11	2.20	0.68	50	1.83	5
	873 NC (C)	3.94	0.14	2.08	0.56	50	1.86	
C-099888	873 NC (B)	2.74	0.31	2.10	0.36	12	0.64	

throughout the life of the swamp, so that a certain amount of oxidation and enhanced decay of vegetal material was possible. The high proportion of vitrinite B relative to vitrinite A is also indicative of an attrital coal, suggesting conditions in the peat swamp favourable for accelerated mechanical and biochemical degradation of plant matter. However, the particular characteristics of the plant communities growing in Viséan time undoubtedly also influenced maceral type and distribution.

Samples 873 NC (C) and 873 NC (D) from Station 5 show even higher contents of inertinite than the HD series. However, because of the higher rank of these coals compared to the HD set, their high level of anisotropy, and the possibility that they may be heat affected, maceral identification was more difficult than with the HD samples.

The data showing a relatively high content of inertinite in these northern Yukon coals are similar to maceral data for three coal samples from the somewhat younger Mattson Formation (Upper Viséan, Serpukovian) collected by B.C. Richards (ISPG) in the Liard River - Nahanni area, District of Mackenzie, Northwest Territories. These samples are at least partially representative of the seams from which they were collected (B.C. Richards, pers. comm., 1986) and they show extraordinarily low vitrinite and correspondingly high inertinite contents. Liptinite is abundant in the Mattson samples and can be detected because of the low rank of these coals (Romax 0.79-0.82).

Reflectance analyses

The reflectance data obtained from these samples are recorded in Table 68.4. As mentioned previously, both maximum (Romax) and minimum (Romin) reflectances were determined on each sample and the bireflectance calculated, that is Romax - Romin. Bireflectance is an indicator of heat affected coals (Goodarzi, 1984); that is, coals whose rank may be increased by igneous thermal activity. Coals so affected have higher bireflectances than coals that have increased in rank by more usual coalification processes.

Reflectances of coal of the HD series and of the coals from Stations 3 and 5 were relatively easy to measure. All contained sufficient vitrinite and, though these coals were collected from outcrop, only occasionally did they show weathering effects. In contrast, measurements on dispersed carbonaceous matter in the black shales were more difficult. Most of the carbonaceous particles in the shales are small, preventing easy identification of vitrinite and restricting the number of particles upon which Romax and Romin could be measured. However, the results appear reasonably reliable because the values obtained on the shale samples from Station 2 agree fairly well with one another and the two values obtained from the two higher rank shales at Station 4 are close.

There are two anomalous results; samples 922 NC (1A) at Station 2, and 873 NC (B) at Station 5 are significantly lower in reflectance than the other samples at their respective stations. A probable reason may be the poorer quality of the carbonaceous matter in these samples rather than a real difference in rank.

The results indicate a high level of maturity for the Kayak samples. They are anthracitic. Nearly all are well above the lower reflectance threshold of 2.50 suggested by Davis (1978) as the boundary between semi-anthracite and anthracite. The samples appear to fall into two populations. Those from Stations 1 and 2 have reflectances ranging from about 2.7 to 3.0, whereas the samples from Stations 3, 4 and 5 in the British Mountains – Malcolm River area have higher values, ranging approximately from 3.5 to 4.0. This higher level of maturity for the latter group of samples is indicative of either exposure to higher temperatures than the beds at Stations 1 and 2 or exposure for a longer period of time at the same temperature. The higher temperature model for the northwestern group of samples could be accomplished by deeper burial or by the thermal effects of intruded igneous bodies of various kinds.

In the discussion of maceral composition it was noted that the coals at Station 5 showed evidence of being thermally affected, that is, they appear to have undergone more rapid upgrading of rank than would be achieved by more normal and slower coalification caused solely by deeper burial. The bireflectance data support this interpretation. Bireflectance values of 1.83 and 1.86 for the two coals at Station 5 are higher than would be obtained on normally coalified material of this rank (Stach et al., 1982; Goodarzi, 1984). Normal bireflectance should be about 1.0, or slightly less. Bireflectance on the other samples of this study appear to be about average for normal coalification.

There is no obvious explanation for the systematically higher ranks of the samples at Stations 3, 4 and 5 over those at Stations 1 and 2. The Mt. Fitton and Mt. Sedgwick granites are some 80 m.y. older than the Kayak Formation and can reasonably be expected to have cooled and crystallized by the time the Kayak was deposited. Moreover, these two intrusions are known to have been uplifted and denuded during the Ellesmerian Orogeny. Nevertheless, the carbonaceous shales at Station 2, near the headwaters of Spring River, are the closest of any of the stations to either of the exposed intrusions, and they are in the population with the lower rank values.

It is possible, however, that the uplifts are cored with younger granite bodies at deeper structural levels and that these granites had not cooled by Viséan time. This concept is supported by the presence of thermally altered conodonts, with a Colour Alteration Index of 5, midway between Stations 2 and 3 on the north flank of Romanzof Uplift (Norris, 1986). The conodonts are about 40 m.y. younger than the granites and about 40 m.y. older than the Kayak coals.

A recent aeromagnetic survey (EMR, unpublished data) reveals a strong spatial correlation between magnetic anomalies and the Mt. Fitton and Mt. Sedgwick stocks. However, there are no obvious anomalies over any of the five stations where the Kayak beds were sampled.

The occurrences of the two populations of reflectance values more or less along strike from one another in the same tectonic element (Romanzof Uplift) suggests a local rather than a regional cause for the thermal upgrading at Stations 3, 4 and 5 relative to Station 2. This local effect may have been a restricted heat source beneath the structurally highest part of the uplift.

Summary and conclusions

Reflectance data on coal and carbonaceous shale from the Kayak Formation in northern Yukon Territory indicate maturity levels well into the anthracite range (>2.5 Romax).

There appear to be two populations in terms of maturity, with those samples from the British Mountains – Malcolm River area more mature than those obtained from sites farther to the southeast. The former population may be, in part, the product of abnormal thermal upgrading, possibly by igneous activity.

An important result of the study was the discovery of a thick seam of anthracite of good quality in the area south of the Barn Mountains. This seam is over 5 m thick, with average ash and sulphur contents of 6.8 per cent and 0.5 per cent, respectively.

The result of this study for northern Yukon would imply that rocks of Mississippian age or older are not attractive prospects for hydrocarbon exploration, particularly for oil, though some may still be within the gas window.

Acknowledgments

The authors wish to thank the following colleagues at ISPG for assistance: R.A. Davidson for chemical analyses, F. Goodarzi for confirmation of heat affected samples, J. Utting for palynological data, and C. Boonstra for typing the manuscript.

References

- American Society for Testing and Materials (ASTM)
1979: Part 26, Gaseous fuels; coal and coke; atmospheric analysis; American Society for Testing and Materials, Philadelphia, Pennsylvania.
- Davis, A.
1978: The reflectance of coal; in *Analytical methods for coal and coal products*, vol. 1, ed. C. Karr; Academic Press, New York, p. 27-81.
- Goodarzi, F.
1984: Organic petrography of graptolite fragments from Turkey; *Marine and Petroleum Geology*, v. 1, p. 202-210.
- Norris, D.K.
1981a: Geology Blow River and Davidson Mountains, Yukon Territory, District of Mackenzie; Geological Survey of Canada, Map 1516A, scale 1:250,000.
1981b: Geology Herschel Island and Demarcation Point, Yukon Territory; Geological Survey of Canada, Map 1514A, scale 1:250,000.
1986: Lower Devonian Road River Formation on the north flank of Romanzof Uplift, northern Yukon Territory; Geological Survey of Canada, Paper 86-1A, p. 801-802.
- Norris, D.K. and Yorath, C.J.
1981: The North American plate from the Arctic Archipelago to the Romanzof Mountains; in *The Ocean Basins and Margins*, ed. E.M. Nairn, M. Churkin, Jr., and F.G. Stehli; v. 5, chap. 3, *The Arctic Ocean*; New York and London, Plenum Press, p. 37-103.
- Stach, E., Mackowsky, M. Th., Teichmüller, M., Taylor, G.H., Chandra, D., and Teichmüller, R.
1982: *Coal Petrology*, Third Edition, Gebrüder Borntraeger, Berlin, Stuttgart.

Comparison of morphology and reflectance of macerals from a tectonically thickened coal seam from Mist Mountain, British Columbia

Project 780006

F. Goodarzi
Institute of Sedimentary and Petroleum Geology, Calgary

Goodarzi, F., Comparison of morphology and reflectance of macerals from a tectonically thickened coal seam from Mist Mountain, British Columbia; in *Current Research, Part B*, Geological Survey of Canada, Paper 86-1B, p. 671-678, 1986.

Abstract

Samples from a tectonically thickened coal seam at Byron Creek Collieries, Mist Mountain, were examined using reflected light microscopy. Petrographic analyses were made and reflectances of macerals were determined.

The coal macerals consist of liptinite, mainly cutinite, three types of vitrinites, two types of semifusinite, two types of fusinite and varieties of heat affected products, including pyrolytic carbons.

Reflectance of coal macerals increases from cutinite toward fusinite with pyrolytic carbon having reflectances in the fusinite range. The boundary between the cutinite and vitrinite group of macerals is sharp, but the boundary between vitrinite and semifusinite is not well defined, and is more dependent on reflectance than the morphology of the macerals.

A maceral with semifusinite morphology may, in fact, be a vitrinite (telinite) and hence might behave as a reactive (fluid) maceral during carbonization.

The heat affected products and pyrolytic carbons are commonly anisotropic.

Résumé

Des échantillons d'une veine de charbon tectoniquement épaissie à Byron Creek Collieries, à Mist Mountain, ont été examinés par microscopie en lumière réfléchie. Des analyses pétrographiques ont été effectuées et la réflectance des macéraux a été calculée.

Les macéraux du charbon sont constitués de liptinite (principalement de la cutinite), trois types de vitrinite, deux types de semifusinite, deux types de fusinite et diverses variétés de produits ayant subi une transformation thermique, y compris des carbones pyrolytiques.

La réflectance des macéraux du charbon augmentait de la cutinite à la fusinite, le carbone pyrolytique ayant certaines réflectances dans la gamme de la fusinite. La limite entre le groupe cutinite et le groupe vitrinite des macéraux était nette, mais celle entre la vitrinite et la semifusinite n'était pas aussi bien définie et dépendait plus de la réflectance que de la morphologie des macéraux.

Un macéral ayant une morphologie semi-fusinitique pourrait effectivement être une vitrinite (télinite) et ainsi, se comporter comme un macéral réactif (fluide) au cours de la carbonisation.

Les produits ayant subi une transformation thermique et les carbones pyrolytiques sont généralement anisotropiques.

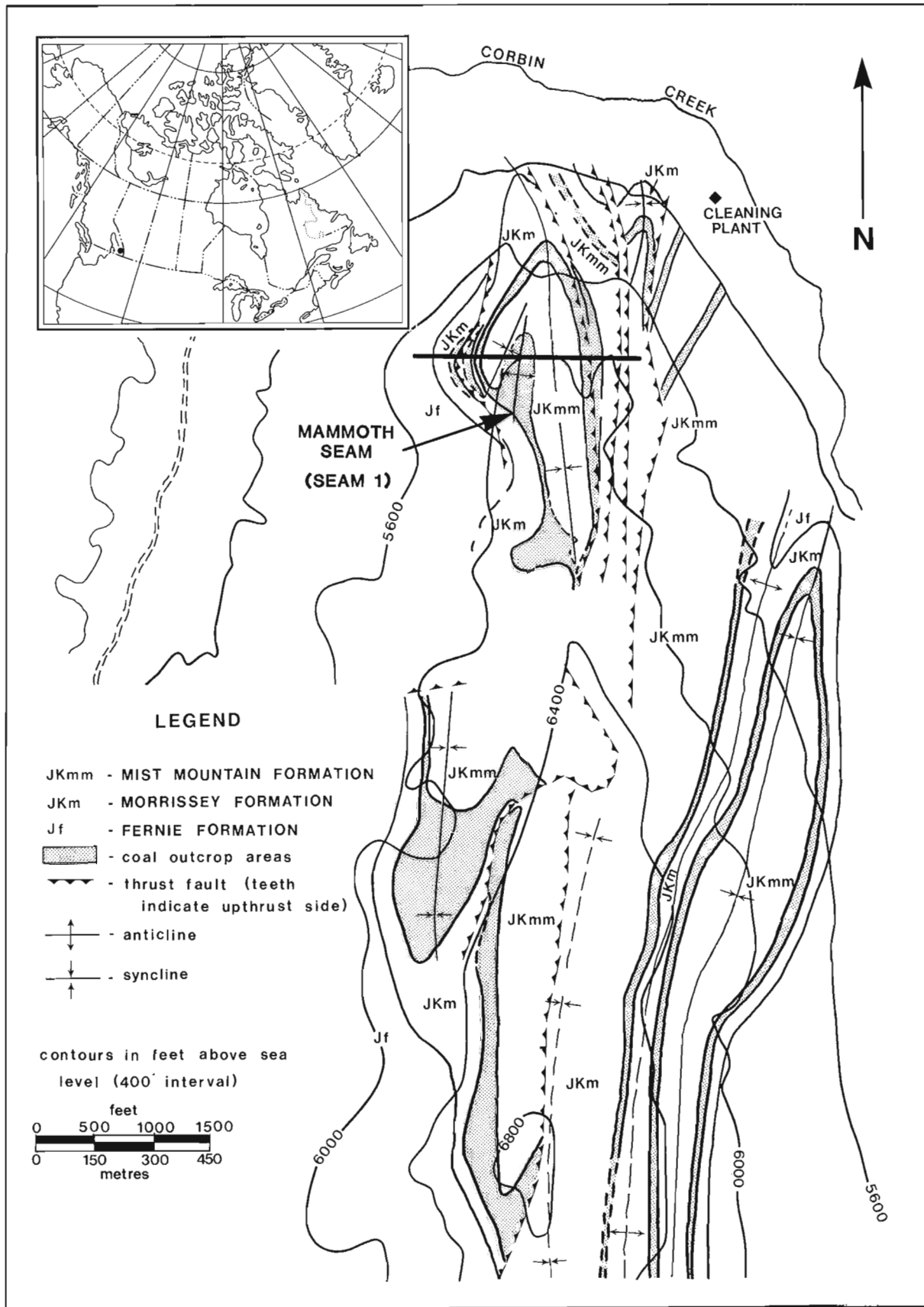


Figure 69.1. Geology of Byron Creek Collieries.

Introduction

The "Mammoth" seam (seam no. 1) which is about 30 m thick (Fig. 69.1) has been structurally thickened, due to folding and faulting, to 100 m in thickness. It lies directly on the Morrissey Formation sandstone (Gibson, 1985). The coal seam occurs in the Mist Mountain Formation, which is folded and faulted and underlain by lower Kootenay Group and Fernie Formation strata (Gibson, 1985).

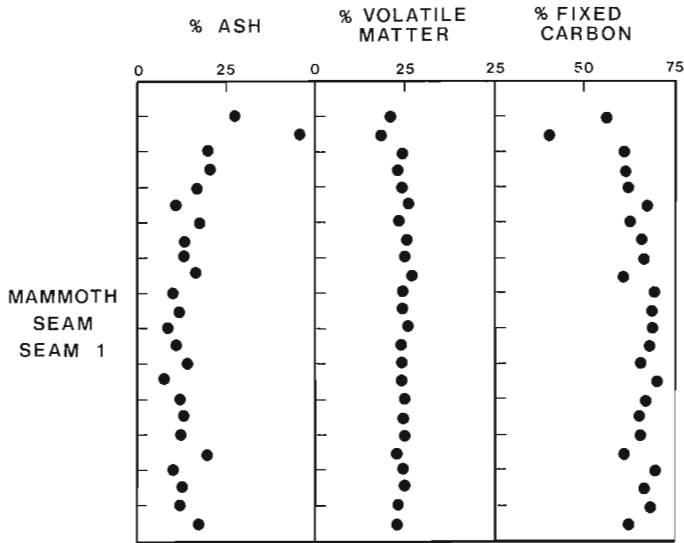


Figure 69.2. Proximate analysis for seam no. 1 from Byron Creek.

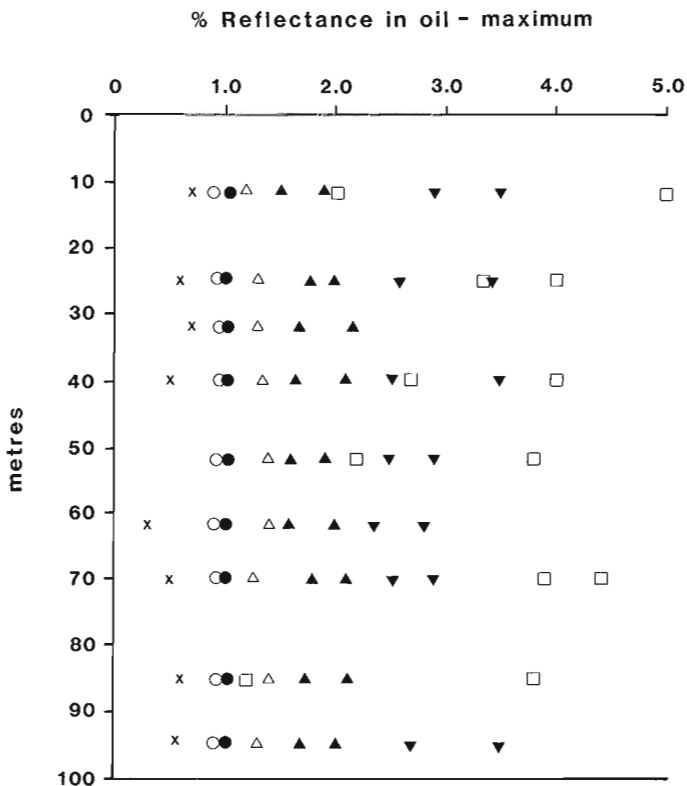


Figure 69.3. Comparison of macerals and heat-affected fragments in seam no. 1 from Byron Creek: cutinite x, vitrinite A O, vitrinite B ●, semifusinite (telinite?) Δ, low reflecting semifusinite ▲, high reflecting semifusinite ▴, fusinite ▼, pyrofusinite ▽, anisotropic granular fragment max. - min. □.

The actual undisturbed thickness of the Mammoth seam is a matter of some dispute. MacKay (1931) thought that it might vary between 4 to 60 m, whereas Norris and Price (1956) have stated that it might vary between 4 to 8 m.

Reflectance studies on the various macerals of single or suites of related coals were carried out in various countries by Bell and Diessel (1970), Alpern (1970), Kosina and Hrnčir (1983), and Cameron (1984). Bell and Diessel (1970) divided the inertinites in Australian coals into low and high reflecting semifusinite, with a reflectance threshold between the two ranging from 1.55 to 2.70; and low and high reflecting fusinite, with a reflectance threshold ranging from 2.8 to 3.0. Alpern (1970) examined European Carboniferous coal and determined the reflectance thresholds for liptinite, vitrinite and inertinite macerals in lignite to anthracite. The reflectance of pyrofusinite remains almost unchanged with increasing rank whereas the reflectance increases moderately for semifusinite and biofusinite and sharply for vitrinite.

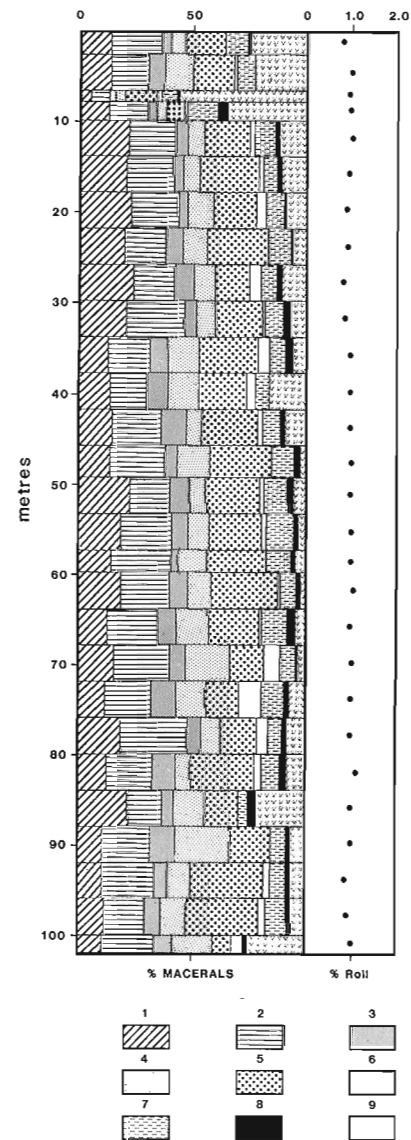


Figure 69.4. Maceral analysis and reflectance for seam no. 1 from Byron Creek: 1. desmocollinite, 2. telocollinite, 3. pseudovitrinite, 4. low reflecting semifusinite, 5. high reflecting semifusinite, 6. fusinite, 7. inertodetrinite and isotropic-anisotropic chars formed due to friction, 8. liptinite, and 9. mineral matter.

PLATES 69.1-69.7

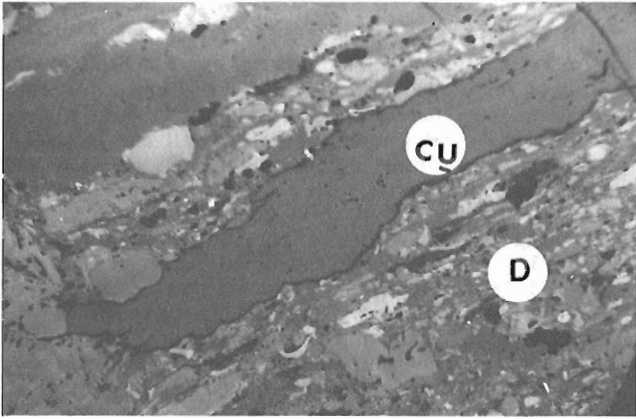


Plate 69.1

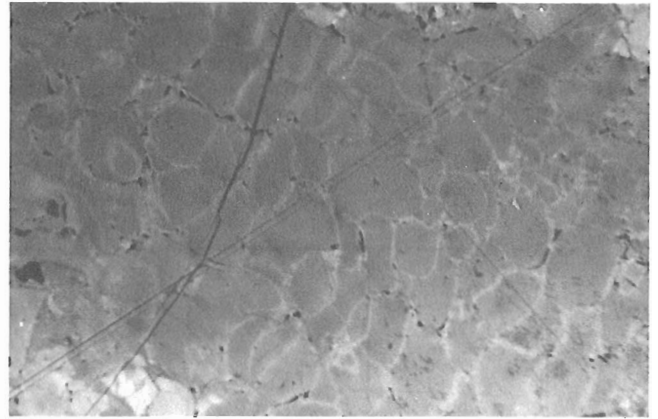


Plate 69.2

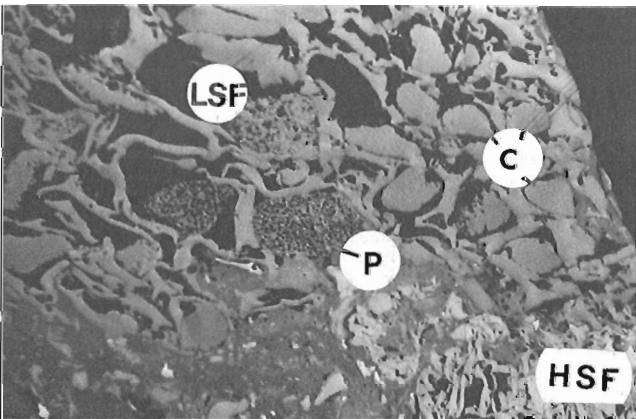


Plate 69.3a

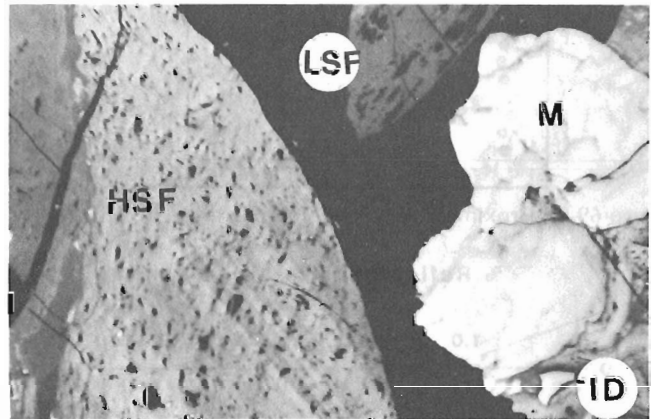


Plate 69.3b

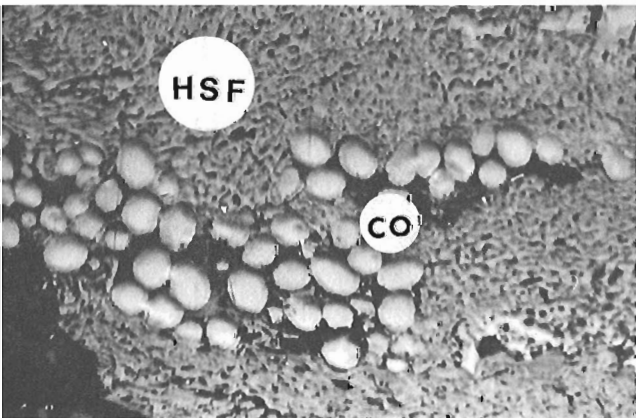


Plate 69.3c

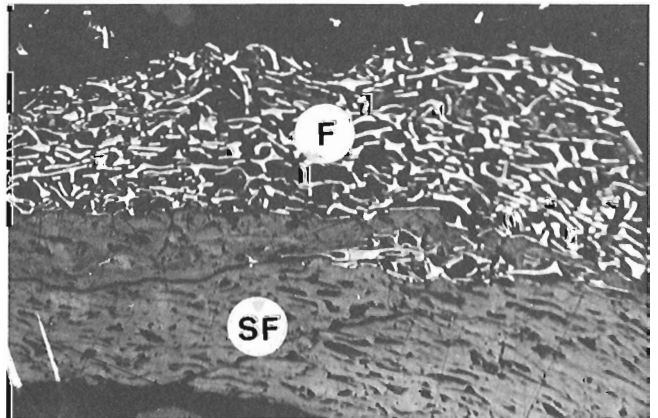


Plate 69.4

Cameron (1984) examined Canadian Kootenay coals and concluded that there is considerable overlap between the reflectance of inertinite macerals and that the reflectance of the majority of the semifusinite in the Kootenay coals is closer to vitrinite.

Byron Creek coal mine is an active coal mine in southeastern British Columbia and covers an area of about 3 km (north-south) by 1.5 km (east-west). The mine contains a very large geological resource (165 MT), of which approximately 45 per cent is economically mineable, high volatile bituminous coal ($R_{oil} = 1.0$).

Seam no. 1 (Mammoth seam) of Byron Creek mine comprises 100 m of tectonically thickened coals of high volatile A bituminous rank ($R_{oil} = 1.0$). In this paper the relationship between morphology and reflectance of macerals is examined, as is the threshold between vitrinite-semifusinite and semifusinite-fusinite macerals.

Acknowledgments

The author wishes to thank Esso Resources Canada Limited for its cooperation and permission to visit the Byron Creek property and to obtain samples, and to Dr. J. Allan, Mr. A. Beaven and Mr. B. Norland of Esso Resources Canada Limited for their assistance in sample collecting. The manuscript benefitted from critical review by Dr. A.R. Cameron of the Geological Survey of Canada, Calgary. The author also acknowledges, with appreciation, the secretarial assistance of Mrs. D. Thompson.

Experimental work

Sampling

Full channel samples were collected every 4 m for coal, and every 2 m for carbargillites. Coal samples were crushed to <20 mesh (840 μ m) for maceral analysis and reflectance measurements. Proximate analyses (Fig. 69.2) were made following the procedures outlined by ATSM (1979).

Microscopy

Macerals were analyzed using a Swift point counter. Macerals included liptinite, as well as vitrinite, which was analyzed in three groups: vitrinite A, vitrinite B, and pseudovitrinite. Inertinites were divided into low and high semifusinites, fusinite, pyrofusinite, heat affected products (chars), and pyrolytic carbons (Fig. 69.3).

Reflectance of coal macerals (Fig. 69.3) was determined by measuring maximum reflectance with a Zeiss MPM II microscope fitted with Zonax microcomputer and printer, under standard conditions, following the procedure outlined in the International Handbook of Coal Petrology (1963). Fifty reflectance measurements were carried out on vitrinite A and vitrinite B, and ten measurements for the other macerals. Reflectance measurements on pyrofusinite and pyrolytic carbons were based on an average of five measurements.

Plates 69.1-69.4

**Macerals from Byron Creek coal; oil immersion; plane polarized light;
magnification: full scale of long axis of photographs = 300 microns.**

- Plate 69.1** Thin wall cutinite (Cu); desmocollinite (D); teleocollinite.
- Plate 69.2** Pseudovitrinite.
- Plate 69.3** Semifusinite.
- Low reflecting semifusinite (LSF); telinite containing corpohuminites (C); corpohuminites with porigelinitic morphology (P); and high reflecting semifusinite (HSF).
 - Low reflecting semifusinite (LSF); high reflecting semifusinite (HSF); macrinite (M); inertodetrinite (ID).
 - High reflecting semifusinite (HSF) containing coprolites (CO).
- Plate 69.4** Fusinite (F) showing bogen structure and semifusinite (SF).

Results

Morphology and maceral analysis

The coal macerals consist of liptinites, mainly resinite and cutinite (Pl. 69.1). Three types of vitrinite – vitrinite A (telocollinite), vitrinite B (desmocollinite; Pl. 69.1), and vitrinite C (pseudovitrinite; Pl. 69.2) – are present. Inertinites consist of low semifusinite (Pl. 69.3a, b), high semifusinite (Pl. 69.3b, c), and fusinite (Pl. 69.4). These coals also contain pyrolytic carbon, and weathered and heat affected chars formed as a result of friction (Pls. 69.5–69.7). There is little variation in the percentage of liptinite and vitrinite within the coal seam. Within the inertinite group, large variations in inertinite macerals were observed (Fig. 69.4).

Reflectance

The reflectance of coal macerals increases from cutinite toward fusinite. The reflectance of vitrinite (vitrinite A and vitrinite B) maintains almost the same value throughout the coal seam (Fig. 69.4). The heat affected chars and pyrolytic carbon are anisotropic and cover a wide range of reflectances throughout the seam (Fig. 69.3).

Discussion

I will discuss the reflectance and morphology of macerals in seam no. 1 by comparing the vitrinite and inertinite maceral groups.

Cameron (1985) stated that much of the inertinite (semifusinite) in Kootenay coal has a reflectance closer to vitrinite macerals than to inertinite macerals, and hence if the macerals were divided into reactive and nonreactive based on their reflectance, the majority of inertinite in Kootenay coals might be reactive. Nandi and

Montgomery (1975) have shown that low reflecting semifusinite is as reactive as vitrinite. Koensler (1980) carbonized some Kootenay coals and found that during carbonization, inertinite with a reflectance 0.2 to 0.3 per cent higher than vitrinite of the same coal, reacts in a manner similar to the vitrinite.

The relationship between the present data and Cameron's data (1985) is interesting. Cameron established that the reflectance of macerals in a high volatile bituminous coal from seam 17, Weary Ridge, British Columbia, was 0.62 per cent for cutinite, 0.95 per cent for vitrinite B, 1.0 per cent for vitrinite A, 1.32 per cent for low and 1.5 per cent for high reflecting semifusinite, and 2.12 per cent for fusinite.

The reflectance of the vitrinite group of macerals in the present study is essentially similar to Cameron's data for seam 17 because of the similarity in rank of both coal seams. In the present study, the reflectance ranged from 0.3 to 0.7 per cent for cutinite (Pl. 69.1), 0.90 per cent for desmocollinite (vitrinite B) (Pl. 69.1), 1.05 per cent for telocollinite (vitrinite A) (Pl. 69.1), 1.2 to 1.4 per cent for low reflecting semifusinite (Pl. 69.3a), 1.5 to 1.8 per cent for medium reflecting semifusinite 1.9 to 2.2 per cent for high reflecting semifusinite (Pl. 69.3b, c), 2.0 to 2.8 per cent for low reflecting fusinite (Pl. 69.4), and 2.8 to 3.5 per cent for high reflecting pyrofusinite. The pyrolytic carbons and anisotropic fragments (Pls. 69.5, 69.8) formed as a result of tectonic friction (Bustin, 1983; Goodarzi, 1986a, b), have a reflectance range of 3.5 to 5.0 per cent.

The low reflecting semifusinite (Fig. 69.3) in this study commonly shows a morphology similar to texto-ulminite in subbituminous coals; for example, it often contains rounded corpocollinite or rounded vesiculated bodies similar to porigelinite in lignite-subbituminous coals (Pl. 69.3a). This type of semifusinite is perhaps telinite, since textinite in

Plates 69.5–69.7

Heat affected chars from Byron Creek coal; oil immersion;
magnification: full scale of long axis of photographs = 200 microns.

- Plate 69.5**
- Heat affected pseudovitrinite showing vacuoles; plane polarized light.
 - Weathered, heat-affected char showing oxidation rim (O) and vacuoles; plane polarized light.
- Plate 69.6**
- Anisotropic chars (C) and desmocollinite (D); partially crossed polars.
 - Anisotropic fragment (A) in desmocollinite; microscope stage rotated to show the anisotropy.
 - Partially crossed polars.
- Plate 69.7**
- Coarse grained mosaic (Mc); strongly anisotropic and isotropic telocollinite (T); partially crossed polars.
 - Pyrolytic carbon (P) showing lamellar structure and anisotropy in desmocollinite (D). Sporinite (S) is present; partially crossed polars.
 - Pyrolytic carbon (P), (anisotropic) in desmocollinite matrix, (isotropic).

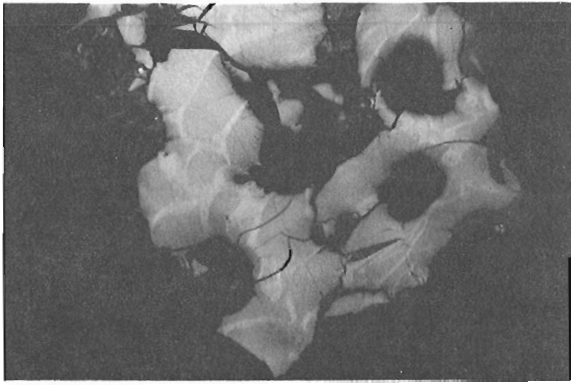


Plate 69.5a

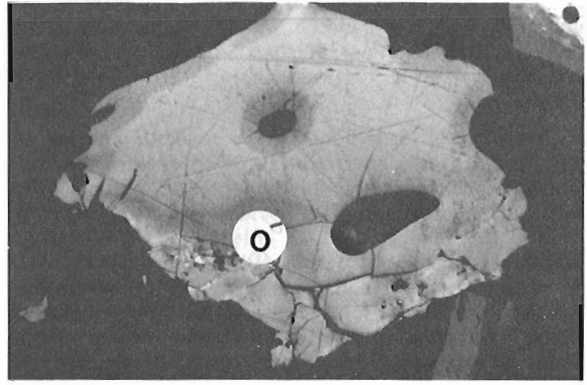


Plate 69.5b

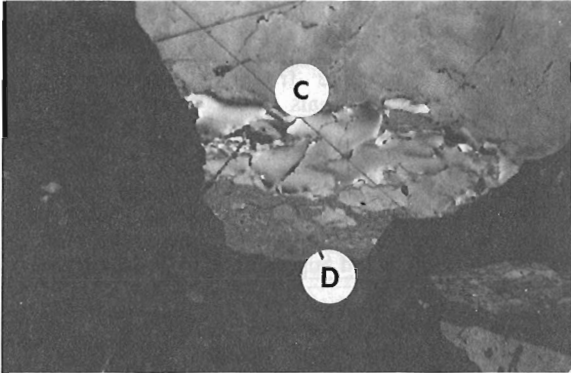


Plate 69.6a

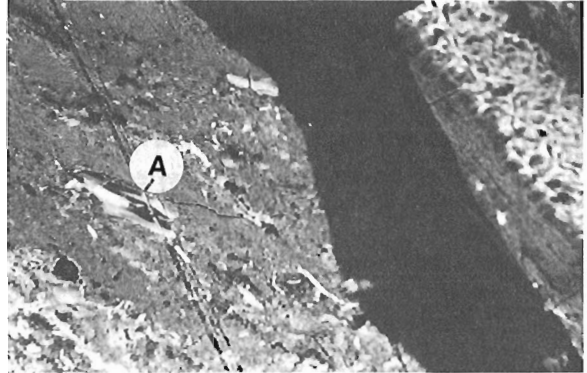


Plate 69.6b

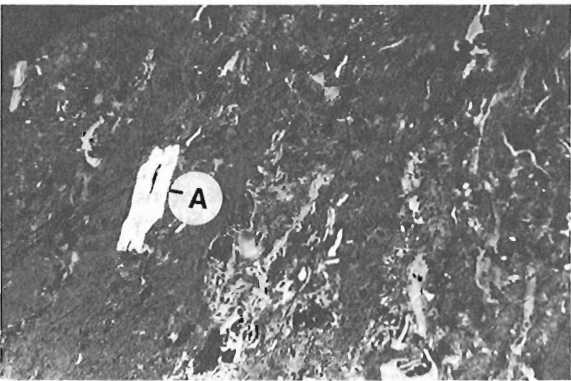


Plate 69.6b_j

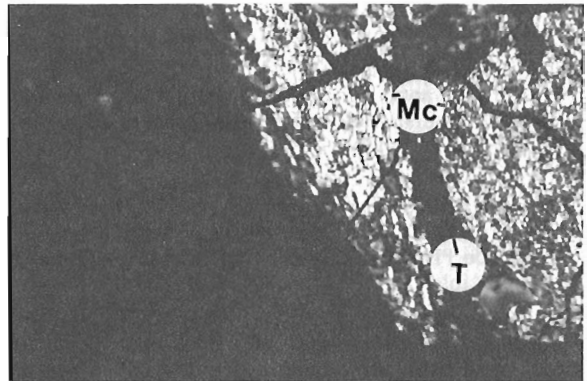


Plate 69.7a

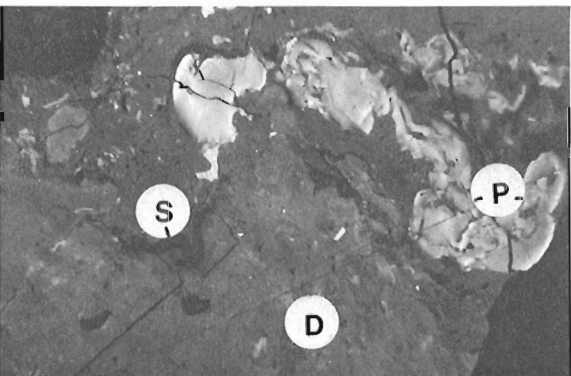


Plate 69.7b

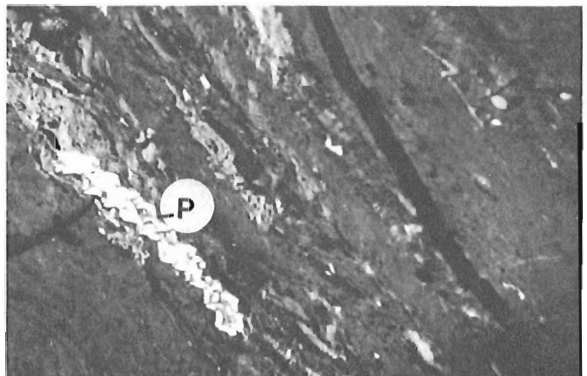


Plate 69.7c

subbituminous coals is the precursor of telinite in bituminous coals (Teichmüller, 1982), and could be classified with reactive coal macerals. Pearson (pers. comm., 1986) also believes that the low reflecting semifusinite from Kootenay coal is reactive.

The heat affected fragments in these coals consist of two groups: 1. isotropic, thermally altered fragments, for example, pseudovitrinite chars showing plastic deformation and devolatilization vacuoles (Pl. 69.5a), or char showing oxidation rims (Pl. 69.5b); and 2. anisotropic chars that include char showing basic anisotropy (Pl. 69.6a, b), char with granular morphology and high anisotropy (Pl. 69.7a), and pyrolytic carbon (Pl. 69.7b, c). Bustin (1983) stated that during faulting, coal in a narrow zone in the interface of a coal layer may experience a temperature of 350° to 600°C. Goodarzi (1986b) has found that coals in tectonically disturbed seams commonly contain isotropic and anisotropic chars and pyrolytic carbon with reflectances greater than those of the macerals that were not affected by heat.

Conclusions

1. The boundary between liptinite and vitrinite macerals is sharp; in contrast, the boundary between vitrinite and inertinite is not well defined.
2. Semifusinite can be divided into a low reflecting type, with %R_{oil} of 1.2 to 1.8; and a high reflecting type, with %R_{oil} of >1.8 per cent.
3. Low reflecting semifusinite, with a reflectance of 1.2 per cent, might, in fact, be vitrinite (telinite) and could be classified with reactive macerals.
4. Weathered and heat affected chars were formed as a result of tectonic friction.
5. Heat affected anisotropic chars have a higher bireflectance than the semifusinites.

References

Annual Book of ASTM Standards

- 1979: Proximate analysis of coal and coke, Part 26, Gaseous Fuels; coal coke; atmospheric analysis, D3172-3173, p. 380.

Alpern, B.

- 1970: Classification pétrographique des constituants organiques fossiles des roches sédimentaires: Revue de l'Institut Français du Pétrole et Annales Combustibles Liquides, v. XXV, p. 1233-1267.

Bell, J.A. and Diessel, C.F.K.

- 1970: Various interpretations of coal petrographic nomenclature and their effects on maceral analyses; Proceeding of Australian Institute of Mining and Mineralogy, no. 234, p. 27-36.

Bustin, R.M.

- 1983: Heating during thrust faulting in the Rocky Mountains; friction or fiction; Tectonophysics, v. 95, p. 309-328.

Cameron, A.R.

- 1964: Comparison of reflectance data for various macerals for coals of the Kootenay Group, southeastern British Columbia; 1984 Symposium on the Geology of Rocky Mountain Coal, Proceedings; North Dakota Geological Society, Bismark, North Dakota, p. 61-75.

Gibson, D.

- 1983: Stratigraphy, sedimentology and depositional environments of the coal-bearing Jurassic-Cretaceous Kootenay Group, Alberta and British Columbia; Geological Survey of Canada, Bulletin 357.

Goodarzi, F.

- 1986a: Characteristics of pyrolytic carbon in Canadian coals; Fuel, v. 64, p. 1672-1676.
- 1986b: Anisotropic fragments in strongly folded and faulted coals from Rocky Mountain area of southeastern British Columbia; Canadian Journal of Earth Science, v. 23, no. 2, p. 254-258.

International Handbook of Coal Petrology

- 1963: International Handbook of Coal Petrology, 2nd Edition; 1971, 1st Supplement to 2nd Edition; 1975, 2nd Supplement to 2nd Edition.

Koensler, W.

- 1980: Des Verhalten des Inertinitis westkanadischer Kreidekohlen bei der Verkokung; Dissertation Techn., Hochsch, Aaschen, 118 p.

Kosina, M. and Hrnecir, J.

- 1983: The properties of macerals in Czechoslovak coals rich in inertinite; International Journal of Coal Geology, v. 3, p. 145-156.

Nandi, B.N. and Montgomery, D.S.

- 1975: Nature and thermal behaviour of semifusinite in Cretaceous coal from Western Canada; Fuel, v. 54, p. 193-196.

Norris, D.K. and Price, R.A.

- 1956: Coal Mountain, Kootenay District, British Columbia; Geological Survey of Canada, Map 4.

Teichmüller, M.

- 1982: Origin of petrographic constituents of coal; in Coal Petrology, ed. E. Stach, M. Th. Mackowsky, M. Teichmüller, G.H. Taylor, D. Chandra and R. Teichmüller; Gebruder Borntraeger, Berlin, p. 233.

Outliers of porphyritic alkaline volcanic rocks of the Christopher Island Formation at Snowbird Lake, N.W.T.

Projects 770055 and 810024

S.M. Roscoe and A.R. Miller
Mineral Resources Division

Roscoe, S.M. and Miller, A.R., Outliers of porphyritic alkaline volcanic rocks of the Christopher Island Formation at Snowbird Lake, N.W.T.; in Current Research, Part B, Geological Survey of Canada, Paper 86-1B, p. 679-683, 1986.

Abstract

Gently dipping, little-metamorphosed volcanoclastic rocks and minor lava occur in isolated outcrops at the north end of Snowbird Lake. They are strikingly similar to the distinctive, phytic, alkaline volcanic rocks and derived sedimentary rocks of the Christopher Island Formation found 150 to 550 km farther north and are considered to be outliers of this formation. The volcanic rocks may have been erupted along late fractures, and subsequently preserved in down-dropped fault blocks, along the margin of a major shear zone that borders the outliers. The occurrences of these volcanic rocks mark an extension, towards the Athabaska region, of the Dubawnt alkaline igneous province and related metallogenic domains.

Résumé

Des roches volcanoclastiques peu métamorphisées et inclinées en pente douce, ainsi que quelques coulées de lave se trouvent dans des affleurements isolés à l'extrémité nord du lac Snowbird. Elles ressemblent à s'y méprendre aux roches volcaniques caractéristiques à nature alcaline et phytique et aux roches sédimentaires dérivées de la formation de Christopher Island, trouvées 150 à 550 km plus au nord; elles sont, en outre, considérées comme des avant-buttes de cette formation. Ces roches volcaniques ont probablement été éjectées le long des fractures tardives et ensuite conservées sous forme de blocs de failles, le long de la marge d'une importante zone de cisaillement qui limite ces avant-buttes. La présence de ces roches volcaniques marque une extension en direction de la région de l'Athabasca de la province ignée alcaline de Dubawnt et des domaines métallogéniques connexes.

Introduction

Gently dipping volcanoclastic conglomerate and sandstone and porphyritic lava were noted by one of us (SMR) at the northeast end of Snowbird Lake (NTS 65D/15) in June 1985. These rocks had been mapped by F.C. Taylor (1963) as the youngest map unit (unit 10) in the Snowbird Lake map sheet (GSC map 1138A) but his descriptions of them as conglomerate, arkose and shale do not convey the important information that most of the pebbles and detrital grains are of volcanic origin. The volcanoclastic sedimentary rocks and massive lava are remarkably similar to the equally distinctive phyrlic alkaline volcanic and sedimentary rocks that form the Christopher Island Formation which underlies extensive areas between Kamilukuak Lake and Baker Lake 150 to 550 km north and northeast of Snowbird Lake (Fig. 70.1). Some of these similarities, which lead us to regard the Snowbird Lake rocks as an outlier of Christopher Island Formation, are outlined and illustrated in this report.

Outcrops of volcanic and volcanoclastic sedimentary rocks

The volcanic-sedimentary rocks outcrop in two places at Snowbird Lake. One is near the north shore of a narrow bay at the northeast corner of the lake ($60^{\circ}54.7'N$, $102^{\circ}38.8'W$; Fig. 70.2). The other is a narrow island 12 km southwest of the lakehead ($60^{\circ}49.8'N$, $102^{\circ}43.3'W$). The island outcrops are flaggy, hematitic, lithic sandstone and volcanic pebble conglomerate (Fig. 70.3). Other small low

islands in the northernmost part of the lake are no doubt underlain by similar rocks as they are composed of piles of thin, reddish, ice heaved rock shingles like the detritus found adjacent to the island outcrops.

The northern outcrops are mainly on a low, northeasterly-elongated hill about 250 m long (Fig. 70.2). Outcrops and extensive areas of frost heaved brown, red and maroon, fine grained, fissile sandstone occur on low ground along the southeast flank of the hill. Buff sandstone and grit outcrops along the southeast side of the hill which is capped by flaggy grit containing poorly sorted volcanic pebbles and widely scattered cobbles and boulders of granite. A thin layer of massive, fine grained, olive porphyritic lava or hypabyssal intrusive rock outcrops sparingly along the northwest flank of the hill.

The outcrop areas are along the west side of a wide, major mylonite zone (Taylor, 1963), part of the Virgin River-Black Lake-Tulemalu shear zone (GSC map 1250A; Tella and Eade, 1985). Volcanic sandstone at the lakehead outcrop area presumably overlies quartzofeldspathic gneiss that outcrops nearby. There are a number of northeasterly-striking topographic lineaments in the extensively drift covered area north of the lake and two of these flank the area of volcanoclastic rocks (Fig. 70.2). It seems likely that they are faults and that the volcanic arenites, rudites and flows were preserved within a system of grabens related to brittle faulting and downdrop along the west side of the mylonite zone. The Black Lake-Tulemalu shear zone extends north

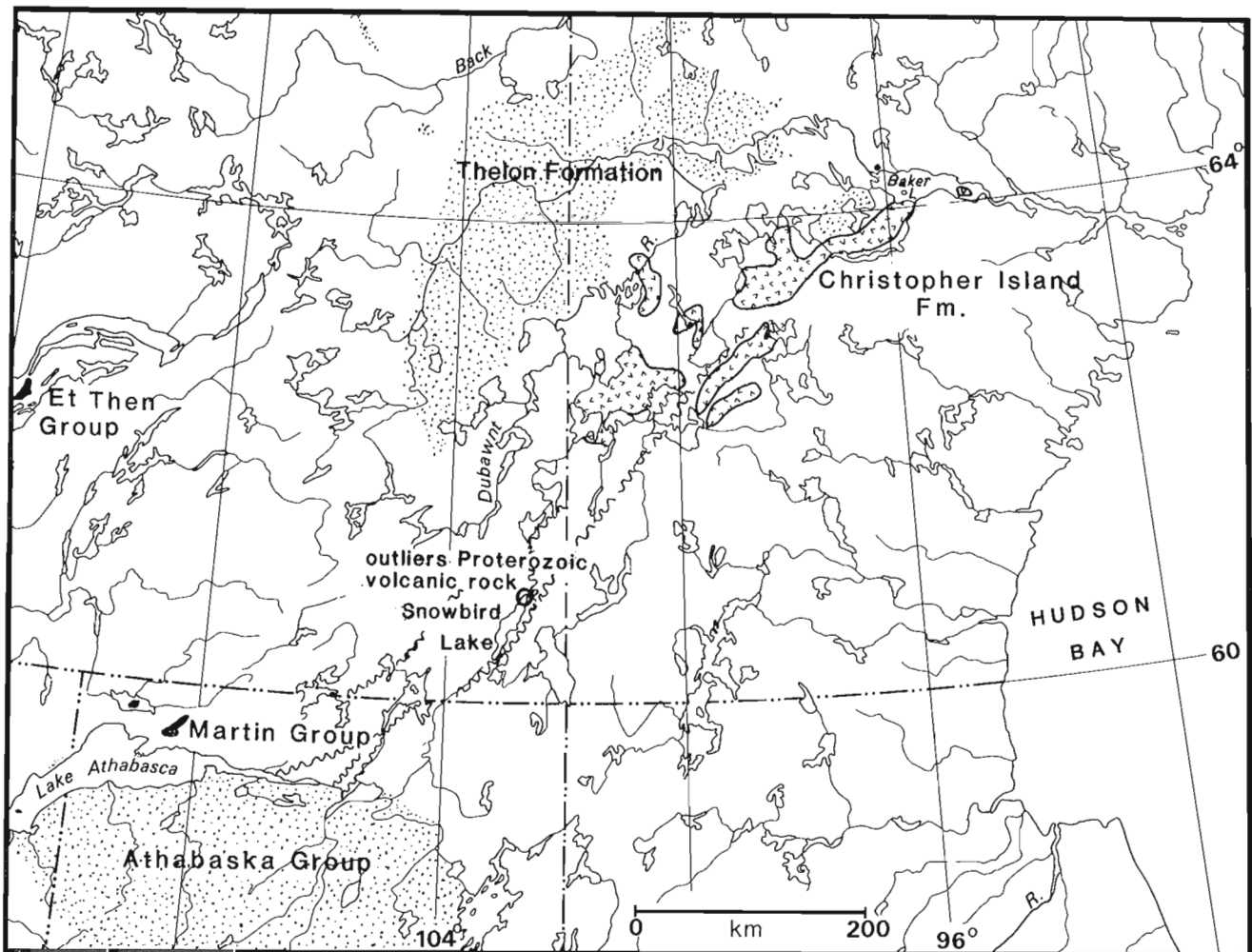


Figure 70.1. Location of Snowbird Lake and areas of Christopher Island Formation and other Neopaphebian and Helikian rocks in Northwest Territories and Saskatchewan.

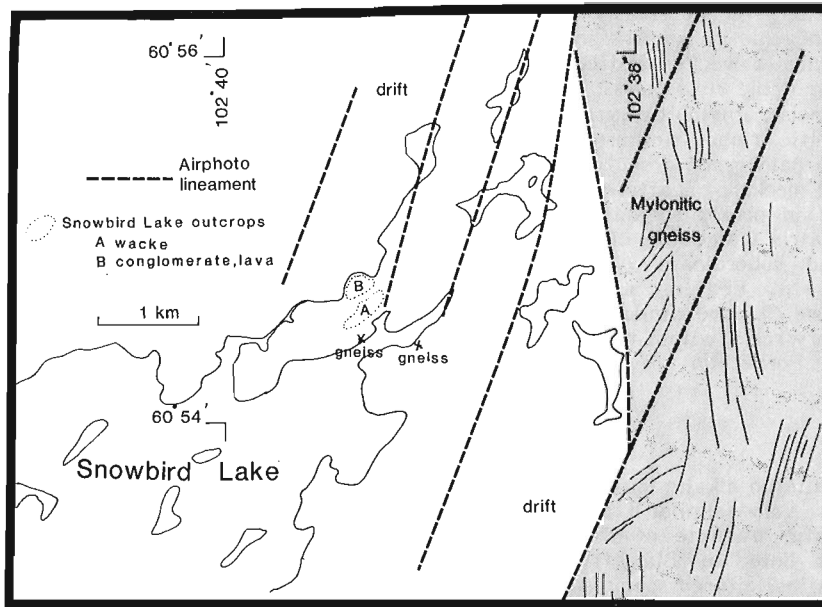


Figure 70.2. Volcanic-sedimentary rocks at northeast end of Snowbird Lake.



Figure 70.3. Conglomerate with porphyritic volcanic pebbles from an island near the northeast end of Snowbird Lake.

into the Baker Lake area, and fracture systems developed along it may have provided loci for eruptions of alkaline volcanic rocks of the Christopher Island Formation as well as being responsible later for the preservation of erosional remnants of these rocks in structural troughs.

Petrographic and mineralogical features

The massive lava contains abundant macrocrysts of phlogopite as well as potassium feldspar. A sample (85RF40) collected at the northern outcrop area shows excellent preservation of textures despite variable replacement of minerals by hematite, dolomite, analcime, chlorite and muscovite. The presence of analcime indicates that the rock was subjected only to zeolite facies metamorphism. Pebbles of similar porphyritic rocks (Fig. 70.4A) are common in conglomerates in both of the outcrop areas. Figure 70.4B is a photomicrograph of part of one such pebble. It is texturally and mineralogically similar to Christopher Island Formation trachyandesites (Blake, 1980; Miller, 1980; Smith et al., 1980). Altered phlogopite contains secondary ferric oxide. Secondary dolomite is present in the matrix and in altered feldspar phenocrysts.

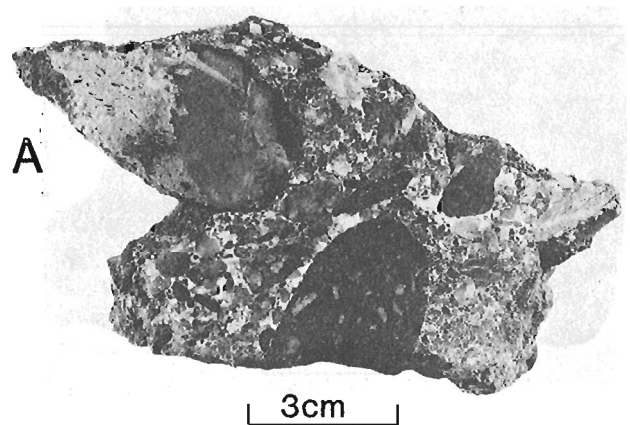


Figure 70.4A. Volcaniclastic conglomerate with feldspar and mica phyrlic trachyte clasts set in a finer, granule-sized matrix which is cemented with carbonate (white).

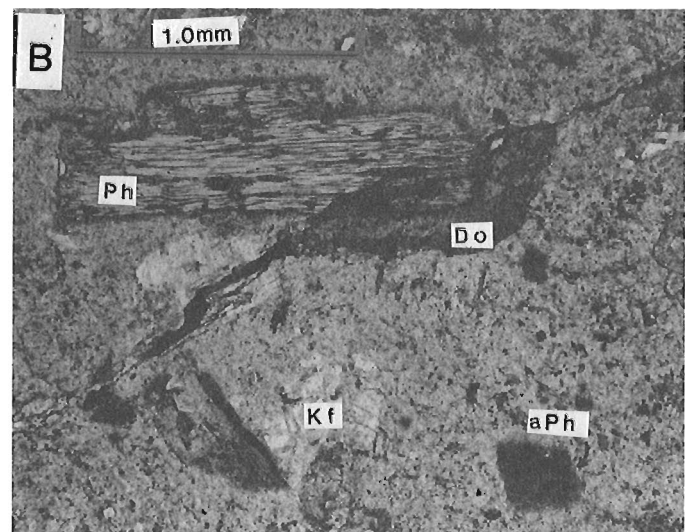


Figure 70.4B. Phlogopite-alkalic feldspar phyrlic trachyte from a pebble in conglomerate at Snowbird Lake. Ph, phlogopite; Kf, alkalic feldspar; Do, dolomite; aPh, ferric oxide after altered phlogopite.

In addition to abundant volcanic clasts and variably rounded and altered volcanogenic phlogopite and potassium feldspar granules, volcanoclastic wackes and conglomerates contain a variety of metamorphic rock clasts: quartz-mica schist, quartz-feldspar gneiss, mylonitic granite, quartz granules displaying mylonitic ribbon texture, quartz and granite. Elongate dark to pale green granules of mica are conspicuous in all clastic rocks. Scattered boulders of granitic rock are present in poorly sorted wacke at the mainland outcrop area. Matrix framework clasts are tightly packed with calcite and subordinate chlorite-analcime mixtures as authigenic cement. Features such as low angle crossbedding shown in Figure 70.5 are similar to those found in volcanoclastic sedimentary rocks within the main areas of the Christopher Island Formation (Tella et al., 1981, Fig. 32.4, 32.8, 32.9).

Chemical composition

A single analysis of altered alkalic lava from Snowbird Lake (sample 85RF40) is very similar to analyses of carbonate-rich altered mafic trachyte of the Christopher Island Formation that are listed by Blake (1980, Table 5, analyses 1, 2, 3, p. 16). A less altered specimen with lower CO₂, H₂O, CaO, and MgO contents and K₂O:Na₂O ratios unaffected by alkali exchange, perhaps like the trachyte

Table 70.1. Chemical analysis of altered alkalic lava, Snowbird Lake (sample 85RF40)

%		ppm	
SiO ₂	45.0	Ag	10
TiO ₂	0.75	Ba	4000
Al ₂ O ₃	10.2	Be	6.1
Fe ₂ O ₃	4.7	Co	40
FeO	1.7	Cr	320
MnO	0.08	Cu	35
MgO	10.2	La	86
CaO	9.03	Ni	310
Na ₂ O	5.63	Pb	60
K ₂ O	1.59	V	100
P ₂ O ₅	1.26	Yb	1.1
CO ₂	3.7	Zn	110
H ₂ O	4.3		
S	0.0		
Total	98.14		

Analyses by ICP, except FeO, H₂O.

Analytical Chemistry Section, Mineral Resource Division, Geological Survey of Canada.

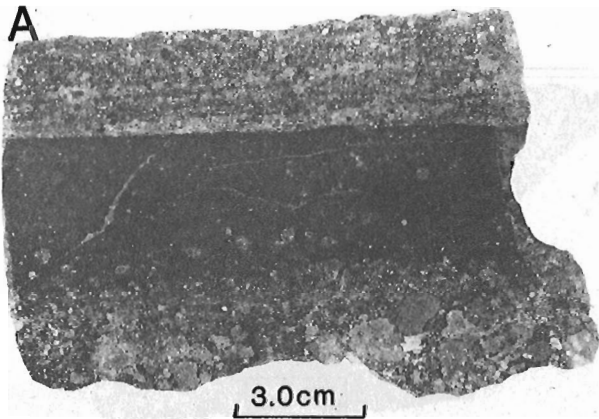


Figure 70.5A. Volcaniclastic wacke with planar bedding and low angle crossbedding.

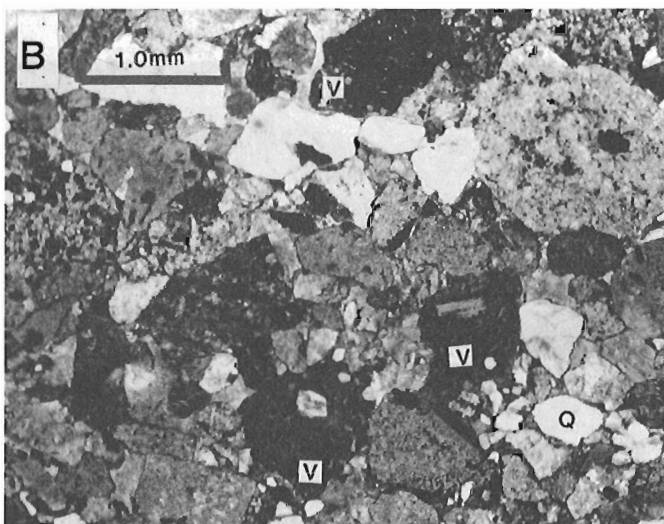


Figure 70.5B. Volcaniclastic wacke, Q, quartz-bearing clasts; V, altered feldspar or mica phyrific volcanic clasts.

pebble shown in Figure 70.3, would likely fall within the same compositional field as trachyandesites from the Christopher Island Formation within the Baker Lake Basin. High TiO₂, P₂O₅, Ba, Cr, and Ni contents (Table 70.1) are similar to those that characterize alkaline lavas of that formation in the Baker Lake-Angikuni Lake area (Blake, 1980; Smith et al., 1980).

Conclusions

Small areas of little deformed, subgreenschist facies volcanic wacke, volcanic conglomerate, and lava at the north end of Snowbird Lake (NTS 65D/15) represent distant outliers of the Christopher Island Formation which consists of alkaline volcanic and volcanoclastic sedimentary rocks in the lower part of the Dubawnt Group of late Aphebian to Helikian age. The outliers are likely erosional remnants of a once much more extensive area of volcanic rocks, possibly contiguous with Christopher Island rocks now preserved in several structural basins in an area extending 150 to 550 km north and northeast of Snowbird Lake.

Conglomerate in the Snowbird outlier includes pebbles of mylonite which indicate that eruption of the volcanic rocks postdated development of the major shear zone which borders them on the east (Taylor, 1963). Eruptive centres of alkaline Christopher Island volcanic rocks may have been developed along late brittle fracture systems that were developed along the shear zone. The preservation of erosional remnants of the volcanic strata may be attributed to fault development of structural troughs along the same system.

The recognition of these outlying occurrences of rocks correlative with the Christopher Island Formation results in a considerable extension of a distinctive alkaline petrogenic province and related metallogenic domains. It also provides a partial bridge between geological domains in the Baker Lake area and similar domains in northern Saskatchewan. The present erosion surface at Snowdrift Lake, and probably through extensive areas north and south of the Lake, nearly corresponds to the surface that existed at the time that the

Christopher Island alkaline volcanic rocks were extruded and derived debris deposited unconformably on the older igneous and metamorphic rocks. There may be possibilities that unconformity-related pitchblende veins could have been formed in this area, analogous to the situation in the Beaverlodge area (Tremblay, 1972) and Baker Lake area (Miller, 1980) where pitchblende veins are found mainly in crystalline rocks below but near unconformities. No evidence has been found, however, for the existence of any mineral concentrations within or near the alkalic igneous rocks and derived sedimentary rocks at Snowbird Lake.

Acknowledgments

Figure 70.1 was draughted by S.B. Green. Alalcime was identified in the volcanic rocks by A.C. Roberts and some occurrences of muscovite confirmed by G.M. LeCheminant of the Mineralogy Section of the Mineral Resource Division. Reviews of an initial manuscript by A.N. LeCheminant resulted in improvements in this paper.

References

- Blake, D.H.
1980: Volcanic rocks of the Paleohelikian Dubawnt Group in the Baker Lake-Angikuni Lake Area, District of Keewatin, N.W.T.; Geological Survey of Canada, Bulletin 309, p. 1-39.
- Miller, A.R.
1980: Uranium geology of the eastern Baker Lake Basin, District of Mackenzie; Geological Survey of Canada, Bulletin 330, 63 p.
- Smith, T.E., Tetley, N., and Hudec, P.P.
1980: Proterozoic mafic syenites from Baker Lake, N.W.T., Canada; Precambrian Research, v. 13, p. 167-179.
- Taylor, F.C.
1963: Snowbird Lake Map-Area, District of Mackenzie; Geological Survey of Canada, Memoir 333, p. 14.
- Tella, S. and Eade, K.E.
1985: The significance of high pressure-temperature granulite inclusions in the Tulemalu Fault Zone, District of Keewatin, N.W.T., Canada; in Program of abstracts, G.A.C.-M.A.C. Fredericton, v. 10, p. A62.
- Tella, S., Eade, K.E., Miller, A.R., and Lamontage, C.G.
1981: Geology of the west half of the Kamilukuak Lake map area, District of Keewatin; a part of the Churchill Structural Province; in Current Research, Part A, Geological Survey of Canada, Paper 81-1A, p. 231-240.
- Tremblay, L.P.
1972: Geology of the Beaverlodge Mining area, Saskatchewan; Geological Survey of Canada, Memoir 367, 265 p.

The Gambier Group in the Sky Pilot area, southwestern Coast Mountains, British Columbia

Project 800028

T.S.T. Heah¹, R.L. Armstrong¹, and G.J. Woodsworth
Cordilleran and Pacific Margin Division, Vancouver

Heah, T.S.T., Armstrong, R.L., and Woodsworth, G.J., The Gambier Group in the Sky Pilot area, southwestern Coast Mountains, British Columbia; in Current Research, Part B, Geological Survey of Canada, Paper 86-1B, p. 685-692, 1986.

Abstract

The Sky Pilot area, in the northern part of the Britannia pendant, is underlain by a homoclinal succession of basalt, dacitic andesite to dacite flows, andesite to dacite tuff, breccia, agglomerate, and argillite. These unfossiliferous rocks belong to the Goat Mountain Formation of the Gambier Group. Plutonic rocks cutting the strata are diorite, quartz diorite, and quartz eye porphyry. An Early Cretaceous age of 114 ± 40 Ma at an initial $^{87}\text{Sr}/^{86}\text{Sr}$ ratio of 0.70325 was obtained from a two-point Rb-Sr isochron. Prehnite-pumpellyite to greenschist facies regional metamorphism is locally overprinted by amphibolite facies contact metamorphism. K-Ar dates on hornblende of 101 ± 4 Ma (from diorite) and 95.1 ± 3.3 Ma suggest contact metamorphism and emplacement of the diorite are mid Cretaceous.

The Goat Mountain basalts are tholeiitic; the dacites are calc-alkaline and sodic. A gabbro-trondhjemite trend and a bimodal basalt-dacite association suggest formation in an extensional area, perhaps a back-arc basin, proximal to an island arc. The petrochemical similarity to Archean greenstone belts is noteworthy.

Résumé

La région du mont Sky Pilot dans la partie nord de l'enclave Britannia, recouvre une succession homoclinale de basaltes, de coulées dont la composition varie de l'andésite dacitique à la dacite, de tuf de nature andésitique à dacitique, de brèches, d'agglomérats et d'argilite. Ces roches non fossilifères appartiennent à la formation de Goat Mountain, du groupe de Gambier. Les roches plutoniques qui coupent les strates se composent de diorite, de diorite quartzique et de porphyre quartzifère. Ces roches datent du Crétacé inférieur, soit de 114 ± 40 millions d'années, avec un rapport initial $^{87}\text{Sr}/^{86}\text{Sr}$ de 0,70325 (datation obtenue à l'aide d'un isochrone Rb-Sr à 2 points). Un métamorphisme régional du faciès à prehnite et à pumpellyite à celui des schistes verts est surimposé par endroits par un métamorphisme de contact à faciès des amphibolites. Les datations établies à l'aide de la méthode K-Ar, de 101 ± 4 millions d'années (à partir de la diorite) et $95,1 \pm 3,3$ millions d'années, indiquent que le métamorphisme de contact et la mise en place de la diorite datent du milieu du Crétacé.

Les basaltes de Goat Mountain sont tholéitiques; les dacites sont calco-alcalines et sodiques. Une tendance gabbro-trondhjemite et une association basalte-dacite bimodale semblent indiquer que leur formation a eu lieu dans une région d'extension, probablement un bassin arqué vers l'arrière, voisin d'un arc insulaire. Il convient de noter la similitude pétrochimique de ces roches avec celles de zones de roches vertes de l'Archéen.

¹ Department of Geological Sciences, University of British Columbia, Vancouver,
British Columbia V6T 2B4

Introduction

The Britannia pendant, about 40 km north of Vancouver, is a body of metamorphosed volcanic and sedimentary rocks surrounded by granitoid rocks of the Coast Plutonic Complex. The pendant is host to the Britannia volcanogenic sulphide deposits. The ore bodies are in a broad, northwest-trending shear zone and are hosted by rocks assigned by Roddick and Woodsworth (1979) to the Early Cretaceous Gambier Group. Most reports on the Britannia pendant have concentrated on the ore bodies, closely associated rocks, and the polyphase deformation within the shear zone (see Payne et al., 1980). Little has been published on the relatively undeformed northern part of the pendant, where this study focuses on the petrology and chemistry of a relatively undisturbed stratigraphic succession. Sample location maps, petrographic descriptions, photographs, supplemental figures, and analytical details are available in the more comprehensive report of Heah (1982).

Stratigraphic nomenclature

The term Gambier Group, originally used for strata on Gambier Island has since been extended to include the Britannia pendant and similar Late Jurassic and Early Cretaceous volcanic and sedimentary rocks and their metamorphosed equivalents in the southern Coast Mountains (e.g. Bostock, 1963; Roddick, 1965). Schofield (1918, 1926) recognized two units in the Britannia pendant: a lower, mainly volcanic unit, the Goat Mountain Formation, and an upper sedimentary unit, the Britannia Formation. James (1929) divided the Goat Mountain Formation into lower, middle and upper members. Contrary to Schofield (1926), James felt that the Britannia Formation is older than the Goat Mountain Formation and was thrust over the Goat Mountain Formation. Britannia mine geologists (e.g. Payne et al., 1980) have tended to use the term Britannia Group for rocks of the Britannia pendant but recognize the equivalence of the Britannia and Gambier groups. In this paper, the term Gambier Group is used for strata of the Britannia pendant because of lithologic similarities with reference sections of the Gambier Group (Roddick, 1965). The term Goat Mountain Formation is used for strata of the Sky Pilot area, which is in the northern part of the pendant.

Goat Mountain Formation

The Goat Mountain Formation can be divided into seven units (Fig. 71.1). These form a gentle southwest-dipping homocline that is disrupted by several steep, north-south trending faults of small displacement. Original volcanic and sedimentary structures and textures are commonly well preserved.

Unit 1, the oldest in the area, is composed of resistant, porphyritic basalt flows, tuff, breccia, argillite, and dacite flows or intrusive sheets. The base was not observed. Basaltic flows (and minor intrusive sheets) are the most abundant rocks of unit 1. Phenocrysts of pyroxene and normally zoned plagioclase, totalling up to 35 per cent of the rock, occur in an aphanitic, dark green matrix. The flows have pilotaxitic to trachytic textures. Hornblende, K-feldspar, and garnet are occasional constituents. Well bedded argillite is abundant in the upper part of the unit. The argillite, which contains light and dark coloured laminae 1 to 4 cm thick, is interbedded with light green dacite flows or intrusive sheets and dark green, vesicular basalt. Dacite is a very fine grained, pilotaxitic rock with about 15 per cent plagioclase phenocrysts and about 20 per cent primary quartz. Sparse primary K-feldspar is present. Tuff, breccia and conglomerate are minor components of the lower parts of unit 1.

Unit 2 conformably overlies unit 1. The contact is well exposed east of Sky Pilot Mountain, where grey-green, vesicular, porphyritic basalt of unit 2 rests on rusty weathering, black argillite of unit 1. Unit 2 is a recessive sequence of vesicular pyroxene basalt flows, reworked breccia, tuff, conglomerate and pillow lava. Columnar jointing is locally present. The basaltic flows are massive, dark grey-green, and commonly vesicular. Some of the flows contain small angular xenoliths of black argillite, presumably derived from unit 1. Pyroxene and plagioclase phenocrysts are set in an aphanitic matrix. Pyroxene in each of the few thin sections examined is either hypersthene or augite and are heavily altered to uralite and actinolite. Subophitic, glomeroporphyritic, and subtrachytic textures are retained in the rocks in spite of the extensive metamorphism.

LEGEND

- EKs Granodiorite and quartz diorite
- EKd Quartz diorite, diorite, dacite quartz-eye porphyry

GOAT MOUNTAIN FORMATION

- IK₆ Massive, vesicular and amygdaloidal pyroxene basalt flows, andesite and dacite tuff, pillow lava, argillite and agglomerate
- IK₅ Dacite tuff, basalt flows, argillite, basalt breccia and agglomerate, sandstone and dacite crystal lapilli tuff
- IK₄ Porphyritic basalt flows, in part amygdaloidal, mafic tuff and flow breccia, argillite
- IK₃ Argillite, andesite tuff, basalt tuff breccia, minor chert
- IK₂ Pyroxene basalt flows, andesitic tuff breccia, tuff, agglomerate, and pillow lava
- IK₁ Basalt flows, argillite, dacite flows, mafic tuff, tuff breccia, and minor agglomerate

SYMBOLS

- Bedding -----
- Fault -----
- Contact (defined / approximate, assumed) -----
- Limit of mapping -----
- Sample for chemical analysis • g
- K-Ar date ----- x 95 Ma

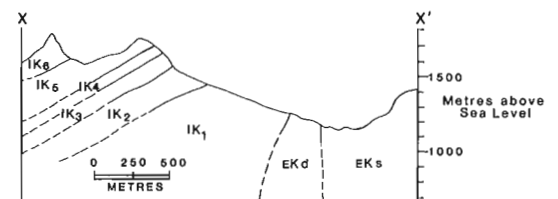
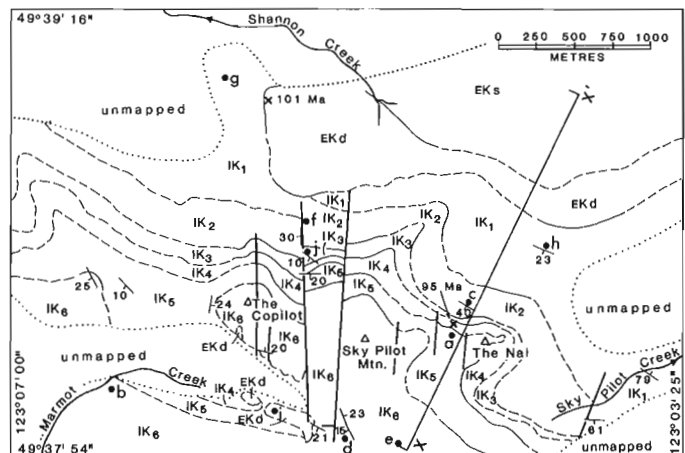


Figure 71.1. Sketch map and cross-section of the Sky Pilot area. The south contact of the Squamish granodiorite (EKs) is taken from Roddick and Woodsworth (1979).

Above the massive pyroxene basalt flows, unit 2 contains (in decreasing order of abundance) reworked breccia, tuff, some with accretionary lapilli, pillow breccia and pillow lava. The reworked breccia contains angular siliceous volcanic fragments up to a centimetre long, and angular clasts of feldspar and quartz. A conspicuous feature of the breccia and tuff is their very well bedded nature. Some centimetre-thick beds are traceable as far as 8 m. Some of the laminations are less than a millimetre thick. Delicate dark green and thicker light grey-green laminations repeat in a cyclic fashion. Small ripple marks are present in some of the reworked tuff. Accretionary lapilli, indicative of subaerial volcanism, are locally present. Because of the angular nature of the clasts in the breccia, reworking was probably slight. Interbedded with, and overlying the breccia and tuff, are pillow lava, pillow breccia, and tuffaceous sandstone. The pillow breccia overlies the pillow lava. The pillows are enclosed in tuffaceous sediments that seem to ooze around the pillows. Laminations in the tuffaceous sediments are convoluted as a result of the loading by the overlying pillow lavas.

Unit 3, best exposed northeast of The Copilot, is characterized by rusty and recessive weathering black argillite, reworked andesite tuff, basalt breccia, and minor silicified tuff or impure chert. The conspicuous bedding is marked by alternating light and dark grey bands in the argillite and reworked andesite tuff. Load casts indicate that the section is upright. Imbricated pebbles of argillite occur subparallel to bedding planes in one outcrop. Asymmetrical sand waves in the reworked tuff indicate that the tuff was waterlain. The well-bedded nature of the tuff, the good sorting, and the extremely fine grain size indicate a low energy environment of deposition, distant from the volcanic source. The black argillite is rusty weathering, hard, and very fine grained, with a conchoidal fracture. The reworked andesite tuff is very fine grained, rusty weathering, well bedded with alternating light and dark green laminae, and likewise have a conchoidal fracture. In thin section, the tuff is seen to consist of plagioclase and volcanic rock fragments set in a very fine grained, cloudy matrix. Outcrops of breccia are grey weathering, with angular clasts of porphyritic basalt, chert and black argillite up to 15 cm across. The clasts are framework supported, the porphyritic clasts being the most abundant. The volcanic rocks could have been eroded from the underlying unit 2, or erupted through it. One thin section of breccia contains an amygdaloidal, glomeroporphyritic basalt clast in contact with what appears to be a welded lapilli breccia. At one locality, 1 m of light grey weathering silicified tuff or impure chert was found.

Unit 4 consists of massive porphyritic basalt flows, mafic breccia, and well bedded argillite. This member is characteristically grey weathering; the best section is northeast of The Copilot. The porphyritic volcanic rocks are dark green on fresh surfaces. Chlorite amygdules are commonly present. In hand specimen, clasts in the breccia are indistinguishable from the porphyritic volcanics. The argillite locally contains subrounded clasts of porphyritic or tuffaceous mafic volcanic rocks.

Unit 5 consists of thin bedded, reworked dacite tuff, interlayered with a few porphyritic, vesicular basalt flows, minor argillite, epiclastic sandstone, basalt breccia and conglomerate, and dacite crystal-lapilli tuff. The best section is in the bowl between Sky Pilot Mountain and The Copilot. There, porphyritic basalt of unit 4 is conformably overlain by rusty-grey weathering, well bedded, reworked green and grey siliceous tuffs and epiclastic sandstone, all containing convoluted bedding indicative of soft sediment deformation. Individual beds range in thickness from 1 to 3 cm. Darker grey-green beds alternate with lighter coloured green-grey beds. Flame structures and graded bedding indicate that beds are upright. Thin sections show

that the green and grey tuffs are composed of subrounded quartz and feldspar fragments. Thin, well sorted laminae are defined by differences in grain size.

Overlying the green and grey tuffs is rusty weathering, black argillite with some interbeds of white tuff. Above the argillite are well bedded, light green tuffs similar to those at the base, minor argillite, and dacite flows or sills. Grey weathering basaltic breccia and conglomerate overlie the light green tuff. One of the volcanic breccias contains accretionary lapilli. Porphyritic, green basalt overlies the breccia and conglomerate, and is capped by 2 m of rusty weathering, black argillite.

The top of the unit consists of well bedded green and grey tuffs with load and flame structures, truncated foreset beds, and convoluted bedding. Individual beds pinch and swell, and are from 1 to 3 cm thick. These tuffs are finer grained than the basaltic tuff of unit 2, and lack the volcanic sandstone, but exhibit the same cyclic dark green-light green banding. In a similar section on Goat Ridge, vesicular porphyritic basalt flows are more abundant. These flows, found towards the top of the section, are 3 to 5 m thick, and are interlayered with well bedded tuff.

Rusty weathering, siliceous volcanic breccia and dacitic, crystal-lapilli tuff forms steep cliffs south-southwest of The Nai. Broken plagioclase and quartz grains are conspicuous in thin section. In Marmot Creek basin, breccias with subangular to angular clasts up to 15 cm across of porphyritic basalt indicate a proximal source. The typical breccia is composed of angular plagioclase, quartz, volcanic rock and chert fragments. The volcanic rock fragments are amygdaloidal and porphyritic basalt.

Unit 6, the uppermost stratified unit in the map area, forms the serrated peaks of Sky Pilot Mountain and The Copilot. The top of the unit was not observed. The lower parts consist of vesicular and amygdaloidal pyroxene basalt flows, andesite and dacite tuff, dacitic-andesite pillow lava, some breccia, and black and grey argillite. The lower part of unit 6 consists of resistant, commonly amygdaloidal, dark green, porphyritic basalt which forms steep, continuous cliffs. The basalt is grey-green weathering, massive and structureless. Plagioclase phenocrysts are conspicuous on weathered surfaces.

In Marmot Creek basin, pillowed dacitic andesite is intercalated with the basal porphyritic basalt. Pillows are typically oval in shape, 40 to 60 cm across, and draped with bedded sandy tuff which oozed between pillows. The bedding in the sandy tuff is locally distorted adjacent to the pillows. Higher in the section, towards the col south of Sky Pilot Mountain, angular clasts of broken pillows, together with the draping sandy tuff, are found. The clasts are set in a layered, sandy or tuffaceous matrix. The pillowed dacitic andesite consists largely of hornblende, hypersthene and augite (partly altered to chlorite and epidote) and plagioclase in a fine grained, altered matrix.

On the ridge west of The Copilot, the base of unit 6 is marked by grey-green weathering, vesicular, porphyritic basalt interbedded with volcanic breccia and minor pillow lava. Clasts in the volcanic breccia are feldspar and pyroxene porphyries. Above the basalt flows and pyroclastics are well bedded chert and siltstone with large asymmetrical sand waves. Crossbeds in siltstone indicate that the section is upright. Similar rocks in the Marmot Creek basin display flame and load structures. One intrusive sheet of dacitic quartz-eye porphyry, locally subparallel to bedding in the sediments, contains xenoliths of porphyritic basalt and cherty tuff, and locally is autoclastic.

Rusty weathering, black and grey argillite forms up to 5 per cent of the lower part of unit 6 and forms good marker horizons. Argillite is finely laminated, very fine grained, and composed largely of subangular quartz and plagioclase clasts.

The rock is inequigranular, with the larger grains being matrix-supported. Bedded rocks above 1785 m were not closely studied.

Granitoid rocks

Dacitic quartz-eye porphyry with conspicuous quartz and plagioclase phenocrysts, and medium grained, equigranular quartz diorite form several resistant outcrops in Marmot Creek basin. The porphyry is similar to dacite dykes described from the mine area (Payne et al., 1980). North of the Britannia pendant and outside the area studied in detail is the Squamish granodiorite, which intruded and contact metamorphosed the pendant. North and east of Sky Pilot Mountain, a previously unmapped older body of diorite is situated between the Squamish granodiorite and the Goat Mountain Formation. Mafic minerals in the diorite are hornblende (about 20%), biotite (about 15%) and (in one sample) clino- and orthopyroxene. Near the contact with the Squamish granodiorite, chlorite, clinozoisite, actinolite, and calcite are abundant alteration products. Minor chlorite and sericite are present away from the contact.

Metamorphism

Rocks of the Goat Mountain Formation are everywhere metamorphosed, the grade ranging from prehnite-pumpellyite to amphibolite facies. Most rocks are mixtures of actinolite, chlorite, epidote, and quartz. Sphene, albite, and clinozoisite are commonly present. The assemblage prehnite + pumpellyite + chlorite + quartz was found in a pillow lava in Marmot Creek basin; the typical greenschist assemblage of epidote or clinozoisite + chlorite + actinolite is common throughout the Goat Mountain Formation. Insufficient work was done to map the distribution of prehnite-pumpellyite and greenschist facies assemblages.

Contact metamorphism on the north side of the area resulted from emplacement of diorite and the Squamish granodiorite. Near the contact with the diorite, the assemblage plagioclase (An₈₀) + garnet + biotite + quartz is present in basalt. With increasing distance from the diorite, the An content of the plagioclase decreases. Near the Squamish granodiorite, the strata are pervasively recrystallized, and mineral assemblages include actinolite + chlorite + epidote/clinozoisite.

Table 71.1. Chemical analyses

Sample	a	b	c	d	e	f	g	h	i	j
Lat.	49°38.0'	49°38.0'	49°38.2'	49°37.8'	49°37.5'	49°38.5'	49°39.0'	49°38.4'	49°37.9'	49°38.4'
Long.	123°04.7'	123°06.5'	123°04.7'	123°05.2'	123°04.9'	123°05.5'	123°05.9'	123°04.1'	123°04.6'	123°05.4'
<u>Oxides (wt %)</u>										
SiO ₂	47.8	48.3	48.5	49.8	52.1	60.1	60.6	64.7	72.4	79.1
TiO ₂	0.98	0.90	0.93	0.95	0.74	0.52	1.03	0.57	0.26	0.19
Al ₂ O ₃	15.3	15.5	15.8	16.2	15.3	14.7	15.5	14.9	13.3	10.6
Fe ₂ O ₃	11.3	9.5	10.4	9.6	8.8	8.7	10.4	5.6	4.48	3.19
MnO	0.17	0.17	0.17	0.17	0.18	0.18	0.18	0.18	0.13	0.11
MgO	11.4	10.9	10.6	7.8	8.7	2.12	2.79	1.73	1.07	1.09
CaO	6.05	10.5	8.9	10.4	9.2	5.88	6.33	5.31	2.36	1.97
Na ₂ O	3.24	1.87	2.31	2.69	2.75	5.75	1.60	6.12	3.79	1.80
K ₂ O	1.21	0.47	0.37	0.43	1.14	0.34	0.27	0.23	1.49	1.22
P ₂ O ₅	0.84	0.79	0.60	1.12	0.61	1.28	1.41	0.48	0.38	0.20
L.O.I.	1.81	0.97	1.03	0.76	0.55	0.23	0.00	0.00	0.30	0.33
H ₂ O ⁻	0.14	0.10	0.43	0.13	0.08	0.18	0.06	0.26	0.10	0.22
<u>Trace Elements (ppm)</u>										
Rb	34	14	10	7	22	3	5	2	21	30
Sr	424	433	466	539	443	258	468	436	266	261
Zr	77	73	60	90	62	140	80	111	98	151
Nb	6	8	2	6	0.1	8	8	9	5	4
Y	25	27	19	25	24	27	31	34	16	19
<p>Pressed powder samples were analysed for major and trace elements using X-ray fluorescence methods described by van der Heyden (1982) and Berman (1979), respectively. H₂O⁻ and L.O.I were determined for 120°C, 6 hours and 990°C, 1 hour, respectively. The major element analyses were normalized to 100% during data processing so the totals are not meaningful.</p>										

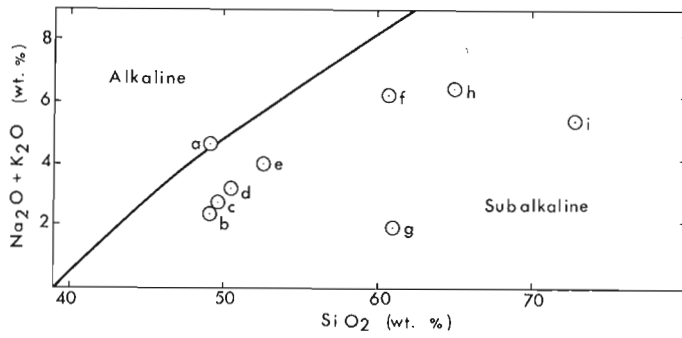


Figure 71.2. Alkalies-silica plot for volcanic rocks of the Goat Mountain Formation. In this and subsequent plots, the letters are those used for sample identification in Table 71.1. Divider after Irvine and Baragar (1971).

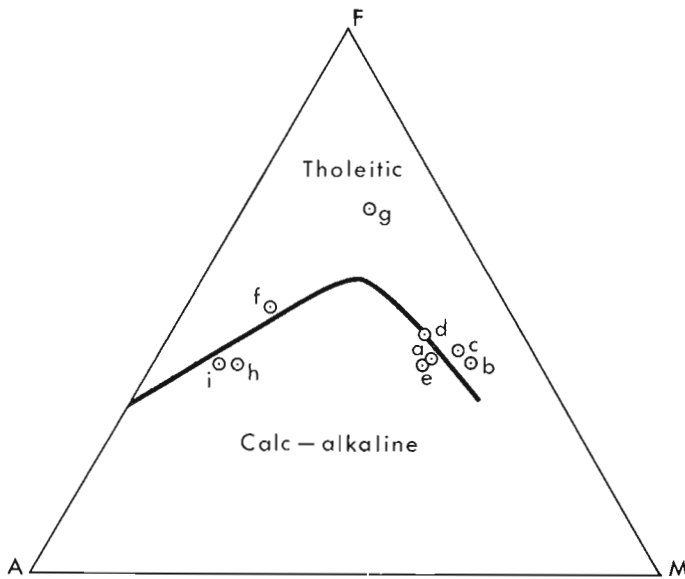


Figure 71.3. AFM diagram for Goat Mountain volcanic rocks. Divider after Irvine and Baragar (1971).

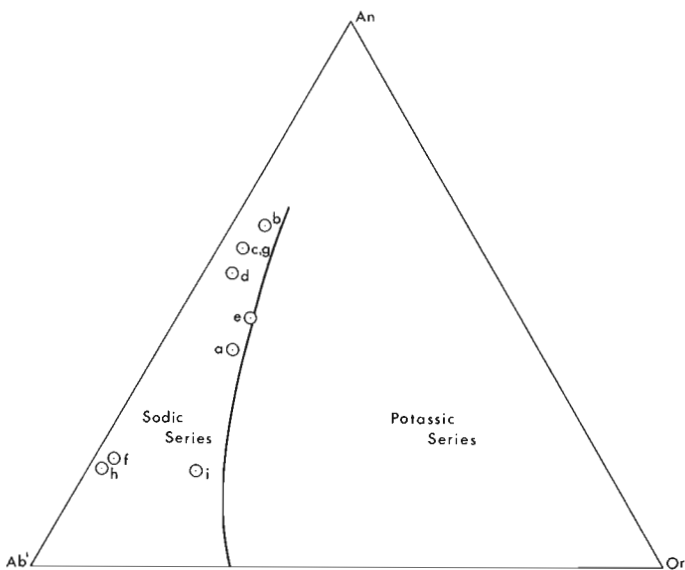


Figure 71.4. Normative anorthite-albite'-orthoclase plot; divider after Barker and Arth (1976).

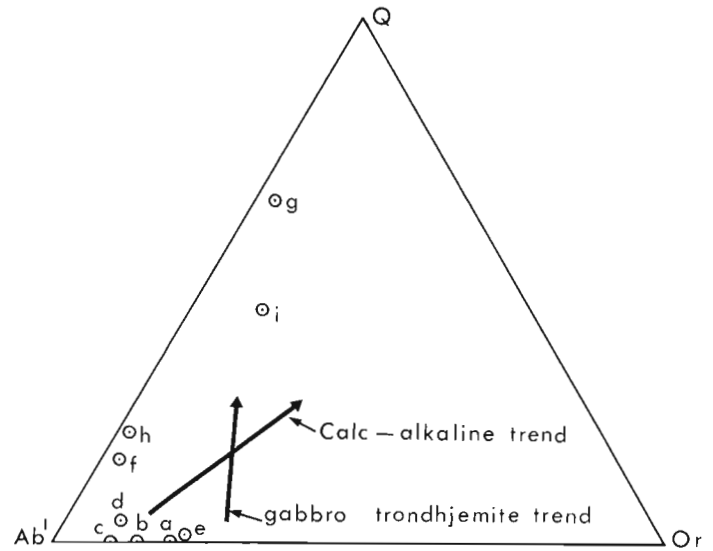


Figure 71.5. Normative quartz-albite-orthoclase plot; trend lines after Barker and Arth (1976).

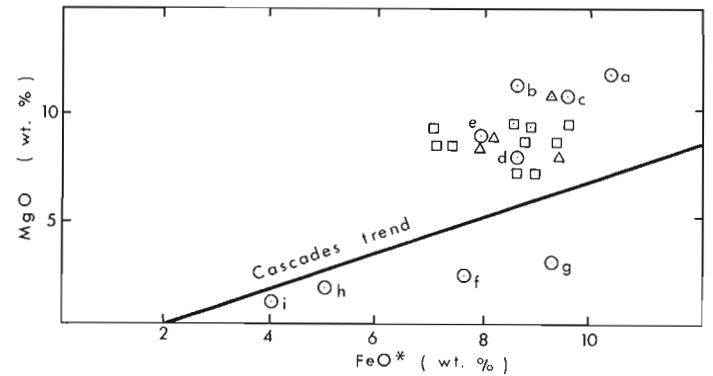


Figure 71.6. MgO-FeO* plot. Circles are Goat Mountain Formation; triangles are Juan de Fuca Ridge basalts (Green, 1977); squares are back-arc basin basalts (Stern, 1980). Cascades trend line from Jakes and Gill (1970).

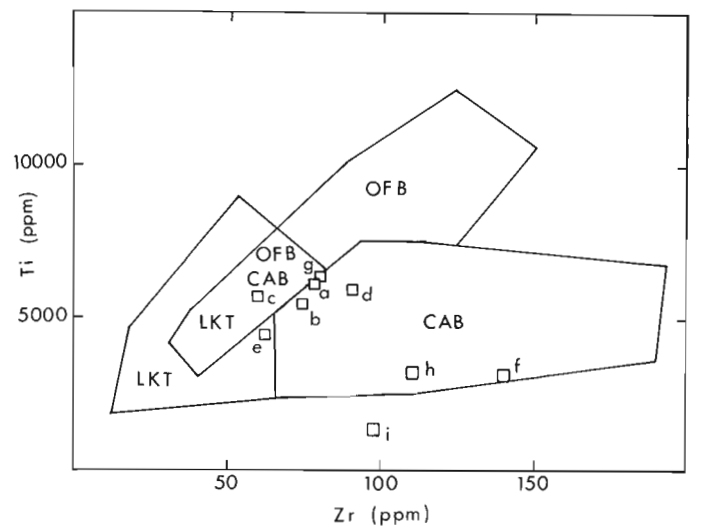


Figure 71.7. Ti-Zr discrimination plot; fields are after Pearce and Cann (1973).

Structure

The Sky Pilot area is on the north limb of an open syncline with a gently-plunging west-northwest axis (Payne et al., 1980). The Goat Mountain Formation in the Sky Pilot area forms an upright homocline dipping southwest about 20° (Fig. 71.1). Steep to vertical faults, mostly north-south trending, disrupt the homocline and give the peaks their craggy and serrated appearance. Movement on these faults appears small, generally only a few metres. On many of the minor faults the west side is down, but others have the east side down.

Major element chemistry

A representative suite of ten of the least altered volcanic rocks, covering as wide a compositional range as possible, was analyzed by X-ray fluorescence (Table 71.1). Only one tuff (sample f) was analyzed; tuffs are more likely to be modified before or during metamorphism. Analysis j, an impure chert or silicified tuff, is not included in the following discussion.

The classification scheme of Irvine and Baragar (1971) was used for the remaining nine analyses. In applying that scheme, Fe₂O₃ was set equal to TiO₂ + 1.5 (weight percent), and the remaining Fe was allotted to FeO. Analysis g, a basalt on the basis of the high An content of the plagioclase, has an unusually high (for basalt) silica content, perhaps due to secondary quartz seen in thin section. The sample is also unusual in its low alkali content relative to other volcanic rocks of the Goat Mountain Formation with roughly the same silica content.

On an alkalis-silica plot (Fig. 71.2) and the alternative OI'-Ne'-Q' plot (shown in Heah, 1982), the Goat Mountain volcanic rocks plot in the subalkaline field. On an Al₂O₃ versus normative plagioclase diagram also shown in Heah (1982) all samples plot in or very near the tholeiitic field. The bimodal distribution of more MgO-enriched basalt and more alkali enriched andesite and dacite in the AFM diagram (Fig. 71.3) reflects a modal anorthite gap in these samples between An₂₂ and An₄₅. A trend towards iron enrichment, typical of non-orogenic suites such as the Mid-Atlantic Ridge, many ocean islands, and orogenic volcanic rocks of some island arcs (Irvine and Baragar, 1971; Stern, 1980; Hawkins, 1977) is indicated in the Goat Mountain basalt. The more felsic rocks straddle the boundary between calc-alkaline and tholeiitic fields, similar to the island arc tholeiite series of Jakes and Gill, 1970. On a normative colour index versus normative plagioclase composition plot (shown in Heah, 1982), the majority of samples plot as basalt, and the rest are dacite or tholeiitic andesite, near dacite.

A distinctly sodic trend is evident from the ternary plot of normative An-Ab'-Or (Fig. 71.4), which shows the relatively low K and high Na contents of the more differentiated Goat Mountain volcanic rocks. Similarly, a plot of Qz-Ab-Or (Fig. 71.5) shows that Goat Mountain rocks follow a gabbro-trondhjemite trend. The gabbro-trondhjemite association is a plutonic equivalent of the extrusive basalt-dacite series typical of many Archean and Proterozoic greenstone belts (Barker and Arth, 1976; Ermanovics et al., 1979). In the Archean the lack of andesites has been explained by some workers as being due to the absence of plate-tectonic processes as we know them today (Barker and Arth, 1976). In the Early Cretaceous, however, the regional setting and history of the Cordillera suggest that plate-tectonic processes were occurring.

On MgO versus FeO* (Fig. 71.6) the bimodal nature of the Sky Pilot volcanic rocks is clear. MgO is positively correlated with FeO* in felsic rocks and sample g; the trend is similar to many moderately Fe-enriched island arc tholeiites. The magnesian basalts cluster above the Cascades

calc-alkaline trend; they are similar to basalts of some back-arc basins (Hawkins, 1977; Stern, 1980) and the Juan de Fuca Ridge (Green, 1981). The lack of andesites, as seen in the Sky Pilot area, has in other circumstances been inferred to indicate an extensional environment such as a back-arc basin (e.g. Snyder et al., 1976).

Major elements thus show the striking similarity of Goat Mountain volcanic rocks with basalt-dacite suites that are common in Precambrian greenstone belts and modern primitive arc and back-arc settings. Bimodal chemistry suggests an extensional, back-arc setting, but Cretaceous paleogeography would make an intra-arc setting more likely. The similarity of Goat Mountain and Precambrian volcanic suites weakens arguments against a subduction origin for Precambrian bimodal greenstone belts.

Trace element chemistry

The incompatible elements, Ti, Zr, Y and Nb, appear to be relatively immobile during metamorphism or other post-depositional alteration processes (e.g. Pearce and Cann, 1973), making them useful in the study of metavolcanic rocks. On the SiO₂ versus Zr/TiO₂ plot of Winchester and Floyd (1977), the classification of all samples, except for the silicified basalt (g), agrees with petrographic and major element classifications. On Zr/TiO₂ versus Nb/Y, only analysis h is anomalous. This sample is petrographically a dacite, has 64.7 per cent SiO₂, but plots in the "subalkaline basalt" field because of its low Zr content. The more felsic rocks have higher K/Rb ratios than the basalts. Nb is variable but generally low. The crude decrease of Nb with increasing Rb is unusual and suggests that Rb has been depleted in some siliceous rocks, possibly during metamorphism.

On a Ti-Zr-Y plot (shown in Heah, 1982), the Goat Mountain basalts fall in a LKT-CAB-OFB field that excludes within-plate settings. Pearce and Cann (1973) found that a better separation for altered samples may be obtained using a Ti versus Zr plot (Fig. 71.7). In this plot, a positive correlation between Ti and Zr is observed. Most basalts plot in the calc-alkaline field, one falls in the low-K tholeiite field, and one in the area of overlap of the CAB-OFB-LKT fields. The normalized incompatible element plot of Sun (1980) (shown in Heah, 1982) shows the jagged distribution typical of volcanic arc basalts.

The trace elements, Zr, Nb and Y, have concentrations intermediate between those of mid-ocean ridges and back-arc basin tholeiites, and the relatively low Ti concentrations are similar to those of island-arc and arc-tholeiites (Pearce and Cann, 1973; Sun, 1980). The moderately high Sr concentrations are similar to those of ocean island tholeiites and island arc rocks (Pearce and Cann, 1973; Sun, 1980). Rb concentrations are low and variable, and overlap the range of calc-alkaline basalts, back-arc basin tholeiites, and island-arc tholeiites (Jakes and Gill, 1970; Stern, 1980).

Trace element results support the inference based on major elements that metamorphism did not confound rock chemistry. The exceptions to this are silica enrichment in sample g, Rb depletion in siliceous rocks, and Zr depletion in dacite sample h. All indications are for a volcanic arc environment, with abundant island-arc tholeiitic basalts, and sodic dacite. The bimodal character and simple local structure (tilting and normal faults) suggest shallow crustal extension within the magmatic arc setting inferred from regional geology.

Geochronometry

Four relatively unaltered volcanic rocks, covering as large a compositional range as possible, were analyzed for Rb, Sr and Sr isotopic composition (Table 71.2). Two of these

samples give a whole-rock Rb-Sr isochron date of 114 ± 40 Ma (Early Cretaceous) with an initial ratio of 0.70325 ± 0.00010 (Fig. 71.8). This result is inaccurate but plausible. The other two samples, are somewhat more altered and widely separated geographically. They do not lie on the isochron just mentioned, but plot, within experimental error, on the Squamish granodiorite isochron of 102 ± 15 Ma at an initial ratio of 0.7035 ± 0.0002 (Fig. 71.8). We see no

Table 71.2. Rb-Sr analytical data

Sample	Lithology	Sr(ppm)	Rb(ppm)	$^{87}\text{Rb}/^{86}\text{Sr}$	$^{87}\text{Sr}/^{86}\text{Sr}$
d	Basalt flow	512	6.6	0.037	0.70331
g	Quartz-basalt flow	477	4.5	0.027	0.70355
h	Dacite flow	442	2.4	0.016	0.70350
i	Dacite quartz-eye porphyry	269	21.3	0.229	0.70362

Rb and Sr were determined by replicate analysis of pressed powder pellets using X-ray fluorescence. U.S. Geological Survey rock standards were used for calibration; mass absorption coefficients were obtained from Mo K α Compton scattering measurements. Rb/Sr ratios have a precision of 2% (1 σ) and concentrations a precision of 5% (1 σ). Sr isotopic composition was measured on unspiked samples prepared using standard ion exchange techniques. The mass spectrometer (60 $^\circ$ sector, 30 cm radius, solid source) is of U.S. National Bureau of Standards design, modified by H. Faul. Data acquisition was digitized and automated using a NOVA computer. Experimental data were normalized to a $^{86}\text{Sr}/^{88}\text{Sr}$ ratio of 0.1194 and adjusted so that the NBS standard SrCO $_3$ (SRM987) gives a $^{87}\text{Sr}/^{86}\text{Sr}$ ratio of 0.71022 ± 2 and the Eimer and Amend Sr a ratio of 0.70800 ± 2 . The precision of a single $^{87}\text{Sr}/^{86}\text{Sr}$ ratio is 0.00013 (1 σ). Rb-Sr dates are based on a Rb decay constant of $1.42 \times 10^{-11} \text{y}^{-1}$. The regressions were calculated using the method of York (1967).

Table 71.3. K-Ar analytical data

Sample Number	TH-HB	TH-19A,B
Latitude	49 $^\circ$ 38.2'	49 $^\circ$ 38.9'
Longitude	123 $^\circ$ 04.6'	123 $^\circ$ 05.7'
Material Analysed	Hornblende	Hornblende
K (wt %)	0.143	0.605
Radiogenic ^{40}Ar ($\times 10^{-6} \text{ cm}^3 \text{g}^{-1}$)		
0.5428	2.436	
% of total ^{40}Ar	41.2	77.2
Date	95.1 \pm 3.3 Ma	101 \pm 4 Ma

K was determined in duplicate by atomic absorption using a Techtron AA4 spectrophotometer and Ar by isotope dilution using an AEI MS-10 mass spectrometer and high purity ^{38}Ar spike. Errors reported are for 1 σ . The constants used are:

$$K\lambda_{\epsilon} = 0.581 \times 10^{-10} \text{y}^{-1}$$

$$K\lambda_{\beta} = 4.962 \times 10^{-10} \text{y}^{-1}$$

$$^{40}\text{K}/\text{K} = 0.01167 \text{ atom percent}$$

special significance in this, but infer that initial ratios of 0.70325 to 0.7035 are typical for the Cretaceous igneous suite of this area.

Two K-Ar dates were obtained (Table 71.3). A date of 95.1 ± 3.3 Ma was obtained for hornblende from a synmetamorphic hornblende vein cutting volcanic rocks north of The Nai. This age is interpreted as the age of crystallization of the vein minerals and consequently of metamorphism of the Sky Pilot area. This date is probably not reset or the result of slow cooling because the metamorphic temperatures probably did not exceed 500 $^\circ\text{C}$, the blocking temperature for Ar in hornblende. A date of 101 ± 4 Ma was obtained for hornblende from diorite south of the Squamish granodiorite. This is not necessarily the age of the diorite; temperatures of metamorphism, indicated by mineral assemblages in volcanic rocks close to the diorite, exceeded 500 $^\circ\text{C}$. The date probably reflects cooling from the metamorphic culmination associated with emplacement of the Squamish granodiorite.

Within experimental uncertainties, the K-Ar dates for the hornblende vein and the diorite are the same as the nearly concordant U-Pb, K-Ar and Rb-Sr dates for the Squamish granodiorite (White, 1968, and unpublished University of British Columbia data). The conclusion is that metamorphism of the Goat Mountain Formation and emplacement of the Squamish granodiorite were synchronous events. The diorite may be somewhat older but was probably associated with the same mid-Cretaceous culmination of thermal activity.

Strontium isotopic composition

In the Sky Pilot area, $^{87}\text{Sr}/^{86}\text{Sr}$ ratios are similar to those of back-arc basins, enriched mid-ocean ridges, island-arc tholeiites and calc-alkaline volcanics in the northeastern Pacific (Faure, 1977; Stern, 1982). The Sr isotopic ratios in these magmas may be increased from the values observed in depleted mid-ocean ridge basalt by several methods, including:

- contamination of the mantle-derived magma with ^{87}Sr from sialic rocks of the underlying crust;
- interaction of the seafloor with seawater before subduction and magma generation; and
- contamination of the magma source with subducted terrigenous sediment. In the Sky Pilot area, many of the volcanics are waterlain and variously altered. Reactions between the volcanic rocks and sea water may have further increased some $^{87}\text{Sr}/^{86}\text{Sr}$ ratios.

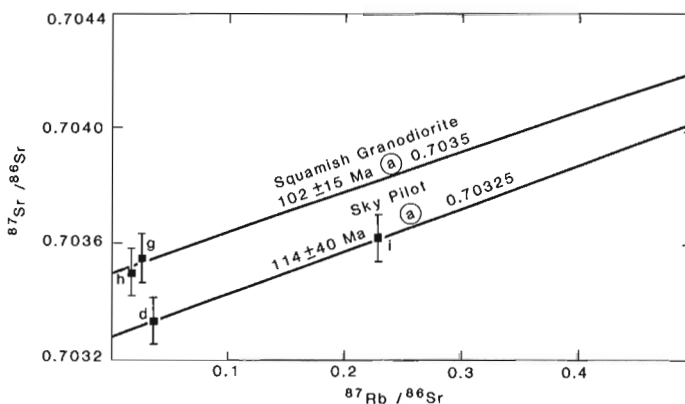


Figure 71.8. Rb-Sr isochron for the Goat Mountain Formation. The Squamish granodiorite isochron is based on unpublished data of R.L. Armstrong.

The low initial $^{87}\text{Sr}/^{86}\text{Sr}$ ratio of 0.70325 ± 0.00010 for the two most likely cogenetic and least altered of the four samples of the Sky Pilot volcanics indicates that they have a very slightly ^{87}Sr enriched upper mantle source. The initial $^{87}\text{Sr}/^{86}\text{Sr}$ ratio of 0.7035 ± 0.0002 for the Squamish granodiorite may be higher due to contamination with ^{87}Sr from the crust, but is not significantly different. The similarity between initial ratios and ages of the Sky Pilot volcanics and the Squamish granodiorite is compatible with a common upper mantle subduction zone source for both. However, the Sr isotopic data do not uniquely identify the source of the small amount of added ^{87}Sr .

Acknowledgments

Assistance in the field was provided by Peter van der Heyden, Pat Whiting, Chris Hrkac, Kevin Cawston, and Jim Beaton. K.L. Scott did the Rb/Sr, K, and Sr isotopic analyses. J.E. Harakal did the Ar analyses. S.J. Horsky supervised X-ray diffraction and fluorescence measurements.

References

- Barker, F. and Arth, J.G.
1976: Generation of trondhjemitic-tonalitic liquids and Archean bimodal trondhjemite-basalt suites; *Geology*, v. 4, p. 596-600.
- Berman, R.G.
1979: The Coquihala volcanic complex, southwestern British Columbia; unpublished M.Sc. thesis, University of British Columbia, 170 p.
- Bostock, H.S.
1963: Squamish Map-area; Geological Survey of Canada, Map 42-1963.
- Ermanovics, I.F., McRitchie, W.D., and Houston, W.N.
1979: Petrochemistry and tectonic setting of plutonic rocks of the Superior Province in Manitoba; in *Trondhjemites, Dacites and Related Rocks*, ed. F. Barker; Elsevier, Amsterdam, p. 323-362.
- Faure, G.
1977: Principles of isotope geology; John Wiley and Sons, Inc., N.Y., 464 p.
- Green, N.L.
1981: Geology and petrology of Quaternary volcanic rocks, Garibaldi Lake area, southwestern British Columbia; *Geological Society of America Bulletin*, Part 2, p. 1359-1470.
- Hawkins, J.W. Jr.
1977: Petrologic and geochemical characteristics of marginal basin basalts; in *Island arcs deep sea trenches and back-arc basins*, ed. M. Talwani and W.C. Pitman; American Geophysical Union, Maurice Ewing Series, Washington, D.C., v. 1, p. 355-365.
- Heah, T.S.T.
1982: Stratigraphy, geochemistry and geochronology of the Lower Cretaceous Gambier Group, Sky Pilot area, southwestern British Columbia; B.Sc. Thesis, University of British Columbia, 97 p.
- Irvine, T.N. and Baragar, W.R.A.
1971: A guide to the chemical classification of the common volcanic rocks; *Canadian Journal of Earth Sciences*, v. 8, p. 523-548.
- Jakes, P. and Gill, J.B.
1970: Rare earth elements and the island-arc tholeiite series; *Earth and Planetary Science Letters*, v. 9, p. 17-28.
- James, H.T.
1929: Britannia Beach map-area, British Columbia; Geological Survey of Canada, Memoir 158, 139 p.
- Payne, J.G., Bratt, J.A., and Stone, B.G.
1980: Deformed Mesozoic volcanogenic Cu-Zn sulfide deposits in the Britannia District, British Columbia; *Economic Geology*, v. 75, p. 700-721.
- Pearce, J.A. and Cann, J.
1973: Tectonic setting of basic volcanic rocks using trace element analyses; *Earth and Planetary Science Letters*, v. 19, p. 290-300.
- Roddick, J.A.
1965: Vancouver North, Coquitlam and Pitt Lake map-areas, British Columbia; Geological Survey of Canada, Memoir 335, 276 p.
- Roddick, J.A. and Woodsworth, G.J.
1979: Geology of Vancouver west half and mainland part of Alberni; Geological Survey of Canada, Open File 611.
- Schofield, S.J.
1918: Britannia map-area; Geological Survey of Canada, Summary Report, part B, p. 56-59.
1926: The Britannia mines, British Columbia; *Economic Geology*, v. 21, p. 271-284.
- Snyder, W.S., Dickinson, W.R., and Silberman, M.L.
1976: Tectonic implications of space-time patterns of Cenozoic magmatism in the western United States; *Earth and Planetary Science Letters*, v. 32, p. 91-106.
- Stern, C.R.
1980: Geochemistry of Chilean ophiolites: Evidence for the compositional evolution of the mantle source of back-arc basin basalts; *Journal of Geophysical Research*, v. 85, p. 955-966.
1982: Strontium isotopes from circum-Pacific intra-oceanic island arcs and marginal basins: Regional variations and implications for magma genesis; *Geological Society of America Bulletin*, v. 93, p. 477-486.
- Sun, S.S.
1980: Lead isotopic study of young volcanic rocks from mid-ocean ridges, ocean islands and island arcs; *Philosophical Transaction of the Royal Society of London*, A 297, p. 409-445.
- Van der Heyden, P.
1982: Tectonic and stratigraphic relationships between the Coast Plutonic Complex and Intermontane Belt, West Central Whitesail Lake map area, British Columbia; unpublished M.Sc. thesis, University of British Columbia, 122 p.
- White, W.H.
1968: Granitic rocks of southwestern British Columbia, in *Guidebook for geological field trips in southwestern British Columbia*; Department of Geology, University of British Columbia, Report No. 6.
- Winchester, J.A. and Floyd, P.A.
1977: Geochemical discrimination of different magma series and their differentiation products using immobile elements; *Chemical Geology*, v. 20, p. 325-343.
- York, D.
1967: The best isochron; *Earth and Planetary Science Letters*, v. 2, p. 479-482.

Metamorphism in the northern Adams River area, northeastern Shuswap Complex, Monashee Mountains, British Columbia

EMR Research Agreement 139

J.H. Sevigny¹ and E.D. Ghent¹
Cordilleran and Pacific Margin Division, Vancouver

Sevigny, J.H. and Ghent, E.D., Metamorphism in the northern Adams River area, northeastern Shuswap Complex, Monashee Mountains, British Columbia; *in* Current Research, Part B, Geological Survey of Canada, Paper 86-1B, p. 693-698, 1986.

Abstract

In the northern Adams River area, Monashee Mountains, British Columbia, metamorphic grade increases from sillimanite-muscovite zone to K-feldspar-sillimanite zone along a northwesterly trend parallel to the structural fabric. Metamorphic isograds mapped in pelitic rocks, in order of increasing grade are: kyanite out; K-feldspar-sillimanite in; and muscovite + quartz out. The metamorphic culmination, delineated by the trace of the last isograd, is characterized by extensive development of migmatite and injection of pegmatite, and the first occurrence of peraluminous granite. Garnet-hornblende Fe-Mg exchange thermometry yields mean temperature estimates of $672 \pm 7^\circ\text{C}$ and $680 \pm 5^\circ\text{C}$ for the sillimanite-muscovite and K-feldspar-sillimanite zones, respectively. Garnet-clinopyroxene geothermometry yields a mean temperature estimate of $675 \pm 11^\circ\text{C}$ for the higher grade zone. Calculated temperatures using garnet-biotite geothermometry exhibit considerable range (e.g., $670 \pm 27^\circ\text{C}$ and $665 \pm 20^\circ\text{C}$ for the above metamorphic zones).

Résumé

Dans la région nord du bassin de la rivière Adams dans les monts Monashee, en Colombie-Britannique, le degré de métamorphisme augmente de la zone à sillimanite et muscovite à la zone à feldspath potassique et sillimanite en direction générale du nord-ouest, parallèlement à l'orientation structurale. Les isogrades du métamorphisme cartographiés dans les roches pélitiques, en ordre de degré croissant, sont: le cyanite à l'extérieur; le feldspath potassique et sillimanite à l'intérieur; et la muscovite + quartz à l'extérieur. La culmination métamorphique délimitée par la trace du dernier isograde est caractérisée par un développement intense de la migmatite et une injection de pegmatite, et par une première manifestation de granite hyperalumineux. La thermométrie d'échange du Fe et du Mg dans les roches à grenat et hornblende donne des températures moyennes de $672 \pm 7^\circ\text{C}$ et $680 \pm 5^\circ\text{C}$ respectivement pour les zones à sillimanite et muscovite et à feldspath potassique et sillimanite. La géothermométrie appliquée aux roches à grenat et clinopyroxène donne une température moyenne de $675 \pm 11^\circ\text{C}$ pour la zone au degré de métamorphisme le plus élevé. Les températures calculées à l'aide de la géothermométrie appliquée aux roches à grenat et biotite font preuve d'une variation considérable (p. ex. $670 \pm 27^\circ\text{C}$ et $665 \pm 20^\circ\text{C}$ pour les zones métamorphiques susmentionnées).

¹ Department of Geology and Geophysics, University of Calgary, Calgary, Alberta T2N 1N4

Introduction

During the 1985 field season, mapping on a scale of 1:24 000 and extensive sampling were carried out in the northern Adams River area (52°N , 119°W), along the northeast margin of the Shuswap Metamorphic Complex, in the northern Monashee Mountains of southeastern British Columbia (Fig. 72.1). The purpose of the present study is twofold. The first is to delineate the metamorphic culmination, mapped in part by Raeside (1982), in the area north of Pat Creek; and the second is an understanding of the metamorphic evolution of this area through a detailed petrological study.

Regional geology

The geological setting of the area shown in Figure 72.1 has been discussed by Campbell (1968), Ghent et al. (1977), Simony et al. (1980), Pell and Simony (1981) and Raeside and Simony (1983). The following discussion summarizes their findings.

The northeast margin of the Shuswap Metamorphic Complex is underlain by approximately 5-6 km of metasedimentary and metavolcanic rocks of the Hadrynian Horsethief Creek Group which structurally overlies the Malton Gneiss, a sheet of tectonically mobilized Archean basement. The Horsethief Creek Group is a miogeoclinal

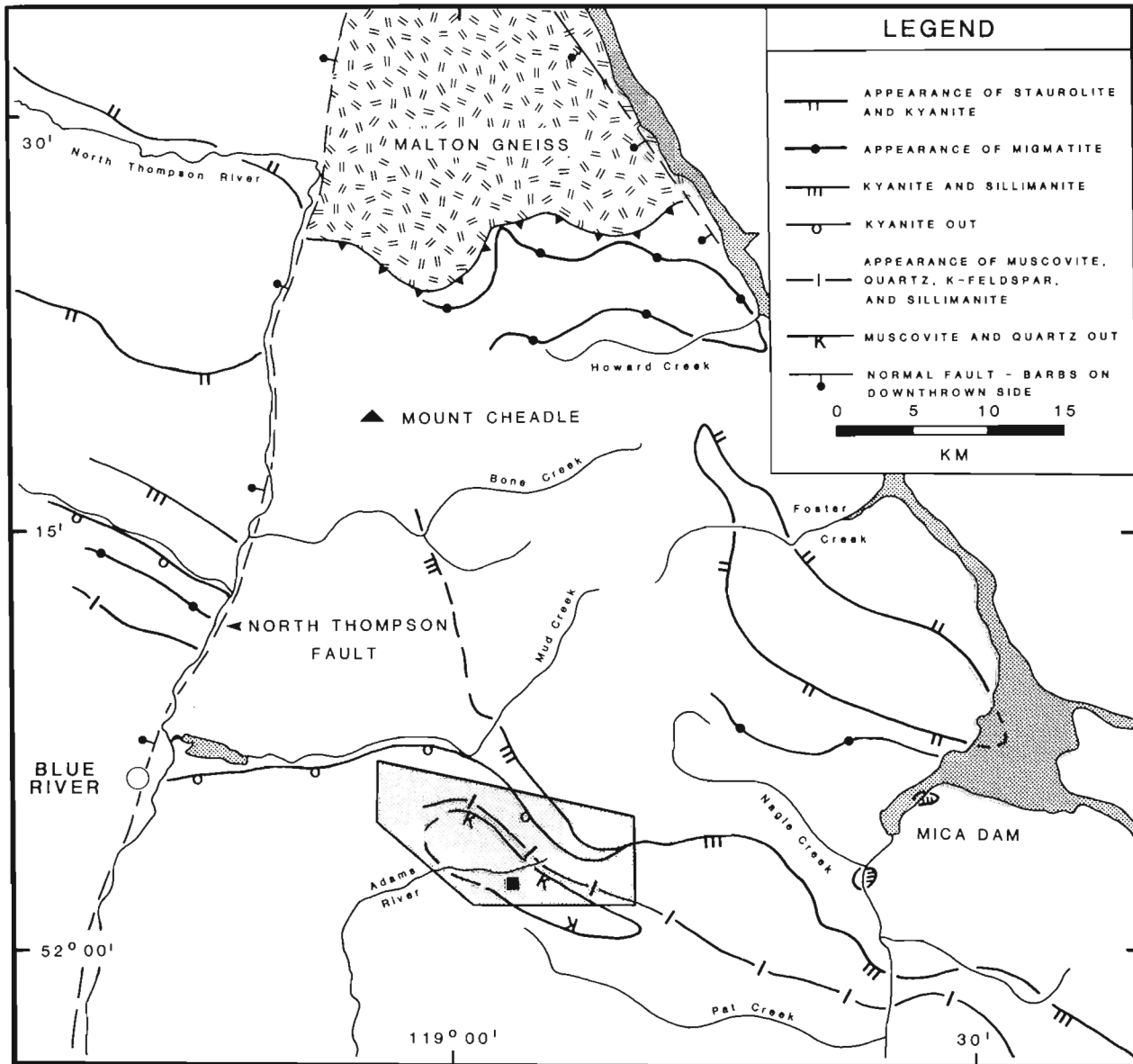


Figure 72.1. Map of the northeastern margin of the Shuswap Metamorphic Complex showing the location of presently mapped isograds in pelitic rocks. The study area is lightly shaded: the location of Figure 72.3 is shown by a filled square within the lightly shaded area. Isograds compiled from Knitter (1979), Leatherbarrow (1981), Pell (1984), Raeside (1982), Robbins (1976), R. Duchesne (personal communication, 1985), P.S. Simony (personal communication, 1985) and unpublished mapping from the senior author.

package characterized by, in descending stratigraphic order: an upper clastic division; the middle marble; a semipelite-amphibolite division; the lower marble or calc-silicate; a lower pelite division; and, at the base, a lower grit unit consisting of psammite, pelite and granule conglomerate. Marble and calc-silicate marker horizons allow the recognition of major structures.

Three major phases of folding (F_1 , F_2 , F_3) have been recognized in rocks of the Horsethief Creek Group in the area shown in Figure 72.1. The first folding episode (F_1) produced west-verging recumbent structures which were refolded by tight, northeast-verging F_2 folds to produce a SW-dipping stack of folds on which third phase folds (F_3) are locally imprinted. F_1 and F_2 folds are the products of superimposed coaxial deformations. Metamorphism, which occurred during the Columbian Orogeny, outlasted F_2 folding. F_3 folds are largely post-metamorphic and fold both earlier structures and metamorphic isograds.

Mesoscopic structures associated with F_1 and F_2 folds include a penetrative, axial-plane schistosity. Only in F_2 fold hinges can S_1 be distinguished from S_2 and, thus, this foliation surface is described as S_{1+2} . F_3 is manifested by folding of the S_{1+2} surface on planar F_2 limbs and is most commonly seen on a large scale.

Major faults shown in Figure 72.1 include the Malton Gneiss décollement and the North Thompson Fault. The latter structure, bounding the western margin of Figure 72.1, is a west-side-down normal fault which has juxtaposed two different metamorphic terranes as indicated by different isograd patterns across the fault. On the basis of a decrease in metamorphic pressure of about 150 MPa (1.5 kbar) westward across the North Thompson Fault, Pell and Simony (1981) argued for offset of about 4.0 km. The Malton décollement is marked by an extensive mylonite zone which represents the sheared contact between cover (Horsethief Creek Group) and basement.

As shown in Figure 72.1, metamorphism along the northeastern margin of the Shuswap Complex is in the amphibolite facies with grade increasing southwestward to a culmination in the northern Adams River area. Pelites of the Horsethief Creek Group are characterized by the development of migmatite and the injection of pegmatite. Mapping during 1985 has revealed that within the metamorphic culmination, as defined by the sillimanite-K-feldspar zone, continuous sheets and small bodies of peraluminous granite occur.

Metamorphism in the northern Adams River area

Metamorphic grade in the northern Adams River area ranges from sillimanite-muscovite zone to K-feldspar-sillimanite zone as shown in Figure 72.1. Metamorphic isograds mapped in pelitic rocks, in order of increasing grade are: kyanite-out; K-feldspar-sillimanite-in; and muscovite + quartz-out (see Ghent et al., 1982).

Rock types

A variety of rock types outcrop in the northern Adams River area including metasedimentary and metavolcanic rocks of the Horsethief Creek Group; pegmatite; and biotite-muscovite granite. As metamorphic grade increases from the sillimanite-muscovite zone to the K-feldspar-sillimanite zone, pelites become less schistose and more gneissic, and the abundance of migmatite and pegmatite increases dramatically, as does the occurrence of granite. In the K-feldspar-sillimanite zone, approximately 40% of the outcrop consists of a medium- to very coarse-grained biotite-muscovite granite.

Metapelites contain the mineral assemblage biotite + garnet + sillimanite + plagioclase + quartz \pm K-feldspar \pm muscovite. Garnet is subidioblastic to xenoblastic and characterized by inclusion-rich cores and inclusion-poor rims which truncate the foliation. In a few of the samples studied the external schistosity can be traced into the garnet rim thereby suggesting that garnet rims crystallized postkinematically. In the K-feldspar-sillimanite zone, metapelites lack primary muscovite, that is, muscovite intergrown with biotite in the plane of schistosity. However, in nearly all samples examined a secondary or retrogressive muscovite is present and overprints S_{1+2} , locally displaying a weak, planar fabric.

Amphibolites contain the mineral assemblage hornblende + plagioclase + ilmenite + sphene + garnet + apatite \pm quartz \pm biotite \pm scapolite \pm clinopyroxene. Bulk composition appears to be the primary factor controlling the mineral assemblage present. For example, in a restricted area of uniform metamorphic grade, amphibolites containing biotite lack clinopyroxene, whereas those with scapolite contain clinopyroxene. All amphibolites studied contain poikiloblastic garnet which range in size from 0.2 to 2.0 mm. Textural relations suggest that garnet grew statically, postdating formation of the metamorphic foliation.

Granite is predominantly medium- to coarse-grained and contains sodic plagioclase ($An_{13 \pm 3}$), perthitic orthoclase, quartz, muscovite, and biotite. Garnet is also common but sillimanite is rare. By far the majority of granitic rocks display a hypidiomorphic-granular texture although a weakly developed metamorphic fabric was observed in two samples and both of these contained coexisting garnet and sillimanite. Granite is chemically peraluminous (e.g., Clarke, 1981) as indicated by: (1) the coexistence of the diagnostic minerals muscovite and biotite and, in some samples, garnet; and (2) normative corundum in the CIPW norm. A suite of granites is currently being studied geochemically in order to understand their petrogenesis.

Field relations

Field relations between the above rock types are well exposed in the alpine areas surrounding the Adams River headwaters. Pegmatite is common and occurs as small, discontinuous lenses and dykes up to ten metres wide. In many localities lenses of pegmatite are difficult to distinguish from migmatite leucosome. Numerous generations of pegmatite can be documented which have intruded all rock types, including granite. Pegmatic intrusions predating F_2 structures are deformed and generally concordant with the metamorphic foliation (S_{1+2}). Other pegmatites cut F_2 structures whereas many have been folded by F_3 (Fig. 72.2A). A few pegmatites crosscut F_3 structures (Fig. 72.2B). The later pegmatites are discordant with respect to S_{1+2} . No significant compositional variations between successive generations of pegmatite were observed.

Granite was first encountered at or close to the muscovite + quartz-out isograd. As shown in Figure 72.3, a detailed geologic sketch map, granite passively intruded the country rock and did not distort the planar metamorphic fabric either on mesoscopic (Fig. 72.4) or on a regional scale in rocks of the Horsethief Creek Group. Intrusive contacts with the country rock are sharp and generally discordant with respect to S_{1+2} (Fig. 72.4). Chilled margins are not developed suggesting intrusion at elevated temperatures possibly at depth. Sheets of granite 5-50 m thick (Fig. 72.5), traceable for over a kilometre along strike, are typical of granitic occurrences. Internally, granite does not exhibit a flow foliation or metamorphic fabric. Granitic sheets are, however, well layered with layers concordant with intrusive contacts. Layering is defined by laterally continuous medium

grained and pegmatitic domains; later domains formed local segregations (Fig. 72.6). Contacts between domains are gradational and display no evidence of crystal settling or multiple injection (Fig. 72.7).

The timing of granitic intrusion, relative to folding is, at present, not well constrained. Granite cuts F_2 structures and appears to cut F_3 structures, however, unambiguous field relations have not been well documented. Thin section examination reveals that granite exhibits internal deformation as shown by strongly undulose quartz, bent or broken plagioclase twins, and kinked mica. Thus, granitic intrusion predates a mild deformational and/or folding event.

Metamorphic zones and isograds

Field mapping and petrographic analyses in conjunction with laboratory study of rocks collected by P. Doucet (see Doucet et al., 1985) have allowed us to: (1) trace isograds mapped by Raeside (1982) in the area north of Pat Creek westward into the northern Adams River area and across to the Mud Lake area, (2) locate the kyanite-out isograd precisely just south of Mud Creek, and (3) define the extent and position of the metamorphic culmination more accurately. Points 1, 2 and 3 are illustrated in Figure 72.1. Continued fieldwork in 1986 will allow us to locate the western and southwestern trace of the muscovite + quartz-out isograd (see dashed line on Fig. 72.1).

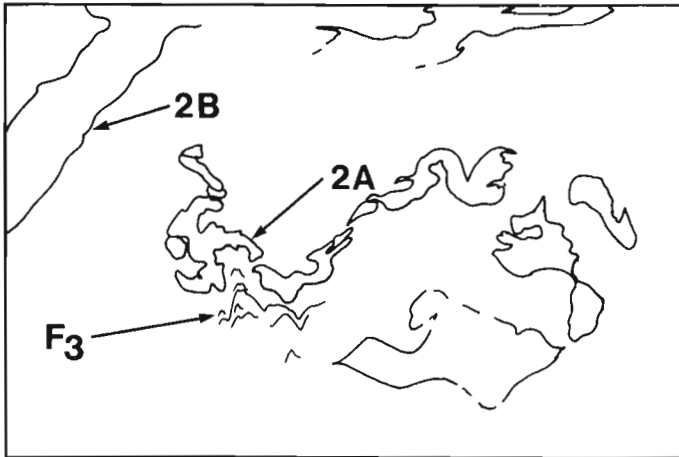


Figure 72.2. Field relations between folds and two generations of pegmatite: (A) folding of pegmatite by F_3 , and (B) intrusion of pegmatite postdating F_3 .

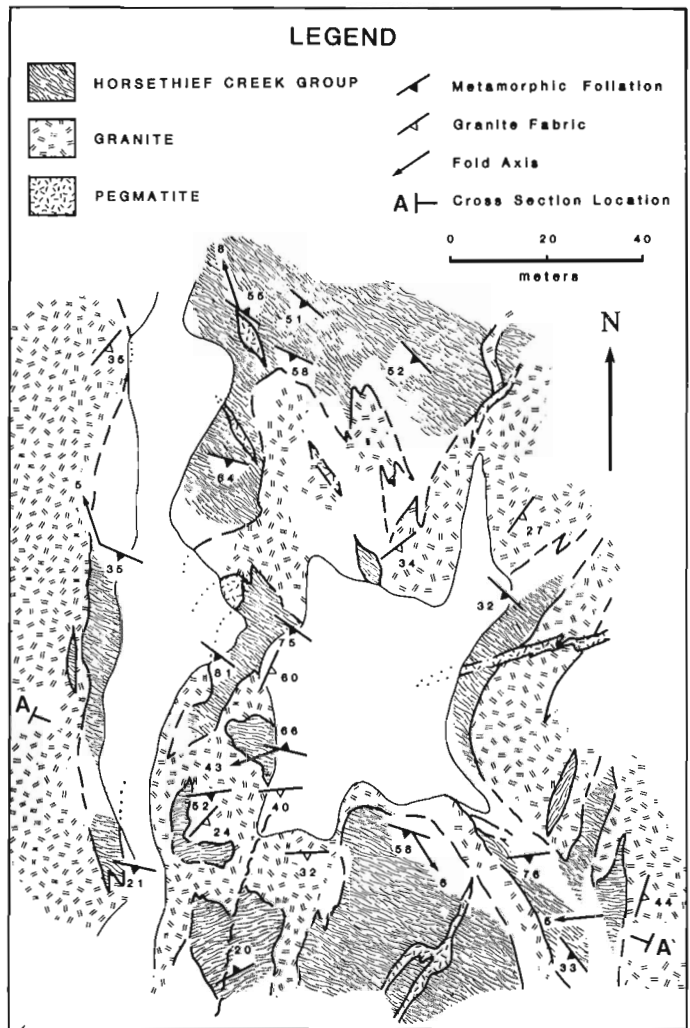


Figure 72.3. Detailed geological sketch map illustrating intrusive relations between granite, pegmatite, and Horsethief Creek Group rocks in the northern Adams River area. Location of Figure 72.3 is shown by the filled square inside the shaded box in Figure 72.1.

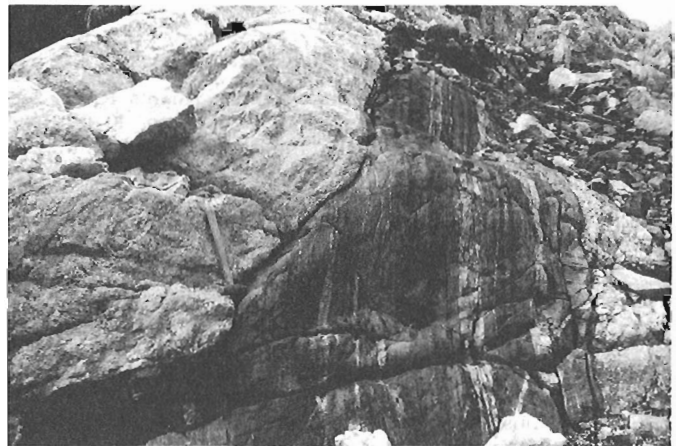


Figure 72.4. Sharp, discordant contact between light coloured granite and darker, gneissic metasedimentary rock in the northern Adams River area. Hammer is 45 cm long.

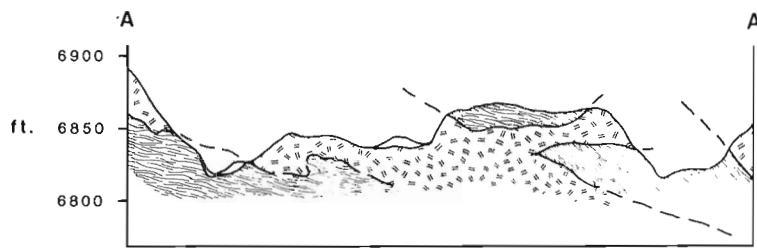


Figure 72.5

Cross-section illustrating intrusive relations between sheets and dykes of granite and country rock. Location of cross-section is shown in Figure 72.3.

Pressure and temperature estimates

Fe-Mg exchange thermometry has been applied to microprobe analyses of coexisting garnet-biotite in pelitic rocks, and garnet-hornblende and garnet-clinopyroxene in garnet amphibolites to estimate metamorphic temperatures. Pressures have been estimated from garnet-plagioclase- Al_2SiO_5 -quartz equilibria. Results of work in progress are briefly summarized below.

In the sillimanite-muscovite zone, the range in calculated garnet rim-biotite temperatures is 600 to 660°C (Thompson, 1976 calibration), 630 to 715°C (Ferry and Spear, 1979 calibration), and 610 to 685°C (Ganguly and Saxena, 1984 calibration). Temperatures were estimated using a pressure of 700 MPa (7.0 kbar). Nearly identical temperatures are recorded in the K-feldspar-sillimanite zone. Temperature estimates obtained using garnet core-matrix biotite compositions are higher by 20 to 45°C, but, in a few samples studied, are up to 95°C greater. Unfortunately, garnet core temperatures estimated with matrix biotite may not have petrological significance due to the possibility of disequilibrium.

Temperature estimates have been obtained from garnet amphibolites using the garnet-hornblende and garnet-clinopyroxene geothermometers of Graham and Powell (1984) and Ellis and Green (1979), respectively. Garnet rim-hornblende pairs yield temperature estimates (mean and one standard deviation) of $672 \pm 7^\circ C$ and $680 \pm 5^\circ C$ for samples in the sillimanite-muscovite and K-feldspar-sillimanite zones, respectively. In all samples studied thus far, garnet core temperatures are about 10-15°C lower than garnet rim temperatures, whereas hornblende inclusions in garnet yield temperatures intermediate between rim and core. Assuming equilibrium between garnet core and matrix hornblende, it appears that garnet grew in a regime of increasing temperature and, based on textural evidence, postdated development of the metamorphic foliation. Garnet rim-clinopyroxene temperature estimates using the calibration of Ellis and Green (1979), calculated at 700 MPa (7.0 kbar), are consistent with garnet-hornblende temperatures when both pyroxene and garnet are corrected for ferric iron (see Ghent et al., 1983, for a discussion of the ferric iron calculation).

In the northern Adams River area, calculated pressures using garnet-plagioclase- Al_2SiO_5 -quartz equilibria (Ghent et al., 1979) range from 680 to 830 MPa (6.8 to 8.3 kbar) with a mean value of 740 MPa (7.4 kbar). These pressure estimates are higher by about 50 MPa (0.5 kbar) than those reported by Ghent et al. (1982) in the Mica Creek area to the east. No structural evidence has been found to substantiate this pressure increase. Pressure estimates ranging from 540 to 590 MPa (5.4-5.9 kbar) have been reported by Ghent et al. (1983) from the Mica Creek area using the plagioclase-clinopyroxene-garnet-quartz geobarometer of Newton and Perkins (1982). Equilibria involving pelitic and basic rocks do not agree precisely although they do bracket the pressure between 550 and 750 MPa (5.5 and 7.5 kbar).

Temperature estimates presented in this study are consistent with published data. Ghent et al. (1982) reported nearly identical garnet core and slightly lower garnet rim

temperatures from pelitic rocks sampled from the eastward extension of the two metamorphic zones discussed in this report. Garnet-clinopyroxene temperature estimates with a mean and standard deviation of $678 \pm 18^\circ C$ were reported by Ghent et al. (1983) from samples at the K-feldspar-sillimanite-in isograd in the Mica Creek area to the east. This estimate is in excellent agreement with the present study suggesting that temperature does not increase westward along this isograd.

Conclusions

Field mapping and extensive sampling during 1985 in the northern Adams River area allowed us to trace isograds westwards thus partly delineating the extent of the metamorphic culmination, as defined by the K-feldspar-sillimanite zone, along the northeast margin of the Shuswap

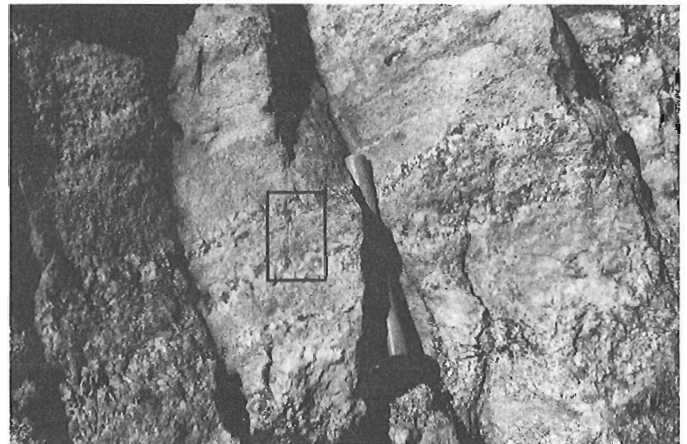


Figure 72.6. Well-layered biotite-muscovite granite in the northern Adams River area. Location of Figure 72.7 is shown by open box. Hammer is 45 cm long.

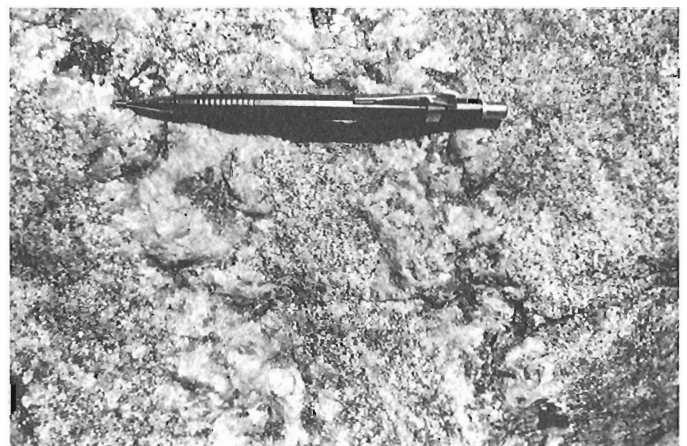


Figure 72.7. Close-up of Figure 72.6 showing the gradational contact between medium grained granite and pegmatitic granite. Location shown by open box in Figure 72.6.

Metamorphic Complex. Metamorphic grade increases from sillimanite-muscovite zone to K-feldspar-sillimanite zone, across the muscovite + quartz-out isograd, along a northwesterly trend parallel to the structural fabric. The metamorphic culmination is characterized by extensive development of migmatite and injection of pegmatite, and the first occurrence of peraluminous granite. Garnet-hornblende Fe-Mg exchange thermometry yields temperature estimates (mean and one standard deviation) of $672 \pm 7^\circ\text{C}$ and $680 \pm 5^\circ\text{C}$ for the sillimanite-muscovite and K-feldspar-sillimanite zones, respectively. Garnet-clinopyroxene geothermometry yields a temperature estimate of $675 \pm 11^\circ\text{C}$ for the higher grade zone. Calculated temperatures using garnet-biotite geothermometry exhibit considerable range (e.g., $670 \pm 27^\circ\text{C}$ and $665 \pm 20^\circ\text{C}$ for the above metamorphic zones).

References

- Campbell, R.B.
1968: Canoe River, British Columbia; Geological Survey of Canada, Map 15-1967.
- Clarke, D.B.
1981: The mineralogy of peraluminous granites: a review; *The Canadian Mineralogist*, v. 19, p. 3-17.
- Doucet, P., Ghent, E.D., and Simony, P.S.
1985: Metamorphism in the Monashee Mountains east of Blue River, British Columbia; in *Current Research, Part A*, Geological Survey of Canada, Paper 85-1A, p. 69-71.
- Ellis, D.J. and Green, D.H.
1979: An experimental study of the effect of Ca upon garnet-clinopyroxene Fe-Mg exchange equilibria; *Contributions to Mineralogy and Petrology*, v. 71, p. 13-22.
- Ferry, J.M. and Spear, F.S.
1979: Experimental calibration of the partitioning of Fe and Mg between biotite and garnet; *Contributions to Mineralogy and Petrology*, v. 66, p. 113-117.
- Ganguly, J. and Saxena, S.K.
1984: Mixing properties of aluminosilicate garnets: constraints from natural and experimental data, and applications to geothermo-barometry; *American Mineralogist*, v. 69, p. 88-97.
- Ghent, E.D., Knitter, C.C., Raeside, R.P., and Stout, M.Z.
1982: Geothermometry and geobarometry of pelitic rocks, upper kyanite and sillimanite zones, Mica Creek, British Columbia; *The Canadian Mineralogist*, v. 20, p. 295-305.
- Ghent, E.D., Robbins, D.B., and Stout, M.Z.
1979: Geothermometry, geobarometry, and fluid compositions of metamorphosed calc-silicates and pelites, Mica Creek, British Columbia; *American Mineralogist*, v. 64, p. 874-885.
- Ghent, E.D., Simony, P.S., Mitchell, W., Perry, J., Robbins, D., and Wagner, J.
1977: Structure and metamorphism in the southeast Canoe River area, British Columbia; in *Report of Activities, Part C*, Geological Survey of Canada, Paper 77-1C, p. 13-17.
- Ghent, E.D., Stout, M.Z., and Raeside, R.P.
1983: Plagioclase-clinopyroxene-garnet-quartz equilibria and the geobarometry and geothermometry of garnet amphibolites from Mica Creek, British Columbia; *Canadian Journal of Earth Sciences*, v. 20, p. 699-706.
- Graham, C.M. and Powell, R.
1984: A garnet-hornblende geothermometer: calibration, testing, and application to the Pelona Schist, Southern California; *Journal of Metamorphic Geology*, v. 2, p. 13-31.
- Knitter, C.C.
1979: Metamorphism and structure of the Soards Creek area, British Columbia; unpublished M.Sc. thesis, University of Calgary, Alberta.
- Leatherbarrow, R.W.
1981: Metamorphism of pelitic rocks from the northern Selkirk Mountains, southeastern British Columbia; unpublished Ph.D. thesis, Carleton University, Ottawa.
- Newton, R.C. and Perkins, D., III.
1982: Thermodynamic calibration of geobarometers based on the assemblage garnet-plagioclase-orthopyroxene (clinopyroxene)-quartz; *American Mineralogist*, v. 67, p. 203-222.
- Pell, J.
1984: Stratigraphy, structure, and metamorphism of Hydrinian strata in the southeastern Cariboo Mountains, B.C.; unpublished Ph.D. thesis, University of Calgary, Alberta.
- Pell, J. and Simony, P.S.
1981: Stratigraphy, structure, and metamorphism in the southern Cariboo Mountains, British Columbia; in *Current Research, Part A*, Geological Survey of Canada, Paper 81-1A, p. 227-230.
- Raeside, R.P.
1982: Structure, metamorphism, and migmatization of the Scrip Range, Mica Creek, British Columbia; unpublished Ph.D. thesis, University of Calgary, Alberta.
- Raeside, R.P. and Simony, P.S.
1983: Stratigraphy and deformational history of the Scrip Nappe, Monashee Mountains, British Columbia; *Canadian Journal of Earth Sciences*, v. 20, p. 639-650.
- Robbins, D.B.
1976: Metamorphism and structure of the Encampment Creek area, British Columbia; unpublished M.Sc. thesis, University of Calgary, Alberta.
- Simony, P.S., Ghent, E.D., Craw, D., Mitchell, W., and Robbins, D.B.
1980: Structural and metamorphic evolution of northeast flank of Shuswap Complex, southern Canoe River area, British Columbia; *Geological Society of America, Memoir 153*, p. 445-461.
- Thompson, A.B.
1976: Mineral reactions of pelitic rocks. I. Predictions of P-T-X (Fe-Mg) phase relations. II. Calculation of some P-T-X (Fe-Mg) phase relations; *American Journal of Science*, v. 276, p. 401-454.

Geology between Harrison Lake and Fraser River, Hope map area, southwestern British Columbia

Project 800029

J.W.H. Monger
Cordilleran and Pacific Margin Division, Vancouver

Monger, J.W.H., Geology between Harrison Lake and Fraser River, Hope map area, southwestern British Columbia; in *Current Research, Part B, Geological Survey of Canada, Paper 86-1B*, p. 699-706, 1986.

Abstract

The southeasternmost one-third of the Coast Plutonic Complex (CPC), near latitude 50°N, contains rocks and structures correlative with those in the Cascade Fold Belt to the south. In the CPC between Harrison Lake and Fraser River, greenschist to amphibolite metamorphic-grade rocks comprise three lithologically distinctive packages which can be correlated with little metamorphosed protolith strata of mainly early Mesozoic age in flanking and along-strike areas. These packages were structurally juxtaposed, metamorphosed, and intruded by syntectonic Spuzzum intrusions of late Early to mid-Cretaceous age, and subsequently were cut by major, steeply dipping and vertical faults trending north-northwest. Strongly developed, shallowly plunging, stretching lineations along these faults, higher metamorphic grade rocks in the hanging walls of faults with possible steep dips, and dip directions of related cleavages, suggest that the faults formed in a transpressive structural regime. All structures are offset 80-100 km by the north-trending, early Tertiary, Fraser River-Straight Creek dextral wrench-fault system.

Résumé

Le tiers le plus au sud du Complexe plutonique côtier (CPC), près du 50° de latitude N, contient des roches et des structures qui correspondent à celles de la zone de plissements Cascade au sud. Dans le CPC, entre le lac Harrison et le fleuve Fraser, les roches métamorphiques qui vont du faciès des schistes verts à celui des amphibolites comprennent trois lithologies distinctes qui peuvent être mises en corrélation avec de petites strates protolithiques de nature métamorphisée datant principalement du Mésozoïque inférieur dans les régions latérales et le long des failles. Ces ensembles ont été juxtaposés, métamorphisés et pénétrés structurellement par des intrusions syntectoniques de Spuzzum de la fin du Crétacé supérieur au Crétacé moyen, et ont ensuite été coupés par d'importantes failles verticales à pente abrupte et d'orientation nord-nord-ouest. Des linéations allongées et très prononcées plongeant peu profondément dans le sol le long de ces failles, des roches à degré métamorphique élevé dans les parois suspendues des failles dont le pendage est parfois abrupt, et les directions de pendage des clivages connexes semblent indiquer que les failles se sont formées dans un système structural transpressif. Toutes les structures ont été déplacées de 80 à 100 km par le réseau de failles de décrochement dextre orienté vers le nord de Fraser River-Straight Creek, datant du début du Tertiaire.

Introduction

This is a progress report, along with accompanying papers by Arthur (1986) and O'Brien (1986), on the preliminary results of fieldwork carried out in 1985 in parts of Hope (NTS 92H) map area.

The west half of Hope map area, between 49 and 50° latitude and 121 and 122° longitude, consists mainly of the Cascade Fold Belt (Roddick et al., 1979) in its southern and eastern parts, and the Coast Plutonic Complex in its northern and western parts (Fig. 73.1). This division is based partly on physiography with a somewhat arbitrary dividing line along the Fraser River (Holland, 1964), and partly on the higher proportion of granitic rock in the Coast Plutonic Complex, but many rock units are common to both. The Cascade Fold Belt consists of a high grade metamorphic and granitic core that formed mainly in Cretaceous time, and is flanked on the east and west by little metamorphosed rocks. To the north, this core forms the southeastern part of the Coast Plutonic Complex between Harrison Lake and Fraser River. East of the core are Permian to Middle Jurassic strata of the Hozameen Group, east of which again are Triassic to Cretaceous mainly sedimentary strata of the Methow Trough (see O'Brien, 1986). West of the core and south of Fraser River are upper Paleozoic strata of the Chilliwack Group, and overlying lower Mesozoic strata of the Cultus Formation (Monger, 1970). To the north, across Fraser River and mainly west of Harrison Lake, are Middle Triassic to Cretaceous strata (see Arthur, 1986). The regional north-northwest-trending fabric which formed in mid-Cretaceous to earliest Tertiary time was disrupted and offset 80-100 km in the Eocene by the north-trending Fraser River-Straight Creek dextral wrench-fault system (Monger, 1985a).

This report mainly outlines the lithology and structural relationships of those rocks in the metamorphic core which lie north of Fraser River, and between Harrison Lake on the west and the Fraser River fault system on the east, and summarizes the regional structural evolution. This area is regionally important in that it is one place where an apparent transition from low to high grade metamorphic rocks can be observed on the west side of the Cascade Fold Belt. Elsewhere, blueschist facies rocks of the Shuksan Metamorphic Suite (Misch, 1966) are juxtaposed to the east against high grade, Barrovian metamorphic rocks of the core across the Straight Creek dextral wrench-fault.

Many detailed studies have been made in this area, in large part as student thesis research, but no recent regional summary incorporating all of these details has been undertaken. Studies prior to 1970 were summarized in the compilation by Monger (1970), which incorporated the regional synthesis of Misch (1966). Since 1970, detailed investigations have been made of granitic rocks (Richards, 1971; Richards and McTaggart, 1976; Vining, 1977), and of metamorphic rocks and structure (Reamsbottom, 1971, 1974; Lowes 1972; Pigage, 1973, 1976; Bartholemew, 1979; Gabites, 1985). Davis et al. (1978) attempted a regional synthesis based partly on stratigraphic correlations, and most recently Cowan and Potter (in press) and Brown (in press) have presented new interpretations of (North) Cascade structure, metamorphism and evolution, based on data acquired mainly south of 49 degrees.

Acknowledgments

In 1985, the writer was ably assisted in the field by Dave Handel, Steve Irwin and Mary Maclean. Independent mapping carried out by Andrew Arthur and Jennifer O'Brien towards M.Sc degrees at, respectively, the Universities of British Columbia and Arizona, was funded by this project, as was radiolarian sampling by Fabrice Cordey, Université Pierre et Marie Curie, Paris.

Lithostructural packages

Within the Cascade Fold Belt in Canada and its extension to the north in the southeastern part of the Coast Belt, and west of the Fraser River-Straight Creek fault system, are five major rock packages, excluding granitic rocks. They are either known to be or are possibly partly coeval with one another, but are lithologically distinct. Some have different structural styles and metamorphic grades from others, and they are separated from one another by faults (Fig. 73.2, 73.3). To avoid the premature use of formal stratigraphic nomenclature for these poorly known rocks, the neutral lithostructural term "package" is used herein. Earlier Monger (1985b) called some of them "small terranes" which lie between the Intermontane superterrane to the east and the Insular superterrane to the west. North of Fraser River, from west to east and in order of increasing metamorphic grade, these packages are called herein Harrison Lake, Slollicum, Cogburn, and Settler packages. South of Fraser River are the Chilliwack-Cultus and Darrington (?) packages.

Harrison Lake package

The Harrison Lake package is exposed on the west side of Harrison Lake and comprises a stratigraphic succession of sedimentary and volcanic rocks which range from Middle Triassic to Early Cretaceous (Fig. 73.2, 73.3). These rock units, described by Arthur (1986), were originally named by

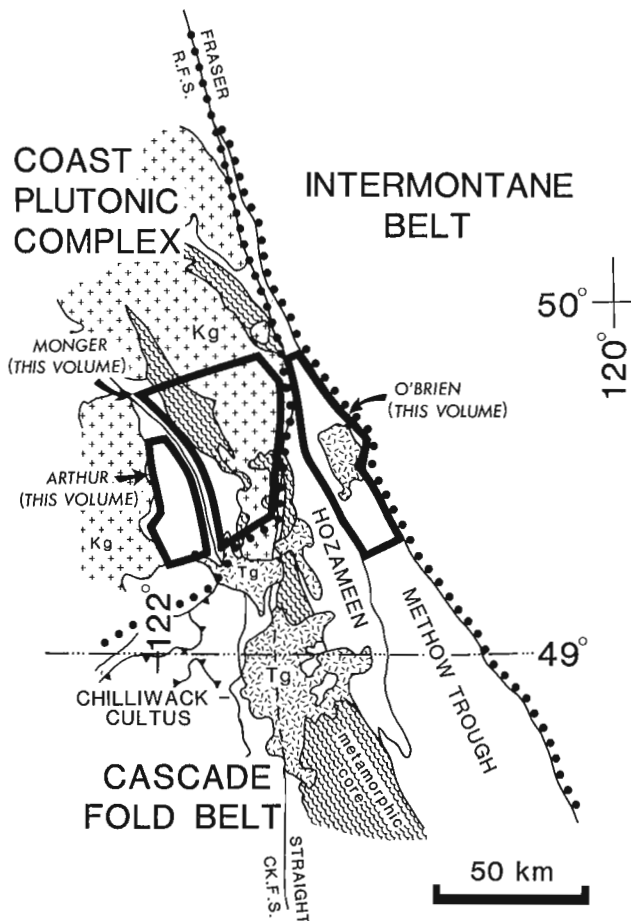


Figure 73.1. Index map of Cascade Fold Belt and southeastern Coast Plutonic Complex, showing geological/physiographic belts, major structural elements and location of areas discussed here and in accompanying papers by Arthur (1986) and O'Brien (1986).

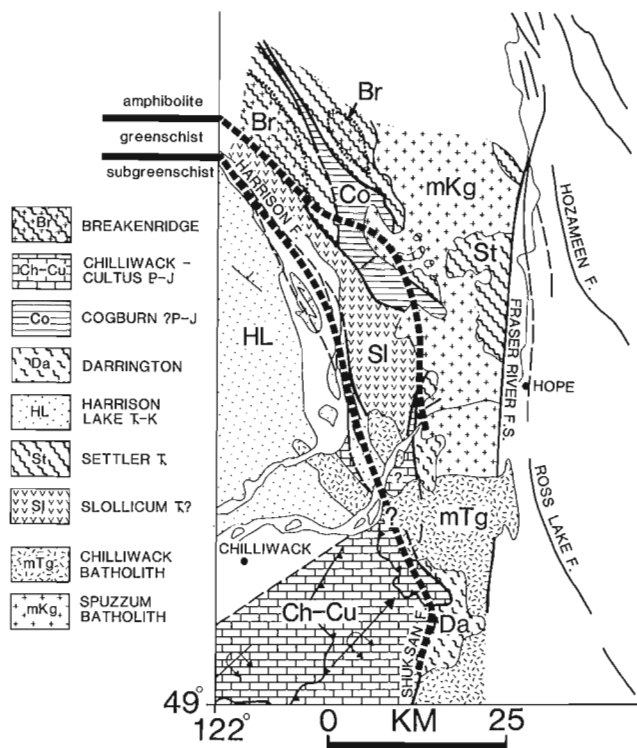


Figure 73.2. Distribution of lithostructural packages in the Cascade Fold Belt, southeastern Coast Belt, west of the Fraser River fault system.

Crickmay (1925, 1930) and are, from base to top: (1) Camp Cove Formation (Middle Triassic, from radiolaria identified by F. Cordey, personal communication, 1986), (2) Harrison Lake and Echo Island formations (Early and Middle Jurassic), (3) Mysterious Creek and Billhook formations (Late Jurassic), and (4) Peninsula and Brokenback Hill formations (Early Cretaceous). The package is penetratively deformed only near its eastern limit, where it lies close to the Harrison Fault. Subgreenschist facies metamorphism is typical of the package as a whole, with local extensive hydrothermal alteration, and lawsonite, a mineral found in many low grade metamorphic rocks west of the Cascade core, is present locally in Cretaceous strata (M. Brandon, personal communication, 1985). The basal conglomerate of the Harrison Lake Formation, of Toarcian age, contains numerous partly decalcified limestone clasts with local Early Permian schwagerinid fusulinids and common rhomboporoid bryozoans, which are forms common in Permian limestone of the Chilliwack Group. These clasts suggest that a stratigraphic linkage existed in Early Jurassic time between rocks west of Harrison Lake and the Chilliwack-Cultus package south of Fraser River.

Slollicum package

The Slollicum package includes those rocks mapped as Chilliwack Group by Lowes (1972) east of Harrison Lake, which Crickmay (1925, 1930) had called Slollicum Series (Fig. 73.2). Since there appears to be little similarity between Chilliwack Group and these rocks, the writer prefers the term "Slollicum".

Slollicum rocks are mainly schistose basic to intermediate and locally felsic flows and volcanoclastics, with pillow structures and volcanic breccias of varying coarseness

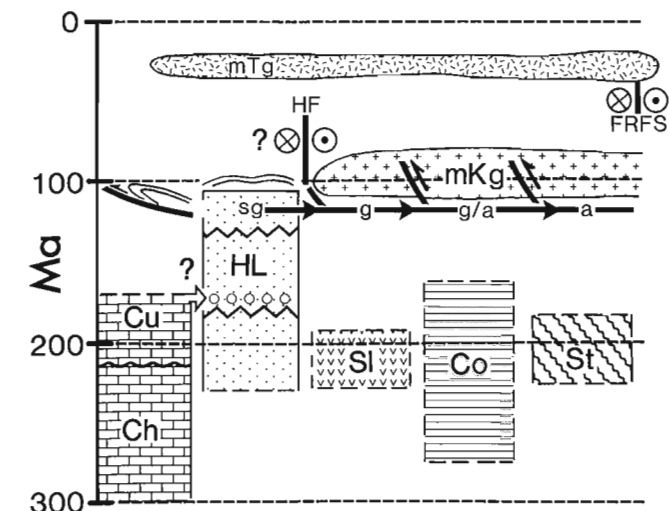
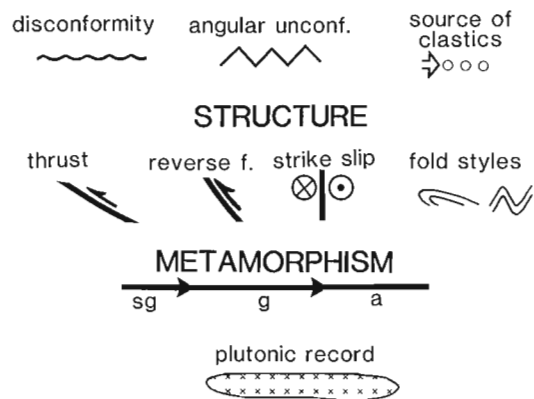


Figure 73.3. Time-space diagram, showing ages, probable ages and relationships between lithostructural packages, granitic intrusions, metamorphism and structure.

preserved in places. Interbedded with the volcanics are dark grey to black pelites, that locally contain conglomerates composed of flattened cobbles and pebbles of carbonate and quartz-eye porphyry in a pelitic matrix. The rocks are typically penetratively deformed and recrystallized, and most are metamorphosed regionally to greenschist facies, with the highest grade rocks in eastern exposures, featuring garnet and biotite, probably belonging to lower amphibolite facies. A strong northeast-trending, northeast-plunging linear fabric is developed locally (Fig. 73.4).

The age of the unit is not known although felsic volcanic rocks were sampled in 1986 for U-Pb dating. In general lithology, and particularly in conglomerate composition, the package most closely resembles the little metamorphosed Upper Triassic Cadwallader Group (Rusmore, 1985), whose type area is 180 km to the north-northwest, more or less along regional strike.

Cogburn package

East of the Slollicum lies a distinctive package of bedded chert, argillite, basic volcanics, ultramafic rocks and minor marble (Fig. 73.2). Lowes (1972) included it within the assemblage he mapped as Chilliwack Group (Slollicum package herein), but Gabites (1985) extracted it as the

Cogburn Creek Group. The rocks range in metamorphic grade from greenschist in the south, to amphibolite grade in the north. The foliation in this unit is typically parallel with compositional layering and generally steeply dipping or vertical. Separating the Cogburn and Slollicum packages in places are metadiorite and metagabbro that Lowes (1972) suggested were lithologically similar to the Yellow Aster Complex of the Washington Cascades (see Misch, 1966); recently Gabites (1985) obtained a highly discordant U-Pb date from the metadiorite, which is supportive but not proof of this suggestion.

The age of the Cogburn package is not known. Gabites (1985) noted, and the writer agrees, that the range of lithologies is similar to that of the Permian to Jurassic Hozameen and Bridge River groups, which flank the metamorphic core on the east side.

Settler package

The Settler Schist (Lowes, 1972; Pigage, 1973, 1976; Bartholemew, 1979; Gabites, 1985) comprises dominant pelitic and quartzofeldspathic schist, amphibolite, locally

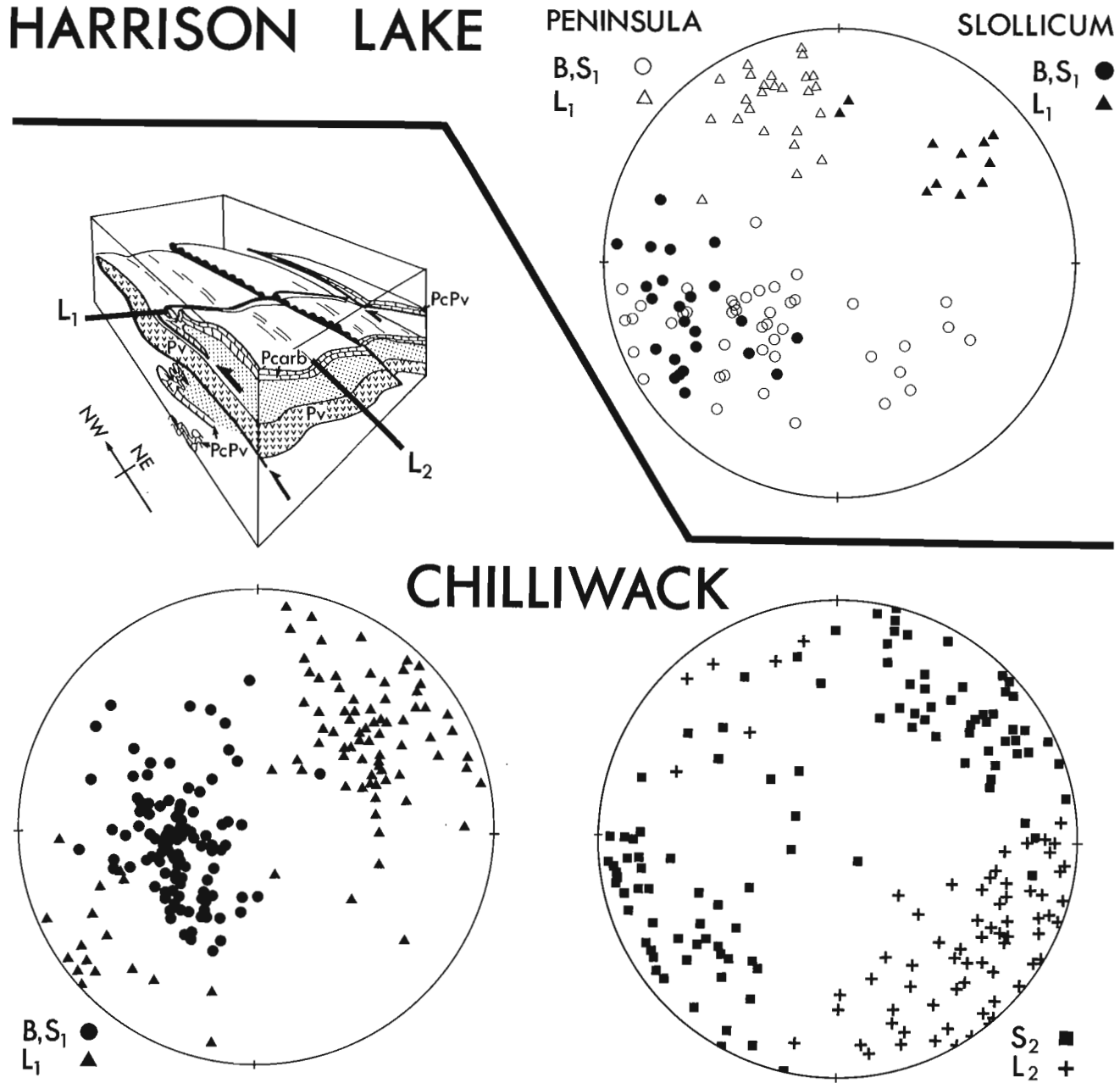


Figure 73.4. Plots of structural elements from Cretaceous rocks of the Harrison Lake, Slollicum, and (from Monger, 1966) Chilliwack-Cultus packages. B=bedding, S1=first (slaty) cleavage; L1=, for Chilliwack, minor first fold axes, bedding/cleavage intersections, L1=, for Harrison Lake, Slollicum, stretching lineations; S2=second (crenulation) cleavage, L2=minor second fold axes, intersections of second cleavage with B and S1. Inset is a sketch of major structures in the Chilliwack valley.

with relict pillow structures, minor quartzite, which is probably metachert, and minor ultramafic rocks. The metamorphic grade is entirely within amphibolite facies, with distinctive high-Al staurolite schist, and extensive kyanite- and sillimanite-bearing schists, with the latter occurring particularly near contacts with the Spuzzum intrusions. The Settler package is structurally conformably underlain by homogenous, typically fine grained, grey gneiss, migmatite, and amphibolite of the Breakenridge Formation (Reamsbottom, 1971, 1974), which outcrops in two domes in the northwestern part of the area (Fig. 73.2).

Rb-Sr isochrons (scatterchons) by Bartholomew (1979) and Gabites (1985) of, respectively, 214 ± 32 Ma and 210 ± 27 Ma are interpreted by Gabites to date either Triassic-Jurassic deposition of the Settler package, or else partial to complete resetting of pre-Jurassic rocks by Mesozoic metamorphism. The protolith of the Settler is generally similar lithologically to little metamorphosed Triassic-Jurassic strata (Spider Peak Formation, Ladner Group) which form the lower part of the succession in the Methow trough to the east (O'Brien, 1986). Lowes (1972) correlated the Settler Schist with the Chiwaukum Schist of the Washington Cascades on the basis of lithological similarity. An additional possible correlation is with quartzose pelites of low metamorphic grade that outcrop along strike south of Fraser River and which speculatively are correlated with the Darrington Phyllite of the Washington Cascades (below), although the age of the latter is considered by Armstrong (1980) to be most probably Jurassic on the basis of Rb-Sr isotope studies.

Chilliwack-Cultus package

The Chilliwack Group (Pennsylvanian-Permian in British Columbia; Devonian to Permian in Washington) and the stratigraphically overlying Cultus Formation (Late Triassic-Early Jurassic) consist of pelite, carbonate, mafic to felsic flows and volcanoclastic rocks (Monger, 1970, 1977). The package is exposed mainly south of Fraser River, but as noted by Crickmay (1930), it extends north of Fraser River near the southeastern extremity of Harrison Lake. There, crinoidal limestone containing mid-Carboniferous conodonts (M.J. Orchard, personal communication, 1985) is associated with pelite and sandstone containing volcanic quartz. At that place, the package lies west of the Harrison Fault, and so apparently is in the same structural block as the Harrison Lake package (Fig. 73.3). South of Fraser River, in the Chilliwack valley, fossiliferous Permian limestone forms a marker within the package which indicates a large structure of northwesterly overturned, northeast-trending recumbent folds, separated by thrust faults (Fig. 73.4; Monger, 1966). The package is penetratively deformed and the orientation of the early fold axes and related linear structures is similar to that of stretching lineations in the Slollicum package (Fig. 73.4). Later folds are crenulations and kink-bands, with a predominantly west-southwest vergence, and north-northwest trend, which is generally similar to that of lineations developed along the Harrison Fault (see below). The metamorphic grade is subgreenschist, and lawsonite is present in both Paleozoic and Mesozoic rocks.

The Chilliwack-Cultus package is bounded on the east by a major fault, which is probably the northward extension of the Shuksan thrust as mapped by Misch (1966). Across the fault are gabbroic rocks and amphibolite, probably correlative with the Yellow Aster Complex of Misch (1966), and rocks tentatively correlated with Darrington Phyllite.

Darrington(?) package

Rocks in Nesakwatch and Foley creeks in the eastern part of the Chilliwack valley, and east of Wahleach Creek south of Fraser River, are dark grey pelites, siltstones, and "grits" with angular quartz fragments in a pelitic matrix. Many of these rocks contain contact metamorphic biotite and andalusite porphyroblasts related to nearby Tertiary granitic intrusions. In places and locally within the same outcrop, these rocks exhibit quartz segregations parallel with bedding, and elsewhere bedding which becomes brecciated. In the Chilliwack Valley they lie east of rocks correlated with the Yellow Aster Complex of Misch (1966; see Monger, 1970; Jewett and Brown, 1985), and are on trend with strata of the Shuksan metamorphic suite; for these reasons and their general lithological similarity, they are considered to be probable correlatives of the Darrington Phyllite.

Structural relationships between packages

Harrison Lake/Slollicum relations

The Harrison Lake package is bounded by the major Harrison Fault on its east side, which was first recognized by Crickmay (1930). Cretaceous strata on the northwest shore of Harrison Lake, on the eastern three-quarters of Long Island, and in the neck of Cascade Peninsula on the east side of Harrison Lake, develop a strong cleavage which dips $50-70^\circ$ to the east (Fig. 73.4). The zone of cleavage development is 1-2 km wide, but has no marked linear fabric within it. East of this is a zone about 1 km wide within which an extremely strong linear fabric is present. Clasts in conglomerates are stretched and Early Cretaceous clamshells are distorted and locally drawn out into cigar-like forms that are only recognizable as fossils because of the gradation between them and less distorted fossils elsewhere. The elongation direction is about $N340^\circ$, with northward plunges $10-30^\circ$ (Fig. 73.4). As noted above, this orientation is similar to that of the later structures in the Chilliwack valley (Fig. 73.4). Immediately east of this are greenschist grade rocks of the Slollicum schist, which typically have northeast-trending mineral and stretching lineations (Fig. 73.4) and are truncated by the fault. It is possible to draw two conclusions from these observations. Firstly, the strong subhorizontal stretching lineations in Cretaceous rocks near the Harrison Fault indicate strike-slip movement on it. Secondly, if the northeast-dipping cleavage in subgreenschist-grade Early Cretaceous strata west of the fault indicates the attitude of the fault, then the juxtaposition of these rocks against higher grade, greenschist, Slollicum rocks, with their northeast-trending lineations, to the east, suggests that the fault as exposed near Cascade Peninsula developed in a transpressive regime which postdates metamorphism of the Slollicum schist and the development of its northeasterly trending fabric.

The Harrison Fault appears to be the westernmost of a family of major north-northwest-trending faults, several of which display along them north-northwest stretching lineations indicative of strike-slip displacements (Fig. 73.5). From west to east, other major, named, faults are: (1) the Ross Lake Fault, on which Haugerud (1985) reported northwest-trending horizontal lineations, and possible northerly segments called the "Kwoiek" (informal name), Bralorne and Tzchaikazan faults, (2) the Hozameen and Yalakom faults, which at the Coquihalla River shows north-northwest stretching lineations with the same orientation as structures on the Harrison Fault, and (3) easternmost, the Pasayten Fault. Evidence for mainly dextral strike-slip displacements has been reported for segments of several of these faults, as summarized by Kleinspehn (1985), although Lawrence (1978) reported petrofabric data indicating sinistral shear on the Pasayten Fault.

The age of these structures would appear to be Late Cretaceous and/or early Tertiary. They clearly postdate regional metamorphism and intrusion of the mid-Cretaceous Spuzzum batholith. In the Methow Trough, rocks as young as early Late Cretaceous are in fault basins bounded by the north-northwest-trending faults, and Haugerud (1985) presented evidence to show that stretching fabrics on the Ross Lake Fault are Eocene.

Slollicum/Cogburn/Settler relations

The Slollicum, Cogburn, and Settler packages appear to be structurally conformable, separated mainly by layer-parallel faults across which there is metamorphic continuity. Although the Slollicum is mainly of greenschist grade and the Settler entirely amphibolite, the metamorphic boundary between the two grades is locally within the easternmost parts of the Slollicum and cuts across the Cogburn package (Figs. 73.2, 73.3). Near Cogburn Creek the contact between Slollicum and Cogburn is marked by the belt of ultramafic rocks (mainly metamorphosed dunite and peridotite) which lies along the southwest side of Talc Creek. To the north, the Cogburn package forms an elongate sliver within a major synform in Settler Schist that lies between the two Breakenridge gneiss domes. In places, the contact between Cogburn and Settler packages, well exposed on ridges west of Mt. Urquhart, is marked by slivers of ultramafic rock, and is generally conformable with the local foliation. To the south the contact between Slollicum, Cogburn and Settler packages is largely obliterated by intrusive rock of the Spuzzum batholith, but locally is exposed near the lower part of Ruby Creek, where Cogburn chert and ultramafics separate Slollicum greenschists and phyllites to the west from Settler pelitic schist and amphibolite to the east. These relationships suggest that the structural juxtaposition of the three packages is related to their fabric and was pre- and syn-metamorphic.

Relationships between the Spuzzum batholith and these rocks are of critical importance in dating their deformation and metamorphism. The batholith yielded U-Pb dates of 110 Ma (R.L. Armstrong, in Irving et al., 1985), and K-Ar dates ranging from 79-103 Ma (Richards and McTaggart, 1976). It intrudes all three packages. Locally, as near Mount Urquhart, the base of the batholith is strongly foliated, and the foliation in it is concordant with that in the underlying Settler Schist. Elsewhere, as near the eastern contact of the batholith on Highway 7, northeast-plunging mineral lineations in the quartz diorite of the batholith parallel those in nearby schist. These field relationships suggest that the batholith is syn- to late-tectonic. Bartholomew (1979), in his detailed study of metamorphism of the Settler Schist, concluded that earliest phases of the Spuzzum batholith preceded the peak of regional metamorphism in which temperatures of about 700°C and pressures of 7-8 kilobars were attained.

South of the area, in Washington, Misch (1966) mapped the Shuksan Thrust, on which blueschist and greenschist grade rocks of the Shuksan Metamorphic Suite were emplaced over lower grade rocks of the Chilliwack Group. This thrust steepens to the east towards a "root zone" which apparently crosses the International Boundary near Slesse Creek, where rocks belonging to the Yellow Aster Complex are exposed. The fault possibly can be traced northwards, across the Fraser River and up Ruby Creek, to the area south of Cogburn Creek, where Lowes (1972) suggested that metadiorite and metagabbro near the southwestern boundary of the Cogburn package were correlative with the Yellow Aster Complex to the south. Thus, the boundary between Cogburn and Slollicum packages probably lies at or near the Shuksan Thrust. Recent work near Slesse Creek (Jewett and Brown, 1985) suggests that the Shuksan Thrust as mapped immediately north of the International Boundary is a post-metamorphic structure, and that lineations there indicate strike-slip movement on it. Speculatively, and based on relationships observed between Harrison Lake and Fraser River to the east, the Shuksan Thrust as mapped by Misch (1966) consists of two discrete sets of structures. An older thrust fault is pre- or syn-metamorphic and places Shuksan on Chilliwack, and Cogburn on Slollicum. A younger strike-slip fault is analogous to, or maybe even links up with, the Harrison Fault (Fig. 73.2).

Conclusions

1. Greenschist to amphibolite grade metamorphic rocks between Harrison Lake and Fraser River are probably metamorphosed from equivalents of strata in surrounding areas. Tentative correlations are Slollicum rocks with the Upper Triassic Cadwallader Group, Cogburn package with Permian to Jurassic Hozameen and Bridge River groups, and Settler Schist with Triassic and Jurassic rocks of the Methow Trough (Spider Peak, Ladner groups) and/or Darrington Phyllite of the Washington Cascades.
2. Juxtaposition of Slollicum, Cogburn and Settler packages occurred on layer-parallel (thrust?) faults, prior to and during regional metamorphism, which was largely coeval with intrusion of the Spuzzum batholith in late Early to mid-Cretaceous time. Structures in the Slollicum schist have similar orientation to early structures in the Chilliwack Group, which are northwesterly overturned recumbent folds and thrusts, suggesting that possibly these structures are of a similar age.

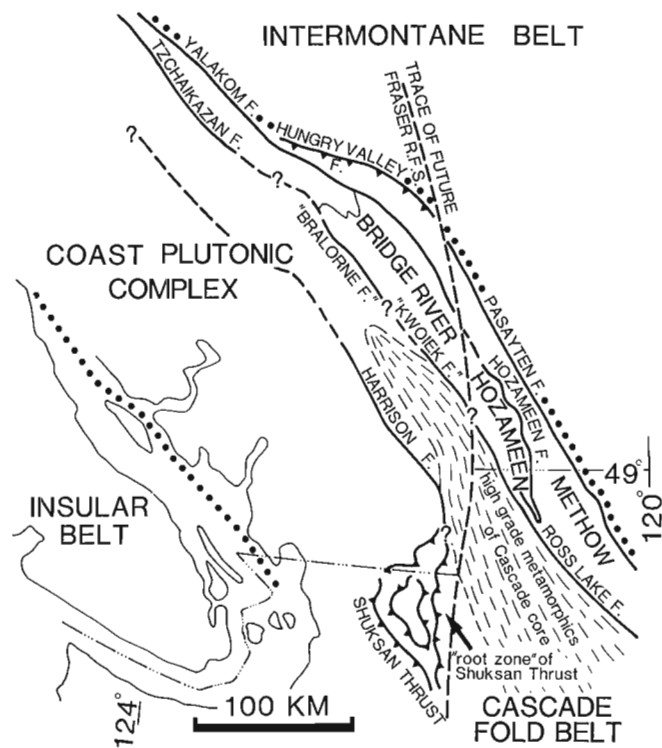


Figure 73.5. Distribution of major north-northwest-trending faults. About 80 km displacement on the Fraser River - Straight Creek fault system has been restored.

- The earlier structures were cut by the north-northwesterly trending Harrison Fault, which is one of a number of major strike-slip faults in the region that largely govern the regional grain and which probably developed in a transpressive regime. Later structures in the Chilliwack Valley have similar trends to cleavages and stretching lineations associated with the Harrison Fault.
- All of these structures were disrupted and offset 80-100 km by the early Tertiary, Fraser River-Straight Creek dextral wrench-fault system.

From these conclusions, the structural evolution of the area can be cartooned as in Figure 73.6. This model draws on earlier models of the Coast Belt as fundamentally a collisional orogen (Davis et al., 1978; Monger et al., 1982; Monger, 1985b), and of the Cascade Belt south of latitude 49° as an enormous accretionary prism (Cowan and Potter, in press), and on the recent emphasis by Brown (in press) on the importance of transcurrent displacements in the evolution of the western part of the Cascades.

The structural and metamorphic evolution of this area appears to have occurred during and following Early Cretaceous closure of an oceanic or marginal basin (whose floor is represented by Bridge River/Hozameen and Shuksan/Darrington rocks and their possible metamorphic equivalents, the Cogburn and Settler packages) which was

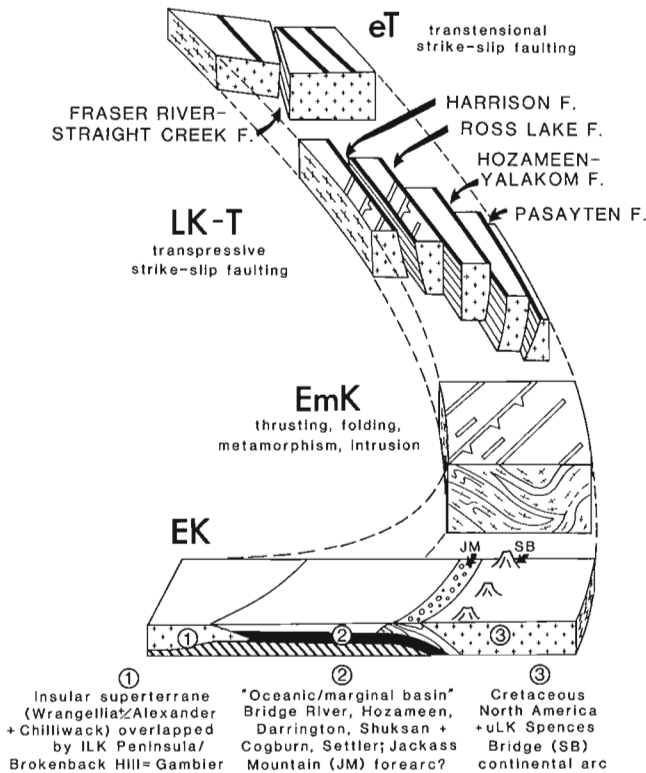


Figure 73.6. Speculative depiction of evolution of structures in the Cascade Fold Belt and southeastern Coast Plutonic Complex. An oceanic/marginal basin was closed in Early Cretaceous time, with the late Early Cretaceous Spences Bridge arc, Jackass Mountain fore-arc (?) on its eastern margin. Final closure/collision produced mid-Cretaceous metamorphic rocks and northeasterly trending structures. These were cut by north-northwest-trending strike-slip faults, with mainly dextral offsets, that were cut in turn by the north-trending, dextral early Tertiary Fraser River-Straight Creek fault system.

trapped between the Insular superterrane (= Wrangell +? Alexander terranes) to the west, and the Cretaceous continental margin to the east (formed by the western edge of the previously accreted Intermontane superterrane). The time of transition between closure by subduction of oceanic crust and terminal collision is difficult to ascertain precisely, but was probably in the later part of the Early Cretaceous. To the south, blueschist metamorphic rocks in the Shuksan metamorphic suite, presumably related to subduction, are dated at about 129 Ma (Armstrong, 1980; Brown et al., 1982). As noted earlier, lawsonite, typical of high pressure, low temperature metamorphism, occurs in earliest Cretaceous rocks west of Harrison Lake. Final closure of the basin by east-dipping subduction is possibly recorded by the late Early Cretaceous Spences Bridge continental arc, which is built on the western edge of the Intermontane superterrane, and whose forearc basin may be represented by the Jackass Mountain Group (Fig. 73.6). Arrival of the Insular superterrane at the subduction zone probably caused collision, manifested by high grade synplutonic metamorphism of latest Early Cretaceous age, and uplift and inversion of the basin in mid- and early Late Cretaceous time. These rocks and early structures were subsequently disrupted in post-mid-Cretaceous and pre-Late Eocene time by transpressional faulting along the Harrison, Ross Lake, Hozameen, and Pasayten faults. Finally, in Late Eocene time, transtensional faulting on the Fraser River-Straight Creek fault system disrupted earlier elements.

References

- Armstrong, R.L.
1980: Geochronometry of the Shuksan metamorphic suite, North Cascades, Washington; Geological Society of America, Abstracts with Programs, v. 12, p. 94.
- Arthur, A.
1986: Stratigraphy along the west side of Harrison Lake, southwestern British Columbia; in Current Research, Part B, Geological Survey of Canada, Paper 86-1B, report 75.
- Bartholemew, P.R.
1979: Geology and metamorphism of the Yale Creek area, B.C.; University of British Columbia, unpublished M.Sc. thesis, 105 p.
- Brown, E.H.
- Metamorphism and structural history of Northwest Cascades; University of California at Los Angeles, Rubey Volume 7. (in press)
- Brown, E.H., Wilson, D.L., Armstrong, R.L., and Harakal, J.E.
1982: Petrologic, structural and age relations of serpentinite, amphibolite, and blueschist in the Shuksan Suite of the Iron Mountain-Gee Point area, North Cascades, Washington; Geological Society of America, Bulletin, v. 93, p. 1087-1098.
- Cowan, D.S. and Potter, C.J.
- Continent:oceanic transect B3: Juan de Fuca spreading ridge to Montana thrust belt; Geological Society of America.
- Crickmay, C.H.
1925: The geology and paleontology of the Harrison Lake district, British Columbia, together with a general review of the Jurassic faunas and stratigraphy of western North America; unpublished Ph.D. thesis, Stanford University, 140 p.
- 1930: The structural connection between the Coast Range of British Columbia and the Cascade Range of Washington; Geological Magazine, v.67, p. 482-491.

- Davis, G.A., Monger, J.W.H., and Burchfiel B.C.
 1978: Mesozoic construction of the Cordilleran "collage", central British Columbia to northern California; in Mesozoic Paleogeography of the Western United States, ed. D.G. Howell and K.A. Douglas; Pacific Section, Society of Economic Paleontologists and Mineralogists, p. 1-32.
- Gabites, J.E.
 1985: Geology and geochronometry of the Cogburn Creek – Settler Creek area, northeast of Harrison Lake, B.C.; unpublished M.Sc. thesis, University of British Columbia, 153 p.
- Haugerud, R.A.
 1985: Ross Lake fault zone in the Maselpanik area, SW B.C., a major crustal shear during the Eocene; Geological Society of America, Abstracts with Programs, v. 17, p. 360.
- Holland, S.S.
 1964: Landforms of British Columbia; British Columbia Department of Mines and Petroleum Resources, Bulletin 48, 138 p.
- Irving, E., Woodsworth, G.J., Wynne, P.J., and Morrison, A.
 1985: Paleomagnetic evidence for displacement from the south of the Coast Plutonic Complex, British Columbia; Canadian Journal of Earth Sciences, v. 22, p. 584-598.
- Jewett, P.D. and Brown, E.H.
 1985: Fault motions in the Pleiades-Slesse Mountain area, North Cascades of Washington and British Columbia; Geological Society of America, Abstracts with Programs, v. 17, p. 364.
- Kleinspehn, K.L.
 1985: Cretaceous sedimentation and tectonics, Tyaughton-Methow Basin, southwestern British Columbia; Canadian Journal of Earth Sciences, v. 22, p. 154-174.
- Lawrence, R.D.
 1978: Tectonic significance of petrofabric studies along the Chewack-Pasayten Fault, north-central Washington; Geological Society of America Bulletin, v. 89, p. 731-743.
- Lowe, B.E.
 1972: Metamorphic petrology and structural geology of the area east of Harrison Lake, British Columbia; unpublished Ph.D. thesis, University of Washington, 162 p.
- Misch, P.
 1966: Tectonic evolution of the Northern Cascades of Washington State; Canadian Institute of Mining and Metallurgy, Special Volume 8, p. 101-184.
- Monger, J.W.H.
 1966: The stratigraphy and structure of the type area of the Chilliwack Group, southwestern British Columbia; unpublished Ph.D. thesis, University of British Columbia, 173 p.
 1970: Hope map-area, west half (92H W 1/2), British Columbia; Geological Survey of Canada, Paper 69-47, 75 p.
- Monger, J.W.H. (cont.)
 1977: Upper Paleozoic rocks of the western Canadian Cordillera and their bearing on Cordilleran evolution; Canadian Journal of Earth Sciences, v.14, p. 1832-1859.
 1985a: Structural evolution of the southwestern Intermontane Belt, Ashcroft and Hope map-areas, British Columbia; in Current Research, Part A, Geological Survey of Canada, Paper 85-1A, p. 349-358.
 1985b: Terranes in the southeastern Coast Plutonic Complex and Cascade Fold Belt; Geological Society of America, Abstracts with Programs, v. 17, p. 371.
- Monger, J.W.H., Price, R.A., and Tempelman-Kluit, D.J.
 1982: Tectonic accretion and the origin of the two major metamorphic and plutonic belts in the Canadian Cordillera; Geology, v. 10, p. 70-75.
- O'Brien, J.
 1986: Jurassic stratigraphy of the Methow Trough, southwestern British Columbia; in Current Research, Part B, Geological Survey of Canada, Paper 86-1B, report 80.
- Pigage, L.C.
 1973: Metamorphism southwest of Yale, British Columbia; unpublished M.Sc. thesis, University of British Columbia, 95 p.
 1976: Metamorphism of the Settler Schist, southwest of Yale, British Columbia; Canadian Journal of Earth Sciences, v. 13, p. 405-421. Reamsbottom, S.B.
 1971: The geology of the Mount Breakenridge area, Harrison Lake, B.C.; unpublished M.Sc. thesis, University of British Columbia, 143 p.
 1974: Geology and metamorphism of the Mount Breakenridge area, Harrison Lake, B.C.; unpublished Ph.D. thesis, University of British Columbia, 155 p.
- Richards, T.A.
 1971: Plutonic rocks between Hope, B.C. and the 49th parallel; unpublished Ph.D. thesis, University of British Columbia, 178 p.
- Richards, T.A. and McTaggart, K.C.
 1976: Granitic rocks of the southern Coast Plutonic Complex and northern Cascades of British Columbia; Geological Society of America, Bulletin, v. 87, p. 935-953.
- Roddick, J.A., Muller, J.E., and Okulitch, A.V.
 1979: Fraser River, British Columbia-Washington; Geological Survey of Canada, Map 1386A, scale 1:1 000 000.
- Rusmore, M.E.
 1985: Geology and tectonic significance of the Upper Triassic Cadwallader Group and its bounding faults, southwestern British Columbia; unpublished Ph.D. thesis, University of Washington, 174 p.
- Vining, M.R.
 1977: The Spuzzum Pluton northwest of Hope, B.C.; unpublished Ph.D. thesis, University of British Columbia, 147 p.

Structure and stratigraphy of the southwestern Fraser River delta: a trial shallow seismic profiling and coring survey

Project 790006

J.L. Luternauer, J.J. Clague¹, T.S. Hamilton², J.A. Hunter¹,
S.E. Pullan¹, and M.C. Roberts³
Cordilleran and Pacific Margin Division, Vancouver

Luternauer, J.L., Clague, J.J., Hamilton, T.S., Hunter, J.A., Pullan, S.E., and Roberts, M.C., Structure and stratigraphy of the southwestern Fraser River delta: a trial shallow seismic profiling and coring survey; in Current Research, Part B, Geological Survey of Canada, Paper 86-1B, p. 707-714, 1986.

Abstract

Shallow seismic reflection profiles of the southwestern part of the Fraser River delta were interpreted with lithologic data from drill holes, an exploratory well, and cores collected specifically for this project. Results of this trial survey show that this technique is an effective and relatively inexpensive method for identifying Tertiary and Quaternary subsurface strata as well as structural, depositional, and erosional features. If such a survey is extended over other parts of the delta our understanding of the apparently complex history of this feature and our ability to assess seismic risk in the area should be markedly enhanced.

Résumé

Des profils de réflexion sismique peu profonde de la partie sud-ouest du delta du fleuve Fraser ont été interprétés à l'aide de données lithologiques obtenues de trous de forage, d'un puits exploratoire et de carottes prélevées principalement aux fins du présent projet. Les résultats de cette étude indiquent que cette technique constitue un moyen efficace et relativement peu coûteux d'identifier les strates souterraines du Tertiaire et du Quaternaire, ainsi que les caractéristiques structurales, de dépôt et d'érosion. L'extension d'un tel levé à d'autres parties du delta améliorerait grandement l'état de connaissances actuel de l'évolution apparemment complexe du delta ainsi que l'aptitude des instances à évaluer les dangers sismiques de cette région.

¹ Terrain Sciences Division, Vancouver

² Pacific Geoscience Centre, Box 6000, Sidney, B.C. V8L 4B2

³ Department of Geography, Simon Fraser University, Burnaby, B.C. V5A 1S6

Introduction

During the past decade major advances have been made in our understanding of the evolution and stability of the Fraser River delta of south-coastal British Columbia (Fig. 74.1) (Hebda, 1977; Byrne, 1978; Clague et al., 1983; Luternauer and Finn, 1983; Styan and Bustin, 1984). But, on the whole, interpretations and conclusions have been of a general nature because of the lack of detailed lithostratigraphic and structural information. In an effort to fill this gap in our knowledge, the Geological Survey of Canada has initiated a project to systematically map the delta's subsurface by means of high resolution seismic profiling and coring. A trial survey to test techniques and determine the feasibility of the project was performed during the summer of 1985.

A preliminary analysis of ground motion produced by the September 1985 earthquakes in Mexico added impetus to this study by indicating that assessments of seismic risk can

be upgraded if the geometry of Quaternary deposits and configuration of the bedrock surface are precisely known, as these can influence the amplitude and period of seismically-induced ground motion. Because the highly urbanized and industrialized Fraser River delta lies in a zone of high seismic risk (Milne et al., 1978), it would be prudent to proceed with the acquisition of these types of data.

Methods

Seismic survey

Shallow seismic reflection profiling was performed with an engineering seismograph (Hunter et al., 1984) over a distance of approximately 6 km along roadways and a causeway on the southwestern part of the Fraser River delta (Fig. 74.2). The "optimum offset" technique (Hunter et al., 1984) was used, with a 20 m source-geophone offset for line 200 (Fig. 74.2) and a 25 m offset for all other lines.

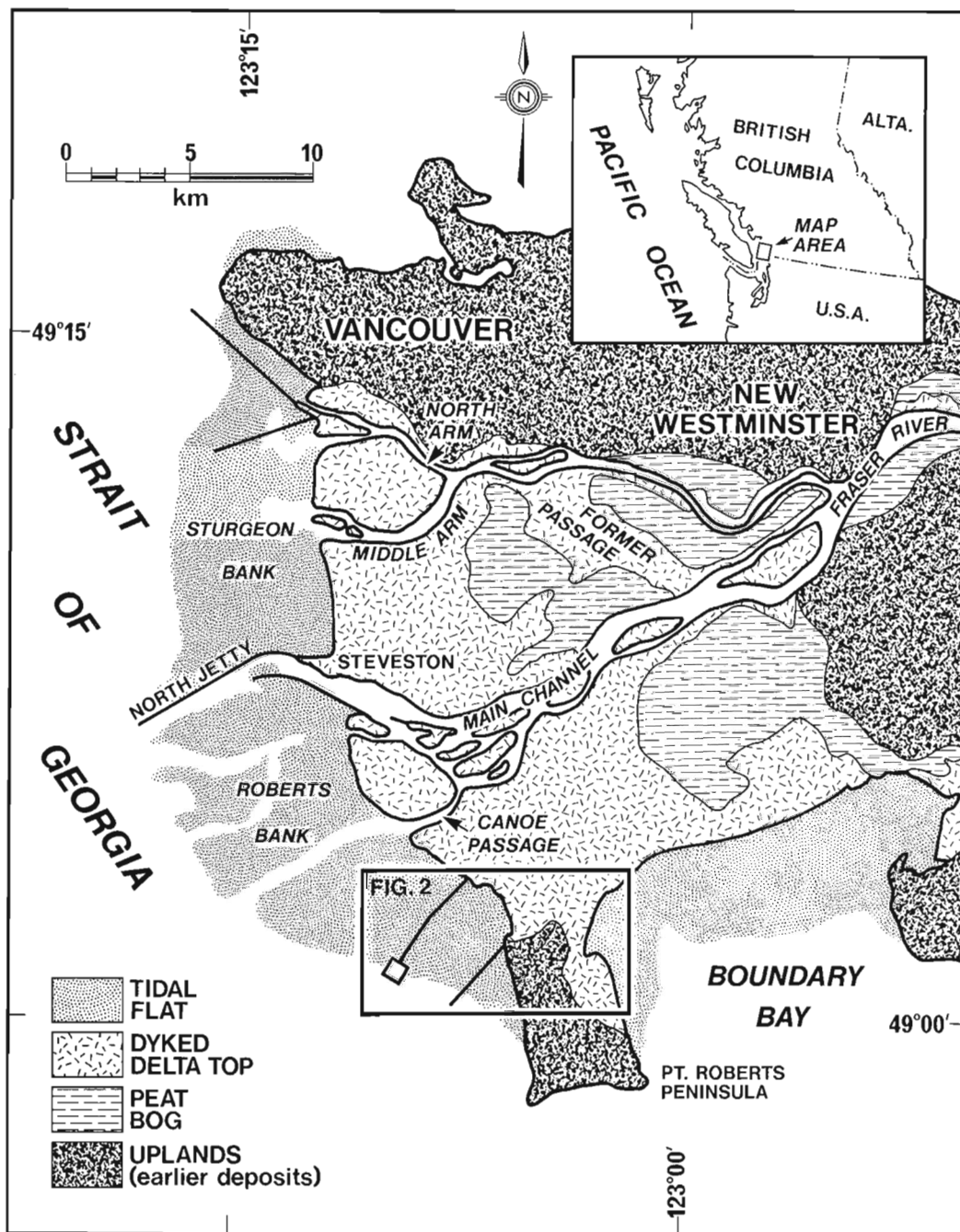


Figure 74.1. Location and geographic setting of study area.

Line 200 was shot using a 100 ms recording scale; other lines were shot with a 200 ms scale, yielding potentially deeper penetration. High frequency phones, with natural frequencies of either 50 Hz or 100 Hz, were used with a 12-channel array, 1 geophone per channel. The recording instrument was a Nimbus 1210F engineering seismograph. A 12-gauge "Buffalo" gun was used exclusively as the energy source in the survey. In this paper, the seismic data are displayed as variable area plots to which an automatic gain control has been applied. The analog field filters were set to record above 300 Hz, and digital filtering was done in the pass-band ranges 250-600 Hz, 400-1000 Hz, 200-600 Hz, 300-800 Hz, and 250-600 Hz for lines 100, 200, 300A-B, 300C-D, and 400, respectively. These data were collected with a non-zero offset so that the first arrival may represent the sum of several different travel paths. As a consequence, the shallowest portion of the record (to 25 ms) contains little if any interpretable geological information. Average velocities in the range 1500-1650 m/s were used to convert travel-times to depths. Calculated depths are thought to be accurate for the upper part of the sequence, but should be regarded as minima for the lower part.

Coring

Cores collected at 3 sites (Fig. 74.2) served as ground truth for the upper part of the sedimentary column represented in the seismic profiles. These were obtained with the Simon Fraser University Concore C-68 research drill rig described by Roberts et al. (1985). Lithology of the cores (Fig. 74.3, 74.4) was logged in the field. For core SFU(D)38 (Fig. 74.3), down-hole gamma, spontaneous potential, and resistivity values were also determined to test these measures as sediment descriptors.

Additional lithologic control was drawn from two sources. The first was a log for an exploratory well (Richfield-Pure 6-3-5) drilled on Point Roberts Peninsula (rig release January 1963) (Fig. 74.2). This well penetrated Pleistocene, Tertiary, and Cretaceous units (Hopkins, 1966). The second source was two logs of boreholes drilled in 1968 in the course of geotechnical investigations for the Roberts Bank coal port (data provided by National Harbours Board). The more westerly of these boreholes reached a depth of 73 m and bottomed out in "till".

Interpretation

On the basis of available lithologic control and seismic signature, we have tentatively identified Tertiary and Quaternary sequences within the records (Fig. 74.5-74.8). The lowest sequence is assigned a Tertiary age on the basis of its probable correlation with a thick Miocene succession present at depth in the Point Roberts well (Hopkins, 1966). The upper limit of the Tertiary sequence is defined in the records by a prominent 200 Hz reflector which represents an erosional surface. The Tertiary sequence in places extends almost to the present delta surface (Fig. 74.7); elsewhere, however, it is covered by thick Quaternary sediments (Fig. 74.5, 74.6, 74.8). Erosion of the Tertiary sequence has produced a northwest-trending ridge, the axis of which extends along the present shoreline in the vicinity of the coal port and the northeast coast of Point Roberts peninsula.

Sediments unconformably overlying the Tertiary bedrock ridge are known to be Quaternary, but it is difficult at this early stage in the study to differentiate Pleistocene and Holocene deposits. It is known, however, from the Point Roberts well record and from surface exposures on Point Roberts peninsula that most of the Quaternary sequence at

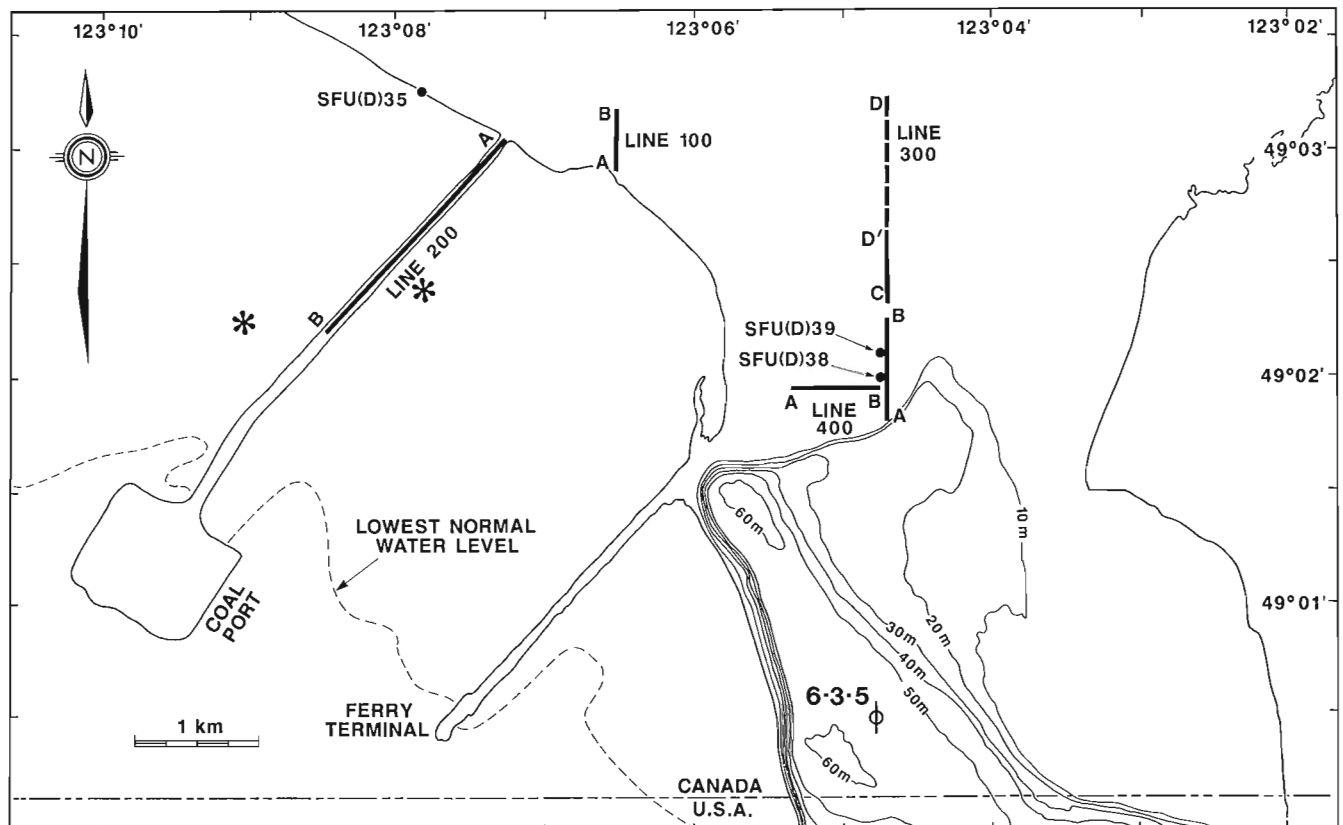


Figure 74.2. Location of seismic survey lines and borehole and coring sites. Asterisks indicate sites of two holes drilled as part of a geotechnical assessment by Swan Wooster Engineering for the National Harbours Board. ϕ is the location of the Richfield-Pure 6-3-5 exploration well (total depth: 4509 m). Solid dots indicate sites where cores described in Figures 74.3 and 74.4 were obtained for this study using a truck-mounted drill rig.

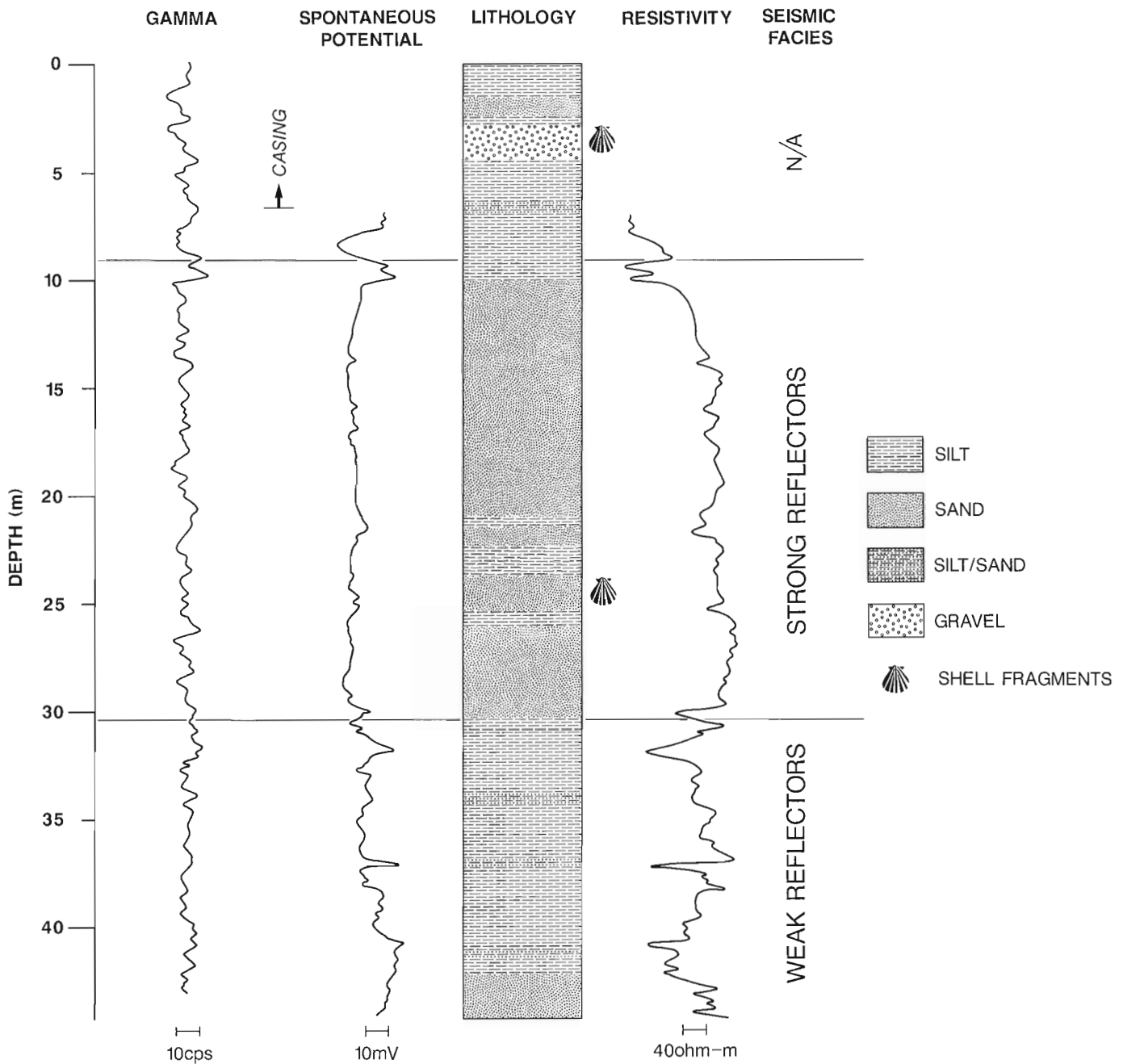


Figure 74.3. Lithology and wireline geophysical logs of gamma, SP, and resistivity for core SFU(D)38. The prominent breaks at about 8 and 30 m delineate lithologically controlled seismic facies (line 300, Fig. 74.7).

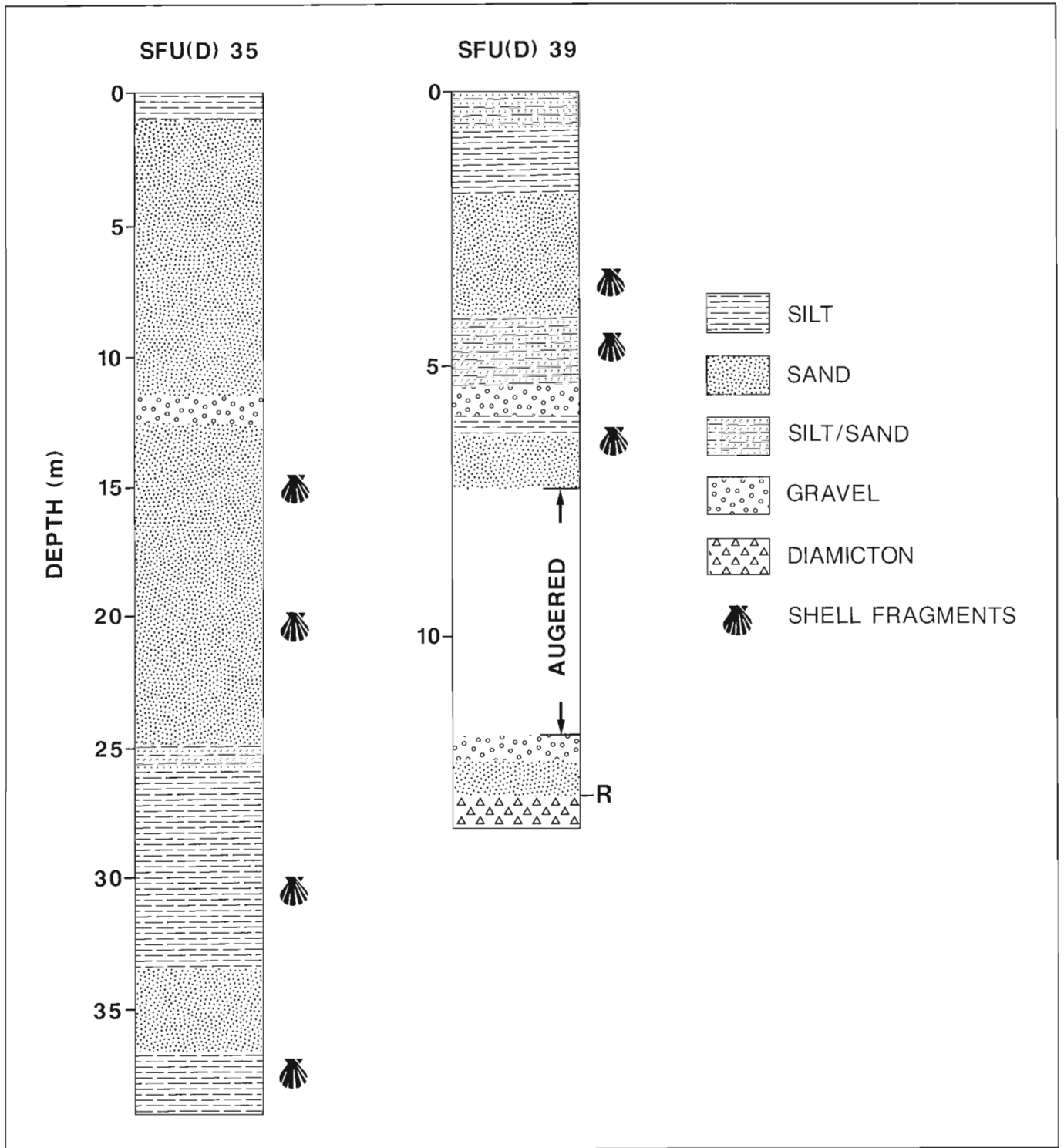


Figure 74.4. Lithology of cores SFU(D)35 and SFU(D)39. Note the different depth scales for the two logs. The letter "R" near the base of SFU(D)39 indicates the probable depth of the strong reflector which marks the attenuated Pleistocene section and the top of what is thought to be Tertiary bedrock (Fig. 74.7).

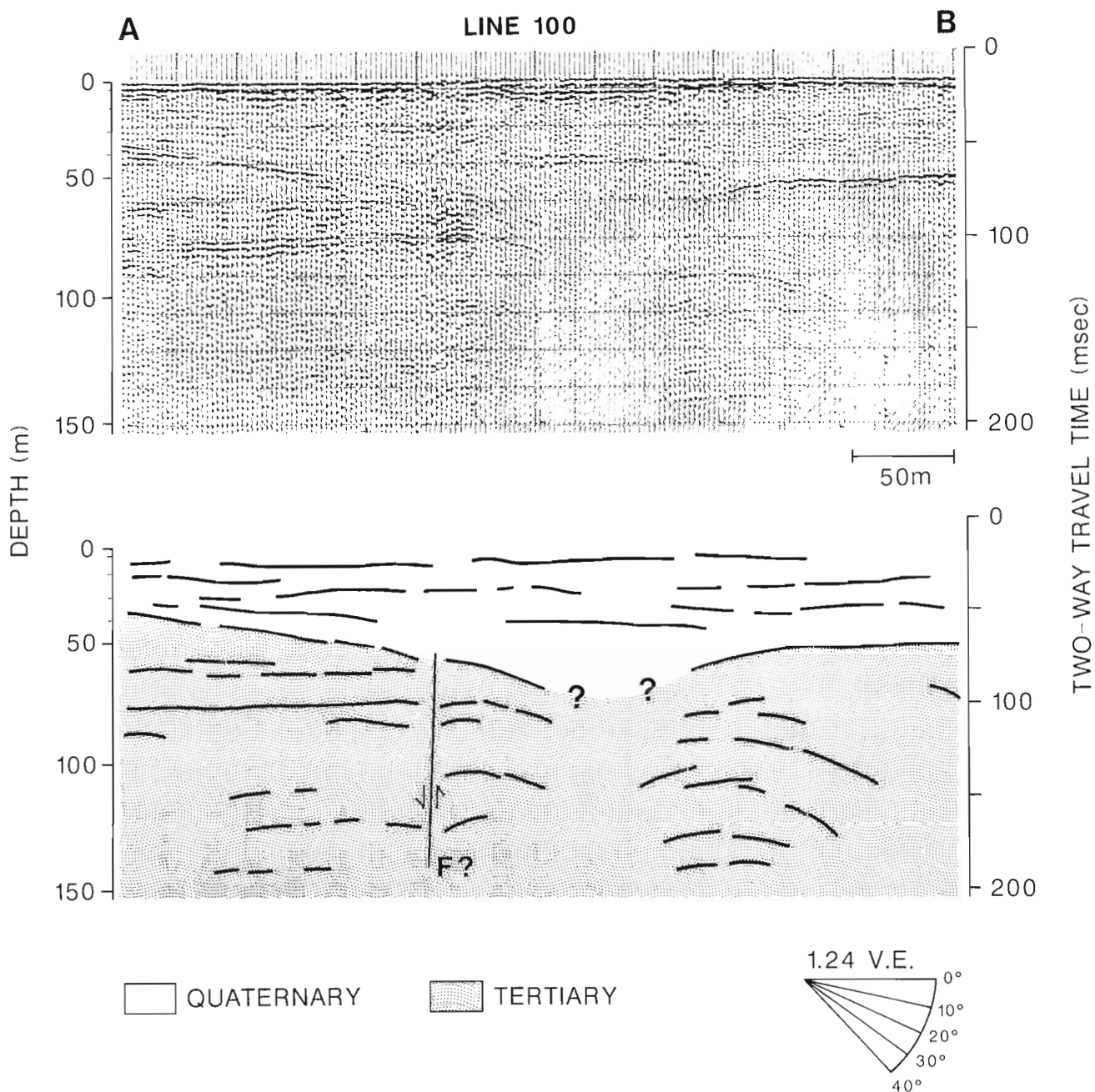


Figure 74.5. Line 100 (A-B is S-N) with seismic reflection record and interpretation.

the south end of line 300 (Fig. 74.7) and along line 400 (Fig. 74.8) is Pleistocene. The presence of till at a depth of 73 m in the borehole near the coal port causeway also suggests that much of the sequence above presumed Tertiary bedrock along line 200 also is Pleistocene (Fig. 74.6). This includes sediment in the northeast half of the section (A end of profile) which displays strong, but discontinuous and irregular reflectors dipping steeply (15-20°) towards the southwest. What are thought to be thick Holocene sediments (mainly silt and sand) occur north of the Tertiary ridge along line 300 (CD', Fig. 74.7) and possibly along line 100 (Fig. 74.5). Thinner Holocene sediments overlie Pleistocene deposits along line 200; but the contact between the two sequences is ill-defined by the seismic method.

Summary and implications

In spite of the limited scope of this survey, it has revealed that the subsurface character of the Fraser River

delta is far more complex than previously thought. We now have evidence that Tertiary basement underlies part of the delta at very shallow depth. Furthermore, it appears that the northwest-trending ridge produced by erosion of the Tertiary sequence has strongly influenced the pattern of growth of the delta during the Holocene and therefore has contributed to its present surface morphology.

This survey has demonstrated that shallow seismic reflection mapping coupled with coring can provide not only geometric and facies control on the Quaternary strata, but also some information on the subjacent bedrock units. Extension of such surveys to other parts of the delta will thus markedly improve our knowledge of the delta's structure and history and may contribute to better assessment of seismic risk in this area.

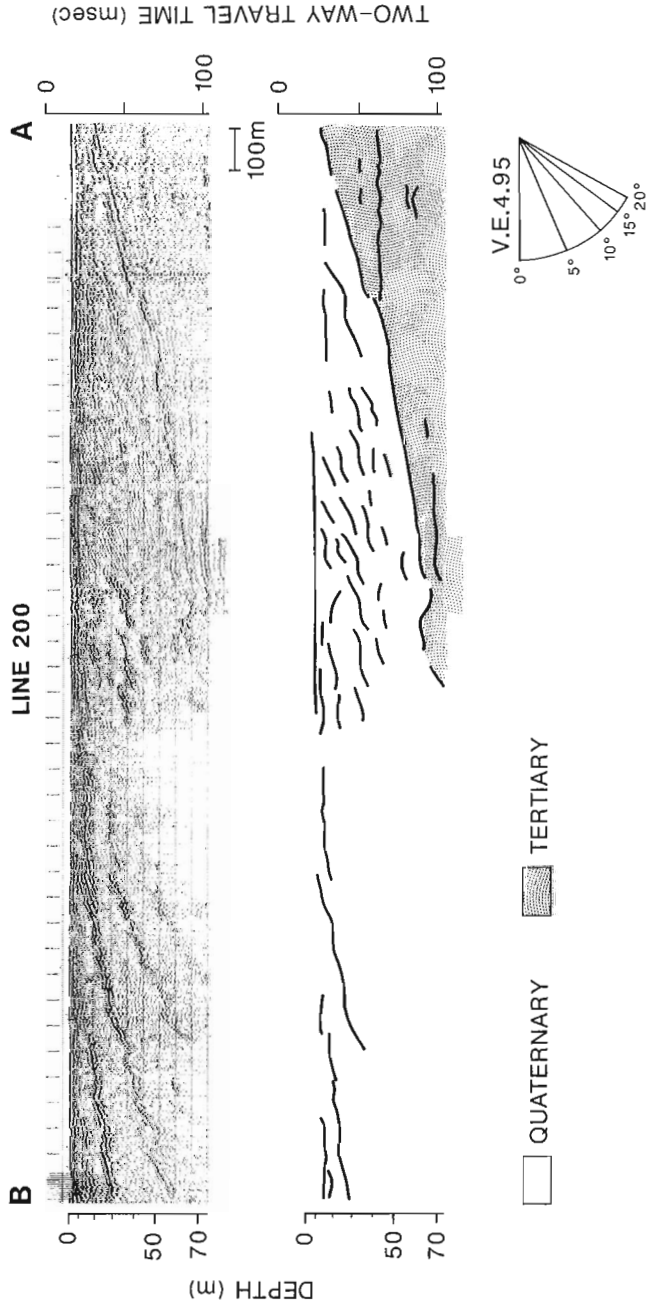


Figure 74.6

Line 200 (B-A is W-E) with seismic reflection record and interpretation.

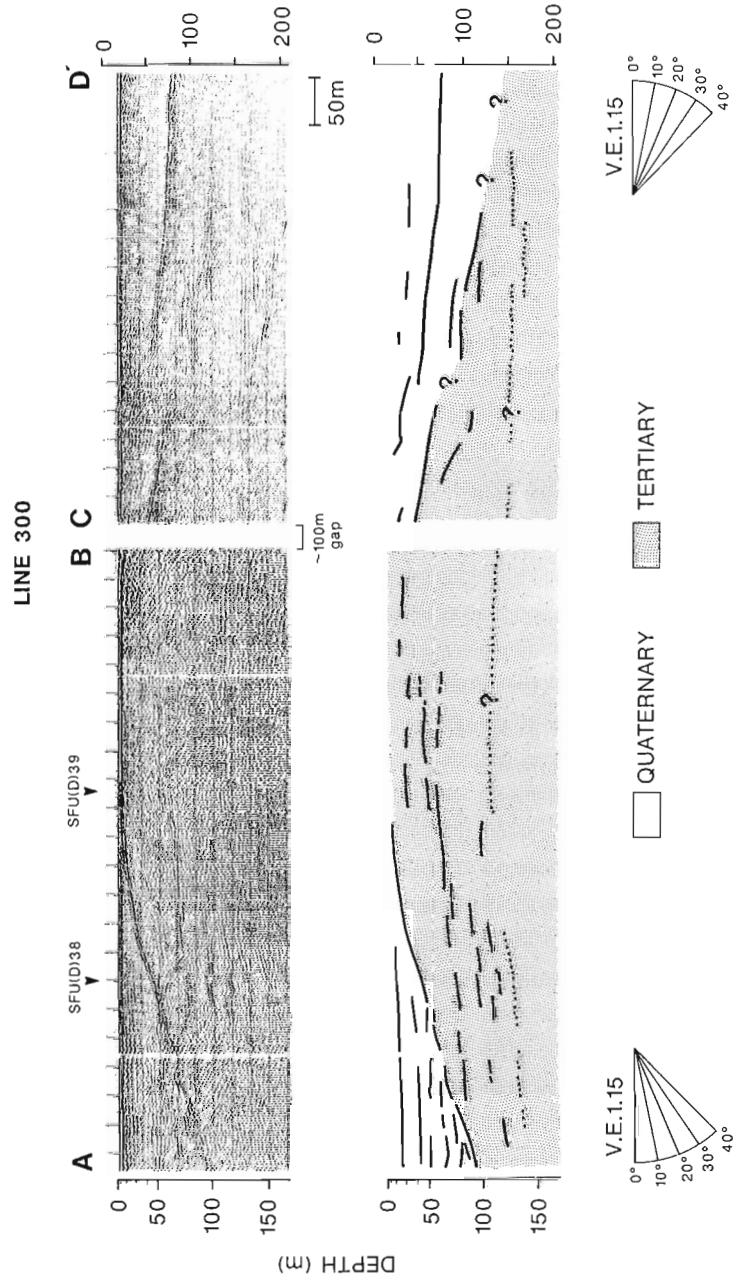


Figure 74.7

Line 300 (A-D' is S-N) with seismic reflection record and interpretation. The interpretation here is constrained by the borehole evidence from SFU(D)38, SFU(D)39, and the Richfield-Pure Point Roberts 6-3-5 exploration well, about 2.5 km to the south. Note the prominent reflector, marking the unconformity at the top of the Upper Tertiary sequence (age inferred from the Point Roberts well tie). Also note that the bedrock ridge which separates two areas of thick Quaternary deposits.

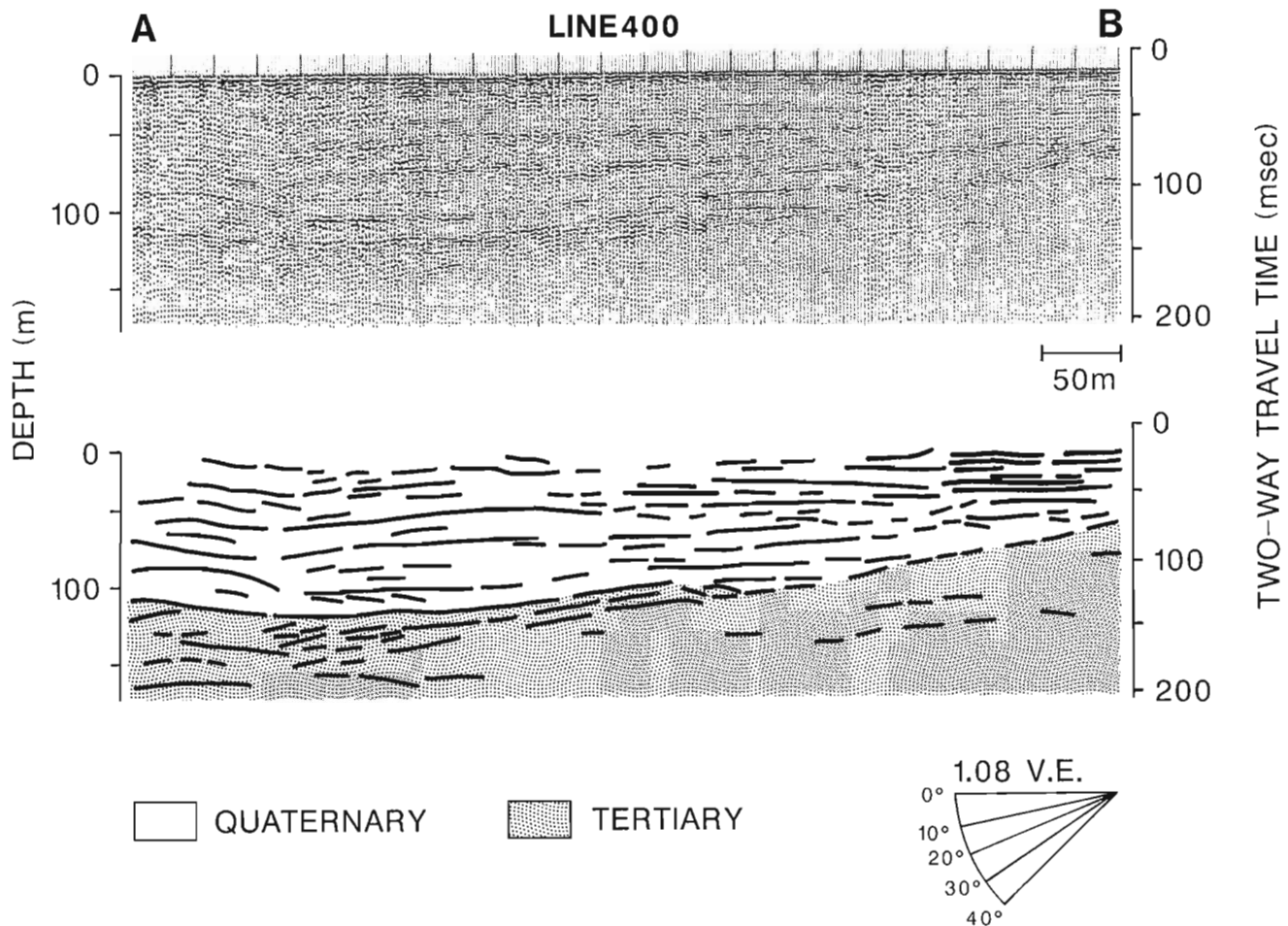


Figure 74.8. Line 400 (A-B is W-E) with seismic reflection record and interpretation. The Quaternary seismic facies in this record is similar to that underlying Pleistocene ridges and banks in the Strait of Georgia (Hamilton and Luternauer, 1983).

References

- Byrne, P.M.
1978: An evaluation of the liquefaction potential of the Fraser Delta; *Canadian Geotechnical Journal*, v. 15, p. 32-46.
- Clague, J.J., Luternauer, J.L., and Hebda, R.J.
1983: Sedimentary environments and postglacial history of the Fraser Delta and lower Fraser Valley, British Columbia; *Canadian Journal of Earth Sciences*, v. 20, p. 1314-1326.
- Hamilton, T.S. and Luternauer, J.L.
1983: Evidence of seafloor instability in the south-central Strait of Georgia, British Columbia: a preliminary compilation; in *Current Research, Part A, Geological Survey of Canada, Paper 83-1A*, p. 471-421.
- Hebda, R.J.
1977: The paleoecology of raised bog and associated deltaic sediments of the Fraser River delta; Ph.D. thesis, University of British Columbia, Vancouver, B.C., 202 p.
- Hopkins, W.S., Jr.
1966: Palynology of Tertiary rocks of the Whatcom Basin, southwestern British Columbia and northwestern Washington; Ph.D. thesis, University of British Columbia, Vancouver, B.C., 184 p.
- Hunter, J.A., Pullan, S.E., Burns, R.A., Gagne, R.M., and Good, R.L.
1984: Shallow seismic reflection mapping of the overburden-bedrock interface with the engineering seismograph - some simple techniques; *Geophysics*, v. 49, p. 1381-1385.
- Luternauer, J.L. and Finn, W.D.L.
1983: Stability of the Fraser River Delta front; *Canadian Geotechnical Journal*, v. 20, p. 603-616.
- Milne, W.G., Rogers, G.C., Riddihough, R.P., McMechan, G.A., and Hyndman, R.D.
1978: Seismicity of western Canada; *Canadian Journal of Earth Sciences*, v. 15, p. 1170-1193.
- Roberts, M.C., Williams, H.F.L., Luternauer, J.L., and Cameron, B.E.B.
1985: Sedimentary framework of the Fraser River delta, British Columbia: preliminary field and laboratory results; in *Current Research, Part A, Geological Survey of Canada, Paper 85-1A*, p. 717-722.
- Styan, W.B. and Bustin, R.M.
1984: Sedimentology of Fraser River delta peat deposits: a modern analogue for some deltaic coals; in *Sedimentology of Coal and Coal-bearing Sequences*, ed. R.A. Rahmani and R.M. Flores; International Association of Sedimentologists, Special Publication No. 7, p. 241-271.

Stratigraphy along the west side of Harrison Lake, southwestern British Columbia

Project 800029

A.J. Arthur¹
Cordilleran and Pacific Margin Division, Vancouver

Arthur, A.J., Stratigraphy along the west side of Harrison Lake, southwestern British Columbia; in *Current Research, Part B, Geological Survey of Canada, Paper 86-1B*, p. 715-720, 1986.

Abstract

A relatively undeformed, fossiliferous, Triassic to Middle Albian section concludes two major volcanic episodes: one during the Middle Jurassic (Harrison Lake Formation) and the other during the Early Cretaceous (Brokenback Hill Formation). They are separated by argillite (Mysterious Creek Formation), volcanoclastic rock (Billhook Creek Formation), and conglomerate and sandstone (Peninsula Formation).

Two and possibly three unconformities were found within the section. The first spans the Triassic-Jurassic boundary between Middle Triassic Camp Cove Formation and Toarcian sediments of the Harrison Lake Formation. The second unconformity lies between Oxfordian Billhook Creek Formation and the Berriasian Peninsula Formation. Evidence for a minor orogenic event during the second hiatus has been noted. The third unconformity is not seen but evidence points to a hiatus spanning the Bathonian.

The Harrison Fault is the dominant structural feature juxtaposing highly deformed, metamorphosed rocks, to the east against the little deformed strata to the west of Harrison Lake.

Résumé

Une coupe fossilifère relativement non déformée et datant du Triassique moyen à l'Albien moyen marque la fin de deux importants épisodes volcaniques: un durant le Jurassique moyen (formation de Harrison Lake) et l'autre au cours du Crétacé inférieur (formation de Brokenback Hill). Elles sont séparées par de l'argilite (formation de Mysterious Creek), des roches volcanoclastiques (formation de Billhook Creek), du conglomérat et du grès (formation de Peninsula).

Il y a deux et probablement trois discordances dans cette section. La première s'étend le long de la limite du Trias et du Jurassique, entre la formation de Camp Cove, qui date du Trias moyen, et les sédiments du Toarcien de la formation de Harrison Lake. La deuxième discordance s'étend entre la formation de Billhook Creek de l'Oxfordien et la formation de Peninsula du Berriasien. On a relevé certaines indications selon lesquelles un événement orogénique peu important aurait eu lieu au cours du second hiatus. La troisième discordance ne se voit pas, mais tout semble indiquer la présence d'une lacune stratigraphique au cours du Bathonien.

La faille Harrison, soit la formation structurale la plus importante de la région, jouxte des roches très déformées et métamorphosées à l'est, ces dernières gisant contre des strates très peu déformées à l'ouest du lac Harrison.

¹ Department of Geology, University of British Columbia, Vancouver, British Columbia V6T 2B4

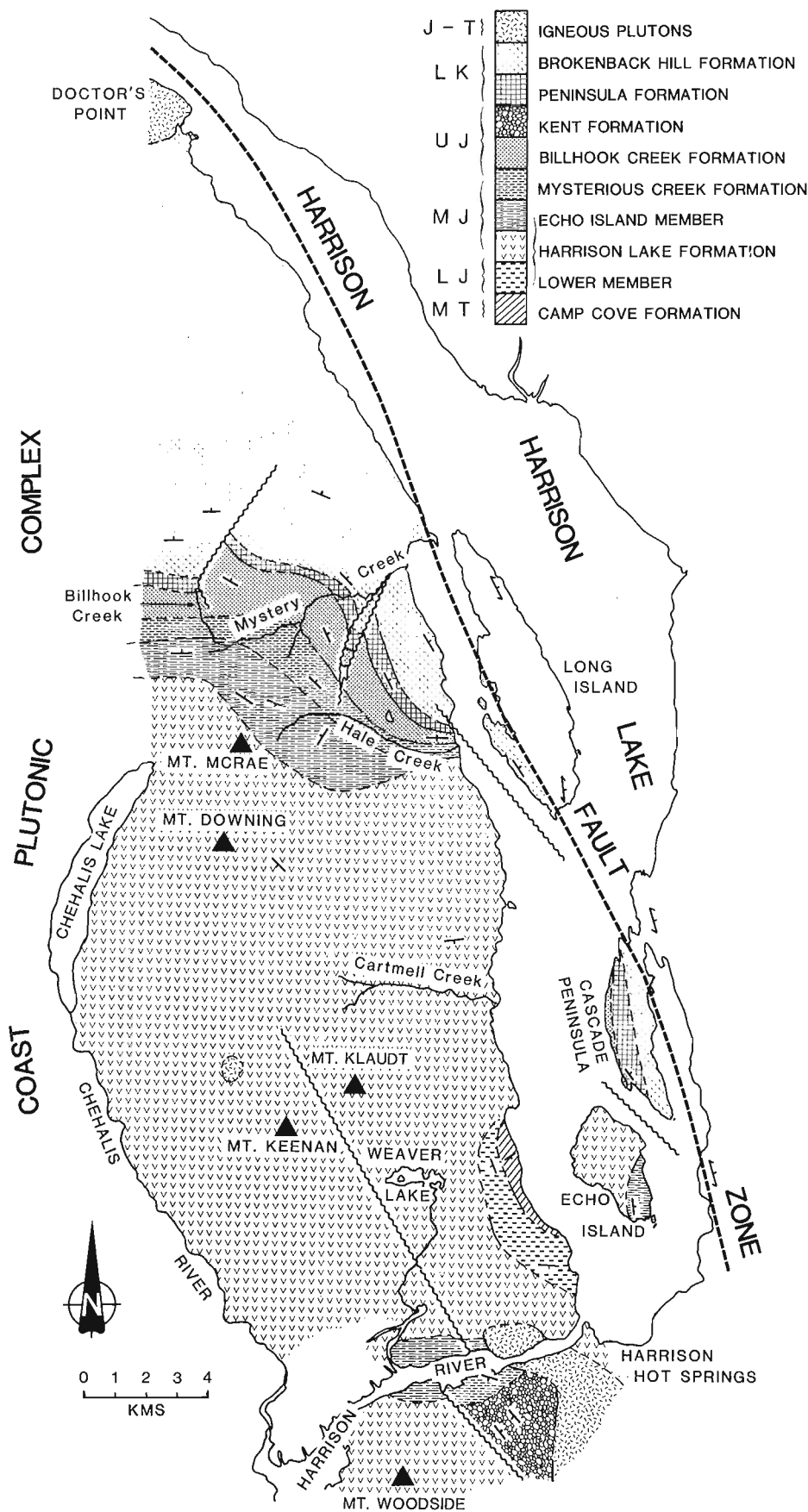


Figure 75.1. Geology of study area west of Harrison Lake (see Monger, 1986, for location map).

Introduction

Field work along the west side of Harrison Lake was undertaken in the summer of 1985 as part of M.Sc. research (at U.B.C.) in an area which contains one of the most complete stratigraphic sections in the southern Coast Mountains. The purpose of this project is to remap the area between Harrison Lake and Chehalis Lake north to Doctor's Point, as it has not been studied as a complete section since 1925 (Crickmay, 1925), with emphasis on lithology, stratigraphy, nomenclature, fossil fauna and environmental setting of the Jura-Cretaceous strata.

The writer is thankful to D. Handel, S. Irwin and M. MacLean for their valuable assistance in the field, and to J.W.H. Monger, H.W. Tipper and P.L. Smith for suggesting the project and offering many stimulating ideas.

Stratigraphy and lithology

The strata along the western shores of Harrison Lake range from Middle Triassic to Middle Albian. In the central part of the map area, around Mystery Creek (Fig. 75.1), the beds dip uniformly at 30-50° towards the northeast but north and south of this area, attitudes become more variable. The stratigraphic section contains two major volcanic episodes, the Lower to Middle Jurassic Harrison Lake Formation to the south and the Early Cretaceous Brokenback Hill Formation to the north. These are separated by shales of the Mysterious Creek Formation, volcaniclastic rocks of the Billhook Creek Formation and sandstones of the Peninsula Formation.

Camp Cove Formation

The Middle Triassic Camp Cove Formation is the oldest unit in the map area (Fig. 75.2) as indicated by radiolaria from a siliceous argillite (Cordey, personal communication, 1985). Conodonts extracted from the same siliceous argillite by the writer had a Middle Triassic age suggested by Orchard (personal communication, 1986) based on the presence of *Neogondolella cf. constricta*. Other lithologies in this formation are green plagioclase porphyry flows, tuffs and sandstones. The base of the Camp Cove was not seen.

Harrison Lake Formation

The Harrison Lake Formation unconformably overlies the Camp Cove Formation. The unconformity is marked by a basal conglomerate and although no fossils were found in the matrix, numerous fossils were found in the clasts. Weathered calcareous clasts within the conglomerate contain abundant rhomboporoid bryozoa and crinoid fragments as well as less abundant rhynchonellid brachiopods and

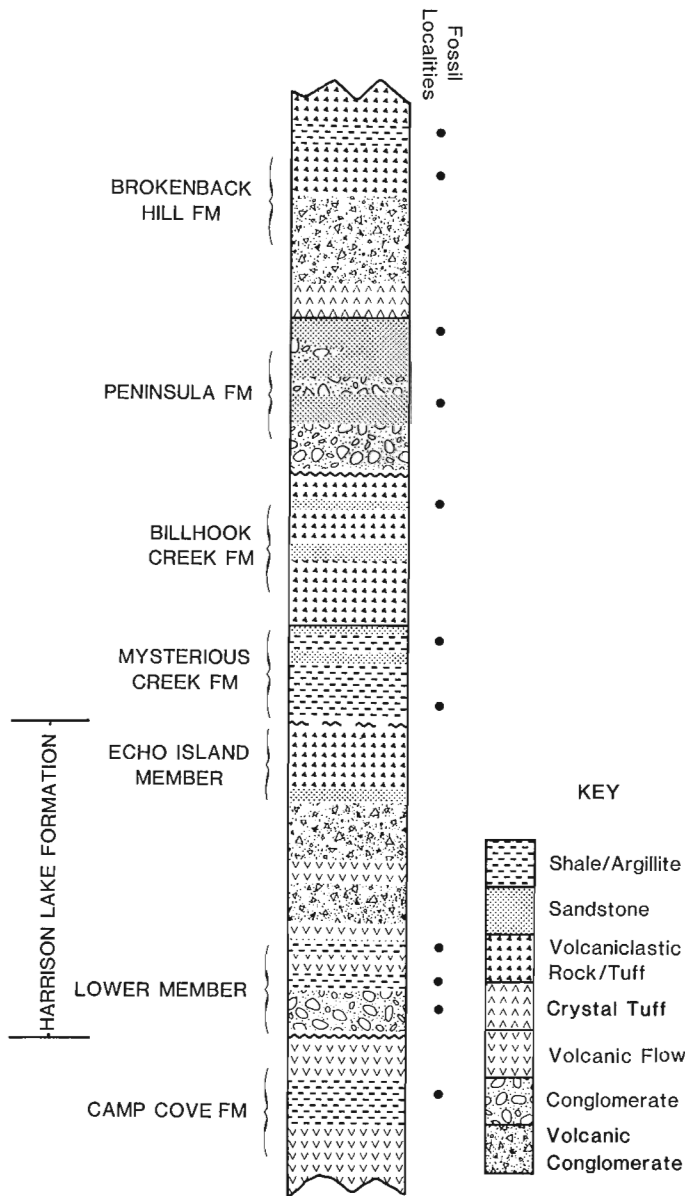


Figure 75.2. Stratigraphy of the Middle Triassic to Middle Albian section on west side of Harrison Lake with fossil localities (section not to scale).

schwagerinid fusulinids (Monger, personal communication, 1985). Light to dark green chert clasts yielded radiolaria and conodonts (*Neohindeodella* sp.) with the latter probably of Middle to Late Triassic age (Orchard, personal communication, 1986). Clasts are well rounded, up to 10 cm across and are predominately chert, limestone and volcanic rock. The matrix is poorly sorted, medium- to coarse-grained and consists of feldspar, quartz and lithic grains.

Immediately overlying the conglomerate is well-indurated calcareous argillite (Fig. 75.2). Near the base of the argillite, Early Toarcian ammonites (*Dactylioceras*, *Harpoceras*) were collected. *Dumortieria* (Tipper, personal communication, 1985) was collected from near the top of the argillite unit and is Late Toarcian. Between the two fossil localities is a volcanic flow which may indicate the onset of Harrison Lake volcanism. The basal conglomerate and overlying argillite comprise the lower member of the Harrison Lake Formation (Fig. 75.2).

Most of the Harrison Lake Formation consists of a thick section of intermediate to acidic volcanic flows (Fig. 75.3) and pyroclastics (Monger, 1970) that cover a large area, from the top of the argillite unit near Harrison Lake, 10 km west to the Chehalis valley and 15 km north to Hale Creek (Fig. 75.1). The Harrison Lake volcanics also cover most of Echo Island and make up much of Mount Woodside to the south. The lensoidal nature of the units, lack of abundant bedding structures and high degree of hydrothermal alteration (especially in the central region) make internal stratigraphic correlation within the volcanics difficult. Crickmay (1925) measured 9240 feet (2816 m) of volcanic material along the west shore of Harrison Lake. The flow rocks include massive, thick dacite, light grey to tan rhyolite and dark green plagioclase porphyry andesite, which are locally amygdaloidal (Thompson, 1972). Pyroclastic rocks exceed flow rocks in abundance (Monger, 1970) and vary from tuffs to volcanic breccias. Fossils are rare within the volcanic sequence of the Harrison Lake Formation, but collections made by Crickmay (1925) were interpreted as Middle Jurassic (Crickmay, 1962).

Echo Island Formation

Northeast of Mount McRae (Fig. 75.1) a thick section of finely banded tuffs and argillites outcrop which were called Echo Island Formation by Crickmay (1925). Similar rocks are also found on the southeast corner of Echo Island, where they are in conformable contact with Harrison Lake volcanics, and along parts of Harrison River. Within the interbedded light and dark coloured tuff and argillite are rare plagioclase porphyry flows and medium grained sandstone beds. The flows are up to 10 m thick and closely resemble the green andesite flows of Harrison Lake volcanics.

Soft-sediment deformation structures are found locally in the interbedded tuff/argillite sequence. Fossils are rare; a single *ex situ* *Trigonia* sp. was found but is not enough to date the sequence. However, Callovian ammonites from the overlying formation suggest that the Echo Island is Middle Jurassic, possibly Bajocian or Bathonian (?).

Because this sequence is closely related to Harrison Lake volcanics, it is better described as the Echo Island Member of Harrison Lake Formation (Fig. 75.2). Beds are commonly lensoidal and the unit is quite variable in thickness and lithology. On the southeast corner of Echo Island, volcanic sandstone is common and some volcaniclastic beds are found but no flows. Northeast of Mount McRae the sequence is finer grained and flow rocks are common.

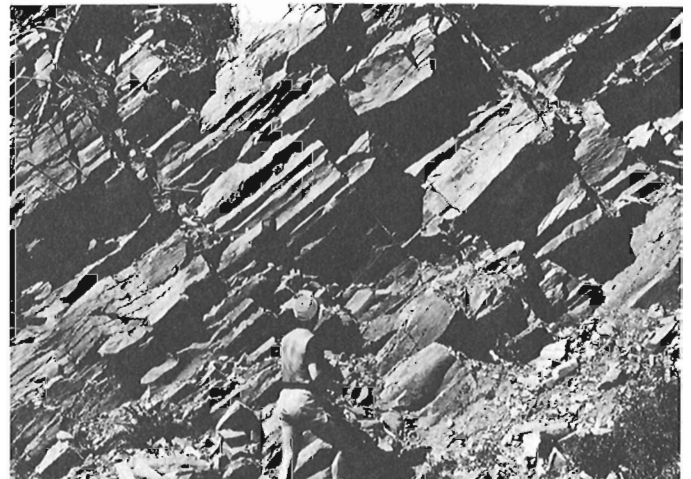


Figure 75.3. Columnar jointing in flows of the Harrison Lake Formation near Mount McRae.

West toward Chehalis valley exposure is poor but volcanic rocks seem to dominate. The Echo Island Member of Harrison Lake Formation marks the waning of Middle Jurassic volcanism in the area as shown by an increase in sediments and a decrease in volcanics (Crickmay, 1925).

Attitudes in the Echo Island Member are highly variable and small scale folding is common. The attitudes of the overlying Mysterious Creek Formation, however, are regular and no small scale folding is apparent. This fact, the lack of Bathonian fossils in collections from this area, and the absence of Bathonian rocks over much of British Columbia (Frebald and Tipper, 1967, p. 8; Tipper, personal communication, 1985) imply a possible hiatus between the Harrison Lake Formation (Echo Island Member) and the overlying Mysterious Creek Formation.

Mysterious Creek Formation

The sediments of the Mysterious Creek Formation are mainly grey to black shale and argillite with interbedded medium grained green sandstone beds near the top of the section. The formation underlies the upper reaches of the Mystery Creek valley (Fig. 75.1) and strikes west to the Chehalis valley, but exposure is poor. A fossil locality 100 m north of the Hale Creek bridge on the B.C. Hydro power line road yielded ammonites *Cadoceras* and *Paracadoceras*, of Callovian age. Ammonites of the same genera were also collected 50 m up from the mouth of Hale Creek. Mysterious Creek Formation also outcrops on the south shore of the Harrison River (Fig. 75.1) where ammonites of the genus *Lilloettia* were collected from Crickmay's locality 8 (Crickmay, 1930). Callovian *Lilloettia* specimens were also collected from localities along Hale Creek. The section south of Harrison River was computed by Crickmay (1925, p. 38) to be 2300-2400 feet (701-731.5 m) thick and the section in Mystery Creek, 2300-2900 feet (701-884 m) thick.

Billhook Creek Formation

The Billhook Creek Formation conformably overlies the Mysterious Creek. The contact between the two is gradational with the green sandstone in the upper section of Mysterious Creek being found in Billhook Creek Formation interbedded with a very characteristic green volcanoclastic rock (Fig. 75.4). The base of the Billhook is placed at the first appearance of the volcanoclastic rock. In Mystery Creek valley, several fossil localities were found within the finer grained sandstone lenses of the Billhook but further work is required before an exact age is assigned to them.

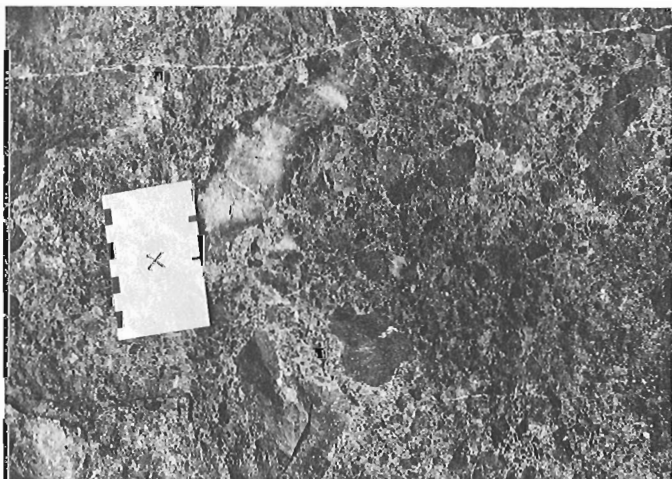


Figure 75.4. Characteristic green volcanoclastic rock of the Billhook Creek Formation.

One locality, however, yielded an abundant collection of ammonites. This locality is equivalent to Brookfield's locality 1 (Brookfield, 1973) from which he obtained *Cardioceras martini* and *Cardioceras ? lilloetense* (see Callomon, 1984, p. 162). The locality is on the west shore of Harrison Lake some 400 m north of the mouth of Hale Creek and the ammonites are Lower Oxfordian (Brookfield, 1973). A locality in argillite and tuffaceous sandstone of the same age (Lower Oxfordian based on *Cardioceras*) occurs on the southwest shore of Cascade Peninsula west of the small bay (Fig. 75.1) (Crickmay's locality 24, 1930; Brookfield's locality 2, 1973). Crickmay placed those rocks in his Agassiz Prairie Formation (Crickmay, 1962), however, the discovery of *Cardioceras* north of Hale Creek indicates that the Peninsula locality can be correlated with the Billhook Creek Formation and the two localities simply show rapid facies changes (Brookfield, 1973).

A sample from a granodiorite pluton 7 km northwest of Weaver Lake collected by J. Monger in 1985 was dated (U/Pb) at 160 ± 2 Ma (P. van der Heyden, personal communication, 1986). This is approximately coeval with the volcanoclastic rocks of Billhook Creek Formation.

Kent Formation

Conglomerate, sandstone and argillite beds form the Kent Formation, which is found in the southern part of the map area on Mount Agassiz (Fig. 75.1). It rests on the Mysterious Creek Formation and a section measured by Crickmay (1925) from the Mysterious Creek-Kent contact to the peak of Mount Agassiz gave a thickness of 3060 feet (933 m). The conglomerate of the Kent is composed of sedimentary clasts (argillite, tuff, sandstone) and some volcanic clasts (probably derived from the Harrison Lake volcanics) that are up to 15 cm across. A notable lack of granitic clasts indicates that the plutons within the present Coast Mountains to the west were not exposed within the provenance of the Kent Formation at this time (Brookfield, 1973). The Kent represents a period of uplift and perhaps minor orogenic deformation which Crickmay named the Agassiz Orogeny (Crickmay, 1931, p. 46).

Because no fossils have been found in the Kent, the lack of granite pebbles becomes important in determining its age. The Kent is older than the Early Cretaceous Peninsula Formation, which contains abundant granite clasts, and it rests on the Mysterious Creek Formation and possibly on a sliver of Billhook (Crickmay, 1962); it is thus younger than Callovian and perhaps younger than Early Oxfordian. Brookfield (1973) bracketted the age of the Kent between the Upper Oxfordian and Tithonian.

The Kent is overlain by a thick sequence of black argillites which Crickmay (1925) called the Agassiz Prairie Formation. Its age is not known, but it is assumed to be younger than the Kent Formation.

Peninsula Formation

The Peninsula Formation unconformably overlies the Billhook Formation west of Long Island and on the west shore of Cascade Peninsula, where the unconformity is well exposed (Fig. 75.5). The basal granite conglomerate of Peninsula Formation west of Long Island is easily recognizable but clast size varies greatly from west to east. In Chehalis valley, granite clasts up to 50 cm across were noted. The size decreases to 20-30 cm in Mystery Creek valley and along the lakeshore, granite clasts are small (2-3 cm) and mixed with beach sands and well-rounded chert pebbles. This indicates a western source from the granitic bodies within the present Coast Mountains, which must have been exposed in the latest Jurassic or earliest Cretaceous in order to supply the granite clasts to the conglomerate.

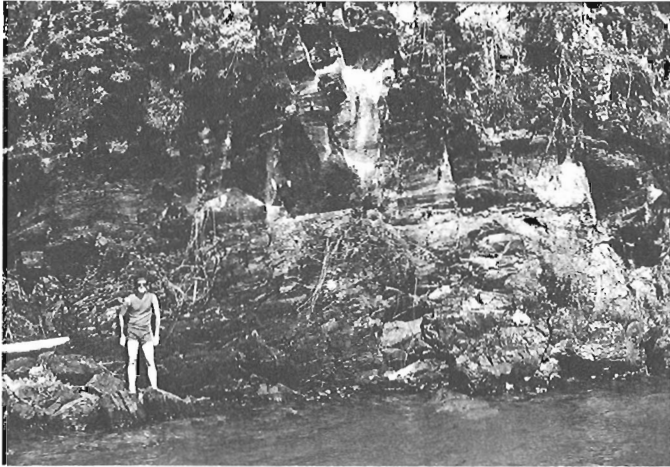


Figure 75.5. Jura-Cretaceous unconformity on southwest shore of Cascade Peninsula. Lower Oxfordian *Cardioceras* collected from cleaved argillites beneath Middle Berriasian calcareous sands containing granite and limestone clasts.

The age of the Peninsula Formation was determined by Crickmay (1925) as early Neocomian based on the bivalve *Buchia*, which is found within this formation in vast numbers. Specimens collected by the writer were studied by J.A. Jeletzky and an age of Lower Berriasian to Lower Valanginian was assigned to them (Jeletzky, personal communication, 1986). Belemnites are also common.

Sandstone in the lower section of the Peninsula Formation is medium- to coarse-grained, moderately to well sorted and have a granitic source. The lithology, sorting and fauna, as well as abundant carbonized wood debris in the sandstones indicate a beach environment for deposition. The upper section of sandstone, however, is darker and commonly tuffaceous. *Buchia*-rich layers are more common and the uppermost part of the formation is marked by a *Buchia* coquina several metres thick. This increase in tuffaceous material marks the beginning of the second major volcanic episode in the area.

Brokenback Hill Formation

Conformably overlying the *Buchia* coquina bed of the Peninsula Formation are crystal tuffs and volcanic conglomerates (Fig. 75.6) of the Brokenback Hill Formation. It covers a large area in the northern part of the map area up to the Doctor's Point pluton (Fig. 75.1). It also forms Brokenback Hill, west of Long Island, and outcrops on the southwest shore of Long Island as well as the eastern side of Cascade Peninsula.

The lower part of the section is composed of green crystal tuff, volcanic conglomerate and tuffaceous sandstone, which give way to volcanic flows, pyroclastics, argillite and sandstone in the upper reaches of the formation. *Buchia* (*B. crassicolis*, *B. keyserlingi*) and ammonite (*Homolosomes quatsinoensis*) specimens collected from the southeast tip of Cascade Peninsula indicate an Upper Valanginian age (Jeletzky, personal communications, 1986). In the area 4 to 8 km west-northwest of the north tip of Long Island, *Homolosomes cf. packardi* and *Inoceramus paraketzovi*, which are Lower Hauterivian (Jeletzky, personal communication, 1986), were collected from tuffaceous sandstone. North of this area, fossils become scarce but an ammonite collected from locally derived float (Ray et al., 1985) near the Doctor's Point pluton indicates a Middle Albian age (Tipper, personal communication, 1985).



Figure 75.6. Volcanic conglomerate from lower section of Brokenback Hill Formation.

Structure

The dominant structural feature in the region is the Harrison Fault Zone (Fig. 75.1). West of the fault is the relatively undeformed Middle Triassic to Middle Albian section just described. On the east side of the fault, highly deformed rocks with a regular foliation and metamorphic rocks of greenschist grade are present (Monger, 1986). The Harrison Fault Zone is marked by highly sheared rocks, which commonly contain stretched conglomerate pebbles and bivalves.

Structures on the west side of Harrison Lake are less distinctive. In the southern part of the map area, broad domes are the dominant feature, with many of the topographic highs (Mount Keenan, Mount Klautd) forming the locus of these domal structures (Thompson, 1972). Faults within the Harrison Lake Formation are difficult to distinguish in the field; however, airphotos show the presence of several linears (one is shown in Fig. 75.1), which trend northwest-southeast. Displacement on these faults is not known but it is thought to be relatively minor (Crickmay, 1925).

To the north, the formations overlying the Harrison Lake Formation are gently warped into a broad syncline and anticline (Fig. 75.1), which plunge towards the northeast. The time of folding is not known, but is possibly concurrent with Harrison Fault. At the lakeshore, Billhook Creek, Mysterious Creek and Peninsula formations strike west and their dip is vertical. On Long Island, only 1 km to the east, the beds of the Brokenback Hill Formation dip 45° towards the northeast and there is no trace of the other three formations. To account for this, a fault has been placed between the two locations. Several other faults cut the formations northwest of this area.

The unconformity between Billhook Creek and Peninsula formations (Fig. 75.2) is important because it marks a period of significant uplift whereby plutons from a site within the Coast Mountains could be unroofed by the Lower Berriasian in order to supply granitic material to the basal conglomerate of the Peninsula Formation. During this uplift in Late Jurassic (post-Callovian) time, the Kent conglomerate was deposited marking Crickmay's Agassiz Orogeny. This uplift can be compared with the inferred Late Oxfordian to early Kimmeridgian uplift of the Taseko Lakes area, which lies to the north (Jeletzky and Tipper, 1968; Brookfield, 1973).

Brookfield (1973) felt that the Kent conglomerate simply indicated uplift, whereas Crickmay (1931) felt orogenic deformation also occurred, and used the name Agassiz Orogeny. On the southwest corner of Cascade Peninsula the *Cardioceras*-bearing argillite of Billhook Creek Formation (Fig. 75.4) is strongly cleaved but the overlying Peninsula Formation lacks this cleavage. Monger (personal communication, 1985) noted the same relationship at an outcrop along the northwest shore of the Cascade Peninsula. This cleavage beneath the Jura-Cretaceous unconformity indicates that some degree of deformation did occur following the Lower Oxfordian. This would lend some credibility to Crickmay's Agassiz Orogeny, although the orogenic event seems to have been relatively minor.

Regional correlations

Numerous correlations between the rocks in the map area with other rocks in southwestern British Columbia and northwestern Washington have been proposed. The Camp Cove Formation was once correlated with the lower section of the Cultus Formation south of the Fraser River (Monger, 1970), however, the Middle Triassic age for the Camp Cove makes this correlation less certain. The Harrison volcanics can possibly be correlated with the few outcrops of volcanic rock in the Cultus Formation, with the volcanics of the Dewdney Creek Group (O'Brien, 1986), which lay to the east, and with the Middle Jurassic Wells Creek volcanics just north of Mount Baker in Washington (Misch, 1966; Monger, 1970).

The age of the black argillite of the Agassiz Prairie Formation, which overlies the Kent Formation, is not known. It was, however, deposited sometime in the Late Jurassic and can probably be correlated with the Oxfordian black shale near Slesse Creek included by Monger (1970) in the Cultus Formation, the lower section of the Nooksack Group of Washington, the lower part of the Fire Lake Group near the north tip of Harrison Lake, and possibly the upper section of Dewdney Creek Group to the east (Monger, 1970).

The Lower Cretaceous Peninsula and Brokenback Hill formations contain an abundant *Buchia* fauna which Jeletzky (1965) used in correlating the two formations with parts of the Nooksack Group to the south. The two formations have also been correlated with parts of the Fire Lake Group (Roddick, 1965; Monger, 1970). The upper section of the Brokenback Hill Formation, around Doctor's Point, may represent a lateral equivalent of the Gambier Group, which is found to the west along the coast (Ray et al., 1985).

References

Brookfield, M.E.

- 1973: Lower Oxfordian (Upper Jurassic) sediments at Harrison Lake, British Columbia, and the age of the 'Agassiz Orogeny'; *Canadian Journal of Earth Sciences*, v. 20, p. 1688-1692.

Callomon, J.H.

- 1984: A review of the biostratigraphy of the post-Lower Bajocian ammonites of western and northern North America; *in* Jurassic-Cretaceous biochronology and biogeography of North America, ed. G.E.G. Westermann; Geological Association of Canada, Special Paper 27, p. 143-174.

Crickmay, C.H.

- 1925: The geology and paleontology of the Harrison Lake District, British Columbia, together with a general review of the Jurassic faunas and stratigraphy of western North America; unpublished Ph.D. thesis, Stanford University, Stanford, California.
- 1930: Fossils from Harrison Lake area, British Columbia; National Museum of Canada, Bulletin 63, p. 33-66.
- 1931: Jurassic history of North America and its bearing on the development of continental structure; *Proceedings American Philosophical Society*, v. 70, p. 15-102.
- 1962: Gross stratigraphy of Harrison Lake area, British Columbia; Published by author (Article 8). Available from Evelyn deMille Books, Calgary, Alberta.

Frebald, H. and Tipper, H.W.

- 1967: Middle Callovian sedimentary rocks and guide ammonites from southwestern British Columbia; Geological Survey of Canada, Paper 67-21, 29 p.

Jeletzky, J.A.

- 1965: Late Upper Jurassic and early Lower Cretaceous fossil zones of the Canadian Western Cordillera; Geological Survey of Canada, Bulletin 103, 70 p.

Jeletzky, J.A. and Tipper, H.W.

- 1968: Upper Jurassic and Cretaceous rocks of the Taseko Lakes map-area and their bearing on the geological history of southwestern British Columbia; Geological Survey of Canada, Paper 67-54, 75 p.

Misch, P.

- 1966: Tectonic evolution of the Northern Cascades of Washington State; Canadian Institute of Mining and Metallurgy, Special Volume 8, p. 101-184.

Monger, J.W.H.

- 1970: Hope map-area, west half, British Columbia; Geological Survey of Canada, Paper 69-47, 75 p.
- 1986: Geology between Horreson Lake and Frose River, Hope map area, southwestern British Columbia; *in* Current Research Part B Geological Survey of Canada, Paper 86-1B, report 73.

O'Brien, J.

- 1986: Jurassic stratigraphy of the Methow Trough, southwestern British Columbia; *in* Current Research, Part B, Geological Survey of Canada, Paper 86-1B, report 80.

Ray, G.E., Coombes, S., MacQuarrie, D.R., Niels, R.J.E., Shearer, J.T., and Cardinal, D.G.

- 1985: Precious metal mineralization in southwestern British Columbia; Geological Society of America, Field Trip 9.

Roddick, J.A.

- 1965: Vancouver North, Coquitlam and Pitt Lake map-area, British Columbia; Geological Survey of Canada, Memoir 335, 276 p.

Thompson, R.I.

- 1972: Harrison, Lucky Jim claims; *in* Geology, Exploration and Mining in British Columbia, British Columbia Department of Mines and Petroleum Resources, p. 102-114.

Stratigraphy, deformation and low grade metamorphism of the Telkwa Formation near Terrace, British Columbia

Project 800028

M.G. Mihalynuk and E.D. Ghent¹
Cordilleran and Pacific Margin Division, Vancouver

Mihalynuk, M.G. and Ghent, E.D., Stratigraphy, deformation and low grade metamorphism of the Telkwa Formation near Terrace, British Columbia; in Current Research, Part B, Geological Survey of Canada, Paper 86-1B, p. 721-726, 1986.

Abstract

Volcaniclastic rocks of the Telkwa Formation (of the Hazelton Group) form the western margin of the Intermontane Belt near Terrace, B.C., and are cut by intrusions of the Coast Plutonic Complex. These rocks outcrop for 25 km in the dip direction of a moderately eastward dipping homoclinal succession.

Development of a gross volcanic stratigraphy within the map area is based on the recognition of (a) mineralogical and compositional trends and (b) rare, but distinctive and widespread tephra. Hydrothermal metamorphism to zeolite and prehnite-pumpellyite facies is stratigraphically controlled, and depends upon both bulk rock composition and depth of burial. Zeolite facies metamorphism predominates in the upper felsic portions of the stratigraphy, while prehnite-pumpellyite-epidote is found in the generally more basic rocks of the lower half of the sequence.

Westward-directed imbricate thrusts in the west, and rotated block faults in the centre and east of the map area resulted in the repetition of the observed stratigraphy. The undisturbed Telkwa section may have been as thick as 6 or 7 km.

Résumé

Les roches volcanoclastiques de la formation de Telkwa (du groupe de Hazelton) forment la limite ouest de la zone Intermontane, près de Terrace (C.-B), et sont coupées par des intrusions du Complexe plutonique côtier. Ces roches affleurent sur une longueur de 25 km dans la direction du pendage d'une succession homoclinale dont la pente s'incline légèrement vers l'est.

Le développement d'une stratigraphie volcanique grossière à l'intérieur de la région cartographiée est basé sur la reconnaissance, a) de tendances minéralogiques et de compositions, et, b) de projections volcaniques (tephra) rares mais distinctes et répandues. La stratigraphie contrôle le degré de métamorphisme hydrothermique, du faciès à zéolites à celui à prehnite et à pumpellyite, et dépend à la fois de la composition de la roche en vrac et de la profondeur de son enfouissement. Le métamorphisme du faciès à zéolites prédomine dans les parties supérieures felsiques de la stratigraphie, tandis qu'un faciès à prehnite et à pumpellyite avec épidote se trouve dans les roches généralement plus basiques de la partie inférieure de cette séquence.

À l'ouest, des poussées imbriquées orientées vers l'ouest, et des blocs faillés pivotés dans le centre et l'est de la région cartographiée, ont entraîné une répétition de la stratigraphie observée. La section non perturbée de Telkwa avait probablement une épaisseur de 6 à 7 km.

¹ Department of Geology and Geophysics, University of Calgary, Calgary, Alberta T2N 1N4

Introduction

Recent remapping of the Terrace (NTS 103I east half) map area by Woodsworth et al. (1985) has produced a stratigraphic subdivision of the Mesozoic rocks consistent with that in common use in west-central B.C. (Tipper and Richards, 1976). The stratigraphy is dominated by the Upper Triassic to Middle Jurassic Hazelton Group, a thick volcanic sequence. In Terrace map area, the Hazelton Group is itself dominated by the Howson subaerial facies (Tipper and Richards, 1976) of the Telkwa Formation. These rocks are mainly subaerial volcanics with thick (20-200 m) epiclastic sequences.

This preliminary description of the Telkwa Formation in the Terrace area is based on fieldwork done in 1984 and 1985, mainly on a well exposed section south of the Copper (Zymoetz) River west of the Clore River (Fig. 76.1 and 76.2) on NTS maps 103I/8 and 93L/5. Equivalent rocks have been studied in detail near Smithers (Dudley, 1983; Tipper and Richards, 1976) where thickness estimates of 2-2.5 km have been made. Within the study area, however, the Telkwa Formation and related volcanics attain a thickness of 6 km. These rocks outcrop as a moderately dipping homoclinal succession for 25 km in their dip direction.

Stratigraphy

The oldest rocks observed within the area are Paleozoic (mainly or entirely Lower Permian) carbonates and underlying cherts and volcanoclastics(?). These are unconformably overlain by Upper Triassic (?) and Lower Jurassic volcanics of the Telkwa Formation (Woodsworth et al., 1985). The Telkwa Formation has been subdivided into four members primarily on the basis of textural, mineralogical, and depositional facies differences.

Paleozoic "basement" rocks

The Mesozoic volcanoclastic rocks rest unconformably atop, or are juxtaposed with, Paleozoic volcanic and sedimentary strata.

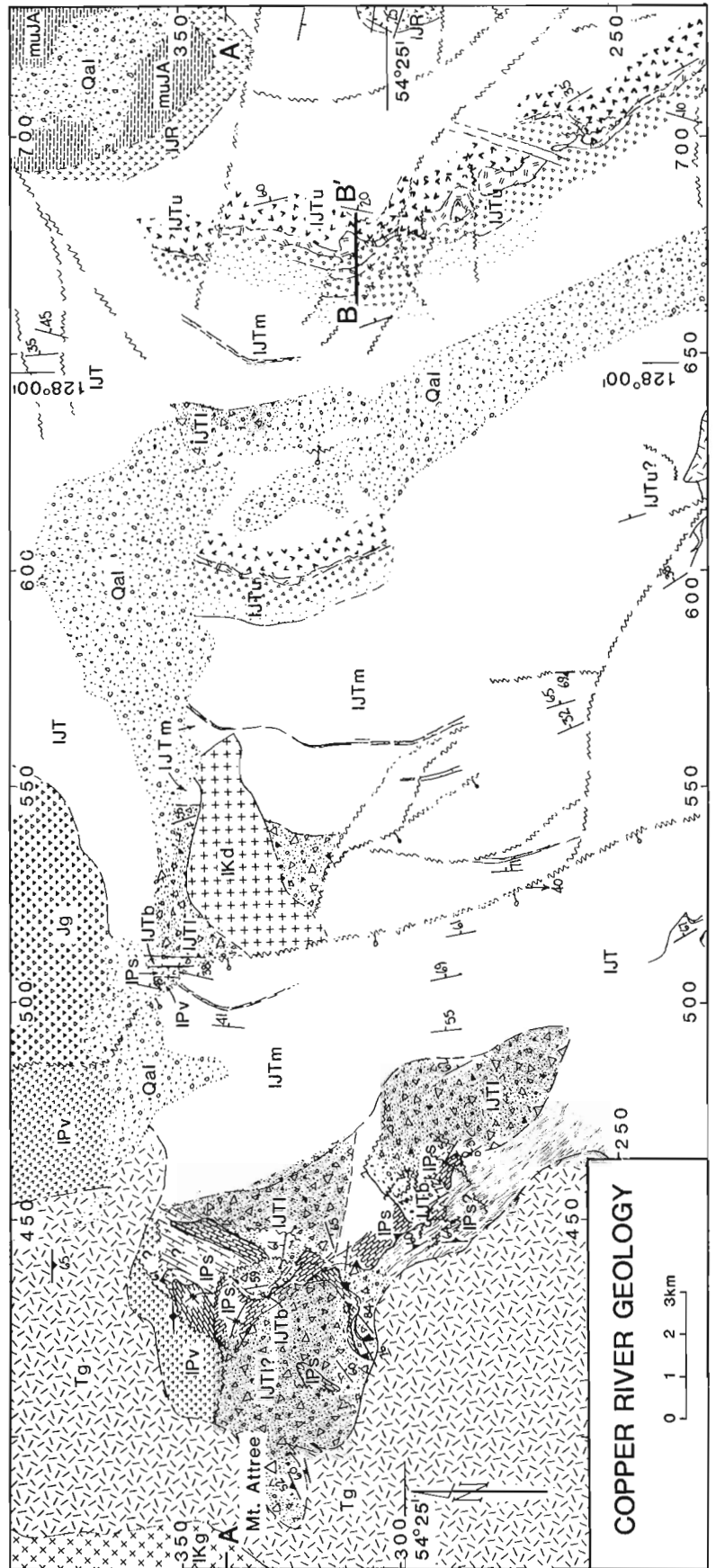


Figure 76.1. Location map. The area indicated by the rectangle is shown in Figure 76.2.

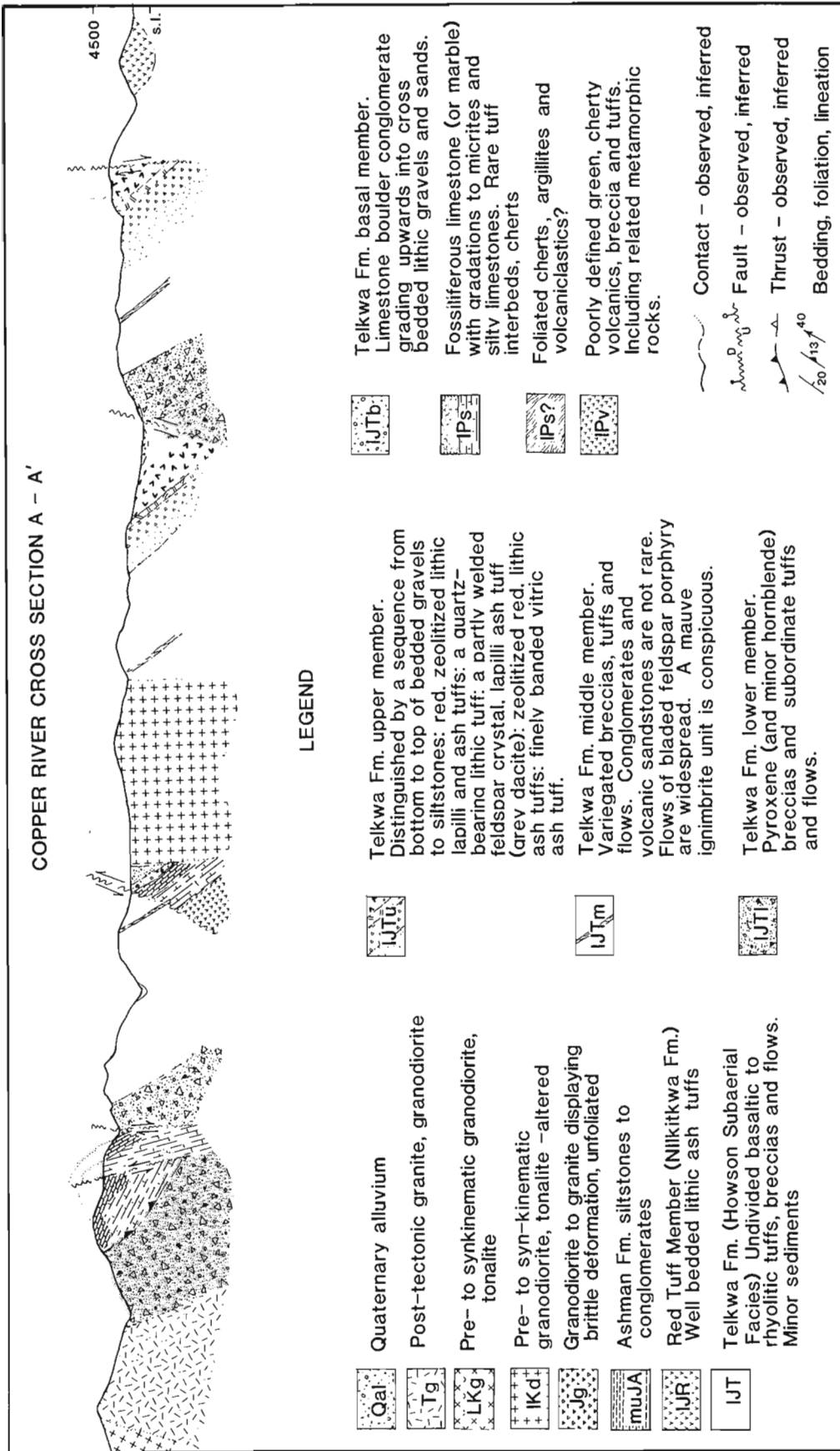


Figure 76.2. Geological map and cross-section of the Copper River area, Terrace, B.C. Geology by Mihalynuk 1984, 1985; Woodsworth et al. (1985); Tipper (1976); Monger (unpublished field data). The grid markers refer to those on NTS maps 1031/8 and 93L/5.

The most common unconformable association is between massive Lower Permian calcarenites and overlying conglomerates, although Triassic argillites are also rarely observed at the Mesozoic-Paleozoic contact.

An indeterminate thickness of highly deformed chert, pelitic chert, and sublitharenites are present about 7 km southeast of Mt. Attree (Fig. 76.2). There, planar bedded, pyritic, muddy chert gravel and sand grade upwards over about 10 m through calcarenite with pebbles outlining crossbedding; into pure, fossiliferous limestone with interbedded chert; and finally massive limestones with ash and lapilli interbeds (up to 20 cm thick).

A typical section of Permian carbonates comprises a lower argillaceous package (250 m) and an upper, thick bedded calcarenite (300 or more m; Monger, 1977).

Basal Conglomerate (15-100 m)

Just north of the immediate map area the Telkwa Formation rests atop Triassic argillite. In most places, however, the base of the Telkwa Formation is a conglomerate resting unconformably atop the Permian unit (the Triassic either never having been present, or having been removed by Late Triassic/Early Jurassic erosion). The conglomerate is 15-100 m thick and is composed of Permian carbonate blocks up to 2 by 0.5 m, but normally less than 20 cm across. The matrix contains iron oxide stained carbonate cement and volcanic debris.

Blocks of soft sediment deformed Upper Triassic (Karnian) argillite (up to 3 m across) occur within this basal member elsewhere in the Terrace map area (Woodsworth, personal communication, 1984). Tipper and Richards (1976) considered the Telkwa Formation to be Pliensbachian to Sinemurian. The probability that some of the basal Telkwa in the Terrace map area is Late Triassic raises a stratigraphic problem not resolved by the present work.

Lower Member

The lower member is between 0.75 and 1.5 km thick and is composed of agglomerate and breccia with subordinate tuff and flows. The most striking characteristic of this unit is the abundance of pyroxene phenocrysts (and to a lesser extent, hornblende, especially near the top) comprising as much as 30% or more of the sample.

Middle Member

The middle member is between 2.5 and 3.5 km thick. It is a highly variable assemblage of breccia, tuff and flows. Epiclastic units (20-50 m thick) are also an important constituent. Bladed-feldspar porphyry flows are widespread (feldspars 2 to 3 cm long). Flows are typically 1-3 m thick, and composite flows reach 55 m in thickness. A mauve ignimbrite in the central part of the middle member is a conspicuous marker horizon. It is typically 15 to 45 m thick, and contains strongly flattened purple pumice blocks up to 80 cm across. In a very general sense, it separates a more basic lower stratigraphy from more felsic, younger volcanics.

Upper Member

The upper member type section is located on the east side of the Clore River (Fig. 76.2). Total thickness of this unit is greater than about 0.75 km. It is distinguished by a sequence of bedded silt- to gravel-sized epiclastics (210 m); overlain by red, zeolitized lithic lapilli and vitric ash tuffs (190 m); a zeolitized, quartz and feldspar rich (15 and 50% respectively) crystal ash tuff (115 m); and 65 m of grey dacite.

The dacite is laterally extensive, thereby constituting a good marker horizon. It is feldspar rich, containing sparse lithic lapilli fragments and flattened feldspar rich pumice blocks (15 cm). Located 25 m from the bottom of the dacite is a 5 m thick red lithic ash tuff which is also laterally continuous. Atop the grey dacite is recessive lithic ash tuff with beds several centimetres to 1.5 m thick. A well indurated and banded (welded?) feldspar crystal, vitric ash tuff (15 m) is included for a composite thickness of 125 m.

Lithology of the topmost part of the upper member differs between the north and south ends of the ridge east of the Clore River. On the north end there are more than 100 m of siliceous mudstones; on the south end, lahars, tuff and rare feldspar porphyry flows are present. Upwards in section these lithologies appear to give way to well bedded lithic lapilli and ash tuffs which may be related to the Red Tuff member (Nilkitkwa Formation) of Tipper (1976).

Rocks shown as the Red Tuff member by Tipper (1976) are poorly exposed where mapped (Fig. 76.2) so that thickness is only crudely estimated at 200-500 m.

Ashman Formation

At the top of the volcanoclastic section are rocks of the Ashman Formation (Tipper, 1976). These are thinly bedded (2-20 cm) argillaceous siltstones to glauconitic sandstones with packstone horizons composed of pelecypods (notably *Trigonia*), brachiopods, and ammonite hash. Ammonites collected from that horizon are Middle Bathonian to Early Callovian based on preliminary identification of *Lilloettia* and *Xenocephalites* by R.L. Hall at the University of Calgary.

Changes in the orientation of bedding from below to above the contact may be due to an angular unconformity. However, abundant slickensided fractures within the volcanic tuffs, as well as slightly undulatory bedding in the marine sediments, point to a faulted contact.

Alteration and metamorphism

Alteration within the volcanic rocks is widespread. Glass and primary ferromagnesian minerals (notably olivine) have, in general, been totally altered. In the lower member, pyroxene and rarely hornblende have survived. Highly indurated lithologies such as flows are most apt to contain surviving ferromagnesian minerals. Even so, olivine can only be inferred to have existed from the presence of iddingsite pseudomorphs. The effects of alteration on the minerals makes it very difficult to accurately classify most flow and pyroclastic units except on a textural basis.

Hydrothermal metamorphism to zeolite and prehnite-pumpellyite facies appears to be regionally developed. Field evidence indicates that facies distribution is in part depth related. In general, the mauve ignimbrite marks an upwards change from prehnite-pumpellyite to zeolite facies. This change not only represents a decrease in depth-related pressure and temperature, but also a change to more acidic compositions higher in the stratigraphy.

In the contact aureoles of Mesozoic stocks and large Tertiary apophyses, rocks of albite-epidote hornfels and greenschist facies are found. Where Permian carbonates are within 2 km of intrusive contacts a well developed skarn assemblage (grossular, tremolite, epidote, ± diopside) is developed, and may locally host lenses (5 cm thick) of chalcopyrite.

Structure

Deformation within the map area is dominated by thrust faulting in the west, and block faulting in the east. Westward-directed thrust faults interleave Permian

limestones with lower member volcanics. About 6.5 km southeast of Mt. Attree, the thrust plane is outlined by 2 m of chlorite schist and a foliation is developed in a zone subparallel to both the intrusive contact and the fault plane. Within this zone, greenschist facies rocks are present; these contain sheared carbonate lenses more than 5 m across.

Aphophyses from granitic dykes related to Tertiary granitic bodies commonly show no chilled contacts, perhaps indicating that moderately high temperature existed within the country rocks prior to dyke intrusion. Although the effect is probably a result of the advancing thermal front associated with a large intruding body, it is obvious from thrust faults crosscut by the intrusion that the volcanic rocks were subjected to an earlier deformation. These dissected thrust faults acted as pathways for fluids associated with the granites and now host a well developed skarn assemblage. The thrusts appear to have been rotated into their present position, dipping steeply to the east. This rotation may be coincident with formation of the homocline that characterizes the regional structure. Minor antithetic(?) block faults crosscut the thrust planes.

Block faults also repeat the stratigraphic section, as can be seen from the repetition of the grey dacite marker on the ridge east of the Clore River (Fig. 76.2 and 76.3). Detailed mapping shows that this repetition was produced by normal faulting (or high angle reverse faulting if deformation was pre-structural tilting). Similarly, block faulting repeats the mauve ignimbrite marker within the central part of the map area. Two major block faults with a stratigraphic throw of some 5 km divide the map area into thirds and result in the repetition of major stratigraphic subdivisions. In this interpretation, the faults are thought to be block faults rather than thrusts because no evidence for the latter was found.

The thermal metamorphic halo associated with a Late Cretaceous dioritic stock about 14 km east of Mt. Attree affects the rocks on both sides of the westernmost major block fault. This suggests that faulting predated Cretaceous intrusion. In addition, the intrusive body likely utilized the structurally weakened zone during emplacement.

Summary and conclusions

The Lower Jurassic Telkwa Formation and related units form a moderately east-dipping homocline, and outcrop for 25 km in their dip direction. The volcanic pile can be subdivided into basal, lower, middle, and upper members.

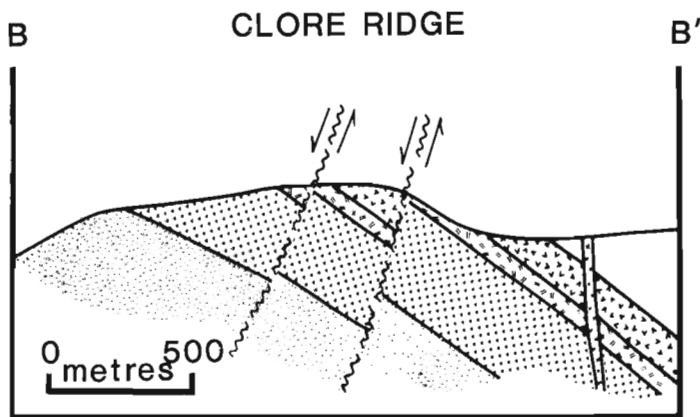


Figure 76.3. East-west cross-section of the ridge east of the Clore River (line B-B' on Fig. 76.2). The style of deformation is dominated by block faulting. Grey dacite marker is a resistant horizon forming the ridgetops. Patterns are the same as on Figure 76.2.

Prehnite-pumpellyite facies metamorphism dominates the lower volcaniclastics whereas zeolites are developed in the upper parts of the volcanic package.

In the field area, the Telkwa Formation consists of pyroclastics (60-70%), flows (20-30%), and epiclastics (10-20%) (Fig. 76.4). The total thickness of 6 km is not geologically unreasonable. For example, 11.3 km of volcanic derived rocks (10% pyroclastics, 90% volcanic sand and siltstones) are found in the Southland Syncline of New Zealand (Boles and Coombs, 1977). Furthermore, the Karmutsen volcanics on Vancouver Island form a volcanic pile 5.5 km thick (Surdam, 1973).

Deformation is dominated by west-directed thrusts in the west, and by block faults in the eastern part of the map area. Thrusts interleave the lower member with Permian carbonates. Block faults produce apparent repetitions of the volcanic stratigraphy causing the 6 km section to outcrop across the map area despite highly consistent dips to the east.

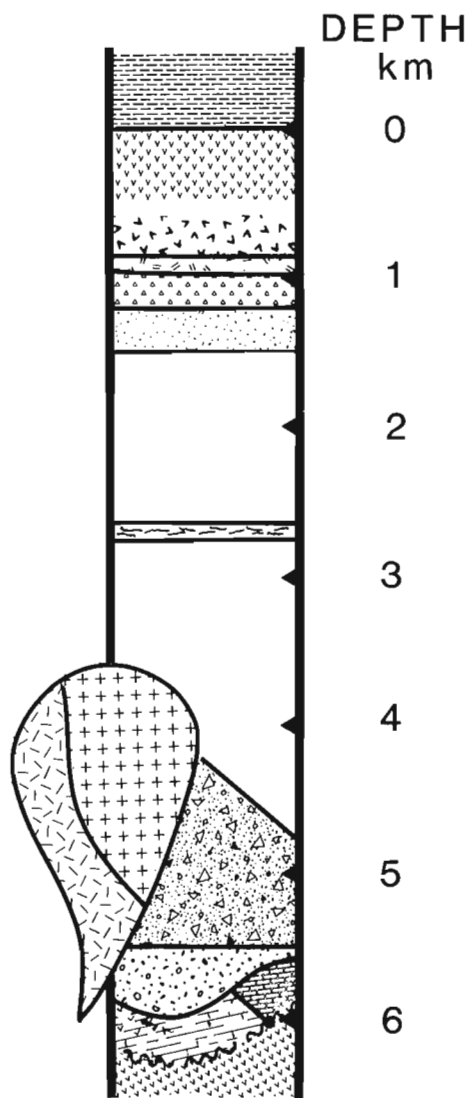


Figure 76.4. Stylized stratigraphic column showing the relationship between the volcaniclastics and adjacent lithologies. Patterns are the same as for Figure 76.2.

References

- Boles, J.R. and Coombs, D.S.
1977: Zeolite facies alteration of sandstones in the Southland Syncline, New Zealand; *American Journal of Science*, v. 277, p. 982-1012.
- Dudley, J.S.
1983: Zeolitization of the Howson Facies, B.C.; unpublished Ph.D. thesis, University of Calgary, 302 p.
- Monger, J.W.H.
1977: Upper Paleozoic rocks of the western Canadian Cordillera and their bearing on Cordilleran evolution; *Canadian Journal of Earth Sciences*, v. 14, p. 1832-1859.
- Surdam, R.C.
1973: Low-grade metamorphism of tuffaceous rocks in the Karmutsen Group, Vancouver Island, British Columbia; *Geological Society of America, Bulletin*, v. 84, p.1911-1922.
- Tipper, H.W.
1976: Smithers, B.C. 93L; Geological Survey of Canada, Open File 351.
- Tipper, H.W. and Richards, T.A.
1976: Jurassic stratigraphy and history of north-central British Columbia; Geological Survey of Canada, Bulletin 270, 73 p.
- Woodsworth, G.J., Hill, M.L., and van der Heyden, P.
1985: Preliminary geological map of Terrace (NTS 103I east half) map area, British Columbia; Geological Survey of Canada, Open File 1136.

Metamorphic pressures and temperatures in the Barkerville and Cariboo terranes, Quesnel Lake, British Columbia: preliminary results

EMR Research Agreement OSB85-00295

D.W.A. McMullin and H.J. Greenwood¹
Cordilleran and Pacific Margin Division, Vancouver

McMullin, D.W.A. and Greenwood, H.J., Metamorphic pressures and temperatures in the Barkerville and Cariboo terranes, Quesnel Lake, British Columbia: preliminary results; in *Current Research, Part B*, Geological Survey of Canada, Paper 86-1B, p. 727-732, 1986.

Abstract

Temperatures and pressures calculated using mineral microprobe analyses on samples collected from the Quesnel Lake area agree in general with the isograds drawn on published maps. In the Ogden Peak and Mt. Watt areas (kyanite-staurolite grade) temperatures range from 530 to 570°C and pressures from 6 to 7 kbar. In the Mt. Wotzke area, however, calcareous lithologies yield temperatures of about 613°C, considerably higher than the garnet grade indicated on the map. Pelitic lithologies which have clearly reached sillimanite grade yield temperatures of about 515°C which are too low, presumably as a result of retrogression or resetting.

Résumé

Les températures et les pressions d'échantillons prélevés dans la région du lac Quesnel, calculées à l'aide d'analyses effectuées au moyen d'une microsonde minérale, correspondent en général aux isogrades du métamorphisme indiqués sur les cartes publiées. Dans la région du pic Ogden et celle du mont Watt (degré du cyanite et staurolite), les températures varient de 530°C à 570°C et les pressions, de 6 à 7 kbar. Dans la région du mont Wotzke cependant, les lithologies calcaires donnent des températures d'environ 613°C, soit beaucoup plus élevées que celle de la roches grenatifère indiquée sur la carte. Les lithologies pélitiques ayant manifestement atteint le degré de sillimanite donnent des températures d'environ 515°C qui sont trop basses, vraisemblablement suite à des épisodes de régression ou de nouvelle compaction du sol.

¹ Department of Geological Sciences, University of British Columbia, Vancouver, B.C. V6T 2B4

Introduction

The northernmost part of the Shuswap Complex has been the focus of much field mapping in recent years. This includes work by the Geological Survey (e.g. Campbell and Campbell, 1969; Campbell, 1978; Struik, 1983) as well as a large number of Ph.D and M.Sc theses both completed and under way at the University of British Columbia (e.g. Getsinger, 1985; Fletcher, 1972; Engi, 1984; Pigage, 1978; Montgomery, 1985; Fillipone, 1985, and others). These studies have, by necessity, concentrated on the stratigraphy and structure of the areas involved. It is now considered appropriate to attempt a synthesis of the metamorphic history.

This study was begun with the collection of samples from four areas between the east and north arms of Quesnel Lake (Fig. 77.1). These localities are referred to here as Ogden Peak area, Mt. Watt area, Northwest Mt. Wotzke area, and Northeast Mt. Wotzke area. These areas fill in a sample gap between the Three Ladies Mountain (Getsinger, 1985), Penfold Creek (Fletcher, 1972) and Niagara River (Engi, 1984) and the areas to the south studied by Montgomery (1985; Fig. 77.1) and Pigage (1978).

Field observations

The areas sampled have been mapped by Campbell (1978) and Struik (1983). The stratigraphic terms used are those defined by Struik.

Ogden Peak area

Struik (1983) assigned the rocks of the Ogden Peak area (Fig. 77.2a) to the Downey succession of the Snowshoe Group. At Ogden Peak the rocks are thinly interlayered, silvery grey or green pelitic to psammitic schist, grey to pink quartzite, buff calcareous schist and marble and dark green amphibolite. Campbell (1978) drew the kyanite-staurolite isograd through the Ogden Peak area (Fig. 77.1). The pelitic to psammitic schist consist of quartz, biotite, garnet \pm muscovite \pm feldspar \pm staurolite \pm kyanite. The quartzite is commonly micaceous (biotite \pm muscovite). Fine grained garnet occurs in some layers. The calcareous schist consists of carbonate and white mica and the amphibolite contains amphibole, feldspar \pm garnet. Only a few outcrops contain staurolite and only one mesoscopic occurrence of kyanite was found in the present study. While this confirms Campbell's (1978) location of the isograd it suggests that the incoming of staurolite \pm kyanite may be very sensitive to the bulk rock composition. The distribution of mineral occurrences does not permit the definition of metamorphic gradient across the area studied.

Mt. Watt area

Struik (1983) indicated that the Pleasant Valley fault outcrops on Mt. Watt (Fig. 77.2b) separating the Barkerville Terrane below from overthrust Cariboo Terrane. The Barkerville Terrane rocks on Mt. Watt belong to the Bralco succession of the Snowshoe Group and to undivided Paleozoic Snowshoe Group. The Cariboo Terrane rocks on Mt. Watt are lithologies characteristic of the Isaac and Cunningham formations. The Bralco succession lies directly on the Downey succession (Fig. 77.2b) with a thick marble unit, the Bralco Marble (P_B), at its base. This is overlain by a pelitic to calcareous schist with some amphibolitic layers and is in turn overlain by a second marble unit, P_{B2} , found only on Mt. Watt (Struik, 1983). This is overlain by the Snowshoe Group.

The Isaac and Cunningham formations thrust on top of the Bralco succession rocks (Struik, 1983) consist of interbedded thin (1-5 m) marble and calcareous schist layers (Isaac Fm.) grading upwards into a massive, coarsely crystalline marble (Cunningham Fm. of Struik, 1983).

The Bralco succession at Mt. Watt is similar to the Downey succession at Ogden Peak. However, it contains the thick Bralco Marble units mentioned above and, in detail, the schists between these two units appear to be less calcareous and have fewer quartzites and more amphibolite units. The Snowshoe Group rocks above the Bralco succession appear to be more pelitic than either the Downey or Bralco successions.

Campbell (1978) mapped the staurolite-kyanite isograd across the Mt. Watt area. Sampling there was over a moderate distance perpendicular to the isograd and, in the pelitic rocks, metamorphic grade appears to increase significantly from northwest to southeast. The mineral assemblages in the various lithologies are the same as those at Ogden Peak. To the southeast the Snowshoe Group contains very abundant, large (1-3 cm) kyanite and staurolite crystals. Closer to Mt. Watt (to the northwest) these diminish in size and abundance though lithologies of suitable bulk composition contain staurolite, if not kyanite.

Northwest Mt. Wotzke area

Struik (1983) mapped all of the rocks in this area as upper Isaac Formation (Fig. 77.2c). The rocks are virtually all calcareous schists and marble with very minor occurrences of pelitic schist and quartzite as well as some rare thin (10 cm +) pegmatite dykes. As in the Ogden Peak and Mt. Watt areas the calcareous schists consist entirely of carbonate and white mica, and the marbles consist of coarsely crystalline carbonate. The pelitic units contain quartz, biotite (\pm muscovite) and locally garnet. Some samples contain biotite-mantled knots of quartz and feldspar (after garnet?). Pegmatite contains quartz, feldspar, muscovite, garnet and tourmaline. Campbell (1978) drew the staurolite-kyanite isograd to the southeast of this area (Fig. 77.1) implying these rocks are garnet grade. The presence of pegmatite dykes would indicate that the thermal regime is higher than garnet grade and that the absence of high grade metamorphic minerals is probably a function of the rock bulk composition.

Northeast Mt. Wotzke area

Struik (1983) indicated that the rocks in this area belong to the lowermost part of the Snowshoe Group (undivided Hadrynian Snowshoe Group; Fig. 77.2d). These are markedly different from the previously described Snowshoe Group rocks (Downey and Bralco successions) in that they contain virtually no calcareous rocks. There is one thin (10 m), discontinuous marble unit (H_{SM}) and some associated calcareous schist. Instead the rocks consist of pelitic schist varying to quartzose and feldspathic psammitic schist. These have been intruded by abundant coarse grained pegmatite (K_G) consisting of quartz, feldspar and muscovite with accessory garnet, tourmaline and beryl.

Campbell (1978) indicated that this area lies within the kyanite-staurolite and sillimanite zones (Fig. 77.1). No outcrop with kyanite or staurolite was found and garnet is rare. The pelitic lithologies consist of coarse grained biotite, muscovite, quartz, feldspar and sparse fine grained garnet. Many samples contain scattered knots of biotite, quartz and feldspar similar to those northwest of Mt. Wotzke. Whether this garnet-out reaction is prograde or retrograde is uncertain. The presence of abundant pegmatite which Fletcher (1972) reported only from sillimanite grade rocks just to the east (Fig. 77.1) suggests that all the rocks in this area are at sillimanite grade.

Petrology

Ogden Peak area

All the samples thin sectioned contained garnet as a porphyroblastic phase set in a strongly foliated matrix of biotite, muscovite and quartz (and commonly plagioclase, zoisite and carbonate in the more calcareous schists). The foliation is strongly flattened around the porphyroblasts. The garnets usually show a helicitic inclusion trail (of quartz and opaque material), S_i , which is discordant to the exterior foliation, S_e . Garnet usually shows two stages of growth indicated by a marked change in inclusion density at the rim. This could indicate either two periods of metamorphism or two periods of garnet growth during a single period of progressive metamorphism. Garnet in most samples shows partial alteration to chlorite.

Staurolite is present in some samples and with one exception is strongly altered to sericite. Where fresh, the textural relationships indicate that staurolite is approximately synchronous with garnet.

Kyanite is present in only two samples and occurs at the interface between very pelitic layers and quartzite. The reason for this mode of occurrence is not fully understood. The paucity of kyanite makes its textural relations difficult to determine. The occurrence of garnet inclusions in a kyanite crystal in one sample shows that kyanite growth is later than some of the garnet growth.

Mt. Watt area

The pelitic rocks at Mt. Watt are similar to those at Ogden Peak, although the presence of biotite as a porphyroblastic phase without garnet at lower grades and the

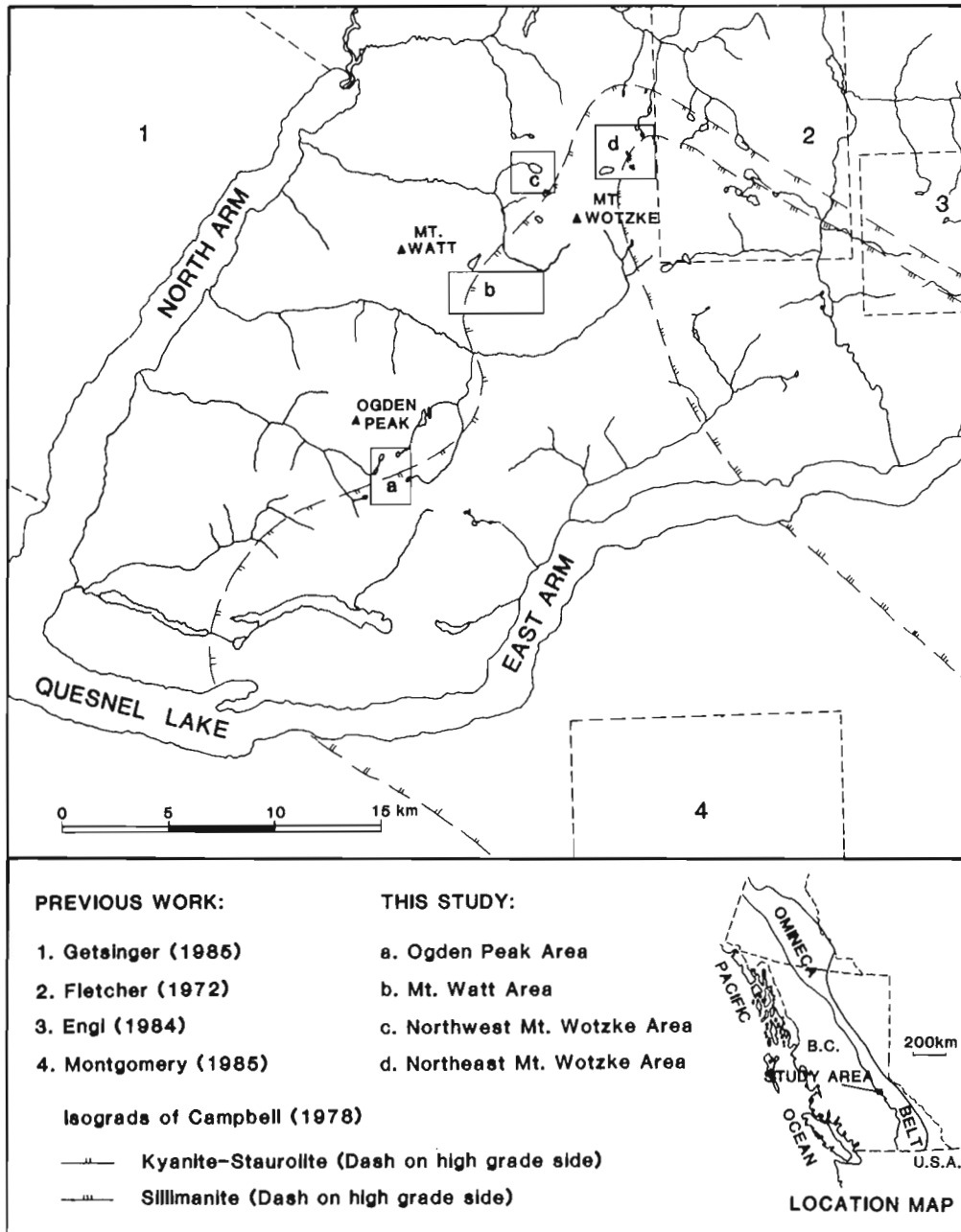


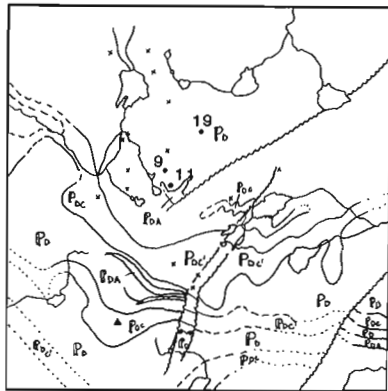
Figure 77.1. Map of Quesnel Lake area showing the location of areas examined in this study and in previous work.

presence of kyanite porphyroblasts at the higher grades makes them appear different. The absence of garnet may be the result of a calcareous bulk composition. The matrix minerals are biotite, muscovite and quartz with zoisite, plagioclase and carbonate in the more calcareous samples. Accessory minerals include ilmenite (sphene in calcareous rocks), tourmaline, zircon and apatite.

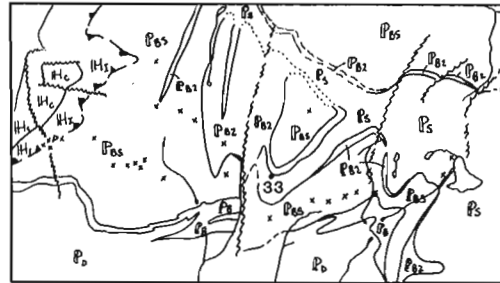
Flattening of the foliation about the garnet and staurolite porphyroblasts is pronounced. Garnets are helicitic with S_i discordant to S_e . Kyanite appears to be later than the garnet and staurolite because S_i within kyanite seems continuous with S_e .

Northwest Mt. Wotzke area

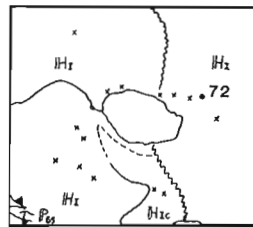
The highly calcareous composition of the rocks from this area generates mineral assemblages which appear, at first glance, to be low grade. Only two of the more pelitic units contain garnet. Assemblages consist of biotite, muscovite, quartz, plagioclase, zoisite, carbonate, sphene (ilmenite or hematite in more pelitic layers), tourmaline and apatite. Sphene and apatite contents are high in many samples and sphene shows at least two stages of growth. Some of the samples are markedly less foliated than others indicating mineral growth during more static conditions. There is no noticeable retrogression.



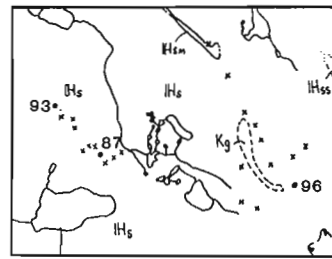
a. Ogden Peak Area



b. Mt. Watt Area



c. Northwest Mt. Wotzke Area



d. Northeast Mt. Wotzke Area



LEGEND (Stratigraphy of Struik, 1983)

BARKERVILLE TERRANE

PALEOZOIC

P_s Undifferentiated Snowshoe Gp.

BRALCO SUCCESSION

P_{B1} Marble

P_{B2} Pelitic - psammitic schist, calc-schist & amphibolite

P_B Marble

DOWNEY SUCCESSION

P_{Da} Amphibolite

P_D Pelitic - psammitic schist, calc-schist, quartzite & amphibolite

P_{Dc} Differentiated marble

HADRYNIAN

H_s Undifferentiated Snowshoe Gp.

CARIBOO TERRANE

HADRYNIAN

H_c Cunningham Fm.

H_i Isaac Fm.

IGNEOUS INTRUSIVE ROCKS (post terranes)

CRETACEOUS

K_g Granite pegmatite

--- Geologic contact (defined: assumed)

~ Fault (defined: assumed)

↖ Thrust

x Sample collected

• Microprobe sample

Figure 77.2. Detailed maps of the areas shown in Figure 77.1. Geology indicated is that of Struik (1983).

The low grade appearance of these rocks is misleading. Some samples contain garnet and one contains rounded knots of biotite, quartz, plagioclase and ilmenite around which the foliation is flattened. These are clearly the products of a garnet-out reaction. Getsinger (1985) noted a similar texture in sillimanite grade rocks north of Quesnel Lake. This confirms the field observation that although the rocks lack kyanite \pm staurolite they probably are of at least this grade.

Northeast Mt. Wotzke area

The apparently low grade of the pelitic rocks from this area is due to the absence of obvious porphyroblasts. Virtually all samples contain microscopic sillimanite. The usual assemblage is quartz, biotite, muscovite, garnet, sillimanite, plagioclase, apatite, ilmenite and occasionally staurolite. There is some retrogression of garnet to chlorite and of staurolite to sericite.

The rocks are clearly higher grade than those at either Ogden Peak or Mt. Watt. Garnets are usually much smaller than those in rocks at lower grades. Staurolite is absent in all but two samples where it is reacting out in favour of sillimanite. Sillimanite is present as fine fibrolite usually associated with biotite around large (old?) garnets and relict staurolite. These rocks also show the garnet breakdown texture seen in thin sections from the Northwest Mt. Wotzke area. Here the garnet is replaced by a fine grained mixture of quartz, biotite, plagioclase, ilmenite \pm garnet \pm sillimanite. Because the rocks from this area are clearly at sillimanite grade it seems possible that the rocks in the Northwest Mt. Wotzke area are also at, or close to, sillimanite grade even though they lack sillimanite.

Temperature and pressure determinations

Methods

Eight samples from the four areas were chosen for microprobe analysis. Three each from the Ogden Peak and Northeast Mt. Wotzke areas were chosen. Only one sample from the Mt. Watt area was chosen because retrogression in the others was too serious and only one sample from the Northwest Mt. Wotzke area was sufficiently pelitic to yield an assemblage suitable for temperature determinations.

Microprobe analyses were done on the ARL electron microprobe at the University of Calgary. A total of nine hundred analyses of biotite, garnet and plagioclase were done and the initial attempts to process some of these data are described here.

Biotite, garnet and plagioclase were analyzed to utilize the geothermometer of Ferry and Spear (1978) and the geobarometer of Ghent (1976). The Ferry and Spear (1978) geothermometer utilizes the temperature dependence of the distribution coefficient of Fe and Mg between garnet (almandine-pyrope) and biotite (annite-phlogopite). The Ghent (1976) geobarometer utilizes the univariant equilibrium $3 \text{ anorthite} = \text{grossular} + 2 \text{ aluminosilicate} + \text{quartz}$. The reaction curve is displaced by solid solution of the anorthite in plagioclase and grossular in garnet allowing the assemblage plagioclase + garnet + aluminosilicate + quartz to exist over a wide range of pressures and temperatures. Corrections to these equilibria for non-ideality in both garnet and plagioclase were derived from Newton and Hazelton (1981), Hodges and Spear (1982) and Ganguly and Saxena (1984) and are described in Getsinger (1985) and Lang and Rice (1985). For this study a computer program was written to calculate the pressure and temperature simultaneously using the expressions given by Getsinger (1985) and Lang and Rice (1985).

In processing the data and interpreting the results it is important to keep in mind some of the limitations that arise from the assumptions made in deriving the formulae used.

Corrections applied to either empirically derived or calculated equilibria will only improve the resulting calculated pressures and temperatures if such corrections are valid over a wide range of compositions, an assumption which is impossible to verify at present. Furthermore, re-equilibration during cooling, uplift and erosion will seriously affect the calculated temperatures and pressures. Because temperature and pressure are calculated using different equilibria the rates of re-equilibration may be different for each set of minerals. This would result in calculated pressures and temperatures which were never simultaneously experienced by the rocks.

Nevertheless, the calculated temperatures and pressures for the various areas tend to confirm the conclusions made from both field and thin section observations. The temperatures given below are those calculated using the Ganguly and Saxena (1984) correction. Other corrections will be applied during extensions to this project. The temperatures and pressures are given below as means and standard deviations (1 sigma) on multiple analyses within the samples. A complete propagation of error from all sources has yet to be made.

Ogden Peak area

Two of the samples from this area give reasonable temperatures. Sample DM-85-9 gives a temperature of $545 \pm 4^\circ\text{C}$ using seven garnet-biotite pairs. The same sample yields pressures of $7.1 \pm 0.6 \text{ kbar}$ (on 3 garnet-plagioclase pairs). This temperature and pressure is consistent with the aluminosilicate phase present (kyanite) using the phase diagram of Holdaway (1971). Sample DM-85-19 gives temperatures of $525 \pm 12^\circ\text{C}$ (5 garnet-biotite pairs) at 7 kbar. No pressure calculations were possible due to the lack of kyanite. The third sample from this area gave a wide range of temperatures (using 17 garnet-biotite pairs) from about 530 up to 955°C calculated at 7 kbar. The source of scatter may be non-equilibrium retrogression of garnet to biotite (i.e. inherited Mg/Fe ratios in the biotite giving high distribution coefficients and therefore high calculated temperatures).

Mt. Watt area

Only one sample (DM-85-33) from this area was suitable for analysis. The temperatures calculated at 6 kbar (no aluminosilicate) reflect the retrograde appearance of these rocks. Temperatures show a marked bimodal distribution. Garnet in contact with coarse grained biotite from the matrix yields temperatures of $573 \pm 14^\circ\text{C}$ (3 garnet-biotite pairs) whereas garnet in contact with much finer grained biotite in pull-aparts give temperatures of $479 \pm 8^\circ\text{C}$ (5 garnet-biotite pairs). The obvious interpretation is that the high temperatures represent prograde conditions and the lower temperatures retrograde conditions. The prograde temperature is consistent with the grade of the rocks (kyanite).

Northwest Mt. Wotzke area

It was demonstrated above that the rocks from this area are probably of higher grade than the garnet grade indicated by Campbell (1978). This is borne out by the temperature determinations for sample DM-85-72. Calculated temperatures are $613 \pm 27^\circ\text{C}$ (13 garnet-biotite pairs) at 7 kbar (no aluminosilicate). Note that the range given here is quite large compared to other samples. The reason for this is not understood.

Northeast Mt. Wotzke area

All the samples from this area yielded temperatures inconsistent with the mineral assemblage. Sample DM-85-87 gave temperatures of $514 \pm 11^\circ\text{C}$ at 7 kbar (no plagioclase).

At this pressure the temperature is much too low for rocks containing sillimanite. However, reducing the pressure and repeating the calculations yields even lower temperatures (about 4° for each kbar). Only at about 4 kbar does the calculated temperature enter the sillimanite field (T approx = 503°C). However, this is too close to the triple point as defined by Holdaway (1971) at 3.75 kbar and 500°C. The interpretation made here is that the sample has re-equilibrated at about 500°C.

Sample DM-85-93 contains plagioclase and sillimanite and is suitable for both pressure and temperature determinations. However, again the calculated temperature is too low (501 and 507°C on 2 garnet-biotite pairs). Pressures are 5.1 and 4.8 kbar. These conditions are well into the kyanite field (Holdaway, 1971) and retrogression is probably responsible for low temperatures. The accuracy of the calculated pressure is unknown because it hinges on the temperature determination.

Sample DM-85-96 also contains both plagioclase and sillimanite and is suitable for pressure and temperature determinations. Calculated temperatures are $511 \pm 8^\circ\text{C}$ (12 garnet-biotite pairs) and calculated pressures are 7.1 ± 0.4 kbar (6 garnet-plagioclase pairs). Like the previous sample these conditions are well within the kyanite field of stability (Holdaway, 1971) and equilibrium retrogression of the garnet-biotite pairs has probably occurred.

It is interesting to note that in the samples from this area there were no indications of higher grade conditions which must have prevailed. It is puzzling why retrogression in this case is complete whereas in some of the previous samples (those from Ogden Peak and Mt. Watt) at least some of the evidence for higher grades remained. The reason may lie in the higher grade attained by these rocks and in the differences in gross bulk composition of the rocks.

Conclusions

Field observations, thin section petrology and pressure and temperature calculations confirm that the rocks at Ogden Peak and Mt. Watt have undergone staurolite-kyanite grade metamorphic conditions ($T = 530$ to 570°C and $P = 6$ to 7 kbar) indicated by Campbell (1978). All the evidence indicates, however, that the rocks at Northwest Mt. Wotzke area have attained sillimanite grade ($T = 610^\circ\text{C}$ at 6 to 7 kbar) rather than the garnet grade shown by Campbell (1978). The rocks at Northeast Mt. Wotzke have attained sillimanite grade as indicated by the thin section observations. However, pressure and temperature calculations are at variance with this presumably as a result of retrogression. Thin section examination of one sample (DM-85-33) from the Mt. Watt area reveals a pull-apart or microboudinage texture which occurred at temperatures below those of the peak of metamorphism. This has important implications for the timing of structural and metamorphic events. There is no evidence to indicate a low pressure phase of metamorphism as yet.

References

Campbell, K.V. and Campbell, R.B.
1969: Quesnel Lake map-area, British Columbia; in Report of Activities, Part A, April to October 1969. Geological Survey of Canada, Paper 70-1A, p. 32-35.

Campbell, R.B.
1978: Quesnel Lake (93A) map-area, British Columbia; Geological Survey of Canada, Open File 574 (map).

Engi, J.E.
1984: Structure and metamorphism north of Quesnel Lake and east of Niagara Creek, Cariboo Mountains, British Columbia; unpublished M.Sc. thesis, University of British Columbia, 137 p.

Ferry, J.M. and Spear, F.S.
1978: Experimental calibration of the partitioning of Fe and Mg between biotite and garnet; Contributions to Mineralogy and Petrology, v. 66, p. 113-117.

Fillipone, J.A.
1985: Structure and metamorphism at the Intermontane-Omineca boundary, near Boss Mountain, east central British Columbia; unpublished M.Sc. thesis, University of British Columbia, 149 p.

Fletcher, C.J.N.
1972: Metamorphism and structure of Penfold Creek area, near Quesnel Lake, British Columbia; unpublished Ph.D. thesis, University of British Columbia, 123 p.

Ganguly J. and Saxena, S.K.
1984: Mixing properties of aluminosilicate garnets: constraints from natural and experimental data, and applications to geothermo-barometry; American Mineralogist, v. 69, p. 88-97.

Getsinger, J.S.
1985: Geology of the Three Ladies Mountain/Mount Stevenson area, Quesnel Highland, British Columbia; unpublished Ph.D. thesis, University of British Columbia, 239 p.

Ghent, E.D.
1976: Plagioclase-garnet- Al_2SiO_5 -quartz: a potential geobarometer-geothermometer; American Mineralogist, v. 61, p. 710-714.

Hodges, K.V. and Spear, F.S.
1982: Geothermometry, geobarometry and the Al_2SiO_5 triple point of the Mt. Moosilauke, New Hampshire; American Mineralogist, v. 67, p. 1118-1134.

Holdaway, M.J.
1971: Stability of andalusite and the aluminum silicate phase diagram; American Journal of Science, v. 271, p. 97-131.

Lang, H.M. and Rice, J.M.
1985: Geothermometry, geobarometry and T-X(Fe-Mg) relations in metapelites, Snow Peak, Northern Idaho; Journal of Petrology, v. 26(4), p. 889-924.

Montgomery, J.R.
1985: Structural relations of the southern Quesnel Lake Gneiss, Isosceles Mountain area, southwest Cariboo Mountains, British Columbia; unpublished M.Sc. thesis, University of British Columbia, 96 p.

Newton, R.C. and Hazelton, H.T.
1981: Thermodynamics of the garnet-plagioclase- Al_2SiO_5 -quartz geobarometer; in Thermodynamics of Minerals and Melts, ed. R.C. Newton, A. Navrotsky, and B.J. Wood; New York, Springer-Verlag, p. 131-147.

Pigage, L.C.
1978: Metamorphism and deformation on the northeastern margin of the Shuswap Metamorphic Complex; unpublished Ph.D. thesis, University of British Columbia, 289 p.

Struik, L.C.
1983: Bedrock geology of Quesnel Lake (93/A10) and part of Mitchell Lake (93A/15) map areas, central British Columbia; Geological Survey of Canada, Open File 962 (map).

Structural style of the northeast margin of the Bowser Basin, Spatsizi map area, north-central British Columbia

Project 770016

C.A. Evenchick
Cordilleran and Pacific Margin Division, Vancouver

Evenchick, C.A., Structural style of the northeast margin of the Bowser Basin, Spatsizi map area, north-central British Columbia; in Current Research, Part B, Geological Survey of Canada, Paper 86-1B, p. 733-739, 1986.

Abstract

Structural style along the northeast margin of the Bowser Basin is dominated by northwest-trending folds and thrust faults with northeasterly vergence. Angular unconformities in the Early Jurassic (Pliensbachian) to Cretaceous (Maastrichtian) strata of the Bowser and Sustut basins are expressions of a long period of interaction between terranes within the Intermontane Belt, and between the Omineca, Intermontane, and Coast belts.

Northeast-trending steeply dipping faults expose different levels of the northwesterly-trending major structures.

Résumé

La géologie structurale le long de la limite nord-est du bassin de la rivière Bowser est dominée par des plis et des failles chevauchantes à tendance nord-ouest, convergeant vers le nord-est. Les discordances angulaires des strates du Jurassique inférieur (Pliensbachien) au Crétacé (Maastrichtien) du bassin des rivières Bowser et Sustut traduisent une longue période d'interaction entre les diverses régions de la zone Intermontane, et entre les zones Omineca, Intermontane et Côtière.

Les failles à pentes abruptes axées vers le nord-est exposent différents niveaux d'importantes structures orientées vers le nord-ouest.

Introduction

In the summer of 1985 mapping at a scale of 1:50 000 was begun in Spatsizi map area (104 H, Fig. 78.1) to gain a better understanding of the structural style and tectonic setting of the northeast margin of the Bowser Basin, an area within the Intermontane Belt of the Canadian Cordillera. In the study area Jurassic (and minor Triassic) volcanic rocks are exposed in a northwest-trending belt flanked by Jurassic marine and nonmarine clastic sediments of the Bowser Basin to the southwest, and Cretaceous nonmarine sediments of the Sustut Basin to the northeast (Fig. 78.2). A structural culmination at the northeast edge of the Bowser Basin permits observation of structural style and key unconformities in rocks with the greatest range in age known in the region.

This report presents structural and tectonic implications obtained from a combination of the detailed mapping with stratigraphic relationships and sedimentological data from the Sustut Basin (Eisbacher, 1974a), and the regional map of Spatsizi map area (Gabrielse and Tipper, 1984). The map of north-central Spatsizi area is modified after Gabrielse and Tipper (1984), and the areas of more detailed mapping are within 5 km of sections B-C, C-D, E-F, and G-H (Figs. 78.2, 78.3).

I appreciate the enthusiastic assistance of Susie Gareau in the field work and an introduction to the geology and subsequent discussions with H. Gabrielse and H.W. Tipper.

Stratigraphy and tectonics

Cold Fish volcanics

Jurassic volcanic rocks in the region were previously (informally) called the Toodoggone volcanics, a name used for similar rocks of the Hazelton Group east of the Sustut Basin. The unit consists of a sequence of rhyolitic, andesitic, and basaltic subaqueous and subaerial flows, breccia, and tuff. Local fossil-bearing members of tuff, sandstone, and limestone have yielded mainly Early Pliensbachian fossils in the region of Figure 78.2, but volcanics in areas to the northwest are as young as Toarcian and Bajocian (Smith et al., 1984). The thickness of the unit is unknown, but assumed to be greater than the 1000 m exposed on ridge walls transecting the Nation Anticline in section B-C.

The areas of volcanics covered by 1:50 000 mapping, chosen for their excellent exposure and well defined layering, are southwest of Cold Fish Lake, crossed by section B-C, and immediately east of Spatsizi River, crossed by section G-H. The unit is undivided on the 1:250 000 scale map of Gabrielse and Tipper (1984). Some areas appear to be underlain by structureless masses of volcanics, but locally, and where exposure is good, individual markers may be traced for several kilometres, delineating the structure (Fig. 78.4, 78.5). Because the lateral extent of markers cannot be assumed with confidence, no attempt has been made to correlate them across faults. In the region of section I-J, steeply dipping markers in the volcanics are truncated by gently dipping sediments of the Bowser Lake Group (Fig. 78.3). Fossils collected during regional mapping indicate a Bathonian/Callovian age for the sediments (H.W. Tipper, personal communication, 1986), and therefore the angular unconformity is evidence for a pre-Bathonian/Callovian phase of deformation. In the Joan Lake Anticline (section A-B) the volcanics are overlain with slight angular discordance by the Spatsizi Group; the absence of Spatsizi Group sediments in section I-J may also be an indication of post-Pliensbachian, pre-Bathonian/Callovian deformation.

Spatsizi Group

The Spatsizi Group is predominantly marine shale and siltstone, with distinctive, well banded tuffaceous beds, and minor sandstone, conglomerate, and limestone. Recognized as a unit distinct from the Bowser Lake Group (Gabrielse and Tipper, 1984; Smith et al., 1984), it has recently been formally named and divided into formations (R.C. Thomson, personal communication). In section B-C, at least 30 m of black shale and siltstone with Early Pliensbachian fossils (H.W. Tipper, personal communication, 1986) overlie Cold Fish volcanics with minor, or no angular discordance. The contacts of the Spatsizi Group in section G-H are not exposed, but are assumed to be faults. The Spatsizi Group is coeval with the Cold Fish volcanics, and the shales are considered to be the basinward facies of the volcanic arc (Smith et al., 1984).

Bowser Lake Group

The Spatsizi Group is unconformably overlain by the Bowser Lake Group, a sequence of dark grey marine shale, chert-pebble conglomerate, and nonmarine clastic rocks (Tipper and Richards, 1976). Macrofossils in the Spatsizi area are Bathonian to Upper Jurassic (Gabrielse and Tipper, 1984). The unit is divided into a lower, Ashman Formation, and an upper unnamed sequence. Dark grey to black shale at the base of the Ashman Formation (Bathonian) is overlain by a relatively continuous layer of massive, chert-pebble conglomerate (Bathonian/Callovian). A Callovian to Oxfordian sequence of black shale with lenses of chert-pebble conglomerate and sandstone (Fig. 78.6) comprise the rest of the Ashman Formation. The marine sequence is overlain by nonmarine, upper Oxfordian to Kimmeridgian or younger, massive chert-pebble conglomerate and sandstone.

Fossil collections from the study area (sections C-D, E-F, and G-H) identified by H.W. Tipper, are Middle Jurassic; no Upper Jurassic strata are known. A study of the radiolarian fauna in the chert clasts, the dominant clasts in the conglomerate, revealed ages as young as Carnian to Norian (Late Triassic) (Currie, 1984). The most likely source for the chert is the Cache Creek Group, and the influx of coarse clastic detritus from the north and northeast (Eisbacher, 1974b) in Bathonian time is considered to mark the collision of the Cache Creek Terrane with Stikinia. The change to a nonmarine environment in the Late Jurassic indicates a rapid filling of the basin.

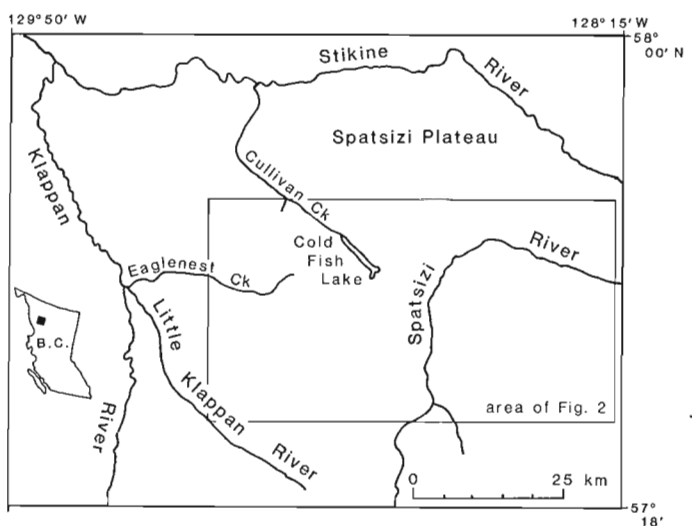


Figure 78.1. Map showing location of the study area.

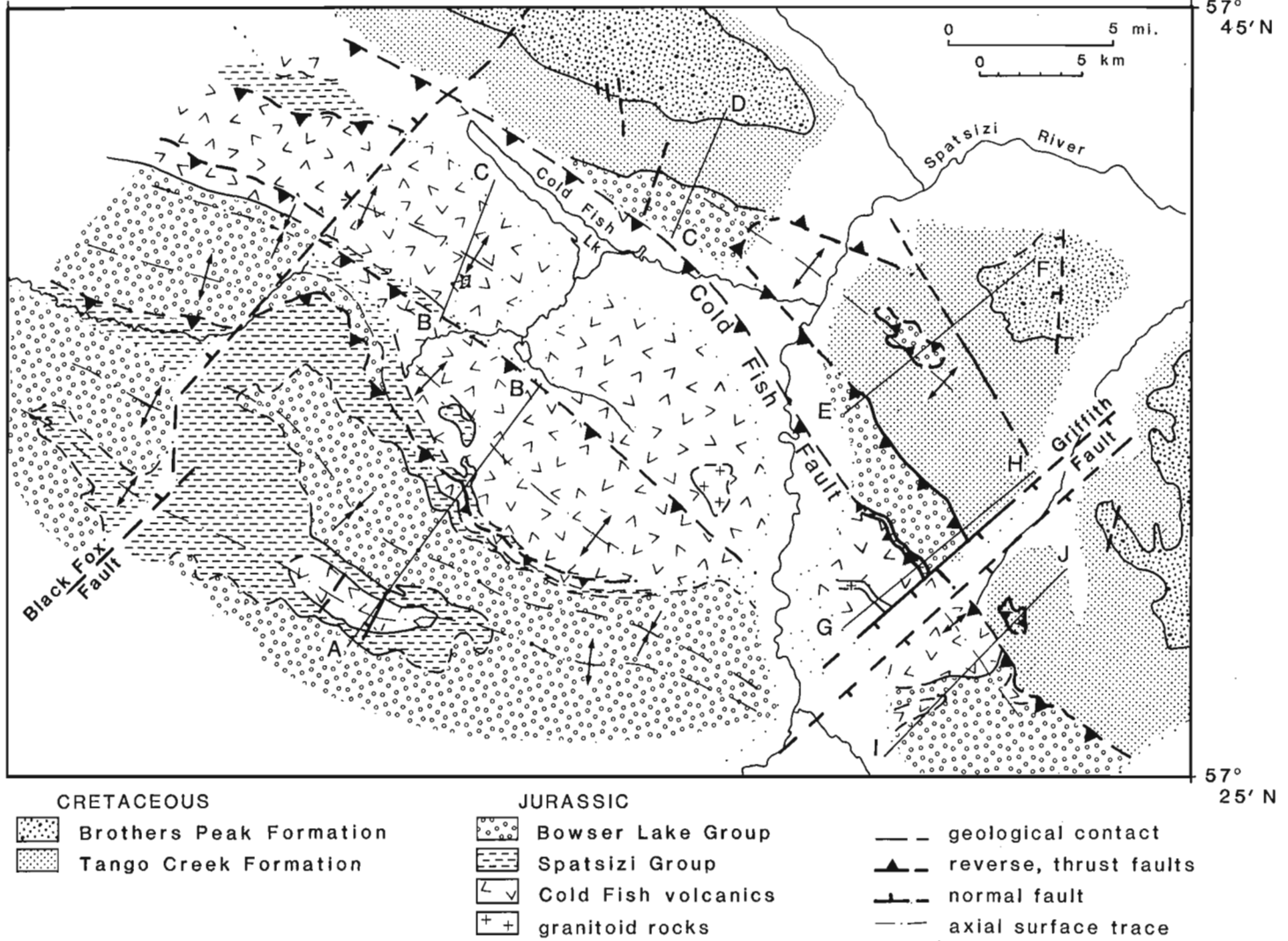


Figure 78.2. Geological map of the study area, modified after Gabrielse and Tipper (1984).

Sustut Group

The Sustut Group is a succession of nonmarine clastics, Middle Albian to Maastrichtian (based on palynology, A.R. Sweet, personal communication), that were deposited in the Sustut Basin along the northeast margin of Bowser Basin. Eisbacher (1974a) subdivided the group into two formations, each of which was further divided into two informal members. The dominant lithologies are sandstone and mudstone in the Tango Creek Formation, and mudstone, tuff, and conglomerate in the overlying Brothers Peak Formation. Eisbacher (1974a) deduced from paleocurrent data that sediments in the lower member of Tango Creek Formation were deposited by rivers that flowed southwest from Omineca Belt, across Sustut Basin, and at least the northern part of Bowser Basin. They brought the first influx of detritus from the rising metamorphosed miogeoclinal strata of Omineca Belt. Large muscovite flakes in the coarse sandstones are distinctive, and mark the base of Tango Creek Formation. Two small outliers of Tango Creek Formation southwest of Sustut Basin are further evidence that the Tango Creek once extended farther to the southwest than the

present exposure of Sustut Basin. One outlier is near Cullivan Creek, where Middle Albian sandstone and conglomerate (A.R. Sweet, personal communication, 1985) unconformably overlie Cold Fish volcanics (Gabrielse and Tipper, 1984). The other outlier is a small outcrop of mica-bearing sandstone in the core of a syncline on the top of the ridge of Bowser Lake Group shown in section G-H. The sandstone overlies a refolded isoclinal fold in Bowser Lake Group and only the later, upright, open fold appears to have affected the Tango Creek. More work needs to be done to confirm the relationships, but it appears that Middle Jurassic rocks were deformed prior to deposition of the Sustut Group. This may also explain the absence of Upper Jurassic rocks in the region. The same relationship occurs in section C-D, where Middle Jurassic conglomerate is overlain directly by Tango Creek Formation.

Paleocurrents in the upper member of Tango Creek Formation and overlying units, indicate a change to longitudinal flow, southeasterly down the axis of Sustut Basin (Eisbacher, 1974a). Eisbacher also noted an increase in the proportion of chert clasts in the upper member, inferred to

be derived from Bowser Lake Group. These data require uplift of part of Bowser Basin, presumably including the lower unit of Tango Creek Formation. Intra-Tango Creek deformation may account for the parts of the Tango Creek that are intensely deformed (Fig. 78.7), in contrast to other parts affected only by minor block faulting. The results of intra-Tango Creek deformation are shown schematically in section C-D, with a thrust fault placing Bowser Lake Group on Tango Creek Formation, a relationship observed by Eisbacher in the area shown in section E-F. Tango Creek sediments overlying Bowser Lake Group, and below the thrust fault are intensely folded. Folded Tango Creek sediments and the thrust fault carrying Bowser Lake Group over the Tango Creek are assumed to be overlain with angular discordance by relatively undeformed sediments of the upper part of Tango Creek Formation and Brothers Peak Formation. This relationship has not been observed, but can be deduced from the structural relationships, and the paleocurrent and sedimentological data of Eisbacher (1974a).

Structure

The structure is dominated by northwest-trending large scale folds and thrust faults. The map pattern is inferred to reflect different levels of the northwest-trending contractional structures juxtaposed by displacement on northeast-trending, steeply dipping, dip-slip faults. Northwest-trending folds occur in all units. Plunges range from 0 to 30 degrees, similar to those reported by Koo (1986) in the Groundhog coalfield 45 km to the south. Northeast-trending folds warp bedding; this trend of folds is associated with more intense deformation in areas to the west and southwest.

North and northeast-trending, steeply dipping extensional and contractional faults with minor (less than 50 m) displacement are common, and affect rocks as young as Brothers Peak Formation. They are also present in the Groundhog coalfield (Koo, 1986). Although most of the faults are relatively minor, two of them significantly affect the map pattern. The Black Fox Fault, northwest of section B-C (Fig. 78.2), offsets Spatsizi and Bowser Lake sediments. Much of the displacement was pre-Brothers Peak because the Tango Creek-Brothers Peak contact is offset 10 m or less. The relative displacement of the Jurassic contact shows that the fault, with unknown but assumed steep dip, had west-side-down displacement. Griffith Fault, on the slope

southeast of section G-H, is assumed to have southeast-side-down displacement because Sustut Group on the southeast side of the fault is in contact with Bowser Lake Group, and one kilometre to the northeast, a southwest dipping contact between members of the Bowser Lake sediments also has apparent southeast-side-down offset. These relationships suggest that the block between the Black Fox and Griffith faults is high-standing with respect to the bounding areas. Recognition of the significance of the Black Fox and Griffith faults allows a more consistent interpretation of the northwest-trending structures.

In section A-B, the Joan Lake Anticline exposes one of the most basinward areas of Cold Fish volcanics. The extent that the volcanics continued to the southwest under the Bowser Basin is unknown. To the northeast is a relatively simple syncline, and on the southwest flank of the Mt. Will Anticline is a thrust fault that repeats a sliver of the Spatsizi Group. A thrust fault to the northwest puts Spatsizi Group on Bowser Lake Group and is inferred to be a higher structural level of the fault shown on section A-B. These were shown as two separate faults by Gabrielse and Tipper (1984). On the northwest side of Black Fox Fault, the same structures are identified, but at a higher stratigraphic level, so that volcanics are not exposed on either of the anticlines, nor in the hanging wall of the thrust fault.

Section B-C crosses a broad faulted anticline, the Nation Anticline. Small outcrops of Spatsizi Group occur on the southwest flank and in a valley on the southwest side of the anticline (Fig. 78.2). The Spatsizi Group (with late Early Pliensbachian fossils, H.W. Tipper, personal communication) unconformably overlies volcanics on the southwest flank of Nation Anticline. Volcanics on the northeast flank of the Mt. Will Anticline are inferred to be thrust over the Spatsizi Group on the southwest flank of Nation Anticline. There, and on the southwest flank of Mt. Will Anticline, faults carrying the Cold Fish volcanics used the shales of the Spatsizi Group as a glide zone; the same level of detachment is assumed for thrust faults postulated to lie below the Nation Anticline. Erosion through one of the faults produced the window shown in Figure 78.2 near section B-C. A fault carrying volcanics over the Nation Anticline, above the level of exposure in section B-C, may explain the presence of volcanics at higher structural levels elsewhere (ie. northwest of Black Fox Fault). Southeast of Griffith Fault, the Cold Fish volcanics close around the southeast-plunging Nation Anticline (sections G-H, I-J).



Figure 78.4. View west obliquely across the northwest-trending Nation Anticline near section B-C, showing the well developed layering, and structural style of the Cold Fish volcanics.



Figure 78.5. View southeast to the well-layered volcanics on the northeast limb of the Nation Anticline. Rocks on the extreme right of the ridge coincide with rocks on the extreme right of the ridge in the foreground of Figure 78.4.

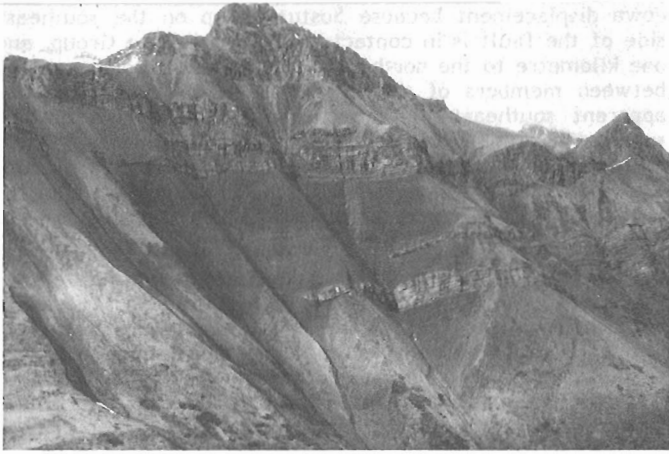


Figure 78.6. View northeast to shale and channel conglomerate in the Ashman Formation northwest of section A-B.



Figure 78.7. View southeast to folded sediments of the Tango Creek Formation, on the ridge crossed by section G-H.

Mesoscopic folds in the volcanics are rare, but well defined large scale folds near section B-C define the crest and northeast limb of the anticline (Figs. 78.4, 78.5). The southwest limb is faulted near section B-C. The fault that cuts the crest of the anticline occurs only on the ridge of section B-C, and seems to have minor displacement. The volcanics in section G-H have consistently steep dips, commonly subvertical in the south. In this area the only fold seen is a tight to isoclinal antiform, overturned slightly to the northeast, with an amplitude of at least 200 m.

The Cold Fish Fault occupies the valley of Cold Fish Lake and is the northeasternmost limit of Cold Fish volcanics. Outcrops are rare in the valley, but one outcrop of volcanics on the slope north of the southeast end of the lake limits the fault to the northeast side of the valley near section C-D. The volcanics are within 500 m of outcrops of the Bowser Lake Group which is exposed in section C-D as a broad anticlinorium. On the steep northeast limb, mica and plant-bearing sandstone and mudstone of Tango Creek Formation unconformably overlie chert-pebble conglomerate of Bowser Lake Group. Folds in Tango Creek Formation are chevron-like, with southwest-dipping axial surfaces. One kilometre north of the contact with Bowser Lake sediments, the Tango Creek is steeply to moderately northeast-dipping, and is affected only by tilting and late block faulting, as is the Brothers Peak Formation. From structural and sedimentological data, the undeformed Tango Creek is inferred to unconformably overlie folded Tango Creek and Bowser Lake sediments.

Low on a hillside southeast of section C-D, below the anticline in the Bowser Lake Group, a discontinuity in stratigraphy was seen from a distance. It may either be an intra-Bowser unconformity like the one observed by Eibacher (1974b) to the southeast, or a thrust fault placing Bowser Lake on Tango Creek. The latter relationship was observed along trend to the southeast by Eibacher (1974a) (section E-F), where a klippe of Bowser Lake Group lies on folded Tango Creek Formation. Further study of that klippe, and a fossil collection, confirmed that the rocks are Middle Jurassic, and that the extent of Bowser Lake sediments is roughly as Eibacher originally showed, not as shown by Gabrielse and Tipper (1984). The thrust fault beneath the klippe is inferred to be the same fault that puts Bowser Lake Group on the Tango Creek at the southwest end on section E-F and in section G-H. A northwest plunge of less than 10 degrees is required to close the thrust fault around the anticline before it reaches the level of exposure on the

ridge in section C-D. On the southeast side of Griffith Fault (section I-J), the thrust fault is interpreted to be lower than the level of erosion. Tango Creek Formation below the thrust is well exposed in sections E-F and G-H, and is intensely deformed; axial surfaces consistently dip to the southwest (Fig. 78.7). Folds in the Bowser Lake Group are commonly large-scale, open to close folds. In section G-H, one isoclinal fold overprinted by an upright open fold occurs below an unconformity with Tango Creek.

The absence of Bowser Lake Group in the footwall of the Cold Fish Fault southeast of Griffith Fault (section I-J), can be explained by southeast-side-down displacement on the fault. If the unconformity on the top of the ridge in section G-H is a gently-dipping surface that cross cuts structures in the Bowser Lake Group, then at higher levels only Tango Creek should occur in the footwall of the Cold Fish Fault. The relationship in the air inferred in section G-H is seen on the ground in section I-J, and implies that Cold Fish Fault is post-Middle Albian.

Regional implications

In a reconnaissance of the stratigraphy and structure of the Groundhog coalfield, southern Spatsizi area, Bustin and Moffat (1983) presented cross sections of the northern margin of the coalfield. A measurement of the length of the contact between the Jackson and Currier units, when compared with the width of the section (p. 241, their Fig. 15) indicates that folding has resulted in 15 per cent shortening. According to Bustin and Moffat, no significant thrust faults occur in the area, but a décollement must occur at depth to accommodate the shortening observed at the surface, and is shown schematically as a fault below the Jackson unit into which all thrust faults sole. Data collected in the summer of 1985, when combined with regional work, show that rocks as old as Pliensbachian are involved in significant contractional deformation. The contact between the Cold Fish volcanics and Spatsizi Group has been shortened approximately 50 per cent. A décollement probably exists in or below the Cold Fish volcanics (or basinal equivalents).

Summary

Northwest-trending folds and faults are an expression of major northeasterly shortening. Dip-slip displacement on northeast-trending faults has resulted in the exposure of different levels of the contractional structures.

From the relationships of structures above and below unconformities it appears that significant deformation occurred during the following times: post-Pliensbachian, pre-Bathonian/Callovian (unknown style and vergence); post-Bathonian/Callovian, pre-Albian (NE contraction); and post-Middle Albian, pre-Campanian (NE contraction). In an area 160 km to the southeast, the Brothers Peak Formation is also involved in deformation, indicating post-basal Brothers Peak deformation (post-Campanian?). The unconformities are an expression of deformation involving a number of terranes over a period of about 100 Ma. Collision of Stikinia with Cache Creek Terrane (Middle Jurassic, Bathonian) initiated coarse clastic deposition in Bowser Basin as chert was derived from Cache Creek Group, and resulted in a stratigraphic link between the two terranes. Subsequent shortening in Bowser Basin predated deposition of the Sustut Group and may have been related to continued convergence between Stikinia and the Cache Creek Terrane. Late Early Cretaceous uplift in the Omineca Belt is reflected by clasts of miogeoclinal rocks and detrital micas that were deposited in the Sustut Basin and across part of the northern Bowser Basin. Northeast-verging folds and thrust faults in Bowser Lake Group and the lowest Sustut Group were associated with uplift of Bowser Basin, confining further sedimentation to Sustut Basin. The deformation reflects interaction between Stikinia and the Coast Belt. Shortening continued into the middle Late Cretaceous and possibly later.

References

- Bustin, R.M. and Moffat, I.
 1983: Groundhog coalfield, central British Columbia: reconnaissance stratigraphy and structure; Bulletin of Canadian Petroleum Geology, v. 31, p. 231-245.
- Currie, L.
 1984: The provenance of chert clasts in the Ashman conglomerates of the northeastern Bowser Basin; unpublished B.Sc. thesis, Queen's University at Kingston, 59 p.
- Eisbacher, G.H.
 1974a: Sedimentary and tectonic evolution of the Sustut and Sifton Basins, north-central British Columbia; Geological Survey of Canada, Paper 73-31, 57 p.
 1974b: Deltaic sedimentation in the northeastern Bowser Basin, British Columbia; Geological Survey of Canada, Paper 73-33, 13 p.
- Gabrielse, H. and Tipper, H.W.
 1984: Bedrock geology of Spatsizi map area (104 H); Geological Survey of Canada, Open File 1005.
- Koo, J.
 1986: Geology of the Klappan coalfield in northwestern British Columbia (104H/2,3,6,7); British Columbia Ministry of Energy, Mines and Petroleum Resources, Geological Fieldwork, 1985, Paper 1986-1, p. 225-228.
- Smith, P.L., Thomson, R.C., and Tipper, H.W.
 1984: Lower and Middle Jurassic sediments and volcanics of the Spatsizi map area, British Columbia; in Current Research, Geological Survey of Canada, Paper 84-1A, p. 117-120.
- Tipper, H.W. and Richards, T.A.
 1976: Jurassic stratigraphy and history of north-central British Columbia; Geological Survey of Canada, Bulletin 270, 73 p.

DC resistivity and CSAMT profiles of the southwestern Fraser River delta, British Columbia

Project 820017

T.S. Hamilton and D.C. Nobes
Cordilleran and Pacific Margin Division, Sidney, B.C.

Hamilton, T.S. and Nobes, D.C., DC resistivity and CSAMT profiles of the southwestern Fraser River delta, British Columbia; in Current Research, Part B, Geological Survey of Canada, Paper 86-1B, p. 741-747, 1986.

Abstract

Geoelectrical sounding profiles were collected on the southwestern part of the Fraser River delta to assess the viability of electrical techniques in a tidal flat environment. It proved to be rapid and relatively inexpensive, and adaptable to the tidal flats of Roberts Bank. Electrical prospecting methods yield resistivity versus depth information which provides a complementary data set to drillholes and seismic reflection records, to give thickness variations, structures and facies changes. This information contributes to our understanding of the Quaternary history of the Fraser River delta, to the geotechnical assessment for foreshore and marine engineering development, and to the evaluation of seismic risk.

Résumé

Des profils de sondages géoélectriques ont été faits dans la partie sud-ouest du delta du fleuve Fraser afin d'évaluer la fiabilité des techniques électriques dans un milieu de zone intertidale. Cette technique s'est avérée rapide et relativement peu coûteuse, et tout à fait adaptable à la zone intertidale du banc Roberts. Les méthodes de prospection électrique fournissent des données de la résistivité par rapport à la profondeur, ce qui permet d'obtenir des données complémentaires à celle des trous de forage et des registres de réflexion sismique; elles renseignent ainsi sur les variations des épaisseurs des strates et les changements de structures et de faciès. Ces renseignements contribuent à une meilleure compréhension de la période du Quaternaire du delta du fleuve Fraser, et contribuent à l'évaluation géotechnique des zones d'avant-plage et marine en vue de travaux de mise en valeur, ainsi qu'à l'évaluation des dangers sismiques.

Introduction

Electrical sounding techniques have been used effectively for shallow prospecting in a variety of engineering and geological applications including foundation studies for major construction projects and the determination of overburden thickness and hydrological studies (Bhattacharya and Patra, 1968). The goal of the survey, in all of these cases, is to determine the thickness and/or lateral extent of a less resistive unconsolidated layer over a more resistive bedrock.

As with other geophysical methods, a sound interpretation relies on a knowledge of the lithologies likely to be present and an appreciation of the possible variation in their physical properties. A general framework has been established for the Quaternary geology of the lower mainland (Armstrong and Hickock, 1976), for the postglacial history of the Fraser delta (Clague et al., 1983) and for the Quaternary section beneath the Strait of Georgia (Hamilton and Luternauer, 1983). Essential borehole control on lithologies of the Fraser delta (Roberts et al., 1985) and the subjacent Tertiary and Cretaceous sedimentary bedrock units (Hopkins, 1966; Richfield Pure Point Roberts 6-3-5 well history report), along with a regional indication of variations in bedrock stratigraphy (Roddick, 1965) provide the necessary geological background for interpreting geoelectrical surveys in the area.

During the 1985 field season, a variety of geological and geophysical studies were performed, directed at improving our understanding of the Quaternary section in the southwestern part of the Fraser delta. These studies were conducted mainly on the subaerial portion of the delta and included shallow high-resolution seismic profiling, coring and geophysical borehole logging (Luternauer et al., 1986). A program of geoelectric profiling was initiated to determine the resistivity structure of the shallow part of the sedimentary column and to demonstrate the utility of the method in the logistically difficult area of Roberts Bank (Fig. 79.1). This area was chosen for study because the tidal flats constitute a significant gap in the regional Quaternary picture, being inaccessible to conventional seismic techniques as practiced in deeper water or on land, and because sufficient groundtruth had already been collected on the shallow lithologies (by the 1968 Swann Wooster/National Harbours Board coring program for the geotechnical assessment of the coalport) to constrain subsurface geophysical interpretations in this area. These studies should also serve as a model for future geoelectrical investigations of the Fraser River delta.

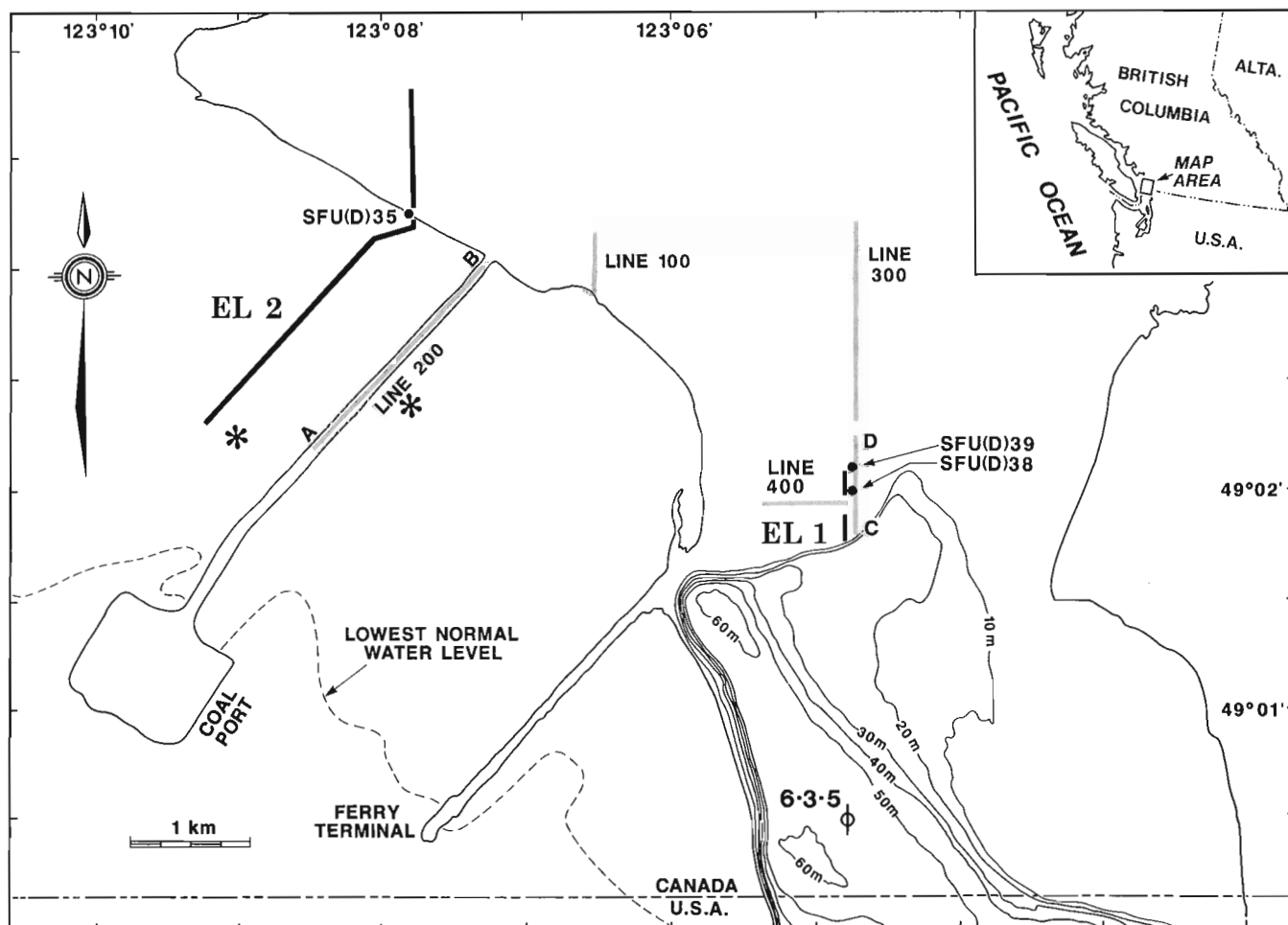


Figure 79.1. Geographic setting of survey area. The electrical survey lines are shown in black, seismic survey lines (100 to 400) in grey and coreholes as dots (SFU(D)35 etc.) of Luternauer et al. (1986). Asterisks denote the locations of geotechnical assessment boreholes (Swann Wooster Engineering/National Harbours Board, 1969). The location of the Richfield-Pure Point Roberts exploration well is given by the dry hole symbol ϕ . For clarity of presentation, the separation of seismic line 300 and resistivity line EL1 has been exaggerated; the true separation was 8 m.

Methods and techniques

The resistivity equipment consisted of Phoenix IPT1 and IPT1B transmitters (maximum output 3 kW at 10 A) and a Huntec M4 receiver. For line EL1 20 m dipole spacings were used with the IPT1B transmitter and with input power ranging from 25 to 60 W. For line EL2 the source and receiver dipoles were 100 m long for the southern part of the line (across the tidal flats), and 50 m long for the northern part of the line (along 34th St.). There, a gasoline generator supplied power to the IPT1 transmitter. The input power ranged from 300 to 750 W for the 100 m dipole and 500 to 2500 W for the 50 m dipole. On all lines, chargeability readings (induced polarizations) were also taken, using 100 ms delay times, 100 ms integration times and 0.125 Hz (8 s period) with 50% duty cycle. Routine readings taken at each station included: Vp (primary voltage), Sp (self potential), total chargeability, number of cycles and 10 chargeability factors.

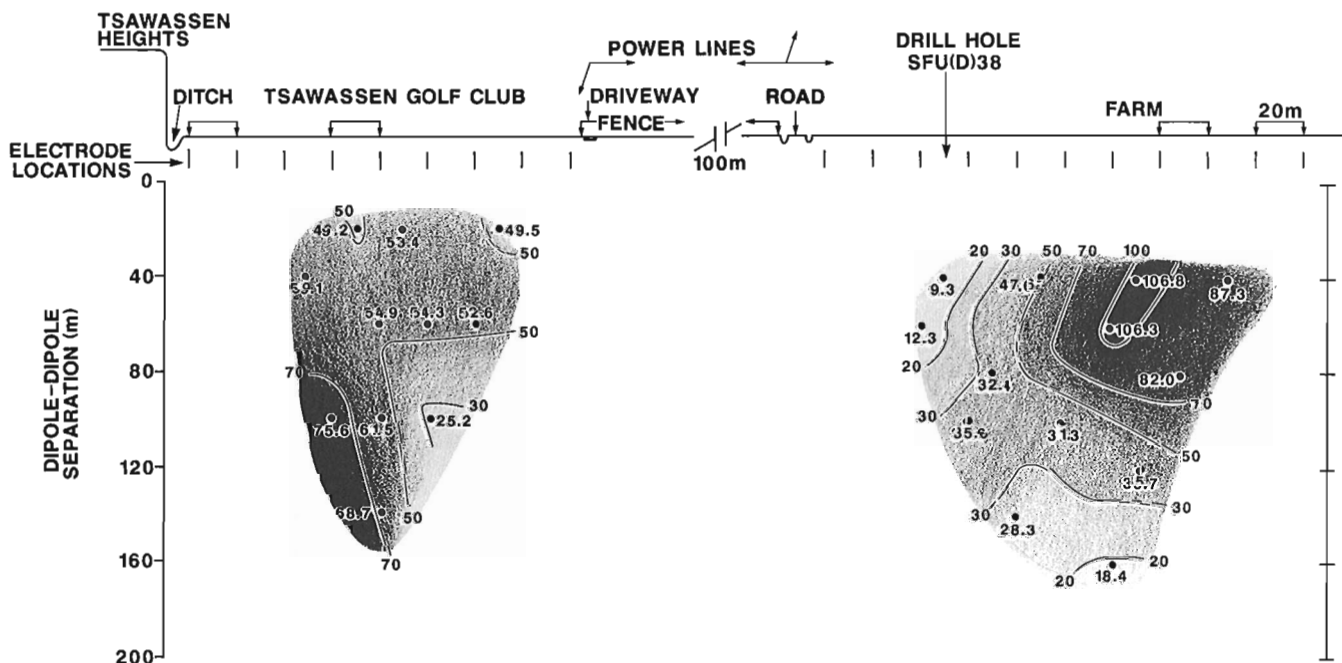
Preceding the actual survey, array tests were performed on Lulu Island (near 123 02.4', 49 09.7') in an area underlain by more than 35 m of fluvial and tidal-facies silts and sands of probable Pleistocene age (based on coring results by M. Roberts and students, personal communication, 1986). For both Wenner and dipole-dipole array configurations, electrical soundings indicated a near surface zone (<10 m) of moderately high apparent resistivities (up to 90 ohm-m), correlating with the upper silt member, overlying a less resistive zone (2 to 6 ohm-m) extending to several tens of metres depth. The contrast picked up in these tests effectively distinguished the top of the water table at the upper silt/sand boundary, revealing it to be an electrical as well as a lithological and a hydrological boundary. These equipment and operations tests indicated the range of apparent resistivities to be expected for the Quaternary sediments, in addition to demonstrating the extent to which the resistivities could be raised in the vadose zone.

Field survey work was performed from 14 to 17 August 1986, chiefly to take advantage of pronounced daytime low tides for the work on Roberts Bank. The decision to conduct the survey directly on Roberts Bank at low tide/subaerial exposure was made to acquire data more directly comparable to on-land results, and to avoid any ambiguity or masking effect imposed by a thin, highly conductive seawater layer. From magnetic observatory records at Victoria, this interval proved to be magnetically quiet and the survey data are considered to be free from natural electrical perturbations. This was also born out by the very low noise levels which were determined when comparative sets of readings were made with the transmitter switched off. Field work proceeded rapidly as the entire electrical survey was completed in four days with a four-person crew, averaging 1 km per day. By comparison, the acquisition of the 5 km of high resolution seismic data (Luternauer et al., 1986) kept a four-person crew occupied for approximately three weeks.

Electrical sounding profiles

Line EL1

The pseudo-section for line EL1 (Fig. 79.2) indicates a complex, non-layered subsurface electrical structure not correlated with either the drillhole or the seismic reflection data of Luternauer et al. (1986). The observed range of apparent resistivities (9.3 to 106.8 ohm-m) is comparable with that observed in the downhole log of borehole SFU(D)38, but markedly lower in the actual position of the drillhole (<25 ohm-m on the line compared to resistivities for individual thin beds of up to 90 ohm-m). This may be due to differences in electrode spacing between the two methods, directional anisotropy, or contamination of the region by the low resistivity salt muds used in drilling.



APPARENT RESISTIVITY PSEUDO-SECTION EL 1

Figure 79.2. Pseudo-section for resistivity line EL1. Due to the presence of power lines, fences, and culverts, the middle portion of the line was not surveyed. Note the 20 m separation for both the current and potential electrodes. Relative depth is plotted as dipole-dipole separation, with no vertical exaggeration. Drillhole SFU(D)38, with a suite of downhole geophysical logs, is indicated.

The high and variable resistivities in the upper part of the northern portion, and all of the southern portion of the line, may be due to facies changes or changes in water content in the Quaternary section. Sediments with a nominal 30% porosity, a relatively fresh (1 ohm-m) formation water and with saturation varying from 33% to 100% would account for the observed apparent resistivities. Regions of drained zones and perched water tables would be expected for the kinds of Quaternary sediments present in the Point Roberts area. Small scale facies changes are indicated by the geological mapping (Armstrong and Hickock, 1976), the lack of lithologic continuity between closely spaced boreholes and the shallow high resolution seismic sections.

The low (<30 ohm-m) apparent resistivities at the deepest part of the north end of the section are thought to represent saturated Tertiary bedrock. Low resistivities and high porosities were determined for the water saturated Tertiary clastic succession in the nearby Point Roberts well (well history report, Richfield Pure Point Roberts 6-3-5). In addition, the major seismic reflector (on line 300) representing the top of the Tertiary shallows in this area and borehole SFU(D)39 was only able to penetrate to 13 m depth, which could also be taken to indicate the proximity of bedrock and the abbreviated nature of the local Quaternary succession (Luternauer et al., 1986). For Tertiary bedrock saturated with relatively fresh formation waters (1 ohm-m) the range of apparent resistivities indicate a range of porosities from 17 to 31%, in keeping with the Point Roberts well.

Line EL2

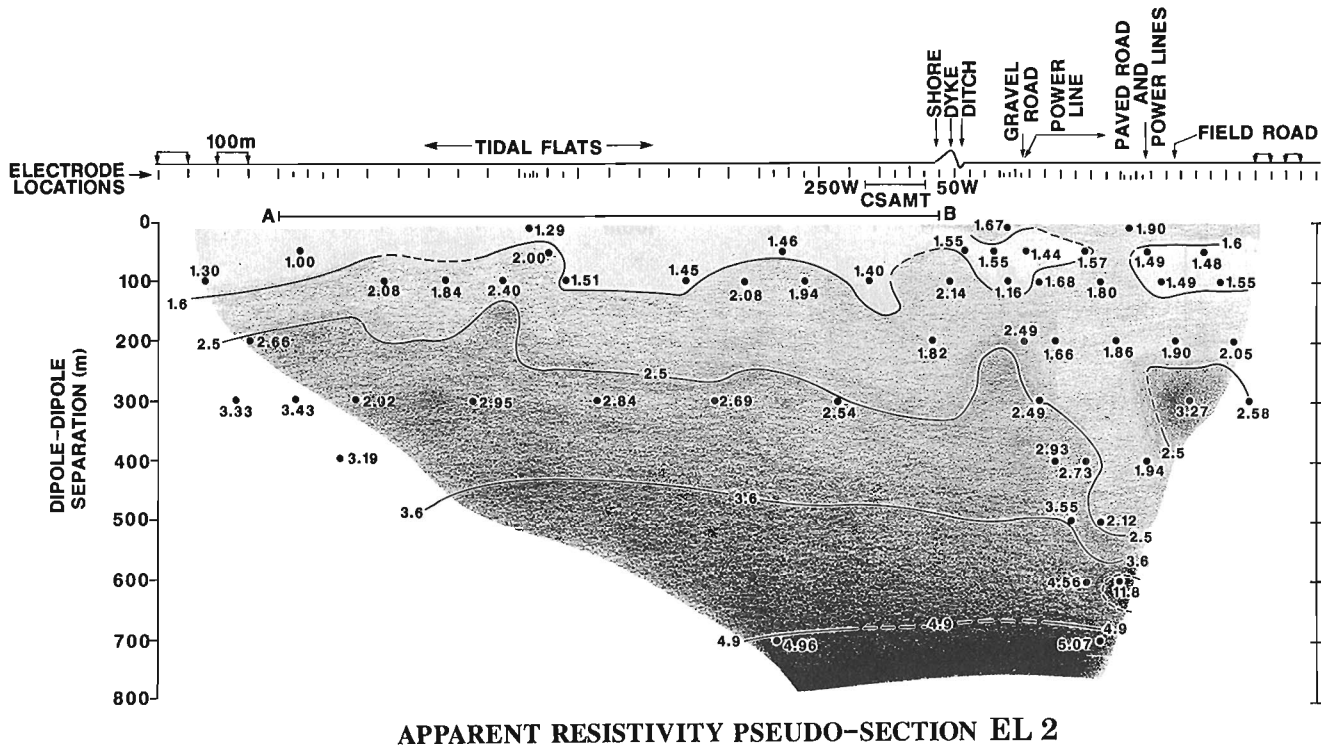
The apparent resistivity structure below the tidal flats and adjacent dyked lowlands is relatively flat and characterized by low values (Fig. 79.3). The low apparent

resistivities are predictable, particularly for the tidal flats where the near-surface sediments (both exposed and in boreholes) are superhydrous marine silts with high porosities and relatively saline formation waters. The relief on the resistivity contours is thought to reflect real subsurface structures such as channels and buried topography due to erosional and constructional features of probably Pleistocene age. Unconformities with relief of this type are frequently seen within glacially dominated parts of the Quaternary section (Hamilton and Luternauer, 1983; Luternauer et al., 1986). On the pseudo-section, the complexity just to the north of the land-sea boundary is marked both by an inversion in the apparent resistivity gradient as a function of depth and by the persistence of low apparent resistivity values at depth. Possible geological explanations for this geoelectrical structure include hydrological effects at the land-sea boundary (freshwater-saltwater mixing) and the influence of a local bedrock high (as indicated by seismic Lines 200 and 100). However, some effect due to the presence of power lines in this vicinity cannot be ruled out.

The CSAMT (Controlled Source Audio Magneto-Tellurics) pseudo-section for the near shore portion of the Roberts Bank line EL2 is presented in Figure 79.4A. Apparent resistivity was directly available as output from the Phoenix system (calculated from E and H fields) while the depth is scaled according to the relationship:

$$h = (\rho_a < T > / 2\pi\mu)^{1/2}$$

(Bostick, 1977); where h represents the depth, T represents the period (inverse frequency), $\rho_a < T >$ is the apparent resistivity as a function of period, μ is the magnetic permeability of free space. An attempt was made to model the CSAMT results using a Bostick transform as described by Jones and Foster (1986). However, because of the large gradients in apparent resistivity at the top and bottom of the



APPARENT RESISTIVITY PSEUDO-SECTION EL 2

Figure 79.3. Pseudo-section for resistivity line EL2. This particular crossing of Roberts Bank was chosen to avoid buried submarine power cables. Principal spacings for both current and potential electrodes were 100 m across the tidal flats and 50 m on land. Relative depth is plotted as dipole-dipole separation with a vertical exaggeration of 2X. The CSAMT line was run by reoccupying stations of the resistivity line for the receiver positions, while the source was positioned along the coalport causeway, about 1 km to the southeast. The projected position of seismic line 200 is shown by A-B.

intermediate layer, the inversion was unstable. Nonetheless, there is good qualitative agreement between the magnetotelluric and the DC resistivity sections and also a general agreement between the electrical and the seismic structure (line 200). In both the CSAMT section (Fig. 79.4A) and the seismic section (line 200) there is an indication that Tertiary basement slopes down to the southwest. In Figure 79.4A, the persistence of relatively low apparent resistivities to about 84 m is best explained by relatively high porosities. This is in keeping with the unconsolidated sand and silt lithologies encountered by shallow boreholes in the immediate area (SFU(D)35) and in the 1968 Swann Wooster/National Harbours Board geotechnical boreholes (see asterisks, Fig. 79.1) and also in keeping with moderately conductive formation waters (0.25 to 1.0 ohm-m).

On the CSAMT pseudo-section, a gross progression from high resistivities to low resistivities and back to high resistivities with increasing depth, imply that induced currents will be channelled in the intermediate more conductive layer. The high apparent resistivities at the highest frequencies on the CSAMT section can be interpreted in terms of partial water saturations (60% or greater) in the shallowest layers. The draining of pore waters and expulsion of gases from the sediments of the tide flats was in fact observed during falling and rising tides over the course of the survey, supporting the possibility of water saturations less than unity. At any depth apparent resistivities decrease in a southwesterly sense. This transverse gradient can be readily interpreted as an increase in salinity from the landward side to the seaward side of the section, because of the fresh water recharge and runoff from the nearby emergent lowlands. The conductivity of brine solutions varies approximately linearly with salinity allowing one to estimate the salinities across

the section according to relatively simple formulae (Dresser Atlas, 1979). Using the layers, temperatures, and porosities of the preferred resistivity model given in Table 79.1, the lateral gradient in apparent resistivities implies that salinities vary by a factor of 1.3 to 3.3 across the 200 m width of the section. Furthermore the salinity gradients appear to be greatest in the intermediate layer with the most saline formation waters.

A simple three layer resistivity structure was determined by comparing the DC data to the reference field curves (apparent resistivity versus apparent resistivity divided by depth) of Bhattacharya and Patra (1968). Considering the relatively flat nature of the pseudo-section (Fig. 79.3), the apparent resistivities given at each depth were averaged to obtain an approximate layered electrical structure that would fit the whole data set. These averages were plotted with errors, given by the actual range of values rather than a standard error of the mean. The theoretical response curves for various configurations of thickness and resistivity contrast were compared to the averaged values for Roberts Bank taking into account the actual range of values. The preferred model, based only on the dipole-dipole data, is presented in Table 79.1 and also in Figure 79.4B, along with the range of acceptable models. The average temperatures in the various layers were estimated from the bottom hole temperature of the Point Roberts well and the local geothermal gradient of about 15 degrees celsius per kilometre. This low geothermal gradient is in keeping with expectations from regional heat flow studies. The estimates of porosity and formation water resistivity are based on the DC data set and Archie's law. Note the general agreement between the data points transcribed from the CSAMT section and the DC models. The first layer in the electrical model is

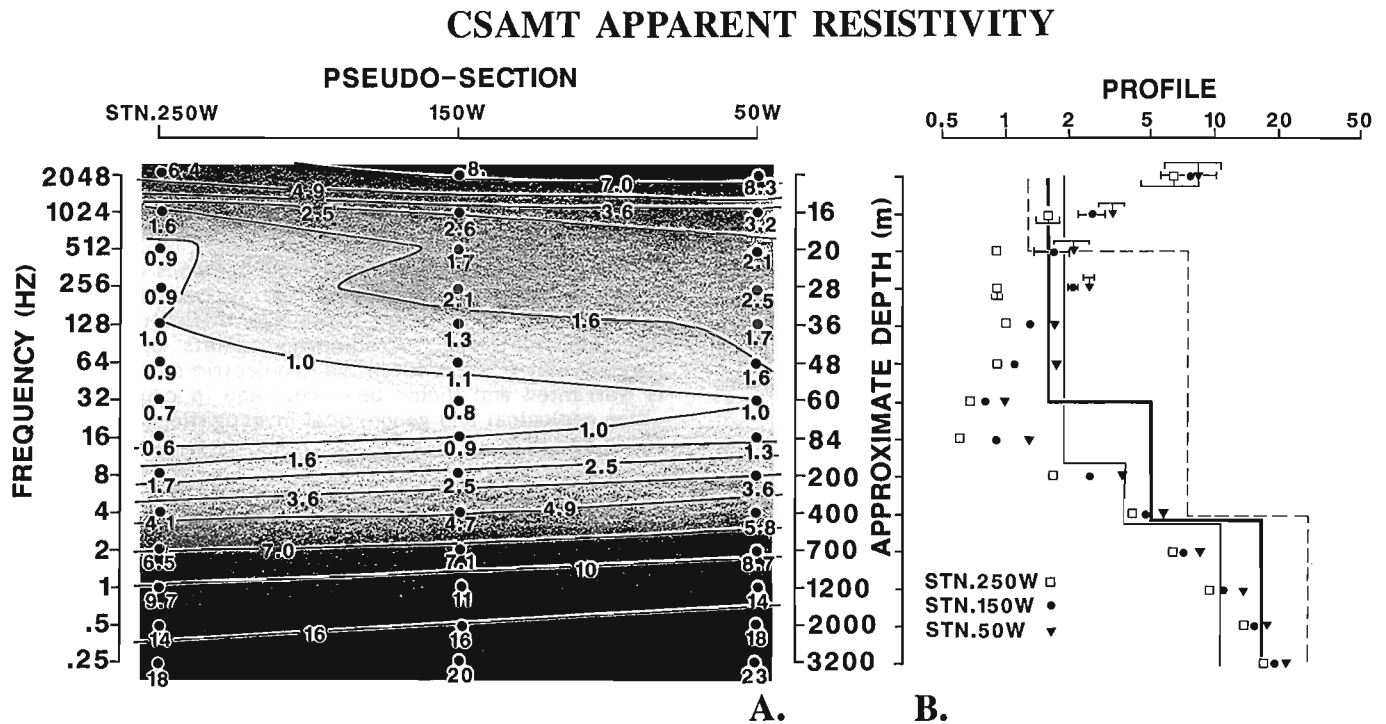


Figure 79.4. A. CSAMT pseudo-section across the nearshore portion of Roberts Bank. Note the logarithmic depth scale. B. Comparison of CSAMT profiles to simple three layer models for the DC resistivity. Apparent resistivity is shown as a function of depth (both on logarithmic scales). Data points for the CSAMT profiles are transcribed from the adjacent pseudo-section. The preferred DC resistivity model is indicated by the bold line, with the range of acceptable models indicated by the dashed and the faint solid lines.

Table 79.1

Layer	Thickness (m)	Layer Resistivity	Pore Fluid Resistivity	Temp (C)	Porosity (%)
Unconsolidated Quaternary Sediments	70 ± 60	1.6 ± 0.3	1.00	9	72 to 88
Transition Zone Pleistocene ± Weathered Bedrock	365 ± 60	7.0 ± 4.0	0.25	10	15 to 29
Tertiary Clastic Sedimentary Bedrock	unresolved	22.0 ± 12.0	0.92	15	16 to 30

equivalent to the Quaternary layer (Holocene plus Pleistocene undifferentiated on seismic line 200). While the resistivity of this shallowest layer is well constrained its thickness is not. The ambiguity in resolving the layer 1-2 boundary and in constraining the resistivity for layer two is simply due to real structural variations (topography on the base of layer one) as is implied by both the contours in Figure 79.3 and the dipping reflectors within and at the base of the Quaternary sediments on seismic line 200. One should interpret the large error bars on the thickness of layer one as an indication of the presence of real structure in the first layer, rather than that the model is poor. The depth to the third layer is well constrained by the model although this is well below the actual top of bedrock as deduced from the seismic data. This layer has resistivities which are very similar to the Tertiary clastic sedimentary succession in the nearby Point Roberts well. The intermediate layer has formation resistivities which are transitional to layer three. The most likely geological explanation for layer two is that it represents a transition zone comprised partially of tighter Quaternary deposits than are found in layer 1 (Pleistocene tills and marine clays etc.) and partly of weathered bedrock or strata with more saline formation waters than are typical for the Tertiary succession below. Alternatively, one could interpret the transition zone in terms of a resistivity gradient representing the closure of porosity with depth.

In the model, layers one and three have relatively fresh formation waters (salinity less than 10 000 ppm) to give the best agreement between observed and expected porosities. If by contrast, layer one were completely saturated with sea water, the estimated porosities would drop to the 40% range but these are still greater than any possible estimates for layer two. Similarly if the formation fluid resistivities and salinities for layer three were more like those of seawater, the porosity estimates would drop to the 13% range but these estimates are still in line with data for the Point Roberts well, and still imply a tighter bedrock than the overlying strata.

Discussion

Conventional DC resistivity and MT surveying techniques have proven useful in defining the shallow geoelectrical structure of the southwestern Fraser River delta and in providing a complementary geophysical data set to the seismic and borehole information. The unconformity at the base of the Quaternary was found to have considerable relief, which was unexpected in this region of subdued surface topography. Of particular interest are the places where the Tertiary bedrock rises to near the surface at the north end of line EL1 and beneath the dyked foreshore along the edge of Roberts Bank. Along line EL2, the apparent

resistivity is interpreted in terms of a three-layer model, with an upper porous hydrated layer composed of unconsolidated Holocene and Pleistocene deposits (sands, silts) overlying a transition zone composed of lower porosity materials (Pleistocene tills, compacted marine clays, and weathered Tertiary bedrock) which in turn overlies less porous Tertiary sedimentary strata which constitute local electrical basement. Subsurface topography between layers 1 and 2 is readily apparent and correlates well with seismic and geotechnical borehole results.

Not only are the resistivity data useful for the interpretation of stratigraphy and structure but also for relative changes in other subsurface petrophysical properties, particularly in the porosity and the salinity of formation waters. On Roberts Bank the porosity of layer one is 72 to 88%, for a pore fluid that consists of seawater mixed with freshwater discharge from the neighboring lowlands. General trends in the CSAMT results support this conclusion. The transition zone has porosities ranging from 15 to 29%, for a pore fluid consisting of seawater, or 30 to 60% for a freshwater-seawater mixture. A porosity gradient most likely exists, decreasing downwards through the transition zone. Porosities in the Tertiary bedrock (layer 3) range from 16 to 30%, in good agreement with results from the Point Roberts well. Apparent resistivities at all depths decrease in a seaward direction correlating with an increase in salinity.

In conclusion, these electrical methods are rapid and relatively inexpensive, and have been successfully adapted to the relatively unknown and logistically difficult region of the intertidal platform. Preliminary results of this survey suggest that a more extensive geoelectric sounding program is warranted and should be undertaken in conjunction with other geological and geophysical investigations on the Fraser River delta.

Acknowledgments

The authors gratefully acknowledge the able assistance of D. Duggan, L. McIntyre and J.L. Luternauer in performing the electrical survey and extend special thanks to Captain John McGrath and the personnel of the Canadian Coast Guard Hovercraft Base at Sea Island for providing logistical support on the tidal flats. The Department of Geophysics and the Astronomy at the University of British Columbia also provided logistical support with the loan of a transmitter and a receiver. Thanks are due P. Cartwright of Phoenix Geophysics for the release of the CSAMT data, to M.C. Roberts of Simon Fraser University for providing access to his drillhole logs, and to J.A. Hunter and S.E. Pullan for providing access to their seismic profiles.

References

- Armstrong, J.E. and Hickock, S.R.
1976: Vancouver Sheet, Surficial Geology; Geological Survey of Canada, Map 1486A, 1:50 000.
- Bhattacharya, R.K. and Patra, H.P.
1968: Direct Current Geoelectric Sounding, Principles and Interpretation; Elsevier, 135 p.
- Bostick, F.X.
1977: A simple almost exact method of MT analysis; in Workshop on Electrical Methods in Geothermal Exploration; United States Geological Survey, Contract no. 14080001-8-359.
- Clague, J.J., Luternauer, J.L., and Hebda, R.J.
1983: Sedimentary environments and postglacial history of the Fraser delta and lower Fraser valley, British Columbia; Canadian Journal of Earth Sciences, v. 20, p. 1314-1326.
- Dresser Atlas
1979: Resistivity (Salinity) of Brine Solutions; in Log Interpretation Charts; Dresser Industries Inc., Houston, 107 p.
- Hamilton, T.S. and Luternauer, J.L.
1983: Evidence of seafloor instability in the south-central Strait of Georgia, British Columbia: a preliminary compilation; in Current Research, Part A, Geological Survey of Canada, Paper 83-1A, p. 417-421.
- Hopkins, W.S., Jr.
1966: Palynology of Tertiary Rocks of the Whatcom Basin, Southwestern British Columbia and Northwestern Washington; unpublished Ph.D. thesis, University of British Columbia, Vancouver, B.C., 184 p.
- Jones, A.G. and Foster, J.H.
1986: An objective real-time data-adaptive technique for efficient model resolution improvement in magnetotelluric studies; Geophysics, v. 51(1), p. 90-97.
- Luternauer, J.L., Clague, J.J., Hamilton, T.S., Hunter, J.A., Pullan, S.E., and Roberts, M.C.
1986: Structure and stratigraphy of the southwestern Fraser River delta: a trial shallow seismic profiling and coring survey; in Current Research, Part B, Geological Survey of Canada, Paper 86-1A report 74.
- Roberts, M.C., Williams, H.F.L., Luternauer, J.L., and Cameron, B.E.B.
1985: Sedimentary framework of the Fraser River delta, British Columbia, preliminary field and laboratory results; in Current Research, Part A, Geological Survey of Canada, Paper 85-1A, p. 717-722.
- Roddick, J.A.
1965: Vancouver North, Coquitlam and Pitt Lake map-areas, British Columbia; Geological Survey of Canada, Memoir 335, p. 69-70.

Jurassic stratigraphy of the Methow Trough, southwestern British Columbia

Project 800029

Jennifer O'Brien¹
Cordilleran and Pacific Margin Division, Vancouver

O'Brien, J., Jurassic stratigraphy of the Methow Trough, southwestern British Columbia; in Current Research, Part B, Geological Survey of Canada, Paper 86-1B, p. 749-756, 1986.

Abstract

The Lower and lower Middle Jurassic Ladner Group consists of Sinemurian(?) to Aalenian(?) thin bedded argillaceous strata with subordinate siltstone, greywacke and conglomerate, which grades upsection and in part laterally into an assemblage of upper Toarcian(?) to lower Bajocian volcanic rocks. These volcanic rocks, referred to herein as the Dewdney Creek Formation, consist predominantly of crystal-lithic tuff, volcanic breccia, tuffaceous siltstone and greywacke, volcanic conglomerate and locally preserved andesitic flows. Recognition of regionally extensive lower Middle Jurassic volcanic rocks within the trough demonstrates that volcanic detritus characteristic of the Jurassic section was likely derived from local volcanic centers. Upper Oxfordian to upper Tithonian volcanic sandstone and sandy argillite, referred to herein as the Thunder Lake sequence, disconformably overlies the Ladner Group.

Résumé

Le groupe de Ladner datant du Jurassique inférieur et du début du Jurassique moyen est composé de minces strates argileuses lithées datant du Sinémurien(?) à l'Aalénien(?); elles contiennent également des quantités variables de grès, de grauwacke et de conglomérat qui passent, vers le haut et en partie latéralement, à un assemblage de roches volcaniques datant du Toarcien supérieur(?) au Bajocien inférieur. Ces roches volcaniques, appelées ci-après formation de Dewdney Creek, se composent principalement de roches pyroclastiques, de brèches volcaniques, d'aleurolite tufacé et de grauwacke, de conglomérat volcanique et de coulées d'andésite préservées par endroits. L'identification dans la dépression de roches volcaniques datant du début du Jurassique moyen, roches d'ailleurs très répandues dans cette région, démontre que les débris pierreux volcaniques de la section jurassique proviennent vraisemblablement de centres volcaniques locaux. Le grès volcanique et l'argilite sableuse datant de l'Oxfordien supérieur au Tithonien supérieur, appelés dans le présent ouvrage la séquence de Thunder Lake, recouvre le groupe de Ladner de façon discordante.

¹ University of Arizona, Tucson

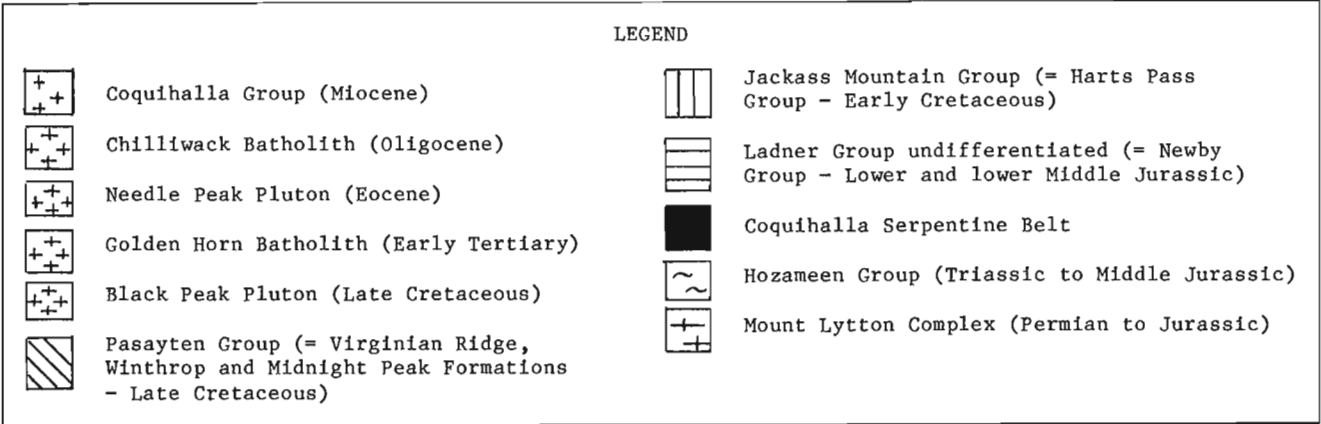
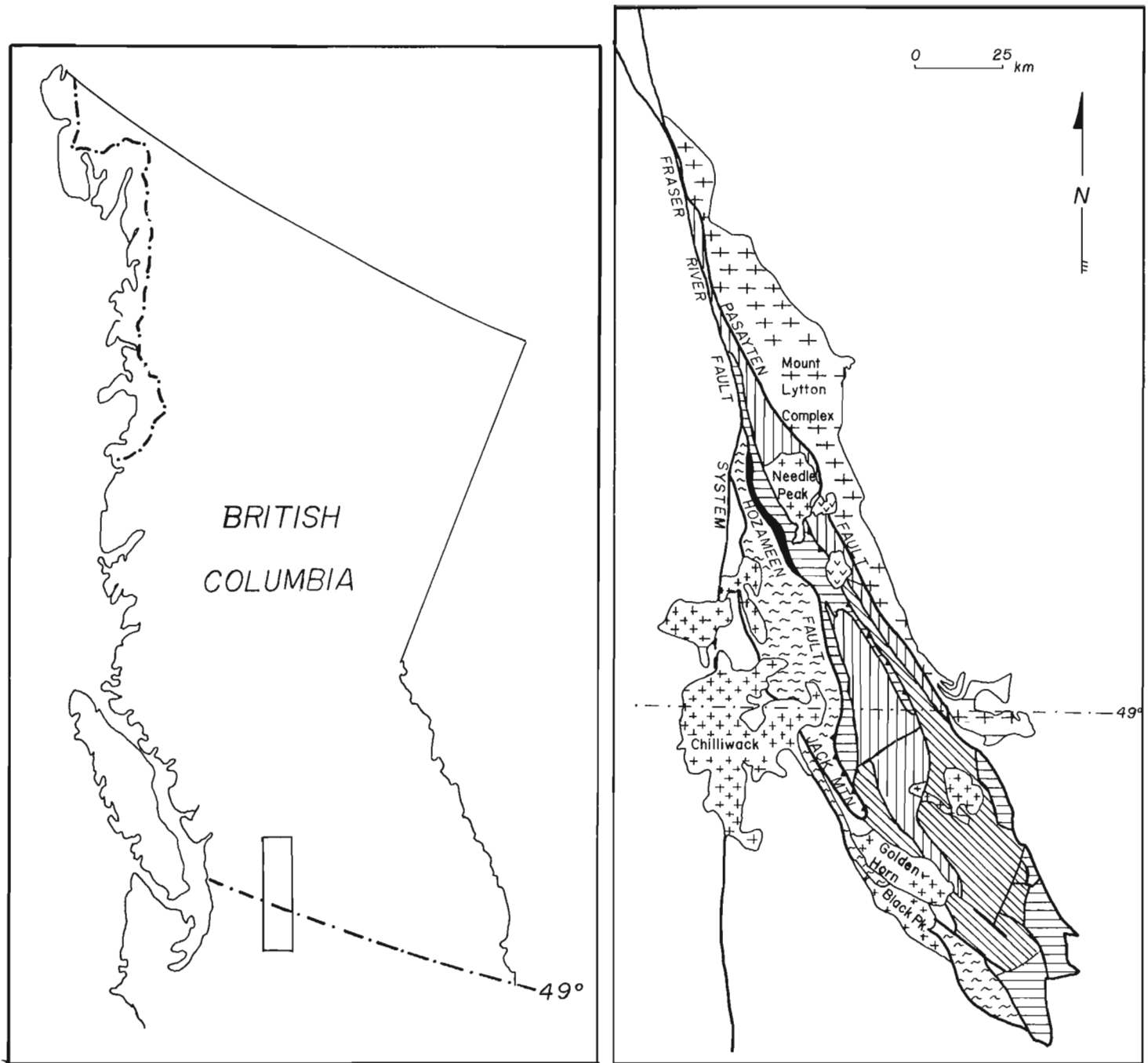


Figure 80.1. Regional geology of the Methow Trough (Compiled from Monger, 1970; Coates, 1972; Roddick et al., 1979; and Trexler and Bourgeois, 1985).

Introduction

Current geological mapping in the Methow Trough (Hope map area (92H)) to study its framework, Jurassic depositional history and stratigraphic nomenclature began in the summer of 1985. Cairnes (1924) originally referred to Jurassic argillaceous rocks in the Methow Trough as the Ladner Series and to Jurassic volcanic rocks as the Dewdney Creek Series. Based on paleontology, Coates (1970) assigned a Lower and lower Middle Jurassic age to both the sedimentary and volcanic rocks and referred to them collectively as the Ladner Group. The name Dewdney Creek Group was applied to a thin and discontinuous Upper Jurassic clastic unit (Coates, 1970). From the present study it is apparent that the Jurassic lithologic units of Cairnes (1924) can be recognized consistently throughout the Trough, and that the Dewdney Creek Group of Coates (1970) is a locally significant biostratigraphic unit. Because of this, the Jurassic units are herein referred to as the Sinemurian(?) to lower Bajocian Ladner Group which includes the Toarcian(?) to lower Bajocian Dewdney Creek Formation, and the Oxfordian to Tithonian Thunder Lake sequence. These divisions are based on Cairnes' lithologic criteria but also take into consideration paleontological data which provide age constraints for the units.

Acknowledgments

The writer gratefully acknowledges able assistance from D. Handel, S. Irwin, and M. MacLean in the field. Discussions in the field with A. Arthur, G. Gehrels, J.A. Jeletzky, J.W.H. Monger, T.P. Poulton, H.W. Tipper, and G.E. Ray are much appreciated. The manuscript was reviewed by P. Coney, G. Gehrels, J.W.H. Monger, and H.W. Tipper.

Regional setting

Extending from north-central Washington into south-western British Columbia, the Methow Trough comprises a fault-bounded sequence of Lower Jurassic through Upper Cretaceous sedimentary and volcanic rocks believed to depositionally overlie Triassic basalt (Fig. 80.1). The present eastern boundary is the Pasayten fault which juxtaposes the Methow stratigraphy against Mesozoic crystalline rocks of the Mount Lytton Complex. To the west, the Permian to Jurassic Hozameen Group is separated from the Methow by the Jack Mountain thrust and Hozameen fault. The Tertiary right-lateral Fraser River Fault System (FRFS) truncates the trough to the northwest (Monger, 1985).

Stratigraphy of Jurassic rocks

Jurassic strata of the Methow Trough are interpreted to overlie a basement of Triassic volcanic greenstone, referred to as the Spider Peak Formation (Ray et al., 1985). Based on detailed mapping (1:20 000) in the Coquihalla and Anderson River areas; reconnaissance mapping (1:50 000) in Manning Park, north of the park boundary and the East Anderson River area (Fig. 80.2); and preliminary paleontological determinations, three lithologically distinct Jurassic units are recognized. These units are the Lower and lower Middle Jurassic Ladner Group which includes the Dewdney Creek Formation, and the Upper Jurassic Thunder Lake sequence. Disconformably overlying the Jurassic strata are Lower Cretaceous shale, arkose and conglomerate of the Jackass Mountain Group (Coates, 1974).

Spider Peak Formation

The Spider Peak Formation is a Lower to Middle(?) Triassic volcanic greenstone sequence which outcrops locally along the Hozameen fault in the Coquihalla area (Fig. 80.3)

(Ray et al., 1985; Ray, in press). It comprises greenstone and gabbro with subordinate interbeds of tuff, argillite, and volcanic sandstone and siltstone. Cairnes (1924) was the first to suggest that this greenstone unit, which he referred to as the Cache Creek Series, represents the basement to the Methow Trough. A conglomerate near the base of the Ladner Group contains volcanic clasts with petrologic similarities to the underlying greenstone. Based on this observation, Cairnes (1924) suggested that the conglomerate represented "local irregularity of sedimentation near the base of the slate belt" possibly marking an unconformity. More recent work in the same area by Anderson (1976), Ray et al. (1985), and Ray (in press) demonstrated that the contact between the Ladner Group and the Spider Peak Formation is a regional unconformity.

Ladner Group

The oldest Jurassic unit recognized is Sinemurian(?) to Aalenian(?) and comprises thin bedded argillaceous strata with subordinate interbeds of tuffaceous siltstone and local conglomerate and greywacke (Fig. 80.4). A poorly sorted conglomerate near the base of the section contains pebble- to boulder-sized clasts of basic to felsic volcanic, granitic and sedimentary rocks in an argillite matrix. Discontinuous lenses of conglomerate higher in the section are different from the basal conglomerate in that greywacke forms the

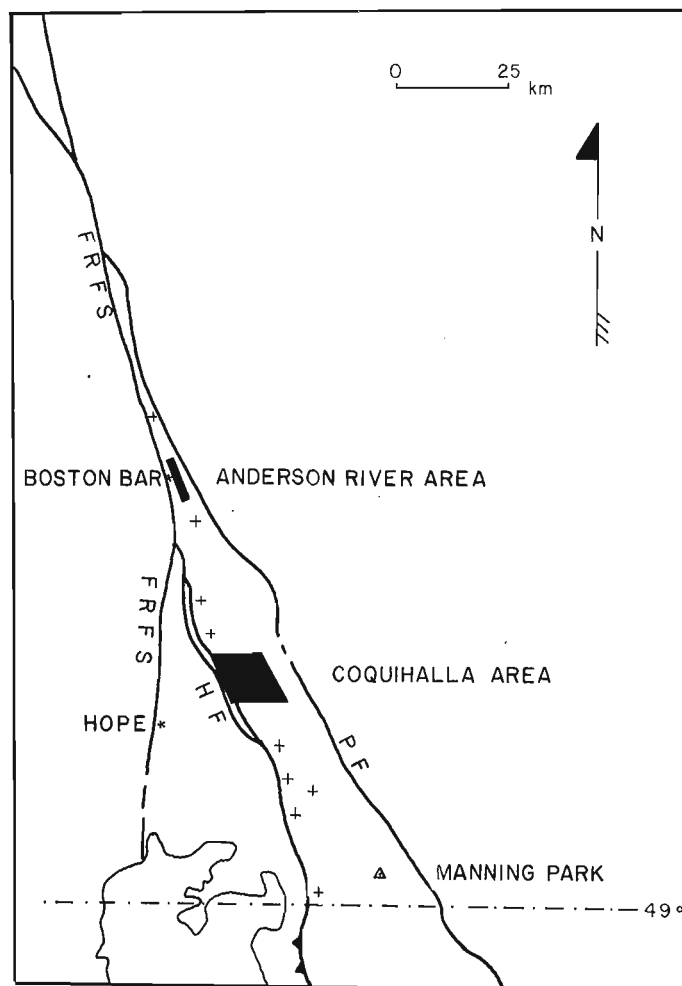


Figure 80.2. Location of areas mapped in detail. Crosses correspond to areas of reconnaissance work. Abbreviations: FRFS = Fraser River Fault System, HF = Hozameen Fault, PF = Pasayten Fault.

matrix and argillite and subordinate intermediate to felsic volcanic rocks form the clasts. Both conglomerates are matrix supported with sub- to well-rounded clasts.

In the Coquihalla area and northward to the Fraser River Fault System, the argillaceous strata display a well developed slaty cleavage. Rarely preserved fold hinges suggest that the unit has undergone indeterminate amounts of structural thickening. Because facing indicators are rare in these rocks, the thickness of the argillaceous strata has probably been overestimated in previous reports. Cairnes originally estimated their thickness to be 2000 m. Ray (in press) suggested a more appropriate figure of 1500 m for the argillaceous strata and 2000 m total for the rocks herein defined as the Ladner Group.

Lower Pliensbachian ammonites from one locality (GSC Loc. C-087352; H.W. Tipper) and a fragment of the bivalve *Weyla*(?) are the only fossils retrieved from the argillaceous unit in the Coquihalla area and north to the Fraser River Fault System. Late Jurassic *Buchia* collected from greywacke near Carolin mine (Coquihalla area) (Report Km-6-1983-JAJ) are herein assigned to the Thunder Lake sequence and are discussed below. In Manning Park, a section of argillite approximately 700 m thick is recognized by Coates (1974) as constituting a lower unit of the western belt of the Ladner Group. Fossils from this unit collected from the Divide Section (Coates, 1974) are late Toarcian to Aalenian with one lower Bajocian ammonite recorded from float.

Dewdney Creek Formation

Lower Jurassic argillaceous strata described above grade upsection and in part laterally into Toarcian(?) to lower Bajocian volcanic strata with subordinate argillaceous interbeds (Fig. 80.4). The volcanic strata consist of crystal-lithic tuff, tuffaceous siltstone and sandstone, conglomerate, volcanic breccia and locally preserved andesitic flows. The present distribution of volcanic rocks (Fig. 80.3) is controlled by regional folds and thrust(?) faults; their original distribution is unknown.

Facies variations in the volcanic rocks reflect local changes in depositional environment. Proximity to volcanic centres active in the early Middle Jurassic is recognized by the association of locally preserved andesitic flows and coarse volcanic breccia. This association occurs in both the Anderson River and Manning Park areas (Fig. 80.3). Elsewhere, the volcanic assemblage is typically interbedded crystal-lithic tuff and tuffaceous strata with laterally discontinuous beds of massive pebble conglomerate and volcanic breccia. The poorly sorted conglomerate contains a variety of sub- to well-rounded clasts of felsic to andesitic volcanic rocks, argillite, and rare limestone and granitic clasts within a tuffaceous greywacke matrix. Clasts range up to 25 cm across in the conglomerate. Andesitic fragments range in size up to 0.5 m in the volcanic breccia.

A diverse Aalenian to Bajocian fauna (H.W. Tipper, personal communication, 1985) was collected from interbeds of argillite and wacke within volcanic strata in the Anderson

Table 80.1. A comparison of Jurassic stratigraphic nomenclature

		COQUIHALLA AREA		MANNING PARK			
		CAIRNES (1924)		COATES (1970)		CURRENT STUDY	
SERIES	STAGE	UNITS		UNITS		UNITS	
		LADNER SERIES	DEWDNEY CREEK SERIES	LADNER GROUP	DEWDNEY CREEK GROUP	LADNER GROUP @ DEWDNEY CREEK FM.	THUNDER LAKE SEQUENCE
CRETACEOUS	BARREMIAN						
	HAUTERIVIAN						
	VALANGINIAN						
	BERRIASIAN		- ? - ? -				
	TITHONIAN		crystal-lithic tuff		vol. ss. sandy arg.		volc. ss. sandy arg
	KIMMERIDGIAN						
JURASSIC	OXFORDIAN		- ? - ? - ? - ? - ? -				
	CALLOVIAN						
	BATHONIAN		arg., minor cgl., tuffaceous greywacke				tuff, breccia, cgl., arg., flows
	BAJOCIAN			volc. ss., arg., cgl., tuff, breccia			
	AALENIAN						
	TOARCIAN						argillite, siltstone, wacke, congl.
	PLIENSBACHIAN						
	SINEMURIAN						
	HETTANGIAN		- ? - ? -				- ? - ? - ? - ? - ?
	NORIAN						
TRIASSIC	CARNIAN		CACHE CREEK SERIES				SPIDER PEAK FORMATION

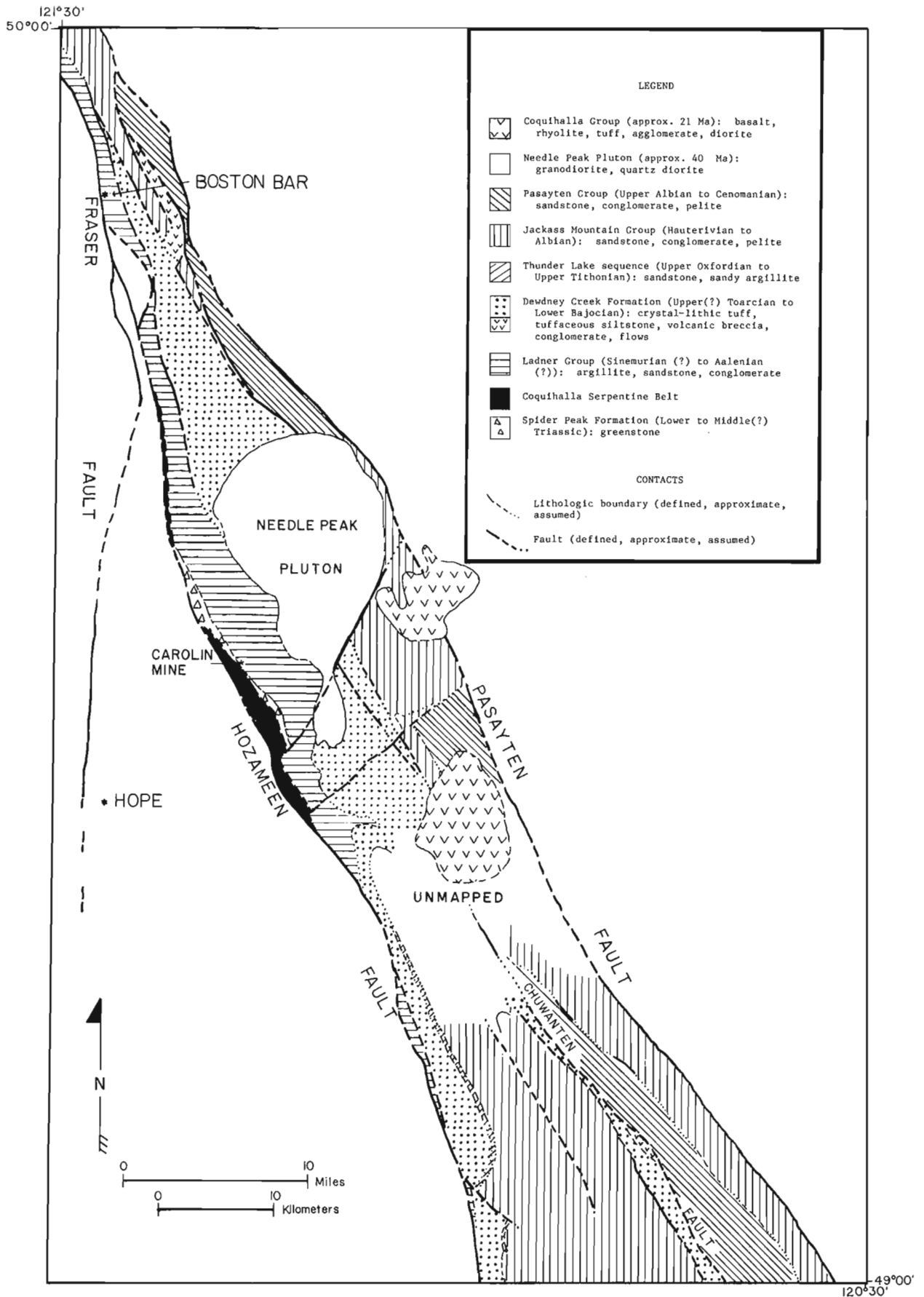


Figure 80.3. Simplified geological compilation of the Methow Trough, southwestern British Columbia. Compiled by author from field work and Monger (1970) and Coates (1974).

River area. In the Coquihalla area, one poorly preserved fragment of an Aalenian(?) ammonite (H.W. Tipper and P.L. Smith, personal communication, 1985) was retrieved from the locally sheared argillaceous interbeds. Belemnites found in coarse volcanic sandstone and pebble conglomerate in this area are either Jurassic or Cretaceous. Lower Bajocian ammonites were collected from volcanic wacke which overlies the more argillaceous strata of the western belt of the Ladner Group in Manning Park (Coates, 1974).

Thunder Lake sequence

Upper Oxfordian to upper Tithonian volcanic sandstone and sandy argillite disconformably overlie the lower Middle Jurassic strata. These beds were observed in a thin- to medium-bedded section less than 350 m thick at the west end of Thunder Lake in Manning Park. The section outcrops as a discontinuous belt north of the park boundary as far as Mount Dewdney (Fig. 80.3). It has not been recognized farther north except for the greywacke beds reported to be part of the Ladner Group (Ray, in press) near Carolin mine (Coquihalla area), but that greywacke appears to this writer to be tectonically incorporated into the argillaceous strata. These beds contain poorly preserved fragments of Upper Jurassic *Buchia concentrica*, which range from late Oxfordian to Kimmeridgian (GSC Report Km-6-1983-JAJ). The rocks are lithologically distinct from the underlying lower Middle Jurassic volcanic strata of the Ladner Group but are distinguished from fine grained sediments of the Lower Cretaceous Jackass Mountain Group only by the presence of diagnostic Jurassic and Cretaceous fossils.

Discussion of stratigraphic nomenclature

The nomenclature used in this report is based on detailed and regional geological mapping, preliminary paleontological determinations (in conjunction with H.W. Tipper), lithologic distinctions and nomenclature originally recognized by Cairnes (1924), and paleontological constraints reported by Coates (1970). The Ladner Series of Cairnes (Table 80.1) was characterized by argillaceous strata whereas his overlying Dewdney Creek Series was characterized by crystal-lithic tuff. Detailed mapping by Coates and paleontological studies (Friebold et al., 1969) in the Manning Park area led to a major revision of the Jurassic stratigraphic nomenclature (Coates, 1970, his Figure 13-4) in which Lower to Middle Jurassic strata were referred to the Ladner Group whereas Upper Jurassic strata were referred to the Dewdney Creek Group.

Coates' Dewdney Creek Group comprises a local biostratigraphic unit with lithologies that are significantly different from those of that unit first described by Cairnes. In this study, Coates' Dewdney Creek Group is consequently referred to informally as the Thunder Lake sequence in reference to the well exposed section at Thunder Lake. Insufficient information on strata near the Jura-Cretaceous boundary in the Methow Trough prevents the proposal of more formal nomenclature at this time.

In the current study the name "Dewdney Creek" is retained as a formation name for the Middle Jurassic volcanic strata described above, in order to restore Cairnes' name for lithologies that he recognized as being distinctive

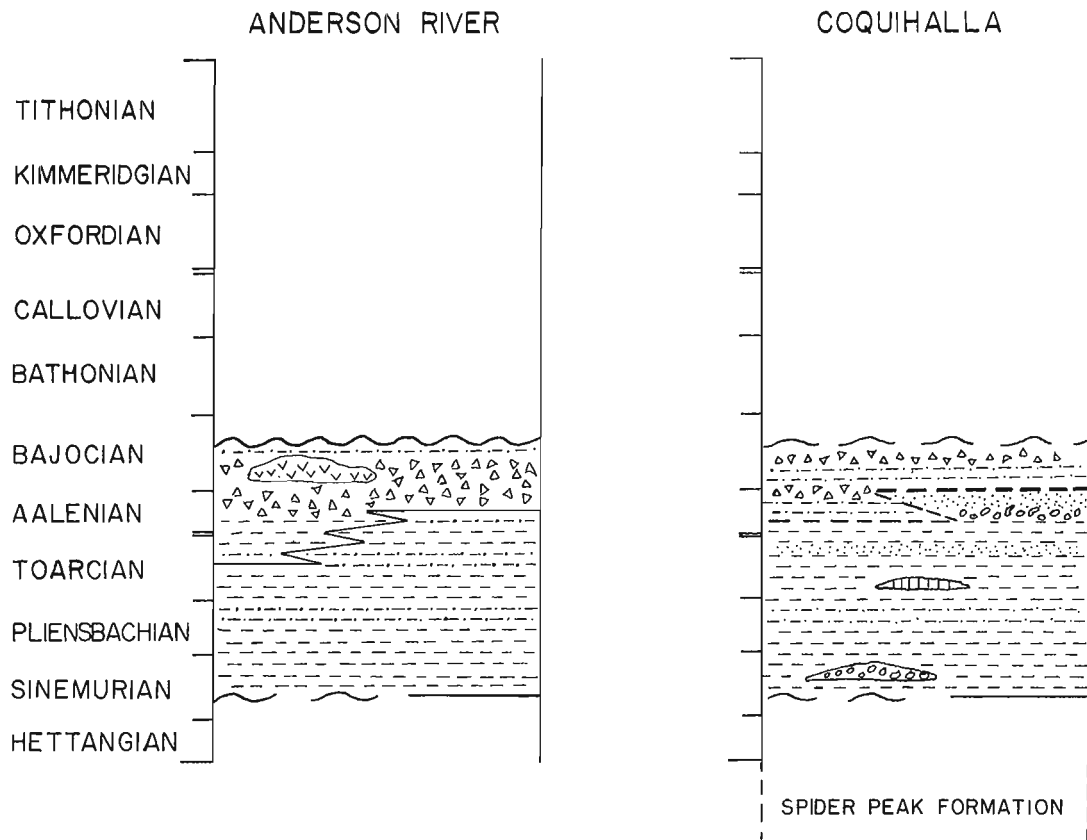
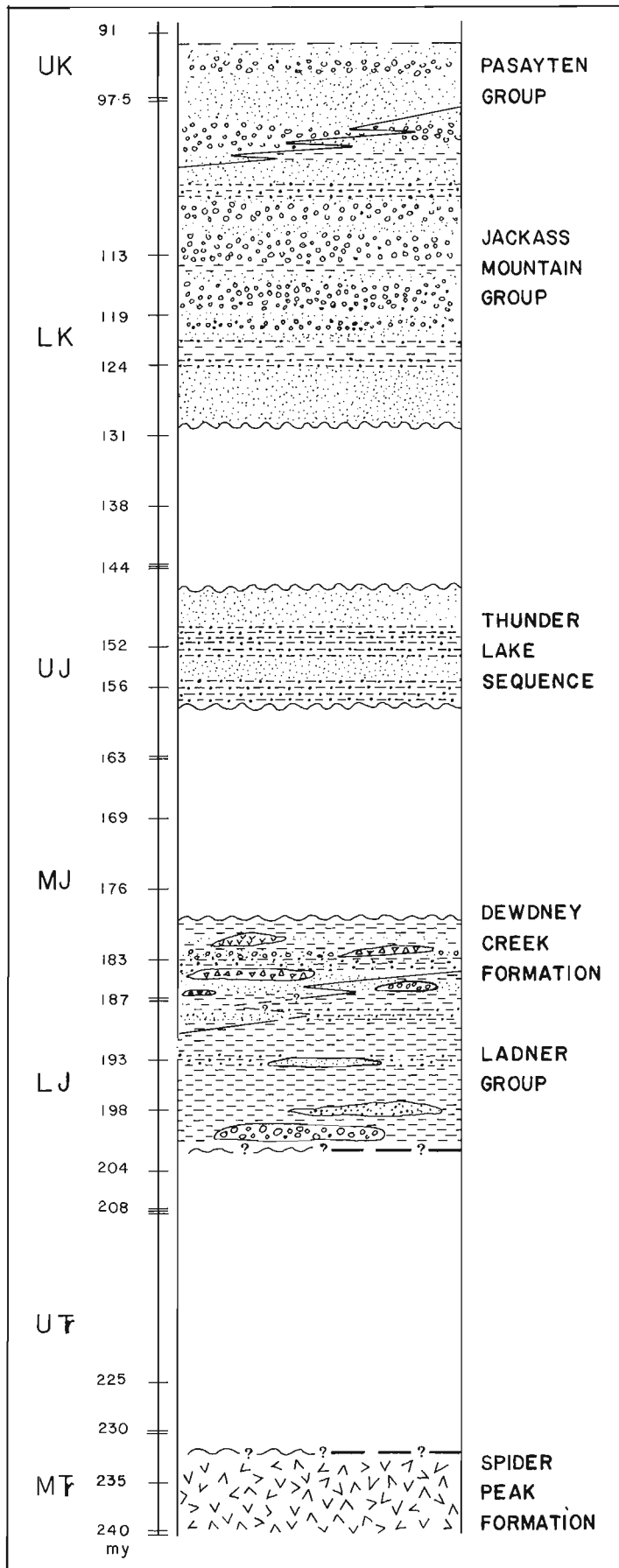


Figure 80.4. Stratigraphic sections of the Ladner Group compiled from detailed mapping and preliminary paleontological determinations from the Anderson River and Coquihalla areas. See Figure 80.5 for legend.



from the Ladner Series. The type locality of the volcanic strata was originally the Dewdney Creek watershed (Cairnes, 1924). Due to the heterogeneity of the unit I suggest that the Dewdney Creek watershed and the Lookout Road section (Manning Park) be recognized as type areas. In this way, both the tuffaceous strata and volcanic breccia and andesitic flows will be represented.

Depositional environment of the Jurassic units

Early Jurassic time as recorded in the Methow strata was a period of regional tectonic quiescence. This is evident from the lack of angular unconformities within the section as well as a predominance of sediments characteristic of low energy depositional environments punctuated by turbidity flows. Subordinate influxes of conglomerate and wacke suggest mass gravity flow and slumping caused by irregularities of the basement depositional surface.

The lower Middle Jurassic volcanic strata overlying the argillite indicate a change in regional tectonic configuration that appears to have caused a local regression and an initiation of volcanic activity within the region. Preliminary fossil identifications of ammonites collected from strata interbedded with volcanic breccia and tuffaceous sediments in the Anderson River and East Anderson River areas (H.W. Tipper, personal communication, 1985) suggest that intermittent volcanism was initiated as early as the Toarcian stage. Synchronous activity that produced more significant accumulations of coarse volcanic breccia and andesitic flows in the Anderson River and Manning Park appear restricted to the lower Bajocian. The presence of pelagic faunas and woody debris (logs) generally within the more argillaceous strata suggest that marine deposition was at least in part proximal to subaerial volcanic edifices.

Upper Jurassic volcanic sandstone and sandy argillite overlie the lower Middle Jurassic strata disconformably. These sediments were derived from an eroding volcanic source region either from within the trough or to the east. This is suggested as there is no evidence of westerly derived sediments until Albian-Campanian (Trexler and Bourgeois, 1985) or Cenomanian (Tennyson and Cole, 1978; Kleinspehn, 1985) time.

Figure 80.5. Stratigraphic section of the Methow Trough compiled from current study and the work of Coates (1974). Time scale from Palmer (1983).

Conclusions

The Jurassic stratigraphy of the Methow Trough in southwestern British Columbia has been redefined in order to clarify relationships between the recognized units and thereby to provide a better understanding of the evolution of the trough in Jurassic time. Three distinct lithologic units are recognized. These include: (1) Sinemurian(?) to Aalenian(?) argillaceous strata which belongs to the Ladner Group, (2) Toarcian(?) to lower Bajocian volcanic strata referred to herein as the Dewdney Creek Formation of the Ladner Group, and (3) Oxfordian to Tithonian volcanic sandstone and sandy argillite which is referred to herein as the Thunder Lake sequence. Stratigraphic and paleontologic relations indicate that the argillaceous strata are overlain by and locally gradational into the volcanic rocks, and that the Thunder Lake sequence disconformably overlies the Sinemurian to lower Bajocian Ladner Group. Based on detailed and reconnaissance mapping, the distribution of these units has been compiled for southwestern British Columbia (Fig. 80.3).

References

- Anderson, P.
1976: Oceanic crust and arc-trench gap tectonics in southwestern British Columbia; *Geology*, v. 4, p. 443-446.
- Armstrong, R.L.
- Mesozoic and Early Cenozoic magmatic evolution of the Canadian Cordillera; *Geological Society of America, Memoir*. (in press)
- Cairnes, C.E.
1924: Coquihalla area, British Columbia; *Geological Survey of Canada, Memoir* 139, 187 p.
- Coates, J.A.
1970: Stratigraphy and structure of Manning Park area, Cascade Mountains, British Columbia; in *Structure of the southern Canadian Cordillera*, ed. J.O. Wheeler; *Geological Association of Canada, Special Paper* 6, p. 149-154.
1974: *Geology of the Manning Park area*; *Geological Survey of Canada, Bulletin* 238, 177 p.
- Dickinson, W.R.
1976: Sedimentary basins developed during evolution of Mesozoic-Cenozoic arc-trench system in western North America; *Canadian Journal of Earth Sciences*, v. 13, p. 1268-1287.
- Eisbacher, G.H.
1974: Evolution of successor basins in the Canadian Cordillera; *Society of Economic Paleontologists and Mineralogists Special Publication* 19, p. 274-291.
- Frebold, H., Tipper, H.W., and Coates, J.A.
1969: Toarcian and Bajocian rocks and guide ammonites from southwestern British Columbia; *Geological Survey of Canada, Paper* 67-10.
- Jeletzky, J.A. and Tipper, H.W.
1968: Upper Jurassic and Cretaceous rocks of the Taseko Lakes map area and their bearing on the geologic history of southwestern British Columbia; *Canadian Geological Survey, Paper* 67-54, 128 p.
- Kleinspehn, K.L.
1985: Cretaceous sedimentation and tectonics, Tyaughton-Methow Basin, southwestern British Columbia; *Canadian Journal of Earth Sciences*, v. 22, p. 154-174.
- Monger, J.W.H.
1970: Hope map-area, west half (92H, W 1/2), British Columbia; *Geological Survey of Canada, Paper* 69-47, 75 p.
1985: Structural evolution of the southwestern Intermontane Belt, Ashcroft and Hope map areas, British Columbia; in *Current Research, Part A*, *Geological Survey of Canada, Paper* 85-1A, p. 349-358.
- Monger, J.W.H., Price, R.A., and Tempelman-Kluit, D.J.
1982: Tectonic accretion and the origin of the two major metamorphic and plutonic belts in the Canadian Cordillera; *Geology*, v. 10, p. 70-75.
- Palmer, A.R.
1983: The Decade of North American Time Scale; *Geology*, v. 11, p. 503-504.
- Price, R.A., Monger, J.W.H., and Roddick, J.A.
1985: Cordilleran cross-section: Calgary to Vancouver; in *Field guides to Geology and Mineral Deposits in the Southern Canadian Cordillera*, ed. D. Tempelman-Kluit; *Geological Society of America*, 85 p.
- Ray, G.E.
- The Hozameen fault system and related Coquihalla Serpentine Belt of southwestern British Columbia; *Canadian Journal of Earth Sciences*. (in press)
- Ray, G.E., Coombes, S., MacQuarrie, D.R., Niels, R.J.E., Shearer, J.T., and Cardinal, D.G.
1985: Precious metal mineralization in southwestern British Columbia; in *Field Guides to Geology and Mineral Deposits in the southern Canadian Cordillera*, ed. D. Tempelman-Kluit; *Geological Society of America, Vancouver*, 31 p.
- Roddick, J.A., Muller, J.E., and Okulitch, A.V.
1979: Fraser River (Sheet 92) British Columbia-Washington; *Geological Survey of Canada, Map* 1386A.
- Tennyson, M.E. and Cole, M.R.
1978: Tectonic significance of upper Mesozoic Methow-Pasayten sequence, northeastern Cascade Range, Washington and British Columbia; in *Mesozoic paleogeography of the western United States*, ed. D.G. Howell and K.A. McDougall; *Society of Economic Paleontologists and Mineralogists, Pacific Coast Paleogeography Symposium*, v. 2, p. 499-508.
- Trexler, J.H. and Bourgeois, J.
1985: Evidence for mid-Cretaceous faulting in the Methow basin, Washington: Tectonostratigraphic setting of the Virginian Ridge Formation; *Tectonics*, v. 4, no. 4, p. 379-394.

Structural control of podiform chromitite in Bay of Islands Ophiolite, Springer Hill area, Newfoundland¹

Contract 27ST. 23233-5-0244

Richard Dahl² and David H. Watkinson²

Dahl, R. and Watkinson, D.H., Structural control of podiform chromitite in Bay of Islands Ophiolite, Springer Hill area, Newfoundland; in *Current Research, Part B, Geological Survey of Canada, Paper 86-1B*, p. 757-766, 1986.

Abstract

A detailed study of a podiform chromitite ore deposit at Springer Hill, in the Lewis Hills Massif of the Bay of Islands Ophiolite Complex has been undertaken to understand the controls of the geometrical distribution of the ore. A preliminary interpretation of the field data indicates that the ore is of a subconcordant tabular type, and consists of chromitite concentration within dunite that was emplaced in harzburgite of the mantle tectonite. The dunite-chromitite body was emplaced syntectonically with an early high temperature deformation (S_1) of the harzburgite. At this stage of the investigation, it cannot be stated whether the chromitiferous dunite body originated by mantle metasomatism, in situ partial melting or by intrusion.

The subconcordant character of the dunite-chromitite body with respect to the S_1 foliation, and the discordancy between various structures in the dunites, harzburgites and chromitites respectively suggest a rotational stress regime (simple shear) during the S_1 deformation.

Subsequent heterogeneous mylonitic deformation (S_2) has overprinted the S_1 structures, and has dismembered the original 400 m-long continuous pod of dunite-chromitite into a series of smaller disconnected pods. This later deformation produced two structural displacements: one steeply dipping to the northwest that is obvious in local exposure; the other involves a subhorizontal displacement that is less obvious in the local exposures of the mapped area. Any extension of the dunite-chromitite body at depth is likely to be approximately parallel to the L_1 lineation, but dislocated by the S_2 structural displacements.

Résumé

Un gisement podiforme de chromitite dans le complexe ophiolitique de Bay of Islands a été cartographié et ses structures analysées, en détail afin de préciser les relations géométriques entre le corps minéralisé et les structures des roches encaissantes. La zone étudiée, Springer Hill, se situe dans le massif de Lewis Hills, à l'ouest de Terre-Neuve. Les données préliminaires démontrent sans équivoque que le gisement de Springer Hill appartient au type structural tabulaire-subconcordant, et consiste en une concentration de chromitite au sein d'une lentille de dunite mise en place syntectoniquement dans les tectonites harzburgitiques. Le processus pétrogénétique à l'origine de la principale lentille de dunite chrométifère ne peut être précisé au stade actuel de l'étude.

Le caractère subconcordant de l'ensemble du gisement par rapport à la foliation⁵, ainsi que les relations discordantes illustrées par les structures et contacts lithologiques des dunites, harzburgites et chromitites semblent indiquer un régime de contrainte rotationnel (cisaillement simple) durant l'épisode de déformation S_1 .

Cette déformation primaire est oblitérée par une seconde phase de déformation mylonitique plus hétérogène, découpant la lentille originale, s'étendant sur une longueur continue d'environ 400 m, en un chapelet de lentilles secondaires plus ou moins reliées. Cette dernière phase tectonique des deux plans structuraux suivants: le premier, à fort plongement vers le nord-ouest, est mis en évidence par la géologie régionale; l'autre, subhorizontal, est moins facile à discerner dans la région à l'étude. Toute extension en profondeur de la masse minéralisée suit sans doute, de façon plus ou moins parallèle, la linéation L_1 , et présente des signes de dislocation suite aux épisodes techniques S_2 .

¹ Contribution to the Canada-Newfoundland Mineral Development Agreement 1984-1989. Project carried by Geological Survey of Canada, Mineral Resources Division, Project 770063.

² Department of Geology, Carleton University, Ottawa, Ontario, K1S 5B6.

Introduction

Chromite is an ubiquitous phase in ophiolitic or alpine peridotites, but seldom occurs in modal concentrations greater than 5%. Exceptions are the irregular or discontinuous lensoidal bodies of chromite concentrations at or near the transition zone from harzburgitic tectonites (upper residual mantle) to mafic and ultramafic cumulates (Thayer, 1964; Coleman, 1977). Depending on whether the chromite concentrations are hosted by the tectonites or the cumulate unit, they are classified as "podiform" (Thayer, 1962) or "ophiolitic stratiform" (Rahgoshay et al., 1981; Dahl and Watkinson, 1985) chromite deposits respectively. The apparent irregular shape of podiform chromites has resulted in a poor understanding of the geometrical forms of the ore, and consequently erroneous estimations of their economic potential.

Recent investigations of podiform chromite deposits in the New Caledonia ophiolitic peridotites (Moutte, 1979; Prinzhofer, 1980; Cassard, 1980; Secher, 1981; Cassard et al., 1981) have provided detailed documentation of the geometrical control of this type of chromite deposit. Cassard et al. (1981) defined three major types of podiform chromite ores based on the geometrical relationship between the general shape of the deposit and the tectonic structures of the associated peridotites. Basically these authors distinguish concordant, subconcordant and discordant chromite pods, depending on whether they are parallel, sub-parallel or discordant to the foliation of the harzburgite and dunite.

The present study follows a similar methodology in defining the geometric and kinematic parameters necessary to formulate a realistic model of the Springer Hill chromite-rich rocks. Preliminary data, based on mapping at a scale of 1:500 and collected during the 1985 summer field season, are presented here.

The area under study is located in the Lewis Hills massif of the Bay of Islands Ophiolite Complex, in western Newfoundland (Fig. 81.1). The regional mapping performed by Karson (1975, 1977, 1979) led to the distinction of two main areas (Karson and Dewey, 1978; Karson, 1984) as shown in Figure 81.1:

- (1) the Coastal complex (CC), including strongly deformed peridotites, metabasites and amphibolites, interpreted as a fossil transform fault; and
- (2) the Bay of Islands complex (BOIC), interpreted as a classical ophiolitic section ranging from ultramafic tectonites into mafic and ultramafic cumulates, is regarded as fossil oceanic crust and upper mantle adjacent to the fracture zone.

The Springer Hill area is located in the southern part of the Bay of Islands complex (Fig. 81.1), near the transition from harzburgitic tectonites to dunitic tectonites. The main lithological and structural features of the Springer Hill area have recently been summarized by Dunsworth et al. (1986).

Mapping technique

A detailed grid was established over an area 600 m by 200 m to include the main chromitite outcrops of the Springer Hill deposit (Fig. 81.2). All exposures in this area were carefully examined, and mapped at a scale of 1:500. Systematic observations included accurate measurement of the strike and dip of all penetrative structures, foliation, lineation and shear-planes, the axes and axial planes of folds, crenulations, boudins, and contacts of the various intrusive dykes and lithological bands. The main results of this mapping are summarized in Figure 81.2.

Lithological units

Four main lithologies were recognized: harzburgite, dunite, chromitite and pyroxenite.

Harzburgite tectonite.

The harzburgite tectonite is a coarse grained, three phase peridotite (60% olivine, 35% orthopyroxene, 0-5% chromite), exhibiting an homogeneous tectonic fabric (S_1 , and equivalent to the S_1 fabric of Dunsworth et al., 1986), and is most obvious as flattened and elongated chromite and orthopyroxene grains. This deformation is assumed to be the result of asthenospheric flow at the time that the ophiolitic slab was close to the oceanic ridge where it was accreted (Malpas, 1978; Girardeau, 1979; 1982; Girardeau and Nicolas, 1981; Casey and Karson, 1981). A secondary deformation (S_2 , and equivalent to the S_2 foliation of Dunsworth et al., 1986) affects the harzburgite heterogeneously (Fig. 81.3e), and is represented by thin mylonitic bands ranging from a few millimetres to about 30 cm wide, which crosscut or transpose the former S_1 foliation. This secondary deformation appears to be typical of a high strain rate and low temperature (<900°C) regime (Gueguen and Nicolas, 1980; Nicolas et al., 1980). Pyroxenitic and numerous dunitic dykes and pods occur in the harzburgite in a concordant to subconcordant attitude, and appear to be approximately contemporaneous with S_1 , but pre-date S_2 , which they never crosscut. Some clinopyroxenitic dykes are clearly discordant to S_1 , and therefore postdate it, but have been affected by mylonitic shears and therefore pre-date the S_2 foliation. No gabbroic dykes were observed.

Dunite

Relatively small pods and bands of dunite are ubiquitous throughout the tectonized harzburgite in the area mapped (Fig. 81.2). These small discontinuous dunitic bodies, which range in width from a few centimetres to several metres and described as "dykelets" by Dunsworth et al. (1986), are not shown in Figure 81.2. This map illustrates only the distribution of the dunite surrounding the main chromitite mineralization and other unusually large dunitic bodies. The dunitic bands are commonly chromitiferous, and both fine grained and coarse grained varieties occur in the area mapped. These dunitic bands were regarded as dyke swarms by Dunsworth et al. (1986), intruded synkinematically with the harzburgite foliation. Preliminary petrographic and chemical data suggest that they should be regarded as in situ products of partial melting of the harzburgite, rather than intrusions or injections from a distal parental source.

The coarser grained variety (Fig. 81.3a) seems to be restricted to pods and bands greater than 1 m in width. Chromite abundance also correlates with the size of the dunitic body, the wider bodies containing the highest chromite concentrations. Coarse grained dunite consists of millimetre-sized, euhedral chromite crystals disseminated throughout an olivine matrix. Primary textures are overprinted by a subsequent tectonic fabric (mainly S_1 type), manifested as the aggregation of chromite grains and a weak elongation of individual crystals or crystal aggregates. This tectonic overprinting is most clearly demonstrated by isoclinal folds in schlieren and seams of massive chromitite (Fig. 81.3b), which form segregations in the dunite pods.

All outcropping chromitite pods in the Springer Hill area are surrounded by a dunitic aureole (Fig. 81.2), which is almost invariably the pattern for chromitite pods and segregations in ophiolites (Coleman, 1977).

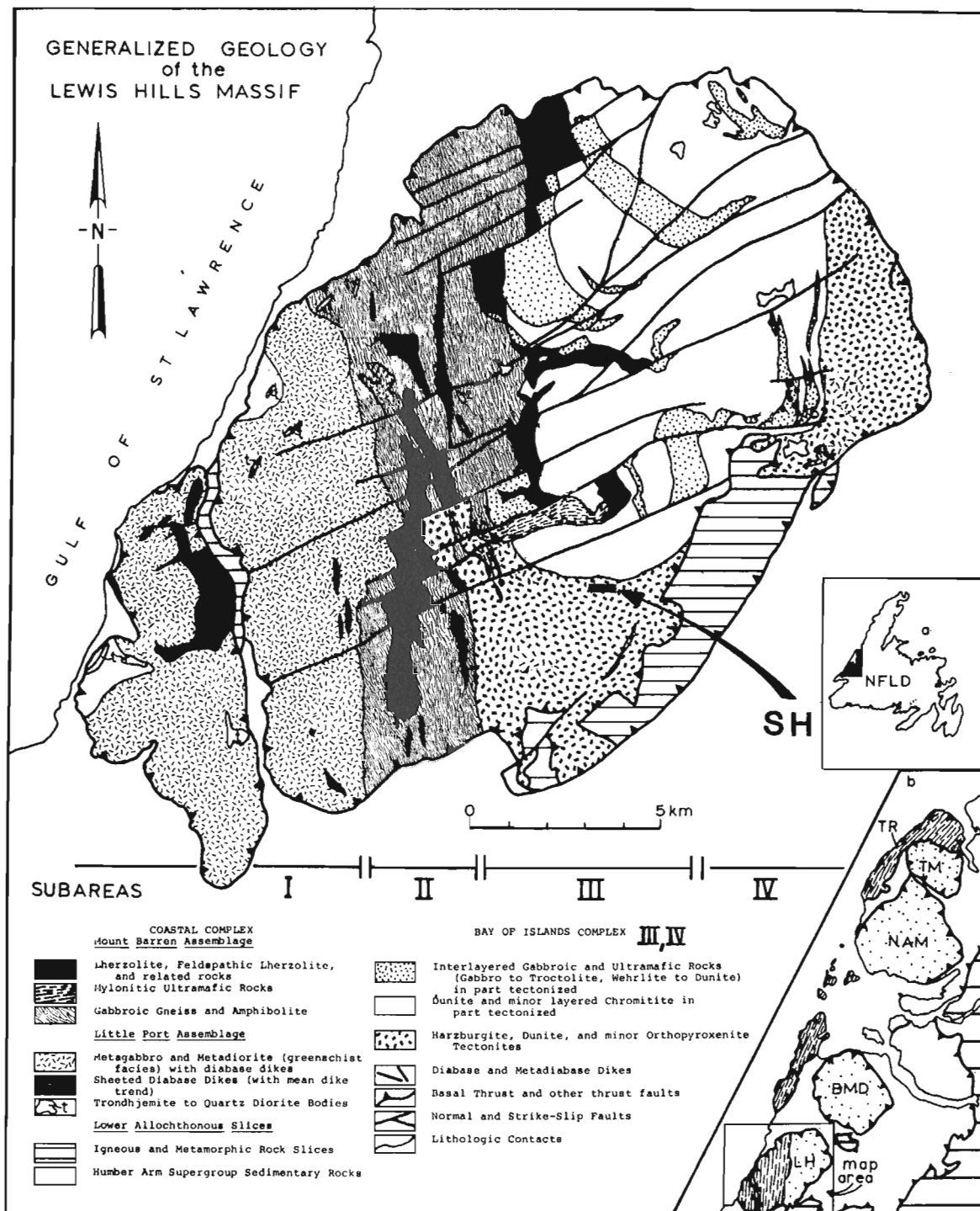


Figure 81.1. Geological map of the Lewis Hills Massif (from Karson, 1977, 1979) showing the location of the Springer Hill area (SH) of the present study. Index maps a and b show the location and tectonic setting of the massif. In b, symbols are as follows: hatched: parautochthonous carbonate terrain; blank: allochthonous clastic sedimentary rocks (Humber Arm Super Group); stippled: Bay of Islands Ophiolite complex massifs (TM, Table Mountain; NAM, North Arm Mountain; BMD, Blow Me Down Mountain; LH, Lewis Hills); dashed lines: Coastal Complex (TR, Trout River).

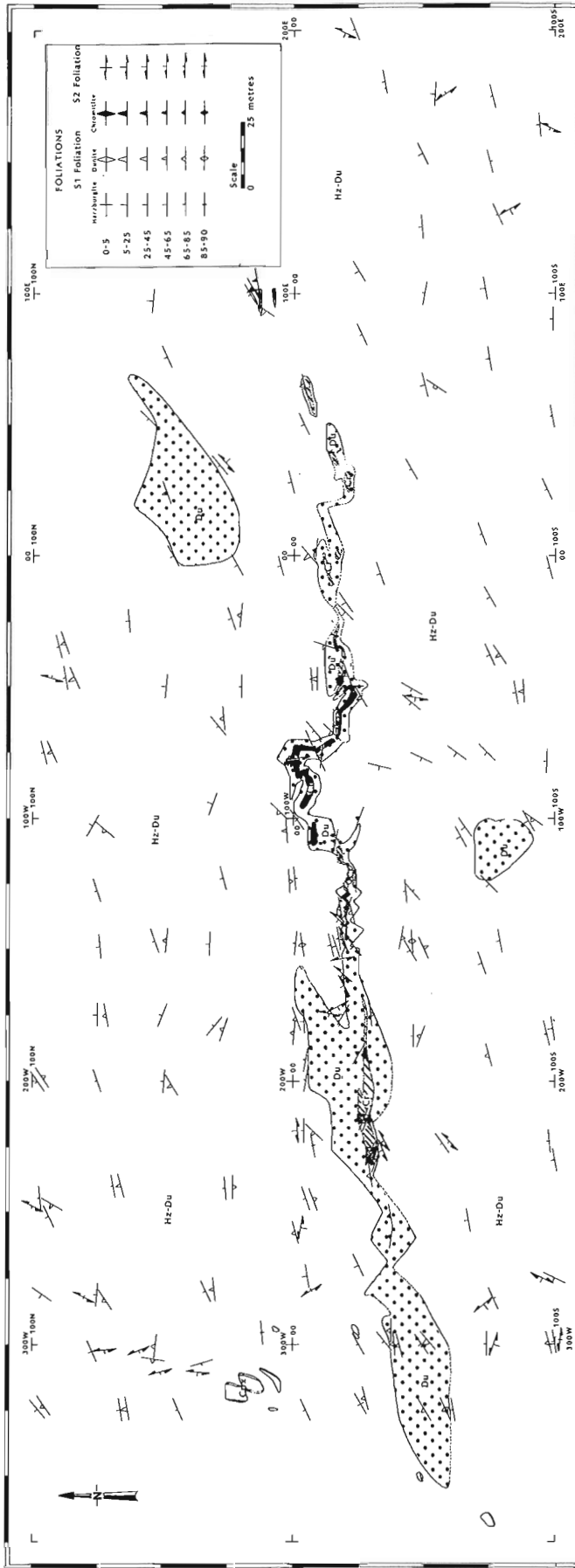


Figure 81.2. Geological map of the main chromitite showing of the Springer Hill area (SH), Lewis Hills Massif, Western Newfoundland. Symbols are as follows: black: outcropping chromitite ore; hatched: non outcropping expected extensions of the chromitite ore; stippled: dunitic aureole and major dunitic pods; white: harzburgite with dunitic and pyroxenitic banding and dykes. All rocks are foliated as indicated.

The length of the dunite aureole surrounding the main chromite showing is about 400 m and its width ranges from less than 2 m in the east, to about 20 m in the west (Fig. 81.2). The thick dunite section near the baseline at point 200W (Fig. 81.2) is an artifact of a local NE-SW trending shear zone. Locally, discordant dunite dykelets or veinlets, which are commonly offset by small shears, cut various lithologies.

Chromitite

Although chromite is ubiquitous in both the harzburgite and dunite, its modal concentration exceeds 5% only in the dunitic pods and bands. Typically, the chromite in these dunitic bodies is concentrated in their central portions where it attains a modal concentration of up to 100%. The main chromitite showing at Springer Hill appears to represent an unusually large example of a chromitiferous dunite dyke or vein. However, preliminary chemical and petrographical results suggest that there are differences in the genesis of the main chromitiferous dunitic body compared to that of the ubiquitous small dunitic dykes or veins. Whereas the latter usually contain up to about 5% orthopyroxene and the range of olivine composition is 91.3-92.4 Fo%, the main chromitiferous body does not contain orthopyroxene and the range of olivine composition is 92.0-93.7 Fo%. Chromite compositions, however, tend to be similar in both the small and main dunitic bodies, differing only in that the massive chromite of the main showing has a higher ferric iron content compared to the chromites of the smaller dunitic bodies. These data suggest that the main chromitiferous dunite body consists of a higher proportion of early crystallization and differentiation products of a harzburgite melt than do the small dunitic bodies.

The most common textures of the main Springer Hill showing are massive chromitite and chromitite containing occluded olivine or disseminated olivine (Fig. 81.3f). The two textural types are spatially associated with the massive chromitite occurring as sigmoidal to lenticular S or Z shaped seams in a matrix of the occluded olivine type chromitite (Fig. 81.3c). We interpret these structures to be indicative of ductile deformation of the chromitite ore.

The main chromitite showing now consists of a series of discontinuous pods, that in some parts may attain widths of up to 6 m (Fig. 81.2). Very thin chromitite seams, the width of which appears to be a function of the width of the dunitic pod and of the intensity of the strain, occur between major chromitite pods and commonly exhibit isoclinal folds. Axial planes of these folds are parallel to S_1 foliation. This suggests that mantle flow may have contributed to the attenuation and boudinage of a formerly more continuous chromitite body into the series of pods that now exist.

As in the case of the dunite and harzburgite, the chromitites have undergone high strain rate (S_2) deformation. This deformation produced multiple offsets of the original chromitite pod, as illustrated on a large scale by the numerous offsets of both the chromitite pod and its dunitic aureole (Fig. 81.2), and, on a smaller scale, by the juxtaposing of dismembered angular fragments (Fig. 81.3d). The cooler temperature conditions of this deformation compared to that of the S_1 deformation is indicated by the extensive fine granulation that affects the chromite grains in the S_2 shears.

In contrast, the Bluff Head chromite deposit located 12 km to the west of the main Springers Hill deposit at the western margin of the Bay of Islands complex, represents a regularly layered "stratiform ophiolitic" chromitite and consists of massive chromite layers with disseminated euhedral olivine crystals (up to 6 mm long) which are intercalated with dunite layers containing disseminated chromite. An example of the Bluff

Head mineralization, which occurs in the transition zone of the ophiolite sequence in the western part of the Lewis Hills, is illustrated in Figure 81.3g.

Pyroxenite

Orthopyroxenitic and clinopyroxenitic dykes or veins occur in the mapped area (Fig. 81.2), mainly in the form of concordant, isoclinally folded bands. Coarse grained to subpegmatitic pyroxenites also occur as diffuse impregnations. Clinopyroxenite is rare, except in the westernmost part of the mapped area, where it occurs as dykes (1.5 m wide) that crosscut the foliation. In most cases, dunite occurs as a thin aureole (10 to 20 cm wide) at the transition from pyroxenite to the harzburgite and as lensoidal patches within the dykes. This lithological distribution pattern may suggest either an in-dyke magmatic differentiation due to a crystallization path that first crosses the olivine solidus and later the clinopyroxene solidus (Sinigoi et al., 1980, 1983), or alternatively clinopyroxene crystallization from a partial melt segregation derived from the surrounding harzburgite ("in situ" dykes of Boudier and Nicolas, 1972 and Boudier, 1972, 1976), in which case the dunite aureole is interpreted as depleted harzburgite.

Structure

High-temperature and slow strain rate structures: S_1 - L_1

A regional homogeneous foliation S_1 , characterized by coarse to porphyroclastic textures of high temperature and slow strain rate conditions, occurs in the Springer Hill area.

The S_1 and associated structures have been systematically measured in both the harzburgite and the dunite pods and bands (Fig. 81.2, 81.4a,b). In the harzburgite, the average foliation plane trends ENE-WSW with a NNW dip. In the dunites, the strike and dip of S_1 related structures are similar, but the data are slightly more dispersed. The reason for this greater dispersion becomes evident from the study of individual exposures, where the foliation of the harzburgite commonly appears to be discordant to the dunite foliation. This discordance suggests a differential strain pattern for the two lithologies, and is probably related to the emplacement process of the dunite bands and pods.

The L_1 lineation (Fig. 81.4b) exhibits a well defined average pole plunging towards the west-northwest, and there is a good concordance between spinel lineation, boudin axis and fold axis.

Axial planes of folds are always parallel to the local average foliation plane (Fig. 81.4c), and therefore were included with foliation in plotting of structural data. Fold axes are plotted separately (Fig. 81.4c) to show the close relationship between high temperature foliation and isoclinal folding.

Low temperature and high strain rate structures: S_2 - L_2

A distinct tectonic style (S_2) occurs in the form of shear zones, mylonitic bands and shear folds, characterized by extensive stretching lineation of the orthopyroxenes and spinels, and a strong penetrative planar fabric. The chromites that have been affected by these structures exhibit fine granulation textures. All these features, together with their very localized and heterogeneous distribution strongly suggest that temperature was lower and strain rate higher for the S_2 fabric than was the case for the S_1 fabric (Gueguen and Nicolas, 1980; Nicolas et al., 1980).

The field relationships strongly suggest that S_2 structures crosscut S_1 structures, and also that the S_1 trend is progressively transposed toward the S_2 average trend. The spatial distribution

of the poles of S_2 foliation planes (Fig. 81.4d) illustrates this situation. The S_2 poles range from the S_1 field (WSW trend, WNW dip), through an intermediate SW trend and NW dip, and a S trend and W dip, to the SE trend and SW dip of the S_2 fabric.

The field data and the structural analysis, indicate that two main active S_2 shear planes have affected the area. The first is subhorizontal, with a shallow westerly dip, and is strongly discordant both to the high-temperature foliation (S_1) and the attitude of the main dunite-chromite pod. The second dips steeply to the northwest, and is responsible for the across-strike offsets of the main dunite-chromite pod (Fig. 81.2). The subhorizontal S_2 shear plane probably caused a similar dismembering of the pod as did the steeply dipping shear planes; however displacements were not observed in outcrops of the main chromite showing, but were observed in areas outside the area of detailed mapping shown in Figure 81.2.

Shear-folds are commonly associated with the S_2 mylonitic bands.

Dykes, veins and pods

The attitude of the dunite bands and pods appears to be entirely controlled by the high-temperature (S_1) deformation, to which they are concordant to subconcordant (Fig. 81.4e). The average trend of the dunitic bodies is E-W, with a dip to the north. The contact of the main dunite-chromite showing with harzburgite is parallel to the average strike of the foliation plane but, in places the dip and trend of internal structures differ from those of the contact zone. The main dunite-chromite pod is therefore classified as the subconcordant tabular type (Cassard et al., 1981).

Most of the pyroxenitic dykes (Fig. 81.4f) have also undergone high-temperature (S_1) deformation, except the clinopyroxenitic dykes in the western area, which are discordant to the S_1 attitude, but have been affected by S_2 shear structures.

Conclusions

The field data relating to the spatial relationship between the successive deformation phases and emplacement processes allows a preliminary interpretation of the control of the chromite mineralization. However, it should be stressed that this interpretation is provisional, pending the acquisition of additional laboratory data.

The main chromite pod and associated dunite aureole was emplaced into the host harzburgite syntectonically with the S_1 deformation. Whether the chromite-dunite pod originated by mantle metasomatism (Dungan and Ave Lallemand, 1977; Whitaker and Watkinson, 1984, in press), "in situ" partial melting during upper mantle flow, or by syntectonic dyke-shape intrusion (Lago et al., 1982) cannot be stated at the present stage of our investigations. However, micro-textural, micro-structural and geochemical investigations carried out to date suggest that processes involving in situ partial melting and proximal amalgamation of the resultant liquid were dominant factors in the genesis of the main chromite-bearing dunitic body. The S_1 deformation appears to be less homogeneous in the chromite pods than in the host harzburgite. Furthermore, dunite and chromite locally show discordant foliation with respect to the harzburgite foliation (Fig. 81.5). These major structural features are thought to be genetically related to upper mantle flow at or near an active spreading ridge axis (Girardeau and Nicolas, 1981; Nicolas and Violette, 1982).

A secondary structural control affects the chromite body and its associated dunite aureole. This consists of a heterogeneous high strain and low temperature (<900°C) deformation (S_2) expressed mainly as thin, subparallel mylonitic bands. This type of deformation dismembered the original continuous pod into a series of smaller pods, which in the eastern part of the zone are now isolated from the main body (Fig. 81.2). The occurrence of both steeply dipping and subhorizontal S_2 systems suggests that the dismembering process occurred along subhorizontal and subvertical planes. Therefore, any original

Figure 81.3. (opposite) Major lithologies and associated structures in study area.

a, part of dunite aureole to main chromite pod with disseminated coarse grained chromite: the texture looks magmatic but exhibits a foliation (70N79 to 95N68) that is subconcordant to the host harzburgite foliation (85N64).

b, concordant dunitic dyke (90N53) with isoclinally folded chromite segregations with slightly discordant axial plane versus the dyke boundaries and local foliation; this suggests a rotational (simple shear) regime of deformation in the dunite bands. Axes of the chromite folds dip northwesterly, concordant to the local lineation attitude.

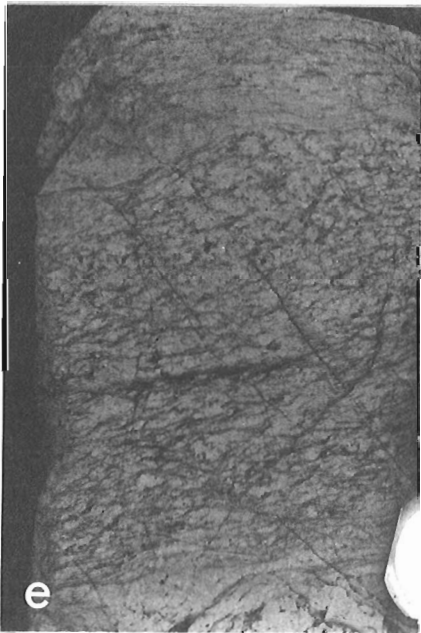
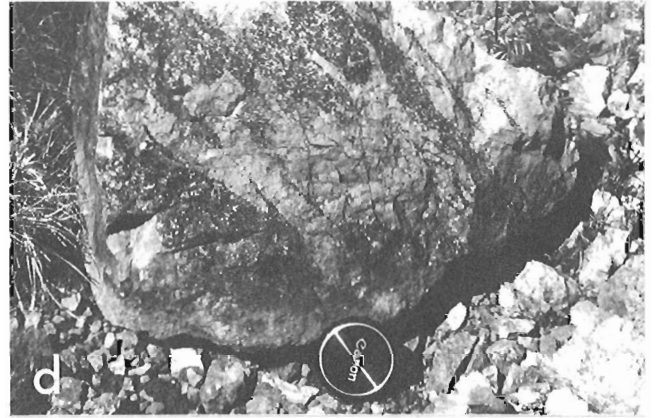
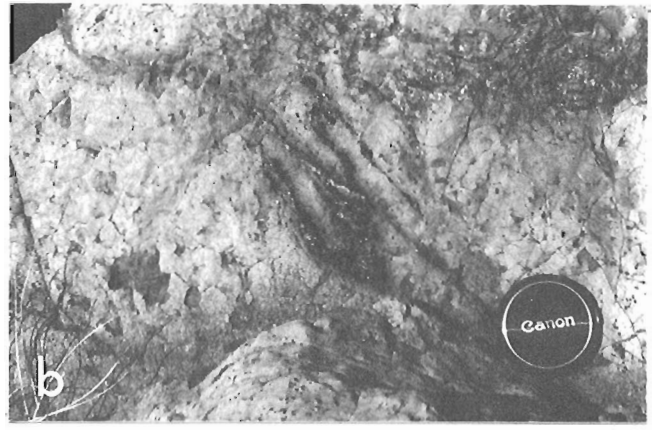
c, deformation features in the chromite: here, massive sigmoidal chromite schlieren in a matrix of disseminated olivine-rich chromite.

d, plastic deformation of alternating chromite-dunite bands, at a decimetric scale: here the banding underwent heterogeneous S_2 deformation, leading to an intensive fragmentation of the chromite layers. Fine grained (high strain rate and low temperature deformation conditions) chromite seams still connect the fragments along the S_2 shears

e, mylonitic shear zones (S_2 : 65N60) at the contact between the dunitic aureole and the host harzburgite. The heterogeneity of the S_2 deformation can be seen where thin mylonitic bands alternate with wider less deformed bands with partially transposed S_1 defoliation. The area affected by that deformation is about 16 m wide, and corresponds to a major NE-SW offset of the dunitic aureole of the main showing. The area is characterized by a strong stretching lineation of the orthopyroxenes, trending and dipping northwesterly (L_2 : 107NW49 and 127NW56).

f, typical texture of the chromite from the main showing: coarse grained massive chromite with 10 to 15% disseminated olivine crystals. A discordant dunite dykelet or veinlet cross-cuts the ore, and is itself offset by a later millimetric S_2 shear.

g, dunite-chromite cumulative layering in the Bluff Head area, Lewis Hills Massif: this chromite mineralization, which is of the "ophiolitic stratiform" type, occurs in basal mafic-ultramafic cumulates of the transition zone. Penetrative deformation, when observed, is weak.



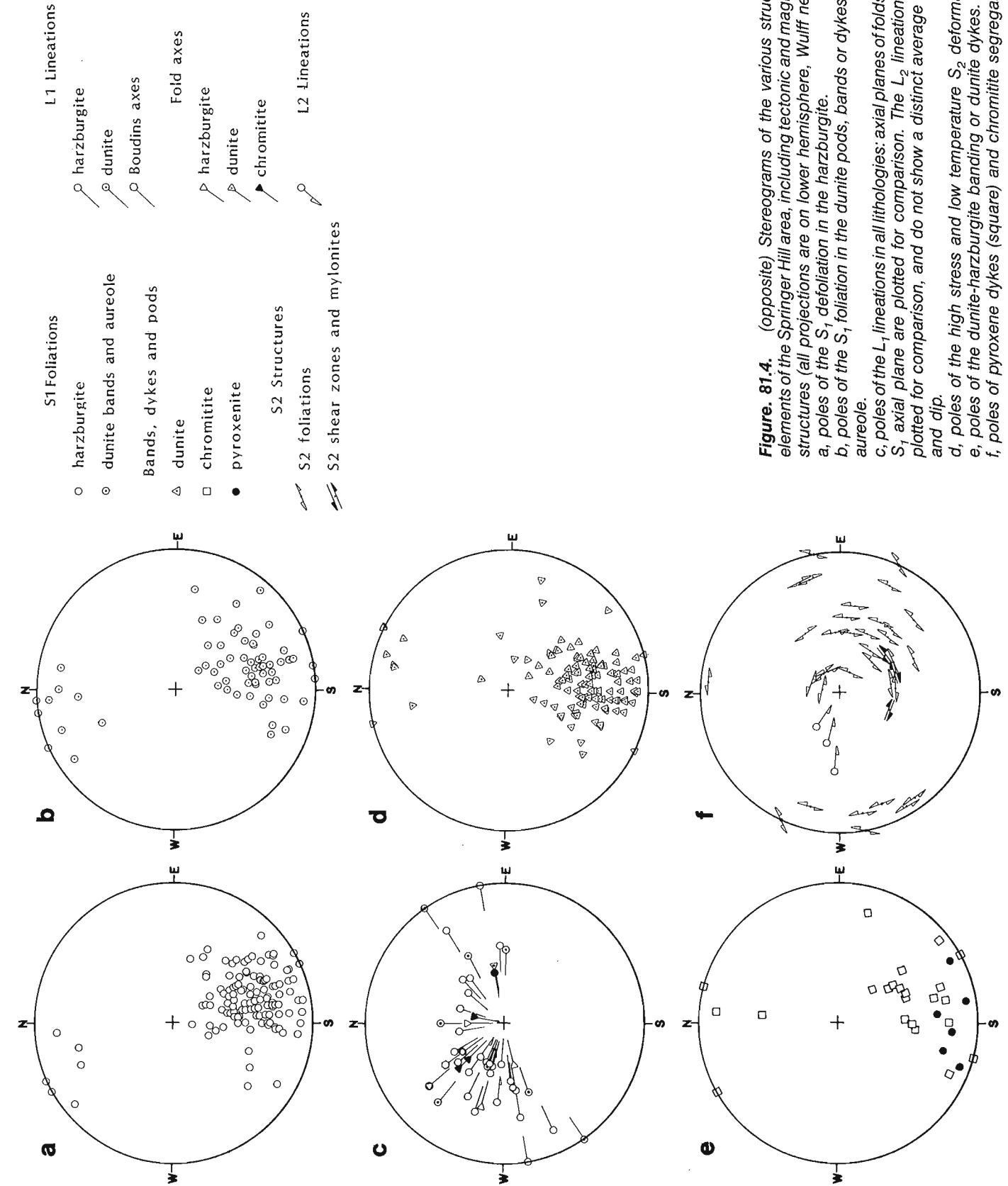


Figure 81.4. (opposite) Stereograms of the various structural elements of the Springer Hill area, including tectonic and magmatic structures (all projections are on lower hemisphere, Wulff net).
 a, poles of the S_1 defoliation in the harzburgite.
 b, poles of the S_1 foliation in the dunitic pods, bands or dykes, and aureole.
 c, poles of the L_1 lineations in all lithologies: axial planes of folds with S_1 axial plane are plotted for comparison. The L_2 lineations are plotted for comparison, and do not show a distinct average trend and dip.
 d, poles of the high stress and low temperature S_2 deformation.
 e, poles of the dunitic-harzburgite banding or dunitic dykes.
 f, poles of pyroxene dykes (square) and chromitite segregations.

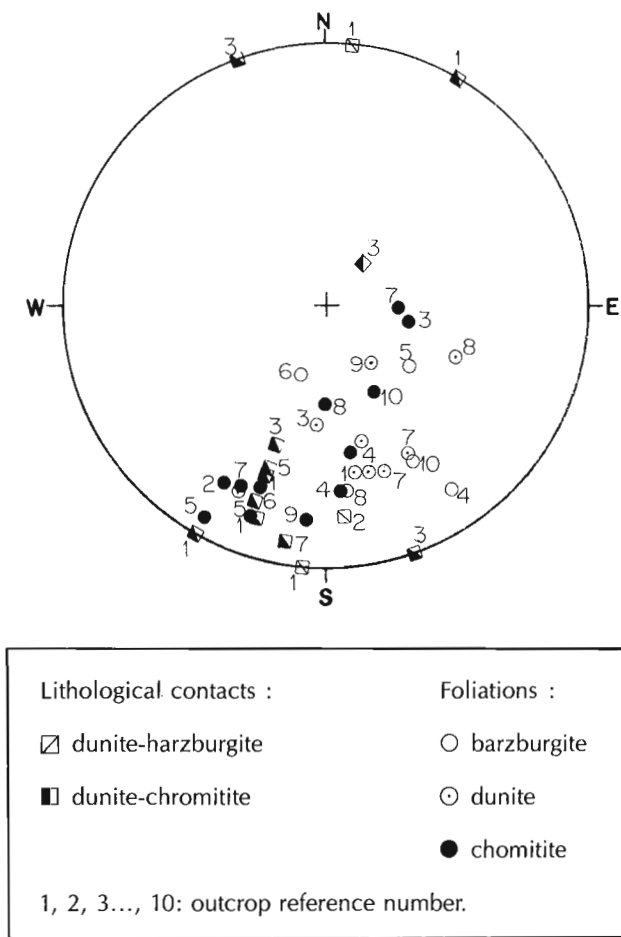


Figure 81.5. Relationships between lithological contacts, intrusive contacts and foliation planes for given outcrops. Numbers are the outcrop references, or a given section.

steeply dipping continuity of the chromitite may have been dislocated by this later tectonic event. This cooler and later phase of deformation probably operated off-axis, and could be related to either of two major processes: a transform-fault (Karson and Dewey, 1978) or early thrusting and shearing related to the initiation of obduction (Girardeau, 1982; Girardeau and Mevel, 1982).

In the light of the structural controls delineated in this study, the geometry of the chromitite deposit becomes an important consideration from the exploration point of view. In particular, the subconcordant attitude of the dunite-chromitite pods of the Springer Hill area, indicates that the trend and dip of $S_1 - L_1$ foliation and lineation should guide exploration efforts to determine any continuation of the chromitite pods with depth. In this regard, it should be noted that the attitude of the lineation corresponds to the direction of the optimal potential extension of a given chromitite pod in the local foliation plane. Thus for the main chromitite of Springer Hill, the optimal potential extension would be along an axis trending $N60^\circ$ and dipping toward the northwest. However, any such extension would be affected by any change in foliation attitude that occurs to the northwest of the outcrop area, and of course may be dislocated by the localized S_2 structures.

Acknowledgments

Discussions in the field with S. Dunsworth, R. Talkington, M. Wawrskow and T. Calon are greatly appreciated. J. Lydon

and R.F.J. Scoates are acknowledged for review of an early draft of this paper. NSERC grant number A7874 to D.H. Watkinson supported part of the study.

References

- Boudier, F.
1972: Relations Iherzolite-gabbro-dunite dans le Massif de Lanzo (Alpes Piemontaises) : exemple de fusion partielle; Thesis 3rd cycle doct., University of Nantes, France, 106p.
1976: Le Massif Iherzolitique de Lanzo (Alpes Piemontaises), etude structurale et petrologique; Thesis doct. d'etat, University of Nantes, France, 163p.
- Boudier, F. and Nicolas, A.
1972: Fusion partielle gabbroique dans la Iherzolite de Lanzo (Alpes Piemontaises); Schweizerische Mineralogische und Petrographische Mitterlungen, v. 52, p. 39-56.
- Casey, J.F. and Karson, J.A.
1981: Magma chamber profiles from the Bay of Islands ophiolite complex: implications for crustal-level magma chambers at mid-ocean ridges; Nature, v. 292, p. 295-301.
- Cassard, D.
1980: Structure et origine des gisements de chromite du Massif du Sud (ophiolites de Nouvelles Caledonie) - Guides de prospection; Thesis 3rd cycle doct., University of Nantes, France, 239p.
- Cassard, D., Nicolas, A., Rabinovitch, M., Moutte, J., Leblanc, L. and Prinzhofer, A.
1981: Structural classification of chromite pods in southern New-Caledonia; Economic Geology, v. 76, no. 4, p. 805-831.
- Coleman, R.G.
1977: Ophiolites, Mineral and Rocks 12, P.J. Wyllie (ed.), Springer-Verlag, 229p.
- Dahl, R. and Watkinson, D.H.
1985: Structural, petrological and geochemical investigations on podiform chromite ore deposits: a review; unpublished Carleton University report, 29p.
- Dungan, M.A. and Ave Lallemand, H.G.
1977: Formation of small dunite bodies by metasomatic transformation of harzburgite in the Canyon Mountain Ophiolite, Northeast Oregon; in Magma Genesis, H.J.B. Dick (ed.), Oregon, Department of Geology and Mineral Industries Bulletin, v. 96, p. 109-128.
- Dunsworth, S., Calon, T. and Malpas, J.
1986: Structural and magmatic controls on the internal geometry of the plutonic complex and its chromite occurrences in the Bay of Islands ophiolite; in Current Research, Part A, Geological Survey of Canada, Paper 86-1A, report 85.
- Girardeau, J.
1979: Structures des ophiolites de l'Ouest de Terre-Neuve et modele de croûte oceanique; These de doctorat de 3eme cycle, Universite de Nantes, France, 154p.
1982: Tectonic structures related to thrusting of ophiolite complexes: the White Hills peridotite, Newfoundland; Canadian Journal of Earth Sciences, v. 19, p. 709-722.

- Girardeau, J. and Mevel, C.
1982: Amphibolitized sheared gabbros from ophiolites as indicators of the evolution of the oceanic crust: Bay of Islands, Newfoundland; *Earth and Planetary Science Letters*, v. 61, p. 151-165.
- Girardeau, J. and Nicolas, A.
1981: The structures of two ophiolites massifs, Bay of Islands, Newfoundland: a model for the oceanic crust and upper mantle; *Tectonophysics*, v. 77, p. 1-34.
- Gueguen, Y. and Nicolas, A.
1980: Deformation of mantle rocks; *Annual Review, Earth and Planetary Sciences*, v. 8, p. 119-144.
- Karson, J.A.
1975: Structural studies in the mafic and ultramafic rocks of the Lewis Hills, western Newfoundland; Masters Thesis, State University of New-York at Albany, 125p.
1977: The geology of the northern Lewis Hills, western Newfoundland, unpublished Ph.D. Thesis, State University of New York at Albany, 474p.
1979: Geology of the Lewis Hills Massif, western Newfoundland; Geological Survey of Canada, Open File 628, 20p.
1984: Variations in structure and petrology in the coastal complex, Newfoundland: the anatomy of an oceanic fracture zone; *Journal of Geological Society, London, Special Publication 13*, p. 131-146.
- Karson, J.A. and Dewey, J.F.
1978: Coastal complex, western Newfoundland, an Ordovician oceanic fracture zone; *Geological Society of America Bulletin*, v. 89, p. 1037-1049.
- Karson, J.A. and Dick, H.J.B.
1983: Tectonics of ridge-transform intersections at the Kane Fracture zone; *Marine Geophysical Research*, v. 6, p. 51-98.
- Lago, B., Rabinovitch, M. and Nicolas, A.
1982: Podiform chromite ore bodies: a genetic model; *Journal of Petrology*, v. 23, 1, p. 103-125.
- Malpas, J.
1978: Magma generation in the upper mantle, field evidence from ophiolite suites, and application to the generation of oceanic lithosphere; *Philosophical Transactions of Royal Society of London, Serie A*, v. 288, p. 527-540.
- Moutte, J.
1979: Le Massif de Tiebaghi, Nouvelle-Caledonie, et see gites de chromite; Thesis doct. Ing. E.N.S.M., Paris, France, 160p.
- Nicolas, A. and Violette, J.F.
1982: Mantle flow at oceanic spreading centers: models derived from ophiolites; *Tectonophysics*, v. 81, p. 319-339.
- Nicolas, A., Boudier, F. and Bouchez, J.L.
1980: Interpretation of peridotite structures from ophiolitic and oceanic environments; *American Journal of Science*, v. 280A, p. 192-210.
- Prinzhofer, A.
1980: Structure et petrologie d'un cortege ophiolitique : le Massif du Sud (Nouvelle-Caledonie). La transition manteau-croûte en milieu oceanique; Thesis Doc. Ing., Ecole des Mines de Paris, France.
- Rahgoshay, M., Juteau, T. and Whitechurch, H.
1981: Kizilyukse Tepe: a special stratiform chromite ore deposit in an ophiolitic complex (Pozanti-Karzanti Massif, Taurus, Turkey); *Comptes Rendus, Academie des Sciences, Paris*, v. 293, II, 10, p. 765-771.
- Secher, D.
1981: Les lherzolites ophiolitiques de Nouvelle-Caledonie et leurs gisements de chromite. Deformation de la chromite; Thesis 3rd cycle doct., University of Nantes, France, 286p.
- Sinigoï, S., Comin-Chiaramonti, P. and Alberti, A.A.
1980: Phase relation in the partial melting of the Baldissero spinel lherzolite (Ivrea-Verbano zone, western Alps, Italy); *Contributions to Mineralogy and Petrology*, v. 75, p. 111-121.
- Sinigoï, S., Comin-Chiaramonti, P., Demarchi, G. and Siena, F.
1983: Differentiation of partial melts in the mantle: evidence from the Balmuccia peridotite, Italy; *Contributions to Mineralogy and Petrology*, v. 82, p. 351-359.
- Thayer, T.P.
1962: Application of structural geology in exploration for podiform chromite deposits. Report of 5th Meeting of the Geologists of the FPR, Beograd, Yougoslavia, p. 295-303.
1964: Geologic features of podiform chromite deposits; in *Methods of Prospection for Chromite*, R. Woodfili and D. Ostle, ed.; Organ. Economic Coop. Devel., Paris, p. 135-146.
- Whittaker, P.J. and Watkinson, D.H.
1984: Genesis of chromitite from the Mitchell Range, Central British Columbia; *Canadian Mineralogist*, v. 22, p. 161-172.
in press: Origin of chromite in dunitic layers of the Mt. Sydney-Williams ultramafic rock complex, British Columbia. (in press).

Electrothermal vapourization as a means of sample introduction into an inductively coupled plasma mass spectrometer: a preliminary report of a new analytical technique

Project 580175

C.J. Park and G.E.M. Hall
Mineral Resources Division

Park, C.J. and Hall, G.E.M., Electrothermal vapourization as a means of sample introduction into an inductively coupled plasma mass spectrometer: a preliminary report of a new analytical technique; in Current Research, Part B, Geological Survey of Canada, Paper 86-1B, p. 767-773, 1986.

Abstract

Development work in the application of electrothermal vapourization as a means of sample introduction into an inductively coupled plasma mass spectrometer is described. Preliminary results obtained in the analysis of various matrices for molybdenum, tungsten, thallium and iron are illustrated by measurement of isotope ratios, and the potential and usefulness of isotope dilution measurement is demonstrated. The anticipated value of such a technique is expected to be seen in the direct analysis of seawater at and below the part-per-billion level and in the determination of elements in geological materials whose natural abundance is below $1 \mu\text{g}\cdot\text{g}^{-1}$. Relative standard deviations in the range of 1-2% at the picogram level are obtained.

Résumé

Le présent rapport fait état de travaux de mise au point dans le domaine de la vaporisation électrothermique en tant que méthode utilisée pour introduire un échantillon dans un spectromètre de masse à plasma couplé par induction. Les résultats préliminaires obtenus au cours de l'analyse de diverses matrices pour y détecter la présence de molybdène, de tungstène, de thallium et de fer, sont illustrés par la mesure des rapports isotopiques; l'utilité et les possibilités que présentent la mesure de la dilution de l'isotope sont également démontrés. On s'attend à voir la valeur réelle d'une telle technique lors de l'analyse directe de l'eau de mer à des niveaux inférieurs ou égaux à une partie par milliard et pour le dosage des éléments de matériaux géologiques, dont l'abondance naturelle est inférieure à un $\mu\text{g}\cdot\text{g}^{-1}$. On obtient des écarts types relatifs de 1 à 2 % au niveau du picogramme.

Introduction

The inductively coupled plasma (ICP) has been used as an excitation source for optical emission spectroscopy for more than 20 years, primarily because of its high temperature (about 7000°K) and available thermal energy. Since most elements of the periodic table are highly ionized by the ICP, it is also a good ion source for atomic mass spectrometry (Houk et al., 1980; Gray, 1985). ICP/mass spectrometry (ICP/MS) has three important advantages over ICP/emission spectrometry (ICP/ES): simpler spectra, superior sensitivity and isotope abundance information (Douglas, 1983). For trace elements in solution, isotope abundances can be determined by ICP/MS with a precision of less than 1% and a measurement time of approximately five minutes per sample. This contrasts with thermal ionization mass spectrometry, where much better precision (0.001-0.1%) is possible but where sample throughput is limited to only a few per day (Heumann, 1982). The ability to carry out isotope abundance measurements with moderate precision but with a high sample throughput is a feature unique to ICP/MS. One of the most successful applications of isotope abundance measurements is the quantitative determination of trace elements by the isotope dilution technique (Schmidt and Northrup, 1986). This technique utilizes an absolute internal standard which can obviate any systematic errors in sample handling, preparation and analysis, thus providing one of the most fundamentally accurate approaches open to the analytical chemist. The isotope dilution technique is, however, correct only if the added isotopes are in chemical equilibrium with those present in the sample. Basically, a known amount of an enriched isotope is added to the sample and the ratio of the enriched isotope to a reference isotope of that element is measured. With a knowledge of the natural isotopic abundance of the element, the concentration can be calculated from a simple equation (Park, 1985). Since only the isotope ratios are used in this equation, good precision obtained in the isotope ratio measurement results in good precision in the quantification of the element.

The efficiency of sample introduction into the ICP is often the critical factor in analytical performance of ICP/ES and ICP/MS. Nebulization of solutions is the most common sample introduction technique for ICP-based analytical instrumentation in use today, and, though convenient, it suffers from the following disadvantages, particularly in ICP/MS:

1. Typically, a minimum volume of 2 mL of sample solution is required for analysis under normal operating conditions and less than 5% of this volume actually reaches the ICP, thus failing to achieve maximum sensitivity.
2. Introduction of water causes specific spectral interferences and significant background spectra.
3. The nebulization of high salt solutions (>1%) generates non-reproducible and significantly suppressed signals due to salt build-up on the capillary of the nebulizer and sometimes on the sample injection tube of the torch. Viscous solutions are not easily nebulized and require matching of calibration standards to equalize nebulization efficiencies which can significantly be affected by viscosity and surface tension properties (McLaren et al., 1985).
4. The introduction of most organic solvents into the ICP produces high plasma noise and a low signal-to-noise ratio.

These problems impede the straightforward analysis of geological materials where high salt solutions are often obtained after fusion or acid attack of the sample, and lengthy separation procedures, such as ion exchange,

extraction and precipitation, are frequently required to eliminate or minimize these effects. It is evident that an alternative sample introduction technique is desirable to overcome these limitations.

There have been many reports (Nixon et al., 1974; Gunn et al., 1978; Kitazume, 1983) describing electrothermal devices to vaporize micro-samples in ICP/ES. An electrothermal vaporizer (ETV) can be used advantageously to introduce microlitre volumes of sample solutions containing high solids (>1%) and organic solvents into the ICP, because sample solutions are dried and ashed before vaporization of analyte elements. In addition to this sample handling capability, an ETV provides improved detection limits (typically an order of magnitude) compared to conventional nebulizers (concentric or cross-flow types) due to relatively high sample transport efficiency (60-80% cf. 1-4%).

In this work, the ETV is employed as a sample introduction device for ICP/MS to determine isotope abundances of picogram amounts of samples in various solutions (4% salt and organic solvents). This work is a preliminary study to demonstrate that ETV/ICP/MS can be used for the quantitative determination of picogram amounts of elements using the isotope dilution technique. Three elements in particular – molybdenum, tungsten and thallium – have been selected for this investigation as their determination limits by other methods (ICP/ES and atomic absorption spectroscopy) are inadequate for geochemical exploration purposes. The application of this technique to seawater analysis is also of immediate interest as present methods entail separation and preconcentration steps which are time-consuming and liable to contamination problems (reagents, glassware etc.). Iron was selected to demonstrate the potential of ETV/ICP/MS in the analysis of seawater. The value of measurement by isotope dilution will be shown by examining isotope ratio data; analyses of international reference materials will be presented in a future publication after receipt of enriched isotope standards.

Experimental

Reagents

High purity argon (Matheson) and Freon 23 (Matheson), trifluoromethane, were used. Sodium carbonate used in preparing the 4% salt solution was 'Baker analyzed' reagent grade. Stock standard solutions ($1000 \mu\text{g}\cdot\text{mL}^{-1}$) of the elements of interest were prepared by dissolution of their reagent-grade salts. A seawater standard (CASS-1) was obtained from the National Research Council of Canada, Ottawa.

Instrumentation

The ICP/MS system used was the ELAN 250 from SCIEX (Division of MDS Health Group Ltd., Thornhill, Ontario). The ETV used in this work was basically a modification of the rhenium filament ETV previously described (Park, 1985). The modified ETV was custom-made at the Geological Survey of Canada to accommodate either a graphite platform or a metal filament, while maintaining the high sample transport efficiency (about 80%) of the rhenium filament ETV. A schematic of the ETV is given in Figure 82.1 and the optimum operating conditions are described in Table 82.1.

The graphite platform is 1.1 cm long, 0.4 cm wide, 0.1 cm thick (Varian, Park Ridge, Illinois, U.S.A.), and can hold about 10 μL of solution. The graphite platform was used only for the determination of the refractory elements (tungsten and molybdenum) which require a high vaporization temperature. These elements however, readily

form carbides when heated on graphite and, therefore, Freon 23 gas (trifluoromethane) was added during heating to prevent carbide formation by preferential formation of volatile fluorides (Kirkbright and Snook, 1979). Introduction of Freon gas into the argon carrier gas did not corrode the nickel sampler orifice as evidenced by the absence of a nickel signal at the mass spectrometer. Freon gas was injected onto the graphite platform via specially-constructed stainless steel tubing located approximately 0.3 cm from the platform. The metal filaments used in this work are made of 0.0085 cm thick tungsten ribbon and 0.005 cm thick rhenium ribbon

(Rembar, Dobbs Ferry, New York, U.S.A.). The centre of the filament has a dimple to hold about 5 µL of solution, and is narrower than its ends to allow intensive localization of heat in the sample. The tungsten filament was chosen for thallium determination because rhenium evaporates from the rhenium filament, particularly when sample solutions contain acid, and forms an oxide, $^{187}\text{Re}^{16}\text{O}$, in the ICP, which is isobaric with ^{203}Tl .

The rhenium filament was chosen for the determination of iron.

The electrodes are made of stainless steel and cooled by water. The graphite platform and metal filaments are resistively heated by a programmable power supply, IL 550 (Instrumentation Laboratory Inc., Lexington, Massachusetts, U.S.A.).

Temperature calibration curves of the graphite platform and rhenium filament for various voltage settings are presented in Figure 82.2.

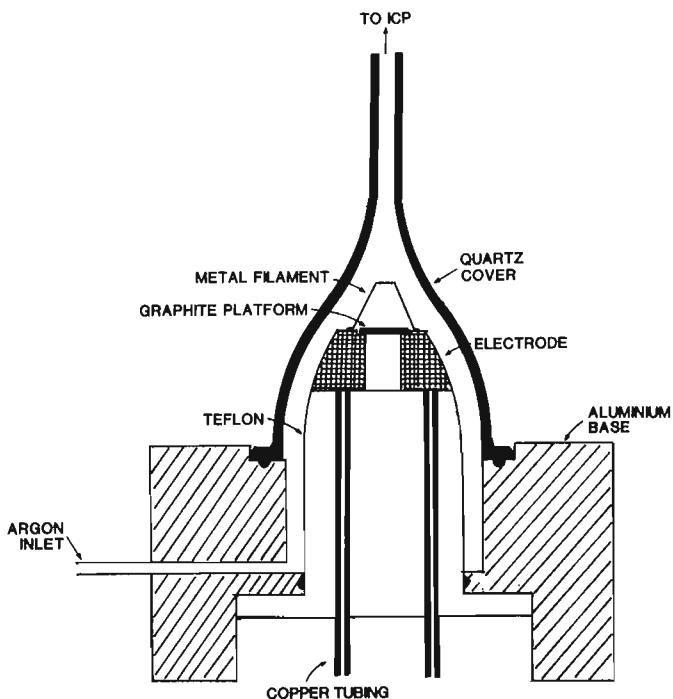


Figure 82.1. Electrothermal vapourizer.

Procedure

A 5 µL aliquot of sample solution is pipetted onto the graphite platform or metal filament. The solution is then dried at about 100°C for 1 minute and ashed at about 1100°C for 1-2 minutes (the ashing step is necessary only for salt solutions). During this operation, the ETV carrier argon flow is diverted to a fume hood vent and an ETV auxiliary argon flow (about 1.5 L/min) bypasses the ETV to the ICP. Just before vapourization, the ETV auxiliary argon flow is turned off and the ETV carrier argon flow is switched to the ICP. The sample is vapourized at 1600-1900°C for 2-5 seconds.

Table 82.1. Operating conditons of the ETV and Elan

RF forward power	1 kW
Reflected power	20 W
Distance from sampling orifice to load coil	2.2 cm
Plasma gas flow rate	13 L min ⁻¹
Auxiliary gas flow rate	2.1 L min ⁻¹
Carrier argon flow rate	1.2 L min ⁻¹
	(graphite platform)
	1.5 L min ⁻¹ (metal filament)
Freon injection rate	1 mL min ⁻¹
Ion lens setting	B = 10
	E1 = 80
	E2 = 20
	S2 = 35 - 40
Vapourization temperature	1600°C (graphite platform)
	1600-1900°C (metal filament)
Measurement parameters (measurements taken in multichannel mode):	
Measurement time	0.05-0.1 s (signal integration)
	0.01 s (peak plotting)
Dwell time	5 ms

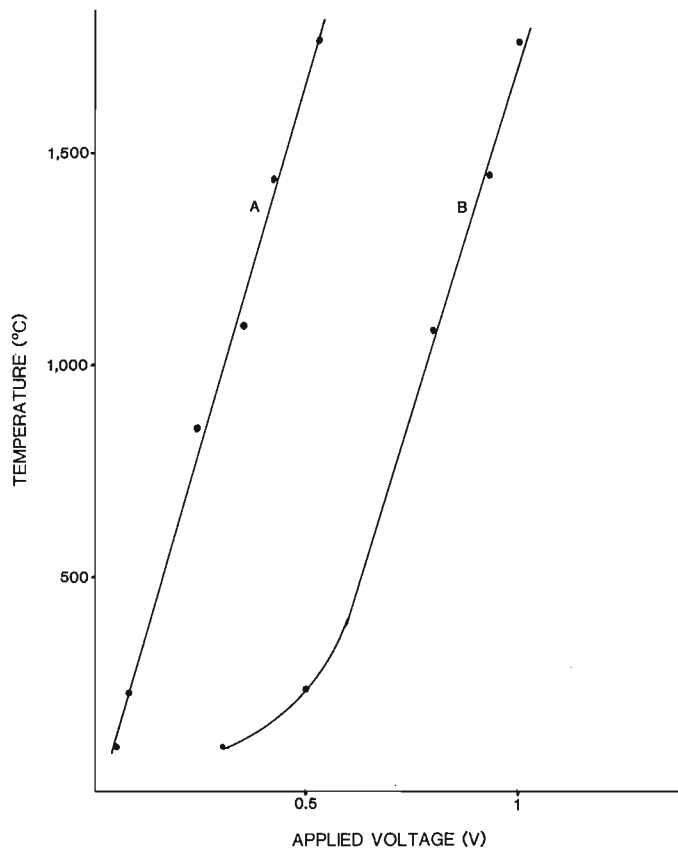


Figure 82.2. Temperature-voltage calibration curve for rhenium filament (A) and graphite platform (B).

In order to determine isotope abundances from transient signals, the mass spectrometer is required to possess the requisite mass stability, fast electronics and computer control, so that rapid mass peak-hopping can be used during the few seconds in which the sample is vapourized. During the peak-hopping, the signal intensity of each isotope is measured for 5 milliseconds (dwell time) and accumulated at buffer registers. The accumulated signals are averaged for each 0.5 seconds and added to get 1 or 2 second-integrated counts, depending on sample solutions. From these integrated counts, isotope abundances are calculated.

Results and discussion

Effect of operating parameters

The most critical parameters affecting sensitivity in the ETV/ICP introduction system comprise: the carrier argon flow rate, the RF power to the ICP, the filament vapourizing temperature, and, when added, the Freon gas injection rate. An example of the various combined settings of

these four parameters and their optimum values is shown in Table 82.2 for tungsten, mass 184. A 5 μL aliquot of a 100 $\text{ng}\cdot\text{mL}^{-1}$ standard was used for optimization. A drastic decrease in signal obtained when changing the carrier argon flow rate from 1.2 to 0.8 L/min or reducing the graphite vapourization temperature from 1600 to 1100°C illustrates the experimentation required to optimize these parameters for each element. The dramatic change in response to varying the ICP parameters is in agreement with Horlick et al. (1985).

Isotope dilution technique

The advantages of using the isotope dilution technique rather than direct calibration at one mass setting are: improvement in precision and reduction in interferences. A disadvantage of the ETV sample introduction system compared to nebulization is that precision is often degraded; this has been evidenced in ICP/ES and atomic absorption spectroscopy studies. Five consecutive determinations of molybdenum and tungsten were made, using 5 μL of a

Table 82.2. Effect of operating parameters on the tungsten signal (^{184}W)

Carrier argon flow rate (L/min)	Freon injection rate (mL/min)	Graphite platform temperature (°C)	RF power (kW)	Relative peak height (normalized to maximum)
1.4	1.0	1600	1.0	0.56
1.2	1.0	1600	1.0	1.00
1.0	1.0	1600	1.0	0.63
0.8	1.0	1600	1.0	0.08
1.2	2.0	1600	1.0	0.46
1.2	0.5	1600	1.0	0.70
1.2	1.0	1400	1.0	0.50
1.2	1.0	1250	1.0	0.28
1.2	1.0	1100	1.0	0.03
1.2	1.0	1600	1.05	0.92
1.2	1.0	1600	0.90	0.88
1.2	1.0	1600	0.80	0.44

Table 82.3. Isotope ratio measurements of Mo and W in 100 $\text{ng}\cdot\text{mL}^{-1}$ standard solution

		Mo				W			
		95	96	97	98	182	183	184	186
1 sec-integrated signal ^a (1000 ions)	mean	79.0	85.6	50.1	126.6	190.6	102.0	216.9	199.0
	SD	10.5	10.9	6.7	16.3	28.0	14.7	31.1	29.2
	RSD (%)	13.27	12.83	13.45	12.90	14.71	14.39	14.34	14.69
Isotope ratio ^a (normalized to the most abundant)	mean	0.624	0.676	0.396	1	0.878	0.470	1	0.917
	SD	0.011	0.01	0.007	0	0.007	0.003	0	0.013
	RSD (%)	1.79	1.54	1.83	0	0.81	0.65	0	1.47
Natural isotope ratio (normalized to the most abundant)		0.652	0.684	0.389	1	0.857	0.466	1	0.932
Difference (%)		-4.3	-1.2	+1.8	0	+2.5	+0.86	0	-1.6

^a Five measurements of 5 μL aliquot
SD Standard deviation
RSD Relative standard deviation

Table 82.4. Matrix effects on thallium measurements at 20 $\mu\text{g}\cdot\text{mL}^{-1}$ Tl

Matrix element	Concentration ($\mu\text{g}\cdot\text{mL}^{-1}$)	$^{203}\text{Tl}_a$		$^{205}\text{Tl}_a$	
		1 s-integrated signal (ions)	Abundance (%)	1 s-integrated signal (ions)	Abundance (%)
-	-	14244 \pm 1280	30.59 \pm 0.27	32336 \pm 3174	69.41 \pm 0.27
Cu	100	18056 \pm 1986	29.88 \pm 1.05	42340 \pm 4310	70.12 \pm 1.05
Na	100	9886 \pm 1583	29.12 \pm 0.68	23412 \pm 2997	70.88 \pm 0.68
Pb	100	44700 \pm 4023	26.87 \pm 0.35	121756 \pm 11445	73.13 \pm 0.35

^a Mean of five measurements \pm standard deviation

100 $\text{ng}\cdot\text{mL}^{-1}$ standard solution, and the signals of four isotopes of each element measured. The results, shown in Table 82.3, indicate the superior relative standard deviation obtained by measuring the isotope ratio (normalized to ^{98}Mo and ^{184}W) rather than the absolute value of ions per second at one mass, thus improving the precision from about 13-14% to 1-2%.

The matrix effects of a 5000-fold excess of sodium, copper and lead on 20 $\text{ng}\cdot\text{mL}^{-1}$ thallium at masses 203 and 205 are shown in Table 82.4. The results are tabulated as integrated signals and as abundances for each isotope. It is evident that sodium causes a suppression while copper and lead cause an enhancement of the thallium signal at both masses. Lead is a particularly serious interferent (three-fold enhancement) at this level. However, if a ratio is measured, as shown in the abundance figures, then the shift encountered due to matrix elements is almost negligible compared to absolute signal depression or enhancement. Hence time-consuming separation of the analyte, such as thallium, from its matrix, would not be necessary. Table 82.4 also gives further evidence of the satisfactory precision (0.5-2.0%) obtainable by isotope dilution in the presence of 5000-fold excess of matrix elements.

Sensitivity

As mentioned previously, the much higher transport efficiency of the analyte into the ICP by the ETV rather than the nebulizer results in a significant increase in sensitivity and lowering of detection limits. In Figure 82.3, the transient signals (ions/s) of four molybdenum isotopes (masses 95, 96, 97, 98) generated from the vapourization of 5 μL of 100 $\text{nL}\cdot\text{mL}^{-1}$ standard solution are plotted. The peak height of the most abundant isotope, ^{98}Mo , is about 240 000 ions/s. This value is approximately ten-fold greater than the steady count rate obtained by conventional nebulization of the same solution.

The data shown in Table 82.5 demonstrate this ten-fold increase in sensitivity of ETV over nebulization introduction for the elements copper, molybdenum, lead, thallium and tungsten. Optimum conditions were used in all cases. These findings are in agreement with Ng and Caruso (1985), using ETV/ICP/ES.

Background spectra with the ETV

When sample solutions are nebulized into the ICP/MS, water is also introduced, typically at 20 $\mu\text{L}/\text{min}$. Dissociation of water in the ICP generates background peaks due to the formation of molecular species such as oxides

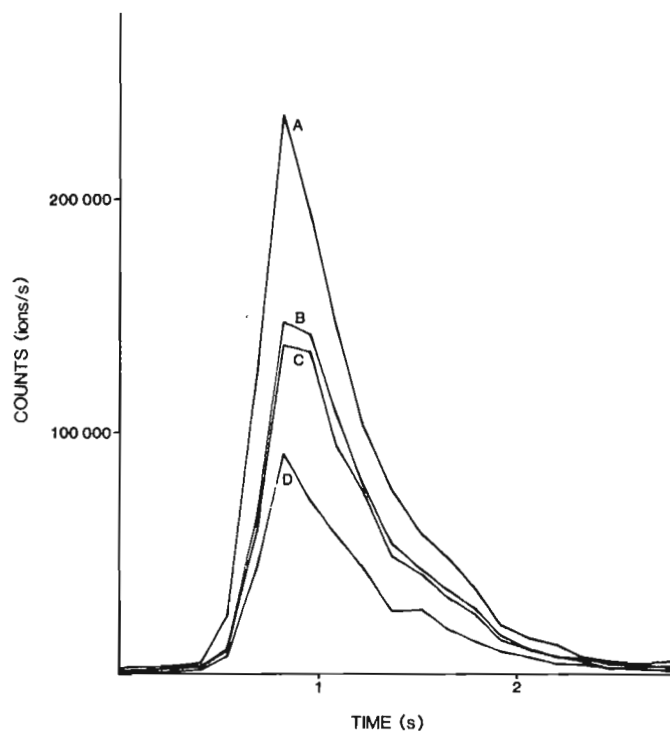


Figure 82.3. Four molybdenum isotope transient signals (m/e ; A = 98, B = 96, C = 95, D = 97) from 5 μL of 100 $\text{ng}\cdot\text{mL}^{-1}$ standard solution.

and hydrides. This actually precludes measurement of some elements such as iron where the molecular ions, $^{40}\text{Ar}^{16}\text{O}^+$ and $^{40}\text{Ar}^{14}\text{N}^+$, overlap the major iron isotopes, ^{56}Fe and ^{54}Fe , respectively. However, with the ETV method of sample introduction, dry argon carrier gas containing sample micro-particulates is injected into the ICP, and hence, concentrations of ions such as oxygen and hydrogen in the axial channel of the ICP are much lower. Background signals at masses 54 and 56 were found to be about 2000 and 3500 ions/s, respectively, while those using nebulization were about 25 000 and 60 000 ions/s, respectively. Thus, direct determination of iron in a matrix such as seawater becomes possible, hitherto unachievable by ICP/MS (McLaren et al., 1985). Five aliquots of the seawater reference material, CASS-1, were injected onto the ETV and the measurements obtained at ^{54}Fe and ^{56}Fe are given in Table 82.6.

Table 82.5. Sensitivity comparison of two sample introduction methods

Sample solution ^a	ETV Peak height (ions/s)	Nebulizer counts (ions/s)
100 ng·ml ⁻¹ Cu	210 000	25 000
100 ng·ml ⁻¹ Mo	240 000	22 000
100 ng·ml ⁻¹ Pb	130 000	12 000
100 ng·ml ⁻¹ Tl	190 000	20 000
100 ng·ml ⁻¹ W	120 000	10 000

^a Measurement at the most abundant isotope

Table 82.6. Direct determination of iron in seawater (CASS-1)^a

Run #	1 sec-integrated signal		ratio ⁵⁶ Fe/ ⁵⁴ Fe
	⁵⁴ Fe	⁵⁶ Fe	
1	9160	176 800	19.30
2	7213	121 900	16.90
3	7132	125 300	17.57
4	5549	103 300	18.62
5	6119	110 700	18.09
Mean	7035	127 600	18.10
SD	1378	28 873	0.93
RSD (%)	19.6	22.6	5.1

^a The recommended concentration of Fe in CASS-1 is 0.873 μg·mL⁻¹

Thus, precision of better than 5% at the 1 ng·mL⁻¹ level can be expected in the direct determination of iron in seawater by isotope dilution ETV/ICP/MS.

High salt solutions

Sample solutions containing a high level of dissolved salts are frequently obtained in the analysis of geological materials after decomposition by fusion or acid attack. For example, a carbonate fusion used to decompose rocks for the determination of boron, molybdenum and tungsten by ICP/ES yields a 4% salt solution (Hall and Pelchat, 1985). Such a solution cannot be nebulized into the ICP/MS as it causes rapid salt deposition at the sample orifice and, hence, erratic data. This salt can, however, be effectively removed before vapourization of a relatively involatile analyte, such as molybdenum or tungsten, by heating the graphite platform to 1100°C for 2 minutes. Isotope ratios, ⁹⁶Mo/⁹⁸Mo and ¹⁸²W/¹⁸⁴W, were measured five times in 4% salt solution at the 50 ng·mL⁻¹ level with a relative standard deviation of

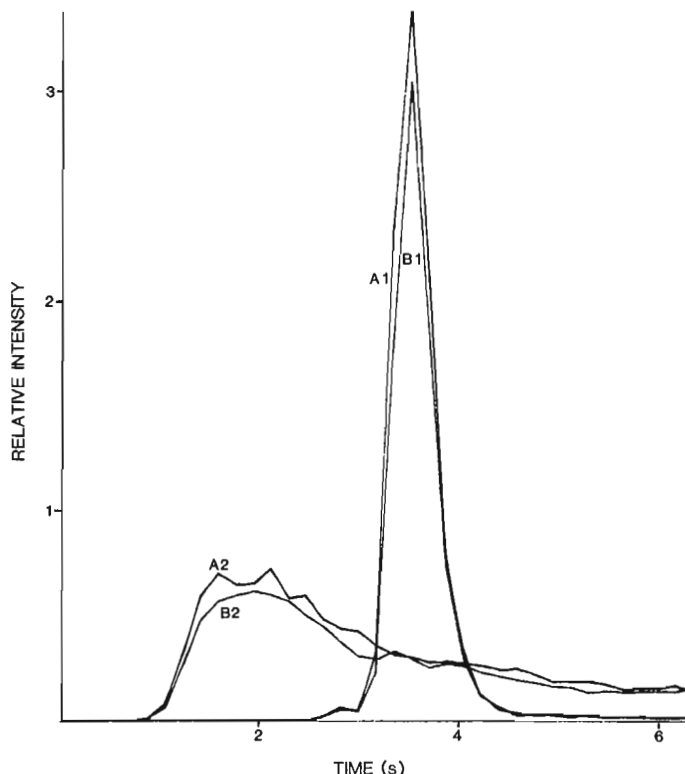


Figure 82.4. Two tungsten isotope transient signals (m/e; A = 184, B = 182) from standard solution (A1, B1) and 4% salt solution (A2, B2) with 2 min ashing at 1100°C.

1.6 and 1.0%, respectively. However, the requirement of the long ashing period at 1100°C to eliminate the salt leads to carbide formation of the analyte. Figure 82.4 illustrates the two tungsten transient signals, ¹⁸²W and ¹⁸⁴W, obtained from a standard solution alone and one containing 4% salt (sodium carbonate) with an ashing stage. It is immediately apparent that the tungsten signals from the salt solution are much broader, require a longer integration time, and hence suffer from a poorer signal-to-noise ratio. This problem could likely be remedied by a higher vapourization temperature (>1600°C) but the present design precludes this possibility due to electrode discharge to the graphite at higher voltages. An improved design of the ETV to allow higher temperatures is currently under construction.

Organic solvents

Although ETV/ICP/MS is extremely sensitive and the isotope dilution method of measurement allows determination of elements in complex matrices, there may still be situations where separation of the analyte remains necessary to achieve determination at the ng·g⁻¹ level in the rock, soil or sediment. Such would be the case in the determination of the platinum-group elements, gallium and thallium, where the natural abundance is below 1 μg·g⁻¹ and large sample weights (>10 g) are not used for digestion. Methylisobutyl ketone (MIBK) is often used as the solvent in which to extract gold or thallium as their chloro-complexes (Hubert and Chao, 1985) or base metals from waters as chelate complexes with ammonium pyrrolidine dithiocarbamate (APDC). MIBK can be injected easily onto the ETV and dried before volatilization of a volatile element such as thallium. Isotope abundances of ²⁰³Tl and ²⁰⁵Tl were determined from five 5 μL aliquots of 2 ng·mL⁻¹ Tl in MIBK and are presented in Table 82.7. The measured abundances are very close to the

Table 82.7. Thallium isotope abundance measurements from 2 ng•mL⁻¹ in MIBK

Run #	²⁰³ Tl	²⁰⁵ Tl
1	29.99	70.01
2	30.56	69.44
3	30.38	69.62
4	28.82	71.19
5	29.82	70.18
Mean	29.91	70.09
SD	0.68	0.68
RSD (%)	2.28	0.97
Natural abundance (%)	29.5	70.5
Difference (%)	+1.4	-0.6

natural values with precision in the range 1-2%, showing promise of this technique for the analysis of geological materials at the ng•g⁻¹ level for thallium.

Conclusions

The data reported have shown that ETV/ICP/MS with isotopic dilution measurement is a promising analytical technique capable of determining picogram amounts of analytes with a relative standard deviation of 1-2% in complex solutions and in organic solvents. The combination of the ETV with ICP/MS measurement is predicted to have considerable impact in analytical chemistry, particularly in the area of seawater analysis and in the determination of metals in geological materials at the ng•g⁻¹ level.

Acknowledgments

The authors thank R. Thibedeau and S. Banzky for construction of the ETV, and N. de Silva and A.G. Plant for critical review of this manuscript.

References

Douglas, D.
1983: ICP/MS. Technologies marry to produce better analysis; Canadian Research, v. 16(3), p. 55-60.

Gray, A.L.
1985: The ICP as an ion source—origins, achievements and prospects; Spectrochimica Acta, v. 40B, p. 1525-1537.

Gunn, A.M., Millard, D.L., and Kirkbright, G.F.
1978: Optical emission spectrometry with an inductively coupled radiofrequency argon plasma source and sample introduction with a graphite rod electrothermal vaporisation device; Analyst, v. 103, p. 1066-1073.

Hall, G.E.M. and Pelchat, J.C.
1985: The determination of boron and other refractory elements in geological materials by inductively-coupled plasma emission spectrometry; in Current Research, Part A, Geological Survey of Canada, Paper 86-1A, p. 89-94.

Heumann, K.G.
1982: Isotopic analyses of inorganic and organic substances by mass spectrometry; International Journal of Mass Spectrometry and Ion Physics, v. 45, p. 87-110.

Horlick, G., Tan, S.H., Vaughn, M.A., and Rose, C.A.
1985: The effect of plasma operating parameters on analyte signals in inductively coupled plasma-mass spectrometry; Spectrochimica Acta, v. 40B, p. 1555-1572.

Houk, R.S. Fassel, V.A., Flesch, G.D., Svec, H.J., Gray, A.L., and Taylor, C.E.
1980: Inductively coupled argon plasma as an ion source for mass spectrometric determination of trace elements; Analytical Chemistry, v. 52, p. 2283-2289.

Hubert, A.E. and Chao, T.T.
1985: Determination of gold, indium, tellurium and thallium in the same sample digest of geological materials by atomic-absorption spectroscopy and two-step solvent extraction; Talanta, v. 32, p. 568-570.

Kirkbright, G.F. and Snook, R.D.
1979: Volatilization of refractory compound forming elements from a graphite electrothermal atomization device for sample introduction into an inductively coupled argon plasma; Analytical Chemistry, v. 51, p. 1938-1941.

Kitazume, E.
1983: Thermal vaporization for one-drop sample introduction into the inductively coupled plasma; Analytical Chemistry, v. 55, p. 802-805.

McLaren, J.W., Mykytiuk, A.P., Willie, S.N., and Berman, S.S.
1985: Determination of trace metals in sea water by inductively coupled plasma mass spectrometry with preconcentration on silica-immobilized-8-hydroxyquinoline; Analytical Chemistry, v. 57, p. 2907-2911.

Ng, K.C. and Caruso, J.A.
1985: Electrothermal vaporization for sample introduction in atomic emission spectrometry; Applied Spectroscopy, v. 39(4), p. 719-726.

Nixon, D.E., Fassel, V.A., and Kniseley, R.N.
1974: Inductively coupled plasma—optical emission analytical spectroscopy, tantalum filament vaporization of microliter samples; Analytical Chemistry, v. 46, p. 210-213.

Park, C.J.
1985: Feasibility study of an electrothermal vaporizer/inductively coupled plasma/mass spectrometry system; unpublished Ph.D. thesis, University of Toronto.

Schmidt, M. and Northrup, M.A.
1986: A cost effective instrument for accurate element analysis; American Laboratory, February, 1986, p. 125-132.

Zircon morphology and U-Pb geochronology in active shear zones:
studies on syntectonic intrusions along
the northwest boundary of the Central Metasedimentary Belt,
Grenville Province, Ontario

Project 830006

O. van Breemen and S. Hanmer
Lithosphere and Canadian Shield Division

van Breemen, O. and Hanmer, S., Zircon morphology and U-Pb geochronology in active shear zones: studies on syntectonic intrusions along the northwest boundary of the Central Metasedimentary Belt, Grenville Province, Ontario; in *Current Research, Part B*, Geological Survey of Canada, Paper 86-1B, p. 775-784, 1986.

Abstract

From field observations, two granite sheets near the base of the Central Metasedimentary Belt Boundary Zone (CMBBZ) are syntectonic w.r.t. NW directed overthrusting. Internal zoning of zircons from these granites show an outward change from regular igneous to irregular discordant patterns and together with numerous synneusis twins is interpreted in terms of crystallization in a dynamic environment. Movement in the lowest structural level occurred at 1060 ± 6 Ma. Younger movements occurred at higher structural levels in the CMBBZ.

Zircon morphology and U-Pb isotope systematics from the Redstone Lake meta-tonalite, the lowest structural slice in the western CMBBZ indicate that this unit was a 1450-1300 Ma old igneous precursor which underwent granulite facies metamorphism during the Grenville Orogeny. Similar zircon U-Pb isotope systematics and morphology have been documented in the Central Gneiss Belt. The age and geometrical relations suggest that the Redstone Lake meta-tonalite structurally underlay the sediments and volcanics of the Central Metasedimentary Belt to the SE and may have been structurally detached from the CGB.

Résumé

D'après les observations faites sur le terrain, deux couches de granite situées près de la base de la partie limitrophe de la Zone métasédimentaire centrale (CMBBZ) présentent un cas de chevauchement syntectonique axé vers le nord-ouest. La zonation interne des zircons de ces granites indique un changement vers l'extérieur des structures ignées régulières à des structures discordantes irrégulières qui sont interprétées, avec de nombreux mâcles, en termes de cristallisation dans un milieu dynamique. Il y a eu un déplacement dans la structure inférieure voilà environ 1060 ± 6 millions d'années. Des mouvements plus récents se sont produits dans les structures supérieures de la CMBBZ.

La morphologie et la classification de l'isotope U-Pb des zircons de la tranche structurale inférieure de la partie ouest de la CMBBZ, soit la métatonalite de Redstone Lake, indique que cette unité a un précurseur igné âgé de 1450 à 1300 millions d'années qui a subi un métamorphisme au faciès des granulites au cours de l'orogène de Grenville. Une classification et une morphologie semblable de l'isotope U-Pb des zircons ont été faites pour la Zone centrale de gneiss. Les rapports âge et géométrie semblent indiquer que la méta-tonalite de Redstone Lake est recouverte de façon structurale par des sédiments et des roches volcaniques de la Zone métasédimentaire centrale au sud-est et qu'elle a probablement été détachée de façon structurale de la Zone centrale de gneiss.

Introduction

The Central Metasedimentary Belt Boundary Zone (CMBBZ) in Ontario is a broad SE dipping belt several tens of kilometres map width, of highly strained gneisses and tectonic mélanges separating the main body of the Central Metasedimentary Belt (CMB) from the Central Gneiss Belt (CGB) to the NW (Fig. 83.1). The internal geometry of the structure of this zone is still not resolved. However, recent mapping in the Haliburton region reveals at least two discrete thrust sheets each 3-4 km thick of foliated meta-tonalite to granodiorite with minor granite and syenite (Hanmer and Ciesielski, 1984; Hanmer et al., 1985). Intervening ductile high strain zones have assemblages of kinematic indicators showing thrusting to the NW along the direction of the extension lineation.

The present geochronological study complements recent U-Pb zircon work in the CGB which provided evidence for igneous basement of 1500-1300 Ma age affected by granulite facies metamorphism and tectonism in the 1160-1030 Ma range (van Breemen et al., 1986). Within the CGB, a SE younging stacking order of thrust structural domains has been proposed (Culshaw et al., 1983) and supported by the above U-Pb zircon study.

The present study attempts to determine the age and order of thrust stacking within the CMBBZ and to this end syntectonic pegmatites and granite sheets have been collected for U-Pb zircon dating both along and across this zone (samples 1-5, Fig. 83.1). In addition, a sample has been collected from the Redstone Lake meta-tonalite bounded by the two lower ductile thrust zones in the Haliburton area (sample 6, Fig. 83.1). Analytical techniques of zircon separation, documentation, purification and isotopic analysis are similar to those described in van Breemen et al. (1986). Regression analyses were done according to the methods of York (1969). Two sigma uncertainties in the isotopic ratios are 0.5% for $^{206}\text{Pb}/^{238}\text{U}$ and $^{207}\text{Pb}/^{235}\text{U}$ and 0.15% for $^{207}\text{Pb}/^{206}\text{Pb}$. U-Pb isotopic data are presented in Table 83.1; they are plotted for the syntectonic intrusions in Figure 83.2 and for the Redstone Lake meta-tonalite in Figure 83.3.

Case studies

Boudined pegmatite, Killaloe (sample 1)

The older of two pegmatites sampled at Killaloe cuts straight gneisses comprising thin continuous amphibolite layers in pink quartzofeldspathic granitic material. This 50 to 100 cm thick intrusion has been boudined and folded and is mildly foliated internally (Fig. 83.4).

Zircons are euhedral to subhedral and are generally fairly coarse and magnetic. By X-ray diffraction they were identified as zircon showing no back reflections. Most of the grains appeared as angular fragments, presumably broken during the crushing. Three fractions have been analyzed of which two were abraded (Table 83.1; Fig. 83.2). The data points fit a chord (MSWD = 0.69) with an upper intercept age of $1029 \pm 14 / -4$ Ma and a lower intercept close to the origin.

Crosscutting pegmatite, Killaloe (sample 2)

This parallel-sided pegmatite crosscuts the same straight gneisses as the boudined pegmatite described above. The pegmatite is not deformed.

Zircons are euhedral to subhedral. Four fractions were analyzed of which two were abraded. Uranium contents were lower than in the zircons from the boudined pegmatite (Table 83.1).

The data points do not fit a chord and the distribution of data suggests a component of older radiogenic lead. Cores were, however, not detected under transmitted light. As the uranium concentrations in zircons from this pegmatite are lower than those from the boudined pegmatite, it is assumed that in this case lead loss also occurred in recent time. According to this model, the lowest $^{207}\text{Pb}/^{206}\text{Pb}$ model age, close to 1010 Ma, represents the maximum age for the intrusion of this pegmatite. Thus the isotopic data indicate that the crosscutting pegmatite is at least 20 Ma younger than the boudined pegmatite, which is consistent with the field relationships.

Hawk Lake granite veins (sample 3)

This weakly foliated granite is part of a swarm of subconcordant sheets, appearing late syntectonic with respect to shearing on the underside of the Redstone Lake thrust sheet. The rock sampled consists of microcline, quartz and plagioclase and in thin section is fresh except for minor sericitic development. There are some late cracks. The grain size varies from 1 to 0.1 mm and some poorly developed quartz stringers are up to several millimetres long. It is clear that this granite has not undergone strong shearing in the solid state.

Zircons are generally ovoid and electron microscope images show their surfaces to be made up of many small facets with rounded edges and there are some depressions which could be interpreted in terms of resorption (Fig. 83.5A). Polished and etched zircons show complex growth histories. Apparent cores viewed in transmitted light turn out to be euhedrally zoned centres which grade outwards into irregularly zoned mantles (Fig. 83.5B). The irregular zones feature many discordances giving a 'cross-laminated' appearance. Many euhedral centres have also been modified by cut-offs and embayments, the latter of which clearly indicate resorption (Fig. 83.5C, D, E).

Two other features characterize this striking zircon population. There is an abundant variety of doubly to multiply twinned grains made up of euhedral to irregular but ovoid shapes (Fig. 83.5H). In addition there are a number of small flat equant grains (Fig. 83.5N). The full significance of all the textural and morphological features of the zircons from the Hawk Lake and Carnarvon granite veins is discussed below.

Only the most characteristic ovoid-prismatic zircons are included in this analysis. Of the four zircon fractions analyzed, three were abraded. A regression line fits the four zircon fractions (MSWD = 0.24) and corresponds to an upper intercept age of 1060 ± 6 Ma and a lower intercept age of 204 ± 52 Ma. The linear array provides no evidence for an older inherited zircon component, supporting the impression gained from the etched sections that the euhedral cores are not xenocrystic.

Carnarvon granite veins (sample 4)

The Carnarvon granite veins occur on the upper side of the Redstone Lake thrust sheet. This leucocratic granite is medium- to coarse-grained and generally well foliated. The granite sheets show clear evidence for branching and comprise a strongly deformed nearly transposed vein array which is now only crosscutting at a low angle to foliated and layered amphibolite straight gneiss (Hanmer and Ciesielski, 1984; Fig. 14.3B). In thin section this granite is like the Hawk Lake granite veins except that quartz stringers are somewhat better developed. One thin section showed cracks up to 20 microns wide which contain both quartzofeldspathic material and secondary alteration products of unidentified minerals.

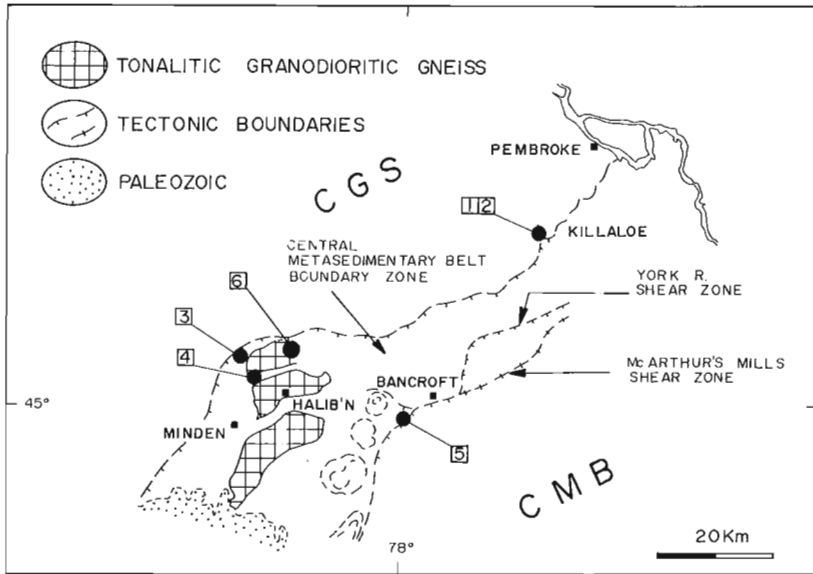


Figure 83.1

Sample locality map of the Central Metasedimentary Belt Boundary Zone shown in relation to the Central Gneiss Belt (CGS) and the Central Metasedimentary Belt (CMB).

Figure 83.2

Isotope ratio plot for zircons from syntectonic pegmatites and granites.

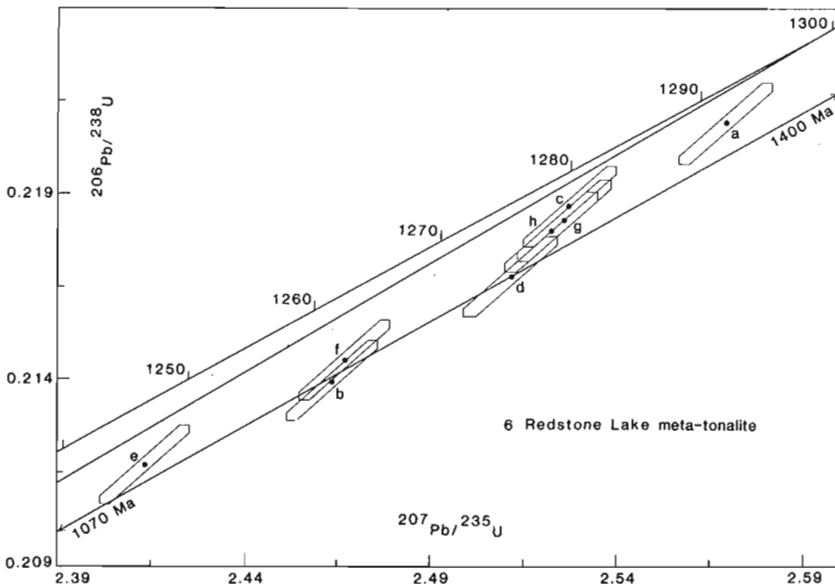
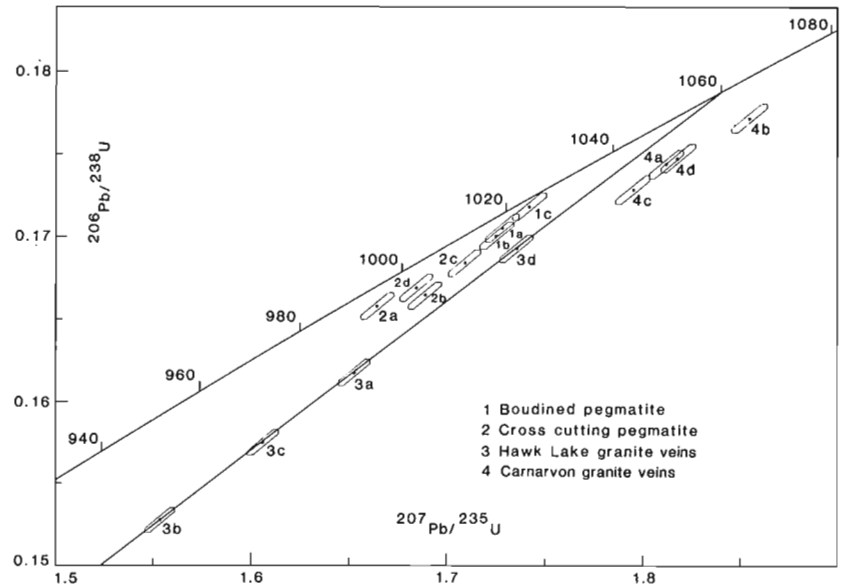


Figure 83.3

Isotope ratio plot for zircons from Redstone Lake meta-tonalite.

Table 83.1. U-Pb zircon isotopic data

Sample and zircon fraction*	Weight (mg)	U (ppm)	Pb** (ppm)	Measured $^{206}\text{Pb}/^{204}\text{Pb}$	^{204}Pb	Atomic abundance ^{208}Pb	$^{206}\text{Pb}/^{238}\text{U}$	$^{207}\text{Pb}/^{235}\text{U}$	$^{207}\text{Pb}/^{206}\text{Pb}$ age (Ma)
1. Bouldined pegmatite, Killaloe									
a, + 149, N	1.54	885.6	155.1	18659	0.031	73.95	0.170507	1.72821	1028.1
b, + 149, N, A	2.43	1010.0	176.0	49835	0.010	73.71	0.170052	1.72520	1029.9
c, - 149 + 105, N, A	1.27	1260.7	220.1	9372	0.082	74.72	0.171811	1.74239	1029.2
2. Cross cutting pegmatite, Killaloe									
a, + 149, N2°, A	1.40	722.5	134.7	8580	0.074	73.87	0.16578	1.6642	1008.6
b, - 149 + 105, N 0°, A	1.46	544.1	95.6	5451	0.134	75.49	0.16644	1.6887	1030.1
c, - 149 + 105, N 0°, A	1.98	299.7	54.2	6375	0.030	74.03	0.16841	1.7090	1030.6
d, + 105, N 0°, A fines	1.39	413.5	76.1	4079	0.158	75.44	0.16690	1.6841	1019.0
3. Hawk Lake granite veins									
a, - 149 + 105, N	1.55	997.1	158.0	4047	0.183	76.71	0.16175	1.6528	1044.4
b, - 149 + 105, M, A	2.06	1214.4	183.1	4016	0.228	76.99	0.15277	1.5532	1034.2
c, - 149 + 105, M, A	1.67	1242.3	195.2	1967	0.479	80.80	0.15745	1.6061	1040.9
d, - 105 + 74, NM, A	2.04	853.0	145.1	5159	0.169	76.78	0.16927	1.7355	1051.3
4. Carnarvon granite veins									
a, - 149 + 105, N 0.5°	4.69	994.9	171.9	20067	0.037	75.89	0.17439	1.8120	1078.2
b, - 149 + 105, N 0.5°, A	2.02	757.6	134.1	21011	0.009	76.05	0.17719	1.8549	1093.1
c, - 105 + 74, N 1.0°	2.82	928.4	159.1	14963	0.040	75.90	0.17281	1.7948	1077.2
d, - 105 + 74, N 1.0°, A	3.28	1177.2	205.0	15630	0.053	76.21	0.17476	1.8182	1080.7
5. Pegmatite in mylonite near Bancroft									
a, + 105, A	0.62	2774	262.2	1610	0.578	75.09	0.086306	0.79469	830.9
b, - 105 + 74, A	0.74	3588	358.5	4059	0.231	70.93	0.095414	0.88948	856.7
c, - 74 + 44 N, A	0.68	3919	504.4	2717	0.240	73.68	0.125240	1.21313	935.7
6. Redstone Lake meta-tonalite									
a, + 149, N 0°, A light	1.23	60.76	13.94	15394	0.022	84.65	0.22090	2.5690	1300.5
b, + 149, N 0°, A strong	0.42	52.48	11.78	2757	0.214	86.52	0.21397	2.4637	1281.1
c, - 149 + 105, N 0°, A light	0.93	74.95	17.08	4388	0.181	86.38	0.21866	2.5273	1288.6
d, - 149 + 105, N 0°, A strong	0.26	59.48	13.65	2873	0.134	85.92	0.21677	2.5116	1293.3
e, - 62, N 0°, A strong	2.58	111.6	24.66	33697	0.009	82.81	0.21171	2.4134	1261.6
f, + 149, M 0°, A light	1.35	74.77	16.64	9734	0.041	83.98	0.21453	2.4671	1278.7
g, + 149, N 0°, A strong	1.33	52.31	12.02	7911	0.039	84.48	0.21826	2.5259	1291.0
h, + 149, N 0°, A light	1.98	55.39	12.75	12413	0.025	84.28	0.21797	2.5223	1290.9
* Sieve size in microns									
** Radiogenic lead									
N,M, Respectively non-magnetic or magnetic at given side slope angle on Frantz magnetic barrier separator, model LB-1, current 1.8 amps. Where side slope angle is not given, N and M refer to original concentrate from Frantz isodynamic separator model L-1, side slope 10° and current 1.8 amps.									
A, abraded									

The zircon population is similar to that of the Hawk Lake granite veins except that etched zircon sections from the Carnarvon granite veins show a range from regularly zoned subhedral zircon to zircons with irregularly zoned mantles (Fig. 83.5F, G). Various twins and flat equant grains are common (Fig. 83.5I, J, K, L, M, O).

U-Pb zircon data points for the Carnarvon granite veins plot close to the concordia (Fig. 83.2). However, the two abraded fractions have moved up parallel to the concordia, indicating a component of inherited zircon. In view of the complexity of internal zonation, such an inherited component would be difficult to identify even in etched sections: but note possible xenocryst in Figure 83.5F. The age cannot be accurately determined. Assuming a similar Pb loss pattern to that of zircons from the Hawk Lake granite veins the age and uncertainty of the Carnarvon granite veins are estimated at 1065 ± 15 Ma. The radiometric evidence thus indicates that shear movements above and below the Redstone Lake thrust sheet were part of the same general event, though precise relative timing is not possible.

Pegmatite in mylonite near Bancroft (sample 5)

Along the upper side of the CMBBZ 12 km southwest of Bancroft, aphanitic, homogeneous flinty mylonites dip moderately SE and carry a strong dip parallel stretching lineation. The mylonites are crosscut orthogonally by an isotropic pegmatite sheet several metres thick. Thin offshoots intruding the mylonites are folded and carry a mild axial planar foliation. The fold axial planes are subparallel to the mylonite foliation in outcrop faces perpendicular to the stretching lineation.

The zircons appear altered and have less altered cores and numerous other mineral inclusions. The crystals are euhedral and there are many twins. Uranium concentrations are extremely high and the discordance of isotope ratios has the unusual relationship of increasing with grain size and decreasing with uranium concentration (Table 83.1). A regression line for the three analyzed fractions does not provide a concordant fit (MSWD = 8.82) and corresponds to an upper intercept age of 990 ± 21 Ma and a lower intercept age of 227 ± 25 Ma.

Redstone Lake meta-tonalite (sample 6)

The Redstone Lake meta-tonalite is a foliated medium- to coarse-grained grey biotite tonalite-granodiorite. Inclusions are few and the rock is strikingly homogeneous.



Figure 83.4. Folded boudined pegmatite (sample 1) cutting straight gneisses at Killaloe.

There are some occurrences of generally concordant continuous narrow amphibolite sheets which appear to be intrusives, either dykes or sills. Hypersthene is locally present. Although not identified at the sample locality, it is present several kilometres along strike.

Abundant zircon is clear with some inclusions. Crystals vary from prismatic with rounded terminations to oval and multifaceted. In transmitted light, many grains show internal euhedral igneous zonation which is discordant to the outer shape. Etched sections also display the inner igneous and outer metamorphic morphology (Fig. 83.5P).

Eight zircon fractions were analyzed which ranged from coarser than 149 microns to less than 62 microns and were either strongly or weakly abraded. The data points are distributed as a linear array close to but subparallel to the concordia from 1245 to 1290 Ma (Fig. 83.3). The array is indicative of a mixing line and in view of the low U concentrations, recent Pb loss is likely to have been limited. If the most discordant data point is omitted (6d in Fig. 83.3), then a regression line can be fitted to the remaining seven data points within their uncertainty limits (MSWD = 2.31) corresponding to an upper intercept age of $1344 +93 -32$ Ma and a lower intercept age of $1016 +143 -193$ Ma.

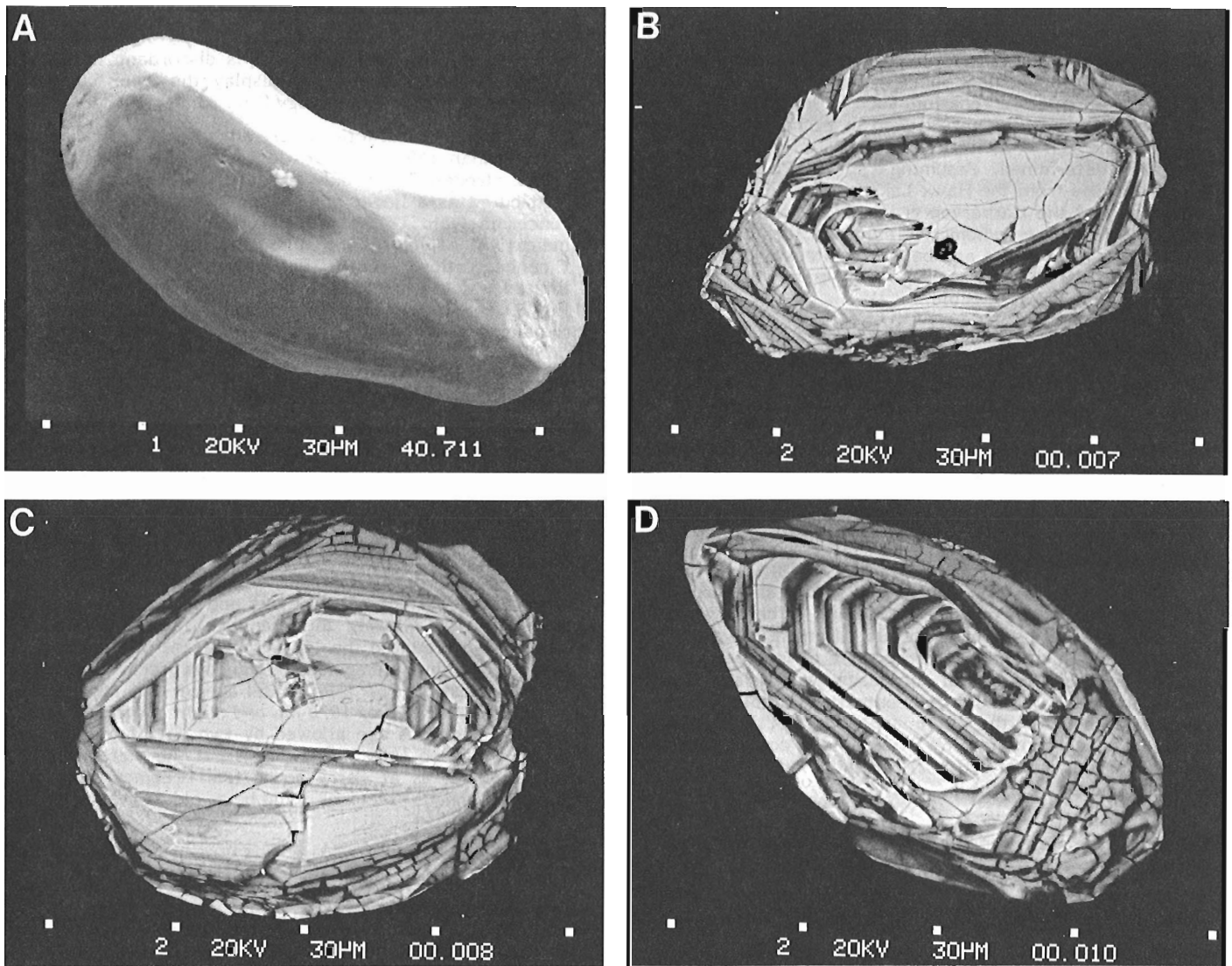
The morphological relationship between euhedral cores and multi-faceted rims suggests a two stage igneous-metamorphic zircon growth history. Both the morphological and isotopic data are comparable to those of granulite facies rocks in the OGB in which young igneous basement was involved in granulite facies metamorphism. The sporadic occurrence of hypersthene in the Redstone Lake meta-tonalite was probably more widespread prior to retrogression associated with upward thrusting and granite intrusion along the CMBBZ. Clearly the granulite facies metamorphism would have predated the 1060 ± 6 Ma age of the Hawk Lake granite. A minimum age for the igneous precursor is likely to be the oldest $^{207}\text{Pb}/^{206}\text{Pb}$ model age of 1300 Ma. Assuming a metamorphic age of 1070 Ma and slight recent Pb loss, the maximum igneous age allowed by two out of the eight data points would be 1400 Ma. However, if the metamorphic age was 1160 Ma as at Parry Sound (van Breemen et al., 1986), then the igneous precursor could be as old as 1450 Ma.

Zircon morphology

Zircon is typically an early phase in granite magmas; in contrast with zircon in a basic magma where it grows conforming to the irregular interstices between earlier formed crystals (Poldervaart, 1956; van Breemen et al., 1986). Therefore the inner euhedral morphology of zircons from the Hawk Lake and Carnarvon granite veins is typical of free growth in a liquid. The irregular zonation of the outer zircon mantles can be explained by interference with already precipitated phases such as feldspar.

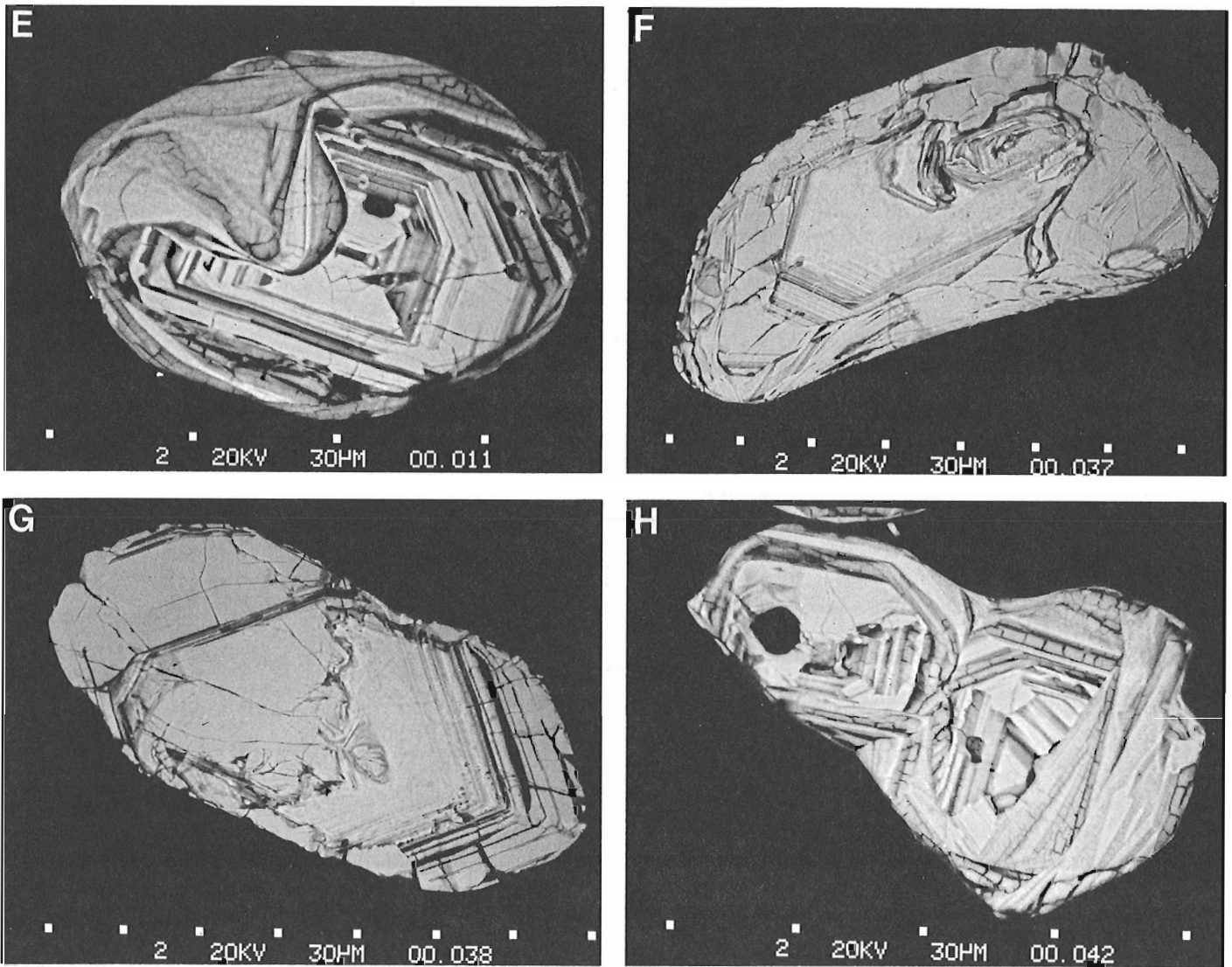
The ovoid zircon shapes are furthermore, suggestive of an abrasion or corrosion process. In this regard the numerous internal cut-offs in the growth zoning are of interest. These discontinuities might be explained in three ways: 1) zoned zircon growing up to the edges of other minerals; 2) fracturing due to grain impingement and 3) resorption on contact with adjacent grains (impingement resorption). Only the last two mechanisms can explain the cut-offs affecting the central euhedrally zoned zircon (Fig. 83.5C, D, E). There is no positive evidence for breaking of the zircons, such as filled or healed cracks or offsets of the zoning. Evidence is only positively conclusive for the case of chemical corrosion; for example, the wavy discontinuity or cut-off featured in Figure 83.5D or the striking resorbed embayment of Figure 83.5E.

Figure 83.5. Scanning electron microscope images of zircons and polished and etched zircon grain mounts from the Hawk Lake granite veins (HLG), Carnarvon granite veins (CAG) and Redstone Lake meta-tonalite. Unless indicated otherwise, images were taken in the backscattered electron mode. Grain mounts were etched with hydrofluoric acid.



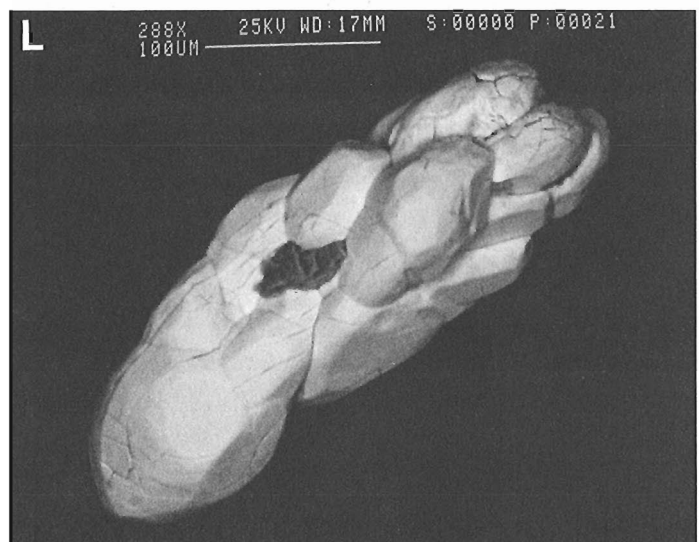
- A. Secondary electron image of multiple faceted zircon showing rounded edges and concave regions (HLG).
- B. Polished and etched section showing change from regular igneous to irregular zoning. Note discordancies in zoning of the outer mantle (HLG).
- C. Prismatic igneous outline changes to outer rounded shape. Note linear cut-off of central igneous zoning (HLG).
- D. Euhedral igneous zoning has been terminated along wavy line (bottom left). Note how bulbous zoning parallel to the inner igneous prism turns to make a 90° discordance with euhedral zoning (HLG).

Figure 83.5 (cont.)



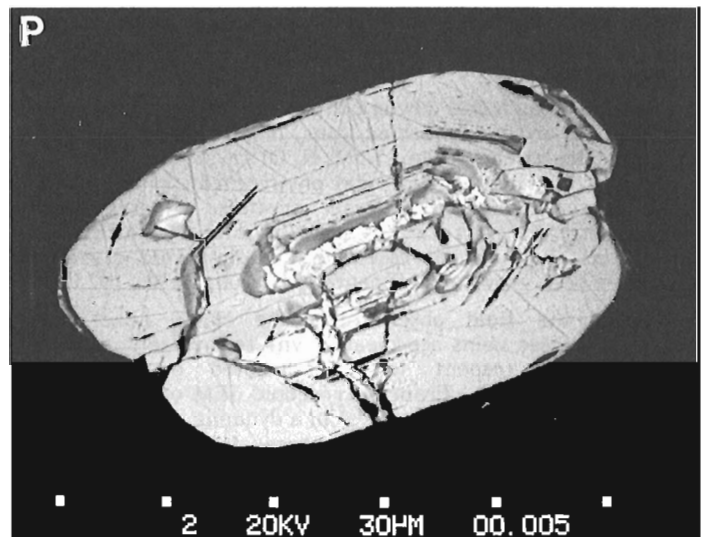
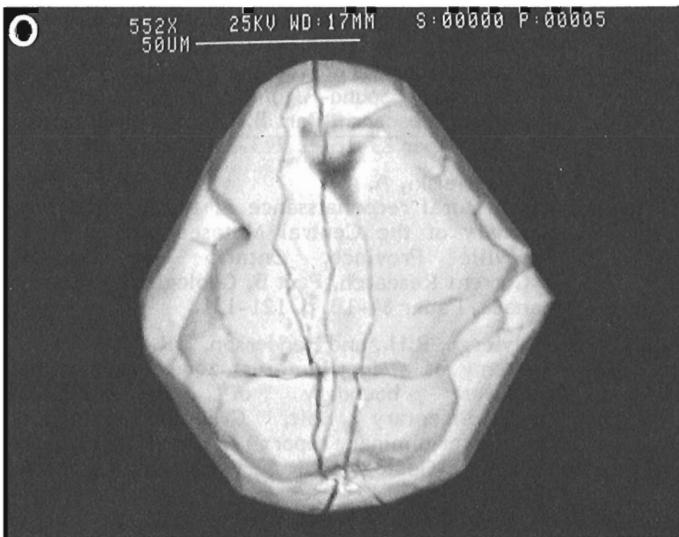
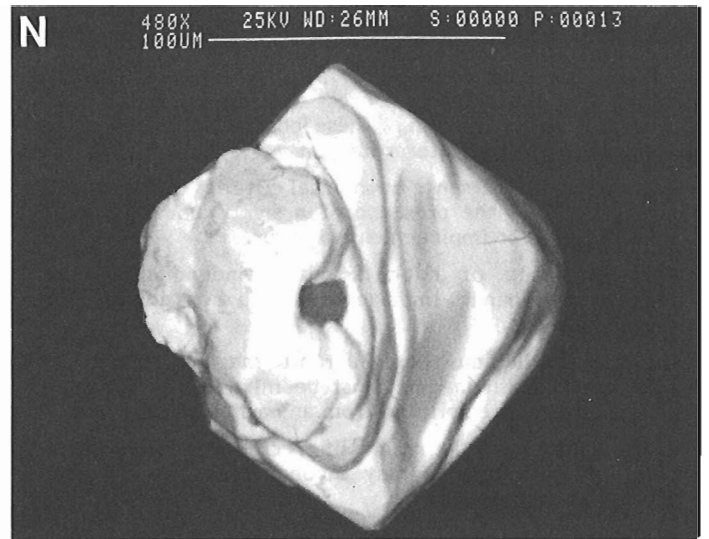
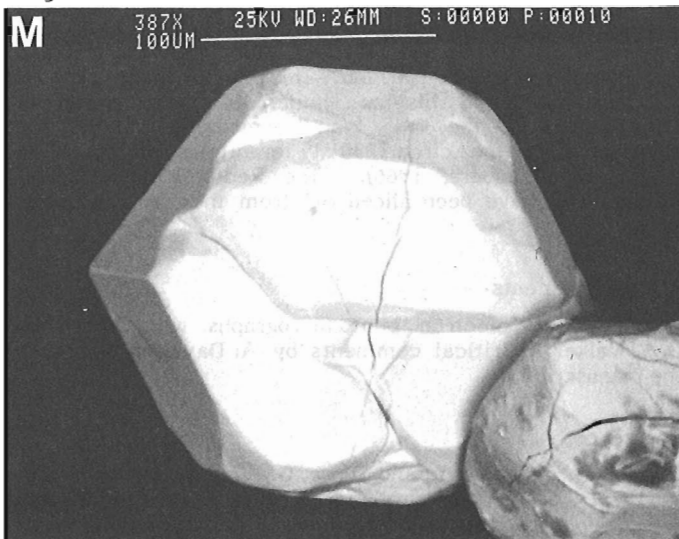
- E. Oval outline contains euhedral igneous centre with deeply resorbed embayment (HLG).
- F. Euhedral igneous centres followed by outer mantles of irregular and discordant zoning also characterize many etched sections of zircons from the Carnarvon granite veins (CAG). Note oval inclusion in euhedral centre which may be xenocrystic.
- G. The Carnarvon granite also contain zircons with little or no irregular outer zoning.
- H. Twins are common in both the Hawk Lake and Carnarvon granites. This section is interpreted in terms of synneusis as the two grains show early independent subhedral growth zones followed by common more irregular zonation (HLG).

Figure 83.5 (cont.)



- I. Twin of two subhedral igneous crystals. Mild resorption is shown by depressions on igneous faces (CAG).
- J. Early free growing euhedral zircon has (100) and (101) faces consistent with formation at high temperature. Later lower temperature (110) prism faces are sites of docking with more irregular zircon. Actively growing faces appear to be favoured for attachment (CAG).
- K. Synneusis of three multi-faceted crystals (CAG).
- L. Multiple twin in which a number of small, irregular, ovoid grains appear to have been stacked up behind a larger plug (CAG).

Figure 83.5 (cont.)



- M. Flat equidimensional zircon showing both a pyramid and a short flat prism. Note transverse fracture perpendicular to the c axis (CAG).
- N. Flat diamond shaped zircon in which a prism has not developed. Note depression with gangue which may have prevented growth perpendicular to photo. The c axis is horizontal (HLG).
- O. Flat zircon with transverse cracks. Note extension perpendicular to the c axis and repetition of partially developed pyramids (CAG).
- P. Zircon from Redstone Lake meta-tonalite featuring euhedral igneous core and multi-faceted metamorphic overgrowth.

Twins in the Hawk Lake and Carnarvon granite veins show good evidence of synneusis (Fig. 83.5H, I, J). Figure 83.5J shows a small irregular-ovoid zircon with impingement controlled faceting docked on a low temperature (110) face (Caruba et al., 1975) of a subhedral crystal, indicating that the twinning process was late compared with the euhedral zircon growth. These observations lead us to the following tentative interpretation:

1. The common occurrence of internal cut-offs in the growth zoning requires the presence of a significant volume of solid phase(s) for impingement to occur.
2. The abundance of cut-offs within individual zircons requires a dynamic impingement with rotation of the growing zircons.
3. If zircon is a liquidus phase in granite magmas, then in the light of (1) fresh magma must be mixed with the solid phases already precipitated from an earlier pulse.
4. In the light of 1-3 the mixing of precipitated solids with a pulse of fresh magma may involve the same dynamic process as suggested by 2.
5. In the light of 1-4 such docking textures as illustrated in Figure 83.5K and L might represent the accumulation of small multi-faceted grains dammed behind a larger zircon in the interconnected space of a solid framework i.e. a filter press.

While the euhedral zircon centres crystallized first, the outer mantles and twins formed later, it is believed that the flat plate-like zircons (Fig. 83.5M, N, O) crystallized last in an almost solid, near static local environment, probably in cracks or fissures between larger crystals. There is no evidence that the flat zircons grew in late hydrothermal solutions as they do not resemble the dipyrmaid crystals which have been grown experimentally (Caruba et al., 1975).

From the field observations the Hawk Lake and Carnarvon granite veins are clearly syn- to late-tectonically emplaced with respect to NW directed overthrusting (Hanmer et al., 1985). From microscopic SEM observations, the zircons of these granites grew in a dynamic crystal mush. In view of the absence of such textures from posttectonic granites elsewhere, we suggest that the dynamics of the crystallizing granites are linked to the regional tectonic deformation: more specifically, they were emplaced into active shear zones and may have facilitated movement along these.

Hypotheses that the granites had moved a considerable distance up the shear zones or were formed in the shear zones are not supported by the absence (Hawk Lake granite veins) or near absence (Carnarvon granite veins) of older inherited zircon. The isotopic evidence indicates that even during the shearing there was little interaction between the granite magma or crystal mush and the country rock.

Regional implications

Although the results of this geochronological study are preliminary, a number of significant conclusions can be drawn. The main ductile thrusting at the base of the CMBBZ near Haliburton occurred at circa 1060 Ma. Movements post-dating the 1029 ± 14 - 4 Ma boudined pegmatite at the base of the CMBBZ near Killaloe are late tectonic. The preliminary 990 ± 21 Ma late-syntectonic pegmatite in mylonite at the top of the CMBBZ near Bancroft suggests that later movements occurred at higher structural levels in this boundary zone.

Both the morphology of the Redstone Lake metatonalite zircons and isotope systematics clearly indicate that this unit is a slice of retrogressed granulite which formed as a crystallized igneous body 1450-1300 Ma years ago and was metamorphosed before 1060 Ma. This allochthonous unit thus shows a geological history similar to the high grade orthogneisses of the CGS (van Breemen et al., 1986) but different from the circa 1230 Ma granitoids of the CMB (Silver and Lumbers, 1966). The Redstone Lake metatonalite may have been sliced off from the Central Gneiss Belt.

Acknowledgments

Scanning electron photomicrographs were taken by D.A. Walker. Critical comments by A. Davidson improved the manuscript.

References

- Caruba, R., Baumer, A., and Turco, G.
1975: Nouvelles synthèses hydrothermal du zircon: substitutions isomorphiques; relation morphologie-milieu de croissance; *Geochemica et Cosmochemica Acta*, v. 39, p. 11-26.
- Culshaw, N.G., Davidson, A., and Nadeau, L.
1983: Structural subdivisions of the Grenville Province in the Parry Sound-Algonquin region, Ontario; in *Current Research, Part B, Geological Survey of Canada, Paper 83-1B*, p. 243-252.
- Hanmer, S. and Ciesielski, A.
1984: A structural reconnaissance of the northwestern boundary of the Central Metasedimentary Belt, Grenville Province, Ontario and Quebec; in *Current Research, Part B, Geological Survey of Canada, Paper 84-1B*, p. 121-131.
- Hanmer, S., Thivierge, R.H., and Henderson, J.R.
1985: Anatomy of a ductile thrust zone: part of the northwest boundary of the Central Metasedimentary Belt, Grenville Province, Ontario (preliminary report); in *Current Research, Part B, Geological Survey of Canada, Paper 85-1B*, p. 1-5.
- Poldervaart, A.
1956: Zircons in rocks. 2. Igneous rocks; *American Journal of Science*, v. 254, p. 521-554.
- Silver, L.T. and Lumbers, S.B.
1966: Geochronologic studies in the Bancroft-Madoc area of the Grenville Province, Ontario; *Geological Society of America, Special Publication 87*, p. 156 (abstract).
- van Breemen, O., Davidson, A., Loveridge, W.D., and Sullivan, R.W.
1986: U-Pb zircon geochronology of Grenville tectonites, granulites and igneous precursors, Parry Sound, Ontario; in *New Perspectives on the Grenville Problem*, ed. J.M. Moore, A. Davidson, and A.J. Baer; *Geological Association of Canada, Special Paper*.
- York, D.
1969: Least squares fitting of a straight line with correlated errors; *Earth and Planetary Science Letters*, v. 5, p. 320-324.

Distribution and origin of alluvial gold in southwest Gaspésie, Quebec¹

Project 840053

**Y.T. Maurice
Mineral Resources Division**

Maurice, Y.T., Distribution and origin of alluvial gold in southwest Gaspésie, Quebec; *in* Current Research, Part B, Geological Survey of Canada, Paper 86-1B, p. 785-795, 1986.

Abstract

An orientation survey conducted in the auriferous lower segment of the Assemetquagan River shows that although gold is preferentially found in crevices and cleavage openings of fissile bedrock on the river bed, moss growing on surfaces of boulders and outcrops also retains significant amounts of detrital gold and is a useful sample medium for exploration. The upper part of gravel deposits on stream banks, however, does not reflect the presence of gold and should be avoided in geochemical exploration surveys based on the detection of particulate gold. Turbulent flow and a sharp bend in the river channel have played a key role in distributing gold and other heavy minerals in this portion of the river.

Regional sampling established that small quantities of alluvial gold occur in some tributaries of the Assemetquagan River but failed to show a continuation upstream of the relatively rich lower segment of the river. These minor occurrences, and similar ones found in several of the other drainage basins in southwest Gaspésie, are probably derived directly from small scattered bedrock sources in the Fortin and Matapédia group sediments which are known to host gold and base metal mineralization. None, however, was found that match the lower 2 km of the Assemetquagan River for its gold content. A tentative explanation for the presence of gold in that segment is that gold was eroded from a bedrock source within Fortin Group sediments by the Laurentide ice sheet as it flowed southeasterly across western Gaspésie. It was then preferentially deposited in the Assemetquagan River valley, along with a large quantity of Shield-derived heavy minerals (almandite garnet and ilmenite), because the valley gorge constituted a major obstacle which impeded advancement of the debris-rich basal part of the ice sheet, thus concentrating the detritus in the river channel.

Résumé

Une étude d'orientation effectuée le long du cours inférieur aurifère de la rivière Assemetquagan a démontré que, quoique l'on retrouve l'or détritique concentré préférentiellement dans les fissures et entre les feuillets de clivage d'affleurements fissiles sur le lit de la rivière, on en retrouve également en quantité substantielle dans la mousse qui croît à la surface d'affleurements et de blocs dans le cours d'eau, phénomène qui la rend utile comme matériau d'échantillonnage aux fins d'exploration. D'un autre côté, la partie supérieure des bancs de gravier sur les berges de la rivière ne contient pas d'or et ne devrait pas être échantillonnée lors de levés géochimiques axés sur la détection de particules d'or. De la turbulence et un coude dans la rivière ont joué un rôle clef dans la répartition de l'or et d'autres minéraux lourds dans cette partie du cours d'eau.

Un échantillonnage régional a indiqué qu'il y a de petites quantités d'or alluvionnaire dans certains tributaires de la rivière Assemetquagan, mais cette étude n'a pas démontré l'existence d'un prolongement en amont des concentrations d'or relativement élevées du cours inférieur de la rivière. Ces quelques petits indices, et d'autres semblables que l'on retrouve dans plusieurs des bassins de drainage du sud-ouest de la Gaspésie, proviennent probablement directement de petites sources dispersées dans les roches des groupes de Fortin et de Matapédia, lesquels renferment manifestement des minéralisations d'or et de métaux communs. Aucun de ces indices alluvionnaires, toutefois, est comparable au tronçon de 2 km de long du cours inférieur de la rivière Assemetquagan pour sa teneur en or. On suggère comme explication possible de la présence d'or dans ce tronçon, que l'or a été érodé d'une source minéralisée dans les sédiments du groupe de Fortin par l'inlandsis des Laurentides lors de son passage en direction sud-est dans la partie ouest de la Gaspésie. L'or, ainsi qu'une bonne quantité de minéraux lourds en provenance du Bouclier canadien (du grenat almandin et de l'ilménite), ont été déposés préférentiellement dans la vallée de la rivière Assemetquagan. La vallée a agi comme un obstacle qui a empêché l'avance de la partie inférieure du glacier, riche en débris, et a provoqué ainsi une accumulation de débris glaciaire dans le chenal de la rivière.

¹ Contribution to the Canada Economic Development Plan for Gaspé and Lower St. Lawrence Mineral Program 1983-1988.

Introduction

The occurrence of alluvial gold near the mouth of the Assemetquagan River, a major tributary of the Matapedia River in southwest Gaspésie, has been known since the 1950s. Mining companies have been slow to explore for placer deposits in this area because of the environmental impact associated with placer mining in a region that thrives on tourism and salmon fishing. With the recent worldwide upsurge in gold exploration activity, however, efforts are being made to learn more about this occurrence in an attempt to trace it back to a bedrock source. To date, the only documented study of the Assemetquagan gold occurrence is by Girard (1985) who reported on the mineralogy and chemistry of auriferous samples collected at the mouth of the river. In addition, Soquem conducted a regional alluvial heavy mineral and lithochemical survey in 1983, to assess the gold potential of a 125 km² area in southwest Gaspésie. Sampling along the Assemetquagan River was restricted due to poor access. The results were not encouraging and no follow-up was undertaken by the company (D. Simoneau, personal communication, 1984).

This paper documents the distribution of gold at both local and regional scales on the basis of samples of alluvium collected from all the major drainage basins over an area of 750 km² of southwest Gaspésie and proposes a mode of origin for the alluvial mineralization. A parallel study is being conducted to investigate the nature, distribution and composition of the Quaternary deposits in the area to increase our understanding of the role of glaciation in shaping dispersal patterns in the region.

Geological framework and mineralization

The Gaspésie Peninsula forms part of the Paleozoic Appalachian Fold Belt (Fig. 84.1). The northern third is occupied by the Cambro-Ordovician Quebec Complex which includes highly contorted greenschist and biotite grade metasediments and metavolcanics (Mattinson, 1964). These rocks contain an abundance of generally small base metal occurrences, mostly copper, which are not known to be auriferous.

Within the study area, the rocks range in age from Upper Ordovician to Middle Devonian. They are mildly fractured and folded and their grade of regional metamorphism does not exceed subgreenschist. About 45% of the study area, including all of the basin area drained by the Assemetquagan River except for a small fringe at the headwaters, is underlain by the Fortin Group, a thick marine sequence of dark slaty mudstones and siltstones. An extensive network of quartz veins, some quite massive, occurs within this unit. Some veins are very lightly mineralized with copper and other metal sulphides and a few contain gold. Some alluvial gold was found in a stream adjacent to one such auriferous quartz vein in the Kempt River basin (Fig. 84.1) (McGerrigle, 1950; Dumont, 1961, 1963).

To the north, and in fault contact with the Fortin, lies a 4 to 6 km wide band of medium grained, grey to greenish grey feldspathic sandstone, the York River Formation. Overlying this unit, in a synclinal fold, is a narrow strip of red Battery Point sandstone, the youngest rocks exposed within the study area (Stearn, 1965). A narrow zone of andesitic volcanics is exposed over a strike length of about 12 km near the Fortin-York River contact on the east side of the Matapedia River. Farther north lies another band of York River sandstone that conformably overlies a thick sequence of limestone and calcareous siltstone belonging to the Saint-Léon, Cap Bon-Ami and Grande Grève formations. None of the above units is known to be mineralized in western Gaspésie.

To the south lies a sequence of limestones and calcareous mudstones and siltstones, the Matapedia Group, which is sepa-

rated from the Fortin Group by a major fault that runs across the entire length of southern Gaspésie (Lachance, 1979). Several base metal occurrences, some auriferous, occur within a few kilometres on either side of this structure which, in recent years, has been the focus of mineral exploration activity (Savard, 1985). Within the study area, several of these occurrences are found to the south of the fault within Matapedia Group rocks and are associated with small felsic dykes and sills. Their genetic relationship to the fault is unclear. The mineralization occurs in thermally and metasomatically altered zones around the intrusives. The alteration consists of bleached and recrystallized limestone, calc-silicates and, in some cases, garnetiferous skarns. The sulphide assemblage includes pyrite, pyrrhotite, chalcopyrite and bornite with minor sphalerite, galena, and molybdenite. (Lachance, 1974, 1977; Savard, 1985). Some occurrences contain sub-economic grades and tonnages and one, near the village of St-Benoit, also contains significant gold values (Lachance, 1979). The large ore deposits of Gaspé Copper Mines, Madeleine Mines and Sullipek, that are located about 150 km to the northeast of the study area, are of this type.

Farther south, the Chaleurs Bay Group consists mainly of calcareous mudstones and siltstones but it includes a thick sequence of porphyritic volcanics and pyroclastics of andesitic composition (Bélanger, 1982). The La Garde Formation, mostly sandstones and conglomerates, is adjacent to these volcanics to the south and forms the lithology along the coast of Chaleur Bay.

Gold distribution in the Lower Assemetquagan River valley

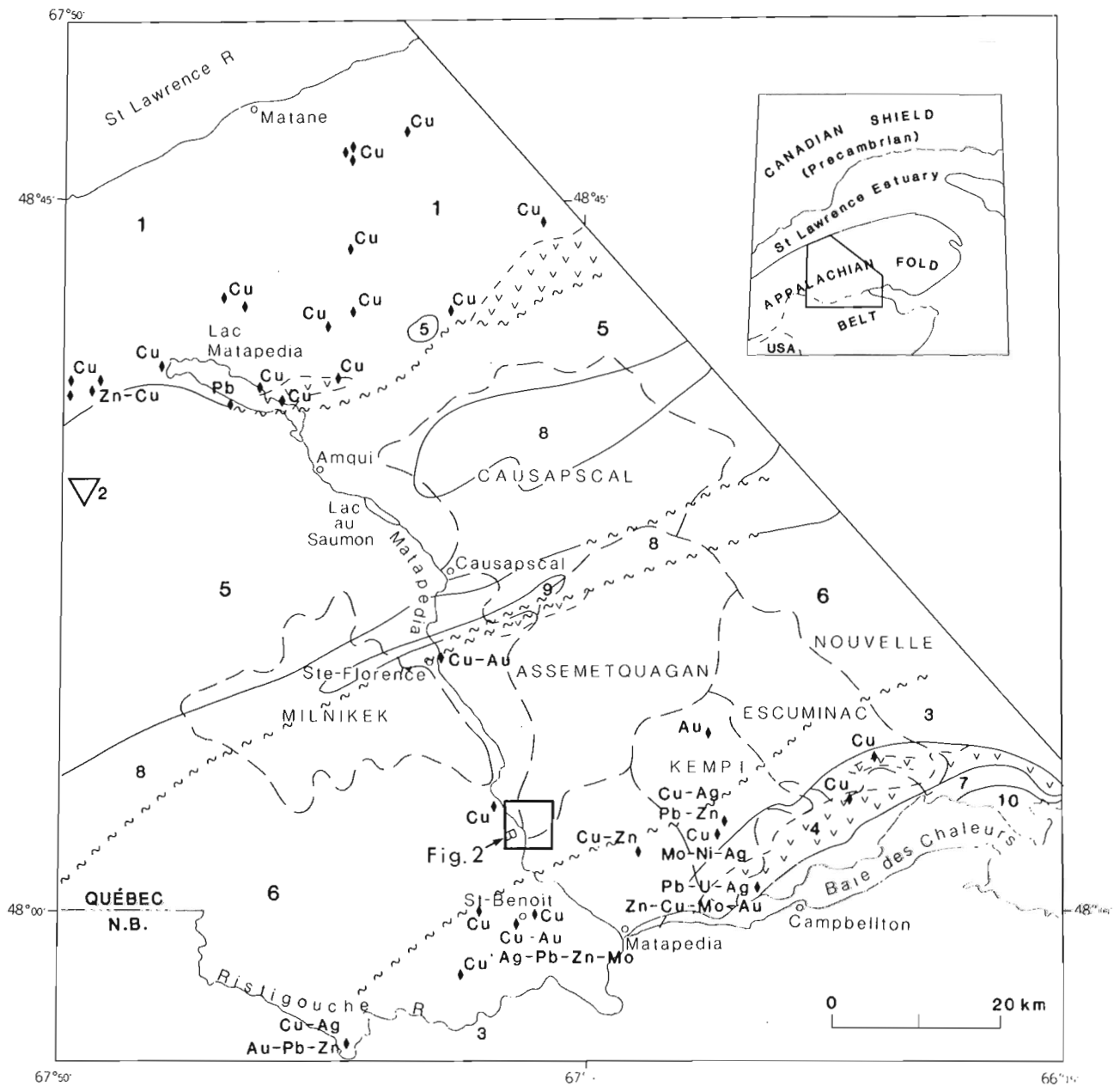
An orientation survey was conducted along the 2 km segment of the lower Assemetquagan River known to contain alluvial gold. The purpose of this study was to establish a suitable sampling procedure to be used in the regional survey and to gather data against which to compare the regional data.

The Assemetquagan, as most rivers in southwest Gaspésie, flows in a narrow, deeply incised V-shaped valley. Its floor is situated between 150 and 300 m below a rolling upland surface with summits about 300 to 450 m above sea level. The lower 900 m segment of the river (segment A, Fig. 84.2) is characterized by swift and turbulent flow. It is actively cutting into bedrock which is almost continuously exposed on both banks. Fortin Group rocks in this area are fissile, with the schistosity forming a narrow angle with the direction of the river channel and dipping from 35° to 60° towards the northwest (Fig. 84.2, 84.3).

Upstream from segment A and for most of the rest of its course, the Assemetquagan River is much wider and shallower, and its flow is relatively tranquil. Outcrops are less frequent and the shores are covered with medium to coarse gravel. The river bed itself is completely littered with a variety of large rounded boulders, mostly Fortin Group rocks and Fortin-derived quartz, but also of other lithologies including the distinctive Val Brillant Quartzite, York River and Battery Point sandstones, Cambro-Ordovician volcanics and sediments, gneisses and anorthosites from the Canadian Shield and a few ultramafics, probably derived from a small plug west of Lake Matapedia (Fig. 84.1).

For the purpose of the study, the lower 2 km of the river were divided into two segments: segment A which corresponds to the turbulent lower 900 m stretch and segment B which extends 1100 m upstream from the previous and is characterized by a relatively gentle flow. Furthermore, the right and left banks of segment A were evaluated separately. The aim of this part of the study was to determine the variation in the gold content and the ability to detect gold in stream sediment samples collected from five different environments. These are:

- a — gravel accumulated on shore and in embayments between outcrops,



- UPPER DEVONIAN AND CARBONIFEROUS
- 10 Bonaventure and Fleurant conglomerates
- LOWER TO MIDDLE DEVONIAN
- 9 Battery Point Formation
- LOWER SILURIAN TO LOWER DEVONIAN
- 8 York Lake Formation
- 7 La Garde Formation
- 6 Fortin Group
- 5 Cap Bon-Ami Limestone, Grande Grève Formation, Saint-Léon Siltstone, Val Brilliant Sandstone, Sayabec Limestone
- 4 Chaleurs Bay Group

- ORDOVICIAN TO SILURIAN
 - 3 Matapedia Group
 - ORDOVICIAN
 - 2 Serpentinite
 - CAMBRIAN TO MIDDLE ORDOVICIAN
 - 1 Quebec Complex
- Volcanics.....
 - Geological boundary.....
 - Geological boundary (faulted).....
 - Outline of drainage basins investigated....
 - Mineral occurrence.....

Figure 84.1. Geology and mineral occurrences of western Gaspésie and location of study area.

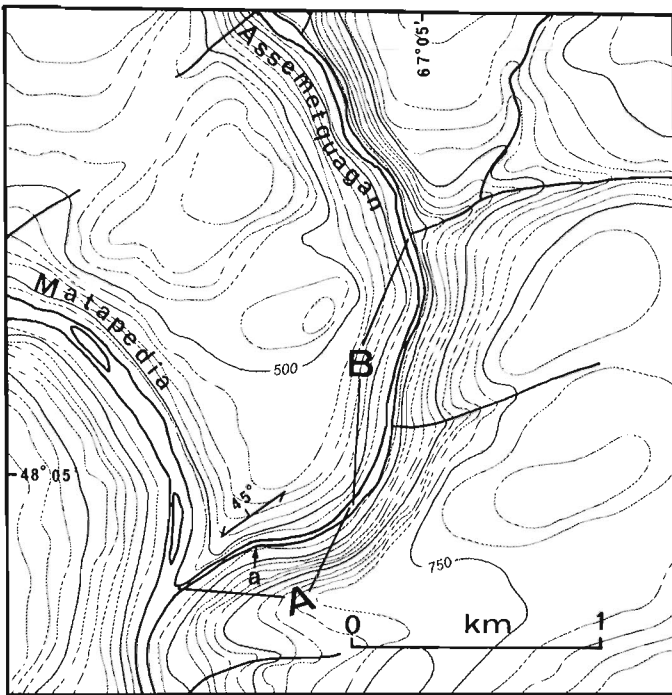


Figure 84.2. Lower Assemetquagan River valley (topographic contour intervals = 50 feet (15.25 m)).

- b – gravel in shallow depressions on outcrop surface (samples include material in contact with outcrop surface),
- c – gravel filling wide bedrock crevices,
- d – silt and sand filling cleavage openings between slate panes (in places mixed with deeply penetrating root-lets of grass-like vegetation),
- e – silt and sand trapped in moss on surfaces of outcrops and boulders.

Several sites representing each environment were selected and at each one, two types of samples were collected:

- 1 – a heavy mineral concentrate obtained from approximately 3 L (5 kg) of minus 4 mm sediment, and
- 2 – a bagful of the same material unprocessed.

All sample sites were located above the low (summer) water line but are submerged each spring. The heavy mineral concentrates were obtained by panning on site to bring the weight of the sediment sample down to about 500 g. At this stage, a preliminary count of gold grains was done. In the laboratory, the heavy minerals were further concentrated using a spiral concentrator (Maurice and Mercier, 1986), the magnetite was removed using a hand magnet and the concentrate was sized to $\pm 250 \mu\text{m}$ (60 mesh Tyler). Each size fraction was then run through a Frantz isodynamic separator at various amperage settings and gold grains in the least magnetic fraction were counted using a binocular microscope. Several hundred minus $250 \mu\text{m}$ heavy mineral grains were mounted on glass slides for mineralogical studies. Microprobe and other grain analyses were carried out as required. Chemical analyses of heavy mineral concentrates were not routinely done because, as will be shown later, a large proportion of the samples obtained during the regional sampling survey did not contain sufficient heavy minerals for chemical analyses.

The combined methods of panning and concentrating the heavy minerals with a spiral concentrator produces a concentrate of minerals of specific gravities greater than about 3.7. The



Figure 84.3. Fortin slates exposed along the lower segment of Assemetquagan River.

technique is only moderately efficient in terms of heavy mineral recovery but it is expected to extract all gold particles larger than 50-100 μm (Mercier and Maurice, 1986).

The unprocessed sediment samples were sized to $\pm 106 \mu\text{m}$ (150 mesh Tyler). A 20 gram subsample of the fine fraction was analyzed for gold by fire assay and atomic absorption. The total coarse fraction, in the order of 100 grams, was analyzed for gold using a Metallic Sieves Analysis technique, a method that ensures representative results from samples containing coarse particulate gold (see Maurice, 1986 for details). A subsample of the plus $106 \mu\text{m}$ fraction was also analyzed for As, W, Cr, Ba, Nb, Ta, Sb and Sn, but these results are not reported here.

The gold data are tabulated in the Appendix and summarized in Table 84.1. The main conclusions to emerge from these results are:

1 – Shallow samples collected from loose gravel deposits on river banks do not reflect the presence of detrital gold (column a, Table 84.1). Samples collected deep into these deposits, however, may show the presence of gold but this has not been tested in the Assemetquagan River. Accumulations of gravel in shallow outcrop cavities, which are periodically washed clean (column b), are also inadequate to detect gold.

2 – Silt and sand filling cleavage openings between slate panes show the best concentrations of gold (column d) but silt and sand trapped in moss (column e) and in wide bedrock crevices (column c) also retain significant quantities of gold. The amount of gold is somewhat correlated to the amount of heavy minerals in the samples (Fig. 84.4). However, the gold to heavy mineral ratio is higher in the bedrock crevices probably because the water current washes out some of the lighter heavies entering the crevice thus causing an enrichment in gold. Note that the gold particles tend to be somewhat coarser in the crevices.

3 – Gold is not equally distributed between the left and right banks (column f) of the river despite the fact that both banks have similar rock exposure providing similar sample material. The higher gold and heavy mineral content of left bank sediments may be related to a decrease in flow velocity due to a sharp left hand bend in the river ("a" in Fig. 84.2). The highest gold grain counts and the largest gold particles were obtained at the bend and about half way between the bend and the mouth where the flow appears to be slowing due to a slight widening of the channel at high water. At those sites, the non-magnetic heavy minerals make up an unusually high proportion of the sediment.

Table 84.1. Gold concentration and particle size in various environments and sample types in lower Assemetquagan River basin

		a	b	c	d	e	f	g
Number of sites		8	4	5	14	9	9	8
Number of gold grains per 3 litres of sediment	range	0 - 1	0	0 - 8	1 - 25	0 - 12	0 - 2	1 - 3
	mean	—	—	4.6	5.7	3.3	0.7	2.5
Dimension (long axis) of gold grains (mm)	range	0.6	—	0.2 - 1.9	0.2 - 3.0	0.1 - 1.5	0.15 - 0.35	0.1 - 0.8
	mean	—	—	0.88	0.70	0.66	0.29	0.53
Weight of non-magnetic minus .85 mm heavy minerals per 3 litres of sediment	range	0.9 - 81.6	0.3 - 8.9	1.5 - 55.9	11.6 - 235.9	7.9 - 155.1	11.1 - 82.6	13.3 - 45.7
	mean	15.0	3.7	29.9	112.8	58.0	32.7	27.9
Gold concentration in minus 106 μm unprocessed sediment (ppb)	range	<5 - 20	<5 - 10	<5 - 15	<5 - 860	<5 - 130	<5 - 900	<5 - 760
	mean*	7.5	6.8	5.5	76.3	18.1	102.5	103.1
Gold concentration in plus 106 μm unprocessed sediment (ppb)	range	<10	<10 - 40	<10 - 4230	<10 - 7390	<10 - 4670	<10 - 150	<10 - 1920
	mean*	—	15.0	891	1888	825	33.3	332

Sampling environments and sample locations (see Fig. 84.2)

- a. Gravel accumulated on shore and in embayments between outcrops, left bank, segment A.
- b. Gravel in shallow depressions on outcrop surface, left bank, segment A.
- c. Sand and gravel filling wide crevices in outcrop, left bank, segment A.
- d. Silt and sand in cleavage openings between slate panes, left bank, segment A.
- e. Silt and sand trapped in moss on surface of outcrops and boulders, left bank, segment A.
- f. Combination of environments c, d and e, right bank, segment A.
- g. Combination of environments c, d and e, right and left banks, segment B.

* For values below analytical detection limit, 1/2 detection limit is used to compute the mean

4 – In segment B (column g), gold is present in concentrations that are higher than on the right bank of segment A, but considerably lower than on the left bank of that same segment. This is probably due to more efficient hydraulic sorting in segment A as a result of greater turbulence. This turbulence is also thought to be responsible for bringing heavier gold particles near the edge of the stream channel where they are accessible to sampling.

5 – On average, there is good correlation between the number of gold particles detected visually and the gold concentrations obtained analytically from the plus 106 μm fraction of the unprocessed sediments (Table 84.1). At individual sites, however, the ability to detect coarse gold is significantly greater by visually counting gold grains in the heavy mineral concentrates (see Appendix). This is due to the much greater initial quantity of sediment from which the heavy minerals are extracted (≈ 5 kg) compared to the amount of plus 106 μm unprocessed sediment used in the analyses (≈ 100 g). This larger quantity of sediment increases the likelihood of at least one gold particle being contained in the sample.

6 – The analyses of the minus 106 μm fraction of unprocessed sediment represents the least reliable method of detecting gold in this area. For example, fine gold was not detected in five of the fourteen auriferous sites in category d on the left bank of segment A (see Appendix). This can be interpreted as being due in part to the relatively coarse nature of the Assemetquagan gold. However, the sample weight analyzed (20 g) is even smaller than the weight analyzed in the coarse fraction,

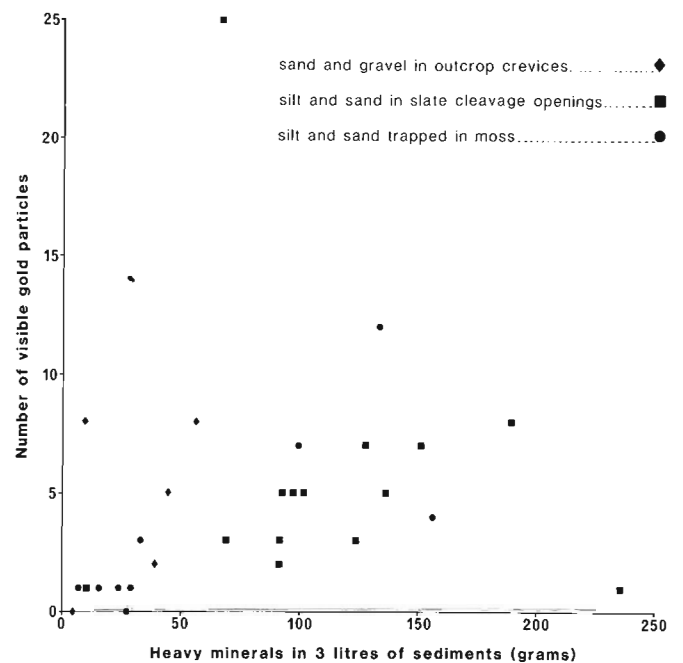


Figure 84.4. Number of gold particles vs heavy mineral content for different sample types, left bank of lower Assemetquagan River.

which further decreases the probability of a sample containing a gold particle. Also, the small particle size in this fraction may produce gold concentrations that are near or below the analytical detection limit. To illustrate this, Table 84.2 shows the effect of a single gold particle of various sizes on the gold concentrations in same size samples as those analyzed in this study. Nevertheless, because fine and coarse gold are likely to be distributed differently in stream alluvium as a result of differences in their response to hydraulic forces, it is advisable to analyze gold in both fractions when conducting this type of geochemical exploration for gold.

Morphology and composition of gold grains

Some of the gold grains found by the author in the lower Assemetquagan River show smooth and regular outlines but the majority are irregular. Some are even delicate with ragged edges. Larger grains often show evidence of having been formed by pressure fusion of two or more smaller grains. The largest grain found by the author is slightly over 5 mm (long axis) and weighs 75 mg.

Some gold grains contain embedded grains of other minerals including quartz, plagioclase, calcite, ferromagnesian minerals, ilmenite, and lithic fragments. Some of these grains appear to have been pressed against the gold grains and may have been acquired during transport. Others are more intimately associated with the gold suggesting a common source. The significance of these inclusions as source indicators is still being investigated.

Microprobe analyses revealed small inclusions of gersdorffite ((Ni, Fe, Co) AsS) in most grains examined and of arsenopyrite (FeAsS) in some. The gold has a fineness (1000 × Au/Au + Ag) ranging from 787 to 938 based on microprobe analyses of a dozen grains. Hg, Co, As, Fe, and Sb were also analyzed but not detected. Some grains exhibit a thin (5-10 μm) rind which contains over 97% Au.

Regional gold distribution

The detailed study near the mouth of the Assemetquagan River has confirmed and quantified a fact that is well known to gold prospectors: irregularities in the bedrock on the streambed provide the best locale for finding particles of native gold. Perhaps what was not as commonly known is that even in a highly auriferous stream, such as the lower 900 m segment of the Assemetquagan River, the upper 30 cm of loose gravel deposits appear to be practically devoid of gold both fine and coarse. The data also show that silt and sand trapped in mosses growing on relatively smooth surfaces of outcrops and boulders reflect the presence of gold in the stream. This is particularly important because many of the sample sites visited during the regional survey did not have appropriately located outcrops but

moss could usually be scraped off the surface of large boulders, fallen tree trunks, etc.

Figure 84.5 shows the regional distribution of visible gold as well as gold detected by analyses of the plus and minus 106 μm fractions of sediments collected mostly from mosses and outcrop fissures. In the regional survey, heavy minerals were extracted from 10 L of sediment instead of 3 L as was the case in the orientation survey.

Very difficult access to the hinterland, particularly in the Assemetquagan River basin, has been a major hinderance in previous attempts to carry out regional sampling for the purpose of evaluating the full extent of the region's placer deposits. For this reason, sample density in the present survey was kept low but sites were carefully selected and samples taken with great care to ensure they were representative.

Sampling in the Assemetquagan River and its tributaries failed to indicate a continuation upstream of the relatively rich lower portion of the river. In fact, an extensive search was conducted about 7 km upstream from the mouth of the river in what was considered ideal sampling conditions (fissile outcrops, etc.) without detecting any gold. However, one small gold flake was found about 3.5 km from the mouth and another in a small tributary that flows into the Assemetquagan from the northwest, about 4.3 km from the mouth. Other small flakes were found in Creux and Castor creeks, both major tributaries of the Assemetquagan (Fig. 84.5). One small flake and a relatively strong geochemical anomaly (210 ppbAu) were detected in the lower Milnikek River, on the west side of the Matapedia, and two flakes were seen in heavy mineral concentrates from Clark Creek, south of the Assemetquagan.

Several gold flakes, usually very small, were found in the basins which drain into Chaleur Bay, most of them in the Kempt and Escuminac systems (Fig. 84.5). As stated previously, one of the tributaries near the headwaters of Kempt River intersects auriferous quartz veins and is known to contain alluvial gold. The area surrounding the two sites in the lower Escuminac River basin, where 300 and 450 ppbAu were detected in the fine fraction of the sediment, should be examined in detail (compare these levels with Tables 84.1 and 84.2).

Heavy mineral distribution and composition

Figure 84.5 shows semiquantitatively the relative abundance of heavy minerals extracted from 10 L of sediment at each sample site. Heavy minerals were extracted in the regional survey in the same manner as in the orientation survey.

On the basis of abundance of heavy minerals alone, the survey area can be divided into two distinct zones along line AA' shown in Fig. 84.5. To the north of the line, more than 5 g of heavy minerals were recovered at most sample sites with large zones producing over 20 g and up to 300 g per 10 L of sediment. In the area to the south of the line, which includes all of the river basins that drain into Chaleur Bay, less than 5 g and, in most cases, less than 2 g of heavy minerals were recovered at each sample site from the same amount of sediment, except in the area underlain by the Chaleurs Bay Group volcanics where the sediments contain a greater proportion of heavy minerals. Another noticeable feature is the near absence of erratics from the Canadian Shield and other indicator lithologies in the southern zone, and a relative abundance of such erratics in the northern zone. A few syenite erratics, that may be derived from New Brunswick, were found near the coast of Chaleur Bay.

The heavy mineral assemblage in the northern zone consists mostly of angular to subrounded ilmenite, garnet (predominantly almandine) and hematite with lesser zircon, chromite, barite, rutile, pyrite and goethite. Barite was found in substantial amounts in parts of the Milnikek and Causapsal

Table 84.2. Effect of one gold flake on gold concentration.*

Size of gold flake		Au concentration (ppb)	
a (μm)	mesh (Tyler)	20 g sample	100 g sample
355	40	—	760
180	80	—	99
106	150	100	20
75	200	36	—
38	400	5	—

* Computed using a square prism-shaped flake with a volume = $a^3/10$ and density = 17 g/cm³.

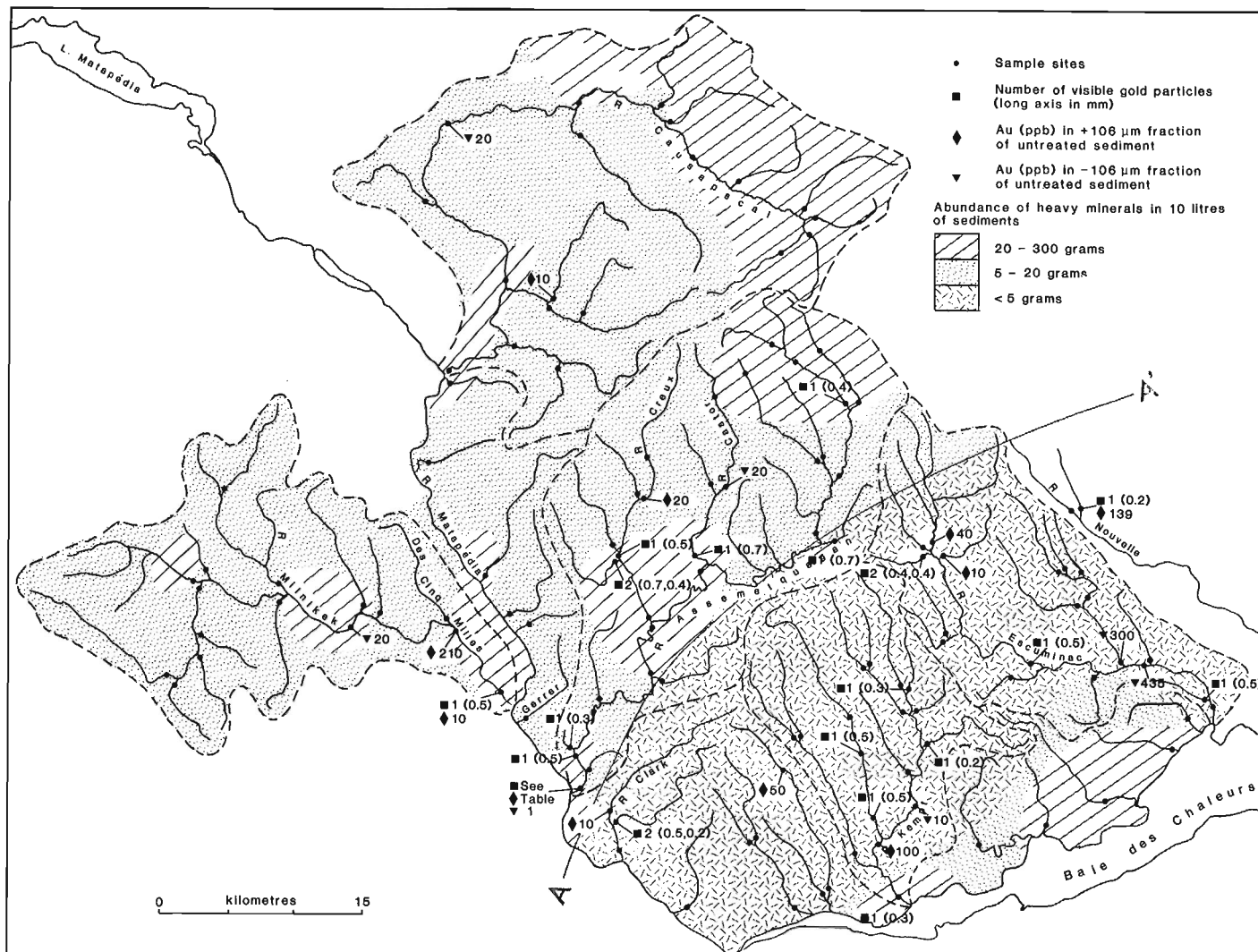


Figure 84.5. Relative abundance of heavy minerals and regional gold distribution in southwest Gaspésie.

basins. Two types of zircons are found in the samples: one type is angular to subangular, and the other is well rounded to almost spherical. The well rounded zircons, which usually account for about 10% of the zircons, may be derived from arenaceous sedimentary rocks within Gaspésie (e.g. York River, Battery Point). Some of the angular zircons, as well as the bulk of the ilmenite and all of the garnet are thought to originate from the Canadian Shield. There are no large expanses of garnetiferous rocks known in Gaspésie that could have supplied the quantity of garnet observed in the streams of the region. Although ilmenite occurs as an accessory mineral in the volcanics and some sedimentary rocks within Gaspésie, its abundance in the samples also precludes a provenance solely from Gaspésie lithologies. On the other hand, vast ilmenite deposits occur across the St. Lawrence estuary, including ilmenite and garnet-rich beach sands along the north shore of the St. Lawrence (Rose, 1969; D. Cossette, personal communication, 1986). Similar deposits in preglacial times would have been particularly vulnerable to glacial erosion. The ilmenite in the heavy mineral samples from the study area is mostly the exsolved ilmenite-hematite varieties that are so common in the north shore deposits (Rose, 1969). Rounded pebbles of ilmenite measuring several centimetres in diameter have been found by the writer near the mouth of the Assemetquagan River further supporting Shield derivation.

In the southern zone, pyrite, mostly as limonite-coated cubes, usually represent from 30 to 50% and, in places, up to 90% of the heavy minerals recovered. Garnet and ilmenite, of the same varieties as those found in the northern zone, continue to be present. Near Chaleur Bay, clinopyroxene is an important constituent which is derived from the volcanics of the Chaleurs Bay Group.

The role of glaciation on heavy mineral dispersal in southwest Gaspésie

During the development of the last glacial maximum, the Laurentide ice sheet extended across the St. Lawrence estuary and flowed southeastward over western Gaspésie Peninsula (David and Leblais, 1985). This glacial advance is responsible for most of the glacial deposits of western Gaspésie which, judging from the composition of the heavy mineral assemblage in the study area, have an important Shield-derived component. Northward ice movements in western Gaspésie during deglaciation may also be responsible for some dispersal imprinted upon the earlier southeastward trend.

Variations in the proportions of three indicator minerals in the heavy mineral assemblages across the survey area define several broad zones illustrated in Figure 84.6.

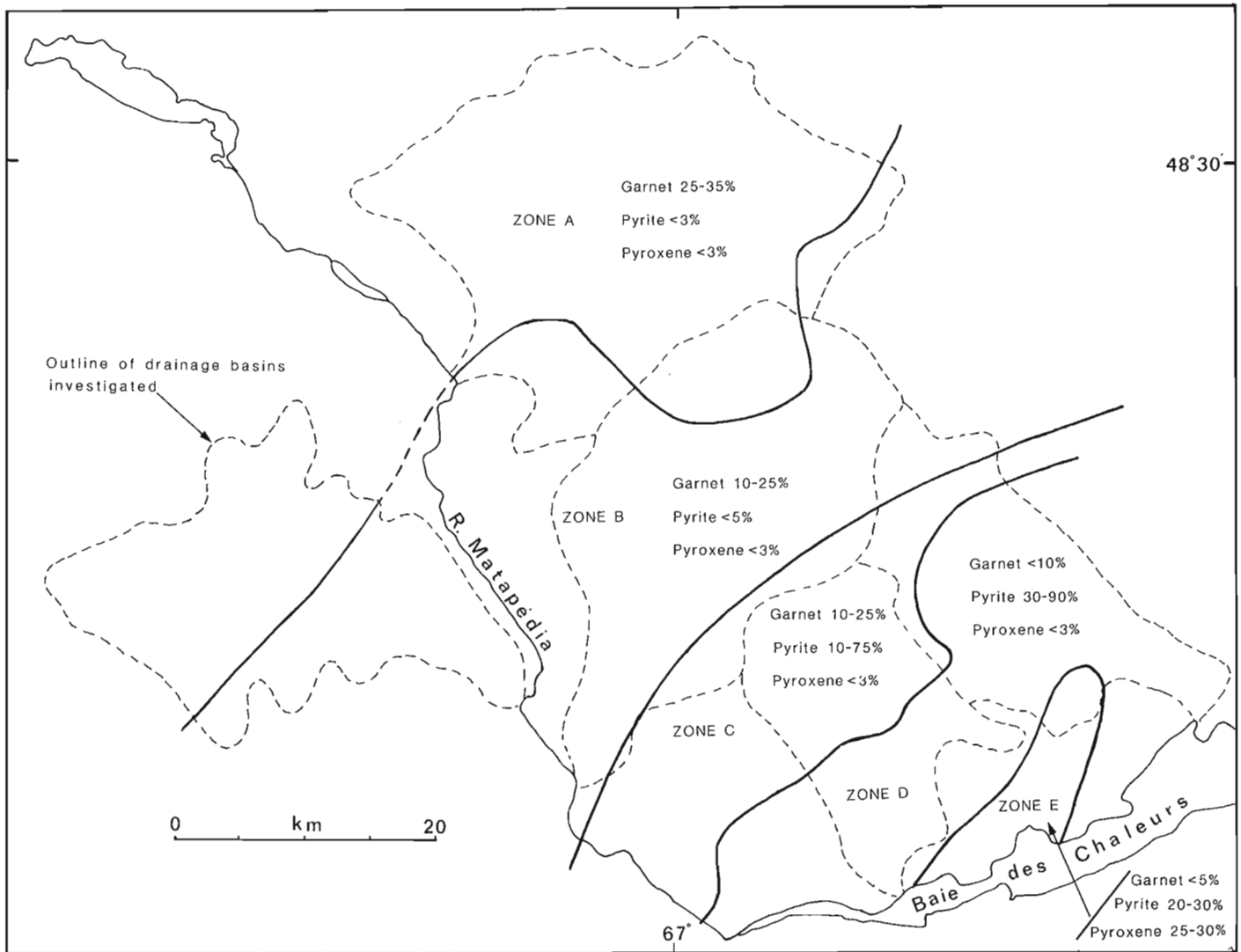


Figure 84.6. Zonal distribution in the proportion of indicator heavy minerals in southwest Gaspésie.

From north to south:

- Zone A: Garnet 25-35%; pyrite <3%; pyroxene <3%
- Zone B: Garnet 10-25%; pyrite <5%; pyroxene <3%
- Zone C: Garnet 10-25%; pyrite 10-75%; pyroxene <3%
- Zone D: Garnet <10%; pyrite 30-90%; pyroxene <3%
- Zone E: Garnet <5%; pyrite 20-30%; pyroxene 25-30%

Garnet shows a steady decrease from north to south corresponding to increasing distance from the source. The sharp increase in pyrite observed from zone B to zone C corresponds to the decrease in heavy mineral abundance discussed earlier. This abrupt change in heavy mineral abundance reflects differences in the amount of debris transported by the ice that flowed over the southern region (zones C and D) and the ice that flowed over the northern region (zones A and B). The Assemetquagan River valley, that seems to separate zones B and C (AA' in Fig. 84.5), may have been a major obstacle to the advancing ice sheet. The gorge itself, and the fact that the south side of the valley is somewhat more elevated than the north side — Figure 84.2 illustrates this for the lower portion of the valley — could have impeded advancement at the base of the glacier and provoked shearing higher up in the ice mass allowing only cleaner ice than is found at the base to continue southward. This would have caused a significant drop in the quantity of heavy minerals derived from northern sources to be deposited in the

southern zones resulting in an increase in the proportion of locally derived pyrite. However, because pyrite and other heavy minerals are not generally abundant in the sedimentary rock formations of southwestern Gaspésie, the concentration of heavy minerals in zones C and D is generally low compared to zones A and B but the proportions between the various mineral species are not drastically different. In zone E, the occurrence of porphyritic basic volcanics causes an increase in the total heavy mineral content with a high proportion of clinopyroxene.

Thick glacial deposits occur in zone A, but zones B, C, and D are characterized by a lack of glacial erosional and depositional features. David and Leblond (1985) suggested that the lack of glacial erosion in parts of southwest Gaspésie was due to frozen basal conditions of the ice sheet during the last glacial maximum. Under these conditions, ice flows by internal deformation above the zone of regelation spreading debris contained in the upper layers of the ice sheet. Upon melting, this debris is deposited as a veneer of melt-out till which has minimal geomorphic relief. In zones C and D, which were overridden by relatively clean ice, such deposits would be expected to be very thin, much thinner than in zone B.

The heavy mineral dispersal mechanism proposed above does not take into consideration dispersal due to postglacial fluvial transport. It is uncertain, for example, what proportion

of heavy minerals in the sediments of the Assemetquagan River and its tributaries (zone B) was transported by alluvial processes from glacial deposit sources in zone A. Experience elsewhere in the Appalachians has shown that fluvial transport of heavy minerals in general and gold in particular, does not cause significant long distance displacement of geochemical anomalies associated with the heavy minerals (Maurice, 1986). Furthermore, the occurrence of almandite garnet in zones C and D is proof that ice carried garnet-bearing debris across the Assemetquagan River valley. No other mechanism could satisfactorily explain the presence of these garnets in the Kempt and Escuminac river systems. Local garnet sources associated with felsic dykes are too scarce and localized to have generated the uniform garnet distribution observed (Fig. 84.6). Furthermore, garnet from these local sources would be expected to be of a calcic variety and not almandite.

In summary, the writer favours glacial dispersal processes to explain the regional distribution of heavy minerals across the study area. Alluvial processes caused local redistribution of the heavy minerals in the streams but had minimal influence on the regional patterns. Supporting data are being sought by studying the region's Quaternary deposits.

The source of gold and exploration guidelines

The regional distribution of gold in the study area does not correlate with the abundance of heavy minerals. In zones C and D (Fig. 84.6), where heavy minerals are not abundant, gold grains were observed in many samples. In zone B, on the other hand, gold tends to occur in areas of high heavy mineral yield even though large areas containing abundant heavy minerals do not appear to be auriferous (Fig. 84.5).

In zones C and D, the absence of glacial erosion and the extreme scarcity of glacial deposits preclude any relationship between gold distribution and glacial action. The lack of glacial deposits in this part of Gaspésie also accounts for the near perfect fit between the geology and the regional stream sediment geochemical data recently published by the Ministère de l'Énergie et des Ressources du Québec (Choinière, 1985). In these zones, alluvial gold tends to be adjacent to, or very near the auriferous bedrock as no glacial transport was involved. The presence of alluvial gold in a stream segment that intersects auriferous veins in the Kempt River basin (see Geological Framework and Mineralization) supports this view. Very fine gold particles, such as the ones seen in our samples (<100 µm), may have undergone some alluvial transport although close scrutiny may reveal nearby sources, possibly quartz veins in the Fortin Group and intrusive contact zones near acid and intermediate dykes in the Matapedia Group.

The gold-bearing lower segment of the Assemetquagan River is situated at the southern edge of zone B where, according to the proposed model, advancement of the debris-rich lower part of the glacier was impeded. Upon melting of the ice sheet, an important volume of glacial debris would have been dumped into the river channel and adjacent ground. This material had a high content of Shield-derived garnet and ilmenite and the strong current in this section of the river contributed to further enrich the heavy minerals by flushing out the lighter components. This material is also believed to have contained the gold that is found in this segment of the river. However, because gold is so concentrated in this relatively short segment, it is thought that the source is relatively near, possibly within Fortin Group rocks. According to David and Lebus (1985), however, all of the Fortin to the northwest of the mouth of the Assemetquagan River was under frozen conditions during the glacial maximum and not likely to have been eroded. On the other hand, the same authors also suggested that there was

probably southward extensions of the freezing (wet) basal conditions (and therefore of erosion) in the valleys. It is possible that the ice sheet collected auriferous debris within the Fortin in a valley up ice from the mouth of the Assemetquagan. Two valleys appear to be appropriately situated and oriented: the Matapedia valley south of the town of Ste. Florence, and the lower 8 km of the Milniket River and its tributary, Cinq Milles Creek (Fig. 84.5). The gold anomalies in the lower Milniket River (Fig. 84.5) could very well represent a trail of this dispersion.

If the source is within the Fortin Group, it is probably associated with quartz veins. Prospecting should be directed at major fracture zones such as the one forming the contact between the Fortin and the York River. One Cu-Au occurrence is known along this contact zone on the east side of the Matapedia River. The presence of gersdorffite and arsenopyrite inclusions in the gold grains suggests that these minerals could also occur at the source. Therefore, As, Ni and Co could be useful pathfinders for this mineralization. Arsenic analyses, done as part of the present survey, did not reveal any anomaly over Fortin Group rocks but Tremblay and Choinière (1978) showed several Ni-Co stream sediment anomalies up ice from the mouth of the Assemetquagan. One group of anomalies that may be significant occurs at the intersection of a major fracture (along which flows Gerrer Creek, see Fig. 84.5) with the Matapedia River, only about 6 km north of the mouth of the Assemetquagan.

A few gold flakes were found elsewhere in the Assemetquagan basin (e.g. Creux and Castor creeks) but they are believed to be locally derived and unrelated to the concentrations at the mouth of the river. These areas should nevertheless be prospected for auriferous quartz veins.

Based on the regional gold distribution within the study area and current knowledge of the region's mineral deposit geology, the Fortin and Matapedia groups are the most likely hosts of the bedrock sources of alluvial gold in southwest Gaspésie. Additional support for this point of view comes from the fact that none of the samples collected in the Causapsal and in the northern part of the Milniket basins, which are situated up ice from the Fortin-York River contact, contained visible gold particles, although two samples revealed traces of gold analytically. Furthermore, Tremblay and Wilhelm (1978) did not report finding any gold during an extensive heavy mineral study in northwestern Gaspésie. Their study area extended from the town of Ste-Florence to the St. Lawrence River (Fig. 84.1).

Nevertheless, the possibility of the source being situated beyond the limits of the Fortin should also be considered. Maurice (1986) has shown that, in the Eastern Townships, gold can be transported over distances as great as 100 km by ice and yet give rise to concentrated placer deposits. In this context, the presence of gersdorffite inclusions in many of the gold grains could suggest an ultramafic affiliation. Therefore, it could prove worthwhile to examine the ultramafic lens southwest of Lake Matapedia for gold. The lens is situated about 70 km up ice from the mouth of the Assemetquagan.

Acknowledgments

Field sampling was conducted under hazardous conditions by Mario Bergeron and Serge Gaudard. Isabelle Poliquin and Andrée Blais carried out the basic mineralogical studies. Microprobe, X-ray diffraction and other studies of specific minerals were done by Dominique Paré, Don Harris and Andy Roberts. Dominique Paré, Jean Veillette and Bruce Ballantyne reviewed the manuscript and provided many useful suggestions. The writer benefitted immensely from discussions with Peter David on the glacial history of western Gaspésie.

References

- Bélanger, J.
1982: Roches volcaniques dévoniennes de la bande de Ristigouche, comté de Bonaventure; Ministère de l'Énergie et des Ressources, Province de Québec, rapport intérimaire, DP-939, 13 p.
- Choinière, J.
1985: Synthèse de la géochimie des sédiments de ruisseaux de la Gaspésie; Ministère de l'Énergie et des Ressources, Province de Québec, MM 84-01.
- David, P.P. and Lebuis, J.
1985: Glacial maximum and deglaciation of western Gaspé, Québec, Canada; Geological Society of America, Special Paper 197, p. 85-109.
- Dumont, P.E.
1961: Rapport sur les Mines Bern-Or Ltée, Canton de Fauvel, Comté de Bonaventure, Province de Québec; Ministère des Richesses Naturelles du Québec, GM-11569, 4 p.
1963: Rapport sur les Mines Bern-Or Limitée, groupe de 13 claims, Canton Fauvel, P. Qué.; Ministère des Richesses Naturelles du Québec, GM-12409, 2 p.
- Girard, A.
1985: Indices d'or alluvionnaire des rivières Assemetquagan et Kempt Nord, Gaspésie; Ministère de l'Énergie et des Ressources, Province de Québec, DP84-35, 23 p.
- Lachance, S.
1974: Géologie de la région de l'Ascension-de-Patapédia, Comté de Bonaventure; Ministère des Richesses Naturelles du Québec, rapport préliminaire, DP-273, 19 p.
1977: Région de St-Alexis-de-Matapédia, Comté de Bonaventure; Ministère des Richesses Naturelles du Québec, DPV-458, 23 p.
1979: Géologie de la région de Saint-André-de-Ristigouche, Comté de Bonaventure; Ministère des Richesses Naturelles du Québec, rapport préliminaire, DPV-667, 19 p.
- Mattinson, C.R.
1964: Région du Mont Logan, Comtés de Matane et de Gaspé-Nord; Ministère des Richesses Naturelles du Québec, Rapport Géologique 118, 102 p.
- Maurice, Y.T.
1986: Interpretation of a reconnaissance geochemical heavy mineral survey in the Eastern Townships of Quebec; in Current Research, Part A, Geological Survey of Canada, Paper 86-1A, p. 307-317.
- Maurice, Y.T. and Mercier, M.M.
1986: A new approach to sampling heavy minerals for regional geochemical exploration; in Current Research, Part A, Geological Survey of Canada, Paper 86-1A, p. 301-305.
- Mercier, M.M. and Maurice, Y.T.
1986: Etude de l'efficacité relative de différentes méthodes de concentration des minéraux lourds; Ministère de l'Énergie et des Ressources du Québec, rapport non-publié, 252 p.
- McGerrigle, H.W.
1950: Gold placer and vein prospect, Fauvel Township, Bonaventure County; Quebec Department of Mines, Mineral Deposits Branch, GM-556, 2 p.
- Rose, E.R.
1969: Geology of titanium and titaniferous deposits of Canada; Geological Survey of Canada, Economic Geology Report 25, 177 p.
- Savard, M.
1985: Indices minéralisés du sud de la Gaspésie; Ministère de l'Énergie et des Ressources, Province de Québec, Rapport ET-83-08, 92 p.
- Stearn, C.W.
1965: Région de Causapscal, Comtés de Matapédia et de Matane; Ministère des Richesses Naturelles du Québec, Rapport Géologique 117, 52 p.
- Tremblay, R.L. and Choinière, J.
1978: Atlas géochimique des sédiments de ruisseau de la Gaspésie; Ministère de l'Énergie et des Ressources, Province de Québec, DPV-563.
- Tremblay, R.L. and Wilhelm, E.
1978: Prospection alluvionnaire (minéraux lourds) en Gaspésie — traitement des données et comparaison avec les résultats géochimiques en sédiments de ruisseaux; bulletin de l'ICM, v. 71, no. 793, p. 88-95.

APPENDIX 84.1

Sample number	Pan concentrates		Unprocessed sediments	
	Heavy minerals/ 3 litres (g)	Number of gold grains	Au (+106 µm) ppb	Au (-106 µm) ppb
a — Gravel accumulated on shore and in embayments between outcrops, left bank, segment A.				
1	2.8	0	< 10	5
2	4.4	0	< 10	< 5
3	3.9	0	< 10	< 5
4	0.9	0	< 10	20
5	12.5	0	< 10	10
6	1.8	0	< 10	10
7	81.6	0	< 10	< 10
8	12.2	1	< 10	< 10
b — Gravel in shallow depressions on outcrop surface, left bank, segment A.				
9	3.9	0	< 10	10
10	0.3	0	40	10
11	1.6	0	10	< 10
12	8.9	0	< 10	< 5
c — Sand and gravel filling wide crevices in outcrop, left bank, segment A.				
13	1.5	0	< 10	15
14	43.8	5	< 10	< 5
15	38.9	2	< 10	< 5
16	9.5	8	4230	< 5
17	55.9	8	210	5
d — Silt and sand in cleavage openings between slate panes, left bank, segment A.				
18	11.6	1	440	< 5
19	188.8	8	1680	< 5
20	100.7	5	490	< 5
21	235.9	1	< 10	< 5
22	135.9	5	5640	130
23	123.3	3	1760	15
24	90.3	2	340	< 5
25	96.4	5	610	10
26	127.3	7	1030	10
27	91.6	3	950	860
28	69.0	3	2010	10
29	92.4	5	710	5
30	150.3	7	3370	10
31	66.0	25	7390	5
e — Silt and sand trapped in moss on surface of outcrops and boulders, left bank, segment A.				
32	155.1	4	1880	5
33	132.4	12	4670	5
34	23.3	1	< 10	< 5
35	32.6	3	< 10	5
36	99.7	7	720	5
37	28.8	1	< 10	130
38	27.2	0	< 10	< 5
39	15.0	1	< 10	< 5
40	7.9	1	130	5
f — Combination of environments c, d, and e, right bank, segment A.				
41 (moss)	11.8	0	20	< 5
42 (crevice)	39.8	1	< 10	< 5
43 (crevice)	11.1	1	< 10	< 5
44 (slate)	19.4	0	150	< 5
45 (slate)	31.2	2	< 10	10
46 (slate)	ND	ND	< 10	< 5
47 (moss)	ND	ND	< 10	< 5
48 (moss)	ND	ND	< 10	< 5
49 (moss)	82.6	0	100	900
g — Combination of environments c, d, and e, right and left banks, segment B. R = right bank; L = left bank.				
50 (moss, R)	45.7	3	< 10	760
51 (moss, R)	ND	ND	< 10	< 5
52 (crevice, R)	26.0	3	< 10	< 5
53 (moss, L)	13.3	3	< 10	< 5
54 (moss, R)	ND	ND	710	< 5
55 (slate, R)	ND	ND	1920	5
56 (moss, R)	ND	ND	< 10	350
57 (slate, R)	26.7	1	< 10	< 5

ND = Not determined

Deformation in the Thompson Belt, central Manitoba: a progress report¹

Contract 24ST.23233-5-0077

F. Fueten², P.-Y. F. Robin² and M.E. Pickering²

Fueten, F., Robin, P.-Y. F. and Pickering, M.E., Deformation in the Thompson Belt, central Manitoba: a progress report. in Current Research, Part B, Geological Survey of Canada, Paper 86-1B, p. 797-809, 1986.

Abstract

Metasediments and underlying gneisses of the Thompson Belt, east of the Churchill-Superior Province boundary record a complex history spanning from the Archean to the Proterozoic. A structural and metamorphic study has been undertaken on a corridor cutting through the belt, from Paint Lake, on the southeast end, to Oswagan Lake and INCO Limited's Pipe 2 open pit mine, on the northwest end.

Several blocks can be defined along the traverse, each characterized by specific compositional and structural features. However, gneissic foliation strikes parallel to the belt in all blocks and is uniformly subvertical or steeply dipping. Stretching lineations parallel the foliation, with variable plunges southwest or northeast; shallow plunges are rare and the lineations become steeply down-dip and more prominent closer to the boundary with the Churchill Province. The latest and dominant tectonic episode along that boundary which is recorded by the foliations and lineations appears to be one of general flattening or of plane strain, with the flattening parallel to the length of the belt and stretching along a direction which is presently vertical. Asymmetric kinematic indicators of sense of shear fail to indicate whether the Churchill or Superior side moved up with respect to the other.

The latest period of metamorphism at the northwest end reached temperatures of 575° to 625°C and pressures corresponding to depths of 7 to 17 km. This metamorphism was contemporaneous with, or later than, the main period of deformation recorded in the rocks.

Résumé

Les métasédiments et les gneiss sous-jacents de la zone de Thompson, située à l'est de la limite entre les provinces de Churchill et du lac Supérieur, révèlent une histoire complexe qui s'étend de l'Archéen jusqu'au Protérozoïque. On a entrepris une étude structurale et métamorphique d'un couloir traversant la zone de Thompson depuis Paint Lake, au sud-est, jusqu'au lac Oswagan et à la mine à ciel ouvert de Pipe 2 (INCO Limited), au nord-ouest.

On distingue plusieurs blocs tectoniques ayant chacun leur composition et structures caractéristiques. Cependant, l'orientation de la foliation gneissique y est relativement uniforme, avec une direction parallèle à la zone et un pendage fortement incliné ou vertical. Les linéations d'allongement sont parallèles à la foliation et d'inclinaisons variables (sud-ouest ou nord-est): rarement horizontales, elles deviennent plus marquées et verticales, près de la limite avec la province de Churchill. Le plus récent événement tectonique responsable de la microstructure le long de cette limite est donc un aplatissement parallèle à la zone et un allongement dans une direction qui est maintenant verticale. Les indicateurs cinématiques du sens de cisaillement ne parviennent pas à déterminer lequel des côtés, Churchill ou du lac Supérieur, s'est déplacé vers le haut par rapport à l'autre.

La dernière période de métamorphisme dans la partie nord-ouest a atteint des températures de 575° à 625°C et des pressions correspondant à une profondeur de 7 à 17 km. Ce métamorphisme a été contemporain ou postérieur à la phase principale de déformation enregistrée par les roches.

¹ Contribution to the Canada-Manitoba Mineral Development Agreement, 1984-1989. Project carried by Geological Survey of Canada, Lithosphere and Canadian Shield Division, Project 850011.

² Department of Geology and J.T. Wilson Research Laboratories, Erindale Campus, University of Toronto, Mississauga, Ontario L5L 1C6

Introduction

During the summer of 1985 a structural mapping project was started in the Thompson Belt. Work was carried out on the Pipe 2 mine property of INCO Metals Company, as well as on Lower Ospwagan Lake, Upper Ospwagan Lake, Mid Lake, Liz Lake and on a 3-km wide strip across Paint Lake. These localities provide a 25-km long cross-section in the northwestern half of the belt. The goal of the project is to study the structures and microstructures of the gneisses in the Thompson Belt and their implications concerning the deformation history of the Churchill-Superior boundary in northern Manitoba. The research focuses on petrofabric indicators (foliation, lineations, kinematic indicators of sense of shear, micro-structures), as expres-

sions of the deformation history, and on metamorphic textures and assemblages.

Regional setting

The Thompson Belt is a linear northwesterly trending belt at the border between the Churchill Province and the Pik-witonei region of the Superior Province (Fig. 85.1). The basement lithologies in the belt are a series of felsic gneisses, with minor amounts of mafic and ultramafic material. These gneisses are considered to be the retrograded equivalents of the Pik-witonei granulites (Scoates et al., 1977; Weber and Scoates, 1978). At the western margin of the belt, they are overlain by a

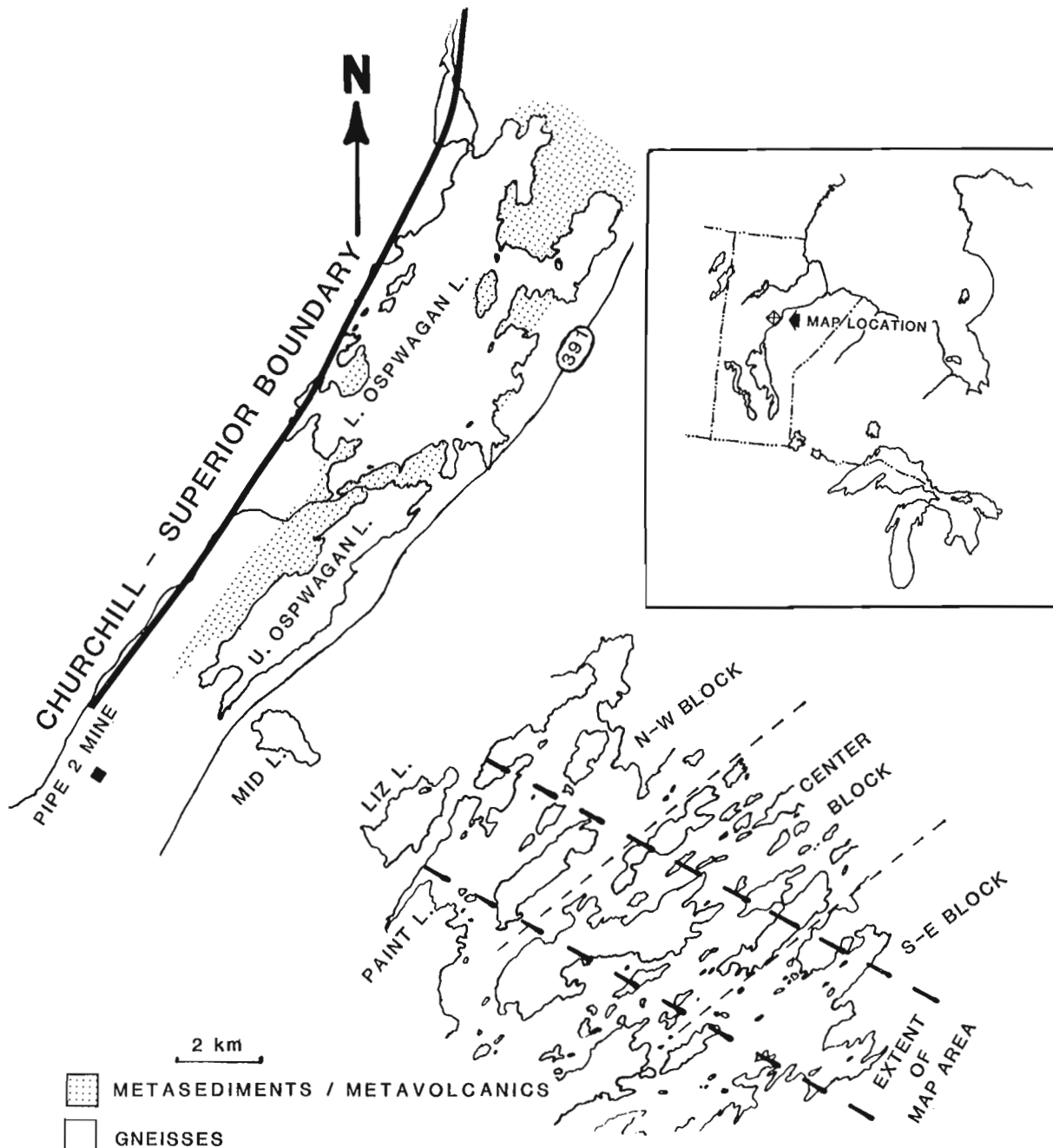


Figure 85.1. Location of the Thompson Belt and extent of area mapped. Stippled pattern shows approximate distribution of metasediments on Ospwagan Lake.

suite of metavolcanic and metasedimentary rocks called the Ospwagan Group by Scoates et al. (1977). Peredery et al. (1982) divided the sedimentary rocks into the Pipe and the Thompson assemblages.

The gneisses are thought to have undergone several deformation events starting in the Archean (Green et al., 1985). The latest evolutionary model of the Thompson Belt, proposed by Green et al. (1985), considered the belt to "... have been successively the site of continental rifting and rupturing, an evolving continental margin, a continent-volcanic island arc "suture" zone and eventually a continental-scale strike-slip fault..." over a period of time spanning from 2.4 Ga to 1.6 Ga. Both gneisses and metasediments probably owe their current structural attitude to the Hudsonian orogeny, dated between 1.9-1.6 Ga in the Thompson Belt (Green et al., 1985).

Pipe 2 mine

The Pipe 2 mine was operated by INCO Metals Company until 1984. The geology of this deposit has been briefly discussed by Peredery et al. (1982) and Gale et al. (1982). The mine is located within a major tight fold plunging 80° to the northeast and opening towards the northeast. Faulting and shearing along, and parallel to, the northwestern limb of the fold complicate its structure and control to some extent the geometry of the ore zone.

The mine pit provides, on the eastern limb of the fold, some of the best outcrops of what has been interpreted as a contact between basement gneisses and metasediments on the western part of the belt. However, definition of that contact is problematic and the gneisses cannot directly be correlated with the gneisses outcropping on Paint Lake. The style of deformation, the attitudes and characteristics of foliations and of lineations, as well as the minor folds, are all very similar in both gneisses and metasediments. Angular discordances are numerous in all rocks but are small (<15°); most are identifiably tectonic in origin, i.e. they can be accounted for by minor faulting and shearing, slip along bedding planes or gneissic layers, and/or by minor folds. The tectonic strain on the eastern limb has not destroyed bedding or bedding continuity in the metasediments, except along the minor faults and shear zones mentioned above, and it has not caused the formation of any significant secondary foliation in them. It seems therefore unlikely that the tectonic strain could have been sufficient to rotate an earlier discordant gneissic banding into parallelism with the bedding. The parallelism between bedding in the metasediments and layering in the gneisses therefore requires the gneissic foliation of the basement to have been approximately horizontal when the sediments were deposited on it, as suggested in Peredery et al.'s (1982) Figure 3. This might explain the difficulty in locating the metasediment-gneiss contact. Alternatively, the "gneisses" at Pipe mine might only be metaquartzitic and meta-arkosic members of the Thompson assemblage rather than unconformably overlain basement gneisses. There is indeed no sharp compositional break between the "gneisses" and the adjacent undisputed metasediment, an impure quartzite (Peredery et al., 1982).

Bedding and foliations (Fig. 85.2a, b) are near-vertical. The predominant lineation is one of vertical extension. A shallow crenulation cleavage is also visible on vertical faces in pelitic metasediments. Minor folds of various scales (50 m to 10 cm) are common on the eastern limb of the major Pipe 2 mine fold; the minor fold axial planes are parallel to the major fold axial plane. The sense of asymmetry associated with the minor folds is consistent with the sense of shear expected for parasitic folds on a major fold.

The western limb of the Pipe 2 mine fold is characterized by a vertical foliation and a very pronounced vertical stretching lineation (Fig. 85.2c). The layering is more disrupted than on the

eastern limb, and some concentric structures could be interpreted as steeply plunging sheath folds, suggesting the strain is higher in the western limb.

The metamorphic assemblages and characteristic minerals of the metasediments at Pipe 2 mine are:

- quartz + sillimanite + biotite + muscovite + garnet + plagioclase
- quartz + sillimanite + biotite + muscovite + plagioclase
- dolomite + diopside + hornblende
- diopside + quartz + biotite + hornblende
- quartz + biotite + hornblende + garnet

Secondary chlorite, exhibiting a weak alignment in some samples, is a common minor constituent. One sedimentary layer within one sample contains andalusite. The foliation is wrapped around the andalusite prophyroblasts which appear to have been affected by the deformation more than the sillimanite. The andalusite is therefore tentatively interpreted as earlier than the sillimanite, which is common in the other metasediments and less deformed. Staurolite, reported by Peredery et al. (1982), has not been found in any of our samples.

The peak pressures and temperatures estimated using the assemblages observed here yield temperatures between 575° and 625°C and pressures between 2.5 kb and 5.75 kb (Fig. 85.3). This pressure corresponds to a depth of 7 to 17 km. The metamorphic temperature is less than that of 700°C obtained at the Thompson mine (Paktunc, 1984).

Ospwagan Lake

The gneisses and metasediments outcropping on Lower Ospwagan Lake have been considered to be the stratigraphic equivalents of the rocks at the Pipe 2 mine. The gneiss-metasediment contact is not clearly exposed on Lower Ospwagan Lake. The gneissic foliation on Upper Ospwagan Lake (Fig. 85.2d) is nearly vertical and strikes between 040° and 075°. On Lower Ospwagan Lake, which is closer to the Superior-Churchill boundary, the average foliation dips approximately 80° to the southeast (Fig. 85.2e). The lineations (Fig. 85.2f) on both lakes are generally steep.

The metamorphic assemblages for the metasediments on Ospwagan Lake are:

- quartz + muscovite + biotite + sillimanite + garnet + plagioclase
- quartz + muscovite + biotite + sillimanite
- quartz + muscovite + biotite + garnet +/- plagioclase
- quartz + muscovite + biotite

Minor, secondary chlorite is common in the metasediments. No andalusite has been seen in any samples from this locality. The metamorphic assemblages on Lower and Upper Ospwagan Lake are thus very similar to the Pipe 2 mine assemblages, and metamorphic grade is therefore also similar to that of the Pipe 2 mine.

Paint Lake

A metamorphic study by Russell (1981) on parts of Paint Lake indicated an older (interpreted as Archean) period of metamorphism, with an estimated temperature of 910 ± 70°C. Russell determined a Hudsonian overprint to have been at conditions of 650 ± 50°C and 4-5 kb.

The limited field work on Paint Lake in 1985 outlined three major gneissic blocks. The north-west block is identical to an area of gneisses with preserved features of Archean metamorphism outlined by Russell (1981). Since the fieldwork was limited to a 3-km wide strip the lateral extent of these blocks is not known.

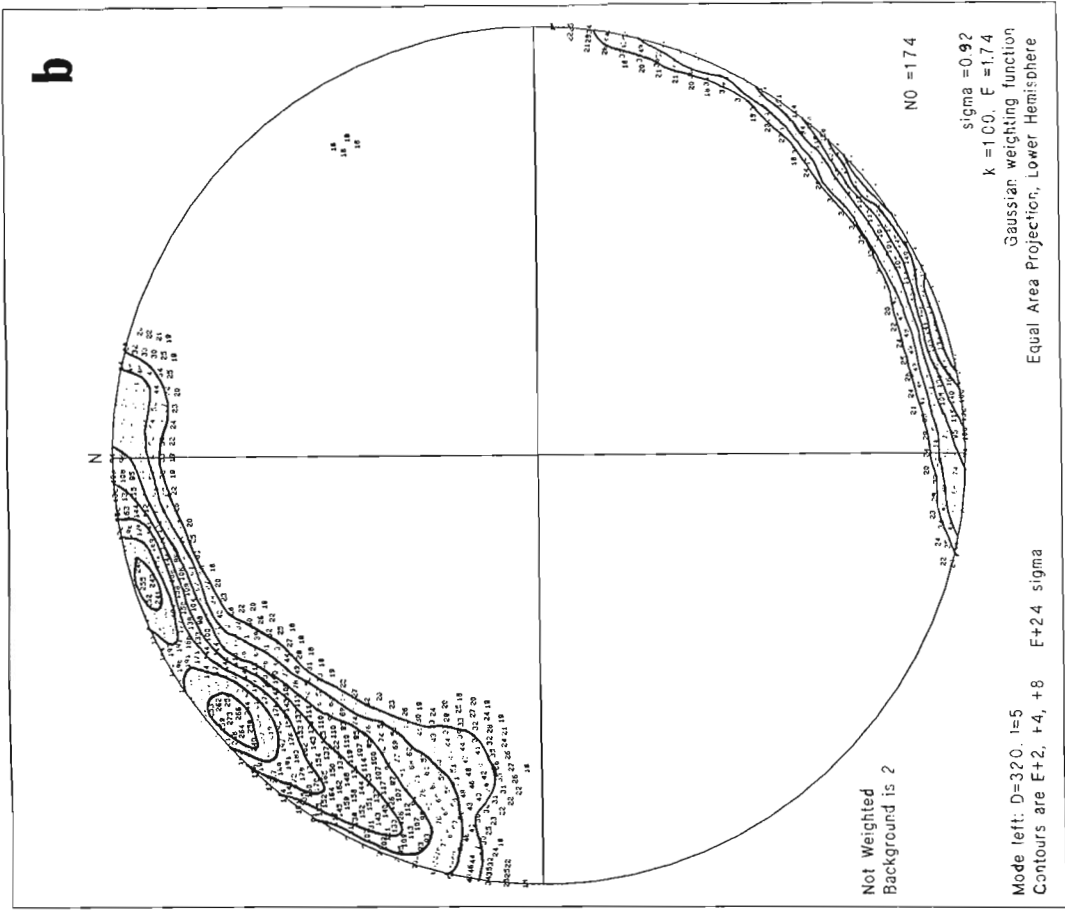
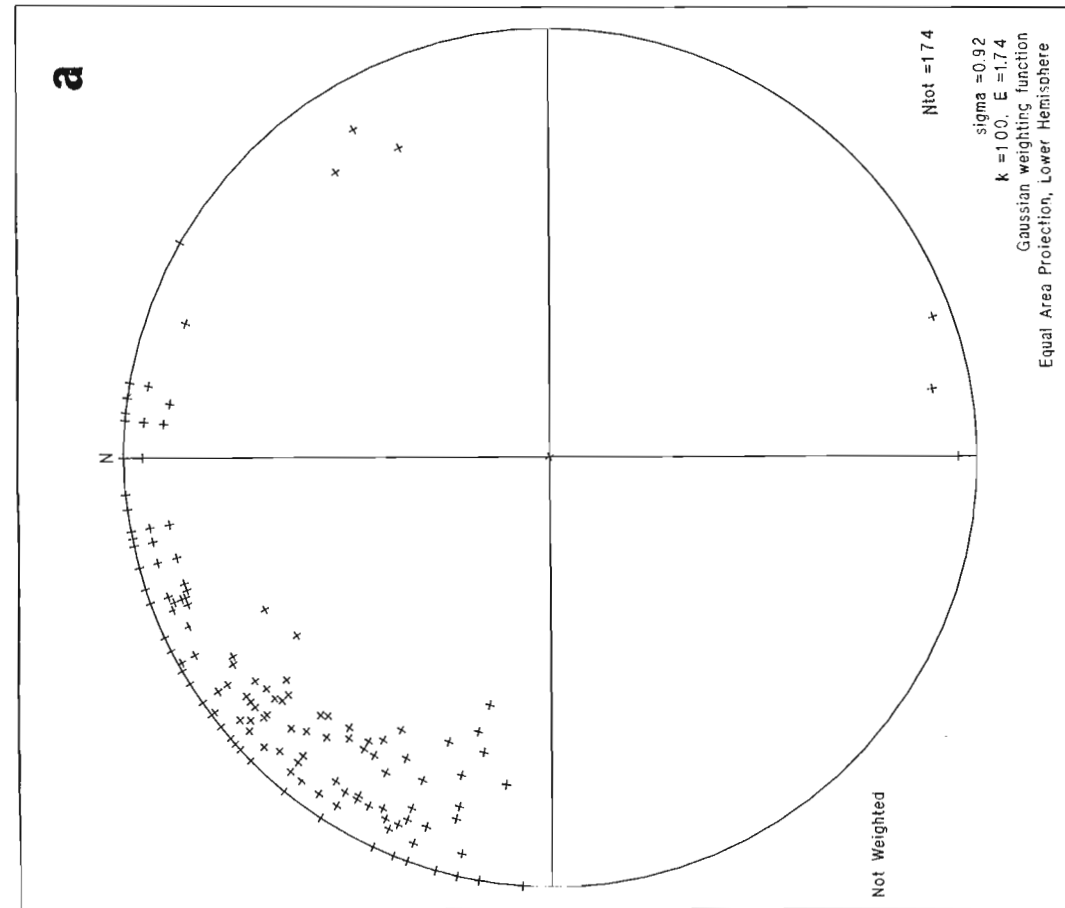
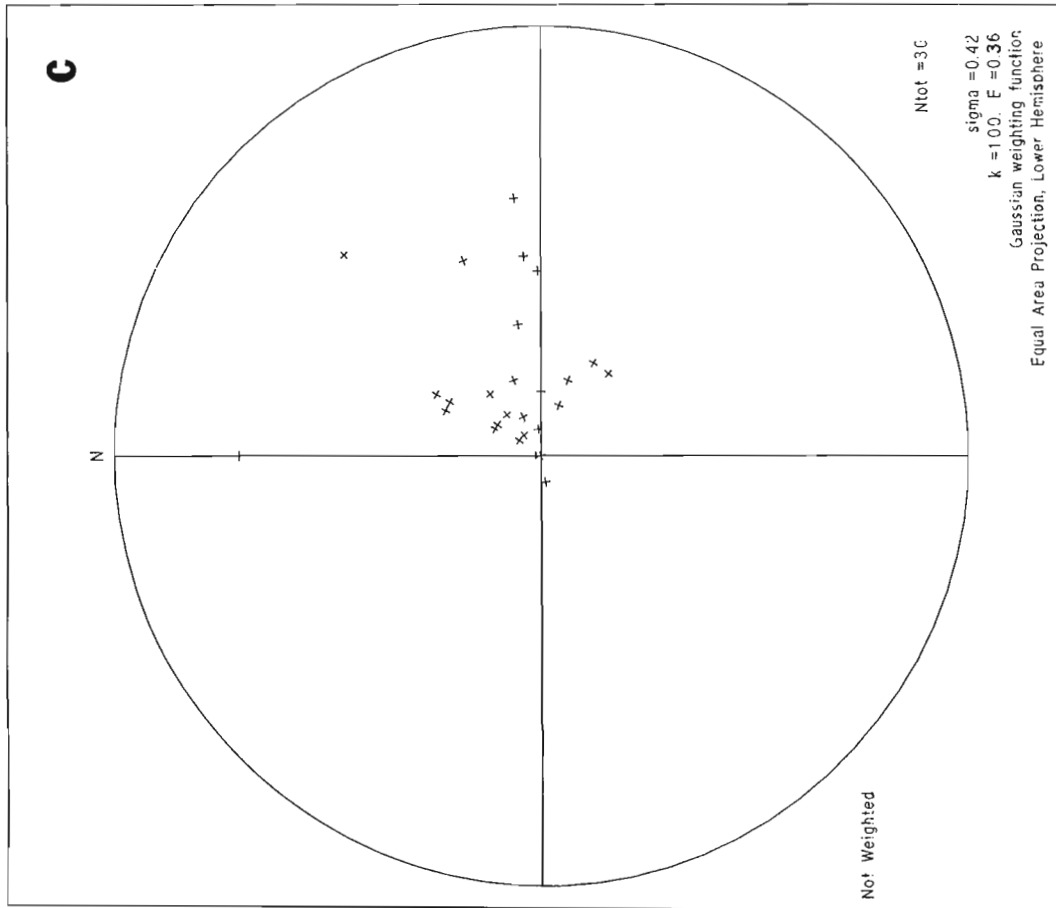


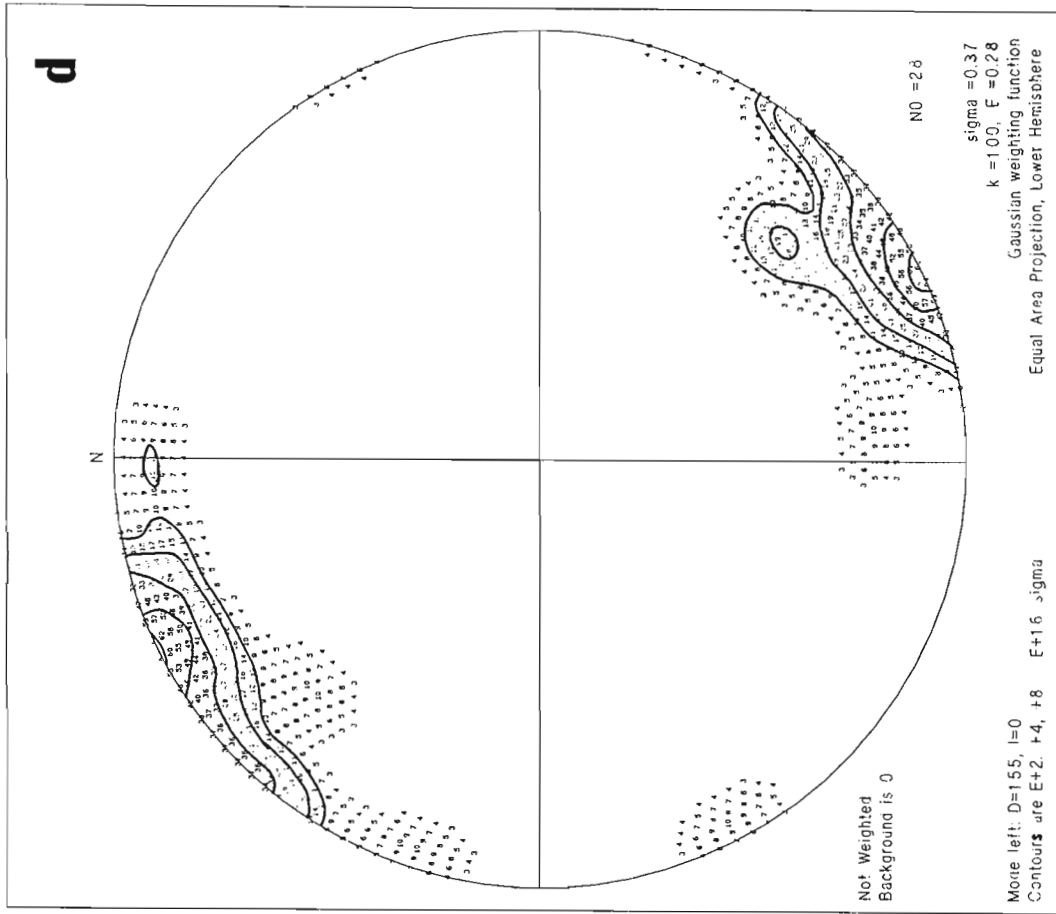
Figure 85.2a. Pipe 2 mine, gneissic foliation data

2b. Pipe 2 mine, gneissic foliation contoured data

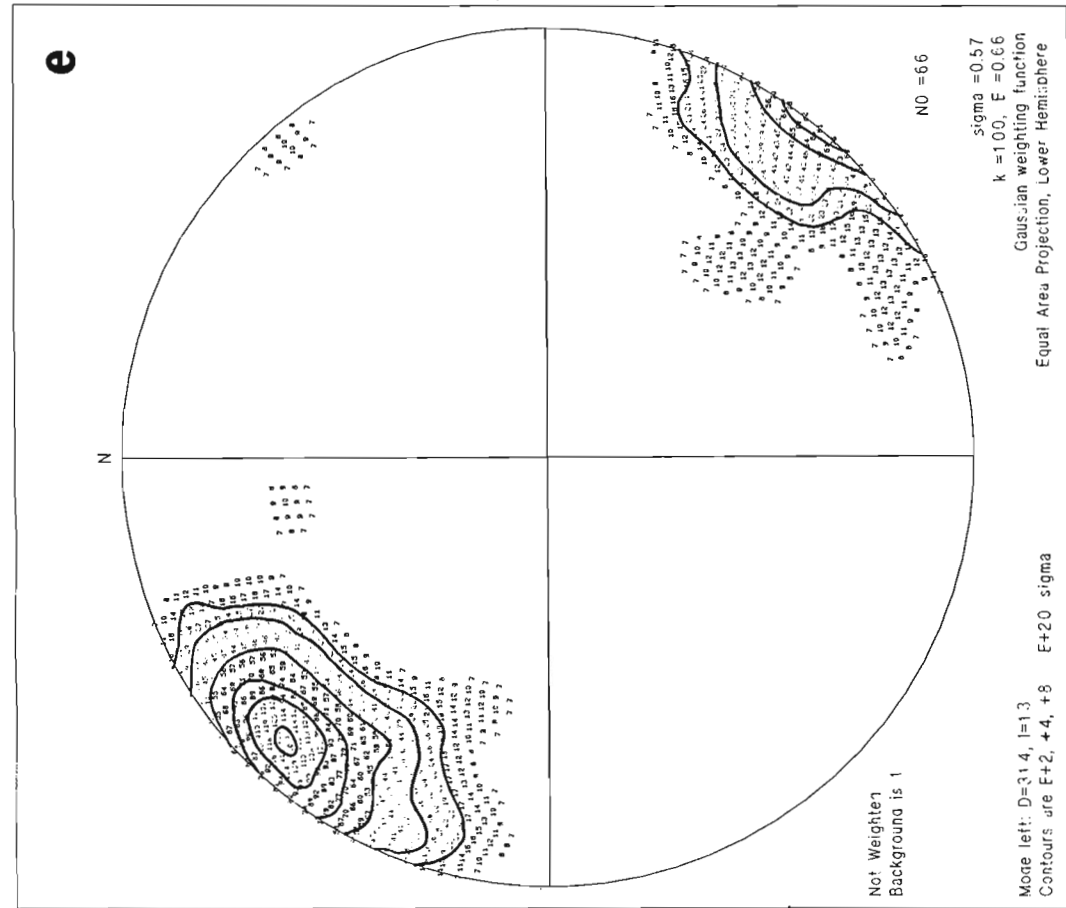
NOTE: All orientation data were plotted and contoured using the program described by Robin and Jowett (1986). Contour intervals are in the number of standard deviations (sigma) given on each graph. Data points and contoured diagrams are presented for the first data set, to allow for a visual comparison, in subsequent diagrams only the contoured diagrams are presented. No contouring was done on linear orientation data since not enough data were available in any one data set to yield statistically significant contours.



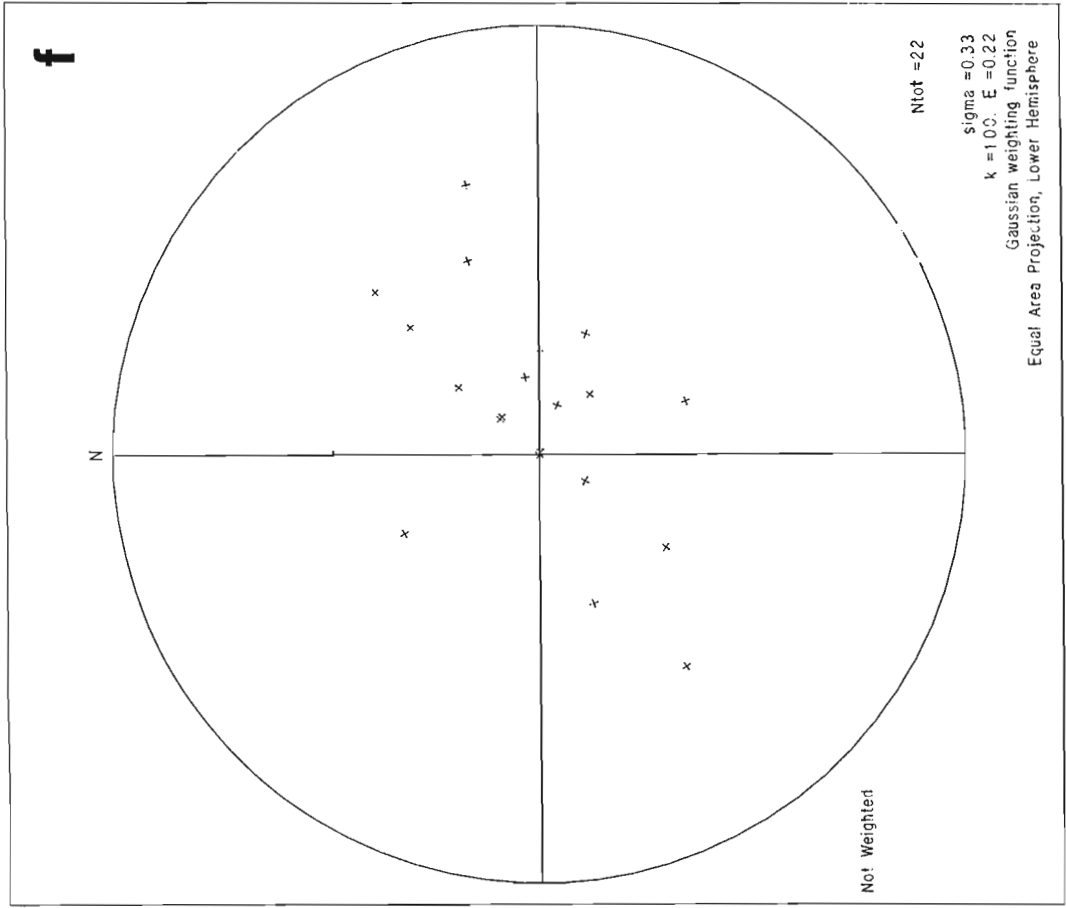
2c. Pipe 2 mine, gneissic lineation



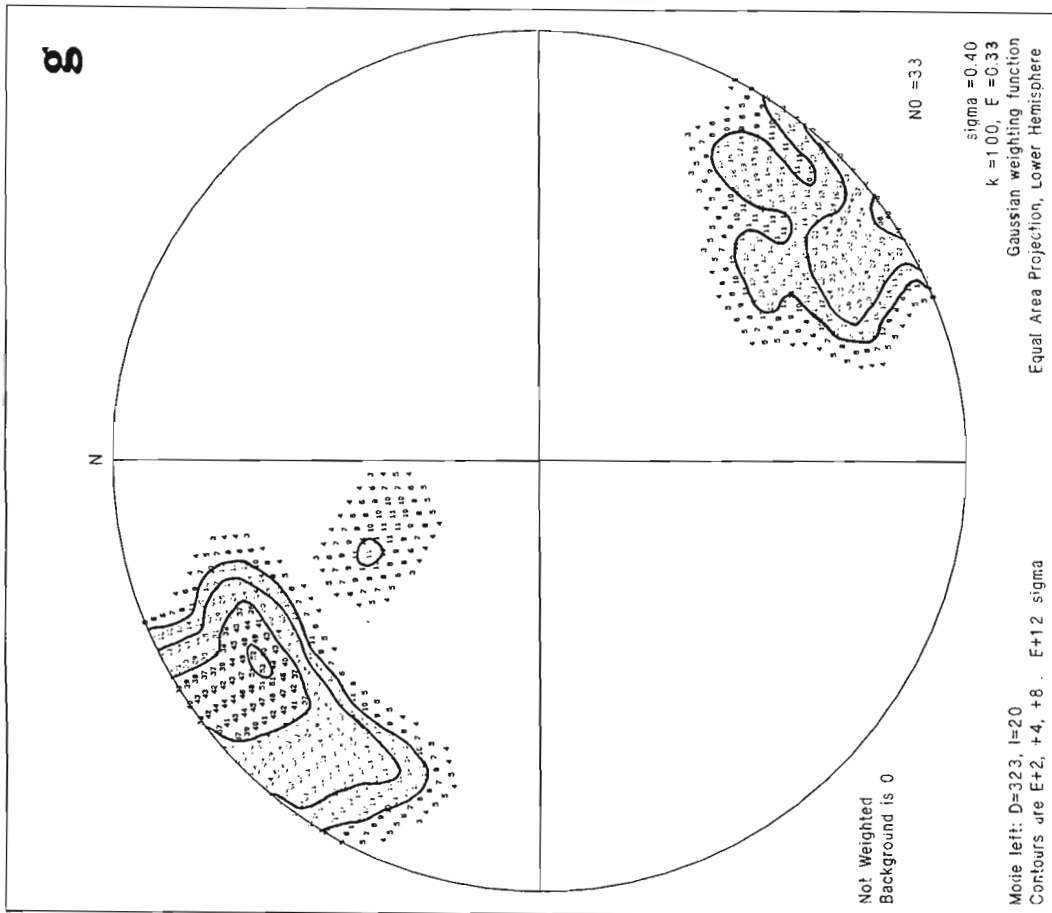
2d. Upper Oswegan Lake, gneissic foliation



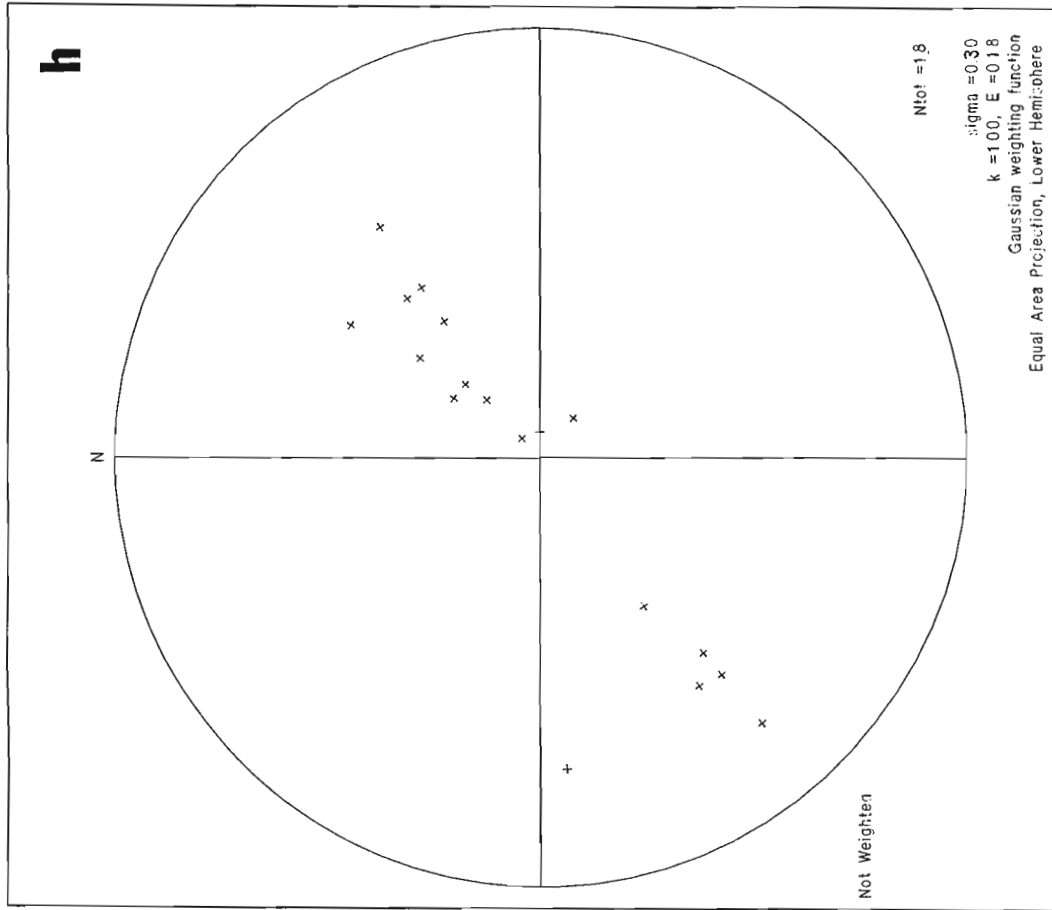
2e. Lower Oswagan Lake, gneissic foliation



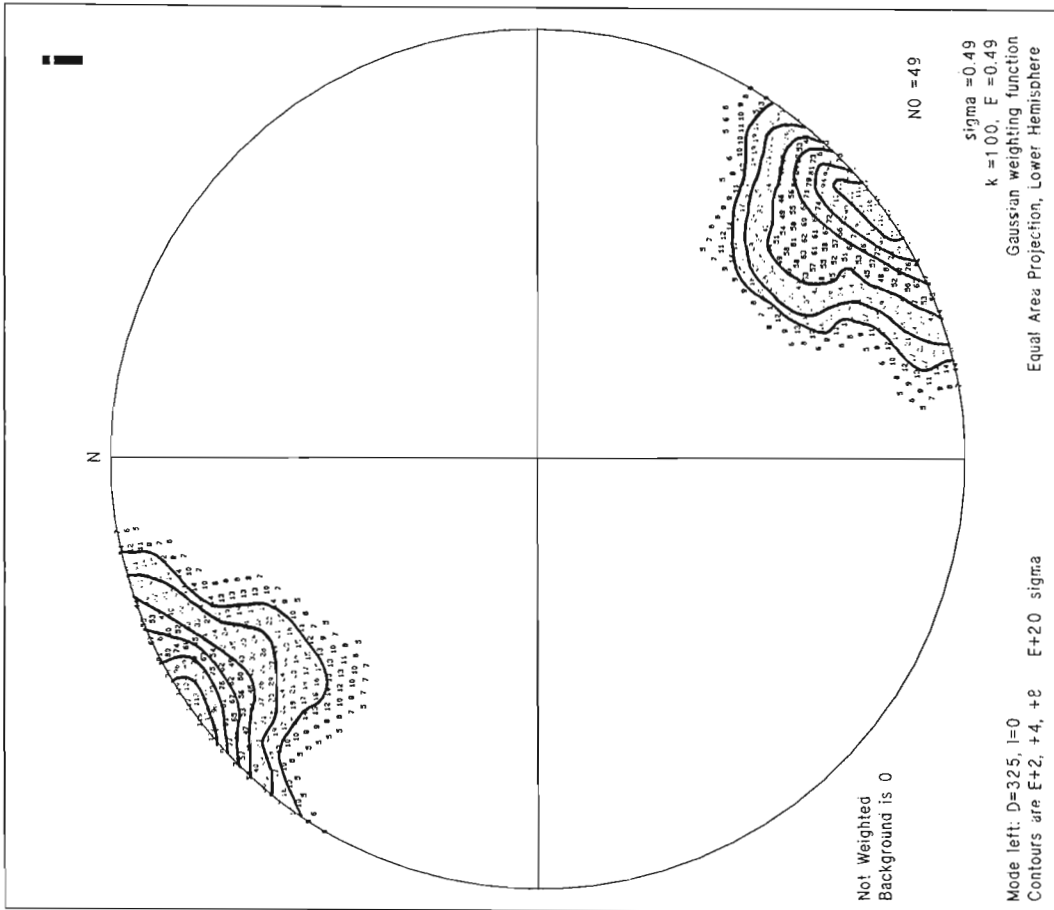
2f. Oswagan Lake, gneissic lineation



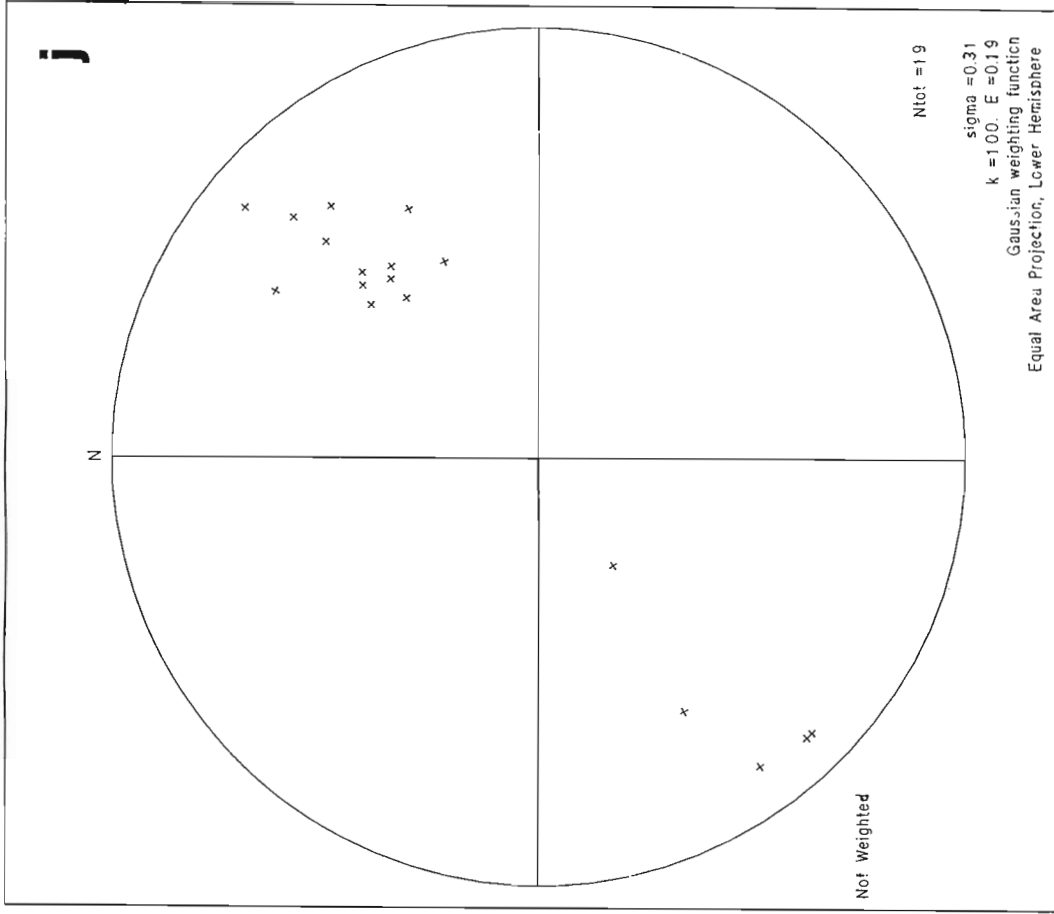
2g. Paint Lake northwest block, gneissic foliation



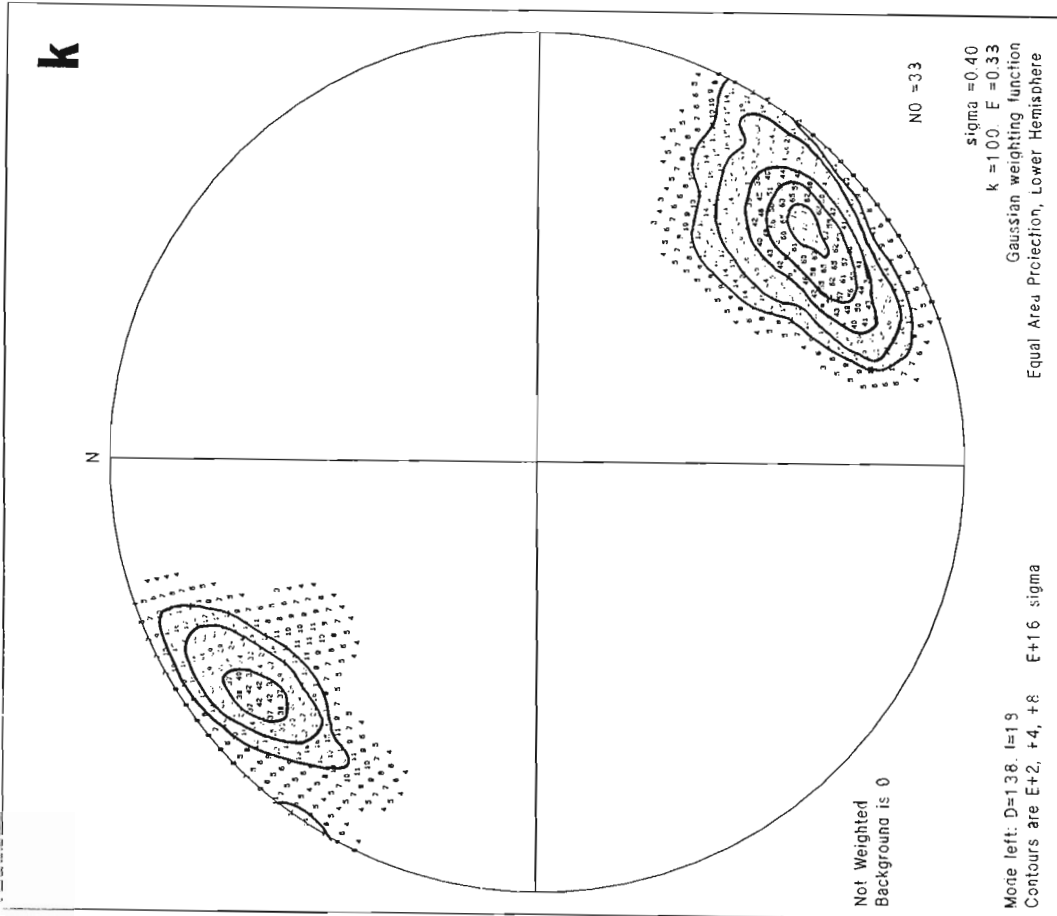
2h. Paint Lake northwest block, gneissic lineation



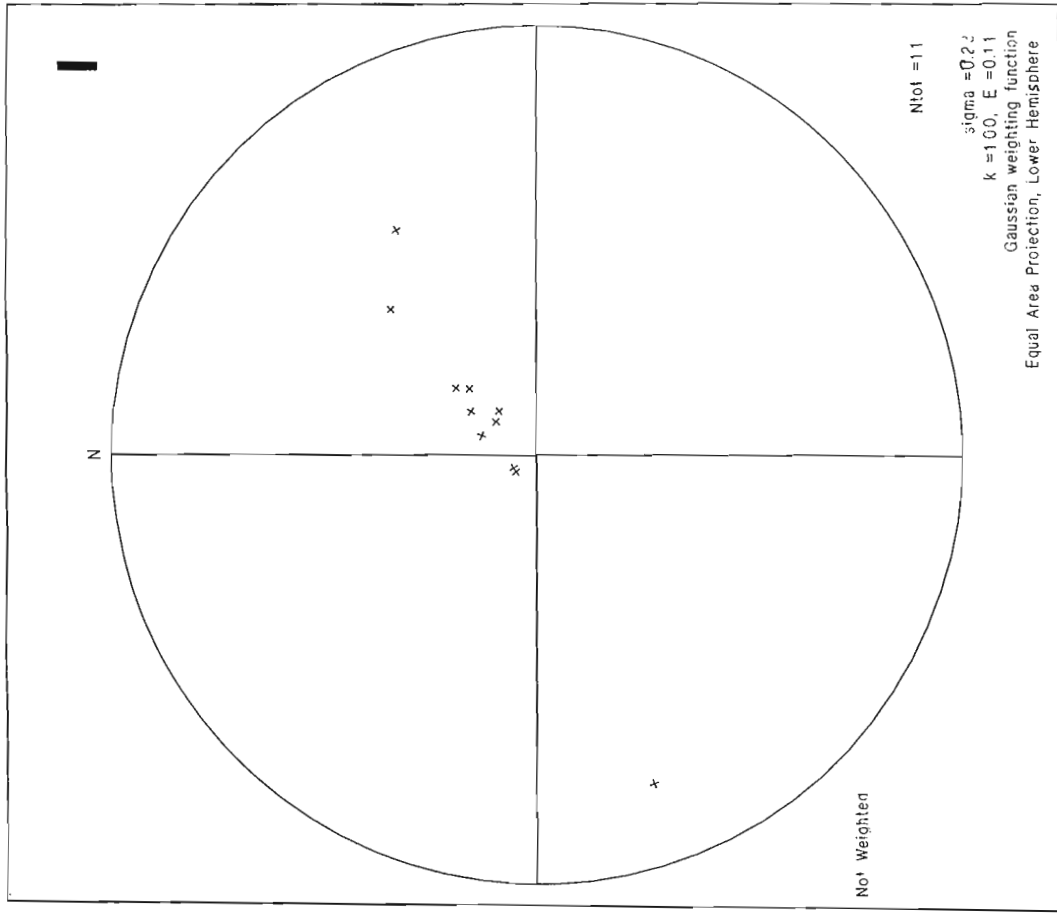
2i. Paint Lake center block, gneissic foliation



2j. Paint Lake center block, gneissic lineation



2k. Paint Lake southeast block, gneissic foliation



2l. Paint Lake southeast block, gneissic lineation

Paint Lake northwest block

The gneisses of this block are of enderbitic composition, containing quartz, plagioclase, orthopyroxene, clinopyroxene, hornblende and biotite (Russell, 1981). The pyroxenes are commonly altered. Outcrops contain 30% pegmatite and variable amounts of amphibolite. The block is bounded to the northwest by a mylonite zone, located on the southwest shore of Liz Lake. The southeastern border of this region is also well defined by the disappearance of enderbitic gneisses.

The gneissic foliation (Fig. 85.2g) shows a pattern very similar to that at Lower Ospwagan Lake, with the average foliation dipping approximately 75° to the southeast. Lineations (Fig. 85.2h) are concentrated in a vertical plane coinciding with the foliation and show a considerable variation in plunge both to the northeast and to the southwest.

The percentage of dynamically recrystallized quartz varies considerably but generally increases towards the northeast. This is tentatively interpreted as resulting from an increase in degree of deformation, although other factors such as differences in thermal history may be involved.

Paint Lake center block

The dominant rock type consists of granodioritic to dioritic gneisses. Rocks consist of biotite, feldspar, rare hornblende and common orthopyroxene altered to various degrees. Completely altered patches, which may be a highly altered clinopyroxene, are present in some samples. The mesoscopic layer thickness varies between 2 and 15 cm. Approximately 25% of pink pegmatite and between 2 and 20% amphibolite are present in the outcrops. At the northwestern part of this block, pyroxenes are rare and highly altered, if present, and the amount of pyroxene in the rock generally increases towards the southeast, suggesting that the Hudsonian overprint becomes weaker in this direction.

Long dimensions of mafic minerals and mafic clots show a preferred orientation which becomes more pronounced toward the northern border of the block. The samples with the strongest preferred orientation do not contain any pyroxene. In these samples, although the quartz is approximately equant, with grain sizes reaching up to 1 mm, interference colours of quartz indicate a strong crystallographic preferred orientation. These rocks thus appear to have been annealed after a strong deformation.

The variation in pyroxene content is therefore consistent with a model of gradual retrogression and disappearance of the pyroxenes towards the northwest as the deformation becomes stronger.

The gneissic foliation in this block shows a maximum dipping steeply to the northwest (Fig. 85.2i). Lineations trend towards the northeast and southwest (Fig. 85.2j) but appear to be shallower than in the northern Paint Lake block. Shallow dipping minor folds are common in the orthopyroxene-bearing gneisses of this block.

The southeast border of this block is defined by the disappearance of orthopyroxene-bearing gneiss.

Paint Lake southeast block

The bulk composition in this block is approximately granodioritic. Pegmatite (mostly white) layers make up between 10 and 30% of the outcrop. Amphibolite layers (10-cm thick) constitute approximately 5% of the rock. Mesoscopic gneissic layering thickness ranges from 5 to 40 cm. Some outcrops are not well layered except for the presence of the pegmatite layers.

Biotite is present in all samples, and hornblende is common. A good clinopyroxene has been found in one coarse-

grained sample (gs. 1 mm). The plagioclase is generally not sericitized except in some strongly foliated samples interpreted as having been sheared. At one location in which biotite and garnet are the mafic minerals, lozenge-shaped, sericitized feldspars are aligned parallel to the foliation. Several of these feldspars appear to be solely contained within single quartz grains (Fig. 85.4). The quartz in this sample reaches a grain size of 2.5 mm in the long diameter, with aspect ratios of up to 4 to 1. A possible explanation is again that this is the result of static annealing of a previously sheared rock.

The gneissic foliation in this block (Fig. 85.2k) shows two maxima although it is uncertain whether they are statistically significantly different. Lineations plunge steeply (Fig. 85.2l).

Kinematic indicators

Foliations and lineations can be used as crude indicators of the strain in the Thompson Belt. The nearly vertical foliations suggest that the dominant strain recorded by the fabric of these rocks was one of general flattening onto a presently vertical plane parallel to the direction of the belt. The steeply plunging lineations suggest furthermore a stretching of the rocks in a direction which is now vertical. We believe that large strains are required to account for uniformly steep foliations and lineations over a large region such as the Thompson Belt, whether the fabric is formed by that strain or merely transposed by it into isoclinal folds. Mylonites and sheath folds also require large strains, at least locally. However, simple strain theory (the 'room problem' argument for high strains in narrow zones) suggests that large strains restricted to narrow zones such as the Thompson Belt require a large component of progressive simple shear. In order to determine the sense of such progressive simple shear one can look for kinematic indicators of the sense of progressive simple shear (henceforth called kinematic indicators, for the sake of brevity).

Mesoscopic and microscopic kinematic indicators sought were asymmetric folds, asymmetric tails or pressure shadows, asymmetrically distorted foliations around porphyroblasts, and S-C fabrics (Berthé et al. 1979).

In general, convincing mesoscopic kinematic indicators are relatively rare in the Thompson belt, and they are mostly found on Ospwagan Lake and near the Pipe 2 mine.

(1) Asymmetric minor folds are present; however, a sense of asymmetry observed in one outcrop is often found to be reversed in the next outcrop. At the Pipe 2 mine, the sense which they indicate is simply explained by their position with respect to major folds.

(2) S-C type fabrics are found in some metasediments (Fig. 85.5) but are rare and not completely convincing.

(3) Even though tails are common on feldspars in the gneisses, and garnets with pressure shadows are common in metasediments, in most samples these structures are either only slightly asymmetric or not at all. Asymmetric tails, which form far less than 1% of tailed feldspars, are usually only weakly asymmetrical and have to be considered suspect if only because of their scarcity.

Of the convincing kinematic indicators, 12 indicate that the Churchill side moved up with respect to the Superior side (Fig. 85.5). However, five other indicators, among the best ones, i.e. showing the most pronounced asymmetry and the least ambiguity, indicate that the Superior side moved up with respect to the Churchill side (Fig. 85.6).

(4) An interesting fabric, developed in several of the gneisses on Lower Ospwagan Lake and at the Pipe 2 mine, can also be interpreted as a kinematic indicator. This fabric consists of two sets of microfaults-microfissures in feldspar-rich patches, approximately perpendicular to each other, both striking paral-

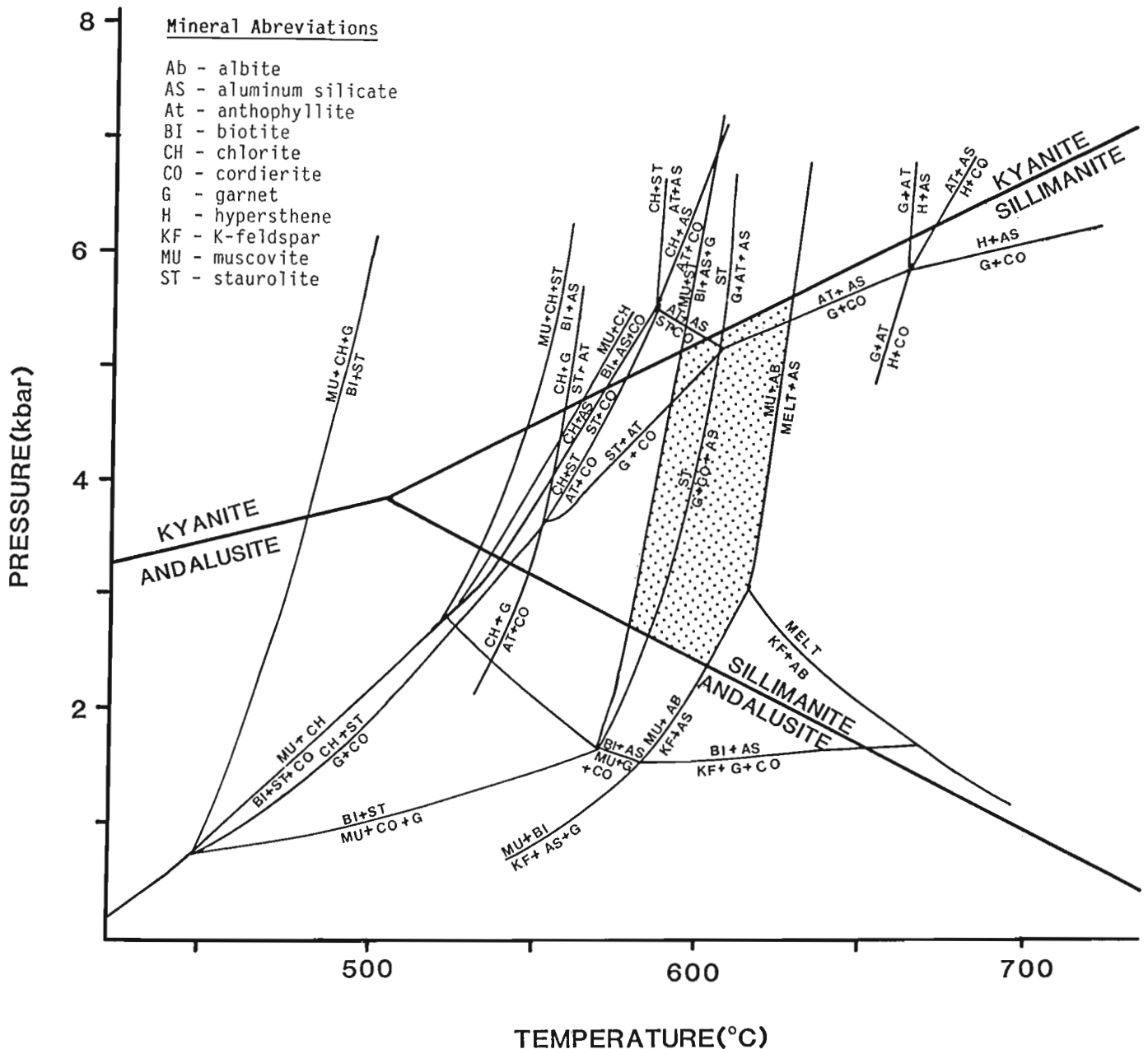


Figure 85.3. Petrogenetic grid for Pipe 2 mine metasediments. The stippled area shows the range of possible peak temperatures and pressures. Petrogenetic grid by D.M. Carmichael (see Bailes, 1980).

lel to the foliation and symmetrically inclined at 45° to it (Fig. 85.7). The microfaults are commonly filled with micas, separating individual rectangular feldspar crystals. This geometry gives a blocky appearance to the feldspar-rich patches. Quartz in these rocks is commonly present in quartz ribbons. A granite gneiss only 2 km from the Superior-Churchill boundary presents an extreme case, almost all of the quartz in the sample is contained in quartz ribbons (Fig. 85.7). Offsets of feldspar grains of similar crystallographic orientations along these microfaults indicate east side up for east dipping ones and west side up for west dipping ones. Neither set appears to dominate over the other. The development of two sets of microfaults symmetric with respect to the foliation is indicative of an environment locally dominated by progressive pure shear. The sense of offset would indicate an overall horizontal compression and vertical extension.

Another interesting microstructural feature which is quite common in the belt is a set of small horizontal, undisplaced micro-fractures segmenting individual mineral grains or monomineralic patches. They appear to become more common towards the Churchill-Superior boundary, although this may be simply a function of a more common suitable lithology. These fractures are best displayed in the sillimanite mats (Fig. 85.8) common in the metasediments exposed on Ospwagan Lake. These fractures show no visible opening or fissure filling under standard optical microscope magnifications; they are interpreted as late tension fractures, with negligible displacement, and are considered to be stress indicators rather than strain indicators. The direction of least compressive stress which they indicate is, nevertheless, in agreement with the vertical stretching direction inferred from mesoscopic lineations and kinematic indicators.

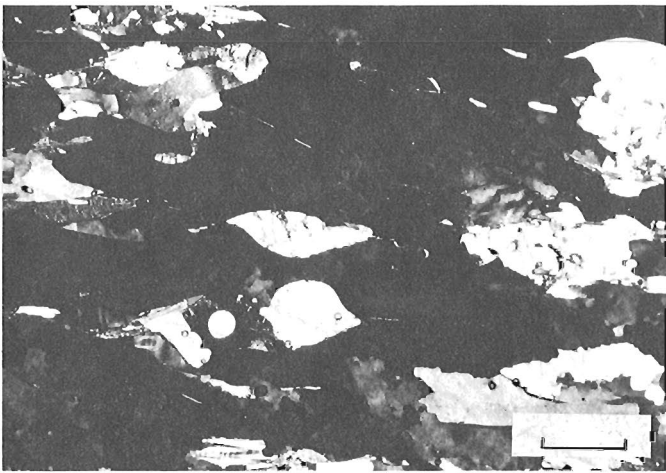


Figure 85.4. Lozenge-shaped feldspars (illuminated) within a single grain of extinct quartz. Bar scale measures 1 mm.

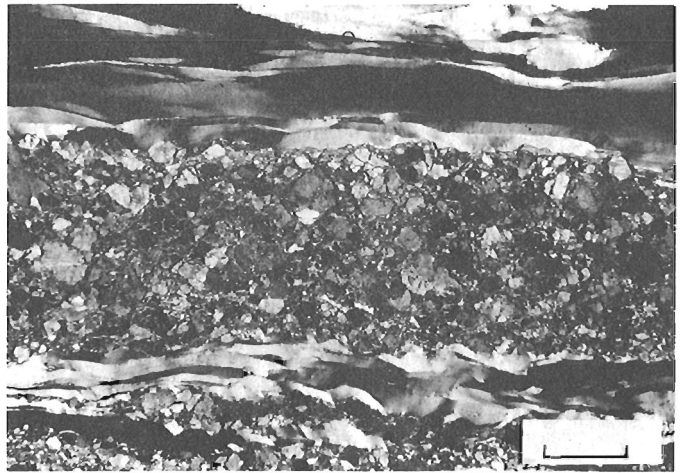


Figure 85.7. Blocky fabric developed in granite gneiss. Feldspars are separated by thin layers of micas. Feldspars and micas are isolated within quartz-free patches. Quartz in this sample is almost exclusively contained within quartz ribbons. Bar scale measures 0.5 mm.

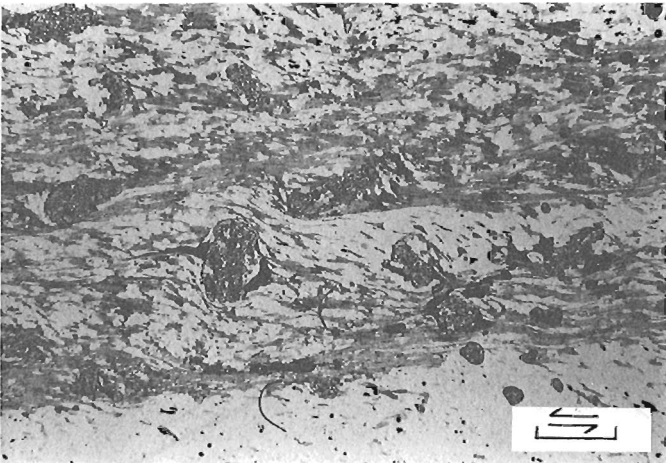


Figure 85.5. Pelitic metasediment showing asymmetric pressure shadows on garnets, S-C type asymmetry and a possible shear band. Foliation and lineation in the sample are near vertical; the sense of asymmetry in the sample suggests that the Churchill side moved up with respect to the Superior side. Bar scale measures 0.5 mm.

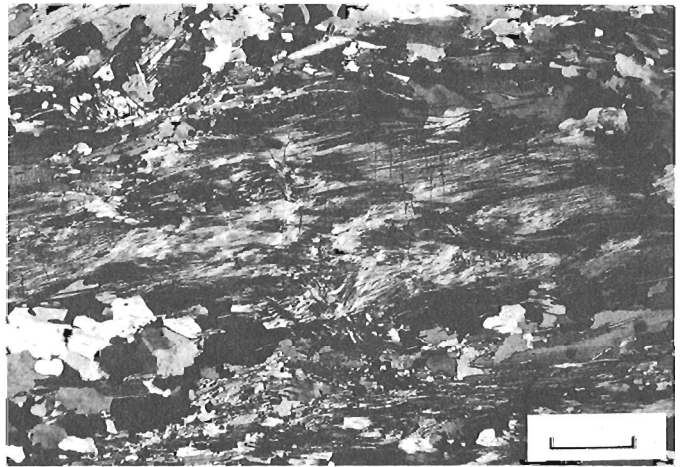


Figure 85.8. Micro-fractures within a sillimanite mat in pelitic metasediment. Fractures are oriented approximately horizontally. Bar scale measures 0.5 mm.

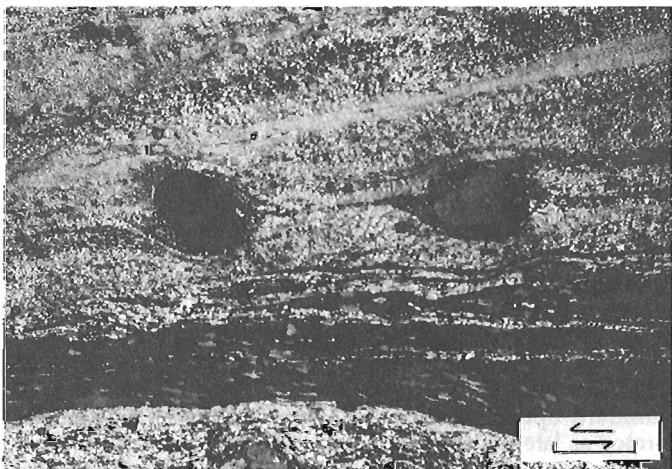


Figure 85.6. Mylonite within a gneiss. Foliation and lineation in the sample are near vertical. Foliation draped around rolled feldspars indicate that the Superior side moved up with respect to the Churchill side. Bar scale measures 0.5 mm.

Summary

The metamorphic grade on the western side of the belt does not appear to be significantly lower than for the main part of the belt. Metamorphic conditions associated with the Hudsonian event are between 575°C and 625°C and 2.5 kb to 5.75 kb for the Pipe 2 mine and Ospwagan Lake, and 650±50°C 4-5 kb for Paint Lake (Russell, 1981).

The gneissic foliation is generally steep everywhere. It becomes subvertical or very steeply inclined to the southeast near the Superior-Churchill boundary. Lineation plunges vary on Paint Lake; they are generally steep close to the boundary.

Several of the gneisses on Paint Lake have textures which have been interpreted as annealed shear textures, in contrast to the pristine shear textures found on Ospwagan Lake and at the Pipe 2 mine. One possible explanation for this is that the annealed textures on Paint Lake are the result of deformation which occurred earlier than that responsible for the pristine textures on Ospwagan Lake. Alternatively, conditions on Paint Lake were sufficiently different from those on Ospwagan Lake to allow shear textures of the same age to anneal on Paint Lake

while they remained pristine on Ospwagan Lake and at the Pipe 2 mine.

The indicators that are present record movements which are now in a vertical direction, consistent with the steeply plunging lineations. This extension may be locally considerable. The last recorded event in the belt was thus one of now vertical extension with NW-SE directed horizontal compression. This is more consistent with converging plates than with the transcurrent faulting proposed by Green et al. (1985).

Acknowledgments

The co-operation and help of the staff of INCO Metals Company, especially R.C. Sommerville, M. Toderian and D. Mundy, were greatly appreciated. Discussions with J.R.F. Scoates and the help of W. Weber proved to be very useful. J.R. Henderson, C.R. van Staal and E. Froese critically read various versions of the manuscript and contributed to significant improvements.

References

- Bailes, A.H.
1980: Geology of the File Lake area; Manitoba Mineral Resources Division, Geological Report 78-1.
- Berthé, P., Choukroune, P. and Jegouzo, P.
1979: Orthogneiss, mylonite and non-coaxial deformation of granites: the example of the South Armorican shear zone; *Journal of Structural Geology*, v. 1, p. 31-42.
- Gale, G.H., Somerville, R.C., Chornoby, J., Haystead, B., Provins, N., Braun, D., Mundy, D. and Walker, A.
1982: Geological setting of the mineral deposits at Ruttan, Thompson, Snow Lake and Flin Flon; Geological Association of Canada, Field Trip Guidebook 14.
- Green, A.G., Hajnal, Z. and Weber, W.
1985: An evolutionary model of the western Churchill Province and western margin of the Superior Province in Canada and the north-central United States; *Tectonophysics*, v. 116, p. 281-323.
- Paktunç, A.D.
1984: Metamorphism of the ultramafic rocks of the Thompson mine, Thompson nickel belt, northern Manitoba; *Canadian Mineralogist*, v. 22, p. 77-91.
- Peredery, W.V. and Geological Staff
1982: Geology and nickel sulphide deposits of the Thompson Belt, Manitoba; in *Precambrian Sulphide Deposits*, ed. R.W. Hutchinson, C.D. Spence and J.M. Franklin; Geological Association of Canada, Special Paper 25, p. 165-209.
- Robin, P.-Y.F. and Jowett, C.E.
1986: Computerized density contouring and statistical evaluation of orientation data using counting circles and continuous weighting functions; *Tectonophysics*, v. 121, p. 207-223.
- Russell, J.K.
1981: Metamorphism of the Thompson nickel belt gneisses: Paint Lake, Manitoba; *Canadian Journal of Earth Sciences*, v. 18, p. 191-209.
- Scoates, R.F.J., Macek, J. and Russell, J.K.
1977: Thompson nickel belt project: Manitoba Mineral Resources Division, Report of Field Activities 1977, p. 47-53.
- Weber, W. and Scoates, R.F.J.
1978: Archean and Proterozoic metamorphism in the northwestern Superior Province and along the Churchill-Superior boundary, Manitoba; Geological Survey of Canada, Paper 78-10, p. 5-16.

Mechanical role of the syntectonic Laloche Batholith in the Great Slave Lake Shear Zone, District of Mackenzie, N.W.T.

Project 830009

S. Hanmer and J.N. Connelly¹
Lithosphere and Canadian Shield Division

Hanmer, S. and Connelly, J.N., Mechanical role of the syntectonic Laloche Batholith in the Great Slave Lake Shear Zone, District of Mackenzie, N.W.T.; in Current Research, Part B, Geological Survey of Canada, Paper 86-1B, p. 811-826, 1986.

Abstract

The Great Slave Lake Shear Zone (GSLSZ) is a crustal scale, lower Proterozoic, dextral, transcurrent shear zone, up to 25 km wide, made of 5 belts of granulite to lower greenschist facies mylonites. The Laloche Batholith, spatially coincident with the site of the GSLSZ, was emplaced incrementally during the tectonic history of the GSLSZ. With time the metamorphic grade decreased, the zone of actively forming mylonites shifted laterally and narrowed. Ductile deformation progressively evolved through the brittle-ductile transition to non-disruptive brecciation and brittle faulting. The history of the GSLSZ represents a single progressive event, which occurred during a period of uplift, unroofing and thermal decay accompanied by ongoing syntectonic acid and mafic magma injection.

Résumé

Le cisaillement du Grand lac des Esclaves est une structure à décrochement dextre, comprenant cinq zones de mylonites, dont la largeur peut atteindre jusqu'à 25 km. Le batholithe de Laloche, qui coïncide cartographiquement avec le cisaillement, s'est mis en place pendant le fonctionnement de ce dernier. La localisation de la mylonitisation en cours s'est déplacée latéralement et s'est rétrécie au fur et à mesure que l'environnement métamorphique passe du faciès granulitique au faciès des schistes verts. La déformation a progressivement évolué de la phase ductile à celle de la déformation cassante. L'histoire de ce cisaillement constitue un seul cycle de tectonisme, de soulèvement, d'érosion et de refroidissement, synchrones d'injection de magmas mafiques et acides.

¹ Department of Geological Sciences, Queen's University, Kingston, Ontario K7L 3N6

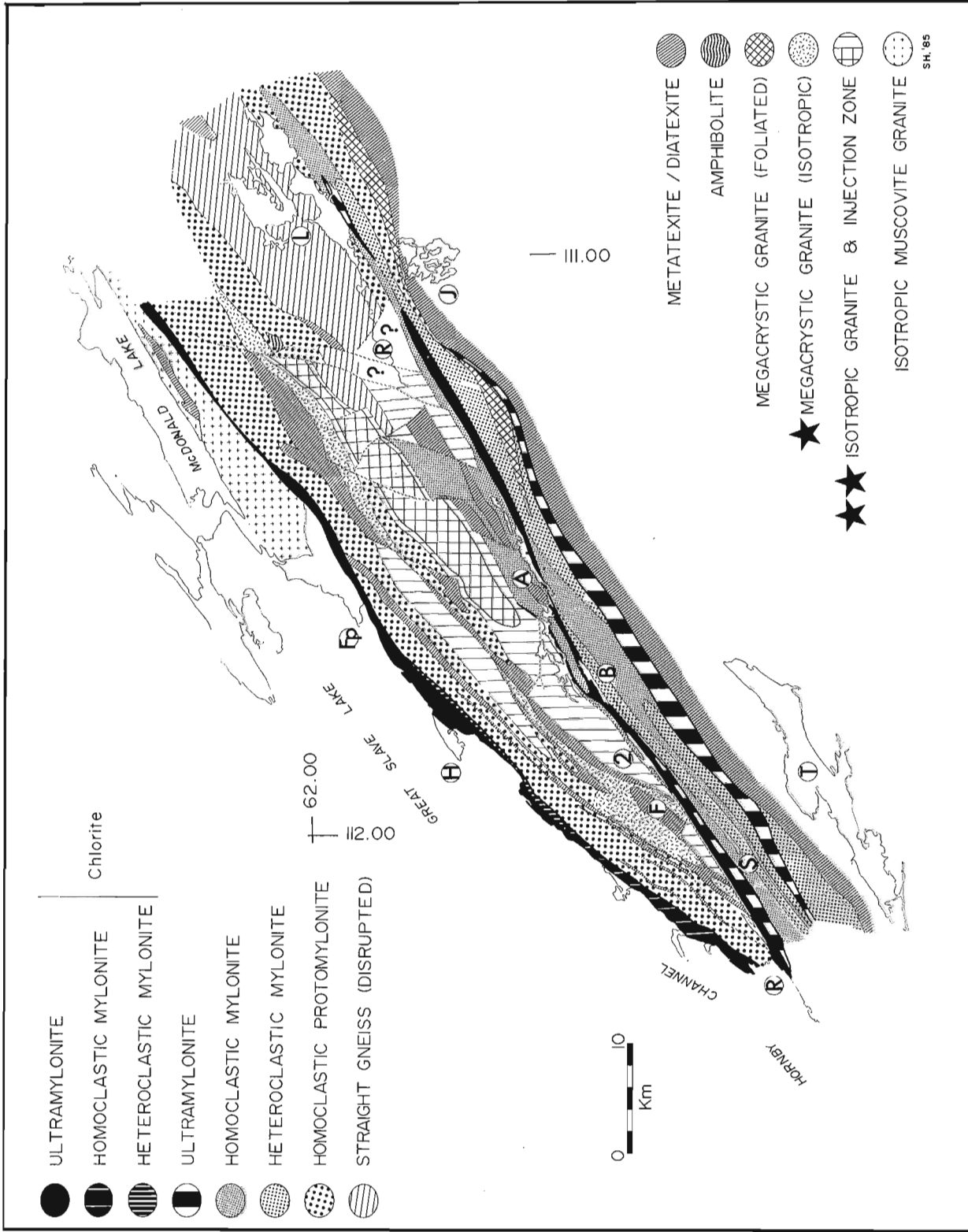


Figure 86.1. Generalized geology of the Great Slave Lake Shear Zone. Mylonite terminology after Hammer and Lucas (1985). (*) Falls Lake granite. (**) Second Lake granite. L, Laloche Lakes; R, Laloche River; J, Jigsaw Lake; A, Avocado Lake; 2, Second Lake; F, Falls Lake; S, Spike Lake; T, Thubun Lakes; Fp, Finger Point; H, Hook Point. See text.

Introduction

The Great Slave Lake Shear Zone (GSLSZ; Hanmer and Lucas, 1985), as mapped in McDonald-Laloche-Great Slave lakes area is a major, crustal scale, NE striking, ductile transcurrent shear zone, up to 25 km wide. It lies close to the contact of Slave Craton and the Churchill Province. Four belts of mylonitic rocks of different metamorphic grade and different age of main preserved structure were identified by Hanmer and Lucas (1985) who found that metamorphic grade decreased with time from granulite facies to lower greenschist facies and that the locus of maximum strain rate shifted laterally within the shear zone. The GSLSZ shows a dextral sense of offset with a subhorizontal movement vector throughout its deformation history. All reference to previous work in this report refers to Hanmer and Lucas (1985), unless otherwise stated.

Our fieldwork in 1985 completed the 1:250 000 to 1:50 000 scale structural and lithological mapping of the McDonald-Laloche-Thubun lakes section of the GSLSZ (Fig. 86.1). Principal new field results are:

1. The GSLSZ is spatially coincident and contemporaneous with a composite granite batholith. The plutons are K-feldspar megacrystic biotite +/-hornblende granites-granodiorites, except for the youngest pluton which is equigranular. From Thubun Lakes to Jigsaw Lake, the southeastern margin of the GSLSZ is a progressive structural boundary coincident with the intrusive contact of the batholith to the northwest with aluminous paragneiss (migmatite) to the southeast. The batholith contrasts compositionally with regionally extensive muscovite leucogranite to the northwest and garnet leucogranite or diatexite to the southeast of the GSLSZ.
2. We have confirmed and completed the delimitation and definitions of the four structural belts previously identified and propose to call them belts no. 1 to 3 and Hornby Channel ultramylonite belt. The distribution of the belts is strongly controlled by the distribution of country rock within the batholith.
3. The long narrow strips of distinctive aluminous and calc-silicate paragneiss with layered amphibolite in belt no. 2 (Supracrustal Assemblage of Hanmer and Lucas, 1985) are metatexites and diatexites (Mehnert, 1968; Brown, 1973), lithologically identical to the extensive migmatites flanking the GSLSZ to the southeast. The youngest diatexite component in belt no. 2 is isotropic to poorly foliated and crosscuts relatively older strongly mylonitized migmatite, thus confirming the suggestion that belt no. 2 mylonites formed under upper amphibolite facies conditions.
4. The presence of retrograde garnet-muscovite-biotite mylonitic paragneiss with relict migmatitic structure in belt no. 3 indicates that this belt was once at the same metamorphic grade as belt no. 2, but has since been syntectonically retrograded. This confirms that the preserved deformation and metamorphism in belt no. 3 is younger than that in belt no. 2.
5. A fifth distinct belt of chlorite grade ultramylonite, the Laloche River ultramylonite belt, separates, and is younger than, the upper greenschist-lower amphibolite belt no. 3 and the upper amphibolite facies belt no. 2. Identification of this new belt allows us to delimit firm boundaries to belts no. 1, 2 and 3.
6. There is very close correspondance between the structural and lithological map units and the 1:250 000 scale aeromagnetic maps of the area (Geological Survey of Canada 1964a, b).

7. Mixed steeply and shallowly plunging extension lineations reported from granulite facies gneisses and mylonites of belt no. 1 are present in tectonites of all metamorphic grades through to chlorite grade in a corridor along the northwest side of belt no. 3. The mixed lineations are spatially rather than temporally controlled.

We use the terminology of Hanmer and Lucas (1985) to describe mylonites throughout this report.

Structural belts

The GSLSZ comprises 5 structural belts. We are now able to propose firm boundaries and relative time relations between the belts. To reflect this and to facilitate description we replace the informal positional labels used previously (Central, Northwestern, Southeastern and External belts) with numbers and names (no. 1, 2, 3 and HCUB respectively: see below). Each belt was derived by the metamorphism and deformation (mylonitization) of similar protolith, but each contains a distinct syntectonic metamorphic mineral assemblage. There are no preserved metamorphic gradients and thus no mineral isograds. The higher the metamorphic grade preserved, the older the metamorphism and deformation i.e. belt no. 1 (granulite), belt no. 2 (upper amphibolite), belts no. 3 (upper greenschist - lower amphibolite), Hornby Channel ultramylonite belt (HCUB; External belt of Hanmer and Lucas, 1985) and Laloche River ultramylonite belt (LRUB; new name), both of lower greenschist facies (Fig. 86.2). Our work this season completed the mapping of the interior and the southeastern margin of the GSLSZ and identified the LRUB along the Laloche River to the southeast of the Laloche Lakes. It marks the boundary between the belts no. 2 and no. 3 and clearly reworks its neighbours structurally and metamorphically, as shown by the rapid, but progressive, strain gradients on either side. We have also completed the mapping of two volumetrically important late-syntectonic elongate granite plutons (Falls Lake and Second Lake granites of Fig. 86.1) which dominate the map pattern of belt no. 2 and strongly affect the microstructural preservation of the adjacent mylonitic rocks. All of the structural and

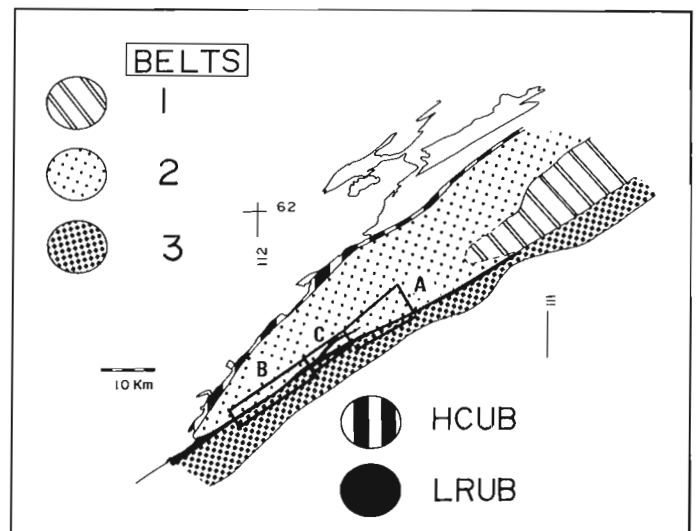


Figure 86.2. Distribution and boundaries of the structural belts of the Great Slave Lake Shear Zone. HCUB = Hornby Channel ultramylonite belt; LRUB = Laloche River ultramylonite belt. Outlined areas locate parts A, B and C of Figure 86.6.

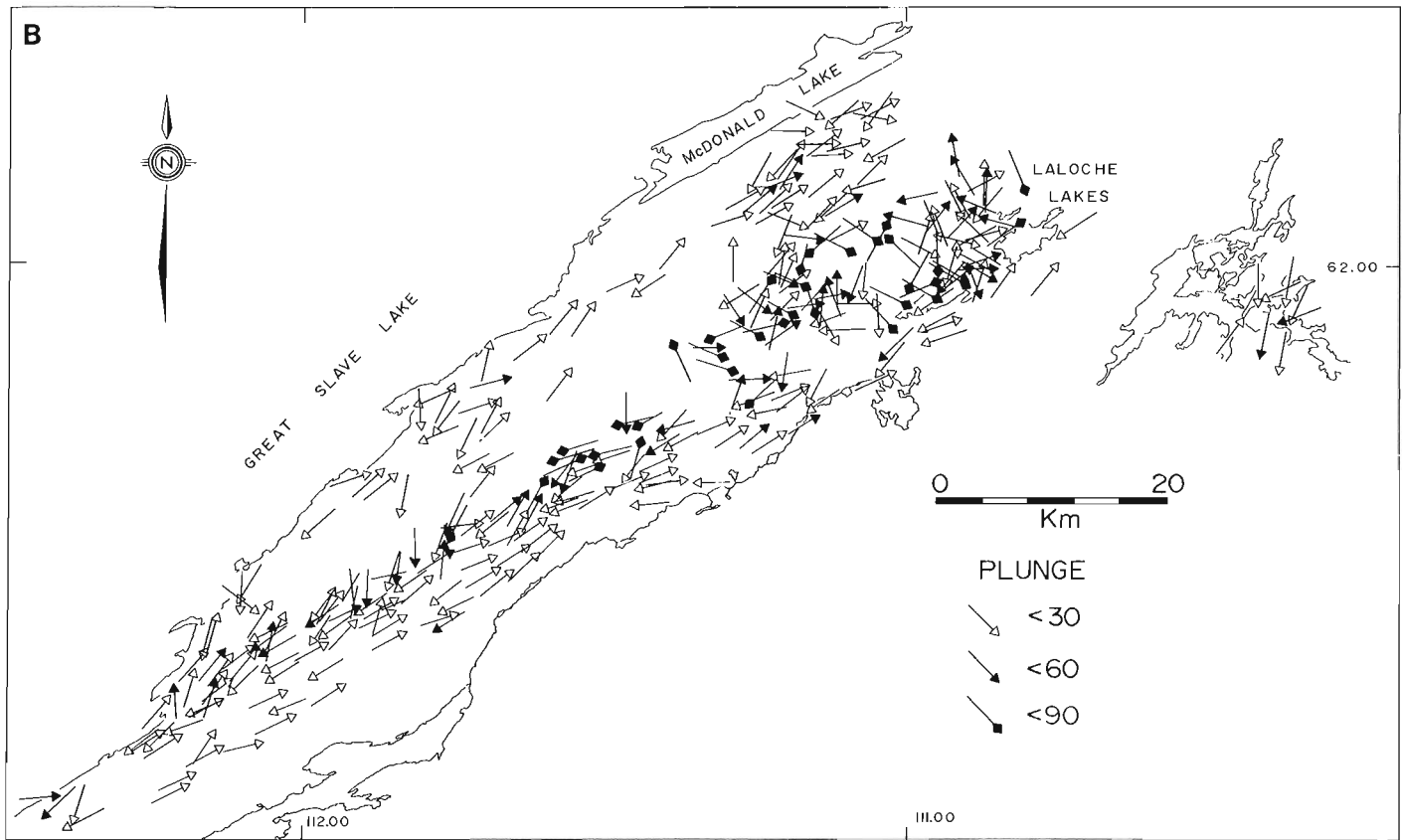
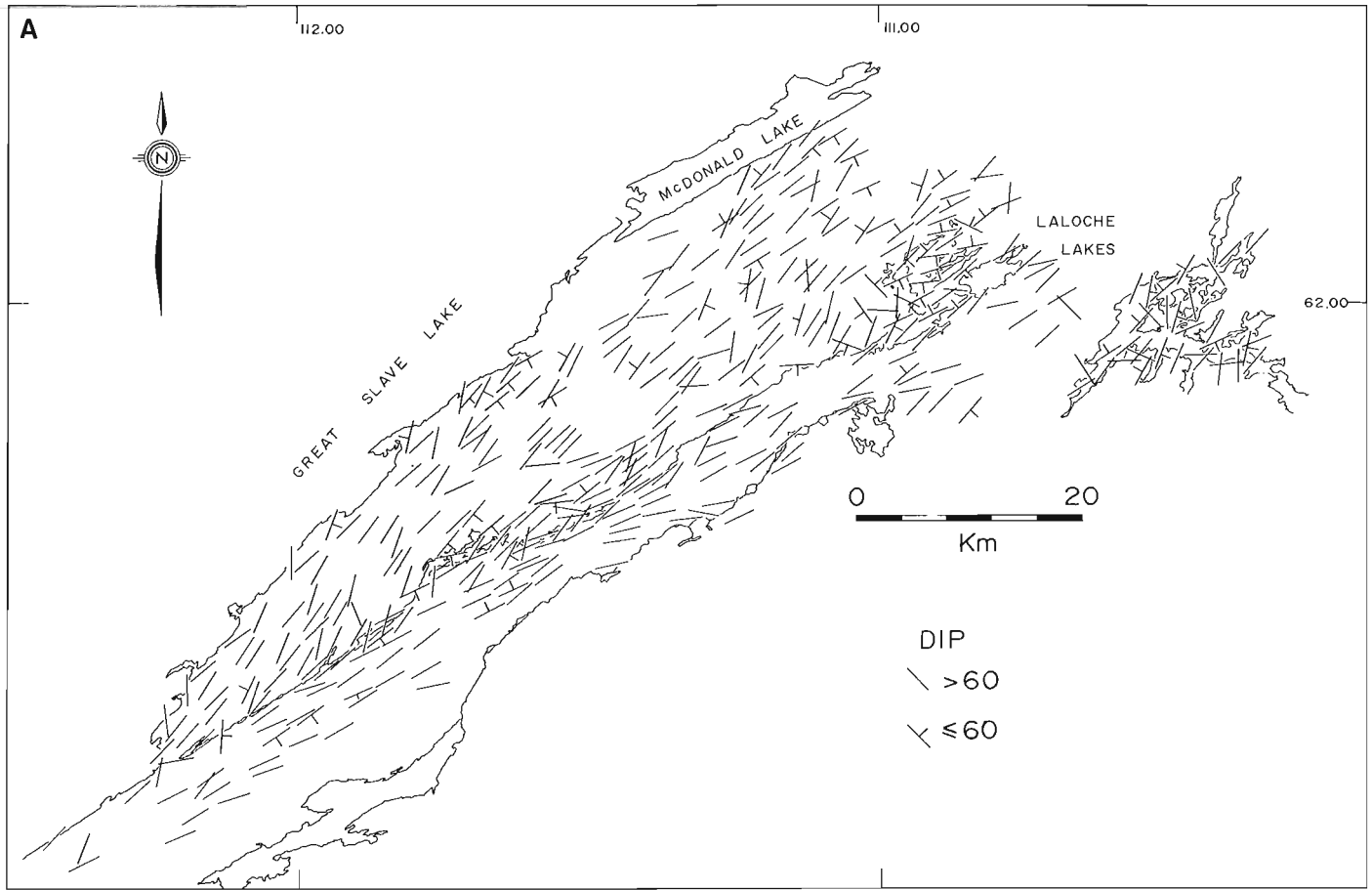


Figure 86.3. Structural geometry of the Great Slave Lake Shear Zone. (A) Foliation. (B) Extension lineation. See text.

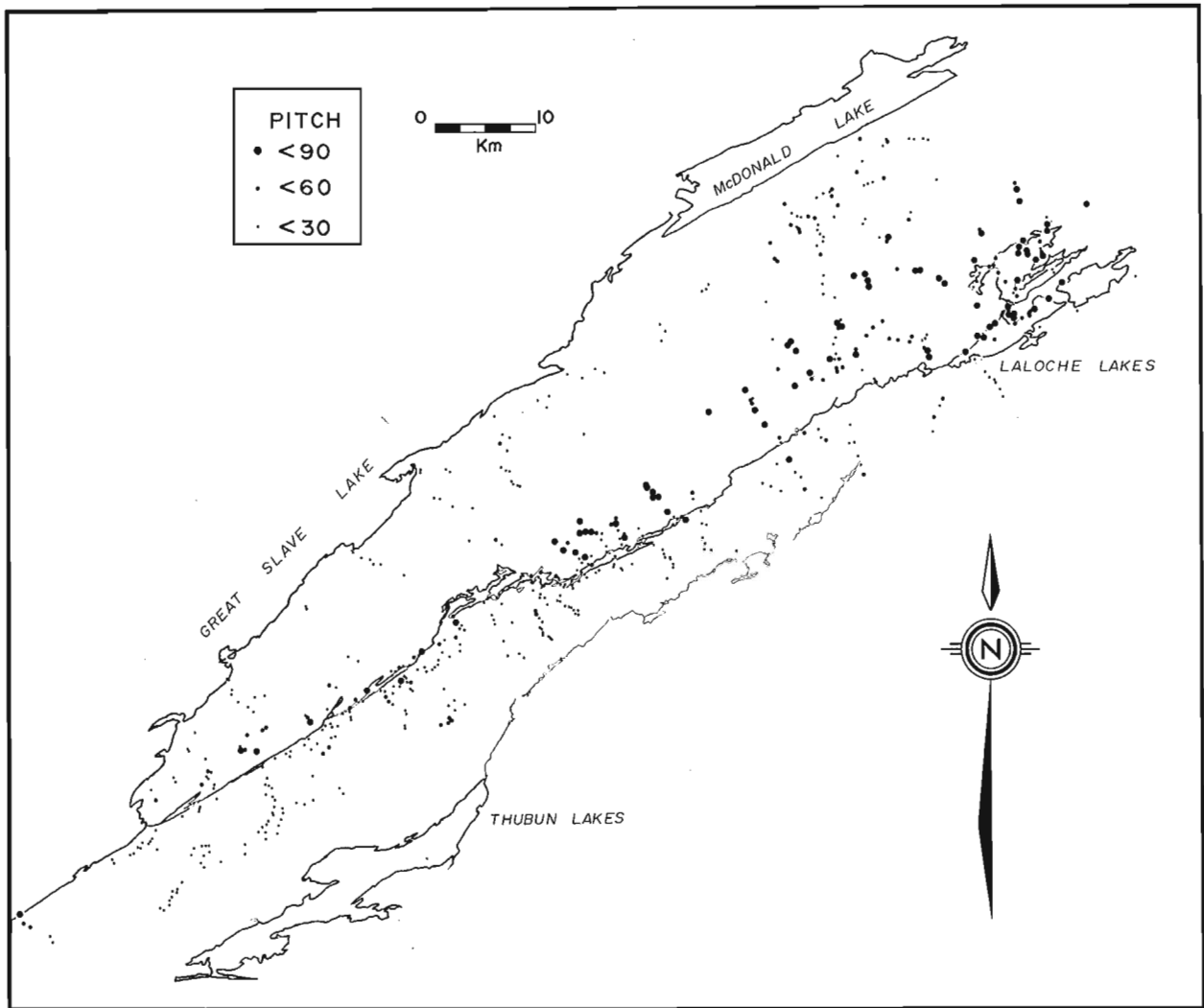


Figure 86.4. Extension lineations in the Great Slave Lake Shear Zone expressed as pitch in the foliation plane. See text.

lithological map units correspond very closely with the anomaly pattern on the 1:250 000 scale aeromagnetic maps of the area (Geological Survey of Canada, 1964a, b).

All of the structural belts show an upright, northeast-striking foliation and layering (Fig. 86.3A) and a shallowly plunging extension lineation (Fig. 86.4B). The main exceptions are (1) the disrupted foliation and layering in the southeast part of belt no. 1 and (2) a corridor of mixed shallow and steep extension lineations located along the Laloche River and widening in the vicinity of Laloche Lakes. The corridor of mixed lineation orientation lies immediately northwest of belt no. 3 and is narrow (5 km wide) within the LRUB and the southeast margin of belt no. 2, widening (10 km) within belt no. 1. We present a map of lineation pitch (Fig. 86.4) to filter out the effects of disruption in belt no. 1 and to highlight our observation that the corridor of mixed extension lineations contains lineations subparallel to foliation dip, while elsewhere lineations are subparallel to strike. It also shows that the corridor of mixed extension lineations is less pronounced southwest of Avocado Lake.

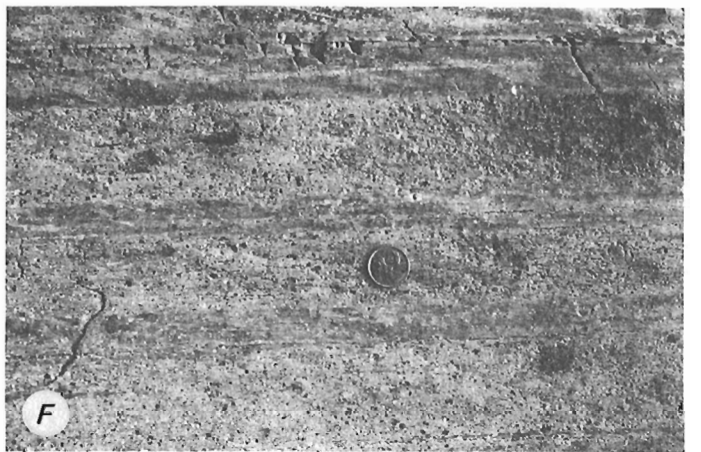
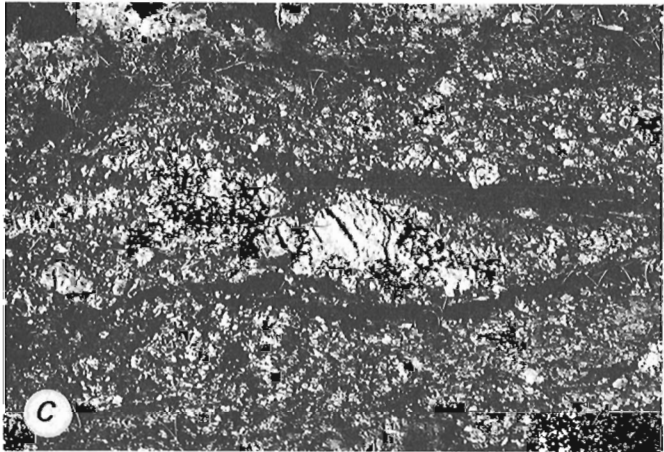
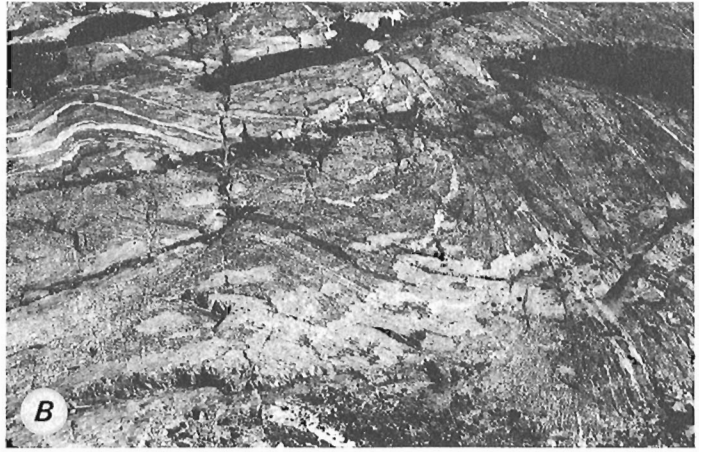
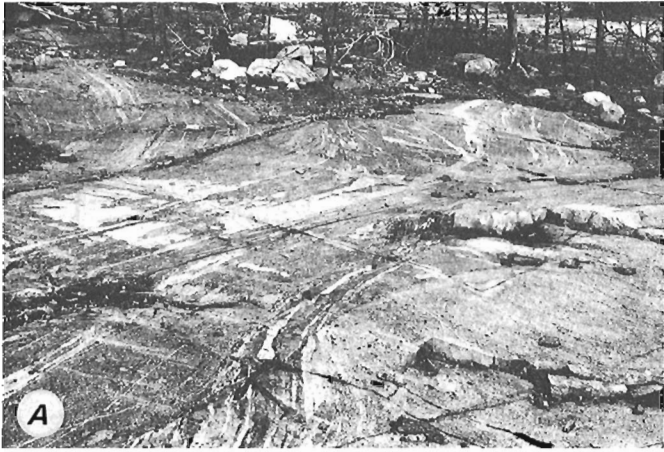
Belt no. 1

Our attempt to firmly establish the southwest limit of the characteristic granulite facies disrupted straight gneisses, mylonites and extensive block gneiss

(unique to this belt) of belt no. 1 was frustrated by the complexity of late brittle faulting along vertical NNE and NW striking planes (Fig. 86.1). Displacement on these faults is usually unknown, but has brought fault bounded areas of obvious belt no. 1 material into the plane of the map, surrounded on all sides by recognizable upper amphibolite facies homogeneous granitic mylonites and mylonitic paragneiss of belt no. 2. This suggests a steep movement vector on at least some of these faults, cutting across a shallowly dipping boundary between the two belts in this area. Is belt no. 1 wedging out southwestwards in both the horizontal and the vertical planes? Locally the fault intercalation is too complex to resolve even at our mapping scale (blank area in Fig. 86.1).

Mylonite, and even sugary (granoblastic) ultramylonite, extensively developed along the northwest boundary of belt no. 1 and derived from relatively homogeneous megacrystic garnet-biotite meta-granite (similar to that commonly containing metamorphic orthopyroxene at Laloche Lakes), are identical to those previously described from within the belt. They lie southwest along strike from the "greasy" suspected granulite facies sugary straight gneisses previously reported along this boundary.

A widespread array of irregular veins and small bodies of 'vein leucogranite' (Hanmer and Lucas, 1985) crosscuts the granulite facies gneisses and mylonites. We have observed



these veins deformed and transposed into the discordant ductile shears responsible, in great part, for the disruption of the straight gneisses and mylonites (Fig. 86.5A, B). This confirms the suggestion that the disruption was due to continued post-granulite movement in the adjacent post 'vein leucogranite' belts no. 2 and 3.

Belt no. 2

This belt is dominated by pink, finely homoclastic protomylonites, commonly passing into mylonites, locally to ultramylonites. However, homoclastic mylonite predominates on the southeastern side of the belt, north of Avocado Lake (Fig. 86.6A). Long, narrow (30-40 km x 0.5-3 km) strips of a supracrustal assemblage of aluminous paragneiss, less aluminous quartz-plagioclase-biotite gneiss, calc-silicate, finely banded amphibolite gneiss and white leucogranite outcrop within the pink granite protomylonites and mylonites. Progressive sheeted contacts between pink granite mylonite and the aluminous paragneisses indicate that the granite protolith intruded the supracrustal rocks.

It was previously speculated that the very clean white leucogranite, containing lilac garnets identical to those in aluminous garnet-cordierite-sillimanite-biotite paragneiss, might be the product of partial melting of the paragneiss. New observations confirm this speculation. (1) The garnet leucogranite is exclusively associated with the aluminous paragneiss in the strips of supracrustal rocks. (2) The full range of metatexite through to diatexite structure, as described by Mehnert (1968) and Brown (1973), is present in the association i.e. intercalation of white garnet leucogranite leucosome in aluminous paragneiss "paleosome", with continuous layering; disrupted and misoriented blocks of the same, isolated in white garnet leucogranite leucosome; white garnet leucogranite with a wispy relict layering of sillimanite-biotite melanosome, plus scattered lilac garnets and common development of isolated, fist-size K-feldspar porphyroblasts (Fig. 86.5C). These migmatites are variably strained. Within a given outcrop, mylonitic to ultramylonitic straight layered gneiss, clearly derived by the tectonic transposition of migmatitic structure, is crosscut by strongly foliated and tightly folded mature metatexite to inhomogeneous (at outcrop scale) diatexite, which is in turn crosscut by isotropic

homogeneous diatexite (Fig. 86.5D) containing few misoriented xenoliths of metatexite. No time correlation between outcrops is implied here. However, it is clear that the process of mylonitization is both preceded and followed by migmatization (in-situ melt production). This re-enforces the contention that the mylonitization of belt no. 2 occurred at upper amphibolite facies conditions.

Two large elongate granite plutons lie within belt no. 2 (Fig. 86.1). They were emplaced post-tectonically with respect to the upper amphibolite facies mylonitization in belt no. 2, but are syntectonic with respect to the later chlorite grade mylonitization in the LRUB (see below). However, since they strongly influence the map pattern and the preservation of mylonitic texture in belt no. 2, it is appropriate to describe these granites here. The larger of the two, the Second Lake granite (new name), is an equigranular, mostly isotropic, medium to coarse, biotite-bearing leucocratic granite. Locally it carries scattered K-feldspar megacrysts up to several centimetres long. Previously it was inadequately described as "zoned". Our work shows that the pluton (30 x 5 km) extends from a line through Hook Point and Avocado Lake northeastwards to its termination south of McDonald Lake. It is flanked on either side by zones, at least a kilometre wide, of progressive outwards increase in the proportion of large misoriented xenoliths/rafts of foliated granite mylonite passing into granite mylonite country rock with abundant veins of isotropic equigranular leucocratic granite and quartz-feldspar pegmatite. These zones are classical vein aureoles, typical of the intrusive contacts between a pluton and its country rock. The lateral vein aureoles coalesce in the plane of the map and the granite sheet passes along strike to the southwest into a single 5 km wide vein aureole extending over 20 km to Second Lake. If the coalescing of lateral vein aureoles represents the transition from the walls to the roof of the pluton, then the 'V'-shaped map pattern suggests that the roof of the elongate pluton dips gently to the southwest and is cut at a very low angle by the present erosion surface. Areal smaller, texturally and compositionally identical vein aureoles occur elsewhere in belt no. 2, principally between Second Lake and the mouth of the Laloche River, and between Hook and Finger points. In each of these areas, veined country rock is volumetrically dominant over concordant sheets (up to 1 km thick) and patches of clean isotropic granite which possibly represent parts of the still buried plutons which the vein aureoles surround.

Figure 86.5. Disrupted straight gneiss from belt no. 1.

- (A) A shear zone (top right to bottom left) cuts across straight gneiss, derived by deformation of megacrystic granite, whose layering (top to bottom) is preserved in 3 shear-bounded pods (top left and right plus bottom right). Hammer for scale (centre right). GSC 204337-C.
- (B) Detail of the shear-bounded margin of a pod of straight gneiss derived by the deformation of megacrystic granite with amphibolite inclusions. Field of view 3m. GSC 204335 H. The straight gneisses and the bounding shears are composed of mylonite in both examples. Migmatites from belt no. 2.
- (C) Very coarse inhomogeneous diatexite with large K-feldspar porphyroblasts and aligned biotite-sillimanite schlieren. GSC 204337-A.
- (D) Metatexite layering cut by near isotropic coarse garnet leucogranite leucosome. GSC 204337-C.
- (E) A vertical sheet of isotropic equigranular granite cutting across the contact between megacrystic Falls Lake granite (upper slope) and garnet-sillimanite-biotite migmatite (lower slope). GSC 204337-B.
- (F) Bands of heteroclastic mylonite derived from grey biotite granodiorite alternate with bands of pink homoclastic granite mylonite, belt no. 3. The textural difference is a function of plagioclase/K-feldspar ratio rather than age of the protolith. GSC 204336-K.

The mylonitic texture of the country rock, present both as xenoliths and as wall rock in the vein aureoles, has been intensely, as well as extensively, modified by the thermal and hydrothermal effects of the equigranular granite and associated pegmatites. Our observations are: (1) The finely homoclastic protomylonites and mylonites, locally carrying strips of transposed paragneiss and amphibolite, which dominate belt no. 2 away from the Second Lake granite, can be traced progressively into an homogeneous, fine grained, granoblastic foliated meta-granite in the vein aureoles, which also contains long, straight, highly attenuated strips of amphibolite. (2) Commonly the meta-granite foliation is weakened by the coarsening of pre-existing quartz and feldspar and by growth of feldspar porphyroblasts. The latter may also form nebulous isotropic veins crosscutting the meta-granite foliation. (3) Within the meta-granite of both the xenoliths and the vein aureoles, mylonitic texture (i.e. a very fine grained matrix containing a macroscopically visible, distinctly coarser grained porphyroblast population) is locally present in irregular patches. These observations indicate that the meta-granite here is a recrystallized and coarsened mylonitic rock, derived from finely homoclastic protomylonite and associated mylonite.

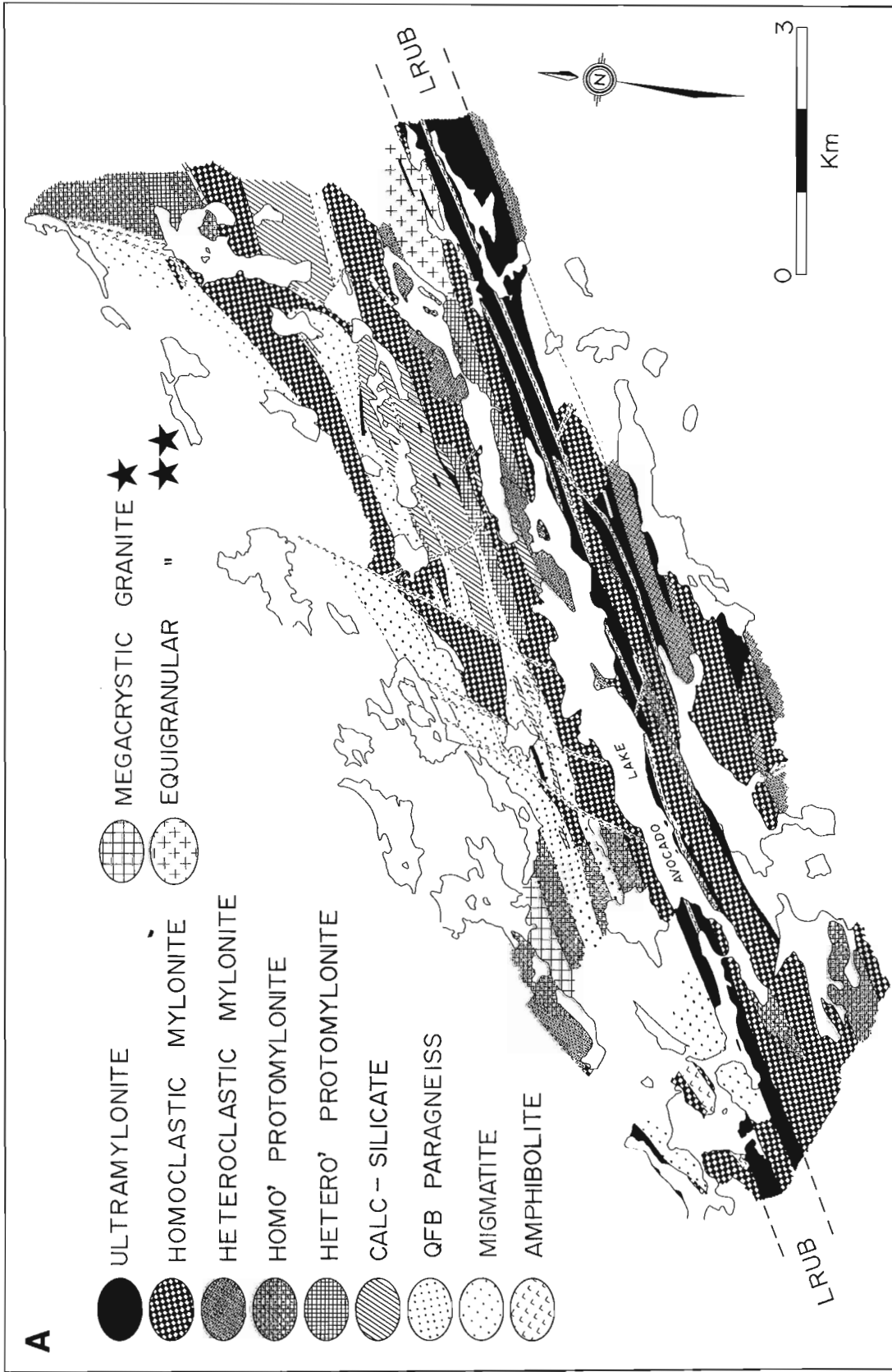
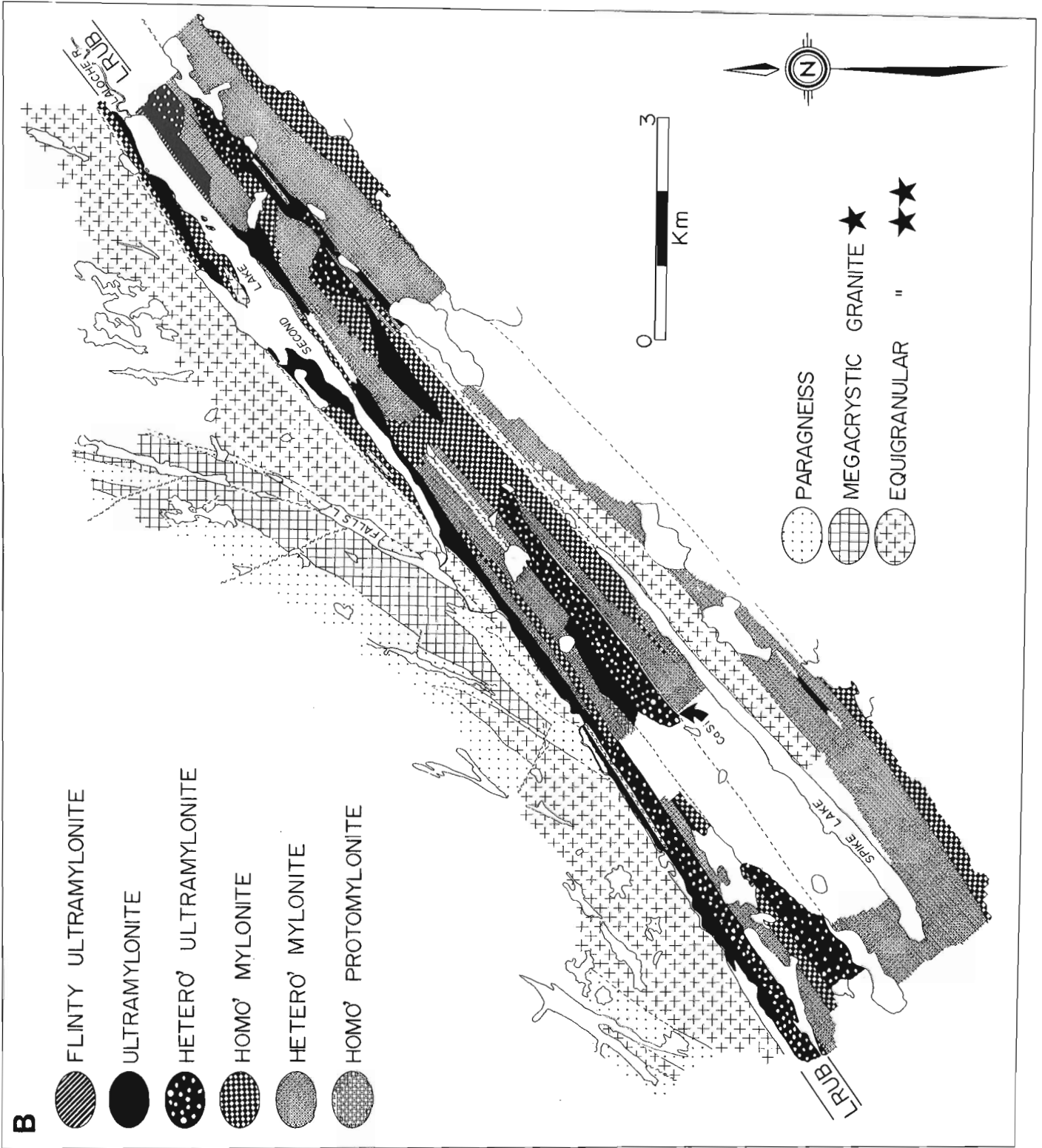


Figure 86.6. (A) and (B) Detailed maps of textural transitions in mylonitic rocks of belt no. 2 and belt no. 3, adjacent to the Laloche River. (★) Falls Lake granite. (★★) Second Lake granite, except along the southwest side of Spike Lake calc-silicate. All faults (broken squiggly lines) have been walked out. See Figure 86.2 for location and text for discussion.



Locally, the meta-granite foliation and thin (10 cm) veins of granite and pegmatite are deformed around steeply to shallowly plunging, moderate to tight folds. An axial planar foliation is common in the pegmatite veins. Whereas folds of mylonitic foliation are not common elsewhere in belt no. 2, they are a characteristic feature of the vein aureoles and, along with the abundant equigranular granite and pegmatite sheets, lend an highly disturbed appearance to the outcrop. We suggest that the thermal effect of the veining, plus the rheological heterogeneity which their emplacement induced, allowed the vein aureole materials to deform in response to, probably fairly weak, regional or local stresses. Previously, such irregular looking tectonites were erroneously interpreted as low strain protolith to the homoclastic protomylonites.

On the northwest side of the Second Lake granite (Fig. 86.1) lies an anastomosing array of vertical sheets, each up to several kilometres thick, of homogeneous, coarse grained, leucocratic, megacrystic biotite granite, the Falls Lake granite (new name). The euhedral K-feldspar megacrysts, up to 10 cm long and set in a very coarse isotropic matrix, may be aligned in a vertical 060° trending plane, indicating magma flow parallel to the regional structural grain. Furthermore, small scale 'Z' folds, 25 cm in amplitude, developed in the contact between aluminous paragneiss and isotropic granite (southwest of Second Lake) suggest that the magma flow was associated with dextral shear along its southeast margin, the significance of which remains ambiguous. The scarcity of xenoliths of wall rock may indicate an highly viscous magma. A tectonic foliation is locally superimposed on this magmatic flow alignment, rounding off the corners of the still monocrystalline megacryst cores. The contacts of the granite with the homoclastic protomylonites, mylonites and the metatexites-diatexites of belt no. 2 are all clearly intrusive. Wherever the isotropic granite divides into two sheets surrounding a pod (up to 3 km wide) of aluminous paragneiss, the foliation and layering of the aluminous paragneiss remain straight and parallel to the regional 060° strike and are cut across by the granite. However, not all of the curved 'V'-shaped, paragneiss/granite contacts are the result of intrusive interdigitation. Just southwest of Second Lake (Fig. 86.6C) the paragneiss layering and the concordant granite contact are both deflected about a moderate, upright, horizontal fold, to which the tectonic foliation developed in granite is axial planar.

Clearly, both the Second Lake granite and the Falls Lake granite were emplaced after the upper amphibolite facies deformation and metamorphism of belt no. 2, but have been subjected to at least local tectonic stresses. The Falls Lake granite is locally cut by 20 m wide, NW trending vertical sheets of isotropic equigranular granite (Fig. 86.5E), several kilometres long and identical to the Second Lake granite. Such veins have not been traced into the main Second Lake granite outcrop, but we suggest that they indicate that the Second Lake granite is younger than the Falls Lake granite. The mylonitic textures of the country rocks in contact with the Falls Lake granite are not markedly modified. However, sillimanite and garnet in the paragneisses are unaltered to within 2 m of the granite contact. This, in conjunction with the paucity of associated pegmatite and the possibly elevated magma viscosity, suggests that the Falls Lake granite was relatively dry throughout its crystallization history and that it had little hydrothermal effect on the wall rocks.

Belt no. 3

Although identified last year by Hanmer and Lucas (1985), most of this belt was mapped this season. We confirm and extend their description. The belt is dominated by

heteroclastic and homoclastic mylonites derived from a remarkably homogeneous leucocratic megacrystic granite. Most striking are the two continuous ultramylonite belts located along the northwest and southeast flanks of belt no. 3. The former, although adjacent to, is quite distinct from the chlorite grade ultramylonites of the LRUB (Fig. 86.6B). Belt no. 3 as a whole is very straight and of constant width (circa 5 km), except for a constriction just west of Jigsaw Lake (Fig. 86.1) where it narrows to about 2 km. Shear sense criteria (Hanmer, 1984a; Hanmer and Lucas, 1985; Hanmer, 1986) are all sinistral in the southwestern part of the constriction. This is the only really significant exception to the dextral shear sense of the GSSLZ and clearly suggests that the constriction is the result of anomalously strong subhorizontal NE-SW extension of this part belt no. 3.

Most of the mylonite and ultramylonite of belt no. 3 is granite in composition and is visibly derived from a coarse leucocratic megacrystic biotite granite which is locally preserved. The one exception observed is the strip of coarse, subsisotropic, equigranular biotite granite protolith along the southeast side of Spike Lake (Fig. 86.6B), very similar to the Second Lake granite. However, not uncommonly, the mylonites are compositionally banded on a 20 cm scale where grey-pink (granodioritic?) mylonites with a somewhat higher plagioclase and biotite content alternate with the pink granite mylonites (Fig. 86.5F). In very few places, e.g. east of Barrier Lake (Fig. 86.6C), these two lithologies occur in pods of relatively low finite strain where it is clear that both are derived from megacrystic granitic protoliths. The granite cuts the granodiorite. We note that superficially the biotite granodiorite resembles the biotite-rich megacrystic granite of belt no. 1 at Laloche Lakes (Hanmer and Lucas, 1985).

Of major importance is the discovery, in the vicinity of Spike Lake (Fig. 86.6B), of two strips of muscovite-bearing aluminous paragneiss and calc-silicate, associated with minor amphibolite gneiss layered on the scale of centimetres, plus sheets of white leucogranite carrying small lilac garnets, which all together constitute a very straight layered gneiss. This gneiss is lithologically identical to the supracrustal assemblage of belt no. 2, although no sillimanite was observed in the field. The association of aluminous paragneiss with garnet leucogranite in a schistose garnet-biotite-muscovite paragneiss suggests that this straight gneiss is the tectonically transposed equivalent of a metatexite. If true, this would support the suggestion that belt no. 3 had earlier undergone a similar tectonometamorphic history to that of belt no. 2 and has since been further mylonitized and metamorphically retrograded.

Over much of its length, the boundaries of belt no. 3 are marked by strips of ultramylonite, 2 km wide along the southeast side and 1 km wide along the northwest side. However, in the Laloche Lakes area, where belt no. 3 is dominated by finely homoclastic protomylonite, the ultramylonites, while still present, are of lesser importance (Fig. 86.1). Does this herald northeastward attenuation of belt no. 3? We note that the ultramylonites on the northwest side here, while discontinuous, are, nevertheless, several hundred metres thick and that the southeastern contact here is poorly exposed and appears to be fairly abrupt. In conjunction with the presence of discontinuous quartz stockwork, this suggests that the latter contact has been modified by later brittle faulting.

Between the Jigsaw Lake constriction and Thubun Lakes, the southeastern boundary of belt no. 3 is well exposed and has been examined in some detail. The structural boundary zone is superimposed on a lithological contact zone. On the northwest side of the contact zone, the ultramylonites

are uniformly pink and of granite composition. On the southeast side they are pink, dark grey or white, in alternating strips. The dark grey mylonites are biotite rich, quartzofeldspathic and contain garnet and muscovite. The white mylonites are leucocratic, quartzofeldspathic and contain lilac pin-head garnets. The lithological contact is effected by progressively increasing intercalation of grey and white mylonite within the pink until the grey and white mylonites become volumetrically dominant. Farther to the southeast the foliation progressively decreases in intensity as the compositional layering becomes more irregular. Within approximately a kilometre of the limit of the ultramylonites, the gneiss is a recognizable, commonly highly contorted, cordierite-garnet-sillimanite-biotite mature metatexite to diatexite, with no pink granite. A poorly foliated homogeneous coarse white granite with sporadic garnets encountered on some traverses, is thought to be the ultimate melt product of these migmatites. We interpret these observations as the progressive sheeted intrusive contact of the megacrystic granite(s) precursor to the belt no. 3 mylonites, emplaced into upper amphibolite facies migmatites. We do not know if the emplacement was syn- or post-migmatization.

The Laloche River ultramylonite belt (LRUB)

The upper amphibolite facies mylonites and aluminous paragneisses of belt no. 2 and the lower amphibolite or upper greenschist facies mylonites of belt no. 3 are everywhere separated by a 1 km wide strip of chlorite-grade pink, grey to grey-green, ultramylonites; the LRUB. The ultramylonite is generally too fine grained for any compositional variation to be readily identified in the field, although colour banding is present. Three textural varieties occur: (1) aphanitic, showing good foliation on weathered surfaces; (2) aphanitic and flinty with no foliation; (3) heteroclastic ultramylonite. The contact of the LRUB with belt no. 2 is faulted at Second Lake, and probably to the southwest where it is occupied by the Laloche River. The bend in the Laloche River northeast of Second Lake (Fig. 86.6C) marks a short splay off of the LRUB cutting into belt no. 2, less than 10 km long. It ends in an area of poor exposure. Between the two branches of the LRUB (Fig. 86.6B), a 50 m scale "mesh structure" (Sibson, 1979), i.e. a zone of strongly heterogeneous deformation, is developed where anastomosing strands of chlorite ultramylonite, up to several metres wide, isolate 10-50 m wide elliptical pods of recrystallized biotite-bearing granite

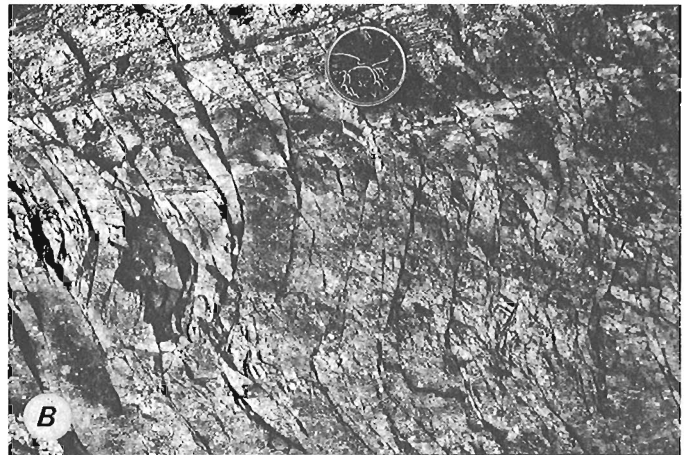


Figure 86.7. Laloche River Ultramylonite belt. (A) Shear bounded pod in 'Mesh' structure. GSC 204337-D. (B) Incipient stage of non-disruptive brecciation of ultramylonite. Note sigmoid geometry of spaced fractures. GSC 204337-F. (C) E-W dextral faults cut mature non-disruptive breccia derived from ultramylonite. Note anticlockwise rotation of the colour banding. GSC 204336-W. (D) Disruptive emplacement of pseudotachylite into fractured and dilated ultramylonite. GSC 204337-G.

mylonite with amphibolite layers and inclusions (Fig. 86.7A). The internal layering of these pods, commonly highly discordant to the enveloping ultramylonite strands, is commonly irregularly folded and may be cut by veins of foliated equigranular granite. To the northeast, the belt no. 2 – LRUB contact lies under Avocado Lake (Fig. 86.6A), to the northeast of which it is occupied by a 25 m wide quartz stockwork in a fault. With the exception of the southeast shore of Barrier Lake (Fig. 86.6C), the belt no. 3 – LRUB boundary is everywhere a progressive contact zone. Pink mylonites, with small scattered amphibolite and biotite-rich metasediment inclusions, pass northwestward into grey/white/green to pink ultramylonite with slivers of fine chlorite phyllite.

Isolated, narrow (several metres) zones of chlorite grade ultramylonite occur within biotite mylonites to the southeast of the LRUB, within the belt no. 2 tectonites and the Second Lake granite. From this we conclude that the LRUB is younger than the tectonites of the adjacent belts. Between Avocado and Second lakes the LRUB ultramylonites are cut by thin sheets of foliated, but non-mylonitic, equigranular granite identical to the adjacent Second Lake granite. Furthermore, as shown above, the Second Lake granite is syntectonic. From this we conclude that the Second Lake granite is syntectonic with respect to the chlorite ultramylonites of the LRUB.

The ultramylonites are pervasively brecciated throughout much of their thickness in both branches of the LRUB. The brecciation resulted in little or no dilation or quartz mineralization and therefore took place at significant confining pressures. Brecciation occurred by the repeated formation of arrays of centimetre-spaced, en-echelon (shear?) fractures, oriented 45° clockwise to the mylonite foliation (Fig. 86.7B). With progressive deformation the central sections of each fracture of the array, and the intervening rock slices, rotated clockwise through the normal to the mylonitic foliation to positions 45° anticlockwise with respect to the undisturbed mylonite foliation. The end sections of the fractures remain undisturbed, as is the mylonite foliation between them, i.e. the mylonite slabs are bent, so brittle and ductile behaviour were coeval. We propose that at a critical angle the rotation of a given set of fractures was no longer able to accommodate the imposed strain rate and a new crosscutting set formed within the same pseudo-coherent volume of rock, effectively delimiting centimetre-scale breccia fragments which do not show evidence for significant angular misorientation (disruption) between near neighbours. We refer to this as non-disruptive brecciation.

The breccia is cut by discrete, straight E-W faults, up to several metres long, fairly regularly spaced at approximately metre intervals, which systematically offset the still coherent layering/colour banding in the brecciated ultramylonite (Fig. 86.7C). The angle made by the faults with the colour banding remained constant as the faults rotated anticlockwise with increasing strain. The faults are sufficiently common to effect a systematic rotation of the ultramylonite foliation from 060° towards an 030° strike (Fig. 86.3A), or may result in local dispersal of foliation dip and strike. Locally the ends of these faults can be traced into similar scale faults parallel to the LRUB trend. No significant quartz mineralization is associated with any of these faults.

The breccias are cut and infiltrated by veins of black pseudotachylyte, varying in width from millimetres to tens of centimetres (Fig. 86.7D). Major, 25m wide, quartz stockworks are associated with late, very long, straight fractures. They cut all of the rocks and structures described above, but may themselves be cut by pseudotachylyte; good examples occur along Avocado Lake. Of particular interest

is the quartz stockwork at the northeast end of Spike Lake, which lies well within belt no. 3 (Fig. 86.6B). It can be traced to the northeast, passing close to Barrier Lake (Fig. 86.6D), into Avocado Lake where it lies within the LRUB (Fig. 86.6A). From here, it projects along the strike of the LRUB through Avocado Lake. Northeast of Avocado Lake it outcrops continuously along the LRUB to give a total strike length of 40 km. Since the stockwork cuts across the LRUB boundary but does not detectably offset it, the fracture in which it lies does not have a significant lateral displacement.

The sequence of structures described from the LRUB, and the changing mechanical nature of the tectonites with time strongly suggest that the LRUB preserves a complete record of the brittle-ductile transition, from ductile ultramylonite, via semi-brittle non-disruptive brecciation (low temperature, significant pressure), to spaced faulting and finally quartz stockworks in dilational fractures. Ductile shear-sense indicators in the ultramylonites are consistently dextral. The rotation of fractures through the normal to the undisturbed mylonitic foliation also indicates a distributed bulk dextral shear along the LRUB foliation direction. Interpreting bulk kinematics from slip on a single set of straight faults is equivocal (Freund, 1974). However, the observations we have presented concerning straight E-W faults are not incompatible with initiation and continued slip of fractures within the shortening quadrant of continuing dextral shear along the LRUB foliation direction, associated with an unknown, but possibly significant, component of shortening across the shear plane.

The Hornby Channel ultramylonite belt (HCUB)

We propose to rename the chlorite grade External Belt of Hanmer and Lucas (1985) the Hornby Channel Ultramylonite belt (the HCUB) in order to emphasise its similarities with the LRUB. Most of the HCUB was mapped last summer. Our work, concentrated at the southwestern end and the Finger Point – McDonald Lake section (Fig. 86.1), confirms and extends the previous results. Of interest is the frequent brecciation of the ultramylonites, very similar to that described for the LRUB, which is especially well developed at the southwestern end of the belt. We note that the LRUB and the HCUB are both chlorite grade dextral transcurrent tectonite belts of similar width. We suggest that they probably formed at the same structural depth, and at about the same time.

Mafic dykes

Two kinds of mafic sheet were previously reported within belt no. 2; (1) deformed and metamorphosed (amphibolite) dykes and (2) half a dozen examples of diabase dykes. We confirm these observations and extend them to belt no. 3. The occurrence of a swarm of diabase dykes, syntectonic with respect to the HCUB, on the northwest side of the GSLSZ, (Hanmer and Lucas, 1985), coupled with the observation that the metamorphosed dykes within the GSLSZ are late syntectonic with respect to deformation in their respective belts, lends support to Hanmer and Lucas' speculation that there were several periods (or a continuum?) of mafic dyke injection throughout the structural life of the GSLSZ.

Laloche Batholith

Megacrystic granite to granodiorite is the main protolith of the extensive mylonites of the GSLSZ (see also Hanmer and Lucas, 1985). The oldest granite protolith is the biotite-rich megacrystic granite of belt no. 1. Its tectonite derivatives are cut by the 'vein leucogranite' which is itself transposed in the younger no. 2 and no. 3 belts (Hanmer and Lucas, 1985). The main leucocratic megacrystic granite

protolith in belt no. 3 contains xenoliths which lithologically resemble belt no. 1 megacrystic granite. Is belt no. 3 leucocratic megacrystic granite protolith the plutonic source of the 'vein leucogranite' in belt no. 1? Since the veins are also present in belt no. 3, is the 'vein leucogranite' a late veining phase of the megacrystic granite? No field age relations with respect to belt no. 1 protolith are available for the leucocratic megacrystic granite protolith of belt no. 2. Lithologically, it closely resembles that in belt no. 3 and bears a similar relationship to the 'vein leucogranite' of belt no. 1. The leucocratic megacrystic Falls Lake granite and the younger equigranular Second Lake granite both postdate the upper amphibolite facies mylonitization in belt no. 2. The Second Lake granite is demonstrably younger than the mylonitization in belt no. 3 since it is syntectonic with respect to the lower greenschist facies the LRUB. There are no post-tectonic granites. Clearly, a volume of granite of batholithic proportions was emplaced into the GSSLZ during the course of its tectonic activity.

We cannot delimit individual plutons within the granite protolith. However, we note that the strips of aluminous paragneiss, included within and intruded by the granite in belt no. 2, are of such dimensions that, even in two dimensions, they appear to have been equal in undeformed size to that expected of an individual pluton (e.g. Pitcher, 1978) in a batholith, rather than deformed included xenoliths. Abundant, smaller inclusions occur in belt no. 1 granites. Similar paragneiss inclusions, while present, are very much smaller and much fewer in number in the granite of belt no. 3. Thus there is clearly a bulk compositional boundary within the protolith of the GSSLZ at the northwest limit of belt no. 3. On account of their size, we suggest that the aluminous paragneiss strips in belt no. 2 are deformed screens of country rock between plutons making up a batholith. This would require that the plutons be sufficiently spaced apart to preserve the country rock screens and, by the same token, suggests that the absence of similar screens in belt no. 3 reflects a closer spacing of the plutons. No megacrystic granite is reported from the Great Slave Lake area northwest of the HCUB (Stockwell, 1932; Wright, 1968a, b; Reinhardt, 1969; Hoffman et al., 1977). We have shown that the southeastern structural boundary of the GSSLZ coincides with the intrusive boundary of the megacrystic granite protolith of belt no. 3. We therefore suggest that the GSSLZ was active during the emplacement of a granite batholith with which it is spatially coincident and which we propose to call the Laloche Batholith.

The local occurrence of hornblende has previously been reported in the Falls Lake and Second Lake granites as well as within the granite tectonites of belt no. 1. We extend this observation to all granitic rocks of all belts. It is clear that the proportion of hornblende contained by the granites is a direct function of the proximity to swarms of amphibolite xenoliths within the otherwise leucocratic biotite granite. Indeed, the margins of the amphibolite xenoliths commonly grade into an amphibole-rich host whose quartzofeldspathic component is of granite composition. We therefore suggest that the hornblende in the granites is a contaminant, xenocrystic or chemical. We note that while the amphibolite xenoliths are commonly in a part "digested" state, suggesting prolonged interaction with granite magma, the contacts of the granite with aluminous paragneiss inclusions are invariably sharp, perhaps suggesting a relatively short period of chemical interaction.

Deformation

Hanmer and Lucas (1985) reported an assemblage of mechanically independent shear sense indicators which, with few exceptions, indicate an history of dextral displacement.

We confirm these observations and can extend them to belt no. 3 and the LRUB (Fig. 86.8). The significant occurrence of sinistral shear in belt no. 3 has already been discussed.

The corridor of mixed steeply and shallowly plunging extension lineations presents a kinematic anomaly within the GSSLZ. Careful observation shows that the slip vector is locally parallel or locally normal to the steep extension lineation in the same outcrop and, where it is parallel, it can show southeast side either up or down. At its widest part, the corridor occurs within the disrupted, heterogeneously deformed granulites of belt no. 1. Southwest of belt no. 1, the corridor lies mostly within the upper amphibolite mylonites and paragneiss of belt no. 2, but also within the lower greenschist ultramylonites of the LRUB. In the former, there are local indications of heterogeneous deformation, mostly in the form of 5-100 m wide nests of 1-10 m wavelength folds deforming the mylonitic foliation, around which the external mylonitic foliation passes. Although much of the LRUB ultramylonite has been subsequently reoriented by the E-W faulting described above, steep lineations are seen where the vertical foliation strikes 060° , i.e. is undisturbed. However, we cannot say that the steep lineations are associated with syn-metamorphic heterogeneous strain as in the other two belts. We emphasise that: (1) The mixed lineations are developed in a corridor of heterogeneous strain within which elliptical relatively stiff pods of lower strain are separated from each other by anastomosing high strain bands. (2) The corridor is more extensively developed in the drier, stronger granulite facies tectonites and is least pronounced in those rocks which deformed under the wetter conditions of the lower greenschist facies. (3) The corridor existed at least as early as the main syn-metamorphic activity in belt no. 2 and was active to the end of ductile deformation in the GSSLZ. (4) The corridor is located along a bulk compositional boundary within the Laloche Batholith.

We therefore suggest that the northwest contact of belt no. 3 represents a rheological interface within the Laloche Batholith and that the heterogeneous strain on its northwestern side is a result of strain incompatibilities across that interface. The steep lineations formed as a result of local shortening across the flow plane (transpression) as elliptical pods of relatively stiff material attempted to move past each other. Such movement may have been lateral, or vertical where relative displacement between two pods squeezed out a third one caught between them. If this is reasonable, then the main plutonic architecture of the batholith was in place even during the high grade early history of the GSSLZ. It is interesting to note that the southeastern, and what would appear to be the northwestern, contacts of the Laloche Batholith have localized the ultramylonites of belt no. 3 and the HCUB. The southeastern boundary of belt no. 3 even contains a narrow (100 m) band of chlorite ultramylonite, just southwest of the constriction west of Jigsaw Lake, suggesting that this contact played a further role in localizing the latest minor ductile movements.

A number of brittle faults of significant length, oriented oblique to regional strike, occur mostly within belt no. 2 and at the southwestern end of belt no. 1 (Fig. 86.1). In other words, they occur between, but do not significantly displace, the LRUB and the HCUB. There are two important orientation sets; NNE-SSW and E-W. An example of the latter occurs near the southwest end of Avocado Lake. Locally it is mylonitic with dextral shear bands, develops dextral en-echelon quartz tension gashes where it is purely brittle and dextrally offsets the Second Lake granite boundary (Fig. 86.1). This fault seems to be a larger scale equivalent to those seen within the LRUB. Good examples of the NNE-SSW set occur north and northeast of Avocado Lake, and sinistrally offset the Second Lake granite boundary

(Fig. 86.1). These two fault sets are geometrically conjugate and are commonly lined with chlorite-bearing non-disruptive breccia. We suggest that they are synchronous with movements on the LRUB and the HCUB into which they root without significantly offsetting them. Furthermore, they may allow semi-brittle distortion (strike-parallel extension) of the rigid belt no. 2, caught between the active LRUB and the HCUB, at least during the brecciation phase of their activity.

Finally we note that throughout the history of the GSLSZ, transcurrent shear appears to be associated with at least local components of extension along the bulk shear plane. At the scale of structures such as the Jigsaw Lake constriction, and perhaps at larger scale too, finite strain is not ideal simple shear. This is comforting, since the presence of shear sense indicators such as shear bands and rotated winged inclusions require boundary conditions which deviate from those of simple shear (see Hanmer, 1984a).

Geochronology

U-Pb geochronological study of zircons from syntectonic granites in the GSLSZ is presently being undertaken by S. Bowring (Washington University, St. Louis, USA). Preliminary ages for the Falls Lake granite and the Second Lake granite fall within the range 1.91-1.95 Ga. The oldest megacrystic granite from belt no. 1 at Laloche Lakes gives a preliminary age of 2.15 Ga. We cannot determine if this granite was syntectonically or pre-tectonically emplaced. We may, however, confidently conclude that the history of the GSLSZ took place entirely within the lower Proterozoic.

Summary

The Great Slave Lake Shear Zone is a crustal scale, lower Proterozoic, dextral, transcurrent shear zone, up to 25 km wide, made of 5 belts of granulite through to lower

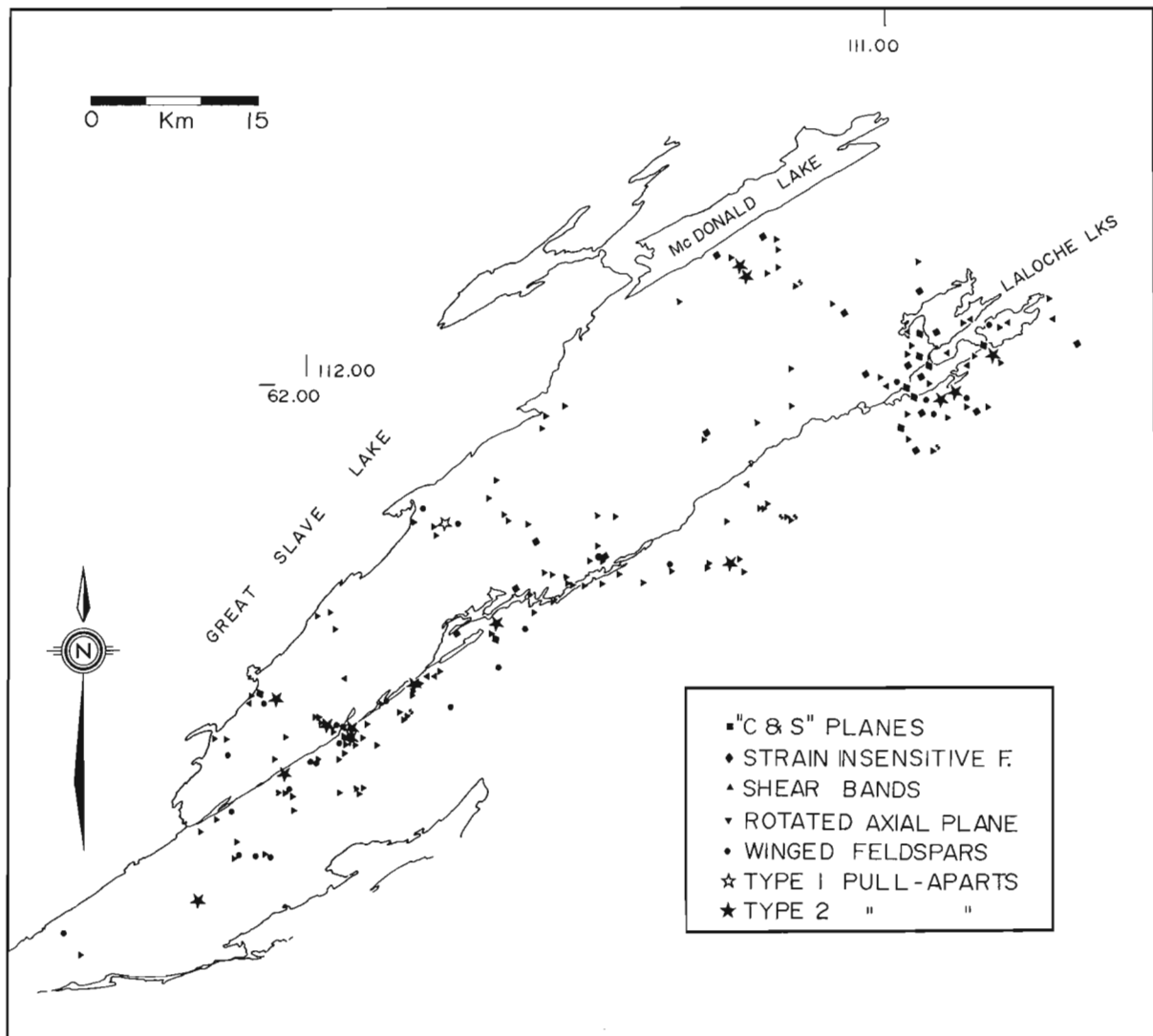


Figure 86.8. Distribution of unequivocal macroscopic shear sense indicators within the Great Slave Lake Shear Zone. The overwhelming majority give a dextral transcurrent sense movement (S = sinistral). The assemblage of mechanically independent structures comprises 'C and S' planes (Berthé et al., 1979), strain insensitive foliation (Means, 1981; Hanmer, 1984b), shear band foliation (White et al., 1980), progressive rotation of fold axial planes with strain, rotated winged inclusions, including feldspars (Hanmer, 1984a) and asymmetrical pull-aparts and foliation fish (Hanmer, 1986).

greenschist facies straight gneisses and mylonites. A batholith, spatially coincident with the site of the GSLSZ, was emplaced incrementally during the major part of the tectonic history of the GSLSZ. With time the metamorphic grade of the actively forming tectonites decreased, the locus of highest strain rate shifted laterally (not centripetally as previously proposed), and the width of the active locus of shearing decreased. Finally deformation passed progressively through the brittle-ductile transition to purely brittle failure. Most of, if not all, the deformation of the GSLSZ represents a single progressive event, which occurred during a period of uplift, unroofing and thermal decay accompanied by on-going syntectonic acid and mafic magma injection.

Acknowledgments

We thank Dianne Paul, Peter Rushforth and Elaine Dodd for their excellent assistance, their unflagging enthusiasm and good company throughout the fieldwork. Special thanks to Martin Irving for excellent expediting. Marc St-Onge and Tony Davidson critically read and much improved the original manuscript.

References

- Berthe, D., Choukroune, P., and Jegouzo, P.
1979: Orthogneiss, mylonite and non-coaxial deformation of granites: the example of the South Armorican Shear Zone; *Journal of Structural Geology*, v. 1, p. 31-42.
- Brown, M.
1973: The definition of metatexis, diatexis and migmatite; *Proceedings of the Geological Association*, v. 84, p. 371-382.
- Freund, R.
1974: Kinematics of transform and transcurrent faults; *Tectonophysics*, v. 21, p. 93-134.
- Geological Survey of Canada
1964a: Taltson Lake, District of Mackenzie, NWT, Geological Survey of Canada, Map 7184G.
1964b: Snowdrift, District of Mackenzie, NWT; Geological Survey of Canada, Map 7189G.
- Hanmer, S.
1984a: The potential use of planar and elliptical structures as indicators of strain regime and kinematic indicators; *in* Current Research, Part B, Geological Survey of Canada Paper, 84-1B, p. 133-142.
- Hanmer, S.
1946b: Strain-insensitive foliations in polymineralic rocks; *Canadian Journal of Earth Sciences*, v. 21, p. 1410-1414.
- Hanmer, S.
1986: Asymmetrical pull-aparts and foliation fish as kinematic indicators; *Journal of Structural Geology*, v. 8, p. 111-122.
- Hanmer, S. and Lucas, S.B.
1985: Anatomy of a ductile transcurrent shear: the Great Slave Lake Shear Zone, District of Mackenzie, NWT (preliminary report). *in* Current Research, Part B, Geological Survey of Canada, Paper 85-1B, p. 7-22.
- Hoffman, P.F., Bell, I.R., Hildebrand, R.S., and Thorstand, L.
1977: Geology of the Athapuscow Aulacogen, East Arm of Great Slave Lake; *in* Current Research, Part A, Geological Survey Paper, 77-1A, p. 117-129.
- Means, W.D.
1981: The concept of steady-state foliation; *Tectonophysics*, v. 78, p. 179-199.
- Mehnert, K.R.
1968: *Migmatites and the origin of granitic rocks*. Elsevier, Amsterdam, 405 p.
- Pitcher, W.S.
1978: Anatomy of a Batholith; Geological Society of London, v. 135, p. 157-182.
- Reinhardt, E.W.
1969: Geology of the Precambrian rocks of Thubin Lakes map area in relationship to the McDonald Fault system, District of Mackenzie (75 E312 and parts of 75 E/13 and 85 H/9); Geological Survey of Canada Paper, 69-21, 29 p.
- Sibson, R.H.
1979: Fault rocks and structure as indicators of shallow earthquake source processes; *in* USGS Open File Report 79/12391, p. 276-304.
- Stockwell, C.H.
1932: Great Slave Lake - Coppermine River area, NWT; Geological Survey of Canada, Summary Report, Pt C, p. 37-63.
- White, S.H., Burrows, S.E., Carreras, J., Shaw, N.D., and Humphreys, F.J.
1980: On mylonites in ductile shear zones. *Journal of Structural Geology*, v. 2, p. 175-187.
- Wright, G.M.
1968a: Christie Bay, District of Mackenzie; Geological Survey of Canada, Map 1122A.
- Wright, G.M.
1968b: Reliance, District of Mackenzie; Geological Survey of Canada, Map 1123A.

Geology of the New Fox alteration zone, Laurie Lake, Manitoba¹

Project 800007

B.A. Barham² and E. Froese
Lithosphere and Canadian Shield Division

Barham, B.A. and Froese, E., Geology of the New Fox alteration zone, Laurie Lake, Manitoba; in Current Research, Part B, Geological Survey of Canada, Paper 86-1B, p. 827-835, 1986.

Abstract

Several occurrences of cordierite-anthophyllite are known in volcanic and sedimentary rocks of the Wasekwan Group in the Dunphy Lakes – Laurie Lake area. The New Fox alteration zone is a particularly well exposed example demonstrating in situ alteration by a systematic relationship of mineral assemblages reflecting progressive calcium-sodium depletion and by a gradual obliteration of primary features. Incipient alteration allows the appearance of cummingtonite in mafic volcanic rocks, in some of which pillows are preserved. Cummingtonite-bearing rocks form zones of varying width, from several centimetres to outcrop size, separating unaltered rocks from those more intensely altered, garnet- anthophyllite and cordierite-anthophyllite rocks. These rocks are very heterogeneous and some very garnet-rich varieties are present. The mineral assemblages are products of medium grade metamorphism. The chemical composition of altered rocks requires chloritic precursors, some very iron-rich, such as are found in hydrothermal alteration zones associated with volcanogenic sulphide deposits.

¹ Contribution to the Canada-Manitoba Mineral Development Agreement 1984-1989. Project carried by Geological Survey of Canada.

² Ottawa-Carleton Centre for Geoscience Studies, Carleton University, Ottawa, Ontario, K1S 5B6

Introduction

Coarse grained rocks of unusual composition, characterized by the presence of garnet, staurolite, cordierite, sillimanite and pale bronze or green amphibole, were noticed in the Dunphy Lakes area by Stanton (1949). One occurrence of such rocks is now known as the New Fox alteration zone. Stanton's (1949) work was incorporated in the report by Milligan (1960); however, the occurrences of these rocks were not shown on the revised maps. Mustard (1974) reported cordierite-anthophyllite rocks from several localities in the Dunphy Lakes – Laurie Lake area, including the Lar deposit, and attributed them to metamorphism of chlorite-rich zones. Lustig (1979) described metamorphosed alteration zones at the Fox Mine. In the recent mapping by Gilbert et al. (1980), some occurrences of rocks of unusual composition reported by Stanton (1949) were recognized as altered volcanic rocks. Other occurrences, including rocks of the New Fox alteration zone, were merely indicated as porphyroblastic schists and their origin was not discussed. Gale (1983) used the designation New Fox occurrence and commented that the genesis of these porphyroblastic schists had not been determined, although he regarded similar rocks at the Lar deposit as constituting an alteration zone. Stewart and Brewer (1984) briefly describe the New Fox occurrence and on an unpublished map by P. Stewart, dated December 1984, an alteration zone is shown. The New Fox occurrence was mentioned by Gunter and Yamada (1985) and dealt with in an oral presentation by Barham (1986). In this paper, the geological relationships observed in outcrops are discussed and a documentation of mineral assemblages is provided. Related studies are the investigations of alteration zones in the Fox Mine area (Olson, 1984) and associated with the Lar deposit (Elliott, 1984; Elliott and Appleyard, 1985).

Regional setting

The Dunphy Lakes – Laurie Lake area lies at the western end of the Lynn Lake greenstone belt (Fig. 87.1). The early geological work in the region, as well as the results of an extensive mapping program by the Manitoba Mines Branch, were summarized in the report by Milligan (1960). More recent revisions and additions, based on a four-year mapping program by the Manitoba Mineral Resources Division, were presented by Gilbert et al. (1980). The presently used stratigraphic framework includes the older Wasekwan Group consisting of volcanic and sedimentary rocks and the younger Sickle Group consisting of sandstone and conglomerate. High grade metamorphic rocks in the southern part of the area shown in Figure 87.1, probably derived from Wasekwan Group rocks, are known as the Burntwood River Metamorphic Suite. Intrusive rocks of pre-Sickle and post-Sickle age are recognized.

Lithology of the New Fox alteration zone

The New Fox alteration zone is developed in interlayered volcanic and sedimentary rocks of the Wasekwan Group in a border zone adjacent to a large intrusion of post-Sickle granodiorite (Fig. 87.1). The border zone is characterized by irregular bodies of granodiorite with intrusive breccia commonly present near the contacts. The central part of the New Fox alteration zone is least disturbed by post-Sickle intrusions and the lithological units, shown in Figure 87.2, form a local stratigraphic succession. Pillow shapes and graded bedding indicate tops facing south. Foliations are subparallel to lithological contacts. Topographic depressions and discontinuities of lithological units suggest two northeasterly trending post-metamorphic faults. In outcrops nearby, small shear zones and a crenulation foliation, parallel to the postulated faults, were observed.

Unit 1 consists of well layered hornblende-biotite psammites. They are overlain by mafic to intermediate volcanic flows and subordinate volcanoclastic rocks constituting unit 2. Centrally zoned pillows and quartz-filled amygdules are common. Unaltered rocks consist of about 55% hornblende, 40% plagioclase, 3% quartz, 2% magnetite and trace amounts of epidote. Unit 3 includes sedimentary and volcanoclastic rocks of variable composition, in a few places displaying graded bedding. Unit 4 consists of rusty-brown layered psammites characterized by zoned hornblende-plagioclase ovoids probably representing calcareous concretions.

Small dykes and sills of foliated tonalite, extensively folded and bodinaged, are thought to be of pre-Sickle age. Younger intrusive rocks, ranging in composition from diorite to granodiorite, cut all older deformed rocks. Brecciated xenoliths near contacts are common. These intrusions are probably related to the large body of post-Sickle granodiorite north of the New Fox alteration zone.

Alteration

Mafic volcanic rocks commonly display epidotized patches, particularly in pillow cores. This alteration is of regional extent in rocks of the Wasekwan Group (Syme, 1985) and appears to be earlier than locally observed silicification and calcium-sodium depletion, e.g. at the New Fox alteration zone.

Quartz-rich rocks, presumably products of silicification are shown along a portion of the contact of units 2 and 3 (Fig. 87.2). In mafic volcanic rocks, patches of quartz-garnet-magnetite (Fig. 87.3) and quartz-plagioclase-filled interpillow areas (Fig. 87.4) are present. Epidote patches in some quartz-magnetite rocks may represent unreplaced pillow cores. In felsic sediments and volcanoclastic rocks, silicification is indicated by lensoid layers of quartz-plagioclase-magnetite rock.

The dominant alteration is marked by progressive depletion in calcium and sodium. The first manifestation is the appearance of cummingtonite, commonly as patches with diffuse contacts (Fig. 87.3) or in pillow margins. Such alteration has also been reported from the Laurie Lake area (Jackson and Gordon, 1985), but not associated with the more advanced stages of alteration. Pervasive alteration leads to the formation of quartz-plagioclase-cummingtonite rocks, in a few places with lenses of coarser garnet and anthophyllite (Fig. 87.5, 87.6) probably developed in interpillow spaces. The proportion of garnet-anthophyllite varies and some outcrops are entirely constituted of garnet-anthophyllite rock which may be very garnet-rich (Fig. 87.7). In transitional rocks, cummingtonite coexists with either hornblende or anthophyllite. Garnet and magnetite are common in cummingtonite-bearing rocks. As well as affecting large bodies of outcrop size, cummingtonite alteration may be limited to narrow zones separating cordierite-anthophyllite-garnet rock from unaltered mafic rock (Fig. 87.8). More intense calcium-sodium depletion allows the appearance of cordierite-anthophyllite-garnet rocks characterized by porphyroblasts of garnet, radiating anthophyllite and aggregates of cordierite (Fig. 87.9, 87.10). These rocks are very heterogeneous, displaying garnet-rich and anthophyllite-rich layers and patches (Fig. 87.11, 87.12). Plagioclase is generally absent and retrograde chlorite is common. Staurolite was observed in one sample as armoured relics in cordierite.

Metamorphism

In the Dunphy Lakes – Laurie Lake area, Gilbert et al. (1980) marked the first appearance of sillimanite in greywacke and the beginning of anatexis (Fig. 87.1). These boundaries approximately define the biotite-sillimanite-almadine zone in pelitic

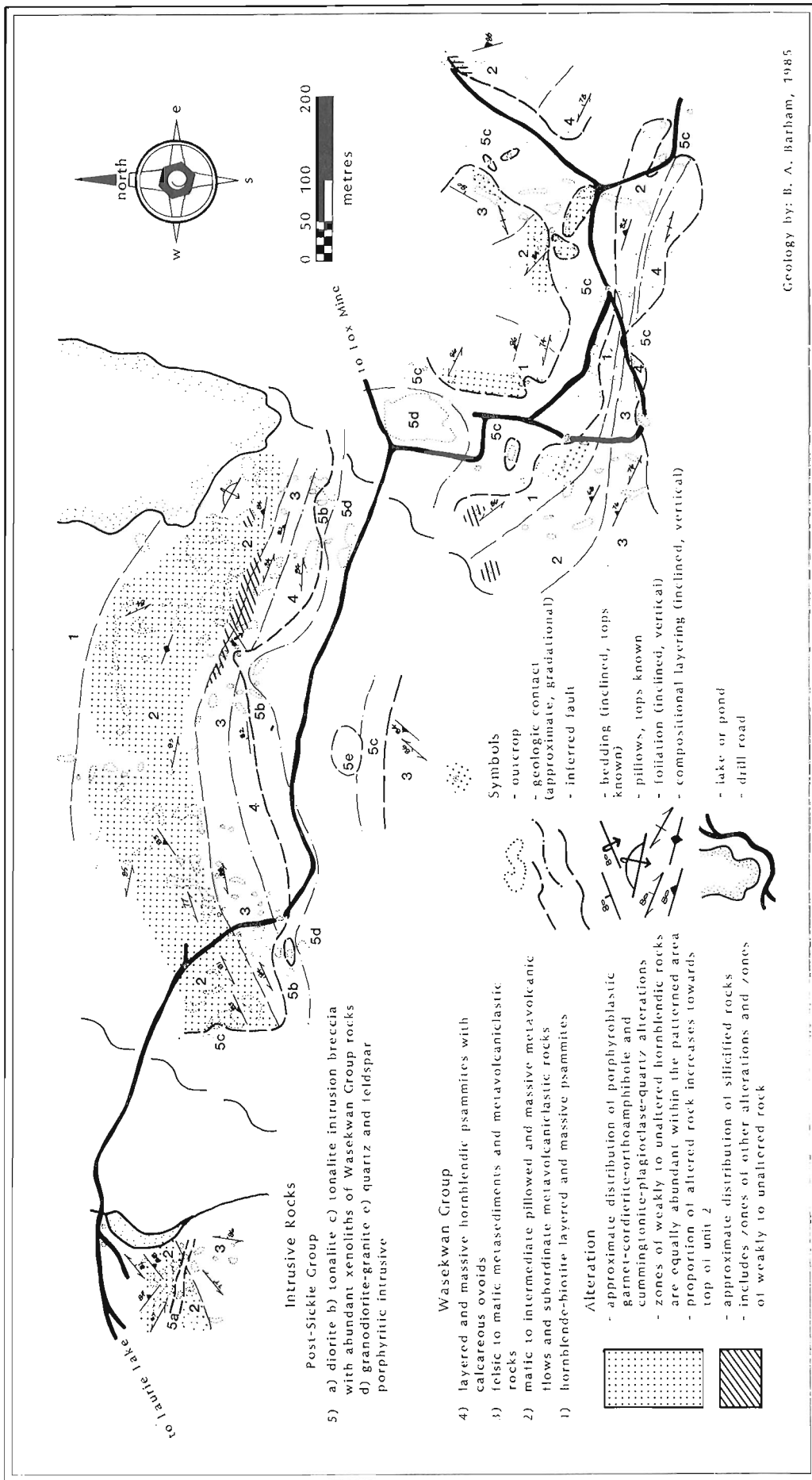


Figure 87.2. Geology of the New Fox alteration zone.

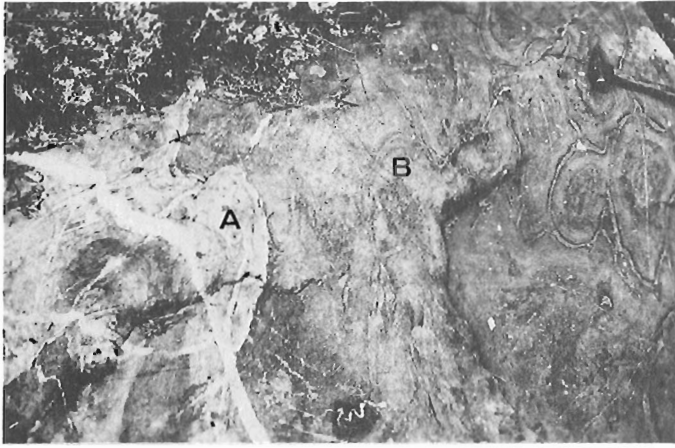


Figure 87.3

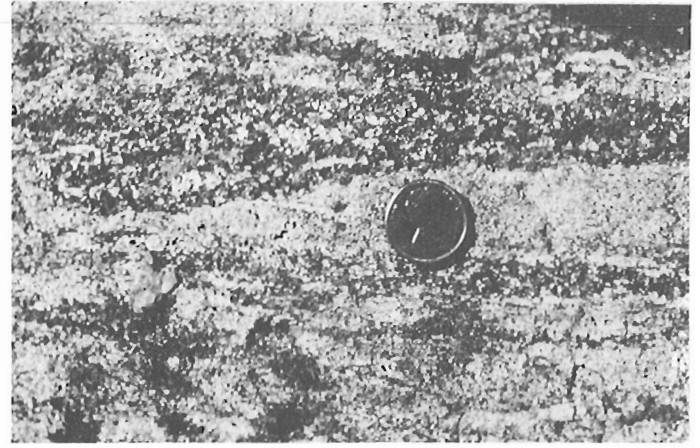


Figure 87.6

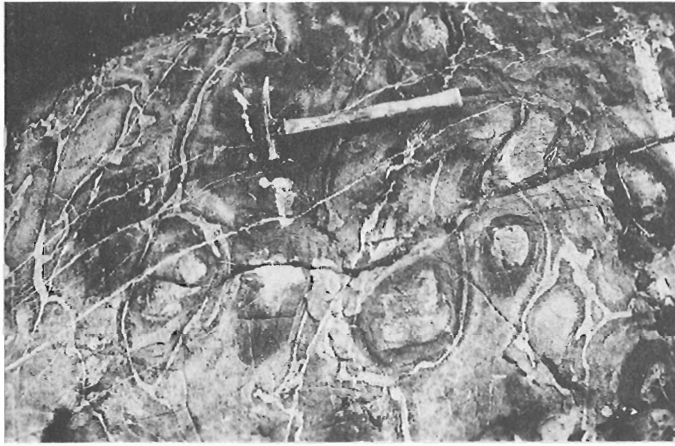


Figure 87.4

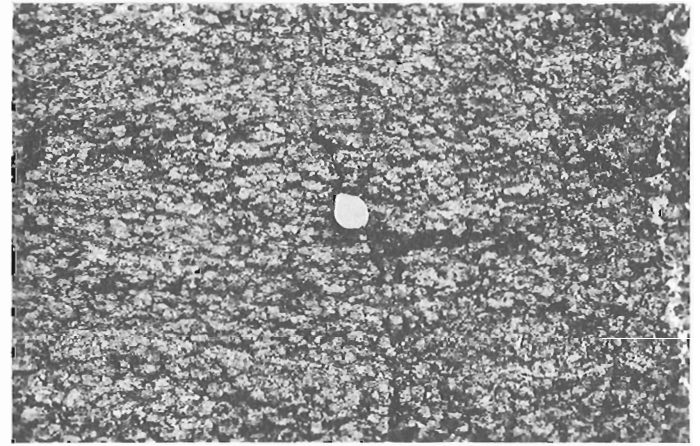


Figure 87.7



Figure 87.5

Figure 87.3. Patches of quartz-garnet-magnetite (A) in mafic volcanic rock with remnant pillows. In lighter-coloured portions of the rock (B) containing cummingtonite, pillows are obscured. GSC 203317-U

Figure 87.4. Mafic volcanic rock with quartz-plagioclase-filled interpillow areas and cummingtonite-rich pillow margins (grey). Dark areas are hornblende-bearing. Some pillows have epidote cores. GSC 203317-V

Figure 87.5. Rock pervasively altered to quartz-plagioclase-cummingtonite. Lenses of coarser garnet-anthophyllite probably occupy interpillow spaces. GSC 203317-W

Figure 87.6. Lens of quartz-plagioclase-cummingtonite rock surrounded by coarser garnet-anthophyllite. GSC 203317-X

Figure 87.7. Very garnet-rich garnet-anthophyllite rock. GSC 203317-Y

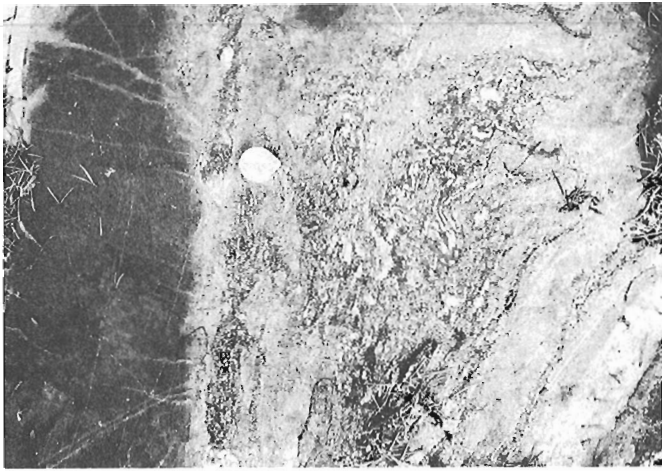


Figure 87.8

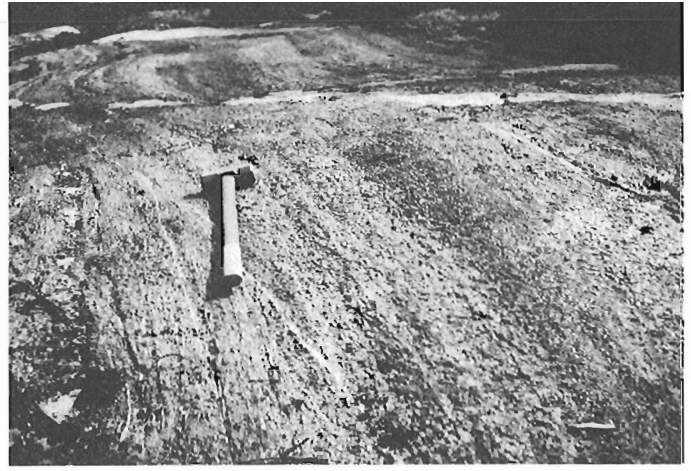


Figure 87.11

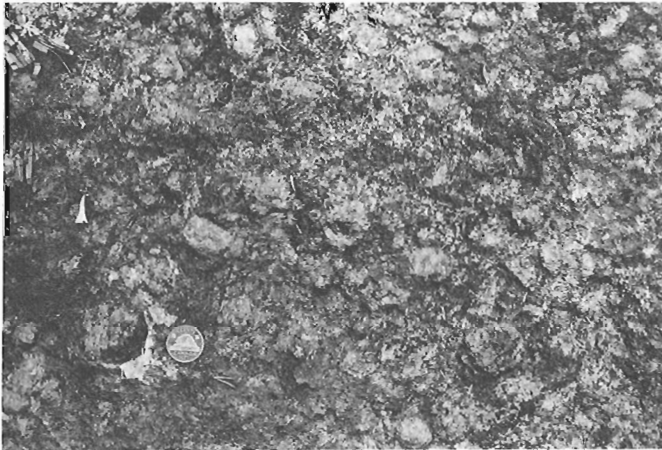


Figure 87.9

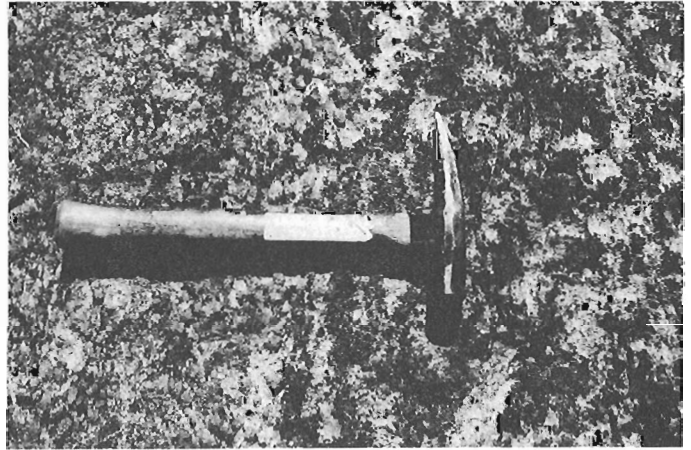


Figure 87.12



Figure 87.10

Figure 87.8. *Cummingtonite-rich rock separating cordierite-anthophyllite-garnet rock from unaltered amphibolite. GSC 203317-Z*

Figure 87.9. *Cordierite-anthophyllite-garnet rock. GSC 201399-K*

Figure 87.10. *Cordierite-anthophyllite rock. GSC 201399-M*

Figure 87.11. *Compositionally layered cordierite-anthophyllite-garnet rock. GSC 201399-L*

Figure 87.12. *Compositionally layered cordierite-anthophyllite-garnet rock. GSC 201399-N*

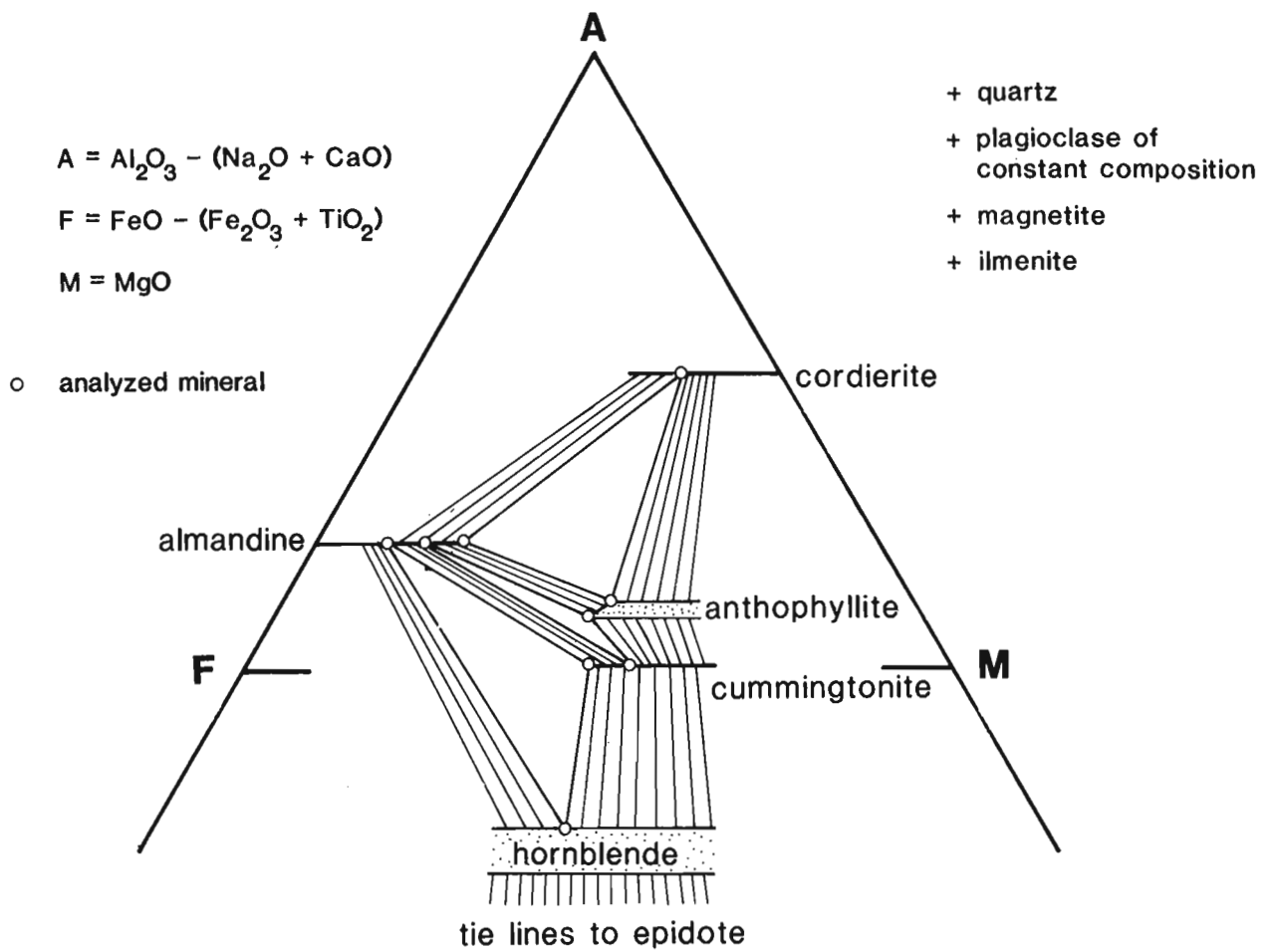


Figure 87.13. Mineral assemblages shown on an AFM diagram.

Table 87.1. Metamorphic mineral assemblages

sample	qz	pl	bi	hb	ep	alm	cum	at	co	st*	mt	ch**
NFF-36	x	x	x	x	x						x	
NFF-35	x	x	x	x								x
NF1-12	x	x	x	x		x					x	x
NFF-8	x	x	x	x			x					x
NFF-10b	x	x	x	x		x	x				x	
NFF-1	x	o		o		o	o				x	
NFF-28	x	o	o			o	o	o		x	x	o
NFF-7	x	x	x				x	x			x	
NFF-26	x	x	x			x		x			x	x
NFFM-3	x		o			o		o	o		x	o
NF3-14	x		x					x	x		x	x
NF3-16	x		x			x		x	x	x		x
Abbreviations:	qz quartz	pl plagioclase	bi biotite	hb hornblende	ep epidote	alm almandine	cum cummingtonite	at anthophyllite	co cordierite	st staurolite	mt magnetite	ch chlorite
*	armoured relic in cordierite											
**	retrograde mineral											
o	analyzed mineral											

Table 87.2. Composition of minerals from sample NFF-1

	hornblende	almandine	cummingtonite
SiO ₂	41.87	36.25	51.92
TiO ₂	0.40	0.08	0.11
Al ₂ O ₃	14.04	19.68	2.28
FeO	20.97	35.42	27.99
MnO	0.09	1.91	0.31
MgO	7.84	3.07	14.92
CaO	10.55	3.33	0.96
Na ₂ O	2.13	0.24	0.02
K ₂ O	0.34	0.01	0.04
	<hr/> 98.23	<hr/> 99.99	<hr/> 98.62

Mineral assemblage: quartz, plagioclase An₃₇, hornblende, almandine, cummingtonite, magnetite

Total iron expressed as FeO. Assuming a ratio of weight % Fe₂O₃ to weight % FeO = 0.2 in hornblende gives 3.55 % Fe₂O₃ and 17.77 % FeO.

Electron microprobe analyses by M. Bonardi, Mineralogy Section, Geological Survey of Canada

rocks (Bailes, 1980; Froese and Moore, 1980) which corresponds to the upper temperature range of Winkler's (1979) medium grade metamorphism. The New Fox alteration zone has been metamorphosed to this grade.

Representative mineral assemblages are listed in Table 87.1 and mineral analyses from three rocks are given in Tables 87.2, 87.3, and 87.4. For the hornblende analysis, a ratio of weight % Fe₂O₃ to weight % FeO of 0.2 has been assumed; this is somewhat lower than ratios ranging from 0.24 to 0.38 reported by Jen and Kretz (1981). An AFM diagram accommodating the observed mineral assemblages and based on the available mineral analyses has been constructed (Fig. 87.13).

The components are defined as follows (Froese, 1969):

$$A = \text{Al}_2\text{O}_3 - (\text{Na}_2\text{O} + \text{CaO})$$

$$F = \text{FeO} - (\text{Fe}_2\text{O}_3 + \text{TiO}_2)$$

$$M = \text{MgO}$$

Relict staurolite in cordierite associated with almandine and anthophyllite suggests that the temperature exceeded that of the reaction

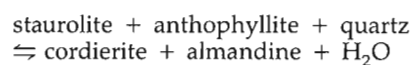


Table 87.3. Composition of minerals from sample NFF-28

	biotite	almandine	cummingtonite	anthophyllite	chlorite
SiO ₃	37.64	36.49	53.08	46.81	25.91
TiO ₂	2.03	0.05	0.06	0.18	0.08
Al ₂ O ₃	17.23	20.08	2.25	9.98	22.13
FeO	16.82	33.51	24.95	25.58	20.22
MnO	0.03	2.84	0.39	0.51	0.04
MgO	13.54	4.42	16.89	13.60	20.50
CaO	0.11	2.49	0.59	0.58	0.02
Na ₂ O	0.57	0.39	0.35	1.23	0.08
K ₂ O	8.29	0.08	0.01	0.03	0.05
	<hr/> 96.26	<hr/> 100.35	<hr/> 98.57	<hr/> 98.50	<hr/> 89.03

Mineral assemblage: quartz, plagioclase An₄₅, biotite, almandine, cummingtonite, anthophyllite, magnetite, chlorite

Total iron expressed as FeO.

Electron microprobe analyses by M. Bonardi, Mineralogy Section, Geological Survey of Canada

Table 87.4. Composition of minerals from sample NFFM-3

	biotite	almandine	anthophyllite	cordierite	chlorite
SiO ₂	38.29	36.96	45.79	49.09	25.01
TiO ₂	1.84	0.03	0.28	0.03	0.12
Al ₂ O ₃	16.88	20.07	11.43	32.05	21.97
FeO	16.20	32.99	23.92	6.63	21.76
MnO	0.02	0.88	0.33	0.07	0.13
MgO	13.89	6.37	14.51	10.06	18.60
CaO	0.13	2.14	0.55	0.04	0.07
Na ₂ O	0.32	0.15	1.20	0.14	0.19
K ₂ O	8.76	0.01	0.05	0.02	0.02
	<hr/> 96.33	<hr/> 99.60	<hr/> 98.06	<hr/> 98.13	<hr/> 87.87

Mineral assemblage: quartz, biotite, almandine, anthophyllite, cordierite, magnetite, chlorite

Total iron expressed as FeO.

Electron microprobe analyses by M. Bonardi, Mineralogy Section, Geological Survey of Canada.

This reaction is shown to terminate at an invariant point at about 600°C and 5 kb ($P_{\text{H}_2\text{O}} = P_{\text{total}}$) on a grid developed by D.M. Carmichael (see Bailes, 1980). The metamorphic pressure imposed on this rock probably was below 5 kb and the temperature around 600°C.

Conclusions

The systematic change in mineral assemblages and gradual obliteration of primary features provide a good example of the effects of progressive in situ alteration. Most cordierite-anthophyllite rocks are now regarded as metamorphic products of rocks that reached an appropriate composition prior to metamorphism (Robinson et al., 1982). Their chemical composition requires a chlorite-rich precursor. Cumingtonite- and anthophyllite-bearing rocks without cordierite probably were derived from less intensely altered rocks with a smaller amount of chlorite. The less severe calcium-sodium depletion in such rocks is reflected in the presence of plagioclase. Iron-rich chlorite probably accounts for the garnet-anthophyllite rocks with a high garnet content.

Most likely precursors of the cordierite-anthophyllite rocks and related compositional variants are the chloritic portions of alteration zones, associated with some volcanogenic sulphide deposits (Lydon, 1984). Trace amounts of pyrrhotite and chalcopyrite were noted in some rocks; however, accumulations of sulphides have not been found.

Acknowledgments

We are grateful to D.A. Baldwin for suggesting this study and taking a continued interest in it. The excellent exposures available in 1985 resulted from earlier extensive moss stripping by P.W. Stewart, K. Brewer, A. Michelsen, and J. Lutz. Access to drill core was provided by Sherritt Gordon Exploration Limited. Support during the course of fieldwork by P.J. Chornoby and R.F. Sawyer is greatly appreciated. L.H. Adamitz was an enthusiastic and competent field assistant.

References

- Bailes, A.H.
1980: Geology of the File Lake area; Manitoba Mineral Resources Division, Geological Report 78-1.
- Barham, B.A.
1986: Cordierite-orthoamphibole-garnet rocks of the New Fox alteration zone, Laurie Lake, Manitoba; Geological Association of Canada, Program with Abstracts, v. 11, p. 43. (abstract).
- Elliott, S.
1984: A study of the alteration zone associated with the Lar deposit; Manitoba Mineral Resources Division, Report of Field Activities 1984, p. 20-22.
- Elliott, S.R. and Appleyard, E.C.
1985: A study of the alteration zone associated with the Lar deposit, Laurie Lake area; Manitoba Mineral Resources Division, Report of Field Activities 1985, p. 32-36.
- Froese, E.
1969: Metamorphic rocks from the Coronation mine and surrounding area; Geological Survey of Canada, Paper 68-5, p. 55-77.
- Froese, E. and Moore, J.M.
1980: Metamorphism in the Snow Lake area, Manitoba; Geological Survey of Canada, Paper 78-27.
- Gale, G.H.
1983: Mineral deposit investigation in the Lynn Lake area; Manitoba Mineral Resources Division, Report of Field Activities 1983, p. 84-87.
- Gilbert, H.P., Syme, E.C., and Zwanzig, H.V.
1980: Geology of the metavolcanic and volcanoclastic metasedimentary rocks in the Lynn Lake area; Manitoba Mineral Resources Division, Geological Paper GP80-1.
- Gunter, W.R. and Yamada, P.H.
1985: Evaluation of industrial mineral occurrences in the Lynn Lake area; Manitoba Mineral Resources Division, Report of Field Activities 1985, p. 41-43.
- Jackson, S.L. and Gordon, T.M.
1985: Metamorphism and structure of the Laurie Lake region, Manitoba; in Current Research, Part A, Geological Survey of Canada, Paper 85-1A, p. 753-759.
- Jen, L.S. and Kretz, R.
1981: Mineral chemistry of some mafic granulites from the Adirondack region; Canadian Mineralogist, v. 19, p. 479-491.
- Lustig, G.N.
1979: Geology of the Fox orebody, northern Manitoba; unpublished M.Sc. thesis, University of Manitoba, Winnipeg.
- Lydon, J.W.
1984: Volcanogenic massive sulphide deposits part 1: a descriptive model; Geoscience Canada, v. 11, p. 195-202.
- Milligan, G.C.
1960: Geology of the Lynn Lake district; Manitoba Mines Branch, Publication 57-1.
- Mustard, J.W.
1974: Geology, metamorphism and structure of the North Laurie Lake area, northern Manitoba; unpublished B.Sc. thesis, Queen's University, Kingston.
- Olson, P.E.
1984: The geology of the Fox Mine area; Manitoba Mineral Resources Division, Report of Field Activities 1984, p. 23-24.
- Robinson, P., Spear, F.S., Schumacher, J.C., Laird, J., Klein, C., Evans, B.W., and Doolan, B.L.
1982: Phase relations of metamorphic amphiboles: natural occurrence and theory; Mineralogical Society of America, Reviews in Mineralogy, v. 9B, p. 1-227.
- Stanton, M.S.
1949: Geology of the Dunphy Lakes area, Granville Lake Division, Manitoba; Manitoba Mines Branch, Report and Map 48-4.
- Stewart, P.W. and Brewer, K.
1984: Mineral deposit studies in the western Lynn Lake greenstone belt; Manitoba Mineral Resources Division, Report of Field Activities 1984, p. 17-19.
- Syme, E.C.
1985: Geochemistry of metavolcanic rocks in the Lynn Lake belt; Manitoba Energy and Mines, Geological Report GR84-1.
- Winkler, H.G.F.
1979: Petrogenesis of Metamorphic Rocks, fifth edition; Springer-Verlag, New York.

Reconnaissance geology of western and central Algonquin Park and detailed study of coronitic olivine metagabbro, central Gneiss Belt, Grenville Province of Ontario

Project 760061

A. Davidson and S.M. Grant¹
Lithosphere and Canadian Shield Division

Davidson, A. and Grant, S.M., Reconnaissance geology of western and central Algonquin Park and detailed study of coronitic olivine metagabbro, Central Gneiss Belt, Grenville Province of Ontario; in Current Research, Part B, Geological Survey of Canada, Paper 86-1B, p. 837-848, 1986.

Abstract

Geological reconnaissance in western and central Algonquin Provincial Park enabled northeastward extension of the formerly established McLintock subdomain and recognition of a new subdivision, Opeongo subdomain, in Algonquin domain. To the northwest, Kiosk domain was found to comprise two parts: a southern belt of highly strained gneiss that delimits the northern extent of granulite facies metamorphism in Algonquin domain, and a northerly region of less regular structure and large metagranitoid plutons. Graphite-bearing pelitic gneiss was traced from Burk's Falls east-northeast through Algonquin Park. As part of a continuing study, coronitic olivine metagabbro bodies and their tectonic setting were examined in parts of Huntsville, Seguin and Rosseau subdomains, southwest Kiosk domain and the Kawagama tectonic zone of Muskoka domain. A previously unidentified cluster of these bodies was found in southeastern Kiosk domain. Results of preliminary analytical chemistry are presented.

Résumé

Un levé géologique de reconnaissance dans les parties ouest et centrale du parc provincial Algonquin nous permet d'étendre le sous-domaine McLintock, déjà établi, vers le nord-est et de définir un nouveau sous-domaine, l'Opeongo, dans le domaine d'Algonquin. Vers le nord-ouest, le domaine Kiosk se présente en deux parties: une zone sud de gneiss fortement déformé qui marque la limite septentrionale du faciès des granulites dans le domaine d'Algonquin, et une zone nord à structure hétérogène qui contient de grands plutons méta-granitoides. Un gneiss pélitique à graphite a été tracé de Burk's Falls vers l'est-nord-est à travers le parc Algonquin. Dans le cadre d'une étude thématique, on a examiné du point de vue de leur caractère pétrologique et structural, des corps de métagabbro à olivine coronitique dans les sous-domaines d'Huntsville, de Séguin et de Rosseau, dans la partie sud-ouest du domaine de Kiosk et dans la zone tectonique de Kawagama (domaine de Muskoka). Un groupe de corps semblables, jusqu'ici inconnu, a été identifié dans la partie sud-est du domaine de Kiosk. Des données chimiques préliminaires sont présentées.

¹ Department of Geology, University of Leicester, Leicester LE1 7RH, England

Introduction

After wide-ranging aerial reconnaissance mapping in 1980, Davidson and Morgan (1981) recognized the Central Gneiss Belt of the Grenville Province in Ontario to be made up of several lithotectonic blocks which they referred to as domains. Subsequent work (Davidson et al., 1982; Culshaw et al., 1983) elaborated this subdivision and showed the nature of the boundaries between domains to be broad zones of ductile shear (Davidson, 1984) along which crustal blocks have been displaced with respect to one another. Kinematic indicators were used to demonstrate a predominant sense of overriding to the northwest where shear zones are oriented northeast, and oblique or lateral displacement with the same sense where they are differently oriented. Culshaw et al. (1983) suggested the stacking order illustrated in Figure 88.1. It was recognized that the lower deck of this stack, in particular, contains folded shear zones that serve to further divide it into subdomains, but relative ages of formation of these smaller lithotectonic units have not been deduced.

Fieldwork in 1985 was undertaken in the western and central parts of Algonquin Provincial Park and adjoining regions, within the area covered by N.T.S. 1:50 000 map

sheets 31E/7 - /11 and /14 - /16. The primary concern was to take a first look at the eastern extension of Algonquin domain, its southern boundary with the eastward continuation of Muskoka domain, and the region to the northwest that had been distinguished previously as Kiosk domain on the basis of differences in metamorphic grade and structural orientation (Davidson and Morgan, 1981). Concurrently, the field component of a study of coronitic olivine metagabbro bodies, initiated in 1984 (Grant, 1985), was concluded in areas south and west of Algonquin domain, and is the subject of the second part of this report.

Acknowledgments

Proficient and companionable assistance was rendered this past season by Léo Nadeau, Louise Corriveau, Terry Needham, Jill Stewart and Chris Robinson. Sincere thanks are extended to George Whitney of the Ontario Ministry of Natural Resources and his Algonquin Park staff, without whose willingly given co-operation the field operation could not have taken place. Thanks are also due to Ross Austin, Radio Observatory at Lake Traverse, for the use of facilities at that establishment.

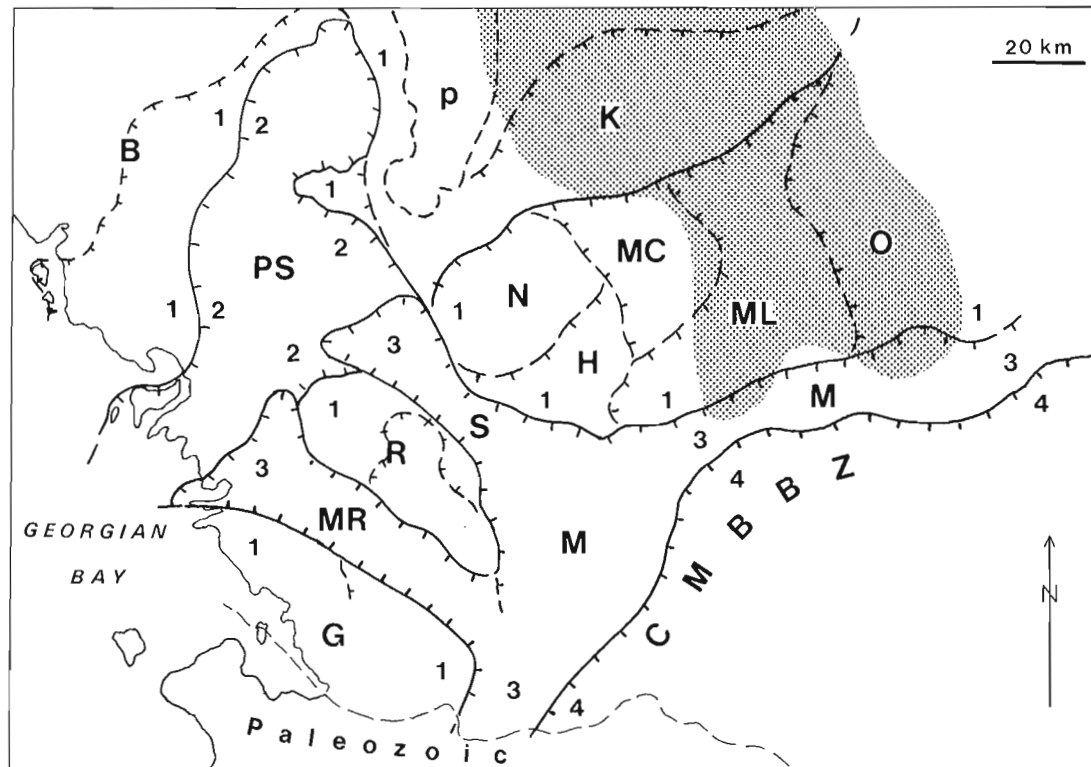


Figure 88.1. Lithotectonic subdivisions of the Central Gneiss Belt east of Georgian Bay. Stacking order is given by numbers. Stack 1: B - Britt, K - Kiosk, R - Rosseau, G - Go Home, N - Novar, H - Huntsville, MC - McCraney, ML - McLintock, O - Opeongo. Stack 2: PS - Parry Sound. Stack 3: M - Muskoka, MR - Moon River, S - Seguin. Stack 4: CMBBZ - Central Metasedimentary Belt boundary zone. Subdomains N, H, MC, ML and O are in Algonquin domain; p is Powassan batholithic complex. Shaded area indicates 1985 field area.

PART I: RECONNAISSANCE MAPPING IN WESTERN AND CENTRAL ALGONQUIN PARK

A. Davidson

In summary, Algonquin domain contains several cell-like subdomains, some with whorl-shaped internal structural map patterns, separated by zones of flaggy gneiss having more regular trends oriented mainly either northeast or northwest with moderate to shallow southeast and northeast dips respectively. The predominant metamorphic grade is granulite facies. A series of broad, en echelon, shallow southerly dipping shear zones forms the southern boundary of this domain from Dorset to Ontario Highway 127 south of Whitney (Fig. 88.2), and includes the previously described Kawagama zone (Culshaw et al., 1983). Deformed migmatitic gneisses, derived at least in part from Algonquin domain rocks, feature largely in this region and are at amphibolite grade. To the northwest, the Kiosk domain appears to be divisible into two parts: 1) a southerly region containing a large proportion of highly grain-refined, strongly lineated gneisses, many of which can be termed mylonitic. Although in part of granulitic aspect, most of these rocks do not contain hypersthene, despite suitable composition; however, clinopyroxene-bearing leucosomes were noted in places. 2) a region to the north, extending beyond the map area boundary (46°N) into previously mapped areas (Lumbers, 1971, 1976), containing large plutons of deformed metamazonite and metagranite with metasedimentary gneisses and strongly deformed, generally more mafic metaplutonic rocks between them.

Structural trends throughout the study region are clearly evident on aeromagnetic maps except in the northern part of Algonquin Park where the strong expression of an east-trending swarm of post-Grenvillian diabase dykes masks the more subdued bedrock trends. Where outcrop is plentiful, as in the southern and western parts of the park and neighbouring areas, ridges and valleys reflect gneissic layering, but some fold-like expressions are found to be caused by valley intersections of relatively planar tracts of gneisses that are very shallowly inclined.

Rock types in Algonquin and Kiosk domains are many and varied, but the combination of high metamorphic grade and the extreme ductile deformation to which they have been subjected makes distinction into mapping units a difficult task at reconnaissance scale. The main reasons for this are: 1) ductile attenuation has given rise to very thin rock units, 2) deformation and metamorphism, whereby original textural characteristics have been completely obliterated, has led certain plutonic and supracrustal rocks with similar compositions to converge toward a common, nondescript derivative gneiss, and 3) complex structure has rendered the continuity of recognizable units unpredictable. The mapper is faced with certain recognition of rocks as metasedimentary only where they contain units of characteristic composition (aluminous, quartzitic, calcareous), and as plutonic only where relict primary texture is preserved; metavolcanic rocks, if present, have not been recognized, and a large proportion of compositionally 'ordinary', fine grained, quartzofeldspathic gneiss and granulite cannot be conclusively assigned to a particular protolith. It has been shown previously that well developed layering in gneissic and granulitic rocks does not necessarily reflect a supracrustal origin, being the result of either severe transposition or metamorphic segregation during ductile deformation.

Much of the investigated region has been stated to be part of the 'Algonquin batholith' (Schwerdtner and Lumbers, 1980), said to be basement to the Grenville Supergroup supracrustal succession that occupies the Central Metasedimentary Belt to the south. Although metaplutonic rocks of various types have been mapped as underlying much

of eastern Algonquin Park and the area to the southeast (Lumbers, 1982), rocks in the current field area to the west are found to include a fair proportion of gneiss and granulite that is metasedimentary in origin. These are most commonly recognized by the presence of aluminous varieties, characterized by their content of graphite and/or pyrite in assemblages such as quartz, two feldspars, violet garnet, biotite and/or hypersthene or sillimanite, and rare green spinel. Associated calcareous rocks include assemblages containing quartz, plagioclase, scapolite, grossularite, diopside and rare wollastonite. Also present locally are rocks containing dark red andradite and iron-rich amphibole and clinopyroxene with calcic plagioclase and scapolite. Calc-silicate-bearing marble is rare, but is present as decimetre-scale layers in some tracts of mafic calc-silicate granulite. Most of these characteristic metasediments occur as thin units within less diagnostic layered quartzofeldspathic gneiss and granulite with variable colour index. The metasedimentary rocks are not mere lenses included within a single plutonic complex; rather, they form linear or sinuous tracts that can be traced for several tens of kilometres.

Unequivocal metaplutonic rocks with composition ranging from gabbro to granite appear to lie as lenticular or tadpole-shaped masses, many of them folded, within a supracrustal or nondescript gneiss matrix. Similar in form to metaplutonic rocks recognized in Britt domain (Davidson et al., 1982), most of these orthogneissic rocks are in continuous strips conformable with the regional gneissosity. Crosscutting contacts have not been recognized. Relict igneous texture is best preserved in quartz-absent rocks, such as gabbro, but coarsely megacrystic (K-feldspar) granitoid rocks retain evidence of their origin where reduced to augen gneiss in which lenticular quartz grains wrap the larger feldspars. The relative state of deformation of the various metaplutonic rocks cannot generally be used as a guide to their relative ages, but it seems likely that some tracts of fairly uniform quartzofeldspathic gneiss or granulite that are interlayered with metasedimentary rocks, together lying between recognizable metaplutonic masses, may represent earlier intrusions.

Algonquin domain

Within Algonquin domain (as defined in Culshaw et al., 1983), McLintock subdomain has been extended northeastward around the eastern side of McCraney subdomain (Fig. 88.2) on the basis of continuity of its internal structure and rock assemblages. It is a terrane of interleaved metasedimentary gneiss and granulite of the types just described and metaplutonic orthogneiss; the latter occurs in relatively small lenticular masses that can be shown to grade along their lengths from orthogneiss with recognizable relict igneous texture, features such as stretched xenoliths, and sharp lateral contacts, to fine grained granulite lacking any such evidence of origin. Regional layering and foliation in this subdomain strikes in undulating fashion between northeast and north-northwest with easterly dips and contains major recumbent folds, such as south of Lake of Two Rivers (Fig. 88.2), with U-shaped closures and axes parallel to the regional lineation. The prevailing lineation plunges mainly to the east, but turns southeasterly in the eastern part of this subdomain.

A marked change in attitude of layering occurs east of Lake of Two Rivers, where a northwest-trending belt of well layered mixed migmatitic and orthogneissic granulites truncates major fold structures of McLintock subdomain, marking the boundary of Opeongo subdomain. Eastward from this 'straight zone', which dips moderately east-northeast and

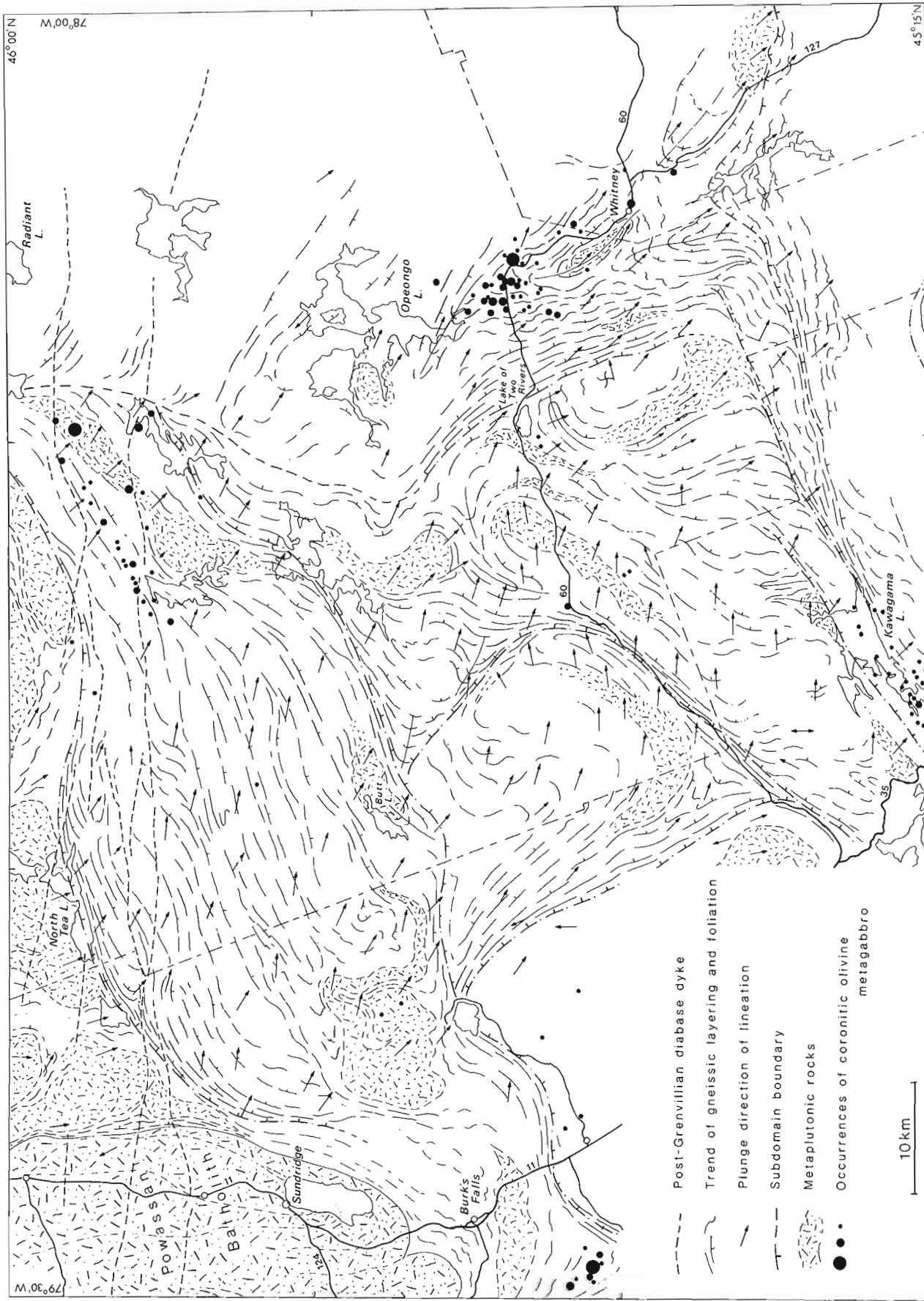


Figure 88.2. Geological sketch map of western and central Algonquin Park and adjoining regions showing predominant trends of gneissic layering and lineations. Some metaplatonic units have been outlined. More highly deformed plutonic rocks are present, but at the present stage of mapping they are not separable from metasedimentary and other gneisses of equivocal origin.

contains a shallowly southeast-plunging stretching lineation, the layering becomes undulatory. Farther east, layering describes major folds whose northwest-elongate map patterns include closures representing domal antiforms overturned to the northwest and inclined either northeast or southwest. Granitoid orthogneiss occupies the core of one such fold west of Whitney, but strips of similar orthogneiss also occur interlayered with metasedimentary granulite in its carapace. A continuous tract of interlayered charnockitic orthogneiss and metasedimentary granulite and gneiss, including marble, outlines another dome southeast of Whitney, clearly expressed by an annular negative aeromagnetic anomaly (Geological Survey of Canada, 1953); its core, however, includes both hypersthene-bearing orthogneiss and graphitic metasedimentary gneiss whose foliation attitudes do not conform to the domal structure of the carapace. Opeongo subdomain contains a large cluster of coronitic olivine metagabbro bodies, featured in Grant (1985, Fig. 57.8) and now extended southeastward on either side of the domal structure west of Whitney.

Kiosk domain

The whorl-like structure of McCraney, the undulating northerly structure of McLintock and the northwesterly structural trend of Opeongo subdomain turn into the continuous, broad, east-northeast-trending straight belt that characterizes southern Kiosk domain. To the west, this belt swings southwestward, conforming to the southern termination of the Powassan batholithic complex, a large, composite metaplutonic mass in places with narrow metasedimentary septa that separate distinctive plutonic phases. South and east of this large complex, smaller, more highly deformed metaplutonic masses characterized by phases similar to those in the Powassan complex, namely garnetiferous metadiorite, garnet-hornblende metamonzonite and meta-quartz monzonite, commonly migmatitic, and biotite leucogranite orthogneiss, extend from west of Ontario Highway 11 to east of Butt Lake (Fig. 88.2). They occur within a matrix of mafic, quartzofeldspathic and pelitic gneisses. The latter locally contains notable amounts of graphite and has been traced east-northeast through Algonquin Park as far as Radiant Lake; it may continue northeastward as far as the Ottawa River in the vicinity of Bissett Creek, where similar rocks are being actively explored for commercial exploitation of their graphite content (D. Villard, Ontario Ministry of Natural Resources, personal communication, 1985). North of this zone, highly flattened and lineated, mainly grey quartzofeldspathic gneisses appear to represent a series of adjacent, now elongate plutons of tonalitic to granodioritic composition. Another cluster of coronitic olivine metagabbro bodies lies within this zone, and scattered, small bodies of meta-ultramafite, leucodioritic and monzonitic orthogneiss are also present. This straight zone is bordered, at least along the south side of North Tea Lake, by mylonitic tectonites similar to those that bound many of the domains and subdomains already described to the south and southwest (see Davidson, 1984). Stretching lineations, commonly manifest as quartz rods, plunge moderately to shallowly east-southeast.

The plutons mapped along the 46th parallel by Lumbers (1971, 1976) continue southward but terminate against the straight zone of southern Kiosk domain. The metasedimentary gneiss assemblage that includes quartzite and pink, sillimanite-bearing, migmatitic quartzofeldspathic leucogneiss, lying north of the more mafic and graphitic pelitic assemblage in the Burks Falls area, does not appear to continue eastward. Instead, this assemblage forms a narrow

septum between the Powassan batholithic complex and the next plutonic mass to the east, and trends northward out of the map area. As previously mentioned, gneisses between the relatively well defined metaplutonic masses in northern Kiosk domain include more highly deformed and modified metaplutonic rocks. Gneissosity trends in this region are quite variable, and lineations plunge more southerly than in the straight belt to the south.

Summary

A further distinctive subdomain has been identified within Algonquin domain and the boundary between Algonquin and Kiosk domains has been found to be the site of a broad belt of highly strained mylonitic gneiss. Estimation of relative sense of displacements between these lithotectonic blocks has not been possible on the basis of field observations and awaits careful micropetrofabric analysis of suitable rocks. It is important to record that most of the rocks in the subdomain boundary zones within Algonquin domain are in granulite facies and exhibit granoblastic texture. The boundary between Algonquin and Kiosk domains appears to mark the northwestern limit of the granulite facies terrane centred in western Algonquin Park, but it is not yet known whether or not this terrane has been displaced northwestward over somewhat lower grade rocks. It is possible that future mapping in more detail will prove a connection between the southern Kiosk straight zone and the zone of similar rocks that bisects Britt domain far to the west, passing around the south end of the Powassan complex and then swinging northward and around the north end of Parry Sound domain.

It is noted that although lineations throughout the study area plunge moderately to gently between east and south with very few exceptions, lineation attitude is much more uniform in the straight zones between subdomains than it is within them (see Fig. 88.2). This suggests that, while a common ductile deformation affected the whole region, later stages of this deformation continued in particular restricted zones, isolating the cell-like subdomains that were then subjected to certain, though undetermined, amounts of internal warping, rotation and mutual displacement, all of this occurring under high grade metamorphic conditions. A study of these conditions, based on thermobarometric estimates deduced from suitable metamorphic mineral assemblages, is currently being undertaken by students and staff of the University of Michigan (see Anowitz and Essene, 1986; Moecher and Essene, 1986). It is hard to reconcile the observed pattern of lineation attitudes with the diapiric model espoused for this region by Schwerdtner and Lumbers (1980) unless it is admitted that structures related to earlier diapirism have been obliterated by subsequent deformation.

PART II: METAGABBROIC ROCKS IN THE CENTRAL GNEISS BELT OF ONTARIO

S.M. Grant

Coronitic olivine metagabbro bodies are common throughout the Central Gneiss Belt in Ontario. They have been found in all domains except Parry Sound domain. Ranging in size from a few metres to rarely as much as one kilometre in long dimension, and usually equant or oblong in plan, they occur singly and in small or large, dispersed or concentrated clusters. Some elongate clusters appear to be associated with domain or subdomain boundary shear zones; others occur within the lithotectonic blocks. Also present are other types of metagabbro that do not exhibit classic corona textures, either because this has been destroyed by thorough recrystallization or because the parent gabbro had a different mineralogy, for example, norite or clinopyroxene-bearing leucogabbro.

The corona textures are apparent to the naked eye in coarse grained metagabbro and are spectacular in thin sections of finer grained rocks (for illustrations see McLelland and Whitney, 1980; Davidson et al., 1982; Emslie, 1983). The coronas are produced by reaction between plagioclase and both olivine and Fe-Ti oxide. Where unreacted olivine remains in the cores of coronas, it is surrounded by successive shells of orthopyroxene, clinopyroxene, aluminous amphibole and garnet; amphibole may not be present, in which case clinopyroxene and garnet may form a symplectic intergrowth along their mutual contact. Where no olivine remains, the corona are mosaics of orthopyroxene; garnet of the outer rim has commonly migrated into the plagioclase, leaving a 'moat' of recrystallized plagioclase behind it (Whitney and McLelland, 1973). Coronas around Fe-Ti oxide grains, now ilmenite but probably once containing a Ti-magnetite phase, are composed

of successive shells of biotite, brown amphibole and garnet. These coronas are themselves subject to further change, normally through hydration by which the rock is finally changed to amphibolite with or without garnet, losing evidence of former igneous texture if there is accompanying deformation. Where hydration is not involved, coronitic metagabbros may recrystallize to a granular mosaic of plagioclase, hypersthene, augite, hornblende and garnet with an equilibrium texture; trains of garnet are generally the only evidence for former coronitic structure, and would not be recognized as such if transitional stages had not been observed.

In the first season of this study, a small cluster of three coronitic olivine metagabbro bodies in Go Home subdomain of Muskoka domain and a large cluster in Algonquin domain (Opeongo subdomain) were examined (Grant, 1985). Last season, elongate, concentrated clusters in the Huntsville-Novar subdomain boundary zone near the town of Huntsville and along the Kawagama zone near the southern margin of McLintock subdomain near Dorset, a dispersed population in northwestern Rosseau subdomain, and small clusters in Sequin subdomain and at the southwest end of Kiosk domain were mapped and extensively sampled for analytical studies. Localities of these and other known occurrences of olivine metagabbro are shown in Figure 88.3. This report concludes with a brief summary of preliminary geochemical results obtained so far at the University of Leicester on samples collected during both field seasons.

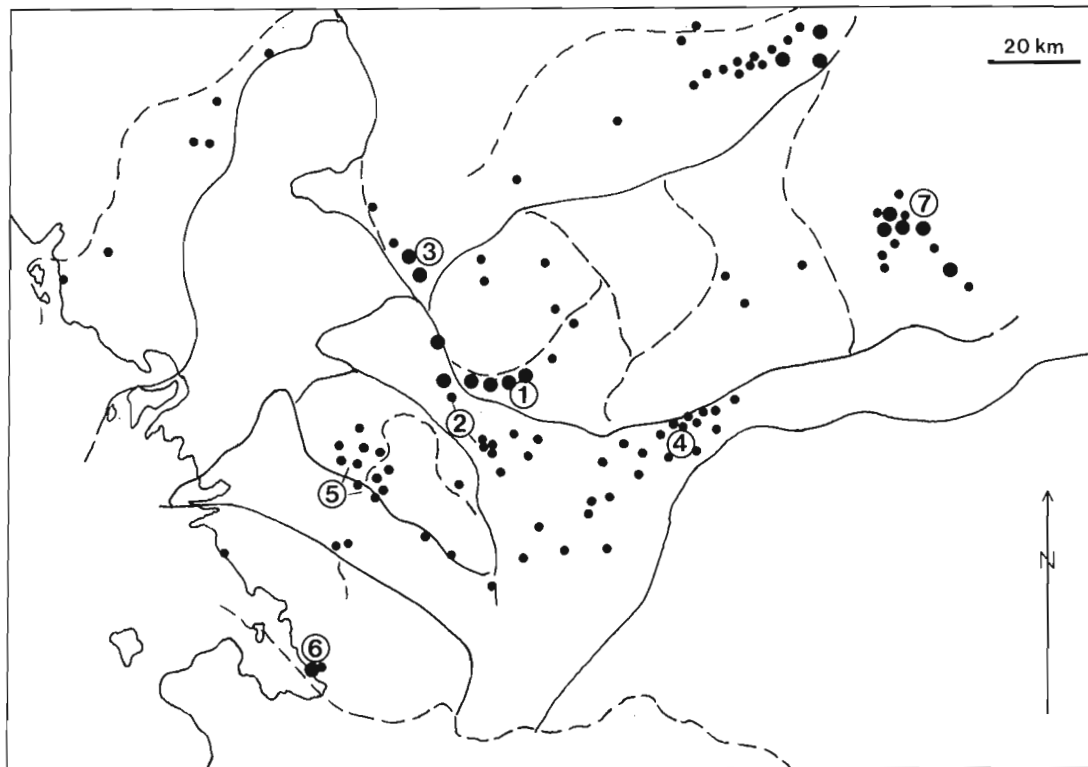


Figure 88.3. Generalized distribution of coronitic olivine metagabbro bodies in part of the Central Gneiss Belt. Outlines of lithotectonic subdivisions are shown (see Fig. 88.1 for nomenclature). Clusters discussed in this paper are: 1, Novar -Huntsville boundary zone, 2, Sequin subdomain, 3, southwestern Kiosk domain, 4, Kawagama zone, and 5, Rosseau subdomain. For 6, Go Home, and 7, Opeongo (Algonquin) occurrences, see Grant, 1985.

Novar-Huntsville boundary zone

Figure 88.4 shows the major concentration of coronitic olivine metagabbro bodies along the boundary between Novar and Huntsville subdomains just west of the town of Huntsville. The boundary zone is characterized by flaggy L-S tectonites which locally include fragments and slivers of anorthositic gneiss. Structures in Novar subdomain are either truncated or transposed into parallelism with the trend of the boundary zone. Nadeau (1985) proposed that the boundary zone was the site of northward-directed ductile thrusting of rocks of Huntsville subdomain over those of Novar subdomain, this having occurred before the emplacement of Seguin subdomain which lies to the south.

The metagabbro bodies vary from small pods about 5 m in diameter to large masses reaching 800 m in longest dimension. They are enveloped by gneisses, with which they are normally in tectonic contact. Possible examples of original, fine grained intrusive margins have been noted in two places, one of which is illustrated in Figure 88.5A, in which it seems likely that two metagabbro pods were once part of a single body with a primary chilled margin. Later deformation led to fragmentation and shearing of this body, accompanied by recrystallization of the gabbro to garnet amphibolite, whereby parts of the body became separated by remobilized, tightly folded and highly strained gneiss. Such small-scale tectonic reworking can also account for the overall map pattern through a combination of bounding and tectonic slicing of a few, formerly larger gabbro intrusions. Boudins of metagabbro are represented in Figure 88.5B; topographically they form knolls separated by valleys containing steeply dipping gneisses. In general the surrounding gneisses are highly strained, fine grained and commonly have isoclinally folded layering adjacent to the metagabbro bodies. Local mobilization at contacts between gneiss and metagabbro has produced chaotic interleaving of migmatitic gneiss, pegmatite and recrystallized gabbro. The gneissic protolith is identifiable in the northwest part of Lake Vernon (Fig. 88.4) as metaplutonic rock (Lake Vernon suite of Nadeau, 1985). To the east the metagabbroic rocks are underlain by highly strained gneiss of uncertain protolith that constitutes most of the subdomain boundary zone. Northwest of Big Island, metagabbroic pods appear to be tectonically

stacked; they have foliated margins truncated by steeply dipping gneiss (Fig. 88.5C) in which rotated feldspar augen indicate a northward transport direction.

Except in the cores of the larger bodies, the gabbroic rocks rarely contain unrecrystallized primary plagioclase, in contrast to many occurrences studied elsewhere in the region. The margins of the metagabbro bodies may be simply retrogressed and reworked to a fine grained garnet amphibolite. Alternatively they may be deformed to a foliated, clot-textured rock in which mafic porphyroclasts of clinopyroxene are surrounded by secondary amphibole. These clots are variably flattened, rotated and wrapped by recrystallized plagioclase. Further deformation has led to the development of attenuated mafic lenses separated by thin layers of fine grained feldspathic material.

Seguin subdomain in the Huntsville area

Metagabbro bodies in Seguin subdomain adjacent to Huntsville subdomain are of several types. West and northwest of Lake Vernon, a few, relatively large bodies of well preserved olivine metagabbro with minimal development of corona reactions occur within migmatitic gneisses. Some smaller bodies, however, although texturally well preserved, exhibit advanced reaction with complete replacement of original olivine, total recrystallization of plagioclase laths and their partial or complete replacement by garnet. South of Huntsville and west of Mary Lake (Fig. 88.6), the larger bodies of a cluster within migmatitic gneiss are predominantly recrystallized with either garnet pseudomorphs after plagioclase in a matrix of intergrown clinopyroxene and plagioclase or a well developed vein network structure. The former appears to be a case of completion of the reaction between olivine and plagioclase under static conditions. In the latter, the vein material is the dry assemblage plagioclase-hypersthene-augite, and surrounds dark cores containing the assemblage plagioclase-biotite-amphibole-garnet. The vein network structure is flattened in places and is locally folded. Its orientation is clearly truncated at the contacts of the metagabbro bodies with quartzofeldspathic gneiss, which are commonly the sites of pegmatite formation. Smaller metagabbro bodies in this

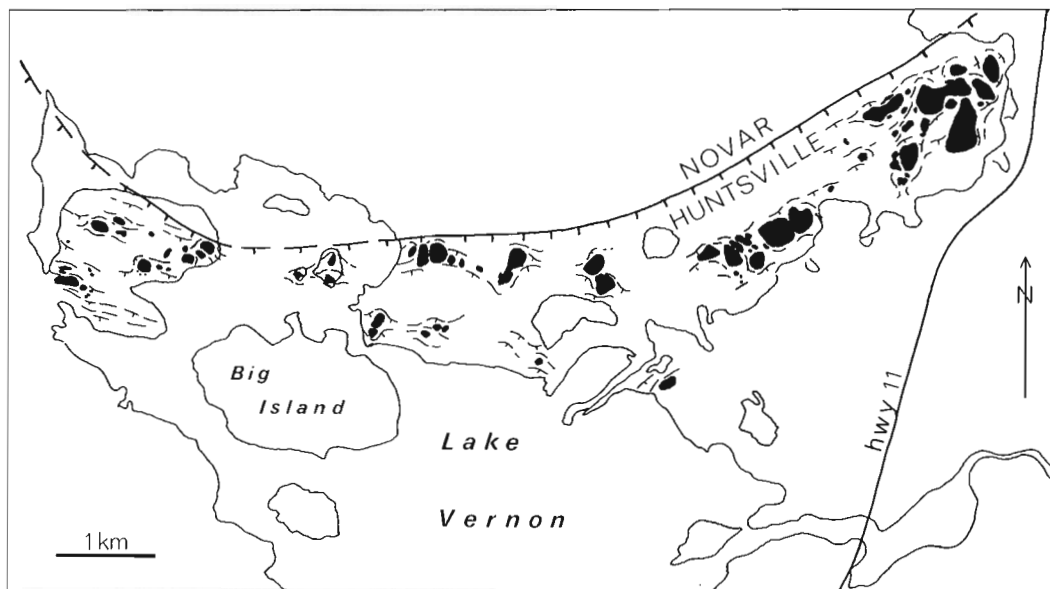


Figure 88.4. Sketch map of distribution of coronitic olivine metagabbro bodies (black) in Huntsville subdomain close to the boundary with Novar subdomain in the vicinity of Lake Vernon.

vicinity are foliated and tectonically interleaved with grey, migmatitic gneiss whose foliation is variable and wraps the included mafic blocks. Less than metre-size, boudin-like amphibolite masses and thin, folded amphibolite layers in migmatitic gneiss may represent the extreme product of tectonic break-up of formerly larger gabbroic masses in a ductile environment. Such small-scale tectonic inclusions are common in the gneisses in many parts of the Central Gneiss Belt.

Southwestern Kiosk domain

In the shear belt east of Parry Sound domain between the northwest margin of Novar subdomain and the village of Magnetawan (Fig. 88.3), well preserved coronitic olivine metagabbro bodies occur singly or in small clusters, particularly near Rainy Lake (Fig. 88.7). The surrounding amphibolite grade gneisses vary from grey, streaky, relatively mafic migmatites to leucocratic migmatites with pink leucosomes. The latter contain rare relict K-feldspar megacrysts in their mesosome and were probably derived from a granitoid plutonic protolith. The southeast margin of the gabbro body immediately northeast of Rainy Lake may be a preserved chilled intrusive contact; gabbro at the contact is fine grained, and coarsens toward the interior of the body. The large body southeast of Rainy Lake is locally very coarse grained, with primary feldspar laths in excess of 2 cm. Coronas around olivine and Fe-Ti oxide grains in these bodies have very narrow garnet rims; this is true even in the fine grained rocks near the contacts. In the cluster northwest of

Rainy Lake the gabbroic bodies show more recrystallization, locally developing to garnet-spotted textures, but some parts do retain a coronitic fabric. The largest gabbro mass occupies a hill on whose north slope the contact with underlying gneiss is exposed. It is a zone approximately 1 m wide of sheared and cataclastic gneiss and gabbro cut by deformed pegmatite. The country rock here is megacrystic (K-feldspar) granitoid orthogneiss. Farther northwest, near Magnetawan, a small coronitic metagabbro body, equant in plan and about 50 m in diameter, contains both well preserved, fine grained gabbro with minimal development of corona texture and garnet-spotted, clinopyroxene-rich derivative rock, the two grading into one another. At its margins the gabbro is heavily amphibolitized and has become detached into masses ranging from a few metres to a few centimetres in a matrix of sheared pegmatitic gneiss.

Kawagama zone

In the vicinity of Kawagama Lake northeast of the village of Dorset (Fig. 88.3), McLintock subdomain of Algonquin domain and the northeastern extension of Muskoka domain are separated by a moderately to shallowly southeast-dipping shear belt up to 4 km in outcrop width (Culshaw et al., 1983). Adjacent McLintock subdomain contains recognizable metasedimentary and granitoid plutonic gneisses interlayered with gneiss and granulite of

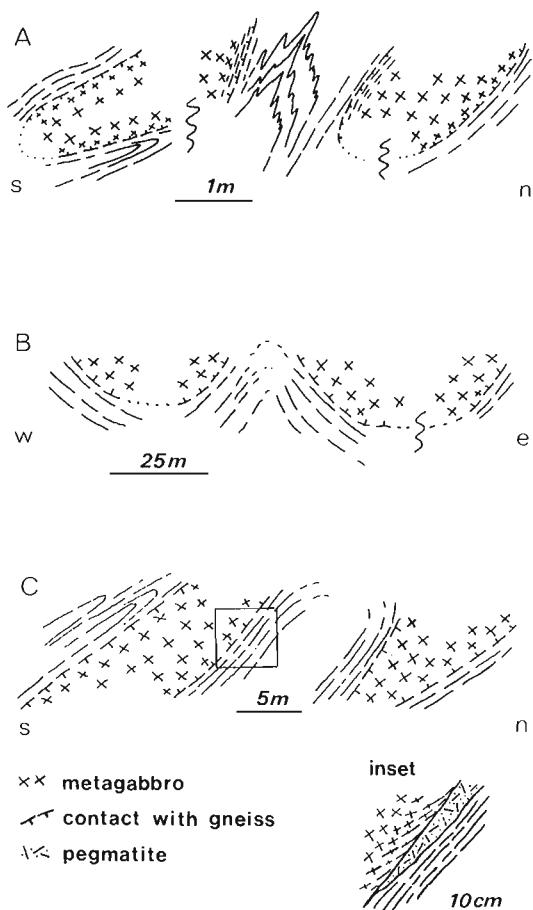


Figure 88.5. Sketches of field relationships of coronitic olivine metagabbro bodies with enclosing gneiss. See text for details.

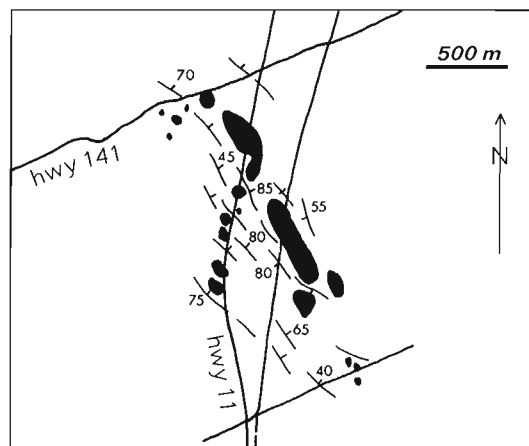


Figure 88.6. Sketch map of distribution of metagabbro bodies within migmatitic gneiss in the core of Seguin subdomain 2 km southwest of Mary Lake.

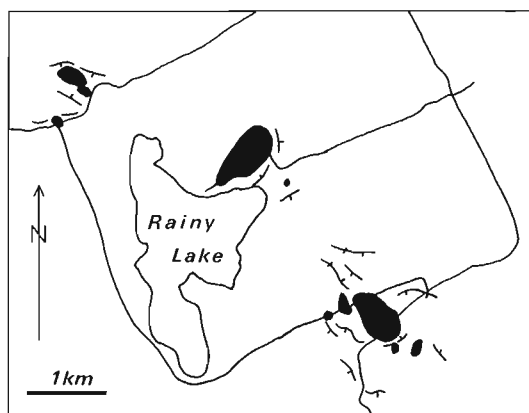


Figure 88.7. Sketch map of distribution of coronitic olivine metagabbro bodies in southwestern Kiosk domain; Rainy Lake is 10 km southwest of Burk's Falls (Fig. 88.2).

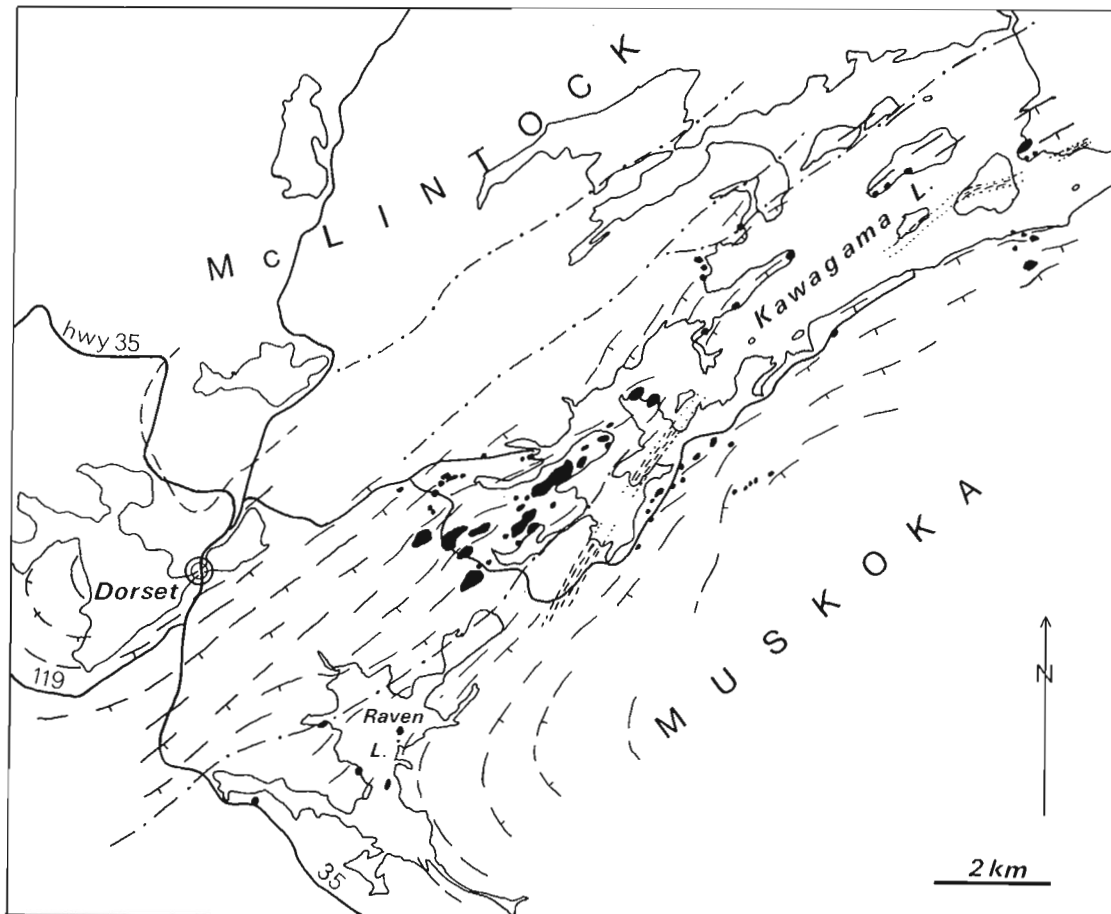


Figure 88.8. Sketch map of distribution of coronitic and amphibolitic metagabbro bodies in the Kawagama tectonic zone at the southwest margin of McIntock subdomain (see Fig. 88.2). Narrow patterned map unit is syenitic orthogneiss; other types of highly strained orthogneiss in long, narrow units are also present within the gneissic tectonites of the Kawagama zone.

unknown affinity. A characteristic orthogneiss is granodioritic and contains feldspar megacrysts or flattened feldspar aggregate augen up to 3 cm long; the rock varies from grey to olive-brown, the latter containing hypersthene. The metasediments include pelitic and semipelitic units and again are hypersthene-bearing in places. Major fold structures are present and are apparently truncated by the Kawagama shear zone.

Muskoka domain southeast of Kawagama Lake is composed predominantly of heterogeneous grey and pink migmatitic gneisses and has not been recognized to contain rocks of clearly metasedimentary origin. Highly deformed metagranitoid rocks are present in places, and include small patches of charnockitic rocks in an otherwise amphibolite facies terrane. Southeast of the Kawagama zone, gneissosity trends swing southward, defining large-scale open folds with gently east-southeast-plunging axes.

The boundary zone at Kawagama Lake (Fig. 88.8) is characterized by a concentration of metagabbro lenses, thin and continuous layers of orthogneiss, and some recognizable metasedimentary units all within a host of flattened migmatitic gneiss. One orthogneiss layer, a characteristic pink quartz syenite, has been traced sporadically for 12 km and is only 100-200 m thick. The gneissic rocks strike northeast, dip southeast between 15 and 30° and contain a strongly developed down-dip lineation. Minor perturbations

of this trend occur around the margins of the metagabbro bodies. Late, small-scale extensional shear folds occur locally near the southwest end of Kawagama Lake. The Kawagama zone contains several topographically defined lineaments parallel to its length. These probably represent particularly high strain zones along which late differential displacement has occurred between Muskoka and Algonquin domains. At River Bay on the northwest side of Kawagama Lake, mylonitic and cataclastic gneiss with pronounced southeast-plunging lineation is exposed. Pseudotachylyte veins cut the gneiss and probably represent the latest tectonic activity along this zone.

The metagabbroic rocks in the Kawagama zone show both greater compositional variety and degree of recrystallization than those previously described, perhaps with the exception of the metagabbros west of Mary Lake. Some have low plagioclase contents and border on ultramafic composition. Others have produced biotite-rich rocks on recrystallization. The largest body retains a coronitic interior with unrecrystallized plagioclase laths. In general, however, the bodies are now amphibolite and vein network metagabbro with patches showing relict recrystallized and clotted, foliated fabrics. All the contacts are tectonic and are usually associated with deformed, syntectonic pegmatite. Relict textures become highly flattened at the margins of the bodies, and vein networks are flattened, foliated, and in

places show isoclinal folds. As in the networks near Mary Lake, the more leucocratic veins have anhydrous assemblages containing pyroxenes and in places garnet. Tectonic stacking has occurred and may be observed on ridges where metagabbro lenses on the lower slopes are separated from those capping the hills by highly strained gneiss. Internal shearing within one metagabbro pod isolated by boudinage may be a small scale example of the overall tectonic pattern in the Kawagama zone (Fig. 88.9A).

Metagabbro bodies have not been recognized in the immediately adjacent part of McLintock subdomain to the northwest. In Muskoka domain to the southwest, however, metagabbro bodies are common, though more widely dispersed than in the Kawagama zone itself. For example, relatively well preserved metagabbro bodies exposed on the shores of Raven Lake (Fig. 88.8) are medium- to coarse-grained, have a patchy relict fabric of mafic coronas now cored by orthopyroxene, and contain recrystallized plagioclase laths with granular garnet in their centres. Some bodies are strongly lineated, and others vary from garnet-spotted amphibolite to vein network metagabbro with two-pyroxene-bearing neosomes. Again, foliation developed in the vein networks may be truncated at the contact with the surrounding gneiss (Fig. 88.9B).

Western Rosseau subdomain and its boundary with Moon River subdomain

Near the southwest shores of Lake Rosseau and Lake Joseph, the structures in Rosseau subdomain are truncated at the margin of Moon River subdomain to the southwest, where highly deformed and flattened migmatitic gneisses dip gently southwest and contain tectonic inclusions of meta-anorthosite (Davidson et al., 1982). Within Rosseau subdomain, an internal high strain zone, marked by a semi-continuous strip of meta-anorthositic gneiss, separates a terrane of metasedimentary and metaplutonic gneisses that verge on granulite facies (metamorphic hypersthene is present locally, particularly in the orthogneiss near Port Carling) from a predominantly migmatitic gneiss terrane to the northwest.

Metagabbro bodies, many of them coronitic, occur in both subdomains and also on either side of the internal high strain zone in Rosseau subdomain (see Davidson et al., 1982, for their distribution). In the northwest part of Rosseau subdomain, they are enveloped by pink migmatitic gneisses with thin amphibolite layers and lenses. With two exceptions they are small and recrystallized; the two larger bodies, however, contain well preserved coronitic olivine metagabbro. The abundant smaller bodies were probably derived by boudinage of larger masses; they are variably recrystallized, ranging from those with relict igneous fabric to those that are now garnet amphibolite. Near the boundary with Moon River subdomain, deformation is apparently more intense and metagabbroic boudins are foliated and sheared into clotted, porphyroclastic rock. Some are completely recrystallized to amphibolite; at one locality a foliated vein network was observed.

Many small lenses and blocks of amphibolite occur within the layering of the marginal Moon River gneissic tectonites. A few of the larger mafic masses preserve what appears to be a deformed coronitic texture. In one body exposed on the highway 2 km southwest of Port Carling, strings of red garnet in a clinopyroxene-rich matrix mark former plagioclase laths; this rocks looks like a flattened equivalent of the well preserved garnet-lath metagabbro already described from west of Mary Lake.

Summary of field relationships

In all the areas studied so far, the distribution of metagabbro bodies can be accounted for by map-scale boudinage of former larger gabbroic masses during ductile deformation within gneissic envelopes. The mechanism was probably progressive in any one area, with initially large boudins continuing to pull apart to form smaller ones as deformation proceeded. It is tempting to suggest that the abundance of smaller amphibolitic boudins in the Kawagama zone and south of it, in the area west of Mary River, and in the Moon River subdomain margin near Port Carling may have resulted from further tectonic reworking of already boudined metagabbro masses such as are present at Lake Vernon and elsewhere. This would accord with the sequence of tectonic stacking suggested by Culshaw et al. (1983; see Fig. 88.1) whereby Seguin and Moon River subdomains and their extension eastward in Muskoka domain were emplaced together after deformation within Algonquin domain and Rosseau subdomain (an inlier of deck 1). However, relatively large and well preserved coronitic metagabbro bodies as well as highly deformed ones do occur within Seguin and Moon River subdomains, and it is therefore possible that gabbroic magma was introduced into the crust throughout a protracted period of perhaps episodic deformation.

Although layering ascribable to a primary igneous origin has been observed in a few of the well preserved metagabbro bodies, it is very rare; more common are patchy segregations of markedly different grain size. It does not seem likely, therefore, that the concentrated clusters of metagabbro bodies were derived by the break-up of layered mafic igneous complexes. The distribution of the coronite bodies shows that they are not restricted to the high strain zones that bound the lithotectonic domains and subdomains. Neither do they appear to be spatially related to any one particular type of host rock. Relatively uniform fine grain size of some bodies, ophitic texture, and the local preservation of what can best be interpreted as former chilled contacts together suggest that these bodies were derived for the most part from relatively small intrusions, perhaps irregular dykes. Although coarse grain size, found in many of the larger bodies, is commonly thought to be a feature of large igneous masses, it may occur in relatively small intrusions if nucleation sites are widely spaced and crystallization is rapid; stellate and feathery plagioclase growth observed in some metagabbro bodies support this contention. It is possible that the gabbroic magma was introduced into a ductile medium deep crust when the surrounding rocks were at conditions of amphibolite or granulite facies metamorphism. Intruded at deep level, subsolidus reactions between olivine and plagioclase, and Fe-Ti oxide and plagioclase (and perhaps interstitial fluid) would occur during cooling from magmatic temperature to ambient metamorphic temperature at high pressure. The other alternative is that the metagabbro bodies represent relatively high level intrusions that were buried during tectonic stacking, the reactions recorded within them being entirely the result of superimposed metamorphism, and separation into tectonically enclosed masses being the effect of Grenvillian deformation. It is hoped that a thorough study of rock and mineral

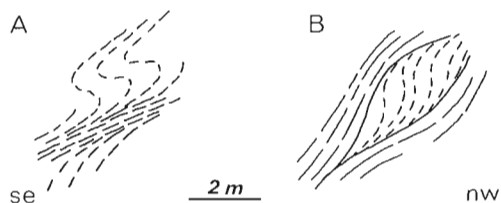


Figure 88.9. Tectonic features associated with deformed metagabbro in the Kawagama tectonic zone.

chemistry will shed some light on the mechanisms of the corona reactions, possibly leading to a resolution of the alternative modes of formation expressed above.

Preliminary analytical results

XRF whole-rock analyses have been made to date on coronitic olivine matagabbros from Go Home (4), Opeongo (10), Huntsville (6) and Seguin (6) subdomains. Analyses were made in order to assess the amount of variation in bulk chemical composition within and between areally distinct clusters. Preliminary results are shown as oxide/oxide plots in Figure 88.10 and approximate ranges for all the analyses are given in Table 88.1. The plots show that, although there is considerable overlap between some clusters,

there are significant differences between them. None of the plots, for example, show any overlap between the Go Home and Opeongo clusters, which are discriminated in particular by the high Fe and Ti contents of the Opeongo metagabbros.

Differences in bulk composition are reflected both by differences in proportions of primary igneous minerals and in mineral compositions. In the first case, for example, the Go Home coronites have a higher plagioclase content than those from any other population, and those from the Opeongo cluster are notably rich in ilmenite and its titanian corona minerals. In the second case, primary olivine ranges from Fo₅₅ (Go Home) to as fayalitic as Fo₂₈ (Opeongo), with comparable differences in primary clinopyroxene and the

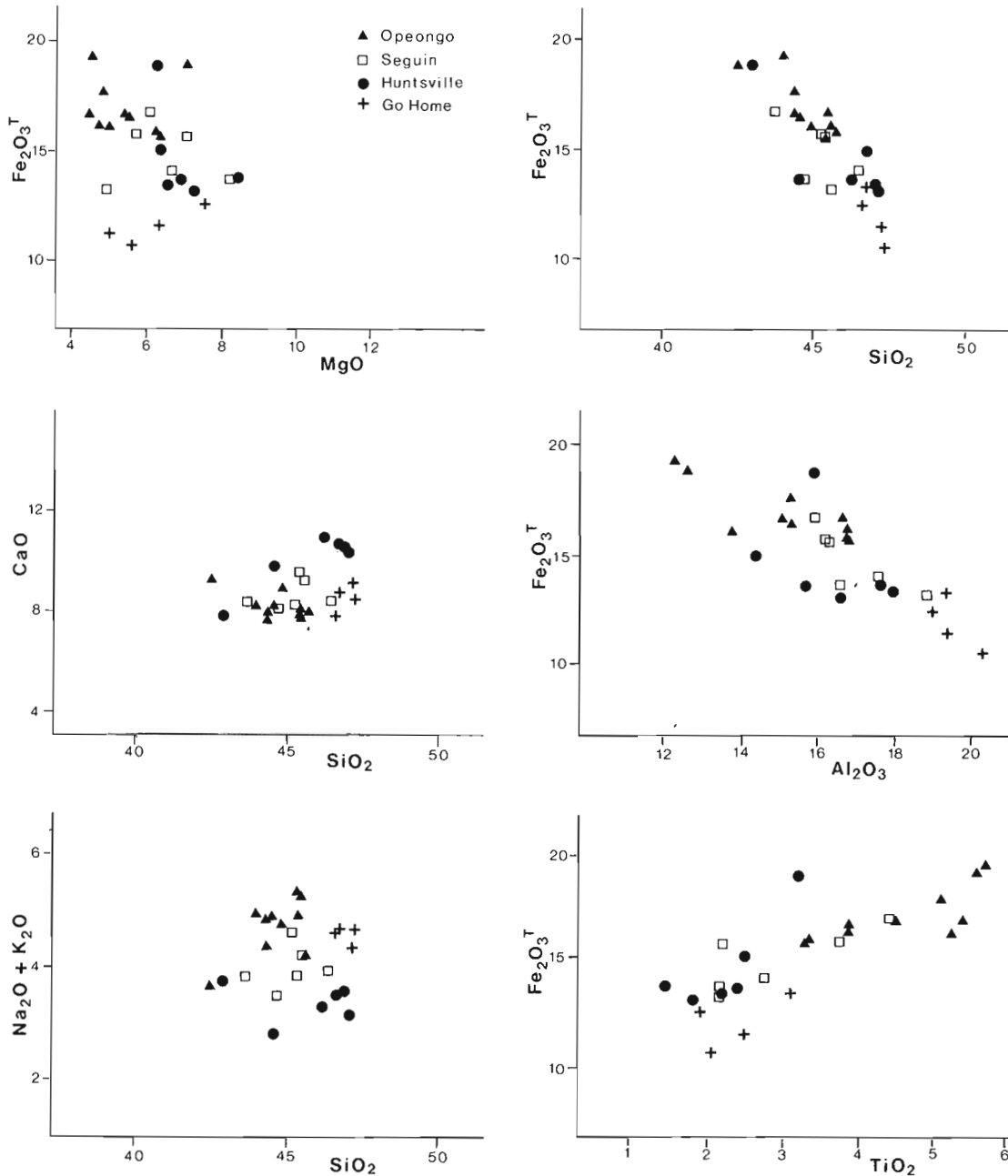


Figure 88.10. Oxide/oxide plots (weight per cent, and with total Fe as Fe_2O_3) showing range of bulk rock composition in coronitic olivine metagabbro from Opeongo, Seguin, Huntsville and Go Home subdomains.

Table 88.1. Range in composition (weight per cent) of coronitic olivine metagabbro from Go Home, Opeongo, Huntsville and Seguin subdomains

SiO ₂	42.2 - 47.2
TiO ₂	1.4 - 5.7
Al ₂ O ₃	12.2 - 20.0
Fe ₂ O ₃ T	10.6 - 19.4
MgO	4.3 - 8.5
CaO	7.6 - 10.9
Na ₂ O	2.5 - 3.6
K ₂ O	0.3 - 1.1

secondary mafic silicates. Garnet compositions, however, do not appear to have as wide a range of Mg:Fe ratios as the other mafic silicates.

It is of interest that the corona minerals formed around ilmenite are notably magnesian, and are only slightly richer in iron than those developed around olivine, attesting to considerable ion mobility at grain scale. In this regard, most coronites do not show any evidence for reaction between primary clinopyroxene and plagioclase, yet where these two minerals are in contact adjacent to olivine or ilmenite coronas, narrow rims of amphibole and garnet in particular have spread along the clinopyroxene-plagioclase interfaces.

Further mineral analytical work will be aimed at carefully evaluating the variations in the corona reactions observed from place to place, and details of the mechanism by which they formed. It is hoped that thermobarometric estimates from coronite assemblages, coupled with those obtained from the surrounding country rocks, will help to solve which of the two mechanisms, primary subsolidus reaction or superimposed metamorphism, is responsible for the reactions, or whether and to what extent both have been involved.

References

- Anowitz, L.M. and Essene, E.J.
1986: Thermobarometry in the Grenville Province, Ontario; Geological Association of Canada, Program with Abstracts, v. 11, p. 41 (abstract).
- Culshaw, N.G., Davidson, A., and Nadeau, L.
1983: Structural subdivisions of the Grenville Province in the Parry Sound-Algonquin region, Ontario; in Current Research, Part B, Geological Survey of Canada, Paper 83-1B, p. 243-252.
- Davidson, A.
1984: Identification of ductile shear zones in the southwestern Grenville Province of the Canadian Shield; in Precambrian Tectonics Illustrated, ed. A. Kröner and R. Greiling; E. Schwartzbart'sche Verlagsbuchhandlung, Stuttgart, p. 263-279.
- Davidson, A. and Morgan, W.C.
1981: Preliminary notes on the geology east of Georgian Bay, Grenville Structural Province; in Current Research, Part A, Geological Survey of Canada, Paper 81-1A, p. 291-298.
- Davidson, A., Culshaw, N.G., and Nadeau, L.
1982: A tectono-metamorphic framework for part of the Grenville Province, Ontario; in Current Research, Part A, Geological Survey of Canada, Paper 82-1A, p. 175-190.
- Emslie, R.F.
1983: The coronitic Michael gabbros, Labrador: assessment of Grenvillian metamorphism in northeastern Grenville Province; in Current Research, Part A, Geological Survey of Canada, Paper 83-1A, p. 139-145.
- Geological Survey of Canada
1953: Whitney; Geological Survey of Canada, Aeromagnetic Map 111G.
- Grant, S.M.
1985: Coronitic gabbro and meta-anorthosite in the Central Gneiss Belt, Grenville Province of Ontario; in Davidson, A., Nadeau, L., Grant, S.M., and Pryer, L.L., Studies in the Grenville Province of Ontario; in Current Research, Part A, Geological Survey of Canada, Paper 85-1A, p. 474-478.
- Lumbers, S.B.
1971: Geology of the North Bay area, Districts of Nipissing and Parry Sound; Ontario Department of Mines and Northern Affairs, Geological Report 94, 104 p.
1976: Mattawa - Deep River area (western half), District of Nipissing; Ontario Division of Mines, Preliminary Map P.1196, Geological Series.
1982: Summary of metallogeny, Renfrew County area; Ontario Geological Survey, Report 212, 59 p.
- McLelland, J.M. and Whitney, P.R.
1980: Compositional controls on spinel clouding and garnet formation in plagioclase of olivine metagabbros, Adirondack Mountains, New York; Contributions to Mineralogy and Petrology, v. 73, p. 243-251.
- Moecher, D.P. and Essene, E.J.
1986: Fluid composition in Grenville gneisses: constraints from scapolite equilibria; Geological Association of Canada, Program with Abstracts, v. 11, p. 102 (abstract).
- Nadeau, L.
1985: Characterization of lithotectonic units and their boundaries in the Huntsville region, Central Gneiss Belt; in Davidson, A., Nadeau, L., Grant, S.M., and Pryer, L.L., Studies in the Grenville Province; in Current Research, Part A, Geological Survey of Canada, Paper 85-1A, p. 464-474.
- Schwerdtner, W.M. and Lumbers, S.B.
1980: Major diapiric structures in the Superior and Grenville provinces of the Canadian Shield; in The Continental Crust and its Mineral Deposits, ed. D.M. Strangway; Geological Association of Canada, Special Paper 20, p. 149-180.
- Whitney, P.R. and McLelland, J.M.
1973: Origin of coronas in metagabbros of the Adirondack Mts., N.Y.; Contributions to Mineralogy and Petrology, v. 39, p. 81-98.

SCIENTIFIC AND TECHNICAL NOTES NOTES SCIENTIFIQUES ET TECHNIQUES

Titaniferous placers on the central continental shelf off western Canada

Project 840033

J.V. Barrie¹ and J.L. Luternauer
Cordilleran and Pacific Margin Division, Vancouver

Barrie, J.V. and Luternauer, J.L., Titaniferous placers on the central continental shelf off western Canada; in Current Research, Part B, Geological Survey of Canada, Paper 86-1B, p. 849-852, 1986.

Abstract

Concentrations of titanium ranging from 0.6-1.1% by volume with associated concentrations of vanadium as high as 0.04% and zirconium as high as 0.2% were found in surficial sediments collected from water depths of approximately 100 m on the northern margin of Cook Bank and southwestern margin of Goose Island Bank in Queen Charlotte Sound. These deposits are of potential economic grade but further surveys must be performed to evaluate their extent, thickness and mineralogical variability.

Résumé

On a trouvé des concentrations de titane variant de 0,6 à 1,1 % en volume avec des concentrations associées de vanadium et de zirconium atteignant respectivement 0,04 et 0,2 % dans les sédiments de surface prélevés sous l'eau, à des profondeurs d'environ 100 m sur la marge nord du banc Cook et sur la marge sud-ouest du banc de l'île Goose dans le détroit de la Reine-Charlotte. Le potentiel économique de ces gisements est évident mais il faudra procéder à des études additionnelles afin d'évaluer leur étendue, leur épaisseur et leur variabilité minéralogique.

¹ C-CORE, Memorial University of Newfoundland, St. John's, Newfoundland A1B 3X5

Introduction

A report on the Late Quaternary history and sedimentation of Queen Charlotte Sound, British Columbia (Luternauer and Murray, 1983) (Fig. 1,2) identified extensive areas with well sorted sands (Fig. 3) from which three samples were collected at 82, 102 and 122 m water depths which contained 22, 28 and 26 wt% heavy mineral concentrations, respectively (Fig. 2). These concentrations are very high when compared to the norm for detrital sediments (Folk, 1974). As part of a more extensive assessment of placer deposits on the central and northern shelf off western Canada these samples were analyzed for their elemental and mineral composition. Attention was focused first on the titanium content of these samples as deposits of titaniferous magnetite had been recognized on the southern shores of Queen Charlotte Sound (Holland and Nasmith, 1958) and because several previously examined samples in the Sound contained high proportions of opaques at least part of which were identified as ilmenite (Wiese, 1969).

Methods

Heavy mineral separation was performed by the standard gravity method using tetrabromoethane and separatory funnels (Carver, 1971). The resultant heavy

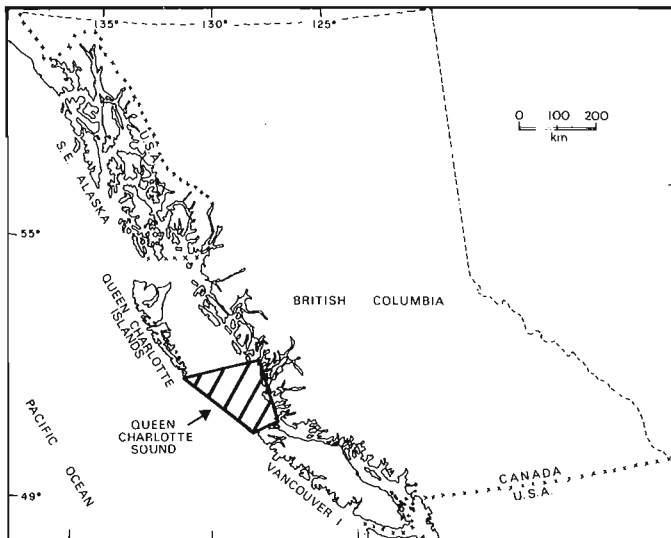


Figure 1. Index map.

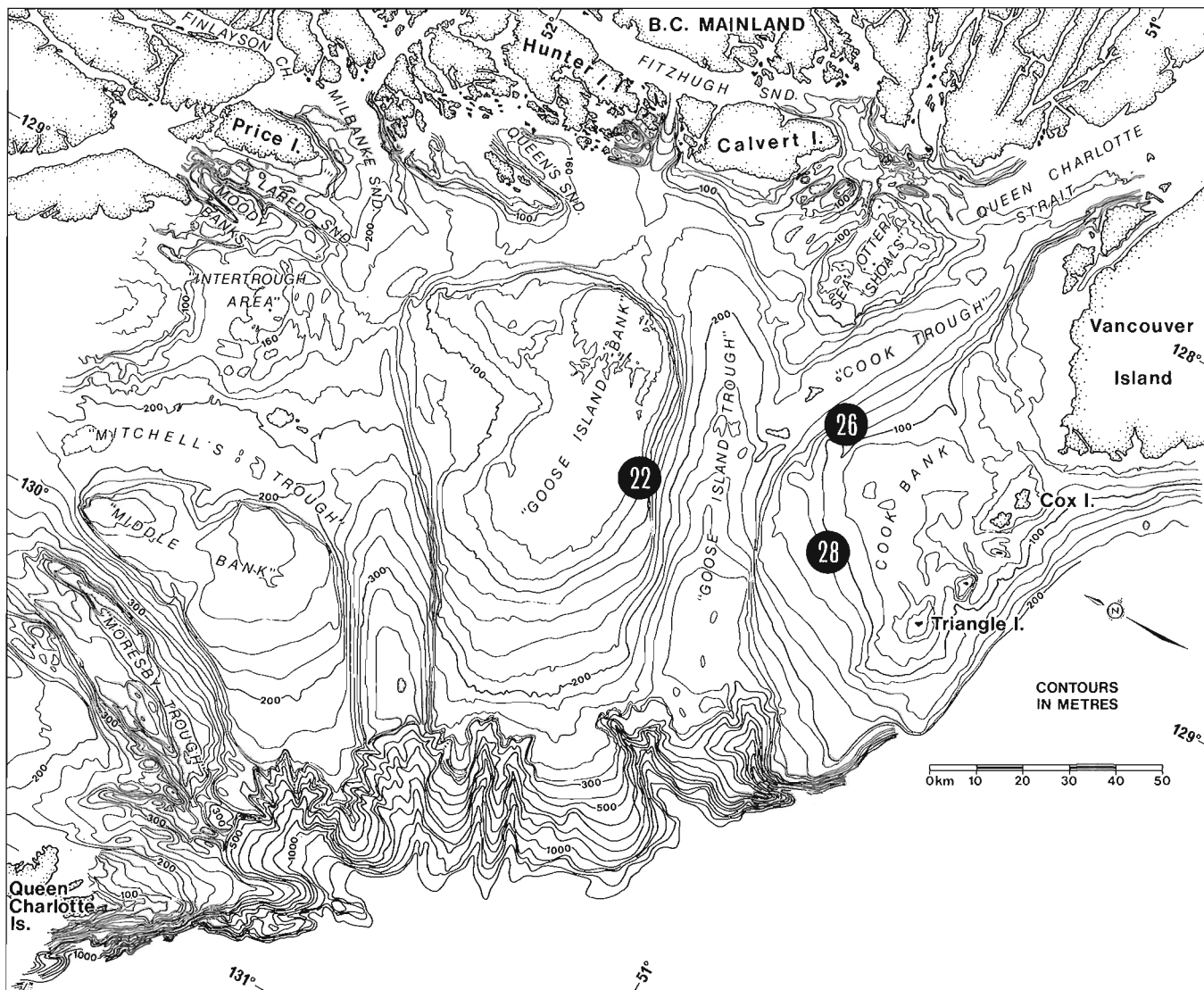


Figure 2. Location and total heavy mineral concentration of analyzed samples in Queen Charlotte Sound.

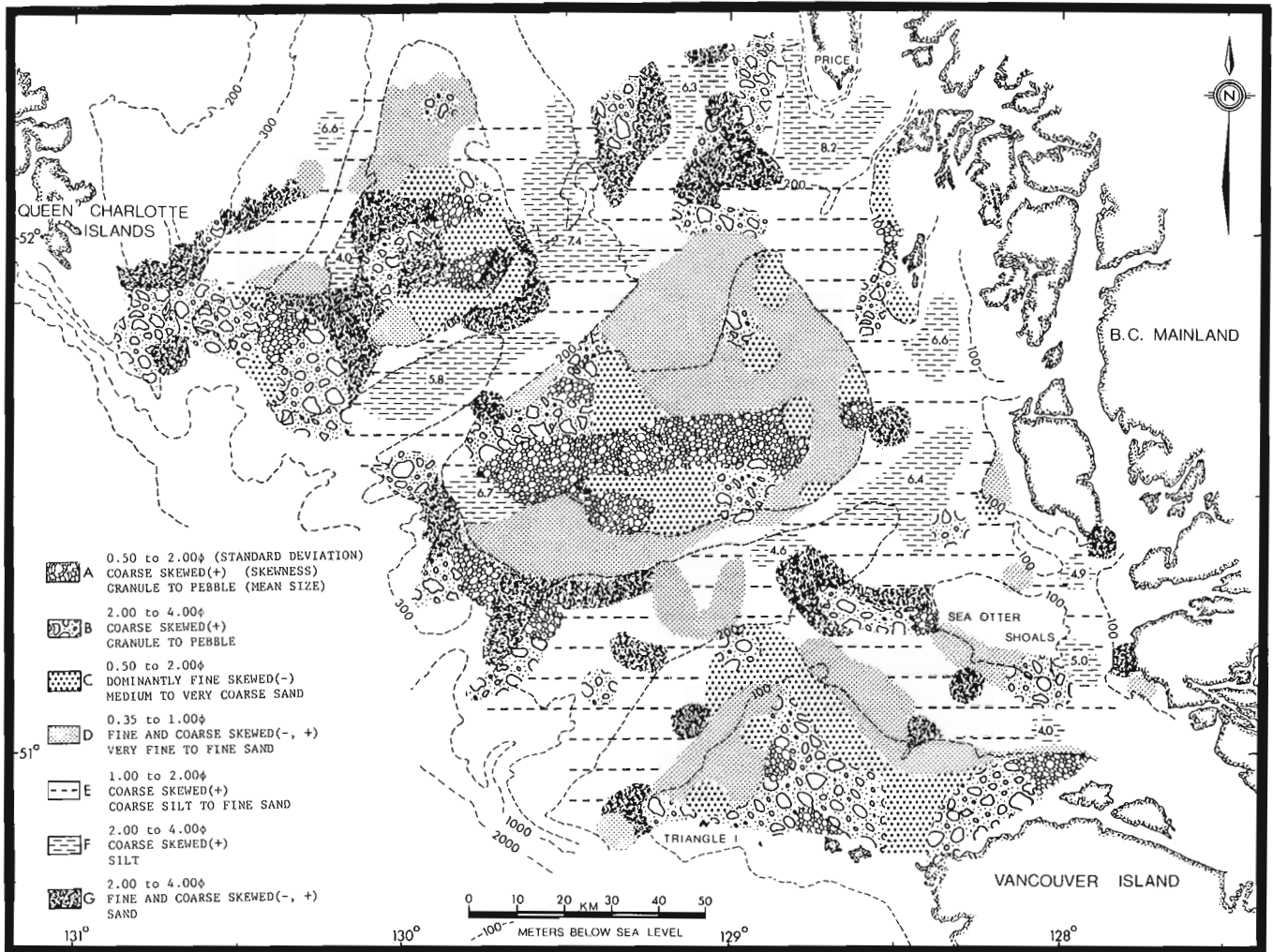


Figure 3. Grain size distribution of sediments in Queen Charlotte Sound. Local minimum mean grain size indicated in areas having type F sediment (from Luternauer and Murray, 1983).

Table 1. Heavy mineral percentages of amphibole, opaques (ilmenite), sphene and magnetite as well as concentrations of manganese, titanium, vanadium, chromium and zirconium. Sample locations shown in Figure 2

Sample Number	Water Depth (m)	Total Heavy Mineral Concentration (wt%)	Specific Heavy Mineral Concentration (wt%)				Specific Element Concentration (PPM)				
			Amp	Op	Sp	Mag	Mn	Ti	V	Cr	Zr
74	102	28	45	21	8	5	235	6500	160	85	350
63	122	26	45	11	8	15	235	10 800	330	120	750
180	82	22	50	4	8	7	205	7400	185	120	1450

residue, after magnetic separation, was split using a microsplitter and mounted in Canada balsam for examination. At least 200 non-opaque minerals were counted per slide using the ribbon method (Galehouse, 1971). Subsamples were also epoxied, thin sectioned, polished and carbon coated for analysis of the elemental concentration of principal heavy minerals, particularly the opaques, by a scanning electron microscope (SEM) element backscatter unit.

Results

The nonmagnetic heavy mineral suite is dominated by amphibole and lesser concentrations of ilmenite and sphene (Table 1). The latter two minerals both contain titanium. Other minerals found in quantities greater than 5 wt% are garnet, epidote, magnetite (including titaniferous magnetite) and chlorite. The individual sand samples have a combined ilmenite, rutile and zircon content as high as 5 wt%. The SEM assay established that the three samples contained anomalously high concentrations of titanium and associated vanadium and zirconium (Table 1).

Discussion and conclusions

The combined ilmenite, rutile and zircon concentrations compare favorably with those of a mined beach deposit along eastern Australia which contains rutile and zircon grades ranging between 0.2-10% (Jones and Davies, 1979). There is, therefore, potential for an economic deposit of titanium in Queen Charlotte Sound. However, further work must be undertaken to define the lateral extent, thickness and variability of these deposits.

References

- Carver, R.E.
1971: Heavy mineral separation; in *Procedures in Sedimentary Petrology*, ed. R.E. Carver; John Wiley and Sons, New York, p. 427-452.
- Folk, R.L.
1974: *Petrology of sedimentary rocks*; Hemphill's, Austin, Texas, 168 p.
- Galehouse, J.S.
1971: Sedimentation analysis; in *Procedures in Sedimentary Petrology*, ed. R.E. Carver; John Wiley and Sons, New York, p. 69-94.
- Holland, S.S. and Nasmith, H.W.
1958: *Investigations of beach sands*; British Columbia Department of Mines, Special Report, p. 3-8.
- Jones, H.A. and Davies, P.J.
1979: Preliminary studies of offshore placer deposits, eastern Australia; *Marine Geology*, v. 30, p. 243-268.
- Luternauer, J.L. and Murray, J.W.
1983: Late Quaternary morphologic development and sedimentation - central British Columbia continental shelf; *Geological Survey of Canada, Paper 83-21*, 38 p.
- Wiese, W.
1969: *Studies on properties, distribution and heavy mineral contents of sediments in northern Queen Charlotte Sound*; unpublished B.Sc. thesis, Department of Geological Sciences, University of British Columbia, 78 p.

Garnetiferous gneisses and a quartz syenite intrusive sheet at Lynx Lake, Northwest Territories

Project 770024

S.S. Gandhi
Mineral Resources Division

Gandhi, S.S., Garnetiferous gneisses and a quartz syenite intrusive sheet at Lynx Lake, Northwest Territories; in Current Research, Part B, Geological Survey of Canada, Paper 86-1B, p. 853-857, 1986.

Abstract

Garnetiferous quartzo-feldspathic gneisses, containing lenses of amphibolite, predominate in a 40 x 40 km area of the Lynx and Howard lakes. They are intruded by a quartz syenite sheet 50 km long and up to 4 km wide in plan. The intrusion has an arcuate outline and occurs at the crest of a 15 km wide antiform plunging gently to the southwest. A vertical sheared and mylonitic zone, up to 6 km wide and trending northeast, occurs on the southeast side of the intrusion.

Résumé

Des gneiss grenatifères de nature quartzo-feldspathique, contenant des lentilles d'amphibolite, constituent le matériau le plus répandu dans une superficie de 40 sur 40 km de la région des lacs Lynx et Howard. Ces roches comprennent une intrusion d'une couche de syénite à quartz de 50 km de long et pouvant atteindre 4 km de large. Cette intrusion a un contour arqué et se trouve sur l'arête d'un anticlinal de 15 km de large, incliné en pente douce vers le sud-ouest. Une zone mylonitique et cisailée à composante verticale, atteignant 6 km de largeur et d'orientation nord-est, se manifeste du côté sud-est de l'intrusion.

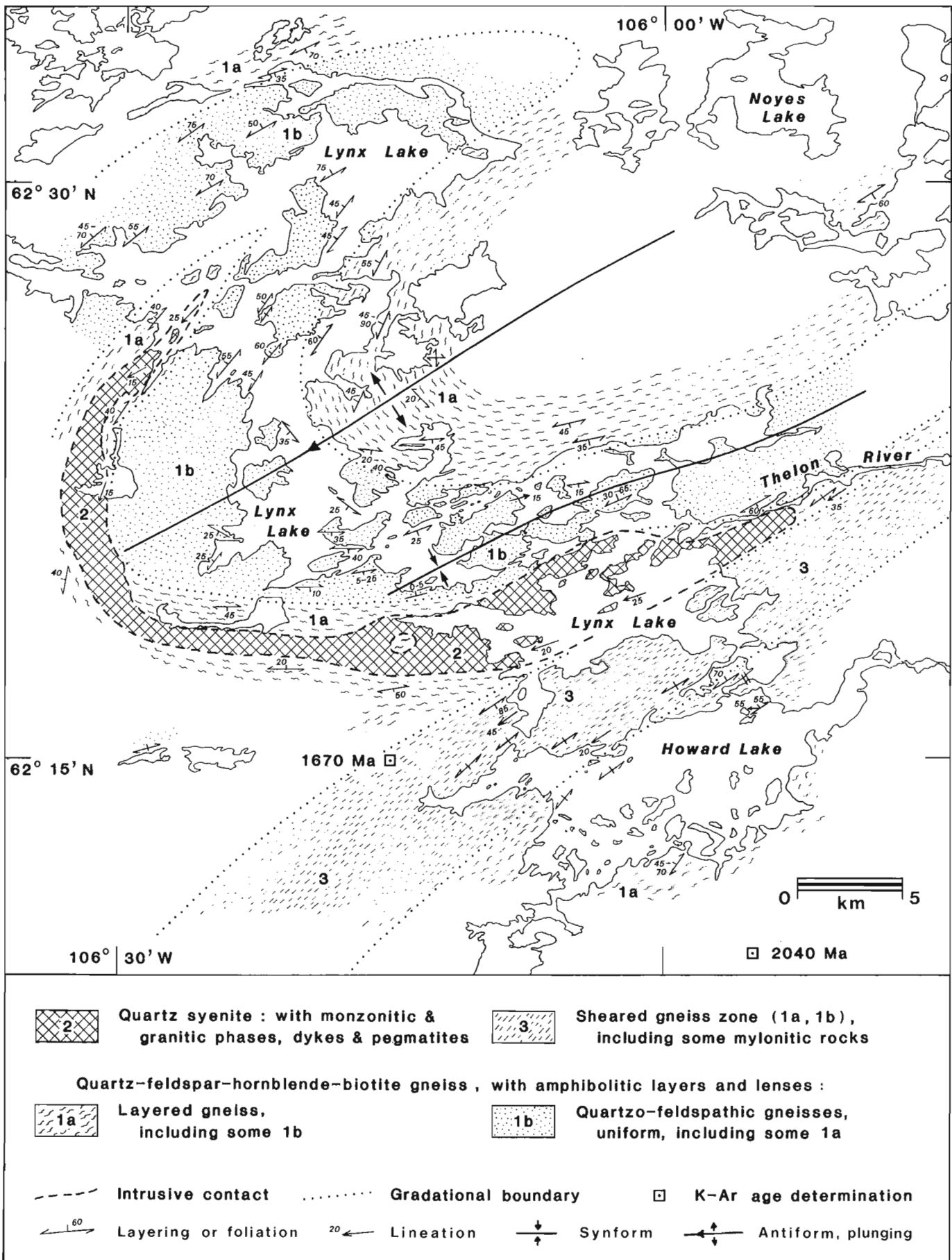


Figure 1. Generalized geological map of the Lynx Lake area, Northwest Territories.

General geology

The Lynx Lake-Howard Lake area (75J) is part of the Aphebian basement, 70 km southwest of the Helikian Thelon sandstone (Wright, 1967). Reconnaissance mapping on scale 1 inch to 8 miles by Wright (1967) showed the granite, granodiorite and allied rocks as predominant in the area, with a 5 km wide zone of gneisses and schists derived from sedimentary and volcanic rocks, trending southwesterly from the south end of Lynx Lake. He reported a K-Ar date of 1670 Ma on a biotite amphibolite on the northwest margin of this zone of gneisses and schists, and another date of 2040 Ma on a gneissic granite south of Howard Lake (Fig. 1).

Observations by the writer in 1985 showed that this zone of gneisses and schists contains highly sheared and mylonitic rocks, and grades into the gneisses that are common throughout the study area (unit 1, Fig. 1). The granitic rocks are limited in extent, represented by a quartz syenite intrusion and related dykes and pegmatites. The gneisses, quartz syenite and the shear zone reveal a sequence of events briefly outlined here.

Quartzo-feldspathic gneisses and amphibolite (unit 1)

Quartz-feldspar-hornblende-biotite gneisses, ranging from felsic to intermediate in composition and containing layers and lenses of amphibolite, can be grouped broadly into two subunits (Fig. 1): (1a) predominantly layered gneisses and (1b) relatively uniform quartzo-feldspathic gneisses with a minor component of layered gneisses. Garnet is commonly present in the two subunits and in the amphibolites. It is generally concentrated along layers up to a few centimetres thick.

The layered gneisses (subunit 1a) have compositionally distinctive layers and lenses due to variation in abundance of the mafic minerals, and also show some variations in texture. The layering is on a centimetre to metre scale. Some of the felsic layers have porphyroblastic feldspar, and resemble subunit 1b. Foliation is parallel to or at low angles to the layering.

The quartzo-feldspathic gneisses (subunit 1b) are of relatively more homogeneous character over widths of several tens of metres. They contain feldspar porphyroblasts 1 to 2 cm long, are well foliated, and locally show well



Figure 2. Highly deformed pegmatite in a quartz-feldspar-biotite layer of unit 1a, on the west shore of Howard Lake; view looking north; north end of the pegmatite layer on the left is cut by an east-northeasterly trending mafic dyke containing garnet; glacial grooves and striae trend westerly (62°13.7'N; 106°6.1'W). GSC 204136-R

developed augen texture. A few of these, in zones several metres thick, contain very coarse feldspar crystals up to 8 cm long. Mafic minerals usually constitute between 10 and 20 per cent of the rock, with hornblende generally predominant over biotite, but biotite is the main mafic constituent in some of the gneisses.

The amphibolite lenses in the two subunits range in size up to several tens of metres in thickness and several hundred metres in length. They lack recognizable volcanic features, and although most are conformable to foliation and layering, some show transgressive relationships. The latter may represent mafic sills and dykes. The amphibolites also occur as a series of boundin-like lenses a few centimetres to several tens of metres long, parallel to foliation and layering.

The gneisses of the two subunits contain pegmatitic veins and lenses that are deformed, and in places they are tightly folded and boundinaged (Fig. 2).

The layering and foliation in the unit define a major antiformal and subsidiary synforms at Lynx Lake.

Quartz syenite (unit 2)

This is a sill-like intrusive body. It is arcuate in plan and continuous for a 50 km length with a width of up to 4 km. It has sharp contacts with gneisses of unit 1, commonly at a low angle to the foliation and layering in the latter. The quartz syenite is medium- to coarse-grained and massive to crudely lineated due to streaky aggregates of mafic minerals. The main minerals are plagioclase, potash feldspar (orthoclase, microcline, perthite), quartz, hornblende and biotite. The accessory minerals are magnetite, apatite, zircon, and fluorite, and rarely garnet at the contacts of the intrusion. The composition varies from monzonitic through quartz syenitic to granitic. The hornblende-rich varieties contain traces of augite in hornblende aggregates. Quartz commonly makes up less than 15 per cent of the rock. Potash feldspar predominates over plagioclase. Zircon is locally abundant, and forms euhedral or subhedral crystals surrounded by radiation haloes. Purple fluorite was observed at several localities.

The intrusion is distinctly radioactive, showing 100-150 counts per second on an Exploranium GRS-101 scintillometer, in contrast to 30 to 60 counts per second for the rocks of unit 1. In addition, numerous dykes and pegmatites related to the intrusion are similarly radioactive. They cut the deformed, less radioactive, older pegmatites in the gneisses. The highest radioactivity (200 to 300 counts per second) was encountered in the reddish sapprolitic material derived from the quartz syenite at Mountain Bay on the west shore of Lynx Lake (62°25'N; 106°40'W).

The intrusion contains xenoliths of the gneissic country rock at several localities. At Mountain Bay, or gneissic xenolith 20 m wide and 75 m long, contains a quartzite lens up to 15 m wide and 50 m long. Quartzite however is not seen in the country rock within the study area. The nearest quartzite exposure is approximately 20 km southwest of Lynx Lake (62°13.5'N; 106°40'W) where it is associated with micaceous schist and quartzo-feldspathic gneiss. It was discovered during the course of this study. It forms a ridge 1.5 km long and up to 200 m wide, trending east-northeast.

Sheared gneissic zone (unit 3)

This is a nearly vertical, northeast trending zone characterized by highly sheared and mylonitic rocks. Compositionally the zone as a whole is similar to the layered gneiss (subunit 1a), but the layering is more pronounced and the layers and lenses are generally thinner (Fig. 3). Some are thinly laminated or fine grained and lineated due to

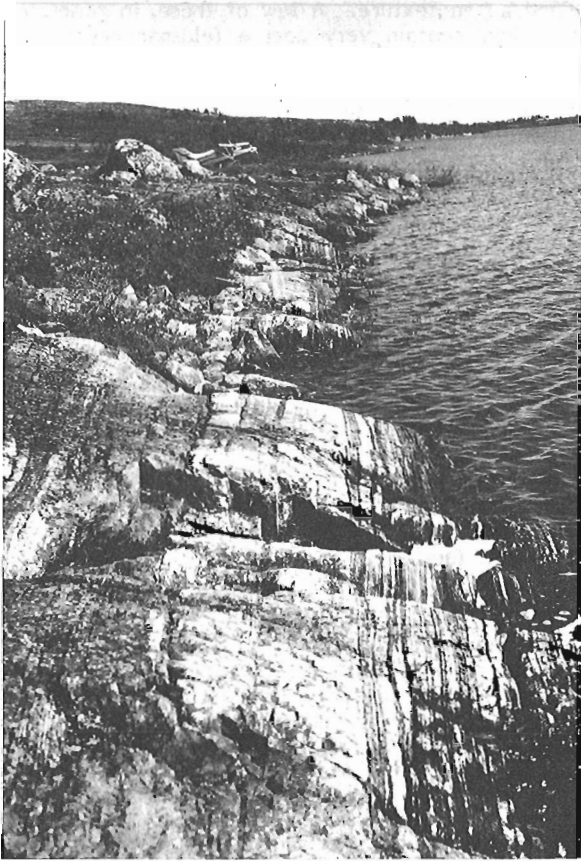


Figure 3. Typical outcrop surface of the highly sheared and mylonitic 'straight' zone (unit 3); 2.5 km west of rapids between Howard and Lynx lakes; looking northeast; pyrite-bearing fractures at the centre of the photograph are radioactive, with two spots reading 600 and 1200 counts per second on the Exploranium GRS-101 scintillometer (62°17'N; 105°58.2'W). GSC 204136-Q

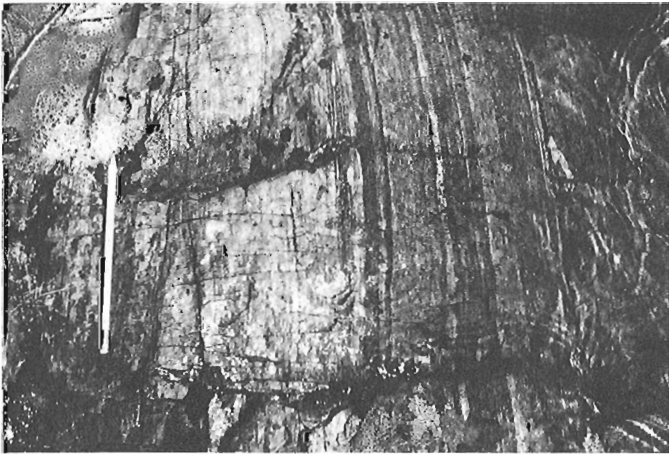


Figure 4. Close-up photograph of the shore outcrop in Figure 3; the darker layers are biotite-rich; the lighter quartzo-feldspathic layer on the left is fine grained and contains quartz streaks of few millimetres thick and more than 10 cm long, indicating its mylonitized character. GSC 204136-T

mylonitization (Fig. 4, 5). Mylonitized character is best represented by fine grained, light pink weathering quartzofeldspathic gneiss layers which contain quartz streaks less than 5 mm wide and more than 10 cm long (Fig. 4). Other features of the zone include an abundance of biotite-rich schistose layers, highly attenuated minor folds several metres in length, and overall straight trend on a regional scale, in contrast to the undulating trend shown by gneisses of unit 1 (Fig. 2, 3). Lineation plunges gently to moderately to the southwest (Fig. 1). Relatively less sheared rocks occur within and at the margin of the zone, which has gradational boundaries with the gneisses of unit 1. Locally, the boundary between the sheared and unsheared equivalent rock is abrupt, as seen on 'Pegmatite Island' on the north shore of Howard Lake (62°15'N; 106°04'W). Large bodies of undeformed pegmatite occur on the island, but along the north shore of the island, the pegmatite has been reduced to highly sheared, fine to medium grained felsic micaceous schist. The undeformed pegmatite shows spotty high radioactivity (130 to 200 counts per second on Exploranium GRS-101 scintillometer) and is believed to be related to the quartz syenite.

Regional geological observations

According to Wright (1967) gneisses and schists derived from sedimentary and volcanic rocks occur 70 km northeast of Lynx Lake, at Boomerang Lake (62°37.5'N; 105°00'W) in a northeast-trending zone 12 km wide and 20 km long. Field observations by the writer showed that these rocks are generally similar to those of unit 1 in the Lynx Lake area, and that some of them are highly sheared. Similar rocks also occur in the intervening region, along the northeasterly region structural trend. Exploration work at Boomerang Lake has revealed the presence of graphitic horizons in garnetiferous metapelites associated with quartz-feldspar-hornblende-biotite gneisses, and of unconformity-related uranium mineralization in the Thelon sandstone above the graphitic horizons (Gibbins, 1983; G.I. Davidson, personal communication, 1985). Garnetiferous metapelites extend for 10 km south of the 12 km wide zone mapped by Wright (1967).

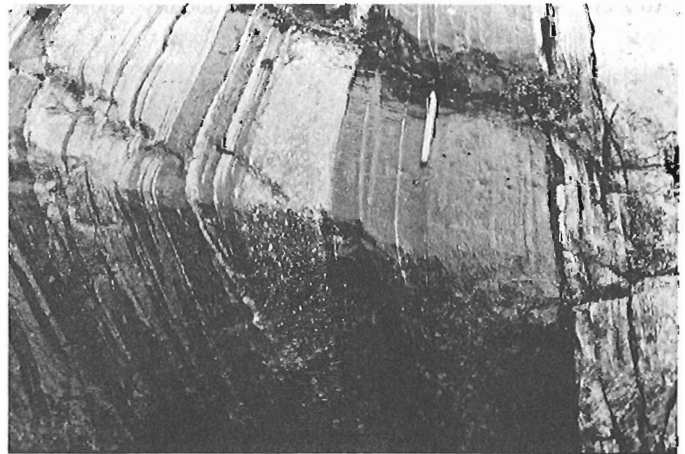


Figure 5. Highly sheared gneiss (unit 3) on the northwest shore of Howard Lake; interlensing of the fine grained felsic and mafic components, and the feldspar 'augen' gneiss lens as seen in centre, are common in unit 3; looking northeast (62°15.4'N; 106°3.3'W). GSC 204136-S

Graphitic horizons have not been found at Lynx Lake, but the layered gneisses contain some layers that are similar to the garnetiferous metapelites south of Boomerang Lake. Association of the metapelitic rocks and the quartz-feldspar-hornblende-biotite gneisses in the region, and the presence of quartzite in the vicinity of Lynx Lake are noteworthy in consideration of the sedimentary origin of these gneisses as visualized by Wright (1967). Quartzite also occurs 150 km northeast of Lynx Lake, near Eyeberry Lake as reported by Wright (ibid).

The sheared and mylonitic zone, according to observations by S.M. Roscoe (personal communication, 1985), extends for over 100 km to the southwest to Manchester Lake, and coincides with a steep southeasterly decreasing magnetic gradient and linear magnetic lows (Geological Survey of Canada, 1981). The boundary of this zone with the quartz syenite intrusion is not exposed, but the intrusion appears to predate the shearing and mylonitization in the zone judging from the observations on 'Pegmatite Island' in Howard Lake. The intrusion was emplaced after the development of the older pegmatites in the gneisses of unit 1 and their deformation. A gentle folding event imparted the arcuate outline in plan to the intrusion.

Acknowledgments

Andrew Stordy provided able assistance during the field work carried out in 1985. Some of the field work was done with S.M. Roscoe of the Geological Survey of Canada. Tom Faess, the owner of the Lynx Tundra Lodge which served as our base at Lynx Lake, his wife Andrea and his father Hank who has prospected the area, provided gracious hospitality and their cooperation is acknowledged.

The paper benefitted from the critical reviews by S.M. Roscoe and R.T. Bell of the Geological Survey of Canada.

References

- Geological Survey of Canada
1981: Magnetic Anomaly Map of Lockhart River; Map 1566A; NTS 75; scale 1:1 000 000.
- Gibbins, W.A.
1983: Southeast Mackenzie District; in *Mineral Industry Report, 1979, Northwest Territories*, EGS-1983-9, ed. J.A. Brophy; Department of Indian and Northern Affairs, Ottawa, p. 129-178.
- Wright, G.M.
1967: Geology of the southeastern barren ground, parts of the Districts of Mackenzie and Keewatin (Operations Keewatin, Baker and Thelon); Geological Survey of Canada, Memoir 350, 91 p.

Sediment transport study at King Point, Yukon Territory

Project 830007

Pete Morgan¹
Atlantic Geoscience Centre, Dartmouth

Morgan, P., Sediment transport study at King Point, Yukon Territory; in Current Research, Part B, Geological Survey of Canada, Paper 86-1B, p. 859-863, 1986.

Abstract

A field study was conducted at King Point to collect sediment transport and coastal zone data. Nearshore directional wave measurements were collected for the first time in the Canadian Beaufort Sea. The data also included wind speed and direction, bottom current velocities and directions, sediment samples and beach and bathymetric profiles. The data will be used to calibrate numerical models to estimate wave climate and alongshore sediment transport rates and directions.

Résumé

Une étude sur le terrain, réalisée à King Point au Yukon, visait à recueillir des données sur le transport des sédiments et sur la zone littorale. C'était la première fois que l'on recueillait des données de mesure sur la direction des vagues dans la mer de Beaufort. Les données recueillies portaient également sur la vitesse et la direction du vent, la vitesse et la direction des courants de fond, les sédiments et les profils littoraux et bathymétriques. Ces données serviront à calibrer les modèles numériques servant à évaluer le régime des vagues et le rythme et la direction du transport des sédiments le long du littoral.

¹ Sea consult, Suite 820, 1200 West 73rd Avenue, Vancouver, British Columbia V6P 6G5

Introduction

As part of the Northern Oil and Gas Action Program (NOGAP), the Beaufort Coastal Project (D1) was established to provide information on the coastal zone as required by government for land use planning and by industry in the design of shore-based facilities. Specific areas of interest include rates of coastline recession, rates and directions of sediment transport and analysis of wave and weather conditions at sites around the Beaufort Sea.

During 1984-85, as part of a collaboration between the Geological Survey of Canada (GSC) and Indian and Northern Affairs Canada (INAC), Keith Philpott Consulting Ltd. of Thornhill, Ontario, performed an extensive numerical modelling study (Pinchin et al., 1985). The study featured a synthesis of available meteorological, wave and geological data, and the application of numerical modelling techniques to predict wave climate and rates and directions of sediment transport at several sites in the Beaufort Sea. The study indicated a growing data base regarding coastal processes in the Beaufort Sea, but also illustrated the lack of pertinent site specific data to aid in the further calibration of the numerical procedures. The required data include both deepwater and nearshore directional wave records, nearshore and beach sediment samples, and beach and bathymetric profiles.

Field work was conducted during the summer of 1985. Part of the work was done under contract by Dobrocky Seatech Ltd. of Sidney, British Columbia. King Point has

been investigated in the course of several research programs on the Beaufort Sea coast (Mackay, 1963; Public Works Canada, 1971; McDonald and Lewis, 1973). It has also been proposed as a site for an onshore terminal to support the offshore oil and gas industry in the Arctic. As such, information on the wave climate, the wind climate and the sediment transport processes is essential in the analysis of coastal processes and sedimentation.

Between 24 August and 16 September 1985, a field camp was established at King Point. The remoteness of the location (200 km northwest of Inuvik) meant that all equipment had to be brought into the camp by barge or float plane.

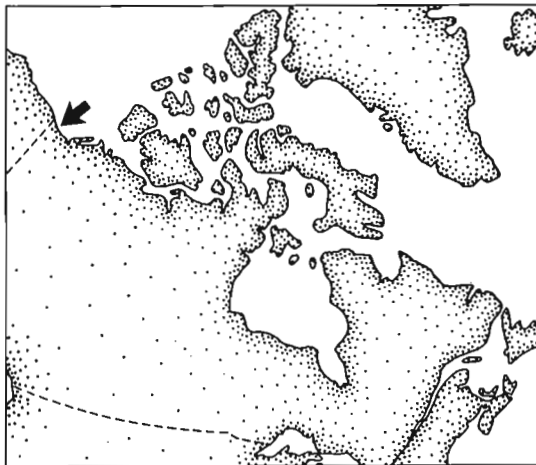
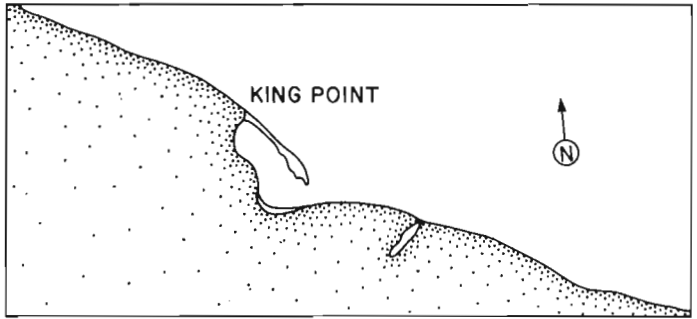
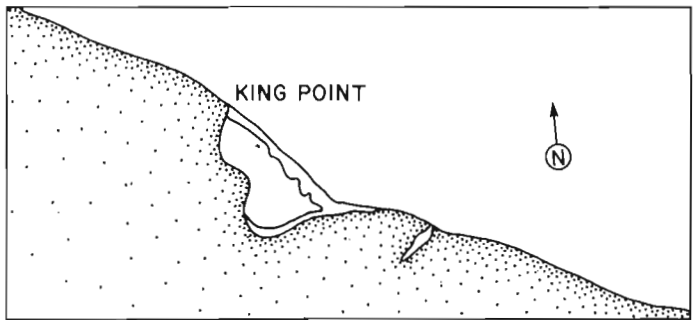


Figure 1. Location map, King Point, Yukon Territory.



1954



1975

Figure 3. Comparison of 1954 and 1975 air photos. The development of the barrier beach since 1954 indicates sediment transport predominantly to the southeast.



Figure 2. Oblique air photo of the King Point area.

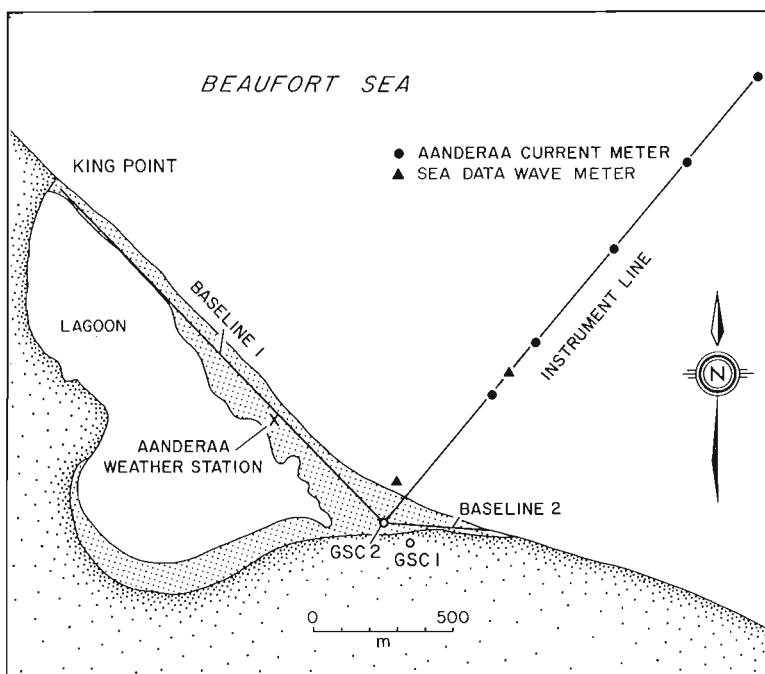


Figure 4. Storm-surge driftwood deposits at the southeast end of the barrier beach.

Site description

King Point is located about 70 km southeast of Herschel Island on the Yukon coast of the Beaufort Sea (Fig. 1). The site features 50 m high ice rich tundra cliffs and a 2 km long barrier beach lying to the southeast of the cliffs (Fig. 2). The barrier beach separates a broad lagoon from the ocean. The depth of the lagoon (to a maximum of 3.5 m) suggests that the lagoon had a thaw lake origin. The lagoon was open to the sea as recently as 1954, but it is now completely landlocked; the barrier beach developed rapidly from a spit between 1954 and 1975 (Fig. 3).

The highest point on the barrier beach lies 2.5 m above sea level. The beach features several lines of storm-surge driftwood deposits (Fig. 4). Overwash patterns at the northwest end indicate that some past storm surges have overtopped portions of the beach, and must have been in the range of 1.5 to 2.0 m.



Oceanographic instrumentation and deployment

Previous coastal sediment transport studies (Gillie, 1984a, b) used remote power cables and micro-computers for wave and current meter operation. In the Beaufort Sea however, the possibility of ice floes becoming grounded in the study area, the maintenance which shore-based acquisition and power supplies require, and the need for a large power supply pointed to the use of instruments featuring self-contained power sources and data loggers. Although the performance of each device during deployment could not be monitored (as with remote micro-computers and instrument to shore cables), the problems of cables becoming buried or broken during storms, or being snagged by ice floes were eliminated.

To measure directional waves and currents, two Sea Data directional wave and current meters (Models 621 and 635-12) were deployed. Both instruments were set to record values every 3 hours for 17.5 minute periods. Model 621 meter was deployed from 28 August to 14 September, 20 m offshore from the still water mark, in 2.6 m of water (Fig. 5). This meter measured breaking waves and longshore currents. The meter was mounted in a tripod 1.5 m in height (Fig. 6) and zero current calibration was performed by placing the current sensor in a drum of water. Divers carried the meter and tripod into place off the beach; sand bags were used to anchor the feet of the tripod. A float was attached to mark the instrument, and a line was attached to shore to support the hose for the suspended sediment sampling pump.

Model 635-12 meter (Fig. 7) was deployed from 29 August to 11 September in 6 m of water, 600 m from shore. This meter measured waves and currents outside of the breaking zone. After the zero check, the meter was by boat. The meter was being supported upright in its descent by a line to the boat. Sandbags were again used to anchor the legs of the tripod.

Model 635-12 meter was recovered 3 days before the model 621 meter, because it was found tipped over on a reconnaissance dive. Although the pressure sensor

Figure 5

Instrument deployment locations and survey control system.

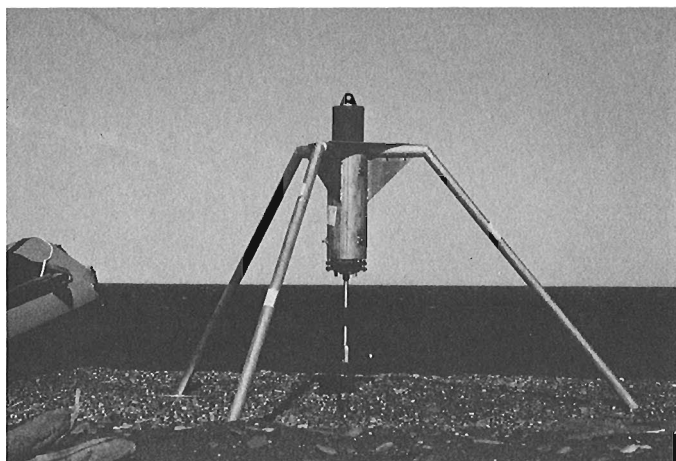


Figure 6. Sea Data 621 directional wave and current meter, in tripod.



Figure 7. Sea Data 635-12 directional wave and current meter, in tripod. This experimental tripod configuration proved less suitable than the configuration of Figure 6 for deployment in the nearshore zone. The meter was overturned after 13 days of deployment during storm conditions.

continued to measure wave heights, the sensor used to measure currents had become uncalibrated. Nevertheless, the deployment of these two instruments has provided the first directional wave measurements in the Canadian Beaufort Sea.

Five Aanderaa current meters were deployed between 30 August and 6 September in 5.0, 7.5, 10.0, 12.5 and 15.0 m of water (Fig. 5). Near-bottom currents (1 m above the bed) were measured every 5 minutes. The meters were mounted on concrete anchors, and each supported by two Vimy floats. These meters were deployed using a Zodiac boat. Divers inspected the Aanderaa meters to check their orientations, and to see that they were operating properly.

Only three of the Aanderaa meters (5.0 m, 10.0 m and 15.0 m) were recovered as the surface markers on the other two meters were lost. Although the data record is not as extensive as hoped for, current velocity and direction comparisons can be made with the data obtained.

Weather station

To obtain site specific weather data, a portable Aanderaa weather station was constructed on the beach (Fig. 8). Wind speed, wind direction and barometric pressure were recorded at 15 minute intervals, 10 m above ground level, from 26 August to 14 September.

These data will enable comparisons to be made with longer wind records from other locations around Beaufort Sea. Such site specific data allow for more effective wave climate hindcasting.

Beach profiling and bathymetric surveying

In order to model shoreline change due to wave attack as accurately as possible, extensive series of beach and bathymetric profiles are required. Since the sediment transport models have been developed chiefly for beaches possessing fine sands and shallow profiles, the steep profiles and coarse sediments found at King Point will provide nontypical input conditions for the numerical models.

A system of co-ordinates for horizontal control was established by locating two steel pins (GSC 1, GSC 2), using the known location of two instrumented boreholes. The two baselines established on the beach are shown in Figure 5.

Station spacing was 100 m along baseline 2, and 100 m along baseline 1 from GSC 2 to the 600 m station, with 200 m spacings from this station to the end of the baseline. The stations were located in this manner to more accurately monitor the higher sediment deposition rates at the southeast end of the barrier beach.

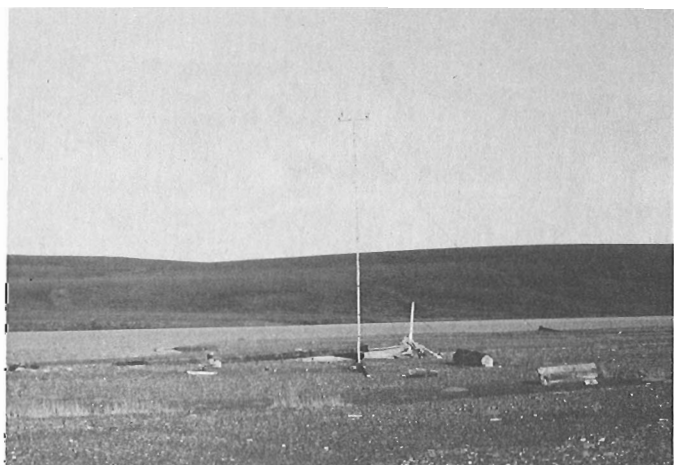


Figure 8. Aanderaa weather station.

Profile lines were then run at right angles to the baselines at each station, running from wading depth on the ocean side, across the barrier beach to either the tundra edge, or the edge of the lagoon. Mean sea level derived from the wave meter records will be used for vertical datum.

Bathymetry both in the lagoon and offshore (to a depth of 7.5 m) was studied by running sounding lines along each of the profile lines; distance was measured electronically and depth by an echo sounder.

Bottom sediment sampling

During the field program 76 bottom sediment samples were collected. A sample was collected at each of the Aanderaa current meter deployment sites, and 3 samples were taken from the swash zone during the collection of suspended sediment samples by hand.

Four samples were taken on each profile line to provide a representative set of sediment samples in the nearshore zone. One was taken at the top of the active beach berm, one in the swash zone, one 20 m offshore from the still water mark, and the final one 50 m offshore from the still water mark. The samples from the active beach berm and the swash zone were gathered by hand; offshore samples were collected using a pipe dredge hand-hauled from a boat.

The samples collected illustrated a wide variation of sediments at the site. The active beach berm and swash zone were made up of coarse sands, granule and pebble sized gravel. Between 5 and 10 m offshore from the still water line, the size increased dramatically, with larger pebbles and



Figure 9. Vibracoring unit.



Figure 10. Active beach (looking southeast), showing seaward storm-surge driftwood deposits. During the storm of 15 September, wave run-up reached the driftwood deposit.

cobbles present. At 20 m offshore, this gave way to coarse sand with scattered pebbles. About 50 m offshore a stiff clay was found in some samples, along with finer sands and silts.

Suspended sediment sampling

Field measurements of suspended sediment concentrations can be used to constrain numerical estimates of sediment transport. Four sets of measurements were taken to coincide with the 17.5 minute sampling intervals of the model 621 meter. A small water pump sampled water from a nozzle strapped to the leg of the current meter tripod at the same elevation as the current sensors. The amount of sediment in the sample along with the currents measured by the meter, will provide a suspended sediment flux which will then be compared to the numerical estimation of suspended flux at that point in the surf zone.

Vibracoring program

The vibracore sampling was carried out by M.J. O'Connor and Associates of Calgary. It was hoped to obtain 3 to 4 m core samples from both onshore and offshore locations at the southeast end of the spit. A new 3.5 inch (8.9 cm) diameter drill stem (Fig. 9) was tested for its penetration ability into heavy gravel, which is abundant at King Point.

The vibracoring program met with limited success. Only four locations had been tested with the unit when the drive cable broke and could not be repaired at the site. At the first three locations, penetration into the surficial sand layers was quick but ended about 1.3 m below ground level when heavier gravels were encountered. At the fourth location on the active beach berm the drive cable broke at a depth of 1.8 m.

Wave and wind conditions

During the deployment period, wave attack was predominantly from the northwest, with the wave height ranging up to about 1.6 m. Due to the very steep beach face, the attacking waves would break within 5 m of the still water mark. Wave heights, however, were extremely variable: 5 second waves of 1.0 m in height could reduce to 0.2 m within a matter of hours.

The largest storm occurred on the morning of 15 September, with an estimated storm surge of at least 0.8 m. The highest waves were approximately 1.5 m in height. The entire width of the active beach to the first major log line was submerged (Fig. 10). The storm lasted only 5 hours.

Along with the predominant direction of wave attack, the wind blew predominantly from the north or northwest, gusting at times up to 40 km/h. However, the strongest winds blew directly from the south, and reached estimated velocities of 70 to 80 km/h on two separate days. During this time, there was no significant wave attack on the beach.

Summary and future work

The field program provided a unique set of synchronous wave, current and sediment data, under a wide range of weather conditions. Observations of beach conditions indicated very active sediment transport processes, with profiles changing daily.

The data are being analyzed and will be used to estimate sediment transport at King Point, and to aid in the calibration of numerical modelling procedures as they apply to the Beaufort coastline.

Acknowledgments

This study was funded by the Northern Oil and Gas Action Program. I thank Rick Gillie and Gar Fisher of Dobrocky-Seatech and Doug Deveau of M.J. O'Connor and Associates for taking part in this study. My appreciation is also extended to the personnel at the Polar Continental Shelf Project in Tuktoyaktuk, and at the Inuvik Scientific Resource Centre for logistic support. As well, the assistance of John Milne and Danny Gordon was greatly appreciated.

References

- Gillie, R.D.
 1984a: Canadian coastal sediment study: site maintenance contract; National Research Council of Canada Canadian Coastal Sediment Study, Report C²S²-8, 109 p.
 1984b: Evaluation of measurement techniques; National Research Council of Canada Canadian Coastal Sediment Study, Report C²S²-9, 30 p.
- Mackay, J.R.
 1963: Notes on the shoreline recession along the coast of the Yukon Territory; Arctic, v. 16, p. 195-197.
- McDonald, B.C. and Lewis, C.P.
 1973: Geomorphic and sedimentologic processes of rivers and coast, Yukon Coastal Plain, Canada; Environmental-Social Committee, Northern Pipelines, Task Force on Northern Oil Development, Report 73-39, 245 p.
- Pinchin, B.M., Nairn, R.B., and Philpott, K.L.
 1985: Numerical estimation of sediment transport and nearshore profile adjustment at coastal sites in the Canadian Beaufort Sea; unpublished contract report to Department of Indian and Northern Affairs and Geological Survey of Canada, 2 volumes.
- Public Works Canada
 1971: Herschel Island: feasibility of a marine terminal; Engineering Programs Branch, Ottawa, 141 p.

Illite crystallinity studies around the Roberts metal deposit, Eastern Townships, Quebec¹

Contract 24ST.23233-5-1469

J.Y. van Bosse², I.M. Samson², and A.E. Williams-Jones³

van Bosse, J.Y., Samson, I.M., and Williams-Jones, A.E., Illite crystallinity studies around the Roberts metal deposit, Eastern Townships, Quebec; in *Current Research, Part B, Geological Survey of Canada, Paper 86-1B*, p. 865-868, 1986.

Abstract

Illite crystallinity (IC) values obtained from sediments within a 4 km radius of the J.A.G. Mines, Saint-Robert Ag, W, Bi deposit, Eastern Townships, Quebec, range from 0.17 to 0.37 °2 θ . Low IC values (<0.23) dominate in the central part of the study area, around the deposit. High IC values (\geq 0.23) occur principally around the margins of the study area and in isolated patches within the central portion. More information is required from outside of the study area to determine whether the higher IC values represent the regional diagenetic-metamorphic grade. If so, the presence of a wide zone of sediments bearing well-crystallized illites (i.e., low IC values) over the deposit area supports the hypothesis that a hidden intrusive body exists at depth.

Chlorite crystallinity patterns parallel those of IC patterns throughout the study area.

Résumé

Les indices de cristallinité de l'illite des roches sédimentaires à l'intérieur d'un rayon de 4 km du dépôt de Ag, W et Bi des mines J.A.G., à Saint-Robert, dans l'Estrie au Québec, donnent des valeurs de 0,17 à 0,37 ° 2 θ . Les valeurs basses (<0,23) dominent dans la partie centrale de la région étudiée, autour du dépôt. Les valeurs élevées (\geq 0,23) se trouvent principalement en périphérie de la région étudiée, et dans des zones isolées à l'intérieur de la partie centrale. Des données supplémentaires provenant de l'extérieur de la région étudiée seront nécessaires pour bien déterminer si les indices élevés de cristallinité de l'illite sont représentatifs du degré métamorphique régional. Si tel est le cas, la présence d'une large zone de roches sédimentaires caractérisées par des illites bien cristallisées (indices faibles) vient appuyer l'hypothèse selon laquelle un amas intrusif est présent en profondeur.

Les configurations cristallines de la chlorite correspondent à celles de l'illite dans la région étudiée.

¹ Contribution to the Federal Asbestos Initiatives, Geoscience Research Program 1984-1987. Project carried by Geological Survey of Canada, Mineral Resources Division, Project 840059.

² Mineral Exploration Research Institute, C.P. 6079, Succ. A, Montreal, Quebec, H3C 3A7

³ Department of Geological Sciences, McGill University, 3450 University Street, Montreal, Quebec H3A 2A7

Introduction

The J.A.G. Mines, Saint-Robert Ag, W, Bi deposit near St. Robert de Bellarmin, Eastern Townships, Quebec, is associated with a magnetic anomaly and a small thermal metamorphic aureole and alteration zone. Cattalani and Williams-Jones (1986) suggested that an intrusive stock at depth produced these features. The objective of this study is to use illite crystallinity values obtained from the host sedimentary sequence to delineate any low-grade thermal aureole which may exist outside of the small, high-grade aureole and alteration zone, centred on the deposit.

Geology

As described by Cattalani and Williams-Jones (1986) the study area lies within the Boundary Mountain Anticlinorium, immediately south of the major fault which separates the anticlinorium from the Gaspé-Connecticut Valley Synclinorium (Fig. 1). The sedimentary rocks are part of the Frontenac Formation, and consist of finely laminated slates, siltstones, sandy schists, quartzites and greywackes (of which some are calcareous), of possible Early Ordovician age (Harron, 1976). Thick (0 to >70 m) Pleistocene glacial till and recent alluvium in the study area severely restrict sampling.

The sedimentary strata were deformed during the Middle Ordovician Acadian Orogeny into tight, upright isoclinal folds trending ENE. A major penetrative cleavage, F_1 , parallels the folding. A weaker subparallel cleavage, F_2 , is represented by crenulation of the shaley units, the F_3 deformation is characterized by open folds with axial traces approximately normal to F_1 and F_2 .

Acadian dyke swarms cut the Frontenac Formation. Granodioritic, granitic and lamprophyric dykes have intruded predominantly along the penetrative cleavage.

Two fault systems are present in the area. The "Main Fault" system, in the centre of the mine property, consists of major, vertical faults, predominantly dip-slip (downthrow to the north) in character, which have a strike length of over 2.5 km. A minor system of later, subvertical faults is found in the western and central portions of the property; these are approximately normal to the Main Fault system.

Metamorphism and alteration

The regional metamorphic grade reported by Cattalani and Williams-Jones (1986) is lower greenschist to greenschist facies. A small thermal aureole is present in the centre of the property. The aureole, 2.5 km by 0.5 km, lies along the Main Fault system and consists of biotite-hornfelses.

A zone of moderate to intense hydrothermal alteration is closely associated with the Main Fault system (and thus also with the thermal aureole) and a magnetic anomaly. Rocks within and near the faults are bleached and friable, and consist mainly of kaolinite. Farther from the fault system (up to 250 m), rocks are a pale grey-green colour where the alteration is phyllic. Another small phyllic alteration zone has been observed to the northwest of the Main Fault system.

Sampling and analyses

The study area is roughly 8 km in diameter (Fig. 2), and is centred on the deposit. Exposure is somewhat sporadic, particularly north and south of the mine property, due to thick glacial till and alluvial cover. Most rocks sampled are siltstones to fine greywackes; a small number of these are calcareous. The siltstones are commonly phyllitic or schistose.

The samples were processed as detailed in Duba (1982) to separate out the less than 2 μm mineral fraction; carbonate was not removed from the samples. Oriented <2 μm fractions were analyzed by X-ray diffraction, using a Siemens diffractometer with a $\text{CuK}\alpha$ source and 1° divergence and scatter slits. The samples were scanned at $1^\circ/20/\text{min}$; the scan was recorded at $1^\circ/20/\text{cm}$.

Mineralogy of the <2 μm fraction

In the majority of samples analyzed, the <2 μm fraction comprises illite, chlorite, quartz and feldspar (predominantly plagioclase). In a given sample one or more of these minerals may be absent with the exception of illite which is present in all samples. Kandites and possibly biotite were only indicated in a few samples. Glycolation of 6 samples with wide peaks near $1.0 \eta\text{m}$ (basal 001 illite peak) resulted in a slight splitting of that peak. No major peak shifts were observed. This suggests that

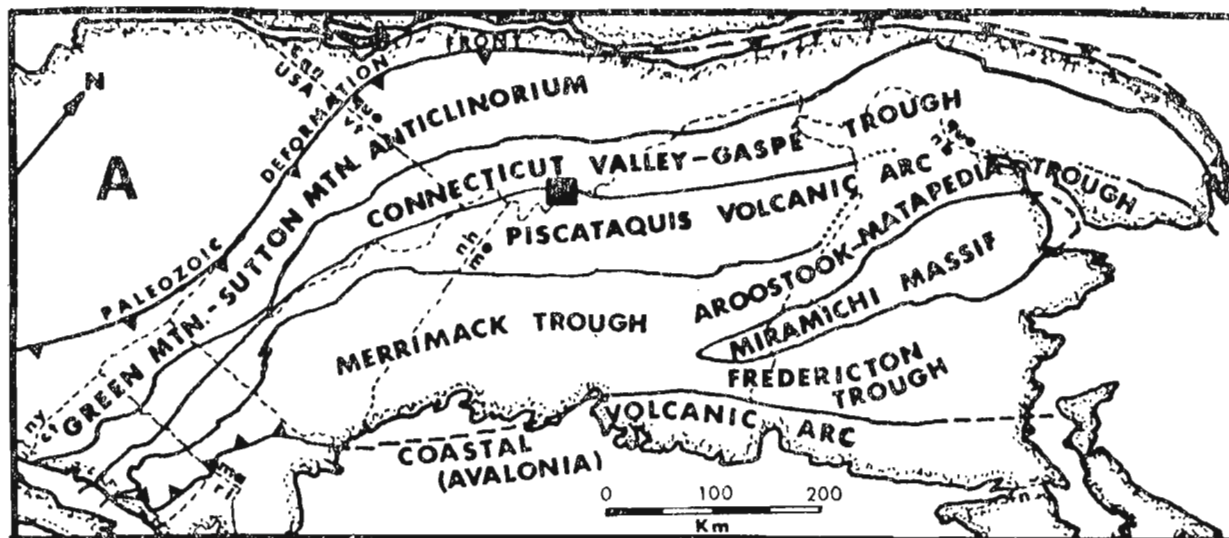


Figure 1. Location of the J.A.G. Mines, St-Robert property. From Cattalani and Williams-Jones (1986).

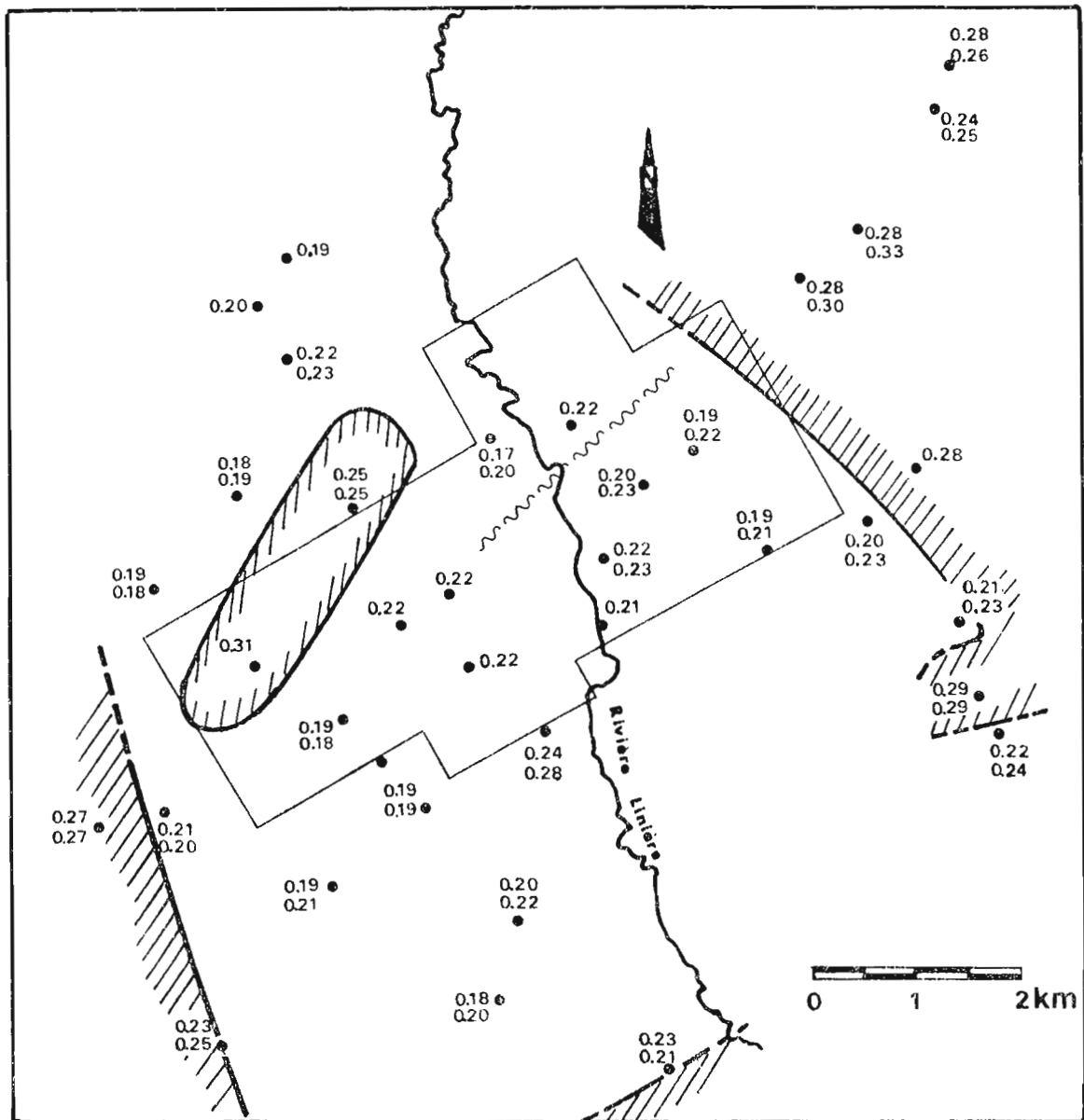


Figure 2. Map of the illite crystallinity values in the St-Robert deposit area. The chlorite crystallinity index, where measurable, is listed below the illite crystallinity index.

smectites are present, but in quantities of less than 10% (cf., Kalkberg examples, Hower, 1981).

Illite crystallinity Index (IC)

Introduction

The progressive ordering of the illite crystallinity structure with increasing diagenetic grade, due to a decrease in the proportion of smectite layers (cf., Hower, 1981) is reflected in the X-ray diffractograms of the $<2 \mu\text{m}$ clay fraction by a narrowing of the illite 001 peak ($1.0 \eta\text{m}$). The illite crystallinity index is defined as the width of this peak at half height, measured in 2θ . In a similar manner, the 001 peak of chlorite ($1.4 \eta\text{m}$) may be measured to obtain the chlorite crystallinity index.

In addition to natural variations, the 001 peak width is dependent on the X-ray diffraction conditions, the roughness of

the specimen surface, and the difficulty of assessing the background (Brindley and Brown, 1980). Duba (1982) concluded that the illite crystallinity index is independent of the carbonate content of the host rock, and noted that chlorite crystallinity generally parallels illite crystallinity.

Result

In most samples, the illite 001 peak is sharp and well-defined. The IC values of the St. Robert samples are low, falling in a range from $0.17\text{-}0.23^\circ 2\theta$, in the area 2-3 km around the deposit in all directions. The few high IC values within this area are from samples which exhibit evidence of fairly pervasive weathering. Consistently higher IC values, $0.23\text{-}0.37^\circ 2\theta$ are found on the margins of the study area (Fig. 2). Chlorite crystallinity indices parallel illite crystallinity indices closely (Fig. 3).

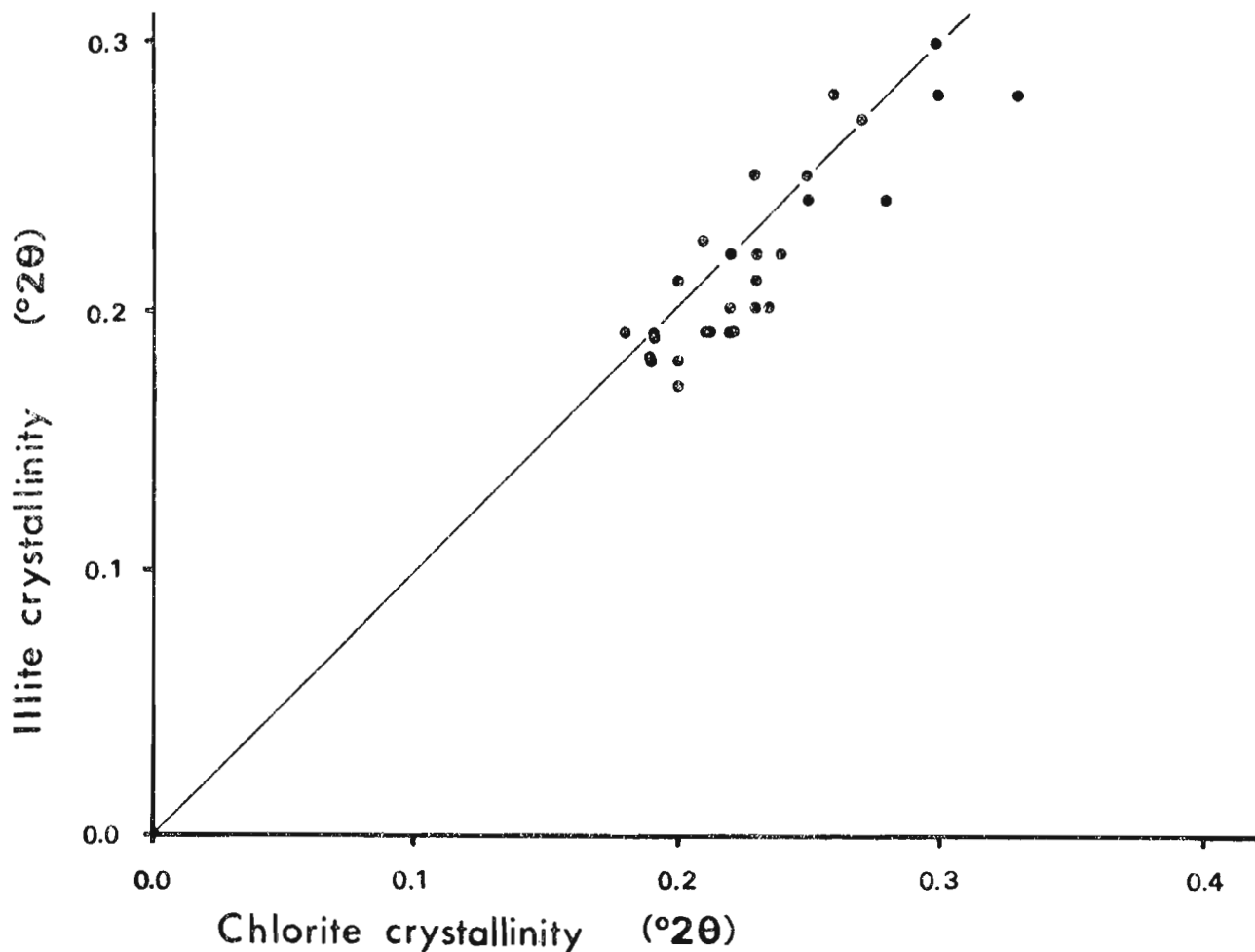


Figure 3. Graph of illite crystallinity versus chlorite crystallinity values for samples containing both minerals. The line indicates the ideal 1:1 correlation between the parameters.

Discussion and conclusions

The generally low IC values and the absence of smectite indicate thermal conditions higher than those associated with diagenesis (the upper limit of which is defined at IC index of $0.38^{\circ}2\theta$ by Kisch, 1980). Illite crystallinity values for rocks outside the study area are required to determine whether the higher IC values represent the regional diagenetic grade. If these high IC values are representative, the wide zone of low IC values (i.e., well-crystallized illite) associated with the deposit would support the hypothesis that a hidden intrusive body exists at depth, and suggests that the body may be larger than anticipated in that most of the chosen study area has undergone low-grade thermal metamorphism.

Acknowledgments

We wish to thank S. Cattalani and J. Clark of McGill University for their assistance.

References

- Brindley, G.W. and Brown, G.
1980: Crystal Structures of Clay Minerals, Second Edition, Mineralogical Society, London.
- Cattalani, S. and Williams-Jones, A.E.
1986: Geological and fluid inclusion studies at the St. Robert Ag. W, Bi deposit, Eastern Townships, Quebec; in Current Research, Part B, Geological Survey of Canada, Paper 86-1A, 365-374.
- Duba, D.
1982: The application of illite crystallinity, organic matter reflectance and isotopic techniques to the exploration for sedimentary-hosted hydrothermal ore deposits, southwestern Gaspé; M.Sc. thesis, McGill University, Quebec, 142 p.
- Harron, G.A.
1976: Metallogeny of sulfide deposits in the Eastern Townships; Ministère des Richesses Naturelles, Quebec, Paper ES-27, 42 p.
- Hower, J.
1981: X-ray diffraction identification of mixed-layer clay minerals; in F.J. Longstaffe, ed., Short Course in Clays and the Resource Geologist, Mineralogical Association of Canada, p. 39-59.
- Kisch, H.J.
1980: Incipient metamorphism of Cambro-Silurian clastic rocks of the Omland Supergroup, Central Supergroup, Central Scandinavian Caledonides, Western Sweden: illite crystallinity and, vitrinite reflectance; Journal of Geological Society, London, v. 1371, p. 271-288.

Géologie du Quaternaire de la région du mont Alexandre, Gaspésie (Québec)¹

Contrat 54SZ. 23233-5-0772

Marc Cloutier² et Paul Corbeil²
Division de la science des terrains

Cloutier, M., et Corbeil, P., Géologie du Quaternaire de la région du mont Alexandre, Gaspésie (Québec); dans Recherches en Cours, partie B, Commission géologique du Canada, Étude 86-1B, p. 869-873, 1986.

Résumé

Un placage de till recouvre une bonne partie du plateau de la région du mont Alexandre. Des régoïlithes d'âge pré- et post-glaciaire tapissent la roche de fond. Les surfaces striées et les erratiques indiquent un écoulement glaciaire vers le sud et le sud-est.

Abstract

A till veneer covers a substantial part of the plateau in the Mont Alexandre area. Regoliths of preglacial and postglacial age cover bedrock. Striated surfaces and transport of erratic blocks indicate glacial flow to the south and to the southeast.

¹ Contribution au Plan de développement économique Canada/Gaspésie et Bas Saint-Laurent, volet mines 1983-1988. Sous la responsabilité de la Commission géologique du Canada, Division de la science des terrains, projet 840035.

² COGÉO Consultants Inc., 405, Les Érables, Laval (Québec) H7R 1B1

Introduction

Un projet de cartographie des formations en surface à l'échelle 1/50 000 a été entrepris à l'été 1985 dans le centre Est de la péninsule gaspésienne : feuillet Mont Alexandre 22 A/11 et 1/3 Est du feuillet Ruisseau-Lesseps 22 A/12 (fig. 1). La campagne de terrain a de plus permis un relevé des marques d'érosion glaciaire et le pointage des erratiques. Cette note présente ces observations et les intègre dans l'histoire glaciaire régionale.

Ce travail s'insère à l'intérieur d'un projet plus vaste, de compilation quaternaire à l'échelle de 1/250 000.

Rappel de l'histoire glaciaire de la Gaspésie

Les premiers auteurs des travaux touchant l'histoire glaciaire de la péninsule ont postulé, d'une part, l'existence d'une calotte glaciaire gaspésienne dans les secteurs les plus élevés et, d'autre part, que l'influence de la calotte continentale sur la péninsule fut réduite au minimum (Bell, 1863; Chalmers, 1886, 1906; Coleman, 1922).

Un peu plus tard, la découverte, dans la région de la Gaspésie, de plusieurs blocs précambriens provenant des régions au nord du Saint-Laurent démontrèrent que l'inlandsis avait, en partie du moins, recouvert la péninsule (Jones, 1934, 1939; Alcock, 1935, 1944; Flint et al., 1942; McGerrigle, 1950, 1952).

Grant (1977) a suggéré pour le Wisconsin supérieur que la limite sud de l'inlandsis à l'est de Saint-Antonin se situait dans le golfe Saint-Laurent et que la péninsule était recouverte partiellement par une calotte régionale se rattachant à celle du Nouveau-Brunswick.

Récemment, David et Lebus (1985) ont synthétisé plusieurs années de travaux (Lebus et David, 1972; Lebus 1973a, 1973b, 1975; Lebus et David, 1977) et proposé un modèle d'englaciation et de déglaciation pour la partie occidentale de la Gaspésie. Ils divisèrent la région en quatre zones (fig. 2) : du nord au sud, l'érosion glaciaire augmente en importance et les dépôts s'épaississent de la zone I à la zone II; ils sont absents dans la zone III et ressurgissent dans la zone IV. Cette zonation est due à des changements de température à la base du glacier : depuis la zone I vers le sud, la partie inférieure de la glace devient de plus en plus froide pour être complètement gelée à la base, dans la zone III. Elle se réchauffe ensuite jusqu'au point de fusion dans la zone IV.

Chauvin (1982, 1983, 1984) et LaSalle (1983, 1984, 1986) qui ont travaillé du nord au sud dans la partie centrale de la péninsule, ont observé un écoulement vers le sud ou le sud-est au pleni-glaciaire. Sur le versant nord, Chauvin (1984) détermine, par une étude de dispersion d'erratiques, que la glace s'écoulait vers le nord-est au tardi-glaciaire en direction de l'ouverture du golfe Saint-Laurent. Suite aux observations sur les surfaces d'érosion, les accumulations de dépôts et les sédiments d'altération, LaSalle suggère que le modèle de David et Lebus (op. cit.) s'applique au plateau central mais avec de légères modifications.

Les travaux de Bail (1983, 1985) sur le versant sud pour la région de New-Carlisle – Paspébiac indique l'existence d'un mouvement vers le nord provenant de la calotte Escuminac.

Cadre physique

Physiographie

Le territoire se situe dans la région physiographique des Appalaches et, pour la majeure partie, dans la division des monts Notre-Dame (fig. 1). La division du bas-plateau des Chaleurs occupe une faible part dans le coin sud-est (Bostock, 1970).

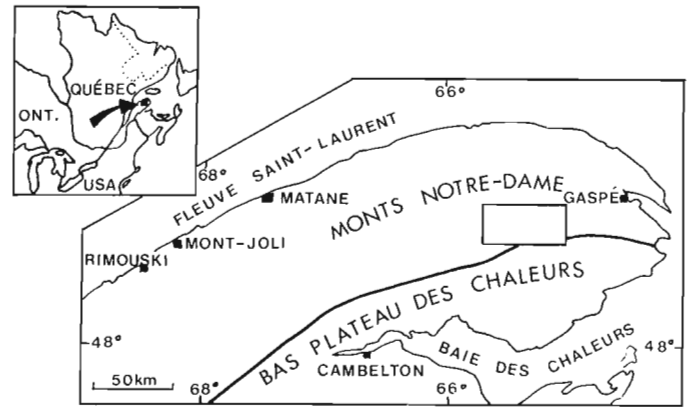


Figure 1. Carte de localisation et divisions physiographiques.

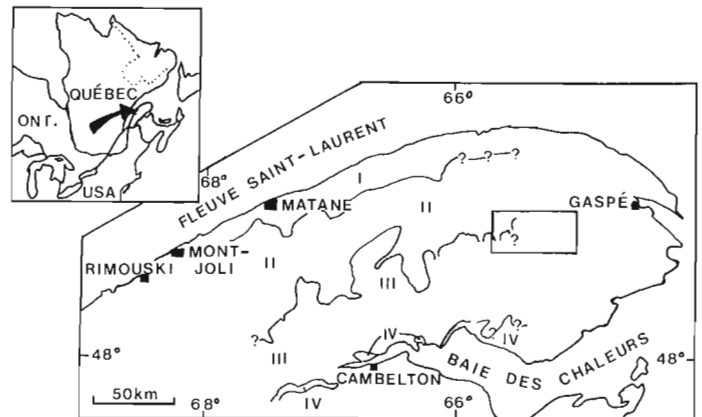


Figure 2. Zones liées au régime thermique à la base du glacier (d'après David et Lebus, 1985). Partant de la zone I vers le sud, la glace devient de plus en plus « froide » et est gelé au substratum dans la zone III.

La région se présente comme un plateau ondulé en pente légère vers le sud, dont l'altitude varie de 550 à 490 m. Seules quelques montagnes, dont le mont Alexandre et le mont de l'Observation atteignent des altitudes supérieures à 700 m. La surface est entaillée de profondes vallées fluviales.

Géologie

La région d'étude s'insère dans l'unité tectonostratigraphique du synclinorium de Gaspé (Poole et Rodgers, 1972). Le substratum est composé essentiellement de roches terrigènes – grès, siltstone, argilites – et calcaires, d'âge siluro-devonien déformées lors de l'orogénie acadienne du Dévonien tardif. Notons un conglomérat calcaire à stromatopores (formation West Point, Bourque 1975) qui peut présenter de bonnes qualités comme indicateur lithologique. La structure (plis et failles principales) de ces formations s'oriente suivant une direction régionale ouest-est (Morin et Simard, 1985).

Des bandes de roches volcaniques, constituées principalement de basalte, viennent s'intercaler dans la séquence sédimentaire. Elles ne peuvent pas toutes être utilisées comme traceurs lithologiques avec le même degré de confiance à cause de leur présence en petites enclaves affleurant un peu partout dans le secteur, en plus de la bande principale exposée dans le synclinal du mont Alexandre. Cependant, l'unité de roche épicaustite – conglomérat volcanique rouge (formation West Point) – constitue le meilleur traceur.

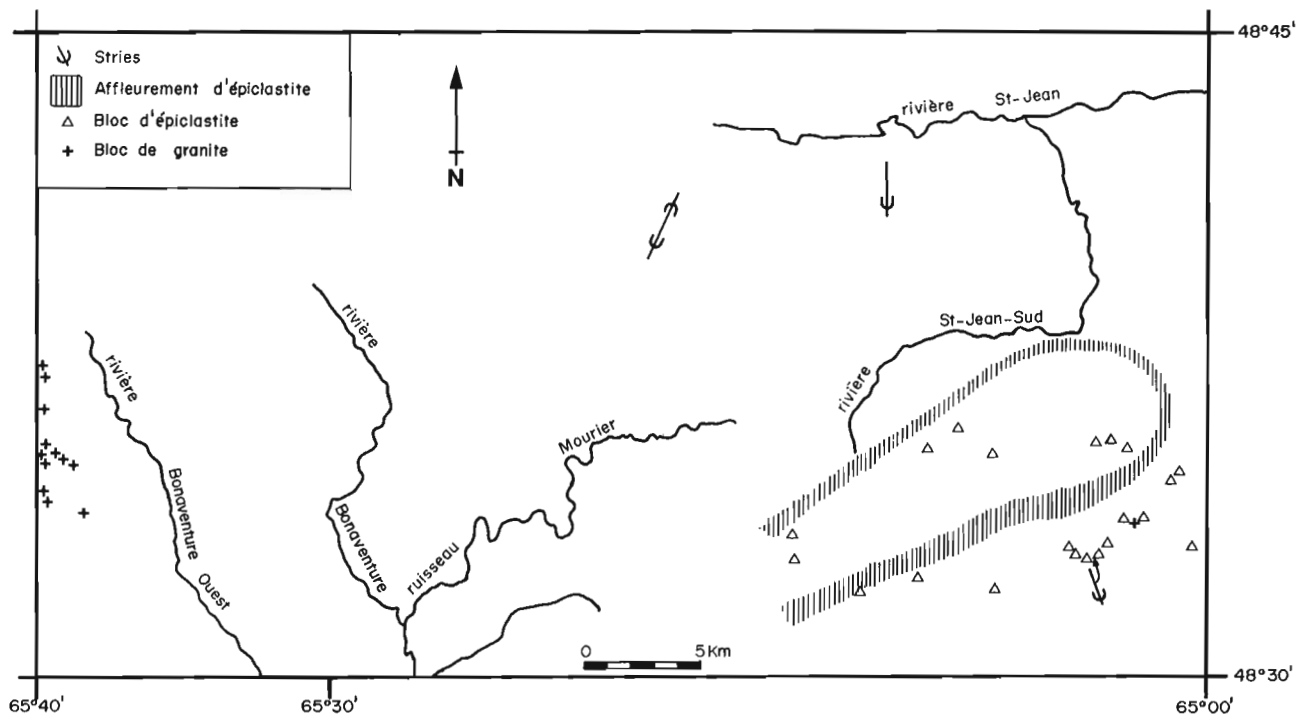


Figure 3. Marques d'érosion glaciaire et blocs erratiques.

Écoulements et transport glaciaire

Le plateau ne présente presque aucun macro-signe d'érosion glaciaire. Les vallées ont des profils en V très encaissés, le réseau de drainage est entièrement contrôlé par la structure de la roche de fond, les interfluvés sont plats. Seules les dépressions topographiques occupées partiellement par des petits lacs et marécages indiquent une érosion glaciaire possible.

Cependant, trois sites de micro et meso formes d'érosion glaciaire ont été retracés (fig. 3).

Une roche moutonnée et deux surfaces striées témoignent de la présence d'une glace active qui s'écoulait vers le sud et le sud-est, et, d'un mouvement orienté NE-SW d'une direction et d'un âge incertains.

Le mouvement vers le sud et le sud-est confirmé par un déplacement vers le sud des traceurs lithologiques :

- plusieurs erratiques de roches épicastites ont été localisés. Ils sont tous situés au sud de leur aire d'affleurement. Aucun ne se retrouve au nord de la bande d'épiclastite située dans le flanc nord du synclinal du mont Alexandre (fig. 3);
- de plus, les erratiques de roches volcaniques sont tous situés au sud des aires d'affleurement.
- seuls quelques blocs erratiques de conglomérat calcaire à stromatopores ont été repérés, toujours au sud des aires d'exposition;
- des blocs granitiques ont été pointés dans la partie sud du 1/3 Est de la carte 22 A/12 (fig. 3). Ces blocs appartiennent à l'extrémité sud-est de la trainée des monts McGerrigle déjà identifiée au nord par Chauvin (1984).

Géologie de surface

Le répartition des sédiments meubles a fait l'objet d'une carte déjà publiée (Cloutier et Corbeil, 1986). Les principales unités sont :

- Régolithe

Il se présente comme un sédiment constitué soit de fragments anguleux mono-lithologiques provenant de l'altération mécanique du roc - « rubble » -, soit un sédiment silto-argileux dérivé de la décomposition chimique du substratum - saprolite -. Entre ces deux extrêmes existent des diamictons monolithologiques dans lesquels des fragments anguleux, souvent pourris, sont englobés dans une matrice silto-argileuse en général oxydée. Ces sédiments reposent directement sur la roche de fond altérée sur des épaisseurs variant de 30 cm à plus de 2 m. De plus, à quelques endroits le long de la route Chandler-Murdochville, nous les avons observés sous le till.

- Till

Le till se présente comme un diamicton, fissile par endroits, variant de compact à lâche. La matrice est silto-argileuse, parfois carbonatée, contenant de nombreux galets anguleux à sub-arrondis et dont plusieurs sont striés. La lithologie variée reflète le substratum de la région avec grès, silstones, calcaires et roches volcaniques, et les apports régionaux avec des granites et skarns venant des secteurs monts McGerrigle et Murdochville au nord. Dans le coin nord-est de la zone d'étude, les galets sont mono-lithologiques, striés et de forme pentagonale. Dans la région étudiée, on trouve une couverture de till sur une grande partie du plateau. Le dépôt est mince, presque toujours d'épaisseur inférieure à 1 m. La couverture est sporadique avec de nombreuses percées rocheuses. Dans les dépressions autour des lacs et marécages, l'épaisseur dépasse 1 m. La topographie ne semble plus contrôlée par le socle mais par la couverture de dépôts. Dans les flancs de vallée comme la rivière Saint-Jean et le ruisseau Sirois, on peut observer de grandes zones de placage de till lâche, sur des dénivelées de plus de 10 m. La couleur du till varie de gris à chamois.

- Sédiments lacustres

Dans le secteur du lac Triangle, on retrouve des silts bruns d'une faible épaisseur (30 cm) surmontant le till. Ces silts sont à plusieurs endroits recouverts d'un très mince placage de matière organique noire. Ils sont d'origine lacustre et ont été déposés dans un bassin un peu plus grand que le lac actuel, en le comblant graduellement.

Mentionnons la présence de marnes qui constituent l'assise du lac Triangle.

- Alluvions

Les alluvions sont constituées surtout de graviers et de sables, fins par endroits, rarement stratifiés, mais plutôt avec des coupures granulométriques. Les graviers et blocs sont sub-arrondis ou arrondis. Ils recouvrent le fond plat des vallées sous forme de plaines alluviales et de terrasses de basse altitude.

À certains endroits (rivière Saint-Jean Sud), l'épaisseur des dépôts atteint plus de 10 m dans le talus de terrasse supérieure. Il s'agit probablement d'alluvions d'origine fluvio-glaciaire lointaine, entaillées par les cours d'eau, lors du relèvement isostatique.

- Colluvion

Les pentes mobilisent les sédiments déjà décrits pour former des colluvions sous forme de talus et cônes.

Discussion

Le relief actuel est typiquement d'origine fluviale. Le patron de drainage est contrôlé soit par la structure ou par une ancienne surface d'érosion. Les vallées qui incisent le plateau présentent toutes le même profil caractéristique en «V». Il semble que des glaces n'ont eu que peu d'effet sur le modèle actuel. Ceci rejoint le modèle de David et Leblond (1985) d'une glace gelée à la base pour la région.

Cependant, les marques d'érosion glaciaire, les trainées de blocs locales – épicastite, roche volcanique, conglomérat calcaire – et l'étendue de la mince couche de till sur la majeure partie du plateau au sud de la rivière Saint-Jean, indiquent que la glace était active – érosion, transport, déposition – pendant un certain temps.

Dans le modèle de David et Leblond, cette activité glaciaire aurait eu lieu soit au début de la glaciation ou lors du retrait de la glace.

Dans une autre optique, l'extension vers l'est de la zone III (fig. 2) où la glace est gelée à la base, ne peut être poursuivie. Déjà LaSalle et David (1984) ont remarqué des signes de glaces actives sur le plateau dans la partie sud de la Gaspésie.

En conformité avec les données au nord (Chauvin 1983) et au sud (LaSalle, 1984), les stries et les trainées d'erratiques indiquent un écoulement de la glace vers le sud ou le sud-est. Aucun erratique provenant du nord du Saint-Laurent n'a été observé. Les granites localisés appartiennent probablement tous à la trainée des monts McGerrigle (Chauvin, 1984).

Durant la déglaciation, des eaux de fonte ont pu mettre en place des sédiments qui ont presque tous été érodés lors de l'encaissement du système fluviale dû au relèvement isostatique. Seules quelques hautes terrasses demeurent au-dessus des terrasses et plaines alluviales actuelles. Les lacs qui ont occupé les dépressions se sont comblés ou bien vidangés par le même réseau fluviale s'encaissant dans les seuils.

Comme LaSalle (1986), nous avons observé le régolithe parfois sous le till, parfois sur des surfaces striées. Les régolithes ont donc été déposés à deux époques différentes : avant et après une glaciation.

Remerciements

Les auteurs remercient monsieur Jean Veillette (CGC) pour son appui comme délégué scientifique et pour ses commentaires et suggestions sur une première version de cette note. M. P. LaSalle du MER nous a fait part de données inédites et fourni de précieux conseils. Nous remercions également M. Rémi Morin pour les informations fournies sur les traceurs lithologiques.

Que M. Pierre Dumas, Mmes Elaine Cousineau et Marie-Claude Lebeuf soient également assurés de notre reconnaissance pour leur soutien technique et administratif.

Bibliographie

- Alcock, F.J.
1935: Geology of Chaleur Bay region; Geological Survey of Canada, Memoir 183, 146 p.
1944: Further information of glaciation in Gaspé; Royal Society of Canada Transactions, section IV, p. 15-21.
- Bail, P.
1983: Problème géomorphologique de l'englacement et de la transgression marine pleistocène en Gaspésie sud orientale; Thèse de doctorat non publiée, Département de géographie, Université McGill, Montréal, 148 p.
1985: Un mouvement glaciaire vers le Nord-Ouest dans la région de Saint-Godefroi, Gaspésie, Québec; Journal Canadian des Sciences de la terre, vol. 22, n° 12, p. 1871-1877.
- Bell, R.
1863: On the surficial geology of Gaspé Peninsula; Canadian Naturalist and Geologist, vol. 8, p. 175-183.
- Bostock, H.S.
1970: Physiographic regions of Canada; Geological Survey of Canada, Map 1254A, scale 1:5 000 000.
- Bourque, P.A.
1975: Lithostratigraphic framework and unified nomenclature for Silurian and basal Devonian rocks in eastern Gaspé Peninsula, Québec; Canadian Journal of Earth Sciences, v. 12, p. 858-872.
- Chalmers, R.
1886: On the glaciation and Pleistocene subsidence of north New Brunswick and south-eastern Quebec; Royal Society of Canada Transactions, section 4, p. 139-145.
1906: Surface geology of eastern Quebec; Geological Survey of Canada, Annual Report for 1904, Volume 16, Part A, p. 250-263.
- Chauvin, L.
1982: Géologie du Quaternaire de la région du Mont-Louis – Grande-Vallée; Ministère de l'Énergie et des Ressources, Québec, DP 82-04.
1983: Géologie du Quaternaire de la région de Ruisseau Lesseps – Murdochville (Partie centrale de la Gaspésie); Ministère de l'Énergie et des Ressources, Québec, DP-83-26.
1984: Géologie du Quaternaire et dispersion glaciaire en Gaspésie, Région de Mont-Louis – Rivière Madeleine; Ministère de l'Énergie et des Ressources, Québec, ET 83-19, 33 p.
- Cloutier, M. et Corbeil, P.
1986: Géologie du Quaternaire, Mont Alexandre (22 A/11), Québec, Commission géologique du Canada, Dossier public 1255.

- Coleman, A.P.
1922: Physiography and glacial geology of Gaspé Peninsula, Quebec; Geological Survey of Canada, Museum Bulletin 34, 52 p.
- David, P.P. et Lebuis, J.
1985: Glacial maximum and deglaciation of western Gaspé, Quebec, Canada; Geological Society of America, Special Paper 197, p. 85-109.
- David, P.P., Chauvin, L., Choinière, J., and LaSalle, P.
1984: Ice flow directions and trace element concentration patterns in stream sediments in Gaspé, Quebec; Geological Association of Canada (abstract), p. 56.
- Flint, R.F., Demorest, M., and Washburn, A.L.
1942: Glaciation of Shickshock Mountains, Gaspé Peninsula; Geological Society of America Bulletin, v. 32, p. 291-317.
- Grant, D.R.
1977: Glacial style and ice limits, the Quaternary stratigraphic record, and changes of land and ocean level in the Atlantic Provinces, Canada; Géographie physique et Quaternaire, v. 31, p. 247-260.
- Jones, I.W.
1934: Région de la rivière Dartmouth, péninsule de Gaspé; Rapport annuel du Service des Mines de Québec pour l'année 1934, partie D.
1939: Rapport géologique sur une partie de l'Est de Gaspé; Bureau des Mines du Québec, RP-130.
- LaSalle, P.
1983: Géologie des sédiments meubles de la région de New Richmond – New Carlisle; Ministère de l'Énergie et des Ressources, Québec, DP 83-29, 1 carte annotée.
- LaSalle, P. and David, P.P.
1984: Glacial erosion and transport in southern Gaspé, Québec; Geological Association of Canada, Program with Abstracts, v. 9, p. 82.
1986: Illinoian and younger diamicts of Eastern Gaspé Peninsula, Québec, Canada; Geological Society of America, Abstracts, v. 18, no. 1, p. 29.
- Lebuis, J.
1973a: Géologie du Quaternaire de la région de Cap-Chat, comtés de Gaspé-Nord, Matane et Matapédia; Ministère des Richesses naturelles, Québec, DP-145, 11 p.
1973b: Géologie du Quaternaire de la région de Matane-Amqui, comtés de Matane et Matapédia; Ministère des Richesses naturelles, Québec, DP-216, 18 p.
1975: Géologie du Quaternaire de la partie occidentale de la Gaspésie; Ministère des Richesses naturelles, DP-327, 32 cartes.
- Lebuis, J. et David, P.P.
1972: Région Courcellette-Tourelle, comtés de Gaspé-Nord et de Matane (géologie du Quaternaire); Ministère de l'Énergie et des Ressources, Québec, DP-63, 25 p.
1977: La stratigraphie et les événements du Quaternaire de la partie occidentale de la Gaspésie, Québec; Géographie physique et Quaternaire, vol. 31, p. 275-296.
- McGerrigle, H.W.
1950: La géologie de l'Est de Gaspé; Ministère des Richesses naturelles, Québec, RG-35, 168 p.
1952: Pleistocene glaciation of Gaspé Peninsula; Royal Society of Canada Transactions, vol. 46, series 3, p. 37-51.
- Morin, R. et Simard, M.
1985: Région de Sirois-Raudin; dans Rapport d'activités 1985, Ministère de l'Énergie et des Ressources, Québec, DV85-12, p. 17-18.
- Poole, W.H. et Rodgers, J.
1972: Appalachian geotectonic elements of the Atlantic provinces and southern Quebec; 24th International Geological Congress (Montreal), Guidebook A63-C63.

CANADA-NEWFOUNDLAND MINERAL DEVELOPMENT AGREEMENT 1884-89

ENTENTE DE MISE EN VALEUR DES MINÉRAUX CANADA-TERRE-NEUVE

- R.R. MILLER: Geology of the Strange Lake Alkalic Complex and the Associated Zr-Y-Nb-Be-REE Mineralization
- A.F. HOWSE: Marble Assessment – Insular Newfoundland
- J. TUACH: Metallogeny of Newfoundland Granites – Studies in the Western White Bay Area and on the Southwest Coast
- B.F. KEAN and D.T.W. EVANS: Metallogeny of the Tulks Hill Volcanics, Victoria Lake Group, Central Newfoundland
- D.T.W. EVANS and B.F. KEAN: Geology of the Jacks Pond Volcanogenic Sulfide Prospects, Victoria Lake Group, Central Newfoundland
- B. RYAN and D. LEE: Gneiss-Anorthosite-Granite Relationships in the Anaktalik Brook-Kogaluk River Area (NTS 14D/1, 8) Labrador
- A. KERR: Plutonic Rocks of the Eastern Central Mineral Belt, Labrador: General Geology and Description of Regional Granitoid Units
- C.F. GOWER, T. VAN NOSTRAND, G. McROBERTS, L. CRISBY, and S. PREVEC: Geology of the Sand Hill River – Batteau Map Region, Grenville Province, Eastern Labrador
- G.A.G. NUNN, R.F. EMSLIE, C.E. LEFEBVRE, N. NOEL, and S. WELLS: The Atikonak River Massif and Surrounding Area, Western Labrador and Quebec
- I. KNIGHT: Ordovician Sedimentary Strata of the Pistolet Bay and Hare Bay Area, Great Northern Peninsula, Newfoundland
- S.J. O'BRIEN, W.L. DICKSON, and R.F. BLACKWOOD: Geology of the Central Portion of the Hermitage Flexure Area, Newfoundland
- M. BATTERSON and P. LEGROW: Quaternary Exploration and Surficial Mapping in the Letitia Lake Area, Labrador

These reports were originally published in Current Research (1986), Mineral Resources Division, Newfoundland Department of Mines and Energy, Report 86-1 and are contributions to the Canada-Newfoundland Mineral Development Agreement 1984-1989. The projects were jointly funded by Newfoundland Department of Mines and Energy and Geological Survey of Canada.

Camera-ready copy of the abstracts was provided by Newfoundland Department of Mines and Energy.

GEOLOGY OF THE STRANGE LAKE ALKALIC COMPLEX AND THE ASSOCIATED Zr-Y-Nb-Be-REE MINERALIZATION

R. R. Miller
Mineral Deposits Section

ABSTRACT

The Strange Lake Alkalic Complex is located on the Quebec-Labrador border in northern Labrador. It contains substantial quantities of Zr, Y, Nb, Be and REE, which are concentrated in lenses and veins of fine grained and pegmatitic granite.

Petrographic and mapping studies have identified three major subdivisions of the riebeckite ± aegirine granite, based on the volume percent of exotic minerals (many of which are ore minerals). These subdivisions are: exotic-poor (<5 percent exotic minerals), exotic (5 to 10 percent exotic minerals) and exotic-rich (>10 percent exotic minerals). The spatial relationships between these subdivisions are illustrated in cross-section and plan views of the complex. Age relationships, as indicated by field evidence, indicate that the exotic mineral contents increase with decreasing age.

The comparative chemistry of the subdivisions reflect the exotic mineral contents, as most incompatible elements, including Zr, Be, Y, Nb, and Th, increase in concentration with differentiation; REE concentrations and patterns also follow this trend.

Mineralization at Strange Lake occurs in the most exotic mineral enriched phases, which are late stage and enriched in incompatible elements. Concentrations of many elements are economically interesting.

MARBLE ASSESSMENT - INSULAR NEWFOUNDLAND

A. F. Howse
Mineral Deposits Section

ABSTRACT

An assessment of Newfoundland's marble deposits was initiated in 1985. The project's aim is to determine the potential value of this marble for such industrial applications as fillers, whiteners and dimension stone.

Marble of potential commercial value occurs at a number of localities in western Newfoundland. At White Bay, deposits exist in the Cambro-Ordovician Coney Arm Group and in the Eocambrian White Bay Group. In the same area, a newly identified unit of marble and calc-silicate rocks occurs within the Precambrian terrane of the Long Range Mountains. White high-purity marble is found in the Ordovician St. George Group at several sites around Canada Bay on the Great Northern Peninsula. In and around Corner Brook, marble deposits are hosted by the St. George Group and Table Head Formation.

METALLOGENY OF NEWFOUNDLAND GRANITES - STUDIES IN THE WESTERN WHITE BAY AREA AND ON THE SOUTHWEST COAST

J. Tuach
Mineral Deposits Section

ABSTRACT

Gold prospects in the Silurian Sops Arm Group, White Bay area, are briefly described, and it is suggested that they may have formed in epithermal-fumarolic environments. In addition, potential exists for gold mineralization associated with carbonate-altered ultramafic rocks along lineaments. A fluorite occurrence is described from the Devils Room Granite.

Molybdenite and fluorite occurrences are briefly described in the Isle Aux Morts Brook and Strawberry granites, southwest coast of Newfoundland. Anomalous radioactivity is present in the Peter Snout and Rose Blanche east granites. The gold-bearing environments in the Cape Ray area are summarized, and additional potential for gold is noted in the Port Aux Basques Gneiss and in the Bay Du Nord Group.

METALLOGENY OF THE TULKS HILL VOLCANICS, VICTORIA LAKE GROUP, CENTRAL NEWFOUNDLAND

B.F. Kean and D.T.W. Evans
Mineral Deposits Section

ABSTRACT

The Tulks Hill volcanics are host to pyritic volcanogenic sulfides and are part of a thick sequence of volcanic and volcanoclastic rocks of the Victoria Lake Group. The group was deposited during the development of an early to middle Ordovician island arc. The volcanic rocks occur within two principal volcanic units, informally termed the Tulks Hill and Tally Pond volcanics. The volcanic rocks consist of intercalated mafic and felsic rocks that are predominantly pyroclastic; mafic pillow lava is more common in the Tally Pond volcanics than in the Tulks Hill volcanics. The felsic volcanic rocks occur as laterally extensive sheets of crystal and crystal-lithic tuff, breccia and minor flows. Sedimentary rocks consist of sandstone, siltstone, shale, argillite, chert and minor interbedded conglomerate. The clastic sedimentary rocks appear to be derived from the adjacent and underlying volcanic rocks of the Victoria Lake Group.

There are six principal volcanogenic sulfide occurrences in the Victoria Lake Group, four in the Tulks Hill volcanics and two in the Tally Pond volcanics. The Tally Pond (Boundary) deposit and Burnt Pond prospect are both massive sulfides in the Tally Pond volcanics. The Tulks Hill, Tulks East and Victoria deposits are both stratiform, pyritic, Zn-Pb-Cu, massive sulfides in the Tulks Hill volcanics. The Jacks Pond deposit also occurs in the Tulks Hill volcanics, but aside from a zone of transported clastic sulfides, it mostly appears to be a stockwork zone. The mineralization is hosted by felsic crystal tuff, lapilli tuff and breccia, and are enveloped by an alteration halo characterized by silicification, sericitization and chloritization. Disseminated and stringer sulfides are also well developed in this halo.

GEOLOGY OF THE JACKS POND VOLCANOGENIC SULFIDE PROSPECTS, VICTORIA LAKE GROUP, CENTRAL NEWFOUNDLAND

D. T. W. Evans
Department of Earth Sciences
Memorial University of Newfoundland
and
B. F. Kean
Mineral Deposits Section

ABSTRACT

The Jacks Pond prospects occur in the felsic volcanic rocks of the Tulks Hill volcanics, Victoria Lake Group. The Tulks Hill volcanics consist predominantly of linear belts of felsic pyroclastics and minor mafic volcanic rocks that are intercalated with mafic to felsic, fine grained, volcanoclastic rocks. The host rocks to the mineralization are variably altered, fine grained, felsic, lapilli tuff, vitric tuff and crystal-vitric tuff.

The Jacks Pond prospects consist of four pyritic, volcanogenic sulfides with low base-metal values. The mineralization occurs mainly as disseminated and stringer sulfides in an alteration stockwork containing minor, exhalative sulfides that exhibit detrital textures. Chloritization, sericitization and silicification are characteristic alteration types.

GNEISS-ANORTHOSITE-GRANITE RELATIONSHIPS IN THE ANAKTALIK BROOK-KOGALUK RIVER AREA (NTS 14D/1, 8), LABRADOR

B. Ryan and D. Lee
Labrador Mapping Section

ABSTRACT

Granulite and amphibolite facies gneisses of the Archean Nain Province and the Early Proterozoic Churchill Province are intruded by Middle-Proterozoic plutons of gabbroid, intermediate and granitoid compositions. Contact aureoles are variably developed, the most widely recognized transformation being a pyroxene hornfels assemblage developed in a Churchill Province, granulite facies, garnetiferous gneiss south and east of Makhavinekh Lake. Gabbroic rocks occur as isolated rafts in younger rocks in the Kogaluk River area, but constitute a large coherent body in the northern half of the project area. Intermediate plutons form irregular intrusive bodies in anorthosite north of Trout Pond, but constitute a flat-lying sheet south of Makhavinekh Lake. Rapakivi granite forms an ovoidal, steep-walled, flat-topped pluton between Makhavinekh Lake and Anaktalik Brook. Field relationships suggest co-existence of gabbroid, intermediate and granitoid compositions. Minerals of economic importance are limited to isolated small occurrences of labradorite in the gabbroids, and graphitic and pyritic gossan zones in the metasedimentary rocks.

PLUTONIC ROCKS OF THE EASTERN CENTRAL MINERAL BELT, LABRADOR: GENERAL GEOLOGY AND DESCRIPTION OF REGIONAL GRANITOID UNITS

Andrew Kerr
Labrador Mapping Section

ABSTRACT

This preliminary report outlines results from a three-year project initiated in late 1984 to assess the potential of granitoid rocks in the eastern Central Mineral Belt for granophile mineralization, and gather information on the major early to middle Proterozoic batholiths of which they form a part.

Granitoid rocks in the area fall into two major groups. An earlier group (Makkovikian granitoids) consists of foliated to gneissic rocks emplaced c.1.85 Ga, contemporaneous with a major period of deformation and metamorphism. These contrast with a younger group of posttectonic intrusions that form the c.1.65 Ga Trans-Labrador batholith, which is generally undeformed or only weakly foliated over much of the study area. Although it includes layered gabbros, monzonites and syenites, the Trans-Labrador batholith is dominated mostly by granites and alkali-feldspar granites. The northern margin of the batholith in this area includes a number of small, leucocratic granite bodies whose outcrop patterns suggest that their upper surfaces are cut by the present erosion surface. Some of these bodies host Mo-Cu mineralization, and others appear to be spatially associated with hydrothermal veins containing Mo and base metal sulfides.

GEOLOGY OF THE SAND HILL RIVER - BATTEAU MAP REGION, GRENVILLE PROVINCE, EASTERN LABRADOR

Charles F. Gower, Timothy Van Nostrand, Gordon McRoberts,
Loretta Crisby and Stephen Prevec
Labrador Mapping Section

ABSTRACT

The Sand Hill River - Batteau map region is subdivided into six structural-lithological entities, namely the 1) Domino domain, 2) Earl Island domain, 3) Paradise metasedimentary gneiss belt, 4) Sand Hill Big Pond gabbro-norite, 5) Paradise Arm pluton, and 6) the White Bear Arm complex. The Domino and Earl Island domains consist of granitoid plutonic rocks and orthogneiss, together with layered mafic intrusions and rare metasedimentary gneiss. The Paradise metasedimentary gneiss belt comprises cordierite-garnet-sillimanite-kyanite pelitic gneiss with minor quartzite, psammitic gneiss, calc-silicate rocks and amphibolite. Sapphirine and orthopyroxene are present in metasedimentary gneiss adjacent to the Sand Hill Big Pond gabbro-norite. The Sand Hill Big Pond gabbro-norite and White Bear Arm complex are both composed of anorthosite, norite, gabbro and monzonite, and are interpreted as having been contiguous prior to the emplacement of the linear Paradise Arm pluton. Other rocks mapped include pre-Grenvillian mafic dikes of various ages, and late Precambrian - early Paleozoic north-northeast-trending mafic dikes.

Regional structures have a consistent west-northwest trend and are associated with tight folds and major strike-slip faults. A north-directed thrust was mapped in the northeast part of the area. Many prominent photolineaments are interpreted to be related to post-Grenvillian faulting and dike emplacement.

The best prospects for economic mineralization are sulfide-rich zones and muscovite-rich pegmatite in the Paradise metasedimentary gneiss belt.

THE ATIKONAK RIVER MASSIF AND SURROUNDING AREA, WESTERN LABRADOR AND QUÉBEC

Nunn G.A.G., Emslie R.F., Lefebvre C.E.,
Noel N. and Wells S.
Labrador Mapping Section
and
Geological Survey of Canada

ABSTRACT

The Atikonak River massif is a suite of troctolitic, noritic and anorthositic rocks in southwestern Labrador. Spatially related pyroxene quartz monzonite and rapakivi-textured quartz syenite to granite occur with the anorthositic rocks in an association that is common to anorthositic suites elsewhere in Labrador. Areas of paragneiss and K-feldspar porphyritic granite also occur in and around the massif.

Magmatic structures and textures are well preserved in the Atikonak River massif and clearly demonstrate that intrusion of the basic magmas was not accomplished as highly crystalline mushes. Widespread development of mineralogical layering, including graded and cross-bedded varieties, attests to the presence of substantial amounts of liquid at the time of intrusion. Evidence of sub-solidus reaction between olivine and plagioclase is common in crystal cumulates in the massif. At present it is unclear to what extent such reactions took place during cooling of the massif from magmatic temperatures, or are the result of later regional metamorphism.

The massif is rimmed on the northwest side by monzonitic and rapakivi-textured rocks, which are in turn adjacent to paragneiss that is intruded by gabbro-noritic and granitoid plutonic rocks. On the southeast side, the anorthositic rocks thermally affect part of a gabbro-norite body. In the southeast of the map area, the anorthositic rocks and the amphibolite equivalents of the gabbro-norite are intruded by a suite of predominantly equigranular or K-feldspar megacrystic granitoid rocks.

ORDOVICIAN SEDIMENTARY STRATA OF THE PISTOLET BAY AND HARE BAY AREA, GREAT NORTHERN PENINSULA, NEWFOUNDLAND

Ian Knight
Newfoundland Mapping Section

ABSTRACT

Autochthonous Ordovician carbonate and siliciclastic rocks occur between Cambrian dolostones in the west and allochthonous sedimentary rocks of the Northwest Arm Formation in the eastern part of the map area. The Lower Ordovician St. George Group comprises four formations, the Watts Bight, Boat Harbour, Catoche and Aguathuna formations. Four lithologic members are delineated in the Catoche Formation within undolomitized parautochthonous strata. The members, in ascending order, are: 1) lower burrowed limestone, 2) middle mound, 3) upper burrowed limestone, and 4) white limestone. The Aguathuna Formation, which is mapped in this area for the first time, is thin and appears to rest disconformably upon the Catoche Formation. The Table Head Group comprises only the Table Point, Black Cove and Cape Cormorant formations. Fenestral limestones form an important member at the base of the Table Point Formation.

A number of erosional disconformities occur near the top of the St. George Group and the base of the Table Head Group. Growth faults breached the platform during the late Arenig, coinciding with regression on the platform and later early Llanvirn transgression. Shale-filled fissures, erosion and cementation at the top of the Table Point limestone, and abundance of Table Head-derived limestone breccias and possible olistoliths, suggest the area preserves the complex final stages of the Ordovician platform. The carbonates were succeeded by Middle Ordovician flysch, which flooded southwestward into the area.

Deformation began with the emplacement of Lower Ordovician mélangé (Northwest Arm Formation) over the flysch basin and westward thrusting of parautochthonous limestones. This was followed by a later phase of compression in which a penetrative cleavage, westward-verging thrusts, northeast-trending, upright to overturned folds, and overthrusting, deformed the eastern half of the carbonate terrane, the flysch basin and the overlying mélangé. The carbonate terrane was later extensively block faulted by northeast-, northwest- and west-trending high-angle faults.

Widespread sphalerite mineralization occurs in the Boat Harbour and Catoche formations within matrix breccias and secondary dolostones. Formation of cavern breccias and widespread dolomitization may have been partly controlled by the growth faulting that dissected the platform during late Arenig regression and karstification.

GEOLOGY OF THE CENTRAL PORTION OF THE HERMITAGE FLEXURE AREA, NEWFOUNDLAND

S.J. O'Brien, W.L. Dickson, and R.F. Blackwood
Newfoundland Mapping Section

ABSTRACT

The oldest known rocks in the region are pre-Middle Ordovician mafic meta-igneous complexes, representing vestiges of either the crust of an ocean basin or the roots of a remnant arc. These rocks form the substrate to a thick succession of silicic volcanic and sedimentary rocks, most of which are of Middle Ordovician age. During the Silurian, the Hermitage Flexure area was affected by a tectono-thermal event, marked by large scale recumbent folding and greenschist to amphibolite facies metamorphism and migmatization. Major synkinematic, multiphase batholiths, containing significant proportions of hornblende-biotite tonalite and granodiorite, were intruded at this time. The granitoids are essentially deformed throughout, and are affected by major D₁ mylonite zones. Thermal relaxation of thickened crust resulted in the production of post D₁, syn D₂ muscovite-bearing granites, possibly by progressive partial melting of peraluminous parental material. The area is host to a variety of mineral occurrences, including volcanogenic base metals and uranium, and granite-hosted uranium, molybdenum, tin and tungsten. The potential for epithermal-fumerolic gold mineralization in the volcanic and comagmatic intrusive rocks is high.

QUATERNARY EXPLORATION AND SURFICIAL MAPPING IN THE LETITIA LAKE AREA, LABRADOR

Martin Batterson and Paul LeGrow
Quaternary Geology Section

ABSTRACT

Investigations in the Letitia Lake area focused on 1:50,000 scale terrain mapping of the northern half of 13L/1 and the southern portion of 13L/8 and detailed Quaternary exploration around Two-Tom Lake. Terrain mapping focused on ground verifying an air photograph interpretation; till sampling and locating ice flow indicators. Evidence of three flows was found, all probably related to the Late Wisconsin, with the latest flow being generally west to east (072-080). Detailed studies followed up a previously reported radiometric anomaly that was confirmed by an airborne scintillometer survey. A ground program, consisting of bedrock and boulder mapping, identified two distinct, mineralized, syenite-gneiss, boulder trains and several areas of previously unmapped mineralized bedrock. In addition, a ground scintillometer survey was used to enhance the airborne survey, and a biogeochemical program was initiated with the aim of defining dispersal patterns.

ERRATA

Geological Survey of Canada, Paper 86-1A

Current Research, Part A

- Report 28:** Submersible observations and origin of an iceberg pit on the Grand Banks of Newfoundland: J.V. Barrie, W.T. Collins, J.I. Clark, C.F.M. Lewis, and D.R. Parrott.
- p. 255: The scale bar in Figure 28.4 should represent 100 m, not 50 m.
 - p. 257: Insert "The result of this loading has been observed to be primarily a bearing capacity failure under an inclined load" between the fifth and sixth sentences of the second paragraph.
- Report 65:** Notes on the Proterozoic Thule Group, northern Baffin Island: G.D. Jackson.
- p. 542: In Figure 65.1, west and southwest of Dundas, the Thule Group pattern should be present on the larger island, north of the fault on the smaller island and by the shore of the smaller island, just north of the same fault.
 - p. 543: In the left column, third line from the bottom, "Cadogan Glacier" should read "Kissel Gletscher".
 - p. 549: The first line after the heading "Dundas Formation" should read "Seen only briefly at Dundas Mountain near Dundas,...".
 - p. 551: In the right column, twelfth line from the top, "Wolstenholme" should read "Northumberland".

Author Index/Index des auteurs

	Page		Page
Al-Aasm, I.S.	201	Hall, D.J.	567
Ames, D.E.	213	Hall, G.E.M.	767
Armstrong, R.L.	685	Hamilton, T.S.	707, 741
Arthur, A.J.	715	Hanmer, S.	775, 811
Ashton, K.E.	305	Hattori, K.	77
Banerjee, I.	383	Heah, T.S.T.	685
Barham, B.A.	827	Helmstaedt, H.	457
Barr, S.M.	179	Henderson, C.M.	411
Barrie, J.V.	849	Hicks, K.	77
Bédard, P.	319	Hillaire-Marcel, C.	11
Beke, G.J.	289	Himmler, I.	85
Bell, R.T.	585	Hughes, J.D.	507
Blake, W., Jr.	239	Hughes, M.D.	85, 417
Blakeney, C.	605, 617	Hunter, J.A.	707
Bolton, T.E.	97, 107	Jackson, L.E., Jr.	257
Bornhold, B.D.	201	Jackson, S.L.	539
Bouchard, M.A.	295	Jamieson, R.A.	1, 179, 191, 557
Brisbin, W.C.	213	Jeletzky, J.A.	351
Cameron, A.R.	665	Jennings, A.	605, 617
Cause, C.	11	Jerzykiewicz, T.	421, 653
Cheel, R.J.	637	Johnston, H.P.	157
Clague, J.J.	707	Jones, R.	567
Clark, P.U.	171	Josenhans, H.W.	171
Clifford, P.M.	147	Kaszycki, C.A.	245
Cloutier, M.	869	Klassen, R.A.	617
Connelly, J.N.	811	Lamothe, M.	279
Connors, K.A.	557	Lau, S.	213
Copeland, M.J.	399	Leckie, D.A.	429, 637
Corbeil, P.	869	Leger, A.	111
Currie, K.L.	157	Lichti-Federovich, S.	263
Dahl, R.	757	Loncarevic, B.D.	85
David, J.	131	Luternauer, J.L.	707, 849
David, P.P.	319	MacLean, B.	605, 617
Davidson, A.	837	MacNeill, D.J.	417
Davies, E.H.	519	Mahony, H.	73
Davies, G.R.	467	Mamet, B.L.	467
DiLabio, R.N.W.	245	Marcotte, C.	295
Dixon, J.	375	Mason, R.	567, 577
Dixon, J.M.	457	Matthews, J.V., Jr.	289
Duk-Rodkin, A.	257	Maurice, Y.T.	785
Edmunds, C.F.	567	McCready, R.G.L.	73
Embry, A.F.	329, 341	McIntyre, D.J.	405
Erdmer, P.	19, 29	McLean, R.A.	443
Evenchick, C.A.	733	McMullin, D.W.A.	727
Fader, G.B.J.	591	Melnik, N.	567, 577
Fahrig, W.F.	65	Mihalynuk, M.G.	721
Foscolos, A.E.	429	Miller, A.R.	679
Froese, E.	827	Miller, R.O.	591
Fueten, F.	797	Monger, J.W.H.	699
Gagnon, Y.D.	1	Moreton, C.	57
Gandhi, S.S.	47, 853	Morgan, P.	859
Gariepy, C.	131	Mortensen, J.K.	141
Ghent, E.D.	693, 721	Mott, J.A.	457
Gibling, M.R.	73	Mott, R.J.	289
Goodarzi, F.	421, 671	Mountain, B.	567
Gordon, T.M.	539	Nassichuk, W.W.	411, 467
Grant, D.R.	289	Neimanis, V.P.	507
Grant, S.M.	837	Nobes, D.C.	741
Green, S.B.	47	Norris, D.K.	665
Greenwood, H.J.	727		
Gregoire, D.C.	39		

O'Beirne-Ryan, A.M.	179, 191
O'Brien, J.	749
Osadetz, K.G.	647
Owen, J.V.	29
Park, C.J.	767
Pedder, A.E.H.	471
Pickering, M.E.	797
Plint, H.E.	557
Poulsen, K.H.	213
Poulton, T.P.	519
Pratt, K.C.	665
Pullan, S.E.	707
Rappol, M.	223
Ravenhurst, C.E.	547
Reynolds, P.H.	547
Ricketts, B.D.	363, 405
Roberts, M.C.	707
Robin, P.-Y.F.	797
Rodkin, O.	257
Roscoe, S.M.	47, 679
Samson, I.M.	865
Sanford, B.V.	617
Sartenaer, P.	489

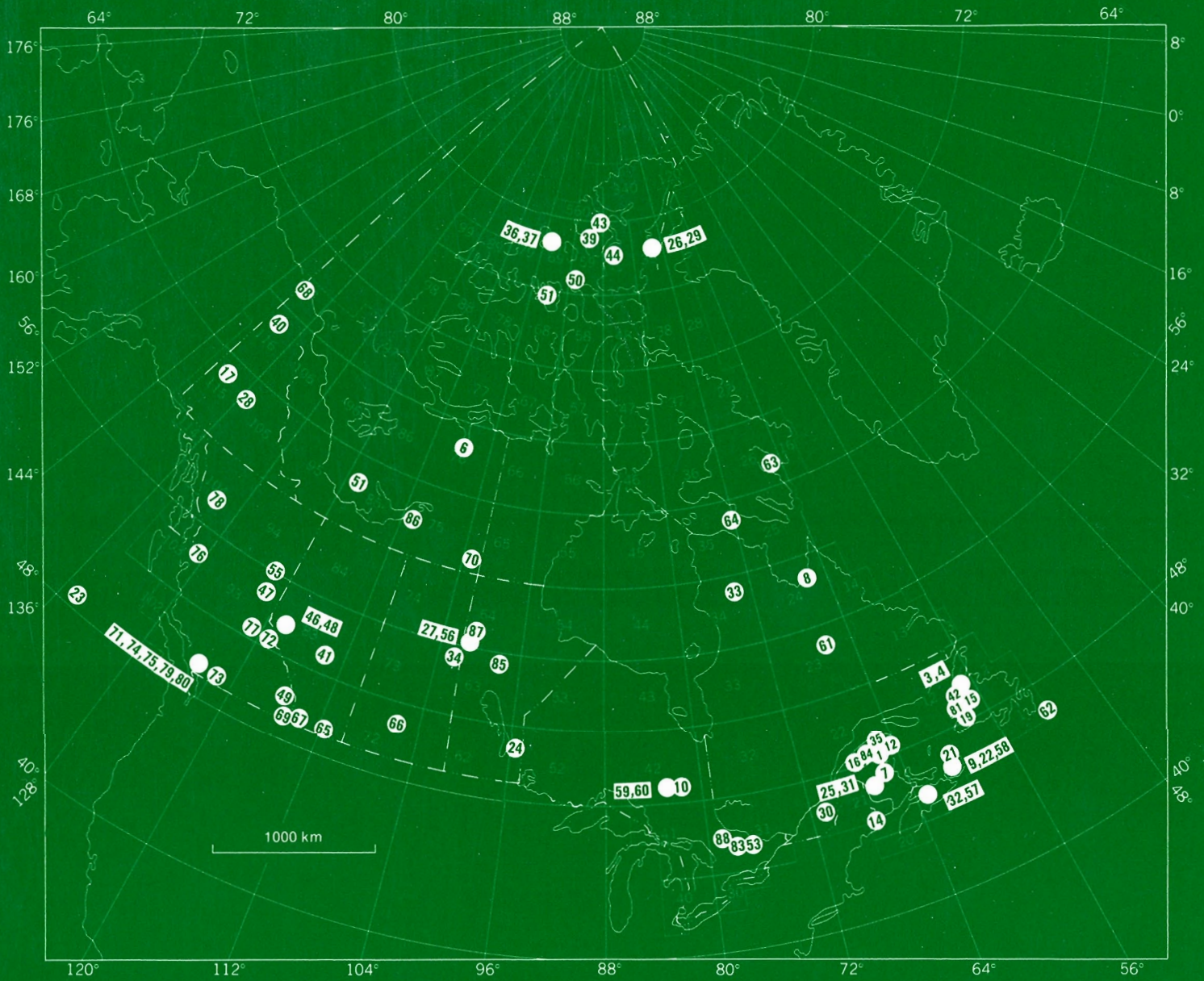
Sevigny, J.H.	693
Shilts, W.W.	271
Smith, S.L.	271
Snowdon, L.R.	647
Steele-Petrovich, H.M.	493
Sweet, A.R.	653
Thorpe, R.I.	585
van Berkel, J.T.	157
van Bosse, J.Y.	865
van Breemen, O.	775
Watkinson, D.H.	757
Watson, P.	417
Whalen, J.B.	121
Wheatley, K.J.	305
William-Jones, A.E.	865
Williams, G.L.	605, 617
Williams, P.F.	57, 111
Woodsworth, G.J.	685
Zentilli, M.	73, 547

NOTE TO CONTRIBUTORS

Submissions to the *Discussion* section of *Current Research* are welcome from both the staff of the Geological Survey and from the public. Discussions are limited to 6 double-spaced typewritten pages (about 1500 words) and are subject to review by the Chief Scientific Editor. Discussions are restricted to the scientific content of Geological Survey reports. General discussions concerning branch or government policy will not be accepted. Illustrations will be accepted only if, in the opinion of the editor, they are considered essential. In any case no redrafting will be undertaken and reproducible copy must accompany the original submissions. Discussion is limited to recent reports (not more than 2 years old) and may be in either English or French. Every effort is made to include both *Discussion* and *Reply* in the same issue. *Current Research* is published in January and July. Submissions should be sent to the Chief Scientific Editor, Geological Survey of Canada, 601 Booth Street, Ottawa, Canada, K1A 0E8.

AVIS AUX AUTEURS D'ARTICLES

Nous encourageons tant le personnel de la Commission géologique que le grand public à nous faire parvenir des articles destinés à la section *discussion* de la publication *Recherches en cours*. Le texte doit comprendre au plus six pages dactylographiées à double interligne (environ 1500 mots), texte qui peut faire l'objet d'un réexamen par le rédacteur en chef scientifique. Les discussions doivent se limiter au contenu scientifique des rapports de la Commission géologique. Les discussions générales sur la Direction ou les politiques gouvernementales ne seront pas acceptées. Les illustrations ne seront acceptées que dans la mesure où, selon l'opinion du rédacteur, elles seront considérées comme essentielles. Aucune retouche ne sera faite aux textes et dans tous les cas, une copie qui puisse être reproduite doit accompagner les textes originaux. Les discussions en français ou en anglais doivent se limiter aux rapports récents (au plus de 2 ans). On s'efforcera de faire coïncider les articles destinés aux rubriques *discussions* et *reponses* dans le même numéro. La publication *Recherches en cours* paraît en janvier et en juillet. Les articles doivent être renvoyés au rédacteur en chef scientifique: Commission géologique du Canada, 601, rue Booth, Ottawa, Canada, K1A 0E8.



Energy, Mines and
Resources Canada

Energie, Mines et
Ressources Canada